FUNDAMENTALS OF BIOCHEMISTRY II - BIOENERGETICS AND METABOLISM



Henry Jakubowski
College of St. Benedict/St. John's University

LibreTexts™

College of St. Benedict/St. John's University

Fundamentals of Biochemistry II - Bioenergetics and Metabolism

Henry Jakubowski

This text is disseminated via the Open Education Resource (OER) LibreTexts Project (https://LibreTexts.org) and like the thousands of other texts available within this powerful platform, it is freely available for reading, printing, and "consuming."

The LibreTexts mission is to bring together students, faculty, and scholars in a collaborative effort to provide an accessible, and comprehensive platform that empowers our community to develop, curate, adapt, and adopt openly licensed resources and technologies; through these efforts we can reduce the financial burden born from traditional educational resource costs, ensuring education is more accessible for students and communities worldwide.

Most, but not all, pages in the library have licenses that may allow individuals to make changes, save, and print this book. Carefully consult the applicable license(s) before pursuing such effects. Instructors can adopt existing LibreTexts texts or Remix them to quickly build course-specific resources to meet the needs of their students. Unlike traditional textbooks, LibreTexts' web based origins allow powerful integration of advanced features and new technologies to support learning.



LibreTexts is the adaptable, user-friendly non-profit open education resource platform that educators trust for creating, customizing, and sharing accessible, interactive textbooks, adaptive homework, and ancillary materials. We collaborate with individuals and organizations to champion open education initiatives, support institutional publishing programs, drive curriculum development projects, and more.

The LibreTexts libraries are Powered by NICE CXone Expert and was supported by the Department of Education Open Textbook Pilot Project, the California Education Learning Lab, the UC Davis Office of the Provost, the UC Davis Library, the California State University Affordable Learning Solutions Program, and Merlot. This material is based upon work supported by the National Science Foundation under Grant No. 1246120, 1525057, and 1413739.

Any opinions, findings, and conclusions or recommendations expressed in this material are those of the author(s) and do not necessarily reflect the views of the National Science Foundation nor the US Department of Education.

Have questions or comments? For information about adoptions or adaptions contact info@LibreTexts.org or visit our main website at https://LibreTexts.org.

This text was compiled on 04/20/2026

TABLE OF CONTENTS

Licensing

About the Authors

12: Bioenergetics and Biochemical Reaction Types

- 12.1: Biochemical Reactions and Energy Changes
- 12.2: Phosphoryl Group Transfers and ATP
- 12.3: The Chemistry and Biochemistry of Dioxygen
- 12.4: Biological Oxidation-Reduction Reactions

13: Glycolysis, Gluconeogenesis, and the Pentose Phosphate Pathway

- 13.1: Glycolysis
- 13.2: Fates of Pyruvate under Anaerobic Conditions- Fermentation
- 13.3: Gluconeogenesis
- 13.4: Pentose Phosphate Pathway of Glucose Oxidation

14: Principles of Metabolic Regulation

- 14.1: Regulation of Metabolic Pathways
- 14.2: Basic Principles of Metabolic Control Analysis (MCA)
- 14.3: The Flux Control Coefficient
- 14.4: Concentration Control and Elasticity Coefficients
- 14.5: Metabolism and Signaling: The Steady State, Adaptation and Homeostasis

15: Glucose, Glycogen, and Their Metabolic Regulation

- 15.1: Insulin Signaling in the Liver
- 15.2: Glycogenesis
- 15.3: Glycogenolysis and its Regulation by Glucagon and Epinephrine Signaling
- 15.4: Regulation of Glycolysis
- 15.5: Regulation of Gluconeogenesis

16: The Citric Acid Cycle

- 16.1: Production of Acetyl-CoA (Activated Acetate)
- 16.2: Reactions of the Citric Acid Cycle
- 16.3: Regulation of the Citric Acid Cycle
- 16.4: Variants of the Citric Acid Cycle

17: Fatty Acid Catabolism

- 17.1: Digestion, Mobilization, and Transport of Fats
- 17.2: Oxidation of Fatty Acids
- 17.3: Ketone Bodies

18: Nitrogen - Amino Acid Catabolism

- 18.1: The Biochemistry of Nitrogen in the Biosphere
- 18.2: Metabolic Fates of Amino Groups
- 18.3: Nitrogen Excretion and the Urea Cycle
- 18.4: An Overview of Amino Acid Metabolism and the Role of Cofactors
- 18.5: Pathways of Amino Acid Degradation

19: Oxidative Phosphorylation

- 19.1: Electron-Transfer Reactions in Mitochondria
- 19.2: ATP Synthesis
- 19.3: Regulation of Oxidative Phosphorylation

20: Photosynthesis and Carbohydrate Synthesis in Plants

- 20.1: Light Absorption in Photosynthesis - An Overview
- 20.2: The Kok Cycle and Oxygen Evolving Complex of Photosystem II
- 20.3: Plant Electron Transport and ATP Synthesis
- 20.4: CO_2 uptake - Calvin Cycle and C3 organisms
- 20.5: CO2 uptake - C4 and CAM Pathways
- 20.6: Biosynthesis of Starch, Sucrose and Cellulose

21: Lipid Biosynthesis

- 21.1: Biosynthesis of Fatty Acids and Eicosanoids
- 21.2: Biosynthesis of Triacylglycerols
- 21.3: Biosynthesis of Membrane Glycerolipids
- 21.4: Biosynthesis of Membrane Sphingolipids
- 21.5: Biosynthesis of Cholesterol and Steroids
- 21.6: Biosynthesis and Metabolism of Isoprenoids

22: Biosynthesis of Amino Acids, Nucleotides, and Related Molecules

- 22.1: Overview of Nitrogen Metabolism - Nitrogenase
- 22.2: Biosynthesis of Amino Acids
- 22.3: Molecules Derived from Amino Acids
- 22.4: Biosynthesis and Degradation of Nucleotides

Index

Glossary

Detailed Licensing

Licensing

*A detailed breakdown of this resource's licensing can be found in **Back Matter/Detailed Licensing**.*

About the Authors

Henry Jakubowski

Dr. Henry Jakubowski is a Professor Emeritus of Chemistry at the College of Saint Benedict/Saint John's University (CSB/SJU) in Minnesota, where he taught for 32 years. Before that, he was a post-doctoral fellow at the Mayo Clinic, where he focused on biophysical techniques to explore protein function. His main expertise in biochemistry is in protein structure/function and enzyme kinetics. His research interests focused on the development and characterization of inhibitors for low molecular weight protein tyrosine phosphatase. While at CSB/SJU, he was active in major curricular reform. It involved replacing all introductory courses in the chemistry curriculum with classes focusing on structure/function relationships that integrated organic, inorganic, and biochemistry content. In addition, he designed novel in-depth chemistry classes in signal transduction and computational biochemistry. He was also actively involved in study abroad, and created a unique research exchange program with Southwest University in China, where he is a visiting Professor of Chemistry. For the last six years, he has become a climate activist and has given many talks and presentations to lay and academic groups. His current efforts focus on introducing climate change into the biochemistry curriculum.

Patricia Flatt

Dr. Patricia Flatt is a Professor of Chemistry at Western Oregon University. She holds a PhD in Biochemistry from Vanderbilt University where her research focused on the response of the p53 signaling pathways to DNA damage. Her current research interests include natural product biosynthesis in microorganisms and their evolutionary origins. She is a strong advocate for the advancement of women and underrepresented minorities pursuing careers in STEM. At WOU, she has served as the PI on a collaborative grant with Oregon State University to develop a STEM Scholars Center for Diversity and Excellence at WOU for the advancement of women and underrepresented minority students pursuing STEM degree paths. She is also serving as a Co-PI on an NSF ADVANCE grant supporting mid career women faculty in STEM, entitled 'ASCEND: Advancing STEM Careers by Empowering Network Development'. She believes that the creation of open education resources (OERs) can help to reduce the barriers to education and improve educational outcomes for underserved populations, as well as promote collaboration and sharing among educators to develop more effective and innovative teaching materials.

CHAPTER OVERVIEW

12: BIOENERGETICS AND BIOCHEMICAL REACTION TYPES

Return to Fundamentals of Biochemistry Search Fundamentals of Biochemistry

12.1: Biochemical Reactions and Energy Changes
12.2: Phosphoryl Group Transfers and ATP
12.3: The Chemistry and Biochemistry of Dioxygen
12.4: Biological Oxidation-Reduction Reactions

This page titled 12: Bioenergetics and Biochemical Reaction Types is shared under a not declared license and was authored, remixed, and/or curated by Henry Jakubowski and Patricia Flatt.

12.1: BIOCHEMICAL REACTIONS AND ENERGY CHANGES

LEARNING GOALS (CHATGPT O3-MINI)

1. **Explain Key Reaction Mechanisms:**
   - Describe the three primary ways to break a C–X bond (leading to carbocations, carbanions, or free radicals) and explain why these intermediates are high in energy.
2. **Interpret Free Energy Diagrams:**
   - Compare free energy profiles for uncatalyzed versus enzyme-catalyzed reactions.
   - Explain how enzymes lower the activation energy without changing the free energies of reactants or products.
3. **Analyze Transition States and Intermediates:**
   - Discuss the relationship between the structure of transition states and the intermediates formed during bond breaking.
   - Relate changes in Gibbs free energy (ΔG) to reaction kinetics and thermodynamics.
4. **Assess Structural Influences on Reactivity:**
   - Evaluate how resonance and inductive effects stabilize reactants, intermediates, and products.
   - Compare the thermodynamic driving forces for reactions based on the relative stability of similar molecules.
5. **Determine Oxidation States and Oxidation Levels:**
   - Apply the rules for calculating oxidation numbers to assess the oxidation of carbon atoms in organic molecules.
   - Use changes in oxidation state to identify and predict oxidation reactions in metabolic pathways.
6. **Describe Nucleophilic Addition Reactions:**
   - Outline the mechanisms by which water, alcohols, and amines add to carbonyl groups, leading to diols, hemiacetals, acetals, and Schiff bases.
   - Understand how acid and base catalysts influence these reactions.
7. **Examine Reactivity of Carboxylic Acid Derivatives:**
   - Compare the relative reactivity of carboxylic acid derivatives (amides, esters, anhydrides, acid chlorides) based on resonance stabilization and leaving group stability.
   - Predict how bond strengths and product stability affect nucleophilic substitution reactions.
8. **Understand C–C Bond Formation Mechanisms:**
   - Describe how aldol and Claisen condensations use enolate intermediates to form new C–C bonds.
   - Explain the roles of electrophiles (e.g., carbonyl carbons) and nucleophiles (e.g., carbanions) in these reactions.
9. **Explore C–C Bond Cleavage Reactions:**
   - Detail the mechanisms of retroaldol reactions and decarboxylation (especially in beta-keto acids), emphasizing the importance of electron sinks.
10. **Integrate Reaction Mechanisms with Metabolic Contexts:**
    - Connect these basic organic and thermodynamic principles to their roles in bioenergetics and metabolic pathways.
    - Prepare to apply these concepts in the more comprehensive studies of reaction mechanisms in Unit 2: Bioenergetics and Metabolism.

These goals are designed to build a strong foundation in both the mechanistic details and the thermodynamic principles that underlie enzyme function and metabolic reactions.

12.1.1: INTRODUCTION

We have already discussed How Enzymes Work and Enzymatic Reaction Mechanisms in great detail in Chapter 6. Here, we will focus on a lighter, less granular review of some key reaction mechanisms and the changes in Gibbs' free energy associated with them, both in an uncatalyzed and enzyme-catalyzed reaction. Consider it a simple review of basic organic reactions and thermodynamics in preparation for the comprehensive focus on reaction mechanisms in Unit 2: Bioenergetics and Metabolism.

12.1.2: BREAKING C-X BONDS

Organic reactions involve making and breaking bonds to carbon. There are three ways to break a bond to a C-X bond, producing either a carbocation, carbanion, or free radical intermediate, all unstable and reactive, as illustrated in Figure **12.1.1**. Both the carbocation and free radical are electron-deficient, and the carbanion, although not electron-deficient, has a negative charge on C, an atom with a relatively low electronegativity.

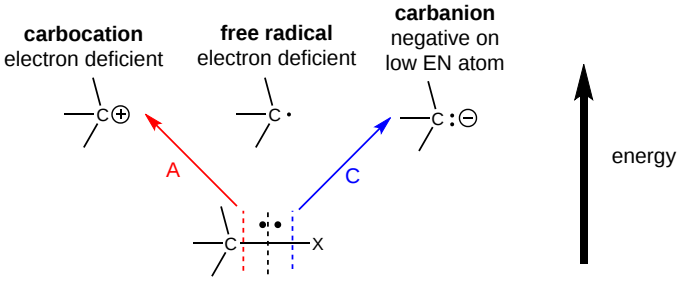


Figure **12.1.1**: Ways to break a C-X bond

These unstable intermediates are higher in energy than the reactants. Hence, the transition state, which is even higher in energy than the intermediates, must have a structure that resembles the intermediates more than the reactants, as shown in Figure **12.1.2**. The charged carbanion and carbocation intermediates have a developing charge in the transition state.

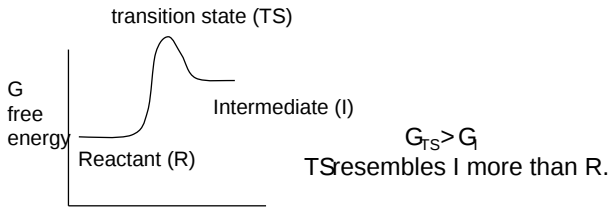


Figure **12.1.2**: Gibbs' free energy of reactants, transition state, and intermediate in breaking a bond.

The thermodynamics of the reactions is determined by the change in free energy between the intermediates and the reactants. In contrast, the kinetics of the reaction is determined by the difference in free energy between the transition states and the reactants, as shown in Figure **12.1.3**. A catalyst lowers the energy of the transition state without affecting the energies of the reactants or intermediates (assuming that these are free and not bound to the catalyst.

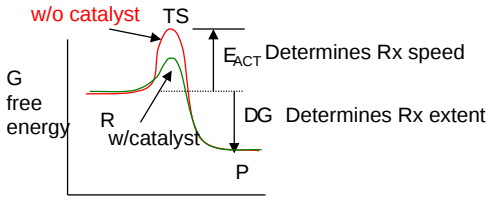


Figure **12.1.3**: Activation energy and ΔG for a simple uncatalyzed and catalyzed reaction

The free energy diagram shown in Figure 3 is very simplistic. We need a diagram that better fits an enzyme-catalyzed reaction using the simple reaction equation below.

$$E + S \leftrightarrow ES \rightarrow EP \leftrightarrow E + P$$

A free energy diagram for the binding of E and S followed by the conversion of bound S to bound and then the free product is shown in Figure **12.1.4**.

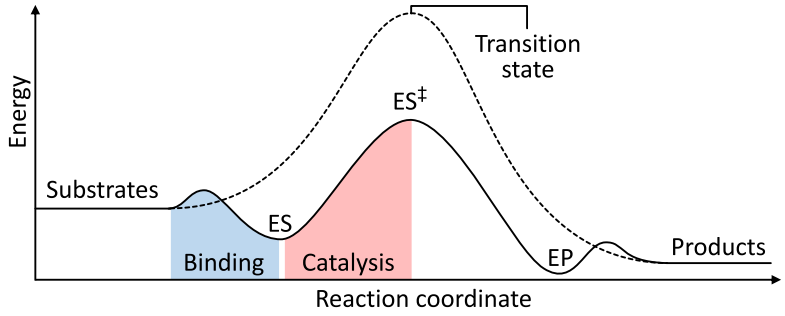


Figure **12.1.4**: Simple free energy curve for the enzyme-catalyzed substrate conversion to product. https://commons.wikimedia.org/wiki/F...y_levels_2.svg

Even this diagram is overly simplified since it suggests that the bound substrate in the ES complex is converted to the bound product in one step with no intermediates.

The free energy diagram should include intermediates along the reaction pathway. An example of this is shown in Figure **12.1.5** for the reversible conversion of a 3-carbon sugar, dihydroxyacetone phosphate (DHAP), to another 3-carbon sugar, glyceraldehyde-3-phosphate, in a reaction catalyzed by the enzyme triose phosphate isomerase (we will study the enzyme in the next chapter).

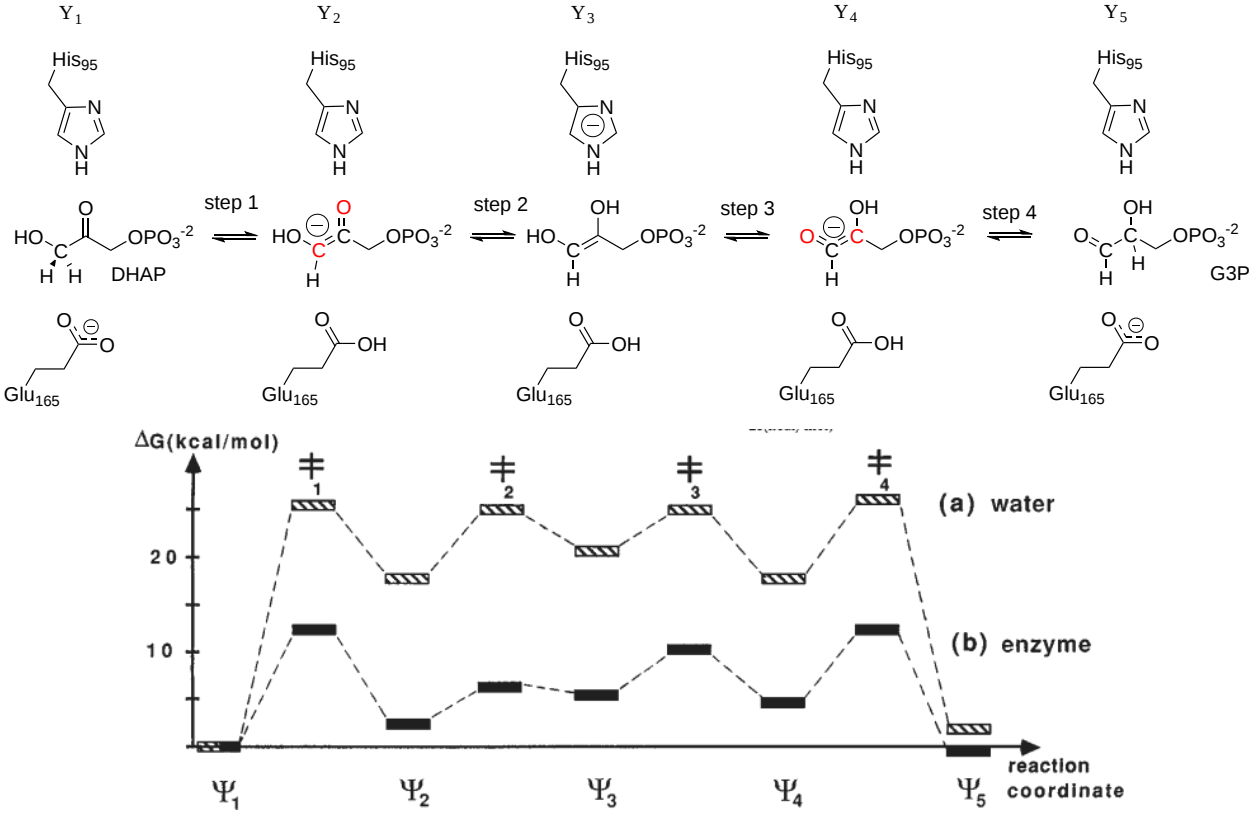


Figure **12.1.5**: Complete free energy profile for all the elementary steps of the triosephosphate isomerase-catalyzed reaction. Aqvist J, Fothergill M. Computer simulation of the triosephosphate isomerase-catalyzed reaction. J Biol Chem. 1996 Apr 26;271(17):10010-6. doi: 10.1074/jbc.271.17.10010. PMID: 8626554. Creative Commons Attribution (CC BY 4.0)

Note that the enzyme lowers the activation energy of each step in the overall reaction. Enzymes can also catalyze reactions by altering the reaction pathway, although in this case, all the intermediates in the conversion are the same in both the uncatalyzed and catalyzed pathways.

A comparison of the thermodynamic reactivity of molecules of similar structures can be made by determining the relative stability of the reactants and products from structural considerations. Consider two reactants, R_1 and R_2, which produce products P_1 and P_2, respectively. Any structural features that preferentially stabilize R2 compared to R1 or P2 compared to P1 but don't stabilize R2 and P2 to the same extent will lead to a greater driving force for R2 → P2 compared to R1. This is shown graphically in Figure **12.1.6**:

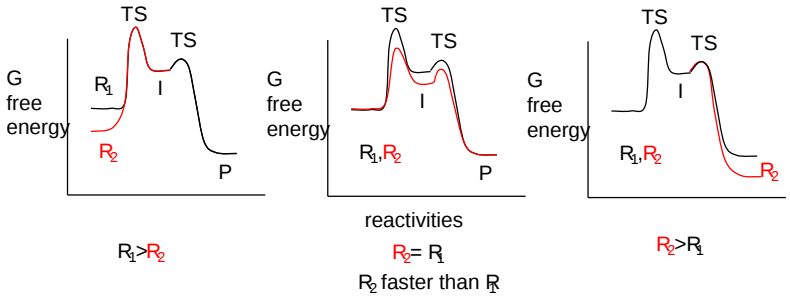


Figure **12.1.6**: Free energy reaction diagrams for two similar molecules

Mechanisms that stabilize a reactant, intermediate, or product include resonance and inductive effects (electron release or withdrawal).

An example of how the comparative acidity of two similar molecules can be determined by comparing their structures is shown below for acetic acid and ethanol in Figure **12.1.7**.

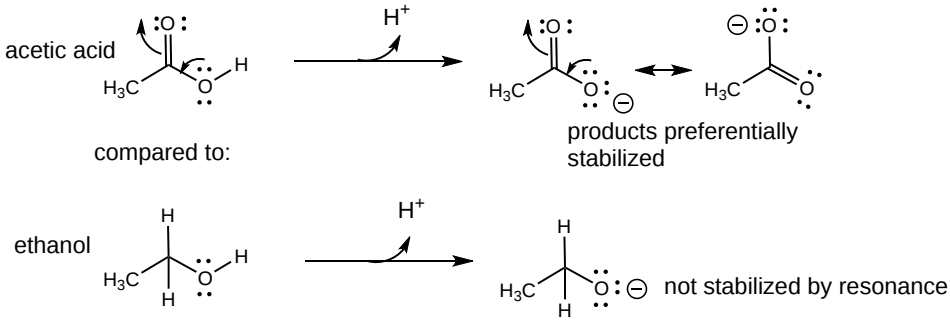


Figure **12.1.7**: Comparative acidity of two similar molecules

The stronger acid, acetic acid, has the more stable (and hence less basic) charged product (the conjugate base)

An example of how an intermediate can be stabilized through resonance is shown in Figure **12.1.8** for the keto-enol tautomerization reaction, which is favored in the direction of the keto form, a weaker acid than the enol.

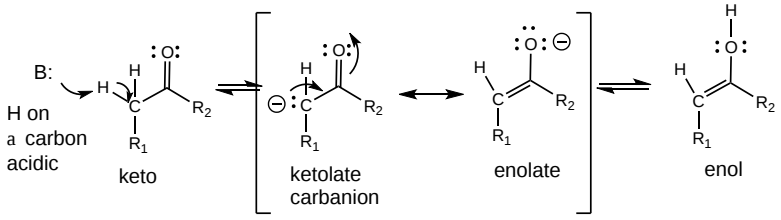


Figure **12.1.8**: Comparative stability of keto and enol intermediates

An example of how the inductive effect (electron release and withdrawal) stabilizes/destabilizes carbocations and cations is shown in Figure **12.1.8**.

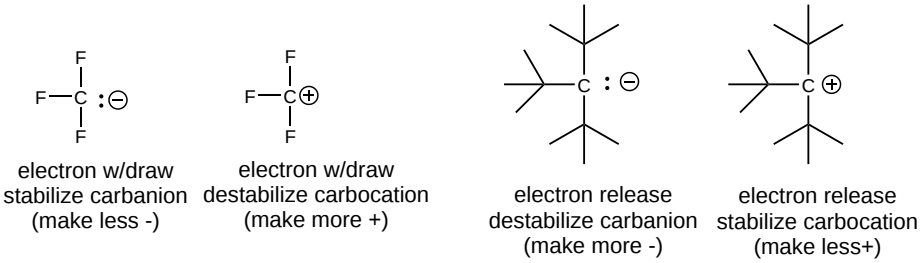


Figure **12.1.8**: Factors contributing to stabilization of carbocations and carbanions

Also, remember that electron-withdrawing by the F's in the negatively charged conjugate base of trifluoracetic acid helps explain its lower pKa than acetic acid.

Lastly, consider how stabilizing a tertiary carbocation below helps explain the preferential formation of the tertiary alcohol over the secondary alcohol, as shown in Figure **12.1.9**.

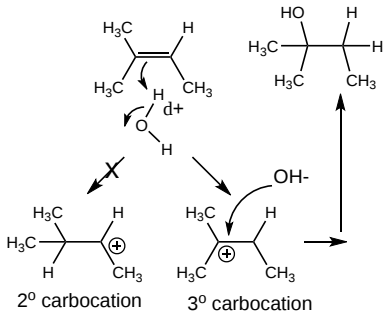


Figure **12.1.9**: Preferential formation of tertiary alcohol

12.1.3: OXIDATION OF ORGANIC MOLECULES

Organic molecules are usually oxidized in two-electron steps. Two methods can be used to determine if a C atom in an organic molecule has been oxidized.

- C is oxidized if the number of bonds from C to oxygen increases or the number of bonds to H decreases. More generally, if the number of bonds from C to a more electronegative atom increases or the number of bonds from C to a less electronegative atom decreases, the carbon is oxidized.
- A more robust method involves determining the oxidation number of the carbon atoms in the reactant and product. If the oxidation number becomes more positive, the C is oxidized.

The general rules for determining the oxidation numbers of the atoms in a molecule are:

1. O is generally 2-
2. H is usually 1+
3. in molecules consisting of one type of atom (like O_2) - i.e., a polyatomic element, the atoms have an oxidation number of 0.
4. the sum of the oxidation numbers of the atoms in a molecule equals the net charge on the molecule or ion.

In general, the oxidation number can be calculated as follows:

1. assign all nonbonded electrons of an atom to that atom
2. assign all bonded electrons to the more electronegative atom of the two atoms bonded
3. assign one electron of a bond to each atom if the two are identical.
4. sum up the assigned electrons from 1-3. Subtract this number from the total number of electrons in the atom's outer shell (the group number). The result is the oxidation number.

An illustration of the sequential two-step oxidation of ethane to acetic acid and assigned oxidation numbers is shown in Figure **12.1.10**. Focus on the **C** with **red** bonds. One electron is assigned to the C for the non-bolded red bond and 2 for the bolded red bond. Remember that C has a higher electronegativity than H, so we assign both electrons in a C-H bond to C to determine C's oxidation number. Each carbon in a C-C bond is assigned one electron from the bond since they have the same electronegativities.

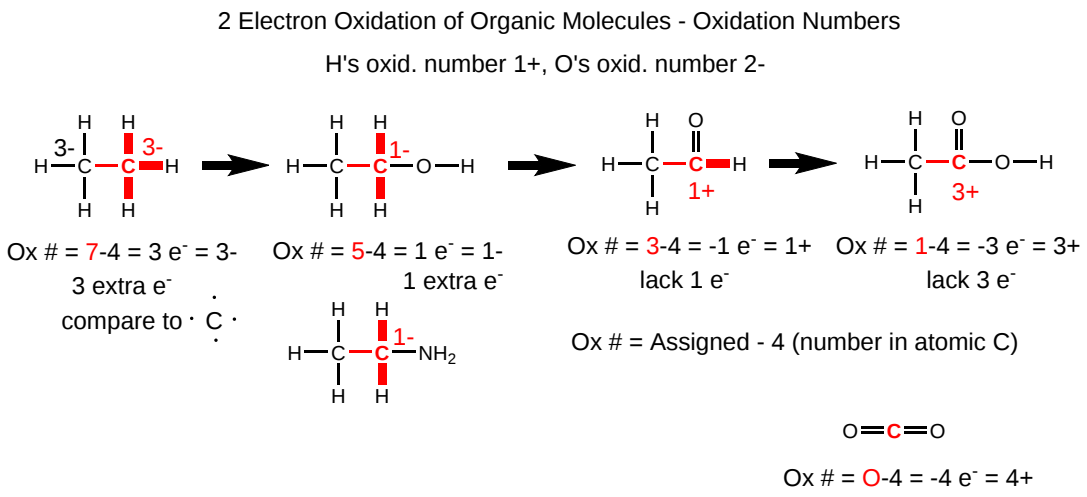


Figure **12.1.10**: Change in oxidation number on the stepwise conversion of ethane to acetic acid

Note that the red carbon connected to the NH_2 in ethylamine has the same oxidation state as the red carbon in ethanol. Hence, converting ethane to ethylamine is an oxidation reaction and requires an oxidizing agent.

Reactions of Carbonyls: Aldehydes and Ketones

When water reacts with an aldehyde in a nucleophilic addition reaction, a 1,1-diol or a geminal diol results. This reaction can be catalyzed by a base, which acts as the nucleophile (it's a stronger nucleophile than water) and adds to the carbonyl C. OH- is regenerated when the alkoxide produced abstracts a proton from water, regenerating OH-.

When an alcohol adds to an aldehyde or ketone, a hemiacetal or hemiketal, respectively, is formed. In the presence of an acid catalyst, the acid protonates the carbonyl oxygen, making the carbonyl more electrophilic. After the alcohol adds and forms the hemiacetal or hemiketal, the acid can protonate the OH group, leading to its expulsion as water in an acid-catalyzed elimination. The carbocation or resonant-form oxonium ion can react with another ROH to form an acetal or ketal. These steps are summarized in Figure **12.1.11**.

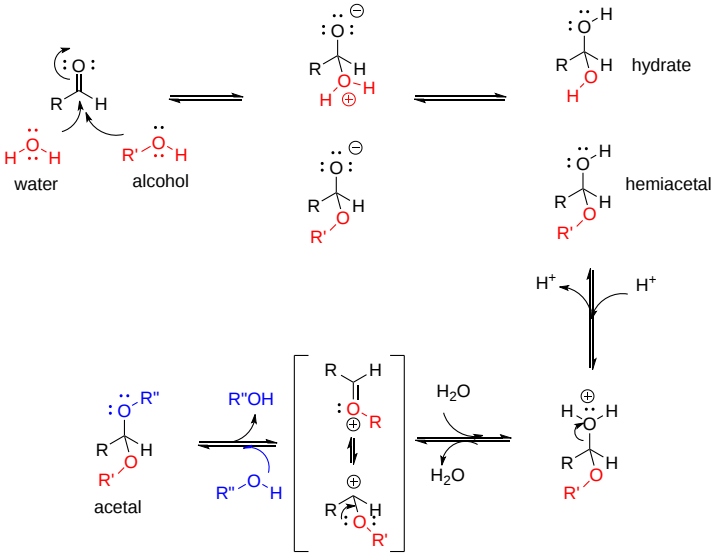


Figure **12.1.11**: Nucleophilic addition to an aldehyde

If the nucleophile is an amine, an addition can occur, followed by an elimination to form an imine or Schiff base, as shown in Figure **12.1.12**.

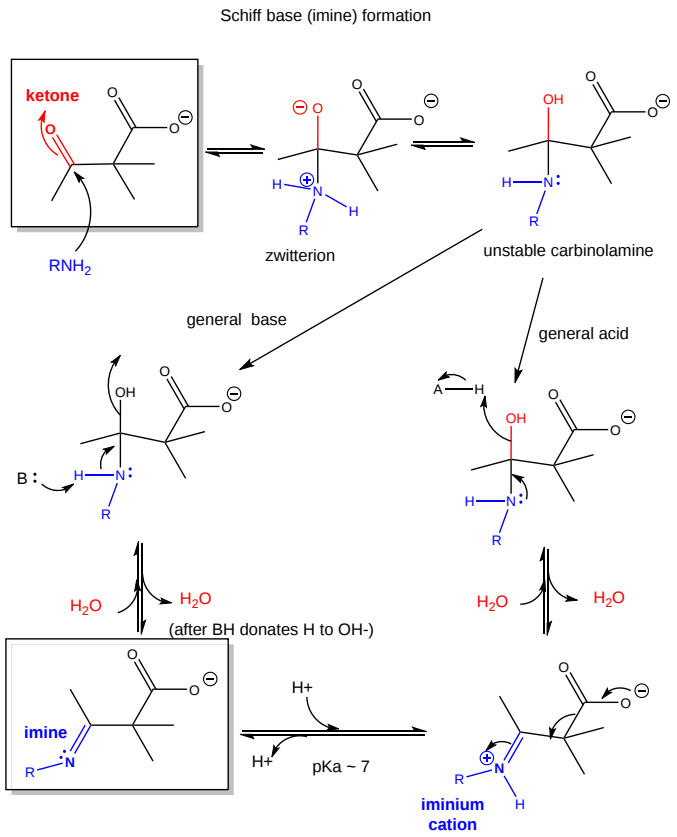


Figure 12.1.12: Schiff base formation

An acetal or ketal is a geminal ether (as water addition to aldehydes or ketones produces geminal diols). As with other ethers, these geminal ethers are stable to base and are often used as protecting groups to keep aldehydes and ketones from undesired reactions in basic solution. Acetal formation is favored by excess anhydrous alcohol in acetic conditions, while high water concentrations and an acid catalyst accelerate acetal breakdown.

Why are ethers and, hence, acetals/ketals resistant to bases? They resist nucleophilic attack, such as by base, since the expelled group (alkoxide) is unstable. (Epoxides, in contrast, will react with OH- nucleophiles since the epoxide ring is strained and of high energy.). Ethers can react with acids, which protonate the ether O to form an oxonium ion. Nucleophilic attack (such as by Br-) on an adjacent C can occur (S_N2), with electrons flowing to the protonated oxonium ion (a great electron sink) as it departs.

12.1.4: REACTIONS OF CARBOXYLIC ACID DERIVATIVES

Carboxylic acid derivatives undergo nucleophilic substitution reactions. They have good leaving groups compared to aldehydes and ketones (which undergo addition reactions). With the substitution reaction, the carbonyl's double bond stability is retained. Two things control the reactivity of these derivatives: the stability of the reactants compared to the products. Figure 12.1.13 shows the relative reactivity of carboxylic acid derivatives.

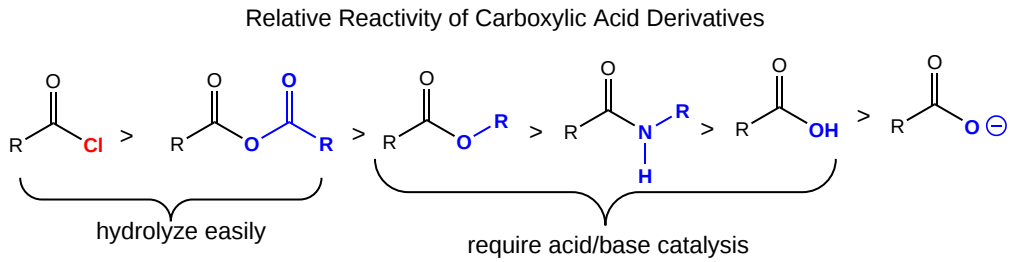


Figure 12.1.13: Relative reactivity of carboxylic acid derivatives

A reactant is less reactive if stabilized by resonance. Hence, the relative reactivity is amide < ester < anhydride < acid chloride.

The nonbonded electron pair on N of the amide, a less electronegative atom than O, can delocalize and form a resonant structure with a double bond between the N and carbonyl C more readily than the O in the ester. An electron pair on the bridging O in the anhydride could delocalize and split between the two carbonyls C (called competing resonances). This process is less stable than with the other carboxylic acid derivatives. The reactant least stabilized by resonance is the acid chloride, since a nonbonded pair of electrons on the larger chlorine molecule can't delocalize as readily, given the C-Cl bond distance.

Notice this order of decreased stability based on resonance stabilization is also the order of increased electrophilicity of the carbonyl C (which is most electrophilic in the absence of electron delocalization from the adjacent N, O, or Cl.

The stability of the products is also important. If the deprotonated leaving group is considered as one of the products (which differentiates the different reactions), then the order of decreased stability of products is Cl^- > $RCOO^-$ > RO^- > RHN^-. This is shown in Figure **12.1.14**. (Note: the pKa of ROH = 16 and R_2NH = 40)

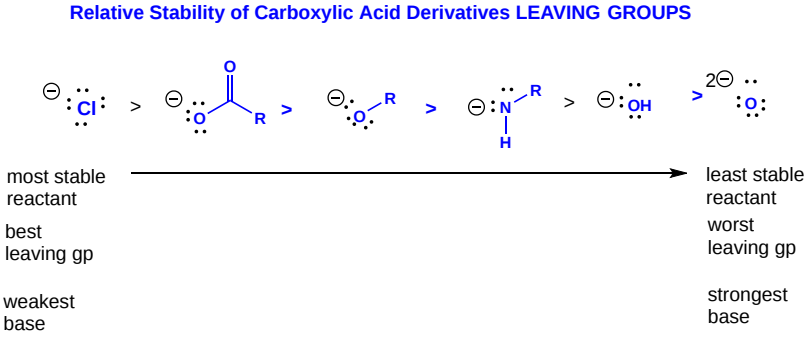


Figure **12.1.14**: Relative stability of carboxylic acid derivative leaving groups

What determines the stability of products compared to reactants is the strength of bonds made and broken during the reaction.

In nucleophilic addition to aldehydes and ketones, the strength of the bond to the nucleophile must be greater than the strength of the pi bond broken in the carbonyl. A C-Cl bond strength is 81 kcal/mol (340 kJ/mol) compared to a pi C-O bond strength of 93 kcal/mol (389 kJ/mol). Hence, a Cl- is not likely to add to a carbonyl C. Consider the hydration of formaldehyde (carbonyl with 2 H's), acetaldehyde (with 1 H and 1 methyl group, and acetone (with 2 methyl groups). The ΔG^o for hydration of these is -19, -1, and +15 kcal/mol (63 kJ/mol), respectively, showing that increased electron release toward the carbonyl C, which makes it less electrophilic and more stable, decreases the reactivity of the carbonyl.

In nucleophilic substitution, the leaving group (anion) must be more stable than the nucleophile.

12.1.5: KINETICS OF REACTIVITY OF CARBONYLS

The relative kinetic reactivity of various carbonyls toward nucleophiles follows the order of electrophilicity of the C. (i.e, the extent of the positive charge on the carbonyl C.) The slow step in a nucleophilic attack is breaking the pi-carbonyl bond. If the reactant is stabilized by resonance in ways that reduce the electrophilicity of the carbonyl C, the reaction is slowed.

Nucleophilicity is a measure of the "affinity" of an atom or ion for an electrophilic C with a nucleophilic lone pair. This is similar to basicity, which is a measure of the "affinity" of an atom or ion for a proton. Halides are not good nucleophiles for reactions with acid derivatives since the halide (like Cl-) is a better leaving group than the actual leaving group.

Making C-C Bonds

Metabolism can be divided into catabolic (breaking down) and anabolic (synthetic) reactions. To obtain energy, sugars and fatty acids are converted to carbon dioxide. Hence, C-C bonds must be broken. In contrast, C-C bonds must be synthesized in photosynthesis. In all reactions, electrons from broken bonds flow to atoms where bonds will be made. Flow is from a source (a pair of electrons possibly with a negative charge) to a sink (a slightly or fully positive atom). Figure **12.1.15** shows a couple of ways to make a C-C bond using either the reaction of two carbon-centered radicals (free radical mechanisms are uncommon biologically) or a carbocation with a carbanion.

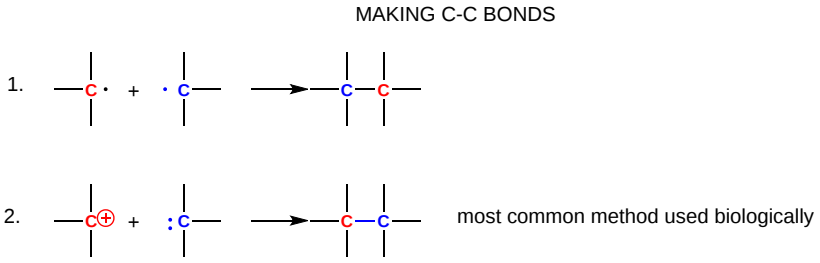


Figure **12.1.15**: Making C-C bonds

A carbocation is unstable unless incorporated into a molecule in which it is stable, so instead of using them, the carbonyl C is used as the electrophilic carbon. (Instability of carbocations is reflected in their propensity to rearrange.) Taking into account the resonance form of the C=O carbonyl bond with a positive charge on C and a negative charge on O, the net charge on the carbonyl is about +0.5. A carbanion, often stabilized as an enolate resonant form, is used as the negatively charged carbon. These features are illustrated in Figure **12.1.16**.

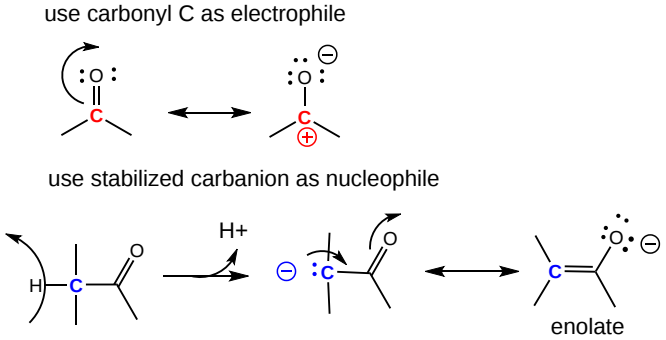


Figure **12.1.16**: Carbonyl carbons as electrophiles and carbanions as nucleophiles

One method of making a C-C bond is an aldol condensation, in which a carbanion formed by the deprotonation of a C-H alpha to a carbonyl (which is stabilized by the enolate resonance form) acts as a nucleophile that adds to a carbonyl C in an aldehyde or ketone. The reaction is illustrated in Figure **12.1.17**.

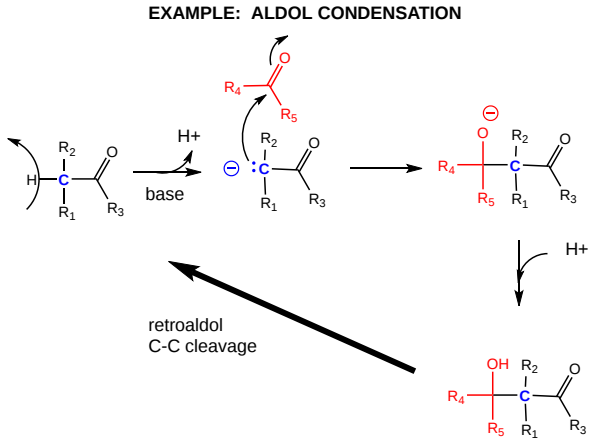


Figure **12.1.17**: Aldol condensation

In another C-C bond synthesis reaction, a Claisen Condensation, a carbanion formed by the deprotonation of a C-H alpha to a carbonyl (which is stabilized by the enolate resonance form) acts as a nucleophile that substitutes at a carbonyl C in a carboxylic ester or thioester. This is illustrated in Figure **12.1.18**.

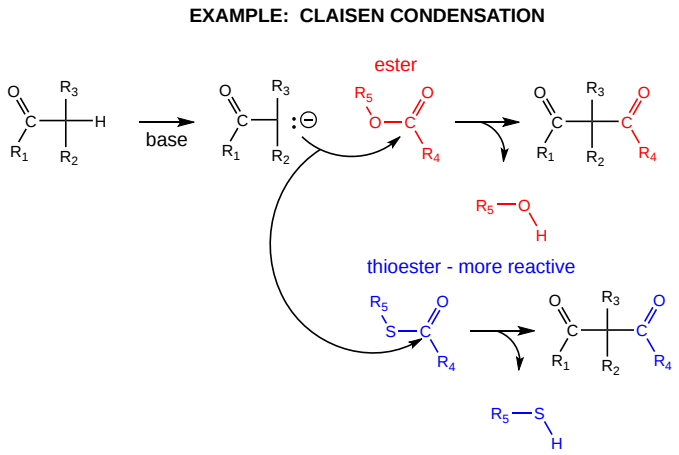


Figure **12.1.18**: Claisen condensation

12.1.6: BREAKING C-C BONDS

In addition to a retroaldol condensation, a common method to break a C-C bond is through a decarboxylation reaction at a beta-keto acid. Notice in Figure **12.1.19** that the analogous reaction at an alpha-keto acid is unlikely since the electrons from the C-C bond that is cleaved have no "sink" to which to flow.

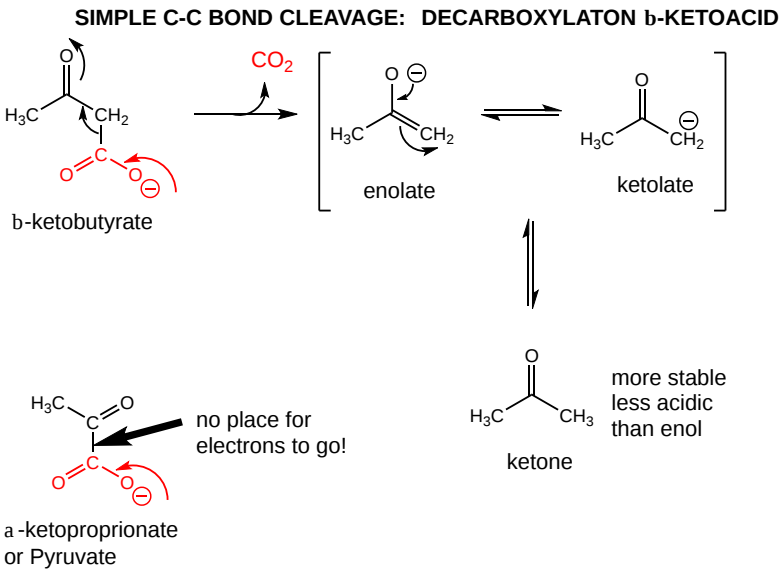


Figure **12.1.19** C-C bond cleavage by decarboxylation of beta-keto acids.

Alpha-keto acids can be decarboxylated using thiamine cofactors as discussed in Chapter 6.

12.1.7: SUMMARY

This chapter provides a concise yet comprehensive review of key organic reaction mechanisms and thermodynamic principles as they pertain to biochemistry. It bridges the detailed understanding of enzyme mechanisms from previous chapters with broader concepts essential for metabolism and bioenergetics. Major topics include:

- **Mechanisms of Bond Breaking:**
  The chapter begins by outlining the three primary pathways for breaking a C–X bond—leading to the formation of carbocations, carbanions, or free radicals. These unstable intermediates, each high in energy, require transition states that resemble the intermediates more than the reactants. This discussion lays the groundwork for understanding reaction kinetics and the factors that determine activation energies.
- **Free Energy Diagrams and Enzyme Catalysis:**
  A series of free energy diagrams illustrate the differences between uncatalyzed and enzyme-catalyzed reactions. Enzymes are shown to lower the activation energy by stabilizing transition states without altering the free energies of the reactants or products. The diagrams

progress from simple representations to more detailed profiles that include intermediates along the reaction pathway, such as in the triose phosphate isomerase reaction.

- **Structural Effects on Reactivity and Thermodynamics:**
  The text reviews how resonance and inductive effects influence the stability of reactants, intermediates, and products. Through comparative analyses (e.g., acetic acid vs. ethanol), it is shown how molecular structure dictates the driving force of a reaction, and how these principles apply to the relative reactivity of similar compounds.
- **Oxidation of Organic Molecules:**
  The oxidation process is explained in terms of electron flow—specifically, how an increase in bonds to more electronegative atoms (or a decrease in bonds to hydrogen) indicates oxidation. The chapter also provides a method for calculating oxidation numbers to determine changes in the oxidation state of carbon atoms during metabolic transformations.
- **Reactions Involving Carbonyls:**
  A detailed look at nucleophilic addition reactions to aldehydes and ketones is presented. The formation of geminal diols, hemiacetals, acetals, and Schiff bases are explained, along with the role of acid and base catalysis in these transformations. This section underscores the importance of reaction conditions in determining product stability.
- **Reactivity of Carboxylic Acid Derivatives:**
  The reactivity order of carboxylic acid derivatives (from amides to acid chlorides) is analyzed in terms of resonance stabilization and leaving group ability. The chapter discusses how bond strengths and product stability influence the outcome of nucleophilic substitution reactions in these derivatives.
- **C–C Bond Formation and Cleavage:**
  The synthesis of new carbon–carbon bonds is illustrated by mechanisms such as aldol and Claisen condensations, where enolate intermediates act as nucleophiles. Conversely, the chapter explains the mechanisms by which C–C bonds are broken, highlighting retroaldol condensations and decarboxylation reactions—particularly the decarboxylation of beta-keto acids, where electron flow has a favorable sink.

Overall, this chapter integrates basic organic reaction mechanisms with thermodynamic concepts to prepare students for advanced studies in bioenergetics and metabolism. It emphasizes how structural features and energetic considerations govern both the direction and rate of biochemical reactions, providing a foundation for understanding metabolic pathways and enzyme-catalyzed processes in living systems.

This page titled 12.1: Biochemical Reactions and Energy Changes is shared under a not declared license and was authored, remixed, and/or curated by Henry Jakubowski and Patricia Flatt.

- **11.2: Diffusion Across a Membrane - Passive and Facilitated Diffusion** by Henry Jakubowski and Patricia Flatt has no license indicated.

12.2: PHOSPHORYL GROUP TRANSFERS AND ATP

LEARNING GOALS (CHATGPT O3-MINI)

1. **Understand the Role of Biological Oxidation in Energy Transduction:**
   - Explain how biological oxidation reactions convert chemical potential energy stored in organic molecules into ATP.
   - Discuss the dual functions of oxidation in generating both new molecules and usable energy for driving endergonic processes.
2. **Describe ATP Structure and Free Energy Characteristics:**
   - Analyze the structure of ATP, including its phosphoanhydride and phosphoester bonds.
   - Explain why ATP is considered to have a high free energy transfer potential (relative to its hydrolysis products) and clarify the misconception of "high-energy bonds."
3. **Explain the Mechanism of Phosphoryl Transfer:**
   - Illustrate the mechanism for ATP hydrolysis and alcoholysis, emphasizing the SN2-like nucleophilic attack on the terminal phosphoryl group.
   - Distinguish between phosphoryl transfer (EC2.7 reactions) and hydrolysis (EC3.6 reactions) in terms of reaction mechanisms and enzyme classifications.
4. **Apply Biochemical Standard State Conditions:**
   - Compare biochemical standard states (pH 7, 1 bar, defined Mg^{2+} concentration, and ionic strength) to standard chemical conditions, and explain their importance in accurately representing cellular reactions.
5. **Assess How ATP Drives Thermodynamically Unfavorable Reactions:**
   - Analyze examples such as glucose phosphorylation and peptide bond synthesis to understand how coupling ATP hydrolysis (exergonic) to otherwise unfavorable reactions (endergonic) shifts the net free energy change.
   - Break down composite reactions into individual steps to show how overall energy balance is achieved.
6. **Evaluate the Energetics of Covalent Bond Cleavage and Formation:**
   - Understand how destabilization of reactants (e.g., in anhydrides or thioesters) versus stabilization of products contributes to large negative $\Delta G°$ values.
   - Discuss the factors (resonance, charge density, hydration) that affect the free energy change upon ATP hydrolysis and related reactions.
7. **Explain the Energy Sources and Mechanisms of Active Transport:**
   - Identify the different energy sources (ATP hydrolysis, oxidation, light, collapse of ion gradients) used by cells to drive active transport against a concentration gradient.
   - Contrast active transport with facilitated diffusion and describe how energy coupling is used to move molecules against their natural chemical potential.
8. **Differentiate Transport Mechanisms in Active Transport:**
   - Define and provide examples of symport, antiport, electrogenic, and electroneutral transport mechanisms.
   - Explain how the coupling of transport processes (e.g., ion gradients driving sugar uptake) contributes to overall cellular function.
9. **Integrate ATP Use in Signal Transduction and Transport Processes:**
   - Describe the role of ATP in powering active transport systems (e.g., Na^+/K^+ ATPase) as well as in signal transduction pathways via protein kinases.
   - Connect the molecular details of phosphoryl transfer to broader physiological processes such as nerve conduction and cellular response to environmental signals.

By achieving these goals, students will gain a comprehensive understanding of how ATP functions as an energy currency in the cell, how its hydrolysis is coupled to both chemical synthesis and active transport, and how these processes are integral to maintaining cellular homeostasis and responding to environmental changes.

12.2.1: ATP AND PHOSPHORYL TRANSFER REACTIONS

Biological oxidation reactions serve two functions, as described in the previous chapter. Oxidation of organic molecules can produce new molecules with different properties. For example, increases in solubility are observed on the hydroxylation of aromatic substrates by

cytochrome P450 (which we will explore in another chapter section). Likewise, amino acids can be oxidized to produce neurotransmitters. Many biological oxidation reactions occur, however, to produce energy to drive thermodynamically unfavored biological processes such as protein and nucleic acid synthesis or motility. Chemical potential energy is not just released in biological oxidation reactions. Instead, it is transduced into a more useful form of chemical energy in the molecule ATP (adenosine triphosphate). We will discuss the properties that make ATP so useful biologically and how exergonic biological oxidation reactions are coupled to the synthesis of ATP.

ATP is used universally as a "carrier" of free energy, which means it has a high free energy compared to its hydrolysis reaction products. Using alternative language, ATP has a high-energy transfer potential. The structure of ATP and a simplified reaction mechanism for the cleavage of the terminal (γ) phosphoanhydride bond by water (hydrolysis) or alcohol (alcoholysis) is shown in Figure **12.2.1** below.

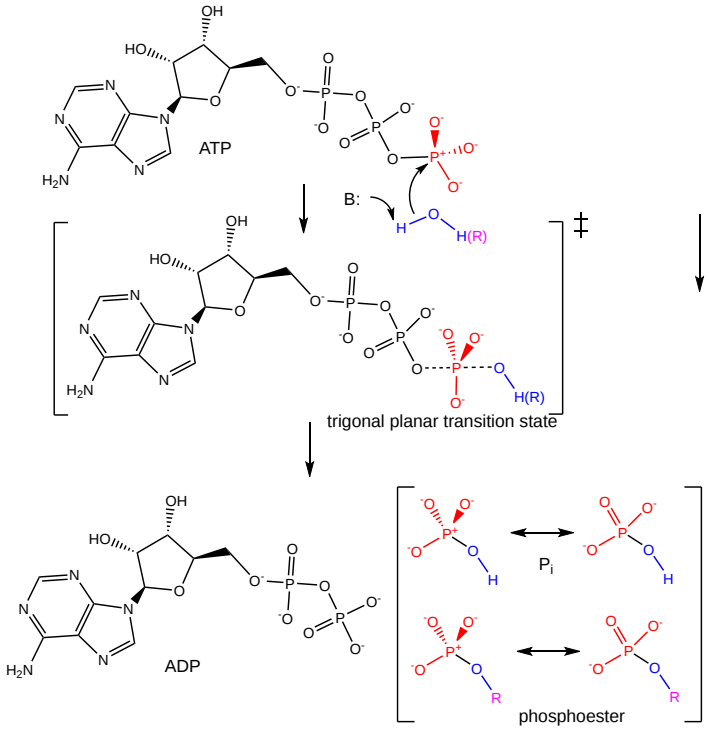


Figure **12.2.1**: Mechanism for the hydrolysis and alcoholysis of the terminal phosphoanhydride bond in ATP

The reaction is also a nucleophilic substitution. Changing perspectives, the water or alcohol is phosphorylated by ATP. Hence, the reaction can also be called a **phosphoryl transfer**. Chapter 6.5 shows that two different Enzyme Commission numbers might apply to reactions involving ATP. These are

- EC2 - transferases: transfer/exchange of a group from one molecule to another. More specifically, they are in category EC2.7 - transferring phosphorus-containing groups.
- EC3- hydrolases: hydrolysis reactions. More specifically, they are in category EC3.6 - acting on acid anhydride.s

Most of the examples in this book would best be classified as **phosphoryl transfer** reactions.

The terminal phosphate is shown in an alternative resonance form with the P atom sp^3 hybridized with tetrahedral geometry and a +1 formal charge. The attack on the electrophilic P atom by the incoming nucleophile leads to the formation of a trigonal planar transition state, with the dashed lines representing bond formation and breaking in an S_N2-like reaction. The final products are ADP, inorganic phosphate (Pi), or a phosphoester.

The hydrolysis reaction can be represented by a chemical equation or by a more typically written "biochemical" equation. Here is the chemical equation as recommended by the IUBMB/IUPAC:

$$\mathrm{ATP^{4-}(aq) + 2\,H_2O\ (l) \rightleftharpoons ATP^{3-}(aq) + HPO_4{}^{2-}(aq) + H_3O^+(aq)}$$

This equation is written to have both charge and mass balance. For example, the sum of charges on the left-hand side (-4) is the same as on the right-hand side (-4).

Of course, this is even a simplified equation since the reaction depends on the pH and the presence of divalent cations such as Mg^{2+}. Other species that could be included just for ATP^{4-} include $HATP^{3-}$, H_2ATP^{2-}, $MgHATP^-$, and Mg_2ATP, for example. The actual equilibrium

constant would depend on the pH, the concentration of $Mg^{2+,}$ and the total ionic strength of the solution. If these were all fixed, the reaction could be written as a simplified biochemical equation as shown below:

$$\mathbf{ATP + H_2O \rightleftharpoons ADP + Pi}$$

We will most often use simplified biochemical equations when discussing metabolism.

Just as there are standard state conditions for chemical reactions (1 bar pressure for a gas, 1 M for a solute in solution), there are biochemical standard states for biochemical reactions. They are pressure = 1 bar, pH = 7 (i.e., H_3O^+=10^{-7} M), Mg^{2+} = 1 mM, and ionic strength of either 0 or 0.25 M.

ATP contains two phosphoanhydride bonds (connecting the three phosphates) and one phosphoester bond (connecting a phosphate to the ribose ring). The pK_as for the reactions $HATP^{3-} \rightarrow ATP^{4-} + H^+$ and $HADP^{2-} \rightarrow ADP^{3-} + H^+$ are about 7.0, so the overall charges of ATP and ADP at physiological pH are -3.5 and -2.5, respectively. Each phosphorous atom is highly electrophilic and can react with nucleophiles like the OH of water or alcohol.

As we discussed earlier, anhydrides are thermodynamically more reactive than esters, which are more reactive than amides. The large negative ΔG^o (-7.5 kcal/mol, -31kJ/mol) for the hydrolysis of one of the phosphoanhydride bonds can be attributed to the relative destabilization of the reactants (ATP and water) and relative stabilization of the products (ADP = Pi). Specifically

- The reactants can not be stabilized to the same extent as the products by resonance due to competing resonance of the bridging anhydride O's.
- The charge density on the reactants is greater than that of the products
- Theoretical studies show that the products are more hydrated than the reactants.

The ΔG^o for hydrolysis of ATP is dependent on the divalent ion concentration and pH, which affect the stabilization and the magnitude of the charge states of the reactants and products.

Carboxylic acid anhydrides are even more unstable to hydrolysis than ATP (-20 kcal/mol, -84 kJ/mol), followed by mixed anhydrides (-12 kcal/mol, -50 kJ/mol) and phosphoric acid anhydrides (-7.5 kcal/mol or -31 kK/mol). The terminal anhydride bond is often called a "high-energy bond." **This is absolutely wrong and has created deep misconceptions about molecules like anhydrides**. What is true is that the anhydride reactants are high-energy but *only compared to the energy of their cleavage products*, such that the reaction proceeds with a large negative ΔG^o.

There is no such thing as a high-energy bond. All covalent bonds lower the energy of a system of two separated atoms. Figure **12.2.2** shows high-energy molecules compared to their hydrolysis products. Think of a graph of free energy. Carboxylic acid anhydrides and water (reactants) have high energy compared to their collective products, two acetic acids.

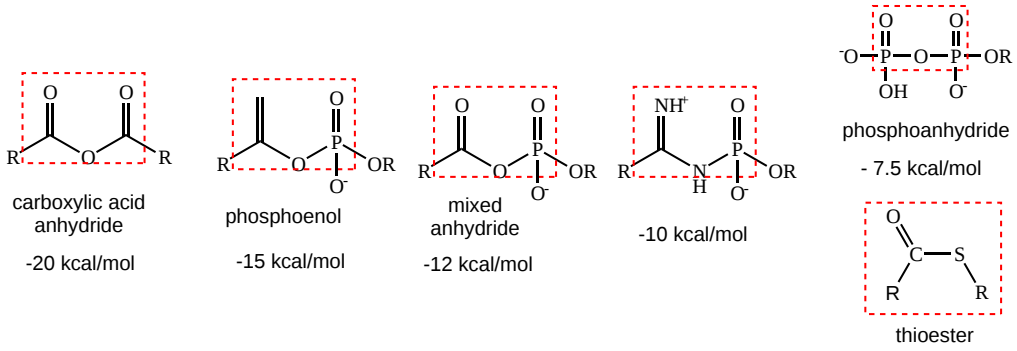


Figure **12.2.2**: Molecules that are high energy *compared to their hydrolysis products*.

Some older books state that the terminal anhydride bond is "high energy." There is no such thing as a "high energy" bond. When a bond forms between two molecules, the energy is lowered. Energy input is required to break any bond.

Each molecule above, except the thioester, has a similar motif outlined with the red dotted rectangle. The thioester is also considered high energy compared to its hydrolysis product since the reactant is effectively destabilized compared to a carboxylic acid ester. This arises because the sulfur atom is larger in the thioester than the oxygen atom in the carboxylic acid ester. Hence, the bond length of C-S (1.82 Å)is larger than for C-O (1.43 Å), so the C-S bond is weaker. In addition, the lone pairs on the S, which is more polarizable than O, are less likely to be shared with the C as part of the resonance stabilization of the ester. Both effects raise the energy of the thioester compared to the carboxylic acid ester. The hydrolysis products of both esters are of similar energy. Hence, the ΔG^o for the hydrolysis of the thioester is more negative and about the same for the hydrolysis of ATP.

How can ATP be used to drive thermodynamically unfavored reactions? First consider how the hydrolysis of a carboxylic acid anhydride, which has a ΔG^o = -12.5 kcal/mol (-52 kJ/mol) can drive the synthesis of a carboxylic acid amide, with a ΔG^o = + 2-3 kcal/mol (+ 4-12 kJ/mol). The reaction is:

anhydride + amine --> amide + carboxylic acid

This can be broken into two reactions, the hydrolysis of the anhydride and the synthesis of the amide, as shown in Figure **12.2.3**.

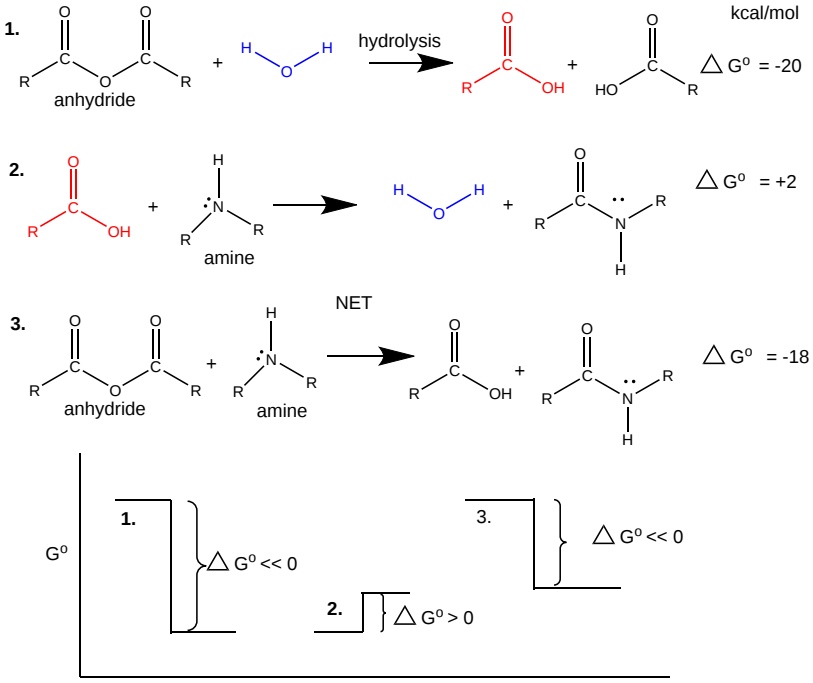


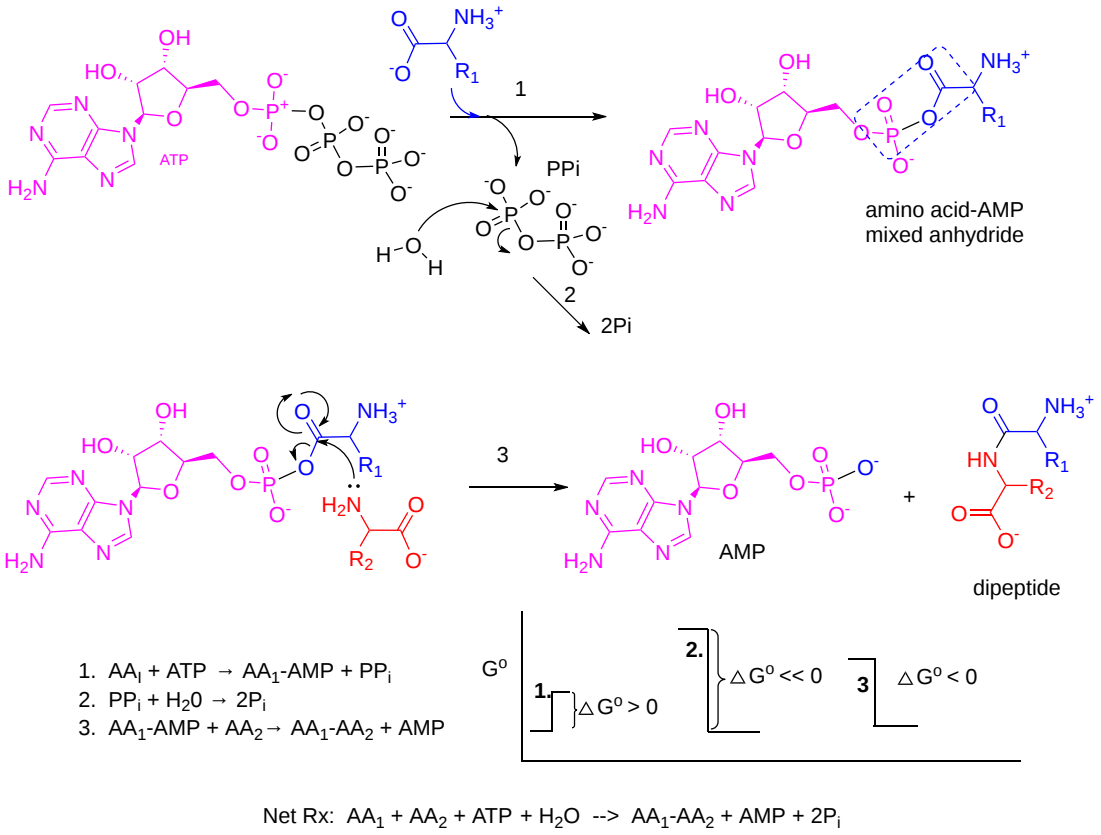
Figure **12.2.3**: Individual and net reactions for the formation of an amide from an anhydride and an amine

Now consider the reaction of glucose + Pi to form glucose-6-P. A phosphoester is formed in this reaction, so that the reaction would proceed with a positive ΔG^o = 3.3. If ATP was used to transfer the terminal (gamma) phosphate to glucose to form Glc-6-P, the reaction proceeds with a ΔG^o = -4.2 kcal/mol (-17.6 kJ/mol). This can be calculated since ΔG and ΔG^o are state functions and path-independent. Adding the reactions and the ΔG^os gives:

- glucose + Pi → glucose-6-P, ΔG^0 = 3.3
- ATP + H_2O → ADP + Pi , ΔG^0 = -7.5
- NET: glucose + ATP -→ Glucose-6-P + ADP, ΔG^o = -4.2

In most biological reactions using ATP, the terminal phosphate of ATP is transferred to a substrate using an enzyme called a kinase. Hence, hexokinase transfers the gamma phosphate from ATP to a hexose sugar. A protein kinase is an enzyme that transfers the gamma phosphate to a protein substrate.

ATP is also used to drive peptide bond (amide) synthesis during protein synthesis. From an energetic point of view, anhydride cleavage can provide the energy for amide bond formation. Peptide bond synthesis in cells is accompanied by cleavage of both phosphoanhydride bonds in ATP in complicated reactions catalyzed by ribosomes in the cells. (This topic is considered in depth in Unit III). Figure **12.2.4** is a grossly simplified mechanism of how peptide bond formation can be coupled to ATP cleavage.



Net Rx: $AA_1 + AA_2 + ATP + H_2O$ --> AA_1-$AA_2 + AMP + 2P_i$

Figure **12.2.4**: Individual and net reactions for forming a dipeptide from separate amino acids coupled with the cleavage of ATP.

In the first reaction, the carboxylic acid end of amino acid 1 is activated to form a mixed carboxylic ester. The leaving group, Pi, is hydrolyzed in reaction 2 to help drive the reaction. An amide bond is formed in reaction 3, with the expulsion of an excellent leaving group, AMP. Phosphorylation reactions using ATP are nucleophilic substitution reactions that proceed through a pentavalent transition state. These reactions are also called phosphoryl transfer reactions.

One last note. ATP exists in cells as just one member of a pool of adenine nucleotides, which consists of not only ATP but also ADP and AMP (along with Pi). These constituents are readily interconvertible. We break down an amount of ATP each day equal to our body weight. Likewise, we make about the same amount from the turnover products. When energy is needed, carbohydrates and lipids are oxidized, and ATP is produced, which can be immediately used for motility, biosynthesis, etc. It is important to realize that although ATP is converted to ADP in a thermodynamically spontaneous process, it is kinetically slow without an enzyme. Hence, ATP is stable in solution. However, its biological half-life is not long since it is used quickly as described above. This recapitulates a theme we have seen before. Many reactions (like oxidation with dioxygen, denaturation of proteins in nonpolar solvents, and ATP hydrolysis) are thermodynamically favored but kinetically slow. This kinetic slowness is a necessary but, of course, insufficient condition for life.

12.2.2: INTRODUCTION TO ACTIVE TRANSPORT

We have previously discussed how chemical potential energy in the form of reduced organic molecules can be transduced into the chemical potential energy of ATP. This ATP can drive reductive biosynthesis and movement (from individual cells to whole organisms). ATP has two other significant uses in the cell.

Active Transport: Molecules must often move across membranes against a concentration gradient - from low to high chemical potential - in a process characterized by a positive ΔG. As protons could be "pumped" across the inner mitochondrial membrane against a concentration gradient, powered by the ΔG associated with electron transport (passing electrons from NADH to dioxygen), other species can cross membranes against a concentration gradient - a process called active transport - if coupled to ATP hydrolysis or the collapse of another gradient. Remember that active transport differs from facilitated diffusion, which we studied earlier, and occurs down a concentration gradient across the membrane. Many such species must be transported into the cell or intracellular organelles against a concentration gradient, as illustrated in Figure **12.2.5**:

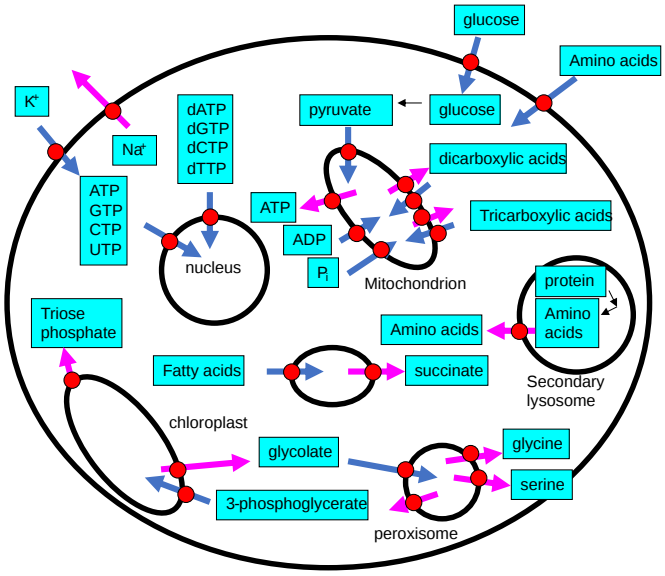


Figure **12.2.5**: Examples of active transport reactions (source unfortunately lost)

Signal Transduction: All cells must know how to respond to their environment. They must be able to divide, grow, secrete, synthesize, degrade, differentiate, cease growth, and even die when the appropriate signal is given. This signal invariably is a molecule that binds to a receptor, typically on the cell surface. (Exceptions include light transduction in retinal cells when the signal is a photon and lipophilic hormones that pass through the membrane.) Shape changes follow binding in transmembrane protein receptors, which effectively transmit the signal into the cytoplasm. We will discuss two main types of signal transduction pathways:

- nerve conduction, in which a presynaptic neuron releases a neurotransmitter, causing a postsynaptic neuron to "fire";
- signaling at the cell surface, which leads to the activation of kinases within the cytoplasm;

We will discuss signal transduction in the final two chapters.

A membrane receptor is required for active transport to occur, which recognizes the ligand to be transported. However, the energy source used to drive transport against a concentration gradient is of major interest to us. The biological world has adapted to use almost any source of energy available.

Energy released by oxidation: We have already encountered the active transport of protons driven by oxidative processes. In electron transport in respiring mitochondria, NADH is oxidized as it passes electrons to a series of mobile electron carriers (ubiquinone, cytochrome C, and eventually dioxygen) using Complexes 1, 3, and 4 in the inner membrane of the mitochondria. Somehow, the energy lost in this thermodynamically favored process was coupled to conformational changes in the complex, which caused protons to be ejected from the matrix into the inner membrane space. One can imagine a series of conformation-sensitive pKa changes in various side chains in the complexes, which lead in concert to the vectorial discharge of protons.

ATP hydrolysis: One would expect that this ubiquitous carrier of free energy would be used to drive active transport. This is one of the predominant roles of ATP in the biological world. 70% of all ATP turnover in the brain is used for the creation and maintenance of a Na and K ion gradient across nerve cell membranes using the membrane protein Na+/K+ ATPase.

Light: Photosynthetic bacteria have a membrane protein called bacteriorhodopsin, which contains retinal, a conjugated polyene derived from beta-carotene. It is analogous to the visual pigment protein rhodopsin in retinal cells. Absorption of light by the retinal induces a conformation change in the retinal and protein, which leads to the vectorial discharge of protons.

Collapse of an ion gradient: The favorable collapse of an ion gradient can be used to drive the transport of a different species against a concentration gradient. We have already observed that the collapse of a proton gradient across the inner mitochondrial membrane (through FoF1ATP synthase) can drive the thermodynamically unfavored synthesis of ATP. The collapse of a proton gradient provides a proton-motive force that can drive the active transport of sugars. Likewise, a sodium-motive force can drive the active transport of metal ions. Since the energy to make the initial ion gradients usually comes from ATP hydrolysis, ATP indirectly powers the transport of the other species against a gradient.

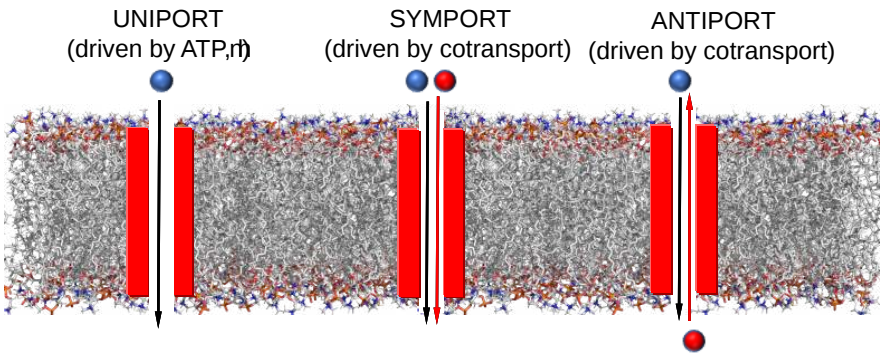


Figure 12.2.6: Types of coupled active transport

Often, one species' transport is coupled to another's transport. If the species are charged, a net change in charge across the membrane may occur. Several terms are used to describe various types of transport, as we saw previously in Chapter 12, and which are illustrated in Figure 12.2.6.

- symport - two species are cotransported in the same direction by the same transport protein
- antiport - two species are cotransported in opposite directions by the same transport protein
- electrogenic - a net electrical imbalance is generated across the membrane by symport or antiport of charged species
- electroneutral - no net electrical imbalance is generated across the membrane by symport or antiport of charged species

12.2.3: SUMMARY

This chapter explores the central role of ATP and phosphoryl transfer reactions in cellular energy transduction and their integration into broader biochemical processes such as active transport and signal transduction. Key topics include:

- **ATP as the Universal Energy Currency:**
  The chapter begins by highlighting how biological oxidation reactions not only modify organic molecules but also convert chemical potential energy into ATP. ATP's structure—with its phosphoanhydride and phosphoester bonds—is examined to explain its high free energy transfer potential relative to its hydrolysis products. The discussion clarifies the common misconception of "high-energy bonds" by emphasizing that ATP's reactivity arises from the relative instability of the reactants compared to the stabilized products formed after hydrolysis.
- **Mechanism of Phosphoryl Transfer Reactions:**
  Detailed mechanisms for ATP hydrolysis and alcoholysis are presented, showcasing a nucleophilic substitution (SN2-like) reaction at the terminal phosphoryl group. This section differentiates between enzyme classes that catalyze phosphoryl transfer (EC2.7 transferases) and those involved in hydrolysis (EC3.6 hydrolases), illustrating how enzymes lower activation energy while maintaining the overall free energy landscape.
- **Thermodynamic Considerations:**
  The chapter emphasizes the importance of biochemical standard states (pH 7, defined Mg^{2+} concentration, etc.) in evaluating reaction energetics. It demonstrates how ATP hydrolysis, with a ΔG° of approximately -7.5 kcal/mol, can drive thermodynamically unfavorable reactions—such as glucose phosphorylation and peptide bond formation—by coupling exergonic and endergonic processes to achieve a net negative ΔG°.
- **Active Transport and Energy Coupling:**
  Building on the role of ATP in metabolism, the text introduces active transport mechanisms that move molecules against their concentration gradients. Various energy sources—ATP hydrolysis, oxidative reactions, light, and the collapse of ion gradients—are discussed as drivers of active transport. Different transport modes are defined, including symport, antiport, electrogenic, and electroneutral processes, illustrating how cells harness these mechanisms to maintain ionic gradients and support cellular functions.
- **Integration with Signal Transduction:**
  Finally, the chapter touches on the dual role of ATP in both energy transfer and signaling. ATP-powered kinases play a key role in transducing extracellular signals by phosphorylating proteins, linking the molecular details of phosphoryl transfer to critical physiological processes such as nerve conduction and cellular communication.

Overall, the chapter integrates detailed molecular mechanisms with thermodynamic principles to illustrate how ATP not only drives biosynthetic reactions and active transport but also underpins the dynamic regulation of cellular signaling and homeostasis.

This page titled 12.2: Phosphoryl Group Transfers and ATP is shared under a not declared license and was authored, remixed, and/or curated by Henry Jakubowski and Patricia Flatt.

- **11.2: Diffusion Across a Membrane - Passive and Facilitated Diffusion** by Henry Jakubowski and Patricia Flatt has no license indicated.

12.3: THE CHEMISTRY AND BIOCHEMISTRY OF DIOXYGEN

LEARNING GOALS (CHATGPT O3-MINI)

1. **Appreciate Oxygen's Unique Role in Chemistry and Biology:**
   - Explain why oxygen is central to molecular diversity and its critical role in forming essential molecules (e.g., water) that serve as solvents, climate moderators, and oxygen sources.
2. **Trace the Geochemical and Biological History of Oxygen:**
   - Describe the early reducing atmosphere, the rise of photosynthetic cyanobacteria, and the Great Oxidation Event.
   - Explain how increasing atmospheric oxygen levels influenced the evolution of eukaryotic life, migration from aquatic to terrestrial environments, and major mass extinctions of anaerobic organisms.
3. **Understand the Molecular Properties of Dioxygen:**
   - Describe the molecular orbital configuration of ground state (triplet) oxygen and excited state (singlet) oxygen.
   - Explain how oxygen's diradical nature and spin restrictions contribute to its kinetic sluggishness in oxidation reactions despite favorable thermodynamics.
4. **Analyze the Stepwise Reduction of Dioxygen and Formation of ROS:**
   - Outline the sequential addition of electrons to dioxygen to form reactive oxygen species (ROS) such as superoxide, peroxide, and hydroxyl radicals.
   - Discuss the factors that govern the formation and stability of these ROS, including electron spin and activation energy barriers.
5. **Examine Cellular Defense Mechanisms Against Oxidative Stress:**
   - Identify and explain the roles of key antioxidant enzymes (e.g., superoxide dismutase, catalase, peroxidase) and small-molecule antioxidants (e.g., glutathione) in detoxifying ROS.
   - Describe how the sequestration of metal ions by proteins such as ferritin and transferrin minimizes ROS generation via reactions like the Fenton reaction.
6. **Evaluate the Impact of Oxidative Modifications on Biomolecules:**
   - Discuss how ROS can oxidatively modify proteins (e.g., carbonylation of lysine), lipids (e.g., lipid peroxidation), and DNA (e.g., formation of 8-oxoguanine).
   - Explain the link between oxidative damage, aging, and the development of diseases such as cardiovascular disease, neurodegenerative disorders, and cancer.
7. **Understand the Role of Iron Homeostasis in Oxidative Stress:**
   - Explain the structure and function of iron-binding proteins (ferritin and transferrin) in iron storage, transport, and prevention of iron-mediated oxidative damage.
   - Analyze how the controlled oxidation of Fe^{2+} to Fe^{3+} within ferritin protects cells from toxic free iron and its associated reactions.
8. **Connect Scavenger Receptors to Oxidative Modification and Disease:**
   - Describe how modifications (e.g., carbonylation) of lipoproteins by ROS lead to recognition and uptake by scavenger receptors.
   - Compare the structural features and functions of receptors such as MARCO (SR-A2) and LOX-1 in the clearance of oxidized low-density lipoprotein (oxLDL) and their roles in atherosclerosis.
9. **Integrate the Dual Nature of Oxygen in Biological Systems:**
   - Discuss how oxygen is both indispensable for energy production via aerobic metabolism and potentially harmful due to the generation of toxic ROS.
   - Evaluate how cells balance these contrasting roles through regulation of oxidative reactions and repair mechanisms.

By achieving these goals, students will gain a comprehensive understanding of oxygen's pivotal role in the evolution of life, its unique chemical behavior, and its profound impact on cellular physiology and pathology.

12.3.1: THE HISTORY OF OXYGEN

Oxygen may be considered one of the most important elements in chemistry. Not counting hydrocarbons, there is a greater diversity of molecules with oxygen than with carbon. Given its role in the molecular world, very little time is spent on the chemistry of oxygen in

undergraduate chemistry classes. Why is oxygen so special?

Oxygen reacts with atoms of all elements except the Noble gases to form molecules. Water is one of the most important molecules in the biological sense. It :

- provides a perfect solvent for biomolecules
- moderates the Earth's climate
- is the source of almost all the dioxygen in the air

From a chemical point of view, water is a(n):

- nucleophile and electrophile
- acid and base
- oxidizing agent and reducing agent
- a protic solvent that can form H-bonds

The formation of the Earth and the development of life:

The gaseous and dusty environment from which the Earth was formed contained metals and water, which, as you remember from introductory chemistry, can react to form hydrogen gas. H_2 reacts with nonmetals (under various conditions of temperature and pressure) to form H_2S, HCl, CH_4, and NH_3, contributing to the reducing nature of the early atmosphere. This kept the transition metals in their lowest oxidation states. Many metals, including the coinage metals (Cu, Ag, and Au) and the platinum group (Ru, Rh, Pd, Pt), were stable in elemental form.

Then, around 2.7-2.8 billion years ago, photosynthetic organisms (blue/green algae- also called cyanobacteria) developed that could oxidize water to form dioxygen. Oxygen was generally unavailable for redox chemistry before then, as photosynthesis, the process that would evolve to oxidize water to produce dioxygen, was unavailable. Remember that oxidizing water to dioxygen, which is a strong oxidizing agent, requires a stronger oxidizing agent than dioxygen and lots of energy. Fossilized remains of cyanobacteria are found in stromatolites. Using knowledge of how atmospheric oxygen can alter the chemistry of different sulfur isotopes of SO_2, it has been shown that O_2 did not exist in the atmosphere above 1 ppm earlier than 2.4 billion years ago, although there might have been isolated pockets with higher concentrations. After that, it rose, presumably as a result of cyanobacteria. Before this, bacteria oxidized a similar molecule, H_2S, to form elemental sulfur. It could do this through the photosynthetic reduction of CO_2 by H_2S. Volcanic gases like H_2 might have kept oxygen levels from rising between 2.7 billion years ago and 2.4 billion years ago when its build-up started. Hydrogen in the form of H2 and methane probably decreased around 2.4 billion years ago as methane, with its hydrogen atoms, escaped to the upper atmosphere and space. Methane levels would also be decreased by its easy reaction with dioxygen in the presence of UV light to form CO2. This would paradoxically lead to a cooling of the Earth and pronounced glaciation as a more potent greenhouse gas, methane, was replaced with a less potent one, carbon dioxide.

Over the next billion years, dioxygen rose to perhaps 0.2 - 2% (compared to the present levels of 20%). Why? Because the early atmosphere was reducing, the added oxygen combined with a large "sink" of reduced metals (like elemental Cu and Fe) or nonmetals (like C and ammonia), preventing a large buildup. Only after these reduced substances were "titrated" did dioxygen build up to present levels. In addition, the oxygen might have increased weathering (by oxidation) of sulfur deposits, which can lead to sulfides entering the ocean, which could precipitate ocean iron ions necessary for cyanobacterial chemistry. This would constrain cyanobacterial growth until dioxygen levels in the atmosphere increased enough, so sulfides were converted to sulfates. This first increase in atmospheric oxygen is often called the Great Oxidation Event, as it correlated and presumably caused one of the greatest mass extinctions (of anaerobic organisms) of all time.

Around 2.3 billion years ago, redox chemistry changed as trace dioxygen had accumulated in the atmosphere, although isotope evidence suggests that little dioxygen was found in water. Around 1.8 - 1.5 billion years ago, the Earth's atmosphere became somewhat oxygenated, coinciding with the development of eukaryotic organisms. Until then, life was restricted to the oceans since no ozone layer could absorb dangerous UV radiation. The buildup of dioxygen in the air must have led to another extinction of anaerobic organisms, since, as we shall see, oxygen metabolism products are very toxic. Some evolved to use dioxygen. Ozone developed, and life could migrate from the sea to the land. It wasn't until around 600 million years ago that animals arose, however. Was this event associated with developing a fully oxygenated (20%) atmosphere? Recent evidence, which shows that substantial oxygen wasn't available in the deep sea until about 600 million years ago, suggests that. Based on an analysis of iron compounds in Newfoundland waters, oxygen was very low in the sea 580 million years ago, during the Gaskiers' glaciation period. Immediately after that, it rose to levels consistent with atmospheric dioxygen levels of 15%, which is necessary for large animals. Similar trends in carbon and sulfur isotopes in marine rocks in Oman also suggest large increases in oxygen at the end of the Gaskiers glaciation period. What caused this second great oxygenation event? One possibility is that organic matter was sequestered from a reaction with atmospheric dioxygen, as clays bound organic molecules in the ocean, and lichens and zooplankton facilitated weather and production of insoluble organic material in the oceans.

Dioxygen is critically important for higher organisms, so understanding its chemistry becomes important. This chapter will show that dioxygen is a ground-state diradical with low solubility in an aqueous solution. It reacts in a kinetically sluggish fashion in the oxidation reaction and forms toxic byproducts upon reduction. Life forms evolved ways to deal with these problems, including ways to increase their solubility (with dioxygen binding and transport proteins) and enzymes (that could activate it kinetically and detoxify oxygen by-products). Dioxygen is toxic to many cells. Obligate aerobes die in an oxygen environment as this excellent oxidizing agent oxidizes many of their cellular components. Several strains of bacteria swim away from high levels of dioxygen. A graph showing the log of survival vs. log pO2 is linear, with a negative slope for various organisms, including mice, fish, rats, rabbits, and insects. Pure oxygen can induce chest soreness, coughs, and sore throats. Premature infants put in pure dioxygen environments often developed blindness due to retrolental fibroplasia (a build-up of fibrous tissue behind the lens). The trade-off for this toxicity is clear. Energy is derived from organic molecules through oxidation. Before dioxygen became available to power aerobic catabolism of reduced molecules like fatty acids and less reduced sugars, such molecules were only partially oxidized. The glycolytic pathway, found in most organisms, oxidizes glucose (6 Cs) to two pyruvate molecules (3 Cs). With the availability of dioxygen, pathways evolved (Krebs Cycle, mitochondrial electron transport/oxidative phosphorylation) that allowed pyruvate to be fully oxidized to carbon dioxide, releasing much more energy.

12.3.2: THE PROPERTIES OF DIOXYGEN

It is important to understand the properties of dioxygen since oxidation reactions using O_2 power not only our bodies but our entire civilization. We will concentrate on biological reactions, but even these show the same characteristics as non-biological ones.

- Oxidation of organic molecules by oxygen is thermodynamically favored but kinetically slow.
- Pure oxygen environments are toxic to cells and organisms.

First, we will try to understand these properties of oxygen, and then we will see how organisms overcome these problems to use dioxygen.

We can understand both of these properties by looking at the molecular orbitals of oxygen and its reduction products, as shown in the diagrams below. Ground-state oxygen is a diradical, which explains the paramagnetic behavior of oxygen. The two unpaired electrons have a spin state of 1/2 for a total resultant spin S of 1, making ground state oxygen a triplet (2S+1) = 3. Organic molecules typically undergo 2-electron oxidation steps. Consider the stepwise oxidation of methane below. The oxidation number of C in methane is -4, -2 in methanol, 0 in formaldehyde, +2 in formic acid, and finally, +4 in carbon dioxide, indicating two electron losses in each step. These states are shown in Figure **12.3.1**.

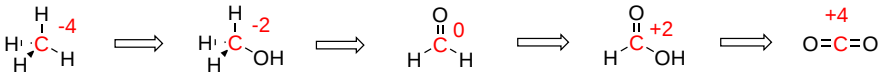


Figure **12.3.1**:

The two electrons lost by the organic substrate are added to oxygen. However, since the two lost electrons are spin-paired, a spin flip must occur to allow the electrons to enter the unfilled oxygen orbitals. Alternatively, energy can be put into ground-state dioxygen to produce excited-state singlet oxygen (S=0, 2S+1 = 1). The source of the large activation energy required (about 25 kcal or 105 kJ/mol) to flip the electron spin accounts for the kinetic sluggishness of reactions of dioxygen with organic reactants.

A traditional Lewis structure for ground-state dioxygen can not be easily written since the electrons are added in pairs, and dioxygen is a diradical. There are 6 electrons in the sigma molecular orbitals from second shell electrons (two each in σ2s, σ2s*, and σ2p,) and 6 electrons in the pi molecular orbitals from second shell electrons (two each in two different π2p orbitals, and one electron each in two different π2p*), so the net number of electrons in bonding orbitals is 4, giving a bond order (or number of 2). In contrast, it is easy to write the Lewis structure of singlet, excited state oxygen since all electrons can be viewed as paired, with two net bonds (1 sigma, 1 pi) connecting the oxygen atoms. Figure **12.3.2** shows the molecular orbital diagram for ground and excited state dioxygen.

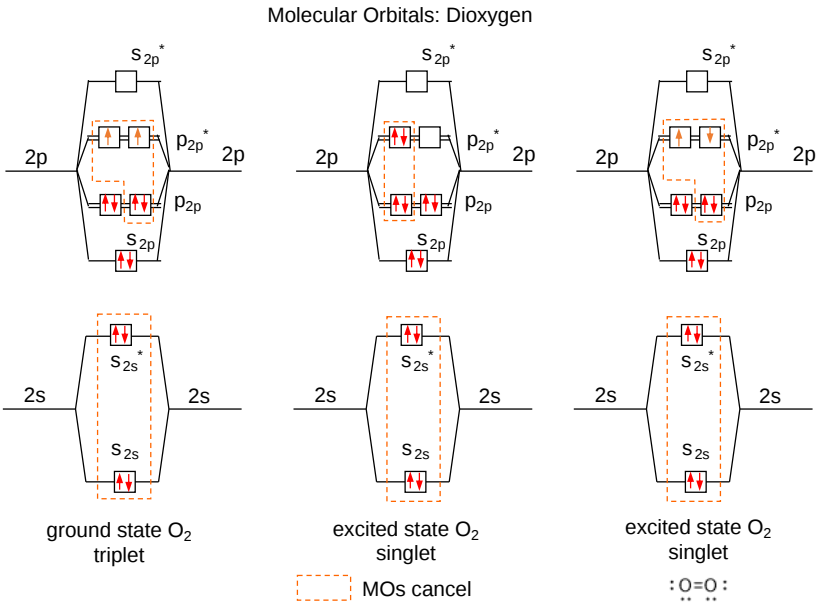


Figure **12.3.2**: Molecular orbital diagram for ground and excited state dioxygen

This Lewis structure will be used to represent singlet, excited oxygen, which should react more quickly with organic molecules. The excited state singlet on the right is unstable and decays to the middle singlet state. The middle state is approximately 94.3 kJ/mol higher in energy than the ground state triplet (on the left). In quantum mechanical parlance, the transition from the ground state triplet to the singlet state is forbidden for several reasons, making it unlikely that absorption of a photon will induce the transition.

12.3.3: THE REDUCTION OF DIOXYGEN

When oxygen oxidizes organic molecules, it is reduced. By adding electrons one at a time to the molecular orbitals of ground-state dioxygen, we produce the step-wise reduction products of oxygen. On the addition of one electron, superoxide is formed. A second electron produces peroxide. Two more produce two separated oxides since no bonds connect the atoms (the number of electrons in antibonding and bonding orbitals is identical). Each of these species can react with protons to produce species such as HO_2, H_2O_2 (hydrogen peroxide), and H_2O. The first two reactive reduction products of dioxygen make it potentially toxic. Figure **12.3.3** shows the MO diagrams for the reduction products of dioxygen.

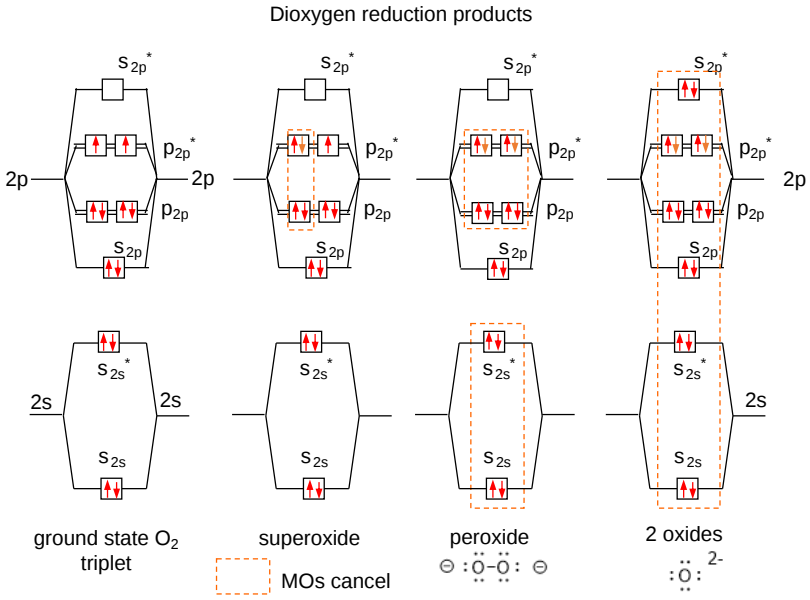


Figure **12.3.3**: MO diagrams for the reduction products of dioxygen

How are the potential problems in oxygen chemistry dealt with biologically?

Kinetic sluggishness: Enzymes that utilize dioxygen must activate it somehow, decreasing the activation energy. Enzymes that use dioxygen are typically metalloenzymes and often heme-containing proteins. Since metals such as Fe^{2+} and Cu^{2+} are themselves free radicals (i.e., they have unpaired electrons), they react readily with ground-state oxygen, which itself is a radical. The molecular orbitals of the metal and oxygen combine to produce new orbitals, which for oxygen are more singlet-like. Likewise, dioxygen reacts more readily with organic molecules, which can form reasonably stable free radicals, such as flavin adenine dinucleotide (FAD), as we shall see later.

Dioxygen toxicity: Since toxicity arises from oxygen reduction products, enzymes that use oxygen have evolved to bind oxygen and its reduction products tightly (through metal-oxygen bonds), so they are not released into the cells, where they can cause damage. In addition, enzymes that detoxify free dioxygen reduction products are widely found in nature. For example:

- superoxide dismutase catalyzes the dismutation (self-redox) of 2 superoxides into dioxygen and hydrogen peroxide;
- catalase converts hydrogen peroxide into water and oxygen;
- peroxidase catalyzes the reaction of hydrogen peroxide with an alcohol to form water and an aldehyde;
- peroxiredoxins react with peroxides and thioredoxin (a small electron donor) to form water and oxidized thioredoxin.

Finally, free radical scavengers such as vitamins A, C, E, and selenium can react with reactive free radicals to produce more stable free radical derivatives of the vitamins and Se. More on this later.

12.3.4: THE REACTIONS OF DIOXYGEN AND ITS REDUCTION PRODUCTS

12.3.4.1: TRIPLET O_2 - GROUND STATE

Here are some reactions for the ground state (triplet O_2):

a. Metal ions - Metal ions are radicals themselves, so they can easily react with dioxygen (think about rust). Here is one example

$$Fe^{2+} + O_2 \rightleftharpoons [\, Fe^{2+}{-}O_2 \rightleftharpoons Fe^{3+}{-}O_2^{-\bullet}] \rightleftharpoons Fe^{3+} + \underbrace{O_2^{-\bullet}}_{\text{superoxide}}$$

b. Autoxidation of organic molecules to produce peroxides - These are multistep reactions that have initiation, propagation, and termination steps.

$$RH \rightarrow R\cdot \text{ (Initiation)}$$
$$R\cdot + O_2 \rightarrow ROO\cdot \text{ (Propagation)}$$
$$ROO\cdot + RH \rightarrow R\cdot + ROOH \text{ (Propagation)}$$
$$R\cdot + R\cdot \rightarrow R\text{-}R \text{ (Termination)}$$
$$ROO\cdot + ROO\cdot \rightarrow ROOR + O_2 \text{ (Termination)}$$
$$ROO\cdot + R\cdot \rightarrow ROOR \text{ (Termination}$$

Figure **12.3.4** summarizes the triplet ground state dioxygen reactions.

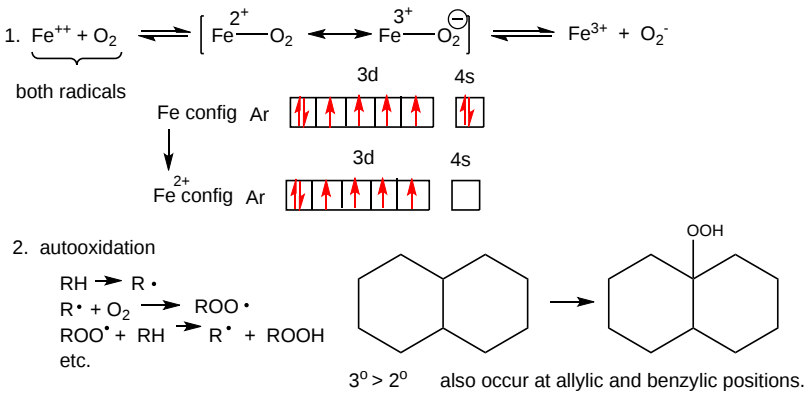


Figure **12.3.4**: Reactions of triplet ground state dioxygen

The initiation step above occurs mostly at C atoms, which can produce the most stable free radicals (allylic, benzylic position, and $3^o > 2^o >> 1^0$ carbons).

12.3.4.2: SINGLE O_2 - EXCITED STATE

Figure **12.3.5** shows some reactions for singlet dioxygen in which dioxygen is shown with a double bond and two lone pairs on each oxygen.

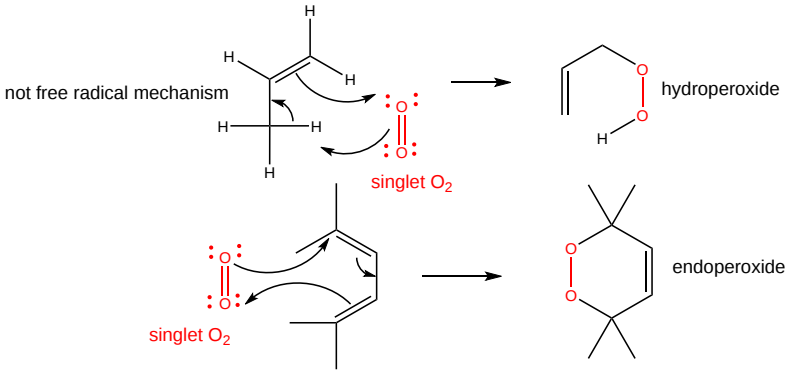


Figure **12.3.5**: Some reactions for singlet dioxygen

Alkenes react with oxygen to form hydroperoxides, potentially through an epoxide intermediate. Dienes react with oxygen in a Diels-Alder pericyclic reaction to form endoperoxides. A molecular orbital perspective (that you may remember from chemistry classes) on this cycloaddition reaction is shown in Figure **12.3.6**.

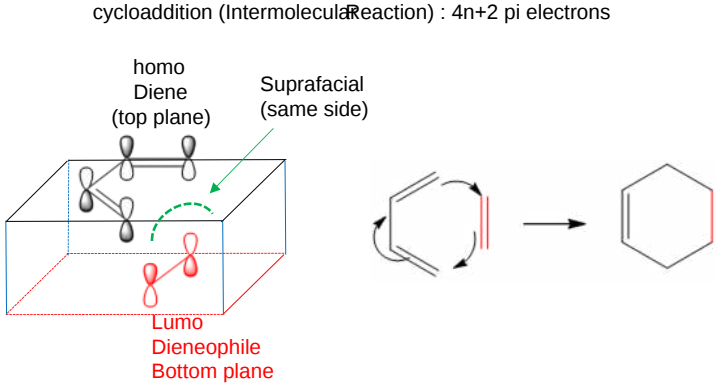


Figure **12.3.6**: Pericyclic cycloaddition reactions using molecular orbitals

Singlet oxygen can be made from triplet oxygen by photoexcitation. Alternatively, it can be made from triplet oxygen through collision with an excited molecule that relaxes to the ground state after a radiationless energy transfer to triplet oxygen to form reactive singlet oxygen. This latter process accounts for the photobleaching of colored clothes when the conjugated dye molecules absorb UV and Vis light and relax to the ground state by transferring energy to triplet oxygen to form singlet oxygen. That can more readily react with the conjugated double bonds in the dye. These processes are summarized in Figure **12.3.7**.

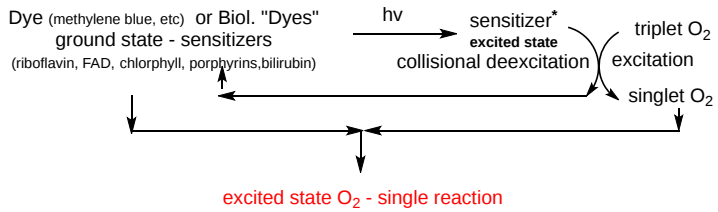


Figure **12.3.7**: Photosensitization and the reaction of dyes with singlet state dioxygen

12.3.4.3: SUPEROXIDE

Common reactions of superoxide are shown below.

a. **Dismutation:** This reaction involves a specified reactant undergoing an oxidation reaction, followed by another molecule of the same reactant undergoing a reduction.

$$O_2^{-\bullet} + O_2^{-\bullet} + 2H^+ \rightleftharpoons H_2O_2 + O_2 \qquad \text{(slow)}$$

$$HO_2^{\bullet} + O_2^{-\bullet} + H^+ \rightleftharpoons H_2O_2 + O_2 \qquad \text{(fast)}$$

b. Acid/Base:

$$HO_2^{\bullet} \rightleftharpoons O_2^{-\bullet} + H^+ \qquad (pKa = 4.8)$$

c. With metal ions:

$$\underbrace{Fe^{3+}}_{\text{as in heme}} + O_2^{-\bullet} \rightarrow O_2 + Fe^{2+}$$

The enzyme superoxide dismutase catalyzes the dismutation reaction. The common eukaryotic cytosolic form contains Cu^{2+} and Zn^{2+} ions coordinated by histidine side chains. The reaction proceeds in two steps or half-reactions. The first is an electron's removal (oxidation) from superoxide ($O_2^{-\cdot}$) through its reduction by Cu^{2+}. This reaction forms Cu^{1+} and nontoxic O_2.

$$Cu^{2+}\text{–SOD} + O_2^{-\bullet} \longrightarrow Cu^{+}\text{–SOD} + O_2$$

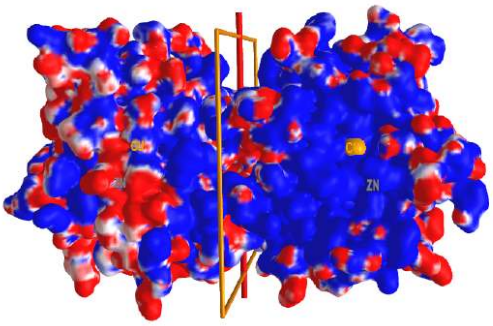
(reduction of Cu; oxidation of superoxide)

The second is the addition (reduction) of an electron from a second superoxide to Cu^{1+} to reform the catalytic Cu^{2+} and, in the process, form the reactive peroxide O_2^{2-} (unfortunately), which when protonated forms H_2O_2.

$$Cu^{+}\text{–SOD} + O_2^{-\bullet} + 2H^{+} \longrightarrow Cu^{2+}\text{–SOD} + H_2O_2$$

(oxidation of copper; reduction of superoxide)

Figure 12.3.8 shows an interactive iCn3D model of the electrostatic potential surface of the superoxidase dismutase dimer showing Cu and Zn ions (2SOD).



NCBI iCn3D Figure 12.3.8: Electrostatic potential surface of the superoxidase dismutase dimer showing Cu and Zn ions (2SOD) (Copyright; author via source). Click the image for a popup or use this external link: https://structure.ncbi.nlm.nih.gov/i...zozKPVKr4MzES9

Two dimers are shown with a C2 axis of rotation separating them. Red indicates the negative surface potential, and blue is the positive. Catalytic Cu^{2+} and Zn^{2+} ions are in each subunit and are shown in orange (Cu) and gray (Zn) spheres and labeled (disregard the label not centered on the orange and gray spheres). Note that the Cu^{2+} and Zn^{2+} ions are in the center of a large blue surface (positive potential), which helps "sweep up" any negatively charged superoxide O_2^- nearby. Rotate the complex around the C2 axis, and you will see another large positive blue patch on the backside. These two positive electrostatic surfaces facilitate the electrostatic attractions and binding of the dangerous superoxide anion from the larger 3D region around the enzyme.

The Zn^{2+} in SOD is not redox active. What is its role? Both metals appear to increase the thermostability of the individual monomer and the dimer. In the presence of metal ions (a holo form of the enzyme), the dimer dissociates into monomers at a higher urea concentration than the apo-dimer. Ion binding reduces the flexibility of groups found in the dimer interface. The protein has a disulfide bond between Cys 57 and Cys 146. This bond stabilizes a metal ion binding loop that contributes to the binding interface in the dimer. The enzyme operates at diffusion-controlled rates (k_{cat}/K_M is between 10^8 and 10^9 $M^{-1}s^{-1}$), partly due to the attraction of any negatively charged superoxide by the electrostatic field around the dimer.

There are two other superoxide dismutases, one that uses either Mn^{2+} or Fe^{2+} (bacterial, mitochondrial, chloroplasts, protists) and another that uses Ni^{2+}(some prokaryotes).

12.3.4.4: PEROXIDE

In contrast to dioxygen, which contains multiple bonds between the O atoms, peroxide has only one bond. It is quite weak and requires only 38 kcal/mol (160 kJ/mol) to break it. Remember, bonds can be broken in a heterolytic way (both electrons in a bond go to one of the atoms or in a homolytic fashion, in which one electron goes to each atom.

Figure 12.3.9 shows typical reactions of peroxides.

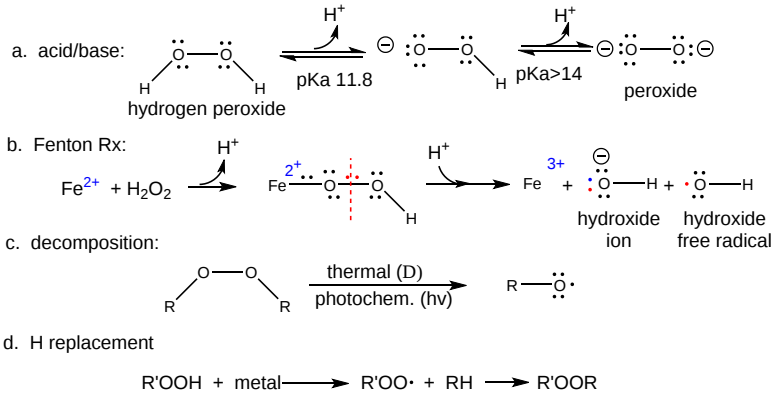


Figure **12.3.9**: Reactions of peroxides

The reaction with Fe^{2+}, the **Fenton Reaction**, is similar to that of triplet O_2 with Fe^{2+}. In this reaction, homolytic cleavage of the O-O bond occurs, generating OH^- and the hydroxy free radical, $OH\cdot$, which will react with any molecule it encounters. Thermal or photochemical homolytic cleavage of peroxide also forms free radicals that react like the hydroxy-free radical.

The enzyme **catalase** facilitates the decomposition of the reactive H_2O_2 to water and dioxygen. As such, it offers protection similar to that against superoxide offered by superoxide dismutase. This is the next reaction catalyzed by the enzyme catalase:

The human enzyme is a homotetramer, with each monomer having a heme at the active site. The tetramer also binds $NADP^+$ (2/tetramer), but its function is unclear. Figure **12.3.10** shows a potential mechanism for catalase.

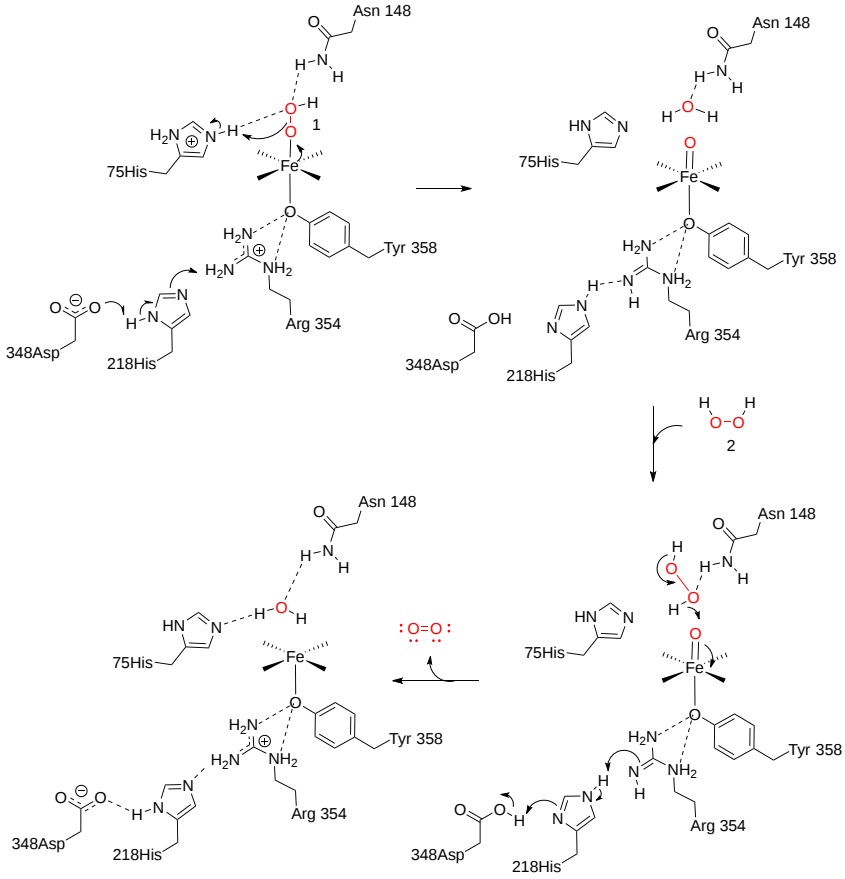
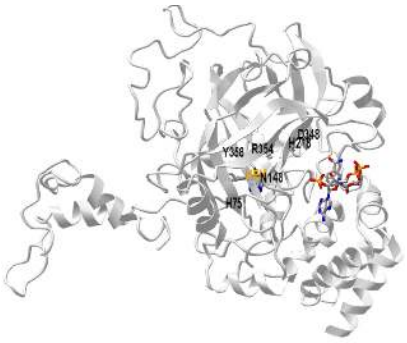


Figure **12.3.10**: Human catalase reaction mechanism (adapted from Putnam et al. J. Mol. Biol. 296, 2000,https://doi.org/10.1006/jmbi.1999.3458)

Figure **12.3.11** shows an interactive iCn3D model of human erythrocyte catalase with bound ligand (CN^-) and NADPH (1DGG)

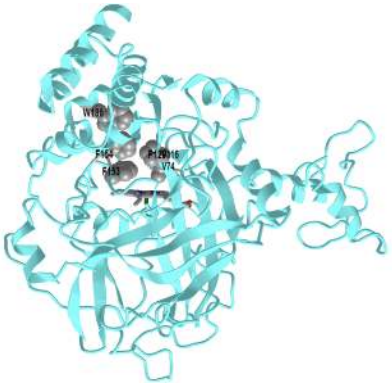


NCBI iCn3D Figure **12.3.11**: human catalase with bound ligand (CN^-) and NADPH (1DGG). (Copyright; author via source). Click the image for a popup or use this external link: https://structure.ncbi.nlm.nih.gov/i...TD7yJsfrNcwSJ7

The cyanide ligands in this structure bind to the heme instead of peroxide. The reaction in mammalian catalases appears to involve a tyrosine radical.

H_2O_2 is very similar in structure to H_2O. How does the enzyme differentiate between them? Both approach the heme through a long 25 Å water channel with a hydrophobic constriction partway into the channel leading to the active site heme. Four waters in the crystal structure are positioned in the constricted opening and in a widened opening just at the heme. The amino acid side chains forming the constriction are Val 74, Val 116, Pro 129, Phe 153, Phe 154, and Trp 186. These allow only small molecules to enter. Two of the four waters form hydrogen bonds to side chains (one to His 75 and Asn 148, and another to Gln 168 and Asp 12. The others don't form hydrogen bonds, are more dynamic, and are more likely to leave the channel. H_2O_2 is bigger and can form bridging hydrogen bonds to side chains that mobile waters can't. They probably leave the opening. H_2O_2 is more polar and has a higher dipole moment (2.26 Debye) than water (1.86 Debye), which implies that hydrogen bonds would be differentially stabilized in this hydrophobic site compared to the less polar water.

Figure **12.3.12** shows an interactive iCn3D model of human erythrocyte catalase (monomer) showing the hydrophobic constriction leading to the active site (1DGF**)**



NCBI iCn3D Figure **12.3.12**: Human erythrocyte catalase (monomer) showing hydrophobic constriction leading to the active site (1DGF**)**. (Copyright; author via source). Click the image for a popup or use this external link: https://structure.ncbi.nlm.nih.gov/i...e48pAa9X4zhcM7

12.3.5: HYDROXYL FREE RADICAL

We won't specifically discuss the reaction of the hydroxyl free radical ($^{\cdot}OH^-$) since it will react with anything nearby to produce another free radical. General reactions of the radical are shown in Figure **12.3.13**.

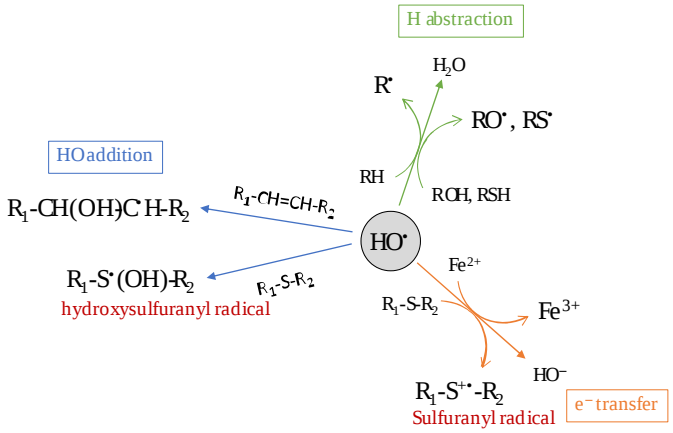


Figure **12.3.13**: Chemical reactions of the hydroxyl radical. Fabrice Collin. Int. J. Mol. Sci. 2019, 20, 2407; doi:10.3390/ijms20102407. Creative Commons Attribution (CC BY) license (http://creativecommons.org/licenses/by/4.0/).

In summary, we reap the benefits of using dioxygen as an oxidizing agent as it allows the aerobic and, hence, complete oxidation of carbohydrates and lipids to CO_2 and H_2O. Yet we pay the price for using O_2 as an oxidizing agent, as its partial reduction products, the superoxide radical, peroxides, and hydroxy free radical, collectively known as **reactive oxygen species (ROS),** can react with and damage proteins, nucleic acids, and lipids, as we will see below. Figure **12.3.13** summarizes their reactions.

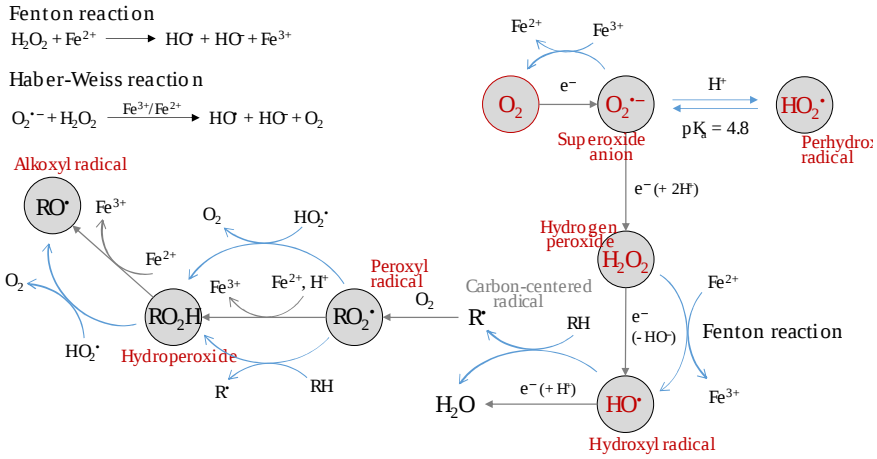


Figure (\PageIndex{14}\): Basis of Reactive Oxygen Species (ROS) generation. Fabrice Collin, ibid.

We have presented the role of superoxide dismutase and catalase in removing ROS in cells. In addition to these elegantly designed proteins, another simpler biomolecule, the tripeptide glutathione (γGlu-Cys-Gly), can reduce ROS in cells and prevent oxidative damage. Glutathione serves as a major antioxidant in cells. It exists in reduced (GSH) and oxidized (GSSG) states, the ratio of which depends on the cellular oxidative stress. It can react with and detoxify peroxides and alkyl free radicals by the following net reactions:

$$2\ GSH + R_2O_2 \rightarrow GSSG + 2\ ROH$$

$$2GSH + 2R^{\cdot} \rightarrow GSSG + 2RH$$

12.3.6: PROTECTION FROM FE^{2+} - FERRITIN AND TRANSFERRIN

The Fenton reaction shows the potential problem with having free Fe^{2+} ions in a chemical state that would easily allow this reaction and the generation of ROS. Hence, much of the Fe^{2+} in the body is sequestered in Fe^{2+} binding cofactors like heme and FeS clusters. It is transported in the blood by the protein **transferrin** and stored in cells, such as erythrocytes, in **ferritin**. The iron ions in transferrin and ferritin are in the +3 oxidation state (Fe^{3+}). This strongly positive cation is quite insoluble in the presence of anions like hydroxide, phosphate, and carbonate. The K_{sp} value for the hydroxide salt of Fe^{3+} is $3.8x10^{-38}$. Let's detour for a bit and look at the structures of ferritin and transferrin and how they work, starting with ferritin.

12.3.6.1: FERRITIN

The biologically functional form of ferritin is a 24-mer. The structure encapsulates a large volume that can hold many Fe ions (up to 4500) in the central cavity. The ions are stored in the more insoluble form, Fe^{3+}, in complexes of oxide and hydroxide. Mammalian ferritin contains both heavy (H) and light (L) chains, so they are hetero 24-mers.

Figure **12.3.15** shows an interactive iCn3D model of ferritin, the intracellular Fe storage protein (1fha).

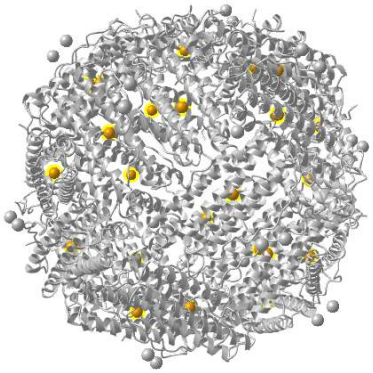


Figure **12.3.15**: Ferritin, the intracellular Fe storage protein (1fha). (Copyright; author via source). Click the image for a popup or use this external link: https://structure.ncbi.nlm.nih.gov/i...MQXAbPAwNnVya8

The ferritin chains are shown in purple. This structure shows only 24 Fe ions (in orange spheres with yellow halo).

Two questions arise. How does Fe^{2+} get into the internal volume of ferritin, and how does it convert to Fe^{3+}? There must be a channel through which Fe^{2+} can diffuse. Its conversion to Fe^{3+} requires catalysis by a Fe cluster in the heavy chain (H) subunits. Figure **12.3.16**s shows a generic diagram outlining the processes of uptake and conversion to Fe^{3+} salts inside the central cavity of ferritin.

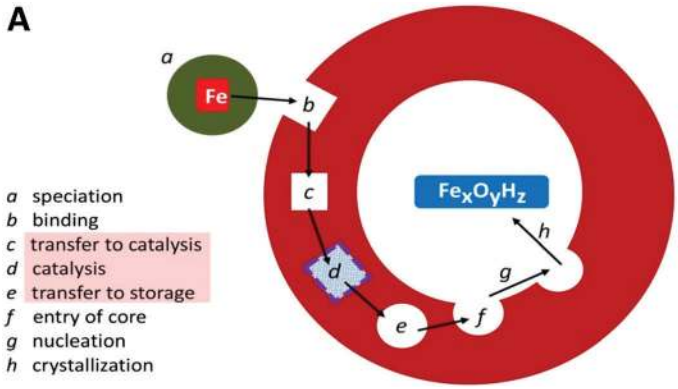


Figure **12.3.16**: (A) Schematic outline of phases involved in the uptake, oxidation, and storage of Fe(II). Hagen et al. *Metallomics*, 9,(2017). https://doi.org/10.1039/c7mt00124j. Creative Commons Attribution Non-Commercial License (https://creativecommons.org/licenses/by/3.0/),

Heart and brain ferritin are enriched in the heavy (H) chain. These two organs require safety from toxic Fe^{2+} ions. Ferritins in organs like the liver and spleen, which store lots of iron, are enriched in the light (L) chain. The two chains are about 50% homologous, but the H chain has a dinuclear **ferroxidase** iron site, which catalyzes the Fe^{2+} to Fe^{3+} conversion. Once inside, the L chain surface provides a nucleation site for the deposition of Fe^{3+} into a ferrihydrite "precipitate" ($(Fe^{3+})_2O_3 \cdot 0.5H_2O$). The general reaction is:

$$2Fe^{2+} + O_2 \rightarrow [Fe^{3+}\text{-O-O-}Fe^{3+}] \rightarrow [Fe^{3+}\text{-O(H)-}Fe^{3+}]$$

Figure **12.3.17** shows a possible generic mechanism for the oxidation of the Fe cluster from Fe^{2+} to Fe^{3+}.

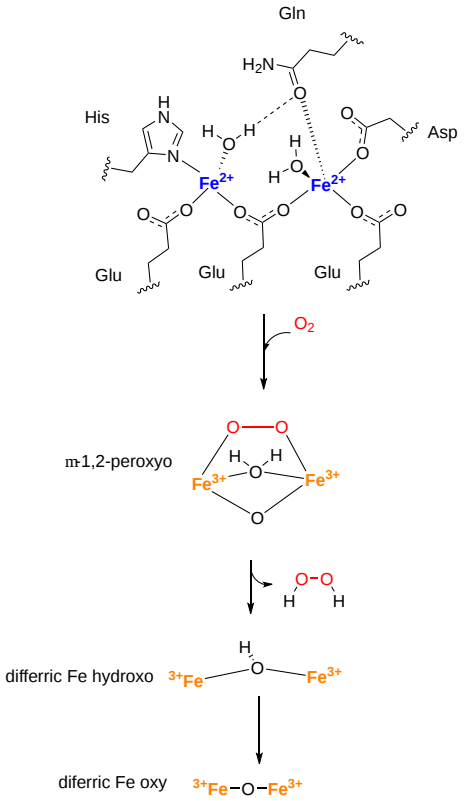


Figure **12.3.17**: Possible mechanism for ferroxidase activity of ferritin heavy chain. (adapted from Hagen et al. *Metallomics*, 9 (2017). https://doi.org/10.1039/c7mt00124j)

It acts as a ferroxidase, suggesting that dioxygen is involved as a ligand in oxidizing the two Fe^{2+} ions in the cluster to Fe^{3+}.

Figure **12.3.18**s shows a closeup of the interactions of the di-Fe cluster and two other Fe ions bound in the human H chain with water ligands.

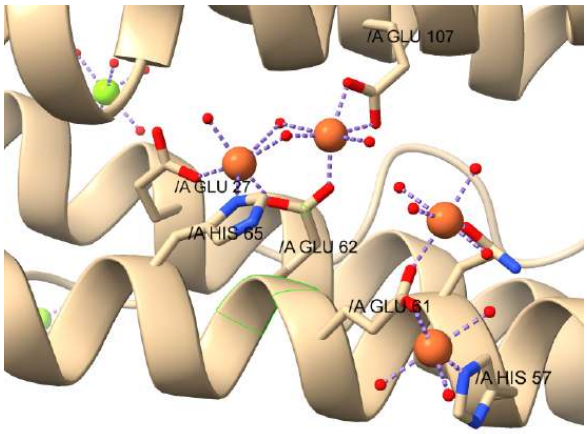
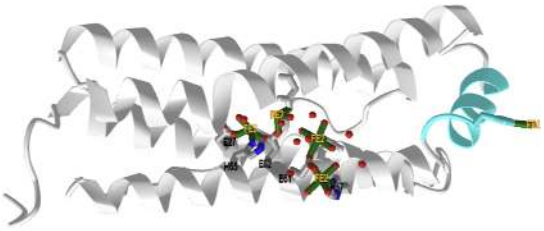


Figure **12.3.18**: Interactions of the diFe cluster and two other Fe ions bound in the site with water ligands (image made with ChimeraX)

The dinuclear Fe core is shown in the central area of the figure.

Figure **12.3.19** shows an interactive iCn3D model of human heavy-chain ferritin monomer with bound Fe (4zjk)



NCBI iCn3D Figure 12.3.19: Human heavy-chain ferritin monomer with bound Fe (4zjk). (Copyright; author via source). Click the image for a popup or use this external link: https://structure.ncbi.nlm.nih.gov/icn3d/share.html?Ux6ED11dT5dyBb2XA

The crystal structure of the full ferritin structure shows multiple binding sites and a channel to the oxidase site.

Now, let's look at how the light chain L might nucleate the formation of the iron precipitates. Crystal structures show how mineralization probably occurs at a specific site on the light chains that present themselves on the inside surface of ferritin. Figure 12.3.20 shows a closeup of the interactions of a di-Fe cluster and two other Fe ions bound in the human L chain with water and peroxide ligands. This site probably represents the nucleation and mineralization site.

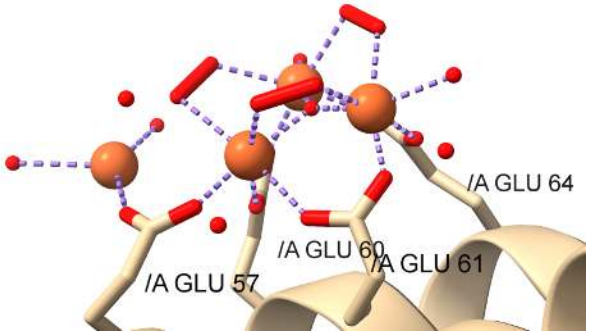
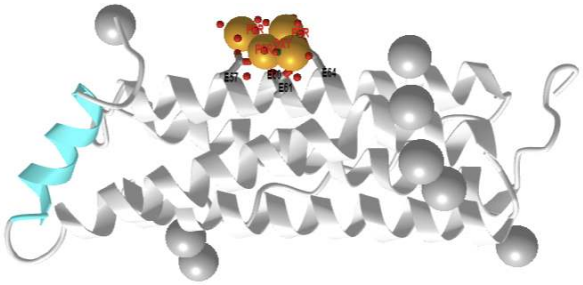


Figure 12.3.20: Closeup of the interactions of a di-Fe cluster and two other Fe ions bound in the human L chain with water and peroxide ligands at the probable mineralization site

Figure 12.3.21 shows an interactive iCn3D model of human light chain ferritin with a possible nuclear site for mineralization (5LG8). The structure was made after 60 minutes of mineralization.



NCBI iCn3D Figure 12.3.21: Human light chain ferritin with a possible nuclear site for mineralization (5LG8). (Copyright; author via source). Click the image for a popup or use this external link: https://structure.ncbi.nlm.nih.gov/i...LKo7WJtoHeLBq9

The structure suggests the presence of a μ(3)-oxo)Tris[(μ (2)-peroxo)] triiron(III) cluster assembled at subsite on the L chains containing the carboxylate ligands Glu60, Glu61, and Glu64 side chains. A Glu57, which is along the incoming path of Fe ions, is involved in Fe delivery and coordination. Figure 12.3.22 shows the electrostatic surface around the nucleation site.

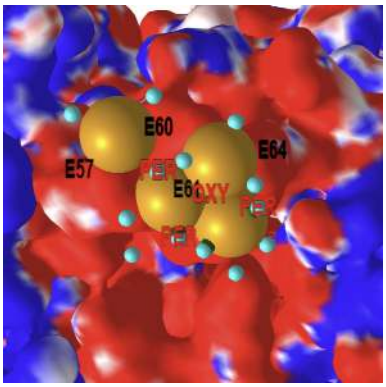


Figure **12.3.22**: Electrostatic surface around the nucleation site in light chain ferritin. Here is a link to an interactive iCn3D model: https://structure.ncbi.nlm.nih.gov/i...9LKs4NFkurnhX8

Note that the Fe ions are embedded in a site of negative electrostatic potential arising partly from the localization of the glutamic acid side chains in the site. this

Why doesn't the heavy chain of ferritin perform the same nucleation function in preparation for the crystallization of ferrihydrite? A comparison of Figures 18 and 20 shows that the H chain (which has the ferroxidase activity) has a His 65 ligand instead of a glutamic acid (position 60) as one of the coordinating ligands. This gives Glu 61 more flexibility, which must inhibit the nucleation and mineralization process.

Figure **12.3.23** shows two top views (left and center image) and one side view of three contiguous subunits of human heavy-chain ferritin monomer with bound Fe (4zjk). The gray/black sphere is actually a Ca^{2+} ion (which is larger than Fe^{2+}) from the crystal structure. This three-monomer cluster would be replicated 8 times to form the full ferritin shell. There is a three-fold C3 axis going through the central calcium in the figure, where all the monomers meet. Fe^{2+} must move through these central ions into the internal cavity.

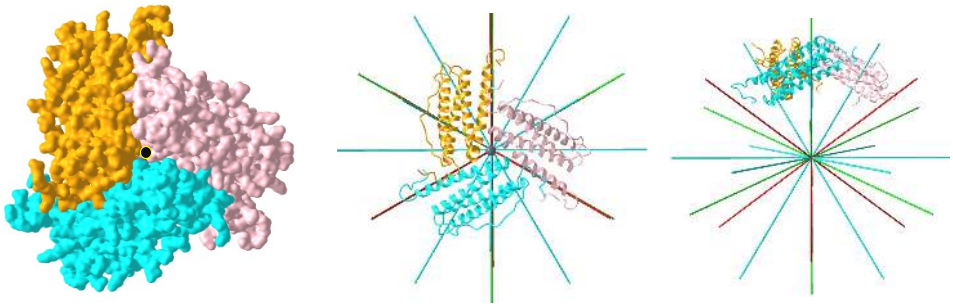


Figure **12.3.23**: Opening in ferritin formed by 3 contiguous subunits of human heavy-chain ferritin monomer (4zjk)

12.3.6.2: TRANSFERRIN

Iron ions are moved in the circulation bound to the iron-binding protein **transferrin**. It binds to a transferrin receptor and can be endocytosed into the cell, where the Fe ions are transferred and stored in ferritin. The transferrin receptor can also bind and internalize circulating ferritin (see pdb 6GSR).

Figure **12.3.24** shows an interactive iCn3D model of transferrin (2N and 2C-lobes) binding to the ectodomain of the transferrin receptor (1SUV).

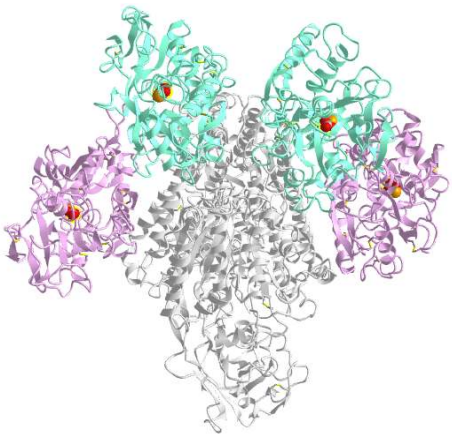


Figure **12.3.24**: Transferrin (2N and 2C-lobes) binding to the ectodomain of the transferrin receptor (1SUV). (Copyright; author via source). Click the image for a popup or use this external link: https://structure.ncbi.nlm.nih.gov/i...cBhTyxoSDQgH47

The transferrin receptor is shown in gray (2 monomers) bound to the N-lobes (cyan) and C-lobes (magenta) of transferrin. Each transfer lobe has a bound CO_3^{2-} (spacefill with CPK colors) and a Fe^{3+} ion (orange).

12.3.7: OXIDATIVE MODIFICATION OF PROTEINS

Many amino acid side chains can be oxidized in cells, as shown in Table **12.3.1**.

Table **12.3.1**: Amino acid side chain oxidation products. Berlett and Stadtman. JBC, 272, 20313-20316 (1997). DOI:https://doi.org/10.1074/jbc.272.33.20313. Creative Commons Attribution (CC BY 4.0)

Amino acids	Oxidation products
Cysteine	Disulfides, cysteic acid
Methionine	Methionine sulfoxide, methionine sulfone
Tryptophan	2-, 4-, 5-, 6-, and 7-Hydroxytryptophan, nitrotryptophan, kynurenine, 3-hydroxykynurinine, formylkynurinine
Phenylalanine	2,3-Dihydroxyphenylalanine, 2-, 3-, and 4-hydroxyphenylalanine
Tyrosine	3,4-Dihydroxyphenylalanine, tyrosine-tyrosine cross-linkages, Tyr-*O*-Tyr, cross-linked nitrotyrosine
Histidine	2-Oxohistidine, asparagine, aspartic acid
Arginine	Glutamic semialdehyde
Lysine	α-Aminoadipic semialdehyde
Proline	2-Pyrrolidone, 4- and 5-hydroxyproline pyroglutamic acid, glutamic semialdehyde
Threonine	2-Amino-3-ketobutyric acid
Glutamyl	Oxalic acid, pyruvic acid

We will focus on one here, the oxidation of the ε-amino group of lysine by H_2O_2 to form α-aminoadipic semialdehyde, where the amine is replaced with an aldehyde. This reaction is called the Fenton reaction. It is actually a **carbonylation** reaction. Figure **12.3.25** shows a hypothetical mechanism for the oxidation of lysine side chains.

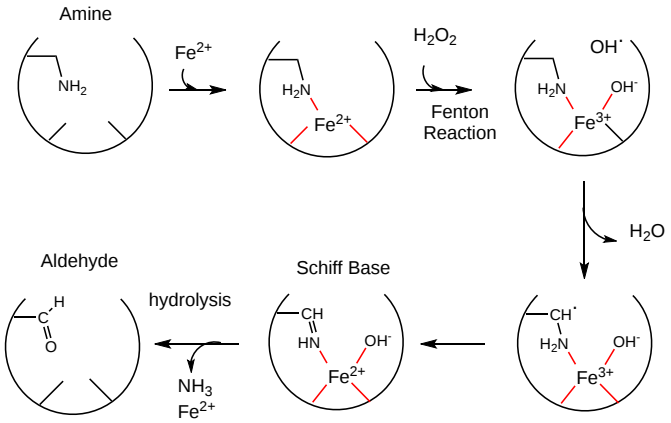


Figure **12.3.25**:

The next result is the oxidation of the lysine ε-amino group to an aldehyde. Oxidized levels of proteins (as evidenced by increased carbonylation levels) increase dramatically with age (especially after age 40). The reactions seem to be catalyzed by metals and may proceed by the generation of hydroxy free radicals. Diseases associated with premature aging (Werner's Syndrome, another link to Werner's Syndrome, Progeria) show very high levels of oxidized proteins at an early age. Fibroblasts from 10-year-old children with progeria have levels of oxidized proteins usually not seen until age 70. Beta-amyloid protein deposits (found in Alzheimer's and Down's Syndrome) cause neurotoxicity and death, partly by increasing superoxide production by endothelial cells, causing vasoconstriction/dilation and, ultimately, disease progression. Beta-amyloid aggregates appear to increase H_2O_2 levels in a process facilitated by Fe^{2+} and Cu^{+}. Free radical scavengers (antioxidants) may help to prevent this damage.

Carbonylation of proteins appears to be irreversible and nonrepairable. Increased carbonylation leads to misfolding and protein aggregation in ways that protein chaperones can not reverse. The graphs in Figure **12.3.26** (the summation of many experiments) show the correlation (negative) of increasing carbonylation of proteins (red line), a measurement of oxidative damage, and the resulting decrease in protein function (green).

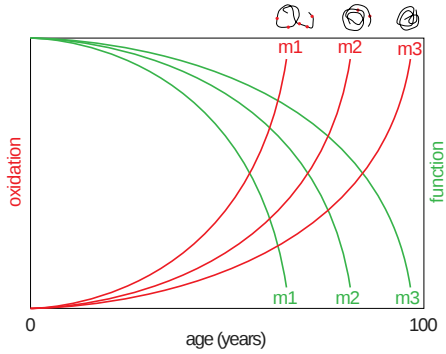


Figure **12.3.26**: Susceptibility of proteoforms to oxidative modifications determines the onset of their oxidation over time and leads to their functional decline. Krisko and Radman, (2019) *Open Biol.***9.** http://doi.org/10.1098/rsob.180249. Creative Commons Attribution License http://creativecommons.org/licenses/by/4.0/.

Red dots in the top representations of protein show carbonylation. Variants of the same protein (proteoforms) that have more intrinsically disordered regions (m1) are more susceptible to carbonylation compared to more ordered variants (m3). Cancer starts to increase around 40 years of age, and the levels of carbonylation correlate with increased cancer rates and may, in part, cause it.

Lou Gehrig's Disease (Amyotrophic Lateral Sclerosis) is a disease of progressive motor neuron degeneration, which affects 1/100,000 people and is 10-15% familial. Of the familial cases, about 25% have a mutation in superoxide dismutase I, a copper-zinc enzyme. About 2-3% of ALS patients carry 1 of 60 dominant mutations in this enzyme. Mutations often decrease the stability of the protein, which decreases Zn^{2+} affinity 5-50 fold. The A4V mutation (valine at amino acid 4 substituted for Ala) has the weakest Zn affinity and causes rapid disease progression. Without Zn^{2+}, the apoprotein somehow seems to induce cell death in neurons. This superoxide dismutase also expresses a second activity. It also acts as a peroxidase, which takes ROH + H_2O_2 to form an RHO (an aldehyde) plus water. In some cases, the enzyme retains normal activity against superoxide but altered peroxidase activity.

Figure **12.3.27**s shows the extent of carbonylation of wild type (WT) and two mutant forms of α-synuclein after exposure (in vitro) to increasing doses of γ-radiation. α-synuclein forms aggregates (Lewy bodies) in Parkinson's Disease.

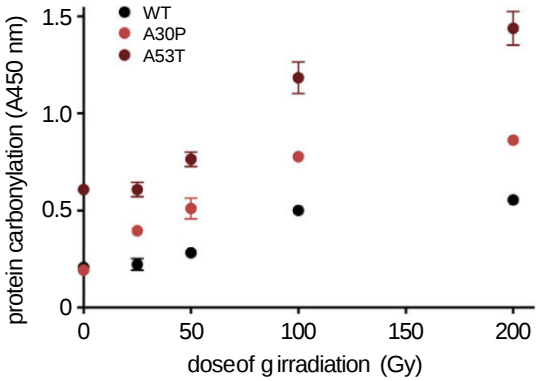


Figure **12.3.27**: Wild-type version of α-synuclein is characterized by the highest oxidation resistance. The plot displays the differential resistance to γ radiation of the human α-synuclein protein isomorph. Krisko and Radman, ibid.

The mutants, especially the A53T one, show significantly high extents of oxidative damage. This particular mutation is associated with the early onset (around 30) of Parkinson's Disease.

Is your hair going white? Wood et al. have shown that millimolar concentrations of hydrogen peroxide build up in hairs that have grayed and whitened. This was associated with a decrease in catalase and increases in Met oxidation (to Met-sulfoxide) in proteins, also associated with a decrease in the repair enzyme Met-sulfoxide reductase, Met 374 in the active site of tyrosinase, an enzyme required for the production of melanin in hair follicles, is also damaged, leading to lack of melanin, a pigment necessary for hair coloration and "senile hair graying".

ROS and Protein Folding

As discussed earlier, the cytoplasm has sufficient concentrations of "β-mercaptoethanol"-like molecules (used to reduce disulfide bonds in proteins in vitro), such as glutathione (γ-Glu-Cys-Gly) and reduced thioredoxin (with an active site Cys), to prevent disulfide bond formation in cytoplasmic proteins. Disulfide bonds in proteins are typically found in extracellular proteins, which keep multisubunit proteins together as they become diluted in the extracellular milieu. These proteins destined for secretion are cotranslationally inserted into the endoplasmic reticulum (see below), which presents an oxidizing environment to the folding protein and where sugars are covalently attached to the folding protein and disulfide bonds are formed (see Chapter 3D: Glycoproteins - Biosynthesis and Function). Protein enzymes involved in disulfide bond formation contain free Cys, forming mixed disulfides with their target substrate proteins. The enzymes (thiol-disulfide oxidoreductases, protein disulfide isomerases) have a Cys-XY-Cys motif and can promote disulfide bond formation or their reduction to free sulfhydryls. They are especially redox-sensitive since their Cys side chains must cycle between free and disulfide forms.

Reactive oxygen species (ROS) can significantly affect redox chemistry and, if present in excess, can place the cell under "oxidative" stress. ROS can indiscriminately oxidize lipids, nucleic acids, and proteins, but more specifically, they may also oxidize proteins involved in creating and maintaining the normal disulfide bond formation in proteins. As the concentration of ROS increases, the concentration of cytoplasmic proteins with incorrect disulfides should increase. Using a two dimension PAGE system (first dimension run under nonreducing and the second reducing conditions) of neural cell proteins derived from cells exposed to normal and differing oxidative conditions (hydrogen peroxide or decreased intracellular glutathione levels, Cumming et al showed that oxidizing stress increased the levels of disulfide bonds in redox-sensitive enzymes and, unexpectedly, among other cytoplasmic proteins involved in many aspects of life, affecting the activity of many cellular processes, suggesting that disulfide bond formation may have not only a structural but regulatory role.

12.3.8: OXIDATIVE MODIFICATION OF LIPIDS:

Figure 4 shows the most likely position in organic molecules that can form stable free radicals (allylic, benzylic position, and $3^o > 2^o >> 1^0$ carbons), which are likely targets for reaction with ROS. Hence, unsaturated fatty acids are extra reactive at the methylene C that separates the double bonds, as shown in Figure **12.3.28**.

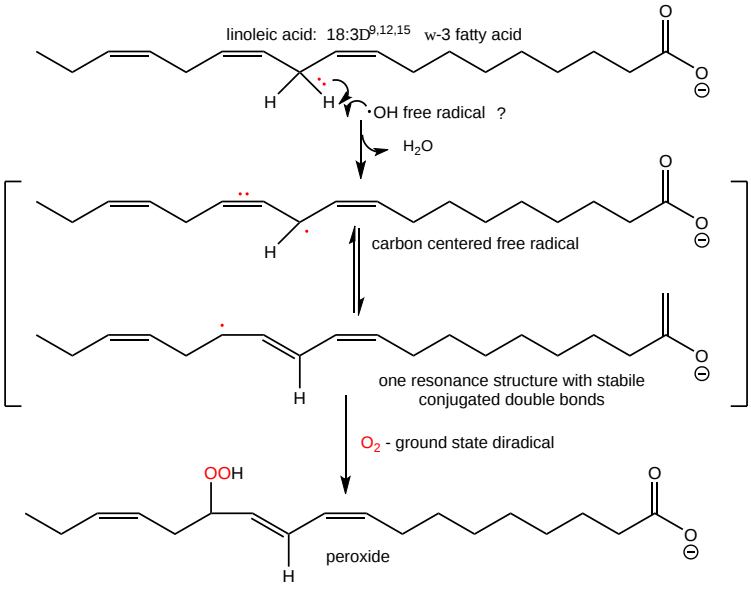


Figure **12.3.28**: Reactions of fatty acids with ROS

12.3.9: LIPID AND PROTEIN OXIDATION - CARDIOVASCULAR DISEASE

The initial stages of cardiovascular disease appear to involve the development of fatty acid streaks under the artery walls. Macrophages are immune cells that have receptors that recognize oxidized lipoproteins in the blood, which they take up. The cells then further differentiate into fat-containing **foam cells,** forming the streaks. Oxidation of fatty acids in lipoproteins could produce lipid peroxides and, along with the Fenton reaction, lead to the oxidation of apoproteins in LDL. Cortical neurons from fetal Down Syndrome patients show 3-4 times higher levels of intracellular reactive oxygen species and increased lipid peroxidation levels than control neurons. This damage is prevented by the treatment of the neurons in culture with free radical scavengers or catalase. Figure **12.3.29** shows key events in atherosclerotic plaque initiation.

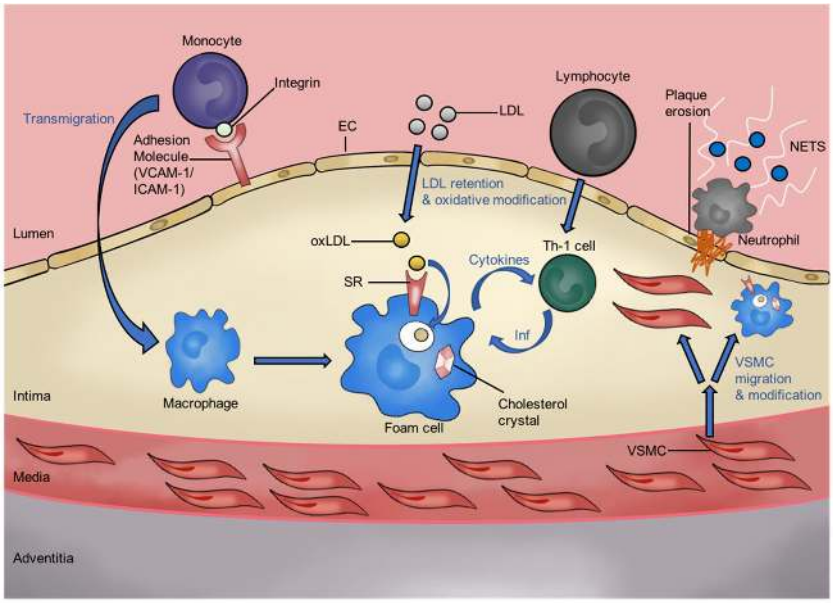


Figure **12.3.29**: Key events in atherosclerotic plaque initiation. Blood LDL can accumulate within the arterial wall, in the sub-endothelial intima. This accumulated LDL can be chemically modified or oxidized: this new lipid particle species (e.g., oxLDL) promotes chronic inflammation, which promotes the trans-endothelial migration of immune cell types and foam cell development. Abbreviations: endothelial cell, EC; intercellular adhesion molecule-1, ICAM-1; interferon-γ, IFNγ; low-density lipoprotein, LDL; Neutrophil extracellular traps, NETS; oxidized low-density lipoprotein, oxLDL; scavenger receptor, SR; T- helper 1 cell, Th1; vascular cell adhesion molecule-1, VCAM-1; vascular smooth muscle cell, VSMC. Cuthbert et al. *Cells* **2020**, *9*(11), 2453; **https://doi.org/10.3390/cells9112453.** Creative Commons Attribution (CC BY) license (**http://creativecommons.org/licenses/by/4.0/**).

How do fatty streaks appear under the endothelial cells? LDL oxidized in the lipid monolayer and, through carbonylation of lysine side chains of the apoproteins in LDL, binds to "scavenger" receptors in macrophages, which have moved into the intima below the endothelial cell barrier. Scavenger receptors were first recognized to bind acetylated LDL (conversion of ε-amino groups of lysines, for example, to acetylated and uncharged derivatives). This mimics, to some degree, the carbonylation of the ε-amino groups to aldehydes, as shown in Figure **12.3.30**.

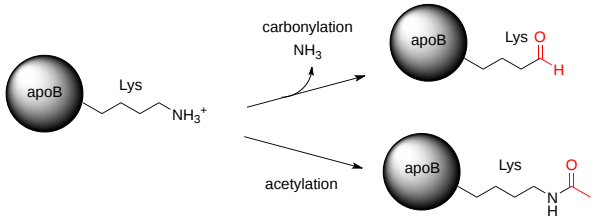


Figure **12.3.30**: Carbonylation and acetylation of lysine side chains

Either modification would make the apoprotein more acidic with a lower isoelectric point since positive lysine side chains are replaced with neutral derivatives. Assuming an asymmetric distribution of the negatively charged side chains (Asp and Glu) on the apoprotein, any pre-modification negative electrostatic potential surfaces would become more negative, enhancing binding to positive clusters displaying positive electrostatic potentials on scavenger receptors. Scavenger receptors often bind polyanions.

Many different classes (A-J) of scavenger receptor classes have been identified. One, class C, is only found in Drosophila. They bind a variety of polyanionic ligands and display broad binding specificity. Many in a single class have multiple names, which makes their designation even more confusing. They bind a diverse set of ligands, including those from bacteria and yeast (in a way similar to pathogen-associated molecular patterns - PAMPs - in the innate immune system) as well as self and modified self ligands (such as oxidized LDL -

oxLDL). Once bound, the ligand and scavenger receptors are taken into the cell by endocytosis to remove and degrade the bound ligand. They can also act in signaling pathways.

The members of the scavenger receptor family are designated as illustrated in this example, **SR-F1.1**, where **S** is Scavenger, **R** is Receptor, **F** is Class, **1** is Order in class, and **1** is an alternatively spliced form. Figure **12.3.31** shows domain structures of the different classes of scavenger receptors.

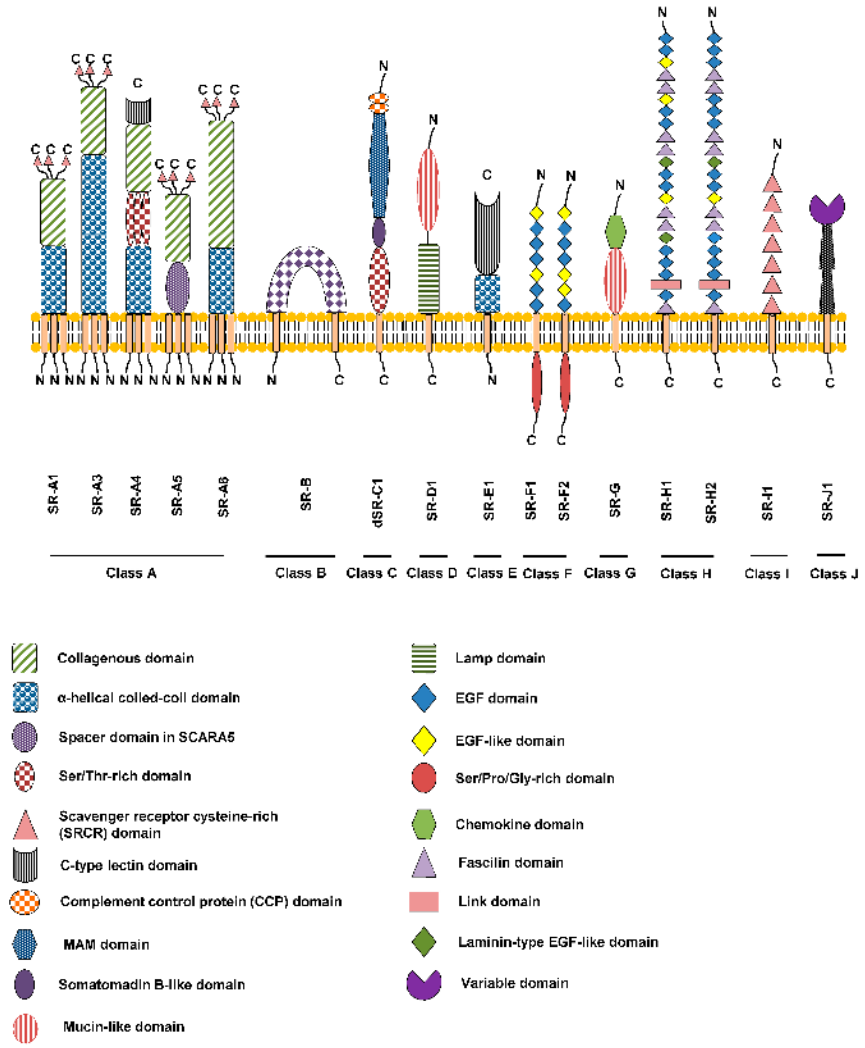


Figure **12.3.31**: Domain structures of the different classes of scavenger receptors. Zani et al. *Cells* **2015**, *4*, 178-201. https://doi.org/10.3390/cells4020178. Creative Commons Attribution 4.0 International

A more detailed cartoon showing examples from a few different scavenger receptor classes involved in cardiovascular disease is shown in Figure **12.3.32**.

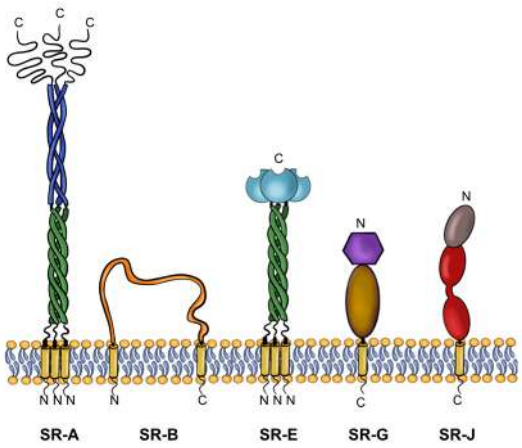


Figure **12.3.32**: Five different SR classes (A, B, E, G, J) are most closely linked to the initiation and progression of atherosclerosis. These molecules are potential biomarkers and therapeutic targets. Their structures are represented in the sketches above. Abbreviations: N-terminus, N; C-terminus, C. Cuthbert et al. ibid.

Modified LDL binds to several different scavenger receptors, including SR-A1 (also called SCARA1 or CD204), SR-A2 (also called MARCO), and SR-E1 (also called Lectin-like oxidized LDL receptor 1 or LOX-1), which binds oxidized and acetylated LDL.

Let's look in greater detail at two scavenger receptors that recognize oxLDL.

SR-A2 (MARCO)

This scavenger receptor is a trimer that binds oxLDL, polyanions, and pathogens. It has an extracellular domain (ectodomain) formed from three **c**ysteine-**r**ich monomers, so it's abbreviated SRCR. A five-stranded antiparallel β sheet and an α helix with a large loop covering it, while the dimer has a larger 8-stranded β-sheet. The polyanion ligands presumably bind to the receptors' surface with a positive (blue in figures) electrostatic potential associated with an arginine cluster. Crystal structures show that the protein also has a region of negative (red in figures) electrostatic potential, which is most likely involved in metal ion binding and in the self-association of monomers to form trimeric receptors.

Given the size of the oxidized LDL (250 Å in diameter), it would not be unexpected that oxLDL binding would promote the formation of clusters of the normal trimer scavenger receptor. This is illustrated in Figure **12.3.33**.

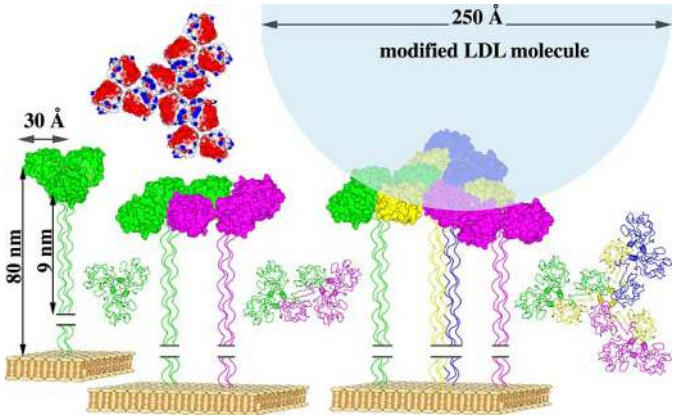


Figure **12.3.33**: Model for dimerization and oligomerization of trimeric MARCO molecules. Ojalaet al. JBC **282,16654**-16666 (2007) DOI:https://doi.org/10.1074/jbc.M701750200. Creative Commons Attribution (CC BY 4.0)

Monomeric, dimeric, and oligomeric forms of **SR-A2 (**MARCO) are shown in the bottom part of the figure. The trimeric receptor molecules can form dimers and multimers by swapping domains. Multiple interactions would promote tighter binding of large ligands such as LDL and bacteria (0.2-2 μm diameter). The assembly could proceed to the formation of oligomers (the *yellow molecule* has swapped domains with three other molecules), thus resulting in the creation of a large surface capable of interacting with large ligands, such as modified LDL (250 Å in diameter) or bacteria (0.2-2 μm). The red and blue surfaces above the trimer represent the negative (red) and positive (blue) electrostatic surface potential of the oligomer.

SR-E1 (Lox1 or Lectin-like oxidized LDLR or Oxidized low-density lipoprotein receptor 1.

LOX-1 is expressed on macrophages, dendritic cells, endothelial cells, platelets, smooth muscle cells, and adipocytes. It binds oxLDL, some bacteria (through their negatively charged cell walls), and even apoptotic cells. Figure **12.3.34** shows an interactive iCn3D model of the

extracellular C-type lectin-like domain of dimeric human Lox-1 (1YPQ)

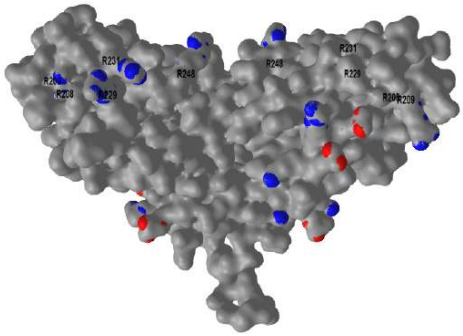


Figure 12.3.34: Extracellular C-type lectin-like domain of dimeric human Lox-1 (1YPQ). (Copyright; author via source). Click the image for a popup or use this external link: https://structure.ncbi.nlm.nih.gov/i...qGY4HBzPjjs7P7

A disulfide bridge connects the dimer in this structure. The two monomers are shown in gray spheres. They come together to form a heart-like structure A series of arginines (with blue spheres for the surface Ns and labeled) are shown in the cradle of the heart shape. These most likely interact with the oxidized apoprotein B of the oxLDL. Other blue (N) and red (O) spheres near each other can form salt bridges and may interact with zwitterion heads of LDL surface lipids such as phosphatidylcholine, sphingomyelin, or phosphatidylethanolamine.

Figure 12.3.35 shows an interactive iCn3D model of an AlphaFold predicted model of human oxidized LDL receptor - LOX (P78380)



Figure 12.3.35: . (Copyright; author via source). Click the image for a popup or use this external link: https://structure.ncbi.nlm.nih.gov/i...rLoi7ZK4K3SsH8

The yellow spacefill indicates the transmembrane segment. Rotate the model along the long axis, and one face of the top domain has a red (negative electrostatic potential) face while the opposite side has a blue (positive potential).

12.3.10: OXIDATIVE MODIFICATION OF DNA

Significant evidence suggests oxygen free radicals are linked to aging and diseases. Mutations caused by hydroxylation reactions (presumably from the generation of hydroxyl free radicals, as shown above) can lead to cancer. A particularly nasty reaction is the hydroxy radical insertion into DNA bases. Figure 12.3.36 shows the hydroxylation at position 8 of guanine to produce 8-oxy-G and at positions 5 and 6 in thymine.

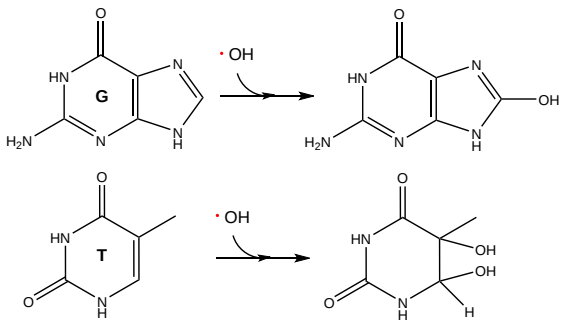
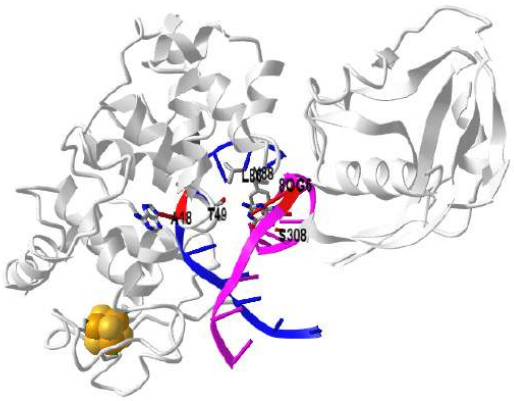


Figure 12.3.36: Hydroxylation of G and T bases by the hydroxyl free radical

Mitochondrial DNA is more susceptible to oxidation than is nuclear DNA. The human mitochondrion has a small genome (16.5 Kb compared to the nuclear genome of 3 Gb), which codes 13 protein subunits involved in respiration, 22 tRNAs, and two ribosomal RNAs. (The mitochondria presumably are vestiges of a bacteria that invaded an early cell and established a symbiotic relationship with the cell). There is an inverse correlation of oxidized mitochondrial DNA [8-oxoG] with the maximal life span of an organism, but this correlation is not seen with nuclear DNA. Presumably, the nuclear DNA is somewhat protected from oxidative damage since it is bound to histone proteins (which form nucleosome core particles with DNA) and by DNA repair enzymes. DNA repair enzymes encoded in the nucleus are found in the mitochondria, and mitochondrial DNA is packaged with mitochondrial transcription factor A (TFAM). Examination of human bladder, head and neck, and lung primary tumors reveals a high frequency of mitochondrial DNA mutations. In addition, most cellular dioxygen use occurs in the mitochondria. Hence, this organelle probably faces the highest concentration of toxic oxygen reduction products. Recently, the crystal structure of an enzyme, adenine DNA glycosylase (MutY), that repairs 8-oxoG modified DNA, has been determined in complex with the oxidatively damaged DNA. If not repaired, the 8-oxyG base pairs with adenine instead of cytosine, causing a GC to AT mutation on DNA replication.

Figure **12.3.37** shows an interactive iCn3D model of adenine mispaired with 8-oxoguanine by MutY adenine DNA glycosylase (1RRQ)



NCBI iCn3D Figure **12.3.37**: Adenine mispaired with 8-oxoguanine by MutY adenine DNA glycosylase (1RRQ) (Copyright; author via source). Click the image for a popup or use this external link: https://structure.ncbi.nlm.nih.gov/icn3d/share.html?4RiEc6TuqmexiW1r7

The protein MutY, which catalyzes the base excision and repair, is shown in gray. The DNA strands are shown in magenta and blue. 8-OxyG on the magenta strand is labeled 8OG7 and is shown in CPK-colored sticks. Its mismatched adenine base pair partner, labeled A18 on the blue strand, is shown in CPK-colored sticks. Notice its orientation is kinked away from the orientation in a canonical base pair. Key amino acid side chains (Thr49, Leu86, Tyr88, and Ser308) interacting with the 8-oxyG are shown in CPK-colored sticks with labels.

Although oxidative damage in mitochondria clearly can promote premature aging, other independent mechanisms may also. Kujoth et al. developed a mouse model that expressed a mutant form of mitochondrial DNA polymerase that was defective in the proofreading activity of the enzyme. These mice displayed premature aging but showed no increased levels of oxidized mitochondrial lipids or hydroxylated G residues in mitochondrial DNA. They did show significant activation of a cytosolic enzyme called caspase-3, which, when active, leads to the programmed death of cells (a process called apoptosis). This calcium-activated aspartic acid protease (with an active site Asp) is activated by binding mitochondrial cytochrome C that has "leaked" into the cytoplasm from its normal location in the intermembrane space in mitochondria. The process is usually associated with DNA damage (mutations, fragmentation) that would arise if the proofreading function of DNA polymerase were defective. This was indeed found in these mice.

Oxidative damage to biomolecules might not initiate aging and disease processes, but rather might be a secondary effect of other initiating events. Reversing or preventing oxidative damage might slow the progression of aging and disease. Aging is a complex feature of organisms and would be expected to have complex causes and biological effects. At the organismal level, aging has been studied in the roundworm C. elegans, which lives for only a few weeks. Genetic analyses can easily find gene alterations associated with premature aging. One hormonal system recently associated with aging in eukaryotes (and in C. elegans) involves the signaling pathways for insulin and insulin growth factor I (IGF-1), which regulate carbohydrate, lipid, and reproductive pathways in C. elegans. Mutations that decrease signaling from this pathway increase C. elegans life span. These mutations lead to increased activity of the DAF16 transcription factor, which upregulates the expression of many genes. In contrast, when exposed to insulin or IGF-1, wild-type organisms decrease the activity of DAF16. Using DNA microarrays, investigators determined which DAF16-controlled genes were upregulated in mutant worms at the mid-life point of the organism. These genes included, among others, peroxisomal and cytosolic catalase, Mn-superoxide dismutase, cytochrome P450s, metallothionein-related Cd-binding protein, and heat shock proteins. In the next section, we will investigate the function of several of these gene products. Still, needless to say, they are all involved in cellular responses to stress, often involving dioxygen metabolites. The

overexpression of mitochondrial catalase in mice increased their lifespan by 20%. Decreased levels of insulin-like growth factor also promote longevity in mice, indicating again that mechanisms in addition to oxidative damage by ROS are involved in aging.

12.3.11: BENEFICIAL OXIDATION OF PROTEINS: OXIDATIVE BURST IN MACROPHAGES

There are cases in which oxidative damage to protein and lipids is desirable. One example involves the role of macrophages in the immune system in eliminating foreign microorganisms. When macrophages recognize and engulf microbes, one mechanism deployed to kill the microorganism is oxidative damage. The stimulated macrophages undergo an oxidative burst, which leads to increased oxygen utilization. One outcome of this is the generation of ROS. Activating the ROS-generating system can also kill the macrophage (which is OK).

In addition, immune function decreases with age. This probably also occurs through damage from ROS. Oxidative stress and irradiation also shorten telomeres at the end of chromosomes. They are enriched in guanine bases with many repeats (thousands) of TTAGGG sequences and, hence, are susceptible to oxidation. However, as you might expect, macrophages have developed ways to limit self-damage by ROS.

In the presence of ROS, the macrophage or mitochondrial kinase Mst1/2 is recruited to their respective membranes from the cytosol. The enzyme acts as a ROS sensor and "attenuator" through the phosphorylation and stabilization of a protein, Keap1, that binds to a transcription factor, Nrf2 (also called NFE2L2). When bound to unphosphorylated Keap1, the transcription factor Nrf2 is a target for proteolysis. Keap1 phosphorylation prevents its binding to Nrf2. Free Nrf2 then can translocate to the nucleus, where it promotes transcription of antioxidant proteins such as glutamate-cysteine ligase catalytic subunit (Gclc), which catalyzes the first step and rate-limiting step of glutathione (γ-glutamyl-cysteinyl-glycine) synthesis. These processes are illustrated in Figure **12.3.38**.

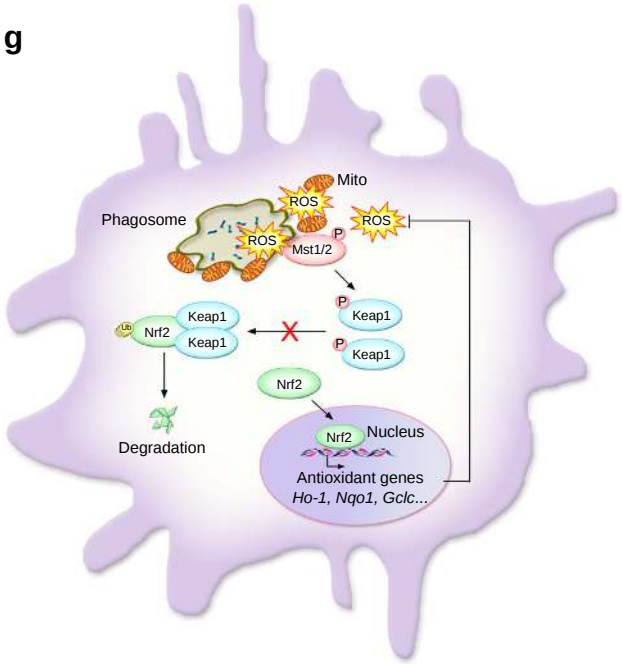


Figure **12.3.38**: A proposed working model for kinases Mst1/2 sense ROS and maintain cellular redox balance by modulating the stability of Nrf2. Wang, P., Geng, J., Gao, J. *et al.* Macrophage achieves self-protection against oxidative stress-induced aging through the Mst-Nrf2 axis. *Nat Commun* **10,** 755 (2019). https://doi.org/10.1038/s41467-019-08680-6. Creative Commons Attribution 4.0 International License. http://creativecommons.org/licenses/by/4.0/.

Phagosomal or mitochondrial ROS release attracts Mst1/2 to the membrane of phagosome or mitochondrion from the cytosol and activates Mst1/2; Mst1/2
phosphorylate Keap1 to stabilize Nrf2 and regulate the expression of antioxidant enzymes to protect the cell against oxidative damage.

12.3.12: SUMMARY

This chapter explores the unique role of oxygen in both chemistry and biology, tracing its evolution from an inert component of early Earth's reducing atmosphere to a key player in modern aerobic metabolism and cellular signaling. The chapter is organized around several core themes:

- **Oxygen's Ubiquity and Chemical Versatility:**
  Oxygen is one of the most abundant and chemically reactive elements, forming a vast array of compounds (with water being the most critical for life) due to its ability to bond with nearly all elements. Its dual roles as a nucleophile/electrophile, acid/base, and oxidizing/reducing agent highlight its versatility in biochemical reactions.

- **Geochemical History and the Great Oxidation Event:**
  The chapter reviews how the early Earth's reducing atmosphere, rich in hydrogen and various reduced compounds, was transformed by the advent of photosynthetic cyanobacteria. This evolutionary milestone—the Great Oxidation Event—led to a gradual increase in atmospheric oxygen, profoundly affecting metal chemistry, mass extinctions among anaerobes, and the eventual rise of eukaryotes and terrestrial life.
- **Molecular Properties and Reactivity of Dioxygen:**
  An in-depth analysis of oxygen's molecular orbital configuration explains its ground state as a triplet diradical—a feature that underlies its paramagnetic properties and kinetic sluggishness despite thermodynamically favorable oxidation reactions. The transition to singlet oxygen, though energetically demanding, significantly alters reactivity and is pivotal in photochemical processes.
- **Formation and Impact of Reactive Oxygen Species (ROS):**
  The stepwise reduction of dioxygen produces various ROS, such as superoxide, peroxide, and the highly reactive hydroxyl radical. While these species are essential for certain biological functions, they also pose a risk to cellular components. The chapter discusses how the generation of ROS is tightly controlled, and how their toxic effects are mitigated.
- **Antioxidant Defenses and Iron Homeostasis:**
  Cells employ a sophisticated network of antioxidant enzymes (e.g., superoxide dismutase, catalase, peroxidases) and small-molecule antioxidants like glutathione to detoxify ROS. In parallel, the chapter highlights the critical roles of iron-binding proteins—ferritin for storage and transferrin for transport—in preventing harmful iron-mediated reactions (such as the Fenton reaction) that can exacerbate oxidative stress.
- **Oxidative Modifications and Disease:**
  Oxygen-derived radicals can modify proteins, lipids, and DNA, leading to carbonylation, lipid peroxidation, and mutagenic DNA lesions like 8-oxoguanine. These modifications are linked to aging and various diseases, including cardiovascular disorders, neurodegeneration, and cancer. The chapter also discusses how the body's scavenger receptors recognize and clear oxidatively modified molecules (e.g., oxidized LDL), processes that are intimately connected with the pathogenesis of atherosclerosis.
- **Beneficial Uses of Oxidative Reactions:**
  Finally, the chapter acknowledges that controlled oxidative processes are not solely detrimental. For example, the oxidative burst in macrophages is a crucial immune defense mechanism that utilizes ROS to destroy pathogens, albeit with protective measures in place to minimize self-damage.

Overall, this chapter integrates historical, molecular, and physiological perspectives to illustrate how oxygen, despite its potential for causing oxidative damage, has been harnessed by living systems to drive complex biochemical processes essential for life.

This page titled 12.3: The Chemistry and Biochemistry of Dioxygen is shared under a not declared license and was authored, remixed, and/or curated by Henry Jakubowski and Patricia Flatt.

- **11.2: Diffusion Across a Membrane - Passive and Facilitated Diffusion** by Henry Jakubowski and Patricia Flatt has no license indicated.

12.4: BIOLOGICAL OXIDATION-REDUCTION REACTIONS

LEARNING GOALS (CHATGPT O3-MINI)

1. **Understand the Fundamentals of Oxidation Reactions:**
   - Describe the general steps of oxidation processes in organic chemistry, including initiation, propagation (and branching), and termination reactions.
   - Compare the mechanisms of combustion (using dioxygen) with those of controlled oxidation using alternative oxidizing agents like permanganate and chromate.
2. **Contrast Chemical and Biological Oxidizing Agents:**
   - Explain why dioxygen is often unsuitable for controlled oxidation in organic synthesis and how alternative oxidizing agents overcome these challenges.
   - Identify the unique challenges of oxidizing organic molecules in biological systems and the specialized oxidizing agents (e.g., NAD^+, FAD, monooxygenases) that are employed instead.
3. **Examine the Chemistry and Function of NAD^+ and FAD:**
   - Illustrate the structures of NAD^+ (and its reduced form, NADH) and FAD (and $FADH_2$), and explain how their chemical properties make them effective two-electron hydride carriers.
   - Discuss the mechanistic basis of hydride transfer reactions catalyzed by dehydrogenases, and how these reactions integrate into metabolic pathways (e.g., conversion of pyruvate to lactate).
4. **Explore the Roles of Dehydrogenases in Biological Oxidation:**
   - Describe how dehydrogenase enzymes use NAD^+ and FAD to oxidize substrates and drive energy production in pathways such as glycolysis and the Krebs cycle.
   - Use standard reduction potentials and the Nernst equation ($\Delta G = -nFE°$) to analyze the thermodynamics of these redox reactions.
5. **Differentiate Among Enzyme Classes that Utilize Dioxygen:**
   - Compare monooxygenases (including hydroxylases) that incorporate one oxygen atom into substrates, dioxygenases that incorporate both atoms, and oxidases that transfer electrons to dioxygen without substrate incorporation.
   - Illustrate the roles of these enzyme classes in diverse biological contexts, such as xenobiotic metabolism, hormone synthesis, and detoxification.
6. **Delve into the Mechanism and Function of Cytochrome P450 Enzymes:**
   - Outline the catalytic cycle of cytochrome P450s, emphasizing the role of the heme cofactor, electron transfer from NADPH via cytochrome P450 reductase, and the activation of dioxygen for substrate hydroxylation.
   - Analyze how cytochrome P450-mediated reactions can both detoxify substrates and, paradoxically, activate procarcinogens.
7. **Understand the Structural Basis for Redox Tuning in Enzymes:**
   - Explain how the protein microenvironment (e.g., ligand identity, hydrophobicity, hydrogen bonding) modulates the redox potential of enzyme-bound cofactors such as FAD and metal centers in cupredoxins like azurin.
   - Evaluate examples where mutations alter redox potential and discuss the implications for enzyme function.
8. **Recognize the Sequential Oxidation of Organic Molecules in Metabolism:**
   - Describe the stepwise oxidation of methane to carbon dioxide in methanotrophs, including the enzymes involved in each oxidation step (e.g., methane monooxygenase, methanol dehydrogenase).
   - Discuss how these sequential reactions illustrate the controlled use of oxidizing agents to extract energy from organic molecules.
9. **Integrate the Role of Heme Proteins in Diverse Redox Processes:**
   - Compare the functions of different heme proteins (hemoglobin, cytochrome C, cytochrome P450) and explain how variations in coordination and protein environment enable them to carry out distinct redox roles.
   - Link structure to function by discussing how differences in heme ligation (e.g., proximal histidine vs. cysteine) determine each protein's reactivity and physiological role.
10. **Explore Transition Metal Homeostasis and Its Impact on Oxidative Reactions:**
    - Discuss the importance of metalloproteins in binding, transporting, and regulating transition metals such as Fe, Zn, and Cu.

- Explain how differences in metal binding affinities and coordination geometries are critical for preventing metal-induced oxidative damage while facilitating essential redox reactions.

These learning goals are intended to help students integrate chemical principles with biological context, enabling a deeper understanding of how oxidizing agents function in both laboratory settings and living systems.

12.4.1: GENERAL OXIDIZING AGENTS

Before considering common biological oxidizing agents, look back at the ones you saw in other chemistry classes. Oxidizing agents are required to oxidize organic molecules. In chemistry labs, you likely never used dioxygen as an oxidizing agent. It is difficult to limit the extent of oxidation using dioxygen. In addition, side reactions are likely given the nature of the reactive oxygen reduction products. The mechanisms of combustion reactions of organic molecules with dioxygen to produce carbon dioxide and water are complicated. Table **12.4.1** shows some key steps in the combustion of methane.

Initiation

$$CH_4 \longrightarrow CH_3^{\bullet} + H^{\bullet}$$

$$O_2 \longrightarrow 2\,O^{\bullet}$$

Propagation

$$CH_4 + H^{\bullet} \longrightarrow CH_3^{\bullet} + H_2$$

$$CH_4 + HO^{\bullet} \longrightarrow CH_3^{\bullet} + H_2O$$

$$CH_3^{\bullet} + O^{\bullet} \longrightarrow CH_2O + H^{\bullet}$$

$$CH_2O + HO^{\bullet} \longrightarrow CHO^{\bullet} + H_2O$$

$$CH_2O + H^{\bullet} \longrightarrow CHO^{\bullet} + H_2$$

$$CHO^{\bullet} \longrightarrow CO + H^{\bullet}$$

$$CO + HO^{\bullet} \longrightarrow CO_2 + H^{\bullet}$$

Branching

$$H^{\bullet} + O_2 \longrightarrow HO^{\bullet} + O^{\bullet}$$

Termination

$$H\cdot + R^{\bullet} + M \longrightarrow RH + M^{*}$$

In chemistry, other oxidizing agents are often used, including permanganate and chromate. Their mechanism of action is illustrated in Figure **12.4.1**.

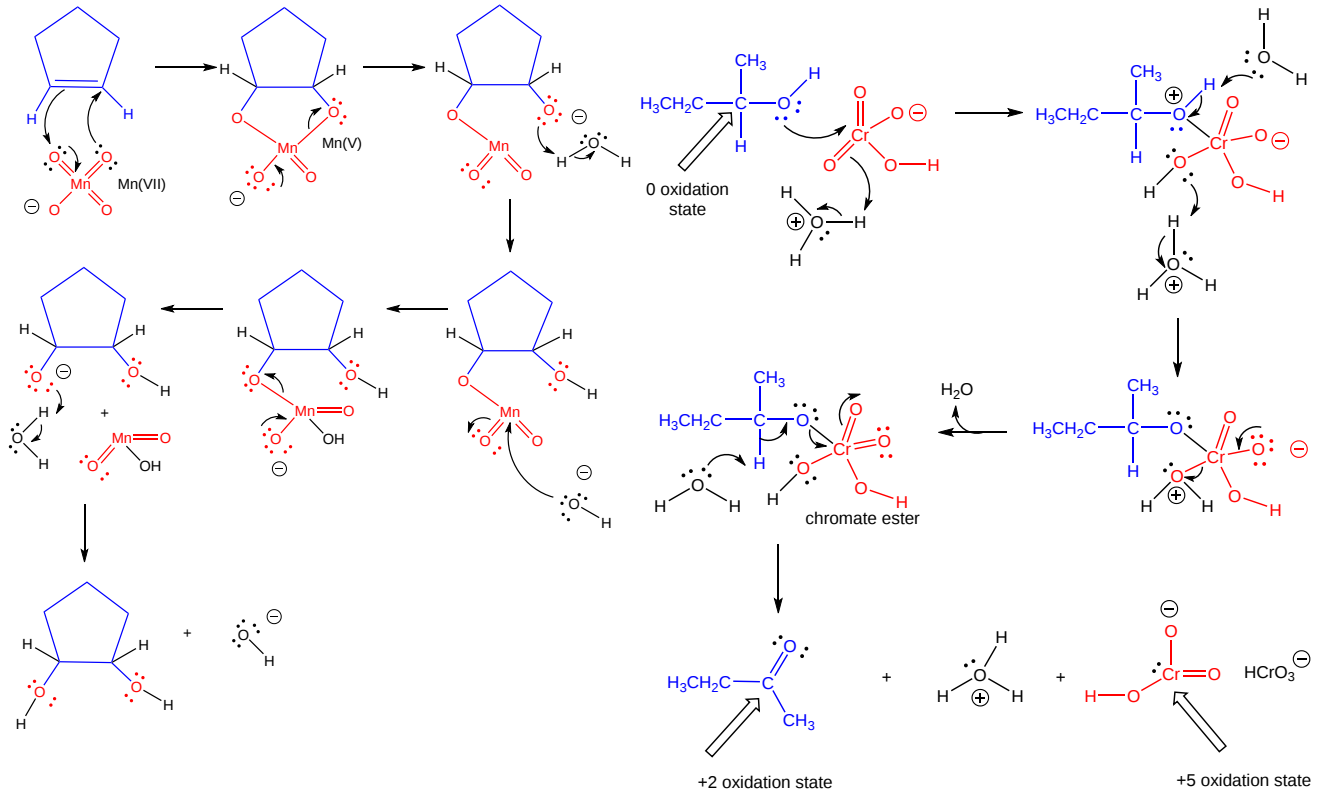


Figure **12.4.1**: Mechanism of oxidation of organic molecules by permanganate and chromate

Oxygen can often be inserted into a molecule in a nonoxidative process by hydration of an alkene to an alcohol (a readily reversible reaction), which could then be oxidized to either an aldehyde/ketone or carboxylic acid using an appropriate oxidizing agent.

Most biological oxidation reactions (such as those found in glycolysis, the Krebs cycle, and fatty acid oxidation) do not use dioxygen as the immediate oxidizing agent. Instead, they use nicotinamide adenine dinucleotide (NAD^+) or flavin adenine dinucleotide (FAD) as oxidizing agents, which are reduced. Enzymes that use these oxidizing agents are usually called **dehydrogenases**. Dioxygen can also introduce oxygen atoms into biological molecules in oxidative reactions. Enzymes that introduce one oxygen atom of dioxygen into a molecule (and the other oxygen into water) are called **monooxygenases**. (Note: some monooxygenases that hydroxylate biomolecules are called **hydroxylases**.) Those that introduce both atoms of dioxygen into a substrate are called **dioxygenases**. These oxygenases are not usually used to oxidize organic molecules for energy production. Instead, they introduce O atoms for other reasons, including increasing the solubility of nonpolar aromatics to facilitate secretion and produce new molecular species with different biological activities. Finally, dioxygen can oxidize biological molecules without adding oxygen atoms to the substrate. Instead, electrons lost from the oxidized substrate are passed via intermediate electron carriers to dioxygen, which gets reduced to superoxide (if one electron is added), hydrogen peroxide (if two electrons are added), or water (if 4 electrons are added). These enzymes are called oxidases. (Note: The letters oxi- or oxygen- are used in all the enzymes that use dioxygen as the oxidizing agent.)

In this chapter section, we will discuss biological oxidation reactions. Most introductory biochemistry texts don't approach oxidation reactions in one cohesive chapter. Probably because of that, when I was learning biochemistry, I found the presentation of these different enzymes involved in redox reactions very confusing. Hopefully, this section will alleviate that problem. First, the chemistry of NAD^+ and FAD will be discussed. Then, the enzymes using dioxygen in oxidative reactions (monooxygenases, dioxygenases, and oxidases) will be explored.

12.4.2: THE CHEMISTRY OF NAD^+ AND FAD

NAD^+ is a nicotinic acid or nicotinamide derivative, as illustrated in Figure **12.4.2**.

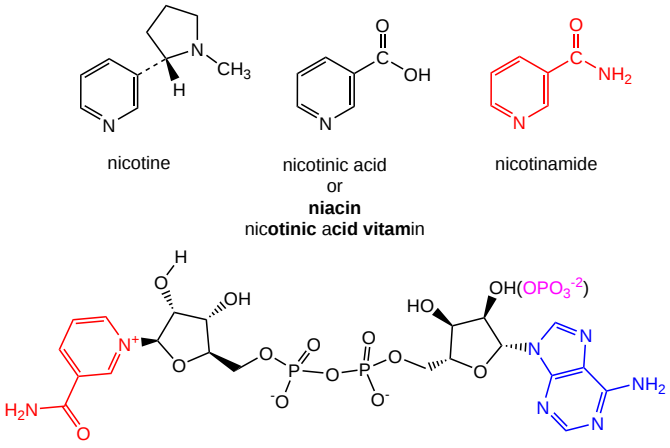


Figure 12.4.2: Structure of niacin derivatives

It and its reduction product, NADH, exist in the cells as interconvertible members of a pool whose total concentration does not vary significantly with time. Hence, if NAD^+ is oxidizing carbohydrates and lipids to produce energy in the form of ATP, levels of NAD^+ would begin to fall as NADH rises. A mechanism must be present to regenerate NAD^+ from NADH if oxidation continues. As we will see later, this happens in the muscle under anaerobic conditions (if dioxygen is lacking, as when you are running a 100 or 200 meter race, or if a saber-toothed tiger is chasing you) when pyruvate and NADH react to form lactate + NAD^+. The reaction is shown in Figure 12.4.3.

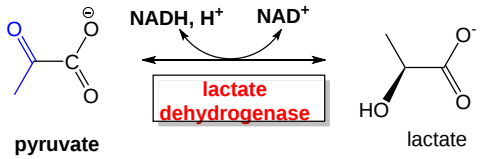


Figure 12.4.3: Conversion of pyruvate to lactate

Under aerobic conditions (sufficient dioxygen available), NADH is reoxidized in the mitochondria by electron transport through various mobile electron carriers, which pass electrons to dioxygen (using the enzyme complex cytochrome C oxidase) to form water.

NAD^+/NADH can undergo two-electron redox steps, in which a hydride is transferred from an organic molecule to the NAD^+, with the electrons flowing to the positively charged nitrogen of NAD^+, which serves as an electron sink. NADH does not react well with dioxygen since single electron transfers to/from NAD^+/NADH produce free radical species that can not be stabilized effectively. All NAD^+/NADH reactions appear to involve 2-electron hydride transfers. Figure 12.4.5 shows both 1 and 2 electrons to NAD^+.

Figure 12.4.4:

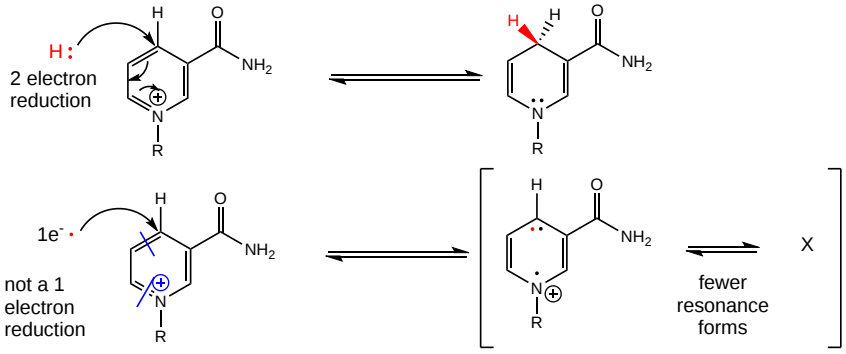


Figure 12.4.4: 1 and 2 electrons to NAD^+

FAD (or flavin mononucleotide-FMN) and its reduction product, $FADH_2$, are derivatives of riboflavin, as shown in Figure 12.4.5.

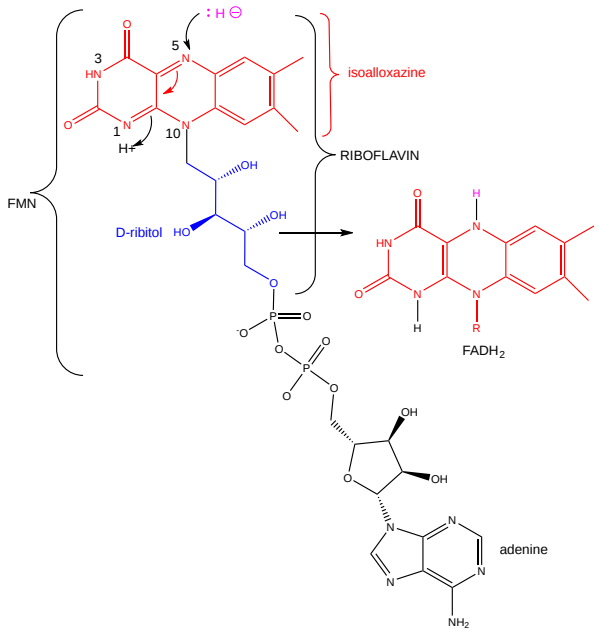


Figure **12.4.5**: Structures of riboflavin, FMN and FAD

$FAD/FADH_2$ differ from NAD^+/NADH since they are bound tightly (K_D approx 10^{-7} - 10^{-11} M) to enzymes that use them. This is because $FADH_2$ is susceptible to reactions with dioxygen since $FAD/FADH_2$ can form stable free radicals arising from single electron transfers. $FAD/FADH_2$ can undergo one or two electron transfers. This is illustrated in Figure **12.4.6**.

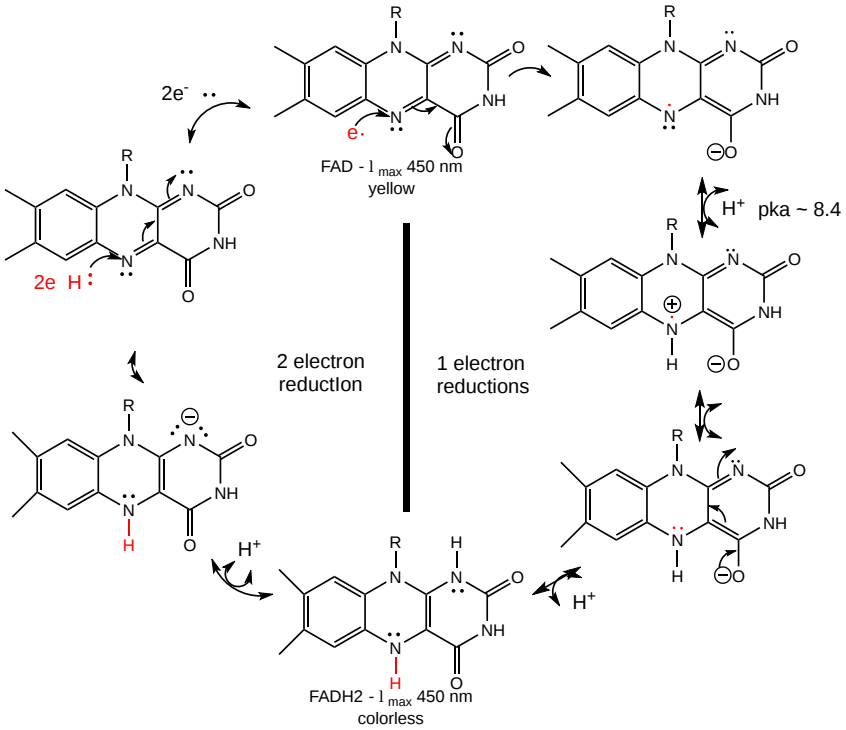


Figure **12.4.6**: 1 and 2 electrons reduction of FAD

$FAD/FADH_2$ are tightly bound to enzymes to control the nature of the oxidizing/reducing agents that interact with them. (i.e., so dioxygen in the cell won't react with them in the cytoplasm.) An enzyme with a tightly bound FAD that oxidizes a substrate would be inactive for further catalytic steps unless another oxidizing agent reoxidizes the bound $FADH_2$.

12.4.3: DEHYDROGENASES

These enzymes use NAD^+/NADH or FAD/$FADH_2$ and are named for the oxidized substrate. For instance, in the reaction:

$$\text{pyruvate} + \text{NADH} \rightleftharpoons \text{lactate} + \text{NAD}^+$$

which is used to regenerate NAD^+ under anerobic conditions, the enzyme is named lactate dehydrogenase. As in acid/base reactions, when the preferred direction for the reaction (from a ΔG^o perspective) is from a stronger acid to a weaker (conjugate) acid, the preferred direction for a redox reaction is in the direction from a stronger to a weaker oxidizing/reducing agent. This can easily be determined from charts of standard reduction potentials and using the equation: $\Delta G^o = -nFE^o$,

- where F is the Faraday constant (96,494 Coulombs/mol e^- = 96, 494 J/(V.mol) = 23.06 kcal/(V·mol) or 96 kJ/(V·mol). One Faraday is the charge per one mol of electrons).
- and E^o, the standard EMF or standard cell potential (total voltage at standard state conditions), which can be determined by adding the standard reduction potentials (**E^o**) for the two appropriate half-reactions after reversing the equation for the half-reaction that represents the oxidation. Hence $E^o = E^o_{reduction} - E^o_{oxidation}$.

When n=2 (number of electrons), which is common for oxidations of organic molecules,

$$\Delta G^o \text{ (kcal/mol)} = -46.12E^o \text{ or approximately } -50E^0 \text{ (or } -193E^o \text{ kJ/mol)}$$

Notice that when $E^o > 0$, $\Delta G^o < 0$, the reaction as written is favored under standard conditions. Note in the table below that many of the half-reactions involve protons. For biological reactions involving free protons, the standard state concentration for the protons is not 1 M as for other solutes in solution but is defined as the hydronium ion concentration at pH 7.0. The E^o and ΔG^o values for the reactions involving hydrogen ions at a standard state of pH 7.0 are usually written as $E^{o'}$ and $\Delta G^{o'}$.

Table **12.4.2** below shows common standard reduction potentials.

Table 12.4.2: Standard reduction potentials for common biomolecules

oxidant	reductant	n (electrons)	$E^{o'}$ (volts), 25ºC
Acetate + carbon dioxide	pyruvate	2	-0.70
succinate + CO_2 + $2H^+$	α−ketoglutarate + H_2O	2	-0.67
acetate	acetaldehyde	2	-0.60
glycerate-3-P	glyceraldehyde-3-P + H_2O	2	-0.55
O_2	O_2^-	1	-0.45
ferredoxin (ox)	ferredoxin (red)	1	-0.43
Carbon dioxide	formate	2	-0.42
$2H^+$	H_2	2	-0.42
α-ketoglutarate + CO_2 + $2H^+$	isocitrate	2	-0.38
acetoacetate	β-hydroxybutyrate	2	-0.35
Cystine	cysteine	2	-0.34
Pyruvate + CO_2	malate	2	-0.33
NAD^+ + $2H^+$	NADH + H^+	2	-0.32
$NADP^+$ + $2H^+$	NADPH + H^+	2	-0.32
FMN (enzyme bound)	$FMNH_2$	2	-0.30
Lipoic acid, ox	Lipoic acid, red	2	-0.29
1,3 bisphosphoglycerate + $2H^+$	glyceraldehyde-3-P + Pi	2	-0.29
Glutathione, ox	Glutathione, red	2	-0.23
FAD (free) + $2H^+$	$FADH_2$	2	-0.22
Acetaldehyde + $2H^+$	ethanol	2	-0.20
Pyruvate + $2H^+$	lactate	2	-0.19
Oxalacetate + $2H^+$	malate	2	-0.17
α-ketoglutarate + NH_4^+	glutamate	2	-0.14
FAD + $2H^+$ (bound)	$FADH_2$ (bound)	2	0.003-0.09
Methylene blue, ox	Methylene blue, red	2	0.01
Fumarate + $2H^+$	succinate	2	0.03
CoQ (Ubiquinone - UQ) + H^+	UQH	1	0.031
UQ + $2H^+$	UQH_2	2	0.06
Dehydroascorbic acid	ascorbic acid	2	0.06
Ubiquinone; ox	red	2	0.10
Cytochrome b2; Fe^{3+}	Cytochrome b2; Fe2+	1	0.12
Cytochrome c1; Fe3+	Cytochrome c1; Fe^{2+}	1	0.22
Cytochrome c; Fe^{3+}	Cytochrome c; Fe^{2+}	1	0.25
Cytochrome a; Fe^{3+}	Cytochrome a; Fe^{2+}	1	0.29
1/2 O_2 + H_2O	H_2O_2	2	0.30
Cytochrome a3; Fe^{3+}	Cytochrome a3; Fe^{2+}	1	0.35
Ferricyanide	ferrocyanide	2	0.36
Cytochrome f; Fe^{3+}	Cytochrome f; Fe^{2+}	1	0.37
Nitrate	nitrite	1	0.42
Photosystem P700	.	.	0.43
Fe^{3+}	Fe^{2+}	1	0.77
1/2 O_2 + $2H^+$	H_2O	2	0.816

The substrate oxidation mechanism by NAD^+ involves concerted hydride transfer to one face of NAD^+. Hydride transfer is possible since water is excluded from the active site. It is facilitated by removing a proton from an oxygen on an alcoholic substituent, for example, adjacent to the departing hydride. The negative charge on the oxide acts as a "source" of electrons, which can then flow through the hydride transfer to the positively charged ring nitrogen of NAD^+, which acts as an electron "sink." This is crudely illustrated in the cartoon shown in Figure 12.4.7, which shows ethanol oxidation by the enzyme alcohol dehydrogenase.

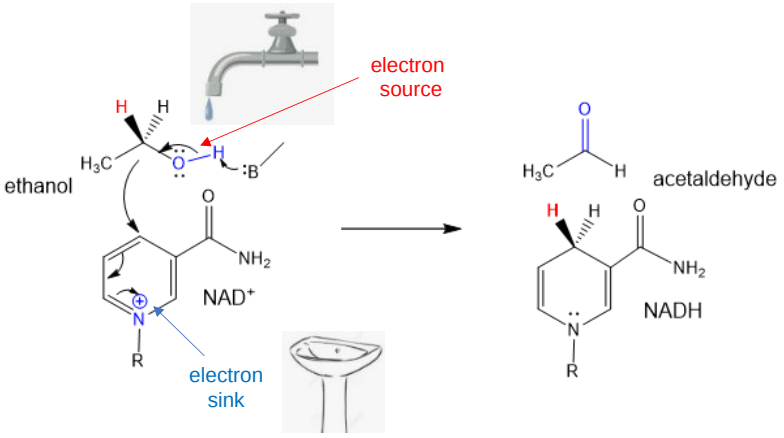


Figure **12.4.7**: Source and sink analogy for hydride transfer in alcohol dehydrogenase

For substrates like ethanol that lose a hydride from a methylene carbon atom that has two hydrogens, only one of them is lost (either the proR or proS) from the prochiral center.

The site on NAD^+ that receives the hydride and the entire ring is planar with sp^2 hybridization. When bound to the enzyme, the hydride is transferred to the RE face of the ring. The same occurs in the reverse reaction when the hydride from NADH is transferred to the RE face of acetaldehyde. Using the Cahn-Ingold rules, RE and SI faces can be determined by prioritizing the substituents attached to the sp^2 carbon. The reversible transfer of the proR hydrogen to the Re faces of the reactants in the reversible conversion of ethanol to acetaldehyde is shown in Figure **12.4.8**.

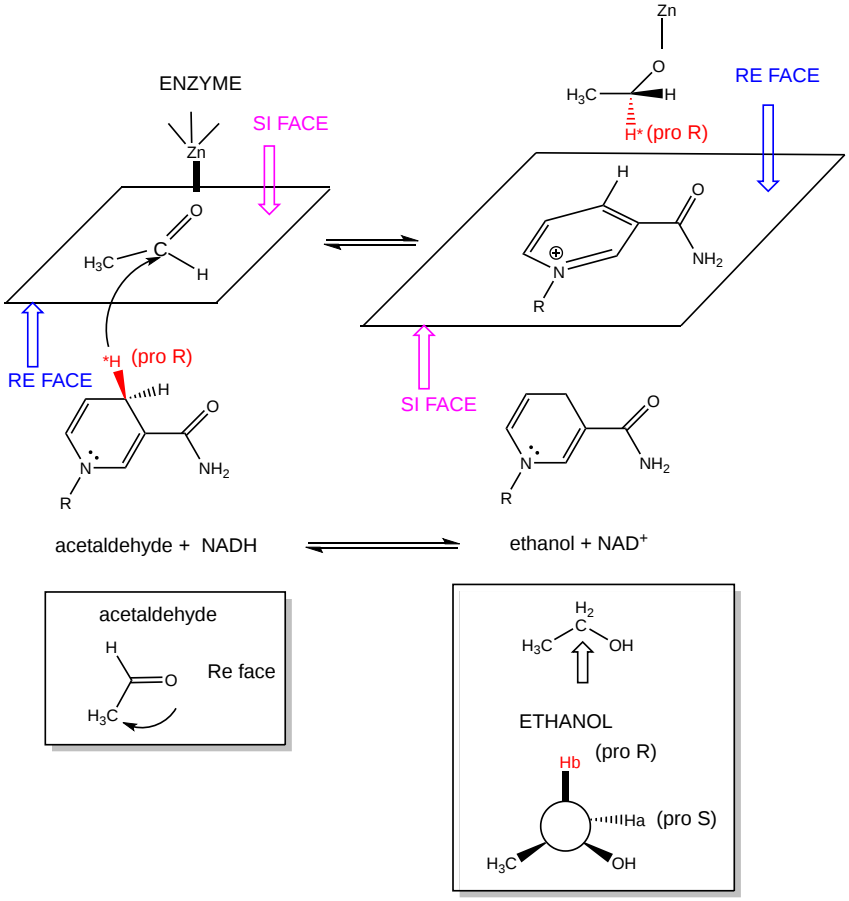


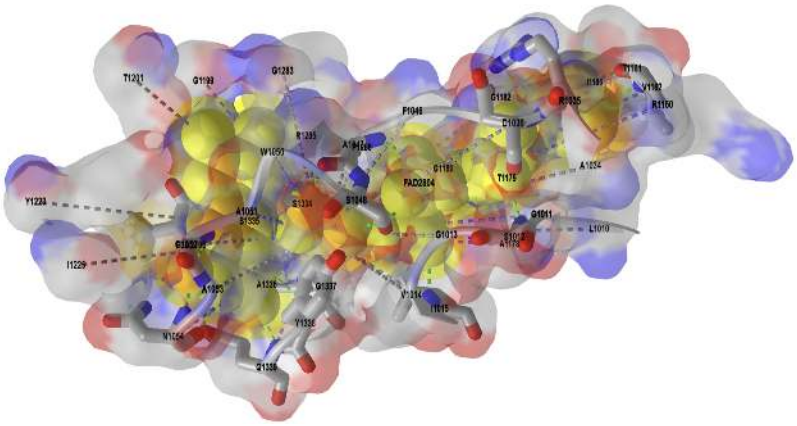
Figure **12.4.8**: Reversible transfer of the proR hydrogen to the Re faces of the reactants in the alcohol dehydrogenase reaction

FAD has a more positive reduction potential than NAD^+, so it is used for more "demanding" oxidation reactions, such as the dehydrogenation of a C-C bond to form an alkene. You will notice on standard reduction potential tables that the potential of FAD is often listed several times and depends on the enzyme. This is because the FAD is tightly bound to the enzyme. Hence, its tendency to acquire

electrons depends on its environment, in much the same fashion as the pKa of an amino acid side chain (which reflects its tendency to release protons), which is affected by the environment of the amino acid side chain in the protein. The standard reduction potential for flavin enzymes varies from -465 mV to + 149 mV. Compare this to the free FAD/FADH^2 reduction potential, which in aqueous solution is -208 mV. The standard reduction potential of the flavin in D-amino acid oxidase, a flavoprotein, is about 0.0 V. Remember, the more positive the standard reduction potential, the more likely the reactant will be reduced and act as an oxidizing agent. Hence, the FAD in D-amino acid oxidase is a better oxidizing agent than free FAD. The K_D for binding of FAD to the enzyme is 10^{-7} M compared to the K_D for binding of $FADH_2$, which is 10^{-14} M. By gaining electrons, the flavin binds more tightly, which preferentially stabilizes the bound $FADH_2$ compared to the bound FAD. This shifts the equilibrium of FAD ↔ $FADH_2$ to the right, making the bound FAD a stronger oxidizing agent.

A mechanism for the 2-electron hydride reduction of FAD is shown in Figure 6 above.

Figure 12.4.9 below shows an interactive iCn3D model of D-amino acid oxidase bound to FAD and a trifluoroalanine (1C0L) .



NCBI iCn3D **Figure 12.4.9:** D-amino acid oxidase bound to FAD and a trifluoroalanine (1C0L). (Copyright; author via source). Click the image for a popup or use this external link: https://structure.ncbi.nlm.nih.gov/i...wYfRAK9TBSt2c8

FAD is shown in spacefill and colored yellow. Only the amino acids interacting with FAD are shown as a surface with underlying CPK-colored sticks. The noncovalent interactions are shown as sticks. If you rotate the molecule, you will see that the FAD is almost completely buried and has extensive interactions with protein, contributing to its low K_D.

Thermodynamically, FAD, especially when covalently or tightly bound (and not released) from an enzyme, has a greater drive to be reduced, making it a stronger oxidizing agent than NAD^+. Hence, it will be used biologically for more difficult oxidation reactions. Converting C-C to C=C is thermodynamically more difficult than converting C-OH to C=O. That can likewise be inferred from standard reduction potential (SRP) values for organic molecules. The standard reduction potential (SRP) generally varies from about +1 to +2.5V for reducing alkenes to alkanes. For reducing an aldehyde to an alcohol, the SRP generally varies from about -2.5 to about 0V.

Hence, reducing an alkene to an alkane is more favored than reducing an aldehyde to an alcohol. So, accordingly, the oxidation of an alkane to an alkene (reverse rx) is less favored than the oxidation of an alcohol to an aldehyde. This makes some intuitive sense since the alcohol is already partially oxidized. So biologically, the tough oxidations use FAD as the oxidizing agent. Of course, one of the toughest, the oxidation of H_2O to O_2 in photosynthesis, requires an even stronger oxidizing agent than O_2 (of course). It is the oxygen-evolving complex, which we will see in the chapter on photosynthesis.

Can the standard reduction potential of a redox-active center in a protein be tuned by changing the environment of that center, much as the pKa of an acid side chain can by changing the polarity of the environment? The answer is yes. The active site of azurin, a cupredoxin, has a redox-active copper ion coordinated by a Cys and two His residues in a trigonal planar fashion. Met 121 serves as a weak axial ligand. Marshall et al. have reported a feasible method to manipulate this active site's redox potential (E^o). The wild-type azurin was mutated to alter the hydrophobicity and hydrogen bonding capabilities while maintaining the overall architecture of the metal binding site. Ser 46 was selected for mutation since it occupied a position similar to Asn in another cupredoxin involved in an important H bond binding two ligand binding loops. An N47S mutation, which strengthened the hydrogen bond between the two ligand-containing loops, increased Eo by ~130 mV while preserving metal binding site architecture as determined by UV-Vis spectroscopy. They also compared a M121Q mutant with wild-type M121 and with a M121L mutant. A plot of E^o vs. log partition coefficient for transfer of the side chain from water to octanol was essentially linear with a positive slope, showing that the standard reduction potential depended on the hydrophobicity of the weakly coordinating ligand in the metal binding region. This behavior extended to double mutants (where one set of mutants involved M121). The investigators were able to tune the E^o over a 700 mV range!

12.4.4: MONOOXYGENASES

An example of monooxygenases is the hydroxylases, which hydroxylate amino acids like tryptophan and tyrosine to form 5-hydroxytryptophan and 3,4-dihydroxyphenylalanine or dopa, respectively. These two substances can be decarboxylated using PLP-dependent enzymes to form the neurotransmitters 5-hydroxytryptamine (5-HT or serotonin) and dopamine. The latter can be hydroxylated again to form norepinephrine and subsequently methylated to form epinephrine. LSD and amphetamine are analogs of serotonin and dopamine, respectively. The derivatives of tryptophan and tyrosine are shown in Figure **12.4.10**.

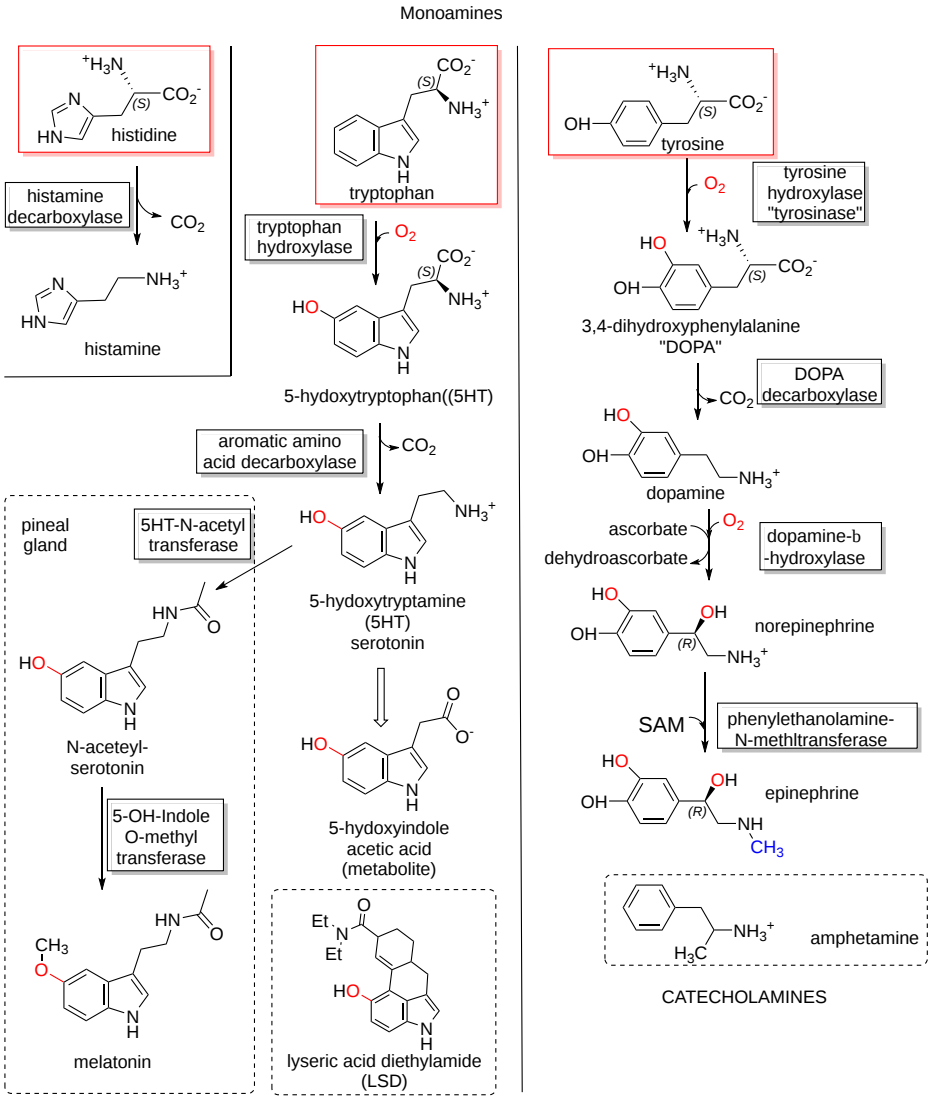


Figure **12.4.10**: Derivative of tryptophan and tyrosine derived from monooxygenases

Since these monooxygenases use dioxygen, you might expect the enzymes to use the motifs described in the previous section to facilitate their reaction with dioxygen. The enzyme contains a metal ion (Fe^{2+}) bound to a heme in the protein. In addition, the reduction products of dioxygen that are eventually used to hydroxylate the substrate stay bound to the enzyme.

Tyrosine 3-monooxygenase (Tyrosine hydroxylase)

Tyrosine hydroxylase is a homotetramer that uses a Fe ion and biopterin cofactor for hydroxylation. Dihydroxyphenylalanine (DOPA) biosynthesis is the rate-limiting step in catecholamine synthesis.

Figure **12.4.11** shows a possible mechanism for the rat enzyme.

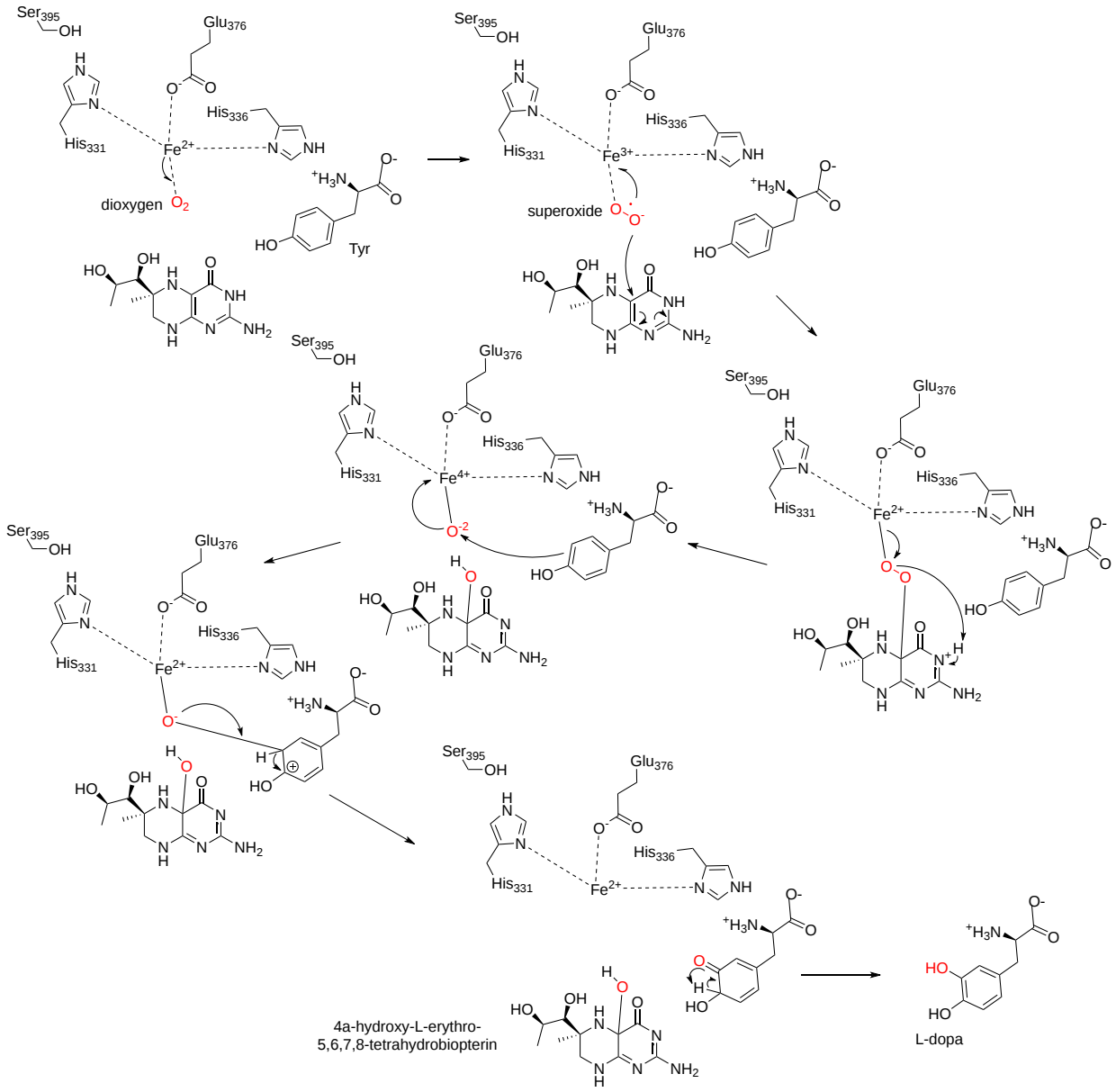


Figure **12.4.11**: A possible mechanism for rat tyrosine hydroxylase, a monooxygenase. https://www.ebi.ac.uk/thornton-srv/m-csa/entry/134/

The Fe^{2+} ion binds O_2. Some mechanisms show a single electron transfer to the bound O_2 from the pterin ring to form Fe^{2+}-O_2^-(bound superoxide) and a radical cation pterin. This is unstable and forms Fe^{2+}-μ-peroxypterin, followed by heterolytic cleavage of the peroxo O-O bond. Ultimately, hydroxpterin and an $Fe^{4+}O$ oxospecies form, which then hydroxylates tyrosine.

Figure 12.4.12 below shows an interactive iCn3D model of rat tyrosine hydroxylase with bound cofactor analog and iron (2TOH).

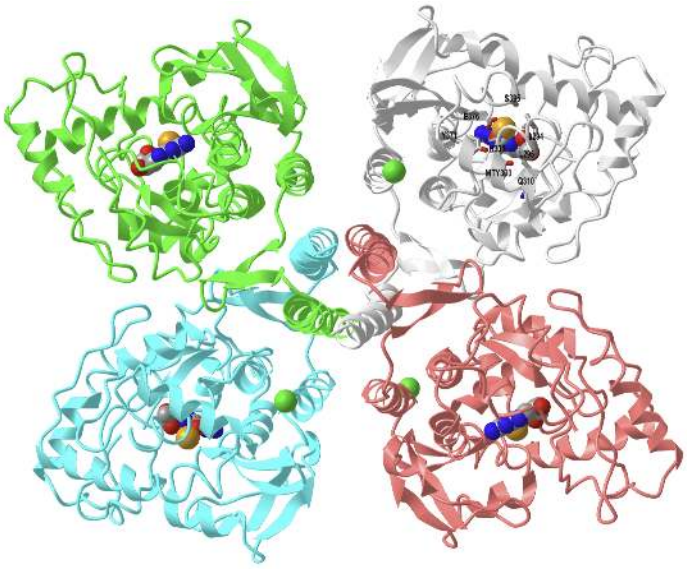


Figure 12.4.12: Rat tyrosine hydroxylase with bound dihydrobiopterin analogue and iron (2TOH). (Copyright; author via source). Click the image for a popup or use this external link: https://structure.ncbi.nlm.nih.gov/i...KeKiLDfmeNFfr7

Four monomers in the homotetramer are shown. The cofactor analog (HBI), 7,8-dihydrobiopterin, is shown in spacefill. Phenylalanine 300 has been self-hydroxylated by the enzyme to produce meta-tyrosine (MTY300), which, along with the other key amino acids in the active site, is labeled in CPK-colored sticks in the gray monomer. The pterin ring interacts through pi stacking with Phe 300, facilitating self-hydroxylation. The Fe ion is far (5.6 Å) from the carbon on pterin. This suggests that O_2 might bridge the reacting pterin C- and the Fe ion in a Fe^{2+}-μ-peroxypterin complex.

Tryptophan hydroxylase

This enzyme also uses a tetrahydropterin cofactor and an Fe ion to form the hydroxylating intermediates. As in the case of tyrosine hydroxylase, both the amino acid substrate and the cofactor must be present for oxygen to be activated. Otherwise, it only oxidizes Fe^{2+} to Fe^{3+}. This serves as a protective mechanism so that O_2 is not activated unnecessarily, which avoids the formation of soluble ROS.

Figure **12.4.13** shows a possible mechanism without catalytic residues for tryptophan hydroxylase.

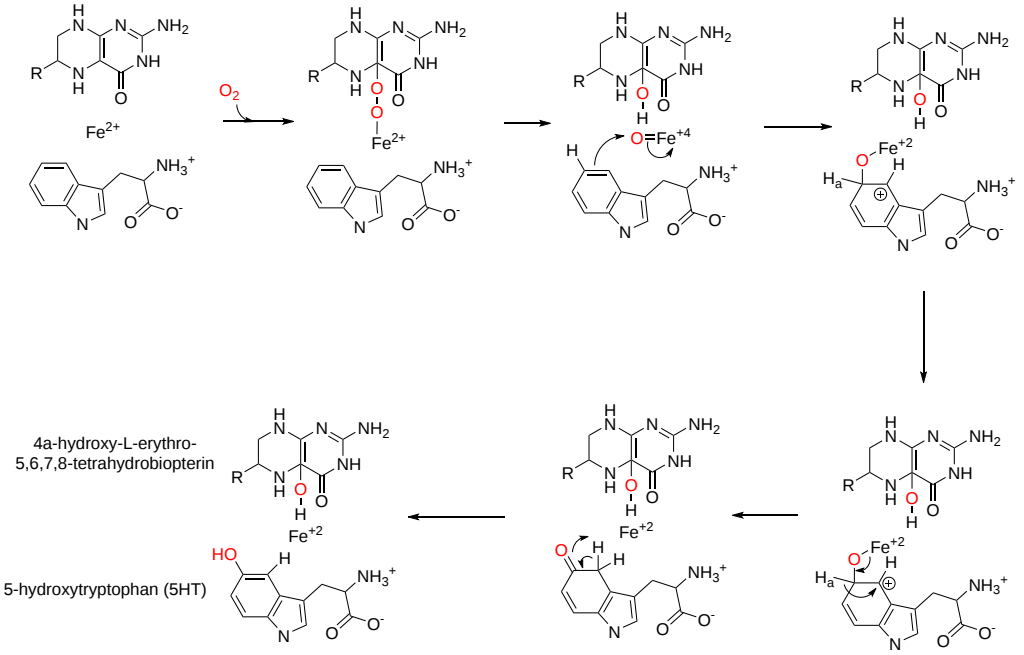


Figure 12.4.13: possible mechanism without catalytic residues for tryptophan hydroxylase, adapted from Kenneth M. Roberts, Paul F. Fitzpatrick, https://doi.org/10.1002/iub.1144

Cytochrome P450s

The **cytochrome P450 (CYP)**consists of a large group of monooxygenases that contain a heme that absorbs maximally at 450 nm. They catalyze the following reaction:

$$RH + NAD(P)H + H^+ + O_2 \rightarrow ROH + NAD(P)^+ + H_2O$$

An example includes cytochrome P450cam, which hydroxylates camphor, a large aromatic, completely nonpolar molecule. The enzyme has been called the"biological equivalent of a blowtorch," as it can, at room temperature, stereospecifically hydroxylate nonactivated hydrocarbons at physiological temperature. This reaction proceeds without stereospecificity only at high temperatures without a catalyst. Remember from the previous chapter section that dioxygen is a ground-state triplet radical that is not reactive with carbon atoms (which are singlets) unless converted to a singlet state, a process that requires significant energy. Cytochrome P450s get around this problem by binding to an Fe ion in the heme to form common intermediates such as oxos, oxides, and peroxides. The molecular orbitals of the bound dioxygen are "singlet-like."

Remember from introductory chemistry that transition metal ligands are named with a specific nomenclature. Some are shown in Figure 12.4.14.

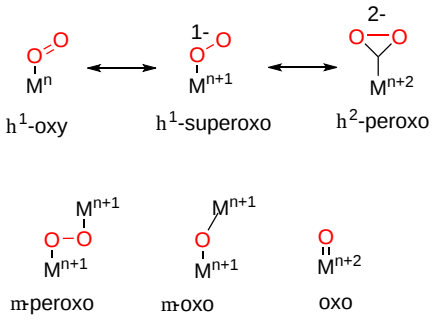


Figure 12.4.14: Common oxygen transition metal ligands

In their names, η is the hapticity (the number of atoms of a ligand attached to a metal), and μ is the number of metal atoms bridged by a ligand. For Fe ions and oxygen ligands, some examples include $Fe^{III}–O_2^-$ (superoxo) and $Fe^{IV}=O$ (ferryl-oxo)

If the aromatic substrate gets oxidized, something must be reduced. That something is, of course, O_2. Electrons for the reduction of O_2 come from the oxidized substrate and input of electrons through NAD(P)H. Cytochrome P450s are microsomal proteins, and most require another protein, **NADPH-cytochrome P450 reductase (CPR)**. Before we look at the structure and mechanism of cytochrome P450, let's look at this microsomal protein first. CPR catalyzes this reaction:

$$NADPH + \text{oxidized CytoP450 } (Fe^{3+}\text{-heme b}) + H^+ \leftrightarrow NADP^+ + \text{Oxidized CytoP450 } (Fe^{2+}\text{-heme b})$$

The protein contains multiple domains and results from a fusion of genes from flavodoxin (which binds FMN) and FAD reductases. In addition, it contains an NADP binding domain. It ultimately accepts a hydride ion (2 electrons) from NADPH and then transfers electrons to FMN (in one-electron steps). These are used to reduce the heme, which then activates dioxygen (oxidation number of 0) for hydroxylation reactions by cytochrome P450. In the hydroxylated organic product and water, oxygen has an oxidation number of -2.

Figure 12.4.15 below shows an interactive iCn3D model of rat NADPH-cytochrome P450 reductase (1AMO).

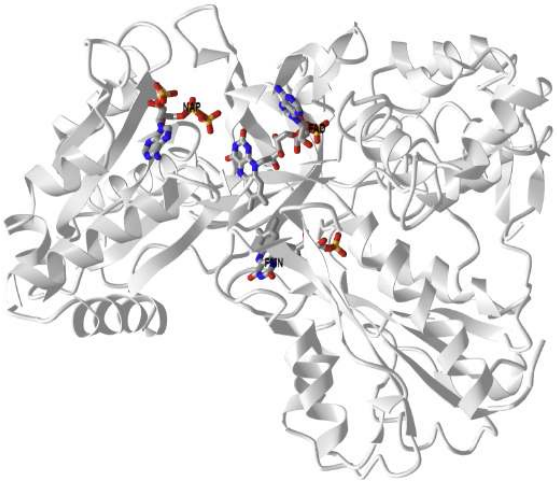


Figure 12.4.15: Rat NADPH-cytochrome P450 reductase (1AMO). (Copyright; author via source). Click the image for a popup or use this external link: https://structure.ncbi.nlm.nih.gov/i...nMh9ByRbsWk4B8

$NADP^+$ is labeled as NAP. The enzyme is unique because it has binding sites for FAD and FMN (similar to nitric-oxide synthase). The flavins are aligned for electron transfer. The cleft in the enzyme presumably binds cytochrome P450. The protein has short (20 amino acids) lumenal sections, followed by a 20 amino acid membrane-spanning helix (not shown in the above structure), followed by a large cytosolic domain, where it can interact with cytochrome P450, which is found in multiple places, including the ER, microsomal, and mitochondrial membranes as well as the cytoplasm.

The cytochromes P450s contain a heme, which, instead of reversibly carrying dioxygen (as in myoglobin and hemoglobin), activates dioxygen for hydroxylation reactions involving aromatic, nonpolar substrates. Hydroxylation of these substrates increases their solubility, facilitating their elimination from the body. Epoxide intermediates and products are often produced, which can open up through nucleophilic attack using an alcohol (sugar derivative), as illustrated in Figure **12.4.16**.

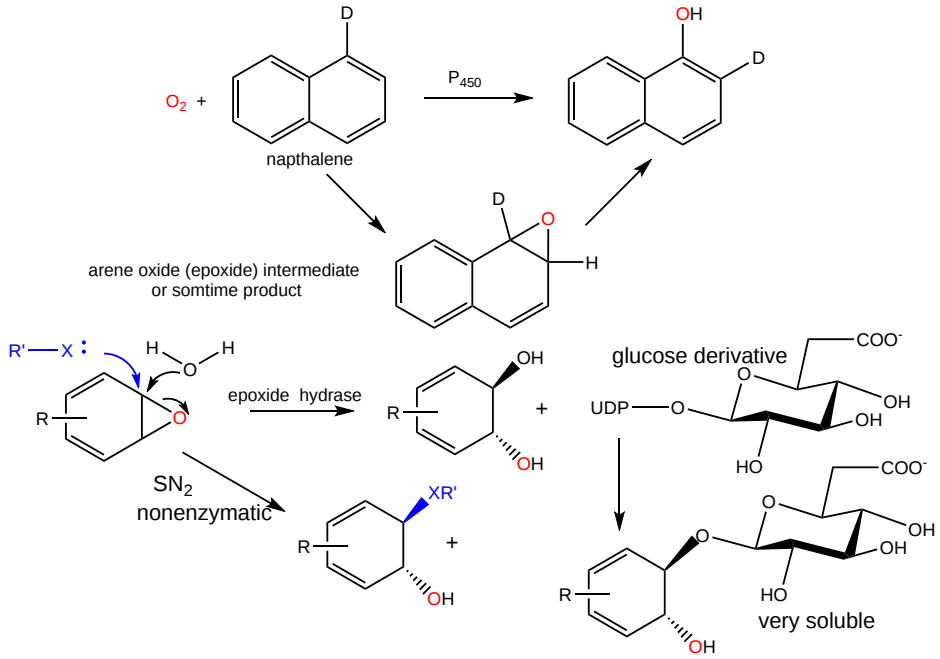


Figure **12.4.16**: Cytochrome P450 hydroxylation reaction to increase target solubility

This type of reaction also converts steroids to different biologically active ones.

The hydroxylation reaction can also lead to reactions with amines, including those on nucleotide bases in DNA, resulting in the formation of large adducts, as illustrated in Figure **12.4.17**.

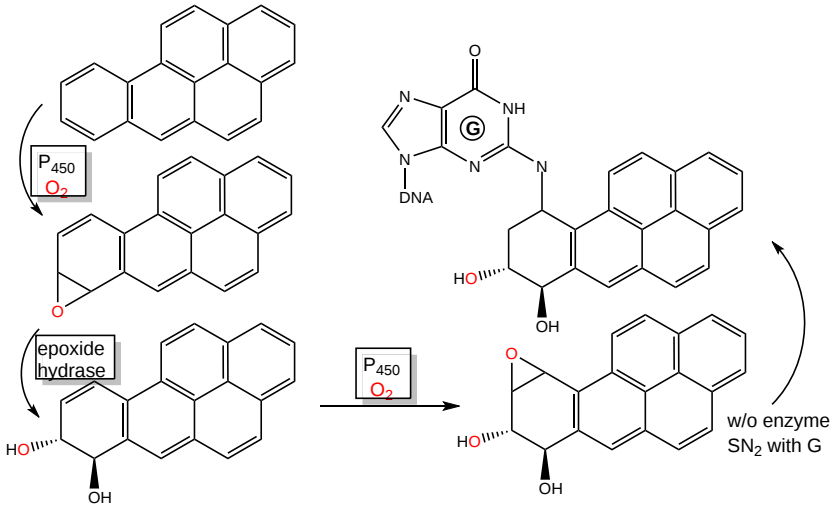


Figure **12.4.17**: Cytochrome P450-mediated formation of carcinogens.

Hence, cytochrome P450 can activate aromatic substrates to become carcinogens.

The cytochrome P450 family of genes/proteins is inducible on exposure to nonpolar aromatic molecules such as dioxin. These nonpolar molecules can enter the cytoplasm, binding to the arylhydrocarbon receptor (AhR), which is bound to a heat shock protein, Hsp90. Upon binding of dioxin, TCDD, for example, the AhR-TCCD complex dissociates from Hsp90 and migrates to the nucleus, where it binds a protein called Amt. The AhR-Amt complex is an enhancer/transcription factor, facilitating the transcription of the cytochrome P450 genes.

Figure **12.4.18** illustrates the activation of cytochrome P450 gene expression on exposure to nonpolar aromatic molecules such as dioxin.

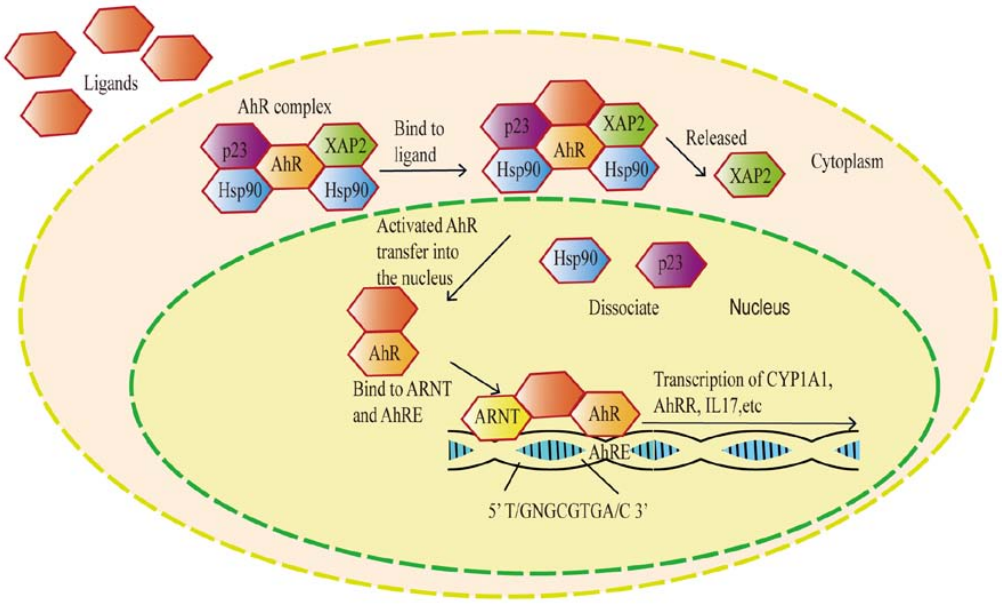


Figure **12.4.18**: Activation of cytochrome P450 and other gene expression on exposure to nonpolar aromatic molecules such as dioxin

On binding to a ligand, the AhR is activated and enters the nucleus, where it binds to ARNT on the aryl hydrocarbon response element (AhRE) and promotes transcription of downstream genes, including cytochrome P450 family 1 subfamily A member 1 (CYP1A1) and interleukin-1 (IL-1). CYP1A1 is in the CYP1A family and promotes the activation of procarcinogens and the hydroxylation of steroid hormones like estrogens. It also participates in the metabolism of steroidal hormones, including estrogens. ARNT is the aryl hydrocarbon receptor nuclear translocator; AhRE the aryl hydrocarbon response element; CYP1A1, XAP2 is the aryl hydrocarbon receptor interacting protein; AHRR is the aryl-hydrocarbon receptor repressor; IL-11 is interleukin 17, Hsp90 is heat shock protein 90, and p23 is prostaglandin E synthase 3

Dioxin has been shown to affect estrogen-mediated activities. Estrogens, small hydrophobic hormones derived from cholesterol, enter cells and bind to cytoplasmic estrogen receptors, which then dimerize and bind to the estrogen response element (ERE), initiating transcription.

Tamoxifen, a drug derived from the yew plant, blocks the biological effects of the estrogen receptor. Although it binds to the estrogen receptor, it doesn't elicit the same conformational changes in the protein, which prevents the bound receptor from binding to the estrogen response element and recruiting other proteins needed for estrogen-dependent gene transcription. It is used in chemotherapy and the prevention of estrogen-dependent breast cancer cells.

How does dioxin interfere with estrogen signaling? Ahr and ARnt contain a basic helix-loop-helix motif, which mediates their interaction with DNA. Upon binding of the complex, detoxification genes are activated. The dioxin-Ahr-Arnt complex can also bind to the estrogen receptor, activating genes containing an estrogen response element (ERE) in the absence of estrogen. However, if estrogen is present, inhibition of gene expression from ERE is observed. Dioxins can be potent dysregulators of estrogen-induced gene expression. Such changes in estrogen activity could help to explain the pro- and inhibitory effects of dioxin on estrogen-mediated cellular responses and the possible effects of dioxin on the immune system and cancer development.

Given the importance of the cytochrome P450s, we'll offer two variant portrayals of their mechanism. Figure **12.4.19** shows the overall catalytic cycle of the enzyme with associated redox changes in the generic substrate, RH, and the Fe heme ion.

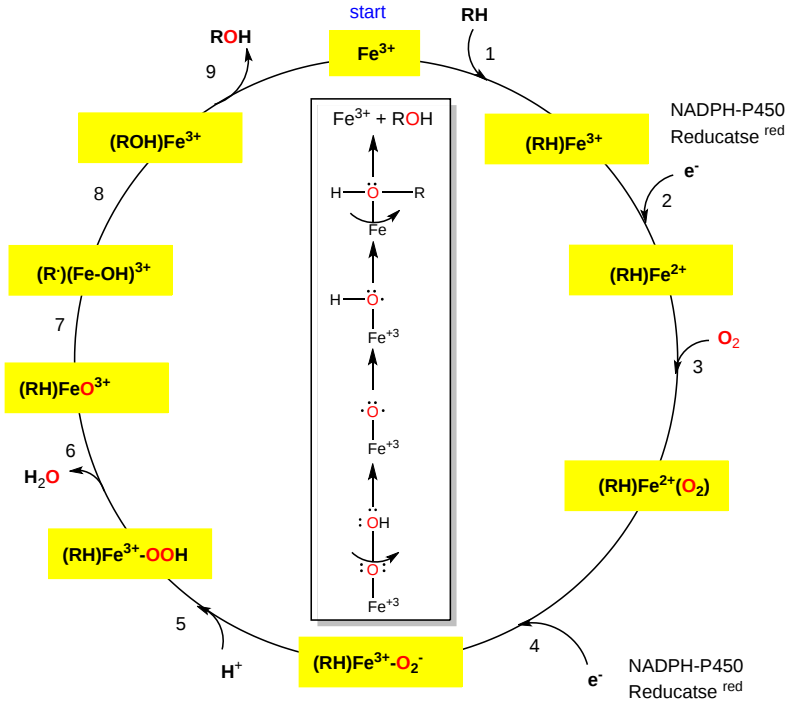


Figure **12.4.19**: Catalytic cycle of cytochrome P450 with the generic substrate RH and the Fe heme ion

The key hydroxylating agent appears to be formal FeO^{3+}, shown in step 7.

A possible mechanism for the hydroxylation of estrone by cytochrome P450 from Bacillus megaterium is shown below in Figure **12.4.20**. It follows the general catalytic cycle shown above.

$$\text{Estrone} + \text{NADH} + H^+ + O_2 \rightarrow \text{2-hydroxyestrone} + NAD^+ + H_2O$$

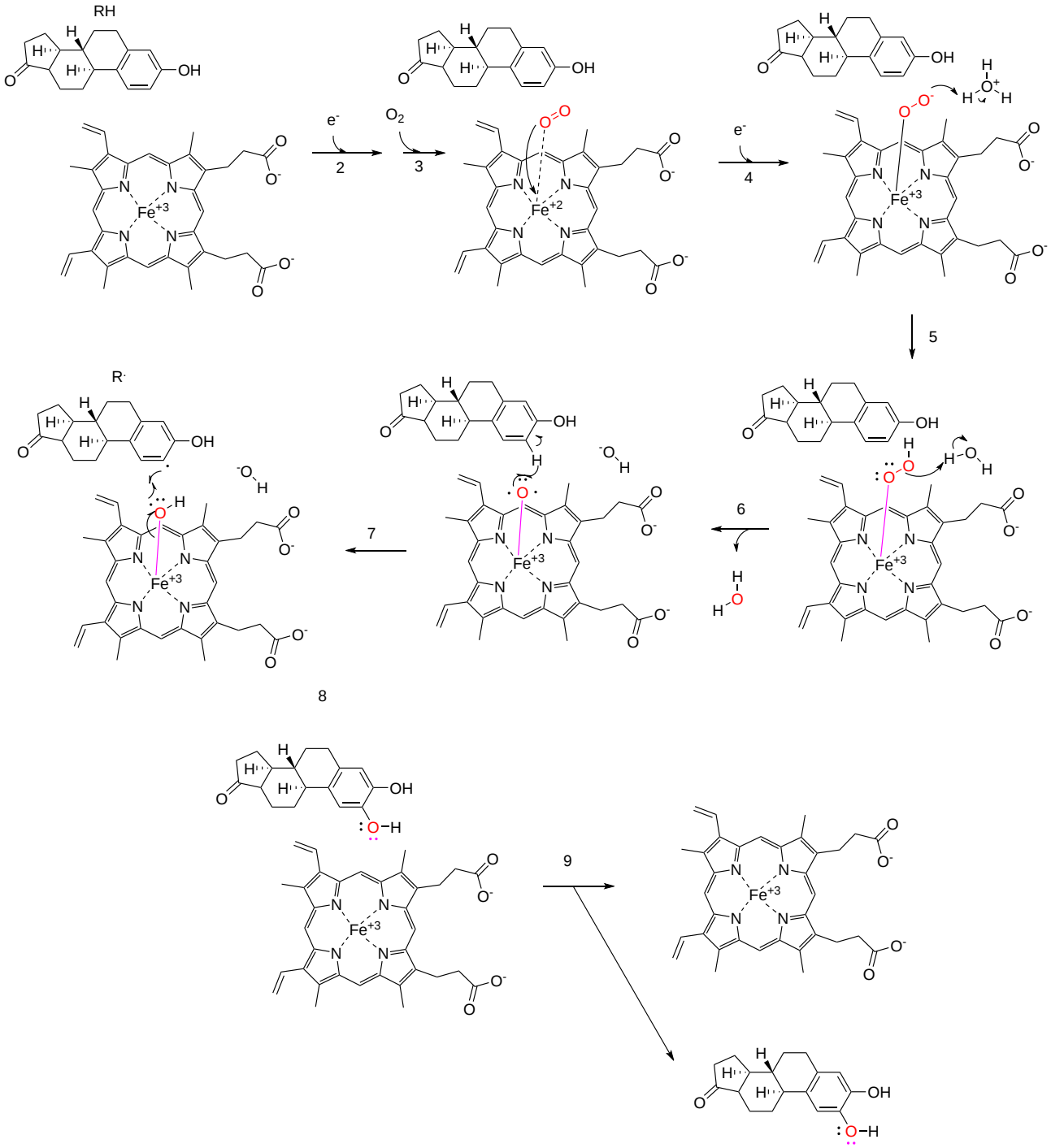


Figure **12.4.20**: Possible mechanism for the hydroxylation of estrone by cytochrome P450 from Bacillus megaterium after https://www.ebi.ac.uk/thornton-srv/m...csa/entry/699/

As with the previous generic mechanism, the two added electrons derive from NADH, which passes a hydride to FAD, which passes single electrons onto FMN, then passes them onto the heme. The exact species for several parts of the mechanism are not completely clear. For instance, a Fe^{4+}-oxo complex has been proposed.

Let's show the structure of a human cytochrome P450 1A1 active in drug metabolism and the activation of benzo[a]pyrene (a fused benzene and α-pyrone ring), a component of cigarette smoke, into a carcinogen. **Figure 12.4.21** below shows an interactive iCn3D model of human microsomal (ER) cytochrome P450 2A6 complexed with coumarin (1Z10). Coumarin is a benzo-α-pyrone found in many plants like tonka beans and some types of cinnamon. It has a sweet, vanilla-like scent and bitter taste.

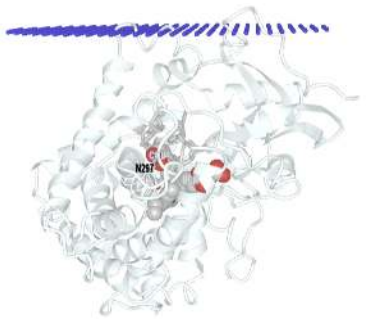


Figure 12.4.21: Human microsomal cytochrome P450 2A6 complexed with coumarin (1Z10). (Copyright; author via source). Click the image for a popup or use this external link: https://www.ncbi.nlm.nih.gov/Structu...J8LxFpEyGdeab6

The heme (heme) and coumarin (COU) are shown in spacefill, CPK colors, and labeled. The amino acids lining the binding pocket for coumarin are shown in CPK-colored sticks and unlabeled, except for Asn 297. The coumarin is bound in a completely nonpolar site but forms one hydrogen bond with Asn 297 (labeled), which helps position it.

12.4.5: DIOXYGENASES

An example of a dioxygenase is the cyclooxygenase activity of prostaglandin synthase. This enzyme, often called cyclooxygenase or COX, is an integral membrane protein found in the ER membrane and a homodimer (with two hemes). It catalyzes two different reactions. One is the addition of two dioxygens to arachidonic acid - 20:4$^{\Delta}$5, 8, 11, 15 (which is liberated from the C2 position of phospholipid membranes by phospholipase A2 upon appropriate signaling) to form prostaglandin PGG2. This molecule, with 5 chiral centers, arises from arachidonic acid, which has one. The cyclooxygenase activity is buried in the membrane, from where the arachidonic acid can readily access its active site. The active site is at the end of a hydrophobic channel (arachidonic acid binding site) and stretches from the membrane-binding region to a buried heme. PGG2 can be further metabolized to PGH2 by the addition of two electrons to PGG2 by the hydroperoxidase activity of the enzyme, located at the other end of the enzyme. This activity forms an alcohol from the peroxide functional group in PGG2. There is one heme per monomer, which acts in both the cyclooxygenase and peroxidase activities. Each monomer of the dimer has both enzymatic activities. A possible abbreviated reaction mechanism is shown in Figure **12.4.22**.

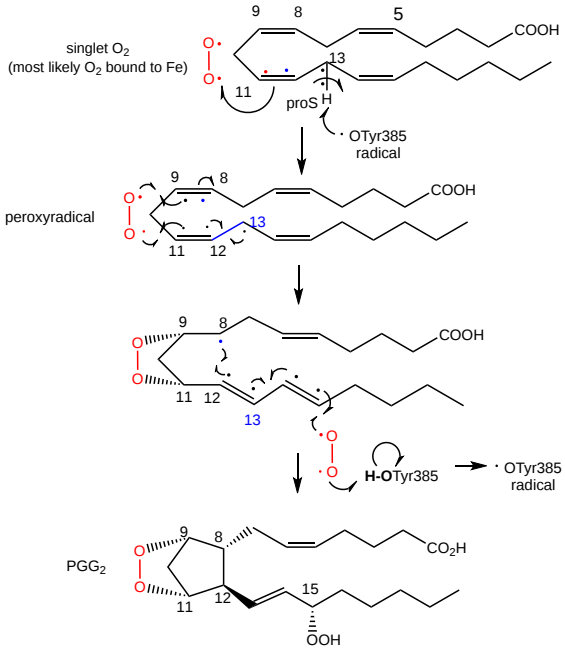


Figure **12.4.22**: A possible abbreviated reaction mechanism for dioxygenase cyclooxygenase.

In summary:

- The carboxylate of arachidonic acid is coordinated to Arg 120 and Tyr 355.
- The C13 pro(S) H atom of arachidonic acid is close to Tyr 385, which allows its abstraction.

- This results in a radical centered on C11 that reacts with dioxygen to form a peroxyl radical.
- Attack by dioxygen at C11 occurs from the side of the substrate opposite to that of hydrogen abstraction.
- The oxygen radical at C11 cyclizes by attacking C9.

The C13 proS hydrogen atom (not proton) is removed from bound arachidonic acid by a free radical form of Tyr 385, which acts as an oxidizing agent. A site-specific mutant in which Phe replaces Tyr 385 is inactive. How is the Tyr free radical formed? Based on the single electron standard reduction potential (0.9 V for Tyr and -0.2 to + 0.2 V for Fe^{3+} in the bound heme), it appears that the heme iron is not a potent enough oxidizing agent to accomplish this task. However, oxygen bound to the heme iron could be converted to a peroxide and form an Fe^{4+}-oxo complex (which has also been proposed for cytochrome P450). The Fe^{4+} ion is a more potent oxidizing agent (standard reduction potential of approximately 1 V, sufficient for oxidation of Tyr 385. Another possibility is that the peroxide activator (in forming the ferryl-oxo ligand) is NO (nitric oxide, a free radical). NO is formed by immune cells (like macrophages) on immune activation. The NO might react with superoxide (also a radical, possibly formed during an oxidative burst in macrophages during immune stimulation) to form peroxynitrite (NO^{3-}). This can donate an oxo group to the Fe^{3+} to form the Fe^{4+}-oxo complex, which could then oxidize Tyr to the free radical form. There might be other mechanisms as well to generate the Tyr free radical, since just adding organic peroxides to the enzyme will generate it.. After abstraction of the proS H atoms, a carbon-centered free radical at C11 results, which reacts with oxygen, as shown below. The exact form of oxygen that reacts is unclear, but presumably is either a peroxy or activated singlet form.

12.4.6: OXIDASES

This class of enzymes does not incorporate dioxygen into an organic substrate. Rather, it accepts electrons released from an organic substrate through intermediate electron carriers (such as ubiquinone and cytochrome C) to form superoxide (as in NADPH-oxidase), hydrogen peroxide (as in xanthine oxidase), or water (as in cytochrome C oxidase). The mechanism of cytochrome C oxidase again supports our expectations about enzymes that use dioxygen. Dioxygen binds to metals in the enzyme. One oxygen atom binds a heme Fe^{2+} of cytochrome a3, which is bound to the enzyme, while the other binds a Cu^{1+} of Cu B. All oxygen reduction intermediates remain bound to the enzyme. Four electrons are added from four different cytochrome C molecules, which serve as mobile carriers of electrons.

We will explore cytochrome C oxidase in detail in Chapter 19.1: Electron-Transfer Reactions in Mitochondria. Figure **12.4.23** shows cartoon versions of several oxidases.

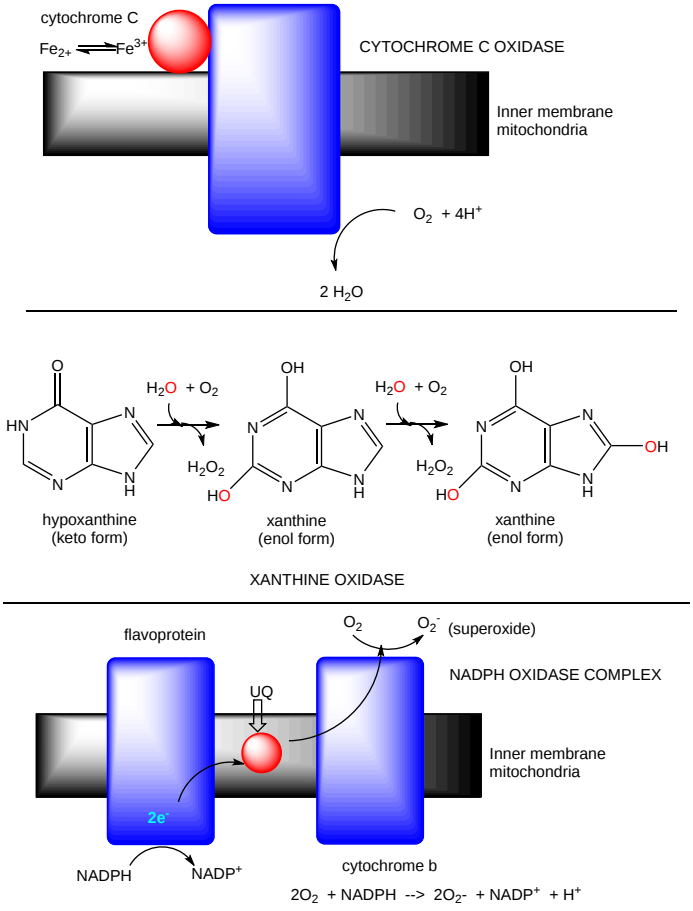


Figure 12.4.23: Examples of oxidases

Another example of an oxidase is monoamine oxidase. Mitochondrial monoamine oxidase catalyzes the oxidative deamination of certain neurotransmitters after post-synaptic neurons have taken them up in the process of inactivation. The reaction is shown in Figure 12.4.24.

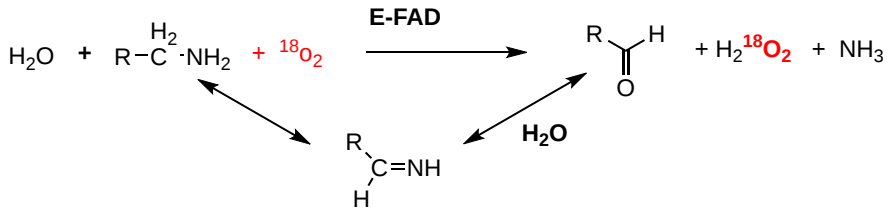


Figure 12.4.24: Monoamine oxidase reaction

A Schiff base is formed, which is then hydrolyzed, incorporating unlabeled oxygen into the oxidized molecule.

12.4.7: BIOLOGICAL OXIDATIONS: METHANE TO CO_2

In the previous chapter section, we discussed the progressive oxidation of methane by 2 electron loses to form methanol, formaldehyde, formic acid, and CO_2, with a progressive increase in oxidation number for the C by +2 (from -4 in methane to +4 in CO_2), as reviewed in Figure 12.4.25.

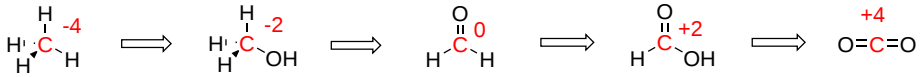


Figure 12.4.25:: Progressive stages in the oxidation of methane

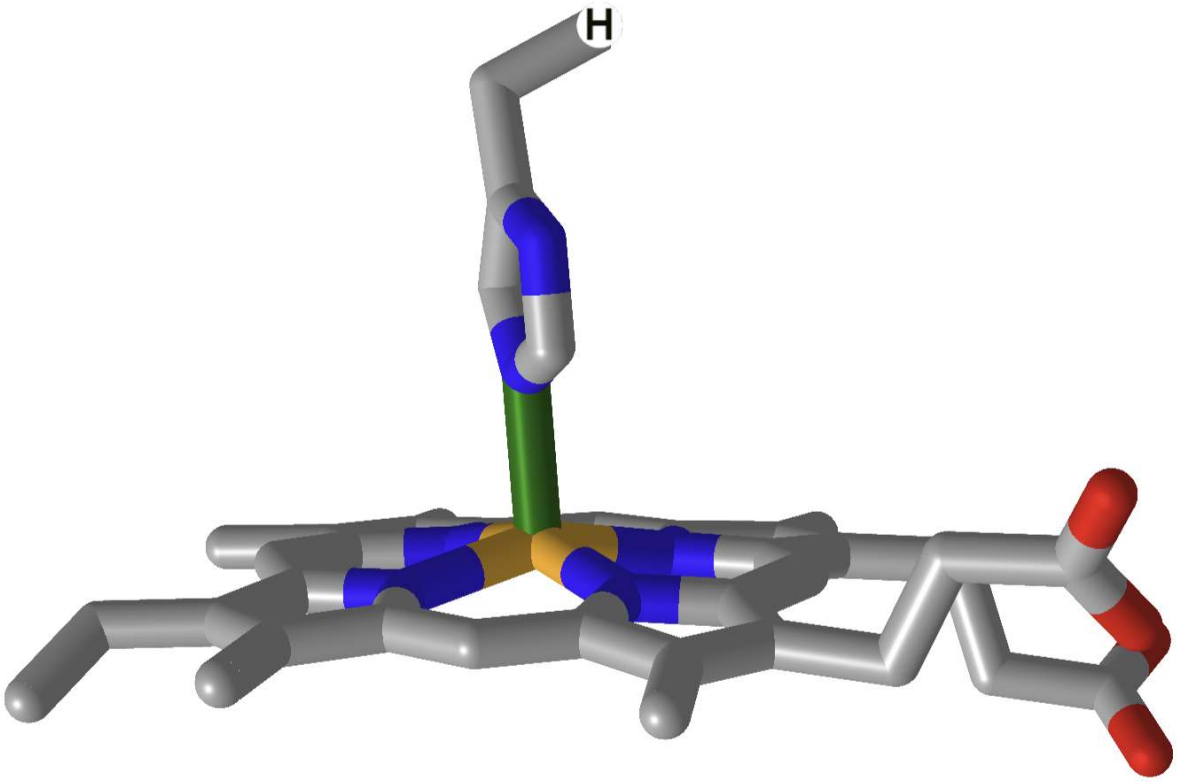
Methanotrophs are aerobic bacteria that use methane as an energy source, converting it in a series of two-electron oxidations, as shown above, to carbon dioxide. The enzymes involved in this sequential process are methane monooxygenase, methanol dehydrogenase, formaldehyde dehydrogenase, and formate dehydrogenase. Methane monooxygenase exists in a soluble and membrane form, both of which are part of a larger complex. Both have a hydroxylase (which uses dioxygen to add O to methane), and the membrane form has recently been shown to be associated with methanol dehydrogenase in a larger complex consisting of trimers of each enzyme (the hydroxylase and the dehydrogenase).

12.4.8: HEME PROTEINS

So far in this course, we have examined three different kinds of heme proteins.

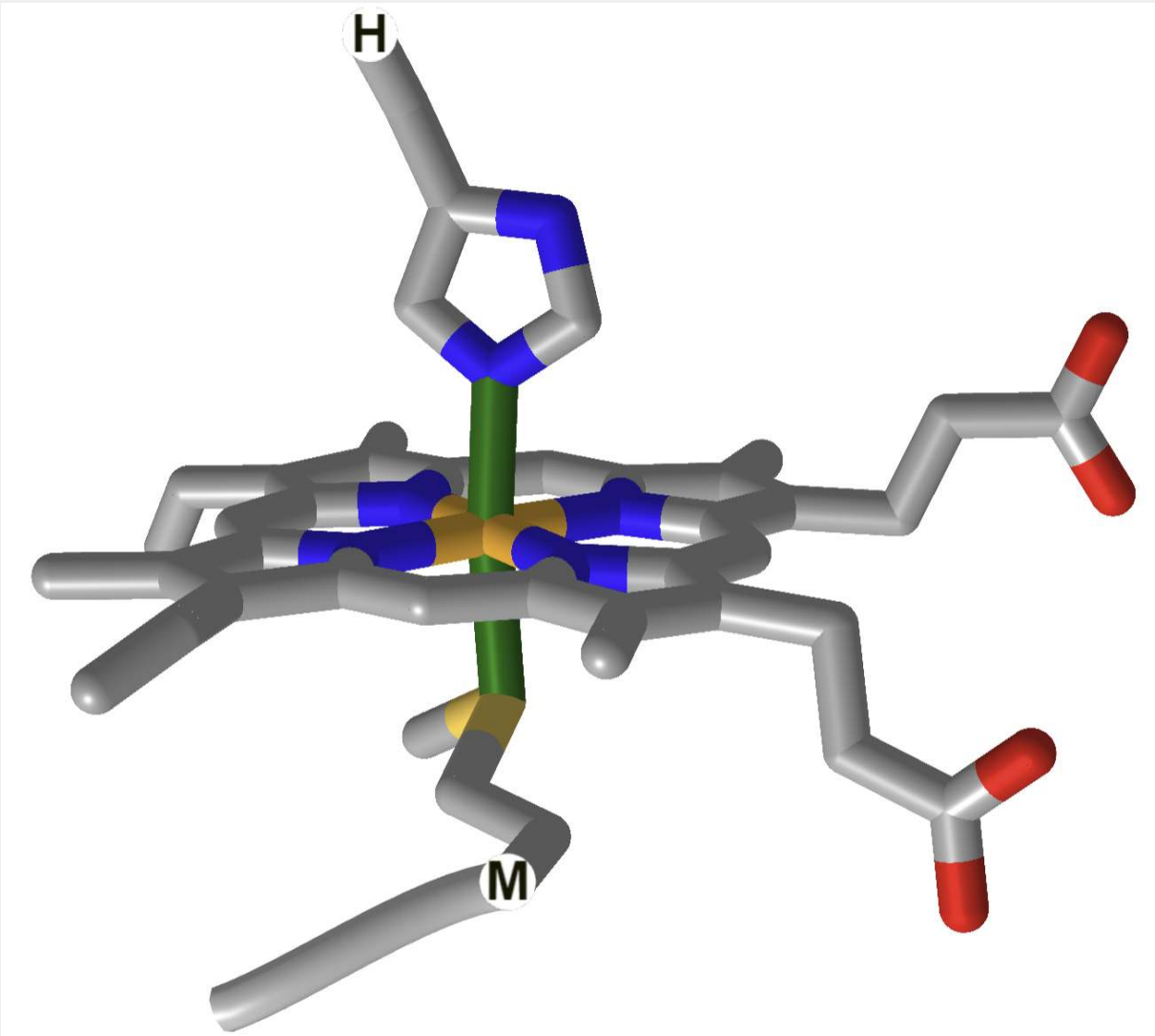
- The first is that hemoglobin and myoglobin serve as carriers of **dioxygen**. Even though they bind one of the best oxidizing agents around (dioxygen), the heme Fe^{2+} is not oxidized to Fe^{3+}. If it does, as in the case of met-Hb, the protein loses its ability to carry oxygen.
- Cytochrome C, conversely, does not bind dioxygen but serves as a carrier of **electrons,** which are passed to dioxygen in Cytochrome C oxidase. As an electron carrier, its Fe ion readily cycles between the 2+ and 3+ states.
- Finally, the Fe^{2+} in the heme of the cytochrome P450s (so named since they have an absorbance maximum at 450 nm when they bind CO) does **both**. It binds dioxygen and cycles between the 2+ and 3+ states, activating dioxygen for hydroxylation reactions.

The heme and amino acid ligands' structure and their absorbance spectra are shown in Table 12.4.3 below.

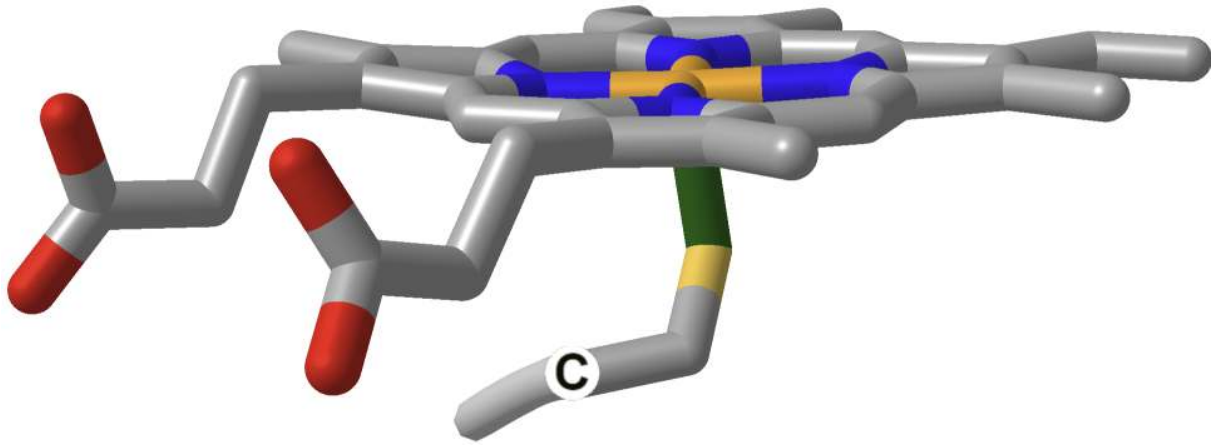


hemoglobin

cytochrome C



Cytochrome P450



P450: Fujishiro et al. J Biol Chem. 2011 Aug 26; 286(34): 29941–29950. Published online 2011 Jun 30. doi: 10.1074/jbc.M111.245225. CC BY license.

Cyto C: Hulko et al. December 2011. Sensors 11(6):5968-80. DOI:10.3390/s110605968. Creative Commons Attribution 3.0 Unported

Hemoglobin: Nitzan et al. July 2014, Medical Devices: Evidence and Research 7(1):231-9. DOI:10.2147/MDER.S47319. Creative Commons Attribution-NonCommercial 3.0 Unported

How could heme serve such diverse functions? We can explain this by referring to one of the course's main themes - structure mediates function. The environment of each heme must be different. The protein ligands coordinating the Fe ions are different. The 5th ligand is the proximal His in hemoglobin, while dioxygen binds to the 6th site. The 5th and 6th ligands in cytochrome C are His and Met, respectively. In cytochrome P450, the 5th site is occupied by Cys, and the 6th by dioxygen. Presumably, the environments surrounding the hemes are different as well. Once again, we have seen an analogous example in which the microenvironment influences chemical properties. The pKa of a given amino acid side chain can vary considerably depending on the polarity of the local environment. Likewise, the standard reduction potential of tightly bound FAD/$FADH_2$ depends on the microenvironment.

As we have seen (from the study of heme proteins and the oxidative enzymes of cells), transition metals such as Fe, Zn, and Cu have vital biological roles as binding sites and cofactors in many reactions. Yet they also pose problems since they can lead to cellular oxidative damage. As we saw with cytoplasmic metallothioneins, which bind to heavy metals and protect the cell from such damage, many proteins are involved in the binding and regulating transition metals in the cell. Integral membrane proteins are required to bind and transport these cations into the cytoplasm. Other proteins act as sensors of transition ion concentration (such as latent transcription factors, which bind heavy metals and become active transcription factors for metallothioneins. Others act as chaperone proteins, which bind metal ions and transfer them to apometalloproteins. Recent work suggested transporters and chaperones are involved in metal ion biology and bind these ions with unusual coordination geometry, presumably facilitating the transfer of the ion to the apo-target protein.

The transition metals Zn and Fe are often found in E. Coli at a concentration of 0.1 mM, compared to Cu and Mn, which are present at 10 to 100 μM concentrations. Also, about one-third of all proteins demonstrate specific binding of metal ions and can be classified as metalloproteins. Mass balance suggests that metal ions would be distributed in proteins with low, intermediate, and high metal binding affinity as well as in free pools, which potentially can be toxic to cells. Depending on their Kd for metal ion binding, metalloproteins would be in various states of ligation. The free concentration of some ions (Cu and Zn) is so low that newly synthesized apoproteins that bind these ions would not obtain the ions from the free pool. In such cases, metal chaperones would be required.

12.4.9: SUMMARY

This chapter provides an integrated overview of the principles and mechanisms underlying oxidation reactions in both chemical and biological contexts. It bridges foundational organic redox chemistry with the sophisticated enzyme-catalyzed processes essential for metabolism and detoxification in living systems.

- **Chemical Oxidation Reactions:**
  The chapter begins by reviewing classical oxidation mechanisms encountered in organic chemistry. It outlines the multi-step process of oxidation—highlighting initiation, propagation (including branching), and termination steps—using the combustion of methane as an illustrative example. In laboratory settings, strong oxidants like permanganate and chromate are employed to achieve controlled oxidation, contrasting sharply with the challenges of using dioxygen, whose uncontrolled reactivity and complex radical intermediates often lead to overoxidation and side reactions.
- **Biological Oxidizing Agents:**
  In biological systems, oxidation is precisely regulated. Rather than relying on dioxygen directly for substrate oxidation, cells use specialized redox carriers such as NAD^+ and FAD. These cofactors mediate two-electron hydride transfers via dehydrogenase enzymes, which are central to energy-yielding pathways like glycolysis, the Krebs cycle, and fatty acid oxidation. The chapter explains the structural basis and mechanistic details of hydride transfer, emphasizing how the planar, electron-deficient nicotinamide ring of NAD^+ acts as an effective electron sink.
- **Enzyme Classes Utilizing Dioxygen:**
  The discussion expands to enzymes that use molecular oxygen in more diverse ways:
  - **Monooxygenases (Hydroxylases):**
    These enzymes incorporate one atom of dioxygen into a substrate while reducing the other to water. Examples include tyrosine and tryptophan hydroxylases, which are critical in neurotransmitter biosynthesis.
  - **Dioxygenases:**
    Unlike monooxygenases, dioxygenases insert both atoms of dioxygen into their substrates. The cyclooxygenase activity of prostaglandin synthase, which converts arachidonic acid to prostaglandin precursors, is presented as a key example.
  - **Oxidases:**
    Oxidases catalyze reactions in which electrons from substrates are transferred to dioxygen, producing reactive oxygen species (ROS)

such as superoxide or hydrogen peroxide. The chapter outlines how enzymes like cytochrome C oxidase and monoamine oxidase harness oxidase activity to facilitate vital cellular processes, including terminal electron transfer and neurotransmitter inactivation.

- **Cytochrome P450 and Electron Transfer Mechanisms:**
  A substantial portion of the chapter is devoted to cytochrome P450 enzymes, the workhorses of xenobiotic metabolism. These heme-containing monooxygenases use electrons supplied by NADPH-cytochrome P450 reductase to activate dioxygen, enabling the hydroxylation of nonpolar, otherwise inert substrates. The catalytic cycle of P450s, with its series of redox intermediates and oxygen-activating steps, is examined in detail, along with discussions of how structural variations in the heme environment govern function.
- **Tuning Redox Potentials and Transition Metal Homeostasis:**
  The chapter highlights the principle that an enzyme's microenvironment can tune the standard reduction potentials of its redox-active centers. Examples include modifications in FAD-binding sites and engineered mutations in cupredoxins (e.g., azurin) that modulate redox potentials by altering hydrophobicity and hydrogen bonding. Additionally, the role of metalloproteins in managing transition metal ions (Fe, Zn, Cu) is discussed. These proteins not only support essential catalytic functions but also prevent metal-mediated oxidative damage by sequestering free ions through high-affinity binding and specialized chaperone systems.
- **Integration into Metabolism and Physiology:**
  Finally, the chapter connects these oxidation mechanisms to the broader context of cellular metabolism. The sequential oxidation of methane by methanotrophs exemplifies how a series of enzyme-catalyzed redox reactions can fully extract energy from an organic substrate. Likewise, the diverse functions of heme proteins—from oxygen transport by hemoglobin to electron transfer by cytochrome C and substrate oxidation by cytochrome P450—underscore the versatility of redox chemistry in biology.

In summary, this chapter underscores how nature has evolved a variety of oxidizing agents and enzymes to precisely control redox reactions. These processes are fundamental not only for energy production and biosynthesis but also for detoxification and metabolic regulation. Understanding these mechanisms is crucial for appreciating how redox chemistry underpins life at the molecular level.

This page titled 12.4: Biological Oxidation-Reduction Reactions is shared under a not declared license and was authored, remixed, and/or curated by Henry Jakubowski and Patricia Flatt.

- **11.2: Diffusion Across a Membrane - Passive and Facilitated Diffusion** by Henry Jakubowski and Patricia Flatt has no license indicated.

CHAPTER OVERVIEW

13: GLYCOLYSIS, GLUCONEOGENESIS, AND THE PENTOSE PHOSPHATE PATHWAY

Return to Fundamentals of Biochemistry Search Fundamentals of Biochemistry

13.1: Glycolysis
13.2: Fates of Pyruvate under Anaerobic Conditions- Fermentation
13.3: Gluconeogenesis
13.4: Pentose Phosphate Pathway of Glucose Oxidation

Thumbnail: Due to its role in the pentose phosphate pathway and the Calvin cycle, D-Ribose-5-phosphate isomerase is highly conserved in most organisms, such as bacteria, plants, and animals. It plays an essential role in the metabolism of plants and animals, as it is involved in the Calvin cycle which takes place in plants, and the pentose phosphate pathway which takes place in plants as well as animals. (CC BY-SA 4.0; Ishikawa, K., Matsui, I., Payan, F., Cambillau, C., Ishida, H. et al. via Wikipedia)

This page titled 13: Glycolysis, Gluconeogenesis, and the Pentose Phosphate Pathway is shared under a not declared license and was authored, remixed, and/or curated by Henry Jakubowski and Patricia Flatt.

13.1: GLYCOLYSIS

LEARNING GOALS (CHATGPT O3-MINI)

1. **Understand Free Energy Concepts in Metabolic Reactions:**
   - Explain how the change in free energy (ΔG) of a reaction depends on reactant/product concentrations and temperature, and why a negative ΔG is required for spontaneity.
   - Describe how Le Chatelier's principle and reaction coupling can drive nonspontaneous steps forward.
2. **Review Historical Perspectives on Glycolysis:**
   - Summarize the historical contributions of Otto Meyerhof and Archibald Hill to our understanding of sugar metabolism and anaerobic/aerobic energy production.
   - Discuss the significance of their work in shaping modern concepts of glycolysis and cellular respiration.
3. **Outline the Glycolytic Pathway:**
   - Identify the 10 key enzymatic reactions that convert glucose into pyruvate, noting the division between energy-consuming and energy-generating phases.
   - Explain how the overall net reaction of glycolysis results in the production of ATP, NADH, and pyruvate.
4. **Analyze Reaction Coupling and Energy Investment:**
   - Illustrate how the initial investment of ATP in the early steps (e.g., hexokinase and phosphofructokinase reactions) enables later substrate-level phosphorylation.
   - Describe the concept of a "committed step" (PFK1 reaction) and how it regulates the glycolytic pathway.
5. **Examine Key Enzymatic Mechanisms:**
   - Detail the mechanism of hexokinase, including the induced-fit conformational change that protects ATP from hydrolysis by water.
   - Explain the isomerization reaction catalyzed by phosphoglucose isomerase, including the role of cis-enediol intermediates.
   - Describe the phosphorylation of fructose-6-phosphate by phosphofructokinase-1, including its allosteric regulation by ATP and ADP.
   - Analyze the aldolase reaction that cleaves fructose-1,6-bisphosphate into DHAP and G3P, and distinguish between Class I and Class II aldolases.
   - Discuss the role of triose phosphate isomerase in converting DHAP to G3P, ensuring that only one 3-carbon molecule proceeds in glycolysis.
   - Examine the oxidation of G3P to 1,3-bisphosphoglycerate by glyceraldehyde-3-phosphate dehydrogenase, focusing on the formation of a high-energy mixed anhydride and the role of NAD^+.
   - Describe substrate-level phosphorylation by phosphoglycerate kinase and the subsequent conversion of 3PG to 2PG (by phosphoglycerate mutase), leading to enolase catalysis that produces PEP.
   - Explain the final ATP-producing reaction catalyzed by pyruvate kinase, including the factors that make this step highly exergonic.
6. **Understand Enzyme Structure–Function Relationships in Glycolysis:**
   - Compare and contrast the structural differences among various hexokinase isozymes and their regulatory mechanisms.
   - Discuss the significance of induced-fit mechanisms and conformational changes (as seen with hexokinase and phosphofructokinase) in ensuring reaction specificity and efficiency.
7. **Integrate Glycolysis with Broader Metabolic Contexts:**
   - Connect how glycolysis links to aerobic respiration via conversion of pyruvate to acetyl-CoA and entry into the Krebs cycle, as well as to anaerobic pathways (e.g., lactate formation).
   - Explain how the balance between ATP consumption and production in glycolysis reflects its role as a central energy-extracting pathway in cells.
8. **Apply Knowledge of Reaction Thermodynamics to Metabolic Regulation:**
   - Use examples from glycolysis to illustrate how cells control metabolic flux by coupling energetically unfavorable reactions with those that release energy.
   - Discuss how changes in substrate availability and product removal can drive the overall pathway toward ATP synthesis.

By achieving these goals, students will develop a detailed understanding of glycolysis from both a mechanistic and thermodynamic perspective, equipping them to appreciate how the oxidation of sugars is coupled to energy production in living cells.

13.1.1: INTRODUCTION

This chapter will provide a historical overview of glycolysis and introduce you to the 10 enzymatic reactions in the pathway. Our main goal is to understand how the oxidation of our major food molecules, sugars in the case of glycolysis, can lead to ATP synthesis.

Before we begin our journey into the glycolytic pathway, reviewing the concept of reaction free energy is useful. For a reaction to be spontaneous, the change in the free energy within the system must be negative. From the equation in **Figure 13.1.1,** you can see that the change in free energy of a reaction depends on the concentration of the reactants and the products, as well as the temperature within the system.

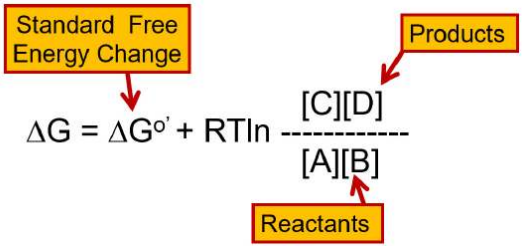


Figure 13.1.1: The Change in Free Energy of a Reaction. The change in the free energy of a reaction is equal to the standard free energy change for the reaction plus the gas constant (R) multiplied by the Temperature in Kelvin (T) and the natural log (ln) of the concentrations of the products of the reaction (noted as C and D in the example) over the concentration of the reactants (noted as A and B in the example).

You will note that some reactions of glycolysis and other metabolic pathways that we will investigate are not favored. Thus, it is necessary to drive the reaction to become spontaneous by either coupling the reaction with a spontaneous reaction that can generate enough free energy to drive the nonspontaneous reaction forward or by using Le Chatelier's principle and removing the products from the enzyme's area as soon as they are made. This will help drive the reaction forward. In this way, a small amount of product can be formed spontaneously. Essentially, the continued removal of the product or the addition of excess reactant will drive the reaction forward. It is worth noting that the temperature of the reaction can also influence the change in free energy. However, in biological systems, temperature changes that will significantly affect the change in free energy are usually incompatible with maintaining most life forms. Thus, it will not be a large consideration in our metabolic discussions here.

When reactions are coupled together to obtain a spontaneous reaction, the overall free energy change for a chemically coupled series of reactions is equal to the sum of the free energy changes of the individual steps, as noted in **Figure 13.1.2.**



Figure 13.1.2: The Coupling of Two Reactions. The top reaction is nonspontaneous, with a positive change in free energy of 21 kJ/mol. This reaction can be driven forward by coupling it with a strongly spontaneous reaction that releases -34 kJ/mol. The overall net reaction has a negative change in free energy and is spontaneous.

The metabolic reactions of carbohydrates and other food molecules play an important role in generating energy in the form of ATP. For carbohydrates, this begins with the metabolic process known as glycolysis (or the breakdown, "lysis," of sugars, "glycol"). At the end of the 1910s, Otto Meyerhof mapped some metabolic conversions by measuring heat trends and oxygen consumption in frog muscles. When the muscle is working, lactic acid is formed from carbohydrates. Otto Meyerhof showed that reprocessing lactic acid to carbohydrates occurs.

Concurrently, Archibald Hill also outlined these processes in frog muscles. In opposition to the prevailing view that mechanical movement and chemical processes were parallel sequences, Hill could show through measurements of heat generated by the mechanical processes that these were delayed compared to the movements. The chemical sequence consists of a work phase, which is not dependent on oxygen supply, and a recovery phase when oxygen is required. Together, their work has opened the door to understanding aerobic and anaerobic metabolism, beginning with glycolysis. They both shared the Nobel Prize in Physiology and Medicine in 1922 for their work in these processes **Figure 13.1.3**.

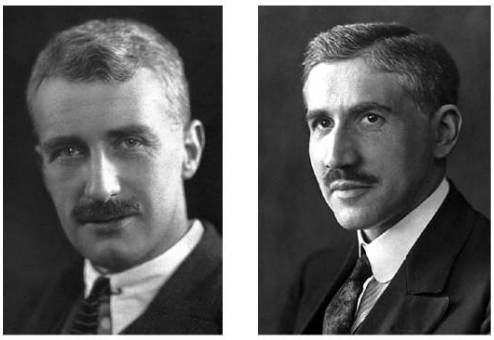


Figure 13.1.3: The Nobel Prize for Physiology and Medicine in 1922. Archibald V. Hill and Otto Fritz Meyerhof received this award for their work on sugar metabolism and breakdown. Photos from Nobel Prize.Org

The glycolytic pathway consists of 10 enzymatic steps that convert glucose to pyruvate. This conversion generates a small amount of energy. The pyruvate can then be converted to lactic acid (lactate) in vertebrates or to ethanol in yeast in an anaerobic (or oxygen-independent) pathway, or it can be fully oxidized to carbon dioxide in an aerobic (or oxygen-requiring) pathway that takes place within the mitochondria (which is shown in green in **Figure 13.1.4:**). Aerobic oxidation yields about 18 times as much energy as the anaerobic pathways, causing them to be favored over anaerobic pathways. Most animal tissues can only survive short anaerobic bursts in isolation and don't involve the entire organism. The aerobic pathway is required to sustain life. Yeast also prefers to grow using the aerobic, mitochondrial pathway. However, if oxygen is unavailable, yeast and other fungi can switch to anaerobic growth and produce ethanol as a byproduct. The production of alcoholic beverages through this fermentation process is quite popular.

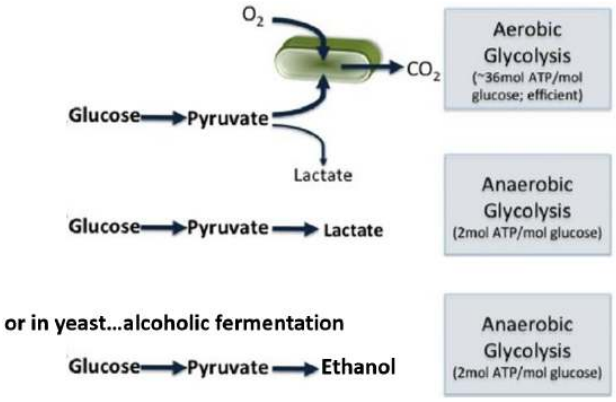


Figure 13.1.4: Overview of Aerobic and Anaerobic Oxidation of Glucose. Figure modified from Kim, Y. et al (2011) PLoS ONE 6(12):e28293

Figure 13.1.5 summarizes the glycolytic pathway coupled to the oxidative phosphorylation pathway that occurs within the mitochondria.

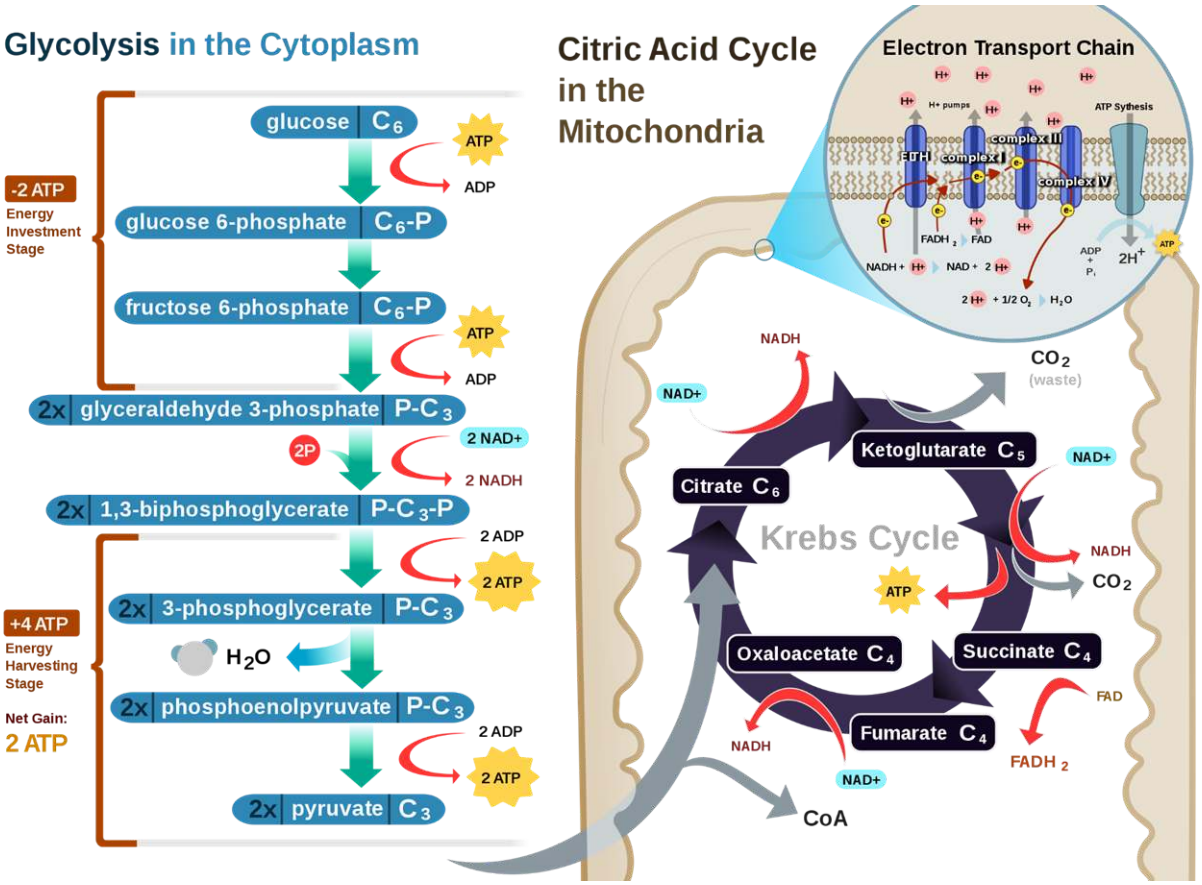


Figure 13.1.5: A Summary of the Glycolytic and Oxidative Phosphorylation Pathways. The glycolytic pathway is shown in blue on the left-hand side. During aerobic metabolism, pyruvate is converted to acetyl-CoA, which then enters the Krebs cycle within the matrix of the mitochondria. Future chapters will focus on the reactions inside the mitochondria. Our focus in this chapter will be on the cytosolic reactions of the glycolytic pathway.

The major reactions of glycolysis are shown in **Figure 13.1.6**. The pathway can be divided into two major sections: (1) the energy-consuming reactions and (2) the energy-generating reactions. An adage states that 'It takes money to make money.' The same can be thought about the glycolytic pathway. The first section requires an energy investment to generate energy in the second half of the reaction pathway. In this pathway, glucose, a 6-carbon hexose, is converted to two 3C molecules - pyruvate. **Figure 13.1.6** shows the entire pathway using Lewis wedge/dash representations plus the anaerobic conversion of pyruvate to lactate.

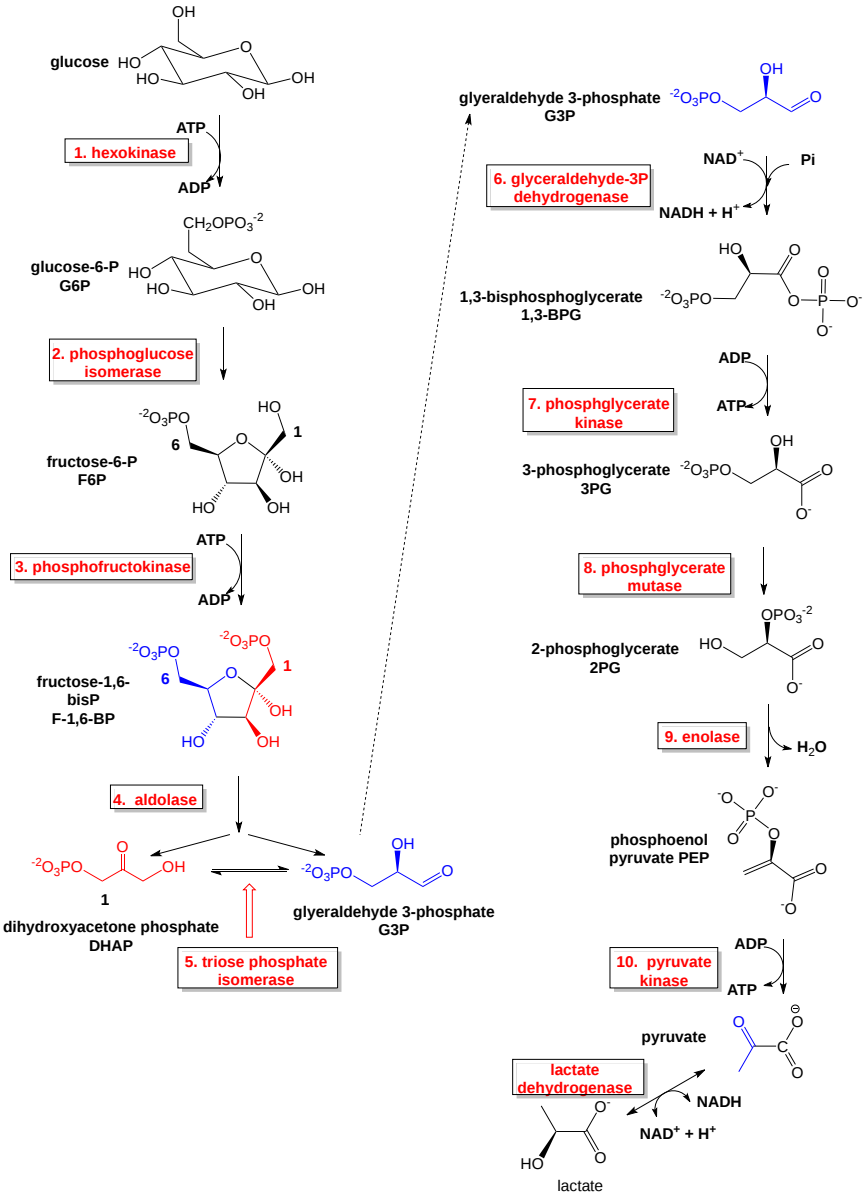


Figure 13.1.6: Glycolytic pathway. The chemical steps of the glycolytic pathway are shown using Lewis wedge/dash representations. Enzymes required at each step are labeled in red. The energy-consuming steps encompass reactions 1 - 3, whereas the energy-producing steps occur in the second half of the pathway from reactions 4 - 10. The conversion of pyruvate to lactate by lactate dehydrogenase represents anaerobic respiration as it occurs within mammalian species.

Glycolysis is the key anaerobic pathway for energy production in all organisms, except in lithotropes that use the oxidation of inorganic molecules for energy production. In aerobic systems, glycolysis releases energy quickly within the body, as glycogen metabolism can quickly release glucose for utilization. Given the centrality of glycolysis to all of life, we will explore each reaction in detail below.

13.1.2: REACTION 1: GLUCOSE → GLUCOSE-6-PHOSPHATE. ΔG^{O}=-4.0 KCAL/MOL (-16.7 KJ/MOL).

The first step in glycolysis is catalyzed by enzymes known as **hexokinases**. The hexokinase family enzymes typically have broad specificity for various hexoses and catalyze the phosphorylation of carbon 6. Hexokinase phosphorylates glucose using ATP as the source of the phosphate, producing glucose-6-phosphate, a more reactive form of glucose. Notably, this reaction prevents the phosphorylated glucose molecule from continuing to interact with the GLUT transport proteins that can shuttle glucose into and out of the cell. Thus, once phosphorylated, glucose can no longer leave the cell. Do note that both sugar forms (the free sugar and the phosphorylated version) can shift back and forth between the ring-closed and ring-opened conformation. Hexokinases require glucose to be in the closed conformation for the phosphorylation reaction. **Figure 13.1.7** shows the reaction, which is catalyzed by **hexokinase** (a kinase that transfers the γ-phosphate from ATP to a hexose in the closed-ring form).

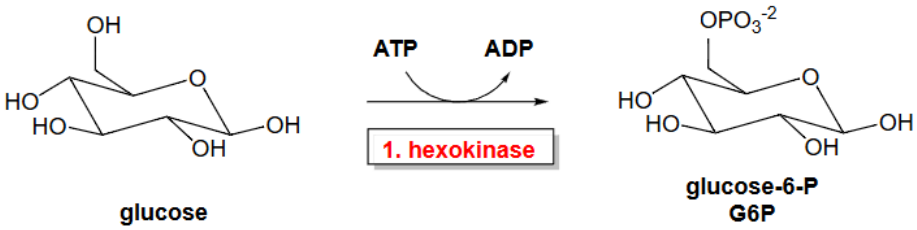


Figure 13.1.7 : Summary reaction - hexokinase

This reaction is a nucleophilic substitution reaction on the gamma phosphate of ATP. A phosphoanhydride bond is broken in ATP as a phosphoester bond is made to form glucose 6-phosphate. Hence, the reaction proceeds with a negative ΔG^o.

Vertebrates have four types of hexokinases, I-IV (also called A-D). The regulation of these enzymes is presented in more detail in Chapter 15.5. Hexokinases I-III bind glucose more tightly, as reflected by low K_M values. Type IV or glucokinase binds it less tightly and is found in high concentrations in vertebrate livers. Yeast has three isozymes: P1, PII or hexokinase B, and glucokinase. Most prokaryotic hexokinases are in the glucokinase (Type IV) class.

In addition to hexokinases, there are many other sugar kinase enzymes. Notably, all sugar kinases must prevent the spurious hydrolysis of ATP by water, which can also be considered a phosphotransfer to water, instead of the preferred transfer of the γ phosphate of ATP to a sugar ROH (alcohol), an "alcoholysis" reaction. Hexokinase does this through an "induced fit" mechanism, in which glucose binding triggers a large conformation change to close off the active site to water.

This conformational change is illustrated in **Figure 13.1.8** below, which shows an interactive iCn3D model of the yeast hexokinase PI in the absence (2YHX) and presence (3B8A) of glucose.

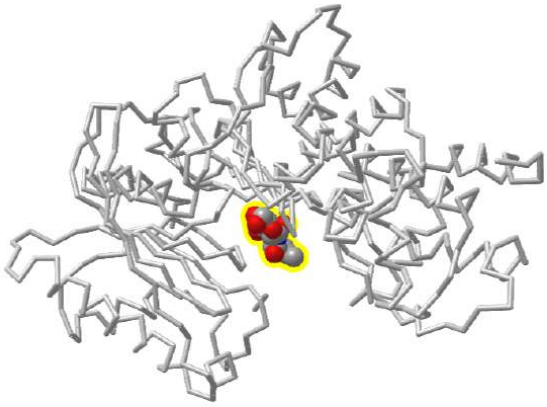


Figure 13.1.8: Yeast hexokinase PI in the absence (2YHX) and presence (3B8A) of glucose. (Copyright; author via source). Click the image for a popup or use this external link: https://structure.ncbi.nlm.nih.gov/i...84YGEd1ob3th7A

Within **Figure 13.1.8,** the gray structure is hexokinase without glucose (2YHX). However, it has a glucose analog bound, o-tolyoylglucosamine (spacefill, yellow highlights), which binds at the glucose binding site but does not cause a subsequent conformation change. The cyan structure (in the actual iCn3D model) shows the enzyme with glucose shown as colored sticks. Note the large conformational change in the actual binding of glucose, a classic example of an "induced fit" mechanism.

Figure 13.1.9 shows the surface of both enzymes using the same color coding as in the above figure. These images better show how the active site of hexokinase is occluded in the glucose-bound form. This prevents water access and hydrolysis of bound ATP instead of "alcoholysis" of ATP (transfer of phosphate to glucose). The gray structure on the left has the glucose analog bound, which doesn't alter the global conformation of the protein.

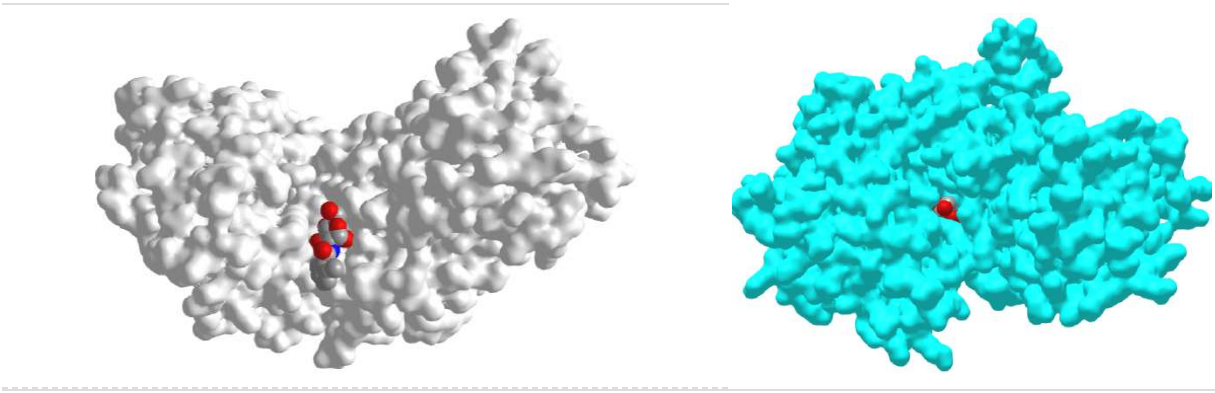


Figure 13.1.9: Surface of human hexokinase I with bound o-tolyoylglucosamine (spacefill, left, 2YHX) and with bound glucose (spacefill, right, 3B8A)

Hexokinase I is the key form in the brain. It forms a complex with porin in the mitochondrial outer membrane and ATP/ADP translocase or carrier protein in the mitochondrial inner membrane, facilitating the hexokinase reaction. Figure 13.1.10 below shows the mechanism for human hexokinase I **reacti**on.

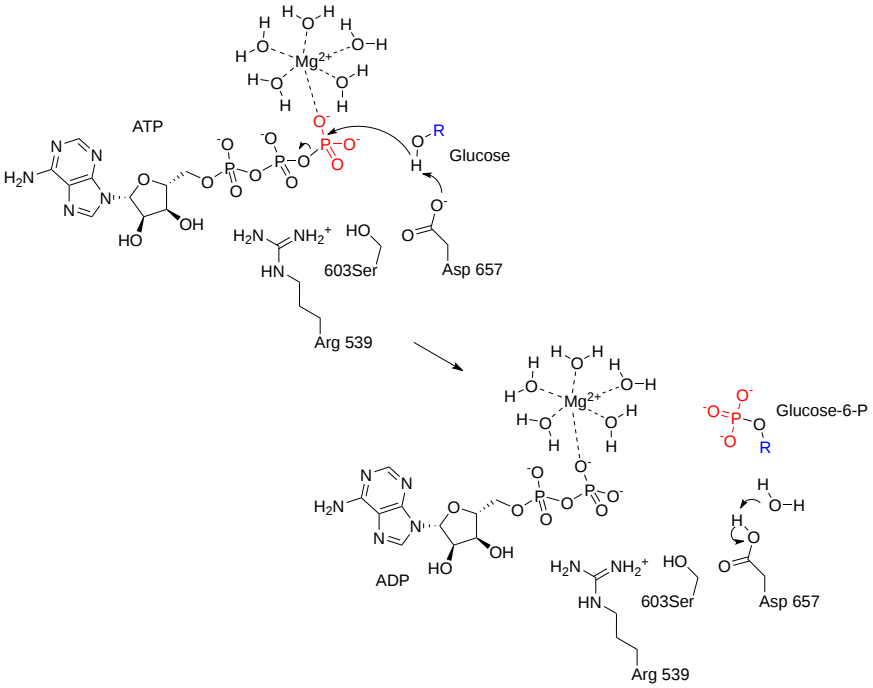


Figure 13.1.10: Mechanism of human hexokinase I.

Ribeiro AJM *et al.* (2017), *Nucleic Acids Res*, **46**, D618-D623. Mechanism and Catalytic Site Atlas (M-CSA): a database of enzyme reaction mechanisms and active sites. DOI:10.1093/nar/gkx1012. PMID:29106569. https://www.ebi.ac.uk/thornton-srv/m-csa/entry/696/. Creative Commons Attribution 4.0 International (CC BY 4.0) License.

Figure 13.1.11 below shows an interactive iCn3D model of human hexokinase I with glucose and ADP in the active site (1dgk).

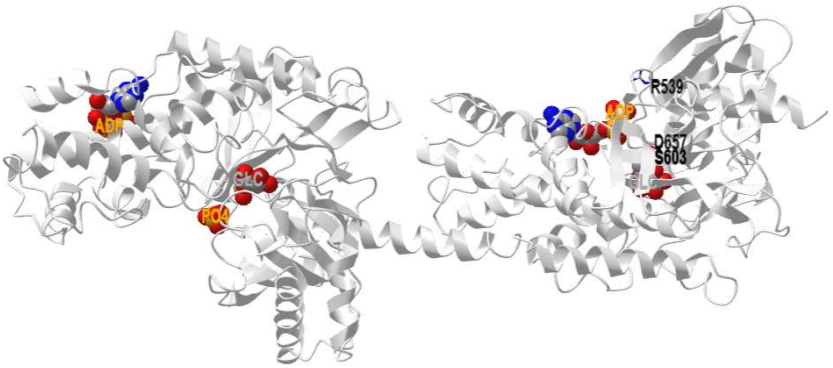


Figure 13.1.11: Human hexokinase I with glucose and ADP in the active site (1dgk). (Copyright; author via source). Click the image for a popup or use this external link: https://structure.ncbi.nlm.nih.gov/i...aQy4gf6A2bWtp8

The key catalytic residues are shown in colored sticks and labeled. Glucose, ADP, and PO_4^{2-} are shown as colored spheres.

Note that hexokinase I and forms II and III have spatially distinct halves similar to those in the yeast enzymes. Forms I-III have a molecular weight of about 100K. Form IV (glucokinase) has a molecular weight of 50K, similar to the distinct halves of I-III. This suggests that I-III arose through gene duplication.

Each half also binds glucose and ADP, but the N-terminal domains of I and III are catalytically inactive. Hexokinase II, with both halves active, is the primary enzyme involved in glycolysis in most mammalian tissues. Another difference is that glucose-6-phosphate, a product, inhibits I-III. PO_4^{2-} relieves G6P product inhibition in form I but not the others. ADP binding at multiple sites in hexokinase I likely causes a conformational change that affects structure and activity.

13.1.3: SUGAR KINASES, IN GENERAL

We will encounter many kinases that use ATP to phosphorylate sugars, so exploring their similarities and differences at the beginning of our studies on carbohydrate metabolism is useful.

Figure 13.1.12 below shows the comparative structures of the five carbohydrate kinase classes.

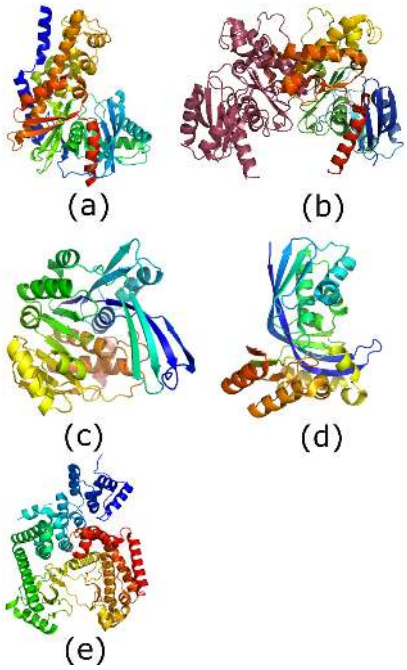


Figure 13.1.12: Structures of the five carbohydrate kinase classes. All images are shown in rainbow format (blue: *N*-terminus, red: *C*-terminus). Roy, S.; Vivoli Vega, M.; Harmer, N.J. Carbohydrate Kinases: A Conserved Mechanism Across Differing Folds. *Catalysts* **2019**, *9*, 29. https://doi.org/10.3390/catal9010029. **Creative Commons Attribution License**

Panel (**a**) shows the structure of human glucokinase (hexokinase class; PDB (protein data bank) ID: 4IWV).

Panel (**b**) shows the structure of *Bacillus subtilis* fructokinase dimer, the second molecule shown in raspberry (ROK kinase class; PDB ID: 1XC3 [17]).

Panel (**c**) shows the structure of *Escherichia coli* ribokinase (ribokinase class; PDB ID: 1RKD; [18]).

Panel (**d**) shows the structure of *Aquifex aeolicus* IspE (GHMP kinase class; PDB ID: 2V2Z; [19]).

Panel (**e**) shows the structure of human PIK3C3 (phosphatidylinositol phosphate kinase class; PDB ID: 3IHY).

Table 13.1.1: Overview of the Five Carbohydrate Kinase Classes.

Carbohydrate Kinase Family	Common Substrates	Native Phosphate Donors (Minor Donors in Parentheses)	Pfam ID
Hexokinase	Glucose, mannose, fructose	ATP (ITP)	PF00349, PF03727, PF02685
ROK Kinase	Glucose, allose, fructose, *N*-acetylglucosamine, *N*-acetylmannosamine	ATP (polyphosphate)	PF00480
Ribokinase	Ribose, 2-deoxy-d-ribose, adenosine	ATP, ADP (GTP, ribonucleotide)	PF00294
GHMP Kinase	Galactose, *N*-acetylgalactosamine,	ATP (GTP, ITP)	PF00288
Phosphatidylinositol kinase	Phosphatidylinositol, phosphatidylinositol phosphates	ATP (GTP)	PF00454, PF01504

ROK is a bacterial **R**epressor, **O**pen reading frame, **K**inase. Ribokinases include adenosine kinases, fructokinases, and phosphofructokinases. GHMP Kinases include Galactokinase, Homoserine kinase, Mevalonate kinase, and Phosphomevalonate kinase. Roy et al. Ibid

Many of these kinases are regulated by the binding of allosteric effectors.

Figure 13.1.13 shows a common mechanism for all, using glucose as an example substrate.

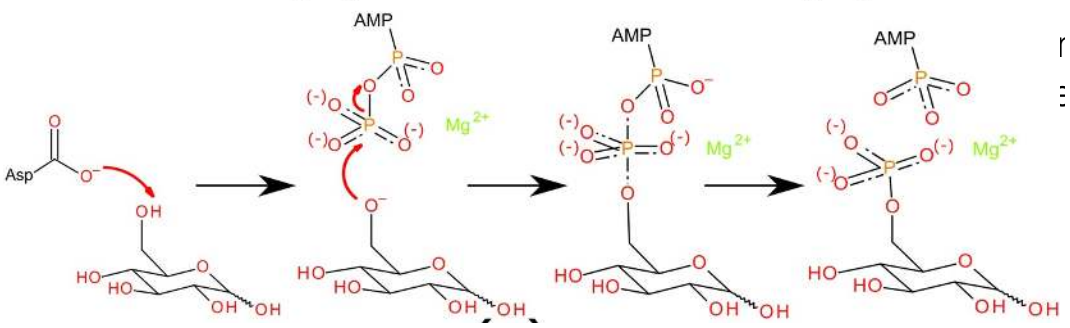


Figure 13.1.13: Generic reaction mechanism for carbohydrate kinases (hexokinase shown). Roy et al., Ibid. The generic reaction is initiated by a catalytic base abstracting a proton from the reactive hydroxyl (left). The oxygen atom then attacks the -phosphate of ATP (second left), forming a pentacoordinate transition state (second right). This is stabilized by a divalent cation and by the protein (not shown). This transition state resolves, leaving ADP and the phosphorylated carbohydrate (right).

13.1.4: **REACTION 2**: **GLUCOSE-6-PHOSPHATE ↔ FRUCTOSE-6-PHOSPHATE**. ΔG^{O}=+0.4 KCAL/MOL (+1.7 KJ/MOL)

In the second step of glycolysis, the **phosphoglucose isomerase (PGI)** converts glucose-6-phosphate into one of its isomers, fructose-6-phosphate. Recall that an isomerase is an enzyme that catalyzes the conversion of a molecule into one of its isomers. In this reaction, the aldose, glucose-6-phosphate, is converted to the ketose, fructose-6-phosphate. This conversion is essential to allow the eventual split of the sugar into two three-carbon molecules. We'll present this reaction, catalyzed by **phosphoglucose isomerase (PGI)**, in several different types of representations (chair, wedge/dash, and Fischer projection), as shown in **Figure \(\PageIndex{14}\)** below.

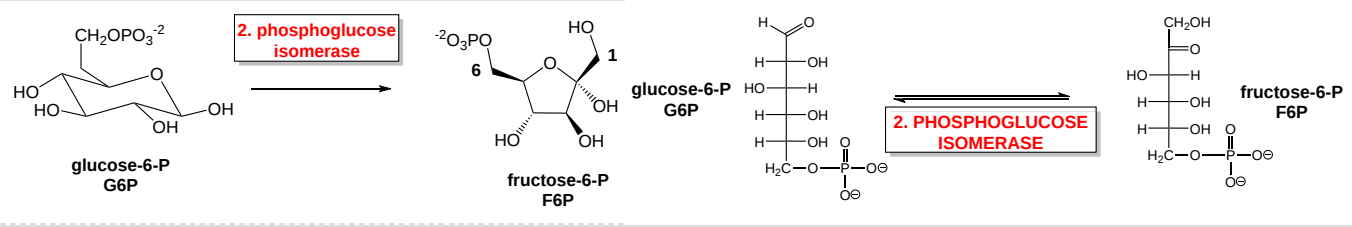


Figure 13.1.14: Summary reaction, phosphoglucoisomerase

From a functional perspective, seen more clearly from the linear Fischer structure, it is evident that the C=O has been moved to the C2 position to create the ketose structure. The carbonyl O is now positioned to be an electron sink, facilitating electron flow for reaction 4. This isomerization reaction would be expected to have a ΔG^o of about 0.

It has been proposed that the mechanism of PGI requires the enzyme to open the Glucose-6-Phosphate ring before the actual isomerization step, which proceeds through the formation of a cis-enediol intermediate and keto-enol tautomers before conversion back to the cyclic form.

Figure 13.1.15 below shows a proposed mechanism for rabbit phosphoglucose isomerase

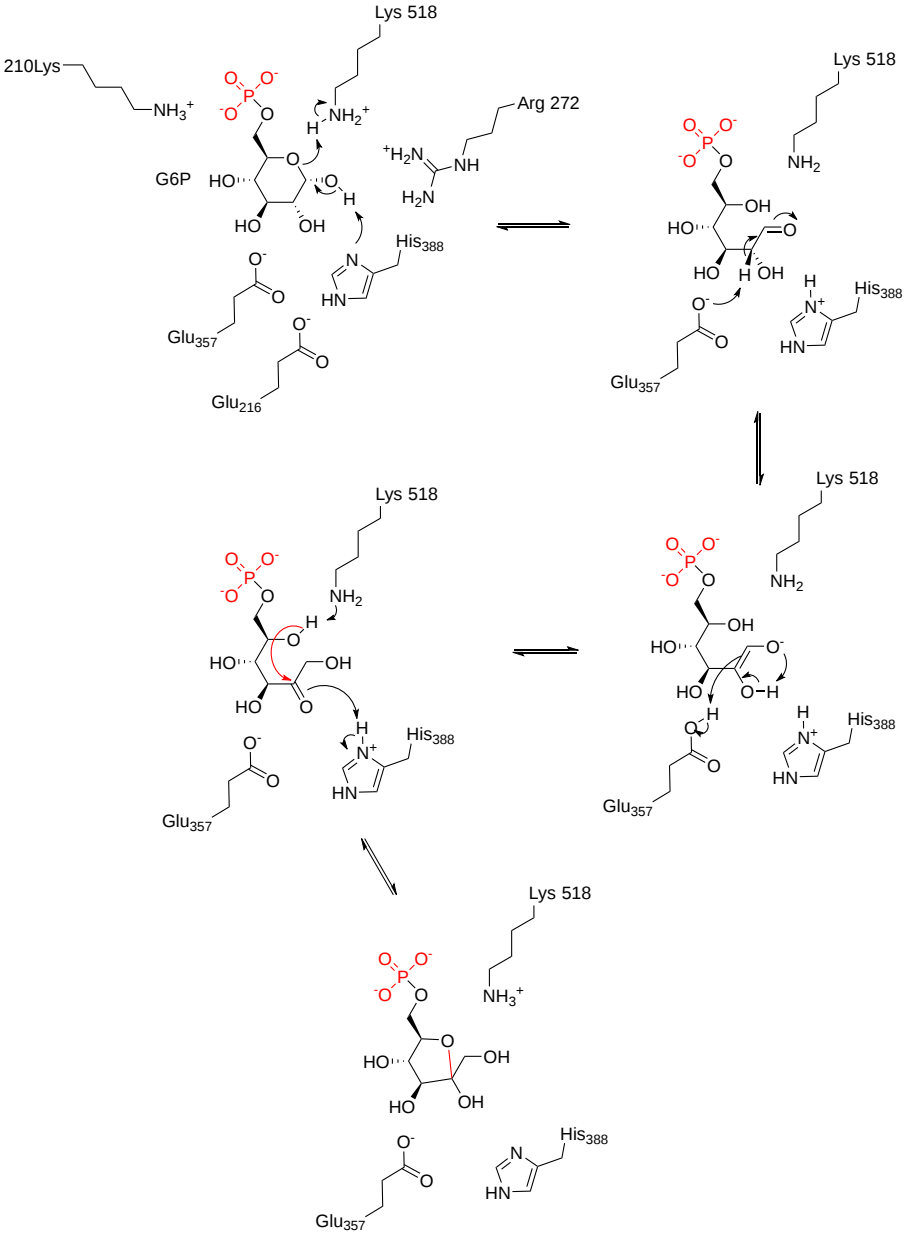


Figure 13.1.15: Mechanism for phosphoglucose isomerase. Ribeiro AJM *et al. Ibid*

Figure 13.1.16 below shows an interactive iCn3D model of rabbit phosphoglucose isomerase with bound 6-phosphogluconic acid (1DQR)

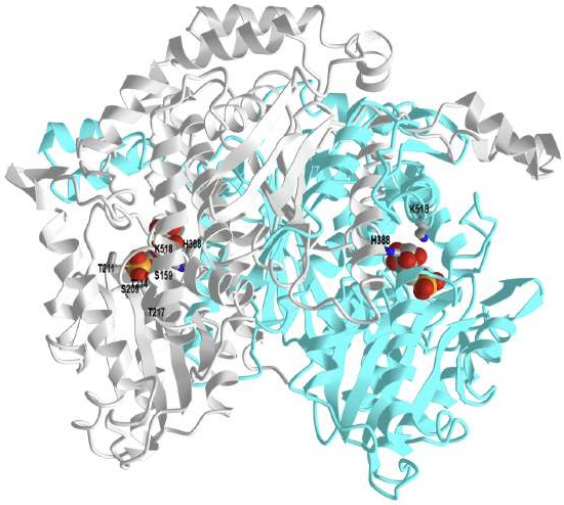


Figure 13.1.16: Rabbit phosphoglucose isomerase with bound 6-phosphogluconic acid (1DQR). (Copyright; author via source). Click the image for a popup or use this external link: https://structure.ncbi.nlm.nih.gov/i...xo1SgF1ZpAySm9

One monomer of the dimer is shown in gray, and the other in cyan. The catalytic residues Lys518 and His388 are shown in both subunits in colored sticks and labeled. Additional residues that contribute to specificity (Ser209, Ser159, Thr214, Thr217, and Thr211) are shown in the gray subunit with color sticks and labeled. 6-phosphogluconic acid, a competitive inhibitor, is shown in color spacefill.

The enzyme also has other functions besides its role in glycolysis, so it is a member of a group called "moonlighting" (a term that refers to working at a secondary job) proteins. Phosphoglucoisomerase acts outside the cell as a nerve growth factor and cytokine. It is also called autocrine motility factor (PGI/AMF), and its cytokine activity is associated with aggressive cancers.

13.1.5: **REACTION 3: FRUCTOSE-6-PHOSPHATE → FRUCTOSE-1,6-BISPHOSPHATE.** ΔG^{O}=-3.4 KCAL/MOL (-14 KJ/MOL)

The third step is the phosphorylation of fructose-6-phosphate, catalyzed by the enzyme **phosphofructokinase-1 (PFK1)**. A second ATP molecule donates a high-energy phosphate to fructose-6-phosphate, producing fructose-1,6-bisphosphate. Bisphosphate is used when two phosphate groups are joined to a molecule at different positions. In this case, one phosphate is at the 1-carbon position, and the other is at the 6-carbon position. This differs from the term diphosphate, which is used when the phosphate groups are joined in a sequence, as in the molecule ADP. In ADP, both phosphate groups are joined in tandem from the 5-carbon position on the ribose ring structure.

In the glycolytic pathway, PFK1 is a rate-limiting enzyme. The mechanism of PFK1 regulation is discussed in greater detail in Chapter 15.5. However, we will introduce the process here. Essentially, the enzyme is sensitive to the energy load within the cell. Recall that ATP is a recycled molecule and exists in a pool of interconverting ATP, ADP, and AMP. A chief outcome of glycolysis is to shift the pool towards increased levels of ATP to drive endergonic processes like muscle contraction. PFK1 activity is sensitive to the ATP:ADP ratio within the cell. PFK1 is more active when the concentration of ADP is high and the concentration of ATP is low, and it is conversely less active when ADP levels are low and the concentration of ATP is high. This is a type of end-product inhibition since ATP is the end product of glucose catabolism. Note, however, that ATP is also a substrate for PFK1. ATP is required in the process as the phosphate donor in the reaction. This is the second energy-intensive step in the glycolytic pathway. At the end of the PFK1 step, 2 ATP molecules have been broken down in the glycolytic pathway.

The PFK1 enzymatic step is also important within the glycolytic pathway as it is the committed step. Glucose-6-phosphate may be used for other purposes within the cell, and the isomerase step that converts glucose-6-phosphate to fructose-6-phosphate is readily reversible. The PFK1 enzyme only works in the forward direction to create fructose 1,6-bisphosphate. It cannot operate in the reverse direction and recover the reactant. Thus, it is considered the committed step in the glycolytic pathway as the fructose-1,6-bisphosphate will predominantly be converted into pyruvate through the remaining enzymatic steps.

The reaction catalyzed by PFK1 is shown in **Figure 13.1.17** below.

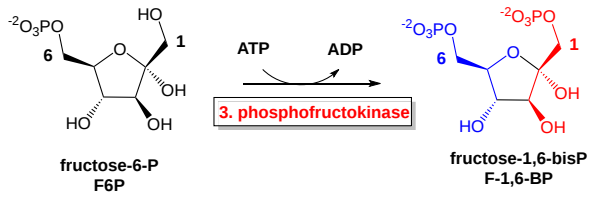


Figure 13.1.17: Summary reaction - phosphofructokinase

By phosphorylating this intermediate, both products of the cleavage of this 6C molecule will be phosphorylated, keeping both more readily inside the cell. This reaction is a nucleophilic substitution reaction on the gamma phosphate of ATP. A phosphoanhydride bond is broken in ATP as a phosphoester bond is made in fructose-1,6-bisphosphate. As in reaction 1, this reaction proceeds with a negative ΔG^{o}.

The PFK1 enzyme exists as a tetramer, and like another "famous" tetramer, hemoglobin, it can exist in T and R symmetry states. Hence, it is an allosteric enzyme and has many allosteric regulators. One important allosteric activator of eukaryotic (not prokaryotic) PFK is fructose-2,6-bisphosphate. This is formed by a separate **phosphofructokinase enzyme named PFK2**. This regulatory pathway will be described in greater detail in Chapter 15.5. Hence, the number 1 is added to the name of the glycolytic enzyme, PFK1, which forms fructose 1,6-bisphosphate, to indicate the position of phosphorylation. Mammals have three isoforms of PFK1: muscle (PFKM), liver (PFKL), and platelet (PFKP).

The mechanism for E. Coli phosphofructokinase is shown in **Figure 13.1.18** below. A metal cofactor (Mg2+) coordinates the positioning of the ATP and stabilizes the gamma phosphate for nucleophilic attack by the fructose alcohol group at position 1. Activation of the fructose alcohol group is mediated by proton abstraction with a coordinated Asp_{127} of PFK1.

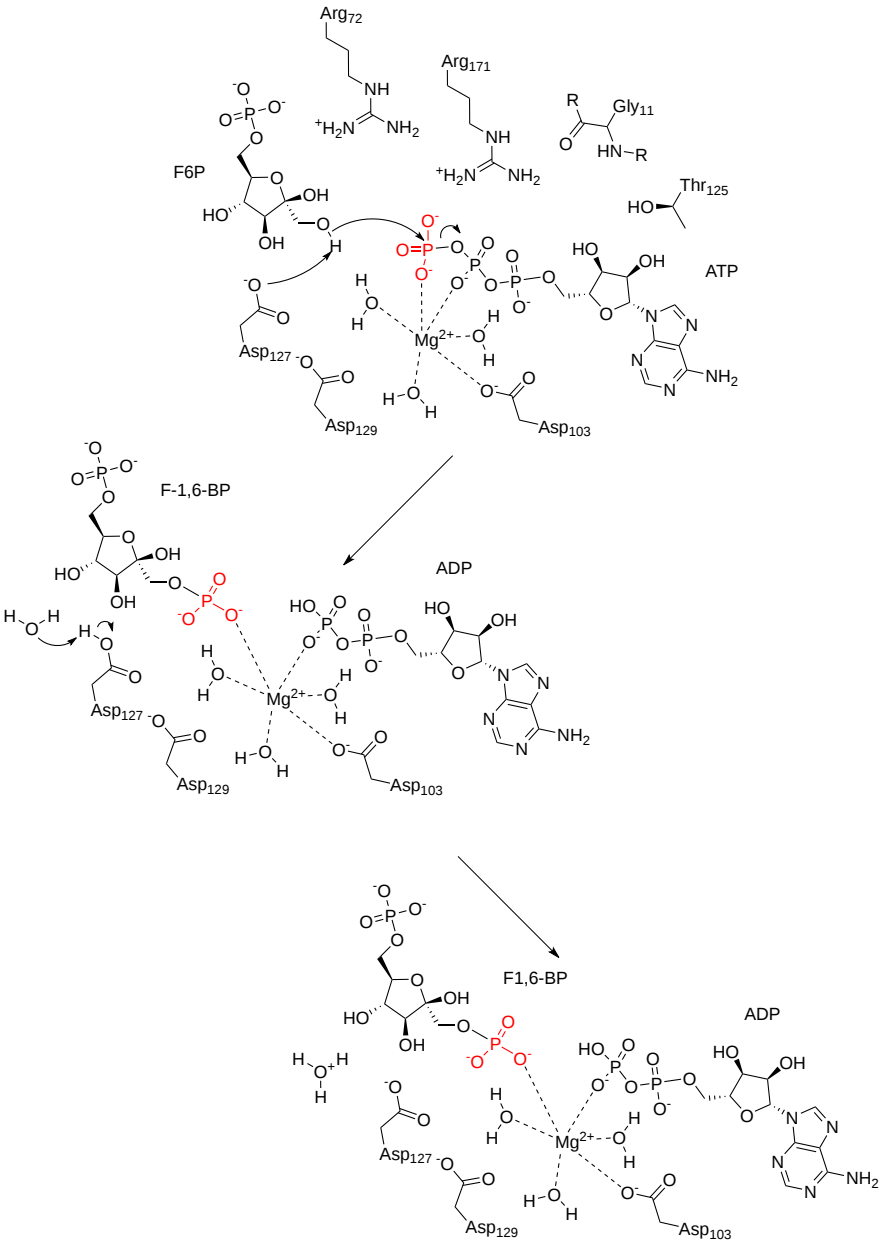


Figure 13.1.18: Proposed mechanism for E. Coli phosphofructokinase. Ribeiro AJM *et al. Ibid*

Figure 13.1.19 below shows an interactive iCn3D model of the *E. Coli* phosphofructokinase with bound F1,6-bisphosphate and ADP products (1PFK). (long load)

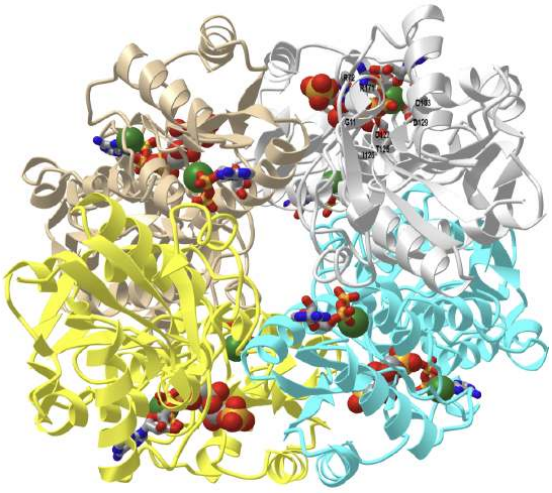


Figure 13.1.19: E. Coli phosphofructokinase with bound F1,6-bisphosphate and ADP products (1PFK). (Copyright; author via source). Click the image for a popup or use this external link: https://structure.ncbi.nlm.nih.gov/i...t4KKgLAGzHrzo8

Each monomer of the tetramer is shown in a different color. The gray monomers show key binding and catalytic residues described in the mechanism above. F1,6-bisphosphate is shown as spacefill, and ADP is shown as sticks.

The structure of the human platelet PFK1 tetramer has been determined in the presence of ATP and ADP. **Figure 13.1.20** below shows an interactive iCn3D model of the human phosphofructokinase-1 dimer (for clarity) in a complex with ATP and Mg (4XYJ). (long load)

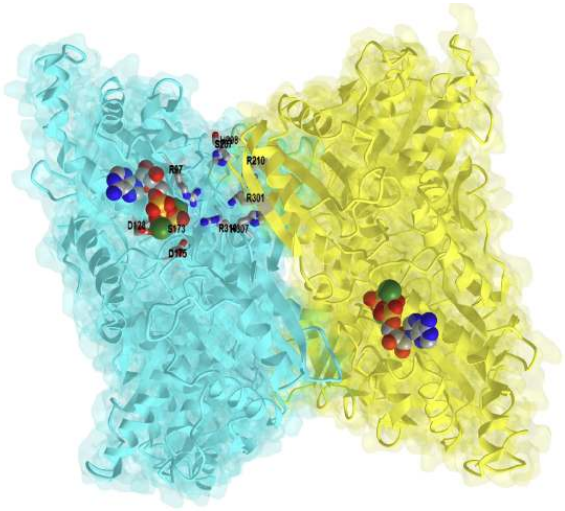
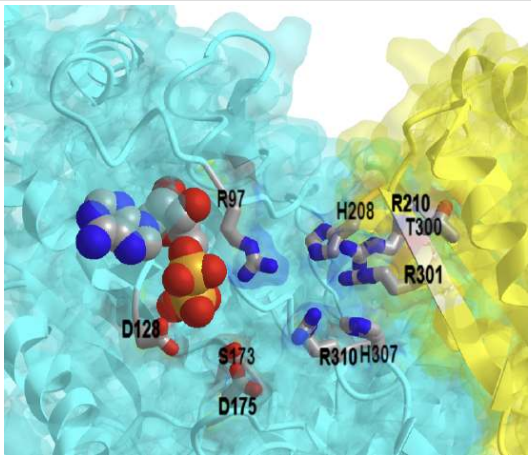


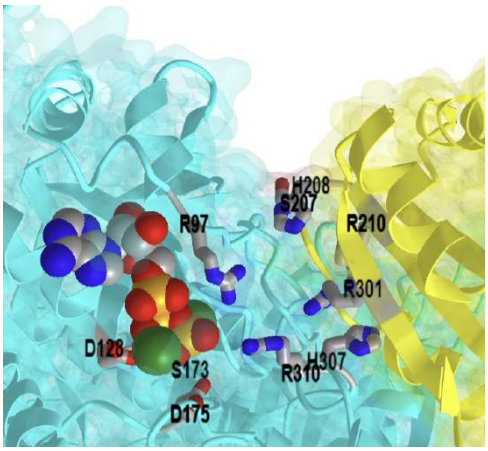
Figure 13.1.20: Human phosphofructokinase-1 dimer in complex with ATP and Mg (4XYJ). (Copyright; author via source). Click the image for a popup or use this external link: https://structure.ncbi.nlm.nih.gov/i...AKfonyGsNq6Cs9 (long load). Here is a link to the ADP bound structure: https://structure.ncbi.nlm.nih.gov/i...N81MBS4PZfSQp9

The monomers are shown as colored surfaces with secondary structures underneath. Note that side chains from each monomer in the dimer contribute to binding and catalysis. The actual PDB structure is tetrameric. The structures have an E173S mutation.

Figure 13.1.21 shows the differences in orientation of the key side chains in the ADP structure (left) and the ATP structure (right) that are key in the conformation changes in the enzyme on substrate binding.



ADP-bound form of human PFK (4XYK)



ATP-bound form of human PFK (4XYJ)

Figure 13.1.21: Conformation changes in the active site of PFK on ATP hydrolysis

13.1.6: REACTION 4: **FRUCTOSE-1,6-BISPHOSPHATE → DIHYDROXYACETONE PHOSPHATE (DHAP) + GLYCERALDEHYDE 3-PHOSPHATE (G3P).** ΔG^{O} = + 5.7 KCAL/MOL (+24 KJ/MOL)

The newly added high-energy phosphates further destabilize fructose-1,6-bisphosphate. The fourth step in glycolysis employs an enzyme, aldolase, to cleave fructose-1,6-bisphosphate into two three-carbon isomers: dihydroxyacetone phosphate and glyceraldehyde-3-phosphate. This reaction is shown in **Figure 13.1.22** below in both wedge dash and Fischer projections.

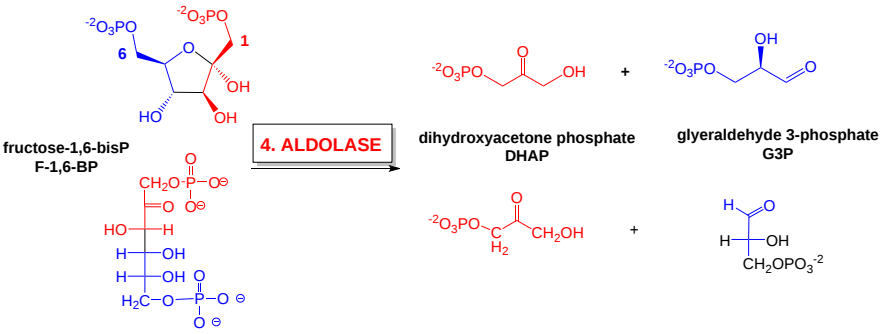


Figure 13.1.22: Summary reaction - aldolase

This is the first C-C bond cleavage within glucose on the path to complete cleavage during aerobic respiration and release of 6 carbon dioxide molecules per glucose metabolized. This reaction is the reverse of an aldol condensation, when an enol or enolate reacts with a carbonyl C to form an adduct. Note that both products are phosphorylated. The reaction is not thermodynamically favored but is pulled in the forward direction by utilizing the product in the next reaction in the pathway.

Table 13.1.2 Characteristics of the Three Classes of Aldolases (I, IA, and II) and the Organisms in Which They are Found.

Aldolase class	Organisms	Characteristics
I	Higher eukaryotes (plants, animals), some protozoans (e.g., Trypanosoma brucei, Leishmania donovani, Plasmodium falciparum), some bacteria, some algae	• Mechanism of action: Schiff base forms substrate intermediate • Structure: Typically forms homo-tetramers, contains TPI β/α-barrel fold
IA	Archaea	• Mechanism of action: Schiff base forms substrate intermediate • Structure: Typically forms homo-octamers/ decamers/higher oligomers, contains TPI β/α-barrel fold
II	“Lower” eukaryotes (some protozoans (e.g., Giardia lamblia), fungi, yeasts, algae), most bacteria, some archaea	• Mechanism of action: Divalent ion forms substrate intermediate, metal-dependent • Structure: Typically forms homo-dimers, contains TPI β/α-barrel fold

Pirovich et al, Frontiers in Molecular Biosciences, 8 (2021), https://www.frontiersin.org/article/...lb.2021.719678. AUTHOR=Pirovich David B., Da’dara Akram A., Skelly Patrick J. **Creative Commons Attribution License (CC BY).**

Class I Aldolase

These enzymes proceed through a Schiff base intermediate between a reactive lysine and the reactant/product. The enzyme is favored in the reverse direction, and it's perhaps easier to see the mechanism presented in that fashion. In rabbits, the muscle Class I aldolase (RAMA) uses Lys-229 to form a Schiff base with DHAP, as shown in a mechanism presented in **Figure 13.1.23** below.

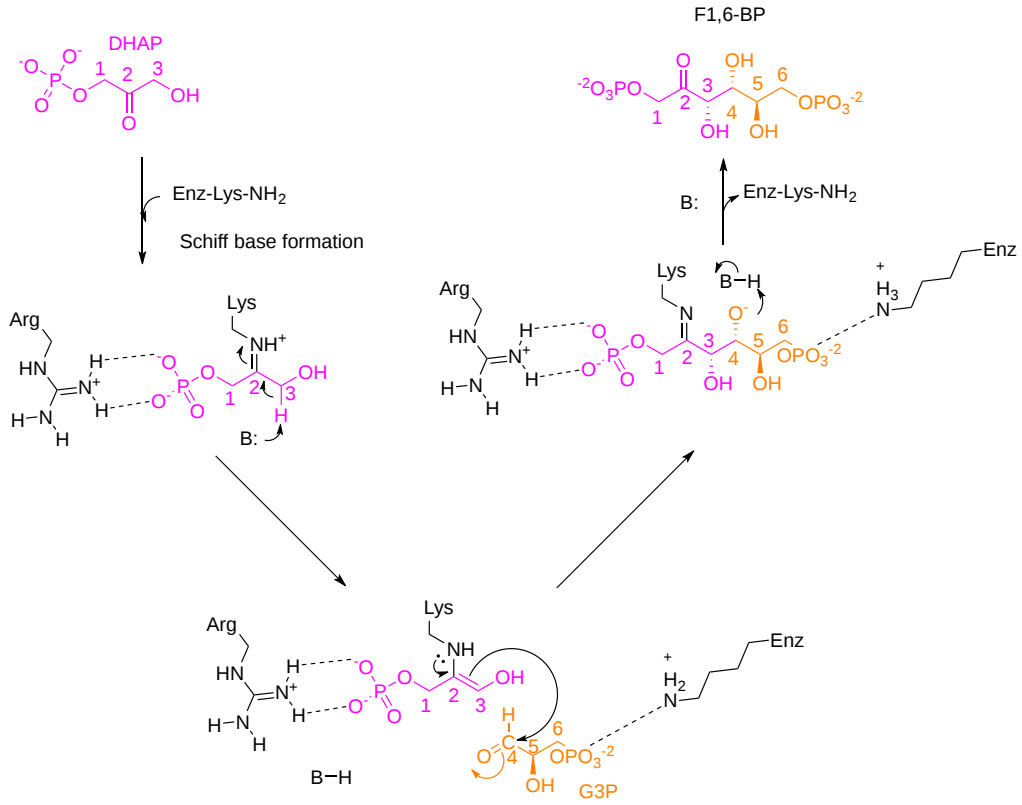


Figure 13.1.23: Class I aldolases - general mechanism (after Bolt et al., Arch Biochem Biophys. 2008 June 15; 474(2): 318–330)

Only the pro(S) proton of the dihydroxyacetone phosphate C3 carbon is removed and effectively exchanged with the glyceraldehyde-3-phosphate substrate. **Figure 13.1.24** below reviews how the pro(R) and pro(S) hydrogens can be visually differentiated by replacing one with

a deuterium and determining the stereochemistry of the now chiral C3.

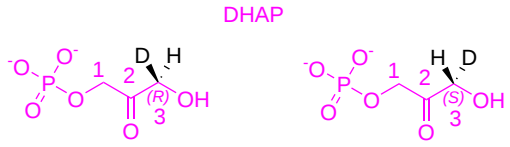


Figure 13.1.24: Visualization of the Pro(R) and Pro(S) hydrogens on DHAP

Figure **13.1.25** shows key active site residues in the active site of a Class I aldolase from rabbit muscle. The first step in Schiff base formation with Lys229 is shown.

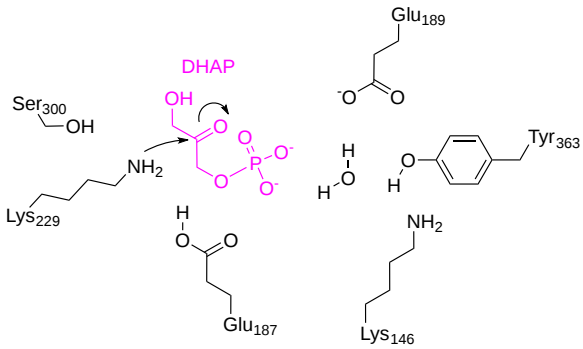
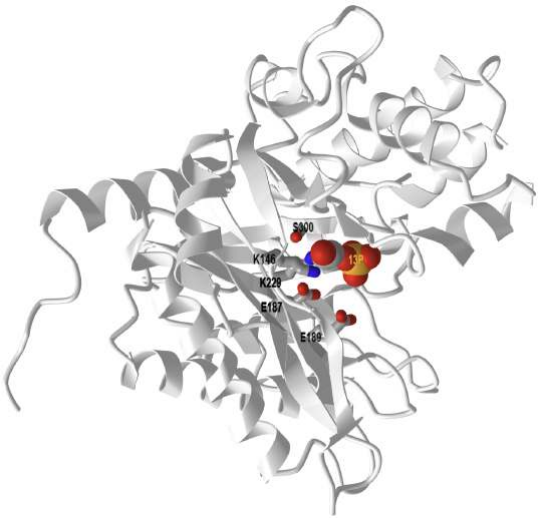


Figure **13.1.25**: Catalytic residues in rabbit muscle Class I enolase.

Figure **13.1.26** shows an interactive iCn3D model of the dihydroxyacetone phosphate enamine intermediate in fructose-1,6-bisphosphate aldolase from rabbit muscle (2QUT)



NCBI iCn3D Figure **13.1.26**: Dihydroxyacetone phosphate enamine intermediate in fructose-1,6-bisphosphate aldolase from rabbit muscle (2QUT). (Copyright; author via source). Click the image for a popup or use this external link: https://structure.ncbi.nlm.nih.gov/i...uR5KZBsfN8QQh9

Only one monomer of the four in the homotetramer is shown. The ligand, 1,3-dihydroxyacetonephosphate, is shown in spacefill with CPK colors. It is in Schiff base linkage with Lys229. The key catalytic residues are shown and labeled.

The reaction proceeds between eneamine and iminium covalent intermediates. A K146M mutation (in the active site) decreases enzyme activity and allows the trapping of the K229 eneamine intermediate. A key tyrosine (Y363) in its deprotonated state, formed in the presence of the iminium phosphate and a local water, appears to abstract the C3 pro(S) proton to form the enamine.

Class II Aldolase

Figure **13.1.27**:

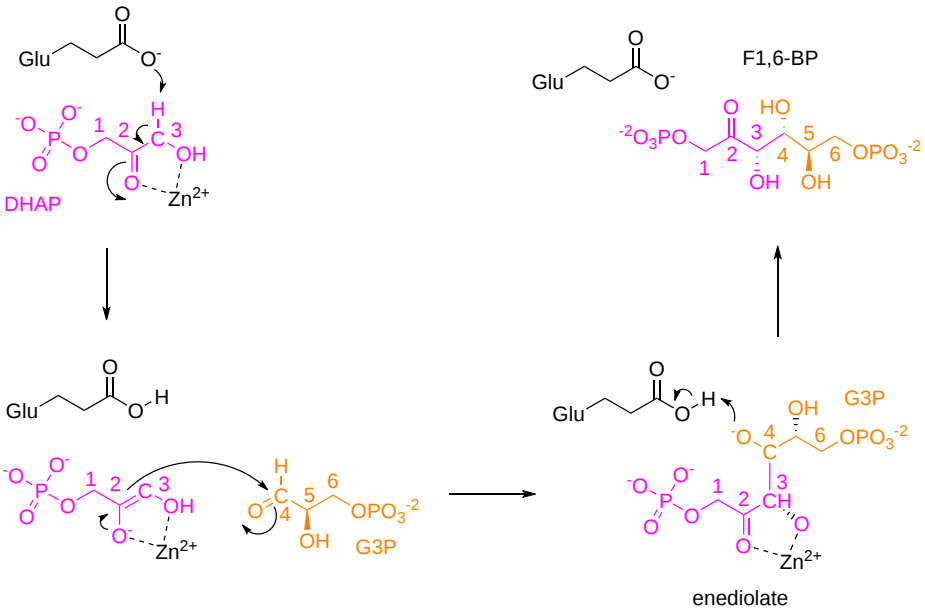


Figure 13.1.27: Class II aldolases - general mechanism (after Bolt et al, ibid)

13.1.7: **REACTION 5: DHAP ↔ G3P**. ΔG^{O}= +1.8 KCAL/MOL (+7.5 KJ/MOL)

This reaction, catalyzed by triose phosphate isomerase (TPI), is shown in Figure 13.1.28.

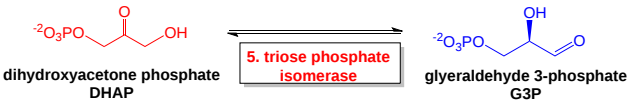


Figure \(\PageIndex{28}\: Summary reaction - triose phosphate isomerase.

This is another simple isomerization reaction. Only one product, glyceraldehyde-3P, continues in glycolysis, so only one enzyme is needed to metabolize the cleavage products of this reaction further. As in other isomerization reactions, the ΔG^{o} is close to 0.

Figure \(\PageIndex{29} below shows a proposed mechanism for this reaction.

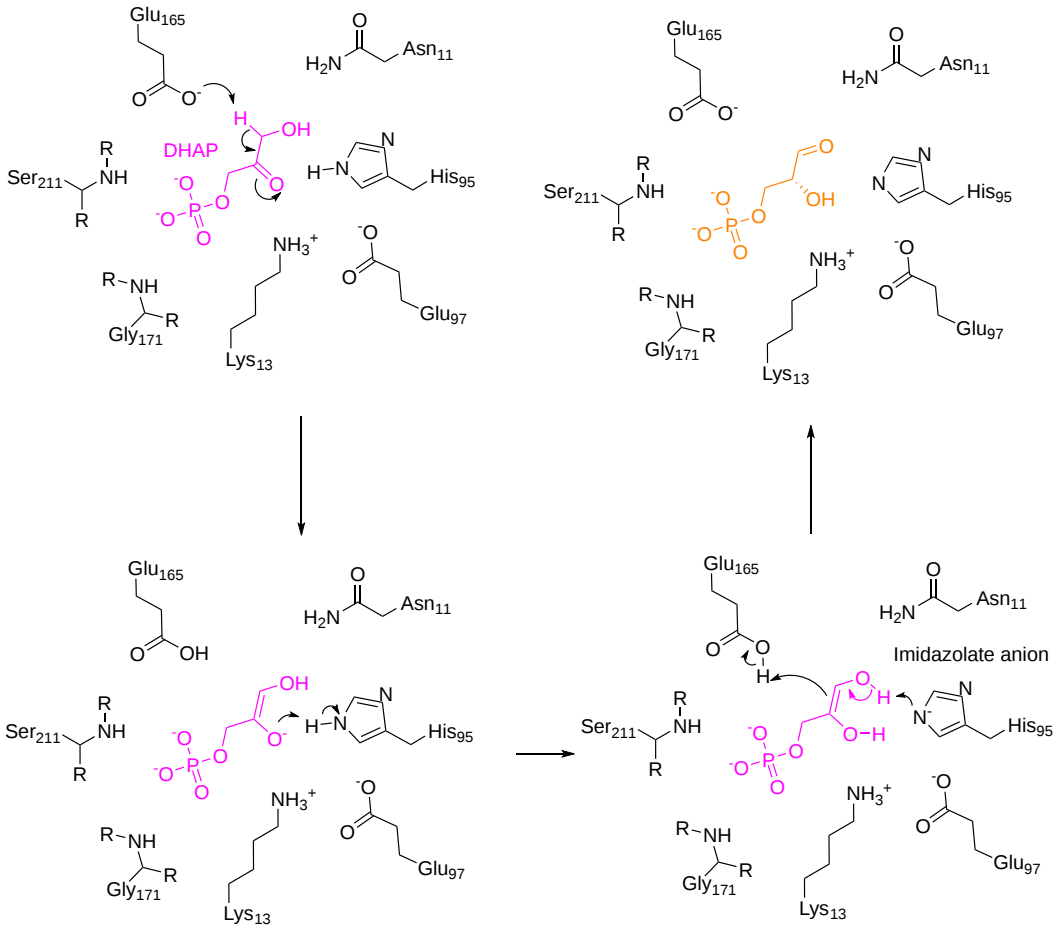


Figure **13.1.29**: Proposed mechanism for triose phosphate isomerase (after Bolt et al., ibid)

Note that the reaction employs the deprotonation of a neutral imidazole side chain to form an imidazolate anion. This would not likely be favorable, given its pKa value.

Four possible conserved proton donors have more reasonable pKas in the active sites of TPIs, including K12, H95, E97, and E165. Mutations of E97 to E97Q and E97D lead to a 4000-fold reduction in k_{cat} (E97Q) but only a 100-fold reduction for E97D suggesting tha30}\) shows an interactive iCn3D model of the chicken triosephosphate isomerase-phosphoglycolohydroxamate complex (1TPH)

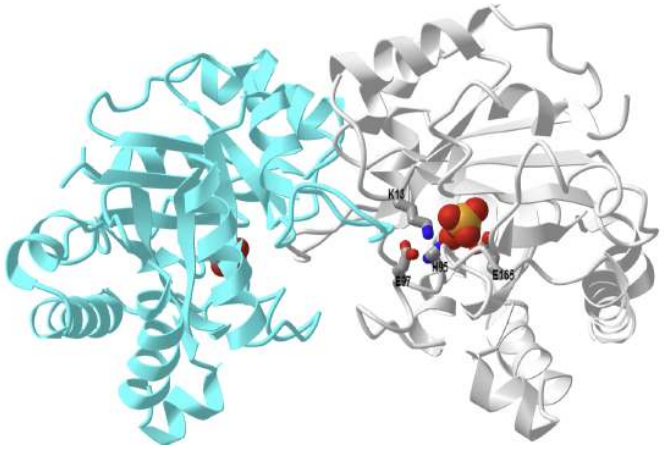


Figure **13.1.30**: Chicken triosephosphate isomerase-phosphoglycolohydroxamate complex (1TPH). (Copyright; author via source). Click the image for a popup or use this external link: https://structure.ncbi.nlm.nih.gov/i...AFXpt9kg5aki5A

The four key conserved residues are shown in the gray monomer of the homodimer.

13.1.8: **REACTION 6: G3P ↔1,3 BPG.** ΔG^{O}= +1.5 KCAL/MOL (+6.1 KJ/MOL)

This reaction, catalyzed by **glyceraldehyde-3-phosphate dehydrogenase**, is shown in Figure **13.1.31**

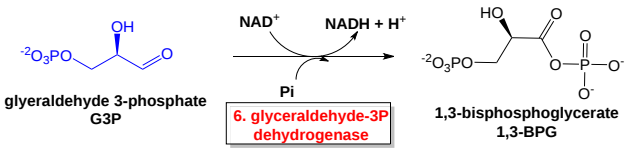


Figure \(\PageIndex{31}\): Summary reaction - glyceraldehyde-3-phosphate dehydrogenase

This is a big reaction! The ΔG^{o} is close to 0, but look at what happened. The carbonyl O in G3P has been oxidized to the form of a mixed anhydride, which can donate a phosphate to ADP (in the next step) to form ATP. This is an oxidation reaction because the carbonyl C in G3P has two bonds to O but three bonds in 1,3 BPG.

To carry out an oxidation reaction, you need an oxidizing agent. In comes NAD^{+}, a modest but very prevalent oxidizing agent in biology. When glucose is oxidized completely by O_2 to CO_2 during combustion, much energy is released, so we can surmise that oxidation reactions, if carried out by powerful oxidizing agents like O_2, proceed with a large negative ΔG^{o}. For every oxidation reaction, the oxidizing agent is reduced. All reactions are potentially reversible, so the formed products are new potential oxidizing and reducing agents. As in acid/base reactions, which proceed from stronger to weaker conjugate acid, redox reactions proceed from a stronger to a weaker oxidizing agent. For reaction 6, we must use tables of redox potentials to calculate the actual ΔG^{o}. It turns out to be close to 0, which is great since a substrate-level phosphorylation reaction (using inorganic phosphate - Pi instead of ATP) occurs in the same reaction. In summary, this reaction catalyzes the first and only glucose oxidation in glycolysis, which has paid (thermodynamically) for the generation of a mixed anhydride whose phosphorylating potential is higher than that of ATP.

Figure **13.1.32** shows a proposed mechanism for glyceraldehyde-3-phosphate dehydrogenase from Trypanosoma cruzi

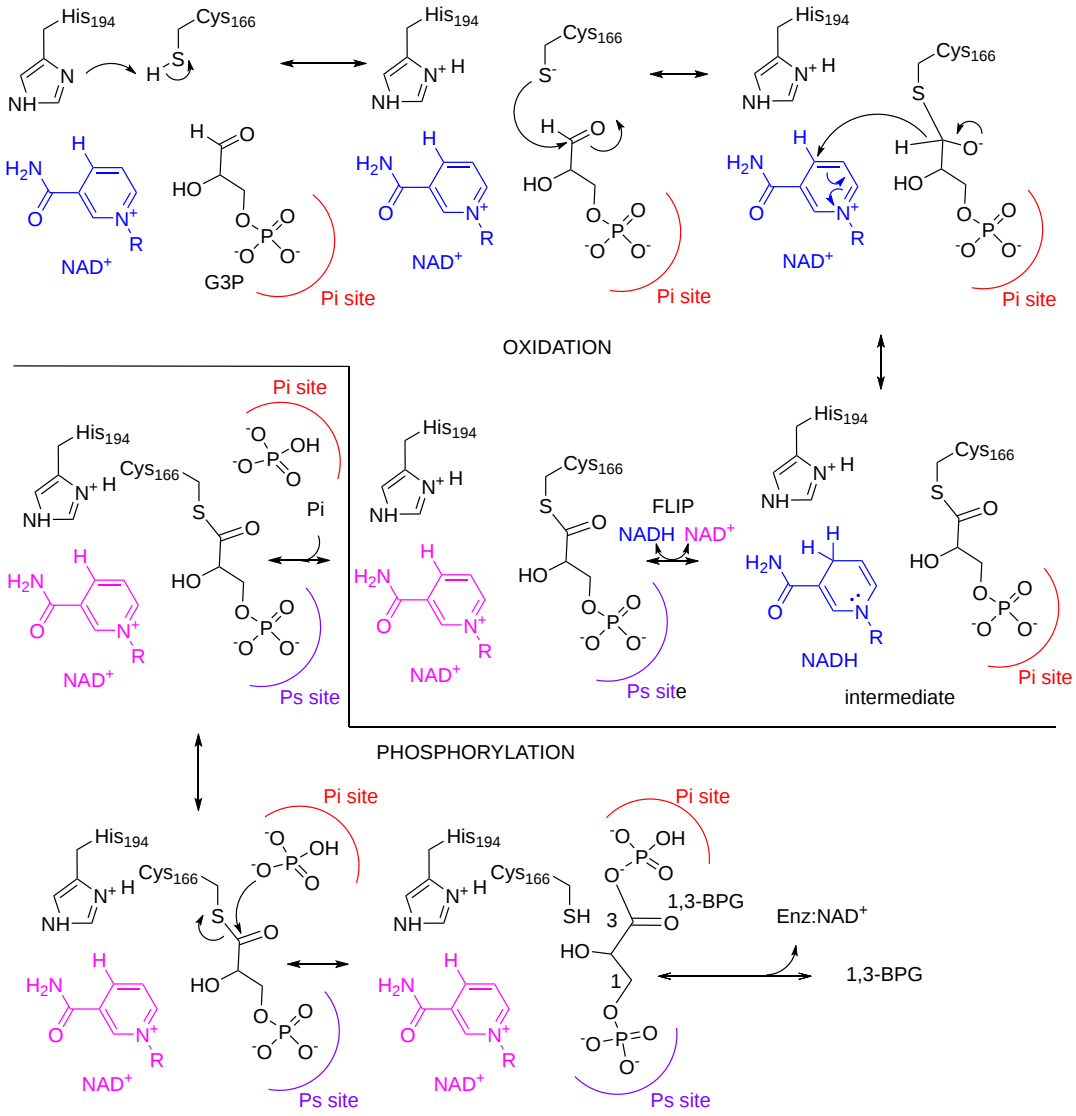
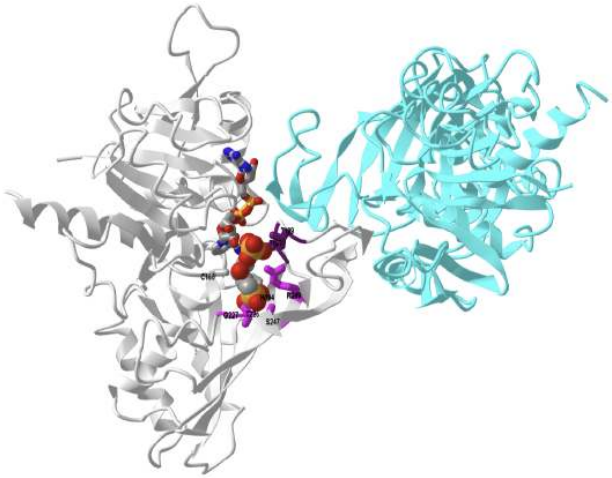


Figure **13.1.32**: Proposed mechanism for glyceraldehyde-3-phosphate dehydrogenase from Trypanosoma cruzi (after Reis et al. Phys. Chem. Chem. Phys., 2013, 15, 3772. https://pubmed.ncbi.nlm.nih.gov/23389436/)

The reaction proceeds in two parts. The first (top section) is the oxidation of glyceraldehyde-3-phosphate (G3P) by NAD^+ to the state of a thioester attached to Cys166. The now reduced NADH dissociates and is replaced by a new NAD^+ for another catalysis cycle. In the meantime, inorganic phosphate, Pi, binds and reacts with the thioester to form 1,3-bisphosphoglycerate (1,3-BPG).

The mechanism is not entirely clear. Two phosphate binding sites, Pi (red) and Ps (purple) interact with phosphate groups on the substrates. The oxidation part of the reactions appears to take place at the Pi site. Pi comprises the side chains of Thr197, Thr199, and the 2-hydroxyl group of the ribose in NAD^+. The Pi site in the T. cruzi enzyme consists of Thr226 and Arg249, Gly227, and Ser247. The mechanism appears to involve a flip of the orientation of substrates and intermediates after the dissociation of NADH from the enzyme.

Figure **13.1.33** shows an interactive iCn3D model of the Trypanosoma cruzi glyceraldehyde-3-phosphate dehydrogenase with bound NAD and a 1,3-bisphosphoglycerate analogue (1QXS)



NCBI iCn3D Figure **13.1.33**: Trypanosoma cruzi glyceraldehyde-3-phosphate dehydrogenase with bound NAD and a 1,3-bisphosphoglycerate analogue (1QXS) . (Copyright; author via source). Click the image for a popup or use this external link: https://structure.ncbi.nlm.nih.gov/i...WnsNSgmA3AJyw6

Only two monomers of the homotetramer are shown for clarity. The Pi site is magenta, and the Ps site is purple. The phosphonic acid analog is shown in spacefill and NAD in sticks. The active site His194 and Cys166 are also shown in sticks and labeled.

13.1.9: **REACTION 7: 1,3 BPG + ADP + H^+ → 3PG + ATP** ΔG^O= -4.5 KCAL/MOL (-19 KJ/MOL)

This reaction, catalyzed by **phosphoglycerate kinase**, is shown in Figure **13.1.34**

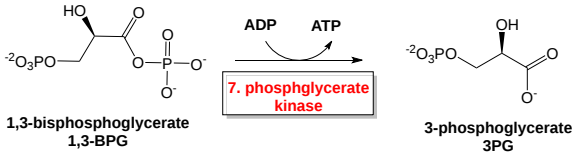


Figure **13.1.34**: Summary reaction - phosphoglycerate kinase

It's finally happened! An ATP has been made for each of the two 1,3-BPG molecules derived from glucose. We've made back the ATP used in steps 1 and 3. A mixed phosphoanhydride bond is broken in 1,3 BPG as a phosphoanhydride bond is made in ATP. As the mixed phosphoanhydride has higher energy than its hydrolysis product compared to the phosphoanhydride in ATP, the reaction proceeds with a negative ΔG^o.

A mechanism for the reaction is shown in Figure **13.1.35**.

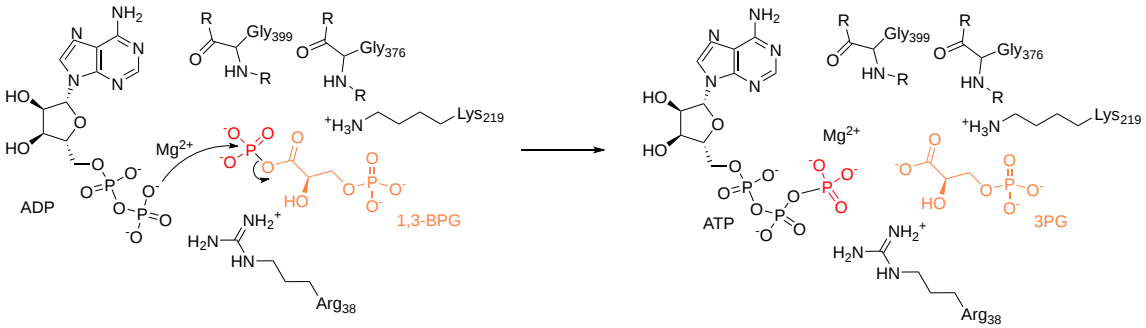
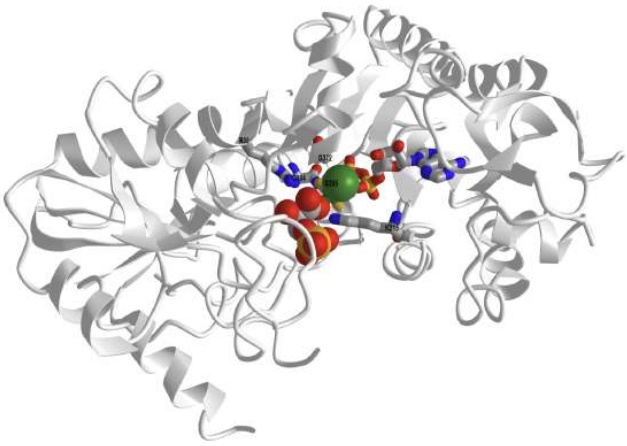


Figure **13.1.35**: Reaction mechanism for phosphoglycerate kinase

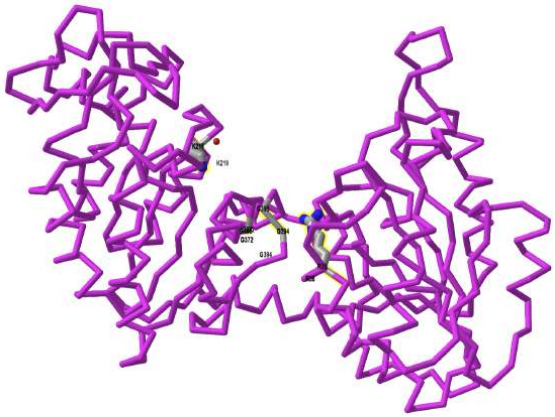
Figure **13.1.36** shows an interactive iCn3D model of human phosphoglycerate kinase in complex with ADP, 3PG, and magnesium trifluoride (2WZB).



NCBI iCn3D Figure **13.1.36**: Human phosphoglycerate kinase in complex with ADP, 3PG, and magnesium trifluoride (2WZB). (Copyright; author via source). Click the image for a popup or use this external link: https://structure.ncbi.nlm.nih.gov/i...w5yvu2VuGhmQXA

3-phosphoglycerate is shown in spacefill with CPK colors. ADP plus the adjacent MgF_3 is a mimetic for the transition state for ATP synthesis. Hence, this structure shows the products/transition state in a closed active site, which, as we have seen before, prevents spurious hydrolysis of 1,3-BPG or ATP.

Figure **13.1.37** shows an interactive iCn3D model of the alignment of the open form of human phosphoglycerate kinase (2XE7) with bound 3PG and ADP with the closed form with bound 3PG, ADP, **and MgF_3** (2WZB).



NCBI iCn3D Figure **13.1.37**: Alignment of the open form of human phosphoglycerate kinase (2XE7) with bound 3PG and ADP with the closed form with bound 3PG, ADP, **and MgF_3** (2WZB). (Copyright; author via source). Click the image for a popup or use this external link: https://structure.ncbi.nlm.nih.gov/i...n5FfsJeYitiWr9

Use the "a" key to toggle back between the open form (magenta) and closed forms (cyan). In the closed state, most closely representing the bond transition state of ATP, the two lobes of the enzyme clamp together.

13.1.10: **REACTION 8: 3PG ↔ 2PG** ΔG^{O}= +1.1 KCAL/MOL (4.6 KJ/MOL)

This reaction, catalyzed by **phosphoglycerate mutase (PGM)**, is shown in Figure **13.1.38**

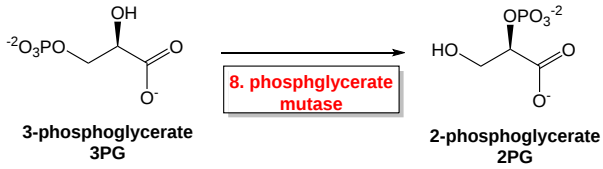


Figure **13.1.38**: Summary reaction - phosphoglycerate mutase

This isomerization reaction proceeds with little thermodynamic barrier. Its function is to locate the phosphate on C2 which on the next reaction (dehydration) will form a molecule whose phosphoryl transfer potential is greater than ATP. It seems so simple, but the enzymes that catalyze this reaction are diverse and quite complicated from a mechanistic perspective.

There are two types of PGMs, bisphosphoglycerate and monophosphoglycerate mutases, that carry out three different reactions involving the shuffling of phosphates from one position to another in 3C sugars or the cleavage of a phosphate from a sugar

- 3-phosphoglycerate ↔ 2-phosphoglycerate (reaction 8 of glycolysis) catalyzed by bisphosphoglycerate and monophosphoglycerate (the glycolytic enzyme) mutases
- 1,3-bisphosphoglycerate ↔ 2,3-bisphosphoglycerate by bisphosphoglycerate mutases
- 2,3-phosphoglycerate ↔ 3-phosphoglycerate + Pi by bisphosphoglycerate mutases

Within the monophosphoglcyerate mutases, and more specifically, the phosphoglycerate mutase (PGM) of glycolysis, there are two types

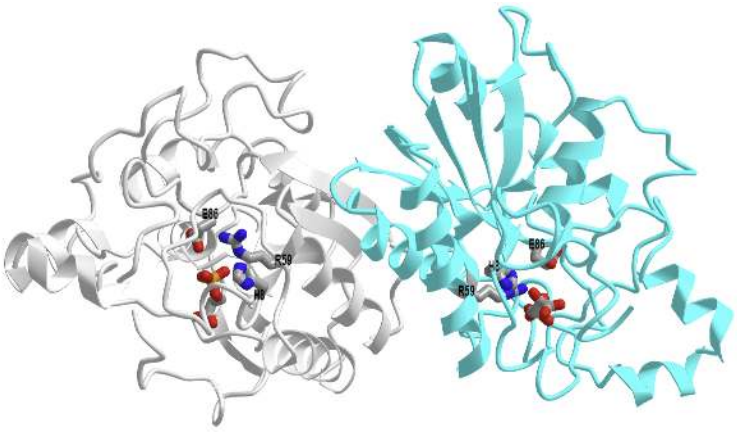
- one that depends on the cofactor 2,3-phosphoglycerate. These are called cofactor-dependent phosphoglycerate mutase (dPGM) and are found in mammals, yeast, and some bacteria. They do not require metal ions.
- one that does not depend on the cofactor 2,3-phosphoglycerate. These are called cofactor-independent phosphoglycerate mutase (iPGM) and are found in plants and some bacteria. These can only interconvert 3PGA and 2PGA. One family of enzymes in the class requires $Mn^{2+,}$ while the other requires Mg^{2+} or Zn^{2+}. These enzymes are often structurally similar to alkaline phosphatases.

The cofactor-independent and cofactor-dependent monophosphoglycerates (such as the phosphoglycerate mutase of glycolysis) are very different structurally and mechanistically so we will look at both types of mechanisms. Within each type, the enzyme sequences are very conserved.

Mechanism of cofactor (2,3-BPG) dependent phosphoglycerate mutase (dPGM)

The reaction is much less complicated than the cofactor-independent PGM. In E. Coli, the reaction involves the transfer of the phosphate on the C3-OH to the nucleophilic nitrogen on histidine 8 (His 10 in other enzymes) in the active site to form a covalent pHis8 intermediate. The phosphate on pHis8 could then be transferred to the O on carbon C2 of the substrate. An active His 181 in E. Coli may also act as a general acid/base and is adjacent to the Glu 88 in the active site.

Figure **13.1.39** shows an interactive iCn3D model of yeast phosphoglycerate mutase (cofactor dependent) bound to 3-phosphoglycerate (1QHF)



NCBI iCn3D Figure **13.1.39**: Yeast phosphoglycerate mutase (cofactor dependent) bound to 3-phosphoglycerate (1QHF). (Copyright; author via source). A dimer of the active tetramer is shown. Click the image for a popup or use this external link: https://structure.ncbi.nlm.nih.gov/i...9F4oc6mmr5DFs9

Mechanism of cofactor-independent phosphoglycerate mutase (iPGM)

Let's consider the mechanism for the Mn^{2+}-requiring iPGM from Geobacillus stearothermophilus. Two Mn^{2+} ions are in the active site. The mechanism for the first half of the cofactor-independent phosphoglycerate mutase (iPGM) reaction is shown in Figure **13.1.40**.

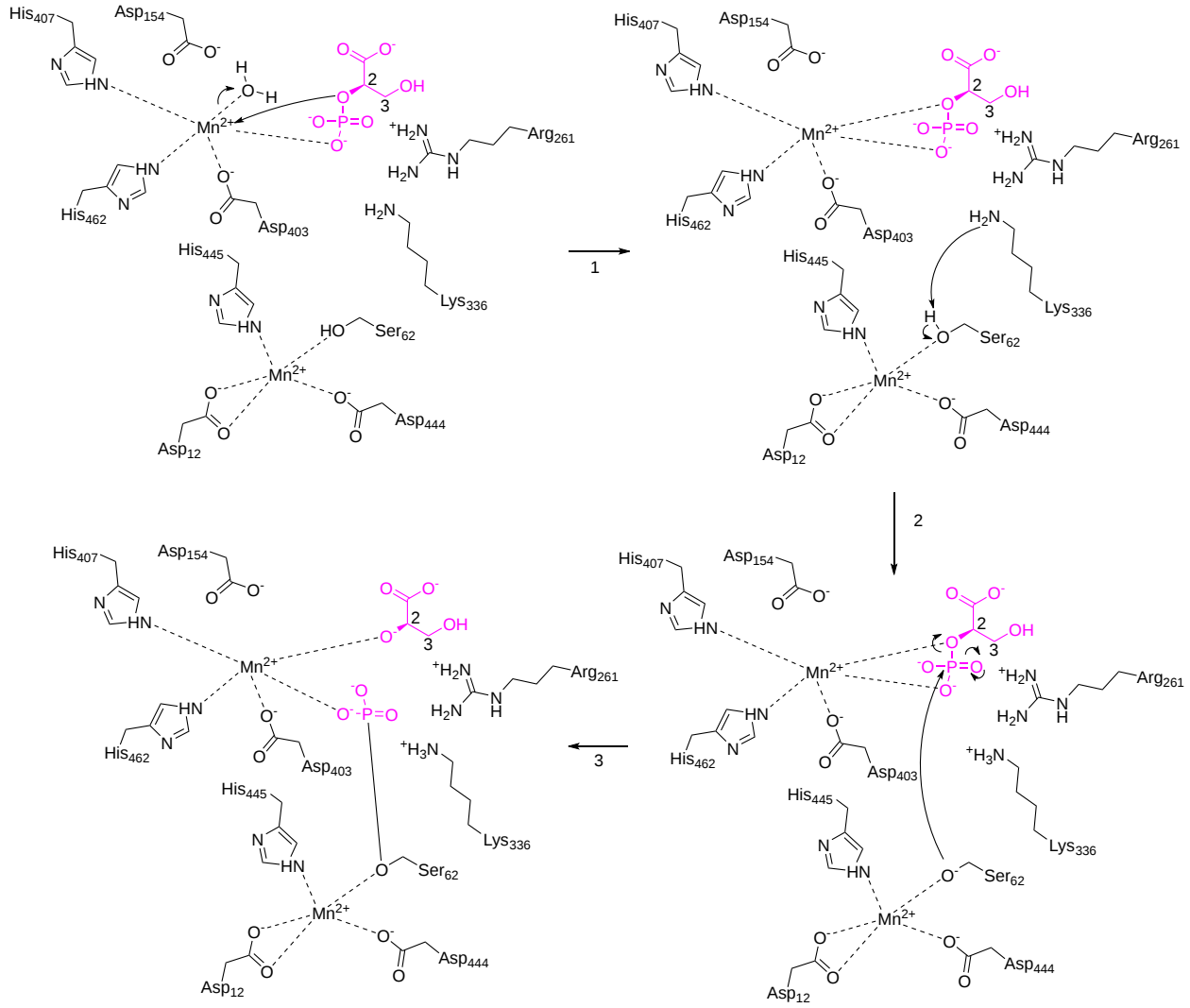


Figure **13.1.40**: Part A - Mechanism for cofactor-independent phosphoglycerate mutase (iPGM) from Geobacillus stearothermophilus (after Bolt et al, ibid)

Arg 261 interacts with the substrate, stabilizing its negative charge and transition state. It also makes the target phosphorus more electrophilic. A Mn^{2+} ion activates Ser 62 to become more nucleophilic after the abstraction of a proton by Lys 336. Reaction 3 probably proceeds through an S_N2 mechanism.

Figure **13.1.41** shows the rest of the mechanism.

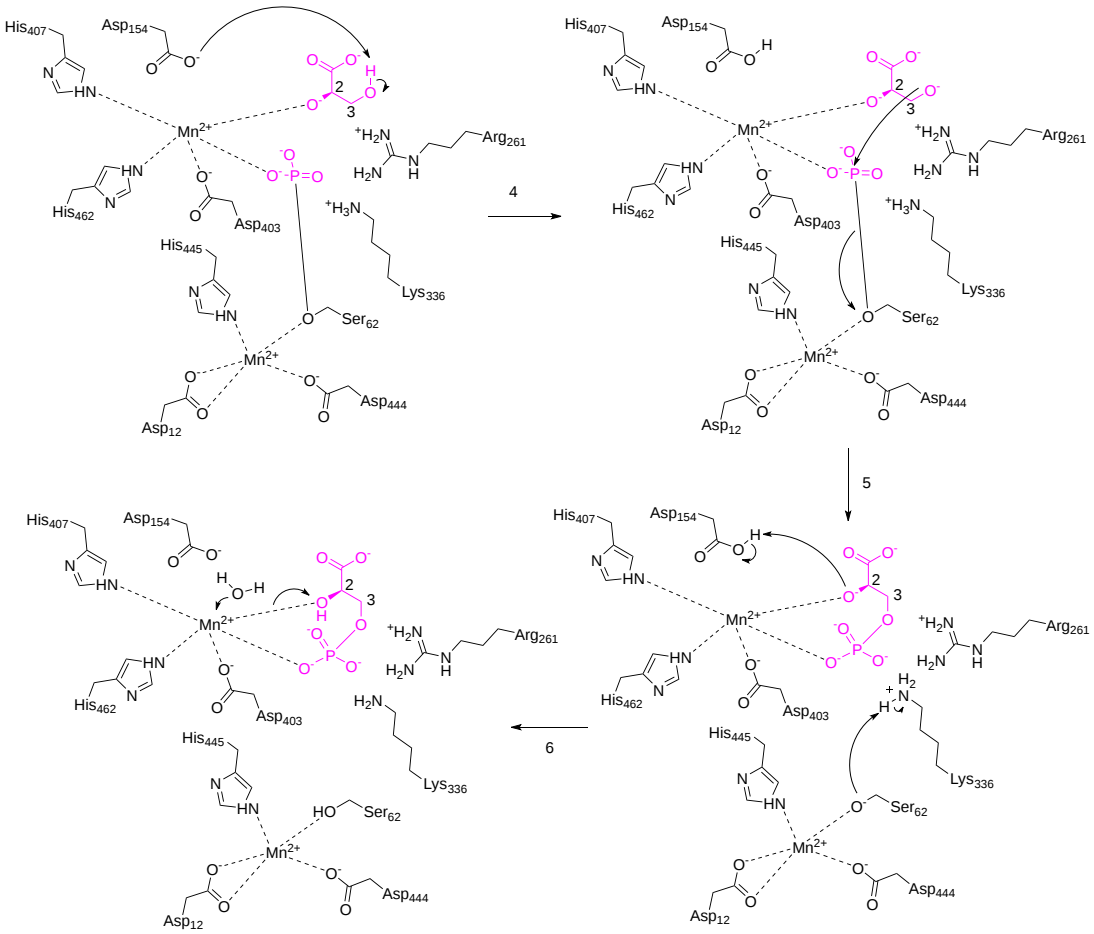


Figure **13.1.41**: Part B - Mechanism for cofactor-independent phosphoglycerate mutase (iPGM) from Geobacillus stearothermophilus (after Bolt et al., ibid)

The iPGMs are monomers with two distinct domains (lobes) containing a substrate binding site separated from an active site. They are connected by flexible sequences that bend to produce either an open or closed form of the enzymes (as we have seen before). In some enzymes, the two sites are merged at the interface between the domains. The active site Ser 62 becomes phosphorylated and then transfers its phosphate to the new site in the substrate, which is oriented differently in the enzyme.

Figure **13.1.42** shows an interactive iCn3D model of the Geobacillus stearothermophilus cofactor-independent Phosphoglycerate Mutase (iPGM) with bound 2-phosphoglycerate (product) (1O98)

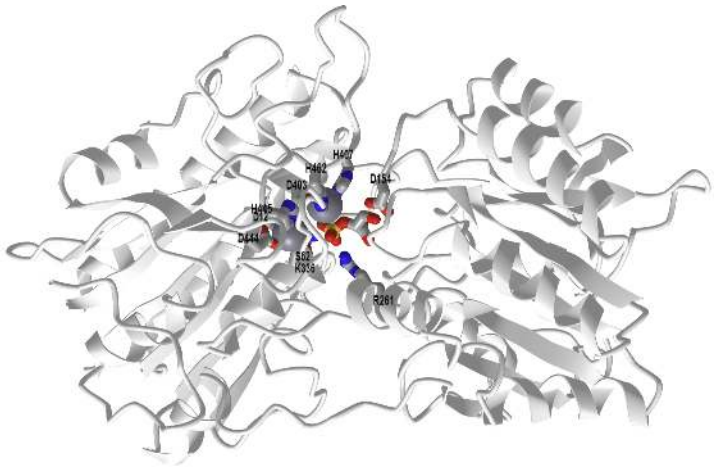


Figure **13.1.42**: Cofactor-Independent Phosphoglycerate Mutase with bound 2-phosphoglycerate (product) (1O98). (Copyright; author via source). Click the image for a popup or use this external link: https://structure.ncbi.nlm.nih.gov/i...71iYHXAEKMGsEA

13.1.11: **REACTION 9: 2PG ↔ PEP + H_2O** ΔG^{O}= +0.4 KCAL/MOL (+1.7 KJ/MOL)

This reaction, catalyzed by **enolase**, is shown in Figure **13.1.43**

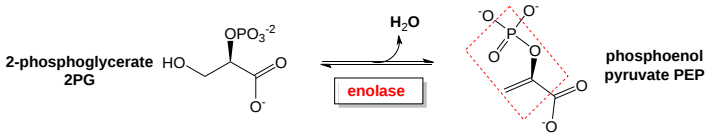


Figure \(\PageIndex{43}\: Summary reaction - enolase

Now you can see the rationale for reaction 8. In a simple dehydration reaction, a molecule with high phosphoryl-transfer potential has been produced, which, in the next and final step of glycolysis, produces ATP.

This enzyme has an active-site $Mg2^{+}$ required for catalysis. Mammals have three forms of the enzyme: α-enolase (ENO-1) found in most tissues, β-enolase (ENO-3) found mostly in muscle, and γ-enolase (ENO-2) found in neurons. Figure **13.1.44** shows a possible mechanism for yeast enolase.

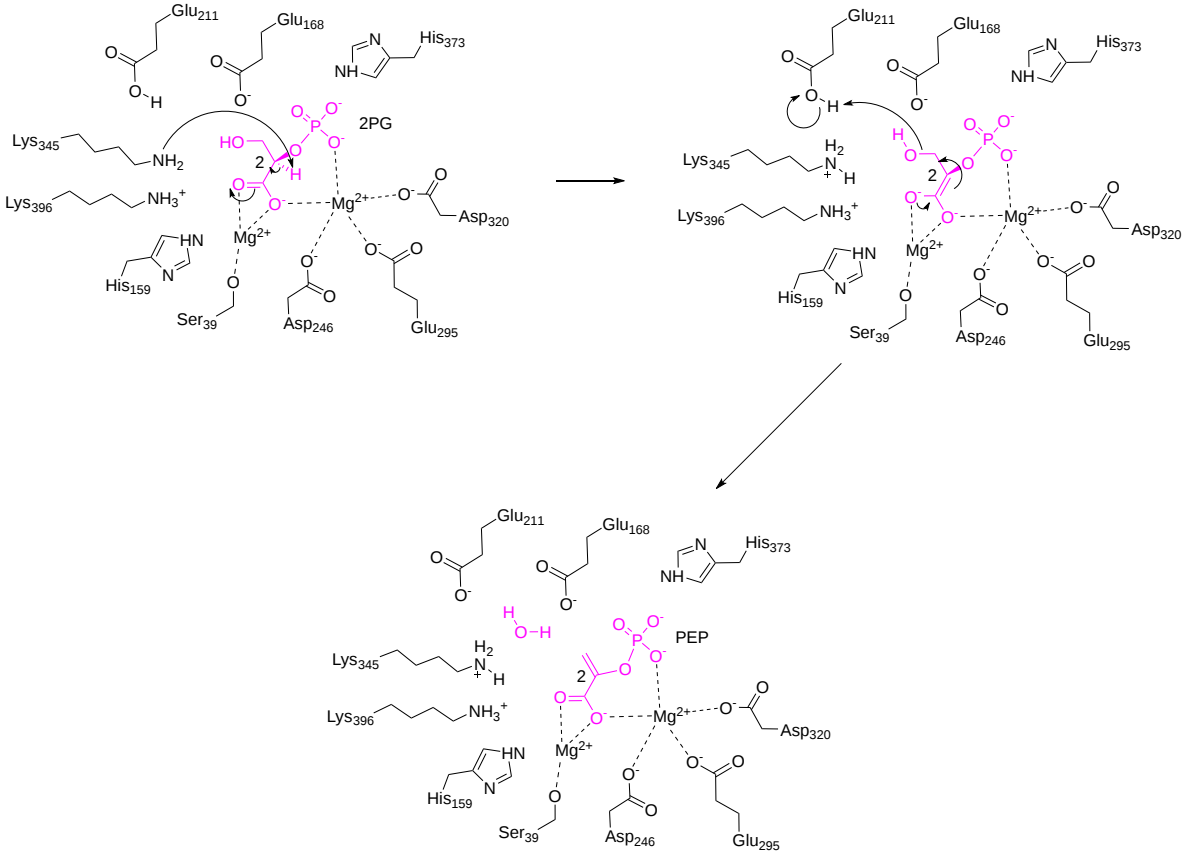
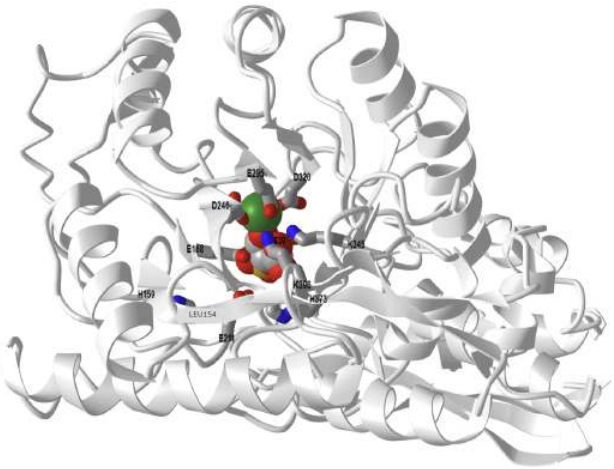


Figure **13.1.44**: A possible mechanism for yeast enolase

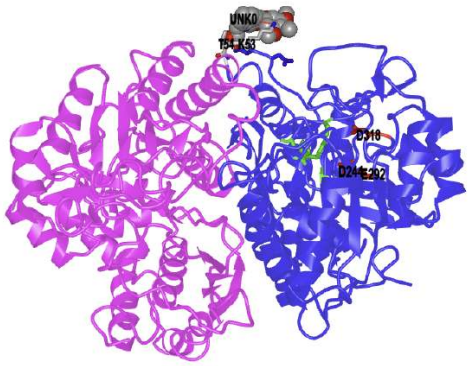
Figure **13.1.45** shows an interactive iCn3D model of Yeast enolase with bound 2-phosphoglycerate (7ENL)



NCBI iCn3D Figure 13.1.45: Yeast enolase with bound 2-phosphoglycerate (7ENL). (Copyright; author via source). Click the image for a popup or use this external link: https://structure.ncbi.nlm.nih.gov/i...TgwYV9vF8cYtPA



Enolase might seem like a nondescript, boring enzyme to some. Yet it and hexokinase have an unlikely role in the growth of tumor cells. Both hexokinase and enolase 1 (ENO1) are overexpressed in these cells, so inhibiting them could slow tumor cell growth and potentially kill them. We will see in several subsequent chapters that cancer cells engage in glycolysis even under aerobic conditions (called the Warburg effect). An inhibitor was recently found that did not bind at the active (orthosteric) site but at an allosteric site. Binding of the drug (SU212, a podophyllotoxin derivative) at an allosteric site did not affect the reaction kinetics but did lead to enzyme degradation. Figure 13.1.45*B* shows an iCn3D model of the drug docked (using Neurosnap) to the allosteric site of human enolase 1 (2PSN).



NCBI iCn3D Figure 13.1.45*B*: Human enolase 1 (2PSN) with SU212 docked at an allosteric site.. (Copyright; author via source).

Two identical subunits of the enolase 1 tetramer are shown (magenta and blue). SU212 is shown in spheres. The active site of the blue subunit is shown in green sticks and the Mg^{2+} binding site in red sticks. Tailor D, Garcia-Marques F, Bermudez A et al., Non-orthosteric inhibition of enolase 1 impedes growth of triple-negative breast cancer. Cell Reports Medicine, 2025; 6

To view the complex in iCn3D, download this PNG file of the protein complex. If the file opens in a browers window and not to your download folder, click on the image and follow prompts to save it.

1. Open iCn3D
2. **File, Open File, iCn3D PNG appendible**

13.1.12: **REACTION 10: PEP + ADP → PYR + ATP** ΔG^{O}= -7.5 KCAL/MOL (-31 KJ/MOL)

This reaction, catalyzed by **pyruvate kinase**, is shown in Figure 13.1.46

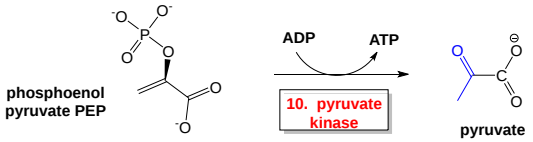


Figure **13.1.46**: Summary reaction - pyruvate kinase

In this step, one more ATP is made for each PEP consumed (hence 2 ATPs for both 3C PEPs). The phosphoryl transfer potential for PEP is higher than for ATP, which allows this reaction to proceed with a large negative ΔG^o (-7.5 kcal/mol, -31 kJ/mol).

The mechanism for rabbit pyruvate kinase is shown in Figure **13.1.47**.

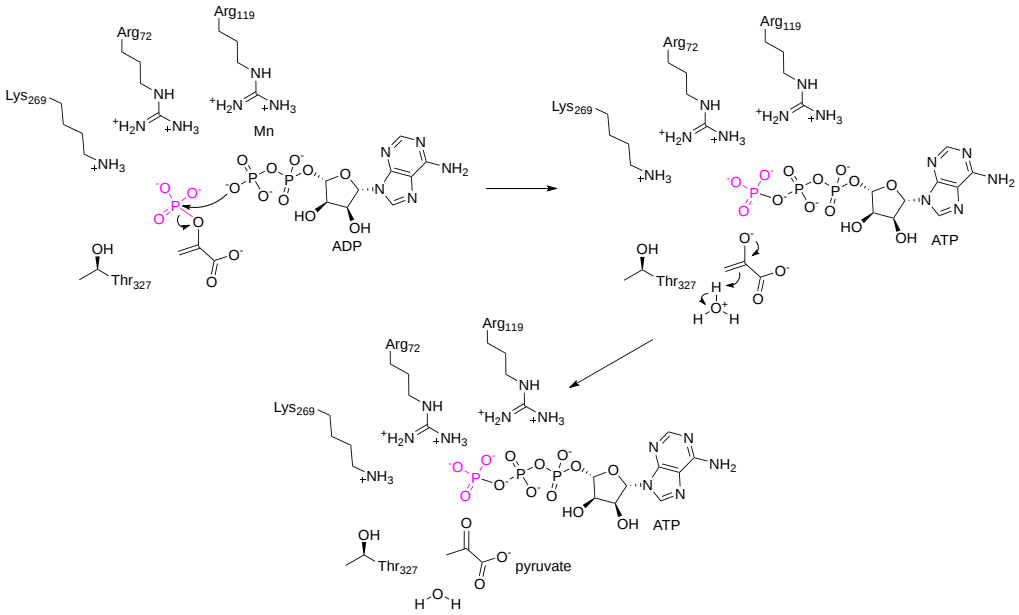
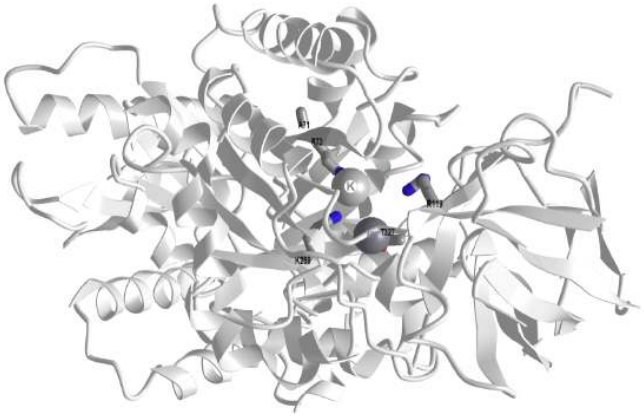


Figure **13.1.47**: Mechanism for rabbit pyruvate kinase

Figure **13.1.48** shows an interactive iCn3D model of rabbit muscle pyruvate kinase complexed with Mn^{2+}, K^+, and pyruvate (1PKN)



NCBI iCn3D Figure **13.1.48**: **Rabbit muscle pyruvate kinase complexed with Mn^{2+}, K^+, and pyruvate (1PKN)**. (Copyright; author via source). Click the image for a popup or use this external link: https://structure.ncbi.nlm.nih.gov/i...cZkm8DdEw2N3C6

We are done! Given that glycolysis is the central anaerobic energy-extracting pathway in all life, we examined each enzyme in detail.

This is the net reaction of the glycolytic pathway:

$$\mathrm{Glc + Pi + 2\,ADP + 2\,NAD^+ \longrightarrow 2\,Pyr + 2\,ATP + 2\,NADH + 2\,H^+ + 2\,H_2O}$$

13.1.13: UNCOUPLING GLYCOLYTIC OXIDATION AND PHOSPHORYLATION (ATP FORMATION)

Since we are most interested in energy transduction, let's consider just two important steps in glycolysis that directly lead to ATP synthesis. Only one oxidative step is found in this pathway, namely the oxidative phosphorylation of the 3C glycolytic intermediate glyceraldehyde-3-phosphate, to 1,3-bisphosphoglycerate, a mixed anhydride (see link below for mechanism). The oxidizing agent is NAD^{+}, and the phosphorylating agent is NOT ATP but rather Pi. The enzyme is named glyceraldehyde-3-phosphate dehydrogenase. It contains an active site Cys, which helps explain how the enzyme can be inactivated with a stoichiometric amount of iodoacetamide. A general base in the enzyme abstracts an H+ from Cys, which attacks the carbonyl C of the glyceraldehyde, forming a tetrahedral intermediate. Instead of the expected reaction (the protonation of the alkoxide in an overall nucleophilic addition reaction at the aldehyde), a hydride leaves from the former carbonyl C to NAD+ in an oxidation step. Notice this is a two-electron oxidation reaction similar to alcohol dehydrogenase. An acyl-thioester intermediate has formed, much like the acyl intermediate that formed in Ser proteases.

Next, inorganic phosphorous, Pi, attacks the carbonyl C of the intermediate in a nucleophilic substitution reaction to form the mixed anhydride product, 1,3-bisphosphoglycerate. Although we have formed a mixed anhydride, we cleaved a sulfur ester, which is destabilized with respect to its hydrolysis products (since the reactant, the thioester, is not stabilized by resonance to the extent of regular esters owing to the poor donation of electrons from the larger S to the carbonyl-like C.) In the next step, catalyzed by the enzyme phosphoglycerate kinase, ADP acts as a nucleophile that attacks the mixed anhydride of the 1,3-bisphosphoglycerate to form ATP. Note that the enzyme is named for the reverse reaction. We have coupled the oxidation of an organic molecule (glyceraldehyde-3-phosphate) to the phosphorylation of ADP by forming a "high" energy mixed anhydride, 1,3-bisphosphoglycerate.

The linkage between the oxidation of glyceraldehyde-3-phosphate and the phosphorylation of ADP by 1,3-bisphosphoglycerate can be artificially uncoupled by adding arsenate, which has a similar structure to phosphate. The arsenate can form a mixed anhydride at C1 of glyceraldehyde-3-phosphate, but since the bridging O-As bond is longer and not as strong as in the mixed anhydride, it is easily hydrolyzed. This prevents the subsequent transfer of phosphate to ADP to form ATP.

Figure **13.1.49** summarizes oxidation and substrate-level phosphorylation in glyceraldehyde-3-phosphate dehydrogenase.

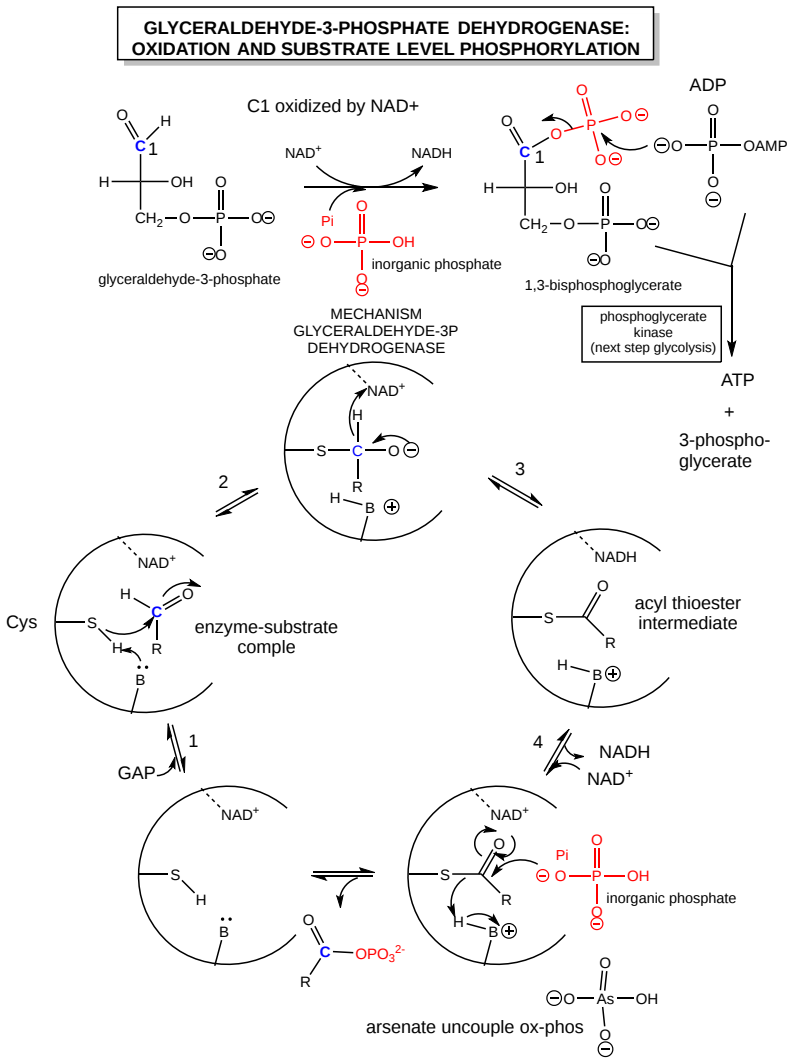


Figure **13.1.49**: Oxidation and substrate-level phosphorylation in glyceraldehyde-3-phosphate dehydrogenase (after Voet and Voet)

Summary: Under anaerobic conditions, glucose (6Cs) is metabolized through glycolysis, which converts it into two pyruvate molecules (3Cs). Only one oxidation step occurs when glyceraldehyde 3-phosphate is oxidized to 1,3-bisphosphoglycerate. To regenerate NAD^+ so glycolysis can continue, pyruvate is reduced to lactate, catalyzed by **lactate dehydrogenase**, as shown in Figure **13.1.50**. These reactions occur in the cytoplasm of cells actively engaged in the anaerobic oxidation of glucose (muscle cells, for example, during sprints).

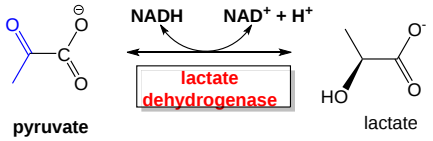


Figure **13.1.50**: Conversion of pyruvate to lactate

We will explore the fate of pyruvate under anaerobic conditions more in the next chapter section.

13.1.14: SUMMARY

This chapter offers a comprehensive overview of glycolysis, tracing its historical discovery and highlighting the biochemical principles that enable the oxidation of glucose to drive ATP synthesis. It integrates the concepts of free energy, reaction coupling, and enzyme regulation to explain how cells extract energy from sugars through a series of ten enzymatic reactions.

- **Foundations of Reaction Free Energy and Coupling:**
  The chapter begins by reviewing the fundamental concept of free energy (ΔG) and its dependence on reactant and product concentrations, temperature, and system conditions. A negative ΔG is essential for spontaneous reactions. Importantly, the chapter

emphasizes how energetically unfavorable steps in metabolic pathways are driven forward by coupling them to strongly exergonic reactions or by continuously removing products (via Le Chatelier's principle).

- **Historical Perspectives and the Emergence of Glycolysis:**
  The pioneering work of Otto Meyerhof and Archibald Hill in the early 20th century is discussed. Their experiments in frog muscles, which correlated heat production, oxygen consumption, and lactic acid formation, laid the groundwork for our current understanding of both aerobic and anaerobic metabolism. Their contributions established glycolysis as the central anaerobic pathway for energy production.
- **The Glycolytic Pathway Overview:**
  Glycolysis is described as a 10-step process that converts one molecule of glucose (a six-carbon sugar) into two molecules of pyruvate (each with three carbons). The pathway is divided into two phases:
  - **Energy Investment Phase (Steps 1–3):** Glucose is phosphorylated by hexokinase to form glucose-6-phosphate, isomerized to fructose-6-phosphate by phosphoglucose isomerase, and then phosphorylated by phosphofructokinase-1 (PFK1) to yield fructose-1,6-bisphosphate. These steps require ATP input and represent the commitment of glucose to the glycolytic pathway.
  - **Energy Payoff Phase (Steps 4–10):** Fructose-1,6-bisphosphate is cleaved by aldolase into two three-carbon intermediates, which are then further processed. Notably, the oxidation of glyceraldehyde-3-phosphate (G3P) by glyceraldehyde-3-phosphate dehydrogenase (GAPDH) forms a high-energy mixed acyl-thioester (1,3-bisphosphoglycerate) that, via substrate-level phosphorylation catalyzed by phosphoglycerate kinase, generates ATP. Subsequent steps include the isomerization by triose phosphate isomerase, dehydration by enolase to form phosphoenolpyruvate (PEP), and finally, the conversion of PEP to pyruvate by pyruvate kinase, yielding additional ATP.
- **Enzymatic Mechanisms and Regulation:**
  Detailed mechanisms for key enzymes are presented to illustrate how structural features and induced-fit conformational changes ensure reaction specificity and efficiency. For example:
  - **Hexokinase** employs an induced-fit mechanism upon glucose binding, thereby protecting ATP from nonproductive hydrolysis.
  - **Phosphofructokinase-1 (PFK1)**, a major regulatory enzyme, is allosterically controlled by cellular energy status (ATP, ADP, and AMP levels), ensuring the glycolytic flux adjusts to the cell's metabolic needs.
  - **GAPDH** couples the oxidation of G3P with the reduction of NAD^+ and the formation of a high-energy mixed anhydride intermediate, which is crucial for substrate-level phosphorylation.
  - **Aldolase** catalyzes the reversible cleavage of fructose-1,6-bisphosphate into two three-carbon sugars, using distinct mechanisms that vary between Class I and Class II enzymes.
  - **Triose phosphate isomerase** rapidly equilibrates dihydroxyacetone phosphate (DHAP) and glyceraldehyde-3-phosphate (G3P), ensuring efficient substrate channeling to downstream steps.
- **Integration with Broader Metabolic Context:**
  The chapter concludes by linking glycolysis to both anaerobic and aerobic metabolism. Under anaerobic conditions, pyruvate is reduced to lactate to regenerate NAD^+, enabling glycolysis to continue in the absence of oxygen. In contrast, under aerobic conditions, pyruvate enters the mitochondria, where it is further oxidized through the Krebs cycle and oxidative phosphorylation, yielding significantly more ATP. This integration highlights glycolysis as a central hub in cellular energy metabolism.

Overall, the chapter not only details the step-by-step enzymatic transformations of glycolysis but also emphasizes the thermodynamic and regulatory strategies cells use to harness the energy stored in sugars. This foundational understanding is essential for appreciating the complexities of energy metabolism in living systems.

This page titled 13.1: Glycolysis is shared under a not declared license and was authored, remixed, and/or curated by Henry Jakubowski and Patricia Flatt.

- **Current page** by Henry Jakubowski and Patricia Flatt has no license indicated.
- **11.2: Diffusion Across a Membrane - Passive and Facilitated Diffusion** by Henry Jakubowski and Patricia Flatt has no license indicated.

13.2: FATES OF PYRUVATE UNDER ANAEROBIC CONDITIONS- FERMENTATION

LEARNING GOALS (CHATGPT O3-MINI)

1. **Explain the Purpose of Fermentation:**
   - Define fermentation as an anaerobic process that enables ATP production when oxygen is limited, emphasizing the critical role of glycolysis and the recycling of NADH to NAD^+.
2. **Describe NAD^+/NADH Recycling in Fermentation:**
   - Explain why recycling NADH to NAD^+ is essential for sustaining glycolysis under anaerobic conditions and compare how this recycling occurs via aerobic pathways (e.g., the citric acid cycle) versus anaerobic fermentation.
3. **Differentiate Between Lactate and Ethanol Fermentation:**
   - Contrast the two major anaerobic fermentation routes: lactate fermentation (conversion of pyruvate to lactate by lactate dehydrogenase) and ethanol fermentation (pyruvate decarboxylation to acetaldehyde followed by reduction to ethanol by alcohol dehydrogenase).
4. **Understand Tissue-Specific Fermentative Pathways:**
   - Identify the physiological contexts in which each fermentation type occurs—for example, lactate production in mammalian muscle and red blood cells, and ethanol production in yeast and certain fish species.
5. **Explain the Cori Cycle and Its Importance:**
   - Describe the Cori cycle, including how lactate produced in muscle is transported to the liver for conversion back to pyruvate and subsequently to glucose via gluconeogenesis, highlighting its role in maintaining energy homeostasis.
6. **Analyze Enzyme Structure and Regulation in Fermentation:**
   - Detail the structural and mechanistic aspects of key enzymes (e.g., lactate dehydrogenase, pyruvate decarboxylase, alcohol dehydrogenase), including their isozyme variations, active site configuration, and allosteric regulation.
7. **Discuss Ethanol Metabolism in Humans:**
   - Outline the sequential metabolism of ethanol in the liver by cytosolic alcohol dehydrogenase (ADH) and mitochondrial acetaldehyde dehydrogenase (ALDH2), and explain how disruptions in these pathways (e.g., accumulation of acetaldehyde) contribute to toxicity.
8. **Evaluate the Effects of Alcohol Consumption:**
   - Assess the concept of hormesis in alcohol consumption, discussing how moderate drinking may be cardioprotective while excessive intake leads to detrimental outcomes such as liver damage, altered gene expression, and increased cancer risk.
9. **Link Fermentative Metabolism to Systemic and Cellular Health:**
   - Connect changes in NADH/NAD^+ ratios during ethanol metabolism to broader metabolic effects, including downregulation of glycolysis and the Krebs cycle, lactic acidosis, and hypoglycemia.
10. **Examine Therapeutic Strategies for Alcohol Abuse:**
    - Understand the mechanism of disulfiram as an inhibitor of ALDH, the rationale behind its use in treating alcoholism, and its role in promoting abstinence through the accumulation of toxic acetaldehyde.

These learning goals are intended to provide a comprehensive framework for understanding fermentation's biochemical basis, its integration with cellular metabolism, and its physiological and clinical implications.

13.2.1: INTRODUCTION TO FERMENTATION

Fermentation occurs when a fuel molecule is broken down anaerobically (or without oxygen) to meet ATP demands. One of the most notable pathways to utilize fermentation is glycolysis, which we have just described. During glycolysis, glucose is converted to pyruvate, yielding 2 ATP energy-rich molecules. This occurs in anoxic conditions (or without the requirement of oxygen). However, the process of glycolysis cannot be sustained if the end product is pyruvate. This is because the production of pyruvate also yields two molecules of reduced NADH in addition to the production of the two ATP molecules. The pool of available NAD^+/NADH is limited within the body, and thus, this electron acceptor/donor molecule must continually be recycled for metabolic pathways to remain functional. For example, if NADH is not oxidized back into NAD^+ in a timely manner, the glycolytic pathway can slow. Therefore, to be able to maintain the process of

energy generation through glycolysis, the pool of NADH needs to be converted from the reduced form back into the oxidized form (NAD^+), where it can then accept electrons from intermediates in the glycolytic pathway. This process of recycling NADH to NAD^+ can occur aerobically through the Citric Acid Cycle, which is described in more detail in Chapter 16, or it can be processed via anaerobic fermentation (Figure 13.2.1).

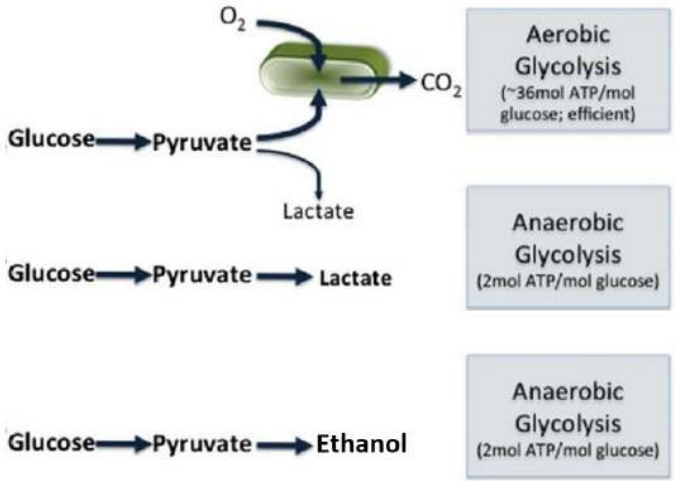
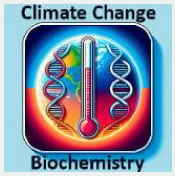


Figure 13.2.1: Fates of Pyruvate via Aerobic or Anaerobic Pathways.

In the 1860s, Louis Pasteur first described fermentation very narrowly as the process yeast uses to convert glucose into ethanol when grown in the absence of air. Subsequently, it was discovered that other microorganisms could convert pyruvate to lactate (or lactic acid) instead of ethanol during anaerobic respiration. These microorganisms became known as lactic acid bacteria and are currently utilized heavily within the food industry to produce a wide array of fermented food products, including cheese, yogurt, and sauerkraut, to name a few. As the enzymes within the glycolytic pathway were discovered, it became apparent that muscle tissue could also engage in anaerobic respiration, producing lactate. Thus, while fermentative processes are most often described in microbial organisms, the definition of fermentation has since been broadened to include any enzymatic, energy-yielding pathways that occur in the absence of oxygen, including the production of lactate in muscle tissue of animals during the glycolytic process.

FERMENTATION IN SYNTHETIC BIOLOGY AND THE FOOD INDUSTRY



Industry is turning to microbes to produce new food products such as animal-free proteins and novel foods, drugs, household products, and chemical feedstocks to produce commercial products like biofuels and even plexiglass, to name just a few. Check out Chapter 32.18: Turning Trees into Plexiglass: Synthetic Biology For Production of Green Foods and Products for more details!

Synthetic biology, using existing and modified metabolic pathways in microorganisms to accomplish these tasks, is revolutionizing manufacturing to make it greener, more sustainable, and with a lower carbon footprint. One major goal is to reduce CO_2 emissions to reduce global warming and its consequences. When the pathways are highly engineered and tailored to specific goals, it is often called precision fermentation. These microbial pathways can also be anaerobic or aerobic, so the original definition of fermentation involving anaerobic reactions has been expanded.

NADH recycling to NAD^+, typically in anaerobic fermentation reactions, occurs by two different routes:

- lactate fermentation (Figure 13.2.1 in bacteria and fungi, such as Lactobacillus, Leuconostoc mesenteroides, Pediococcus cerevisiae, Streptococcus lactis, and Bifidobacterium bifidus) and, of course, the muscles of animals. Yogurt is the product of the anaerobic fermentation of milk by microorganisms such as Lactobacillus delbrueckii subsp. bulgaricus and Streptococcus thermophilus.
- ethanol fermentation in yeast and some bacteria, such as Zymomonas mobilis.

We will focus on the details of these two systems here.

13.2.2: LACTATE FERMENTATION

In lactate fermentation, pyruvate is converted to lactate by the enzyme lactate dehydrogenase. In the process, NAD^+ is regenerated. The reaction catalyzed by lactate dehydrogenase (LDH) is shown in Figure 13.2.2.

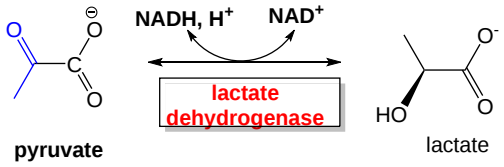


Figure 13.2.2: Reaction catalyzed by lactate dehydrogenase

It is named for the reverse reaction, which uses NAD^+ as an oxidizing agent, as with other dehydrogenases. The reaction is reversible with the ΔG^0 for conversion of pyruvate to lactate of -3.76 kcal/mol (-15.7 kJ/mol). Under anaerobic conditions, when glycolysis is the major source of ATP, pyruvate levels increase, further driving the reaction towards lactate formation and NAD^+ regeneration so glycolysis can continue.

The enzyme is found in the cytoplasm, but a mitochondrial form also exists. It is most abundant in muscle, liver, and kidney, and it is also found in erythrocytes. Interestingly, mature red blood cells are enucleated and do not contain any mitochondria. Their lifespan is limited to approximately two weeks. During this time, their primary energy resources are generated through anaerobic fermentation via the glycolysis-lactate pathway.

The active enzyme is a tetramer of various compositions of two different subunits, the heart (H) and muscle (M) forms. The quaternary structures contain five different isozyme forms containing the H and M subunits. LDH-1, found most abundantly in the heart, is a tetramer of 4H subunits (H_4). The other forms are as follows: LDH-2 (H_3M, prevalent in red blood cells), LDL-3 (H_2M_2, prevalent in lungs), LDH-4 (HM_3, prevalent in the kidney), and LDH-5 (M_4, prevalent in muscle).

During anaerobic metabolism, lactate is produced by muscle tissue and released into the bloodstream, where it can travel back to the liver. Once in the liver, lactate is converted back into pyruvate and can be utilized to produce glucose through a pathway called gluconeogenesis. The liver can export glucose into the blood. There, it is taken up by the muscle and used for ATP production. This cycle is called the **Cori cycle, illustrated** in Figure 13.2.3.

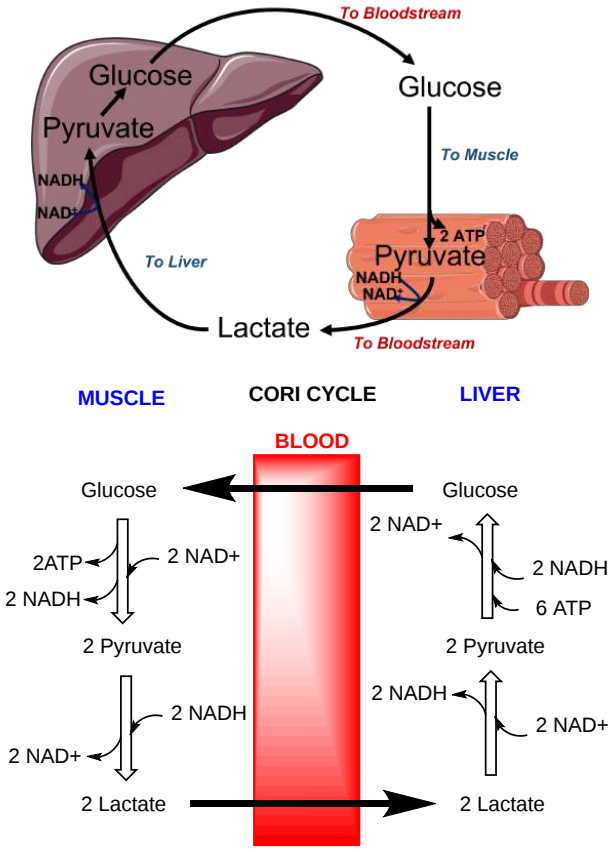


Figure 13.2.3: Cori cycle. The *Upper diagram* is a cartoon image of the Cori cycle, and the *lower diagram* demonstrates the recycling of NAD+/NADH in different locations within the body. Figure modified from Servier Medical Art

Notably, animal anaerobic metabolism can only be sustained for short periods due to its high energy demand. Aerobic respiration is required to maintain an adequate ATP supply. However, the production of lactate by certain tissues, such as white or fast-twitch muscle cells, occurs regularly and releases lactate into the bloodstream, which can be taken up and used as an energy source by neighboring tissues, such as red, slow-twitch muscle. Brain tissue can also effectively use lactate as an energy source. Within these 'consumer' tissues, lactate is converted back into pyruvate using the mitochondrial LDH enzyme. It can be converted to pyruvate and used in aerobic respiration to produce high levels of ATP.

Thus, lactate production can be considered a response during metabolic stress, such as intense cardiovascular exercise. It has also been noted that after an injury or head trauma, the activation of epinephrine will cause an increase in lactate production, and blood levels of lactate will increase. Thus, it has been hypothesized that lactate may play a role in the repair of damaged tissue. Clinical trials and experiments are currently underway to determine if lactate can help in the healing and recovery process for conditions such as traumatic brain injury, myocardial infarction, and sepsis. Early studies have shown that lactate can increase the production of Brain-Derived Neurotropic Factor (BDNF), which supports neuronal growth, providing further support for the role of lactate in recovery and repair.

Spectroscopy analyses show that the geometry and electrostatics of the active sites of LDHs from different organisms are essentially the same. The mechanism for the reverse oxidation of lactate by NAD^+ by spiny dogfish lactate dehydrogenase (LDH) is shown in Figure **13.2.4**

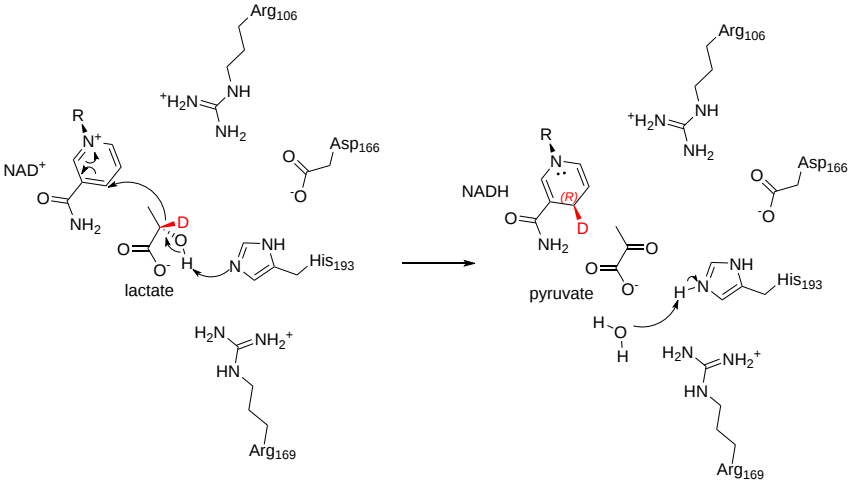


Figure 13.2.4: Mechanism for the reduction of lactate by NAD^+ by spiny dogfish lactate dehydrogenase (LDH)

Lactate is shown with a deuterium (D), which moves as a deuteride to NAD^+ to form NADH, to illustrate the stereochemistry of the reaction. In the reverse reaction, reducing pyruvate to lactate (to regenerate more NAD^+ so anaerobic glycolysis can continue), the deuterium (or the proR H of non-deuterated NADH) is removed.

Figure **13.2.5** shows an interactive iCn3D model of dogfish M4 apo-lactate dehydrogenase (1LDM).

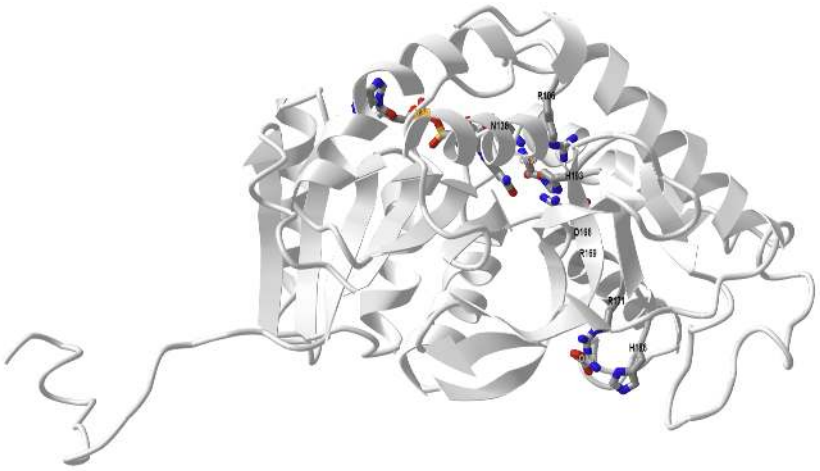


Figure 13.2.5: Dogfish M4 apo-lactate dehydrogenase (1LDM).(Copyright; author via source). Click the image for a popup or use this external link: https://structure.ncbi.nlm.nih.gov/i...FBzuqJ2gEPUHM8

Only the monomer of the active tetramer is shown. Oxamic acid (labeled) is structurally similar to lactate/pyruvate and is a competitive inhibitor of the enzyme. His193, the active site general base/acid, is near Arg 169, and also to Asp 166 and Asn 138, which are hydrogen bonded to the inhibitors.

LDH exists in two major conformational states, the T (inactive) and R (active) states, as seen with other allosteric proteins. Figure **13.2.6** shows an interactive iCn3D model of the T state (2ZQY) and R state (2ZQZ) of Lacticaseibacillus casei L-lactate dehydrogenase.

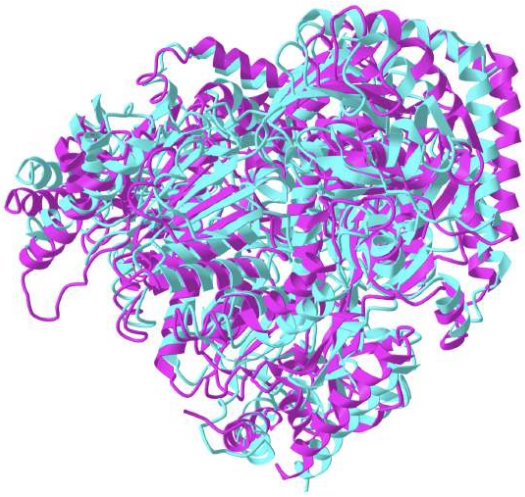


Figure 13.2.6: T state (2ZQY) and R state (2ZQZ) of Lacticaseibacillus casei L-lactate dehydrogenase. (Copyright; author via source). Click the image for a popup or use this external link: https://structure.ncbi.nlm.nih.gov/i...zjrtVYjLXdhDp8

Toggle between the magenta T and cyan R states using the "a" key. Orient the proteins to see the best view of the allosteric changes caused by binding regulators. The spheres show Arg 171, whose disposition changes significantly in the T and R states. Pyruvate (a reactant/product) activates the enzyme (conversion of T to R state) and is considered a **homotropic regulator** since it is a substrate. This is similar to hemoglobin's allosteric "activation" by its ligand O_2, which preferentially binds to the R state and promotes the T-to-R state transition. Fructose 1,6-bisphosphate, a glycolytic intermediate, also activates the Lacticaseibacillus casei L-lactate dehydrogenase, and since it is not a reactant/product of the enzyme, it is considered a heterotropic allosteric regulator. Hence, the substrate concentration (pyruvate) and NADH levels effectively regulate the enzyme. High concentrations of ethanol consumption lead to high levels of NADH through the activity of alcohol dehydrogenase. High levels of NADH would lead to increased lactate production as well.

13.2.3: ETHANOL FERMENTATION IN YEAST

In this process, pyruvate is decarboxylated first to acetaldehyde by the thiamine pyrophosphate (TPP)-requiring enzyme **pyruvate decarboxylase**. The resulting product, acetaldehyde, is then reduced by NADH to form ethanol by the enzyme **ethanol dehydrogenase** in a process that reforms NAD^+. Yeast is a facultative (not obligate) anaerobe in that it can produce energy by glycolysis and ethanol fermentation in the absence of oxygen. Figure **13.2.7**:. Of course, in the presence of oxygen, the pyruvate produced from glycolysis in yeast is preferentially converted to acetyl-CoA, which enters the citric acid cycle and oxidative phosphorylation pathways to maximize ATP production.

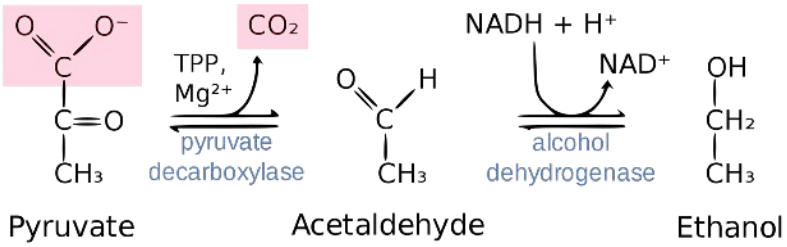


Figure 13.2.7: Summary of Ethanol Fermentation in Yeast. Figure from Thomas Baldwin

Pyruvate decarboxylase

Pyruvate decarboxylase catalyzes the first step in the alcoholic fermentation pathway, converting pyruvate into acetaldehyde and carbon dioxide. Interestingly, in addition to yeast, some fish species, such as goldfish and carp, have a homologous enzyme that allows for ethanol production when oxygen is scarce. Pyruvate decarboxylase is tetrameric, occurring as a dimer of dimers with two active sites shared

between the monomer subunits of each dimer. The decarboxylation reaction requires two cofactors, thiamine pyrophosphate (TPP) and magnesium (Figure **13.2.8**). Within the active site, the acidic Glu-477 and Glu-51 residues and the Mg^{2+} cofactor interact with and stabilize the TPP cofactor. The aminopyrimidine ring on TPP acts as a base and enables the formation of the TPP nucleophile by removing the C2 proton. The protonation of Glu-51 stabilizes this reaction. The nucleophilic attack of pyruvate causes the release of carbon dioxide. The acetaldehyde intermediate is still covalently attached to the TPP cofactor following the release of carbon dioxide.

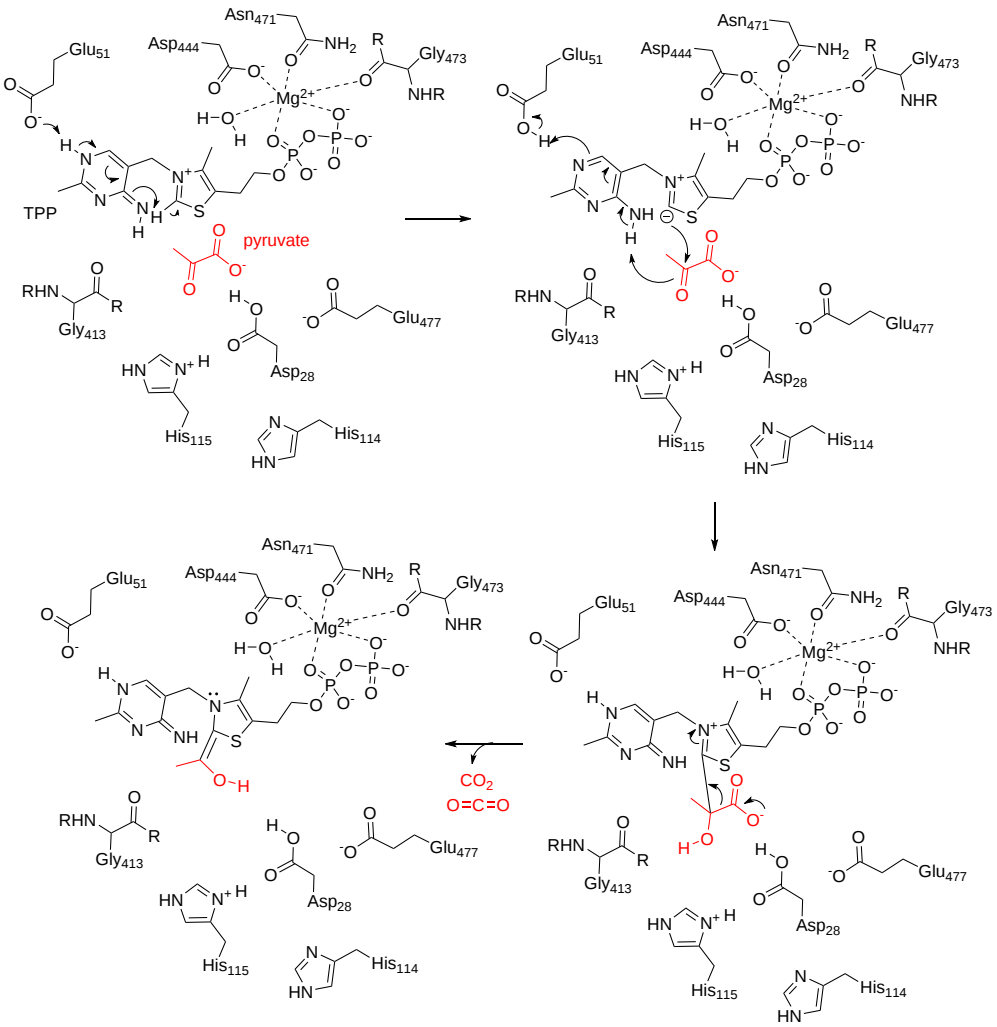


Figure 13.2.8: Part 1 Pyruvate Decarboxylase mechanism - decarboxylation

Once carbon dioxide diffuses away from the active site, the double bond of the enol intermediate abstracts a proton from Asp-28, which is stabilized by a neighboring His-115 residue. TPP can then serve as a good leaving group during the formation of the carbonyl functional group and causes the release of acetaldehyde (Figure **13.2.9**:).

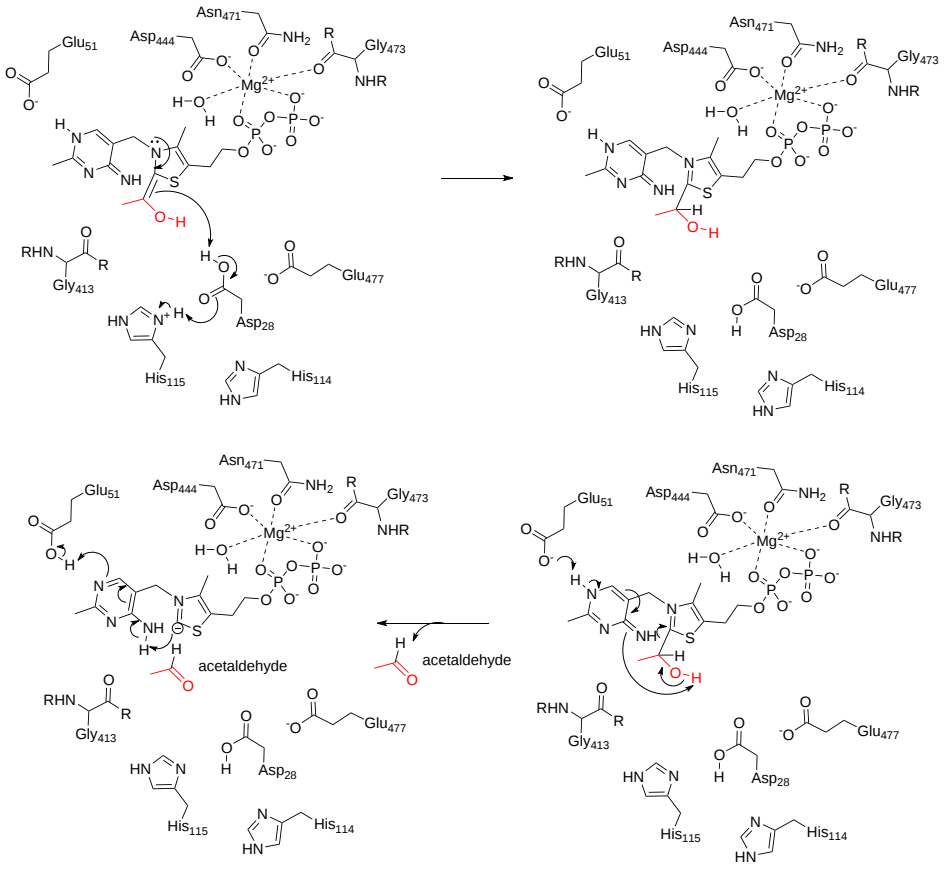
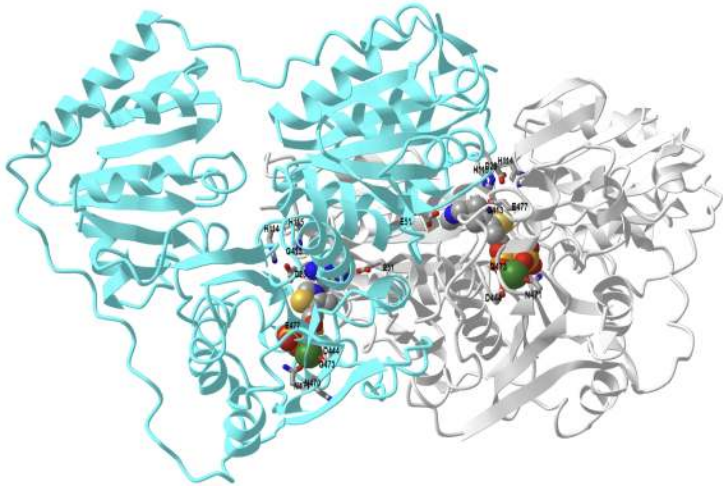


Figure 13.2.9: Part 2 Pyruvate Decarboxylase mechanism - acetaldehyde generation

Figure 13.2.10 shows an interactive iCn3D model of the thiamin diphosphate-dependent enzyme pyruvate decarboxylase from the yeast Saccharomyces cerevisiae (1PVD).



NCBI iCn3D Figure 13.2.10: Thiamin diphosphate-dependent enzyme pyruvate decarboxylase from the yeast Saccharomyces cerevisiae (1PVD).(Copyright; author via source). Click the image for a popup or use this external link: https://structure.ncbi.nlm.nih.gov/i...DMM4gjodX4q1G9 TTP is shown in spacefill. The enzyme is a homotetramer.

Alcohol dehydrogenase (ADH)

Alcohol dehydrogenase enzymes catalyze the interconversion of aldehydes or ketones with alcohol functional groups. In humans and other animals, they are utilized to break down ingested alcohols and participate in the biosynthesis of numerous metabolites. There are at least five classes of alcohol dehydrogenases that use NAD^+ as an oxidizing agent to convert alcohols to aldehydes or ketones. We are mainly

concerned with the yeast ADH, a member of Family I, that is involved in ethanol fermentation. Figure **13.2.11** shows the reaction catalyzed by alcohol dehydrogenase.

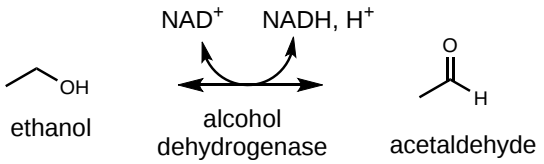


Figure 13.2.11: Reaction catalyzed by alcohol dehydrogenase

Figure **13.2.12*A*** below shows a mechanism for yeast alcohol dehydrogenase (ADH1). ADH1 requires zinc as a metal cofactor and utilizes NADH as the reducing agent in converting acetaldehyde into ethanol.

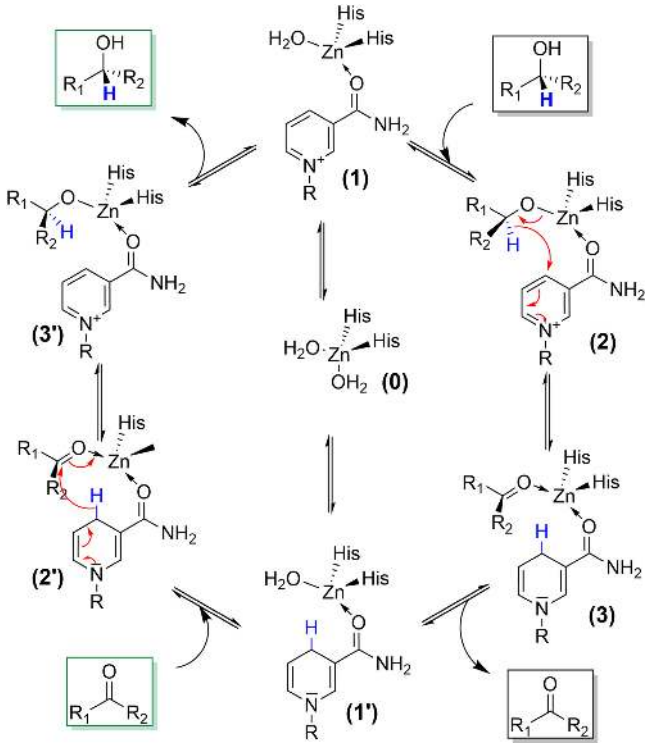


Figure 13.2.12*A*: Simplified catalytic mechanism of ADH reactions. Upon binding of both substrates (e.g., NAD(P)+ and alcohol; 0->1->2), a hydride transfer occurs from the alcohol-carbon atom to the oxidized nicotinamide moiety, yielding the Zn-coordinated carbonyl product and NAD(P)H (3). Both can dissociate from the active site, yielding apo-ADH (0). Alternatively, only NAD(P)H stays bound, and the reduced ADH can undergo a reductive conversion (1'->2'-> 3'-> 1). Amanda Silva de Miranda, et al. Front. Catal., 10 May 2022. Sec. Biocatalysis. https://doi.org/10.3389/fctls.2022.900554. Creative Commons Attribution License (CC BY).

Figure **13.2.12*B*** shows key amino acids in the active site of yeast ADH1. Note that in this figure, two cysteines are the coordinating ligands.

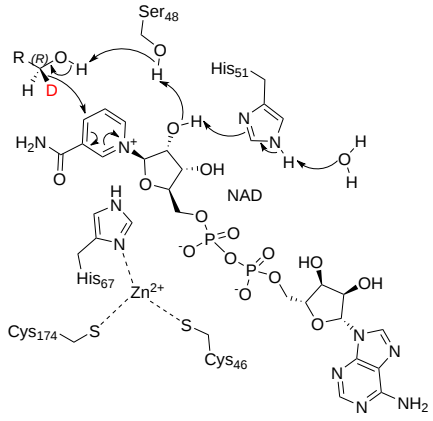


Figure 13.2.12*B*: Abbreviated mechanism for yeast alcohol dehydrogenase (ADH1)

If you look at the reverse reduction reaction, the acetaldehyde (or a ketone for 2^0 alcohols) carbonyl is sp^2 hybridized and planar, so the hydride could be added to either of the two faces, re or si, of the plane (using the same rules used to define R or S enantiomers). Likewise, the methylene carbon atom with two hydrogens, one of which is transferred as a hydride, is prochiral. Hence, four different stereochemical hydride transfer pathways are possible, as shown below in **Figure 13.2.13*A***. Hydride transfers from the prochiral aldehyde/ketone si-face result in (*R*)-configured alcohols, whereas hydride attacks from the *re*-face yield (*S*)-alcohols. In both cases, the hydride transferred can stem from either the *re*- or *si*-face of the nicotinamide ring.

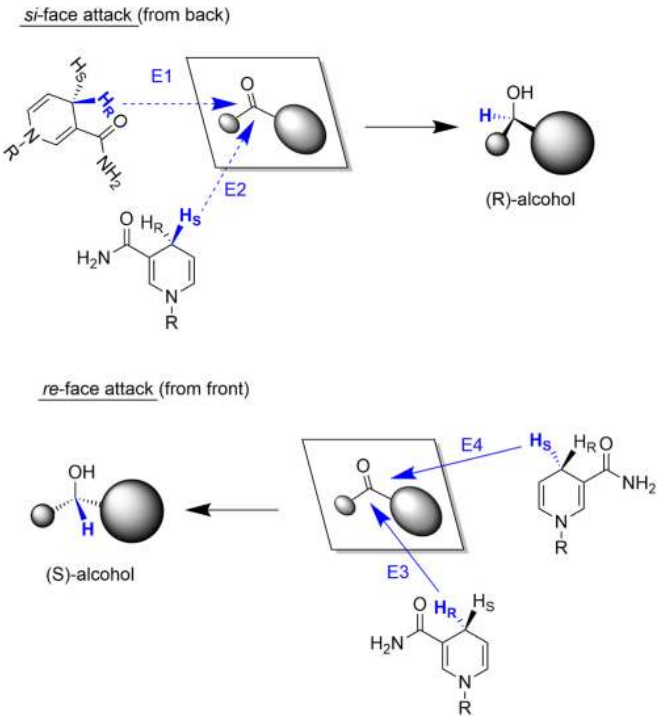


Figure 13.2.13*A*: Possible stereochemical courses of the hydride transfer from NAD(P)H to the ketone. Attacks from the *si*-face of the ketone result in (*R*)-alcohols (E1 and E2), whereas hydride attacks from the *re*-face (E3 and E4) result in (*S*)-alcohols.

ADHs catalyzing hydride addition from the *re*-face of the ketone (or abstraction of a hydride from (*S*)-alcohols) are termed Prelog-selective ADHs, whereas those ADHs attacking from the *si*-face (or abstracting a hydride from the (*R*)-alcohol) are termed *anti*-Prelog ADHs. Different ADHs are available for the different reaction stereochemistries.

The stereochemistry for the reaction of ADH1 with ethanol is shown in **Figure 13.2.13*B*** below**.** Deuterium (**D**) is shown in the figure to illustrate the reaction's stereochemistry better. With the **deuterium** label, the carbon is now chiral, and the enantiomer shown is the R isomer. The enzyme removes the corresponding **H** in the undeuterated and prochiral form of ethanol, as shown in Figure **13.2.13*B*** below.

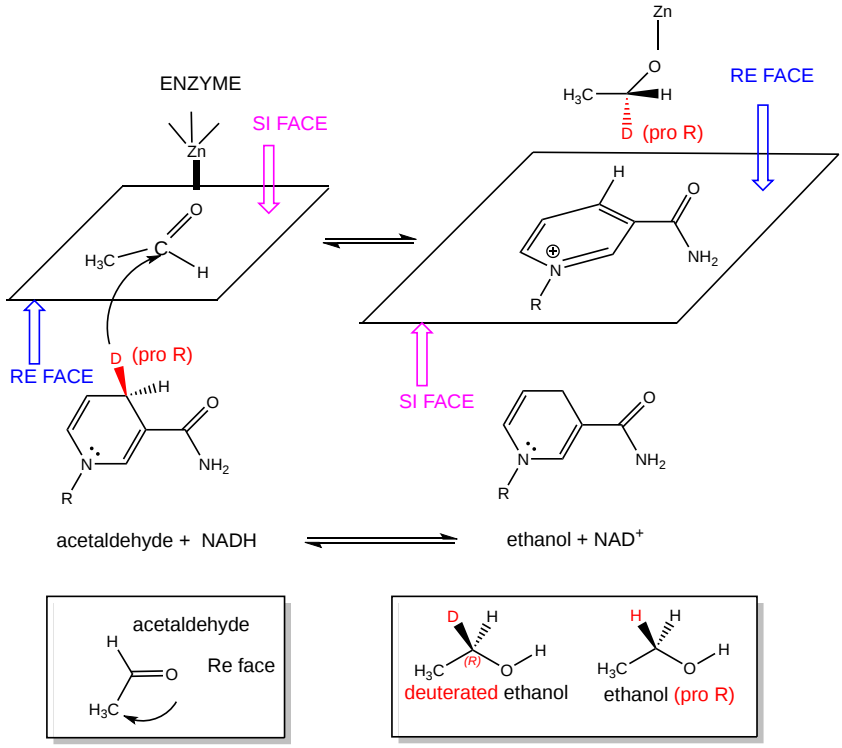


Figure 13.2.13*B*: Stereochemistry of human alcohol dehydrogenase reaction.

Figure 13.2.14 shows an interactive iCn3D model of the Yeast alcohol dehydrogenase (ADH I) with bound substrate analogs- ADH1 (4W6Z).

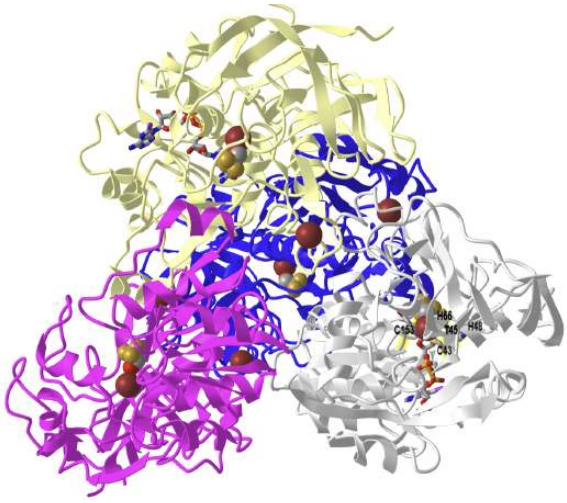


Figure 13.2.14: Yeast alcohol dehydrogenase structure with bound substrate analogs (4W6Z). (Copyright; author via source). Click the image for a popup or use this external link: https://structure.ncbi.nlm.nih.gov/i...feE7toF6wU6MB9

All four monomers of the homotetramer are shown. The light gray subunit has the key catalytic and binding residues shown in sticks and labeled. The numbering of key residues differs slightly from the mechanism shown above. The cofactor analog, nicotinamide-8-iodo-adenine-dinucleotide, is shown in sticks, and the substrate analog, trifluoroethanol, is shown in spacefill.

Only two subunits (a homodimer) have both bound cofactor and substrate. The substrate trifluoroethanol in these subunits is ligated to the catalytic Zn^{2+} through its oxygen, with the other ligands provided by the side chains of Cys 43, Cys 153, and His 66. The other two monomers (the other homodimer) have a different conformation and use Glu 67 to coordinate the Zn^{2+} instead of His 66, and no substrate is bound. This may be an intermediate in the process that displaces water bound to Zn^{2+} with the substrate.

13.2.4: ALCOHOL METABOLISM IN HUMANS:

When ethanol is consumed, it is oxidatively metabolized primarily in the liver. Cytosolic Alcohol Dehydrogenase (ADH) and mitochondrial Acetaldehyde Dehydrogenase 2 (ALDH2) are the main enzymes involved in this metabolic pathway, first converting ethanol to acetaldehyde and then acetaldehyde to acetate **(Figure 13.2.15:)**. Liver mitochondria have a limited capacity to use the acetate in the Kreb cycle because the enzyme needed to convert acetate to acetyl-CoA (acetyl-CoA synthase 2) is almost absent in the liver but is abundant in the heart and skeletal muscles. Thus, most of the acetate resulting from ethanol metabolism escapes the liver into the blood circulation and is eventually metabolized to CO_2 by way of the Krebs cycle in cells with mitochondria that contain enzymes to convert acetate to acetyl-CoA, such as the heart, skeletal muscle, and brain.

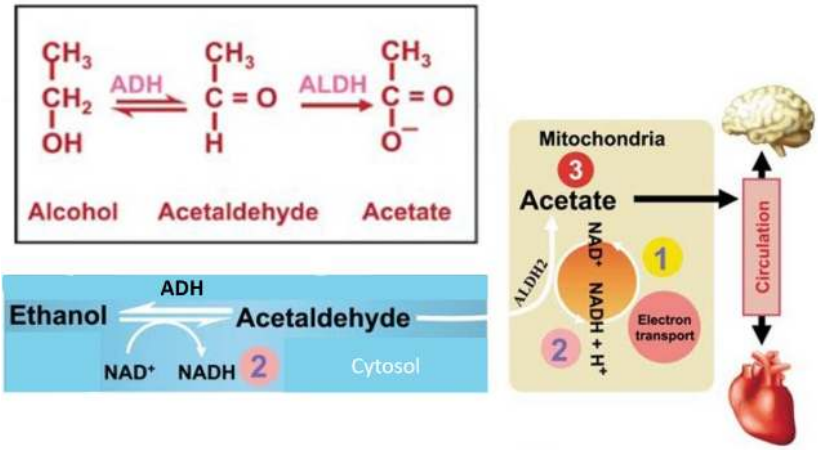


Figure 13.2.15: Summary of Ethanol Metabolism in Humans. Figure modified from Zakhari, S. (2013) Alcohol Research: Current Reviews 35(1):6-16

Like many substances, alcohol can be both beneficial and detrimental, depending on the quantity and frequency of consumption. This is known as a hormetic response (Figure **13.2.16**:). At low doses (up to two daily drinks for men and one daily drink for women), the consumption of alcohol may be cardioprotective. At higher consumption rates, the detrimental effects of alcohol consumption become apparent and include cardiotoxicity, liver damage, and increased cancer risk, not to mention the debilitation that can accompany addiction.

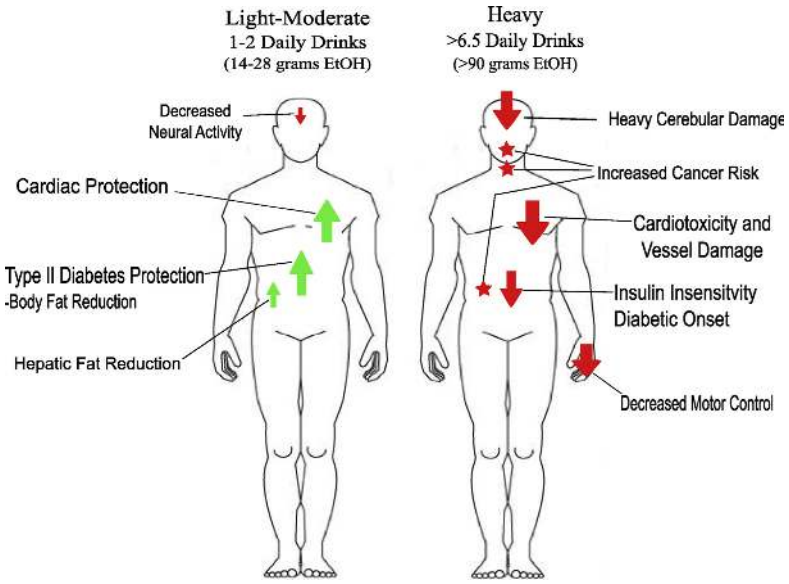


Figure 13.2.16: Alcohol Consumption and Hormesis. Figure from Adamson, S.S., et al (2017) Translational Medicine of Aging 1:18-23.

The graph in Figure **13.2.17** exemplifies the hormetic nature of alcohol consumption. The data show that having one drink per day lowers overall mortality, but after that, there is a sharp rise.

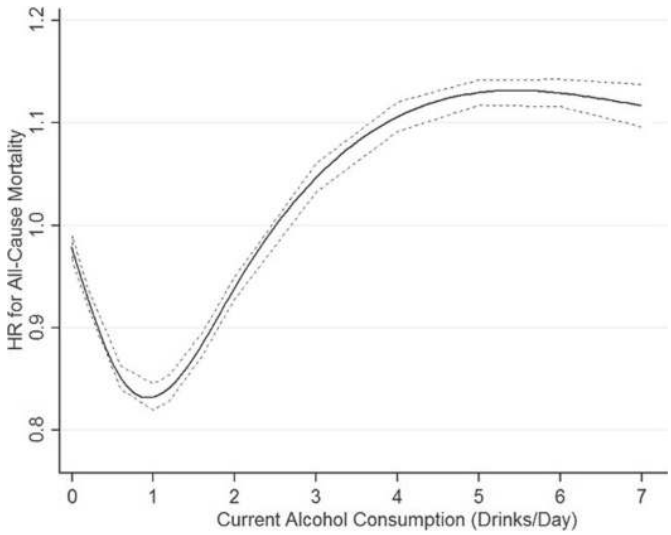


Figure 13.2.17: Risk of Mortality and Alcohol Consumption. Tian, Y., Liu, J., Zhao, Y. *et al.* Alcohol consumption and all-cause and cause-specific mortality among US adults: prospective cohort study. *BMC Med* **21**, 208 (2023). https://doi.org/10.1186/s12916-023-02907-6. Creative Commons Attribution 4.0 International License. http://creativecommons.org/licenses/by/4.0/.

Dose–response relationship between alcohol consumption and risk of mortality from all causes. A nonlinear relationship of current alcohol consumption (as a continuous variable) with all-cause mortality ($p < 0.05$ for the nonlinear test), using maximally adjusted estimates (adjusted for sex, age, race/ethnicity, education, marital status, body mass index, physical activity, smoking, and physician-diagnosed diseases (heart disease, stroke, cancer, diabetes, hypertension, asthma, emphysema, and chronic bronchitis). That indicates that alcohol consumption had a J-shaped association with risk of all-cause mortality. HR, hazard ratio.

The Centers for Disease Control estimates that alcohol abuse leads to approximately 80,000 deaths annually in the United States and that up to 40% of deaths related to liver disease are caused by alcohol abuse. Harvard Medical School has evaluated thousands of studies and developed a method for alcohol risk assessment. They categorize low-risk drinking behavior for men as no more than four drinks in a single day or 14 drinks in a week, and no more than three drinks in a single day or a total of seven drinks in a single week for women. Women have lower drinking tolerance due to their smaller size but also due to metabolic differences. Women have less ADH and typically higher fat levels, which cause ethanol to disperse and be retained longer. Addiction and damage to the liver tend to occur more quickly in women as well. Harvard ranks people at increased risk if their drinking is above either the single-day or the weekly limit (which is estimated at 29% of drinkers). High-risk drinkers break both the daily and weekly limits (estimated at 14% of drinkers).

During ethanol metabolism, when circulating ethanol is in the millimolar range, acetaldehyde is in the micromolar range, and acetate is in the millimolar range **(Figure 13.2.18:)**. When heavy drinking or chronic drinking occurs, the acetaldehyde dehydrogenase enzyme cannot keep up with the Alcohol Dehydrogenase enzyme, and the pool of Acetaldehyde increases. This aldehyde has many toxic effects within biological systems **(Figure 13.2.19:)**.

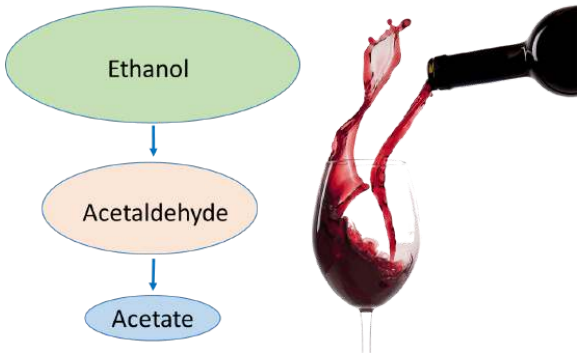


Figure 13.2.18: The Effects of Binge or Chronic Drinking on Ethanol Metabolites. Figure modified from Zakhari, S. (2013) Alcohol Research: Current Reviews 35(1):6-16

Acetaldehyde can form adducts with proteins. For example, acetaldehyde adducts on cytoskeletal components such as microtubulin lead to the swelling of hepatocytes (liver cells). If secreted from the cell, these protein adducts can also be recognized as foreign by the immune

system and cause an autoimmune response, causing further inflammation and damage to the liver. Acetaldehyde also causes oxidative damage to lipids and DNA and can alter mitochondrial function. Overall, the liver is stressed and unhappy when too much ethanol is consumed.

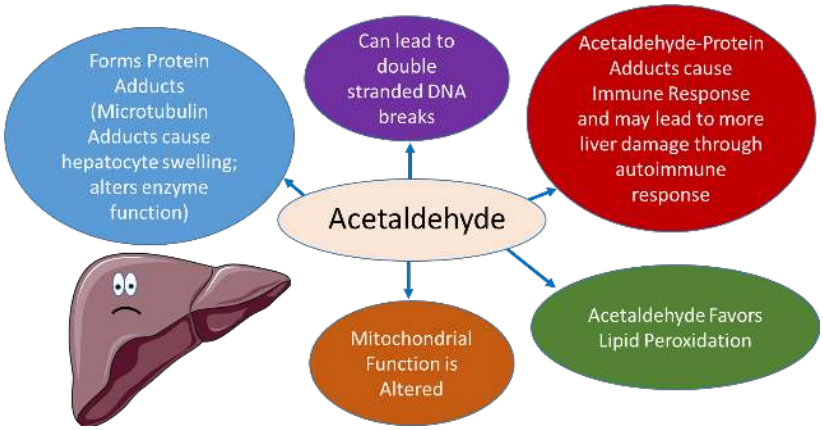


Figure 13.2.19: Acetaldehyde Toxicity. Figure modified from Servier Medical Art

Heavy chronic drinking can also lead to epigenetic modifications that alter protein expression patterns within the cell. Due to the oxidation of alcohol to acetate, alcohol metabolism also increases the NADH: NAD^+ ratio, altering carbohydrate metabolism. Heavy ethanol consumption promotes the formation of reactive oxygen species and can also promote apoptosis. Overall, heavy drinking is extremely hard on liver function. It can lead progressively from the formation of a fatty liver to liver cirrhosis and increased risk of liver cancer. The risk for several other types of cancer is also heightened with heavy alcohol use.

Chronic heavy alcohol use can also alter gene expression, especially in the liver. Figure 13.2.20 is a schematic representation of DNA methylation, which converts cytosine to 5′methyl-cytosine via the actions of DNA methyltransferase (DNMT). DNA methylation typically occurs at cytosines that are followed by a guanine (i.e., CpG motifs). Within the liver, chronic heavy drinking reduces pools of S-adenosylmethionine (SAM) while increasing homocysteine and S-adenosylhomocysteine (SAH). SAH further inhibits DNA methyltransferases (DNMTs) by negative feedback inhibition, ultimately resulting in the global hypomethylation of DNA. This hypomethylation leads to the inappropriate expression of many genes, especially within the liver tissue.

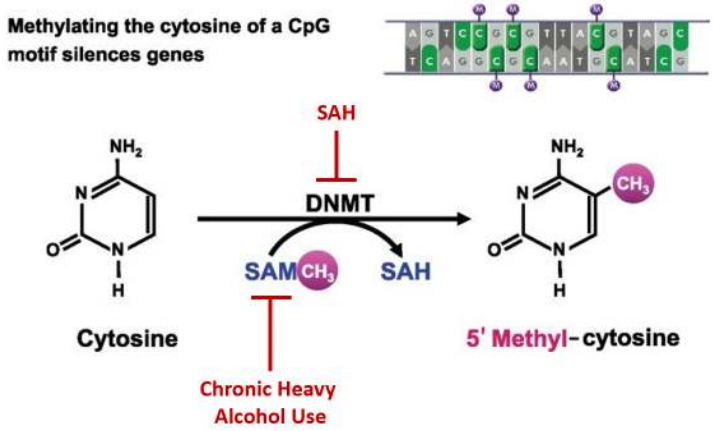


Figure 13.2.20: Effects of Chronic Alcohol Use on DNA Methylation. Figure modified from Zakhari, S. (2013) Alcohol Research: Current Reviews 35(1):6-16

Two upregulated genes due to this hypomethylation encode catalase and the p450 oxidoreductase, CYP2E1. Both of these enzymes are involved in oxidative pathways of alcohol metabolism that produce the toxic acetaldehyde intermediate (Figure 13.2.21). Expression of both of these proteins becomes more prevalent in chronic alcohol consumption or when blood alcohol levels are high, as in cases of binge or heavy drinking. The activity of these enzymes can also lead to the formation of reactive oxygen species that contribute to global cellular damage (lipid peroxidation, DNA damage, protein damage, etc).

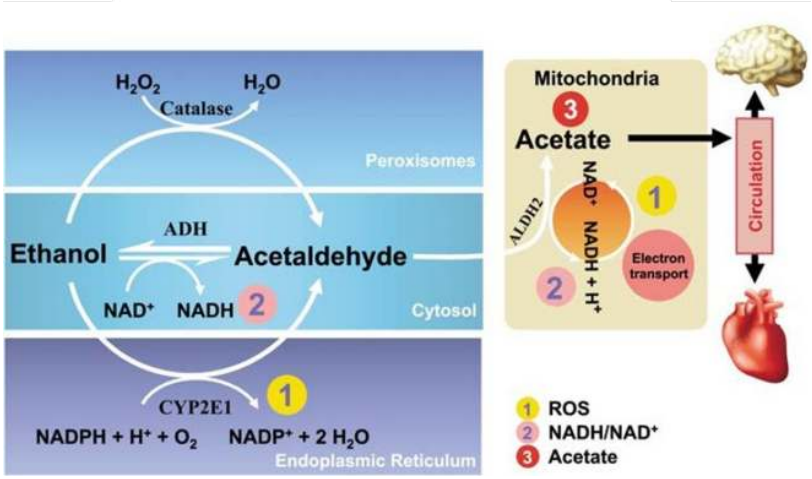


Figure 13.2.21: Oxidative Pathways of Alcohol Metabolism

Figure from Zakhari, S. (2013) Alcohol Research: Current Reviews 35(1):6-16

Gene regulation in other areas of the body is also affected in response to chronic heavy alcohol consumption. This is due to the production of acetate during the metabolic pathway of alcohol, which is released from the liver into the bloodstream. In other areas of the body, acetate is converted to acetyl-CoA by the enzyme Acetyl-Coenzyme A (acetyl-CoA) synthetase (AceCS). AceCS is activated by Sirtuin 1, also known as NAD-dependent protein deacetylase (SIRT1). Acetyl-CoA is used by histone acetyltransferase (HAT) to acetylate the lysine residues in histone proteins. Histone acetylation causes these proteins to release the bound DNA, allowing regions to be opened up for transcription (Figure 13.2.22). Thus, higher levels of acetate promote histone acetylation and increased gene expression.

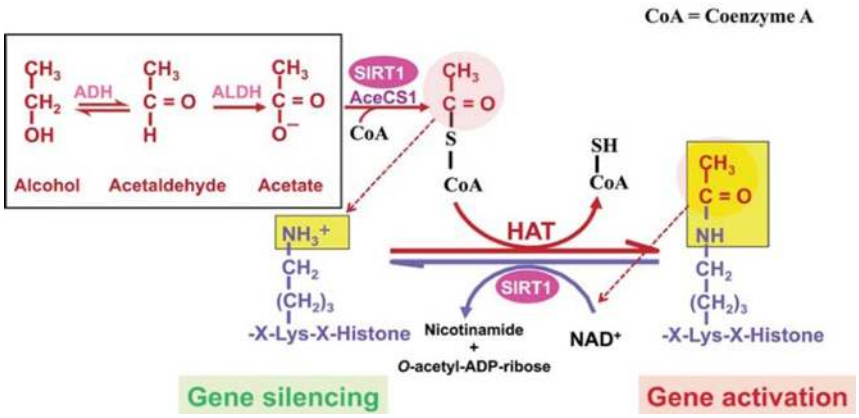


Figure 13.2.22: The Effects of Chronic Alcohol Consumption on Histone Acetylation. Note in the diagram shown, that SIRT1 also deacetylates histones, resulting in gene silencing. Thus, SIRT1 is a sensor that balances gene activation and silencing in the cell based on the cell's energy status. Alcohol metabolism results in acetate formation, which is used in ***extrahepatic tissues*** to produce acetyl-CoA, upregulating histone acetylation within those tissues. NOTES: AceCS1 = Acetyl-CoA synthase 1; ADH = alcohol dehydrogenase; ALDH = Aldehyde dehydrogenase. Figure from Zakhari, S. (2013) Alcohol Research: Current Reviews 35(1):6-16

In addition to these effects, both ADH and ALDH utilize the cofactor nicotinamide adenine dinucleotide (NAD+), which is reduced to NADH; as a consequence, during ethanol oxidation, the ratio NADH/NAD^+ is significantly increased, altering the cellular redox state and triggering several adverse effects related to alcohol consumption. Glycolysis and the Kreb Cycle are downregulated due to low NAD+ levels. This results in lower pyruvate levels and lower conversion of pyruvate to acetyl-CoA and also causes a decrease in gluconeogenesis (ie, there is not enough pyruvate to drive glucose production). Thus, the pyruvate that does form favors anaerobic conversion to lactate and can result in lactic acidosis or lowering of the blood pH levels. Low rates of gluconeogenesis can also contribute to hypoglycemia, which can be seen during binge drinking.

Hyperuricemia or an increase in blood levels of uric acid can also occur due, in part, to the increased production of ketone bodies and lactic acid. Both the ketone bodies and lactate can compete with uric acid for excretion into the urine within the kidney. The uric acid gets retained and heightens blood levels.

Ketone bodies typically form during periods of starvation when carbohydrate stores have been depleted. When the liver can no longer efficiently maintain blood glucose levels, it will break down fatty acids into ketone bodies and secrete these into the bloodstream (Figure **13.2.23**). Ketone bodies, such as acetoacetate, acetone, and D-beta-hydroxybutyrate (which isn't a real ketone, but is still referred to as a ketone body), are released into the bloodstream to compensate for the reduced glucose levels. Brain, heart, and skeletal muscle tissue can utilize ketone bodies as an energy source. This is a good short-term solution to starvation. However, the formation of lactate and ketone bodies can severely reduce blood pH levels and induce a life-threatening state known as ketoacidosis. In addition to starvation, heavy alcohol consumption can induce ketogenesis inappropriately.

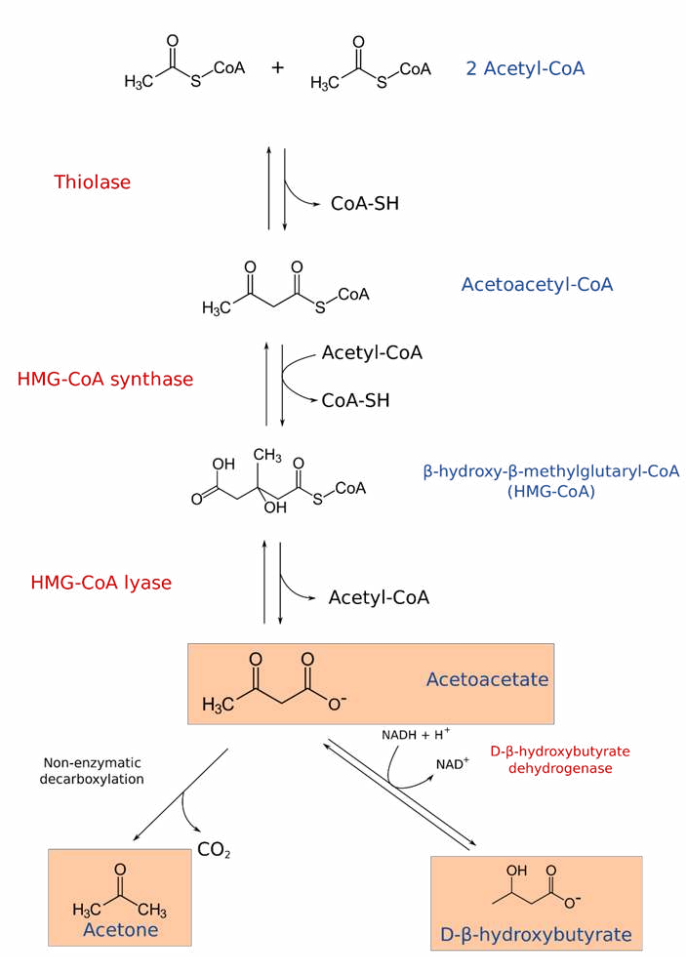


Figure 13.2.23: Formation of Ketone Bodies. Figure from Sav vas

As noted before, high levels of lactate and ketone bodies within the bloodstream can result in dehydration and reduced excretion of uric acid, leading to hyperuricemia. Over time, high uric acid levels can cause uric acid to precipitate, especially in joints, where it causes painful gout flare-ups (Figure **13.2.24**).

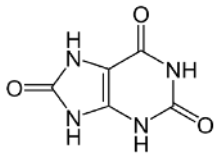




Figure 13.2.24: Hyperuricemia and Gout. Image from www.scientificanimations.com

According to the American Cancer Society, excessive alcohol use can also increase the risk for several different forms of cancer.

- **Cancers of the mouth, throat, voice box, and esophagus:** Alcohol use raises the risk of these cancers. Drinking and smoking together raise the risk of these cancers even more than drinking or smoking alone. This might be because alcohol can help harmful chemicals in tobacco get inside the cells that line the mouth, throat, and esophagus. Alcohol may also limit how these cells can repair damage to their DNA caused by the chemicals in tobacco.
- **Liver cancer:** Long-term alcohol use has been linked to an increased risk of liver cancer. Regular, heavy alcohol use can damage the liver, leading to inflammation and scarring. This might raise the risk of liver cancer.
- **Colon and rectal cancer:** Alcohol use has been linked with a higher risk of cancers of the colon and rectum. The evidence for this is generally stronger in men than in women, but studies have found the link in both sexes.
- **Breast cancer:** Even a few drinks a week are linked with an increased risk of breast cancer in women. This risk may be especially high in women who do not get enough folate (Vitamin B12) in their diet or through supplements. Alcohol can also raise estrogen levels in the body, which may explain some of the increased risks. Cutting back on alcohol may be an important way for many women to lower their risk of breast cancer.

So how does alcohol consumption contribute to increased risks of cancer? Alcohol may help other harmful chemicals, such as those in tobacco smoke, enter the cells lining the upper digestive tract more easily. This might explain why the combination of smoking and drinking is much more likely to cause cancers in the mouth or throat than smoking or drinking alone. In other cases, alcohol may slow the body's ability to break down and get rid of some harmful chemicals. Alcohol might affect the body's ability to absorb some nutrients, such as folate. Folate is a vitamin needed as a cofactor for enzymes involved in amino acid biosynthesis. Absorption of nutrients can be even worse in heavy drinkers, who often have low levels of folate. These low levels may play a role in the risk of some cancers, such as breast and colorectal cancer. Alcohol can raise the levels of estrogen, a hormone important in the growth and development of breast tissue. This could affect a woman's risk of breast cancer. Too much alcohol can also add extra calories to the diet, which can contribute to weight gain in some people. Being overweight or obese is known to increase the risk of many types of cancer.

Overall, heavy ethanol consumption produces a wide spectrum of hepatic lesions (Figure **13.2.25**). Fatty liver (i.e., steatosis) is the earliest, most common response that develops in more than 90 percent of problem drinkers who consume 4 to 5 standard drinks per day. With continued drinking, alcoholic liver disease can proceed to liver inflammation (i.e., steatohepatitis), fibrosis, cirrhosis, and even liver cancer (i.e., hepatocellular carcinoma). Heavy drinking can also damage other organs, such as the pancreas and the brain, and can raise blood pressure. It also increases the risk of heart disease and stroke. In pregnant women, alcohol use, especially heavy drinking, may lead to birth defects or other problems with the fetus.

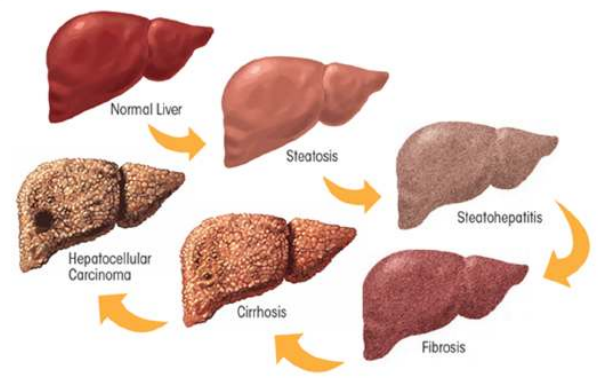


Figure 13.2.25: The Effects of Heavy Chronic Drinking on the Liver. Figure from Osna, N.A. et al (2017) Alcohol Research: Current Reviews 38(2)

In 1951, the FDA approved disulfiram for the treatment of alcoholism in the US (Figure **13.2.26**). Initially, the drug was prescribed in very high doses, often as high as 3,000 mg per day. The high doses led to reports of severe reactions to alcohol, some of which were fatal. It is an inhibitor of the ALDH-2, which will lead to an even higher increase in acetaldehyde concentration if alcohol is consumed. Thus, alcoholics who are taking this drug to quit drinking need to maintain sobriety. If they drink while taking this drug, they will become very ill due to the accumulation of acetaldehyde. Overall, the use of this drug supports abstinence, which is often hard to achieve realistically.

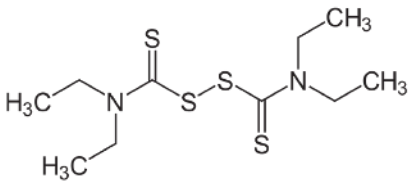


Figure 13.2.26: Disulfiram

At one time, it was thought that before prescribing disulfiram to people, patients should experience mixing the drug with alcohol in a supervised setting. Researchers felt it was important for the individuals to have full knowledge of what would happen if they mixed disulfiram and alcohol. This practice is no longer used, but every person must be educated on the reactions of combining alcohol with disulfiram before a prescription is written. Along with these effects, alcohol may contribute to cancer growth in other, unknown ways.

In other mammals, various ADHs are used to metabolize ethanol to acetaldehyde oxidatively (also toxic), which is converted to acetate by the enzyme aldehyde dehydrogenase, which catalyzes the following reaction:

$$\mathbf{CH_3CHO + NAD^+ + H_2O \rightarrow acetate + NADH + H^+}$$

They can also convert methanol to the very toxic and reactive formaldehyde, which makes methanol poisoning so dangerous, if not fatal. Mammalian enzymes are dimers of up to nine different monomers.

13.2.5: SUMMARY

This chapter provides an in-depth exploration of fermentation as an anaerobic metabolic process that sustains ATP production when oxygen is scarce. It begins by emphasizing that glycolysis, which converts glucose into pyruvate while yielding 2 ATP and 2 NADH molecules, must be coupled with NADH oxidation to regenerate NAD^+. Without this regeneration, glycolysis would eventually stall due to the limited pool of NAD^+ available.

Two primary fermentative pathways are described in detail:

- **Lactate Fermentation:**
  In animal cells, particularly in muscle tissues under anaerobic conditions, pyruvate is reduced to lactate by lactate dehydrogenase (LDH). This reaction not only regenerates NAD^+ but also allows glycolysis to continue during intense exercise or oxygen deficiency. The chapter reviews the enzyme's structure, isozyme variations (e.g., LDH-1 in the heart, LDH-5 in muscle), and its reversible nature. Additionally, the Cori cycle is introduced as the mechanism by which lactate produced in muscles is transported to the liver, converted back to pyruvate, and ultimately used for gluconeogenesis, thereby linking peripheral anaerobic metabolism with hepatic aerobic processes.
- **Ethanol Fermentation in Yeast:**
  Yeast and some other organisms utilize a two-step anaerobic process where pyruvate is first decarboxylated to acetaldehyde by thiamine pyrophosphate-dependent pyruvate decarboxylase, and then reduced to ethanol by alcohol dehydrogenase (ADH), regenerating NAD^+ in the process. This pathway enables yeast to survive in oxygen-limited environments and underpins the industrial production of alcoholic beverages.

The chapter further extends its discussion to human alcohol metabolism, where ethanol is oxidized in the liver by cytosolic ADH to acetaldehyde, which is then further oxidized by mitochondrial acetaldehyde dehydrogenase (ALDH2) to acetate. This metabolism not only affects the cellular $NADH/NAD^+$ ratio—impacting glycolysis, the Krebs cycle, and gluconeogenesis—but also has clinical significance. Excessive ethanol consumption leads to acetaldehyde accumulation, which is toxic and can cause liver damage, promote oxidative stress, and even contribute to cancer risk. The concept of hormesis is introduced to illustrate how moderate alcohol consumption may confer some cardioprotective effects, while chronic heavy drinking has severe detrimental consequences.

Lastly, the chapter touches on therapeutic strategies such as disulfiram, a drug that inhibits ALDH, thereby reinforcing abstinence by causing adverse reactions when alcohol is consumed.

Overall, the chapter weaves together the biochemical, physiological, and clinical aspects of fermentation and ethanol metabolism, underscoring their critical roles in energy production, metabolic regulation, and human health.

This page titled 13.2: Fates of Pyruvate under Anaerobic Conditions- Fermentation is shared under a not declared license and was authored, remixed, and/or curated by Henry Jakubowski and Patricia Flatt.

- **Current page** by Henry Jakubowski and Patricia Flatt has no license indicated.
- **11.2: Diffusion Across a Membrane - Passive and Facilitated Diffusion** by Henry Jakubowski and Patricia Flatt has no license indicated.

13.3: GLUCONEOGENESIS

LEARNING GOALS (CHATGPT O3-MINI)

1. **Define and Contextualize Gluconeogenesis:**
   - Explain what gluconeogenesis is and why it is essential for maintaining blood glucose levels during fasting, starvation, low-carbohydrate diets, or intense exercise.
   - Differentiate gluconeogenesis from glycogenolysis in terms of substrates, regulation, and tissue distribution.
2. **Identify Substrates and Cellular Locations:**
   - List the primary non-carbohydrate precursors (lactate, glycerol, and glucogenic amino acids) that feed into gluconeogenesis.
   - Describe where gluconeogenesis predominantly occurs in animals (mainly in the liver, and to a lesser extent in the kidney cortex).
3. **Understand Energy Requirements and Thermodynamics:**
   - Illustrate how gluconeogenesis is a highly endergonic process, highlighting key energy-consuming steps (e.g., conversion from phosphoenolpyruvate to glucose-6-phosphate requiring ATP).
   - Explain the principle of reaction coupling and how unfavorable reactions are driven forward by coupling with strongly exergonic steps.
4. **Describe the Bypass Reactions of Gluconeogenesis:**
   - Outline the key bypass steps that reverse irreversible reactions of glycolysis, focusing on the conversion of pyruvate to phosphoenolpyruvate and the dephosphorylation steps involving fructose-1,6-bisphosphatase and glucose-6-phosphatase.
   - Explain the roles of pyruvate carboxylase, PEP carboxykinase, and the transport mechanisms (including the malate-aspartate shuttle) that link mitochondrial and cytosolic reactions.
5. **Examine Enzyme Mechanisms and Cofactor Roles:**
   - Describe the catalytic mechanism of pyruvate carboxylase, emphasizing the role of biotin (its structure, attachment to the enzyme, and function in carbon fixation) and the subsequent transfer of CO_2 to pyruvate to form oxaloacetate.
   - Discuss the reaction mechanism of phosphoenolpyruvate carboxykinase (PEPCK) in converting oxaloacetate to phosphoenolpyruvate, including the use of GTP and the removal of CO_2.
6. **Understand Metabolic Integration and Regulation:**
   - Explain how intermediates from the citric acid cycle, amino acid metabolism, and lipid metabolism (via glycerol) can be channeled into gluconeogenesis.
   - Discuss the regulatory mechanisms that ensure gluconeogenesis is activated when blood glucose levels are low and inhibited when energy is abundant, including the impact of ketosis and insulin-sensitizing agents (e.g., metformin).

By achieving these goals, students will develop a comprehensive understanding of gluconeogenesis—from substrate selection and enzyme mechanisms to its regulation and integration into overall energy metabolism.

13.3.1: INTRODUCTION

Gluconeogenesis is a metabolic pathway that results in the generation of glucose from non-carbohydrate carbon substrates such as lactate, glycerol, and glucogenic amino acids. It is one of the two main mechanisms humans and many other animals use to keep blood glucose levels from dropping too low (hypoglycemia). The other means of maintaining blood glucose levels is glycogen degradation (glycogenolysis). Gluconeogenesis is ubiquitous in plants, animals, fungi, bacteria, and other microorganisms. In animals, gluconeogenesis occurs mainly in the liver and, to a lesser extent, in the cortex of the kidneys. This process occurs during fasting, starvation, low-carbohydrate diets, or intense exercise and is highly endergonic. For example, the pathway leading from phosphoenolpyruvate to glucose-6-phosphate requires six molecules of ATP. Gluconeogenesis is often associated with ketosis. Gluconeogenesis is also a therapy target for type II diabetes, such as metformin, which inhibits glucose formation and stimulates cell uptake.

Lactate is transported back to the liver, which converts it into pyruvate by the Cori cycle using lactate dehydrogenase. Pyruvate, the first designated substrate of the gluconeogenic pathway, can then be used to generate glucose (Figure **13.3.1**). All citric acid cycle intermediates, through conversion to oxaloacetate, amino acids other than lysine or leucine, and glycerol can also function as substrates for gluconeogenesis. Transamination or deamination of amino acids facilitates the entry of their carbon skeleton into the cycle directly (as

pyruvate or oxaloacetate) or indirectly via the citric acid cycle. Glycerol, a part of the triacylglycerol molecule, can be used in gluconeogenesis.

Gluconeogenesis is a pathway consisting of eleven enzyme-catalyzed reactions. Depending on the substrate being used, the pathway can begin in the mitochondria or cytoplasm. Many of the reactions are the reversible steps found in glycolysis (Figure **13.3.1**). In humans, gluconeogenesis is restricted to the liver and, to a lesser extent, the kidney.

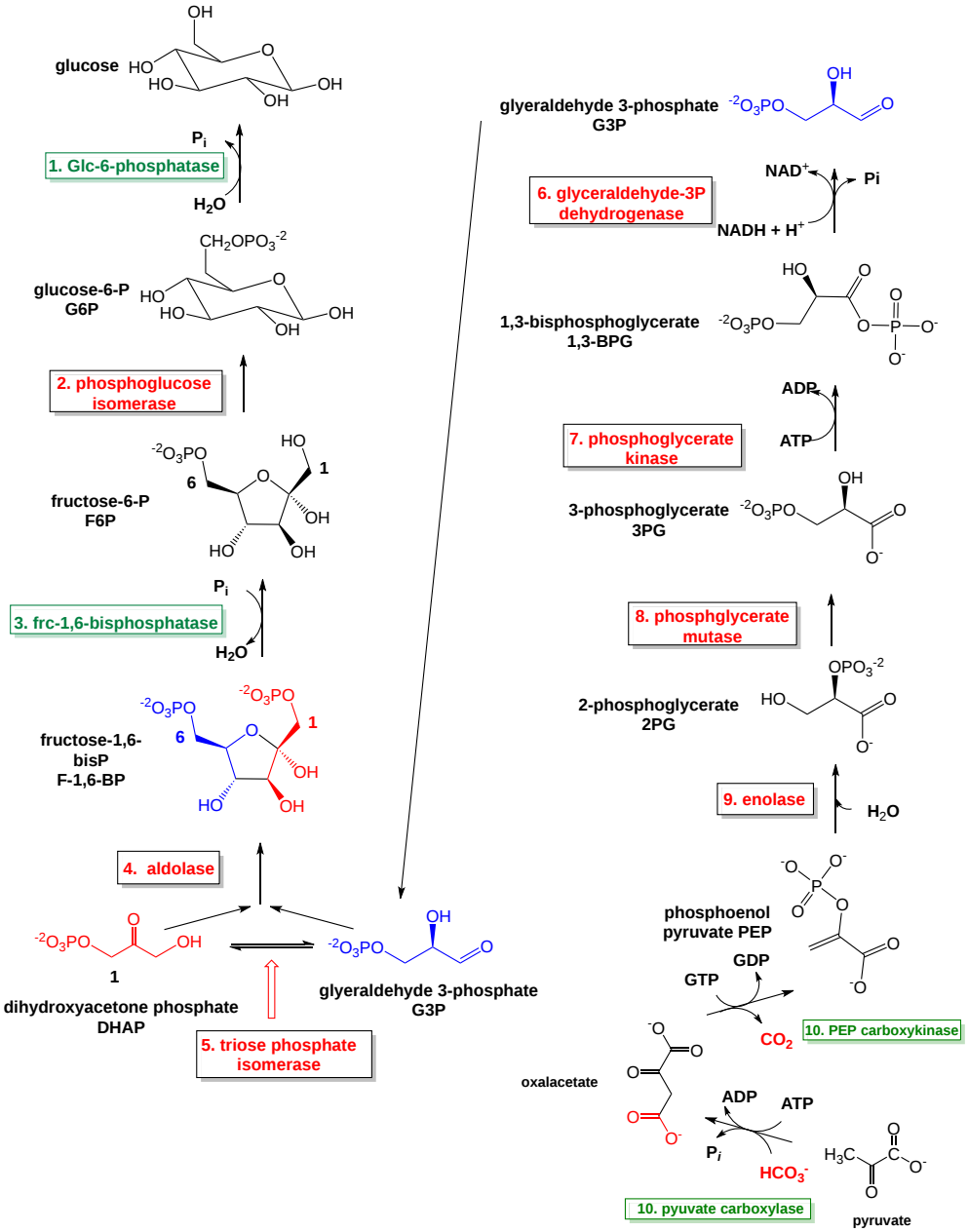


Figure13.3.1: Gluconeognesis

13.3.2: BYPASS I (REVERSE OF STEP 10 IN GLYCOLYSIS): PYRUVATE TO PHOSPHOENOLPYRUVATE

The conversion of pyruvate into phosphoenolpyruvate requires two enzymatic steps, with the formation of oxaloacetate as the intermediate. In all species, the formation of oxaloacetate from pyruvate and any other TCA cycle intermediates is restricted to the mitochondrion, and the enzymes that convert PEP to glucose are found in the cytosol. The location of the enzyme that links these two parts of gluconeogenesis by converting oxaloacetate to PEP, PEP carboxykinase, varies by species: it can be found entirely within the mitochondria, entirely within the cytosol, or dispersed evenly between the two, as it is in humans. Dedicated transport proteins move PEP across the mitochondrial

membrane; however, no such proteins exist for oxaloacetate. Therefore, in species that lack intra-mitochondrial PEP, oxaloacetate must be converted into malate or aspartate, exported from the mitochondrion, and converted back into oxaloacetate to allow gluconeogenesis to continue.

Here is the net reaction: Pyruvate + ATP + HCO_3^- + GTP → PEP + ADP + GDP + CO_2, $\Delta G^{o'}$ = +0.2 kcal/mol (0.8 kJ/mol)

Figure 13.3.2 shows the overall reaction for converting pyruvate to phosphoenol pyruvate.

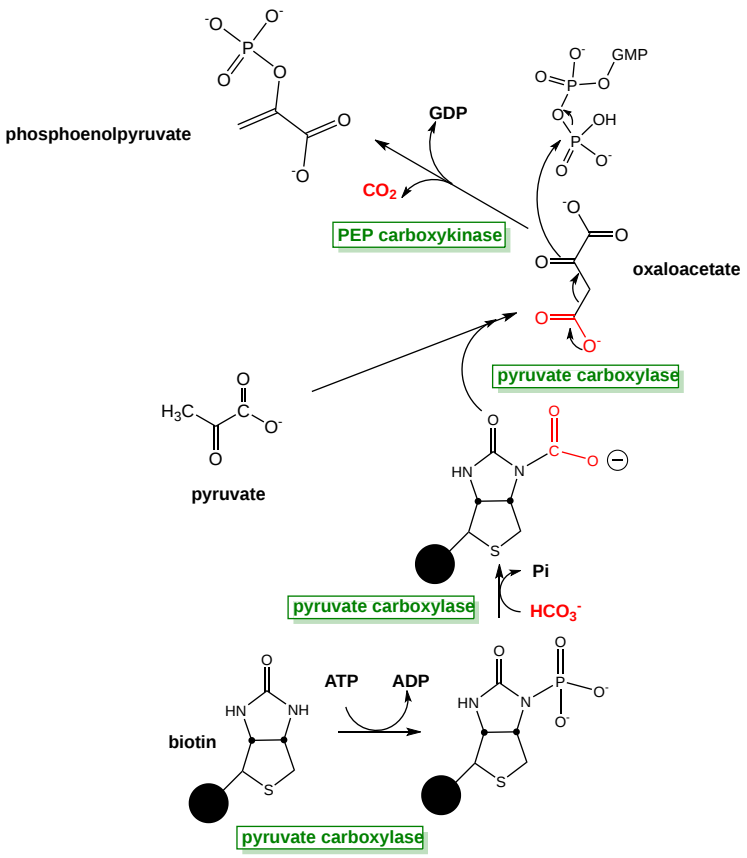


Figure 13.3.2: Overall reaction for the conversion of pyruvate to phosphoenol pyruvate

In systems that produce oxaloacetate in the mitochondria and then need to transport it to the cytosol to be converted into phosphoenolpyruvate, three enzymes are needed for the process: pyruvate carboxylase (PC) located in the mitochondrial matrix, aspartate aminotransferase (AAT), located in the matrix and the cytosol, and the phosphoenolpyruvate carboxykinase (PCK) located in the cytosol. Oxaloacetate and aspartate are intermediate compounds formed in the process.

In the first reaction, pyruvate carboxylase converts pyruvate into oxaloacetate, based on the following reaction:

Pyruvate carboxylase: pyruvate + HCO_3^- + ATP → oxaloacetate + ADP + P_i

The pyruvate carboxylase enzyme requires biotin as a cofactor. It has two major enzymatic functions: 1) carbon dioxide is fixed or attached to biotin, and 2) a carbon transferase activity, moving the fixed carbon dioxide to pyruvate to create oxaloacetate. Figure (\PageIndex{3}\) shows the biotin cofactor. Biotin is a water-soluble vitamin (D-biotin or vitamin B7) and a cofactor in enzymatic reactions involving carboxylation (or carbon fixation reactions). It is part of the vitamin B2 complex and is an essential vitamin for mammals—a deficiency results in dermatitis, loss of hair, and neurologic symptoms.

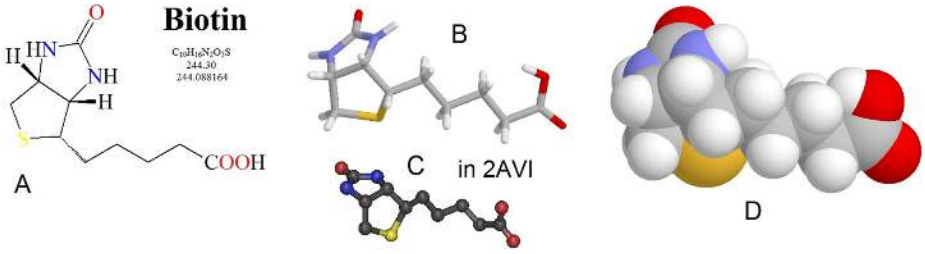


Figure (\PageIndex{3}\): Chemical Structure of Biotin. Biotin is shown in several different renderings: (A) line structure, (B) stick model, (C) ball and stick model, and (D) spacefilling model. Figure from: Biosynthesis

The biotin cofactor forms an amide linkage with the pyruvate carboxylase enzyme at a lysine residue (Figure (\PageIndex{4}\)). This creates a flexible linker region within the pyruvate carboxylase capable of dipping the biotin cofactor into the different catalytic domains of the enzyme for the expression of catalytic activity. Attaching the biotin to the enzyme requires the energy of ATP.

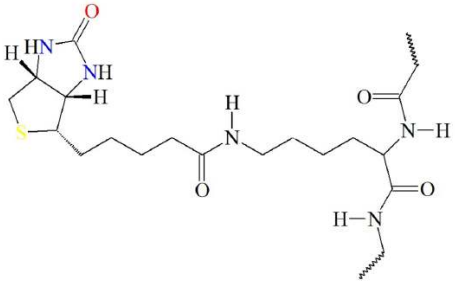


Figure (\PageIndex{4}\) Attachment of Biotin Cofactor to Lysine Residue in Pyruvate Carboxylase. Image from: Biosynthesis

The pyruvate carboxylase enzyme is a tetramer that contains four functional protein subunits, as shown in Figure **13.3.5**. The BCCP flexible arm can extend into the biotin carboxylation (BC) domain, where biotin is first carboxylated. Then, the BCCP shifts to the carboxyl transferase (CT) domain, where the fixed carbon dioxide can be transferred to pyruvate, forming oxaloacetate.

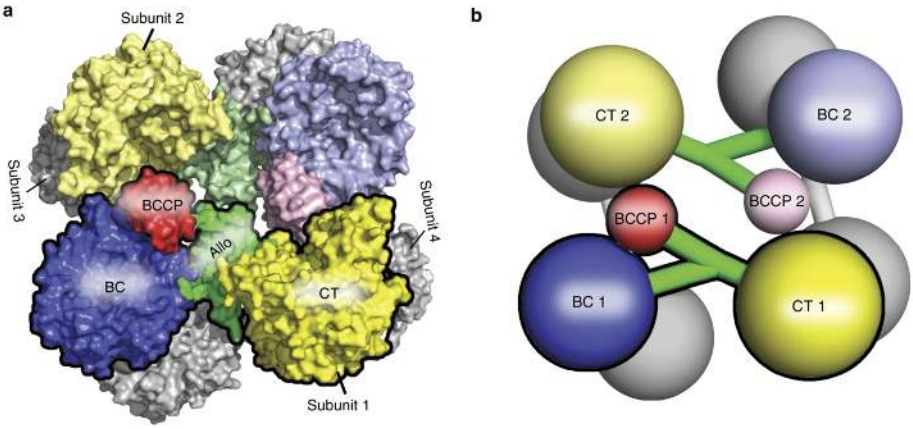


Figure 13.3.5 Structure of the Pyruvate Carboxylase Enzyme. The Pyruvate carboxylase's overall structure is a tetramer containing four functional protein subunits. Two subunits are shown in color, with the other two indicated in gray at the back of the structure. (a) shows the space-filling model while (b) shows the major domains as a cartoon graphic. Each subunit contains a biotin carboxylase (BC) domain shown in blue, a carboxytransferase (CT) domain shown in yellow, and the biotin-carboxyl carrier protein (BCCP) domain shown in red and green. Figure modified from Liu, Y., et al (2018) Nat Commun 9:1384

In the first part of the reaction, the biotin cofactor is carboxylated using bicarbonate as a substrate with ATP to drive the formation of a molecule with high energy with respect to its hydrolysis product intermediate. (**Remember, there is no such thing as a "high energy" bond.**) Thus, biotin acts as an intermediate carrier of the carboxy group that will be added to pyruvate during the formation of oxaloacetate. This occurs in the biotin carboxylase domain (BC), where biotin is bound to a biotin carboxyl carrier protein (BCCP) domain. The carboxyl

group is then transferred to pyruvate to form oxaloacetate in the carboxyl transferase (CT) domain. Let's break up the enzyme mechanism from *Rhizobium etli* into three figures.

Figure**13.3.6** below shows the first steps in the carboxylation of biotin in the biotin carboxylase domain, using bicarbonate as a substrate. In Figure**13.3.6**, you can see that oxygen from bicarbonate mediates nucleophilic attack on the outer phosphate group of the ATP molecule, forming the carbonyl-phosphate intermediate + ADP. The carbonyl-phosphate decomposes to release carbon dioxide and phosphate. The negatively charged phosphate activates the biotin cofactor to enable a nucleophilic attack on the carbon of the carbon dioxide, producing the carboxybiotin intermediate, shown in the upper part of Figure**13.3.7**.

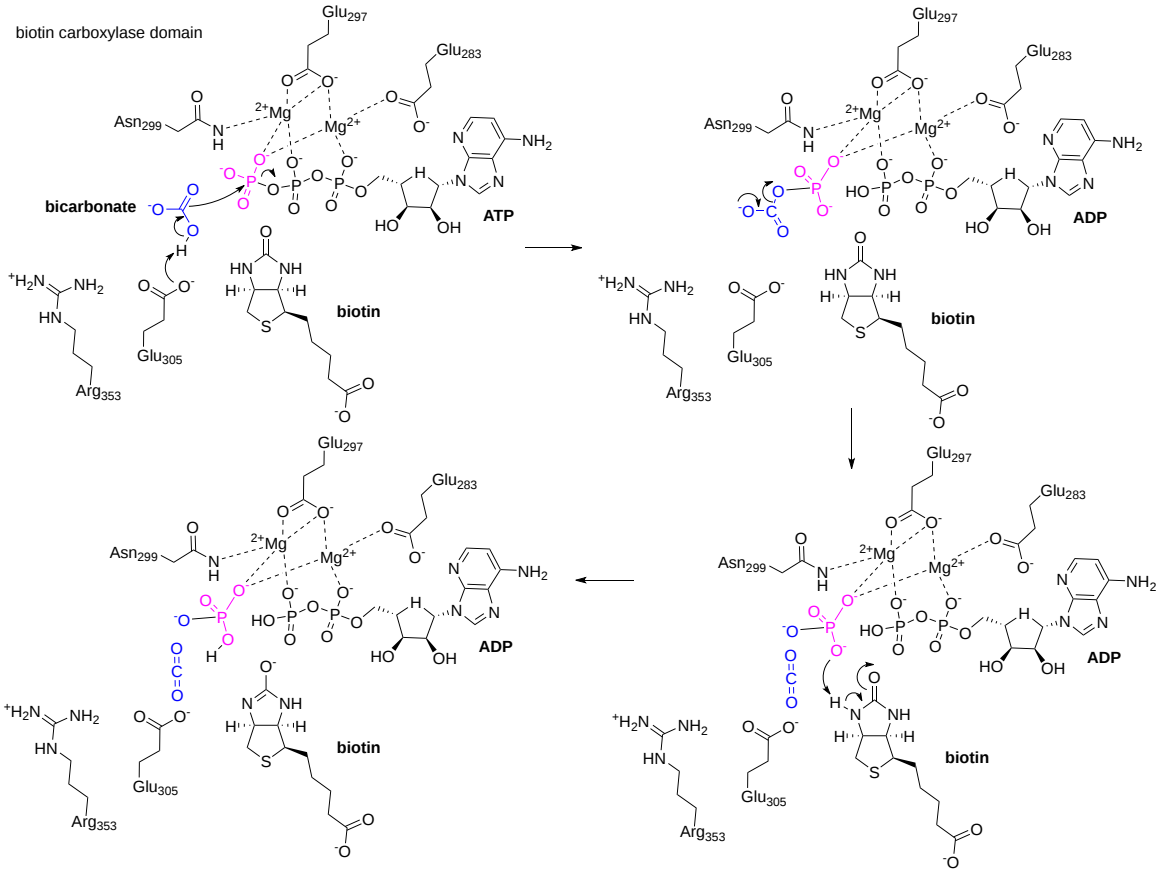


Figure 13.3.6: The Carboxylation of Biotin during the Pyruvate Carboxylase Reaction Mechanism. Bicarbonate, shown in blue, enters the active site of the enzyme and reacts with the terminal phosphate of ATP, forming a phosphorylated intermediate. Two Mg^{2+} cofactors stabilize this reaction. The carboxyphosphate intermediate decomposes to release carbon dioxide and phosphate.

Image modified from Ribeiro AJM *et al.* (2017), *Nucleic Acids Res*, **46**, D618-D623. Mechanism and Catalytic Site Atlas (M-CSA): a database of enzyme reaction mechanisms and active sites. DOI:10.1093/nar/gkx1012. PMID:29106569. https://www.ebi.ac.uk/thornton-srv/m-csa/entry/223/. Creative Commons Attribution 4.0 International (CC BY 4.0) License.

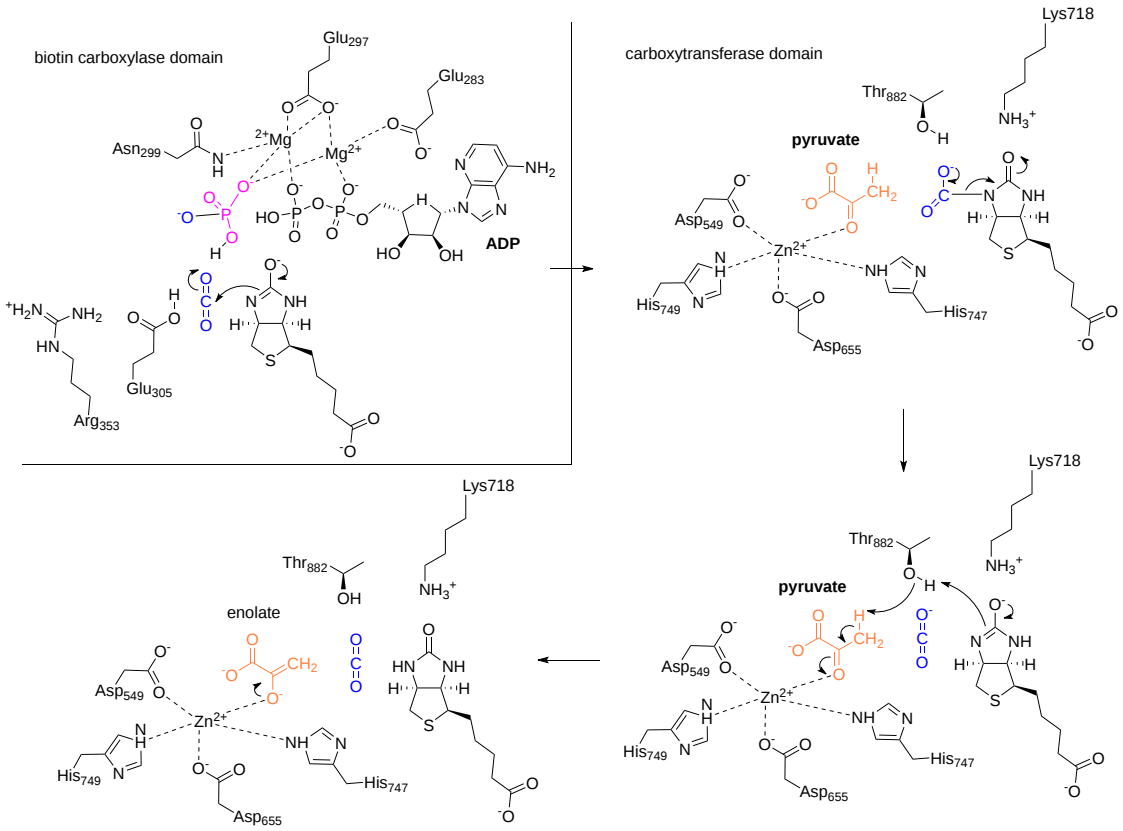


Figure13.3.7: Carboxylation of biotin in pyruvate carboxylase. The upper diagram shows the actual carboxylation of biotin, which occurs in the BC domain. The carboxybiotin intermediate shifts on the flexible arm and enters the carboxytransferase (CT) domain. Pyruvate enters the active site, and this begins the steps involved in the carboxylation of pyruvate to form oxaloacetate. Ribeiro, ibid

The carboxyltransferase activity is housed in the CT domain of the enzyme. It requires the formation of a carbanion intermediate on the pyruvate molecule to make it reactive enough to cause the addition of the carboxyl group. A base from the enzyme eliminates a proton from the C3 position of pyruvate, causing the formation of an enol reaction intermediate. As the electrons on the oxygen from the pyruvate molecule reform the carbonyl group, the electrons from the carbon-carbon double bond shift onto the carbon, creating a reactive carbanion intermediate. The carboxybiotinyl complex swings into the CT domain, providing the carboxyl group that will be incorporated into pyruvate. The carbanion intermediate mediates a nucleophilic attack onto the carboxyl carbon from the BCCP complex, and carbon dioxide is transferred to the pyruvate, creating oxaloacetate. The biotin cofactor is restored by the donation of a proton from a basic residue in the enzyme. This also restores the pyruvate carboxylase enzyme for another round of activity.

Figure**13.3.8** below shows the carboxylation of the enolate form of pyruvate to form oxaloacetate.

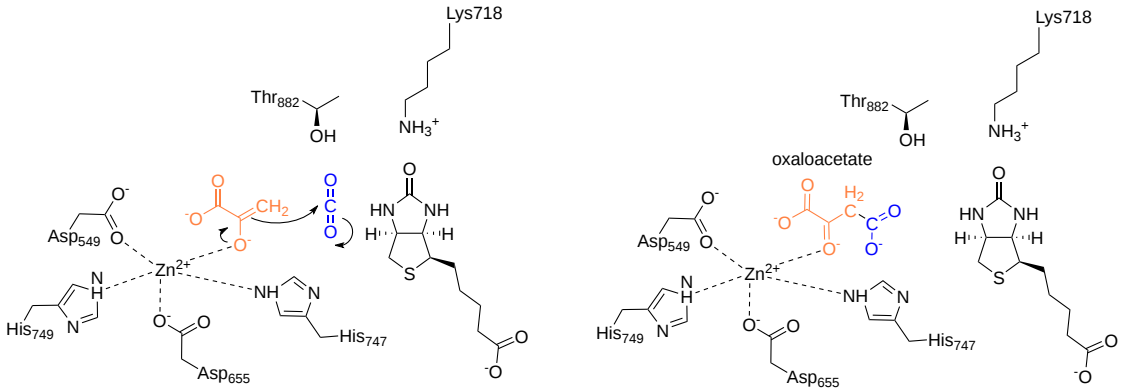
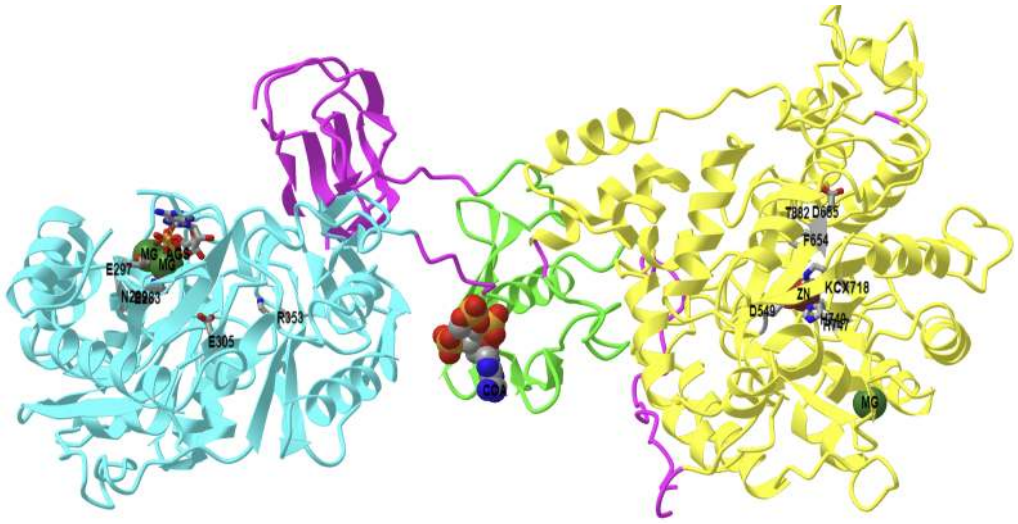


Figure13.3.8: Carboxylation of the enolate form of pyruvate to form oxaloacetate by pyruvate carboxylase. Ribeiro et al, ibid

Figure**13.3.9** below shows an interactive iCn3D model of the biotin-dependent multifunctional enzyme pyruvate carboxylase from Rhizobium etli (2QF7)

https://bio.libretexts.org/@go/page/15007



NCBI iCn3D **Figure13.3.9: Biotin-dependent multifunctional enzyme pyruvate carboxylase from Rhizobium etli (2QF7).** The enzyme is a homotetramer with C2 symmetry, but only one subunit chain is shown for clarity. The biotin carboxylase domain (BC) is shown in cyan, the carboxytransferase domain (CT) in yellow, a C-terminal biotin carboxyl carrier protein (BCCP) domain (disconnected in parts) in magenta, and the allosteric domain in green. AGS in the cyan domain is a phosphothiophosphoric acid-adenylate ester, an ATP analog. It is shown interacting with the 2 Mg^{2+} ion, and it is represented in sticks and labeled. Acetyl-CoA and a nonhydrolyzable analog, ethyl-CoA, are allosteric activators. CoASH (ethyl group not shown) is illustrated in spacefill bound to the green allosteric domain. Acetyl-CoA binding leads to a conformational change that decreases the distance between the two active sites on the BT (cyan) and CT (yellow) domains. Biotin, not shown, is tethered in the BCCP domain, which transfers biotin between the two catalytic domains, not within a single monomer (as shown above), but between different monomers in the homo 4-mer.

(Copyright; author via source). Click the image for a popup or use this external link: https://structure.ncbi.nlm.nih.gov/i...7g91JmzJMad4r9

Figure**13.3.10** shows the flexible nature of the biotin flexible arm of the enzyme during the catalytic process.

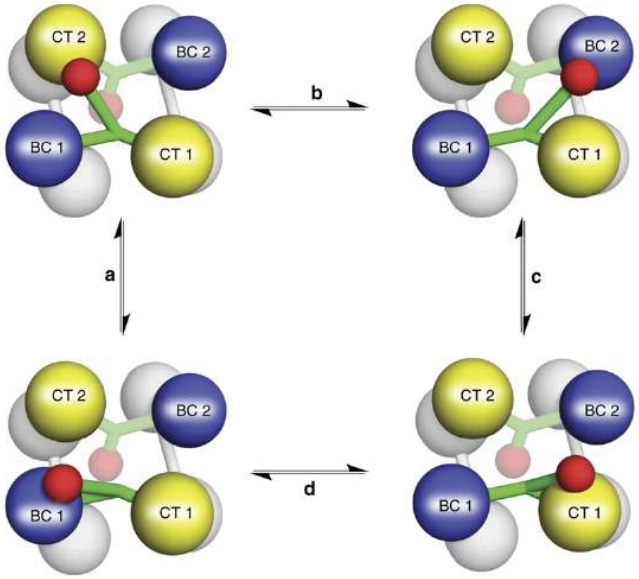


Figure13.3.10 The Catalytic Activity of Pyruvate Carboxylase. The Biotin-Carboxyl Carrier Protein Domain (BCCP) is a flexible arm of the protein structure that can swing from one catalytic domain to the other during the reaction process. As shown in the diagram, the BCCP domain of subunit 1 will be fixed with carbon dioxide at the biotin carboxylase domain from subunit 1 (BC1). The BCCP will then translocate to the carboxyltransferase domain from subunit 2 (CT2), creating one molecule of oxaloacetate and resetting the biotin cofactor. The BCCP will then swing into the BC2 domain, where carbon fixation will occur. BCCP then shifts to the CT1 domain, creating a second oxaloacetate molecule and resetting the biotin. While this happens with the BCCP from subunit 1, the other BCCP arms from subunits 2, 3,

and 4 are also active. Thus, one full sequence of the enzyme activity will produce eight oxaloacetate molecules. Image from: Liu, Y., et al (2018) Nat Commun 9:1384

The next reaction in the process requires the conversion of oxaloacetate to phosphoenolpyruvate by phosphoenolpyruvate carboxykinase (PEPCK). However, the major human PEPCK enzyme, PCK1, resides in the cell's cytoplasm. Thus, the oxaloacetate produced in the matrix of the mitochondria by pyruvate carboxylase must be transported into the cytosol. However, there are no oxaloacetate transporters that can mediate the transfer directly. To leave the mitochondrial matrix, oxaloacetate must first be converted to aspartate by the aspartate aminotransferase enzyme (AAT). It can then be transported to the intermembrane space of the mitochondria through an antiporter that transports one molecule of aspartate out of the matrix and one molecule of glutamate into the matrix Figure**13.3.11**. Once in the intermembrane space, the aspartate can pass freely through a pore in the outer mitochondrial membrane. When it reaches the cytoplasm, aspartate is reconverted to oxaloacetate using the cytoplasmic aspartate aminotransferase enzyme (AAT). Oxaloacetate can then be used as a substrate by the phosphoenolpyruvate carboxykinase enzyme (PEPCK).

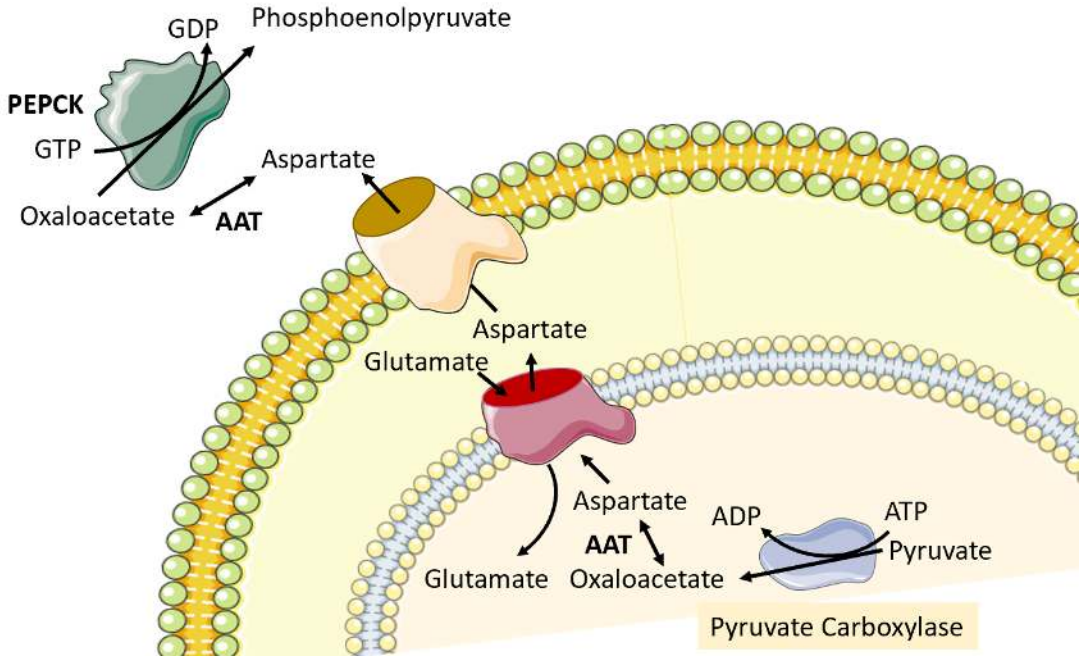


Figure13.3.11 Conversion of Oxaloacetate to Aspartate and Transfer to the Cytoplasm. Image modified from SMART Servier Medical Art

The glutamate/aspartate transporter has some additional complexities associated with it. It cannot function on its own. It requires the coordinated functioning of the malate/alpha-ketoglutarate antiporter. Together, these antiporters are known as the Malate-Aspartate Shuttle System.

The Malate-Aspartate Shuttle System is dependent on the functioning of two enzymatic processes. The first is the aspartate aminotransferase indicated more simplistically in Figure**13.3.11**. The aspartate aminotransferase enzyme can utilize glutamate as an amine donor to generate aspartate from oxaloacetate. Alpha-ketoglutarate is also formed in this process. This enzyme can also work in the reverse reaction to produce glutamate and oxaloacetate, depending on substrate concentrations and other regulatory mechanisms. In a different reaction using malate dehydrogenase, oxaloacetate can be reduced to form malate using a molecule of NADH as the electron donor.

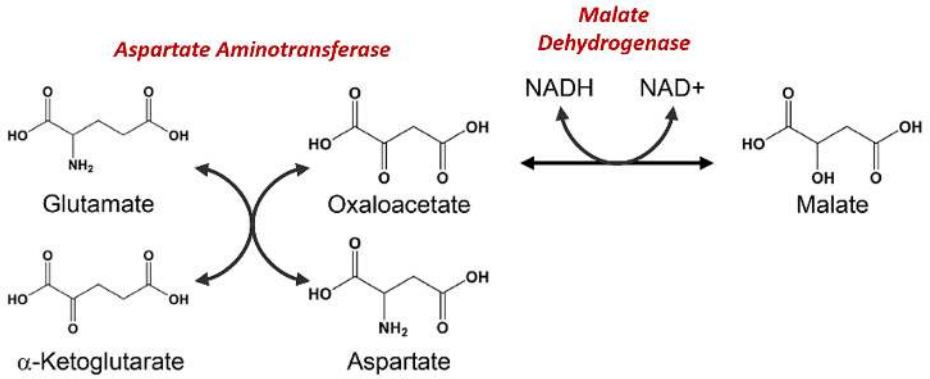


Figure13.3.12 Chemical Reactions of the Malate-Aspartate Shuttle System

Figure modified from Son, H.F. and Kim, J-J. (2016) PLoS One 10.1371

The malate dehydrogenase enzyme is expressed at high levels in the cytoplasm of liver cells and in the matrix of the mitochondria. This enzyme is a component of the Krebs cycle, where it mediates the formation of oxaloacetate in the last step of the cycle. Within the cytoplasm, it predominantly converts oxaloacetate to malate. The malate can then be shuttled into the matrix of the mitochondria through the malate/alpha-ketoglutarate antiporter (Figure**13.3.13**). In this antiporter, malate moves into the mitochondrial matrix while alpha-ketoglutarate moves into the intermembrane space (and subsequently into the cell's cytosol). Together with aspartate, it can be used by cytoplasmic aspartate aminotransferase to produce glutamate and oxaloacetate. This oxaloacetate pool is then utilized in the gluconeogenic pathway when PEPCK is active. The glutamate generated from this reaction is transported back into the matrix of the mitochondria through the aspartate/glutamate antiporter. The aspartate pool in the matrix of the mitochondria is supplied by the reaction of the aspartate aminotransferase enzyme, which completes the reverse reaction from the one seen in the cytoplasm. In the matrix, aspartate aminotransferase uses glutamate and oxaloacetate as substrates to generate aspartate and alpha-ketoglutarate. This enables the transport of aspartate and glutamate through their specific antiporter. Within the gluconeogenic pathway, heightened levels of oxaloacetate are produced in the matrix of the mitochondria. Oxaloacetate is then converted to aspartate and transported across the inner membrane, where it can subsequently be converted back into oxaloacetate and used for glucose production.

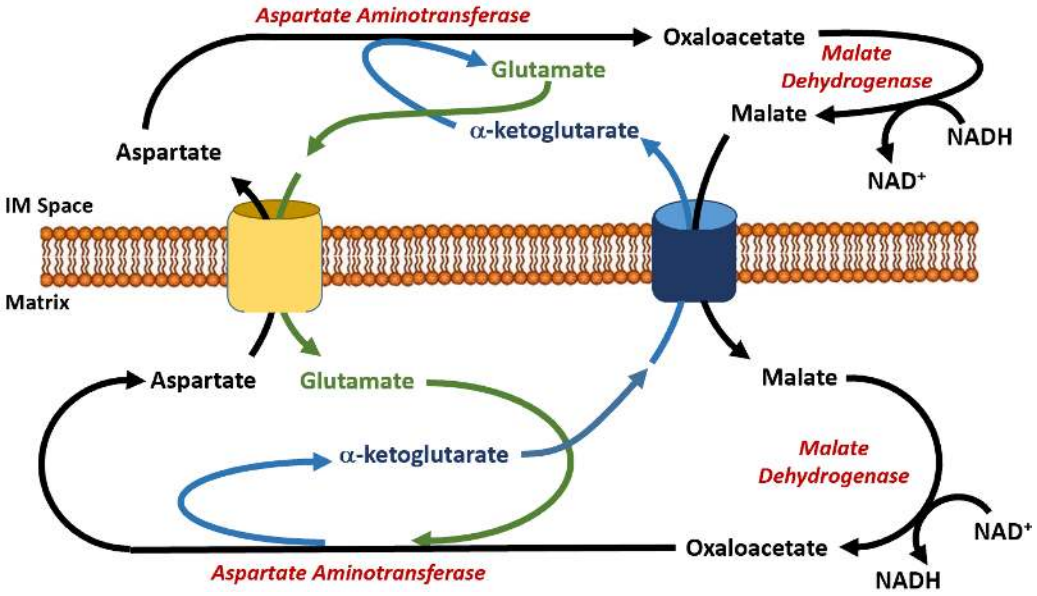


Figure13.3.13: The Malate-Aspartate Shuttle System.

Once oxaloacetate has been effectively transported via the Malate-Aspartate Shuttle into the cytoplasm, it is converted to phosphoenolpyruvate (PEP) by the PEP carboxykinase (PEPCK). The overall reaction mediated by PEPCK is:

PEP carboxykinase (PEPCK): oxaloacetate + GTP → phosphoenol pyruvate + GDP

PEPCK is classified as a lyase enzyme and exists in two isozymes: a cytoplasmic PEPCK and a mitochondrial PEPCK. The cytoplasmic form is predominantly used in the gluconeogenic pathway and requires the action of the Malate-Aspartate Shuttle. However, small amounts of PEP can be made directly by the mitochondrial PEPCK and transported across the mitochondrial membrane. The conversion of

oxaloacetate to phosphoenolpyruvate by PEPCK mediates the removal of carbon dioxide and the addition of a phosphate group. A molecule of GTP is used during this process as the phosphate donor, and magnesium ions serve as a cofactor. Figure **13.3.14** shows the reaction mechanism for the human PEP carboxykinase.

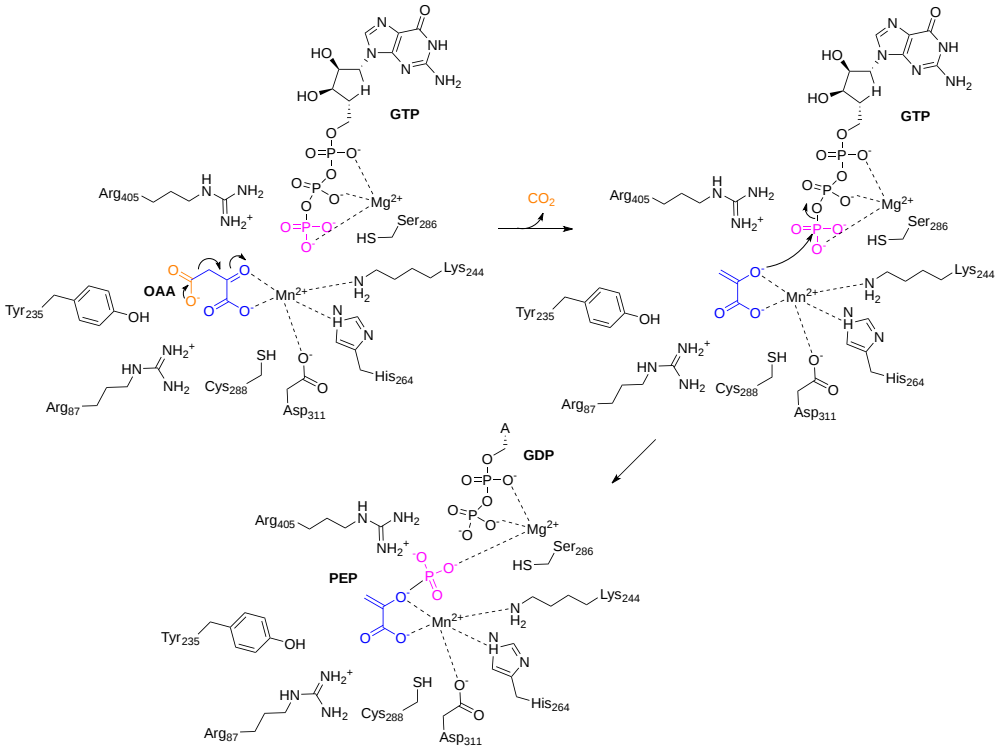
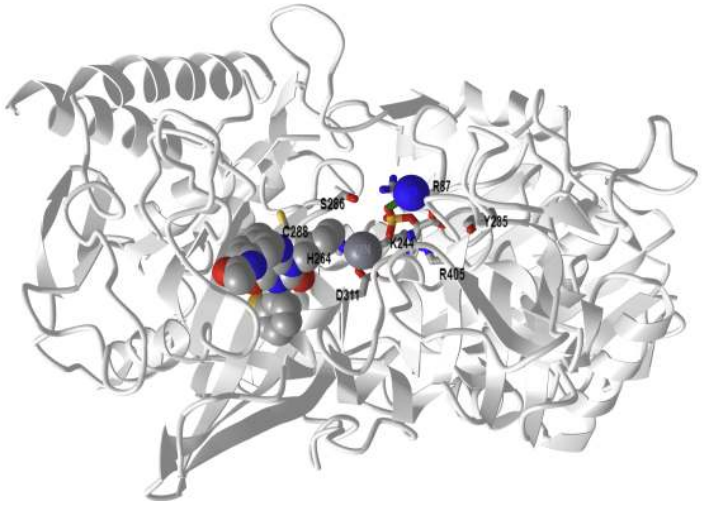


Figure 13.3.14: Reaction mechanism for human PEP carboxykinase (PEPCK)

Figure13.3.15 below shows an interactive iCn3D model of phosphoenolpyruvate carboxykinase (PEPK) with a bound PEP and GTP-competitive inhibitor (1NHX).



NCBI iCn3D **Figure 13.3.15: Phosphoenolpyruvate carboxykinase (PEPK) with a bound PEP and GTP-competitive inhibitor (1NHX).** PEP is shown in colored sticks. The competitive inhibitor is shown in colored spacefill. The active site residues from the human PEPCK mechanism are shown as labeled sticks. (Copyright; author via source). Click the image for a popup or use this external link: https://structure.ncbi.nlm.nih.gov/i...QFcTssCJbuW2K7

13.3.3: PHOSPHATASE REACTIONS OF GLUCONEOGENESIS (REVERSE OF STEPS 1 AND 3 IN GLYCOLYSIS):

The last two unique enzymes of the gluconeogenic pathway are both phosphatase enzymes. Fructose 1,6-bisphosphatase converts fructose 1,6-bisphosphate to fructose 6-phosphate. The phosphoglucoisomerase used in glycolysis can convert fructose 6-phosphate back into glucose 6-phosphate. A unique glucose 6-phosphatase enzyme will then convert glucose 6-phosphate to free glucose. Figure**13.3.16** shows the unique phosphatase reaction.

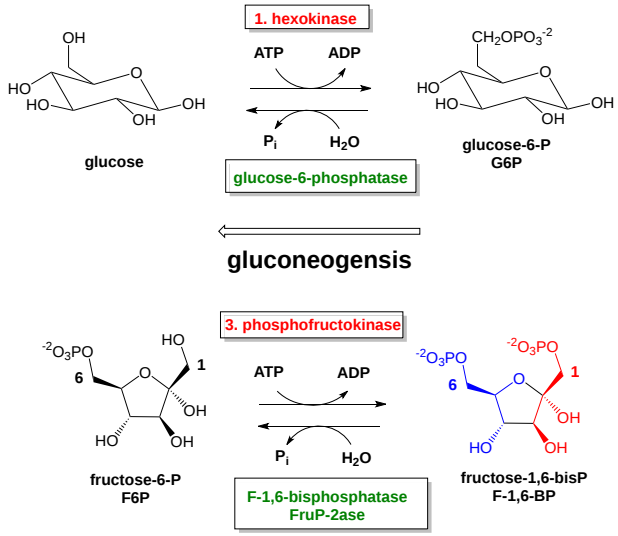


Figure 13.3.16: Phosphorylase Enzymes utilized during Gluconeogenesis

First, let's consider the dephosphorylation of fructose 1,6-bisphosphate. The gluconeogenic enzyme is named fructose-1,6-bisphosphatase (FBP or FBPase-1). FBP requires a metal cofactor and is competitively and allosterically regulated. Fructose 2,6-bisphosphate and low-energy load (AMP and ADP) inhibit the enzyme. The overall reaction is shown below:

Fructose-1,6-bisphosphatase: F1,6BP + H_2O → F6P + P_i

Figure **13.3.17** shows the mechanism of mouse fructose,1-6-bisphosphatase (FBPase-1)

https://bio.libretexts.org/@go/page/15007

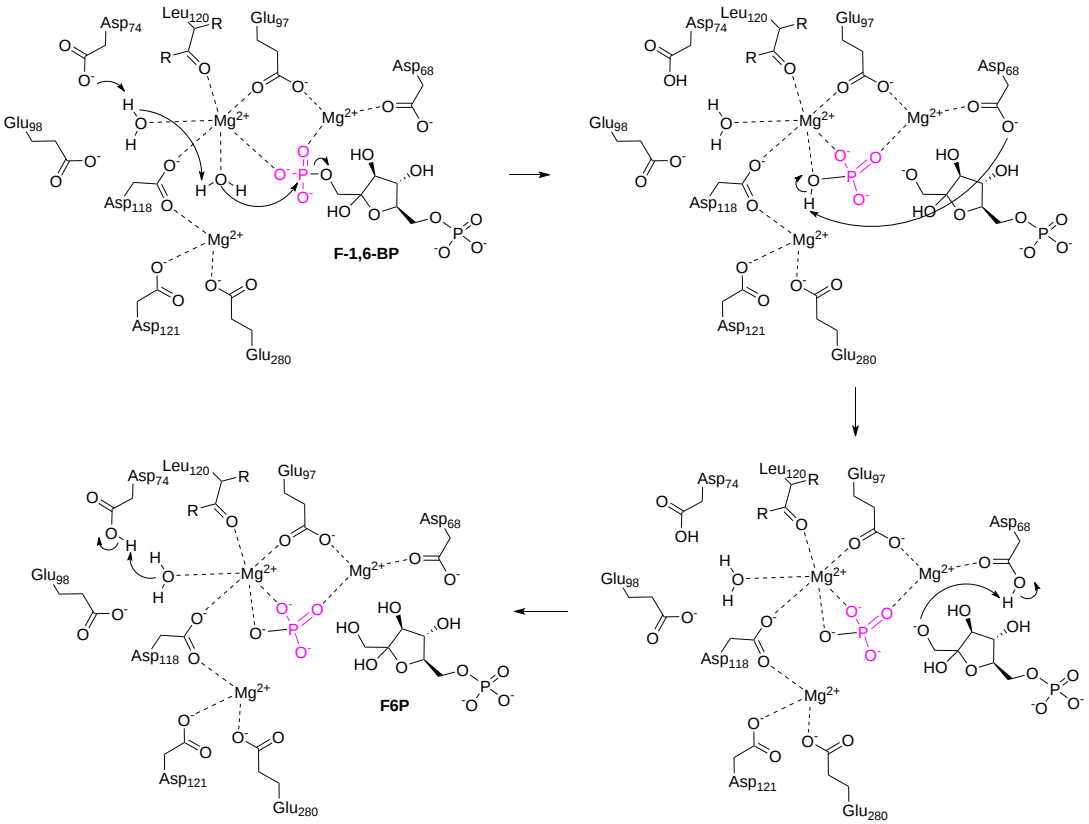
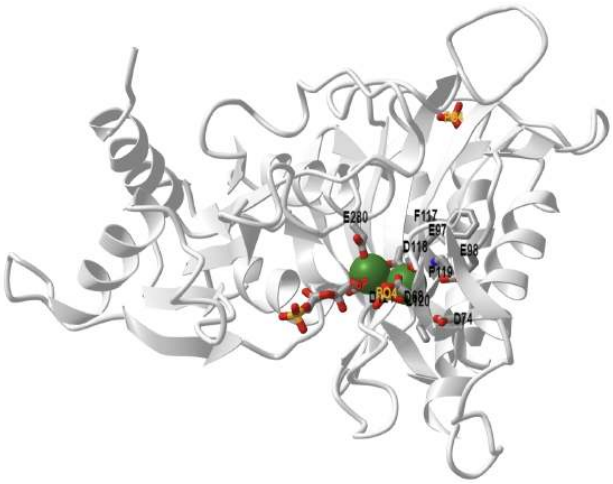


Figure 13.3.17: Mechanism of mouse fructose,1-6-bisphosphatase. Mg^{2+} ions coordinate the positioning of F-1,6-BP near an activated water molecule that mediates nucleophilic attack on the 1-position phosphate group. This leads to the cleavage of the phosphate group from the sugar molecule, F6P, which can then leave the active site.

Figure**13.3.18** below shows an interactive iCn3D model of pig fructose-1,6-bisphosphatase with bound Mg^{2+}, fructose-6-phosphate, and phosphate in the R state (1EYI).



NCBI iCn3D **Figure 13.3.18: Fructose-1,6-bisphosphatase with bound Mg, fructose-6-phosphate and phosphate in the R state (1EYI).** (Copyright; author via source). Click the image for a popup or use this external link: https://structure.ncbi.nlm.nih.gov/i...DbWMHBRTdPGhJ8

FBP is an allosteric homotetramer and can exist in a tense (T) and relaxed (R) state. The enzyme has the highest catalytic activity when it is in the R state. Figure**13.3.18** shows only one monomer of the R state with bound ligands and substrates for clarity.

Figure **13.3.19** shows an interactive iCn3D model of tetrameric FBP enzyme in the T state with bound Mg^{2+}, fructose-6-phosphate, phosphate, and AMP, an allosteric inhibitor, in the T state (1EYJ).

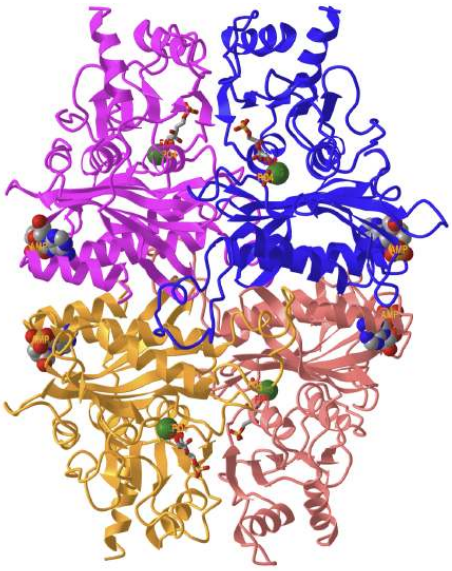


Figure 13.3.19: Tetrameric fructose-1,6-bisphosphatase in the T state with bound Mg^{2+}, fructose-6-phosphate, phosphate and AMP in the T state (1EYJ). (Copyright; author via source). Click the image for a popup or use this external link: https://structure.ncbi.nlm.nih.gov/i...UAbjNtkPsoBdA9

FBPase is inhibited by AMP and fructose-2,6-bisphosphate and activated by ATP. Allosteric changes control the catalytic activity of the enzyme and the transition from the T to the R state or vice versa. Figure 13.3.17 shows that FBP has three metal binding sites. The mechanism is shown in Figure 13.3.17. All the binding sites in the model are filled with Mg^{2+}; however, Zn^{2+} can also play a role. In the presence of AMP, only one site is occupied by Mg^{2+}, as shown in the model of the T state in Figure 13.3.19. The T-state form of FBP has a disordered loop (52-72). In the R state (no AMP), the loop interacts with the active site, and 1 Zn^{2+} and 2 Mg^{2+} ions are bound in the three sites. The binding of AMP leads to the dissociation of two of the bound metal cofactors and causes a decrease in enzyme activity.

The resulting fructose 6-phosphate is isomerized to glucose 6-phosphate. Glucose 6-phosphate is then converted by the last unique gluconeogenic enzyme, glucose 6-phosphatase, to generate free glucose. The overall reaction is shown below:

Glucose-6-phosphatase: G6P + H_2O → glucose + P_i

The dephosphorylation of glucose only occurs appreciably in liver cells, as this is the primary location for regulating blood glucose levels. This serves as the final step in the gluconeogenic pathway. The glucose 6-phosphatase enzyme is a transmembrane protein that resides in the inner membrane of the endoplasmic reticulum. Thus, for glucose 6-phosphate to be dephosphorylated, it must first be transported from the cytoplasm into the lumen of the endoplasmic reticulum (ER) through transporter 1 (T1) (Figure 13.3.20). The glucose 6-phosphatase (G-6-Pase) then cleaves the phosphate from the substrate, releasing inorganic phosphate (P) and glucose (red molecule). The inorganic phosphate is then transported back into the cytoplasm through transporter 2 (T2), and glucose is transported through Transporter 3 (T3). Free glucose is then transported back into the bloodstream through a glucose (GLUT) transporter (not shown in Figure 13.3.20).

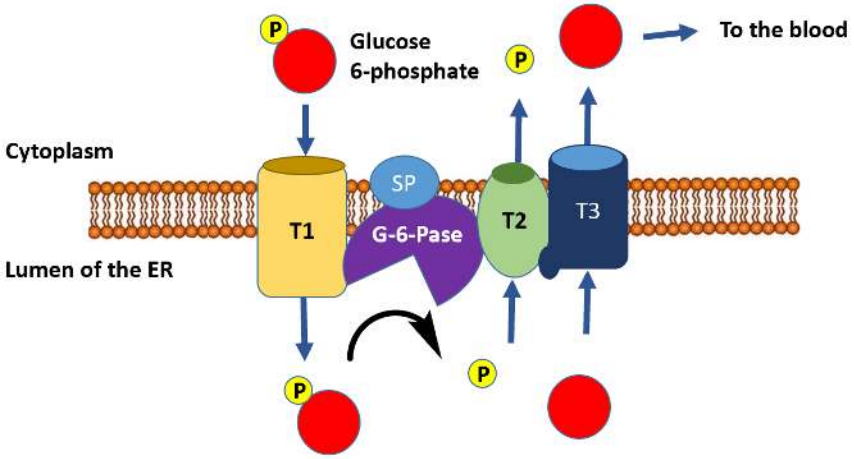


Figure13.3.20 Dephosphorylation of Glucose 6-Phosphate in the Lumen of the Endoplasmic Reticulum.

The catalytic site of this hydrolase enzyme uses Lys76, Arg83, His119, Arg170, and His176. His 176 acts as a nucleophile that attacks the phosphorus of G6P in an S_N2-like reaction to form a His-PO_3^{2-} intermediate. Hydrolysis follows, restoring the enzyme to its original state. Figure **13.3.21** shows an abbreviated mechanism for the reaction.

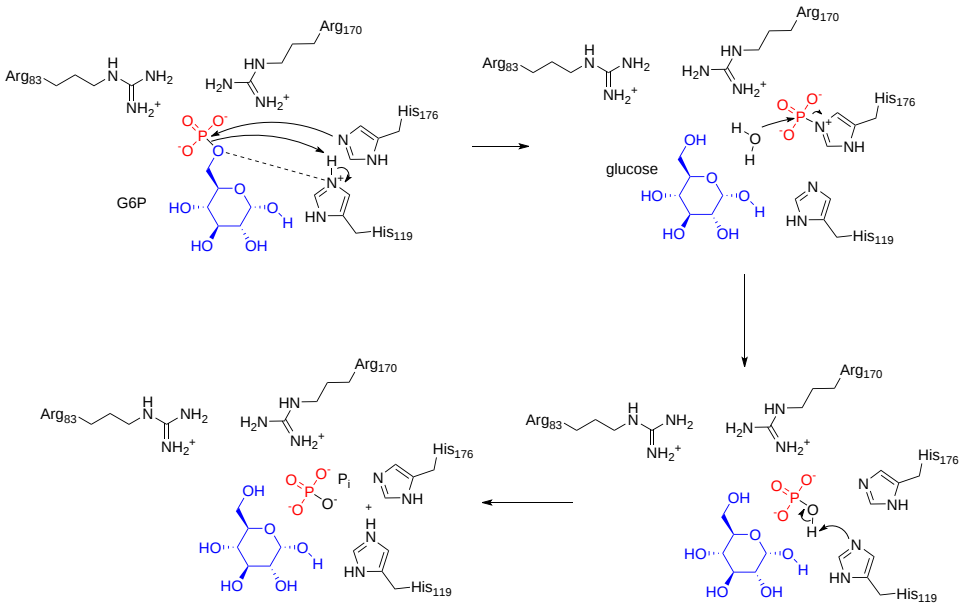
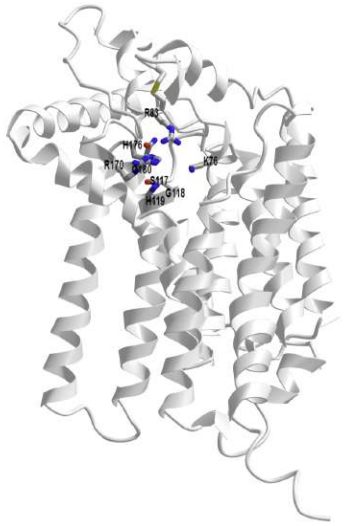


Figure 13.3.21: Abbreviate mechanism for human glucose-6-phosphatase

Figure **13.3.21** shows an interactive iCn3D model of the AlphaFold predicted structure of human glucose-6-phosphatase (P35575). The enzyme contains nine transmembrane helices that dock the protein in the inner membrane of the ER. The active site faces the ER lumen.



NCBI iCn3D Figure **13.3.14**: AlphaFold predicted structure of human glucose-6-phosphatase (**P35575)**(Copyright; author via source). Click the image for a popup or use this external link: https://structure.ncbi.nlm.nih.gov/i...jmcQAo49eZ8p16

13.3.4: SUMMARY:

This chapter provides an in-depth exploration of gluconeogenesis, a crucial metabolic pathway responsible for generating glucose from non-carbohydrate substrates—such as lactate, glycerol, and glucogenic amino acids—to maintain blood glucose levels, especially during fasting, starvation, or prolonged exercise. Gluconeogenesis, which occurs predominantly in the liver (with minor contributions from the renal cortex), complements glycogenolysis as a mechanism for preventing hypoglycemia.

Key topics covered include:

- **Metabolic Importance and Energy Considerations:**
  The chapter emphasizes that gluconeogenesis is a highly endergonic process requiring significant energy input—for instance, converting phosphoenolpyruvate to glucose-6-phosphate consumes six ATP molecules. This energy investment is critical for driving the formation of glucose, especially when carbohydrate availability is low.
- **Substrate Utilization and Integration:**
  Multiple non-carbohydrate substrates feed into the gluconeogenic pathway. Lactate produced in peripheral tissues during anaerobic glycolysis is recycled back to pyruvate via the Cori cycle. Additionally, intermediates from the citric acid cycle and amino acid metabolism can be converted into oxaloacetate, while glycerol from triacylglycerol breakdown can also serve as a substrate.
- **Mitochondrial and Cytosolic Reactions:**
  The pathway bridges reactions occurring in both the mitochondria and the cytosol. The conversion of pyruvate to phosphoenolpyruvate (PEP) is a two-step process: first, pyruvate carboxylase converts pyruvate into oxaloacetate in the mitochondrial matrix—an enzyme that requires biotin as a cofactor—and then, PEP carboxykinase (PEPCK) converts oxaloacetate to PEP, a reaction that may take place in the cytosol. Due to the impermeability of the mitochondrial inner membrane to oxaloacetate, intermediates such as malate or aspartate are used to transport carbon skeletons between these compartments via the malate-aspartate shuttle.
- **Enzyme Mechanisms and Cofactor Roles:**
  Detailed mechanisms are discussed for key gluconeogenic enzymes, such as pyruvate carboxylase and PEPCK. Pyruvate carboxylase utilizes ATP and bicarbonate to carboxylate pyruvate into oxaloacetate, with biotin acting as an essential carrier of the activated CO_2. The structural dynamics of this multifunctional enzyme—including its tetrameric organization and the flexible movement of its biotin-carboxyl carrier protein domain—are highlighted to explain its catalytic efficiency.
- **Phosphatase Steps and Final Glucose Production:**
  The final steps of gluconeogenesis involve unique phosphatase enzymes that reverse the irreversible steps of glycolysis. Fructose-1,6-bisphosphatase dephosphorylates fructose-1,6-bisphosphate to fructose-6-phosphate, and glucose-6-phosphatase, a transmembrane protein located in the endoplasmic reticulum, converts glucose-6-phosphate to free glucose. These dephosphorylation reactions are pivotal for releasing glucose into the bloodstream.
- **Physiological and Therapeutic Implications:**
  The chapter concludes by connecting the biochemical details of gluconeogenesis to its broader physiological significance in blood glucose homeostasis and energy balance. It also touches on the clinical relevance, noting that gluconeogenesis is a target for type II diabetes therapies, such as metformin, which work by inhibiting excessive glucose production.

Overall, this chapter integrates enzyme mechanisms, cellular compartmentalization, and regulatory strategies to illustrate how gluconeogenesis is finely tuned to meet the body's energy demands and maintain metabolic homeostasis during periods of carbohydrate scarcity.

13.3.5: REFERENCES

Principles of Biochemistry/Gluconeogenesis and Glycogenesis. (2019, February 8). *Wikibooks, The Free Textbook Project*. Retrieved 22:01, August 11, 2022, from https://en.wikibooks.org/w/index.php?title=Principles_of_Biochemistry/Gluconeogenesis_and_Glycogenesis&oldid=3515124.

This page titled 13.3: Gluconeogenesis is shared under a CC BY-SA 4.0 license and was authored, remixed, and/or curated by Henry Jakubowski and Patricia Flatt.

- **Current page** by Henry Jakubowski and Patricia Flatt is licensed CC BY-SA 4.0.
- **11.2: Diffusion Across a Membrane - Passive and Facilitated Diffusion** by Henry Jakubowski and Patricia Flatt has no license indicated.

13.4: PENTOSE PHOSPHATE PATHWAY OF GLUCOSE OXIDATION

LEARNING GOALS (CHATGPT O3-MINI)

1. **Define the Pentose Phosphate Pathway (PPP) and Its Role in Metabolism:**
   - Explain the overall purpose of the PPP as a branch of glucose metabolism that does not generate ATP but instead produces NADPH and ribose 5-phosphate (R5P).
   - Discuss the significance of NADPH in biosynthetic reactions, antioxidant defense, and cellular redox balance, and R5P in nucleotide and nucleic acid synthesis.
2. **Differentiate the Oxidative and Non-Oxidative Branches:**
   - Outline the steps of the oxidative branch, including the reactions catalyzed by glucose-6-phosphate dehydrogenase (G6PD), 6-phosphogluconolactonase (6PGL), and 6-phosphogluconate dehydrogenase (6PGD), emphasizing the irreversible production of NADPH and ribulose-5-phosphate.
   - Describe the non-oxidative branch, detailing how enzymes such as ribose 5-phosphate isomerase (RPI), ribulose 5-phosphate epimerase (RPE), transketolase (TKT), and transaldolase (TALDO) catalyze reversible reactions that interconvert sugar phosphates to supply glycolytic intermediates.
3. **Analyze Enzyme Mechanisms and Cofactor Roles:**
   - Explain the catalytic mechanism of key PPP enzymes (e.g., the role of $NADP^+$ in G6PD and the formation of enediol intermediates in transketolase and transaldolase reactions).
   - Discuss the structural features of these enzymes, including cofactor binding sites, and how these features contribute to their catalytic functions.
4. **Understand the Integration of PPP with Glycolysis and Other Pathways:**
   - Illustrate how the non-oxidative branch links the PPP to glycolysis and gluconeogenesis by providing fructose 6-phosphate (F6P) and glyceraldehyde 3-phosphate (G3P).
   - Explain how metabolic intermediates from the PPP can be redirected based on cellular energy and biosynthetic demands.
5. **Examine Regulation of the PPP:**
   - Describe how the ratio of $NADP^+$ to NADPH regulates the flux through the oxidative branch, with high $NADP^+$ levels stimulating G6PD activity.
   - Discuss how the cellular demand for ribose 5-phosphate versus NADPH influences the reversible reactions of the non-oxidative branch, and how this allows cells to adapt to varying metabolic needs.
6. **Discuss Tissue-Specific PPP Activity and Physiological Relevance:**
   - Compare PPP activity in different tissues (e.g., high in adipose tissue for lipid biosynthesis and low in skeletal muscle, which relies more on glycolysis for energy production).
   - Relate the importance of PPP-derived NADPH in protecting cells against oxidative stress, particularly in red blood cells that lack mitochondria.
7. **Identify Clinical and Therapeutic Implications:**
   - Explain how mutations or deficiencies in PPP enzymes (e.g., G6PD deficiency) affect redox balance and can lead to conditions like hemolytic anemia.
   - Discuss how targeting PPP enzymes might provide therapeutic avenues for diseases involving oxidative stress or cancer.

By achieving these goals, students will gain a comprehensive understanding of the pentose phosphate pathway's structure, function, regulation, and its integration with broader metabolic networks essential for cell survival and proliferation.

13.4.1: INTRODUCTION

The pentose phosphate pathway (PPP), or the pentose phosphate shunt, is an important part of glucose metabolism. The PPP branches after the first step of glycolysis and consumes the intermediate glucose 6-phosphate (G6P) to generate fructose 6-phosphate (F6P) and glyceraldehyde 3-phosphate (G3P) through the oxidative and non-oxidative branches of the PPP. Unlike glycolysis and glucose aerobic oxidation, the PPP does not provide adenosine 5′-triphosphate (ATP) to meet cells' energy demands. Instead, it supplies NADPH and ribose 5-phosphate (R5P). These two metabolites are vital for the survival and proliferation of cells. R5P is a building block for nucleic acid synthesis. NADPH offers the reducing power required to synthesize fatty acids, sterols, nucleotides, and non-essential amino acids.

Moreover, the NADPH-derived conversion of oxidized glutathione (GSSG) to reduced glutathione (GSH) *via* glutathione reductase is important for cellular antioxidant defenses. Interestingly, NADPH also serves as the substrate of NADPH oxidases (NOXs), which produce reactive oxygen species (ROS).

Both the oxidative branch and non-oxidative branch of the PPP take place in the cytosol (Figure **13.4.1**). Glucose 6-phosphate dehydrogenase (G6PD) is the rate-limiting enzyme of the oxidative PPP, determining the flux of G6P directed into the pathway. G6PD catalyzes the conversion of G6P to 6-phosphogluconolactone, accompanied by NADPH production. 6-phosphogluconolactonase (6PGL) is the enzyme that hydrolyzes 6-phosphogluconolactone to produce 6-phosphogluconate (6PG). 6-phosphogluconate dehydrogenase (6PGD) converts 6-PG to ribulose 5-phosphate (Ru5P) and generates NAPDH (Figure **13.4.1**). The largest contributor to cytosolic NADPH is the oxidative PPP in mammalian cells.

The non-oxidative branch consists of a series of reversible transfer reactions of chemical groups. Ribose 5-phosphate isomerase (RPI) and ribulose 5-phosphate epimerase (RPE) catalyze reversible reactions converting Ru5P to R5P and xylulose 5-phosphate (Xu5P), respectively. TKT catalyzes two reversible reactions. One is the conversion of Xu5P and R5P to G3P and sedoheptulose 7-phosphate (S7P). The other is the conversion of Xu5P and erythrose 4-phosphate (E4P) to G3P and F6P. Therefore, TKT can bi-directionally regulate the carbon flux between the non-oxidative PPP and glycolysis or gluconeogenesis. Transaldolase (TALDO) reversibly converts G3P and S7P to E4P and F6P. The non-oxidative branch not only replenishes metabolites of the oxidative branch (by their reversal), but also regulates the flux of glycolysis or gluconeogenesis by providing F6P and G3P (Figure **13.4.1**).

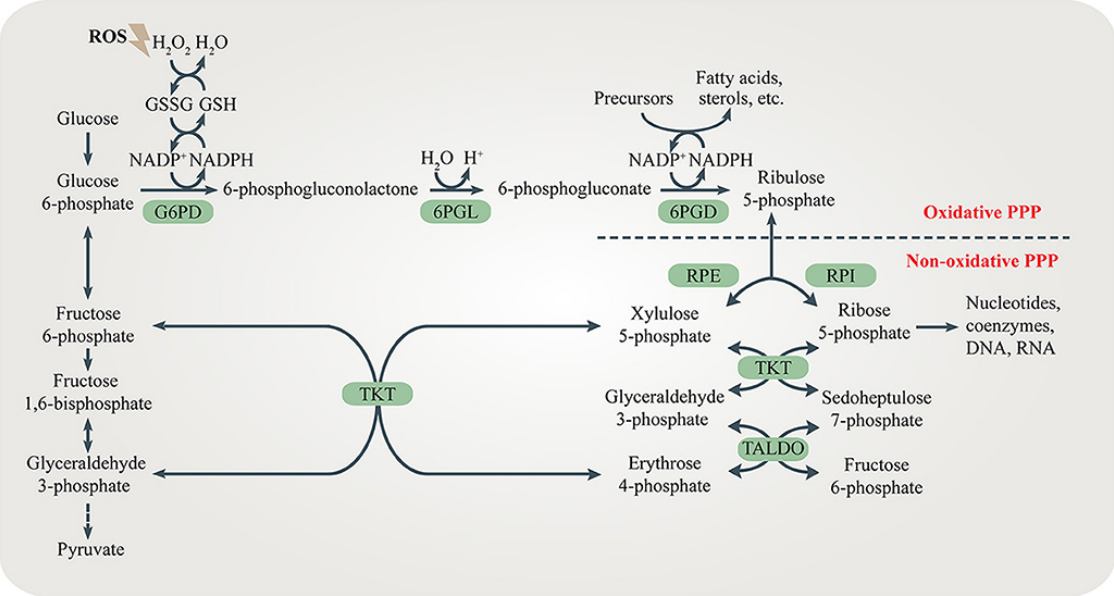


Figure 13.4.1: The pentose phosphate pathway (PPP). The PPP branches after the first step of glycolysis and goes back to fructose 6-phosphate and glyceraldehyde 3-phosphate in the glycolytic and gluconeogenic pathway. The PPP produces R5P and NADPH for biosynthesis and redox regulation. Enzymes in the oxidative and non-oxidative PPP are shaded in green. Figure from: Ge, T., et al. (2020) Cellular Endocrinology DOI:10.3389

13.4.2: OXIDATIVE BRANCH

The oxidative branch of PPP (ox-PPP) is a non-reversible metabolic pathway where glucose-6-phosphate (G6P) is transformed into 6-phosphoglucono-δ-lactone by glucose-6-phosphate dehydrogenase (G6PD) and, subsequently, to ribulose-5-phosphate by 6-phosphogluconate dehydrogenase (6PGD) with the concomitant production of nicotinamide adenine dinucleotide phosphate (NADPH). The resulting ribulose-5-phosphate is then converted to ribose-5-phosphate and used for the biosynthesis of nucleotides (Figure**13.4.2**).

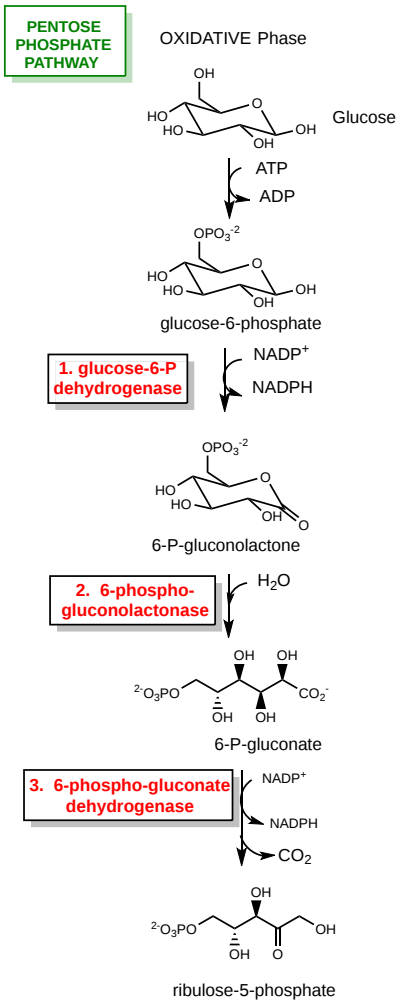


Figure 13.4.2: Summary of the oxidative branch of phosphopentose pathway

The first enzyme in the oxidative branch is the glucose-6-phosphate dehydrogenase enzyme. It is also the first committed enzyme in the pathway and is involved in the regulation. PPP metabolizes 5 to 30% of glucose depending on the tissue type. The enzymatic reaction is:

1. Glucose-6-phosphate dehydrogenase: Glc6P + $NADP^+$ → 6-phosphogluconolactone + NADPH

The oxidative branch produces NADPH for reductive biosynthesis, and it also maintains the reducing condition of the cell to protect it against oxidative stress, which is especially important in erythrocytes (Figure**13.4.3**). It also starts the pathway to produce 5-carbon sugars for nucleotide biosynthesis.

G6PDH AND ROS

G6PDH is very important for protection against free radicals in red blood cells since they don't have mitochondria that could provide another source of NADPH for protection. NADPH is involved in protection against ROS through the three cycles shown in Figure **13.4.3**.

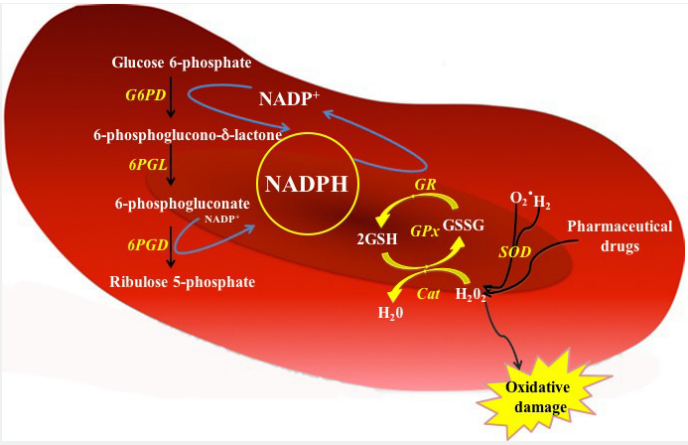


Figure 13.4.3: Function of G6PD enzyme in the PPP from red blood cells. In G6PD-normal red cells, the NADPH is produced by the action of glucose 6-phosphate dehydrogenase (G6PD) and 6-phosphogluconate dehydrogenase (6PGD) enzymes. The NADPH serves as a proton donor to regenerate the GSSG. Cat = Catalase; GPx = Glutathione peroxidase; GR = Glutathione reductase; G6PD = glucose 6-phosphate dehydrogenase; 6PGL = 6-phosphogluconolactonase; 6GPD = 6-phosphogluconate dehydrogenase; SOD = Superoxide dismutase; GSH = Reduced glutathione; GSSG = Oxidized glutathione; H_2O_2 = Peroxide; O_2^- = Superoxide. Gomez-Manzo et al. Int J Mol Sci. 2016 Dec; 17(12): 2069. doi: 10.3390/ijms17122069. Creative Commons Attribution (CC-BY) license (http://creativecommons.org/licenses/by/4.0/).

NADPH can keep glutathione in its reduced form, which, as a substrate for catalase, can help rid the cell of hydrogen peroxide and indirectly other ROS.

The enzyme is active as a dimer or tetramer. Each monomer in the complex has a substrate binding site that binds to G6P and a catalytic coenzyme binding site that binds to $NADP^+$/NADPH. For some higher organisms, such as humans, G6PD contains an additional $NADP^+$ binding site, called the $NADP^+$ structural site, that does not seem to participate directly in the reaction catalyzed by G6PD. The evolutionary purpose of the $NADP^+$ structural site is unknown; however, it does play a role in the overall stability of the enzyme.

Mutations that cause dysfunction or deficiencies are very common, especially in males and in Africa, Asia, the Mediterranean, and the Middle East, in a geographic distribution that parallels the incidence of malaria. Interestingly, many of the mutations occur near the $NADP^+$ structural site. Glucose-6-phosphate dehydrogenase deficiency is very common worldwide and causes acute hemolytic anemia in the presence of simple infection, ingestion of fava beans, or reaction with certain medicines.

An abbreviated mechanism for glucose-6-phosphate dehydrogenase from *Leuconostoc mesenteroides* is shown in Figure 13.4.4.

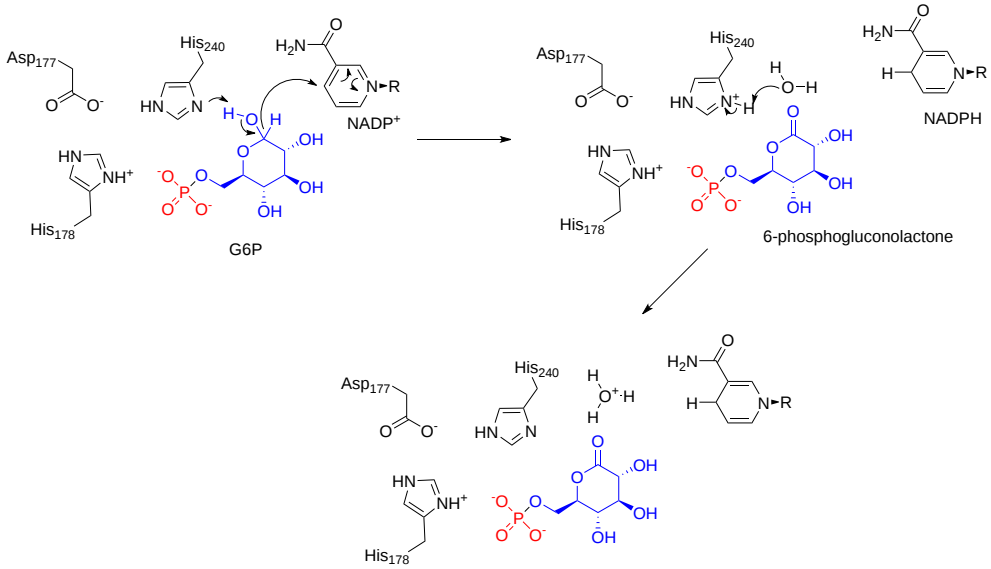


Figure 13.4.4: Mechanism of *Leuconostoc mesenteroides* glucose-6-phosphate dehydrogenase. Ribeiro AJM *et al.* (2017), *Nucleic Acids Res*, **46**, D618-D623. Mechanism and Catalytic Site Atlas (M-CSA): a database of enzyme reaction mechanisms and active sites.

DOI:10.1093/nar/gkx1012. PMID:29106569 https://www.ebi.ac.uk/thornton-srv/m-csa/entry/843/. Creative Commons Attribution 4.0 International (CC BY 4.0) License.

Figure **13.4.5** shows an interactive iCn3D model of the glucose 6-phosphate dehydrogenase from Leuconostoc mesenteroides (1DPG).

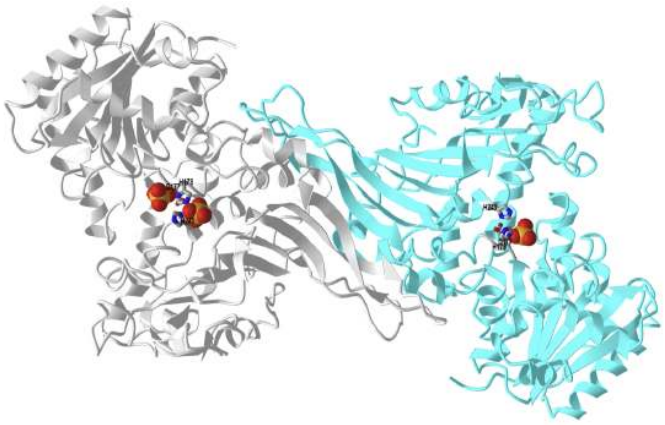


Figure 13.4.5: Glucose 6-phosphate dehydrogenase from Leuconostoc mesenteroides (1DPG). (Copyright; author via source). Click the image for a popup or use this external link: https://structure.ncbi.nlm.nih.gov/i...m8NCXiBuQbTQb7

Interestingly, this bacterium has an incomplete glycolytic pathway and can use this enzyme with either $NADP^+$ for anabolism or NAD^+ for catabolism.

Each monomer can bind two $NADP^+$, one at a site that promotes structure integrity and stability and the other at the catalytic site where $NADP^+$ serves as a substrate (or cofactor). The other substrate, glucose-6-phosphate, binds between the two.

Figure **13.4.6** shows an interactive iCn3D model of the human glucose 6-phosphate dehydrogenase with bound structural and substrate $NADP^+$ (2BH9).

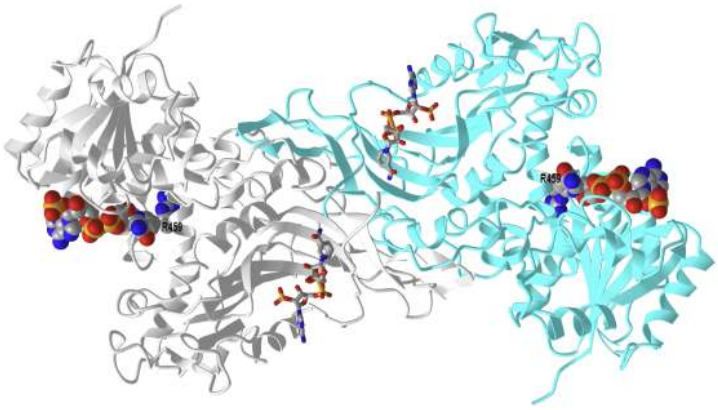


Figure 13.4.6: Human glucose 6-phosphate dehydrogenase with bound structural and substrate NADP (2BH9). (Copyright; author via source). Click the image for a popup or use this external link: https://structure.ncbi.nlm.nih.gov/icn3d/share.html?NFJnS7UtUt3Uwu2D7

The biological unit shown is a dimer. The structural $NADP^+$ is shown in spacefill bound in the N-terminal end of each monomer, while the substrate (cofactor) $NADP^+$ is shown in sticks. Arg 459 is shown in spacefill.

A common disease-causing mutation of G6PDH is the Canton R459L mutation. It's common in China and Southeast Asia. The enzyme's activity is significantly decreased, and the enzyme is less able to form tetramers. It unfolds at a lower temperature. This suggests that the mutation causes a significant conformation change. The Arg459 is shown in the above model. Its contribution to interhelical noncovalent attractions between it and D181 and N185. D181 is shown in proximity to Arg459 in the above model.

Figure **13.4.7**s shows a static image of glucose 6-phosphate dehydrogenase with bound structural and substrate $NADP^+$ as well as glucose-6-phosphate.

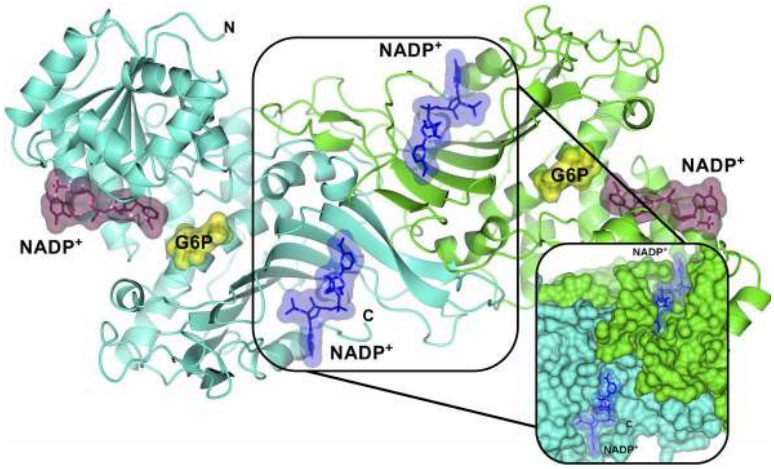


Figure 13.4.7: Glucose 6-phosphate dehydrogenase with bound structural and substrate $NADP^+$ as well as glucose-6-phosphate (2BHL and 2BH9). Structural $NADP^+$ (**blue** molecular surface), catalytic $NADP^+$ (dark **purple** molecular surface), and G6P substrate (**yellow** molecular surface) in the dimer are shown. The two monomers are shown in **cyan** and **green**. Right inset, close-up of the dimer interface and both structural $NADP^+$ molecules. Gomez-Manzo et al., ibid.

The second reaction of the oxidative branch is mediated by the phosphogluconolactonase (6PGL, PGLS) enzyme. The overall reaction is shown here:

2. 6-phosphogluconolactamase: 6-phosphogluconolactone + H_2O → 6-phosphogluconate

6PGL is a cytosolic enzyme found in all organisms that catalyzes the hydrolysis of 6-phosphogluconolactone to 6-phosphogluconic acid in the oxidative phase of the pentose phosphate pathway. 6PGL hydrolysis of 6-phosphogluconolactone to 6-phosphogluconic acid has been proposed to proceed via proton transfer to the O5 ring oxygen atom (Figure **13.4.8**). The reaction is initiated via the attack of a hydroxide ion at the C5 ester. A tetrahedral intermediate forms, and the elimination of the ester linkage follows, aided by the donation of a proton from an active site histidine residue.

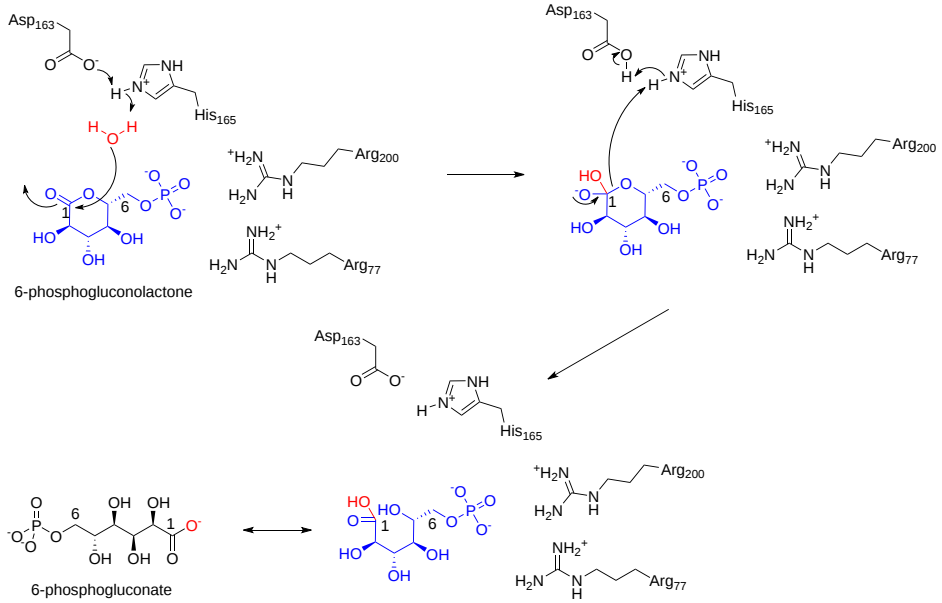


Figure 13.4.8: Mechanism for 6-phosphogluconolactamase. His 165 and Asp 163 appear involved in a proton relay scheme. His 163 is conserved in lactonase. Arg 77 and 200 are involved in binding the substrate.

Figure **13.4.9** shows an interactive iCn3D model of the 6-phosphogluconolactonase from Trypanosoma brucei complexed with 6-phosphogluconic acid (3E7F). This enzyme is a target for developing drug treatment strategies for African sleeping sickness.

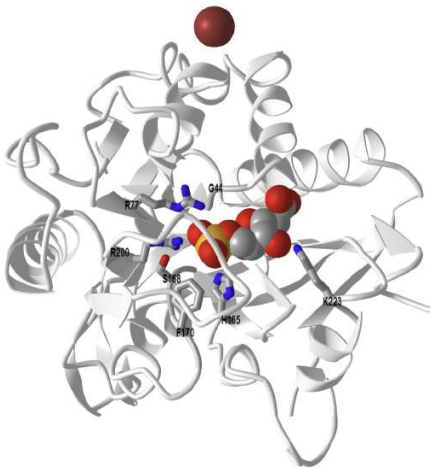
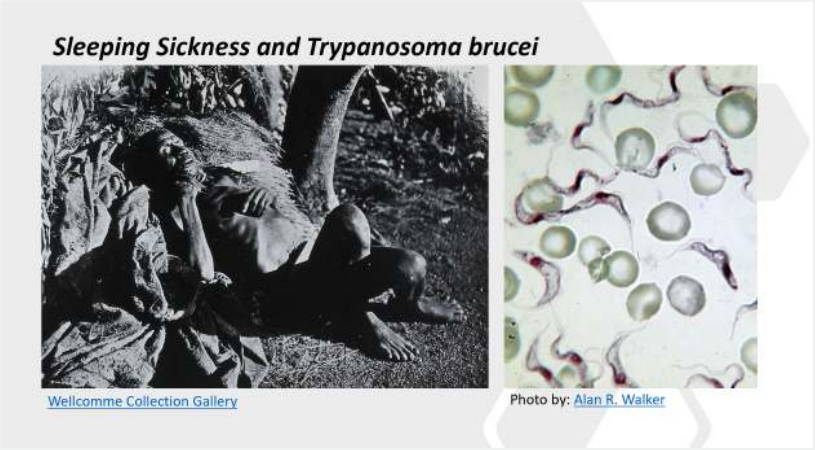


Figure 13.4.9: 6-phosphogluconolactonase from Trypanosoma brucei complexed with 6-phosphogluconic acid (3E7F). The key residues involved in binding and the charge-relay system are shown in sticks and labeled. The product, 6-phosphogluconic acid, is shown in spacefill. The single sphere is a Zn^{2+}, which does not appear to be involved in catalysis. (Copyright; author via source). Click the image for a popup or use this external link: https://structure.ncbi.nlm.nih.gov/icn3d/share.html?jRgi1nfrSGGgTYWo8

GLYOXOSOMES AND GLYCOSOMES



Trypanosomiasis is a disease usually referred to as African human trypanosomiasis or African sleeping sickness. This infectious disease is caused by the parasites *Trypanosoma brucei gambiense or Trypanosoma brucei rhodesiense*, which the tsetse fly transmits.

The vector tsetse fly, *Glossina*, carries the trypanosome within the midgut after a blood meal. These protozoa then migrate to the salivary glands of the fly, which can be transmitted during the next feeding. After inoculation within the host, the parasite can live freely within the bloodstream and evade mammalian host defenses through variable surface glycoproteins (VSG). The clinical disease has two stages. These are characterized by an early/first hemolymphatic stage and a late /second meningoencephalitis stage with an invasion of the central nervous system (CNS). In stage 1, systemic symptoms develop, including intermittent fever, headache, pruritus, and lymphadenopathy. Undulating fevers reflect parasites multiplying within the blood. Less frequent hepatosplenomegaly may occur in the early stage. In the late/second stage, CNS symptoms manifest as sleep disturbances or neuropsychiatric disorders. A sleep disorder is the most common symptom of the second stage, and it is from this that the term “African sleeping sickness” was ascribed.

13.4.3: NEW DRUG TARGETS:

Enzymes involved in the pentose phosphate pathway provide a new set of drug targets to help combat parasitic infections such as those caused by trypanosomes. In this context, new therapeutics have focused on the disruption of glycosomes within these organisms. Glyoxosomes are specialized peroxisomes found in plants and some fungi. They all have enzymes for the glyoxylate shunt and can

hence create some glucogenic intermediates. In trypanosomes and Leishmania, another internal organelle called the glycosome is found. This houses most of the glycolytic enzymes and also the oxidative enzymes of the pentose phosphate pathway. This makes the enzymes in the glycosome unique drug targets.

The third enzyme utilized in the oxidative branch of the PPP is 6-phosphogluconate dehydrogenase (6PGDH). The overall reaction is shown here:

3. 6-phosphogluconate dehydrogenase: 6-phosphogluconate + $NADP^+$ ↔ ribulose-5-phosphate + NADPH + CO_2

6PGDH catalyzes a reversible oxidative decarboxylation reaction, as shown in Figure **13.4.10**. Oxidation, followed by decarboxylation, forms an enediol intermediate, followed by conversion to the product. Notably, $NADP^+$ serves as an electron acceptor in the reaction, producing a second molecule of NADPH. Essentially, an active center lysine abstracts a proton from the substrate, 6-phosphogluconate, and NADP+ is reduced, causing the formation of a ketone intermediate. Decarboxylation leads to the formation of the enediol intermediate. The active site lysine abstracts a proton in the second half of the reaction, causing the formation of ribulose 5-phosphate. The abstracted proton is transferred to the active site Glu_{190}, resetting the enzyme for another catalytic cycle.

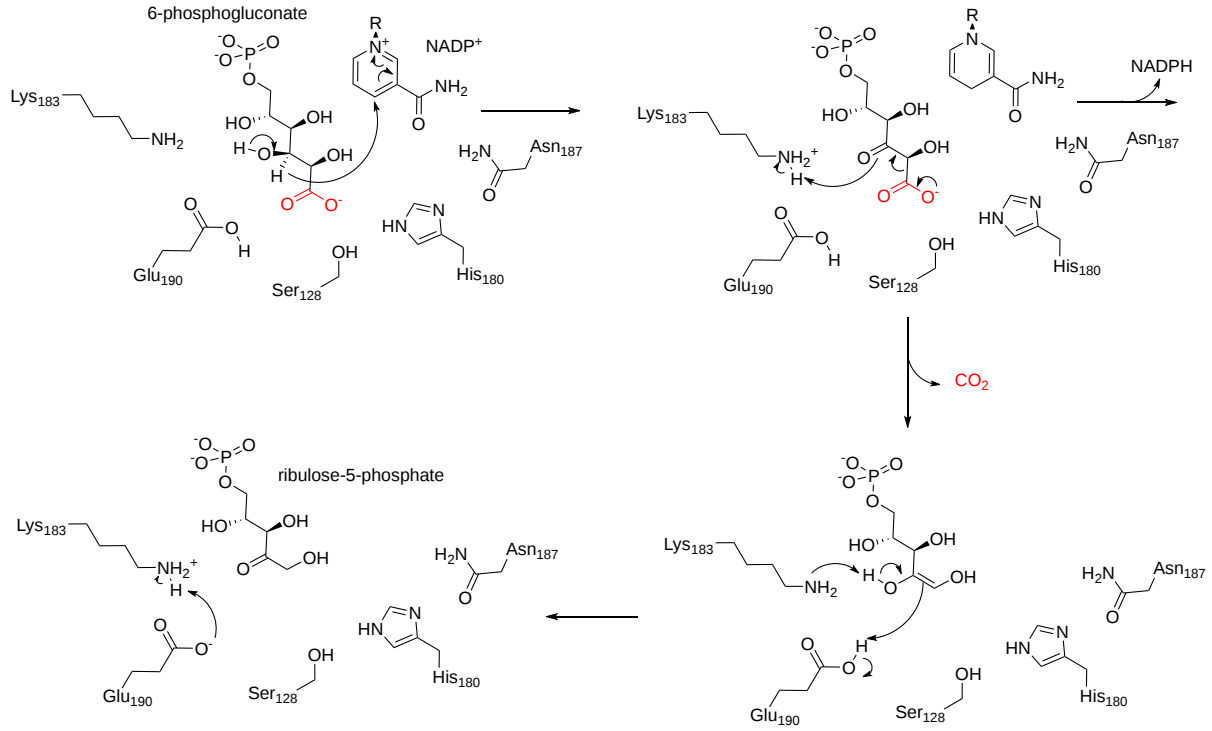
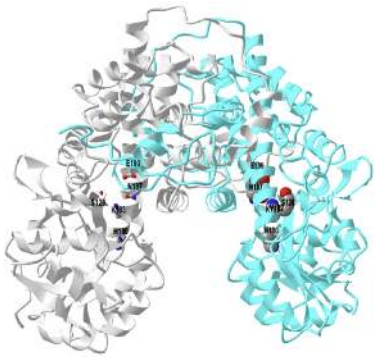


Figure 13.4.10: Mechanism of 6-phosphogluconate dehydrogenase.

Figure **13.4.11** shows an interactive iCn3D model of sheep 6-phosphogluconate dehydrogenase (2PGD).



NCBI iCn3D **Figure 13.4.11: Sheep 6-phosphogluconate dehydrogenase (2PGD).** (Copyright; author via source). Click the image for a popup or use this external link: https://structure.ncbi.nlm.nih.gov/i...DqosWmFg1DqK16

The protein is a homodimer in which the monomers act independently: each contains a large, mainly alpha-helical domain and a smaller beta-alpha-beta domain, containing a mixed parallel and anti-parallel 6-stranded beta-sheet. $NADP^+$ is bound in a cleft in the small domain, and the substrate binds in an adjacent pocket.

13.4.4: NONOXIDATIVE BRANCH

The non-oxidative branch of the pentose phosphate pathway (nonox-PPP) is responsible for forming simple sugars within the cell and maintaining these building blocks in appropriate concentrations. The enzymes utilized in this pathway mediate a set of reversible reactions that lead to the production of ribose-5-phosphate, xylulose-5-phosphate, sedoheptulose 7-phosphate, and erythrose 4-phosphate, as well as intermediates utilized in the glycolytic pathway, including glyceraldehyde-3-phosphate and fructose-6-phosphate Major enzymes utilized include transketolase (TKT) and transaldolase (TALDO), as well as important isomerase and epimerase enzymes.

Ribose 5-phosphate is an important building block for the biosynthesis of nucleotides, and erythrose 4-phosphate is used to synthesize aromatic amino acids. When these simple sugars are in excess, they can also be converted into glycolytic intermediates and utilized for energy production.

The nonoxidative branch of the phosphopentose pathway is shown in Figure **13.4.12**.

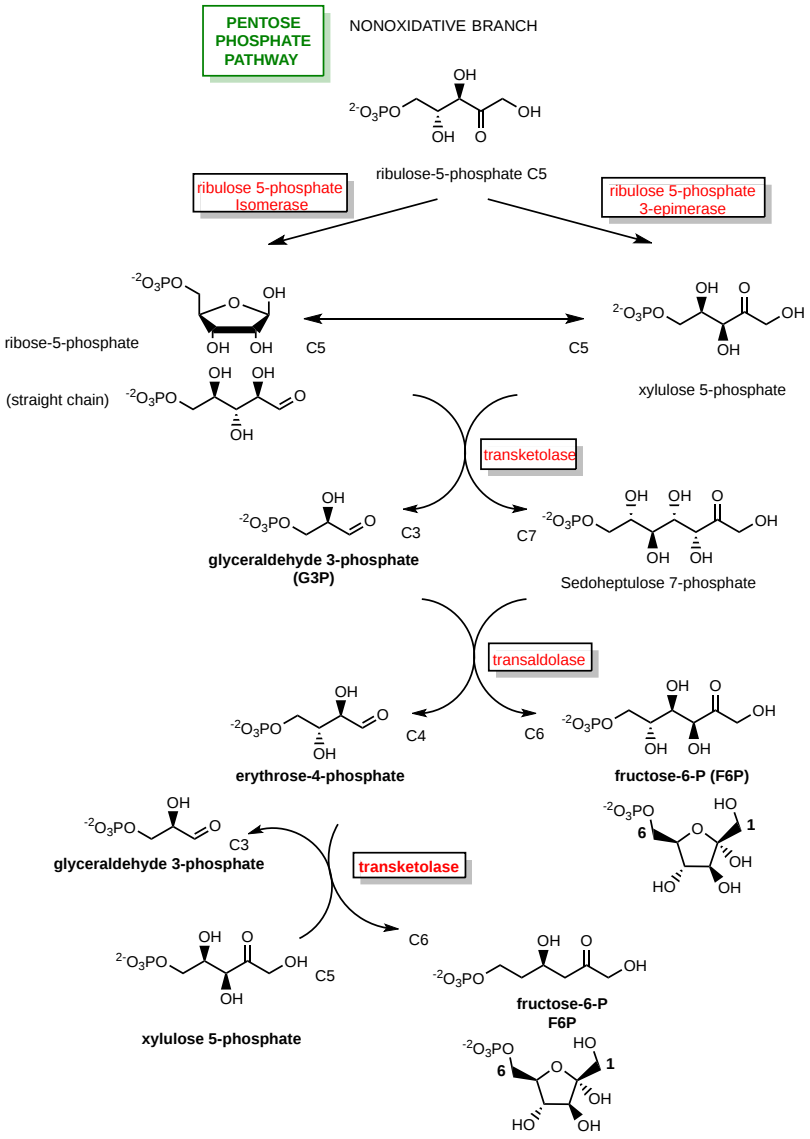


Figure 13.4.12: Nonoxidative branch of the phosphopentose pathway

Now, let's examine the individual enzymes. Ribulose 5-phosphate is the starting place for the non-oxidative portion of the PPP. It can be converted down two different pathways, either to ribose-5-phosphate or to xylulose-5-phosphate. The ribose 5-phosphate isomerase is involved in the ketose-aldose conversion and will be the first enzyme discussed.

Ribose-5-phosphate isomerase (Rpi)

This enzyme is fully reversible and is usually referred to as ribose-5-phosphate isomerase. However, it can also be known as ribulose 5-phosphate isomerase, as it mediates the transition between this aldose-ketose pair. In addition to the PPP, this enzymatic reaction is also required in the Calvin cycle in photosynthesis.

There are two different Rpi enzymes, RpiA and RpiB, with little sequence or structural similarity and distinct mechanisms. RpiA is found in all three kingdoms of life and is highly conserved due to its role in the PPP and the Calvin Cycle of photosynthesis. RpiB, on the other hand, is only found in some bacteria and protozoans. Thus, RpiB is a potential therapeutic target for treating diseases such as African Sleeping Sickness, Chagas disease, and leishmaniasis. While RpiA and RpiB are structurally very different, both enzymes catalyze the isomerization reaction through an enediol intermediate using the linear form of the sugar. The reaction mechanism of RpiB is detailed below.

Figure **13.4.13** shows a mechanism for *Escherichia coli* RpiB.

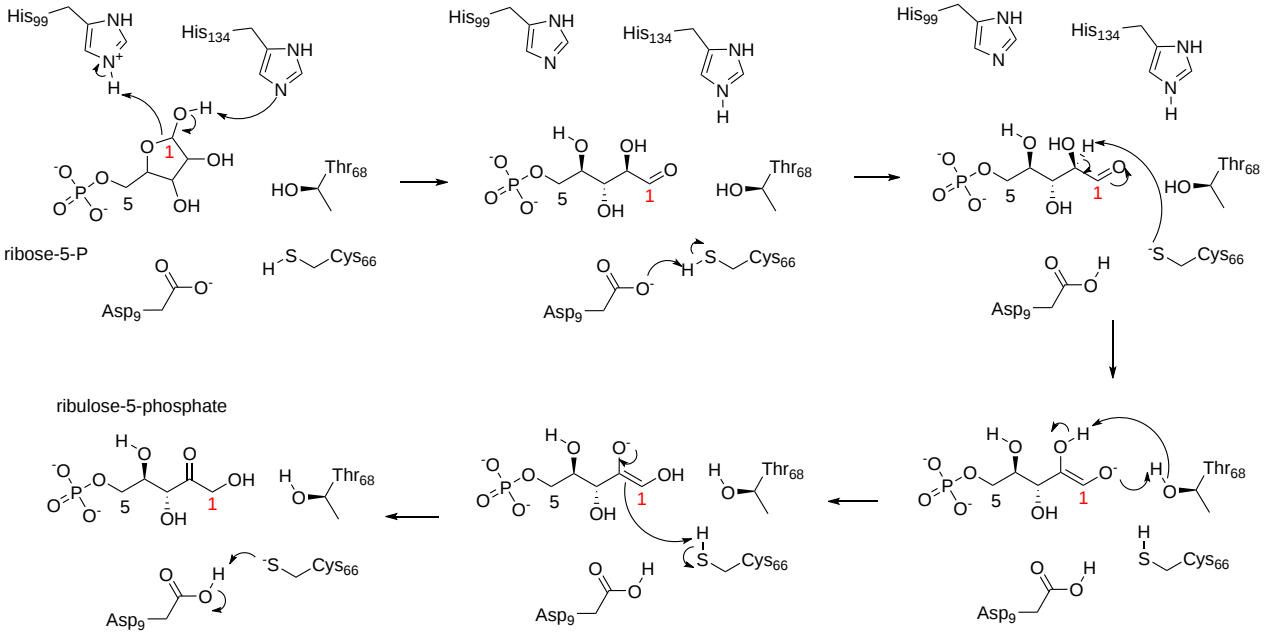
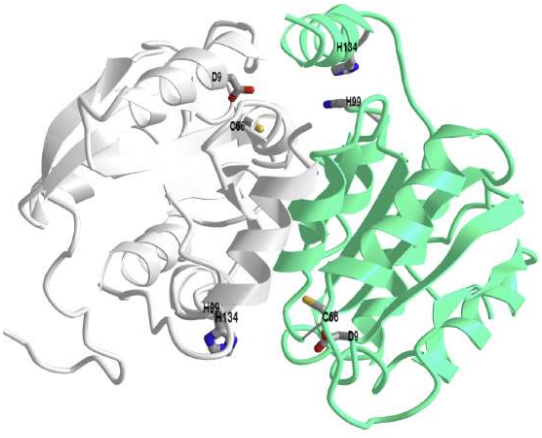


Figure 13.4.13: Mechanism for *Escherichia coli* RpiB. https://www.ebi.ac.uk/thornton-srv/m-csa/entry/680/. Creative Commons Attribution 4.0 International (CC BY 4.0) License.

RpiB is a homodimer that can form a tetramer. The monomer subunits are coordinated in a head-to-tail format, such that there are two active sites per dimer where side chains from each monomer contribute to each active site (Figure **13.4.14**). The reaction mechanism requires two major steps: (1) ring opening of the furanose form of the sugar, and (2) isomerization through an enediol intermediate (Figure **13.4.13**). Figure **13.4.14** shows an interactive iCn3D model of Ribose-5-phosphate isomerase (RPIB_AlsB) from Escherichia coli (1NN4).



NCBI iCn3D **Figure 13.4.14: Ribose-5-phosphate isomerase (RPIB_AlsB) from Escherichia coli (1NN4).**Active site residues are indicated in each of the monomer subunits. (Copyright; author via source). Click the image for a popup or use this external link:

https://structure.ncbi.nlm.nih.gov/i...ByuLUqhhs9B8c9

The other major pathway for ribulose 5-phosphate conversion involves the ribulose 5-phosphate (3) epimerase (RPE) and the conversion to xylulose 5-phosphate.

Ribulose-5-phosphate (3) epimerase (RPE)

This enzyme is also called pentose-5-phosphate 3-epimerase or PPE. Sugar epimerase enzymes alter the stereochemistry of the sugar at one of the alcohol positions, creating a different epimer. The RPE enzyme has a Zn^{2+} cofactor; however, its requirement for enzyme activity is not essential. A Zn^{2+} independent form can still function and stabilize an oxyanion intermediate with adjacent and conserved methionines. A mechanism of the Zn^{2+}-dependent form of the enzyme is shown in Figure **13.4.15**.

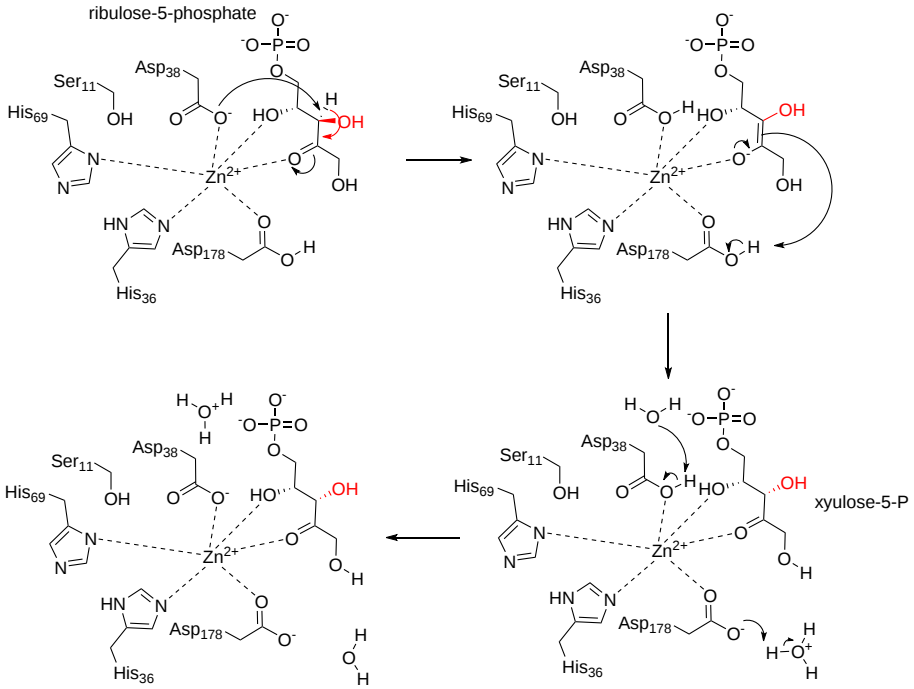


Figure 13.4.15: Mechanism for rice ribulose-5-phosphate epimerase

The enzyme utilizes an acid/base catalytic mechanism that mediates the formation of a trans-2,3-enediol phosphate intermediate. Key aspartic acid residues act as proton donors and acceptors during the reaction. A zinc metal cofactor helps stabilize charges during the reaction.

Figure **13.4.16** shows an interactive iCn3D model of cytosolic D-ribulose-5-phosphate 3-epimerase from rice (1h1z).

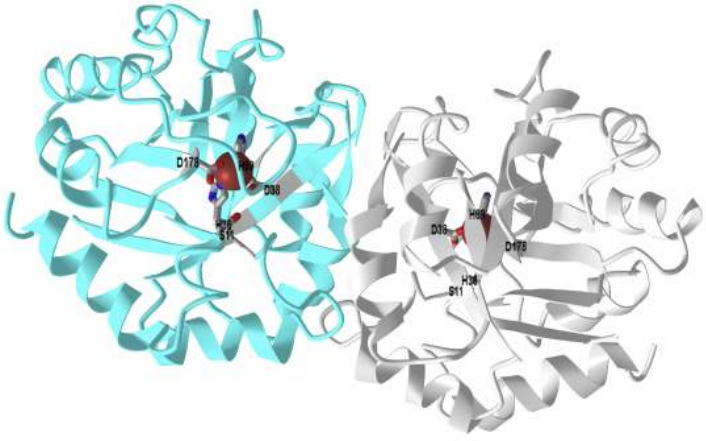


Figure 13.4.16: Cytosolic D-ribulose-5-phosphate 3-epimerase from rice (1h1z). (Copyright; author via source). Click the image for a popup or use this external link: https://structure.ncbi.nlm.nih.gov/i...AH7uS2T8hsnpXA

Transketolase (TK)

The pool of ribose 5-phosphate created can be utilized for nucleotide production, or some of it can react with the xylulose 5-phosphate created in the RPE reaction. The transketolase enzyme converts two five-carbon sugars (ribose 5-phosphate and xylulose 5-phosphate) into a 3-carbon and a 7-carbon sugar (glyceraldehyde 3-phosphate and sedoheptulose 7-phosphate). Transketolase enzymes transfer ketone functional groups from ketoses to aldoses, effectively creating a new ketose that is two-carbon atoms larger. The ketose donor then becomes an aldose with two fewer carbons. The basic transketolase reaction shown in Figure **13.4.17**

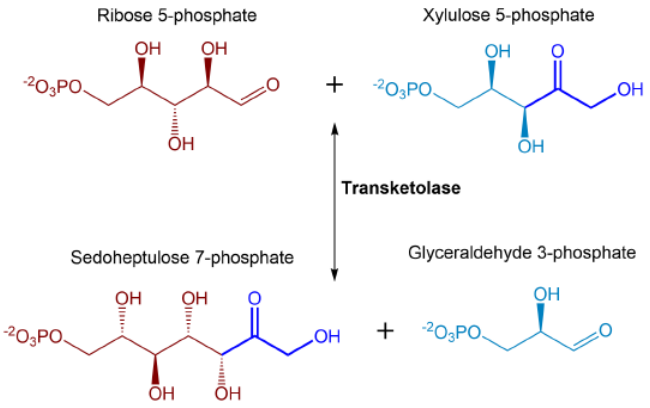


Figure 13.4.17: Transketolase reaction. The reaction shows the reversible conversion of ribose 5-phosphate and xylulose 5-phosphate to sedoheptulose 7-phosphate and glyceraldehyde 3-phosphate.

Note the number of carbons in the reactants and products: 5C + 5C ↔ 3C + 7C. For this reversible reaction, the enzyme uses the cofactor thiamine pyrophosphate (TPP) and a divalent cation. The enzyme transfers a 2C ketol group from xylulose-5-phosphate to ribose-5-phosphate, an aldose. Glyceraldehyde-3-phosphate, the other product, is a glycolytic intermediate that can be used in the glycolytic pathway.

The mechanism for the reverse reaction (yeast numbering system) is shown in Figure **13.4.18**. In this reaction, sedoheptulose 7-phosphate binds with the enzyme, and the TPP cofactor is activated to form a carbanion. The carbanion mediates nucleophilic attack on the carbonyl carbon of the substrate, forming a covalent intermediate. His_{263} serves as a base and abstracts a proton, enabling bond cleavage and the formation of ribose 5-phosphate. Ribose 5-phosphate leaves the active site, and glyceraldehyde 3-phosphate enters. The two-carbon intermediate (covalently bound to the TPP) mediates nucleophilic attack on the glyceraldehyde 3-phosphate, enabling the formation of xylulose 5-phosphate and the restoration of the enzyme.

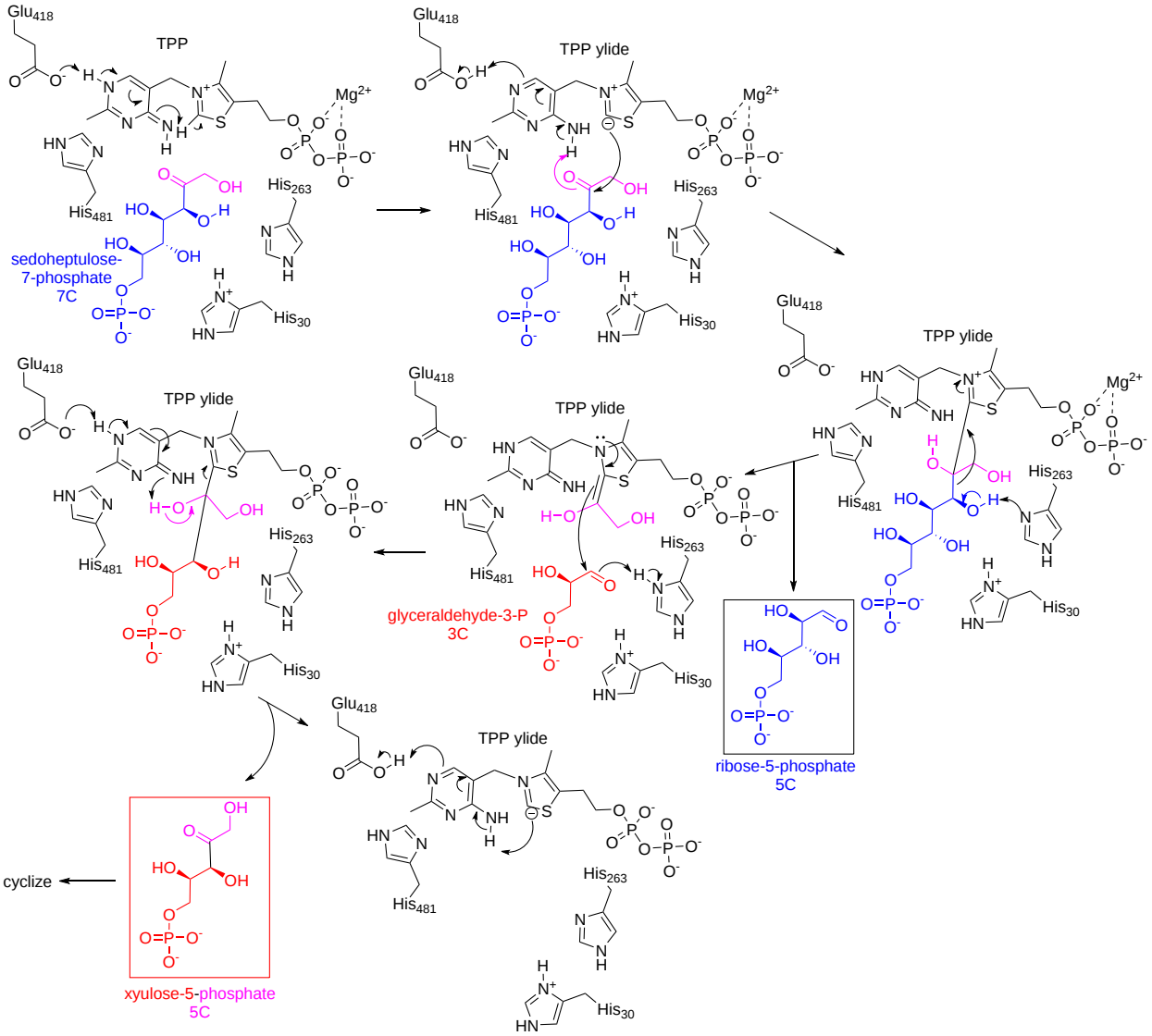


Figure 13.4.18: Mechanism of the transketolase reaction during the pentose phosphate pathway.

https://www.ebi.ac.uk/thornton-srv/m-csa/entry/219/

Figure **13.4.19** shows an interactive iCn3D model of Human transketolase in a covalent complex with donor ketose D-xylulose-5-phosphate (4kxv).

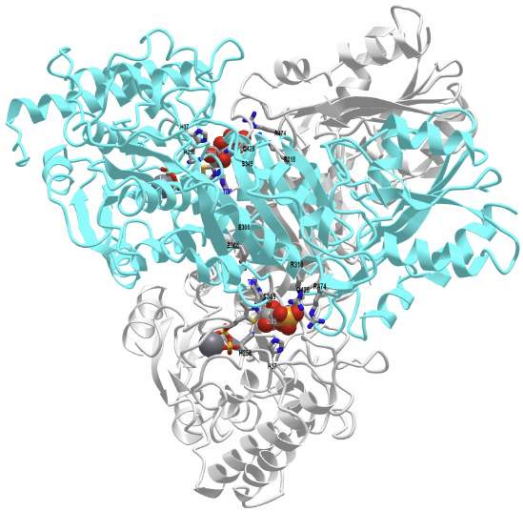


Figure 13.4.19: Human transketolase in covalent complex with donor ketose D-xylulose-5-phosphate (4kxv). (Copyright; author via source). Click the image for a popup or use this external link: https://structure.ncbi.nlm.nih.gov/i...WtGtQ7mKA6UYx7

The enzyme is a dimer (gray and cyan coloring). Numbering of key residues compared to the yeast mechanism:

Human	Yeast
E366	E418
Q428	H481
H258	H262
H38	H30

Also shown are human active site residues H474, R318, and S345. The covalent xylulose-5-phosphate adduct is shown in spacefill and labeled DX5 (xylitol-5-phosphate). TPP is shown in sticks and labeled. The metal ion is Ca^{2+}. Structural analyses show a 20^0 distortion in the planarity of the cofactor-substrate bond and a lengthening of the C-C bond in the substrate, which breaks.

Transaldolase

In addition to being used as a resource in the glycolytic pathway, glyceraldehyde 3-phosphate can also be used as a substrate in a transaldolase reaction along with the sedoheptulose 7-phosphate produced in the previous reaction. This results in the formation of erythrose 4-phosphate and fructose 6-phosphate. A summary of the reaction is shown in Figure **13.4.20**.

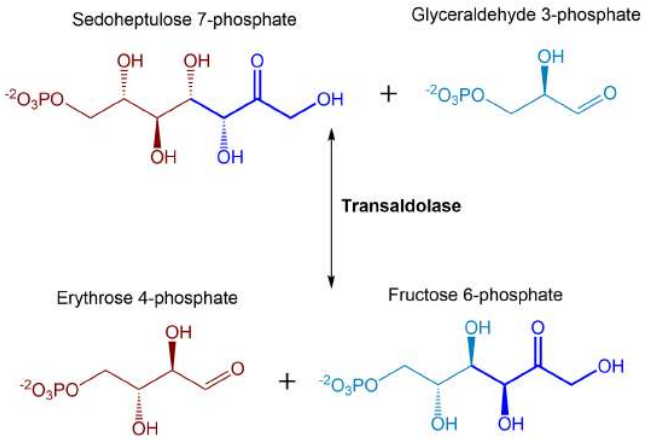


Figure 13.4.20: Summary of transaldolase reaction

As with transketolase, the transaldolase enzyme is reversible. Again, note the number of carbons in the reactants and products: 3C + 7C ↔ 4C + 6C. Unlike the transketolase used in the last reaction, the transaldolase enzyme does NOT use TPP as a cofactor. Instead, it forms a Schiff base intermediate similar to the aldolase enzyme in the glycolytic pathway. The enzyme removes a 3C ketol group

(dihydroxyacetone) from sedoheptulose 7-phosphate and transfers it to glyceraldehyde 3-phosphate, forming fructose 6-phosphate. Erythrose 4-phosphate is left from the original sedoheptulose 7-phosphate.

We will explore the mechanism of the *E. Coli* enzyme in the reverse direction. The first part of the mechanism of transaldolase is shown in Figure **13.4.21**.

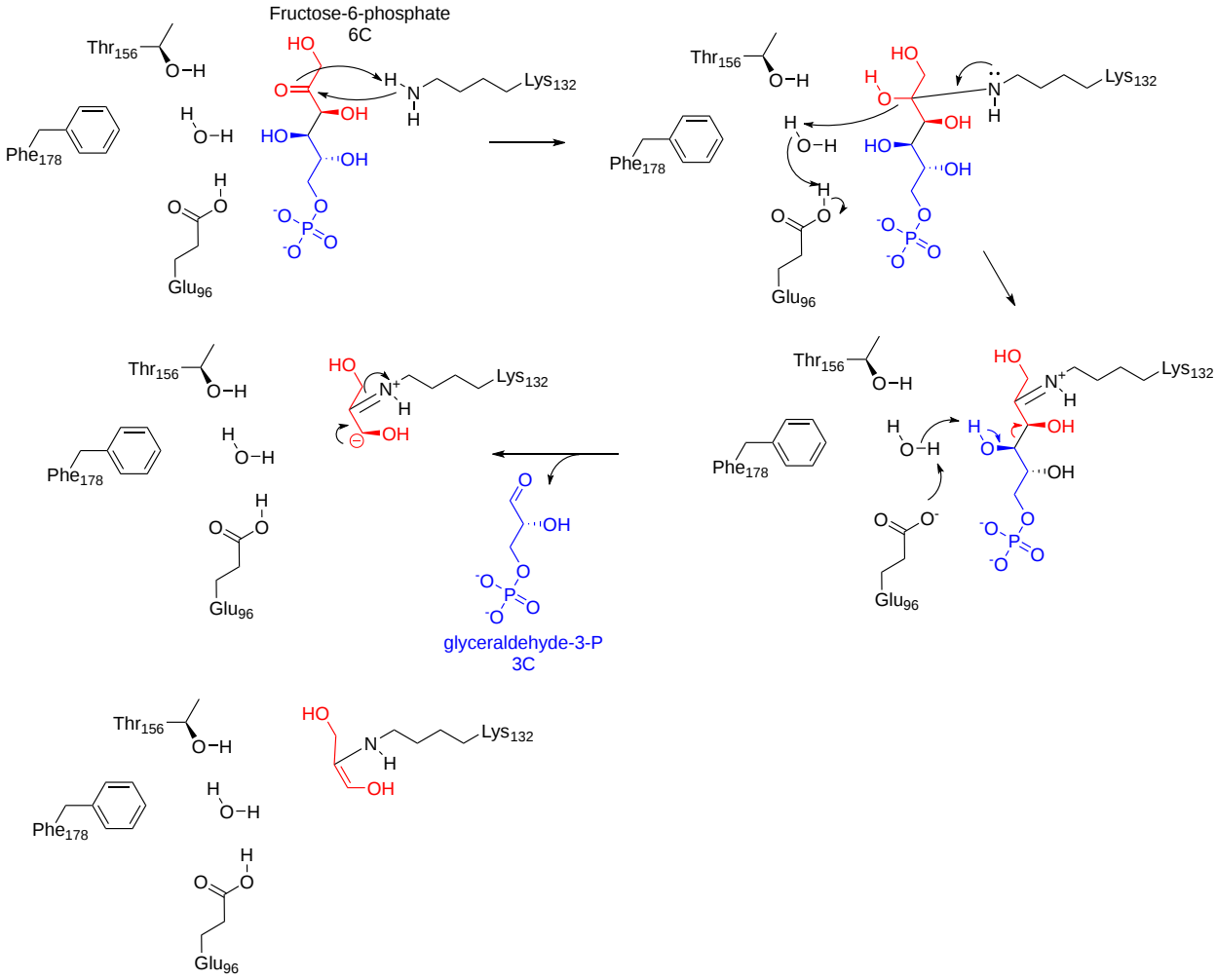


Figure 13.4.21: Mechanism for the first half of the transaldolase reaction. https://www.ebi.ac.uk/thornton-srv/m-csa/entry/148/

In the first part of the reaction, fructose 6-phosphate binds to the enzyme's active site, where an active site lysine residue mediates nucleophilic attack on the carbonyl carbon and forms a covalent intermediate with the enzyme. Formation of the Schiff base leads to dehydration of the intermediate. The Schiff base nitrogen becomes protonated, leading to the oxidation of the C4 hydroxyl group and subsequent bond cleavage, releasing glyceraldehyde 3-phosphate. The remaining ES-complex rearranges to form an enol intermediate.

Figure **13.4.22** shows the mechanism for the second half of the transaldolase reaction.

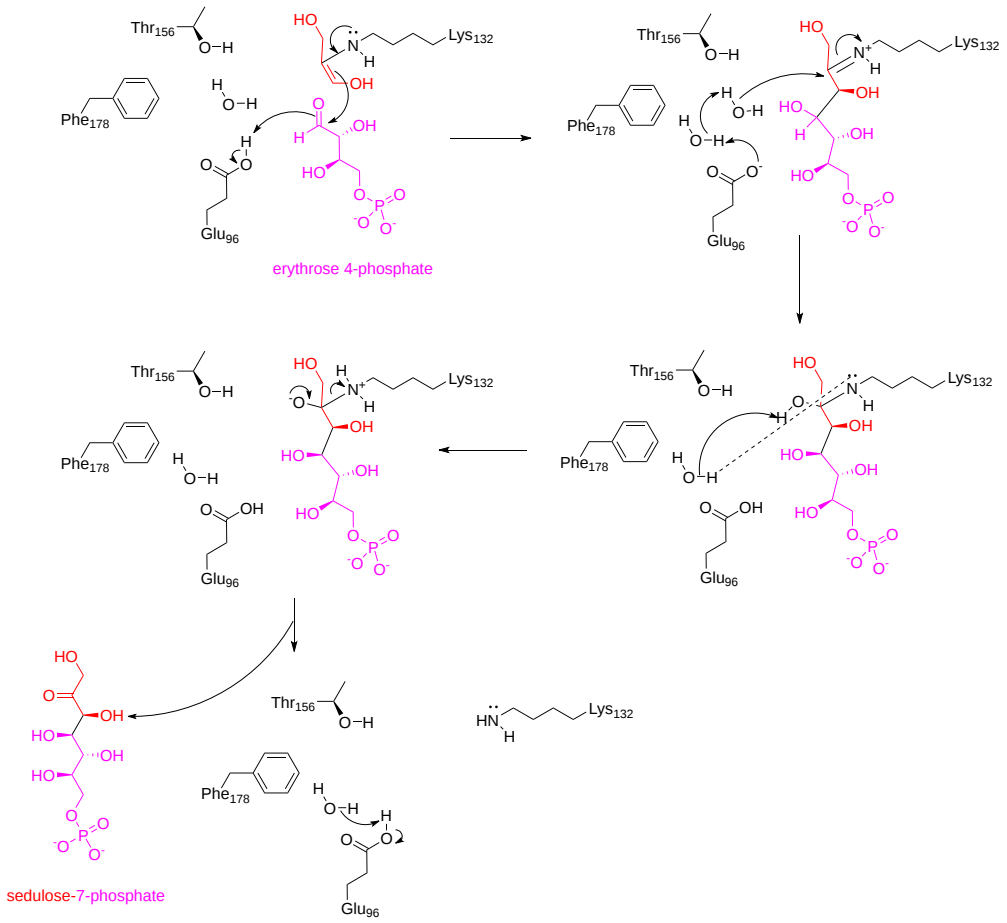


Figure 13.4.22: Mechanism for the second half of the transaldolase reaction. https://www.ebi.ac.uk/thornton-srv/m-csa/entry/148/

Once glyceraldehyde 3-phosphate has left the enzyme's active site, erythrose 4-phosphate can bind. The enol from the ES intermediate mediates nucleophilic attack on the aldehyde carbonyl group of erythrose 4-phosphate. This results in the formation of a Schiff base intermediate. Hydration at the Schiff base carbon atom ensues, followed by the oxidation of the newly incorporated alcohol to form a ketone functional group. The formation of the ketone causes bond cleavage between the enzyme and the newly formed ketose, sedoheptulose 7-phosphate.

Figure 13.4.23 shows an interactive iCn3D model of transaldolase B from Escherichia coli (1ONR).

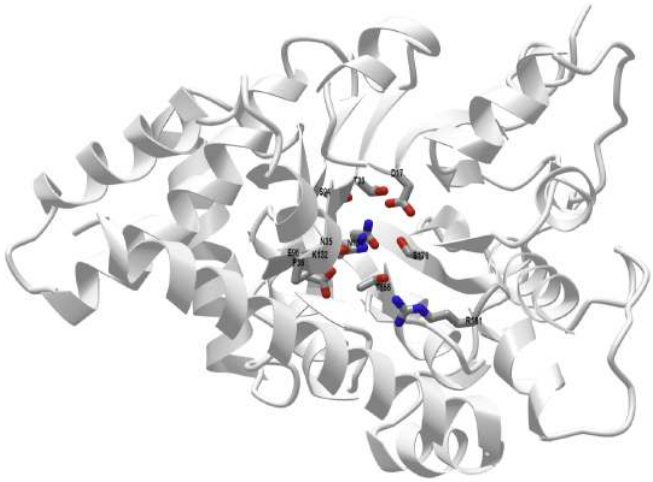


Figure 13.4.23: 3D structure of Transaldolase B from E. coli (1ONR). (Copyright; author via source). Click the image for a popup or use this external link: https://structure.ncbi.nlm.nih.gov/i...7swLZVpNPe3eU9

Transketolase

As seen above, fructose 6-phosphate is a product of the transaldolase enzyme during the nonoxidative branch of the PPP. This sugar can feed back into the glycolytic cycle. The formation of fructose 6-phosphate can also occur using the transketolase enzyme when it transfers a 2C ketol group from xylulose 5-phosphate to the aldose, erythrose 4-phosphate. This reaction is summarized in Figure **13.4.24**.

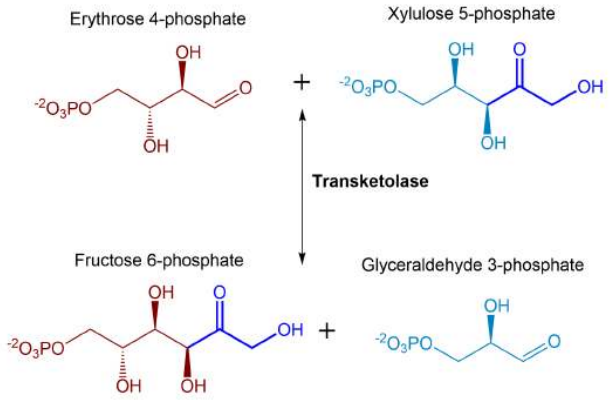


Figure 13.4.24 Summary of the second transketolase reaction during the pentose phosphate pathway.

Both products of this final transketolase reaction can be utilized in energy formation through glycolysis. Thus, there are clear metabolic ties of the PPP with the energy-producing glycolytic pathway, and intermediates from both pathways can easily be exchanged through the activity of these reversible enzymes. The PPP provides key intermediates, including ribose 5-phosphate, which is used in the biosynthesis of nucleotides and, ultimately, nucleic acids, as well as other important metabolic molecules such as FAD, NAD^+, $NADP^+$, and Coenzyme A. In addition to being a biosynthetic source for these molecules, the PPP is also the primary source for reducing $NADP^+$ to NADPH during the oxidative reactions. NADPH is utilized in many biosynthetic processes as an electron donor. For example, the biosynthesis of many lipid molecules requires NADPH, including the production of triacylglycerols, phospholipids, and steroids. NADPH is also required for the biosynthesis of some amino acids (such as glutamate and proline) and is involved in reducing ribonucleotides and deoxyribonucleotides during the synthesis of RNA and DNA. NADPH is also utilized by many oxidoreductases involved in detoxification reactions within the body. Within the immune system, NADPH oxidases or NOX enzymes are involved in producing superoxide and are utilized to damage invading pathogens nonspecifically. $NADP^+$/NADPH ratios also can play a regulatory role in cellular metabolic processes and are utilized as allosteric effectors for several enzymes and oxidation sensor proteins.

13.4.5: REGULATION OF THE PENTOSE PHOSPHATE PATHWAY

The cellular demand for the two major products of the PPP (ribose 5-phosphate and reduced NADPH) can differ depending on the cell type or the current cellular environment, such as increased metabolic demand or oxidative stress. Thus, the two major products may need to be produced independently and in different quantities. For example, we can imagine times when the needs for ribose 5-phosphate and NADPH are in balance with the standard PPP reactions. However, we can also imagine times when the demand for ribose 5-phosphate may be much higher than the demand for NADPH, or vice versa, the demand for NADPH may be much greater than the demand for ribose 5-phosphate. Thus, regulatory strategies are in place that enable the production of these different pools to be regulated independently of one another and adapt to cellular needs. This ability largely depends on producing metabolic intermediates that can be easily interchanged within the glycolytic pathway.

For example, the ratio of $NADP^+$/NADPH serves as a key regulator of the oxidative branch of the PPP. The first enzymatic step of the pathway mediated by the glucose 6-phosphate dehydrogenase (G6PD) is regulated in this fashion. It helps control the pool of glucose 6-phosphate utilized within the PPP to produce reduced NADPH. Low levels of $NADP^+$ inhibit the G6PD enzyme. The G6PD reaction is essentially irreversible and serves as the committed step for glucose to enter the PPP's oxidative part. Thus, the regulation of this enzymatic step is key in the regulation of NADPH levels within the cell. When the ratio of $NADP^+$/NADPH increases, G6PD becomes more active, and the reduction of $NADP^+$ to NADPH increases.

When ribose 5-phosphate is in high demand, its cellular concentration will decrease, pulling the ribose 5-phosphate isomerase reaction forward by mass action. This enzyme will then convert ribulose 5-phosphate, generated in the oxidative branch of the pentose phosphate pathway, into ribose 5-phosphate to replenish the pool and meet biosynthetic needs. However, suppose cellular demand for ribose 5-phosphate exceeds the amount generated by the oxidative branch. In that case, additional ribose 5-phosphate can be produced in the nonoxidative branch of the pentose phosphate pathway through the rearrangement of glycolytic intermediates.

The opposite also occurs when there is a high need for NADPH in the cell but a low need for ribose 5-phosphate. In this situation, ribose 5-phosphate is converted to fructose and glyceraldehyde 3-phosphate and can be incorporated into the glycolytic pathway.

In addition, the activity of the PPP varies depending on the tissue type and location within the body. For example, skeletal muscle has very low PPP activity, as this tissue requires more energy production and activity of the glycolytic pathway. On the other hand, the PPP is highly active in adipose tissue due to the heightened requirement for intermediates needed for lipid biosynthesis.

13.4.6: SUMMARY

Chapter Summary: The Pentose Phosphate Pathway (PPP)

This chapter provides a detailed overview of the pentose phosphate pathway (PPP), a crucial branch of glucose metabolism that diverges from glycolysis at the level of glucose 6-phosphate (G6P). Unlike glycolysis, which generates ATP for cellular energy, the PPP is primarily devoted to biosynthesis and redox regulation. The pathway is divided into two interconnected branches:

- **Oxidative Branch:**
  In this irreversible segment of the PPP, G6P is oxidized by glucose-6-phosphate dehydrogenase (G6PD), the pathway's rate-limiting enzyme, to form 6-phosphogluconolactone while reducing $NADP^+$ to NADPH. Subsequent hydrolysis by 6-phosphogluconolactonase (6PGL) and decarboxylation by 6-phosphogluconate dehydrogenase (6PGD) yield ribulose 5-phosphate and an additional NADPH molecule. NADPH produced here is vital for reductive biosynthetic processes (e.g., fatty acid and sterol synthesis) and for maintaining cellular antioxidant defenses through glutathione reduction.
- **Non-Oxidative Branch:**
  This branch comprises a series of reversible reactions that interconvert sugar phosphates. Enzymes such as ribose 5-phosphate isomerase (RPI) and ribulose 5-phosphate epimerase (RPE) convert ribulose 5-phosphate into ribose 5-phosphate (R5P) and xylulose 5-phosphate (Xu5P). Transketolase (TKT) and transaldolase (TALDO) then catalyze carbon-shuffling reactions that generate glycolytic intermediates, including fructose 6-phosphate (F6P) and glyceraldehyde 3-phosphate (G3P). This flexibility allows the PPP to adjust the production of R5P for nucleotide synthesis or divert carbon into glycolysis/gluconeogenesis as needed.

Regulation and Physiological Significance:
The PPP is tightly regulated based on the cellular demand for NADPH and R5P. For example, high $NADP^+$/NADPH ratios stimulate G6PD activity, boosting NADPH production to support anabolic reactions and antioxidant defenses. Conversely, when R5P demand is high, flux through the non-oxidative branch is adjusted to favor its production. Tissue-specific variations exist: skeletal muscle, which prioritizes ATP production, exhibits low PPP activity, whereas adipose tissue, with its high lipid biosynthetic needs, shows elevated PPP flux.

Clinical Relevance:
Mutations in G6PD, the key enzyme of the oxidative branch, can lead to G6PD deficiency, a common enzymopathy associated with hemolytic anemia, particularly under conditions of oxidative stress (e.g., infection, ingestion of fava beans, or certain medications). The widespread importance of NADPH in cellular metabolism underscores the significance of the PPP in health and disease.

Overall, this chapter integrates the biochemical mechanisms, regulatory strategies, and physiological roles of the PPP, emphasizing its critical function in maintaining cellular redox balance and providing essential precursors for biosynthesis.

13.4.7: REFERENCES:

Edwards et al.: Structural characterization of a ribose5-phosphate isomerase B from the pathogenic fungus Coccidioides immitis. BMC Structural Biology 2011 11:39. https://www.ncbi.nlm.nih.gov/pmc/articles/PMC3212906/

Ge T, Yang J, Zhou S, Wang Y, Li Y and Tong X (2020) The Role of the Pentose Phosphate Pathway in Diabetes and Cancer. *Front. Endocrinol.* 11:365. doi: 10.3389/fendo.2020.00365

Polat, I.H., Tarrado-Castellarnau, M., Bharat, R., Perarnau, J., Benito, A., Cortes, R., Sabatier, P., and Cascante, M. (2021) Oxidative Pentose Phosphate Pathway Enzyme 6-Phosphogluconate Dehydrogenase Plays a Key Role in Breast Cancer Metabolism. *Biology* 10(2):85. **https://doi.org/10.3390/biology10020085**

Wikipedia contributors. (2022, March 6). Glucose-6-phosphate dehydrogenase. In *Wikipedia*, *The Free Encyclopedia*. Retrieved 22:01, August 12, 2022, from https://en.wikipedia.org/w/index.php?title=Glucose-6-phosphate_dehydrogenase&oldid=1075517394

Wikipedia contributors. (2021, August 29). 6-phosphogluconolactonase. In *Wikipedia*, *The Free Encyclopedia*. Retrieved 23:05, August 12, 2022, from https://en.wikipedia.org/w/index.php?title=6-phosphogluconolactonase&oldid=1041297267

Wikipedia contributors. (2022, March 28). 6-Phosphogluconate dehydrogenase. In *Wikipedia*, *The Free Encyclopedia*. Retrieved 05:50, August 14, 2022, from https://en.wikipedia.org/w/index.php?title=6-Phosphogluconate_dehydrogenase&oldid=1079702040

Wikipedia contributors. (2022, July 4). Ribose-5-phosphate isomerase. In *Wikipedia, The Free Encyclopedia*. Retrieved 05:33, August 15, 2022, from https://en.wikipedia.org/w/index.php?title=Ribose-5-phosphate_isomerase&oldid=1096406233

This page titled 13.4: Pentose Phosphate Pathway of Glucose Oxidation is shared under a not declared license and was authored, remixed, and/or curated by Henry Jakubowski and Patricia Flatt.

- **Current page** by Henry Jakubowski and Patricia Flatt has no license indicated.
- **11.2: Diffusion Across a Membrane - Passive and Facilitated Diffusion** by Henry Jakubowski and Patricia Flatt has no license indicated.

CHAPTER OVERVIEW

14: PRINCIPLES OF METABOLIC REGULATION

Return to Fundamentals of Biochemistry Search Fundamentals of Biochemistry

14.1: Regulation of Metabolic Pathways
14.2: Basic Principles of Metabolic Control Analysis (MCA)
14.3: The Flux Control Coefficient
14.4: Concentration Control and Elasticity Coefficients
14.5: Metabolism and Signaling: The Steady State, Adaptation and Homeostasis

Thumbnail: Overview of regulatory interactions involved in metabolic regulatory networks. The function of metabolic networks are governed by constraints. The regulation of a metabolic network involves a tight interplay between different cellular networks such as signalling and gene networks and by interactions with its environment. The enzyme capacity is the net result of the amount of enzyme expressed and its activity as dictated by post-translational modification and allosteric regulation. Metabolite pools and fluxes are considered as the outputs of metabolic reaction networks and can be involved in various regulatory feedback loops to other networks within the metabolic reaction networks as indicated by the dashed arrows. (CC BY 3.0; Jan Berkhout, Frank J. Bruggeman, and Bas Teusink via MDPI)

This page titled 14: Principles of Metabolic Regulation is shared under a not declared license and was authored, remixed, and/or curated by Henry Jakubowski and Patricia Flatt.

14.1: REGULATION OF METABOLIC PATHWAYS

LEARNING GOALS (CHATGPT O3-MINI)

1. **Explain the Importance of Metabolic Regulation:**
   - Describe how cells balance metabolite flux to meet biological demands and conserve energy (ATP).
   - Compare the cellular consequences of unregulated versus tightly controlled metabolic pathways.
2. **Differentiate Between Regulatory Mechanisms:**
   - Distinguish between regulation by changing the activity of preexisting enzymes and altering the enzyme concentration.
   - Provide examples of each mechanism in cellular metabolism.
3. **Analyze Enzyme Kinetics in Regulation:**
   - Interpret the significance of substrate concentration relative to the Km in determining enzyme activity.
   - Explain how substrate availability affects the velocity of an enzymatic reaction.
4. **Evaluate Inhibition Strategies:**
   - Illustrate how product inhibition and end-product feedback serve as regulatory mechanisms to prevent unnecessary enzyme activity.
   - Discuss the physiological benefits of these inhibition mechanisms.
5. **Understand Allosteric Regulation and pH Effects:**
   - Explain how binding of effectors at allosteric sites can modulate enzyme conformation and activity.
   - Analyze the dual impact of pH on overall enzyme conformation versus specific active site protonation states.
6. **Discuss Covalent Modifications:**
   - Identify common post-translational modifications (e.g., phosphorylation, acetylation) and explain how they alter enzyme function.
   - Use the example of ERK2 phosphorylation to illustrate how covalent modifications can change enzyme conformation and activity.
7. **Examine the Concept of Enzyme Condensates:**
   - Describe how the assembly of enzymes into condensates (or supramolecular complexes) can coordinate pathway regulation.
   - Analyze the role of enzyme polymerization in regulating flux through metabolic pathways.
8. **Assess Regulation at the Transcriptional and Translational Levels:**
   - Explain how extracellular signals affect the transcription of enzyme-coding genes.
   - Discuss the role of mRNA degradation and co/post-translational modifications in controlling enzyme concentration and activity.
9. **Integrate Thermodynamic Principles in Metabolic Regulation:**
   - Relate the concepts of ΔG and ΔG° to enzyme-catalyzed reactions, particularly in reactions far from equilibrium.
   - Evaluate why enzymes catalyzing irreversible or “committed” steps are prime targets for regulation.
10. **Apply Analogies to Understand Metabolic Flux:**
    - Use the water flow (pipe and valve) analogy to explain how cells regulate the flow of metabolites through a pathway.
    - Critically assess how this analogy aids in understanding the dynamics of metabolic control.

These learning goals will not only help students grasp the molecular and kinetic details of enzyme regulation but also encourage them to integrate structural, thermodynamic, and systems biology perspectives into their understanding of metabolism.

Exquisite mechanisms have evolved to control the flux of metabolites through metabolic pathways, ensuring that the output of these pathways meets biological demand and that energy in the form of ATP is not wasted by having opposing pathways run concurrently in the same cell.

Enzymes can be regulated by changing the activity of a preexisting enzyme or the amount of an enzyme.

14.1.1: CHANGING THE ACTIVITY OF A PRE-EXISTING ENZYME

The quickest way to modulate the activity of an enzyme is to alter the activity of an enzyme that already exists in the cell. The list below, illustrated in the following figure, outlines common methods for regulating enzyme activity.

1. Substrate availability: Substrates (reactants) bind to enzymes with a characteristic affinity (characterized by a dissociation constant) and a kinetic parameter called Km (units of molarity). If the actual concentration of a substrate in a cell is much less than the Km, the enzyme's activity is very low. If the substrate concentration is much greater than Km, the enzyme's active site is saturated with substrate, and the enzyme is maximally active.
2. Product inhibition: A product of an enzyme-catalyzed reaction often resembles a starting reactant, so it should be clear that the product also binds to the active site, albeit with probably lower affinity. Under conditions in which the product of a reaction is present in high concentration, it would be energetically advantageous to the cell if no more product were synthesized. Product inhibition is hence commonly observed. Likewise, it is energetically advantageous to a cell if the end product of an entire pathway could likewise bind to the initial enzyme in the pathway and inhibit it, allowing the whole pathway to be inhibited. This type of feedback inhibition is commonly observed. Figure **14.1.1** shows product and end-product inhibition.



Figure **14.1.1**: Product and end product inhibition of an enzyme

3. Allosteric regulation: As many pathways are interconnected, it would be optimal if the molecules of one pathway affected the activity of enzymes in another interconnected pathway, even if the molecules in the first pathway are structurally dissimilar to reactants or products in a second pathway. Molecules that bind to sites on target enzymes other than the active site (allosteric sites) can regulate the activity of the target enzyme. These molecules can be structurally dissimilar to those that bind at the active site. They do so by conformational changes that activate or inhibit the target enzyme's activity.
4. pH and enzyme conformation: Changes in pH that accompany metabolic processes, such as respiration (aerobic glycolysis, for example), can alter the conformation of an enzyme and, consequently, its activity. The initial changes are covalent (change in the protonation state of the protein), which can alter the delicate balance of forces that affect protein structure.
5. pH and active site protonation state: Changes in pH can affect the protonation state of key amino acid side chains in the active site of proteins without affecting the local or global conformation of the protein. Catalysis may be affected if the mechanism involves an active site nucleophile (for example) that must be deprotonated for activity.
6. Covalent modification: Many, if not most, proteins undergo post-translational modifications, which can alter enzyme activity through local or global shape changes by promoting or inhibiting binding interactions between substrates and allosteric regulators. They can also change the location of the protein within the cell. Proteins may be phosphorylated, acetylated, methylated, sulfated, glycosylated, amidated, hydroxylated, prenylated, or myristoylated, often in a reversible manner. Some of these modifications are reversible. Regulation by phosphorylation, through the action of kinases, and dephosphorylation, by phosphatases, is extremely common. Control of the phosphorylation state is mediated through signal transduction processes starting at the cell membrane, leading to the activation or inhibition of protein kinases and phosphatases within the cell.

Figure **14.1.2** illustrates methods for regulating the activity of pre-existing enzymes.

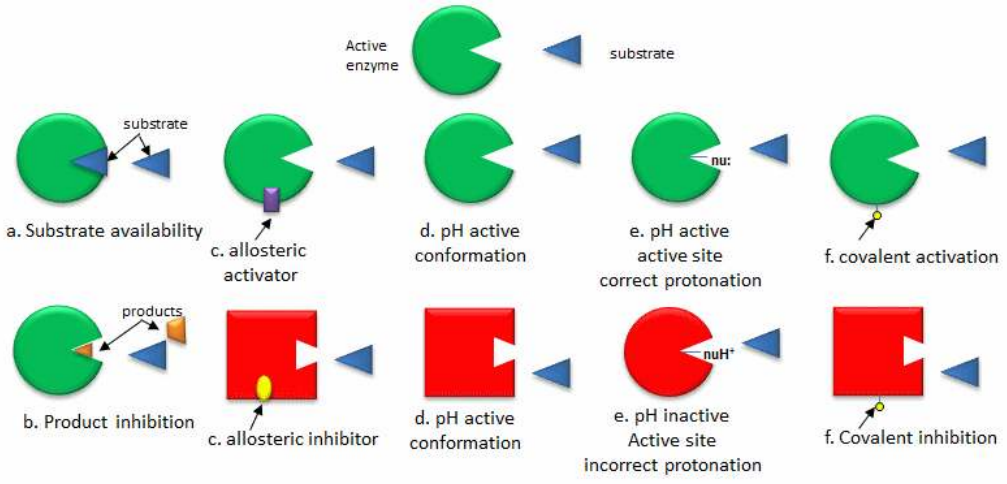
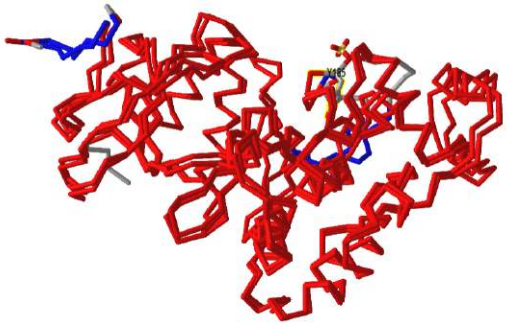


Figure **14.1.2**: Ways to regulate the activity of pre-existing enzymes

Extracellular regulated kinase 2 (ERK2), also known as mitogen-activated protein kinase 2 (MAPK2), plays a vital role in cell signaling across the cell membrane. Phosphorylation of ERK2 on Threonine 183 (Thr183) and Tyrosine 185 (Tyr185) leads to a structural change in the protein and regulates its activity.

Figure **14.1.3** shows an interactive iCn3D model showing the structural alignment of ERK2 in the dephosphorylated (5UMO) and phosphorylated (pY185) forms (2ERK). Toggle back and forth between the two structures with the "a" key.



NCBI iCn3D Figure **14.1.3**: Structural alignment of ERK2 in the dephosphorylated (5UMO) and phosphorylated (pY185) forms (2ERK). (Copyright; author via source). Click the image for a popup or use this external link:https://structure.ncbi.nlm.nih.gov/i...8iMQUVBbmMTRJ6

The residues that change significantly in conformation on phosphorylation are shown in blue. The side chain of tyrosine 185 in the unphosphorylated form is shown in CPK-colored sticks and labeled.

14.1.2: REGULATION OF SINGLE ENZYMES OR ENTIRE PATHWAYS: ENZYME CONDENSATES

Single enzymes or all the enzymes of a given pathway can be coordinately regulated to maximize end-product output by organizing the enzymes in one large complex built from soluble enzymes that produce a "condensate" through a process similar to phase separation. Such condensates are shown for a series of enzymes in Figure **14.1.4**.

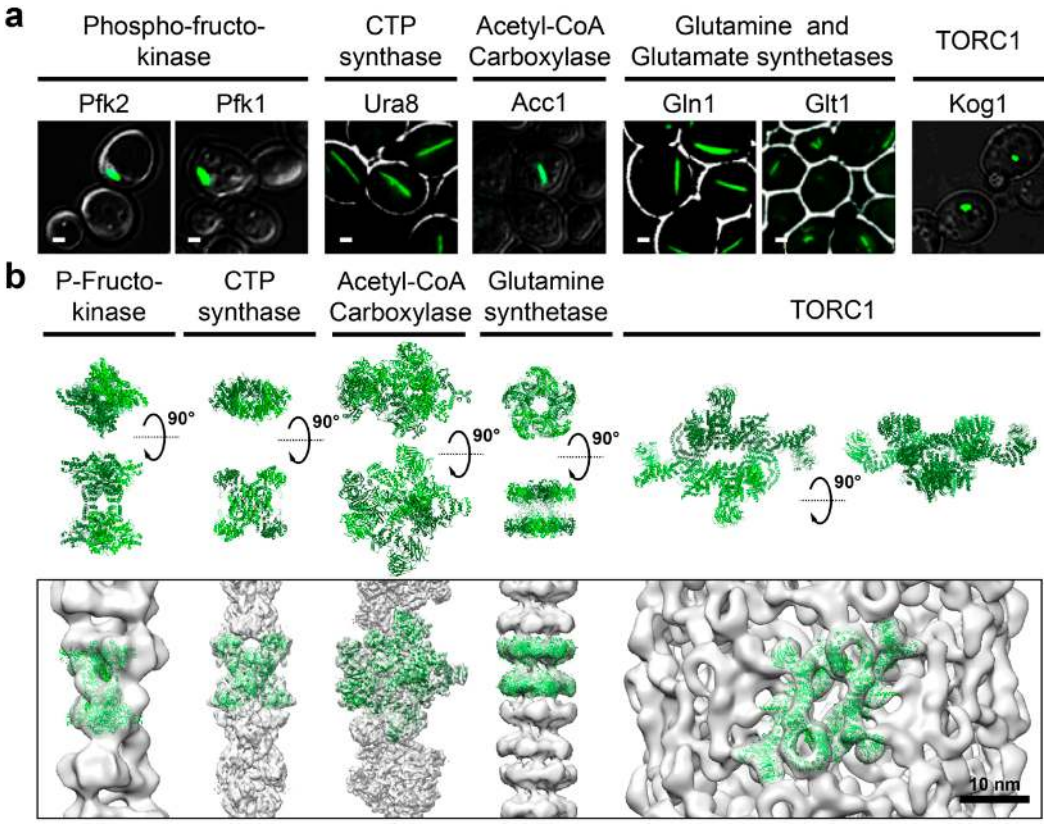


Figure **14.1.4**: Supramolecular assembly of enzyme condensates. Prouteau and Loewith. *Biomolecules* **2018**, *8*(4), 160; https://doi.org/10.3390/biom8040160. Creative Commons Attribution (CC BY) license (http://creativecommons.org/licenses/by/4.0/).

The figure shows metabolism-related enzymes that form polymers in various organisms.

Panel (**a**) shows examples of metabolic enzymes observed to coalesce into cytosolic condensates.

Panel (**b**) top shows structures of metabolic enzymes that polymerize into filaments. The protomer of the polymer is shown above and placed into the filament below. These include P-Fructo-Kinase (4XYJ), cytidine triphosphate synthase (5U03), acetyl-CoA carboxylase (6G2D), glutamine synthetase (3FKY), mTORC1 (5FLC) from PDB files.

Panel (**b**) bottom shows the same structures from the Electron Microscopy Data Bank, including P-Fructo-Kinase filament (emd-8542), human CTP synthase filament (and-8474), human acetyl-CoA carboxylase with citrate (emd-4342), and the yeast glutamine synthetase filament.

14.1.3: CHANGING THE AMOUNT OF AN ENZYME

Another method to modulate the activity of an enzyme is to alter the activity of an existing enzyme in the cell. Figure **14.1.5** shows how enzyme concentrations are regulated.

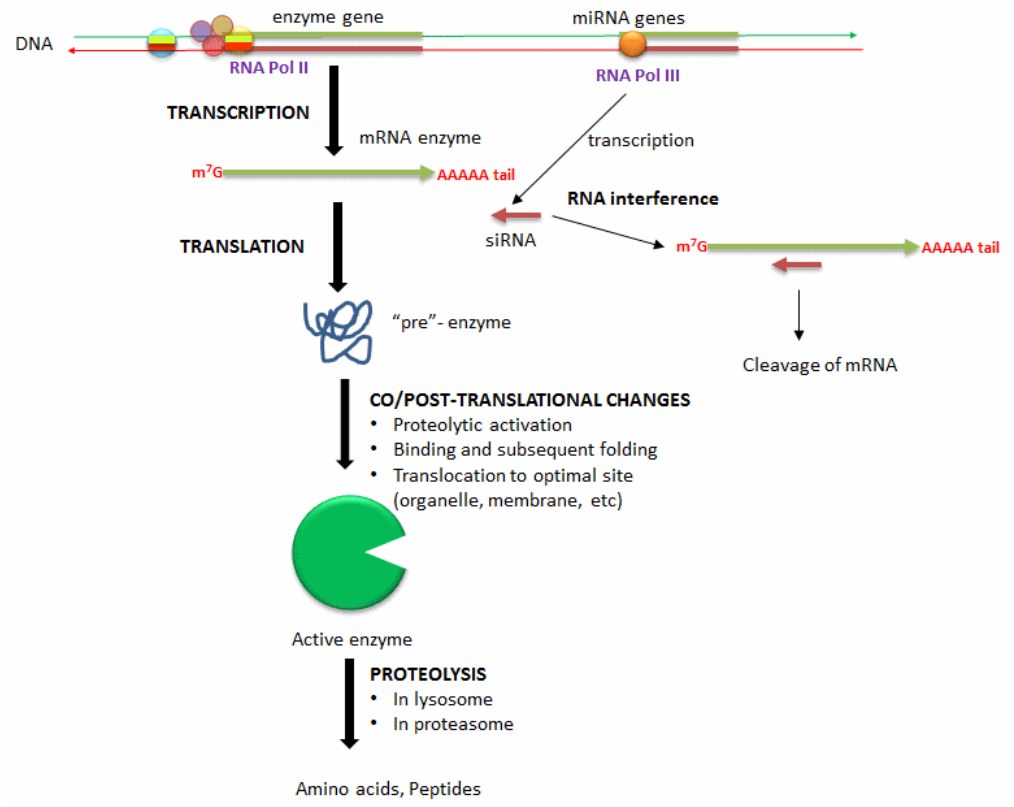


Figure **14.1.5**: Ways to regulate the concentration of an enzyme

Methods include:

1. Alterations in the transcription of an enzyme's gene: Extracellular signals (hormones, neurotransmitters, etc.) can lead to signal transduction responses and ultimately activate or inhibit the transcription of the gene for a protein enzyme. These changes result from the recruitment of transcription factors (proteins) to DNA sequences that regulate the transcription of the enzyme gene.
2. Degradation of messenger RNA for the enzyme: The levels of messenger RNA for a protein directly determine the amount of that protein synthesized. Two key proteins are involved in an RNA interference (RNAi) pathway. The RNase **Dicer** produces 21–25 nt small single-stranded RNAs (siRNAs or miRNAs) which can bind the protein **Argonaute.** The bound siRNA (a guide RNA) finds a complementary sequence on a specific mRNA, leading to the chemical modification or cleavage of the mRNA, silencing its translation into a protein.
3. Co/Post-translational changes: Once a protein enzyme is translated from its mRNA, it can undergo many changes that regulate its activity. Some proteins are synthesized in a "pre" form, which proteases must cleave in a targeted and limited fashion to activate the protein enzyme. Some proteins are not fully folded and must bind to other cellular factors to adopt a catalytically active form. Finally, a

fully active protein can be fully proteolyzed by the proteasome, a complex within cells or in lysosomes, organelles within cells that contain proteolytic enzymes.

The concentrations of all proteins are affected by their relative rates of synthesis and degradation. However, some enzymes positioned at key points in metabolic pathways are ideal candidates for regulation, as their activity can affect the output of entire pathways. These enzymes typically have two common characteristics: they catalyze reactions far from equilibrium, and they catalyze early committed steps in pathways.

14.1.4: WHICH ENZYMES TO REGULATE: REACTIONS NOT AT EQUILIBRIUM

The optimal enzymes for regulation are those located at the beginning of pathways that catalyze thermodynamically favored reactions. Why is the latter so important? These enzymes control the flux of metabolites through pathways; therefore, to understand their regulation, we can use the analogy of water flow (or flux) from one container to another, as illustrated in Figure **14.1.6**.

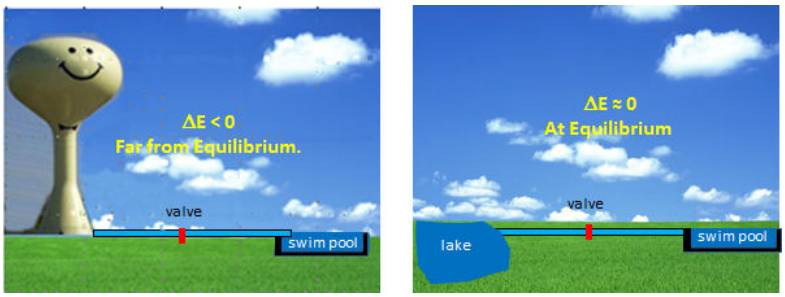


Figure **14.1.6**: Regulation of water flow in pipe

Let's say you wish to fill a swimming pool to a desired height, and you have two options to do so (see the figure below). You could open a valve that controls the flow from your town's water tower to the pool. In this, the reaction (flow of water) is energetically (thermodynamically) favored given the difference in height of the water levels and the potential energy difference between the two. Even though flow (or flux) is flavored, you can regulate it, from maximal flow to no flow, by opening and closing the valve (analogous to activating and inhibiting an enzyme). In the other scenario, where you fill the pool from a lake, your options are limited. It would be hard to fill the water to the desired level (especially if it were an above-ground pool). It would be hard to regulate the flow.

By analogy, the best candidates for regulation are those enzymes whose reactions are thermodynamically favored (i.e., not at equilibrium) but can be controlled by the mechanisms discussed in the previous section.

Which reactions are commonly not at equilibrium? Let's quickly review a key thermodynamic equation for the reversible conversion of reactants A and B to products P and Q:

$$\Delta G = \Delta G^0 + RT \ln \frac{[P][Q]}{[A][B]} = \Delta G^0 + RT \ln Q_{rx} \tag{14.1.1}$$

In reactions that are favored in the forward direction, $\Delta G < 0$. If $\Delta G^o < 0$, the forward reaction is favored unless the ratio of products to reactants is too high. $\Delta G^o < 0$ if the reactants are chemically unstable compared to the products. Several types of reactions often fit these criteria.

14.1.4.1: HYDROLYSIS (OR SIMILAR REACTIONS) OF ANHYDRIDE OR ANALOGOUS MOTIFS.

Figure 7 below shows molecules with similar "anhydride" motifs and the $\Delta G°$ for the hydrolysis of these molecules. Those with more negative ΔG^0 values can transfer their phosphate group to ADP to make ATP, which is necessary to drive unfavorable biological reactions. Metabolic reactions that involve hydrolysis (or other types of transfer reaction of these groups) usually proceed with a negative ΔG^0 and ΔG, making them prime candidates for pathway regulation. Many textbooks label these molecules as having "high-energy" bonds. This confuses many students as bonds between atoms lower the energy compared to when the atoms are not bonded. It takes energy to break the "high" energy phosphoanhydride covalent bond. The hydrolysis of the molecules below is exergonic because more energy is released during bond formation in the new products than was required to break the bonds in the reactants. In addition, other effects, such as preferential hydration of the products, lower charge density, and fewer competing resonances in the products, all contribute to the thermodynamically favorable hydrolysis of the reactants.

Figure **14.1.7** shows the structures of thermodynamically unstable metabolites (compared to their reaction products in aqueous solutions) and their $\Delta G^0_{hydrolysis}$.

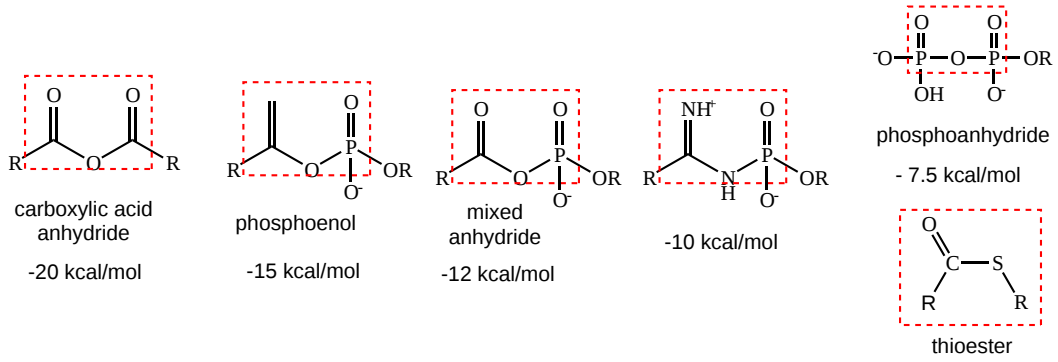


Figure **14.1.7**: Metabolites that are thermodynamically unstable compared to their hydrolysis products and their $\Delta G^0_{hydrolysis}$

14.1.4.2: THIOESTERS

Thioesters (such as Acetyl-SCoA) are also included in Figure 7, as they have the same negative ΔG° of hydrolysis as ATP, even though they lack an "anhydride" motif. Thioesters are destabilized compared to their hydrolysis products (a carboxylic acid and a thiol) compared to esters made with alcohol, since the C-S bond in the reactant is weaker. The S atom is larger than an O atom, so the C-S bond length is longer than a C-O bond. The lone pair on the S can't delocalize as readily to form a C=S double bond in the reactant through resonance. This destabilizes the reactant, the thioester, compared to a regular carboxylic acid ester. This, in turn, increases the ΔG° of hydrolysis of the thioester compared to the product, the free thiol.

14.1.4.3: REDOX REACTIONS

Most students likely recall that redox reactions are thermodynamically favored if the oxidizing agent deployed is strong enough. The full oxidation reactions of hydrocarbons, sugars, and fats by dioxygen are clearly exergonic (think burning of wood!). What about redox reactions with less powerful oxidants? NAD^+ is frequently used as a biological oxidizing agent. Are all these reactions as favored as combustion? Hardly so. Remember that in every redox reaction, an oxidizing and reducing agent react to form another oxidizing and reducing agent. Consider the following reaction:

$$\text{Pyruvate} + \text{NADH} \leftrightarrow \text{Lactate} + NAD^+$$

This reaction can proceed in either direction and is reversible. The above form is written in the favored direction in anaerobic metabolism when both Pyr and NADH levels are high. Although the ΔG^0 favors lactate oxidation, given the high concentration of Pyr and NADH, the reaction is driven in the opposite direction and proceeds as shown. To determine if a redox reaction is favored and likely to occur (and possibly be regulated), the ΔG^0 for a redox reaction should be calculated from standard reduction potentials, using the formula $\Delta G^0 = -nFE^0$.

14.1.5: WHICH ENZYMES TO REGULATE: THOSE CATALYZING COMMITTED STEPS IN PATHWAYS

The best enzymes for regulation catalyze the first committed step in the reaction pathway. The committed step proceeds with a $\Delta G^0 < 0$ and is essentially irreversible. These reactions often occur from key metabolic intermediates immediately before or proximal to branches in reaction pathways. Two examples of key intermediates at branch points of metabolic pathways are shown in Figure **14.1.8**, which illustrates the reactions involved in the production and utilization of the intermediate glucose-6-phosphate.

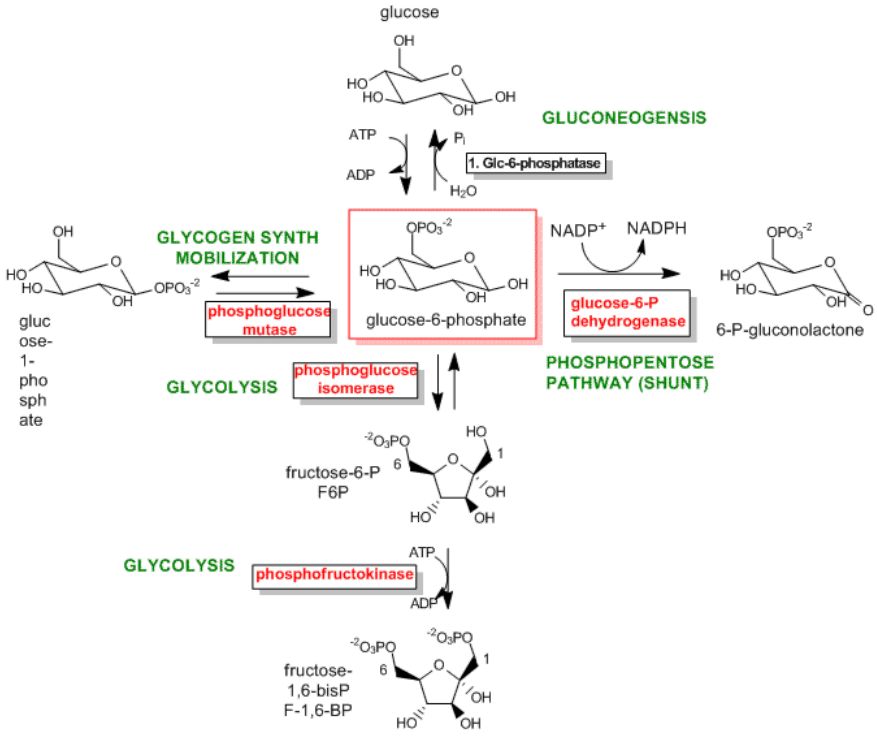


Figure **14.1.8**: Reactions for the production and use of the intermediate glucose-6-phosphate

Figure **14.1.10** shows reactions for producing and using the intermediate acetyl-CoA.

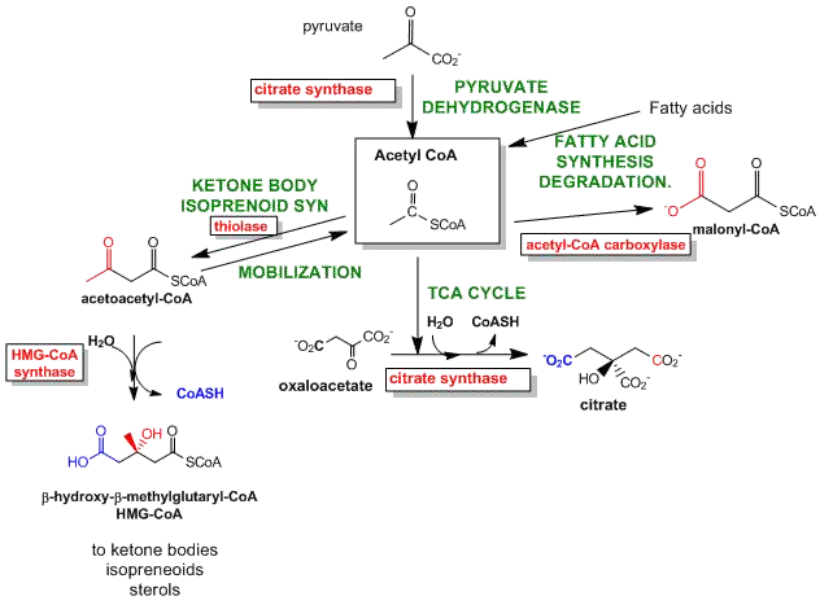


Figure **14.1.10**: Reactions for the production and use of the intermediate acetyl-CoA

In reality, metabolic regulation is more complex and is distributed to many steps in a reaction pathway in ways that might not be evident without detailed mathematical analyses. We will discuss that in the following sections on metabolic control analysis.

14.1.6: SUMMARY

This chapter provides an in-depth look at the sophisticated regulatory mechanisms that control metabolic pathways, ensuring that cells meet their energetic and biosynthetic demands without wasting resources. Key points include:

- **Balancing Metabolic Flux:**
  Cells utilize exquisite regulatory strategies to direct metabolite flux, thereby matching pathway outputs to biological needs while

conserving ATP.

- **Two Main Regulatory Approaches:**
  1. **Modulating Enzyme Activity:**
     - **Substrate Availability:** Enzyme activity is influenced by how substrate concentration compares with the enzyme's Km.
     - **Product Inhibition:** End-products or intermediates can bind to enzymes, reducing further product formation and saving energy.
     - **Allosteric Regulation:** Binding of effectors at sites other than the active site induces conformational changes that either activate or inhibit enzymes.
     - **pH Effects:** Changes in pH can alter both the overall conformation of enzymes and the protonation states of key active site residues, thus modulating catalytic activity.
     - **Covalent Modifications:** Post-translational modifications (e.g., phosphorylation, acetylation) can rapidly alter enzyme activity, as exemplified by the phosphorylation-induced conformational change in ERK2.
  2. **Adjusting Enzyme Concentration:**
     - **Transcriptional Control:** Extracellular signals can activate or repress the transcription of genes coding for metabolic enzymes.
     - **mRNA Stability:** Regulation of mRNA degradation through mechanisms such as microRNA binding directly influences enzyme levels.
     - **Co/Post-Translational Processing:** Activation or inactivation of enzymes through proteolytic cleavage or folding, and their eventual degradation via proteasomes or lysosomes, further fine-tune enzyme abundance.
- **Enzyme Condensates:**
  The formation of supramolecular assemblies or condensates allows for the coordinated regulation of multiple enzymes within a pathway, enhancing the efficiency and responsiveness of metabolic control.
- **Thermodynamic Considerations:**
  Enzymes catalyzing reactions far from equilibrium ($\Delta G < 0$) and those that mediate the committed, irreversible steps of metabolic pathways are optimal control points. This chapter explains how the hydrolysis of "high energy" bonds (e.g., in ATP or thioesters like Acetyl-SCoA) and redox reactions drive these irreversible steps.
- **Practical Analogy:**
  An analogy comparing metabolic regulation to controlling water flow with a valve illustrates how precise regulation of enzyme activity can control the "flow" of metabolites in a pathway, ensuring the right output without waste.

Overall, the chapter integrates structural, kinetic, and thermodynamic perspectives, providing a comprehensive framework that junior and senior biochemistry majors can build upon to understand metabolic control and its importance in cellular physiology.

This page titled 14.1: Regulation of Metabolic Pathways is shared under a not declared license and was authored, remixed, and/or curated by Henry Jakubowski and Patricia Flatt.

- **11.2: Diffusion Across a Membrane - Passive and Facilitated Diffusion** by Henry Jakubowski and Patricia Flatt has no license indicated.

14.2: BASIC PRINCIPLES OF METABOLIC CONTROL ANALYSIS (MCA)

LEARNING GOALS (CHATGPT O3-MINI)

1. **Conceptualize Metabolic Control Analysis (MCA):**
   - Define MCA and explain why enzyme kinetics in complex metabolic pathways require a systems-level approach.
   - Describe the challenges posed by the multiple steps, rate constants, and chemical species involved in enzyme-catalyzed reactions.
2. **Differentiate Between Equilibrium and Steady-State Conditions:**
   - Contrast equilibrium conditions (where no net change in reactant or product concentrations occurs) with steady state in open systems (where input equals output).
   - Explain the significance of steady state in cellular metabolism and why it is more relevant to in vivo conditions than equilibrium.
3. **Apply Differential Equations to Model Metabolic Reactions:**
   - Write ordinary differential equations (ODEs) for simple and complex reaction schemes, including unimolecular and bimolecular reactions.
   - Interpret the ODEs used to describe the time-dependent concentration changes of reactants, intermediates, and products in metabolic pathways.
4. **Understand and Analyze Enzyme Kinetics Using Simulation Tools:**
   - Utilize computational programs such as VCell and COPASI to simulate progress curves (concentration vs. time) for enzyme-catalyzed reactions.
   - Compare simulation results for isolated enzyme reactions with those embedded in metabolic "mini-pathways" and evaluate how pathway context alters apparent equilibrium constants.
5. **Relate In Vitro vs. In Vivo Kinetics:**
   - Explain how experimental approaches (varying substrate or inhibitor concentrations in vitro) differ from the dynamic conditions encountered in vivo, where flux and steady-state concentrations govern enzyme behavior.
   - Discuss how the concept of flux (J) provides a more accurate description of pathway kinetics in a cellular context.
6. **Interpret the Mathematical Derivation of Net Reaction Rates:**
   - Follow the derivation of the reversible Michaelis–Menten equation under rapid equilibrium conditions and understand the roles of dissociation constants (K_S and K_P).
   - Explain why the net forward rate of a reversible reaction cannot be determined by a simple subtraction of forward and reverse rates.
7. **Analyze the Impact of Inhibitors on Enzyme Kinetics:**
   - Distinguish between simple enzyme kinetics and competitive inhibition models by comparing their derived equations.
   - Apply knowledge of inhibition parameters (K_I) to understand how inhibitors alter the net rate of enzymatic reactions.
8. **Examine the Role of Computational Models in Systems Biology:**
   - Discuss how complex pathways, such as yeast glycolysis, are modeled computationally using curated databases (e.g., Biomodels) and the integration of experimental data.
   - Evaluate how branching reactions and additional pathway components improve the accuracy of simulations relative to experimental in vivo fluxes.
9. **Develop Practical Skills in Parameter Variation and Sensitivity Analysis:**
   - Practice modifying kinetic parameters (e.g., rate constants, substrate concentrations) in simulation programs to observe their effects on the time-course graphs of metabolite concentrations.
   - Interpret how changes in model parameters influence the steady-state and overall flux of the pathway.
10. **Integrate Theoretical and Practical Aspects of Metabolic Control:**
    - Synthesize the mathematical derivations, computational simulations, and experimental differences to build a comprehensive understanding of how metabolic pathways are regulated at the systems level.
    - Critically assess the limitations of in vitro enzyme kinetics when applied to the dynamic conditions of living cells.

These learning goals aim to guide students through the theoretical underpinnings and practical applications of metabolic control analysis, equipping them with the skills necessary to bridge the gap between individual enzyme behavior and the integrated function of metabolic networks.

14.2.1: INTRODUCTION TO METABOLIC CONTROL ANALYSIS

Enzyme kinetics is difficult, in part due to the complicated mathematical derivations, the number of chemical species involved (an enzyme and all its substrates and products), the number of steps in the mechanism, and numerous rate, kinetic, and dissociation constants. An example of such a "complicated" reaction explored earlier is shown in Figure **14.2.1**.

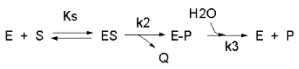


Figure **14.2.1**: Chemical Equations for an enzyme-catalyzed reaction with a covalent E-intermediate

$$v = \frac{\frac{k_2 k_3}{k_2+k_3}(E_0)(S)}{\left[\frac{k_3}{k_2+k_3}\right]K_S + S} = \frac{k_{cat}(E_0)(S)}{K_M + S} \tag{14.2.1}$$

But single enzymes rarely act in isolation. They are components of complex pathways with many steps, many of which are regulated. To fully understand a reaction, it is important to study the concentrations of all species in the entire pathway as a function of time. Imagine deriving the equations and determining all the relevant concentrations and constants of a pathway such as glycolysis!

To study enzyme kinetics in the lab, you have to spend much time developing assays to measure how the concentration of species changes as a function of time, to be able to measure the initial velocities of an enzyme-catalyzed reaction. However, in networks of interconnected metabolic reactions, the concentration of certain species in the system may remain constant. How can this happen? Two simple examples might help explain how.

Example 1: There is no change in input or output from a given reaction. This would occur in a closed system for a reversible reaction at equilibrium.

For a reversible reaction of reactant R going to product P (R ↔ P) with forward and reverse first-order rate constants, the following equation can be written at equilibrium:

$$v_f = k_1 R = k_2 P$$
$$K_{eq} = \frac{P_{eq}}{R_{eq}} = \frac{k_1}{k_2} \tag{14.2.2}$$

At equilibrium, $\boldsymbol{R}$ and $\boldsymbol{P}$ don't change.

Example 2: Consider the reaction as part of a pathway of reactions (like an open system). Now, imagine a nonzero input to form reactant R and a nonzero output that consumes product P, as shown in Figure **14.2.2**.

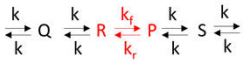


Figure **14.2.2**: Reactant R conversion to Product P with preceding and following steps

If the input and output rates are the same, the concentrations of R and P would remain constant over time. This would lead to a **steady state** but not equilibrium species concentrations.

14.2.1.1: THE STEADY STATE - A THRESHOLD BIOCHEMISTRY CONCEPT

Students often struggle to understand the concept of steady state and recognize when it may prevail under specific conditions.

IN VITRO VS. IN VIVO

In his book Fundamentals of Enzyme Kinetics, Cornish-Bowden discusses the key differences between enzyme kinetics performed in test tubes (*in vitro*) and what occurs in cells (*in vivo*). We've discussed this previously, but it's essential to revisit it now. The conditions under which the enzymes are studied (*in vitro*) and operate (*in vivo*) are very different.

- *In vitro* (in the lab), the enzyme is held at a constant concentration while the substrate is varied (i.e, the substrate concentration is the independent variable). The substrate concentration determines the velocity. When inhibition is studied, the substrate varies while the inhibitor is held constant at several different fixed concentrations.
- *In vivo* (within the cell), the velocity may be maintained at a relatively constant level in a pathway. This means that the velocity determines the **substrate** concentration! *You may have to repeat this sentence many times in your mind to realize its significance, as it seems to contradict all the kinetics you studied in many courses!* To avoid a bottleneck in flux, the substrate can't build up at the enzyme; therefore, the enzyme processes it in a steady-state fashion to produce the product, as determined by the Michael-Menten equation.

These differences are vastly underappreciated and not widely understood by students and instructors alike.

Additionally, we confound our efforts in helping students understand the steady state by focusing **alm**ost exclusively on presenting initial rate v_0 vs [S] curves when the substrate concentration is changed. Then, instructors expect students to magically understand the steady state when substrate levels in pathways don't change. It's a big leap out of this box. We can help students better understand the steady state by shifting to progress curves (concentrations vs time), which are easily constructed using programs such as VCell and Copasi.

Let's use Vcell to analyze a very simple reversible enzyme in isolation, S ↔ P. Then we will place that same enzyme into a "mini" pathway, A ↔ S ↔ P ↔ Q, in which there is one preceding reactant, A, and one following product, Q, that help control S and P levels. We must start the simulation at a specified concentration, so the default for the simulations is set such that [S] and [A] at time t = 0, S_0 and A_0, are both 5, and the rest are set to 0. Hence, as the simulation begins, concentrations will be adjusted until equilibrium or steady-state concentrations are reached. Table **14.2.1** shows the reaction diagrams and their parameters. Here is the equation for both.

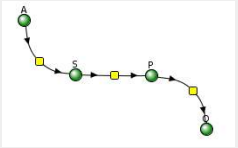
$$\frac{\left(\frac{S \cdot VmaxFwd}{KmFwd} - \frac{P \cdot VmaxRev}{KmRev}\right)}{\left(1.0 + \frac{S}{KmFwd} + \frac{P}{KmRev}\right)} \tag{14.2.3}$$

A reversible enzyme in isolation, S ↔ P



Parameter	Description	Value
J	Reaction rate	S↔P Eq3
KmFwd	Km forward	10.0
VmaxFwd	Max forward rate	10.0
KmRev	Km reverse	20.0
VmaxRev	Max reverse rate	5.0
Size	Size	50000.0
InitConc	Initial concentration for S	5.0

A reversible enzyme for S ↔ P in a mini-pathway A ↔ S ↔ P ↔ Q



Parameter	Description	
J for S↔P	Reaction rate S ↔ P, Eq 3 above	
KmFwd	Km forward	
VmaxFwd	Max forward rate	
KmRev	Km reverse	
VmaxRev	Max reverse rate	
J for P↔Q	Reaction rate	(K
Kf	Forward rate constant	
Kr	Reverse rate constant	
J for A↔S	Reaction rate	(K
Kf	Forward rate constant	
Kr	Reverse rate constant	
Size	Size	
initConc	Initial concentration for S	
initConc	Initial concentration for P	
initConc	Initial concentration for Q	
initConc	Initial concentration for A	

Figure **14.2.3**: Reaction schemes and parameters for a simple enzyme-catalyzed reversible reaction (left) and the same reaction embedded in a "mini" pathway (right).

Vcell simulation for the isolated enzyme

Remember that an enzyme doesn't change the thermodynamics of a given reaction and hence doesn't alter K_{eq}. It just speeds up both the forward and the reverse reactions. Hence, you can calculate the K_{eq} for the reaction condition from the Vcell model time course graph:

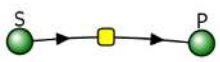
$$K_{eq} = \frac{[P]_{eq}}{[S]_{eq}} = \frac{4}{1} = 1 \tag{14.2.4}$$

Now you observe that in this reaction, S does change from its initial value, $S_0 = 5$ (since $P_0 = 0$). Soon, however, the reaction reaches a dynamic equilibrium, in which both S and P don't change over time.

You could choose a different initial concentration of S and P, rerun the simulation, and calculate K_{EQ} for the new conditions using the CSV-downloaded spreadsheet data from each run you make. They should be the same.

VCell MODEL

Reversible reaction E + S ↔ ES ↔ EP ↔ E + P



Initial values

Name	Description	Global	
J	reaction rate		$\frac{(\frac{S \cdot VmaxFwd}{KmFwd} - \frac{P \cdot VmaxRev}{KmRev})}{(1.0 + \frac{S}{KmFwd} + \frac{P}{KmRev})}$
KmFwd	Km forward		10.0
VmaxFwd	max forward rate		10.0
KmRev	Km reverese		20.0
VmaxRev	max reverse rate		5.0
S	Species Concentration	☑	Variable
P	Species Concentration	☑	Variable

Select Load [model name] below

Load EnzymeRevIsolated

Select **Start** to begin the simulation.

Select **Plot** to change Y axis min/max, then **Reset** and **Play** | Select **Slider** to change which constants are displayed | Select **About** for software information.

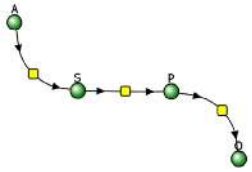
Move the sliders to change the constants and see changes in the displayed graph in real-time.

Time course model made using Virtual Cell (Vcell), **The Center for Cell Analysis & Modeling**, at **UConn Health**. Funded by NIH/NIGMS (R24 GM137787); Web simulation software (miniSidewinder) from Bartholomew Jardine and Herbert M. Sauro, University of Washington. Funded by NIH/NIGMS (RO1-GM123032-04)

Vcell simulation for the enzyme in a "mini-pathway"

Now compare this same reaction, but in which S and P are part of the "mini-pathway" A ↔ S ↔ P ↔ Q, as shown in the Vcell model below. The enzyme kinetic parameters for S ↔ P ($K_{M\ forward}$, $V_{M\ forward}$, $K_{M\ reverse}$, $V_{M\ reverse}$) in the A ↔ S ↔ P ↔ O pathway were made the same as for the simple S ↔ P reaction, since it's the same enzyme. How do the A ↔ S and P ↔ Q reactions affect the apparent K_{EQ}? Run the Vcell model with the defaults automatically set to the values in the table above!

VCell MODEL



Initial Values

Name	Description	Global	
J	reaction rate		$(Kf \cdot A - Kr \cdot S)$
Kf	forward rate constant		2.0
Kr	reverse rate constant		2.0
A	Species Concentration	☑	Variable
S	Species Concentration	☑	Variable

Name	Description	Global	
J	reaction rate		$\frac{(\frac{S \cdot VmaxFwd}{KmFwd} - \frac{P \cdot VmaxRev}{KmRev})}{(1.0 + \frac{S}{KmFwd} + \frac{P}{KmRev})}$
KmFwd	Km forward		10.0
VmaxFwd	max forward rate		10.0
KmRev	Km reverese		20.0
VmaxRev	max reverse rate		5.0
S	Species Concentration	☑	Variable
P	Species Concentration	☑	Variable

Name	Description	Global	
J	reaction rate		$(Kf \cdot P - Kr \cdot Q)$
Kf	forward rate constant		20.0
Kr	reverse rate constant		2.0
P	Species Concentration	☑	Variable
Q	Species Concentration	☑	Variable

Select Load [model name] below

Load EnzymeRev_Constant_S_Premoved

Select **Start** to begin the simulation.

Select **Plot** to change Y axis min/max, then **Reset** and **Play** | Select **Slider** to change which constants are displayed | Select **About** for software information.

Move the sliders to change the constants and see changes in the displayed graph in real-time.

Time course model made using Virtual Cell (Vcell), **The Center for Cell Analysis & Modeling**, at **UConn Health**. Funded by NIH/NIGMS (R24 GM137787); Web simulation software (miniSidewinder) from Bartholomew Jardine and Herbert M. Sauro, University of Washington. Funded by NIH/NIGMS (RO1-GM123032-04)

As in the first simulation, constant values for S and P are soon reached. Both are significantly lower than in the simple reaction of S ↔ P since P is being pulled toward Q faster than Q is converted back to S. Note also that Q reaches a higher concentration than either A or S, but remember that the sum of the initial values of A and S is 10.

Run the simulation again, but this time, set k_f=200 for the P ↔ Q reaction.

Now, calculate the "$K_{EQ\ apparent}$" for the different k_f values of the conversion of P → Q from this equation. Again, use the CSV-downloaded spreadsheet data for each run you make.

$$K_{eq\ apparent} = \frac{[P]_{steady\ state}}{[S]_{steady\ state}} \tag{14.2.5}$$

Do they equal 4 as in case 1? No, they do not! You should see that the "$K_{EQ\ apparent}$" value deviates most from 4 (lower number) when the rate constant for removal of P is highest (k_f=200).

14.2.2: ANIMATIONS

Now, let's look at some animations of these reactions as an additional way to understand their dynamics. Click the image in Figure **14.2.4** to view (in a new window) the animation of the chemical species and an inserted graph showing concentration vs time for the reversible enzyme-catalyzed Reaction S ↔ P

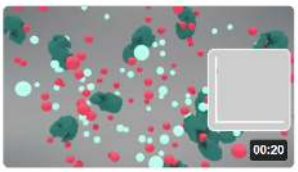
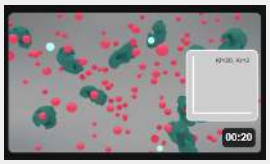


Figure **14.2.4**: Animation of the reversible enzyme-Catalyzed Reaction: S ↔ P

Pay attention to the disappearance of S (red) and the appearance of P (light blue) species after interacting with the enzyme (green).

Now here are two animations for the S ↔ P reaction when it's embedded in the "minipathway" A ↔ S ↔ P ↔ Q, when k_f for the reaction P ↔ Q is **20** (left) and 200 (right). Click the images in Figure **14.2.5** to view (in a new window) an animation of the chemical species and inserted graphs showing concentrations vs time.

"mini-pathway" A ↔ S ↔ P ↔ Q, k_f for the reaction P ↔ Q = **20**



"mini-pathway" A ↔ S ↔ P ↔ Q, k_f for the reaction P ↔ Q = **200**

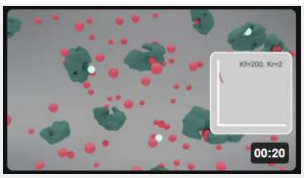


Figure **14.2.5**: Animation of the reversible enzyme-catalyzed Reaction embedded in a "minipathway" A ↔ S ↔ P ↔ Q when k_f for the reaction P ↔ Q is **200.** S (red), P (light blue), and enzyme (green).

These animations should reinforce your understanding of the differences between equilibrium and steady-state conditions, although you can calculate the actual $K_{EQ\ apparent}$ from the insert graphs without numerical data.

Understanding a pure enzyme in vitro and in vivo requires different approaches. Biochemists isolate and purify an enzyme found in some tissues and study its mechanism of action. When performing thermodynamic measurements to determine equilibrium constants (K_{eq}) or dissociation constants (K_D), from which ΔG^0 can be calculated, a protein concentration is usually held constant as the binding ligand concentration is varied (independent variable). A dependent variable signal (often spectroscopic) is measured. Measurements are made when equilibrium is reached.

As we mentioned above (but it bears repeating), for enzyme kinetic measurements *in vitro*, the enzyme concentration is usually held constant as substrate and modifiers are varied (independent variables) to determine how velocity (dependent variable) changes. The substrate concentration determines the velocity. When inhibition is studied, the substrate concentration varies while the inhibitor concentration remains constant at several different fixed levels.

In vivo, the substrate concentration is determined by the reaction's velocity. For sets of reactions in pathways, flux (J) is used instead of velocity. In the steady state, the in and out fluxes for a given reaction are identical. Flux J is used to describe the rate of the system, whereas the rate or velocity v is used to describe the rate of an individual enzyme in a system.

Computer programs can find steady-state concentrations by finding the solution to the ordinary differential equations (ODE) when set to zero ($v_f = v_r$). To model a process at very low concentrations, programs can also use probabilistic or stochastic simulations to model probability distributions for species and their change with time for a finite number of particles. In such simulations, concentrations (in mM) are replaced with the number of particles/unit volume. ODEs don't work well to describe these conditions since changes in concentrations are not continuous.

Now, let's return to our earlier rhetorical question of deriving the equations and determining all the relevant concentrations and constants for a pathway such as glycolysis. This has been done by Teusink et al. for glycolysis in yeast. Many complicated metabolic and signal transduction pathways have been mathematically modeled to understand cellular and organismal responses better. Quantitatively modeling and predicting concentrations, inputs, and outputs of all species in complex pathways is the basis of systems biology.

14.2.2.1: BASIC PRINCIPLES OF METABOLIC CONTROL ANALYSIS - GLYCOLYSIS

Let's use a more complex example, glycolysis, to illustrate the powers of computational modeling of entire pathways. The reference for this model is shown below.

Can yeast glycolysis be understood in terms of the in vitro kinetics of the constituent enzymes? Testing biochemistry, Bas Teusink, Jutta Passarge, Corinne A. Reijenga, Eugenia Esgalhado, Coen C. van der Weijden, Mike Schepper, Michael C. Walsh, Barbara M. Bakker, Karel van Dam, Hans V. Westerhoff, and Jacky L. Snoep, 2000, *European Journal of Biochemistry*, 267, 5313-5329. PubMed ID: 10951190.

Databases containing curated models with all the above information have been developed for many pathways. The yeast glycolysis model described in the reference above and the material below is found in the Biomodels Database. The model, BIOMD0000000064, can be downloaded as a Systems Biology Markup Language (SBML) file and imported into any of the programs described above.

A variety of inputs are required for such computational analyses:

a. **Defined pathways.** These are available in many databases. An example from the KEGG pathways for yeast glycolysis is shown in the left panel of Figure **14.2.6** below. The right panel shows a more familiar representation, with glucose on the outside of the cell (Glc_o) entering the cell.

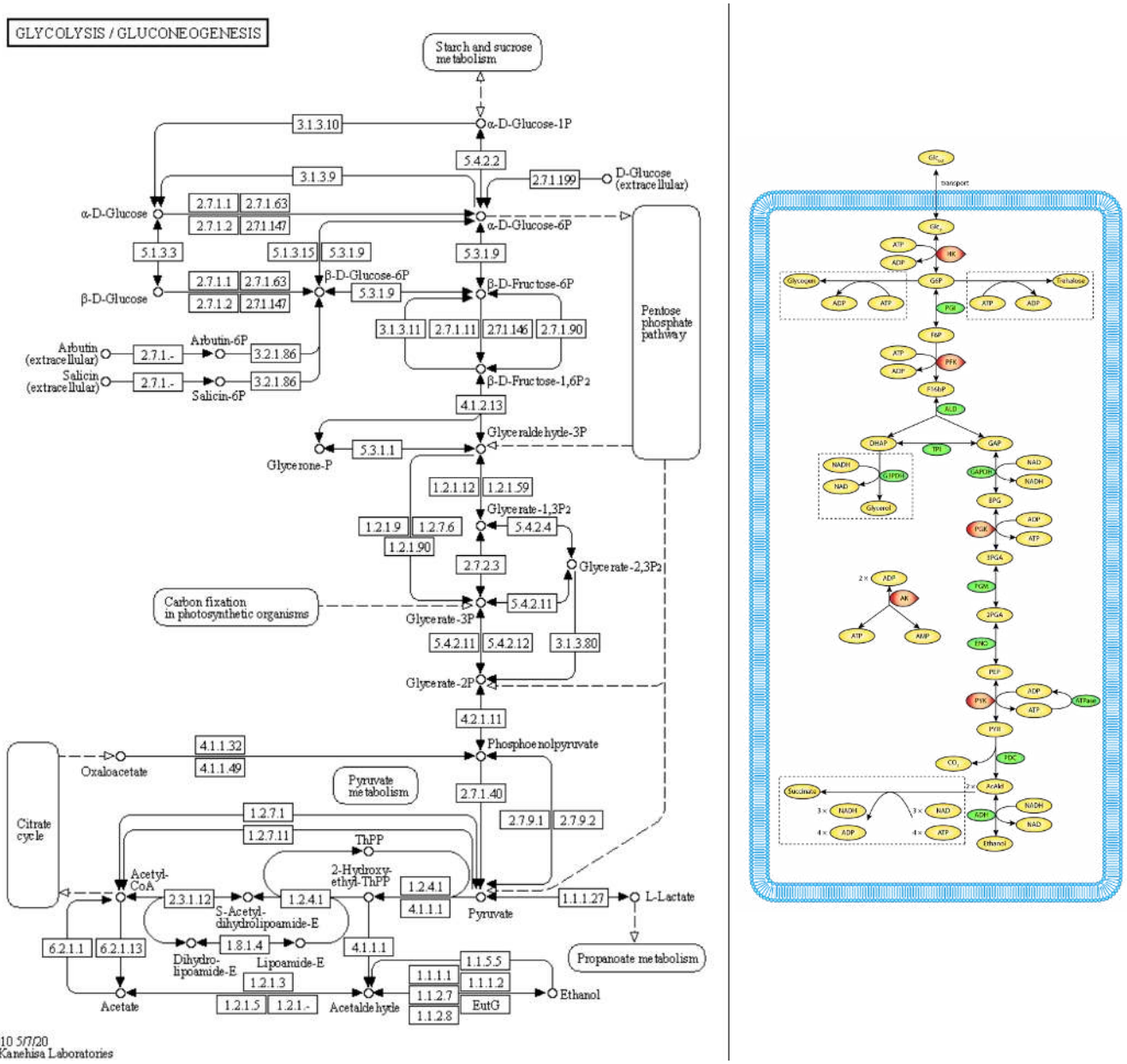


Figure **14.2.6**: Left - Glycolysis Pathway from KEGG. http://www.genome.jp/dbget-bin/www_bget?pathway:sce00010; Right - Teusink Glycolysis Model based on BIOMD0000000064. https://models.physiomeproject.org/e/72/. 6:43am 23st April 2023. CellML author(s): Catherine Lloyd. Creative Commons Attribution 3.0 Unported License.

b. A **computational modeling program** to input all parameters, equations, and models and calculate concentrations for all species as a function of time. We have been using Vcell throughout this book. A **reaction diagram** is constructed that connects all the species involved. Two are shown in Figure **14.2.7** below.

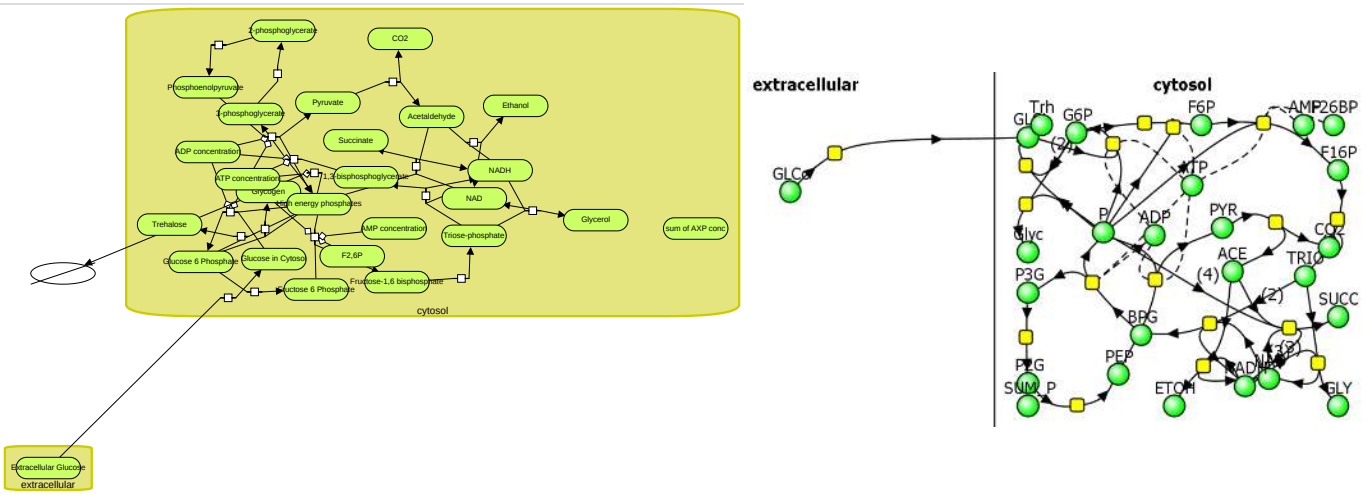


Figure **14.2.7**: Reaction Scheme for Yeast Glycolysis. Left made using NEWT Pathway Viewer using Systems Biological Graphical Notation (SBGN) for BIOMD0000000006. Right is a reaction diagram using Vcell. P represents ATP and ACE acetaldehyde.

The computational results from the analyses for yeast glycolysis were able to fit experimental data only if corrected by the addition of several branching reactions (shown in the figures above and Figure **14.2.8**) and in the dotted boxes in Figure 6 (Right)

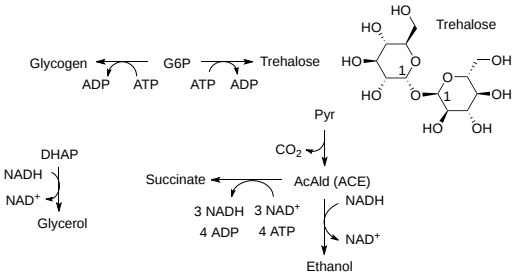


Figure **14.2.8**: Branching reactions for Yeast Glycolysis model (Teusink)

Trehalose is the non-reducing disaccharide Glc-(α 1,1)-Glc. It is a reserve carbohydrate that also protects yeast against the effects of stress (desiccation, dehydration, temperature extremes) and lethal levels of ethanol. These effects arise from its impact on protein stability, which is likely due to its preferential exclusion from the hydration sphere of proteins. A similar mechanism accounts for the stabilizing effect of glycerol on protein stability, as described in Chapter 4.9.

c. Table 2 below shows a list of all reactions as shown in Figure **14.2.10** for glycolysis and branching reactions (taken from COPASI).

Reaction	Name	Structure
ACE + NADH → NAD + ETOH	vADH	cytosol
F16P → 2TRIO	vALD	cytosol
P →	vATP	cytosol
P2G → PEP	vENO	cytosol
TRIO + NADH → NAD + GLY	vG3PDH	cytosol
NAD + TRIO → NADH + BPG	vGAPDH	cytosol
P + GLci → G6P	vGLK	cytosol
GLCo → GLci	vGLT	extracellular
G6P + P → Glyc	vGLYCO	cytosol
PYR → ACE + CO2	vPDC	cytosol
P + F6P → F16P	vPFK	cytosol
G6P → F6P	vPGI	cytosol
BPG → P + P3G	vPGK	cytosol
P3G → P2G	vPGM	cytosol
PEP → P + PYR	vPYK	cytosol
3NAD + 4P + 2ACE → 3NADH + SUCC	vSUC	cytosol
2G6P + P → Trh	vTreha	cytosol

Table **14.2.2**: List of reactants and concentrations for yeast glycolysis. P is ATP, ACE is acetaldehyde, a reactant/product of the enzyme alcohol dehydrogenase.

d. **Parameters** (concentrations, rate, enzyme kinetics, and equilibrium constants) of all species. Table **14.2.3** below shows the initial concentrations for the glycolysis model.

Species	Structure	Clamped	Conc (mM)
GLCo	extracellular	TRUE	50
GLCi	cytosol	FALSE	0.087
G6P	cytosol	FALSE	2.45
F6P	cytosol	FALSE	0.62
F16P	cytosol	FALSE	5.51
TRIO	cytosol	FALSE	0.96
BPG	cytosol	FALSE	0
P3G	cytosol	FALSE	0.9
P2G	cytosol	FALSE	0.12
PEP	cytosol	FALSE	0.07
PYR	cytosol	FALSE	1.85
ACE	cytosol	FALSE	0.17
P	cytosol	FALSE	6.31
NAD	cytosol	FALSE	1.2
NADH	cytosol	FALSE	0.39
Glyc	cytosol	TRUE	0
Trh	cytosol	TRUE	0
CO2	cytosol	TRUE	1

Table **14.2.3**: Initial concentrations for the glycolysis model. Clamped TRUE means concentrations were fixed.

e. **Equations** that can be used to compute the change in concentrations of all species with time. These are usually ordinary differential equations (ODEs) as described in Chapter 6B - Kinetics of Simple and Enzyme-Catalyzed Reactions, Sections B1: Single Step Reactions.) ODEs are easy to write but require a computer to solve as the number of interacting species increases.

For a quick review, consider the relatively simple reaction scheme shown in Figure **14.2.12** below. The set of ODEs for each species is shown below.

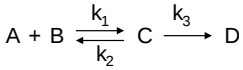


Figure **14.2.12**: Chemical reactions for ODEs

This set of ODEs for each species can be written.

$$\begin{aligned}\frac{d[A]}{dt} &= -k_1[A][B] + k_2[C] \\ \frac{d[B]}{dt} &= -k_1[A][B] + k_2[C] \\ \frac{d[C]}{dt} &= +k_1[A][B] - k_2[C] - k_3[C] = +k_1[A][B] - (k_2 + k_3)[C] \\ \frac{d[D]}{dt} &= +k_3[C]\end{aligned} \tag{14.2.6}$$

If a reaction removes species X, the right side of the ODE for the disappearance of that species has a – sign for that term. Likewise, if a reaction increases the concentration of species X, the right-hand side has a positive sign. The above examples illustrate unimolecular (C to D, C to A + B) and bimolecular (A + B to C) reactions.

Now, let's examine the equations specifically for the change in the concentration of glucose-6-phosphate. Two reactions can form it, and four reactions can remove it (check arrows for reversibility), as shown in Figure **14.2.13** below.

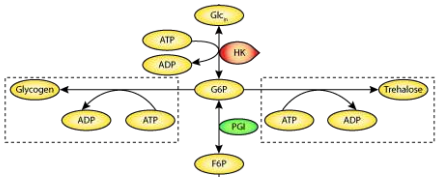


Figure **14.2.13**: The reactions that change [G6P] in the Teusink yeast glycolysis model

An ODE can be written for the change in the concentration of glucose-6-phosphate.

$$d[G6P]/dt = v_{HK} - v_{PGI} - 2v_{trehalose} - v_{glycogen}) \tag{14.2.7}$$

where HK is hexokinase and PGI is phosphoglucoisomerase. Note their is a coefficient of 2 for the formation of trehalose since it takes 2 G6Ps to make 1 trehalose.

Let's look at the terms and how they are written in Vcell.

Formation of G6P

Only one reaction goes towards G6P. It's the reaction catalyzed by hexokinase (G + ATP → G6P + ADP). In the Vcell reaction diagram, ATP is represented by P. Flux J =

$$\frac{VmGLK \cdot \left(GLCi \cdot ATP - \frac{G6P \cdot ADP}{KeqGLK}\right)}{KmGLKGLCi \cdot KmGLKATP \cdot \left(1.0 + \frac{GLCi}{KmGLKGLCi} + \frac{G6P}{KmGLKG6P}\right) \cdot \left(1.0 + \frac{ATP}{KmGLKATP} + \frac{ADP}{KmGLKADP}\right)} \quad (14.2.8)$$

Removal of G6P

3 reactions go away from G6P.

i. G6P → F6P. Flux J =

$$\frac{VmPGI\_2 \cdot \left(G6P - \frac{F6P}{KeqPGI\_2}\right)}{KmPGIG6P\_2 \cdot \left(1.0 + \frac{G6P}{KmPGIG6P\_2} + \frac{F6P}{KmPGIF6P\_2}\right)} \quad (14.2.9)$$

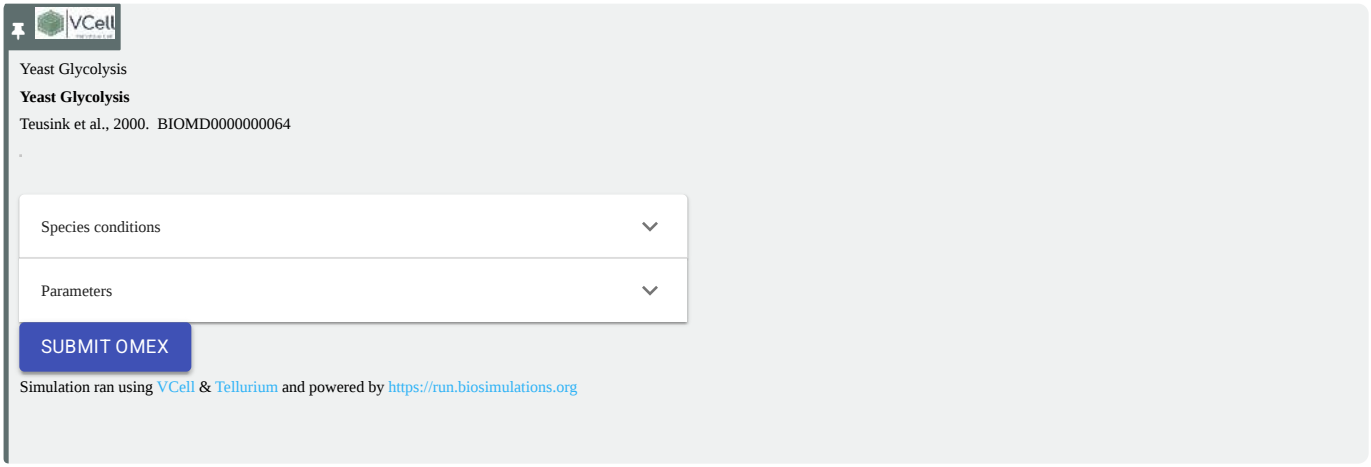
ii. G6P → Glycogen

Flux J = KGLYCOGEN_3

iii. G6P → Trehalose

Flux J = KTREHALOSE

Now let's run a simulation of the model of yeast glycolysis (*Teusink,B et al.: Eur J Biochem 2000 Sep;267(17):5313-29*). The actual model is available from Biomodels (BIOMD0000000064).



For Figure **14.2.14** below, the model was run, and the CSV file was used to plot the concentration vs time plots for each species. Two species, EtOH (50 mM) and GLCo - glucose outside (50 mM), have fixed concentrations much larger than the rest, so they are omitted from the graph for clarity. When you run the simulation above, repeat the process by downloading the CSV file and plotting the progress curves. Also, note that the y-axis values are not shown correctly when you run the simulation. Rescale them in the spreadsheet based on the correct values of EtOH and GLC0, which were held constant (clamped) throughout the time course at 50 mM.

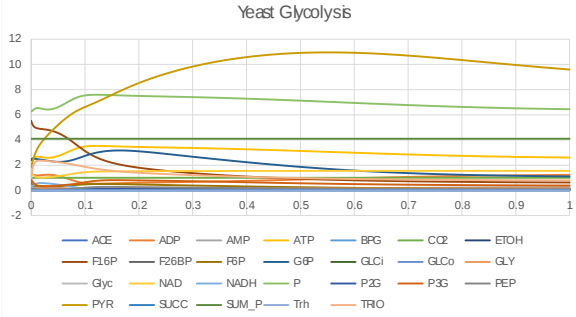


Figure **14.2.14**: Time course graphs of all glycolytic species vs time

How closely does simulation replicate fluxes found experimentally in vivo? As mentioned above, without the addition of the branch reaction, a steady state was not achieved in the simulation. Fluxes in the model were within a factor of two for only about half of the enzymes, indicating that the model requires improvement. Other discrepancies could be attributed to differences in kinetics in vivo compared to in vitro measurements. Additional products (glycogen, trehalose, glycerol, and succinate) were derived from glucose, which mainly entered glycolysis and was converted to ethanol, highlighting the complexity of modeling even a relatively "simple" pathway like glycolysis.

14.2.2.2: METABOLIC CONTROL ANALYSIS AND SIMPLE ENZYME INHIBITION

Biochemists model complex enzyme-catalyzed reactions in the presence and absence of modifiers (either activators or inhibitors) to develop reaction mechanisms. The following kinetic parameters are experimentally determined by fitting the initial velocity (vo) vs substrate concentration ([S]) through nonlinear fitting algorithms.

- K_m – the Michaelis Constant, the concentration of substrate at half-maximal velocity;
- V_m – the velocity at saturating substrate concentration;
- k_{cat} - the turnover number for conversion of bound reactant to product;
- K_{ix} – inhibition dissociation constants.

An example of competitive inhibition, shown in Figure **14.2.15**, illustrates a common type of analysis for such reactions.

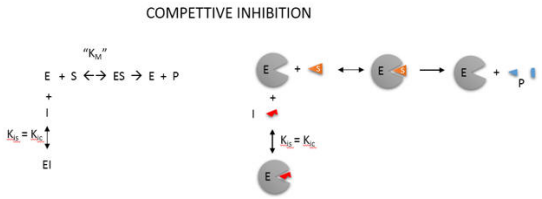


Figure **14.2.15**: Chemical reactions for competitive inhibition

One modern pictorial depiction of a simple irreversible, enzyme-catalyzed reaction of substrate S going to product P with inhibition by the product and by an added inhibitor is shown in Figure **14.2.16**. The square, a "node" in the reaction diagram, represents the enzyme.

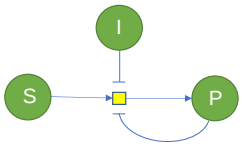


Figure **14.2.16**: Pictorial Description for product and separate competitive inhibitor

Consider the simple enzyme-catalyzed reaction for a reversible conversion of substrate S to product P that has three reversible steps, as shown in Figure **14.2.17**

$$E + S \underset{k_{-1}}{\overset{k_1}{\rightleftharpoons}} ES \underset{k_{-2}}{\overset{k_2}{\rightleftharpoons}} EP \underset{k_{-3}}{\overset{k_3}{\rightleftharpoons}} E + P$$

Figure **14.2.17**: Three step reversible enzyme-catalyzed reaction

If the forward (f) and reverse (r) chemical reaction steps were irreversible and written separately, simple Michaelis-Menten equations could be written for each.

$$\begin{aligned} v_f &= \frac{V_f S}{K_{MS} + S} = \frac{\frac{V_f S}{K_{MS}}}{1 + \frac{S}{K_{MS}}} \\ v_r &= \frac{V_r P}{K_{MP} + P} = \frac{\frac{V_r P}{K_{MP}}}{1 + \frac{P}{K_{MP}}} \end{aligned} \tag{14.2.10}$$

For the actual reversible reactions, the net forward rate cannot be found by simple subtraction of the two equations above as the differential equations describing the simple forward and reverse rates don't account for the reverse steps

$$v \neq \left[\frac{\frac{V_f S}{K_{MS}}}{1 + \frac{S}{K_{MS}}} - \frac{\frac{V_r P}{K_{MP}}}{1 + \frac{P}{K_{MP}}} \right] \tag{14.2.11}$$

A simple derivation (assuming rapid equilibrium for both forward and reverse steps) can be made for the net forward reaction. Again, consider the following enzyme-catalyzed reaction (Figure 17 above):

$$E + S \underset{k_{-1}}{\overset{k_1}{\rightleftharpoons}} ES \underset{k_{-2}}{\overset{k_2}{\rightleftharpoons}} EP \underset{k_{-3}}{\overset{k_3}{\rightleftharpoons}} E + P$$

? A DERIVATION OF THE RAPID EQUILIBRIUM, FULLY REVERSIBLE MICHAELIS-MENTEN EQUATION CONVERSION OF SUBSTRATE S TO PRODUCT P

Here it is if you wish to see it!

Derivation

You may remember that for the isolated E + S ↔ ES and for the E + P ↔ EP reactions, the simple dissociation constants, K_S and K_P are given by

$$\begin{aligned} K_S &= \frac{E_{eq} S_{eq}}{ES_{eq}} = \frac{k_{-1}}{k_1} \text{ or } ES = \frac{[E][S]}{K_S} \\ K_P &= \frac{E_{eq} P_{eq}}{EP_{eq}} = \frac{k_3}{k_{-3}} \text{ or } EP = \frac{[E][P]}{K_P} \end{aligned} \tag{14.2.12}$$

The rapid equilibrium assumption states that the rate of dissociation of ES and EP, which are both physical steps, is much faster than the rate of the chemical conversion steps for each complex. Hence, $k_{-1} \gg k_2$ and $k_3 \gg k_{-2}$, so the relative amounts of ES and EP can be determined from the dissociation constants as shown above.

Mass conservation of enzymes gives

$$E_0 = E + ES + EP = E + \frac{[E][S]}{K_S} + \frac{[E][P]}{K_p} = E\left[1 + \frac{[S]}{K_S} + \frac{[P]}{K_p}\right] \tag{14.2.13}$$

From this, we can get the fractional amount of both ES and EP

$$\begin{aligned} \frac{ES}{E_0} &= \frac{\frac{[E][S]}{K_S}}{E\left[1 + \frac{[S]}{K_S} + \frac{[P]}{K_p}\right]} \text{ or } ES = \frac{E_0 \frac{[S]}{K_S}}{\left[1 + \frac{[S]}{K_S} + \frac{[P]}{K_p}\right]} \\ \frac{EP}{E_0} &= \frac{[E][P]}{E\left[1 + \frac{[S]}{K_S} + \frac{[P]}{K_P}\right]} \text{ or } EP = \frac{E_0 \frac{[P]}{K_P}}{\left[1 + \frac{[S]}{K_S} + \frac{[P]}{K_P}\right]} \end{aligned} \tag{14.2.14}$$

Now, we can derive the rate equation for the net forward reaction for the rapid equilibrium case:

$$v = k_2[ES] - k_{-2}[EP] = k_2 \frac{E_0 \frac{[S]}{K_S}}{\left[1 + \frac{[S]}{K_S} + \frac{[P]}{K_p}\right]} - k_{-2} \frac{E_0 \frac{[P]}{K_p}}{\left[1 + \frac{[S]}{K_S} + \frac{[P]}{K_p}\right]} \tag{14.2.15}$$

Knowing that k_2E_0 and $k_{-2}E_0$ represent the maximal velocities, V_f and V_r, respectively, the equation becomes:

$$v = k_2[ES] - k_{-2}[EP] = \frac{V_f \frac{[S]}{K_S}}{\left[1 + \frac{[S]}{K_S} + \frac{[P]}{K_p}\right]} - \frac{V_r \frac{[P]}{K_p}}{\left[1 + \frac{[S]}{K_S} + \frac{[P]}{K_p}\right]} = \frac{V_f \frac{[S]}{K_S} - V_r \frac{[P]}{K_p}}{\left[1 + \frac{[S]}{K_S} + \frac{[P]}{K_p}\right]} \tag{14.2.16}$$

Here is the derived equation.

$$v = k_2[ES] - k_{-2}[EP] = \frac{V_f \frac{[S]}{K_S}}{\left[1 + \frac{[S]}{K_S} + \frac{[P]}{K_P}\right]} - \frac{V_r \frac{[P]}{K_P}}{\left[1 + \frac{[S]}{K_S} + \frac{[P]}{K_P}\right]} = \frac{V_f \frac{[S]}{K_S} - V_r \frac{[P]}{K_P}}{\left[1 + \frac{[S]}{K_S} + \frac{[P]}{K_P}\right]} \tag{14.2.17}$$

An equation of a similar form can be derived from the steady state assumption. Hence, the net forward rate can't be determined by the simple subtraction of the backward rate from the forward rate, as shown in Equation 10 above.

14.2.3: COMMON FORMS OF KINETIC EQUATIONS

Programs like COPASI and VCell have many built-in equations for the velocities of many enzyme-catalyzed reactions with similar forms. Two are shown below:

Reversible Michaelis-Menten:

$$\frac{\frac{V_f[\text{substrate}]}{K_{Ms}} - \frac{V_r[\text{product}]}{K_{Mp}}}{1 + \frac{[\text{substrate}]}{K_{Ms}} + \frac{[\text{product}]}{K_{Mp}}} \tag{14.2.18}$$

Competitive Inhibition Reversible:

$$\frac{\frac{V_f[\text{substrate}]}{K_{Ms}} - \frac{V_r[\text{product}]}{K_{Mp}}}{1 + \frac{[\text{substrate}]}{K_{Ms}} + \frac{[\text{product}]}{K_{Mp}} + \frac{[\text{inhibitor}]}{K_I}} \tag{14.2.19}$$

What is most important for readers to understand is not detailed derivations or how to solve the differential equations on their own. However, you should be able to:

- write the differential equation of a given reaction.
- recognize the common equations used for nonenzyme-catalyzed reactions (mass action) and enzyme-catalyzed ones;
- change parameters in programs that use numerical methods to solve systems of linked differential equations for a system, and see how the time course graphs are affected.

14.2.4: SUMMARY

This chapter introduces the fundamentals of metabolic control analysis (MCA) by exploring the complexities of enzyme kinetics within metabolic pathways. It begins by addressing the challenges inherent in studying enzyme-catalyzed reactions, including the involvement of multiple chemical species, numerous rate and dissociation constants, and complex reaction mechanisms. Key highlights include:

- **Complexity in Enzyme Kinetics:**
  The chapter outlines the difficulties in deriving kinetic equations for enzyme-catalyzed reactions, using an example that demonstrates how multiple reaction steps and intermediates can be mathematically described by ordinary differential equations (ODEs).
- **Equilibrium vs. Steady State:**
  Two scenarios are contrasted: a closed system reaching equilibrium (with no net change in reactant or product concentrations) and an open system achieving a steady state where inputs equal outputs. The steady state concept is emphasized as more relevant to in vivo conditions, where enzymes operate under continuous flux rather than static equilibrium.
- **In Vitro vs. In Vivo Kinetics:**
  A significant portion of the chapter is devoted to understanding the differences between controlled laboratory experiments (in vitro) and the dynamic environment of the cell (in vivo). The discussion highlights that while in vitro assays focus on initial rate measurements with varying substrate concentrations, in vivo systems are governed by steady-state fluxes that maintain balanced metabolite levels.
- **Simulation and Modeling Tools:**
  The use of computational tools like VCell and COPASI is introduced to simulate progress curves (concentration versus time) for enzyme reactions. These simulations illustrate how embedding an enzyme within a “mini-pathway” alters its apparent equilibrium constant compared to when it is studied in isolation.
- **Derivation of Kinetic Equations:**
  The chapter walks through the derivation of a net forward rate equation for reversible enzyme reactions under rapid equilibrium assumptions. It explains why the net rate cannot simply be determined by subtracting the reverse rate from the forward rate, and extends the discussion to include the impact of enzyme inhibitors.
- **Modeling Complex Pathways:**
  Using yeast glycolysis as a model system, the chapter demonstrates how complex pathways are mathematically modeled. It covers the integration of branching reactions, parameterization with experimental data, and the construction of reaction schemes to account for the dynamic behavior of metabolites.

Overall, this chapter equips students with both the theoretical framework and practical skills necessary for analyzing and modeling metabolic networks. By combining mathematical derivations with computational simulations, junior and senior biochemistry majors gain a comprehensive understanding of how enzyme kinetics and pathway dynamics are integrated within the broader context of systems biology.

This page titled 14.2: Basic Principles of Metabolic Control Analysis (MCA) is shared under a not declared license and was authored, remixed, and/or curated by Henry Jakubowski and Patricia Flatt.

- **11.2: Diffusion Across a Membrane - Passive and Facilitated Diffusion** by Henry Jakubowski and Patricia Flatt has no license indicated.

14.3: THE FLUX CONTROL COEFFICIENT

LEARNING GOALS (CHATGPT O3-MINI)

Below is a series of learning goals designed for junior and senior biochemistry majors to master the concepts presented in the introduction to metabolic control analysis:

1. **Define Metabolic Control Analysis (MCA):**
   - Explain MCA and its relevance in understanding the dynamic behavior of complex metabolic and signal transduction systems.
   - Describe how external inputs, outputs, pools, and reservoirs interact with internal enzymatic processes.
2. **Differentiate Between Local and System-Level Properties:**
   - Contrast traditional enzyme parameters (e.g., K_M and V_M) with system-level control parameters such as control coefficients.
   - Use analogies (e.g., emergent properties like consciousness) to illustrate why a system's behavior cannot be predicted solely from isolated components.
3. **Understand the Flux Control Coefficient (FCC):**
   - Define the FCC also represented as (C_{Ei}^{J}), as the ratio of the fraction change in flux (dJ/J) to the fractional change in the enzyme "i" concentration/activity (dE_i/E_i or dU_i/U_i), and explain its mathematical representation.
   - Interpret the significance of the FCC in quantifying how changes in the activity or concentration of a single enzyme affect overall pathway flux.
4. **Apply the Summation Theorem:**
   - Demonstrate that the sum of all individual flux control coefficients in a pathway equals 1 or $\sum_{i=1}^{n} C_{Ei}^{J} = 1$
   - Discuss the implications of shared flux control across multiple enzymes and why the concept of a single "rate-limiting" enzyme can be misleading.
5. **Analyze Sensitivity in Metabolic Pathways:**
   - Explain how sensitivity analyses reveal the impact of small perturbations (e.g., 1% changes) in enzyme activities on overall pathway flux.
   - Evaluate experimental and computational data showing that even enzymes with high thermodynamic driving forces (e.g., HK, PFK, PK) may have minor flux control in steady-state conditions.
6. **Interpret System-Level Control Parameters:**
   - Identify and distinguish between different control coefficients, such as the Flux Control Coefficient, Concentration Control Coefficient, and Elasticity Coefficient.
   - Discuss which parameters have the greatest impact on pathway output, system resilience, or fragility, and the importance of accurate measurement.
7. **Explore Flux Control in Aerobic Glycolysis:**
   - Describe how the Warburg effect is quantified (e.g., $W=J_{Lac}/J_{ox}$) and its implications for energy and biosynthetic demands in proliferating cells.
   - Analyze the experimental and modeling evidence that highlights the central role of enzymes like GAPDH in regulating the balance between anaerobic and aerobic pathways.
8. **Integrate Computational and Experimental Approaches:**
   - Explain how computational models (using tools such as VCell) are used to simulate metabolic pathways and validate them against experimental flux measurements.
   - Discuss the process of using sensitivity analyses and FCC measurements to refine models of complex systems like yeast glycolysis.
9. **Assess the Impact of Enzyme Regulation on Flux Distribution:**
   - Evaluate how feedback inhibition, allosteric regulation, and changes in enzyme concentration or activity contribute to the distributed control of metabolic flux.
   - Discuss examples where alterations in one enzyme's activity affect the entire pathway, underscoring the interconnected nature of metabolic control.
10. **Critically Evaluate the Concept of "Rate Limiting":**

- Reconsider the traditional notion of a “rate-limiting” enzyme in light of quantitative MCA, where flux control is shared among multiple steps.
- Analyze how computational and experimental studies challenge and refine our understanding of enzyme control in metabolic networks.

These learning goals aim to provide students with a comprehensive framework for understanding and applying metabolic control analysis in both theoretical and practical contexts, bridging isolated enzyme kinetics with whole-system behavior.

14.3.1: INTRODUCTION

Metabolic control analysis (MCA) is one method used to address the complexity of dynamic changes of species in a complex metabolic system. As such, an understanding of MCA would apply to complex signal transduction pathways and other emerging areas in systems biology. In MCA, external inputs (source) and outputs (exits), and pools and reservoirs exist. These are connected to the internal metabolic enzymes, reactants, and products of the pathway connecting the two external reservoirs.

In studying complex metabolic systems, what is interesting to know is not just the K_M or V_M of particular enzymes (such as those far from equilibrium or catalyzing “rate-limiting” steps based on in vitro studies), but rather the control parameters, known as **control coefficients**, for the system. These coefficients are properties of the whole pathway as an emerging system with properties different from those of the individual steps. Another example of an emergent property is consciousness. It must emerge from the incredible assembly of around 90 billion neurons in the brain, forming around 10^{15} synapses. It cannot simply be predicted from the properties of isolated neurons. Three especially relevant parameters are used in metabolic control analyses: the Flux Control Coefficient, the Concentration Control Coefficient, and the Elasticity Coefficient.

To understand how a pathway is regulated and how scientists modify it to meet their demands, one needs to understand these coefficients. In particular, we would like to know which:

- parameters have the greatest effect (increase or decrease) on a preferred outcome;
- properties of the system make it most resilient or fragile;
- parameters should be measured most accurately

14.3.2: THE FLUX CONTROL COEFFICIENT

The **Flux Control Coefficient** (C_{Ei}^{J}) gives the relative fractional change in pathway flux J (dJ/J) (a system variable) with fractional change in concentration or activity of an enzyme Ei (du_i/u_i). The change in the concentration of an enzyme can arise from increased synthesis or degradation of the enzyme, a change in a modifier (an inhibitor or activator), a covalent modification, the presence of inhibitor RNA, mutations, etc. Again, the word flux J is used to describe the rate of the system, whereas rate or velocity v is used to describe an individual enzyme in the system. Think of u as “units” of activity.

The **Flux Control Coefficient** (C_{Ei}^{J}) can also be written as

$$C_{Ei}^{J} = \frac{dJ}{du}\frac{u}{J} \tag{14.3.1}$$

The dJ/du in Equation 14.3.1 suggests that the C_{Ei}^{J} is equal to the slope of a plot of J vs u multiplied by u/J at that point. Alternatively, it is the slope of an ln-ln plot of $\ln J$ vs $\ln u$. A more formal definition would be obtained using partial derivatives (a normal derivative like dy/dx with every other variable held constant) - in this case, all other enzyme concentrations or activities other than the one under study:

$$C_{Ei}^{J} = \frac{\dfrac{\partial J}{J}}{\dfrac{\partial u}{u}} = \frac{\partial \ln J}{\partial \ln u_i} \tag{14.3.2}$$

C_{Ei}^{J} clearly shows how the system flux changes with changes in the activity of a single enzyme. The variable ui is a property of an enzyme (a local property), but J and concentrations (for the concentration coefficient – see below) are system variables. Hence, every enzyme in a pathway has a flux control coefficient. How are they related? It makes sense that the sum of all of the individual $C_{Ei}^{J} = 1$ as the fractional change in flux, $\partial J/J$, is equal in magnitude to the fractional change in all enzyme activities. This relationship, shown below, is called the **Summation Theorem**.

$$\sum_{i=1}^{n} C_{Ei}^{J} = 1 \tag{14.3.3}$$

This equation would predict that if one magical enzyme X were truly rate-limiting and completely controlled that rate, then $C^{J}_{Ex} = 1$ for that enzyme and 0 for all the other enzymes. Yet this is counterintuitive since if all the enzymes are linked, their responses should also be linked.

Hence, all enzymes share control of flux.

Another way to consider this is to consider a linear set of connected reactions. For these enzymes, C^J_{Ei} would vary between 0 and 1. If one enzyme was completely rate limiting, its C^J_{Ei} = 1 indicating that the fractional change in flux, $\partial J/J$, is equal to the fractional change in enzyme concentration (or activity) u, $\partial u/u$, for enzyme X. This implies that all change in flux is accounted for by the change in the concentration of enzyme X. This is a bit difficult to believe so it would make sense to think of the control of a pathway as being distributed over all the enzymes in the pathway. Plots of flux J vs enzyme activity u are similar to rectangular hyperbolas. Hence, the flux coefficient changes with enzyme activity and flux, so at different fluxes, different enzyme flux coefficients would also change. “Control” gets redistributed in the pathway.

Textbooks often describe that, ideally, the first step of a linear pathway would be the committed step and be rate-limiting. But think of this. If the end product of a pathway feeds back and inhibits the first enzyme in the pathway, then the last enzyme influences the first enzyme, although the last is not considered “rate-limiting”. Now, if another enzyme removes the last product and hence the first enzyme's feedback inhibitor of the pathway, that enzyme also determines flux. This again shows that flux control is distributed throughout the system. The classical “rate-limiting” enzyme might still have the largest C^J_{Ei} of the pathways, but if the system is in a steady state, all enzymes have the same rate. Hence, the term “rate-limiting” is somewhat misleading in a pathway. Analysis of flux control coefficients gives a truly quantitative analysis of the system pathway.

Phosphofructokinase is said to be a “key” enzyme in glycolysis as it is one of three enzymes in the pathway that is characterized by a large negative free energy difference. Figure **14.3.1**:

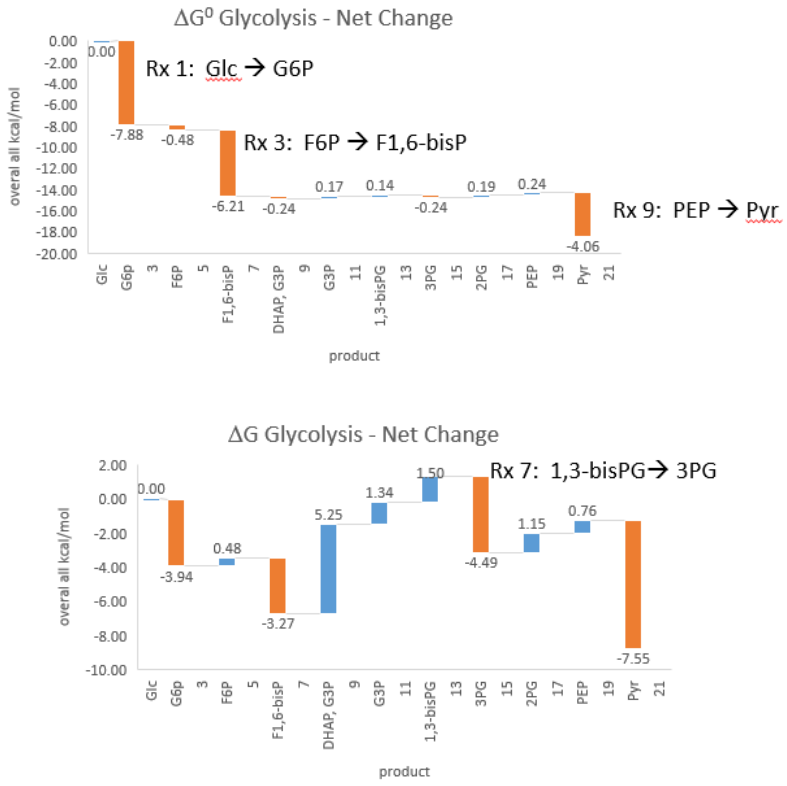


Figure **14.3.1**: ΔG^0 and ΔG values for enzymes in glycolysis

It is also highly regulated. However, Heinisch et al. (Molecular and General Genetics, 202, 75-82) found that increasing its concentration 3.5-fold in fermenting yeast did not affect the flux of ethanol production.

Here are some results of "sensitivity analyses" of yeast glycolysis showing the effect of small changes (up to 5%) on the flux control coefficients of glycolytic enzymes. The changes in the enzymes for these analyses are 1%. The numbers are scaled values that represent a relative change. A value of + 0.5 means that if the parameter is increased by 10%, the target value will increase by 5%. A column shows the rate of a reaction that is changed, and the row indicates the flux of the reaction that has been affected. Green represents positive values and red, negative, with the intensity of the color correlating with the extent of the change. The table is split, with column 1 headings of the first table applying to tables 2 and 3 as well.

	(Hexokinase)	(Glucose-6-phosphate is...	(Glycogen synthesis)	(Trehalose 6-phosphate ...	(Phosphofructokinase)	(Aldolase)
(Hexokinase)	0.155598	0.00218158	-0.0213366	-0.0147151	0.0016614	0.000351121
(Glucose-6-phos...	0.177323	0.00248618	-0.101886	-0.0788257	0.00189337	0.000400147
(Glycogen synth...	0	0	1	0	0	0
(Trehalose 6-pho...	0	0	0	1	0	0
(Phosphofructok...	0.177323	0.00248618	-0.101886	-0.0788257	0.00189337	0.000400147
(Aldolase)	0.177323	0.00248618	-0.101886	-0.0788257	0.00189337	0.000400147
(Glyceraldehyde ...	0.188586	0.0026441	-0.107526	-0.0833339	0.00201363	0.000425563
(Phosphoglycera...	0.188586	0.0026441	-0.107526	-0.0833339	0.00201363	0.000425563
(Phosphoglycera...	0.188586	0.0026441	-0.107526	-0.0833339	0.00201363	0.000425563
(Enolase)	0.188586	0.0026441	-0.107526	-0.0833339	0.00201363	0.000425563
(Pyruvate kinase)	0.188586	0.0026441	-0.107526	-0.0833339	0.00201363	0.000425563
(Pyruvate decarb...	0.188586	0.0026441	-0.107526	-0.0833339	0.00201363	0.000425563
(Succinate synth...	0.0928625	0.00130199	-0.0595875	-0.0450188	0.00099154	0.000209553
(Glucose transpo...	0.155598	0.00218158	-0.0213366	-0.0147151	0.0016614	0.000351121
(Alcohol dehydr...	0.19398	0.00271972	-0.110228	-0.0854928	0.00207122	0.000437735
(Glycerol 3-phos...	0.0928625	0.00130199	-0.0595875	-0.0450188	0.00099154	0.000209553
(ATPase activity)	0.268522	0.00376484	-0.292486	-0.202286	0.00286714	0.000605945

Table, part 2, continued:

	(Glyceraldehyde 3-phosp...	(Phosphoglycerate kinase)	(Phosphoglycerate muta...	(Enolase)	(Pyruvate kinase)	(
(Hexokinase)	0.0132581	0.000377931	0.00030863	0.000840434	0.000428631	(
(Glucose-6-phosphate isomerase)	0.0151093	0.0004307	0.000351723	0.000957781	0.000488479	(
(Glycogen synthesis)	0	0	0	0	0	(
(Trehalose 6-phosphate synthase)	0	0	0	0	0	(
(Phosphofructokinase)	0.0151093	0.0004307	0.000351723	0.000957781	0.000488479	(
(Aldolase)	0.0151093	0.0004307	0.000351723	0.000957781	0.000488479	(
(Glyceraldehyde 3-phosphate dehy...	0.0476129	0.00135724	0.00110836	0.00301819	0.00153931	(
(Phosphoglycerate kinase)	0.0476129	0.00135724	0.00110836	0.00301819	0.00153931	(
(Phosphoglycerate mutase)	0.0476129	0.00135724	0.00110836	0.00301819	0.00153931	(
(Enolase)	0.0476129	0.00135724	0.00110836	0.00301819	0.00153931	(
(Pyruvate kinase)	0.0476129	0.00135724	0.00110836	0.00301819	0.00153931	(
(Pyruvate decarboxylase)	0.0476129	0.00135724	0.00110836	0.00301819	0.00153931	(
(Succinate synthesis)	-0.228632	-0.0065173	-0.00532223	-0.014493	-0.00739161	-
(Glucose transport)	0.0132581	0.000377931	0.00030863	0.000840434	0.000428631	(
(Alcohol dehydrogenase)	0.0631784	0.00180094	0.0014707	0.00400489	0.00204254	(
(Glycerol 3-phosphate dehydrogen...	-0.228632	-0.0065173	-0.00532223	-0.014493	-0.00739161	-
(ATPase activity)	0.165497	0.0047176	0.00385254	0.0104909	0.00535047	(

Table, part 3, continued

	(Pyruvate decarboxylase)	(Succinate synthesis)	(Glucose transport)	(Alcohol dehydrogenase)	(Glycerol 3-phosphate d...	(ATPase activity
(Hexokinase)	.000256363	-0.0178963	0.984936	0.00560057	-0.0289301	-0.08292
(Glucose-6-phosphate isomerase)	.000292158	-0.0203951	1.12246	0.00638256	-0.0329695	-0.0944978
(Glycogen synthesis)		0	0	0	0	0
(Trehalose 6-phosphate synthase)		0	0	0	0	0
(Phosphofructokinase)	.000292158	-0.0203951	1.12246	0.00638256	-0.0329695	-0.0944978
(Aldolase)	.000292158	-0.0203951	1.12246	0.00638256	-0.0329695	-0.0944978
(Glyceraldehyde 3-phosphate dehy...	.00092066	-0.0681563	1.19375	0.0213292	-0.110646	-0.0946468
(Phosphoglycerate kinase)	.00092066	-0.0681563	1.19375	0.0213292	-0.110646	-0.0946468
(Phosphoglycerate mutase)	.00092066	-0.0681563	1.19375	0.0213292	-0.110646	-0.0946468
(Enolase)	.00092066	-0.0681563	1.19375	0.0213292	-0.110646	-0.0946468
(Pyruvate kinase)	.00092066	-0.0681563	1.19375	0.0213292	-0.110646	-0.0946468
(Pyruvate decarboxylase)	.00092066	-0.0681563	1.19375	0.0213292	-0.110646	-0.0946468
(Succinate synthesis)	0.00442091	0.337761	0.587821	-0.1057	0.549517	-0.0933806
(Glucose transport)	.000256363	-0.0178963	0.984936	0.00560057	-0.0289301	-0.08292
(Alcohol dehydrogenase)	.00122164	-0.0910284	1.2279	0.0284869	-0.147844	-0.0947182
(Glycerol 3-phosphate dehydrogen...	0.00442091	0.337761	0.587821	-0.1057	0.549517	-0.0933806
(ATPase activity)	.00320011	-0.240966	1.69975	0.0754091	-0.39165	-0.116635

Some things to note:

- almost everything has changed in each column, which shows that a change in one enzyme affects all enzymes;
- 2 adjacent rows often have identical numbers since they describe two connected reactions (without branches), so their steady state fluxes will be the same;
- the sum of the C_{Ei}^{J} values across the same row in both tables is 1 (summation theorem);
- perturbations of the "big 3" enzymes for steps 1,3, and 10 in glycolysis (hexokinase, phosphofructokinase, and pyruvate kinase), all of which proceed with a significant $-\Delta G^0$ and $-\Delta G$, have **minor effects** on the flux.

It should be clear from these results that you can't predict the enzymes that control the flux without this kind of mathematical analysis. Don't rely on just your "biochemical intuition."

14.3.3: FLUX CONTROL IN AEROBIC GLYCOLYSIS

Let's look at another pathway to run a full simulation using Vcell - aerobic glycolysis. We have mostly encountered glycolysis as a central anaerobic pathway in almost all organisms. In some cases, it can also run aerobically. One prime example is cancer cells, which require both energy in the form of ATP and anabolic building blocks to proliferate - a hallmark of cancer cells. Warburg noted aerobic glycolysis, and this effect now bears his name.

Aerobic glycolysis has been modeled in yeast cells. The pathway is shown in Figure **14.3.2** below.

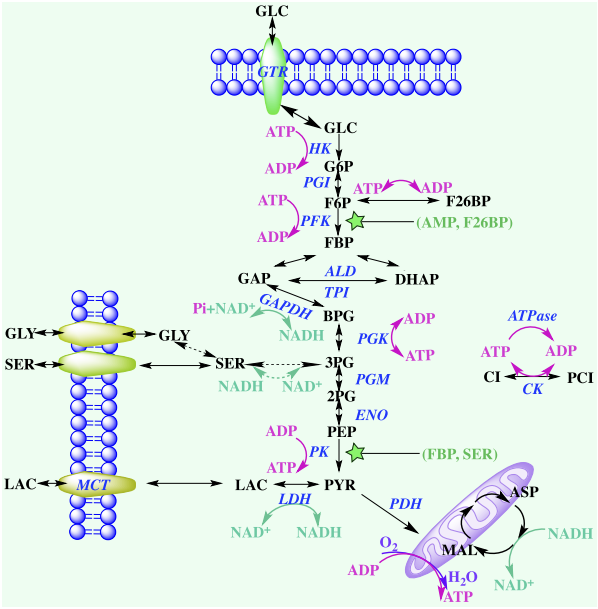


Figure **14.3.2**: Schematic of the glycolysis model with chemical reactions and allosteric points of regulation described. Alexander A Shestov et al. (2014) Quantitative determinants of aerobic glycolysis identify flux through the enzyme GAPDH as a limiting step. eLife 3:e03342. https://doi.org/10.7554/eLife.03342. Creative Commons Attribution License

Abbreviations: GLC—glucose, G6P—glucose-6-phosphate, F6P—fructose-6-phosphate, FBP—fructose-1,6,-bisphosphate, F26BP—fructose-2,6,-bisphosphate, GAP—glcyceraldehyde-3-phosphate, DHAP—dihydroxyacetone phosphate, BPG—1,3 bisphosphoglycerate, 3PG—3-phosphoglycerate, 2PG—2-phosphoglycerate, PEP—phosphoenolpyruvate, PYR—pyruvate, SER—Serine, GLY—glycine, Lac—lactate, MAL—malate, ASP—aspartate, Pi—inorganic phosphate, CI—creatine, PCI—phosphophocreatine, GTR—glucose transporter, HK—hexokinase, PGI—phosphoglucoisomerase, PFK—phosphofructokinase, ALD—aldolase, TPI—triosephosphoisomerase, GAPDH—glyceraldehyde-phosphate dehydrogenase, PGK—phosphoglycerate kinase, PGM—phosphoglycerate mutase, ENO—enolase, PK—pyruvate kinase, LDH—lactate dehydrogenase, MCT—monocarboxylate transporter, PDH—pyruvate dehydrogenase, CK—creatine kinase.

The Warburg Effect **W** can be quantitatively described by the ratio of the flux of pyruvate to lactate (J_{Lac}) compared to the flux of pyruvate entry into the mitochondria and subsequent consumption of O_2 by mitochondrial oxidative phosphorylation (J_{ox}), so $\mathbf{W} = J_{Lac}/J_{ox}$).

Usually, in normal conditions for healthy cells, W <0.10, so less than 10% of glucose is converted (or diverted) to lactate. On average, for different tissues, W < 0.3. Hence, some lactate is always being made. High values of W (> 1) mean that most of the glucose is diverted to lactate synthesis. The W values is determined by lots of factors that determine the energy state of cells, including rates of glucose uptake, ATP hydrolysis, and biosynthesis, as well as the balance of cytoplasmic and mitochondrial NAD^+/NADH, hence the redox state of the cell. Key to the balance leading to aerobic glycolysis is the need to reoxidize cytosolic NADH back to NAD^+ under aerobic conditions so glycolysis can continue under conditions when there is a high growth rate.

How does a cell know which path to take, pyruvate to lactate (anaerobic), pyruvate to CO_2 with ATP synthesis (aerobic), or some of both? Regarding metabolic control analysis, what controls the flux of pyruvate through these paths? This is where computational modeling informed by experimental data helps. We can determine the flux control coefficient (C^J_{Ei}), more easily written as **FCC**, for each enzyme in glycolysis to help us understand what controls the flux. Figure **14.3.3** metaphorically describes these different paths. In a way, the flux of pyruvate through these three choices, anaerobic, aerobic, and both (as reflected by the Warburg effect W) is then perhaps the best example to use to discuss flux control since the readers are likely very familiar with the concept of anaerobic and aerobic metabolism and the "switch" between them when running short sprints vs marathons.

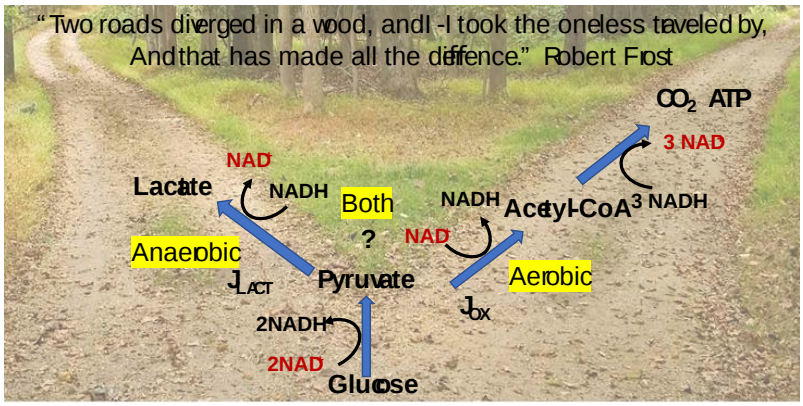


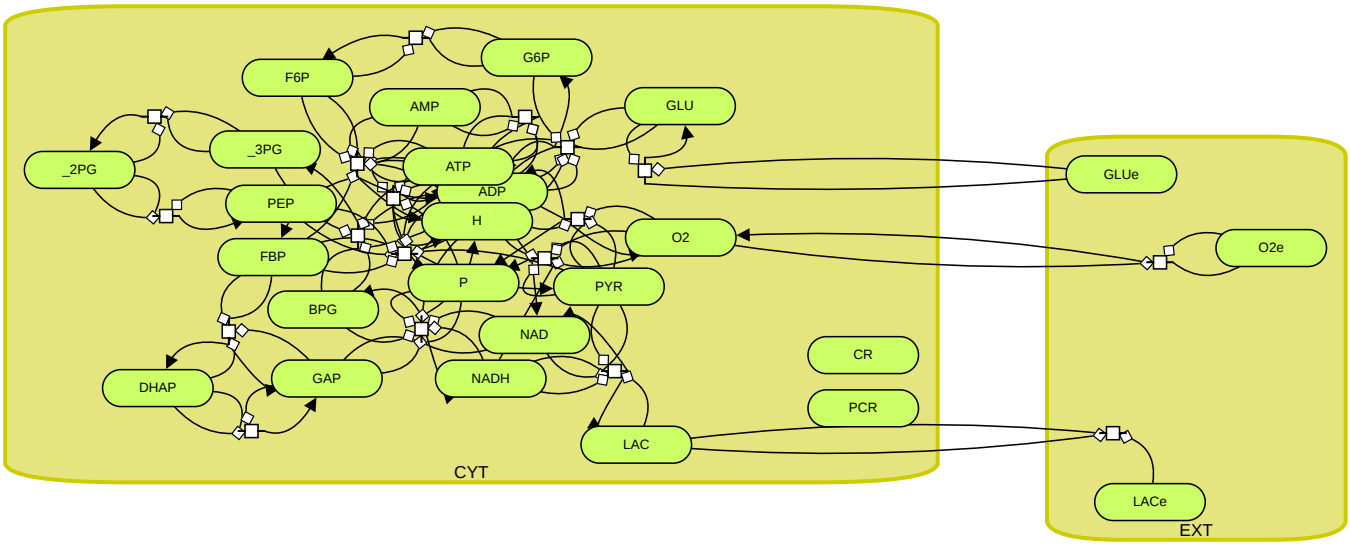
Figure **14.3.3**: Fluxs of pyruvate through multiple paths

Now let's run the Vcell model for aerobic glycolysis in yeast.

VCell MODEL

AerobicGlycolysis

Quantitative determinants of aerobic glycolysis identify flux through the enzyme GAPDH as a limiting step. .Shestov AA, Liu X, Ser Z, Cluntun AA, Hung YP, Huang L, Kim D, Le A, Yellen G, Albeck JG, Locasale JW. *eLife* , 7/ 2014 , Volume 3 , PubMed ID: 25009227. Biomodel MODEL1504010000



Select Load [model name] below

Load AerobicGlycolysis

Select **Start** to begin the simulation.

Select **Plot** to change Y axis min/max, then **Reset** and **Play** | Select **Slider** to change which constants are displayed | Select **About** for software information.

Move the sliders to change the constants and see changes in the displayed graph in real-time.

Time course model made using Virtual Cell (Vcell), **The Center for Cell Analysis & Modeling**, at **UConn Health**. Funded by NIH/NIGMS (R24 GM137787); Web simulation software (miniSidewinder) from Bartholomew Jardine and Herbert M. Sauro, University of Washington. Funded by NIH/NIGMS (RO1-GM123032-04)

Where did all the parameters in the model come from? They are derived experimentally, and the goal of modeling is to produce a computational model that is consistent with the experimental findings that are fed into the model.

The result of the model suggests that the Warburg effect is determined by the growth rate of the cells as well as the activity of mitochondria. The model does **not** support the idea that aerobic glycolysis balances energy needs and new biosynthesis as cells proliferate. Rather, the cells that proliferate the most have the most active mitochondria and, hence, lower levels of lactate production. Redox balance is key in pushing cells toward lactate synthesis and aerobic glycolysis.

A key step is catalyzed by glyceraldehyde-3-phosphate dehydrogenase (**GAPDH**), the glycolytic enzyme that separates the top and bottom halves of glycolysis. Experimental data show that flux through this enzyme is rate-limiting, with the levels of F1,6-BP also being very important. Some key steps that were thought to be rate-limited had negative fluxes. Negative flux control coefficients were found and confirmed for several steps thought to be rate-limiting in glycolysis.

The flux control coefficients, given by the formula

$$C_{Ei}^{J} = \frac{\frac{\partial J}{J}}{\frac{\partial u}{u}} = \frac{\partial \ln J}{\partial \ln u_i} \tag{14.3.4}$$

were calculated for each enzyme in the glycolytic pathway. The authors of the study used this equation for the Flux Control Coefficient:

$$FCC = \frac{d \ln [J_{LACT}]}{d \ln [E_i]} \tag{14.3.5}$$

The fluxes were measured for lactate production using 13C-labeled lactate to get the absolute lactate concentration. Fluxes were then measured by changes in ^{13}C-lactate production with time. The FCC of each enzyme could be calculated using these data and the selective inhibition by small drugs of each step in glycolysis to alter the "concentration/activity of the enzyme". The results are shown in Figure **14.3.4** below.

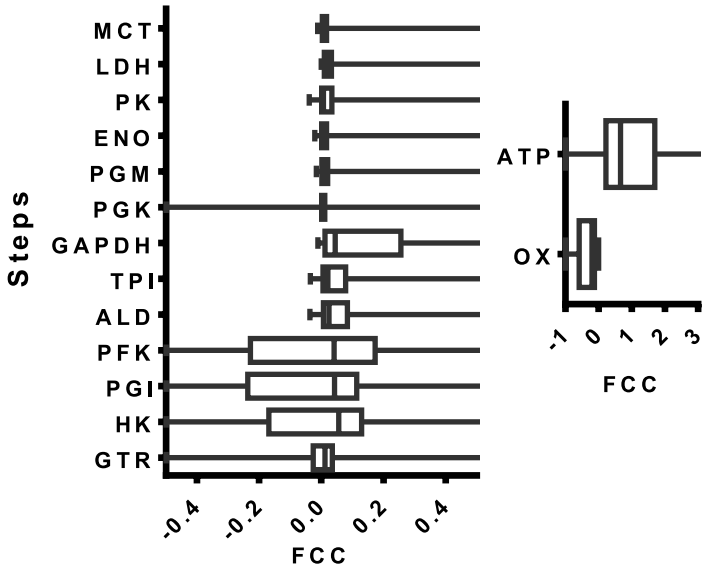


Figure **14.3.4**: (left) Box plots of flux control coefficient (FCC) for lactate production for each enzymatic step in glycolysis (FCC = $dlnJ_{lac}/dln\ E_i$) where J_{lac} is the rate of pyruvate conversion to lactate, and E_i is the ith enzyme in glycolysis for each step of glycolysis. (right) Box plots of flux control coefficient (FCC) for lactate production, oxygen consumption (OxPhos), and ATP consumption (ATP). Shestov et al., ibid

The left-hand side of Figure 4 shows that two of the key enzymes that are thermodynamically favored in glycolysis, PFK (phosphofructokinase) and HK (hexokinase), both driven by ATP hydrolysis, have essentially *negative* flux coefficients, so they are **NOT** key in driving flux toward lactate. Only one enzyme, GAPDH, is characterized by a positive flux coefficient. (Remember, we are talking about flux coefficients, not the Warburg effect factor W.)

Also important, as mentioned above, is the concentration of F1,6BP (FBP in the figure below). The model and data show that high levels of FBP and associated higher concentrations of the reactants in the first half of glycolysis (denoted by ↑↑ a large font size). A corresponding depletion of substrates in the bottom half (denoted by ↓↓) actually causes a bottleneck in glycolysis and inhibits flux through GADPH. Hence, GADPH determines the flux through glycolysis. This "bottleneck" is associated with the redox and energy states of the cell. These outcomes are illustrated in Figure **14.3.1** below.

Figure **14.3.5**:

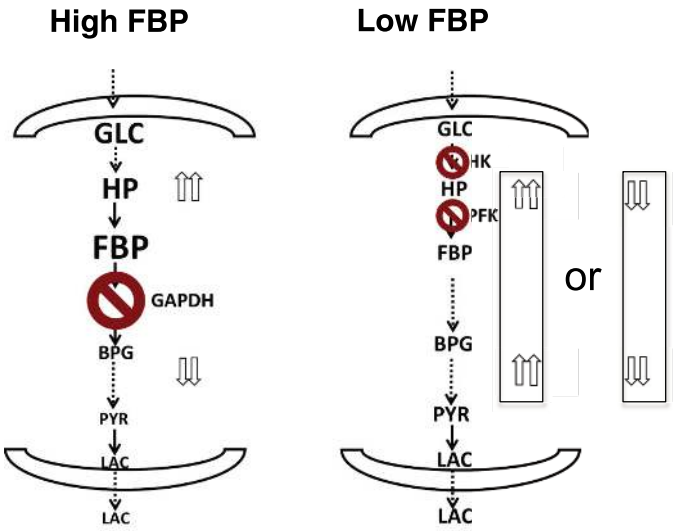


Figure **14.3.5**: **A unified model of aerobic glycolysis.** Shestov et al., ibid

When there is a balance of metabolites in the top and bottom halves of glycolysis (right hand size), including both high levels in both top and bottom (denoted by ↑↑ and font size) or low levels in both (denoted by ↓↓ and font size), no bottleneck at GAPDH exists and flux through glycolysis is determined by the usual "suspects", hexokinase and phosphofructokinase.

The results described above are those predicted by computational modeling. Do experimental data support the model? The only way to know is to test the model. This was done by using drugs to inhibit each of the enzymes in glycolysis. This offers an effective way to change the "effective" concentration or activity in the enzyme. From this data, flux changes due to changes at each step could be determined. These data supported the computation results - GADPH regulates aerobic metabolism in normal and proliferative conditions. When the top half substrates were elevated, the blockade of flux was determined by GADPH. In Chapter 13, we studied the glycolytic enzymes and the myriad of small molecules that control the activity of the three major enzymes with the biggest thermodynamic push, HK, PFK, and PK. GADPDH appears to be equally important. It is known to be regulated by many mechanisms, including post-translational modifications, such as nitrosylation, and the modification of its active site cysteine with ROS. Perhaps this helps regulate the balance between anaerobic and aerobic glycolysis. Also, there are high levels of expression of GADPH in cells engaged in aerobic glycolysis.

14.3.4: SUMMARY

This chapter introduces Metabolic Control Analysis (MCA) as a systems-level approach to understanding the dynamic regulation of complex metabolic networks and signal transduction pathways. Unlike traditional enzyme kinetics that focus on individual parameters such as K_m and V_m, MCA examines how changes in enzyme activities influence overall pathway behavior. Key points include:

- **Systems Perspective:**
  MCA considers both external inputs/outputs and internal enzyme-mediated reactions, emphasizing that emergent properties (like flux control) arise from the entire network rather than isolated steps.
- **Control Coefficients:**
  The chapter explains the concept of control coefficients, particularly the Flux Control Coefficient or FCC (also represented as C_{Ei}^{J}), which quantifies the relative change in pathway flux in response to a fractional change in the activity of a specific enzyme. This is mathematically defined as

$$C_{Ei}^{J} = \frac{dJ}{du}\frac{u}{J}$$

- **Summation Theorem and Distributed Control:**
  A fundamental property of MCA is the Summation Theorem, which states that the sum of all individual flux control coefficients in a pathway equals 1:

  $\sum_{i=1}^{n} C_{Ei}^{J} = 1$

  This illustrates that flux control is distributed among multiple enzymes rather than being governed by a single “rate-limiting” step.
- **Sensitivity Analysis:**
  The chapter presents sensitivity analyses showing how small perturbations in enzyme activities affect the entire pathway. These analyses highlight that even enzymes traditionally viewed as key (due to large free energy changes) may exhibit minimal flux control when the system is in steady state.
- **Application to Aerobic Glycolysis:**
  The chapter extends MCA concepts to the study of aerobic glycolysis—an important metabolic phenotype in cancer cells. It introduces the Warburg effect, quantified as the ratio of lactate flux (J_{Lac}) to mitochondrial oxidative flux (J_{ox}), and discusses how computational modeling, alongside experimental data, can identify critical control points in glycolysis. Notably, the enzyme GAPDH emerges as a key regulator, while enzymes like hexokinase and phosphofructokinase, despite their significant thermodynamic roles, show negative or minor flux control coefficients.
- **Integration of Computational Models and Experimental Data:**
  By leveraging computational tools (such as VCell) to simulate metabolic networks, the chapter underscores how models are refined using experimental data. This integrated approach helps pinpoint which enzymes and parameters most effectively modulate pathway flux, contributing to our understanding of cellular resilience and fragility.

Overall, the chapter lays the groundwork for using MCA to quantitatively analyze metabolic pathways, shifting the focus from isolated enzyme kinetics to a holistic view of pathway regulation and control. This framework is essential for exploring both normal cellular metabolism and altered states such as those observed in cancer.

This page titled 14.3: The Flux Control Coefficient is shared under a not declared license and was authored, remixed, and/or curated by Henry Jakubowski and Patricia Flatt.

- **11.2: Diffusion Across a Membrane - Passive and Facilitated Diffusion** by Henry Jakubowski and Patricia Flatt has no license indicated.

14.4: CONCENTRATION CONTROL AND ELASTICITY COEFFICIENTS

LEARNING GOALS (CHATGPT O3-MINI)

1. **Define Concentration Control Coefficients:**
   - Explain the concept of a concentration control coefficient ($C_{E_i}^{S}$) as a measure of how changes in an enzyme's activity affect the concentration of a system metabolite.
   - Interpret the equation ($C_{E_i}^{S} = \frac{\frac{\delta S_i}{S_i}}{\frac{\delta u_i}{u_i}} = \frac{\partial \ln S_i}{\partial \ln u_i} = \frac{\partial S_i}{\partial u_i}\frac{u_i}{S_i}$), emphasizing its role as a system-level property.
2. **Understand the Summation Theorem for Concentration Coefficients:**
   - Demonstrate why the sum of all individual concentration control coefficients in a pathway equals zero, $\sum_{i=1}^{n} C_{Ei}^{S} = 0$
   - Discuss the implications of this theorem for the redistribution of control within a metabolic network.
3. **Interpret the Impact of Enzyme Activity Changes on Metabolite Concentrations:**
   - Analyze how a decrease in enzyme activity (e.g., due to a mutation) can lead to compensatory changes in substrate concentrations, using the example of a low [S] scenario where [S] must increase to maintain constant flux.
4. **Define and Calculate Elasticity Coefficients:**
   - Describe the elasticity coefficient (ε_S^v) as a local property that quantifies how sensitive an enzyme's rate (v) is to changes in substrate concentration (S).
   - Explain the elasticity equation ($\varepsilon_S^v = \frac{\frac{\delta v}{v}}{\frac{\delta S}{S}} = \frac{\partial \ln v}{\partial \ln S} = \frac{\partial v}{\partial S}\frac{S}{v}$),
5. **Relate Elasticity Coefficients to Enzyme Kinetics:**
   - Explain how elasticity coefficients can be determined from the slope of a velocity vs. substrate concentration curve at a specific tangent point and why they must be evaluated under in vivo steady-state conditions.
   - Differentiate between elasticities for substrates, products, and other modifiers, noting that values can be positive or negative depending on whether the species increases or decreases the reaction rate.
6. **Connect System-Level and Local Control Parameters:**
   - Explain the rationale behind linking global system control coefficients (like flux and concentration control coefficients) to local properties (elasticity coefficients) via the Connectivity Theorem: ($\Sigma_{i=1}^{n} C_{vi}^{J} e_s^{vi} = 0$)
   - Analyze how this theorem integrates multiple enzyme influences at branch points and complex network nodes.
7. **Apply Computational Tools for Parameter Analysis:**
   - Use software such as COPASI to analyze and interpret tables of elasticity coefficients and concentration control coefficients from experimental data.
   - Evaluate how changes in kinetic parameters (K_m, V_m, K_{ix}) affect system flux and metabolite concentrations, reinforcing the connection between theory and practical measurements.
8. **Critically Assess the Role of Control Coefficients in Metabolic Regulation:**
   - Evaluate how concentration control coefficients differ from flux control coefficients in terms of their magnitude, range (negative to positive for concentration coefficients vs. 0 to 1 for flux coefficients), and overall impact on pathway regulation.
   - Discuss real-world examples and experimental findings that illustrate the importance of these coefficients in maintaining metabolic homeostasis.

These learning goals are designed to guide students through both the theoretical derivations and practical implications of concentration control and elasticity coefficients, equipping them with a deeper understanding of how enzyme kinetics shape the behavior of entire metabolic systems.

14.4.1: CONCENTRATION CONTROL COEFFICIENTS

The **Concentration control coefficient** ($C_{E_i}^{S}$), a global property of the system, gives the relative fractional change in metabolite concentration $S_j(dS_j/S_j)$, where S_j is the concentration of any metabolite in the system and as such is a system variable, with fractional change in concentration or activity of enzyme $E_i(du_i/u_i)$. Similar equations to section 15.3 apply.

$$C_{E_i}^{S} = \frac{\frac{\partial S_i}{S_i}}{\frac{\partial u_i}{u_i}} = \frac{\partial \ln S_i}{\partial \ln u_i} = \frac{\partial S_i}{\partial u_i}\frac{u_i}{S_i} \tag{14.4.1}$$

It can be shown that the sum of all of the individual $C_{E_i}^{S} = 0$ (another summation theorem) is not 1, as in the case of flux control coefficients. This again would make sense in the steady state. Flux coefficients usually vary from 0 to 1, but concentration coefficients can vary from negative to positive and from small to large.

$$\sum_{i=1}^{n} C_{Ei}^{S} = 0 \tag{14.4.2}$$

A simple example shows that the concentration control coefficients can have large values. For a given enzyme, at low [S], for example, when [S] << Km,

$$v = \frac{V_m S}{K_M + S} = \frac{V_m S}{K_M} = \frac{k_{cat} E_{tot} S}{K_M} \text{ when } S \ll Km \tag{14.4.3}$$

If the enzyme had only 0.1x of its normal activity (due to a mutation, for example), then to maintain constant flux, the [S] would have to increase 10-fold.

The tables below show the C^{S}_{Ei} values for incremental changes in the substrate (1%).

	(Hexokinase)	(Glucose-6-phosphate is...	(Glycogen synthesis)	(Trehalose 6-phosphate s...	(Phosphofructokinase)	(Aldolase)
High energy pho..	0.149291	0.00209315	-0.162615	-0.112466	0.00159405	0.000336889
Glucose 6 Phosp..	0.718017	-0.834548	-0.581964	-0.420826	-0.635556	-0.134319
Triose-phosphate	0.290279	0.0040699	-0.192953	-0.144737	0.00309946	0.000655043
NAD	0.000899872	1.26168e-05	-0.000702168	-0.000511095	9.60839e-06	2.03065e-06
Acetaldehyde	0.0928625	0.00130199	-0.0595875	-0.0450188	0.00099154	0.000209553
2-phosphoglycer..	0.579779	0.00812887	-0.417532	-0.308373	0.00619059	0.00130833
1,3-bisphosphog..	1.00165	0.0140438	-0.889801	-0.63383	0.0106951	0.00226032
Fructose 6 Phos...	0.946321	0.013268	-0.825856	-0.589942	-1.06108	-0.224249
Glucose in Cytoso	-2.15363	-0.0301953	0.295321	0.203672	-0.0229954	-0.00485988
Phosphoenolpyr...	0.751848	0.0105414	-0.614078	-0.44347	0.00802786	0.00169662
Pyruvate	0.458649	0.00643055	-0.261508	-0.202671	0.00489723	0.00103499
Fructose-1,6 bis...	0.567903	0.00796236	-0.369069	-0.278109	0.00606379	-0.525832
3-phosphoglycer..	0.535653	0.0075102	-0.37565	-0.27884	0.00571944	0.00120875
NADH	-0.0312961	-0.000438791	0.0244203	0.017775	-0.000334164	-7.06227e-05

table, part 2:

	(Glyceraldehyde 3-phosp...	(Phosphoglycerate kinase)	(Phosphoglycerate mutas...	(Enolase)	(Pyruvate kinase)	(Pyruvate decarboxylase)
High energy pho..	0.092012	0.00262286	0.00214191	0.00583266	0.00297472	0.00177918
Glucose 6 Phosp..	-0.194066	-0.00553197	-0.00451758	-0.0123019	-0.00627409	-0.00375253
Triose-phosphate	-0.968588	-0.0276102	-0.0225473	-0.061399	-0.0313141	-0.0187289
NAD	-0.00695116	-0.000198147	-0.000161813	-0.000440635	-0.000224729	-0.00013441
Acetaldehyde	-0.228632	-0.0065173	-0.00532223	-0.014493	-0.00739161	-0.00442091
2-phosphoglycer..	0.207334	0.00591018	0.00482644	-1.19124	-0.607546	-0.363372
1,3-bisphosphog..	0.47628	-0.337666	-0.275748	-0.750894	-0.382964	-0.22905
Fructose 6 Phos...	-0.344437	-0.00981839	-0.008018	-0.0218339	-0.0111355	-0.00666015
Glucose in Cytoso	-0.183506	-0.00523095	-0.00427175	-0.0116325	-0.00593269	-0.00354833
Phosphoenolpyr...	0.319778	0.00911547	0.00744398	0.0202708	-1.29924	-0.777074
Pyruvate	0.115796	0.00330085	0.00269558	0.00734036	0.00374367	-2.4298
Fructose-1,6 bis...	-1.5751	-0.0448992	-0.0366661	-0.0998459	-0.0509225	-0.0304567
3-phosphoglycer..	0.184471	0.00525847	-0.352935	-0.961081	-0.490162	-0.293165
NADH	0.24175	0.00689123	0.0056276	0.0153246	0.0078157	0.00467456

table, part 3

	e kinase)	(Pyruvate decarboxylase)	(Succinate synthesis)	(Glucose transport)	(Alcohol dehydrogenase)	(Glycerol 3-phosphate d...	(ATPase activity)
High energy pho..		0.00177918	-0.133971	0.945013	0.0419254	-0.217747	-0.620819
Glucose 6 Phosp..		-0.00375253	-0.338999	4.54506	0.106088	-0.620486	-1.57602
Triose-phosphate		-0.0187289	-0.0705359	1.83747	0.0220739	-0.280221	-0.339013
NAD		-0.00013441	-0.0177345	0.0056962	0.00554992	0.016672	-0.00178363
Acetaldehyde		-0.00442091	-0.662239	0.587821	-0.1057	0.549517	-0.0933806
2-phosphoglycer..		-0.363372	-0.299326	3.67001	0.0936725	-0.486218	-0.903552
1,3-bisphosphog..		-0.22905	-0.691066	6.34045	0.216266	-1.12294	-2.74768
Fructose 6 Phos...		-0.00666015	-0.53586	5.99023	0.167695	-0.986943	-2.49168
Glucose in Cytoso		-0.00354833	0.247704	0.208505	-0.0775176	0.400422	1.1477
Phosphoenolpyr...		-0.777074	-0.463155	4.75921	0.144942	-0.752507	-1.68334
Pyruvate		-2.4298	-0.165759	2.90326	0.0518733	-0.269095	-0.230185
Fructose-1,6 bis...		-0.0304567	-0.126035	3.59483	0.039442	-0.475374	-0.603896
3-phosphoglycer..		-0.293165	-0.266111	3.39069	0.0832782	-0.432242	-0.763605
NADH		0.00467456	0.616777	-0.198105	-0.193017	-0.579826	0.0620318

14.4.2: ELASTICITY COEFFICIENT

The **Elasticity Coefficient**, (ε_S^v), in contrast to the flux and concentration control coefficients, which are properties of the system, is a local property and can be measured using isolated enzymes and substrates. It makes sense that some kinetic property of the isolated enzyme would affect its propensity to affect system flux. The elasticity coefficient gives a measure of how much a substrate S (or other substance) can change the reaction rate (v) of an isolated enzyme. (Note that we use v and not flux J, which describes a system property.) Hence

$$\varepsilon_S^v = \frac{\frac{\partial v}{v}}{\frac{\partial S}{S}} = \frac{\partial \ln v}{\partial \ln S} = \frac{\partial v}{\partial S}\frac{S}{v} \tag{14.4.4}$$

PRICE ELASTICITY

The term elasticity is also used in economics and is especially useful when inflation is high. If the price of your favorite product, such as a Starbucks Latte, goes up, consumers might buy it less frequently or opt for a cheaper alternative from a competitor. If a small rise in price for a Starbucks latte leads to a large drop in demand, the Starbucks latte is characterized by a high elasticity. However, if people don't change their latte buying behavior when there is a big price rise on the latte, the product is inelastic. If you are the CEO of a company, it is good to know the elasticity of your products to maximize your profits.

Hence, the elasticity coefficient can be determined using basic enzyme kinetics of the isolated enzyme. Note that the coefficient at each S concentration is the slope of the v vs S curve multiplied by the S/v at that tangent point. The elasticity coefficient must be evaluated at the same enzyme and substrate concentration as in vivo in the steady state. Velocity (v), not flux, is used. In the above case, S is the substrate, but it could be a product or modifier. There is a different elasticity coefficient for each parameter. There is no summation theory for elasticities. Values can be positive for species that increase the velocity or negative for those that decrease it. Hence, there can be multiple elasticities.

The tables below show the elasticity coefficients (relative or scaled) for yeast glycolysis determined using COPASI.

	High energy phos...	Glucose 6 Phosphate	Triose-phosphate	NAD	Acetaldehyde	2-phosphoglycerate	1,3-bisphosphogly...	Fructose 6 Phosph...
(Hexokinase)	1.02118	-0.0166	0	0	0	0	0	0
(Glucose-6-..	0	1.18397	0	0	0	0	0	-0.710951
(Glycogen s..	0	0	0	0	0	0	0	0
(Trehalose 6..	0	0	0	0	0	0	0	0
(Phosphofr...	-3.20462	0	0	0	0	0	0	0.93355
(Aldolase)	0	0	-3.10067	0	0	0	0	0
(Glyceralde...	0	0	0.919332	0.145002	0	0	-0.0811565	0
(Phosphogl...	-9.63644	0	0	0	0	0	2.84704	0
(Phosphogl...	0	0	0	0	0	-2.261	0	0
(Enolase)	0	0	0	0	0	0.8303	0	0
(Pyruvate ki...	-1.82687	0	0	0	0	0	0	0
(Pyruvate d...	0	0	0	0	0	0	0	0
(Succinate s..	0	0	0	0	1	0	0	0
(Glucose tra..	0	0	0	0	0	0	0	0
(Alcohol de..	0	0	0	-3.03483	3.19545	0	0	0
(Glycerol 3-..	0	0	0.38368	-0.36338	0	0	0	0
(ATPase act...	1.79865	0	0	0	0	0	0	0

table, part 2

	phoglycerate	1,3-bisphosphogly...	Fructose 6 Phosph...	Glucose in Cytosol	Phosphoenolpyruv...	Pyruvate	Fructose-1,6 bisph...	3-phosphoglycerate	NADH
(Hexokinase)		0	0	0.457337	0	0	0	0	0
(Glucose-6-..		0	-0.710951	0	0	0	0	0	0
(Glycogen s..		0	0	0	0	0	0	0	0
(Trehalose 6..		0	0	0	0	0	0	0	0
(Phosphofr...		0	0.93355	0	0	0	-0.400941	0	0
(Aldolase)		0	0	0	0	0	1.89712	0	0
(Glyceralde...		-0.0811565	0	0	0	0	0	0	-0.0921294
(Phosphogl...		2.84704	0	0	0	0	0	-2.28602	0
(Phosphogl...		0	0	0	0	0	0	2.79933	0
(Enolase)		0	0	0	-0.389446	0	0	0	0
(Pyruvate ki...		0	0	0	0.763604	-0.245925	0	0	0
(Pyruvate d...		0	0	0	0	0.411178	0	0	0
(Succinate s..		0	0	0	0	0	0	0	0
(Glucose tra..		0	0	-0.072249	0	0	0	0	0
(Alcohol de..		0	0	0	0	0	0	0	3.19614
(Glycerol 3-..		0	0	0	0	0	0	0	0.581052
(ATPase act...		0	0	0	0	0	0	0	0

Things to note:

- the columns show substrates, not enzymes;
- green cells (with positive elasticities) are generally substrates for their target enzymes (for example, glucose-6-phosphate for phosphoglucomutase);

Other "generic" sensitivities can be determined as well. For example, incremental changes in K_m, V_m, or K_{iz} for specific enzymes could affect fluxes in a pathway.

A link between system control coefficients and local coefficients:

You would think there should be some relationship between a system variable, such as the flux control coefficient, and a local variable, such as the elasticity coefficient. There is, and it is expressed by the **Connectivity Theorem** (below). If a substrate S is acted upon by many different enzymes ($i \ldots \ldots n$), which is very likely, especially for branch points in metabolic pathways, then it can be shown that

$$\sum_{i=1}^{n} C_{vi}^{J} e_{s}^{vi} = 0 \qquad (14.4.5)$$

14.4.3: SUMMARY

This chapter delves into two key concepts in metabolic control analysis: concentration control coefficients and elasticity coefficients. It begins by defining the concentration control coefficient ($C_{E_i}^S$) as a system-level parameter that quantifies the relative change in a metabolite's concentration in response to a fractional change in the activity or concentration of an enzyme. Mathematically, it is expressed as

$$C_{E_i}^S = \frac{\frac{\partial S_i}{S_i}}{\frac{\partial u_i}{u_i}} = \frac{\partial \ln S_i}{\partial \ln u_i} = \frac{\partial S_i}{\partial u_i}\frac{u_i}{S_i},$$

which highlights its dependence on both local enzyme properties and global metabolite levels. A critical insight is provided by the summation theorem for concentration coefficients, which states that the sum of all individual concentration control coefficients within a pathway equals zero ($\sum_{i=1}^{n} C_{E_i}^S = 0$). This result underscores the idea that changes in enzyme activities are balanced across the system, reflecting the interconnected nature of metabolic networks.

The chapter then introduces the elasticity coefficient (ε_S^v), a local property that measures how sensitively an enzyme's reaction rate (v) responds to changes in the concentration of a substrate or modifier. Defined as

$$\varepsilon_S^v = \frac{\frac{\partial v}{v}}{\frac{\partial S}{S}} = \frac{\partial \ln v}{\partial \ln S} = \frac{\partial v}{\partial S}\frac{S}{v},$$

the elasticity coefficient is determined by the slope of the vv versus SS curve at a given point. It must be evaluated under conditions that mimic the in vivo steady state. Unlike system-level control coefficients, elasticity coefficients can have both positive and negative values, reflecting whether a substrate acts to enhance or inhibit enzyme activity.

An important connection between local and global properties is established through the Connectivity Theorem, which links flux control coefficients and elasticity coefficients by the relation.

$$(\Sigma_{i=1}^{n} C_{vi}^J e_s^{vi} = 0)$$

This theorem integrates the local responsiveness of individual enzymes with the overall control exerted on the system flux, emphasizing that the effects of enzyme modifications are distributed throughout the network.

Overall, the chapter provides a comprehensive framework for understanding how local enzyme kinetics (as measured by elasticity coefficients) relate to and influence the global behavior of metabolic systems (as characterized by concentration control coefficients). By combining theoretical derivations with computational analyses, students gain a nuanced perspective on how changes at the molecular level can impact whole-pathway dynamics, offering valuable insights into metabolic regulation and system robustness.

This page titled 14.4: Concentration Control and Elasticity Coefficients is shared under a not declared license and was authored, remixed, and/or curated by Henry Jakubowski and Patricia Flatt.

- **11.2: Diffusion Across a Membrane - Passive and Facilitated Diffusion** by Henry Jakubowski and Patricia Flatt has no license indicated.

14.5: METABOLISM AND SIGNALING: THE STEADY STATE, ADAPTATION AND HOMEOSTASIS

LEARNING GOALS (CHATGPT O3-MINI)

1. **Differentiate Binding and Kinetic Responses:**
   - Describe the characteristics of hyperbolic binding curves for simple ligand–macromolecule interactions versus sigmoidal curves observed in allosteric binding (using the Hill Equation).
   - Compare these binding interactions to the hyperbolic and sigmoidal plots of initial enzyme velocity versus substrate concentration.
2. **Analyze System Responses to Stimuli:**
   - Distinguish between linear, hyperbolic, and sigmoidal responses in biochemical systems by interpreting the corresponding reaction schemes and steady-state equations.
   - Derive and explain the steady-state equations for simple linear responses (e.g., synthesis and degradation of a protein) and enzyme-catalyzed reactions leading to hyperbolic responses.
3. **Understand Adaptation and Homeostasis:**
   - Define adaptation in the context of cellular signaling and metabolic regulation, emphasizing the return to a basal state following a transient stimulus.
   - Explain the concept of homeostasis and its biological importance, relating it to steady-state conditions in metabolic pathways.
4. **Explore Circuit Motifs for Adaptive Responses:**
   - Identify and describe different network motifs—including negative feedback loops, incoherent feedforward systems, and state-dependent inactivation (Types A and B)—that enable perfect or near-perfect adaptation.
   - Evaluate how these motifs integrate to modulate responses to pulsed or stepwise stimuli and maintain cellular homeostasis.
5. **Develop Mathematical and Computational Modeling Skills:**
   - Formulate ordinary differential equations (ODEs) to model the dynamics of linear, hyperbolic, and sigmoidal responses in biochemical systems.
   - Use computational tools (e.g., VCell) to simulate reaction diagrams and interpret time course graphs for adaptive systems, linking theoretical predictions to simulated experimental data.
6. **Critically Evaluate Response Sensitivity and Robustness:**
   - Analyze how varying stimulus inputs (e.g., continuous versus pulsed signals) influence the overall response of the system and the degree of adaptation achieved.
   - Discuss the criteria for achieving parameter-independent return to baseline, highlighting the robustness of control mechanisms in biological networks.
7. **Integrate Theoretical Concepts with Physiological Contexts:**
   - Relate the mathematical descriptions of binding and kinetic responses to real-world biological phenomena such as sensory adaptation (e.g., taste attenuation, chemotaxis) and cellular signaling pathways.
   - Discuss the implications of perfect or near-perfect adaptation in the context of disease states or abnormal cellular responses (e.g., uncontrolled proliferation in tumor cells).

These learning goals aim to build a comprehensive understanding of how binding interactions, enzyme kinetics, and network motifs contribute to the regulation of cellular responses and the maintenance of homeostasis.

14.5.1: INTRODUCTION

We have studied binding interactions in Chapter 5, kinetics in Chapter 6, and principles of metabolic control in this chapter. We've learned the following:

Binding Reactions

- for simple binding of a ligand to a macromolecule, graphs of fractional saturation of the macromolecule vs free ligand concentration are hyperbolic and demonstrate saturation binding. In the initial part of the binding curve, when [L] << K_D, the fractional saturation shows a linear dependence on free ligand concentration. Figure **14.5.1** shows [ML] vs L, which is the same basic equation as a plot of Y vs L.

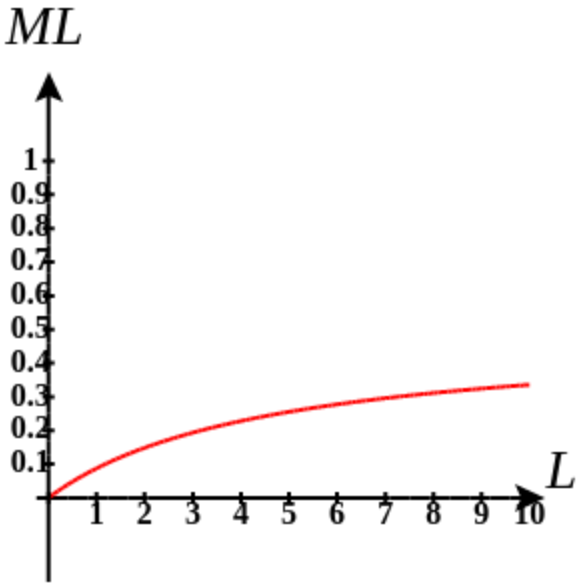


Figure 14.5.1

- for allosteric binding of a ligand to a multimeric protein, graphs of fractional saturation vs free ligand concentration are sigmoidal and also display saturation binding. In the first parts of the binding curve, the fractional saturation is much more sensitive to ligand concentration than in simple binding of a ligand to a macromolecule with one binding site. Figure 14.5.2 below shows graphs for the allosteric binding of a ligand to a macromolecule using the Hill Equation (instead of the MWC equation we used to model O_2 binding to tetrameric hemoglobin).

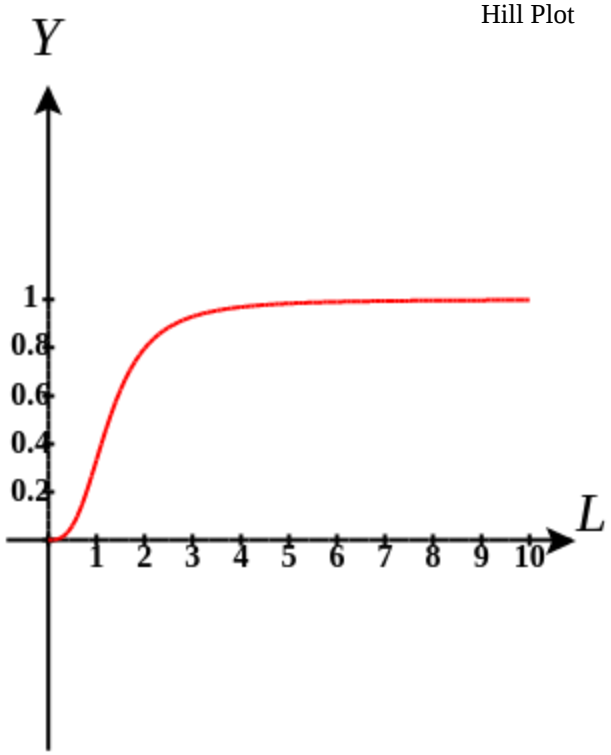


Figure 14.5.2

In these two plots, the system (in this case, a single macromolecule) displays different sensitivities to ligand concentration, allowing the system to respond differently to changes in physiological conditions.

Binding and Chemical Reactions

As with the case for binding interactions, we have seen hyperbolic and sigmoidal plots of initial velocity (v_0) vs [substrate] for enzyme-catalyzed reactions. These also allow appropriate responses to a single substrate in a physiological setting.

But what if you put the same macromolecule and ligand into a larger metabolic or signal transduction pathway in vivo? What kinds of responses would they make to a change in input? As we have just seen in our discussion of the steady state, the ligand or substrate concentration might not change at all as flux continues through the pathway. One could imagine many scenarios with different inputs and optimal outputs. For example, what if the input (a reactant or small signaling molecule) comes in pulses? Ultimately, a system should return to its basal state since a prolonged response (such as cell proliferation) could harm the organism's health.

Let's examine some simple examples and see how different inputs lead to specific outputs. We'll construct some very simple reaction diagrams in Vcell and see how varying them leads to different outputs. Here are two simple cases for **isolated** chemical species and reactions, analogs to the simple binding reactions described above.

Linear Response: A Signal S and a Response R; S → R

If no enzyme is involved, the rate doubles as the signal (substrate) doubles since dR/dt = k[S] for the first-order reaction. If S is the stimulus and R is the response, a plot of R vs S is linear. Hence, the system responds linearly with increasing S. Here is the simple chemical equation

$$S \underset{k_2}{\overset{k_1}{\rightleftarrows}} R \tag{14.5.1}$$

As a concrete example, consider the synthesis and degradation of a protein, characterized by the following equation derived from mass action.

$$\frac{dR}{dt} = k_0 + k_1 S - k_2 R \tag{14.5.2}$$

where S is the signal (ex., concentration of mRNA) and R is the response (ex, concentration of the transcribed protein). A constant k_0 has been added to account for any basal rate of the reaction. (This is a vastly oversimplified way to model a complex process like mRNA translation to a protein, as it omits 100s of steps.)

Here is the simplified derivation under steady state (SS) conditions typically found for enzymes embedded in a pathway.

$$\begin{aligned} \frac{dR_{SS}}{dt} &= k_0 + k_1 S - k_2 R = 0 \\ R_{SS} &= \frac{k_0 + k_1 S}{k_2} \end{aligned} \tag{14.5.3}$$

The equation is a linear function of S.

Hyperbolic Response: E+S ↔ ES → E + R

In a simple enzyme-catalyzed reaction with a fixed enzyme concentration, as S increases, the initial velocity saturates. Hence, there is a limit on the response, so the response R is a hyperbolic function of S. Increasing S ever more after saturation won't lead to more R (in a given amount of time).

As a concrete example of this, consider the phosphorylation/dephosphorylation of a protein R. R_P represents the phosphorylated and active form of the protein R with concentration $[R_P]$. The reaction is simply written as R ↔ R_P, where R_P is the response. Mass action shows the total amount of R, $R_T = R + R_P$. A simple mass action equation can be derived.

Here is the chemical equation

$$\mathrm{R} + \mathrm{S} \underset{k_2}{\overset{k_1}{\rightleftarrows}} \mathrm{R_P} \tag{14.5.4}$$

Here is the math equation, again for the steady state (SS), when $dR_P/dt = 0$. (We derived the same equation for the steady-state version of the Michaelis-Menten equation in Chapter 6.

$$\frac{dR_P}{dt} = k_1 S (R_T - R_P) - k_2 R_P \tag{14.5.5}$$

? DERIVATION: STEADY STATE HYPERBOLIC RESPONSE TO A STIMULUS S

Click below to see the derivation

Derivation

$$\frac{dR_P}{dt} = k_1 R[S] - k_2 R_P \tag{14.5.6}$$

then in the steady state:

$$\begin{aligned} \frac{dR_P}{dt} &= k_1 S (R_T - R_P) - k_2 R_P = 0 \\ k_2 R_{P,SS} &= k_1 S (R_T) - k_1 S (R_{P,SS}) \\ k_2 R_{P,SS} + k_1 S (R_{P,SS}) &= k_1 S (R_T) \\ R_{P,SS} (k_2 + k_1 S) &= k_1 S (R_T) \end{aligned} \tag{14.5.7}$$

Finally, we get

$$R_{P,Ss} = \frac{k_1 S (R_T)}{(k_2 + k_1 S)} = \frac{(R_T) S}{\left(\frac{k_2}{k_1} + S\right)} \tag{14.5.8}$$

In the steady state, $dR_P/dt = 0$, and the steady state equation can be written as:

$$R_{P,ss} = \frac{k_1 S (R_T)}{(k_2 + k_1 S)} = \frac{(R_T) S}{\left(\frac{k_2}{k_1} + S\right)} \tag{14.5.9}$$

Sigmoidal Response

Consider this simple reaction for a homotetramer in which each monomer can bind a substrate S: nS + E_n ↔ E_nS_n → E_n + nR: If E_n is a multimeric allosteric enzyme, as S increases, the initial velocity also saturates, but the response R is a sigmoidal function of S (in analogy to

the above example). The equation is too complicated to derive here, but the result reproduces a sigmoidal curve for the steady state, much as the Hill equation does for cooperative binding.

14.5.2: ADAPTATION AND HOMEOSTASIS

The above examples show that the response of proteins or enzymes to increasing levels of a stimulus like a ligand or a substrate can be linear, hyperbolic, or sigmoidal, with varied outcomes. However, an ever-increasing or increasing and plateauing response might be too much in many biological conditions. The cell needs a way to turn off the response and settle back to a basal state, even when there is constant or changing stimuli. This allows the **adaptation** of a system to a stimulus and the maintenance of **homeostasis**. Every system needs to be able to respond and return to a homeostatic basal level. The maintenance of homeostasis is critical to life.

HOMEOSTASIS - ASBMB

The American Association for Biochemistry and Molecular Biology (ASBMB) describes both homeostasis and evolution as key underlying concepts for all biology. Homeostasis shapes both form and function from the molecular to the organismal levels. Homeostasis is needed to maintain biological balance. The steady state at the molecular to organismal levels in metabolic and signaling pathways is a hallmark of homeostasis. Here are the learning goals for homeostasis designated by the ASBMB

1. Biological need for homeostasis

Biological homeostasis is the ability to maintain relative stability and function as changes occur in the internal or external environment. Organisms are viable under a relatively narrow set of conditions. As such, there is a need to tightly regulate the concentrations of metabolites and small molecules at the cellular level to ensure survival. To optimize resource use and maintain conditions, the organism may sacrifice efficiency for robustness. The breakdown of homeostatic regulation can contribute to the cause or progression of disease or lead to cell death.

2. Link steady-state processes and homeostasis

A system that is in a steady state remains constant over time, but that constant state requires continual work. A system in a steady state has a higher level of energy than its surroundings. Biochemical systems maintain homeostasis via the regulation of gene expression, metabolic flux, and energy transformation but are never at equilibrium.

3. Quantifying homeostasis

Multiple reactions with intricate networks of activators and inhibitors are involved in biological homeostasis. Modifications of such networks can lead to the activation of previously latent metabolic pathways or even to unexpected interactions between components of these networks. These pathways and networks can be mathematically modeled and correlated with metabolomics data and kinetic and thermodynamic parameters of individual components to quantify the effects of changing conditions related to either normal or disease states.

4. Control mechanisms

Homeostasis is maintained by a series of control mechanisms functioning at the organ, tissue, or cellular level. These control mechanisms include substrate supply, activation or inhibition of individual enzymes and receptors, synthesis and degradation of enzymes, and compartmentalization. The primary components responsible for the maintenance of homeostasis can be categorized as stimulus, receptor, control center, effector, and feedback mechanism.

5. Cellular and organismal homeostasis

Homeostasis in an organism or colony of single-celled organisms is regulated by secreted proteins and small molecules, often functioning as signals. Homeostasis in the cell is maintained by regulation and by the exchange of materials and energy with its surroundings.

In the rest of the chapter, we will describe chemically and mathematically simple biological circuits/motifs that allow perfect or near-perfect adaptation to a stimulus, a hallmark of homeostasis. We define adaptation as a complete or almost complete return to a basal state after introducing a stimulus. In all the cases below, we will consider not a single application of a stimulus but a pulse application (a repetitive step wave function). The pulsed stimuli could be of constant magnitude or an increasing/decreasing pulse of a signal, such as a substrate. All responses must be transient to avoid uncontrolled responses such as proliferation (a hallmark of tumor cells) or cell death.

Adaptation is commonly found in sensory systems like vision, hearing, pressure, taste, etc. Think of eating your favorite cookie. The first bite is delicious, but by the tenth bite, there is significant attenuation in the positive sensory response, which helps keep most from adding significant weight continually.

Ma et al. conducted simulations on three-component/node (protein, enzyme) systems to see which might display the potential for perfect or near-perfect adaptation. The simple 3-component motifs or circuits were modeled using simple mass action kinetic equations, ordinary

differential equations (which we learned to write in Chapter 6.2), or a combination of both. The systems that displayed adaptation had to conform to three criteria:

1. The stimulus had to induce a response of high magnitude initially
2. The system had to return to a basal or near basal state.
3. The return to a basal state had to be mostly parameter-independent. That is, the return to the basal state must occur for many different combinations of parameters.

The possible 3-component components (nodes) and the links among the nodes are shown in Figure **14.5.3** below.

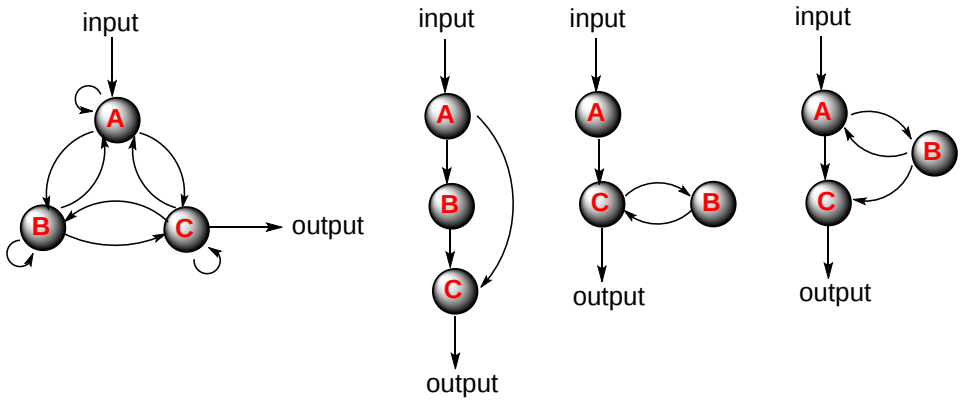


Figure **14.5.3**: Possible 3-component components (nodes) and the links among the nodes. After Ma et al. Cell Theory,138, 760-773 (2009) https://www.cell.com/fulltext/S0092-8674(09)00712-0. DOI:https://doi.org/10.1016/j.cell.2009.06.013.

Out of over 16,000 models, several hundred were found that met the criteria. Most were variations of simple motifs that we will show below. The most common motifs were the **negative feedback loop** and the **incoherent feedforward system**.

Much of the discussion, models, and equations used below are from two articles:

- John J Tyson, Katherine C Chen, Bela Novak, Sniffers, buzzers, toggles and blinkers: dynamics of regulatory and signaling pathways in the cell, Current Opinion in Cell Biology, Volume 15, Issue 2, 2003, Pages 221-231, https://doi.org/10.1016/S0955-0674(03)00017-6.
- James E. Ferrell, Perfect and Near-Perfect Adaptation in Cell Signaling, Cell Systems, Volume 2, Issue 2, 2016, Pages 62-67, https://doi.org/10.1016/j.cels.2016.02.006.

Adding a third component to form a mini pathway can change the response R to a stimulus S from linear or hyperbolic/sigmoidal in the steady state to one that exhibits perfect or near-perfect adaptation. Again, we see this kind of response in signaling pathways in sensation and in chemotaxis, in which a cell moves toward a stimulus (a chemoattractant molecule).

14.5.2.1: SIMPLE 3-NODE MOTIF/CIRCUIT FOR PERFECT ADAPTATION

Figure **14.5.4** below shows our first example of a 3-component system that displays perfect or near-perfect adaptation. The right-hand side shows a Vcell reaction diagram. In this example, a stimulus S (a reactant, neurotransmitter, mRNA, etc.) leads to the synthesis of X and R, a response molecule. Both X and R get degraded. The yellow squares represent the nodes through which the flux of S to X and R proceeds. Each node has an equation for the flux, J, through the node. The left part of Figure 4 shows the periodic pulse of stimuli S that increases the concentration of S from an initial value of S_0 = 1 μM to S + 0.2 μM for each step. Note that the flux equations for J are very simple and are based on mass action and are not derived through Michaelis-Menten kinetic equations.

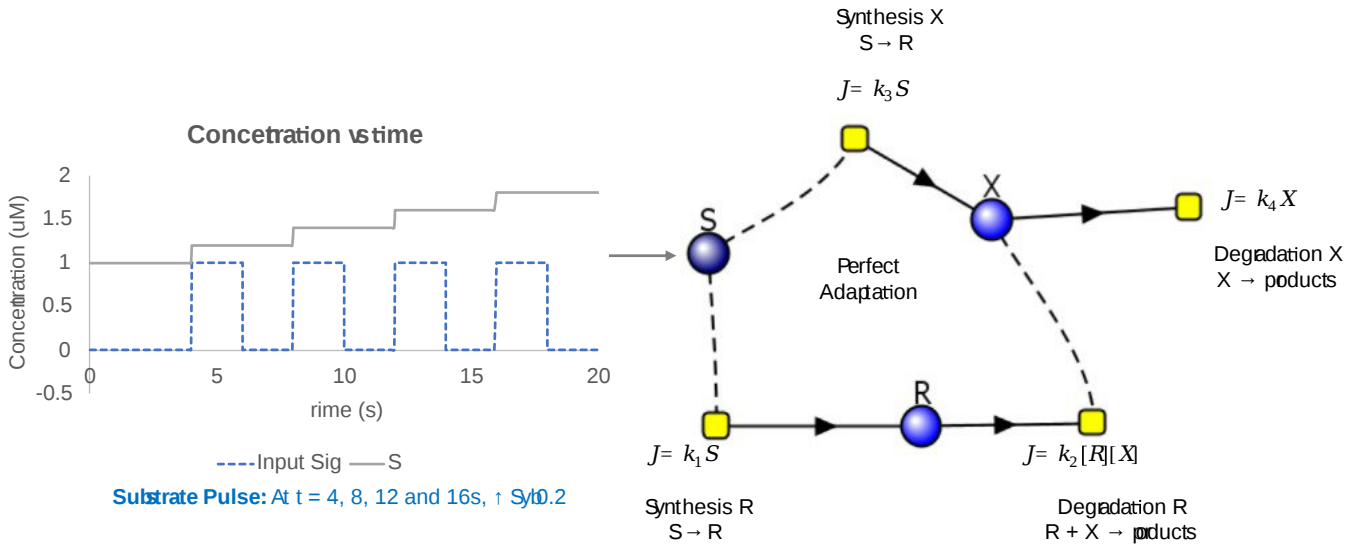


Figure **14.5.4**: Simple 3-component system that displays perfect or near-perfect adaption.

Note that S, the stimulus (or substrate for example) is a square wave step function varying from 0 to 1 over the time interval shown in the graph. The dotted blue line simply shows when the pulse is delivered. The initial S concentration is 1 µM and increases by 0.2 µM for each step (as shown in the gray line). Hence, S increases in a stepwise fashion.

Figure **14.5.5** below is a time course graph that shows the stepwise (=0.2 uM) increase in S from 1 µM and the concentration of R (the response) over 20 seconds. Even though S continues to increase in a stepwise fashion, R rises substantially only from the initial input of S (1 µM), and subsequent increases in S with each increment of S are damped out!

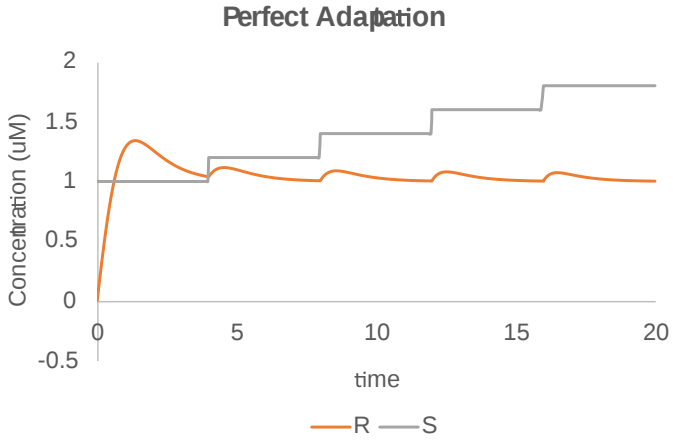


Figure **14.5.5**: Time course for a 3-component Perfect Response system. Model by ModeBrick from VCell: CM-PM12648679_MB4:Perfect_Adaptation; Biomodel 188456707

RUNNING ADAPTIVE VELL MODELS IN THIS BOOK

The present version of Vcell release (as of 4/28/23) does not yet allow the export of a file compatible with the software used to run simulations with this book. The Vcell model includes an "event" that allows for the production of stepwise changes in stimuli. A future release will allow users to run the simulations within this book (as is the case for the other Vcell simulations throughout the book).

14.5.2.2: NEGATIVE FEEDBACK LOOP

The negative feedback loop is one of the simplest circuits/motifs to generate perfect or near/perfect adaptation. It has only two nodes (yellow dots) and two proteins. An example is bacterial chemotaxis. Figure **14.5.6** below shows a Vcell reaction diagram (left), another representation (middle), and the time course graphs for all species. This model works especially well with certain parameters assigned.

Figure 14.5.6

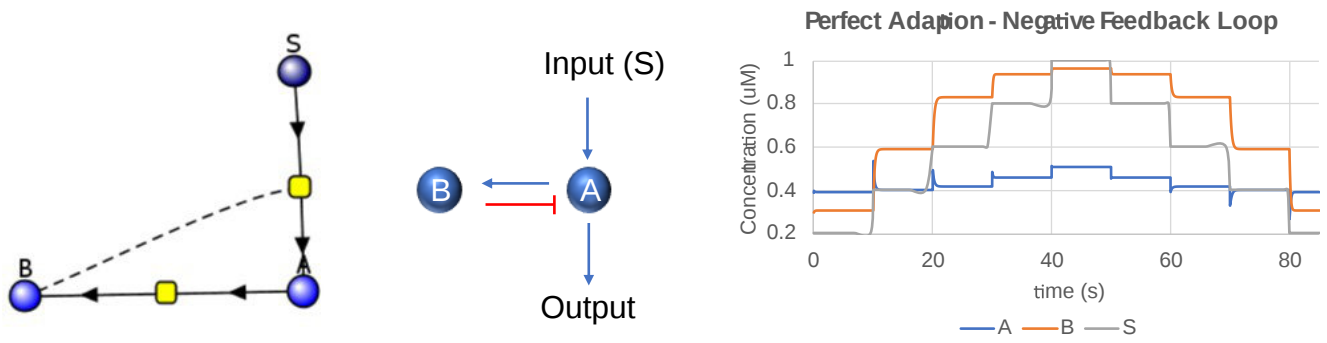


Figure 14.5.6: Near-Perfect Adaptation from Negative Feedback. Adapted from Ferrell (ibid)

The gray line in the graph is the stimulus S (substrate). The blue line is the response, designated in this model as A. B acts as an inhibitor (note the dotted line to the input node in the left diagram and the blunt-ended red bar in the middle diagram. Note that the stimulus goes from 0.2 μM (initial concentration) at t=0 to 1 μM (a 5-fold increase) at 40 seconds, but the response A increases at most from 0.4 (initial condition) to 0.5 (a 1.25-fold increase).

If we say [A] is the output, then the differential equation for dA/dt is given by

$$\frac{dA}{dt} = k_1 S \cdot (1 - A) - k_2 A \cdot B \tag{14.5.10}$$

dB/dt is given by

$$\frac{dB}{dt} = k_3 A \frac{1 - B}{K_3 + 1 - B} - k_4 \frac{B}{K_4 + B} \tag{14.5.11}$$

The constants for the graph (right) produced by the Vcell model are:

- $k_1 = k_2 = 200$
- $k_3 = 10$; $k_4 = 4$
- $K_3 = K_4 = 0.01$

14.5.2.3: INCOHERENT FEEDFORWARD SYSTEMS

In this circuit/motif, the stimulus S increases the concentration of A (the output) but also forms a negative modulator, B, which, with a bit of a time lag, decreases the concentration of A through inhibition. There is no feedback inhibition from A in this simple system. If you're reading carefully, you'll see that the reaction scheme and inhibition are identical to the first circuit/motif we introduced. Here, we simplify the diagram and give it an official name. The word incoherent in the name makes sense since the stimulus S is converted both to the output A and to the inhibitor B, which on the surface seems like a crazy (incoherent) thing to do.

Figure 14.5.7 below shows the Vcell reaction diagram (left) and a more classical reaction diagram (middle), and progress curves showing S, the stimulus, A, the output or response, and B, the inhibitor. The dashed line in the left diagram from B to the reaction node for the S → A reaction shows that B affects the rate of that reaction. The equations used account for the inhibitory effect of B.

Figure 14.5.7: Near-Perfect Adaptation from an Incoherent Feedforward System. Adapted from Ferrell (ibid)

Note that the response A goes up or down a bit with each new step in the concentration of S, but to a very minimal degree. The system is certainly almost perfectly adapted.

The differential equation for dA/dt (where A is the response) is

$$\frac{dA}{dt} = k_1 \mathrm{S} \cdot (1 - A) - k_2 A \cdot B \tag{14.5.12}$$

The equation for dB/dt (the inhibitor generated from A) is

$$\frac{dB}{dt} = k_3 \ \mathrm{S} \ \frac{1 - B}{K_3 + 1 - B} - k_4 B \tag{14.5.13}$$

The constants for the graph (right) produced by the Vcell model are:

- $k_1 = 10$; $k_2 = 100$
- $k_3 = 0.1$; $k_4 = 1$
- $K_3 = 0.001$

14.5.3: STATE-DEPENDENT INACTIVATION SYSTEMS.

Two simple circuits/motifs in this system were found after the initial analyses that showed all possible interactions in a 3-component system (see Figure 3). The motif was patterned after the inhibition of proteins in neuron stimulation, specifically in ion channels in neural cell membranes that open up on a change in the transmembrane potential but then close again quickly to avoid constant neuronal stimulation (or inhibition). The Na^+ ion channel has both fast (1-2 ms) and slow (100 ms) inactivation mechanisms. The fast one allows for repetitive firing, the development of action potentials, and the control of the excitation of neurons and at the neuromuscular junction. Neuronal signaling is discussed in Chapter 28.9. Figure **14.5.8** below shows a simplified model for one type of inactivation of the Na^+ ion channel

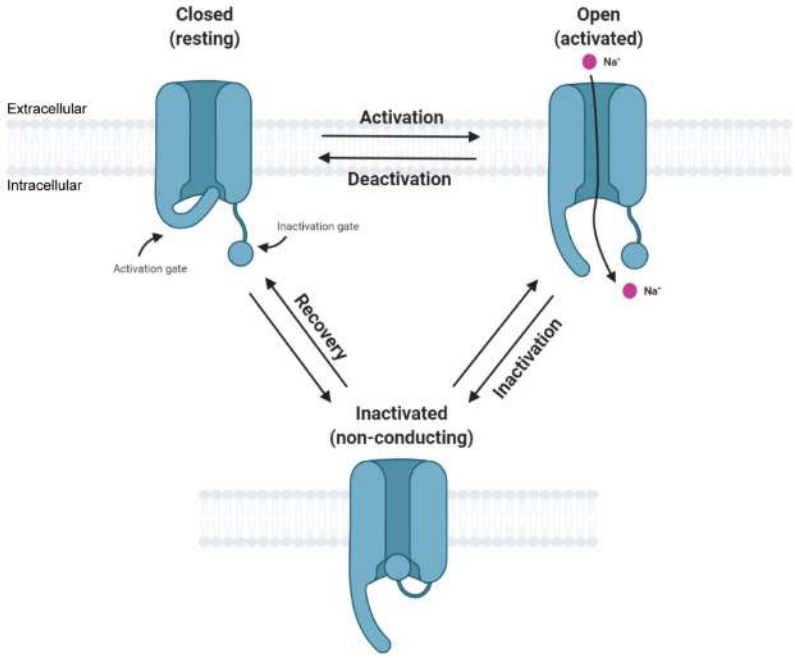


Figure **14.5.7**: Simplified state transition model of voltage-gated sodium channels featuring closed, open, and inactivated states. Zybura, A. et al. *Cells* **2021**, *10*, 1595. https://doi.org/10.3390/cells10071595. Creative Commons Attribution (CC BY) license (**https://creativecommons.org/licenses/by/4.0/**).

The figure implies at least three conformational states of the channel, so the inactivation for the channel and the circuit/motif for adaptation we will discuss are called **state-dependent inactivations**. The slow return to the original state is observed in many ion channels and in the return of G protein-coupled receptors to the normal state after desensitization. Also, some protein kinases (which use ATP to phosphorylate protein substrates) can be inactivated by internalizing the membrane kinase into vesicles, which can be reactivated and returned to the plasma membrane slowly.

For the construction of a perfect or near-perfect adaption state, we will assume the protein A exists in an off state (A_{off}) which binds the stimulus (B or S), an on state (A_{on}) which is viewed as the response (or A produces the response), and an inactivated state (A_{in}) which slowly reverts to the A_{off} state which can be activated again. The inactive state can be produced by conformational transitions with the protein itself or another molecule produced downstream of it in a metabolic or signaling pathway. For example, a GPRC could be phosphorylated or bind to another species to produce an inactive state.

Two different circuits/motifs can produce state-dependent inactivation. We'll refer to these as Type A and Type B.

Type A

Figure 14.5.9 shows the Vcell reaction diagram (top left), a classical reaction diagram (bottom left) and time course graphs for Type A state-dependent inactivation.

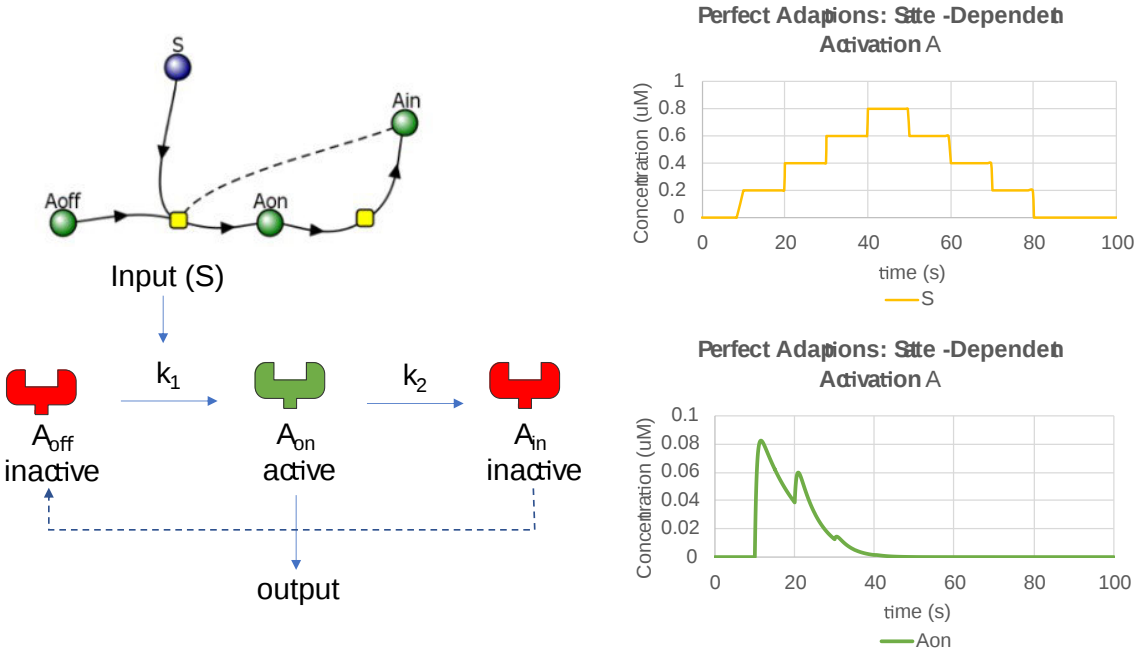


Figure 14.5.9: Perfect Adaptation for Type A State-Dependent Inactivation. Adapted from Ferrell (ibid).

A_{on} represents the active state of the protein. This mechanism applies well to the Na^+ channel. The differential equations for dA_{on}/dt and dA_{off}/dt are shown below.

For dA_{on}/dt

$$\frac{dA_{on}}{dt} = k_1 \text{Input} \cdot (1 - A_{on} - A_{in}) - k_2 A_{on} \tag{14.5.14}$$

dA_{in}/dt

$$\frac{dA_{in}}{dt} = k_2 A_{on} \tag{14.5.15}$$

with constants $k_1 = k_2 = 1$.

Again, as with the other cases, the stimulus S is pulsed. The different colors in the bottom left reaction diagram imply an off and inactive red state and a green active state, each of different conformations. The graphs were produced using Vcell. A slight anomaly in the graph of Aon shows two additional small peaks as the system returns to the basal state. This contrasts with just one peak, which returns to the basal state in a simple exponential fashion as described in the Ferrell paper. We are uncertain as to the source of the discrepancy.

Type B

In this case, the periodic stimulus, abbreviated as B, is a binding partner for A_{off}, which produces an active complex B-A_{on}. Figure 14.5.10 below shows the Vcell reaction diagram (top left), a classical reaction diagram (bottom left), and time course graphs for Type B state-dependent inactivation.

Figure 14.5.10

Figure 14.5.10: Perfect Adaptation for Type B State-Dependent Inactivation. Adapted from Ferrell (ibid)

BA_{on} represents the active state of the protein bound to B, while BA_{in} represents the inactive complex.

The equation of dBA_{on}/dt for the formation of the active state is

$$\frac{dBA_{on}}{dt} = k_1 \left(B_{tot} - BA_{on} - BA_{in}\right) * \left(1 - BA_{on} - BA_{in}\right) - k_2 BA_{on} \tag{14.5.16}$$

and the equation for dBA_{in}/dt for the formation of the inactive state is

$$\frac{dA_{in}}{dt} = k_2 AB_{on} \tag{14.5.17}$$

with constants $k_1 = k_2 = 4$.

The graphs (note the different time concentration scales on the left) show a fairly quick return to the basal state after each stimuli pulse (B).

14.5.4: SUMMARY

This chapter integrates foundational concepts in binding interactions, enzyme kinetics, and metabolic control to explain how biological systems generate varied responses and maintain homeostasis. Key topics include:

- **Binding Interactions:**
  The chapter contrasts simple binding—where the fractional saturation of a macromolecule by a ligand follows a hyperbolic curve—with allosteric binding, which produces sigmoidal curves. These different binding behaviors, modeled by the Hill equation among other models, illustrate how macromolecules can respond with varying sensitivities to changes in ligand concentration.
- **Enzyme Kinetics and Response Curves:**
  Building on the binding principles, the discussion shifts to enzyme-catalyzed reactions. It explains how initial velocity (v_0) vs. substrate concentration plots can be hyperbolic or sigmoidal, depending on the underlying reaction mechanisms. Two key scenarios are examined:
  - **Linear Response:** A simple system where a stimulus S is directly converted to a response R, yielding a linear relationship between S and R.
  - **Hyperbolic Response:** In enzyme-catalyzed reactions with saturable kinetics, increases in substrate S lead to a hyperbolic response in product formation, reflecting the inherent limits of enzyme activity.
  - **Sigmoidal Response:** For systems involving allosteric enzymes or cooperative binding, the response curve becomes sigmoidal, allowing for more sensitive regulation under physiological conditions.
- **Systems-Level Responses in Pathways:**
  The chapter emphasizes that, within metabolic or signaling pathways, the behavior of individual reactions may differ from that observed

in isolation. For instance, even when inputs (such as substrates or signaling molecules) change, a pathway may exhibit steady-state behavior due to internal regulatory mechanisms.

- **Adaptation and Homeostasis:**
  A central theme is how cells achieve adaptation—returning to a basal state following a transient stimulus—to maintain homeostasis. The concept of homeostasis is underscored as a critical aspect of life, requiring the fine-tuning of gene expression, enzyme activity, and metabolic fluxes. The chapter reviews:
  - The biological necessity of maintaining stable internal conditions.
  - How adaptation prevents overreaction to persistent stimuli, thus avoiding detrimental outcomes like uncontrolled cell proliferation or cell death.
- **Adaptive Circuit Motifs:**
  The latter part of the chapter presents several simple circuit motifs that can generate perfect or near-perfect adaptation:
  - **Negative Feedback Loops:** Systems in which a product inhibits its own production, thereby dampening responses to sustained stimuli.
  - **Incoherent Feedforward Systems:** Circuits where a stimulus drives both a direct positive response and a delayed negative response via an inhibitor, yielding transient responses that return to baseline.
  - **State-Dependent Inactivation:** Models based on the behavior of ion channels and receptors, where proteins transition between active, inactive, and off states to prevent continuous signaling.

Through mathematical derivations, simulations (using tools like VCell), and graphical illustrations, the chapter provides a framework for understanding how biochemical systems modulate responses to diverse inputs. It bridges molecular interactions with systems-level behavior, emphasizing the interplay between binding, kinetics, and regulatory circuit design in achieving adaptive homeostasis.

This page titled 14.5: Metabolism and Signaling: The Steady State, Adaptation and Homeostasis is shared under a not declared license and was authored, remixed, and/or curated by Henry Jakubowski and Patricia Flatt.

- **11.2: Diffusion Across a Membrane - Passive and Facilitated Diffusion** by Henry Jakubowski and Patricia Flatt has no license indicated.

CHAPTER OVERVIEW

15: GLUCOSE, GLYCOGEN, AND THEIR METABOLIC REGULATION

Return to Fundamentals of Biochemistry Search Fundamentals of Biochemistry

15.1: Insulin Signaling in the Liver
15.2: Glycogenesis
15.3: Glycogenolysis and its Regulation by Glucagon and Epinephrine Signaling
15.4: Regulation of Glycolysis
15.5: Regulation of Gluconeogenesis

This page titled 15: Glucose, Glycogen, and Their Metabolic Regulation is shared under a not declared license and was authored, remixed, and/or curated by Henry Jakubowski and Patricia Flatt.

15.1: INSULIN SIGNALING IN THE LIVER

LEARNING GOALS (CHATGPT O3-MINI)

1. **Understand Glycogen Structure and Function:**
   - Describe the molecular structure of glycogen, including alpha $1 \rightarrow 4$ main chain linkages, alpha $1 \rightarrow 6$ branch points, and the role of glycogenin at the reducing ends.
   - Explain the physiological roles of glycogen storage in liver versus skeletal muscle and its significance in energy metabolism.
2. **Appreciate the Importance of Blood Glucose Homeostasis:**
   - Discuss how liver glycogen reserves help maintain blood glucose levels critical for brain function and overall energy balance.
   - Explain the consequences of impaired glucose homeostasis on neuronal function and organismal survival.
3. **Describe Glycogen Metabolism Pathways:**
   - Outline the process of glycogen breakdown (glycogenolysis) and its conversion to glucose 1-phosphate and subsequently to glucose 6-phosphate.
   - Connect glycogenolysis to broader metabolic pathways, such as glycolysis, anaerobic lactate production, and aerobic respiration.
4. **Differentiate Hormonal Regulation of Glucose:**
   - Compare the roles of insulin and glucagon in the regulation of blood glucose levels.
   - Explain how insulin promotes glucose uptake and storage, while glucagon stimulates gluconeogenesis and glycogenolysis.
5. **Trace Insulin Biosynthesis and Maturation:**
   - Describe the synthesis of insulin from preproinsulin to proinsulin and its conversion to mature insulin with the release of the C-peptide.
   - Recognize the clinical significance of C-peptide measurements in distinguishing endogenous insulin production from exogenous administration.
6. **Explain the Structure and Activation of the Insulin Receptor:**
   - Describe the molecular architecture of the insulin receptor, emphasizing its receptor tyrosine kinase activity, dimerization, and autophosphorylation.
   - Illustrate how insulin binding induces conformational changes that enable downstream signaling.
7. **Outline the Insulin Signaling Cascade:**
   - Map the key steps of the insulin signaling pathway, including the recruitment of IRS-1, activation of PI3-kinase, conversion of PIP2 to PIP3, and subsequent activation of PDK and Akt.
   - Explain how Akt activation leads to the phosphorylation of downstream targets (e.g., AS160 and GSK-3), resulting in GLUT4 translocation and activation of glycogen synthase.
8. **Connect Insulin Signaling to Glucose Uptake and Glycogen Synthesis:**
   - Explain the mechanism by which insulin signaling increases the number of GLUT4 transporters at the plasma membrane, facilitating rapid glucose uptake.
   - Describe how insulin-induced inactivation of GSK-3 via Akt leads to activation of glycogen synthase, thereby promoting glycogen synthesis.
9. **Integrate the Role of Hexokinase in Glucose Metabolism:**
   - Understand how hexokinase phosphorylates glucose to form glucose 6-phosphate, effectively trapping glucose within the cell for energy production or storage.
   - Discuss how this phosphorylation step is essential for both glycolysis and glycogen synthesis.
10. **Evaluate the Physiological and Clinical Relevance:**
    - Discuss how the integrated processes of insulin signaling, glucose uptake, and glycogen synthesis contribute to maintaining energy homeostasis.
    - Evaluate the implications of dysregulation in these pathways in metabolic diseases such as diabetes.

These learning goals aim to provide a comprehensive framework that connects molecular mechanisms with systemic physiological outcomes, equipping students with the knowledge to understand and analyze insulin-mediated regulation of glucose metabolism.

15.1.1: INTRODUCTION

In this section, we will discuss insulin signaling and glycogen synthesis. Insulin is released in the fed state and leads to glucose uptake, where it can be stored, if not needed, for glycogen synthesis. Recall that glycogen is a large polymer of glucose residues connected in the main chain by alpha 1 → 4 linkages and with branching side chains about every 12 – 15 residues at the alpha 1 → 6 positions. The reducing ends of the carbohydrate (two for each polymer) are connected to the glycogenin dimeric protein at the center of the macromolecule (Figure **15.1.1**). With the branching nature of the polymer, many non-reducing ends of the molecule are present, allowing easy access and fast release of glucose for energy utilization.

Most of the body's glycogen pools are stored in the liver, with 10% of the liver biomass in glycogen granules, and in the skeletal muscle, with glycogen comprising 2% of the muscle biomass. Each glycogen polymer may have upwards of 30,000 glucose residues, making it visible using standard microscopic techniques. The muscle cells use glycogen stored within muscle tissue as a source of energy to fuel muscle contraction. In the liver, the purpose of glycogen storage is different. Glycogen stored at this location maintains the homeostatic balance of blood glucose levels. The liver is the primary organ that can actively transport glucose into the bloodstream. Our only other major source of glucose within the blood is our diet.

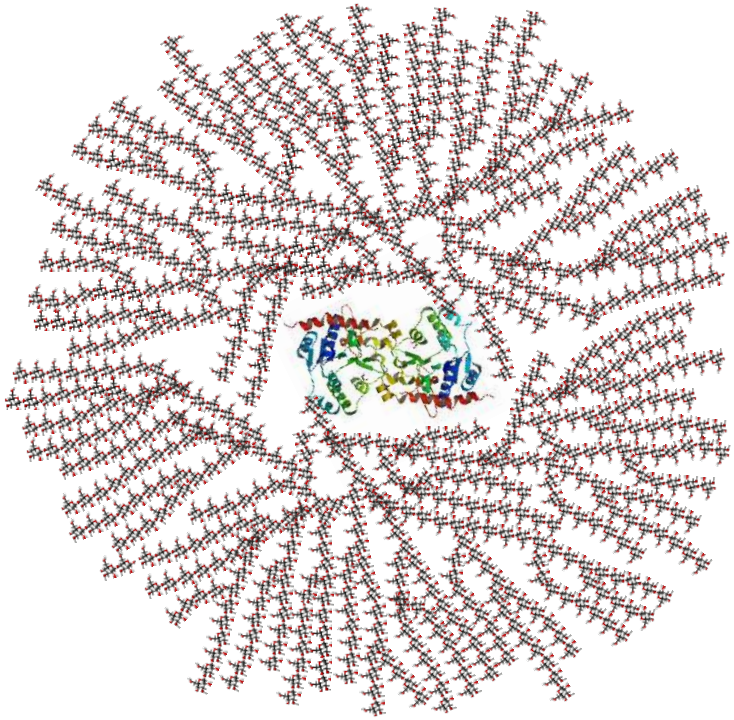


Figure **15.1.1**: The Glycogen Polymer. The glycogen-reducing ends of the glycogen polymer are connected with the dimeric glycogenin protein shown at the center of the diagram using the ribbon projection. The polymer is constructed predominantly of glucose monomers connected through alpha 1 --> 4 linkages. Alpha 1 --> 6 branches are apparent about every 12 - 15 residues. (Public Domain; Mikael Häggström via Wikipedia.

Blood glucose homeostasis is critical for brain function (Figure **15.1.2**). The brain has a huge energy demand but nearly zero storage of key energy molecules required for ATP production. Furthermore, glucose and ketone bodies are the only energy sources that can pass the blood-brain barrier and be utilized by the brain for ATP production. Note that ketone bodies are only produced during starvation or disease states such as diabetes and are not a regular energy source for the brain. Thus, glucose is critical for brain function. The brain uses nearly 10% of the whole body's energy for nerve impulse transmission. If the blood flow carrying critical oxygen and glucose to the brain is impeded, people will lose consciousness within approximately 20 seconds! Brain death/permanent damage occurs within 4 minutes of blood flow cessation. This exemplifies the importance of the liver in maintaining blood glucose levels, as well as the importance of oxygen maintenance.

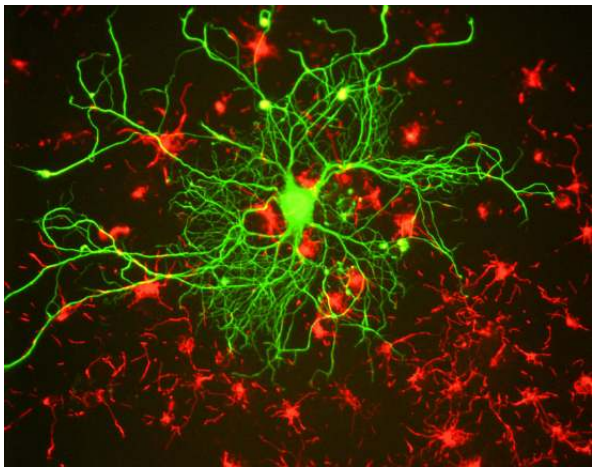


Figure 15.1.2: Cortical neuron stained with antibody to neurofilament subunit NF-L in green. In red are neuronal stem cells stained with antibodies to alpha-internexin. Image created using antibodies from EnCor Biotechnology Inc. (CC BY-SA 3.0 Unported; GerryShaw via Wikipedia)

Glycogen in the liver or muscle can be broken down into glucose 1-phosphate (Figure 15.1.3). This can be converted to glucose 6-phosphate, which is readily used in many cellular processes. The glycolysis (or the breakdown of glucose into pyruvate) occurs in all cells and produces a small amount of ATP. Further processing of pyruvate can occur anaerobically (or in the absence of oxygen) to produce lactate, or the process can continue to occur in the aerobic pathway to complete oxidation to carbon dioxide and water in the Krebs cycle. Note that oxygen from breathing is used to create the water within this pathway. This fuels the process of oxidative phosphorylation within the mitochondria and produces large quantities of ATP (from 30-36 molecules/glucose). Within the liver, glucose can be freed from glycogen and released into the bloodstream to maintain homeostatic levels. Glucose 6-phosphate can also be utilized as a precursor for other major macromolecules such as ribose and deoxyribose, as well as the hexosamine compounds commonly found cushioning joints or attached to plasma membrane proteins.

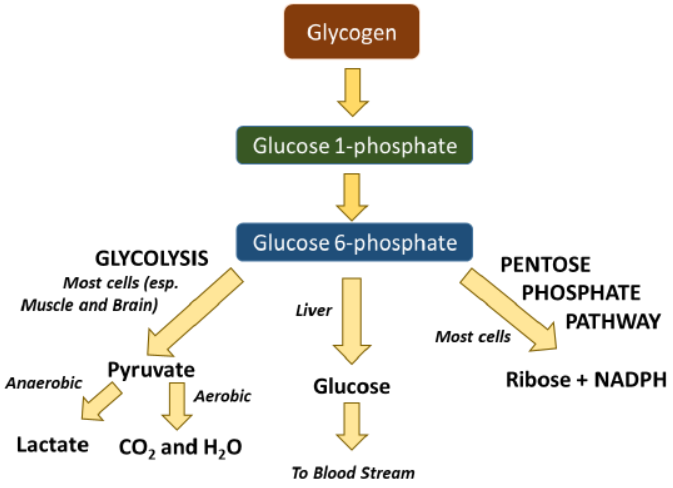


Figure 15.1.3: Pathways of Glycogen Utilization.

In healthy individuals, hormone signaling is critical to maintaining blood glucose homeostasis. Within this system, the hormones glucagon and insulin work together to maintain normal plasma glucose levels (Figure 15.1.4). During hyperglycemia, pancreatic beta (β) cells release insulin, which stimulates glucose uptake by energy-consuming cells and glycogen formation in the liver. During hypoglycemia, pancreatic alpha (α) cells release glucagon, which stimulates gluconeogenesis and glycogenolysis in the liver and the release of glucose to the plasma.

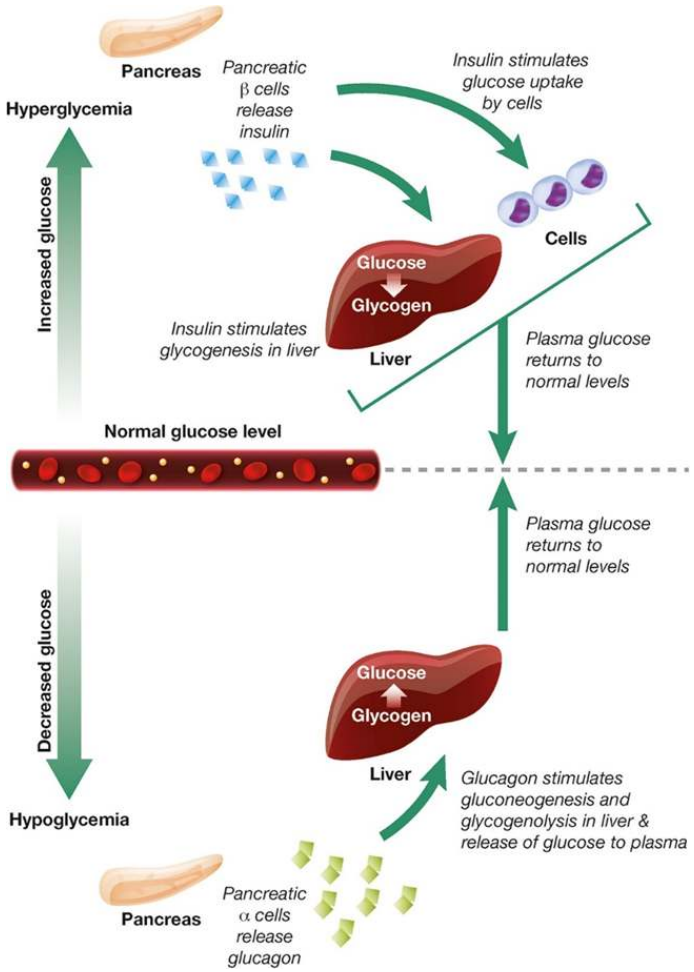


Figure **15.1.4**: Hormone Signaling Involved in Blood Glucose Homeostasis. The hormones glucagon and insulin, released by the pancreas, are critical for regulating the liver's release or uptake of glucose from the bloodstream. In the *upper diagram*, beta cells within the pancreas secrete the insulin hormone when blood glucose levels rise. Insulin signaling causes the liver to increase glucose uptake from the bloodstream and promotes its storage as glycogen. Alternatively, alpha cells in the pancreas release the hormone glucagon when blood glucose levels are low, as shown in the *lower diagram*. Glucagon signaling in the liver leads to the breakdown of glycogen and the release of stored glucose into the bloodstream. Hædersdal, S., et al (2018) Mayo Clinic Proceedings 93(2):217-239

The first area we will focus our attention on is the mechanism insulin utilizes to reduce blood glucose levels. Figure **15.1.5** shows the structure of the pancreas and its anatomical relationship with the liver and the stomach. The pancreas is the sensor organ that detects blood glucose levels. It is responsible for signaling the liver to remove or release glucose in response to changing levels. Notably, the pancreas also produces most of the digestive enzymes utilized by the body, including proteases, amylases, and lipases.

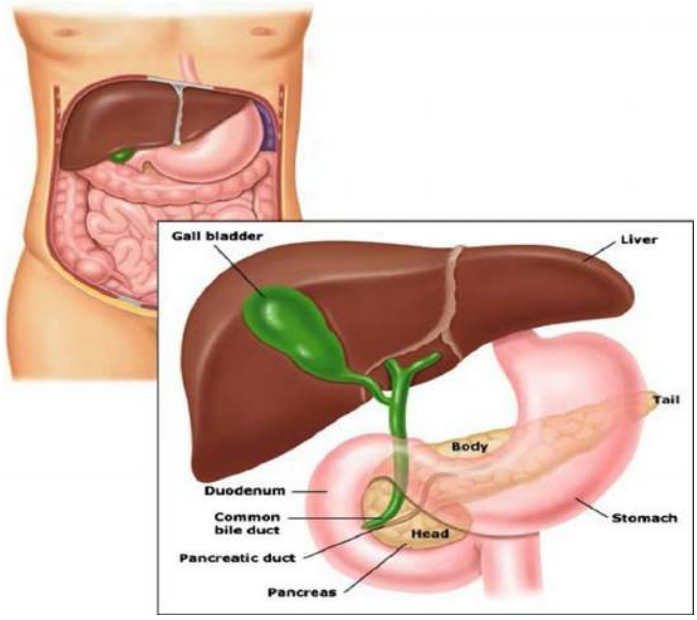


Figure 15.1.5: The Anatomy of the Liver and Pancreas. Akinlade, A., et al (2014) Int. Archives of Med 7(50):28

Figure 15.1.6 shows a light microscope image of the pancreatic islet cells. They are responsible for the production of glucagon and insulin. The islets are distinguished from the surrounding tissue by a continuous connective tissue capsule and extensive vascularity.

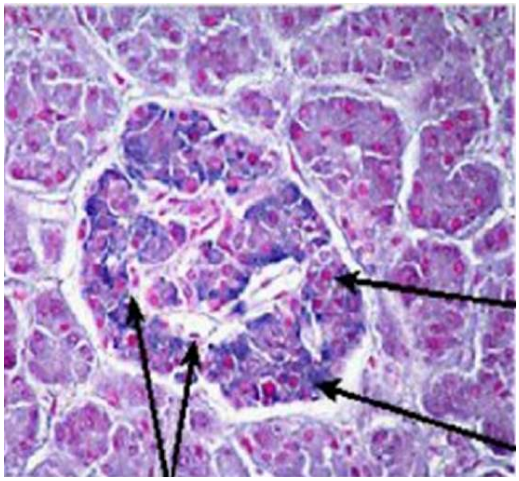


Figure 15.1.6: Pancreatic Islet Cells. In this diagram, the islet cells that secrete glucagon (known as alpha cells) are stained in red, while the beta cells that produce insulin are stained in blue. Akinlade, A., et al (2014) Int. Archives of Med 7(50):28

Insulin is a peptide hormone composed of 51 amino acids, as shown in Figure 15.1.7. It is initially synthesized as preproinsulin, which is converted to proinsulin after removing the signal peptide. Two disulfides are made in the ER (catalyzed by protein disulfide isomerase) along with selective proteolytic cleavage to form insulin. Mature insulin consists of A and B chains that are connected in proinsulin by the C-peptide.

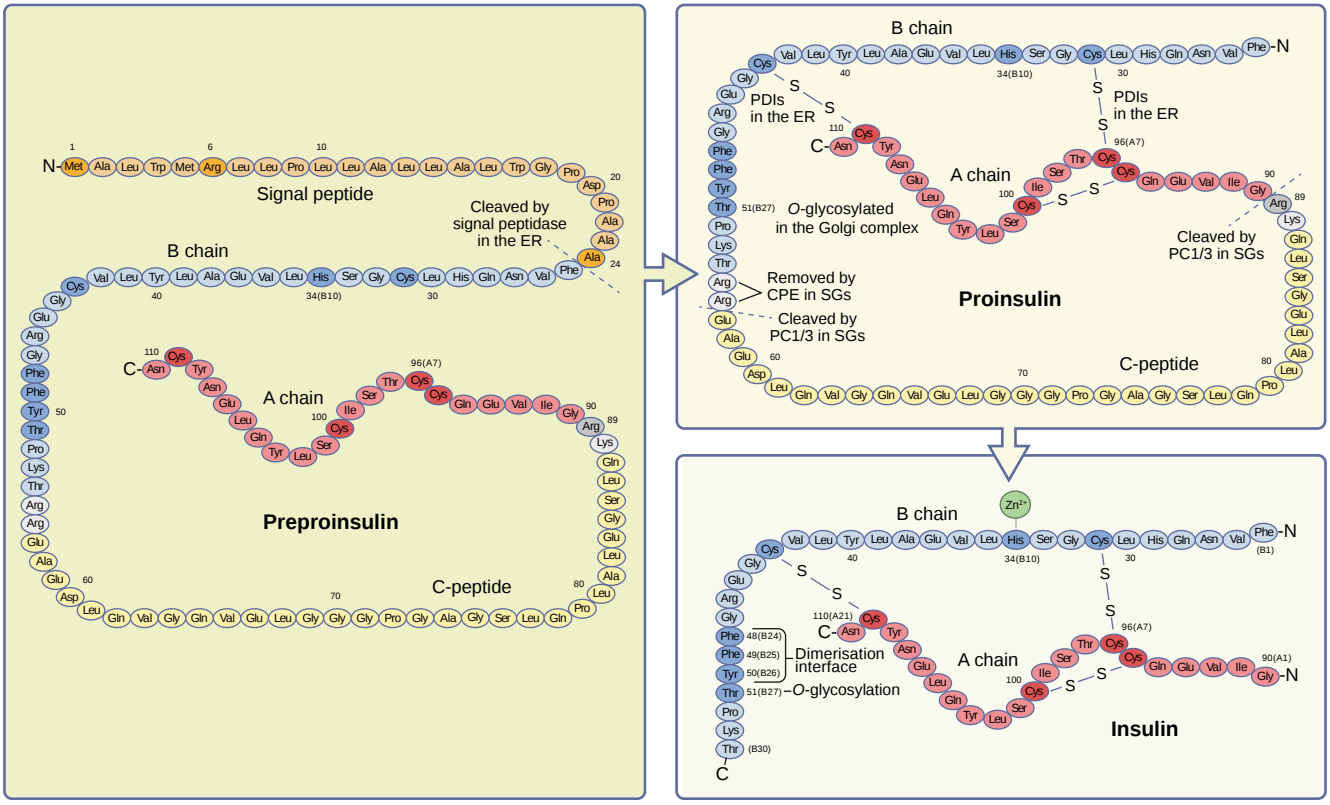
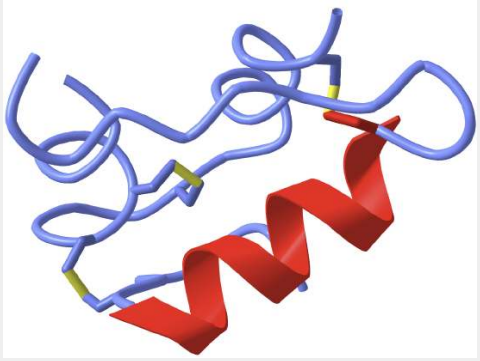
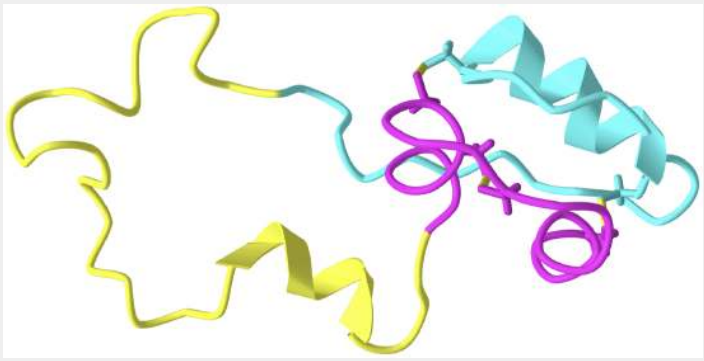


Figure 15.1.7: Conversion of preproinsulin to mature insulin. Vasiljević, J. *et al. Diabetologia* **63**, 1981–1989 (2020). https://doi.org/10.1007/s00125-020-05192-7. http://creativecommons.org/licenses/by/4.0/.

Figure 15.1.8 shows interactive iCn3D models of human insulin (3I40) and human proinsulin (2KQP). (Copyright; author via source). Click the image for a popup or use the external link provided:

Human insulin (3I40)	Human Proinsulin (2KQP)
	
Colored code to show secondary structure External link: https://structure.ncbi.nlm.nih.gov/i...A3QZdZpfEMxR17	The "future" A chain in mature insulin is shown in magenta, the C-peptide connecting the A and B chains is shown in yellow, and the future B chain is in cyan. External link: https://structure.ncbi.nlm.nih.gov/i...nQJXhrEfHD1GH9

The maturation of preproinsulin to insulin is shown in more detail in Figure 15.1.9. The peptide is first translated on ribosomes linked to the rough endoplasmic reticulum (ER), where a signal peptide docks the peptide to the ER membrane. The proinsulin is folded, and the signal peptide is cleaved. It is transported to the Golgi, where it is further packaged into secretory vesicles. Within the secretory vesicles, the proinsulin is cleaved to release the C-peptide. The A and B peptides are held together by disulfide bridges and form the active insulin component.

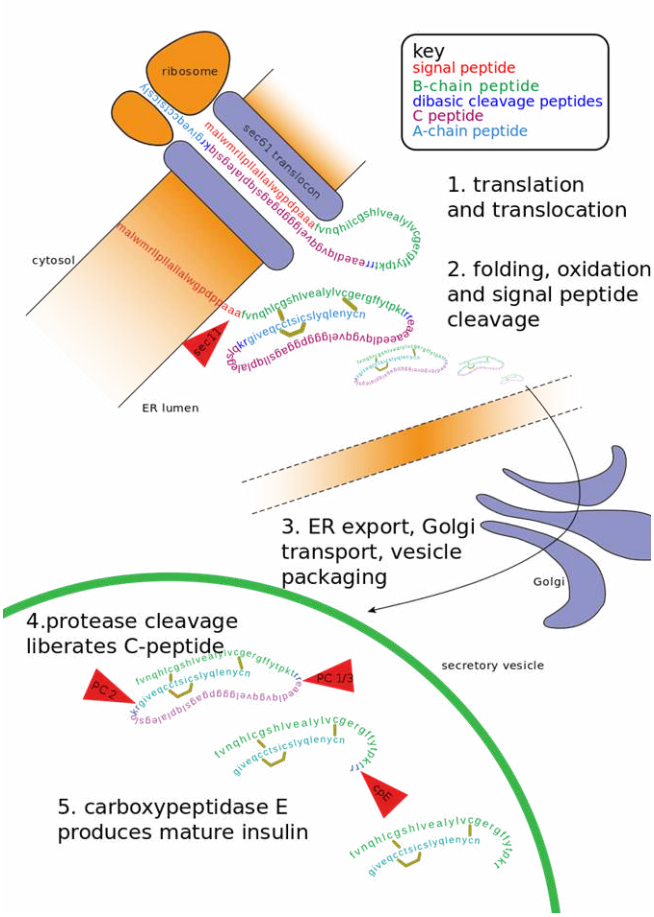


Figure **15.1.9**: Insulin Production. The process of insulin production includes the translation of the insulin mRNA into the rough endoplasmic reticulum. The peptide is transported through the Golgi and packaged into secretory vesicles, where protease cleavage by carboxypeptidase E produces the mature insulin peptide and peptide C. Image from Fred the Oyster

The C-peptide is a bioactive peptide secreted simultaneously and in equal amounts to the insulin hormone. It also has a longer half-life than insulin and is excreted by the kidneys into the urine, making detection easy. Furthermore, it allows for detecting patient-produced insulin, even if they are receiving insulin injections. Thus, C-peptide detection is often utilized to help distinguish between patients with type 1 diabetes and patients with type 2 diabetes (or maturity-onset diabetes). Details about the different forms of diabetes will be discussed later.

Once insulin is released from the pancreas, it travels throughout the body and binds with cellular targets that contain the insulin receptor. The Insulin Receptor is a tyrosine kinase receptor that dimerizes upon insulin binding, as shown in Figure **15.1.10**. Insulin receptors are located on most cell types throughout the body, causing pleiotropic effects during insulin response. The primary targets of insulin action are the liver, which promotes the uptake of glucose and the production of the glycogen storage molecule, as well as skeletal muscle and fat. The receptor's tyrosine kinase portion, located on the plasma membrane's internal side, is quite flexible.

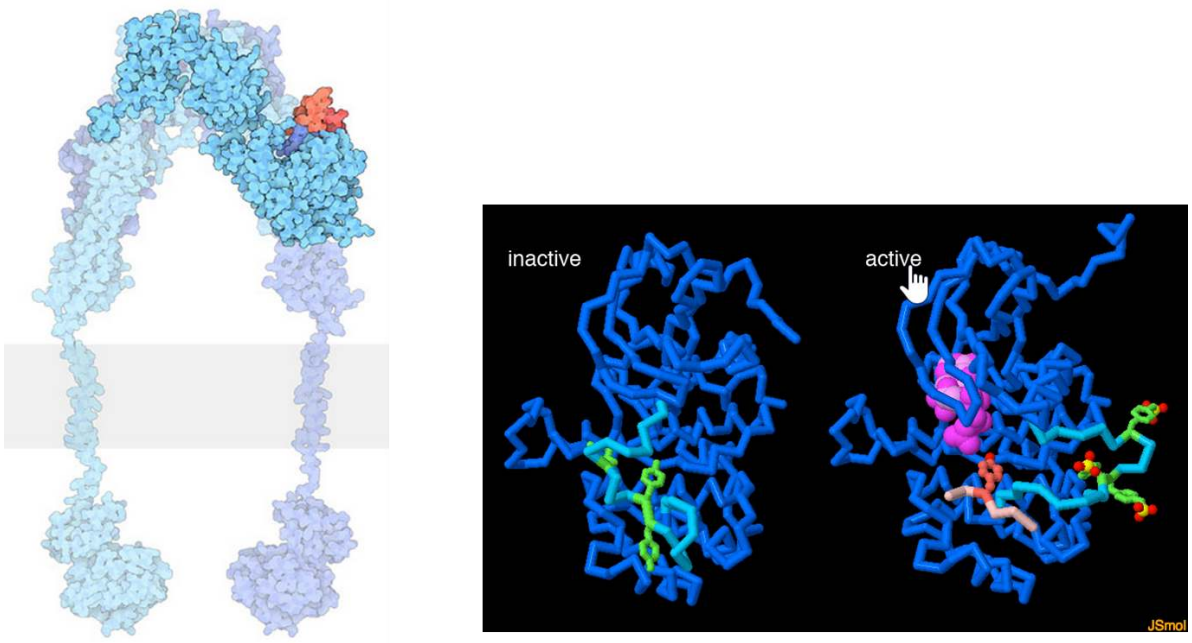


Figure 15.1.10: The Insulin Receptor. Images from Goodsell, D., et al (2015) RCSB PDB-101 'Molecule of the Month'

The left-hand diagram shows a space-filling model of the activated insulin receptor dimer embedded into the plasma membrane (the gray bar). The tyrosine kinase portion of the receptor is shown on the inside of the cell, whereas the insulin binding domain is present on the external side of the plasma membrane. The *middle and right-hand diagrams* show the inactive *(middle)* and active forms *(far right)* of the tyrosine kinase domain of an insulin receptor monomer. When activated, the tyrosine kinase domain binds to ATP (hot pink) and phosphorylates downstream targets, including several of its tyrosine residues (green). In the inactive state (middle), a mobile loop (turquoise) binds in the ATP binding site and prevents ATP association. When the insulin receptor is activated, the mobile loop opens, allowing for the binding of ATP and self-phosphorylation of tyrosine residues and other signaling proteins (a small peptide from one is shown in light pink).

Figure 15.1.11 below, which shows an interactive iCn3D model of the **Full-length mouse insulin receptor bound to four insulins (7SL7)**.

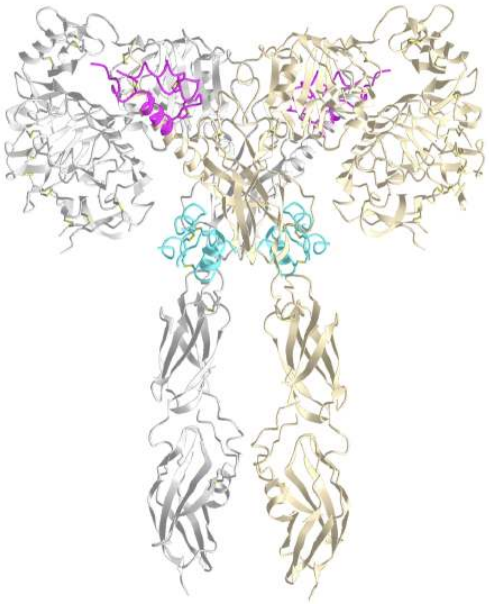


Figure 15.1.11: Full-length mouse insulin receptor bound to four insulins (7SL7). (Copyright; author via source). Click the image for a popup or use this external link: https://structure.ncbi.nlm.nih.gov/i...gkTrtvaqQF6o2A

The receptor is a dimer (one monomer gray and the other light brown). Four insulins are bound in maximally activated insulin receptors. Two insulins (magenta) are bound at the same respective place in each monomer (site-1, the primary site), and the two others are

bound at a second parallel site (site-2). The full active state is a symmetric T-shape. Less active receptors have fewer bound insulins, with receptor geometry more asymmetric (one insulin bound at site 1 gives a Γ-shaped conformation, while two produce a T-shaped conformation as the second insulin binds). When four insulins are bound at both sites, the asymmetric conformation can't be formed. Although the structure is described as full-length, both monomers end at amino acid 910. The single membrane-spanning alpha-helix occurs at amino acids 947-967 and is NOT shown in the model.

Activation of the insulin receptor in the liver when insulin is present initiates a phosphorylation signaling cascade, as shown in Figure **15.1.12**. One of the proteins activated is Rab10. Rab 10 promotes the fusion of GLUT4-containing secretory vesicles (GSVs) with the plasma membrane, allowing for increased surface expression of GLUT4. GLUT4 is a glucose transporter protein. Thus, an increased protein concentration in the plasma membrane results in the upregulation of glucose import into the cell. Having GLUT4 proteins stored within secretory vesicles makes them available more readily than having to activate gene transcription pathways and production of the protein *de novo*. This allows a faster response to help lower blood glucose levels. The result is increased glucose uptake from the bloodstream into liver cells and other cellular targets, reducing blood glucose levels.

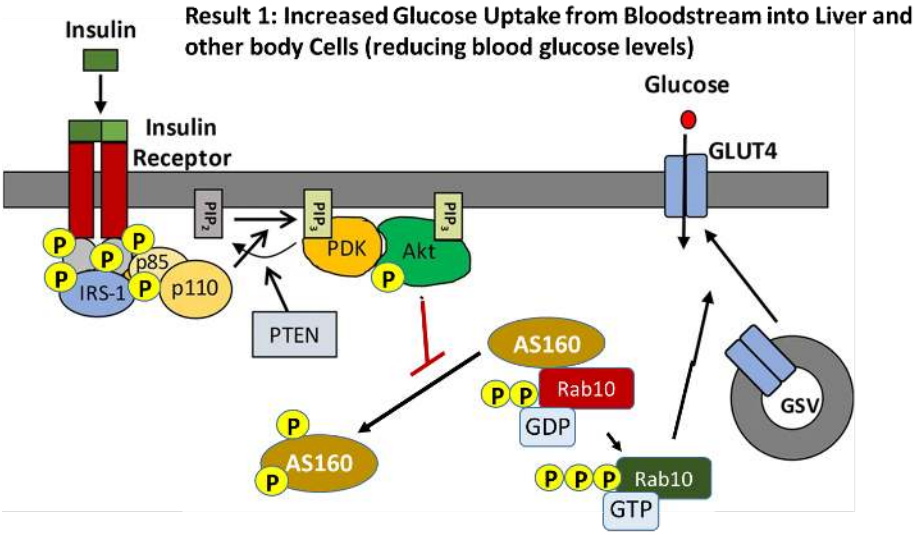


Figure **15.1.12**: Insulin Activation of Liver Cells and Glucose Uptake. Image from Carmichael, R.E., et al (2019) Scientific Reports 9:6477

The insulin receptor is a receptor tyrosine kinase, which undergoes dimerization and autophosphorylation of Tyr residues upon insulin binding. The phosphorylated receptor also recruits and phosphorylates the insulin receptor substrate 1 (IRS-1) on tyrosine residues, which then recruits dimeric Phosphoinositol (PI)3-kinase (p85/p110 in the diagram above) and phosphorylates the p85 regulatory subunit. The PI3 kinase catalyzes the phosphorylation of phosphatidylinositol bisphosphate (PIP2) within the plasma membrane to form phosphoinositol, 3,4,5-triphosphate (PIP3). PIP3 recruits PIP3-dependent kinase (PDK), which phosphorylates and activates Akt. Once activated, Akt dissociates from the membrane into the cytosol, where one of its downstream targets is AS160. AS160 is a GTPase that binds typically with Rab10 (a G-protein), causing the cleavage of GTP to GDP. Thus, AS160 downregulates the activity of Rab10. In the phosphorylated state, AS160 cannot bind or inhibit Rab10, enabling Rab10 to release GDP and bind with a molecule of GTP. In the activated state, Rab10 helps promote the fusion of GLUT4-containing secretory vesicles (GSVs) with the plasma membrane.

Figure **15.1.13** provides a deeper look at some of the initial activation steps in the insulin signaling pathway. This step shows the phosphorylation of Phosphoinositol 4,5-bisphosphate (PIP2) to Phosphatidylinositol 3,4,5-triphosphate (PIP3). PIP2 is a common phospholipid within the lipid bilayer structure. In future lectures, we will see the utilization of this phospholipid in other signaling pathways as well.

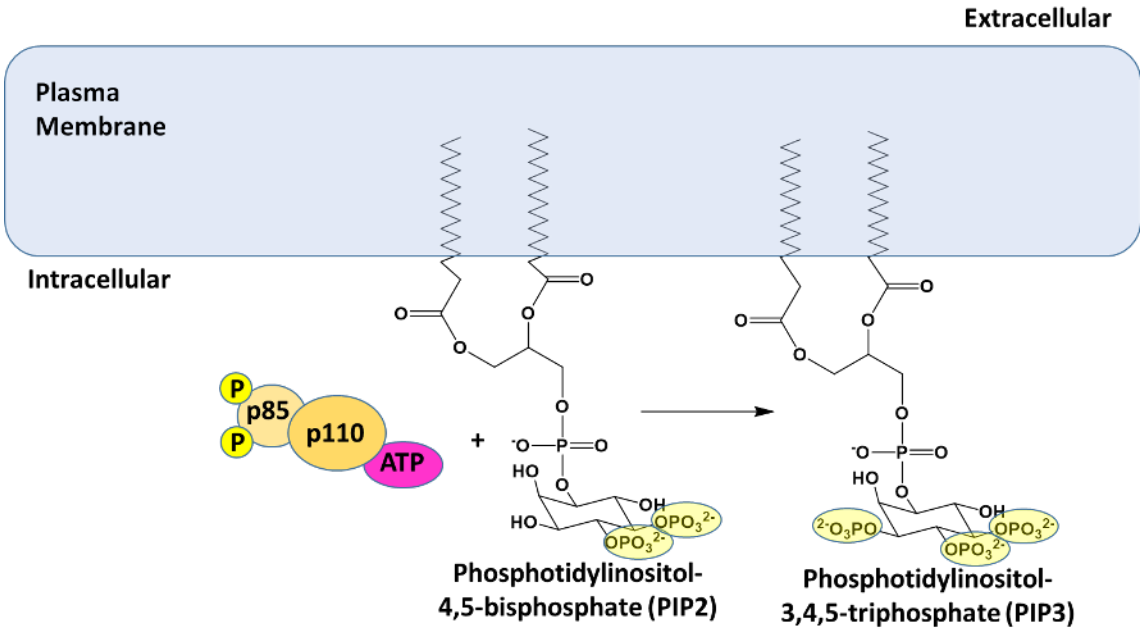


Figure **15.1.13**: Phosphorylation of phosphotidylinositol-4,5-bisphosphate During Insulin Signaling.

Once glucose enters a cell, it is rapidly converted to glucose 6-phosphate via the enzyme hexokinase, as shown in Figure **15.1.14** below. This enzyme is covered in more detail in our section on glycolysis. Importantly, phosphorylation traps the glucose inside the cell, preventing its redistribution back into the bloodstream. This helps to maintain the homeostasis of glucose within the bloodstream. In addition, glucose 6-phosphate is the first step in many glucose pathways, including energy utilization and the formation of building blocks such as ribose and deoxyribose used in RNA and DNA synthesis.

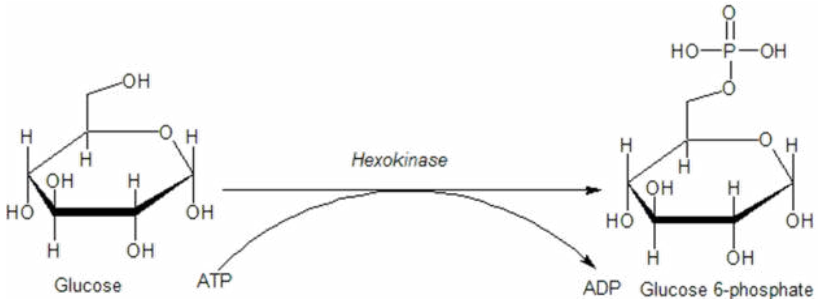


Figure **15.1.14**: Conversion of Glucose to Glucose-6-Phosphate by Hexokinase. Image from Jmun7616

Insulin signaling increases the number of GLUT4 transporters in the plasma membrane, causing an increased uptake of glucose into the cell. If glucose is not required for energy or other metabolic intermediates within liver and muscle tissue, it is then converted to glycogen for storage. The primary enzyme necessary for glycogen synthesis is also activated via insulin signaling, as shown in Figure **15.1.15**. In addition to phosphorylating the AS160 protein, Activated Akt also phosphorylates the Glycogen Synthase Kinase enzyme (GSK-3), which inactivates this protein. This allows protein phosphorylase 1 (PP1) to dephosphorylate the Glycogen Synthase enzyme, shifting it into a more active state and causing glycogen synthesis to commence.

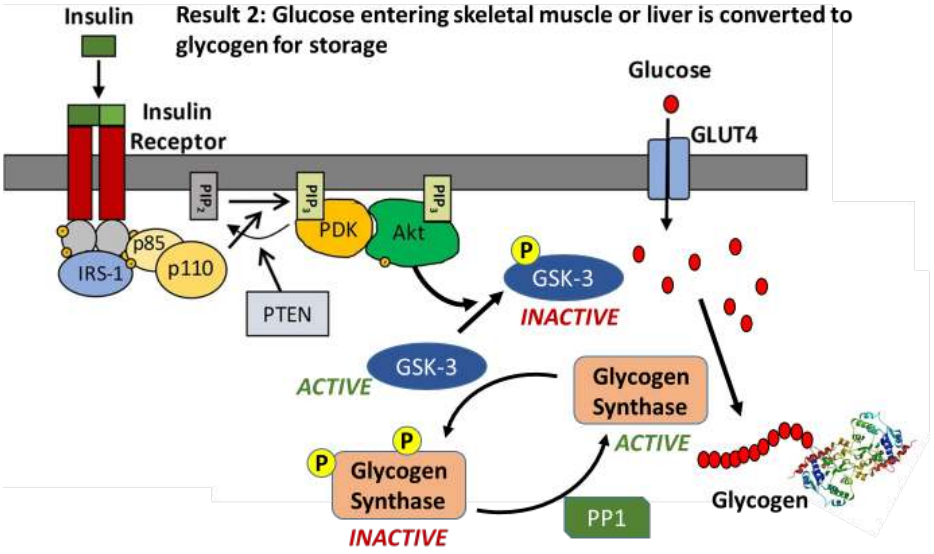


Figure **15.1.15**: Activation of Glycogen Synthase During Insulin Signaling. Image modified from Carmichael, R.E., et al (2019) Scientific Reports 9:6477

In this section, we have covered two pathways activated during the cellular response to insulin signaling, and I am sure you are feeling a bit overwhelmed with the complexity. However, biological processes are incredibly complex, and signaling pathways have multiple pleiotropic downstream effects. We have only touched the tip of the iceberg for insulin signaling, as evidenced in Figure **15.1.16**. This figure gives a more complete representation of the chemical changes induced within a liver cell in response to insulin signaling. For our purposes, we will restrict coverage to the two downstream effects: an increase in GLUT4 transporters in the plasma membrane and increased glycogen synthase activity.

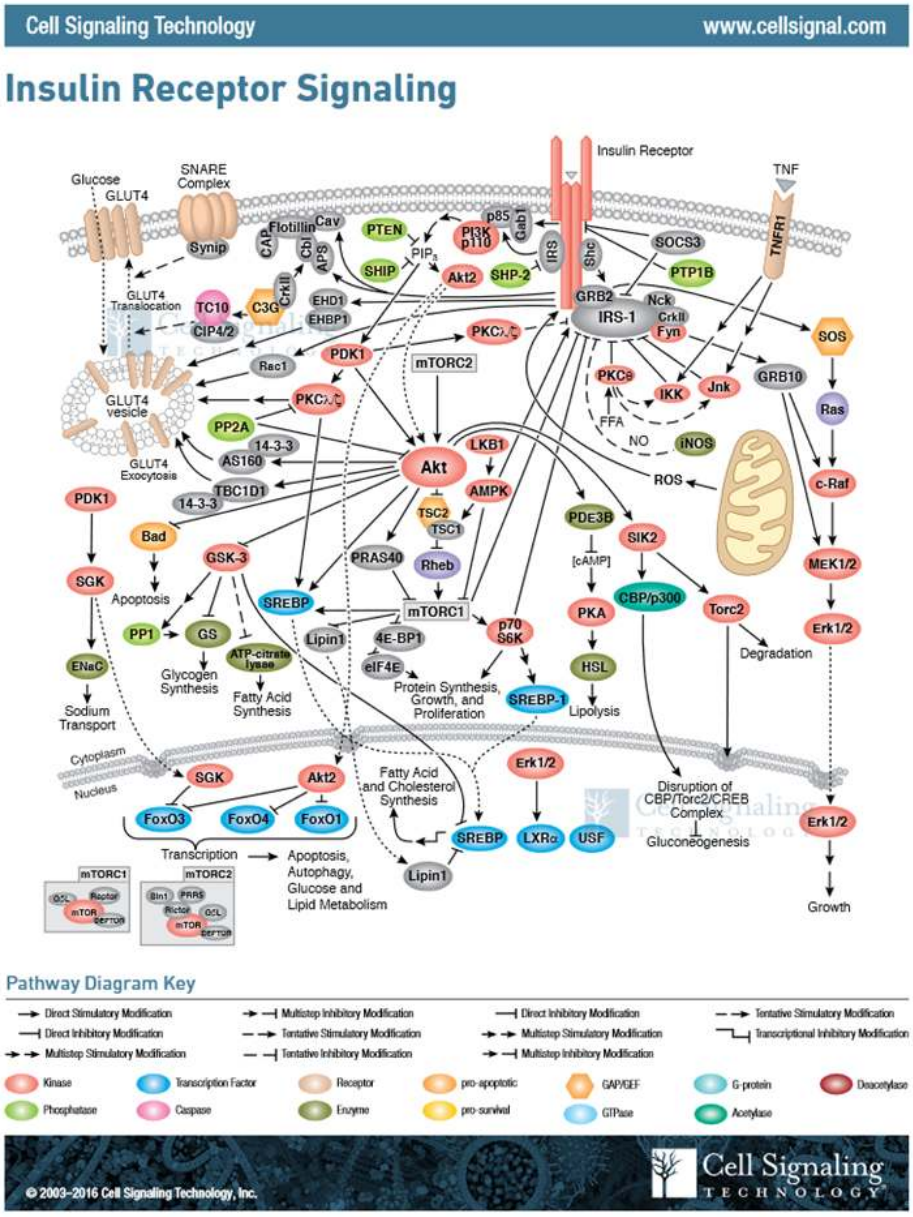


Figure **15.1.16**: Insulin Signaling Pathway. Image by Cell Signaling Technology

15.1.2: SUMMARY

This chapter explores the critical role of insulin signaling in regulating glucose uptake and glycogen synthesis, emphasizing how these processes maintain blood glucose homeostasis and overall energy balance in the body.

Glycogen Structure and Function:

The chapter begins with an overview of glycogen—a large, highly branched polymer of glucose residues. Glycogen's structure, characterized by alpha 1→4 linkages in the main chain and alpha 1→6 branch points approximately every 12–15 residues, allows for rapid mobilization of glucose. Glycogen is predominantly stored in the liver and skeletal muscle, where it serves distinct purposes: the liver maintains blood glucose levels for systemic homeostasis, while muscle glycogen provides an immediate energy source during contraction.

Hormonal Regulation and Blood Glucose Homeostasis:

Maintaining blood glucose levels is essential for proper brain function and overall cellular energy balance. The chapter outlines the complementary roles of insulin and glucagon—hormones secreted by the pancreatic islet cells—in regulating blood glucose. During hyperglycemia, insulin is released from beta cells to promote glucose uptake and glycogen synthesis, whereas during hypoglycemia, glucagon from alpha cells stimulates glycogenolysis and gluconeogenesis, ensuring a steady supply of glucose.

Insulin Biosynthesis and Structure:

Insulin is synthesized initially as preproinsulin, then processed to proinsulin and finally to mature insulin, with the C-peptide being cleaved off in the process. The chapter emphasizes the importance of the C-peptide not only as a marker for endogenous insulin production but also for distinguishing between type 1 and type 2 diabetes.

Insulin Receptor and Signaling Cascade:

Central to insulin's action is its receptor—a receptor tyrosine kinase that dimerizes and autophosphorylates upon insulin binding. This activation initiates a cascade of events: the receptor phosphorylates IRS-1, which then recruits PI3-kinase. The kinase catalyzes the conversion of PIP2 to PIP3, leading to the activation of PDK and Akt. Activated Akt phosphorylates multiple downstream targets such as AS160 and GSK-3. Phosphorylation of AS160 facilitates the translocation of GLUT4-containing vesicles to the plasma membrane, thereby increasing glucose uptake, while the inactivation of GSK-3 promotes glycogen synthase activity and subsequent glycogen synthesis.

Integration of Glucose Uptake and Metabolism:

Once inside the cell, glucose is rapidly phosphorylated by hexokinase to form glucose 6-phosphate, a metabolic "trapping" step that commits glucose to intracellular pathways including glycolysis and glycogen synthesis. This integration ensures that, in the fed state, excess glucose is efficiently stored as glycogen, helping to maintain stable blood glucose levels.

Physiological and Clinical Implications:

The chapter underscores the physiological importance of these interconnected processes. In the liver, glycogen storage and release are vital for sustaining blood glucose levels, particularly for brain function, which relies almost exclusively on glucose under normal conditions. The discussion also hints at the clinical relevance of these pathways in the context of metabolic diseases such as diabetes, where dysregulation of insulin signaling can lead to severe systemic effects.

Overall, the chapter provides a comprehensive view of how insulin signaling orchestrates a series of molecular events—from receptor activation to metabolic regulation—ensuring efficient energy storage and maintaining homeostasis in the body.

This page titled 15.1: Insulin Signaling in the Liver is shared under a not declared license and was authored, remixed, and/or curated by Henry Jakubowski and Patricia Flatt.

- **11.2: Diffusion Across a Membrane - Passive and Facilitated Diffusion** by Henry Jakubowski and Patricia Flatt has no license indicated.

15.2: GLYCOGENESIS

LEARNING GOALS (CHATGPT O3-MINI)

1. **Describe the Enzymatic Steps of Glycogenesis:**
   - Outline the six-step process of glycogen synthesis, identifying the roles of hexokinase, phosphoglucomutase, glycogen synthase (GS), UDP-glucose pyrophosphorylase (UGPase), glycogenin (GN), and glycogen branching enzyme (GBE).
2. **Explain the Role of Glycogen Synthase in Glycogen Assembly:**
   - Discuss how GS extends the glycogen main chain via the formation of alpha $1 \rightarrow 4$ glycosidic bonds using UDP-glucose and how its activity is regulated by insulin signaling and allosteric effectors such as glucose-6-phosphate.
3. **Understand the Function and Mechanism of UDP-Glucose Pyrophosphorylase (UGPase):**
   - Describe how UGPase catalyzes the reversible conversion of glucose 1-phosphate and UTP into UDP-glucose and inorganic pyrophosphate, emphasizing the enzyme's dependency on divalent cations (e.g., Mg^{2+}) and the key active site residues and loops involved in catalysis.
4. **Explain the Role of Glycogenin in Priming Glycogen Synthesis:**
   - Illustrate how glycogenin self-catalyzes its glycosylation to provide the primer required for GS activity, including the role of Mn^{2+} and critical aspartate residues in coordinating UDP-glucose.
5. **Analyze Glycogen Branching Enzyme (GBE) Function and Structure:**
   - Describe the mechanism by which GBE introduces alpha $1 \rightarrow 6$ branches into the glycogen molecule, increasing the number of non-reducing ends, and discuss the domain organization and structural features that distinguish eukaryotic GBE from its prokaryotic counterparts.
6. **Integrate Enzyme Cooperation in Glycogen Synthesis:**
   - Explain how glycogenin and glycogen synthase interact within a multi-enzyme complex, detailing the conformational states (closed/inactive, partially open, and open/active) that regulate their cooperative activity during glycogen assembly.
7. **Examine the Regulation of Glycogen Synthase Activity:**
   - Discuss the dual regulation of GS via allosteric activation by glucose-6-phosphate and reversible phosphorylation (and dephosphorylation), including the role of GSK-3, phosphatases, and the structural basis for the inactive (T) and active (R) states.
8. **Assess the Impact of Mutations and Post-translational Modifications:**
   - Analyze how mutations in critical regions (e.g., the 309-loop of UGPase, the arginine cradle in GS) and post-translational modifications influence enzyme activity and overall glycogen synthesis.
9. **Utilize Structural Models to Understand Enzyme Function:**
   - Interpret interactive structural models (e.g., iCn3D models of human UGPase, glycogenin-GS complexes, and GBE) to correlate structural features with catalytic mechanisms and regulatory interactions.
10. **Synthesize the Overall Pathway of Glycogen Synthesis and Its Regulation:**
    - Integrate the individual enzymatic steps and regulatory mechanisms into a comprehensive overview of glycogen synthesis, emphasizing how the cooperative and coordinated activities of these enzymes contribute to cellular energy storage and metabolic homeostasis.

These learning goals will guide students through both the mechanistic details and the regulatory complexities of glycogenesis, preparing them to analyze and interpret experimental data and structural information in this critical area of metabolic biochemistry.

15.2.1: INTRODUCTION

The process of forming glycogen is called **glycogenesis,** and it requires the activity of six enzymes, as illustrated in Figure **15.2.1**. We have already discussed several, including hexokinase, which phosphorylates the 6'-OH of glucose, and phosphoglucomutase, which converts glucose-6-phosphate to the glucose-1-phosphate isomer. This section will discuss the remaining four enzymes and their role in glycogen biosynthesis. They are Glycogen Synthase, UDP-Glucose Pyrophosphorylase (preferred name UTP-glucose-1-phosphate uridylyltransferase), glycogenin, and glycogen branching enzyme.

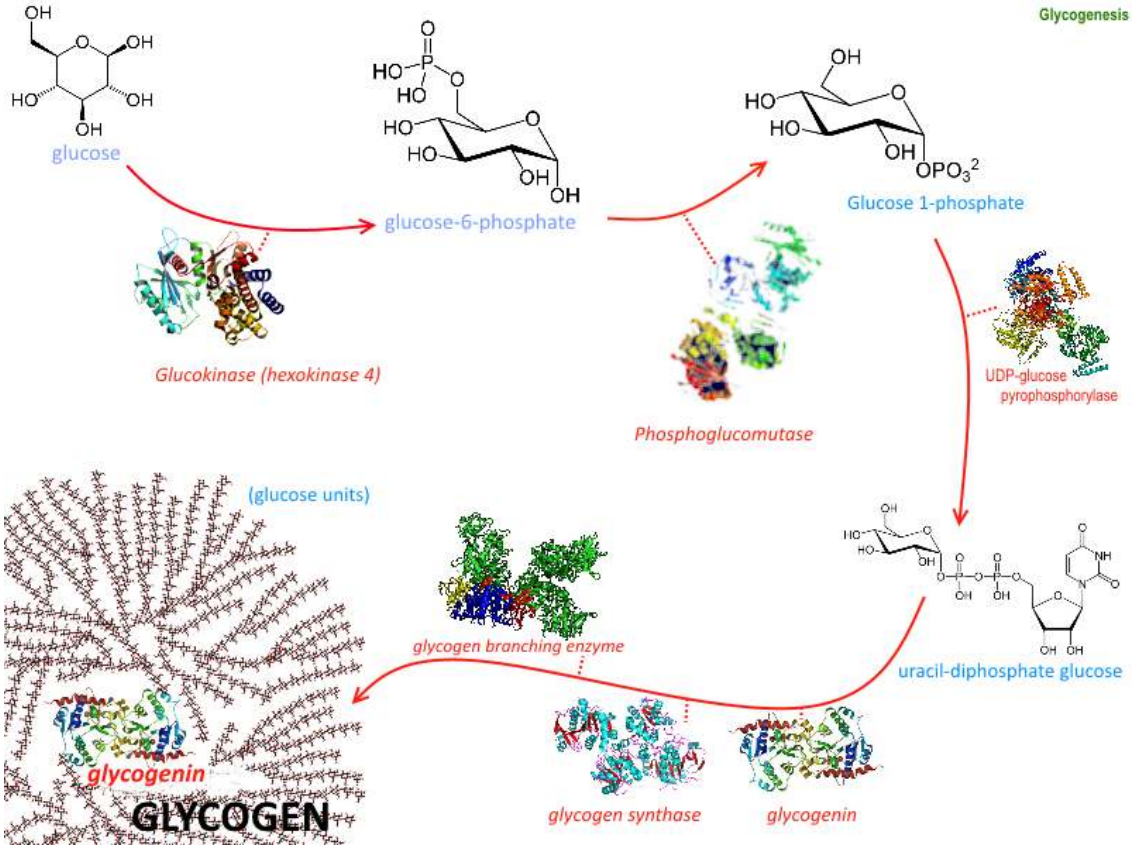


Figure **15.2.1**: Enzymes involved in Glycogenesis. Image from Mark Cidade

Given their importance in synthesizing the second main energy storage molecule, we must probe them in detail.

Glycogen synthase (GS) is a key enzyme whose activity is highly regulated. In Chapter 15.1, we have already explored how insulin signaling upregulates the activity of this enzyme by inhibiting phosphorylation by GSK-3. Other effectors include the allosteric binding of glucose-6-phosphate, which also increases the activity of the GS. In a later section, we will also see that the hormone glucagon can also regulate the activity of the GS through protein kinase A (PKA) in a fashion that decreases glycogen synthesis and increases glycogen breakdown.

In the glycogenesis pathway, GS is responsible for building most of the main α-1 → 4 chain glucose acetal linkages. The GS requires a primer of 4-6 glucose residues linked together by α-1 → 4 bonds to initiate synthesis. Since GS can only form α-1 → 4 linkages in the main chain, it CANNOT create the α-1 → 6 branches inherent to the core structure of glycogen.

GS uses the glycogen primer and glucose activated through covalent attachment to uridine diphosphate (UDP) at the 1-position to build the glycogen main chain. Upon completion of one round of synthesis, the 1 position of the incoming UDP-glucose is covalently attached to the 4-position of the nascent glycogen molecule, releasing the UDP as a leaving group.

$$\text{Glycogen}_{(n)} + \text{UDP-glucose} \rightarrow \text{Glycogen}_{(n+1)} + \text{UDP}$$

15.2.2: UTP--GLUCOSE-1-PHOSPHATE URIDYLYLTRANSFERASE (OR UDP-GLUCOSE PYROPHOSPHORYLASE)

The formation of the UDP-glucose required for the synthesis of the main chain of glycogen is mediated by **UTP-glucose-1-phosphate uridylyltransferase (preferred name), which is also called UDP-glucose pyrophosphorylase** (GalU or UGPase; EC 2.7.7.9). UGPase catalyzes the reversible reaction of glucose 1-phosphate and UTP into UDP-glucose and inorganic pyrophosphate (PP_i) (Figure **15.2.2**). Enzymes of the UGPase family are ubiquitous and can be found in the tree of life.

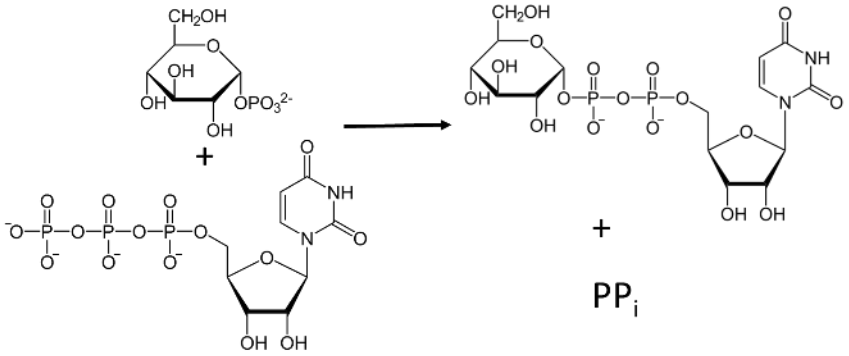


Figure **15.2.2**: Formation of UDP-Glucose

UDP-glucose is an activated form of glucose used to synthesize other glycans, including sucrose, cellulose, starch, and glycogen, and the glycan parts of glycoproteins, glycolipids, and proteoglycans. Hence, it is a key metabolite that gives more importance to understanding UGPase.

Like many other nucleotidyl transferases, UGPase requires divalent cations to promote the reaction (Figure **15.2.3**). In most cases, magnesium ions are employed. The reaction mechanism follows a sequential bi-bi-mechanism, starting with the binding of UTP to the active site in the presence of a magnesium ion, followed by the binding of glucose 1-phosphate. The octahedral coordination sphere of magnesium positions the substrates correctly and enables the nucleophilic attack of glucose 1-phosphate on UTP. A lysine, an aspartate, and several water molecules within the active site help stabilize the position of the substrates and cofactor for the proper nucleophilic attack of the phosphoryl oxygen of glucose 1-phosphate on the α-phosphorus atom of UTP. Finally, PP_i is released from the UGPase/Mg^{2+}/UDP-glucose complex. UDP-Glucose then dissociates from the complex, restoring the enzyme's active site for another round of synthesis.

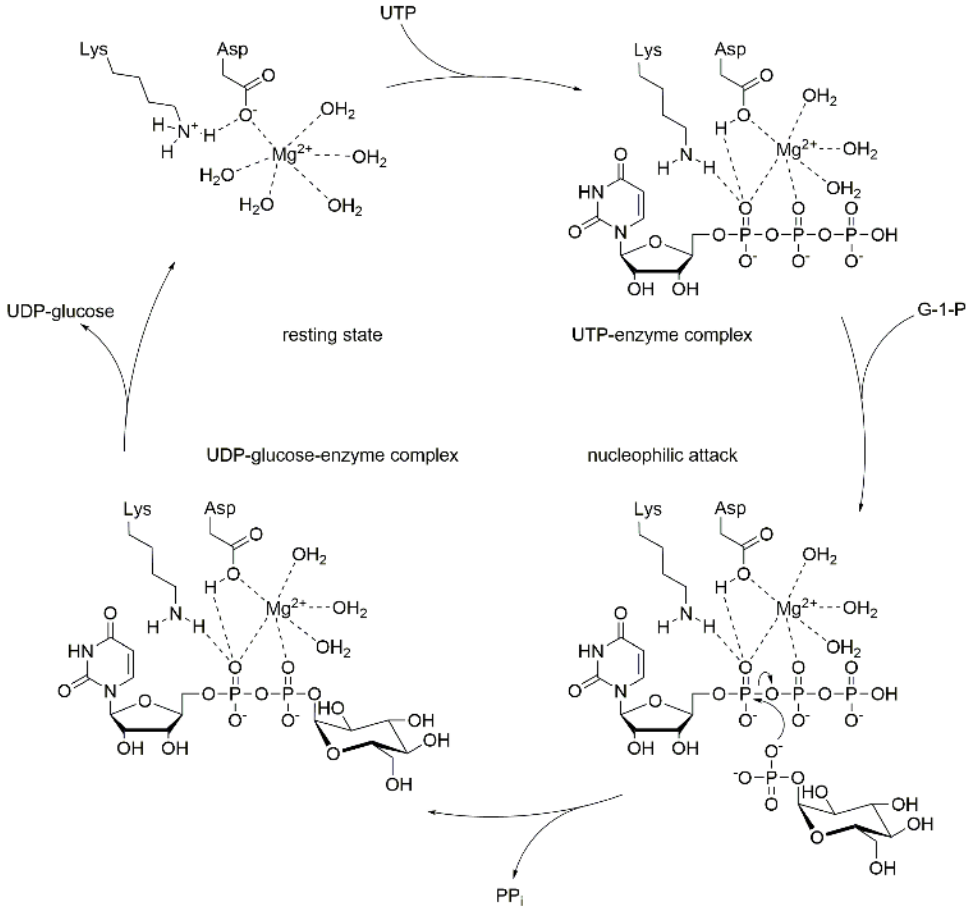


Figure **15.2.3**: Proposed Reaction Mechanism of UTP--glucose-1-phosphate uridylyltransferase (UDP-Glucose Pyrophosphorylase). Image from Kumpf, A., et al. (2019) *Int. J. Mol. Sci. 20(22)* 5809; https://doi.org/10.3390/ijms20225809

Figure **15.2.4** shows an interactive iCn3D model of the human UDP-glucose pyrophosphorylase tetramer (3R2W).

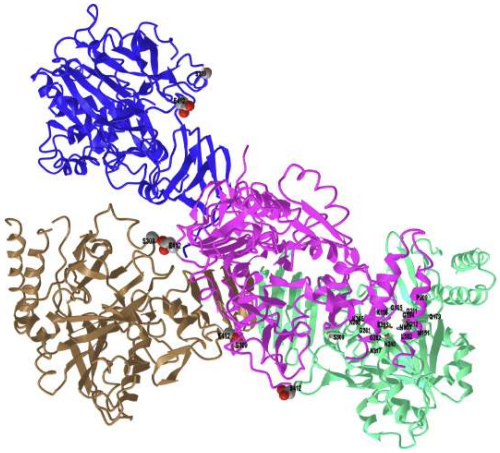


Figure **15.2.4**: Human UDP-glucose pyrophosphorylase tetramer (3R2W). (Copyright; author via source). Click the image for a popup or use this external link: https://structure.ncbi.nlm.nih.gov/icn3d/share.html?9yq9STPGvq87Wnbt8

Substrate binding and active site residues are shown as CPK-colored sticks and labeled in one of the subunits. Three key loops whose correct positioning is required for catalysis are colored as follows:

- Latch Loop: 406-416, yellow, which contains Glu 412 (shown in spacefill)
- SB Loop: 275-282, red
- 309 Loop: 309-311, cyan, which contains Ser 309 (shown in spacefill).

For clarity, only four of the eight subunits are shown. Note the proximity of the interacting loops positioned between the brown and magenta subunits. The SB and 309 loops at that location are part of the brown subunit, while the yellow latch loop is part of the magenta subunit. The latch loop is between the SB and 309 loops. The cyan 309 loop is prevented from interacting with the substrate and the movements of the SB and 309 loops needed for catalysis. In other species, it has been observed that the SB loop moves down to bind UDP-glucose at the active site. The structure above represents the apo-enzyme, which is inactive and in its **closed** form without a bound substrate.

Mutations in the 309 loop (S309N/S311R) still had 84% of normal activity. Glu412 in the latch loop is highly conserved in vertebrates (but not in yeast). Mutations in Glu 412 didn't affect the formation of oligomers of the enzyme but did affect activity.

- replacing E412 with a short aspartate (E412D) significantly increases activity (176%)
- E412Q, which eliminates the charge while retaining the approximate size of the side chain, showed just a marginal increase in activity (19%)
- E412K, which flips the charge and increases the length of the side chain, decreased activity to 22%.

These mutations generally suggest that steric effects in the region of subunit interaction are most important in activity.

15.2.3: GLYCOGEN SYNTHASE

UDP-glucose is then utilized by **glycogen synthase** (GS) to extend the main chain of glycogen by one glucose residue. In this reaction, the 4'-OH group of the glycogen main chain attacks the anomeric carbon of UDP-glucose (Figure **15.2.5**). The UDP functional group serves as a good leaving group, allowing for the formation of the alpha 1 --> 4 bond.

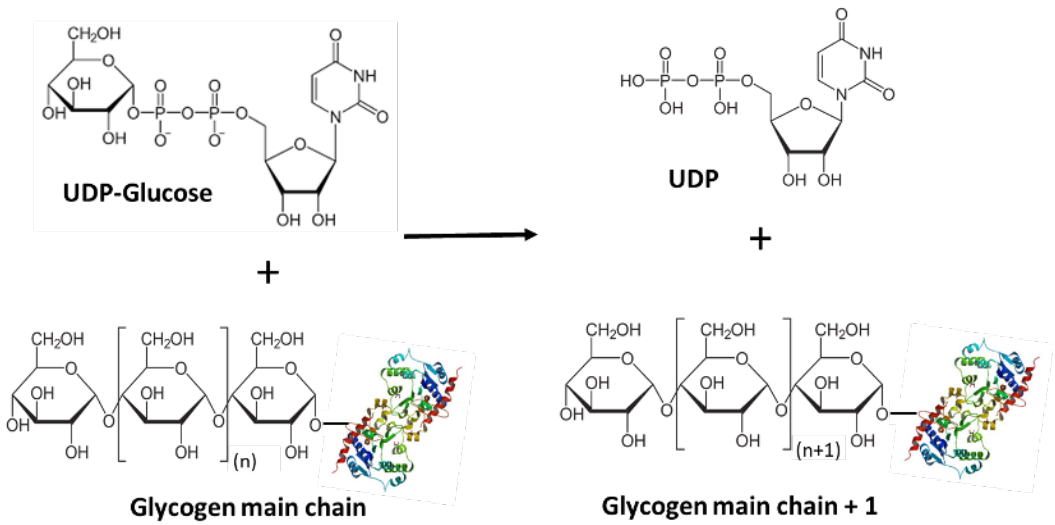


Figure **15.2.4**: Formation of the Glycogen Mainchain by Glycogen Synthase. Image modified from Mikael Häggström

Glycogen synthase has two isoforms: GS1, which is expressed in tissues where glycogen is present (for example, muscle), and GS2, which is expressed only in the liver. We will explore its mechanism more fully below.

15.2.4: GLYCOGENIN

Previously, we mentioned that GS requires a glycogen primer of 4 – 6 glucose residues to add new residues to the main chain. The small docking protein, **Glycogenin (GN or GYG)**, provides this primer. This protein is a homodimer that self-catalyzes its own glycosylation at amino acid Tyr-194. In this reaction, UDP-glucose is coordinated by a Mn^{2+} metal cofactor and critical aspartate residues (Figure **15.2.6**). The –OH group of Tyr-194 then mediates nucleophilic attack on the anomeric carbon of UDP-glucose. Thus, glycogenin is tethered to the reducing end of the glycogen molecule.

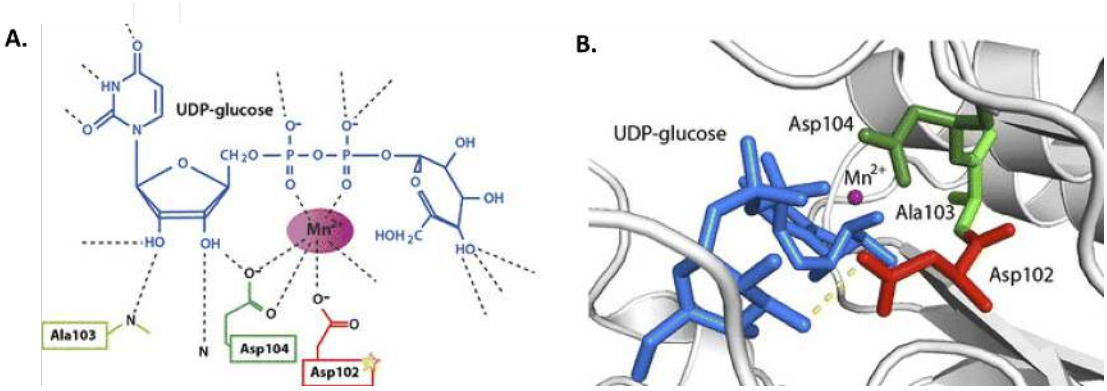


Figure **15.2.6**: Coordination of UDP-Glucose by Glycogenin. Critical aspartic acid residues and a manganese ion cofactor are required for the coordination of UDP-glucose by glycogenin. Image from Hedberg Oldfors, C., Glamuzina, E., Ruygrok, P. and Anderson, L. (2016) *J. Inherit. Met. Dis.* 40(1) DOI: 10.1007/s10545-016-9978-1

As with glycogen synthase, glycogenin (GN or GYG) has two isoforms, with GN2 (or GYG2) mainly expressed in the liver, pancreas, and heart.

15.2.5: MECHANISMS FOR GLYCOGEN SYNTHESIS BY GLYCOGENIN AND GLYCOGEN SYNTHASE

How do glycogenin and glycogen synthase cooperate in the synthesis of glycogen? Structures of the complex of glycogenin-1 (GYG1), which seeds the molecule by starting glycogen synthesis by autoglucosylation, and glycogen synthase-1 (GS1 or GYS1), which extends the molecule, show allosteric transitions between three primary states, the closed/inactive, partially open, and open active complex, as shown in Figure **15.2.7**:

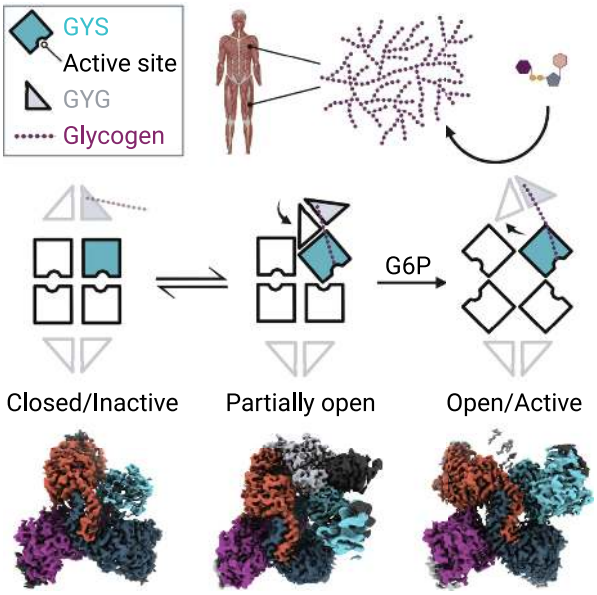


Figure 15.2.7: GYS1 chains A, B, C, and D are colored orange, turquoise, purple, and navy, respectively. GYG1 globular domains and the GYG1-tail fragment are colored in gray shades for all chains. The bottom left structure shows the apo GYS1:GYG1 mobile complex. The bottom middle structure is the apo GYS1:GYG1 ordered complex. The bottom right structure is the +G6P GYG1:GYS1 complex. Fastman et al., 2022, Cell Reports 40, 111041 July 5, 2022, 2022. https://doi.org/10.1016/j.celrep.2022.111041. Creative Commons Attribution (CC BY 4.0)

It makes sense that both enzymes bind to each other and cooperate in the synthesis of glycogen. In the closed state, GS (GYS) is a tetramer, which, like hemoglobin, can be described as a T or closed/inactive state. In a slight difference, one of the GS (GYS) subunits appears to display an asymmetric conformation, which leads to close interactions with GN (GYG), allowing the glycogen seed polymer on GN (GYG) to move to GS (GYS) for elongation (a partially open state). Multiple conformations of the complex have been resolved. Further conformational changes lead to the open/active state, resulting in a more open binding groove for GN (GYG).

Figure 15.2.8 shows an interactive iCn3D model of the Human glycogenin-1 and glycogen synthase-1 complex in the presence of glucose-6-phosphate (8CVX). Glucose-6-phosphate is an allosteric activator of glycogen synthase.

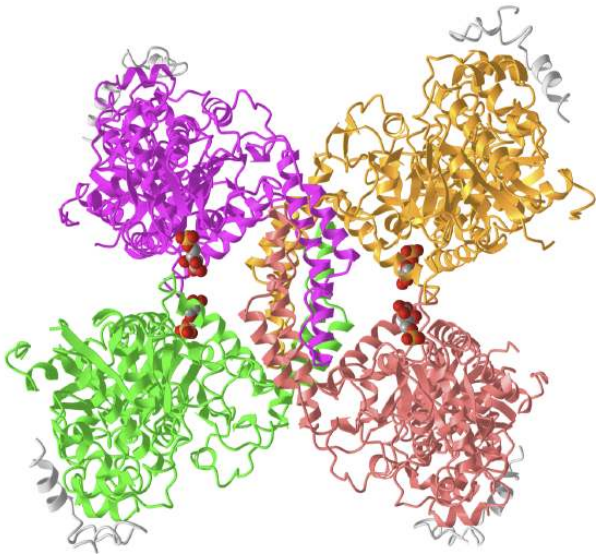


Figure 15.2.8: Human glycogenin-1 and glycogen synthase-1 complex in the presence of glucose-6-phosphate (8CVX). (Copyright; author via source). Click the image for a popup or use this external link: https://structure.ncbi.nlm.nih.gov/i...ivh4gZCupGcXZ7

The larger glycogen synthase subunits in the tetramer are shown in various colors, while the glycogenin fragments bound to each GS (GYS) monomer are shown in gray.

Figure **15.2.9** illustrates the conformational changes induced on the binding of glucose-6-phosphate to glycogen synthase.

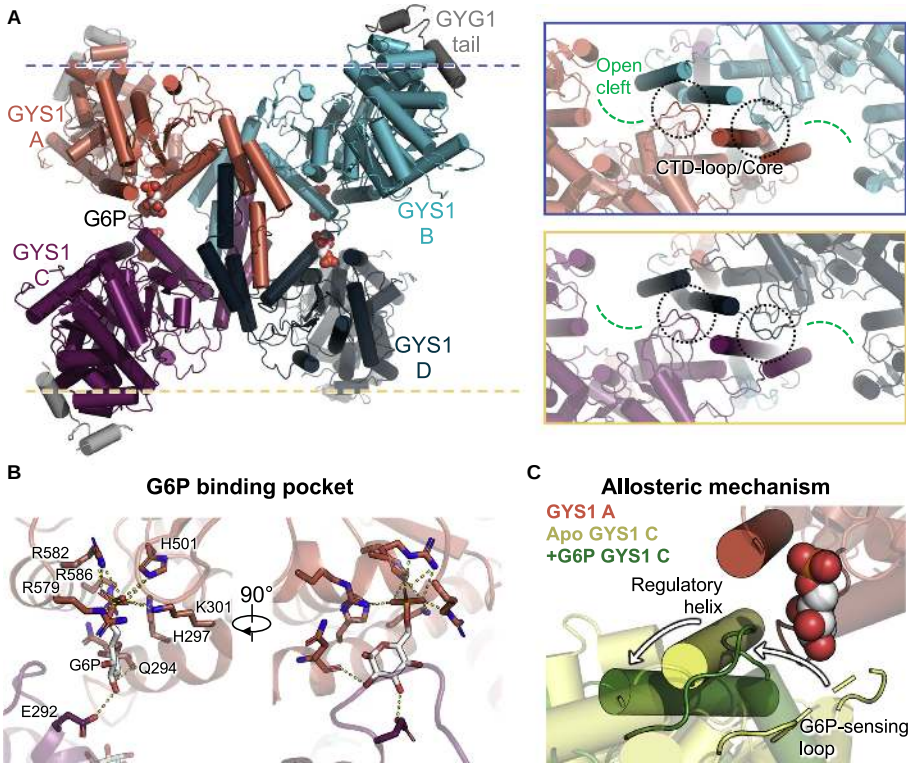


Figure **15.2.9**: G6P binding induces a conformational change across the GYS1 tetramer, leading to an open conformation for all four active sites. Fastman et a.l, ibid.

Panel (A) shows a cartoon representation of the +G6P GYS1:GYG1 complex (left) with GYS1 and GYG1 chains colored as in the previous figure. G6P is shown as spheres colored by heteroatom. Blue and yellow lines and boxes (right) indicate relative positions for perpendicular views. A black dotted circle indicates the oligomeric interface between the CTD-loop region and tetramerization core domains. The CTD-loop, residues 484–488, forms cross-protomer interactions on the other side of the active site. Green dashed semicircles indicate open active sites.

Panel (B) shows G6P-binding site interactions. G6P (white) and proximal interacting residues are shown as sticks and colored by heteroatom. Yellow dotted lines indicate polar interactions.

Panel (C) shows changes at the G6P-binding site across conformations. A G6P-bound protomer is highlighted in orange, with G6P shown as spheres. The adjacent active state protomer (chain C) is shown as a green cartoon. A basal state protomer (chain C) is modeled relative to the orange G6P-bound protomer and shown in yellow. Key changes to the G6P-sensing loop and a regulatory helix are highlighted by outline and non-transparent representation with arrows indicating the relevant motions. The rest of each chain is shown in a transparent cartoon representation.

We will return to the mechanism after exploring the last enzyme in the pathway.

15.2.6: GLYCOGEN BRANCHING ENZYME

The final enzyme, the **glycogen branching enzyme** (GBE), catalyzes the hydrolytic cleavage of an α(1→4) glycosidic linkage and subsequent inter- or intra-chain transfer of the non-reducing terminal fragment to the C6 hydroxyl position of an α-glucan (Figure **15.2.10**). In this example, an inter-chain transfer is occurring. At the top of the scheme, above the arrow, you can see that the GBE enzyme transiently removes several glucose residues (usually around 7) from one linear glycogen chain and then attaches it as an alpha 1 → 6 branch to the other chain. In this process, an additional non-reducing end is created, which can act as a primer site for Glycogen Phosphorylase (the main enzyme that breaks down glycogen). Thus, glucose residues can be released very quickly when needed.

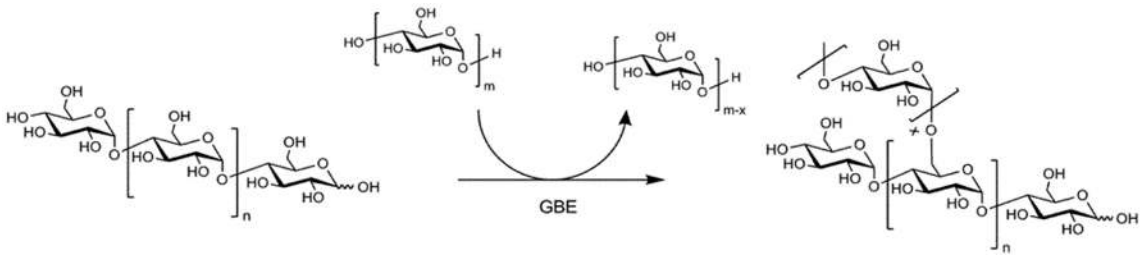


Figure 15.2.10: Formation of Glycogen alpha 1 --> 6 Branches. Image from van der Vlist, J., et al (2012) Polymers 4(1) 674-690. DOI: 10.3390/polym4010674

Details of the structure and domain organization of the human glycogen branching enzyme are shown in Figure 15.2.11. The four domains include N1, CBM48, the catalytic domain, and the C-terminal domain.

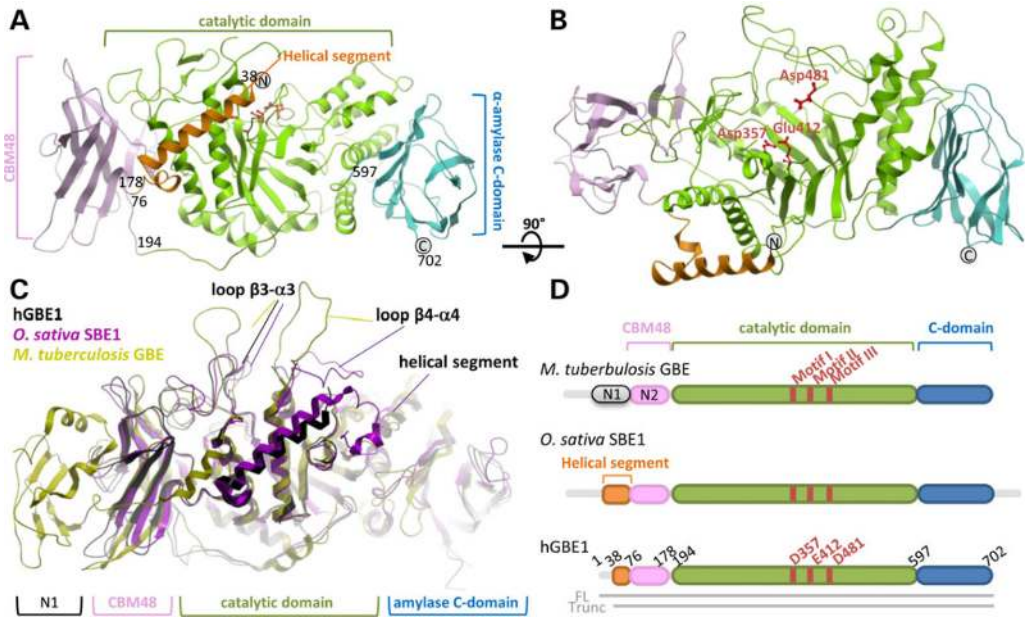


Figure 15.2.11: Crystal structure of hGBE1. Froese et al. *Human Molecular Genetics*, Volume 24, Issue 20, 15 October 2015, Pages 5667–5676, https://doi.org/10.1093/hmg/ddv280. Creative Commons Attribution License (http://creativecommons.org/licenses/by/4.0/)

Panels (**A** and **B**) show orthogonal (perpendicular) views of hGBE1 showing the N-terminal helical segment (orange), CBM48 (pink), central catalytic domain (green), and C-terminal domain (blue). The catalytic triad Asp357-Glu412-Asp481 is shown as red sticks. Numbers refer to domain boundaries. N- and C-termini are labeled as grey spheres.

Panel (**C**) shows the superposition of branching enzyme structures from human (hGBE1, this study), *O. sativa* SBE1, and *M. tuberculosis* GBE, highlighting the conserved domain architecture and three regions of structural variation.

Panel (**D**) shows the domain organization of hGBE1, *O. sativa* SBE1, and *M. tuberculosis* GBE, revealing differences in the N-terminus between prokaryotic and eukaryotic polypeptides. Prokaryotic GBEs contain two N-terminal carbohydrate-binding domains (N1, N2,) whereas eukaryotes contain only one (CBM48) and replace the prokaryotic N1 domain with a helical extension.

Figure 15.2.12 shows an interactive iCn3D model of the **human glycogen branching enzyme (GBE1)**

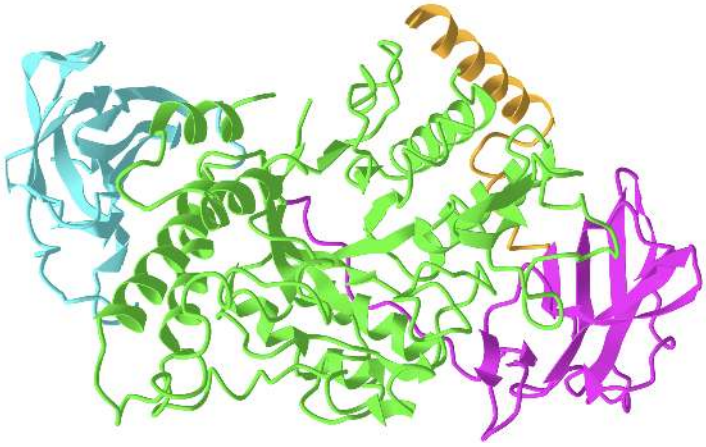


Figure 15.2.12: **human glycogen branching enzyme (GBE1)**. (Copyright; author via source). Click the image for a popup or use this external link: https://structure.ncbi.nlm.nih.gov/i...47aqw5qto8hkU7

The domains in the iCn3D module are colored similarly to the previous figures.

The enzyme core is similar to amylase with the conserved active site. Diseases of glycogen storage often result from mutations in the amylase core domain. For example, late-onset adult polyglucosan body disease (APBD) arises from a common mutation, Y329S. The effect of this mutation may arise from misfolding. A tetrapeptide, Leu-Thr-Lys-Glu, administered to patients, increased activity twofold, likely by acting as a chaperone to facilitate proper protein folding.

15.2.7: PUTTING IT ALL TOGETHER: GLYCOGEN SYNTHESIS AND ITS REGULATION

Figure 15.2.13 shows the steps involved in the addition of glucose from the donor UDP-glucose to glycogenin and through glycogen synthase to the growing glycogen polymer, which becomes branched through the activity of the glycogen branching enzyme.

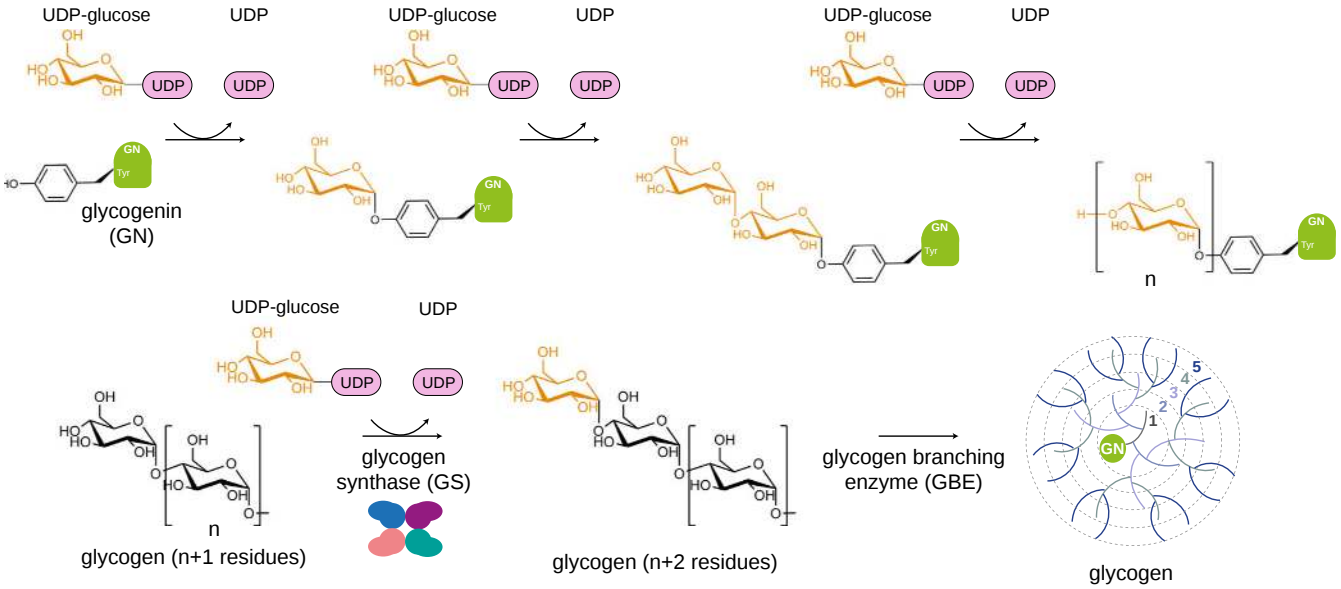


Figure 15.2.13: Summary of glycogen synthesis. Marr, L., Biswas, D., Daly, L.A. *et al. Nat Commun* **13**, 3372 (2022). https://doi.org/10.1038/s41467-022-31109-6. Creative Commons Attribution 4.0 International License. http://creativecommons.org/licenses/by/4.0/

The top reaction shows the step catalyzed by glycogenin (GN), while the bottom reactions are those catalyzed by glycogen synthase and the glycogen branching enzyme.

The regulation of glycogen synthesis occurs in part through the phosphorylation of key residues in both GS (GYS) and GN (GYG). Those sites are shown in Figure 15.2.14.

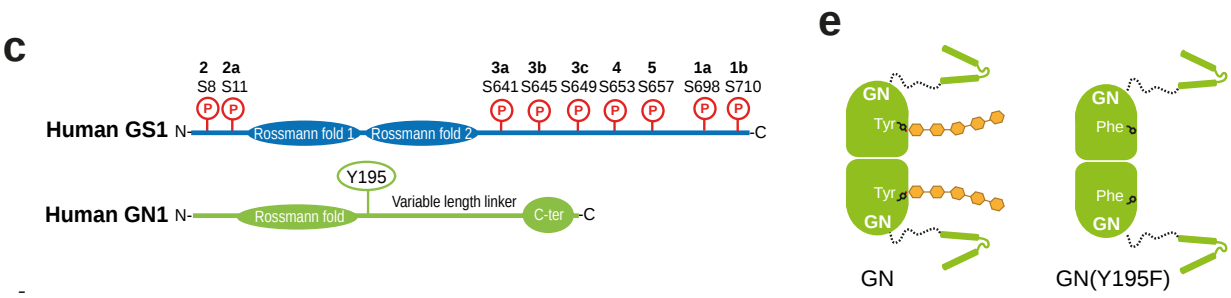


Figure **15.2.14**: Domain and phosphorylation sites for glycogen synthase 1 (GS1) and glycogenin 1 (GN1). Marr et al., ibid.

Panel c shows the domain architecture of human GS (top) and GN (bottom). Known in vivo phosphorylation sites of GS are shown in red and labeled with the corresponding residue number and classical nomenclature (in bold). GN tyrosine 195, which becomes auto-glucosylated and was mutated to phenylalanine (Y195F) in this study, is indicated. Not to scale. **Panel e** shows the cartoon representation of GN WT and Y195F.

As we showed above, glycogen synthase is allosterically activated on the binding of glucose-6-phosphate, which can be thought to activate the enzyme by a T to R state change. The enzyme is inactivated by phosphorylation at multiple sites, as shown above. Activation can also occur through dephosphorylation. Phosphorylation of a site can create a binding site that facilitates additional phosphorylations. This can lead to a flexible "spike" of hyperphosphorylated residues forming from two monomers. Particularly important is pSer641 (site 3A), which interacts with a series of arginine residues in a regulatory helix of glycogen synthase. This arginine cluster has been referred to as the arginine cradle. The interaction sites are illustrated in Figure **15.2.15**.

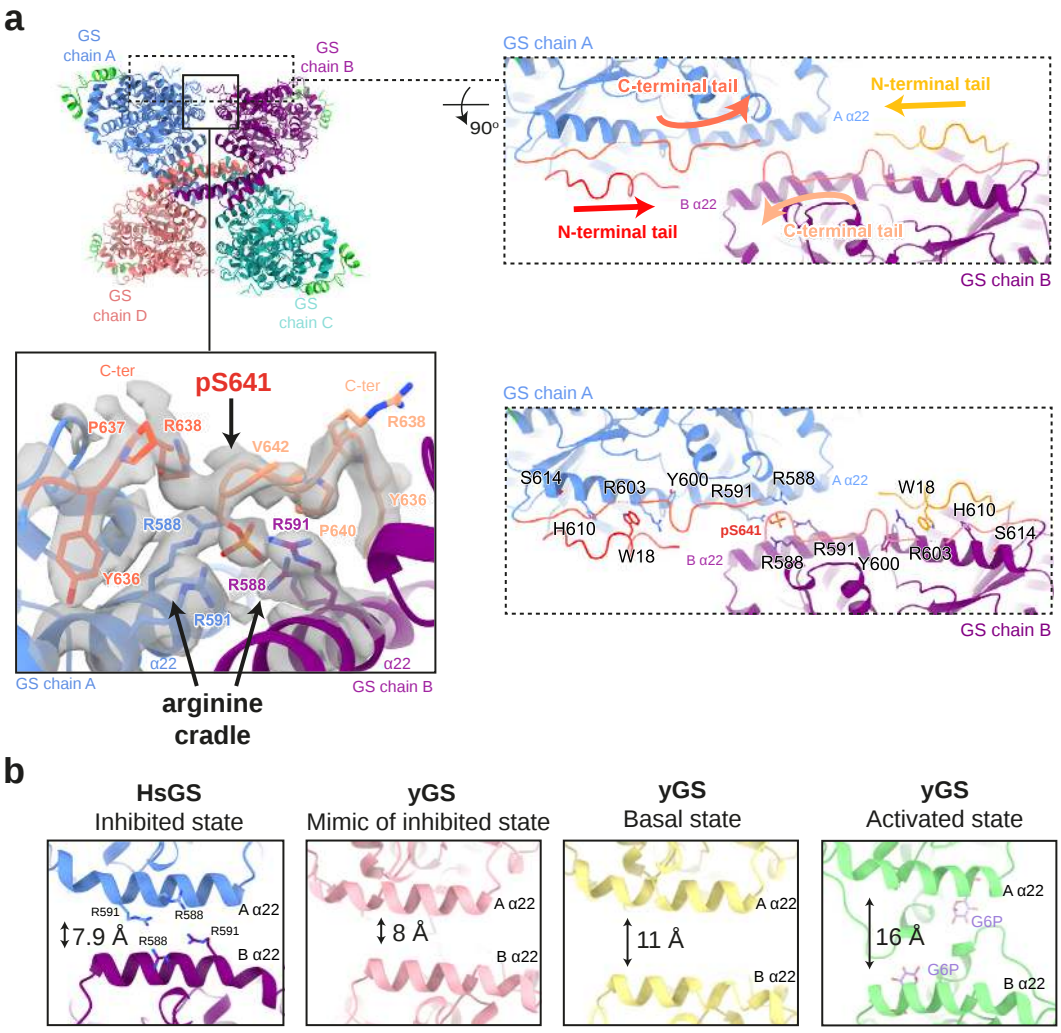


Figure **15.2.15**: **The phosphoregulatory region of human GS.** Marr et al, ibid

Panel a shows the human (Hs)GS-GN[34] structure in ribbons (top left). The N- and C-terminal tails of one GS protomer (chain A) lie next to one another and move towards the adjacent protomer, meeting the N- and C-terminal tails from chain B. Arrows indicate a continuation of cryo-EM density (top right). Electron density (C1 symmetry) for phosphorylated S641 (pS641) interacting with R588 and R591 on the regulatory helices α22 (bottom left). Residues interacting with the N- and C-terminal tails that are mutated in this study are shown (bottom right).

Panel b shows a comparison of distances between regulatory helices of adjacent monomers of HsGS (reported here), low activity inhibited mimic (PDB ID 5SUL), basal state (PDB ID 3NAZ), and G6P-activated (PDB ID 5SUK) yeast GS (yGS) crystal structures. Quoted distances were measured from Cα of Arg591 (chain A) and -Cα of Arg580 (chain B) of HsGS and corresponding yeast residues.

The strong electrostatic arginine-pSer interactions lock the tetramer into the inactive T state.

A cartoon model illustrating the regulation of glycogen synthase by phosphorylation/dephosphorylation and interconversion between T and R state is shown in Figure **15.2.16**.

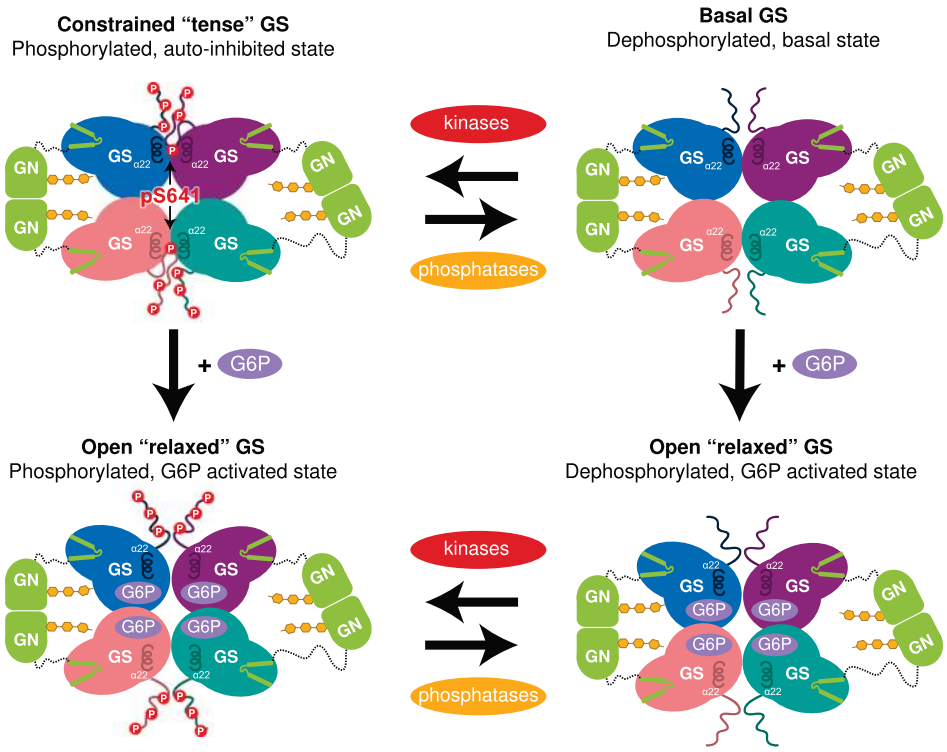


Figure **15.2.16**: **GS and GN cooperate to synthesize glycogen.** Marr et al, ibid

The inhibition by phosphorylation can be relieved by binding the allosteric effector glucose-6-phosphate and does not require phosphatases,

15.2.8: SUMMARY

This chapter provides a comprehensive overview of glycogenesis—the process by which cells synthesize glycogen, the primary storage form of glucose. It builds on earlier discussions of hexokinase and phosphoglucomutase, focusing on the four key enzymes that complete the pathway: Glycogen Synthase (GS), UDP-Glucose Pyrophosphorylase (UGPase), Glycogenin (GN), and Glycogen Branching Enzyme (GBE).

Glycogen Synthase (GS):

GS is the central enzyme responsible for elongating the glycogen main chain by forming α(1→4) glycosidic bonds using UDP-glucose as the activated donor. Its activity is intricately regulated—upregulated by insulin signaling (which inhibits phosphorylation by GSK-3) and further enhanced allosterically by glucose-6-phosphate. Despite its pivotal role, GS requires a preformed glycogen primer (4–6 glucose residues) provided by glycogenin, and it cannot generate the branch points in glycogen.

UDP-Glucose Pyrophosphorylase (UGPase):

UGPase catalyzes the reversible conversion of glucose-1-phosphate and UTP into UDP-glucose and inorganic pyrophosphate. This reaction, which requires divalent cations (typically Mg^{2+}) and involves key active site loops (the latch, SB, and 309 loops), is crucial for generating the activated glucose needed for glycogen synthesis. Structural studies reveal how substrate positioning and specific residue interactions, such as those involving Glu412 and Ser309, influence enzyme activity and regulation.

Glycogenin (GN):

GN acts as the primer for glycogen synthesis by self-catalyzing the addition of a short glucose chain via autoglucosylation at a specific tyrosine residue. Coordinated by a Mn^{2+} cofactor and essential aspartate residues, glycogenin provides the initial oligosaccharide that glycogen synthase can then extend, ensuring that glycogen synthesis can be efficiently initiated.

Glycogen Branching Enzyme (GBE):

GBE introduces α(1→6) branches into the glycogen molecule by cleaving α(1→4) bonds and transferring a short glucan fragment to a C6 hydroxyl group on a neighboring chain. This branching increases the number of non-reducing ends, which is critical for rapid mobilization of glucose during energy demand. Structural analyses of human GBE (hGBE1) illustrate its domain organization and active site features, and highlight the differences between prokaryotic and eukaryotic enzymes.

Integration and Regulation:

The chapter concludes by integrating these enzymes into the broader context of glycogen synthesis. It explains how glycogenin and glycogen synthase cooperate through conformational transitions—shifting from closed/inactive to open/active states—to extend the glycogen molecule, while the branching enzyme remodels the structure to optimize storage and mobilization. Additionally, the regulation of glycogen synthesis is underscored by reversible phosphorylation events and allosteric mechanisms that fine-tune enzyme activities in response to cellular energy status.

Overall, this chapter elucidates the molecular mechanisms and regulatory networks underlying glycogenesis, providing students with a detailed understanding of how glucose is stored and mobilized in cells—a fundamental aspect of energy metabolism and homeostasis.

15.2.9: REFERENCES

1. Kumpf, A., Partzsch, A., Pollender, A., Bento, I., and Tischler, D. (2019) Two Homologous Enzymes of the GalU Family in *Rhodococcus opacus* 1CP-*Ro*GalU1 and *Ro*GalU2. *Int. J. Mol. Sci.* 20(22), 5809. https://doi.org/10.3390/ijms20225809

This page titled 15.2: Glycogenesis is shared under a not declared license and was authored, remixed, and/or curated by Henry Jakubowski and Patricia Flatt.

- **11.2: Diffusion Across a Membrane - Passive and Facilitated Diffusion** by Henry Jakubowski and Patricia Flatt has no license indicated.

15.3: GLYCOGENOLYSIS AND ITS REGULATION BY GLUCAGON AND EPINEPHRINE SIGNALING

LEARNING GOALS (CHATGPT O3-MINI)

1. **Understand the Overall Process of Glycogenolysis:**
   - Describe the stepwise breakdown of glycogen into glucose-1-phosphate and free glucose, and explain how the end products differ between liver (glucose release into circulation) and skeletal muscle (glucose-6-phosphate for glycolysis).
2. **Identify the Key Enzymes in Glycogenolysis:**
   - Explain the roles of glycogen phosphorylase and glycogen debranching enzyme in catalyzing the sequential breakdown of glycogen, including how glycogen phosphorylase acts on alpha $1 \rightarrow 4$ linkages and the debranching enzyme resolves alpha $1 \rightarrow 6$ branches.
3. **Analyze the Mechanism of Glycogen Phosphorylase:**
   - Detail the reaction mechanism of glycogen phosphorylase, including the function of the pyridoxal phosphate (PLP) cofactor (attached via a Schiff base with a lysine residue) and how inorganic phosphate is utilized to cleave glycosidic bonds.
4. **Examine the Function of Glycogen Debranching Enzyme:**
   - Outline the dual catalytic activities of the glycogen debranching enzyme (glycosyl transferase and glucosidase) that enable the enzyme to process branch points and allow continuous glycogen breakdown.
5. **Discuss Hormonal Regulation of Glycogenolysis:**
   - Compare and contrast the roles of glucagon and epinephrine in activating glycogenolysis, including their effects on liver and skeletal muscle.
   - Explain how glucagon signaling downregulates glycogen synthesis and promotes glycogen breakdown in the liver, while epinephrine activates glycogenolysis in both liver and muscle tissues.
6. **Understand the Glucagon Signaling Cascade:**
   - Describe the glucagon receptor as a G-protein-coupled receptor and outline the signaling cascade that leads to cAMP production, activation of protein kinase A (PKA), and the subsequent phosphorylation of key regulatory proteins.
7. **Examine the Regulation of Glycogen Synthase and Phosphorylase:**
   - Detail how PKA-mediated phosphorylation inactivates glycogen synthase (and its associated protein phosphatase PP1) while activating phosphorylase kinase, which in turn phosphorylates and activates glycogen phosphorylase.
8. **Evaluate Allosteric and Isozyme Regulation in Glycogenolysis:**
   - Discuss the allosteric regulation of glycogen phosphorylase by metabolites such as glucose (in liver) and AMP (in skeletal muscle) that shift the enzyme between active (R) and inactive (T) states.
   - Compare the tissue-specific differences between liver and muscle isozymes of glycogen phosphorylase in terms of their regulatory properties.
9. **Connect Glycogenolysis to Overall Glucose Metabolism:**
   - Integrate how glucose-1-phosphate, produced from glycogen breakdown, is converted to glucose-6-phosphate and directed into glycolysis, gluconeogenesis, or other metabolic pathways.
   - Relate these processes to the body's energy homeostasis and the role of the liver in maintaining blood glucose levels.
10. **Understand the Clinical Implications:**
    - Explain how deficiencies in glycogen phosphorylase (as in McArdle's Disease) affect muscle metabolism, leading to exercise intolerance, muscle cramping, and potential secondary complications (e.g., myoglobinuria and kidney damage).

These learning goals are designed to build a detailed understanding of the enzymatic mechanisms, regulatory pathways, and physiological significance of glycogenolysis and its hormonal control in maintaining metabolic balance.

In the previous section, you learned that glucagon signaling down-regulates glycogen synthesis. Now, let's look at glycogen breakdown, called glycogenolysis, and its control by two hormones, glucagon and epinephrine. Only two enzymes are required for the breakdown of glycogen: the glycogen phosphorylase enzyme and the glycogen debranching enzyme.

15.3.1: GLYCOGENOLYSIS: AN OVERVIEW

Two key enzymes are required for the stepwise catabolism of glycogen: glycogen phosphorylase and glycogen debranching enzyme. In the liver, the ultimate end product is glucose-1-phosphate, which is dephosphorylated in the liver to enable the export of free glucose into the circulation. In contrast, in the respiring skeletal muscle, it is converted to glucose-6-phosphate for glycolysis. Glycogenolysis is also activated by the hormones glucagon and epinephrine.

15.3.1.1: GLYCOGEN PHOSPHORYLASE

Glycogen phosphorylase (GP) catalyzes the release of glucose 1-phosphate from the alpha 1→ 4 non-reducing glycogen ends. Figure **15.3.1** shows an overview of this reaction.

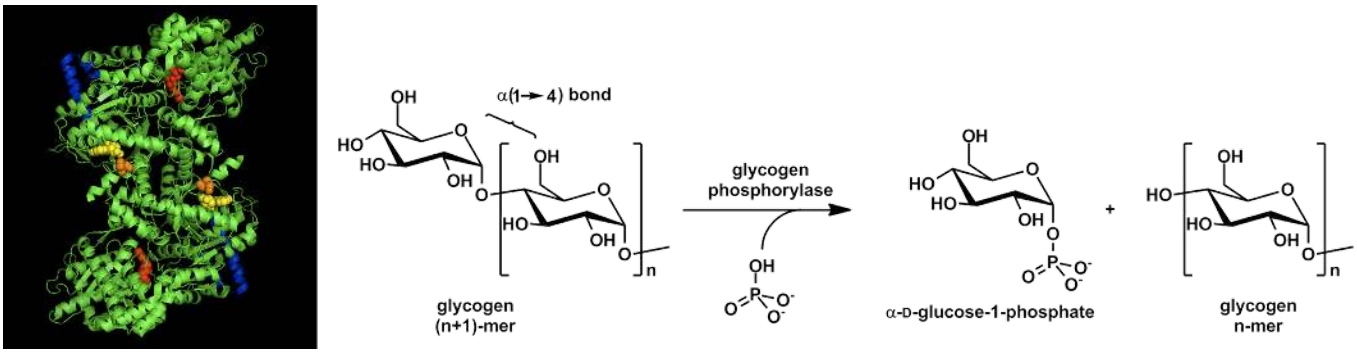


Figure **15.3.1**: Overview of Glycogen Phosphorylase Reaction. Images from Ascherer730 and Michal Sobkowski

Glycogen phosphorylase is a homodimer with two active sites. It also requires a cofactor, pyridoxal phosphate (PLP) to be functional (Figure **15.3.2**). The PLP is derived from Vitamin B6. You may have previously heard that low B vitamin levels are associated with lethargy or a lack of energy. We will continue to see that the B vitamins provide essential cofactors for enzymes involved in the production of ATP. Thus, lacking B vitamins means you are not efficiently producing ATP. The PLP cofactor of GP is attached covalently to the enzyme through a Schiff-base linkage with a Lysine (K) residue.

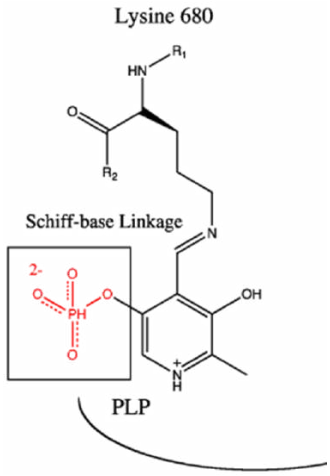


Figure **15.3.2**: Pyridoxyl Phosphate Cofactor Associated with Glycogen Phosphorylase Image modified from Ascherer730

The reaction mechanism of glycogen phosphorylase is detailed in Figure **15.3.3**. When glycogen phosphorylase binds with glycogen, a free inorganic phosphate anion is positioned by the PLP and the enzyme active site in proximity with the anomeric carbon position of the non-reducing end residue of the glycogen molecule. The oxygen in the glycosidic bond attacks the partially charged hydrogen associated with the phosphate ion, leading to the cleavage of the glycosidic bond. The cleaved glycogen chain leaves the active site, and one of the phosphate oxygens attacks the carbocation intermediate created during the cleavage. This results in the release of the terminal glucose residue as glucose 1-phosphate

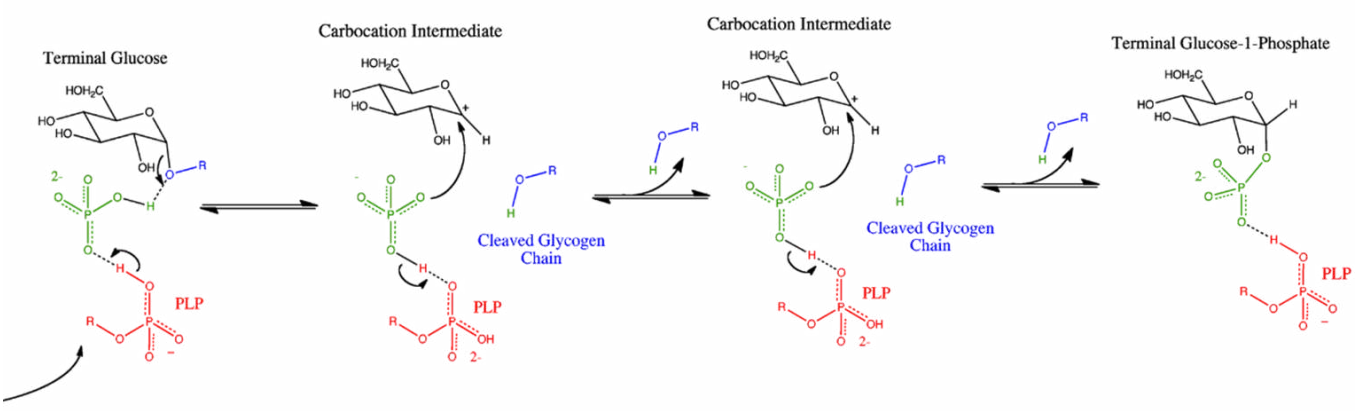
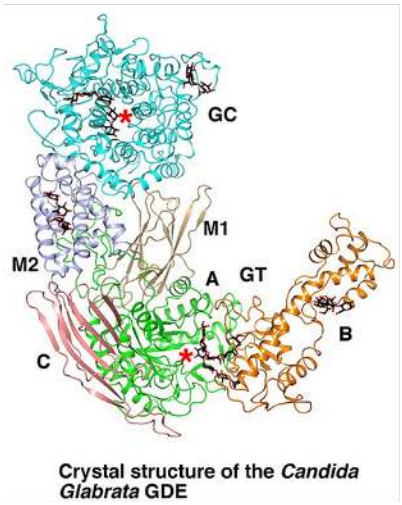


Figure **15.3.3**: Glycogen Phosphorylase Reaction Mechanism. Image from Ascherer730

15.3.1.2: GLYCOGEN DEBRANCHING ENZYME

Glycogen phosphorylase cannot cleave the alpha 1 → 6 linkages. It also cannot cleave α,1 → 4 linkages that are within four residues of an α,1→ 6 linkage (the glycogen chain will no longer fit into the active site of the enzyme). The Glycogen Debranching Enzyme (GDE) has two catalytic activities that enable it to deal with this problem. The first catalytic activity is a Glycosyl Transferase (GT) activity. In this process, the three remaining alpha 1 → 4 extended units on the branch site (colored in green) are clipped off of the branch site and attached to a straight chain of alpha 1 → 4 extended glucose residues. The second part of the reaction requires glucosidase (GC) activity, which mediates the hydrolysis of the α,1 → 6 glycosidic bond and releases free glucose in the process. Glycogen phosphorylase can then resume the breakdown of the remaining alpha 1 → 4 chain. Figure **15.3.4** shows an overview of glycogen breakdown.



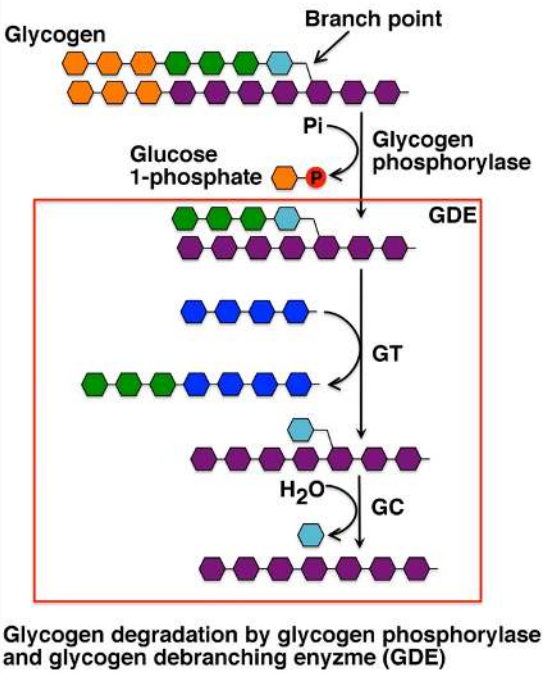


Figure **15.3.4**: Biological Activity of the Glycogen Debranching Enzyme. Image modified from XiangSong

15.3.1.3: DEPHOSPHORYLATION OF GLUCOSE 1-PHOSPHATE

Following the activation of glycogenolysis, the liver cell has now released large quantities of glucose 1-phosphate from glycogen and a smaller amount of free glucose from the clipped branch residues. The free glucose can be transported to the bloodstream straight away, but the glucose 1-phosphate must be dephosphorylated before release (Figure **15.3.5**).

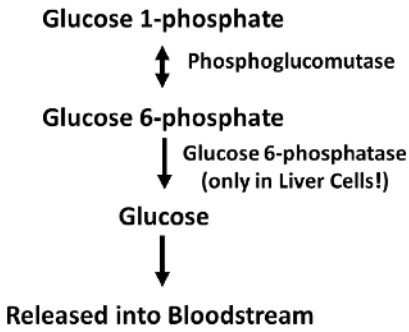


Figure 15.3.5: Process of Glucose Dephosphorylation in Liver Cells

The dephosphorylation of glucose only occurs in liver cells, as this is the primary location for regulating blood glucose levels. Free glucose can exit the cell, whereas phosphorylated forms are trapped inside. Figure 15.3.6 outlines the process of glucose dephosphorylation in the liver. To mediate the dephosphorylation of glucose, glucose 6-phosphate is transported from the cytoplasm into the lumen of the endoplasmic reticulum (ER) through transporter 1 (T1). The glucose-6-phosphatase (G-6-Pase) then cleaves the phosphate from the substrate, releasing inorganic phosphate (P) and glucose (represented by the red molecule). The inorganic phosphate is then transported back into the cytoplasm through transporter 2 (T2), and glucose is transported through Transporter 3 (T3). Free glucose is then transported back into the bloodstream through a glucose (GLUT) transporter in the plasma membrane.

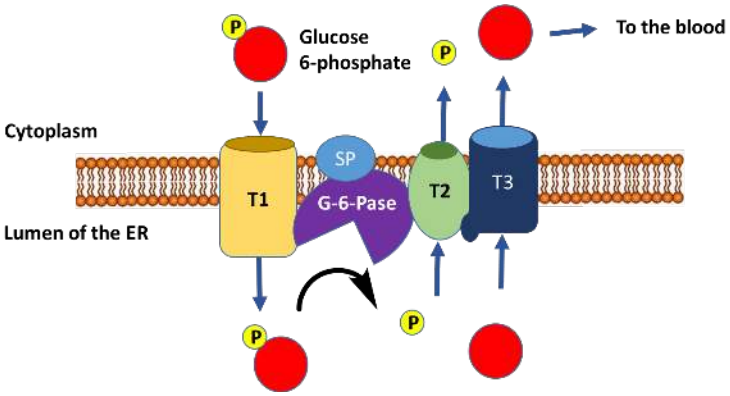


Figure 15.3.6: Dephosphorylation of Glucose 6-phosphate in Liver Cells.

15.3.2: HORMONAL CONTROL OF GLYCOGEN BREAKDOWN

In the previous sections, we've discussed insulin signaling and the process of building glycogen (glycogenesis) in detail. Now, look at the other side of the homeostatic balance, which begins with glucagon signaling. During hypoglycemia (or low blood glucose levels), pancreatic alpha (α) cells release the hormone peptide, glucagon, which stimulates gluconeogenesis (the formation of glucose) and glycogenolysis (the breakdown of glycogen) in the liver, resulting in the release of glucose to the plasma, and the raising of blood glucose levels, as shown in Figure 15.3.7.

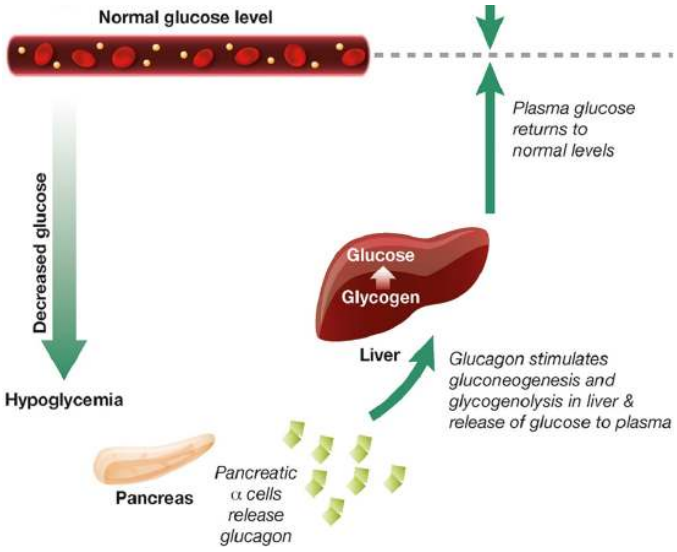


Figure **15.3.7**: Summary of Glucagon Signaling During Low Blood Glucose Levels. Image from Hædersdal, S., et al (2018) Mayo Clinic Proceedings 93(2):217-239

Let's review a few terms before we begin. In the previous section, we were introduced to glycogenesis, the process of synthesizing glycogen. We saw that this pathway was activated during insulin signaling. In glucagon signaling, this pathway is inhibited and the opposite pathway, glycogenolysis (glycogen breakdown) is activated. Glucagon signaling in the liver also downregulates glycolysis (the utilization of glucose for energy production), as the liver attempts to utilize glucose to maintain blood glucose levels. It doesn't utilize it for its own energy needs during this time. Instead, liver cells can use lipids to generate ATP, and in fact, glucagon signaling increases lipolysis or the breakdown of lipids. Finally, glucagon also up-regulates gluconeogenesis, or the generation of glucose from non-sugar metabolites. In a later section, we will address the mechanisms of glycolysis and gluconeogenesis regulation. Here, we will only take a cursory look at these pathways and focus more on the process of glycogenolysis.

15.3.2.1: OVERVIEW OF GLUCAGON SIGNALING

Glucagon signaling begins when the hormone binds with its receptor on liver cells, as shown in Figure **15.3.8**. Glucagon receptors are not as widespread within the body as insulin receptors. Since the purpose of this hormone is to cause the release of glucose back into the bloodstream, this process is highly controlled, and only the liver can deliver glucose back into the bloodstream to maintain homeostasis. Thus, other target tissues, such as skeletal muscle, do not require these receptors to be expressed and are therefore not sensitive to glucagon signaling.

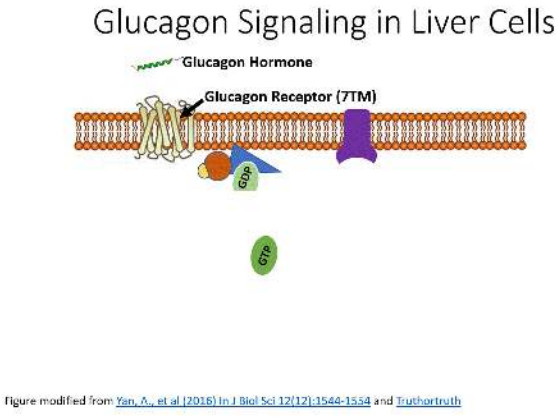


Figure **15.3.8**: Overview of Glucagon Signaling Cascade

The glucagon receptor is a G-protein-coupled receptor, also called a 7TM receptor (as it contains seven transmembrane helices that span the plasma membrane). This family of receptors is widespread throughout the body and is responsible for many of the pharmaceutical mechanisms of action seen in our treatment of different disease conditions. With this pathway, once glucagon binds to the receptor, the receptor moves laterally in the plasma membrane. It binds with a G-protein, an intracellular peripheral protein. The G-protein consists of

three major domains: the alpha, beta, and gamma domains. The alpha domain is capable of binding to the GDP/GTP cofactor. When the G-protein is inactive, all three subunits stay together, and the alpha subunit remains inactive and bound to GDP.

When the G-protein associates with an activated receptor, the alpha subunit exchanges GTP for the bound GDP cofactor, and the gamma and beta subunits dissociate into the cytoplasm. The activated alpha subunit moves laterally on the periphery of the plasma membrane until it contacts the adenylyl cyclase enzyme (also called adenylate cyclase). This activates the adenylyl cyclase, which converts ATP into cyclic adenosine monophosphate (cAMP). cAMP production is an amplification step within this pathway. That means that more cAMP is produced than G-proteins are activated.

After some time, a G-protein hydrolase causes the hydrolysis of the GTP to GDP and inactivates the G-protein. At this point, the G-protein associates with the gamma and beta subunits, reforming its inactive state. Another glucagon signaling event will be required to reactivate the process. The cyclic AMP produced in the process serves as a second messenger and activates a myriad of downstream targets. We will focus on two of the major targets.

The first is Protein Kinase A, which becomes activated upon binding with cAMP. The second target is a cAMP Response Element-Binding *Protein* (CREB). The CREB protein is also activated when bound to the cAMP molecule. This causes the CREB protein to translocate from the cytosol into the mitochondria and the nucleus. In both locations, the activated CREB binds to specific response element sequences in the DNA and activates the transcription of genes involved in gluconeogenesis. These genes and their encoded proteins have been discussed in more detail in Chapter 14. What is important to note is that glucagon signaling in the liver results in the upregulation of glucose production *de novo* from non-carbohydrate precursors. This is NOT a favored pathway in the body. It is energetically expensive for the liver to manufacture glucose. In fact, the cost of ATP is more expensive than can be produced from the newly formed molecule. However, organs like the brain can only utilize free glucose as an energy source. Thus, the liver will use this energy deficit to build glucose for use by the brain and other cellular targets.

Glucagon signaling also leads to the downregulation of glycolysis, which we will cover in more depth in Section 15.4, as well as glycogenesis. It also leads to an increase in glycogenolysis, or the breakdown of glycogen. Let's examine the regulation of both of these processes in more detail.

15.3.3: REGULATION OF GLYCOGENESIS

Since glycogen synthase (GS) is the primary enzyme required for glycogenesis, it is also the primary target for regulating this pathway. Recall that GS is active in the dephosphorylated state. Thus, PKA down-regulates the activity of this enzyme through the phosphorylation of GS, as shown in Figure **15.3.9**. Phosphorylation of GS causes it to shift into its inactive conformation, inhibiting glycogenesis.

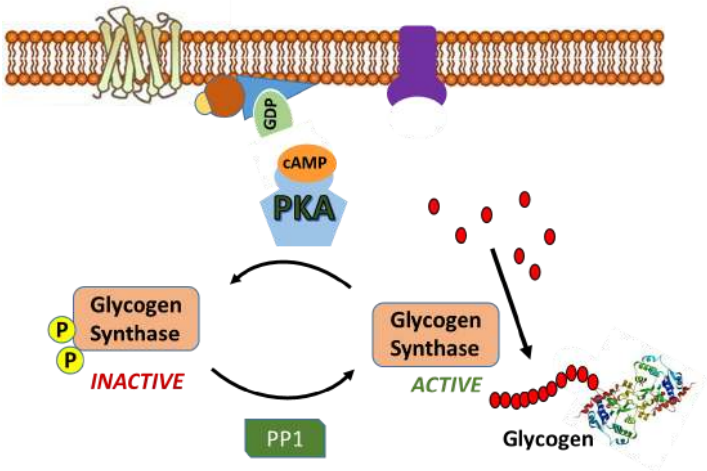


Figure **15.3.9**: Inactivation of Glycogen Synthase through Phosphorylation. When bound to cAMP, protein kinase A (PKA) phosphorylates and inactivates the glycogen synthase enzyme. The activity of protein phosphorylase 1 (PP1) is required to dephosphorylate GS and restore its activity. Image modified from Yan, A., et al (2016) In J Biol Sci 12(12):1544-1554 and Servier Medical Art

Additionally, activated PKA phosphorylates the protein phosphatase 1 (PP1) enzyme, resulting in the inactivation of the phosphatase. PP1 normally dephosphorylates GS, helping to retain the active conformation of GS. Thus, phosphorylation of PP1 by PKA helps to maintain the GS in the phosphorylated, inactive state. The inhibition of PP1 is quite complicated, as shown in Figure **15.3.10**. PP1 contains a regulatory domain and a catalytic domain. Normally, the regulatory domain of PP1 binds to glycogen, keeping the molecule close to the location where GS is present. Thus, when GS is near its substrate, it can bind with PP1 and be dephosphorylated into its active state. This is more efficient than diffusing in the cell and trying to find the PP1 randomly. When PKA phosphorylates the regulatory domain of PP1, it dissociates from the catalytic domain, causing the catalytic domain to float away from the glycogen molecule. This makes PP1 less efficient

at dephosphorylating GS because it is more difficult for the molecules to interact randomly. Thus, PP1 is less active. PKA further reduces this activity by phosphorylating an allosteric inhibitor (I) of PP1. In the phosphorylated state, the inhibitor can bind to PP1, inactivating the phosphatase. Both phosphorylation events need to be reversed to regain full PP1 activity.

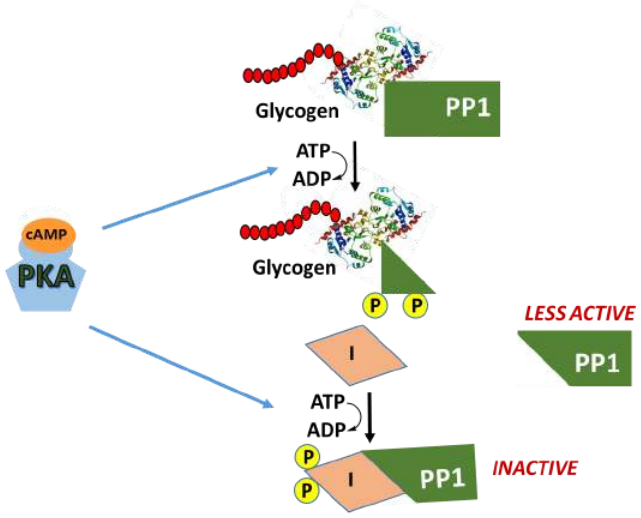


Figure 15.3.10: Inactivation of Phosphorylase 1 (PP1) by Protein Kinase A (PKA). PKA phosphorylates PP1 causing it to dissociate from glycogen and become less active. PKA also phosphorylates an allosteric inhibitor (I) of PP1 which increases its binding affinity for PP1. The phosphorylated inhibitor maintains PP1 in an inactive conformation. Image Modified from Yan, A., et al (2016) In J Biol Sci 12(12):1544-1554 and Servier Medical Art

In summary, glucagon signaling in the liver downregulates glycogenesis by activating PKA. PKA phosphorylates GS directly, inactivating the enzyme, and maintains it in the inactive state by also inhibiting the PP1 responsible for dephosphorylating GS.

15.3.4: ACTIVATION OF GLYCOGENOLYSIS

In addition to phosphorylating GS and PP1 during the inactivation of glycogenesis, PKA also phosphorylates the enzyme **Phosphorylase Kinase**, which is upstream of glycogen phosphorylase, the primary enzyme involved in glycogen breakdown. As its name implies, phosphorylase kinase is a protein kinase that phosphorylates the enzyme to activate it. Figure 15.3.11 offers a first view of the phosphorylation cascade required for glycogen phosphorylase activation.

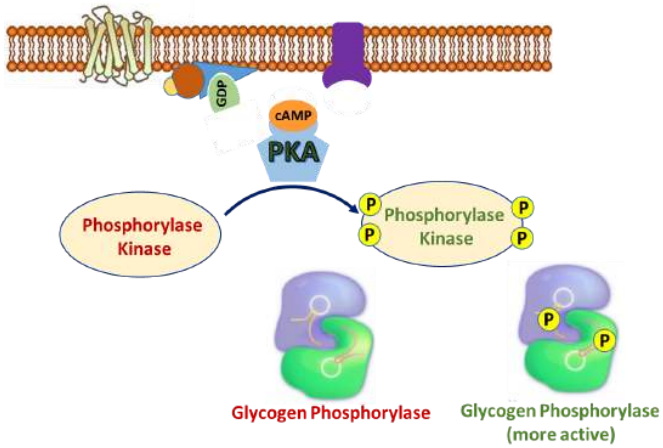


Figure 15.3.11: Activation of Glycogen Phosphorylase by Protein Kinase A (PKA) Signaling. PKA upregulates the activity of Phosphorylase Kinase through direct phosphorylation. The activated kinase enzyme phosphorylates its downstream target, Glycogen Phosphorylase (GP). In the phosphorylated state, GP is more active. Image modified from Yan, A., et al (2016) In J Biol Sci 12(12):1544-1554 and Llavero, F., et al (2019) Int. J. Mol. Sci. 20(23):5919

The phosphorylase kinase enzyme is a complex enzyme that is a tetramer of a tetrameric complex, αβγδ, so the full holoenzyme has an $(\alpha\beta\gamma\delta)_4$ structure. It is large, with a molecular weight of around 1.3×10^6. As expected, it is highly regulated in multiple ways, including phosphorylation by PKA, ADP (an allosteric effector), divalent cations like Ca^{2+}, and pH. The α and β are regulatory subunits that affect activity through their phosphorylation. The δ is calmodulin, a calcium-binding protein we discussed in Chapter 12.7, and its binding of

calcium affects the holoenzyme activity. The γ subunit has kinase activity, an N-terminal catalytic domain, and a C-terminal calmodulin-binding domain. This is primarily regulated by phosphorylation through the PKA pathway, as shown in Figure 15.3.5.

"PHK is one of the largest of the protein kinases and is composed of four types of subunit, with stoichiometry $(\alpha\beta\gamma\delta)_4$, and a total molecular weight. wt of 1.3×10^6 Da. Activity is regulated by cyclic AMP-dependent protein kinase phosphorylation, autophosphorylation, allosteric effectors (e.g., ADP), metal ion concentration (Ca^{2+} and Mg^{2+}), proteolysis, and pH (Pickett-Gies and Walsh, 1986). The α and β subunits are regulatory and are the targets for control by phosphorylation. The δ subunit is essentially identical to calmodulin and confers Ca^{2+} sensitivity. The 386 amino acid γ subunit is the catalytic subunit, which comprises an N-terminal kinase domain (residues 1–298) and a regulatory calmodulin-binding domain (residues 299–386)."

Calcium, an allosteric regulator, may be present within cellular targets due to nerve impulse firing, muscle contraction, or hormone signaling. Calcium in the cell generally indicates a high cellular energy demand at that time, indicating that energy production is needed. Thus, calcium binding to the phosphorylase kinase is a positive effector of the enzyme, upregulating its activity. The enzyme's maximal activity is achieved through combined phosphorylation and calcium binding. Thus, phosphorylase kinase can exist in 4 different activity states as shown in linked equilibria in Figure **15.3.12**.

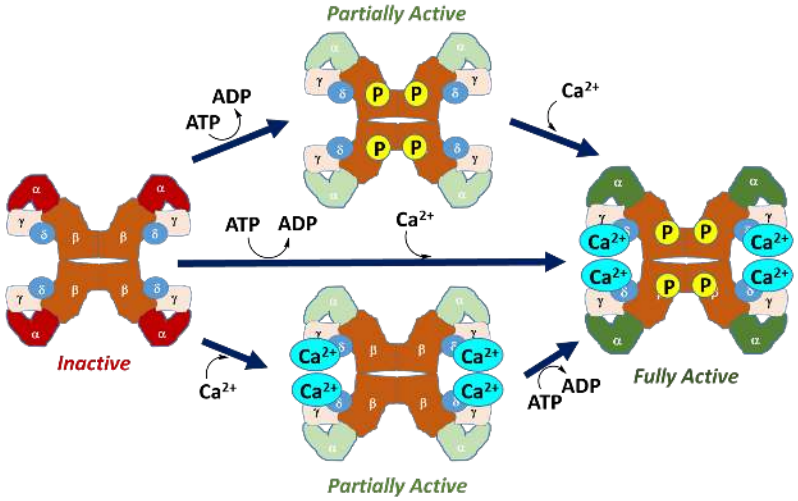


Figure **15.3.12**: Activation States of Phosphorylase Kinase (PK). In the left-hand diagram, PK is in the inactive state, with the kinase-containing alpha domains shown in red. The upper diagram shows the activation of PK through phosphorylation by Protein Kinase A during hormone signaling. This leads to a partially active enzyme. Similarly, calcium binding, shown in the lower diagram, also results in a partially active enzyme. Calcium plays a particularly important role in the activation of this enzyme in skeletal muscle. The process of muscle contraction causes the release of high levels of calcium into the cytoplasm. Thus, the presence of calcium within the cytoplasm of muscle cells indicates high energy demand, as the muscle is being called into action. This activates PK and stimulates the breakdown of glycogen within muscle tissue, helping to meet energy demands. Maximal activity is obtained with both calcium binding and phosphorylation.

This diagram should be quite familiar by now. It is yet another example of a tetrameric enzyme (where the "enzyme" composition is αβγδ) existing in two major states: an inactive T state and an active R state. The interconversion is regulated by allosteric effectors (Ca2+) and is post-translationally phosphorylated.

A mechanism for the phosphorylation of a Ser in a substrate target protein (i.e, glycogen phosphorylase) by the catalytic domain of the γ subunit of phosphorylase kinase is shown in Figure **15.3.13**.

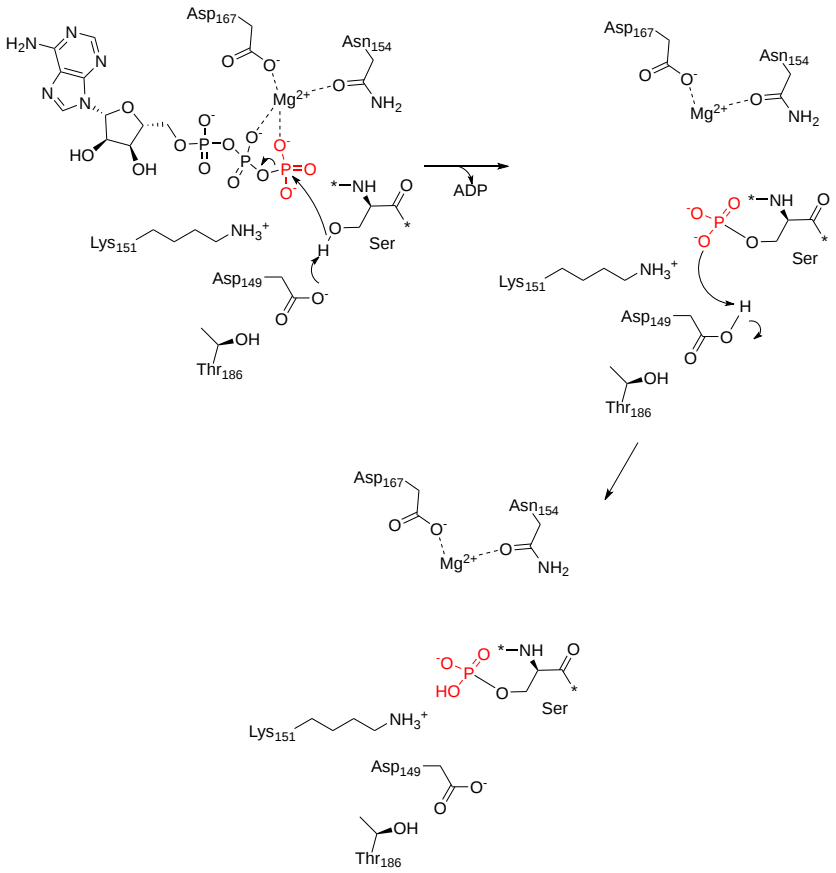


Figure **15.3.13**: A mechanism for the phosphorylation of a Ser in a substrate target protein (i.e, glycogen phosphorylase) by the catalytic domain of the γ subunit of phosphorylase kinase. https://www.ebi.ac.uk/thornton-srv/m-csa/entry/35/. Creative Commons Attribution 4.0 International (CC BY 4.0) License.

The * in the mechanism denotes the serine of the target protein.

Figure **15.3.14** below shows an interactive iCn3D model of a truncated form of the rabbit phosphorylase kinase gamma subunit dimer bound to a peptide substrate complex (2PHK).

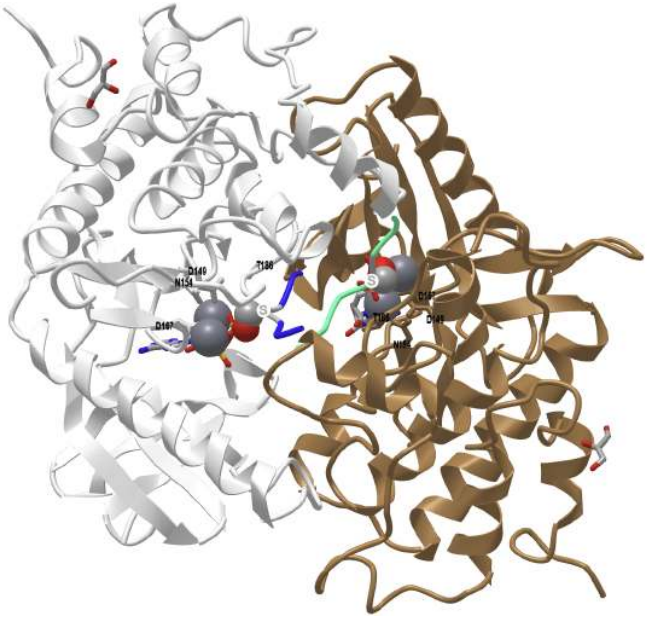


Figure 15.3.14: Rabbit phosphorylase kinase gamma subunit dimer bound to a peptide substrate complex (2PHK). (Copyright; author via source). Click the image for a popup or use this external link: https://structure.ncbi.nlm.nih.gov/i...3wHapyHWEy7qi9

The phosphorylase kinase dimer is shown (gray and brown subunits). A non-hydrolyzable ATP analog (adenylyl imidodiphosphate, AMPPNP) in each subunit is shown as CPK-colored sticks. The backbone of two identical peptide substrates (blue and cyan) with the sequence RQMSFRL (similar to the target sequence in glycogen phosphorylase and an ideal peptide substrate) is shown as a backbone trace, with the central Ser, which gets phosphorylated, represented as CPK-colored spheres. Active site residues are shown as CPK-colored sticks and labeled in each subunit.

We have been primarily discussing the regulation of glycogenolysis in the liver. However, in considering the activity of PK and its reactivity with Ca^{2+} ions, we should also consider the activation of glycogenolysis in skeletal muscle. Notably, glycogenolysis in liver tissue and skeletal muscle has many differences. First, the G-protein-coupled pathway is activated by different hormones. Liver tissue is responsive to Glucagon stimulation and stimulation through the Epinephrine hormone signaling pathway. Glycogenolysis in skeletal muscle tissue, on the other hand, is only activated by the Epinephrine signaling pathway, but not by glucagon. This is because the liver is the primary organ responsible for regulating blood glucose levels. Thus, due to low blood glucose levels, pancreatic signaling primarily targets glycogenolysis within the liver tissue. Both systems are responsive to epinephrine, which is described in more detail below.

15.3.5: EPINEPHRINE SIGNALING

Epinephrine is a small amino acid-derived hormone (can you guess the amino acid?? Yes, it is tyrosine!!), as shown in Figure **15.3.15**. It is also known as adrenaline, which is secreted by the adrenal glands located above the kidneys during the fight-or-flight response. It is also secreted during heavy or sustained exercise. Epinephrine has pleiotropic effects in the body, including the activation of glycogenolysis in the liver and skeletal muscles. Epinephrine also promotes fat breakdown in adipose tissue, which releases this energy reserve into the bloodstream for utilization by muscle tissue. It also causes the relaxation of smooth muscles in the lungs and respiratory tract, allowing for improved oxygen absorption. Cardiac contractility is also increased to increase blood flow to skeletal muscles. This supports the generation of ATP from glucose and fatty acids for sustained muscle utilization. It also reduces blood flow to the skin and causes the contraction of smooth muscles in the ski,n causing goosebumps.

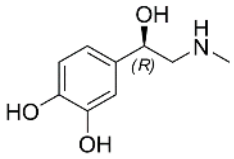


Figure **15.3.15**: Structure of Epinephrine

Within the liver and skeletal muscle, the epinephrine signaling pathway overlaps with the glucagon signaling pathway, which is also present in the liver. The epinephrine receptor is also a G protein-coupled receptor related to the glucagon receptor. However, it is specific for epinephrine and cannot bind with glucagon. It does activate the same G-protein pathway leading to Protein Kinase A activation, as shown in Figure **15.3.16**. The body is very efficient at reusing machinery in different parts of the body; in this case, it does so under different regulatory parameters.

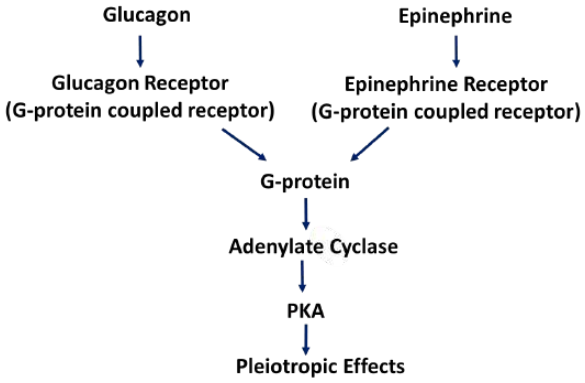


Figure **15.3.16**: Similarities of Glucagon and Epinephrine Signaling Pathways

The glycogen phosphorylase enzymes are also encoded by different genes within the liver and skeletal muscle. These are known as isozymes. Recall that isozymes have the same biological function, but since they are expressed from different genes, they have different enzyme kinetics and they are regulated in different and unique ways within each tissue.

The liver and skeletal muscle forms of Glycogen Phosphorylase share approximately 90% sequence identity. Both isozymes can exist in two major conformations, the a-form and the b-form. The protein adopts the a-form when it is phosphorylated at Ser 12 by phosphorylase kinase, as shown in Figure **15.3.17**. The Glycogen Phosphorylase enzyme can also be in two different states: the relaxed, flexible state,

which is the active form of the enzyme, and the tense or rigid state, which is inactive. When the protein is in the a-conformation, it favors the relaxed and active state of the protein. Therefore, the phosphorylation of Glycogen Phosphorylase leads to an increase in the enzyme's activity. This is depicted in the following diagram.

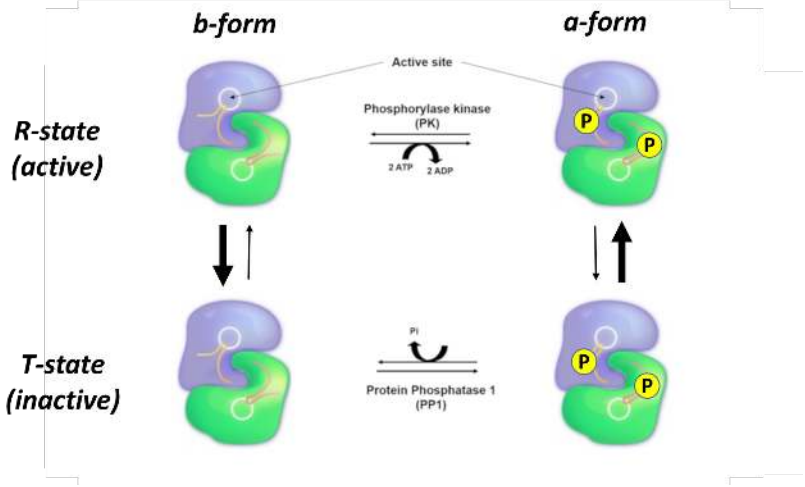


Figure 15.3.17: Enzymatic States of Liver and Skeletal Muscle Glycogen Phosphorylase. Both isozymes of Glycogen Phosphorylase are responsive to phosphorylation by phosphorylase kinase. Phosphorylation of Glycogen Phosphorylase causes it to shift from the b-form to the a-form of the protein. The a-form of the protein favors the relaxed, active state of the protein, whereas the b-form of the protein favors the tense and inactive state. Image modified from Llavero, F., et al (2019) Int. J. Mol. Sci. 20(23):5919

Another way to think about these four different enzyme states is that they exist in a dynamic equilibrium, with the population of each state determined by the phosphorylation state AND the presence of allosteric inhibitors and activators, which we will explore below. In Figure 17 above, the R state is positioned at the top, and the T state is positioned at the bottom. The vertical arrows indicate the equilibrium between just those two states. The thickness of the arrows indicates the preferred direction of the reversible reaction. In the absence of phosphorylation (left-hand vertical states), the equilibrium favors the T or inactive form. When phosphorylated (right-hand vertical states) on Ser12 by the enzyme phosphorylase kinase, the R or active form is favored. The horizontal equilibria show the phosphorylation of Ser12 by phosphorylase kinase (top, shown reversibly, but the enzyme is not acting physiologically to remove phosphate) and dephosphorylation of Ser 12 by the enzyme protein phosphatase 1 (which acts physiologically only as a phosphatase).

Different tissue-specific allosteric effectors also regulate the different isozymes of the Glycogen Phosphorylase enzyme. Within the liver, glucose acts as a negative regulator of Glycogen Phosphorylase, which is logical, given the role of this pathway in liver tissue, which is to promote the release of glucose into the bloodstream. The presence of free glucose in the cytoplasm of the liver would indicate either the fed state, when blood glucose levels are high, or that high levels of glycogenolysis have released substantial glucose. Within liver tissue, the presence of free glucose causes the a-form of Glycogen Phosphorylase to shift to the Tense state, reducing enzyme activity. This is shown in Figure 15.3.18.

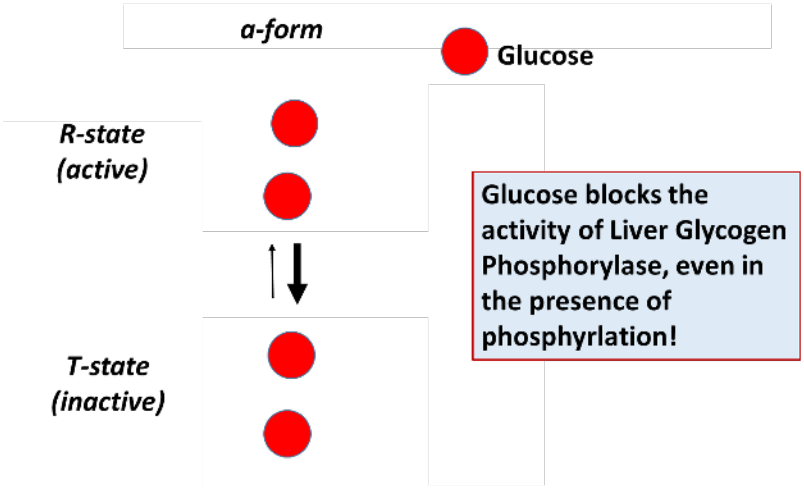


Figure **15.3.18**: Regulation of Liver Glycogen Phosphorylase by Free Glucose. When the liver isoform of Glycogen Phosphorylase is in the a-form (phosphorylated), it can be shifted into the Tense state in the presence of high levels of free glucose. This blocks the glycogen binding site of the enzyme, essentially serving as a competitive inhibitor. Image modified from Llavero, F., et al (2019) Int. J. Mol. Sci. 20(23):5919

Skeletal muscle glycogen phosphorylase (or Myophosphorylase, as it is sometimes called) is more responsive to allosteric effectors that indicate the energy state of the cell. This makes sense, as the primary purpose of glycogen breakdown in muscle tissue is to meet the energy demands of the muscle tissue. Thus, the energy housed in glucose will be used to produce ATP within these cells. The presence of either glucose 6-phosphate or ATP within skeletal muscle indicates high energy levels. Thus, glycogen breakdown will be inhibited. On the other hand, the presence of AMP indicates a low-energy state and serves as an activator of Glycogen Phosphorylase. This is shown in Figure **15.3.19** to Figure **15.3.21**below.

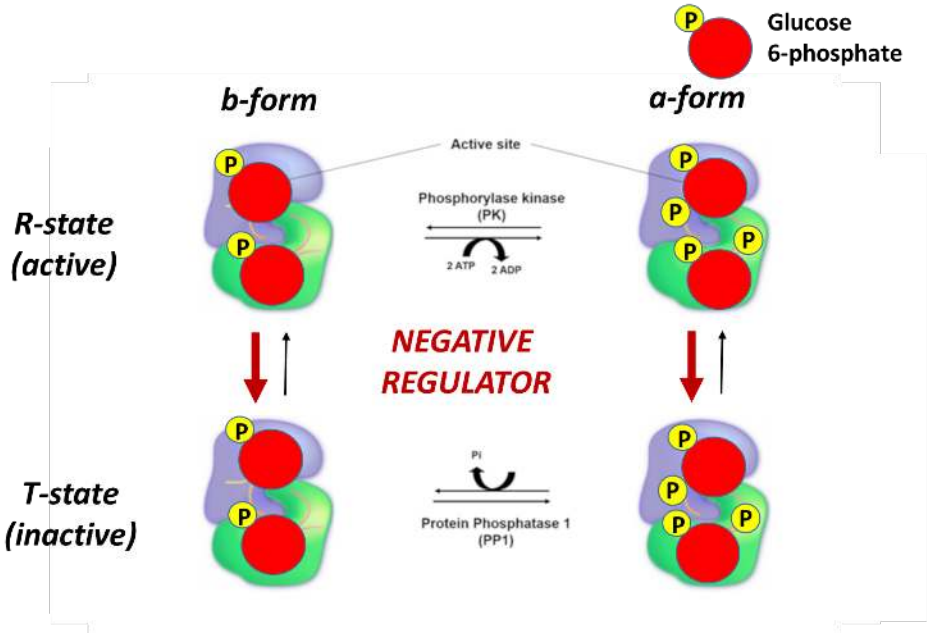


Figure **15.3.19**: Regulation of Skeletal Muscle Glycogen Phosphorylase by Glucose 6-phosphate. The presence of high levels of Glucose 6-phosphate negatively regulates Muscle Glycogen Phosphorylase. Regardless of the form (a or b) the enzyme is shifted into the Tense state. Image modified from Llavero, F., et al (2019) Int. J. Mol. Sci. 20(23):5919

Again, note that the bold red arrows point downward, showing that the addition of glucose-6-phosphate favors the T state (inactive) even if glycogen phosphorylase has been phosphorylated.

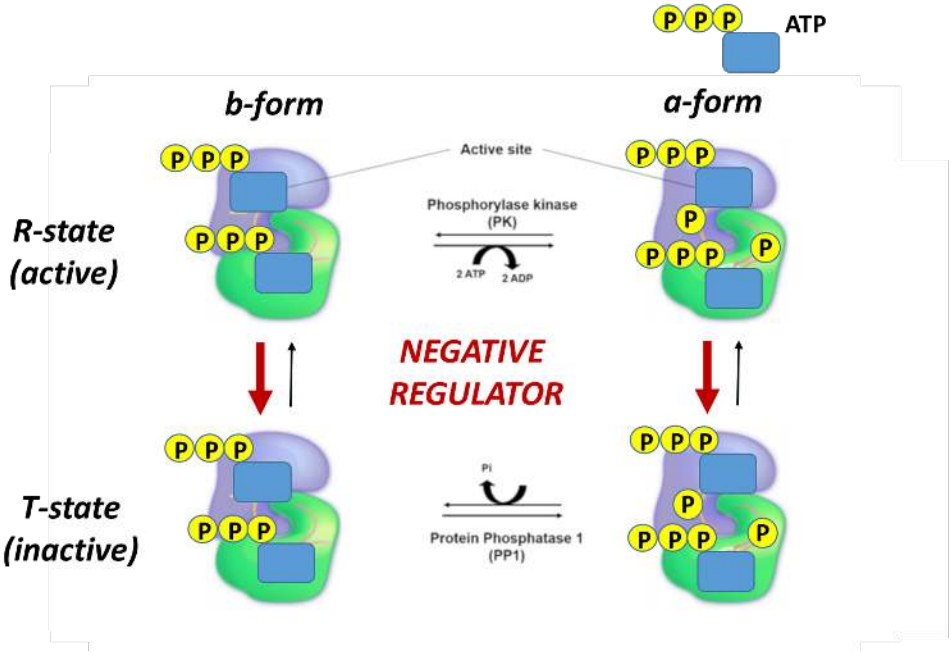


Figure **15.3.20**: **Regulation of Skeletal Muscle Glycogen Phosphorylase by ATP.** In the presence of high levels of ATP, GP is converted to the Tense state, showing the inhibition of the enzyme in the presence of high levels of energy. Image modified from Llavero, F., et al (2019) Int. J. Mol. Sci. 20(23):5919

Again, note that the bold red arrows point downward, indicating that when ATP levels are high, the T state (inactive) is favored, even if glycogen phosphorylase has been phosphorylated. Again, under conditions of a high energy state (as reflected by high ATP), there is no need to cleave glycogen to enter glycolysis.

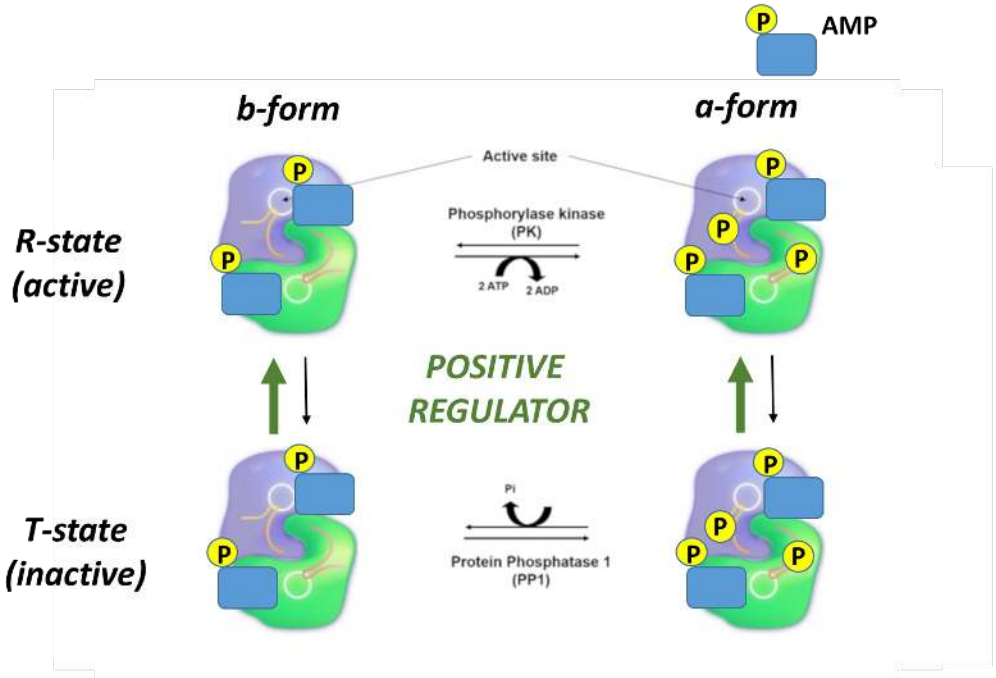


Figure **15.3.21**: Regulation of Skeletal Muscle Glycogen Phosphorylase by AMP. In the presence of low-energy indicators, such as AMP, the glycogen phosphorylase enzyme is activated, even in the absence of phosphorylation. Thus, when AMP is bound, the b-form of glycogen phosphorylase is converted into the relaxed and active state. Image modified from Llavero, F., et al (2019) Int. J. Mol. Sci. 20(23):5919

In contrast, note that the bold green arrows point upward, showing that when the AMP levels are relatively high, the R state is active. Higher levels of AMP reflect a need to activate glycogen breakdown to increase ATP production.

A mechanism for the phosphorolysis of Glc_{n+1} to Glc_n and glucose-1-phosphate is shown in Figure **15.3.22**. Note the unusual presence of a molecule of pyridoxal phosphate covalently attached through a Schiff base linkage to Lys 568 (rabbit phosphorylase).

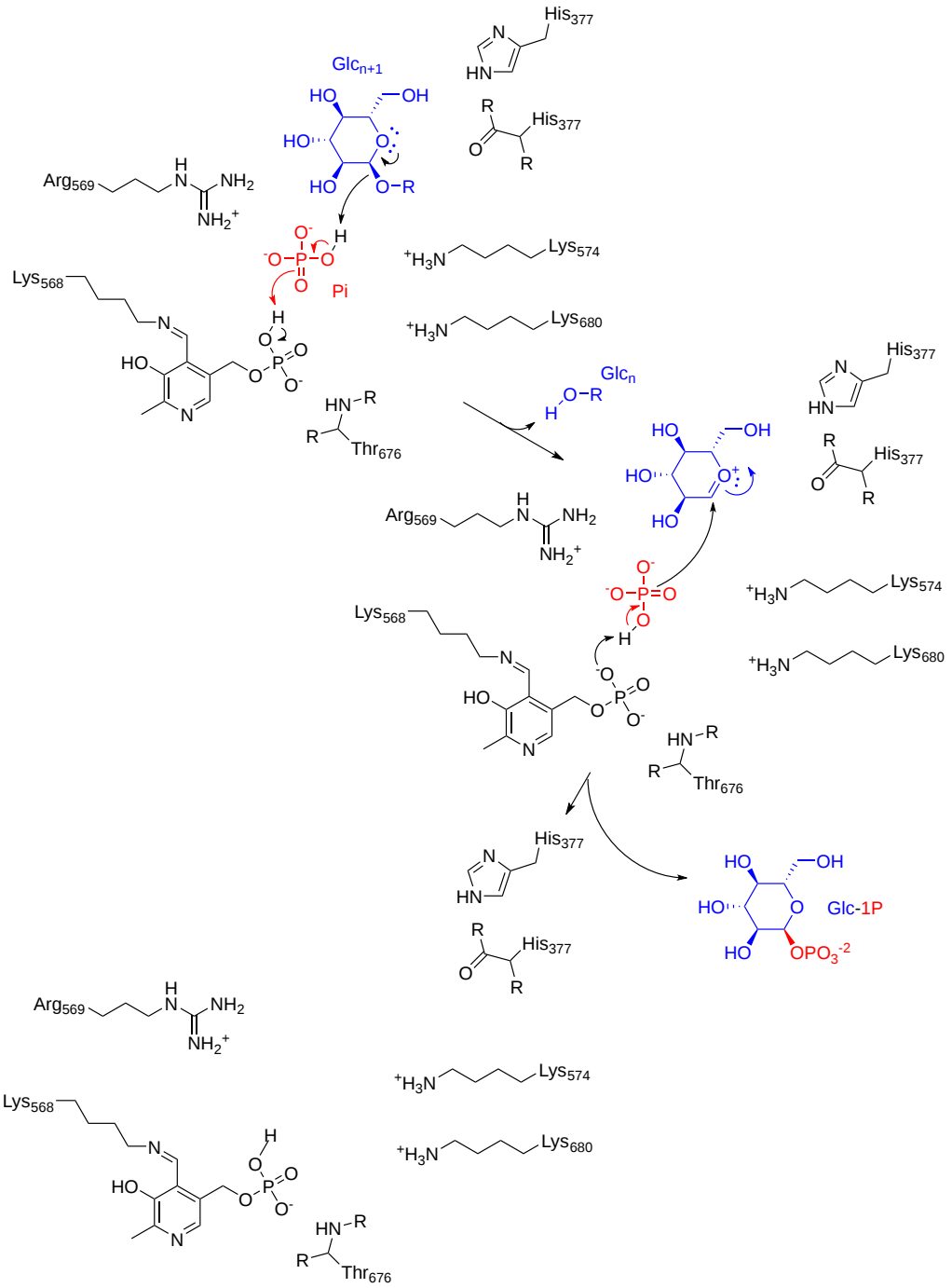


Figure **15.3.22**: A mechanism for the phosphorolysis of Glc_{n+1} to Glc_n and glucose-1-phosphate. https://www.ebi.ac.uk/thornton-srv/m-csa/entry/205/. Creative Commons Attribution 4.0 International (CC BY 4.0) License

PLP, which is covalently attached through a Schiff base, functions in this enzyme as a general acid and base and not as a cofactor that facilitates covalent bond cleavage in amino acid substrates that are covalently attached to it (Chapter 6.8: Cofactors and Catalysis - A Little Help From My Friends).

It is essential to note that the reaction is a phosphorolysis, not a hydrolysis, which would result in the release of free glucose. This glucose would then be more readily available to leave the cell, making it less accessible for cellular energy needs and less available for glycolysis.

Figure **15.3.23** below shows an interactive iCn3D model of a dimer of rabbit glycogen phosphorylase (1GDB).

https://bio.libretexts.org/@go/page/77731

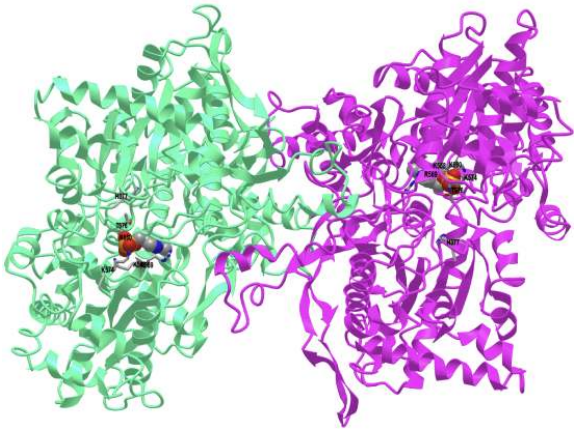


Figure 15.3.23: Dimer of rabbit glycogen phosphorylase (1GDB). (Copyright; author via source). Click the image for a popup or use this external link:https://structure.ncbi.nlm.nih.gov/i...s1LosR5TJLjru9

The subunits in the dimeric form are shown in different colors. PLP is shown in spacefill. Active site residues are shown in both subunits as CPK-colored sticks and labeled.

Let's look at a monomer (from the tetramer) of 2 nonphosphorylated states of glycogen phosphorylase. Since they are both unphosphorylated, they both represent the **b state**. One (**2GPB**) has glucose bound, so it represents the inactive (T state). The other (**3E3N**) has AMP bound, so it represents the active (the R state). Figure **15.3.24** shows the conformation differences between the monomeric states



Figure **15.3.24**: Conformational differences between the monomeric unphosphorylated b state of glucose-bound GP (T state, inactive) and AMP-bound GP (R state, active)

Now, let's examine the conformations of two different GPs activated by distinct means. In one, the nonphosphorylated form of GP (the b state and inactive T state) binds AMP, an allosteric activator (pdb 8GPA), and converts to the active b state (unphosphorylated R state). Let's compare its active conformation to a form of GP activated by phosphorylation (the phosphorylated **a** state and active R state) to which just SO_4^{2-} is also bound. In the 1st case, GP-b T state is driven to the active Gp-b R state by binding the allosteric activator AMP. In the second case, GP-a is already in the R active state since it is phosphorylated. Figure **15.3.25** compares their conformations.

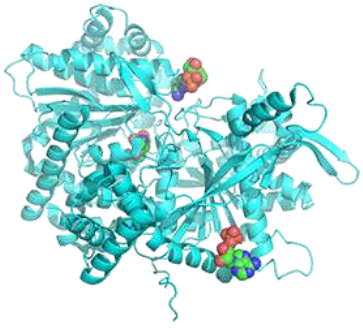


Figure **15.3.25**: Comparison of the conformations of two active forms of GP - phosphorylase b bound to the allosteric activator AMP (R state) and phosphorylase a activated by phosphorylation of Ser 14.

The cyan monomer is glycogen phosphorylase b, which is not phosphorylated but is driven into the **R state** upon the binding of AMP (note that two AMP molecules are bound at the periphery). The dark blue monomer is glycogen phosphorylase A, which is phosphorylated at Ser14 (a different number in this crystal file, as shown in spacefill and labeled SEP-14), also in the R state. It also has two SO_4^{2-} bound, which help stabilize the state. Look carefully! The conformations are very similar, in contrast to those for the T and R states shown in Figure 24.

Figure 15.3.26 below shows an interactive iCn3D model of unphosphorylated (b state) rabbit glycogen phosphorylase with bound glucose (inactive T state, **2GPB).**

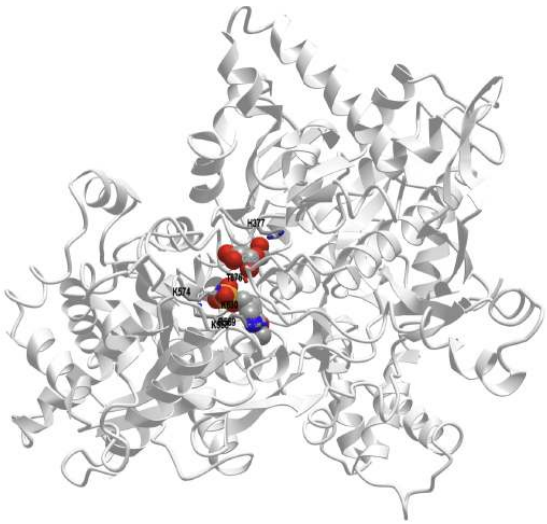


Figure 15.3.26: Unphosphorylated (b state) rabbit glycogen phosphorylase with bound glucose (inactive T state, 2GPB). (Copyright; author via source). Click the image for a popup or use this external link: https://structure.ncbi.nlm.nih.gov/i...eXQciAPczmQpLA

Only 1 monomer of the tetramer is shown. PLP and glucose are shown in spacefill, CPK colors, and labeled. Key active site residues are shown as colored sticks and labeled.

Figure 15.3.27 below shows an interactive iCn3D model of unphosphorylated (b state) rabbit glycogen phosphorylase with bound AMP (active R state, 3E3N).

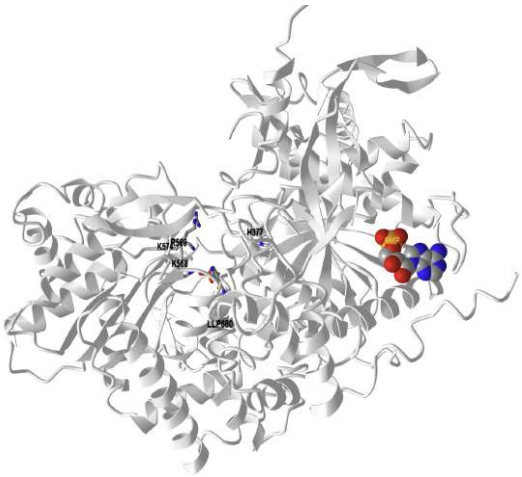


Figure 15.3.27: Unphosphorylated (b state) rabbit glycogen phosphorylase with bound AMP (active R state, 3E3N). (Copyright; author via source). Click the image for a popup or use this external link: https://structure.ncbi.nlm.nih.gov/i...WDZJc1CcpFqEG7

Note the different locations for the binding site of the allosteric activator AMP compared to the inhibitor glucose in the previous model.

MCARDLE'S DISEASE

McArdle's Disease, also referred to as myophosphorylase deficiency or type V glycogen storage disease, is a recessive inherited disorder characterized by an inability to metabolize glycogen due to the absence of a functional myophosphorylase (PYGM). In Figure **15.3.28** shown below, the normal functional pathway is shown in blue on the left, while the mutant pathway is shown on the right in red. Patients with this disease lack sufficient glucose-1-phosphate (G1P) monomers for glycolysis and the hexosamine biosynthetic pathway (HBP). This results in lower ATP and, consequently, lower muscle contraction and lower post-translational modifications by O-GlcNAcylation compared to normal conditions. This is especially pronounced during extended or heavy workouts, where people with McArdle's Disease will sustain painful cramping of their muscle tissue during workouts, can have dark red/brown urine, and can easily tire during activity. Some patients also experience a second-wind phenomenon during workouts, as the body shifts from carbohydrates to lipids as its primary energy source. The urine's dark red/brown color happens if muscle tissue is damaged during the workout. The damaged muscle releases the protein myoglobin into the bloodstream. This is filtered out by the kidneys and excreted in the urine, causing the color change. The severe, uncontrolled disease can cause life-threatening kidney problems.

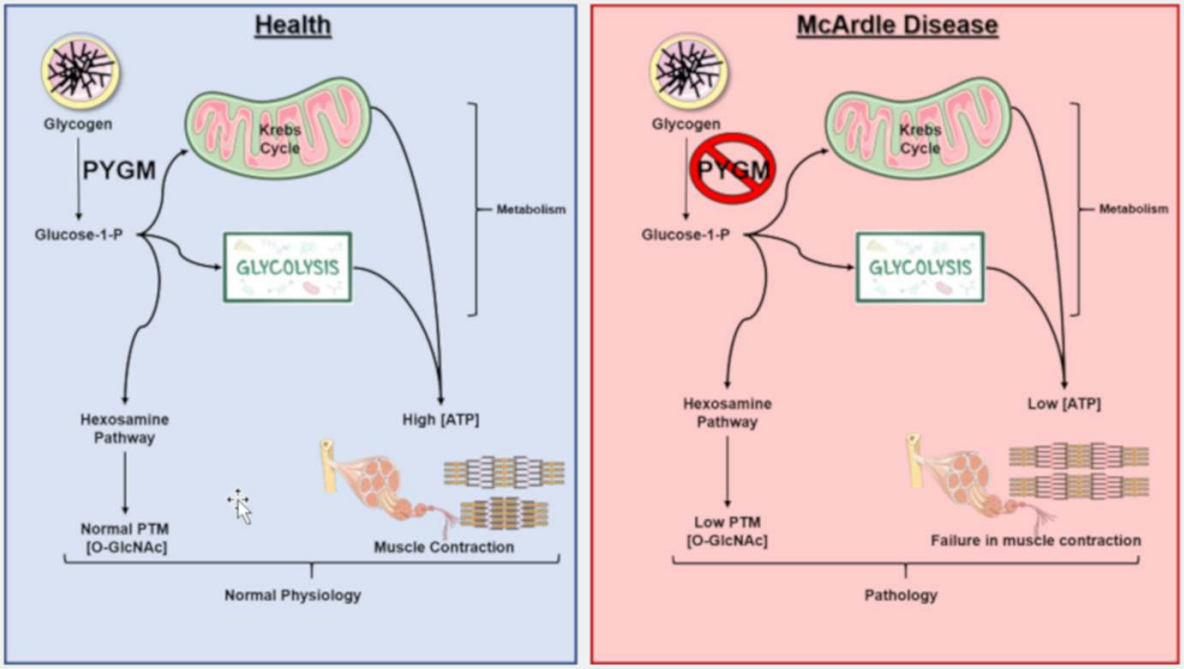


Figure **15.3.28**: McArdle's Disease. *The left-hand side (blue)* represents the normal pathway, whereas the *right-hand side (red)* notes the deficiency of muscle glycogen phosphorylase. Image from Llavero, F., et al (2019) Int. J. Mol. Sci. 20(23):5919

Figure **15.3.29** presents an overview of glucose metabolism in skeletal muscle. Both glucose-1-phosphate (G1P) released from the intracellular glycogen stores by glycogen phosphorylase (GP), as well as the glucose introduced into the cell through glucose transporters (GLUT), are converted to glucose-6-phosphate (G6P) by phosphoglucomutase (PGM) and hexokinase (HK), respectively. The G6P can be directed to different destinations. One is the pentose phosphate pathway, which is used for forming nucleic acid building blocks (ribose and deoxyribose). Another is in the formation of ATP. Here, G6P enters the glycolysis metabolic pathway. The glycolytic reactions culminate in the production of pyruvate and adenosine triphosphate (ATP). Pyruvate can be fermented to lactate by lactate dehydrogenase (LDH) catalysis during anaerobic muscle exercise.

On the other hand, pyruvate can be used to obtain ATP through full oxidation in the Krebs Cycle. In total, oxidative phosphorylation produces between 30-36 molecules of ATP (depending on the organism and tissue), six molecules of carbon dioxide (CO_2), and six molecules of water (H_2O) from 1 glucose molecule. Glycolysis alone only produces two net ATP molecules per glucose. Glucose, in addition to being the main fuel of the cell's energy metabolism, is also used by the cellular machinery as a vitally important substrate for the production of key intermediaries of the hexosamine biosynthetic pathway (HBP) forming O-GlcNAc, β-linked N-acetylglucosamine. And finally, in times of plenty, glucose is utilized by glycogen synthase (GS) to form glycogen.

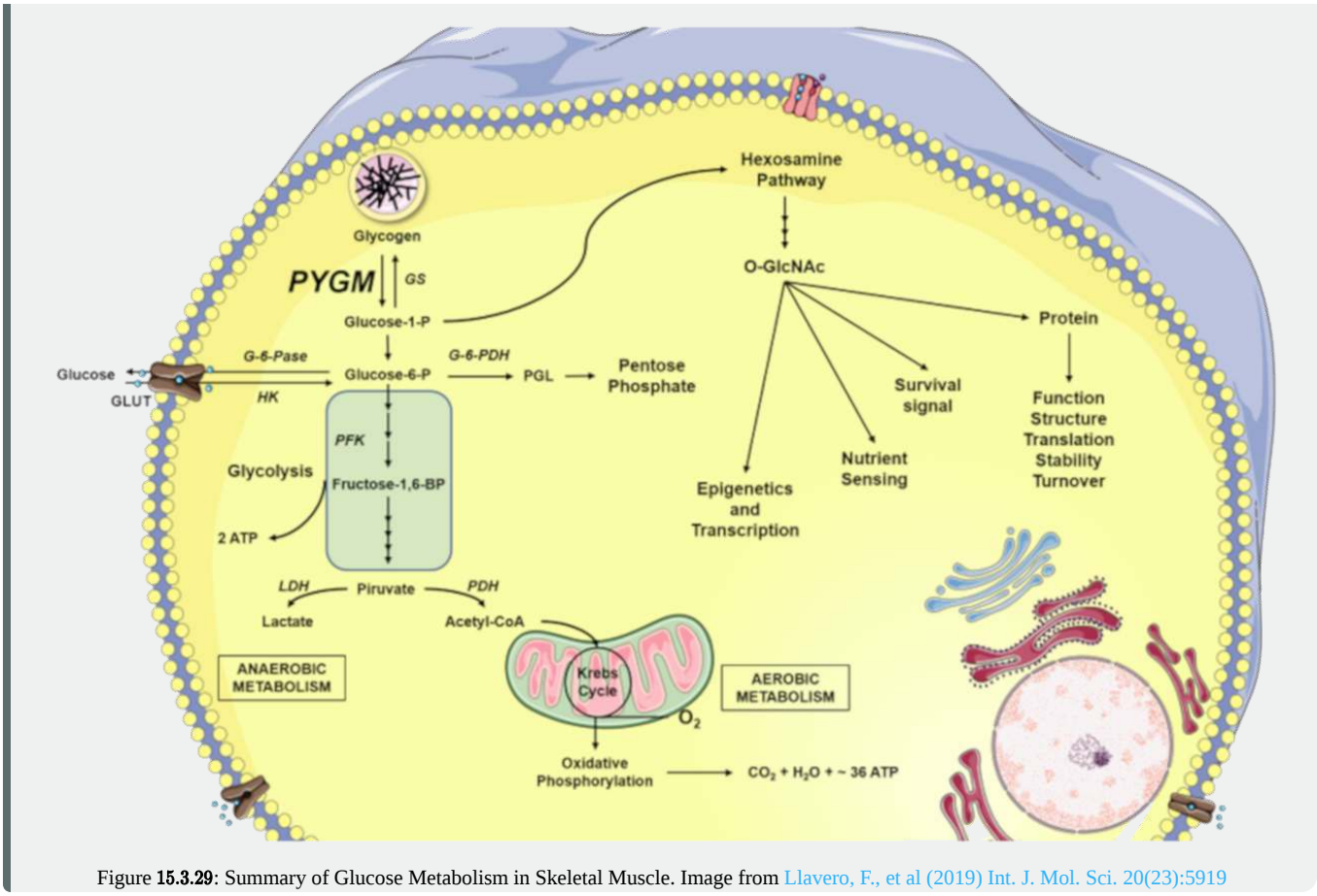


Figure **15.3.29**: Summary of Glucose Metabolism in Skeletal Muscle. Image from Llavero, F., et al (2019) Int. J. Mol. Sci. 20(23):5919

15.3.6: SUMMARY

This chapter provides an in-depth exploration of glycogenolysis—the enzymatic breakdown of glycogen—and its regulation by the hormones glucagon and epinephrine, highlighting key differences between liver and skeletal muscle metabolism.

Overview of Glycogenolysis:

The process of glycogenolysis is initiated by two key enzymes: glycogen phosphorylase and the glycogen debranching enzyme. Glycogen phosphorylase cleaves α(1→4) glycosidic bonds at the non-reducing ends of glycogen, releasing glucose 1-phosphate. In contrast, the debranching enzyme overcomes the limitations imposed by branch points (α(1→6) linkages) by transferring and hydrolyzing short glucan fragments, allowing for continued degradation of glycogen.

Mechanism of Glycogen Phosphorylase:

Glycogen phosphorylase is a homodimer that requires pyridoxal phosphate (PLP) as a cofactor, which is covalently linked to the enzyme via a lysine residue. The enzyme positions a free inorganic phosphate in its active site, facilitating the nucleophilic attack on the glycosidic bond, thereby releasing glucose 1-phosphate. This reaction is critical for generating substrates for further metabolic processes.

Hormonal Regulation and Tissue Specificity:

Hormonal signals tightly regulate glycogenolysis. In the liver, glucagon is released during hypoglycemia, triggering a signaling cascade via its G-protein-coupled receptor. This cascade leads to an increase in cyclic AMP (cAMP), activation of protein kinase A (PKA), and subsequent phosphorylation of key enzymes:

- **Inactivation of Glycogen Synthase (GS):** PKA phosphorylates GS, shifting it into an inactive state and preventing glycogen synthesis.
- **Activation of Glycogen Phosphorylase:** PKA also activates phosphorylase kinase, which in turn phosphorylates glycogen phosphorylase, converting it from the less active b form to the active a form. Additionally, calcium binding further enhances phosphorylase kinase activity, particularly in skeletal muscle.

Skeletal muscle, however, responds primarily to epinephrine rather than glucagon. Epinephrine also activates the cAMP/PKA pathway but, in muscle, glycogenolysis is regulated by allosteric effectors:

- **Inhibition by ATP and Glucose 6-Phosphate:** High levels indicate abundant energy and downregulate enzyme activity.

- **Activation by AMP:** High AMP levels signal low energy, promoting the active state of glycogen phosphorylase.

Conformational States and Allosteric Regulation:
Glycogen phosphorylase exists in dynamic equilibrium between inactive (T) and active (R) conformations. The enzyme's activity is modulated by phosphorylation and by binding of allosteric effectors. Structural models illustrate how binding of inhibitors (e.g., free glucose in the liver) or activators (e.g., AMP in muscle) shifts the equilibrium, thereby finely tuning the enzyme's catalytic performance.

Integration with Overall Glucose Metabolism:
The products of glycogenolysis serve different roles in liver and muscle tissues. In the liver, glucose 1-phosphate is eventually dephosphorylated to free glucose for release into the bloodstream, crucial for maintaining blood glucose levels and supporting brain function. In skeletal muscle, glucose 6-phosphate enters glycolysis to meet immediate energy demands.

Clinical Relevance:
The chapter concludes by highlighting the clinical implications of defective glycogenolysis. For instance, McArdle's Disease (myophosphorylase deficiency) disrupts muscle energy metabolism, leading to exercise intolerance, muscle cramping, and potential kidney complications due to myoglobinuria.

Overall, this chapter bridges the molecular mechanisms of enzyme action with hormonal regulation and systemic metabolic balance, offering a comprehensive understanding of how glycogen breakdown is finely controlled to meet the energy demands of the body.

This page titled 15.3: Glycogenolysis and its Regulation by Glucagon and Epinephrine Signaling is shared under a CC BY-NC-SA 4.0 license and was authored, remixed, and/or curated by Henry Jakubowski and Patricia Flatt.

- **11.2: Diffusion Across a Membrane - Passive and Facilitated Diffusion** by Henry Jakubowski and Patricia Flatt has no license indicated.

15.4: REGULATION OF GLYCOLYSIS

LEARNING GOALS (CHATGPT O3-MINI)

1. **Identify Major Glycolytic Control Points:**
   - Describe the roles of hexokinase, phosphofructokinase-1 (PFK1), and pyruvate kinase as the primary regulatory enzymes in glycolysis.
2. **Understand Hormonal Regulation of Glycolysis:**
   - Compare the effects of glucagon and insulin on glycolysis in the liver, highlighting that glucagon (under low serum glucose) inhibits glycolysis and promotes gluconeogenesis and glycogenolysis, whereas insulin (under high serum glucose) stimulates glycolysis and glycogen synthesis.
3. **Examine Isozyme Diversity in Hexokinase Regulation:**
   - Explain how different hexokinase isozymes (HKI, HKII, HKIII, and HKIV/Glucokinase) vary in their kinetic properties, subcellular localization, and regulatory mechanisms, and how this diversity tailors glucose phosphorylation to the specific metabolic needs of different tissues.
4. **Link Hexokinase Activity to Metabolic Fates of Glucose 6-Phosphate:**
   - Outline the multiple metabolic fates of glucose 6-phosphate (energy production via glycolysis and oxidative phosphorylation, glycogen synthesis, nucleotide biosynthesis via the pentose phosphate pathway, and hexosamine synthesis) and discuss how hexokinase activity influences these pathways.
5. **Analyze Allosteric Regulation of PFK1:**
   - Discuss the structure and regulatory properties of PFK1, including its allosteric sites for activators (e.g., ADP, AMP, and fructose 2,6-bisphosphate) and inhibitors (e.g., ATP and citrate), and explain how these modulators reflect cellular energy status.
6. **Understand Tissue-Specific Composition of PFK1 Isozymes:**
   - Describe how the subunit composition of PFK1 tetramers (composed of muscle, liver, and platelet subunits) varies among tissues and affects the enzyme's kinetic and regulatory properties.
7. **Examine the Role of Pyruvate Kinase in Glycolysis:**
   - Detail the reaction catalyzed by pyruvate kinase, its regulation by feedforward activation (by fructose 1,6-bisphosphate) and feedback inhibition (by ATP and alanine), and the tissue-specific expression of its isozymes (L, R, M1, and M2).
8. **Explore Hormonal Control of Pyruvate Kinase:**
   - Explain how glucagon signaling in the liver, via protein kinase A (PKA), leads to the phosphorylation and inhibition of the liver isozyme of pyruvate kinase, thereby redirecting metabolites toward glucose production rather than glycolysis.
9. **Evaluate the Fructose Regulatory Bypass:**
   - Describe the alternative pathway for fructose metabolism in the liver and kidneys, where fructose is converted to fructose-1-phosphate and then cleaved by Aldolase B, bypassing key regulatory steps (hexokinase and PFK1) and potentially contributing to metabolic dysregulation.
10. **Integrate Hormonal and Cellular Energy Signals:**
    - Synthesize how local indicators of cellular energy (ATP, AMP) and systemic hormonal signals (insulin, glucagon, epinephrine) coordinate to regulate the glycolytic pathway, ensuring that glucose utilization is appropriately matched to both the energy demands of individual cells and the overall metabolic state of the organism.

These learning goals aim to provide students with a comprehensive understanding of how glycolysis is tightly regulated at multiple levels—through enzyme isozymes, allosteric modulation, and hormonal signaling—to maintain metabolic homeostasis.

There are three major enzymatic control points within the glycolytic pathway. These include the reactions of hexokinase, phosphofructokinase, and pyruvate kinase. Key drivers for regulating the pathway are energy demand:

- within the cell, as determined by local indicators such as ATP and AMP
- within the organism as a whole, under the influence of hormone signaling pathways.

We will also observe that the regulation of the pathway can vary depending on the cell type and its cellular needs.

Here is a quick review of some key hormonal effects before we proceed.

Under low serum glucose conditions:

- Glucagon is secreted. This activates glucose synthesis and glycogen breakdown, while inhibiting glycolysis in the liver. Glucose is then exported into the blood and restores a higher glucose concentration.

Under high serum glucose:

- Insulin is secreted, which promotes glucose uptake in the liver and muscle for energy use. Glycolysis is activated, gluconeogenesis is inhibited, and storage by glycogen synthase is activated.

15.4.1: HEXOKINASE REGULATION

One of the primary mechanisms that regulates the hexokinase step in glycolysis is the presence of different hexokinase enzymes in various cellular types. Essentially, these are proteins encoded by different genes but perform the same function within the cell. They are known as isozymes. Isozymes can have different enzyme kinetics, tissue expression patterns, and post-translational modifications, and bind with different allosteric effectors. This allows the body to have differential control over the same processes in different locations within the body. Four important hexokinase isozymes within vertebrates vary in subcellular locations and kinetic parameters. This allows the differential phosphorylation of hexoses depending on local conditions and physiological function. They are designated hexokinases I, II, III, and IV. All of the hexokinases can use multiple hexoses as substrates in addition to glucose. These include mannose, fructose, and 2-deoxyglucose. Hexokinase IV, also known as glucokinase, is specifically expressed in the liver and pancreas.

Recall that hexokinase enzymes mediate the first step in the glycolytic pathway with the formation of glucose 6-phosphate, as shown in Figure **15.4.1** below. They also require ATP as a cofactor in the process.

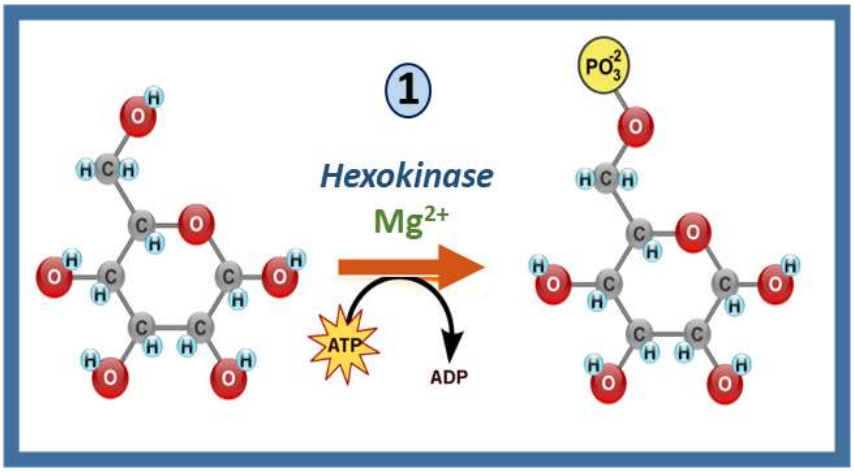


Figure **15.4.1**: Glucose Phosphorylation by Hexokinase Enzymes. Figure modified from YassineMrabet

Recall that glucose-6-phosphate (G6P) has several potential fates within the body, as shown in Figure **15.4.2**. It can serve as an energy source through both glycolysis and aerobic respiration pathways. Short bursts of anaerobic respiration can also be sustained in animals that convert pyruvate into lactate. G6P can also be dephosphorylated in the liver and released back into the bloodstream to maintain homeostatic balance. The pancreas uses G6P as a sensor to determine when to secrete insulin and glucagon. The G6P can also serve as a building block for anabolic processes. It can be converted to ribose through the Pentose Phosphate Pathway, where it will be used to synthesize nucleotide monomers. It can also form hexosamines used in the formation of proteoglycans and glycoproteins.

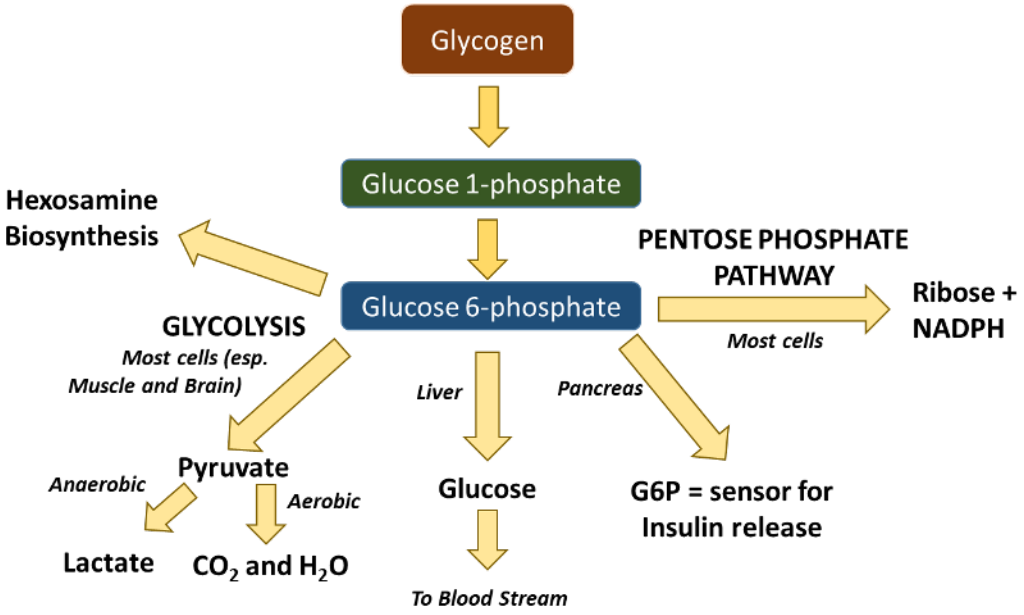


Figure **15.4.2**: Cellular Fates of Glucose 6-Phosphate

Now, let's look at the different isozymes of hexokinase in a little more detail. Hexokinase I (HKI) is widely distributed throughout the body and is the main form expressed in brain tissue and red blood cells, as shown in Figure **15.4.3**. In brain cells, this protein is localized to the mitochondria. This colocalization facilitates the efficient coupling of glycolysis and the Krebs cycle/oxidative phosphorylation pathways within the mitochondria. It also ties the activity of HKI to oxidative phosphorylation and energy load, as HKI preferentially uses mitochondrially derived ATP in its reaction mechanism. HK's association with the mitochondria also has a protective effect on the cell, reducing the potential for programmed cell death or apoptosis.

On the other hand, red blood cells (RBCs) are highly differentiated cells with a very short lifespan. They are replaced in humans approximately every two weeks. RBCs are enucleated and do not have mitochondria, and thus, only generate ATP through glycolysis. The HKI protein is free-floating in the cytoplasm of this system. HKI has a low Km, indicating a high affinity for glucose and activity at low substrate concentrations. It is also inhibited by the product glucose-6-phosphate (G6P) in ***negative feedback inhibition.*** Essentially, you do not want to waste time and energy making more than you need. Low to moderate levels of free inorganic phosphate can overcome this negative feedback inhibition.



Figure **15.4.3**: Localization of Hexokinase I. Hexokinase I (HKI) is found widely throughout the body and is the primary hexokinase found in brain tissue and red blood cells. Within the brain tissue, HKI is localized to the mitochondria. Images from Smart Servier Medical Art and Jessica Polka

HKI and HKII are expressed in skeletal and cardiac muscles, as well as insulin-sensitive tissues. While it is thought that HKI primarily provides a catabolic role for the use of G6P in energy production, HKII may play a more significant role in anabolic processes, providing G6P for conversion to G1P and subsequent utilization in Glycogenesis. Both HKI and HKII are localized to the outer membrane of the mitochondria. However, 95% of HKI is associated with mitochondria, and only about 70% of HKII is, with the remaining HKII fractionating with the cytosolic proteins. This could help to explain the heightened role of HKII in anabolic glycogenesis processes within skeletal muscle and why it is not found in brain tissue. HKII is also often overexpressed in tumor cells, which is associated with higher

mortality rates. It has also been linked with the processes of metastasis and with the development of drug resistance. Similar to HKI, HKII also has a low Km and is inhibited by G6P, although the presence of inorganic phosphate does not release this inhibition.

Not much is known about HKIII's functions. It may be an inactive gene duplication or remnant. Under basal conditions, it is not expressed to appreciable levels in any major tissues, and studies on its biological activity show that it is inhibited by glucose at physiological concentrations. However, some studies suggest that it may be expressed during cellular stress responses, such as hypoxia, although its function in these responses remains unclear.

Hexokinase IV or glucokinase is specifically expressed within the liver and pancreas. HKIV is cytoplasmic and not tethered to the mitochondria. Activity within the pancreas serves as a sensor for insulin release, and in the liver, it produces glucose-6-phosphate (G6P) that fuels glycogen production. HKIV has a higher Km than HKI and HKII, thus it does not work efficiently at low glucose concentrations. However, it is NOT inhibited by the product, G6P. Thus, it will continue to make G6P, even when levels are high. This helps explain the high levels of glycogen stored within the liver but not elsewhere in the body. This also ensures that the sensor system in the pancreas will accurately read blood glucose levels.

The four isozymes of HK share high homology with one another and appear to have arisen from gene duplication events, as shown in Figure **15.4.4**. The left-hand panel of Figure 15.5.4 shows the linear protein domains of the different HK isozymes. HKI and HKII contain an N-terminal domain that localizes the protein to the mitochondrial membrane. HKI, II, and III contain two repeating catalytic domains in the N- and C-termini. However, mutations in the N-terminal domain in HKI and HKIII render them inactive. Both catalytic domains in HKII retain activity. HKIV (Glucokinase) is the most truncated isozyme, only containing the C-terminal catalytic domain. The lower right diagram shows the ribbon diagram of HKIV. Upstream promoter regions of HKIV (not shown in this diagram) also differ, allowing for controlled expression in the liver and pancreas. Feedback inhibition in HKI and HKII occurs through the N-terminal catalytic domain. The upper diagram on the right shows an HKI dimer complex with an ATP analog, glucose, G6P, and Mg^{2+} ion. HKI dimerizes when the concentration of the inhibitor, G6P, is high enough. Dimerization reduces the biological activity of the enzyme in brain tissue. Dimerization of HKI can be reversed in the presence of low levels of inorganic phosphate.

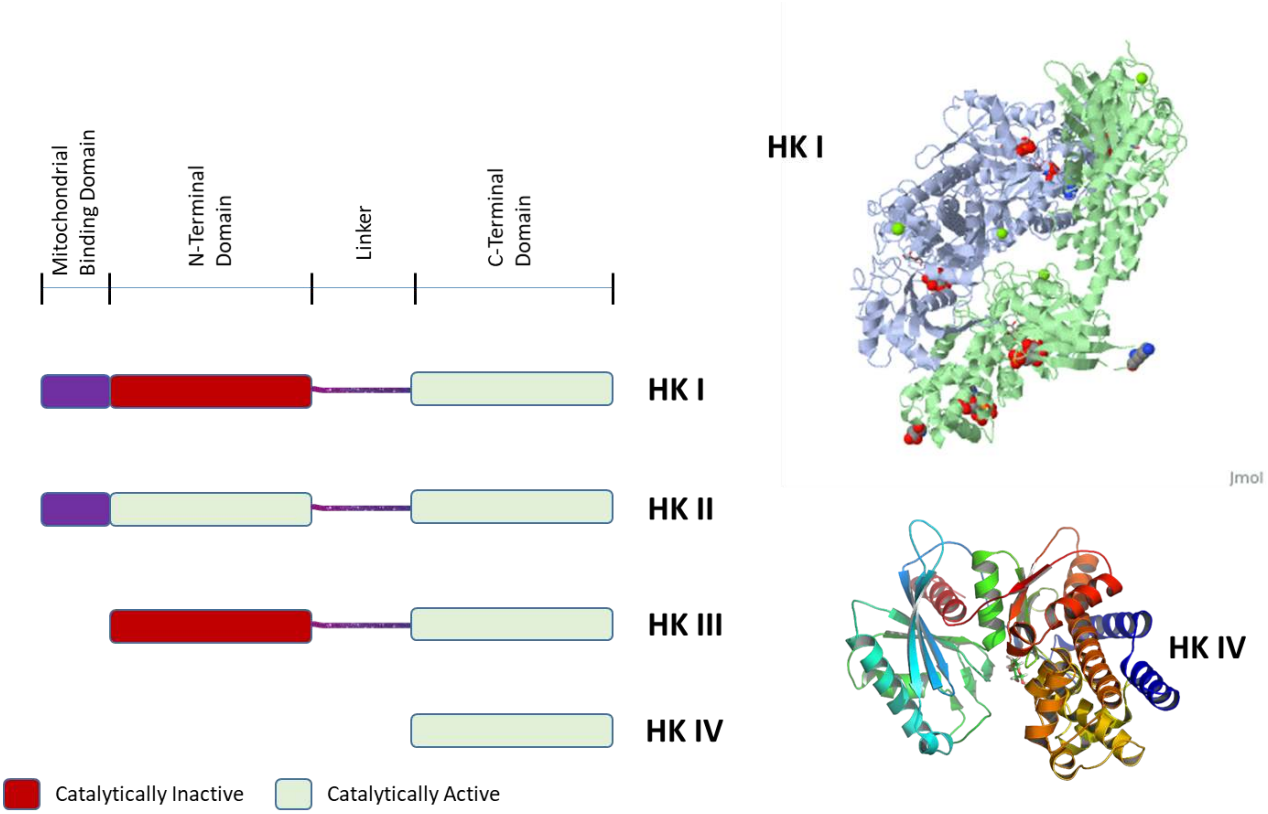


Figure **15.4.4**: Protein Comparison of the Four Major Hexokinases in Vertebrates. The left-hand panel shows the linear protein domains of the hexokinases I - IV. The upper right diagram shows a dimer of HKI complexed with an ATP analog, glucose, glucose 6-phosphate, and Mg^{2+}. The lower panel depicts a ribbon diagram of HKIV. Figures modified from Proteopedia and JAG123

HKIV is also a good model for understanding enzyme conformational changes during the reaction. HKs change shape by induced fit upon substrate binding. HKIV has a large induced fit motion that closes over the substrates ATP and xylose, as shown in Figure **15.4.5**. The binding sites are shown in blue, substrates in black, and the Mg^{2+} cofactor in yellow (PDBs:2E2N,2E2Q).

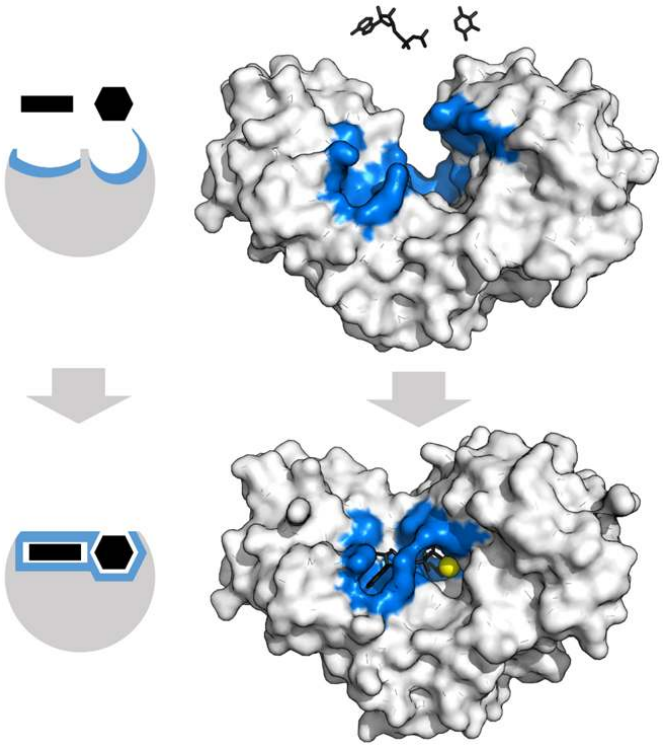


Figure 15.4.5: HKIV Conformational Change During Substrate Binding. The upper diagram shows the enzyme before substrate binding whereas the lower diagram shows the conformational change upon binding with xylose, ATP, and the Mg^{2+} cofactor. Mg^{2+} is shown in yellow and the substrate binding pocket in the enzyme in blue. Xylose and ATP are shown in black. Figure from Thomas Shafee

In summary, the isozyme expression patterns of HKs differentially regulate the fate of glucose within those tissues. Within brain tissue and red blood cells, where only HKI is present, glucose is predominantly used in the glycolytic pathway for energy production. In muscle tissue, the presence of HKII enables the increased utilization of glucose to form glycogen. HKIV expression in the pancreas and liver enables the homeostatic regulation of blood glucose levels and the storage of glucose as glycogen.

15.4.2: PHOSPHOFRUCTOKINASE-1 REGULATION

Recall that phosphofructokinase-1 (PFK1) mediates the third step in the glycolytic pathway with the conversion of fructose 6-phosphate to fructose 1,6-bisphosphate, as shown in Figure 15.4.6. The PFK1 reaction is the first irreversible reaction of glycolysis. It also represents the committed step within the pathway. The phosphorylation of fructose-6-phosphate (F6P) to fructose-1,6-bisphosphate (F1,6BP) commits the F1,6BP to continue through the glycolytic pathway. It cannot be utilized for any other purpose at that point. F6P, on the other hand, could be converted back into glucose-6-phosphate and used for many different purposes (ie, glycogen synthesis, nucleotide synthesis, or hexosamine synthesis). Because of the committed nature of this step, PFK1 is one of the most important control points in the glycolytic pathway.

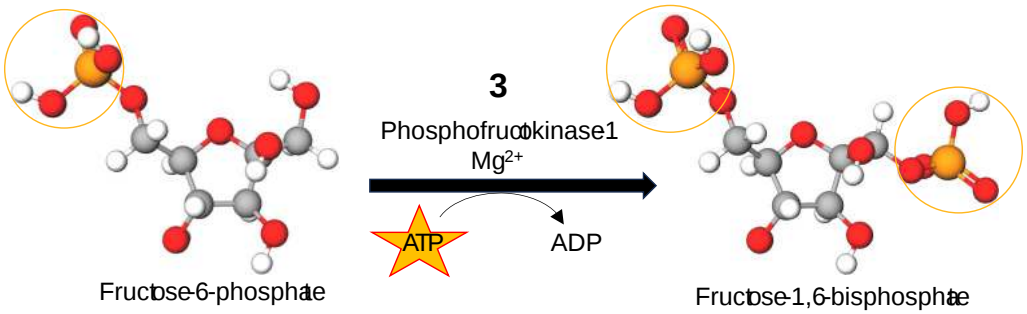


Figure 15.4.6: Phosphofructokinase-1 Activity During Glycolysis. (CC BY 4.0; Henry Jakubowski via LibreTexts)

The PFK1 enzyme is composed of a tetramer that can contain different combinations of three types of subunits: muscle (M), liver (L), and platelet (P). The composition of the PFK1 tetramer differs according to the tissue type in which it is present. For example, mature muscle expresses only the M isozyme; therefore, the muscle PFK1 is composed solely of homotetramers of the M4 isozyme. The liver and kidneys express predominantly the L isoform. In erythrocytes, both M and L subunits randomly form tetramers, including M4, L4, and the three hybrid forms of the enzyme (ML3, M2L2, M3L). As a result, the kinetic and regulatory properties of the various isoenzyme pools depend

on subunit composition. Tissue-specific changes in PFK1 activity and isoenzyme content contribute significantly to the diversities of glycolytic and gluconeogenic rates, which have been observed for different tissues.

PFK1 is an allosteric enzyme with a structure similar to that of hemoglobin insofar as it is a dimer of a dimer, as shown in Figure **15.4.7**. One half of each dimer contains the ATP binding site, whereas the other half has the substrate (fructose-6-phosphate) binding site and a separate allosteric binding site that can bind with ADP or AMP. The allosteric binding of ADP or AMP activates all isoforms of PFK1. This indicates a low-energy state within the cell and the need for glycolysis and energy generation. Allosteric inhibitors include high levels of ATP and Citrate. Note that ATP is a substrate of this enzyme and has the normal substrate binding site. When there is sufficient ATP present, it can also bind allosterically to the enzyme, acting as an inhibitor. Citrate, the first molecule in the Krebs' Cycle (Citric Acid Cycle), can also act as an allosteric inhibitor of PFK-1. At high citrate levels, pyruvate is not needed to generate ATP through oxidative phosphorylation. We will also see that Fructose 2,6-bisphosphate is predominantly a regulator of PFK1 in Liver Cells, where it serves as an activator.

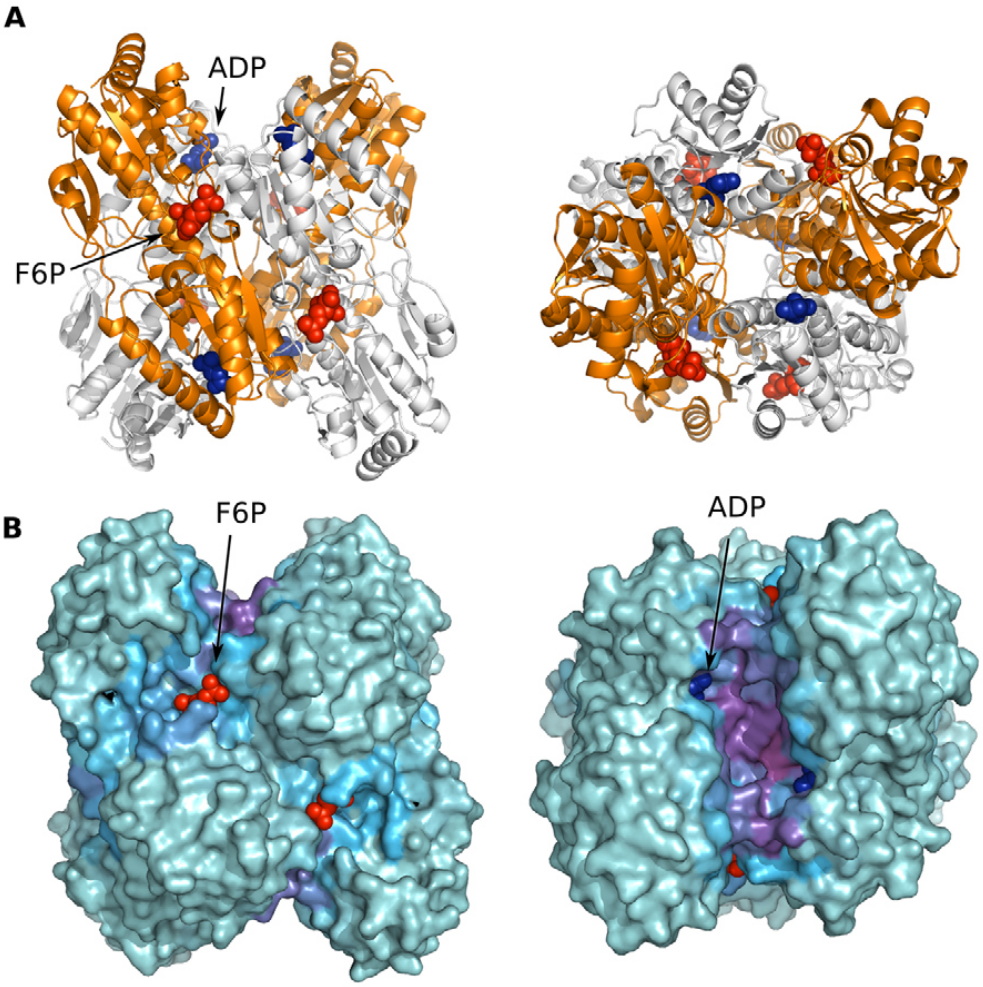


Figure **15.4.7**: Structure of Phosphofructokinase-1. The left-hand diagrams show the ribbon and space-filling models from a side view, whereas the right-hand diagrams have been rotated 90 degrees to show the top-down view. The ATP binding sites are in dark blue, and the fructose 6-phosphate binding sites are in red. A separate allosteric binding site for ADP is also shown. Image modified from Mitternacht, S., and Berezovsky, I.N. (2011)

Before we discuss the formation and use of Fructose 2,6-bisphosphate and its role in the regulation of PFK1, let's review opposing glucose utilization/production pathways within the liver, as shown in Figure **15.4.8**. Two opposing pathways within the liver are glycolysis (the breakdown of glucose) and gluconeogenesis (the formation of glucose). It would be unproductive to have both of these pathways operating simultaneously. Thus, if one pathway is needed, the other must be turned off. We previously saw this same type of control for glycogenesis (the formation of glycogen) and glycogenolysis (the breakdown of glycogen). When one of these pathways is upregulated, the other must be downregulated.

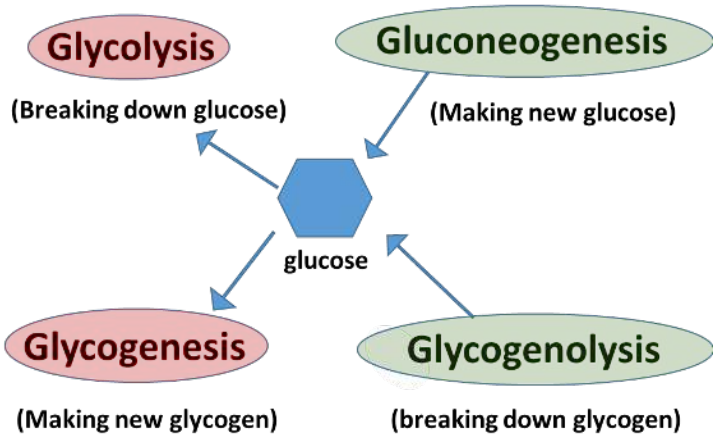


Figure 15.4.8: Opposing Pathways of Glucose in the Liver. Image modified from Yan, A., et al (2016) In J Biol Sci 12(12):1544-1554 and Servier Medical Art

In the resting state of the liver, when blood glucose levels are within the homeostatic range, gluconeogenesis is shut off, as it is very expensive to produce glucose. The liver will only invest in glucose production if blood glucose levels fall critically low (i.e., during extreme exercise or long-term fasting). In the resting state, the liver utilizes the glycolytic pathways to supply normal levels of ATP energy, thereby maintaining housekeeping processes. Glycogenesis and glycogenolysis will be in balance or equilibrium as needed to augment the supply of glucose entering the system from the bloodstream.

If glucose in the blood drops below homeostatic levels, the pancreas releases glucagon, initiating a hormone-signaling pathway that prompts the liver to release glucose into the bloodstream. Thus, glucagon signaling leads to the downregulation of glycolysis and glycogenesis, shunting glucose pools into the bloodstream. It also leads to an increase in glycogenolysis, or the breakdown of glycogen. During this time, liver cells predominantly generate ATP from lipids rather than carbohydrates. Thus, glycolysis can be inhibited to promote the release of glucose into the bloodstream.

If cellular demand for glucose is high, liver cells will also turn on the gluconeogenesis pathway and make glucose from non-carbohydrate precursors (which it then exports into the bloodstream for delivery to tissues). This is an energy-intensive pathway. The major site of gluconeogenesis is the liver, with a small amount also taking place in the kidneys. Little gluconeogenesis occurs in the brain, skeletal muscle, or cardiac muscle. It doesn't make sense to do that! It costs more energy for cells to synthesize glucose than they can obtain by breaking it down through oxidative phosphorylation. This cost can be addressed by utilizing the liver to process it and then releasing it into the bloodstream to fuel activities in the brain, heart, and skeletal muscles.

To do this, glucagon stimulates that lovely signaling pathway that you are all now familiar with (reviewed in Figure 15.4.9)! It activates the G-protein-coupled receptor within the liver, which activates the downstream G-protein. Adenylate Cyclase is activated and produces the second messenger, cAMP. cAMP binds with the CREB protein and activates the transcription of proteins involved in gluconeogenesis. The cAMP also binds with Protein Kinase A and upregulates glycogen phosphorylase activity, resulting in glycogen breakdown. It also downregulates the activity of glycogen synthase, thereby inhibiting glycogenesis. In this section, we will also examine how PKA activation downregulates the activity of the glycolytic pathway.

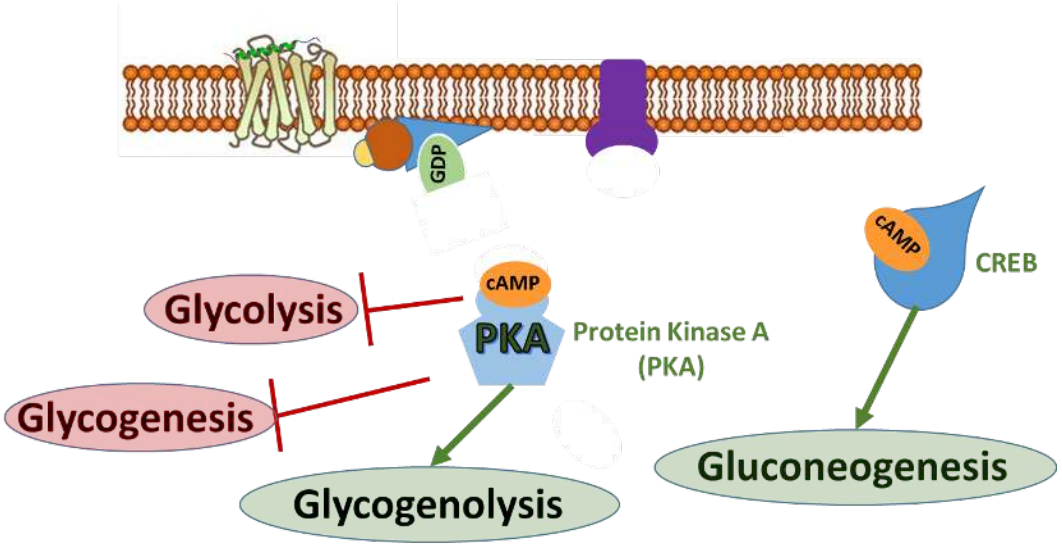


Figure **15.4.9**: Overview of Glucagon Signaling Pathways within the Liver. Image modified from Yan, A., et al (2016) In J Biol Sci 12(12):1544-1554 and Servier Medical Art

Regulation of the glycolytic pathway in response to this signaling occurs through the regulation of the PFK-2/FBPase-2 Enzyme. The activity of this enzyme is controlled through the PKA signaling cascade. This enzyme is responsible for phosphorylating fructose 6-phosphate to form fructose 2,6-bisphosphate. Note that this bisphosphate form of fructose is ***DIFFERENT*** than the bisphosphate form utilized in the glycolytic pathway. The glycolytic pathway requires fructose 1,6-bisphosphate, which is formed from the PFK1 enzyme (or Step 3 of the glycolytic pathway). The PFK-2/FBPase-2 is a separate enzyme not directly involved in the glycolytic pathway. However, we noted previously that fructose 2,6-bisphosphate can be an allosteric activator of the PFK1 enzyme.

The PFK-2/FBPase-2 Enzyme is a dual-purpose enzyme, as shown in Figure **15.4.10**. Half of the protein has kinase activity and can phosphorylate fructose-6-phosphate to fructose-2,6-bisphosphate. The other half of the enzyme contains a phosphatase that can hydrolyze the phosphate group from the 2-position, thereby restoring fructose-6-phosphate. Note that both activities are not functional at the same time! The phosphorylation state determines the activity of the enzyme. When the protein is dephosphorylated, the PFK-2 enzyme is active, leading to the production of fructose-2,6-bisphosphate. This molecule can bind with PFK-1 in the glycolytic pathway and increase its activity. If PKA phosphorylates the protein during glucagon signaling, the FBPase is activated, and the kinase activity is inhibited. This leads to the dephosphorylation of fructose at the 2-position, resulting in the release of fructose-6-phosphate.

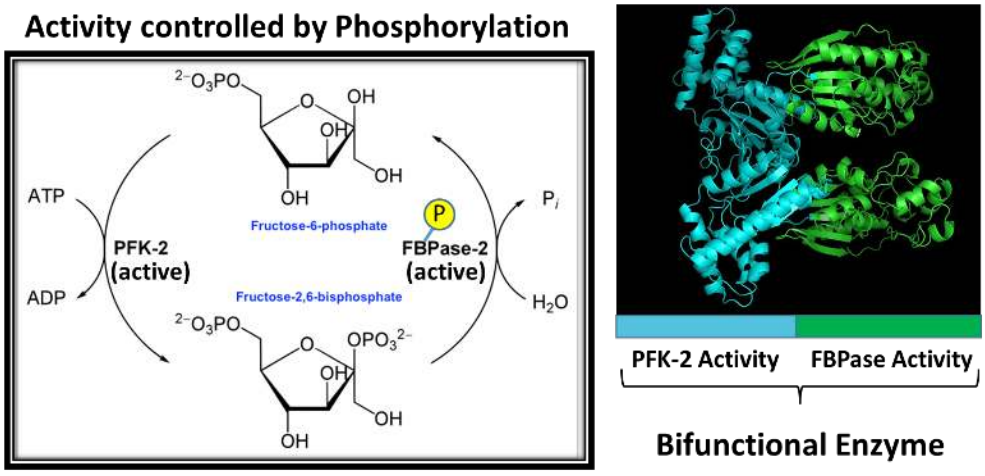


Figure **15.4.10**: Biological Activity of the PFK-2/FBPase-2 Enzyme. The PFK-2/FBPase-2 is a dual functional enzyme capable of phosphorylating the 2'-position of fructose 6-phosphate using the kinase activity. In contrast, the FBPase activity can remove the phosphoryl group from position 2' of fructose 2,6-bisphosphate, yielding fructose 6-phosphate. The PFK-2 component is active when the protein is dephosphorylated, while the FBPase remains inactive. However, the FBPase component becomes active following phosphorylation, and the kinase domain is inhibited. Image modified from Kedrosolan and Hyunsuky

As shown in Figure 15.5.10, the PFK-2/FBPase-2 Enzyme is responsible for phosphorylating fructose 6-phosphate to the fructose 2,6-bisphosphate form. Note again that this bisphosphate form of fructose is ***DIFFERENT*** than the bisphosphate form utilized in the glycolytic pathway. The glycolytic pathway requires fructose-1,6-bisphosphate, which is formed by the PFK1 enzyme (or Step 3 of the glycolytic pathway). If there is a lot of fructose-6-phosphate around (ie, you just drank high fructose corn syrup in your sugary energy drink), it can support both the formation of fructose 1,6-bisphosphate by PFK1 and the production of fructose 2,6-bisphosphate by PFK-2. Fructose 2,6-bisphosphate will bind with PFK1 and increase its activity, converting fructose 6-phosphate into fructose-1,6-bisphosphate, as shown in Figure **15.4.11**.

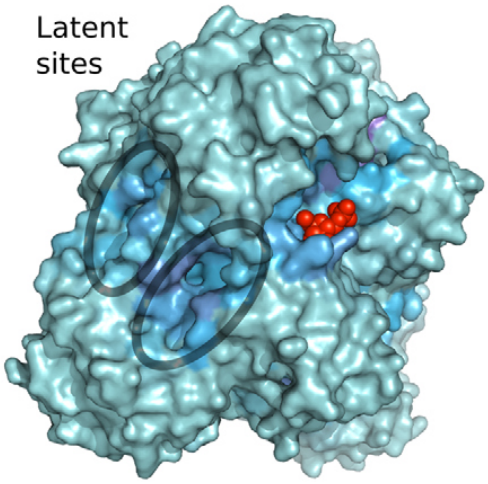


Figure **15.4.11**: Fructose 2,6-bisphosphate is a positive allosteric effector of the PFK1 Enzyme**.** The upper diagram shows a space-filling model of PFK1 with the fructose 2,6-bisphosphate binding sites indicated. Mitternacht, S., and Berezovsky, I.N. (2011), ibid.

However, during glucagon signaling, you must shut down this fast-track upregulation of PFK1 by fructose-2,6-bisphosphate and turn down the glycolytic pathway. To achieve this, Protein Kinase A phosphorylates the PFK-2/FBPase-2 enzyme, thereby altering its activity. The kinase activity is inhibited, and the phosphorylase activity is turned on. Figure **15.4.12** summarizes this pathway control. In the presence of glucagon, PKA phosphorylates the PFK-2/FBPase-2 enzyme, causing its kinase activity to be inhibited and its phosphatase activity to be activated. Dephosphorylation of fructose-2,6-bisphosphate recovers fructose-6-phosphate (F6P). F6P, through the reverse isomerase reaction, can be converted back to glucose-6-phosphate (G6P). G6P will then be transported to the rough endoplasmic reticulum, where it will be dephosphorylated, and free glucose can be released back into the blood.

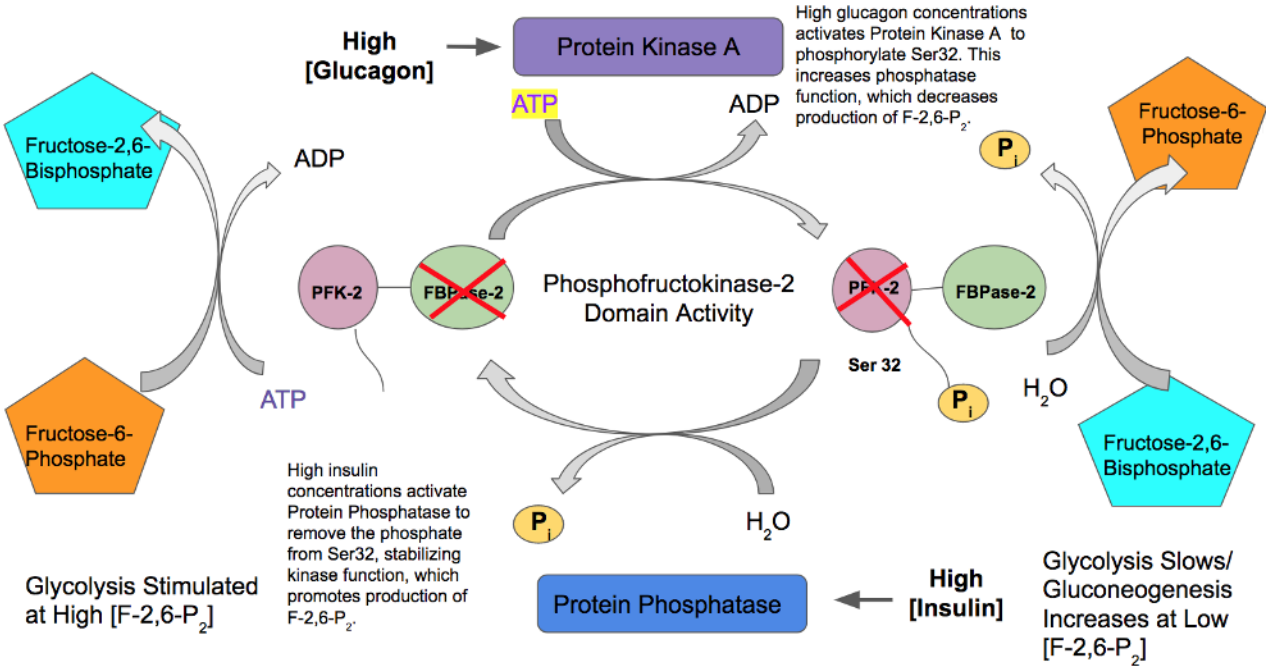


Figure **15.4.12**: Allosteric Regulation of PFK1 in the Liver in Response to Glucagon Signaling. Image from Kedrosolan

The opposite holds for insulin signaling. High insulin concentrations activate protein phosphatase, leading to the dephosphorylation of the PFK-2/FBPase-2 enzyme. In the dephosphorylated state, PFK-2 activity is high, and the FBPase-2 activity is low, stimulating PFK1 and the glycolytic pathway.

15.4.3: PYRUVATE KINASE

Recall that pyruvate kinase mediates the final reaction during glycolysis, producing pyruvate and ATP, as shown in Figure **15.4.13**. Like PFK1, this enzyme is a key regulatory component within the pathway.

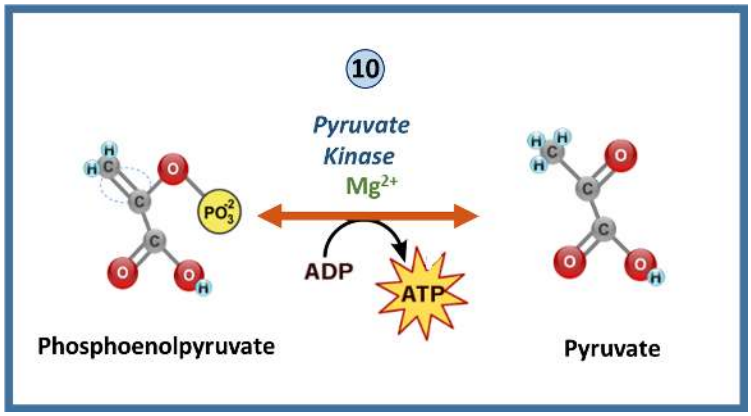


Figure **15.4.13**: Review of the Pyruvate Kinase Reaction. Image modified from YassineMrabet

The pyruvate kinase enzyme is active as a tetramer composed of different isozymes expressed in various tissues. There are three major isozymes of pyruvate kinase: the L form that is predominantly found in the liver, the R form that is predominantly found in erythrocytes, the M1 form in muscle and brain, and the M2 form that is expressed in fetal tissue and at some level in most adult tissues. The L and R forms are splice variants that arise from the same gene locus, and the M1 and M2 forms are also splice variants that arise from the same gene locus.

We will focus on some general regulatory mechanisms common to most pyruvate kinase isozymes, starting with the activator, fructose 1,6-bisphosphate (FBP). Because FBP is an earlier product within the same metabolic cascade, the activation of pyruvate kinase enzymes by FBP is known as ***feedforward stimulation***. All the isozymes, except for the M1 form, are stimulated by the binding of FBP to the enzyme. Similarly, all pyruvate kinase isozymes are inhibited by the product of the reaction, ATP (or a high-energy load), and high levels of alanine. Alanine can be converted to pyruvate in one enzymatic step. Thus, pyruvate serves as a metabolic intermediate in the formation of alanine. High levels of alanine indicate a high energy load within the cell (i.e., the cell is full of building blocks to make new macromolecules and does not require more energy). Thus, high levels of alanine serve as a negative regulator of the pyruvate kinase family of enzymes.

The liver isozyme of pyruvate kinase is also regulated through protein phosphorylation, as shown in Figure **15.4.14**. Like the PFK-2 activity of the PFK-2/FBPase-2 enzyme, the liver isozyme of Pyruvate Kinase is also downregulated during glucagon signaling. Protein kinase A phosphorylates Pyruvate Kinase, inhibiting its activity and preventing the conversion of phosphoenolpyruvate to pyruvate. The dual regulation of the glycolytic pathway during glucagon signaling helps to ensure that glucose resources will be diverted away from cellular use by the liver and released into the bloodstream to restore homeostatic blood glucose levels.

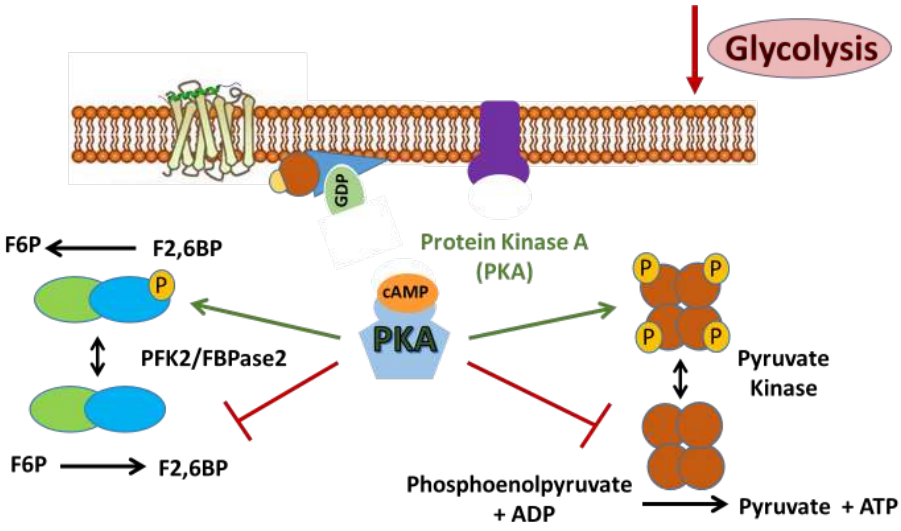


Figure **15.4.14**: Glucagon Signaling in Liver Cells Down Regulates PFK2 Activity and Pyruvate Kinase Activity. Image modified from Yan, A., et al (2016)

15.4.4: FRUCTOSE REGULATORY BYPASS

Other sugars from the diet can also enter the glycolytic pathway, as shown in Figure **15.4.15**. Galactose is converted into glucose-6-phosphate through a four-step process, and mannose can be converted into fructose-6-phosphate. Within most of the body's tissues, fructose can also be converted into fructose-6-phosphate by hexokinase. However, in the liver and kidneys, there is an alternative route that fructose from the diet can take to enter the glycolytic pathway. This pathway is concerning because it bypasses two of the major regulatory steps of the glycolytic pathway, the hexokinase step and the PFK1 step. Within the liver and kidneys, fructose can also be converted into fructose-1-phosphate by the enzyme fructokinase. The other isozyme of aldolase, aldolase B, can cleave fructose-1-phosphate into two three-carbon units: dihydroxyacetone phosphate and glyceraldehyde. Dihydroxyacetone phosphate can be converted to glyceraldehyde 3-phosphate by Triose Isomerase and then continue into the glycolytic cascade. Glyceraldehyde can be phosphorylated to Glyceraldehyde 3-phosphate by Triokinase. This unregulated system can flood the Krebs Cycle with high levels of pyruvate if high levels of fructose enter the cell (i.e., from high fructose corn syrup, sucrose, and other sweeteners common to the Westernized diet). The excess pyruvate can then be shunted into fatty acid biosynthesis for long-term storage as triglycerides. If the pathway is overutilized by consuming too much sucrose and high fructose corn syrup, this can lead to hypertriglyceridemia (or the heightened increase of body fat). With this, we conclude our discussion of glycolysis. In the next section, we will look at the complementary and opposite pathway, gluconeogenesis.

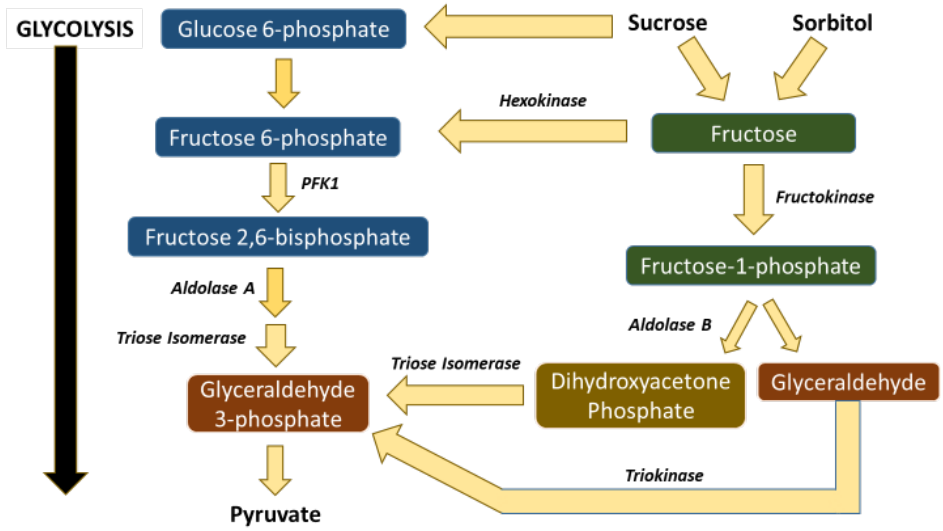


Figure **15.4.15**: Alternate Sugar Sources for Glycolysis

15.4.5: SUMMARY

This chapter explores the intricate regulation of the glycolytic pathway, emphasizing its key control points and how both cellular energy status and hormonal signals coordinate to optimize glucose metabolism. Three major enzymatic steps—mediated by hexokinase, phosphofructokinase-1 (PFK1), and pyruvate kinase—are highlighted as the primary control nodes in glycolysis.

Hexokinase Regulation:
The chapter begins with an overview of hexokinase isozymes, which catalyze the first committed step of glycolysis by phosphorylating glucose to form glucose-6-phosphate (G6P). The four hexokinase isozymes (HKI-IV) exhibit distinct kinetic properties, subcellular localizations, and regulatory behaviors tailored to specific tissue functions. For example, HKI in brain tissue is tightly associated with mitochondria for efficient ATP use, while HKIV (glucokinase) in the liver and pancreas acts as a sensor for blood glucose levels due to its higher Km and lack of product inhibition.

Phosphofructokinase-1 (PFK1) Regulation:
As the first irreversible and committed step of glycolysis, PFK1 converts fructose-6-phosphate to fructose-1,6-bisphosphate. The enzyme functions as an allosteric regulator and exists as a tetramer composed of different subunit combinations that vary among tissues. Its activity is modulated by cellular energy indicators: it is activated by ADP, AMP, and fructose 2,6-bisphosphate (an important regulator in liver cells), while high levels of ATP and citrate serve as inhibitors, thereby aligning glycolytic flux with the cell's energy demands.

Pyruvate Kinase Regulation:
Pyruvate kinase catalyzes the final step of glycolysis, generating pyruvate and ATP. This enzyme is also subject to complex regulation, including feedforward activation by fructose-1,6-bisphosphate and inhibition by ATP and alanine. Its isozymes, which differ between tissues such as liver (L form), erythrocytes (R form), and muscle/brain (M1 and M2 forms), ensure that glycolytic output matches both energy production and biosynthetic requirements. In the liver, pyruvate kinase activity is further downregulated by glucagon-mediated phosphorylation via protein kinase A (PKA).

Hormonal Influence on Glycolysis:
The chapter underscores the role of systemic hormonal signals in modulating glycolysis. Under high serum glucose conditions, insulin promotes glycolysis and glycogen synthesis by enhancing glucose uptake in tissues like liver and muscle. Conversely, during low serum glucose, glucagon triggers a cascade that inhibits glycolysis, promotes gluconeogenesis and glycogenolysis, and ultimately increases blood glucose levels. Epinephrine, primarily affecting skeletal muscle, also activates glycolysis and glycogenolysis to meet immediate energy demands during stress or exercise.

Fructose Regulatory Bypass:
An important additional concept discussed is the fructose regulatory bypass. In the liver and kidneys, dietary fructose can be metabolized via an alternative pathway that bypasses the key regulatory steps catalyzed by hexokinase and PFK1. This unregulated pathway can lead to excessive production of pyruvate and its subsequent shunting into lipogenesis, contributing to metabolic disorders such as hypertriglyceridemia.

Integration and Homeostasis:
Overall, the chapter illustrates how multiple layers of regulation—ranging from tissue-specific enzyme isozymes and allosteric modulation to hormonal signaling—are integrated to finely tune the glycolytic pathway. This integration ensures that glucose metabolism is dynamically adjusted to satisfy both cellular energy requirements and whole-body metabolic homeostasis.

By linking molecular details with systemic regulation, this chapter provides a comprehensive framework for understanding the complexity of glycolysis and its critical role in energy metabolism and disease.

This page titled 15.4: Regulation of Glycolysis is shared under a not declared license and was authored, remixed, and/or curated by Henry Jakubowski and Patricia Flatt.

- **11.2: Diffusion Across a Membrane - Passive and Facilitated Diffusion** by Henry Jakubowski and Patricia Flatt has no license indicated.

15.5: REGULATION OF GLUCONEOGENESIS

LEARNING GOALS (CHATGPT O3-MINI)

1. **Describe the Gluconeogenic Conversion Process:**
   - Explain how pyruvate is converted to phosphoenolpyruvate via an oxaloacetate intermediate, outlining the roles of pyruvate carboxykinase and phosphoenolpyruvate carboxykinase (PEPCK) in this process.
2. **Analyze Allosteric Regulation of Pyruvate Carboxykinase:**
   - Identify the major allosteric effectors (Acetyl-CoA and ADP) that regulate pyruvate carboxykinase activity.
   - Explain how Acetyl-CoA serves as an activator under high-energy conditions and how ADP acts as an inhibitor under low-energy conditions.
3. **Explain Transcriptional and Allosteric Regulation of PEPCK:**
   - Describe the transcriptional regulation of cytoplasmic PEPCK in response to increased cAMP, glucocorticoids, and thyroid hormones, including the role of the CREB transcription factor.
   - Discuss how ADP serves as an allosteric inhibitor of PEPCK, linking its activity to cellular energy status.
4. **Discuss the Dual Regulation of Fructose 1,6-Bisphosphatase:**
   - Explain the competitive inhibition of fructose 1,6-bisphosphatase by fructose 2,6-bisphosphate and its effect on the enzyme's Km.
   - Describe how low-energy indicators (AMP and ADP) further inhibit fructose 1,6-bisphosphatase allosterically, ensuring that gluconeogenesis is downregulated when cellular energy is scarce.
5. **Integrate Hormonal and Energy Signals in Gluconeogenesis Regulation:**
   - Evaluate how systemic hormonal signals (e.g., glucagon during hypoglycemia) and local cellular energy indicators (ATP, ADP, and AMP levels) coordinate to regulate the activity of key gluconeogenic enzymes.
   - Discuss the overall significance of these regulatory mechanisms in maintaining blood glucose homeostasis and metabolic balance.

These learning goals aim to provide students with a comprehensive understanding of the multiple layers of control governing gluconeogenesis, linking enzyme kinetics, allosteric regulation, transcriptional control, and hormonal signaling to the broader context of metabolic homeostasis.

Within the regulation of the gluconeogenic pathway, three of the major enzymatic steps are regulated. The first two are the pyruvate carboxykinase enzyme and the phosphoenolpyruvate carboxykinase (PEPCK). Recall that these two enzymes are required to convert pyruvate back into phosphoenolpyruvate via an oxaloacetate intermediate, as shown in Figure **15.5.1**. The third enzyme regulated in this pathway is fructose 1,6-bisphosphatase, which converts fructose 1,6-bisphosphate into fructose 6-phosphate. We will explore the regulation of these three enzymes in more detail.

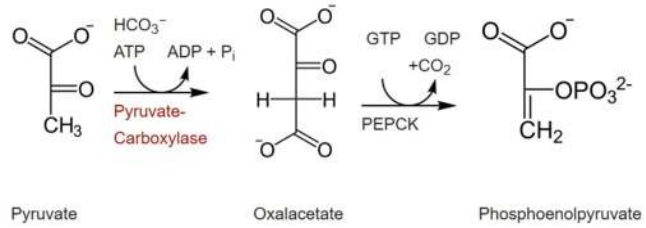


Figure **15.5.1**: Conversion of Pyruvate to Phosphoenolpyruvate during Gluconeogenesis. Image modified from Principles of Biochemistry (2019) Wikibooks

15.5.1: PYRUVATE CARBOXYKINASE

Pyruvatecarboxykinase is one of the primary regulatory points. It is primarily regulated by two allosteric effectors, acetyl-CoA and ADP, as shown in Figure **15.5.2**. When pyruvate enters the Krebs Cycle, it is first converted to acetyl-CoA. If abundant pyruvate is present, an ample supply of acetyl-CoA will also be available, indicating a high energy load for the cell. Acetyl-CoA can bind with pyruvate carboxylase and

act as a protein activator, stimulating the production of oxaloacetate. ADP, on the other hand, is a low-energy indicator and an inhibitor of the enzyme. The next section will illustrate how oxaloacetate enters the cytoplasm.

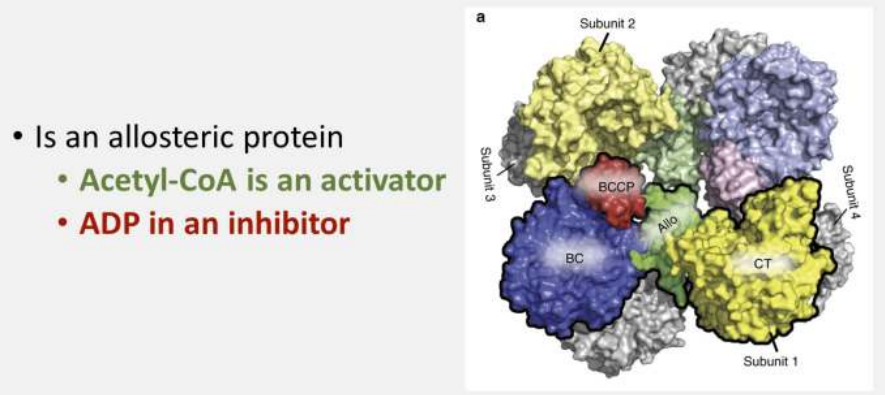


Figure **15.5.2**: Allosteric Regulation of Pyruvate Carboxykinase. Figure modified from Liu, Y., et al (2018) Nat Commun 9:1384

15.5.2: PHOSPHOENOLPYRUVATE CARBOXYKINASE

Cytoplasmic PEPCK is largely regulated at the transcriptional level. Increases in gene expression are seen in response to elevated cAMP levels, glucocorticoids, and thyroid hormone levels, as shown in Figure **15.5.3**. The activated CREB transcription factor plays a role in this response. Alternatively, decreased gene expression is caused by insulin signaling. ADP also acts as an allosteric effector of the protein, causing it to have lower activity. This indicates that when energy is low, the cell cannot afford to use its reserves to remake glucose, so gluconeogenesis is inhibited.

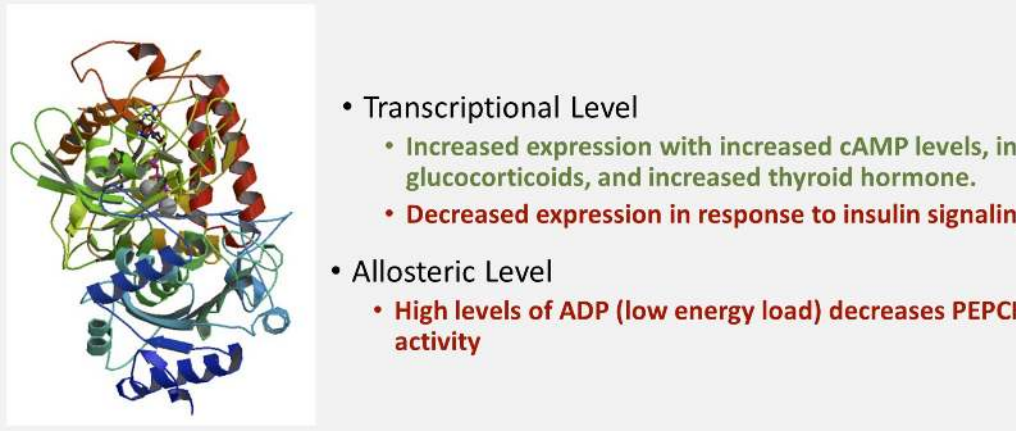


Figure **15.5.3**: Regulation of Phosphoenolpyruvate Carboxykinase at the Transcriptional and Allosteric Levels. Image from ProteinBoxBot

15.5.3: FRUCTOSE 1,6-BISPHOSPHATASE

Fructose 1,6-bisphosphatase is both competitively and allosterically regulated, as shown in Figure **15.5.4**. Fructose 2,6-bisphosphate serves as a competitive inhibitor of the enzyme, reducing the overall activity of the enzyme for fructose 1,6-bisphosphate. Competitive inhibitors bind within the active site and compete with the regular substrate for binding. Thus, they lower the overall Km of the reaction, making the enzyme less effective at lower substrate concentrations. However, the Vmax of the enzyme remains unaffected during the process.

In addition to competitive inhibition, low-energy loads (AMP and ADP) also inhibit the enzyme. ADP and AMP bind allosterically to the enzyme, inhibiting its activity.

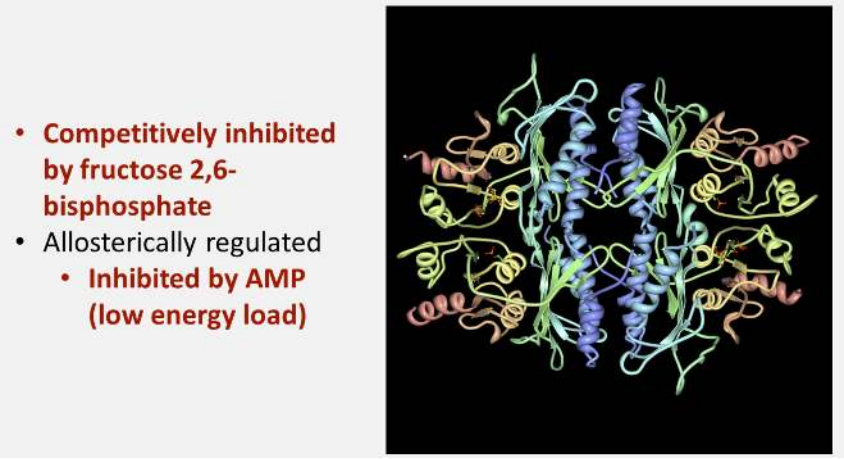


Figure 15.5.14: Regulation of Fructose 1,6-Bisphosphatase by Competitive Inhibition and Allosteric Effectors. Image from Jslipscomb

15.5.4: SUMMARY

This chapter delves into the regulatory mechanisms governing key control points of the gluconeogenic pathway, highlighting how enzymatic activity is finely tuned by both hormonal signals and cellular energy status. Three major enzymes are discussed:

- **Pyruvate Carboxykinase (PCK):**
  This enzyme catalyzes the conversion of pyruvate to oxaloacetate—a crucial step in converting pyruvate back to phosphoenolpyruvate (PEP). Its activity is modulated allosterically: Acetyl-CoA acts as an activator, signaling a high-energy state, while ADP serves as an inhibitor under low-energy conditions. This regulation ensures that the pathway is activated only when necessary.
- **Phosphoenolpyruvate Carboxykinase (PEPCK):**
  Predominantly regulated at the transcriptional level, PEPCK expression is increased in response to elevated cAMP, glucocorticoids, and thyroid hormones, with the CREB transcription factor playing a key role. Additionally, ADP acts as an allosteric inhibitor of PEPCK, linking its activity to the cell's energy balance and ensuring that glucose synthesis is downregulated when energy is scarce.
- **Fructose 1,6-Bisphosphatase (FBPase):**
  FBPase catalyzes the dephosphorylation of fructose 1,6-bisphosphate to fructose 6-phosphate, effectively opposing the action of phosphofructokinase-1 in glycolysis. Its activity is regulated through two mechanisms: competitive inhibition by fructose 2,6-bisphosphate, which reduces substrate binding efficiency, and allosteric inhibition by AMP and ADP, reflecting low cellular energy.

Collectively, these regulatory strategies integrate hormonal signals—such as those mediated by glucagon during hypoglycemia—with intracellular energy cues to modulate gluconeogenesis. This dynamic control ensures that glucose production is enhanced during energy deficits and conserved when energy is abundant, thereby maintaining overall metabolic and blood glucose homeostasis.

By linking enzyme regulation to both systemic and cellular energy demands, this chapter provides a comprehensive framework for understanding how gluconeogenesis is precisely controlled to meet the metabolic needs of the organism.

This page titled 15.5: Regulation of Gluconeogenesis is shared under a not declared license and was authored, remixed, and/or curated by Henry Jakubowski and Patricia Flatt.

- **11.2: Diffusion Across a Membrane - Passive and Facilitated Diffusion** by Henry Jakubowski and Patricia Flatt has no license indicated.

CHAPTER OVERVIEW

16: THE CITRIC ACID CYCLE

Return to Fundamentals of Biochemistry Search Fundamentals of Biochemistry

The citric acid cycle – also known as the TCA cycle or the Krebs cycle – is a series of chemical reactions to release stored energy through the oxidation of acetyl-CoA derived from carbohydrates, fats, and proteins.

16.1: Production of Acetyl-CoA (Activated Acetate)
16.2: Reactions of the Citric Acid Cycle
16.3: Regulation of the Citric Acid Cycle
16.4: Variants of the Citric Acid Cycle

This page titled 16: The Citric Acid Cycle is shared under a not declared license and was authored, remixed, and/or curated by Henry Jakubowski and Patricia Flatt.

16.1: PRODUCTION OF ACETYL-COA (ACTIVATED ACETATE)

LEARNING GOALS (CHATGPT O3-MINI)

1. **Understand the Role of PDC in Metabolism:**
   - Explain how the pyruvate dehydrogenase complex catalyzes the oxidative decarboxylation of pyruvate to form acetyl-CoA, linking glycolysis to the Krebs cycle and overall aerobic respiration.
2. **Describe the Structural Organization of PDC:**
   - Identify the three major enzymatic components of the PDC (E1, E2, and E3) and describe their subunit composition and overall architecture (e.g., E1 as an $\alpha_2\beta_2$ heterodimer, E2 forming a large oligomeric core, and E3 as a smaller, tightly-bound enzyme).
3. **Detail the Reaction Mechanism of the E1 Component:**
   - Explain the mechanism of oxidative decarboxylation catalyzed by pyruvate dehydrogenase (E1), including the formation of the TPP-ylide intermediate, nucleophilic attack on pyruvate's carbonyl carbon, and the role of allosteric stabilization in enabling decarboxylation.
4. **Examine the Role of Cofactors in PDC Catalysis:**
   - List and describe the five essential cofactors involved in PDC activity (TPP, lipoic acid/lipoamide, Coenzyme A, FAD, and NAD^+), including their chemical structures, sources (e.g., thiamine, riboflavin, niacin, and pantothenic acid), and how they contribute to the reaction mechanism.
5. **Compare Thioester and Ester Chemistry:**
   - Analyze the differences in resonance stabilization and bond lengths between carbon-oxygen and carbon-sulfur bonds, and explain why thioesters (like acetyl-CoA) are considered "high-energy" intermediates in metabolism.
6. **Detail the E2 Catalyzed Transacetylation Reaction:**
   - Describe how the dihydrolipoyl acetyltransferase (E2) transfers the acetyl group from the TPP intermediate to Coenzyme A, forming acetyl-CoA, and discuss the role of the lipoamide "swinging arm" in facilitating substrate channeling within the complex.
7. **Understand the E3 Reaction and Enzyme Regeneration:**
   - Explain the function of dihydrolipoyl dehydrogenase (E3) in reoxidizing the reduced lipoamide via FAD and NAD^+, thereby regenerating the oxidized cofactor necessary for continuous PDC activity.
8. **Utilize Structural Models to Visualize PDC Components:**
   - Engage with interactive iCn3D models (e.g., PDB IDs 6CFO, 1ZMD, 6CT0) to identify key active site residues, cofactor binding sites, and structural domains in E1, E2, and E3, enhancing understanding of how structure relates to function.
9. **Integrate Multistep Reaction Mechanisms:**
   - Synthesize the sequential reactions from pyruvate decarboxylation, acetyl group transfer, and cofactor regeneration to explain the overall net reaction catalyzed by the pyruvate dehydrogenase complex.
10. **Discuss the Biological Significance of PDC Regulation:**
    - Evaluate why nature has evolved such a large and complex enzyme system for the conversion of pyruvate to acetyl-CoA, considering factors such as substrate channeling, regulation by cofactors, and the integration of multiple catalytic activities to ensure efficient energy production.

These learning goals aim to guide students through both the mechanistic intricacies and the structural organization of the pyruvate dehydrogenase complex, linking detailed biochemical principles with broader metabolic contexts and energy homeostasis.

16.1.1: INTRODUCTION

Let's briefly review the metabolic processes for energy extraction from glucose oxidation (i.e., glycolysis). Glycolysis is a universal pathway to extract energy from glucose anaerobically. In this linear pathway, 2-3 carbon molecules of pyruvate are formed as glucose is cleaved and converted to two molecules of glyceraldehyde-3-phosphate, formed through an oxidation reaction using the oxidizing agent NAD^+. As glycolysis continues, NADH builds up. Using lactate dehydrogenase, pyruvate, the end product of glycolysis, can be converted to lactate, regenerating NAD^+ so the pathway can continue. The reactions are illustrated in Figure **16.1.1**.

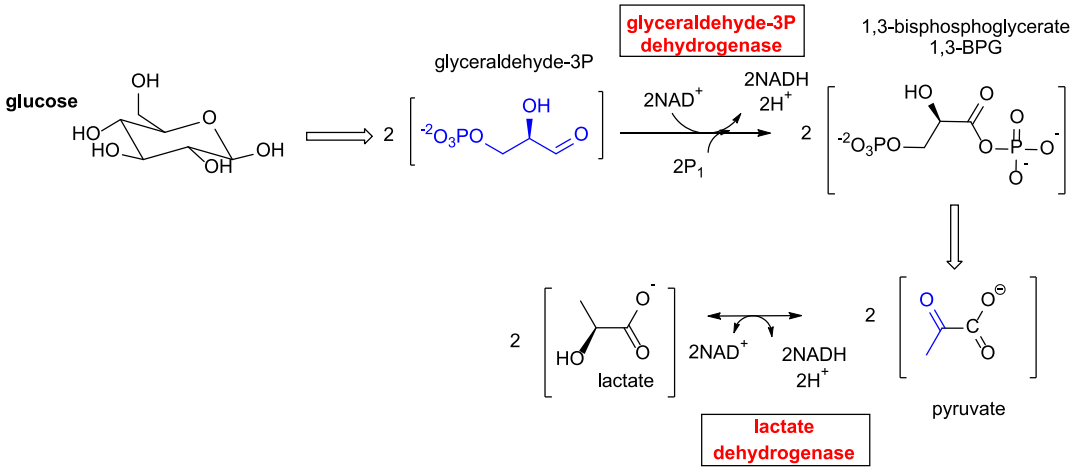


Figure **16.1.1**: Anaerobic production of pyruvate and lactate

A careful glance at the structure of the 3-carbon pyruvate molecule reveals that much more energy could be extracted from it, presumably through oxidative decarboxylation reactions, which convert the carbons into 3 CO_2 molecules. A problem arises immediately when examining pyruvate. It is an α-ketoacid, and there is no easy route to decarboxylate it as an electron "sink" is not available to receive the electrons and stabilize the transition state and intermediate in the reaction. In contrast, the decarboxylation of β-keto acids has a built-in electron "sink", an electronegative carbonyl carbon, to receive the electrons. This is illustrated in Figure **16.1.2**.

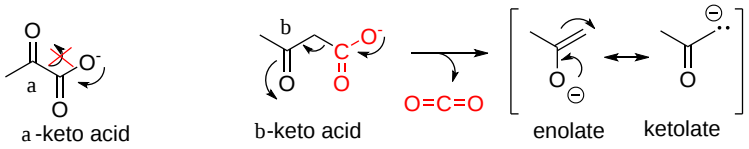


Figure **16.1.2**: Comparison of the decarboxylation of α and β keto acids

To begin the complete oxidation of the remnants of glucose, pyruvate enters the mitochondria and starts the process of oxidative decarboxylation by interacting with the pyruvate dehydrogenase complex (PHC). This catalyzes a complex reaction in which an electron "sink" beta is attached to the carboxylate, which is subsequently released as CO_2. The end products of the PHC oxidative decarboxylation reaction are the two-carbon acetyl-CoAs, NADH, and CO_2. The acetyl-CoA then enters a cyclic, non-linear pathway called the citric acid cycle, tricarboxylic acid (TCA) cycle, or Krebs cycle, named after Hans Krebs, who discovered it. We'll talk about that in section 16.2.

A glance reveals that we have taken glucose a small fraction towards completely oxidizing every carbon into CO_2 and H_2O. Complete oxidation happens under aerobic conditions in the Krebs cycle. Pyruvate formed in glycolysis enters the mitochondrial matrix, where it gets oxidatively decarboxylated while reacting with a small thiol, Coenzyme A (abbreviated either as CoA or CoASH) to form a 2C "activated acetate" acetyl group connected through a thioester link to CoASH, forming acetyl-CoA. Coenzyme A is often abbreviated as CoASH to emphasize that it has a free nucleophile thiol (-SH) group.

The third carbon from pyruvate is released as CO_2. The reaction is catalyzed by the enzyme **pyruvate dehydrogenase complex (PDC)**.

16.1.1.1: PYRUVATE DEHYDROGENASE MECHANISM

This enzyme complex is enormous. The *E. Coli* complex has a molecular weight of almost 4 million with at least 16 chains of three different enzymes catalyzing part of the reaction. The components are pyruvate dehydrogenase (E1), dihydrolipoamide dehydrogenase (E2), and dihydrolipoamide dehydrogenase (E3). The molecular weight of the bovine complex is almost 8 million, and it has 22 E_1, 60 E_2, and 6 E_3 subunits. Nature often uses the same solution for identical problems. For example, many proteases have an active site nucleophilic serine, which works in conjunction with histidine and aspartate to cleave peptide bonds. There are three α-ketoacid dehydrogenase complexes in many organisms. Each has a common E3 but specific E1 and E2 enzymes. Figure **16.1.3** shows an image of the structure so you can get an overview before we dive into the activity of each of the substrates.

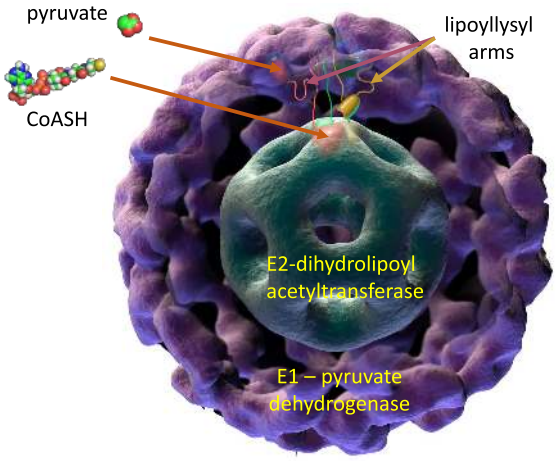


Figure **16.1.3**: View of pyruvate dehydrogenase. https://electron.med.ubc.ca/2018/07/...dehydrogenase/

The E3 subunit is not readily seen in the image above. Why has nature produced such a monstrous enzyme complex to catalyze the oxidative decarboxylation of a small three-carbon molecule? We will explore that at the end of this section.

The complex also employs five substrates/cofactors derived from vitamins collectively.

- Thiamine in the form of thiamine pyrophosphate (TPP), which is covalently attached to E1
- lipoic acid, in the form of lipoamide, which is covalently attached to a lysine side chain in E2
- riboflavin in the form of flavin adenine dinucleotide (FAD/$FADH_2$), which is bound very tightly (and not released) to E3
- pantothenic acid, incorporated into the structure of CoASH/Acetyl-CoA, a substrate/product pair for the reaction
- niacin, nicotinic acid, in the form of NAD^+/NADH, a substrate/product pair for the reaction

The structures for the five are shown in Figure **16.1.4**, along with some additional descriptions that summarize some of the chemistry of these molecules.

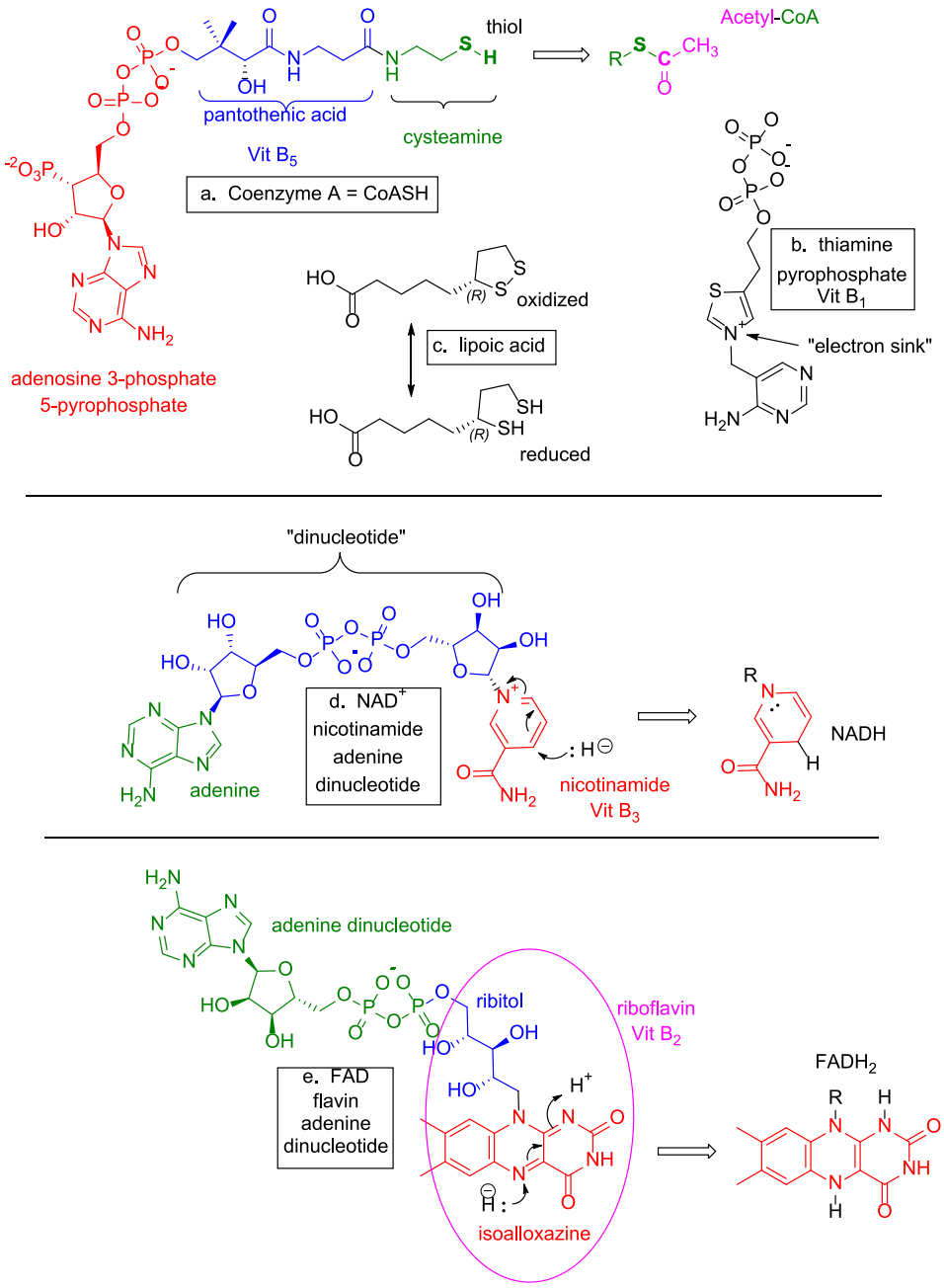


Figure **16.1.4**: Structure of the cofactors in pyruvate dehydrogenase

Figure **16.1.5** shows a schematic of the overall reaction.

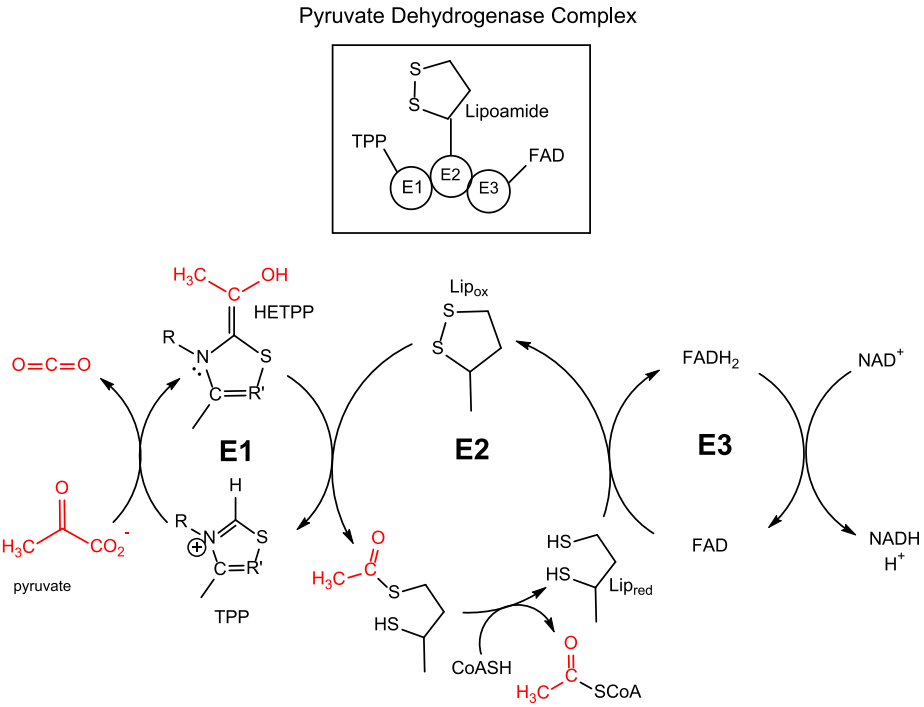


Figure **16.1.5**: Overall reactions catalyzed by pyruvate dehydrogenase

The net reaction is

$$\mathbf{pyruvate + CoASH + NAD^+ \longrightarrow Acetyl\text{—}CoA + CO_2 + NADH + H^+}$$

16.1.2: PART 1: OXIDATIVE DECARBOXYLATION - PYRUVATE DEHYDROGENASE (E1P)

So let it begin. We need to eliminate one carbon as CO_2 and transfer the other two carbons of pyruvate to CoASH to form acetyl-CoA, the thioester of CoASH. Thioesters are "high energy" with respect to their hydrolysis products, as the thioester is destabilized compared to a normal carboxylic acid ester. (**Remember, there is no such thing as a "high energy" bond.**) Since the sulfur atom is larger than the O in the C-S and C-O bond in their respective esters, the thioester as a reactant can not be stabilized well, as the C-S single bond length is longer, as shown in Table **16.1.1** below.

bond	length (Angstroms)
C-O	1.43
C=O	1.21
C-S	1.82
C=S	1.56

Table **16.1.1**: Bond lengths of carbon-oxygen and carbon-sulfur single and double bonds

This minimizes resonance stabilization compared to the carboxylic acid ester, as shown in the figure below. The hydrolysis products of both a carboxylic and a thiol ester are of comparable energy. Hence, only the thioester is relatively destabilized compared to its hydrolysis product, with the $\Delta G^0_{\text{ hydrolysis}}$ = -7.5 kcal/mol (-31 kJ/mol), the same as for the hydrolysis of a phosphoanhydride bond of ATP. Additionally, a resonance structure shows a positive charge on the carbonyl carbon and a negative charge on the oxygen, making the carbonyl carbon more electrophilic. Another, more sophisticated reason for the relative destabilization of the thiol ester is that the overlap between the carbonyl carbon p orbital and the larger sulfur p orbital is less, hindering the delocalization of electrons needed to stabilize the thiol ester.

Figure **16.1.6** illustrates these points.

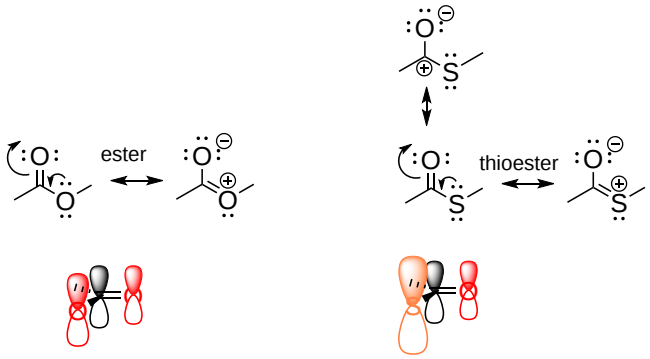


Figure **16.1.6**: Comparison of resonance stabilization of carboxylic esters and thioesters

Now, we can explore the mechanism of CO_2 release and acetyl-CoA production by E_1. The carbon atom directly between the N and S in the thiamine ring has a reduced pKa, allowing it to be deprotonated and form a carbanion. The negative charge can't be stabilized by resonance but is adjacent to the positively charged nitrogen, which can. This zwitterion is called a **ylide**, a net-neutral species with a positive charge (usually on a nitrogen, phosphorus, or sulfur) and a negative charge (usually on a carbon) on adjacent atoms.

The carbanion on the ylide attacks the electrophilic C=O of pyruvate, forming a TPP intermediate with an excellent electron sink (N^+) beta to the carboxyl carbonyl C. This is the essence of the entire reaction, as this enables the decarboxylation event. The remaining reactions catalyzed by E2 and E3 enable the release of the other two carbon atoms of pyruvate as acetyl-CoA (E2) and the return of the enzyme to its original state (E2 and E3).

Figure **16.1.7** shows the reaction mechanism of E1.

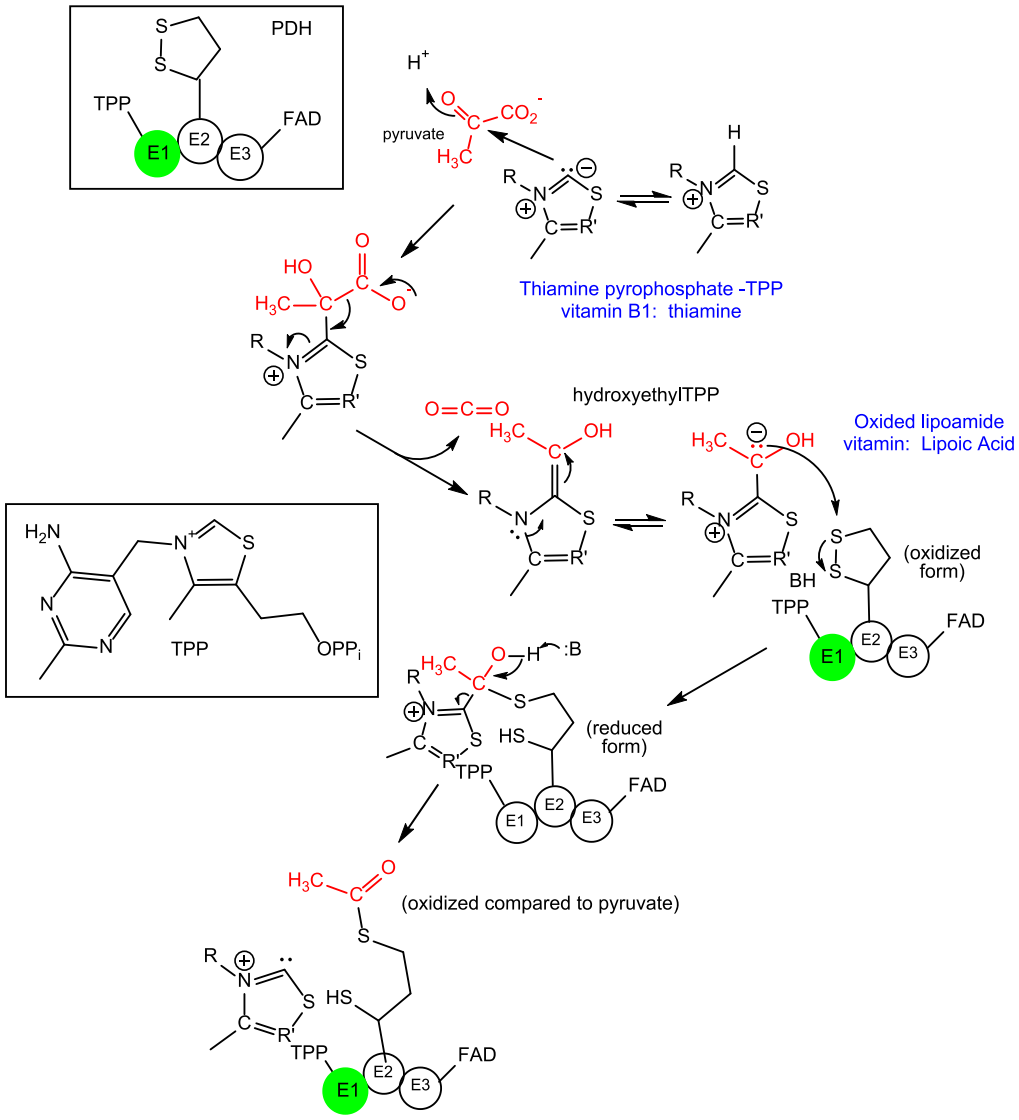
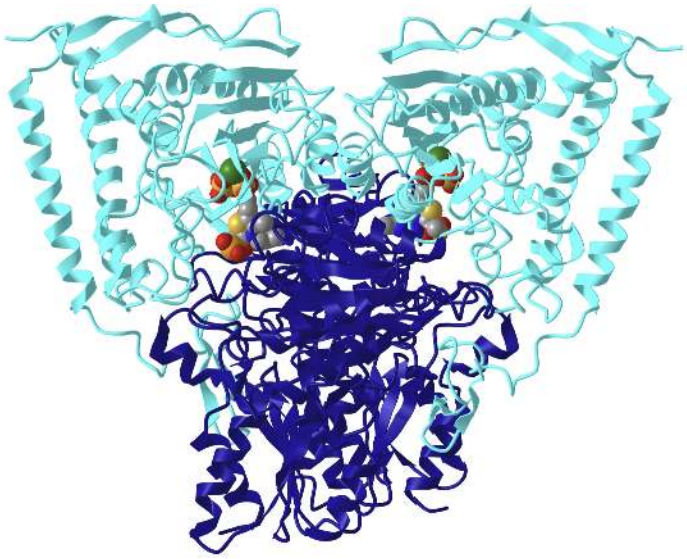


Figure **16.1.7**: Reaction mechanism of E1 of pyruvate dehydrogenase

Note that the carbonyl C in pyruvate has two single bonds to two other carbon atoms, while in the final covalently attached form, it has one bond to carbon and one to sulfur. Sulfur is under oxygen in the periodic table. By analogy, replacing one C-C bond with a C-S bond is an oxidation reaction, which requires an oxidizing agent. The covalently attached ring of the lipoamide with an S-S bond similar to that of a disulfide bond, an oxidized form of sulfur, is the oxidizing agent. On the formation of acetyl-lipoamide, the S-S bond is cleaved, and a thioester is formed. Other sulfur is a free reduced thiol.

There are 22 E1 subunits in the bovine PDC. Here is an iCn3D model of one human pyruvate dehydrogenase E1 component complex with TPnP (TDP acetyl phosphonate, a TPP analog, covalently attached (PDB ID: 6CFO). One E1 subunit is an $\alpha_2\beta_2$ heterodimer. The two alpha chains are cyan, while the beta chains are dark blue. Orient the model to view along the C2 rotational symmetry axes shown.

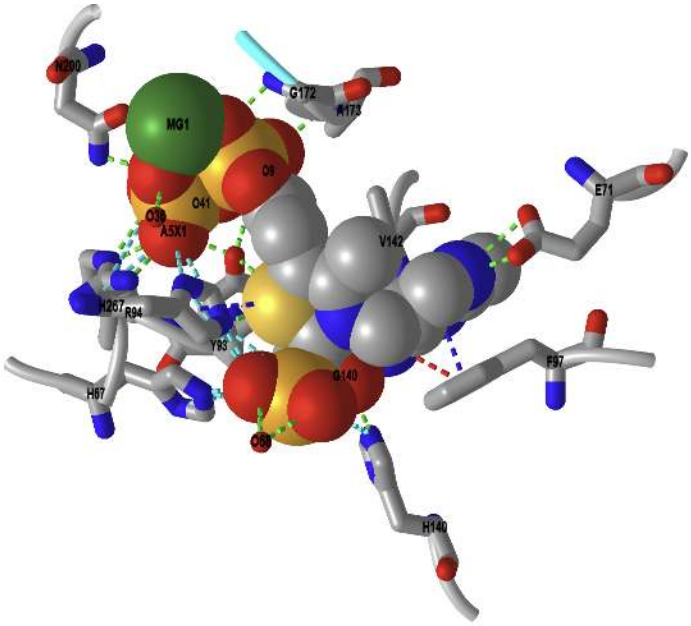
Figure **16.1.8** shows an interactive iCn3D model of the human pyruvate dehydrogenase E1 covalently bound to TDP acetyl phosphonate (TpnP), a TPP analog (6CFO)



NCBI iCn3D Figure **16.1.8**: Human pyruvate dehydrogenase E1 covalently bound to TDP acetyl phosphonate (TpnP), a TPP analog (6CFO). (Copyright; author via source). Click the image for a popup or use this external link: https://structure.ncbi.nlm.nih.gov/i...7FJ2GE47tvS6g7

A heterotetramer consisting of two α (cyan) and two β chains (dark blue) is shown.

Figure **16.1.9** shows an interactive iCn3D model of the TPP analog covalently bound to E1 of pyruvate dehydrogenase (6CFO)



NCBI iCn3D Figure **16.1.9**: TPP analog covalently bound to E1 of pyruvate dehydrogenase (6CFO) . (Copyright; author via source). Click the image for a popup or use this external link: https://structure.ncbi.nlm.nih.gov/i...SNf5sC7SqmQkc8

The dotted lines show the interactions between the TPP analog, color-coded as shown in the legend below.

Hydrogen Bonds		3.8 A	Salt bridge/ion-ion		6 A	Contacts/interactions	4 A
Halogen Bonds		3.8 A	π-Cation		6 A	π-stacking	5.5 A

16.1.2.1:

16.1.3: PARTS 2 AND 3: ACETYL-COA (E2) FORMATION AND REGENERATION OF THE ACTIVE COMPLEX.

The next part of the reaction produces acetyl-CoA (E2). After that, the enzyme is "dead" as it no longer has an oxidized form of lipoamide to serve as an oxidizing agent (which gets reduced) in another round of catalysis. To regenerate enzyme activity, the reduced lipoamide, after the release of the attached acetyl group, must be reoxidized by another oxidizing agent. That oxidizing agent is FAD, which is covalently attached to E3 and is converted to $FADH_2$. It must be reoxidized back to FAD to restore activity to the enzyme complex. The final oxidizing agent used is NAD^+, which the enzyme releases as a product. So it's a bit complicated. Three oxidizing agents are used in the PDH. Two are covalently attached to the enzyme (oxidized lipoamide on E2 and oxidized FAD on E3).

Figure **16.1.10** shows the transacetylation reaction and formation of reduced lipoamide

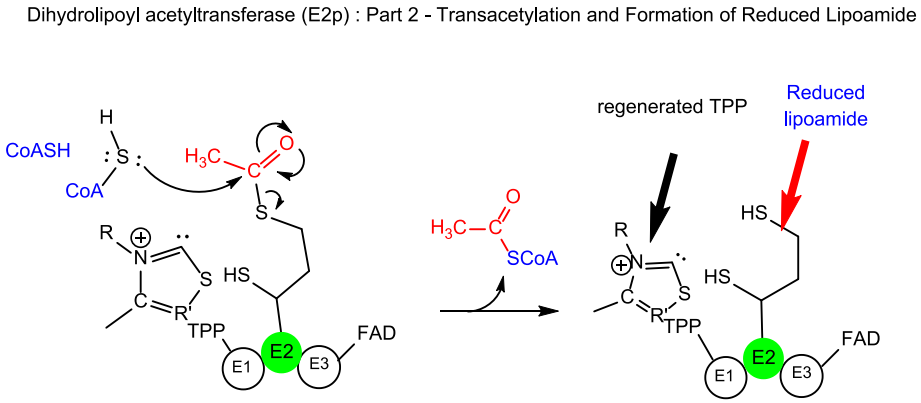


Figure **16.1.10**: Transacetylation reaction and formation of reduced lipoamide by pyruvate dehydrogenase E2

The reaction of E3 follows to restore the fully catalytic enzyme, as shown in Figure **16.1.11**.

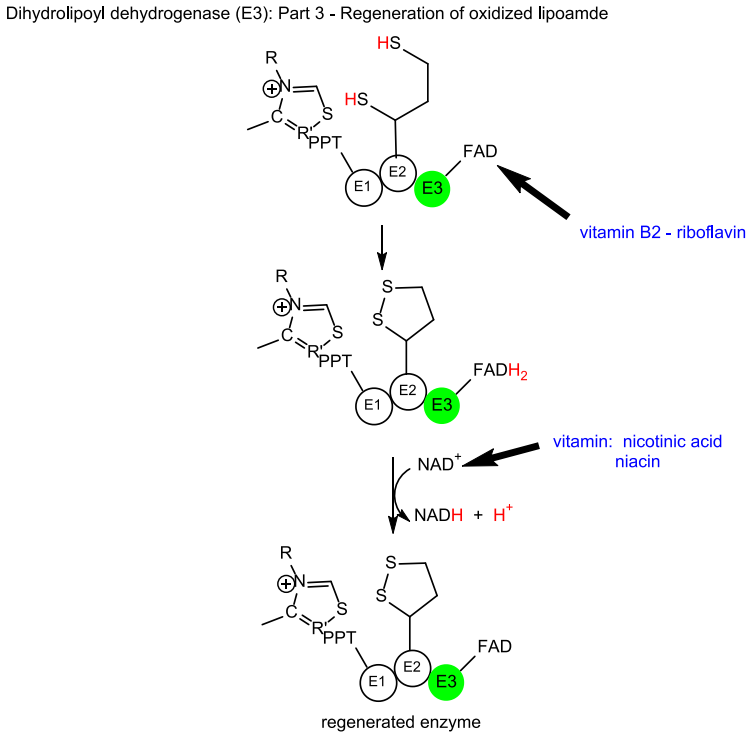


Figure **16.1.11**: Regeneration of oxidized lipoamide by pyruvate dehydrogenase E3.

Let's look in greater detail at the structures of both E2 and E3.

16.1.4: E2: DIHYDROLIPOYL ACETYLTRANSFERASE -

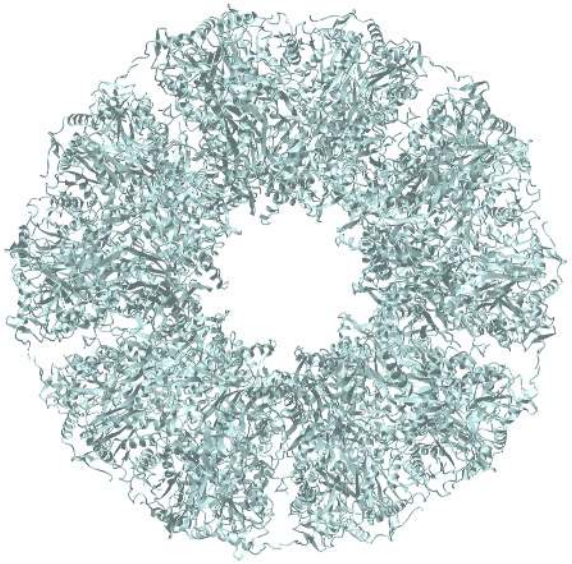
In the mammalian complex, 60 E2 subunits arrange into a pentagonal dodecahedron. Most gram-negative bacteria's E2 subunits arrange into a cube of 24 monomers. Figure **16.1.12** shows a simple view of a pentagonal dodecahedron with 12 equivalent faces.



Figure 16.1.12: Pentagonal dodecahedron. 1. Rotating dodecahedron: https://commons.wikimedia.org/wiki/F...decahedron.gif. User Cyp on en.Wikipedia, CC BY-SA 3.0 <http://creativecommons.org/licenses/by-sa/3.0/>, via Wikimedia Commons

First, let's consider a single E2 monomer. It has a longer disulfide redox domain followed by a smaller dimerization domain, which allows the assembly of multiple subunits into the dodecahedron. In greater detail, the monomer consists of two lipoyl domains, a small domain that facilitates binding to E1, and a C-terminal catalytic domain.

Figure **16.1.12** shows an interactive iCn3D model of E2 inner core 60-mer of human pyruvate dehydrogenase (pdb 6CT0). Symmetry axes are not shown.



NCBI iCn3D Figure **16.1.12**: E2 inner core 60-mer of human pyruvate dehydrogenase (pdb 6CT0). (Copyright; author via source). Click the image for a popup or use this external: https://structure.ncbi.nlm.nih.gov/i...zs6pwfKNuJ2VS6

Each of the 60 subunits is shown in light cyan. To see the C symmetry axes:

- select the menu ☰
- Choose/Check in order: **Analysis, Symmetry, From PDB, 1(global), apply**
- When you see just a single monomeric chain, choose **Cl**ear

The symmetry axes will then appear.

16.1.5: E3: DIHYDROLIPOYL DEHYDROGENASE

The sole function of this subunit is the reoxidation of the now-reduced lipoamide with the free sulfhydryl to the cyclic disulfide form so the enzyme can engage in further catalysis. FAD covalently bound to the E3 subunit is the oxidizing agent. This is our first encounter with FAD. Similar to NAD $^+$, this dinucleotide gains a hydride ($:H^-$) but also, in contrast to NAD^+, a proton to form $FADH_2$.

Another way that the $FAD/FADH_2$ differs from NAD^+/NADH is that the $FAD/FADH_2$ or their mononucleotide analog ($FMN/FMNH_2$) pairs are either covalently attached (in about 10% of flavoproteins) or bound with such a low K_D (often in the nanomolar range) that they don't dissociate from the enzyme during catalysis. Hence, after oxidizing a bound substrate, the reduced $FADH_2$ must be reoxidized by another oxidizing agent, often NAD^+, which can diffuse into the active site to do its job and then dissociate from the complex in the form of NADH, leaving the enzyme competent for another round of catalysis. (DOI: 10.1002/chem.201704622)

Figure **16.1.13** shows an interactive iCn3D model of E3 bound to both FAD (noncovalently) and NADH (NAI) (1ZMD) in the B chain of E3. Symmetry axes are not shown.

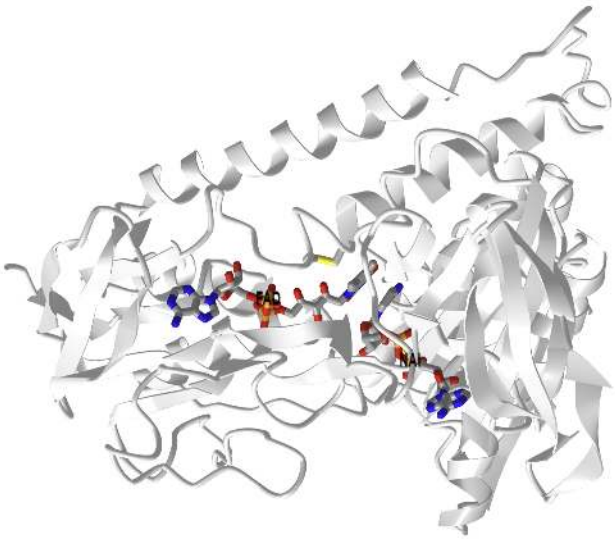


Figure 16.1.13: E3 bound to both FAD (noncovalently) and NADH (NAI) (1ZMD). (Copyright; author via source). Click the image for a popup or use this external: https://structure.ncbi.nlm.nih.gov/i...LAMqAS3Tx9SPE8.

Figure 16.1.14 shows an interactive iCn3D model highlighting the noncovalent interactions stabilizing bound FAD and NADH (NAI) in the E3 subunit of pyruvate dehydrogenase (1ZMD).

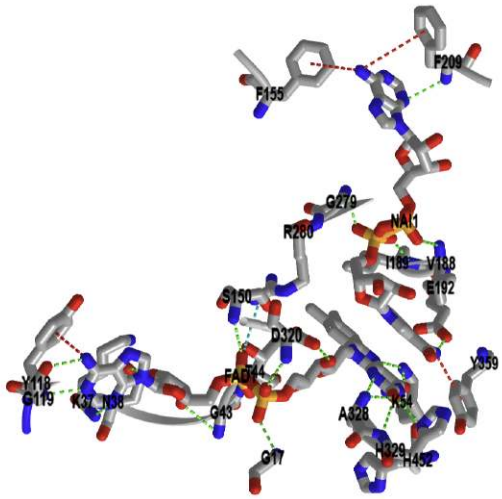


Figure 16.1.14: Noncovalent interactions stabilizing bound FAD and NADH (NAI) in the E3 subunit of pyruvate dehydrogenase (1ZMD). (Copyright; author via source). Click the image for a popup or use this external:https://structure.ncbi.nlm.nih.gov/i...gUED1ZrJVjKcD8

Let's put it all together! Figure 16.1.15 shows a video of the pyruvate dehydrogenase complex from the HHMI.



Figure 16.1.15: Video of the pyruvate dehydrogenase complex

16.1.6: SUMMARY

This chapter provides an in-depth look at how cells extract energy from glucose beyond glycolysis by focusing on the pyruvate dehydrogenase complex (PDC), a critical enzyme system that links glycolysis to the citric acid cycle. Key topics include:

- **From Glycolysis to Acetyl-CoA:**
  Glycolysis converts glucose into pyruvate, a three-carbon molecule. Although glycolysis is efficient for anaerobic energy extraction, pyruvate can be further oxidized under aerobic conditions. The chapter explains that the direct oxidative decarboxylation of pyruvate is challenging due to its α-ketoacid structure lacking a built-in electron sink. PDC overcomes this limitation by using a series of cofactors to facilitate decarboxylation and the formation of acetyl-CoA.
- **Structural Organization of the Pyruvate Dehydrogenase Complex:**
  PDC is a massive multienzyme complex composed of three key components:
  - **E1 (Pyruvate Dehydrogenase):** Functions as an $\alpha_2\beta_2$ heterodimer that uses thiamine pyrophosphate (TPP) to form a reactive ylide intermediate, enabling the decarboxylation of pyruvate.
  - **E2 (Dihydrolipoyl Acetyltransferase):** Transfers the acetyl group from the TPP intermediate to Coenzyme A (CoA) via a "swinging arm" mechanism using lipoamide as a carrier.
  - **E3 (Dihydrolipoyl Dehydrogenase):** Reoxidizes the reduced lipoamide using FAD and NAD^+, regenerating the oxidized form necessary for continued catalysis.
- **Cofactor Utilization and Chemical Basis:**
  The complex requires five key cofactors, each derived from essential vitamins:
  - **Thiamine pyrophosphate (TPP)** – from vitamin B_1
  - **Lipoic acid (as lipoamide)** – critical for substrate channeling
  - **Coenzyme A (CoA)** – derived from pantothenic acid
  - **Flavin adenine dinucleotide (FAD)** – from riboflavin
  - **Nicotinamide adenine dinucleotide (NAD^+)** – from niacin
    These cofactors orchestrate a sequence of redox reactions that not only decarboxylate pyruvate but also generate high-energy thioester bonds in acetyl-CoA, an intermediate vital for entry into the citric acid cycle.
- **Mechanistic Insights:**
  Detailed discussion is provided on the reaction mechanism of E1, emphasizing the formation of a TPP-bound ylide that initiates nucleophilic attack on pyruvate. The subsequent steps involve transacetylation (mediated by E2) and the reoxidation of lipoamide (mediated by E3), underscoring how electron transfer and decarboxylation are tightly coupled within the complex. The chapter also highlights the chemical rationale behind the "high-energy" nature of thioester bonds in acetyl-CoA, drawing comparisons with oxygen-based esters.
- **Structural Visualization:**
  The chapter incorporates interactive structural models (iCn3D) of PDC components, allowing students to explore the spatial arrangement of active sites, cofactor binding domains, and subunit organization. These models help illustrate how the large, multi-subunit architecture of PDC facilitates efficient substrate channeling and coordinated catalysis.

- **Biological Significance:**
  Finally, the chapter discusses why such a complex enzyme system is necessary for cellular energy metabolism. The PDC not only ensures the efficient conversion of pyruvate to acetyl-CoA, but its regulation through multiple cofactors and subunit interactions also allows fine control over metabolic flux into the citric acid cycle, ultimately influencing ATP production and overall energy homeostasis.

In summary, this chapter bridges detailed enzymatic mechanisms with broader metabolic integration, offering students a comprehensive understanding of how the pyruvate dehydrogenase complex serves as a critical nexus between anaerobic glycolysis and aerobic respiration.

This page titled 16.1: Production of Acetyl-CoA (Activated Acetate) is shared under a not declared license and was authored, remixed, and/or curated by Henry Jakubowski and Patricia Flatt.

- **Current page** by Henry Jakubowski and Patricia Flatt has no license indicated.
- **11.2: Diffusion Across a Membrane - Passive and Facilitated Diffusion** by Henry Jakubowski and Patricia Flatt has no license indicated.

16.2: REACTIONS OF THE CITRIC ACID CYCLE

LEARNING GOALS (CHATGPT O3-MINI)

1. **Describe the Overall Function and Importance of the CAC:**
   - Explain how the citric acid cycle serves as a central hub in aerobic metabolism by oxidizing acetyl-CoA to CO_2 while generating high-energy electron carriers (NADH and $FADH_2$) that fuel oxidative phosphorylation.
2. **Explain the Rationale Behind the Cycle's Structure:**
   - Understand why the CAC is cyclic rather than linear, including how the regeneration of oxaloacetate ensures that key intermediates are maintained despite their withdrawal for biosynthetic purposes (anaplerotic reactions).
3. **Outline the Net Stoichiometry and Energy Yield:**
   - Summarize the overall reaction of the CAC and its energy yield, emphasizing that although only one ATP (or GTP) is produced per cycle, the generation of multiple NADH and $FADH_2$ molecules drives substantial ATP synthesis through the electron transport chain.
4. **Detail the Chemical Mechanisms of Key Enzymatic Steps:**
   - Describe the reaction mechanisms of the primary CAC enzymes (e.g., citrate synthase, aconitase, isocitrate dehydrogenase, α-ketoglutarate dehydrogenase, succinyl-CoA synthetase, succinate dehydrogenase, fumarase, and malate dehydrogenase), highlighting how each step contributes to both carbon oxidation and electron transfer.
5. **Analyze the Role of Cofactors and Electron Carriers:**
   - Explain how cofactors such as NAD^+/NADH, FAD/$FADH_2$, and the formation of a thioester bond in acetyl-CoA facilitate the oxidation-reduction reactions within the cycle and drive the thermodynamically unfavorable steps.
6. **Integrate Structural and Mechanistic Perspectives:**
   - Utilize interactive molecular models (e.g., iCn3D) to visualize enzyme active sites, conformational changes, and key residue interactions that facilitate substrate binding and catalysis, such as those seen in citrate synthase and aconitase.
7. **Discuss the Regulation and Interconnectedness of the Cycle:**
   - Evaluate how the CAC is regulated both by substrate availability and by the need to balance catabolic and anabolic processes, including the role of anaplerotic reactions that replenish cycle intermediates.
8. **Relate the Citric Acid Cycle to Broader Metabolic Pathways:**
   - Explain how the CAC integrates with glycolysis, oxidative phosphorylation, and various biosynthetic pathways, underscoring its central role in overall energy homeostasis and cellular metabolism.
9. **Interpret Experimental and Structural Data:**
   - Critically analyze experimental approaches (e.g., isotope labeling and structural studies) that have been used to elucidate the pathway's intermediates, enzyme mechanisms, and regulatory features.
10. **Reflect on Evolutionary and Energetic Considerations:**
    - Discuss why the cycle evolved to include multiple steps for oxidizing a two-carbon unit, emphasizing the advantages of a cyclic pathway that can adapt to the withdrawal of intermediates for biosynthesis while maximizing energy extraction.

These learning goals are intended to provide a comprehensive framework for understanding the citric acid cycle, integrating detailed chemical mechanisms, structural insights, and regulatory strategies to reveal how this central metabolic pathway supports cellular energy production and overall homeostasis.

16.2.1: INTRODUCTION

The acetyl-CoA formed by the pyruvate dehydrogenase complex (PDC) now enters a cyclic, non-linear pathway called the citric acid cycle, tricarboxylic acid (TCA) cycle, or the Krebs cycle, after Hans Krebs, who discovered it. The cycle is shown in Figure **16.2.1** in wedge/dash form with stereochemistry included.

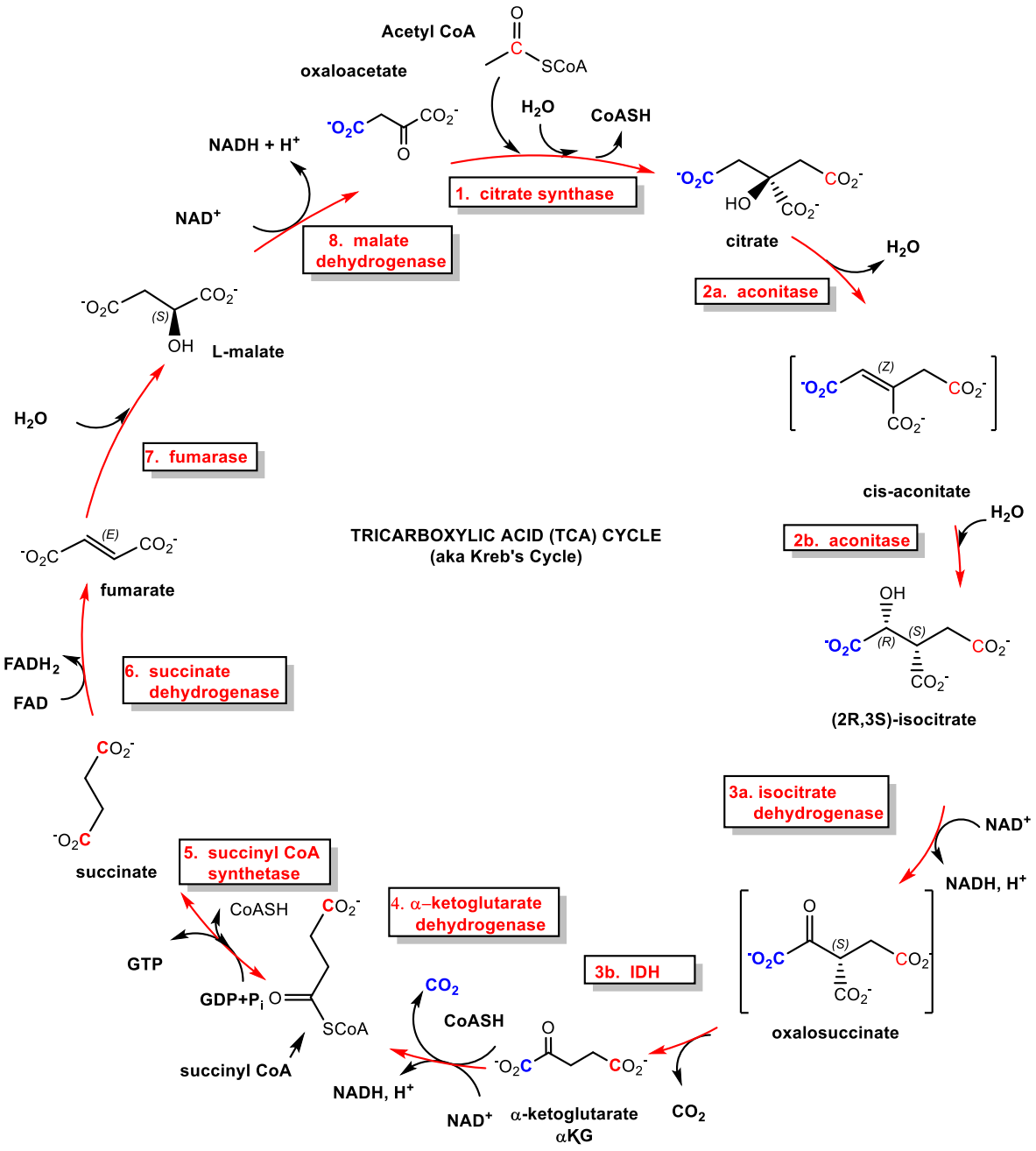


Figure **16.2.1**: Citric Acid Cycle

Why a cycle?

Why is this pathway cyclic and not linear, as we have seen for glycolysis? A simple answer is that it evolved that way, but why would that be advantageous? It turns out that some of the key "intermediates" in the pathway are pulled away for the biosynthesis of other biomolecules. If the citric acid cycle were linear and intermediates pulled off for other reactions, the linear pathway would taper off, which would not be optimal for a key energy production pathway. Of course, removing intermediates from a cyclic pathway would also slow down the process. Still, when this happens, enzymes outside the cycle are used to produce key reaction intermediates that keep the cycle going. The replenishing reactions are called **anaplerotic.**

Look at Figure 1. 2 Cs enter at the top as $CH_3(C{=}O)$-SCoA. At the bottom, 2 Cs depart as CO_2s. Also, 2 Hs leave as 2 NADHs, which are generated on the right-hand side of the cycle along with some protons. Those have to be put back into the cycle for the next round. Krebs thought the input was from pyruvate, $CH_3(C{=}O)CO_2^-$, the end product of glycolysis. Pyruvate also comes from the metabolism of some amino acids.

In his detailed analysis of the enzymes involved in "intermediary" metabolism, Krebs used radioisotope-labeled reactants to trace carbon atoms in respiring tissue. He found that when radiolabeled pyruvate and oxaloacetate were added to muscle tissue *in vitro*, radiolabeled citrate was formed.

$$\text{Pyruvate} + \text{Oxaloacetate} \rightarrow \text{citrate} + CO_2$$

His first version of the cycle had pyruvate as the incoming 2C molecule. But pyruvate is a 3C molecule, so something was amiss. Another CO_2 likely was released. But from what?

Left out of this equation is the initial reaction of pyruvate with CoASH to form acetyl-CoA (an oxidative decarboxylation reaction, discovered by Fritz Lipmann in 1947), which then enters the pathways at the top by reacting with oxaloacetate to form citrate. Oxaloacetate, which would be the pathway's end product if the pathway were linear, reacts with another incoming acetyl-CoA to reform citrate, restarting the cycle. He correctly surmised that the pathway was circular.

Krebs used minced pigeon flight muscles for his experiments. It was a good choice, as these have a very high metabolic rate, allowing him to detect changes in the system after adding specific metabolites. Note that the last four species in the cycle are 4 C carboxylic acids, as shown in Figure **16.2.2** below. Carboxylic acids are inherently not very reactive.

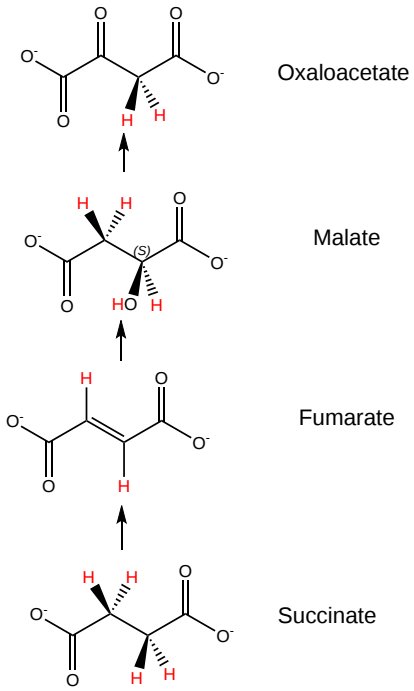


Figure **16.2.2**: Structure of the 4 C carboxylic acids of the citric acid cycle

? EXERCISE 16.2.1

In separate experiments, Krebs and others added four different 4-carbon carboxylic acids to minced pigeon muscle. Each separately sped up the generation of CO_2, but interestingly, none of the added carboxylic acids were further metabolized, so their concentrations remained the same. Explain how this could occur.

Answer

In a linear pathway, added reactants would be consumed unless all steps are equally reversible. The latter seems unlikely in actively respiring flight muscle. The only reasonable explanation is that the pathway was not linear but cyclic, so each species was regenerated in the next turn of the cycle. By definition, each of the 4 C organic acids acted as a general **catalyst** - their addition sped up the reaction, but they were not themselves consumed! Each increased the rate not just of the reaction in which they were a substrate, but all of the reactions. Krebs showed that each species acted not as "hydrogen carriers" but as reaction intermediates.

In Figure 2, each of the successive intermediates differs by **2 Hs**.

? EXERCISE 16.2.2

Account for the changes in Hs at each step, as succinate is converted to oxaloacetate.

Answer

Each step, except the second, involves an oxidation reaction. In the first step (succ → fum), FAD goes to FADH_2. In step 3 (mal → oaa), NAD^+ → NAD**H** + H^+. In step 2 (fum → mal), H_2O is added in a hydration (addition) reaction across the double bond.

It may seem unimportant to focus on Hs, but they are a key to the cycle. Let's revisit glucose and its metabolism. The empirical formula of glucose is $C_6H_{12}O_6$ or $C_6(H_2O)_6$. If the 4 C carboxylic acids were just shuttling Hs, removing 6 H_2 equivalents would also mean removing 6 CO_2s from the complete respiration of glucose. That is what happens in the presence of oxygen when the cycle is running full tilt, and those Hs are passed to Os to form water. If the 4 C acids were just carriers for Hs (and not intermediate in chemical reactions), then if you added lots more of the 4 C acids, even in the absence of oxygen, all of the C atoms in glucose would be fully oxidized to CO_2. That doesn't happen. Oxygen is required, so these 4 C carboxylic acids are not just passive shuttles but active intermediates.

Why are there so many steps involved in simply oxidizing 2 C atoms in pyruvate?

The next obvious question is this: Why are eight reactions required to oxidize just 2 Cs in pyruvate? Partly, this is a matter of evolution again, as the early evolutionary pathway likely served both oxidative (clockwise) and reductive (counterclockwise) reactions, based on the cell's needs. Part of the chemistry in the cycle produces β-keto acids, which are relatively easy to oxidatively decarboxylate. The other part converts an α-ketoacid to a molecule with a better electron sink at the carbon β to the departing CO_2. After the two carbon atoms added to the cycle from acetyl-CoA are released as two CO2s, the remaining reactions are used to regenerate oxaloacetate, allowing the cycle to continue.

Of course, the ultimate goal of an energy-extractive oxidative pathway is not just to form CO_2 but to form ATP or its equivalent (i.e., GTP). Notice that 3 NAD^+s are used and converted to 3 NADH. In addition, a new, more potent oxidizing agent, FAD, is used and is converted to $FADH_2$. NAD^+ and FAD are replenished by reoxidation of NADH and $FADH_2$ (the reduced forms) back to NAD^+ and FAD, through mitochondrial electron transport (oxidation) reactions, in which electrons are passed to stronger and stronger oxidizing agents, the last being O_2. In this thermodynamically favored process, lots of ATPs are made. We will explore those reactions in the next section.

We will go through each step of the citric acid cycle separately and show how the pathway is regulated (section 16.3). Why such detail? There are only eight steps. Given that the citric acid cycle is a hub that, along with glycolysis, controls metabolic flow through many interconnected metabolic pathways, we will examine each carefully.

Other issues

The PDC and citric acid cycle reactions occur in the mitochondrial matrix. Cytoplasmic pyruvate and NAD^+ must be transported from the cytoplasm into the matrix. Additionally, some enzymes in the citric acid cycle have both cytoplasmic and mitochondrial variants. Some homologous pairs are differentiated using NAD^+ or $NADP^+$ as an oxidizing agent. The ones in the cytoplasm are not part of the cycle. You would expect these enzyme pairs to have similar tertiary structures and active site chemistry. Prokaryotic forms of these enzymes are structurally similar to their eukaryotic counterparts, so the interactive molecular models shown below depict enzymes from different organisms. Finally, many variants, shunts, and bypasses of the citric acid pathway are used in different organisms. We will explore this topic in section 16.4.

Additionally, dogma suggests that the cycle proceeds clockwise, in an oxidative direction. Can it return counterclockwise in a reductive fashion? And if so, under what conditions? We'll explore that elsewhere as well.

We will attempt to pair reaction mechanism diagrams that illustrate the flow of electrons during bond formation and bond breaking with interactive molecular models of the active site. You should rotate the models to align and identify key amino acids and ligands (substrate, substrate analogs, inhibitors, activators) shown in the static 2D mechanism diagrams. Since the active sites are often conserved across prokaryotic and eukaryotic versions, our choice of PDB structures depends on which best illustrates a conceptual point.

NOTE

There are several ways to write abbreviated chemical equations that show NAD^+/NADH, FAD/FAD_2, and hydrogen ions in reactions. To make sense of them, consider a simplified mechanism for ethanol oxidation by alcohol dehydrogenase, as shown in Figure **16.2.3**. Note the 2 Hs on the substrate (ethanol) that are removed, one as a hydride (**H**) and the other as a proton (H^+).

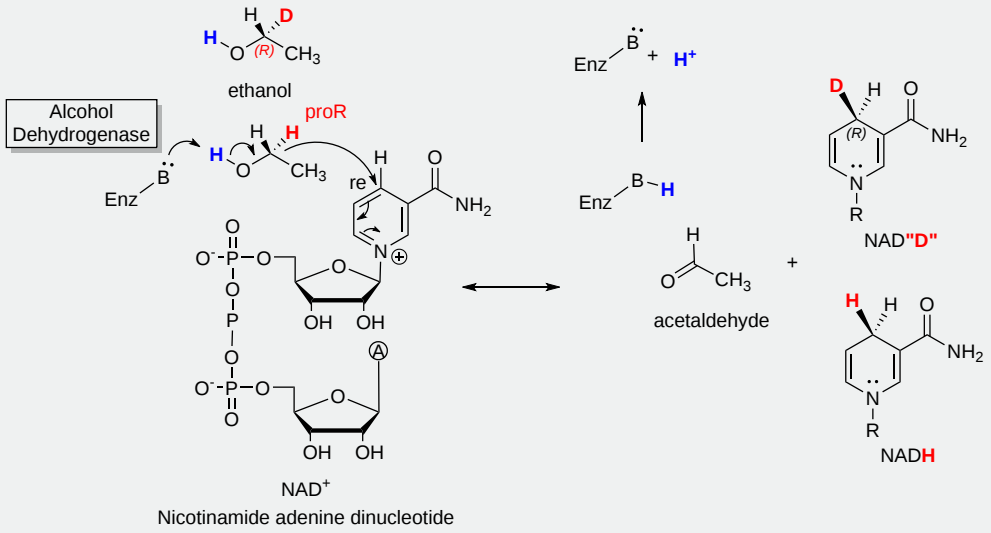


Figure **16.2.3**: Oxidation of ethanol using NAD^+

Here is a list of different and seemingly contradictory ways to write a chemical equation to show changes in NAD^+/NADH and hydrogen ions:

1. $NAD^+ + :H^- \rightarrow NADH$. This chemical equation is charge-balanced and shows just the changes to the NAD^+/NADH pair but not the proton (H^+) lost from the substrate.
2. $NAD^+ + 2e^- + H^+ \rightarrow NADH$. This is the same as equation (1) but with the hydride separated into an electron pair and a proton. The equation is charge-balanced.
3. $NAD^+ + H^+ \rightarrow NADH$. This is balanced for Hs but not for the + charge, as it doesn't explicitly show the electron pair from the hydride added to NAD^+.
4. $NAD^+ \rightarrow NADH + H^+$. This is balanced for charge but not for Hs. The extra H^+ is the proton from the oxidized substrate.

We will use example 4 above throughout this book. That equation is most useful for accounting for the change in the number of protons in the individual reactions and entire pathways. We will also write simplified chemical equations involving FAD (in which 2Hs from the substrate are added) as:

$$FAD \rightarrow FADH_2.$$

Now, let's look at each step in detail.

16.2.2: 1. CITRATE SYNTHASE (CS)

$$\text{Oxaloacetate} + \text{Acetyl-CoASH} + H_2O \rightarrow \text{Citrate} + \text{CoASH}\ \Delta G^o = -7.5\ \text{kcal/mol}\ (-31\ \text{kJ/mol})$$

Acetyl CoA is a thioester. Hence, it is "high energy" compared to its hydrolysis products. (**Remember, there is no such thing as a "high energy" bond.**) The free energy released in its hydrolysis is used to drive the reaction forward. This is important. Otherwise, citrate would not be formed readily. This reaction feeds the end product of glycolysis into the citric acid cycle. It is summarized in Figure **16.2.4**.

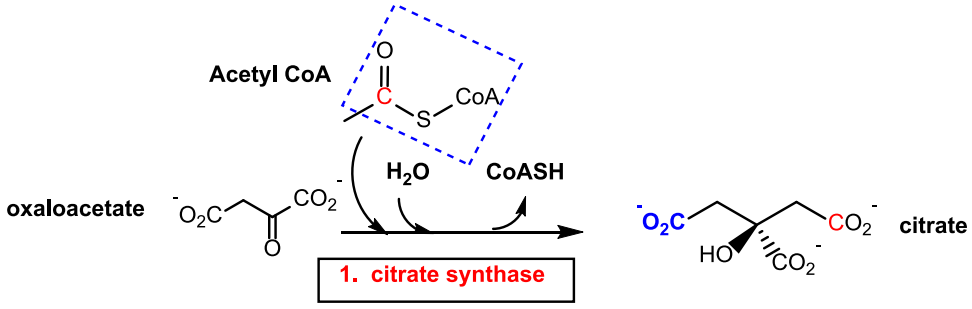


Figure **16.2.4**: Summary reaction - Citrate Synthase

The enzyme exists in two major conformations: an open and a closed conformation. The open form binds oxaloacetate and then acetyl-CoA. The complex then shifts to the closed conformation. These changes sequester the bound substrates, exclude water, and prevent spurious hydrolysis of acetyl-CoA. The binding occurs sequentially, so the kinetics follow a sequentially ordered mechanism.

Figure 16.2.5 left shows an animated gif of the conformational changes between the citrate-bound version (open, green) and the citrate and CoASH-bound form (blue). The image below right shows a smoother transition between the open and closed form without bound ligands (1cts, 2cts)



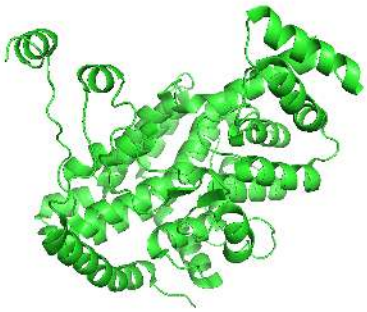


Figure 16.2.5: Conformational changes in citrate synthase on binding substrate

For a more detailed description of the enzyme view, the Regulation of Citrate Synthase.

The mechanism below is from https://chem.libretexts.org/Bookshel...trate_Synthase, with Contributors and Attributions from:

- Dr. Dietmar Kennepohl FCIC (Professor of Chemistry, Athabasca University)
- Prof. Steven Farmer (Sonoma State University)
- Organic Chemistry With a Biological Emphasis by Tim Soderberg (University of Minnesota, Morris)

In this reaction, a C-C bond must form between the substrates. One way to achieve this is to form a nucleophilic carbanion ion from the alpha carbon of acetyl-CoA. Remember, this is not a decarboxylation reaction, so we don't have to worry about an electron "sink" on the β carbon. Forming the carbanion would be possible since the negative charge on the carbon can be withdrawn to the carbonyl oxygen to form an enolate. The enolate becomes even more stable if the negative oxygen is protonated. This reaction is an aldol condensation, which involves adding an enolate to an aldehyde or ketone. The carboxylate group of aspartic acid 375 on citrate synthase removes the acidic alpha proton on acetyl-CoA. At the same time, histidine 274 donates a proton to form the neutral enol, a much more stable molecule than the enolate anion. His 274 continues to stabilize the enol during the reaction. Bound oxaloacetate is stabilized in part by Arg 329. In the next part of the mechanism, a second histidine (320) protonates the carbonyl oxygen of oxaloacetate, activating the carbonyl carbon for nucleophilic attack by the enol in the next step to form (S)-citryl CoA. The hydrolysis of CoASH occurs when His 320 deprotonates a water molecule, facilitating nucleophilic attack on the carbonyl carbon bonded to -SCoA, thereby forming citrate.

A plausible mechanism is shown in Figure 16.2.6.

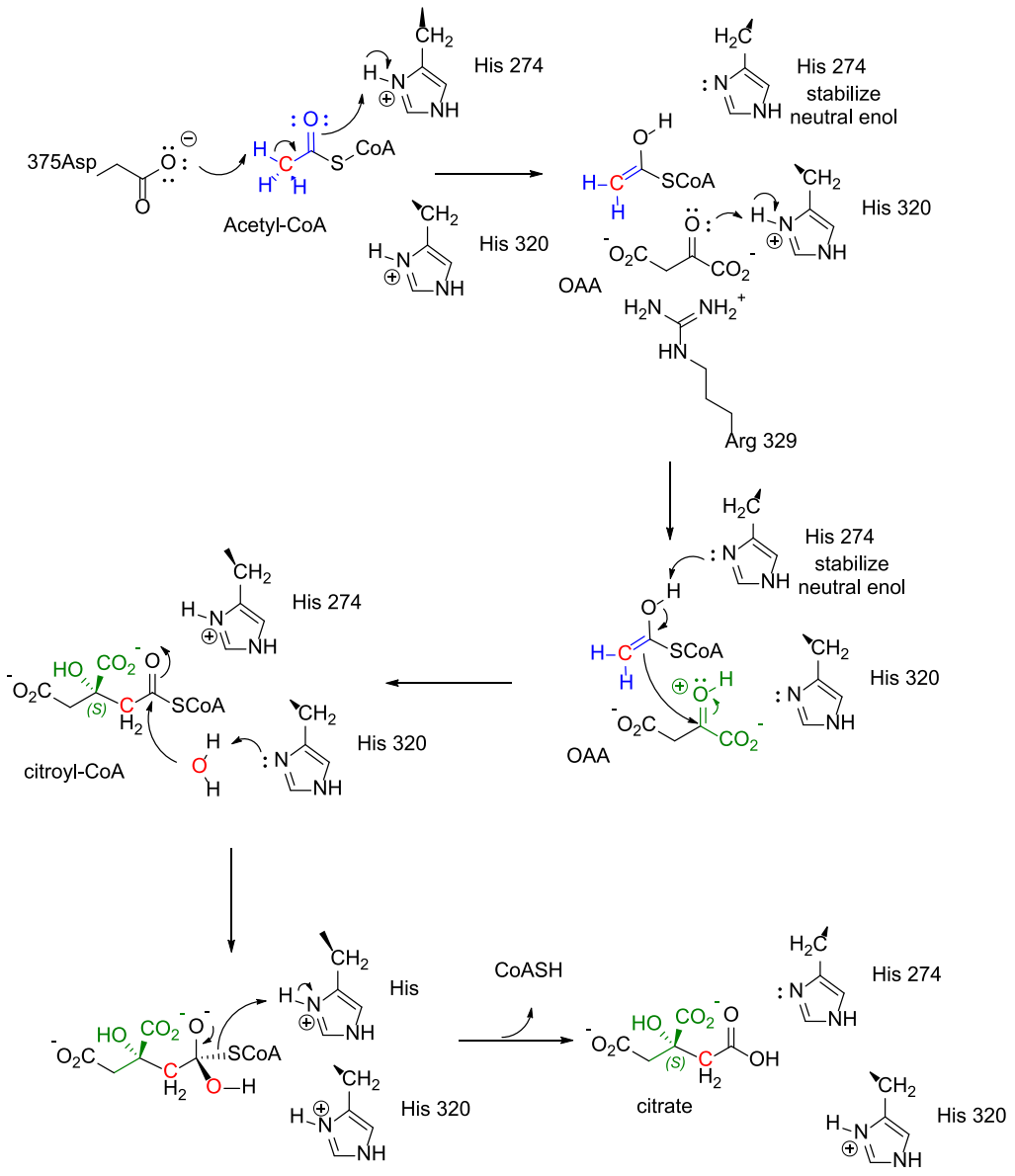


Figure **16.2.6**: Citrate synthase mechanism

Figure **16.2.7** shows an interactive iCn3D model of the pig citrate synthase bound to CoASH and citrate (2CTS)

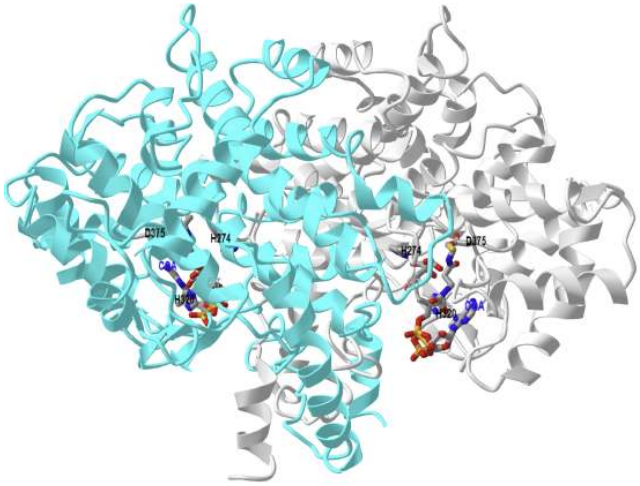


Figure **16.2.7**: pig citrate synthase bound to CoASH and citrate (2CTS). (Copyright; author via source). Click the image for a popup or use this external link: https://structure.ncbi.nlm.nih.gov/i...WXqcEsu336tcL7

The enzyme is a dimer, with its monomers depicted in different colors. Citrate and CoASH are shown as sticks and labeled. The active site residues in each subunit are shown as sticks and labeled.

16.2.3: 2. ACONITASE

Citrate ↔ Isocitrate ΔG^o = +2 (rx 2a), -0.5 (rx 2b) kcal/mol; net ΔG^o = + 1.5 kcal/mol (+6.3 kJ/mol)

Thinking like a chess player, who must anticipate future moves, the chemical rationale for this reaction is to move an OH to a beta position, which in a subsequent step is converted to a β C=O, so it can act as an electron sink to facilitate decarboxylation in a following reaction! The reaction is readily reversible (note the small ΔG^o value) since the reactant and product are simple isomers of each other. Figure **16.2.8** shows the summary reaction.

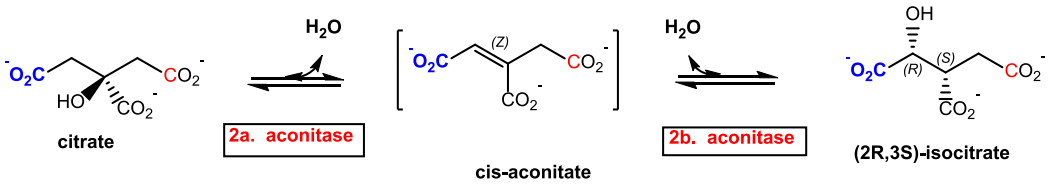


Figure **16.2.8**: Summary reaction of aconitase

The enzyme has an inorganic Fe_4S_4 cluster. Each Fe in the cluster coordinates to 4 S^{2-} in a cubane structure, but when either citrate or isocitrate is bound, one of the Fe ions interacts with both the Os of a substrate carboxylate. The other two carboxylates of isocitrate are stabilized through ion-ion interactions by Arg 446 and 663.

Figure **16.2.9** below shows a plausible partial mechanism. An active site deprotonated serine abstracts a proton at the S carbon. This is followed by the formation of the C-C double bond and the release of the resulting cis-aconitate from one bond to the FeS cluster.

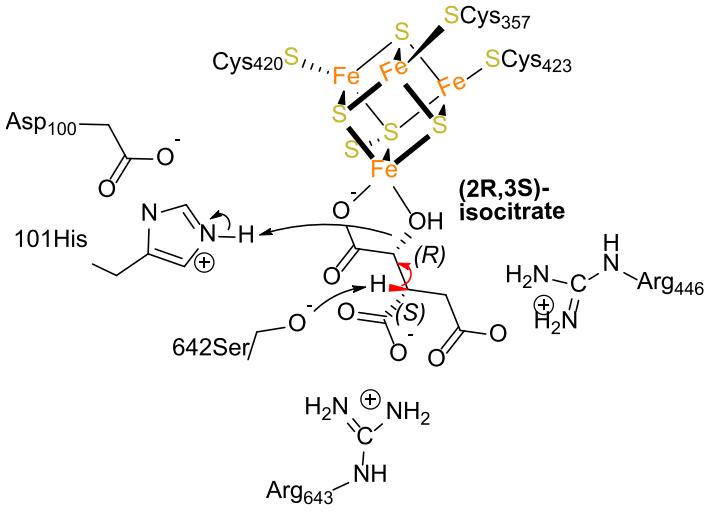
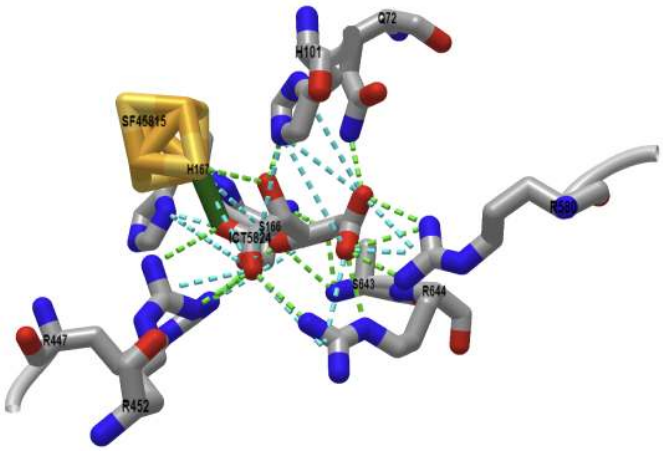


Figure **16.2.9**: Mechanism of aconitase

Figure **16.2.10** shows an interactive iCn3D model of the bovine S642A aconitase with bound citrate (1C97).



NCBI iCn3D Figure **16.2.10**: Bovine S642A aconitase with bound citrate (1C97). (Copyright; author via source). Click the image for a popup or use this external link: https://structure.ncbi.nlm.nih.gov/i...iJJRGaFoCDnhf7

This cis-aconitate intermediate in the interconversion of citrate and isocitrate undergoes a 180^0 flip around the C=C double bond. This is followed by rehydration to form the other isomer. The deprotonated His 101 abstracts a hydrogen from a water-bound to the FeS cluster, with the hydroxide acting as a nucleophile, which, along with the redonation of a hydrogen ion on the protonated Ser 642, the alpha-carbon, completes the rehydration step in the formation of the other isomer.

Exercise 16.2.3

Why was the S642A mutant used to produce the structure shown in the above iCn3D model?

Answer

It allows the binding of substrate/product, in this case, isocitrate, to an inactive enzyme, as the active site serine was mutated to a non-nucleophilic alanine of similar size. Hence, no bond-making/breaking occurs in the complex.

References:

https://collab.its.virginia.edu/acce...-_-/index.html

16.2.4: 3. ISOCITRATE DEHYDROGENASE (IDH)

Isocitrate + NAD^+ → α-ketoglutarate + NADH + H^+ ΔG^o = -2.0 kcal/mol (-8.4 kJ/mol)

The chemical rationale should be clear. In this step, the CO_2 is removed as NADH is produced through an oxidative decarboxylation. The NADH will be reoxidized back to NAD^+ in the electron transport chain, resulting in ATP production (see next section). The reaction is summarized in Figure **16.2.11**.

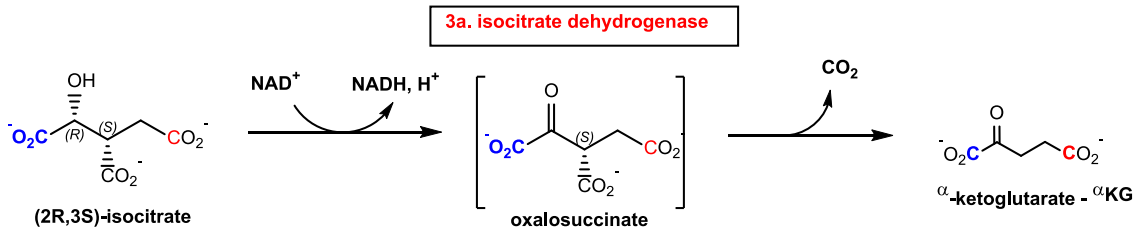


Figure **16.2.11**: Summary reaction: isocitrate dehydrogenase

Exercise 16.2.4

Why must the oxidation reaction precede the decarboxylation reaction?

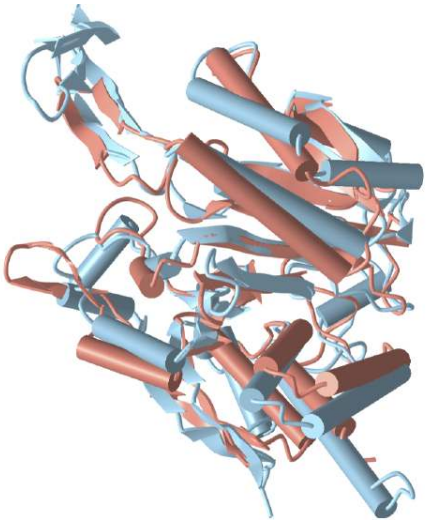
Answer

First, a β-ketoacid intermediate must form, allowing easy intermediate decarboxylation. The β carbonyl provides an electron "sink" to facilitate the decarboxylation.

There are two forms of this enzyme (IDH), a cytoplasmic ($NADP^+$) form and a mitochondrial (NAD^+) form. The cytoplasmic forms from various organisms are homodimers and have a common mechanism of catalysis. In contrast, yeast mitochondrial IDH has two subunits: IDH1 (regulatory, which binds the allosteric activators citrate and AMP) and IDH2 (catalytic, which binds isocitrate and NAD^+).

Mammalian NAD-IDHs are even more complex than yeast NAD-IDH. These enzymes are composed of three types of subunits, α, β, and γ, which share about 40–52% sequence identity. The α and β form an αβ dimer, while the α and γ subunits form αγ. These then interact to form the $\alpha_2\beta\gamma$ heterotetramer, which effectively forms the holoenzyme. It can also form an active heterooctamer. The αγ heterodimer is regulated by citrate and ADP. A conformational change occurs upon citrate binding to the allosteric site, thereby enhancing isocitrate binding. ADP enhances the binding of the allosteric regulator citrate. The α chain is the catalytic subunit.

Figure **16.2.12** shows an interactive iCn3D model that shows the superposition of the α chains of cytoplasmic IDH (NADP, sky blue, 4L03) and mitochondrial IDH (NAD) (6KDY, salmon).



NCBI iCn3D Figure **16.2.12**: Superposition of the A chains of cytoplasmic IDH (4L03) and mitochondrial IDH (NAD) (6KDY) (Copyright; author via source). Click the image for a popup or use this external link: https://structure.ncbi.nlm.nih.gov/i...zy9yn4NaF9g1c9

Click the 3-bar menu (hamburger, ☰) icon (top left) in the model in the window and toggle the "a" key to move between the two forms. Although the structures of the alpha chains are not identical, they align well.

Figure **16.2.13** shows a probable mechanism for the reaction based on the conserved catalytic site shown in the model above.

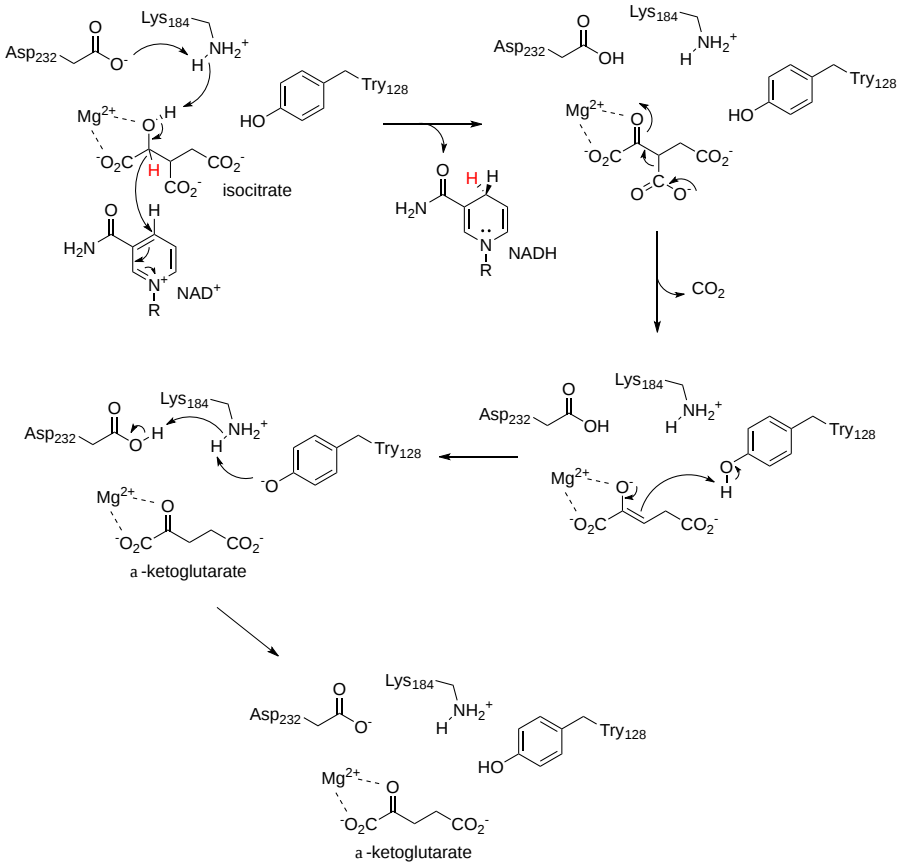
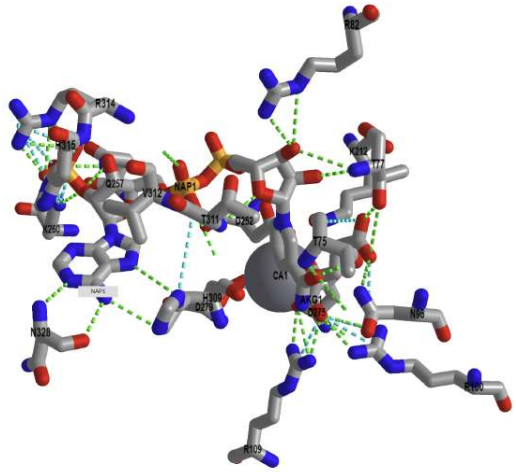


Figure **16.2.13**: Mechanism of isocitrate dehydrogenase (after https://www.ncbi.nlm.nih.gov/pmc/articles/PMC3706558/)

Figure **16.2.14** shows an interactive iCn3D model of the active site of the cytoplasmic human IDH1 in complex with $NADP^+$ and Ca^{2+}/α-ketoglutarate (4L03).



NCBI iCn3D Figure **16.2.14**: Active site of the cytoplasmic human IDH1 in complex with $NADP^+$ (NAP1) and Ca^{2+}/ alpha-ketoglutarate (4L03) (Copyright; author via source). Click the image for a popup or use this external link: https://structure.ncbi.nlm.nih.gov/i...P9DqLoPowEV2d9

Figure **16.2.15** shows an interactive iCn3D model of the active site of the αβ heterodimer of human IDH3 (6kdy) in complex with NAD^+.

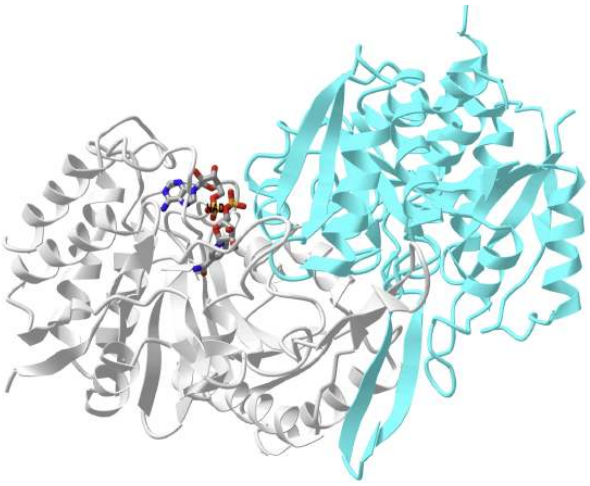


Figure **16.2.15**: αβ heterodimer of human IDH3 (6kdy) in complex with NAD^+(6kdy) . (Copyright; author via source). Click the image for a popup or use this external link: https://structure.ncbi.nlm.nih.gov/i...hyyJiMFEqwktB7

The α subunit is shown in gray and the β in cyan.



Gliomas, a type of brain cancer, are the most common brain tumors in adults under 50. These contain mutations in isocitrate dehydrogenase (IDH). IDH mutations in glial progenitor cells appear to play a key role in glial tumor development. Jung Won Park *et al.* IDH-mutant gliomas arise from glial progenitor cells harboring the initial driver mutation. *Science***391**,eadt0559(2026). DOI:10.1126/science.adt0559

16.2.5: 4. A-KETOGLUTARATE DEHYDROGENASE

$$\alpha\text{-ketoglutarate} + NAD^+ + CoASH \rightarrow \text{succinyl CoA} + CO_2 + NADH + H^+ \quad \Delta G^o = -7.2 \text{ kcal/mol } (-30 \text{ kJ/mol})$$

In the last reaction, α-ketoglutarate is formed. Oh no, you might say! It would have been nice to form a β-ketoacid, which could easily undergo decarboxylation. No worries, though. We spent section 16.1 explaining the biochemistry used to decarboxylate another α-ketoacid, pyruvate. The same chemistry is used to accomplish the oxidative decarboxylation of α-ketoglutarate. Hence, we won't expand on the mechanism here. The reaction is shown in Figure **16.2.16**.

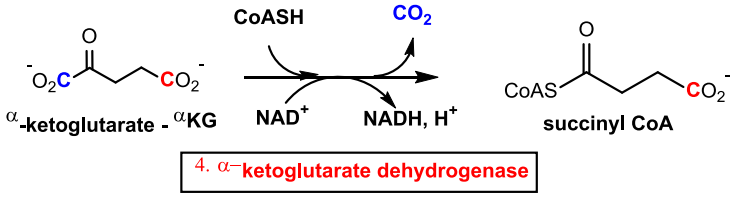


Figure **16.2.16**: Summary reaction for α-ketoglutarate dehydrogenase

16.2.6: 5. SUCCINYL-COA SYNTHETASE (SCS)

$$\text{succinyl CoA} + GDP + P_i \rightarrow \text{succinate} + CoASH + GTP \quad \Delta G^o = -0.8 \text{ kcal/mol } (-3.3 \text{ kJ/mol})$$

This is the first step in which the energy change in the cycle is explicitly captured in the form of a high-energy (with respect to its hydrolysis product) phosphoanhydride bond in the form of GTP (ATP in some organisms). From a chemical step, the cleavage of the thermodynamically unstable thioester is coupled to the endergonic synthesis of GTP. This can transfer its terminal phosphate to ADP to make ATP in a reaction with a $\Delta G^o \approx 0$ kcal/mol. The reaction is shown in Figure **16.2.17**.

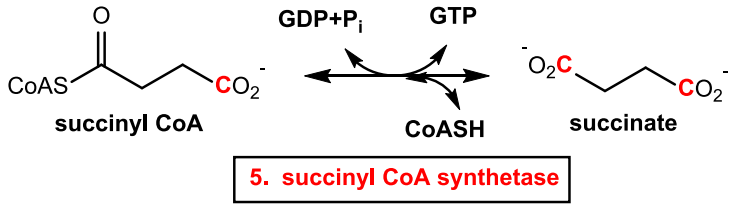


Figure **16.2.17**: Summary reaction for succinyl-CoA synthetase

Succinyl-CoA synthases have two subunits, α and β. The enzyme in E. coli is a tetramer ($\alpha_2\beta_2$) with the catalysis occurring at the αβ interface. The alpha-subunits interact only with the beta-subunits, whereas the beta-subunits interact to form the dimer of alpha beta-dimers with CoA bound in each α subunit to a nucleotide-binding loop.

Two histidines, His 246 and His 142, are involved in the reaction, with His 246 becoming phosphorylated to form an intermediate. A mutation of His 142 to an asparagine (H142N) essentially abolishes enzyme activity. Different SCSs have different specificities for purine nucleoside triphosphates. Organisms, including mammals, may have two different isoforms, one that binds ADP and one that uses GDP (as shown in most diagrams of the citric acid cycle). In E. coli, the α subunit binds CoASH and contains His246, which gets phosphorylated. The β subunit determines the specificity for either GTP or ATP. In E. coli, the ATP binding site (Site II "in the ATP-grasp fold") is quite distant from the CoASH site (Site II), so phospho-His 246 must move between the sites in the dimer interface.

The three steps in the reaction are shown below, where E is the free enzyme, a · indicates a noncovalent complex, and a - represents a covalent bond (after Biochemistry 2002, 41, 537-546)

1. E + succinyl-CoA + P_i ↔ E · succinyl-PO_3 + CoASH
2. E · succinyl-PO_3 ↔ E-PO_3 + succinate
3. E-PO_3 + NDP ↔ E + NTP

Figure **16.2.18** shows an abbreviated mechanism that shows only the involvement of His 246.

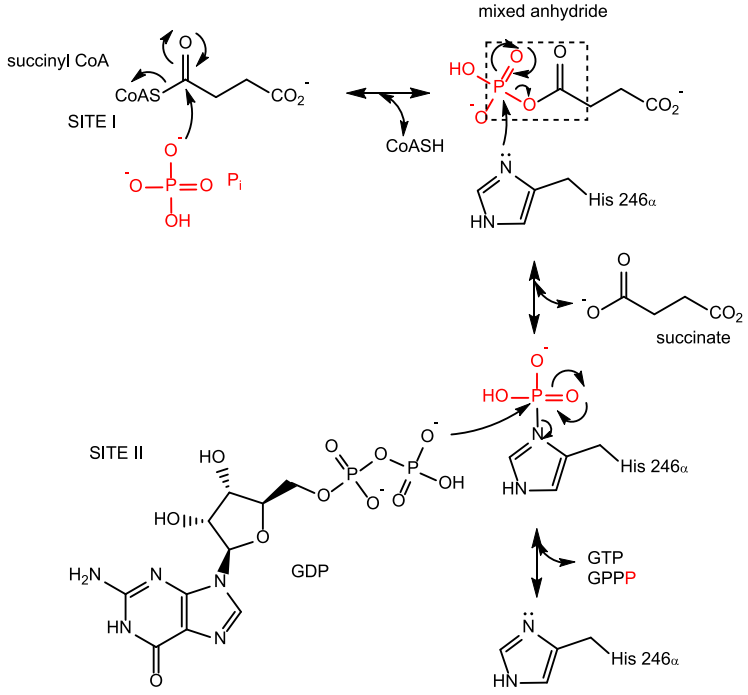


Figure **16.2.18**: Abbreviated mechanism for succinyl-CoA synthase

Kinetic analysis suggests that the three substrates bind in a specific order, catalysis occurs, and then the three products leave. This type of reaction is called an ordered ter ter (tertiary - 3 reactants - in both the forward and reverse) and is shown in Figure **16.2.19**.

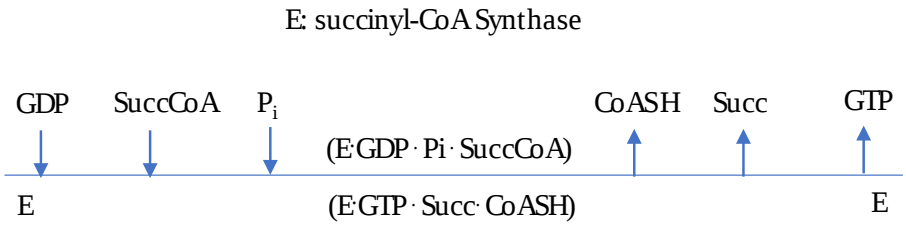
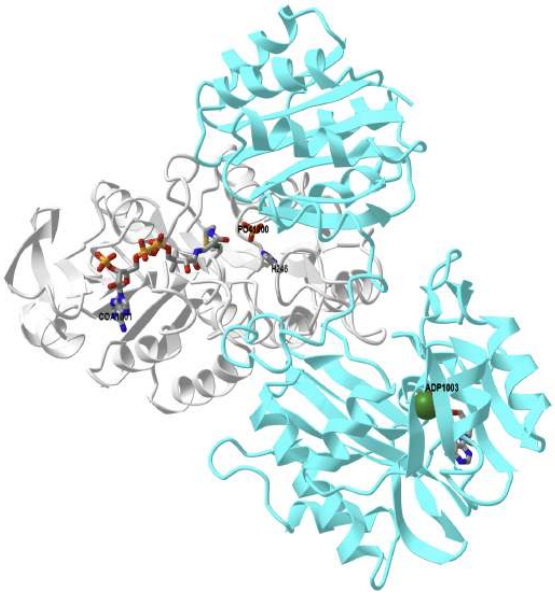


Figure **16.2.19**: Ordered ter ter reaction for succinyl-CoA synthase

The iCn3D model below shows key α-chain residues in the active site, including the phosphorylated His246 and the bound CoASH. Use iCn3D to visualize 1CQJ, the nonphosphorylated form.

Figure **16.2.20** shows an interactive iCn3D model of the complex of ADP and Mg^{2+} with Dephosphorylated E. Coli Succinyl-CoA Synthetase (1CQI)



NCBI iCn3D Figure **16.2.20**: Complex of ADP and Mg^{2+} with Dephosphorylated E. Coli Succinyl-CoA Synthetase (1CQI). (Copyright; author via source). Click the image for a popup or use this external link: https://structure.ncbi.nlm.nih.gov/i...BssxsabV1S9cz6

Just one αβ dimer is shown. The α subunit is shown in gray and the β in cyan. Bound P_i and CoASH are labeled. The active site His246 in the α chain is shown in sticks and labeled.

Figure **16.2.21** shows an interactive iCn3D model of the active site of pig GTP-specific succinyl-CoA synthetase in complex with succinate and CoASH (5CAE).

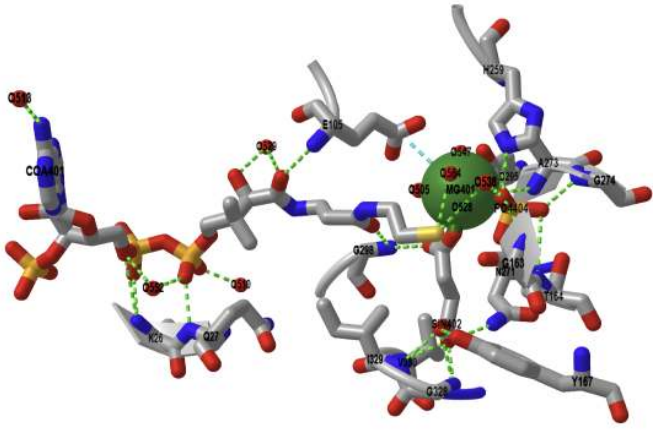


Figure **16.2.21**: Active site of pig GTP-specific succinyl-CoA synthetase in complex with succinate and CoASH (5CAE). (Copyright; author via source). Click the image for a popup or use this external link: https://structure.ncbi.nlm.nih.gov/i...HjH9ER5wLqb1T7

16.2.7: 6. SUCCINATE DEHYDROGENASE

$$\text{succinate} + \text{FAD} \leftrightarrow \text{fumarate} + FADH_2 \quad \Delta G^o = 0 \text{ kcal/mol}$$

The enzyme is yet another step in closing the cycle to reform oxaloacetate. It is also our first encounter with FAD as an oxidizing agent. Its reduction product, $FADH_2$, will be reoxidized in the electron transport chain (mitochondrial inner membrane for eukaryotes), producing energy for ATP. Hence, it can be considered a proxy ATP-generating reaction. The reaction is shown in Figure **16.2.22**.

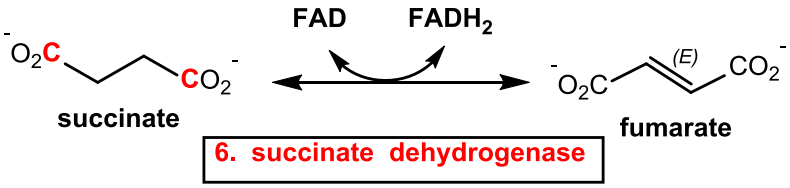


Figure **16.2.22**: Summary reaction for succinate dehydrogenase

The succinate dehydrogenase enzyme is part of the larger Complex II of the electron transport chain. Complex II utilizes numerous cofactors in its overall function. It also utilizes an iron-sulfur cluster cofactor, similar to aconitase, to produce a C=C double-bond intermediate. We will discuss it in greater detail in the chapter on electron transport. Let's concentrate on this new cofactor and oxidizing agent, FAD. Many enzymes use $FAD/FADH_2$ in redox chemistry.

In contrast to NAD^+/NADH, the $FAD/FADH_2$ pair stays tightly bound to the enzyme and doesn't readily dissociate. This means that after one cycle of catalysis (after FAD is converted to $FADH_2$), the enzyme is functionally "dead". Another oxidizing agent must bind to the enzyme and reoxidize $FADH_2$ back to FAD. The dissociation constants for $FAD/FADH_2$ and its protein binder in a flavoprotein are often in the nanomolar range. In around 10% of flavoproteins, $FAD/FADH_2$ are covalently bonded to the enzyme.

Figure **16.2.23** shows an interactive iCn3D model of the Avian respiratory complex II FAD binding subunit with FAD and a malate-like intermediate (1YQ3).

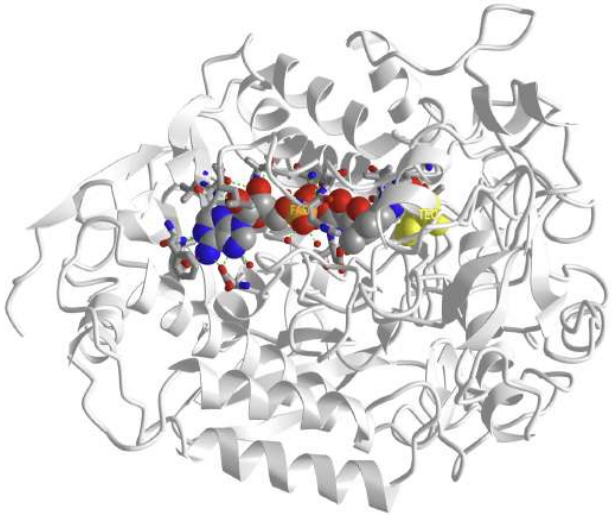


Figure 16.2.23: Avian respiratory complex II FAD binding subunit with FAD and a malate-like intermediate (1YQ3). (Copyright; author via source). Click the image for a popup or use this external link: https://structure.ncbi.nlm.nih.gov/i...SGac3NuN4XBWk7

Note how deeply buried the FAD is within the dehydrogenase subunit. The malate-like intermediate (TEO) is shown next to the FAD in yellow spacefill.

Exercise 16.2.51

Succinate dehydrogenase is irreversibly inhibited by the toxin 3-nitropropionic acid (3np) made by some plants and fungi. Eating moldy sugar cane has led to reported deaths.

1. Draw the Lewis structures of succinate and 3-nitropropionic acid. Compare them and the total number of valence electrons in each.

2. Here is a link to an iCn3D model showing the interaction of 3np with the enzyme. Explain the mode of action of the toxin.

https://structure.ncbi.nlm.nih.gov/i...cja9VKU2ZMCac9

Answer

These molecules are structurally similar and isoelectronic (the same number of electrons in their Lewis structures.

The inhibitor 3np forms a covalent adduct through the guanidino group of Arg 297. This is a key catalytic residue that acts as a general base that accepts a proton from succinate in the reaction.

Figure 16.2.24 (top) shows a very general and abbreviated mechanism for the enzyme for the immediate reaction of succinate with FAD. The bottom part of the image shows the amino acids surrounding succinate in the avian (bird) version of the enzyme (pdb 1yq4)

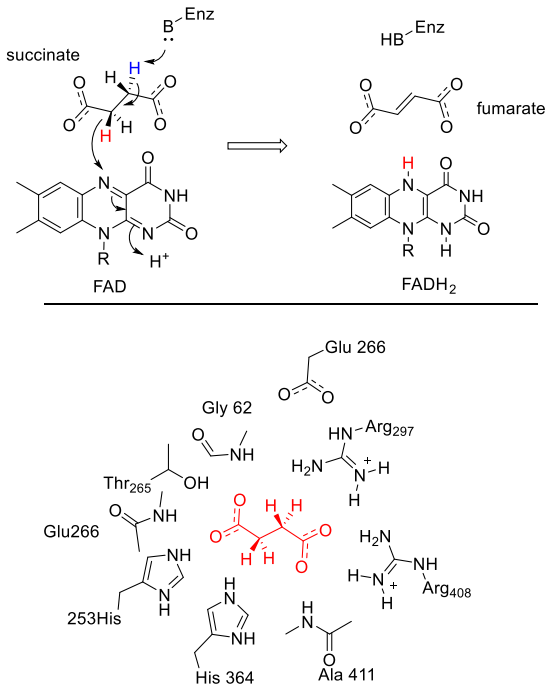


Figure **16.2.24**: Top - a very general and abbreviated mechanism for the enzyme's immediate reaction of succinate with FAD. Bottom - amino acids surrounding succinate in the avian (bird) version of the enzyme (1yq4)

Exercise 16.2.6

One of the amino acids surrounding succinate in the figure above acts as a general base and abstracts a proton from succinate as a hydride is transferred (from a plane above) to FAD. Go to this iCn3D of the active site bound to FAD. Which amino acid is the likely general base? (Note: the figure below shows general protonated states of side chains and not necessarily those involved in the proton abstraction. Go to **Analysis**, **Distance,** and **Distance between 2 atoms** to find the likely general base.

Answer

Arg 297

16.2.8: 7. FUMARASE

$$\text{fumarate} + H_2O \leftrightarrow \text{L-malate}\ \Delta G^o = -0.9\ \text{kcal/mol}\ (-3.8\ \text{kJ/mol})$$

The chemical rationale for this reaction is clear. It is the penultimate step in the resynthesis of oxaloacetate, one of the reactants that start the cycle. This reaction introduces oxygen through hydration, which can be subsequently oxidized in the next step to produce NADH for electron transport and ATP production. The reaction is shown in Figure **16.2.25**.

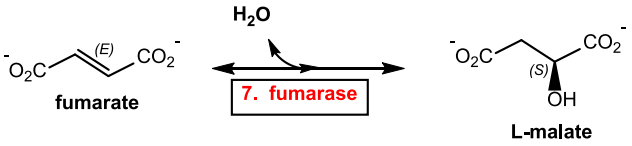


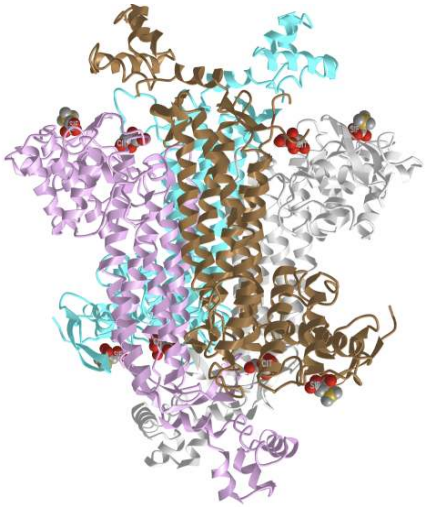
Figure **16.2.25**: Summary reaction for fumarase

There are Class I (dimers containing an unstable FeS cluster, examples A and B) and Class II (tetramer, no bound iron, oxygen stable, example C) fumarases. Humans possess both cytoplasmic and mitochondrial type II fumarases, which result from the alternative transcription of the fumarase genes. We will consider type II fumarase C from *E. Coli*.

The tetramer consists solely of α-helices and random coils, featuring two distinct binding sites. Site A appears to be the active site and contains a buried water molecule. Site A, formed from three subunits, binds competitive inhibitors such as citrate and β-(trimethylsilyl)maleate, a cis substrate for fumarase, and is buried. 12 Å away is site B, which is found in only one of the subunits near a pi-

helix (H129 through N135) and is more surface-exposed. Each site has a histidine, but mutation of only H188N in the A site disrupts enzyme activity. Both sites bind multi-carboxylates. The role of site B is a bit unclear, but it is most likely an allosteric site involved in the transfer of product (malate) from the buried site to the surface for ultimate dissociation.

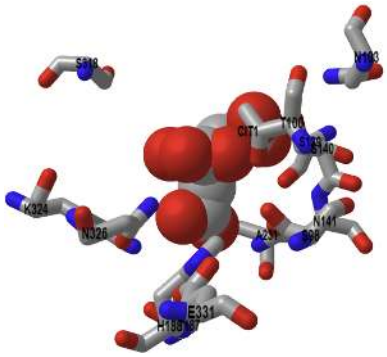
Figure **16.2.26** shows an interactive iCn3D model of the fumarase with beta-(trimethylsilyl)maleate and citrate (1fuq).



NCBI iCn3D Figure **16.2.26**: Fumarase with beta-(trimethylsilyl)maleate and citrate (1fuq). (Copyright; author via source). Click the image for a popup or use this external link: https://structure.ncbi.nlm.nih.gov/i...MewEQFebi4VL48

The monomers in the tetramer are shown in different colors. Citrate (Cit) and beta-(trimethylsilyl)maleate (SIF) are shown in spacefill.

Figure **16.2.27** shows an interactive iCn3D model of the binding site of citrate, a competitive inhibitor of fumarase (1FUQ).



NCBI iCn3D Figure **16.2.27**: Binding site of the competitive inhibitor citrate in fumarase (1FUQ). (Copyright; author via source). Click the image for a popup or use this external link: https://structure.ncbi.nlm.nih.gov/i...yfPc5iPWbExr86

Figure **16.2.28** shows a plausible mechanism for the trans-addition of water to fumarate.

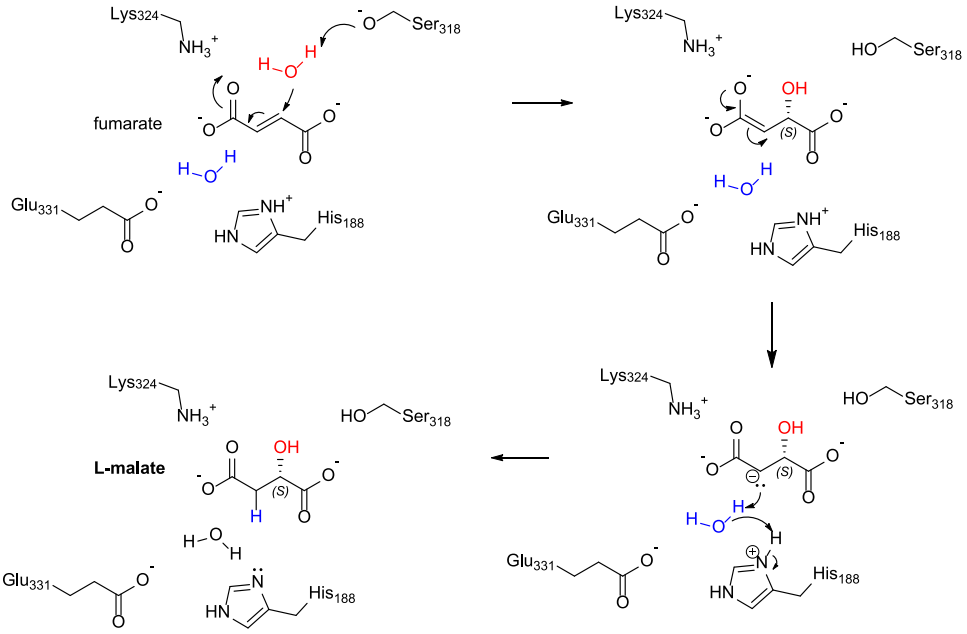


Figure **16.2.28**: Mechanism for fumarase

16.2.9: 8. MALATE DEHYDROGENASE (MDH)

L-malate+ NAD^+ ↔ oxaloacetate + NADH + H^+ ΔG^o = +7.1 kcal/mol (30 kJ/mol)

We are finally there! This last reaction of the citric acid cycle produces oxaloacetate, the starting reactant, allowing the cycle to continue. It also produces NADH for mitochondrial e-transport/ATP production. Notice that the reaction is thermodynamically unfavorable (in the standard state), but the reaction is pulled to citrate formation by the next (and first step of the cycle, citrate synthase. The reaction is shown in Figure **16.2.29**.

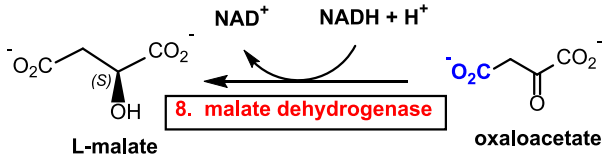


Figure **16.2.29**: Summary reaction for malate dehydrogenase

Malate dehydrogenases are located in the cytoplasm, part of the aspartate-malate shuttle that transports cytoplasmic malate (and, indirectly through MDH, NADH) into the mitochondria. It is also found in the mitochondria, part of the citric acid cycle. There are also NAD^+- and $NADP^+$-dependent forms. Malate can undergo two oxidation reactions, one using NAD^+ and producing oxaloacetate and another, an oxidative decarboxylation, producing pyruvate and CO_2, using $NADP^+$. The latter is sometimes referred to as the **malic enzyme**.

Humans have two forms (MDH 1 and MDH 2) that use NAD^+. The enzyme is a homodimer in humans, with binding sites on both subunits. Its activity is allosterically

regulated by citrate, and ATP, ADP, AMP, fumarate, and aspartate inhibit it. High concentrations of oxaloacetate also inhibit it.

The enzyme is similar to lactate dehydrogenase, which we encountered in glycolysis. Kinetic analyses show that NAD^+ binds first, followed by malate.

Figure **16.2.30** shows an interactive iCn3D model of NAD^+ and malate bound to human malate dehydrogenase 2 (4wlu).

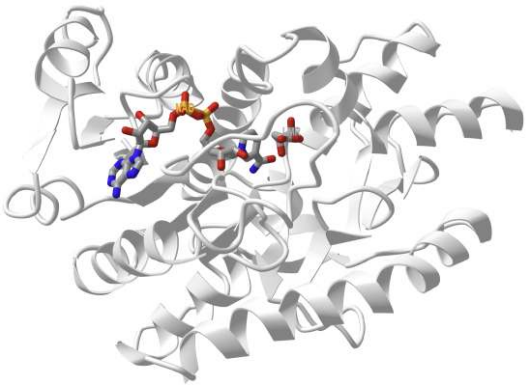


Figure **16.2.30**: NAD^+ and malate bound to human malate dehydrogenase 2 (4wlu). (Copyright; author via source). Click the image for a popup or use this external link: https://structure.ncbi.nlm.nih.gov/i...DrAXBdu64GPzx8

Just one monomer is shown. NAD^+ and malate (LMR) are shown in sticks and labeled.

Figure **16.2.31** shows an abbreviated mechanism for malate dehydrogenase. The numbers refer to the *E. Coli* enzyme.

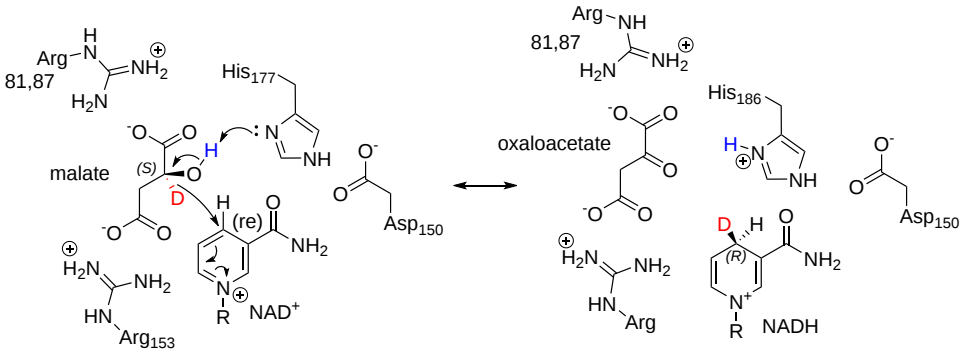


Figure **16.2.31**: Abbreviated mechanism for malate dehydrogenase

Note that the hydride transferred from the malate is shown in red as a deuterium (D). Deuterium (D) was used to indicate the stereochemistry of the removed "H" and to assign that "H" to the proR position in NADH. (Remember that the carbon with the deuterium in NADH is prochiral. D has a higher priority than H in the Cahn/Ingold designation system. It is transferred to the re face of NAD^+ to form NADH. In the reverse reaction, the D atom, which is above the plane of the ring, occupies the proR position. The proR deuterium is transferred back in this reversible reaction.

Figure **16.2.32** shows an interactive iCn3D model of the active site of the E. Coli malate dehydrogenase with bound citrate and NAD^+ (1EMD).

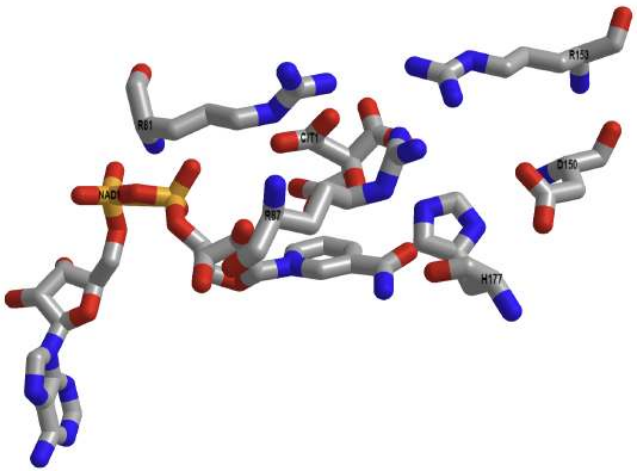


Figure **16.2.32**: Active site of the E. Coli malate dehydrogenase with bound citrate and NAD^+ (1EMD). (Copyright; author via source). Click the image for a popup or use this external link: https://structure.ncbi.nlm.nih.gov/i...mHhmeFQyPpZj18

We have shown many renderings of the enzymes involved in the cycle. Yet another one is shown below. Figure **16.2.33** shows an interactive iCn3D model of the electrostatic surface potential of malate dehydrogenase (4WLU).

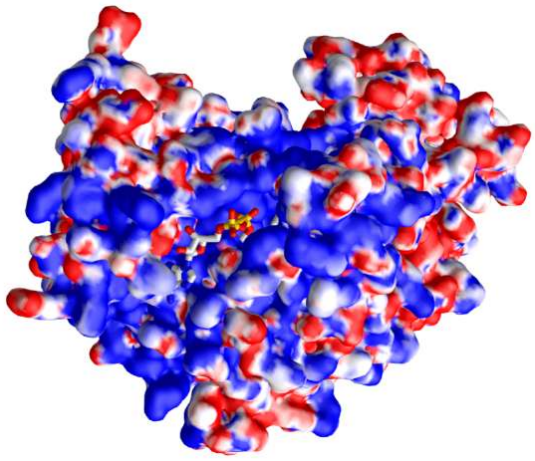


Figure **16.2.33**: Electrostatic surface potential of malate dehydrogenase (4WLU)with bound NAD^+ (4WLU). (Copyright; author via source). Click the image for a popup or use this external link: https://structure.ncbi.nlm.nih.gov/icn3d/share.html?izf2dsWXTw2bE8YD7

The displayed surface is the electrostatic surface potential map of the enzyme. Red shows the more anionic surfaces with a negative electrostatic potential to which cations would be attracted. At the same time, blue represents more cationic surfaces to which anions would be attracted. Note that the bound NAD^+, which has many oxygens that are slightly or entirely negative, is bound in a blue, positive electrostatic potential region.

SUMMARY OF THE CYCLE

Let's do some stoichiometry for the full cycle. Here is the net reaction (assuming that the GTP produced by succinyl-CoA synthetase is equivalent to 1 ATP).

$$\text{Acetyl-CoA} + 3NAD^+ + FAD + ADP + P_i + 2H_2O \rightarrow 2CO_2 + 3NADH + FADH_2 + ATP + 2H^+ + CoASH$$

It must seem like a lot of work to produce just 1 ATP, especially since the partial anaerobic oxidation of glucose in glycolysis produces 2 ATPs in net fashion. The key is to realize that 3 NADHs and 1 FADH2 are produced, which, when reoxidized in mitochondrial electron transport/oxidative phosphorylation, will produce multitudes of ATP.

As was true for glycolysis, this main energy-extracting pathway is highly regulated. We will discuss this in the next section.

Figure **16.2.34** highlights (colored boxes) some key features of molecules involved in the citric acid cycle.

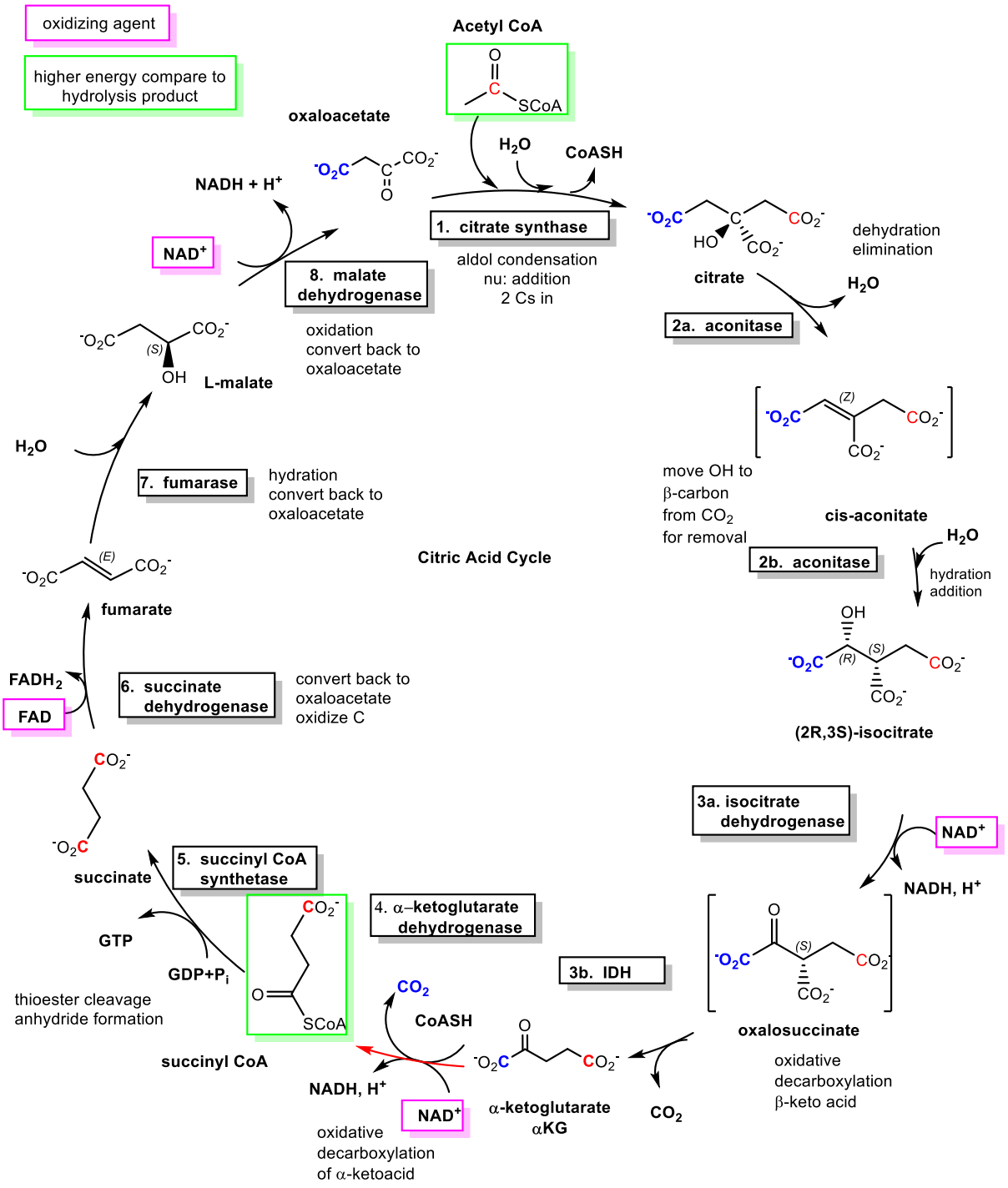


Figure 16.2.34: Summary of the citric acid cycle.

16.2.10: SUMMARY

This chapter provides a detailed examination of the citric acid cycle (CAC), also known as the tricarboxylic acid (TCA) cycle or Krebs cycle, which is central to aerobic metabolism. It bridges the oxidative decarboxylation of pyruvate (via the pyruvate dehydrogenase complex) to the complete oxidation of acetyl-CoA, ultimately linking glycolysis to the electron transport chain and ATP production.

Why a Cycle?

The cyclic nature of the CAC ensures that key intermediates are continuously regenerated, even when they are withdrawn for biosynthetic purposes. This design maintains the flux of the pathway despite the loss of intermediates, a feature that would be unsustainable in a linear pathway.

Key Reactions and Mechanisms:

- **Citrate Synthase:**
  Acetyl-CoA reacts with oxaloacetate to form citrate, a process driven by the high-energy thioester bond of acetyl-CoA. The enzyme undergoes conformational changes—from an open to a closed state—to sequester substrates and prevent unproductive hydrolysis.
- **Aconitase:**
  Citrate is isomerized to isocitrate through the formation of cis-aconitate. The enzyme, which utilizes an iron-sulfur (Fe_4S_4) cluster, catalyzes this reversible hydration/dehydration reaction, critical for repositioning hydroxyl groups for subsequent oxidation.
- **Isocitrate Dehydrogenase:**
  Oxidative decarboxylation of isocitrate produces α-ketoglutarate, NADH, and CO_2. This step requires the formation of a β-ketoacid intermediate that facilitates decarboxylation.
- **α-Ketoglutarate Dehydrogenase:**
  This multienzyme complex further decarboxylates α-ketoglutarate, producing succinyl-CoA, NADH, and CO_2, using a mechanism similar to that of pyruvate dehydrogenase.
- **Succinyl-CoA Synthetase:**
  The high-energy thioester bond of succinyl-CoA is hydrolyzed to drive the substrate-level phosphorylation of GDP to GTP (or ADP to ATP), capturing energy in a readily usable form.
- **Succinate Dehydrogenase:**
  Oxidation of succinate to fumarate generates $FADH_2$. This enzyme, a component of Complex II in the electron transport chain, plays a dual role in the CAC and respiratory chain.
- **Fumarase:**
  Fumarate is hydrated to L-malate in a reaction that is near equilibrium, setting the stage for the final oxidation step.
- **Malate Dehydrogenase:**
  Oxidation of malate produces oxaloacetate, NADH, and a proton, thereby regenerating the cycle's starting material and linking the CAC to NADH-dependent electron transport.

Energy and Regulation:

Although the CAC directly produces only a small amount of ATP (or GTP) per cycle, it generates multiple NADH and $FADH_2$ molecules. These reduced cofactors drive oxidative phosphorylation in the mitochondria, resulting in the production of a large number of ATP molecules. The chapter emphasizes that every step in the cycle is finely tuned, not only by substrate availability and product inhibition but also through the interplay with other metabolic pathways. Anaplerotic reactions replenish intermediates withdrawn for biosynthesis, ensuring the continuity of the cycle.

Structural and Mechanistic Insights:

Interactive molecular models and detailed reaction mechanisms illustrate the precise positioning of substrates, cofactors, and key active-site residues. These visualizations help to explain how enzymes like citrate synthase and aconitase achieve substrate specificity and catalytic efficiency through conformational changes and coordinated electron flow.

In summary, this chapter elucidates the complexity and elegance of the citric acid cycle—a central metabolic pathway that integrates energy extraction, biosynthesis, and regulation. By understanding both the chemical mechanisms and the structural biology of the enzymes involved, students gain a comprehensive view of how cells orchestrate efficient energy production and maintain metabolic balance.

This page titled 16.2: Reactions of the Citric Acid Cycle is shared under a not declared license and was authored, remixed, and/or curated by Henry Jakubowski and Patricia Flatt.

- **Current page** by Henry Jakubowski and Patricia Flatt has no license indicated.
- **11.2: Diffusion Across a Membrane - Passive and Facilitated Diffusion** by Henry Jakubowski and Patricia Flatt has no license indicated.

16.3: REGULATION OF THE CITRIC ACID CYCLE

LEARNING GOALS (CHATGPT O3-MINI)

1. **Integrate Pathway Overview and Energy Extraction:**
   - Explain how the entry of pyruvate into the citric acid cycle supports aerobic energy production and supplies biosynthetic intermediates.
   - Describe the role of the pyruvate dehydrogenase complex (PDC) in converting pyruvate to acetyl-CoA and how this links glycolysis to the citric acid cycle.
2. **Understand Regulatory Mechanisms in the CAC and PDC:**
   - Identify the various regulatory strategies (substrate availability, product inhibition, allosteric effectors, and post-translational modifications) that control key enzymes in these pathways.
   - Discuss how energy status—reflected by the mitochondrial NAD^+/NADH and ATP/ADP ratios—modulates enzyme activity within the cycle.
3. **Analyze Allosteric and Covalent Regulation of PDC:**
   - Describe the allosteric regulation of PDC by substrates (pyruvate and NAD^+) and products (acetyl-CoA, NADH, and ATP).
   - Explain the role of pyruvate dehydrogenase kinase (PDK) and pyruvate dehydrogenase phosphatase (PDP) in covalent modification (phosphorylation/dephosphorylation) of PDC, including the effects of modulators such as dichloroacetate, TPP, Ca^{2+}, and pyruvate.
4. **Examine the Regulation of Key Citric Acid Cycle Enzymes:**
   - Detail how citrate synthase is regulated by its substrates (acetyl-CoA and oxaloacetate) and inhibited by NADH, citrate, and succinyl-CoA, including the structural conformational changes (open vs. closed states) that facilitate its function.
   - Summarize the regulatory features of other CAC enzymes (e.g., isocitrate dehydrogenase, α-ketoglutarate dehydrogenase) with emphasis on the impact of energy carriers and metabolite levels.
5. **Evaluate the Concept and Function of Metabolon Formation:**
   - Define what a metabolon is and describe how physical interactions among citric acid cycle enzymes (such as MDH, CS, and aconitase) enhance metabolic flux by channeling substrates directly from one enzyme to the next.
   - Analyze how alterations in the NAD^+/NADH ratio can modulate the activity of enzymes within a metabolon, thereby influencing the overall rate of the cycle.
6. **Relate Hormonal Regulation to Metabolic Flux:**
   - Compare the effects of hormonal signals (insulin and glucagon) on glycolytic enzymes and the PDC, and explain how these signals indirectly affect the flux through the citric acid cycle.
   - Discuss how hormonal conditions can shift metabolic priorities (e.g., promoting glucose oxidation versus glucose conservation).
7. **Synthesize Structure-Function Relationships:**
   - Use interactive molecular models to visualize active sites, conformational changes, and electrostatic surface potentials of key enzymes (e.g., citrate synthase and isocitrate dehydrogenase).
   - Relate structural features to their regulatory functions, such as how binding of acetyl-CoA or NADH alters enzyme conformation and activity.

These learning goals will guide students to develop a comprehensive understanding of how the citric acid cycle and pyruvate dehydrogenase complex are intricately regulated in response to both cellular energy demands and systemic hormonal signals, ensuring balanced energy production and metabolic homeostasis.

16.3.1: OVERVIEW

The entry of pyruvate into the citric acid cycle, leading to the aerobic production of energy and intermediates for biosynthesis, is a key metabolic step. Hence, both the pyruvate dehydrogenase complex and key enzymes in the cycle are targets for regulation. This occurs through substrate availability, product inhibition, allosteric effectors, and post-translational modifications of key enzymes in the pathway. Figure 16.3.1 shows a summary figure of key regulators.

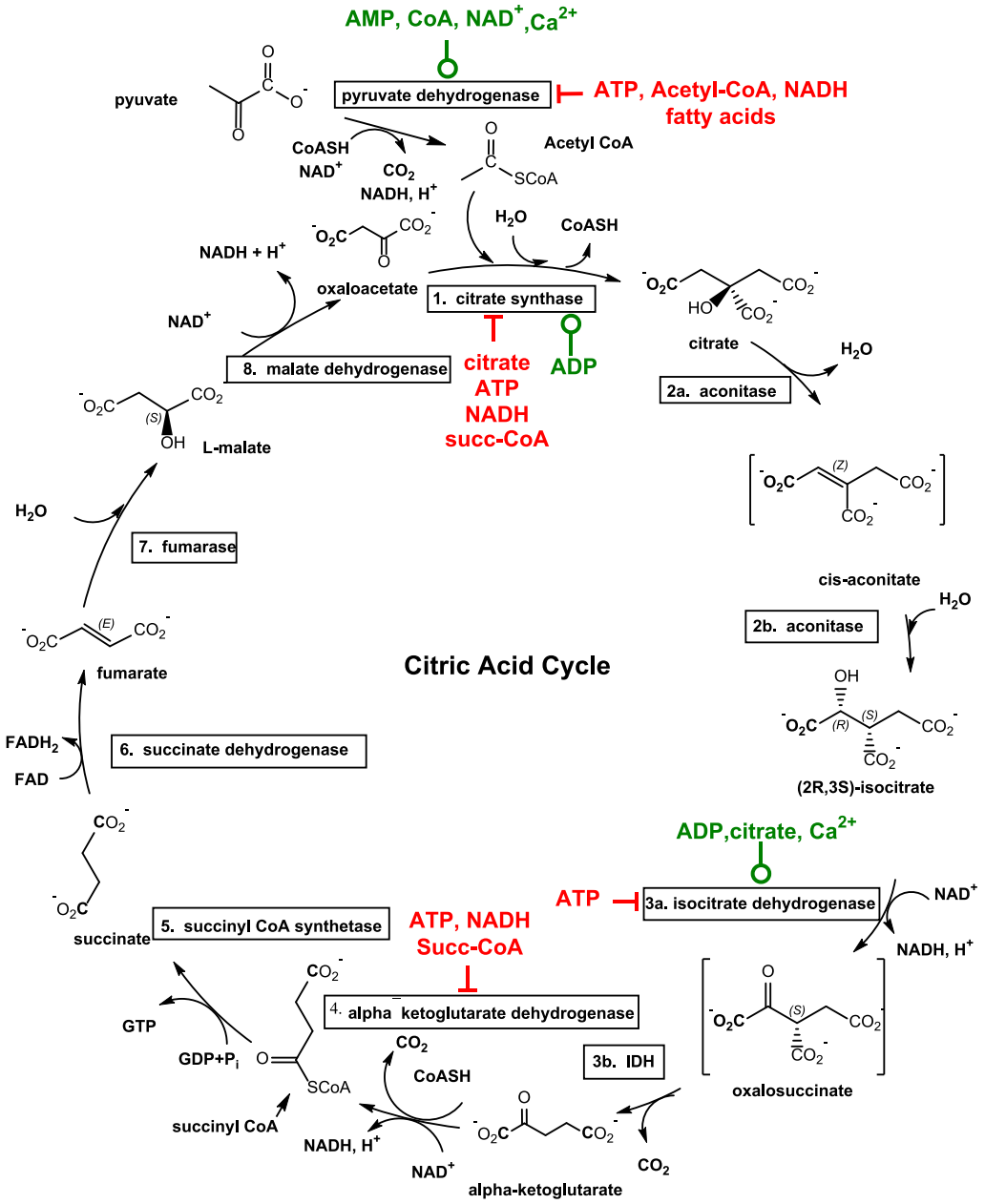


Figure **16.3.1**: Regulation of the citric acid cycle

https://www.nature.com/articles/s41598-021-98314-z

Note that the key steps are primarily regulated by the ratio of mitochondrial NAD+/NADH, which is highly influenced by the ATP/ADP ratio. High NADH inhibits the regulatory enzymes. High levels of acetyl-CoA, derived from pyruvate dehydrogenase and also through fatty acid catabolism, increase flux through the cycle, in part by allosterically activating the first enzyme in the pathway, citrate synthase.

The material below is derived from Renée LeClair, Ph.D., ***Cell Biology, Genetics, and Biochemistry for Pre-Clinical Students.*** https://med.libretexts.org/@go/page/37584. openly licensed (CC BY-NC-SA 4.0

16.3.2: REGULATION OF THE PYRUVATE DEHYDROGENASE COMPLEX (PDC)

Under aerobic conditions, the pyruvate produced by glycolysis will be oxidized to acetyl-CoA using the pyruvate dehydrogenase complex (PDC) in the mitochondria (note: its genes are encoded in the nucleus). As this enzyme is a key transition point (the gatekeeper) between cytosolic and mitochondrial metabolism and is highly exergonic ($\Delta G^{0'}$ = -7.9 kcal/mol, -38 kJ/mol), it is highly regulated by both covalent

and allosteric regulation. Deficiencies of the PDC are X-linked and present with symptoms of lactic acidosis after consuming a meal high in carbohydrates. This metabolic deficiency can be overcome by delivering a ketogenic diet and bypassing glycolysis altogether.

Allosteric and covalent regulations regulate the PDC. The complex itself can be allosterically activated by pyruvate and NAD^+. Elevation of the substrate (pyruvate) will enhance flux through this enzyme, as will the indication of low-energy states triggered by high NAD^+ levels. The PDC is also inhibited by acetyl-CoA and NADH directly. Product inhibition is a common regulatory mechanism, and high NADH levels signal sufficient energy, thereby decreasing PDC activity. Figure **16.3.2** summarizes the regulation. (Adapted from Marks' Medical Biochemistry)

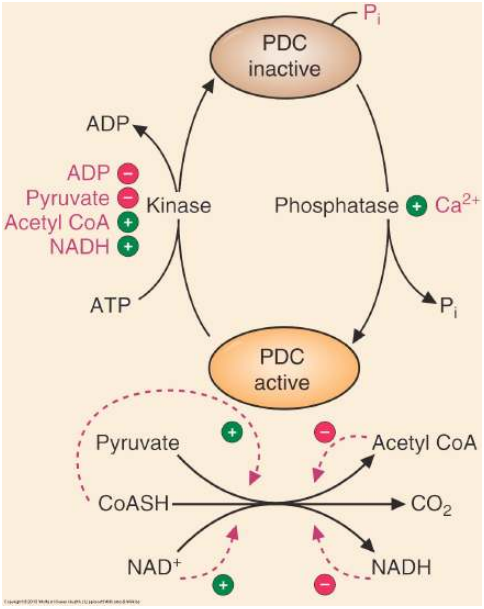


Figure **16.3.2**: Regulation of pyruvate dehydrogenase.

The PDC is also regulated through covalent modification. Phosphorylation of the complex's E1 subunits decreases the enzyme's activity.

The enzyme responsible for the phosphorylation of the PDC is **pyruvate dehydrogenase kinase**. The kinase is regulated inversely to the PDC, as shown in Figure 1 above. The kinase is most active when acetyl-CoA, NADH, and ATP are high. These compounds will stimulate the kinase to phosphorylate and inactivate the PDC. Dichloroacetate, TPP, Ca^{2+}, and pyruvate inhibit PDK. A calcium-mediated phosphatase, PDP, can dephosphorylate the PDC. Starvation and diabetes increase phosphorylation and inhibition of the complex, which impairs glucose oxidation.

Phosphorylation occurs on Serine 264 of the α subunit (site 1), Ser271 (site 2), and Ser203 (site 3), which are located on a conserved phosphorylation loop. Sites 1 and 2 (in loop A) stabilize TPP in the active site, while Ser 203 in the adjacent loop B binds $Mg^{2+,}$ stabilizing PP on bound TPP. All it takes to inhibit is phosphorylation of just one of the Ser side chains. Phosphorylation prevents the ordering of the loop that occurs on TPP binding, which hinders the binding of the lipoyl domains of the PDC core to E1p, which inhibits the flow of metabolites in the PDC.

The specific PDK inhibitor dichloroacetate prevents PDC phosphorylation, increasing levels of reactive oxygen species in mitochondria. This promotes the expression of a mitochondria-K^+ channel axis, leading to cellular apoptosis and the inhibition of tumor growth.

Figure **16.3.3** shows a summary of pathway regulation.

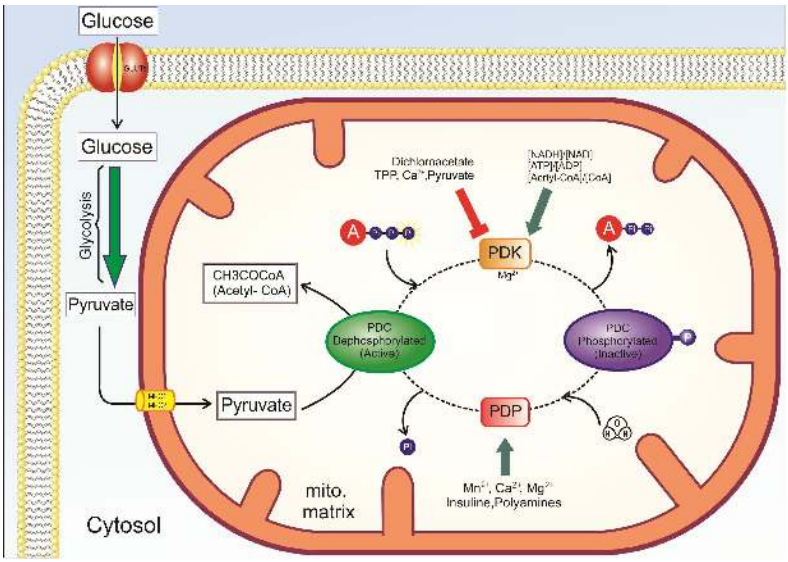


Figure **16.3.3**: Summary of the regulation of pyruvate dehydrogenase

In general, PDC is activated through its substrates CoASH and NAD^+, and kinase inhibition or phosphatase activation (PDP) (dichloroacetate, TPP, Ca^{2+}, and pyruvate) is inhibited by its products, acetyl-CoA and NADH, as well as activation of the kinase (PDK). Abbreviations : PDC: pyruvate dehydrogenase complex, PDK: pyruvate dehydrogenase kinase, PDP: pyruvate dehydrogenase phosphatase, TPP: thiamine pyrophosphate.

The complex is also acetylated and succinylated.

Here is a brief review of general hormonal effects leading up to acetyl-CoA production:

Under low serum glucose conditions

- glucagon is secreted. This activates glucose synthesis and glycogen breakdown, while inhibiting glycolysis in the liver. Glucose is then exported into the blood, restoring a higher glucose concentration.

Under high serum glucose

- Insulin is secreted, promoting glucose uptake in the liver and muscle for energy use (glycolysis is activated, gluconeogenesis is inhibited) and storage (glycogen synthase is activated).

Table **16.3.1** below shows a summary of the regulation of pyruvate in glycolysis and pyruvate dehydrogenase, and also shows the effect of insulin. Glucagon leads to phosphorylation and inactivation of the designated enzymes, the opposite effect of insulin.

Metabolic Pathway	Major Regulatory Enzyme(s)	Allosteric Effectors	Post-translational modifications	Hormonal Effects
Glycolysis	hexokinase; glucokinase (liver)	Glucose 6P (-)		
	PFK-1	Fructose 2,6BP, AMP (+) Citrate (-)		↑ Insulin leads to dephosphorylation of PFK2 and increases production of F2,6BP, which activates PFK-1
	Pyruvate Kinase (PK)	Fructose 1,6BP (+) ATP, Alanine (-)		↑ Insulin leads to dephosporylation and activation of PK
Pyruvate Dehydrogenase Complex	PDC	Pyruvate, NAD^+ (+) Acetyl CoA, NADH, ATP (-)	dephosphorylation by PDP (+) phosphorylation by PDK (-)	↑ Insulin leads to dephosphorylation and activation of PDC

Table **16.3.1**: Summary of the regulation of pyruvate through glycolytic enzymes and pyruvate dehydrogenase

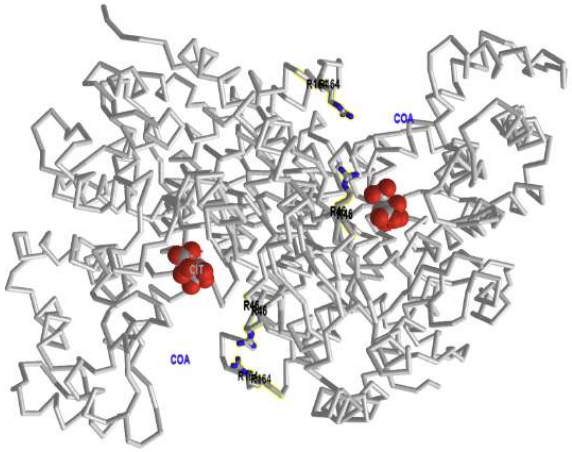
Now, let's focus directly on the regulation of enzymes in the citric acid cycle.

16.3.3: REGULATION OF CITRATE SYNTHASE

Citrate synthase (ΔG^o = -7.5 kcal/mol, -31 kJ/mol), Isocitrate dehydrogenase (ΔG^o = -2.0 kcal/mol, -8.4 kJ/mol), and alpha-ketoglutarate dehydrogenase (ΔG^o = -7.2 kcal/mol, -30 kJ/mol) are all exergonic and likely candidates for regulation. Indeed, they are. Let's start with citrate synthase.

Citrate synthase is regulated in part by the availability of substrate acetyl-CoA and oxaloacetate. It is inhibited by NADH and citrate, a competitive inhibitor of oxaloacetate binding. Succinyl-CoA, a downstream product of the citric acid cycle, is a competitive inhibitor of acetyl-CoA binding.

Figure **16.3.4** shows an interactive iCn3D model of a structural comparison of pig citrate synthase with bound citrate (1CTS) and with bound citrate and CoASH (2CTS)



NCBI iCn3D Figure **16.3.4**: Structural comparison of pig citrate synthase with bound citrate (1CTS) and with bound citrate and CoASH (2CTS). (Copyright; author via source). Click the image for a popup or use this external link: https://structure.ncbi.nlm.nih.gov/i...94UeRDsFyGTcdA

Toggle the "a" key back and forth to change from the open structure (gray) with bound citrate (1CTS) to the closed structure (cyan) after CoASH binds (2CTS).

Citrate and CoASH are the products of the citrate synthase reaction, but observing how they interact with the protein gives clues into catalysis. When both are bound, the enzyme is in a closed conformation, which prevents spurious hydrolysis of the actual acetyl-CoA during the reaction that proceeds to citrate formation. In the presence of citrate, the enzyme is in open form, allowing the release of citrate as a product. The binding of the reactant oxaloacetate triggers the conversion to the closed form. NADH is reported to be an allosteric inhibitor of bacterial citrate synthases, but no entries are available for binding NADH to mammalian enzymes.

The effects of binding acetyl-CoA on the structure of citrate synthase are shown in Figure **16.3.5**:

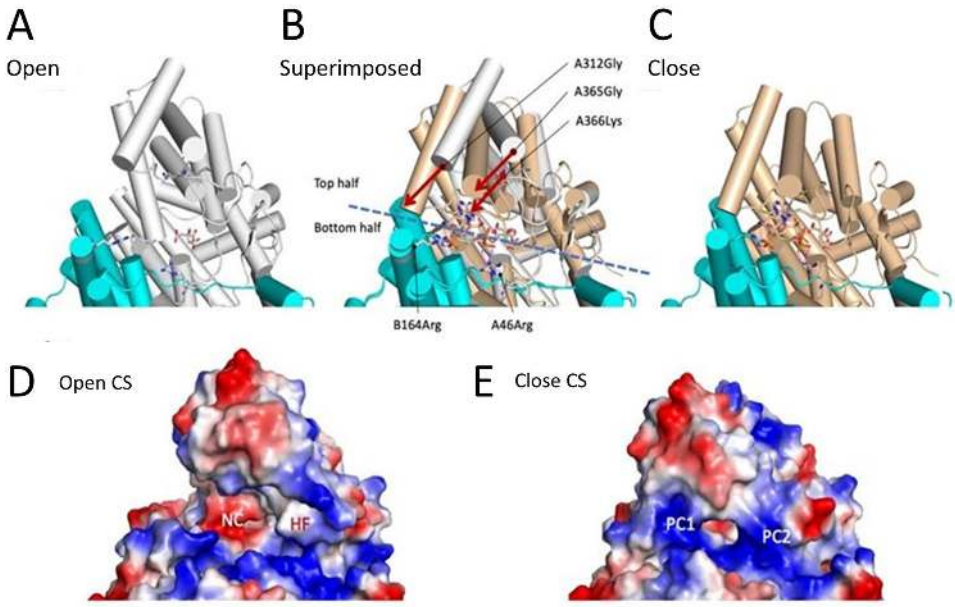


Figure **16.3.5**: Effect of acetyl-CoA binding on CS structure. Omini, J., Wojciechowska, I., Skirycz, A. *et al.* The association of the malate dehydrogenase-citrate synthase metabolon is modulated by intermediates of the Krebs tricarboxylic acid cycle. *Sci Rep* **11,** 18770 (2021). https://doi.org/10.1038/s41598-021-98314-z. Creative Commons Attribution 4.0 International License. http://creativecommons.org/licenses/by/4.0/.

Panel (**A**) shows the open format of CS (PDB ID, 1cts) in a cartoon model, with cylindrical α-helices containing a citrate molecule in a stick model. Subunits A and B are colored white and cyan, respectively. The side chains of key residues, A266Lys, A46Arg, and B164Arg, are shown in the sticks. The residues are shown in the order of the chain name, residue number, and amino acid. The dimeric structure was generated using crystallographic symmetry. One active site domain composed mainly of the A-chain is shown.

Panel (**B**) shows the superimposed model between the open (1cts; white) and closed (2cts; wheat) formats. The citrate molecule is at the same location with a slight rotation. The CoA molecule is present only in the closed format. The molecular domain shown can be divided into the movable upper half and the rigid bottom half. In the bottom domain, A45Arg and B146Arg are shown in the stick model. The locations of those two Cα in Arg are almost consistent between the open and closed formats. The top half of the domain is movable. The motion is visible as the rotation of α-helices represented by A312Gly and A365Gly, indicated by arrows. The A366Lys moves inward and forms a hydrogen bond network A366Lys (NZ):: A438COA(O8A):: B164Arg(NH1).

Panel (**C**) shows the closed format of CS (PDB ID, 2cts) with citrate and CoA molecules in stick models.

Panel (**D**) shows the surface electrostatic potential of the open-format CS, excluding ligands. Calculations were performed in a vacuum environment and ranged between -71 and +71. Red and blue represent the negative and positive potentials. The domain shown corresponds to panel A. Patches of negative charge (**NC**) and hydrophobic area (**HF**) are observed.

Panel (**E**) shows the surface electrostatic potential of the closed format CS, excluding ligands. The domain shown corresponds to panel D. Patches of positive charge (PC1, PC2) are observed.

At the end of this chapter, we will see how citrate synthase's electrostatic surface potential enables it to interact with other enzymes in the citric acid cycle to form a metabolon.

16.3.4: REGULATION OF ISOCITRATE DEHYDROGENASE

In the previous section, structures of the αγ and αβ heterodimer building blocks of the protein were described. The α subunits contain the catalytic site, while the β and γ subunits are the regulatory subunits that bind allosteric effectors. Citrate and ADP allosterically activate both the $\alpha_2\beta\gamma$ heterotetramer and αγ heterodimer. They bind next to each other in the allosteric site, along with Mg^{2+}. Conformational changes in binding citrate lead to a change in the activation of the catalytic subunit α. The binding of ADP enhances this effect.

The domain and cartoon structure of the αγ heterodimer of human NAD-IDH are shown in Figure **16.3.6**.

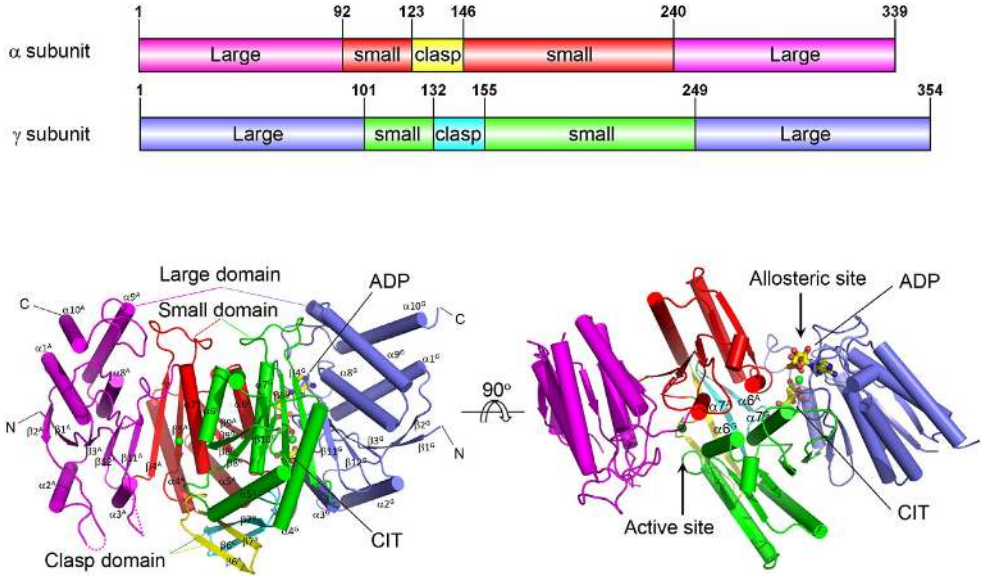


Figure 16.3.6: Domain and cartoon structure of the αγ heterodimer of human NAD-IDH. Ma, T., Peng, Y., Huang, W. *et al.* Molecular mechanism of the allosteric regulation of the αγ heterodimer of human NAD-dependent isocitrate dehydrogenase. *Sci Rep* **7,** 40921 (2017). https://doi.org/10.1038/srep40921. Creative Commons Attribution 4.0 International License. http://creativecommons.org/licenses/by/4.0/

The top panel shows the domain structure of the two monomers. The bottom panel shows two views of the dimer. The color coding is the same as in the top panel.

Figure 16.3.7 shows bound citrate and ADP in the allosteric binding site in the γ subunit of IDH.

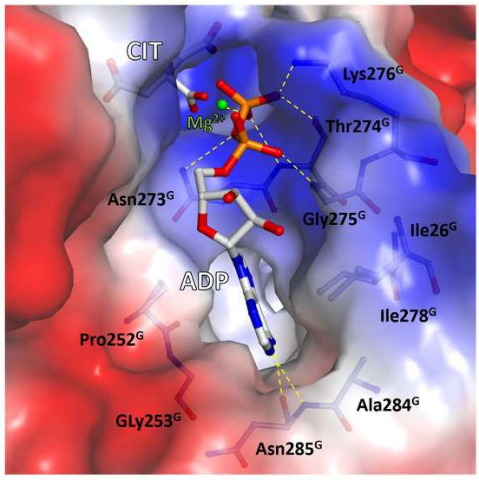


Figure 16.3.7: Bound citrate and ADP in the allosteric binding site in the γ subunit of IDH**.** Ma et al., ibid.

The color represents the site's electrostatic surface potential, with blue indicating a more positive potential and red indicating a more negative potential. Note that both allosteric activators bind adjacent to each other. The binding of ADP does not change the conformation after the citrate is bound.

The proposed molecular mechanism for allosteric regulation of IDH is shown in Figure 16.3.8.

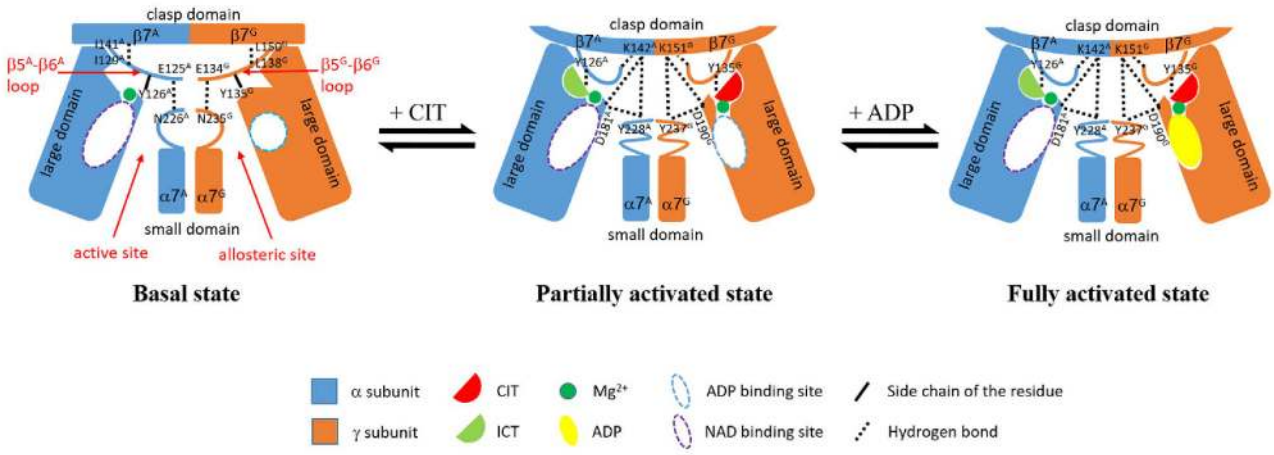


Figure 16.3.8: Mechanism of allosteric regulation of the αγ heterodimer of IDH. Ma et al., ibid.

Legend: In the absence of any activators, the active site adopts an inactive conformation unfavorable for the ICT binding, and the enzyme is in the basal state with a high $S_{0.5,\mathrm{ICT}}$ with a low catalytic efficiency. The binding of CIT induces conformational changes at the allosteric site, which are transmitted to the active site through conformational changes of the structural elements at the heterodimer interface, including the β5–β6 loop, the α7 helix, and the β7-strand in both the α and γ subunits, leading to the conversion of the active site from the inactive conformation to the active conformation favorable for the ICT binding. Hence, the enzyme assumes the partially activated state, which has a moderately decreased $S_{0.5,\mathrm{ICT}}$ (lower substrate concentration for half-maximal activity) with a moderately increased catalytic efficiency. The binding of ADP in the presence of CIT does not induce further conformational changes at the allosteric and active sites. Still, it establishes a more extensive hydrogen-bonding network among CIT, ADP, and the surrounding residues through the metal ion, which conversely enhances or stabilizes the CIT binding. Hence, the binding of CIT and ADP together has a synergistic activation effect, and the enzyme assumes the fully activated state with a substantially decreased $S_{0.5,\mathrm{ICT}}$ with a significantly increased catalytic efficiency.

16.3.5: REGULATION OF A-KETOGLUTARATE DEHYDROGENASE

α-ketoglutarate dehydrogenase and pyruvate dehydrogenase complex both catalyze the oxidative decarboxylation of α-ketoacids. They employ a common mechanism involving three enzymes, E1, E2, and E3, in a large complex. The regulation of α-ketoglutarate dehydrogenase activity is shown in Figure 16.3.9.

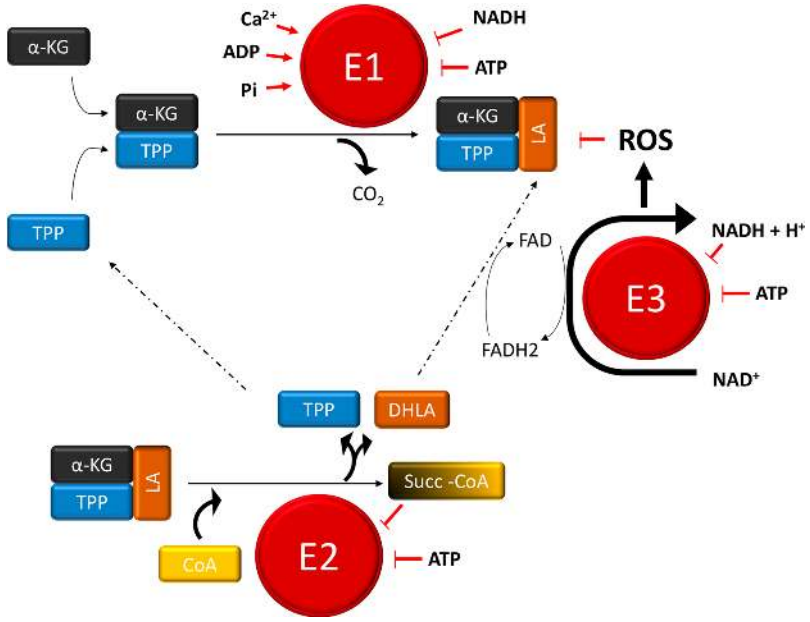


Figure 16.3.9: Regulation mechanisms of α-ketoglutarate dehydrogenase complex (α-KGDC). Vatrinet, R., Leone, G., De Luise, M. *et al.* The α-ketoglutarate dehydrogenase complex in cancer metabolic plasticity. LS and DHLA are lipoamide and dihydrolipoamide,

respectively. TPP is thiamine pyrophosphate. *Cancer Metab* **5,** 3 (2017). https://doi.org/10.1186/s40170-017-0165-0. Creative Commons Attribution 4.0 International License (http://creativecommons.org/licenses/by/4.0/),

As with the other key regulatory enzymes, α-KGDC is regulated by the ratios of ATP/ADP and NADH/NAD^+. The product, succinyl-CoA, inhibits the reaction at the E2 stage. The mitochondria are reservoirs for Ca^{2+} ions. These ions increase the activity of pyruvate, isocitrate, and α-ketoglutarate dehydrogenases, with α-ketoglutarate dehydrogenase being the most affected. Calcium effects also depend on ATP/ADP and NADH/NAD^+ ratios.

16.3.6: REGULATION BY METABOLON FORMATION

Several citric acid cycle enzymes interact to form a metabolon, which allows enhanced flux through pathways as substrates and products are channeled directly from one enzyme to another in the complex. This "facilitated" diffusion minimizes the dissociation of substrates/products and enhances catalysis. Three enzymes in the citric acid cycle —citrate synthase, malate dehydrogenase, and aconitase —form a metabolon, as demonstrated by chemical cross-linking and docking studies. The linkages between malate dehydrogenase, which produces oxaloacetate, and citrate synthase, which utilizes it, are important because concentrations of oxaloacetate are low and would result in reduced flux in the citric acid cycle if it were not channeled directly into citrate synthase. Malate dehydrogenase is also not favored to produce oxaloacetate based on standard free energy and K_{eq} values so pulling the reaction towards citrate synthase in the metabolon also helps the flux.

$$\text{L-malate} + NAD^+ \leftrightarrow \text{oxaloacetate} + NADH + H^+ \quad \Delta G^o = +7.1 \text{ kcal/mol } (+30 \text{ kJ/mol})$$

Figure **16.3.10** shows models of malate dehydrogenase (MDH) and the open and closed forms of citrate synthase (CS). Electrostatic interactions are key.

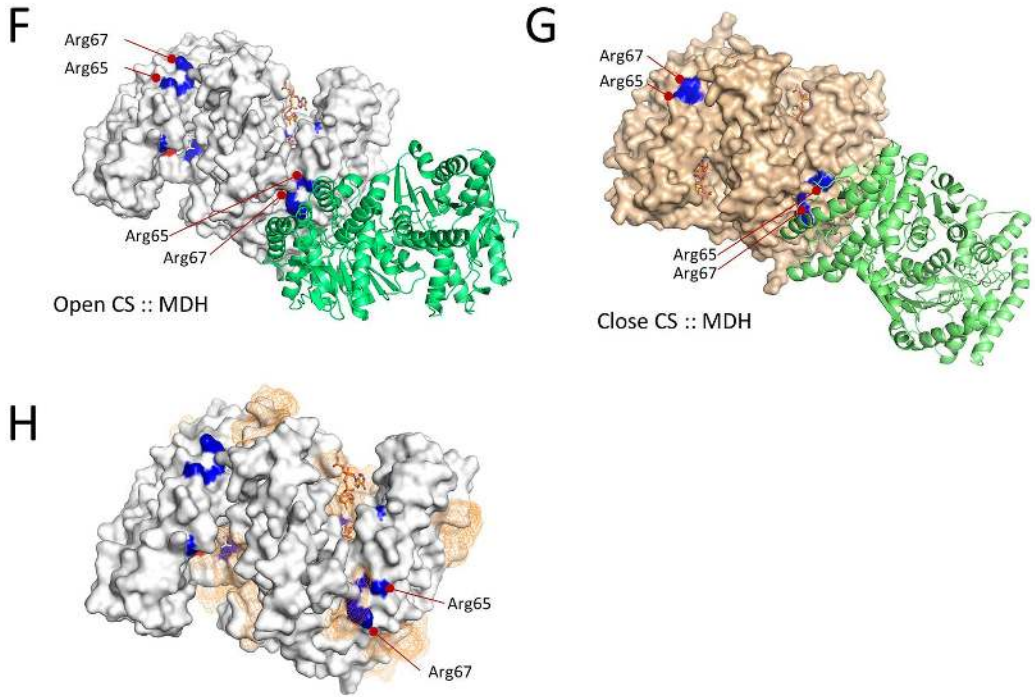


Figure **16.3.10**: Models of malate dehydrogenase (MDH) and the open and closed forms of citrate synthase (CS). Omini, J., Wojciechowska, I., Skirycz, A. *et al.* Association of the malate dehydrogenase-citrate synthase metabolon is modulated by intermediates of the Krebs tricarboxylic acid cycle. *Sci Rep* **11,** 18770 (2021). https://doi.org/10.1038/s41598-021-98314-z. http://creativecommons.org/licenses/by/4.0/.Creative Commons Attribution 4.0 International License.

Panels (**F**) and (**G**) show simulated interactions between MDH (green) and CS in its open (white) form (panel F) and between MDH (green) and CS in its closed (wheat) format (panel G). The 65Arg and 67Arg residues involved in the MDH-CS interaction are highlighted in blue. Active site residues, His274 and His320 (blue), and Asp375 (red), were shown.

Panel (**H**) Predicted acetyl-CoA binding sites in CS apoenzyme. The white surface model of the CS apoenzyme is shown in the open format. The 274His, 320His, 65Arg, and 67Arg residues are highlighted in blue. The orange mesh indicates the positions of acetyl-CoA at the predicted binding sites. White and orange stick models indicate the citrate and CoA in the reported crystal structure.

Does the activity of citrate synthase change when it is complexed to malate dehydrogenase in a metabolon? The results of studies probing that question show that it is affected. The results of such studies show that it does, as illustrated in Figure **16.3.11**.

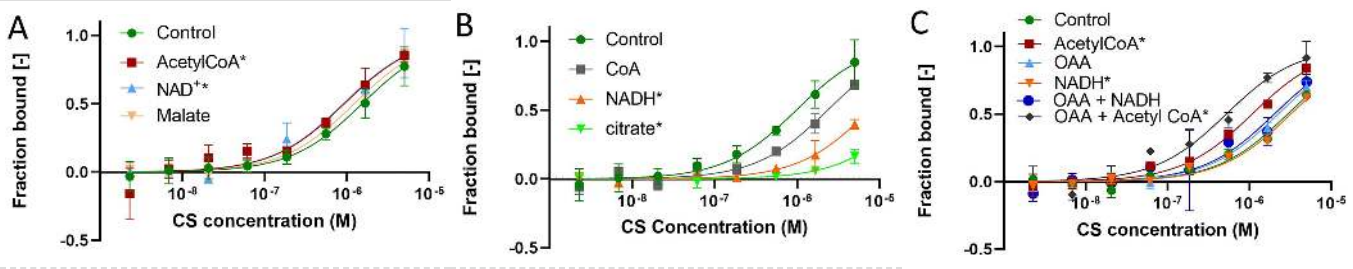


Figure 16.3.11: Effects of metabolites involved in the MDH and CS reactions on the affinity of the MDH-CS multi-enzyme complex. Omini et al., ibid.

Curves represent the response (fraction bound) against CS concentration (M). The interaction was assessed in the MST buffer (control, green) or those with 10 mM of metabolites. Error bars represent the standard deviations of three measurements. Asterisks indicate the conditions that showed significant K_d differences with no K_d confidence overlap with the control.

Panel (**A**) shows the effects of the reaction substrates of MDH and CS. The MDH-CS interaction was assessed in the presence of acetyl-CoA (red), NAD^+ (blue), or malate (brown).

Panel (**B**) shows the reaction's effects on CS and MDH products. The MDH-CS interaction was assessed in the presence of CoA (grey), NADH (orange), or citrate (green).

Panel (**C**) shows the effects of oxaloacetate (OAA) in combination with other CS substrates. The effects of sole substrates, acetyl-CoA (red), OAA (blue), and NADH (orange), as well as their combinations, OAA/acetyl-CoA (purple) and OAA/NADH (gray), were analyzed.

These curves clearly demonstrate how the ratio of NADH to NAD^+ affects the activity of citrate synthase when it is part of a metabolon. NAD^+ increases activity (Panel A) while NADH decreases it (Panel B).

16.3.7: SUMMARY

This chapter explores the complex regulation of energy extraction via the citric acid cycle (CAC) and the pyruvate dehydrogenase complex (PDC), emphasizing how these pathways are finely tuned to meet cellular and systemic energy demands.

Key Concepts in Pathway Regulation:

- The entry of pyruvate into the CAC, after its conversion to acetyl-CoA by the PDC, is a critical junction linking glycolysis to aerobic respiration. Both the PDC and several key enzymes within the CAC are subject to multiple layers of regulation, including substrate availability, product inhibition, allosteric effectors, and post-translational modifications.
- **Energy Status and Allosteric Control:**
  The regulation of these pathways is largely determined by the mitochondrial NAD^+/NADH and ATP/ADP ratios. High levels of NADH and ATP signal an energy-rich state, leading to inhibition of key regulatory enzymes, whereas elevated NAD^+ levels and low energy conditions promote enzyme activity.

Regulation of the Pyruvate Dehydrogenase Complex (PDC):

- The PDC is a highly exergonic and critical "gatekeeper" enzyme that channels pyruvate from glycolysis into the CAC.
- Its activity is modulated both allosterically and by covalent modification. Substrates like pyruvate and NAD^+ activate the complex, while products such as acetyl-CoA and NADH inhibit it.
- Covalent regulation involves phosphorylation of the E1 subunit by pyruvate dehydrogenase kinase (PDK), which inactivates the complex, and dephosphorylation by pyruvate dehydrogenase phosphatase (PDP), which reactivates it. Hormonal cues, such as increased insulin or glucagon levels, further influence these modifications.

Regulation of Key Citric Acid Cycle Enzymes:

- **Citrate Synthase:**
  The first enzyme in the CAC, citrate synthase, catalyzes the condensation of acetyl-CoA with oxaloacetate to form citrate. Its activity is modulated by substrate levels and inhibited by NADH, citrate, and succinyl-CoA. Conformational changes—between open and closed states—play a key role in its catalytic efficiency and regulation.
- **Other Regulatory Nodes:**
  Enzymes such as isocitrate dehydrogenase and α-ketoglutarate dehydrogenase are also regulated by cellular energy levels, ensuring that the cycle adapts to fluctuations in metabolic demand.

Metabolon Formation and Enhanced Flux:

- The chapter introduces the concept of a metabolon—a multi-enzyme complex where enzymes like malate dehydrogenase, citrate synthase, and aconitase physically interact to channel substrates directly from one enzyme to the next.
- This spatial organization minimizes substrate loss, enhances reaction rates, and allows for more precise regulation by modulating local concentrations of intermediates and allosteric effectors.

Hormonal Influence and Systemic Integration:

- Systemic hormonal signals, particularly insulin and glucagon, have profound effects on these pathways. Insulin promotes glucose oxidation and energy storage, while glucagon triggers pathways that conserve and release glucose into the bloodstream.
- These hormonal cues coordinate with intracellular energy sensors to regulate the flux through glycolysis, PDC, and the CAC, thereby maintaining metabolic homeostasis.

In summary, this chapter provides a comprehensive understanding of how the citric acid cycle and the pyruvate dehydrogenase complex are intricately regulated. By integrating structural, enzymatic, and hormonal perspectives, the chapter illustrates how cells coordinate multiple regulatory mechanisms to optimize energy production and biosynthetic output while maintaining metabolic balance.

This page titled 16.3: Regulation of the Citric Acid Cycle is shared under a not declared license and was authored, remixed, and/or curated by Henry Jakubowski and Patricia Flatt.

- **Current page** by Henry Jakubowski and Patricia Flatt has no license indicated.
- **11.2: Diffusion Across a Membrane - Passive and Facilitated Diffusion** by Henry Jakubowski and Patricia Flatt has no license indicated.

16.4: VARIANTS OF THE CITRIC ACID CYCLE

LEARNING GOALS (CHATGPT O3-MINI)

1. **Differentiate Pathway Variants:**
   - Explain the differences between the canonical citric acid cycle and its shunts/bypasses, including the glyoxylate shunt, GABA shunt, and the α-ketoglutarate bypass.
2. **Understand the Glyoxylate Shunt:**
   - Describe the metabolic rationale for the glyoxylate shunt, including how it bypasses the decarboxylation steps of the TCA cycle to allow net carbon assimilation from acetate.
   - Outline the key reactions that convert oxaloacetate and acetyl-CoA into succinate and glyoxylate, and then how glyoxylate is converted to malate.
3. **Analyze the GABA Shunt:**
   - Detail the formation and metabolism of GABA as it relates to the TCA cycle, including the decarboxylation of glutamate and subsequent transamination reactions that reintegrate glutamate into the cycle.
4. **Examine the α-Ketoglutarate Bypass:**
   - Explain how organisms, such as cyanobacteria, bypass the α-ketoglutarate dehydrogenase step by converting α-ketoglutarate directly into succinate using alternative enzymatic reactions.
   - Discuss the physiological significance of this bypass in terms of energy production and biosynthesis.
5. **Evaluate Metabolic Flexibility and Evolution:**
   - Discuss how variations in the TCA cycle, including differences in enzyme cofactor usage (e.g., NAD^+ vs. $NADP^+$) and alternative pathways in prokaryotes versus eukaryotes, contribute to metabolic flexibility.
   - Explore evolutionary perspectives, including the proposed prebiotic “TCA-like” pathways that may have preceded the modern cycle, and how these could have set the stage for the evolution of more complex metabolic networks.
6. **Integrate Regulatory and Biosynthetic Considerations:**
   - Analyze how shunts such as the glyoxylate cycle enable organisms to channel acetyl-CoA into biosynthesis (e.g., for gluconeogenesis) without losing carbon as CO_2, contrasting this with the energy-extractive but carbon-loss–prone full citric acid cycle.
   - Assess how these metabolic adaptations support survival under different environmental and nutritional conditions.

By achieving these learning goals, students will gain a comprehensive understanding of the versatility of the citric acid cycle, the role of alternative metabolic pathways in diverse organisms, and the evolutionary context that has shaped these critical energy-yielding processes.

Evolution has allowed variants in the citric acid cycle to produce new functionalities in organisms. Let's consider a few shunts and bypasses.

16.4.1: GLYOXYLATE SHUNT

What if you were a microorganism that has evolved to use acetate (2C) as a source (if not the sole source) of energy? Remember that the citric acid cycle is also used to generate metabolites for anaplerotic reactions (from the Greek ἀνά= 'up' and πληρόω= 'to fill'). In the full citric acid cycle, activated acetate (2C) reacts with oxaloacetate (4) to produce the 6C molecule citric acid. As the cycle continues back to oxaloacetate, 2 Cs are lost as CO_2, so in sum for one turn of the cycle:

$$\text{oxaloacetate (4C)} + \text{acetyl-CoA (2C)} \rightarrow \text{Citrate (6C)} \rightarrow \rightarrow \rightarrow \text{succinate (4C)} + 2\ CO_2\ \text{(2C)}.$$

During this process, oxidation reactions occur, resulting in the formation of NADH and $FADH_2$. The metabolites formed can be utilized for biosynthesis (OAA, α-KG, and succinyl-CoA).

An alternative "cycle" would be to eliminate the two decarboxylation reactions and generate a 4C molecule (succinate) and one 2C metabolite (glyoxylate), which could react with another activated acetate (acetyl-CoA) to form oxaloacetate (or, more precisely, malate, which can be oxidized to it). Hence, two acetates are required; however, if you are an organism adapted to utilize this as a metabolic energy source, it's no problem. Here is the next reaction

$$\text{oxaloacetate (4C)} + \text{acetyl-CoA (2C)} \rightarrow \text{Citrate (6C)} \rightarrow \rightarrow \text{succinate (4C)} + \text{glyoxylate (2C)};$$

$$\text{glyoxylate (2C)} + \text{acetyl-CoA (2C)} \rightarrow \text{malate (4C)}$$

This reaction would act as a metabolic shunt, altering the flow of metabolites by bypassing part of the citric acid cycle. The shunt, which is found in many microorganisms and some plants, is called the **glyoxylate shunt**, which is shown in Figure **16.4.1**.

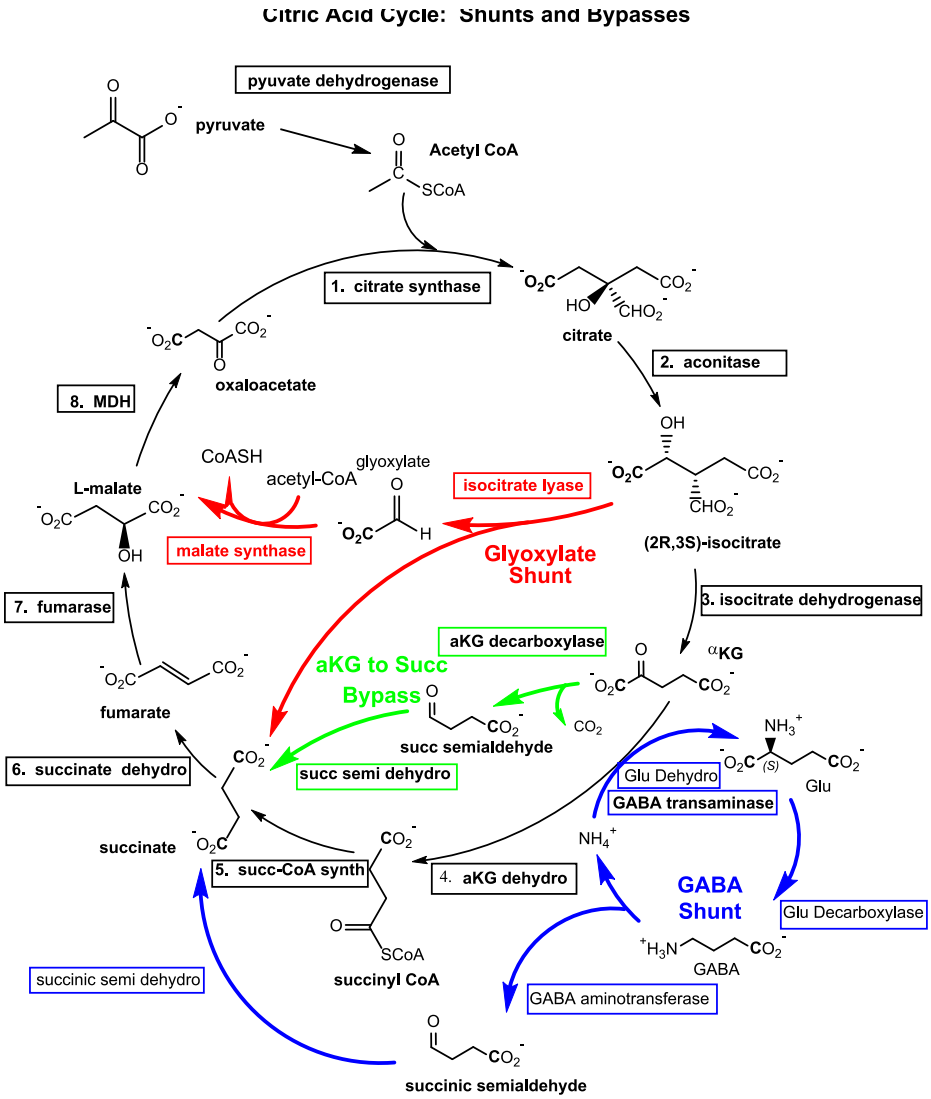


Figure **16.4.1**: Citric Acid Cycle Shunts and Bypasses. (Copyright; author via source)

Why is this so cool? First, consider this observation about the citric acid cycle. One acetate, in the form of acetyl-CoA, is needed to form one oxaloacetate in one turn of the cycle, which is needed for another turn of the cycle. Hence, acetyl-CoA cannot, in a net fashion, be used to synthesize oxaloacetate. We previously observed that oxalate is an intermediate in the synthesis of phosphoenolpyruvate from pyruvate during gluconeogenesis. Hence, acetate can not be used to form glucose in a net fashion. (Note: pyruvate dehydrogenase is not reversible). Another way to think about this is that 2Cs enter the cycle as acetyl-CoA and two leave as CO_2, so that no net synthesis can occur. And you are in trouble if you draw off oxaloacetate as well as α-ketoglutarate and succinate for anaplerotic reactions in biosynthesis, as they are needed metabolites for a cycle that consumes and produces one of each of these, and will be depleted if withdrawn.

Now, you have no worries if you are an organism (many bacteria and plants) with the glyoxylate shunt. A mini cycle still occurs when isocitrate is converted to glyoxylate, then to malate, and back to oxaloacetate and citrate (for energy production), with the net output of 1 succinate (for biosynthesis). The only carbon atoms "lost" from the mini cycle are in the form of succinate, so they are not lost as the two CO2s in the citric acid cycle, since they are used for biosynthesis.

The next reaction for the glyoxylate cycle is:

$$2 \text{ Acetyl-CoA} + 2 \text{ NAD}^+ + 2 \text{ H}_2\text{O} \rightarrow 2 \text{ succinate} + 2 \text{ NADH} + 2 \text{ CoASH} + 2 \text{ H}^+ .$$

In plants, this reaction occurs in organelles called Glyoxysomes. The succinate can be converted through its continuation through the citric acid to oxaloacetate, which can then form glucose and other carbohydrates through gluconeogenesis. Hence, organisms with the glyoxylate

shunt (or cycle) can synthesize carbohydrates in a net fashion from acetate, which can be derived from fatty acid degradation, as we will see in a subsequent chapter.

To operate the glyoxylate cycle efficiently, you need to activate the carboxyl end of acetate. Plants and other organisms that can grow on acetate can produce acetyl-CoA needed for the above pathways from the following reaction catalyzed by acetyl-CoA synthase (i.e., not pyruvate dehydrogenase)

$$\text{Acetate} + \text{CoASH} + \text{ATP} \rightarrow \text{Acetyl-CoA} + \text{AMP} + \text{PP}_i$$

Note that one phosphoanhydride bond is cleaved, and one thioester bond is formed. These molecules are both high-energy compared to their hydrolysis products, so this reaction alone is not thermodynamically favored in any significant way (remember that there is no such thing as a high-energy bond). The hydrolysis of pyrophosphate (PP_i) drives this reaction forward. An analogous reaction drives the creation of peptide bonds in proteins, as it also utilizes ATP to form an activated mixed anhydride from the free carboxyl end.

16.4.2: GABA SHUNT

Now, let's move to the brain, where there is a lot of chemistry happening as you read this page. Relatively high concentrations of key neurotransmitters are required for neural function, and these need to be maintained against metabolic losses. Glutamate is the principal excitatory neurotransmitter, and GABA (δ-aminobutryic acid) is the principal inhibitory neurotransmitter. Both are maintained at high concentrations and are principal players in the GABA shunt. Figure **16.4.2** shows a part of the large pathway shown above, but in a more expanded form.

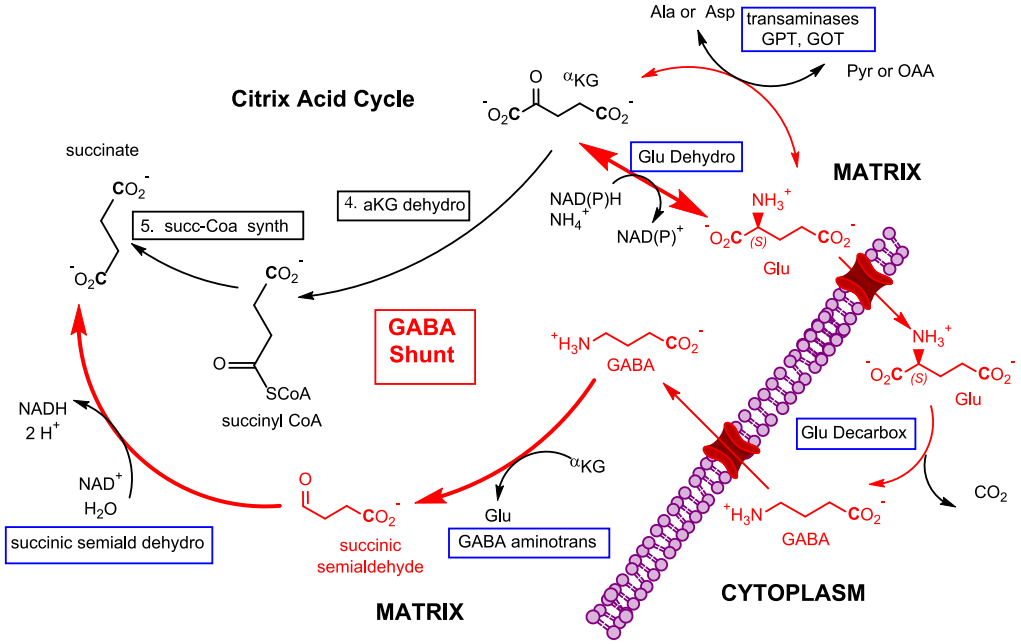


Figure **16.4.2**: Expanded view of GABA shunt. (Copyright; author via source)

GABA is formed in the cytoplasm by decarboxylation of Glu by the enzyme glutamate decarboxylase, which appears to be expressed predominantly in neural tissue. It is metabolized by GABA transaminase but only if the compound from which the shunt starts, α-ketoglutarate, is present abundantly. This conserves the supply of GABA in the neuron. Stated in another way, the breakdown product of GABA, succinic semialdehyde, is formed only if GABA's precursor is present. Inhibitors of GABA aminotransferase are used to treat epilepsy. Another function of the shunt is to allow glutamate to loop into the cycle effectively.

16.4.3: A-KETOGLUTARATE ↔ SUCCINATE BYPASS

In anticipation of the section below, one could ask, what happens when a step in the cycle is impaired or missing? Cyanobacteria, a key player in atmospheric O_2 production and drawdown of natural and anthropogenic atmospheric CO_2, were thought to have an incomplete citric cycle as they lack α-ketoglutarate dehydrogenase. They circumvent this issue by directly converting α-ketoglutarate to succinate through the action of two enzymes: α-ketoglutarate decarboxylase and succinic semialdehyde dehydrogenase, as illustrated below. The first enzyme catalyzes a non-oxidative decarboxylation of the substrate to succinic semialdehyde. This bypass is shown in Figure **16.4.3**. Additionally, cyanobacteria utilize the GABA shunt as a bypass for α-ketoglutarate dehydrogenase.

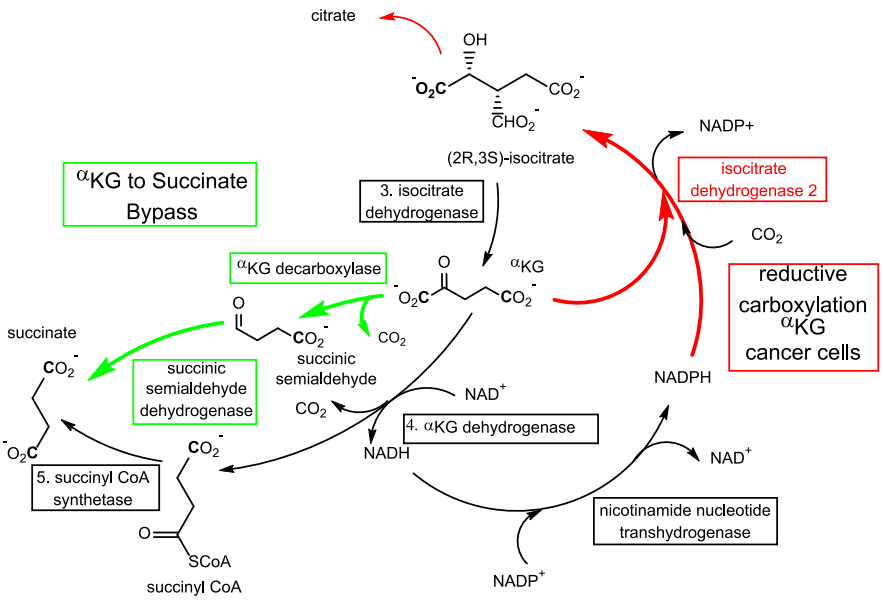


Figure **16.4.3** : α-ketoglutarate to succinate bypass. (Copyright; author via source)

Here is yet another example. Each member of the cycle is a crucial component. Let's consider the first one, citrate. It is formed in the key step, coupling the output of anaerobic glucose metabolism, pyruvate, with the formation of citrate in the citric acid cycle. What happens if aerobic metabolism is impaired, as it would in hypoxic and anoxic conditions, or if mitochondrial function is compromised or in disease states such as cancer? Is there an alternative way to form citrate? Turns out that there is. And it centers on α-ketoglutarate again. This is illustrated in the figure above.

Let's consider cancer, which is characterized by the rapid proliferation of cells. This requires energy and metabolic precursors to synthesize carbohydrates, lipids, and proteins. The citric acid cycle offers both. To accommodate this demand for the withdrawal of citric acid cycle intermediates for reductive biosynthesis, large fluxes of glutamate (derived from abundant glutamine) into the cycle occur in the form of α-ketoglutarate. In another anaplerotic reaction, citrate can be cleaved by citrate lyase to form acetyl-CoA, which is used for fatty acid synthesis required by rapidly proliferating cells. To replenish citrate, cancer cells convert α-ketoglutarate through reductive carboxylation to isocitrate, a process facilitated by isocitrate dehydrogenase 2, which utilizes NADPH for the reduction reaction. That NADPH comes from the enzyme nicotinamide nucleotide transhydrogenase, which can interconvert matrix pools of NADH and NADPH using the collapse of a protein gradient across the mitochondria's inner membrane (which we will study in a subsequent chapter).

$$H^+_{(in)} + NAD^+ + NADPH \leftrightarrow H^+_{(out)} + NADH + NADP^+$$

This process occurs in both oxidative (α-ketoglutarate to succinyl CoA) and reductive reactions (α-ketoglutarate to isocitrate).

16.4.4: VARIANTS OF THE TCA CYCLE IN MICROORGANISMS

It's very easy to be anthropocentric in constructing a biochemistry text, as many who take the course are interested in human medicine. Since humans are an ecosystem of organisms with an expansive microbiome on their skin and in their gut, even from a human health perspective, it is important to compare the same pathway in different organisms. It's also important to understand our role as a small part of a vast biosphere where our survival depends on other organisms, large and small.

In that light, let's consider the citric acid cycle of other organisms. It seems that most organisms have the anaerobic and universal glycolytic pathway. How about the aerobic citric acid cycle? These days of single-cell genomic analysis make it simple to analyze the citric acid cycle genes of any organism. Variants of it are found in almost all aerobic organisms, as well as in some anaerobic ones. Some subtle differences exist between eukaryotic and prokaryotic organisms. NAD^+ is used as a substrate in the mammalian form of isocitrate dehydrogenase, while prokaryotes use $NADP^+$. In mammals, an NAD^+-dependent malate dehydrogenase is utilized, whereas some prokaryotes employ a different enzyme, a $NADP^+$-dependent malate-quinone oxidoreductase. Lastly, different enzymes (and unfortunately with varying names) are used to convert succinyl-CoA to succinate. Plants and fungi use ADP as a substrate; mammals have two enzymes, often named differently for the reverse reaction: succinate-CoA ligase (ADP-forming) and succinate-CoA ligase (GDP-forming).

Analyses have shown that few bacteria have complete cycles. Of those with incomplete cycles, the early steps are least conserved, while the latter are most conserved. The cycle is used for the oxidative production of energy and the generation of metabolites (α-ketoglutarate, oxaloacetate, and succinyl-CoA), which are pulled from the cycle for biosynthesis. Autotrophs that don't have a complete cycle can make

those products from pyruvate. Consider α-ketoglutarate. Some organisms make it through the clockwise oxidative reaction from citrate to α-ketoglutarate, while some methanogenic Archaea undergo counterclockwise reduction reactions. Comparative genomic analyses suggest that the citric acid cycle likely evolved from "linear" oxidative pathways leading to α-ketoglutarate and a reductive pathway leading to succinyl-CoA. Understanding the pathways in individual microorganisms can aid in the rational design of new antibiotics. Figure **16.4.4** below, adapted from Huynen et al., shows a geometric analysis diagram of the citric acid cycle and variants in other organisms.

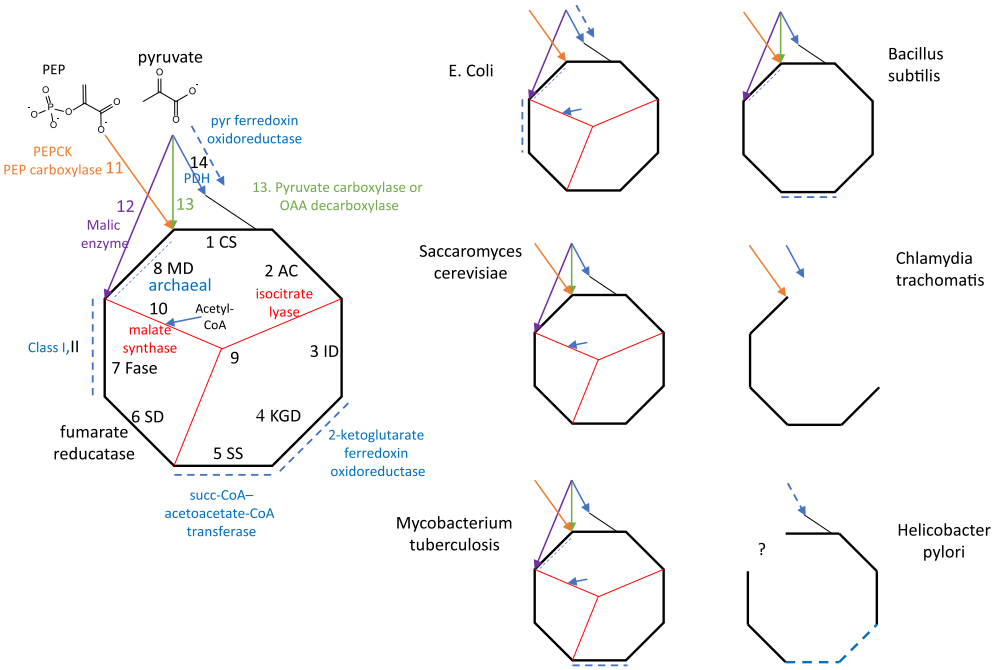


Figure **16.4.4**: Geometric analysis diagram of the citric acid cycle and variants in other organisms. (Copyright; author via source)

16.4.5: THE A-KETOACID PATHWAY - A PRIMORDIAL, PREBIOTIC ANABOLIC "TCA-LIKE" PATHWAY

After studying the complexity of pyruvate dehydrogenase and the citric acid cycle, you might wonder how the cycle might have originated. As discussed above, clues are derived from comparative genome analysis of genes encoding enzymes for the reactions in many organisms. Examining evolutionary changes in genes and functions for these reactions provides insight into the first enzymes that evolved in the pathway. But what about an abiotic pathway that might have arisen before the first biological one? Stubbs et al. have demonstrated that the elementary molecules glyoxylate and pyruvate can react under mild aqueous conditions (pH 7 in 0.5 M phosphate buffer, heated to 50 °C) to form, in a single pot, α-ketoacids similar to those present in the citric acid cycle. From a kinetic perspective, they were formed in the **reverse, counterclockwise reductive direction** compared to the citric acid cycle (clockwise, oxidative). No metals or "enzymes" were needed for the transformations. Glyoxylate acts as a reducing agent and is simultaneously the source of carbon atoms. Once these α-ketoacids form, they could be theoretically converted by transamination reactions to amino acids, as they should be characterized by a $K_{eq} \approx 1$ and a $\Delta G^0 \approx 0$.

The citric acid cycle is filled with carboxylic acids. Only the α-ketoacids (α-ketoglutarate and oxaloacetate) can readily form carbanions at the alpha carbons as their Hs are slightly acidic due to resonance stabilization of the carbanion through an enolate tautomer. The others are electron-rich, so they are less acidic at the alpha carbons, which discourages deprotonation without the use of harsh catalysts. So perhaps alternative functional groups were present in abiotic precursors. Perhaps they contained α-ketoacids similar to α-ketoglutarate, oxaloacetate, and, of course, pyruvate. In addition, α-ketoacids have an electrophile in the form of the carbonyl carbon for C-C bond formation.

Figure **16.4.5** shows the reductive, counter-clockwise pathway (Stubbs et al.). Note that in both the glyoxylate "cycle," which has also been proposed as an abiotic pathway, and the α-ketoacid reductive pathway, no CO_2 is lost in any step. That suggests that the actual decarboxylation steps, although often favored thermodynamically, required the development of catalysts to facilitate the process. The two α-ketoacids substrates in this pathway, glyoxylate (2Cs) and pyruvate (3Cs) are the smallest and most likely formed acids.

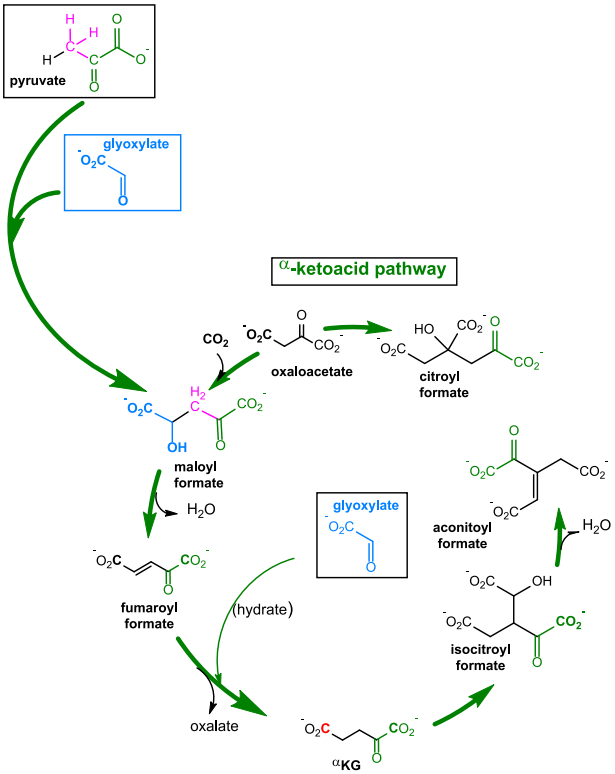


Figure 16.4.5: Proposed prebiotic alpha-keto acids pathway. (Copyright; author via source)

Figure 16.4.6 is an animation that shows the entire citric acid cycle (catabolic, oxidative, running clockwise), the glyoxylate shunt, which bypasses many steps in the citric acid cycle, and the proposed prebiotic anabolic alpha-ketoacid pathway (bold green arrows), which essentially runs counterclockwise and is reductive.

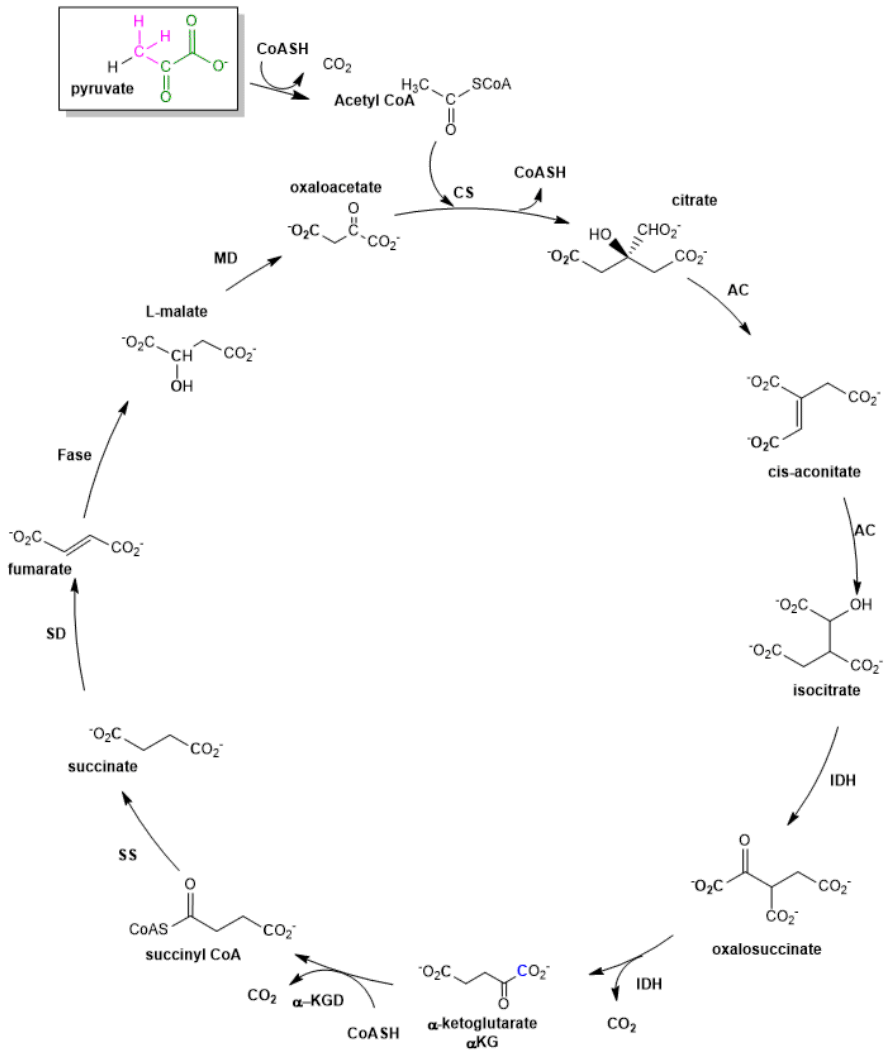


Figure **16.4.6**: Animation of the citric acid cycle (catabolic, oxidative, clockwise), the glyoxylate shunt (which bypasses many steps in the citric acid cycle), and the proposed prebiotic anabolic alpha-ketoacid pathway (bold green arrows). (Copyright; author via source)

16.4.6: SUMMARY

This chapter explores the evolutionary and functional diversity of the citric acid cycle (CAC) by examining various shunts and bypasses that enable organisms to adapt their metabolism to specific environmental and nutritional conditions. Key points include:

- **Evolutionary Adaptations of the CAC:**
  The canonical CAC is not a fixed pathway but has evolved into variants that serve different metabolic needs. Organisms ranging from microorganisms to plants have developed alternative routes that bypass certain decarboxylation steps, allowing them to conserve carbon for biosynthesis. These adaptations are critical when using acetate as a sole or primary carbon source.
- **Glyoxylate Shunt:**
  The glyoxylate shunt is a modified version of the CAC that bypasses the two decarboxylation reactions, thereby preventing the loss of carbon as CO_2. Instead of releasing two CO_2 molecules per cycle turn, this shunt produces succinate and glyoxylate. Glyoxylate can then combine with acetyl-CoA to form malate, which replenishes the cycle. This pathway enables net synthesis of carbohydrates from acetate, a function that is particularly important in microorganisms and plants growing on acetate or fatty acids.
- **GABA Shunt:**
  In the brain, where maintaining high levels of inhibitory neurotransmitters is essential, the GABA shunt provides an alternative route to funnel glutamate into the CAC. This pathway not only supports neurotransmitter balance but also recycles α-ketoglutarate, linking amino acid metabolism with energy production.
- **α-Ketoglutarate Bypass:**
  Some microorganisms, such as cyanobacteria, lack the conventional α-ketoglutarate dehydrogenase enzyme. These organisms use a

bypass that converts α-ketoglutarate directly to succinate through non-oxidative decarboxylation followed by oxidation of succinic semialdehyde. This adaptation ensures continued flux through the cycle despite the absence of a key enzyme.

- **Prebiotic Anabolic Pathways:**
  The chapter also considers hypotheses on the origin of the CAC, discussing the possibility of a primordial, prebiotic α-ketoacid pathway. Under mild conditions, simple molecules like glyoxylate and pyruvate can form α-ketoacids, potentially serving as the precursors to the modern CAC. This perspective provides insight into how early metabolic pathways might have evolved before the advent of sophisticated enzymatic catalysis.
- **Regulatory and Biosynthetic Implications:**
  Beyond energy extraction, the CAC is a hub for biosynthetic precursors. The evolution of these shunts and bypasses reflects a balance between energy production and the need to conserve carbon skeletons for anabolic processes. Regulatory mechanisms—such as substrate availability and allosteric effectors—ensure that these pathways operate efficiently under varying cellular conditions.

In summary, this chapter illustrates how the citric acid cycle is not a static pathway but a versatile network that has evolved diverse variants to meet the metabolic demands of different organisms and environmental conditions. By integrating shunts like the glyoxylate and GABA shunts, and understanding bypass mechanisms and prebiotic pathways, students gain a comprehensive view of the CAC's role in both energy production and biosynthesis, as well as its evolutionary significance in the broader context of metabolism.

This page titled 16.4: Variants of the Citric Acid Cycle is shared under a not declared license and was authored, remixed, and/or curated by Henry Jakubowski and Patricia Flatt.

- **Current page** by Henry Jakubowski and Patricia Flatt has no license indicated.
- **11.2: Diffusion Across a Membrane - Passive and Facilitated Diffusion** by Henry Jakubowski and Patricia Flatt has no license indicated.

CHAPTER OVERVIEW

17: FATTY ACID CATABOLISM

Return to Fundamentals of Biochemistry Search Fundamentals of Biochemistry

Fatty acid catabolism is the mechanism by which the body accesses energy stored as triglycerides.

17.1: Digestion, Mobilization, and Transport of Fats
17.2: Oxidation of Fatty Acids
17.3: Ketone Bodies

Thumbnail: Idealized representation of a molecule of a typical triglyceride, the main type of fat. Note the three fatty acid chains attached to the central glycerol portion of the molecule. (Public Domain; Benjah-bmm27 via Wikipedia)

This page titled 17: Fatty Acid Catabolism is shared under a not declared license and was authored, remixed, and/or curated by Henry Jakubowski and Patricia Flatt.

17.1: DIGESTION, MOBILIZATION, AND TRANSPORT OF FATS

LEARNING GOALS (CHATGPT O3-MINI)

1. **Differentiate Sources and Roles of Fatty Acids:**
   - Explain the two primary sources of fatty acids—dietary (e.g., triacylglycerols from food) and de novo synthesis from acetyl-CoA—and describe their respective roles in energy production and membrane composition.
2. **Describe Lipid Storage in Various Tissues:**
   - Compare the functions of white adipose tissue (WAT) and brown adipose tissue (BAT) in lipid storage and energy expenditure, including the roles of lipid droplets, hormone regulation, and the thermogenic protein uncoupling protein 1 (UCP1).
3. **Outline Lipoprotein Structure and Classification:**
   - Summarize the structural organization of lipoproteins, emphasizing the single phospholipid monolayer, lipid core, and associated apolipoproteins.
   - Classify lipoproteins by density (chylomicrons, VLDL, IDL, LDL, and HDL) and explain how differences in size, composition, and apolipoprotein content affect their function in lipid transport.
4. **Explain the Role of Apolipoproteins in Lipid Transport:**
   - Describe the functions of key apolipoproteins (e.g., apoB100, apoB48, apoA-I, apoE, and apoA-IV) in stabilizing lipoprotein particles, mediating receptor interactions, and facilitating lipid exchange among particles.
   - Discuss how structural features such as tandem amphiphilic helices contribute to the lipid-binding and membrane-associating properties of these proteins.
5. **Understand the Mechanisms of Lipoprotein Assembly and Uptake:**
   - Illustrate how dietary lipids are hydrolyzed and reassembled into lipoproteins (e.g., chylomicrons and VLDL) in the intestine and liver, including the roles of microsomal triglyceride transfer protein (MTP) and apolipoprotein processing.
   - Explain the receptor-mediated uptake of LDL via the LDL receptor, including the structural domains involved in ligand binding and the role of accessory proteins (e.g., PCSK9) in receptor recycling and degradation.
6. **Describe the Function and Regulation of Lipoprotein Lipase (LPL):**
   - Detail how LPL, in association with GPIHBP1 and heparan sulfate, catalyzes the hydrolysis of TAGs in circulating chylomicrons and VLDL to release free fatty acids for uptake by tissues.
   - Explain the structural features of LPL, including its catalytic triad, and how calcium ions stabilize its active dimeric form.
7. **Examine Albumin's Role in Fatty Acid Transport:**
   - Discuss how human serum albumin (HSA) binds multiple fatty acids and various small hydrophobic drugs, influencing their bioavailability and transport in the bloodstream.
8. **Analyze the Impact of Lipoproteins on Cardiovascular Health:**
   - Compare the roles of LDL (and its variant Lp(a)) and HDL in cardiovascular risk, emphasizing how LDL levels are associated with atherogenesis, while HDL is involved in reverse cholesterol transport and is generally cardioprotective.
9. **Evaluate the Effects of Lipid Remodeling Enzymes:**
   - Describe the function of enzymes such as lecithin-cholesterol acyltransferase (LCAT), phospholipid transfer protein (PLTP), and cholesterol ester transfer protein (CETP) in the assembly, maturation, and remodeling of lipoproteins.
10. **Integrate Metabolic Regulation with Hormonal Control:**
    - Summarize how hormonal states (e.g., fed vs. fasting) influence the balance between lipid storage and lipolysis in adipocytes and liver cells, including the roles of insulin, glucagon, and epinephrine.
11. **Connect Structural Characteristics with Functional Outcomes:**
    - Utilize interactive molecular models to visualize and analyze the structural determinants of lipid-binding in apolipoproteins and the conformational properties of lipoprotein particles, linking these insights to their physiological functions and implications in diseases such as atherosclerosis.

By achieving these learning goals, students will develop a comprehensive understanding of how fatty acids and lipoproteins are processed, transported, and regulated in the body, and how these processes impact energy metabolism and cardiovascular health.

17.1.1: INTRODUCTION

This chapter will discuss the breakdown of fats to produce ATP. Most of the available chemical energy stored in fats is in the form of highly reduced fatty acids. One form of fatty acid-containing lipids comes from our diet, which includes triacylglycerols (TAGs) and membrane lipids. Fatty acids, mainly in TAGs, are moved in the circulation by large lipid-carrying vesicles called **lipoproteins**. Lipids can be imported into cells for storage and energy utilization.

Another source of fatty acids comes from those synthesized within cells from the small molecule acetyl-CoA. Fatty acids are synthesized by an enzyme complex called **fatty acid synthase**. This enzyme is most prevalent in adipose (fat) tissue and the liver. Additionally, it is highly expressed in the brain, lungs, and mammary glands.

TAGs, stored in lipid droplets, are found in most cells. The central tissue used for TAG storage is adipose (fat) tissue, whose volume consists primarily of lipid droplets. Given the large muscle tissue mass, a considerable amount of TAGs is stored as small lipid droplets in muscle cells. However, skeletal muscle cells don't synthesize fatty acids. They possess the genes for fatty acid synthase but do not transcribe them into RNA, so no enzyme is produced. They can, however, import them for catabolism. Muscle TAGs can be oxidized for energy, especially during endurance exercise.

TAGs are also stored in the liver in lipid droplets. The liver also assembles lipoproteins, which are then released into the bloodstream. Excess TAGs are stored in the liver in various diseases, including alcoholism and nonalcoholic fatty liver disease (NAFLD), which can progress into nonalcoholic steatohepatitis (NASH), a much worse disease.

WHITE AND BROWN ADIPOSE TISSUES

Two major forms of triacylglycerol-storing fat tissues exist: **white adipose tissue (WAT)** and **brown adipose tissue (BAT)**. The more abundant WAT stores triacylglycerols in a single large lipid droplet within the cell and releases fatty acids through processes controlled by the hormones insulin and epinephrine. This simple role can mask the fact that adipose tissue is a major player in the endocrine system, playing a crucial role in cell signaling and systemic control of metabolism. Adipose tissue releases the key hormones **leptin** and **adipisin**, which, in analogy to the hormones and signaling agents released by immune cells (cytokines, lymphokines), can be called **adipokines**. They also secrete other adipokines, including tumor necrosis factor α (TNF-α), adiponectin, and resistin.

In contrast, BAT specializes not in storing and releasing fatty acids but rather in oxidizing fatty acids in ways that maximize heat production, preventing hypothermia. They have multiple smaller lipid droplets, displaying a larger surface area for lipolysis, the hydrolytic cleavage of fatty acids from the TAGs. A particular mitochondrial protein, uncoupling protein 1 (UCP1), is expressed in brown but not white adipocytes, allowing a "futile" metabolic cycle that leads to the dissipation of heat instead of ATP synthesis. The relative abundance of white and brown adipocytes is crucial in diseases such as obesity and type 2 diabetes. BAT tissue is especially important for thermoregulation in small animals (and newborns). The surface area-to-volume ratio for smaller organisms is greater than that for larger animals, allowing for more efficient heat loss. The ratio of surface area AS per volume V for a sphere is given by:

$$\frac{\mathrm{SA_{sphere}}}{\mathrm{V_{sphere}}} = \frac{4\pi r^2}{\left(\frac{4}{3}\right)\pi r^3}$$

Let's assume an average large adipocyte is a sphere with a diameter of 100 μm. Compare this to a large sphere with a 100 times greater diameter (10,000 μm). The smaller sphere has 1/100 of the diameter but a surface area-to-volume ratio 100 times greater than that of the large sphere.

Just for fun: Many know the formula for the volume of a sphere:

$$V(r) = \frac{4}{3}\pi r^3 \tag{17.1.1}$$

The derivative of the volume with respect to the radius r, dV/dr, gives the volume of an infinitesimal shell around the sphere. Here is the relevant equation:

$$\frac{dV}{dr} = \frac{d}{dr}\left(\frac{4}{3}\pi r^3\right) = 4\pi r^2 \tag{17.1.2}$$

The area of the infinitesimal sphere is:

$$A = 4\pi r^2 \tag{17.1.3}$$

The volume of the infinitesimal sphere is the above equation multiplied by dr! This is a cool application of first-semester calculus!

An intermediate type of fat tissue consists of "bright" adipocytes. White adipocytes can be coaxed to differentiate into beige and brown cells, which could be a potential treatment for obesity.

In this chapter, we will follow the fate of fatty acids from dietary lipids cleaved from TAGs, loaded into chylomicrons, a lipoprotein assembled in the small intestine, secreted into the circulation, and taken up by the liver. The liver can store the incoming fatty acids in TAGs or release them back into the circulation in the form of another lipoprotein, very low-density lipoproteins (VLDL). Circulating VLDL can exchange lipids with other circulating lipoproteins. Lipoproteins deliver fatty acids to cells after interaction with the cell surface of target cells. The fatty acids move into the cell through either the cleavage of TAGs by cell membrane-associated enzyme lipase, followed by fatty acid uptake, or by endocytosis of lipoproteins into the cells.

17.1.2: LIPOPROTEINS

Before examining the individual steps in lipid processing, let's first consider the various lipoproteins. These large vesicular structures transport fats, which are very insoluble molecules, in the circulation. Unlike normal liposomes or vesicles with a lipid bilayer surrounding an interior aqueous compartment, lipoproteins have only a single monolayer of phospholipids encapsulating a nonaqueous interior filled with TAGs, cholesterol, and cholesterol esters. The protein part of the lipoprotein consists of one or several proteins bound on the outside of the particle. The proteins help solubilize the lipoprotein, confine its size, and prevent the aggregation of lipoproteins, which would pose a health risk. The structure of a typical lipoprotein is shown in Figure **17.1.1**.

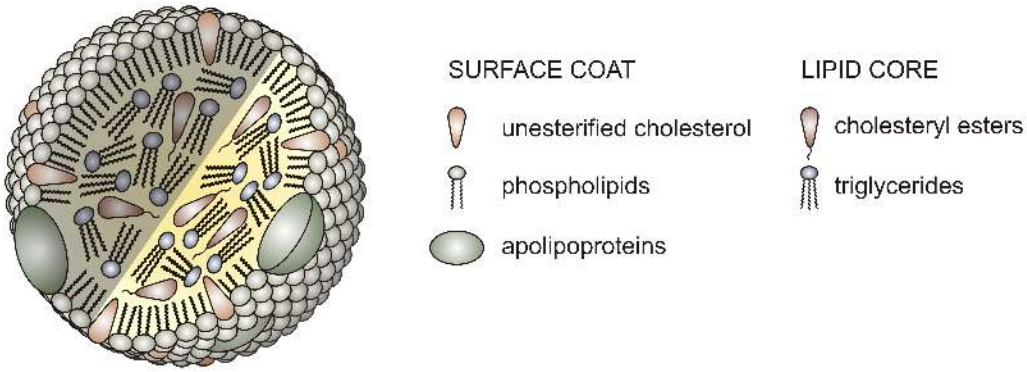


Figure **17.1.1**: Lipoprotein particles are composed of a lipid core containing cholesteryl esters and triglycerides and a surface coat of phospholipids, unesterified cholesterol, and apolipoproteins. (CC BY-SA 3.0 Unported; AntiSense via Wikipedia)

Lipoproteins are classified based on density. The lowest density one, chylomicrons, is the largest and contains the most lipids (mostly triacylglycerols, or TAGs) in its interior compartment. Very large density lipoproteins (VLDL), intermediate density lipoproteins (IDL), low density lipoproteins (LDL), and high density lipoproteins (HDL) have decreasing size, fewer encapsulated lipids, and increasing density. The relative sizes are shown in Figure **17.1.2**.

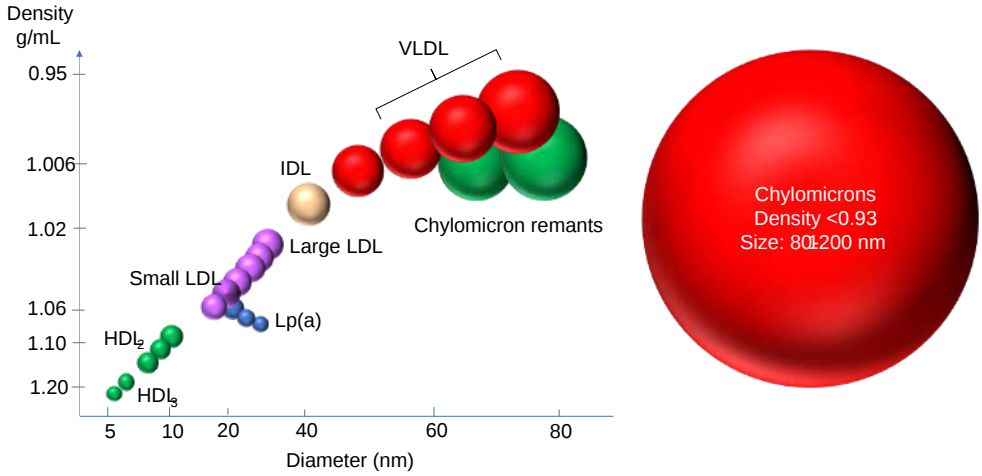


Figure **17.1.2**: Modified and used with permission from Endotext.org.

Lipoproteins (except chylomicrons) can be classified as nanoparticles, which typically vary in size from 1 to 100 nm. Larger lipoproteins and chylomicrons form emulsions in the blood, much as milk (also cloudy) is an emulsion of lipid/protein particles. The serum of people with high levels of lipids (hyperlipidemia) can look milky white, especially after eating foods rich in TAGs, when levels of chylomicrons are very high. Figure **17.1.3** shows the blood of a patient with hyperlipidemia after the addition of EDTA (which binds Ca^{2+} and prevents clotting) that has settled (without centrifugation). The milky white plasma on top (lower density) likely has high concentrations of chylomicrons and/or LDL. The lower layer primarily consists of red blood cells.



Figure **17.1.3**: This is a standard EDTA (cell count) tube, as may be used to obtain a full blood count or iron studies. The tube was set upright for four hours - it was not centrifuged. (Public Domain; Mark-shea via Wikipedia)

No X-ray structures of lipoproteins are available. However, the structure of a nascent HDL particle (3k2s) has been determined using small-angle neutron scattering. Figure **17.1.4** shows an interactive iCn3D model of it.

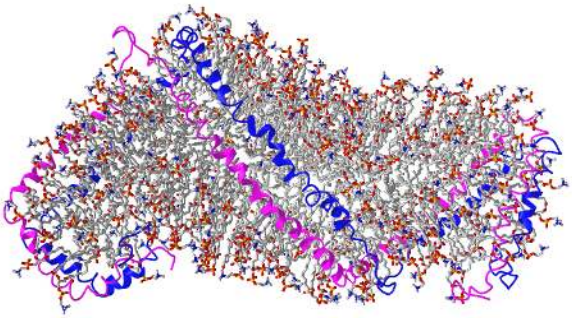


Figure **17.1.4**: Nascent HDL (3k2s) (Copyright; author via source). Click the image for a popup or use this external link: https://structure.ncbi.nlm.nih.gov/i...fF85h11SpeYJg6

The major protein in HDL, a lipoprotein that protects against cardiovascular disease, is apolipoprotein A-I (apoA-I). Figure **17.1.4** shows that it adopts an antiparallel double superhelix as it wraps around the nascent HDL. The more hydrophobic surfaces of apo A-I are oriented inward, allowing interactions with hydrophobic lipids in the core. It is probably prototypical for nascent lipoproteins. It will give you an idea of how proteins wrap around the outside of the particle. Mature lipoproteins are most likely spherical. This nascent HDL in the model contains 200 1-palmitoyl-2-oleoyl-sn-glycero-3-phosphocholines (POPC) molecules, 20 cholesterol, and a single copy of apolipoprotein A-I (apoA-I).

Figure **17.1.5** below shows a cartoon image of VLDL, assembled from lipids synthesized/taken up by and released from the liver, and chylomicrons, assembled from dietary fats and released from enterocytes in the small intestine (size of the lipoproteins is not to scale). VLDL has one copy of Apo B-100, while chylomicrons have one copy of Apo B-48.

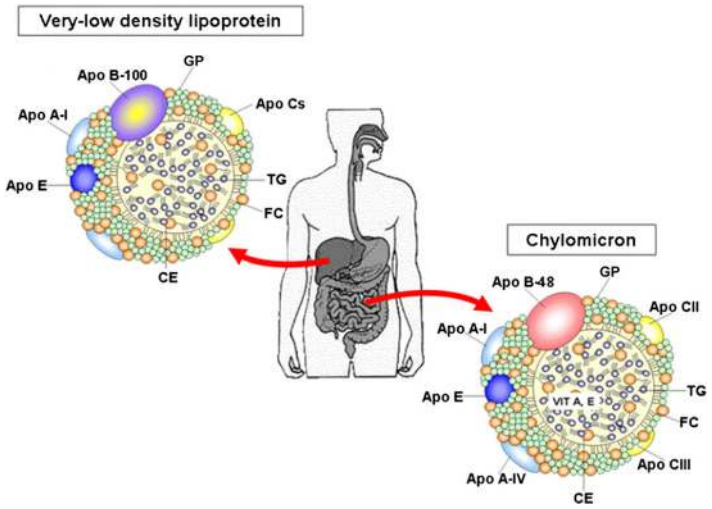


Figure **17.1.5**: Emile Levy, Journal of Lipid Research. 56, 945-962, 5/2015. DOI:https://doi.org/10.1194/jlr.R052415. Creative Commons Attribution (CC BY 4.0)

All lipoproteins, except HDL, are members of the **B**eta-lipoprotein family as they contain an apo-**B** protein. The liver synthesizes apo B100, which becomes a permanent part of VLDL (i.e, it is not exchangeable with other lipoproteins) and its metabolic derivatives, so any lipoprotein containing apo B100 arose from the liver. Other proteins on lipoproteins are exchangeable. In contrast, enterocytes in the small intestine produce apo B-48 (48% the size of apo B100), so this protein marks the lipoproteins (chylomicrons and chylomicron remnants) assembled in the small intestine. Apo B100 has over 4500 amino acids and a molecular mass of 555kDa. The gene for intestinal apo B48 is the same as that for apo B100, except that it contains a premature stop codon, resulting in a shorter, truncated apo B-48.

Apoproteins bind to specific receptors on cells, allowing the uptake of the lipoprotein. For example, the LDL receptors bind to the apo B-100 protein on a region removed (by proteolytic processing) from the apo B48 protein of chylomicrons. They also bind ApoE, which is predominantly found on HDL and VLDL, but some are also present in LDL. The LDL receptors are also called the ApoB/ApoE receptor.

Over 90% of the apoB-containing particles in circulation are LDL. In addition, chylomicrons are present in circulation only after eating. Some apoproteins can act as cofactors and inhibitors for lipoprotein processing.

LIPOPROTEINS AND CARDIOVASCULAR RISK

High concentrations of LDL are associated with increased cardiovascular risk. Chylomicron levels, given their transient and lower concentration levels, do not pose a health risk unless the enzyme required to remove fatty acids from them, lipoprotein lipase, is missing or defective, or if another apoprotein component, apo CII, which mediates the interaction with lipoprotein lipase, is missing. LDL-C (a term used to describe the total cholesterol in LDL particles, which is routinely measured in clinical labs) can be lowered by a healthy diet centered around plant foods. Drugs like statins decrease endogenous cholesterol synthesis, lower LDL levels, and decrease cardiovascular risk.

However, another protein, lipoprotein, also called Lp(a) or LP "little a," is an independent cardiovascular risk factor. Its blood concentration is regulated by genetics and not by diet. In addition to apo B100, these particles contain apo (a), a protein with a unique repeating structure (up to 40 times) called a **kringle**, which is also found in some proteins involved in the blood coagulation system. People whose genes encode apo (a) with the fewest number of kringles express lots of that protein, and their Lp(a) particles are smaller. This confers a greater cardiovascular risk compared to those expressing proteins with many kringle domains. Figure **17.1.6** (from Amgen) shows models of Lp(a) with different numbers of repeating kringle (kinked) domains.

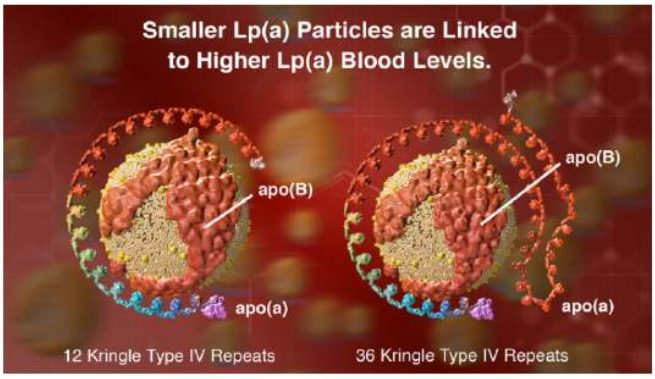


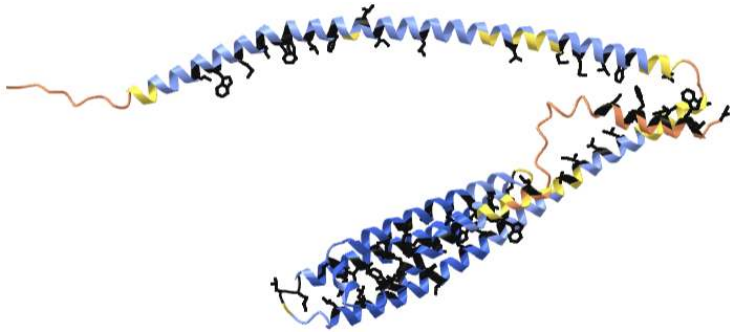
Figure **17.1.6**: https://www.amgenscience.com/feature...-lipoproteina/

From a biochemical perspective, exploring the differences in apolipoprotein binding to single-leaflet-encapsulated lipid nanoparticles is interesting compared to the interaction of peripheral and integral membrane proteins with intact bilayers (which have two leaflets, as studied in Chapter 12.1). As mentioned above, the more nonpolar surfaces of apo AI in HDL are oriented inward toward the nonpolar lipid core. Presumably, apo B proteins in chylomicrons and LDL also wrap around the entire lipid surface.

HDL's major organizing scaffolding protein is apoA-I (see iCn3D model above). It presumably plays a role similar to apoB in chylomicrons and LDL, but it is exchangeable. (Note: ApoA-I is also found in chylomicrons.) It is also a cofactor for the enzyme lecithin:cholesterol acyl transferase (LCAT), which converts free cholesterol in the single bilayer into esterified cholesterol esters within HDL. In its apo-form, it also interacts with the cell surface transporter ATP-binding cassette A1 (ABCA1), which plays a role in assembling HDL particles. HDL also has apoC and apoE proteins, all of which are exchangeable.

Given their heterogeneity and size, it is difficult to determine the structure of lipoproteins. Apolipoproteins have hydrophobic surfaces that promote self-association and aggregation. Apolipoproteins in the A, C, and E classes have repeating amphiphilic helices that embed to some degree in the lipid particles. In addition, the proteins exhibit significant disorder and can adopt multiple bound conformations.

Figure **17.1.7** shows an interactive iCn3D model of the AlphaFold predicted structure of human Apo E (**P02649**) (**P06727**)



NCBI iCn3D Figure **17.1.7**: AlphaFold predicted structure of human Apo E (**P02649).** Copyright; author via source). Click the image for a popup or use this external link: https://structure.ncbi.nlm.nih.gov/i...5GtKt3QWaTZ519

The blue cartoon color represents high certainty in the AlphFold predicted structure, while yellow to orange represents low certainty. The hydrophobic side chains are shown as sticks, helping illustrate the structure's amphiphilic nature.

Figure **17.1.8** shows an interactive iCn3D model of the AlphaFold predicted structure of human Apo A4 (**P02649)**

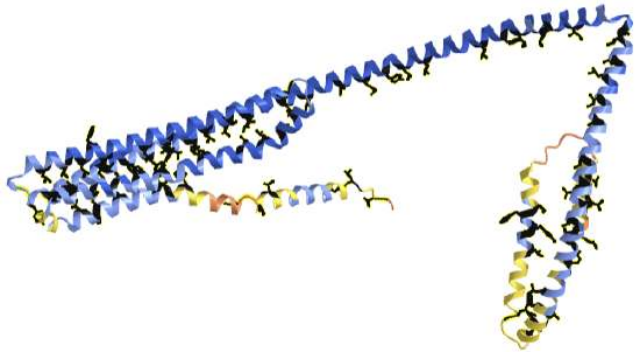


Figure **17.1.8**: AlphaFold predicted structure of human Apo A4 (**P02649).** Copyright; author via source). Click the image for a popup or use this external link:https://structure.ncbi.nlm.nih.gov/i...jSw8wSX1MtpcB8

The blue cartoon color represents high certainty in the AlphFold predicted structure, while yellow to orange represents low certainty. The hydrophobic side chains are shown as sticks. Again, note the amphiphilic nature of the structure.

The exchangeable apolipoproteins have similar genetic sequences (four exons and three introns) and similar amino acid sequences. They have 11-mer amino acid tandem repeats, and some (A-I, A-IV) have 22-mer tandem repeats. These repeats form amphiphilic helices as determined by sequence analysis. The first amino acid in the amphiphilic helix is often positively charged, and a negative one is often found in the middle. Proline, a helix breaker, is often but not always found between the helices.

Figure **17.1.9** shows the primary sequence of apoA-I. An 11-mer repeat is highlighted in yellow. The other highlighted stretches (in different colors) are 22-mer repeats. Note that the repeats are not of identical sequences but rather of sequences that can form amphiphilic helices (i.e., secondary structure repeats).

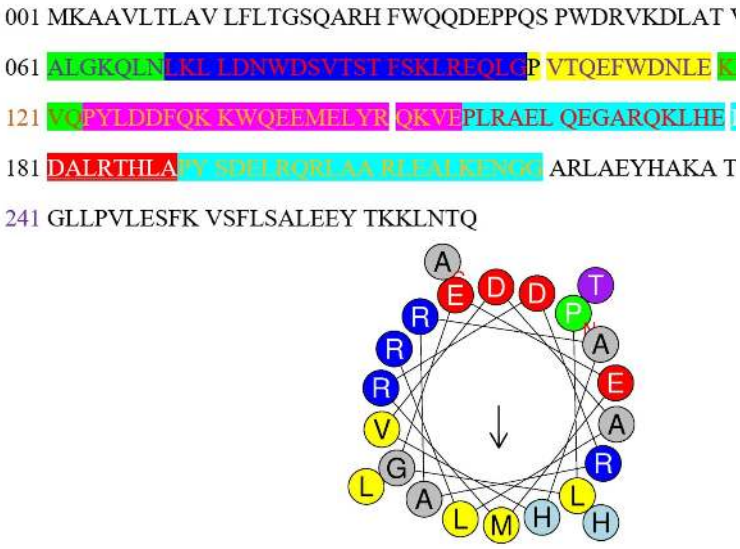


Figure **17.1.9**.belows shows the primary sequence of apoA-I. An 11-mer repeat is highlighted in yellow. The other highlighted stretches (different colors) are 22-mer repeats. Note that the repeats are not of identical sequences but rather of sequences that can form amphiphilic helices (i.e., secondary structure repeats).

The bottom part of Figure **17.1.9**shows a helical wheel projection (using Heliquest) of the red-highlighted 22-mer repeat. The arrow shows the hydrophobic moment with the arrowhead pointing to the more nonpolar face. The particular amphiphilic helix shown may or may not facilitate the binding of the bound conformation of the protein.

The relative areas of the hydrophilic and hydrophobic faces in the amphipathic helices influence the lipid-associating properties of the exchangeable apolipoproteins. The arrangement of tandem repeating amphipathic helices is another factor that might influence the lipid-binding ability of exchangeable apolipoproteins.

Actual amphiphilic helices would bind to the membrane in a parallel fashion, with the nonpolar face anchoring the protein to the lipid surface. Other experimental techniques are used to study how a peptide or protein that can form amphiphilic helices interacts with the lipid

surface. These include site-directed mutagenesis studies coupled with spectroscopic (CD, fluorescence) and binding assay methods (using liposomes).

The properties of a membrane-bound amphiphilic helix are affected by the exact size and distribution of the polar/charged and nonpolar side chains. On binding, they sense or cause membrane curvature, interact with specific lipids, and stabilize specific membrane conformations (such as spherical for lipoproteins). Figure **17.1.10** shows how different proteins with amphiphilic membranes interact with membrane surfaces.

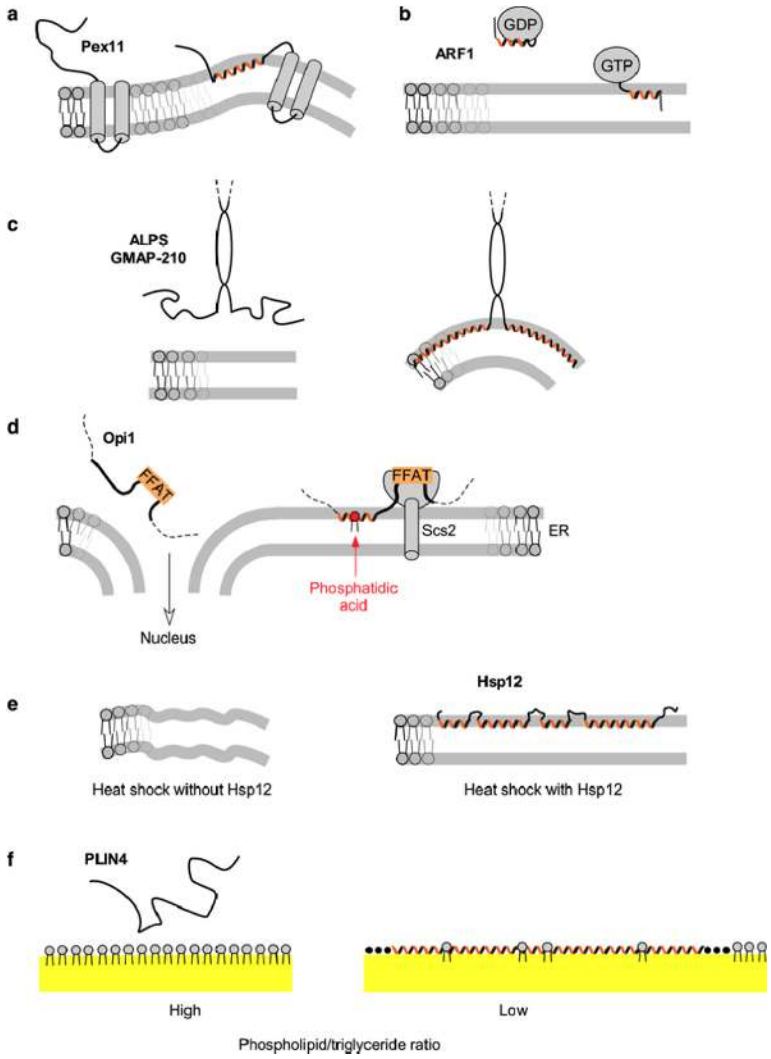


Figure **17.1.10**: Interactions of amphiphilic helices with membranes. Manuel Giménez-Andrés et al. Biomolecules. 2018 Sep; 8(3): 45. doi: 10.3390/biom8030045. Creative Commons Attribution (CC BY) license (http://creativecommons.org/licenses/by/4.0/)

A key point to note is the large conformational changes that occur as the protein or parts of it go from the free, more disordered state to the bound state with lipid-associating amphiphilic helices. The following proteins are depicted in the figure.

a. The peroxisomal membrane protein Pex11 amphiphilic helix distorts the membrane;
b. ARF1 is a small G protein in which only the GTP form localizes and binds through an amphiphilic helix to the membrane;
c. The ALPS motif of the golgin GMAP-210 binds to only highly curved vesicles;
d. The yeast transcriptional repressor Opi1 binds to the endoplasmic reticulum (ER) membrane in part through an amphiphilic helix;
e. The heat shock protein Hsp12 has a long amphiphilic helix, which helps stabilize the membrane;
f. The extremely long amphiphilic helix of perilipin 4 coats lipid droplets and stabilizes them, even in the absence of phospholipids.

17.1.3: DIETARY UPTAKE AND RELEASE INTO THE CIRCULATION

Now, how are the lipid nanoparticles assembled? We'll start with the dietary lipids: TAGs, glycerophospholipids, and cholesterol esters. The figure below shows key steps which are described in Figure **17.1.11**

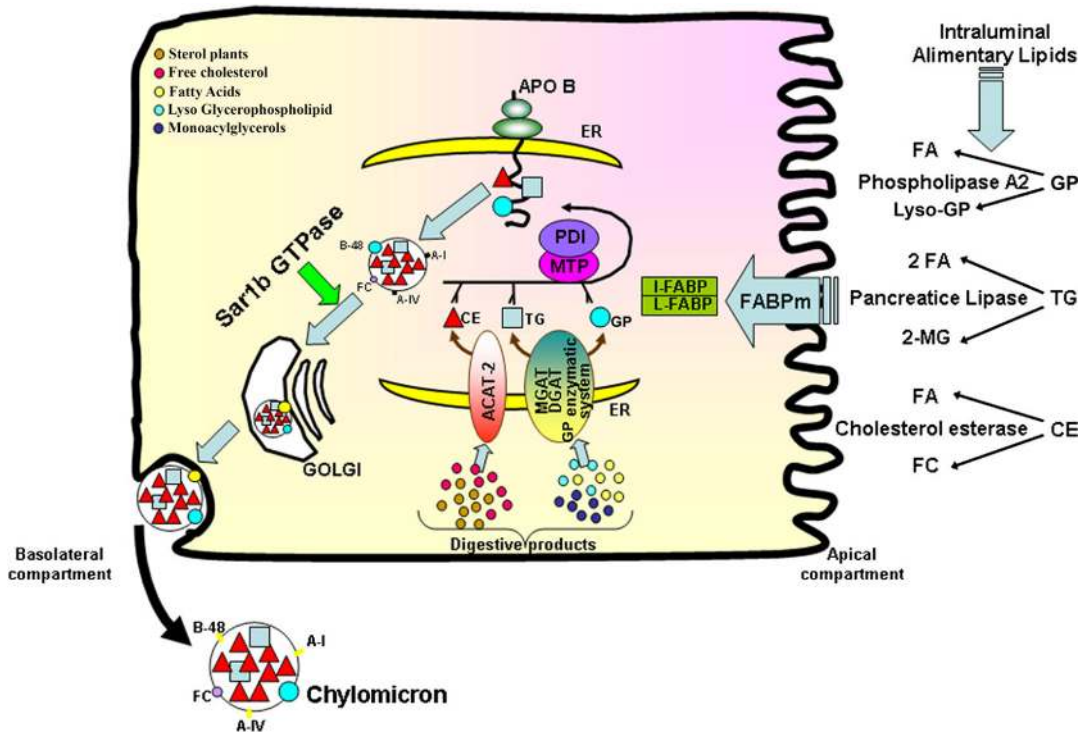


Figure **17.1.11**: Emile Levy, Journal of Lipid Research. 56, 945-962, 5/2015. DOI:https://doi.org/10.1194/jlr.R052415. Creative Commons Attribution (CC BY 4.0)

Here are some key steps depicted in the figure:

- hydrolysis (lipolysis) of TAGs by pancreatic lipase, cholesterol esters (CE) by cholesterol esterase, and glycerophospholipids (GP) by phospholipase A2 in the lumen of the intestine. These enzymes interact at the interface of the lipid substrates and aqueous surroundings;
- the resulting products, which include free fatty acids (FA), 2-monoacylglycerol (MG), free cholesterol (FC), and lyso-glycerolphospholipids (lyso-GP), aggregate with the help of bile salts to form emulsions (like oil drops in water), which can be taken up by diffusion or possibly endocytosis when present in high amounts. Alternatively, membrane transporters (like FABPs and other proteins) can move them into the cell by facilitated diffusion;
- cytoplasmic transporters like fatty acid binding proteins move the lipolysis product to the ER where free fatty acids are reesterified. The enzymes involved include mono- and diacylglycerol acyltransferases (MGAT, DGAT) and sterol O-acyltransferase 2, also known as acyl-coenzyme A:cholesterol acyltransferase (ACAT-2). Multiple enzymes are involved in the resynthesis of glycerophospholipids);
- Apo B-48 is synthesized by ribosomes bound to the ER and interacts with a heterodimer of **microsomal triglyceride transfer protein large subunit two (MTP)** and protein disulfide isomerase (PDI). This facilitates the folding of apo B48 and loading of lipids using MTP into pre-chylomicrons;
- pre-chylomicron vesicles move to the Golgi with the help of Sar1b, a small G-protein (and GTPase) where the particle assembles to the full chylomicron, which is released from the cells as the mature large lipid nanoparticle.

An intriguing feature of lipases is that they work at the interface between the aqueous and nonaqueous (in this case, lipid nanoparticle) environments. Let's briefly consider the hydrolysis mechanism of TAGs by the equine pancreatic mechanism. This enzyme employs the same mechanism observed earlier for the hydrolysis of a peptide bond by serine proteases. A catalytic triad of Asp 176, His 263, and Ser 152 as a nucleophilic catalyst is shown in the partial reaction displayed in Figure **17.1.12**.

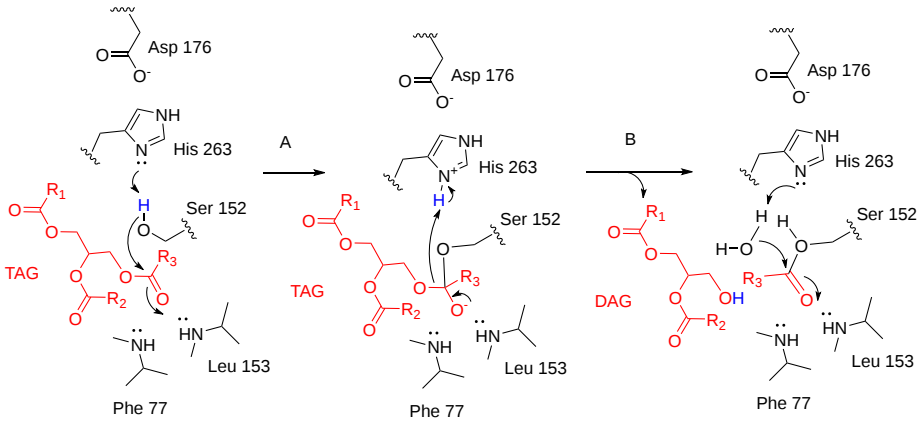


Figure **17.1.12**:

An acyl-Ser intermediate forms in step B (above) to form the product diacylglycerol after the collapse of an oxyanion intermediate in step A. In the second half of the reaction (not shown in its entirety), water cleaves the acyl-Ser intermediate through a hydrolysis reaction, reforming the active enzyme as it releases the free fatty acid, R_3CO_2H. Other lipases also employ the same catalytic triad.

Figure **17.1.13** shows an expanded diagram showing the flow and fate of lipoproteins.

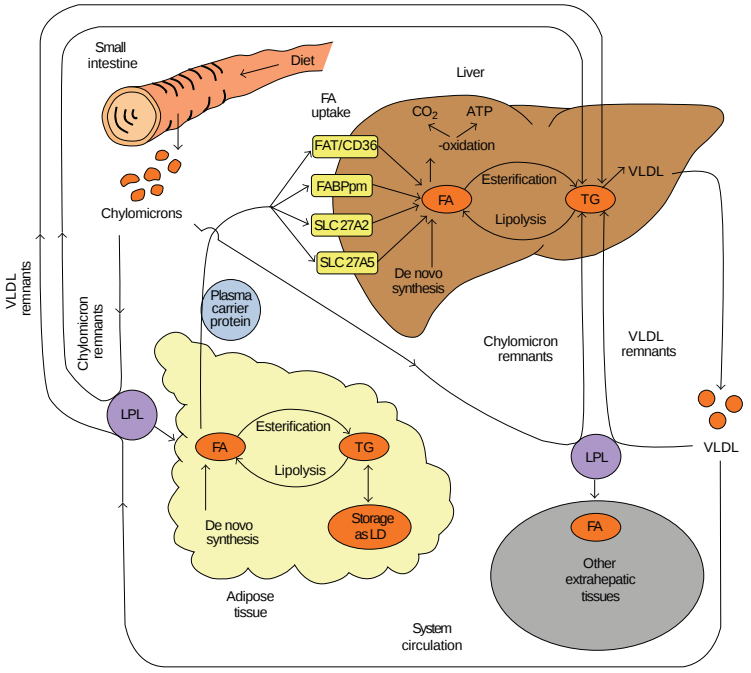


Figure **17.1.13**: Merilin Al Sharif et al. PPAR Research. Volume 2014, Article ID 432647, http://dx.doi.org/10.1155/2014/432647. Creative Commons Attribution License.

Chylomicrons interact with lipoprotein lipase (LPL), which also uses an Asp-His-Ser catalytic triad, to cleave fatty acid esters, allowing the delivery of free fatty acids to adipose cells. The adipocytes can also undergo de novo fatty acid synthesis. Fatty acids (FA) can also be produced by lipase-mediated lipolysis of stored TGs. These free fatty acids (FA) in the adipocyte have two fates. They can be reesterified to glycerol to form TAGs (TG in the figure) or be exported from the cell, where they bind to a plasma carrier protein and are transported to the liver for storage. There, the fatty acids can be taken up by various membrane protein importers, as indicated in the figure by the yellow boxes. As in adipose cells, fatty acids can be reesterified to form TAG stores, which can then be packaged into VLDL particles for export. The fatty acid delivered (or synthesized) could also be used for ATP production through the citric acid cycle and oxidative phosphorylation.

VLDL in circulation can undergo lipolysis by lipoprotein lipase to produce fatty acids for uptake in "extrahepatic" tissue (bottom right of the diagram). As fats are removed from VLDL, their density increases as it forms IDL and LDL, which could be considered VLDL "remnants". VLDL is very enriched in TAGs, but after metabolic processing, the resulting LDL is depleted in TAGs and enriched in cholesterol/cholesterol esters. LDL (not shown in the above figure) can be taken up (endocytosed) by the liver and other cells after binding

to LDL receptors, which recognize apo-B100 and other apoproteins. This allows the delivery of predominantly cholesterol and cholesterol esters to tissues.

How do adipocytes and hepatocytes determine if free fatty acids should be esterified for storage or released for energy use by other tissues? We'll discuss that in a subsequent section. Still, the short answer is that in healthy fasting and exercise states, hormones (glucagon, epinephrine) activate lipolysis in the liver and adipose cells. In contrast, in the fed state, insulin promotes the storage of fatty acids as triacylglycerols.

Adipose cells don't assemble and release lipoproteins. Instead, they release free fatty acids into the circulation, which are carried by albumin, the major protein in serum or plasma. The iCn3D Figure **17.1.14** shows an interactive iCn3D model of the complex of human serum albumin (HSA) binding seven $20{:}4^{\Delta 5,8,11,14}$ - arachidonic acids (1gnj).

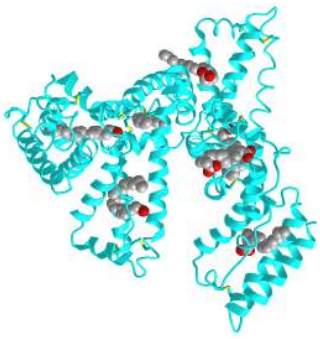


Figure **17.1.14** Human Serum Albumin/Arachidonic Acid complex (1gnj). Click the figure for a popup or use this external link: https://structure.ncbi.nlm.nih.gov/icn3d/share.html?WL7BxK4B23m2p3Z19 (Copyright; author via source)

Given the multiple binding sites for fatty acids in albumin, it should come as no surprise that albumin also binds a host of small drugs, including medicinal drugs and toxins such as warfarin (blood thinner), diazepam, ibuprofen, indomethacin, and amantadine. These appear to bind preferentially at two primary drug binding sites. This binding is likely to be beneficial in delivering drugs through the circulation, but may not be effective if they aren't delivered to the target tissue.

We discussed the structure of micelles, spherical assemblies of single-chain amphiphiles that act as detergents. Oil from your clothes can enter the nonpolar interior of the detergent micelle and effectively solubilize the nonpolar molecule in the micelle, which is effectively a nanoparticle with a diameter of 5-15 nm. You should not be surprised to discover that lipoproteins can also carry fat-soluble vitamins, steroid-like endocrine-disrupting substances, and drugs.

17.1.4: LIPOPROTEIN LIPASE

The enzyme that breaks now TAGs in circulating chylomicrons and VLDL is **lipoprotein lipase (LPL)**. It is a soluble protein secreted by adipocytes and muscle cells, but is made by many cell types. It works at the luminal side of blood vessel endothelial cells. It is recruited to that membrane surface by binding to the **glycosylphosphatidylinositol-anchored high-density lipoprotein-binding protein 1 (GPIHBP1)** and the proteoglycan heparan sulfate at the cell surface.

What is so interesting is that GPIHBP1 is only synthesized by endothelial cells. When lipoprotein lipase is secreted from cells, it binds to the extracellular matrix heparan sulfate but dissociates on the cleavage of heparan sulfate by heparinases. GPIHBP1 is highly acidic with an intrinsically disordered N-terminal domain containing a sulfated tyrosine and is highly enriched in glutamates and aspartates, which are often sequential. Here is the single-letter sequence for amino acids 25-50 of the human version of GPIHBP1: EEEEEDEDHGPDDYDEEDEDEVEEEE. This sequence would have electrostatic and binding properties similar to the highly negatively charged heparan sulfate to which it also binds.

LPL also binds Ca^{2+}, stabilizing the active dimeric form of the protein. Its enzymatic activity is activated by apoC-II. Like pancreatic lipase, it employs a Ser-132, Asp-156, and His-241 triad in its hydrolytic action on TAGs.

Figure **17.1.15**l below shows an interactive iCn3D model of LPL in complex with GPIHBP1, shown in brown (6E7K). The calcium ion is shown (grey spacefill) as well as the catalytic triad (labeled, sticks, CPK colors). The highly negatively charged stretch of amino acids in GPIHBP1 was not present in the crystal structure.

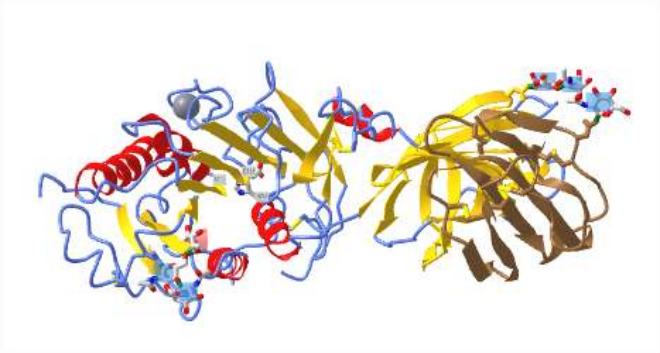


Figure 17.1.15: Lipoprotein Lipase/GPIHBP1 Complex (6E7K)). The calcium ion is shown (grey spacefill) as well as the catalytic triad (labeled, sticks, atom colors). The HPIHBP1 protein is shown in brown. The highly negatively charged stretch of amino acids in GPIHBP1 was not present in the crystal structure. Click the image for a popup or use this external link: https://structure.ncbi.nlm.nih.gov/i...VQmAikgmf7nC67 (Copyright; author via source) Kumari, A.; Kristensen, K.K.; Ploug, M.; Winther, A.-M.L. The Importance of Lipoprotein Lipase Regulation in Atherosclerosis. Biomedicines 2021, 9, 782. https://doi.org/10.3390/biomedicines9070782. Creative Commons Attribution (CC BY) license (https://creativecommons.org/licenses/by/4.0/).

17.1.5: LDL: RECEPTOR AND UPTAKE

Lipoproteins are taken up into cells through receptor-mediated processes. Given its role in cardiovascular disease, let's focus on the LDL receptor. Remember that LDL is the primary carrier of cholesterol. The receptor is found in the cell membranes in most tissues. It has many domain repeats, as illustrated in the Figure 17.1.16 calculated by SMART.

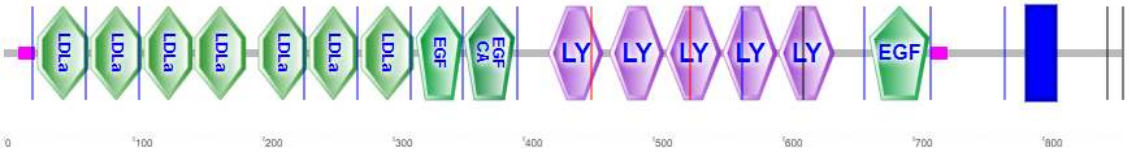


Figure 17.1.16: Domain strucuture of the LDL receptor

They include the N-terminal region cysteine-rich LDLa domains, which bind LDL, epidermal growth factor domains, LY (or LDLb) domains, and a transmembrane domain (blue rectangle).

Figure 17.1.17s shows an interactive iCn3D model of the extracellular domain of the LDL receptor (1n7d).

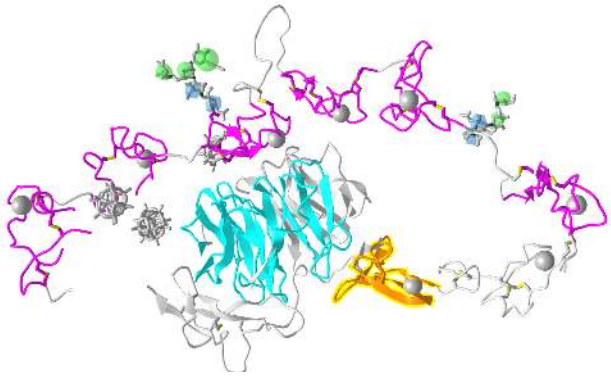


Figure 17.1.17: Click the figure for a popup model or use this external link: https://structure.ncbi.nlm.nih.gov/i...aT7M6ti5iDAbj8 (Copyright; author via source)

Four tandem LY (LDLb) domains are in cyan, LDLa domains in magenta, and the EGF domain in dark orange. Glycans are represented in symbolic nomenclature. Zoom into the structure to see the two disulfide bonds in each LDLa domain and the Ca^{2+} ions that stabilize the domains.

LDL binds its receptor at a broad binding interface with multiple LDLa domains. This may explain why it can bind to lipid nanoparticles with apo B100 or apo E. The binding triggers a series of signaling events that lead to the internalization of the receptor by endocytosis through pits coated with the protein clathrin. These eventually fuse with lysosomes, where they are degraded and cholesterol is delivered to the cell. The steps are described in Figure 17.1.18.

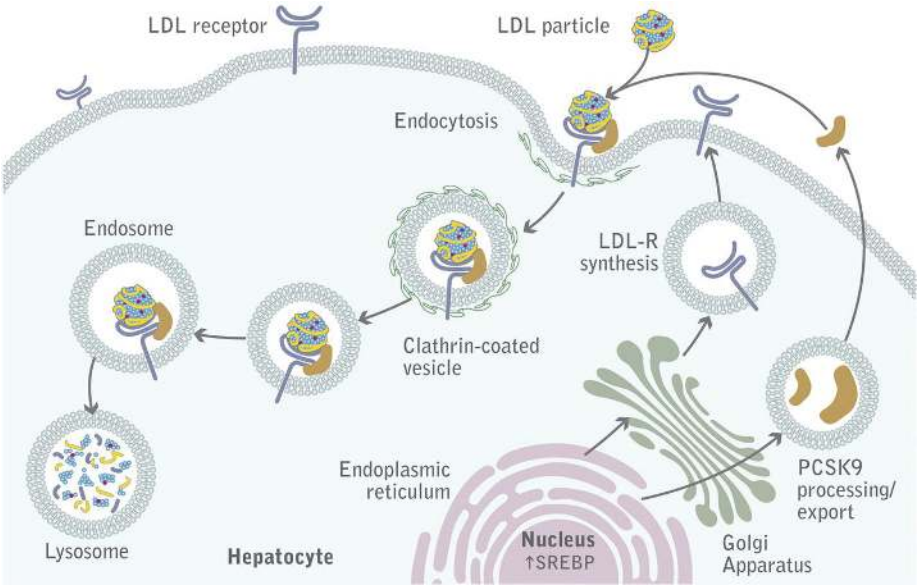


Figure **17.1.18**: Gilles Lambert et al. J. Lipid Research, 53, 2515-2524 (2012) DOI:https://doi.org/10.1194/jlr.R026658. Creative Commons Attribution (CC BY 4.0)

The LDL receptor escapes lysosomal degradation and is continually delivered to the plasma membrane, along with newly synthesized receptors. A key protein, **proprotein convertase subtilisin kexin type 9 (PCSK9)**, a serine protease secreted by the liver, promotes the enzymatic degradation of the receptor and prevents its recycling to the membrane. It also binds to VLDLR and apolipoprotein E receptors, promoting their degradation. Its action reduces LDL clearance from the blood, increasing cardiovascular risk, so inhibitors of its action might be potent drugs to decrease circulating LDL.

The LDL receptor is just one member of the LDL receptor family. Other family members are illustrated in Figure **17.1.19**.

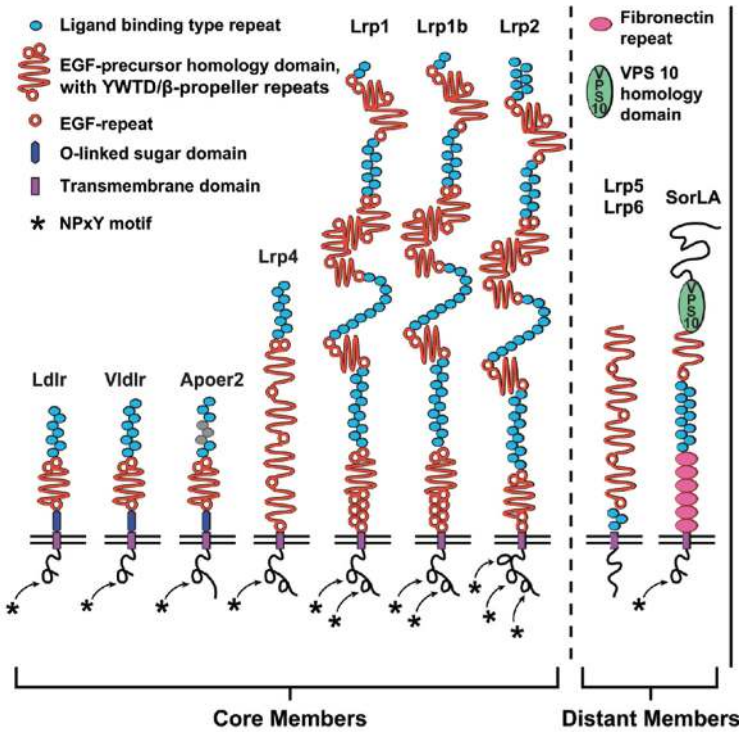


Figure **17.1.19**: LDL Receptor Family. Adapted from Theresa Pohlkamp et al. Front. Mol. Neurosci., 01 March 2017 | https://doi.org/10.3389/fnmol.2017.00054. Creative Commons Attribution License (CC BY)

These include the LDL receptor (abbreviated Ldlr in Figure **17.1.17**, as well as the VLDL receptor (Vldlr), apolipoprotein E2 receptor (Apoe2), and LDL receptor-related proteins (Lrp)1-4. These also have an NPxY-motif (asterisk in the cytoplasmic domain) and a YWTD/β-propeller domain. Given the similarity in domain structure for the LDL family of receptors, the conformational flexibility of the

apolipoproteins (at least free in solution), and similar structures for the exchangeable apolipoproteins, it shouldn't be surprising that the LDL receptor would interact with different classes of lipoproteins, albeit with different affinities.

As mentioned, apoE is found abundantly on HDL and VLDL/chylomicrons and their remnants. It is a ligand that binds to members of the LDL receptor family (remember that LDL generally binds the LDL receptor through apo B100).

APO E AND ALZHEIMER

Apolipoprotein E has three major variants (alleles) named ε2, ε3, and ε4 (also called ApoE2, 3, and 4). ApoE3 is the most prevalent. ApoE4 is found in only 15% of people, but in more than 50% with Alzheimer's Disease (AD), so it's a risk factor for this disease. AD affects the brain, which also contains up to 30% of the body's cholesterol, so aberrations in cholesterol transport and uptake in the brain are not unexpected in neurodegenerative diseases like AD.

ApoE is secreted by brain microglia (immune) cells and astrocytes (specialized glial cells). It assembles lipids into lipoproteins (HDL-like) and becomes the major vehicle for binding to and importing into neurons in a process initiated by the apoE receptor. The major apoE receptor for the clearance of lipoproteins in the brain is sortilin (SorLA in Figure **17.1.17**).

AD is characterized by the accumulation of a toxic amyloid prion protein called amyloid beta (Aβ). It is derived from selective but abnormal proteolysis of the neural integral membrane protein amyloid precursor protein (APP). Aβ aggregates to form insoluble neurotoxic extracellular Aβ amyloid plaques. Figure **17.1.20** shows the process in normal and diseased cells.

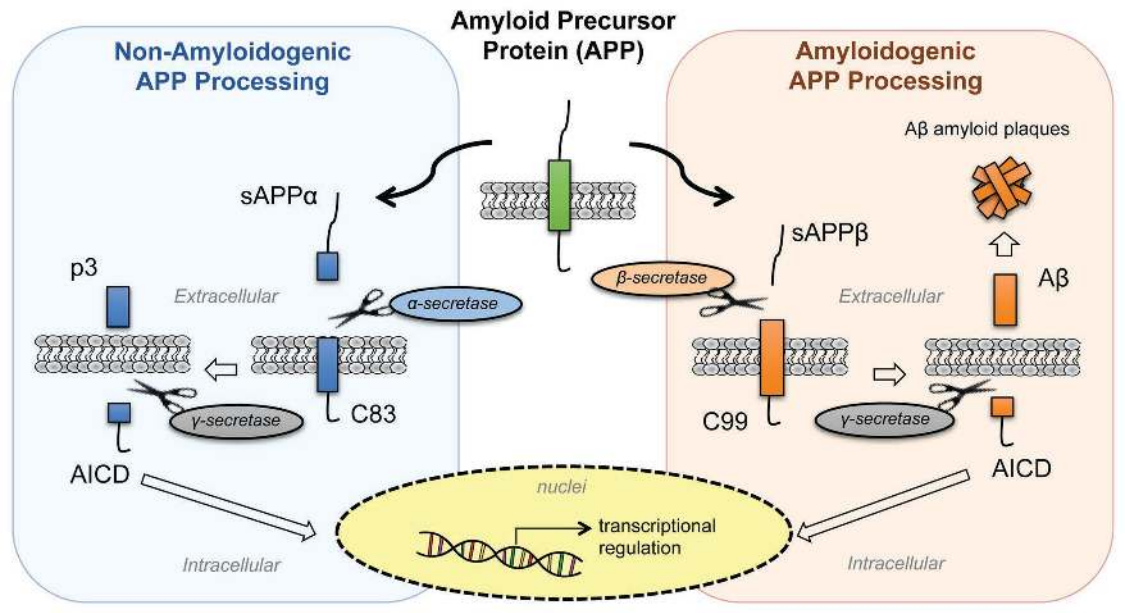


Figure **17.1.20** Processing of amyloid precursor protein (APP). Emma Ristori et al. Front. Physiol., 27 August 2020 | https://doi.org/10.3389/fphys.2020.01056. Creative Commons Attribution License (CC BY).

The figure illustrates the normal (left) and aberrant processing of APP, as well as the family of proteases (secretases) involved. While the LDLR doesn't appear to bind to APP or influence its proteolytic processing, it does bind to Aβ. LRP1 is much bigger than LDLR, binds many ligands, and can be cleaved with the same enzymes as APP. It is expressed in the liver and especially in the brain and can regulate the removal of Aβ.

Immune cells in the brain, known as microglia, remove Aβ plaques (which are extracellular) through a process called phagocytosis. ApoE4 increases the inflammatory response (as measured by cytokine release) of the microglia (a good thing if the responses prevent infection or rid Aβ plaques) but also inhibits their ability to phagocytose the Aβ plaques and their metabolic activity.

An additional note: Having one ApoE4 allele appears to increase the risk of severe COVID-19 5-fold, while being homozygous for E4 leads to a 17-fold increased risk of severe disease.

17.1.6: SCAVENGER RECEPTORS

Patients with homozygous familial hypercholesterolemia (FH) have very high levels of LDL derived from defects in binding and uptake. Patients display fatty acid streaks under the vascular endothelial cells, morphing into calcified plaques and lesions filled with fat. Monocytes/macrophages, which migrate to sites of vascular injury, take up LDL and eventually differentiate into foam cells filled with

lipids. Somehow, they have receptors that can bind and internalize LDL when the "normal" LDL receptor can't. Brown and Goldstein found that a specific chemical modification of LDL, acetylation, was necessary for the rapid uptake of "modified" LDL into macrophage receptors. These receptors are now called scavenger receptors (SRs).

There is a large family of scavenger receptors. It consists of classes A-J proteins that share functional but not sequence homology. They are found on macrophages and endothelium. They bind to and help remove "damage" signals, including damage-associated molecular patterns (DAMPs) and chemical species chemically modified by reactive oxygen species. The ligands are often polyanions, end-stage glycans, and extracellular matrix proteins. One such example is oxidized-LDL (produced in vivo or by chemical oxidative modification with malondialdehyde), which binds to the same scavenger receptor, **SR-A1**, also called **Macrophage scavenger receptor type I**, as acetylated-LDL. Figure **17.1.21** shows the domain structure of the SR family.

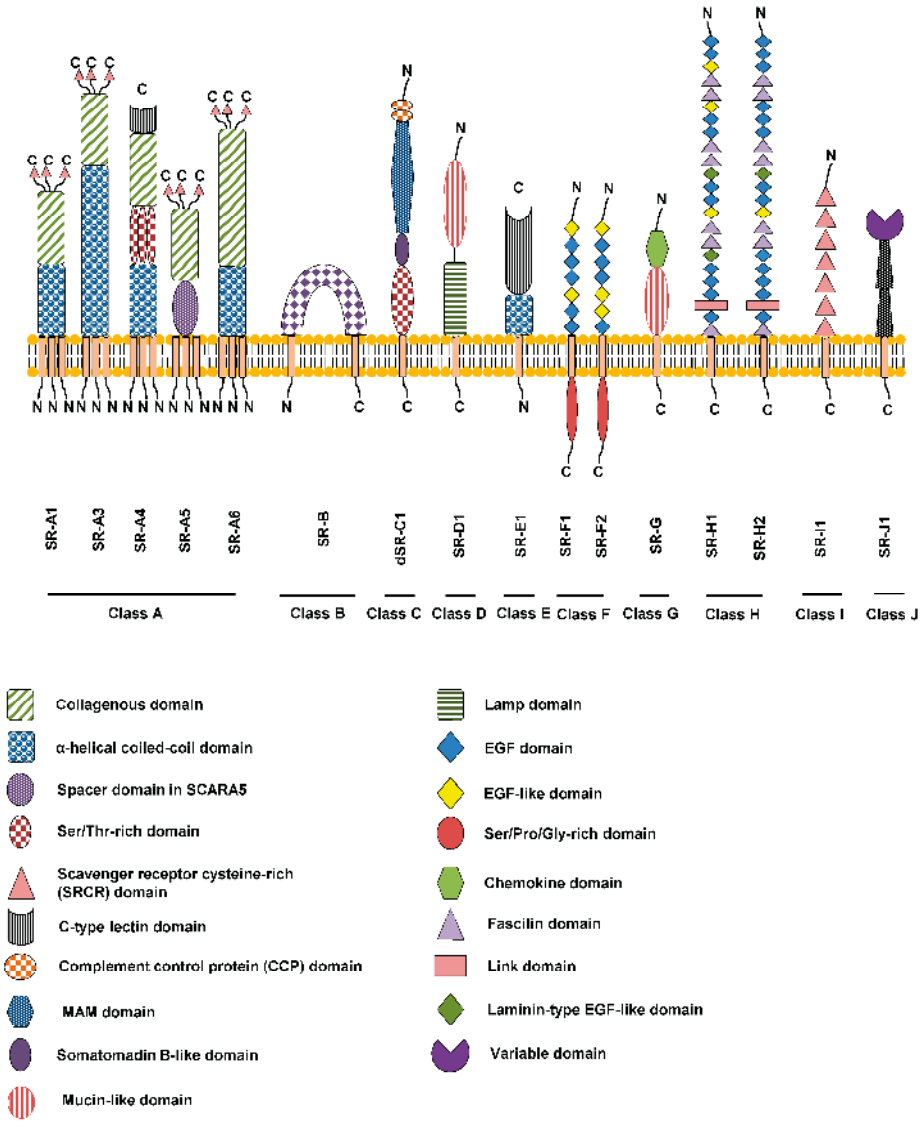


Figure **17.1.21**: Domain Structure of the Scavenger Receptor Family. Izma Abdul Zani et al. Cells 2015, 4(2), 178-201; https://doi.org/10.3390/cells4020178. Creative Commons Attribution license (http://creativecommons.org/licenses/by/4.0/)

SR-A1/MSR1 binds acetylated and oxidized LDL and β-amyloid (42), heat shock proteins (43), and PAMPs from some bacteria and viruses.

It's an enormous task to conceptualize all possible combinations of binding interactions among biological molecules. For visual learners and others, it's extremely useful to portray information on structures and interactions visually. An example using STRING, a database of known and predicted protein interactions, for the domain structure and protein:protein interactions of SR-A1/MSR1, is shown in Figure **17.1.22**.

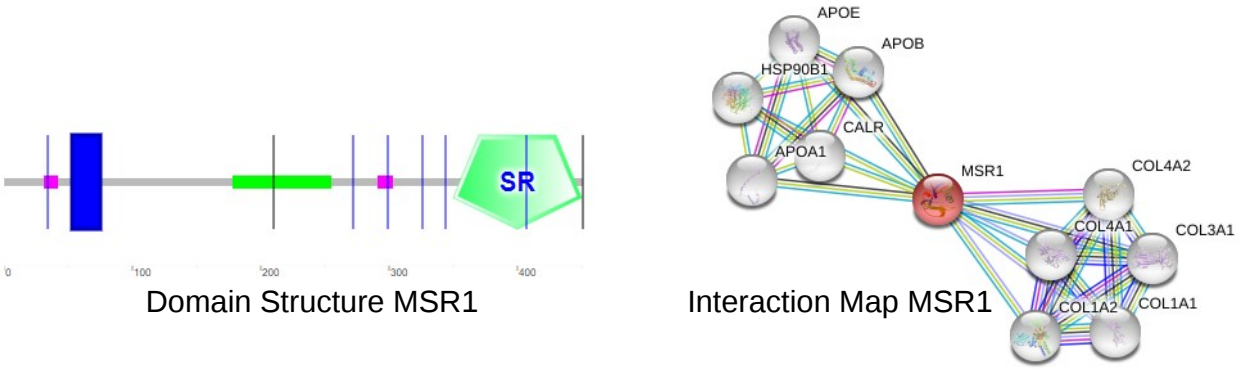


Figure **17.1.22**: Visualization of Domain Structure and Interaction Map of Macrophage Scavenger Receptor 1

Note the interactions with apolipoproteins, apoB, apoE, and apoA1. The right-hand side of the figure also illustrates interactions with the **collagen alpha-2(IV) chain** (COL4A2), which is present in the extracellular matrix.

17.1.7: HDL METABOLISM: THE GOOD CHOLESTEROL

High LDL (and Lp(a)) levels pose a cardiovascular risk. In contrast, high levels of HDL and apo A-I are cardioprotective. HDL is involved in "reverse" cholesterol transport as it is taken up by the liver and sent to the intestines for elimination from the body. We have shown earlier in Figure 2 that HDL exists in many variants, reflecting the assembly and remodeling of HDL by enzymes and lipid transfer proteins. Figure **17.1.23** shows the lifecycle of HDL.

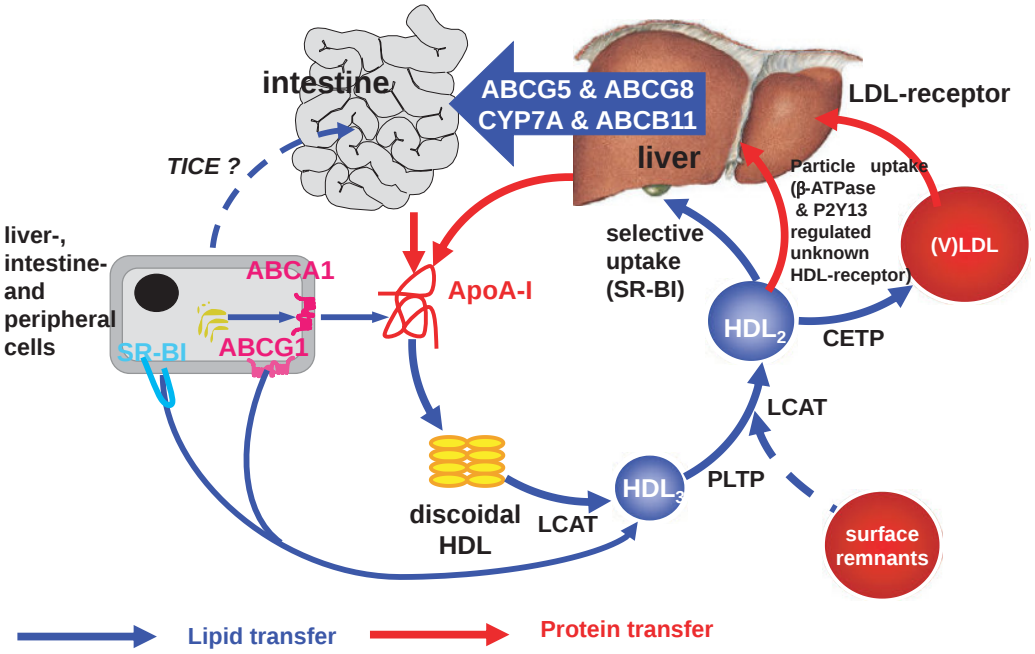


Figure **17.1.23**: Arnold von Eckardstein. Tachometer for Reverse Cholesterol Transport? August 2012. Journal of the American Heart Association 1(4):e003723. DOI: 10.1161/JAHA.112.003723. License CC BY 2.5/. Open Access article under the terms of the creative Commons Attribution Noncommercial License

Secreted apo A-1 accretes lipids in the circulation through the transport and delivery of phospholipids and cholesterol from cell membranes by the ATP-binding cassette transporters (ABC) A1 and G1. Another protein, the **scavenger receptor BI (SR-BI)**, a polytopic integral membrane protein, is also involved. It acts as a receptor for various "lipid" ligands, including phospholipids, cholesterol esters, phosphatidylserine (an outer membrane marker for cell apoptosis), and lipoproteins such as HDL.

Other proteins are also involved in the assembly and remodeling of HDL. The lipolytic enzyme lecithin-cholesterol acyltransferase (LCAT) removes a fatty acid from phospholipids and adds it to free cholesterol in the HDL to form cholesterol esters. Two major lipid transfer

proteins, **phospholipid transfer protein (PLTP)** and **cholesterol ester transfer protein (CETP)**, move lipids between HDLs and other lipoproteins. Cholesterol ester transport protein is made and secreted from the liver. It appears to exchange cholesterol esters from HDL for the return of TAGs from VLDL. Other enzymes (lipoprotein lipase and hepatic lipase) also form free fatty acids.

In the final step, HDL can deliver cholesterol ester and cholesterol to the liver by binding to the liver scavenger receptor BI (SR-BI) mediated by apo A-I. The liver, adrenal gland, endothelial cells, macrophages, and many other tissues express the protein. The liver does **not** primarily take HDL up by endocytosis. In contrast, LDL is taken up by endocytosis mediated by the LDL receptor. SR-BI facilitates the transfer of cholesterol esters from bound HDL to the liver cell.

HDL AND CARDIOVASCULAR RISK

Unlike the widespread use of statins, which reduce LDL-C concentrations and clinically reduce cardiovascular disease risk, drugs such as fibrates, niacin, and inhibitors of cholesterol ester transfer protein (CETP), which raise HDL levels, don't seem to lead to significant decreases in cardiovascular risk. The cholesterol delivered in excess to macrophages can form foam cells under the endothelial layer. Foam cells are proinflammatory and convert over time to cholesterol plaques. In contrast, HDL-C appears to have a direct atherogenic effect.

17.1.8: SUMMARY

This chapter examines the critical roles of fats and lipoproteins in energy metabolism, focusing on the breakdown, transport, and storage of fatty acids and the complex regulation of lipid homeostasis.

Fatty Acid Metabolism and Storage:
The chapter begins by outlining the two primary sources of fatty acids—those derived from the diet (mainly as triacylglycerols, or TAGs) and those synthesized de novo from acetyl-CoA. TAGs are stored in specialized lipid droplets found predominantly in adipose tissue and, to a lesser extent, in muscle and liver cells. The discussion highlights the unique functions of white adipose tissue (WAT), which stores energy and plays an endocrine role by secreting adipokines such as leptin and adiponectin, and brown adipose tissue (BAT), which specializes in heat production through fatty acid oxidation facilitated by uncoupling protein 1 (UCP1).

Lipoprotein Structure and Function:
The transport of hydrophobic fatty acids in the aqueous bloodstream is achieved by lipoproteins—complex particles consisting of a lipid core (composed of TAGs, cholesterol esters, and free cholesterol) surrounded by a single phospholipid monolayer embedded with specific apolipoproteins. The chapter details how lipoproteins are classified by density (chylomicrons, VLDL, IDL, LDL, and HDL), and how their size, composition, and apolipoprotein content determine their metabolic fates. Key apolipoproteins such as apoB100, apoB48, apoA-I, and apoE are discussed in terms of their roles in stabilizing the particle, mediating receptor interactions, and influencing lipid exchange.

Lipoprotein Assembly, Uptake, and Remodeling:
The assembly of lipoproteins begins in the intestine (chylomicrons) and liver (VLDL), where dietary or endogenously synthesized lipids are packaged with apolipoproteins. The chapter explains how lipoproteins are processed in circulation through the action of lipoprotein lipase (LPL), which hydrolyzes TAGs to release free fatty acids for uptake by peripheral tissues. The uptake of lipoproteins into cells occurs via receptor-mediated endocytosis, primarily through the LDL receptor for apoB100-containing particles. Scavenger receptors, which bind modified LDL, and the regulatory role of proteins such as PCSK9 in receptor recycling, further illustrate the complexity of lipid clearance and its impact on cardiovascular risk.

Albumin and Fatty Acid Transport:
The role of serum albumin as the major plasma protein for binding and transporting free fatty acids is also discussed. Albumin's ability to bind various hydrophobic molecules—including drugs and toxins—demonstrates its critical role in maintaining lipid solubility and bioavailability in circulation.

Cardiovascular Implications:
Finally, the chapter connects lipid metabolism to human health by examining the impact of LDL and HDL on cardiovascular risk. High levels of LDL, especially modified forms such as Lp(a), are linked to atherosclerosis and cardiovascular disease, while HDL is protective through its role in reverse cholesterol transport. The structure-function relationships of apolipoproteins, such as the amphiphilic helices in apoA-I and apoE, are emphasized as key determinants of lipoprotein behavior and interactions with cellular receptors.

In summary, this chapter integrates the biochemical pathways of fatty acid oxidation and lipoprotein metabolism, revealing how the body orchestrates the storage, transport, and utilization of lipids. It underscores the intricate regulation of these processes by hormonal signals, enzyme activities, and structural properties of macromolecular complexes, ultimately linking lipid metabolism to energy homeostasis and cardiovascular health.

This page titled 17.1: Digestion, Mobilization, and Transport of Fats is shared under a not declared license and was authored, remixed, and/or curated by Henry Jakubowski and Patricia Flatt.

- **Current page** by Henry Jakubowski and Patricia Flatt has no license indicated.
- **11.2: Diffusion Across a Membrane - Passive and Facilitated Diffusion** by Henry Jakubowski and Patricia Flatt has no license indicated.

17.2: OXIDATION OF FATTY ACIDS

LEARNING GOALS (CHATGPT O3-MINI)

1. **Describe Fatty Acid Oxidation Pathways:**
   - Explain the stepwise β-oxidation of fatty acids in the mitochondria, including the sequential reactions catalyzed by acyl-CoA dehydrogenase, enoyl-CoA hydratase, β-hydroxyacyl-CoA dehydrogenase, and thiolase, and how these reactions yield acetyl-CoA, NADH, and $FADH_2$.
   - Outline the differences between mitochondrial and peroxisomal β-oxidation, emphasizing the roles of acyl-CoA oxidase (which produces H_2O_2) and the metabolism of very long-chain and branched-chain fatty acids.
2. **Explain the Mechanisms of Fatty Acid Transport:**
   - Describe the carnitine cycle, including the roles of CPT-1, carnitine-acylcarnitine translocase (CACT), and CPT-2 in importing fatty acyl-CoAs into the mitochondrial matrix.
   - Discuss the regulatory function of malonyl-CoA in inhibiting CPT-1 to coordinate fatty acid synthesis and oxidation.
3. **Analyze the Oxidation of Unsaturated and Odd-Chain Fatty Acids:**
   - Detail how unsaturated fatty acids are processed via enoyl-CoA isomerase and 2,4-dienoyl-CoA reductase to convert cis double bonds into a form suitable for β-oxidation.
   - Explain the metabolic fate of odd-chain fatty acids, including the conversion of propionyl-CoA to succinyl-CoA via carboxylation, epimerization, and mutase reactions, highlighting the role of vitamin B12 (cobalamin) as a cofactor.
4. **Explore Alternative Oxidative Pathways:**
   - Compare and contrast α-oxidation and ω-oxidation with β-oxidation, focusing on their roles in metabolizing branched-chain fatty acids (e.g., pristanic acid) and very long-chain fatty acids, and their cellular localization (peroxisomes vs. endoplasmic reticulum).
5. **Understand Peroxisomal Function and Protein Import:**
   - Summarize the structure and functions of peroxisomes, including their role in oxidizing VLCFAs and branched-chain fatty acids, as well as in detoxifying hydrogen peroxide.
   - Describe the protein import mechanism into peroxisomes via peroxisome targeting signals (PTS) and the interaction with PTS receptors.
6. **Examine Lipoprotein Structure and Lipid Transport:**
   - Describe the composition and classification of lipoproteins (chylomicrons, VLDL, IDL, LDL, and HDL), and how their structural features (monolayer phospholipid coat, core lipids, and associated apolipoproteins) facilitate the transport of hydrophobic lipids in blood.
   - Explain how apolipoproteins (e.g., apoB100, apoB48, apoA-I, and apoE) mediate receptor interactions and contribute to the assembly, remodeling, and clearance of lipoproteins.
7. **Detail the Role and Mechanism of Lipoprotein Lipase (LPL):**
   - Outline how LPL, with the help of accessory proteins like GPIHBP1 and heparan sulfate, hydrolyzes TAGs from chylomicrons and VLDL to release free fatty acids for uptake by tissues.
   - Explain the significance of the catalytic triad in LPL and how its activity is regulated by Ca^{2+} and apolipoprotein C-II.
8. **Integrate Hormonal Regulation of Lipid Metabolism:**
   - Summarize how hormones such as insulin, glucagon, and epinephrine regulate the balance between fatty acid oxidation and storage, influencing processes like lipolysis in adipose tissue and fatty acid uptake in muscle and liver.
   - Discuss the physiological contexts (fed vs. fasting, exercise) in which these hormonal signals modulate fatty acid metabolism.
9. **Link Fatty Acid Oxidation to Energy Production:**
   - Connect the production of acetyl-CoA from fatty acid oxidation to its entry into the citric acid cycle and subsequent ATP generation via oxidative phosphorylation.
   - Evaluate how the high reduction state of fatty acids makes them an efficient energy source.
10. **Identify and Explain Diseases Related to Fatty Acid Metabolism:**

- Describe the biochemical basis and clinical manifestations of metabolic disorders such as MCAD deficiency, Zellweger syndrome, X-linked adrenoleukodystrophy (X-ALD), and Refsum disease.
- Discuss how deficiencies in specific enzymes or transport proteins lead to the accumulation of fatty acid intermediates and the resulting pathological consequences.

These learning goals will guide students through an integrated understanding of fatty acid catabolism, lipid transport mechanisms, and the associated regulatory and pathological aspects, emphasizing both molecular mechanisms and physiological significance.

17.2.1: INTRODUCTION

Fatty acids, esterified to glycerol in triacylglycerols, are organisms' major source of stored energy. As we burn fossil fuels to produce energy to drive our society, so can we "burn" fatty acids to ultimately produce heat and ATP to drive biosynthetic reactions and to do work. As discussed in an earlier chapter, fatty acids are highly reduced, so their oxidation by dioxygen is highly favored both enthalpically (exothermic reaction) and entropically. Of course, biological oxidation reactions occur stepwise, not directly using O_2, but with less potent oxidizing agents, such as NAD^+ and FAD. We'll focus first on fatty acid oxidation in animals (humans).

As discussed in the previous section, fatty acids released from triglyceride stores in response to signaling by epinephrine and glucagon during exercise and between meals are utilized for energy when glycogen stores are low, without breaking down protein in muscles to produce energy. Some fatty acids are broken down in the normal process of membrane turnover and removal of xenobiotic lipids.

Most fatty acids are oxidized in the mitochondria, where the oxidation reaction occurs at the beta-carbon of the acyl chain, as shown in Figure **17.2.1**.

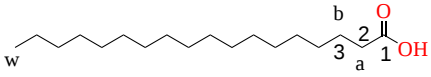


Figure **17.2.1**: α and β carbons of fatty acids

This pathway is called **β-oxidation**. Fatty acids are oxidized in a step-wise fashion by this pathway. In each repetitive cycle of this pathway, acetyl-CoA and one CO_2 are released. In addition, oxidation can occur at α- and β-carbons when oxidized in the peroxisome. The **α-oxidation** pathway is used for fatty acids branched at the β-carbon (C3), releasing one CO_2 until the β-oxidation pathway can be used. The peroxisome degrades fatty acids that can't be oxidized in the mitochondria. These include very long-chain fatty acids (VLCFAs) such as 24:0 and 26:0, and in addition, branched-chain fatty acids (BRCHAs), including some fatty acids from dietary sources such as pristanic acid (an odd-chain 15:0 fatty acid methylated at carbons 2, 6, 10, and 14). The α-oxidation pathway can't be used to completely oxidize fatty acids in the peroxisome. At some point in the oxidative stepwise pathway, the resulting shorter fatty acids are exported to the mitochondria for β-oxidation. Additionally, enzymes in the endoplasmic reticulum facilitate the **ω-oxidation** pathway, which oxidizes fatty acids at the omega or terminal carbon. The enzyme used is the monooxygenase cytochrome P_{450}, which uses one oxygen from O_2 to hydroxylate the ω-carbon.

PEROXISOMES - AN UNDERAPPRECIATED ORGANELLE

These organelles, initially referred to as microbodies, are crucial to cellular metabolism and overall health. In people with Zellweger syndrome spectrum, there is a severe disorder in the formation of peroxisomes, which is often lethal. They are important metabolically in lipid metabolism, the synthesis of myelin sheath lipids, and the metabolism of reactive oxygen species like peroxides. The enzymes catalase and urate oxidase are found in such high concentrations that they often form crystal "bodies" in the peroxisome matrix. Additional roles include responses to pathogens and viruses. Effectively, they are a protective organelle.

In contrast to mitochondria, peroxisomes, like most other organelles, have a single bilayer and no DNA, from which transcription of RNA and translation of proteins occur. Hence, all proteins are imported from the cytoplasm after synthesis on free ribosomes. Imported proteins have a peroxisome targeting sequence (PTS) of serine-lysine-leucine (SKL) near their C-terminus, which facilitates the binding of these proteins to a PTS receptor in the peroxisome membrane. These organelles oxidize very long-chain fatty acids (VLFA), make and break down hydrogen peroxide (hence the name), and synthesize plasmalogens. The enzymes involved in the stepwise cycle of reactions in the peroxisomal β-oxidation pathway utilize enzymes different from those used in the mitochondrial β-oxidation pathway.

For those more inclined towards chemistry than biology, another organelle with its structures and function may seem like one too many. However, this less-discussed organelle is critically important in its own right. Figure **17.2.2** shows the features of peroxisomes and their proteins.

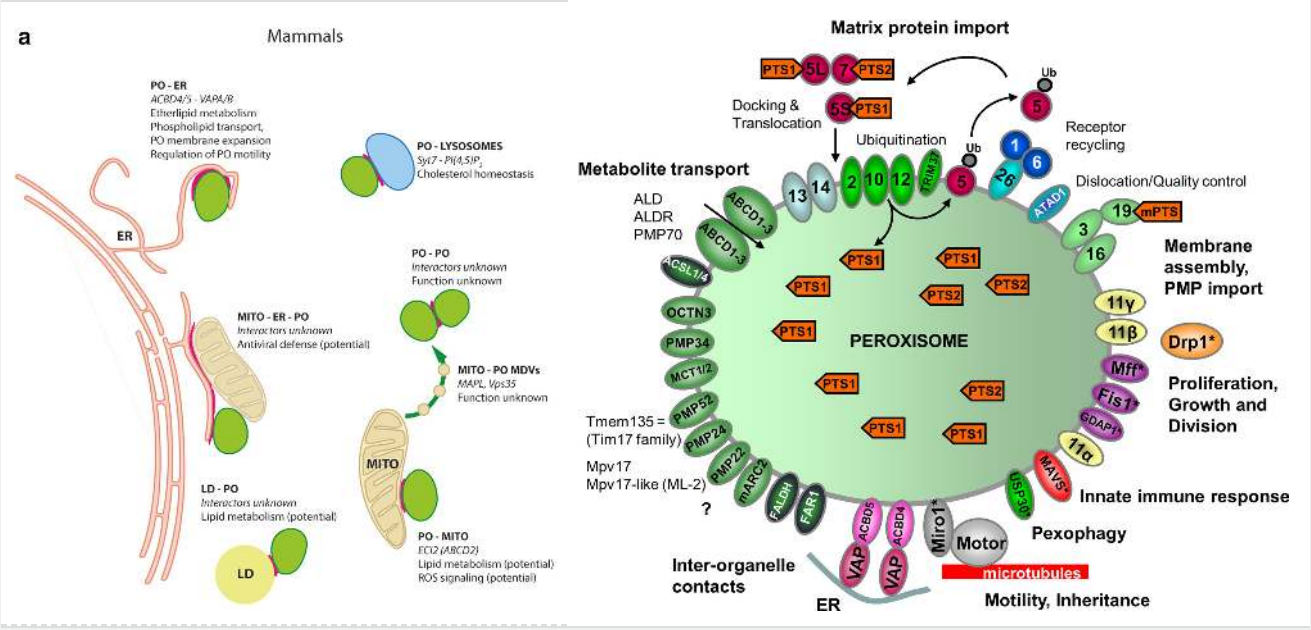


Figure **17.2.2**: Features of peroxisomes and their proteins. Islinger, M., Voelkl, A., Fahimi, H.D. *et al.* The peroxisome: an update on mysteries 2.0. *Histochem Cell Biol* **150,** 443–471 (2018). https://doi.org/10.1007/s00418-018-1722-5. Creative Commons Attribution 4.0 International License (http://creativecommons.org/licenses/by/4.0/)

One interesting feature is its relationship with different cell organelles, as shown in the left panel of Figure 2. Some proteins involved in organelle functions are also shown (right panel).

The peroxisome (PO, green) has binding interactions (red interfaces) with the endoplasmic reticulum (ER), lysosomes, mitochondria, lipid droplets (a pseudo-organelle), and also itself (left figure). Some of the key membrane proteins (which we have discussed previously) involved in peroxisome function include the ABC transporter proteins ABCD1-3 for fatty acids transport, OCTN3 for organic and cation/carnitine transport, and MCT1/2 for monocarboxylate transport. In addition, peroxisomes have receptors for protein import, mediated by PTSs, and for peroxisome movement along microtubules within the cell.

17.2.2: MITOCHONDRIAL B-OXIDATION

Mitochondrial β-oxidation in muscle generates acetyl-CoA, which enters the citric acid cycle for subsequent production of ATP through mitochondrial electron transport and oxidative phosphorylation. In the liver, the generated acetyl-CoA is used for ketone body production under fasting states. Figure **17.2.3** shows the β-oxidation pathway for palmitic acid (16:0), a saturated fatty acid, starting with its import from the cytoplasm.

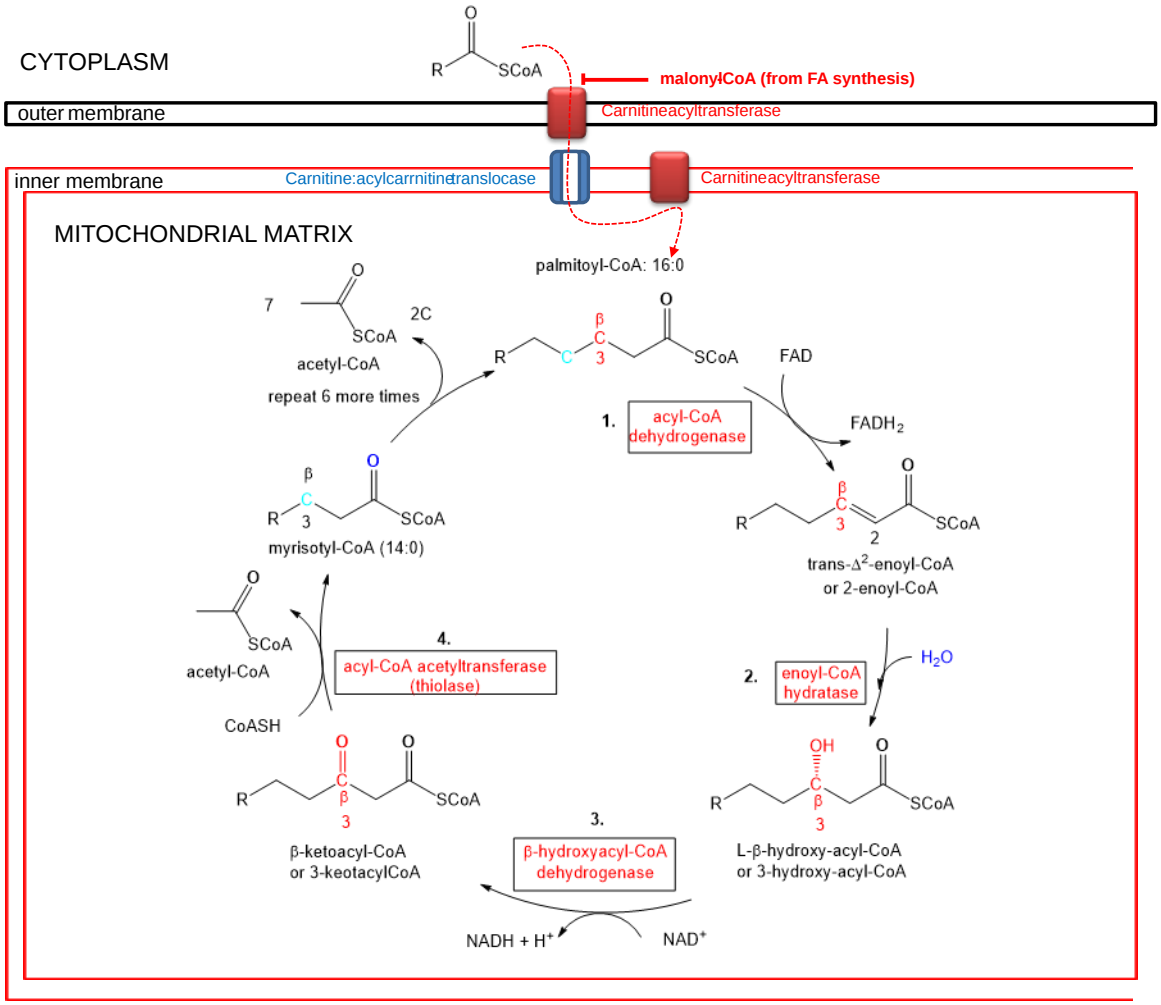


Figure **17.2.3**: Mitochondrial β-oxidation of palmitic acid (16:0)

The pathway involved the cyclic removal of 2-carbon units until 16:0 is cleaved seven times, producing eight 2-carbon acetyl-CoAs. The net chemical equation for the beta-oxidation of 16:0 is shown below.

$$\mathrm{C_{16} - CoA + 7NAD^+ + 7FAD + 7CoASH + 7H_2O} \\ \mathrm{\rightarrow 8Acetyl - CoA + 7NADH + 7FADH_2 + 7H^+} \qquad (17.2.1)$$

Figure **17.2.4** shows an abbreviated comparison of the β-oxidation pathways in the mitochondria and peroxisomes. Peroxisomal beta-oxidation is used to metabolize very-long-chain fatty acids (VLCFAs), which are composed of 24-26 carbon units, and branched-chain fatty acids (BRCHAs).

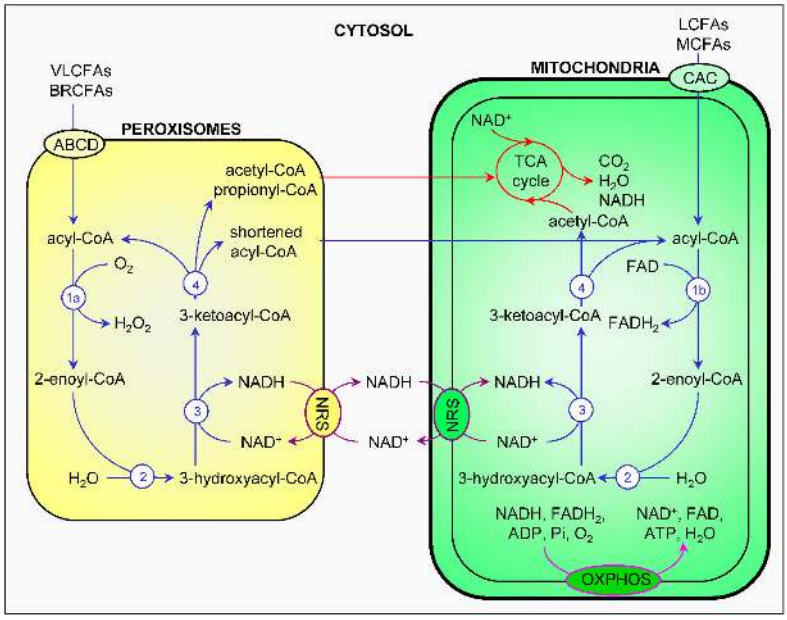


Figure **17.2.4**: Comparison and interplay of peroxisomal and mitochondrial fatty acid β-oxidation. Fatty acid β-oxidation, the NAD(H) redox shuttles, the tricarboxylic acid cycle, and the electron transfer chain are depicted in blue, purple, red, and pink, respectively. 1a, acyl-CoA oxidase; 1b, acyl-CoA dehydrogenase; 2, enoyl-CoA hydratase; 3, 3-hydroxyacyl-CoA dehydrogenase; 4, 3-ketoacyl-CoA thiolase. ABCD, ATP-binding cassette transporters of subfamily D; ADP, adenine dinucleotide phosphate; BRCFA, branched-chain fatty acid; CAC, carnitine-acylcarnitine carrier; FAD, flavin adenine dinucleotide; $FADH_2$, reduced FAD; LCFA, long-chain fatty acid; MCFA, medium-chain fatty acid; NAD, nicotinamide adenine dinucleotide; NADH, reduced NAD; NRS, NAD(H) redox shuttles; OXPHOS, oxidative phosphorylation; TCA, tricarboxylic acid; VLCFA, very-long-chain fatty acid. Fransen et al. International Journal of Molecular Sciences. 18. 1126. 10.3390/ijms18061126. DOI: 10.3390/ijms18061126. Commons Attribution (CC BY) license (http://creativecommons.org/licenses/by/4.0/).

It should be noted that a likely NAD^+/NADH mitochondria transporter, a multi-pass inner mitochondrial membrane protein, has just been identified. The transporter, MCART1, is also called SLC25A51,

17.2.3: B-OXIDATION - MECHANISMS

Fatty acids are imported into the matrix from the cytoplasm through their acyl-CoA derivatives. Two different proteins are required for their import. **Carnitine palmitoyltransferase-1(CPT-1)** transfers the acyl group from CoASH to a carrier protein carnitine. The acylcarnitine is translocated through the inner membrane by the carrier protein **carnitine-acylcarnitine translocase (CACT)**. Once inside the matrix, the acyl group is transferred back to CoASH by **carnitine palmitoyltransferase-2 (CPT-2)**. This **carnitine cycle** is illustrated in Figure **17.2.5**.

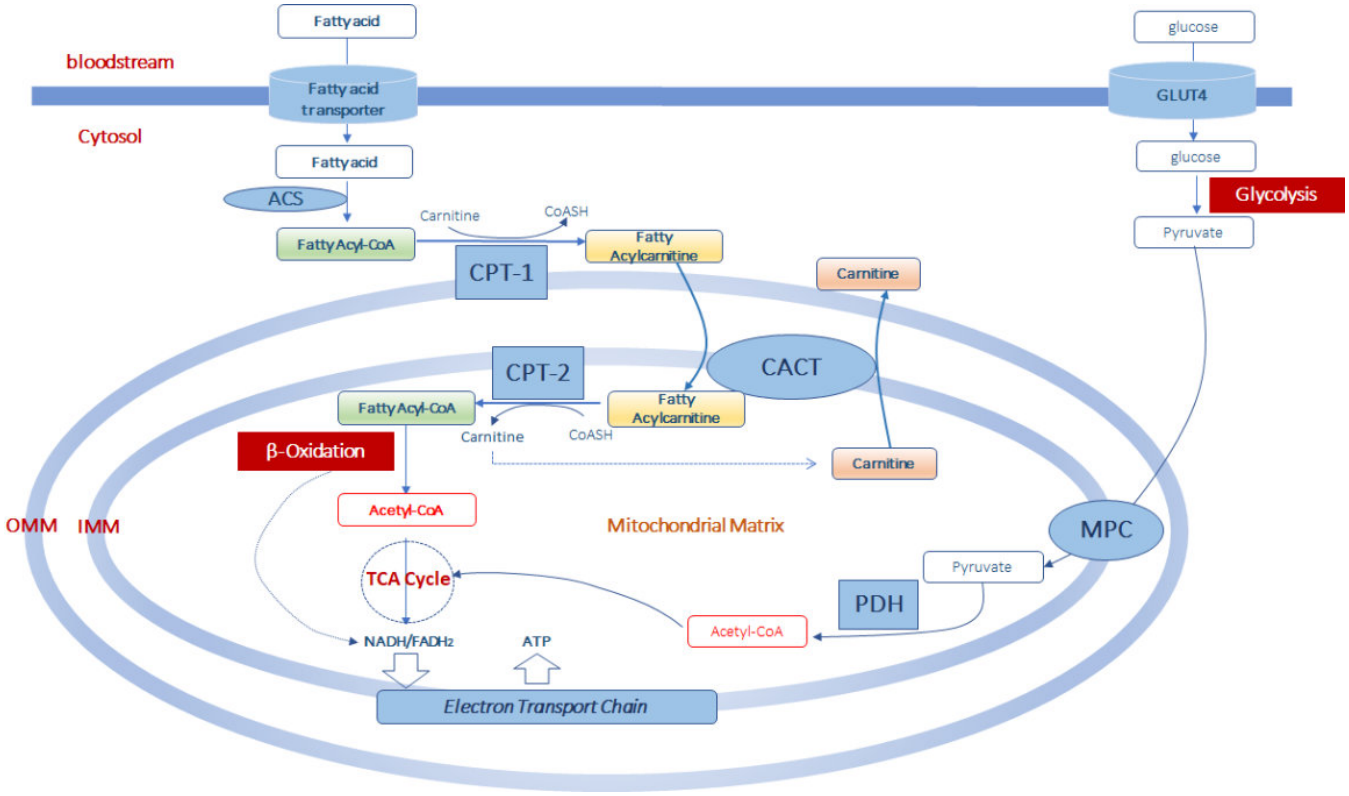


Figure **17.2.5**: Carnitine cycle and the connections between major catabolic pathways.

At the outer mitochondrial membrane (OMM), fatty acyl-CoAs become linked to carnitine through carnitine palmitoyltransferase-1 (CPT-1). The complex is translocated across the inner mitochondrial membrane (IMM) via carnitine-acylcarnitine translocase (CACT). In the mitochondrial matrix, CPT-2 converts fatty acylcarnitines back to fatty acyl-CoAs, which enter the β-oxidation pathway. Free carnitine moves back into the cytoplasm through exchange with acyl-carnitines with CACT. β-Oxidation in the matrix produces acetyl-CoA, which is also formed from glycolytic pyruvate through the action of pyruvate dehydrogenase. Hence, acetyl-CoA links both glycolysis and fatty acid oxidation. The resulting acetyl-CoA can enter the TCA cycle when energy is needed.

The mitochondrial carnitine/acylcarnitine carrier protein helps transport acylcarnitines of different lengths across the mitochondrial inner membrane for β-oxidation into the mitochondrial matrix. Figure **17.2.6** shows an interactive iCn3D model of the human mitochondrial carnitine/acylcarnitine carrier protein AlphaFold model (O43772)

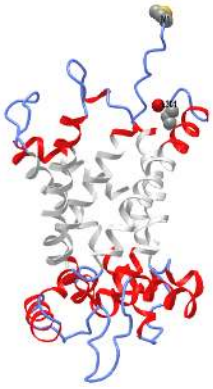


Figure **17.2.6**: Mitochondrial carnitine/acylcarnitine carrier protein AlphaFold model (O43772). (Copyright; author via source). Click the image for a popup or use this external link: https://structure.ncbi.nlm.nih.gov/i...DdDNu9xVJGg2i9

The transmembrane helices are shown in gray. The N- (Met 1) and C-terminal (Leu 301) amino acids are shown in spacefill color CPK.

Malonyl-CoA, produced in the first committed step in fatty acid synthesis, inhibits CPT1. This should make biological sense, as fatty acid oxidation should not occur when fatty acids are being synthesized. Palmitoyltransferase II (CPT II), which converts acylcarnitine to fatty acyl-CoA, traps the molecules within the mitochondrial matrix.

In contrast to this regulated transport mechanism, very long-chain fatty acids (VLCFAs) and branched-chain fatty acids are transported into peroxisomes by the ABCD1-3 transporters through an ATP-dependent process.

The mitochondrial β-oxidation of fatty acids has four steps in the mitochondrial matrix. In those steps, a 16:0 fatty acid (for example) is converted to a (14):0 fatty acid and the 2C molecule acetyl-CoA. The (14):0 fatty acid undergoes six more rounds of the β-oxidation cycle until the entire 16:0 fatty acid is fully converted to 8 acetyl-CoAs.

Step 1: Acyl-CoA dehydrogenase

There are long-chain acyl-CoA dehydrogenases (LCAD), medium-chain acyl-CoA dehydrogenases (MCAD), and short-chain acyl-CoA dehydrogenases (SCAD), which catalyze the first oxidative step in the β-oxidation pathway. These enzymes catalyze the formation of a trans double bond between the α and β carbons (C2 and C3) on the acyl-CoA substrates. A stronger oxidizing agent than NAD^+ is required to form an alkene between the two methylene groups, so FAD is used. Eventually, the reduced $FADH_2$ produced will produce 1.5 equivalents of ATP in the mitochondrial electron transport chain/oxidative phosphorylation.

Figure **17.2.7** shows the key oxidative step in the mechanism of acyl-CoA dehydrogenase to 2-enoyl-CoA by acyl-CoA dehydrogenases

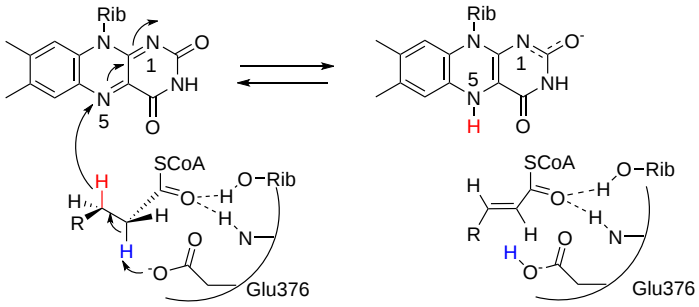
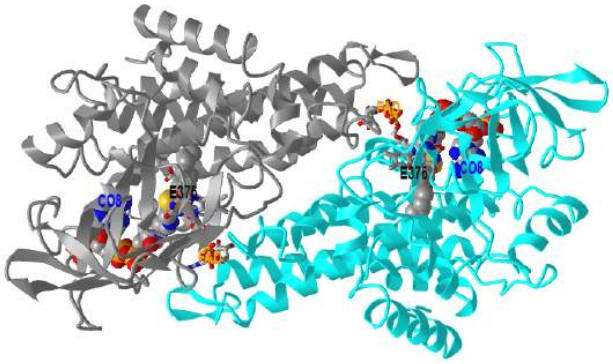


Figure **17.2.7**: Mechanism for conversion of acyl-CoA to enoyl-CoA by acyl-CoA dehydrogenase. (after Ghisla and Thorpe. Eur. J. Biochem. 271, 494–508 (2004) doi:10.1046/j.1432-1033.2003.03946.x)

Figure **17.2.8** shows an interactive iCn3D model of the medium-chain acyl-CoA dehydrogenase from pig liver mitochondria with octanoyl-CoA, a substrate (3MDE)



NCBI iCn3D Figure **17.2.8**: Medium-chain acyl-CoA dehydrogenase from pig liver mitochondria with octanoyl-CoA substrate (3MDE). (Copyright; author via source). Click the image for a popup or use this external link: https://structure.ncbi.nlm.nih.gov/i...SiAZExwXVV2TG6

Two subunits of the biologically active tetramer are shown (dark gray and cyan). FAD is shown in each subunit (sticks, CPK colors, labeled). A bound substrate, octanoyl-CoA (spacefill, CPK colors, labeled CO8) is also shown in each subunit. The catalytic base, Glu 376, is depicted in sticks, with CPK colors and labeled.

The structures of the unliganded and acyl-CoA forms of the enzymes are very similar, so there are no large conformational changes on binding octanoyl-CoA. The ligand binds to the enzyme at the FAD's rectus (re) face with the acyl chain buried. The fatty acyl chain of the thioester substrate is buried inside the polypeptide, and the 3'-AMP moiety is close to the surface of the tetrameric enzyme molecule. The carbonyl oxygen of octanoyl-CoA interacts with the ribityl 2'-hydroxyl group of the FAD and the main-chain carbonyl oxygen of Glu-376. Glu-376 acts as a general base, removing the alpha proton in the reaction.

Step 2. Enoyl CoA hydratase

This enzyme catalyzes a hydration step of the double bond between the α and β carbons (C2 and C3), adding an OH group to the β carbon, in a reaction that poses a low energy barrier. Figure **17.2.9** shows a likely mechanism for enoyl-CoA hydratase.

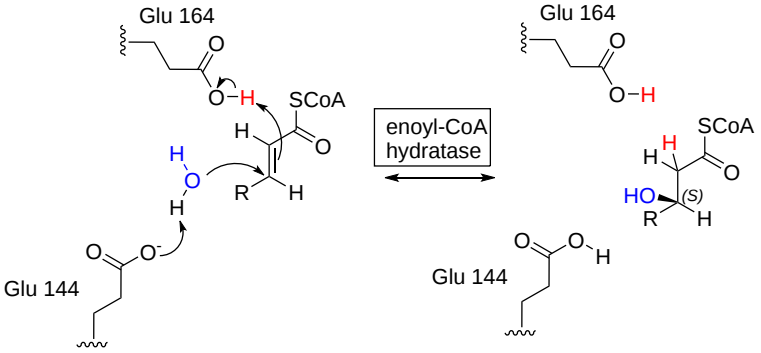
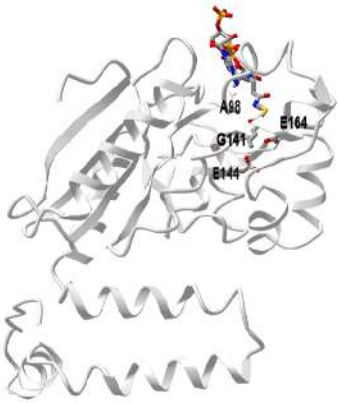


Figure **17.2.9**: Mechanism for enoyl-CoA hydratase

Figure **17.2.10** shows an interactive iCn3D model of the rat enoyl-CoA hydratase in complex with hexadienoyl-CoA (1MJ3)



NCBI iCn3D Figure **17.2.10**: Rat enoyl-CoA hydratase in complex with hexadienoyl-CoA (1MJ3). (Copyright; author via source). Click the image for a popup or use this external link: https://structure.ncbi.nlm.nih.gov/i...byx3eEKewEeEz9

For clarity, only one subunit of the biological hexamer is shown. Two glutamic acids (141 and 164) appear to activate a water molecule for the hydration reaction. Alanine 98 and Gly 141 are also in the oxyanion hole, stabilizing the transition state and intermediate.

The addition of the water is syn since the proton and OH group are added to the same size of the double bond. The glycine amide NH provides a strong hydrogen bond to the carbonyl of the substrate, hexadienoyl-CoA, helping to polarize the ene-one. The substrate trans-2-crotonyl-CoA is converted to the 3(S) alcohol instead of the 3(R) alcohol by a huge factor. The cis and trans isomers of a substrate analog (hexadienoyl-CoA) can bind to the enzyme, but only the cis isomer is polarized. Since the transition state is polarized as well, the bound cis isomer is also strained and destabilized, suggesting that its binding is an example of transition-state binding catalysis.

Step 3. Beta-hydroxyl acyl CoA dehydrogenase

After the addition of the OH on C3 (beta) OH during the hydration reaction, the resulting ROH is oxidized to a ketone, β-ketoacyl-CoA, by the oxidizing agent NAD^+ using the enzyme β-hydroxyl acyl CoA dehydrogenase. The resulting NADH is reoxidized to NAD^+ through the mitochondrial electron transport chain, ultimately leading to 2.5 molecules of ATP for each NADH. Figure **17.2.11** shows a plausible mechanism for the beta-hydroxyl acyl CoA dehydrogenase-catalyzed reaction.

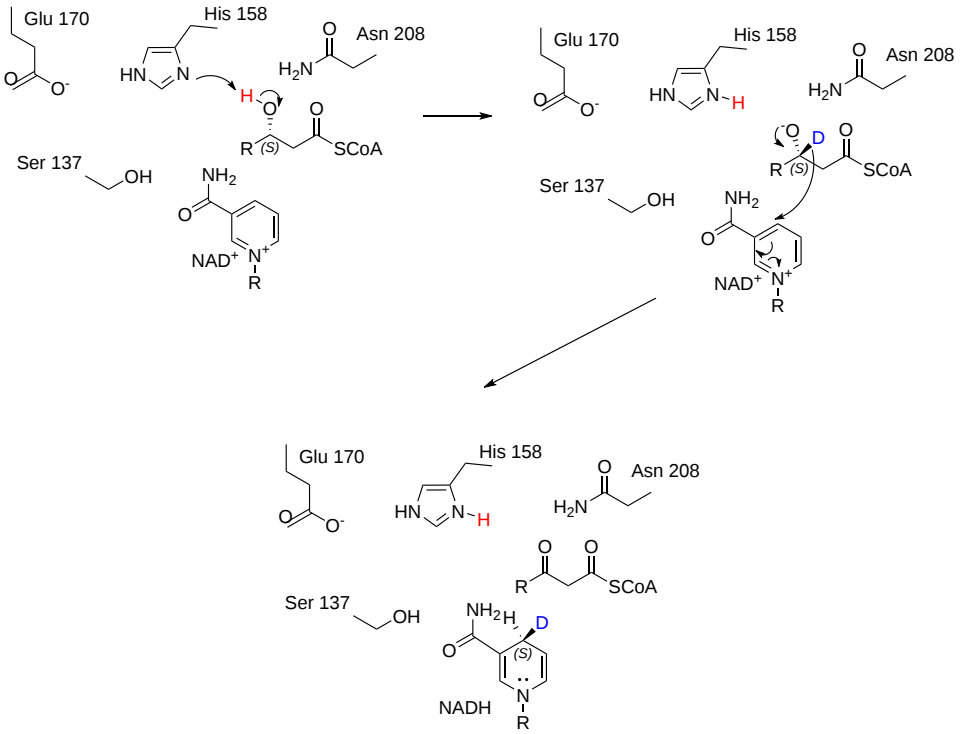


Figure **17.2.11**: Mechanism for production of β-ketoacyl-CoASH by b**eta-hydroxyl acyl CoA dehydrogenase**

His 158 acts as a general base, and Glu 170 increases its basicity. The other group is involved in H-bond and electronic stabilization interactions.

Step 4. **Acetyl-CoA acetyltransferase, mitochondrial - ACAT1** (also called 3-ketoacyl-CoA **thiolase**)

The final step in the beta-oxidation pathway involves cleavage of the bond between the alpha and beta carbon by CoASH. This step is catalyzed by beta-keto thiolase and is a thiolytic reaction (as opposed to cleavage by water, a hydrolysis reaction). The reaction produces one molecule of acetyl-CoA and a fatty acyl-CoA that is two carbons shorter. The process repeats until the even-chain fatty acid is completely converted into acetyl-CoA. The enzyme's activity is reversible, and it can also catalyze the Claisen condensation of two acetyl-CoA molecules into acetoacetyl-CoA, as we will see in the synthesis of ketone bodies in the next chapter section.

The reaction begins with the acylation of the nucleophilic Cys 89 by the carbonyl group of the 3-oxoacyl-CoA, accompanied by the concomitant release of acetyl-CoA. This forms a Cys 89-acyl covalent intermediate. In the next step, Cys 378 acts as a general base to facilitate the nucleophilic attack of free CoASH on the acyl-intermediate. His 348 acts as a general acid and protonates the thiolate leaving group. The amino acids (Cys89, Cys378, and His348) are generally conserved in thiolases (Bhaskar et al. 2020). Kinetically, this mechanism is a ping-pong reaction. A reaction mechanism is shown in Figure **17.2.12**.

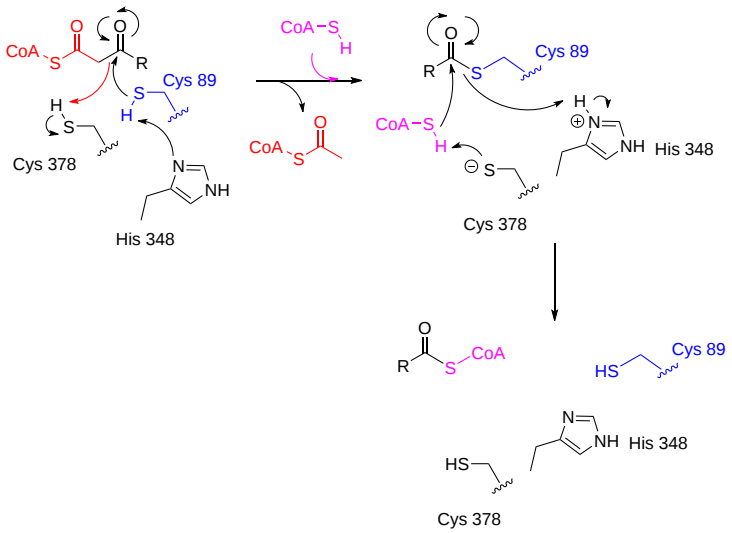
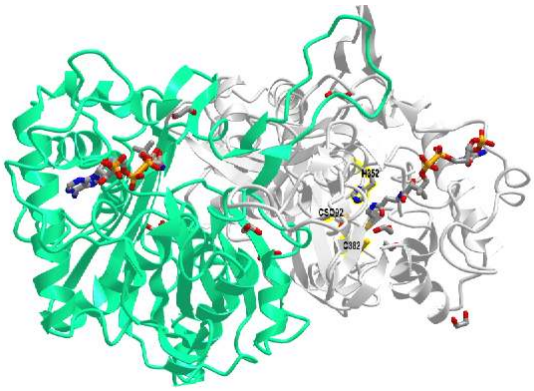


Figure **17.2.12**: Reaction mechanism for mitochodrial acetyl-CoA acetyltransferase (ACAT1, thiolase T1)

Figure **17.2.13** shows an interactive iCn3D model of Human Mitochondrial 3-Ketoacyl-Coa Thiolase (T1) (4C2J)



NCBI iCn3D Figure **17.2.13**: Human Mitochondrial 3-Ketoacyl-Coa Thiolase (T1) (4C2J). (Copyright; author via source). Click the image for a popup or use this external link: https://structure.ncbi.nlm.nih.gov/i...dzAHKEY77WpNi7

Two subunits in the biological function dimer are shown (cyan and gray). The active site is shown in the gray subunit as CPK-colored sticks and labeled. The numbers are a bit different than those shown in the mechanistic figure. CoASH is shown in each subunit as sticks. The fatty-acyl tail appears to bind in a tunnel.

17.2.4: A FEW MORE ENZYMES ARE NEEDED.

Steps 1 through 4 outlined above apply to the beta-oxidation of a saturated fatty acid with an even-numbered carbon skeleton. Unsaturated fatty acids, such as oleate (18:1) and linoleate (18:2), contain cis double bonds that must be isomerized to the trans configuration by the enzyme **enoyl CoA isomerase** or reduced by the 2,4-dienoyl CoA reductase (24DCR), using NADPH.

Enoyl CoA isomerase

This enzyme catalyzes the isomerization of cis double bonds to the trans form, which mimics those formed by acyl-CoA dehydrogenase using FAD in step 1. Figure **17.2.14** shows a plausible mechanism for converting cis double bonds to their trans isomer.

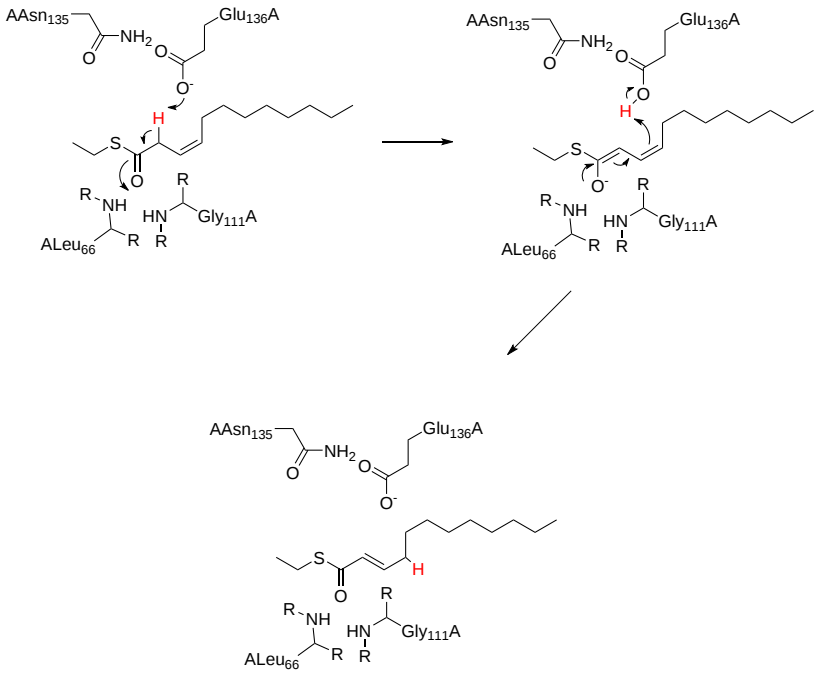


Figure **17.2.14**: Cis to trans isomerization by enoyl-CoA isomerase (https://www.ebi.ac.uk/thornton-srv/m-csa/entry/341/)

Glu 136 acts as a general base, while the amide Hs of Leu 66 and Gly 111 stabilize the intermediate oxyanion and, hence, the developing charge in the transition state. They are optimally situated in the oxyanion hole.

Figure **17.2.15** shows an interactive iCn3D model of the Human mitochondrial Δ^3-Δ^2-enoyl-CoA isomerase (1SG4)

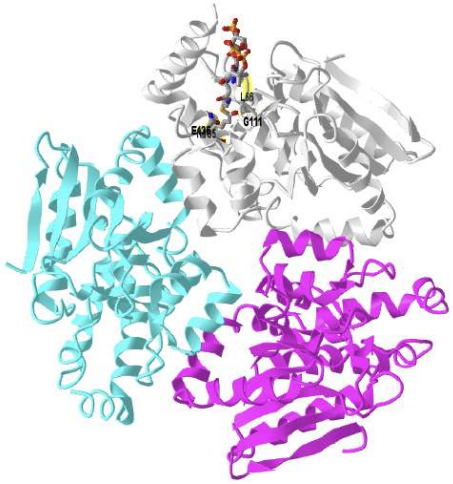


Figure **17.2.15**: Human mitochondrial Δ^3-Δ^2-enoyl-CoA isomerase (1SG4) (Copyright; author via source). Click the image for a popup or use this external link:https://structure.ncbi.nlm.nih.gov/i...H6LxEzBKajq8b7

The three subunits are shown in different colors. The substrate analog octanoyl-CoA is shown in spacefill CPK colors bound to the gray subunit. The catalytic residues are shown in sticks with CPK colors and labeled. The distal omega end binds in a hydrophobic tunnel.

2,4-dienoyl CoA reductase or **24DCR**

An alternative way to deal with the cis double bond is to reduce it, in this case, with NADPH. This enzyme is used on all C=C at even-numbered positions and more at odd-numbered positions. A mechanism for the reduction is shown in Figure **17.2.16**.

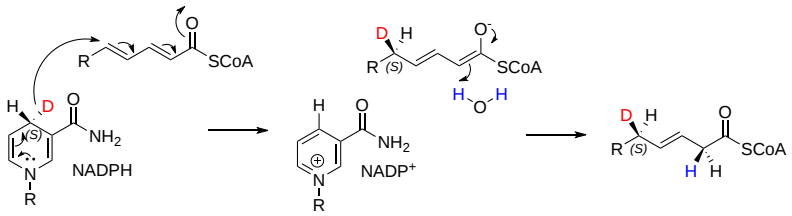
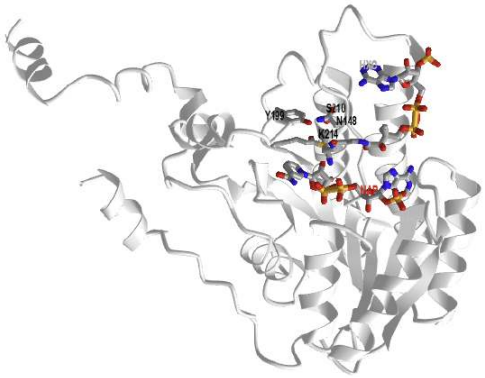


Figure **17.2.16**: a mechanism for the reduction of double bonds in unsaturated fatty acids (after Fillgrove and Anderson, B*iochemistry* (2001) https://doi-org.ezproxy.csbsju.edu/10.1021/bi0111606

Figure **17.2.17** shows an interactive iCn3D model of a monomer of the homotetrameric human mitochondrial 2,4-dienoyl-Coa reductase (1W6U)



NCBI iCn3D Figure **17.2.17**: Monomer of the homotetrameric human Mitochondrial 2,4-Dienoyl-Coa Reductase (1W6U) (Copyright; author via source). Click the image for a popup or use this external link: https://structure.ncbi.nlm.nih.gov/i...pQueKc84sFqzt7

The model shows bound $NADP^+$ and the substrate trans-2,trans-4-dienoyl-CoA. The active site is sufficiently open to accommodate fatty acids of varying lengths. Tyr-199 and Asn-148 stabilize the enolate and the oxidized nicotinamide.

For odd-number chain fatty acids, propionyl-CoA to succinyl-CoA

Although most fatty acids of biological origin have even numbers of carbons, not all do. The oxidation of fatty acids with odd numbers of carbons ultimately produces an intermediate with three carbons, propionyl-CoA, which cannot be oxidized further in the beta-oxidation pathway. These additional steps are necessary:

1. carboxylation to make (S)-methylmalonyl-CoA;
2. isomerization to (R)-methylmalonyl-CoA;
3. rearrangement to form succinyl-CoA. The last step of the process utilizes the enzyme methylmalonyl-CoA mutase, which uses the B12 coenzyme in its catalytic cycle. Succinyl-CoA can then be metabolized in the citric acid cycle.

Figure **17.2.18** shows the pathway for converting propionyl-CoA to succinyl-CoA.

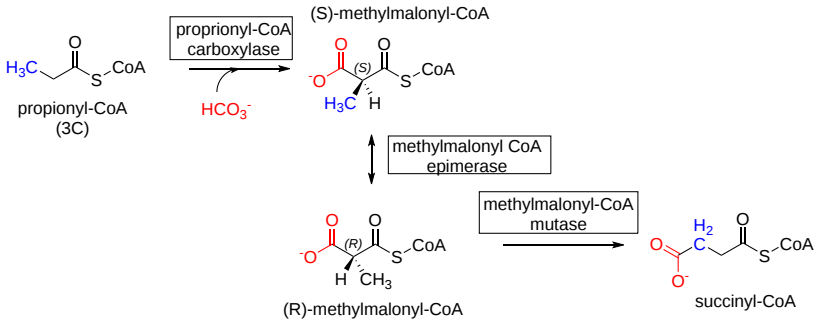


Figure **17.2.18**: Conversion of propionyl-CoA to succinyl-CoA

Mechanisms for conversion of propionyl-CoA to succinyl-CoA.

We will look at each of the enzymes in turn.

Propionyl-CoA carboxylase

The net reaction for this enzyme is shown in Figure 17.2.19 below.

$$\text{Propionyl-CoA} + \text{ATP} + HCO_3^- \rightarrow \text{(S)-methylmalonyl-CoA} + \text{ADP} + P_i + H^+$$

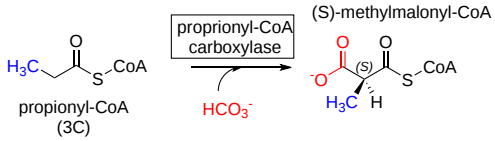


Figure 17.2.19: Propionyl-CoA carboxylase reaction

The enzyme has three subunits. The alpha subunit has a biotin carboxyl carrier protein and biotin carboxylase domains. The beta subunit has carboxytransferase activity. The *Streptomyces coelicolor* propionyl-CoA carboxylase (PCC) mechanism is shown in two parts below.

In Part 1, biotin is carboxylated by HCO_3^- to form an activated bicarbonate derivative (similar to an anhydride) that is high energy in comparison to its hydrolysis product, as shown in Figure 17.2.20 below. This reaction takes place in the alpha subunit.

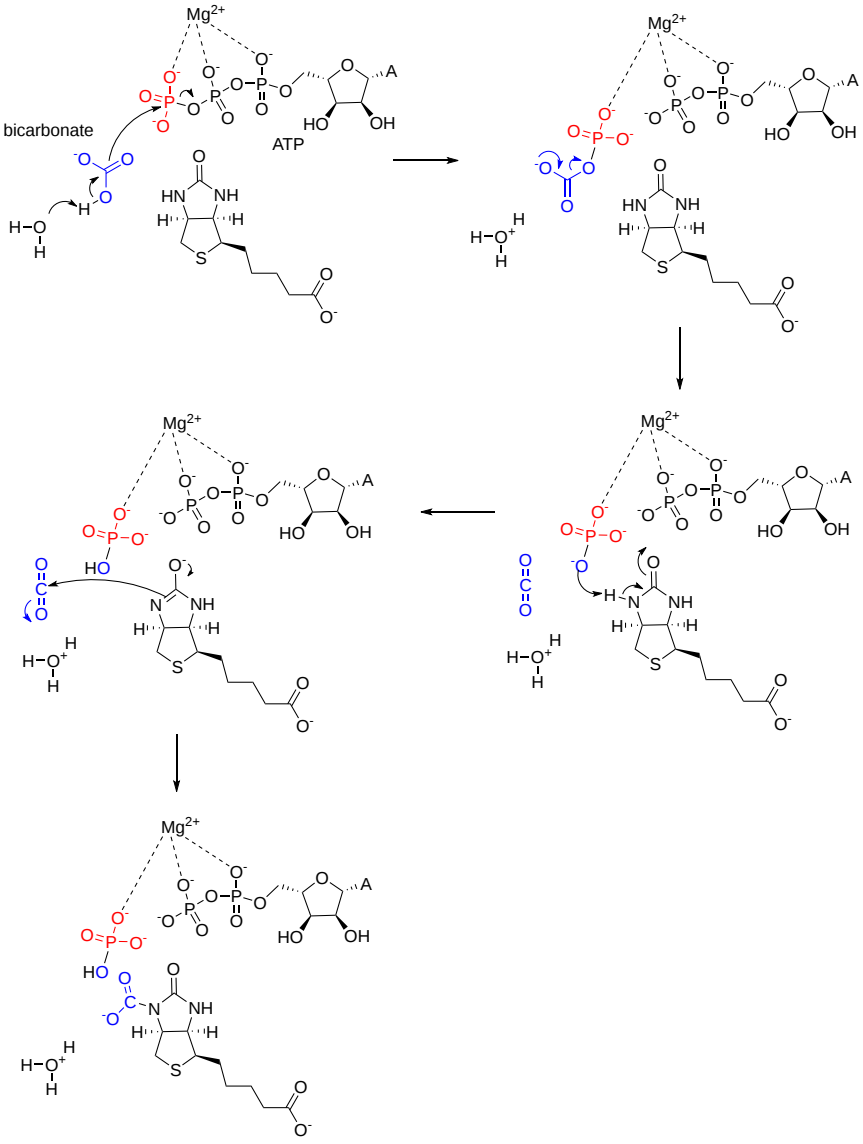


Figure 17.2.20: Formation of carboxylated biotin by propionyl-CoA carboxylase - Part 1. M-CSA. Gemma L. Holliday, Daniel E. Almonacid, Jonathan T. W. Ng. Creative Commons Attribution 4.0 International (CC BY 4.0) License

In Part 2, shown in Figure 17.2.21 below, the carboxyl group on biotin is transferred to propionyl-CoA to form methymalonyl-CoA. This reaction occurs in the beta subunit.

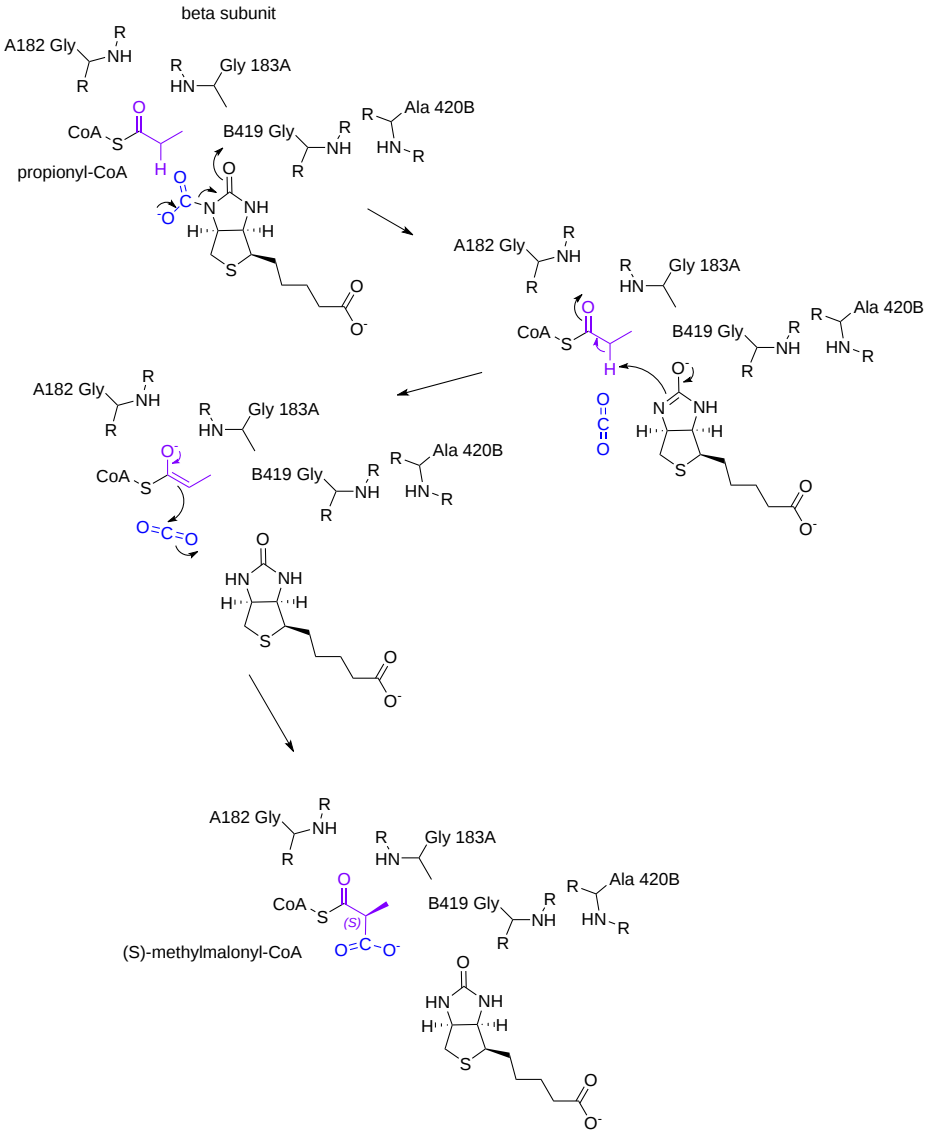


Figure **17.2.21**: Part 2 - Formation of (S)-methylmalonyl-CoA by activated CO_2 transfer from carboxybiotin by propionyl-CoA carboxylase. Holliday et al. ibid.

The roles of the main chain atoms of Ala 182 and Gly 183 in the alpha subunit are to stabilize the propionyl-CoA, while the backbone atoms of Gly 429 and Ala 430 in the beta subunit are to stabilize the oxyanion of carboxylated biotin.

Figure **17.2.22** shows an interactive iCn3D model of biotin and propionyl-CoA bound to Acyl-CoA Carboxylase Beta Subunit from S. coelicolor (1XNY)

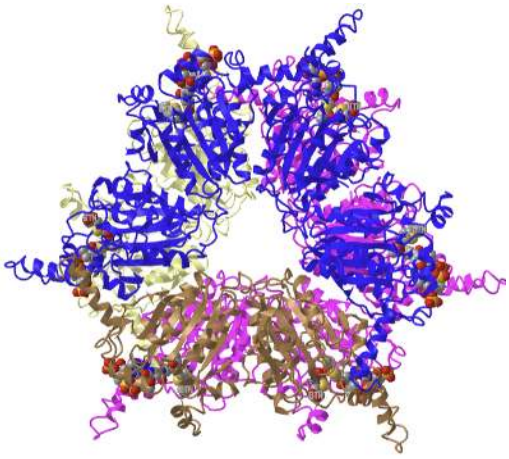


Figure 17.2.22: Monomer of the biotin and propionyl-CoA bound to Acyl-CoA Carboxylase Beta Subunit from S. coelicolor (1XNY). (Copyright; author via source). Click the image for a popup or use this external link: https://structure.ncbi.nlm.nih.gov/i...K46r5EdZezF4o6

Biotin (labeled BTN) and propionyl-CoA are shown in spacefill in CPK colors.

Methylmalonyl-CoA Epimerase

The net reaction is shown in Figure **17.2.23** below.

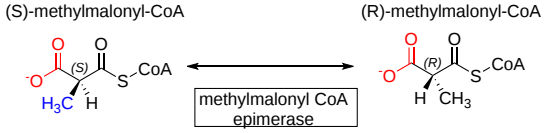
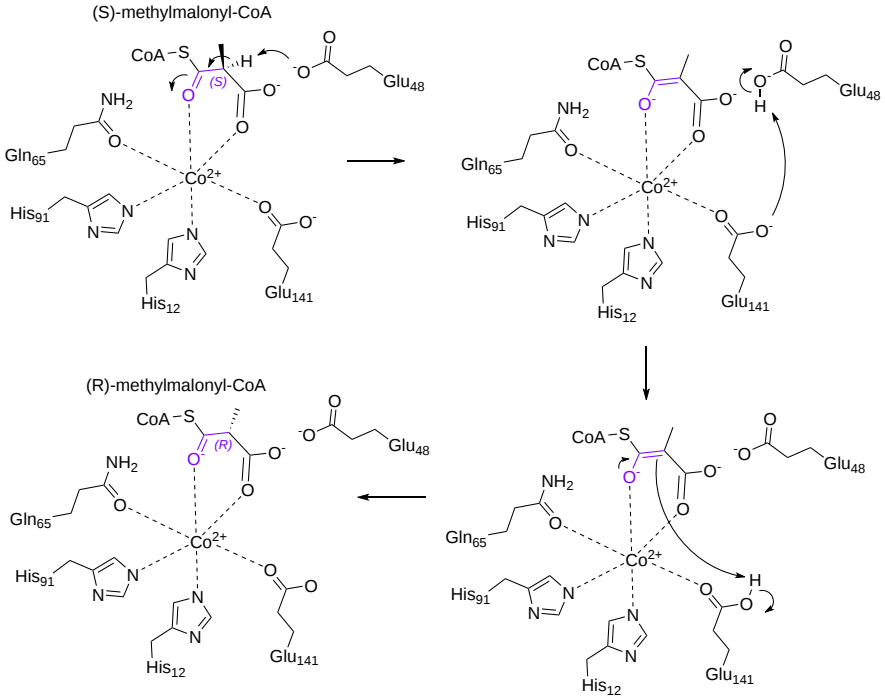


Figure 17.2.23: Methylmalonyl-CoA Epimerase reaction

This reaction proceeds through an enolate intermediate after an abstraction of a proton from the chiral center of the methylmalonyl-CoA, as shown in the reaction mechanism for the enzyme from Propionibacterium freudenreichii subsp. shermanii is shown Figure **17.2.24** below. The reaction is readily reversible.

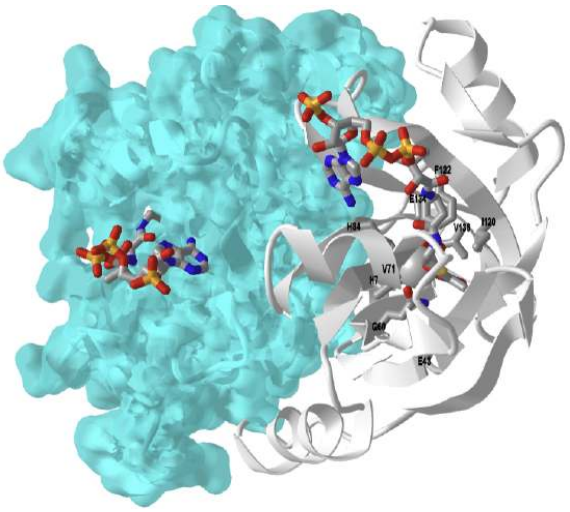


https://bio.libretexts.org/@go/page/15026

Figure 17.2.24: Mechanism for methylmalonyl-CoA Epimerase. Gemma L. Holliday et al. https://www.ebi.ac.uk/thornton-srv/m-csa/entry/33/. Creative Commons Attribution 4.0 International (CC BY 4.0) License

Note the presence of a Co^{2+} ion in the active site.

Figure 17.2.25 shows an interactive iCn3D model of Methylmalonyl-CoA epimerase in complex with 2-nitronate-propionyl-CoA from S. coelicolor (6WFI)



NCBI iCn3D Figure 17.2.25: Methylmalonyl-CoA epimerase in complex with 2-nitronate-propionyl-CoA from S. coelicolor (6WFI). (Copyright; author via source). Click the image for a popup or use this external link: https://structure.ncbi.nlm.nih.gov/i...Sqc98CCjAvzkp7

The enzyme is a dimer with two identical subunits and is catalytic. One of the subunits is shown with a blue transparent surface containing the bound 2-nitronate-propionyl-CoA inhibitor. The other is shown in a gray cartoon, with the key side chains involved in substrate binding and catalysis shown as color sticks and labeled.

Methylmalonyl-CoA Mutase

In this reaction, a methyl group is removed from (R)-methylmalonyl-CoA to form succinyl-CoA, as shown in Figure 17.2.26 below.

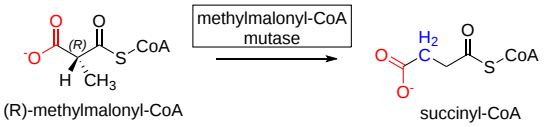


Figure 17.2.26: Methylmalonyl-CoA reaction

This reaction, going in the opposite direction, is an example of a methyltransferase. Another similar enzyme (which we will see in Chapter 18.4 - Amino Acid Degradation) catalyzes a methyl transfer from homocysteine to a new cofactor, **cobalamin**, which transfers it to cysteine to form methionine in a reaction catalyzed by methionine synthase. Cobalamine and its methylated form are derivatives of Vitamin B12. We will leave the details of cobalamin biochemistry to the next chapter and present a mechanism for methylmalonyl-CoA mutase here.

We present the reaction for the reverse reaction, the conversion of succinyl-CoA to (R)-methylmalonyl-CoA by the enzyme from *Propionibacterium freudenreichii subsp. shermanii* in two parts below. The enzyme is a heterodimer composed of an alpha and a beta subunit, and it has a cofactor, adenosylcobalamin (coenzyme B12). In contrast, the human mutase, a homodimer, is similar to the alpha subunit.

First, a free radical is formed from the adenosyl group on the cofactor. This promotes a free-radical rearrangement of succinyl-CoA to (R)-methylmalonyl-CoA (or the reverse for the pathway of interest here). The reaction is shown in two parts for optimal viewing.

Figure 17.2.27 below the first parts of the reaction for the conversion of succinyl-CoA to (R)-methylmalonyl-CoA by the mutase from *Propionibacterium freudenreichii subsp. shermanii*.

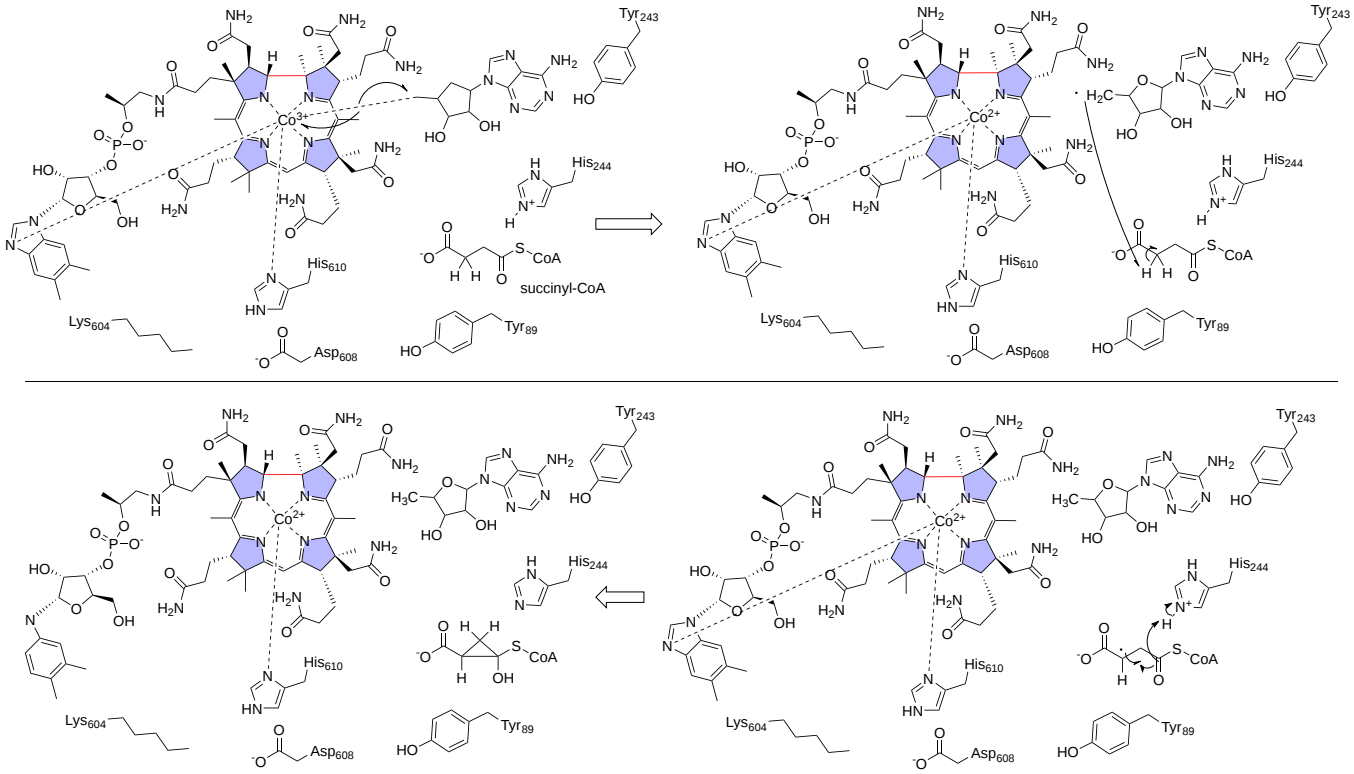


Figure **17.2.27**: Part 1 of the conversion of succinyl-CoA to (R)-methylmalonyl-CoA by methylmalonyl-CoA mutase. Gemma L. Holliday, Gail J. Bartlett, Daniel E. Almonacid. M-CSA. https://www.ebi.ac.uk/thornton-srv/m-csa/entry/62/. Creative Commons Attribution 4.0 International (CC BY 4.0) License

Figure **17.2.28** below shows the rest of the reaction for the conversion of succinyl-CoA to (R)-methylmalonyl-CoA.

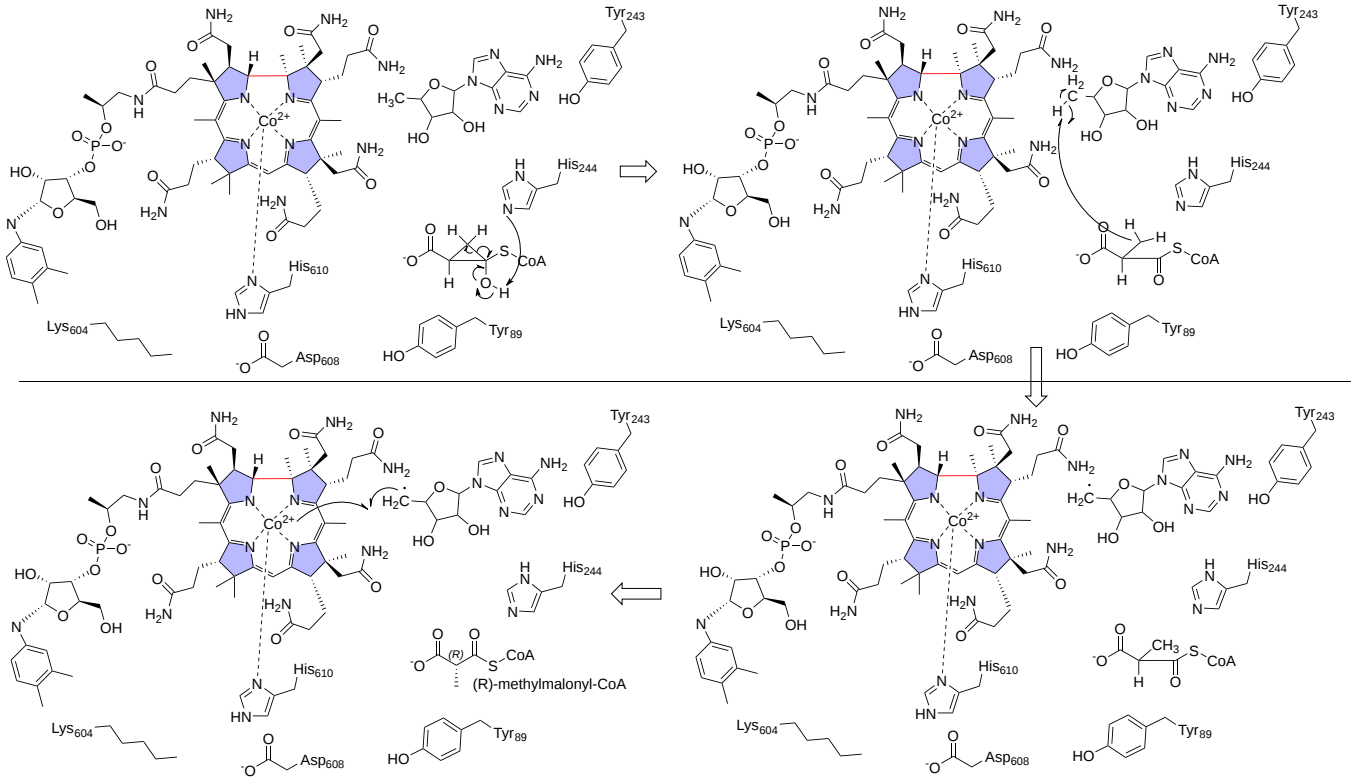


Figure 17.2.28: Part 2 of the conversion of succinyl-CoA to (R)-methylmalonyl-CoA by methylmalonyl-CoA mutase. Gemma L. Holliday et al. ibid.

The last product from the bottom left reaction, the reformed active adenosylcobalamin cofactor, is not shown. The enzyme facilitates the hemolytic cleavage of the Co-C bond. A free-radical rearrangement follows this.

Figure 17.2.29 shows an interactive iCn3D model of the methylmalonyl-coenzyme A mutase from *Propionibacterium freudenreichii subsp. shermanii* (1REQ)

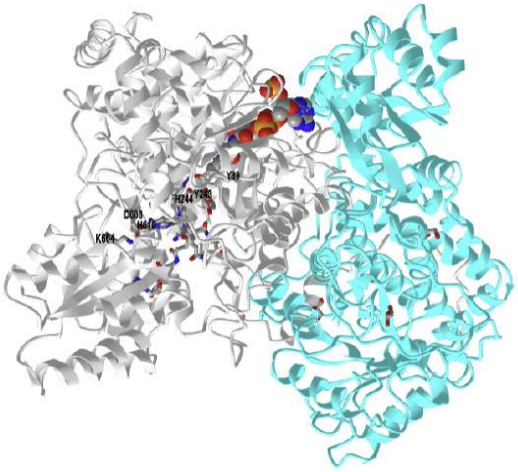


Figure 17.2.29: Methylmalonyl-coenzyme A mutase from *Propionibacterium freudenreichii subsp. shermanii* (1REQ). Click the image for a popup or use this external link: https://structure.ncbi.nlm.nih.gov/i...qPYm2sXjraCuN8

An analog of CoASH, desulfo-CoA (DCA), is shown in spacefill, CPK colors, and labeled. Adenosylcobalamin is shown in colored sticks and labeled B12. The alpha subunit is gray, with the key amino acids from the enzyme mechanism presented above shown as colored sticks and labeled. The beta subunit is shown in blue.

Propionyl-CoA is also produced as a product of methionine, valine, isoleucine, and threonine oxidation. (See the amino acid metabolism chapter for more details on mechanisms.)

17.2.5: VERY LONG CHAIN OXIDATION

In contrast to the oxidation of short and medium-chain fatty acids, which under beta-oxidation require four different discrete enzymes, the oxidation of very long-chain fatty acids (VLCFs) is carried out by two proteins, with the second protein expressing three enzyme activities. The first step, analogous to step 1 in beta-oxidation described above, is carried out by a very long-chain acyl-CoA dehydrogenase (VLCAD). A single trifunctional protein (TFP) with two subunits carries out the next three reactions. The α-subunit carries out the hydration (2-enoyl-CoA hydratase, ECH) and next oxidation step (3-hydroxyl-CoA dehydrogenase (HAD), while the β-subunit has 3-ketothiolase (KT) activity. Deficiencies of TFP can cause significant disease and even death.

TFP is a heterotetramer of two α and two β subunits, with the beta subunits forming a central homodimer. The two alpha units bind at each end, and the whole complex forms an arc. A "tunnel" appears to allow substrate transfer after each step. This minimizes premature intermediate release. Figure 17.2.30 shows an interactive iCn3D model of the human mitochondrial trifunctional protein, a fatty acid beta-oxidation metabolon (6DV2)

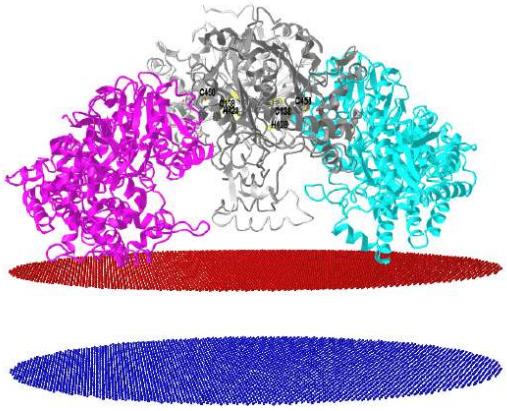


Figure 17.2.30: Human mitochondrial trifunctional protein fatty acid beta-oxidation metabolon (6DV2). Click the image for a popup or use this external link: https://structure.ncbi.nlm.nih.gov/i...XiUXru4vkRVh87

- Grays: two thiolase subunits: reversible thiolytic cleavage of 3-ketoacyl-CoA into acyl-CoA and acetyl-CoA, a 2-step reaction involving a covalent intermediate formed with a catalytic cysteine. The catalytic residues (C138, C458, and H428) are shown as sticks with CPK colors.
- Cyan and magenta subunits: enoyl-CoA hydratase (EC 4.2.1.17) and 3-hydroxyacyl-CoA dehydrogenase (EC 1.1.1.35)
- The red dots represent the inner leaflet of the inner mitochondrial membrane, where proteins reside in the mitochondrial matrix.

17.2.6: REGULATION OF BETA-OXIDATION

We observed that the metabolic decision to utilize carbohydrate energy reserves (glycogen) is a highly regulated process. Glycogen breakdown occurs during fasting and periods of high energy need. Fatty acids, our largest energy stores, are released from triglyceride reserves in adipose cells through extracellular epinephrine and glucagon activation of pathways that activate intracellular hormone-sensitive lipase. Released fatty acids are bound to the serum protein albumin, which transports them to the tissues. Additionally, as mentioned above, malonyl-CoA inhibits the transport of fatty acids into the mitochondria. Malonyl-CoA is the first committed product of fatty acid biosynthesis. Each acyl-CoA product of the four enzymes engages in product inhibition for the enzyme that produced it. 3-ketoacyl-CoA also inhibits enoyl-CoA hydratase and acyl-CoA dehydrogenase [17]. The NADH/NAD^+ and acetyl-CoA/CoA ratios also influence the beta-oxidation pathway through allosteric regulation. For example, the acetyl-CoA/CoA ratio affects the activity of ketoacyl-CoA thiolase.

Fatty acids also bind to the transcription factors called peroxisome proliferator-activated receptors (PPARs) and coactivator PGC-1α, which regulate the transcription of enzymes in the beta-oxidation pathways. PPARs and the retinoid X receptor form heterodimers that bind to the PPAR response element in key promoter sites involved in fatty acid degradation. These include CPT1, long-chain acyl-CoA dehydrogenase (LCAD), medium-chain acyl-CoA dehydrogenase (MCAD), and acyl-CoA synthetase (ACS). The PPARs have tissue specificity. We will discuss PPARs in more detail in the chapter on fatty acid synthesis.

17.2.7: PEROXISOMAL **A**-OXIDATION

Alpha oxidation of fatty acids occurs in the peroxisome, where the metabolism of phytanic acid (3,7,11,15-tetramethyl hexadecanoic acid) in dairy products, animal fat, and some fish occurs. Phytanic acid is produced in ruminants on the degradation of plant material and derives from phytol, an isoprenoid alcohol esterified to chlorophyll. Phytol is first converted to phytanic acid.

Fatty acid β-oxidation can also occur in peroxisomes. In animals, peroxisomes are believed to be important in the initial breakdown of very long-chain fatty acids and methyl-branched fatty acids [11]. The enzymes involved in fatty acid oxidation in peroxisomes differ from those in mitochondria. An important difference is acyl-CoA oxidase, the first enzyme in peroxisome β-oxidation, which transfers the hydrogen to oxygen, producing H_2O_2 instead of $FADH_2$. The H_2O_2 is broken down to water by catalase. The fatty acyl-CoA intermediates formed during β-oxidation are the same in peroxisomes and mitochondria. Peroxisomes also contain the enzymes for α-oxidation, which are necessary to oxidize some fatty acids with methyl branches.

Branched-chain fatty acids also require additional enzymatic modification to enter the alpha-oxidation pathway within peroxisomes. Phytanic acid (3,7,11,14-tetramethylhexadecanoic acid) requires additional peroxisomal enzymes to undergo beta-oxidation. Phytanic acid initially forms phytanyl CoA, which is then hydroxylated at the alpha carbon by phytanyl CoA hydroxylase (alpha-hydroxylase), encoded by the PHYH gene. The alpha carbon-hydroxyl bond then undergoes two successive rounds of oxidation to pristanic acid. Pristanic acid undergoes beta-oxidation, which produces acetyl-CoA and propionyl-CoA in alternative rounds. As with peroxisomal beta-oxidation of VLCFAs, this process generally ends when the carbon chain length reaches 6-8 carbons. At this point, the molecule is shuttled to the

mitochondria by carnitine for complete oxidation to carbon dioxide and water. Figure **17.2.31** shows the steps in the catabolism of phytanic acid (3,7,11,14-tetramethylhexadecanoic acid).

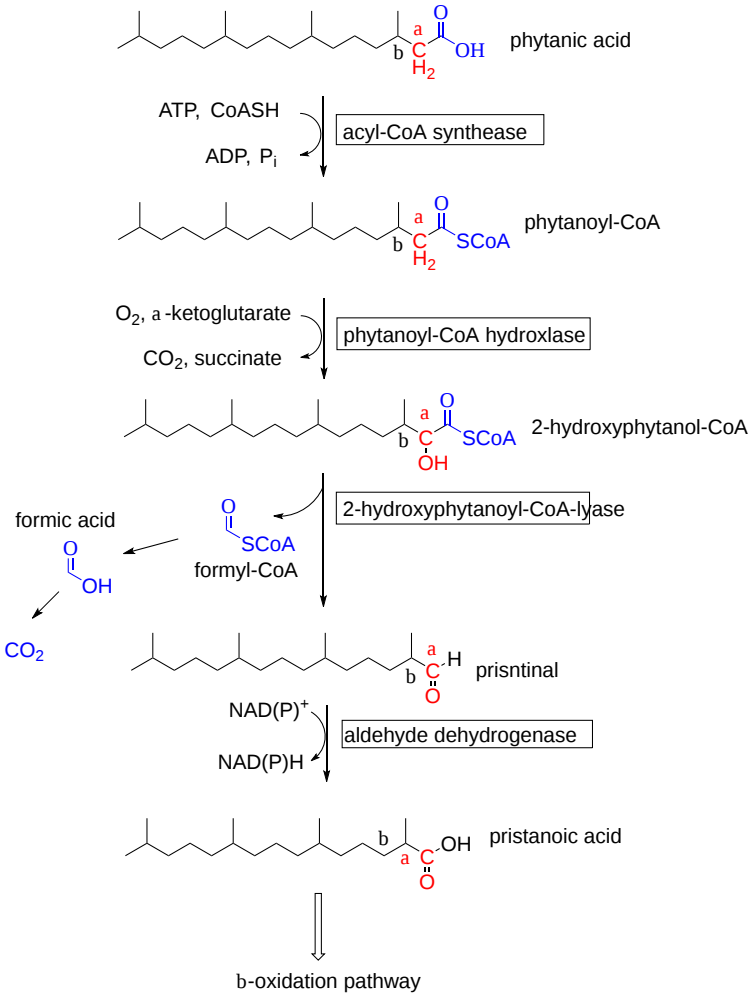


Figure **17.2.31**: Alpha oxidation pathway of catabolism of phytanic acid (3,7,11,14-tetramethylhexadecanoic acid)

17.2.8: OMEGA-OXIDATION

The omega-oxidation pathway occurs in the endoplasmic reticulum and is used to metabolize larger fatty acids, which, due to their hydrophobicity, can damage cells in high concentrations. In this pathway, the fatty acids are metabolized to dicarboxylic acids, which increases their water solubility for excretion in the urine. The first step utilizes cytochrome P450 enzymes, which also modify xenobiotic compounds with dioxygen, thereby increasing their solubility. Figure **17.2.32** shows the omega oxidation pathway.

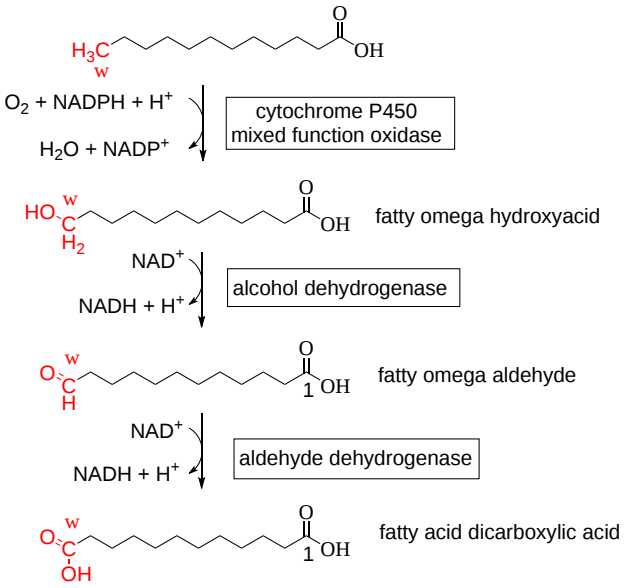


Figure **17.2.32**: The ER omega oxidation pathways for catabolism of fatty acids

Three subfamily members of the cytochrome P450s (CYPs) show a preference for the hydroxylation of short-chain fatty acids (C7-C10, CYP4B), medium-chain (C10-C16, CYP4A), and long-chain (C16-C26, CYP4F) fatty acids, which can be saturated, unsaturated, and branched. Figure **17.2.33** shows a summary of the alpha, beta, and omega oxidation pathways

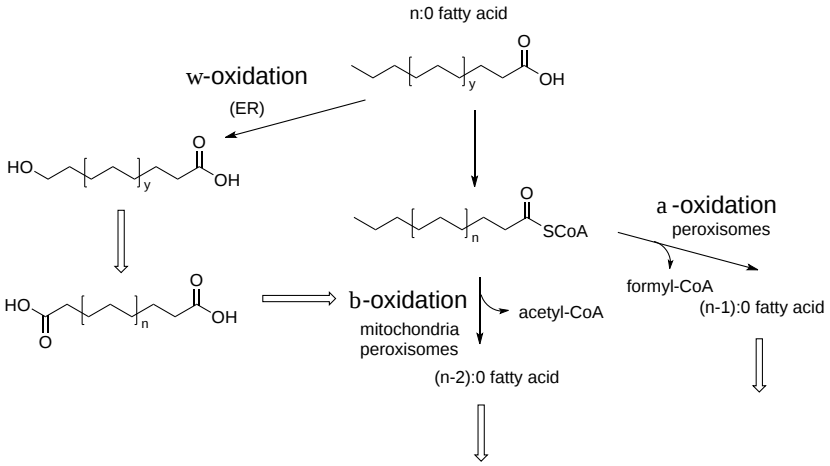


Figure **17.2.33**: https://febs.onlinelibrary.wiley.com...8.2010.07947.x

17.2.9: DISEASES OF FATTY ACID METABOLISM

A few select diseases listed below directly involve defective fatty acid metabolism through intrinsic enzyme deficiencies or indirectly prevent the proper functioning of fatty acid metabolism through extrinsic enzyme deficiencies. Many, but not all, deficiencies of enzymes involved in fatty acid oxidation result in abnormal neurological development and/or function early in life; a brief list of signs and symptoms appears under the selected diseases mentioned.

MCAD Deficiency

Medium-chain acyl dehydrogenase is the most common inherited defect of fatty acid oxidation in people. As expected, medium-chain, 6-8 carbon molecules accumulate in this disease. Clinical manifestations of MCAD deficiency primarily present during fasting conditions and include lethargy, weakness, sweating, and hypoglycemia, most commonly in children under the age of 5. Serum measurements of octanoyl carnitine are usually elevated in these patients and can aid in the diagnosis. These abundant molecules then undergo oxidation by the cytochrome P450 system, which is involved in omega-oxidation, resulting in dicarboxylic acidemia and dicarboxylic aciduria.

Zellweger Syndrome

Zellweger syndrome results from autosomal recessive mutations in the PEX genes, which code for peroxin proteins essential for assembling peroxisomes. Almost 70% of all peroxisomal biogenesis disorders (PBDs) result from a PEX1 gene mutation. Many different fatty acid

compounds, including VLCFAs and phytanic acid, can accumulate without the oxidative machinery of peroxisomes. Manifestations of this disease generally include the brain, kidneys, and skeleton.

X-Linked Adrenoleukodystrophy (X-ALD)

X-ALD is a genetic deficiency of the ABCD transporters in the membrane of peroxisomes, as mentioned previously. It results in the pathological accumulation of phytanic acid and VLCFAs within cells and is most clinically significant when the ABCD1 transporter is absent. The disease presents with neurodegenerative and adrenal abnormalities.

Refsum Disease

Refsum disease results from a genetic deficiency of the enzyme phytanyl CoA 2-hydroxylase, which, as previously mentioned, is involved in the alpha-oxidation of phytanic acid, a breakdown product of chlorophyll. Notable clinical manifestations of Refsum disease include cardiac malfunction and defective functioning of the olfactory and auditory nerves due to the accumulation of phytanic acid.

17.2.10: SUMMARY

This chapter provides a comprehensive exploration of fatty acid metabolism, detailing the catabolic pathways that convert stored lipids into ATP and the specialized mechanisms by which lipids are transported in the body. The chapter begins by outlining how triacylglycerols (TAGs) serve as the major energy reserve, with fatty acids stored in lipid droplets and transported in the circulation via lipoproteins. Key topics include:

- **Fatty Acid Oxidation Pathways:**
  The primary pathway for energy extraction from fatty acids is mitochondrial β-oxidation, where fatty acyl-CoA molecules are systematically broken down to produce acetyl-CoA, NADH, and $FADH_2$. This process, driven by a series of enzymes (acyl-CoA dehydrogenase, enoyl-CoA hydratase, β-hydroxyacyl-CoA dehydrogenase, and thiolase), enables efficient ATP production through subsequent oxidation in the citric acid cycle and electron transport chain. Additionally, the chapter discusses alternative oxidation pathways such as peroxisomal β-oxidation for very-long-chain and branched-chain fatty acids, as well as α- and ω-oxidation pathways, which allow for the metabolism of lipids that cannot be handled by mitochondria alone.
- **Peroxisomes and Their Role:**
  Peroxisomes are highlighted as vital organelles that perform unique oxidative reactions—most notably, the oxidation of VLCFAs and the metabolism of reactive oxygen species. Their functions extend beyond lipid catabolism to include synthesis of specific lipids and maintenance of cellular homeostasis.
- **Lipid Transport and Lipoprotein Metabolism:**
  The chapter details the structure and function of lipoproteins, which transport hydrophobic lipids through the aqueous bloodstream. It explains how different classes of lipoproteins (chylomicrons, VLDL, IDL, LDL, and HDL) are assembled, modified, and cleared from circulation, with a focus on the roles of apolipoproteins (such as apoB, apoA-I, and apoE) in mediating receptor interactions and lipid exchange.
- **Enzymatic Mechanisms and Regulation:**
  Special attention is given to the mechanisms by which enzymes like lipoprotein lipase (LPL) hydrolyze TAGs at the endothelial surface, releasing free fatty acids for cellular uptake. The chapter also covers the regulation of fatty acid oxidation by factors such as the carnitine shuttle, where enzymes like CPT-1 and CPT-2 facilitate the transport of fatty acyl groups into mitochondria, and how malonyl-CoA acts as a key inhibitor to balance fatty acid synthesis and oxidation.
- **Physiological and Pathological Implications:**
  The interplay between fatty acid oxidation, energy production, and lipoprotein metabolism is linked to broader physiological contexts, including the roles of white and brown adipose tissue in energy storage and thermogenesis. The chapter concludes by discussing metabolic disorders resulting from defects in these pathways, such as MCAD deficiency, Zellweger syndrome, X-linked adrenoleukodystrophy, and Refsum disease, as well as the impact of dysregulated lipoprotein metabolism on cardiovascular risk.

In summary, this chapter integrates detailed biochemical mechanisms with physiological regulation and disease relevance, providing a deep understanding of how fatty acids are oxidized for energy, how lipids are transported within the body, and how these processes are coordinated to maintain metabolic homeostasis.

This page titled 17.2: Oxidation of Fatty Acids is shared under a CC BY 4.0 license and was authored, remixed, and/or curated by Henry Jakubowski and Patricia Flatt via source content that was edited to the style and standards of the LibreTexts platform.

- **Current page** by Henry Jakubowski and Patricia Flatt is licensed CC BY 4.0. Original source: https://www.ncbi.nlm.nih.gov/books/NBK556002/.
- **11.2: Diffusion Across a Membrane - Passive and Facilitated Diffusion** by Henry Jakubowski and Patricia Flatt has no license indicated.

17.3: KETONE BODIES

LEARNING GOALS (CHATGPT O3-MINI)

1. **Describe the Structures and Types of Ketone Bodies:**
   - Identify and draw the structures of acetoacetate, D-β-hydroxybutyrate, and acetone.
   - Explain the chemical differences between these molecules, including their pKa values, and how these properties influence their physiological roles.
2. **Understand the Conditions Favoring Ketone Body Formation:**
   - Explain how high concentrations of acetyl-CoA, derived from fatty acid β-oxidation, promote ketogenesis in the liver.
   - Describe metabolic conditions that lead to ketone body synthesis, such as fasting, starvation, and diabetes, particularly when carbohydrate metabolism is compromised.
3. **Outline the Pathways of Ketogenesis and Ketolysis:**
   - Summarize the key reactions and enzymes involved in ketogenesis (e.g., thiolase, HMG-CoA synthase, and HMG-CoA lyase) and how these reactions lead to the production of ketone bodies.
   - Describe ketolysis and how ketone bodies are converted back into acetyl-CoA for entry into the citric acid cycle in extrahepatic tissues.
4. **Explain Hormonal Regulation of Ketone Metabolism:**
   - Discuss the role of insulin, glucagon, cortisol, and catecholamines in modulating fatty acid mobilization, ketogenesis, and ketolysis.
   - Analyze how a low-insulin state triggers increased fatty acid oxidation and ketone body production, and how hormonal signals help maintain energy balance during fasting.
5. **Evaluate the Role of Ketone Bodies in Energy Homeostasis:**
   - Explain why ketone bodies are critical for brain energy supply when fatty acids cannot cross the blood-brain barrier.
   - Discuss the advantages of ketone bodies as an alternative fuel source during prolonged fasting or in diabetic states.
6. **Relate Ketone Body Metabolism to Clinical Conditions:**
   - Define and contrast nutritional ketosis (as seen with ketogenic diets) versus diabetic ketoacidosis, noting the underlying biochemical mechanisms and clinical consequences.
   - Describe the symptoms and metabolic disturbances associated with diabetic ketoacidosis and how they relate to impaired glucose utilization and increased ketone body production.
7. **Integrate Fatty Acid Oxidation with Ketone Body Synthesis:**
   - Explain the biochemical link between fatty acid oxidation, the accumulation of acetyl-CoA, and the activation of ketogenesis in the liver.
   - Discuss how changes in metabolic flux through the citric acid cycle (due to depletion of intermediates for gluconeogenesis) promote ketone body production.

These learning goals aim to ensure that students not only understand the molecular mechanisms underlying ketone body synthesis and utilization but also appreciate the broader physiological and clinical contexts in which these processes operate.

Much of the material below derives from Kolb et al. BMC Medicine (2021) 19:313 https://doi.org/10.1186/s12916-021-02185-0. Creative Commons Attribution 4.0 International License, http://creativecommons.org/licenses/by/4.0/.

17.3.1: INTRODUCTION

Ketone bodies are the name given to two molecules, acetoacetate (a ketone) and D-β-hydroxybutyrate (its reduction product), that derive from the condensation of acetate in the form of acetyl-CoA. Their structures are shown in Figure **17.3.1**.



Figure **17.3.1**: Structure of ketone bodies

They are synthesized when acetyl-CoA concentrations are high. That would occur under a couple of conditions:

- fatty acids are being mobilized in adipocytes and broken down into acetyl-CoA through β-oxidation in the mitochondria;
- the acetyl-CoA produced can not enter the Krebs cycle, leading to the buildup of acetyl-CoA in the matrix.

The latter condition arises when carbohydrate metabolism is compromised, slowing the citric acid cycle. This occurs when the citric acid cycle intermediate oxaloacetate is diverted from the cycle for the gluconeogenic synthesis of glucose. Pyruvate, another source of acetyl-CoA (through pyruvate dehydrogenase), is also depleted in gluconeogenesis. Of course, we are describing conditions in the liver, the major site of gluconeogenesis and ketone body synthesis.

These conditions are also met in the underfed or starving state, when glycogen supplies are exhausted and fatty acid reserves are utilized for energy. Likewise, these conditions are met in diabetes when glucose might be abundant in the circulation, but its entry into the cell is compromised by problems with insulin signaling.

Fatty acids released by adipocytes into the blood are bound to serum albumin for transport to tissues. However, with its bound fatty acids, albumin does not cross the blood-brain barrier. Ketone bodies are small and water-soluble, allowing them to cross the blood-brain barrier and deliver a soluble equivalent of fatty acids to the brain and other tissues during times of energy need. Ketone bodies can be considered solubilized and easily transportable equivalents of fatty acids. They have low pKa values of 3.6 (acetoacetate) and 4.7 (D-β-hydroxybutyrate), so they can lead to "ketoacidosis" in diabetics. Acetone is a non-acidic, sweet-smelling molecule that can be detected in the breath of diabetics. It is produced spontaneously and also catalytically through the decarboxylation of the beta-keto acid acetoacetate. It is also considered a ketone body.

BLOOD-BRAIN BARRIER

The blood-brain barrier (BBB) protects the entire nervous system (CNS). Endothelial cells line the surface of all blood vessels. In the CNS, additional structures prevent the entry of many molecules. Tight and adherence junctions form between endothelial cells, preventing the movement of solutes between the cells. The basement membrane, glial cells, and pericytes provide additional protection. Additionally, drug efflux transporters (ABC transporters) facilitate the movement of xenobiotics (foreign toxic molecules) back across the barrier.

Nonpolar molecules like dioxygen and low-molecular-weight nonpolar molecules can cross the BBB by simple diffusion. Other polar molecules, such as glucose and amino acids, are moved across by transporters. Larger substances can move in through receptor-mediated endocytosis. Albumin, the major carrier of free fatty acids, like other proteins, does not readily pass through the barrier. Neither do albumin:ligand complexes.

Figure **17.3.2** represents the blood-brain barrier.

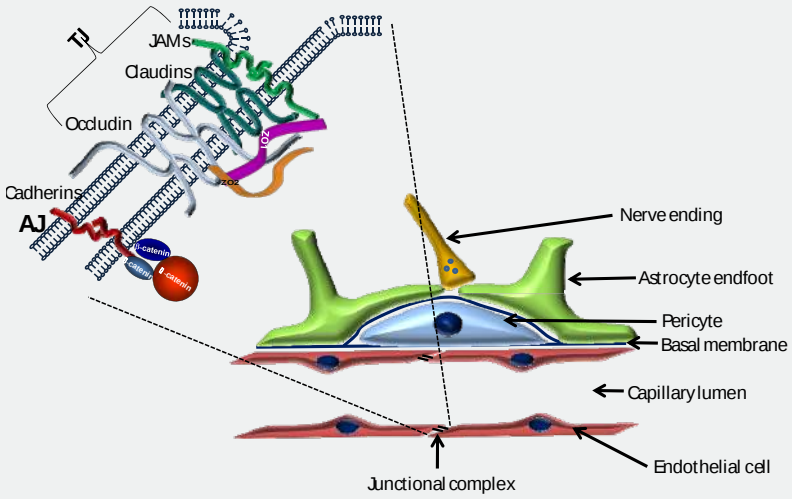


Figure **17.3.2**: Structure of the blood-brain barrier. Wilhelm et al. Int. J. Mol. Sci. 2013, 14, 1383-1411; doi:10.3390/ijms14011383. Creative Commons Attribution License (http://creativecommons.org/licenses/by/3.0/).

In this section, we will explore the synthesis and utilization of ketone bodies. The synthesis pathway is known as **ketogenesis**, and the degradation pathway is referred to as **ketolysis**. Ketone body production and utilization are closely tied to fatty acid metabolism, making it

appropriate to discuss them immediately after fatty acid oxidation. An overview of both ketogenesis and ketolysis is shown in Figure **17.3.3**.

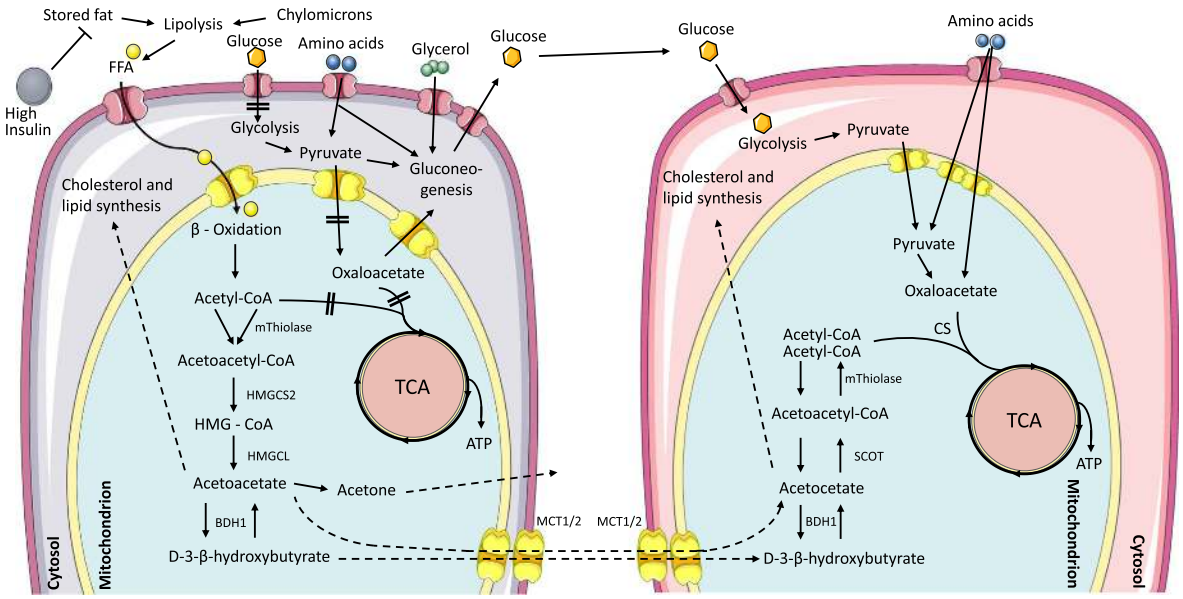


Figure **17.3.3**: Overview of the ketogenesis (left) and ketolysis (right) pathways. FFA, free fatty acids; mThiolase, mitochondrial thiolase; HMGCS2, hydroxy methylglutaryl-CoA synthase; HMGCL, HMG-CoA lyase; BDH1, mitochondrial βOHB dehydrogenase; MCT1/2, monocarboxylate transporter 1 and 2; SCOT, succinyl-CoA:3-oxoacid-CoA transferase; CS, citrate synthase. Kolb et al. BMC Medicine (2021) 19:313
https://doi.org/10.1186/s12916-021-02185-0 Creative Commons Attribution 4.0 International License. http://creativecommons.org/licenses/by/4.0/.

Most acetoacetate is converted to its reduction product, β-hydroxybutyrate, for blood transport. It can be spontaneously or enzymatically converted to acetone, as it is a β-ketoacid with a built-in electron sink that stabilizes the negative charge in the transition state and intermediate. When ketone bodies enter cells, the β-hydroxybutyrate is converted back to acetoacetate and eventually to acetyl-CoA.

17.3.2: KETOGENESIS: THE DETAILS

Figure **17.3.4** shows the chemical structures of all intermediates in synthesizing ketone bodies.

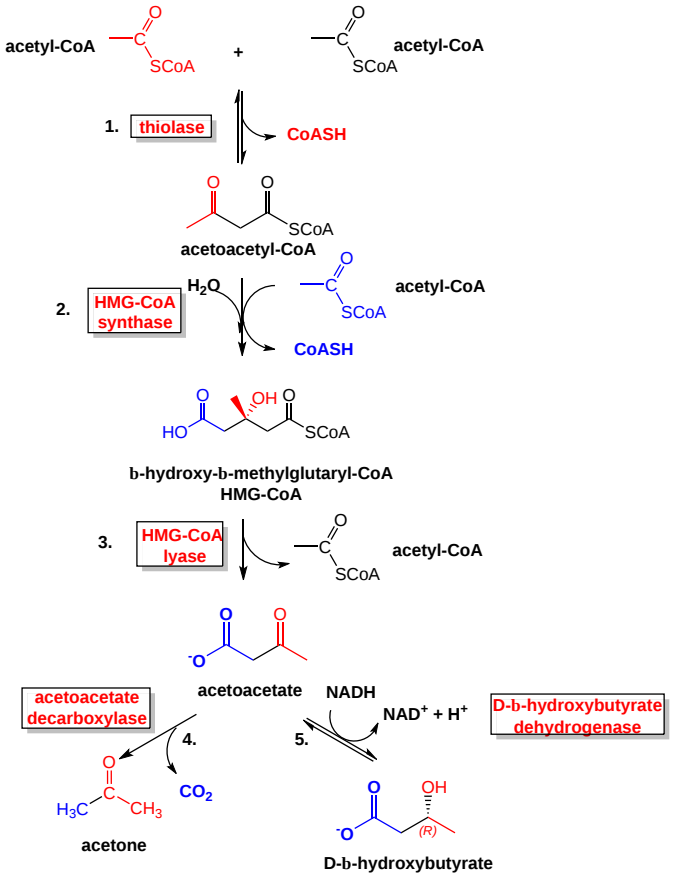


Figure **17.3.4**: Ketogenesis

We'll study three of the reactions in ketogenesis in more detail below.

Reaction 1: Thiolase

We have presented the mechanism of thiolase in Step 4 of mitochondrial β-oxidation of fatty acids using the enzyme **acetyl-CoA acetyltransferase (ACAT1),** also known as 3-ketoacyl-CoA **thiolase**. The final step in the beta-oxidation pathway involves cleavage of the bond between the alpha and beta carbon by CoASH. This step is catalyzed by beta-keto thiolase and is a thiolytic reaction (as opposed to cleavage by water, a hydrolysis reaction). The reaction produces one molecule of acetyl-CoA and a fatty acyl-CoA that is two carbons shorter. The process repeats until the even-chain fatty acid is completely converted into acetyl-CoA. The activity of the enzyme is reversible, and it can also catalyze the Claisen condensation of two acetyl-CoA molecules into acetoacetyl-CoA. This reaction occurs in the first step of ketogenesis. This step makes a C-C bond.

Reaction 2: HMG-CoA Synthase

This enzyme catalyzes the condensation of acetoacetyl–CoA (AcAc-CoA) and acetyl–CoA (Ac-CoA) to form 3-hydroxy-3-methylglutaryl (HMG)-CoA, through the formation of a C-C bond. Forming C-C bonds is critical to all biosynthesis. It's not a simple process. As we saw with pyruvate dehydrogenase, cofactors such as thiamine pyrophosphate are often used. The reverse process, breaking a C-C bond, is also difficult unless the atoms are activated. One way to activate a carbon atom is to oxidize it through hydroxylation, often using dioxygen in reactions catalyzed by the cytochrome P450 enzyme. Likewise, C-C bond formation often occurs through the reaction of radicals in hemolytic reactions or through the rearrangement of key ionic intermediates. Radical reactions can occur between a carbon-free radical and heme derivatives. Radical reactions involve heme cofactors (as in P450), non-heme iron proteins (where the iron ion can cycle between different oxidation states), flavoproteins (in which the flavin can undergo both 1 and 2 electron redox steps), radical *S*-adenosylmethionine (SAM) enzymes, and cobalamins.

HMG-CoA synthase is somewhat unique in forming a C-C bond by activating the methyl group of acetyl-cysteine. The acetyl group comes from an acyl-CoA "donor". The enzyme catalyzes the first committed step in forming complex isoprenoids (like cholesterol) and ketone bodies. The product, 3-hydroxy-3-methylglutaryl HMG–CoA, can either be reduced by HMG-CoA reductase to form mevalonate, which leads to cholesterol synthesis, or cleaved by the enzyme HMG-CoA lyase to produce acetoacetate, a ketone body.

Since it catalyzes the first step in cholesterol synthesis, the enzyme HMG-CoA reductase has been a primary target of drug therapy aimed at reducing high serum cholesterol levels, which are often associated with cardiovascular disease. Over 200 million people worldwide are on statins, the primary drugs used to block HMG-CoA reductase activity. Luckily, statins don't affect HMG-CoA lyase. Gram-positive bacteria also require the mevalonate pathway.

HMG-CoA synthase catalyzes a bisubstrate reaction that displays ping-pong kinetics, which is characteristic of a covalent enzyme intermediate. The first substrate binds to the enzyme and transfers an acetyl group to a nucleophilic Cys 111 in the active site to form an acetyl-Cys 111 intermediate. Free CoA departs. Next, the second substrate, acetoacetyl-CoA, binds and condenses with the acetyl group donated by acetyl-Cys 111. This condensation involves an enolate. Figure **17.3.5** shows a plausible reaction mechanism.

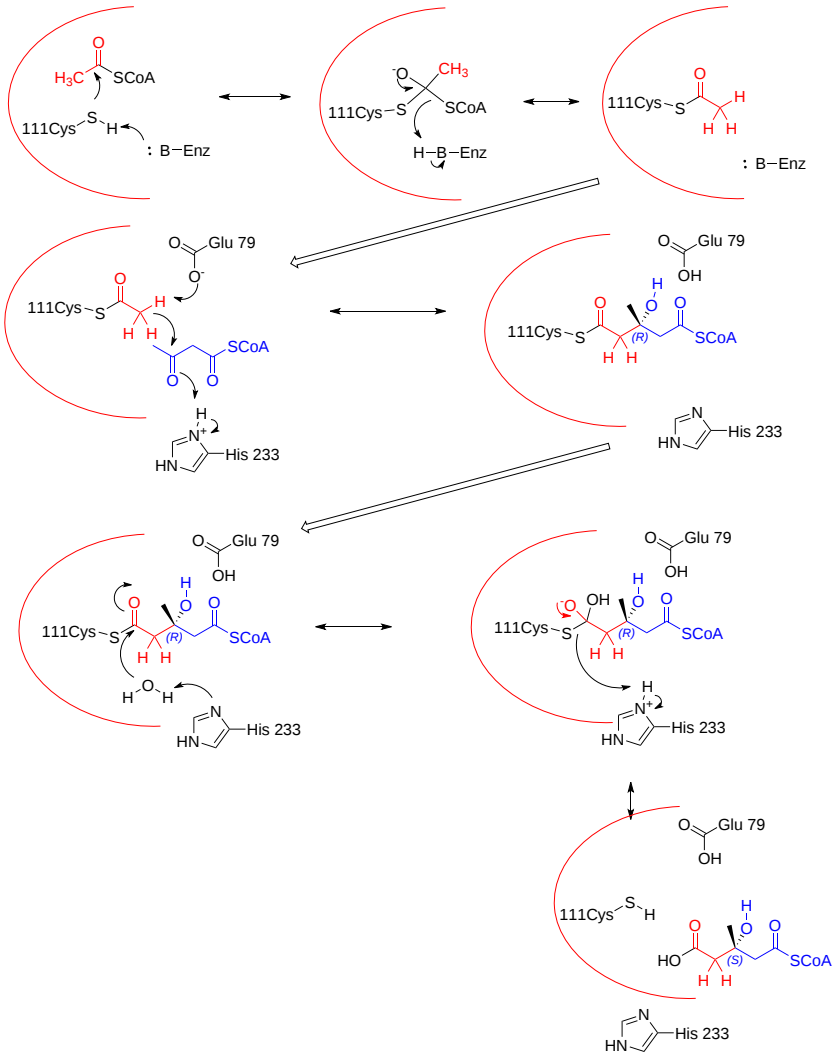
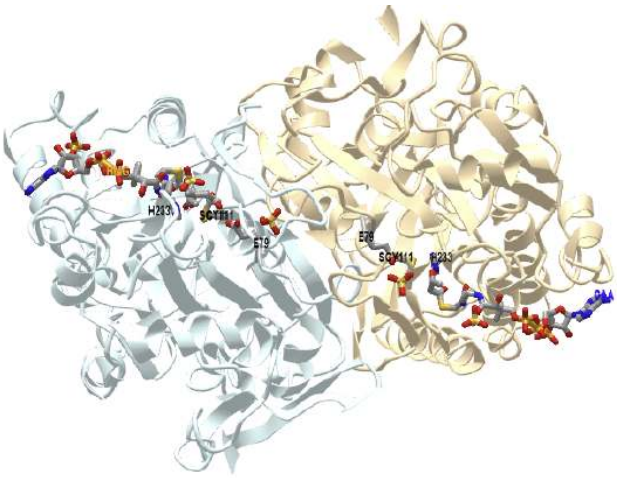


Figure **17.3.5**: Reaction mechanism for HMG-CoA synthase

Hence, the reaction consists of three parts: acetylation/deacetylation, condensation/cleavage involving an enolate intermediate, and C-C bond formation and hydrolysis/dehydration. Figure **17.3.6** shows an interactive iCn3D model of the Staphylococcus aureus HMG-COA Synthase with bound HMG-CoA and acetoacetyl-CoA (1XPK)

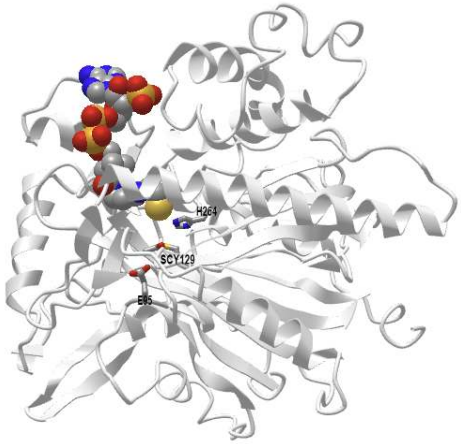
https://bio.libretexts.org/@go/page/15027



NCBI iCn3D Figure **17.3.6**: Staphylococcus aureus HMG-COA Synthase with bound HMG-CoA and acetoacetyl-CoA (1XPK). (Copyright; author via source). Click the image for a popup or use this external link: https://structure.ncbi.nlm.nih.gov/i...deiFs7JceE5H76

The biologically active unit (homodimer) is shown, with each monomer shown in a different color. The A chain (light cyan) has bound HMG-CoA (HMG) while the B chain (light gold) has acetoacetyl-CoA (CAA) bound. The Glu 79, Cys 111, and His 233 in each subunit are shown in CPK sticks and labeled. Note that Cys 111 is covalently modified in each subunit.

Figure **17.3.7** shows an interactive iCn3D model of the human 3-hydroxy-3-methylglutaryl CoA synthase I with bound CoASH (2P8U)



NCBI iCn3D Figure **17.3.7**: Human 3-hydroxy-3-methylglutaryl CoA synthase I (monomer) with bound CoASH (2P8U). (Copyright; author via source). Click the image for a popup or use this external link: https://structure.ncbi.nlm.nih.gov/i...xxEoUfecTk3eL6

The active site side chains are numbered differently (Glu 95, Cys 129, and His 264) than the S. aureus protein. Only the monomer is shown in this model.

Reaction 3: HMG-CoA Lyase

The lyase reaction involves the cleavage of a C-C bond to produce acetyl-CoA and acetoacetate. A gene knockout of this gene in mice is lethal. Figure **17.3.8** shows a plausible mechanism for the reaction.

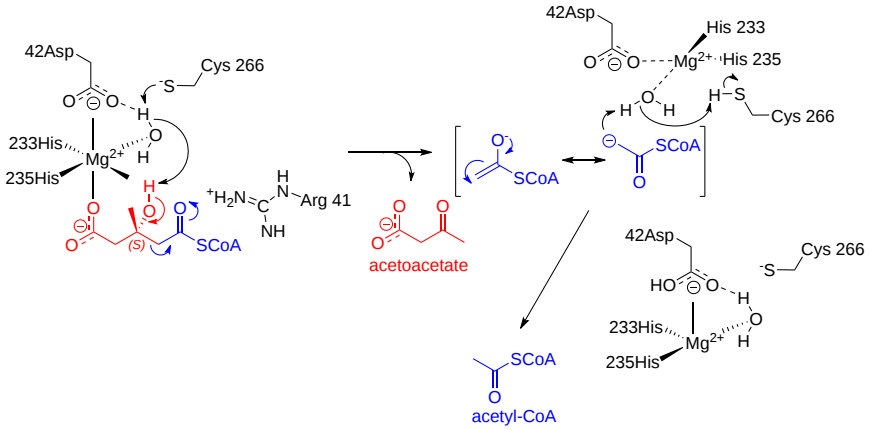


Figure **17.3.8**: Mechanism for HMG-CoA lyase of HMG-CoA. (after Fu et al. The Journal of Biological Chemistry, 285, 26341–26349, August 20, 2010)

Figure **17.3.9** shows an interactive iCn3D model of the human HMG-CoA lyase with the competitive inhibitor hydroxyglutaryl-CoA (HG-CoA)(3MP3)

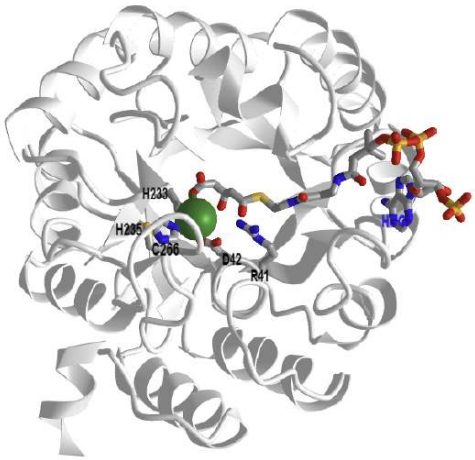


Figure **17.3.9**: Human HMG-CoA lyase with inhibitor HG-CoA (3MP3). (Copyright; author via source). Click the image for a popup or use this external link: https://structure.ncbi.nlm.nih.gov/i...VJBWxXpcKQyij8

Only one subunit of the homodimer is shown. The key residues involved in catalysis and binding (Arg41, Asp42, His233, His235, and Cys266) are shown in sticks, with CPK colors and labels. The competitive inhibitor, 3-hydroxyglutaryl-CoA (without the methyl group), is shown in CPK-colored sticks. The S-stereoisomer of HMG-CoA or inhibitor binds, not the R-isomer. Water may shuttle protons between Asp 42 and the C3 hydroxyl of HMG-CoA. Arg 41 facilitates the proper enol/keto tautomer in the enolization of the product. Mutation of Arg 41 drastically reduces catalysis.

We won't discuss the remaining enzymes in detail since we have encountered variants of NAD^+/NADH dehydrogenase reactions before. The acetoacetate decarboxylase hastens the already spontaneous decarboxylation of the β-keto ester acetoacetate.

Regulation of Ketogenesis

Hormones such as glucagon, cortisol, thyroid hormones, and catecholamines can upregulate ketogenesis, leading to the mobilization of fatty acids. Insulin is the primary hormonal regulator of this process.

Insulin regulates many key enzymes in the ketogenic pathway, and a state of low insulin triggers the process. A low insulin state leads to:

- Increased free fatty acids (FFAs) arising from decreased inhibition of hormone-sensitive lipase
- Increased uptake of FFAs into the mitochondria arising from decreased activation of acetyl-CoA carboxylase, decreasing malonyl-CoA, which disinhibits Carnitine Palmitoyltransferase 1 (CPT1)
- Increased production of ketone bodies arising from increased HMG-CoA activity

17.3.3: KETOLYSIS: UTILIZATION OF KETONE BODIES

Figure **17.3.10** shows the chemical steps in using ketone bodies.

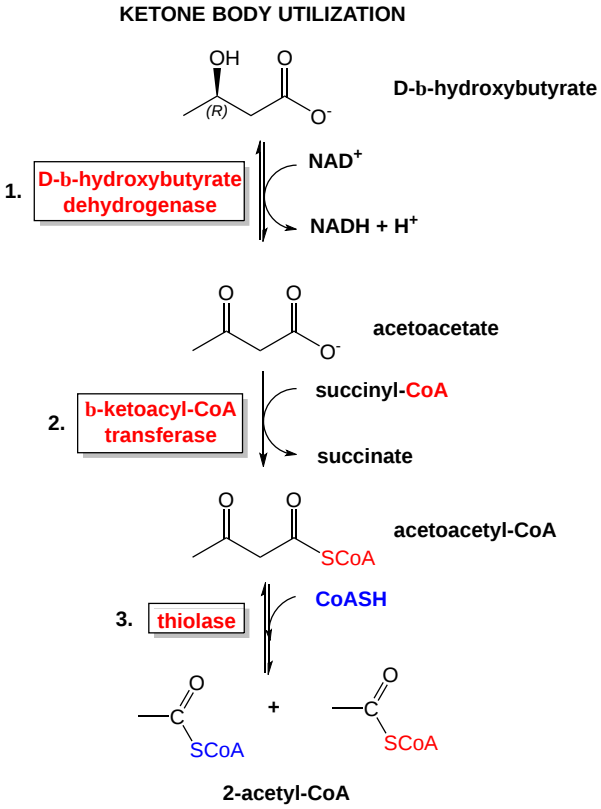


Figure **17.3.10** shows the chemical structures in the utilization of ketone bodies.

Since we have encountered similar reactions, we will not discuss their detailed mechanisms.

Most organs and tissues can utilize ketone bodies as an energy source. They are a major energy source for the brain when glucose is unavailable. That makes sense because fatty acids can't cross the blood-brain barrier. The heart prefers fatty acids for energy but can also use ketone bodies. The liver produces but does not utilize them, as the gene for step 2, β-ketoacyl-CoA transferase, is not transcribed. D-β-hydroxybutyrate is first converted to the other ketone body, acetoacetate, for the pathway to continue. The net result is the formation of two acetyl-CoAs that can then enter the citric acid cycle for ATP production. Acetone is a dead-end ketone body and is excreted in the urine or eliminated in the breath.

17.3.4: CLINICAL SIGNIFICANCE

An overproduction of ketone bodies through increased ketogenesis can cause ketoacidosis (given the pKas of the ketone bodies). One type is diabetic ketoacidosis (DKA) in Type I and II diabetes, which impairs glucose use. This leads to liver gluconeogenesis and the resulting depletion of oxaloacetate and pyruvate, impacting the ability of acetyl-CoA to enter the citric acid cycle.

Upon presentation, patients are often severely dehydrated due to hyperglycemia. High glucose levels in the blood result in increased osmotic pressure in the vessels and decreased water reabsorption in the kidneys. They often have accompanying symptoms like confusion, nausea, vomiting, and abdominal pain. Due to the acidosis, patients often breathe deeply and rapidly to eliminate carbon dioxide, which can lead to respiratory alkalosis. Ketoacidosis can also occur with severe alcoholism and prolonged starvation.

KETOGENIC DIET

The ketogenic diet, characterized by high-fat and low-carbohydrate consumption, can lead to weight loss. It shifts metabolism to more closely resemble the state of fasting. Its long-term effects are not clear, but some have suggested the use of ketone-based drugs to mimic the effect of ketone bodies. Fasting can also lead to a ketogenic state, and it has been used for the treatment of epilepsy before the drug became available. It is important to differentiate this attempt to induce a ketogenic state from diabetic ketoacidosis.

17.3.5: SUMMARY

This chapter explores the synthesis and utilization of ketone bodies—a critical metabolic adaptation that enables energy production during states of low carbohydrate availability. The key points covered include:

- **Ketone Body Structures and Formation:**
  The two main ketone bodies, acetoacetate and D-β-hydroxybutyrate, are synthesized in the liver from acetyl-CoA. Acetone, a minor, nonacidic product, is formed spontaneously from acetoacetate. These compounds are produced when acetyl-CoA accumulates, either due to enhanced fatty acid β-oxidation during fasting, prolonged exercise, or when carbohydrate metabolism is impaired (as in diabetes).
- **Regulatory Conditions for Ketogenesis:**
  Ketone body synthesis is favored under conditions where fatty acids are mobilized from adipose tissue and the citric acid cycle is limited, often due to the withdrawal of oxaloacetate for gluconeogenesis. This metabolic shift ensures that excess acetyl-CoA is diverted to ketogenesis rather than accumulating in the mitochondria.
- **Physiological Role and Transport:**
  Ketone bodies are water soluble and can readily cross the blood–brain barrier, providing an essential energy source for the brain when glucose is scarce. They serve as "solubilized fatty acid equivalents," ensuring that energy production can continue in vital tissues during prolonged fasting or in diabetic conditions.
- **Ketogenesis and Ketolysis Pathways:**
  The chapter outlines the biochemical pathways of ketogenesis (the formation of ketone bodies) and ketolysis (their utilization). Key enzymes in ketogenesis include thiolase, which catalyzes the reversible condensation of acetyl-CoA molecules, HMG-CoA synthase, which forms 3-hydroxy-3-methylglutaryl-CoA (HMG-CoA), and HMG-CoA lyase, which cleaves HMG-CoA to produce acetoacetate. In ketolysis, ketone bodies are converted back to acetyl-CoA to fuel the citric acid cycle.
- **Hormonal Regulation and Metabolic Balance:**
  Hormonal signals play a central role in controlling ketogenesis. Low insulin levels—typical during fasting or in uncontrolled diabetes—trigger the mobilization of fatty acids and increase ketone body production. Conversely, high insulin levels favor carbohydrate utilization and inhibit ketogenesis. These hormonal cues ensure that ketone body production is finely tuned to meet the organism's energy needs without causing metabolic derangements.
- **Clinical Implications:**
  While ketone bodies serve as an essential alternative energy source, excessive production can lead to ketoacidosis—a dangerous condition characterized by metabolic acidosis. The chapter also distinguishes between nutritional ketosis (as seen with ketogenic diets) and diabetic ketoacidosis, underscoring the clinical importance of balanced ketone metabolism.

In summary, this chapter integrates biochemical pathways with hormonal regulation to illustrate how ketone bodies are synthesized and utilized during energy shortage, highlighting their crucial role in maintaining energy homeostasis and their clinical significance in metabolic diseases.

This page titled 17.3: Ketone Bodies is shared under a CC BY 4.0 license and was authored, remixed, and/or curated by Henry Jakubowski and Patricia Flatt via source content that was edited to the style and standards of the LibreTexts platform.

- **Current page** by Henry Jakubowski and Patricia Flatt is licensed CC BY 4.0. Original source: https://doi.org/10.1186/s12916-021-02185-0.
- **11.2: Diffusion Across a Membrane - Passive and Facilitated Diffusion** by Henry Jakubowski and Patricia Flatt has no license indicated.

CHAPTER OVERVIEW

18: NITROGEN - AMINO ACID CATABOLISM

Return to Fundamentals of Biochemistry Search Fundamentals of Biochemistry

18.1: The Biochemistry of Nitrogen in the Biosphere
18.2: Metabolic Fates of Amino Groups
18.3: Nitrogen Excretion and the Urea Cycle
18.4: An Overview of Amino Acid Metabolism and the Role of Cofactors
18.5: Pathways of Amino Acid Degradation

This page titled 18: Nitrogen - Amino Acid Catabolism is shared under a not declared license and was authored, remixed, and/or curated by Henry Jakubowski and Patricia Flatt.

18.1: THE BIOCHEMISTRY OF NITROGEN IN THE BIOSPHERE

LEARNING GOALS (CHATGPT O3-MINI)

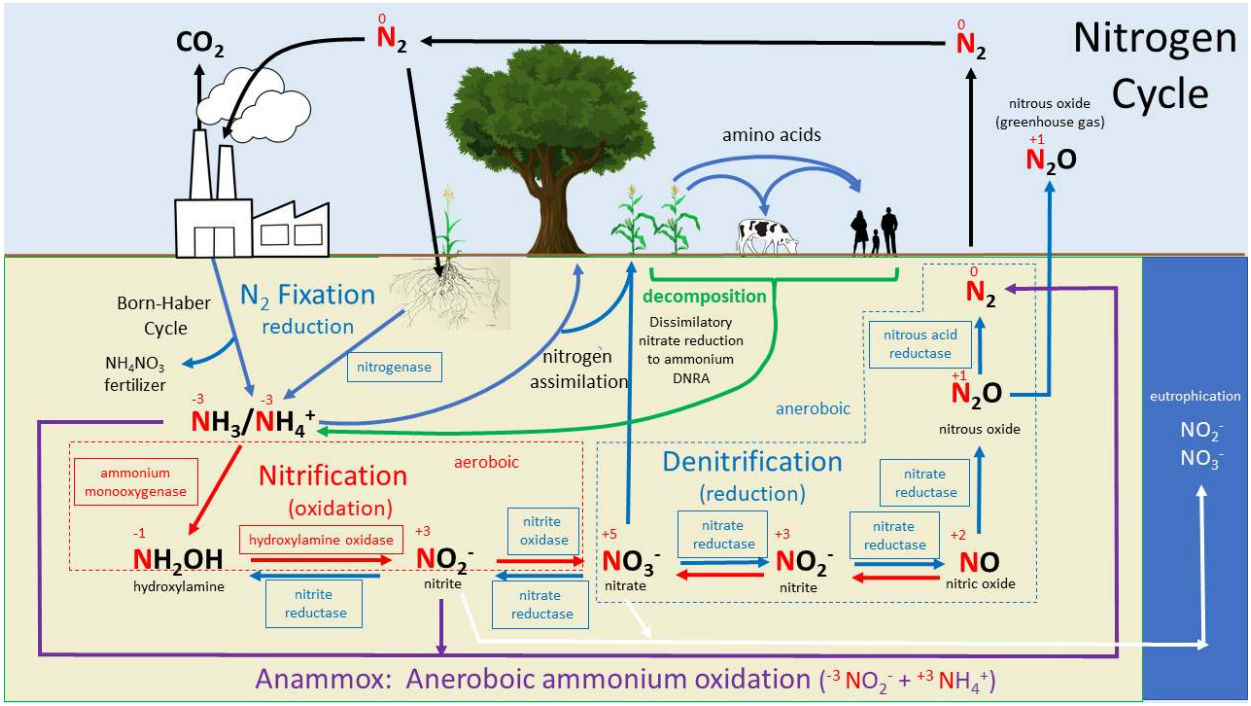
1. **Understand the Broader Scope of Organic Chemistry:**
   - Explain why the traditional definition of organic chemistry as the study of carbon-containing molecules is limited, and describe the importance of nitrogen and oxygen in the structure and function of biomolecules.
2. **Describe the Biological Nitrogen Cycle:**
   - Outline the key steps of the nitrogen cycle, including nitrogen fixation, nitrification, denitrification, anammox, and ammonification.
   - Identify the roles of both inorganic nitrogen species (ammonium, nitrite, nitrate) and organic nitrogen compounds (amino acids, nucleotides) in the cycle.
3. **Compare Biological and Industrial Nitrogen Fixation:**
   - Explain how atmospheric dinitrogen (N_2) is converted to ammonium (NH_4^+) by nitrogenase in certain microorganisms, and contrast this with the industrial Haber-Bosch process, including the thermodynamic and kinetic challenges involved.
4. **Analyze Thermodynamic Considerations in Nitrogen Fixation:**
   - Discuss the thermodynamic parameters ($\Delta H°$, $\Delta S°$, $\Delta G°$) associated with the conversion of N_2 and H_2 to ammonia and explain why, despite being thermodynamically favorable at room temperature, the reaction is kinetically slow.
5. **Evaluate the Ecological and Biospheric Impact of the Nitrogen Cycle:**
   - Analyze the importance of nitrogen-containing metabolites as essential nutrients for plants, and discuss how these compounds regulate primary productivity and biodiversity in ecosystems.
6. **Integrate Nitrogen Metabolism with Energy and Biosynthesis:**
   - Compare how different organisms (e.g., plants as primary producers, carnivores, and omnivores) use nitrogen-containing biomolecules for energy production and biosynthetic pathways.
   - Explain why excess protein cannot be stored like carbohydrates or lipids, and how amino acid catabolism must be tightly regulated to manage toxic ammonium levels.
7. **Link Amino Acid Oxidation to Metabolic Regulation:**
   - Discuss the oxidative metabolism of amino acids in animals, including the removal of the amino group (forming NH_4^+) and the subsequent conversion of the carbon skeleton into ketoacids that feed into glycolysis or the TCA cycle.
   - Understand the mechanisms by which ammonium is recycled or eliminated, emphasizing its toxicity and the need for precise regulation.

These learning goals will equip students with a comprehensive understanding of the nitrogen cycle's key reactions, its interplay with broader metabolic processes, and its ecological significance.

18.1.1: INTRODUCTION

Organic chemistry is usually described as the chemistry of carbon-containing molecules. But isn't that definition a bit carbon-centric, especially since the prevalence of oxygen-containing molecules is staggering? What about nitrogen? We live in a dinitrogen-rich atmosphere (80%), and all classes of biomolecules (lipids, carbohydrates, nucleic acids, and proteins) contain nitrogen. Dinitrogen is very stable due to its triple bond and nonpolar nature. We rely on a few organisms to fix N_2 from the atmosphere to form ammonium (NH_4^+), which, through nitrification and denitrification, can form nitrite (NO_2^-), nitrate (NO_3^-), nitric oxide (NO), and nitrous oxide (N_2O), the latter being a potent greenhouse gas. In the next section, we'll concentrate on the metabolic fate of amino groups in amino acids and proteins. Before exploring their fates, examine the figure below, which provides an overview of the biological nitrogen cycle. The study of biochemistry should encompass more than homo sapiens and expand to the ecosystem in which we are such a small but damaging part.

Let's break down the diagram from a biochemical perspective. There are aerobic and anaerobic processes (conducted by bacteria). Nitrogen-containing substances include inorganic (ammonium, nitrate, nitrite) and organic (amino acids, nucleotides, etc) molecules. The reactions shown are both oxidative and reductive (note: the oxidation numbers of the nitrogen atoms in the molecules are shown in red). Most of the reactions are carried out underground by bacterial and Archaeal microorganisms.



Here are some of the major reactions:

- **N_2 fixation (a reduction)**: N_2 from the air is converted by bacteria to ammonium (NH_4^+) by the enzyme nitrogenase of soil prokaryotes. The energetically unfavorable reaction requires a lot of ATP. Ammonium that has been made can then be taken up by primary producers, such as plants, and incorporated into biomolecules like amino acids, which animals consume. Consider this for those who may still believe that people have marginal effects on our biosphere. We may soon fix more N_2 (to NH_3) through the industrial Haber-Bosch reaction (used for fertilizer and explosive production) than all the N_2 fixed by the biosphere. A significant portion of the nitrogen used comes from the Haber-Bosch reaction. The excess NH_4^+ (upwards of 50%) produced industrially and which enters the soil in fertilizers (mostly as NH_4NO_3) has overwhelmed nature's ability to balance the nitrogen cycle and is not taken up by plants. It is metabolized by microorganisms to nitrite and nitrate.

HABER-BOSCH FIXATION OF N_2

Dinitrogen, N_2, has a triple bond, making N_2 extraordinarily stable, which explains why we can breathe an atmosphere containing 80% N_2 without dying. You may recall from introductory chemistry that high pressure and temperature are required in the Haber-Bosch process to convert N_2 and H_2 into ammonia, NH_3. As with any scientific advance, the Haber-Bosch process has brought both harm (it's used for explosive weapons) and benefit (in the form of fertilizers). This process now fixes enough N_2 in the form of fertilizers to support half of the world's population, with nitrogenase supporting the rest. Efforts are underway to genetically modify plants to produce nitrogenase, eliminating the need for fertilizers, but this may create unforeseen problems.

You might be surprised that the equilibrium constant favors ammonia formation at room temperature; hence, $\Delta G^0 < 0$. The reaction is favored enthalpically as it is exothermic at room temperature. It is disfavored entropically, as should be evident from the balanced equation:

$$\mathrm{N_2\,(g) + 3\,H_2\,(g) \longrightarrow 2\,NH_3\,(g).}$$

The thermodynamic parameters for the reaction (per mol NH_3 produced) are $\Delta H° = –46.2$ kJ, $\Delta S° = –389$ J K–1, and $\Delta G° = –16.4$ kJ (-3.9 kcal) at 298 K

The entropy is negative since the reaction proceeds from four molecules to two molecules. From an enthalpy perspective, raising the temperature of an exothermic reaction reverses it. Increasing the pressure shifts the equilibrium to the side with the fewest molecules.

If the reaction is favored thermodynamically at room temperature, why doesn't it proceed readily? This story sounds familiar, as this same descriptor applies to the oxidation of organic molecules with dioxygen. There, we showed using MO theory that the reaction is kinetically slow. The same is true for NH_3 formation. A superficial way to view this is that we must break bonds in the stable N_2 to initiate the reaction, resulting in a high activation energy and sluggish reaction kinetics.

One could jump-start the reaction by raising the temperature to overcome E_{act}, but as the reaction is exothermic, this favors the reverse reaction. The Keq and ΔG^0 are functions of temperature, and for this reaction, the reaction becomes disfavored at higher temperatures. The solution Haber found was high pressure, forcing the reaction to the side with fewer gas molecules, and high temperature to overcome the activation energy barrier and make the reaction kinetically feasible. A complex metal catalyst (magnetite - Fe_3O_4 -with metal oxides like CaO and Al_2O_3, which prevent reduction of the Fe with H_2) provides an absorptive surface to bring reagents together and facilitate bond breaking in H_2 and N_2.

- **Nitrification**: Ammonium is converted to nitrite by ammonia-oxidizing aerobic microorganisms and further to nitrate by a separate group of nitrite-oxidizing aerobic bacteria. Here are the reactions (Rx 1 and 2) to produce nitrate through a hydroxylamine intermediate, followed by nitrate formation (Rx 3).

$$\mathrm{NH_3 + O_2 + 2\,e^- \longrightarrow NH_2OH + H_2O} \quad \textbf{(Rx 1)}$$

$$\mathrm{NH_2OH + H_2O \longrightarrow NO_2^- + 5\,H^+ + 4\,e^-} \quad \textbf{(Rx 2)}$$

$$\mathrm{NO_2^- + \tfrac{1}{2}\,O_2 \longrightarrow NO_3^-} \quad \textbf{(Rx 3)}$$

These added ions exceed soil capacity and end up in runoff water, polluting our rivers and lakes.

- **Denitrification**: This anaerobic reaction pathway produces N_2 from nitrate. Here is the net reaction:

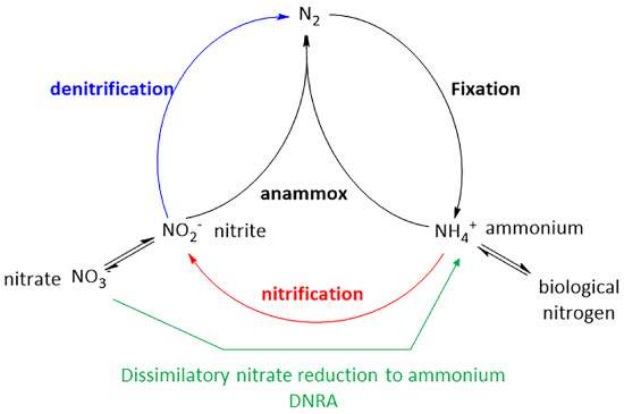
$$\mathrm{2\,NO_3^- + 10\,e^- + 12\,H^+ \longrightarrow 2\,N_2 + 6\,H_2O}$$

- **Anammox reaction**: This recently discovered bacterial anaerobic reaction pathway converts ammonium and nitrate to N_2. Here is the net reaction

$$\mathrm{NO_2^- + NH_3^+ \longrightarrow N_2 + 2\,H_2O}$$

- **Ammonification:** This occurs when plants and animals decompose, which returns ammonium to the soil for reuse by plants and microbes.

These reactions are shown in the abbreviated Nitrogen Cycle below.



Nitrogen metabolites are essential nutrients for plants and perhaps the most important in regulating plant growth (primary productivity) and biodiversity in the biosphere. All living organisms require feedstocks to produce energy and as substrates for biosynthetic reactions. The types used depend on the organism. Plants are primary producers, so they use their synthesized carbohydrates for energy production and biosynthesis. For carnivores, proteins and their derived amino acids are the source of energy (through oxidation) and serve as biosynthetic precursors. For omnivorous organisms, the energy source depends on the "fed" state. With abundant food resources, carbohydrates and lipids serve as the primary sources of energy. Unlike carbohydrates and lipids, which can be stored as glycogen and triacylglycerols for future use, excess protein and its associated amino acids can not be stored, so amino acids can be eliminated or used for oxidative energy.

In the fed state, carbohydrates are the main energy source, while lipids take a predominant role in the unfed state. Under starving conditions, the organisms' own proteins are broken down and used for oxidative energy production and for any remaining biosynthesis. In diseased states like diabetes, which can be likened to a state of starvation in the presence of abundant carbohydrates, both lipids and amino acids become sources of energy.

How are amino acids in animals oxidatively metabolized? Several pathways could be employed to achieve this. Still, it would seem logical that NH_4^+ would be removed, and the carbons in the remaining molecule would eventually enter glycolysis or the TCA cycle in the form of ketoacids. NH_4^+ is toxic in high concentrations. Ammonium is not oxidized to nitrite or nitrates in humans, unlike what occurs in the soil through the action of microorganisms. It can be recycled back into nucleotides or amino acids, eliminating excess amounts from the organism. Both processes must be highly controlled. We will turn our attention to the oxidation of amino acids in the next section.

18.1.2: SUMMARY

This chapter broadens the scope of organic chemistry by emphasizing that life is not only based on carbon compounds but also relies heavily on nitrogen and oxygen. It presents a comprehensive overview of the biological nitrogen cycle, detailing both inorganic and organic transformations and highlighting the intricate interplay between microorganisms and the biosphere.

Key topics covered include:

- **The Biological Nitrogen Cycle:**
  The chapter outlines the major processes—nitrogen fixation, nitrification, denitrification, anammox, and ammonification—that convert atmospheric dinitrogen (N_2) into bioavailable forms such as ammonium (NH_4^+), nitrite (NO_2^-), and nitrate (NO_3^-). These processes are carried out by specialized bacteria and archaea, both aerobically and anaerobically, ensuring that essential nitrogen is incorporated into biomolecules.
- **Thermodynamics and Kinetics of Nitrogen Fixation:**
  Although the conversion of N_2 to ammonia is thermodynamically favorable at room temperature ($\Delta G° < 0$), the reaction is kinetically hindered due to the high stability of the N≡N triple bond. This necessitates the use of energy-intensive processes—such as the biological nitrogenase system in microbes or the industrial Haber-Bosch process—to overcome the activation energy barrier.
- **Impact of Industrial Nitrogen Fixation:**
  The chapter contrasts biological nitrogen fixation with the Haber-Bosch process, discussing how the latter has dramatically increased the amount of fixed nitrogen available globally, with significant ecological consequences such as nutrient runoff and eutrophication.
- **Integration with Ecosystem Function:**
  Nitrogen metabolites serve as crucial nutrients for plant growth, influencing primary productivity and ecosystem diversity. The chapter emphasizes that while plants synthesize carbohydrates for energy, animals rely on proteins and amino acids both as energy sources and for biosynthesis, making the efficient cycling of nitrogen vital for all life.
- **Amino Acid Metabolism and Nitrogen Handling:**
  In animals, the breakdown of proteins for energy requires the removal of the amino group to prevent toxic accumulation of ammonium. The resulting carbon skeletons are converted into ketoacids, which then enter central metabolic pathways like glycolysis and the citric acid cycle. The regulation of ammonium levels through recycling into biomolecules or elimination is crucial for maintaining metabolic balance.

Overall, the chapter illustrates how the study of the nitrogen cycle extends biochemistry beyond the confines of human metabolism to encompass broader ecological and environmental contexts. It sets the stage for further exploration of amino acid oxidation, emphasizing the necessity of understanding nitrogen metabolism to appreciate the full complexity of biological systems.

This page titled 18.1: The Biochemistry of Nitrogen in the Biosphere is shared under a not declared license and was authored, remixed, and/or curated by Henry Jakubowski and Patricia Flatt.

- **11.2: Diffusion Across a Membrane - Passive and Facilitated Diffusion** by Henry Jakubowski and Patricia Flatt has no license indicated.

18.2: METABOLIC FATES OF AMINO GROUPS

LEARNING GOALS (CHATGPT O3-MINI)

1. **Protein Digestion and Amino Acid Liberation:**
   - Describe the stepwise breakdown of dietary proteins beginning in the stomach (via pepsin) and continuing in the small intestine (via trypsin, chymotrypsin, carboxypeptidases, and aminopeptidases), leading to the formation of free amino acids and small peptides.
   - Explain how the acidic environment of the stomach aids in protein unfolding and facilitates enzymatic cleavage.
2. **Proteasomal Degradation and Amino Acid Recycling:**
   - Explain the role of the proteasome and ubiquitin tagging in degrading intracellular proteins, and how this process contributes to the amino acid pool available for metabolism.
3. **Integration of Amino Acid Catabolism into Central Metabolism:**
   - Summarize how different amino acids are catabolized to yield key intermediates (e.g., pyruvate, acetyl-CoA, oxaloacetate, and α-ketoglutarate) that feed into glycolysis and the citric acid cycle.
   - Differentiate between glucogenic and ketogenic amino acids and discuss their respective roles in energy production and biosynthesis.
4. **Transamination and PLP-Dependent Reactions:**
   - Describe the mechanism of transamination reactions, including the role of pyridoxal phosphate (PLP) as a cofactor in facilitating the reversible transfer of amino groups.
   - Compare the functions of aspartate transaminase (AST/GOT) and alanine transaminase (ALT/GPT) in linking amino acid metabolism with carbohydrate metabolism.
5. **Glutamate and Glutamine in Nitrogen Metabolism:**
   - Explain how glutamine and glutamate serve as key nitrogen carriers in the body, facilitating the safe transport of ammonia (NH_3/NH_4^+) and preventing its toxic accumulation.
   - Describe the role of glutaminase in converting glutamine to glutamate and the function of glutamate dehydrogenase in oxidative deamination to form α-ketoglutarate and release ammonium.
6. **The Glucose-Alanine Cycle:**
   - Illustrate the glucose-alanine cycle, detailing how alanine is formed in muscle via transamination, transported to the liver, and then converted back to pyruvate for gluconeogenesis.
   - Contrast the glucose-alanine cycle with the Cori cycle, noting the different substrates and metabolic fates involved in each.
7. **Regulation and Toxicity of Ammonia:**
   - Discuss why high concentrations of ammonia are toxic to cells and the biochemical strategies used to mitigate this toxicity, such as incorporation into glutamine.
   - Explain how the liver processes ammonia, either by converting it to urea, incorporating it into amino acids, or recycling it for biosynthesis.
8. **Integration of Nitrogen Metabolism with Energy Homeostasis:**
   - Analyze how amino acid catabolism interconnects with central energy metabolism, emphasizing how the breakdown of amino acids supplies intermediates for ATP production and biosynthetic pathways.
   - Evaluate the physiological relevance of amino acid catabolism in different nutritional states (fed, fasting, or diabetic conditions).

By achieving these learning goals, students will gain a comprehensive understanding of how amino acids are derived, metabolized, and integrated into central metabolic pathways, as well as the regulatory mechanisms that ensure efficient nitrogen handling and energy homeostasis in living organisms.

From the previous section on the nitrogen cycle, it should be clear that NH_3/NH_4^+ has a central role in metabolism. Nature's plant fertilizer is derived from ammonium, which originates from bacterial nitrogenase and the human-derived Haber-Bosch process. Animals get their ammonia mostly from ingested plants (primary producers) and animal protein. In vertebrates, proteins are digested into small peptides and amino acids, starting in the stomach, where pepsin cleaves proteins after aromatic and Leucine side chains into smaller fragments. The low pH in the stomach (1-2) facilitates protein unfolding, allowing for easy access to buried side chains for pepsin cleavage. As the ingested

materials move into the small intestine, the protein fragments are further cleaved into small peptides by trypsin and chymotrypsin and then into individual amino acids by carboxypeptidases (which cleave C-terminal amino acids) and aminopeptidases (which cleave at the N-terminal end). The individual amino acids are then adsorbed (along with di- and tripeptides) into the epithelial cells lining the small intestine. Peptidases cleave short peptides, and amino acids are moved into the blood through cell membrane transporters, which are coupled to sodium ion intake. Amino acids are taken up by tissues for use in protein synthesis and specifically by the liver of vertebrates for metabolic processing. The gut proteolytic enzymes are secreted into the gut lumen as precursors (proenzymes), where they are activated either autocatalytically or by other proteases into their mature form.

Amino acids are also derived from the degradation of cellular proteins by a supramolecular assembly called the proteasome. Proteins designated for cleavage are covalently modified by ubiquitin, a short ubiquitous protein, which targets them to the proteasome.

18.2.1: DEGRADATION OF AMINO ACIDS TO PRODUCE AMMONIUM

Here is some good advice on giving a seminar: tell what you will tell them, tell them, and tell them what you told them. These words suggest that repetition is a key to learning. So look at Figure **18.2.1**, which shows an overall view of the glycolytic and TCA pathways, and see how amino acid catabolism fits into what you already know!

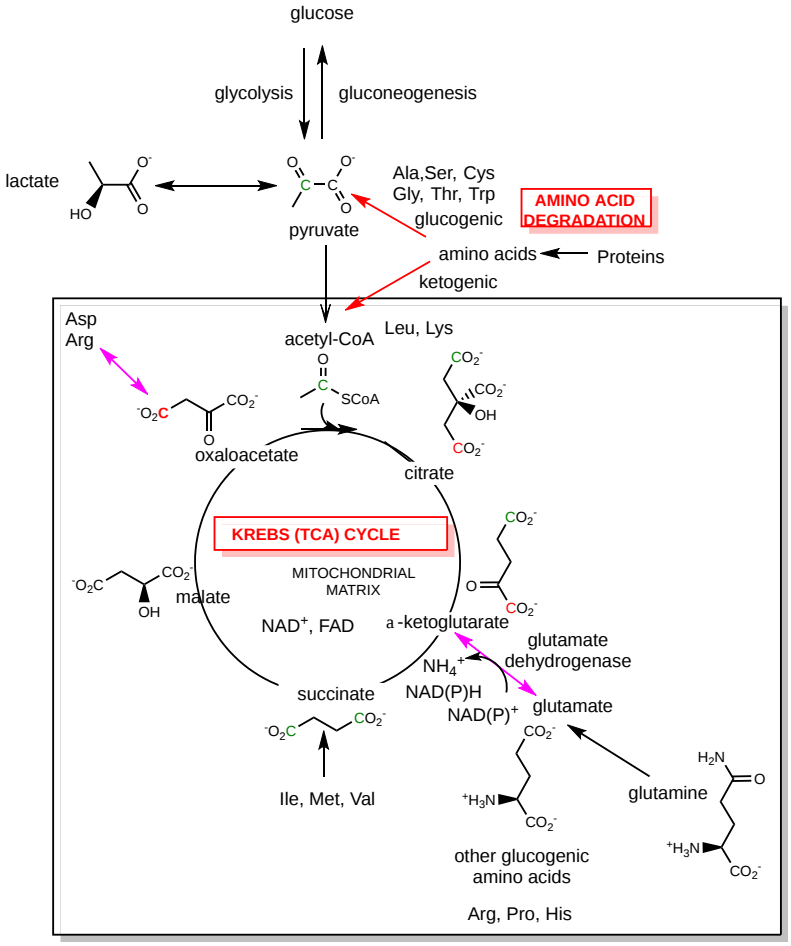


Figure **18.2.1**: Amino acids and their involvement with the glycolytic and TCA pathways

A summarizing principle is that amino acids degrade to form intermediates that fit into these two common pathways, which can be utilized for ATP production and biosynthesis. Those that form pyruvate are **glucogenic** amino acids, while those that form acetyl-CoA are **ketogenic** (form ketones and could form ketone bodies). Many form direct intermediates in the TCA cycle.

This chapter will focus on glutamine/glutamic acid, alanine (which forms pyruvate), and aspartic acid. In this section, we will focus on the role of amino acid catabolism in producing ammonium. When new students confront the structures, properties, and reactions of amino acids, they are undoubtedly daunted. Even biochemists would be if amino acid metabolism is outside their active research area. Perhaps some interesting biological properties of **free** amino acids might pique your interest. For example, did you know that ...

- glutamate and glutamine are the most abundant amino acids in red blood cells;

- alanine and glutamine are the most abundant amino acids in the body;
- glutamic acid, glutamine, and alanine are the most abundant amino acids in the cerebrospinal fluid CSF (50-55% of total amino acids);
- glutamine is the most abundant amino acid in blood serum;
- In contrast, leucine is the most abundant amino acid in **proteins**, and free leucine is a prime regulator of protein synthesis through its interaction with the mTOR kinase complex. The other top three amino acids in proteins are serine, lysine, and glutamic acid.

From the above list, Glu and Gln appear to play special roles in metabolism and signaling. They also play major roles in ammonium metabolism as the pair is a major source of NH_4^+ production in cells. Gln has two Ns (an amine and an amide), so it's not an unexpected source of nitrogen:

- Glutamine can give up its amide nitrogen to form NH_4^+ on conversion to glutamic acid, a reaction catalyzed by **glutaminase**
- Glutamic acid can undergo oxidative deamination to form α-ketoglutarate (a TCA intermediate) and free NH_4^+, a reaction catalyzed by **glutamate dehydrogenase**
- Glutamic acid can also give up its ammonia nitrogen to a ketoacid like pyruvate to form α-ketoglutarate (a TCA intermediate) and another amino acid (alanine if pyruvate was used as the keto acid), a reaction catalyzed by a class of enzymes called **transaminases** (makes sense again), which are also called **aminotransferases**. In this case, free NH_4^+ is not formed but is passed to a keto acid to form another amino acid.

In vertebrates, free amino acids are metabolized in the liver. Amino acids that enter the liver transfer their ammonia group to α-ketoglutarate (aka 2-oxoglutarate) to form glutamic acid, which enters the mitochondria and can be cleaved by glutamate dehydrogenase to form α-ketoglutarate and free ammonium. The NH_4^+ produced is either recycled or excreted as NH_4^+ in fish, urea, $H_2N(C{=}O)NH_2$ in vertebrates, and uric acid in birds and reptiles. Excess amino acids (which cannot be stored for energy) in other organs pass their ammonia group to glutamic acid to form glutamine, which then travels to the liver for processing. Glutamine becomes a safe way to transfer 1-2 ammonium equivalents through the blood.

Alanine and aspartic acid also play secondary roles. Ala is one transamination step away, through the removal of its amine group, from pyruvate. Pyruvate is a crucial α-ketoacid end-product of glycolysis and entry reactant for the TCA cycle (after pyruvate dehydrogenase). In muscle, excess amino acids pass their ammonia groups to pyruvate to form alanine, another "safe" carrier of ammonium, which heads to the liver for processing. Likewise, aspartic acid is one transamination step away, through the removal of its amino group, to form oxaloacetate, another TCA α-ketoacid.

Figure **18.2.2** shows the key α-keto acids, which are also intermediates of the TCA cycle or feed into it (pyruvate) and their respective transamination amino acid products. Their structures immediately show a link between amino acid and carbohydrate metabolism.

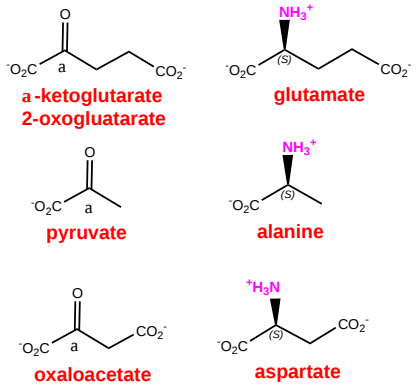


Figure **18.2.2**: α-ketoacids and their transamination amino acid products

We will focus most of our attention on glutamine and glutamic acid. Figure **18.2.3** summarizes the important enzymatic steps in the conversion of Gln ↔ Glu ↔ α-KG

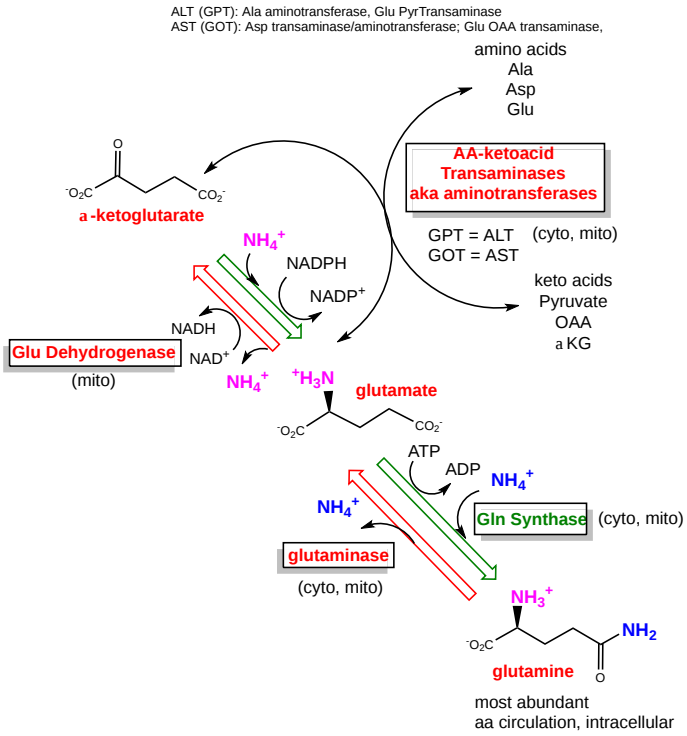


Figure **18.2.3**: Important enzymatic steps in the conversion of Glutamine ↔ Glutamic acid ↔ α-ketoglutarate

18.2.2: PYRIDOXAL PHOSPHATE AND TRANSAMINATION REACTIONS

Most free amino acids initiate their metabolic degradation in the liver through transamination reactions, utilizing PLP as a cofactor. PLP enables other biochemical reactions of amino acids, including racemizations, decarboxylation, and dehydration (of serine). PLP is covalently attached to a Lys through a Schiff base linkage in the enzyme during the reaction cycle, so it is not considered a substrate but rather a cofactor that returns to its original state after the reaction.

Figure **18.2.4** shows the structure of PLP and the imine formed on reaction with an amino acid. The reaction is readily reversible through hydrolysis, which would presumably not be present in the active site of PLP-dependent enzymes. A lysine amine group in the enzyme forms a covalent adduct with PLP to form an imine. The imine in the figure below is referred to as an **internal aldimine**. Internal implies that the source of the N in the imine link is a Lys internal to the protein. If you replace the N in the imine with an O, the functional group with the C=O would be an aldehyde. Hence, the imine shown is an aldimine.

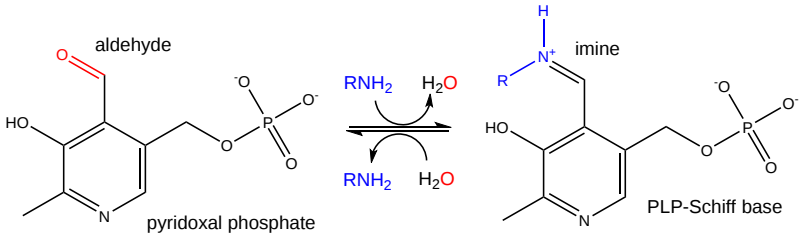


Figure **18.2.4**: PLP and its imine-protein conjugate

William Jencks, in his classic text, Catalysis in Chemistry, describes the mechanistic beauty of PLP-dependent enzymes:

> *"It has been said that God created an organism especially adapted to help the biologist find an answer to every question about the physiology of living systems; if this is so, it must be concluded that pyridoxal phosphate was created to provide satisfaction and enlightenment to those enzymologists and chemists who enjoy pushing electrons, for no other coenzyme is involved in such a wide variety of reactions, in both enzyme and model systems, which can be reasonably interpreted in terms of the chemical properties of the coenzyme. Most of these reactions are made possible by a*

> *common structural feature. That is, electron withdrawal toward the cationic nitrogen atom of the imine and into the electron sink of the pyridoxal ring from the alpha carbon atom of the attached amino acid activates all three of the substituents of this carbon for reactions which require electron withdrawal from this atom."*

When PLP-dependent enzymes react with an **external** amino acid acting as a substrate, the amine of the incoming amino acid replaces the amine from the enzyme's active Lys to produce an **external** imine. The figure below shows an external amino acid in an imine linkage to PLP, and in the form shown, it is an aldimine.

Each PLP-dependent reaction involves a protonated and positively charged pyridinium N as an electron sink, facilitating cleavage of **each bond** around the C_α of the covalently attached amino acid. Bond cleavage would leave a lone pair and a negative charge on the α-carbon, with no place to stabilize it through resonance. On forming a Schiff base with a pKa of around 7.0, the imine nitrogen, especially in its protonated form, is an excellent stabilizer of the negative charge. The continued delocalization of the lone pair and negative charge to the positive pyridinium nitrogen further facilitates stabilization, thereby enhancing the reaction. Figure **18.2.5** shows the cleavage of bonds around the C_α of an amino acid-PLP Schiff base.

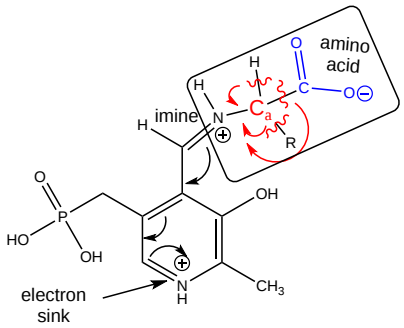
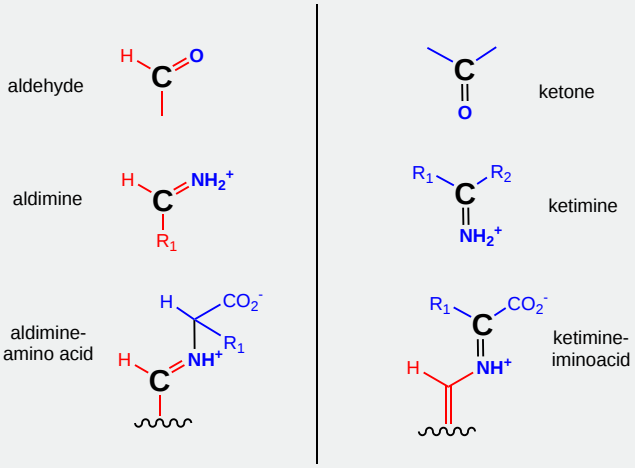


Figure **18.2.5**: Cleavage of bonds around the C_α of an amino acid-PLP Schiff base

ALDIMINES AND KETIMINES

We will encounter two similar types of structures, aldimines and ketimines, when we discuss the chemistry of PLP. They look very similar but are named differently, so it's easy to confuse them. Here they are:



Aldehyde/aldimine and ketone/ketimine structures

It's easy to differentiate them by looking at the **C** atom connected to a =O or =NR. If the **C** atom has an R and H group attached, it's an aldehyde or aldimine. It is a ketone or a ketimine if it has 2 R groups attached.

Figure **18.2.6** shows the mechanism for a transamination reaction using PLP as a cofactor. This is, of course, the reaction most relevant to this chapter. The amino acid substrate is first shown in an aldimine linkage to PLP. Also, note the conversion of an aldimine to a ketimine in the next step.

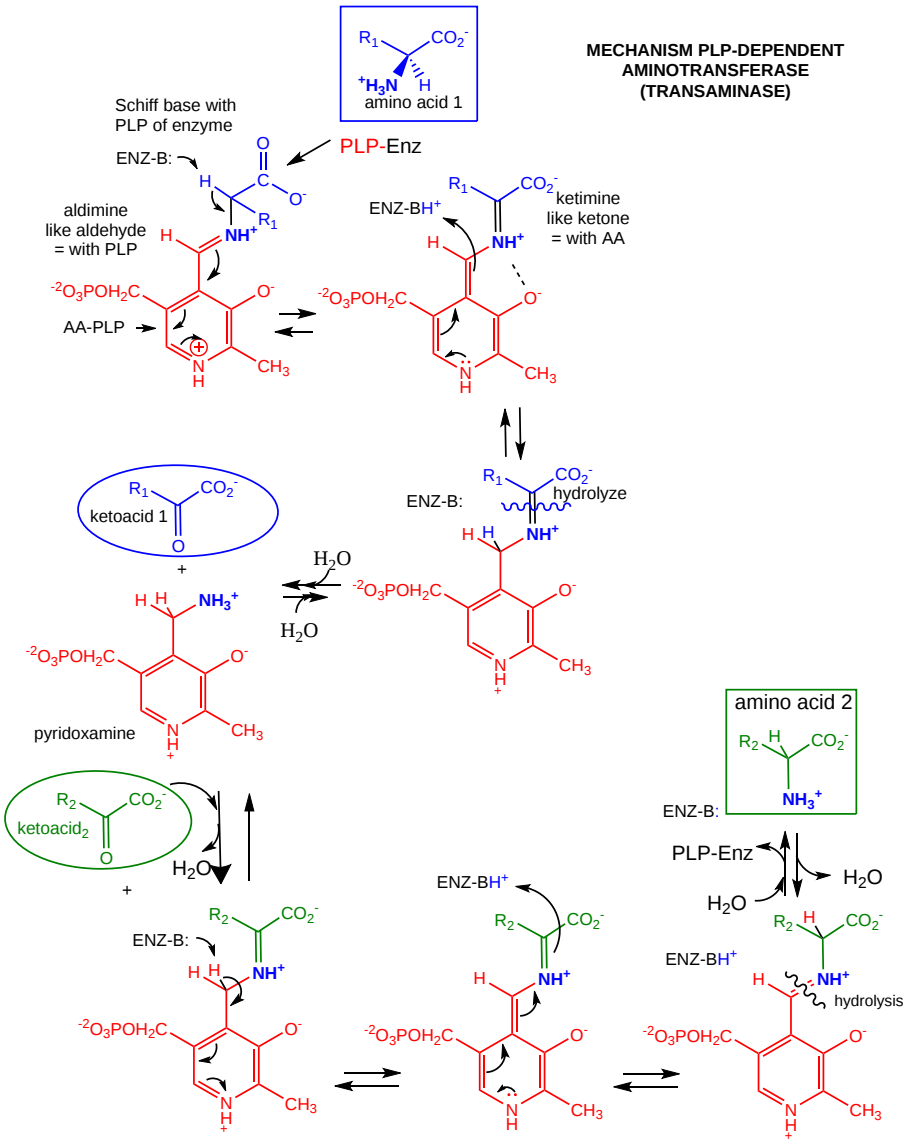
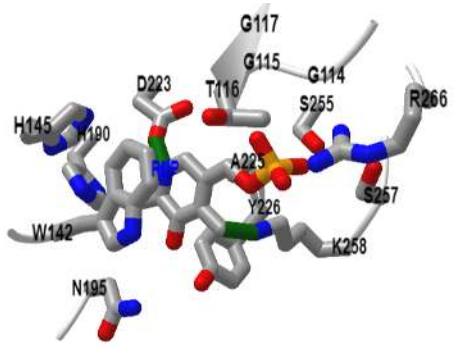


Figure **18.2.6**: Mechanism for a transamination reaction using PLP as a cofactor

The model below shows the active site of aspartate transaminase from E. coli (PDB code 1aam) with PLP in a Schiff base linkage with lysine 258. Three amino acids critical for enzyme function (Trp 142, Asp 223, and Lys 258) and all side chains within 5 angstroms from the active site defined by those amino acids are shown. Lys 258 forms the Schiff base with the PLP cofactor and acts as a general acid/base in the interconversion between the aldimine and ketamine forms (see figure above). The ring of Trp 142 forms pi-stacking interactions with the aromatic ring of PLP, helping to position it. Asp 223 acts as a general acid/base in the catalytic cycle, facilitating the deprotonation of the amine group of the substrate Asp, making it a potent nucleophile in forming the external aldimine.

Figure **18.2.7** shows an interactive iCn3D model of the active site of aspartate transaminase from E. Coli with PLP (1aam)



NCBI iCn3D Figure **18.2.7**: Active site of aspartate transaminase from E. Coli with PLP (1aam). (Copyright; author via source). Click the image for a popup or use this external link: https://structure.ncbi.nlm.nih.gov/i...YeQ6kah4EuERT9

The various names and abbreviations for transaminases/aminotransferases (which are reversible) can be confusing. Two key ones whose levels are used to assess liver toxicity in clinical tests are AST (GOT) and ALT (GPT).

- **AS**partate Amino **T**ransferase (**AST)** is the same enzyme as **G**lutamate **O**xalacetate **T**ransaminase (**GOT**), named for the reverse reaction:

$$\text{aspartate} + \alpha\text{−ketoglutarate} \leftrightarrow \text{oxalacetate} + \text{glutamate}$$

- **AL**anine Amino **T**ransferase (**ALT**) is the same enzyme as **G**lutamate **P**yruvate **T**ransaminase (**GPT**), named for the reverse reaction:

$$\text{alanine} + \alpha\text{−ketoglutarate} \leftrightarrow \text{pyruvate} + \text{glutamate}$$

We will consider other reactions of PLP-dependent enzymes when needed.

To summarize, different amino acids in the liver can donate their amine groups to α-ketoglutarate to form glutamic acid in a reaction catalyzed by a transaminase/aminotransferase.

18.2.3: PRODUCTION OF NH_3 - GLUTAMATE DEHYDROGENASE

Now that we have made glutamic acid from various amino acids, we can break it down to make α-ketoglutarate and ammonium again. The overall reversible reaction catalyzed by the enzyme glutamate dehydrogenase in mitochondria is shown in Figure **18.2.8**. Mammalian livers can also use $NADP^+$ as an oxidizing agent.

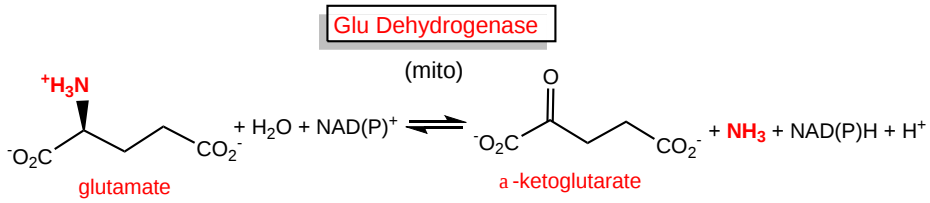


Figure **18.2.8**: Overall reversible reaction catalyzed by the enzyme glutamate dehydrogenase in mitochondria

Humans have two isozymes. GluDH1 is expressed at high levels in the liver, brain, pancreas, and kidney, while GluDH2 is found in the retina, testes, and brain. GluDH1 can use both NAD^+ and $NADP^+$ in both anabolic and catabolic reactions.

The reaction/product pairs again show this reaction as a link between protein and carbohydrate metabolism. Figure **18.2.9** shows just the first step in the glutamate dehydrogenase reaction.

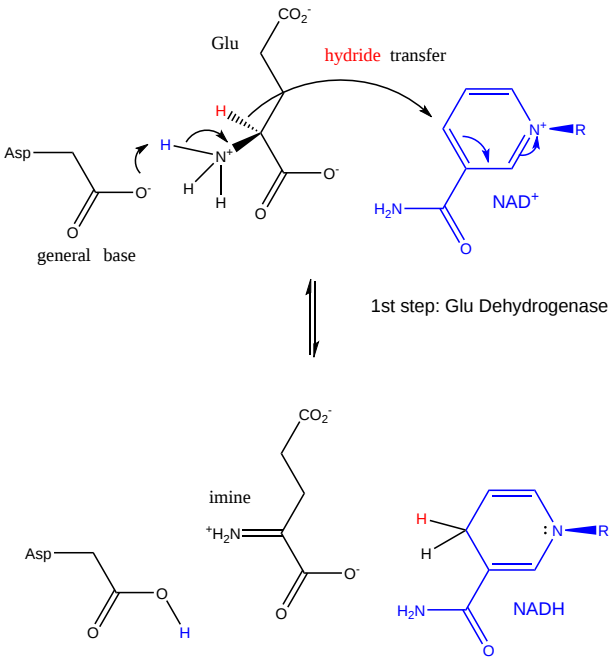


Figure **18.2.9**: First step in the reaction of glutamate dehydrogenase

The C-N bond in Glu becomes a C=N bond in the imine intermediate. You should recognize this as an oxidation step even if the obvious oxidizing agent, $NAD(P)^+$, was not shown. That should also be evident since a hydride (H^-) with a lone pair is removed from glutamic acid, not an H^+ as in an acid/base reaction. Subsequent steps include a nucleophilic attack by water (enhanced by a proximal Lys acting as a general base) on the imine carbon, followed by ammonia release during alpha-ketoglutarate formation. The overall reaction is an **oxidative deamination**.

NH_3/NH_4^+ are toxic in high concentrations. One possible reason is that the NH_4^+ cation might compete with the transport of other ions across neural membranes, altering transmembrane potentials and, hence, neural function. Given this toxicity, one would expect glutamate dehydrogenase to be highly regulated in mammals. The mammalian enzyme is a hexamer of identical subunits, suggesting allosteric regulation of activity (much like tetrameric hemoglobin). ADP and leucine are allosteric activators, whereas GTP, palmitoyl-CoA, and ATP act as inhibitors. The GTP/ADP regulation is consistent with the notion that the enzyme is regulated by the cellular energy demand (note that GTP is formed in the TCA cycle).

Although this reaction is written above in the direction of NH_3 formation, the reaction is reversible, even though the ΔG^0=-6.2 kcal/mol (-26 kJ/mol), and although the human enzymes have a high Km for ammonia (12-62 mM, Brenda Database). As the pH decreases from 8 to 7, the Km for ammonia increases from around 12 to 60 mM. This implies that, in the case of glutamate uptake and in acidotic conditions, the reaction proceeds exclusively in the direction of NH_3 release, acting as an oxidative deamination reaction.

18.2.4: TRANSPORTING AMMONIUM EQUIVALENTS IN THE BLOOD - GLUTAMINE AND ALANINE

NH_3/NH_4^+ are toxic in high concentrations, so mechanisms must be used to transport them in the blood. Ideally, it would be transported in a nontoxic form. Glutamic acid is a key metabolic molecule, so glutamine is the preferred molecule for safe "NH_3/NH_4^+" transport from tissue to the liver, while alanine is the choice for muscle tissue. This less-toxic mode of transport is similar in principle to using soluble ketone bodies to transport the energy equivalent of the less soluble fatty acids in the blood.

A key enzyme for this process is **glutamine synthetase**, which catalyzes this reaction:

$$NH_4^+ + ATP + Glu \rightarrow Gln + ADP + HPO_4^{2-} + H^+$$

This reaction is important as most ingested glutamine is converted to glutamate on absorption.

NH_3/NH_4^+ produced in the intestine and kidneys enters the circulation, where it is directed to the liver to produce urea ultimately.

Figure **18.2.10** shows the Glucose-Alanine Cycle compared to the Cori cycle we discussed in a previous chapter.

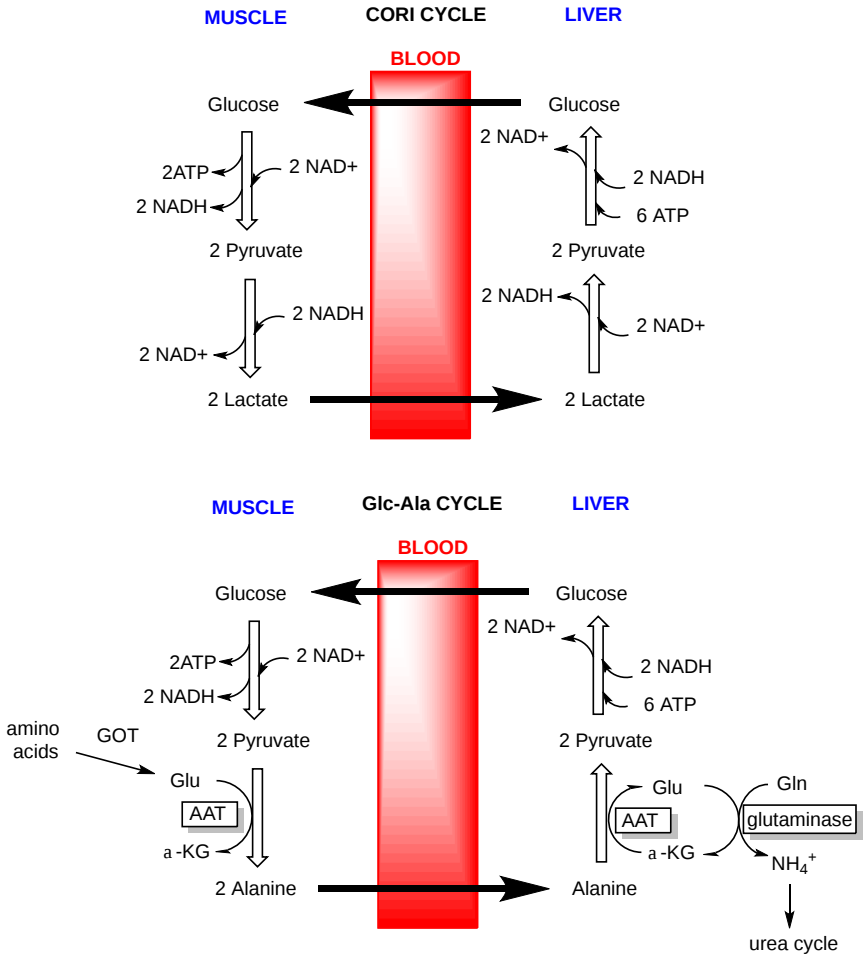


Figure 18.2.10: Glucose-Alanine Cycle in comparison to the Cori cycle

18.2.5: PRODUCTION OF NH_3 - GLUTAMINASE

Most amino acids arriving in the liver for degradation go through two enzymes, transaminases, to form glutamic acid, followed by glutamate dehydrogenase to form a TCA intermediate (alpha-ketoglutarate) and ammonia. Glutamine carries excess ammonia in the bloodstream (see below). When it arrives in the liver, it can lose its amide NH_2 as ammonium as it is converted to glutamic acid by the enzyme **glutaminase.** This nonoxidative enzyme is expressed in the liver, brain, and kidney. Some glutamates can lose ammonia through the enzyme glutamate dehydrogenase, but most are reserved for protein synthesis or the creation of anabolic precursors.

As mentioned above, glutamine is the most abundant free amino acid in the body and cells. It can donate its amide N through reactions catalyzed by **amido**transferase (not to be confused with aminotransferase), incorporating nitrogen into many biomolecules.

18.2.6: METABOLIC SUMMARY

- Glutamine is both a carrier of ammonia and a carbon backbone used in metabolism when converted to α-ketoglutarate. It can be metabolized for energy and used in biosynthesis for nucleotides and neurotransmitters. Its levels are controlled by glutamine synthase and glutaminase. When we get to synthetic pathways, you will find that glutamine is a NH_3/NH_4^+ donor for synthesizing other amino acids and nucleotides, amino sugars, and NAD^+.
- Glutamine absorbed in the intestines is mostly converted to glutamic acid in the intestinal epithelial cells and transported by the blood. The rest heads to the liver for processing. Hence, most glutamine must be synthesized by glutamine synthase, a cytosolic enzyme found in most mammalian cells. However, it is most abundant in muscle, liver, and adipose cells, which express little glutaminase and from which it can be exported. Glutaminase in the liver and kidney leads to ammonium production.
- Glutamine is a source of energy and carbon for biosynthesis by tumor cells, which require energy and intermediates for rapid cell proliferation. Aerobic glycolysis ("Warburg effect") allows that to occur.

18.2.7: SUMMARY

This chapter explores the metabolic fate of proteins and amino acids, emphasizing how nitrogen is managed and integrated into central metabolism. It begins by detailing the process of protein digestion, which starts in the acidic environment of the stomach and continues in the small intestine with enzymes such as trypsin, chymotrypsin, carboxypeptidases, and aminopeptidases. These enzymes break proteins into peptides and amino acids, which are then absorbed through the intestinal epithelium.

In addition to dietary protein breakdown, the chapter describes the intracellular degradation of proteins by the proteasome. Proteins destined for degradation are tagged with ubiquitin, directing them to the proteasome where they are systematically cleaved into amino acids.

The catabolism of these amino acids is integrated into central metabolic pathways. Transamination reactions—catalyzed by PLP-dependent enzymes such as aspartate transaminase (AST/GOT) and alanine transaminase (ALT/GPT)—transfer amino groups to ketoacids, forming key intermediates like oxaloacetate and pyruvate. These reactions not only facilitate the use of amino acids for energy production via the TCA cycle but also play a critical role in biosynthesis.

Glutamate and glutamine are highlighted as central players in nitrogen metabolism. Glutaminase converts glutamine to glutamate, and glutamate dehydrogenase then catalyzes the oxidative deamination of glutamate to produce α-ketoglutarate and ammonium. Because free ammonia (NH_3/NH_4^+) is toxic, the body employs safe transport mechanisms—using glutamine and alanine as non-toxic carriers—to shuttle nitrogen from peripheral tissues to the liver, where ammonia is ultimately converted to urea for excretion.

By linking protein digestion, intracellular proteolysis, transamination, and deamination processes, this chapter illustrates how amino acid catabolism is seamlessly integrated with carbohydrate metabolism to support both energy production and biosynthetic demands. Overall, the chapter underscores the delicate balance of nitrogen metabolism and its vital role in maintaining cellular and systemic homeostasis.

This page titled 18.2: Metabolic Fates of Amino Groups is shared under a not declared license and was authored, remixed, and/or curated by Henry Jakubowski and Patricia Flatt.

- **11.2: Diffusion Across a Membrane - Passive and Facilitated Diffusion** by Henry Jakubowski and Patricia Flatt has no license indicated.

18.3: NITROGEN EXCRETION AND THE UREA CYCLE

LEARNING GOALS (CHATGPT O3-MINI)

- **Explain the Overall Role of the Urea Cycle:**
  Understand how the urea cycle detoxifies excess ammonia generated from amino acid catabolism and why urea is a preferred end product for nitrogen excretion.
- **Describe the Key Enzymes and Their Functions:**
  Identify and explain the roles of the main enzymes (CPS1, OTC, ASS1, ASL, ARG1) in the urea cycle, including their specific reaction steps and contributions to overall cycle function.
- **Analyze Enzyme Mechanisms and Structural Features:**
  Evaluate the reaction mechanisms of enzymes like carbamoyl phosphate synthetase I and arginase, including details such as ATP consumption, active site architecture, substrate tunnels, and the role of cofactors (e.g., N-acetyl-glutamate).
- **Discuss Regulation and Allosteric Control:**
  Understand how key regulators, such as N-acetyl-glutamate, control the rate-limiting step of the urea cycle, and explore how enzyme activity is modulated in response to metabolic demands and dietary protein levels.
- **Examine Experimental Evidence for a Cyclic Pathway:**
  Assess how experiments—like the addition of ornithine—demonstrate the cyclic nature of the urea cycle and the concept of catalytic regeneration within the cycle.
- **Connect the Urea Cycle to Broader Metabolism:**
  Explore how the urea cycle is linked to the tricarboxylic acid (TCA) cycle, particularly through intermediates such as fumarate and aspartate, and understand the role of metabolic shuttles (e.g., malate–aspartate shuttle) in integrating these pathways.
- **Evaluate Energetic and Metabolic Implications:**
  Quantify the energy cost of urea synthesis (in terms of ATP expenditure) and discuss how the cycle's integration with the TCA cycle helps compensate for this energetic demand.
- **Apply Structural Biology to Enzyme Function:**
  Utilize interactive molecular models to gain insights into enzyme structure, such as the tunnel formation in CPS I or the multimeric organization of argininosuccinate lyase, and connect these structures to their catalytic functions.
- **Interpret Clinical Relevance and Disorders:**
  Link the biochemical details of the urea cycle to clinical scenarios, such as hyperammonemia, and discuss how defects in specific enzymes can lead to metabolic disorders, highlighting the importance of enzyme localization and gene regulation.
- **Compare Cyclic versus Linear Metabolic Pathways:**
  Contrast the urea cycle with linear metabolic processes by examining the efficiency, regulation, and "recycling" nature of cyclic pathways, drawing parallels with broader concepts like the circular economy.

These goals aim to integrate mechanistic understanding, regulatory insights, structural biology, and clinical applications, providing a comprehensive framework for mastering the urea cycle and its connections to overall metabolism.

18.3.1: THE UREA CYCLE

Now, we can see what happens to excess NH_3/NH_4^+ that accumulates in the liver mitochondria. The ammonia formed in the liver through oxidative deamination by glutamate dehydrogenase ends up in urea. Alternatively, it can be added to glutamic acid to form glutamine, which can be transported to the kidney. There, after sequential actions of glutaminase (a deamidation reaction) and glutamate dehydrogenase, it forms ammonia for direct excretion in the urine. If your diet is high in proteins and hence amino acids, since they can't be stored as proteins per se, they are metabolized for energy, and the metabolic products can be converted to fat or carbohydrates. That leaves excess nitrogen, which is mainly excreted as urea.

Urea is a highly water-soluble, non-toxic molecule that biochemists use in the lab to chemically denature proteins (at concentrations of 3-6 **M**). Clinical blood urea concentrations are expressed as Blood Urea **Nitrogen** (BUN), which ranges from 7 to 20 mg/dL N, equivalent to 2.5 to 7.1 **mM** urea. Serum levels depend predominantly on the balance between urea synthesis in the liver and its elimination by the kidney. Normal cellular urea concentrations should be similar.

Urea is produced through a cyclic pathway known as the **urea cycle**. You are familiar with perhaps the most favorite biochemical cycle, the tricarboxylic (citric or Krebs) cycle. Krebs also discovered the urea cycle before conceiving the citric acid cycle. He concluded that the urea formation pathway was a cycle using the same logic he deployed for the citric acid cycle. After your first view of the full urea cycle, we'll explain how, as shown in Figure 18.3.1.

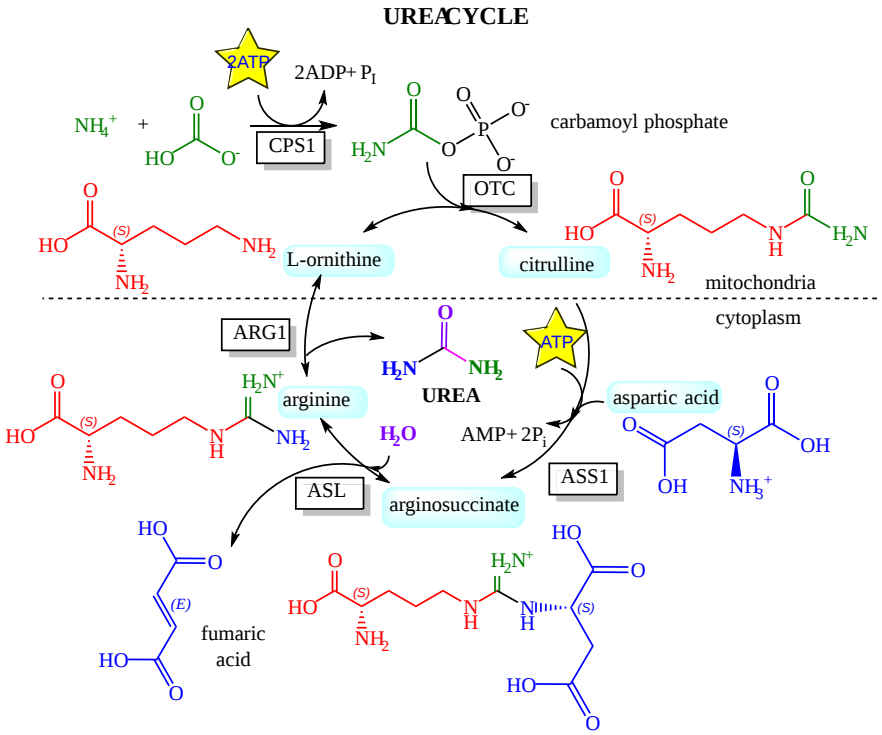


Figure 18.3.1: The Urea Cycle

The enzyme names are:

- CPS1: carbamoyl phosphate synthase I
- OTC: ornithine transcarbamoylase
- ASS1: arginosuccinate synthase 1
- ASL: arginosuccinase lysase (aka arginosuccinase)
- ARG1: arginase

It is color-coded to designate the sources of the C and N atoms. One N comes from ammonia (or indirectly from the amido N of glutamine), while the C atom comes from carbonate. The other comes from the amine of aspartate. Note that three ATPs are used to power the cycle. Also note that the guanidino group of arginine ($NH(NH_2^+)NH_2$) is the immediate donor of the 2 N atoms in the step that produces urea. Knowing that one amino acid was the immediate donor of the N atoms in urea, you would easily predict that.

Let's start with the first step, the cleavage of arginine to produce ornithine and urea. What happens to the ornithine derived as a "waste" product of urea formation? Experimentally, one might add more ornithine to a system running the urea formation pathway and ask what happens to the rate of urea synthesis. If it were a one-step process, you might expect, based on mass action, that adding ornithine, a product, would slow that reaction rate by driving it backward. Krebs found the opposite: adding more ornithine increased the rate of urea formation, but in a way that did **not** alter the ornithine concentration. Hence, ornithine was not consumed per se in a subsequent step. Ornithine appeared to act as a traditional catalyst, speeding up the reaction without being consumed. To do so, it must generate more arginine. The way to account for this was a cyclic pathway, not a linear or branched one. In a cycle, none of the participants is consumed in a net fashion.

Now, let's examine some of the steps, starting with those powered by ATP, which also incorporate nitrogen into the urea precursors.

18.3.2: CARBAMOYL PHOSPHATE SYNTHASE I (CPS I)

This enzyme catalyzes the first "committed" step of the pathway and makes carbamoyl phosphate, the reactant that enters the cycle. It requires a specific cofactor, N-acetylglutamate (NAG), produced by the acetylation of glutamate by acetyl-CoA through the action of NAG synthase, which is activated by arginine. The reaction is not part of the cycle but provides input.

A cytosolic version of this enzyme, CPS II, synthesizes arginine and pyrimidine nucleotides using glutamine as a donor of NH_4^+, which reacts with carboxyphosphate to produce carbamoyl phosphate. NAG does not regulate it.

CPS I provides a way to form a $(C{=}O)NH_2$ unit for urea by condensing bicarbonate and ammonia to form a carbamate, which contains a high-energy "motif" with respect to its hydrolysis product. (Note: This does not imply that the broken bond is high-energy, a misnomer found in many books.) Hence, the reaction is powered by 2 ATPs as an energy source. Urea is a molecule that "carries" both NH_3/NH_4^+ and carbonate.

A reaction mechanism for carbamoyl phosphate synthase is shown in Figure **18.3.2**.

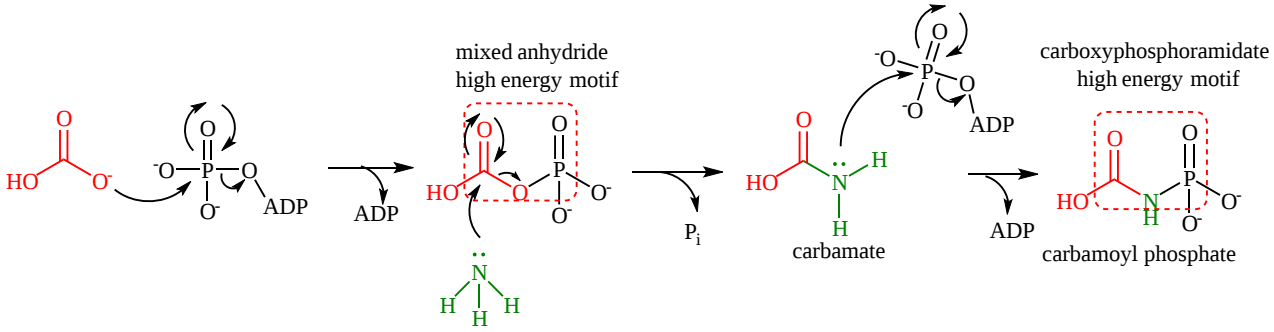


Figure **18.3.2**: Reaction mechanism for carbamoyl phosphate synthase

The two high-energy motif molecules (again with respect to their hydrolysis products) are protected from nonspecific hydrolysis as the mixed anhydride passes along a sequestered tunnel to a more distal phosphorylation site in the multimeric enzyme.

Figure **18.3.3** shows an interactive iCn3D model of the human carbamoyl phosphate synthetase I with bound ADP and N-acetyl-glutamate (5DOU).

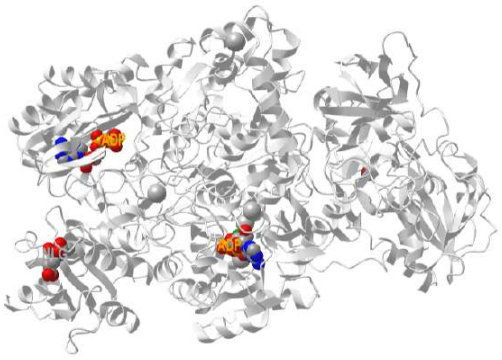


Figure **18.3.3**: Human carbamoyl phosphate synthetase I with bound ADP and N-acetyl-glutamate (5DOU). (Copyright; author via source). Click the image for a popup or use this external link: https://structure.ncbi.nlm.nih.gov/i...yV8fW3mW9idy6A

The model shows one chain of the multimer. The two ADPs and single N-acetylglutamate (NLG) are shown in spacefill and labeled. Additional bound ions are shown (unlabeled).

The protein exists in a monomer-dimer equilibrium mixture. Each monomer has 1 NAG and 2 ADPs in the two binding sites required for the two phosphorylation steps, as shown in the reaction above. The two phosphorylation sites are connected by a tunnel allowing passage of the mixed anhydride to the carbamate phosphorylation site. The NAG is an allosteric modifier as it is not bound near the phosphorylation sites. On binding to the apo form of the enzyme, it elicits a large conformation change, allowing a competent enzyme conformation with a complete tunnel to predominate.

An image of the tunnel for one monomer of the human carbamoyl phosphate synthetase I is shown in Figure **18.3.4**.

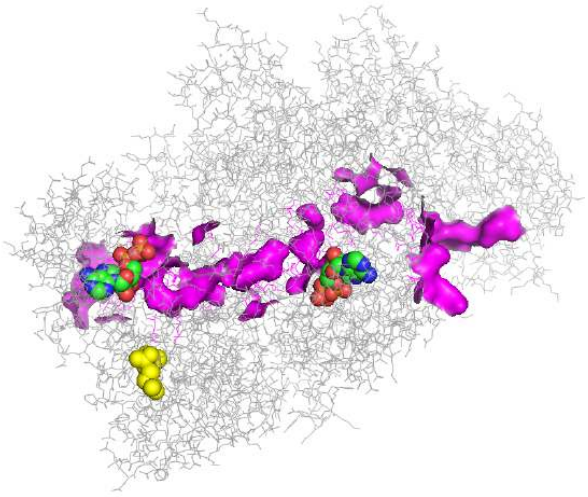


Figure 18.3.4: Tunnel for one monomer of the human carbamoyl phosphate synthetase I enzyme.

Two ADPs are shown below in spacefill with CPK color. The tunnel between the two ADP sites is highlighted in magenta. The yellow molecule is NAG, which again exerts its activation effect by binding to an allosteric site, effectively opening up the tunnel.

Figure 18.3.5 shows the enzyme monomer in a different orientation with a tunnel made using ChExVis: a tool for molecular channel extraction and visualization. The large red and green spheres show the surface openings.

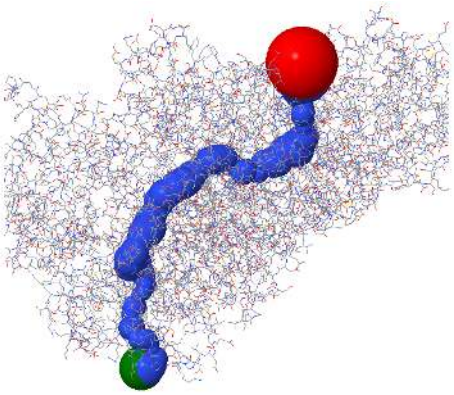


Figure 18.3.5: Second view of the tunnel in human carbamoyl phosphate synthetase I

The top panel in Figure 18.3.6 shows the radius in Angstroms of the tunnel going from the Red sphere to the Green sphere in the image above. The bottom panel measures the hydrophobicity (red)//hydrophilicity (blue) of the amino acids surrounding the tunnel.

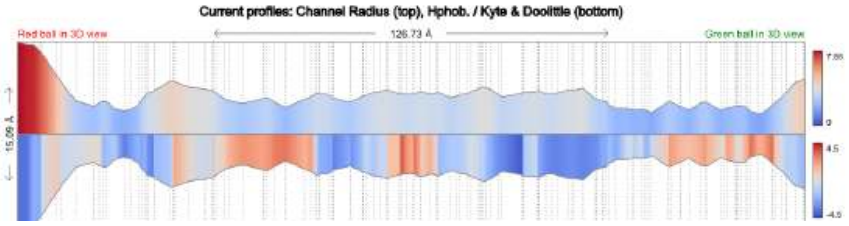


Figure 18.3.6: Tunnel size and polarity profile in human carbamoyl phosphate synthetase I

18.3.3: ASS1: ARGINOSUCCINATE SYNTHASE 1

Another ATP is cleaved to convert citrulline to arginosuccinate, as shown in Figure 18.3.7. The product could easily be cleaved in the next step to form the amino acid arginine.

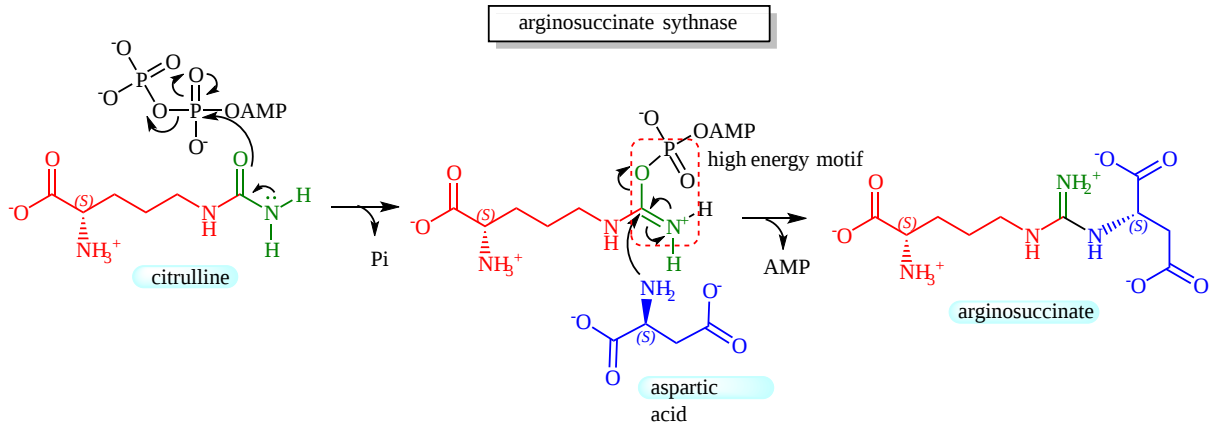


Figure **18.3.7**: ATP cleavage drives the conversion of citrulline to arginosuccinate

18.3.4: ASL: ARGINOSUCCINASE LYASE (AKA ARGINOSUCCINASE)

This enzyme catalyzes a beta-elimination reaction, which may proceed through an E2 or E1 mechanism. A general but very abbreviated mechanism showing a two-step (E1) elimination proceeding through a carbanion intermediate is shown in Figure **18.3.8** below.

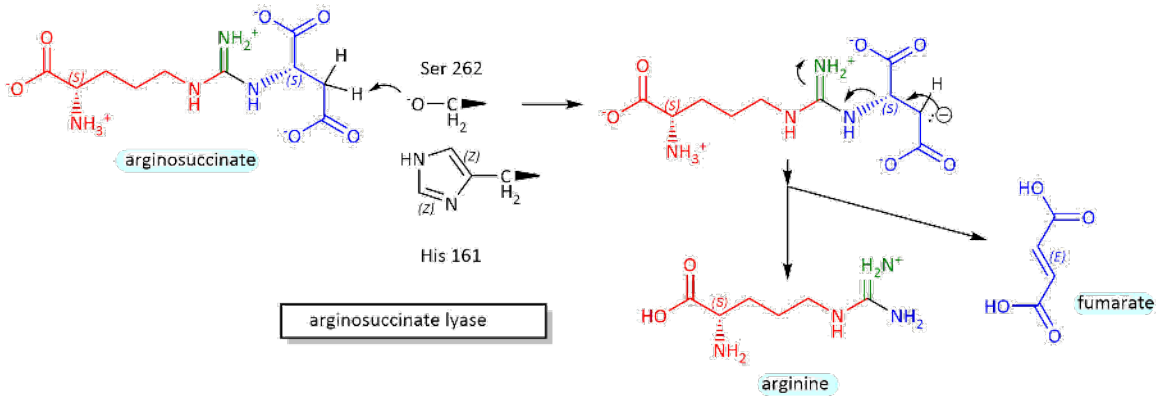


Figure **18.3.8**: Mechanism for conversion of arginosuccinate to arginine and fumarate

Figure **18.3.9** shows an interactive iCn3D model of the tetrameric arginosuccinate lyase (ASL) from *Mycobacterium tuberculosis* (6IEN).

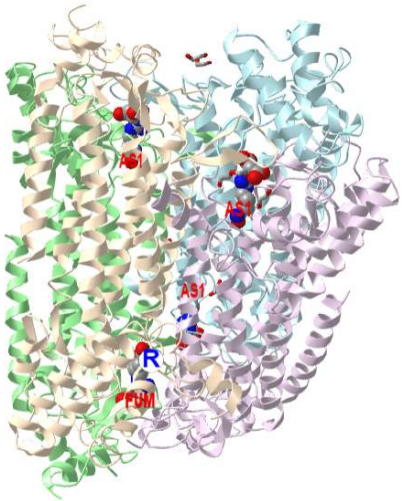


Figure **18.3.9**: Tetrameric arginosuccinate lyase (ASL) from *Mycobacterium tuberculosis* (6IEN). (Copyright; author via source). Click the image for a popup or use this external link: https://structure.ncbi.nlm.nih.gov/i...32EuouGQ6xMVk6

Each monomer of the four monomers is shown in a different color. Three arginosuccinates (substrates) and fumarate, as well as arginine (products), are shown in spacefill with CPK colors and labeled. Each monomer has an N-, M-, and a C-domain. The four binding sites

consist of residues from three monomers. The products are in the fourth site. Catalytic residues probably include a serine and a histidine acting as general acids/bases with a deprotonated lysine, making the serine a general base.

18.3.5: ORNITHINE TRANSCARBAMOYLASE

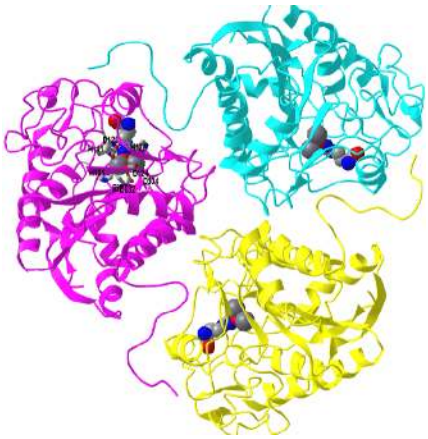
The reaction mechanism is quite simple here. The carbamoyl phosphate is an activated electrophile in which a deprotonated amino group of ornithine attacks the carbonyl C to produce citrulline. The gene is found on the X chromosome in humans, so mutations in males lead to a "hyperammonemia coma" and death. Heterozygous females are either asymptomatic or have problems arising from defects in pyrimidine biosynthesis, which a low-protein diet can alleviate with the addition of arginine.

18.3.6: ARGINASE

There are two general variants of this enzyme. Arginase I is a cytosolic enzyme expressed in the liver and is involved in urea synthesis. Arginase II is a mitochondrial enzyme involved in arginine metabolism more generally. Arginase I converts arginine to ornithine and urea. The enzyme has 2 Mn ions in the active site. A hydroxide ion bridges the two Mn ions and acts as a nucleophile, attacking the arginine guanidino group and forming a tetrahedral intermediate. An active site aspartate (Asp 128) acts as a general acid, protonating the amino leaving group to form ornithine and urea. Water then re-adds to the Mn dinuclear cluster and ionizes, donating a proton to the solvent through an intermediary His 41 as it reforms the active enzyme.

The model below depicts the trimeric human arginase I (3KV2) in complex with the inhibitor N(omega)-hydroxy-nor-L-arginine, in which one of the guanidino nitrogens is replaced with an OH group. The two gray spheres are Mn ions.

Figure **18.3.10** shows an interactive iCn3D model of the trimeric human arginase I in complex with the inhibitor N(omega)-hydroxy-nor-L-arginine (3KV2)**.**



NCBI iCn3D Figure **18.3.10**: Trimeric human arginase I in complex with the inhibitor N(omega)-hydroxy-nor-L-arginine (3KV2)**.** (Copyright; author via source). Click the image for a popup or use this external link:
https://structure.ncbi.nlm.nih.gov/i...QaAQpt5t2KKic6

Figure **18.3.11** show an active site water (#480) near the Mn ions.

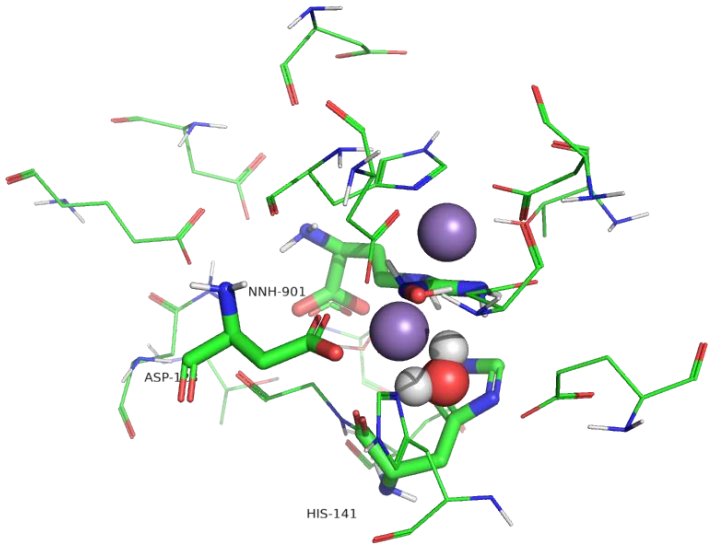


Figure 18.3.11: Active site of human arginase I with an active site water

Water molecules can act as ligands and bind transition-state metal ions through a coordinate covalent bond. The pKa of the bound water shifts to a lower value, making it more likely to deprotonate to form OH^-, which is both a better base and nucleophile. Water 480 in the active site appears to form a coordinate covalent bond to the Mn ion, forming an active site hydroxide that attacks the guanidino group of arginine, leading to the formation of urea and ornithine.

18.3.7: REGULATION

If excess amino acids/proteins are consumed, a change in gene expression can increase levels of the enzymes in the urea cycle. In the short term, the activity is regulated by the enzyme that provides access into the cycle, carbamoyl phosphate synthase, whose activity is regulated by N-acetylglutamic acid and which catalyzes the rate-limiting step. As shown above, the enzyme is functionally inactive in the absence of the allosteric regulator, NAG. The levels of NAG are determined by the enzyme NAG synthase, which is regulated by free arginine, the immediate precursor of urea in the cycle. Supplemental arginine is given to patients with urea cycle disorder, and its effect probably occurs through the regulation of NAG synthase.

18.3.8: THE LINK BETWEEN THE UREA CYCLE AND THE TCA CYCLE

Two major pathways you have explored, the TCA and urea cycles, are not linear but cyclic. What advantages do "circular" pathways offer over linear ones? Perhaps a comparison to economic pathways offers a clue. In a linear economy, raw materials are used to produce a product, which is eventually discarded as trash. Unfortunately, linear pathways dominate our world at a great cost to our environment. To reduce the inefficiencies in a linear economy, make it more viable, and decrease environmental damage and associated climate change, the world should move to a circular economy. A circular economy is characterized by what has been referred to as the 3Rs: reduce, reuse, and recycle. This saves resources and energy. These characteristics also apply to circular biochemical pathways, as reduced levels of metabolites are reused and recycled.

Given this, it should not be surprising that the urea and TCA cycles are linked, especially given that fumaric acid is a product of the urea cycle and a cyclic metabolite of the TCA cycle. In addition, aspartic acid is one transamination step away from oxaloacetate. The interconnections between the urea and TCA cycles are shown in Figure 18.3.12, along with two additions, the malate aspartate shuttle and the aspartate arginosuccinate shunt.

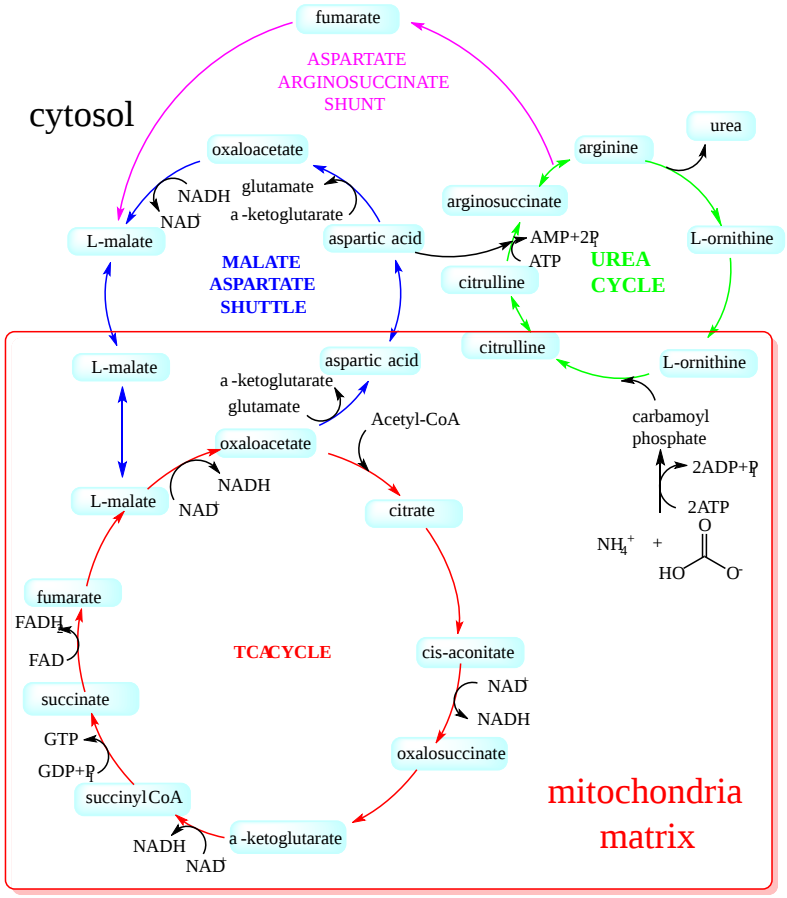


Figure **18.3.12**: Urea and TCA cycles linked by the malate aspartate shuttle and the aspartate arginosuccinate shunt.

One of the nitrogens in urea comes from the amine of aspartate, which can be formed through the transamination of oxaloacetate from the TCA cycle to form aspartate. Since the TCA cycle is a cycle, an equivalent of one oxaloacetate must return to the cycle. It does so indirectly from fumarate, a TCA intermediate produced as a by-product of the urea cycle, but the fumarate is produced in the cytoplasm. There, it gets converted to malate, which can be transported into the mitochondria by a transport protein, mitochondrial 2-oxoglutarate/malate transporter, that is part of yet another cycle shown in the figure above, the **aspartate arginosuccinate shunt. Fumarate is introduced into the shuttle** through the **aspartate-argininosuccinate shunt**, as shown in the figure above**.** Once malate enters the mitochondrial matrix, it can be directly converted to oxaloacetate.

Note that these linked cycles require both mitochondrial and cytoplasmic forms of several enzymes and a balance between two key amino acids across the mitochondrial divide, glutamate and aspartate. One such key enzyme is **as**partate amino**t**ransferase (**AST), also known as g**lutamate **o**xaloacetate **t**ransaminase (**GOT**), named for the reverse reaction of aspartate + α-ketoglutarate ↔ oxaloacetate + glutamate. As mentioned in the previous chapter section, this key enzyme can be detected in the blood if the liver is damaged, so its levels are routinely used in medical tests to assess impaired liver function.

Another key function of the malate-aspartate shuttle is to bring into the mitochondria reduced "equivalents" of NADH produced in the cytoplasm from glycolysis and fatty acid oxidation. There is no membrane transporter for NAD^+ or NADH. Instead, cytoplasmic malate, produced by NADH's cytosolic reduction of oxaloacetate, can be transported into the matrix, which can reform mitochondrial NADH on reconversion to oxaloacetate. The NADH can then power ATP production through mitochondrial electron transport/oxidative phosphorylation pathways.

From an energetic perspective, four phosphoanhydride bonds in 3 ATP molecules are used to produce one urea molecule. This large energy expenditure is partially compensated for by ATP made from the "fumarate equivalents" that enter the mitochondria through the aspartate arginosuccinate and aspartate arginosuccinate shunts and the passage of NADH through oxidative phosphorylation.

18.3.9: SUMMARY

The urea cycle is a central metabolic pathway that detoxifies excess ammonia produced during amino acid catabolism, converting it into urea—a water-soluble, nontoxic molecule suitable for excretion. In the liver, ammonia is generated primarily via oxidative deamination, and

excess nitrogen from a high-protein diet is ultimately processed through this cyclic pathway. The cycle uses energy, consuming three ATP molecules per urea molecule synthesized, a cost partially offset by the integration with other metabolic pathways.

Key Enzymes and Mechanisms:

The cycle involves several critical enzymes:

- **Carbamoyl Phosphate Synthetase I (CPS I):** Initiates the cycle by condensing bicarbonate with ammonia (using N-acetyl-glutamate as an allosteric activator) to form carbamoyl phosphate. The enzyme's structure features a substrate tunnel that channels high-energy intermediates between phosphorylation sites.
- **Ornithine Transcarbamoylase (OTC):** Catalyzes the reaction between carbamoyl phosphate and ornithine to form citrulline, highlighting the cycle's regenerative nature.
- **Argininosuccinate Synthase (ASS1) and Argininosuccinate Lyase (ASL):** Work in tandem to combine citrulline with aspartate (which donates one of the nitrogen atoms) to form argininosuccinate, and then cleave it into arginine and fumarate. The reaction mechanisms here involve ATP cleavage and may proceed via elimination reactions.
- **Arginase (ARG1):** Converts arginine into urea and ornithine, the latter being recycled back into the cycle. The active site of arginase includes a dinuclear Mn center, which plays a crucial role in the hydrolytic mechanism.

Regulation and Metabolic Integration:

The urea cycle is tightly regulated at multiple levels:

- **Allosteric Regulation:** CPS I is dependent on N-acetyl-glutamate (NAG), whose levels are regulated by arginine, linking enzyme activity directly to nitrogen load.
- **Gene Expression:** Long-term adaptations to high protein intake involve changes in the expression of urea cycle enzymes.
- **Connection to the TCA Cycle:** Metabolic interconnections are significant. Fumarate produced in the cycle feeds into the TCA cycle, while aspartate—derived from oxaloacetate via transamination—links back to nitrogen metabolism. Additionally, shuttles like the malate-aspartate shuttle help transport reducing equivalents and maintain metabolic balance across cellular compartments.

Structural Insights:

Advances in structural biology have illuminated the architecture of key enzymes in the cycle. For example, interactive models of CPS I reveal how a conformational change induced by NAG binding opens a tunnel necessary for efficient substrate channeling, while studies on argininosuccinate lyase and arginase illustrate the multi-subunit organization and active site features that facilitate catalysis.

Clinical and Biochemical Significance:

Defects in any step of the urea cycle can result in severe metabolic disorders, such as hyperammonemia. Understanding the cycle's regulation and its integration with other metabolic pathways is essential for appreciating how disruptions in enzyme activity or localization may impact overall metabolic health. Moreover, the cyclic nature of the pathway provides a model for understanding the efficiency of metabolic recycling, drawing parallels to broader concepts such as circular economies.

Overall, the urea cycle is not only a key detoxification pathway but also an exemplary model of metabolic regulation, enzyme mechanism, and the integration of cellular pathways in response to dietary and physiological demands.

This page titled 18.3: Nitrogen Excretion and the Urea Cycle is shared under a not declared license and was authored, remixed, and/or curated by Henry Jakubowski and Patricia Flatt.

- **11.2: Diffusion Across a Membrane - Passive and Facilitated Diffusion** by Henry Jakubowski and Patricia Flatt has no license indicated.

18.4: AN OVERVIEW OF AMINO ACID METABOLISM AND THE ROLE OF COFACTORS

LEARNING GOALS (CHATGPT O3-MINI)

- **Classify Amino Acids by Their Degradation Products:**
  • Identify which amino acids are purely glucogenic, purely ketogenic, or both, and explain the structural features that determine these classifications.
  • Compare the carbon skeleton fate (conversion to pyruvate, acetyl-CoA, or TCA intermediates) with respect to the number of carbon atoms in the amino acid side chains.
- **Trace the Metabolic Fate of Carbon Skeletons:**
  • Describe how deaminated amino acid carbon skeletons enter central metabolic pathways such as glycolysis and the TCA cycle.
  • Explain the concepts of anaplerotic reactions and how certain amino acids replenish TCA intermediates to support biosynthesis.
- **Understand Energy Production and Biosynthesis Integration:**
  • Evaluate how the breakdown of amino acids contributes to both energy production and the synthesis of new biomolecules.
  • Discuss the metabolic rationale behind why acetyl-CoA generated from amino acid degradation is ketogenic rather than glucogenic.
- **Examine the Role of Cofactors in Amino Acid Catabolism:**
  • Identify key cofactors (e.g., pyridoxal phosphate, NAD(P)+/NAD(P)H, tetrahydrofolate, and S-adenosylmethionine) and their roles in facilitating amino acid degradation reactions.
  • Analyze the importance of cofactors in stabilizing transition states, mediating electron flow, and transferring one-carbon units during catabolic reactions.
- **Explore One-Carbon (1C) Metabolism and Folate Chemistry:**
  • Explain how tetrahydrofolate (FH4) and its derivatives serve as carriers for one-carbon units in various oxidation states.
  • Describe the interconversion of FH4 derivatives and the role these reactions play in both nucleotide synthesis and amino acid metabolism.
- **Integrate the Methionine Cycle and SGOC Metabolism:**
  • Illustrate how methyl groups are transferred from N5-methyl FH4 to form methylcobalamin and then to homocysteine, culminating in methionine synthesis.
  • Understand the significance of the Serine Glycine One Carbon (SGOC) cycle in coordinating amino acid metabolism with anabolic processes, particularly in rapidly proliferating cells.
- **Connect Metabolic Pathways to Physiological and Clinical Contexts:**
  • Evaluate how alterations in amino acid degradation and one-carbon metabolism can affect overall metabolic homeostasis and lead to clinical conditions (e.g., megaloblastic anemia resulting from vitamin B12 deficiency).
  • Discuss the broader metabolic interconnections that minimize waste and maximize energy extraction from amino acids, reinforcing the concept of metabolic integration.

These learning goals are intended to help students not only memorize pathways and enzyme functions but also develop a deep, integrated understanding of how amino acid catabolism interlinks with other metabolic processes and its broader physiological significance.

18.4.1: AMINO ACID DEGRADATION

In the previous chapter, we saw how nitrogen is removed from amino acids to produce urea or NH_4^+. What are the fates of the remaining carbon skeletons? This section is where students might get overwhelmed by the diversity of amino acid degradation pathways, so it helps to realize that the carbon skeletons of deaminated amino acids can be used for biosynthesis or energy production and are converted to key glycolytic and TCA intermediates that you have seen many times before. Everything is interconnected, which makes the study of metabolism both daunting and fascinating, as organisms strive to extract all the energy and molecule-building atoms from a metabolite while minimizing waste.

Here are some key features of amino acid catabolism:

- some are converted to pyruvate, the end product of glycolysis and the start reactant of gluconeogenesis. Hence, these amino acids are **glucogenic**.
- some are converted to acetoacetyl-CoA and or acetyl-CoA. Both can be converted to ketone bodies (acetoacetate/β-hydroxybutyrate), which are considered **ketogenic**. Since the two carbons of the acetyl group of acetyl-CoA are lost as CO_2 in the TCA cycle, and there is no reverse for the pyruvate dehydrogenase reaction (pyr → acetyl-CoA), acetyl-CoA formed by amino acid degradation can not be used to create glucose in a net fashion.
- some are metabolized to form TCA intermediates. Since they are added in a **net** fashion to the TCA cycle and don't remove the existing pool of TCA intermediates, they can produce, in a **net** fashion, directly or indirectly, molecules that can be used to produce glucose. These entry reactions to the TCA, which replenish or add to TCA intermediates, are called **anaplerotic** (replenishing) reactions. Hence, these amino acids are also **glucogenic**.
- some have multiple ways to be degraded and can produce both acetyl-CoA and pyruvate, so they are **both glucogenic and ketogenic.**

Let's get more explicit:

- purely ketogenic: only Leu and Lys (the only amino acids whose name starts with **L,** and you have to **L**ove them since there are only two amino acids in this category)
- both: 5 including the aromatics - Trp, Tyr, Phe - and Ile/Thr
- purely glucogenic: the rest

General hints if an amino acid is glucogenic and/or ketogenic are derived from its structure.

Fully or Partly Ketogenic Amino Acids: Amino acids, except for Arg, that have a **continuous chain** of 3 or more carbon atoms in their **side chains** and hence are more "fat-like" are ketogenic or ketogenic/glucogenic. These include Lys, Leu, Ile, and the aromatic amino acids Phe, Trp, and Tyr, excluding Val. (note: Thr, both ketogenic and glucogenic, doesn't fit this rule). The wholly or partly ketogenic amino acids are shown in Figure 18.4.1.

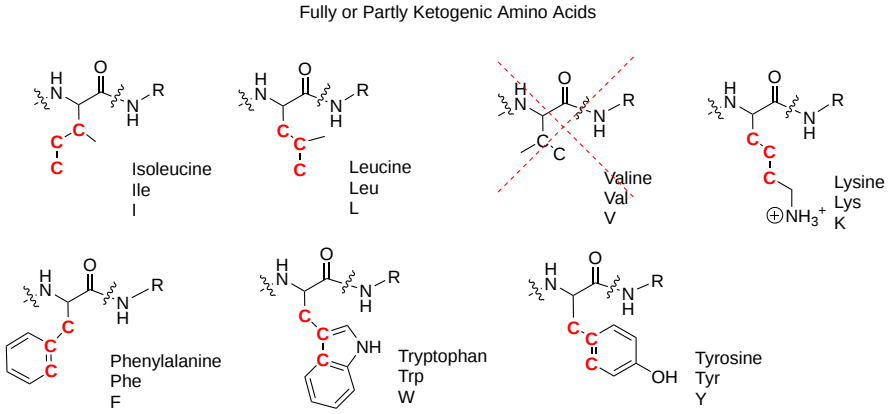


Figure 18.4.1: Fully or Partly Ketogenic Amino Acids

Purely Glucogenic Amino Acids (for Pyr and/or TCA intermediates): Which amino acids produce which intermediate? Except for glycine, it's pretty easy to remember. The number of carbons in the intermediate formed is the same as the number of carbons in the longest chain in the amino acid.

These amino acids form the 5C TCA intermediate alpha-ketoglutarate (2-oxoglutarate) and are shown in Figure 18.4.2.

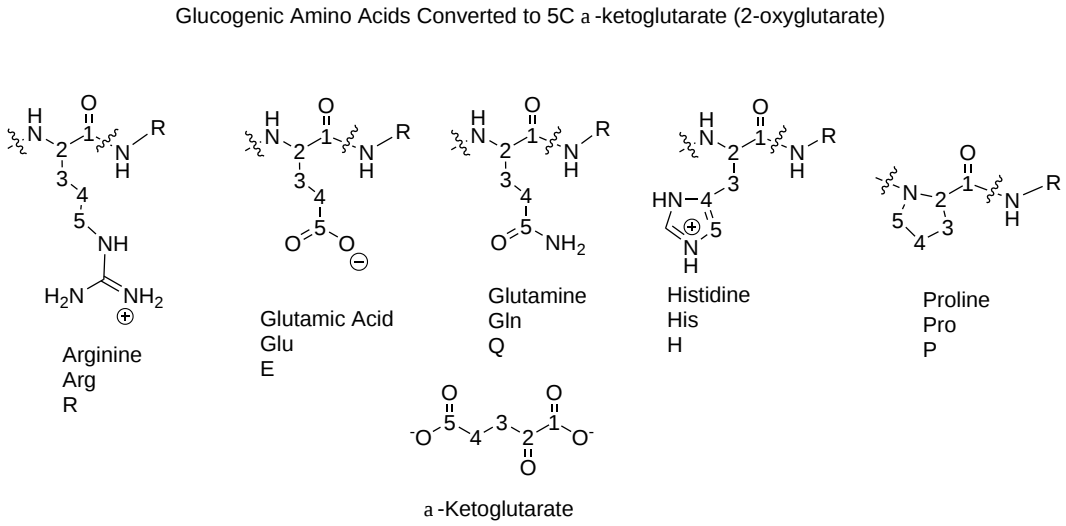


Figure **18.4.2**: Glucogenic Amino Acids Converted to 5C α-ketoglutarate (2-oxoglutarate)

These amino acids form either the 4C TCA intermediate succinate or oxaloacetate. Amino acids with more oxidized 4C atoms in the continuous chain produced oxaloacetate (which is more oxidized than succinate), while the least oxidized ones produced succinic acid (which is more reduced than oxaloacetate). These amino acids are shown in Figure **18.4.3**.

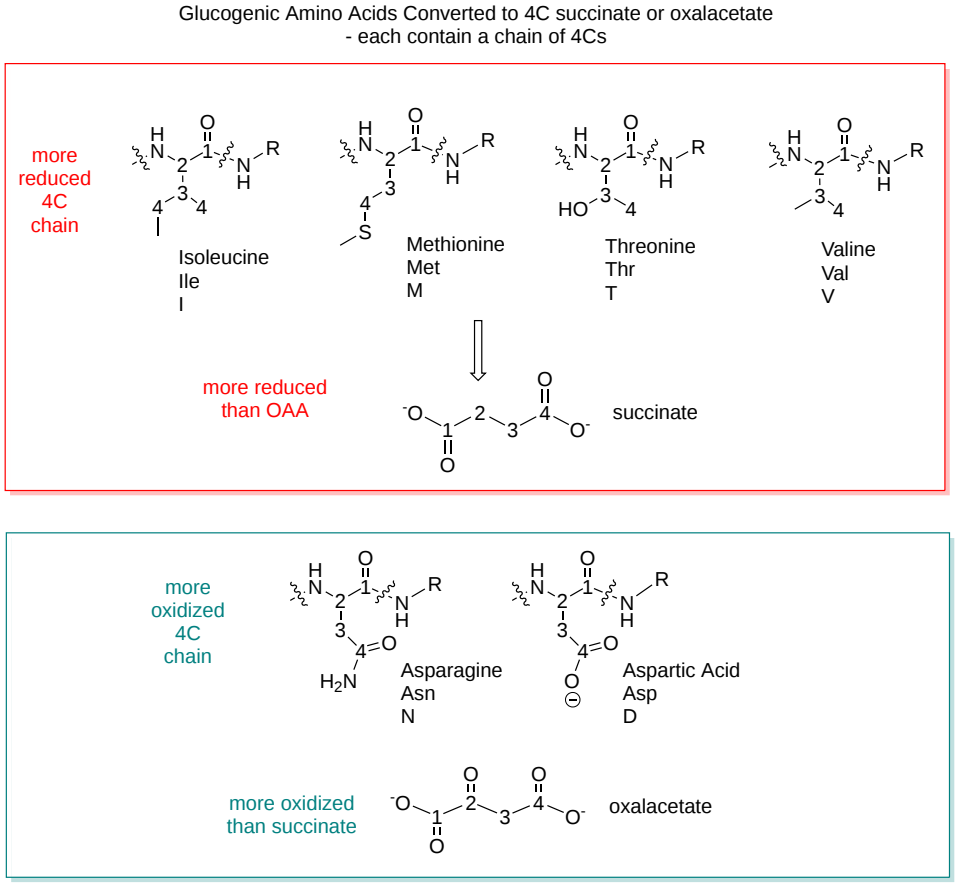


Figure **18.4.3**: Glucogenic Amino Acids Converted to 4C oxaloacetate and succinate

The 3C amino acids, Ser, Ala, and Cys, form pyruvate, as shown in Figure **18.4.4**. The only 2C amino acid, glycine, does as well.

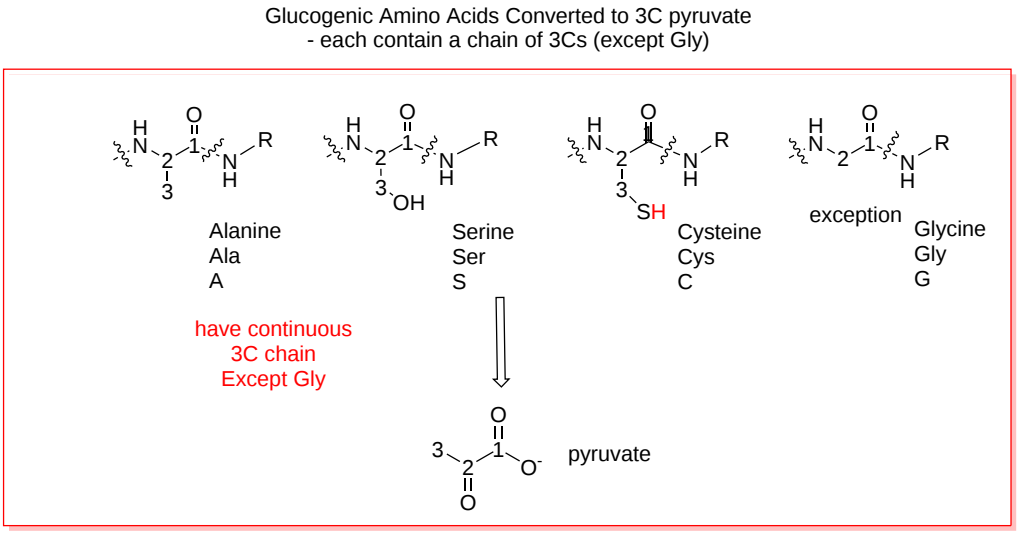


Figure 18.4.4: Glucogenic Amino Acids Converted to 3C pyruvate

A full figure summarizing everything above is shown in Figure 18.4.5!

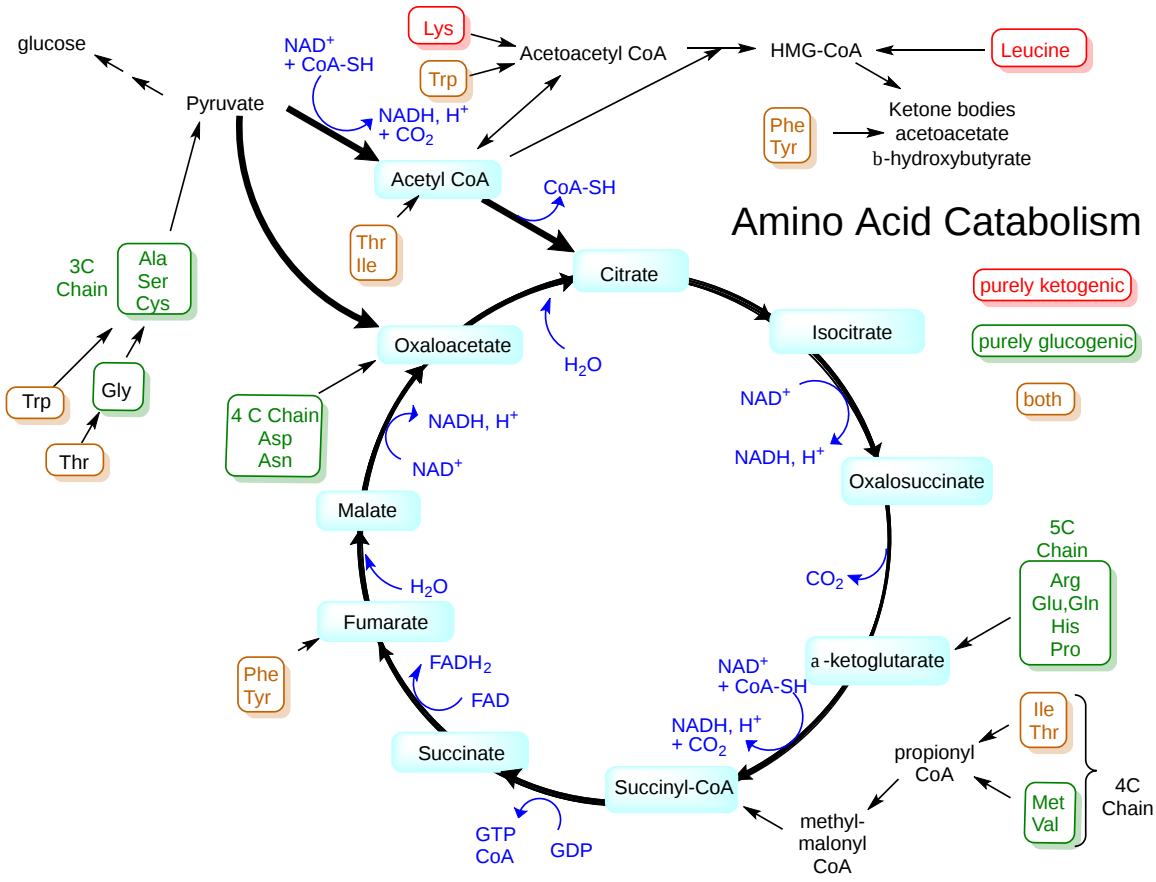


Figure 18.4.5: Summary of amino acid breakdown products

18.4.2: WITH A LITTLE HELP FROM MY FRIENDS: COFACTORS AND AMINO ACID CATABOLISM

The myriad of breaking, making, and rearranging carbon atoms in amino acid catabolism is daunting. As with all reactions, a pathway for a flow of electrons and stabilization of transition states and intermediates must be in place for the reactions to occur. All methods of catalysis (general acid/base, covalent/nucleophilic, electrostatic/metal ion, and preferential stabilization of the transition state) occur. Yet some reactions need additional "helpers" or "cofactors" to facilitate electron flow and shuttle small motifs (from electrons in redox reactions to

methyl groups in methylases) from one molecule to another. In the previous section, we've seen the important role of pyridoxal phosphate in transaminations/aminotransferases. Even the terminology cofactor is a bit confusing since analogous terms are used in different contexts:

- cofactors - nonprotein small molecules or ions (divalent ions, transition metal ions, and Fe/S clusters, for example) that must bind to an enzyme but usually stay put once bound. That is, they don't dissociate during the catalytic cycle. For instance, PLP must initially bind to an enzyme but then becomes covalently attached through a Schiff base through the epsilon amino group of a Lys in the catalytic site. For example, that linkage might be swapped with an incoming amino acid substrate but reform in the catalytic cycle, allowing the enzyme to remain functional.
- coenzyme - a vitamin derivative, organic cofactor, as compared to inorganic ions. Coenzyme is a poor historical name that persists.
- prosthetic group - this is usually a coenzyme that is either covalently bound (like PLP) or noncovalently bound with such a low K_D (like FAD/$FADH_2$-containing enzymes) that they stay bound
- cosubstrate - these bind as substrate (for example, NAD^+), and depart as products (for example, NADH).

Here is a table of common nonmetallic cofactors.

Cofactor	Vitamin Derivative	Carrier
biotin	H - biotin	1 C - CO_2 (most oxidized)
tetrahydrofolic acid (FH_4 or THF)	B9 - folic acid	1C - formyl, -(C=O)H, methylene (-CH_2) (more reduced) and methyl -CH_3
cobalamin	B12 - cobalamin	methyl CH_3
thiamine pyrophosphate	B1 - Thiamine	2C group
coenzyme A	B5 - pantothenic acids	acetyl (CH_3-C=O) and acyl (R-C=O)
pyridoxal phosphate	B6 - pyridoxine	amino and carboxyl groups
NAD^+/$NADP^+$	B3 - Niacin	electrons
FAD/FMN	B2 - riboflavin	electrons

Other non-vitamin cofactors include S-adenosylmethionine (SAM or adoMet), a carrier of methyl groups; Coenzyme Q, a carrier of electrons; tetrahydrobiopterin, a carrier of oxygen and electrons; and heme, a carrier of electrons.

We've already described amino acid deamination reactions using PLP. Now let's consider the biochemistry of two of these cofactors involved in 1 C transfers in amino acid metabolism in more detail, tetrahydrofolate (FH_4) and SAM.

18.4.3: TETRAHYDROFOLATE (FH_4)

Tetrahydrofolate (FH_4) is a key cofactor in the metabolism of amino acids and the biosynthesis of nucleotides. It is also commonly abbreviated as THF, especially in the names of enzymes that use it. To avoid confusion with chemists' use of THF for tetrahydrofuran, it will be referred to mostly here as FH_4; however, the enzymes will be named as derivatives of the abbreviation XHF (X = D for dihydro and T for tetrahydro).

FH_4 is a carrier of 1 C units in various oxidation states. It receives 1C units and then transfers them to other species. The structure of FH_4 and derivatives carrying 1 C units with different oxidation numbers (indicating their oxidation state) are shown in Figure **18.4.6**.

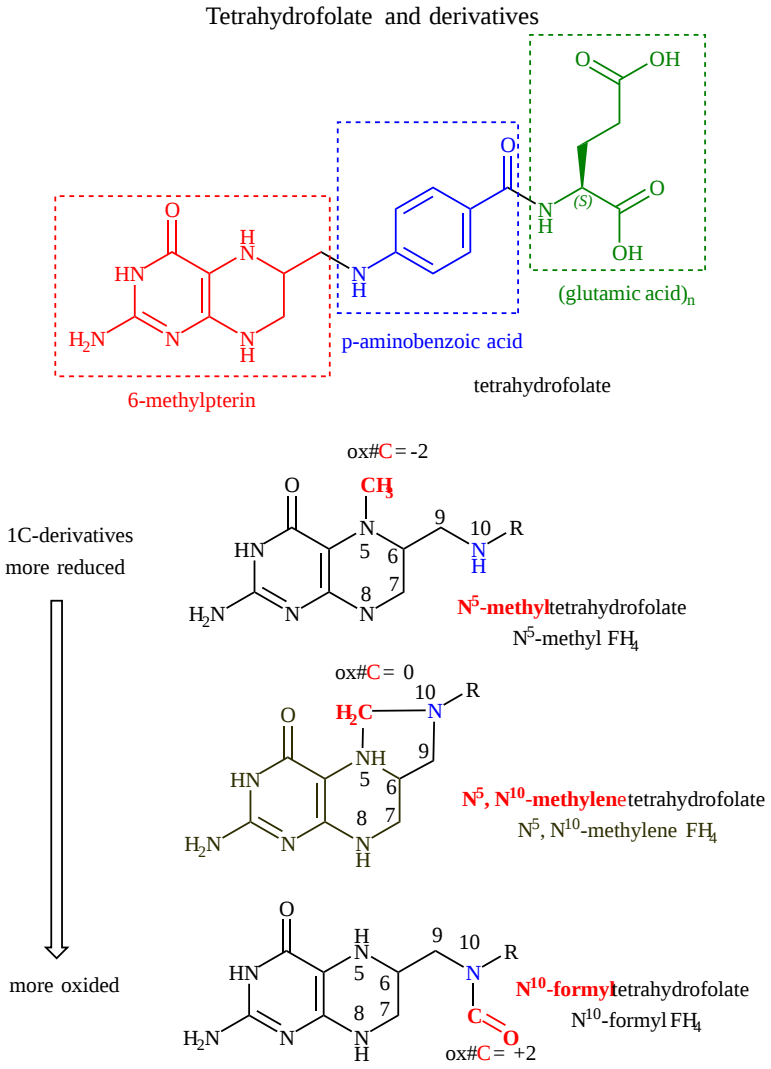
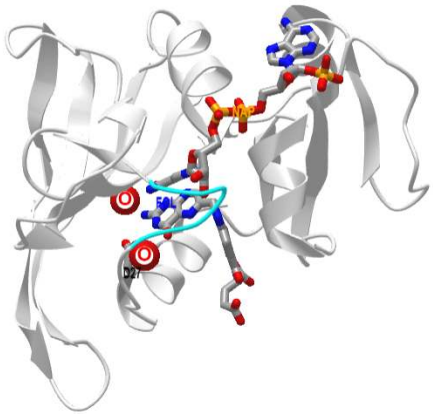


Figure **18.4.6**: 1C derivatives in different oxidation states for tetrahydrofolate

FH_4 is made from the vitamin folate (bacteria, fungi, and most plants can synthesize it), which is first converted to dihydrofolate (FH_2) and then tetrahydrofolate (FH_4) by the enzyme dihydrofolate reductase, using NADPH as a reducing substrate "cofactor." The model below depicts this small enzyme complexed with NADPH ($NADP^+$), folate, and DHFR (7dfr). Folate (FOL) is shown in salmon space fill, while NADPH is shown in cyan.

Figure **18.4.7** shows an interactive iCn3D model of dihydrofolate reductase with bound NADPH ($NADP^+$) and folate (7dfr).



NCBI iCn3D Figure **18.4.7**: Dihydrofolate reductase with bound $NADP^+$ and folate (7dfr). (Copyright; author via source). Click the image for a popup or use this external link: https://structure.ncbi.nlm.nih.gov/i...ojdpBZuQH8Lm96

Folate (FOL) and $NADP^+$ (NAP) are shown in spacefill and CPK colors. The side chain of Asp 27 is shown in sticks and CPK colors. The oxygen atoms of two water molecules interacting with folate are shown as red spheres. A disordered and, hence, mobile loop (residues 16-20) that binds the nicotinamide is shown in cyan.

As FH_4 is a key substrate in many reactions, including nucleotide synthesis (as we shall see later), this enzyme is a key target for chemotherapy to kill cancer cells, which require robust nucleotide synthesis for rapid cell proliferation. One such drug, which inhibits the enzyme, methotrexate, is shown in Figure **18.4.8**.

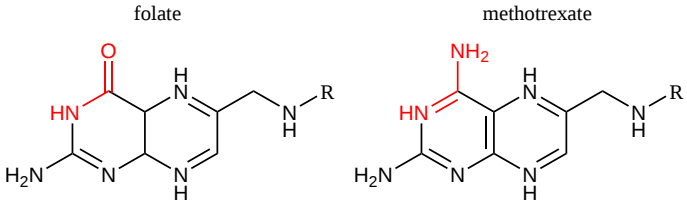


Figure **18.4.8**: A structural comparison of the chemotherapeutic drug methotrexate and folate

Before getting into the nitty-gritty of amino acid degradation and tetrahydrofolate chemistry, let's take a look at the mechanism by which dihydrofolate reductase, DHFR, catalyzes the sequential reduction by 2 NADPH molecules of folate to tetrahydrofolate. This is illustrated in Figure **18.4.9**.

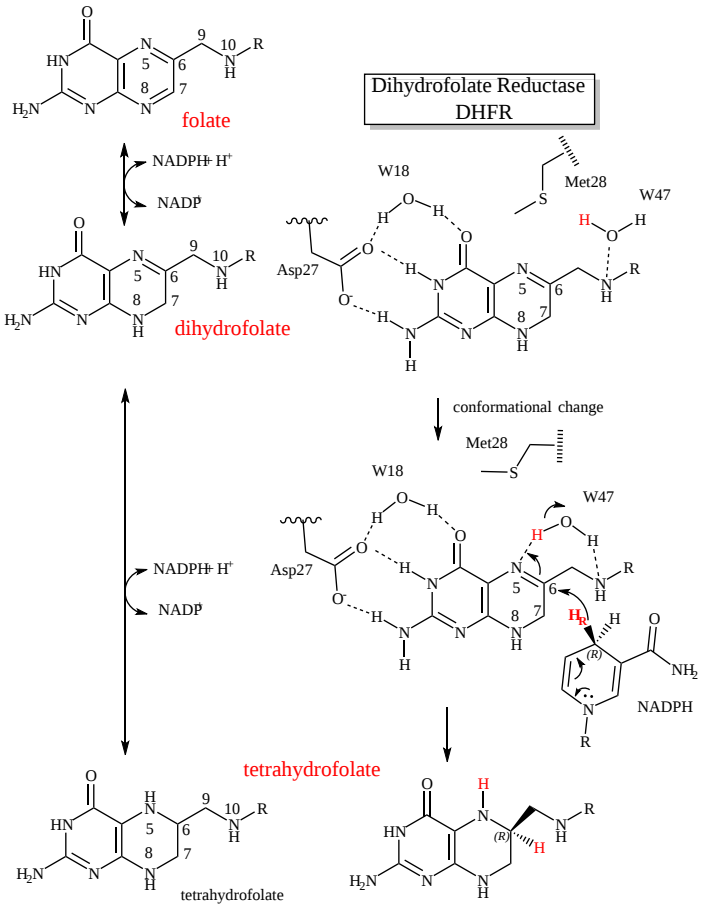


Figure **18.4.9**: Conversion of folate to tetrahydrofolate by dihydrofolate reductase

18.4.4: ONE CARBON CHEMISTRY: THE INTERCONVERSION OF FH_4 1C DERIVATIVES

Tetrahydrofolate is a carrier for 1C units in metabolism. As such, it is intimately involved in many anabolic and catabolic reactions. These include thymidine and purine biosynthesis and amino acid metabolism through reactions involving serine, glycine (both with 1C in their

side chains), and methionine (with 1C after the sulfur in the side chain). Reactions occur in both the cytoplasm and mitochondria. FH_4 is involved directly or indirectly in the epigenetic control of DNA expression, as methylation of both DNA and histones is critical to gene expression. The myriad of 1C derivatives of FH_4 makes the biochemistry complex. Since the transfer of 1C is a critical job in the breakdown of amino acids' carbon skeleton and biosynthesis, we need to explore it. The complexity is simplified by noting that the 1C derivatives have only three different oxidation states (+2, 0, and -2), as noted in Figure **18.4.10**.

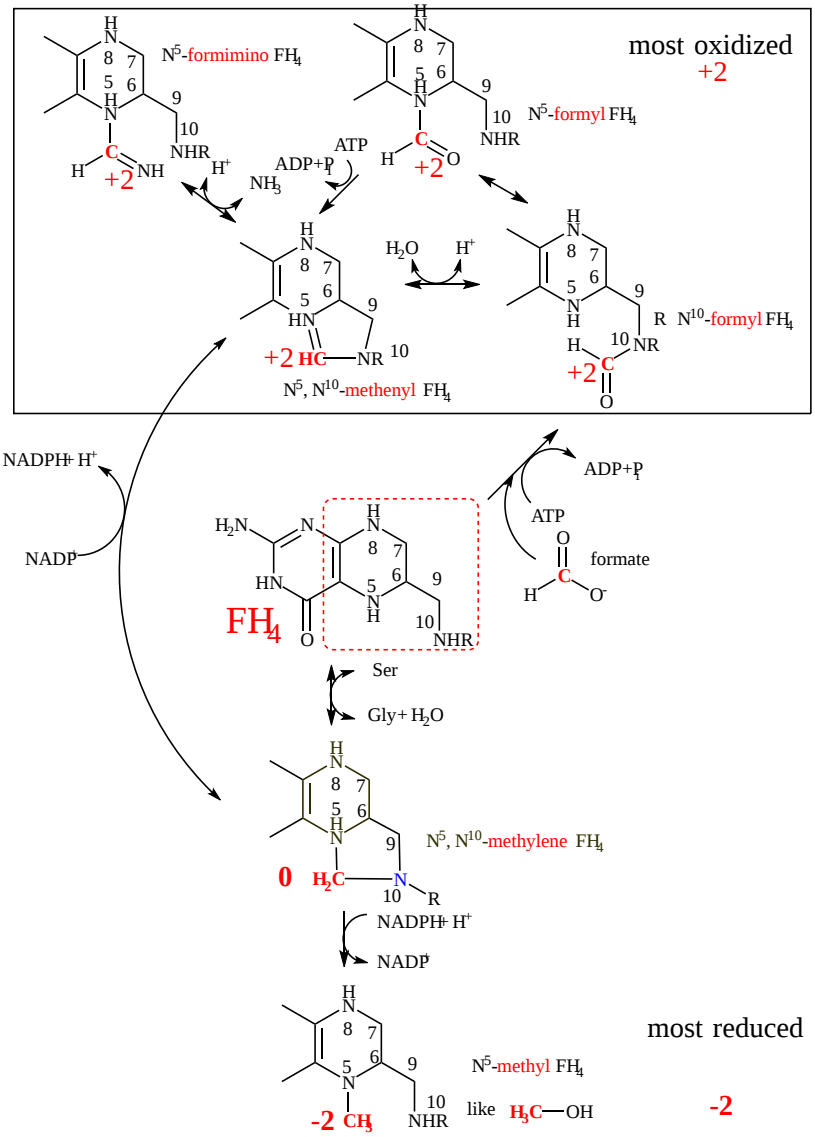


Figure **18.4.10**: Interconversion of 1C derivatives of tetrahydrofolate. The oxidation number of the 1C addition is shown in red. (after http://education.med.nyu.edu/mbm/aminoAcids/folate.shtml)

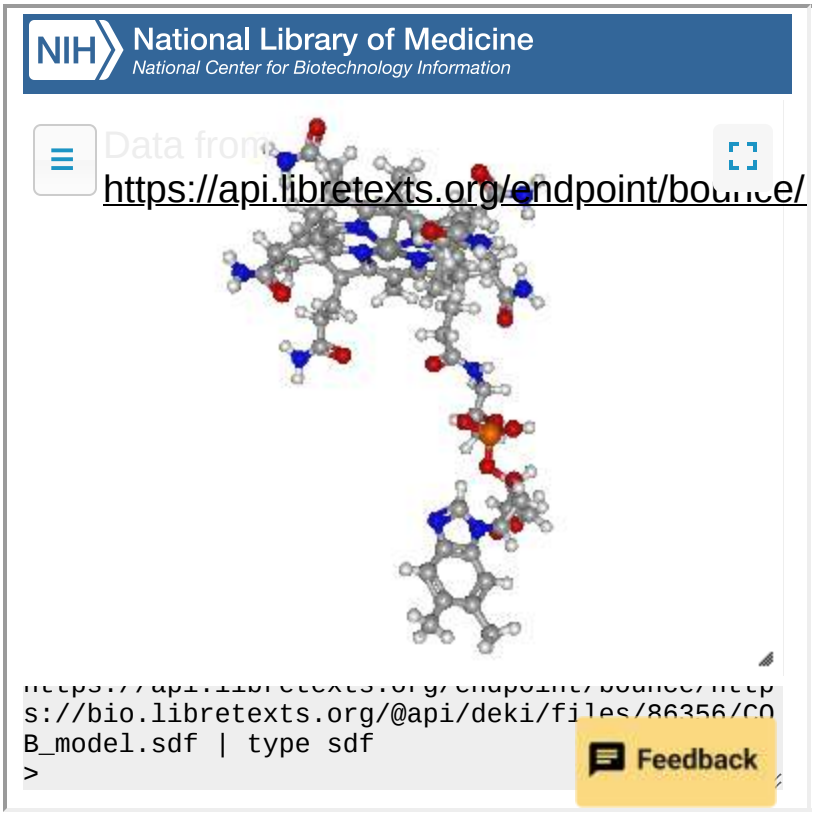
1C units usually enter FH_4 as the N^5,N^{10} methylene unit. This is made in the cytoplasm and mitochondria since 1C-derivatized FH_4 appears not to cross the mitochondrial membranes. The methylene derivative (with a 1C oxidation # = 0) can be reduced to form methyl (oxidation # -2) or oxidized to methenyl or formyl groups (oxidation # +2).

We will revisit some of these reactions in chapters that deal with amino acid and nucleotide biosynthesis. That's not a bad thing—learning occurs best when material is repeated in different contexts.

Methylcobalamin and ^{5}N-methyl FH_4

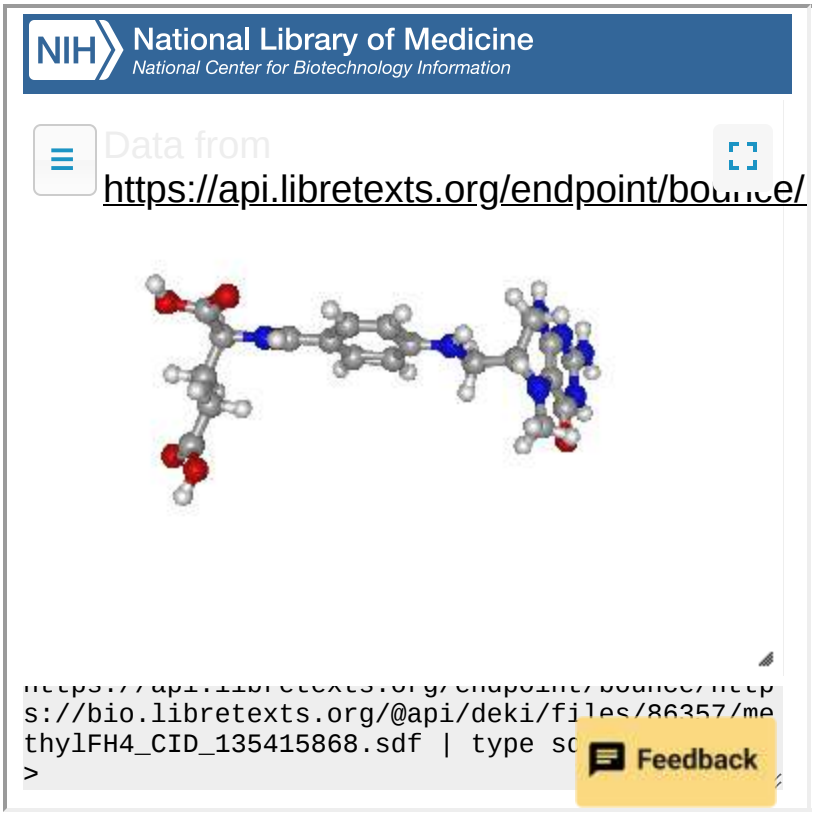
Methyl groups can be stored and transferred from ^{5}N-methyl FH_4 to another cofactor, cobalamine, to form methylcobalamin (Vitamin B12). The $-CH_3$ can then be transferred to homocysteine (the side chain is the same as for Cys but with one extra $-CH_2$ methylene group) to form methionine. This adds to the complexity of 1C transfer, but the iCn3D models below should help you to differentiate the chemical structures of each.

Here is a model of methylcobalamin (vitamin B12) in ball-and-stick form.



Note that the -CH_3 is connected to the center cobalt in the macrocyclic ring.

In contrast, here is the structure of N^5-methyl FH_4.



The -CH_3 here is connected to a ring N5 of FH_4.

18.4.5: SERINE HYDROXYMETHYLTRANSFERASE (SHMT): A COMPLEX REACTION NEEDS TWO COFACTORS - PLP AND FH_4

Let's examine one mechanism that illustrates how a 1C methylene is added to tetrahydrofolate (FH_4). The mechanism shown is for serine dehydratase, also known as serine hydroxymethyltransferase. The enzyme not only uses tetrahydrofolate as a substrate but also PLP, which, as we have seen previously, forms bonds to the alpha-carbon of amino acids that are labile to cleavage. In this case, the amino acid serine dehydrates through an alpha-elimination reaction. Here is the overall reaction.

$$\text{Serine} + FH_4 \leftrightarrow \text{Glycine} + N^5,N^{10}\text{-}CH_2\text{-}FH_4 + H_2O$$

Figure **18.4.11** shows the dehydration reaction and formation of glycine, using PLP as a cofactor. Figure B shows how the released formaldehyde reacts with FH_4 to form N^5,N^{10}-methylene FH4, using FH_4 as a cofactor. As this is needed in purine and thymidylate synthesis, SHMT is also a target for malaria treatment.

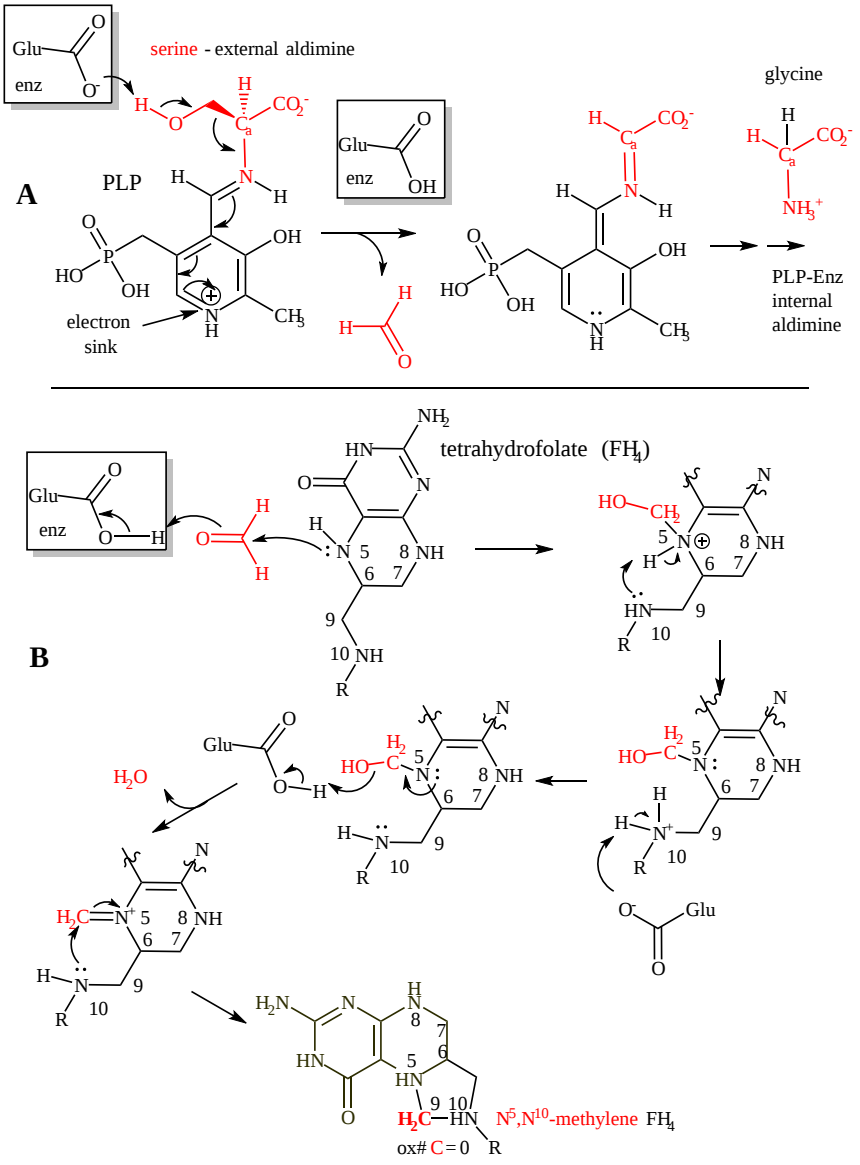


Figure **18.4.11**: Serine hydroxymethyltransferase reaction mechanism

Glu 57 plays a key role as a general acid/base throughout the catalytic cycle of the enzyme.

Pathway diagrams showing a myriad of reactants, products, and enzymes can be very confusing. It's helpful to think about them and see them in different ways. Here is another way to present the conversion of FH_4 and its various 1C intermediates. Figure **18.4.12** concentrates on the **outputs** of 1C FH_4 derivatives (shown in blue eclipses).

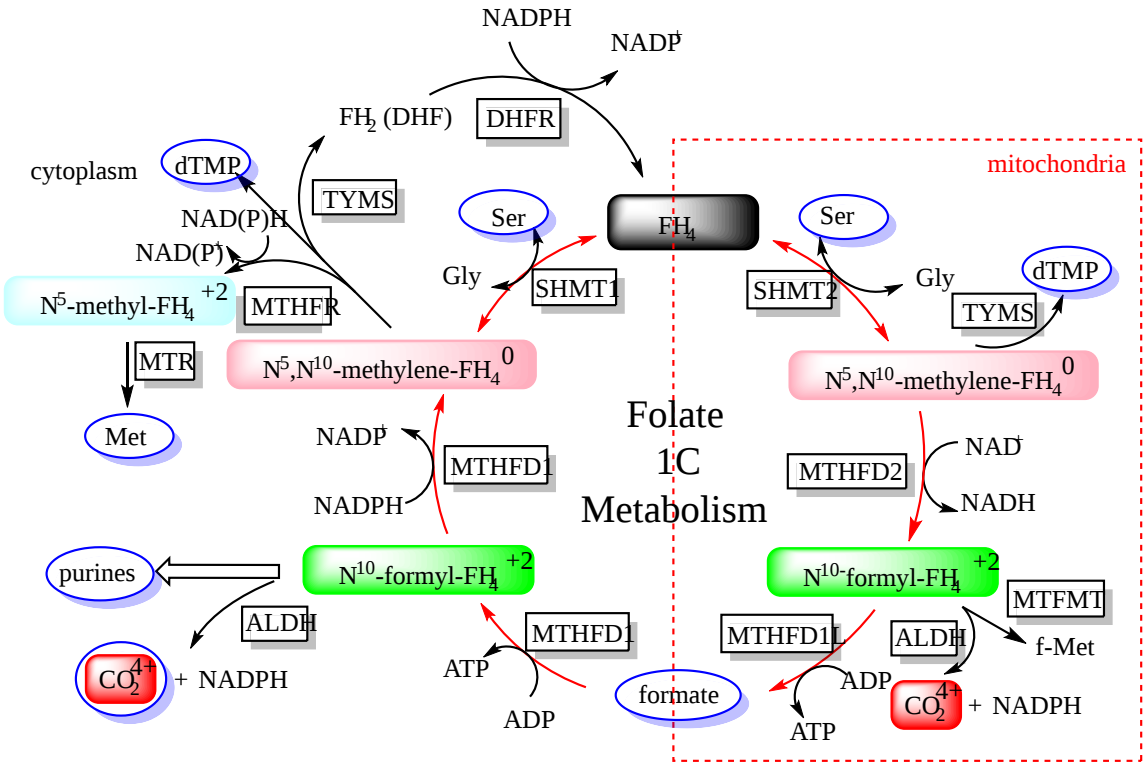


Figure **18.4.12**: Folate 1C Metabolism - Cyclic Presentation after Ducker and Rabinowitz, Cell Metab. 2017 January 10; 25(1): 27–42. doi:10.1016/j.cmet.2016.08.009

The enzymes catalyzing these reactions are shown in the table below. This figure applies to both catabolic and anabolic reactions using FH_4 derivatives. Oxidation numbers for the 1C adducts are shown. Any reaction that changes the redox state must use $NAD(P)^+$/NAD(P)H as a redox reagent.

- N^5,N^{10}-methylene FH_4 gives thymidine and serine
- N^5-methyl FH_4 gives methionine
- N^{10}-formyl FH_4 gives formate, purines, and CO_2
- N^5-formyl serves more as a passive reservoir of 1C units.

Table **18.4.1**: Enzymes catalyzing interconversions of THF derivatives

Abbreviation	Enzyme Name
ALDH	10-formyltetrahydrofolate((aldehyde) dehydrogenase.
DHFR	Dihydrofolate reductase
MTHFD	methylenetetrahydrofolate dehydrogenase
MTHFD1	C-1-tetrahydrofolate synthase, cytoplasmic
MTHFD1L	monofunctional tetrahydrofolate synthase, mitochondrial
MTHFD2/L	methylenetetrahydrofolate dehydrogenase 2/2-like
MTFMT	mitochondrial methionyl-tRNA formyltransferase
MTHFR	methylenetetrahydrofolate reductase
MTR	methionine synthase
TYMS	thymidylate synthetase

A key enzyme in these reactions, methylene-THF reductase (MTHFR), irreversibly removes 1C from the cycle depicted above as it forms N^5-methyl FH_4. As this reaction is a reduction, it requires a reducing agent (NADPH in yeast and animals and NADH in plants). As we will see next, this irreversible removal would deplete the cycle shown; therefore, it is allosterically regulated (inhibited) by another methylating agent, S-adenosylmethionine (SAM, also known as adoMet). Plant versions of the enzyme are reversible, so SAM does not need to regulate them in this feedback loop process.

18.4.6: S-ADENOSYLMETHIONINE (SAM), ALSO KNOWN AS ADOMET

N^5-methyl FH_4 appears to have one function: to methylate a molecule called homocysteine (same as Cys but with an extra -CH_2 in the side chain) to methionine. This is adenosylated (not phosphorylated!) with ATP to produce S-adenosylmethionine (SAM), a more potent methylating agent than N^5-methyl FH_4. SAM is, hence, part of a cycle involving N5-methyl-FH4. The methyl group of N^5-methyl FH_4 reacts with homocysteine to produce methionine, catalyzed by the enzyme methionine synthase, which requires cobalamin (vitamin B12) as a cofactor. The combined Figure **18.4.13** adds the Met and Folate cycles (showing the outputs of the 1C Folate metabolism cycle.

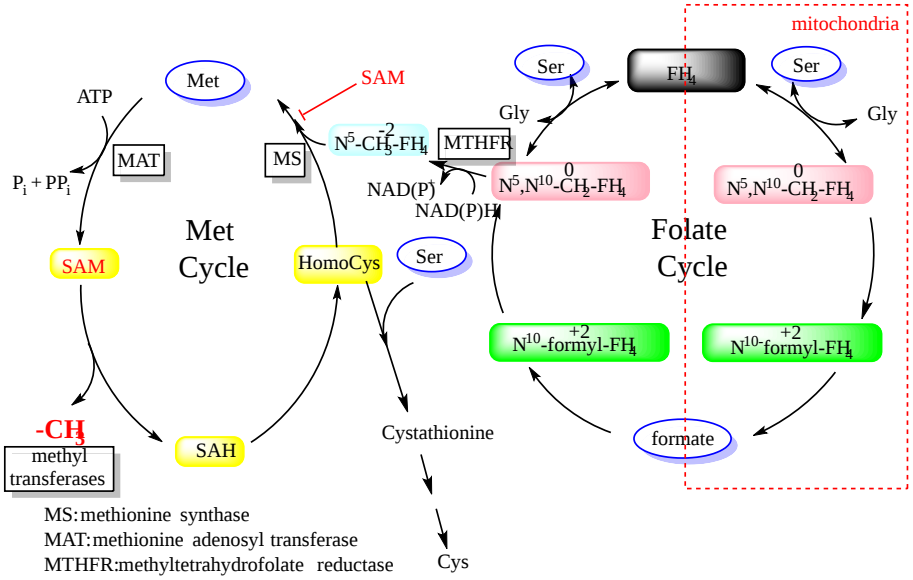


Figure **18.4.13**: Folate and Methionine Cycle (after Ducker and Rabinowitz, Cell Metab. 2017 Jan 10; 25(1): 27–42.)

Figure 18.4.14 shows the structures of molecules in the Met Cycle.

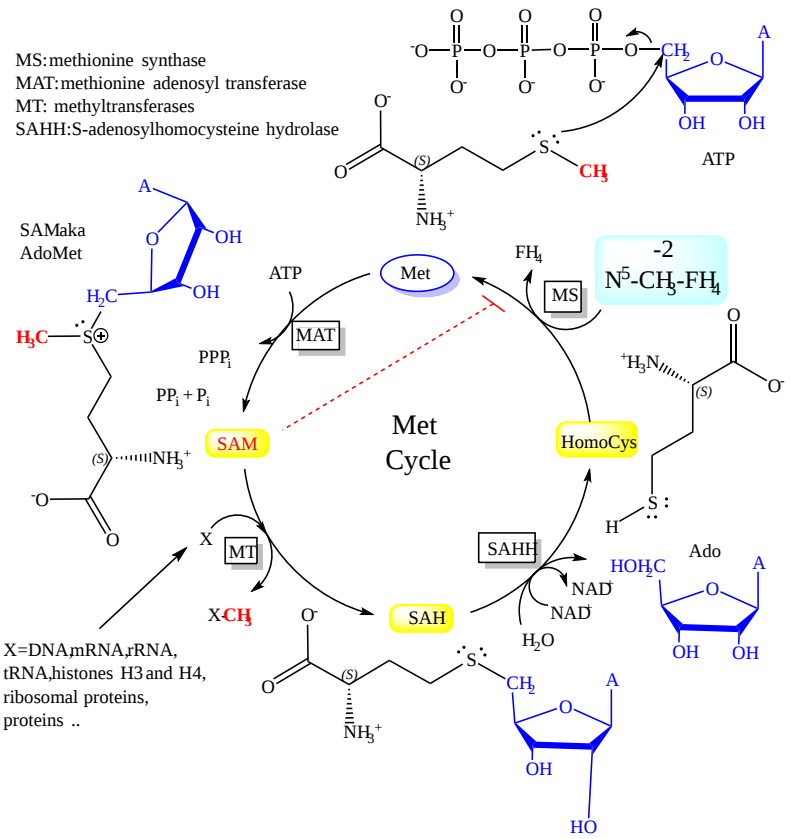
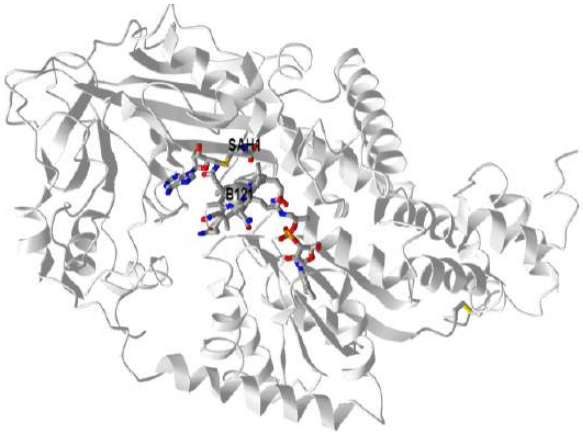


Figure **18.4.14**: The Met Cycle and Methylations by SAM

The mechanism of methyl transfers using SAM as the -CH_3 donor involves an SN_2 attack by a nucleophile of the substrate on the CH_3 of SAM, with the electron pair from the C-S bond going to the positively charged sulfonium sulfur, a great "electron sink". An analogous nucleophilic attack on the terminal CH_3 of plain old methionine would not be readily enabled. Hence, SAM, with its charged S, has a much higher methyl transfer potential than N^5-CH_3-FH_4.

In the actual reaction catalyzed by methionine synthase (MS) in mammals, the methyl-CH_3 from N^5-methyl FH_4 is first transferred to cobalamin, a derivative of vitamin B12, to form methylcobalamin, which then transfers it to homocysteine. The structure of the C-terminal half of B_{12}-dependent Methionine Synthase from *E. Coli* with bound adenosylhomocysteine (3iva) is shown below and in this link:

Figure **18.4.15** shows an interactive iCn3D model of the C-terminal half of B_{12}-dependent Methionine Synthase from *E. Coli* with bound adenosylhomocysteine bound (3iva)



NCBI iCn3D Figure **18.4.15**: C-terminal half of B_{12}-dependent Methionine Synthase from *E. Coli* with bound adenosylhomocysteine (3iva). (Copyright; author via source). Click the image for a popup or use this external link:

https://structure.ncbi.nlm.nih.gov/i...E7jTsdvVvx1M1A

In mammals, vitamin B_{12} is a key cofactor in only two enzymes. One is methionine synthase. The other catalyzes the conversion of methylmalonyl-CoA (derived from the metabolism of Ile, Thr, Val, and Met (as we will see in the next chapter section) to succinyl-CoA in the citric acid cycle. If vitamin B_{12} is lacking, N^5-methyl FH_4 builds up when it can't be transferred to cobalamin to form methylcobalamin, the direct methylating agent in methionine synthesis catalyzed by methionine synthase. Hence, homocysteine builds up as it can't form methionine. Since the enzyme that converts N^5,N^{10}-methylene FH_4 to N^5-methyl FH_4, methylenetetrahydrofolate reductase (MTHFR), is irreversible, levels of N^5-methyl FH_4 are high. You can view N^5-methyl FH_4 as a storage form of folate, so if there is a lack of B12, the use of this storage form of folate becomes impaired. The results of B12 deficiency include megaloblastic anemia.

18.4.7: THE SERINE GLYCINE ONE CARBON (SGOC) METABOLIC CYCLE

Figure 12 illustrates the coupled Folate and Methionine cycles, highlighting the intermediates involved in the 1C-CH_3 transfer reaction, a crucial aspect of amino acid metabolism and other anabolic and catabolic processes. Interpreting metabolic figures is complicated. Each is designed to emphasize certain selected features. Another way to present Figure 12 is to emphasize the metabolites involved in 1C chemistry. Figure **18.4.145** shows what has been called the **Serine Glycine One Carbon (SGOC)** metabolic cycle. It is simply a redrawn version of Figure 12, with attention drawn to non-FH4 molecules involved in 1C transfers, specifically serine, glycine, and formate.

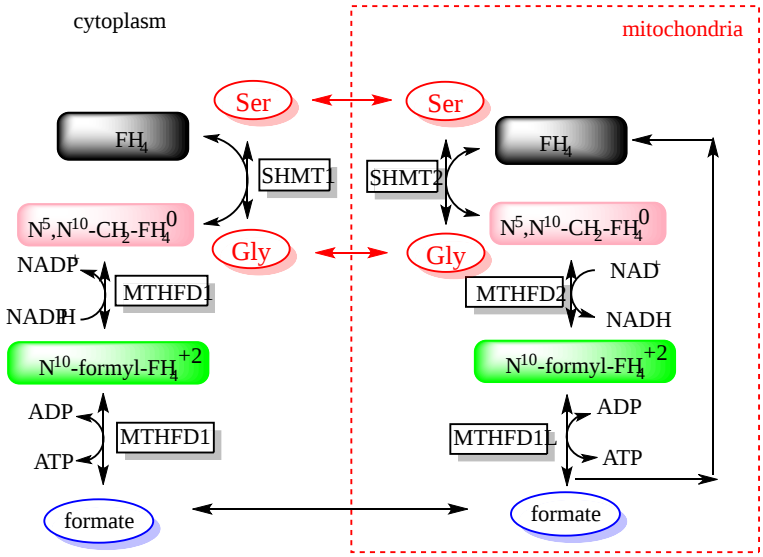


Figure **18.4.15**: The Ser-Gly One Carbon (SGOC) Cycle

This cycle, along with its key substrates serine and glycine, integrates numerous metabolic pathways and regulates the conversion of serine and glycine into essential outputs for other pathways. We will see this cycle again in the chapter on the biosynthesis of amino acids. The pathway is especially important in tumor cells, which need precursors for nucleic acid, protein, and lipid synthesis.

18.4.8: SUMMARY

Amino acid degradation not only provides a mechanism to dispose of excess nitrogen (via urea or direct NH_4^+ excretion) but also channels the remaining carbon skeletons into central metabolic pathways. This chapter explores how deaminated carbon skeletons are converted into key intermediates for energy production and biosynthesis, emphasizing the following core concepts:

Fates of Carbon Skeletons:

- **Glucogenic Pathways:**
  Many amino acids are broken down into intermediates such as pyruvate, oxaloacetate, succinate, or α-ketoglutarate, which can enter the TCA cycle. These pathways can ultimately contribute to gluconeogenesis, replenishing blood glucose levels.
- **Ketogenic Pathways:**
  A smaller subset of amino acids (notably leucine and lysine) is converted to acetyl-CoA or acetoacetyl-CoA. These intermediates can be used to form ketone bodies, since acetyl-CoA's carbons are lost as CO_2 in the TCA cycle and cannot be net used for gluconeogenesis.
- **Dual Role Amino Acids:**
  Some amino acids can give rise to both glucogenic and ketogenic products, reflecting their diverse metabolic fates.

Structural Determinants:
Amino acids with longer, continuous carbon chains in their side groups tend to be ketogenic or both, while those yielding intermediates with the same carbon number as their longest chain tend to be glucogenic. These distinctions are crucial for understanding metabolic flexibility and energy extraction.

Role of Cofactors in Catabolism:
Enzyme-catalyzed degradation of amino acids relies on various cofactors that:

- **Stabilize Transition States:** For example, pyridoxal phosphate (PLP) is essential in transamination reactions.
- **Mediate Electron and Group Transfers:** $NAD(P)^+$/NAD(P)H, as well as other cofactors like coenzyme A, are critical for oxidation–reduction and acyl group transfers during the breakdown of carbon skeletons.

One-Carbon Metabolism and Folate Chemistry:
The chapter delves into the importance of one-carbon (1C) transfers, primarily mediated by tetrahydrofolate (FH_4) and its derivatives:

- **Diverse 1C Forms:** FH_4 can carry one-carbon units in various oxidation states (e.g., methylene, methyl, formyl), which are central to both nucleotide biosynthesis and amino acid metabolism.
- **Interconnected Cycles:** The interconversion between FH_4 derivatives underpins the folate and methionine cycles. For instance, the conversion of N5,N10-methylene FH_4 to N5-methyl FH_4 is an irreversible step catalyzed by methylenetetrahydrofolate reductase (MTHFR) and is tightly regulated.
- **Methyl Group Transfer:** Methylcobalamin (a derivative of vitamin B_{12}) plays a crucial role in transferring methyl groups from N5-methyl FH_4 to homocysteine, thereby generating methionine. This interrelationship is central to epigenetic regulation and metabolic control.

The Serine Glycine One-Carbon (SGOC) Cycle:
An emerging concept discussed is the SGOC cycle, which integrates serine and glycine metabolism with 1C transfers. This cycle is pivotal not only for maintaining nucleotide pools and redox balance but also for supporting the anabolic demands of rapidly proliferating cells, such as those found in tumors.

Overall Integration and Physiological Impact:
The degradation of amino acids illustrates the broader theme of metabolic integration—how the body efficiently recycles carbon skeletons for energy and biosynthesis while ensuring minimal waste. These pathways, their regulation by cofactors, and the integration of 1C metabolism underscore the elegance and complexity of metabolic control, with direct implications for understanding metabolic disorders and therapeutic interventions (e.g., targeting DHFR in cancer chemotherapy).

In summary, this chapter provides a comprehensive look at how amino acid catabolism is interwoven with central metabolic pathways, emphasizing the structural, enzymatic, and regulatory mechanisms that govern the fate of carbon skeletons and one-carbon units in cellular metabolism.

This page titled 18.4: An Overview of Amino Acid Metabolism and the Role of Cofactors is shared under a not declared license and was authored, remixed, and/or curated by Henry Jakubowski and Patricia Flatt.

- **11.2: Diffusion Across a Membrane - Passive and Facilitated Diffusion** by Henry Jakubowski and Patricia Flatt has no license indicated.

18.5: PATHWAYS OF AMINO ACID DEGRADATION

LEARNING GOALS (CHATGPT O3-MINI)

- **Differentiate Amino Acid Fates:**
  • Categorize amino acids as purely glucogenic, purely ketogenic, or both, and explain the structural reasons behind these classifications.
  • Identify which amino acids are converted to pyruvate, acetyl-CoA (or acetoacetate), TCA cycle intermediates (e.g., α-ketoglutarate, succinyl-CoA), or have multiple fates.
- **Trace Metabolic Pathways:**
  • Map the key pathways for converting amino acid carbon skeletons into central metabolites, such as the conversion of alanine to pyruvate or threonine to glycine, propionyl-CoA, and ultimately succinyl-CoA.
  • Explain how different pathways (e.g., the VOMIT pathway for valine, isoleucine, threonine, and methionine) replenish the TCA cycle via anaplerotic reactions.
- **Understand Enzymatic Reactions and Cofactor Roles:**
  • Describe the role of PLP-dependent enzymes in transamination and deamination reactions that facilitate the conversion of amino acids to pyruvate and other intermediates.
  • Identify the key cofactors (such as PLP, NAD^+/NADH, tetrahydrobiopterin, and biotin) involved in these pathways and explain their specific functions.
- **Analyze Pathway Integration:**
  • Explain how the degradation of amino acids integrates with gluconeogenesis, ketogenesis, and the TCA cycle, emphasizing the importance of metabolic flexibility.
  • Discuss the interplay between amino acid degradation and energy metabolism, including the implications for fasting states and overall metabolic homeostasis.
- **Explore Specific Pathway Examples:**
  • Detail the conversion of tryptophan to alanine and acetoacetate, highlighting the branching of pathways that contribute to both glucogenic and ketogenic outcomes.
  • Compare and contrast the metabolism of amino acids like lysine (via saccharopine and acetoacetyl-CoA formation) with the pathways leading from branched-chain amino acids (Val, Ile, and Leu) to succinyl-CoA or acetyl-CoA.
- **Relate Metabolic Pathways to Physiology:**
  • Interpret how these catabolic processes contribute to overall cellular metabolism and the maintenance of energy balance, especially during protein breakdown or fasting.
  • Evaluate the significance of amino acid catabolism in the context of systemic nitrogen and carbon balance as well as its clinical implications, as highlighted by integrated pathway diagrams like the Reactome summary.

These learning goals are designed to help students build a comprehensive understanding of how amino acid carbon skeletons are processed during degradation, reinforcing both the biochemical mechanisms and the broader physiological context of these pathways.

18.5.1: INTRODUCTION

In previous sections, we saw how nitrogen is removed from amino acids to produce urea or NH_4^+, that some amino acids are glucogenic, ketogenic, or both, and the role of tetrahydrofolate derivatives and S-adenosylmethionine in 1C transfer reactions. Now, we can focus on how the carbon skeletons of amino acids are processed during degradation.

Here are some key features of amino acid catabolism that were discussed in the previous section.

- some are converted to pyruvate, the end product of glycolysis and the start reactant of gluconeogenesis. Hence, these amino acids are **glucogenic**;
- some are converted to acetoacetate-CoA and or acetyl-CoA. Both can be converted into ketone bodies (acetoacetate and β-hydroxybutyrate), which are considered **ketogenic**. Since the two carbons of the acetyl group of acetyl-CoA are lost as CO_2 in the TCA cycle, and there is no reverse for the pyruvate dehydrogenase reaction (pyr → acetyl-CoA), acetyl-CoA formed by amino acid degradation can not be used to create glucose in a net fashion;
- some are metabolized to form TCA intermediates. Since they are added in a **net** fashion to the TCA cycle and don't remove the existing pool of TCA intermediates, they can produce, in a **net** fashion, either directly or indirectly, molecules that can be used to produce

glucose. These entry reactions to the TCA, which replenish or add to TCA intermediates, are called **anaplerotic** (replenishing) reactions. Hence, these amino acids are also **glucogenic**.

- some have multiple ways to be degraded and can produce acetyl-CoA and pyruvate, so they are **both glucogenic and ketogenic.**

Let's get more explicit:

- purely ketogenic: only Leu and Lys (the only amino acids whose name starts with **L,** and you have to **L**ove them since there are only two amino acids in this category)
- both: 5 are, including the aromatics - Trp, Tyr, Phe - along with Ile/Thr
- purely glucogenic: the rest

Figure **18.5.1**, also shown in the previous sections, summarizes the fates of the 20 amino acids in their catabolic reactions

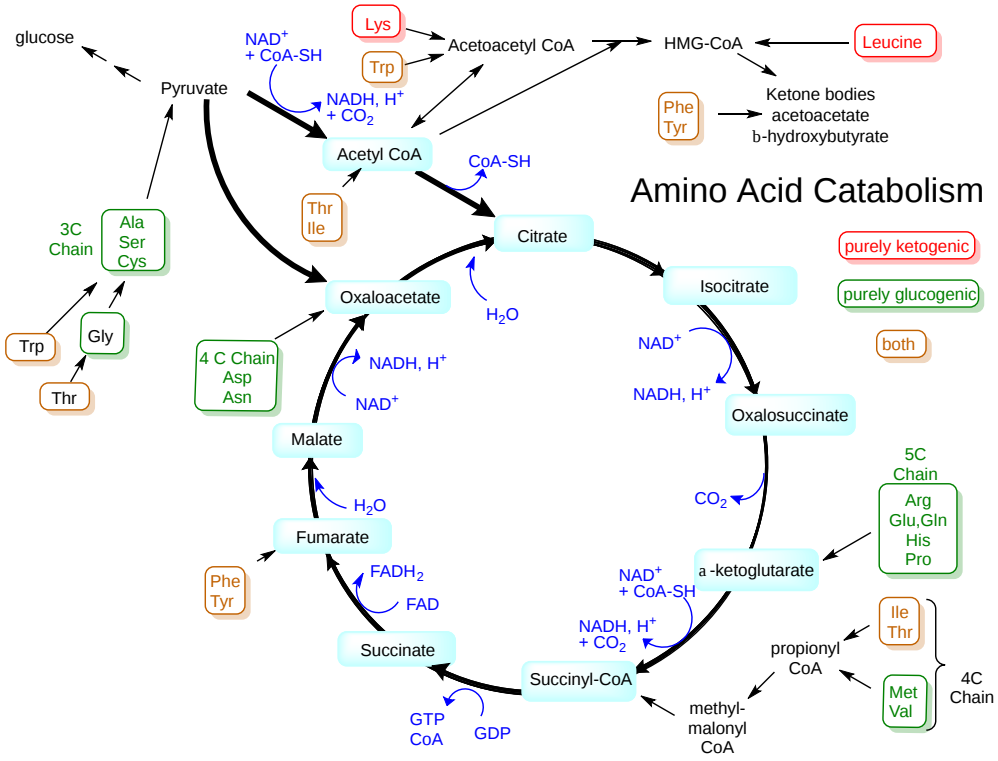


Figure **18.5.1**: Fates of the 20 amino acids in their catabolic reactions

Given the myriad of enzymes and pathways involved, we won't delve into the mechanisms for the reactions or the structures of the enzymes, except one for lysine metabolism.

18.5.2: CONVERSION TO PYRUVATE: ALA, TRP, CYS, SER, GLY, THR

We concluded Section 18.3 with a discussion of the Ser Gly One Carbon Cycle (SGOC), so some of this will be a review.

Figure **18.5.2** shows an overview of the conversion of amino acids to pyruvate. More details are provided for each step below.

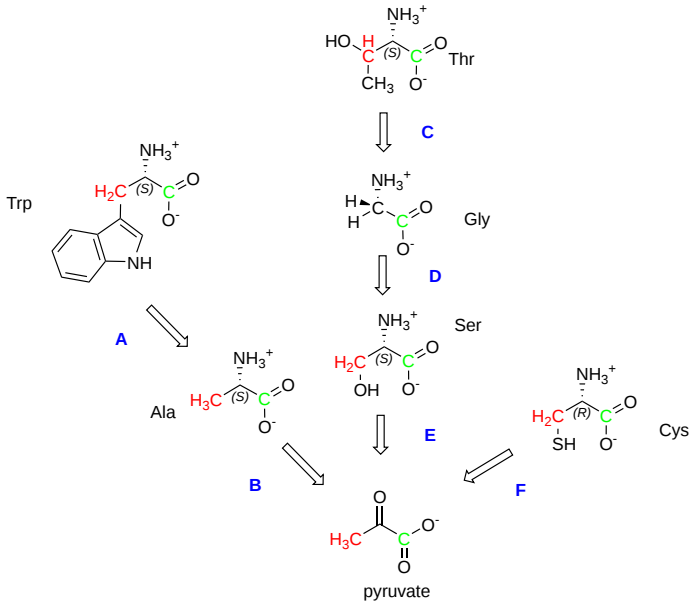


Figure **18.5.2**: Overview of conversion of amino acids to pyruvate

The metabolic steps for the chemical transformations shown in A-F are described in more detail below.

18.5.2.1: TRYPTOPHAN TO ALANINE AND ON TO ACETOACETATE

This is a multistep process, as shown in Figure **18.5.3**.

A. Trp to Ala (and to acetoacetate and NAD^+)

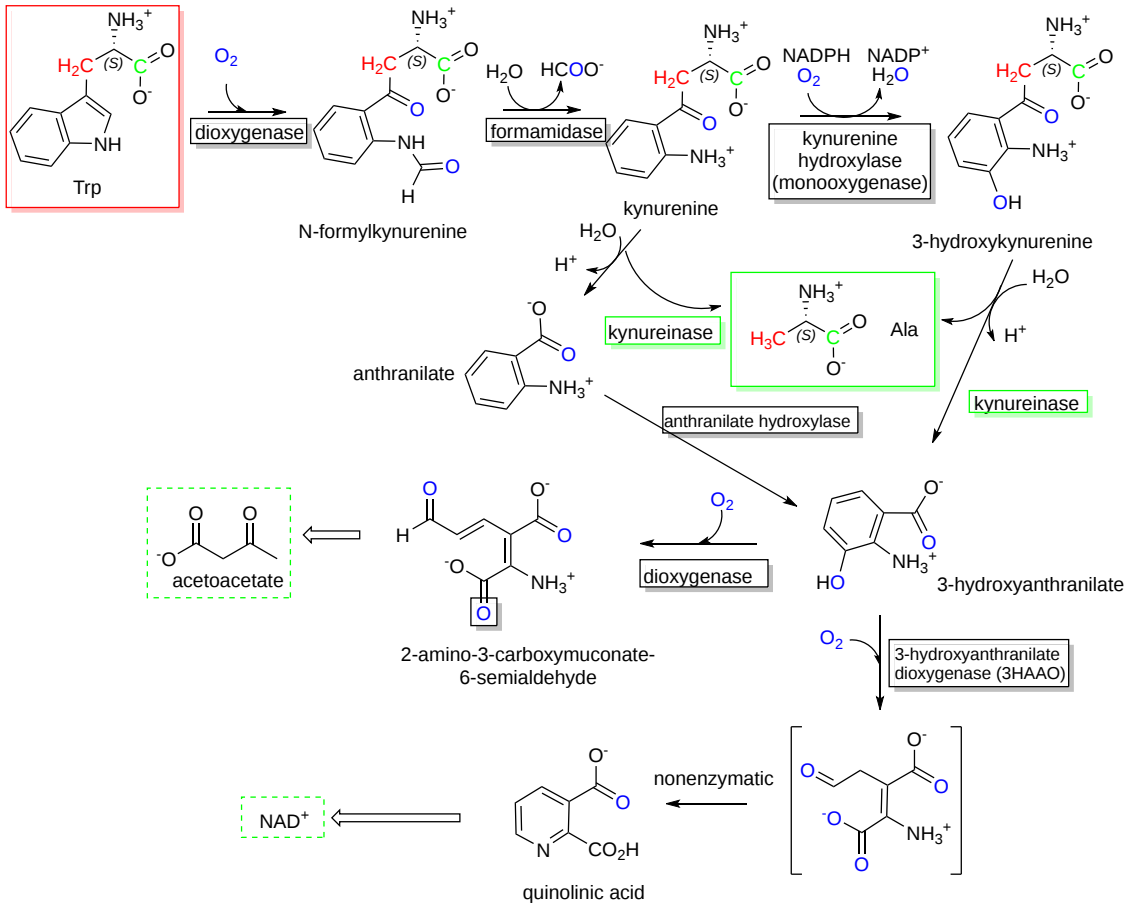


Figure 18.5.3: Conversion of Tryptophan to Alanine and to acetoacetate

The starting material, tryptophan, is highlighted in a red box while the end product of specific interest, Ala, is highlighted in a green box. No reaction occurs in isolation in a cell, but rather as part of a more complex pathway. In the figure above, Ala is presented almost as a side product as the modified aromatic ring found in either anthranilate or 3-hydroxyanthranilate continues to form either acetoacetate, a ketone body which can break down to acetyl-CoA (making tryptophan ketogenic as well as glucogenic) or NAD^+.

18.5.2.2: ALANINE TO PYRUVATE

As described in 18.2 and shown in Figure 18.5.4, the PLP-dependent enzyme **AL**anine Amino **T**ransferase (**ALT**), also known as **G**lutamate **P**yruvate **T**ransaminase (**GPT**), catalyzes this simple transamination reaction:

alanine +α−ketoglutarate ↔ pyruvate + glutamate

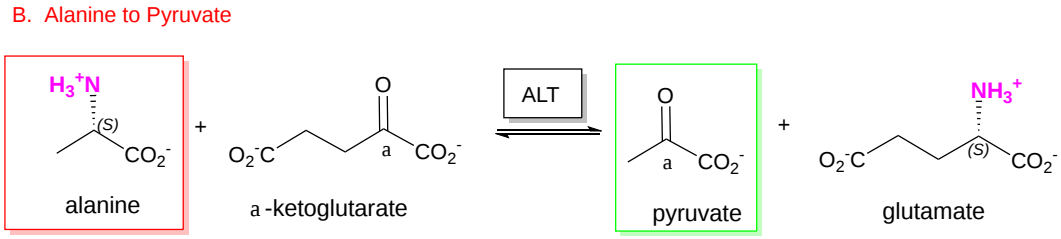


Figure 18.5.4: Alanine to pyruvate

The glutamate produced in this reaction can be oxidatively deaminated to give NH_4^+ and α-ketoglutarate again, as shown below:

glutamate + H_2O + NAD^+ → α-ketoglutarate + NADH + H^+

The sum (net) of the two reactions is:

Alanine + H_2O + NAD^+ → pyruvate + NADH + H^+

18.5.2.3: THREONINE TO GLYCINE

There are several pathways for this conversion.

One involves the conversion of Thr to 2-amino-3-ketobutyrate by **threonine-3-dehydrogenase**.

Rx: Thr + NAD^+ ↔ 2-amino-3-ketobutyrate + NADH

This is followed by the conversion of 2-amino-3-ketobutyrate to glycine by the enzyme **2-amino-3-ketobutyrate coenzyme A ligase.**

Rx: 2-amino-3-ketobutyrate + CoASH ↔ Gly + acetyl-CoA

The net of these reactions is

Rx: Thr + NAD^+ + CoASH ↔ Gly + acetyl-CoA + NADH

These reactions are illustrated in Figure 18.5.5.

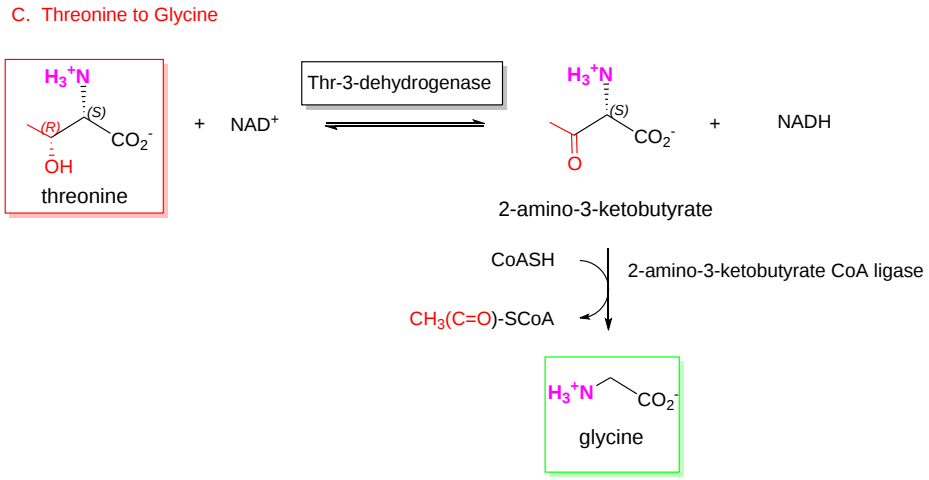


Figure 18.5.5: Threonine to glycine

A second and predominant reaction involves the conversion of Thr to NH_4^+ and α-ketobutyrate by the PLP-dependent enzyme **Ser/Thr dehydratase** (also called threonine ammonia-lyase). We saw this enzyme in the previous section. Note this reaction does NOT produce glycine but is an intermediate, α-ketobutyrate.

$$\text{Rx: Thr} \leftrightarrow NH_4^+ + \text{α-ketobutyrate}$$

α-ketobutyrate can then be converted to propionyl-CoA.

$$\text{Rx: α-ketobutyrate} + NAD^+ + \text{CoASH} \leftrightarrow \text{propionyl-CoA} + \text{NADH} + CO_2 + H^+$$

This reaction, catalyzed by the inner mitochondrial membrane branched-chain α-ketoacid dehydrogenase complex (BCKDC or BCKDH complex), is an oxidative decarboxylation reaction. BCKDC is a member of two other enzymes, pyruvate dehydrogenase and alpha-ketoglutarate dehydrogenase, both of which act on short alpha-keto acids to produce key Kreb cycle metabolites.

Propionyl-CoA is then converted, in several mitochondrial steps, to succinyl-CoA for entry into the TCA cycle. Three enzymes are required for this conversion: propionyl-CoA carboxylase, methylmalonyl-CoA epimerase, and methylmalonyl-CoA mutase. Propionyl carboxylase, like another alpha-keto acid carboxylase (pyruvate carboxylase), requires **A**TP, **B**iotin, and **C**O_2 (as a substrate) for the carboxylation reaction and hence is often referred to as an **ABC** enzyme.

The three-step conversion pathway of propionyl CoA to succinyl CoA is also used for the degradation of **V**aline, **O**dd-chain fatty acids (which form multiple 2-carbon acetyl CoA units and 1 3-C propionyl CoA unit), **M**ethionine, and **I**soleucine, along with **T**hreonine. This three-step pathway is sometimes referred to as the **VOMIT** pathway.

The third pathway, which we just saw in the previous section, is catalyzed by serine hydroxymethyltransferase (SHMT) (but also called glycine hydroxymethyltransferase or threonine aldolase) and requires the use of both PLP and tetrahydrofolate as cofactors. A 1C methylene is added to tetrahydrofolate (FH_4). PLP forms bonds to the alpha-carbon of amino acids that are labile to cleavage. In this case, the amino acid threonine dehydrates through an alpha-elimination reaction. However, threonine has an extra CH_3 group, which is released as acetaldehyde. Here is the overall reaction.

$$\text{Rx: Thr+ } FH_4 + \leftrightarrow \text{ Glycine + } N^5,N^{10}\text{-}FH_4 + \text{acetaldehyde + } H_2O$$

The literature is a bit unclear about the enzymes involved in this reaction. SHMT appears to act on Thr at a lower rate, but a second enzyme, threonine aldolase, which seems to be afunctional in mammals, acts in other organisms.

18.5.2.4: GLYCINE TO SERINE

As mentioned above, this reversible reaction is catalyzed by serine hydroxymethyltransferase (SHMT) (see the mechanism in section 18.4) and uses tetrahydrofolate and PLP as cofactors. Here is the overall reaction, the reverse of the Gly ↔ Ser we saw in 18.4.

$$\text{Rx: Glycine + } N^5,N^{10}\text{-}CH_2\text{-}FH_4 + H_2O \leftrightarrow \text{ Serine + } FH_4$$

Figure **18.5.6** shows the serine dehydratase reaction presented in Chapter 18.4. Figure A below shows the dehydration reaction and formation of glycine. using PLP as a cofactor. Figure B shows how the released formaldehyde reacts with FH_4 to form N^5,N^{10}-methylene FH_4, using FH_4 as a cofactor.

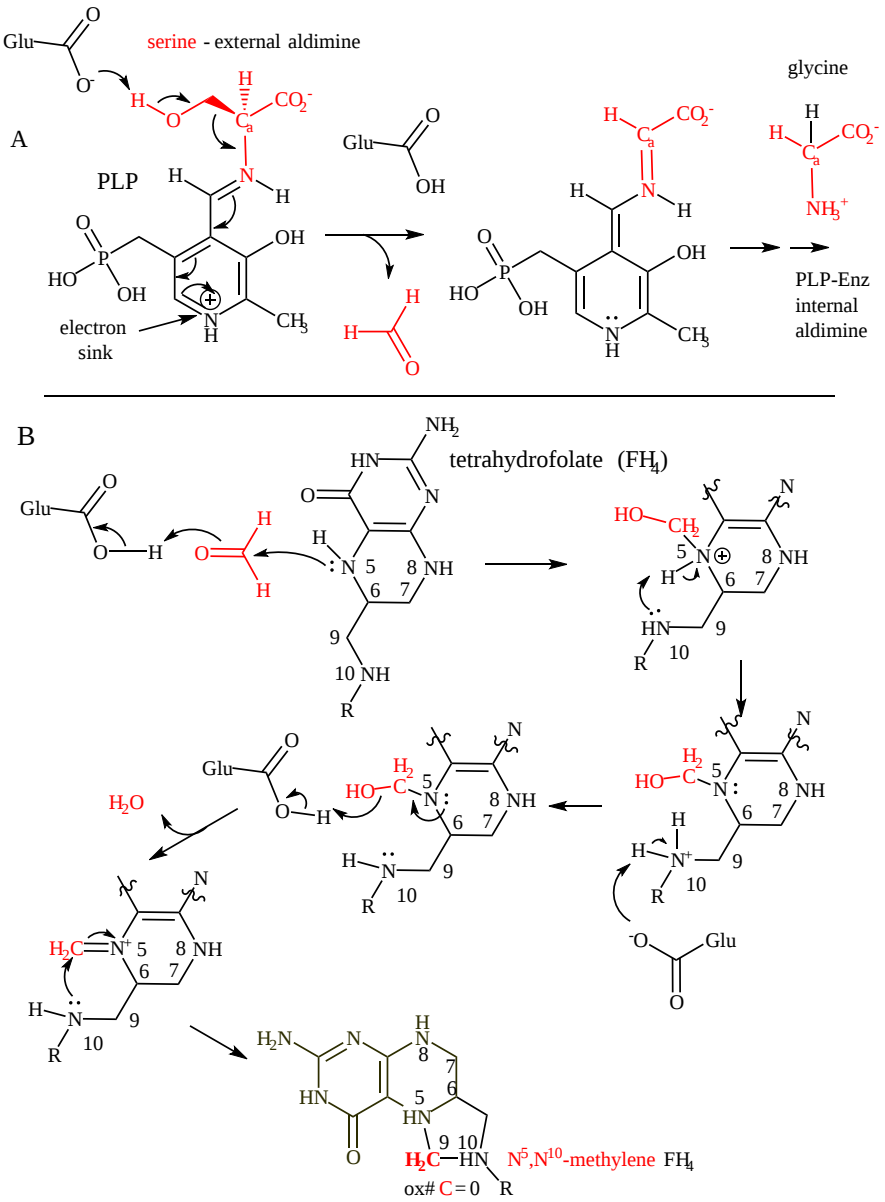


Figure 18.5.6: Reversible reaction of Serine to Glycine

18.5.2.5: SERINE TO PYRUVATE

This reaction is analogous to the Ala → Pyr reaction in Rx B above and is catalyzed by the PLP-dependent enzyme serine/threonine dehydratase/threonine deaminase.

$$\text{Rx: Serine} \leftrightarrow \text{Pyr} + NH_4^+$$

The enzyme is found in the cytoplasm and is mainly involved in gluconeogenesis.

18.5.2.6: CYSTEINE TO PYRUVATE

The overall reactions for this conversion are shown in the figure below. The aspartate aminotransferase used in the production of 3-sulfinylpyruvate is cytosolic and not the same as the more abundant version in the mitochondria.

The reaction pathway is shown in Figure 18.5.7.

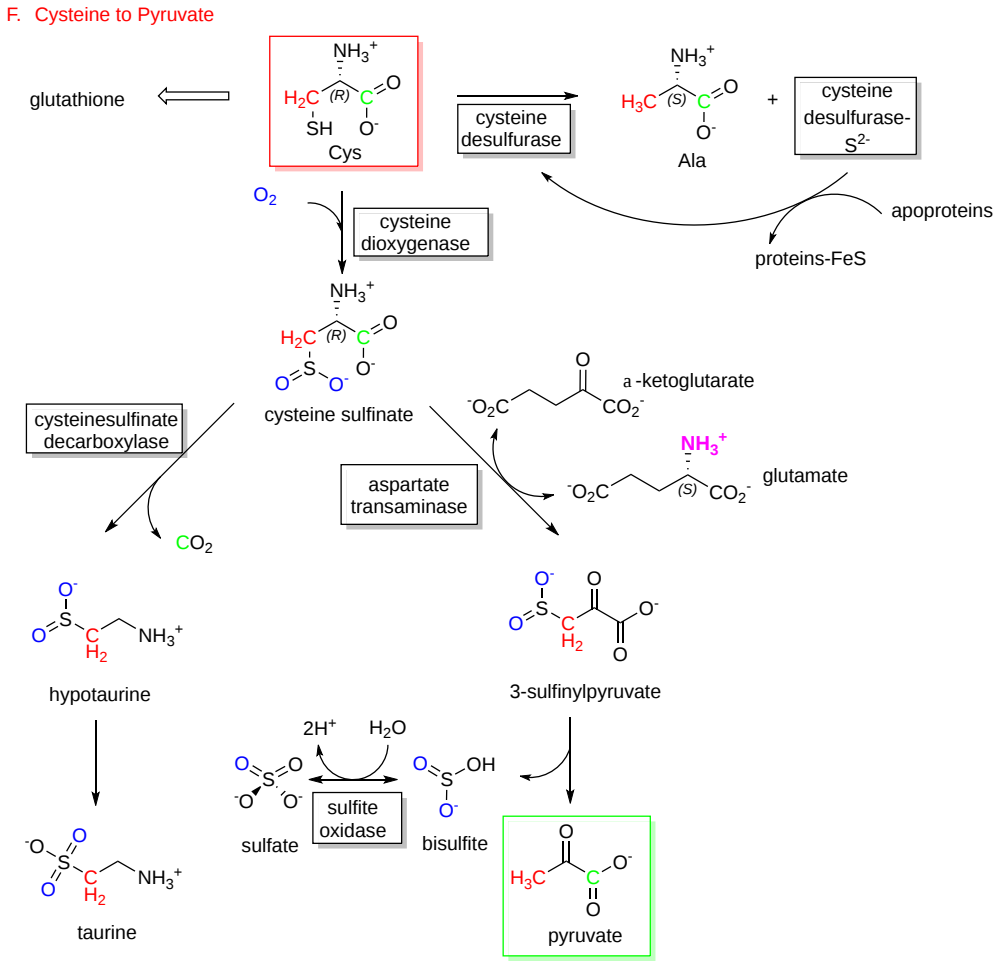


Figure 18.5.7: Cysteine to pyruvate

Other important metabolites are made from cysteine catabolic pathways. One is taurine, the most abundant free amino acid in the body. It is especially abundant in development and early milk. It is synthesized predominantly in the liver. It is unclear if hypotaurine is converted to taurine in a non-enzymatic fashion or by an oxidase/dehydrogenase.

The sulfate produced in these pathways is utilized to synthesize an interesting derivative of ATP, 3′-phosphoadenosine-5′-phosphosulfate (PAPS), which is subsequently used to produce sulfated sugars essential for glycolipid and proteoglycan synthesis. This is illustrated in Figure 18.5.8.

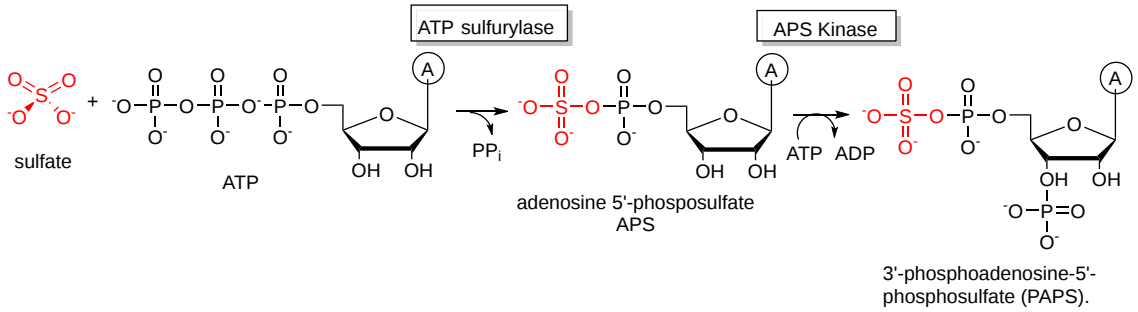


Figure 18.5.8: Sulfate conversion to PAPS

18.5.3: CONVERSION TO ACETYL-COA: TRP, LYS, PHE, TYR, LEU, ILE, THR

An overview of the many reactions in ketogenic amino acid degradation is shown in Figure 18.5.9. The red-boxed amino acids are those that form either acetoacetate (a ketone body) or acetyl-CoA directly (green boxes). Some of the carbons are color-coded red or green to indicate where they end up.

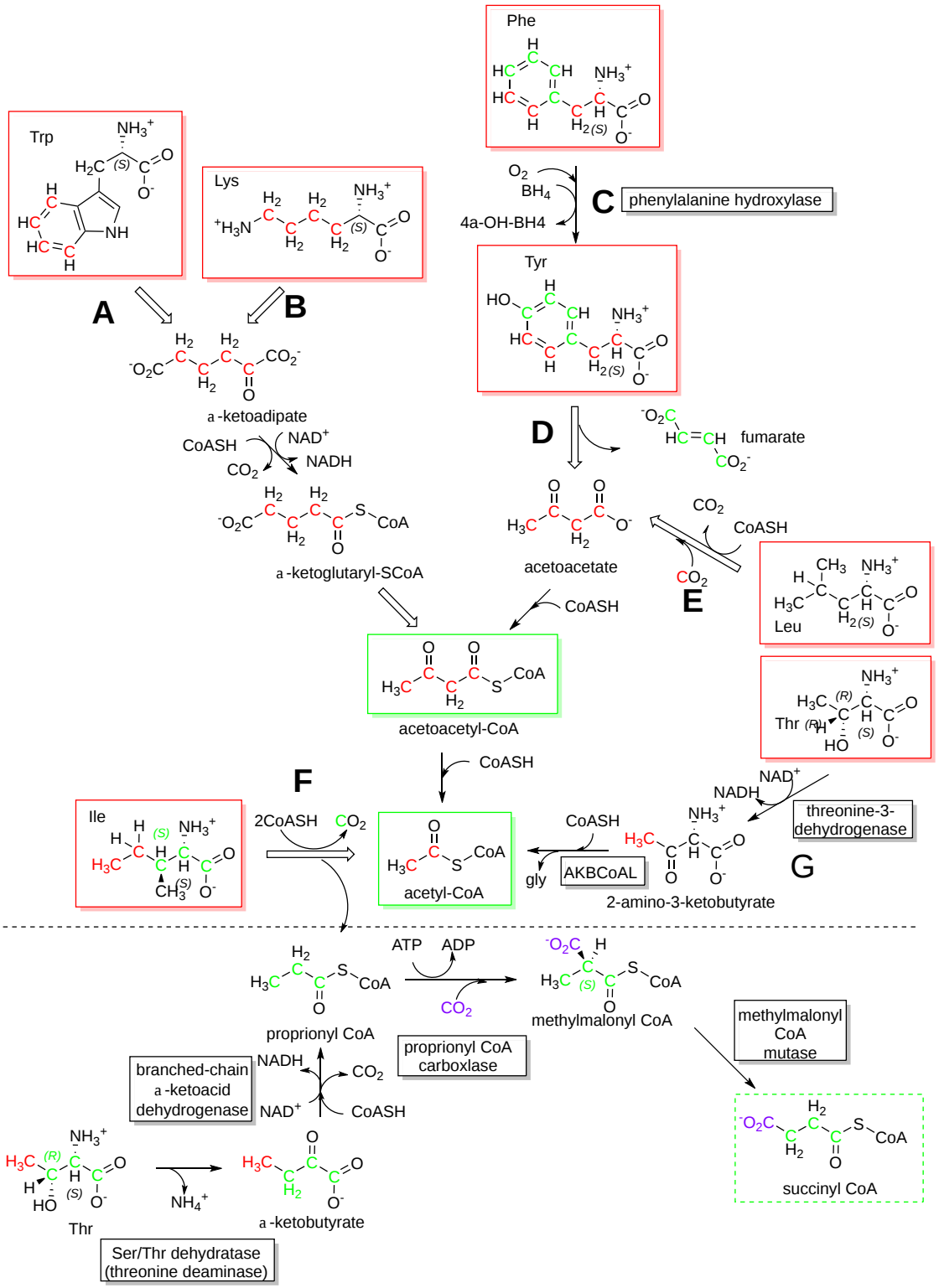


Figure 18.5.9: Ketogenic amino acid pathway

18.5.3.1: TRP TO ACETYL-COA

Fortunately, we have explored the conversion of the non-ring part of tryptophan to alanine and a precursor of acetoacetyl CoA (2-amino-3-carboxymuconate 6-semialdehyde - ACMS) and to NAD^+ (quinolinate). ACMS, through the action of ACMS decarboxylase, leads to acetoacetyl CoA and then to acetyl-CoA as shown in Figure 18.5.10. As Trp is a ketogenic amino acid, it seems appropriate to show the steps that lead to acetyl-CoA even at the risk of providing too much detail.

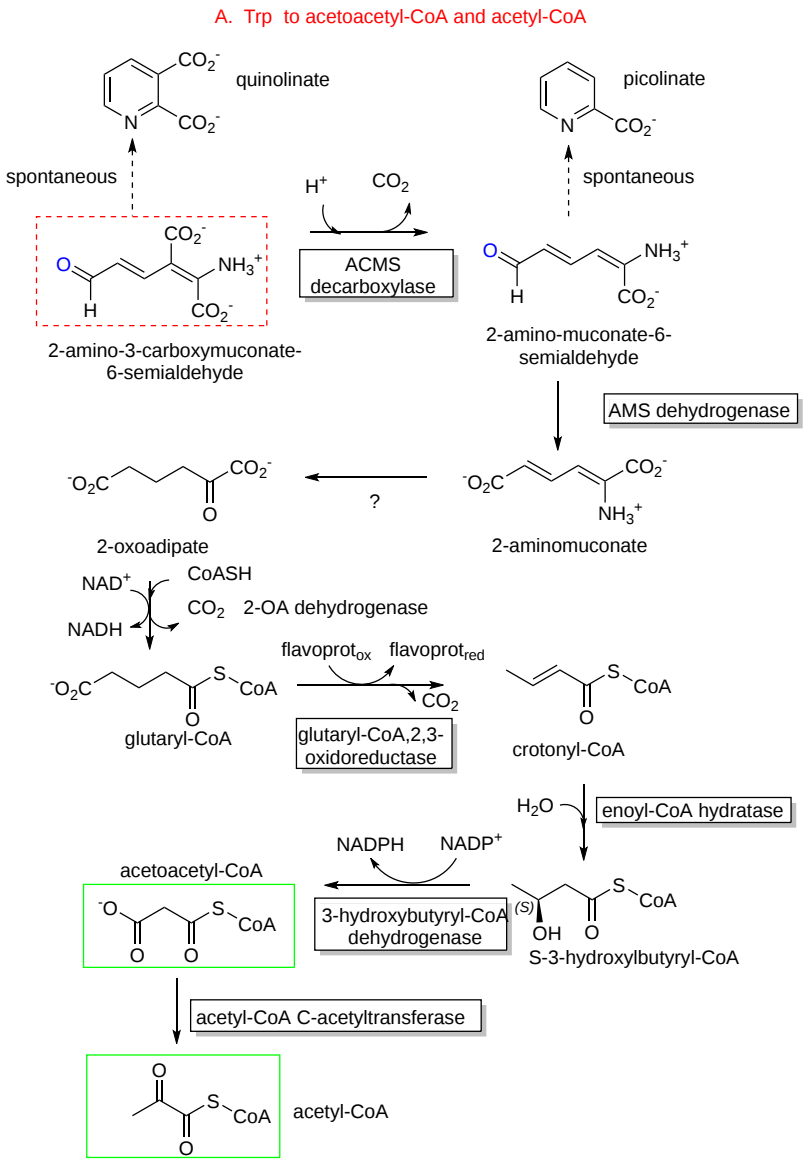


Figure 18.5.10: Part 2 - Tryptophan to acetyl-CoA

18.5.3.2: LYS METABOLISM

In the liver, the main pathway (of several) starts with the formation of saccharopine from the transamination reaction of lysine and α-ketoglutarate, allowing the ε-amino group of lysine to enter the nitrogen metabolic pool. This transamination does not use pyridoxal phosphate (PLP). The first two steps of the reaction are catalyzed by an enzyme, α-aminoadipic semialdehyde synthase, with two activities (condensation/reduction and hydrolysis/oxidation). Lysine is an essential amino acid since the transamination is not reversible. Figure **18.5.11** shows pathways for the conversion of lysine to acetoacetyl-CoA and acetyl-CoA.

B. Lys to acetoacetyl-CoA and acetyl-CoA

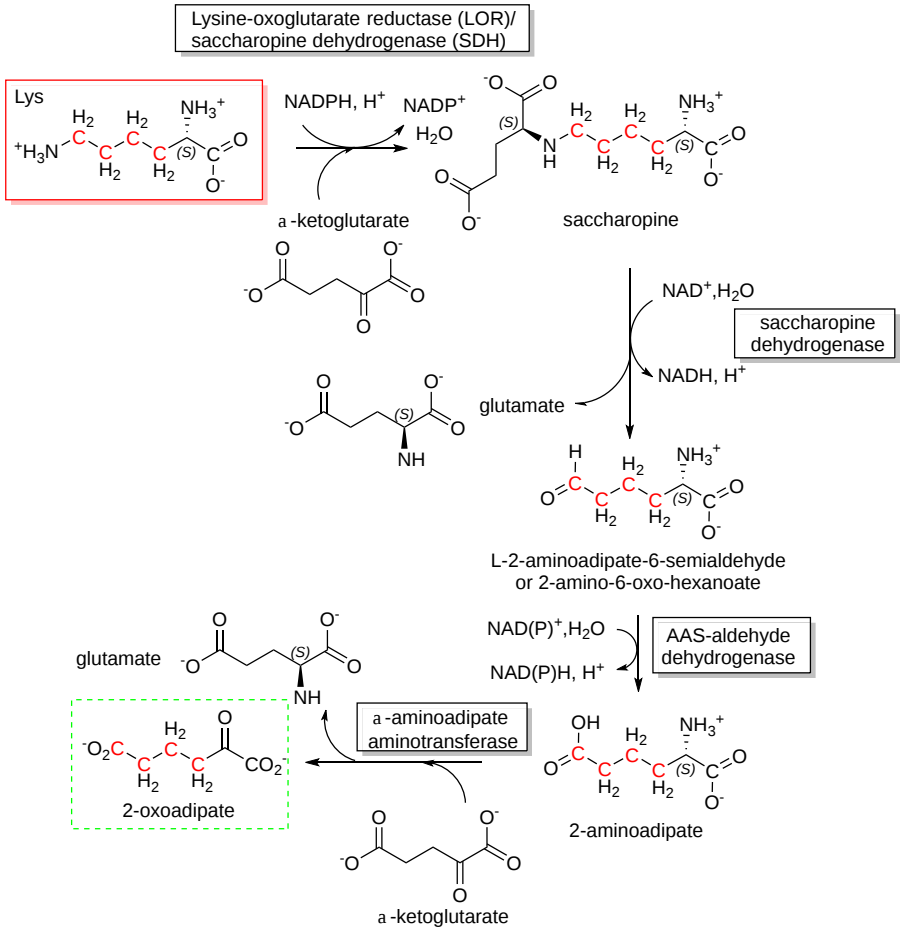
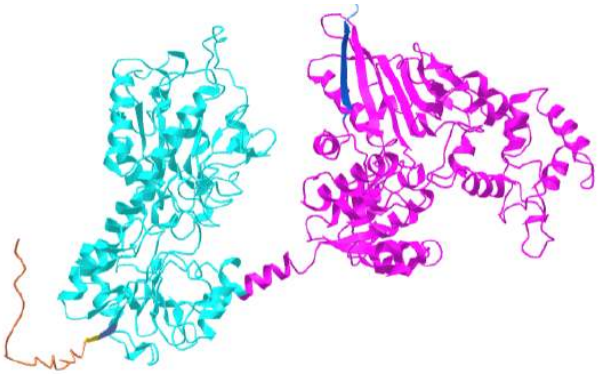


Figure 18.5.11: Pathways for conversion of lysine to acetoacetyl-CoA and acetyl-CoA.

The lysine-oxoglutarate reductase (LOR) and saccharopine dehydrogenase (SDH) are found in a single bifunctional enzyme, often referred to as aminoadipic semialdehyde synthase.

Figure 18.5.12 shows an interactive iCn3D model of the AlphaFold predicted structure of aminoadipic semialdehyde synthase (Q9UDR5)



NCBI iCn3D Figure 18.5.12: AlphaFold predicted structure of aminoadipic semialdehyde synthase (Q9UDR5). (Copyright; author via source). Click the image for a popup or use this external link: https://structure.ncbi.nlm.nih.gov/i...Pi1c7Y5A9DmLa8

The cyan domain represents the lysine-oxoglutarate reductase (LOR) domain, which is connected by an alpha helix to the magenta saccharopine dehydrogenase (SDH) domain.

18.5.3.3: PHENYLALANINE IS CONVERTED TO TYROSINE AND CONTINUES TO ACETOACETATE

We'll follow the conversion of phenylalanine to tyrosine, which proceeds to acetoacetate, resulting in both phenylalanine and tyrosine (ketogenic amino acids), and subsequently produces fumarate. They can enter the TCA cycle, leading to the net production of oxaloacetate, which can be pulled off into gluconeogenesis, making both Phe and Try glucogenic as well.

A new cofactor is required that facilitates electron flow in the conversion of Phe to Try in the first step, catalyzed by the enzyme tyrosine hydrolase. That cofactor is **tetrahydrobiopterin** (BH_4). The reaction involves the hydroxylation of BH_4, followed by its transfer to phenylalanine. Figure **18.5.13** shows a possible mechanism for the conversion of phenylalanine to tyrosine with tetrahydrobiopterin (BH_4).

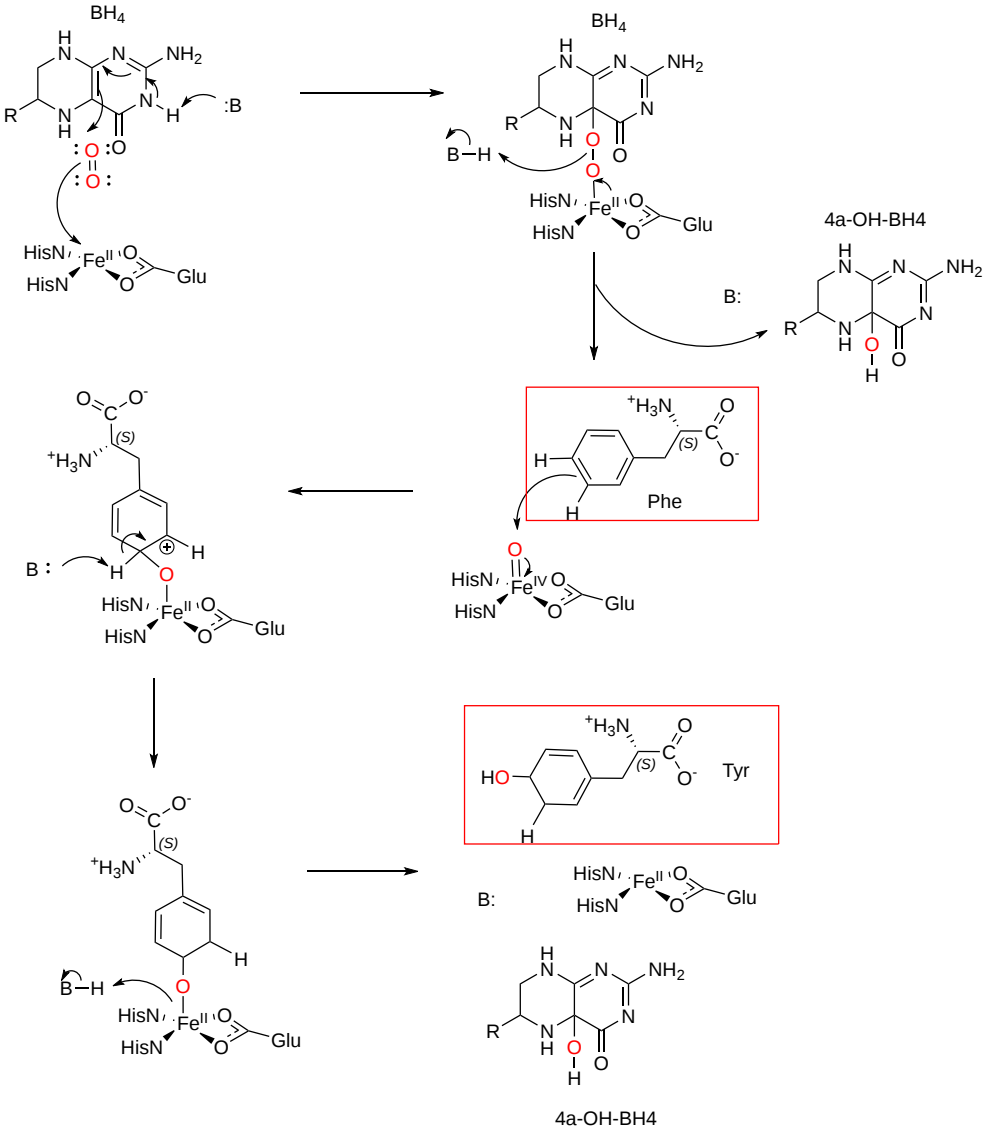


Figure **18.5.13**: Conversion of phenylalanine to tyrosine with tetrahydrobiopterin (BH_4)

As in the case of converting dihydrofolate back to tetrahydrofolate (FH_4) by dihydrofolate reductase, the 4a-OH-BH4 is converted to dihydrobiopterin and then to tetrahydrobiopterin by dihydrobiopterin reductase.

Figure **18.5.14** shows the full pathway for the conversion of Phe and Tyr to acetoacetate and fumarate.

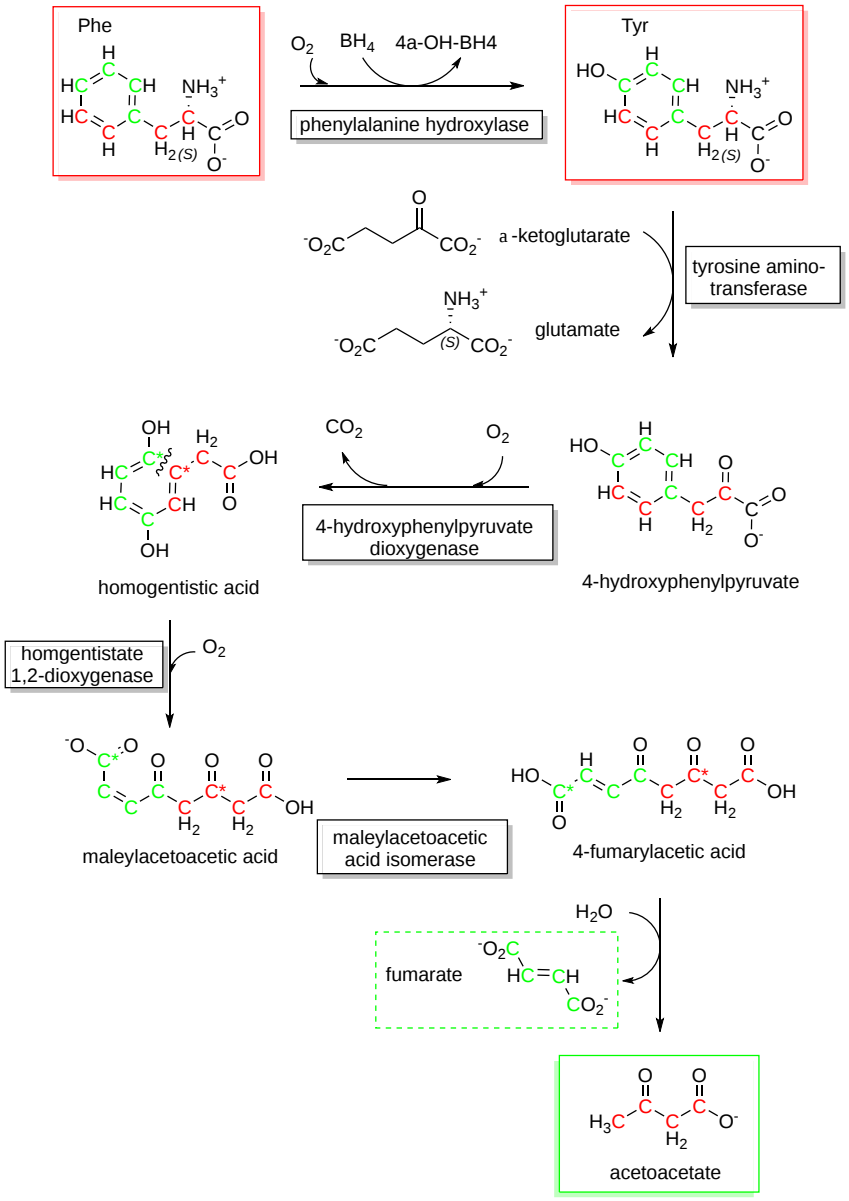


Figure 18.5.14: Conversion of phenylalanine and tyrosine to acetoacetate and fumarate

18.5.3.4: LEU TO ACETOACETATE

The conversion of leucine to acetoacetate is shown in Figure 18.5.15.

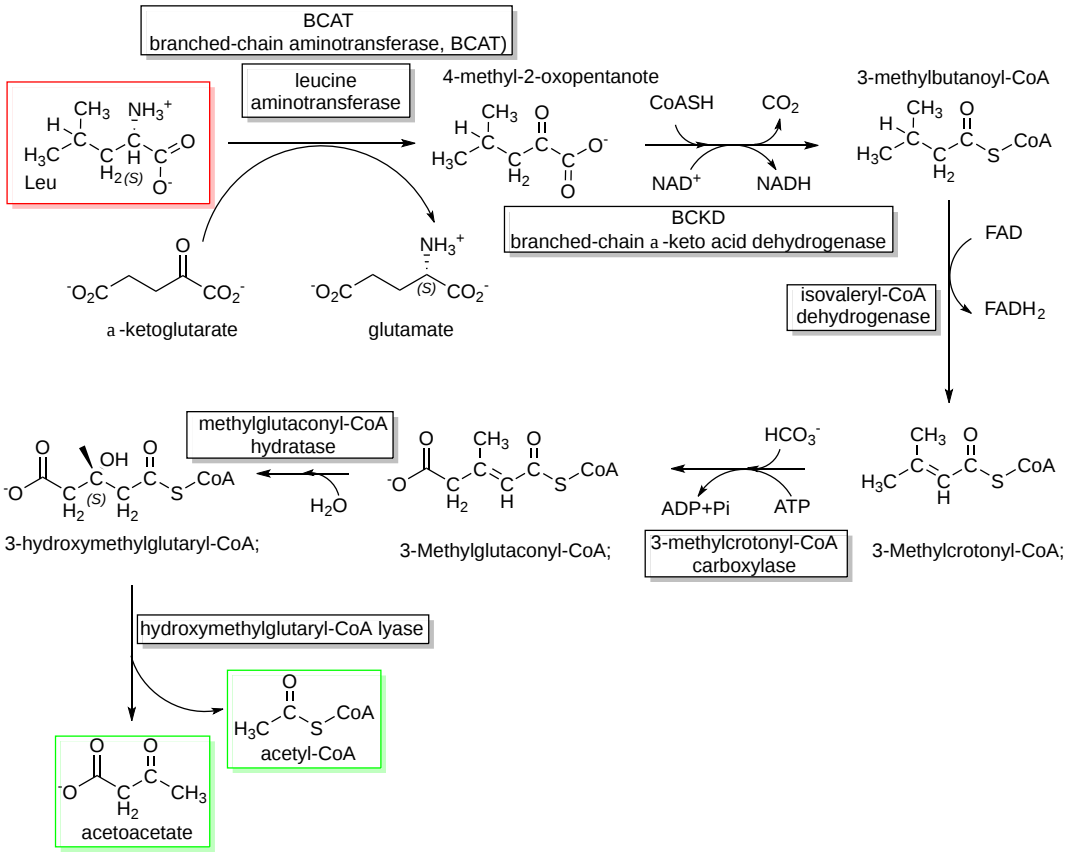


Figure **18.5.15**: Conversion of leucine to acetoacetate

The first reaction is a transamination using the PLP-dependent branched-chain aminotransferase (BCAT) with α-ketoglutarate.

18.5.3.5: ISOLEUCINE TO ACETYL-COA

Figure **18.5.16** shows the pathway for the conversion of isoleucine to acetyl-CoA.

E: Ile to Acetyl-CoA

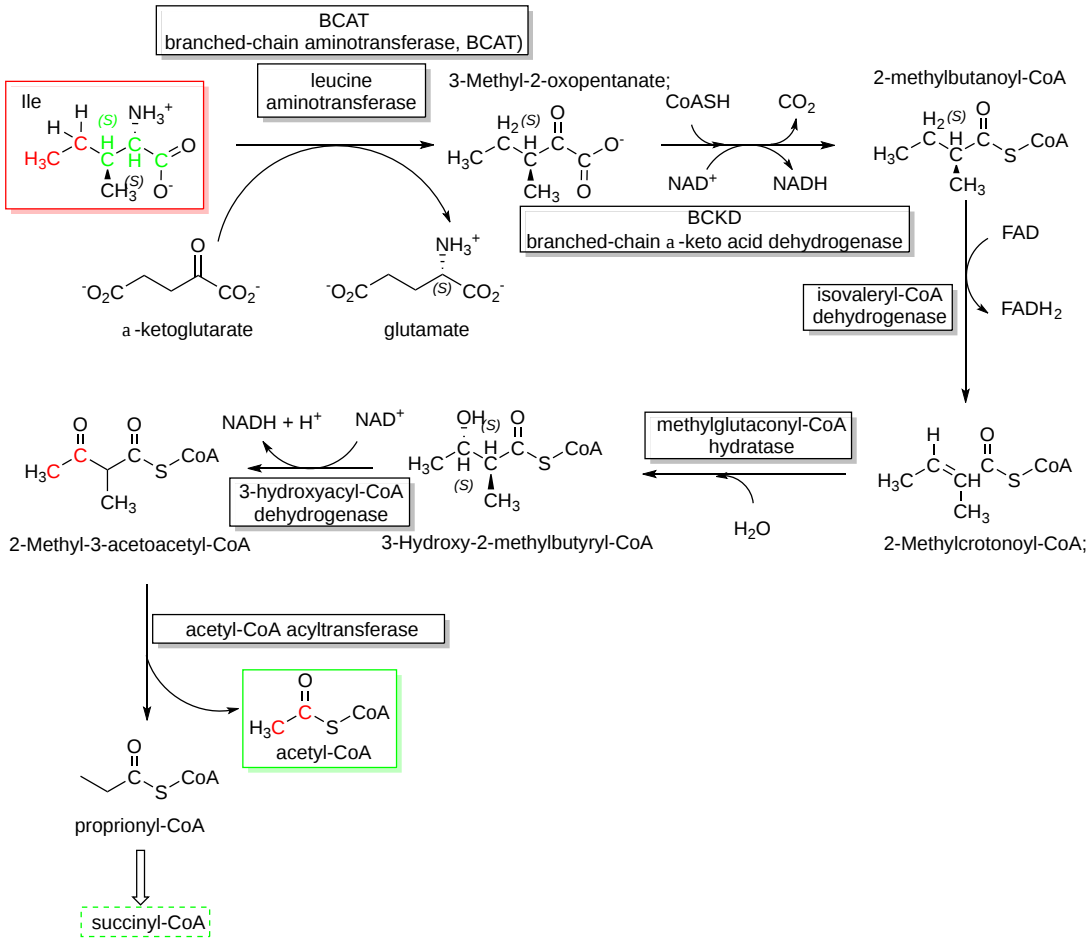


Figure 18.5.16: Pathway for converting isoleucine to acetyl-CoA.

18.5.4: CONVERSION TO A-KETOGLUTARATE: PRO, GLU, GLN, ARG,HIS

18.5.4.1: PROLINE AND ARGININE

The conversion of proline (bottom left) to glutamate (top left) is shown in Figure 18.5.17.

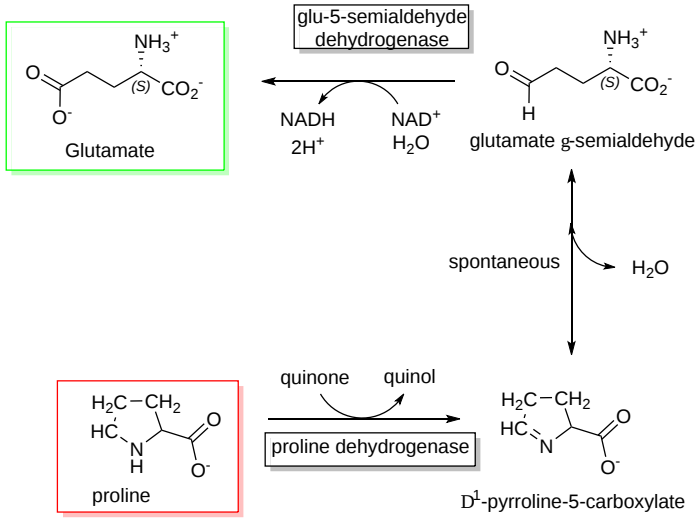


Figure 18.5.17: Conversion of proline (bottom left) to glutamate (top left)

Glutamate can then form α-ketoglutarate, so the reaction is glucogenic.

The conversions of arginine (and proline) to α-ketoglutarate are shown in Figure 18.5.18.

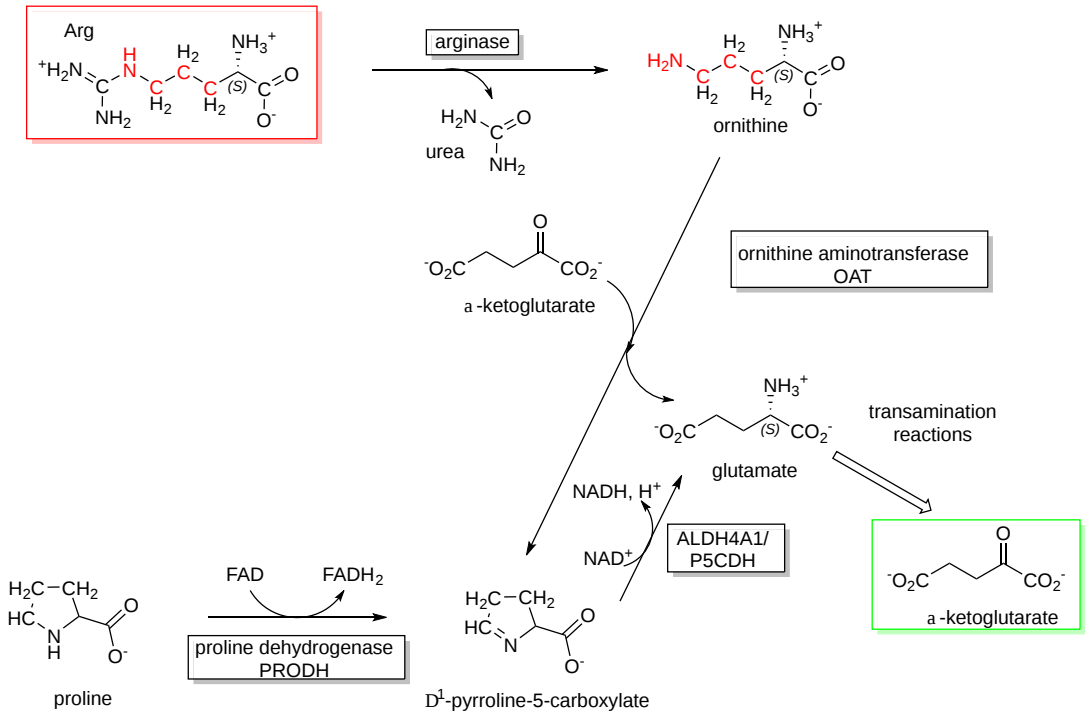


Figure 18.5.18: Conversion of arginine and proline to α-ketoglutarate

18.5.4.2: HISTIDINE

The conversion of histidine to α-ketoglutarate is shown in Figure 18.5.19.

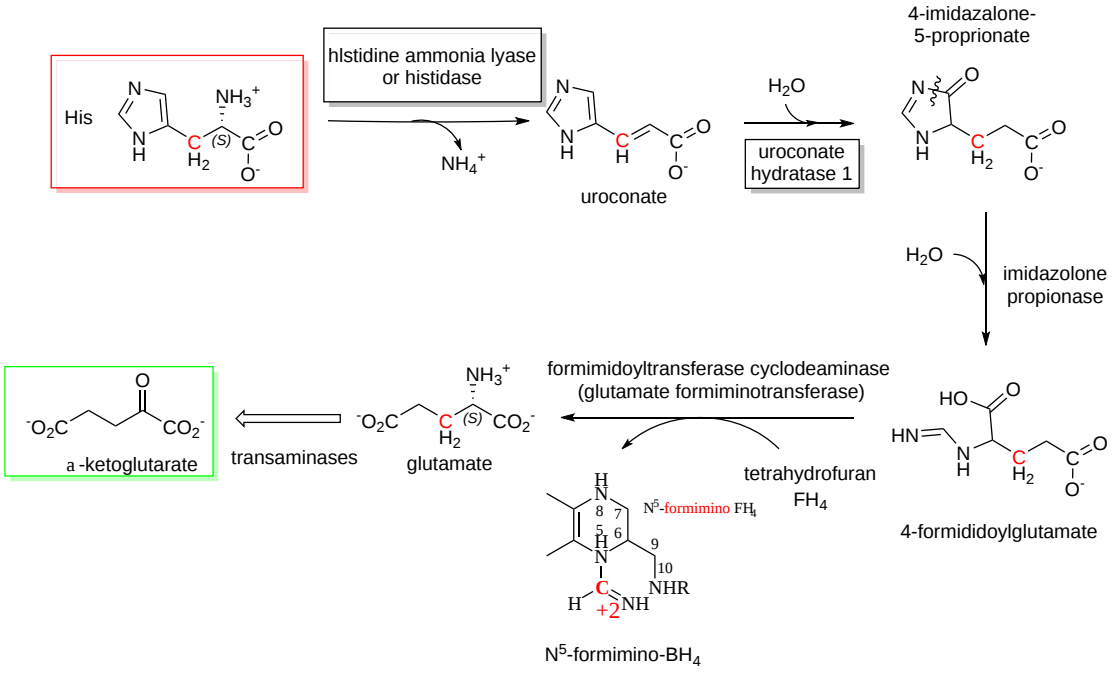


Figure 18.5.19: Conversion of histidine to α-ketoglutarate

As described in the reactions above, histidine can be converted to α-ketoglutarate through transamination reactions. Additionally, we described in a previous section how glutamine can be deaminated through the action of glutaminase to form glutamate, which can subsequently form α-ketoglutarate, a gluconeogenic intermediate.

18.5.5: CONVERSION TO SUCCINYL-COA: MET AND THE BRANCHED-CHAIN AMINO ACIDS ILE, THR, VAL

We have just seen that two branched-chain amino acids, Leu and Ile, are converted to acetyl-CoA and, therefore, are ketogenic (E and F above). The branched-chain hydrophobic amino acids, Val and Leu, can be converted to succinyl-CoA, which can be converted to α-ketoglutarate in the Krebs' cycle in a net fashion and hence are glucogenic amino acids. We saw in the introduction to amino acids that produce acetyl-CoA that threonine and isoleucine, two branched-chain amino acids, also form propionyl-CoA, which goes on to succinyl-CoA. So, let's consider Val, another branched-chain amino acid, before we consider Met, both of which have three C atoms in their side chains.

18.5.5.1: VALINE

The conversion of valine to succinyl-CoA is shown in Figure **18.5.20**.

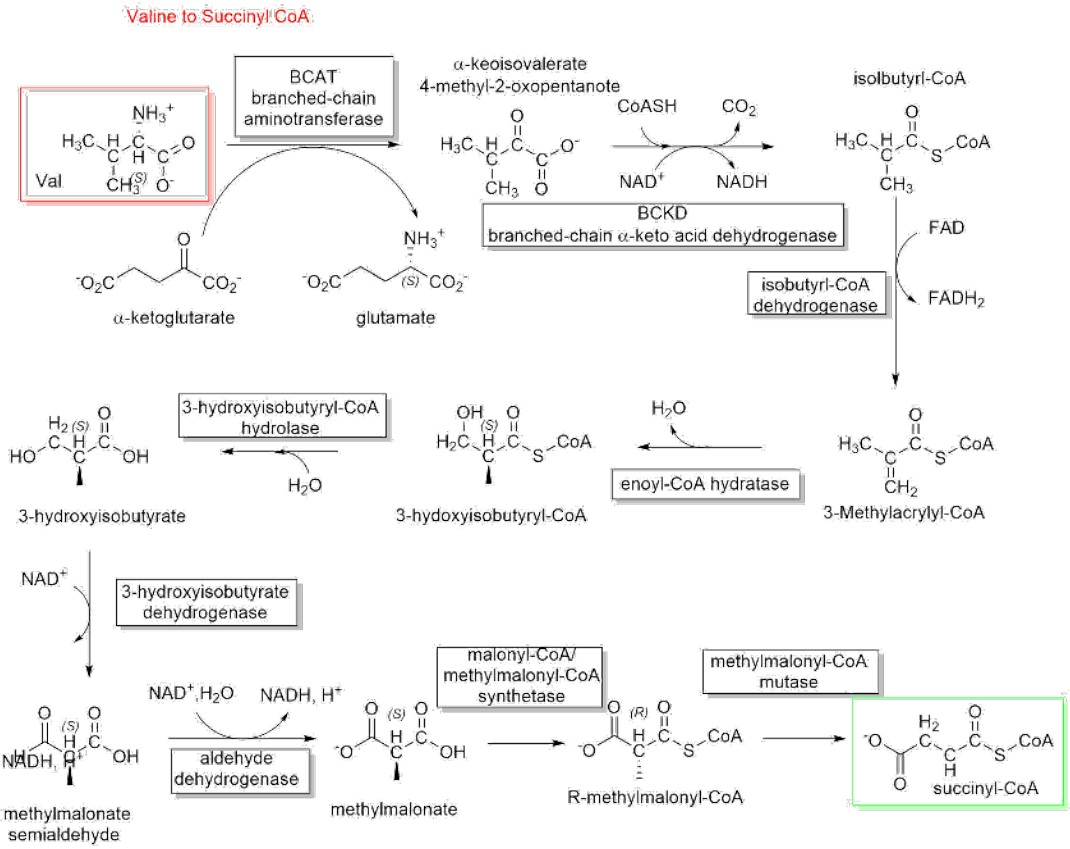


Figure **18.5.20**: Conversion of valine to succinyl-CoA

The other two amino acids with branched-chain carbon chains (isoleucine and leucine) use the same enzymes as valine to enter the degradation pathway. They start with branched-chain transaminases (BCATc or BCATm) followed by oxidative decarboxylation reactions catalyzed by branched-chain ketoacid dehydrogenase (BCKD). Three different enzymes are required for the following dehydrogenase reaction. These are short/branched-chain acyl-CoA dehydrogenase (SBCAD) for isoleucine, isovaleryl-CoA dehydrogenase (IVD) for leucine, and isobutyryl-CoA dehydrogenase (IBD) for valine.

18.5.5.2: METHIONINE

Methionine can be metabolized to S-adenosylhomocysteine (SAM) and on to cysteine and α-ketobutyrate, which can also be produced by a transsulfuration reaction that produces cysteine. That product is metabolized using branched-chain dehydrogenases to produce succinyl-CoA, a key intermediate in the TCA cycle. Three enzymes are needed to convert the α-ketobutyrate to succinyl-CoA. Propionyl-CoA carboxylase uses ATP, biotin, and CO_2, while the methylmalonyl-CoA mutase requires vitamin B12. An additional enzyme is involved in an epimerase reaction, in which D-methylmalonyl-CoA is converted into L-methylmalonyl-CoA. The conversion of propionyl-CoA to succinyl-CoA also occurs for branched-chain amino acids (**V**al, **I**le, **T**hr) as well as **M**et, and in addition, **O**dd number fatty acids. This odd assortment of substrates for conversion to succinyl-CoA leads to the name **VOMIT** pathways. These reactions are illustrated in Figure **18.5.21**.

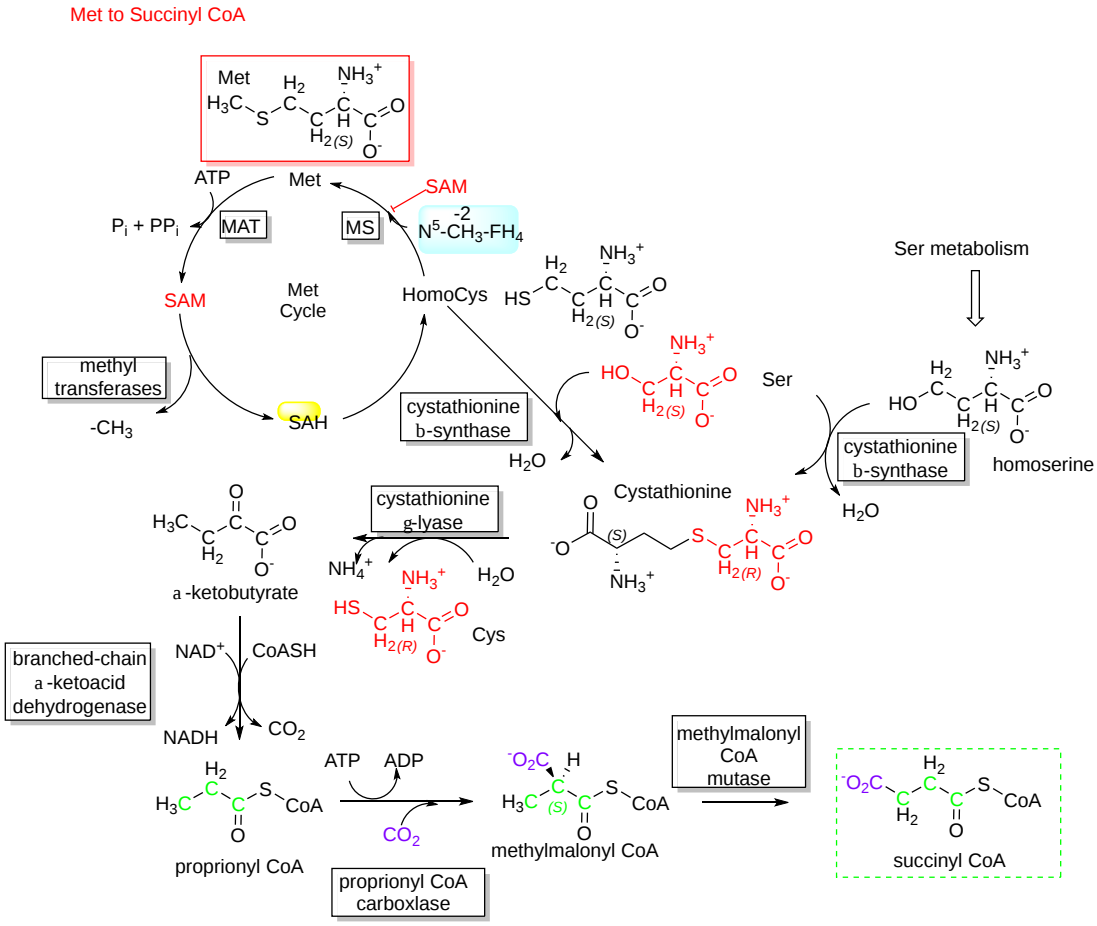


Figure 18.5.21: Methionine conversion to succinyl-CoA

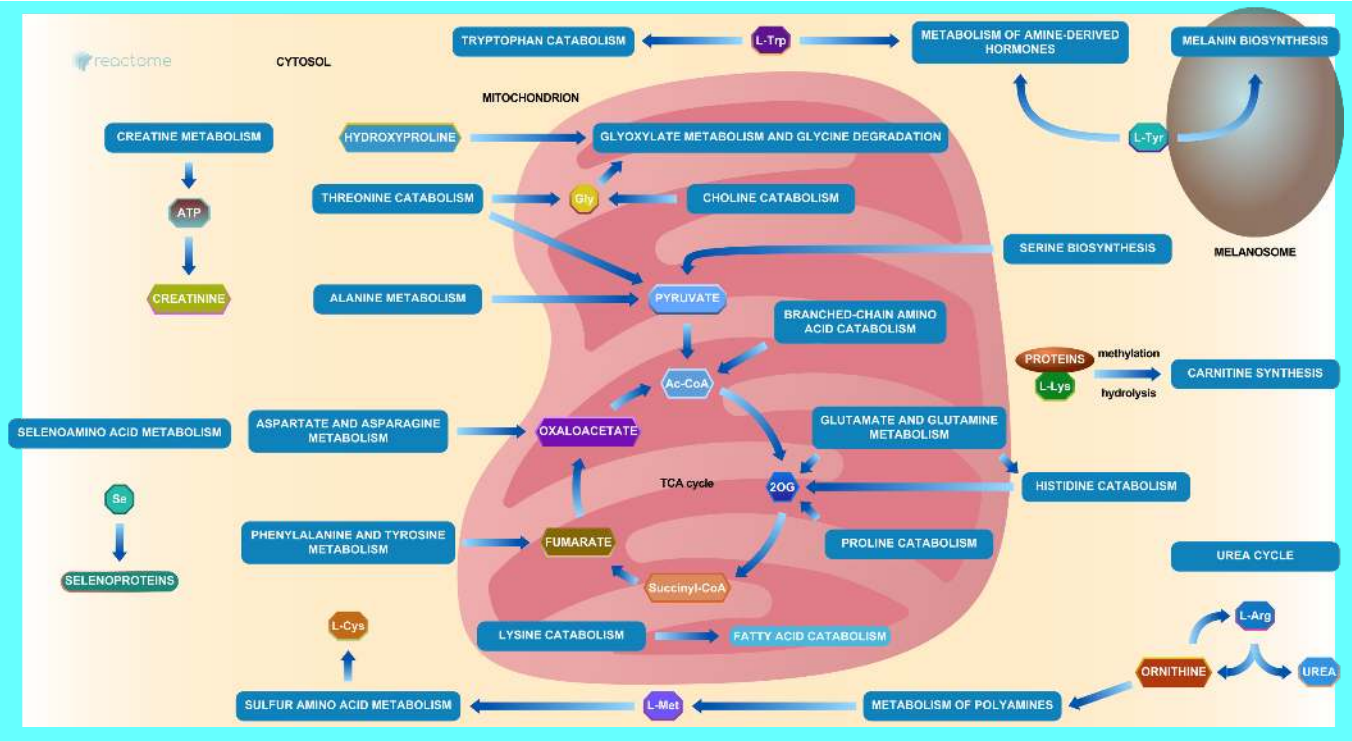
18.5.6: FINALLY, ASPARTATE AND ASPARAGINE

Using the enzyme L-asparaginase, asparagine is converted to NH_3 and aspartate. Aspartate is then used in a transamination reaction to form oxaloacetate, a reactant in gluconeogenesis. Aspartate participates in the urea cycle, which helps eliminate nitrogen. Glutamate also acquires NH_3 through the reaction catalyzed by glutamine synthase.

Both amino acids serve as substrates for transamination reactions, which produce TCA intermediates. Glutamate dehydrogenase can lead to alpha-ketoglutarate.

Glutamate and aspartate play important roles in collecting and eliminating amino nitrogen through glutamine synthetase and the urea cycle, respectively. The catabolic path of the carbon skeletons involves simple 1-step aminotransferase reactions that directly produce net quantities of a TCA cycle intermediate. The glutamate dehydrogenase reaction operating in the direction of 2-oxoglutarate (α-ketoglutarate) production provides a second avenue leading from glutamate to gluconeogenesis.

This SUMMARY GRAPHIC From Reactome shows "Cellular metabolism of amino acids and related molecules includes the pathways for the catabolism of amino acids, the biosynthesis of the nonessential amino acids (alanine, arginine, aspartate, asparagine, cysteine, glutamate, glutamine, glycine, proline, and serine) and selenocysteine, the synthesis of urea, and the metabolism of carnitine, creatine, choline, polyamides, melanin, and amine-derived hormones. The metabolism of amino acids provides a balanced supply of amino acids for protein synthesis. In the fasting state, the catabolism of amino acids derived from the breakdown of skeletal muscle protein and other sources is coupled to the processes of gluconeogenesis and ketogenesis to meet the body's energy needs in the absence of dietary energy sources."



Provided by Reactome. Citation Accessed on Wed, May 15, 2024. Fabregat A, Sidiropoulos K, Viteri G, Marin-Garcia P, Ping P, Stein L, D'Eustachio P, Hermjakob H. Reactome diagram viewer: data structures and strategies to boost performance. Bioinformatics (Oxford, England). 2018 Apr;34(7) 1208-1214. doi: 10.1093/bioinformatics/btx752. PubMed PMID: 29186351. PubMed Central PMCID: PMC6030826. Image: https://reactome.org/PathwayBrowser/#/R-HSA-71291&PATH=R-HSA-1430728

18.5.7: SUMMARY

This chapter builds on earlier discussions of nitrogen removal and one-carbon metabolism by focusing on the fate of amino acid carbon skeletons after deamination. It explores how these carbon fragments are channeled into central metabolic pathways, illustrating their diverse roles in energy production and biosynthesis.

Key Concepts:

- **Classification of Amino Acids by Catabolic Fate:**
  Amino acids are categorized based on their degradation products:
  • **Glucogenic Amino Acids** produce pyruvate or TCA cycle intermediates (e.g., α-ketoglutarate, oxaloacetate), which can be used for gluconeogenesis.
  • **Ketogenic Amino Acids** yield acetyl-CoA or acetoacetyl-CoA, precursors for ketone body formation.
  • **Dual-Function Amino Acids** provide both glucogenic and ketogenic intermediates.
- **Major Pathways for Carbon Skeleton Conversion:**
  • **Conversion to Pyruvate:**
  Amino acids such as alanine, tryptophan, cysteine, serine, glycine, and threonine are converted to pyruvate via transamination and deamination reactions. This process is crucial for fueling gluconeogenesis and energy production.
  • **Conversion to Acetyl-CoA and Acetoacetyl-CoA:**
  Several amino acids, including tryptophan, lysine, phenylalanine, tyrosine, leucine, isoleucine, and threonine, are degraded into acetyl-CoA or acetoacetyl-CoA. These intermediates serve as building blocks for ketone bodies, although the irreversible loss of acetyl carbons as CO_2 prevents their net use in glucose synthesis.
  • **Anaplerotic Reactions and TCA Cycle Replenishment:**
  Amino acids such as proline, arginine, histidine, glutamate, aspartate, and asparagine contribute carbon to the TCA cycle by forming intermediates like α-ketoglutarate, succinyl-CoA, or oxaloacetate. These reactions help replenish the cycle's intermediates, supporting both energy generation and biosynthetic pathways.

- **Detailed Metabolic Pathways:**
  • Pyruvate Formation:
  - **Alanine to Pyruvate:** Catalyzed by alanine aminotransferase (ALT/GPT), producing pyruvate and glutamate.
  - **Threonine Pathways:** Threonine can be converted to glycine (via threonine dehydrogenase or serine hydroxymethyltransferase) or deaminated to form α-ketobutyrate, which feeds into further metabolic steps. **• Conversion to Acetyl-CoA:**
  - **Tryptophan:** Undergoes a complex multi-step pathway yielding both alanine and a precursor for acetoacetyl-CoA.
  - **Lysine:** Metabolized via saccharopine formation and further processing to yield acetoacetyl-CoA and acetyl-CoA.
  - **Aromatic Amino Acids (Phe/Tyr):** Convert to acetoacetate and eventually to acetyl-CoA, with tetrahydrobiopterin (BH_4) facilitating key hydroxylation reactions. **• Entry into the TCA Cycle:**
  - **Branched-Chain Amino Acids (Val, Ile, Leu) and Methionine:** Degraded via pathways (sometimes grouped under the VOMIT pathway) that generate propionyl-CoA and ultimately succinyl-CoA, replenishing the TCA cycle.
  - **Glutamate, Aspartate, and Related Amino Acids:** Directly produce TCA intermediates through transamination reactions and subsequent dehydrogenase activity.
- **Metabolic Integration and Physiological Implications:**
  The degradation of amino acid carbon skeletons is tightly integrated with gluconeogenesis, ketogenesis, and the TCA cycle, ensuring that cells maximize energy extraction and maintain metabolic balance during fasting or high-protein conditions. These interconnected pathways exemplify metabolic flexibility and the efficient recycling of carbon, which is critical for overall cellular homeostasis.
- **Visual Integration:**
  A comprehensive diagram (e.g., from Reactome) illustrates the interconnected nature of these pathways, emphasizing how amino acid degradation contributes to the broader network of cellular metabolism.

In summary, this chapter provides a detailed overview of how amino acid carbon skeletons are transformed and integrated into central metabolism. It underscores the dual role of these pathways in energy production and biosynthesis, highlighting the sophisticated regulatory mechanisms that maintain metabolic balance in response to varying physiological demands.

This page titled 18.5: Pathways of Amino Acid Degradation is shared under a not declared license and was authored, remixed, and/or curated by Henry Jakubowski and Patricia Flatt.

- **11.2: Diffusion Across a Membrane - Passive and Facilitated Diffusion** by Henry Jakubowski and Patricia Flatt has no license indicated.

CHAPTER OVERVIEW

19: OXIDATIVE PHOSPHORYLATION

Return to Fundamentals of Biochemistry Search Fundamentals of Biochemistry

19.1: Electron-Transfer Reactions in Mitochondria
19.2: ATP Synthesis
19.3: Regulation of Oxidative Phosphorylation

This page titled 19: Oxidative Phosphorylation is shared under a not declared license and was authored, remixed, and/or curated by Henry Jakubowski and Patricia Flatt.

19.1: ELECTRON-TRANSFER REACTIONS IN MITOCHONDRIA

Search Fundamentals of Biochemistry

LEARNING GOALS (CHATGPT O3-MINI)

- **Describe the Role of NADH and $FADH_2$:**
  • Explain how these reducing agents, generated in the citric acid cycle, donate electrons to the electron transport chain.
  • Differentiate between the roles of NADH and FADH2 in electron transport under aerobic conditions.
- **Understand the Overall Process of Electron Transport and Oxidative Phosphorylation:**
  • Summarize how electrons flow from NADH and $FADH_2$ through a series of membrane-bound complexes to dioxygen, forming water.
  • Explain how the energy from electron transfer is used to pump protons across the mitochondrial inner membrane, establishing a proton gradient that drives ATP synthesis via ATP synthase (Complex V).
- **Detail the Structure and Function of Each Mitochondrial Complex:**
  • Identify and describe the key features and functions of Complexes I, II, III, and IV.
  • Discuss the role of mobile electron carriers—ubiquinone (UQ) and cytochrome C—in shuttling electrons between complexes.
- **Explain the Mechanisms of Electron Transfer:**
  • Describe the sequence of redox reactions in Complex I, including the roles of FMN and iron–sulfur (FeS) clusters.
  • Outline the Q cycle in Complex III and the importance of its dual electron pathways.
- **Analyze Proton Pumping and Its Coupling to Electron Transfer:**
  • Explain how electron flow through Complexes I, III, and IV is coupled with proton translocation to generate the electrochemical gradient across the inner mitochondrial membrane.
  • Discuss the structural features (e.g., antiporter-like domains, water channels, and conformational changes) that facilitate proton movement.
- **Evaluate Redox Potentials and Their Influence on Electron Flow:**
  • Understand how the standard reduction potentials (E_0 values) of various electron carriers drive the directionality of electron transfer.
  • Relate changes in the redox environment to the formation of reactive oxygen species (ROS).
- **Examine the Impact of Inhibitors and ROS Formation:**
  • Identify common inhibitors of Complex I (e.g., rotenone, piericidin A) and describe their effects on electron transport and ROS production.
  • Explain how disruptions in electron flow can lead to increased ROS, potentially resulting in cellular damage.
- **Discuss the Concept and Significance of Supercomplexes:**
  • Describe how the organization of complexes into supercomplexes (respirasomes) optimizes electron transfer and minimizes electron leak that can form ROS.
- **Integrate Mitochondrial Electron Transport with Cellular Metabolism:**
  • Explain how the mitochondrial electron transport chain links to broader metabolic pathways (e.g., the citric acid cycle) to support cellular energy production.
  • Discuss the physiological importance of maintaining efficient electron transport and proton gradients in aerobic metabolism.

These goals aim to provide students with a deep, integrative understanding of mitochondrial electron transport, from the molecular details of each complex to the overall coupling of electron flow and ATP synthesis in cellular respiration.

19.1.1: AN OVERVIEW OF MITOCHONDRIAL ELECTRON TRANSPORT

The primary oxidizing agent utilized during aerobic metabolism in the citric acid cycle is NAD^+ (although FAD is employed in one step). In the process, these oxidizing agents get reduced to form NADH (and $FADH_2$). Unless NAD^+ is regenerated, glycolysis and the citric acid cycle will halt. This occurs under anaerobic conditions when NADH formed in glycolysis is reoxidized to NAD^+ by pyruvate, which is converted to lactate.

Under aerobic conditions, we continually breathe one of the best oxidizing agents, dioxygen. NADH is oxidized back to NAD^+ not directly by dioxygen, but indirectly as electrons flow from NADH through a series of electron carriers to dioxygen, which is then reduced to water. This process is called electron transport. No atoms of oxygen are incorporated into NADH or any intermediary electron carrier. Hence, the

enzyme involved in the terminal electron transport step, in which electrons pass to dioxygen, is an oxidase. The citric acid cycle enzymes and electron transport are localized in mitochondria, which is shown in Figure **19.1.1**.

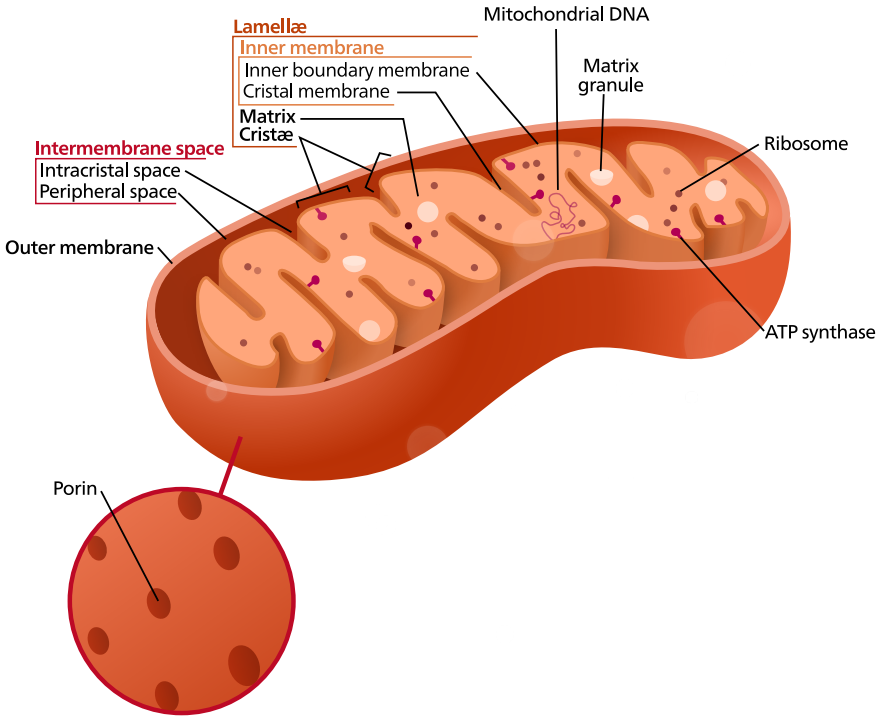


Figure **19.1.1**: Mitochondrion. (Public Domain; Kelvinsong via Wikipedia)

By analogy to the coupling mechanism under anaerobic conditions, it would be useful from a biological perspective if this electron transport from NADH to dioxygen, a thermodynamically favorable reaction (ΔG of about -55 kcal/mol, -230 kJ/mol), were coupled to ATP synthesis. It is! For years, scientists tried to find a molecule with "high energy" (with respect to its hydrolysis product) phosphorylated intermediate similar to 1,3-bisphosphoglycerate (formed by glyceraldehyde-3-phosphate dehydrogenase in glycolysis), which could drive ATP synthesis in the mitochondria. (**Remember, there is no such thing as a "high energy" bond.**) None could be found. Peter Mitchell put forward a startling hypothesis, which was proven correct, and he was awarded the Nobel Prize in Chemistry in 1978. The immediate source of energy to drive ATP synthesis was shown to come not from a phosphorylated intermediate but from a proton gradient across the mitochondrial inner membrane. All the enzyme complexes in electron transport are localized in the inner membrane of the mitochondria, as opposed to the cytoplasmic enzymes of glycolysis. A pH gradient is formed across the inner membrane in respiring mitochondria. In electron transport, electrons are passed from mobile electron carriers through membrane complexes back to another mobile carrier.

Four inner mitochondrial membrane complexes are involved in the flow of electrons to dioxygen. The first, **Complex I**, transfers two electrons from NADH to a flavin derivative, FMN, covalently attached to Complex I. The oxidation of NADH occurs, as expected, by hydride transfer. The reduced form of FMN then passes electrons in single electron steps (characteristic of FAD-like molecules, which can undergo 1 or 2 electron transfers) through the complex to the lipophilic electron carrier, **ubiquinone, UQ,** as shown in Figure **19.1.2**.

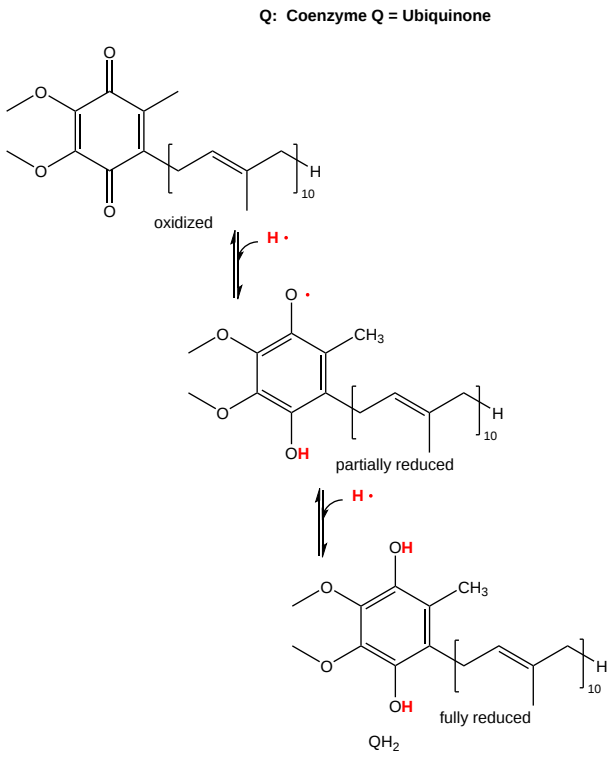


Figure **19.1.2**: lipophilic electron carrier, ubiquinone, UQ (Copyright; author via source)

This then passes electrons through **Complex III** to another mobile electron carrier, a small protein, cytochrome C. This protein has a covalently attached heme with a central iron ion that can undergo one-electron redox reactions (Fe^{3+} + $1e^{-}$ ↔ Fe^{2+}). Reduce cytochrome C (Fe^{2+}), which passes electrons through **Complex IV**, **cytochrome C oxidase**, to dioxygen to form water. At each step, electrons are passed to stronger oxidizing agents, as indicated by their increasing positive standard reduction potentials. Hence, the oxidation at each complex is thermodynamically favored. Four electrons must be added to dioxygen and four H^{+} ions to form water.

$$\mathbf{O_2 + 4\,e^- + 4\,H^+ \longrightarrow 2\,H_2O.}$$

What happened to Complex II? **Complex II** (also called succinate:quinone oxidoreductase) contains the citric cycle enzyme succinate dehydrogenase, which catalyzes the oxidation of succinate to fumarate by FAD. The bound $FADH_2$ does not dissociate from the enzyme, which is functionally dead for further formation of fumarate until it is oxidized back to FAD by additional components of Complex II. In this process, electrons from $FADH_2$ are passed to the same lipophilic mobile electron carrier from Complex I, ubiquinone. Reduced ubiquinone can then transfer electrons to cytochrome C through Complex III.

For Complex I, III, and IV, the energy released by the oxidative event is used to drive protons from the matrix to the intermembrane space of the mitochondria. The oxidative energy released is not used to form a "high-energy" mixed anhydride, as seen in the glyceraldehyde-3-phosphate dehydrogenase reaction from glycolysis. The resulting proton gradient collapses in a thermodynamically favorable process that energetically drives the endergonic synthesis of ATP by the last inner membrane complex, **ATP synthase,** which is sometimes called **Complex V**. This aerobic coupling of electron transfer (from NADH to dioxygen) and ATP synthesis is shown schematically in Figure **19.1.3**. Electron transfer is often referred to as electron transport, which might suggest that it requires energy, as is the case with active transport. However, it does not, since it is strongly favored thermodynamically with dioxygen as the final electron acceptor.

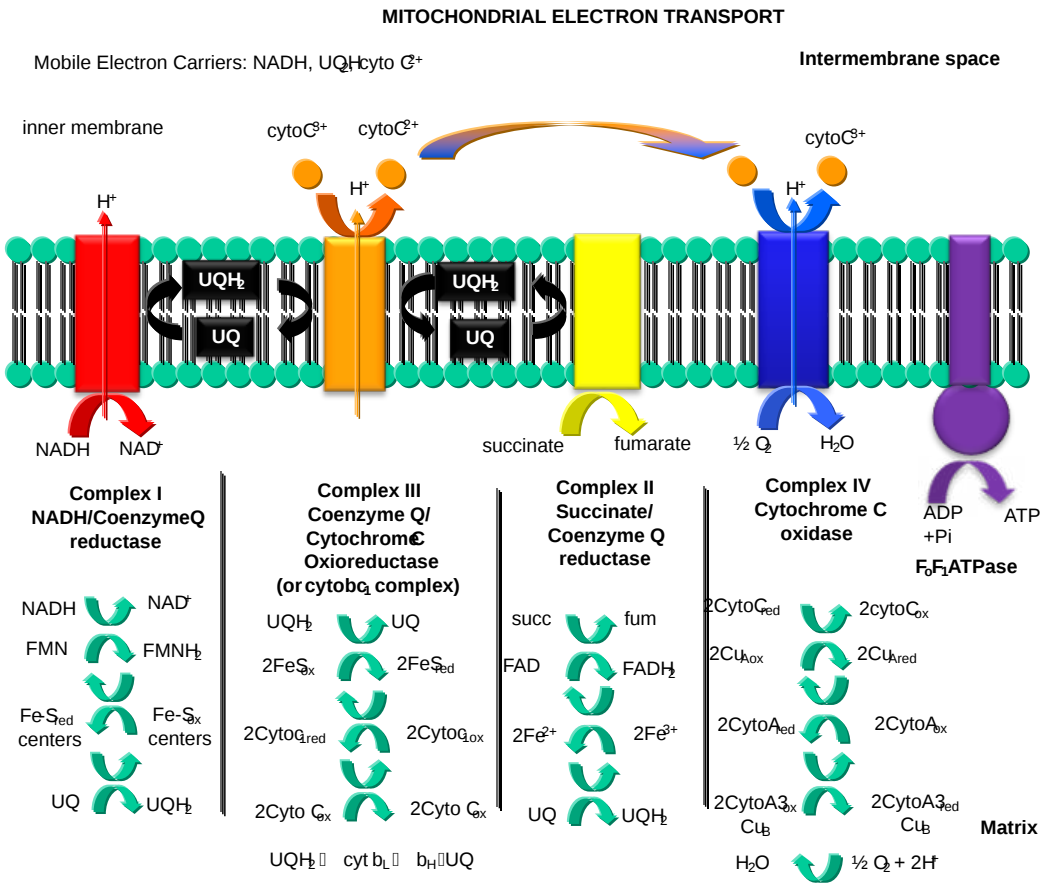


Figure **19.1.3**: ELECTRON TRANSPORT AND PROTON GRADIENT FORMATION IN THE MITOCHONDRIA (after Voet and Voet)

You may wish to question the need for such a complicated series of reactions to move the simple electron from one chemical species to another, and a simple H^+ from one side of a membrane to another to form a proton gradient that collapses anyway. The movers of these species are aligned in the membrane to optimize the processes and allow the vectorial, nonrandom flow of electrons and protons. This is what evolution has produced. One reason must be to maintain optimal control over the efficiency of the coupled reaction. Another powerful explanation is to reduce dangerous side reactions. In redox chemistry, this process involves the formation of highly reactive free radicals that can react quickly and uncontrollably with any nearby species. This is especially true when dioxygen is involved (see Chapter 13.4 - The Chemistry and Biology of Dioxygen). It takes 4 electrons to reduce dioxygen to water. If this process is interrupted, highly reactive oxygen species (ROS), such as superoxide and peroxide, can form, damaging membranes, proteins, and nucleic acids.

Before we explore each complex in more detail, let's get a lower-resolution view of the entire mitochondrial electron transport and ATP synthesis (often called **oxidative phosphorylation or ox-phos**), which is shown in cartoon form in Figure **19.1.4**.

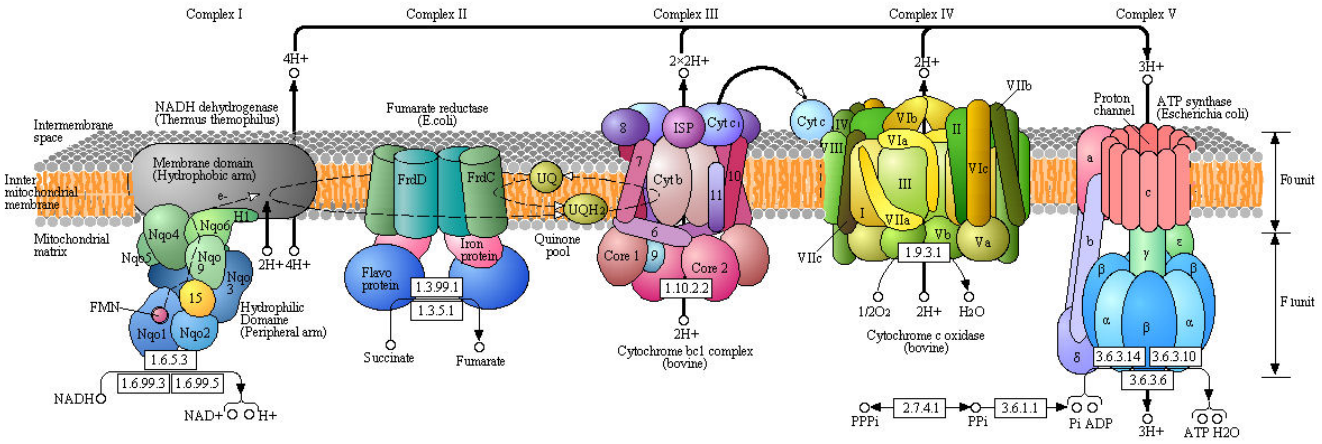


Figure **19.1.4**: Overview of coupled electron transport and ATP synthesis (reprinted with permission from Kanehisa Laboratories and the KEGG project: www.kegg.org). Numbers represent Enzyme Commission Numbers. Original KEGG Map with embedded links.

Especially note:

- the subunit complexity of each Complex;
- the location of the subunits (many integral membrane proteins, others more hydrophilic and located in the polar matrix);
- the mobile electron carriers NADH/NAD^+, lipophilic UQH_2/UQ used for both complex I and II, cytochrome C (a protein), and O_2;
- the number of H^+s moved from the matrix to the intermembrane space through Complexes I, III, and IV and back through ATP synthase.

Also note that the prokaryotic structures are displayed, even though they are placed within the mitochondrial membrane. Bacteria do not have organelles like mitochondria, but have the same complexes inserted into their plasma membranes. For bacteria, protons are ejected into the periplasmic space, which lies between the plasma membrane and the cell wall.

Diagrams like the one shown in Figure **19.1.4** are useful in simplifying complex biological systems. At the same time, they constrain our ideas about how, in this case, the individual complexes are arranged in the membrane. Much evidence suggests that Complex I, III, and IV (those that pump protons) form a large supercomplex called the **respirasome,** which has approximately 80 subunits in mammals**.** Clustering the subunits in a supercomplex increases the likelihood that shared mobile electron carriers will not diffuse away but continue passing electrons along the electron transport chain. As mentioned, some reactions generate reactive oxygen species, which must be kept in the complex to avoid their toxic effects. The stability of the individual complexes is also likely to be increased in the larger aggregate.

Using cryoelectron microscopy (cryoEM), the structures of two large super- and megacomplexes have been solved, revealing the arrangement of all the respiratory complexes. Two different structures showing the SuperComplex-$I_1III_2IV_1$ ($SCI_1III_2IV_1$) and MegaComplex-$I_2III_2IV_2$ ($MCI_2III_2IV_2$) are shown below in Figure **19.1.5**.

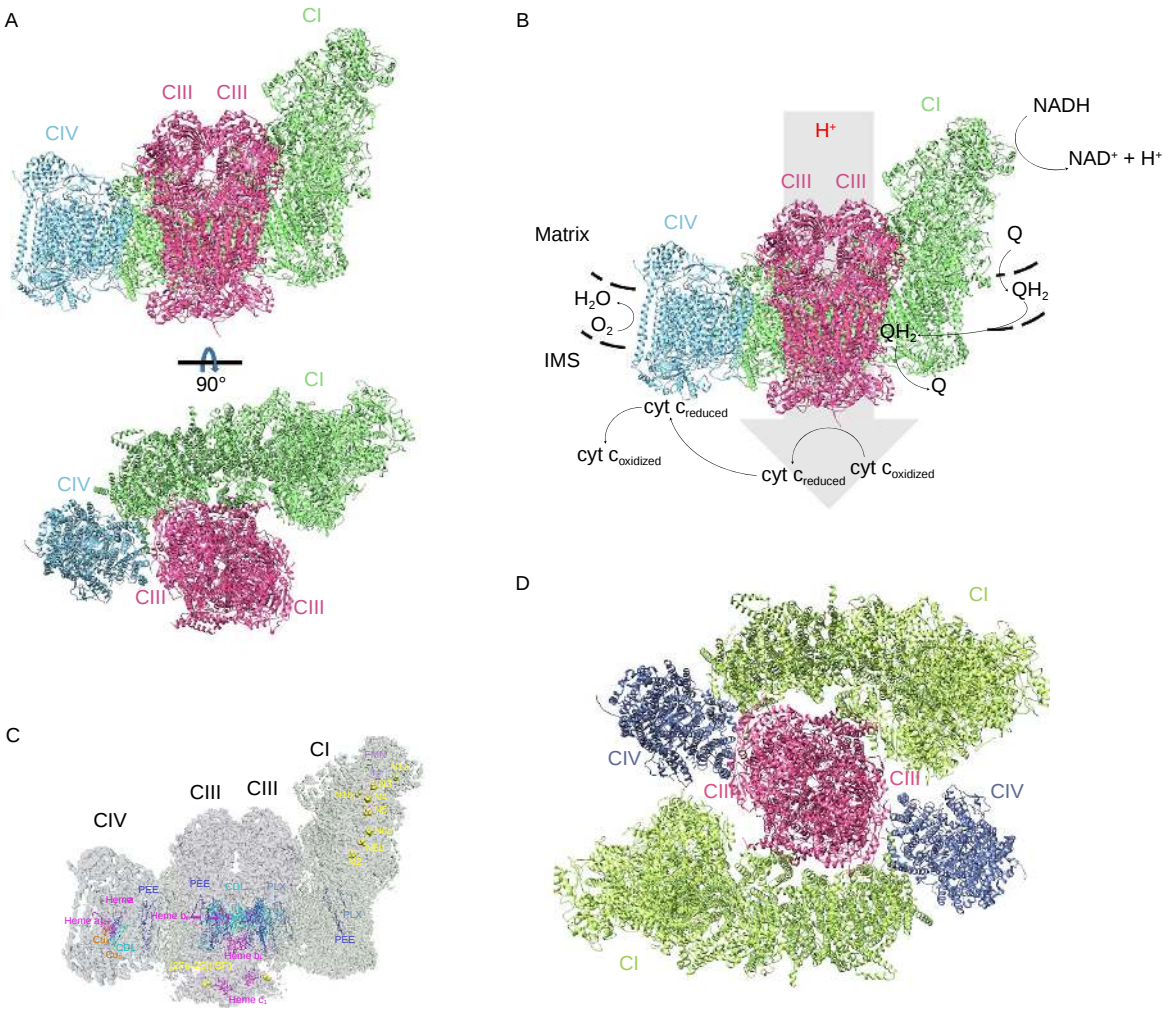


Figure 19.1.5: Structures of Mammalian SCI1III2IV1 and MC I2III2IV2. Meng Wu et al. Protein Cell 2020, 11(5):318–338. https://doi.org/10.1007/s13238-019-00681-x. Creative Commons Attribution 4.0 International License, https://creativecommons.org/licenses/by/4.0/.

Panel (A) shows human SCI1III2IV1 (PDB ID: 5XTH) in side view (along the inner membrane) and a top-down view. Note that CI is adjacent to CIII (located in the center), which is adjacent to CIV. This is the expected orientation, given the flow of electrons from NADH to dioxygen. In panel (B), substrates and products are included in the side view, along with the flow of H^+ (from all of the complexes) into the matrix. Panel C shows the added cofactors (FeS clusters, FMN, hemes, etc). Panel (D) shows a beautiful top-down view of the human megacomplex, which has two copies of each subunit. Again, note the centrality of Complex III.

Figure 19.1.6a shows another model of the megacomplex with Complex II (CII, which does not translocate protons across the membrane) added. It also shows a tetramer of Complex V (ATP synthase)

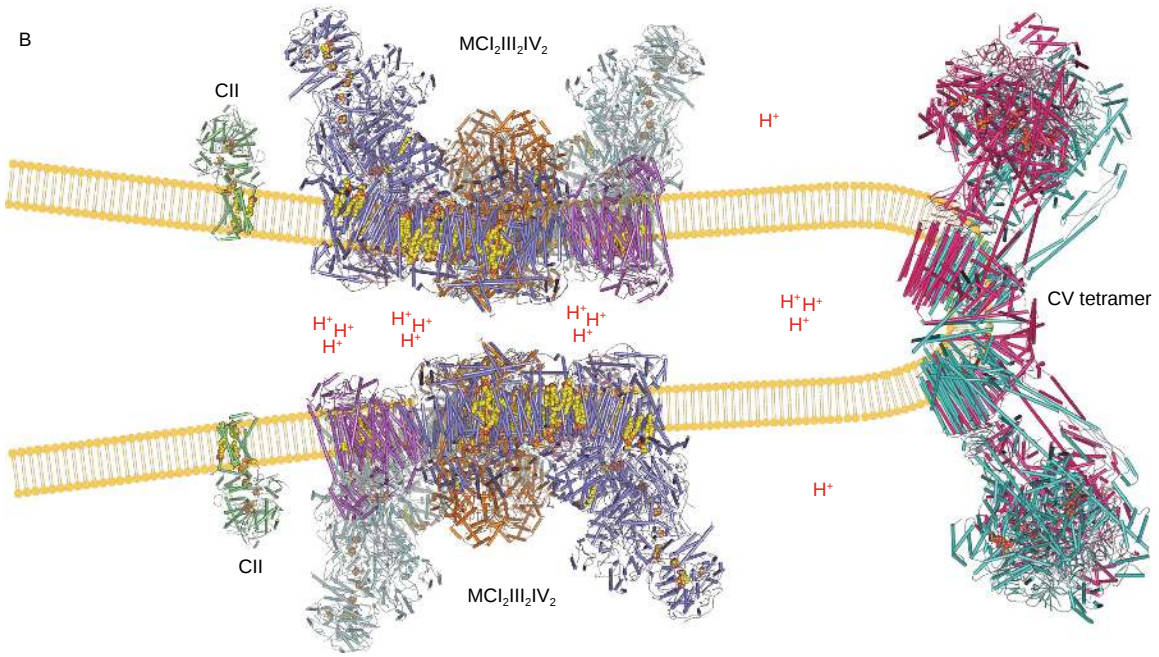


Figure **19.1.6*a***: Arrangement of CII, MCI2III2IV2, and CV tetramer on mitochondrial cristae. (PDB ID of CII: 1ZOY. PDB ID of MCI2III2IV2: 5XTI. PDB ID of SCI1III2IV1: 5XTH. PDB ID of CV: 6J5K. Meng Wu et al. Protein Cell 2020, 11(5):318–338. https://doi.org/10.1007/s13238-019-00681-x. Creative Commons Attribution 4.0 International License, https://creativecommons.org/licenses/by/4.0/.

Recently, Cryo-electron tomography and electron microscopy were used to determine the structures of the respirasome supercomplex in *Chlamydomonas reinhardtii* (green algae). A model (similar but different from the one shown in Figure 6a) was constructed, which is shown in Figure **19.1.6*b*** below.

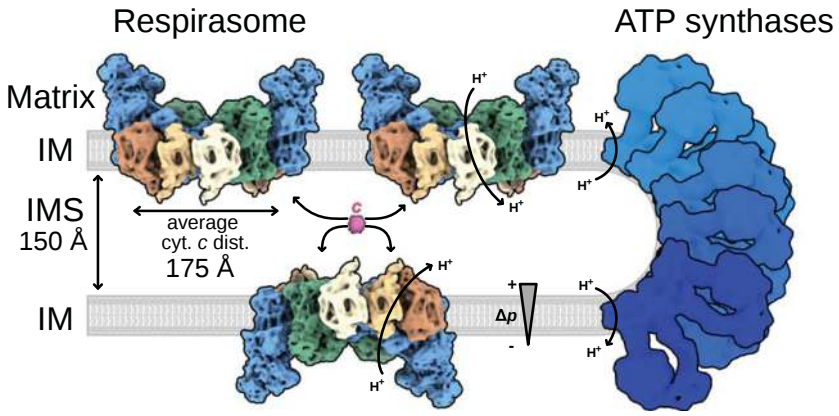


Figure **19.1.6*b***: Schematic side view of a crista in Chlamydomonas reinhardtii. From Florent Waltz *et al.* In-cell architecture of the mitochondrial respiratory chain. *Science* **387**,1296-1301(2025).DOI:10.1126/science.ads8738. Reprinted with permission from AAAS.

IM (transparent gray); Blue, complex I; green; complex III; red-orange/yellow/light yellow, complex IV monomers, respectively. Cytochrome C is depicted as a labeled, reddish circle labeled 'c'.

Complexes I, III, and IV assemble in the flat membrane region of mitochondrial cristae. At the same time, multiple copies of ATP synthase (also called Complex V) are found in the curved membrane connecting the two flat cristae inner membranes. ATP synthase likely induces the curvature of the cristae membrane.

Cytochrome C is a substrate/product of complexes III and IV (see Figure 4 above). Given the membranes and complexes' spacing, cytochrome C likely diffuses freely between copies of supercomplexes of I, III, and IV instead of channeling between multiple complexes in a faster than 3D diffusional search for its binding sites. No free complex I and III were observed, suggesting they are in supercomplexes (i.e., respirasomes). Hence, the respirasomes appear to create the geometry of the cristae and membranes, with the small spacing (150 Å) between the inner membranes facilitating proton flux to the curved membrane occupied by ATP synthase for efficient respiration.

Now, let's explore each complex in more detail.

19.1.2: COMPLEX I - NADH-QUINONE OXIDOREDUCTASE

Complex I is located in the inner mitochondrial membrane in eukaryotes and the plasma membrane of bacteria. Bacteria have only 14 subunits, while the mammalian Complex I has 45, including the core 14 found in bacteria. Another 31 are termed **supernumerary** (in excess of the "normal number") subunits that support the function of the core. The significance of the extra mammalian subunits is still unclear. A cartoon model with the actual crystal structure of the Thermus thermophilus (bacterial) complex is shown in Figure **19.1.7**. The hydrophilic or peripheral domain catalyzes electron transfer, while the membrane domain (encoded by mitochondrial DNA) is involved in the active transport of protons. It is one of the biggest "enzymes" around, making it exciting to try and understand!

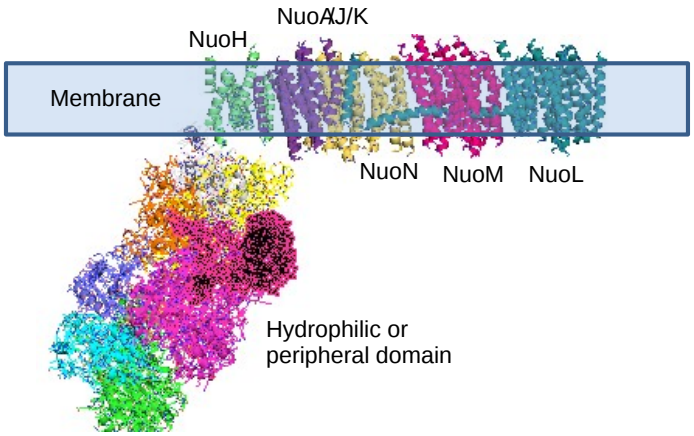
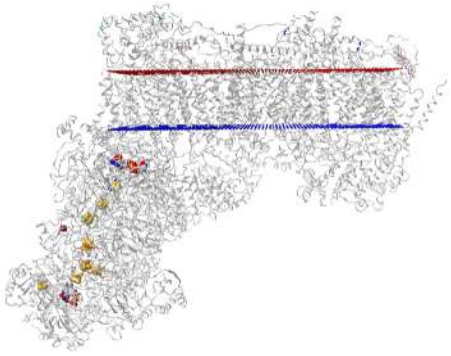


Figure **19.1.7**: Detailed view of Complex I from Thermus Thermophilus (Copyright; author via source)

Figure **19.1.8** shows an interactive iCn3D model of the mammalian respiratory complex I (5LDW)



NCBI iCn3D Figure **19.1.8**: Mammalian respiratory complex I (5LDW). (Copyright; author via source).

Click the image for a popup or use this external link: https://structure.ncbi.nlm.nih.gov/i...xVjRPLLgaLCi17 (both load slowly given the size of the structures). For the external link, use the mouse scroll to zoom the structure to see the labeled FeS clusters and FMN.

The red and blue parallel "dummy" atoms represent the boundary of the mitochondrial inner membrane.

19.1.2.1: ELECTRON TRANSFER IN COMPLEX I

Electron flow occurs from NADH to UQ through a series of one-electron carriers in the hydrophilic or peripheral domain of Complex I. The initial handoff of electrons occurs to a flavin cofactor, FMN, and then through a series of Fe/S clusters to ubiquinone. These electron acceptors include tetranuclear (Fe_4S_4) and binuclear (Fe_2S_2) iron-sulfur clusters, a FMN flavin mononucleotide, and a Mn (II) ion. These are shown in Figure **19.1.9**.

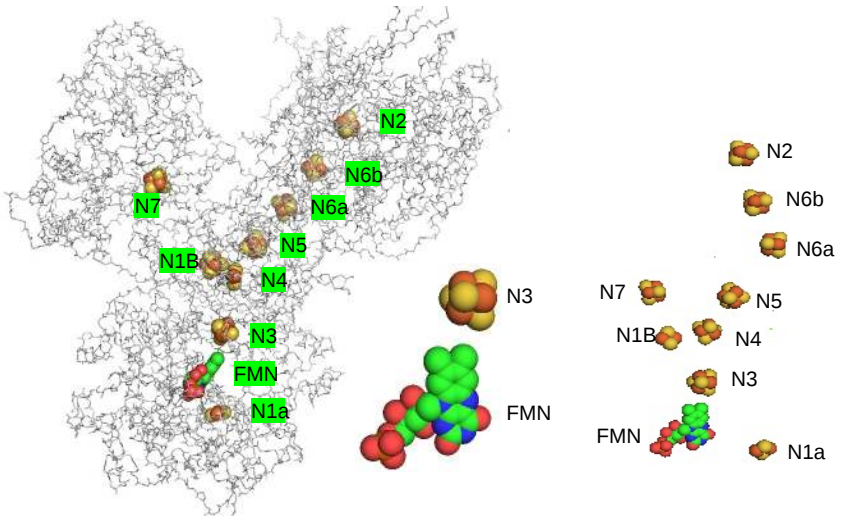


Figure **19.1.9**: Electron Flow in Complex I from T. Thermophilus (Copyright; author via source)

The tetranuclear Fe_4S_4 cluster is based on the cubane structure with Fe and S occupying alternating corners of a square in a tetrahedral geometry. Each Fe is also coordinated to thiolate (RS^-) groups from coordinating cysteines, as well as sulfide (S^{2-}) anions. The actual structure is a distorted cube, as shown in Figure **19.1.10**, along with that of the binuclear Fe_2S_2 cluster, whose bond angles also deviate from those in a perfect tetrahedron.

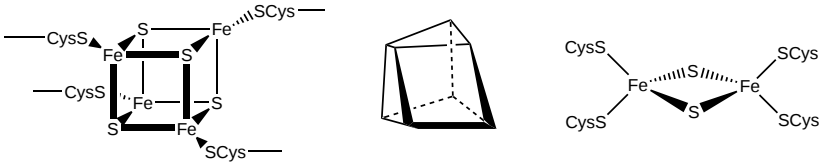


Figure **19.1.10**: Fe/S Clusters in Complex I (Copyright; author via source)

Many micro-redox states with different standard reduction potentials are possible for tetranuclear Fe_4S_4 clusters, much as polyprotic acids have multiple pKa values. The two relevant to the tetranuclear clusters in Complex I are shown below:

a. $Fe(II)Fe(III)_3/S_2(CysS)_2^{1-} + e^- \leftrightarrow Fe(II)_2Fe(III)_2/S_2(CysS)_2^{2-}$ (less positive standard reduction potential)

b. $Fe(II)_2Fe(III)_2/S_2(CysS)_2^{2-} + e^- \leftrightarrow Fe(II)_3Fe(III)/S_2(CysS)_2^{3-}$ (more positive standard reduction potential)

PK$_A$S AND E^0 VALUES

You have studied Bronsted acids in many courses and are familiar with the factors that affect the pKa of **structurally similar acids**. These include the initial charge on a potential proton donor. The relative strength of a series of structurally similar acids can be predicted by examining the factors that stabilize the negative charge on the resulting conjugate base. The more stable the conjugate base, the more acidic the parent acid. Factors that stabilize a negative conjugate base are the electronegativity of the atom holding the negative charge, resonance, which might delocalize the charge, the inductive/electron release effect of substituents, and the hybridization of the atom holding the charge (sp anions are more stable due to more s character with electrons pulled more closely to the nucleus).

What about a single acid? The pKa of a given acid is a constant for a given set of conditions (temperature, solvent polarity, etc), but it can be altered by changing conditions. The diagram below in Figure **19.1.11** shows ways to "tip" the pKa of a given acid (in this case, a simple carboxylic acid) to a lower value, making the acid stronger in the new set of conditions.

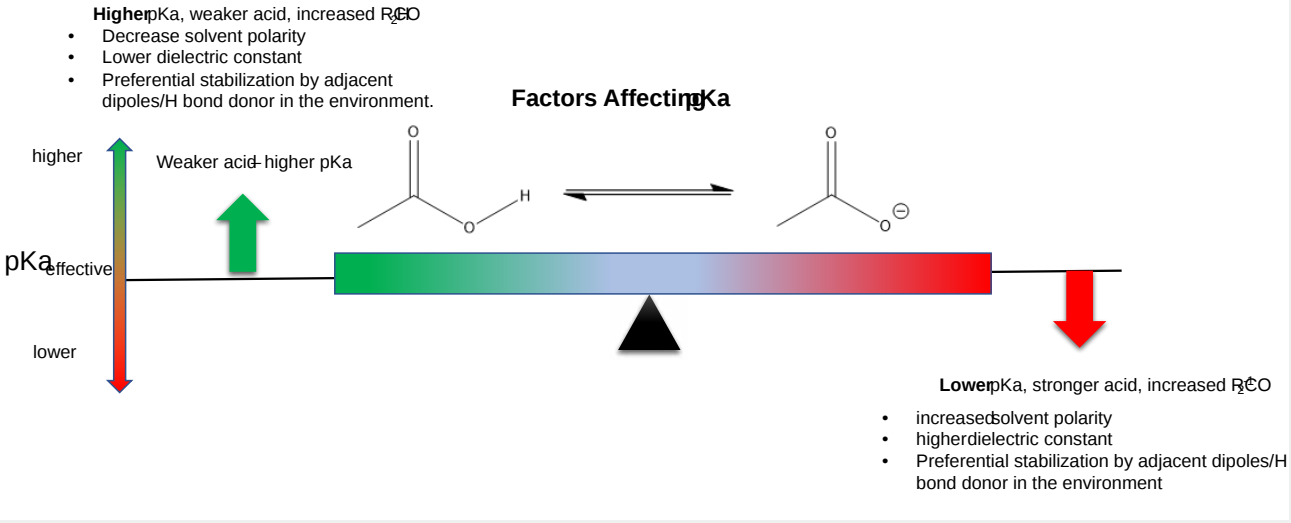


Figure 19.1.11: Factors affecting pKa of a given acid

The same ideas apply to the strength of a potential oxidizing agent (electron acceptor) as described by the E^0 value (higher for stronger oxidizing agents/electron acceptors). Figure 19.1.12 shows the factors that could alter the E^0 value for a binuclear FeS cluster. In this case, changes in coordinating ligands, analogous to changes in substituents for an acid) are included since most students have probably spent more time thinking about pKa values than E^0 values.

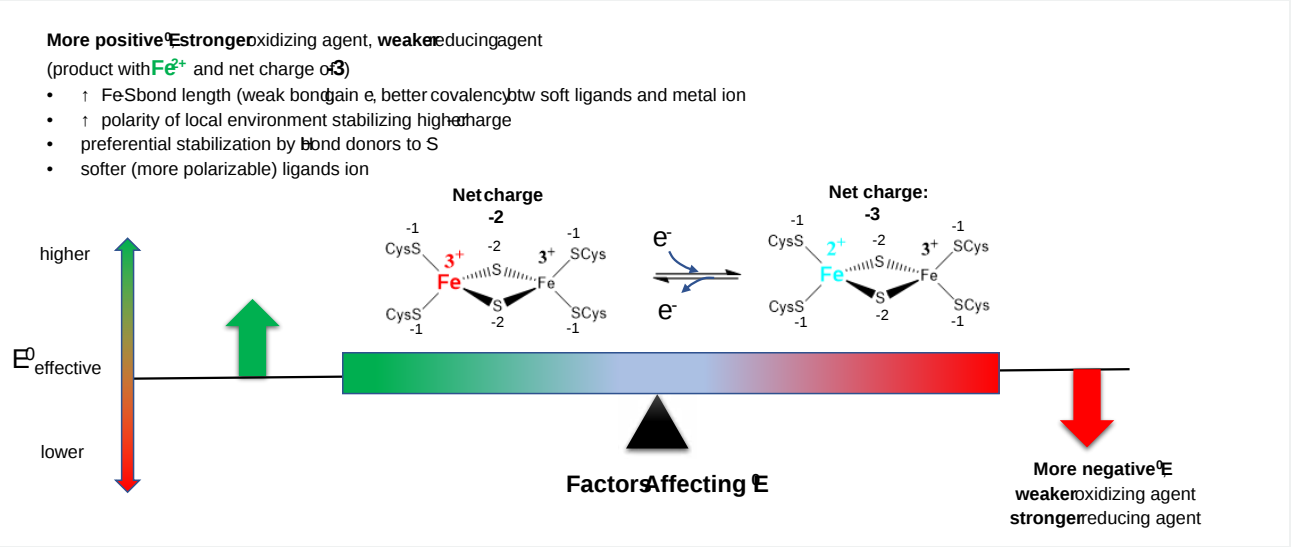


Figure 19.1.12: Factors affecting E^0.

In both acid/base and oxidizing agent/reducing agent cases, the balance of the reactions can be understood through Le Chatelier's principle. The chemical equilibrium can be shifted to the right (deprotonating) for a stronger acid with a lower pKa, or (accepting an electron) for a strong oxidizing agent with a higher E^0. In both cases, this is achieved by preferentially stabilizing products over the initial reactants.

Electrons are passed singly to oxidized UQ in one-electron steps to form UQH_2.

Fe-S clusters are synthesized predominantly in the mitochondria, serving as redox cofactors in electron transport, as described above. They are ubiquitous in all life forms and serve additional roles beyond being redox cofactors. They serve structural roles in proteins and are utilized in redox signaling within the cell, as they change oxidation states. Many proteins interacting with DNA (repair enzymes, polymerases, and helicases) contain an FeS cluster.

Evidence suggests that they played critical roles in the abiotic evolution of life, where oxygen was absent as a terminal electron acceptor in exergonic oxidation reactions. When oxygen became more readily available, it became toxic to the cell as free Fe^{2+} could participate in reactions (such as the Fenton reaction), leading to deleterious reactive oxygen species (such as superoxide). To prevent toxicity from the iron ions themselves, they are carried and delivered to the cytoplasm and nucleus by cytoplasmic iron-sulfur assembly (CIA) proteins.

Figure **19.1.13** shows models of the complex and paths for electron flow.

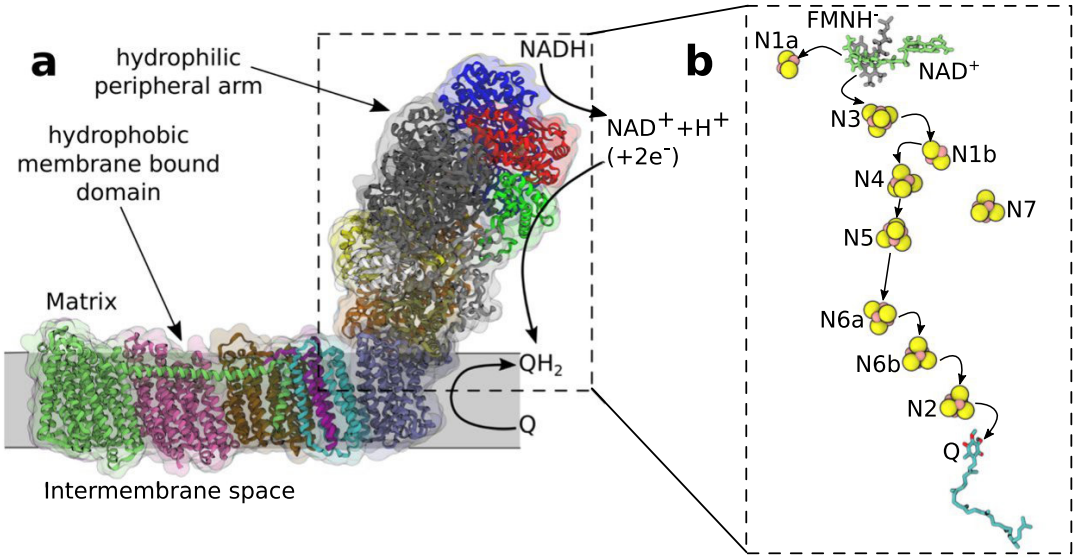


Figure **19.1.13**: Complex I and electron transfer. Martin, D.R., Matyushov, D.V. Electron-transfer chain in respiratory complex I. *Sci Rep* **7,** 5495 (2017). https://doi.org/10.1038/s41598-017-05779-y. Creative Commons Attribution 4.0 International License, http://creativecommons.org/licenses/by/4.0/.

Electrons "tunnel" from one cofactor to another in Complex I through quantum mechanical "hops". Since all redox cofactors after the favored hand-off of electrons from NADH to FMN are FeS clusters with similar E^0 values (modulated only by local environments), there is no significant thermodynamic barrier to electron flow. The final N2 FeS cluster has an E0 value about 100 mV higher than the initial clusters; this final electron acceptor most readily accepts an electron.

The separation of the hydrophilic mitochondrial matrix domains, where electron transfer occurs, from the transmembrane domains, where proton transfer occurs, is an elegant design that keeps the key and reactive particles, e^- and H^+, from reacting with each other. The electrons stay on one side of the membrane, as the protons move to the other side (until the return in the last step when Complex V produces ATP).

19.1.2.2: PROTON TRANSFER IN COMPLEX I

Proton transport occurs in the membrane domain. Available evidence suggests that 4 protons move from the cytoplasm to the periplasmic space against a concentration gradient during a catalytic cycle of Complex I in bacteria and other organisms.

Figure **19.1.14** shows multiple views of both the key electron transfer step and H^+ ejection from the matrix into the intermembrane space. The key to proton transport is the discrete membrane domains shown in the bottom left part of Panel (a). There are four such domains involved from left to right, each one associated with the transport of $1H^+$. The individual membrane domains have different names and abbreviations depending on the organism. They are from left to right:

- Nqo12, NuoL or ND5
- Nqo13, NuoM, or ND4
- Nquo14, NuoN or ND2
- Nqo8, NuoH, or ND1.

The Nqo8, NuoH, or ND1 domain is proximal and closely linked to the site for the reduction of UQ to UQH_2.

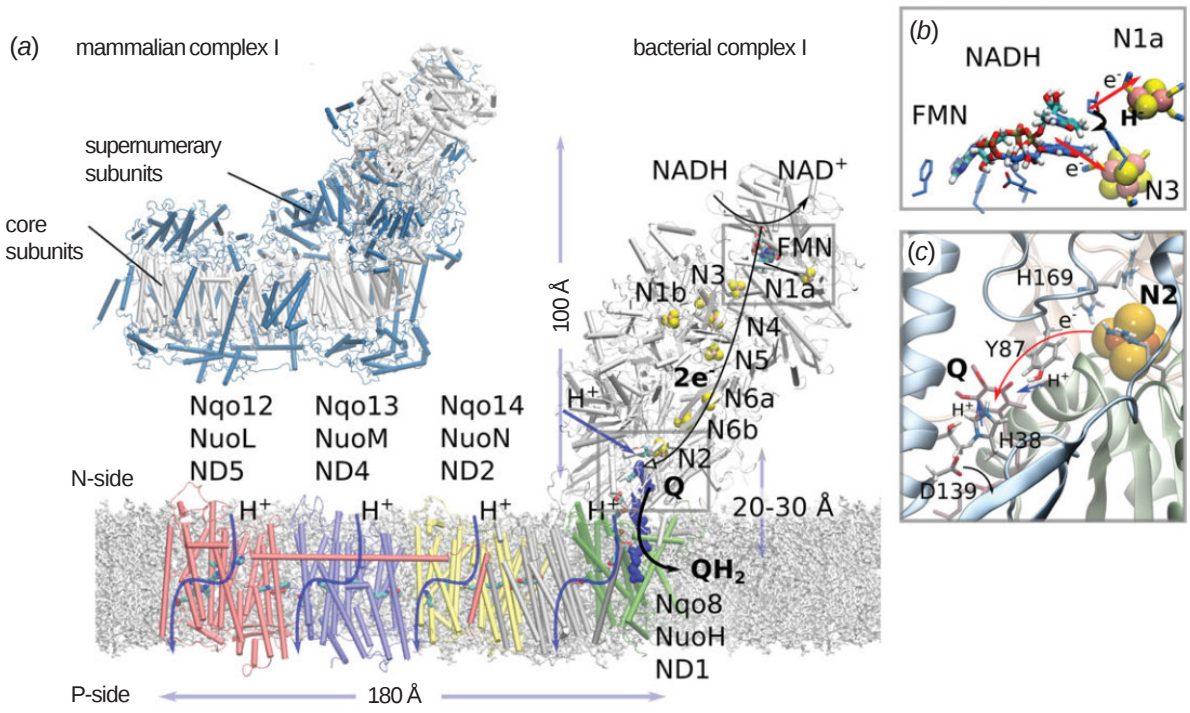


Figure **19.1.14**: Structure and function of complex I. Panel (a) shows a large structural model of complex I from Thermus thermophilus (4HEA) showing the flow of electrons in the hydrophilic domain, while the mammalian complex (5LC5), with its supernumerary subunits in blue, is shown at the top left. Panel (b) shows the NADH/FMN site (3IAM) and its close proximity to the N3 tetranuclear cluster. Panel (c) shows the N2/Q reduction site with pi-stacking interactions of the ubiquinone ring with the aromatic His 38 ring. The P (positive side) accumulated H^+s while the N (negative side) becomes depleted in them. Kaila VRI. 2018 Long-range proton-coupled electron transfer in biological energy conversion: towards mechanistic understanding of respiratory complex I. J. R. Soc. Interface 15: 20170916. http://dx.doi.org/10.1098/rsif.2017.0916. Creative Commons Attribution License http://creativecommons.org/licenses/by/4.0/,""

The NuoN/Nqo14/ND2, NuoM/Nqo13/ND4, and NuoL/Nqo12/ND5 domains act as and are structurally similar to antiporters. Note also a very long helix that crosses the left three-most antiporter domains. This helix runs parallel to the membrane and likely acts as a lever, allowing for coupled conformational changes in the three H^+ transporters. We examined transporters in a previous chapter, and it was demonstrated in both cartoon and structural models that they alternated between inward- and outward-open conformations.

Figure 19.1.15 details the antiporter domains and the unique structural features allowing proton transport. Each antiporter domain consists of two 5-helix bundles, displaying pseudo-symmetry, with transmembrane helices numbered TM4-8 and TM9-13. The next-to-last helix in each bundle (7 and 9) is interpreted, with unbroken parts of the helices numbered TM7a/b and TM12a/b. Running along the middle of each of the antiporter-like domains of the membrane domain is a series of conserved charged amino acids (aspartate, glutamate, lysine, and histidine) that participate in a hydrogen bonding network. Molecular dynamics simulations show water molecules (panel b), represented by red dots (for the oxygen atoms), transiently occupying a hydrogen-bonded water network that serves as a conduit for H^+ flow. An unbound "naked" proton (H^+) would not persist long in any aqueous biological system. Panel C shows the conformational flexibility in broken interrupted helices that presumably gates the proton pore open and closed.

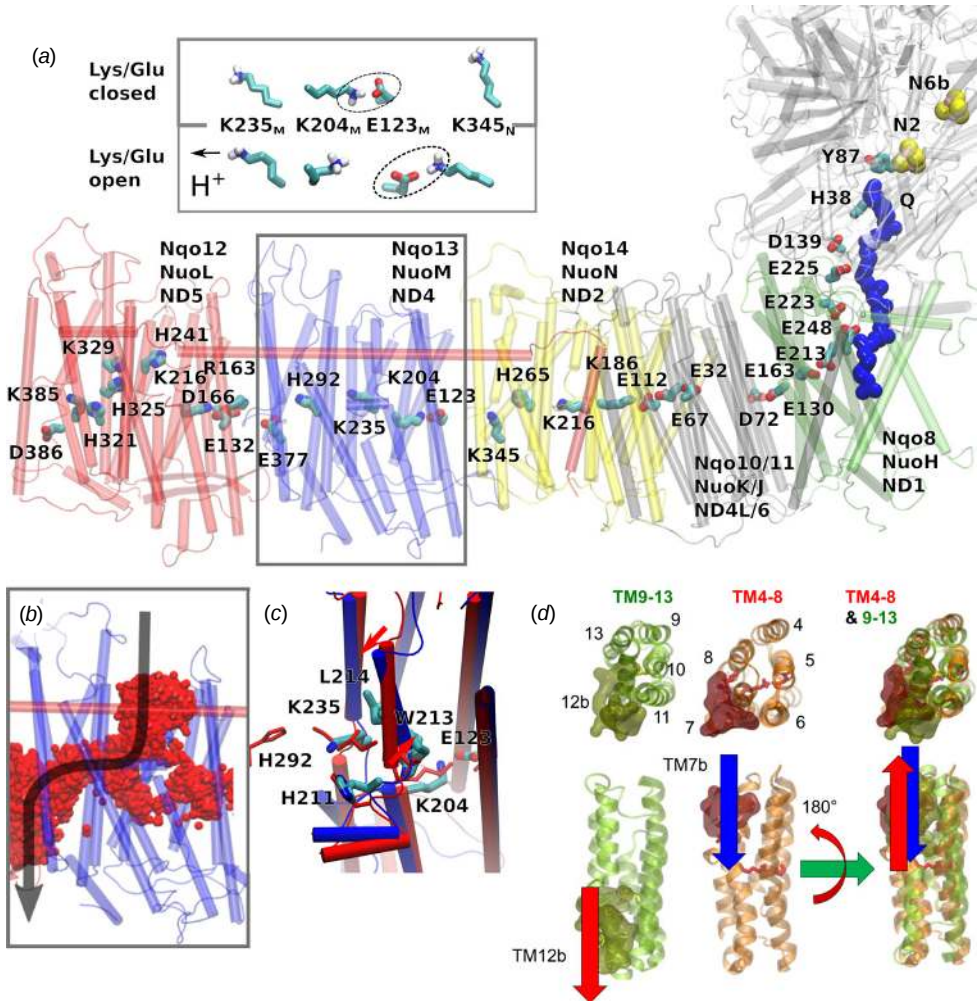


Figure **19.1.15**: Structure of the proton-pumping membrane domain in complex I.

(a) The membrane domain of complex I has conserved buried charged/hydrophilic residues. NuoL (red); NuoM (blue); NuoN (yellow); NuoH (green); Ubiquone - Q (blue van der Waals representation). Inset: The conformation of the Lys/Glu ion pair (here Lys-204M/Glu-123M) can modulate the pKa of the middle Lys (Lys-235M).

(b) The NuoM antiporter-like subunit with water molecules (red dots). The arrow indicates the flow of protons through a hydrogen-bond-linked network of water molecules that "visit" the structure during a μs molecular dynamics simulation.

(c) Snapshot of structures obtained from molecular dynamic simulations of open (in blue) and closed (in red) proton channels from the N-side in Nqo13 (NuoM/ND4), showing conformational changes in the broken helix element.

(d) The structural symmetry of the antiporter-like subunits with an N-side input channel near broken helix TM7b and an output channel near broken helix TM12b.

Kaila VRI. 2018 Long-range proton-coupled electron transfer in biological energy conversion: towards mechanistic understanding of respiratory complex I. J. R. Soc. Interface 15: 20170916. http://dx.doi.org/10.1098/rsif.2017.0916. Creative Commons Attribution License http://creativecommons.org/licenses/by/4.0/,

How is the reduction of ubiquinone and proton transport coupled? The mechanism likely involves conformational changes in flexible regions at the interface of the complex's hydrophilic and membrane domains.

19.1.2.3: INHIBITION OF COMPLEX I

Complex I is inhibited by more than 60 different families of compounds. They include the classic Complex I inhibitor rotenone and many other synthetic insecticides/acaricides. The classes include Class I/A (the prototype of which is Piericidin A), Class II/B (the prototype of which is Rotenone), and Class C (the prototype of which is Capsaicin). They appear to bind at the same site. Figure **19.1.16** shows their structures. From the structure of the three prototypes, what are the characteristics of the pharmacophore, the “ideal binding ligand”? Where are they likely bound? How “promiscuous” is the binding site?

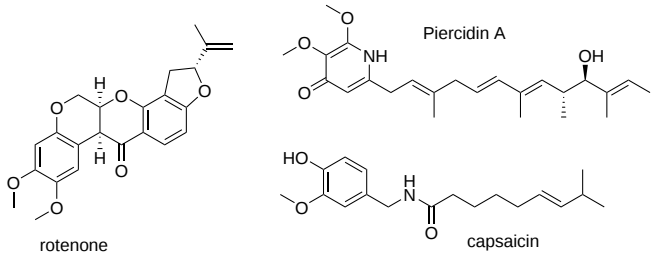


Figure **19.1.16**: Inhibitors of Complex I (Copyright; author via source)

Many devastating neurological diseases are associated with defects in Complex I. In addition to major problems with oxidative ATP production, reactive oxygen species (ROS) increase. Complex I and Complex III are the major sites for generating ROS. Given the locations of the electron carriers at the periphery and internal within the protein complex, which electron carriers might most readily leak electrons to dioxygen? What ROS is likely to form in the process?

Inhibitors might block access to UQ or conformational changes necessary for the final reduction of the ubiquinone free radical. Class A inhibitors dramatically increase ROS production. The actual site of ROS production in Complex I is a bit controversial. One possible electron donor to dioxygen is FMN since both can engage in 1 e^- transfers. Mutants that lack N2 iron-sulfur cluster showed ROS production.

In submitochondrial preparations, normal Complex I activity occurs (which leads to the formation of a sustained proton gradient). Also, reverse electron transport, powered by an artificial proton gradient, can occur, which leads to the reduction of NAD^+, as shown in Figure **19.1.17**.

Figure: Normal and Reverse Electron Transport Complex I

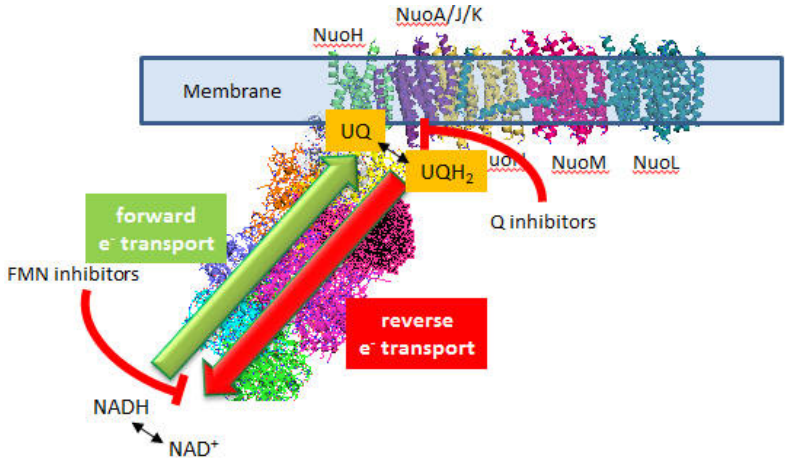


Figure **19.1.17**: Overview of forward and reverse electron transport in Complex I.

A summary of the findings on superoxide production by Complex I shows that:

- flavin site inhibitors inhibit superoxide production but not Q site inhibitors.
- reverse electron transport leads to NAD^+ and O_2 reduction
- Reverse electron transport superoxide production is inhibited by both flavin and Q site inhibitors

Figure **19.1.18** shows an expanded view of electron transport and sites where ROS production is enhanced. Refer to the legend for details.

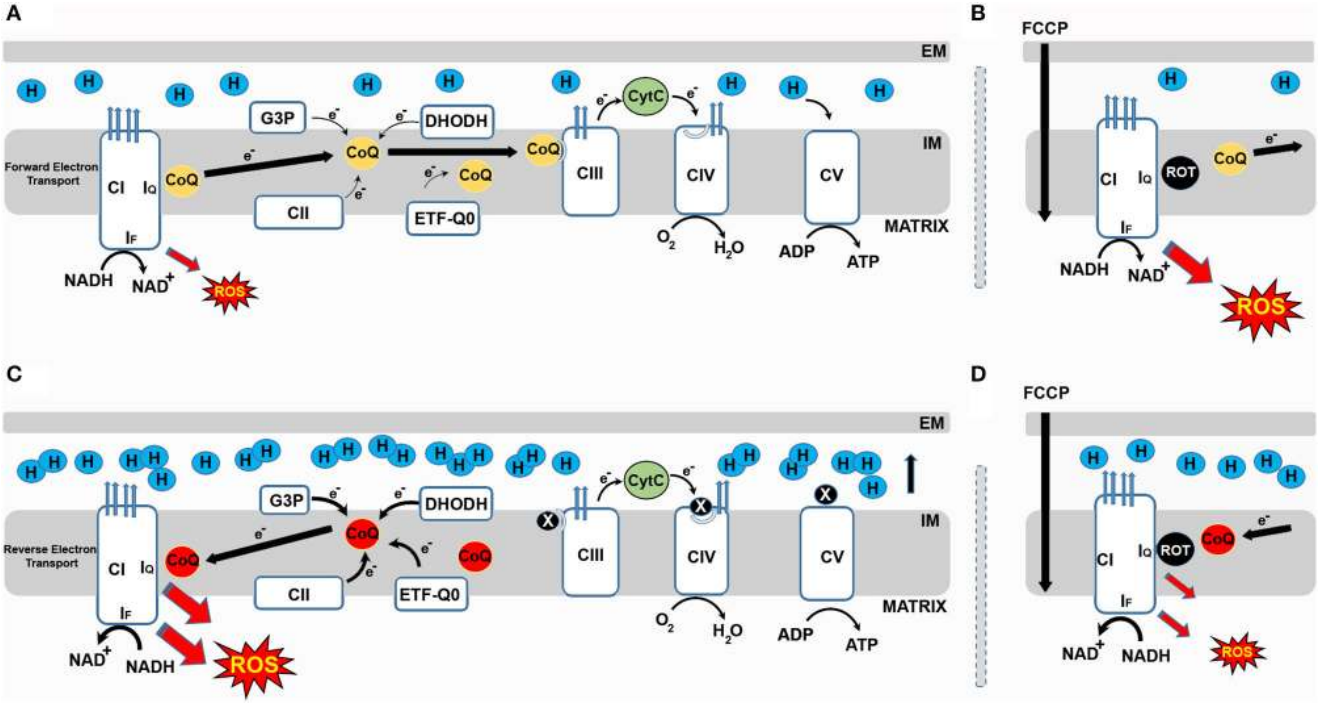


Figure **19.1.18**: Complex I (CI) produces ROS in both the forward and reverse directions. Scialò Filippo et al. Frontiers in Physiology (8), 2017. https://www.frontiersin.org/article/...hys.2017.00428. DOI=10.3389/fphys.2017.00428. **Creative Commons Attribution License (CC BY)**.

(A) During **forward electron transfer (FET)**, ubiquinone, also called Coenzyme Q (CoQ), receives electrons from complexes I and II, glycerol-3-phosphate dehydrogenase (G3P), electron-transferring flavoprotein (ETF-QO), or dihydroorotate dehydrogenase (DHODH). During this process, electrons mainly leak to produce superoxide from the FMN binding site (I_F) of CI during the oxidation of NADH to NAD^+.

(B) In these conditions, if rotenone blocks the ubiquinone binding site (I_Q), electrons cannot be transferred to CoQ, so they leak and generate ROS. FCCP, a molecule that collapses the H^+ gradient by simple diffusion across the membrane, bypassing Complex V - ATP synthase. This also increases mitochondrial ROS generation during FET.

(C) When the CoQ pool becomes over-reduced, a high membrane potential favors the reverse transfer of electrons from ubiquinol to CI in a process called **reverse electron transport (RET)**. During RET, electrons leak at either IF or IQ, generating a significant amount of superoxide.

(D) Blocking the I_Q site with rotenone during RET prevents CoQ from transferring electrons back to CI and reduces ROS production. Similarly, FCCP reduces ROS by dissipating membrane potential.

19.1.3: COMPLEX III

Complex III is a complicated, multisubunit protein at the heart of the respirasome. The subunits involved in electron transfer are cytochrome b, cytochrome c_1, and the Rieske iron-sulfur protein (ISP). Cytochrome b has two hemes. One is **cyto b_{562}**, which is also known as the **low-potential heme** or **cyto b_L**. The other is **cyto b_{566}**, the **high-potential heme or cyto b_H**. The cytochrome c_1 subunit has one heme. The Rieske iron-sulfur protein contains a Fe_2S_2 cluster. Figure **19.1.19** shows the relative position of the bound mobile electron carrier, cytochrome C, and the internal ones, the Rieske Fe/S cluster and cytochrome b_L and b_H. The molecule stigmatellin A also binds to the site where UQ becomes reduced (called the Qo site) and inhibits the complex. This shows that UQ/UQH_2 are in a position to react readily with the Rieske center and cytochrome b_L heme.

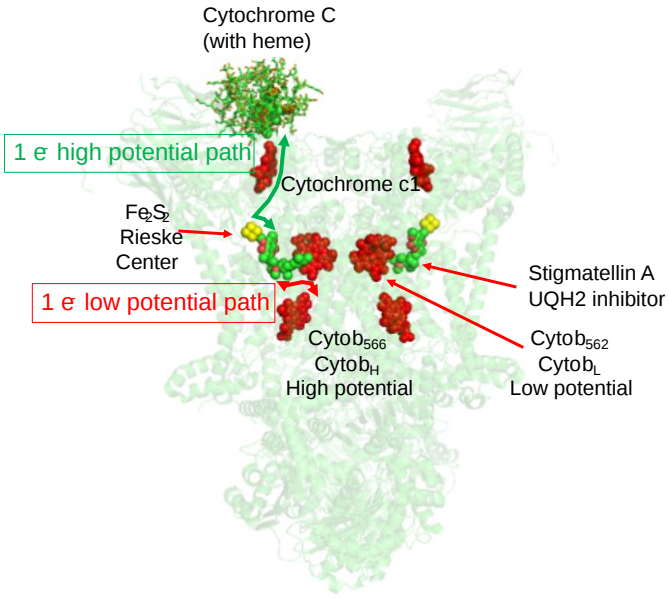
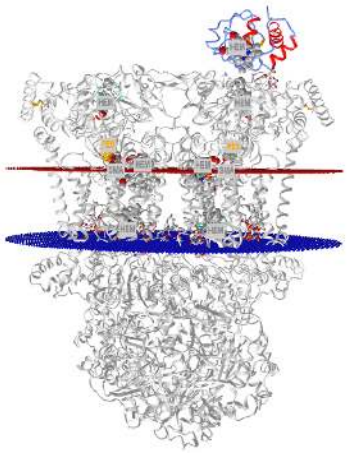


Figure **19.1.19**:

Figure **19.1.20** shows an interactive iCn3D model of a eukaryotic respiratory complex III (3CX5)



NCBI iCn3D Figure **19.1.20**: eukaryotic respiratory complex III (3CX5). (Copyright; author via source).
Click the image for a popup or use this external link:https://structure.ncbi.nlm.nih.gov/i...5riT4GSSGhCHfA. (loads slowly, given the size of the structures).

The Rieske iron-sulfur protein has a Fe_2S_2 iron-sulfur cluster, which differs from other such clusters in that each Fe is also coordinated to two His side chains, as shown in Figure **19.1.21**. Alterations in H bonds to the histidines and the sulfurs in the complex can dramatically affect the standard reduction potential of the cluster.

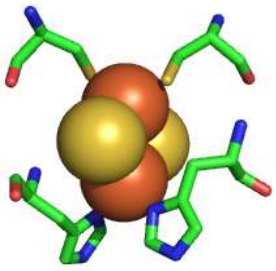


Figure **19.1.21**: The Rieske Fe_2S_2 cluster

As with Complexes I and IV, proton and electron transfer are coupled processes. However, in contrast to Complex I, in which protons pass through protein domains that have homology to K^+/H^+ antiporters, and Complex IV, in which they pass through a combination of a water channel and the H-bond network, the protons in Complex III are carried across the intermembrane space by ubiquinone itself. Two reduced ubiquinones (UQH_2) from complex I pass their four matrix-derived protons into the intermembrane space. In the process, four electrons are removed in a multiple-step process called the Q cycle.

The two electrons from each UQH_2 take different paths. One electron moves to a Fe/S Rieske cluster and the other to cytochrome b_L. The electrons moved to the Rieske center, then moved to cytochrome c1, and then to the mobile electron carrier cytochrome C, which is bound to the complex in the intermembrane space. The electrons moved to cytochrome b_L are transferred to cytochrome b_H in the complex. Through this latter path, two electrons (from two UQH_2) are moved to oxidized UQ, and two matrix protons are added to reform one UQH_2. Hence, only one UQH_2 participates in the net reaction shown below.

$$QH_2 + 2 \text{ cyto } c^{3+} + 2H^+_{matrix} \rightarrow Q + 2 \text{ cyto } c^{2+} + 4H^+_{IMS}$$

Figure **19.1.22** illustrates this net overall reaction, called the **Q cycle**.

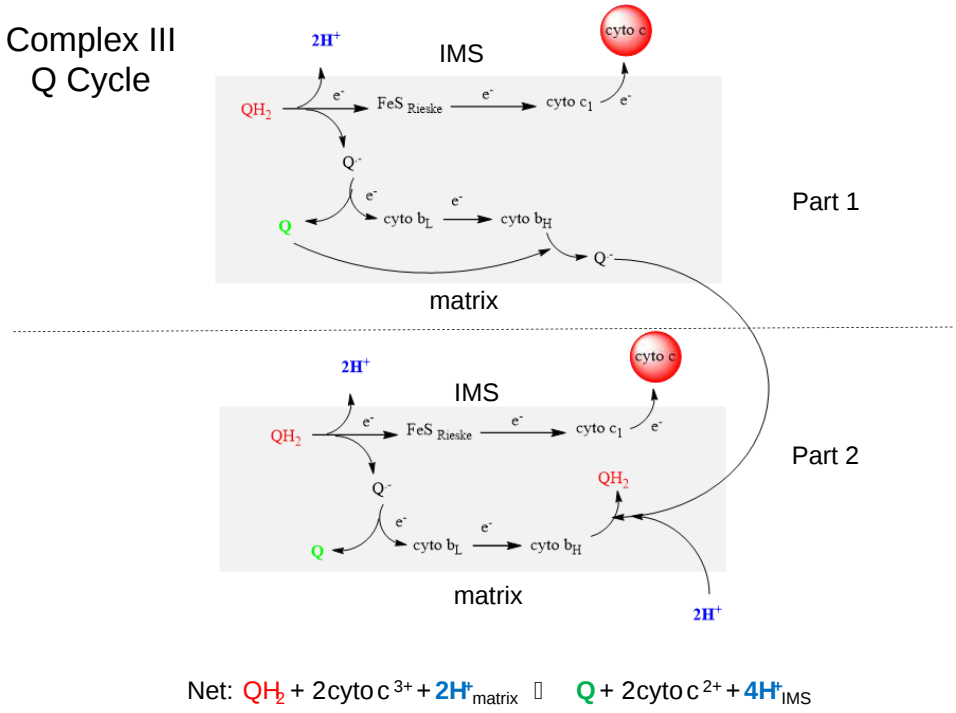


Figure **19.1.22**: Q cycle of Complex III

Once again, the protein has no “proton” channels or hydrogen-bonded networks for proton transfer across the inner membrane.

Another way to think about the electron transfer process from UQH_2 to cytochrome C is that the two electrons from UQH2 take two different paths: one a high-potential path to the Rieske center and on to cytochrome C, and another a low-potential path to the b_L heme and on to the b_H heme and then to UQ to reform UQH2 (see figure above).

Complex III, as did Complex I, can also produce unwanted reactive oxygen species (ROS). Only three of the protein subunits, cytochrome b (with the b_L and b_H hemes), cytochrome c_1, and the Rieske iron-sulfur protein (ISP) are involved in electron transfer, so one of those is most likely involved in ROS production. Experiments and mathematical models support a mechanism that involves a reduction of UQ by adding one electron from cytochrome bL to form $UQ^{\cdot}$, which then passes its electron to dioxygen to form superoxide (O_2^{-}.).

As two ubiquinones must bind to the complex, there must be two proximal sites. One is the Qi site, where oxidized UQ binds and receives an electron, and the other is the Qo site, where UQH_2 binds.

From a kinetic perspective, the first UQH_2 binds and transfers two electrons, one to the Rieske cluster (and on to cytochrome c_1 and then to cytochrome C) and one to cytochrome b_L (and on to heme b_H) and then to an oxidized UQ bound at the Qi site. The $UQ^{\cdot}$ radical is stabilized by the adjacent b_H heme, which has a lower affinity for electrons. A second UQH_2 binds to the Qo site, transferring two electrons (one via the Rieske cluster and the second through cytochrome b_L and b_H) to the $UQ^{\cdot}$ radical present at the Qi site. This forms UQH_2 after two protons are transferred to it from the matrix.

Antimycin A, an extremely toxic drug, binds to the UQ Qi site and hence blocks electron transfer from cytochrome b_L to b_H at the Qi site. Heme b_L can then pass its electron to dioxygen to produce superoxide.

Before we leave Complex III, think about this. The complex has two identical cytochrome b subunits, each with a b_L and b_H heme. The standard reduction potential of the b_L and b_H hemes in a subunit differ. This is another example that shows that the standard reduction potential, E^0, depends on the environment of the electron acceptor/donor, just as the pKa of an acid depends on its environment.

Figure **19.1.23** shows an interactive iCn3D model of just the cytochrome b subunits and all the hemes in the eukaryotic respiratory complex III (3CX5) to give more clarity to the differing environments of the hemes in the two identical cytochrome b subunits.

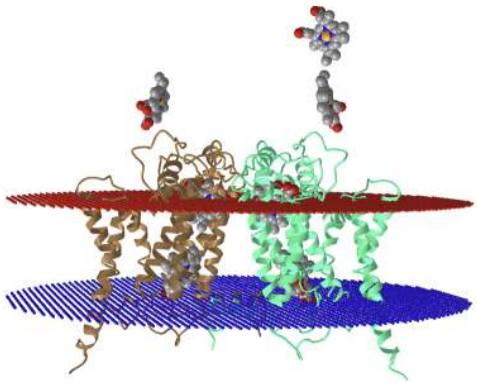


Figure **19.1.20**: Cytochrome b subunits and all the hemes in the eukaryotic respiratory complex III (3CX5). (Copyright; author via source).
Click the image for a popup or use this external link: https://structure.ncbi.nlm.nih.gov/i...BaLQH2KwahNFt9

https://structure.ncbi.nlm.nih.gov/i...BaLQH2KwahNFt9

19.1.4: COMPLEX IV - CYTOCHROME C OXIDASE (CCOX)

This is the final complex in the electron transport chains. It passes 4 electrons and 4 "substrate" protons to dioxygen to produce water. Additionally, it transports as many as 4 H^+ ions from the matrix to the intermembrane space, resulting in a net change of 8 H^+ ions. Here is a modified version of Equation 1 that represents the transported Hs.

$$O_2 + 4e^- + 4H^+ + 4H^+_{(in)} \longrightarrow 2H_2O + 4H^+_{(out)}.$$

The structure of complex IV is shown in Figure **19.1.24**. KEGG pathways (with permission).

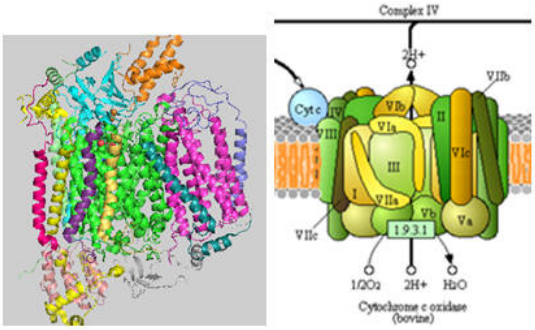


Figure **19.1.24**: Cytochrome C Oxidase structure (left) and cartoon model (right) showing subunits (taken KEGG pathways with permission). (Copyright; author via source)

The 4 H^+s moved across the membrane are not transported by protein domains that are structural equivalents of antiporters, as in Complex I. Rather, elaborate H-bonded water channels with contributions from a space of polar backbone and side chain H-bond donors and acceptors are involved in proton transport. Hence, a key question to understand is how electron transfer is coupled to H^+ transfer through this hydrogen-bonded network. Since it's quite complicated, we will present multiple figures of varying resolutions to help explain this coupled process.

Figure **19.1.25** shows an interactive iCn3D model of the 14-subunit human cytochrome c oxidase (5z62) with bound cofactors required for electron transfer. Note that it does not show cytochrome C.

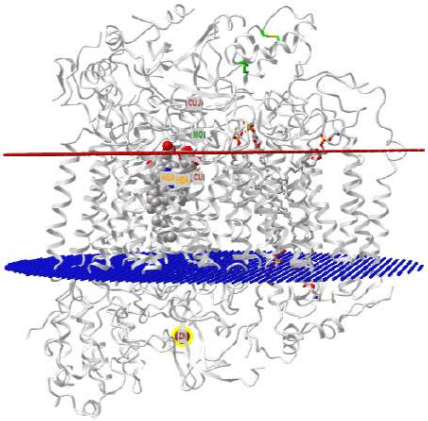


Figure 19.1.25: 14-subunit human cytochrome c oxidase (5z62). (Copyright; author via source).
Click the image for a popup or use this external link:https://structure.ncbi.nlm.nih.gov/i...XoHRyCkpeRN917. (loads slowly, given the size of the structure).

Reduced cytochrome C, a mobile electron carrier protein, binds to Complex IV in the intermembrane spaces and singly passes 4 electrons to a series of electron carriers (oxidizing agents) in the protein, eventually to dioxygen as the terminal electron acceptor. Figure 19.1.26 shows the arrangement of the electron acceptor cofactors in Complex IV. Electron transfer presumably occurs through quantum mechanical tunneling.

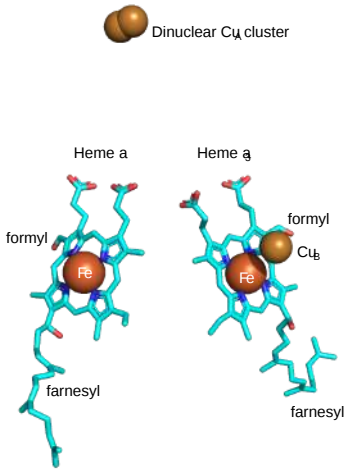


Figure 19.1.26: Electron acceptor cofactors in Complex IV.

Cytochrome C, the initial “substrate” of this complex, delivers electrons from its heme cofactor to a dinuclear copper cluster, Cu A, where the copper ions are collectively coordinated to two histidines and two cysteines and a methionine. Figure 19.1.27 shows an interactive iCn3D model of the coordinating ligands for Cu A cluster in Complex IV (5z62)

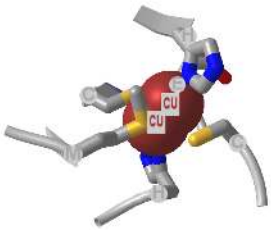
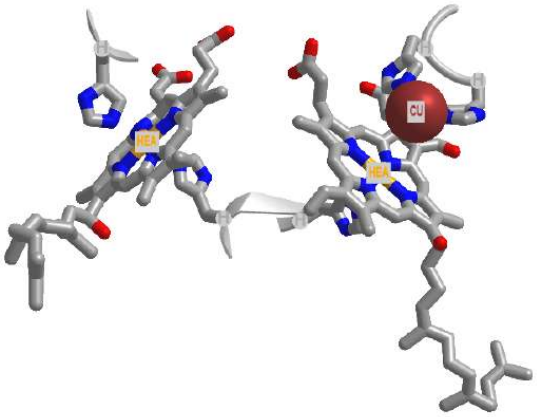


Figure 19.1.27: coordinating ligands for Cu A cluster in Complex IV (5z62). (Copyright; author via source).
Click the image for a popup or use this external link: https://structure.ncbi.nlm.nih.gov/i...7ARphDU4oyDS4A

From there, electrons flow to an adjacent **heme a** (low spin), with two coordinating histidine ligands. This heme hence does not bind dioxygen. From there, electrons move to another heme, **heme a$_3$** (high spin), and then finally to dioxygen, which is coordinated to the Fe in

heme a_3 and to an adjacent Cu B. Heme a_3 has only one coordinating histidine ligand, which allows dioxygen binding to the unligated site. The heme a_3 Fe:Cu dinuclear cluster is unique among all hemes. Figure **19.1.28** shows an interactive iCn3D model of the coordinating ligands for the hemes and Cu B in Complex IV (5z62)



NCBI iCn3D Figure **19.1.28**: coordinating ligands for CuB, heme a, and heme a_3 in Complex IV (5z62). (Copyright; author via source). Click the image for a popup or use this external link: https://structure.ncbi.nlm.nih.gov/i...4EUooXkwh13Fm8

First, let's consider the transfer of electrons from heme a to heme a_3 and then to dioxygen (we will consider the entry of electrons into the complex later). If dioxygen, a substrate for the reaction, dissociated from the heme a_3 Fe before it was completely reduced, toxic ROS would result. This suggests a reason for the evolution of this key enzyme to have produced the unique heme a_3 Fe:Cu dinuclear cluster.

Heme a and a_3 vary from the heme in hemoglobin as they both have a formyl group replacing a methyl and a hydroxyethylfarnesyl group added to a vinyl substituent. Its structure is shown in Figure **19.1.29**. What is the overall charge of the heme in its reduced state? In its oxidized state?

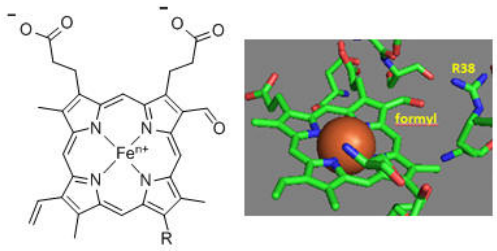


Figure **19.1.29**: Heme-Formyl group of Cytochrome C Oxidase

As hemes are prosthetic groups, they must bind to the apoprotein. The hydroxyethylfarnesyl group, with its nonpolar tail, facilitates the binding of the heme to both the Fe^{+2} and Fe^{+3} forms by about 6.3 kcal/mol (26 kJ/mol). The formyl group in heme a increases the E^0 value (i.e., makes the heme a better oxidizing agent) by about 179 mV (4.1 kcal/mol, 17 kJ/mol). The effect appears to be mediated by the binding of the heme group to the protein again, but only in this case is there a differential effect. The formyl group preferentially stabilizes the binding of the Fe^{+2} heme compared to the Fe^{+3} heme, which, in a thermodynamic cycle, would promote the binding of an electron to Fe^{+3}-heme (increasing its E^0 value) to form the more stably bound Fe^{+2} heme.

The key challenge has been to understand the redox coupling to H^+ transport. How is this done? The electrostatic environment of the hemes must be taken into account. In heme a, the two axial ligands are uncharged imidazole side chains of histidines. The overall charge on Fe^{2+}-heme is zero, as the two propionates cancel the charges on Fe^{2+}. However, there is a net +1 charge in the Fe^{3+}-heme. This charge could be delocalized within the conjugated pi electrons of the planar heme, contributing to the deprotonation of a side chain near heme a in a process that would couple redox and H^+ movement. The formyl group of heme a is coplanar with the heme ring in both Fe^{3+}-heme and Fe^{2+}-heme, allowing it to participate in the π-conjugated electron system of the ring. As the formyl group forms an H bond with Arg 38, changes in oxidation might affect Arg 38 as well.

Many other amino acids are also involved. One is Asp-51 of subunit I, which contains heme a. This undergoes a conformational change, causing it to move to the surface of the inner membrane upon reduction. It is near the matrix in the oxidized state. Hence, it is likely involved in a proton transport pathway. Crystal structures of oxidized and reduced Complex IV show water channels and small "cavities," which calculations show can hold 1-3 water molecules. Hence, groups around the heme, including R38, are accessible to water. Water is involved in H^+ transport through the "handshaking" transfer of protons via a hydrogen-bonded network of waters and selective side chains.

Some of the amino acid residues associated with the water channels are shown in Figure **19.1.30**: and include R38 (the one hydrogen bonded to the formyl group of the heme), S34, T424, S461, S382, and H413.

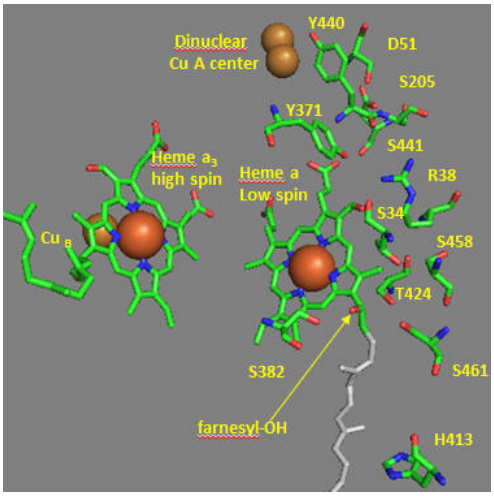


Figure **19.1.30**: Possible amino acids involved in H^+ transport through a hydrogen-bonded network in Complex IV

Another consequence of electron transfer to heme a involves the interaction of S382 and the farnesyl OH group, which are close in space and proximal to a water cavity. On reduction of the heme, a conformation change occurs, which increases the standard reduction potential of the S382-farnesyl OH group. How would this affect the interaction of the two and the S382-L381-Val380 localized conformation? A new water cavity appears to emerge in this region upon reduction. How might this impact proton transfer from the matrix?

Now, let's consider the entry site of electrons into the complex and how they might influence proton transport. As mentioned above, Asp 51 (D51) plays a key role. It is shown in Figure **19.1.29** above and also in Figure **19.1.30** below. In the oxidized state, D51 interacts with two OH side chains (S205 and S441) and amide NH backbone groups but is not exposed to water. On reduction, D51 lies on the surface in an aqueous environment. Near D51 is Y440-S441. The backbone carbonyl group between 440 and 441 forms an "indirect" interaction with R38 (right panel in Figure **19.1.31**), which we showed earlier is affected by the redox state of heme a. They are too far apart to form H bonds. Add two water molecules and envision a bridging interaction between the carbonyl O and the side chain R38 via Y371. Likewise, in your mind, add a water molecule to allow a bridged hydrogen bond interaction between Y371, which also forms a H bond, and the heme a propionate.

Figure: Role of Amino Acids near D51 in Cytochrome C Oxidase

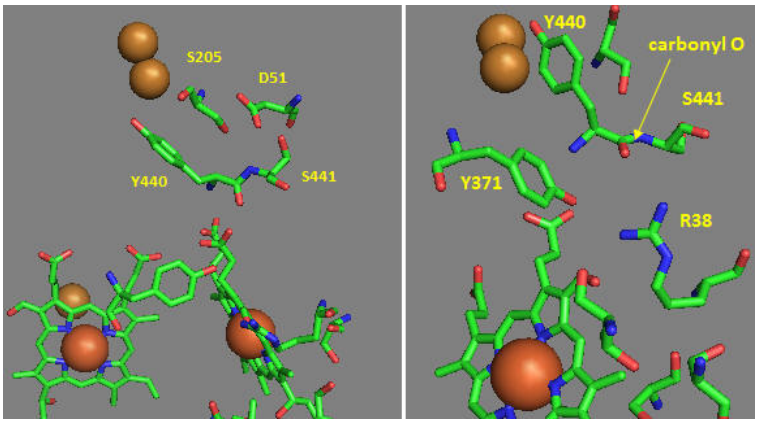


Figure **19.1.31**: Local environment of D51, R38 in hemes in Complex IV

A more nuanced understanding of the mechanism and linkage between H^+ and e^- movement derives from the high-resolution structures that were determined by Yano et al (2016). In their model (shown in the figures below based on the oxidized form of the protein, pdb 5b1a), protons from the negative (matrix) N side of the complex enter through a water channel and proceed to the positive (intermembrane side) through a H bond network (as described above and depicted below). These comprise the **H-Pathway** for H^+ transfer across the membrane. Two other H^+ transfer pathways, the **D- and K-pathways,** are used as a source of substrate H^+ for the 4 H^+s added to dioxygen to form $2H_2Os$.

Directional movement is mediated by proton-proton repulsion, aided by an increase in positive charge on heme a when it transfers an electron to heme a_3. Of course, proton:proton repulsion would move protons in both directions. A conformational change on oxygen binding

that closes the channel prevents reverse flow back through the water channel.

Ultimately, four electrons are transferred from cytochrome Cs (in single-electron steps) to the dicopper cluster, CuA, and then sequentially to heme a to heme a_3 (near the copper B ion) to dioxygen to form water. The motion of electrons and protons is coupled through electrostatic interactions.

Figure **19.1.32** gives an overview of these movements. The small red dots are the oxygen atoms of internal water molecules (the rest have been removed using Pymol). Given the number and location of the internal water molecules, it should be apparent that many would be involved in the proton translocation pathways.

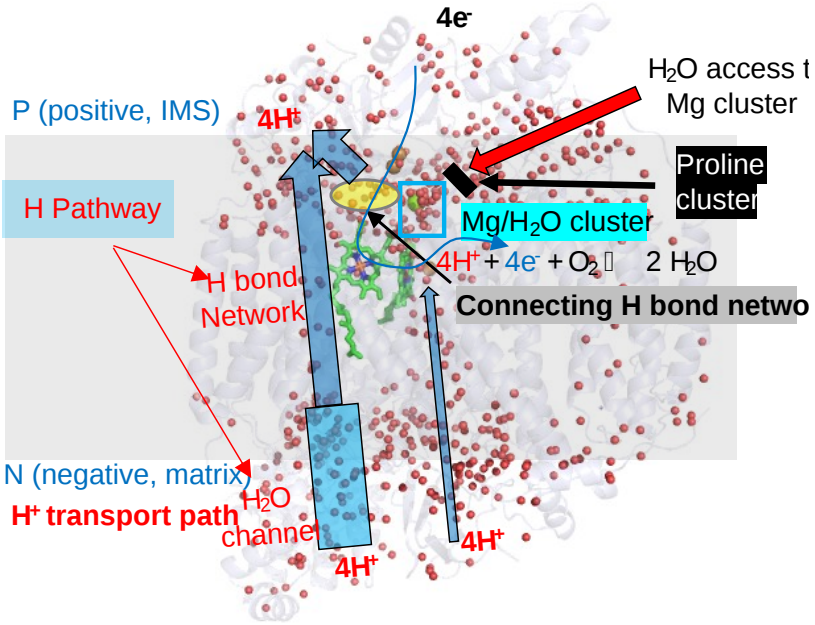


Figure **19.1.32**: Cartoon showing movement of H^+s and e^-s in Complex II

What's so interesting about this model is the detailed description of two types of protons: the ones that add to dioxygen and end up in water (substrate protons) and those that are vectorially (directionally) transported to the IMS. In their model, the H^+s that end up being transported move through the water and H-bond network via a connecting H-bond link region to a Mg^{2+}/water cluster. Since oxygen binding leads to structural changes that close off the water channel, all protons to be transported to the IMS must be bound in the cluster before dioxygen binding.

Figure **19.1.33** shows that, initially, 4 H^+s move through the H system to the Mg^{2+}/H_2O cluster. Oxygen binding then closes the water channels. This buildup of positive charges would certainly lead to enhanced electrostatic attractions for the next phase of the reaction, the movement of electrons into the heme cofactors. Additionally, the 4 H^+s in the cluster are likely prevented from leaking to the P side through proximal waters (see above figure) by a proline cluster, which presumably restricts the dynamic motion of the protein in that region necessary for proton movement. The figure does not show changes in the charge of the electron carriers.

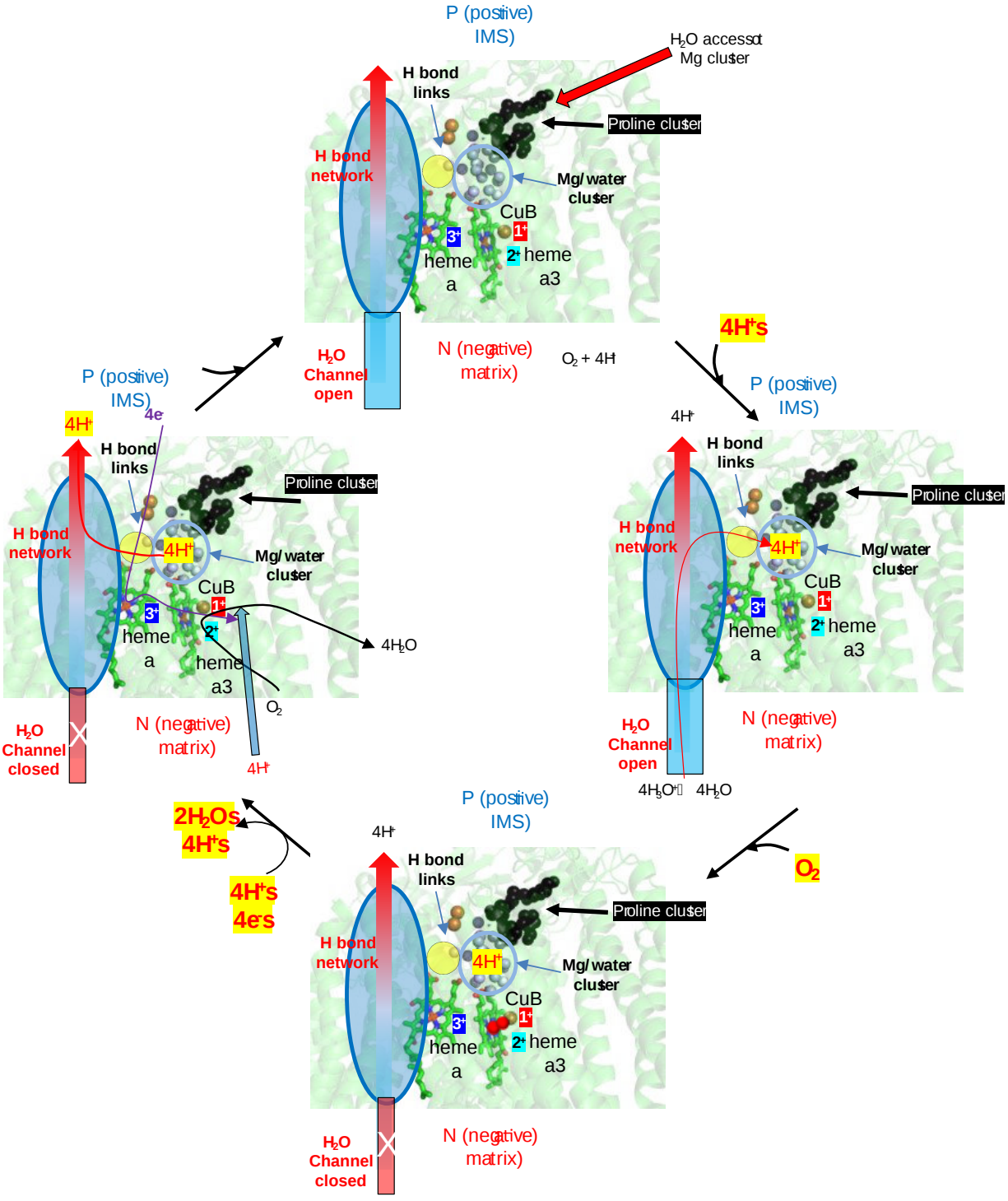


Figure 19.1.33: Proton movement in Complex IV

The figure below breaks down the mechanism to show the addition of the first electron to the CuA (dicopper cluster), delivered from cytochrome C, and the subsequent transport of one proton from the fully proton-loaded Mg^{2+}/water cluster after dioxygen binding. This figure does show the stepwise redox changes in the electron carriers.

After CuA receives an electron from cytochrome C, it donates it to heme a and not to heme a_3, even though both are close. The extra negative charge on heme a facilitates proton pumping through the H pathways shown.

Figure 19.1.34s shows a cartoon description of the movement of protons and electrons through Complex IV.

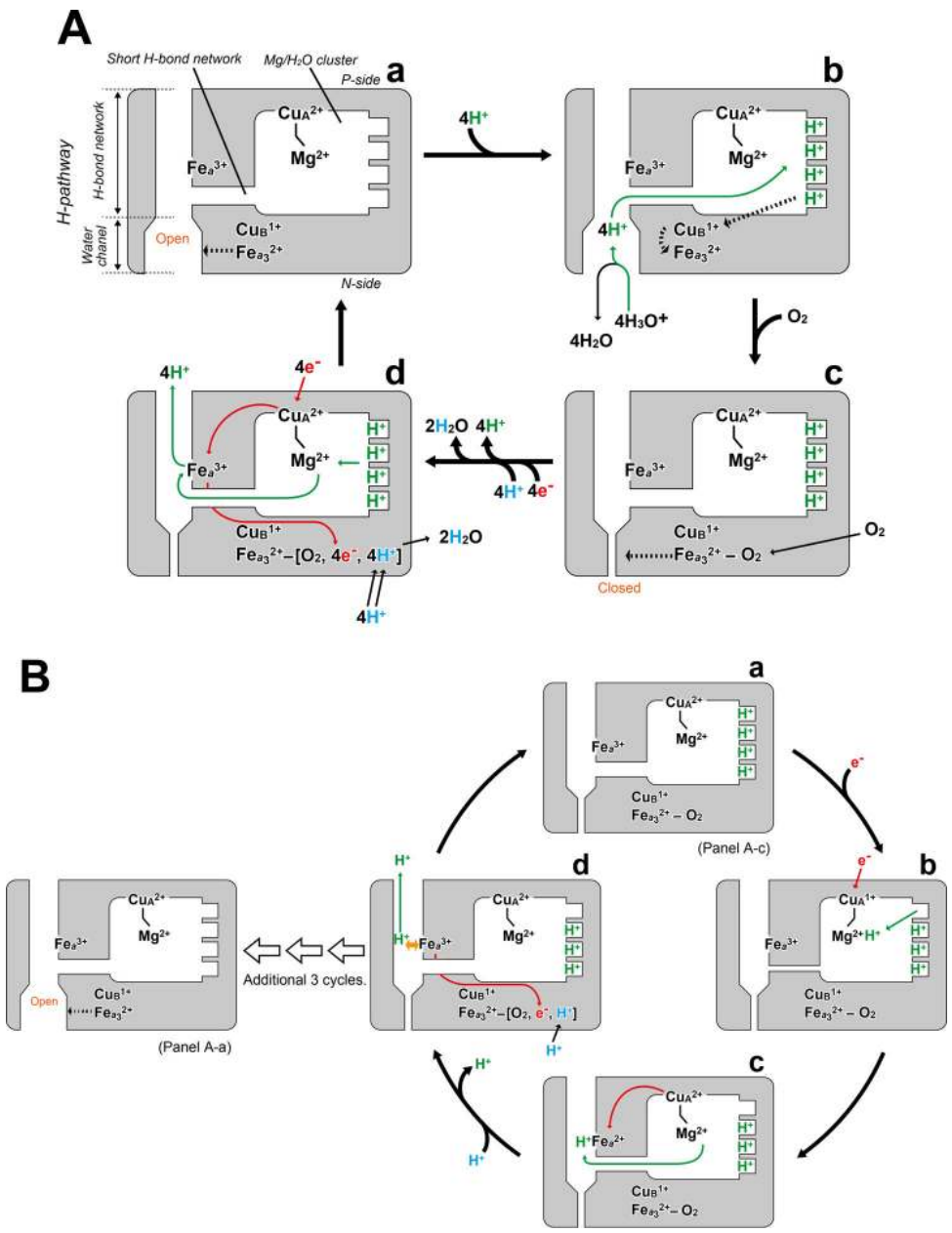


Figure **19.1.34**: **A schematic representation of the role of the Mg/H_2O cluster in the proton-pumping mechanism of bovine heart CcO.** Yano N et al. J Biol Chem. 2016 Nov 11;291(46):23882-23894. doi: 10.1074/jbc.M115.711770. Epub 2016 Sep 7. PMID: 27605664; PMCID: PMC5104913. Creative Commons Attribution (CC BY 4.0)

The Mg/H_2O cluster and the H-pathway are connected with the short hydrogen bond network, as *labeled* in *A* (*a*). The location of heme a is shown by Fe_a^{3+} or Fe_a^{2+} attached to the hydrogen bond network of the H-pathway. The Cu_A site is on the water-accessible surface of the Mg/H_2O cluster. The conformation of the Cu_A-Mg^{2+} complex is shown by the *shape* of a *line* connecting the two metal ions. The *four hollows* on the water-accessible surface of the Mg/H_2O cluster show the proton-accepting sites. Cu_B^{1+} and Fe_{a3}^{2+} indicate the O_2 reduction site. The pumping and chemical (water-forming) protons are *labeled* in *green* and *blue*, respectively. Red curves show electron transfers. *A*, overall catalytic cycle of CcO. *B*, a typical single electron transfer from Cu_A to the O_2 reduction site, coupled with the uptake and release of protons. For the sake of simplicity, the uptake of one chemical proton equivalent (the average number) is given in *B*. Various oxidation and ligand binding states in both Cu_B and Fe_{a3} in the intermediate states shown by *A* (*d*) and *B* (*d*) are not included for the sake of simplicity.

Figure **19.1.35** converts the schematic representation into a "structural cartoon" representation showing one cycle of coupled electron and proton transfer into Complex IV.

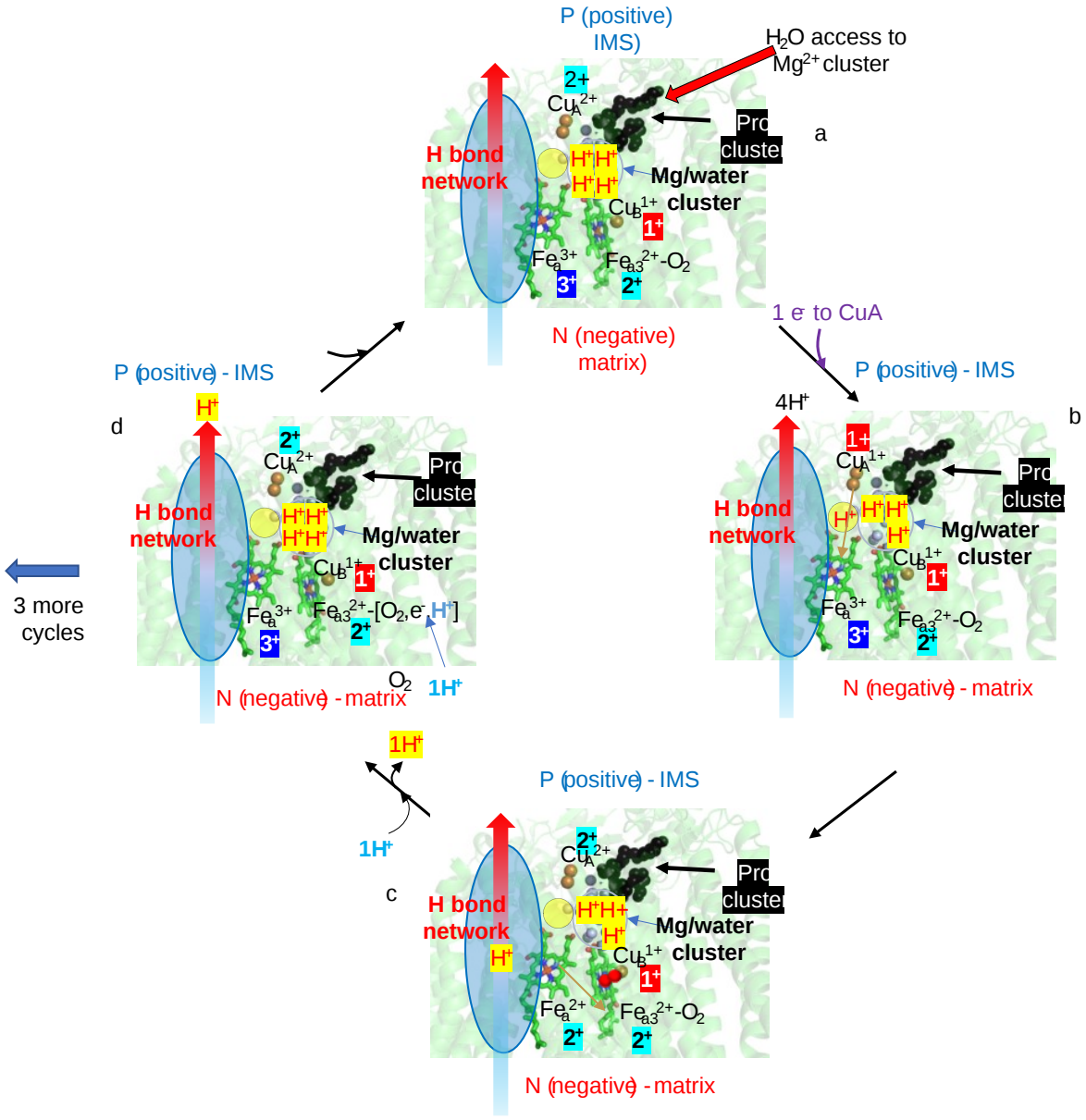


Figure **19.1.35**: Structural cartoon representation showing one coupled electron and proton transfer cycle of Complex IV.

The H- (for transport of $4H^+$s across the membrane) and the D- and K-pathways (sources of substrate $4H^+$s for water synthesis from O_2 are shown in Figure **19.1.36**.

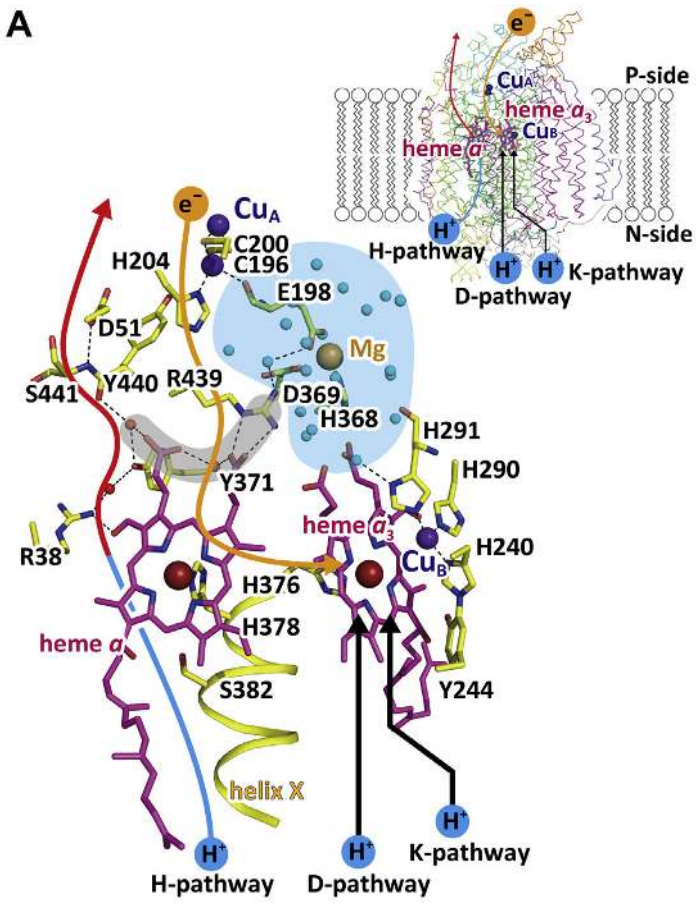


Figure **19.1.36**: The H-, D-, and K-pathways in bovine heart Complex IV (5B1A). Atsuhiro Shimada et al. J. Biol. Chem.(2021) 297(3) 100967. Creative Commons. https://creativecommons.org/licenses/by/4.0/

Two black arrows show the D- and K- for substrate H^+s that form water, while the blue arrow shows the H-pathway for the hydrogen bonding network of water in the water channel. The Mg/H_2O cluster (blue area) is attached to the hydrogen-bond network of the H-pathway via a short hydrogen-bond network (gray area with water shown as a blue sphere). The formyl group and one of the propionate groups of heme a are hydrogen-bonded with Arg38 and a fixed water molecule in the hydrogen-bond network of the H-pathway. Compare this diagram to the ones presented in the figures above it. Again, we present multiple representations to give readers numerous opportunities to conceptualize this complex concept.

19.1.5: COMPLEX II - SUCCINATE:UBIQUINONE OXIDOREDUCTASE (SQR) - SUCCINATE DEHYDROGENASE

You've seen complex II before, but it has another name: succinate dehydrogenase from step 6 of the citric acid cycle, which catalyzes the following reaction.

$$\text{succinate} + \text{FAD} \leftrightarrow \text{fumarate} + \text{FADH}_2 \quad \Delta G^o = 0 \text{ kcal/mol}$$

The ΔG^o for this reaction is about 0 kcal/mol, making it readily reversible.

However, something vital is left out of this description. The above reaction suggests that both FAD and $FADH_2$ are readily diffusable and bind and unbind after catalysis. That's not true. Instead, $FAD/FADH_2$ are covalently attached to the enzyme, so after one cycle of enzyme catalysis, the enzyme is dead. Another substrate/product pair must interact with enzymes to reconvert the covalently attached $FADH_2$ to FAD so catalysis can continue. The other pair is ubiquinone (UQ/UQH_2). Figure **19.1.37** gives a better description of the reaction equation. Complex II links the tricarboxylic acid cycle to electron transport!

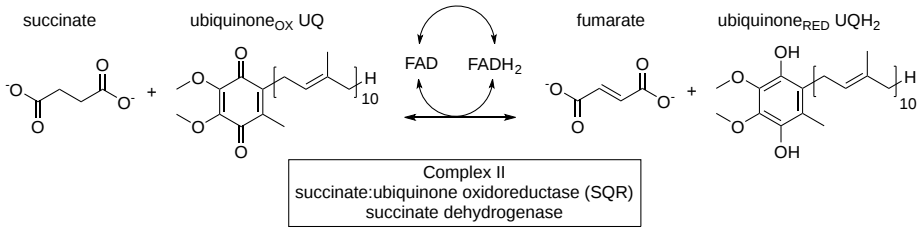


Figure **19.1.37**: Complex II - Succinate Dehydrogenase Reaction

Complex II is a multisubunit integral membrane protein, as with the other mitochondrial electron transport complexes. The hydrophilic section protruding into the matrix contains two proteins, a flavin-binding protein (Fp) and an iron/sulfur protein (Ip). The transmembrane domain has two "cytochrome binding proteins", a lighter one (CybL) and a heavier one (CybS). The complex has binding sites for dicarboxylic acids (succinate/fumarate) and two binding sites for ubiquinone, a proximal, higher-affinity site (Qp) on the matrix side, closer to the succinate binding site, and a distal, lower-affinity site (Qd). The ubiquinone sites bind 2-thenoyltrifluoroacetone (TTFA), which acts as an inhibitor of ubiquinone reduction. 3-nitropropionate - $(NO_2)(CH_2)_2CO_2^-$ is structural similar to succinate - $(CO_2^-)(CH_2)_2CO_2^-$ and is an inhibitor of succinate oxidation.

Figure **19.1.38** shows an interactive iCn3D model of the Mitochondrial Respiratory Complex II from porcine (pig) heart (1ZOY). The chains are:

- hydrophilic FAD-binding protein (lavender)
- hydrophilic FeS protein (blue)
- integral membrane large cytochrome binding protein (brown)
- integral membrane small cytochrome binding protein (green)

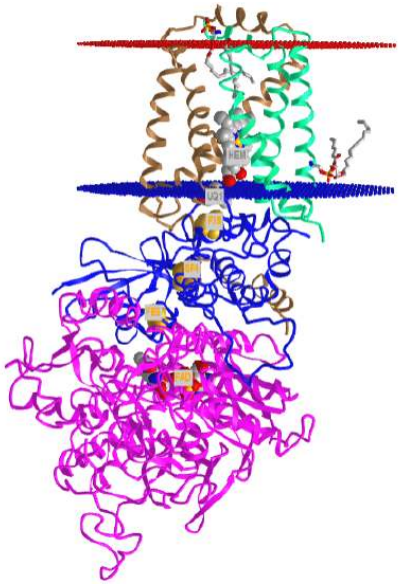


Figure **19.1.38**: Mitochondrial Respiratory Complex II from porcine heart (1ZOY) . (Copyright; author via source). Click the image for a popup or use this external link: https://structure.ncbi.nlm.nih.gov/icn3d/share.html?KKPWG9dW1ARq3wQf9. (loads slowly given the size of the structure).

Given the role of the enzyme in both the mitochondrial citric acid and electron transfer pathways, you would expect high electron transfer rates between the dicarboxylic acid and the ubiquinone binding sites. Any disruptions in electron transfer (by inhibitors or mutations) could produce toxic reactive oxygen species (ROS). The binding of an inhibitor to the proximal Qp site would lead to a buildup of $FADH_2$, which could transfer electrons in single-electron steps to dioxygen to produce ROS. This would occur if the dicarboxylic site were empty.

As there is no H^+ transfer from the matrix to the intermembrane space for Complex II, we'll only focus on electron transfer from succinate to FAD and on to ubiquinone.

The transfer of electrons from succinate to ubiquinone takes two steps.

Step 1: Succinate + FAD ↔ Fumarate + $FADH_2$. Figure **19.1.39** shows a plausible mechanism using a histidine in the active site as a general base. This is a simple hydride ($2e^-$) transfer reaction to FAD. Note that no FeS cofactors are required.

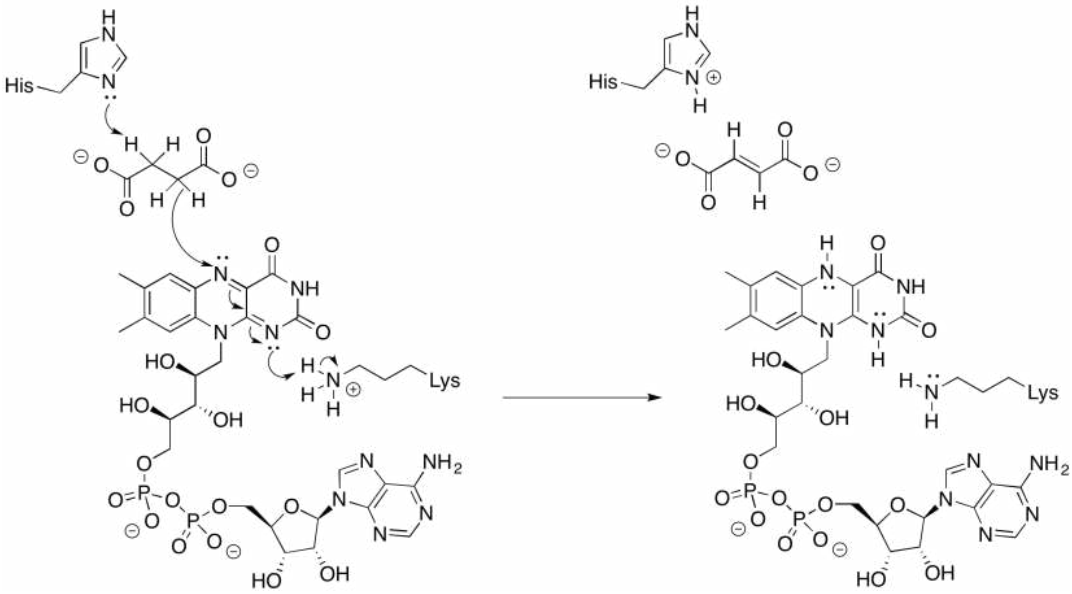


Figure **19.1.39**: A mechanism for Succinate oxidation by FAD to Fumarate and $FADH^2$ (after Schaller, LibreText)

Step 2: $FADH_2$ + UQ ↔ FAD + UQH_2. This does not proceed by transfer of 2 e^- from $FADH_2$ directly to UQ. Rather, it occurs through a series of the FeS cofactors (Fe_2S_2, Fe_4S_4, and Fe_3S_4 clusters) and heme. First, let's consider the path of electron transfer, which will occur in single-electron steps through the intermediary FeS clusters to ubiquinone, as shown in Figure **19.1.40**. The standard reduction potential E^0 is shown for each step. Note that FAD is shown instead of the actual electron donor, $FADH_2$, to correspond to the standard reduction E^0 values in tables.

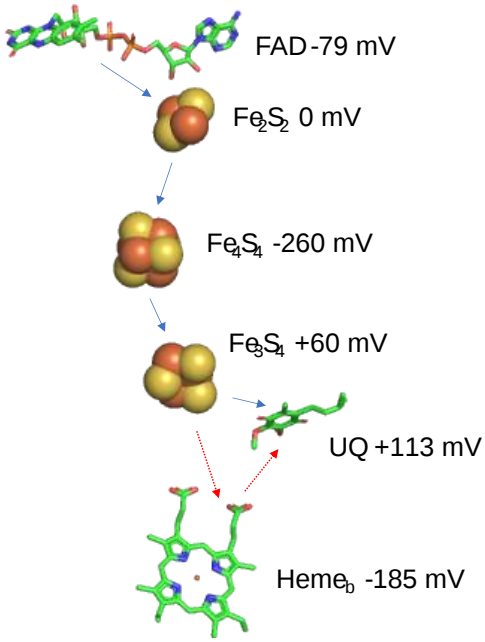


Figure **19.1.40**: Pathway for electron transfer in Complex II

Electrons flow from $FADH_2$ (lowest, most negative E^0 value, -79 mV) to UQ (highest, most positive value E^0 value, +113 mV) or from weakest to strongest oxidizing agent. Electron transfer also depends on distance. The transfer of electrons to heme $_b$ is not likely, given the presence of the closer UQ with the most positive E^0 value. Hence, the function of heme $_b$ is unclear. However, if electrons are transferred to it, it will quickly and favorably send them on to UQ. The FeS clusters have progressively more positive E^0 values except for Fe_4S_4, whose E^0 = -260 mV. Its E^0 is depressed by the presence of charged/polar groups, which would make the transfer of a negative electron less likely. The net transfer standard potential is favored thermodynamically. As the E^0 and corresponding G^0 values are state functions, the final ΔG^0 doesn't depend on the path. The high value of E^0 for Fe_4S_4 presents an activation energy barrier for transfer in both directions and probably prevents reverse electron transport in this complex.

The membrane domains have two polar (Asn, Ser) and five polar-charged (Asp, Glu, and Lys) side chains.

Now, let's look at the terminal step in the transfer of electrons from Fe_3S_4 to ubiquinone. Figure **19.1.41** shows a plausible mechanism. Ubiquinone is shown in black. TTFA, which binds to the ubiquinone site and inhibits electron transfer, is shown in brackets. Tyrosine 91, Serine 41, and Histidine 216 are likely candidates for involvement in catalysis, as shown below. Arginine 46 and aspartate 90 might be involved in the protonation steps of UQH_2.

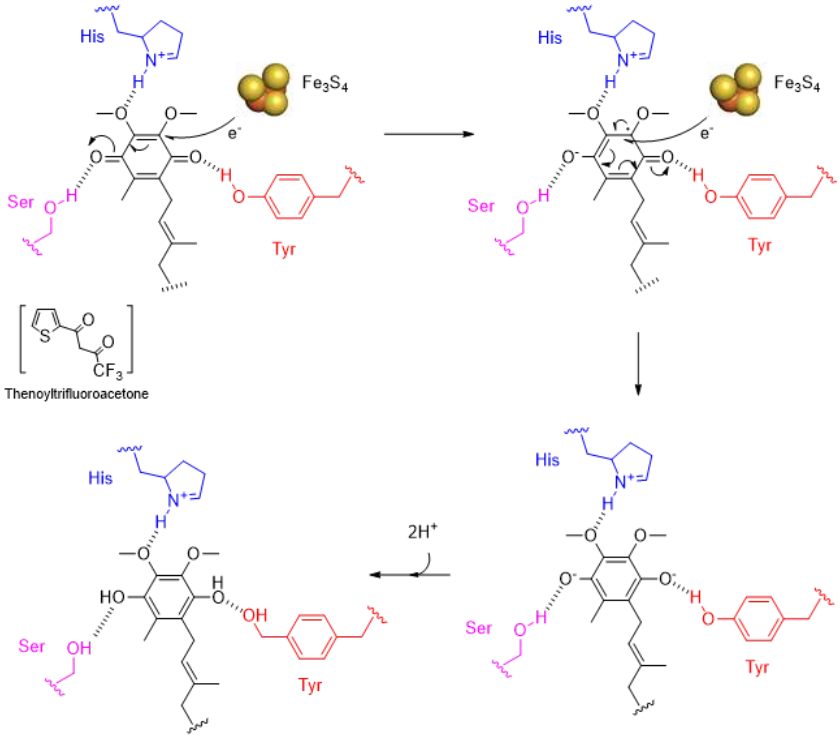
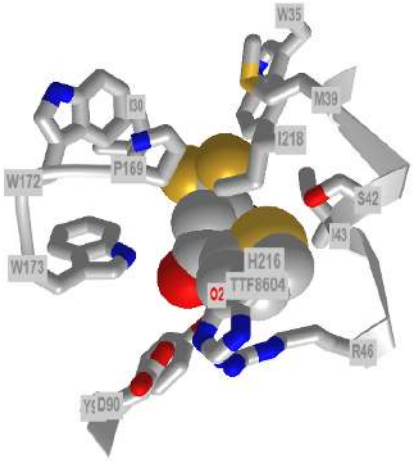


Figure **19.1.41**: Terminal step in the transfer of electrons from Fe_3S_4 to ubiquinone

Figure **19.1.42** shows an interactive iCn3D model of the iCn3D TTFA1 binding site (where ubiquinone binds).



NCBI iCn3D Figure **19.1.42**: Mitochondrial Respiratory Complex II bound with 2-thenoyltrifluoroacetone (1zp0). (Copyright; author via source).

Click the image for a popup or use this external link: https://structure.ncbi.nlm.nih.gov/icn3d/share.html?dY3niSfLVa9WiNNe7

Recent Updates: 10/2/2025

19.1.6: AGING AND SLEEPING: EFFECTS OF MITOCHONDRIAL DAMAGE FROM REACTIVE OXYGEN SPECIES

The ability to use O_2 allowed eukaryotes to extract much more energy from sugars and fatty acids than from simple anaerobic metabolism. As described above, this came with the price of generating reactive oxygen species (such as superoxide, O_2^-), which can accelerate the aging process and tumor formation. Recently, mitochondrial damage has been suggested as the cause of sleep "pressure", which causes us to become sleepy and fall asleep. Mitochondrial changes in "sleep-control" neurons, specifically **dorsal fan-shaped body neurons (dFBNs)**, have been studied in fruit flies, linking energy metabolism to the need for sleep.

In the sleep-deprived Drosophila brain, when there is pressure to fall asleep (sleep pressure), there is a significant increase in expression of genes for mitochondrial respiration and ATP production in the dFBNs. These include components of complexes I–V, ATP/ADP carriers, and enzymes of the TCA cycle (e.g., citrate synthase, succinate dehydrogenase, malate dehydrogenase). These findings link oxidative metabolism in the mitochondria with the regulation of sleep.

Other genes are affected. Sleep pressure is associated with a decrease in transcription of the gene responsible for neuronal communication, linking nerve activity to sleep regulation. Also, with increasing sleep pressure, mitochondria in the dFBNs fragment and undergo mitophagy, a process that removes and recycles damaged mitochondria. Increased contacts between mitochondria and the endoplasmic reticulum are also observed. These changes are reversible with sleep. What is happening at the molecular level? As you continue reading, you'll have to consider both the neural activity and the metabolic activities of the dFBNs. For the rest of the discussion, remember that in the wake state, the neural activity of the dFBNs is inhibited, but they are metabolically active.

To understand, we first need to discuss the effects of the neurotransmitter dopamine on the dFBNs, which lead to the inhibition of neural activity. Neurochemistry and nerve conduction are discussed in detail in Chapter 28.9. Neurotransmitters that act on a very short timescale bind to closed plasma membrane ion channels. Upon binding, the transmitters are "gated" open, allowing the rapid flow of ions within the cell and leading to a neural response. Other neurotransmitters, such as dopamine, act more slowly by inducing conformational changes in a neuroreceptor transmembrane protein. This leads to changes in other membrane and cytoplasmic neural proteins. This process of dopamine signaling of dFBNs involves the following steps:

1. Dopamine binds to its receptor on dFBNs. The receptor is not an ion channel, but a complex membrane protein, a **G-protein coupled receptor (GPCR)**, with seven transmembrane helices. This GPCR then activates, through changes in the binding of an intracellular small G protein (with GTPase activity), an enzyme, **adenylate cyclase**, that converts ATP into cyclic AMP (cAMP).

2. Intracellular cAMP binds to and activates a protein called protein kinase A. The kinase phosphorylates two key membrane proteins that are active transporters, which require ATP to power the movement of ions across the membrane against a concentration gradient or membrane potential. These proteins are the plasma membrane protein Na^+/K^+ ATPase and the plasma membrane Ca^{2+}-ATPase, as well as the endoplasmic reticulum membrane protein SERCA (Sarco/Endoplasmic Reticulum Calcium ATPase). The membrane ATPases are inhibited by phosphorylation. In addition, some voltage-gated Na^+ and Ca^{2+}channels are also inhibited. Most of the ATP used in neurons is used to maintain transmembrane ion concentration gradients, which are necessary for neural cells to function properly. Hence, ATP levels increase as its consumption to maintain and restore ion gradients is reduced.

3. ATP consumption decreases in the wake state, dopamine-inhibited dFBNs. However, its synthesis with high caloric intake increases during the wake state, leading to high ATP levels. Oxidative metabolism continues, however, as NADH builds up when the transport of electrons through the respiration chain stalls due to the high ATP levels. Both ATP and NADH become elevated during the wake state, and this imbalance begins to build up, causing sleep pressure. If the neurons were stimulated (active) to mimic sleep, ATP levels fall.

Now let's turn our attention to mitochondrial electron balance. Typically, electrons flowing from NADH at the start of electron transport in Complex I make it all the way to O_2 in Complex IV, so few superoxide are produced from leakage at Complex I and ubiquinone pool (a one and two-electron mobile electron carrier). However, if there are both high levels of NADH (high levels of electrons) AND high levels of ATP (i.e., they are out of syn), the leakage becomes significant. This leakage is also reinforced by a large protonmotive force (Δp) and high ATP. Reactive oxygen species, like superoxide, damage membrane lipids. ATP levels in the dFBN neurons are about 20% higher than in adjacent neurons after one night of sleep deprivation.

This electron (redox) imbalance is sensed in a somewhat unclear way by the protein **Hyperkinetic**, which is the regulatory β subunit of the voltage-gated potassium channel Shaker in Drosophila. This protein is also a reductase for the reversible reaction of aldehydes/ketones ↔ alcohols (so it is an aldo-keto reductase). It is effectively a $NADP^+$/NADPH sensor, whose ratio is affected by the redox state (or availability of electrons) in the electron transport chain. As an **A**ldo-**K**eto **R**eductase, it possesses an **AKR** domain, which binds to key molecules produced from the degradation of damaged peroxidized lipids formed by ROS (see Chapter 12.3.8 for a review of how peroxidized fatty acids are generated). Two of the degradation products are malondialdehyde (MDA) and 4-hydroxynonenal (4-HNE). Their structures are shown below in Figure 19.1.43.

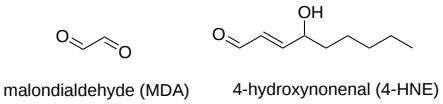


Figure **19.1.43**: Structures of MDA and 4-HNE

These reactive aldehyde-containing species, primarily produced from the peroxidation of omega-6 fatty acids, such as arachidonic and linoleic acids, can react with proteins (through Arg/Lys side chains) via Schiff base formation, as well as with Cys, His, and Lys through a Michael addition. Aldo-keto reductase can help detoxify them to alcohols. It's presumed but not completely confirmed that Hyperkinetic also reduces the bound aldehyde, as other aldo-keto reductases do. However, binding alone, accompanied by confirmations in the protein, is likely sufficient to regulate the Shaker K^+ channel. Changes in the NADPH/$NADP^+$ ratio (if hyerkinetic is catalytically active) may also regulate Shaker. However, mutations in Hyperkinetic appear to affect total sleep duration and have a lesser effect on sleep pressure.

In dFBNs, there was a 20% higher concentration of ATP compared to other neuron types after one night of sleep deprivation. ATP levels in dFBNs sharply increased when a heat stimulus led to increased dopamine levels that inhibited the dFBNs, mimicking the wake state. If the dFBNs were stimulated (not inhibited as by dopamine) directly to mimic sleep, ATP levels fell below baseline. Expressing an alternative oxidase (AOX) from *Ciona intestinalis*, which forms water by reducing O_2, allows extra electrons to be used without ROS production, relieving sleep pressure. Providing further evidence to support this mismatch hypothesis, increasing ATP synthesis through a proton pump (mito-dR) driven by photons results in increased sleep pressure.

Figure **19.1.43** below shows another overview of electron transport oxidative phosphorylation, showing the key players.

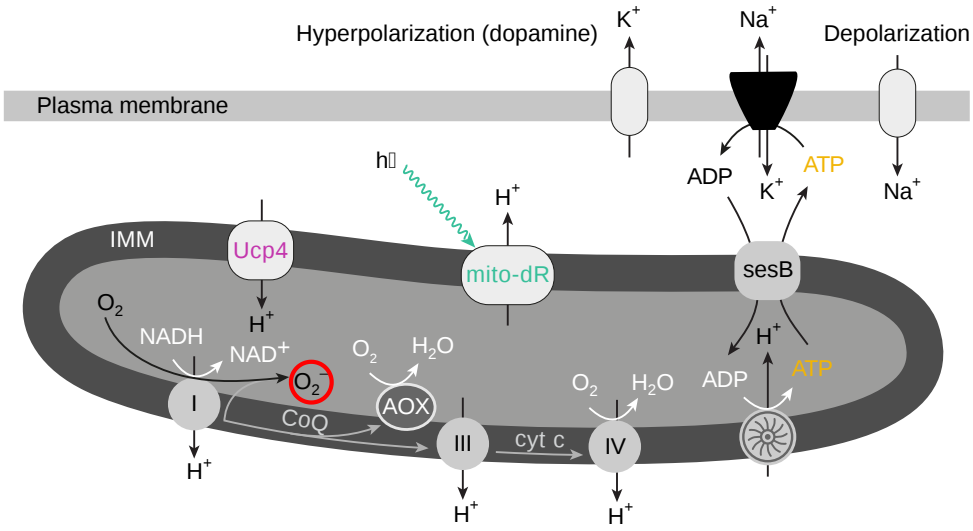


Figure **19.1.43**: Proton-pumping complexes I, III, and IV convert the energy of electron transfers from NADH to O_2—through intermediates CoQ and cytochrome *c* (cyt *c*)—into a proton electrochemical gradient, Δp, across the intermitochondrial membrane (IMM). Ucp4 discharges, whereas illumination ($h\nu$) of mito-dR charges the IMM. The return of extruded protons to the matrix spins the blades of the ATP synthase, producing ATP, which then leaves the matrix via the sesB channel in exchange for cytoplasmic ADP. Neuronal ATP consumption is activity-dependent, in part because the plasma membrane Na^+–K^+ ATPase must restore ion gradients dissipated by action and excitatory synaptic currents. An oversupply (relative to ATP demand) of electrons to CoQ increases the risk of single-electron reductions of O_2 to O_2^- at complexes I and III. AOX mitigates this risk. Sarnataro, R., Velasco, C.D., Monaco, N. *et al.* Mitochondrial origins of the pressure to sleep. *Nature* **645**, 722–728 (2025). https://doi.org/10.1038/s41586-025-09261-y. Creative Commons Attribution 4.0 International License. http://creativecommons.org/licenses/by/4.0/.

Now, let's return to the more macroscopic changes in mitochondria that occur with sleep deprivation. These changes are likely mediated by ROS damage to membrane lipids. A variety of proteins control mitochondrial dynamics and orchestrate the balance between fission and fusion. **Dynamin-related protein 1 (Drp1)** facilitates the fission of the membrane by forming oligomers that surround the mitochondria, and through constriction, severs the mitochondrial membrane. GTP hydrolysis is required for this process. Sleep loss causes the recruitment of Drp1 from the cytoplasm to the mitochondria to initiate fission. This protein belongs to the dynamin family, which comprises GTPase proteins used for membrane fission during endocytosis, where they form helical "collars" around budding vesicles.

This process is reversible since small mitochondria (or fragments) can fuse to form larger ones. Two mitochondrial integral membrane GTPases are involved in mitochondrial fusion: **optic atrophy 1 (Opa1)** and **mitofusin,** also known as mitochondrial assembly regulatory

factor (Mfr). Oligomerization of these proteins promotes fusion. These proteins and their functions are illustrated in Figure **19.1.43** below.

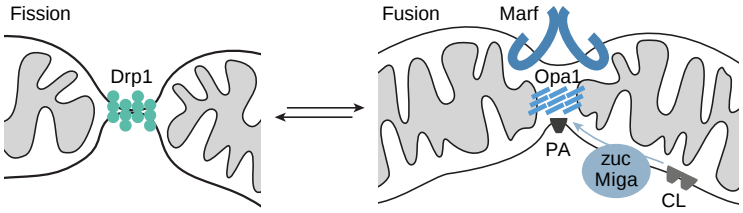


Figure **19.1.44**: The mitochondrial fission (green) and fusion machineries (blue) comprise Drp1, the outer and inner membrane proteins Marf and Opa1, and the mitoPLD zuc, which releases phosphatidic acid (PA) from cardiolipin (CL). Miga stimulates zuc activity and/or supplies phosphatidic acid from other membranes. Sarnataro et al., ibid.

It appears that the reversible fission ↔ fusion process in mitochondria occurs as a response to the imbalance in ATP demand and electrons supplied by NADH. Agents that decrease fragmentation and increase fusion in dFPNs increase sleep depth and duration.

- Overexpression of Drp1 or depletion of Opa led to increased mitochondrial fission, decreased sleep, and reduced ATP concentration.
- IF Drp1 is depleted or Opa1 is increased, fusion occurs, resulting in increased sleep .

These effects were specific to the dFBNs.

Fission followed by mitophagy, which occurs after sleep deprivation, likely facilitates the removal of damaged mitochondria. Increases mitochondrial contact with the ER likely help replace damaged peroxidized mitochondrial lipids with undamaged ER membrane lipids. The upregulation of gene transcripts for the citric acid cycle and electron transport gene is likely an additional attempt to repair and rejuvenate mitochondria in sleep-derived brains.

19.1.7: SUMMARY

This chapter provides a comprehensive look at the mitochondrial electron transport chain (ETC), a critical component of aerobic metabolism that links the oxidation of reducing equivalents (NADH and $FADH_2$) to the production of ATP. It explains how electrons derived from the citric acid cycle are transferred through a series of membrane-bound protein complexes, ultimately reducing molecular oxygen to water, and how the energy released during these redox reactions is harnessed to pump protons across the mitochondrial inner membrane.

Key Components and Electron Carriers:

The ETC is composed of four major complexes (I, II, III, and IV) embedded in the inner mitochondrial membrane, along with mobile electron carriers such as ubiquinone (UQ) and cytochrome c. Complex I (NADH-quinone oxidoreductase) initiates electron transfer by oxidizing NADH through a series of cofactors including FMN and multiple iron–sulfur clusters. Complex II (succinate dehydrogenase) links the citric acid cycle to the ETC by oxidizing succinate to fumarate and transferring electrons from $FADH_2$ to ubiquinone. Complex III (cytochrome bc_1 complex) employs the Q cycle to bifurcate electrons from reduced ubiquinone, directing them to cytochrome c and simultaneously contributing to the proton gradient. Finally, Complex IV (cytochrome c oxidase) receives electrons from cytochrome c and catalyzes the four-electron reduction of oxygen to water while pumping additional protons, further establishing the proton motive force.

Coupling Electron Transport to ATP Synthesis:

Rather than relying on a high-energy phosphorylated intermediate, the ETC couples electron transfer to the active transport of protons from the mitochondrial matrix to the intermembrane space. This proton gradient (proton motive force) is then exploited by ATP synthase (Complex V) to drive the endergonic synthesis of ATP from ADP and inorganic phosphate.

Structural and Functional Integration:

The chapter emphasizes the intricate structural organization of the ETC complexes, including the formation of supercomplexes (respirasomes) that optimize electron transfer and reduce the risk of electron leakage, which can lead to the formation of reactive oxygen species (ROS). Detailed discussions on the electron carriers within Complex I, the Q cycle mechanism of Complex III, and the elaborate water channels and proton pathways in Complex IV illustrate the fine-tuned mechanisms by which the system minimizes side reactions and maximizes efficiency.

Regulation and Inhibition:

Understanding the ETC also involves appreciating its regulation and vulnerabilities. The text reviews how inhibitors, such as rotenone for Complex I and antimycin A for Complex III, can disrupt electron flow, leading to enhanced ROS production and potential cellular damage. These insights underscore the physiological importance of maintaining efficient and tightly controlled electron transport for cellular energy homeostasis.

In summary, this chapter integrates structural, mechanistic, and regulatory aspects of the mitochondrial electron transport chain, providing a detailed view of how electron flow is coupled to proton pumping and ATP synthesis. The material underscores the evolutionary sophistication of the ETC in harnessing energy while minimizing harmful side reactions, a concept central to understanding cellular respiration in aerobic organisms.

This page titled 19.1: Electron-Transfer Reactions in Mitochondria is shared under a not declared license and was authored, remixed, and/or curated by Henry Jakubowski and Patricia Flatt.

- **Current page** by Henry Jakubowski and Patricia Flatt has no license indicated.
- **11.2: Diffusion Across a Membrane - Passive and Facilitated Diffusion** by Henry Jakubowski and Patricia Flatt has no license indicated.

19.2: ATP SYNTHESIS

Search Fundamentals of Biochemistry

LEARNING GOALS (CHATGPT O3-MINI)

- **Describe the Overall Structure and Localization:**
  • Identify the two main components of ATP synthase (Fo and F1) and explain their locations in mitochondria, chloroplast thylakoid membranes, or bacterial cell membranes.
- **Explain the Dual Motor Functionality:**
  • Distinguish between the proton-driven rotary "electrical motor" function of the Fo subunit and the ATP-driven "chemical motor" function of the F1 subunit, including the reversibility of the enzyme.
- **Understand the Structural Organization:**
  • Describe the quaternary structure of the F1 portion (a3β3 hexamer with a central γ subunit) and the role of the rotor (γ, ε, δ) and stator components in facilitating ATP synthesis.
- **Illustrate the Rotary Catalytic Mechanism:**
  • Explain Boyer's three-state (Loose, Open, Tight) conformational model for ATP synthesis and how the rotation of the γ subunit induces cyclic conformational changes in the β subunits to drive catalysis.
- **Evaluate Experimental Evidence for Rotation:**
  • Summarize key single-molecule experiments (e.g., fluorescently labeled actin filaments attached to the γ subunit) that directly demonstrated the rotation of the F1 motor during ATP hydrolysis and synthesis.
- **Describe Proton Translocation and Its Coupling:**
  • Explain how the proton gradient (proton-motive force) across the inner mitochondrial membrane powers the rotation of the Fo subunit and, in turn, ATP synthesis in F1.
  • Identify key residues (e.g., Glu 59 in bovine, Asp 61 in E. coli) involved in proton binding and translocation through the c-ring and Fo channel.
- **Discuss Inhibition and Mechanistic Probes:**
  • Describe the effects of classical inhibitors like oligomycin and dicyclohexylcarbodiimide (DCCD) on the Fo proton channel and explain how these inhibitors provide insight into the enzyme's mechanism.
- **Integrate Thermodynamic Principles:**
  • Derive and explain the equations that link proton concentration (ΔpH) and electrical potential (Δψ) to the overall free energy change driving ATP synthesis, culminating in the concept of the proton-motive force.
- **Relate Structural Dynamics to Function:**
  • Connect the rotational movement of the Fo c-ring and its interaction with subunit a to the generation of a directional force that facilitates conformational changes in the F1 portion necessary for ATP production.
- **Synthesize Concepts of Reversibility:**
  • Discuss how the same molecular machinery can operate in reverse—hydrolyzing ATP to pump protons against their gradient—and the significance of this reversibility in cellular energy homeostasis.

These goals aim to integrate the structural, mechanistic, and thermodynamic aspects of ATP synthase, fostering a deep understanding of how this remarkable nanomotor couples proton flow to the synthesis (and hydrolysis) of ATP.

19.2.1: INTRODUCTION

ATP synthase, also called F_1F_oATPase, is a rotary motor enzyme. This enzyme is found in the inner membrane of mitochondria, the analogous thylakoid membranes of chloroplasts, and the cell membrane of bacteria. The enzyme consists of two parts: the membrane-bound Fo, a proton translocator, and the F_1 part, which has catalytic (ATP synthesis or hydrolysis activity. The F_o part can be considered a rotary electrical motor powered by proton flow, while the F_1 part acts as a rotary chemical motor powered (in reverse) by ATP hydrolysis. The $F_{\mathbf{o}}$ part is named since it is sensitive to **o**ligomycin (note that it should theoretically be read as $F_{\text{litter o}}$ and not F_{zero}). The F_1 part is named after its elution in **F**raction **1** from a column chromatography column.

Many, but especially Paul D. Boyer and John E. Walker, elucidated its mechanism and structure. They, along with Jen Skou, who studied the mechanism of the analogous Na/K-ATPase, were awarded the Nobel Prize for their work.

Let's begin with the known structure of this complex membrane-bound rotary enzyme and then work towards understanding how it functions. The structure of the bovine $F_1F_oATPase$ is shown in Figure **19.2.1**.

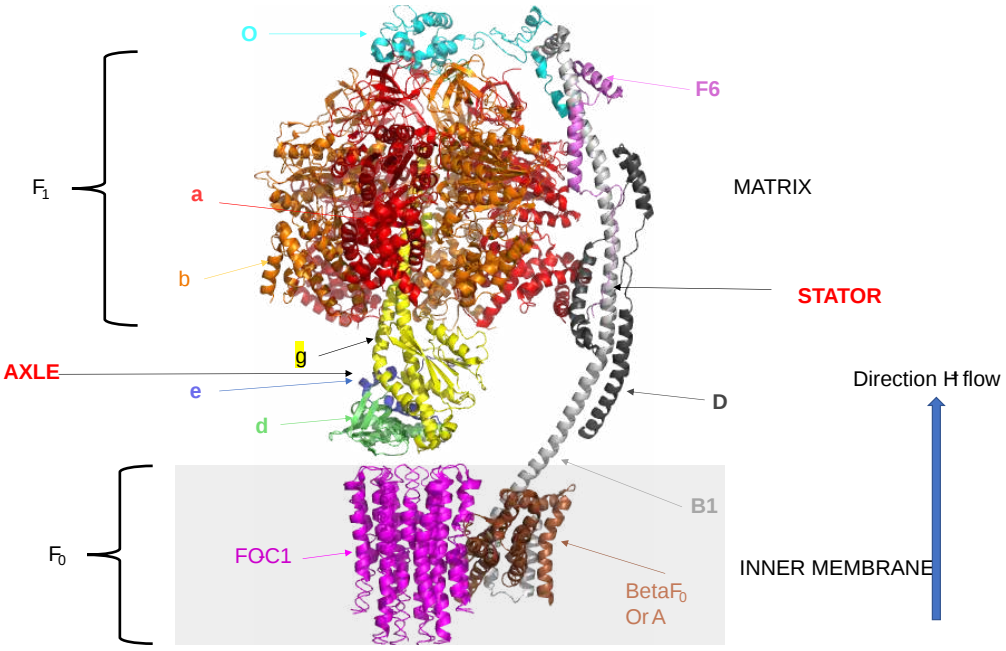


Figure **19.2.1**: Bovine $F_1F_oATPase$.

In the previous section, we discussed how oxidative electron transport in the mitochondria is accompanied by proton transport against a concentration gradient from the matrix through the inner membrane to the intermembrane space. The synthesis of ATP from ADP and P_1 is endergonic and requires an energy source. That energy source is provided by the thermodynamically favored collapse of the pH gradient across the mitochondrial inner membrane. Protons flow through the F_o membrane spanning C helices from the intermembrane space (not shown in Figure 1) to the matrix. This powers the synthesis of ATP from ADP and P_i by the F_1 part of the enzyme in the matrix lumen.

Figure **19.2.2** shows an interactive iCn3D model of the entire bovine mitochondrial ATP synthase (5ARA). The subunits are shown in the same color as Figure 1 above.

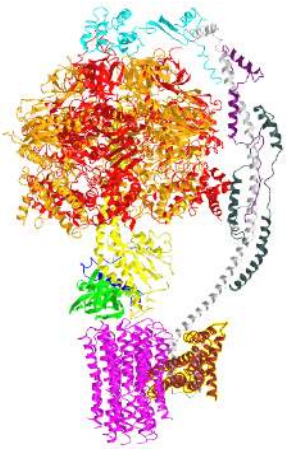


Figure **19.2.2**: Bovine mitochondrial ATP synthase (5ARA). (Copyright; author via source). Click the image for a popup or use this external link: https://structure.ncbi.nlm.nih.gov/i...3YUBWrX91nnua9

The enzyme is reversible. If protons flow down a concentration gradient through F_o, ATP is synthesized by F_1. Alternatively, ATP hydrolysis by F_1 leads to the transport of protons through F_o and against a concentration gradient. Isolated F_1 can only break down ATP and not synthesize it.

We called this structure a rotary enzyme, so what rotates? A rotary "axle" protein complex comprised of the γ, ε, and δ subunits (some also describe the γ, ε, and δ subunits as part of F_1) rotates. Its interactions with the multimeric complex of c alpha helices (shown in purple in the figures above) in the main F_o complex cause the "c-ring complex" complex in F_o to rotate as well. The F_1 part does not rotate because of the

conformational stability of the β subunit and the connection to the long alpha helices of the D and B1 proteins, which comprise the "stator (the stationary) part of an electric motor", which keeps F_1 stationary.

Hence, the enzyme acts like an electric motor, whose components are shown in Figure **19.2.3**.

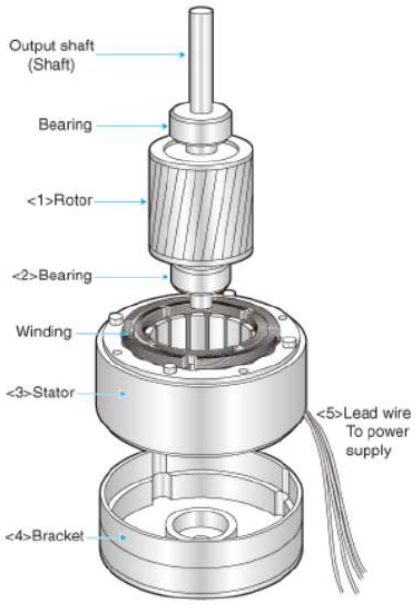


Figure **19.2.3**: Electric motor with rotor, shaft, and stator. http://www.cdmmotor.com/en/article-22982-28485.html

Now, let's examine the mechanisms and evidence for each part of this remarkable enzyme.

19.2.2: F_1

The F_1 unit (with a quaternary structure of $a_3\beta_3$ forming a hexagonal ringed structure with a central cavity occupied by a gamma subunit)is about 80 angstroms from the Fo subunit, and both are connected to the rod-shaped γ subunit, which spans the center of the $a_3\beta_3$ ring. Energy transduction (necessary to capture the negative free energy change associated with the collapse of the proton gradient to drive the positive free energy change for ATP synthesis) occurs between the two subunits.

Figure **19.2.4** shows a top view of the α (red) and β (green) subunits in the $a_3\beta_3$ F_1 complex.

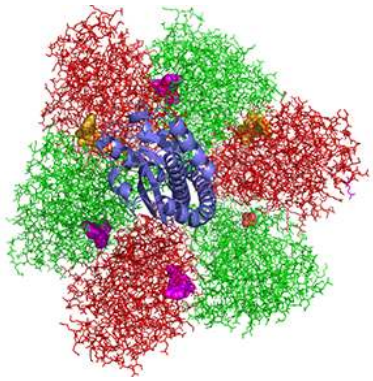


Figure **19.2.4**: Top view of the α (red) and β (green) subunits in the $a_3\beta_3$

The γ subunit is shown coming out of the plane of the ring. ATP is shown in gold spheres, ADP in purple, and the smaller SO_4^{2-} (from a crystallizing agent) is shown in CPK spheres. They are sandwiched between the α and β subunits.

Boyer, in the absence of the complete structure of the F_1F_o ATP synthase, was able to deduce from experimental evidence that the $a_3\beta_3$ complex, which can be viewed as three aβ dimers (with catalysis occurring between subunits of individual dimers where ATP and ADP bind), has three different, interconvertible conformation defined as a Loose (L), Open (O) and Tight (T) states, with names describing the strength of substrate binding in each dimer.

- O - open state with very low affinity for substrates and has no catalytic activity;
- L - loose state with low affinity for substrates and also no catalytic activity;

- T - tight state with high affinity for substrates and with catalytic activity.

The three states rotate not physically with respect to some central axis but conformationally, depending on their interaction with the γ subunit, which binds perpendicularly in the central junction of the $a_3\beta_3$ ring. Changes in the orientation of the central γ subunit due to its rotation with respect to the $a_3\beta_3$ ring cause the conformation of the O, L, and T states to change in situ with the orientation of the rotating γ subunit

The conversion of the LOT conformations, their binding of substrates (ADP and P_i), the conversion of bound ADP and P_i, and the release of the product (ATP) proposed by Boyer are shown in Figure **19.2.5**.

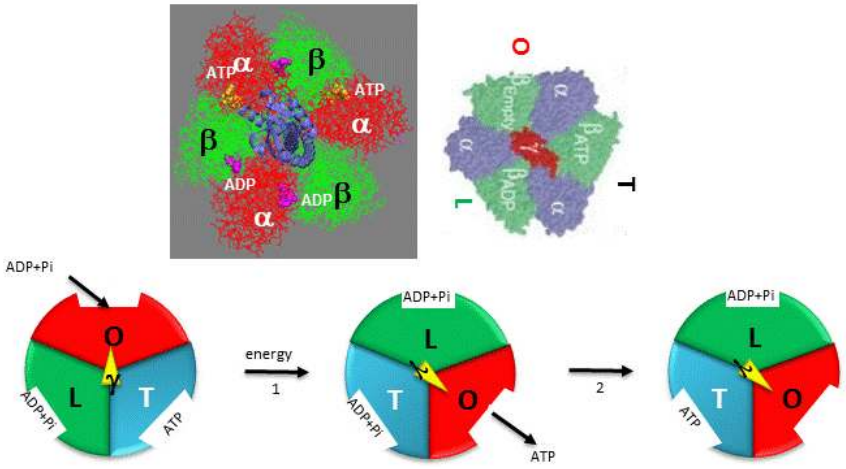


Figure **19.2.5**: Boyer's three-state conformational model (L-O-T) for ATP synthesis

The collapse of the proton gradient (i.e., the proton-motive force) causes the γ subunit to rotate like a crankshaft relative to the F1 subunit, forcing the β subunit to change conformation from the T to the O (releasing ATP) and then to the L (binding ADP and Pi) states. The γ subunit does not appear to undergo any significant conformational change on ATP hydrolysis, as evidenced by tritium exchange studies of amide protons.

To prove that the γ subunit rotates, you'd have to observe a single molecule. Since the γ subunit was too small to discern its rotation visually, Noji et al. covalently attached a fluorescein-labeled actin filament to the γ subunit (near where F_o would bind). The entire F1 molecule was fixed to a glass slip through a His-tag such that the $a_3\beta_3$ ring was immobilized. The γ subunit was free to rotate, which could be detected by observing the fluorescence from the attached actin filament using a microscope. Figure **19.2.6** describes this experiment and the outcomes.

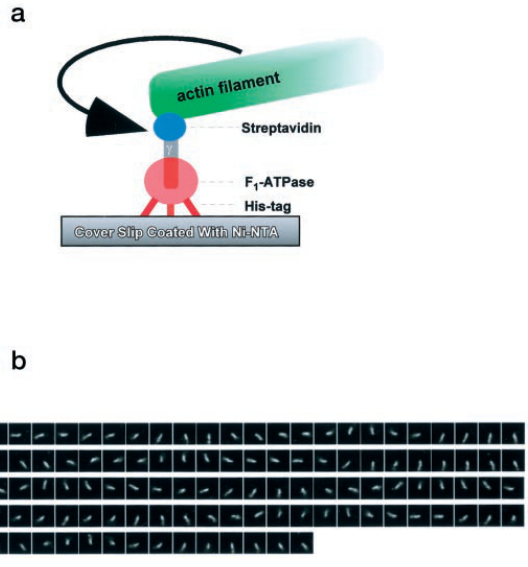


Figure **19.2.6**: The direct observation of the γ rotation in the F_1 motor. Noji and Yoshida. JBC (2001)
DOI:https://doi.org/10.1074/jbc.R000021200. Creative Commons Attribution (CC BY 4.0)

Panel **A** illustrates the experimental setup for observing γ rotation using an optical microscope. The F_1 motor, tagged with 10 His residues at the N terminus of the β subunit, was immobilized upside down on a coverslip coated with nickel-nitrilotriacetic acid (*Ni-NTA*). An actin filament (*green*) labeled with fluorescent dyes and biotins was attached to the biotinylated γ subunit (*gray*) through streptavidin (*blue*).

Panel **B** shows the rotary movement of an actin filament observed from the bottom, the membrane side, with an epifluorescent microscope. Length from the axis to tip, 2.6 μm; rotary rate, 0.5 revolutions per second; the time interval between images, 133 ms.

The actin filament rotated only in the presence of ATP. It rotated only counterclockwise, indicating that the motion was not random but a specific motion of the γ subunit. At extremely low concentrations of ATP, rotation occurred only in 120 ^{o} increments, implying one step per molecule of ATP hydrolyzed. (Remember the β subunits are separated by 120 $^{\circ}$.) As the rotation occurs, there is viscous resistance to the movement of the actin filament. He calculated that for a single 120 ^{o} step caused by hydrolysis of a single ATP molecule, the amount of work was 80 piconewtons, which is approximately the free energy of hydrolysis of a single ATP molecule.

Later experiments in which a colloidal gold nanoparticle (40 nm diameter, with less frictional resistance to movement) was used instead of an actin filament showed the same result. At low [ATP], the motor rotates in 120° steps. At high [ATP], the rotation rate becomes continuous and saturates (with Michaelis/Menten kinetics) at 130 revolutions per second.

Other experiments using immobilized ATPase and magnetic tweezers have investigated the timing of substrate binding and product release when the enzyme operates in reverse (ATP hydrolysis). On rotation of the γ subunit, the three binding sites change properties. In hydrolysis, ATP binds to the open site and helps promote the 120-degree rotation. In the next step, ATP is hydrolyzed. In the final step, products dissociate. Pi dissociation occurs last from the third site. Hence, each of the three beta-binding sites has a different role. One binds the substrate, one performs catalysis, and the third releases products. Assuming the synthesis pathway is the reverse of the ATPase reaction, the final release of Pi in ATP cleavage predicts that Pi binds first in the synthetic direction. This would, in turn, preclude the binding of ATP, which is critical since its concentration during synthesis can be 10 times higher than that of ADP. As Pi is bound first, only ADP, not ATP, can bind next.

The γ subunit rotation plays a "catalytic" role as its rotation induces cyclic conformational changes in the β subunit of the synthase. Can ATP synthesis occur without the gamma subunit by a mechanism that involves a less proficient, but a concerted set of cyclic changes in beta subunit conformation? It can! Uchihashi et al. have used high-speed atomic force microscopy (AFM) to study the $a_3\beta_3$ ring from the F1 subunit without the gamma subunit. They found that upon ATP hydrolysis, the beta subunits underwent conformational changes in the same counterclockwise rotary direction as when the gamma subunit was present. This is illustrated in Figure **19.2.7**.

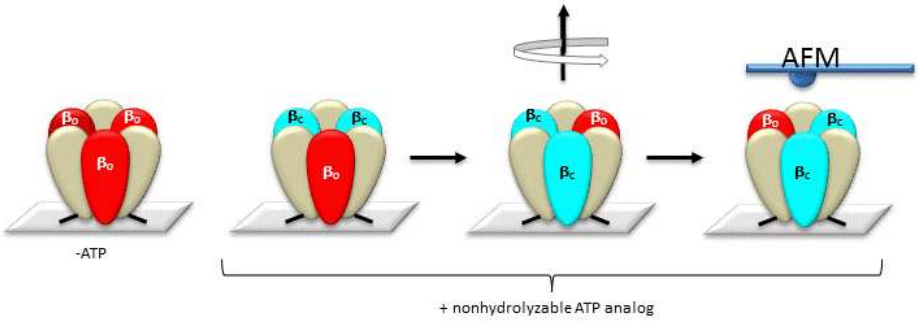


Figure **19.2.7**: AFM Study of Conformational Changes in F1 "gammaless" subunit

These experiments conclusively show that the F1 subunit is effectively a rotary motor with the gamma subunit acting as a rotor in the stationary hexagon ring composed of the three pairs of alpha/beta subunits, which acts as the stator (the stationary part of an electric rotary motor).

The actual amino acids involved in the ATP synthesis/hydrolysis mechanism are still not clearly defined, but Glu 190 on the beta subunit acts as a general base. Figure **19.2.8** shows bound ADP and the proximity of Glu 188. Ala 158 is thought to move towards the active site after a conformational change, with the nonpolar methyl side chain displacing an adjacent water molecule, which could leave as a product of ATP synthesis.

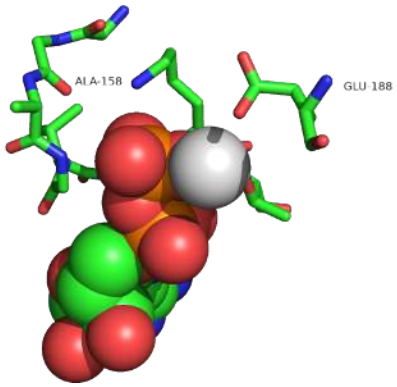


Figure **19.2.8**: Active site residues for the synthesis of ATP. ADP is shown in spacefill, and CPK colors. Mg^{2+} is shown as a gray sphere (1E79).

19.2.3: F_O AND PROTON TRANSFER

The mechanism by which the proton gradient drives ATP synthesis involves a complex coupling of the F_o and F_1 subunits. Proton translocation occurs through the interface of the inner mitochondrial (or cell membrane of bacteria) membrane proteins C1 and A (or beta), whose structures from the bovine enzyme are shown again in Figure **19.2.8**.

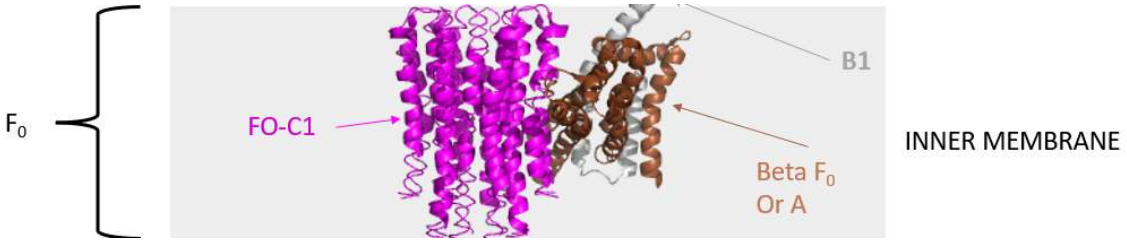


Figure **19.2.8**: Inner membrane proteins C1 and A (or beta)

For protons to translocate through the membrane, there must be an aqueous channel on the matrix and lumenal sides (bounded by the inner and outer mitochondrial membranes). So we have two understand two features:

- How does the rotary axle part of the complex interact with the C1 hexameric ring, causing the ring to rotate in the membrane?
- The nature of the water channels and the pathway for proton translocation.

The number of c monomers in the c-ring can vary between 8 and 17. For example, the bovine ATP synthase in Figures 1 and 2 has eight c-monomers. Each has a critical proton donor and acceptor near the a or beta-F_o chain. In the bovine case, it is glutamate 58. (The side chains in the bovine structure presented in Figure 2 do not show since they were not resolved in the cryoEM structure.) In E. Coli, which we will explore further below, it is aspartate 61. In yeast, it is at position 59. They are positioned near the center of the membrane helices. Mutations in these residues cause significant decreases in enzyme activity. An E56Q mutation in some bacilli species prevents proton pumping and ATP synthesis. Another key charged group, arginine, in the a or beta F_o protein is also key.

Figure **19.2.9** shows an interactive iCn3D model of the E. Coli A_1-C_{12} subcomplex of F_1F_O ATP Synthase (1C17).

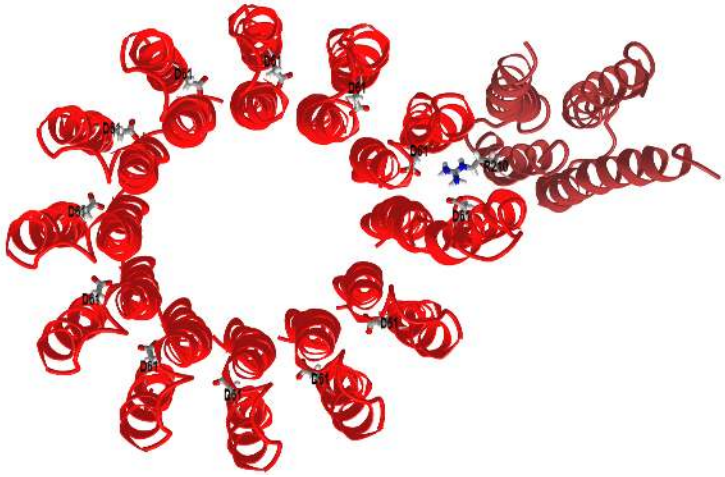


Figure **19.2.9**: E. Coli A_1-C_{12} Subcomplex OF F_1F_O ATP Synthase (1C17). (Copyright; author via source). Click the image for a popup or use this external link: https://structure.ncbi.nlm.nih.gov/i...sfRJBHEBiC5sy9

The key aspartate 61 (sticks and labeled) in each C ring subunit (red) and the proximity of two of the aspartate 61s to arginine 210 in the A subunit (brown) are evident.

Two classic inhibitors (structures shown below) of ATP synthase interact with the F_o subunit. One, oligomycin A, binds between the a and c subunits and blocks the proton transport activity of the F_o subunit. The O protein at the top of the F_1 complex is called the Oligomycin-sensitivity-conferring protein (OSCP), even though oligomycin does not bind there. The soluble F_1 by itself is not sensitive to oligomycin, but when it's linked to F_o in part through the O or OSCP peripheral stalk protein, it becomes sensitive to oligomycin.

Another inhibitor, dicyclohexylcarbodiimide, reacts with a protonated Asp 61 in c subunits of F_o. It does so even at pH 8.0, indicating that the pKa of Asp61 is significantly higher than usual. This might occur if the Asp is in a very hydrophobic environment. Modifying one Asp 61 in only one c-subunit is necessary to stop F_o activity. The protonated carboxyl group donates a proton to a nitrogen atom in DCCD, which then reacts with the deprotonated Asp to form an O-acyl isourea derivative. Figure **19.2.10** shows the structures of oligomycin A and DCCD, inhibitors of proton transport by F_o.

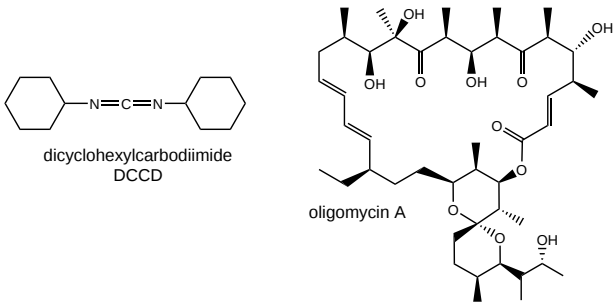


Figure **19.2.10**: structures of oligomycin A and DCCD

Figure **19.2.11** shows an interactive iCn3D model of the F_1F_oATPase c10 ring with bound oligomycin (4F4S)

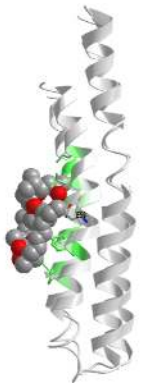


Figure **19.2.11**: E. Coli A_1-C_{12} Subcomplex OF F_1F_O ATP Synthase (1C17). (Copyright; author via source). Click the image for a popup or use this external link: https://structure.ncbi.nlm.nih.gov/i...pJw1pFr8jTPmK8

Only two of the c-subunits are shown interacting with one oligomycin. The actual complex has 10 c-subunits and eight oligomycins bound. The oligomycin is shown in spacefill with CPK colors. The two c-subunits are shown in gray. The side chains from the two c-subunits interacting with oligomycin are shown as CPK-colored sticks. They are conserved between humans and yeast. Note the single H bond between the critical Glu 59 and oligomycin. The green colors indicate hydrophobic parts of the c-subunits, which interact with the mostly nonpolar parts of the antibiotic.

How do these key Asp or Glu side chains participate in proton translocation across the membrane and c-ring rotation, and how do they access the matrix and lumenal water channels?

We can start to understand the answer to these question by examining the structure of the c-ring and its interaction with the a-chain from *Bacillus* PS3 ATP synthase, as shown in Figure **19.2.12**, which show the key Glu59 residues in each of the c subunits of the 10-mer ring along with Arg 176 and two other glutamates (Glu 223 and Glu 162) in the A ring.

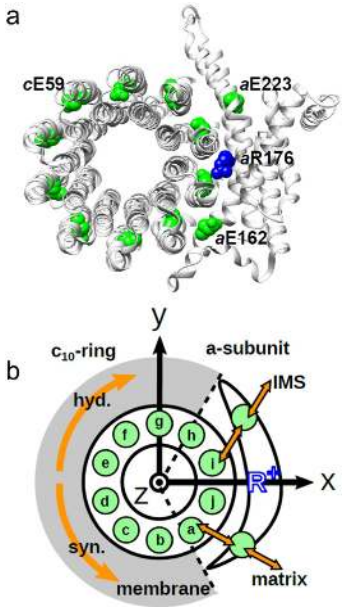


Figure **19.2.12**: Schematic picture of the *a*-subunit and *c*-ring of F_o. Mitome et al. (2022). *eLife* **11**:e69096. https://doi.org/10.7554/eLife.69096. Creative Commons Attribution License

Panel (**a**) shows the ac_{10} part of the F_o region, with the key amino acids represented as colored spheres (numbered based on the yeast protein).

Panel (**b**) shows a cartoon of a simulation model developed by Mitome et al (ibid). The Glu 59s are shown as green circles and labeled a-j. The gray represents the membrane.

Protons move between the protonated Glu 59 in c subunits proximal to the deprotonated Glu 223 and Glu 162 in a hydrogen bond "handshake". The Glu 59s in the c chains in the 10-mer ring are likely to be protonated, given their position in the center of the membrane.

In contrast, the proximal Glu 223 and 162 are more likely to be initially deprotonated, given their proximity to aqueous channels, where they "hand off" their protons to complete the translocation from the intermembrane luminal space to the matrix. Now, once a c-ring Glu59 is deprotonated, it has a negative charge.

Simulations suggest that 2-3 deprotonated Glu 59 have a negative charge proximal to the a-subunit. One is likely to take up a proton, leading to ATP synthesis. The orange arrows show the direction of proton flow. ATP is hydrolyzed if the c-ring rotates clockwise, while counter-clockwise rotation leads to ATP synthesis.

Let's look at the water channel forming at the interface between the c-ring and a-subunit and an additional protein, ASA6, from the unicellular green alga *Polytomella sp*. Figure **19.2.13** shows the interactions and nature of the water channels.

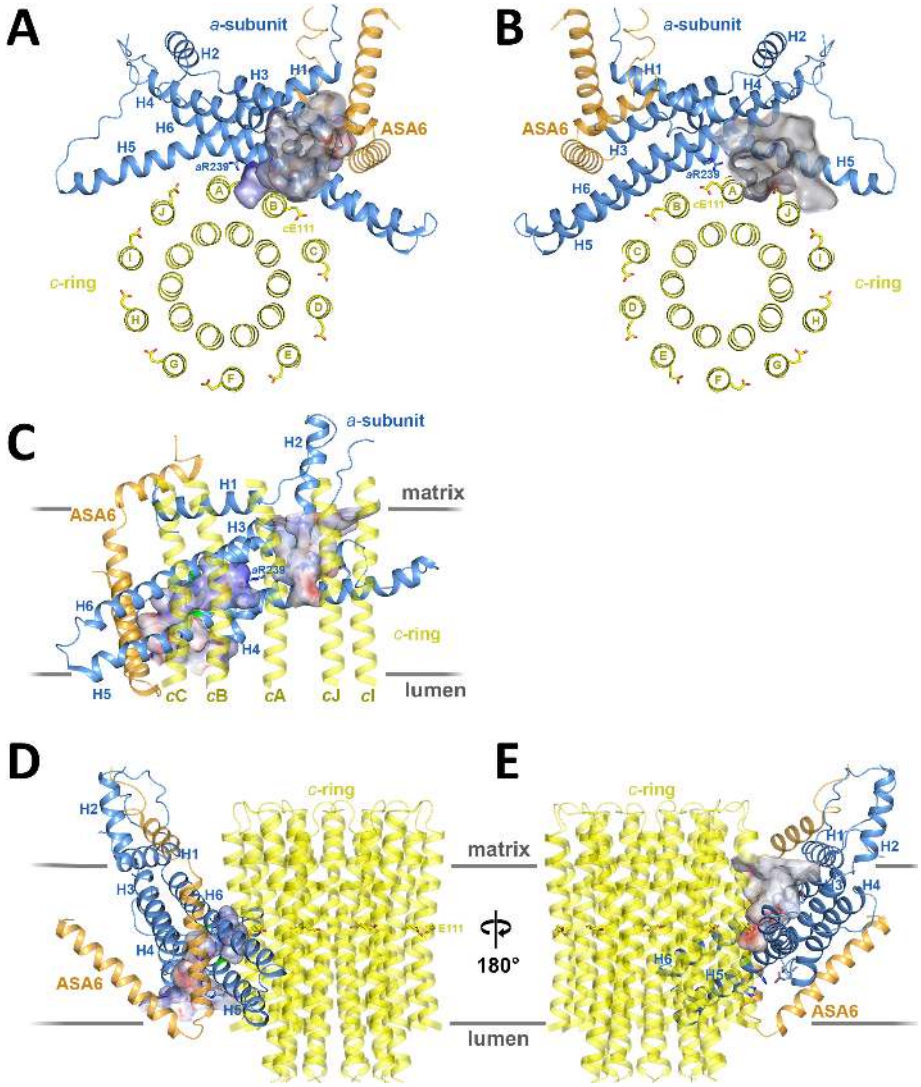


Figure **19.2.13**: Two aqueous channels in F_o. Niklas Klusch, Bonnie J Murphy, Deryck J Mills, Özkan Yildiz, Werner Kühlbrandt (2017) Structural basis of proton translocation and force generation in mitochondrial ATP synthase eLife 6:e33274. https://doi.org/10.7554/eLife.33274. Creative Commons Attribution License

Subunit a is shown in blue, the c_{10}-ring in yellow, and the associated ASA 6 protein in brick. The channels are shown as potential surfaces (red, negative; blue, positive; grey, neutral). (**A**) and (**B**) display a 5 Å slice of the c_{10}-ring at the level of the protonated *c*Glu111.

Panel(**A**) shows a 5 Å slice of the c_{10}-ring at the level of the protonated c-chain Glu111, with the lumenal channel seen from the crista lumen.

Panel (**B**) shows a 5 Å slice of the c_{10}-ring at the level of the protonated c-chain Glu111, with the matrix channel seen from the matrix.

Panel (**C**) shows a side view of both channels, as seen from the *c*-ring, with outer *c*-ring helices represented in transparent yellow. Lumenal channel, left; matrix channel, right. The strictly conserved a-chain Arg239 in helix 5 (H5) separates the lumenal and matrix channels.

Panel (**D**) shows that the lumenal channel passes through the H5/H6 hairpin at the small sidechains *a*Ala246, *a*Gly247 (H5), and *a*Ala292 (H6) (green).

Panel (**E**) shows H4, the N-terminal half of H5, and the connecting H4/H5 loop at the matrix channel.

Figure **19.2.14** a probable proton pathway through the F_o subcomplex

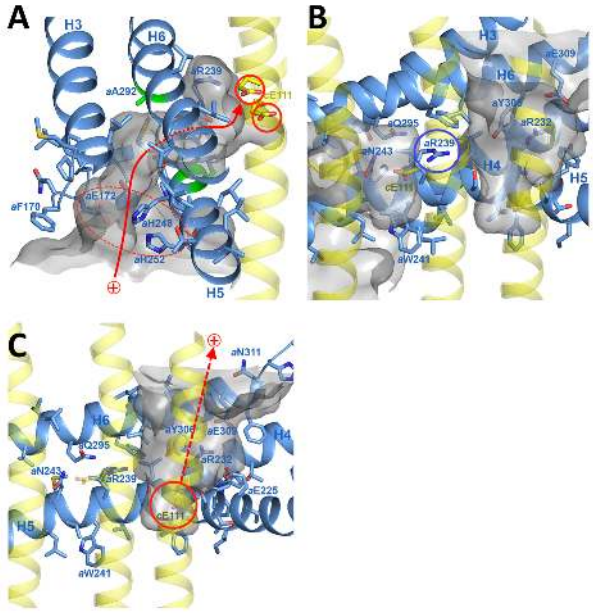


Figure **19.2.14**: Proton pathway through the F_o subcomplex. Klusch et al, ibid.

The a-subunit is shown in blue, the adjacent *c*-ring helices in transparent yellow, and the aqueous channels in translucent grey.

Panel (**A**) shows the movement of protons (red arrow) in the lumenal channel. They likely move between Glu172, His248, His252, and Glu288 in the a-chain (dashed red ellipse) through the H5/H6 helix hairpin at the small sidechains of a-chain Ala246 and Gly247 (H5) and Ala292 (H6) (green) to c-chain Glu111 in the rotor ring *c*-subunits (red circles).

Panel (**B**) shows that a-chain Arg239 (blue circle) is located halfway between the lumenal channel on the left and the matrix channel on the right, forming a seal to prevent proton leakage. *c*-ring helices (transparent yellow) with *c*Glu111 are seen in the foreground.

Panel (**C**) shows the movement of protons (dashed red arrow) in the matrix channel as they pass directly from the deprotonated c-chain Glu111 to the pH 8 matrix.

A final summary view showing c-ring rotation powered by the collapse of the pH between the lumenal (intermembrane space) channel (pink) and matrix channel (light blue) is shown in Figure **19.2.15**.

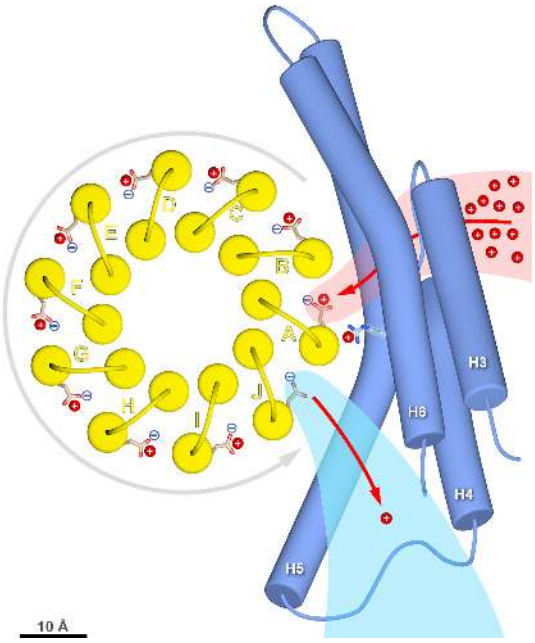


Figure 19.2.15: c-ring rotation is powered by the potential gradient between the lumenal channel (pink) and the matrix channel (light blue). Klusch et al, ibid

The *c*-ring (yellow) and the membrane-intrinsic four-helix bundle of subunit *a* (blue) are drawn to scale, as seen from the matrix. Protons (red) pass from the cristal lumen below the projection plane through the lumenal channel between H5 and H6 to protonate Glu111 of *c*-subunit *A*. *S*ubunit *J* is deprotonated by the higher pH of the matrix channel. The positively charged a-chain Arg239 will likely interact with the deprotonated c-chain Glu111 during its short passage to the lumenal channel. The lumenal and matrix channels approach one another to within 5–7 Å. A protonmotive force of 200 mV between the closely spaced channels creates a local electrostatic field in the range of 40 million to 100 million V/m, depending on the protein dielectric. The field exerts a force on the deprotonated c-chain Glu111, resulting in a net counter-clockwise rotation of the *c*-ring (grey arrow). Scale bar, 10 Å.

Click the images below to view a series of stunning videos (in a new window) showing proton translocation across the channel. (Niklas Klusch, Bonnie J Murphy, Deryck J Mills, Özkan Yildiz, Werner Kühlbrandt (2017) Structural basis of proton translocation and force generation in mitochondrial ATP synthase eLife 6:e33274. https://doi.org/10.7554/eLife.33274. Creative Commons Attribution License)

The three-dimensional arrangement of subunit *a* (blue), *c*-ring (yellow), with the lumenal channel in pink and matrix channel in light blue.

Arrangement of channel-lining sidechains for the lumenal channel.
Sidechains in stick representation are colored as subunit *a*, blue; *c*-ring, yellow; ASA 6, brick; lipids, grey. Channels are shown as potential surfaces (red, negative; blue, positive; grey, neutral).

Arrangement of channel-lining sidechains for the matrix channel.
Sidechains in stick representation are colored as subunit *a*, blue; *c*-ring, yellow; ASA 6, brick. Channels are shown as potential surfaces (red, negative; blue, positive; grey, neutral).

In summary, F_1F_oATP synthase is a rotary enzyme that ultimately couples the collapse of a proton gradient (a chemical potential gradient contributing to the transmembrane electrical potential) to a chemical (phosphorylation) step. The rotor, which is in contact with both the F_o proton pore and the F_1 synthase, moves with respect to both subunits, which couples them. Both the axle and c-ring of F_o rotate. The interaction of the delta protein with the F_1 $a_3\beta_3$ hexamer does not cause $a_3\beta_3$ to rotate as a whole, as does the c-ring. Rather, it causes a sequential rotation in the conformation of the three aβ dimers, transitioning from the Loose to the Open to the Tight (LOT) conformations. The F_o pore can hence be considered an electrical motor and the F_1 synthase a chemical motor. Carrying the analogy of a motor even further, the F_o electrical motor turns the F_1 chemical motor into a generator, not of electricity but of ATP. The figure and link below, taken from the Protein Data Bank, provide more in-depth information about this nanomotor.

The concerted movement of the c-ring and axle protein with respect to the not physically rotating $a_3\beta_3$ F_1 part can be seen in Figure 19.2.16, which is derived from the cryoEM structure of different rotated states of bovine ATP synthase.



Figure **19.2.16**: Structure and conformational states of the bovine mitochondrial ATP synthase (5ARA, 5ARE, 5ARH, 5ARI, 5FIJ, 5FIK, 5FIL)

A phenomenal video is available showing the detailed steps in ATP synthesis by ATP synthesis Click on Figure **19.2.17** to get the link to the video.

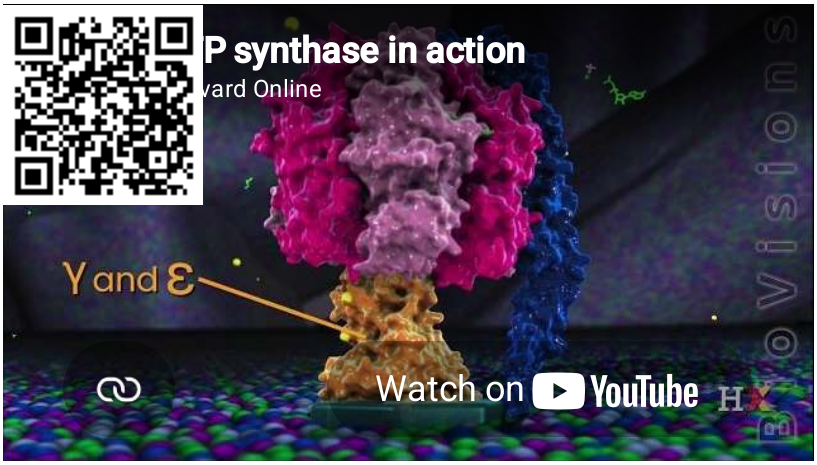


Figure **19.2.17**: ATP synthase in action. Muzzey and Lue, HHMI Institute. For educational and non-commercial use only.

This amazing enzyme and bacteriorhodopsin can be purified and reconstituted in a lipid vesicle. If these proteins are oriented correctly, light can cause proton translocation into the lumen of the vesicle, creating a transmembrane potential. The proton gradient can collapse as protons move from the lumen through the F_o part of F_1F_o ATP synthase, causing ATP synthesis from ADP and Pi in the outside solution. This is shown in Figure **19.2.18**.

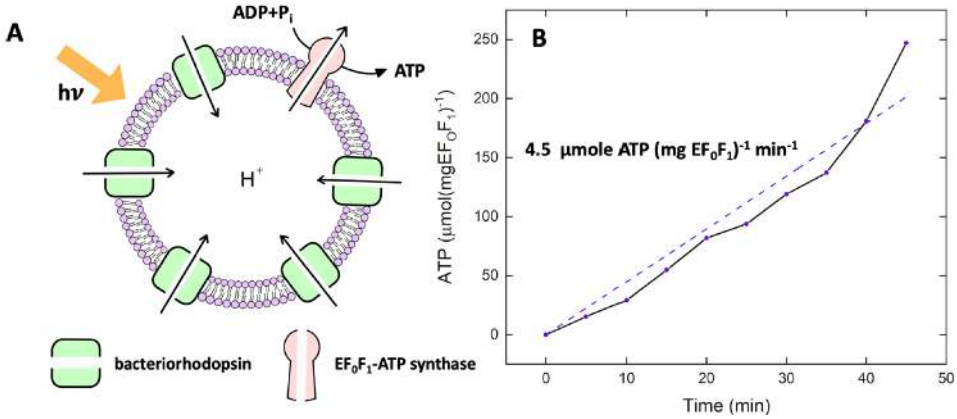


Figure 19.2.18:. Light-driven ATP production. Ahmad et al. *ACS Synthetic Biology* 2021. https://pubs.acs.org/doi/10.1021/acssynbio.1c00071. https://creativecommons.org/licenses/by/4.0/

Panel(A) shows a cartoon of the light-driven ATP synthesis in lipid vesicles. Panel (B) shows the increase in [ATP] over time.

19.2.4: PROTON GRADIENT COLLAPSE AND ATP SYNTHESIS - THERMODYNAMICS

Mathematical analyses indicate that the free energy change associated with the collapse of the proton gradient can readily power the endergonic synthesis of ATP. Consider a typical pH gradient (-1.4 pH units) across the inner membrane of respiring mitochondria (with the outside having a lower pH than the inside, making the inside more depleted in protons). There is a chemical potential difference in protons across the membrane. However, another factor determines the thermodynamic driving force for proton translocation across the membrane. A transmembrane potential exists across the inner membrane of the mitochondria, as it does across most membranes. The source of the membrane potential will be discussed in the signal transduction chapter (Chapter 28). The inside is more negative than the outside, creating a transmembrane electrical potential across the membrane of about -0.14 V. Clearly, protons would be attracted to the other side of the membrane (into the matrix) by this potential difference, which then augments the chemical potential difference. A simple mathematical derivation shows that, indeed, a proton gradient can supply enough energy for ATP synthesis, especially when coupled to a transmembrane electrical potential. We reshow a small image of the complex and its activities in Figure 19.2.19 to help you through this section

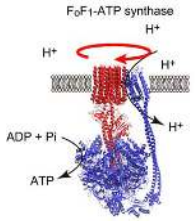


Figure 19.2.19: ATP synthase and its activities. Noji, H., Ueno, H. & Kobayashi, R. Correlation between the numbers of rotation steps in the ATPase and proton-conducting domains of F- and V-ATPases. *Biophys Rev* **12,** 303–307 (2020). https://doi.org/10.1007/s12551-020-00668-7. Creative Commons Attribution 4.0 International License. http://creativecommons.org/licenses/by/4.0/.

Chemical Potential (use G instead of μ)

Since most students use free energy rather than chemical potential (which is the free energy/mol at constant T and P), we will derive these equations using free energy G.

Let's consider the free energy of the protons on the outside (low pH, higher concentration) and in the inside (matrix, higher pH, low concentration):

$$\mathrm{H^+_{out}} \longrightarrow \mathrm{H^+_{in}}\ \mathrm{G} = \mu = \text{ chemical potential (kcal/mol)} \tag{19.2.1}$$

Now express this as the change in free energy, ΔG

$$\Delta G_{\mathrm{chem}} = G_{\mathrm{in}} - G_{\mathrm{out}} = G^0 + RT \ln \left[H^+\right]_{\mathrm{in}} - \left(G^0 + RT \ln \left[H^+\right]_{\mathrm{out}}\right) \tag{19.2.2}$$

This can be rewritten as:

$$\Delta G_{\mathrm{ohem}} = \mathrm{RT|n} \frac{[H^+]_{\mathrm{in}}}{[H^+]_{\mathrm{out}}} = 2.303RT\left[-\log\left[H^+\right]_{\mathrm{out}} - \left(-\log\left[H^+\right]_{\mathrm{in}}\right)\right] \tag{19.2.3}$$

Hence

$$\Delta \mathrm{G_{chem}} = 2.303\mathrm{RT}\left(\mathrm{pH_{out}} - \mathrm{pH_{in}}\right) = 2.303\mathrm{RT}\Delta\mathrm{pH} \tag{19.2.4}$$

In respiring mitochondria, ΔpH = -1.4, so

$$\begin{aligned} \Delta \mathrm{G_{chem}} &= 2.303\mathrm{RT}\Delta\mathrm{pH} \\ &= 2.303(1.99\mathrm{cal/mol \cdot K})(298\ \mathrm{K})(-1.4) = -1.91\mathrm{kcal/molH^+} \end{aligned} \tag{19.2.5}$$

Electrical Potential

Consider the relationship between ΔG and the transmembrane electrical potential

$$\Delta G_{\mathrm{elect}} = +ZF\Delta\psi \tag{19.2.6}$$

where Δψ is the transmembrane potential, Z=+1 (charge on a proton) and F is the Faraday constant

This equation is similar to

$$\Delta G \text{ elect } = -nF\Delta E \tag{19.2.7}$$

where ΔE is the cell potential or EMF. If ΔE is + and Δψ is -, then ΔG is -.

In respiring mitochondria, Δψ = -0.140 V (remember that 1 V = 1 J/C). This might seem small, but consider this. It is equivalent on a larger scale to an electrical field strength of approximately 30 million Volts per Meter. Compare this to an electric field right before a lightning strike of about 3,000,000 V/m. Hence

$$\begin{aligned}\Delta G_{\text{elect}} &= +ZF\Delta\Psi = 1(96.485\text{C/mol})(-0.140\text{ J/C}) \times (1\text{cal}/4.18\text{ J}) \\ &= -3.23\text{kcal/molH}^{+}\end{aligned} \tag{19.2.8}$$

Electrochemical potential

Now, let's add the equations to get the full driving force, the electrochemical potential:

$$\Delta G_{\text{tot}} = 2.303\text{RT}\Delta\text{pH} + \text{ZF}\Delta\psi = -5.15\text{kcal/molH}^{+} \tag{19.2.9}$$

This gives

$$\frac{\Delta G_{\text{tot}}}{F} = \frac{2.303RT\Delta pH + +zF\Delta\psi}{F} \tag{19.2.10}$$

Hence

$$\Delta p = \Delta\psi + \frac{2.303RT\Delta pH}{F} = \Delta\psi + 0.059\Delta pH = 0.224\text{ V} \tag{19.2.11}$$

where Δp is the protonmotive force.

19.2.5: SUMMARY

ATP synthase, also known as F₁F₀-ATPase, is a remarkable rotary motor enzyme that plays a central role in cellular energy metabolism. This enzyme is embedded in the inner membranes of mitochondria, in the thylakoid membranes of chloroplasts, and in bacterial cell membranes, where it couples the energy of a proton gradient to the synthesis of ATP from ADP and inorganic phosphate.

Dual Component Structure and Function:

ATP synthase consists of two major components:

- **F₀ (Fo) Subunit:** This membrane-embedded portion functions as a proton translocator. As protons flow down their electrochemical gradient—from the intermembrane space (or lumen) into the matrix (or stroma)—the Fo complex, which includes a ring of c subunits, rotates like the rotor of an electric motor. Key acidic residues (such as Glu 59 in bovine or Asp 61 in E. coli) are critical for binding and translocating protons.
- **F₁ (F1) Subunit:** This catalytic component protrudes into the mitochondrial matrix and is composed of a hexameric ring (α₃β₃) with a central γ subunit. The F₁ part operates as a rotary chemical motor, where the rotation of the central γ subunit induces conformational changes in the β subunits. These changes follow Boyer's three-state (Loose, Open, Tight) model, sequentially binding ADP and Pi, catalyzing ATP formation, and then releasing ATP.

Mechanism of Energy Conversion:

The enzyme harnesses the free energy released by the collapse of the proton-motive force—comprising both a chemical (ΔpH) and an electrical (Δψ) component—to drive the mechanical rotation of the Fo c-ring. This rotary motion is mechanically coupled to conformational shifts in the F₁ catalytic domain, ensuring that the binding and conversion of substrates occur in a cyclic, highly efficient manner. The reverse operation is also possible: ATP hydrolysis can drive proton pumping, underscoring the enzyme's reversibility and its pivotal role in maintaining cellular energy balance.

Experimental Validation and Structural Insights:

Key experiments, such as those using fluorescently labeled actin filaments attached to the γ subunit, have provided direct visualization of the rotational mechanism at the single-molecule level. These studies demonstrated that, at low ATP concentrations, the motor rotates in discrete 120° steps corresponding to the three catalytic sites in the F₁ hexamer. Structural studies, including cryo-electron microscopy and interactive models (e.g., iCn3D), have further revealed the intricate arrangement of subunits and the dynamic nature of the rotor–stator interactions.

Thermodynamic Considerations:

The driving force for ATP synthesis is derived from the proton-motive force, which is the sum of the proton concentration gradient and the

transmembrane electrical potential. Mathematical analyses show that even modest gradients (e.g., $\Delta pH \approx -1.4$ and $\Delta\psi \approx -0.14$ V) can supply sufficient free energy (approximately –5.15 kcal/mol per proton) to power the endergonic phosphorylation of ADP to ATP.

Conclusion:

This chapter integrates structural, mechanistic, and thermodynamic perspectives to provide a detailed overview of ATP synthase. The enzyme stands as a prime example of nature's ingenuity—a highly efficient, reversible nanomotor that converts the energy stored in an electrochemical gradient into chemical energy, essential for sustaining life.

This page titled 19.2: ATP Synthesis is shared under a not declared license and was authored, remixed, and/or curated by Henry Jakubowski and Patricia Flatt.

- **Current page** by Henry Jakubowski and Patricia Flatt has no license indicated.
- **11.2: Diffusion Across a Membrane - Passive and Facilitated Diffusion** by Henry Jakubowski and Patricia Flatt has no license indicated.

19.3: REGULATION OF OXIDATIVE PHOSPHORYLATION

LEARNING GOALS (CHATGPT O3-MINI)

- **Understand the Primary Function and Regulation of Oxidative Phosphorylation:**
  • Explain that oxphos is chiefly responsible for ATP production under aerobic conditions and that its regulation depends mainly on the cellular energy state (i.e., the ADP/ATP ratio).
  • Compare oxphos regulation with that of glycolysis and the citric acid cycle, noting the lack of allosteric or hormonal control in oxphos.
- **Describe the Key Reactants and Their Roles:**
  • Identify the primary substrates (NADH, $FADH_2$, O_2, ADP, and Pi) and explain how, assuming constant O_2 levels, ADP becomes the critical regulator of oxphos rate.
- **Explain Coupling and Uncoupling Mechanisms:**
  • Describe how electron transport and ATP synthesis are normally coupled through the proton gradient (protonmotive force).
  • Define proton leak and uncoupling, distinguishing between basal (non-regulated) leaks and inducible leaks via proteins like ANT and UCPs, and explain how these processes can lead to heat generation or ROS formation.
- **Evaluate Methods to Measure Oxphos Efficiency:**
  • Outline the experimental approaches used to determine the ADP/O ratio, including the use of coupled spectrophotometric assays (e.g., hexokinase/glucose-6-phosphate dehydrogenase assay).
  • Discuss how state 3 and state 4 respiration are measured to assess the coupling efficiency between electron transport and ATP synthesis.
- **Understand Proton "Slippage" and Its Impact on ATP/O Ratio:**
  • Explain the concept of "redox slippage" at Complex IV and "slippage" at ATP synthase, and how alterations in these processes affect the proton translocation and overall efficiency of ATP production.
  • Discuss how changes in the efficiency of proton pumping (due to enzyme concentration changes or regulatory molecules like reactive nitrogen species) can influence ATP synthesis.
- **Explore the Role of Uncoupling Proteins (UCPs):**
  • Describe the function of UCP1, its activation by fatty acids, and its role in thermogenesis.
  • Compare proposed models (protonophoretic vs. H^+-shuttling) for how UCP1 facilitates proton transport across the mitochondrial membrane.
- **Integrate Mitochondrial and Nuclear Regulation of Oxphos:**
  • Explain the interplay between the mitochondrial genome and nuclear genes in encoding proteins required for oxphos, and how these proteins are imported into the mitochondria.
  • Describe the bidirectional signaling between mitochondria and the nucleus (including retrograde signaling) and its role in coordinating mitochondrial function with cellular energy demands.
- **Discuss Key Signaling Pathways Involved in Energy Homeostasis:**
  • Identify and describe the roles of AMPK and mTOR as cellular energy sensors that modulate ATP synthesis, substrate utilization, and mitochondrial biogenesis in response to changes in the ADP/ATP ratio and other metabolic signals.

These learning goals aim to provide a comprehensive understanding of how oxidative phosphorylation is regulated at multiple levels—from kinetic and structural factors to mitochondrial-nuclear communication—emphasizing its central role in cellular energy metabolism.

19.3.1: INTRODUCTION

The primary function of oxidative phosphorylation (oxphos) is to produce, under aerobic conditions, lots of ATP. It should make sense that, to a first approximation, the regulation of oxphos depends primarily on the cell's energy state, which is reflected by the ADP/ATP ratio. In contrast to glycolysis and the citric acid cycle, which produce NADH, the primary and first electron carrier in oxphos, the regulation does not depend on binding allosteric effectors to key enzymes in the pathway. Likewise, hormonal regulation is not involved. Perhaps this occurs because the oxphos pathway is downstream from the glycolytic and citric acid pathways, where allosteric and hormonal regulation robustly affect their outputs.

If you consider the primary reactants in electron transport to be NADH, $FADH_2$, O_2, ADP, and P_i, and if you assume that O_2 levels are constant, ADP appears to be the main molecule that determines the rate of the oxphos reactions. This follows what we have previously described: AMP, ADP, and ATP levels regulate many of the key enzymes in the glycolytic and citric acid pathways, as reviewed in Figure 19.3.1.

Coordinate regulation of ATP production:

Regulation by:

- [ATP]
- [ADP]- the "PO_4" acceptor
- Mass action ratio, [ATP]/[ADP][P

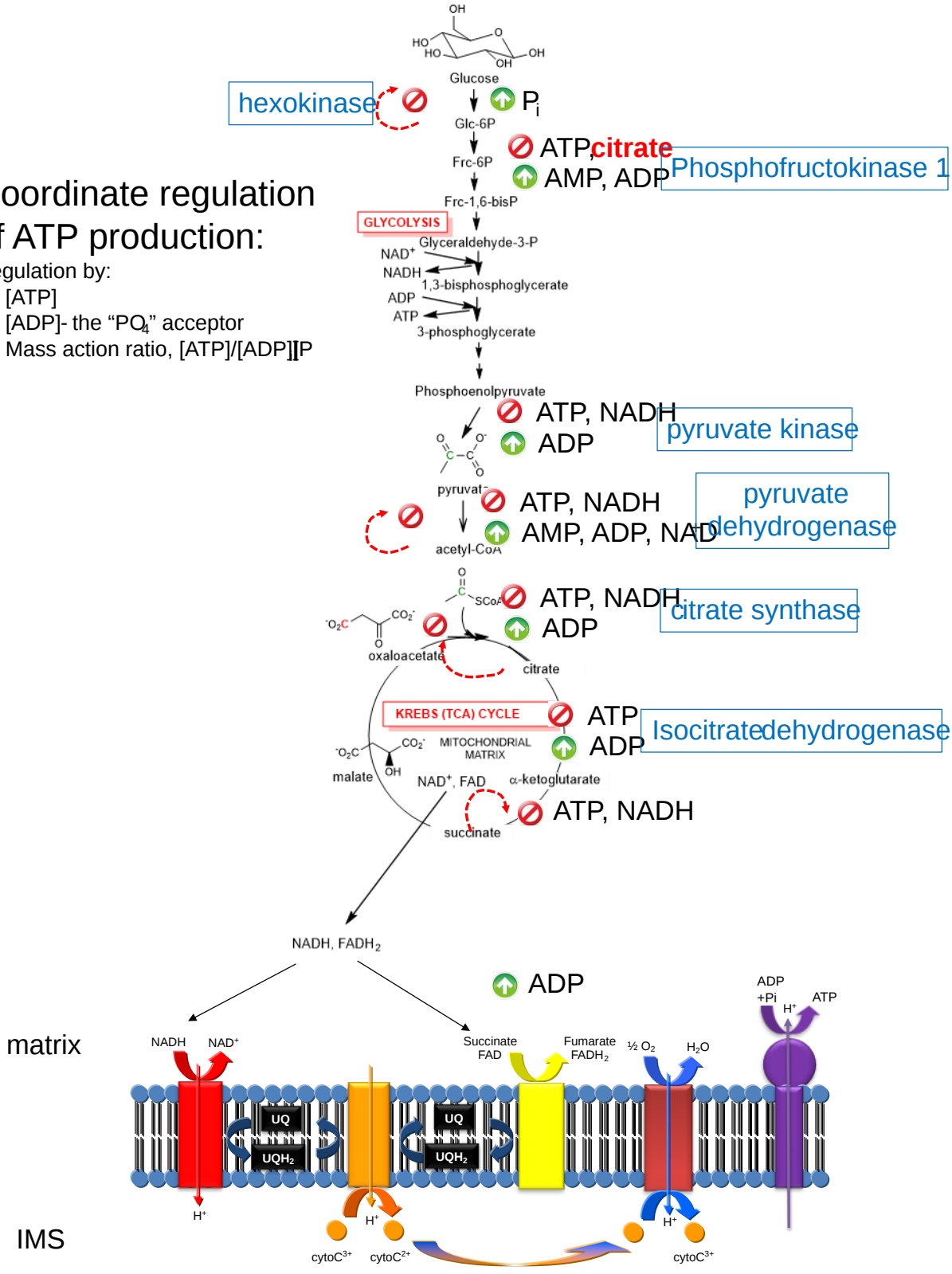


Figure **19.3.1**: Regulation of glycolysis, the citric acid cycle, and oxphos by ATP, ADP, and AMP.

Overall, there are several levels of oxphos regulation, which occur in the kinetics of the electron transport chain complexes, the efficiency of electron and proton transfer, the structure of the mitochondria, and mitochondria formation and their degradation.

19.3.2: COUPLING AND UNCOUPLING OF ELECTRON AND PROTON TRANSPORT

The key is that oxidation (electron transport) is coupled to the regulation of ATP synthesis (phosphorylation). These processes can also be uncoupled if electrons "leak" away from their transfer from NADH to O_2, which produces harmful reactive oxygen species (ROS) such as superoxide. Protons can also "leak" away from the proton gradient if they bypass the ATP synthase complex and pass through the inner membrane with the help of specific carriers and protein uncouplers, as shown in Figure **19.3.2**.

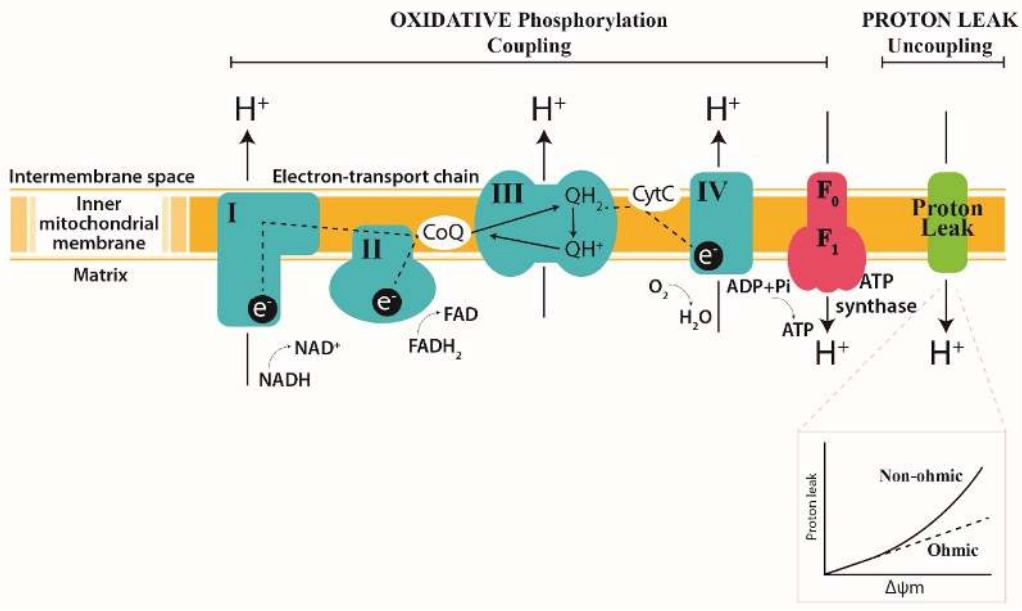


Figure **19.3.2**: Coupling and uncoupling of oxidative phosphorylation. Eyenga, P.; Rey, B.; Eyenga, L.; Sheu, S.-S. Regulation of Oxidative Phosphorylation of Liver Mitochondria in Sepsis. *Cells* **2022**, *11*, 1598. https://doi.org/10.3390/cells11101598. **Creative Commons Attribution License**

The far right light green proton and the insert show the proton leak's kinetics. The dotted line indicates the electron pathways.

There are two types of proton leaks:

- a basal leak through mitochondrial anion carriers in a non-regulated and minor process.
- an inducible leak through specific proteins, adenine nucleotide translocase (ANT), and uncoupling proteins (UCPs), leading to the loss of energy as heat. Fatty acids, as well as ROS, can activate them. A particular UCP, UCP1, is found most abundantly in brown fat in mammals.

The basal leak occurs in the presence of inhibitors of ANT (carboxyatractylate) and UCP1 (GDP). It can be significant (about 25% of the resting metabolic rate of liver cells and up to 50% in respiring skeletal muscle cells). It is less understood than inducible leaks and does appear to be attributed to ANT in some fashion.

When oligomycin, which inhibits the collapse of the proton gradient through ATP synthase, is added to mitochondria, the proton gradient (protonmotive force, Δp) decreases. The leakage rate increases exponentially with increasing Δp, representing **non-Ohmic leakage**. Ohmic leakage would give a linear dependence on Δp. This can be seen by rearranging Ohm's Law (V = IR) to give I = V/R = conductance(V), where V is voltage, I is the current (analogous to the leak), R is resistance, and 1/R is conductance. The exponentially increasing non-Ohmic leakage (usually measured by O_2 uptake in the presence of oligomycin) shown in the inserted graph in Figure 2, is not associated with non-specific membrane damage.

A particular uncoupling membrane protein, UCP1, is especially prevalent in hibernators, small mammals, and human infants, which enables them to maintain their body temperature. The UCP family is activated by fatty acids, which may act as required cofactors for the protein or as antagonists of the inhibition of UCPs by nucleotide diphosphates.

Two methods are used to determine the efficiency of the coupling of oxidation and phosphorylation.

- One is to determine the ADP/O ratio, as both are substrates for oxphos, where O represents the amount of O_2 consumed in converting a defined amount of ADP to ATP when ADP is at high levels (which might not be physiologically relevant). This would give the maximum

phosphorylation rate (defined as state 3).

- A second is to measure ATP (or ADP)/O ratio directly through methods that give spectrophotometric signals, such as the production of NADH by a coupled hexokinase/glucose-6-phosphate dehydrogenase assay in which ATP is used in the following reactions to make NADH, as shown in Figure **19.3.3**.

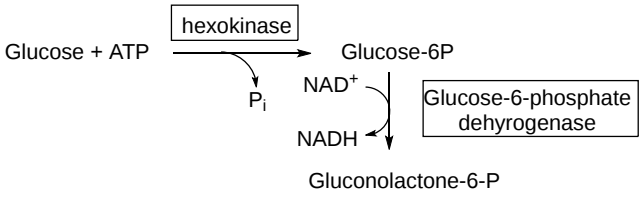


Figure **19.3.3**: Generation of NADH on the combined reaction of hexokinase and glucose-6-phosphate dehydrogenase.

In this coupled assay, one ATP is used to produce one NADH, which absorbs at 340 nm. Additionally, the ATP used as a substrate in the coupled reaction must have left the mitochondria for it to have access to hexokinase, so the internal ratios of ADP/ATP in the respiring mitochondria remain unchanged during the time course of the reaction. This method also allows the measurement to be made under nonsaturating ADP concentrations.

Uncoupling of electron transport and ATP synthesis can occur through a combination of mechanisms, including proton loss at ANT and UCPs, at the complexes in electron transport that transport electrons and protons, and through ATP synthase itself.

Other mechanisms would include substrate depletion or effects on the **mitochondrial permeability transition pore (mPTP)**, an inner membrane transmembrane protein that is gated open by increases in matrix Ca^{2+}, decreases in adenine nucleotide, and increases in Pi. It is also a voltage-gated channel. When the mitochondrial membrane opens, it depolarizes, ATP is depleted, and cell death can be triggered. We'll discuss this complex later.

Figure **19.3.4** shows the chemistry used to analyze the efficiency of oxphos and their graphical results.

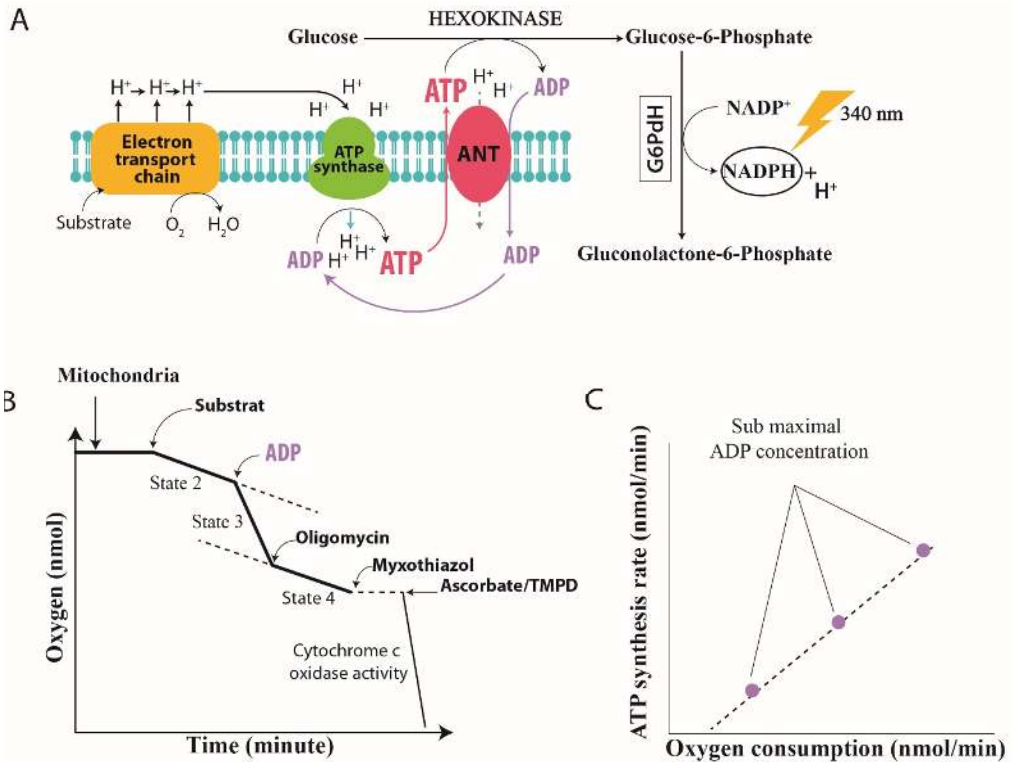


Figure **19.3.4**: Measurement of coupling efficiency in respiring mitochondria. Eyenga et al. Ibid.

Panel (**A**) shows the chemistry involved in determining the ATP/O ratio to measure coupling efficiency. Note that this step allows the regeneration of ADP, and efficiency can be measured at any ADP concentration.

Panel (**B**) shows changes in O_2 with time. The slope of the curve gives the respiration rate. Until a substrate is added, oxygen levels remain constant. Upon the addition of substrate, O_2 is consumed during electron transport, resulting in a linear decline in O_2 levels. When

ADP is added, the rate of O_2 consumption increases, which is reflected in a steady linear decline in O_2 levels. This state, which is at fixed ADP levels (as illustrated in Panel (A)), is called state 3 (maximum ATP synthesis at a given ADP level). When oligomycin, an inhibitor of proton flow across ATP synthase which inhibits ATP synthesis (and ADP use) is added, state 4 ensues with shows decreased O_2 consumption when ATP synthesis is stopped. Note the parallel lines for stages 2 and 4. The Cytochrome c oxidase activity at the end of the curve is the maximal respiration with ascorbate (as an oxidizing agent) and N,N,N′N′-tetra methyl-p-phenylenediamine (TMPD) as a substrate.

Panel (**C**) shows a graph of the rate of ATP synthesis vs. the rate of O_2 consumption. The slope indicates the rate of ATP generation relative to O_2 consumption (i.e., the ATP/O ratio). Note that the graph is linear over a range of fixed, non-saturating ADP concentrations.

19.3.3: CHANGES IN PROTON GRADIENT FROM "SLIPPAGE"

Slippage in the electron transport chains: Redox Slipping

Proton translocation from the matrix to the inner membrane space is an integral part of the function and activity of the electron transport chains that establish the pH gradient and, hence, the Δp. These components are Complexes I, III, and IV. Complex IV (cytochrome C oxidase - CCO) appears to be especially important. CCO removes protons from the matrix on the reduction of O_2 to H_2O. This requires exactly 4 electrons and 4 protons, so the stoichiometry is fixed.

Additionally, the CCO moves protons into the inner membrane space to establish the pH gradient. The electron-to-proton ratio may vary depending on redox and coupling conditions. Alterations in CCO or even decreases in its concentration would also impact the movement of protons. Instead of calling these alterations in nominal proton translocation leakages, they are called slippage since an ordinary function of CCO is proton translocation. Slippages through CCO would decrease proton transport and ATP/O. Reactive nitrogen species (NO and peroxynitrite) can also decrease ATP/O.

Slippage at ATP synthase

Proton leakage at ATP synthase would also result in a decreased ATP/O ratio. This occurs especially if nucleotides are low or if the holoenzyme is compromised by low subunit availability. ATP synthase forms dimers and other multimers to form supercomplexes, and this affects (or is determined by) the formation of invaginations in the inner membrane which form cristae.

Given that the multimeric c-ring of F_0 effectively moves protons across the inner membrane, it is a likely source of slippage. It most likely occurs through a modified version of the F_0 ATP synthase unit known as the **ATP synthase c-subunit leak channel (ACLC).** This differs from the mitochondrial permeability transition pore (mPTP) mentioned above. Alternatively, it may be that the ACLC is part of the leak channel of the mitochondrial permeability transition (MPT) pore discussed above. Studies show that the c-ring can form large conductance channels that are voltage-gated, even in the absence of regulatory subunits. In addition, the added F_1 subunit inhibits it. In neurons stimulated by the excitatory neurotransmitter glutamate, F_1 dissociates from the F_1F_0 complex, allowing the c-ring to slip protons through the membrane. Finally, the knockdown of the c-subunit eliminates high conductance. Hence, the c-ring is part of a type of mPT that is regulated by cyclophilin D (CypD), which is a mitochondrial peptidyl-prolyl cis-trans isomerase that regulates the mitochondrial permeability transition pore (PTP).

In vitro, c-rings incorporated into vesicles form a large voltage-gated channel that is inactivated by the addition of F_1. Also, in neurons stimulated with the excitatory neurotransmitter glutamate, which leads to increases in cytoplasmic Ca^{2+}, binding and ensuring conformational changes in the complex lead to dissociation of F_1 from the complex, freeing F_0 for proton "slippage" and transport uncoupled from ATP synthesis.

A Proposed “bent-pull-twist” model of ACLC gating in physiological and pathological conditions is shown in Figure 19.3.5.

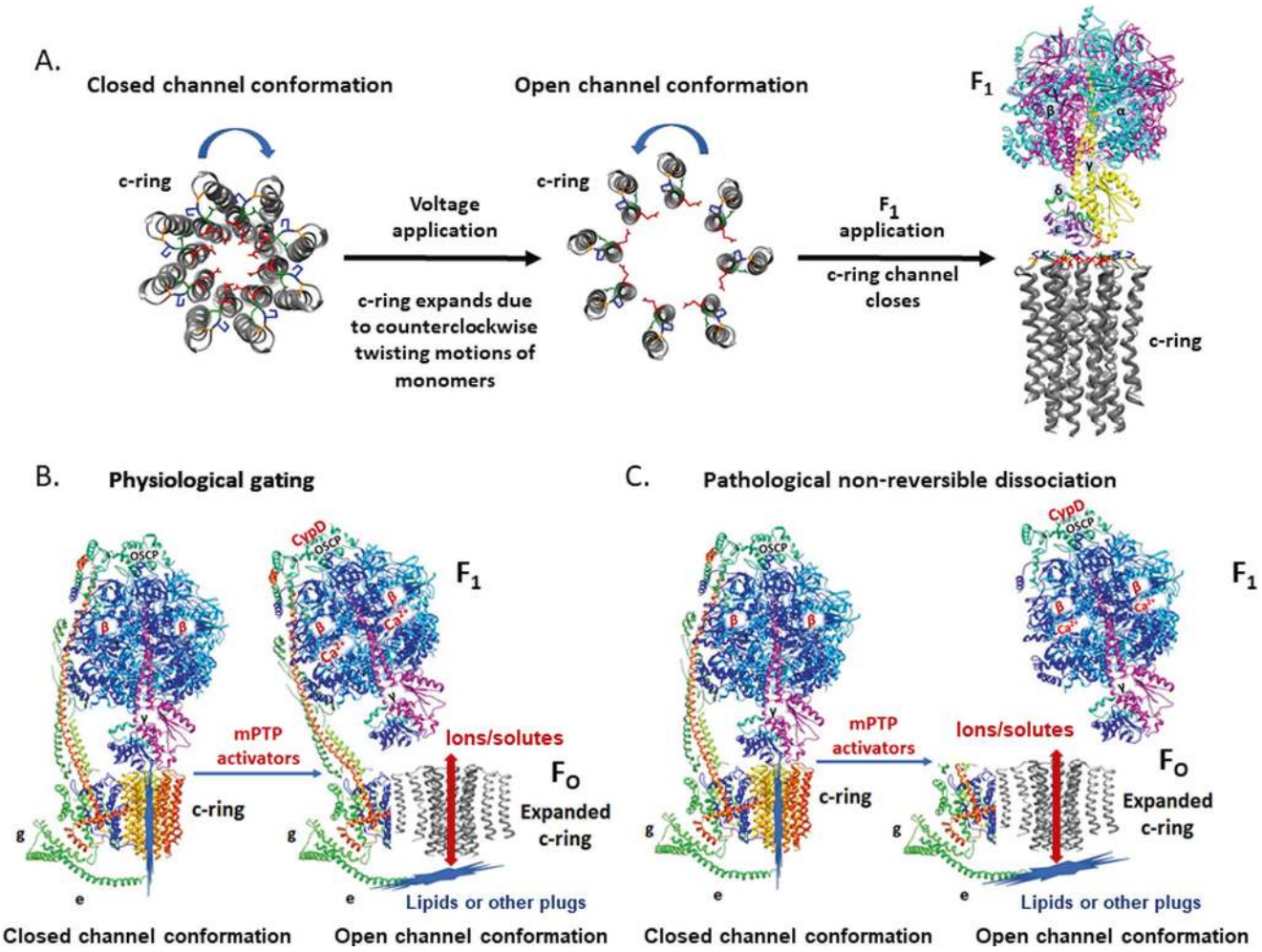


Figure **19.3.5**: **Bent-pull-twist model of ACLC gating in physiological and pathological conditions.** Mnatsakanyan, N., Park, HA., Wu, J. *et al.* Mitochondrial ATP synthase c-subunit leak channel triggers cell death upon loss of its F_1 subcomplex. *Cell Death Differ* (2022). https://doi.org/10.1038/s41418-022-00972-7. Creative Commons Attribution 4.0 International License. http://creativecommons.org/licenses/by/4.0/.

Panel A shows c-ring diameter changes during the electrophysiology recordings, upon the application of voltage and F_1. F_1 added during c-ring recordings probably inactivates the channel due to the specific interactions between F_1 and c-ring that induce twisting motions in c-subunit monomers in a clockwise direction, to stabilize the ring, reduce the pore diameter, and close the channel.

Panel B shows reversible brief openings of ACLC in physiological conditions.

Panel C shows that non-reversible dissociation of F_1 from F_O occurs during long-lasting openings of the c-ring channel in severe pathology. For simplicity, only ATP synthase monomer is shown. ATP synthase subunits are drawn as ribbon representations (modified PDB ID code: 6J5I) [14]. In **B** and **C**, red arrows indicate the ion flow path through the channel. Closed and open conformations of the channel are noted.

19.3.4: A CLOSER LOOK AT UNCOUPLER PROTEIN 1 (UCP1)

UCP1 is an inner membrane protein in the mitochondria that bypasses the movement of protons through the c-ring of F_1. UCP1 is activated by fatty acids and inhibited by purine nucleotides. The mechanism of proton translocation is unclear. It could arise from a "handshake" of protons through a series of linked hydrogen bond donors and acceptors in the membrane. Evidence suggests that what moves are bound and protonated fatty acids, which flip across the inner membrane where the carboxyl group deprotonates on the high-pH side of the membrane.

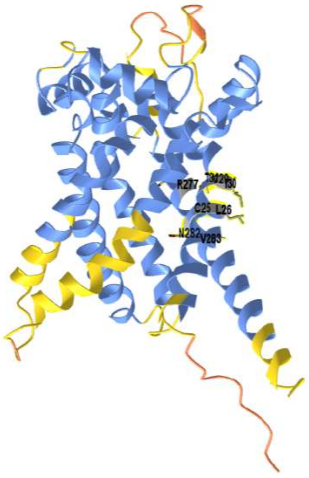
The role of UCP1 in this process may be to facilitate the reuptake of the deprotonated fatty acid across the membrane. This model is known as the protonophoretic model, in which the fatty acid acts as a "protonophore," much like valinomycin, which transports K^+ across the membrane and is classified as an ionophore. UCP1 doesn't interact with H^+ directly but flips the deprotonated fatty acid to continue the cycle. This model would give a stoichiometry of one flipped negatively charged fatty acid per proton transferred.

In the second "H^+-shuttling" model, UCP1 is considered a fatty acid/H^+ symporter (carries both species in the same direction). In this model, a fatty acid is strongly bound to UCP1, with its head group positioned within a cavity in the protein. Both models required UCP1 to carry deprotonated fatty acids back across the membrane.

The NMR structure of a similar protein, UCP2, is known. It can bind fatty acids with the acyl tail near the matrix side. However, UCP2 does not appear to be involved in thermogenesis and doesn't uncouple oxidative phosphorylation (oxphos). It binds and catalyzes the exchange of malate, oxaloacetate, and aspartate for phosphate and H^+ and has other metabolic roles. UCP 1 and 2 are approximately 60% homologous, but they share similar alpha-helical structures, as determined by modeling.

Perturbation of NMR signals from assigned side chains was used to show that the fatty acids bind to UCP1 and are closer to the matrix than the inner membrane space. Two key lysines (K56 on helix 1 and K269 at the matrix side of helix 6) probably bind with the carboxylate end of the fatty acid. UCP1also has a hydrophobic grove (T31, F32, L34, D35, L278, G279, S280, W281, and V283) to accommodate the fatty acid. In addition, UCP1 and UCP2 transport/flip alkyl sulfonates, analogs of fatty acids. This is consistent and required with both models.

Figure **19.3.6** shows an interactive iCn3D model of the predicted AlphaFold model of human UCP1 (P25874). The subunits are shown in the same color as Figure 1 above.



NCBI iCn3D Figure **19.3.6**: Predicted AlphaFold model of human UCP1 (P25874). (Copyright; author via source). Click the image for a popup or use this external link: https://structure.ncbi.nlm.nih.gov/i...Qf8W1MgVH6u546

The blue colors represent assigned structures with the highest predicted confidence, and the red the lowest. The amino acid side chains that are implicated in binding to fatty acids based on perturbation of NMR signals on fatty acid binding (http://dx.doi.org/10.1016/j.str.2017.07.005) are shown in sticks, with CPK colors and labeled. The membrane would be positioned perpendicular to the average vertical orientation of the helices in the above orientation.

19.3.5: ADDITIONAL CONTROLS

From the perspective of moving electrons into the electron transport pathway, the key deliverers of electrons are NADH, derived from integrated multiple pathways at Complex I (as illustrated in Figure 1), and $FADH_2$ from the citric acid cycle at Complex II. Hence, if intermediates in the citric acid cycle are low, the flux through electron transport is compromised. Flux through Complex I seems to determine the rate-limiting steps for oxygen use.

In the previous chapter section, we calculated the total chemical potential driving force across the membrane. A pH difference of 1.4 across the membrane provides a -1.9 kcal/mol (-8 kJ/mol) H^+ chemical potential compared to the -3.23 kcal/mol (13.5 kJ/mol) from the transmembrane potential, $\Delta\psi_m$. Both contribute to the thermodynamically favorable movement of H^+ across the inner membrane in respiring mitochondria, but $\Delta\psi_m$ is a large contributor. Hence, $\Delta\psi$m and ATP synthesis are also coupled, with maximal synthesis occurring between -100 and -150 mV. At values around -200 mV, there is an increase in permeability for protons (which decreases Δp) and the production of superoxide and peroxides. Hence, $\Delta\psi_m$ is also regulated.

ADP levels also control ATP synthesis, with higher concentrations leading to increased ATP synthesis and a decrease in Δp. Decreased ATP synthesis resulting from increased Δp affects coupling and slippage in cytochrome c oxidase, as well as heat generation.

The reduction of O_2 to water by stepwise addition of electrons involves the generation of superoxide, O_2^-. As shown in an earlier section, superoxide formed by Complex I would move to the matrix, while that formed by Complex III would move to both sides of the membrane. Hydrogen peroxide can also form from monoamine oxidase and α-ketoglutarate dehydrogenase, which produces increased peroxides with

increasing NADH concentrations. Respiratory state 4 (when proton transport is blocked by oligomycin) leads to higher levels of ROS. Hence, ROS levels are also determined by the respiratory state and Δp.

Other control mechanisms may be derived from protein subunits that bind to the complex within a lipid bilayer. These include A6L, DAPIT (diabetes-associated protein in insulin-sensitive tissues), and the proteolipid 6.8PL. Another is the ATPase inhibitory factor 1 (IF1), a significant regulator. When the $\Delta\psi_m$ falls too low, IF1 inhibits ATP depletion, which leads to ATP hydrolysis by the complex to move protons from the matrix to the inner membrane space. The interaction of IF1 with ATP synthase is shown in Figure **19.3.7**.

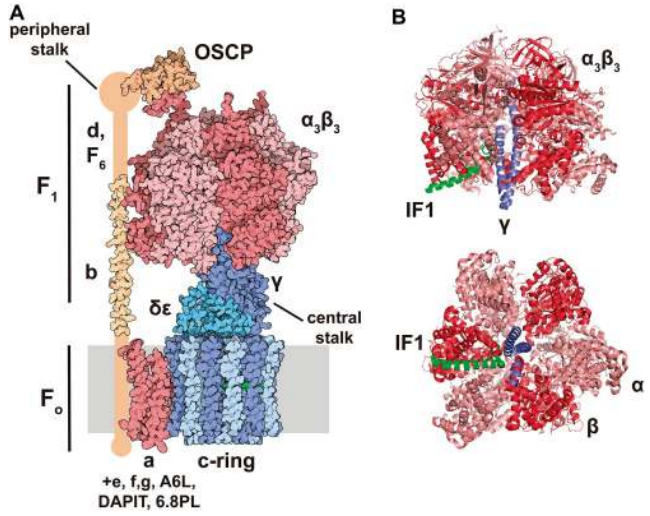


Figure **19.3.7**: Structure of the bovine H^+-ATP synthase and binding site of IF1. Esparza-Moltó, P.B., Nuevo-Tapioles, C. & Cuezva, J.M. Regulation of the H^+-ATP synthase by IF1: a role in mitohormesis. *Cell. Mol. Life Sci.* **74,** 2151–2166 (2017). https://doi.org/10.1007/s00018-017-2462-8. Creative Commons Attribution 4.0 International License (http://creativecommons.org/licenses/by/4.0/)

Panel **(a)** shows the soluble F_1-ATPase domain composed by the 3α3β subassembly (*salmon*/*red*) and γ (*dark blue*), δ and ε (*light blue*) subunits, while the membrane-embedded F_o domain is formed by subunit a (*red*) and a ring of 8c subunits (*light*/*dark blue*). Both domains are linked by a central stalk (γ, δ, ε subunits of the F_1 domain) and a peripheral stalk (b, d F6, A6L, OSCP subunits, in *orange*). The 3D structure of the peripheral stalk is not fully resolved. Except for the A and A6L subunits, the remainder is encoded in the nucleus. (model comprised of multiple PDB structures)

Panel **(b)** shows the lateral and basal view of the bovine F_1 domain (α subunit is shown in salmon, β in *red*, and γ in *blue*) complexed with a fragment of IF1 (*green*). IF1 binds to the αβ interface through residues 1–37 and also contacts the γ subunit. (PDB: 1OHH)

IF1 has an intrinsically disordered N-terminal domain that binds to ATP synthase between the α and β subunits of the F_1, where it adopts an alpha-helical conformation. It can dimerize through self-interactions with the C-terminal domain. Interestingly, bound IF1 inhibits both ATP synthesis and hydrolysis as well as H^+ translocation through the complex. These activities are illustrated in Figure **19.3.8**.

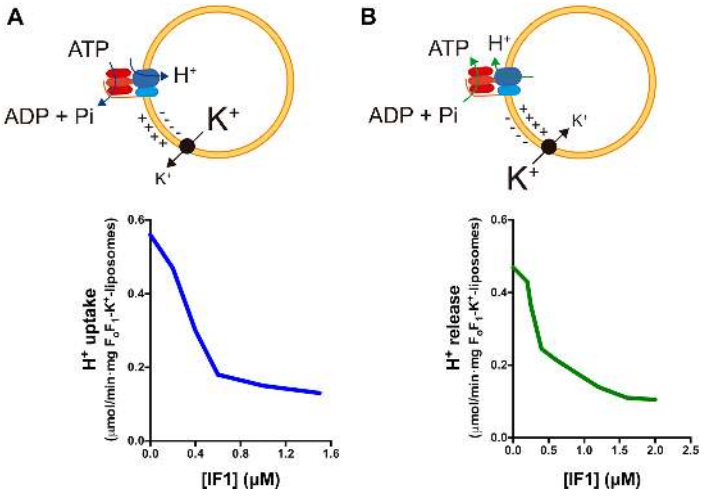


Figure **19.3.8**: IF1 inhibits H^+ translocation through the H^+-ATP synthase in synthetic and hydrolytic modes. Esparza-Moltó, ibid.

Panel **(a)** shows H^+ uptake is induced by valinomycin-mediated K^+ release from F_oF_1-K^+ liposomes with the H^+-ATP synthase functioning in the hydrolytic mode.

Panel **(b)** shows H^+ release is induced by valinomycin-mediated K^+ uptake in F_oF_1-K^+ liposomes with the H^+-ATP synthase functioning in the synthetic mode. The rates of H^+ uptake **(a)** and H^+ release **(b)** are reduced when the liposomes are incubated with increasing concentrations of isolated IF1. *Black circle* valinomycin.

Five key histidines in IF1 play a role in inhibiting the ATPase activity and the oligomerization of IF1. When the pH gradient collapses and the matrix becomes more acidic (as seen in hypoxia and ischemia), IF1 forms dimers that inhibit ATP hydrolysis. At higher pHs, IF1 forms a dimer of IF1 dimers, or effectively a tetramer, which prevents its binding to ATP synthase and the inhibition of ATP synthesis. An IF1-H49K mutant is an active inhibitor even at higher pHs. These properties are illustrated in Figure **19.3.9**.

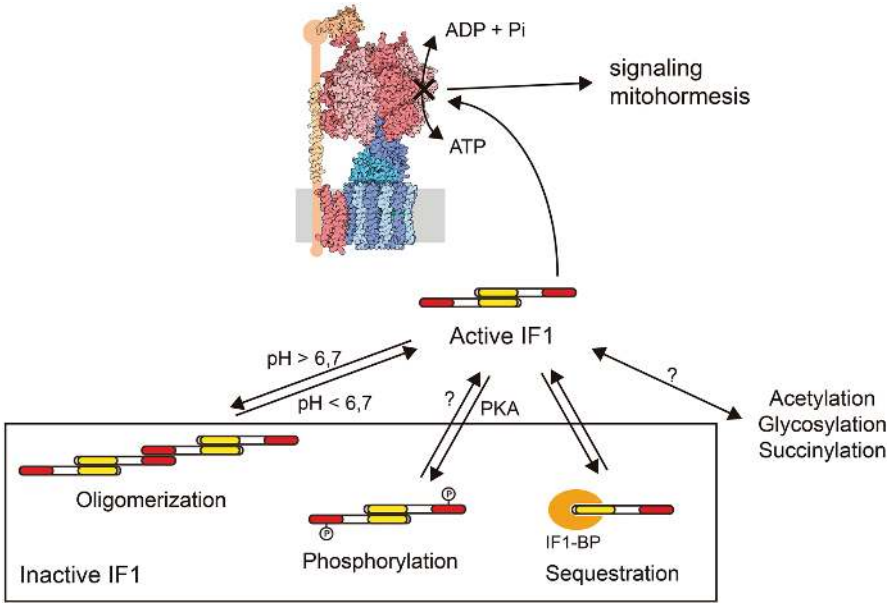


Figure **19.3.9**: Post-translational regulation of IF1 activity. Esparza-Moltó, ibid.

IF1 inhibition of ATP hydrolysis is not only relieved by pH-dependent oligomerization as illustrated above, but also by phosphorylation by a mitochondrial Protein kinase A-like molecule, or by its interaction with yet another protein, BP. A conserved serine 39 is important in its inhibitory action. When dephosphorylated, IF1 binds to ATP synthase and inhibits both ATP synthesis and hydrolysis. When phosphorylated, it can't bind and hence can't inhibit ATP synthase.

19.3.6: MITOCHONDRIA - NUCLEAR SIGNALING

We would be remiss not to include the role of the mitochondrial genome and its relationship to the nuclear genome in controlling mitochondrial function, including oxidative phosphorylation. Mitochondria arose from the internalization of a distant bacterium into a eukaryotic cell. They developed an endosymbiotic relationship in which some of the genes from the original bacterial species are still present in mitochondria today. The mitochondrial genome is shown in Figure **19.3.10**.

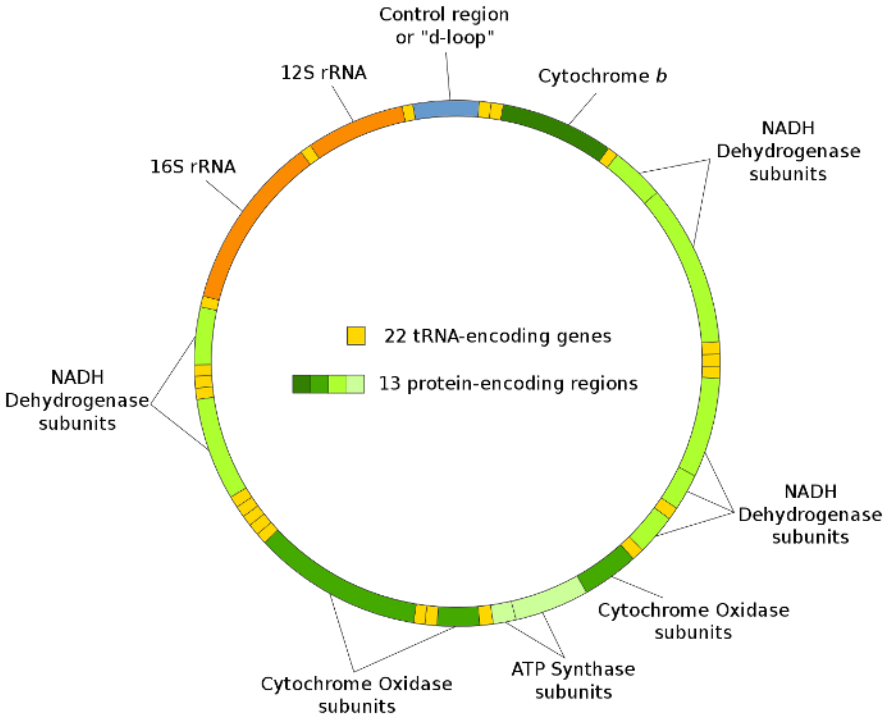
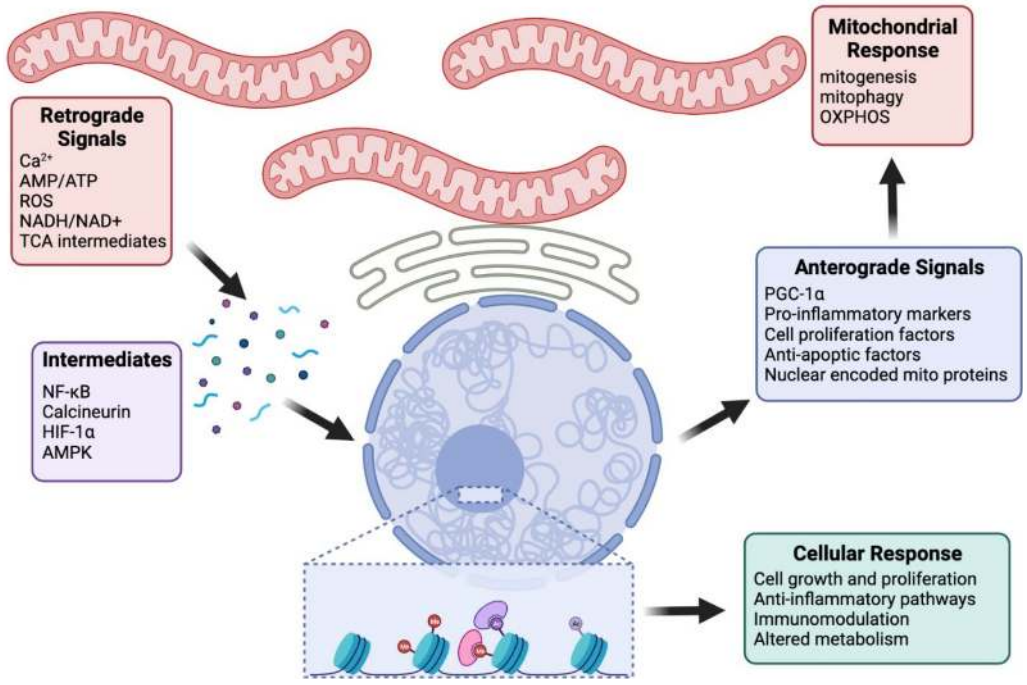


Figure **19.3.10**: Mitochondrial genome. https://commons.wikimedia.org/wiki/C...ial_DNA_en.svg

Mitochondrial DNA is a double-stranded molecule of 16.5 kilobases. It encodes some proteins and its own tRNA and ribosomal RNAs. Each cell has many copies (100s to 1000s) of the circular genome.

Some (actually 13), but not all of the genes for proteins required for oxidative phosphorylation are found in the mitochondrial genome. The rest reside in the nuclear genome, and after transcription and translation, the resulting protein must be imported into mitochondria. In fact, over 95% of mitochondrial proteins are encoded by nuclear genes. Mitochondria move within cells, guided by the internal cytoskeleton, to sites where energy (ATP) is needed. They also participate in buffering intracellular Ca^{2+} ions in the cell, like the ER, with which mitochondria form intimate membrane contacts. The ER also makes contact with the outer nuclear membrane, so, likely, the mitochondria can closely associate with the nucleus as well.

Hence, the respective genomes must be regulated to produce the correct type and amounts of proteins required for oxidative phosphorylation. To accomplish this, bidirectional regulated signaling is used between the two organelles. Direct signaling between the nucleus and mitochondria, as well as retrograde signaling in the opposite direction, exists. Signals and processes affected in these signaling pathways are shown in Figure **19.3.10**.



jdjkfj

Figure **19.3.11**: Signaling from the mitochondria to the nucleus. Brittni R. Walker **and** Carlos T. Moraes**.** *Biomolecules* **2022**, *12*(3), 427; https://doi.org/10.3390/biom12030427**.** Creative Commons Attribution (CC BY) license (https://creativecommons.org/licenses/by/4.0/)

Signals originating from the mitochondria, including calcium, reactive oxygen species (ROS), and AMP/ATP, often stimulate pathways that lead to transcriptional changes in the nucleus. Nuclear responses can involve upregulating cell proliferation and anti-apoptotic factors, as well as proteins involved in mitogenesis, such as PGC-1α and nuclear-encoded mitochondrial proteins. The levels of other molecules, such as TCA intermediates Acetyl CoA and α-ketoglutarate, can influence the epigenome by modifying methylation and acetylation and, consequently, the cell physiology.

We've encountered several key enzymes involved in the regulation of metabolism, including:

- AMP-activated protein kinase (AMPK) senses the cell's energy state (AMP/ATP ratio). When ATP is low (AMP is high), it activates pathways to produce ATP and inhibits pathways that require ATP. AMPK has been found at or near the mitochondrial membrane and may also be found in it. AMPK also promotes mitochondrial biogenesis (mitogenesis)
- mTOR (mammalian target of rapamycin) is a serine/threonine kinase that regulates protein synthesis and other anabolic pathways based on the energy status of the cell. processes in response to growth factors, energy status, and oxygen levels. It also simulated mitogenesis.

19.3.7: SUMMARY

This chapter examines the regulation of oxidative phosphorylation (oxphos), the primary pathway for ATP production under aerobic conditions, and emphasizes how its control is intimately linked to the cellular energy state.

Overview of Oxphos Regulation:

Oxidative phosphorylation is driven by the oxidation of electron carriers (primarily NADH and $FADH_2$) and the reduction of oxygen, which together fuel the synthesis of ATP. Unlike earlier steps in metabolism (e.g., glycolysis and the citric acid cycle), oxphos is not significantly regulated by allosteric effectors or hormones. Instead, the ADP/ATP ratio—reflecting the cell's energy state—is the key determinant of oxphos activity. When ADP levels are high, the electron transport chain accelerates to regenerate NAD^+ and produce ATP.

Coupling and Uncoupling Mechanisms:

A critical aspect of oxphos is the tight coupling between electron transport and ATP synthesis. As electrons flow from NADH (and $FADH_2$) to oxygen, protons are pumped across the inner mitochondrial membrane to generate a proton-motive force (Δp). This force drives protons back into the matrix through ATP synthase, powering ATP formation. However, this coupling can be compromised by "leaks" where:

- **Basal proton leaks** occur through mitochondrial anion carriers in a non-regulated manner.
- **Inducible leaks** occur via specific proteins, such as adenine nucleotide translocase (ANT) and uncoupling proteins (UCPs, notably UCP1 in brown fat), leading to energy dissipation as heat and, in some cases, increased production of reactive oxygen species (ROS).

Measuring Oxphos Efficiency:
Efficiency is often quantified using the ADP/O ratio, which represents the number of ADP molecules phosphorylated per oxygen atom consumed. This measurement can be made using coupled assays (e.g., hexokinase/glucose-6-phosphate dehydrogenase reactions that generate NADH) to monitor ATP production under controlled, non-saturating conditions.

Proton "Slippage" and Its Impact:
Proton "slippage" refers to situations where the expected coupling between electron transport and proton translocation is lost due to inefficiencies or modifications in the proton pumping machinery (e.g., at Complex IV or ATP synthase). Such slippage reduces the ATP/O ratio and can contribute to heat production and enhanced ROS formation, particularly when the protonmotive force (Δp) becomes too high.

Mitochondrial-Nuclear Communication:
Although many oxphos components are encoded by nuclear DNA, a subset of essential proteins is encoded by the mitochondrial genome. Effective oxphos requires tight coordination between these two genomes, achieved through bidirectional signaling. Mitochondria communicate with the nucleus via retrograde signals (e.g., calcium, ROS, AMP/ATP ratios) that influence nuclear gene expression and promote mitochondrial biogenesis, ensuring that protein supply matches metabolic demand.

Key Energy Sensors and Regulators:
The cellular energy state is monitored by key signaling molecules:

- **AMP-activated protein kinase (AMPK):** Activated by high AMP/ATP ratios, AMPK promotes ATP-generating pathways and mitochondrial biogenesis while inhibiting ATP-consuming processes.
- **mTOR (mammalian target of rapamycin):** mTOR integrates signals related to nutrient availability, energy status, and growth factors, coordinating protein synthesis and other anabolic processes with mitochondrial function.

Conclusion:
In summary, the regulation of oxidative phosphorylation is primarily driven by the cell's energy requirements, as indicated by ADP and ATP levels, rather than by direct allosteric or hormonal control. The efficiency of oxphos is modulated at multiple levels, including electron and proton transport kinetics, proton leakage and slippage, and the coordinated expression of mitochondrial proteins through mitochondrial-nuclear signaling. These mechanisms collectively ensure that energy production is finely tuned to meet cellular demands while minimizing the production of harmful reactive oxygen species.

This page titled 19.3: Regulation of Oxidative Phosphorylation is shared under a not declared license and was authored, remixed, and/or curated by Henry Jakubowski and Patricia Flatt.

- **Current page** by Henry Jakubowski and Patricia Flatt has no license indicated.
- **11.2: Diffusion Across a Membrane - Passive and Facilitated Diffusion** by Henry Jakubowski and Patricia Flatt has no license indicated.

CHAPTER OVERVIEW

20: PHOTOSYNTHESIS AND CARBOHYDRATE SYNTHESIS IN PLANTS

Return to Fundamentals of Biochemistry Search Fundamentals of Biochemistry

20.1: Light Absorption in Photosynthesis - An Overview
20.2: The Kok Cycle and Oxygen Evolving Complex of Photosystem II
20.3: Plant Electron Transport and ATP Synthesis
20.4: CO_2 uptake - Calvin Cycle and C3 organisms
20.5: CO2 uptake - C4 and CAM Pathways
20.6: Biosynthesis of Starch, Sucrose and Cellulose

This page titled 20: Photosynthesis and Carbohydrate Synthesis in Plants is shared under a not declared license and was authored, remixed, and/or curated by Henry Jakubowski and Patricia Flatt.

20.1: LIGHT ABSORPTION IN PHOTOSYNTHESIS - AN OVERVIEW

LEARNING GOALS (CHATGPT O3-MINI)

- **Understand the Thermodynamic Basis of Energy Transduction:**
  • Explain how the energy from the oxidation of carbohydrates is stored as ATP and how this process is effectively reversed during photosynthesis, an inherently uphill thermodynamic reaction.
- **Identify the Key Requirements for Photosynthesis:**
  • Describe why a strong oxidizing agent is necessary for water oxidation, the importance of high concentrations of NADPH for reductive biosynthesis, and the need for ample ATP to drive CO_2 fixation.
- **Describe Chloroplast Structure and Functional Organization:**
  • Identify the major structural features of chloroplasts—including the outer membrane, thylakoid membranes (and grana), and stroma—and explain how these compartments separate the light reactions from the dark (Calvin cycle) reactions.
- **Outline the Core Components of the Light Reactions:**
  • Detail the roles of Photosystem II (PSII), cytochrome b_6f, and Photosystem I (PSI) in converting light energy into chemical energy, including the generation of NADPH, ATP, and O_2.
- **Explain the Mechanism of Light Absorption and Energy Transfer:**
  • Describe how pigments such as chlorophylls and carotenoids absorb sunlight, undergo exciton (resonance) energy transfer, and facilitate the creation of an excited state leading to charge separation in the reaction centers.
- **Analyze the Role of Reaction Centers in PSII:**
  • Explain the function of the P680 chlorophylls, the subsequent electron transfer to pheophytin, and how this charge separation initiates water splitting at the oxygen-evolving complex (OEC).
- **Understand the Structural Organization of Light-Harvesting Complexes:**
  • Illustrate the composition of the PSII–LHCII supercomplex, including the arrangement and role of core subunits (e.g., D1, D2, CP43, CP47) and peripheral antenna complexes, and how they optimize light capture.
- **Evaluate Mechanisms of Photoprotection and Energy Regulation:**
  • Discuss how plants prevent damage from excess light through nonphotochemical quenching mechanisms involving PsbS, xanthophyll cycle carotenoids (e.g., zeaxanthin), and state transitions that redistribute light-harvesting complexes between PSII and PSI.
- **Compare Light and Dark Reactions in Photosynthesis:**
  • Explain how the products of the light reactions (ATP, NADPH, O_2) are utilized in the dark reactions to fix CO_2 into carbohydrates, completing the cycle of energy transduction.
- **Integrate the Concept of Energy Conversion Across Biological Systems:**
  • Contrast the mechanisms of ATP synthesis via oxidative phosphorylation in mitochondria with those of the light reactions in chloroplasts, highlighting similarities (e.g., proton gradients) and differences in regulation and energy sources.

These goals are intended to help students develop a deep, integrated understanding of how light energy is captured, transferred, and converted into chemical energy in photosynthesis, and how this process is intricately regulated to support life on Earth.

20.1.1: INTRODUCTION

We have seen how we can transduce the chemical potential energy stored in carbohydrates into the chemical potential energy of ATP. This occurs by coupling the energy released during the thermodynamically favored oxidation of carbon molecules through intermediaries (high-energy mixed anhydride in glycolysis or a proton gradient in aerobic metabolism) to the thermodynamically uphill synthesis of ATP. There is a situation that occurs when we wish to reverse the entire process:

$$\mathbf{CO_2 + H_2O \longrightarrow carbohydrate + O_2}$$

This process is photosynthesis, which occurs in plants, certain photosynthetic bacteria, and algae. Given that this process must, by nature, be an uphill thermodynamic battle, let us consider the major requirements that must be in place for it to occur:

- A **strong oxidizing agent** must be formed to oxidize water to dioxygen. We know that redox reactions occur in the direction of a stronger to a weaker oxidizing agent (just as acid/base reactions are thermodynamically favored in the direction of a

stronger to a weaker acid). Somehow, we must generate a stronger oxidizing agent than product dioxygen, which often has the most positive standard reduction potential in common tables.

- Plants must have high concentrations of a **reducing agent** for the reductive biosynthesis of glucose from CO_2. NADPH is the reducing agent used for most biosynthetic reactions in nature, which differs from NADH only by adding a phosphate to the ribose ring. This phosphate differentiates the pool of nucleotides in the cells used for reductive biosynthesis ($NADPH/NADP^+$) from those used for oxidative catabolism ($NADH/NAD^+$)
- Ultimately, plants require a plentiful source of **ATP,** which is essential for reductive biosynthesis.

The *light reaction* of photosynthesis produces three molecules: O_2, NADPH, and ATP. We will explore the light reaction in the next few sections of this chapter. The **dark reaction**, which, as the name implies, can occur in the dark, involves the actual fixation of carbon dioxide into carbohydrates using the ATP and NADPH produced in the light reaction.

The energy to power the light reactions comes directly from sunlight. Clue two is that plants have an organelle that animal cells don't - the chloroplast. Its structure is similar to that of mitochondria, in that it has an outer membrane, an intermembrane space, and an inner membrane. In addition, it has a series of stacked, interconnected compartments called thylakoids, bounded by a thylakoid membrane that surrounds a lumen. A schematic is shown in Figure **20.1.1** below.

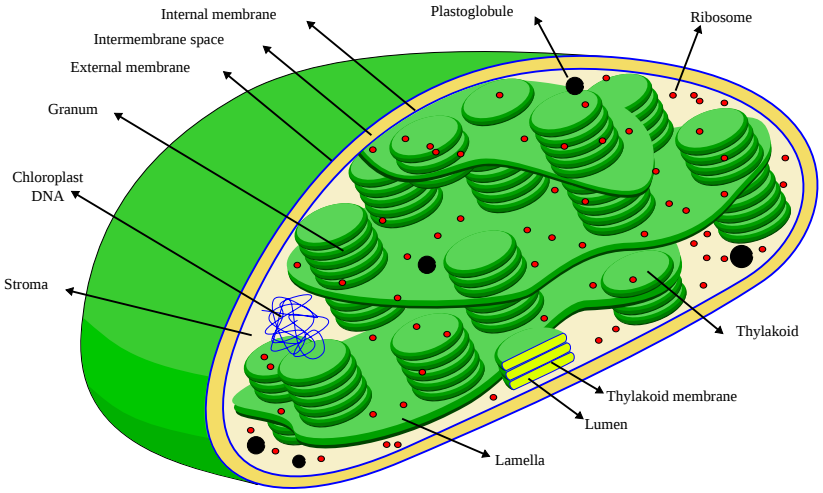


Figure **20.1.1**: The chloroplast. chloroplast: https://commons.wikimedia.org/wiki/F...roplast-en.svg. Creative Commons Attribution-Share Alike 4.0

Stacks of thylakoids are called grana. Each thylakoid represents one granum. The thylakoids are where the **light reactions** occur. In contrast, the stroma contains the enzymes for the **dark reactions** of photosynthesis.

The enzyme complexes involved in the light reaction are aligned in the thylakoid membrane just as the membrane complexes involved in mitochondrial electron transport/oxidative phosphorylation were aligned in the mitochondrial inner membrane. That process uses Complex I, Complex III, Complex II (succinate dehydrogenase), and Complex IV to transfer electrons from NADH and $FADH_2$ to increasingly potent oxidizing agents (ubiquinone, cytochrome C), ending with dioxygen. The energy released during this thermodynamically favored process was captured by forming a proton gradient, which was then collapsed through the F_0F_1ATPase to drive ATP synthesis.

For the light reaction, three complexes, the **Light Harvesting ComplexII -Photosystem II** (also called the **LHC-PSII supercomplex**), **cytochrome b_6f,** and the **light-harvesting complex Photosystem I** (called the LHC-PSII supercomplex) are used to carry out the light reactions of photosynthesis. These include the photooxidation of water to produce O_2 and the transfer of the lost electrons through a series of mobile electron carriers (plastoquinone and plastocyanin) to a terminal acceptor, $NADP^+$, to form the reducing agent NADPH needed for carbohydrate synthesis in the dark reaction. The energy released during the electron transfer process is likewise captured in a proton gradient as protons are moved from the chloroplast stroma to the thylakoid lumen. The collapse of the resulting proton gradient powers ATP synthesis. These reactions are shown in Figure **20.1.2**.

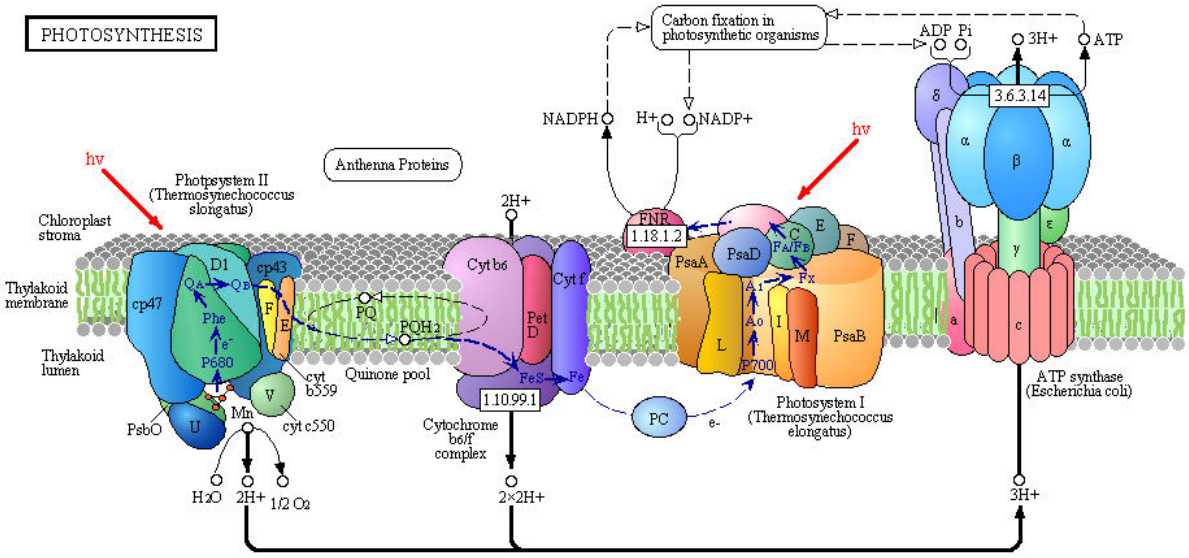


Figure **20.1.2**: Light reaction of photosynthesis. The boxed numbers represent Enzyme Commission Number. Original KEGG Map with embedded links. (reprinted with permission from Kanehisa Laboratories and the KEGG project: **www.kegg.org**)

In this section, we will explore light absorption by the light-harvesting complex (LHCII) of the LHC-PSII supercomplex. Before we get into too much detail, let's start with a simplified review of light absorption in the LHCII.

20.1.2: ABSORPTION OF LIGHT

Plants have many pigments (chlorophylls, phycoerthryins, carotenoids, etc.) whose absorption spectra overlap that of the solar spectra. The primary pigment, chlorophyll, has a protoporphyrin IX ring (the same as in heme groups) with Mg2+ at its center, instead of Fe^{2+}. When the chlorophyll absorbs light, the excited electrons must eventually relax to their ground state. It can do this by either radiative or nonradiative processes. In radiative decay, a lower energy photon is emitted after some vibrational energy loss. Photon release occurs through either fluorescence or phosphorescence. In nonradiative decay, the energy of an excited electron can be transferred to another similar molecule (in this case, other chlorophyll molecules) in a process that excites the electron in the second molecule to the same excited state. It is as if a photon is released by the first excited molecule, which is then absorbed by an electron in a second molecule, exciting it to the same excited state. However, no photon is involved in the energy transfer. In this fashion, energy is transferred from one chlorophyll to another. This type of energy transfer is called resonance energy transfer or **exciton** transfer, as shown in Figure **20.1.3**.

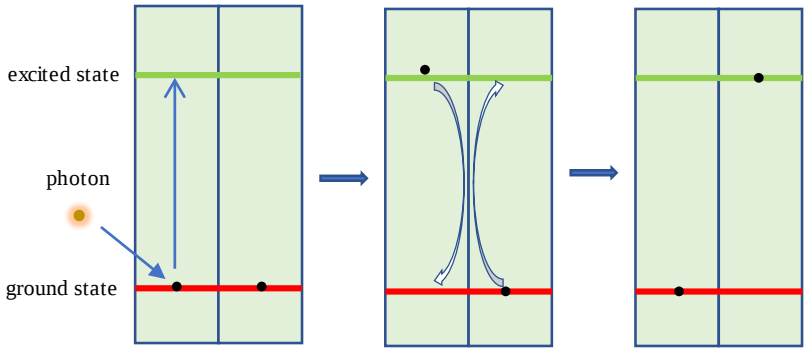


Figure **20.1.3**: Resonance Energy (Exciton) Transfer

Due to its unique environment, one type of chlorophyll exhibits slightly different characteristics. The energy level of the first excited state in the chlorophyll reaction center is lower than in the rest of the chlorophyll molecules, in much the same way that pKa values of amino acid side chains differ with the local and solvent environment and the standard reduction potential of FAD molecules that are tightly bound to enzymes differ due to the different environment of bound $FAD/FADH_2$.

Instead of a radiationless energy transfer to this special chlorophyll, an electron from the excited state chlorophyll is transferred, which, by definition, is a redox reaction. The electron donor (the excited chlorophyll) loses an electron (an oxidation

reaction) as the recipient molecule gains one (a reduction). This charge (electron) transfer reaction produces charge separation in the formation of a positively charged chlorophyll (now an oxidizing agent) and a negatively charged chlorophyll (now a reducing agent). The chlorophylls directly involved in this final process are collectively referred to as the **reaction center.** This process is shown in Figure 20.1.4 below.

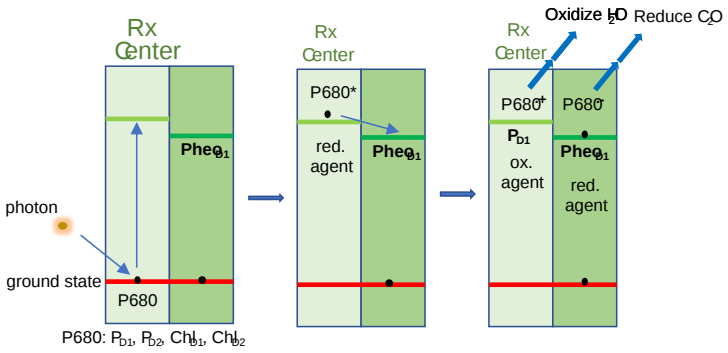


Figure 20.1.4: Reaction Center

The reaction center chlorophylls absorb light at 680 nm; therefore, they are sometimes labeled P680. Four unique chlorophylls (PD1, PD2, ChlD1, and ChlD) are the main players in the reaction center. Both sets of labels are shown in the figure above.

Figure 20.1.5 shows a cartoon of the absorption of photons and subsequent handoff of energy to "antennae" chlorophylls leading to photoexcitation of the reaction center and subsequent transfer of an electron to the special chlorophyll which has a lower first excited state energy. This molecule is named pheophytin A. It is identical to chlorophyll A but lacks the central Mg^{2+} ion.

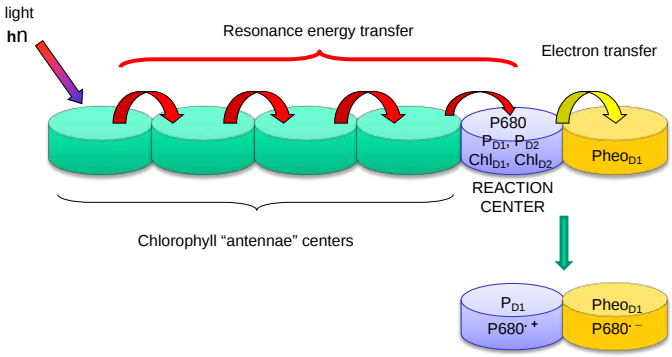


Figure 20.1.5: Photoexcitation and electron transfer of chlorophylls

Photosystems I and II contain many chlorophyll molecules that act as antennas, transferring energy to the reaction centers. The "antenna" proteins involved in photon adsorption and energy transfer in Photosystems I and II are shown in Figure 20.1.6 below. Note the D1, D2, cp47, and cp43 protein subunits in the figure below are also shown in the figure above. The D1 and D2 subunits contain the reaction center chlorophylls.

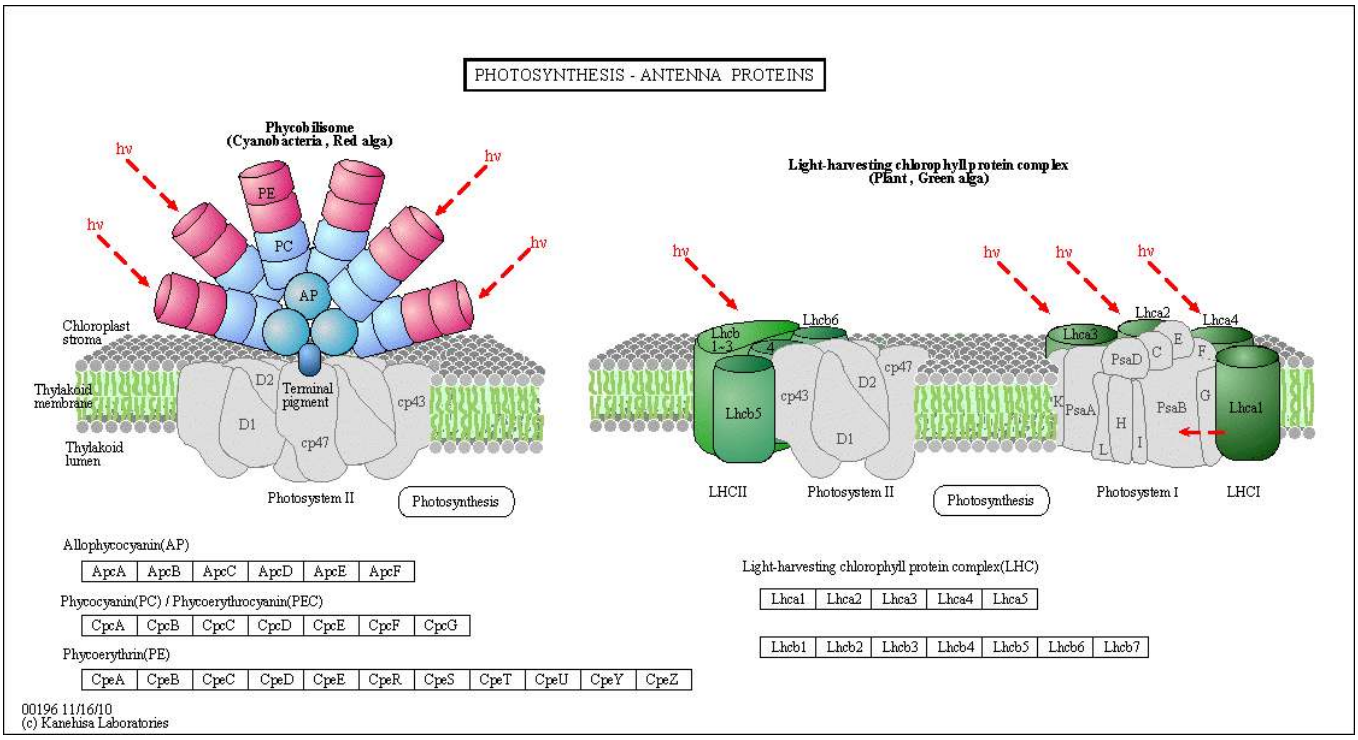


Figure **20.1.6**: Antennae Proteins (reprinted with permission from Kanehisa Laboratories and the KEGG project: **www.kegg.org**)

The different chlorophylls have absorption spectra that overlap reasonably well with the solar spectrum, as illustrated in Figure **20.1.7**.

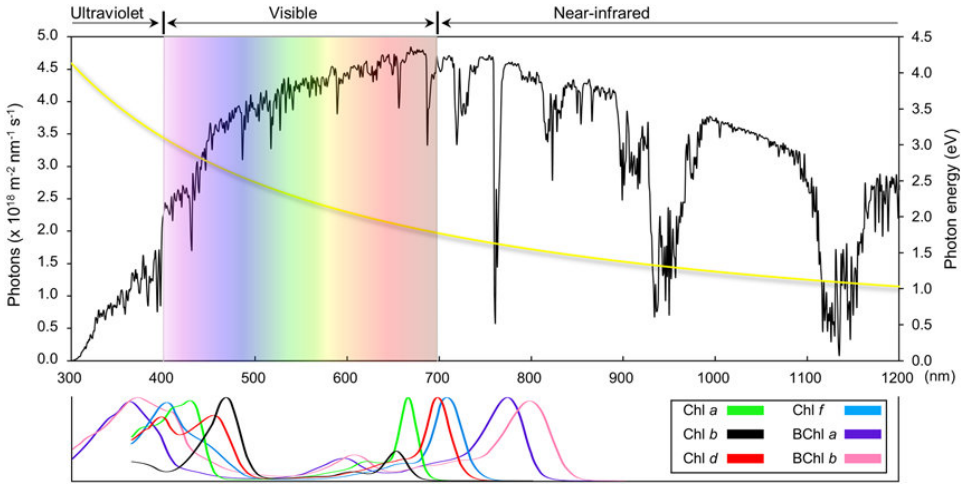


Figure **20.1.7**: Solar spectrum and absorption profiles of chlorophyll and bacteriochlorophyll pigments**.** Cardona T, Shao S, Nixon PJ. Enhancing photosynthesis in plants: the light reactions. *Essays Biochem*. 2018;62(1):85-94. Published 2018 Apr 13. doi:10.1042/EBC20170015Creative Commons Attribution License 4.0 (CC BY).

The black lines represent the solar flux spectrum (photons per square meter per wavelength) from 300 to 1200 nm. The yellow line represents the photon energy ($E = hc/\lambda$) at each wavelength. The absorbance spectra of the chlorophyll species are normalized to the same maximal value.

Suppose you use the energy required to produce glucose from CO_2 and H_2O as a standard. In that case, approximately 95% of the incoming solar energy is wasted, as not all incident light photons have the correct wavelength. Waste also occurs due to reflectance and heat generation.

20.1.3: THE LIGHT HARVESTING COMPLEX (LHCII) - PHOTOSYSTEM II (PS II) SUPERCOMPLEX

Now, let's look more at the chloroplast thylakoid membrane complex that interacts with light and results in water oxidation to form O_2. The first structure is called the **Light-Harvesting Complex II (LHCII) - Photosystem II (PSII) Supercomplex**. It is a super complex (a pun)

to understand. The supercomplex has a **PSII core complex** interacting with a variable number of light-harvesting complex IIs (**LHCIIs)** complexes. Sometimes, the entire supercomplex is more simply referred to as Photosystem II. The supercomplex consists of

- a PSII core **C** with a Mn_4CaO_5 cluster called the oxygen-evolving complex (OEC or OEX) that oxidizes water to O_2;
- peripheral antennae complexes **M** and **S**, also called light-harvesting complexes II (LCHIIs)

The core part of the Photosystem II supercomplex contains the key to the existence of aerobic organisms, as it produces the dioxygen in our atmosphere. Its chemistry is phenomenal. Many seek to modify it to produce, instead of H_2, a green energy source. In the next section, we will explore the mechanisms for water oxidation to O_2 by a PSII-bound inorganic Mn_4CaO_5 cluster, the oxygen-evolving complex (OEC). Let's first look at PSII in light of the discussion above. Where are all the chlorophylls? The mystical "reaction center"?

The PSII Core Complex (within the supercomplex) has over 20 subunits. These include:

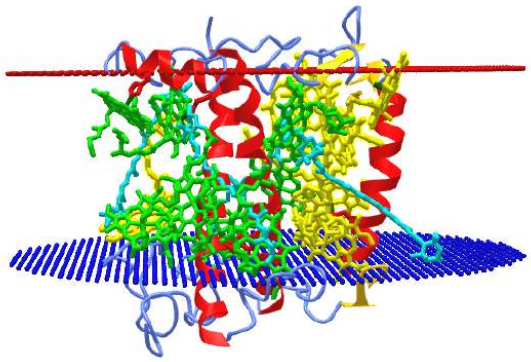
- reaction center subunits D1 and D2
- inner antennae subunits CP43, CP47
- many other small protein subunits
- peripheral subunits that project into the lumen that interact with the OEC

The peripheral antennae complexes (light-harvesting complexes - LHCIIs M and S - consist of proteins encoded by six different Lhcb genes (1-6).

- Lhcb1-3 monomers form trimeric (homo- or hetero) LHCIIs (Lhcb1-3). An example is $(Lhcb3)_3$. That trimer is often referred to as the M-LHCII. There is also an S-form trimer as well as L- and N-forms. **S** is **s**trongly associated with the reaction center, **M** for **m**oderate, and **L** for **l**oose.
- Lhcb4-6 are the minor components and consist of the monomeric proteins **CP29, CP26, and CP24**, respectively.

20.1.4: LIGHT-HARVESTING COMPLEX PROTEINS

Each Lhc apoprotein consists of 3 alpha-helices and binds eight chlorophyll a, six chlorophyll b, and four carotenoid molecules. Figure **20.1.8** shows an interactive iCn3D model of the monomeric pea chlorophyll a-b binding protein AB80 (LHCII type I CAB-AB80) (2BHW)



NCBI iCn3D Figure **20.1.8**: Monomeric pea chlorophyll a-b binding protein AB80 (LHCII type I CAB-AB80) (2BHW). (Copyright; author via source). Click the image for a popup or use this external link: https://structure.ncbi.nlm.nih.gov/i...QtEEWeQ5Y9n2i8

The color scheme is as follows:

- protein - secondary structure colors
- Chlorophyll a - Green
- Chlorophyll b - yellow
- carotenoids - cyan

Now, let's look at a trimeric form of the same protein. of LHCII, the chlorophyll-binding protein, from PSII. It's also called LHCII type I CAB-AB80. We showed the role of the LHCII trimer in the figures above. The subunits function to absorb light for the light reaction. The energy is sent through resonance energy transfer to reaction centers in PSII and PSI. Figure **20.1.9** shows an interactive iCn3D model of the trimeric Light Harvesting Complex (LHC_II) from pea photosystem II (2bhw).

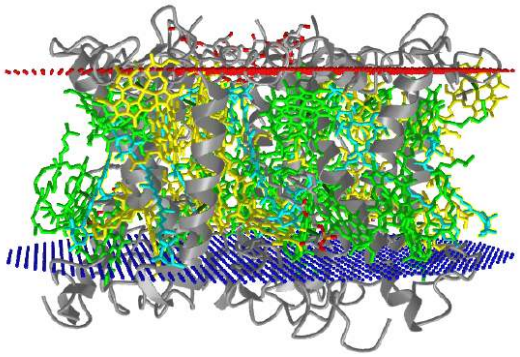


Figure 20.1.9: Light Harvesting Complex (LHC_II) from pea photosystem II (2bhw). (Copyright; author via source). Click the image for a popup or use this external link: https://structure.ncbi.nlm.nih.gov/i...BK6WvzrxABPDh6

The protein is shown in gray. To simplify the model, chlorophyll A molecules are shown in magenta, and chlorophyll B isomeric variants are shown in green. Note the large number of chlorophylls (42) in the LHCII complex, which differentiates it from most protein complexes, which might have just a few ligands bound.

Photosynthetic bacteria and plants have a wide range of molecules that interact with visible light. The main one in PS II is chlorophyll a, whose structure is shown in Figure \(\PageIndex{10}\) below, along with the variant, chlorophyll b. Remember that pheophytin A is identical to chlorophyll A but lacks the central Mg^{2+} ion.

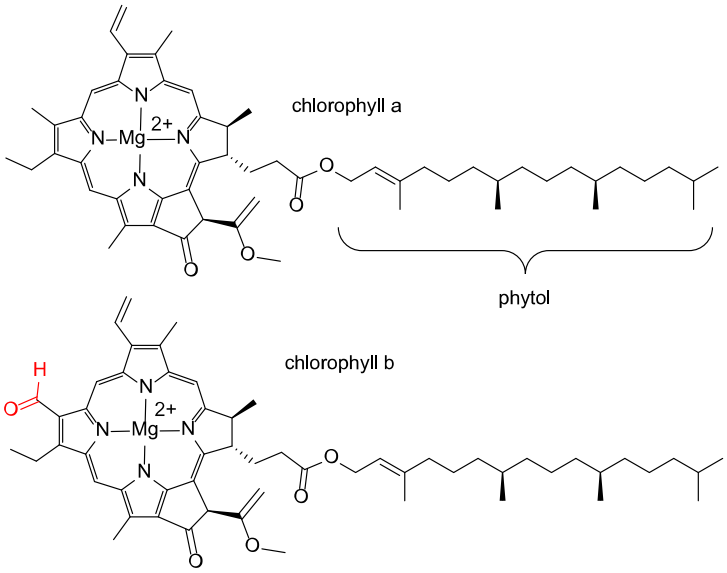


Figure 20.1.10: Chlorophyll a and b

20.1.5: PHOTOSYSTEM II (PS II) SUPERCOMPLEX STRUCTURES

The most common version of the supercomplex is a dimer. A simplified cartoon of the monomeric version of the **PSII-LHCII supercomplex** is shown in Figure 20.1.11. The PSII core is shown in the blue rectangle. The CP29, CP26, and CP24 in the peripheral antennae complexes (light-harvesting complexes - LCHIIs) are shown outside the blue-outlined rectangle. They surround the PSII core.

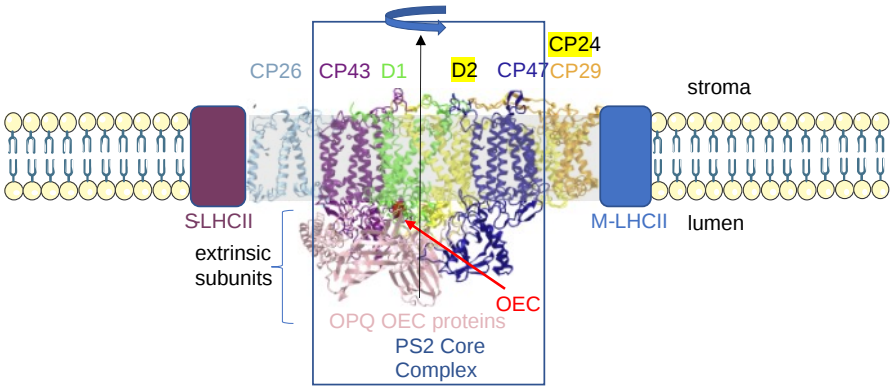


Figure **20.1.11**: Cartoon of the monomeric PSII-LHCII supercomplex structure of the PSII-LHCII supercomplex from Pisumsativum

- The PSII core **C** (outlined in the blue box) contains two reaction center subunits, D1 and D2, and two inner antennae subunits, CP43 and CP47. The core also contains extrinsic subunits (pink) surrounding the OEC (red spacefill)
- A **S**trongly bound LHCIIs protein, **S -LHCII**, left (maroon rectangle), interacting with CP26. The S-LHCii complex is a trimer of individual Lhcb monomers.
- A **M**oderately bound LHCIIs protein complex, **M-LHCII,** right (lighter blue rectangle), interacting with the CP24/CP29 dimer. The M-LHCII complex is a trimer of 3 lcbh-3 subunits $(Lcbh3)_3$.

There can be a variable number of LHCIIs in the complex. The predominant form of the supercomplex is the $\mathbf{C_2S_2M_2}$ complex. There are also many other proteins in the supercomplex that are not shown in Figure 11. A cartoon showing the top-down view of the actual supercomplex dimer, $C_2S_2M_2$, is shown in Figure **20.1.12**.

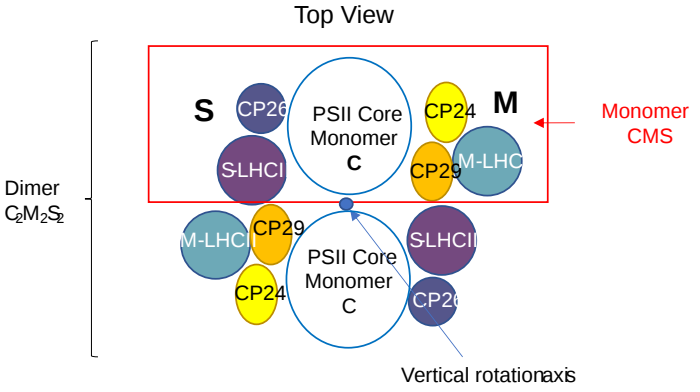
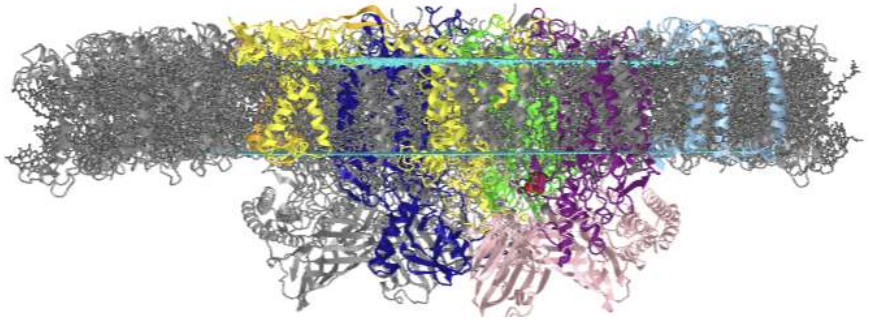


Figure **20.1.12**: Top town view of the **PSII-LHCII supercomplex dimeric complex.**

You could imagine forming the dimer by spinning the monomer CSM 180^0 and reproducing the monomer there.

Figure **20.1.13** shows an interactive iCn3D model of the full C2S2M2-type PSII-LHCII supercomplex from Pisum sativum (5XNL). (long load time)



NCBI iCn3D Figure **20.1.13**: C2S2M2-type PSII-LHCII supercomplex from Pisum sativum (**5XNL).** (Copyright; author via source). Click the image for a popup or use this external link: https://structure.ncbi.nlm.nih.gov/i...F4WFfHoevxaVV8 (long load time)

Only a single CSM monomer of the C2S2M2 dimeric supercomplex is colored. The colors match those in Figures 8 and 9. The molecules shown in gray sticks that outline a bilayer include chlorophyll Bs (98 of them), chlorophyll As (216), and carotene or its derivatives (88) as well. The different proteins in the supercomplex are colored, as shown below.

- CP47 Rx Center (inner antenna protein) Dark Blue
- CP43 Rx Center (inner antenna protein) - Purple
- D1: green
- D2: yellow
- OEC: spacefill Red
- O, P, Q - OEC peripheral: Light pink
- CP24 (peripheral antenna protein): yellow
- CP29 (peripheral antenna protein): orange
- CP26: Light blue
- LHCIIs (S and M) - not shown
- membrane bilayers - cyan spheres

(A quick load version of the C2S2M2-type PSII-LHCII supercomplex with different coloring than above)

20.1.6: PSII SUPERCOMPLEX REGULATION

Plants have evolved a great ability to absorb light over the entire visible range of the spectrum. Can they absorb too much energy? The answer is yes, so plants have developed many ways to protect themselves. IF too much light is absorbed, the pH gradient developed across the thylakoid membranes becomes greater. This is sensed by a protein, PsbS, and through subsequent conformational changes transmitted through the light-harvesting antennae, the excess light energy is dissipated as thermal energy. Mutants lacking PsbS showed decreased seed yield, a sign that they became less adaptable under stress conditions (such as exposure to rapidly fluctuating light levels). Molecules called xanthophylls and other carotenoids, such as zeaxanthin, are also important in excess energy dissipation. These molecules appear to cause excited chlorophyll (a singlet-like excited state dioxygen) to become deexcited. Without the xanthophylls, the excited state chlorophyll could deexcite by transferring energy to ground state triplet dioxygen, promoting it to the singlet, reactive state, which could also be converted to superoxide through electron acquisition. These reactive oxygen species (ROS) can lead to oxidative damage to proteins, lipids, and nucleic acids, as well as alterations in gene transcription and even programmed cell death. Carotenoids can also act as ROS scavengers. Hence, both heat dissipation and the inhibition of ROS formation (by molecules such as vitamin E) are mechanisms of defense against excessive solar energy.

Given that both plants and animals must be protected from ROS, antioxidant molecules made by plants protect humans from diseases such as cancer, cardiovascular disease, and general inflammatory diseases, all of which have been shown to involve oxidative damage to biological molecules. Humans, who can't synthesize the variety and amounts of antioxidants found in plants, are healthier when they consume large amounts of plant products. These phytomolecules also possess other properties, including the regulation of gene transcription, which can have a significant impact on disease propensity.

Plants have to respond to different qualities and quantities of light. When light levels are low, they strive to maximize light capture. Too much light could damage a plant, so molecular adaptations are made to prevent it. Part of the regulation occurs in the supercomplex's stoichiometry by altering the composition of the antenna proteins (the LHCs). The most abundant components of the complex are $C_2S_2M_2$ and C_2S_2M. C_2S and C_2S_2 increase as an adaptation to increasing levels of light.

Light levels can also promote the association of grana membranes mediated by interactions between a PSII-LHCII supercomplex (PSII-LHCIIsc) on one thylakoid membrane and a PSII-LHCIIsc on an adjacent thylakoid membrane, forming a large PSII-LHCIIsc dimer. The structure and properties of paired PSII-LHCIIsc are illustrated in Figure **20.1.14**.

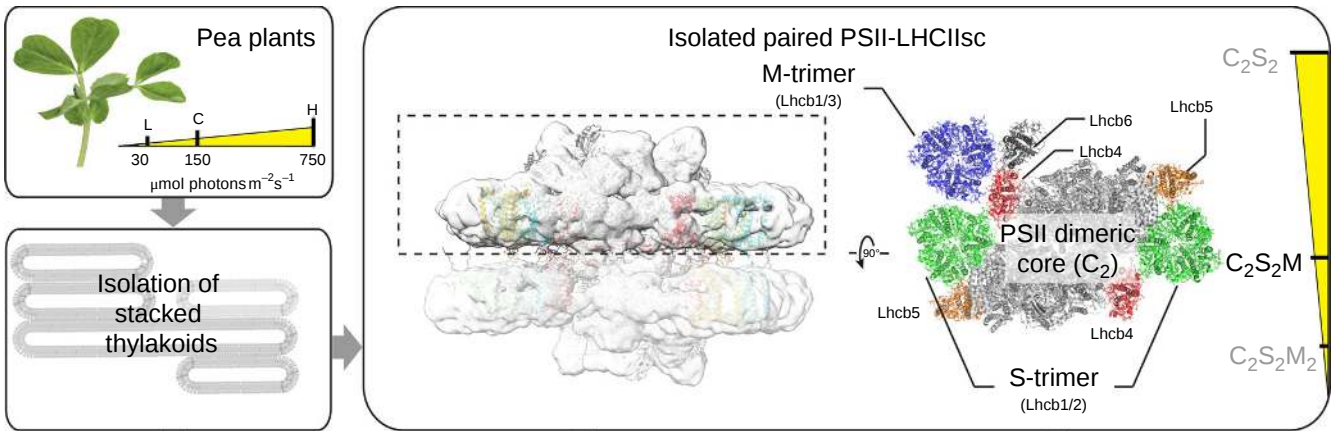


Figure **20.1.14**: Light-driven modulation of paired PSII–LHCIIsc. Heterogeneous mixtures of PSII–LHCIIsc from pea plants grown at different light intensities (L, low; C, moderate used as control; H, high) were isolated and analyzed. Albanese et al. Nature Communications | (2020) 11:1361 | https://doi.org/10.1038/s41467-020-15184-1. Creative Commons Attribution 4.0 International License. http://creativecommons.org/ licenses/by/4.0/.

The figure also shows the variation in the PSII–LHCIIsc with light intensity. At low light, $C_2M_2S_2$ prevails, while at high light intensity, C_2S_2 is most abundant. The system regulates activity by increasing the abundance of LHCIIs in low light and decreasing them in high light intensities.

Figure 1 shows the stacking of individual grana in the chloroplasts. The stacking is maintained at various light levels and is mediated by loops of the LHCII trimers that are exposed in the stroma, as well as Lhcb4 subunits on adjacent membranes. The stromal surfaces are flat and tightly stacked in grana. Stacking is a dynamic process that depends on cross-membrane interactions between and reorganization of the PSII -LHCIIsc.

The PSII–LHCIIsc is regulated through light-dependent post-translational phosphorylation, particularly on LHCII, as well as acetylation, which further regulates energy distribution. In plants, the core proteins CP43, D1, and D2, and PsbH are phosphorylated by the kinase Stn8. Stn7 phosphorylates the peripheral antenna LHCII proteins. Phosphorylation of PSII is not seen in cyanobacteria and red algae. Higher light levels promote higher levels of core protein phosphorylation. Stn7 appears to be inhibited at high light levels. Figure **20.1.15** shows putative Stn8 phosphorylation sites in the PSII -LHCIIsc

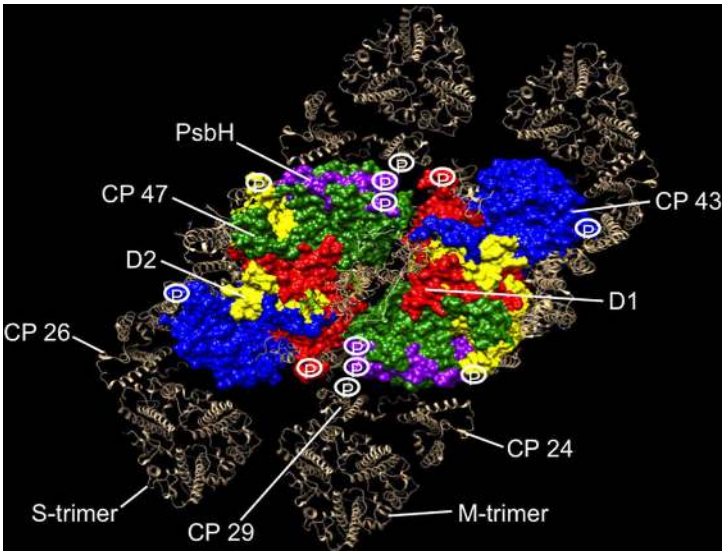


Figure **20.1.15**: **Phosphorylation map of the C2S2M2 supercomplex as catalyzed by the Stn8 kinase**. Puthiyaveetil Sujith and Kirchhoff Helmut, Frontiers in Plant Science, 4 ,2013. https://www.frontiersin.org/article/...pls.2013.00459. DOI=10.3389/fpls.2013.00459. **Creative Commons Attribution License (CC BY)**

The structure is a model pieced together from multiple pdb files. It shows the approximate positions of the phosphorylation sites of D1, D2, CP43, PsbH, and CP29.

Most free N-terminal loops in LHCII can be phosphorylated. Both phosphorylation and lysine acetylation on Lhcb2 N-terminal loops help regulate the redistribution of LHCII from PSII (in grana stacks) to PSI (in single-layered thylakoid regions). Grana stacking by N-terminal

loop association between facing PSII–LHCIIsc and their N-terminal acetylation appears to strengthen grana stacking.

How does PSII respond when the wavelength (not the intensity) of light is changed? For this, we must briefly discuss photosystem I (**PSI**), which we will explore in more detail in Chapter 20.3. Both PSII and **PSI** work together to transduce light into chemical energy, so you would expect that their activities are regulated in a linked fashion. They also have different absorbance spectra characteristics, with PSI absorbing more in the red region. If the effective absorbance (normalized for concentrations and LHCIIs) were the same, you would predict that the effective absorbance ratio over a broad wavelength range for the two photosystems, **PSI**/(**PSI**+PSII) would be 0.5. This is approximately the case over the entire spectral wavelength, except for the range between 670-730 nm, where the ratio is close to 1, indicating that PSI absorbance and activity are skewed toward the red end of the absorbance spectrum. Changes in light characteristics (i.e., wavelength) would then affect each photosystem differently and could cause imbalances in their activities and states, leading to a restorative balance. When exposed to far-red light, the systems move to state I. The major mobile antenna proteins (LHCIIs) move to PSII to restore a "photoabsorption" balance in this state. When exposed to light depleted in the high end of the visible spectrum, the system transitions to state II, where mobile LHCIIs migrate to PSI. What an interesting reciprocal way to balance activity, even if it is hard to conceptualize regulation involving the movement of membrane proteins. Of course, such movement is often seen in the clustering of ligand-bound membrane receptors.

As mentioned above, the location and, hence, movement of the LHCII are regulated by phosphorylation by LHCII kinase. We'll explore that more in Chapter 20.3, when we discuss PSI in more detail.

20.1.7: A CLOSER VIEW OF THE REACTION CENTER AND ITS LOCAL ENVIRONMENT

Let's look at the structure of a simpler PSII complex from Thermostichus vulcanus (3WU2). It has 70 chlorophyll a molecules, four special chlorophylls, four pheophytin As (PHOs), 20 beta-carotenes, four plastoquinol-9s (PL9s), four hemes, and two caroten-3-ols. Figure **20.1.16** shows the arrangement of chlorophyll molecules in the CP47 and CP44 (not CP43, as shown in several of the above diagrams) antennae subunits of PSII from T. vulcanus (3WU2).

.

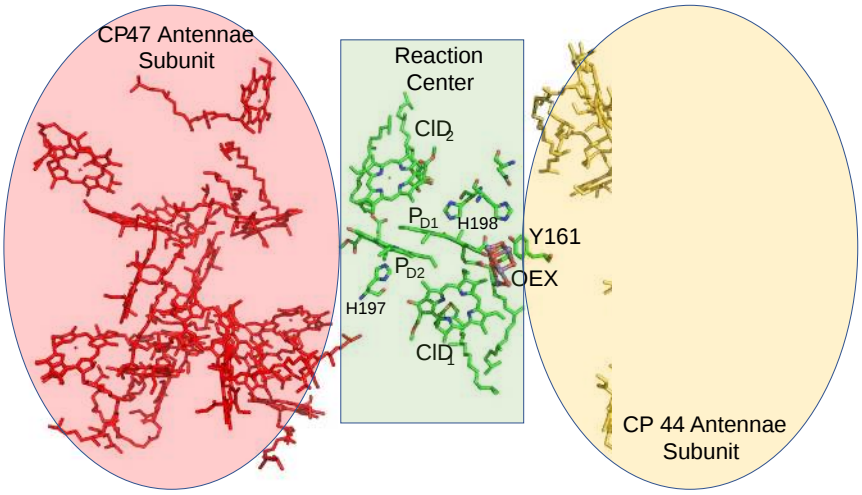


Figure **20.1.16**: Reaction Center with special chlorophylls sandwiched between antennae subunits

- CP44 is the **Photosystem II CP44 reaction center protein, psbC gene,** Photosystem II 44 kDa reaction center protein;
- CP47 is the **Photosystem II CP47 reaction center protein, psbB gene;** Photosystem II CP47 chlorophyll apoprotein

Sandwiched in between them is the reaction center containing the four special chlorophylls, the inorganic metal cluster called the oxygen-evolving complex (OEC or OEX), and a key amino acid near the OEC, Tyr 161 (pdb 3ARC).

Two special chlorophylls, $ChlD_1$ and $ChlD_2$, accompanied by partner chlorophylls, P_{D1} and P_{D2}, which are coplanar with each other, are found near the OEC and are the key chlorophylls in the reaction center that convert the OEC into a powerful enough oxidant to oxidize H_2O.

A special reaction center chlorophyll/pheophytin absorbs a photon of light at 680 nm, so the species that absorbs the photon is labeled P680. On absorption, it forms the excited state, P680*. This transfers the excited state electron to pheophytin, which forms a pheophytin radical anion, while the electron donor P680* becomes $P680^{\cdot+}$, a radical cation. The radical cation, an unstable species, can oxidize another molecule to regain stability, and in a series of addition-linked oxidation steps, water is oxidized (O in water has an oxidation state of 2-) to

O2 (in which each oxygen has an oxidation state of 0). This process occurs through the oxygen-evolving complex, which we will examine in the next section.

Which of the chlorophyll molecules absorbs the light (i.e, which is P680)? The answer is probably all four chlorophylls in the reaction center, P_{D1}, P_{D2}, Chl_{D1}, and $Chl_{D2,}$ through a delocalization of the excited electron, which would be described by a wave function for the combined chlorophylls. When donating the electron from P680*, the positive charge, which can also be described as a "hole" (similar to transistors), becomes delocalized. Quantum mechanical calculations show a coupling between P_{D1} and P_{D2}, such that 80% of the positive charge and radical character is situated on P_{D1} and 20% is on P_{D2}.)

Figure **20.1.17** shows the four chlorophylls in the reaction center of T. Vulcanus. P_{D1} appears closest to the OC.

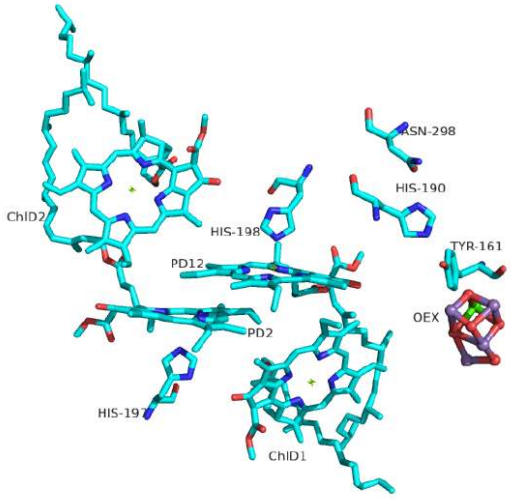
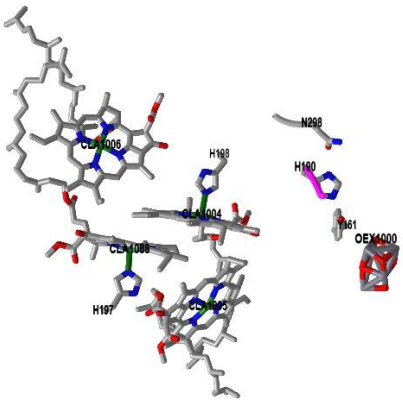


Figure **20.1.17**: Closeup of the reaction center chlorophylls and OEC

Figure **20.1.18** shows an interactive iCn3D model of the key chlorophylls and OEC of photosystem II from Thermostichus vulcanus (3WU2)



NCBI iCn3D Figure **20.1.18**: Key chlorophylls and OEC of photosystem II from Thermostichus vulcanus (3WU2). (Copyright; author via source). Click the image for a popup or use this external link: https://structure.ncbi.nlm.nih.gov/i...qYxWN5sKcquGK7

In any enzymatically catalyzed reaction mechanism, the enzyme must return to the beginning state, and a path for electron flow must be apparent. How does the radical cation $P680^{\cdot+}$ return to the ground state? As we will see in the next section, it "grabs" an electron from the nearby Y161 (also known as **YZ**), forming a radical cation, $Y^{\cdot+}$. This returns to the ground state by capturing an electron from the OEC, which ultimately grabs one from water. This process repeats four times to remove the four electrons from two waters needed to form dioxygen.

Figure **20.1.19** shows the first step in the process of reforming P680 and the formation of the Y161 radical cation.

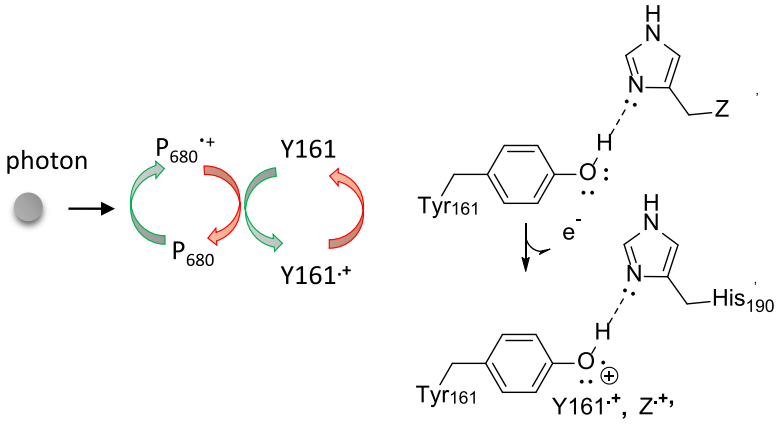


Figure 20.1.19: First step in the process of reforming P680 and formation of the Y161 radical cation.

A different process occurs to remove electrons from the radical anion, $P680^{-\cdot}$. This is passed on to a series of other electron acceptors/carriers as part of the Z scheme for the light reaction of photosynthesis. The electron is ultimately passed on to $NADP^+$ to form NADPH, which is used in the reductive biosynthesis of carbohydrates.

Light is also absorbed in photosystem I, which does not form O_2. Rather, it receives electrons from a mobile electron carrier and passes them on to $NADP^+$ to form NADPH, a reducing agent needed for the reductive biosynthesis of carbohydrates. It also helps produce a proton gradient, which helps drive ATP synthesis.

With this background, we can now explore in greater detail the key reactions that enable the evolution of aerobic organisms.

20.1.8: SUMMARY

This chapter provides a comprehensive overview of how plants and certain photosynthetic organisms convert sunlight into chemical energy, reversing the processes that generate ATP during carbohydrate oxidation. Photosynthesis is presented as a highly orchestrated, thermodynamically uphill process that relies on three key outputs—O_2, NADPH, and ATP—to drive the reductive synthesis of carbohydrates from CO_2 and water.

Thermodynamic Foundations and Key Requirements:

- **Energy Reversal:** The process of photosynthesis reverses the oxidation of carbohydrates (which generates ATP) by coupling the absorption of light energy to the endergonic synthesis of carbohydrates.
- **Essential Molecules:** A strong oxidizing agent is required to extract electrons from water (producing O_2), while high concentrations of NADPH and ATP are generated to fuel the dark reactions (CO_2 fixation).

Chloroplast Architecture and Functional Compartments:

- **Organellar Structure:** Chloroplasts are delineated by an outer membrane and an inner membrane, with thylakoid membranes forming stacks (grana) where the light reactions occur, and a surrounding stroma that houses the enzymes for the dark reactions (Calvin cycle).
- **Spatial Organization:** The segregation of the light and dark reactions within the chloroplast allows for specialized environments that optimize light capture and subsequent energy conversion.

Light Reactions – Capturing and Converting Solar Energy:

- **Pigment Absorption and Energy Transfer:**
  - **Chlorophyll and Carotenoids:** Various pigments absorb specific wavelengths of sunlight. Chlorophyll, with its protoporphyrin IX ring and central Mg^{2+}, is the primary pigment responsible for capturing light energy.
  - **Resonance (Exciton) Transfer:** Energy absorbed by pigment molecules is transferred non-radiatively between chlorophylls until it reaches the reaction center, where charge separation occurs.
- **Photosystem II (PSII) and the Reaction Center:**
  - **P680 and Charge Separation:** In PSII, the reaction center chlorophylls (collectively termed P680) absorb light and become excited. This excited state drives the transfer of an electron to pheophytin, creating a charge-separated state that is critical for water oxidation.
  - **Oxygen-Evolving Complex (OEC):** Adjacent to the reaction center, the Mn_4CaO_5 cluster (OEC) catalyzes the oxidation of water, releasing electrons, protons, and dioxygen—a process fundamental to maintaining aerobic life on Earth.
- **Electron Transport and Proton Gradient Formation:**

- **Z Scheme:** Electrons are transferred through a series of mobile carriers (plastoquinone, plastocyanin) and through cytochrome complexes (cytochrome b_6f and Photosystem I), ultimately reducing $NADP^+$ to NADPH.
- **ATP Synthesis:** The energy from electron flow is harnessed to pump protons across the thylakoid membrane, creating a proton gradient (proton motive force) that drives ATP synthesis via ATP synthase.

Structural Complexity and Regulation of the PSII–LHCII Supercomplex:

- **Supercomplex Organization:**
  - **Core and Antenna Complexes:** The PSII core, containing reaction center proteins (D1, D2, CP43, CP47) and the OEC, is surrounded by peripheral light-harvesting complexes (LHCIIs) that contain multiple chlorophylls and carotenoids. These antenna complexes enhance light absorption and funnel energy efficiently to the reaction center.
  - **Stoichiometric Adaptations:** Plants adjust the composition and organization of these supercomplexes in response to varying light intensities. Under high light, mechanisms such as non-photochemical quenching (mediated by proteins like PsbS and carotenoids like zeaxanthin) dissipate excess energy as heat, thereby protecting the photosystems from damage.
- **State Transitions and Energy Redistribution:**
  - **Balancing PSI and PSII Activity:** The movement of antenna complexes between PSII and PSI (state transitions) helps balance excitation energy between the two photosystems, ensuring efficient use of the absorbed light across the spectrum.

Integration with Carbon Fixation (Dark Reactions):

- **Utilization of Light Reaction Products:** The ATP and NADPH produced in the light reactions are used in the Calvin cycle to fix CO_2 into carbohydrates. This coupling of light-dependent and light-independent reactions completes the cycle of energy transduction, from sunlight to stored chemical energy.

Conclusion:

Overall, this chapter highlights the intricate interplay between structural organization, energy conversion, and regulation within the photosynthetic apparatus. By exploring how plants harness sunlight to produce the critical molecules (O_2, NADPH, ATP) for carbon fixation, we gain insights into the fundamental processes that sustain aerobic life and the adaptive mechanisms that protect these systems under variable environmental conditions.

This page titled 20.1: Light Absorption in Photosynthesis - An Overview is shared under a not declared license and was authored, remixed, and/or curated by Henry Jakubowski and Patricia Flatt.

- **Current page** by Henry Jakubowski and Patricia Flatt has no license indicated.
- **11.2: Diffusion Across a Membrane - Passive and Facilitated Diffusion** by Henry Jakubowski and Patricia Flatt has no license indicated.

20.2: THE KOK CYCLE AND OXYGEN EVOLVING COMPLEX OF PHOTOSYSTEM II

LEARNING GOALS (CHATGPT O3-MINI)

- **Mechanism of Photoexcitation and Charge Separation:**
  • Explain how photoexcitation of non–reaction center chlorophyll transforms it into a strong reducing agent that donates an electron to the reaction center, resulting in the formation of the oxidized, strongly oxidizing $P680^+$.
  • Describe the overall process by which the light reactions generate NADPH, emphasizing the role of sequential electron transfers.
- **Understanding the Z Scheme of Electron Transport:**
  • Outline the flow of electrons through Photosystem II (PSII) and Photosystem I (PSI) as depicted in the Z scheme, including the roles of mobile electron carriers such as plastoquinone and plastocyanin.
  • Compare the electron transport pathway in the light reactions to that of mitochondrial electron transport, noting similarities and differences in the direction of proton gradients and electron acceptor roles.
- **Structure and Function of Photosystem II:**
  • Identify key structural components of PSII (e.g., P680, pheophytin, the oxygen-evolving complex) and describe their roles in the oxidation of water and initiation of electron flow.
  • Explain the net reaction catalyzed by PSII, including the oxidation of water to O_2 and the reduction of plastoquinone to plastoquinol.
- **The Kok Cycle and Water Oxidation Mechanism:**
  • Describe the Kok cycle, including the sequential S-states (S_0–S_4) of the oxygen-evolving complex (OEC), and explain how these states correlate with the stepwise removal of electrons from water.
  • Discuss the significance of the Mn_4CaO_5 cluster structure in the OEC and its role in facilitating the four-electron oxidation required to form O_2.
- **Role of Water Channels and Proton Networks:**
  • Explain how water channels and associated hydrogen-bond networks in PSII provide access for substrate water to the OEC and help remove protons to the thylakoid lumen, thereby contributing to the formation of a proton gradient.
  • Describe how the movement of protons is coupled with electron transfer to drive ATP synthesis.
- **Electron Transfer Beyond PSII:**
  • Detail how electrons are transferred from the radical anion $P680^-$ (pheophytin A^-) to plastoquinone, setting the stage for downstream electron transport and NADPH formation.
  • Evaluate the role of mobile electron carriers in maintaining the flow of electrons and in preventing deleterious charge recombination events.
- **Regulation and Avoidance of Harmful Side Reactions:**
  • Discuss the potential for charge recombination within the PSII reaction center and how safe recombination pathways are favored to minimize the production of reactive oxygen species (e.g., singlet oxygen).
  • Compare the thermodynamic challenges faced by PSII (e.g., the uphill oxidation of water) and how absorbed photon energy overcomes these challenges.

These learning goals aim to develop a comprehensive understanding of the light reactions in photosynthesis—from the molecular events of photoexcitation and electron transfer in PSII to the broader implications for energy conversion, regulation, and protection against oxidative damage.

20.2.1: INTRODUCTION

We have just seen how photoexcitation of the non-reaction center chlorophyll turns that molecule into a good reducing agent, which transfers its electron to the nearest excited state level of the reaction center chlorophyll. If you count both steps together, the non-reaction center chlorophyll gets "photooxidized" in the process, producing the "strong" oxidizing agent, which is the positively charged chlorophyll derivative. The extra electron passed onto the second molecule will eventually be passed on to $NADP^+$ to produce NADPH.

These reactions occur in the presence of light and hence are called the **light reactions**. The light reactions of photosynthesis in green plants are shown in Figure **20.2.1**, along with the standard reduction potentials of the participants, the Z scheme.

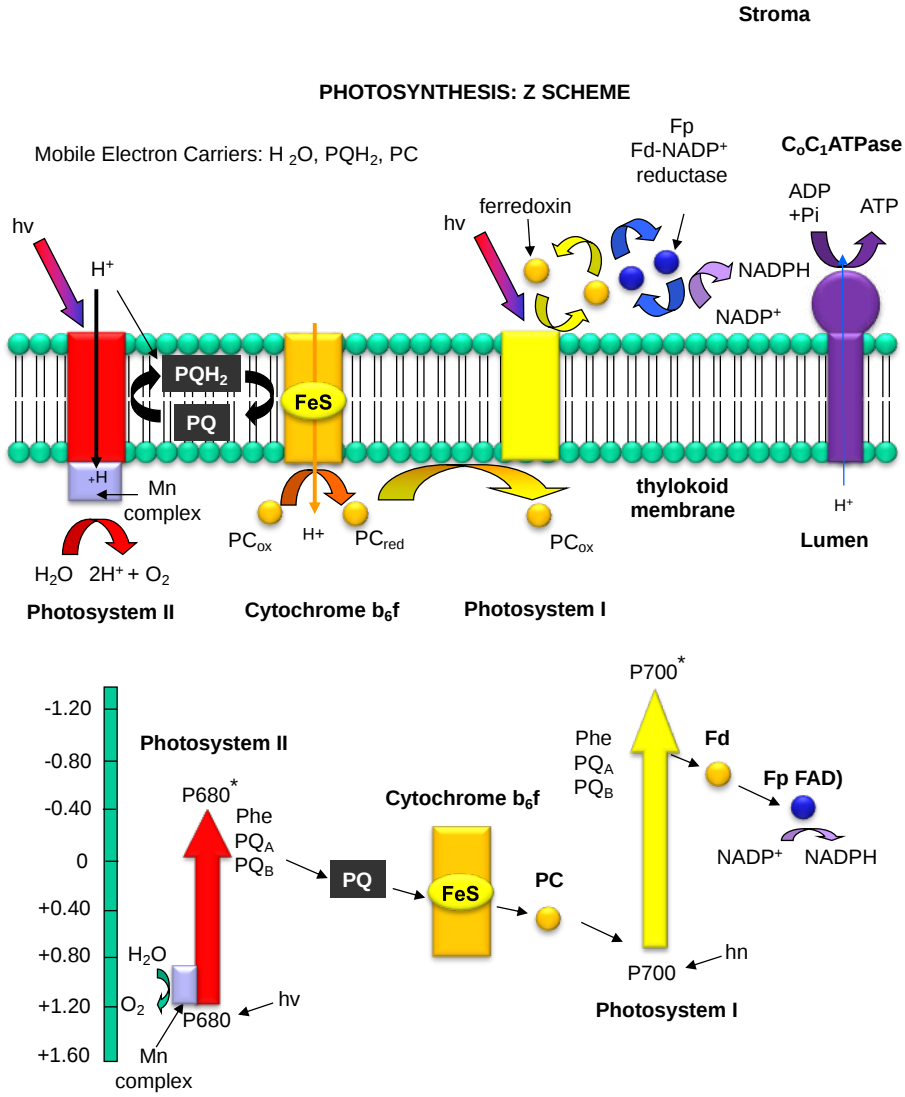


Figure **20.2.1**: Light reaction of photosynthesis and associated standard reduction potentials

The combined processes of PSII and PSI resemble a "Z" scheme (rotate the standard reduction potential figure 90 degrees clockwise in your mind). In an organization reminiscent of electron transport in mitochondria, water is oxidized by **photosystem II (PSII)**. Electrons from water are moved through PSII to a mobile, hydrophobic molecule, plastoquinone (PQ), to form its reduced form, PQH_2. Another photosystem, **photosystem I (PS1)**, is next in the electron transport pathway. It takes electrons from another reduced mobile carrier of electrons, plastocyanin (PC_{red}), to ferredoxin, which becomes a strong reducing agent. Ferredoxin is a protein with an Fe-S cluster (Fe-S-Fe-S in a 4-membered ring, with two additional cysteine residues coordinating each Fe). It ultimately passes its electrons along to $NADP^+$ to form NADPH. Note the complexes that produce a transmembrane proton gradient. In contrast to mitochondria, the lumen (compared to the mitochondrial matrix) becomes more acidic than the stroma. Protons then can move down a concentration gradient through the C_0C_1ATPase to produce the ATP required for the reductive biosynthesis of glucose.

Figure **20.2.2** shows a more detailed view of the molecular players in the light reaction.

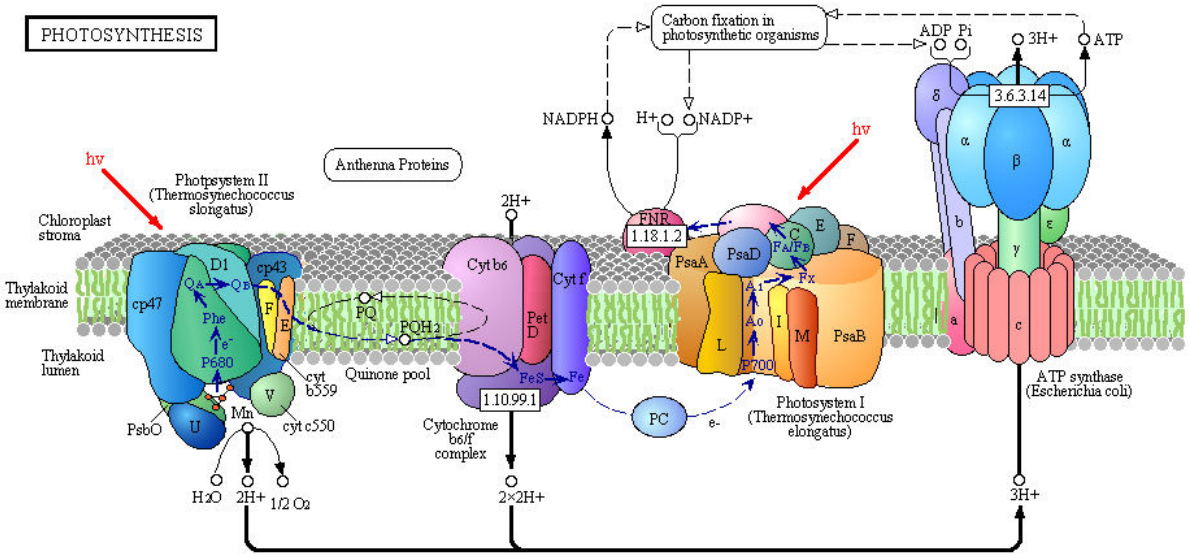


Figure **20.2.2**: Detailed View of Light Reaction of Photosynthesis (reprinted with permission from Kanehisa Laboratories and the KEGG project. The boxed numbers represent the Enzyme Commission Number. Original KEGG Map with embedded links.

20.2.2: PHOTOSYSTEM II

PSII has a complex structure comprising multiple polypeptide chains, chlorophylls, and Mn, Ca, and Fe ions. A Mn cluster, called the **oxygen-evolving complex, OEC** (also called the OEX), is directly involved in the oxidation of water. Two key homologous 32 kDa protein subunits, D1 and D2, in PSII are transmembrane proteins at the heart of the PSII complex. It has been said of PSII that "Of all the biochemical inventions in the history of life, the machinery to oxidize water — photosystem II — using sunlight is surely one of the grandest". (Sessions, A. et al., Current Biology 19 (2009)

The net reaction carried out by PSII is water oxidation and plastoquinone reduction.

$$2PQ + 2H_2O \rightarrow 2PQH_2 + O_2\,(g)$$

The oxidation number of oxygen in water is -2, and 0 in O_2, indicating a loss of electrons or oxidation of the water. Note that water is not converted to $2H_2 + O_2$, as it is in the electrolysis of water. Instead, the Hs are removed from the water as protons in the lumen of the chloroplast since the part of PSII that oxidizes water is near the lumenal end of the transmembrane complex. Protons from the stroma are required to protonate the reduced (anionic) form of plastoquinone to form PQH_2, an activity of PSII. That being said, researchers are actively trying to develop a photosynthetic scheme or mimic that does produce H_2 for use as a clean and essentially boundless fuel source to replace climate-warming fossil fuels.

A quick look at standard reduction potentials (SRP) shows that the passing of electrons from water (dioxygen SRP = +0.816 V) to plastoquinone (approx SRP of 0.11) is **not** thermodynamically favored. The process is driven thermodynamically by the energy of the absorbed photons.

The crystal structure of PSII from a photosynthetic cyanobacterium consists of 17 polypeptide subunits with metal and pigment cofactors and over 45,000 atoms. The **P680 chlorophyll reaction center** is of particular interest, consisting of four monomeric chlorophylls adjacent to a key Tyr 161 side chain. When H_2O oxidizes to form dioxygen, 4 electrons must be removed by photoactivated P680. In PSII, this process occurs in four single-electron steps, with the electrons first being transferred to the oxygen-evolving complex. The electrons that passed through the Mn complex are delivered to P680 by a photoactive **Tyr 161 (Tyr Z or YZ)** free radical.

Five discrete intermediates of the OEC, S_0-S_4, are suggested from the experimental data and are consistent with the Kok cycle, which we will discuss below. These were postulated from experiments in which spinach chloroplasts were illuminated with short light pulses. A pattern of dioxygen release was noted, and it was repeated after four flashes. Ultimately, light absorption by P680 forms the excited state P680*, which donates an electron to **pheophytin**, which passes it to quinones. Hence, P680 gets photooxidized as it forms the cationic $P680^+$. This removes an electron from Tyr 161 (YZ), producing the tyrosine radical cation, **Tyr 161**$^{\cdot+}$. Given its positive charge and its reactive nature as a free radical, as well as its proximity to Mn ions in the OEC, it pulls an electron from a Mn ion in the OEC. This process repeats itself 4 times for the oxidation of two H_2Os, which injects 4 electrons back into the OEC to return to the basal state.

The mechanism is very complicated and still not fully understood. It is perhaps easiest to imagine it involving a series of sequential electron and proton transfers, along with their accompanying changes in charge and redox states. Most biochemistry students have a limited understanding of transition state complexes and chemical kinetics, and even experts struggle with the underlying mechanism.

In summary, for PSII in plants:

1. a pair of chlorophylls (P680) in the D subunits absorb light (maximum absorbance around 680 nm) and reach an excited state
2. an electron transfer from P680 to a nearby chlorophyll with a lower energy level for the excited state electron occurs, which produces an anionic chlorophyll. This chlorophyll has 2 H^+ ions in the chlorophyll instead of Mg^{2+} (again, note the charge balance). After the electron transfer, P680 now becomes the cation $P680^+$.
3. This "anionic" chlorophyll transfers an electron to oxidized plastoquinone.
4. The $P680^+$, a strong oxidizing agent, removes one electron from an adjacent Tyr 161 to reform P680 and the radical cation **Tyr 161$^{\cdot+}$**. Its proximity to the OEC leads it to remove an electron from the OEC, making it a more potent oxidizing agent.
5. This process repeats four times to fully oxidize two water molecules, producing one O_2, with the four electrons removed from water being added back to the metal centers of the OEC.

This suggests that there are five states of the OEC: an initial state, which we will call S_0, and four other states (S_1, S_2, S_3, and S_4). S_1 forms after removing one electron from the OEC by the adjacent radical cation **Tyr 161$^{\cdot+}$** (formed after absorption of one photon). S_2, S_3, and S_4 are sequentially formed after removing one electron by a newly regenerated **Tyr 161$^{\cdot+}$** after another round of photoexcitation. S_4 then returns to its original state, S_0. This series of reactions is called the Kok cycle, which is shown in Figure **20.2.3**.

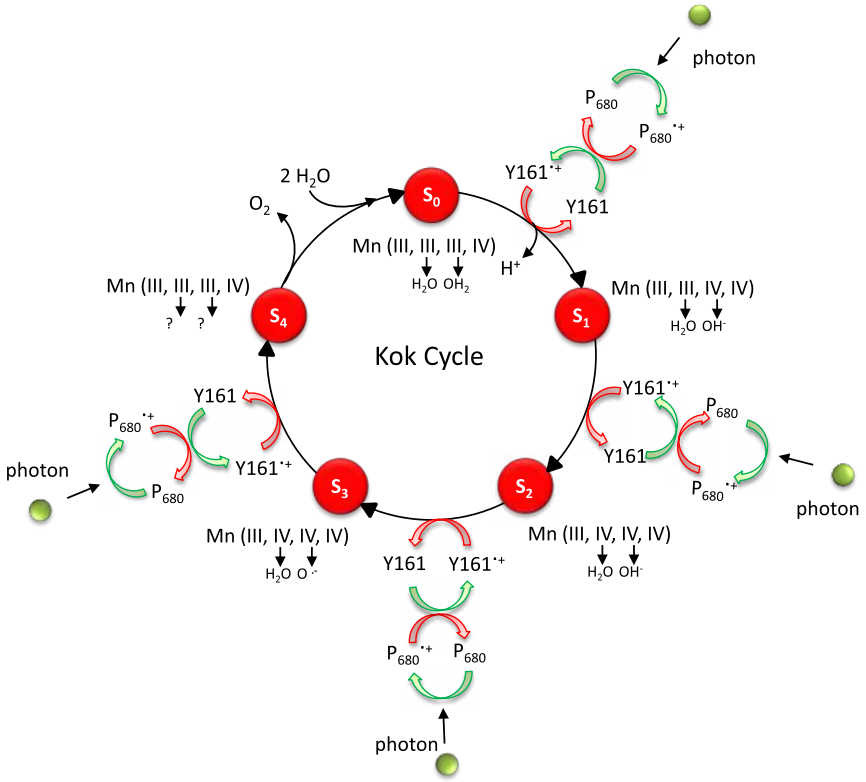


Figure **20.2.3**: The Kok cycle

No structural information is given in the above figure. What is shown instead are possible and consistent oxidation numbers of the four Mn^{n+} ions in the OEC that are consistent with charge balance and the changes in the oxidation number (-2) of the oxygen atom in water as it progresses to O_2 with an oxidation number of 0. The Mn ion states in the Kok diagram denote different discrete oxidation states, where n is the number of oxidative “equivalents” stored in the OEC during cycle progression. Think of the OEC as the key catalyst interacting with substrate H_2O molecules. We start with the S_0 state and must return to it at the end of the full cycle.

Remember that when O_2 acts as an oxidizing agent in combustion reactions, it forms $2H_2O$. That requires the addition of four electrons. If done sequentially, the oxygen intermediates include superoxide, peroxide, and oxide, the latter of which, when protonated, is water. Hence,

two water cycles and four cycles are required to remove the four electrons needed to produce dioxygen. Intermediate but transient oxygen states are also likely to be important in this mechanism.

A similar mechanism is found in PSI, except that plastocyanin, rather than dioxygen, is oxidized, with electrons being transferred to ferredoxin. This process is also challenging, as the reduction potential for oxidized plastocyanin (the form that can act as a reducing agent) is +0.37, whereas for ferredoxin, it is -0.75. This transfer of electrons is an uphill thermodynamic battle, as the more positive the standard reduction potential, the better the oxidizing agent, and the more likely the agent becomes to be reduced. What drives this uphill flow of electrons? Of course, it is the energy input from photons. We won't go into more detail about PSI, as it is very similar to PSII but lacks the OEC.

20.2.3: THE OXYGEN EVOLVING COMPLEX - OEC

Although this is not a bioinorganic textbook, we must move beyond the "simple" Kok cycle diagram and examine the actual structure of the minicatalyst, the OEC, and the protein and water (substrate) environment surrounding it to understand the mechanism. The mechanism of the OEC is still not fully understood. It's experimentally challenging to unravel, given its complexity, as the intermediates are highly labile, and the x-ray-induced transient alterations in the structure of OEC further complicate matters. Paradoxically, it is quite simple overall. Here is the essential reaction:

$$2H_2O + 4 \text{ photons} \rightarrow 4 H^+(\text{lumen}) + 4 e^- + O_2.$$

The crystal structure of PS2 from T. vulcanus has significantly improved our understanding of the OEC and electron flow on water oxidation. We will concentrate on developing an understanding of the amazing Photosystem II from Thermosynechococcus vulcanus, a cyanobacterium (19 subunits with 35 chlorophylls, two pheophytins, 11 beta carotenes, two plastoquinones, two heme irons, one non-heme iron, four Mn ions, 3-4 Ca ions, three Cl ions, one carbonate ion, and around 2800 water molecules).

Nature appears to have evolved a single gene for the central protein in PSII that binds the OEC. The Mn_4CaO_5 cluster appears identical in all photosynthetic organisms, as shown below. Researchers were surprised to find that the Ca ion was an integral part of the basic geometric "framework" of the OEC instead of a Mn, which was found to be "dangling" from the basic geometric framework. A detailed structure of the OEC from T. vulcanus is shown in Figure **20.2.4**.

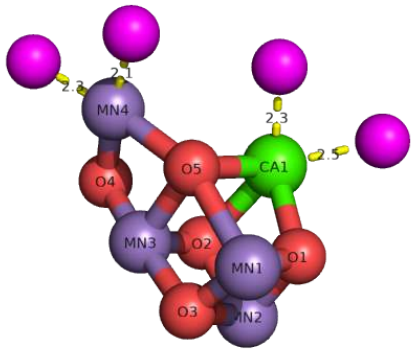
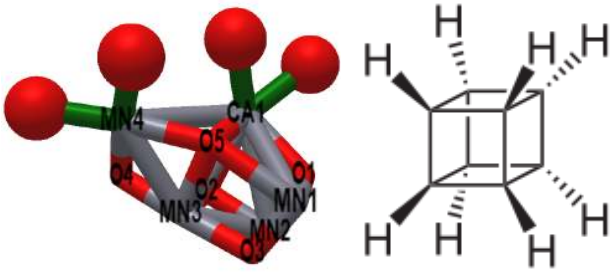


Figure **20.2.4**: Structure of the OEC

Note that the basic structure is a distorted cube, with metal ions at every other corner separated by oxides. Again, it was a surprise that not all of the 4 Mn^{2+} ions were in the cubic structure. Note one "dangling" Mn^{2+} with the other last metal site in the distorted cube occupied by Ca^{2+}. Four oxygens (presumably from water) interact with MN4 and CA1.

It isn't easy to visualize this structure correctly from a 2D figure. Figure **20.2.5** shows an interactive iCn3D model of the OEC with bound water of photosystem II from Thermostichus vulcanus (3WU2), which should help in visualizing this structure.



NCBI iCn3D Figure **20.2.5**: OEX with bound water of photosystem II from Thermostichus vulcanus (3WU2). (Copyright; author via source). Click the image for a popup (followed by Style, Background, White) or use this external link: https://www.ncbi.nlm.nih.gov/Structu...abEp67sSM1y1J9

The shape outlined by O5-CA-O1-MN1 and MN3-O2-MN2-O3 is similar to that of a cubane (shown above right). Four oxygen atoms from bound H_2O, two each for MN4 and CA1, are attached to the OEX. This model does not show the bond between O5 and MN1, so draw it in your mind to see the full distorted cubane.

Now, let's zoom out and view some of the amino acid side chains that interact with the OEC from T. vulcanus. These are shown in Figure **20.2.6**.

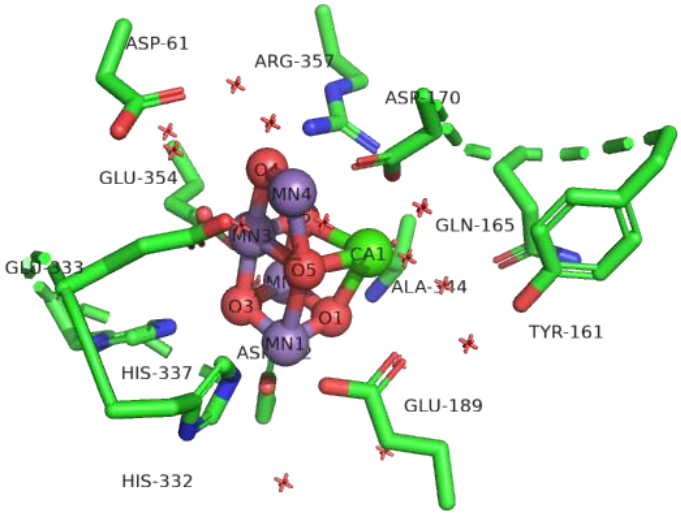
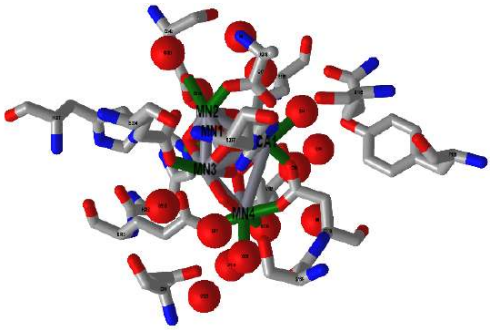


Figure **20.2.6**: OEC and surrounding amino acids from T. vulcanus

The coordination number for all the Mn ions (including those interacting with water) is identical. Note the proximity of Tyr 161, which is involved in electron removal from the OEC after it becomes the radical cation **Tyr 161$^{\cdot+}$** in the primary photooxidation event.

Figure **20.2.7** shows an interactive iCn3D model of the OEX with surrounding amino acids and water in photosystem II from Thermostichus vulcanus (3WU2), presented to once again help you better understand the 2D structure shown above.



NCBI iCn3D Figure **20.2.7**: OEX with surrounding amino acids and water in photosystem II from Thermostichus vulcanus (3WU2). (Copyright; author via source). Click the image for a popup or use this external link: https://www.ncbi.nlm.nih.gov/Structu...YGtFkmyGL1NjC9. Zoom in to see the labels on the amino acids. (Again, this model does not show the bond between O5 and MN1.)

The OEC can be considered a distorted cubane with a MN3-O4-MN4-O5 back. Bonds to O5 are longer than the other bonds, which suggests they are weaker than the other metal-oxygen bonds. This could indicate that it may not be an oxo (O^{2-}) ligand, but rather another variant, such as OH^- (lower charge), which may imply involvement in the splitting of dioxygen in the reaction mechanism. From a mechanistic perspective, an **O-O bond must form between two waters**. Both sets of bound "waters" (purple spheres in Figure 4 and red spheres in Figure 5, shown without Hs attached if they are present) are close to O5.

It is essential to recall that electrons removed from the metal ions in the OEC by **Tyr 161$^+$** must be replenished to the OEC to enable the catalytic cycle to continue. These electrons come from the waters that get oxidized. Such a reversible loss and gain

of electrons most readily occur from the transition state Mn ions, which you all remember from introductory chemistry, have multiple oxidation states. To bring back introductory chemistry again, we present the standard reduction potentials of different Mn ions in Table **20.2.1** below.

Reduction reaction	Standard Reduction Potential
Mn^{2+} (aq) + 2 e^- → Mn (s)	-1.185
MnO_4^- (aq) + 2 H_2O (l) + 3 e^- → MnO_2 (s) + 4 OH^-	+0.595
MnO_2(s) + 4H^+ + e^- → Mn^{3+} + 2H_2O	+0.95
MnO_2(s) + 4H^+ + 2e- → Mn^{2+} + 2H_2O	+1.23
MnO_4- (aq) + 8 H^+ (aq) + 5 e^- → Mn^{2+} (aq) + 4 H_2O (l)	1.507
MnO_4^- (aq) + 4 H^+ (aq) + 3 e^- → MnO_2 (s) + 2 H_2O (l)	1.679
$HMnO_4^-$ + 3H^+ + 2^{e-} → MnO_2(s) + 2H_2O	+2.09
O_2(g) + 4H^+ + 4e^- → 2H_2O +1.229	+1.229

Table **20.2.1**: Standard reduction potentials for Mn ions compared to O_2.

You should be able to determine the oxidation number of the Mn ion in each compound. Based on standard reduction potentials, which oxidation states might be sufficient for the oxidation of H_2O in the OEC?

How does this translate into structural/chemical changes in the OEC? Figure **20.2.8** provides a recent mechanism consistent with each of the Kok states (S_0-S_4).

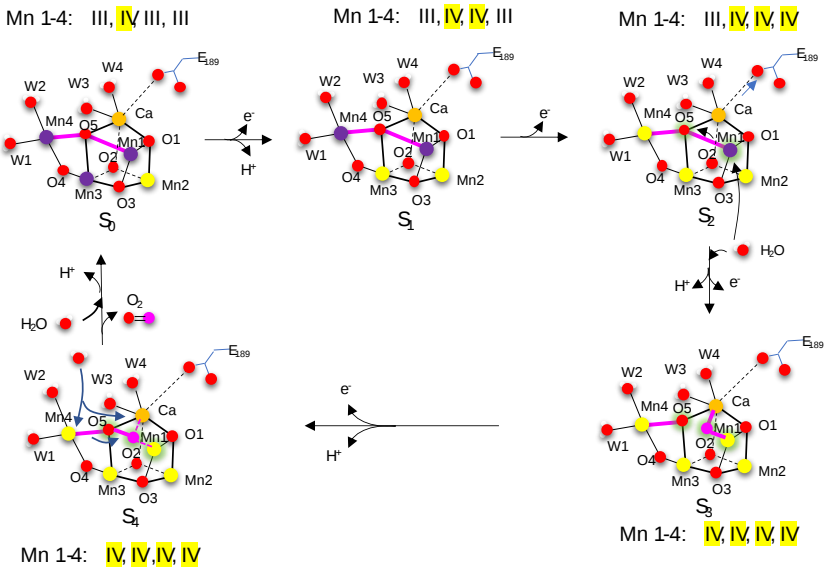


Figure **20.2.8**: Mechanism for water oxidation and O_2 formation through the OEC consistent with the Kok cycle (adapter from Britt & Marchiori, 10.1126/science.aaz4522)

The proposed change in redox state for each Mn ion is illustrated with Mn (III) ions in purple and Mn (IV) ions in yellow. Note the change in the oxidation state of the 4 Mn ions from (III, IV, III, and III) in S_0 to (IV, IV, IV, and IV) for all of them in S_3 and S_4. A flip in the side chain of E180 in S_2 allows the binding of Mn1 through an oxy link to Ca. There are many possible forms of oxygen in the structure, including waters, oxides (bridging oxos and possibly terminal oxides), and hydroxides, and the exact form at some sites remains uncertain. Note also the elegance of having a Mn_4 cluster to catalyze the four-electron oxidation of 2 water through losing 4 electrons. Also, the redox state change in the Mn ions differs from the Kok diagram in Figure 3.

Additionally, the final O_2-producing step, which transitions from S_4 → S_0, remains uncertain. The above mechanism is based on X-ray structures of intermediates and quantum calculations. In it, S_4 has an Mn(IV)$O^{\cdot}$ that bonds with the bridging O5 to form O_2.

20.2.4: WATERS

As water is a reactant in PSII, water channels leading to the OEC must provide a pathway for water to enter and for protons to be removed and directed to the lumen, thereby developing a proton gradient. Another rendering of the Kok cycle, the position of the OEC in PSII on the

luminal side of the membrane, and the presence of water channels (Cl1, O4, O1) and the Yz network, which connects Tyr 161 (Yz) to the lumen, are shown in Figure **20.2.9**.

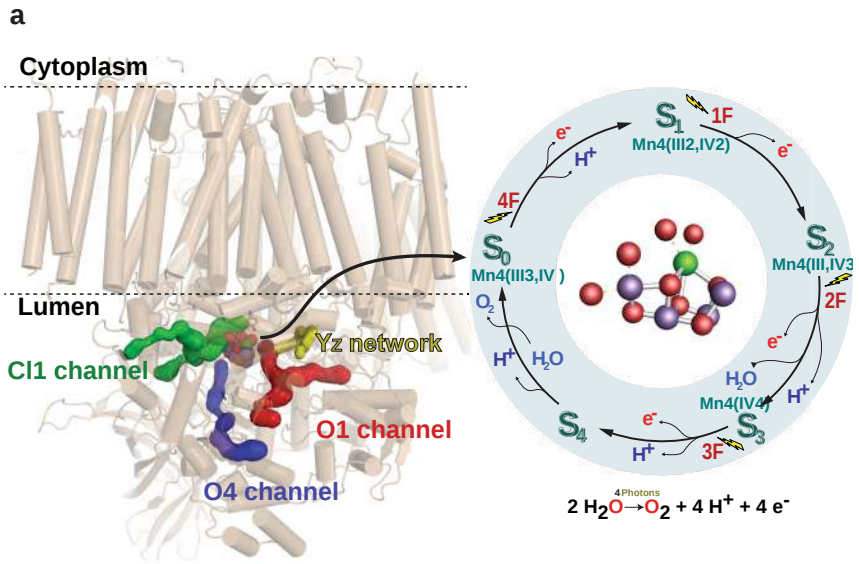


Figure **20.2.9**: An overview of Photosystem II and the main water channels and networks from the OEC to the lumenal side. Hussein, R., Ibrahim, M., Bhowmick, A., *et al.* Structural dynamics in the water and proton channels of photosystem II during the S_2 to S_3 transition. *Nat Commun* **12,** 6531 (2021). https://doi.org/10.1038/s41467-021-26781-z. Creative Commons Attribution 4.0 International License. http://creativecommons.org/ licenses/by/4.0/.

The left part of the figure illustrates the structure of PS II, showing the membrane-embedded helices and the extrinsic subunits in beige. The OEC and the water channels, in addition to the Yz network, are shown in color. The Kok cycle of the water oxidation reaction, triggered by the absorption of photons, is shown on the right and highlighted with a blue circle. F represents a photon.

A more detailed representation of water channels and the Yz networks is shown in Figure **20.2.10**.

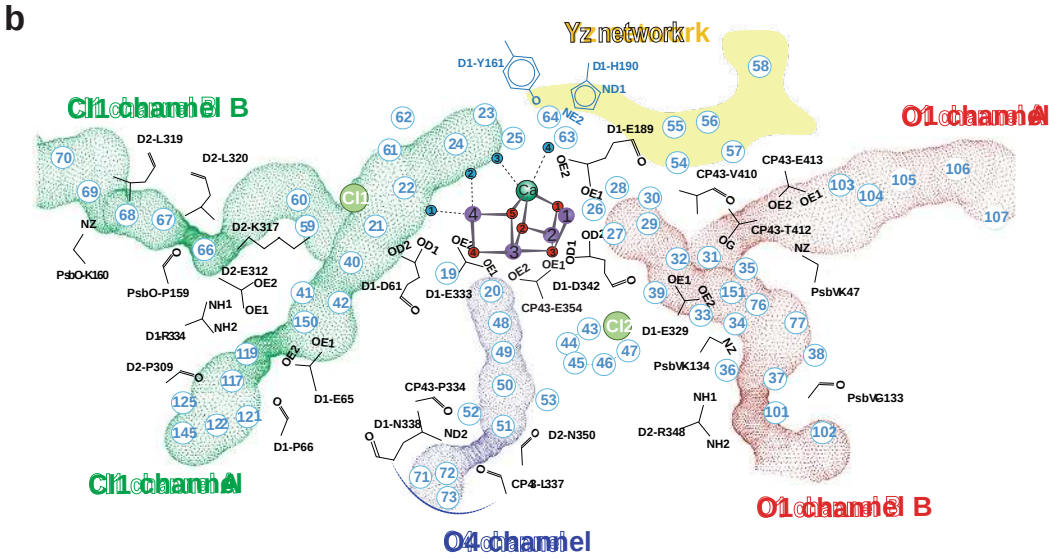


Figure **20.2.10**: A detailed view of the water channels showing the waters within each channel (O1 Channel red dotted, O4 Channel blue dotted, and Cl1 Channel green dotted). The region highlighted with solid yellow represents the Yz network. Residues involved in forming bottlenecks in the channels are shown in black. Water molecules found in the crystal structures are labeled with blue numbers in the channel. Hussein, R., Ibrahim, M., Bhowmick, A., *et al.*, ibid.

These structures show that there is no direct water pathway from across the OEC and that all channels restrict water movement to some degree. The O4 and Cl1 channels are narrower than the O1 channel, so water in those is less mobile. In the O4 channels, waters 50-53 are near charged groups and are close to a major bottleneck (residues D1-N338, D2-N350, and CP43-P334, -L334).

Based on the X-ray structures and molecular dynamics simulations, the O1 channels appear to allow water access to the OEC. The more rigid Cl1 channel A may be involved in H^+ transfer during $S_2 \rightarrow S_3$.

20.2.5: THE LAST STEP: ELECTRON TRANSFER TO PLASTOQUINONE

We are almost ready for the next section, in which we will present the flow of electrons away from PSII through mobile electron carriers, leading to the synthesis of NADPH for the reductive biosynthesis of carbohydrates. Before we leave PSII, let's look at what happens to the radical anion $P680^-$, also known as $PheA^-$ (**pheophytin A**) or $PheA_{D1}$ (the reaction center chlorophyll without a central Mg^{2+} ion), which received an electron from photooxidation of the reaction center P680, as summarized again in Figure **20.2.11**.

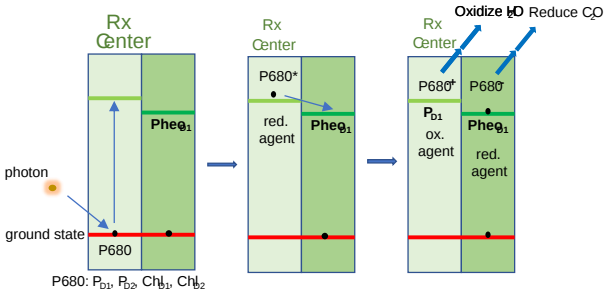
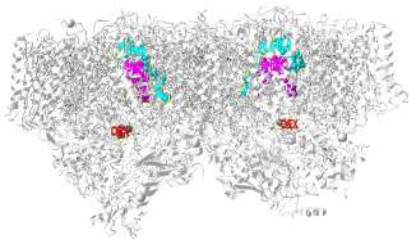


Figure **20.2.11**: The reaction center electron transfer reactions in PSII.

Pheophytin A passes its electron to plastoquinone A (in PSII), which passes it on to the lipophilic mobile electron carrier in the thylakoid membrane, plastoquinone. This is similar to the mobile electron carrier in mitochondrial electron transport, ubiquinone. Ultimately, these are passed to $NADP^+$ to form NADPH, which is used for reductive biosynthesis.

Figure **20.2.12** shows an interactive iCn3D model highlighting just the OEX, pheophytin A (PHO), and plastoquinone A (PL9) in photosystem II from Thermostichus vulcanus (3WU2). (long load time).



NCBI iCn3D Figure **20.2.12**: the OEX, pheophytin A (PHO), and plastoquinone A (PL9) in photosystem II from Thermostichus vulcanus (3WU2). (long load time). (Copyright; author via source). Click the image for a popup or use this external link: https://www.ncbi.nlm.nih.gov/Structu...eamDFQNb2ZLKh7

The OEX (OEC) is shown in spacefill, CPK colors, PHO in spacefill magenta, and PL9 in spacefill cyan. Note the proximity of PHO and PL9 for easy electron transfer to plastoquinone A.

Given the number and proximity of high-energy reactive species in the reaction center, it should not be surprising that side reactions can occur. These would decrease the efficiency of light energy transduction and also could damage molecular components of PSII (and similarly PSI)

Figure **20.2.13**s shows a standard reduction potential diagram for the **P**680 - **Phe**ophytin A - Plasto**Q**uinone **A** triad (abbreviated P Phe Q) in PSII.

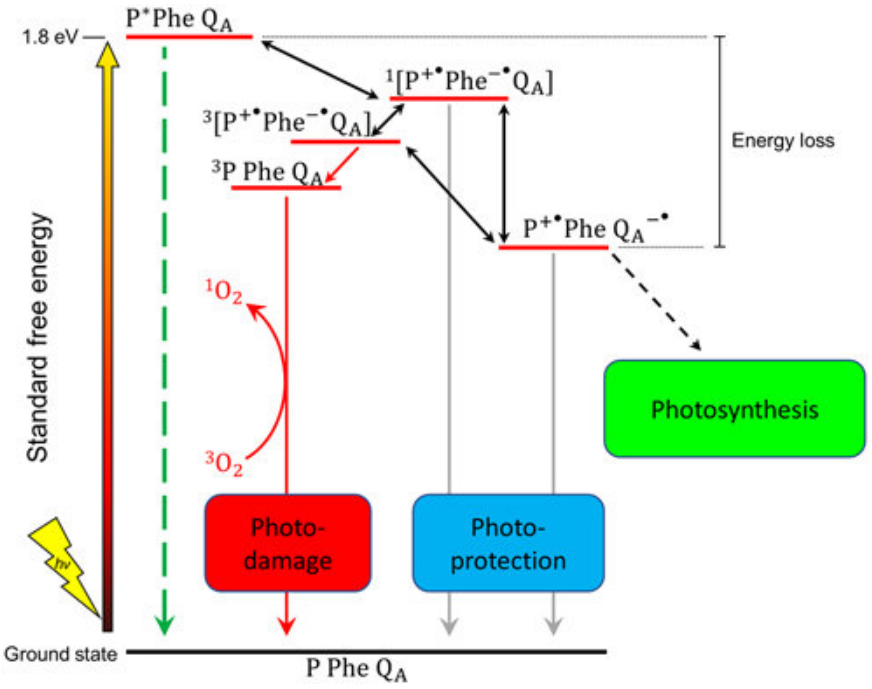


Figure **20.2.13**: Charge recombination pathways in PSII (The energy gaps are not drawn to scale). Cardona T, Shao S, Nixon PJ. Enhancing photosynthesis in plants: the light reactions. *Essays Biochem*. 2018;62(1):85-94. Published 2018 Apr 13. doi:10.1042/EBC20170015Creative Commons Attribution License 4.0 (CC BY).

Safe routes for charge recombination between P^+ and Q_A^- are indicated in blue, the damaging route producing $^1O_2$ in red, and the radiative pathway in green. Stabilizing the $P^+PheoQ_A^-$ state helps prevent reverse electron flow to form $P^+Pheo^-Q_A$ and subsequent charge recombination to form $PPheoQ_A$. For clarity, the details of the additional electron transfer steps, including water oxidation and plastoquinone reduction to plastoquinol by PSII, collectively referred to as photosynthesis, are omitted. Abbreviations: P, primary electron donor of PSII; Pheo, pheophytin electron acceptor; Q_A, primary plastoquinone electron acceptor; $^1O_2$, singlet oxygen; $^3O_2$, triplet oxygen; ^3P, triplet excited state of P.

20.2.6: SUMMARY

This chapter delves into the fundamental processes that convert light energy into chemical energy during photosynthesis, with a focus on the intricate events occurring in Photosystem II (PSII) and their integration into the overall electron transport chain of the light reactions.

Photoexcitation and Charge Separation:

- The chapter begins by explaining how light absorption by non–reaction center chlorophyll molecules transforms them into potent reducing agents. These excited chlorophylls transfer electrons to the reaction center, effectively “photooxidizing” themselves and generating the strongly oxidizing $P680^+$.
- This initial electron transfer sets the stage for the subsequent redox reactions, where the extra electron eventually contributes to the reduction of $NADP^+$ to NADPH.

The Z Scheme and Electron Flow:

- The light reactions are organized into a “Z scheme,” which details the stepwise flow of electrons from water through PSII and PSI to $NADP^+$.
- In PSII, water is oxidized by the oxygen-evolving complex (OEC), a Mn_4CaO_5 cluster, to produce O_2, with the electrons transferred via pheophytin and plastoquinone.
- In PSI, electrons from plastocyanin are passed to ferredoxin, ultimately reducing $NADP^+$.
- The energy released during these electron transfers is harnessed to pump protons from the stroma into the thylakoid lumen, generating a proton gradient that drives ATP synthesis.

Structure and Function of Photosystem II:

- PSII is a complex, multi-subunit assembly featuring key components such as the P680 reaction center, the D1 and D2 proteins, and a series of chlorophylls and carotenoids.

- The chapter highlights the role of the OEC in the oxidation of water, describing how the process proceeds through four sequential electron removals, a cycle summarized by the Kok cycle (S_0 to S_4 states).
- The unique arrangement and redox properties of the Mn ions, together with a key tyrosine residue (Tyr 161), facilitate the extraction of electrons from water, a process that is both thermodynamically challenging and essential for O_2 evolution.

Water Channels and Proton Transfer:

- Detailed structural insights reveal the presence of specialized water channels and hydrogen-bond networks within PSII. These channels guide substrate water molecules to the OEC and facilitate the efficient removal of protons to the thylakoid lumen, contributing to the proton motive force necessary for ATP synthesis.

Regulation and Protection Against Damage:

- The chapter also discusses the potential for unwanted side reactions, such as charge recombination, which can generate reactive oxygen species (ROS) like singlet oxygen.
- It outlines the strategies by which PSII minimizes these harmful reactions, including the establishment of safe charge recombination pathways and the stabilization of the charge-separated state.

Integration into Overall Photosynthetic Energy Conversion:

- Finally, the chapter ties these processes together by explaining how the light reactions generate the three critical products—O_2, ATP, and NADPH—which are subsequently used in the dark reactions (Calvin cycle) for the reductive biosynthesis of carbohydrates.
- A brief comparison is made with PSI, which shares similar photochemical processes but lacks water oxidation, emphasizing the complementary roles of the two photosystems in balancing energy and electron flow.

In summary, this chapter provides an in-depth examination of the light reactions of photosynthesis, focusing on the molecular mechanisms that drive water oxidation, electron transfer, and proton gradient formation. Through detailed structural and mechanistic insights, students gain an appreciation of how these processes underpin the conversion of solar energy into the chemical energy required for life.

This page titled 20.2: The Kok Cycle and Oxygen Evolving Complex of Photosystem II is shared under a not declared license and was authored, remixed, and/or curated by Henry Jakubowski and Patricia Flatt.

- **Current page** by Henry Jakubowski and Patricia Flatt has no license indicated.
- **11.2: Diffusion Across a Membrane - Passive and Facilitated Diffusion** by Henry Jakubowski and Patricia Flatt has no license indicated.

20.3: PLANT ELECTRON TRANSPORT AND ATP SYNTHESIS

Search Fundamentals of Biochemistry

LEARNING GOALS (CHATGPT O3-MINI)

1. **Outline the Photosynthetic Electron Transport Chain:**
   - Describe the linear flow of electrons from photosystem II (PSII) to photosystem I (PSI) through intermediates (plastoquinone, cytochrome b6f, plastocyanin, and ferredoxin) and explain how these events drive the synthesis of NADPH and ATP.
2. **Explain the Function and Mechanism of Cytochrome b6f:**
   - Detail the role of cytochrome b6f as a rate-limiting enzyme in electron transport, its operation via the Q cycle, and its contribution to the generation of the proton gradient across the thylakoid membrane.
3. **Differentiate Linear and Cyclic Electron Flow:**
   - Compare and contrast the pathways and outcomes of linear photophosphorylation versus cyclic electron flow, emphasizing the conditions under which each pathway is favored and how they affect the ATP/NADPH ratio.
4. **Interpret Structural Models of Photosynthetic Complexes:**
   - Use interactive models (e.g., iCn3D visualizations) to analyze the structural features of key complexes such as the cytochrome b6f complex, the PSI-LHCI supercomplex, and the NDH–PSI–LHCI-2 supercomplex, linking structure to function.
5. **Assess the Role of Light-Harvesting Complexes (LHCs):**
   - Explain how the spatial arrangement and phosphorylation state of LHCII proteins regulate the distribution of excitation energy between PSI and PSII, particularly under varying light conditions.
6. **Relate Electron Flow to Proton Gradient and ATP Synthesis:**
   - Illustrate how electron transfer events are coupled to proton translocation and how the resulting electrochemical gradient is harnessed by the chloroplast ATP synthase to synthesize ATP.
7. **Examine the Structure and Regulation of Chloroplast ATP Synthase (CF1FO):**
   - Describe the rotary mechanism of ATP synthase, focusing on the role of the γ subunit in redox regulation, and explain how light-driven changes modulate its activity to prevent wasteful ATP hydrolysis at night.
8. **Analyze the Integration of Electron Transport with Carbon Metabolism:**
   - Evaluate how the electron transport chain interfaces with carbon fixation (via Rubisco) and how feedback mechanisms regulate the balance between electron transport and the demands of the dark reactions.
9. **Explore the Mechanism of Redox Control in Photosynthesis:**
   - Discuss how redox-sensitive processes (e.g., the activation/inactivation of LHCII kinase and the reduction of thioredoxin) serve as rapid feedback mechanisms to adjust photosynthetic efficiency and protect the system from photodamage.
10. **Apply Kinetic and Regulatory Concepts to Model Photosynthetic Efficiency:**
    - Use models (such as the transistor analogy for cytochrome b6f regulation) to predict how changes in light intensity affect electron transport kinetics, excitation balance, and overall photosynthetic performance.

These learning goals are designed to help students integrate structural, mechanistic, and regulatory perspectives of the photosynthetic machinery and understand how these systems work together to support energy conversion in plants.

20.3.1: INTRODUCTION

In the previous sections, we studied light absorption by chlorophylls, the transfer of energy to the reaction center of photosystem II, the oxidation of H_2O by the oxygen-evolving complex (OEC), and the transfer of electrons from these events to the lipophilic electron carrier, plastoquinone. Now, we are ready to see how the process continues as electrons are passed on from reduced plastoquinone to the cytochrome b_6f complex, through photosystem I (which has no OEC), and on to the terminal electron acceptor $NADP^+$, which forms NADPH. This is used for the reductive biosynthesis of glucose after fixation of atmospheric CO_2 by ribulose bisphosphate carboxylase (RuBisCo). As we saw in mitochondrial electron transport, the passage of electrons is accompanied by the movement of protons from the lumen to the stroma, with the ultimate collapse back into the lumen through a rotary ATP synthase, forming the ATP required for reductive biosynthesis. Figure **20.3.1** reviews the light reactions of photosynthesis again.

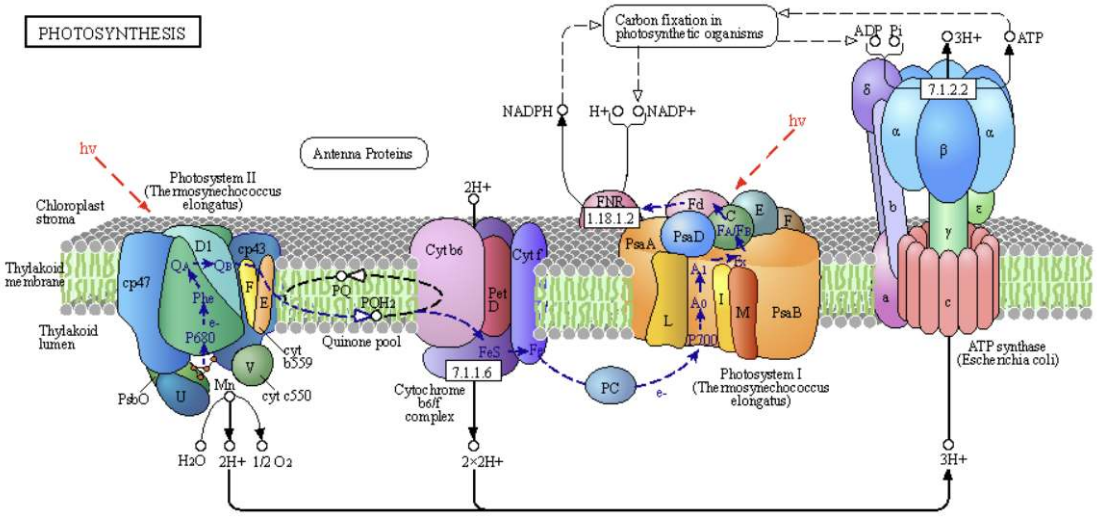


Figure **20.3.1**: Light reactions of photosynthesis

The pathway shows a **"linear"** sequential flow of electrons from:

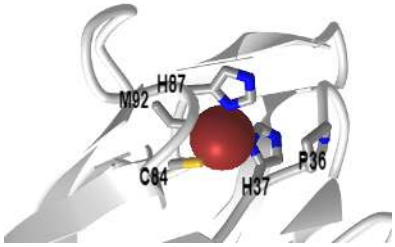
- PSII to a mobile electron carrier, plastoquinone (PQ/PQH_2), then to
- the membrane complex Cytochrome b_6f complex to the mobile carrier plastocyanin (PC), then to
- PSI to the mobile carrier flavodoxin (Fd), then to
- FNR (Ferredoxin-$NADP^+$ Reductase (FNR), a peripheral membrane protein, passes electrons from bound reduced flavodoxin to the mobile electron acceptor, $NADP^+$.

Accompanying this linear flow of electrons is a linear flow of protons (H^+), forming a proton gradient that collapses through ATP synthase to produce ATP. Hence, these linear flows of electrons and protons couple NADPH and ATP synthesis. This sequence of events is also called **linear photophosphorylation,** which leads to an ATP/NADPH ratio ≈ 1.3.

We'll see an alternative **"circular"** electron flow below and see the advantages of each.

20.3.2: CYTOCHROME B_6F

This complex moves electrons from the mobile lipophilic electron carrier reduced plastoquinol (PQH_2), an isoprenoid quinone, to the mobile Cu-containing protein **plastocyanin**, which plays an analogous role to the mobile protein carrier in mitochondrial electron transport, cytochrome C. It catalyzes the rate-limiting step in electron transport in the light reactions. Figure **20.3.2** shows an interactive iCn3D model of the spinach plastocyanin (1AG6)



NCBI iCn3D Figure **20.3.2**: Spinach plastocyanin (1AG6). (Copyright; author via source). Click the image for a popup or use this external link: https://structure.ncbi.nlm.nih.gov/i...DwSDDrYMUb9Xn7

The complex that mediates electron transfer between reduced plastoquinone and the protein plastocyanin, cytochrome b_6f, is centrally positioned between the two photosystems. In addition, it moves 2 H^+s from the stroma into the lumen. These are joined by 2 H^+s from water oxidation by the OEC (on the luminal side of PSII) to create a transmembrane proton gradient, which powers ATP synthesis.

Electron transfer with cytochrome b6f occurs through the quinol (Q) cycle, similar to Complex III in mitochondrial electron transport; therefore, we will not delve into the details here. Figure **20.3.3** shows a summary diagram with electron and proton flow.

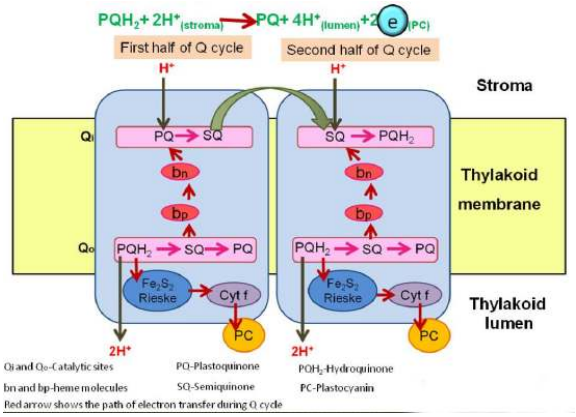


Figure **20.3.3**: Q cycle in the cytochrome b6f complex of photosynthesis. https://twitter.com/BiologyNowadays/...232768/photo/1

Figure **20.3.4** shows another version of the Q cycle as an alternative representation.

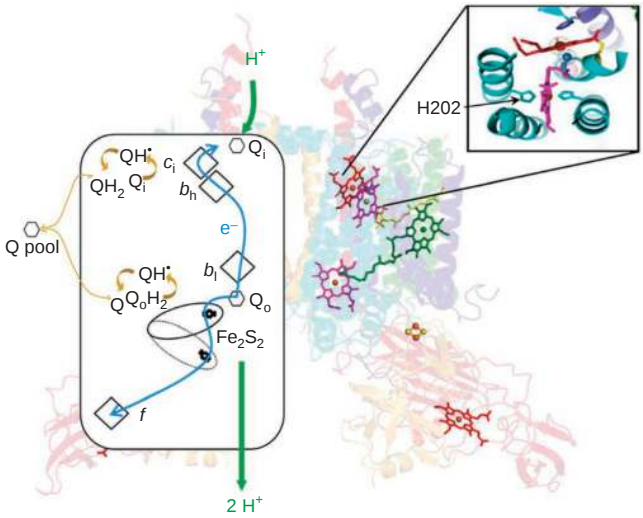


Figure **20.3.4**: Alternative version of the photosynthetic cytochrome b_6f Q cycle. Malnoë et al. *Nat Commun* **2,** 301 (2011). https://doi.org/10.1038/ncomms1299. Creative Commons Attribution-NonCommercialShare Alike 3.0 Unported License. http://creativecommons.org/licenses/by-nc-sa/3.0/

The left box shows the b_6f complex transfers two protons (green arrows) per electron transferred (blue arrows) along high (Fe_2S_2 cluster, cytochrome $_f$) and low potential chains (b_l, bh, c_i hemes) as well as Quinol (QH_2) oxidation at Q_o site, Quinone (Q) reduction at Q_i site. The right structure depicts haems *b* (purple), c_i and f (red), Fe_2S_2 cluster (yellow and orange ball-and-stick model), cytochrome b_6 (cyan), subunit IV (blue), Rieske subunit (yellow), cytochrome *f* (red), PetG, L, M and N subunits (green). Magnification of Q_i site comprising b_h and c_i haems.

Both cytochrome bc1 and cytb_6f are dimeric complexes with 2 Fe_2S_2 clusters, two cytochrome bs, and a cytochrome c. The cytb_6f complex also contains 9-cis β-carotene and an additional c1 heme. The electrons move from PQH_2 through the complex in a similar fashion to that of the bc1 complex.

PQH_2 is oxidized at the Q_p site with a bifurcation of electrons:

- one electron moves through the high-potential Fe_2S_2 center and cyt f pathway (bottom left in pathway diagram of Figure 3), with the electron moving to the soluble peripheral protein plastocyanin and one to photosystem I.
- the other moves through the low potential b_l, bh, c_i hemes pathway (top left in pathway diagram of Figure 3), with the electron moving to a plastoquinone at the Qn site near the stroma. A second round of oxidation of PQH_2 at the Q_p site eventually donates another electron to a plastoquinone$^{-\cdot}$ which regenerates PQH_2 after addition of 2 H^+ from the stroma.

Two successive oxidations of PQH_2 result in twice the number of protons moving into the lumen, and in the process, 2 H+ ions move into the lumen. Cytochrome b_6f is also a redox sensor of the plastoquinol/plastoquinone pool's status.

Figure **20.3.5** shows an interactive iCn3D model of the spinach cytochrome b6f complex (6RQF)

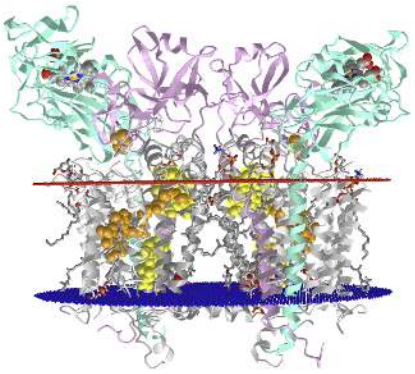


Figure 20.3.5: Spinach cytochrome b6f complex (6RQF). (Copyright; author via source). Click the image for a popup or use this external link: https://structure.ncbi.nlm.nih.gov/i...tgUhjekB4Tndw6

The region away from the red leaflet represents the lumen side of the complex. The FeS cluster and heme C are in the luminal domains. The coloring scheme is as follows:

- cytochrome bcf subunits 4, 5, 6, 7, and 8: light gray
- cytochrome b6: dark gray
- cytochrome b6 FeS subunit: plum
- cytochrome F: cyan
- chlorophylls: orange spacefill, labeled
- FeS clusters: CPK spacefill, labeled
- HEC - Heme C: CPK spacefill, labeled
- heme - porphoryin IX containing Fe: yellow spacefill

Cytochrome b6f is the rate-limiting step for electron flow, but what is its role in regulating the photosynthetic pathway (light reaction plus the dark reaction of carbon metabolism? Data suggest that the complex regulates electron transport in low light conditions but affects a switch to carbon metabolism under saturating light. We'll see that below when we discuss circular electron flow.

20.3.3: PLANT PHOTOSYSTEM I-LHCI SUPER-COMPLEX

If the goal of the photosystem complexes is to transduce light energy delivered by photons into electrons that can be used for reductive biosynthesis of glucose from atmospheric carbon capture of CO_2, then PSI is quite amazing. It has a "quantum efficiency" close to 1, which implies that one absorbed photon produces 1 electron that can be used to reduce $NADP^+$. This occurs because the transfer of photon energy to other molecules in PSI is so rapid compared to non-radiative decay processes for the excited-state chlorophylls.

The same excitation and electron (charge) transfer process we saw in PSII occurs in PSI, with the chlorophyll in the reaction center involved in charge transfers. The light-absorbing molecules of PSI enable light to be absorbed at the far red end of the spectrum. The complex contains 16 proteins, 155 chlorophyll molecules, and 35 carotene derivatives. As with PSII, there is a core complex that is similar to cyanobacterial PSI. The supercomplex has, in addition, light-harvesting complex I proteins surrounding one side of the complex (looking down on it), which comprise four LHCI proteins (Lhca 1-4), allowing for increased light absorption. They have 57 chlorophylls and 13 carotene derivatives.

The apoproteins that bind the chlorophylls, including the LHCI proteins, have similar but slightly different topologies, allowing for tuning the absorbance spectra of the bound chromophores. Seven of the chlorophylls, when bound, have local environments that allow the absorption of far-red light. These are not found in PSII. Far red light would be more abundant in the low parts of the plant canopies, as photons of lower wavelengths would be more filtered out by upper leaves in the canopy.

Due to the complexity of PSI, we will provide several different iCn3D models to illustrate the various features of the **photosystem I-LHCI super-complex**. As with PSII, PSI has a core surrounded by a light-harvesting complex (LHCI). Figure 20.3.6 shows an interactive iCn3D model of the Plant (pea) photosystem I-LHCI super-complex (4XK8)

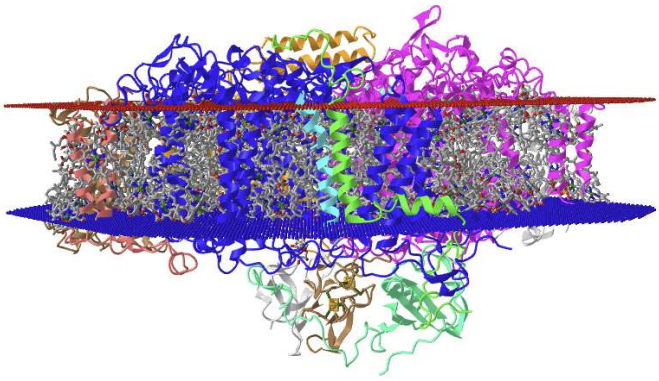


Figure 20.3.6: C. (Copyright; author via source). Click the image for a popup or use this external link: https://structure.ncbi.nlm.nih.gov/i...uWBzFrVBUDHHQ6 (long load time)

Again, the red leaflet represents the lumen side of the complex, while the gray represents the chlorophyll and other lipid molecules in the membrane.

Figure \PageInde.x7 shows an interactive iCn3D model highlighting the chlorophylls, beta carotene derivatives, and FeS clusters of Plant photosystem I-LHCI super-complex (4XK8)

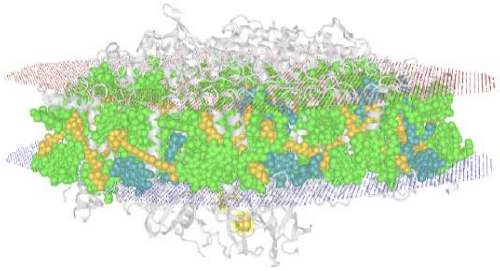


Figure 20.3.7: Chlorophylls, beta carotene derivatives, and FeS clusters of Plant photosystem I-LHCI super-complex (4XK8). (Copyright; author via source). Click the image for a popup or use this external link: https://www.ncbi.nlm.nih.gov/Structu...BecS9cgNqdr8J6 (long load time)

The proteins in the complex are shown in gray cartoons. Chlorophylls A and B are shown in green and teal spacefill, respectively. Beta-carotene derivatives are shown in orange spacefill.

Figure 20.3.8 shows an interactive iCn3D model of the ApoA1 protein with surrounding chlorophyll and other components from plant photosystem I-LHCI super-complex (4XK8)

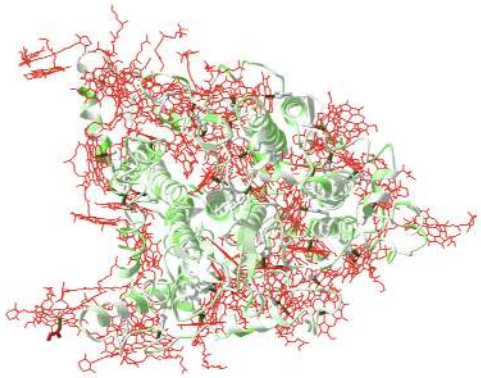


Figure 20.3.8: ApoA1 protein with surrounding chlorophyll and other components from plant photosystem I-LHCI super-complex (4XK8). (Copyright; author via source). Click the image for a popup or use this external link: https://structure.ncbi.nlm.nih.gov/i...L6tsJ3oMDZ2YQA (long load time)

ApoA1 is shown in a cartoon and colored according to hydrophobicity. The chlorophylls, carotenes, and other components within 5 Å are shown in red. Rotate the image to see how the chlorophyll and other lipids encircle the membrane protein components.

Figure **20.3.9** shows an interactive iCn3D model of the Plant (pea) photosystem I-LHCI super-complex, highlighting LHCIs (4XK8)

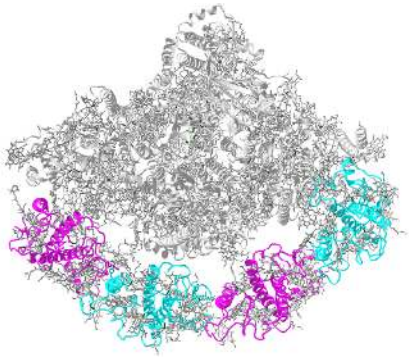


Figure **20.3.9**: Plant (pea) photosystem I-LHCI super-complex highlighting LHCIs (4XK8). (Copyright; author via source). Click the image for a popup or use this external link: https://structure.ncbi.nlm.nih.gov/i...9vHynkRTLxAct7 (long load time)

The LHCI subunits (Lhca 1-4) are shown in alternating magenta and cyan cartoon structures surrounding one side of the core complex. The view in the model above is a top-down view.

We discussed in Chapter 20.1 that PSI absorbance is tilted toward the red end of the spectra, with the effective absorbance ratio over a broad wavelength range for the two photosystems, **PSI**/(**PSI**+PSII), deviating from around 0.5 at the red/far red end of the spectrum (670-730 nm), where the ratio is close to 1. When exposed to far-red light, the systems move to state I. In this state, the major mobile antenna proteins (LHCIIs) move to PSII to restore a "photoabsorption" balance. When exposed to light depleted in the high end of visual spectra, the system moves to state II, where mobile LHCIIs move to PSI.

The location of LHCs is regulated by the phosphorylation of LHCs, which is controlled by the levels of plastoquinone, making excellent biological sense. When the concentration of plastoquinones in the reduced state, PQH_2 (plastoquinol), is high, it would be optimal to increase the activity of PSI to relieve the high concentration of the substrate for cyto b_6f and shift the system to higher PSI activity and continue electron flow. This regulation is mediated by the phosphorylation of LHCs by LHCII kinase (a Ser/Thr kinase), which is activated by high concentrations of reduced PQH_2. Phosphorylation of LHCs leads to their movement from PSII to PSI. When the oxidized form of plastoquinone is high, LHCII kinase is inactivated by dephosphorylation, causing the mobile LHC to move back to PSII to increase output (PQH_2) from PSII. These events occur in low light. In high-light conditions, when the system is functioning at a high level, the LHCII kinase is inhibited by stromal thioredoxin. Specifically, the phosphorylation status of Lhcb1 and Lhcb2 in LHCII homo- or heterotrimers determines the movement between PSII and PSI. The chloroplastic serine/threonine-protein kinase (STT7, also known as STN7) is another LHCII kinase.

Recent Updates: 4.7.25

Linear vs Cyclic Flow of Electrons in Photosynthesis

Sometimes, the flow of electrons from PSI does not go through ferredoxin to $NADP^+$ using Ferredoxin-$NADP^+$ Reductase (FNR). Instead, the electrons are repeatedly shunted repeatedly from reduced ferredoxin (FdH_2) back to PSI through cytochrome b_6f in a **circular flow**, which is often called **cyclic photophosphorylation**. If this happens, NADPH is not made. Yet, protons continue to flow across the membrane, leading to increased ATP synthesis. Here are several reasons this occurs:

- NADPH is in excess, and it's not needed
- $NADP^+$ is low and must be regenerated
- prevention of damage to the photosystems by excess light

This cyclic flow essentially uncouples NADPH and ATP production, allowing the continuous production of ATP.

The actual return of electrons in this circular flow occurs through a thylakoid membrane enzyme called **NAD(P)H dehydrogenase (Ndh)**. This enzyme is structurally very similar to mitochondrial Complex I, also known as NADH:ubiquinone oxidoreductase or Type I NADH dehydrogenase. As the name implies, Complex I binds NADH and passes electrons from it in a dehydrogenation reaction to another mobile electron carrier, ubiquinone (UQ), which forms ubiquinol (UQH_2).

$$\text{NADH} + \text{ubiquinone (UQ)} \leftrightarrow \text{NAD}^+ + \text{UQH}_2$$

The chloroplastic Ndh, however, does not bind NADPH, which is confusing given the name. Rather, it binds reduced ferredoxin from PSI and transfers electrons to plastoquinone (PQ), which, when reduced, can pass electrons to Cyto b6f and then to PSI. Ferredoxin is considered the principal electron donor. The redox state does not change in a net fashion. Note that the cyclic electron pathway, once

started, does not need PSII, so water oxidation is not needed. Hence, the enzyme Ndh binds ferredoxin and plastquinones/ols at distinct sites.

Essentially, FNR makes NADPH and ATP for biosynthesis, while Ndh boosts ATP and helps modulate the NADPH/ATP ratio.

Spinach NDH has many subunits. Ndh A-G are in the membrane arm and are similar to subunits (ND1-ND6) in the analogous arm of mitochondrial complex I. Ndh H-K in the peripheral arm are similar to the Q (ubiquinone) reduction part of complex I. Instead of having a binding site for NADH, it interacts with ferredoxin. Other subunits include NdhL-O and S-V. NdhC, I, J, L, M, O, and U form a plastoquinone binding site. Other subunits (PnsL1–PnsL5 and PnsB1–PnsB5) are found in the spinach chloroplast NDH but not in cyanobacteria.

NDH used for cyclic electron flow is part of a much larger **NDH–PSI–LHCI-2 supercomplex.** The structure of a larger supercomplex in spinach, composed of NDH, PSI, and LHCI-2, determined by cryoelectromicroscopy, is shown in Figure **20.3.10** below.

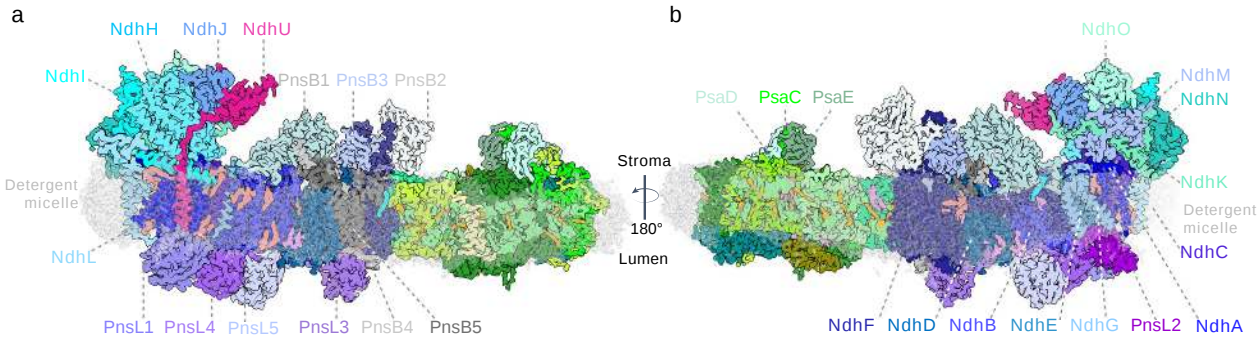


Figure **20.3.10**: **Cryo-EM structure of the NDH–PSI–LHCI-2 supercomplex from *S. oleracea*.** Introini, B., Hahn, A. & Kühlbrandt, W. Cryo-EM structure of the NDH–PSI–LHCI supercomplex from *Spinacia oleracea*. *Nat Struct Mol Biol* (2025). https://doi.org/10.1038/s41594-024-01478-1. Creative Commons Attribution 4.0 International License. http://creativecommons.org/licenses/by/4.0/.

Lateral (**a**,**b**) views of the cryo-EM map of the supercomplex (contour level: 0.38). Shades of cyan (module SubA, NdhH–NdhO) and magenta (module SubE, NdhU) indicate the NDH peripheral arm. The membrane arm is drawn in shades of blue (module SubM, NdhA–NdhG). Lumenal SubL subunits (PnsL1–PnsL5) are shown in shades of purple, and subunits of the stromal SubB (PnsB1–PnsB5) are in shades of gray. PSI–LHC-2 is colored in shades of green. Cryo-EM densities of lipids are salmon (PG), violet (MGDG), pink (SQDG) or green (DGDG). Carotenoids are orange, and chlorophylls are bright green. The detergent belt is transparent gray.

Figure **20.3.11** below shows a proton flow model for the spinach complex—Subunits A-G form transmembrane modules. B, D, and F form antiporters subunits for H+ translocation, and each has two discontinuous helices, TMH7 and TMH12. These homologous antiporter structures are also found in mitochondrial Complex I. Subunits A, C, E, and G from the plastoquinone binding site and the early part of the proton translocation machinery.

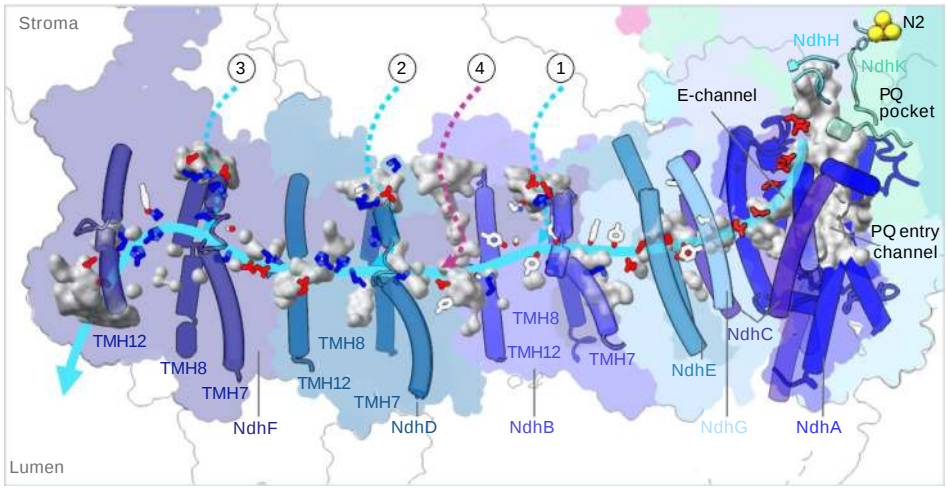
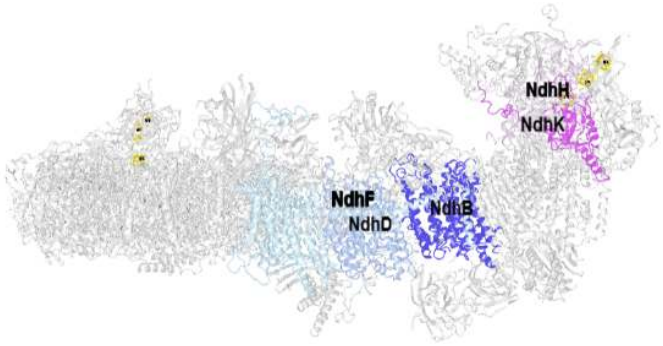


Figure **20.3.11**: Proposed proton transfer path in the membrane arm of S. oleracea NDH. Introini, B. et al., ibid.

Side view of NDH. From right to left, NdhA helices and NdhH and NdhK loops contributing to the formation of the platoquinon (PQ)-binding pocket (gray surface), NdhC TMH1–TMH2, NdhG TMH3, NdhE TMH2–TMH3, and discontinuous TMHs of NdhB, NdhD and NdhF are shown as solid cylinders. Other subunits are shown as outlines. The 4Fe–4S N2 cluster (upper right) is indicated. Charged residues of NdhA–NdhG and residues involved in proton translocation that are conserved between spinach NDH and *A. thaliana* complex I are shown as stick models and are color-coded. Positively charged residues are blue, negatively charged residues are red and key aromatic residues are white. PQ pocket, voids, channels, and depressions within NDH are likely to be relevant for proton translocation and are shown as gray surfaces. The light-blue arrow delineates a continuous hydrophilic path from the Q-binding site to NdhF. Stromal half-channels above NdhB, NdhD and NdhF are indicated as dotted cyan arrows and labeled 1–3; the channel between NdhB and NdhD (magenta) is labeled 4.

Figure **20.3.12** shows an interactive iCn3D model the complex of NDH and the PSI-LHCI-2 supercomplex from *S.* oleracea (9GRX).



NCBI iCn3D Figure **20.3.12**: **NDH–PSI–LHCI-2 supercomplex from *S. oleracea*** (9GRX) (Copyright; author via source). Click the image for a popup or use this external link: ttps://www.ncbi.nlm.nih.gov/Structur...kJXW3YGGrM9sQA

NdhP, D, and B are the antiporters involved in H^+ translocation. Ndh H and K show the region of the PQ binding pocket. Yellow highlights show FeS complexes (spacefill)

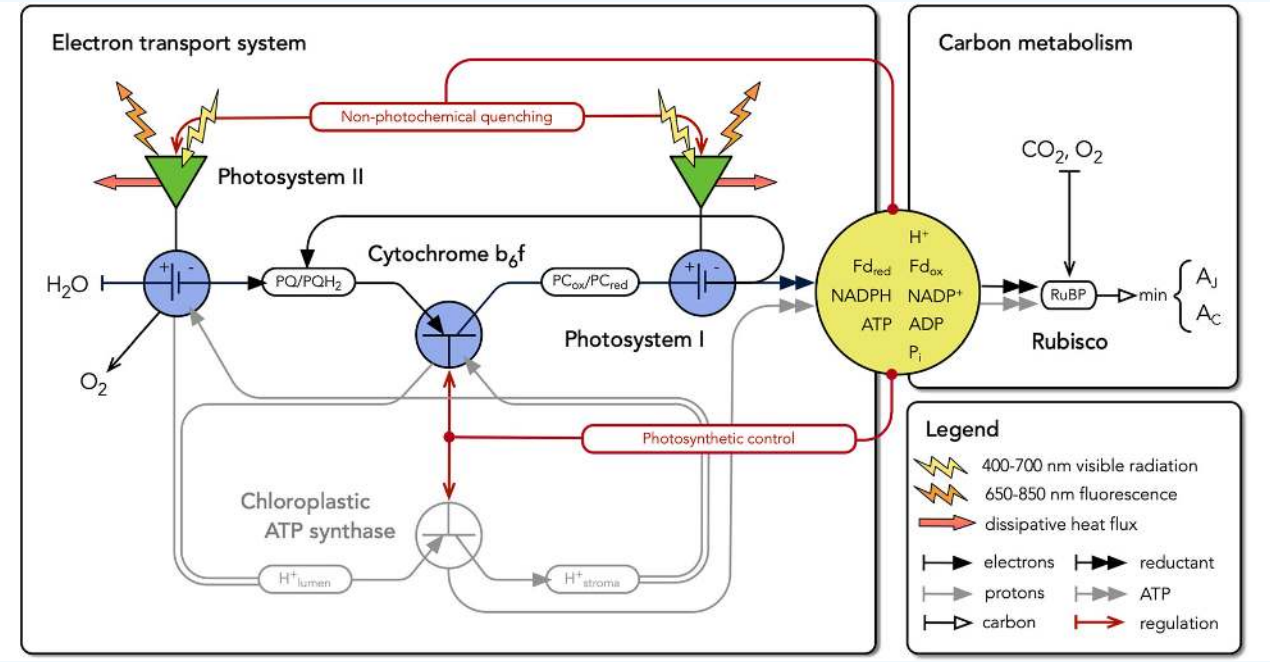
The charged side chains in Complex I involved in proton flow are also found in NDH, supporting the idea that NDH in chloroplasts and Complex I in mitochondria have identical functions resulting from homologous structures.

? REGULATION OF CYTOCHROME B_6F AND RUBISCO: A LARGE CIRCUIT BOARD

Electronic regulation of an enzyme complex

Click here

Johnson and Berry have analyzed electron flow with carbon metabolism in a fashion analogous to transistors in a circuit board, as illustrated in the figure below.



Electron transport system as an electrical circuit (and associated text below). Johnson and Berry. Photosynthesis Research (2021) 148:101–136. Creative Commons Attribution 4.0 International License. http:// creativecommons.org/ licenses/by/4.0/.

They define a transistor as a regulated circuit element that utilizes variable conductance to control the flow of current. The linear flow of electrons from water to reductant is viewed as a light-driven current under the control of many regulatory feedbacks stemming from carbon metabolism. In limiting light, Cyt b_6f presents maximal conductance to flow, and feedback from carbon metabolism adjusts the excitation of PS I and PS II in such a way as to balance the relative rates of **linear and cyclic** electron flow to the NADPH, Fd, and ATP requirements of the sinks. When the light becomes saturating, feedback from carbon metabolism also decreases the apparent conductance of Cyt b_6f, controlling the linear flow of electrons through the plastoquinone pool and the associated flow of protons into the thylakoid lumen. In this way, the regulation of Cyt b_6f simultaneously permits efficient photosynthesis and protects the system from photodamage.

This model is organized around the idea that the distribution of excitation between PS II and PS I is regulated in such a way as to minimize losses of absorbed light and maximize potential electron transport through Cyt b_6f. The expression for the potential electron transport rate has the form of a Michaelis-Menten expression for a single substrate (i.e., light). Still, it describes the kinetic behavior of the entire electron transport chain (i.e., including both photochemical and biochemical reactions). It predicts that electron transport has a hyperbolic dependence on irradiance, with maximum efficiency realized at the limit where absorbed irradiance approaches zero and maximum speed realized at the limit where absorbed irradiance approaches infinity.

The trade-off between the speed and efficiency of potential electron transport is driven by the need for the supplies of reduced plastoquinone and oxidized plastocyanin to be balanced to sustain Cyt b_6f turnover at the maximum catalytic rate. This causes progressive closure of the PS II and PS I reaction centers, with PS II accumulating in a reduced state and PS I in an oxidized state. As the excitation pressure on PS II and PS I increases, the closure of the reaction centers causes the photochemical yields of PS II and PS I, as well as the absorbed quantum yield, to decrease as the potential electron flow through Cyt b_6f and the potential photosynthetic rate increase.

The key prediction of the expression for the potential electron transport rate is that the maximum activity of Cyt b_6f defines the upper limit for the theoretical maximum speed of electron transport. The expressions describing feedback control over Cyt b_6f activity are based on the idea that Cyt b_6f functions like a transistor, i.e., a component of an electrical circuit that uses variable conductance to control the flow of current.

The fact that Cyt b_6f can modulate its conductance to linear electron flow within milliseconds of a perturbation in light suggests that photosynthetic control is the first line of defense against overexcitation, protecting the acceptor side of PS I from being flooded with highly reduced intermediates.

In response to a sustained increase in light, the induction of photosynthetic control is followed by the induction of PQ_N. As NPQ alleviates the electron overpressure in the PQ pool, photosynthetic control progressively relaxes. The two forms of regulation

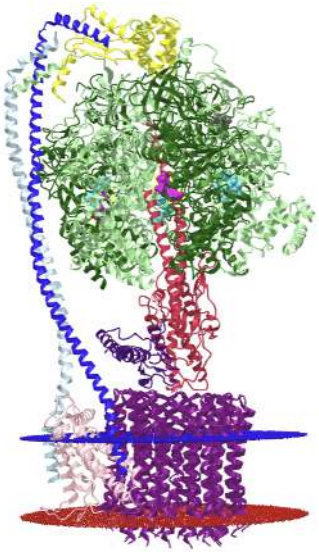
gradually settle into a steady state at the new light intensity. This interaction appears to enable electron transport to proceed at the Cyt b_6f-limited rate under low light intensities, then smoothly transitions to the Rubisco-limited rate once the light intensity is high enough to become saturating. It also appears to enable photosynthesis to operate safely and efficiently in a wide range of biochemical environments, from those characteristic of natural variation in photosynthetic capacity (with balanced electron transport and carbon metabolism) to those resulting from genetic manipulations (with imbalances in electron transport and carbon metabolism).

In this framework, the excitation balance of PS II and PS I, as well as the maximum activities of Cyt b_6f and Rubisco, emerge as key limits on system dynamics. For example, the trade-off between the speed and efficiency of electron transport is shown to be controlled by the excitation balance of PS II and PS I, as well as the maximum activity of Cyt b_6f. The development of PQ_N is shown to be controlled by the excitation balance of PSII and PSI, as well as the demand for linear electron flow (LEF) through the light reactions and circular electron flow (CEF) around PSI. The onset of photosynthetic control depends on the maximum activities of Cyt b_6f and Rubisco.

20.3.4: CHLOROPLAST ATP SYNTHASE - CF_1F_OATPASE

Finally, let's look at the ATP synthase in chloroplasts. It is similar in structure and function to mitochondrial FoF1ATPase so we won't spend much time on the mechanism. Like its mitochondrial counterpart, it is a rotary enzyme that transduces the free energy of a proton gradient collapse into chemical energy in the form of ATP. One difference is that light levels should regulate the rotary enzyme, decreasing its activity at night. This is accomplished in higher plants by conversion between a reduced and oxidized state, an effective redox switch, in one subunit (γ) of the ATP synthase. Deactivation is important at night, as if the rotary enzyme runs in reverse, ATP hydrolysis will occur.

Figure 20.3.13 shows an interactive iCn3D model of the reduced R1 state of chloroplast ATP synthase (R1, CF1FO) (6VON). It should look familiar to you given its similarity to mitochondrial ATP synthase.



NCBI iCn3D Figure 20.3.13: Reduced R1 state of chloroplast ATP synthase (R1, CF1FO) (6VON) (Copyright; author via source). Click the image for a popup or use this external link: https://www.ncbi.nlm.nih.gov/Structu...HT8YZefdWN5XM7 (long load)

- alpha - light green
- beta - dark green
- gamma - yellow
- gamma - crimson
- epsilon - indigo
- b - blue
- b' - light blue
- a - light pink
- c ring - purple
- ATP - spacefill, cyan
- TENTOXIN (TTX) - space fill gray
- ADP - spacefill magenta

In the oxidized state, a disulfide in the γ subunit inhibits torsion by stabilizing two β hairpins. This constraint is relieved on reduction, and rotation is enhanced. In the reduced structure, tentoxin, an uncompetitive inhibitor, is present, which allowed the structure to be determined.

below Yang, JH., Williams, D., Kandiah, E. *et al.* Structural basis of redox modulation on chloroplast ATP synthase. *Commun Biol* **3,** 482 (2020). https://doi.org/10.1038/s42003-020-01221-8. Creative Commons Attribution 4.0 International License. http://creativecommons.org/licenses/by/4.0/.

At night, the enzyme is in the low-activity form. When light becomes available in the day, the pH gradient collapse leads to the release of tightly bound ATP from the oxidized state of the enzyme. PSI can engage in photon-induced electron transfer to ferredoxin. This binds to NADP reductase, leading to the formation of NADPH. These processes are illustrated in Figure **20.3.14**.

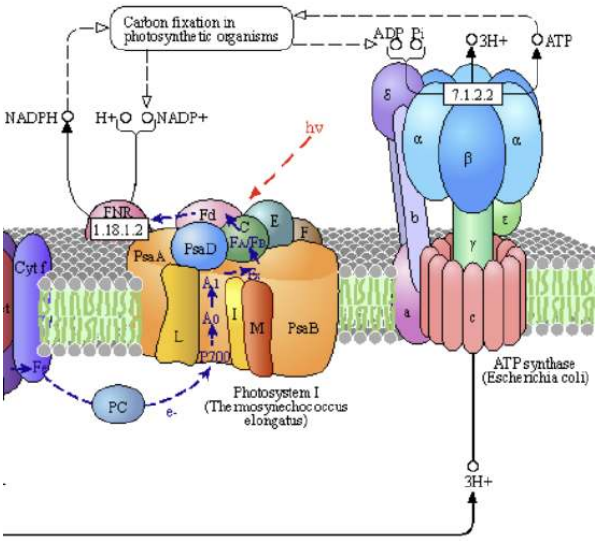


Figure **20.3.14**: Fd bound to PSI is ferredoxin, and FNP is ferredoxin NADP reductase.

Increased reduced ferredoxin leads to the formation of reduced thioredoxin, a small redox protein involved in redox signaling and protection of cells from oxidative stress. A similar process activates the enzyme sedoheptulose-1,7-bisphosphatase (SBPase), found in the dark reaction of the Calvin cycle in photosynthesis. Its activation is illustrated in Figure **20.3.15**.

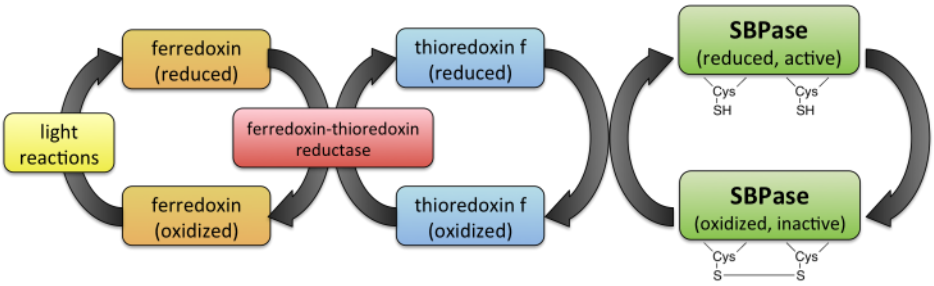


Figure **20.3.15**: SBPase regulation by ferredoxin-thioredoxin system. https://commons.wikimedia.org/wiki/F...xin_system.png. Creative Commons Attribution-Share Alike 3.0 Unported l

Reduced thioredoxin also reduces and activates chloroplastic ATP synthase.

Figure **20.3.16** the activities and structures of the ATP synthase (CF_1F_O)

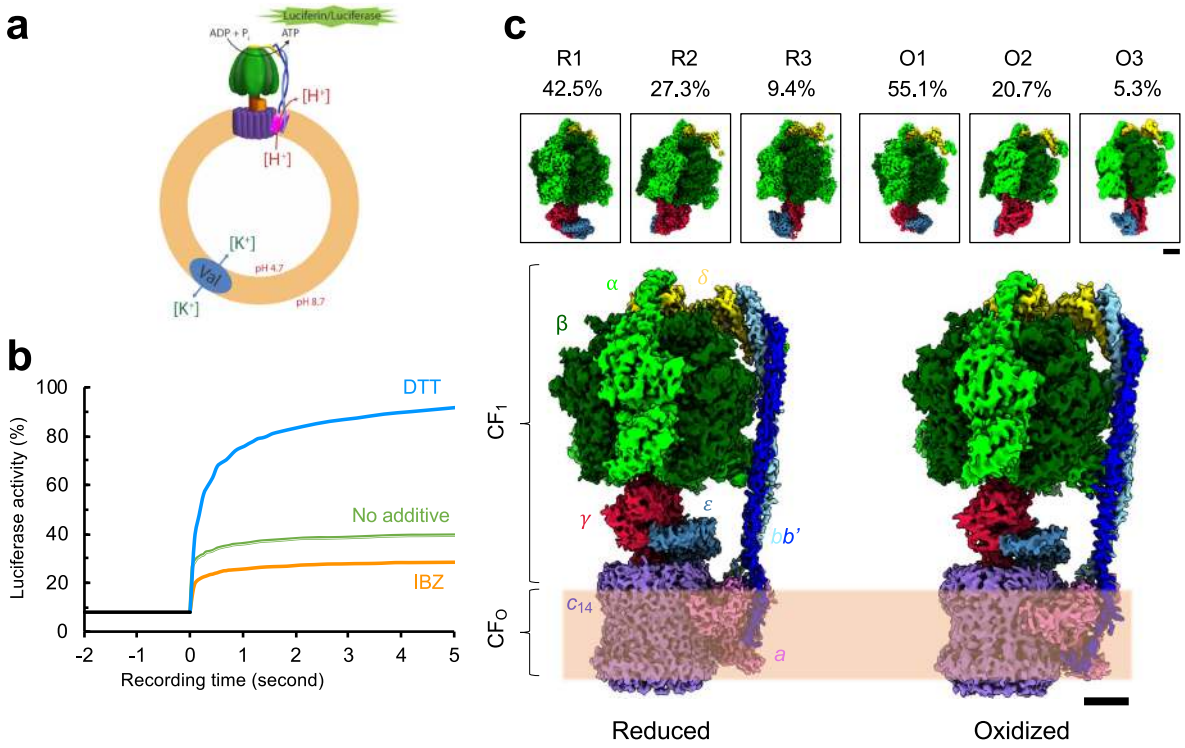


Figure **20.3.16** the activities and structures of the ATP synthase (CF_1F_O). Yang, JH., Williams, D., Kandiah, E. *et al*. Structural basis of redox modulation on chloroplast ATP synthase. *Commun Biol* **3,** 482 (2020). https://doi.org/10.1038/s42003-020-01221-8. Creative Commons Attribution 4.0 International License. http://creativecommons.org/licenses/by/4.0/.

Panel a: For the experiments, purified CF_1F_O was reconstituted into a liposome (orange) mixed with phosphatidylcholine and phosphatidic acid lipids. The generated pH gradient across the membrane drove the reconstituted CF_1F_O to synthesize ATP molecules, which were detected using a luciferin/luciferase assay (green). Val indicates valinomycin.

Pane b: The activity of the enzyme is shown in the reduced state (in the presence of dithiothreitol - DTT, blue curve), oxidized state (in the presence of iodosobenzoate - IBZ, orange curve, and with no additive (green curve). Note that the activity is reduced by about 80% in the oxidized state.

Panel c: The images are from Cryo-EM density maps of the oxidized and reduced forms of the CF_1F_O. The color codes are as follows: α (light green), β (dark green), δ (yellow), *bb'* (blue and light blue), γ (crimson), ε (indigo), *a* (light pink), and *c* ring (purple). R indicates a reduced state, and O indicates an oxidized state. The three-dimensional (3D) reconstructions are categorized into three rotary states (1, 2, and 3). The upper insets are the density maps of the F_1 domains.

Figure **20.3.17** shows the conformation changes in the γ subunit between the oxidized and reduced forms.

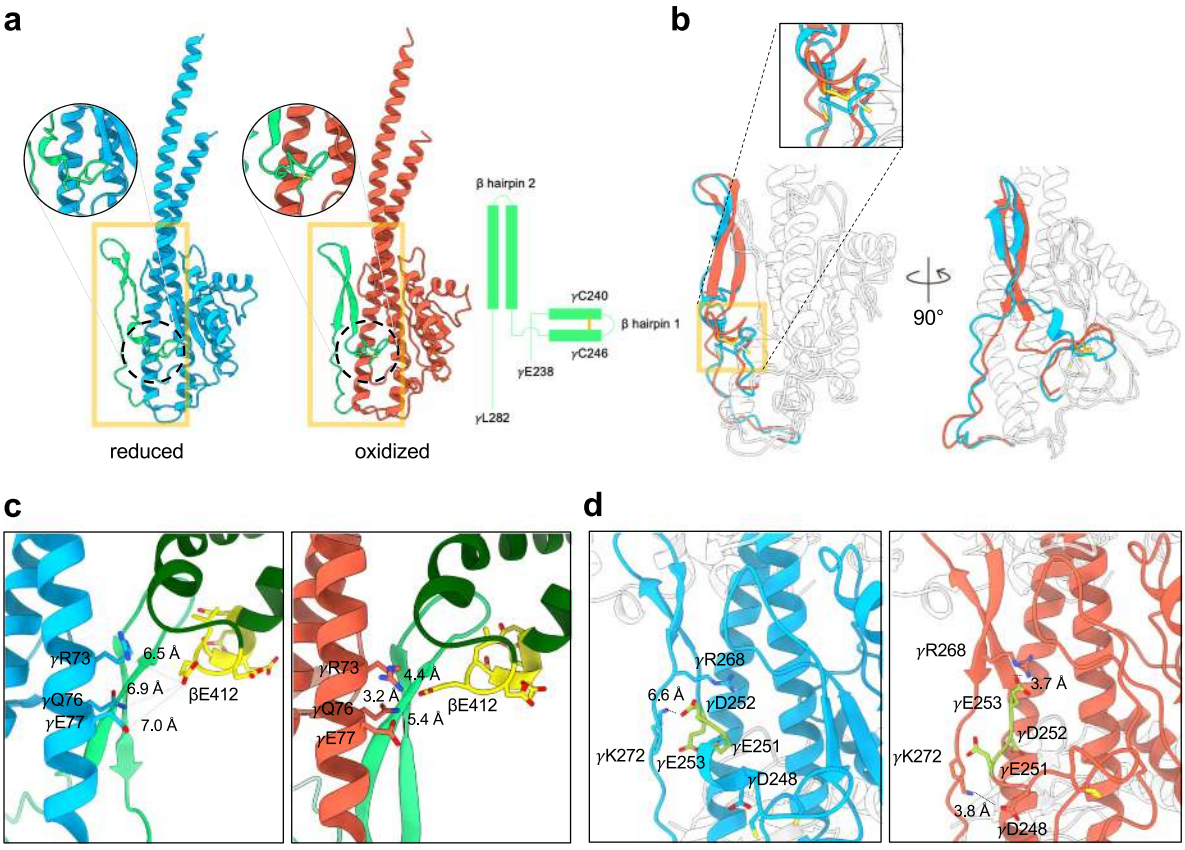


Figure **20.3.17**: Conformation changes in the γ subunit between the oxidized and reduced forms, Yang, JH., Williams, D., Kandiah, E. *et al. Ibid.*

Panel a: Structures of the reduced (light blue) and oxidized (orange) γ subunits. Two β hairpin structures (from γGlu238 to γLeu282) are shown in light green, and the two cysteines of the redox switch are shown in yellow in circular, enlarged views. The diagram on the right shows the topology of the two β hairpin structures.

Panel b Superposition of the reduced and oxidized γ subunits (RMSD 1.016 Å). The two β hairpins are shown in light blue and orange for the reduced and oxidized forms, respectively. Other regions are shown in white.

Panel c Interaction networks of the β hairpin 2 and βDELSEED motif. The left and right panels are the reduced (γ subunit in light blue) and oxidized (γ subunit in orange) forms. Light green represents the β hairpin 2, dark green for the β subunit, and yellow for the βDELSEED motif. The distances connecting the residues of the γ coiled-coil (γArg73, γGln76, and γGlu77) with the βGlu412 are labeled.

Panel d Interaction of the EDE motif with the γ subunit. The EDE motif (yellow) does not interact with any part of the reduced γ subunit but forms an extensive interaction network with its neighborhood when the γ subunit is oxidized.

Figure **20.3.18** shows a cartoon model illustrating the structures of the overall oxidized and reduced states of ATP synthase

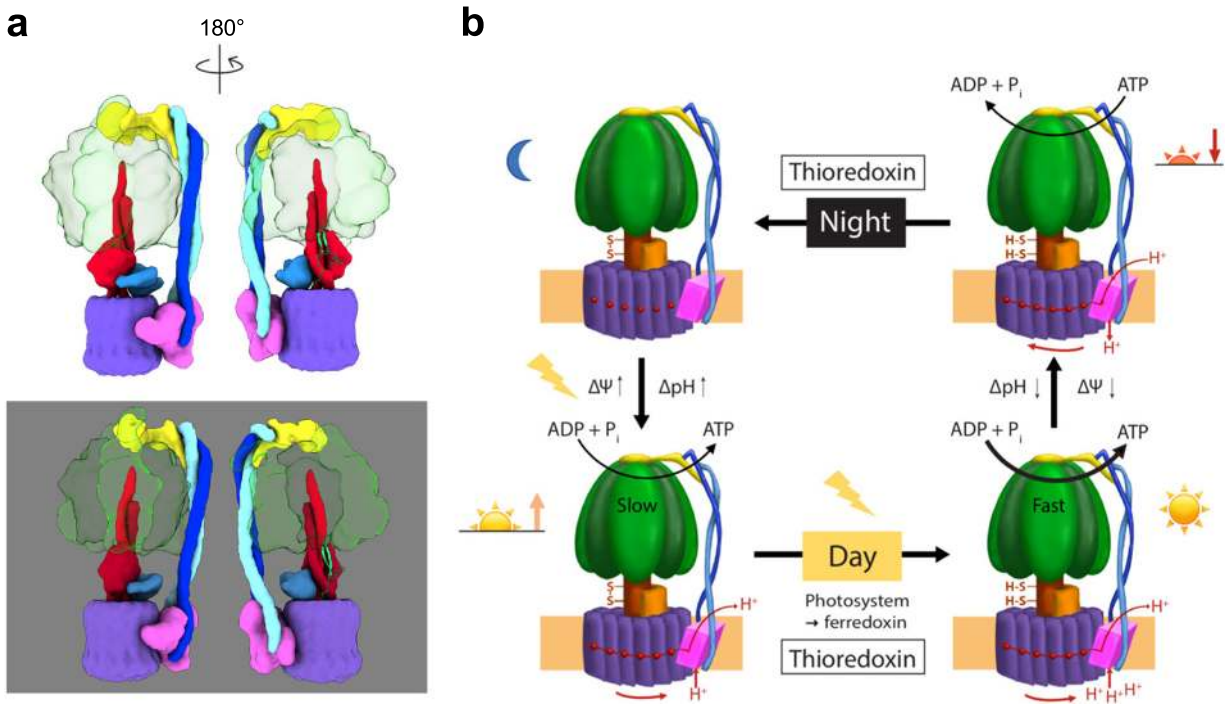


Figure **20.3.18**: Cartoon model illustrating the structures of the overall oxidized and reduced states of ATP synthase. Yang, JH., Williams, D., Kandiah, E. *et al. Ibid.*

Panel a: This shows a cartoon schematic of the redox modulation. The upper and lower models are the reduced and oxidized states, respectively. Color codes are the same as in Fig. 1c, and the β hairpin structures of the γ subunit are shown in light green. The two redox states are aligned in the same view.

Pane b: At night, no energy input from light is available for the photosynthetic electron transport chain, and thus, no electrochemical potential (ΔΨ) and proton gradient (ΔpH) are generated. The oxidized γ subunit prevents CF_1F_O from hydrolyzing ATP. During the day, light induces charge separation, developing an electrochemical potential across the membrane. Although the CF_1F_O begins to synthesize ATP molecules, the γ subunit is still oxidized while ΔΨ is small. The rate of ATP synthesis is not at its maximum. At sunrise, thioredoxin subsequently reduces the γ subunit, fully activating CF_1F_O. The molecular motor, consisting of the γ-ε central shaft and the c_{14}-ring, can rotate at full speed to maximize its ATP synthesis activity. Three ATP molecules per rotation of the c_{14} ring are produced. At sunset, the membrane becomes de-energized, resulting in small ΔΨ and ΔpH, and ATP hydrolysis occurs. To prevent ATP loss from excess ATP hydrolysis, the γ subunit is then oxidized again. Light regulation and redox modulation on the CF_1F_O will cycle daily.

20.3.5: SUMMARY

This chapter integrates detailed mechanistic insights and structural perspectives of the photosynthetic electron transport chain, emphasizing both linear and cyclic pathways. Designed for junior and senior biochemistry majors, the chapter provides an in-depth look at the flow of electrons and protons that drive energy conversion in chloroplasts.

Key Points:

- **Linear Electron Flow:**
  - Electrons are sequentially transferred from PSII through a series of mobile carriers—plastoquinone, cytochrome b6f, plastocyanin, and ferredoxin—to PSI.
  - The terminal acceptor, $NADP^+$, is reduced to NADPH, which along with ATP, fuels the reductive biosynthesis of glucose during the Calvin cycle.
  - This electron movement is coupled to the translocation of protons, establishing an electrochemical gradient that powers ATP synthase.
- **Cytochrome b6f Complex and the Q Cycle:**
  - The cytochrome b6f complex serves as a critical, rate-limiting step in the electron transport chain.
  - It employs a Q cycle mechanism to transfer electrons from reduced plastoquinol to plastocyanin, simultaneously contributing to the proton gradient.

- Structural models illustrate the complex's organization, including its dimeric nature and key prosthetic groups (e.g., Fe2S2 clusters, various hemes).

- **Photosystem I (PSI) and the PSI-LHCI Supercomplex:**
  - PSI exhibits near-unity quantum efficiency by converting absorbed photon energy directly into electrons.
  - The PSI-LHCI supercomplex features an extensive network of chlorophylls and carotenoids that extend its absorption into the far-red region.
  - The dynamic association of light-harvesting complexes (LHCs) between PSI and PSII is modulated by phosphorylation, optimizing energy distribution based on light conditions.
- **Cyclic Electron Flow and NDH Complex:**
  - Under certain physiological conditions, electrons from PSI are redirected in a cyclic pathway via the NDH complex back to the plastoquinone pool.
  - This process, which bypasses $NADP^+$ reduction, enhances ATP production and helps balance the cellular NADPH/ATP ratio.
  - The NDH complex shares structural and mechanistic similarities with mitochondrial Complex I, further emphasizing the conservation of energy conversion strategies.
- **Regulation of Electron Transport and Carbon Metabolism:**
  - The chapter presents an analogy of the electron transport chain as an "electronic circuit board," where cytochrome b6f acts like a transistor, adjusting its conductance in response to light intensity.
  - Feedback mechanisms link the redox state of the plastoquinone pool and the phosphorylation status of LHCs to optimize the balance between electron flow and carbon fixation.
- **Chloroplast ATP Synthase (CF1FO):**
  - Similar to its mitochondrial counterpart, the CF1FO ATP synthase operates as a rotary enzyme that synthesizes ATP by harnessing the proton motive force.
  - Its activity is tightly regulated by redox modulation, primarily via conformational changes in the γ subunit, ensuring that ATP hydrolysis does not occur during periods of low light.
  - Structural models highlight the conformational differences between the oxidized and reduced states of the enzyme, linking these changes to functional regulation.

Overall, the chapter provides a comprehensive view of how structural components and regulatory mechanisms are interwoven to ensure efficient and safe photosynthetic energy conversion. This integration of biophysical, biochemical, and structural data illustrates the complexity of photosynthetic regulation and its adaptation to varying environmental conditions.

This page titled 20.3: Plant Electron Transport and ATP Synthesis is shared under a not declared license and was authored, remixed, and/or curated by Henry Jakubowski and Patricia Flatt.

- **Current page** by Henry Jakubowski and Patricia Flatt has no license indicated.
- **11.2: Diffusion Across a Membrane - Passive and Facilitated Diffusion** by Henry Jakubowski and Patricia Flatt has no license indicated.

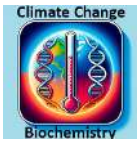
20.4: CO_2 UPTAKE - CALVIN CYCLE AND C3 ORGANISMS

LEARNING GOALS (CHATGPT O3-MINI)

- **Differentiate Between Light and Dark Reactions:**
  • Explain the overall flow of energy from the light reactions (which produce ATP, NADPH, and O_2) to the dark reactions (which fix CO_2 into carbohydrates).
  • Describe why the term “dark reactions” is used despite these reactions occurring in the light.
- **Outline the Calvin (C3) Cycle:**
  • Describe the three phases of the Calvin cycle—carbon capture (CO_2 fixation), reduction (conversion of 3PG to G3P), and regeneration (reformation of RuBP)—and how they combine to produce triose phosphates for carbohydrate synthesis.
  • Explain the stoichiometry of the cycle, including the overall consumption of ATP and NADPH per CO_2 fixed.
- **Examine the Role and Mechanism of RuBisCo:**
  • Detail the dual enzymatic activities (carboxylase and oxygenase) of Rubisco and explain how it catalyzes the fixation of CO_2 into ribulose 1,5-bisphosphate (RuBP) to yield 3-phosphoglycerate.
  • Discuss the structural composition of Rubisco, including the large (chloroplast-encoded) and small (nucleus-encoded) subunits, and how multimer formation (e.g., the Rubiscosome) influences its catalytic efficiency.
- **Understand Rubisco's Limitations and the Problem of Photorespiration:**
  • Explain the competitive oxygenase activity of Rubisco that leads to the formation of 2-phosphoglycolate and 3-phosphoglycerate, outlining the factors (e.g., CO_2 and O_2 concentrations, temperature) that affect this competition.
  • Discuss the kinetic parameters (KM for CO_2 vs. O_2) of Rubisco and how these contribute to the enzyme’s reduced efficiency under current atmospheric conditions.
- **Describe the Glycolate (Photorespiration) Pathway:**
  • Outline the steps of the glycolate salvage pathway, including the conversion of 2-phosphoglycolate to glycine, the subsequent formation of serine, and the regeneration of 3-phosphoglycerate.
  • Discuss the cellular compartments involved in photorespiration (chloroplast, peroxisome, mitochondria) and the overall energetic cost of the process.
- **Explore Plastid Diversity and Interconversion:**
  • Identify different types of plastids (e.g., chloroplasts, amyloplasts, etioplasts, chromoplasts) and explain their roles in photosynthesis and storage.
  • Describe the process of “greening” (conversion of proplastids or etioplasts to chloroplasts) and “de-greening” (transition to leucoplasts or gerontoplasts) in response to developmental cues and environmental signals.
- **Understand Metabolite Exchange and Carbon Partitioning:**
  • Explain the function of the triose phosphate/phosphate translocator (TPT) in exchanging triose phosphates from the chloroplast with inorganic phosphate (Pi) from the cytosol, and its role in balancing carbohydrate synthesis and energy production.
  • Describe how the products of the Calvin cycle are used in the cytosol for the synthesis of sucrose and other metabolites.
- **Connect CO_2 Fixation to Global Carbon Cycling and Climate Impacts:**
  • Discuss the role of Rubisco in capturing atmospheric CO_2 and its significance for global primary production.
  • Evaluate how changes in atmospheric CO_2 concentrations and rising global temperatures might influence Rubisco’s carboxylase versus oxygenase activities, with implications for plant productivity and nutrient content.
- **Analyze Experimental Approaches and Data Interpretation:**
  • Interpret data from deuterium NMR studies that examine changes in isotopomer ratios (e.g., D6S/D6R) of photosynthetically generated glucose, linking these changes to shifts in Rubisco’s activity under different CO_2 levels.
  • Discuss how kinetic measurements and structural studies (including iCn3D models) contribute to our understanding of Rubisco’s function and regulation.

These learning goals aim to provide a comprehensive framework for understanding how the dark reactions of photosynthesis integrate with light reactions, the critical role of Rubisco in CO_2 fixation, and the challenges posed by photorespiration, all within the broader context of plant metabolism and environmental impact.

The source for the organization and some of the text derives from: Sindayigaya and Longhini. https://www.peoi.org/Courses/Courses...chem/biochem18 CC - https://creativecommons.org/licenses...sa/3.0/deed.en



Everything in the chapter is related to climate change. For more general information on biochemistry and climate change, visit Chapter 32 Biochemistry and Climate Change. For more details on carbon fixation or capture, visit Chapter 32.16: Part 4 - Fixing Carbon Fixation.

20.4.1: INTRODUCTIONS

We focused on the light reactions of photosynthesis. Now, let's turn our attention to the dark reactions, which fix CO_2 from the air and reduce it with NADPH produced, along with O_2, in the light reactions, to produce carbohydrates. The dark reactions don't just occur in the dark. The term differentiates them from the light-driven reactions using PSII and PSI. What is so interesting about plants is that they produce fuel from CO_2 using photons as a source of energy (autotrophs) and consume the fuel they make, using both anaerobic and aerobic respiration pathways. Their biosynthetic reactions occur mostly in the chloroplast, a type of plastid, a subcellular organelle with specific functions such as photosynthesis or metabolite synthesis and storage. Plants also can not move to acquire fuel and nutrient molecules. They are subject to many growing conditions (differential light qualities and quantities, temperatures, and rainfall levels). Also, plant cells have cell walls in addition to a cell membrane. Figure **20.4.1** shows a simple cartoon showing the major photosynthesis motifs.

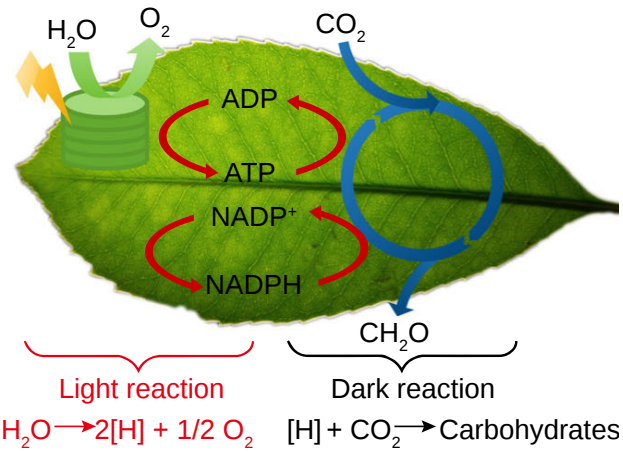


Figure **20.4.1**: **a** Schematic depiction of the light and dark reactions in natural photosynthesis. Li, Y., Hui, D., Sun, Y. *et al*. Boosting thermo-photocatalytic CO_2 conversion activity by using photosynthesis-inspired electron-proton-transfer mediators. *Nat Commun* **12,** 123 (2021). https://doi.org/10.1038/s41467-020-20444-1 Creative Commons Attribution 4.0 International License.

In this section, we will discuss how CO_2 from the atmosphere is "fixed" or "captured" in the formation of the simplest sugars (3 carbon molecules like glyceraldehyde-3-phosphate) in a process called the **C3 or Calvin Cycle**, which is also called the Calvin–Benson–Bassham (CBB) cycle, or the reductive pentose phosphate cycle (RPP cycle). Plants that utilize the C3 cycle are referred to as C3 plants. There are two other major types of carbon capture pathways, the C4 and CAM pathways, which we discuss in the next section. All use a key enzyme, **ribulose 1,5-bisphosphate carboxylase (RuBisCo)**, to covalently fix CO_2 into small carbohydrates, 3-phosphoglycerate. **RuBisCo** is the most abundant protein in the biosphere. Recent estimates suggest that there are approximately 0.7 gigatons (Gt = 10^{12} tons) of it, with over 90% in the leaves (about 3% of their weight) of terrestrial plants. It captures about 120 Gt of atmospheric CO_2 each year. This enzyme has a second competing enzymatic activity. It is also an **oxygenase**, which fixes O_2 at the active site, decreasing its ability to fit O_2. That activity captures about 100 Gt of atmospheric O_2 each year. Hence, the enzyme is often referred to as **ribulose 1,5-bisphosphate carboxylase/oxidase** (but still abbreviated as RuBisCo).

We will devote most of this chapter section to this most important enzyme. Along with RuBisCo, plants have pathways to convert the fixed CO_2 to 3C sugars and then through a unique pentose pathway, which runs in a reductive fashion, ultimately produce the sugar-containing molecules in plants we are most familiar with: sucrose and the glucose polymer starch.

20.4.2: PLASTIDS

There are several types of these organelles. Photosynthesis occurs in chloroplasts, which have their own genome, similar to that of mitochondria. Another common type is the amyloplast, which lacks pigmented molecules (i.e., it is colorless) and has no inner membrane. Rather, they are filled with starch. Chloroplasts and amyloplasts can interconvert. Chloroplasts are abundant in green leaves, while

amyloplasts are predominantly found in locations like potato tubers, where starch is stored. Light can drive the interconversion of plastids, as shown in Figure **20.4.2**.

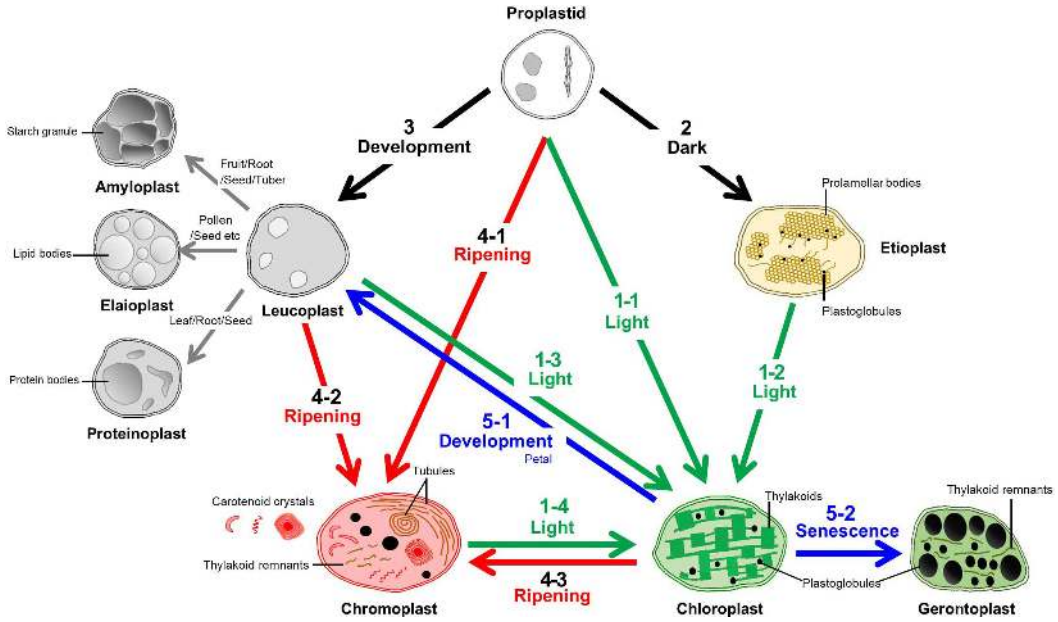


Figure **20.4.2**: Transition pathways among various plastids. Choi et al. Frontiers in Plant Science. 12 (2021). https://www.frontiersin.org/article/...ls.2021.692024. DOI=10.3389/fpls.2021.692024 . **Creative Commons Attribution License (CC BY)**

Arrows show the characteristics and plastid interconversion pathways of the plastids. The transition to a chloroplast is called “Greening” and is identified with the number “1”. This transition is mainly triggered by light signals from proplastids, etioplasts, leucoplasts, and chromoplasts. Etioplasts can develop from proplastids in dark conditions, as indicated by the number “2”. The number “3” indicates leucoplast development triggered by diverse development processes to generate starch, lipid, and protein-enriched sub-types called amyloplasts, elaioplasts, and proteinoplasts, respectively. Mainly during the ripening stage, diverse types of carotenoid crystals were generated within the plastids called chromoplasts from the proplastids, leucoplasts, and chloroplasts, and this is identified with the number “4”. Together with etioplast and leucoplast development (2,3), chromoplast development (4) was identified as a “Non-greening” plastid transition. The loss of green color from the chloroplasts is called “De-greening”. It is identified by the number “5”, and these chloroplasts are then transitioned into leucoplasts or gerontoplasts by developmental regulation or during senescence, respectively.

20.4.3: CO_2 CAPTURE AND THE C3 CYCLE

These processes are used in the synthesis of the simplest carbohydrates (3-carbon polyhydroxy aldehydes and ketones):

1. Carbon capture or fixation phase. We prefer the term carbon capture, as it is now used to describe how the world is seeking new ways (other than planting billions of trees) to "capture" excess CO2 emitted through the burning of fossil fuels. In a reaction catalyzed by RuBisCo, atmospheric CO_2 ultimately reacts with a 5-carbon acceptor molecule, ribulose 1,5-bisphosphate (Ru1,5-BP, six carbons in total), to form two molecules of 3-phosphoglycerate (3PG), which contains three carbons.
2. Reduction phase: 3-phosphoglycerate is reduced to glyceraldehyde-3-phosphate (G3P). Three CO_2s are captured on reaction with 3 Ru1,5-BP to form 6 glyceraldehyde-3-phosphates (G3P). These can readily interconvert to the keto form, dihydroxyacetone phosphate (DHAP).
3. Regeneration phase: Five of the six G3Ps (15 Cs) react to form 3 three molecules of ribulose 1,5-bisphosphate (15 C2) to allow the catalytic C3 cycle to continue. The other G3P moves into the stroma as DHAP, which can be utilized in gluconeogenesis (the reductive biosynthesis of glucose). This can be converted to polymer starch and the disaccharide sucrose (which we will discuss in a future session).

An overview of the Calvin or C3 cycle is shown below in Figure **20.4.3**.

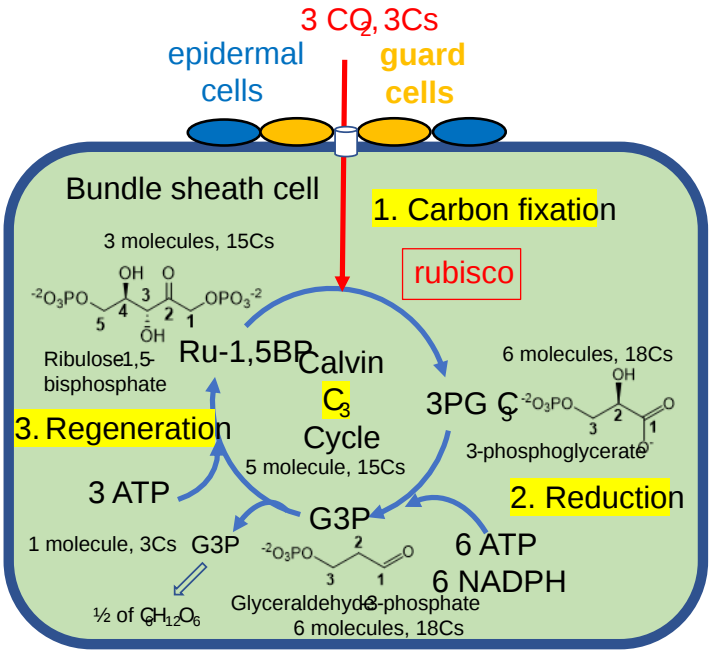


Figure **20.4.3**: C3 or Calvin Cycle. The three stages of the cycle in C3 plants and organisms are shown. Three CO_2s are captured for the net synthesis of one molecule of glyceraldehyde 3-phosphate.

The stoichiometry can be confusing until you count the number of carbon atoms and realize that the cycle must run three times to enable the production of three carbon atoms from three CO_2 molecules, resulting in one net glyceraldehyde-3-phosphate (G3P). The G3P leaves the C3 cycle at the low left for glucose synthesis. The conversion of the 5 G3Ps that reform Ru1,5-BP requires ATP, as shown below:

$$\mathbf{5\,glyceraldehyde\text{-}3\,P + 3\,ATP \longrightarrow 3\,ribulose\text{-}1,5 - 2\,P + 3\,ADP + 2\,P_i}$$

with $\mathbf{P_i}$ indicating inorganic phosphate. Hence, the net equation for three turns of the cycle, sufficient to produce one G3P is:

$$\mathbf{3\,CO_2 + 6\,NADPH + 6\,H^+ + 9\,ATP + 5\,H_2O \longrightarrow glyceraldehyde\text{-}3\text{-}phosphate\ (G_3P) + 6\,NADP^+ + 9\,ADP + 8\,P_i}$$

Even though glucose is not a product of the Calvin cycle, some texts use the following equation to show the stoichiometry to run the C3 cycle enough times (6) to fix 6 $\mathbf{CO_2}$ molecules, enough to make 1 glucose from a simple carbon atom counting perspective.

$$\mathbf{6\,CO_2 + 12\,NADPH + 12\,H^+ + 18\,ATP + 10\,H_2O \longrightarrow 2\,glyceraldehyde\text{-}3\text{-}phosphate\ (G_3P) + 12\,NADP^+ + 18\,ADP + 16\,P_i}$$

Remember that NADPH and ATP are produced in the light reactions in about the same ratio used in the C3 cycle (2NADPH/3ATPs). The net 8 P_is made as products will react with 8 ADP to regenerate 8 ATP in the light reaction. The 9th Pi is incorporated in a triose-phosphate in the light reaction, so one Pi must be imported from the cytoplasm by an inner membrane triose-phosphate/phosphate translocator, which we will discuss below. In the dark, when ATP and NADPH are not produced, CO_2 capture is also inhibited.

A more detailed diagram showing the detailed reactions to regenerate ribulose 1,5-bisphosphate (Ru1,5BP) is shown in Figure **20.4.4**.

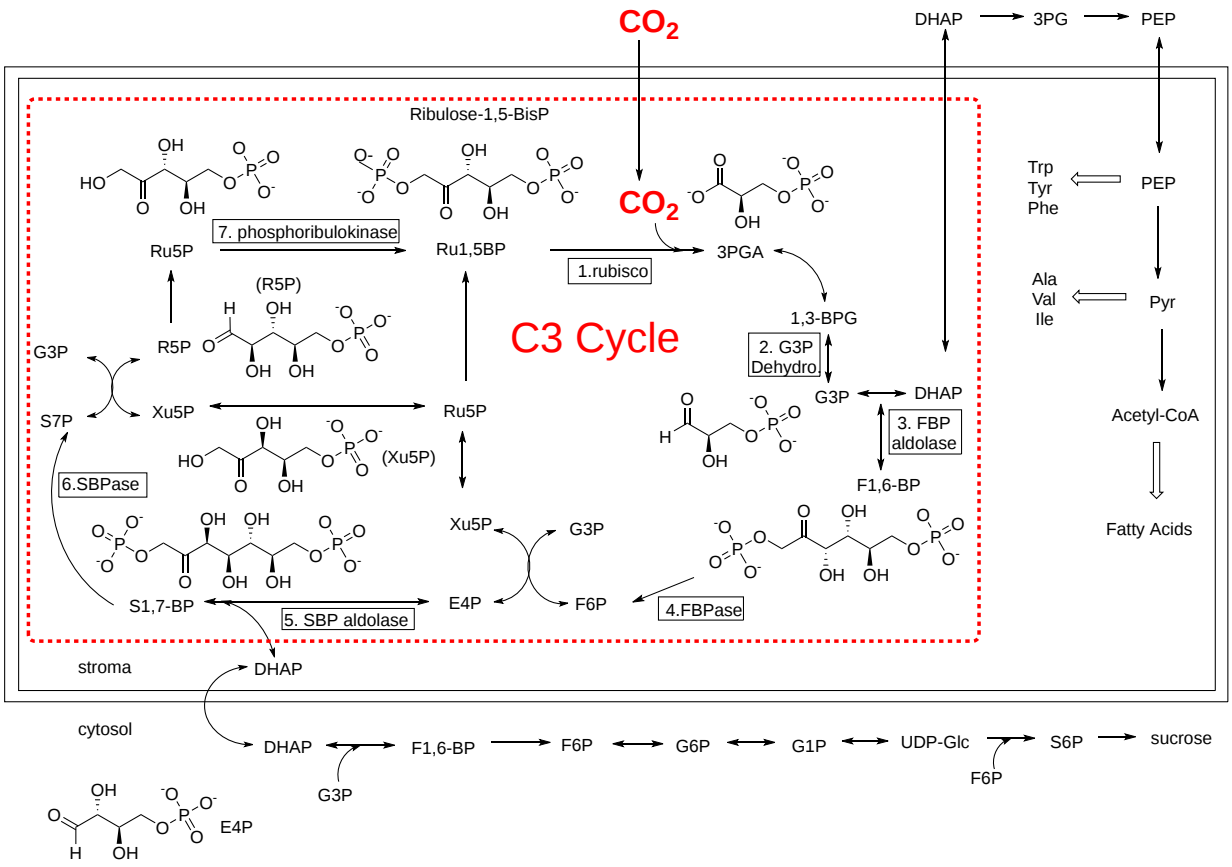


Figure **20.4.4**: Detailed reaction diagram for the Calvin (C3) cycle (after Hashunuma et al. Journal of Experimental Botany, 61 (2010). doi:10.1093/jxb/erp374. Creative Commons Attribution Non-Commercial License (http://creativecommons.org/licenses/bync/2.5)

Abbreviated reactions for synthesizing sucrose, glucogenic amino acids, and fatty acids are also shown.

You should note the reactions for the conversion of the 6C sugar molecule fructose-6-P (F6P) (glycolytic and gluconeogenic intermediate) to the 5C molecule Ru5P and Ru1-5BP are analogous to the reactions of the nonoxidative part of the pentose phosphate pathway (PPP), which generates 5C sugars for the synthesis of nucleotides, nucleic acids, and some amino acids. Hence, we won't discuss them further.

20.4.4: CARBON CAPTURE OF CO_2 INTO 3-PHOSPHOGLYCERATE - RUBISCO

This key enzyme requires a Mg^{2+} ion and proceeds through a carbamoylated lysine side chain, which acts as an "activator CO_2". The Mg^{2+} ion orients key side chains. The resulting 6C molecule cleaves into two molecules of 3PG.

Rubisco is composed of two proteins: a large subunit (around 55 kDa) whose gene is located in the chloroplast, and a small subunit (around 12 kDa) whose genes are found in the nucleus. The large chain, which dimerizes, binds the ribulose-1,5-bisphosphate substrate between monomers in the dimer. Four dimers of the large chain (8 subunits) interact with eight small chains to form a 16-mer in cyanobacteria, red and brown algae, and higher plants. Multimeric units other than 16 are also found, with the large chain dimer being the smallest active unit.

Rubiscos exist in 4 forms:

- Form I: The 16-mer described above
- Form II: Multimers of the large chain dimer, $(L_2)_n$, where n = 1-4
- Form III: Archaeal L_2 or $(L_2)_5$
- Form IV: Rubisco-like protein with no CO_2 or O_2 fixing activities

Figure **20.4.5** shows an interactive iCn3D model of spinach ribulose-1,5-bisphosphate carboxylase/oxygenase (8RUC). The eight large subunits are colored in varying shades of magenta/purple. The eight small subunits are in varying shades of cyan.

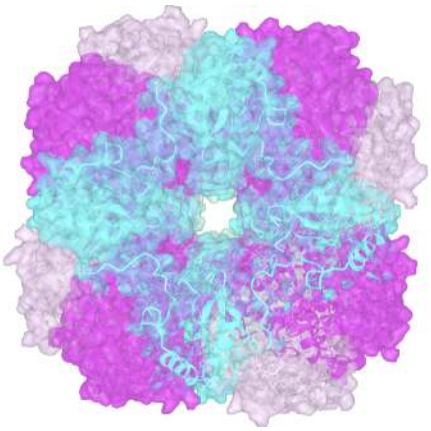


Figure **20.4.5**: Spinach ribulose-1,5-bisphosphate carboxylase/oxygenase (8RUC). (Copyright; author via source). Click the image for a popup or use this external link: https://www.ncbi.nlm.nih.gov/Structu...X2s7BDc8xQ5r19. (Long load time)

A possible mechanism of RuBisCo from *Synechococcus elongatus*, a unicellular cyanobacterium, is shown in Figure **20.4.6**.

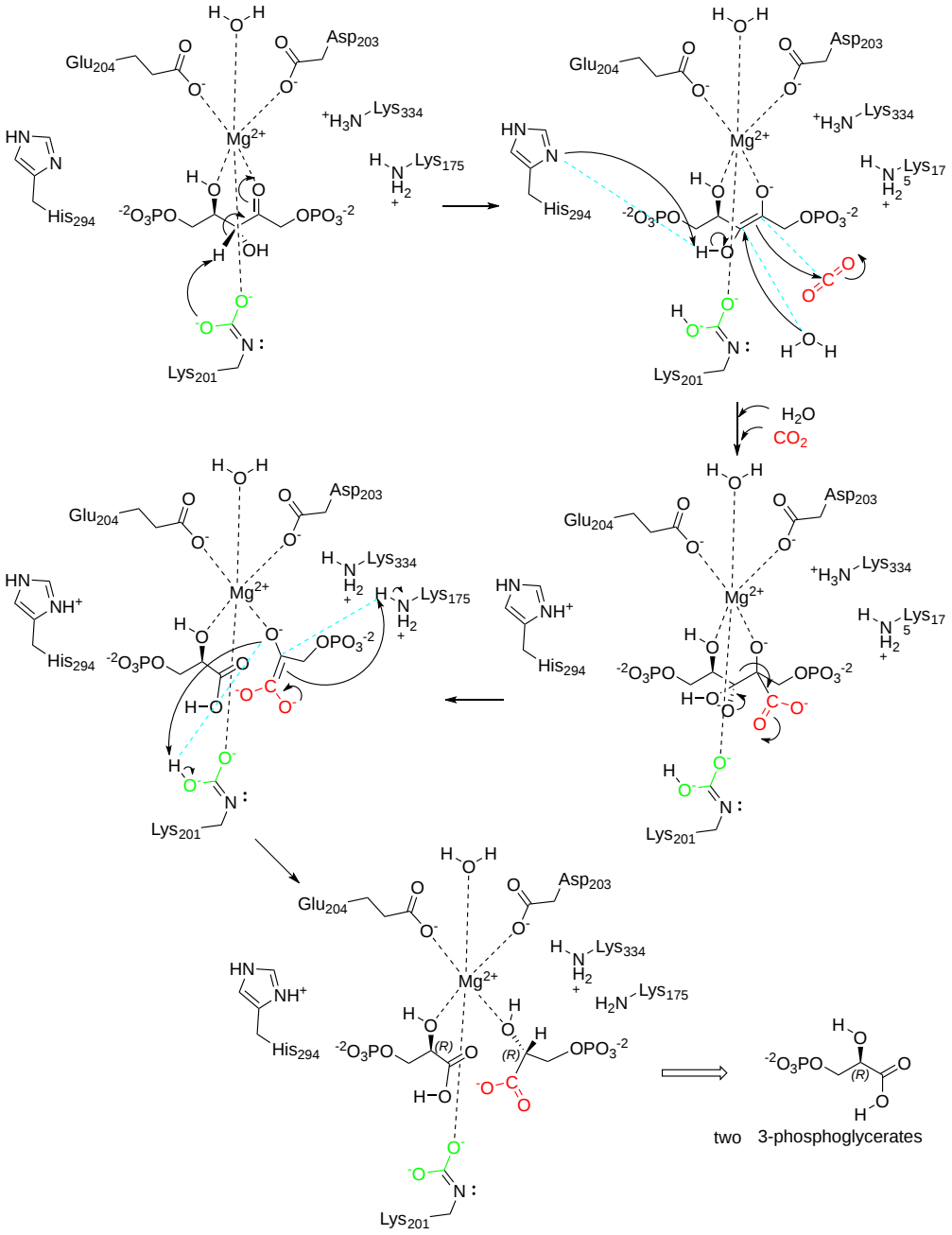
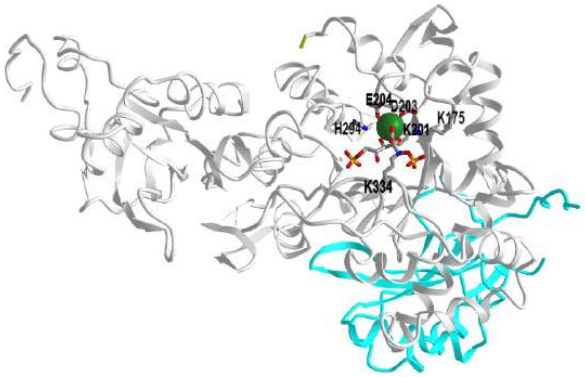


Figure **20.4.6**: Mechanism of ribulose-bisphosphate carboxylase (type I) (after https://www.ebi.ac.uk/thornton-srv/m-csa/entry/907/. Creative Commons Attribution 4.0 International (CC BY 4.0) License)

The green shows the carbamoylated lysine side chain ("activator CO_2"). Ribulose 1,5-bisphosphate is converted to an enediolate, which engages in a nucleophilic attack on the CO_2 to form a 6C sugar. Hydroxylation at C-3 of this sugar is followed by aldol cleavage. Ultimately, two 3PGs are produced, one containing the carbon atom from CO_2 (red). The "activator CO2" (the carboxylated lysine) is hydrolyzed and removed at night, inactivating the enzyme.

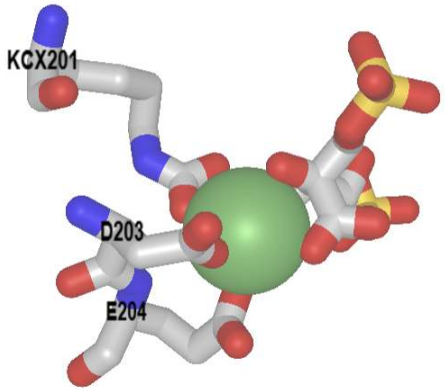
Figure **20.4.7** shows an interactive iCn3D model of a single heavy and light chain of ribulose 1,5-bisphosphate carboxylase/oxygenase (RuBisCo) from Synechococcus PCC6301 (1RBL). (long load time)



NCBI iCn3D Figure **20.4.7**: Ribulose 1,5-bisphosphate carboxylase/oxygenase (RuBisCo) from Synechococcus PCC6301 (1RBL). (Copyright; author via source). Click the image for a popup or use this external link: https://structure.ncbi.nlm.nih.gov/i...BkwkrBmYVwRJ6A

The light chain is shown in cyan, and key residues in the heavy chain are shown in CPK-colored sticks and labeled. Bound to the heavy chain is a substrate analog/inhibitor, 2-carboxyarabinitol-1,5-diphosphate. It is produced in plants, and in the dark, it inhibits the enzyme. As the light increases, its concentration decreases.

Figure **20.4.8** shows one active site of spinach ribulose-1,5-bisphosphate carboxylase/oxygenase complexed with 2-carboxyarabinitol bisphosphate (8RUC). showing the "activator CO_2" bound in a Schiff base link to a lysine side chain (KCX201). The bound activated substrate analog, 2-carboxyarabinitol bisphosphate, contains a $-CO_2^-$ group that coordinates with the Mg^{2+} ion (green sphere) instead of the actual CO_2 (O=C=O) substrate, which would be fixed.



NCBI iCn3D Figure **20.4.8**: Active site of spinach ribulose-1,5-bisphosphate carboxylase/oxygenase complexed with 2-carboxyarabinitol bisphosphate (1RUC). (Copyright; author via source). Click the image for a popup or use this external link: https://www.ncbi.nlm.nih.gov/Structure/icn3d/share.html?PTo2P4jRp3HJrHb99

20.4.5: RUBISCO REACTS WITH BOTH CO_2 AND O_2

Rubisco is a slow carboxylase with a k_{cat} of around 2-10 CO_2/sec. In addition, it can bind another substrate, O_2, and engage in a competing reaction of **photorespiration** (oxidation) of ribulose 1,5-bisphosphate to form one molecule of 3-phosphoglycerate (3PG) and one molecule of 2-phosphoglycolate (2PG), as shown in Figure **20.4.9** below. (Note that **2-phosphoglycolate** is not 2-phosphoglycerate!) In contrast to most oxygenases, no cofactor is required for the RuBisCo/Oxygenase activity. It takes just a simple Mg^{2+} ion. *A more detailed mechanism is shown in Figure 20.*

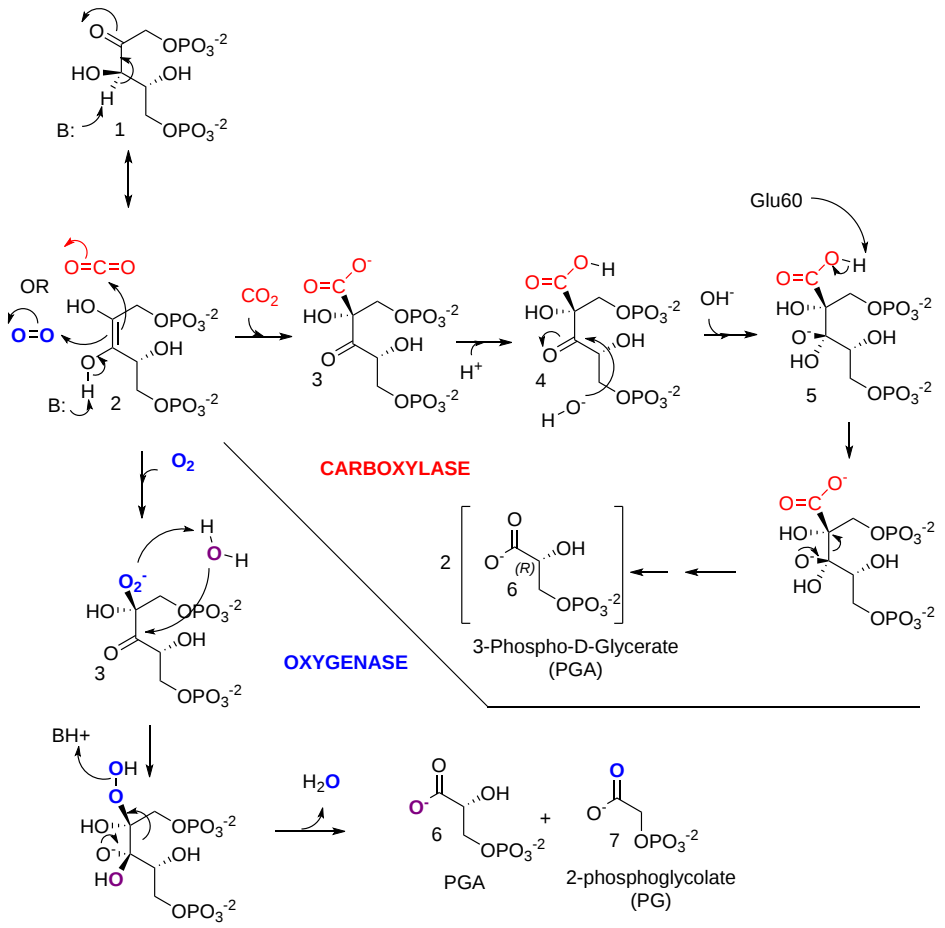


Figure **20.4.9**: RuBP conversion by Rubisco through the carboxylase (a) and the oxygenase (b) reactions. Tommasi, I.C. The Mechanism of Rubisco Catalyzed Carboxylation Reaction: Chemical Aspects Involving Acid-Base Chemistry and Functioning of the Molecular Machine. *Catalysts* **2021**, *11*, 813. https://doi.org/10.3390/catal11070813. CC BY) license (https://creativecommons.org/licenses/by/4.0/

Following RuBP (1) enolization, the 2,3-enol(ate) intermediate (2) may react with CO2(a) or O2(b) co-substrates. The carboxylase reaction produces the 2-carboxy-3-keto-arabinitol 1,5-bisphosphate intermediate (3), which undergoes protonation to form the 2-carboxylic acid before hydration. The C2-C3-scission reaction in C3-gemdiolate (5) occurs in a concerted mechanism upon P1 protonation, producing two molecules of 3-phospho-D-glycerate (3PGA, 6). The oxygenase reaction produces 3-phospho-D-glycerate (3PGA,6) and 2-phosphoglycolate (2PG,7).

The competing reaction with O_2 became a potential problem only after widespread photosynthesis increased the O_2 concentration in the air to 20%. Species evolved to help minimize this problem. Before we describe those adaptations, let's first examine how Rubisco can distinguish between the two nonpolar substrates, CO_2 and O_2. Given the symmetric arrangement of δ^+ and δ^-charges in CO_2, it has a net zero dipole, as does O_2, so it would not align/orient in a field generated by two poles (+ and -). However, CO_2, but not O_2, would align in a field generated by four charged poles, so it has a **quadrupole moment**, as shown below in Figure **20.4.10**.

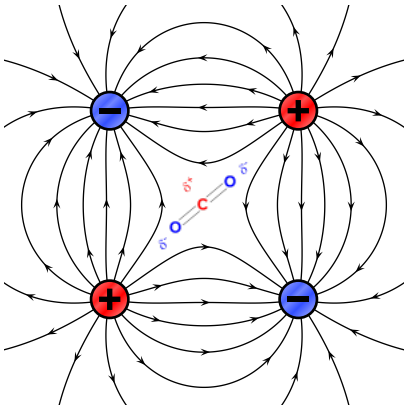


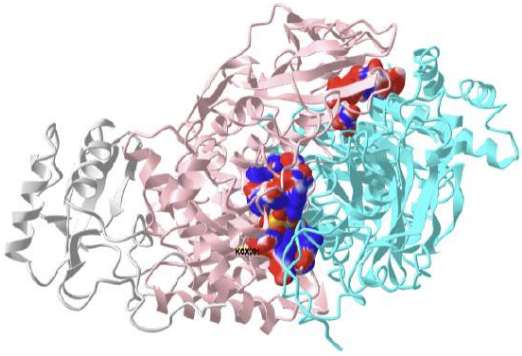
Figure 20.4.10: CO_2 aligning in a quadrupole field. (field lines from https://commons.wikimedia.org/wiki/F...quadrupole.svg)

The dipole unit is the debye, and the quadrupole unit is the debye·Angstrom. Table 20.4.1 below shows some dipole and quadrupole moments values for simple gases. CO_2 has the highest quadrupole moment of all these simple gases.

Molecule	Dipole moment (D)	Quadrupole moment (D Å)
CO_2	0.000	4.30
CH_4	0.000	0.02
H_2	0.000	0.66
O_2	0.000	0.39
CO	0.112	2.5
N_2	0.000	1.52

Table 20.4.1: Dipole and Quadrupole moments for some simple gases. Castro-Muñoz, R., Fíla, V., 2018. Progress on Incorporating Zeolites in Matrimid®5218 Mixed Matrix Membranes towards Gas Separation. Membranes 8, 30. https://doi.org/10.3390/membranes8020030

The active site of Rubisco exhibits a high electrostatic field gradient in its dimeric form. Figure 20.4.11 shows an interactive iCn3D model showing the electrostatic potential surface in the active site between two heavy chains of spinach ribulose 1,5-bisphosphate carboxylase/oxygenase (RuBisCo) (8RUC). It is complex.



NCBI iCn3D Figure 20.4.11: Electrostatic potential surface in the active site between two heavy chains of spinach ribulose 1,5-bisphosphate carboxylase/oxygenase (RuBisCo) (8RUC). (Copyright; author via source). Click the image for a popup or use this external link: https://structure.ncbi.nlm.nih.gov/i...2JG3x4csVnEq67

Two heavy chains are shown in light pink and cyan, and one light chain is shown in gray. The active site regions are depicted as an electrostatic surface potential, with blue representing positive and red representing negative. The model has an activated substrate analog, 2-carboxyarabinitol bisphosphate, shown spacefill (hard to see given the electrostatic surface potential). The residue labeled 201KCX is the carbamate of Lys201.

Presumably, the electrostatic field in the active site facilitates the subtle interaction of the quadrupole CO_2 compared to O_2.

The mechanisms that differentiate the binding of CO_2 and O_2 must also overcome the high intracellular concentration of O_2 (around 250 μM) compared to CO_2 (7–8 μM in C3 plants and 80 μM in C4 plants). The enhanced affinity for CO_2 (about 30-fold) compared to O_2 helps overcome these concentration barriers. No classic "binding pocket" exists for CO_2 and O_2, so diffusion and binding are likely guided

by the electrostatic potential gradients along the diffusion surface. Figure **20.4.12** below the electrostatic potential molecular surface of O_2 and CO_2 (top), calculated from electron density measurement using quantum mechanics, and the electrostatic surface of their binding pockets.

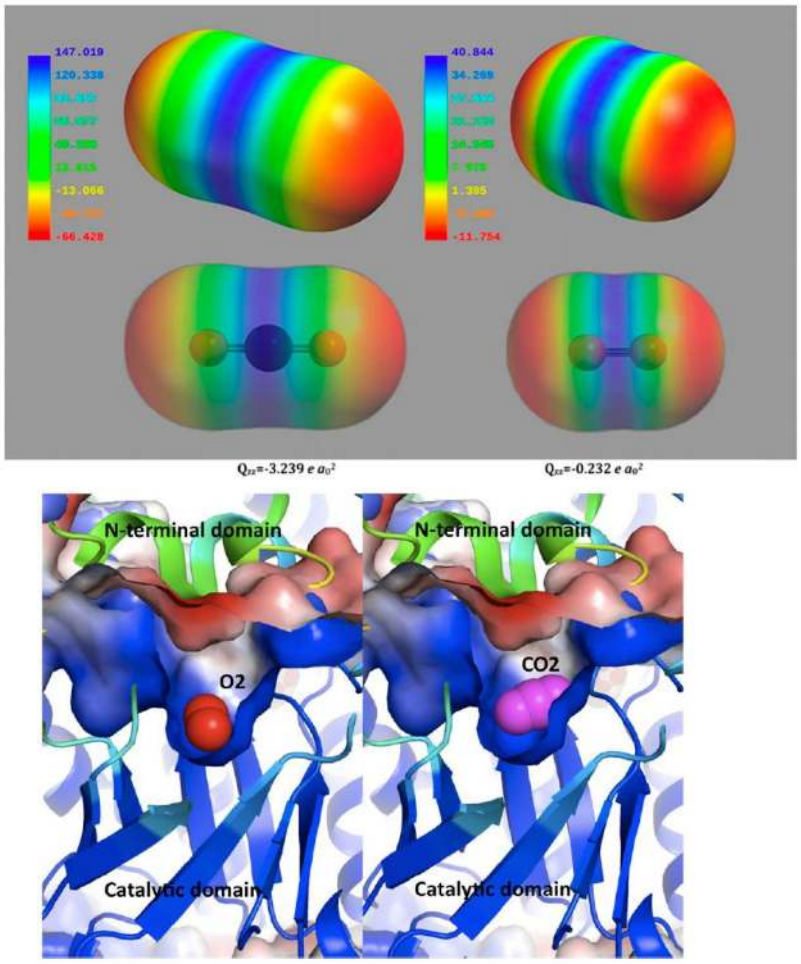


Figure **20.4.12**: Electrostatic potential molecular surface of O_2 and CO_2 (top) and the electrostatic surface of their binding pockets. Tommasi, I.C. et al., ibid.

(**top**) Computed electrostatic potential molecular surfaces of CO_2 (left) and O_2 (right). The color scheme follows commonly accepted conventions: blue, positive; red, negative. The value of the Qzz component of the quadrupole moment, as calculated by Stec, is −3.239 e a_0^2 for CO_2 and −0.232 e a_0^2 for O_2. Note that the ratio of these values is about 14, about equal to the earlier quadrupole moments discussed above, with units of debeye·Å)

(**bottom**) a ribbon representation of the catalytic domain with bound gaseous ligands and surfaces colored by the electrostatic potential. O_2 (in red) and CO_2 (in purple) lie in a positively charged cavity (blue) of the TIM barrel. (Figure from ref. [15], used by permission of PNAS (copyright © 2012).

Both CO_2 and O_2 are situated in a tiny "cavity" that is blue (positive potential, C-terminal domain) and red (negative potential, N-terminal domain) just above it. The quadrupole moment of CO_2 is 10-15x that of O_2, which helps explain its higher affinity in the localized electrostatic potential gradients around the gas molecules.

Molecular dynamics (MD) simulations reveal a preference for interaction with CO_2. There are many subunit-subunit interfaces, and all appear in MD to preferentially interact with CO_2, which probably moves from the solvent through large:small subunit interface to the active site. The CO_2 does not localize at any residues for a long time but seems to occupy areas instead. Since CO_2 has no dipole, it moves closer to the small hydrophobic side chains (Ala, Val, Leu, Ile) and the main chain. CO_2 has more interactions in every active site and in the large:large subunit interface (whose electrostatic potential in the active site is shown above) and in the large:small subunit interface.

In efforts to quantify the preference of CO_2 over O_2 using MD, investigators found that over many different species of Rubisco, the relative distribution of CO_2 and O_2 to the small and large subunits was, on average, 1.8 for CO_2 and 1.4 for O_2, with the number of oxygen bound to

either subunit lower. This is true even though CO_2 has a lower solvation energy than O_2 in water, so additional energy must be spent to desolvate CO_2 differentially. The hydrophobic interactions likely facilitate the movement of CO_2 to the active site, where electrostatic-based potentials favor the binding of CO_2. These results suggest that the small subunit acts like a "mini reservoir" for O2, which then diffuses to the large subunit region of the active site. From a simple thermodynamic perspective, CO_2 would be favored to move along the surface and through spaces in the protein guided by transient interactions with water. The active site in Rubisco is not located in a deep pocket, but rather in shallow grooves near the surface. Although the enzyme is slow (2-10 CO_2/s), it's not much slower than the average enzyme. The median turnover number, kcat (under saturating conditions), of enzymes is approximately 10 s-1, with most values falling between 1 and 100. Its concentration is very high in chloroplasts, which helps increase the fixation of CO_2.

20.4.6: REGULATION OF RUBISCO BY MULTIMER FORMATION AND PHASE SEPARATION

As mentioned above, Rubisco can exist as multimers, including dimers, tetramers, hexamers, octamers, and 16-mers. Different multimers don't seem to significantly differentiate between the competing substrates, CO_2 and O_2, per se. Higher multimers can be induced in the presence of small ligands. The functional complex is often called the **Rubiscosome,** and its aggregation state varies across evolution. Figure **20.4.13** shows structures of the different multimers of Rubisco.

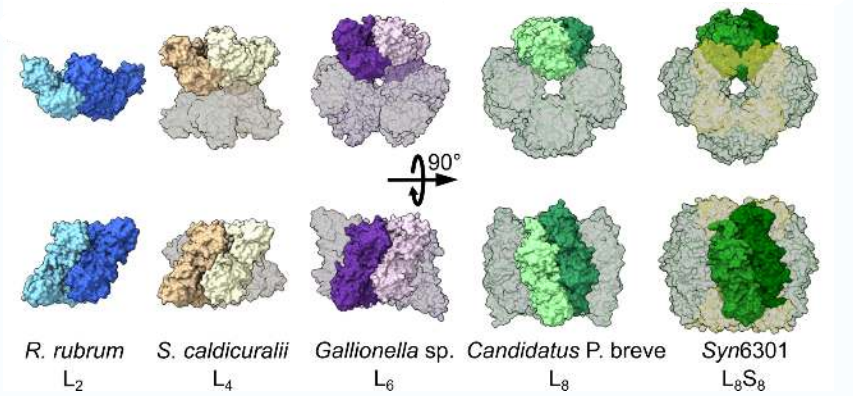


Figure **20.4.13**: **Crystal structure of a tetrameric RuBisCO.** Comparison of RuBisCO oligomeric states illustrating dimer positioning within a multimer. Form II dimer, tetramer, and hexamer are shown alongside form I′ octamer and form I hexadecamer. Protein Data Bank (PDB) codes (left to right): 5RUB, 7T1C, 5C2C, 6URA, and 1RBL. Albert K. Liu *et al.* Structural plasticity enables evolution and innovation of RuBisCO assemblies. *Sci. Adv.***8**, eadc9440(2022). DOI:10.1126/sciadv.adc9440. Creative Commons Attribution License 4.0 (CC BY). https://creativecommons.org/licenses/by/4.0/

These different multimeric structures have evolved to meet the environmental and biochemical needs of their respective organisms. These examples illustrate how, surprisingly, different aggregation states can evolve without great changes in active site requirements. Indeed, the active site is formed between two catalytic large chain monomers. A large chain dimer has two active sites per dimer.

Genomics and phylogenetic analyses show that Rubisco originated about 3 billion years ago when the competing substrate O_2 in the atmosphere was barely present and CO_2 concentrations were 10K% higher than now. Hence, the enzyme evolved when O_2 increased and CO_2 decreased. Key events in the evolution of different forms of Rubisco are shown in Figure **20.4.14** below.

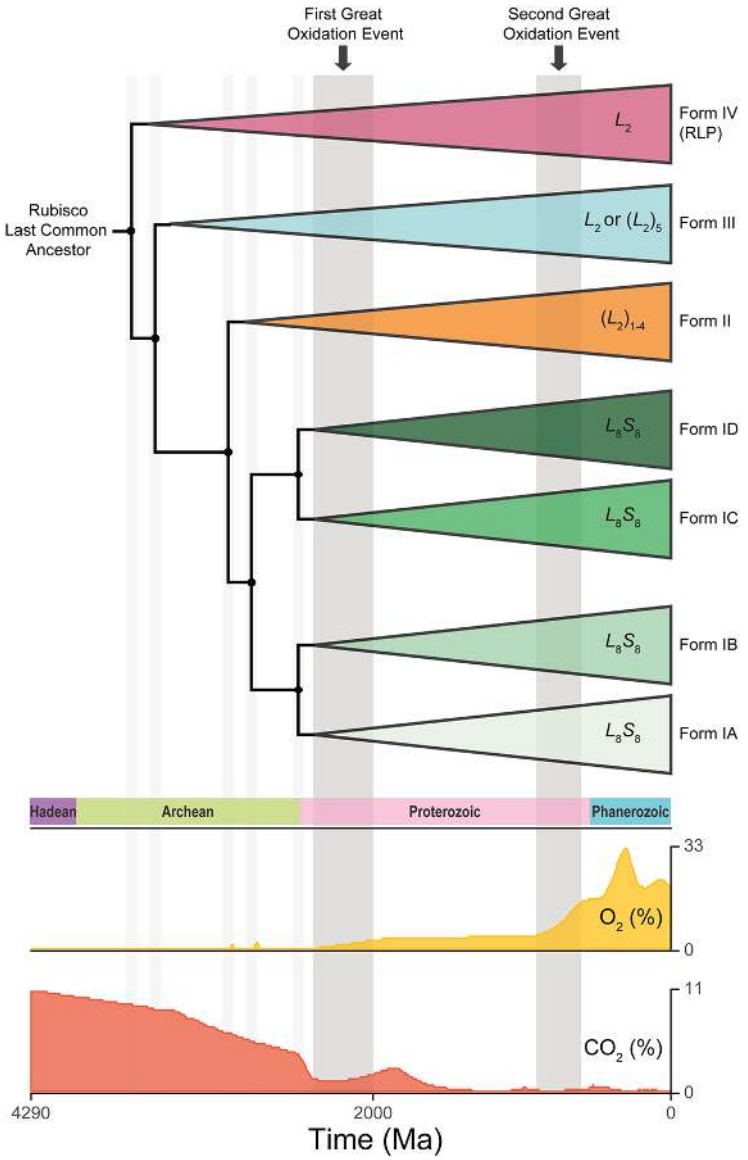


Figure **20.4.14**: The evolutionary history of Rubisco in the context of atmospheric CO_2 (%) and O_2 (%) following divergence from the ancestral Rubisco-like protein (RLP). Bouvier JW, Emms DM, Kelly S. Rubisco is evolving for improved catalytic efficiency and CO_2 assimilation in plants. Proc Natl Acad Sci U S A. 2024 Mar 12;121(11):e2321050121. doi: 10.1073/pnas.2321050121. Epub 2024 Mar 5. PMID: 38442173; PMCID: PMC10945770. Creative Commons Attribution License 4.0 (CC BY).

Gray vertical bars indicate important branch points in the phylogeny at which Rubisco diverged into different evolutionary lineages. To provide additional context, the time period during which the First and Second Great Oxidation events occurred along this evolutionary trajectory is also labeled and referenced as gray vertical bars. Graphics of atmospheric CO_2 and O_2 levels were adapted from the *TimeTree* resource [http://www.timetree.org].

Although the small subunit lacks catalytic activity, its presence enhances enzymatic activity and facilitates the formation of multimers. The multiple forms of Rubisco and evolutionary changes in the enzyme haven't had a huge effect on the specificity of the enzyme for CO_2 compared to O_2. However, evidence suggests there have been slow increases in the activity and specificity of the enzyme for CO_2. The enzyme has evolved more slowly than over 98% of enzymes throughout life, so other strategies are deployed to increase carbon capture. These include increasing Rubisco production in cells, localizing Rubisco near the site of CO_2 import/formation, and phase separation of Rubisco into aggregates.

Rubisco kinetics in extinct and living angiosperms show increases in CO_2/O_2 specificity ($S_{C/O}$), carboxylase turnover rates (k_{catC}), and carboxylation efficiencies (k_{catC}/K_C) in angiosperms, as shown in Table **20.4.2** below.

Rubisco	$S_{C/O}$ (mol mol^{-1})	k_{catC} (s^{-1})	k_{catC}/K_C (s^{-1} μM^{-1})	K_C (μM)	K_C^{air} (μM)	K_O (μM)	K_C/K_O (μM μM^{-1})
Last common angiosperm ancestor	81.1 ± 1.9	2.6 ± 0.3	0.16 ± 0.02	16.3 ± 2.1	24.8 ± 2.8	484.1 ± 56.4	0.034 ± 0.004
Extant angiosperms	87.1 ± 0.5	3.4 ± 0.1	0.20 ± 0.01	17.6 ± 0.5	26.4 ± 0.7	517.2 ± 14.7	0.035 ± 0.001

Table **20.4.2**: Rubisco kinetics in extinct and extant angiosperms. Bouvier JW et al., ibid.

Another mechanism helps Rubisco differentiate between CO_2 and O_2 as competing substrates in some photosynthetic organisms, such as the unicellular algae *Chlamydomonas*. High local concentrations of Rubisco can lead to its phase separation. Such a regulation would aim to increase the localized concentration of CO_2, enabling the enzyme to operate closer to its maximum velocity. This would occur if the phase-separated condensate were located near the source of CO_2 or included in a heterogeneous mixture of condensates. One example is the **carboxysome** in prokaryotes, which contains both Rubisco and carbonic anhydrase, which converts CO_2 (g) into bicarbonate, HCO_3^-. These proteins are encapsulated in an icosahedral protein shell consisting of hexamers of a protein called CcmK2. Click this link for an iCn3D model showing part of the shell from the marine cyanobacterium Prochlorococcus (8WXB). CO_2 is converted to HCO_3^- using carbonic anhydrase in the cytosol, which traps the now anionic carbon in the cell. Bicarbonate can then be transported into the carboxysome and reconverted to CO_2 by encapsulated carbonic anhydrase. The CO_2 is hence delivered to Rubisco at a high concentration and with minimal O_2 as a competitor for Rubisco.

Figure **20.4.15** below shows a model representing the selective permeability of the carboxysome shell to confine metabolite flux for driving the CBB cycle

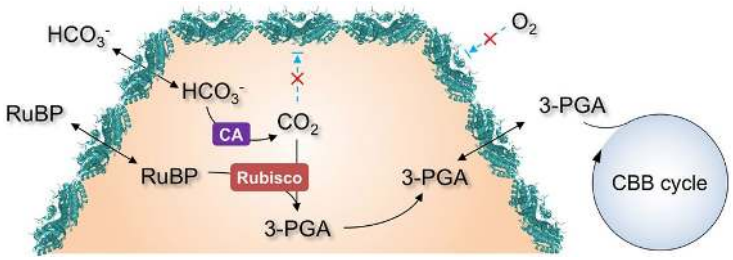


Figure **20.4.15**: Schematic model representing the selective permeability of the carboxysome shell to confine metabolite flux for driving the CBB cycle. Faulkner, M., Szabó, I., Weetman, S.L. *et al.* Molecular simulations unravel the molecular principles that mediate selective permeability of carboxysome shell protein. *Sci Rep* **10**, 17501 (2020). https://doi.org/10.1038/s41598-020-74536-5Creative Commons Attribution 4.0 International License. http://creativecommons.org/licenses/by/4.0/.

CcmK2 hexamers have a concave side facing outwards to the cytoplasm and a convex side facing inwards to the lumen. Based on the positive electrostatic charge of the central pore, CcmK2 acts as a tunnel for HCO_3^- influx and a barrier to O_2 and CO_2, precluding O_2 influx and leakage of CO_2 from the carboxysome lumen to the cytoplasm. Larger molecules like RuBP and 3-PGA can likely pass through CcmK2 but require a conformational change in the CcmK2 pore involving a flip of the Ser39 side chain.

Microalgae (eukaryotic) contain **pyrenoids,** condensates containing Rubisco surrounded by a covering of starch. They are found in the stroma of chloroplasts. They can be connected by tubes containing carbonic anhydrase. Figure **20.4.16** shows the CO_2 concentrating function of pyrenoids in Chlamydomonas and Hornwort, a land plant. In Chlamydomonas, **EPCY1** (similar to **LCI5 with Uniprot ID Q94ET8)**, a linker protein that binds to the small subunit of Rubisco, phase-separates with Rubisco. The pyrenoid accounts for about 30% of global CO_2 fixation.

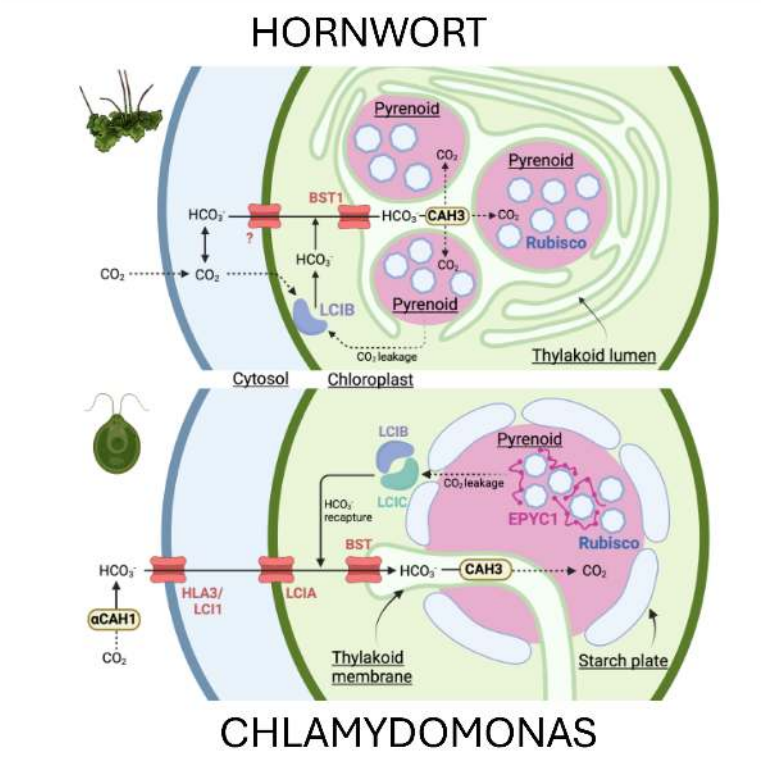


Figure **20.4.16**: CO_2 concentrating function of pyrenoids. Mary Williams. Characterization of the pyrenoid-based CO2-concentrating mechanism in hornworts. July 26, 2024. https://plantae.org/characterization...-in-hornworts/. Creative Commons A-NC 2.0 License.

There is no listing for EPYC1 in Uniprot. Another protein (**LCI5,** UniProt ID: Q**94ET8)** from **Chlamydomonas reinhardtii** with a closely related sequence is listed. An analysis of the amino acid sequence of **LCI5 using** PhaSePro, a database of proteins driving liquid-liquid phase separation (LLPS) in living cells, confirms that the protein contains four mostly identical 60-amino-acid tandem repeats between amino acids 52 and 291, which can drive LLPS. It also states that the common name for LCI5 is **EPYC1**. An analysis of the amino acid sequence using PSIPRED Workbench shows at least five regions of disorder in the protein as illustrated in Figure **20.4.17** below.

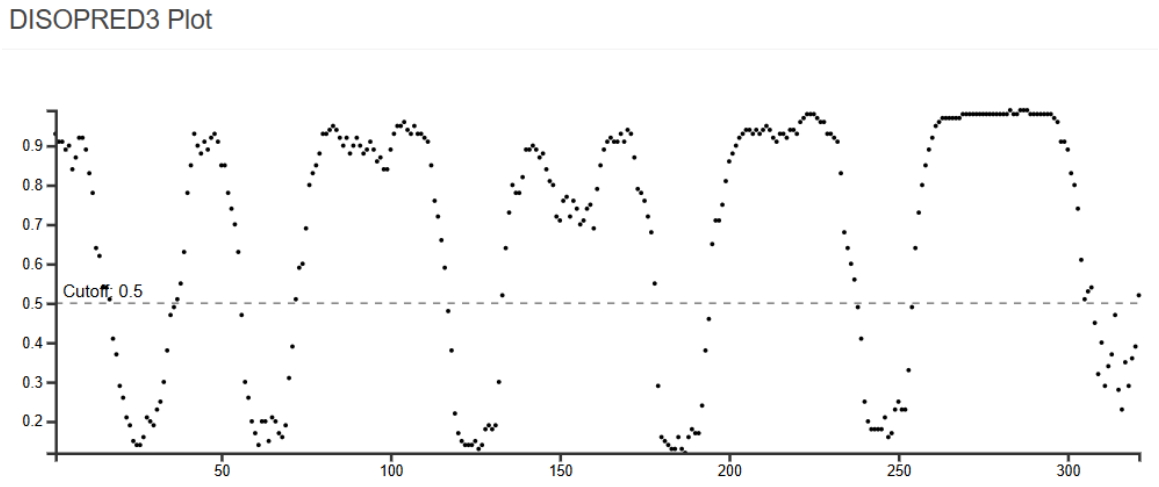
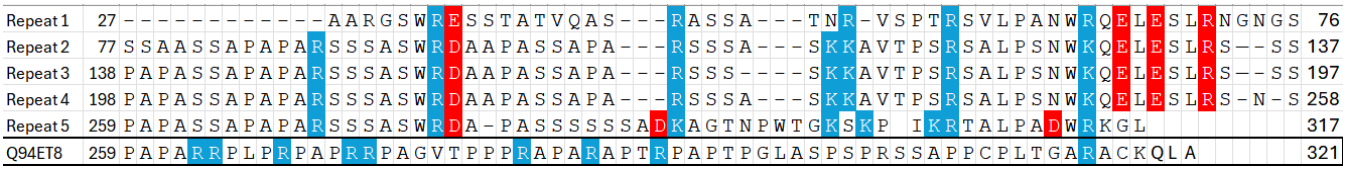


Figure **20.4.17**: **Disorder Plot for LCI5 (Uniprot ID Q94ET8).** PSIPRED Workbench.

Most analyses for tandem disordered repeats in **EPYC1** in the literature show 4-5 such repeats. However, in those plots, the sequence for amino acids 259 to the end is NOT the same as in the Uniprot sequence for LCI5 (aka EPYC1). Two different ways to align the sequence of the literature amino acid sequence and the Uniprot sequences are shown in Figure **20.4.18** below.

Top Panel



Bottom Panel

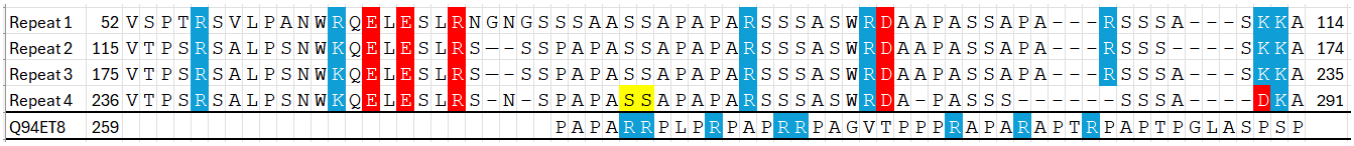
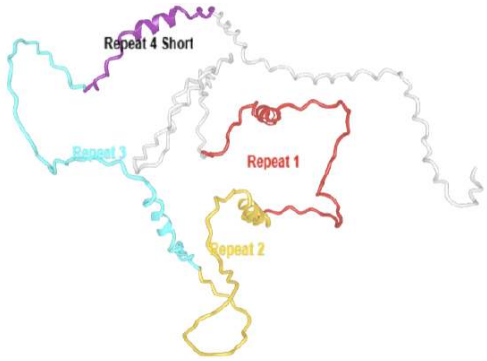


Figure **20.4.18**: sequence of the tandem repeats in LCI5 (aka EPYC1) for literature and Uniprot amino acid sequences. Top panel fromhttps://pmc.ncbi.nlm.nih.gov/articles/PMC7736253/ , bottom panel from https://pmc.ncbi.nlm.nih.gov/articles/PMC7736253/ and https://pmc.ncbi.nlm.nih.gov/articles/PMC6793452/.

In either case, there are at least four tandem repeats in which there is a clear alignment of hydrophobic, polar, and charged (Red for D, E and Blue for R, K)

Figure **20.4.19** shows an interactive iCn3D model of the AlphaFold structure of LCI5 with tandem repeats from Chlamydomonas reinhardtii (Q94ET8). The four internal repeats from the bottom panel above are shown and labeled in Red, Orange, Cyan, and Brown.

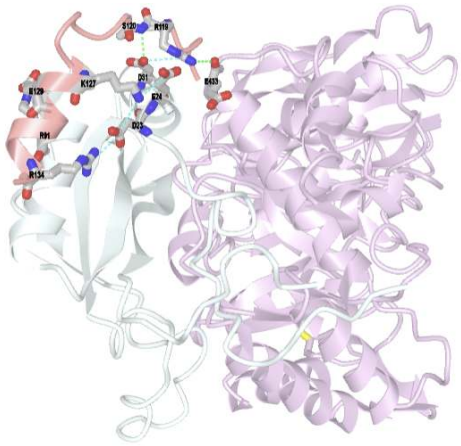


NCBI iCn3D Figure **20.4.19**: AlphaFold structure of LCI5 (EPYC1) with tandem repeats from Chlamydomonas reinhardtii (Q94ET8). (Copyright; author via source). Click the image for a popup or use this external link: https://www.ncbi.nlm.nih.gov/Structure/icn3d/share.html?7m6GBaZBbJWV9USw6

Color code the basic sidechain (R and K) blue and the acidic sidechains (D and E) in red sticks in iCn3D as follows:

- Click on the external link
- **Select, advanced**
- Input this expression to select all the Lysines: $Q94ET8.A:K
- Name the selection All_Lysines
- Repeat for the other amino acids (R, D, and E) and name them appropriately
- Ctrl-click the selections you just made in the Selected Sets window, then choose the following: **Style, Side Chains, Stick**
- Color each as follows: Choose the named selection and then choose the following: **Color, Unicolor,** then blue for Ks and Rs, and red for Ds and Es.

8 EPYC1 proteins bind to 8 sites on the small subunits of Rubisco in Form I Rubisco (L_8S_8) multimer. Figure **20.4.20** shows an interactive iCn3D model of the EPYC1(106-135) peptide-bound large-small chain Rubisco dimer (7JSX)



NCBI iCn3D Figure 20.4.20: EPYC1(106-135) peptide-bound Rubisco (7JSX). (Copyright; author via source). Click the image for a popup or use this external link: https://www.ncbi.nlm.nih.gov/Structu...VWZB2C5pyZrLw6

The small chain is shown in light cyan, and the large chain is in light magenta. The EPYC1 peptide binds largely through ion..ion interactions mostly to the small unit.

Indeed, if EPYC1 is added to Rubisco in vitro, it forms liquid droplets. EPYC1 doesn't act as a scaffold per se to which Rubisco attaches and phase separates. Rather, it is through multiple low-affinity interactions that the interactions of EPYC1 and Rubisco lead to phase separation. It occurs even at low concentrations of both. The linker protein EPYC1, with multiple arginines and lysines, is positively charged. They interact with negative side chains in the small Rubisco subunit. Accordingly, their interactions and phase separation are dependent on the salt.

CIDER (**C**lassification of **I**ntrinsically **D**isordered **E**nsemble **R**egions) was used to calculate the charge distribution of side chains in the large and small subunits of Rubisco and EPYC1. These parameters were calculated.

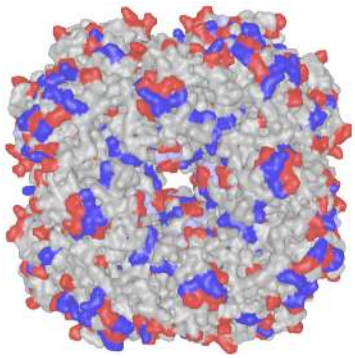
- **κ (kappa, 0-1)**: A measure of the extent of charge segregation in a sequence. All three proteins are weak polyampholytes, characterized by small fractions of positive and negative side chains. As such, they all form globular-like structures that are less dependent on the protein's charge distribution. Low **κ** values are found when charges are mixed along the chain and not highly segregated. This minimizes self-aggregation and the formation of hairpins in EPYC1 with itself, for example. Even strong polyampholytes with low **κ** values form more random coil structures.
- **FCR**: The fraction of charged residues in a sequence
- **NCPR**: The net charge per residue (can be positive or negative)
- **Hydropathy**: The mean hydropathy of a sequence, calculated as the average of a 0-9 using the Kyte-Doolittle hydrophobicity scale.
- **Fraction disorder promoting**: The fraction of residues that promote disorder.

The results are shown in Table 20.4.3:below

seq	length	κ	FCR	NCPR	Hydropathy	Fraction disorder-promoting
LCI5 (aka EPYC1)	321	0.137	0.184	0.109	3.883	0.841
small Rubisco	185	0.169	0.189	0.038	4.464	0.589
large Rubisco	475	0.138	0.240	-0.013	4.274	0.623

Table 20.4.3: Charge Distribution in Rubisco and LCI5 (EPYC1)

Figure 20.4.21 shows an interactive iCn3D model of the surface of spinach ribulose-1,5-bisphosphate carboxylase/oxygenase (8RUC) colored by charge.



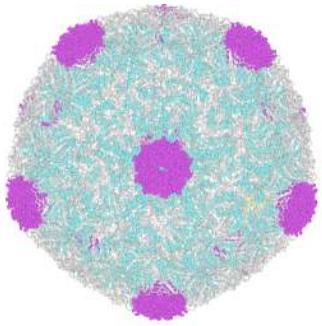
NCBI iCn3D Figure 20.4.21: Surface of spinach ribulose-1,5-bisphosphate carboxylase/oxygenase (8RUC) colored code by charge. Red indicates negative charge and blue positive. (Copyright; author via source). Click the image for a popup or use this external link: https://www.ncbi.nlm.nih.gov/Structu...7QgFy3UMqyLPy5

The full-length linker protein LCI5 (also known as EPYC1), which has highly disordered links, forms a multitude of low-affinity, polyvalent electrostatic interactions with the Rubisco 16-mer, promoting aggregation and phase separation.

Here is a potential model showing these interactions: (Figure 6E from https://pmc.ncbi.nlm.nih.gov/articles/PMC7736253/#F7) - Awaiting permission for use of the actual image instead of this link: https://cdn.ncbi.nlm.nih.gov/pmc/blobs/d65f/7736253/6c90be375842/nihms-1640018-f0006.jpg

It should be noted that Rubisco in the carboxysome also interacts with an intrinsically disordered linker protein CsoS2 (Carboxysome assembly protein CsoS2B), which leads to Rubisco's phase separation together with carboxysomal carbonic anhydrase (CsoSCA) in α-cyanobacteria.

Figure 20.4.22 shows an interactive iCn3D model of the carboxysomal mini-shell icosahedral assembly from CsoS1A and CsoS2 from Halothiobacillus neapolitanus (8B12). The major carboxysome shell protein CsoS1A is in the gray cartoon, the carboxysome shell vertex protein CsoS4A in the purple spacefill, and CsoS2 is in the cyan cartoon.



NCBI iCn3D Figure 20.4.22: Carboxysomal mini-shell icosahedral assembly from CsoS1A and CsoS2 from Halothiobacillus neapolitanus (8B12). (Copyright; author via source). Click the image for a popup or use this external link: https://www.ncbi.nlm.nih.gov/Structure/icn3d/share.html?mE2g19pAtcMaAoiy6.

Carboxysomes self-assemble in a process guided by the intrinsically disordered linker protein CsoS2, which connects multiple shell proteins, carbonic anhydrase, and Rubisco to form the ultimate phase-separated carboxysome. Interactions are mediated in part by a repetitive Ile(Val)-Thr-Gly ([IV]TG) motif in CsoS2 and the β-strand in CsoS1A through His79 and main chain hydrogen bonds in the main chain. The domain and tandem repeat structures of CsoS2 and its interactions with CsoS1A are illustrated in Figure 20.4.23 below.

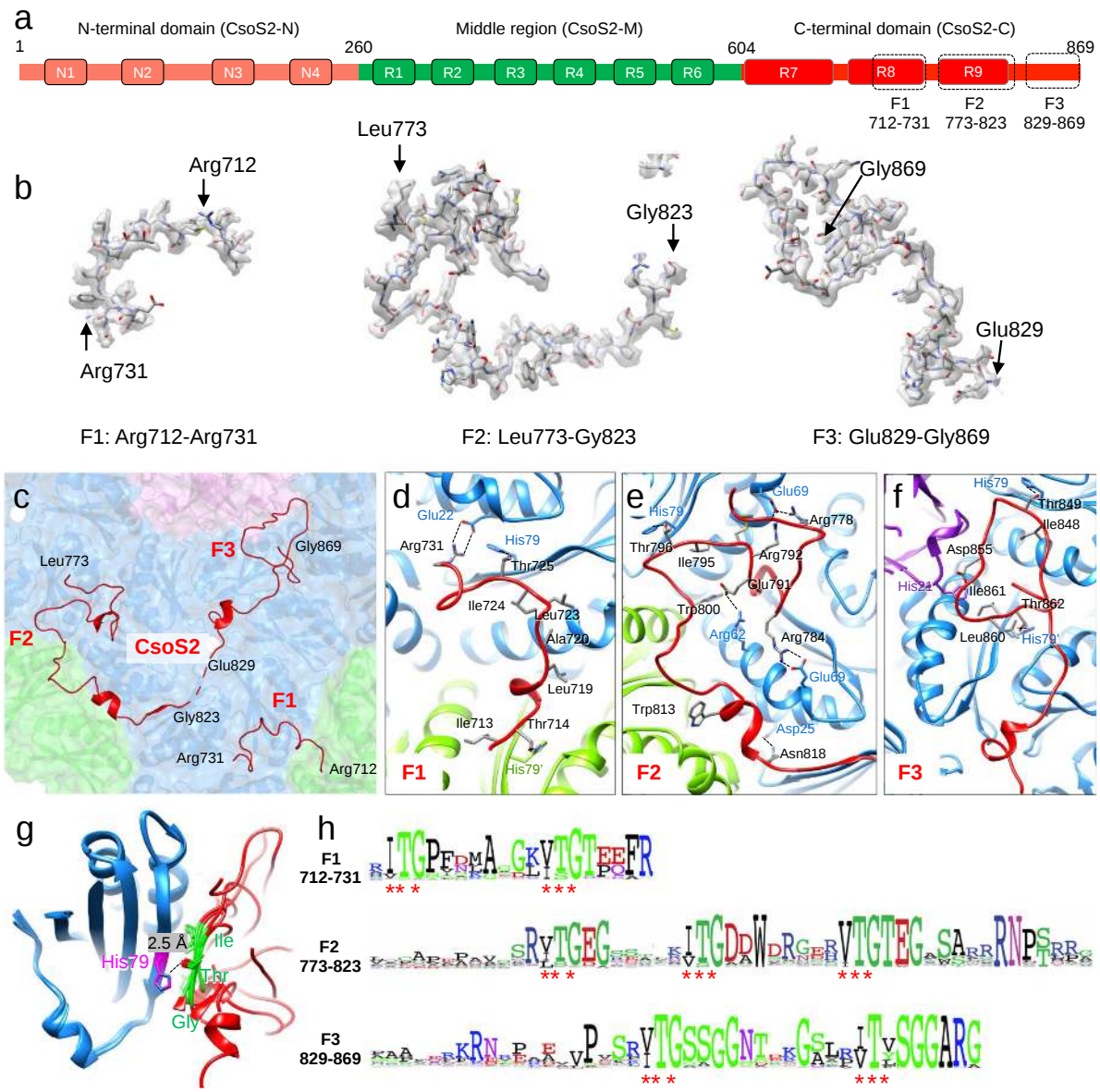


Figure **20.4.23: CsoS2 binds to the shell through multivalent interactions with shell proteins and highly conserved interfaces via novel [IV]TG repeats.** Ni, T., Jiang, Q., Ng, P.C. *et al.* Intrinsically disordered CsoS2 acts as a general molecular thread for α-carboxysome shell assembly. *Nat Commun* **14**, 5512 (2023). https://doi.org/10.1038/s41467-023-41211-y. Creative Commons Attribution 4.0 International License. http://creativecommons.org/licenses/by/4.0/.

Panel a shows the domain arrangement of CsoS2. The N-terminal, Middle and C-terminal domains are colored in pink, green and red, respectively. Three dashed boxes indicate the structured fragments resolved in $T = 9$ shell.

Panel b shows the CryoEM densities of F1-F3 with atomic models. **c** CsoS2 interactions with shell components, viewed from inside. Three structured fragments in the C-terminal domain, F1, F2 and F3, are identified and labelled.

Panels d–f: Interaction interfaces between CsoS2 F1 (**d**), F2 (**e**) and F3 (**f**) fragments with shell components, CsoS1A (blue/green) and CsoS4A (purple).

Panel g shows the alignment of CsoS2-CsoS1A interacting motifs, showing the CsoS2 [IV]TG motif (green) in contact with CsoS1A His79.

Panel h shows the consensus sequences of CsoS2 C-terminal F1, F2 and F3 fragments from 100 CsoS2 sequences, plotted with Weblog. Asterisks indicate the conserved repeating [IV]TG motif present in each fragment.

Figure **20.4.24** below shows a summary representation of phase-separated Rubisco, which preferentially interacts with CO_2 if localized near high concentrations.

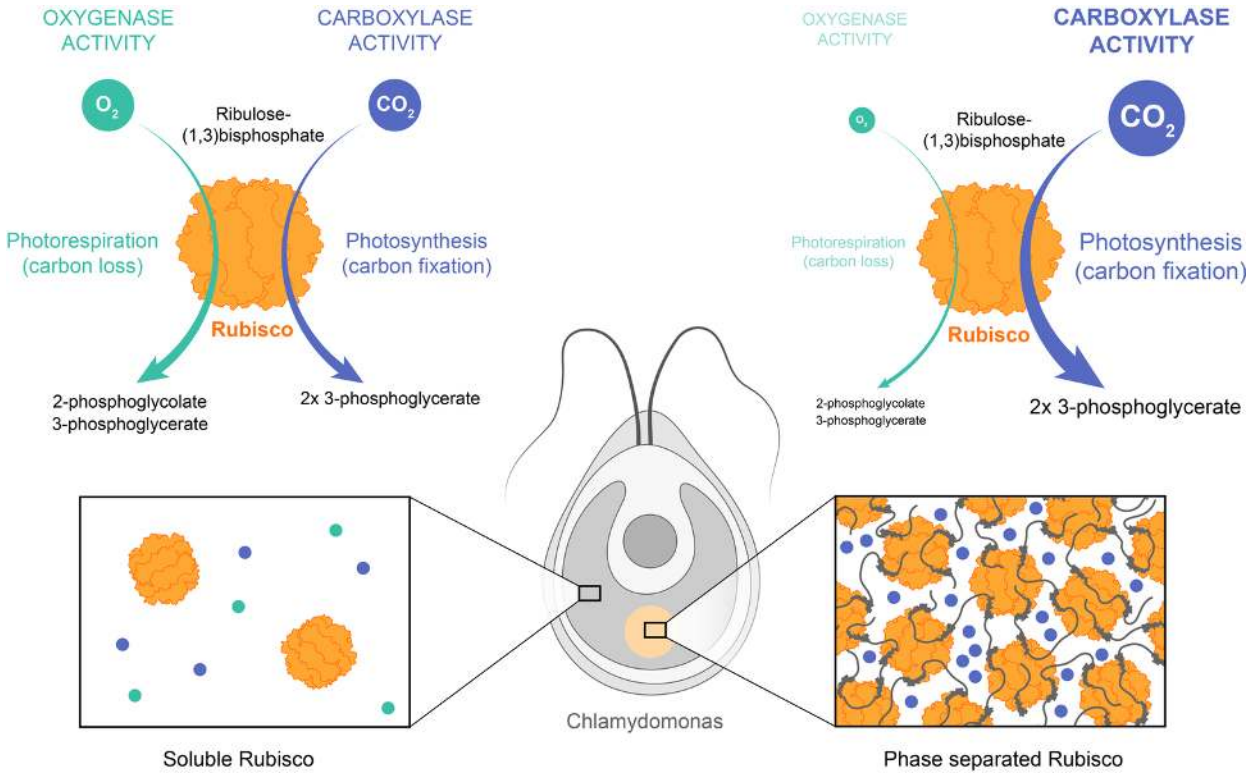


Figure 20.4.24: Phase Separation of Rubisco. PHASE SEPARATION 101. Animation Lab. Margot Riggi, Janet Iwasa, et al. Creative Commons Licensing CC BY 4.0 - https://creativecommons.org/licenses/by/4.0/

Recent Updates: 2/27/25



THE SKEPTICS - BUT ISN'T THE CO_2 WE EMIT INTO THE ATMOSPHERE JUST PLANT FOOD?

This argument is used by many who say that we shouldn't worry about dumping CO_2 from burning fossil fuels into the atmosphere. As with some arguments, there is partial truth in the statement. Of course, CO_2 is plant "food," as Rubisco fixes it in photosynthesis, so increasing CO_2 in very controlled experiments (in which all other conditions are fixed) will increase its fixation as it outcompetes O_2 as a substrate. This is true only for C3 plants. Experiments have shown that increasing CO_2 for C4 plants (discussed in the next chapter section), which have a mechanism for preconcentrating CO_2 as bicarbonate, will not result in the same increase in CO_2 fixation. A complete analysis shows that this description of CO_2 as plant food is incomplete and misleading —an example of a logical fallacy. Several applicable logical fallacies are described below:

- **Half-truth (Cherry-picking Fallacy)** – The argument selectively presents only one fact (that CO_2 benefits plants) while ignoring other relevant facts, such as how excessive CO_2 contributes to global warming, ocean acidification, and extreme weather, which can harm ecosystems, including plants.
- **Hasty Generalization** – Just because CO_2 benefits plants in some cases doesn't mean that increasing CO_2 indefinitely is beneficial. It overlooks the complex ecological and climatic consequences.
- **Oversimplification** – The argument reduces a complex scientific issue to a single, misleading cause-and-effect relationship for climate change.
- **Straw Man Fallacy** (in some contexts) – If this argument is used to dismiss concerns about climate change without addressing the broader scientific consensus, it misrepresents the issue and creates a weaker version of the opponent's position

Other, indirect factors not discussed by those who use the simple argument that CO_2 is simply plant food are listed below (summarized from an excellent video by Andrew Dressler on this topic).

- Weed growth, which competes for sun, nutrients, and water, would increase, necessitating even more toxic herbicides. This is especially true for C4 plants like corn and sorghum, which gain no advantage from elevated CO_2 levels. In addition, studies show that they can become more resistant to herbicides as they experience more optimal growing conditions.
- The effects of increased CO_2 on plants do not persist, as they adapt at the biochemical level to the increased levels. For example, C3 plants decrease the amount of Rubisco they make, especially over longer time periods.
- Plants also need other nutrients, such as nitrogen and phosphorus, so increasing CO_2 alone will not increase plant growth when other nutrients become rate-limiting.
- Stomata opening size and frequency decrease with increasing CO_2, a logical outcome given increased CO_2 availability. This means less CO_2 enters the cell per unit time, but also less O_2 and H_2O (g) leaves. Plants need H_2O primarily for cooling, which occurs with the evaporation as H_2O (l) → H_2O (g), an exothermic and exergonic process that requires heat from the plant. This cooling in plants is analogous to sweating in animals. In field studies, plants getting extra CO_2 are warmer than adjacent plants that aren't. So plants can benefit from extra CO_2 when water-stressed, but they are disadvantaged by the heat stress accompanying global and localized warming.
- Also, as less water enters the roots when stomata are closed, fewer soil nutrients are taken up by the plant. The result of plants growing faster due to increased CO_2 is less nutritious plants that contain more nonstructural sugars, which are deleterious to human health. Hence, all foods—plant and animal alike—will provide less nutrition. This also includes proteins, such as Rubisco, the main protein in consumed plants, which is decreased.
- Metal ions (the ionome), such as iron, zinc, and calcium, are also decreased, as are vitamins. Total mineral content is reduced by around 8% in C3 plants like rice and wheat.
- Faster-growing plants have reduced tolerance to insect and fungal pests. At higher CO_2, the number of aphids significantly increases. The best previous geological example of a rapid increase in atmospheric CO_2 with no preceding warming of the climate is the **Paleocene/Eocene thermal maximum (PETM)**, which occurred about 56 million years ago. Plant fossils from that time show significant insect damage.
- Higher CO_2 levels increase global temperatures, which can lead to excessive and extreme precipitation events that cause flooding, as well as increased droughts. Droughts decrease crop yield. Elevated temperatures in the absence of drought are also bad for plants. Large yield decreases in wheat and rice are observed with increased temperature and CO_2.

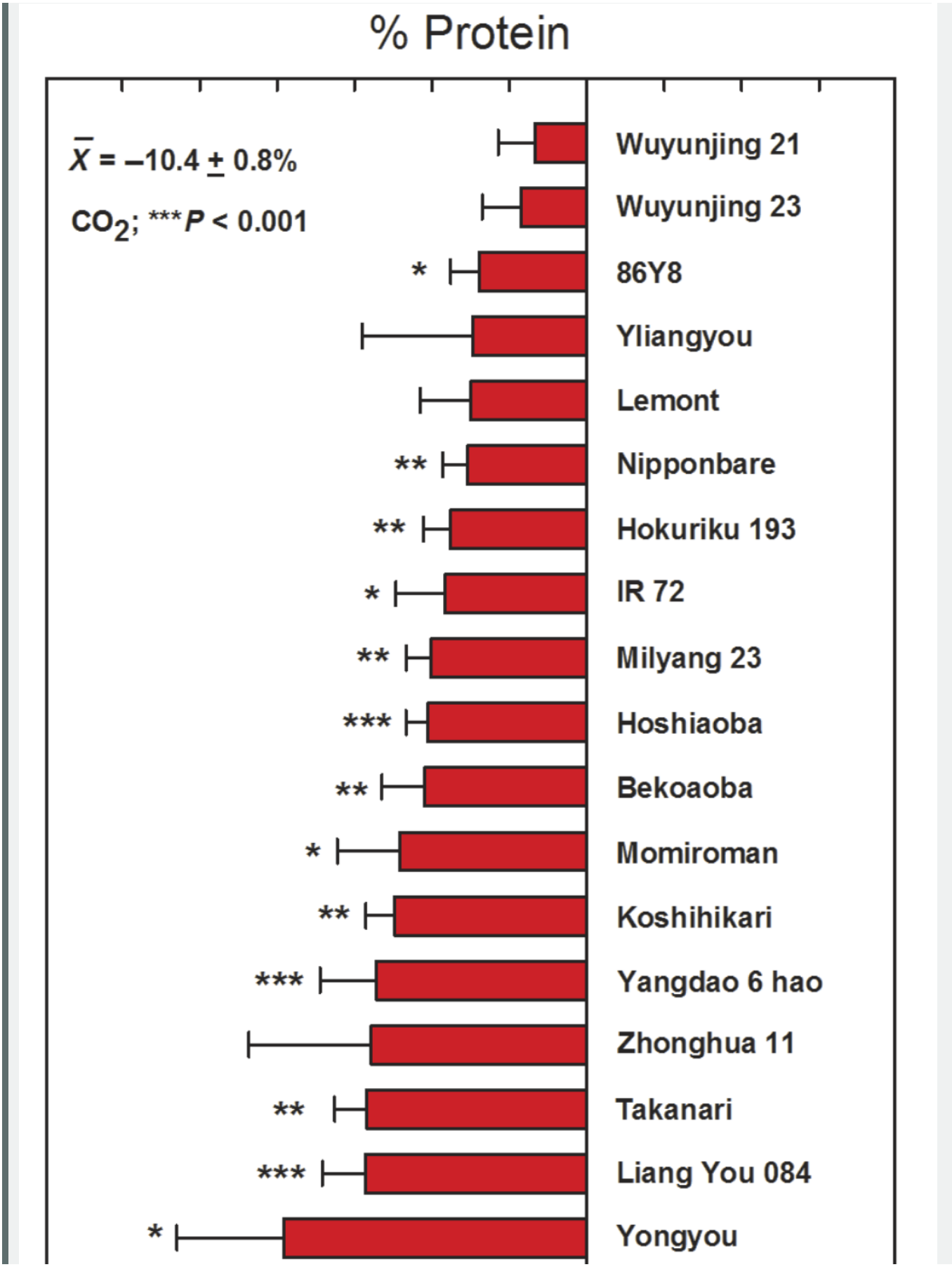
In short, for C3 plants, a rise in CO_2 might be temporarily beneficial for plants but destructive for us.

Three recent studies have quantified these effects and shown that the positive growth response of C3 plants to increased CO_2 has already turned negative. as the Earth warms. Here are links to the three studies.

1. Transition from positive to negative indirect CO_2 effects on the vegetation carbon uptake
2. Shifts in vegetation activity of terrestrial ecosystems attributable to climate trends
3. Inhibitive Effects of Recent Exceeding Air Temperature Optima of Vegetation Productivity and Increasing Water Limitation on Photosynthesis Reversed Global Greening

Finally, data presented in Figure **20.4.25** below clearly show the reduction in plant protein and micronutrients at elevated $CO_{2\ atm}$ levels (568 to 590 ppm compared to present levels of 427 on 2/27/25). The data were obtained through a multiyear study at free-air CO_2 enrichment (FACE) facilities under field conditions in China and Japan. In this technique, rings of pipes or towers are set up around plots of crops, forests, or grasslands. These release controlled amounts of CO_2 into the air, raising the concentration around the plants (often to levels expected later this century) while leaving other environmental factors — like sunlight, wind, temperature, and rainfall — unchanged. The names to the right in the bar graph are particular rice lines (cultivars). The decreased availability of nutrients for herbivores will affect the entire food chain.

https://bio.libretexts.org/@go/page/15050



https://bio.libretexts.org/@go/page/15050

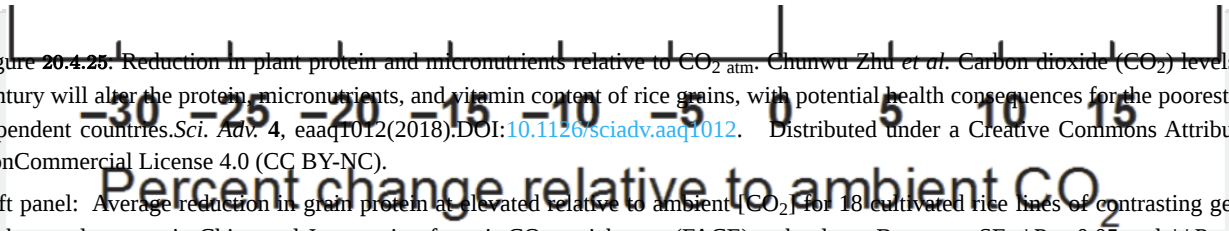


Figure **20.4.25**. Reduction in plant protein and micronutrients relative to $CO_{2\ atm}$. Chunwu Zhu *et al.* Carbon dioxide (CO_2) levels this century will alter the protein, micronutrients, and vitamin content of rice grains, with potential health consequences for the poorest rice-dependent countries.*Sci. Adv.* **4**, eaaq1012(2018).DOI:10.1126/sciadv.aaq1012. Distributed under a Creative Commons Attribution-NonCommercial License 4.0 (CC BY-NC).

Left panel: Average reduction in grain protein at elevated relative to ambient [CO_2] for 18 cultivated rice lines of contrasting genetic backgrounds grown in China and Japan using free-air CO_2 enrichment (FACE) technology. Bars are ±SE. **P* < 0.05 and ***P* < 0.01 (see Methods for additional details).

Right Panel: Average reduction in grain micronutrients, iron (Fe), and zinc (Zn) concentration at elevated relative to ambient [CO_2] for 18 cultivated rice lines of contrasting genetic backgrounds grown in China and Japan using FACE technology. Bars are ±SE. **P* < 0.05 and ***P* < 0.01 for a given cultivar. CO_2; ***P* < 0.01 is based on all cultivars (see Methods for additional details).

Similar effects were seen for B vitamin content.

The box below

? $D6^S/D6^R$ ISOTOPIC ANALYSIS OF RUBISCO CATALYIS

Click here for detailed analysis.

Recent studies have shown that increasing $CO_{2\ atm}$ increases plant carbon capture. Of course, it would, since it is a substrate for Rubisco, which does not operate at V_{max} at current CO_2 atmospheric concentrations. The carboxylation rate would increase compared to the enzyme's oxidase rate. Studies documenting this effect use deuterium NMR.

As you learned in Organic Chemistry, protons (^1H) have characteristic NMR shifts from 1-12 ppm. The proton resonates at a frequency of 100 - 800 MHz. Deuterium (^2H or simply D, with a natural abundance of 0.015%) has a broader signal because it has a small magnetic dipole moment. It has an optimal resonant frequency of 61 MHz. Samples for ^1H NMR experiments are typically dissolved in D_2O or CD_3OD, as the Ds are mostly invisible at the frequencies used. Nevertheless, D-NMR is useful, for instance, for distinguishing stereoisomers of D-substituted molecules. These isomers are called **isotopomers**. Figure **20.4.26** illustrates two isotopomers of deuterium-labeled glucose, an end product of photosynthesis.

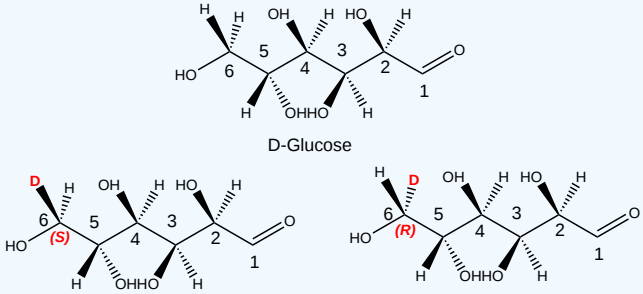


Figure **20.4.26**: Two C6 deuterium isomers of D-glucose (straight chain).

The two C6Hs on glucose in the top panel are identical substituents, so the C6 carbon center does not exist as stereoisomers. However, if each were separately substituted with deuterium, two stereoisomers, known as **isotopomers**, would exist. The original unsubstituted glucose is prochiral at C6, with one of the hydrogens being pro-R and the other pro-S.

Rubisco exhibits both carboxylase and oxygenase activities, and the ratio of $D6^S/D6^R$ isotopomers can provide insight into the relative rates of these activities. As the $CO_{2\ atm}$ increases, the products of carboxylase activity should increase, while those from oxygenase decrease or remain unchanged. The $D6^S/D6^R$ isotopomer ratio change is seen experimentally in glucose form sunflower leaf starch grown in different concentrations of $CO_{2\ atm}$, as shown in Figure **20.4.27** below. The individual D-NMR peaks of glucose from plants grown at higher CO_2 atmospheres have lower NMR shifts (ppm). In addition, the $D6^R$ peak for glucose from leaves exposed to high $CO_{2\ atm}$ is higher in amplitude, indicating increased concentrations of the $D6^R$ isotopomer. As $CO_{2\ atm}$ increases, $D6^S/D6^R$ decreases.

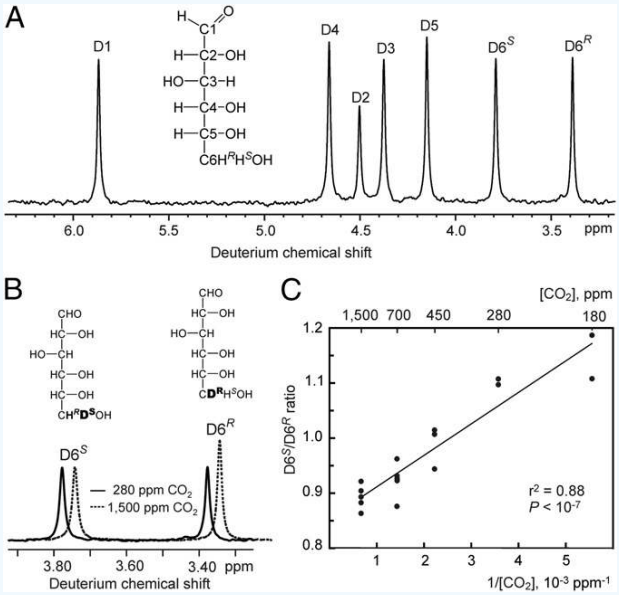


Figure **20.4.27**: Effect of $[CO_2]$ on the $D6^S/D6^R$ isotopomer ratio of photosynthetically generated glucose moieties in sunflower (H. annuus). I. Ehlers, A. Augusti, T.R. Betson, M.B. Nilsson, J.D. Marshall, & J. Schleucher, Detecting long-term metabolic shifts using isotopomers: CO2-driven suppression of photorespiration in C3 plants over the 20th century, Proc. Natl. Acad. Sci. U.S.A. 112 (51) 15585-15590, https://doi.org/10.1073/pnas.1504493112 (2015). This article is freely available online through the PNAS open access option, for which there is permission for the general reuse of figures for non-commercial and educational purposes without requesting permission.

Panel (A): Deuterium NMR spectrum of a glucose derivative displaying one signal for each of the seven glucose isotopomers. The signals' integrals are proportional to the isotopomer abundances.

Panel (B): Excerpts of deuterium NMR spectra of glucose prepared from sunflower leaf starch, showing signals from the $D6^S$and $D6^R$ isotopomers of the $C6H_2$ glucose group. The solid and dashed spectra were acquired from glucose formed at $CO_{2\ atm}$ levels of 280 ppm and 1,500 ppm CO_2, respectively. The dashed spectrum has been shifted to the right to facilitate comparison.

Panel (C): Note: This plot has been linearized by plotting $1/[CO_{2\ atm}]$ on the bottom x-axis. The Dependence of the $D6^S/D6^R$ ratio of glucose from sunflower leaf starch on $1/[CO_2]$ (in units of 10^{-3} ppm^{-1}) during growth [r^2 = 0.88, slope 0.057 ±0.006 (SEM), $P < 10^{-7}$, n = 17, individual plants except for 180 and 280 ppm, where material from two to four plants had to be pooled for each sample].

A similar relationship between $D6^S/D6^R$ and $1/[CO_2]$ was seen in beet sucrose samples obtained from 1890 to 2012.

Mechanistically, this decrease in $D6^S/D6^R$ in leaves grown at high $CO_{2\ atm}$, arising from the increase in $D6^R$ peak, can be explained by the metabolic pathways for the carboxylase and oxygenase reactions in C_3 metabolism. In photooxidation (photorespiration), one G3P is produced along with one 2-phosphoglycolate, a 2-carbon molecule, as CO_2 was not fixed (see The Glycolate Pathway at the end of the chapter). This can be converted to G3P via distinct sets of reactions in the chloroplast and peroxisome. Given the complexity of the isotope effect in enzyme reactions, it has been consistently observed that different sets of reactions yield distinct isotopomer distributions for a common reactant. The carbon group added to 2-phosphoglycolate to form 3-phosphoglycerate originates from serine via peroxisomal serine hydroxymethyltransferase. Serine purchased commercially was synthesized using that enzyme and exhibits a unique, strong isotopomer signal at C3.

Changes in the $D6^S/D6^R$ ratio in tree rings in tropical Toona ciliata trees in Asia and Australia over ≈ 100 years have been observed with increasing $CO_{2\ atm}$ and tree diameter, a measure of irradiance at the tree's crown. The photosynthetic efficiency (increased carboxylation, decreased photorespiration) increased with CO_2 atm but decreased with tree diameter, probably reflecting limitations on water movement to the canopy and reduced leaf CO_2 at high irradiance. (Note: the $D6^S/D6^R$ saturates with tree height and, at some point, no longer increases.) This also correlates with the biosphere primary production increase (carbon fixation into glucose) between 1981-2020.

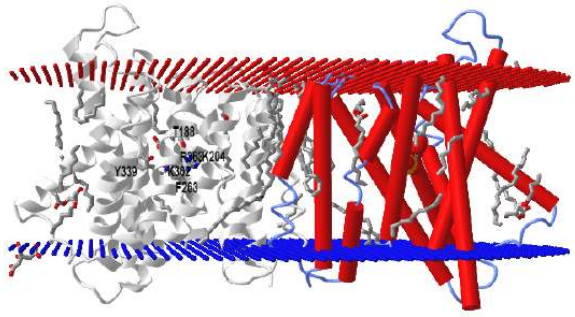
20.4.7: THE NEXT STEP: 3-PHOSPHOGLYCERATE TO GLYCERALDEHYDE 3-PHOSPHATE AND DIHYDROXYACETONE PHOSPHATE

The 3PG produced by RuBisCo is converted to the triose glyceraldehyde-3-P (G3P) (which can readily isomerize to dihydroxyacetone phosphate) using typical glycolytic enzymes run in reverse, except that NADPH is used as a reductant instead of NADH. Additionally, the stromal and cytosolic enzymes are encoded by distinct genes. The G3P not used for resynthesizing ribulose 1,5-bisphosphate can be used to synthesize starch, sucrose, etc., as illustrated in Figure 4 above.

20.4.8: EXCHANGE OF TRIOSES AND PHOSPHATE ACROSS THE INNER MEMBRANE

The inner chloroplast membrane contains a **triose-phosphate/phosphate translocator (TPT)**, an antiporter that transports Pi into the stroma in exchange for a triose phosphate, specifically dihydroxyacetone phosphate or 3-phosphoglycerate. The importance of this was discussed above. The exported triose can be used to synthesize sucrose, which can be transported around the plant as a carbon source. Trioses within the chloroplast can also be converted to glucose and into glycogen as the organelle becomes an amyloplast. If the translocator is inhibited, Pi would decrease in the chloroplast, decreasing ATP and starch synthesis.

The structure of TPT has been determined with bound ligands, 3-phosphoglycerate and inorganic phosphate, in an occluded conformation from *Galdieria sulphuraria, a*n extremophilic unicellular red alga species. Figure **20.4.28** shows an interactive iCn3D model of a triose-phosphate/phosphate translocator from the red algae (5Y78).



NCBI iCn3D Figure **20.4.28**: Triose-phosphate/phosphate translocator from red algae (5Y78). (Copyright; author via source). Click the image for a popup or use this external link: https://structure.ncbi.nlm.nih.gov/i...mVNeFkXibxXr39

The model shows two monomers, one with red cylindrical alpha helices and spacefill 3-phosphoglycerate. The other subunit is gray, with the 3PG in colored sticks and conserved residues (T188, K204, F263, Y339, K362, R363) that interact with both Pi and 3PG. An outward- and inward-open conformation would presumably be triggered on ligand binding.

20.4.9: ACTIVITY REGULATION BY LIGHT

Given their role in photosynthesis, you would expect even the dark reaction enzymes to be regulated by light. Indeed, four C3 cycle enzymes are. They are ribulose 5-phosphate kinase, fructose 1,6-bisphosphatase, sedoheptulose 1,7-bisphosphatase, and glyceraldehyde 3-phosphate dehydrogenase. The regulation is affected by photon-induced disulfide bond formation between two cysteine side chains in the enzymes. When oxidized (in the disulfide bond form), the enzymes are inactive. Under light conditions, PSII, cytochrome b6f, and PSI participate in electron transport to move electrons from H_2O to ferredoxin and then onto a small soluble protein, thioredoxin, which contains a disulfide bond. The enzyme catalyzing this last step is **ferredoxin-thioredoxin reductase.** On reduction, the disulfide in thioredoxin is cleaved, and the now free sulfhydryls in thioredoxin are used to cleave the disulfide in the four enzymes mentioned above in a similar fashion to how β-mercaptoethanol in excess can cleave disulfides in proteins**.** This leads to conformational changes in the four enzymes that activate them. The process reverses in the absence of light, and the enzymes are inhibited. At night, plants mobilize starch for energy.

A simple mechanism to show how thioredoxin catalyzes disulfide bond reduction in target proteins is shown in Figure **20.4.29**.

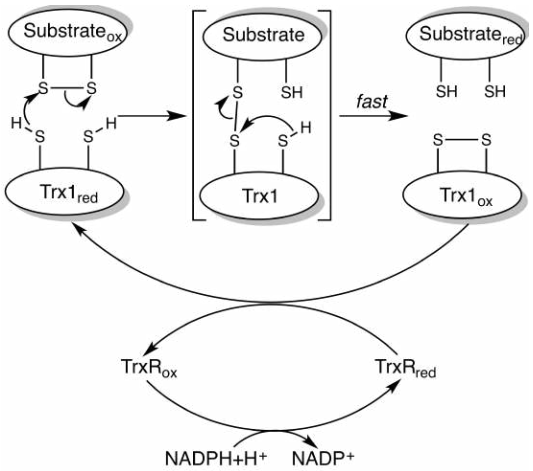
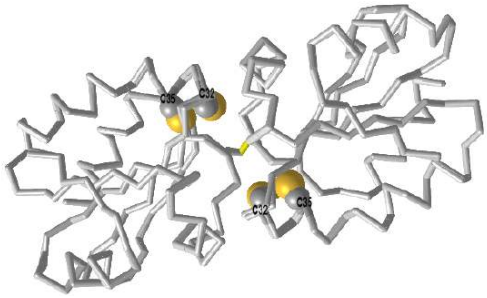


Figure **20.4.29**: Mechanism of thioredoxin reduction of target proteins. https://en.Wikipedia.org/wiki/Thiore...le:FigMech.png

The first enzyme in the oxidative branch of the pentose pathway, glucose 6-phosphate dehydrogenase, uses $NADP^+$ as an oxidizing agent, producing NADPH. In the light, there is a lot of NADPH produced from the light reactions of photosynthesis, so it makes biological sense that under these conditions, glucose 6-phosphate dehydrogenase activity is inhibited. It is also regulated by the cleavage of a critical disulfide bond; however, in this case, it results in enzyme inactivation.

We saw the role of thioredoxin in the previous chapter section when we discussed the regulation of photosynthesis and the chloroplast's ATP synthase.

Figure **20.4.30** shows an interactive iCn3D model showing a comparison of the structures of oxidized (1ERU) and reduced (1ERT) human thioredoxin.



NCBI iCn3D Figure **20.4.30**: Comparison of the structures of oxidized (1ERU) and reduced (1ERT) human thioredoxin. (Copyright; author via source). Click the image for a popup or use this external link: https://structure.ncbi.nlm.nih.gov/i...XPVsErV2JWxdA6.

The two subunits of thioredoxin, linked by a disulfide, are shown in gray. Press the "a" key to toggle between the oxidized form, with Cys32-Cys35 disulfide shown as a yellow stick, and the reduced form with the reduced and separated Cys 32 and Cys 35 shown in colored spheres. Not that the hydrogen covalently attached to the free cysteine side chain does not show in a crystal PDB structure.

20.4.10: SUMMARY

Photosynthesis in vascular plants takes place in chloroplasts. In the CO_2-assimilating reactions (the Calvin cycle), ATP and NADPH are used to reduce CO_2 to triose phosphates. These reactions occur in three stages: the fixation reaction, catalyzed by Rubisco; reduction of the resulting 3-phosphoglycerate to glyceraldehyde 3-phosphate; and regeneration of ribulose 1,5-bisphosphate from triose phosphates. Rubisco condenses CO_2 with ribulose 1,5-bisphosphate, forming an unstable hexose bisphosphate that splits into two molecules of 3-phosphoglycerate. Rubisco is activated by covalent modification (carbamoylation of Lys201) catalyzed by Rubisco activase. It is inhibited by a natural transition-state analog, whose concentration rises in the dark and falls during daylight. Stromal isozymes of the glycolytic enzymes catalyze the reduction of 3-phosphoglycerate to glyceraldehyde 3-phosphate; each molecule reduced requires one ATP and one NADPH. The cost of fixing three CO_2 into one triose phosphate is nine ATP and six NADPH, which are provided by the light-dependent reactions of photosynthesis. An antiporter in the inner chloroplast membrane exchanges Pi in the cytosol for 3-phosphoglycerate or dihydroxyacetone phosphate produced by CO_2 assimilation in the stroma. Oxidation of dihydroxyacetone phosphate in the cytosol generates ATP and NADH, thus moving ATP and reducing equivalents from the chloroplast to the cytosol. Four enzymes of the Calvin cycle are

activated indirectly by light. They are inactive in the dark so that hexose synthesis does not compete with glycolysis—which is required to provide energy in the dark.

20.4.11: PHOTORESPIRATION - RUBISCO/OXYGENASE AND THE GLYCOLATE CYCLE - ANOTHER LOOK

As autotrophs, plants make their fuels. They use that fuel to make ATP to power endergonic reactions like protein synthesis, cell division, etc. As eukaryotic cells, they have mitochondria and can use both aerobic and anaerobic respiration to produce ATP. In the dark, when photons are absent, they carry out mitochondrial aerobic respiration as they break down carbohydrates to CO_2 and water, the reverse of photosynthesis.

They also use O_2 in another process that is driven by light. As we detailed above, the enzyme that captures carbon, RuBisCo, has oxygenase activity. RuBisCo uses O_2 in a process called **photorespiration**, which produces CO_2 in a competing reaction. The final products of the reaction with CO_2 using RuBisCo are two 3C molecules, 3-phosphoglycerate (3PG). Using O_2 as a substrate produces 1 molecule of the 3C 3PG and 1 molecule of a 2C analog, **2-phosphoglycolate** (not 2-phosphoglycerate). 2-phosphoglycolate is also named **carboxymethylphosphate**. About one out of every four turnovers of the enzyme produced this metabolic dead product. Given this non-trivial side reaction, the enzyme should be called **ribulose 1,5-bisphosphate carboxylase/oxygenase**.

Compare the K_M values (9 μM for CO_2 and 350 μM for O_2 or 39x higher for O_2) for the enzyme and the equilibrium concentrations of the gases in aqueous solution (11 μM for CO_2 and 250 μM for O_2 or 23x higher for O_2). Oxygen's greater solubility nearly offsets the higher K_M for O_2, so modern conditions lead to a significant waste of the CO_2 capture efficiency of RuBisCo/Oxy. At higher temperatures in a warming world, the equilibrium ratio of solution concentrations of O_2/CO_2 increases, as does the affinity (based crudely on K_M values) of CO_2. Both of these exacerbate the effect of wasteful oxygenase activity. Finally, as the enzyme captures CO_2 is captured by the enzyme, the ratio of the local concentrations of O_2/CO_2 also goes up. All of these factors make RuBisCo's efficiency worse.

Figure 20.4.28 shows another mechanism for the reaction of both CO_2 and O_2 with RuBisCo/Oxygenase.

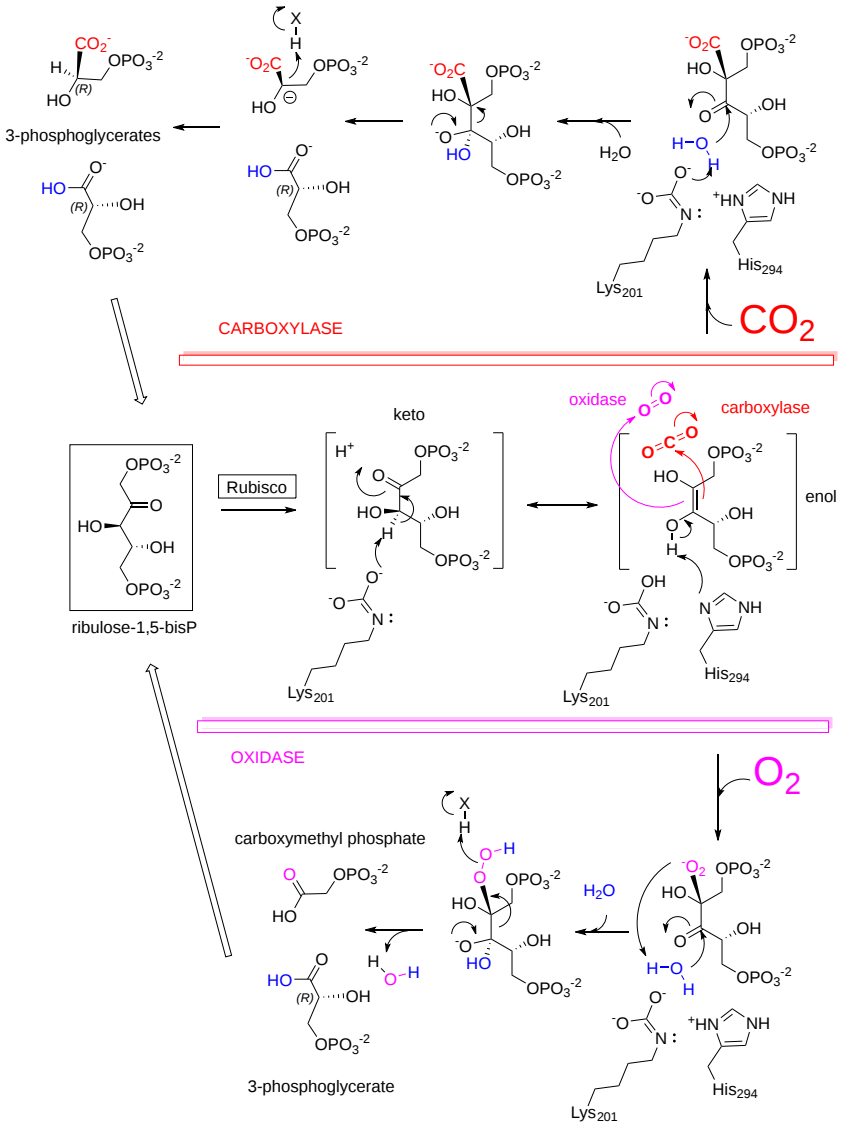


Figure **20.4.28**: Mechanism for the reaction of both CO_2 and O_2 with RuBisCo/Oxygenase. (after Kannappan et al. J. Phys. Chem. B 2019, 123, 2833−2843)

Note again that in contrast to most oxygenases, no cofactor is required for the RuBisCo/Oxygenase.

20.4.12: THE GLYCOLATE PATHWAY

The 2-phosphoglycolate (carboxylmethyl phosphate) "waste" product of the oxygenase activity of RuBisCo/Oxygenase is recycled through a complex pathway that is called "photorespiration". It occurs in three different organelles, the chloroplast, the peroxisome, and the mitochondria. Part of the generalized pathway is shown in Figure **20.4.29**.

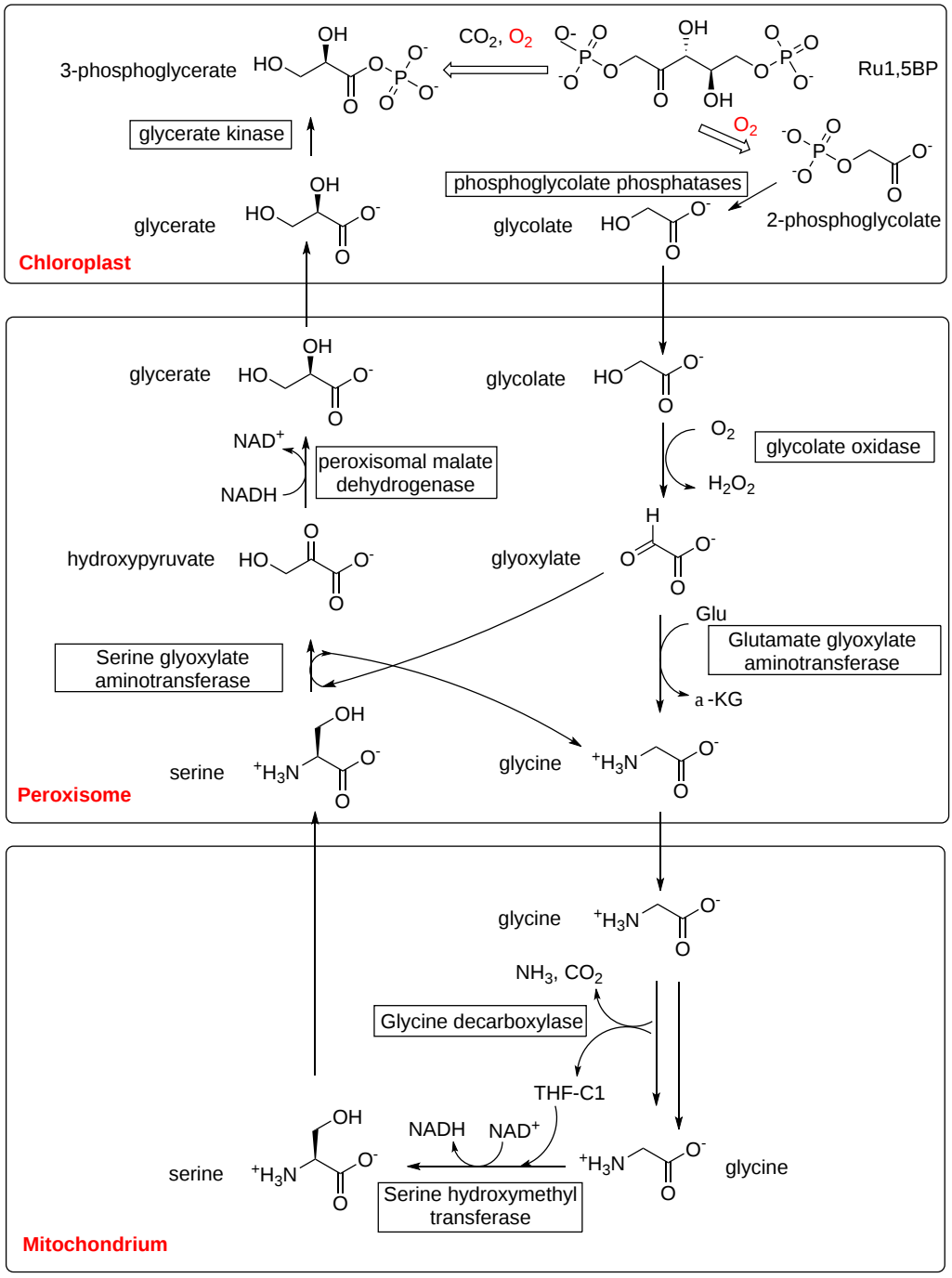


Figure **20.4.29**: The glycolate photorespiration salvage pathway (adapted from Hu et al. *Plant Cell*. 2012;24.doi:10.1105/tpc.112.096586)

Multiplying the stoichiometry represented in the figure by 2 shows that 2 molecules of 2-phosphoglycolate produce 2 molecules of glycine. These get converted to two molecules of serine. We will see the mechanisms for some of these reactions in the chapter on amino acid metabolism. The net reaction is:

$$\mathbf{2\,Glycine + NAD^{++}\ H_2O \longrightarrow serine + CO_2 + NH_3 + NADH}$$

The serine is eventually converted to 3-phosphoglycerate, which can be used again in the C3 cycle. Note that CO_2 is produced in the glycolate pathways that started with the use of O_2 as a substrate by RuBisCo/Oxygenase. Hence, the whole system uses O2 and produces one CO_2, so the combined reactions are usually called **photorespiration**. It's not an ideal term since it is wasteful compared to mitochondrial respiration. Some prefer to call the combined pathway of Rubisco oxygenase and the glycolate pathways the **C2 cycle**.

20.4.13: SUMMARY

This chapter shifts focus from the light-dependent reactions of photosynthesis to the “dark reactions,” a series of biochemical pathways that fix CO_2 into organic compounds, primarily through the Calvin (C3) cycle. Although termed “dark reactions,” these processes occur during the day and are distinguished from the light reactions by their independence from direct photon absorption.

Calvin Cycle Overview:

- **CO_2 Capture and Fixation:**
  Atmospheric CO_2 is fixed by ribulose 1,5-bisphosphate carboxylase/oxygenase (Rubisco) into ribulose 1,5-bisphosphate (RuBP), producing an unstable 6-carbon intermediate that splits into two molecules of 3-phosphoglycerate (3PG).
- **Reduction and Regeneration:**
  3PG is then reduced to glyceraldehyde-3-phosphate (G3P) using ATP and NADPH generated during the light reactions. Most G3P molecules are recycled to regenerate RuBP, while a fraction is used for the synthesis of carbohydrates such as starch and sucrose.

Rubisco: Structure, Function, and Limitations:

- **Dual Activity:**
  Rubisco catalyzes both the carboxylase and oxygenase reactions. Its primary role is to fix CO_2; however, it also reacts with O_2, leading to photorespiration—a process that diverts energy and fixed carbon away from carbohydrate synthesis.
- **Structural Composition and Evolution:**
  The enzyme is composed of large subunits (encoded by the chloroplast genome) and small subunits (nuclear-encoded), forming multimeric complexes (often a 16-mer in higher plants). Rubisco’s slow catalytic rate and competing oxygenase activity are attributed to its evolutionary origin in a high-CO_2, low-O_2 environment, which has become suboptimal under modern atmospheric conditions.
- **Mechanistic Insights:**
  Detailed structural studies reveal how the enzyme’s active site, including a carbamoylated lysine and a bound Mg^{2+} ion, facilitates CO_2 fixation. Despite its inefficiency, high cellular concentrations of Rubisco ensure sufficient carbon fixation.

Photorespiration and the Glycolate Pathway:

- **Competing Reaction with O_2:**
  When Rubisco acts as an oxygenase, it produces one molecule of 3PG and one molecule of 2-phosphoglycolate. The latter is a “waste” product that enters the glycolate salvage pathway (photorespiration), a multi-organellar process spanning the chloroplast, peroxisome, and mitochondrion.
- **Energetic and Metabolic Costs:**
  Photorespiration consumes energy and releases CO_2, thus reducing the overall efficiency of photosynthetic carbon fixation, especially under conditions of high O_2 and elevated temperatures.

Plastid Dynamics and Metabolite Transport:

- **Plastid Diversity and Interconversion:**
  The chapter discusses various plastids—chloroplasts for photosynthesis, amyloplasts for starch storage, and others—and how they interconvert based on developmental and environmental signals.
- **Triose Phosphate/Phosphate Translocator (TPT):**
  The TPT exchanges triose phosphates from the chloroplast with inorganic phosphate from the cytosol, linking the dark reactions with cytosolic carbohydrate metabolism.

Regulation by Light and Redox Control:

- **Enzymatic Regulation:**
  Key Calvin cycle enzymes are modulated by light through the ferredoxin–thioredoxin system. In the light, reduced thioredoxin activates these enzymes by cleaving regulatory disulfide bonds, ensuring coordination between the light and dark reactions.
- **Balancing Carbon Fixation and Photorespiration:**
  The enzyme’s competing activities are influenced by substrate concentrations and environmental conditions, with plants employing mechanisms (e.g., phase separation of Rubisco in carboxysomes or pyrenoids) to increase local CO_2 concentrations and enhance fixation efficiency.

Environmental and Global Implications:

- **Impact of Elevated CO_2 and Climate Change:**
  Changes in atmospheric CO_2 levels affect Rubisco kinetics and plant nutrient composition. Although higher CO_2 can boost carbon

fixation, it may also lead to imbalances in nutrient content (e.g., reduced protein and micronutrient levels) in crops, with broader implications for food security.

- **Photorespiratory Flux and Plant Productivity:**
  The efficiency of the dark reactions is a critical determinant of overall photosynthetic performance, influencing how plants adapt to changing environmental conditions and how global carbon cycles are maintained.

In summary, this chapter integrates the biochemical mechanisms underlying CO_2 fixation, the regulation and limitations of Rubisco, and the metabolic consequences of photorespiration. It highlights the complexity of plant metabolism, emphasizing how dark reactions, though indirectly driven by light, are finely tuned to optimize carbon assimilation and respond to environmental challenges.

This page titled 20.4: CO_2 uptake - Calvin Cycle and C3 organisms is shared under a CC BY-NC-SA 4.0 license and was authored, remixed, and/or curated by Henry Jakubowski and Patricia Flatt.

- **Current page** by Henry Jakubowski and Patricia Flatt is licensed CC BY-NC-SA 4.0.
- **11.2: Diffusion Across a Membrane - Passive and Facilitated Diffusion** by Henry Jakubowski and Patricia Flatt has no license indicated.

20.5: CO2 UPTAKE - C4 AND CAM PATHWAYS

LEARNING GOALS (CHATGPT O3-MINI)

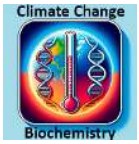
Below are a series of learning goals tailored for junior and senior biochemistry majors based on the provided information about the C4 pathway and associated topics:

- **Distinguish C3 and C4 Photosynthetic Pathways:**
  • Explain how photorespiration in C3 plants, driven by Rubisco's competing oxygenase activity and the glycolate salvage (C2) pathway, reduces photosynthetic efficiency.
  • Describe how the C4 pathway circumvents these inefficiencies by initially capturing CO_2 as bicarbonate (HCO_3^-) and converting it into a 4-carbon (4C) compound prior to RuBisCo fixation.
- **Outline the Initial Steps of the C4 Pathway:**
  • Describe the role of phosphoenolpyruvate (PEP) carboxylase in mesophyll cells in converting HCO_3^- and PEP into oxaloacetate (OAA), a 4C intermediate.
  • Explain subsequent reactions where OAA is converted either to malate (via malate dehydrogenase) or aspartate (via transamination) and how these intermediates transport CO_2 to bundle sheath cells.
- **Examine the Role of Malate Decarboxylation and CO_2 Release:**
  • Discuss how, in the bundle sheath cells, malate is decarboxylated by NADP-malic enzyme to release CO_2 for fixation by RuBisCo, thereby locally saturating RuBisCo with CO_2 and suppressing its oxygenase activity.
- **Understand the Function and Mechanism of Pyruvate Phosphate Dikinase (PPDK):**
  • Describe the reaction catalyzed by PPDK, including its net reaction, formation of high-energy phosphorylated intermediates, and the overall cost of ATP (equivalent to two ATPs per CO_2 fixed in the C4 pathway).
  • Analyze the domain organization of PPDK (nucleotide-binding, central catalytic, and PEP/pyruvate binding domains) and explain how conformational "swiveling" enables sequential phosphotransfer events.
- **Compare Energy Costs and Thermodynamic Trade-offs:**
  • Contrast the ATP requirements for fixing CO_2 in the C4 pathway (approximately 5 ATPs per CO_2 fixed) with those in the C3 pathway (approximately 3 ATPs per CO_2 fixed).
  • Discuss how temperature influences Rubisco affinity for CO_2 and the relative efficiencies of C3 versus C4 pathways.
- **Explore the Role of Carbonic Anhydrases:**
  • Describe the function and distribution of the three classes of carbonic anhydrase (α, β, and γ) in plants, emphasizing their role in interconverting CO_2 and HCO_3^- in different cellular compartments (chloroplast, cytosol, mitochondria) and in the CO_2-concentrating mechanisms of C4 and CAM plants.
- **Introduce Crassulacean Acid Metabolism (CAM):**
  • Outline the CAM pathway, highlighting its adaptation to water-limited environments through nocturnal CO_2 capture and daytime decarboxylation of stored malic acid, and compare its metabolic organization to that of C3 and C4 plants.
- **Discuss Plastid Diversity and Interconversion:**
  • Explain the various types of plastids (chloroplasts, amyloplasts, etioplasts, chromoplasts) and the processes (e.g., "greening" and "de-greening") by which plastids interconvert in response to environmental and developmental cues.
- **Examine Rubisco Aggregation and Phase Separation Mechanisms:**
  • Describe how the enzyme Rubisco, despite its slow turnover, is present in high concentrations and can undergo phase separation with intrinsically disordered linker proteins (such as EPYC1/LCI5 in algae or CsoS2 in carboxysomes) to enhance local CO_2 concentrations. • Understand the roles of protein-protein interactions, tandem repeats, and charge distribution in promoting phase separation and the formation of structures like pyrenoids and carboxysomes.
- **Evaluate the Evolutionary and Ecological Implications:**
  • Discuss the evolutionary history of Rubisco, including its adaptation from a high-CO_2, low-O_2 environment to current atmospheric conditions, and the strategies (e.g., C4 and CAM pathways) that have evolved to mitigate its inefficiencies.
  • Consider how rising atmospheric CO_2 and global warming might impact plant metabolism, photosynthetic efficiency, and ultimately food security through changes in nutrient composition.
- **Relate Plant Photosynthetic Efficiency to Thermodynamic Models:**
  • Compare the thermodynamic efficiencies of C3/C4 photosynthesis with energy conversion in internal combustion engines (e.g.,

the Otto cycle), highlighting how plants use concentration and storage mechanisms to optimize carbon fixation under varying environmental conditions.

These learning goals are designed to help students integrate structural, mechanistic, and regulatory aspects of the C4 pathway and related carbon fixation processes, as well as appreciate their significance in plant physiology and global carbon cycling.

The source for the organization and some of the text derives from Sindayigaya and Longhini. https://www.peoi.org/Courses/Courses...chem/biochem18 CC - https://creativecommons.org/licenses...sa/3.0/deed.en



Everything in the chapter is related to climate change. For more general information on biochemistry and climate change, visit Chapter 32 Biochemistry and Climate Change. For more details on carbon fixation or capture, visit Chapter 32.16: Part 4 - Fixing Carbon Fixation.

20.5.1:

20.5.2: THE C4 PATHWAY

Photorespiration, caused by the oxygenase activity of RuBisCo/Oxygenase and the ensuing glycolate salvage (C2) pathway, significantly diminishes the efficiency of photosynthesis in C3 plants. Rest assured, some plants have found a way around the problem by adding a few steps before RuBisCo. The altered pathway is known as the C4 pathway, and plants that utilize it are referred to as C4 plants. The initial steps involve the temporary capture of CO_2 in the form of HCO_3^-, into a 4C, not 3C sugar. Plants that utilize the C4 pathway include maize, sorghum, sugarcane, and many tropical plants. An overview of the pathways emphasizing the steps that precede RuBisCo is shown in Figure **20.5.1**.

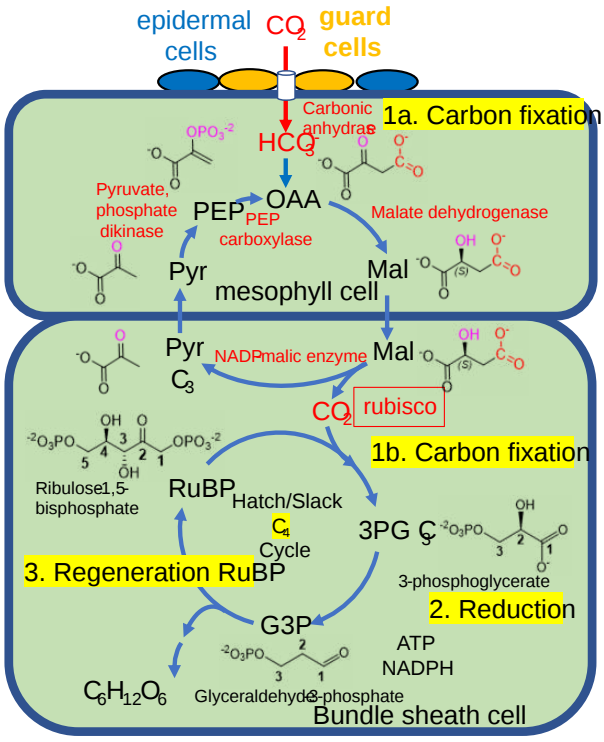


Figure **20.5.1**: Carbon assimilation in C4 plant

This extra step (compared to C3 plants) concentrates CO_2 and effectively decrease the competing substrate O_2 to increase the efficiency of Rubisco.

Experimental evidence shows that radiolabeled $^{14}CO_2$ is captured into the 4C molecule, oxaloacetate (OAA), a citric acid cycle and gluconeogenic intermediate, through the enzyme phosphoenolpyruvate carboxylase, which uses HCO_3^- as a substrate. The reaction takes place in mesophyll cells. OAA can be reduced by NADPH using malate dehydrogenase or converted to aspartate through a transamination (not shown in the figure). Malate moves into the bundle sheath cell. It is then decarboxylated by the NADP-malic enzyme to pyruvate. Pyruvate can move back into the mesophyll cell and be converted to phosphoenolpyruvate (PEP) and then back to OAA by the **pyruvate phosphate dikinase** and **PEP carboxylase**. CO_2 from the decarboxylation of malate is delivered as a substrate to RuBisCo.

Pyruvate dikinase is used in bacteria, protozoa, C4 plants, and another type, Crassulacean, discussed below. Its non-plant function is to produce ATP, similar to pyruvate kinase. The net reaction is:

ATP + phosphate + pyruvate = AMP + PP_i + H^+ + phosphoenolpyruvate

Figure **20.5.2** shows a simplified mechanism for the reaction

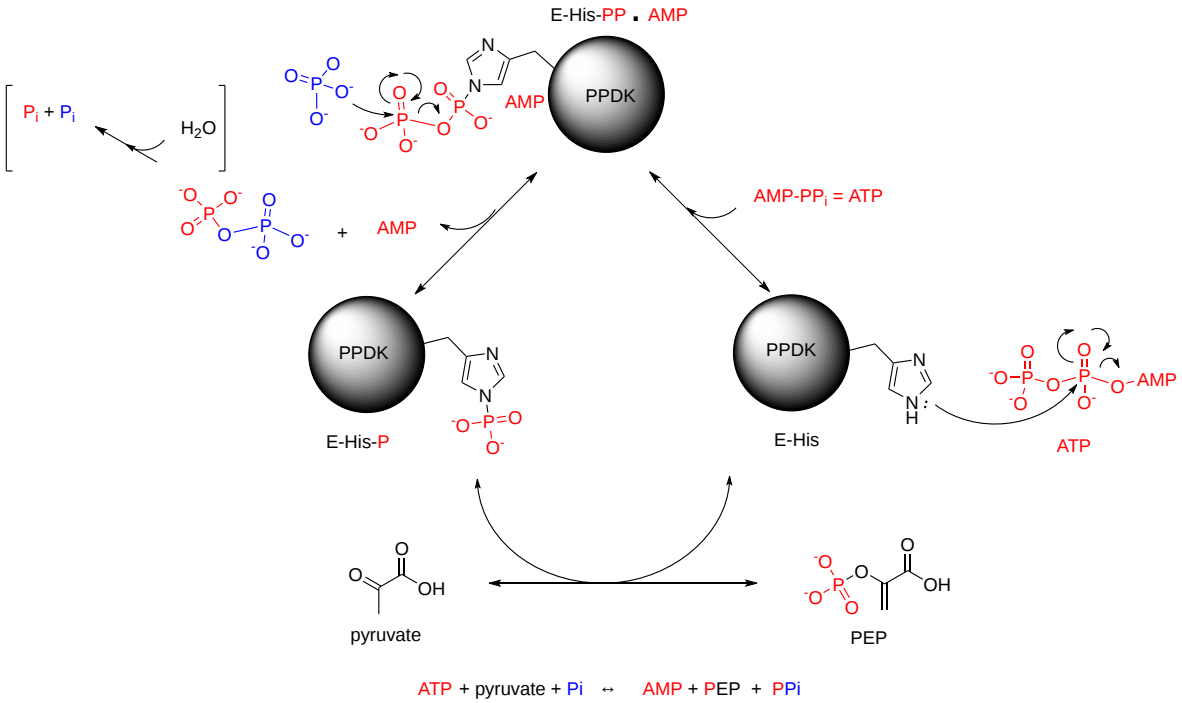


Figure **20.5.2**: Mechanism of pyruvate phosphate dikinase

The net reaction shows that in C4 plants, two molecules are phosphorylated by ATP. One is pyruvate, and the other is inorganic phosphate (Pi). Hence the name dikinase. The reverse reaction of ATP synthesis occurs in bacteria and protozoans. There are two phosphorylated intermediates, an Enz-His-P and an Enz-His-PP_i. These are "activated" phosphate carriers in the phosphotransfer reactions to pyruvate and P_i, respectively. If PP_i is not hydrolyzed to $2P_i$, as illustrated in the top left of Figure 2 above, the reaction is fully reversible.

In C4 plants, there are three reactions

1. Pyr + E-His-P ↔ PEP + E-His
2. E-His + ATP ↔ E-His-PP ·AMP (· indicates a noncovalent interaction)
3. E-His-PP ·AMP + P_i ↔ E-His-P + AMP + PP_i

When PP_i is hydrolyzed, the net input of ATP to phosphorylated pyruvate is two ATP equivalents.

In the next step, PEP is carboxylated in a carbon capture reaction by PEP carboxylase, which, as mentioned above, uses HCO_3^- as a substrate, not CO_2 per se. PEP carboxylase also lacks competing oxidase activity. The product is malate, which releases locally high "saturating" concentrations of CO_2 in the bundle sheath cells, significantly suppressing the oxygenase activity of RuBisCo.

Pyruvate phosphate dikinase undergoes a very large conformational change in domain organization during the catalytic cycle. The two kinase activities are located at different sites in the enzyme. The phosphorylation of Pi occurs in the N-terminal domain, while the phosphorylation of pyruvate occurs in the C-terminal domain. The central domain, which links to the N- and C-terminal domains via associated "tethers," is the site of the catalytic histidine involved in phosphotransfer. A swiveling of domains occurs to allow sequential phosphotransfers.

Figure **20.5.3** shows the Pfam domain structure for the protein.



Figure **20.5.3**: The green represents the AMP/ATP nucleotide-binding domain (NBD), the blue the PEP/pyruvate binding domain (PBD), and the red the central domain which catalyzes the phosphotransfer from ATP to pyruvate and from PEP to AMP through phosphorylated histidine intermediates. The NBD has three subdomains.

Figure **20.5.4** shows an interactive iCn3D model of an AlphaFold-predicted model of chloroplast pyruvate, phosphate dikinase from *Flaveria brownii (Brown's yellowtops) (*Q39734)

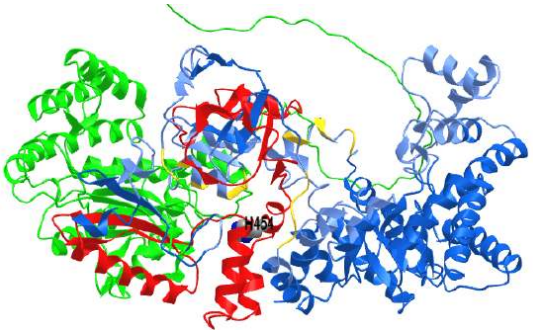


Figure **20.5.4**: AlphaFold-predicted model of chloroplast pyruvate, phosphate dikinase from *Flaveria brownii (Brown's yellowtops) (*Q39734). (Copyright; author via source). Click the image for a popup or use this external link: https://structure.ncbi.nlm.nih.gov/i...VB6Aywuc2bLD38

The green represents the N-terminal NBD, the red is the central domain with the catalytic His (side chain shown as CPK-colored spheres and labeled), and the blue is the PEP/Pyr PBD.

Figure **20.5.5** illustrates the conformation changes that occur in the central domain (yellow in this figure) and the N-terminal nucleotide-binding domain (NBD, green) in various ligand-bound states.

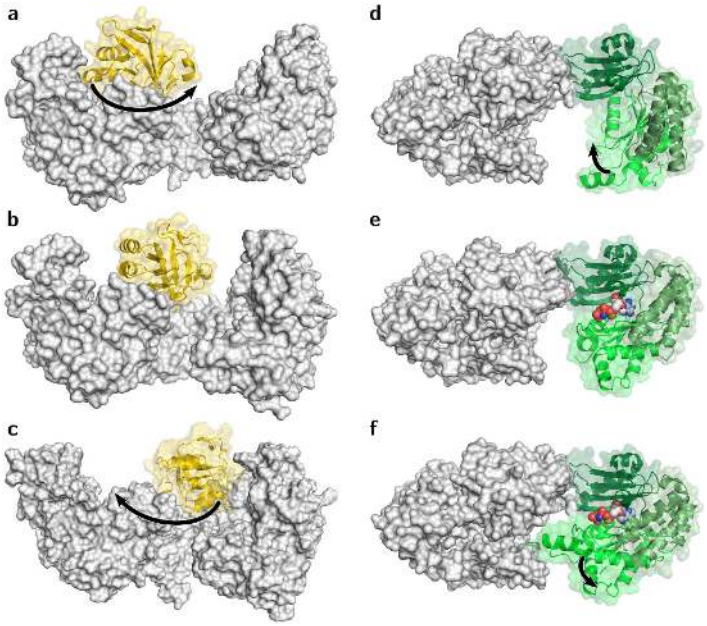


Figure **20.5.5**: **Movement of the PPDK domains**

Panel a–c show movement of the central domain (yellow). In (**a**), it swivels to face the PBD domain (PDB 5JVL/C), and in (**c**), it faces the NBD domain (*Tb*PPDK (PDB 2X0S)). In (**b**) it is in an intermediate position.

Panels d-f show the movement of the NBD (three greens depict the three subdomains). Pane (**d**) is the state without bound nucleotide (PDB 5JVJ/A), while panel (**f**) shows the fully closed, nucleotide-bound state (PDB 5JVL/A). Panel (**e**) shows a semi-closed, nucleotide-bound state (PDB 5JVL/C). Minges, A., Ciupka, D., Winkler, C. *et al.* Structural intermediates and directionality of the swiveling motion of Pyruvate Phosphate Dikinase. *Sci Rep* **7,** 45389 (2017). https://doi.org/10.1038/srep45389. Creative Commons Attribution 4.0 International License. http://creativecommons.org/licenses/by/4.0/

Figure 20.5.6 shows the interactions of bound substrates in different conformation states of PPDK.

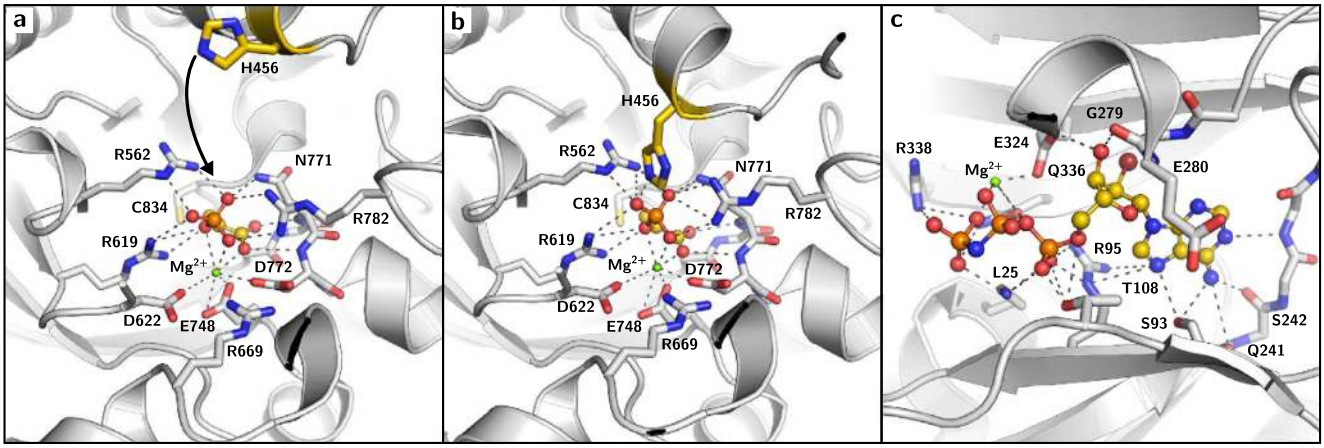


Figure 20.5.6: **Substrate binding sites of *Ft*PPDK.**

Panel (**a**) shows the semi-closed state of the PEP binding site (PDB 5JVL/A) with the catalytic H456 (yellow) pointing away from PEP.

Panel (**b**) shows the closed state of the PEP binding site (PDB 5JVL/C), showing interactions between PEP and surrounding residues, including the catalytic H456 (yellow).

Panel (**c**) shows the closed state of the nucleotide-binding site of 5JVL/D occupied with 2'-Br-dAppNHp, a nonhydrolyzable ATP analog. Interacting residues are highlighted. Minges, A et al. ibid.

After CO_2 is delivered from malate in the bundle sheath cell using RuBisCo, the remaining reactions are the same as in the C3 pathways.

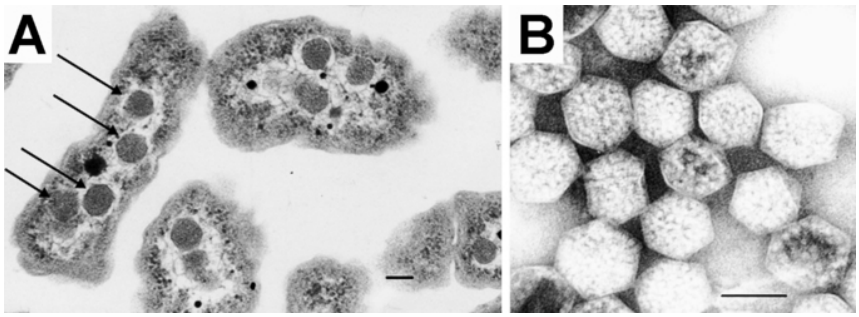
Once CO_2 is fixed into 3-phosphoglycerate in the bundle-sheath cells, the Calvin cycle's other reactions occur exactly as described earlier. Overall, the C4 pathways require more ATP. A molecule of PEP is required for each CO_2 fixed in the C4 pathway, which takes the equivalent of two ATPs. So, each CO_2 fixed in the C4 pathway takes five ATPs compared to three ATPs in the C3 pathway. As mentioned above, the affinity (estimated from the KM) of CO2 for RuBisCo decreases with increasing temperature, thereby decreasing the energetic efficiency of carbon capture. At higher temperatures (28-30 °C), the extra energy cost for the C4 pathway balances out the extra energy cost for the C3 pathway at higher temperatures.

20.5.3: CARBONIC ANHYDRASES

We first encountered carbonic anhydrase when we discussed its mechanism in Chapter x.xx. We'll now discuss its function and activity in the C4 pathway in detail. Given that we are facing a climate crisis due to the increasing levels of CO_2 in the atmosphere arising from the burning of fossil fuels, removing CO2 from the atmosphere —a process called carbon sequestration for climate purposes —becomes even more important. Understanding the role of carbonic anhydrase in CO2 sequestration also becomes crucial.

Plants have three genes for carbonic anhydrase (α, β, and γ). Each can be differentially spliced, resulting in plants having many different isoforms of this protein. They are most abundant in the chloroplast, cytoplasm, and mitochondria, and they have many additional roles outside of fixing CO_2 in C4 (and CAM) plants. In autotrophic (make their own "food") bacteria (such as cyanobacteria, also known as blue-green algae), there are no internal organelles. However, there are **carboxysomes,** which are protein-bounded vesicles (much like a bacteriophage head), which contain not nucleic acid but RuBisCo and carbonic anhydrase in their internal compartment. The carbonic anhydrase converts HCO_3^- to CO_2 for reaction with RuBisCo. The carboxysome thus concentrates the CO_2-producing and fixing enzymes for photosynthesis.

Figure 20.5.7:



F

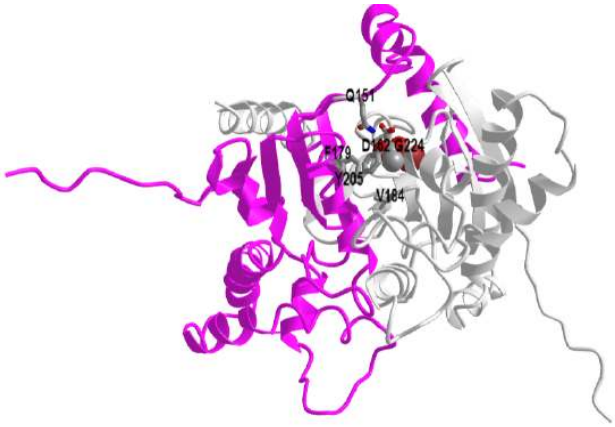
Figure **20.5.7**: **Electron Micrograph of a carboxysome**: (A) A thin-section electron micrograph of H. neapolitanus cells with carboxysomes inside. In one of the cells shown, arrows highlight the visible carboxysomes. (B) A negatively stained image of intact carboxysomes isolated from H. neapolitanus. The features visualized arise from the distribution of stains around proteins that form the shell, as well as around the RuBisCO molecules that fill the carboxysome interior. Scale bars indicate 100 nm. BioLibreText

In C3 plants, CO_2 (aq), which is dissolved CO2, is the actual substrate for RuBisCo, so available HCO3—is converted to CO2 by carbonic anhydrase. In C4 and CAM plants, CO2 (aq) is first converted to bicarbonate by carbonic anhydrase. HCO3- (aq) is then used as the actual substrate for the "carbon fixation" step. Hence, carbonic anhydrase has roles in C3, C4, and CAM plants.

All of the carbonic anhydrases have a Zn^{+2} at the active site. The most prominent alpha form in plants was discovered in erythrocytes and is typically active as a monomer. It has one large 10-strand beta sheet surrounded by seven alpha helices. Three histidine side chains and water form a tetrahedral coordination around the Zn^{2+} ion. **Gamma** carbonic anhydrase is a trimer with three active sites at the interface between pairwise monomers with the Zn-coordinating histidine side chains from two different subunits.

Beta carbonic anhydrase in plants is typically an octamer of identical subunits. Two cysteines, one histidine, and water coordinate the Zn ion. The monomer has four beta strands in a beta-sheet surrounded by alpha helices. An additional beta-strand is involved in monomer interactions. As the active site is located at the interface of two subunits, the functional biological unit is the dimer; however, a tetramer and even an octamer are typically formed. The substrate binding groups have a one-to-one correspondence with the functional groups in the alpha-carbonic anhydrase active site, with the corresponding residues being closely superimposable by a mirror plane of symmetry. Therefore, despite differing folds, alpha- and beta-carbonic anhydrases have converged upon a similar active site design and are likely to share a common mechanism.

Figure **20.5.8** shows an interactive iCn3D model of beta-carbonic anhydrase from Pisum sativum (pea) with bound acetate (1EKJ).



NCBI iCn3D Figure **20.5.8**: Beta-carbonic anhydrase from Pisum sativum (pea) with bound acetate (1EKJ). (Copyright; author via source). Click the image for a popup or use this external link: https://structure.ncbi.nlm.nih.gov/i...VZTEJPy1hPxK27

For the sake of simplicity, only two subunits (A - gray and B - magenta) of the octamer are shown. Acetate, a proxy for HCO_3^{-2}, is shown in spacefill binding between the two subunits in CPK-colored spheres. The side chains involved in Zn^{2+} binding, Cys 160, His 220, and Cys 223 (unlabeled), are on the A chain. The amino acids that bind acetate are distributed between the A chain (Asp 162, Gly 224, Val 184) and the B chain (Gln 151, Phe 169, and Tyr 205) and are labeled. The same groups are involved in substrate binding in alpha carbonic anhydrase, but in a mirror image orientation (with the normal L-amino acids).

Beta carbonic anhydrase is highly expressed in leaves and is found in chloroplasts, mitochondria, and the cytoplasm. Many plants have it in the cytoplasm and chloroplasts.

- β-carbonic anhydrase (βCA) in C3 plants: Most of the βCA in leaves is in chloroplasts in mesophyll cells and may comprise up to 2% of leaf protein. Yet studies have shown that you can delete the gene for it with minimal effect on the maximal rate of photosynthesis. However, by interference, plant development was affected, so the enzyme is probably most needed to produce HCO_3^- for biosynthesis.
- β-carbonic anhydrase (βCA) in C4 plants: Most of the βCA is found in the cytoplasm of mesophyll cells. There, it catalyzes the first reaction of the C4 pathway, CO_2 (aq) to HCO_3^- (aq). Mitochondrial (βCA) and γCA probably function to fix CO_2 arising from oxidative respiration.

20.5.4: CRASSULACEAN ACID METABOLISM (CAM) PATHWAY

Plants that encounter the chronic stress of low water availability have evolved another pathway to adapt to these conditions. Stomata in C3 plants are open during the day to allow carbon capture from CO_2, but they can close when water is limited. This obviously will inhibit plant growth. In the CAM pathway, the stomata remain open at night, allowing for carbon capture when water loss through the stomata is lower. The incoming CO_2 is fixed through carbonic anhydrase and then a series of several enzymes to form malic acid, which is transported for storage and use during the light in vacuoles. This CAM pathway is described in Figure **20.5.9**.

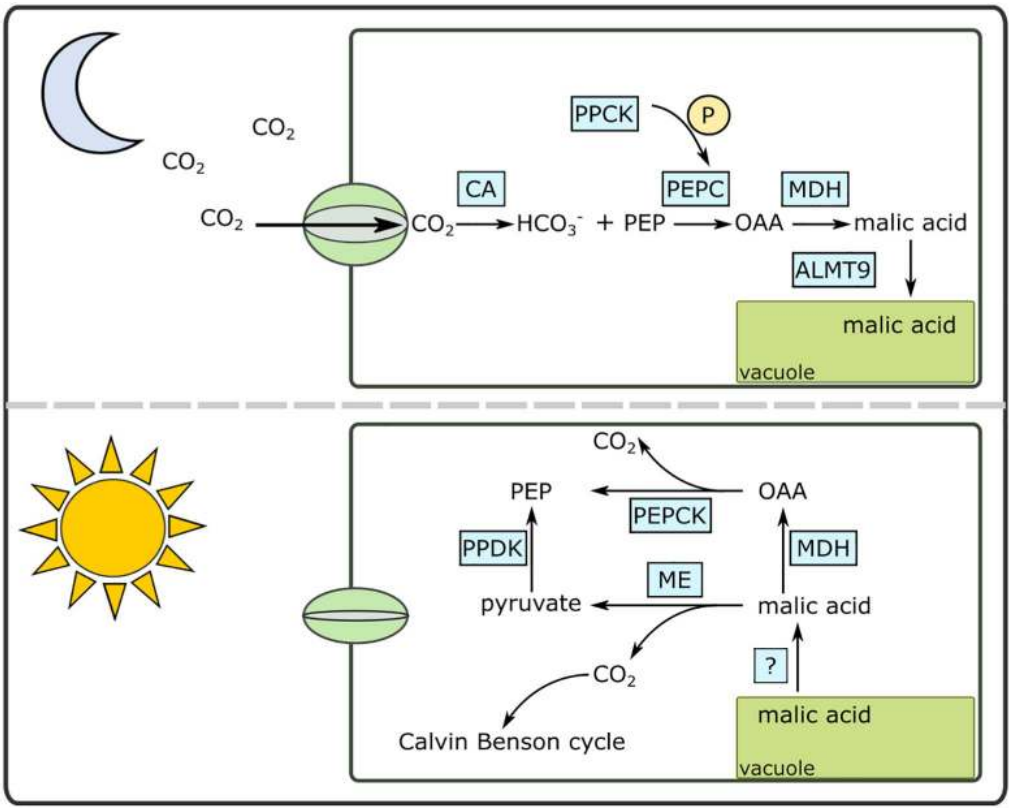


Figure **20.5.9**: A simplified diagram of the Crassulacean acid metabolism (CAM) pathway under day and night conditions. Heyduk Karolina, et al. Frontiers in Plant Science.2019. https://www.frontiersin.org/article/...pls.2018.02000. DOI=10.3389/fpls.2018.02000. **Creative Commons Attribution License (CC BY)**.

The proteins and intermediates in the CAM pathways are ALMT9, aluminum-activated malate transporter; CA, carbonic anhydrase; MDH, malate dehydrogenase; OAA, oxaloacetate; ME, malic enzyme (NAD or NADP); P, phosphate; PEPC, phosphoenolpyruvate carboxylase; PEPCK, PEP carboxykinase; PPCK, PEPC kinase; PPDK, pyruvate, phosphate dikinase.

During the day, malic acid moves back into the cytoplasm, where it is decarboxylated by malic enzyme, releasing locally high CO_2 concentrations for use by RuBisCo in the C3 cycle. In plants that use CAM, other changes occur, including modifications to leaf structure and the activation of additional regulatory processes that coordinate metabolic gene expression.

Figure **20.5.10**s shows more details of the CAM cycle.

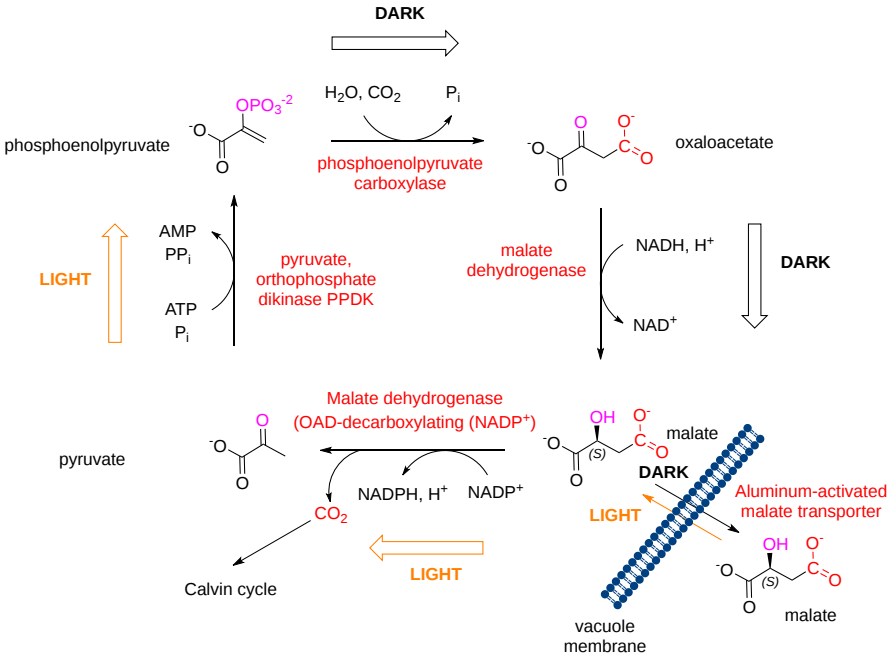


Figure **20.5.10**: Details of the CAM cycle

20.5.5: THERMODYNAMIC COMPARISON BETWEEN THE C3/C4 PATHWAYS AND THE OTTO CYCLE

It is interesting to compare the thermodynamic efficiencies of plants to that of the internal combustion engines, which is governed by the thermodynamic Otto cycle. In the cycle, chemical energy in the form of gasoline and O_2 is converted to thermal energy, which is then converted into mechanical energy. Both photosynthesis (the conversion of the energy of photons into chemical energy) and the Otto cyclehave limited efficiencies.

- In internal combustion engines, power is partly limited by air uptake and different efficiencies when running at non-constant speeds (like stop-and-go).
- In the C3 pathway, efficiency is limited by the oxygenase activity of RuBisCo/Oxygenase (given the much higher concentration of atmospheric O_2 compared to CO_2) and the ensuing photorespiration pathway.
- Water availability also plays a role, as the net reaction of photosynthesis and glucose production, in simplified form, is $6CO_2 + 6H_2O \rightarrow 6C(H_2O_6)$, so in high heat and low humidity, the process efficiency decreases.

Figure **20.5.11** shows a comparison of three stages, the storage component, the basic cycle, and a concentration mechanism, in photosynthesis and the internal combustion engine (ICE).

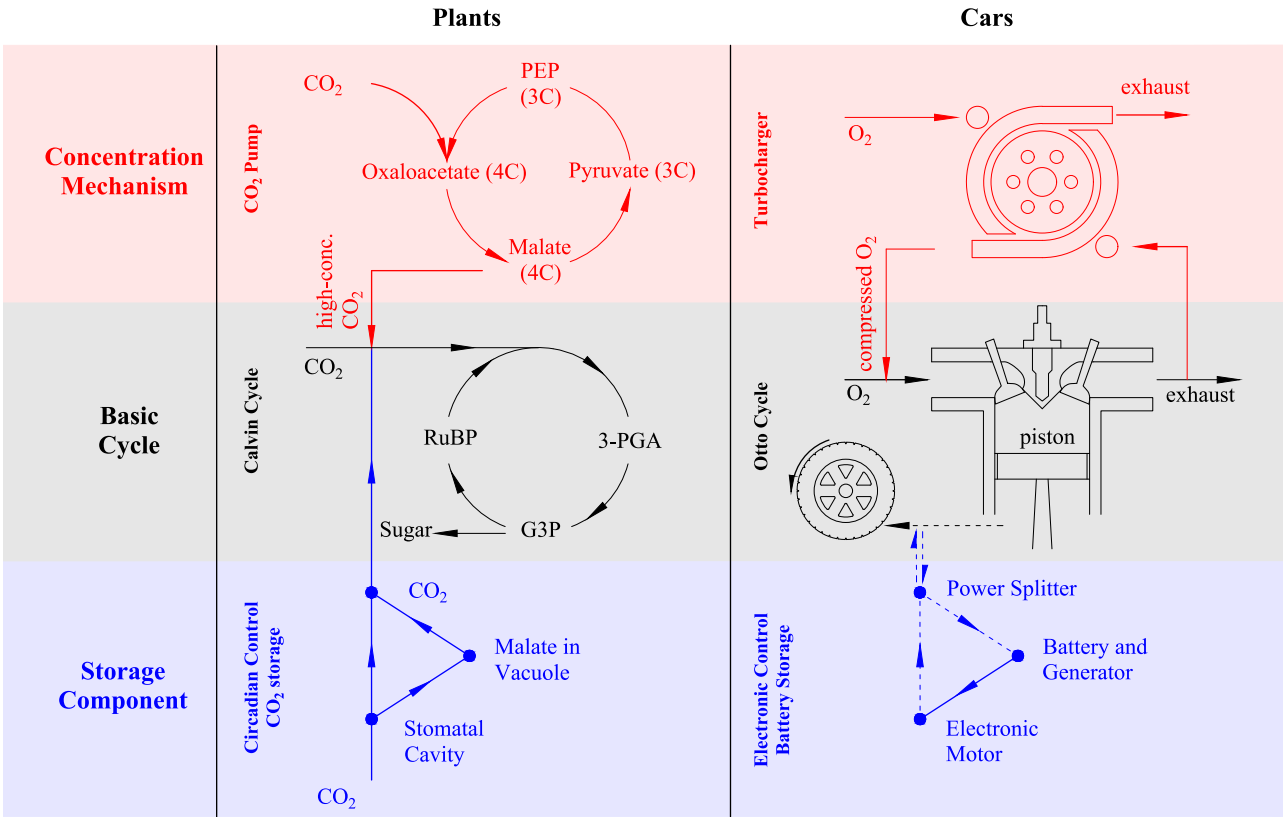


Figure **20.5.11**: A comparison of plant photosynthesis and car engine functioning illustrates how the core processes interact with the additional components. Hartzell S, Bartlett M, Yin J, Porporato A (2018). Similarities in the evolution of plants and cars. PLoS ONE 13(6): e0198044. https://doi.org/10.1371/journal.pone.0198044. Creative Commons Attribution License,

A concentrating mechanism in C4 plants and turbocharged cars provides concentrated CO_2 and oxygen, respectively, to the core cycle (upper row). A storage mechanism in CAM plants allows carbon dioxide to be stored as malic acid at night and then passed to the Calvin cycle during the day, while a storage mechanism in hybrid electric vehicles (HEVs) allows energy to be stored in the battery during braking and then passed to the motor to power the drivetrain in parallel with the engine (bottom row).

20.5.6: SUMMARY

This chapter examines how certain plants overcome the inefficiencies of photorespiration inherent in the C3 pathway by employing the C4 pathway and related adaptations. In C3 plants, Rubisco's dual carboxylase/oxygenase activity leads to significant energy losses due to photorespiration. The C4 pathway, utilized by plants such as maize, sorghum, and sugarcane, introduces additional steps before CO_2 fixation to concentrate CO_2 and suppress Rubisco's oxygenase activity.

Key Elements of the C4 Pathway:

- **Initial CO_2 Capture:**
  In mesophyll cells, atmospheric CO_2 is first converted to bicarbonate (HCO_3^-) and then rapidly fixed by phosphoenolpyruvate (PEP) carboxylase to form a 4-carbon compound, oxaloacetate (OAA). OAA may be reduced to malate or converted to aspartate, which then transports the captured carbon to the bundle sheath cells.
- **CO_2 Release and Concentration:**
  Within bundle sheath cells, malate is decarboxylated by NADP-malic enzyme, releasing CO_2 near Rubisco. This localized, high concentration of CO_2 effectively minimizes Rubisco's competing oxygenase activity and enhances carboxylation efficiency.
- **Role of Pyruvate Phosphate Dikinase (PPDK):**
  PPDK regenerates PEP from pyruvate in the mesophyll cells. This enzyme undergoes significant conformational changes during its catalytic cycle, transferring high-energy phosphate groups via phosphorylated histidine intermediates. The process consumes two ATP equivalents per CO_2 fixed, which, while energetically more demanding than the C3 cycle, is offset by improved carbon fixation efficiency under conditions where photorespiration would otherwise dominate.

Associated Enzymes and Plastid Adaptations:

- **Carbonic Anhydrases:**
  These enzymes (α, β, and γ forms) facilitate the rapid interconversion between CO_2 and HCO_3^-, ensuring efficient substrate availability for PEP carboxylase in C4 and CAM plants. In C3 plants, carbonic anhydrases help generate CO_2 from dissolved bicarbonate for direct fixation by Rubisco.
- **Crassulacean Acid Metabolism (CAM):**
  As an adaptation to water-limited conditions, CAM plants open their stomata at night to fix CO_2 into malic acid, which is stored in vacuoles. During the day, malic acid is decarboxylated to release CO_2 for the Calvin cycle, reducing water loss while maintaining photosynthetic activity.
- **Plastid Interconversion:**
  The dynamic nature of plastids, such as the conversion between chloroplasts and amyloplasts, supports the diverse metabolic needs of the plant. These transitions are regulated by light and developmental signals, optimizing both photosynthesis and storage functions.

Integration with Overall Plant Metabolism and Global Impact:

- **Energy and Carbon Efficiency:**
  The C4 pathway requires additional ATP (approximately 5 ATP per CO_2 fixed compared to 3 ATP in the C3 cycle) due to the extra steps in carbon fixation. However, under high-temperature and high-light conditions, the enhanced CO_2 concentration at Rubisco's active site improves overall photosynthetic efficiency, making the C4 pathway advantageous in tropical and arid environments.
- **Evolutionary Adaptation:**
  The evolution of the C4 pathway represents a critical adaptation to declining atmospheric CO_2 and increasing O_2 levels over geological time, addressing the inherent limitations of Rubisco's carboxylase/oxygenase activity in C3 plants.
- **Implications for Global Climate and Food Security:**
  Changes in atmospheric CO_2 levels and global warming can affect the balance between CO_2 fixation and photorespiration. Although increased CO_2 may boost carbon assimilation in some contexts, rising temperatures and altered water availability can reduce nutrient content in crops, impacting food security worldwide.

In summary, this chapter details the biochemical and structural adaptations that enable C4 plants—and to some extent CAM plants—to more efficiently fix CO_2 and overcome the limitations of the C3 pathway. It integrates discussions of enzyme mechanisms (PEP carboxylase, PPDK, carbonic anhydrases), plastid dynamics, and the evolutionary and ecological implications of these pathways, providing a comprehensive view of advanced carbon fixation strategies in plants.

This page titled 20.5: CO2 uptake - C4 and CAM Pathways is shared under a not declared license and was authored, remixed, and/or curated by Henry Jakubowski and Patricia Flatt.

- **Current page** by Henry Jakubowski and Patricia Flatt has no license indicated.
- **11.2: Diffusion Across a Membrane - Passive and Facilitated Diffusion** by Henry Jakubowski and Patricia Flatt has no license indicated.
- **20.4: CO_2 uptake - Calvin Cycle and C3 organisms** by Henry Jakubowski and Patricia Flatt is licensed CC BY-NC-SA 4.0.

20.6: BIOSYNTHESIS OF STARCH, SUCROSE AND CELLULOSE

LEARNING GOALS (CHATGPT O3-MINI)

- **Characterize Sucrose Structure and Function:**
  • Explain the structure of sucrose as a nonreducing disaccharide formed by an acetal linkage between glucose and fructose.
  • Describe why sucrose is an ideal transport carbohydrate in plants compared to reducing sugars that can lead to glycation (e.g., HbA1c formation).
- **Outline Sucrose Synthesis Pathways:**
  • Illustrate the pathway for sucrose synthesis in the plant cytosol, including conversion of G1P to UDP-glucose and the subsequent reaction with fructose-6-phosphate to form sucrose-6-phosphate.
  • Explain the enzymatic steps involved in the dephosphorylation of sucrose-6-phosphate to yield free sucrose.
- **Discuss Regulatory Mechanisms of Carbohydrate Partitioning:**
  • Analyze how the Calvin cycle output (triose phosphates) is partitioned between sucrose and starch synthesis.
  • Describe the regulatory roles of key enzymes, such as fructose 1,6-bisphosphatase and PPi-dependent phosphofructokinase, and how modulators like fructose 2,6-bisphosphate adjust metabolic flux in response to photosynthetic activity.
- **Examine Glycosyltransferase Mechanisms:**
  • Describe the general role of glycosyltransferases in transferring activated sugars (from nucleotide sugars) to acceptor molecules, forming glycosidic bonds.
  • Compare the different reaction mechanisms (retaining vs. inverting) and discuss the importance of metal ion coordination (e.g., Mn^{2+}) in these enzymes.
- **Understand Starch Biosynthesis:**
  • Outline the biochemical pathway for starch synthesis in plastids, including the formation of ADP-glucose from G1P and ATP, and its subsequent incorporation into the starch polymer by starch synthases.
  • Differentiate between processive and distributive mechanisms in polymer extension, and explain the regulatory influence of redox changes (e.g., disulfide bonds) on starch synthase activity.
- **Explore Cellulose Synthesis:**
  • Describe the synthesis of cellulose by members of the CesA (cellulose synthase) and cellulose synthase-like (Csl) families, emphasizing the formation of β(1,4) linkages using UDP-glucose as the donor.
  • Explain how the rosette-shaped cellulose synthesis complex (CSC) assembles and synthesizes multiple cellulose strands that form protofibrils in the cell wall.
- **Integrate Carbohydrate Metabolism in Plant Physiology:**
  • Discuss how sucrose is transported to sink tissues, either intact or after hydrolysis by invertases, and how these sugars are utilized in energy production and as precursors for other biomolecules.
  • Explain how carbohydrate synthesis (sucrose, starch, cellulose) is coordinated with plant growth, development, and response to environmental signals.
- **Compare and Contrast Carbon Storage Strategies:**
  • Evaluate the distinct roles of sucrose (transport and immediate energy use), starch (temporary storage), and cellulose (structural support) in plant metabolism.
  • Discuss how differences in enzyme regulation and compartmentalization contribute to the efficiency and flexibility of carbohydrate synthesis.

These goals are intended to guide your exploration of how plants synthesize, regulate, and utilize their major carbohydrate products, linking enzyme mechanisms and regulatory strategies to overall plant physiology and adaptation.

Now that we have seen how carbon is captured and fixed into 3C trioses, which can be converted to fructose and glucose and their derivative, we can now explore the synthesis of the key plant carbohydrates we all know, sucrose, starch, and cellulose.

The source for the organization and some of the text derives from Sindayigaya and Longhini. https://www.peoi.org/Courses/Courses...chem/biochem18. Creative Commons - https://creativecommons.org/licenses...sa/3.0/deed.en

20.6.1: SUCROSE SYNTHESIS

Sucrose is a disaccharide of glucose and fructose with an acetal link between the anomeric carbons to form the nonreducing sugar O-α-D-glucopyranosyl-(1→2)-β-D-fructofuranoside. Its structure is shown in Figure **20.6.1**.

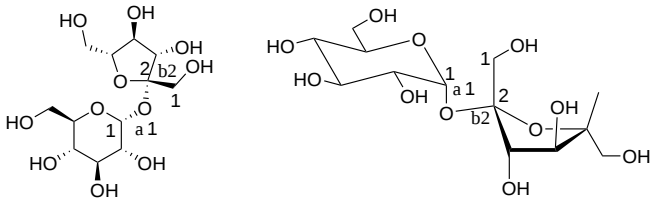


Figure **20.6.1**: Sucrose, a disaccharide of glucose and fructose

Sucrose can be considered a transport form of carbon, much like ketone bodies, which are transport forms of fatty acids. As noted above, the link between the sugars is between the anomeric C-1 link of glucose and the anomeric C-2 link of fructose. As such, it is not cleaved by typical carbohydrate-cleaving enzymes, such as amylases. Additionally, it doesn't react with proteins like other sugars with free cyclic hemiacetals, which can open and form reactive aldehydes. For example, the cyclic monosaccharide glucose, with its anomeric carbon in a readily reversible hemiacetal link, can form covalent bonds to amine groups in proteins such as hemoglobin, which forms the glycosylated version of HbA1c, as shown in Figure **20.6.2**.

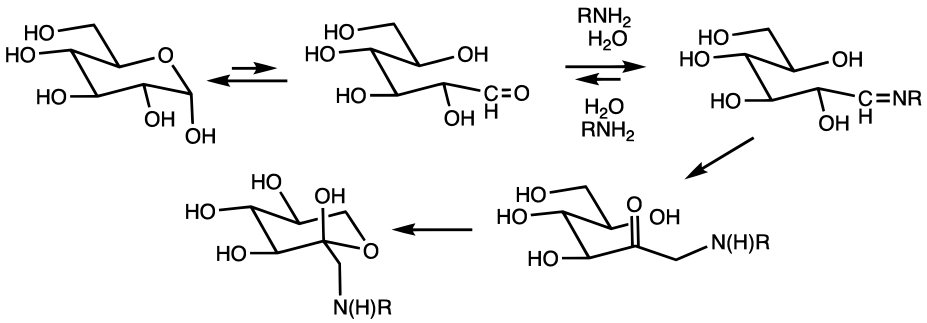


Figure **20.6.2**: Reactions of cyclic hemiacetal sugars with amines. https://en.wikipedia.org/wiki/Glycated_hemoglobin. Creative Commons Attribution-ShareAlike License 3.0

The reaction proceeds through forming a Schiff base, followed by a rearrangement. HbA1c is a marker of diabetes. These features of sucrose may explain its choice as a key form of synthesized carbohydrate in plants.

Sucrose is synthesized in the cytosol, as shown in Figure **20.6.3**.

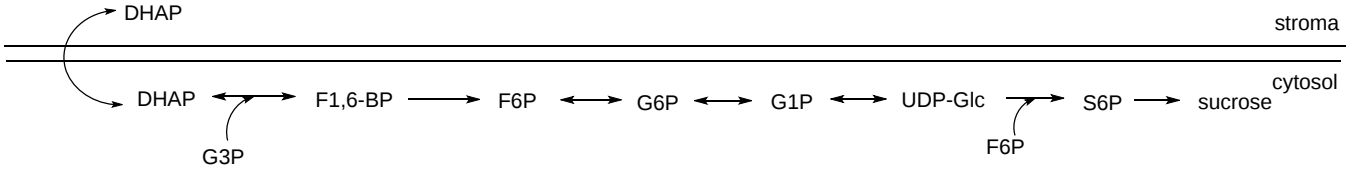


Figure **20.6.3**: Synthesis of sucrose in plants.

We have seen the enzymes that catalyze these reactions through the formation of G1P before in the glycolytic and gluconeogenesis pathways. Glucose-1-phosphate is then converted to UDP-glucose, which reacts with fructose-6-phosphate to form sucrose 6-phosphate and UDP, catalyzed by the enzyme **sucrose 6-phosphate synthase.** The last reaction is the hydrolysis of sucrose 6-phosphate by sucrose 6-phosphatase, which allows the export and transport of sucrose.

In the reaction scheme above, G1P is converted to UDP-Glc through the following reaction:

$$G1P + H^+ + UTP \leftrightarrow UDP\text{-}Glc + P_i$$

This reaction is just mildly favored thermodynamically.

Before studying the enzyme's structure, we will first discuss the regulation of the sucrose synthesis pathway and the general mechanism of glycosyltransferases.

20.6.2: REGULATION

Carbon capture in the light reaction of photosynthesis results in the production of sucrose (for transport) and starch synthesis. The product(s) that result depend on key regulatory steps. Remember the six trioses formed in the Calvin cycle; five are returned into the cycle for the synthesis of ribulose 1,5-bisphosphate, and only one is used to synthesize sucrose and starch. If too much is removed, the cycle slows. If not enough is used for starch and sucrose synthesis, P_i, which is transported into the stroma from the cytoplasm by an important translocator (see Section 20.3), would become depleted.

The key cytosolic regulatory step is catalyzed by **fructose 1,6-bisphosphatase** (FBPase-1) and a unique plant enzyme, **PPi-dependent phosphofructokinase** (PP-PFK-1)**,** which catalyzes the reverse reaction of F6P → F1,6BP in regulatory steps similar to those found in glycolysis and gluconeogenesis.

- **fructose 1,6-bisphosphatase** (FBPase-1) is inhibited by the allosteric modulator **fructose 2,6-bisphosphate** (F2,6BP)
- **PPi-dependent phosphofructokinase (**PP-PFK-1) is activated by **fructose 2,6-bisphosphate**

The coordinate regulation of these two enzymes is shown in Figure **20.6.4**.

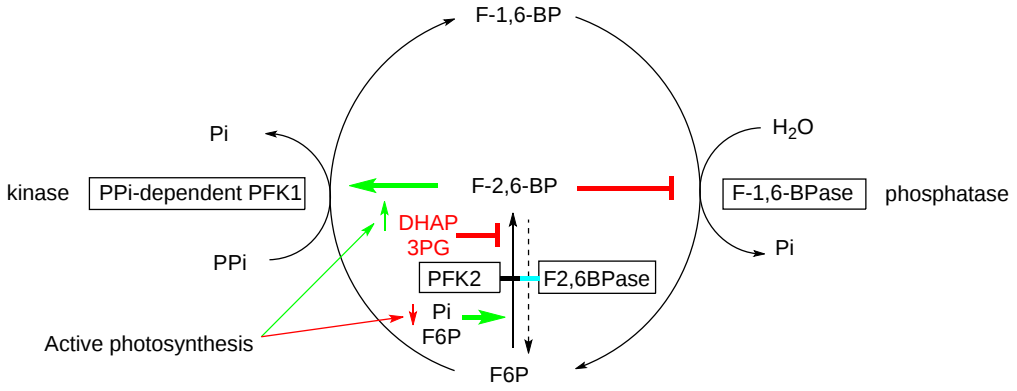


Figure **20.6.4**: Regulation of sucrose synthesis at the formation of fructose-6-phosphate

The substrate for the PPi-dependent phosphofructokinase (PP-PFK-1) is PPi, which serves as a phospho-donor. In the plant cytosol, no pyrophosphatase exists to catalyze the cleavage of PP_i into P_i. Also note that Fru-2,6-P_2 itself is synthesized and degraded by the bifunctional enzyme phosphofructokinase 2/fructose-2,6-bisphosphatase, which we studied before in the regulation of the same step in glycolysis/gluconeogenesis.

The levels of F2,6-BP depend on the rate of photosynthesis:

- When photosynthesis is high (in light conditions), [DHAP] and [3PG] increase, which inhibits PFK2, which decreases F26BP, which causes a differential increase in F1,6BPase activity over PP-PFK-1, which increases F6P for sucrose synthesis as well as Pi for the continuation of the light reactions. This allows sucrose synthesis when excess DHAP and 3PG occur in the light reactions, which makes great biological sense.
- When photosynthesis is low (in dark conditions), the same regulations lead to an increase in F2,6BP, which leads to the preferential activation of the glycolytic enzyme PPi-dependent phosphofructokinase-1 (PP-PFK1) and inhibition of the gluconeogenic enzyme fructose 1,6-bisphosphatase (FBPase-1)

We will see later that the main regulatory step in starch synthesis is **ADP-glucose pyrophosphorylase.** In contrast to the inhibition by 3PG of PFK2, 3PG (which increases in active photosynthesis) activates ADP-glucose pyrophosphorylase while Pi inhibits it. Pi increases when the synthesis of ATP from ADP and Pi (by ATP synthase in the light reaction) slows (such as in darker conditions). If sucrose synthesis slows and sufficient 3PG persists, the activation of ADP-glucose pyrophosphorylase stimulates starch synthesis.

20.6.3: GLYCOSYLTRANSFERASES (GTS)

Glycosyltransferases are crucial enzymes, as they play a vital role in synthesizing most of the planet's biomass. They catalyze the transfer of a monosaccharide from a donor that has been activated by the attachment of a nucleotide in the form of a nucleotide sugar (NDP-sugar) or dolichol-(pyro)phosphate sugar to acceptors. These include other sugars, lipids, and proteins, which are glycosylated on alcoholic side chains (Ser, Thr) or amides (Asn). Over 500,000 different GTs are known and deposited in the Carbohydrate-Active enZYmes Database (CAZy database2). Based on sequence and structure, there are over 114 different families. Although they depart significantly in primary sequence, only three major folds are predominant (GT-A, -B, and -C)

As shown in the reaction below, a glycosyl transferase reaction is required to transfer glucose from a donor, such as UDP-glucose, to an acceptor, like fructose, to form sucrose.

NDP-Glc (donor) + F6P (acceptor) → Sucrose-6-P + NDP

Perhaps now is a good time to study their generic reaction mechanisms before progressing to starch synthesis.

About 65% of glycosyltransferase reactions use nucleotide sugars as donors. These enzymes are called Leloir transferases. They are nucleotide-dependent. The activated NDP-sugar donor binds first to the enzyme, followed by the acceptor, to form a ternary complex. A conformational change enables catalysis, facilitating the sequential release of the products. Hence, the enzyme follows a sequential ordered bi-bi mechanism.

The reaction could proceed with either retention or inversion of the anomeric carbon of the NDP-sugar donor. This is illustrated for the reaction of a C1 α-NDP donor monosaccharide with a monosaccharide acceptor to produce the α(1,4) link with retention of configuration or the β(1,4) link with inversion as shown in Figure **20.6.5**.

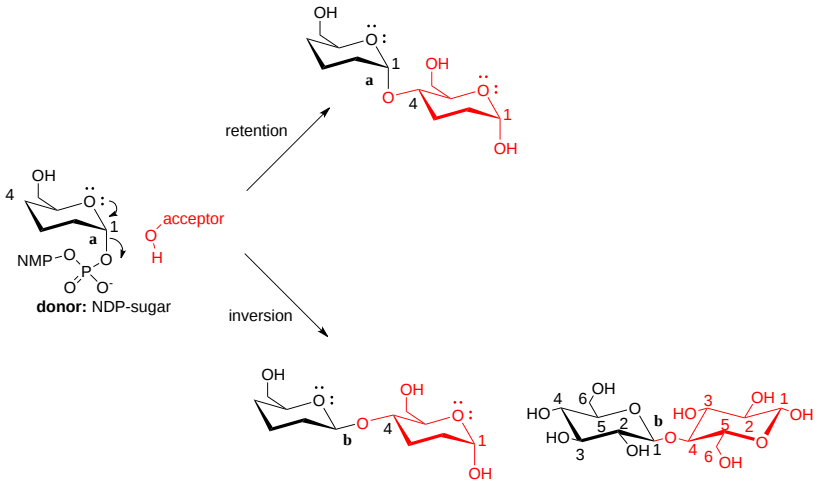


Figure **20.6.5**: Reaction of a donor NDP-monosaccharide and an acceptor monosaccharide with retention or inversion of configuration at the anomeric carbon of the donor

The same stereochemical outcomes can occur in the hydrolysis of acetal bonds by glycosyl hydrolases.

Reactions that proceed with inversion react in an S_N2 reaction, similar to the nucleophilic attack on alkyl halides. The glycosyl transferase that proceeds with inversion makes the attacking nucleophile on the acceptor more nucleophilic by general base catalysis by a deprotonated glutamic or aspartic acid.

The glycosyl transferase that proceeds with the retention of configuration is less understood. Several alternative mechanisms have been proposed for inverting and retaining glycosyltransferase in general, as illustrated in Figure **20.6.6**.

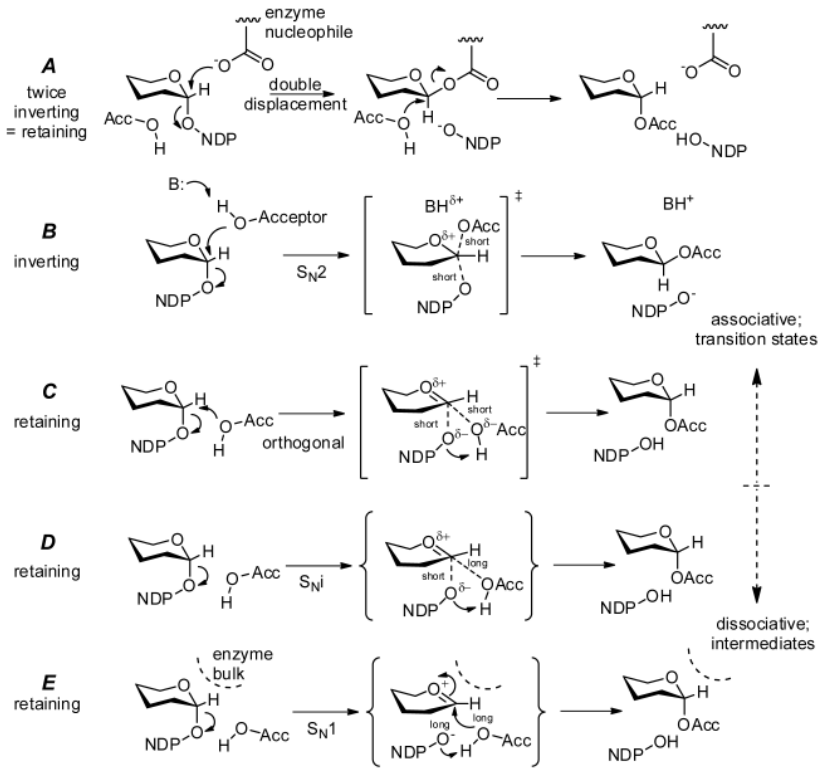


Figure **20.6.6**: .Proposed glycosyltransferase mechanisms. Schuman et al. PLOS One (2013). doi:10.1371/journal.pone.0071077.g001. Creative Commons Attribution License

They include the following possible mechanisms:

Panel (A): A double displacement mechanism utilizing two inversions with net retention of stereochemistry involving a covalent glycosyl-enzyme intermediate. The individual steps are inverting via (B) an S_N2 process.

Panel (B): Inverting Leloir glycosyltransferases promote a backside nucleophilic attack on C1 by the acceptor from an inline (usually equatorial) position, resulting in inversion of the anomeric bond stereochemistry.

Panel (C): An orthogonal mechanism consisting of nucleophilic attack on C1 by the acceptor concurrent with leaving group loss from a position approximately at right angles to the C1-leaving group axis.

Panel (D): An S_N1 mechanism involving an intermediate with oxocarbenium character, followed by rapid internal nucleophilic attack by the acceptor nucleophile; or

Panel (E): An S_N1 mechanism involving a discrete oxocarbenium intermediate. All mechanisms require proton transfers of the hydroxyl hydrogen of the acceptor to an enzymatic base or the departing leaving group.

From your chemistry studies, you will remember that S_N1 reactions are dissociative and form a positively charged carbocation intermediate. In an S_N-1 reaction, the intermediate has a cation character but is not fully charged. In the case of glycosyltransferase, the intermediates would be oxycarbeniums. (Carbenium ion can be considered carbocations with three bonds to the carbon). S_N1 reaction will occur only if the formation of the ion is activated and they are stabilized. A protic solvent is typically required for stabilization if the reaction occurs in solution. An appropriate arrangement of negative or partially negative atoms in the backbone and side chain is required to stabilize S_N1 mechanisms in the enzyme's anhydrous active site.

The double replacement reactions (Panel A) require a side chain nucleophile, and likely candidates in retaining glycosyltransferase are not positioned for such a task. The evidence seems to support the orthogonal mechanism. It appears that the binding of the donor is similar in retaining transferases, such that it is in a 90^0 position of nucleophilic attack by the acceptor, which leads to a trigonal bipyramidal transition state with the nucleophile axial and the leaving group equatorial (orthogonal).

The donor NDP-monosaccharides typically are Mn^2-containing proteins with the inverting and retaining transferase having different coordination geometries for Mn^{2+} binding, as illustrated in Figure **20.6.7**.

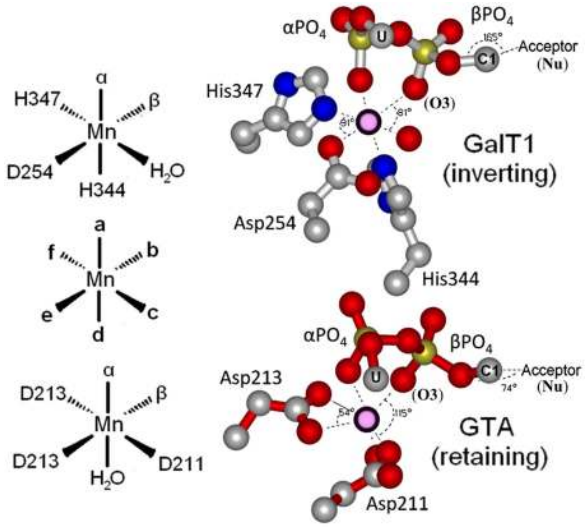


Figure **20.6.7**: Coordination geometries for Mn^{2+} binding in glycosyltransferase. Shuman, ibid.

Inverting enzymes such as GalT1 (top) achieve nearly perfect octahedral geometry about the coordinated metal ion (displayed angles of 81° and 91° compared to ideal octahedral 90° bond angles) with subsequent "inline" (approaching 180°) placement of the acceptor nucleophile for classic inverting S_N2 backside attack. Retaining enzymes, such as GTA (bottom), however, utilize an arrangement of acidic residues, often with acute bidentate Asp coordination, which severely skews the metal geometry (displayed angles of 54° and 115°) and allows sufficient room between phosphate oxygens for orthogonal attack from the acceptor. **U**is uridine, **C1**is donor galactose **C1**.

Figure **20.6.8** shows a possible mechanism for transferring a monosaccharide from the donor ADP-sugar through an oxycarbenium intermediate to an acceptor.

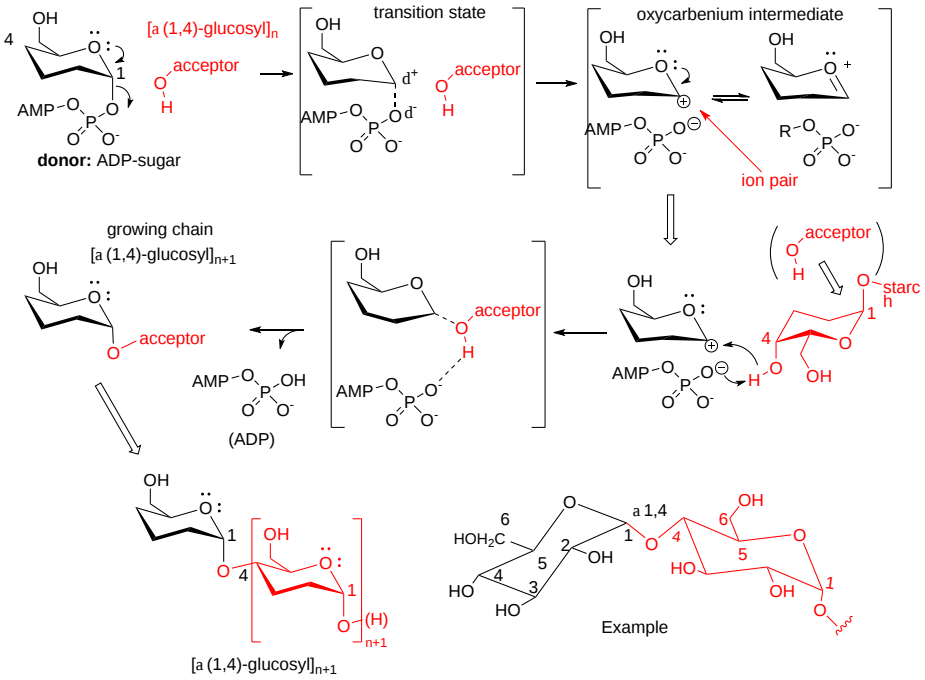


Figure **20.6.8**: Possible mechanism for the transfer of a monosaccharide from the donor ADP-sugar through an oxycarbenium intermediate to an acceptor (example - a growing starch chain). Schuman B, Evans SV, Fyles TM (2013) Geometric Attributes of Retaining Glycosyltransferase Enzymes Favor an Orthogonal Mechanism. PLoS ONE 8(8): e71077. doi:10.1371/journal.pone.0071077. Creative Commons Attribution License

As mentioned above, glycosyltransferases are classified into three major folds: GT-A, GT-B, and GT-C. Different representations of the GT-A fold core structure predicted through analysis by neural networks and deep learning are shown in Figure **20.6.9**.

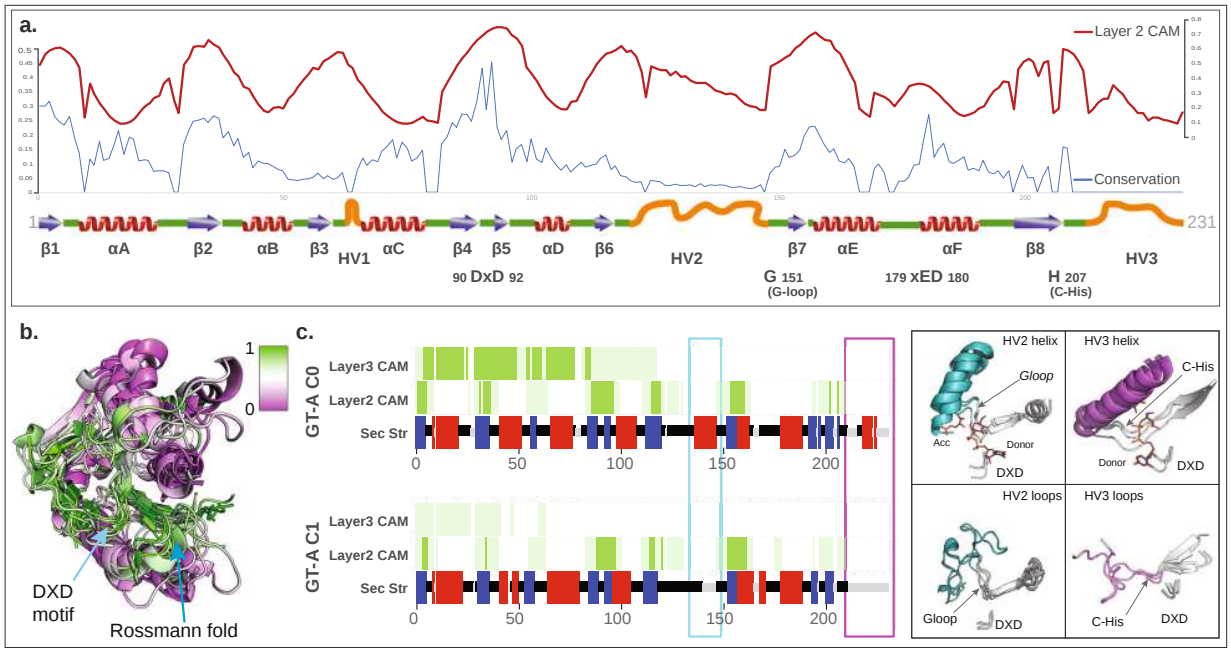


Figure **20.6.9**: Fold core of GT-As. Taujale, R., Zhou, Z., Yeung, W. *et al*. Mapping the glycosyltransferase fold landscape using interpretable deep learning. *Nat Commun* **12,** 5656 (2021). https://doi.org/10.1038/s41467-021-25975-9. Creative Commons Attribution 4.0 International License. http://creativecommons.org/licenses/by/4.0/.

This computational modeling of structure utilizes simple secondary structure representations derived from primary sequences to predict folds independently of the sequence. GT folds are accurately predicted by learning secondary structure features free of primary sequence alignments.

Panel (a) shows a linear map of the conserved secondary core structures (below) and graphs (top). The blue line represents a conservation score, and the red is a CAM score. CAM values correspond to residue positions that distinguish them the most from other class labels (folds and families).

Panel (b) shows the core's structural alignment with the CAM values mapped onto it. The conserved regions have a high CAM value, indicated by a high intensity of green and a low CAM value of purple.

Panel (c) shows the consensus secondary structure on the left for the aligned positions in the two GT-A fold clusters (blue: beta-sheets; red: helices; green: loops). Average CAM values from using different "layers" of analysis are shown for each aligned position (higher intensity of green corresponds to a higher CAM value). Cyan and magenta boxes highlight the secondary structure differences between the two clusters near the hypervariable HV2 and HV3 regions, respectively. The conserved DXD motif, G-loop, and C-His are indicated for reference. Donor and acceptor substrates for GT-A0 are shown as sticks.

This figure provides readers with a sense of the complexity of the analysis required to understand and differentiate the structure-function features of these structurally similar but complex enzymes.

20.6.4: STRUCTURE AND ENZYMATIC ACTIVITY OF SUCROSE SYNTHASE (SUSY)

These enzymes are usually homotetramers with a monomeric molecular weight of around 90,000. The monomers typically have an N-terminal domain that directs the enzyme's targeting to a specific location and a C-terminal GT-B domain. It can be regulated by phosphorylation at a serine near position 12 in the N-terminal domain, which presumably affects its cellular location, and another near position 170 that impacts its degradation. Two glutamates in the C-terminal GT-B domain (E678 and E686) and phenylalanine (680) are essential for the catalytic activity. Sucrose synthase is reversible, as is the synthesis of sucrose-6-P from F6P and UDP-glucose, which can be reversed in the presence of UDP. The enzyme can also use ADP-glucose as a donor.

The structure of the *Thermosynechococcus elongatus* sucrose phosphate synthase with bound UDP and sucrose-6-Phosphate has been solved and along with other studies a reaction mechanism proposed as shown in Figure **20.6.10**.

Figure **20.6.10**: Catalytic model of TeSPS. Yuying et al. Co-crystal Structure of Thermosynechococcus elongatus Sucrose Phosphate Synthase With UDP and Sucrose-6-Phosphate Provides Insight Into Its Mechanism of Action Involving an Oxocarbenium Ion and the Glycosidic Bond. Frontiers in Microbiology, 11, 2020. https://www.frontiersin.org/article/...icb.2020.01050. **Creative Commons Attribution License (CC BY)**.

(A) The state before the reaction is shown. **(B)**The glucose residue of UDPG forms hydrogen bonds between/among the phosphate groups, His158, Glu331, and F6P. Due to the formation of these hydrogen bonds, the pyranose ring of the glucose becomes negatively charged to promote C1 to form an oxocarbenium ion. **(C)**The relatively weak hydrogen bond formed by His158 and O6 is broken, which causes the pyranose ring to lose some negative charge character and forces the C1 oxocarbenium ion to form a covalent bond with the F6P oxygen atom. **(D)**UDP and S6P are released from the catalytic center.

A 2D view of the active site residues is shown in Figure **20.6.11**.

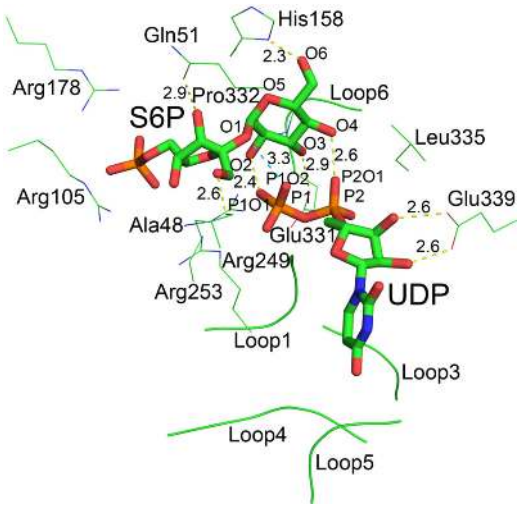
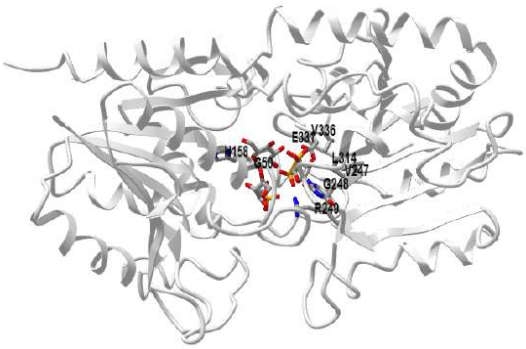


Figure **20.6.11**. The catalytic center of TeSPS. Yuying et al. ibid.

The catalytic center of TeSPS. Loops 1, 3, 4, and 5 form a cave that binds to the uracil moiety of UDP. Glu339 stabilizes the ribose ring via the formation of two hydrogen bonds. Leu335 forces two phosphate groups in UDP to reorient. Several basic amino acids, including Arg105, Arg178, Arg249, and Arg253, interact with the phosphate groups of UDP and S6P via ionic bonds. Pro332 at the turn of loop 6 interacts with the pyranose ring via CH/π bonds. All hydroxyl groups (O2, O3, O4, and O6) of the glucose moiety of S6P form hydrogen bonds with phosphate groups or the side chains of various amino acids. “O2” forms a hydrogen bond with P1O1 of the P1 phosphate group of UDP. “O3” forms a hydrogen bond with the carboxyl group of Glu331. “O4” forms a hydrogen bond with P2O1 of the P2 phosphate

group of UDP. “O6” forms a hydrogen bond with the imidazole side chain of His158. The distances between groups are indicated in the figure.

Figure 20.6.12 shows an interactive iCn3D model of the Thermosynechococcus elongatus Sucrose Phosphate Synthase With UDP and Sucrose-6-Phosphate (6KIH)



NCBI iCn3D Figure 20.6.12: Thermosynechococcus elongatus Sucrose Phosphate Synthase With UDP and Sucrose-6-Phosphate (6KIH) (Copyright; author via source). Click the image for a popup or use this external link: https://structure.ncbi.nlm.nih.gov/i...1kCnQ9pxcJjdy7

20.6.5: METABOLISM OF SUCROSE

Sucrose is a primary synthesis product of photosynthesis and is transported to other plant "sink" tissues where it is used for both energy and biosynthetic precursors. Suc transporters can move it from the phloem to the apoplast. It can enter sink cells through sucrose transporters or be hydrolyzed by cell-wall invertase (cwINV) to yield glucose (Glc) and fructose (Fru), which enter the cells through hexose transporters. Suc can also pass directly from the phloem to sink cells through plasmodesmata (physical connections between cells). Inside sink cells, sucrose (Suc) can be metabolized or transported to the vacuole, where it can be stored as sucrose, transformed into fructans by fructosyltransferases (FTs), or hydrolyzed by vacuolar invertase (vINV) and stored as hexoses. To be metabolized, Suc must be hydrolyzed by either cytosolic invertase (INV) into glucose and fructose or by the reversible reaction of sucrose synthase (SuSy) using UDP instead of water to yield fructose and UDP-G. These processes are illustrated in Figure 20.6.13.

20.6.5.1:

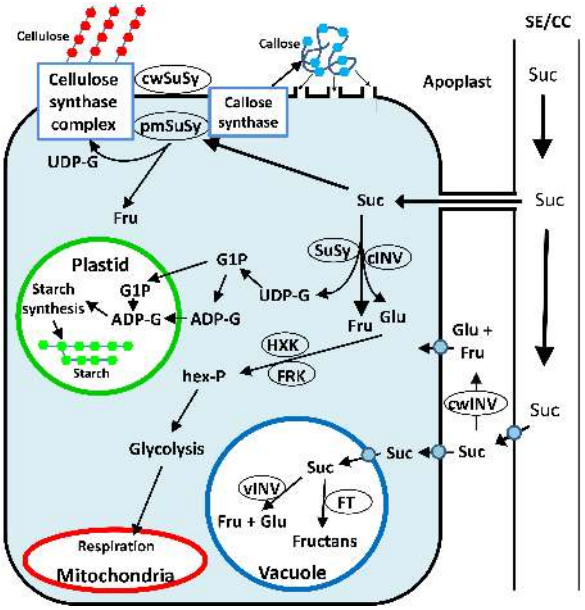


Figure 20.6.13: Simplified schematic presentation of sugar metabolism in sink tissue cells toward cellulose, callose, and starch synthesis. Stein and Granot. Frontiers in Plant Science (10). 2019. https://www.frontiersin.org/article/...pls.2019.00095. DOI=10.3389/fpls.2019.00095 https://www.frontiersin.org/articles...019.00095/full

The hexoses (glucose and fructose) can be phosphorylated to hexose phosphates (hex-P), directed to starch synthesis in the plastid or glycolysis, and then respiration in the mitochondria or directed to other metabolic pathways. Plasma membrane-associated SuSy (pmSuSy)

and cwSUS can generate UDP-G, which is used to synthesize cellulose for cell walls and callose for plugging plasmodesmata. Callose is a polysaccharide in the form of β-1,3-glucan with some β-1,6-branches in the cell walls of a wide variety of higher plants.

20.6.6: BIOSYNTHESIS OF STARCH

During active photosynthesis in bright light, a plant leaf produces more carbohydrates (as triose phosphates) than it needs to generate energy or synthesize precursors. The excess is converted into sucrose and transported to other plant parts for storage or use as fuel. In most plants, starch is the primary storage form, but in a few plants, such as sugar beet and sugarcane, sucrose is the primary form. The synthesis of sucrose and starch occurs in different cellular compartments (the cytosol and plastids, respectively), and these processes are coordinated by various regulatory mechanisms that respond to changes in light levels and photosynthetic rates.

20.6.6.0.1: STARCH SYNTHESIS

Starch, like glycogen, is a homopolymer of D-glucose in (α1,4) linkage with (α1,6) branches. Glycogen is found in all three domains of life: Archaea, Bacteria, and Eukarya. In contrast, starch is found in photosynthetic algae, land plants, and some cyanobacterial species.

Starch is synthesized by starch synthase in chloroplasts for temporary storage and in amyloplasts in seeds, roots, and underground stems (such as tubers) for long-term storage. As with the synthesis of glycogen, the glycosyltransferase catalyzes the addition of an activated ADP-glucose to the acceptor, the elongating starch polymer.

$$\text{ADP-α-D-glucose-1-phosphate (donor)} + [(1\rightarrow4)\text{-α-D-glucosyl}]_{(n)}\ \text{(acceptor)} \leftrightarrow [(1\rightarrow4)\text{-α-D-glucosyl}]_{(n+1)} + \text{ADP} + H^+$$

The ADP-glucose donor is formed in the following reaction:

$$\text{Glucose 1-phosphate} + \text{ATP} \leftrightarrow \text{ADP-glucose} + \text{PPi}$$

There is a pyrophosphatase in plastids (but not in the cytosol), making the reaction irreversible. Hence, the next overall reaction is

$$\text{Starch}_n + \text{glucose 1-phosphate} + \text{ATP} \rightarrow \text{starch}_{n+1} + \text{ADP} + 2\text{Pi}$$

Taking into account the hydrolysis by inorganic pyrophosphatase of the PPi produced during ADP-glucose synthesis, the overall reaction for starch formation from glucose 1-phosphate is:

$$\text{Starch}_n + \text{glucose 1-phosphate} + \text{ATP} \rightarrow \text{starch}_{n+1} + \text{ADP} + 2\text{Pi};\ \Delta G'^{o} = -50\ \text{kJ/mol} = -12\ \text{kcal/mole}\ (-50\ \text{kJ/mol})$$

$$\Delta G'^{o} = -50\ \text{kJ/mol} = -12\ \text{kcal/mol}$$

In glycogen synthesis, the donor is UDP-glucose, and it is added to the reducing end (C1) of the growing glycogen polymer (with the C1 OH acting as a nucleophile) so the polymer extends from that end. Kinetic models suggest that starch synthases, which use ADP-glucose, may use two different active sites that appear to alternately add glucose to the nonreducing C4 end (with the C4 OH acting as a nucleophile), with the reducing end of the linear α(1,4) polymer being alternately covalently attached to one site, then the other, with the attachment activating that end for reaction with C4-OH of the polymer at the other site.

Figure **20.6.14** shows a very simplified structure of the starch synthase using two different active sites as the reaction proceeds through the first steps.

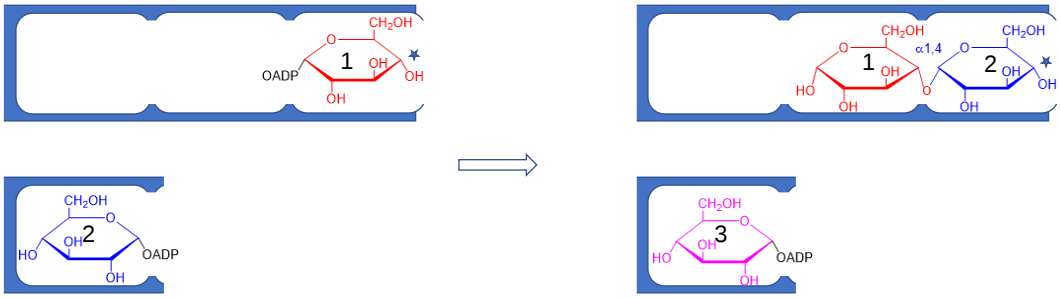


Figure **20.6.14** shows a simplified structure of the starch synthase using two active sites

Note that additional glucose units are added to the nonreducing C4 end, denoted by a star. α(1,6) branches are added by branching enzymes, as in the case of glycogen. Bacteria starch is made like glycogen but uses ADP-glucose, as does plant starch synthase. Structural models show that the protein has one active site, so the kinetic models suggesting the use of two active sites may refer to a movement of chains between different monomers in oligomeric forms of the protein.

Both the donor (ADP-Glc) and product ($starch_{n+1}$) have their participating electrophile (ADP) and now substituted nucleophile (C4-O-R) in the α-anomeric form, so they are retaining glycosyltransferases. The enzymes could act in two different ways:

- a processive mechanism: the acceptor ($starch_n$) stays bound to the enzyme after each addition of the next glucose from the donor ADP-glc, and one chain extends quickly
- a distributive mechanism: the enzyme dissociates from the product ($starch_{n+1}$) after the addition of the glucose from ADP-glc and must rebind to catalyze the next addition, so many new chains start, and the growth of each chain is slow

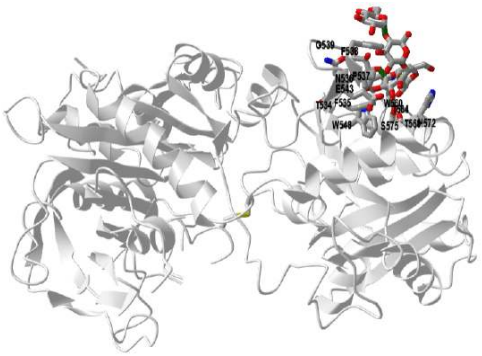
Kinetic evidence suggests that some starch synthases are processive and others are distributive. Along with starch synthase, three other enzymes are involved: ADP-glucose pyrophosphorylase (AGPase), starch branching enzyme (SBE), and starch debranching enzyme (DBE)

Starch synthesis is regulated by gene transcription, phosphorylation, and redox conditions. A key regulatory enzyme is an ADP-glucose pyrophosphorylase (AGPase). This enzyme catalyzes the formation of ADP-glucose (the donor) and PPi from glucose 1-phosphate and ATP. Dithiothreitol, a reducing agent, increases starch synthesis by inactivating AGPase. We will see below that a key disulfide bond is present in some starch synthases that must be reduced (cleaved) to open an active site cleft between the N-terminal and C-terminal lobes of the catalytic domain. In vivo, thioredoxins are probably involved in redox regulation.

20.6.7: STRUCTURES OF STARCH SYNTHETASES (SS)

There are four classes of soluble starch synthetases (SSI-SSIV) and one starch granule-bound one (GBSS). As noted in the mechanism above, all have two catalytic domains except SSII, which has 3 CHO binding domains. GBSS appears to form amylose and long chains of amylopectins (amylose with around 5% α(1,6) branching. Loss-of-function mutants of GBSS have much-reduced amylose concentrations. SSI-SSIII produces most of the amylopectin. SSI is most active with stands (outer ones in branched structures) with around 7-9 glucose units. In leaves, it generates chains of up to 10 residues in amylopectin. The SSs can be chloroplastic or amyloplastic.

Figure **20.6.15** shows an interactive iCn3D model of barley starch synthase I in complex with maltooligosaccharide (4HLN).



NCBI iCn3D Figure **20.6.15**: Barley starch synthase I in complex with maltooligosaccharide (4HLN). (Copyright; author via source). Click the image for a popup or use this external link: https://structure.ncbi.nlm.nih.gov/i...LGwFUeJAMskBcA

The protein is shown in gray in an open conformation with a glucose 5-mer bound on the outside. It has a GT-B fold with distinct N- and C-terminal Rossmann-like domains and a central linker. Side chains within 5 Å of oligosaccharide are shown in sticks and labeled. Note especially the disulfide bridge between cysteines 126 and 506 in the central part of the protein that prevents the formation of the active site. This clearly shows the importance of redox signaling in activating the enzyme.

The maltose is not bound in the active site but at a surface secondary binding site (SBS). The role of this site is somewhat unclear, but it may be involved in carbohydrate-carbohydrate interactions. Specifically, they may assist in recruiting starch chains for further elongation. SBSs are found in many but not all starch synthases. Note that in this structure, there is only one occluded active site and not two, as suggested in Figure 14 above.

Figure **20.6.16** shows an interactive iCn3D model of the catalytic domain of starch synthase IV from Arabidopsis thaliana bound to ADP and acarbose (6GNE).

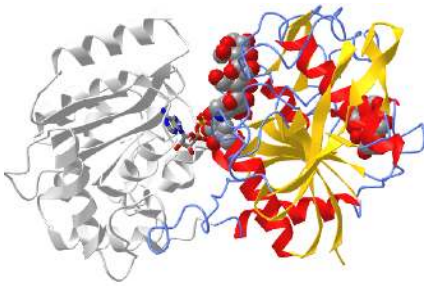


Figure **20.6.16**: Catalytic domain of starch synthase IV from Arabidopsis thaliana bound to ADP and acarbose (6GNE) https://structure.ncbi.nlm.nih.gov/i...MioUaKM73M3Wd9

This structure is just the catalytic domain (representing about half of the total protein sequence). The N-terminal domain is colored by secondary structure. Acarbose (spacefill, CPK colors) again occupies both the donor and acceptor sites in the active site (central regions). The structure has a secondary binding site (SBS) occupied by the disaccharide maltose. Again, there are not two active sites, but the migration of starch chains between monomers in oligomeric forms could support the model shown in Figure 14.

The structure of beta-acarbose, an inhibitor, is shown in Figure **20.6.17**.

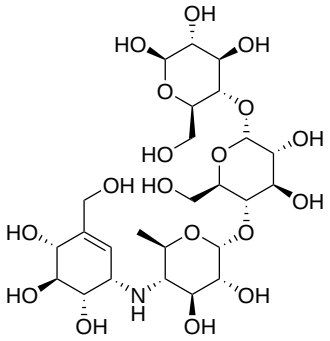


Figure **20.6.17**: structure of beta-acarbose

Figure **20.6.*x*18** below shows an interactive iCn3D model of the Granule Bound Starch Synthase from Cyanobacterium sp. CLg1 bound to acarbose and ADP (6GNF)

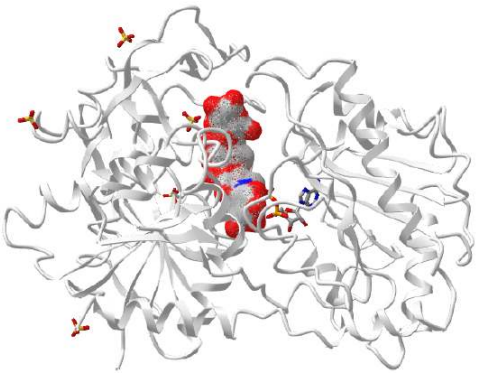


Figure **20.6.18**: Granule Bound Starch Synthase from Cyanobacterium sp. CLg1 bound to beta-acarbose and ADP (6GNF). (Copyright; author via source). Click the image for a popup or use this external link: https://structure.ncbi.nlm.nih.gov/icn3d/share.html?F1tJBDAh6QRhxpH88

ADP, which occupies part of the donor site that would usually bind NTP-Glc, is shown in CPK-colored sticks. Beta-acarbose occupies the rest of the donor site (where Glc of NTP-Glc would bind) and the acceptor site (growing starch chain). It is shown in the CPK-colored wire-frame surface. Histidine 181, which probably stabilizes an " oxocarbenium-like anomeric carbon in the transition state," is shown in balls and sticks with CPK colors.

20.6.8: CELLULOSE SYNTHESIS

We can't leave plant carbohydrate metabolism without considering the synthesis of cellulose, which is catalyzed in plants by members of the superfamily cellulose synthase (CesA) and cellulose synthase-like (CsI) enzymes, which are part of the glycosyltransferase GT2 family and have similar structures. Cellulose and hemicellulose are the chief components of the 1^0 and 2^0 cell walls. Members of the CesA family have a conserved motif (DDDQxxRW) and a zinc-finger domain. Different members catalyze the synthesis of the 1^0 and 2^0 cell walls. Members of the Csl family are involved in additional cell wall glycans, including (1,4)-β-D-mannan (CsIA) and xyloglucan cytoskeleton (CslC). UDP-glucose is the donor in creating the β(1,4) acetal linkages between glucose monomers.

Plant growth must respond to environmental triggers through a balance of cell expansion and cell division. A key regulator of these processes is the flexibility of the cell walls, which can maintain turgor pressure by expansion. Nonexpanding cells (for example, those that line the xylem vessels and are in woody tissue) have secondary cell walls beneath their primary walls.

We have previously discussed the primary and secondary cell wall structure in Chapter 7.3. In brief, the primary cell walls contain cellulose, hemicellulose, and pectins. Cellulose, the main component that provides strength, is synthesized by CesA, which forms a very large rosette-shaped complex (CSC). These complexes appear to regulate the movement of intracellular microtubules, which guide the synthase complex through interactions with microtubule-associated cellulose synthase compartments (MASCs), whose numbers increase during stress. Likewise, there are uncoupling proteins that inhibit microtubule movement from the CSC. These protein complexes stay aligned during cell growth. Hence, the cell wall plays a key role in signal transduction, facilitating growth and cell division.

The structure of the rosette-shaped complex (CSC) has been determined by cryoEM and is shown in Figure **20.6.19**.

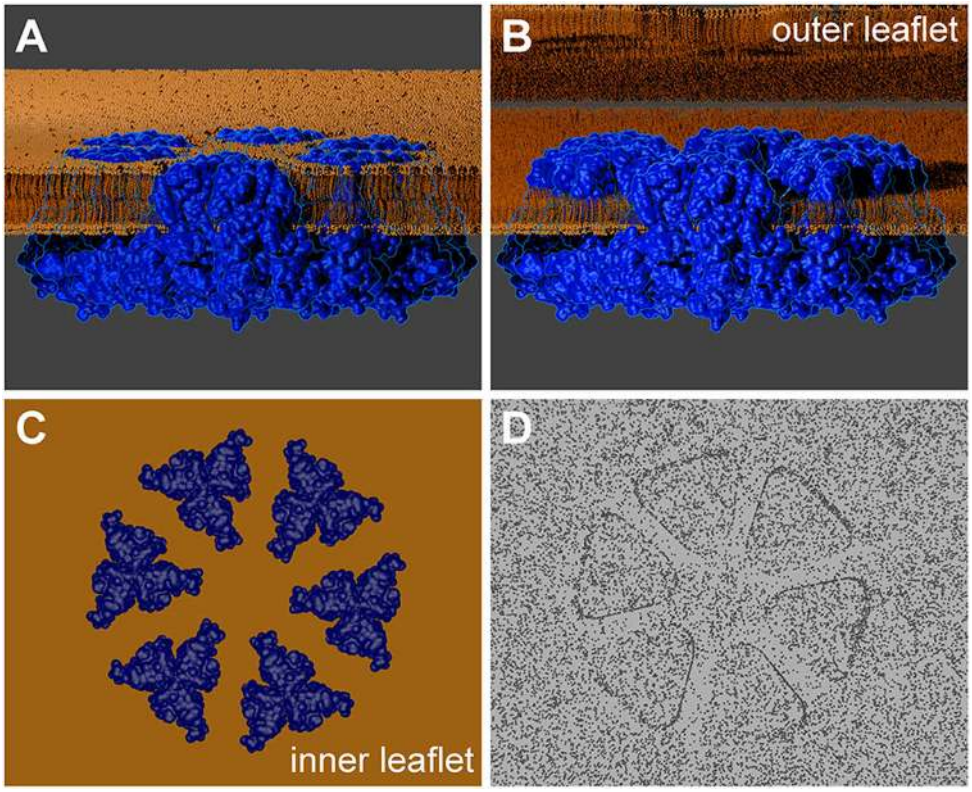


Figure **20.6.19**: Structural cartoons of the CESA CSC complex. Nixon, B., Mansouri, K., Singh, A., *et al.* Comparative Structural and Computational Analysis Supports Eighteen Cellulose Synthases in the Plant Cellulose Synthesis Complex. *Sci Rep* **6,** 28696 (2016). https://doi.org/10.1038/srep28696. Creative Commons Attribution 4.0 International License. http://creativecommons.org/licenses/by/4.0/

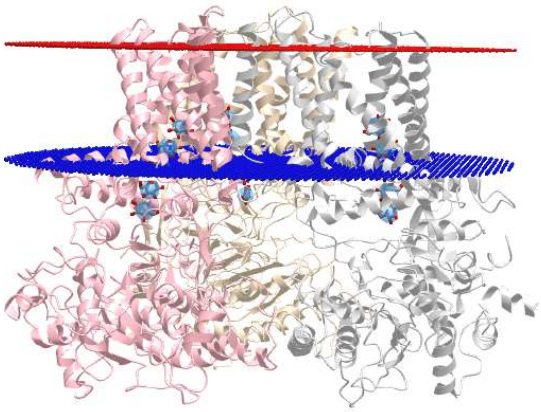
Panel (A) shows the complex as a series of trimers of CESAs, with each monomer spanning the membrane with 7 alpha helices. The catalytic domain is in the cytoplasm.

Panel (B) shows the CSC complex with the top leaflet removed

Panel (C) shows a top-down view of 6 sets of trimers of CESA.

Panel (D) shows a metal replica viewed in the TEM after the biological material has been removed.

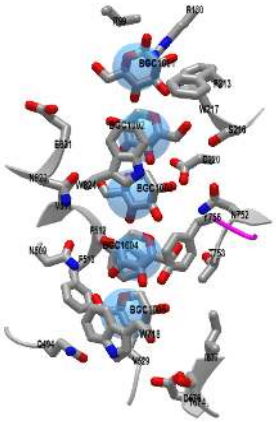
Each trimer synthesizes a cellulose strand. There are 18 trimers in the complex allowing the concomitant synthesis of cellulose strands that can easily self-associate through hydrogen bonding to form near the extracellular surface cellulose protofibrils.Figure **20.6.20** shows an interactive iCn3D model of the catalytically active homotrimeric poplar cellulose synthase (6WLB)



NCBI iCn3D Figure **20.6.20**: Catalytically active homotrimeric poplar cellulose synthase (6WLB). (Copyright; author via source). Click the image for a popup or use this external link: https://structure.ncbi.nlm.nih.gov/i...zCm6fYSwAFA897

Each of the monomers within the trimers is given a different color. A 5 residue β(1,4) glycan is shown in cartoon form emerging into the middle of the membrane complex.

Figure **20.6.21** shows an interactive iCn3D model of the homotrimeric poplar cellulose synthase isoform glycan binding site (6WLB).



NCBI iCn3D Figure **20.6.21**: Homotrimeric poplar cellulose synthase isoform glycan binding site (6WLB. (Copyright; author via source). Click the image for a popup or use this external link: https://structure.ncbi.nlm.nih.gov/i...HqYhTQfuw857PA

The actual transmembrane channels start just above the active site. Key amino acid side chains (Trp 718, Phe 513, Val 529, and Gln 494) help form the portal opening. The actual channel is lined with both aromatic and hydrophilic residues, which supply sufficient but not too strong noncovalent interactions that allow sequential movement of the continually synthesized cellulose as it ratchets forward toward the extracellular side of the membrane. The aromatic residues interact through π-stacking with the glucose residues and through interactions with the equatorial OH groups on the β-glucose polymer. Remember that cellulose is especially stable from a steric perspective since all its OH groups and the acetal linkage are equatorial.

20.6.9: SUMMARY

This chapter explores how plants convert fixed carbon into the major carbohydrates—sucrose, starch, and cellulose—that serve distinct physiological functions such as energy transport, storage, and structural support.

Sucrose Synthesis and Regulation:

- **Structure and Function:**
  Sucrose is a nonreducing disaccharide composed of glucose and fructose linked through their anomeric carbons. Its nonreducing nature prevents unwanted side reactions (e.g., glycation), making it ideal for carbon transport.

- **Biosynthetic Pathway:**
  Sucrose is synthesized in the plant cytosol. Glucose-1-phosphate (G1P) is first converted to UDP-glucose, which then reacts with fructose-6-phosphate via sucrose 6-phosphate synthase to form sucrose-6-phosphate. The final dephosphorylation step, catalyzed by sucrose 6-phosphatase, releases free sucrose.
- **Regulatory Mechanisms:**
  The balance between sucrose and starch synthesis is tightly controlled. Key regulatory enzymes such as fructose 1,6-bisphosphatase and PPi-dependent phosphofructokinase respond to modulators like fructose 2,6-bisphosphate, ensuring proper allocation of carbon based on photosynthetic activity and inorganic phosphate (Pi) availability.

Starch Biosynthesis:

- **Pathway Overview:**
  Excess triose phosphates produced in the Calvin cycle are converted to glucose-1-phosphate, which, with ATP, is transformed into ADP-glucose by ADP-glucose pyrophosphorylase (AGPase). ADP-glucose then serves as the activated donor for starch synthases, which elongate the growing starch polymer by adding glucose residues predominantly at the nonreducing end.
- **Mechanistic and Structural Insights:**
  Starch synthases operate via glycosyltransfer reactions, and kinetic studies suggest they may function via processive or distributive mechanisms. Structural models reveal a GT-B fold with distinct N- and C-terminal domains, where redox-sensitive disulfide bridges can regulate enzyme activity, linking starch synthesis to the cellular redox state.

Cellulose Synthesis:

- **Enzymatic Machinery:**
  Cellulose, the primary structural component of plant cell walls, is synthesized by the cellulose synthase (CesA) family of enzymes. These enzymes, part of the GT2 family, utilize UDP-glucose to form β(1,4)-linked glucan chains.
- **Complex Assembly and Function:**
  CesA enzymes aggregate into rosette-shaped complexes (CSC) in the plasma membrane. Each CSC synthesizes multiple cellulose strands concurrently, which self-associate via hydrogen bonding and π-stacking interactions among aromatic residues, forming robust cellulose microfibrils that contribute to cell wall strength.

Integration of Carbohydrate Metabolism:

- **Carbon Partitioning:**
  The chapter emphasizes that the products of photosynthesis are partitioned among sucrose, starch, and cellulose pathways according to the plant's developmental and environmental needs. Sucrose is typically used for long-distance transport, starch serves as a storage carbohydrate, and cellulose provides structural integrity.
- **Regulatory Coordination:**
  Complex regulatory networks involving enzyme activity modulation by allosteric effectors, phosphorylation, and redox status ensure that carbohydrate synthesis is finely tuned. Transporters such as the triose-phosphate/phosphate translocator further coordinate the exchange of metabolites between the chloroplast and the cytosol, linking carbohydrate synthesis with overall energy metabolism.

In summary, this chapter provides a comprehensive view of plant carbohydrate metabolism—from the assembly of sucrose, starch, and cellulose at the molecular level to the sophisticated regulatory mechanisms that balance carbon allocation, energy storage, and structural development in plants.

This page titled 20.6: Biosynthesis of Starch, Sucrose and Cellulose is shared under a not declared license and was authored, remixed, and/or curated by Henry Jakubowski and Patricia Flatt.

- **Current page** by Henry Jakubowski and Patricia Flatt has no license indicated.
- **11.2: Diffusion Across a Membrane - Passive and Facilitated Diffusion** by Henry Jakubowski and Patricia Flatt has no license indicated.

CHAPTER OVERVIEW

21: LIPID BIOSYNTHESIS

Return to Fundamentals of Biochemistry Search Fundamentals of Biochemistry

21.1: Biosynthesis of Fatty Acids and Eicosanoids
21.2: Biosynthesis of Triacylglycerols
21.3: Biosynthesis of Membrane Glycerolipids
21.4: Biosynthesis of Membrane Sphingolipids
21.5: Biosynthesis of Cholesterol and Steroids
21.6: Biosynthesis and Metabolism of Isoprenoids

This page titled 21: Lipid Biosynthesis is shared under a not declared license and was authored, remixed, and/or curated by Henry Jakubowski and Patricia Flatt.

21.1: BIOSYNTHESIS OF FATTY ACIDS AND EICOSANOIDS

LEARNING GOALS (CHATGPT O3-MINI)

- **Overall Fatty Acid Synthesis Pathway:**
  • Describe the net reaction for fatty acid synthesis, including the conversion of eight acetyl-CoA molecules, NADPH, and ATP into palmitate and by-products.
  • Explain how the use of acetyl-CoA in fatty acid synthesis explains why most fatty acids have an even number of carbons.
- **Types of Fatty Acid Synthase (FAS) Complexes:**
  • Compare and contrast Type I FAS (found in yeast, mammals, and higher eukaryotes as large multienzyme complexes) with Type II FAS (found in plants, most bacteria, and mitochondria as separate enzymes).
  • Summarize key structural differences between the yeast FAS complex (an $\alpha_6\beta_6$ heterododecamer) and mammalian FAS (an α_2 homodimer), including differences in molecular weight and domain organization.
- **Mechanistic Insights into Fatty Acid Synthesis:**
  • Outline the role of acetyl-CoA carboxylase in converting acetyl-CoA to malonyl-CoA via an ATP-dependent, biotin-mediated carboxylation reaction.
  • Explain the iterative cycle of fatty acid chain elongation by the FAS complex, emphasizing the condensation (driven by malonyl-CoA decarboxylation), reduction, dehydration, and a second reduction steps.
  • Describe how the acyl carrier protein (ACP) and its tethered 4'-phosphopantetheine arm shuttle intermediates between the multiple catalytic domains within the FAS complex.
- **Domain Organization and Catalytic Mechanisms:**
  • Identify the various enzymatic domains within FAS (e.g., ketosynthase, ketoreductase, dehydratase, enoyl reductase, malonyl/acetyltransferase, and phosphopantetheinyl transferase) and explain their individual roles in fatty acid synthesis.
  • Discuss the conformational changes and domain “swiveling” observed in enzymes like pyruvate phosphate dikinase, drawing parallels to the dynamic movements required in FAS.
- **Regulation of Fatty Acid Synthesis:**
  • Explain how acetyl-CoA carboxylase is regulated through allosteric effectors (e.g., citrate) and post-translational modifications (e.g., phosphorylation by AMPK or PKA).
  • Describe the mechanisms by which the activity of key enzymes is modulated to balance energy status with the need for fatty acid synthesis.
- **Fatty Acid Elongation and Desaturation:**
  • Outline the additional steps of fatty acid elongation in the endoplasmic reticulum, including the roles of ELOVL enzymes in incorporating two-carbon units from malonyl-CoA.
  • Describe the process of fatty acid desaturation by enzymes such as stearoyl-CoA desaturase, highlighting the role of metal centers, electron donors, and radical intermediates in introducing double bonds into fatty acyl chains.
- **Mitochondrial Fatty Acid Synthesis:**
  • Compare mitochondrial fatty acid synthesis with cytosolic synthesis, focusing on differences in enzyme composition and the ultimate production of octanoate and its conversion to lipoic acid.
- **Eicosanoid and Prostaglandin Biosynthesis:**
  • Explain how arachidonic acid, derived from membrane phospholipids, is converted by cyclooxygenase (COX) enzymes into prostaglandin intermediates (PGG_2 and PGH_2).
  • Discuss the dual enzymatic activities (cyclooxygenase and peroxidase) of COX, the role of heme cofactors, and the significance of radical intermediates in these reactions.
  • Compare the substrate specificities and regulatory mechanisms of COX-1, COX-2, and COX-3, and their implications for the action of drugs such as aspirin and ibuprofen.
- **Physiological Implications of Polyunsaturated Fatty Acids (PUFAs):**
  • Describe the biosynthesis and nutritional importance of ω-3 and ω-6 fatty acids, including their roles as precursors for signaling molecules such as prostaglandins and leukotrienes.
  • Explain how dietary ω-3 fatty acids (e.g., EPA and DHA) influence membrane composition, inflammation, and gene expression via interactions with nuclear receptors like PPARs.

- **Membrane Receptor Signaling by Unsaturated Fatty Acids:**
  • Detail how ω-3 fatty acids act as ligands for G protein-coupled receptor 120 (GPCR120), and describe the downstream signaling pathways (via Gαq, Gαi, Gαs, and β-arrestin) that contribute to anti-inflammatory and metabolic effects.

These learning goals are designed to help you integrate knowledge of fatty acid synthesis, regulation, and metabolism with broader physiological and pharmacological contexts, ensuring a comprehensive understanding of how lipid biochemistry influences cell structure, energy homeostasis, and health.

21.1.1: INTRODUCTION

We present the full fatty acid synthase pathway based on the structure of the yeast fatty acid synthase (FAS) complex, whose full structure is known. Then, we will explore each step in more detail. The mammalian FAS complex is a bit different, and we will summarize those differences next. We will end with a summary of the bacterial pathway.

Let's look at the net reaction first and then return to the structure and mechanism. Equation 1 below shows the net reaction.

$$\begin{aligned} &\text{8 Acetyl-CoA (2C)} + 14\text{NADPH} + 14\text{H}^+ + 7\text{ATP} \rightarrow \text{1 Palmitate (16 : 0)} + 8\text{CoA} \\ &+ 6\text{H}_2\text{O} + 14\text{NADP}^+ + 7\text{ADP} + 7\text{Pi} \end{aligned} \tag{21.1.1}$$

Eight 2C-acetyl-CoAs condense to make the 16:0 fatty acid palmitate. That acetyl-CoA is used to synthesize and elongate fatty acids suggests an immediate explanation for the fact that most fatty acids have an even number of carbon atoms. The net reaction is a reductive biosynthesis, making one long molecule from multiple short ones. Hence, an energy source must drive the reaction (7 ATPs) and a reducing agent (typically NADPH). This reaction occurs in the cytosol and uses the nicotinamide-based redox pair (NADPH/$NADP^+$). These factors differentiate fatty acid synthesis from beta-oxidation, which occurs in the mitochondria and which uses the redox pair NAD^+/NADH.

From a chemical perspective, the acetyl-CoAs, high-energy molecules with respect to their hydrolysis products, must be activated using ATP in some way to drive C-C bond formation. That reaction is catalyzed by the enzyme **acetyl-CoA carboxylase**, which uses the ATP already mentioned and the bound cofactor biotin that adds CO_2 to acetyl-CoA to form malonyl-CoA. Neither malonyl-CoA nor CO_2 is shown in the above equation since they are present on both sides of the net reaction and cancel out from the final balanced equation. C-C bond formation occurs in the reaction of the growing acyl group with the 3C malonyl group, driven by the release of CO_2. The malonyl-CoA produced by acetyl-CoA carboxylase feeds into the fatty acid synthesis cycle.

Only one other enzyme complex is required for the entire reaction, the **fatty acid synthase (FAS) complex**. Don't let that fool you into thinking the mechanism is simple, though! There are two types of fatty acid synthase complexes, I and II. Type II FAS is found in plants, most bacteria, and mitochondria. (Its presence in the mitochondria might seem odd since fatty acid oxidation occurs there. We will discuss that in a bit.) Multiple separate enzymes catalyze the synthesis of fatty acids in the Type II FAS systems. We won't discuss those. Instead, we will focus on the **Type I FAS complex** in some bacteria, fungi like yeast, and higher eukaryotes. The Type I FAS is one very large complex. It consists of two α chains with a total molecular weight of 540,000 in mammals. In yeast, it is an $\alpha_6\beta_6$ heterododecamer with a molecular weight of 2.6 million. The alpha and beta chains in either complex have multiple enzyme catalytic domains.

Large enzymatic complexes typically allow bound substrates to proceed to products without dissociation, with the bound intermediates moving through "channels" to the next active site. In the case of Type I FAS, the growing intermediate, which eventually reaches the end product size of 16:0, is tethered to an **acyl-carrier protein (ACP)**. The tethered intermediate can "swing" from one active site to another to allow the iterative stepwise chemical reactions to complete before adding another 2C acetyl CA to the growing chain. The extra 2Cs come from the 3C malonyl-CoA (formed by the extracyclic - outside of the pathway - enzyme acetyl-CoA carboxylase) and the immediate release of CO_2, which helps drive the reaction forward.

Now we can introduce the fatty acid synthase cycle and feeder acetyl-CoA carboxylase reaction in its entirety, as shown in Figure **21.1.1** for yeast FAS1.

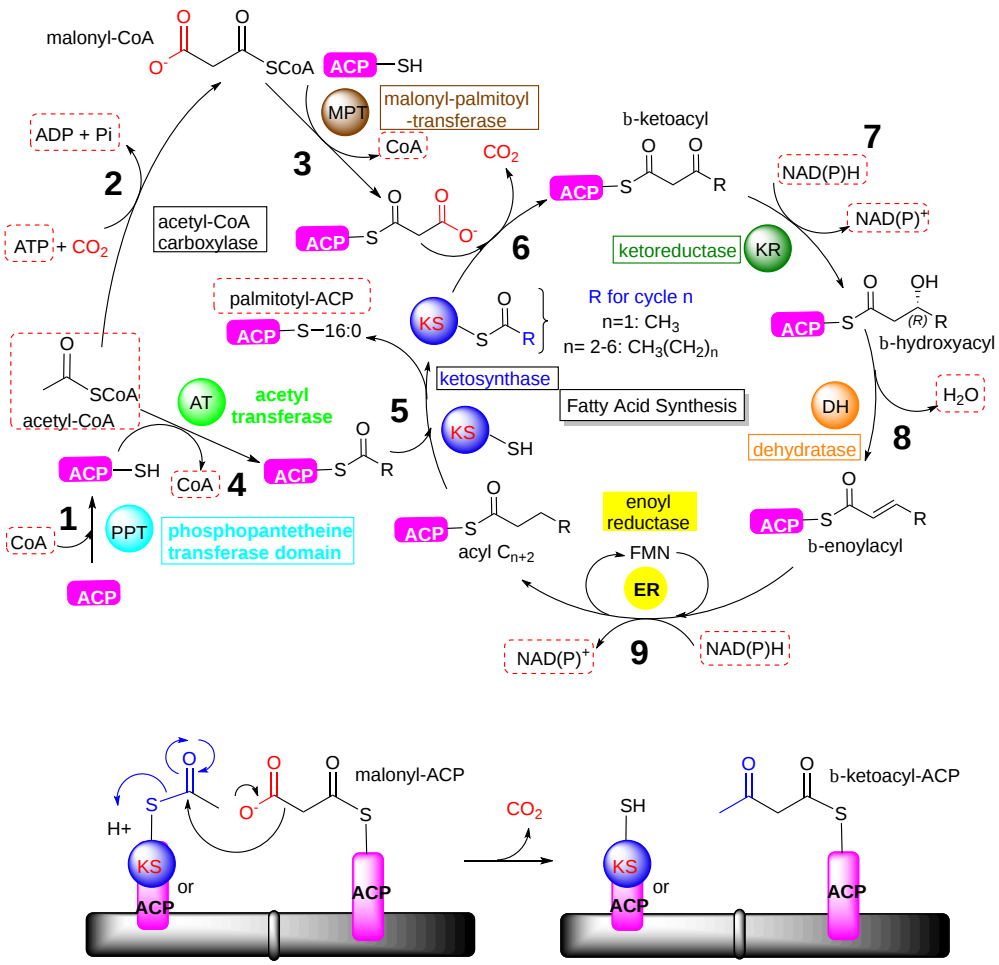


Figure **21.1.1**: The Yeast Fatty Acid synthesis cycle with the feeder acetyl-CoA carboxylase reaction. The bottom part of the figure shows a mechanism for the condensation between acetyl-CoA attached to ACP or KS and malonyl-CoA, driven by the release of CO_2. (adapted from Singh et al. Cell, 180 (2020), https://doi.org/10.1016/j.cell.2020.02.034 and Fischer et al. *Sci Rep* **10,** 895 (2020). https://doi.org/10.1038/s41598-020-57418-8. Creative Commons Attribution 4.0 International License. http://creativecommons.org/licenses/by/4.0/

This figure is difficult to understand, but keep in mind that it scales down the complexity of FAS1 enormously. Let's deconstruct the figure to make it more understandable.

The dotted red boxes show the substrates and products that match chemical equation 1. The substrate acetyl-CoA comes into the cycle in two places, as shown in the extracyclic section to the upper left. It comes in as acetyl-CoA from **reaction 4** after attachment to the acyl carrier protein (part of FAS1). It also comes in "effectively" after it has been carboxylated by acetyl-CoA carboxylase in **reaction 2** to malonyl-CoA, which enters the cycle as malonyl-ACP after **reaction 3**. The other substrates/products include CoAs, the NAD(P)H/NAD(P)$^+$ couples, and H_2O, shown around the right-hand side of the circular fatty acid synthesis cycle (2 -6 o'clock positions) as well as the final product, 16:0-ACP (9:30 clock position), which forms 16:0-SCoA.

The individual enzymatic domains in the $\alpha_6\beta_6$ hetero-dodecamer yeast FAS1 are shown in colored spheres as shown in Figure **21.1.2**.

Domain	Chain	Name
ACP	α FAS2	acyl carrier protein
PPT	α FAS2	Phosphopantetheine transferase
AT	β FAS1	acetyl transferase
MPT	β FAS1	malonyl-palmitoyl transferase
KR	α FAS2	keto reductase
DH	β FAS1	dehydratase
ER	β FAS1	Enoyl reductase
KS	α FAS2	ketosynthase

Figure **21.1.2**: Enzymatic domains in the $\alpha_6\beta_6$ heterododecamer yeast FAS1

Figure **21.1.3** pictorially summarizes the repetitive Claisen condensation reactions of acetyl-ACP and malonyl-ACP in the first step and the growing acyl-ACP chain and malonyl-CoA in the next two cycles.

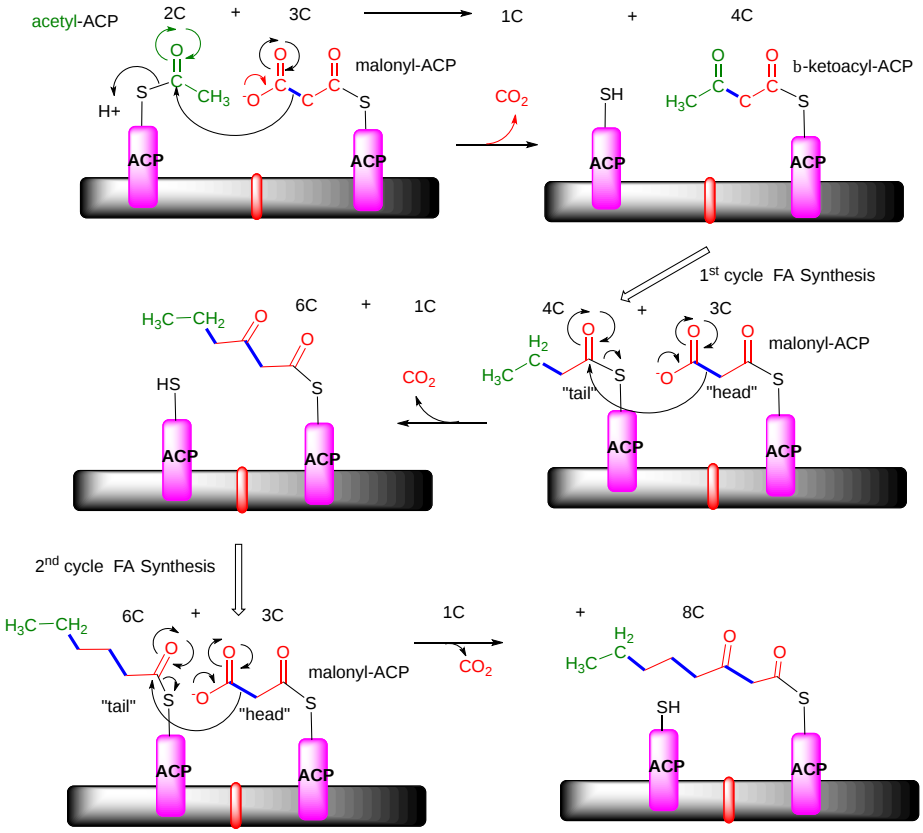


Figure **21.1.3**: Pictorial summary of the first three condensation reactions in fatty acid synthesis. Each acyl group is shown connected to ACP for simplicity.

In each step, the condensation (C-C bond formation) is driven by the decarboxylation of malonyl-CoA. (Of course, earlier expenditure of ATP in step 1 is required). Electrons in malonyl-CoA that form a bond with acetyl-ACP in the first condensation step and acyl-ACP in subsequent condensations are shown as **bold blue lines**. Note that the condensation is from the head of the malonyl-ACP to the tail of the elongating acyl chain. The ACP or equivalent chains are in the interior of the complex, which allows movement of the acyl groups attached to pantetheine chains to interactively reach nearby catalytic domains for each step in the cycle.

21.1.2: MECHANISM OF INDIVIDUAL REACTIONS

Now, we can explore some of the reactions in more detail. Then, we will look at the structure of yeast FAS and its domain organization.

21.1.2.1: REACTION 1: PHOSPHOPANTETHEINE TRANSFERASE

Holo-(acyl carrier protein) synthase (AcpS) from *Bacillus subtilis* is a member of the phosphopantetheinyl transferase superfamily. AcpS post-translationally modifies ACP to its holo form to activate it. AcpS catalyzes the transfer of the 4'-phosphopantetheinyl (P-pant) moiety of coenzyme A to a serine residue on the ACP. This gives the activated ACP enzyme and adenosine 3'5'-bisphosphate as products. This process is important as ACP enzymes play important roles in several biosynthetic pathways, such as the synthesis of fatty acids and vitamins, and the initiation of the biosynthesis of fatty acids, polyketide antibiotics, and non-ribosomal peptides.

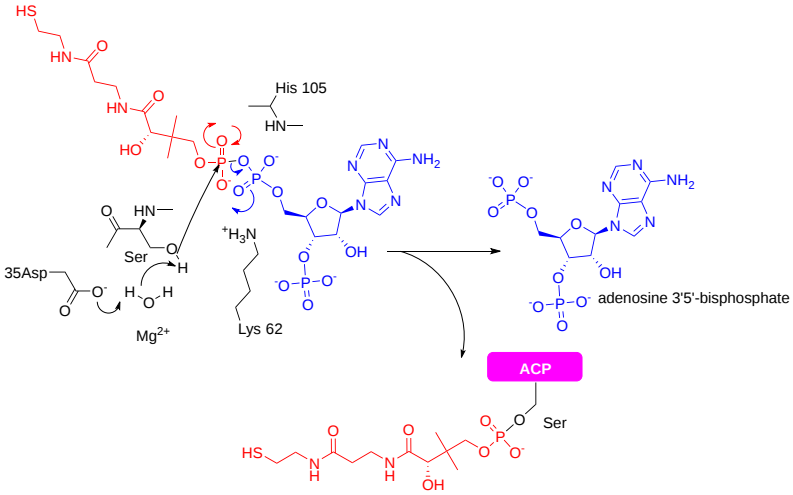


Figure **21.1.4**: https://www.ebi.ac.uk/thornton-srv/m-csa/entry/152/

21.1.2.2: REACTION 2: ACETYL-COA CARBOXYLASE (ACC)

This enzyme catalyzes the carboxylation of acetyl-CoA to malonyl-CoA, which then enters the fatty acid synthesis cycle. This is a key enzyme, the rate-limiting step, and is regulated. The reaction has two steps:

- carboxylation of biotin on the enzyme's biotin carboxyl carrier domain at the expense of ATP hydrolysis. The carboxylation, using bicarbonate as a substrate, leads to the formation of a molecule with high energy (with respect to its hydrolysis product), the carboxylated biotin intermediate. (**Remember, there is no such thing as a "high energy" bond.**)
- transfer of the carboxyl group to acetyl-CoA to form malonyl-CoA requires the formation of a C-C covalent bond.

Biotin, an essential nutrient and cofactor, "carries" activated carboxyl groups for transfer. It is a carboxyl (not acetyl) donor. It is linked through an amide link to a lysine side chain in the protein.

The enzyme is downregulated by 16:0-SCoA, the end product of the pathway for fatty synthesis by FAS, and by phosphorylation by kinase activation through the cAMP pathways from glucagon binding. You don't want to synthesize fatty acids when your energy state is low (signaled by increases in glucagon). Its activity is upregulated by the binding of citrate to an allosteric site. This makes sense since high citrate, a citric acid cycle intermediate, signifies abundant energy reserves are available so that fatty acids would be synthesized for future needs. The dephosphorylated form of the enzyme would signify the need to increase fatty acid synthesis.

Figure **21.1.5** shows a few steps in the carboxylation of biotin and the subsequent transfer of the carboxy group to acetyl-CoA, forming malonyl-CoA.

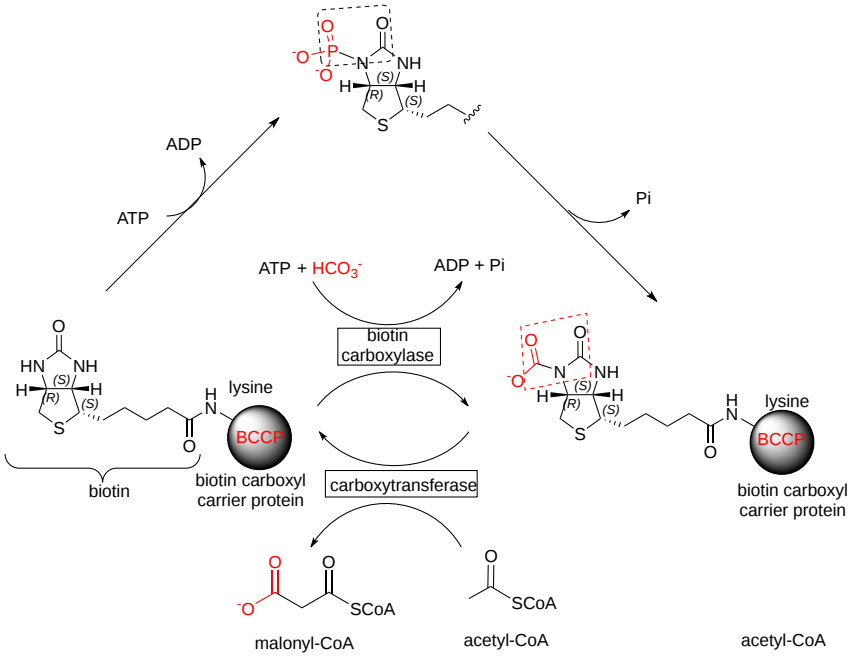


Figure 21.1.5: Simplified reactions of acetyl-CoA carboxylase

BCCP represents the biotin carboxyl carrier domain of acetyl-CoA carboxylase.

Biotin carboxylases are found in many enzymes and pathways, not just fatty acid synthesis. Scientists are trying to devise new pathways and enhanced carboxylases to pull CO_2 from the air into biosynthetic reactions, producing fuels that could be burned. This would release CO2 back into the atmosphere, in a process that would theoretically, but perhaps not practically, be carbon neutral with respect to greenhouse gas emissions.

The abbreviated mechanism shown above shows two of the three activities of acetyl-CoA carboxylase: **biotin carboxylase (BC)** and **carboxyltransferase (CT)** activity. The third is the **biotin carboxyl carrier protein (BCCP)**, which links biotin to it through a lysine side chain. Different enzymes have different acceptors (acetyl-CoA, pyruvate, etc.) of the activated carboxy group, so the structure of those centers varies significantly. The BC and BCCP components are structurally similar for different carboxylases.

A mechanism for the E. Coli biotin carboxylase component of the reaction is shown in Figure 21.1.6.

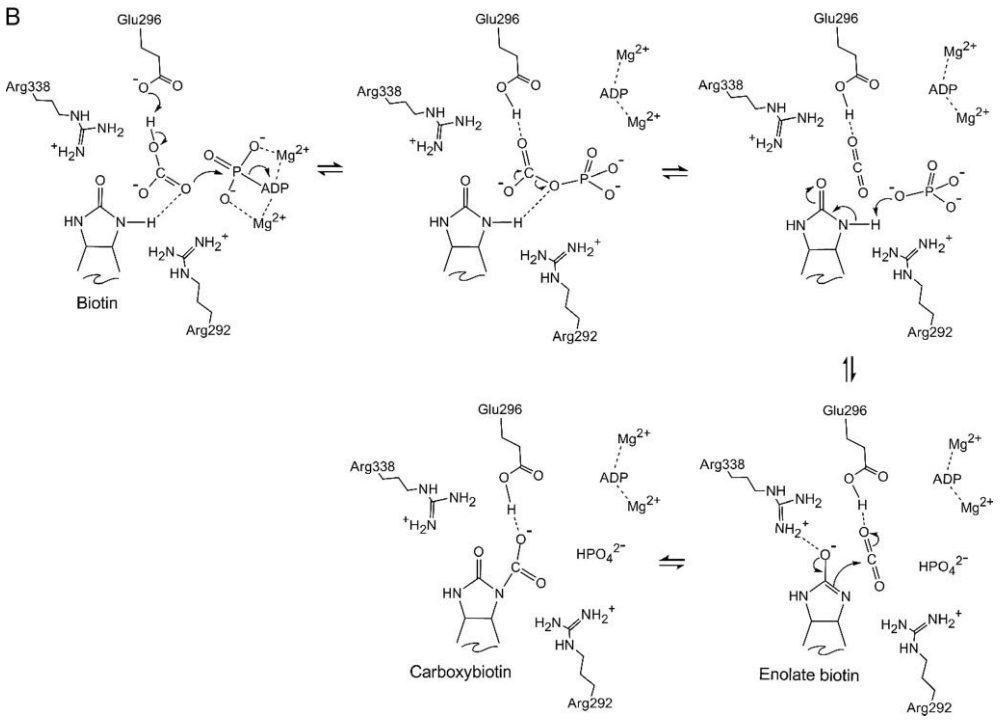


Figure 21.1.6 Reaction mechanism for E. Coli biotin carboxylase. Chou et al. J Biol Chem. 2009 Apr 24; 284(17): 11690–11697. doi:10.1074/jbc.M805783200. Creative Commons Attribution (CC BY 4.0)

Glu 296 acts as a general acid/base, while Arg 338 stabilizes the negative charge in intermediates and transition states.

Structure of acetyl-CoA carboxylase (ACC)

There are two forms of ACC, soluble cytosolic ACC1 and mitochondrial membrane-associated ACC2 (the latter of which regulates the beta-oxidation of fatty acids). The overall domain structure of yeast acetyl-CoA carboxylase is in Figure 21.1.7.

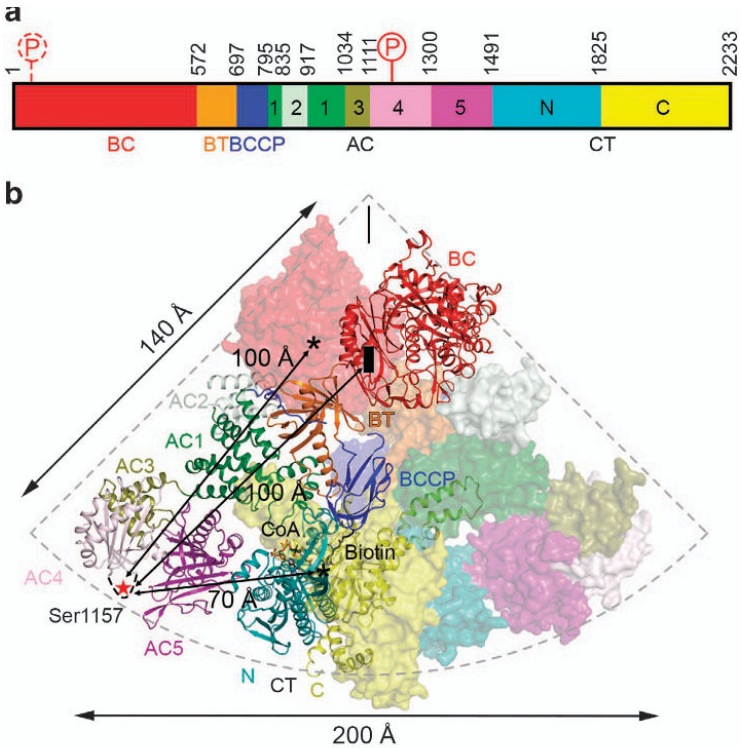


Figure 21.1.7: Overall structure of yeast acetyl-CoA carboxylase (ACC) (ScACC). Wei et al. Cell Discovery (2016) 2, 16044; doi:10.1038/celldisc.2016.44. Creative Commons Attribution 4.0 International License. http://creativecommons.org/licenses/by/4.0/.

Panel (a) shows ScACC's domain organization. The domains are labeled and given different colors. The five domains of ACC Central (AC1–AC5) are labeled 1–5. The phosphorylation site in the central region is indicated. The phosphorylation site before the biotin carboxylase (BC) domain core is indicated with the dashed lines, as it is absent in ScACC.

Panel (b) shows the structure of the ScACC holoenzyme dimer [7]. One protomer is shown as ribbons, while the other is shown as a surface. The domains in the monomers are colored according to panel (a) and labeled. Ser1157 (red star) is located in a loop missing in the structure (dashed lines), and its distances to the BC and carboxyltransferase (CT) active sites (black asterisks) and the BC dimer interface (black rectangle) in the holoenzyme are indicated.

A chain domain structure 5CSKA_Yeast Acety-lCoA Carboxylase is shown in Figure **21.1.8**.

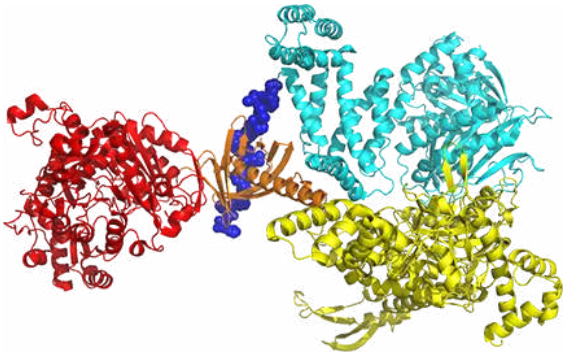


Figure **21.1.8**: General domain structure of yeast acetyl-CoA carboxylase A monomer

The colors used to show the domains are matched to Figure **21.1.*x*** above and are as follows:

- Red - BC, biotin carboxylase (has enzymatic activity)
- Gold - BT, an interaction domain
- Blue - BCCP (biotin carboxyl carrier protein (disordered blue spheres)
- Cyan - AC (central bridging noncatalytic domain comprising AC1-AC5).
- Yellow - CT, carboxyl transferase (has enzymatic activity), comprising the N and C subdomains

A similar domain structure is found in human ACC1. The central bridging domain in human ACC1 is called the Central Domain (CD) with four parts, CD_N, CD_L, $CD_{C1,}$ and CD_{C2}.

Regulation of ACC

ACC1 activity is regulated by product inhibition, allosteric effectors, and phosphorylation by different kinases. The enzyme is inhibited by its product, malonyl-CoA, and the end product of fatty acid synthesis, 16:0-CoA.

The protein is inactive as a monomer and is active as a dimer. Anything that can perturb that equilibrium can affect ACC activity. Phosphorylation generally inhibits the protein by promoting the dissociation of the active dimer. In the presence of the allosteric activator citrate, the active dimer can aggregate to form fibrils, which are even more active than the dimer.

The protein is post-translationally modified by phosphorylation at several sites, but a few stand out. AMP-activated protein kinase (AMPK) phosphorylates human ACC at Ser 80 (in the BC domain). In yeast, the kinase SNF1 (equivalent to human AMPK) does not phosphorylate Ser 80 but phosphorylates a key Ser 1157 in the AC subdomain AC4 in yeast.

- In humans, phosphorylation at Ser 80 in the BC domain prevents dimerization of the protein through the BC domain and hence inhibits activity;
- In yeast, phosphorylation at Ser 1157 in AC subdomain AC4 produces a conformational change in the BC domain region that appears to lead to dimer dissociation.

Human ACC is phosphorylated at many sites, with Ser 80 and 1201 (which is phosphorylated by both AMPK and PKA) being the most important in regulation. In addition, it is phosphorylated at Ser 1263 by a cyclin-dependent protein kinase (CDK). When phosphorylated, the pSer 1263 facilitates the binding of BRAC1, the tumor suppressor protein, which, when mutated, can dramatically increase breast cancer. The binding of BRAC1 leads to an inactive fibril form of ACC. Figure **21.1.9** summarizes the regulation of human CoA carboxylase.

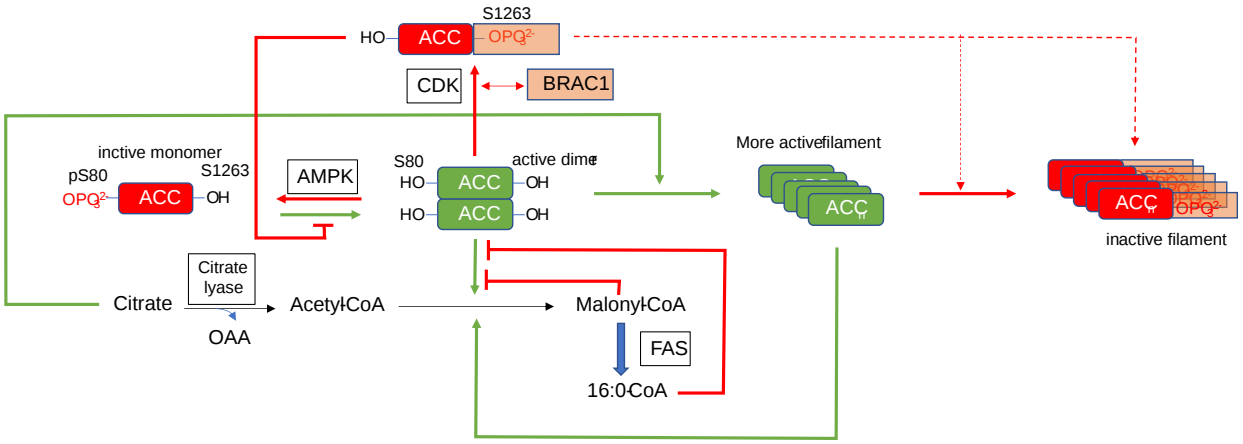


Figure **21.1.9**: Regulation of human acetyl-CoA carboxylase. Red indicates inactive states or inactivating reactions, while green indicates active states and activating reactions.

21.1.2.3: 3. MALONYL-PALMITOYL TRANSFERASE (MPT)/MALONYL-COA-ACYL CARRIER PROTEIN TRANSACYLASE (MAT)

These protein activities are found in the yeast (MPT) and human (MAT) domains. The mechanism is shown in Figure **21.1.10**.

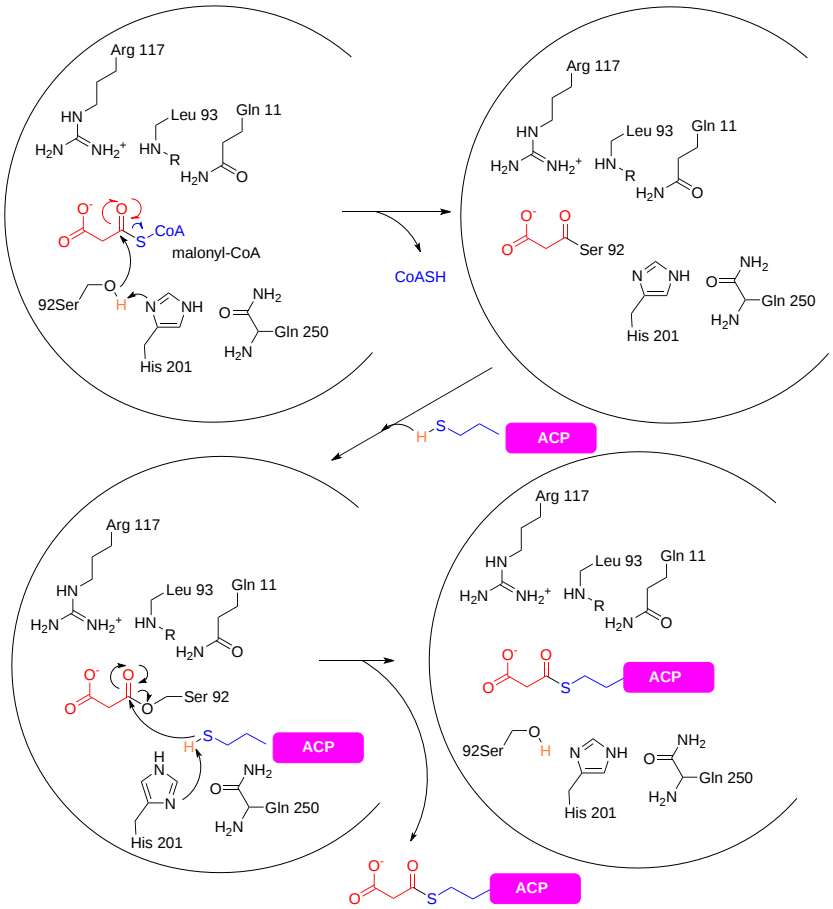


Figure **21.1.10**: Reaction mechanism for Malonyl-Palmitoyl Transferase (MPT)/Malonyl-CoA-acyl carrier protein transacylase (MAT). (after https://www.ebi.ac.uk/thornton-srv/m-csa/entry/291/, Creative Commons Attribution 4.0 International (CC BY 4.0) License.

Two key catalytic residues, Ser 92 and His 201, are involved in the acylation/deacylation of the catalytic serine.

The mechanism is shown in Figure **21.1.11**.

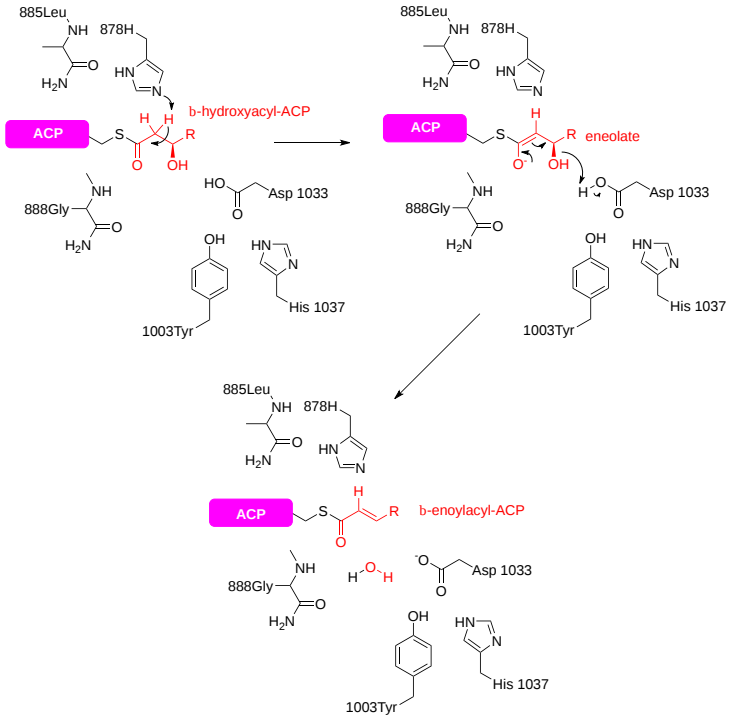
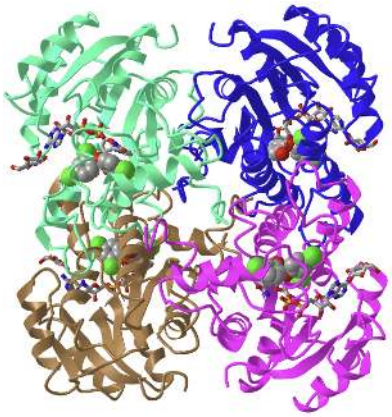


Figure **21.1.11**: Reaction mechanism for β-ketodehydratase (after https://www.ebi.ac.uk/thornton-srv/m-csa/entry/972/, Creative Commons Attribution 4.0 International (CC BY 4.0) License.

21.1.2.4: REACTION 9. ENOYL REDUCTASE

This is the last reaction in the fatty acid synthase cycle, which, of course, repeats until a 16:0-SCoA is made. The yeast enzyme is different in that it has a tightly bound FMN, which is involved in electron transfer (reduction) along with NADPH. The mechanism is likely ping-pong, with $NADP^+$ released before the enoyl acyl-CoA binds.

Figure **21.1.12** shows an interactive iCn3D model of the enoyl-acyl carrier protein reductase (ER) in complex with NAD^+ and triclosan (1QSG)



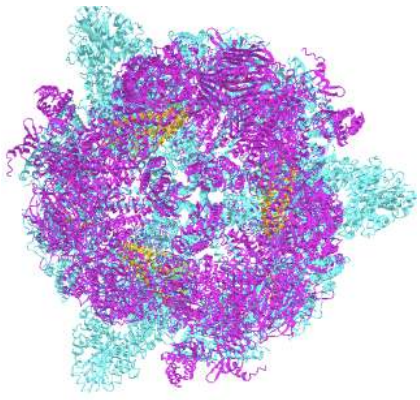
NCBI iCn3D Figure **21.1.12**: enoyl-acyl carrier protein reductase (ER) in complex with NAD^+ and triclosan (1QSG) (Copyright; author via source). Click the image for a popup or use this external link: https://structure.ncbi.nlm.nih.gov/i...Z2ZCQaTYabQWa9

Triclosan is used in many commercial products, even soaps, as it has broad-spectrum antimicrobial activity. However, in a world with increasing antibiotic resistance, it is unwise to use triclosan in soaps since evidence shows that soaps' surfactant properties are sufficient to remove bacteria from the skin. Triclosan is an active site inhibitor of bacterial enoyl-reductases, but in humans, it appears to be an allosteric inhibitor since it is bound at a protein-protein interface and not the active site.

21.1.3: STRUCTURE OF YEAST FATTY ACID SYNTHASE I (FAS1)

Now, you have enough background to explore the actual structure of fatty acid synthase. Animal FAS1 is an α_2 homodimer, some bacterial FASs are α_6 hexamers, while fungal FASs are $\alpha_6\beta_6$ dodecamers. In both cases, the monomers are multi-domain proteins, with each domain having a different catalytic activity. Another type of fatty acid synthase II (FAS2) consists of separate enzymes, each with its catalytic function. Type II FAS is found in plants, most bacteria, and mitochondria.

We'll explore the "more interesting" Type I and start with yeast (Saccharomyces cerevisiae) FAS (6QL5), whose structure has been solved with a regulatory γ subunit that 2.8 angstrom 6QL5. Figure **21.1.13** shows an interactive iCn3D model of the fatty acid synthase complex with bound gamma subunit from Saccharomyces cerevisiae (6QL5) very long load time.



NCBI iCn3D Figure **21.1.13**: Fatty acid synthase complex with bound gamma subunit from Saccharomyces cerevisiae 6QL5. (Copyright; author via source). Click the image for a popup or use this external link: https://structure.ncbi.nlm.nih.gov/i...YnMNSaTbTXYGe7 (very long load time).

The alpha subunits are shown in cyan, the beta subunits in magenta, and the regulatory γ subunit in orange.

The six alpha subunits are arranged in an equatorial wheel or disk. The beta subunits are arranged in trimer top and bottom "domes" that cover the alpha subunit disk. Inside are three spaces or chambers where the reactions occur. Five openings allow outside substrate access, and six openings allow internal metabolite access. The FAS is more porous than other large structures with encapsulated volumes like the proteasome or viral capsids. It is more similar to pyruvate dehydrogenase. The ACP protein domain is found inside the structure. It is tethered and "swingable" to allow the internal transfer of acyl intermediates to the different enzymatic functional domains of the complex.

Figure **21.1.14** shows animated images of yeast fatty acid synthase complex, which should give you a sense of the arrangement of the equatorial alpha-helical wheel, the two beta subunit domes, and the interior and interior volumes available for reaction chemistry and intermediate movement. They switch between the full structure, followed by separate views of the alpha (cyan), beta (magenta), and regulatory (orange) chains.

fatty acid synthase complex - side view

fatty acid synthase complex - top view

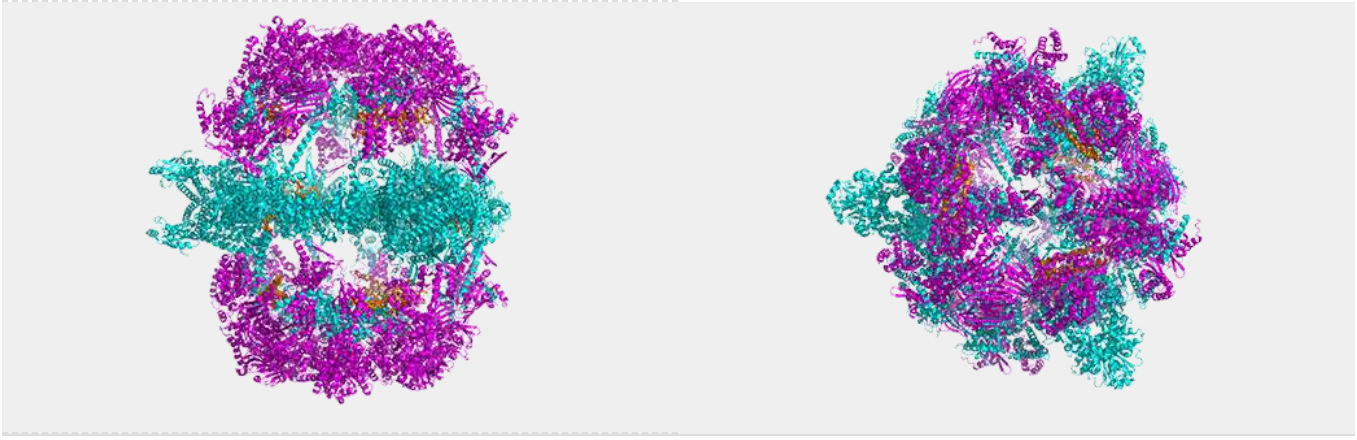


Figure **21.1.14**: Alpha chains (cyan), beta chains (magenta), regulatory (orange)

The α and β monomers are multi-domain proteins, with different domains having different catalytic properties. Simply color-coding the monomers in a single color doesn't provide insight into the remarkable catalytic properties of each chain. Figure **21.1.15** shows color-coded domain and protein structures for yeast $\alpha_6\beta_6$ dodecamer. The color-coding for the domains of each subunit, as shown at the bottom of panel A, is also applied to the domain structures within the actual protein structures.

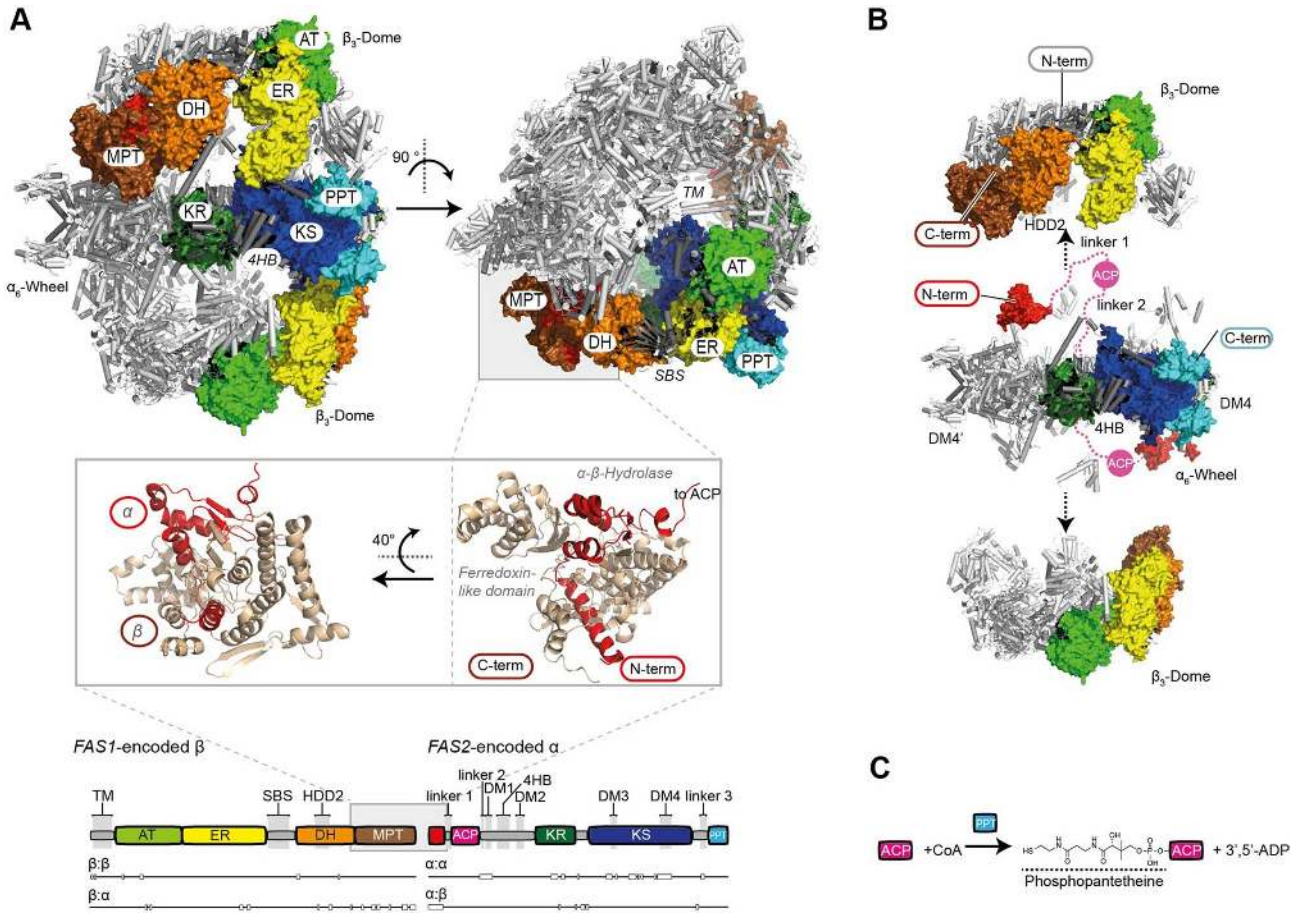


Figure **21.1.15**: Structure of yeast FAS.

Panel (**A**) shows the structure of *S. cerevisiae* FAS (3hmj). The side (left) and top view (right) with two β-subunits and two α-subunits are shown. Note that ACP is in the FAS interior, but is not shown. The MPT fold is comprised of both subunits and shown in cartoon representation (β part in brown and its α part in red). Nomenclature: acetyltransferase (AT), enoyl reductase (ER), dehydratase (DH), malonyl-palmitoyl-transferase (MPT), an acyl carrier protein (ACP), ketoacyl reductase (KR), ketoacyl synthase (KS) and phosphopantetheine transferase domain (PPT). Insertion elements are highlighted in grey: trimerization module (TM), 6-stranded β-sheet (SBS), hotdog-domain 2 (HDD2), dimerization module 1–4 (DM1-4), 4-helical bundle (4HB)). Please note that DM2 is not visible in this structure.

Panel(**B**) shows three yeast FAS barrels as a central D3-symmetric α hexamer (α_6-wheel) and two C3-symmetric β trimers (β_3-domes). β_3-domes have been shifted for clarity (see arrows). ACP domains are shown for two α-subunits and are modeled by spheres in magenta. Dashed lines indicate ACP linkers.

Panel (**C**) shows the post-translational modification of ACP. For phosphopantetheinylation, ACP and PPT have to interact physically. Fischer, M., Joppe, M., Mulinacci, B. *et al.* Analysis of the co-translational assembly of the fungal fatty acid synthase (FAS). *Sci Rep* **10,** 895 (2020). https://doi.org/10.1038/s41598-020-57418-8. Creative Commons Attribution 4.0 International License. http://creativecommons.org/licenses/by/4.0/

In Figure **21.1.16**, we connect the domain structures of each monomer to the actual catalytic cycle of yeast FAS.

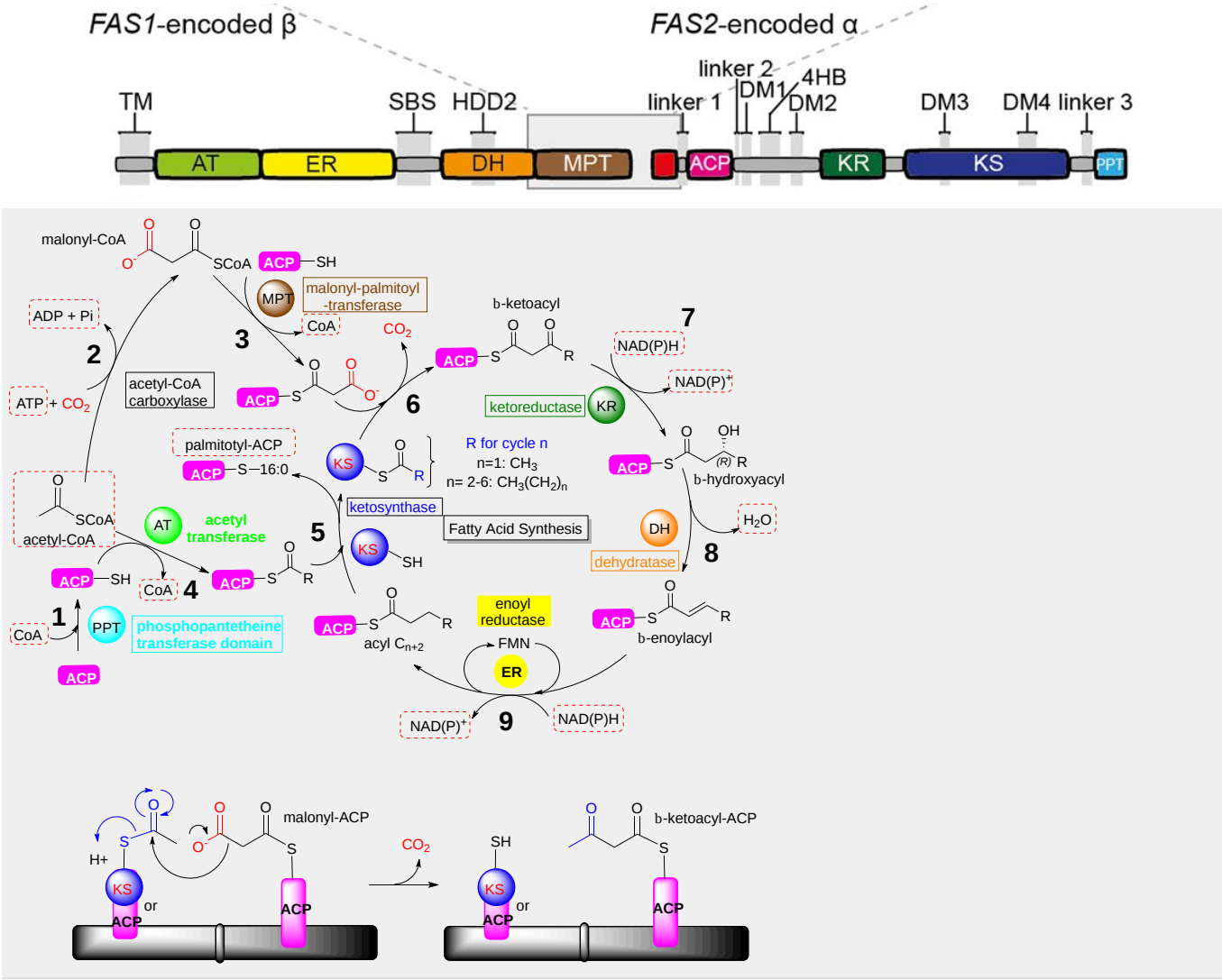


Figure **21.1.16**: Domain structure and the catalytic cycle of yeast fatty acid synthase (adapted from Singh et al. Cell, 180 (2020), https://doi.org/10.1016/j.cell.2020.02.034 and Fischer et al. *Sci Rep* **10,** 895 (2020). https://doi.org/10.1038/s41598-020-57418-8. Creative Commons Attribution 4.0 International License. http://creativecommons.org/licenses/by/4.0/

Figure **21.1.17** shows the actual structure of the isolated α and β monomers. The color coding of the domains is the same as used above.

Fatty acid synthase 1 (FAS1) beta subunit (FAS1) (6U5U G chain)

Fatty acid synthase 2 (FAS2) alpha subunit (2UV8A - P19097 AlphaFold)

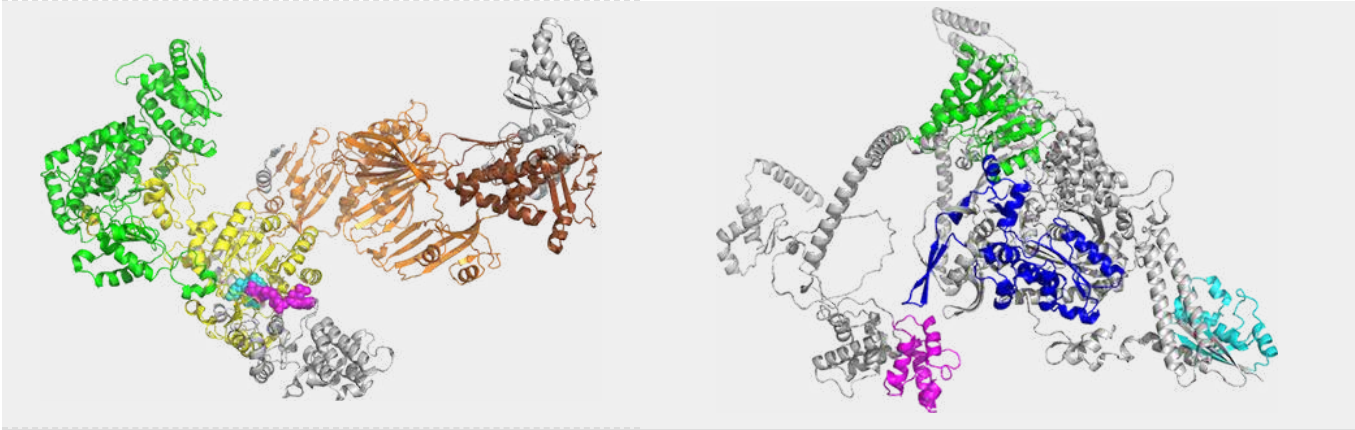


Figure **21.1.17** shows the approximate domain structures and locations for the yeast **fatty acid synthase 1 (FAS1) beta** subunit (6U5U G chain) and fatty acid synthase 2 (FAS2) alpha subunit**.**

The color coding for the domains in each subunit is as follows: FAS1 beta subunit: AT, ER, DH, MPT, flavin mononucleotide (FMN) spacefill cyan NADP nicotinamide-adenine dinucleotide phosphate (NAP), spacefill magenta; FAS2 alpha subunit: ACP, KR, KS, PPT

Now, let's zoom in to see the actual interactions of bound 4'-phosphopantetheine and flavin mononucleotide (FMN). Phosphopantetheine is bound between the alpha (cyan) and beta (magenta) subunits, as shown in Figure **21.1.18**.

4'-phosphopantetheine between alpha (cyan) and beta (magenta) subunits

flavin mononucleotide (FMN) within beta (FAS1) subunit



Figure **21.1.18**:

The γ subunit crosses the entire inner cavity of FAS, interfering with the activities of the reductases.

A central difference in the FAS1 found in humans and other animals occurs in the first reaction, in which the acetyl group of acetyl-CoA is transferred to the pantetheine sulfhydryl of the acyl carrier protein (ACP) domain, catalyzed by the malonyl-/acetyltransferase (MAT) domain. It is then transferred to the active site cysteine of the β-ketoacyl synthase (KS) domain. This allows the malonyl group to be transferred to the now free ACP domain for a second transfer reaction. A Claisen condensation reaction driven by the decarboxylation of the malonyl-ACP occurs to form the β-ketoacyl intermediate bond to the KS domain. Figure **21.1.19** shows an alternative view of the mammalian fatty acid cycle.

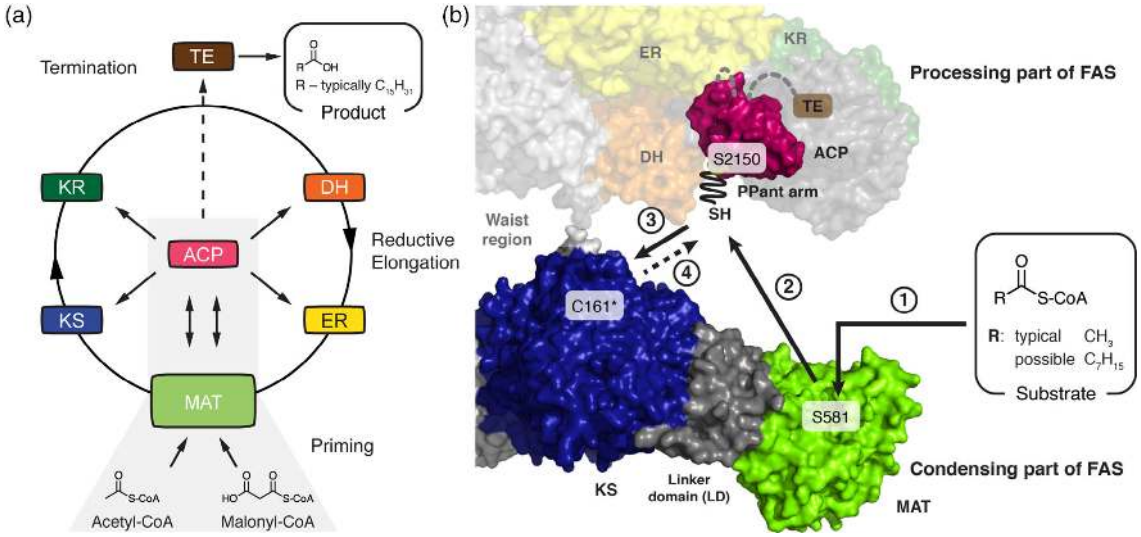


Figure **21.1.19**: Mammalian fatty acid synthase cycle. Rittner et al. Protein Sci. 2020 Feb; 29(2): 589–605. doi:10.1002/pro.3797. Creative Commons Attribution License. http://creativecommons.org/licenses/by/4.0/

Panel (a) shows the priming of animal fatty acid synthesis. Panel (b) shows how, in the first step, the substrate is selected by the MAT domain and transferred to the ACP domain (Step 2), from where it is passed on to the KS domain (Step 3). Important active site residues are highlighted, and C161 is marked with an asterisk. The porcine FAS structure (2png) is shown. Domains of one protomer of the FAS homodimer are colored. ACP, acyl carrier protein; DH, dehydratase; ER, enoyl reductase; FAS, fatty acid synthase; KR, ketoreductase; KS, ketosynthase; MAT, malonyl-/acetyltransferase; PPant arm, expand fully in the figure; TE, thioesterase

Figure 21.1.20 shows the yeast FAS cycle (as a proxy for the mammalian cycle) placed in context with the mitochondrial matrix pathways that feed acetyl-CoA and NADPH into the fatty acid synthesis pathway.

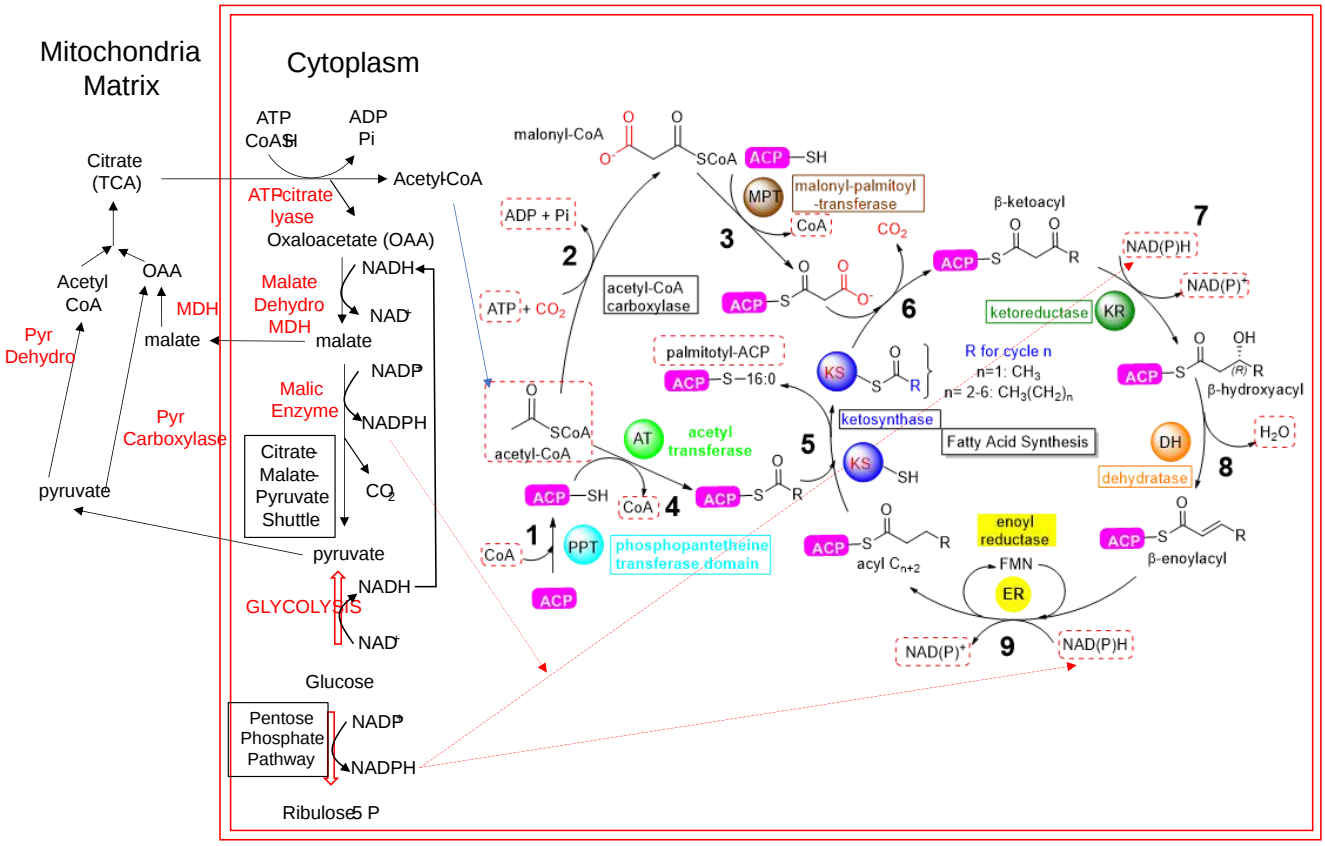


Figure 21.1.20: Yeast FAS cycle (as a proxy for the mammalian cycle) placed in context with the mitochondrial matrix pathways that feed acetyl-CoA and NADPH into the fatty acid synthesis pathway.

21.1.4: FATTY ACID ELONGATION AND DESATURATION

21.1.4.1: OVERVIEW

The elongation of fatty acids occurs in the endoplasmic reticulum of mammals from 16:0, made through fatty acid synthase in the cytoplasm. As with the synthesis of 16:0 by FAS, the elongation consists of two carbon additions driven by the decarboxylation of a malonyl-CoA substrate. Elongation is carried out by a family of **ELOngation of Very Long-chain fatty acid enzymes (ELOVLs)**. Desaturation is catalyzed by **Stearoyl-CoA Desaturases (SCD1 and SCD2**) and **Fatty Acid Desaturases (FADS1 and FADS2)**.

Figure 21.1.21 shows an overview of de novo fatty acid synthesis with elongation and desaturation in mammals and the elongation and desaturation of dietary fatty acids.

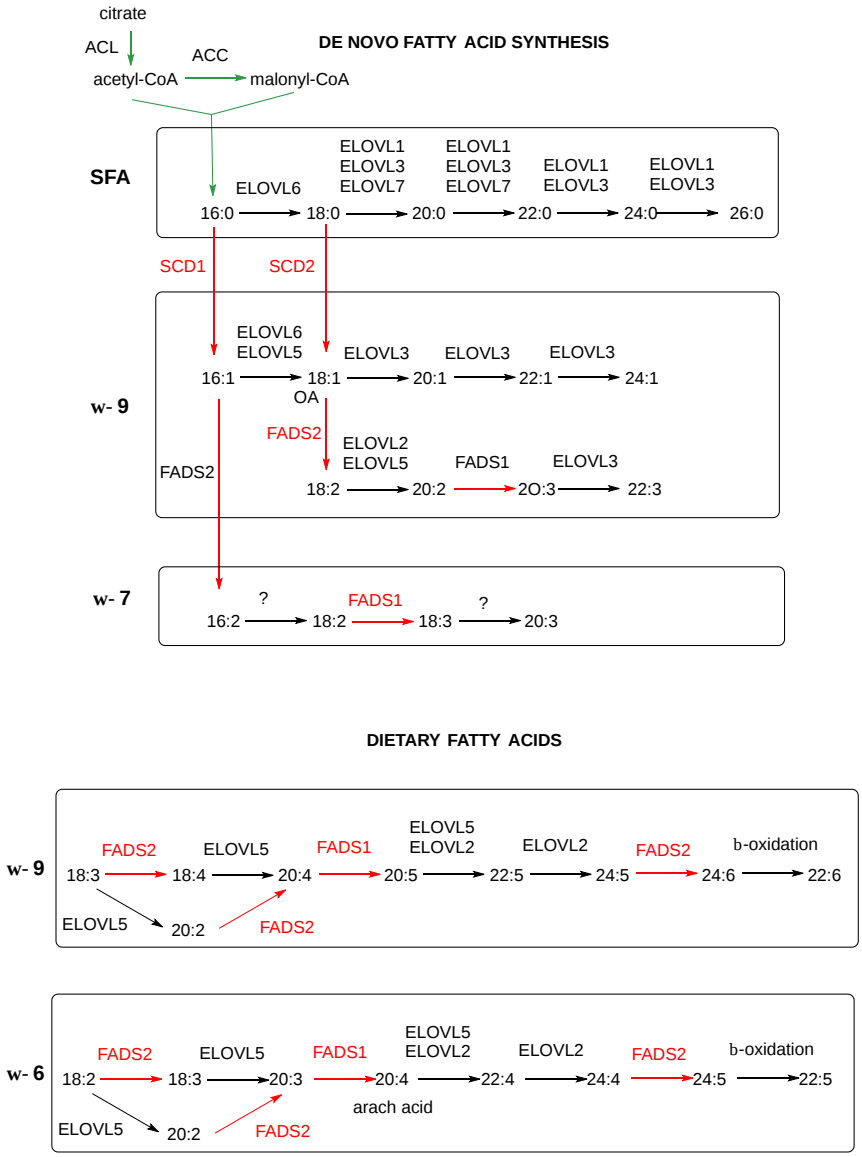


Figure **21.1.21:** Scheme of FA synthesis in mammals. After *Corrales et al. Int. J. Mol. Sci.* **2021**, *22*(15), 8159; **https://doi.org/10.3390/ijms22158159.** Creative Commons Attribution (CC BY) license (https://creativecommons.org/licenses/by/4.0/)

FAs are elongated (ELOVL1–7) and/or desaturated (SCD, FADS) to generate complex FAs. Long-chain saturated FAs (LCSFA) and unsaturated FAs of ω9 and ω7 can be synthesized from palmitic acid (PA, C16:0) produced by the *de novo* FA synthesis. Long-chain unsaturated FAs of the ω6 and ω3 series can only be synthesized from essential diet-derived FAs (OA, oleic acid; NA, nervonic acid; ALA, α-linolenic acid; DHA, docosahexaenoic acid; LA, linoleic acid; ARA, arachidonic acid). SFA are saturated fatty acids.

21.1.4.2: ELONGATION

Mammals use very long-chain fatty acid enzymes (ELOVLs) in the endoplasmic reticulum. There appear to be seven mammalian enzymes with different substrate specificities, as shown in the figure above. The nomenclature for fatty acids is a bit strange. Those with 11-20 carbons are called long-chain FAs (LCFAs), and those with more than 20 are very long-chain FAs (VLCFAs). Those with more than 26 carbons are called ultra long-chain FAs (ULCFAs) found in the skin, retina, meibomian gland, testis, and brain. The same four steps (condensation, reduction, dehydration, and reduction) used in FAS are used in elongation. The enzymes are abbreviated a bit differently (3-ketoacyl-CoA reductase or KAR, 3-hydroxyacyl-CoA dehydratase or HACD, *trans*-2-enoyl-CoA reductase or TER, and LCFA). The enzyme is separate and not part of a multifunctional complex like FAS. The elongation cycle is shown in Figure **21.1.22**.

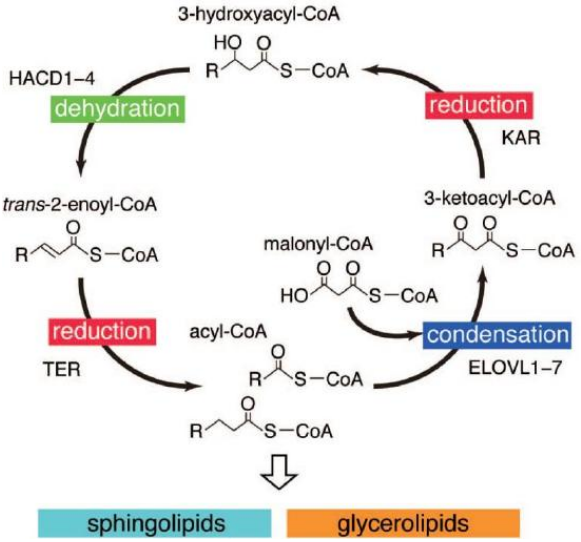


Figure 21.1.22: Mammalian FA elongation cycle. In each cycle, acyl-CoA incorporates two carbon units from malonyl-CoA. Sassa et al. Biomol Ther (Seoul). 2014. http://dx.doi.org/10.4062/biomolther.2014.017. Creative Commons Attribution Non-Commercial License (http://creativecommons.org/licenses/by-nc/3.0/)

Figure 21.1.23 shows fatty acid composition in sphingomyelins, which typically have long fatty acids.

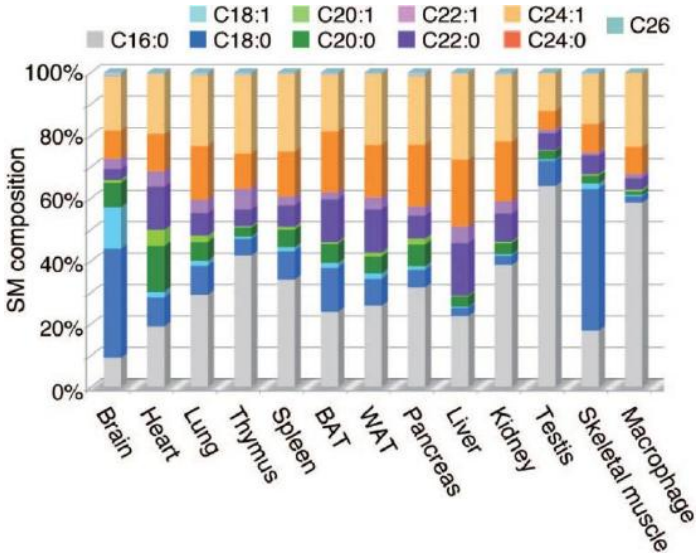


Figure 21.1.23: FA compositions of SM. FA compositions of SM in the indicated mouse tissues, as determined by liquid chromatography-mass spectrometry analysis, are illustrated. SM: sphingomyelin; BAT: brown adipose tissue; WAT: white adipose tissue

21.1.4.3: MECHANISM OF ELOVL7

ELOVL condensing enzymes have a long hydrophobic tunnel and an active site nucleophilic histidine. More traditional nucleophiles like serine or cysteine were eliminated as potential candidates for the active site nucleophile since none were in proximity. The active site with a key HxxHH motif lies deep in the membrane. Nucleophilic catalysis leads to an N-acyl intermediate consistent with the observed ping-pong kinetics. An alternative reaction for a "bisubstrate" reaction is forming a ternary complex with both substrates. The narrow size of the binding pockets precludes this mechanism, so one product must dissociate after it is formed before the next substrate can bind. ELOVL7 preferentially catalyzes the elongation of C18-CoA, presumably arising from the size of the acyl-binding product.

A plausible mechanism for human long-chain fatty acid enzyme 7 (ELOVL7) elongation is shown in Figure 21.1.24 and Figure 21.1.25. Figure 21.1.24 shows the beginning acylation step of the reaction.

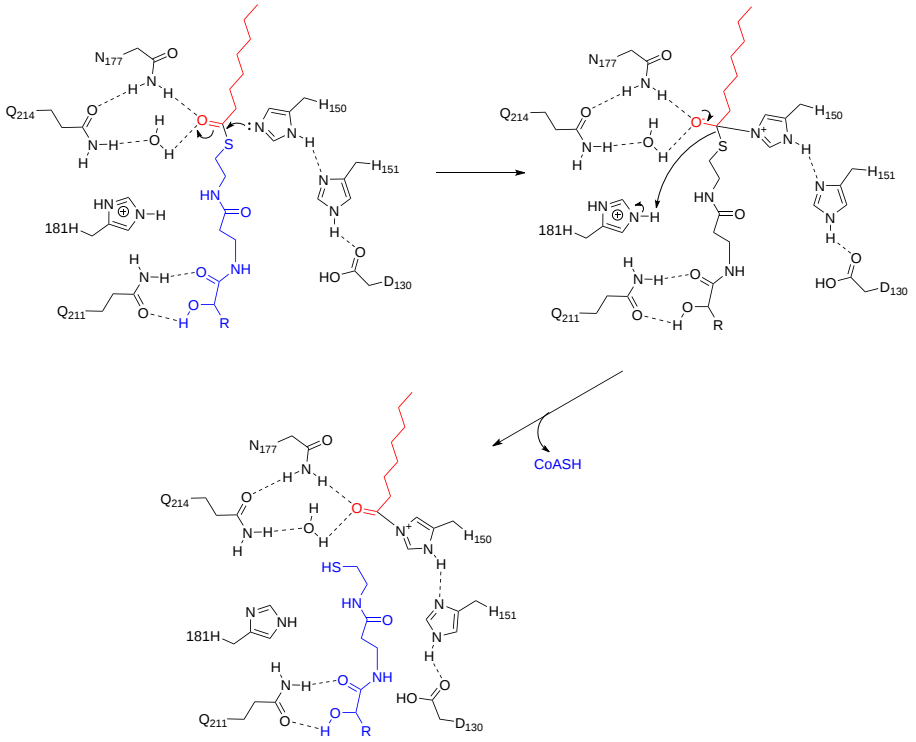


Figure **21.1.24**: Acylation step in the human long-chain fatty acid enzyme 7 (ELOVL7) elongation reaction

Figure **21.1.25** shows the condensation (with the elimination of CO_2), followed by the reduction and dehydration of human ELOVL7.

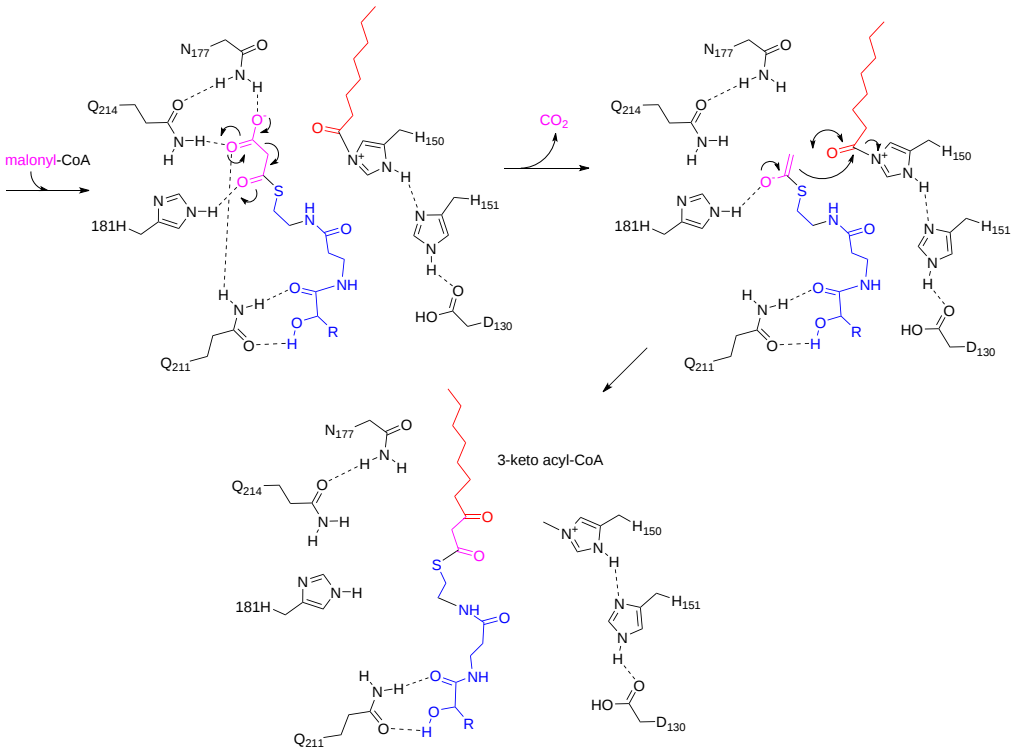
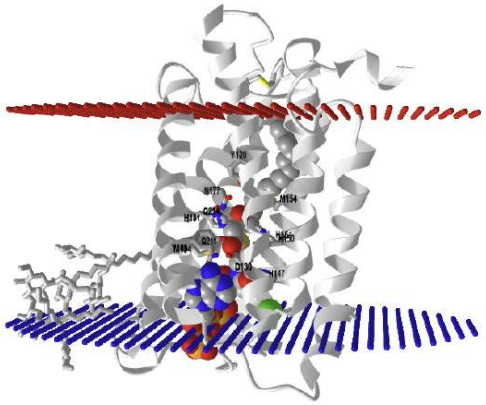


Figure **21.1.25**: Part 2 - Plausible mechanism for mammalian fatty acid elongase 7 (ELOVL7) - condensation (with the elimination of CO_2), followed by reduction and dehydration. (adapted from Nie et al. *Nat Struct Mol Biol* **28,** 512–520 (2021). https://doi.org/10.1038/s41594-021-00605-6)

Figure **21.1.26** shows an interactive iCn3D model of the human ELOVL fatty acid elongase 7 (ELOVL7) with bound 3-keto eicosanoyl CoA (6Y7F).



NCBI iCn3D Figure **21.1.26**: Human ELOVL fatty acid elongase 7 (ELOVL7) with bound 3-keto eicosanoyl CoA (6Y7F). (Copyright; author via source). Click the image for a popup or use this external link: https://structure.ncbi.nlm.nih.gov/i...eajMeiRgfHd9s9

The bound 3-keto eicosanoyl CoA is shown in spacefill, CPK colors. Key amino acids involved in catalysis are shown in sticks, CPK colors, and labeled.

21.1.4.4: DESATURATION

Introducing double bonds requires a different set of enzymes, acyl-coenzyme A (CoA) desaturases. Mammals have desaturases that can produce double bonds at Δ^9, Δ^6, and Δ^5. There are two types: stearoyl-CoA desaturases (SCDs), which introduce a double bond at C9 of saturated fatty acids, and fatty acid desaturases (FADS), which work on unsaturated fatty acids. These are shown in Figure **21.1.20**. Plants, but not mammals, have Δ^{12} and Δ^{15}-desaturases, so they, but not mammals, can synthesize ω6 and ω3 fatty acids. The diet must supply these as they are essential fatty acids. They are precursors for the synthesis of longer fatty acids like arachidonic acid ($20{:}4^{\Delta 5,8,11,14}$), necessary for prostaglandin synthesis (see below), and docosahexaenoic acids (DHA). A plausible mechanism for the stearoyl-CoA desaturase from castor seeds is shown below in Figures 27-30. The mechanisms and explanations are adapted from https://www.ebi.ac.uk/thornton-srv/m-csa/entry/136/. Creative Commons Attribution 4.0 International (CC BY 4.0) License

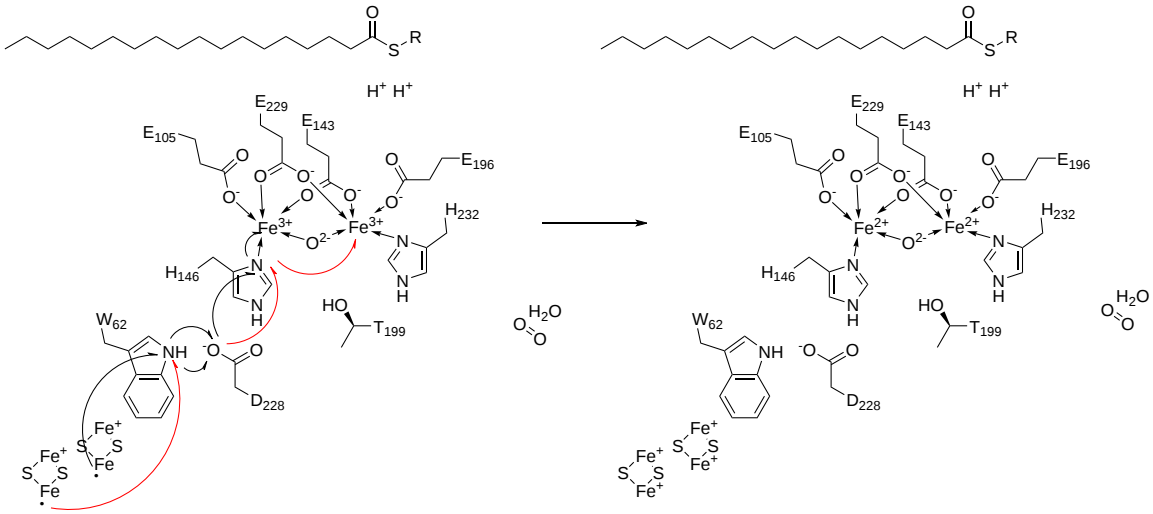


Figure **21.1.27**: Part 1 of the stearoyl-CoA desaturase

At the start of the reaction, ferredoxin, a small iron-sulfur protein, donates a single electron through Trp62, Asp228, and His146 to one of the Fe(III) centers in the desaturase. Ferredoxin then donates a second single electron, through Trp62, Asp228, and His146, to the second Fe(III) center. Both of these are shown in Figure **21.1.27**

Part 2 of the reaction is shown in Figure **21.1.28**.

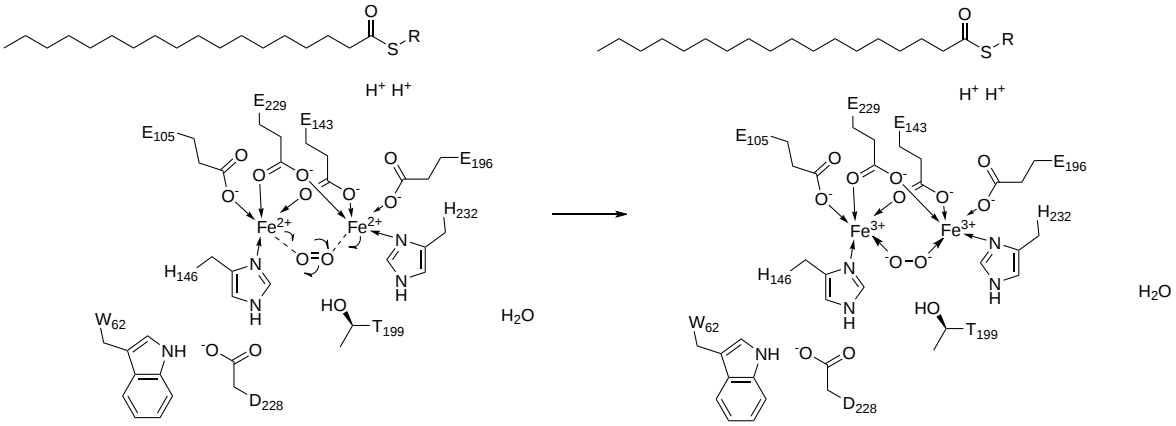


Figure **21.1.28**: Part 2 of the stearoyl-CoA desaturase

The reduced charges on the Fe ions lead to loss of the oxide bridging ion (O^{2-}) and its replacement with dioxygen. Water coordinates to one of the Fe(II)s, which causes it to donate a single electron to the dioxide molecule. This starts the first of two homolytic additions of the dioxygen molecule to both Fe(II) centers, and the second Fe(II) center also donates a single electron to the dioxygen bridge.

Part 3 of the stearoyl-CoA desaturase mechanism is shown in Figure **21.1.29** below.

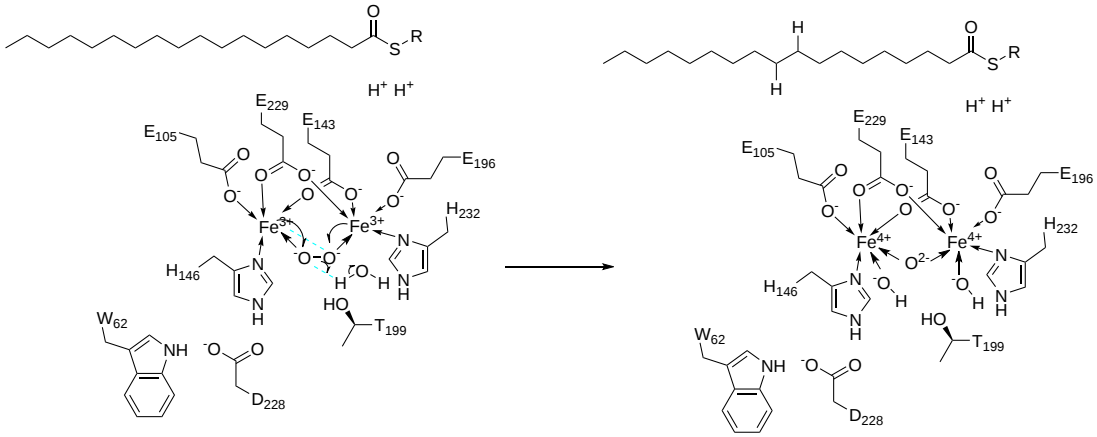


Figure **21.1.29**: Part 3 of the stearoyl-CoA desaturase

Part 4 of the stearoyl-CoA desaturase is shown in Figure **21.1.30**.

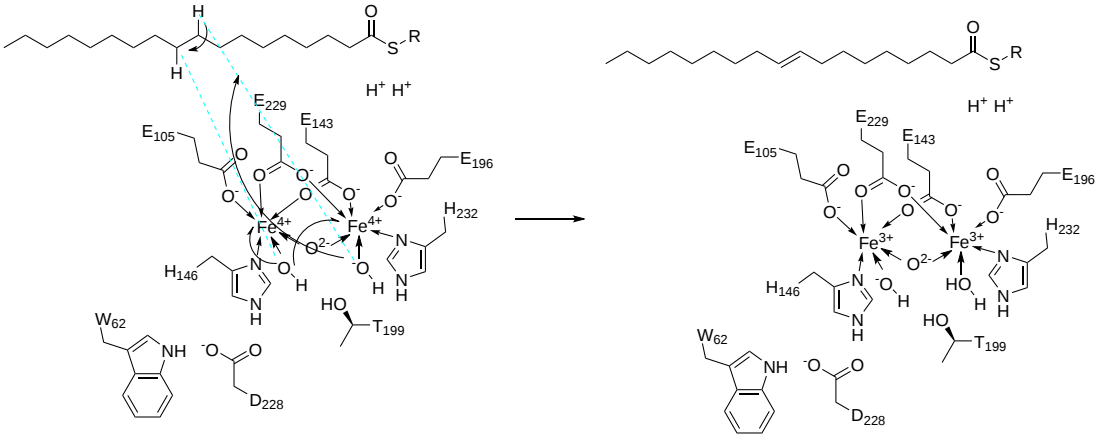
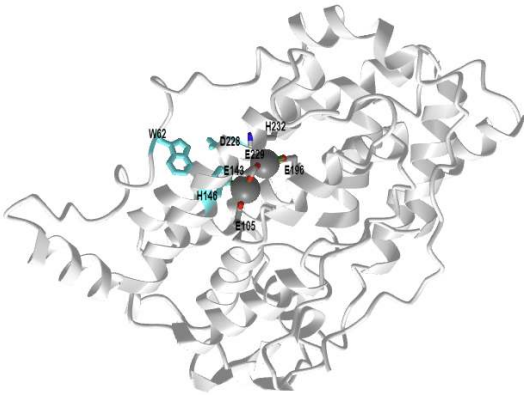


Figure **21.1.30**: Part 4 of the stearoyl-CoA desaturase

In this reaction, the hydroxide on the first Fe(IV) center deprotonates the stearoyl-[acyl-carrier protein] substrate, initiating the elimination of a hydride ion, which attacks the second Fe(IV) bound hydroxide. The excess electrons are donated singly to both Fe(IV) centers, regenerating the enzyme.

Figure **21.1.31** shows an interactive iCn3D model of the Stearoyl-acyl-carrier protein desaturase from castor seeds (1afr)



NCBI iCn3D Figure **21.1.31**: Stearoyl-acyl-carrier protein desaturase from castor seeds (1afr) (Copyright; author via source). Click the image for a popup or use this external link: https://structure.ncbi.nlm.nih.gov/i...UonrwyWfcg9wU8

An electron transport chain carries an electron from ferredoxin to one of the iron centers via several residues. A second electron is then carried to the second iron center. Several redox reactions involve oxygen, water, and iron centers, resulting in the substrate's deprotonation and the formation of a double bond.

There are two possible paths for the electron transport chain. The one described here has been chosen because it is analogous to what has been suggested for *E. coli* ribonucleotide reductase protein R2.

21.1.5: MITOCHONDRIAL FA SYNTHESIS

Mitochondria also engage in limited fatty acid synthesis. They use separate discrete enzymes (at least 6), as do most bacteria. They don't employ a multienzyme complex described above for yeast and mammals. Nevertheless, there are commonalities. Synthesis proceeds by adding two carbon units to a growing acyl-ACP chain using malonyl-CoA and the release of CO_2 to drive the condensation process (in addition to ATP cleavage). The cytoplasmic fatty acid synthesis produces 16:0 (palmitate).

In contrast, mitochondrial FAS produces two major products, 8:0 (octanoate). This is then converted to the 8C derivative lipoic acid. Their structures are shown in Figure **21.1.32**.

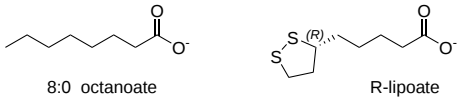


Figure **21.1.32**: Structure of octanoate and R-lipoate

We have seen lipoic acid before as a cofactor in pyruvate dehydrogenase and α-ketoglutarate dehydrogenase, two enzymes that catalyze the more difficult decarboxylation of α-ketoacids (which don't have a built-in electron sink at a β carbon adjacent to the departing carboxyl group). It is also used in branched-chain amino acid dehydrogenases. The absence of lipoic acid is lethal in mice.

Figure **21.1.33** shows the mitochondria's fatty acid synthesis pathway.

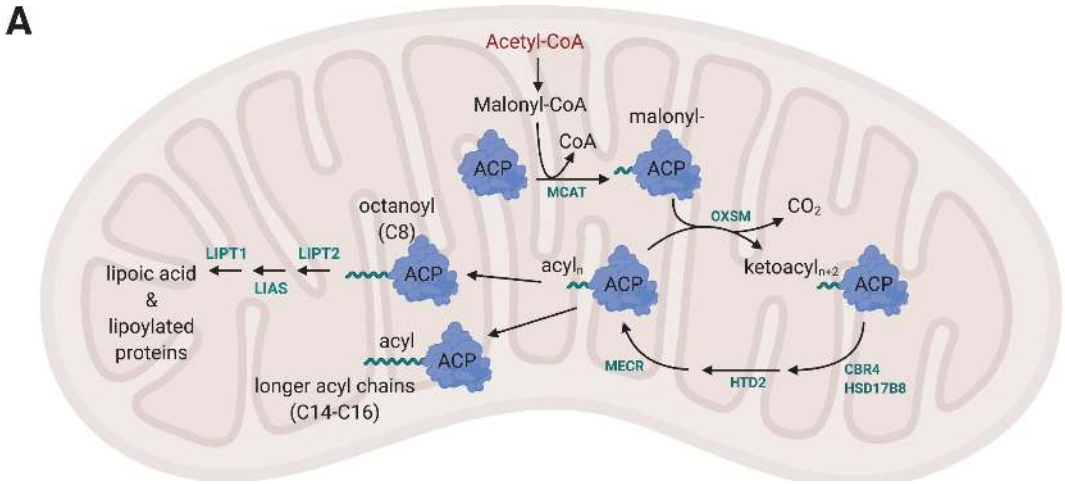


Figure **21.1.33**: mitochondrial fatty acid synthesis pathway and downstream lipoic acid synthesis. Nowinski et al. eLife 2020;9:e58041. DOI: https://doi.org/10.7554/eLife.58041. Creative Commons Attribution License

Some of the enzymes in the pathway include the following: **Mcat** is malonyl-CoA ACP transacylase, and **Ox**sm is beta-ketoacyl synthase that catalyzes the Claisen condensation of malonyl-ACP with the growing acyl chain. **CBR4** is 3-oxoacyl-[acyl-carrier-protein] reductase. **HSD17B8** is (3R)-3-hydroxyacyl-CoA dehydrogenase. **HTD2** is hydroxyacyl-thioester dehydratase type 2). **Mecr** is the terminal enoyl-[acyl-carrier-protein] reductase. **LIPT2** is lipoyltransferase 2. **LIAS** is lipoyl synthase. **LIPT1** (Lipoyltransferase 1) catalyzes the terminal step in lipoic acid and lipoylated protein synthesis.

It now appears that longer fatty acyl chains (up to 14C) are synthesized in mitochondria. Mutations in key enzymes above have been made that don't affect lipoic acid synthesis but impair mitochondrial function.

21.1.6: EICOSANOID AND PROSTAGLANDIN SYNTHESIS

As shown in Figure 20, arachidonic acid, $20{:}4^{\Delta 5,8,11,14}$, an ω-6 fatty acid (5,8,11,14-eicosatetraenoic acid), is synthesized from linoleic acid, $18{:}2^{\Delta 9,12}$, another ω-6 polyunsaturated fatty acid, through a series of elongation and desaturation steps. Arachidonic acid is released from membrane phospholipids on activation of phospholipase A2 and converted to a class of molecules called prostaglandins, which have powerful hormone-like effects.

The prostaglandins are part of a group of icosanoids derived from cleavage of membrane ω-3 ($20{:}5^{\Delta 5,8,11,14,17}$, eicosapentaenoic acid) and ω-6 C_{20} fatty acids, which are metabolized to form leukotrienes (LTs), prostaglandins (PGs), prostacyclins (PCs), and thromboxanes (TXAs). These have differing and sometimes opposing physiological effects in animals. Prostaglandins have been found in almost every tissue in humans and other animals

Ω-3 AND Ω-3 FATTY ACIDS

The most common polyunsaturated fats (PUFAs) in our diet are the ω-3 and ω-6 classes. The most abundant in the ω-6 class in plant food is linoleic acid (18:2 ω-6, or $18{:}2^{\Delta 9,12}$), while linolenic acid (18:3 ω-3 or $18{:}3^{\Delta 9,12,15}$) is the most abundant in the ω-3 class. These fatty acids are essential because they are biological precursors for other PUFAs. Specifically,

- linoleic acid (18:2 ω-6, or $18{:}2^{\Delta 9,12}$) is a biosynthetic precursor of arachidonic acid (20:4 ω-6 or $20{:}4^{\Delta 5,8,11,14}$)
- linolenic acid (18:3 ω-3, or $18{:}3^{\Delta 9,12,15}$) is a biosynthetic precursor of eicosapentaenoic acid (EPA, 20:5 ω-3 or $20{:}5^{\Delta 5,8,11,14,17}$) and to a much smaller extent, docosahexaenoic acid (DHA, 22:6 ω-3 or $22{:}6^{\Delta 4,7,10,13,16,19}$).

These essential precursor fatty acids are substrates for intracellular enzymes such as elongases, desaturases, and beta-oxidation type enzymes in the endoplasmic reticulum and another organelle, the peroxisome (involved in the oxidative metabolism of straight chain and branched fatty acids, peroxide metabolism, and cholesterol/bile salt synthesis). Animals fed diets high in plant 18:2(n-6) fats accumulate 20:4(n-6) fatty acids in their tissues, while those fed diets high in plant 18:3(ω-3) accumulate 22:6(ω-3). Animals fed diets high in fish oils accumulate 20:5 (EPA) and 22:6 (DHA) at the expense of 20:4(n-6).

Figure **21.1.34** below shows the proinflammatory and immunoregulatory roles of eicosanoids in T cells.

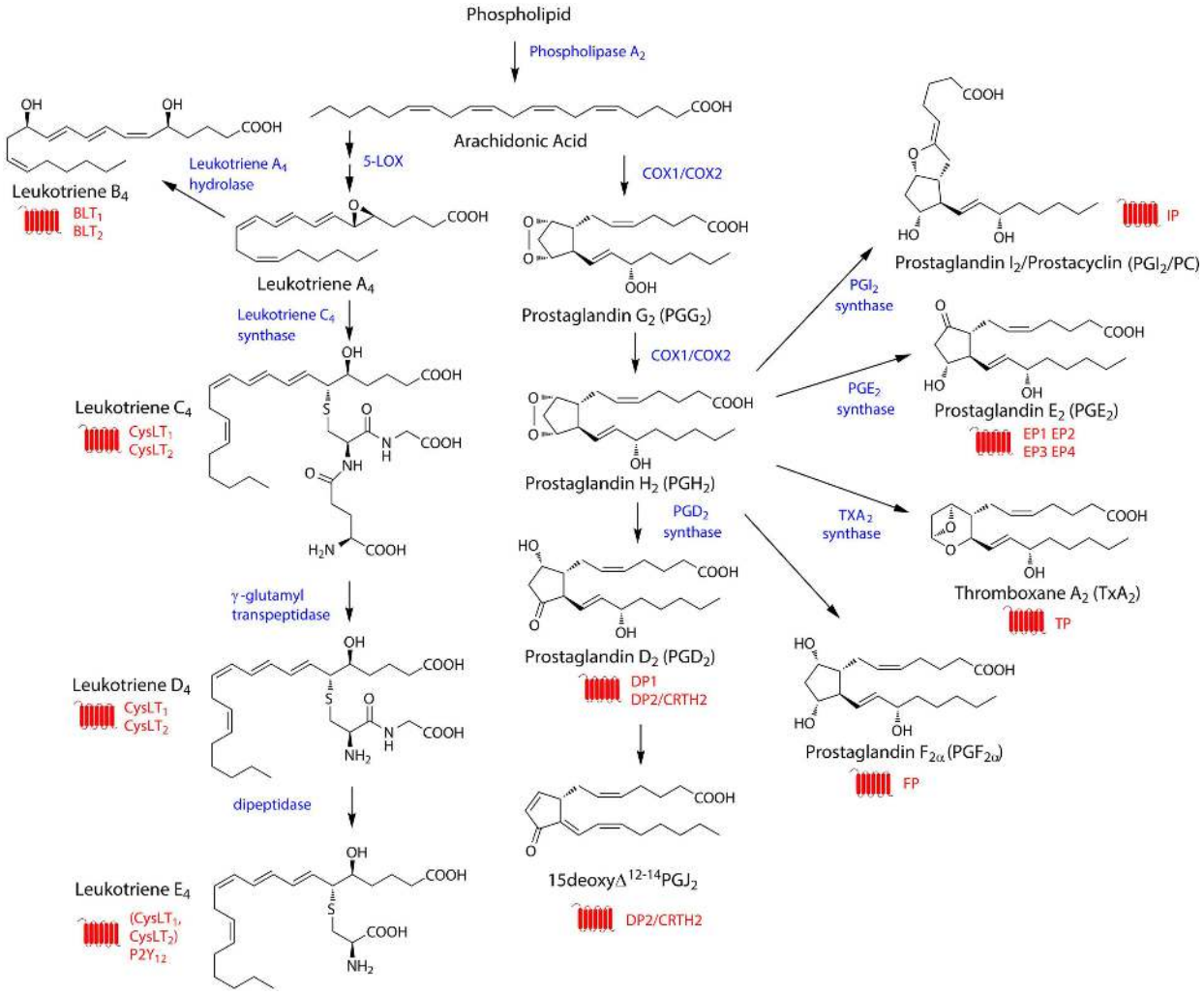


Figure **21.1.34**:Lone, Anna & Taskén, Kjetil. (2013). Proinflammatory and Immunoregulatory Roles of Eicosanoids in T Cells. Frontiers in immunology. https://doi.org/10.3389/fimmu.2013.00130. https://creativecommons.org/licenses/by/3.0/

We will focus our attention on the conversion of arachidonic acid (20:4 ω-6 or $20{:}4^{\Delta 5,8,11,14}$) to prostaglandin G_2 (PGG_2) and H_2 (PGH_2) by the enzyme cyclooxygenase I and II. These enzymes are also called by their more formal names, prostaglandin endoperoxide H synthases (PGHSs) I and II. COX-1 prefers arachidonic acid as a substrate, while COX-2 has a broader substrate specificity and can use eicosapentaenoic acid (EPA, 20:5 ω-3 or $20{:}5^{\Delta 5,8,11,14,17}$) and even neutral substrate derivatives of arachidonic acid, including 2-arachidonoylglycerol and anandamide, both ligands for cannabinoid receptors.

COX 1/2 use two dioxygens and 2 electrons to make PGH_2. Two different, separate but connected catalytic sites are used to catalyze the two steps (shown in Figure **21.1.34**)

1. Arachidonic acid ($20{:}4^{\Delta 5,8,11,14}$) is converted to PGG_2. A **bis-oxygenase** domain catalyzes this step. The word oxygenase is used since both atoms of dioxygen are added to the reactant. Bis indicates that two different molecules of dioxygen are added. Since one of the dioxygens added forms an endoperoxide cyclic bridge in PGG2, this enzymatic domain and the entire enzyme are usually called **cyclooxygenase** (COX). The second dioxygen is added as a peroxide (both oxygen atoms of dioxygen added);
2. Prostaglandin G_2 (PGG_2) is then converted to prostaglandin H_2 (PGH_2), in which the noncyclic peroxide form in the first step is converted to hydroxide. This is also a **reduction** step since the oxidation numbers of the oxygen atoms in the peroxide, -1, change to -2 (a gain of electrons) in the hydroxide in PGH_2. This reaction is catalyzed by the enzyme's peroxidase (POX) activity. A cofactor, heme, in the POX site facilitates catalysis.

The COX reaction proceeds through radical intermediates. The heme activation of peroxide is required at the POX site. We'll show two different mechanisms for both reactions (COX and POX) catalyzed by the enzyme prostaglandin endoperoxide H synthase, which we will also call COX.

The first mechanism shown below in Figure **21.1.35** emphasizes the free radical nature of the reactions. It shows just one amino acid (Tyr 385) involved in the reaction. Note that the first step in the reaction shows the added dioxygen as an excited state "singlet" O_2. Still, it is parenthetically noted that it most likely involves O_2 binding to and being activated by the heme iron in the POX site.

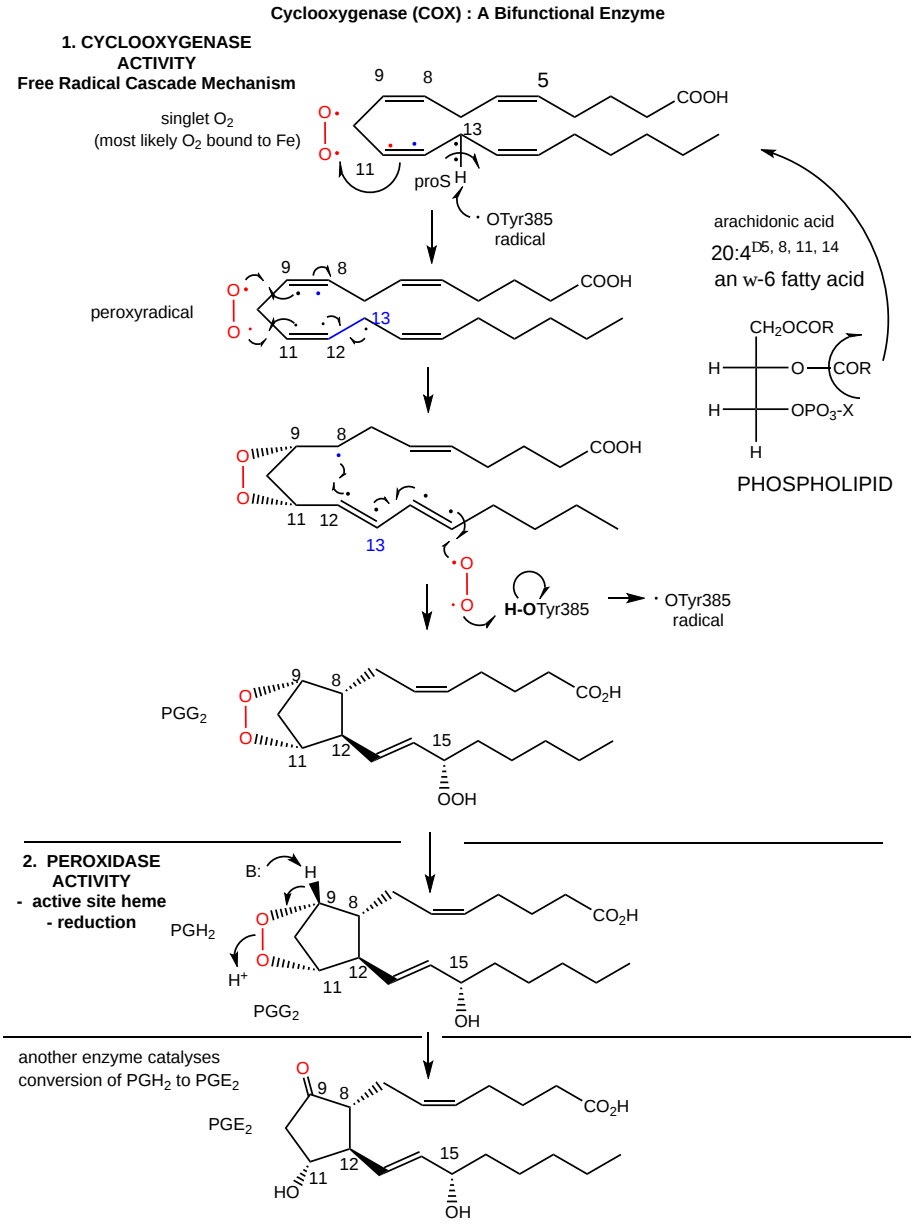


Figure **21.1.35**: Simplified mechanism of prostaglandin endoperoxide H synthase (COX) emphasizing the radical nature of the mechanism.

A more detailed reaction mechanism for the synthesis of PGG_2 by prostaglandin endoperoxide H synthase (COX), emphasizing the role of active site amino acid and the heme in the POX site, is shown in Figures 36-38 below. (The mechanism and its explanation are adapted from https://www.ebi.ac.uk/thornton-srv/m-csa/entry/37/. Creative Commons Attribution 4.0 International (CC BY 4.0) License)

The first step involves a peroxide (denoted H-O-O*), but it might also be a ROO peroxide or NO. The generation of a Tyr-385 free radical in the COX site is critical for the reaction. The heme radical cation in the POX site precedes this.

Figure \(\PageIndex{36}\ below shows the first step in which His 207 deprotonates the alkyl peroxide, which then coordinates to the heme Fe(III) in the POX site.

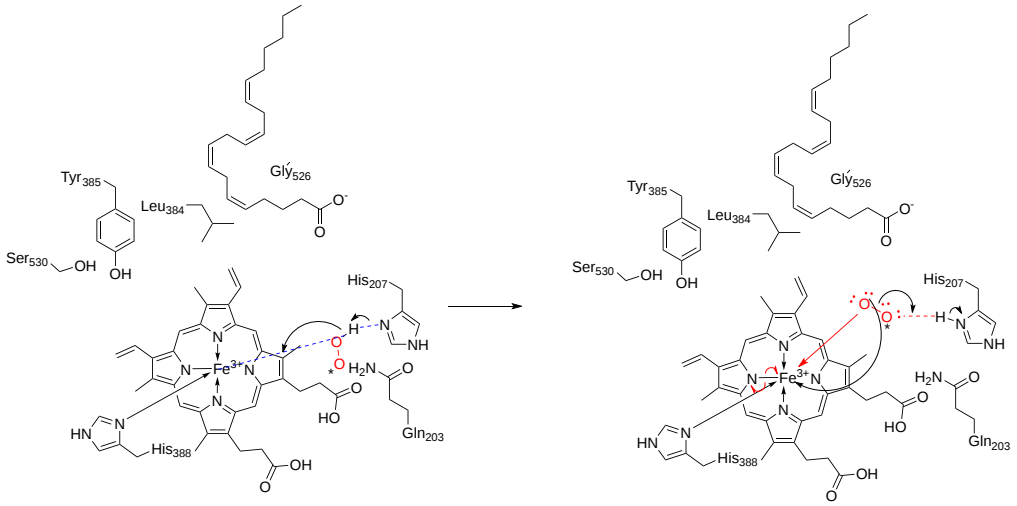


Figure **21.1.36**: First step in the prostaglandin endoperoxide H synthase (COX) reaction.

In the next step, the peroxy bond donates two electrons to the heme Fe(III), one of which moves into the heme ring, forming Fe(IV). The heme ring then removes an electron from Tyr 385. This then removes an H· from the substrate, arachidonic acid. These steps are illustrated in Figure **21.1.37**.

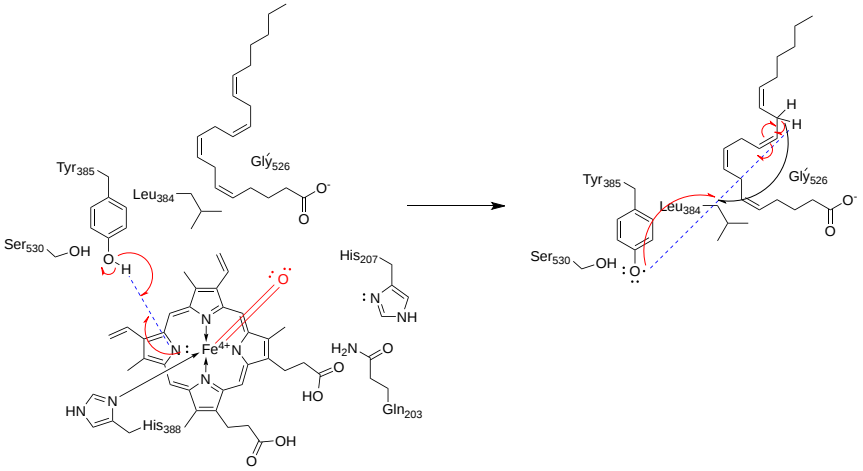


Figure **21.1.37**: Next steps in the prostaglandin endoperoxide H synthase (COX) reaction.

The heme site is not shown in the next steps. Next, the reactive dioxygen, a ground-state diradical, forms a bond to the carbon-free radical in arachidonic acid. The rest of the reaction ensues, as shown in Figure **21.1.38**.

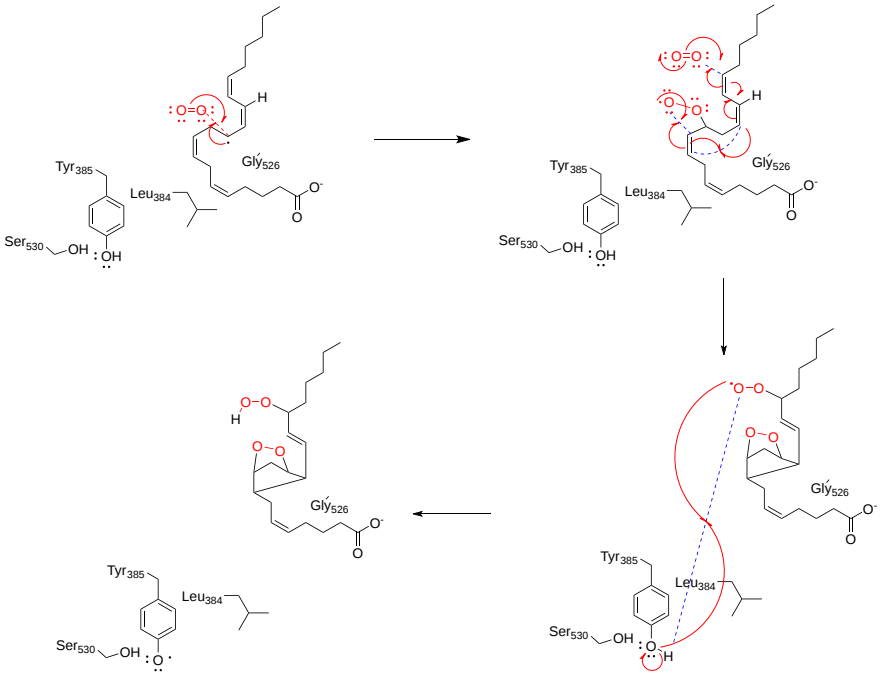
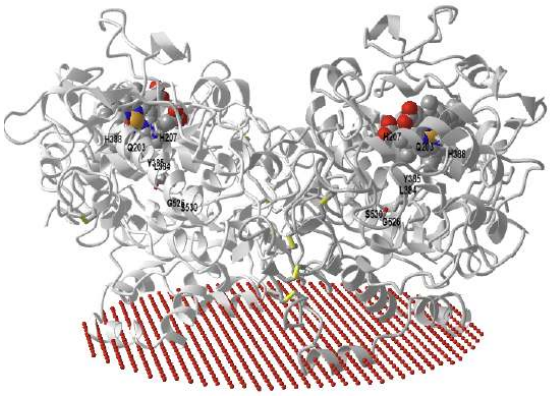


Figure **21.1.38**: Figure **21.1.37**: Final steps in the formation of PGG_2 by prostaglandin endoperoxide H synthase (COX) reaction.

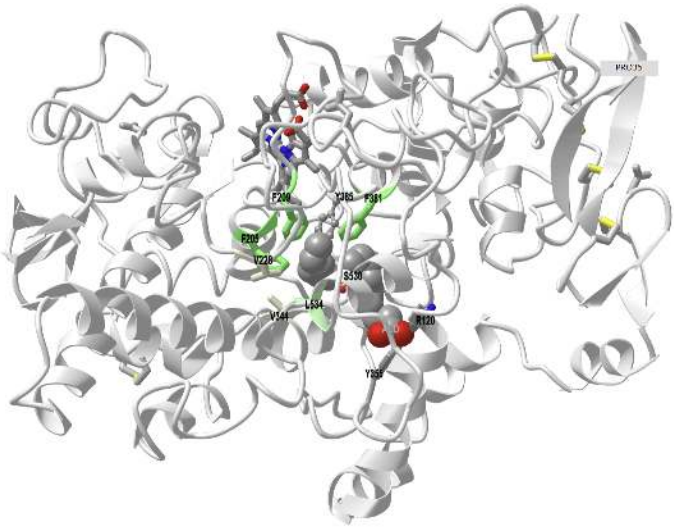
Figure **21.1.39** shows an interactive iCn3D model of the mouse cyclooxygenase 2 (5COX)



NCBI iCn3D Figure **21.1.39**: mouse cyclooxygenase 2 (5COX) (Copyright; author via source). Click the image for a popup or use this external link: https://structure.ncbi.nlm.nih.gov/i...wt9ECkgsyu4Vs8

Here is a model of human cyclooxygenase 1 structure (6Y3C): https://structure.ncbi.nlm.nih.gov/i...joK7oV63vLSi1A

Figure **21.1.39** shows an interactive iCn3D model of the mouse COX-2 with bound arachidonic acid (3KRK)



NCBI iCn3D Figure **21.1.39**: Mouse COX-2 with bound arachidonic acid (3KRK) (Copyright; author via source). Click the image for a popup or use this external link: https://structure.ncbi.nlm.nih.gov/i...yAtJnTkTmuNreA

The following key binding and catalytic residues are shown and labeled:

- Arg-120 and Tyr-355 are close to the carboxylate of AA
- Phe205, Phe209, Val228, Val344, Phe381, and Leu534 form a hydrophobic groove for the ω-end of AA.
- Ser 530, which is above this, gets acetylated by aspirin
- Tyr 385, near C13 in arachidonic acid, forms the free radical that removes a single electron from C13

Prostaglandins, which were first isolated from prostate glands, serve as powerful but labile local hormones that are mediators of pain, inflammation, and immune and clotting activity. The cyclooxygenase activity is inhibited by aspirin, which probably accounts for most of its anti-inflammatory and analgesic properties. Aspirin, acetylsalicylic acid, acetylates a reactive Ser 530 in the active site. Another nonsteroidal anti-inflammatory drug (NSAID) with similar properties is Ibuprofen (Advil). Acetaminophen (Tylenol) is also considered a member of this drug class, even though it doesn't have anti-inflammatory properties. The question has arisen as to why. It now turns out that there are three different types of COX: I, II, and III. COX III is expressed in the brain and might be involved in pain pathways. Acetaminophen appears to work on this COX, as shown in Table **21.1.1** below (Bazan et al.).

Cyclooxygenase Activities

COX	Expression	Function	Inhibitors
COX 1	constitutively	organ pain, platelet function, stomach protection	NSAIDs including aspirin
COX 2	induced by growth factors, neurotransmitters, inflammatory cytokines, oxidative stress, and injury. Constitutively in the brain and the kidney	Inducible COX2: inflammation, pain, fever Constitutive COX2: synaptic plasticity	NSAIDs, COX 2 inhibitors, including celecoxib (Celebrex), which has few GI problems associated with its use
COX 3	constitutively, high in the brain, heart	pain pathways, not inflammation pathways	acetaminophen (no GI problems, great fever reducer), some NSAIDs

21.1.7: FISH Ω-3 FATTY ACIDS AND HEALTH

We mentioned the importance of arachidonic acid in signal transduction in the lipid chapter. In addition, the importance of ω-3 fatty acids to health was discussed as well. As mentioned above, arachidonic acid is cleaved from the C2 or sn-2 position of membrane phospholipids and modified by cyclooxygenase or lipoxygenase to form prostaglandins and leukotrienes, both potent local biological mediators. Linoleic acid and 22:6ω-3 (DHA or docosahexaenoic acid) are also found in membrane phospholipids at the sn-2 position. What is the mechanism for the health-protective effects of ω-3 fatty acids like DHA?

In human tissue, DHA, 22:6ω-3 or $22{:}6^{\Delta 5,8,11,14,17,20}$ is the most abundant ω-3 polyunsaturated fatty acid (PUFA). Since it is synthesized from linolenic acid (as is EPA), a deficiency of linolenic acid in the diet will lead to lowered levels of 22:6ω-3 in tissues, with ensuing health effects. Since these lipids are involved in membrane structure, signal transduction, and hormone synthesis, diverse effects of dietary ω-3 PUFA deficiency will be observed. 50% of all fatty acids in the sn1 and sn2 position of membrane phospholipids of rod outer segments

(in the retina) are 22:6(ω-3). Cognitive dysfunctions (loss of memory, etc.) have been linked to decreased levels of 22:6(ω-3) in the brain. This fatty acid binds to retinoid X receptors, which then activate (through linked binding reactions) nuclear receptors, leading to alterations in gene transcription in the CNS.

In other tissues, 22:6(ω-3) rarely exceeds 10% of membrane fatty acids, but this percentage can be increased in cells with increases in a precursor, 20:5(ω-3). DHA might affect lipid rafts in the membrane, affecting the movement of important membrane protein receptors (and associated proteins), altering cell response to environmental stimuli. DHA and EPA affect arachidonic acid conversion to prostaglandins and leukotrienes. EPA binds less tightly to cyclooxygenase I and is a poor substrate for the enzyme, both effects which inhibit the formation of prostaglandins and the signaling processes mediated by them. This explains why ω-3 fatty acids have anti-inflammatory effects.

In addition, ω-3 fatty acids have noticeable effects on gene transcription, which remain as long as these fatty acids are present in high levels in the diet. These and other fatty acids bind to fatty acid-activated transcription factors called PPARs (peroxisome proliferator receptors - alpha, beta, and gamma 1 and 2). These receptors regulate proteins involved in lipid metabolism through alterations in gene expression. Other fatty acid-dependent transcription factors are known as well. PPARs bind 20:5(ω-3) with a micromolar Kd and change the conformation of the protein to a form that can bind other proteins, ultimately altering gene expression.

Table **21.1.2**: Some biological effects of ω-3 polyunsaturated fatty acids EPA (20:5) and DHA (22:6). Adapted from Jump D. The Biochemistry of ω-3 Polyunsaturated fatty acids. J. Biol. Chem. 277, pg 8755 (200)

Organ(s)	Effect	Mechanism acts through
central nervous system	improve cognitive function	membrane composition; retinoic X receptor alpha
retina	improve acuity	membrane composition
immune	immunosuppressive; anti-inflammatory	membrane composition; rafts
cardiovascular	anti-arrhythmia; anti-clotting	membrane composition; rafts; eicosanoids
serum lipids	lowers triglycerides (a risk factor for cardiovascular disease)	peroxisome proliferator receptor alpha and gamma
liver	decrease lipid synthesis; increase fatty acid oxid. decrease VLDL synthesis	sterol reg. element bind. protein; PPAR alpha PPAR alpha

21.1.8: RECOGNITION OF UNSATURATED FATTY ACIDS BY MEMBRANE G-PROTEIN-COUPLED RECEPTORS

The positive health effects of the ω-3 fatty acids appear to involve those fatty acids acting as hormones that bind to a special membrane receptor called G protein-coupled receptor 120 (GPCR120). We will discuss GPCRs in greater detail in Chapter 28.2. When a hormone binds to the membrane GPCR (a transmembrane protein with seven membrane-spanning helices), the intracellular domain of the GPCR alters how it interacts with various binding partners inside the cell. The GPCRs are given that name since most interact with heterotrimeric G proteins inside the cell. These G proteins have a β, γ, and a variety of different α subunits (α_q, α_i, α_s). Activation of different α subunits leads to different downstream effects as part of an elaborate signaling system in the cell. When the health-promoting polyunsaturated ω-3 fatty acids bind to GPCR120, there are some beneficial health effects on metabolism, as outlined in Table **21.1.3** below.

Protein involved in GPCR120 signaling	Downstream effect
$G\alpha_q$	Increases Ca^{2+} levels in the cell, which act as a second signal (messenger) Increases GLUT4 (glucose transporter) translocation to the cell membrane; Increases secretion of glucagon-like peptide 1 (GLP1)
$G\alpha_i$	Increases insulin secretion Inhibits Ghrelin (hunger hormone) secretion
$G\alpha_s$	Controls fat synthesis
non G protein GPCR kinase (GRK)/β-arrestin 2	Inhibits the NLRP3 inflammasome and is ant-iinflammatory

Figure **21.1.40** below summarizes the data in the table above.

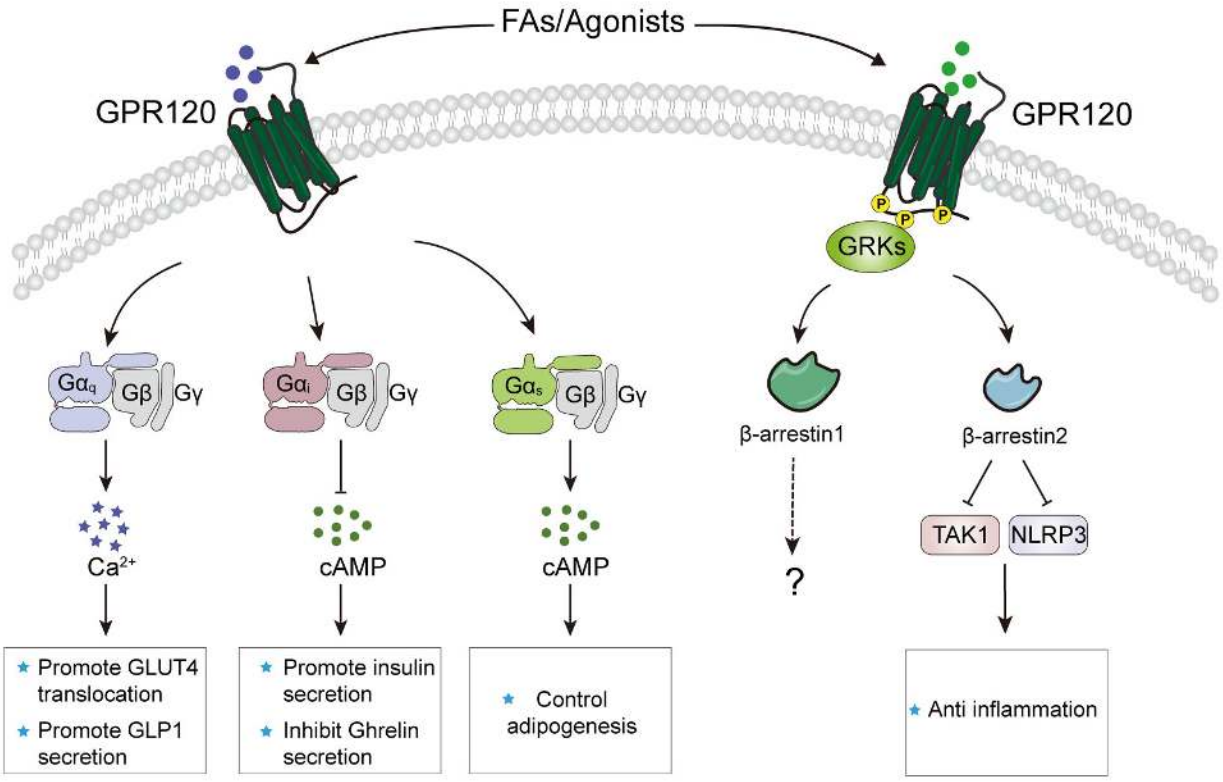


Figure **21.1.40**: Schematic overview of G protein–and arrestin–mediated GPR120 signaling and related functions. Chunyou Mao et al. *Science* **380**, eadd6220 (2023). https://www.science.org/doi/10.1126/science.add6220. With permission from the AAAS.

GPCR120 differentiates fatty acids based on the number and position of the double bonds in the acyl chain of the ligand. Although saturated fatty acids can bind to GPCR 120, only the ω-3 fatty acids elicit health effects.

CryoEM structures show the fatty acids buried in an L-shaped conformation in the GPCR. The protein engages in noncovalent interactions, specifically π:π interactions, with the double bonds in acyl chain. These interactions, which depend on the number of double bonds in the ω-3 fatty acid, differentially bias the GPCR towards specific effects for each different fatty acid.

Figure **21.1.41** shows an interactive iCn3D model of the eicosapentaenoic acid bound GPR120-Gi complex (8ID9).

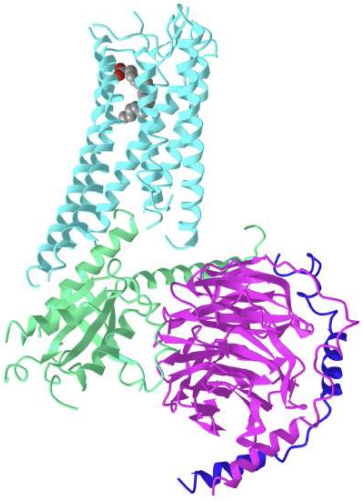


Figure **21.1.41**: Eicosapentaenoic acid bound GPR120-Gi complex (8ID9). (Copyright; author via source). Click the image for a popup or use this external link: https://structure.ncbi.nlm.nih.gov/i...vgMGJRTr3emNj7

The color coding is as follows:

- GPCR120 - cyan (the membrane would be perpendicular across the seven membrane helices) with the bound EPA
- Gβ - magenta
- Gγ - blue
- EPA -spacefill

Figure **21.1.42** shows an interactive iCn3D model showing the nonpolar environment of eicosapentaenoic acid bound to GPR120 (8ID9).

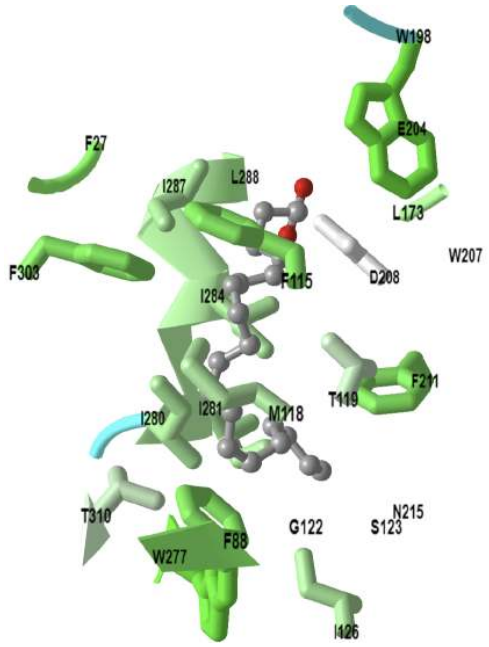


Figure **21.1.42**: Nonpolar environment of eicosapentaenoic acid bound to GPR120 (8ID9). (Copyright; author via source). Click the image for a popup or use this external link: https://structure.ncbi.nlm.nih.gov/i...SszD1K3B9ieND7

Dark green shows the hydrophobic amino acids.

21.1.9: SUMMARY

This chapter provides a comprehensive overview of fatty acid synthesis and its integration with downstream metabolic pathways, drawing upon structural and mechanistic insights from yeast, mammalian, and bacterial systems.

Fatty Acid Synthase (FAS) Pathway Overview:

The synthesis of palmitate (16:0) involves the iterative condensation of eight acetyl-CoA molecules, requiring NADPH, ATP, and protons, to form a long-chain fatty acid. The net reaction highlights that the process is a reductive biosynthesis where acetyl-CoA, a high-energy substrate, is activated (via ATP-dependent carboxylation by acetyl-CoA carboxylase) to form malonyl-CoA, which then condenses with acyl intermediates. In Type I FAS complexes (found in yeast, fungi, and higher eukaryotes), the multifunctional enzyme contains multiple catalytic domains that channel the growing acyl chain, tethered to an acyl carrier protein (ACP), through a series of reactions (condensation, reduction, dehydration, and further reduction).

Structural Organization and Mechanism:

In yeast, the FAS complex is organized as an $\alpha_6\beta_6$ heterododecamer, whereas in mammals it is an α_2 homodimer. These large complexes facilitate substrate channeling, with intermediates shuttled between catalytic sites via a flexible phosphopantetheine arm on ACP. Key domains include the malonyl/acetyltransferase (MAT), ketosynthase (KS), ketoreductase (KR), dehydratase (DH), enoyl reductase (ER), and phosphopantetheinyl transferase (PPT) domains. Structural models and animated visualizations illustrate how the α and β subunits form a central wheel and domes, creating internal chambers for the reactions, while regulatory subunits modulate the complex's activity.

Regulation of Fatty Acid Synthesis:

Acetyl-CoA carboxylase (ACC) plays a critical role as the rate-limiting enzyme in converting acetyl-CoA to malonyl-CoA. ACC is tightly regulated by allosteric effectors (e.g., citrate activates, while palmitoyl-CoA inhibits), product inhibition, and phosphorylation (by AMPK, PKA, or CDKs). These regulatory mechanisms ensure that fatty acid synthesis is coordinated with the cell's energy status and metabolic demands.

Fatty Acid Elongation and Desaturation:

Beyond de novo synthesis, the chapter covers elongation and desaturation pathways that modify fatty acid chain length and saturation. In

the endoplasmic reticulum, ELOVL enzymes catalyze the addition of two-carbon units from malonyl-CoA to form very long-chain fatty acids (VLCFAs), using a mechanism involving a nucleophilic active site histidine. Desaturation reactions, catalyzed by enzymes such as stearoyl-CoA desaturase and fatty acid desaturases, introduce double bonds into fatty acyl chains via radical-mediated mechanisms that depend on electron donors like NADPH and redox-active metal centers.

Mitochondrial Fatty Acid Synthesis:

Mitochondria engage in a limited fatty acid synthesis pathway that produces shorter-chain fatty acids (e.g., octanoate), which serve as precursors for lipoic acid—a vital cofactor for key mitochondrial enzyme complexes. Although this system uses separate enzymes (Type II FAS), it shares the core principles of chain elongation via malonyl-CoA and decarboxylative condensation.

Eicosanoid and Prostaglandin Biosynthesis:

The chapter also examines the metabolism of arachidonic acid, derived from membrane phospholipids, into prostaglandins via the cyclooxygenase (COX) pathway. COX enzymes (PGHS-1 and PGHS-2) convert arachidonic acid to prostaglandin endoperoxides (PGG_2 and PGH_2) through radical intermediates facilitated by a heme cofactor. This pathway is pivotal for producing potent local hormones that mediate inflammation, pain, and other physiological processes.

Nutritional and Signaling Roles of Polyunsaturated Fatty Acids (PUFAs):

Essential ω-3 and ω-6 fatty acids, derived from dietary sources, are crucial for maintaining membrane structure and function. These fatty acids influence the production of signaling molecules and modulate gene expression via nuclear receptors (e.g., PPARs). Additionally, ω-3 fatty acids bind to GPCR120, triggering anti-inflammatory signaling cascades, which contribute to the health benefits associated with fish oils and plant-derived ω-3 PUFAs.

Integration and Physiological Implications:

Throughout the chapter, the discussion emphasizes how fatty acid synthesis and subsequent modifications are finely tuned processes that link cellular energy metabolism with membrane biosynthesis, energy storage, and signaling. The structural complexity of FAS and its regulatory controls highlight the sophisticated nature of lipid biosynthesis, while the evolution of elongation, desaturation, and prostaglandin pathways underpins their critical roles in human physiology and disease.

In summary, this chapter provides an in-depth look at the biochemistry of fatty acid synthesis, from the assembly of long-chain fatty acids by the multifunctional FAS complex to the intricate regulatory mechanisms governing lipid modification and signaling. These processes are essential for cellular function and have broad implications in health, disease, and metabolic regulation.

This page titled 21.1: Biosynthesis of Fatty Acids and Eicosanoids is shared under a not declared license and was authored, remixed, and/or curated by Henry Jakubowski and Patricia Flatt.

- **Current page** by Henry Jakubowski and Patricia Flatt has no license indicated.
- **11.2: Diffusion Across a Membrane - Passive and Facilitated Diffusion** by Henry Jakubowski and Patricia Flatt has no license indicated.

21.2: BIOSYNTHESIS OF TRIACYLGLYCEROLS

by William (Bill) W. Christie and Henry Jakubowski.

This section is an abbreviated and modified version of material from the Lipid Web, an introduction to the chemistry and biochemistry of individual lipid classes, written by William Christie.

LEARNING GOALS (CHATGPT O3-MINI)

1. **Understand TAG Biosynthesis Pathways:**
   - Outline the major biosynthetic routes for triacylglycerol production, including the Kennedy pathway (sn-glycerol-3-phosphate pathway), the dihydroxyacetone phosphate pathway, the monoacylglycerol pathway (in enterocytes), and the alternative diacylglycerol transacylase pathway.
   - Describe the sources of the glycerol backbone (from glycolysis and glyceroneogenesis) and how fatty acyl-CoA substrates are incorporated into glycerolipids.
2. **Enzymatic Mechanisms and Regulation in TAG Synthesis:**
   - Identify and explain the catalytic roles of key enzymes in TAG synthesis, such as glycerol-3-phosphate acyltransferase (GPAT), acylglycerophosphate acyltransferase (AGPAT), phosphatidic acid phosphohydrolases (PAPs, including lipins), and diacylglycerol acyltransferases (DGATs).
   - Discuss how these enzymes are regulated by factors such as insulin, AMP-activated protein kinase (AMPK), and product inhibition, linking enzyme activity to the cell's energy status.
3. **Structure and Function of Lipid Droplets:**
   - Describe the formation of cytoplasmic lipid droplets from the endoplasmic reticulum, including the role of seipin in stabilizing nascent droplets.
   - Explain the composition of lipid droplets (triacylglycerols, cholesterol esters, phospholipid monolayer, and associated proteins like perilipins or oleosins) and how these structures serve as dynamic organelles involved in lipid storage, trafficking, and signaling.
4. **TAG Metabolism and Lipolysis:**
   - Outline the sequential steps of TAG hydrolysis (lipolysis) mediated by adipose triacylglycerol lipase (ATGL), hormone-sensitive lipase (HSL), and monoacylglycerol lipase (MGL).
   - Analyze how regulatory proteins (e.g., CGI-58, G0S2) and hormonal signals (e.g., β-adrenergic stimulation) modulate lipolysis and control the release of free fatty acids and glycerol.
5. **Tissue-Specific TAG Metabolism and Transport:**
   - Compare TAG synthesis and breakdown in different tissues: in the intestines (formation of chylomicrons), liver (VLDL secretion and storage versus oxidation), and the mammary gland (synthesis of milk fat globules).
   - Discuss how the regiospecific structure of dietary TAGs can influence fatty acid uptake and further metabolism.
6. **Role of Lipid Droplets in Cellular Function and Stress Response:**
   - Explain how lipid droplets function beyond energy storage by sequestering potentially toxic free fatty acids and other hydrophobic molecules, thereby protecting cells from lipotoxicity.
   - Describe how lipid droplets are involved in cellular processes such as autophagy (lipophagy), protein sequestration, and regulation of intracellular signaling (including the release of lipokines and adipokines).
7. **Integration with Systemic Metabolism and Endocrine Function:**
   - Discuss the endocrine roles of adipose tissue, focusing on the synthesis and secretion of hormones (e.g., leptin and adiponectin) and their effects on systemic energy balance, insulin sensitivity, and inflammation.
   - Analyze the impact of adipocyte hypertrophy, differences between subcutaneous and visceral fat depots, and their correlation with metabolic diseases such as obesity, type 2 diabetes, and cardiovascular disorders.
8. **Comparative TAG Metabolism in Plants, Yeasts, and Prokaryotes:**
   - Summarize the similarities and differences in TAG biosynthesis and storage between eukaryotes (plants and yeasts) and prokaryotes, including the unique adaptations in Mycobacteria and the formation of lipid inclusions in different organisms.
   - Highlight how the regulation and structural organization of TAG metabolism support different physiological roles across species.

These learning goals aim to guide your understanding of the biochemical pathways involved in TAG synthesis, the complex regulation of lipid storage and mobilization, and the broader physiological implications of lipid metabolism in health and disease.

21.2.1: INTRODUCTION

All eukaryotic organisms and even a few prokaryotes can synthesize triacylglycerols. In animals, many cell types and organs have this ability, but the liver, intestines, and adipose tissue are most active with most of the body stores in the last of these. Within all cell types, even those of the brain, triacylglycerols are stored as cytoplasmic '**lipid droplets**' enclosed by a monolayer of phospholipids and hydrophobic proteins such as the perilipins in adipose tissue or oleosins in seeds. These lipid droplets are now treated as distinctive organelles with their own characteristic metabolic pathways and associated enzymes - no longer boring blobs of fat. However, they are not unique to animals and plants, as Mycobacteria and yeasts have similar lipid inclusions.

The lipid serves as a store of fatty acids for energy, which can be released rapidly on demand, and as a reserve of fatty acids for structural purposes or as precursors for eicosanoids. In addition, lipid droplets serve as a protective agency in cells to sequester any excess of biologically active and potentially harmful lipids, such as free fatty acids, oxylipins, diacylglycerols, cholesterol (as cholesterol esters), retinol esters, and coenzyme A esters.

While triacylglycerols are essential for normal physiology, an excessive accumulation in human adipose tissue and other organs results in obesity and other health problems, including insulin resistance, steatohepatitis, and cardiomyopathy. Accordingly, there is considerable pharmaceutical interest in drugs that affect triacylglycerol biosynthesis and metabolism.

21.2.2: BIOSYNTHESIS OF TRIACYLGLYCEROLS

Three main pathways for triacylglycerol biosynthesis include the *sn*-glycerol-3-phosphate and dihydroxyacetone phosphate pathways, which predominate in liver and adipose tissue, and a monoacylglycerol pathway in the intestines. In maturing plant seeds and some animal tissues, a fourth pathway has been recognized involving a diacylglycerol transferase.

The most important route to triacylglycerols is the *sn*-glycerol-3-phosphate or **Kennedy pathway**, first described by Eugene Kennedy and colleagues in the 1950s, from which more than 90% of liver triacylglycerols are produced. Figure **21.2.1** shows the pathway from glycerol-3-phosphate to triacylglycerols (the Kennedy pathway) and some preceding reactions that generate glycerol-3-phosphate.

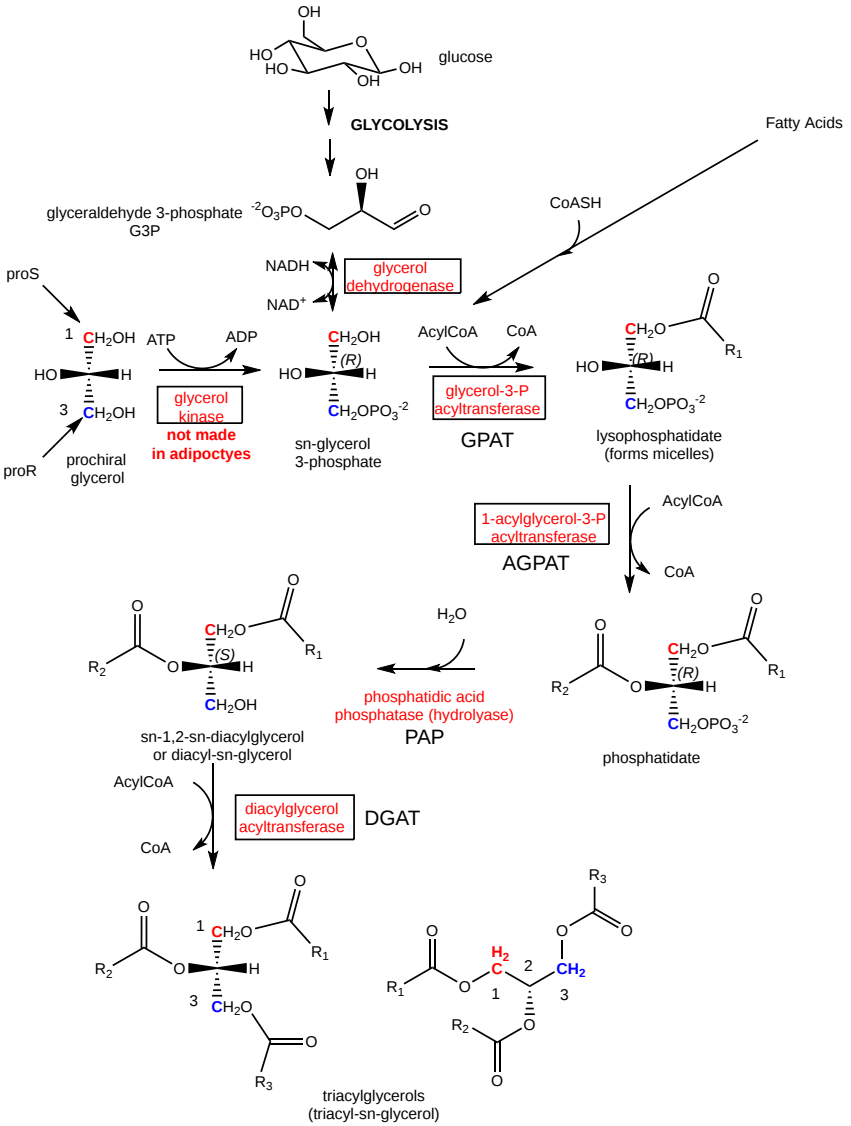


Figure **21.2.1**: Synthesis of triacylglycerols from glycerol-3-phosphate (Kennedy pathway) and some preceding reactions that generate glycerol-3-phosphate.

In this pathway, the main source of the glycerol backbone has long been believed to be *sn*-glycerol-3-phosphate produced by the catabolism of glucose (glycolysis) or, to a lesser extent, by the action of the enzyme glycerol kinase on free glycerol. However, there is increasing evidence that a significant proportion of glycerol is produced *de novo* by a process known as glyceroneogenesis via pyruvate. Indeed, this may be the main source in adipose tissue.

Subsequent reactions occur primarily in or at the endoplasmic reticulum. First, the precursor *sn*-glycerol-3-phosphate is esterified by a fatty acid coenzyme A ester in a reaction catalyzed by a glycerol-3-phosphate acyltransferase (GPAT) at position *sn*-1 to form lysophosphatidic acid, and this is in turn acylated by an acylglycerophosphate acyltransferase (AGPAT) in position *sn*-2 to form a key intermediate in the biosynthesis of all glycerolipids - phosphatidic acid. Numerous isoforms of these enzymes are known; they are expressed in specific tissues and membrane distributions and regulated in different ways.

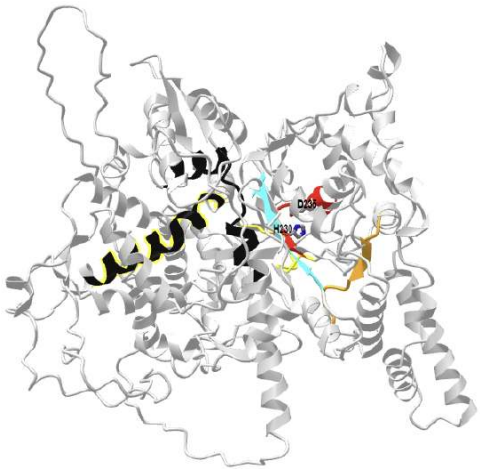
Let's look at some of the enzymes involved in key reactions synthesizing triacylglycerols.

GPAT Enzymes

Glycerol-3-phosphate acyltransferase (GPAT) catalyzes the first step in the pathway in most tissues. From an enzymatic perspective, it can be considered rate-limiting for the pathways since its specific activity is slow. In mammals, there are four isoforms (GPAT1 in the outer membrane of the mitochondria, GPAT2 also in the mitochondria, and GPAT3 and 4, both in the ER. The activity of GPAT1 is activated by insulin, presumably through phosphorylation, and inhibited by AMP-activated protein kinase (AMPK).

Fatty acyl-CoA in the outer membrane could be used for TAG synthesis through the Kennedy pathway in times of energy abundance or imported into the matrix through the carnitine-acyl-CoA cycle in times of energy need. The overexpression of GPAT1 in liver cells increases TAG synthesis and decreases β-oxidation. GPAT1-deficient mice, in contrast, have higher levels of β-oxidation.

Figure **21.2.2** shows an interactive iCn3D model of the AlphaFold predicted structure of human mitochondrial glycerol-3-phosphate acyltransferase 1 - GPAT1 (Q9HCL2).



NCBI iCn3D Figure **21.2.2**: AlphaFold predicted structure of human mitochondrial glycerol-3-phosphate acyltransferase 1 - GPAT1 (Q9HCL2). (Copyright; author via source). Click the image for a popup or use this external link: https://structure.ncbi.nlm.nih.gov/i...kuvBTPo5mNK8p9

Four conserved motifs are involved in catalysis (red and cyan) and binding (orange and yellow). Significant sections are still disordered in the model. Two highly conserved amino acids, His 230 and Asp 235 in the red catalytic motif, are shown in CPK-colored sticks. The black helices are predicted outer mitochondrial membrane transmembrane helices. Both the N- and C-terminal amino acids project into the cytoplasm.

Phosphatidic acid phosphohydrolases (PAPs or 'phosphatidate phosphatases' or 'lipid phosphate phosphatases').

PAPs are also important as they produce *sn*-1,2-diacylglycerols, which are essential intermediates in the biosynthesis of not only triacylglycerols but also phosphatidylcholine and phosphatidylethanolamine (and monogalactosyldiacylglycerols in plants). This is a key branch point in lipid biosynthesis as it may dictate the flow of lipids for storage or membrane biogenesis.

Much of this phosphatase activity leading to triacylglycerol biosynthesis in animals resides in three related cytoplasmic proteins, termed **lipins**, i.e., lipin-1, lipin-2, and lipin-3, which have tissue-specific roles in glycerolipid synthesis. Unusually, these were characterized and named before the nature of their enzymatic activities was determined. Each lipins appears to have distinctive expression and functions, but lipin-1 (PAP1) in three isoforms (designated 1α, 1β, and 1γ) accounts for most of the PAP activity in adipose tissue and skeletal muscle in humans. Lipin 2 is the most abundant in the liver but is also expressed substantially in the small intestine, macrophages, and some regions of the brain, while lipin 3 activity overlaps with that of lipin 1 and lipin 2 and is found in the gastrointestinal tract and liver. Lipins are cytosolic enzymes but associate transiently with membranes to access their substrate, i.e., they are translocated to the endoplasmic reticulum in response to elevated levels of fatty acids within cells. However, they do not have trans-membrane domains. Lipin-1 activity requires Mg^{2+} ions and is inhibited by *N*-ethylmaleimide. In contrast, the membrane-bound activity responsible for synthesizing diacylglycerols as a phospholipid intermediate is independent of Mg^{2+} concentration and is not sensitive to the inhibitor.

Perhaps surprisingly, lipin-1 has a dual role in that it operates in collaboration with known nuclear receptors as a transcriptional coactivator to modulate lipid metabolism (lipin 1α). Lipin 1β is associated with the induction of lipogenic genes such as fatty acid synthase, stearoyl-CoA desaturase, and DGAT. They can have profound effects on signaling in a variety of cell types. Abnormalities in lipin-1 expression are involved in some human disease states that may lead to metabolic syndrome and inflammatory disorders. Lipin 2 is a similar phosphatidate phosphohydrolase regulated dynamically by fasting and obesity (in mice).

PAP depend on divalent Mg^{2+} ions and are sensitive to N-ethylmaleimide. Lipin has an N-Lip (N-terminal) and a C-Lip (C-terminal) domain. The crystal structure of lipin with a 250 amino acid region between the two domains removed has been solved. The domain structures of humans, the yeast Saccharomyces cerevisiae (SC) and its truncated form (Tt-Pah2), and the structure of the Tt-Pah2 truncated fragment of the enzyme from Tetrahymena thermophila are shown in Figure **21.2.3**.

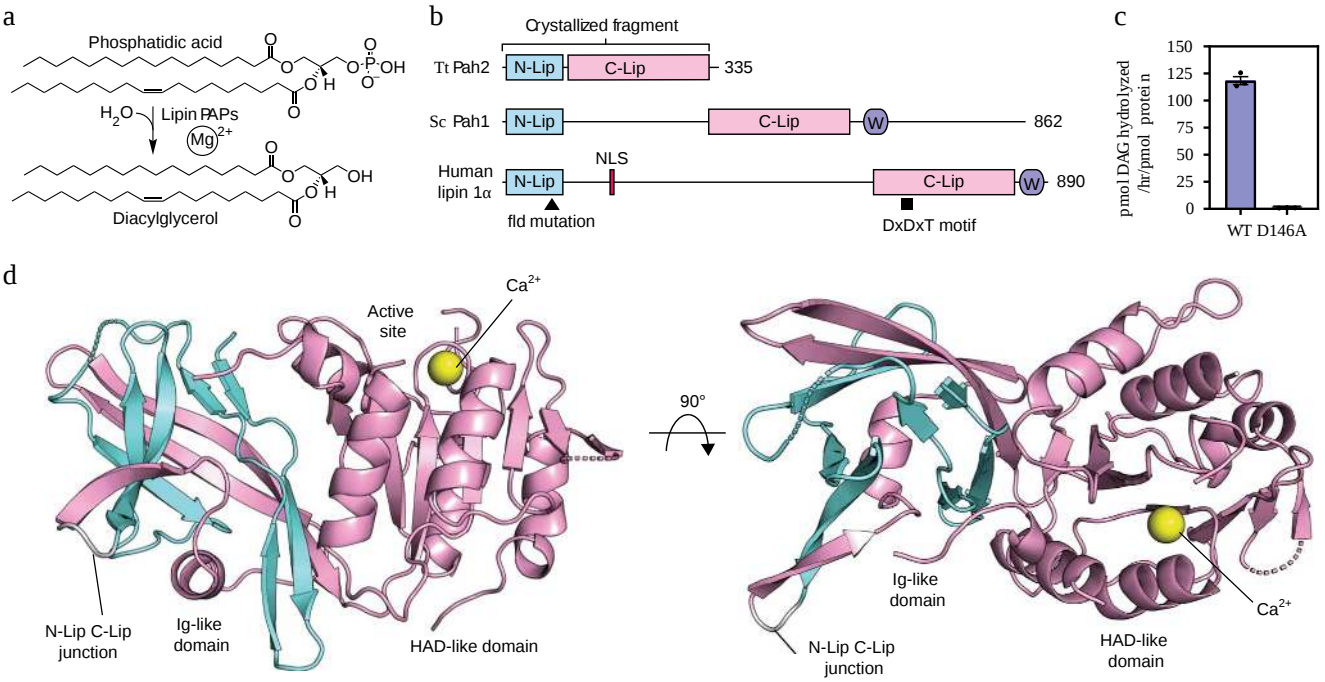


Figure **21.2.3**: The domain structures of human, yeast Saccharomyces cerevisiae (SC) and a truncated form (Tt-Pah2) of the Tetrahymena thermophila enzyme. Khayyo, V.I., Hoffmann, R.M., Wang, H. *et al.* Crystal structure of a lipin/Pah phosphatidic acid phosphatase. *Nat Commun* **11,** 1309 (2020). https://doi.org/10.1038/s41467-020-15124-z. Creative Commons Attribution 4.0 International License. http://creativecommons.org/licenses/by/4.0/.

Panel (a) shows the PAP-catalyzed dephosphorylation reaction.

Panel (b) shows the domain architecture of PAPs drawn to scale. The positions of the nuclear localization signal (NLS), conserved Trp-motif (purple W), catalytic DxDxT motif, and fatty liver dystrophy (fld^{2J}) mutation are indicated.

Panel (c) shows the wild-type (WT) *Tt* Pah2 is catalytically active, and the D146A mutant of the DxDxT motif eliminates activity.

Panel (d) shows the overall structure of *Tt* Pah2, which contains an immunoglobulin-like (Ig-like) domain and a HAD-like catalytic domain. The Ig-like domain is formed by the N-Lip (cyan) and C-Lip (pink) regions connected by a short linker (gray loop) that would be replaced by the extended 500-residue linker in human lipins and a 250-residue linker in *Sc* Pah1. A calcium ion (Ca^{2+}, yellow sphere) is bound in the active site of the HAD-like catalytic domain. The top view (right) of the enzyme shows the N-Lip co-folding with the C-Lip to form the Ig-like domain.

Figure **21.2.4**s shows a closeup of the active site of *Tt* Pah2 and a mechanism for hydrolytic phosphate removal from phosphorylated DAG.

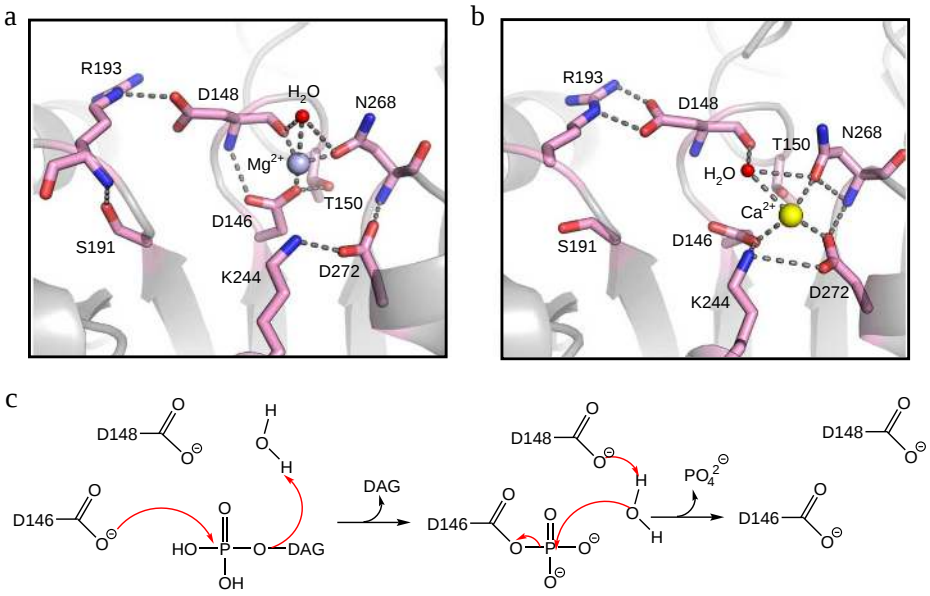
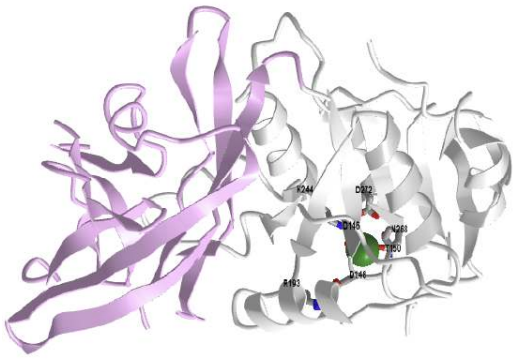


Figure **21.2.4**: **a** Detailed view of the *Tt* Pah2 active site with magnesium bound (light blue sphere). Gray dashes indicate polar contacts. **b** Detailed view of the structural rearrangement of key residue interactions in the active site with calcium bound (yellow sphere). **c** Proposed schematic of lipin/Pah PAPs catalytic mechanism. Catalysis proceeds through a trigonal bipyramidal intermediate. Khayyo, V.I. et al, ibid.

Figure **21.2.5** shows an interactive iCn3D model of the Tetrahymena Thermophila lipin phosphatidic acid phosphatase with magnesium (6TZZ).



NCBI iCn3D Figure **21.2.5**: Tetrahymena Thermophila lipin phosphatidic acid phosphatase with magnesium (6TZZ). Click the image for a popup or use this external link: https://structure.ncbi.nlm.nih.gov/i...GTusCCDP5eRrt7

The N-terminal domain is lavender, and the C-terminal domain is gray. Key amino acids in the active site are shown in CPK-colored sticks and labeled.

Diacylglycerol acyltransferases (DGAT)

In the final step in this pathway, the 1,2-diacyl-*sn*-glycerol intermediate is acylated by **diacylglycerol acyltransferases (DGAT)**, which can utilize a wide range of fatty acyl-CoA esters to form the triacyl-*sn*-glycerol. There are two DGAT enzymes, which are structurally and functionally distinct. In animals, DGAT1 is located mainly in the endoplasmic reticulum and is expressed in skeletal muscle, skin, and intestine, with lower levels of expression in the liver and adipose tissue. It is believed to have dual topology contributing to triacylglycerol synthesis on both sides of the endoplasmic reticulum membrane, but esterifying only pre-formed fatty acids of exogenous origin. Perhaps surprisingly, DGAT1 is the only one present in the mammary gland's epithelial cells that synthesizes milk fat. DGAT1 can also utilize a wider range of substrates, including monoacylglycerols, long-chain alcohols (for wax synthesis), and retinol, and is reported to play an important role in protecting the endoplasmic reticulum from the lipotoxic effects of high-fat diets. Orthologs of this enzyme are present in most eukaryotes other than yeasts, and they are especially important in plants.

Figure **21.2.6** shows an interactive iCn3D model of Human Diacylglycerol Acyltransferase 1 in complex with oleoyl-CoA (6VP0)

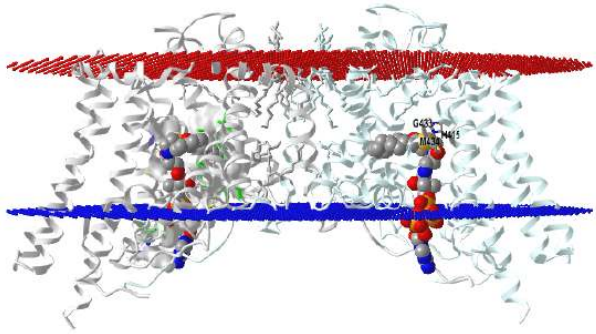


Figure 21.2.6: Human Diacylglycerol Acyltransferase 1 in complex with oleoyl-CoA (6VP0) (Copyright; author via source). Click the image for a popup or use this external link: https://structure.ncbi.nlm.nih.gov/i...adyWg9fy2hh8r8

The red layer is the extracellular leaflet, and the blue is the intracellular leaflet. The protein is a dimer with one subunit in gray and one in light. A substrate, oleoyl-CoA, is shown in spacefill with CPK colors in both monomers. The acyl chain with a clear kink induced by the double bond in the oleoyl acyl group is clearly in the hydrophobic interior of the bilayer. The gray monomer shows the atoms within 4 Å from the oleoly-CoA as surface color-coded by hydrophobicity, with the green being the most hydrophobic. The active site His 415 and Met 434, which hydrogen bonds to it, are shown in the light cyan subunit in sticks, CPK colors, and labeled. Three other conserved polar side chains, Asn378, Gln437, and Gln465, which are in the active site region, are also shown.

Each monomer in the homodimer has nine transmembrane helices, with eight forming a unique fold called the MBOAT, which encloses a chamber with catalytic side chains. The substrates, fatty acyl-CoA and DAG, have different entrances to the chamber, with the acyl-CoA occupying a cytosolic tunnel. The cytosolic face interacts with the CoA, and the acyl chain extends into the ER membrane. The channel appears bent, which probably allows the acylation of DAGs and long-chain alcohols but not cholesterol, a rigid, planar molecule that is acylated to form an ester by a different enzyme, acyl-CoA:cholesterol acyltransferases. Hence, it appears that DAG, the acyl-acceptor, binds in a hydrophobic tunnel from within the bilayer, and the acyl-CoA binds in another tunnel, allowing the transfer of the acyl group.

DGAT2 is the main form of the enzyme in hepatocytes and adipocytes (lipid droplets), although it is expressed much more widely in tissues. It is associated with distinct regions of the endoplasmic reticulum, at the surface of lipid droplets, and in mitochondria, and it esterifies fatty acids of both endogenous and exogenous origin. DGAT2 is believed to have a targeting domain that enables it to tether between the endoplasmic reticulum and lipid droplet, thereby channeling triacylglycerols from the synthesis site in the endoplasmic reticulum to the nascent lipid droplet, where they accumulate and lead to the expansion of the latter (see **below**). Both enzymes are important modulators of energy metabolism, although DGAT2 appears to be especially important in controlling the homeostasis of triacylglycerols *in vivo*. As the glycerol-3-phosphate acyltransferase (GPAT) has the lowest specific activity of these enzymes, this step may be the rate-limiting one. However, DGATs are the dedicated triacylglycerol-forming enzymes, and they are seen as the best target for pharmaceutical intervention in obesity and attendant ailments; clinical studies of DGAT1 inhibitors are at an early stage.

In a second pathway for triacylglycerol biosynthesis, dihydroxyacetone-phosphate in peroxisomes or endoplasmic reticulum can be acylated with fatty acid CoA esters by a specific acyltransferase to form 1-acyl dihydroxyacetone-phosphate, which is reduced by dihydroxyacetone-phosphate oxidoreductase to lysophosphatidic acid; this can then enter the pathway above to triacylglycerols. The precursor dihydroxyacetone-phosphate is also important as part of the biosynthetic route to **plasmalogens**, and neutral plasmalogens can be significant components of cytoplasmic droplets in many mammalian cell types, but not in adipose tissue.

Figure 21.2.7: Biosynthesis of triacylglycerols from dihydroxyacetone-phosphate

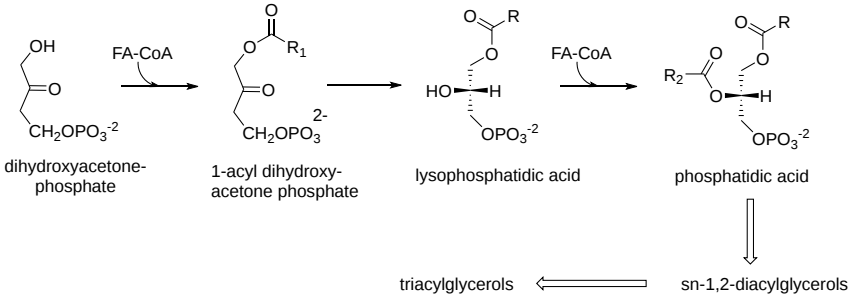


Figure 21.2.7: Biosynthesis of triacylglycerols from dihydroxyacetone-phosphate

In prokaryotes, the glycerol-3-phosphate pathway of triacylglycerol biosynthesis is sufficient. In yeast, glycerol-3-phosphate and dihydroxyacetone-phosphate can be the primary precursors, and synthesis occurs in cytoplasmic lipid droplets and the endoplasmic

reticulum. In plants, the glycerol-3-phosphate pathway is most important.

In the enterocytes of the intestines after a meal, up to 75% of the triacylglycerols are formed via a monoacylglycerol pathway. In this pathway, the enterocytes take up 2-monoacyl-*sn*-glycerols and free fatty acids released from dietary triacylglycerols by the action of pancreatic lipase within the intestines (see below). There, the monoacylglycerols are first acylated by an acyl-coenzyme A:monoacylglycerol acyltransferase with the formation of *sn*-1,2-diacylglycerols mainly as the first intermediate in the process, though some *sn*-2,3-diacylglycerols (~10%) are produced. In addition, 1-monoacylglycerols can be synthesized by the acylation of glycerol for further acylation. There are three isoforms of the monoacylglycerol acyltransferase in humans, of which MGAT2 is most active in the intestines, but also in the liver, where the monoacylglycerol pathway forms an appreciable proportion of the triacylglycerols, while MGAT1 functions in adipose tissue; the role of MGAT3 is not clear. Finally, the acyl-coenzyme A:diacylglycerol acyltransferase (DGAT1) reacts with the *sn*-1,2-diacylglycerols (not the *sn*-2,3 form) to produce triacylglycerols (DGAT1 can also acylate monoacylglycerols). Figure **21.2.8** shows the biosynthesis of triacylglycerols from monoacylglycerols.

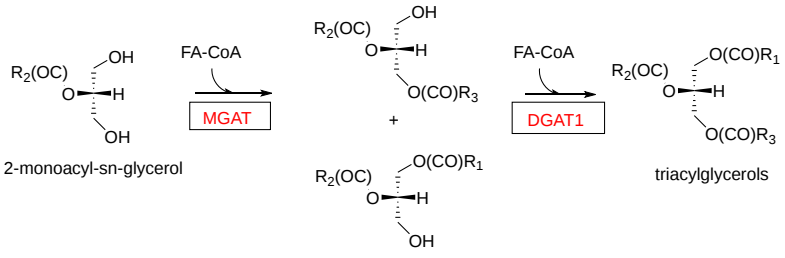


Figure **21.2.8**: Biosynthesis of triacylglycerols from monoacylglycerols

Other pathways: In a fourth biosynthetic pathway, which is less well known, triacylglycerols are synthesized by a transacylation reaction between two racemic diacylglycerols that are independent of acyl-CoA. The reaction was first detected in the endoplasmic reticulum of intestinal microvillus cells and is catalyzed by a diacylglycerol transacylase. Both diacylglycerol enantiomers participate in the reaction with equal facility to transfer a fatty acyl group to form triacylglycerols and a 2-monoacyl-*sn*-glycerol. A similar reaction has been observed in seed oils. Figure **21.2.9**: Biosynthesis of triacylglycerols from diacylglycerol transacylases

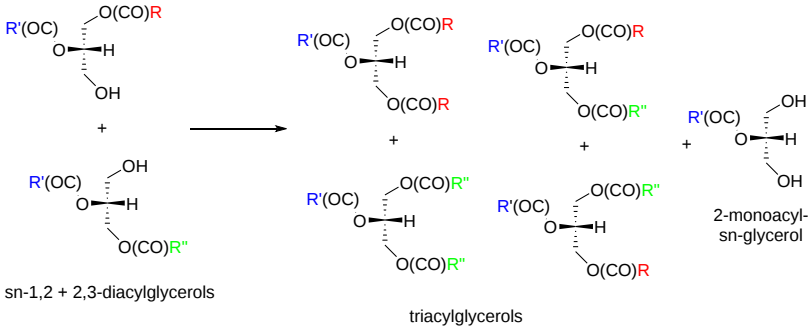


Figure **21.2.9**: Biosynthesis of triacylglycerols from diacylglycerol transacylases

It has been suggested that this enzyme may function in remodeling triacylglycerols post-synthesis, especially in oil seeds, and it may be involved in similar processes in the liver and adipose tissue, where extensive hydrolysis/re-esterification is known to occur. There is evidence for selectivity in the biosynthesis of different molecular species in various tissues and organisms, which may result from the varying biosynthetic pathways. Also, in adipose tissue, fatty acids synthesized *de novo* are utilized in different ways from external sources in that they enter positions *sn*-1 and 2 predominantly. In contrast, a high proportion of the oleic acid synthesized in the tissue by desaturation of exogenous stearic acid is esterified to position *sn*-3.

Among other potential routes to the various intermediates, lysophosphatidic acid and phosphatidic acid can be synthesized in mitochondria. Still, they must then be transported to the endoplasmic reticulum before entering the triacylglycerol production pathway. 1,2-Diacyl-*sn*-glycerols are also produced by the action of phospholipase C on phospholipids and can be utilized for triacylglycerol biosynthesis.

In the glycerol-3-phosphate and other pathways, the starting material has defined stereochemistry, and each of the enzymes catalyzing the various steps in the process is distinctive and can have preferences for particular fatty acids (as their coenzyme A esters) and for particular fatty acid combinations in the partially acylated intermediates. It should not be surprising, therefore, that natural triacylglycerols exist in enantiomeric forms with each position of the *sn*-glycerol moiety esterified by different fatty acids.

21.2.3: TRIACYLGLYCEROL METABOLISM IN THE INTESTINES, LIVER, AND MAMMARY GLAND

Fat comprises up to 40% of the energy intake in the human diet in Western countries, and a high proportion of this is triacylglycerols. The process of fat digestion begins in the stomach with acid-stable gastric or lingual lipases, the extent of which depends on species but may be important for efficient emulsification. However, this is insignificant in quantitative terms compared to the reaction with pancreatic lipase, which occurs in the duodenum. The entry of triacylglycerol degradation products into the duodenum stimulates the synthesis of the hormone cholecystokinin. It causes the gall bladder to release **bile acids**, which are strong detergents and act to emulsify the hydrophobic triacylglycerols, thus increasing the available surface area. In turn, cholecystokinin stimulates the release of the hydrolytic enzyme pancreatic lipase with a co-lipase, which is essential for the enzyme's activity. Pancreatic lipase, co-lipase, bile salts, and calcium ions act together in a complex at the surface of the emulsified fat droplets to hydrolyze the triacylglycerols. The process is regiospecific and results in the release of the fatty acids from the 1 and 3 positions and the formation of 2-monoacyl-*sn*-glycerols, as shown in Figure **21.2.10**.

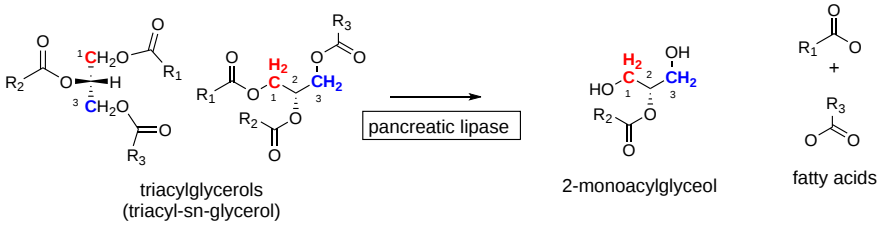


Figure **21.2.10**: Hydrolysis of triacylglycerols in the intestines

Spontaneous isomerization of the latter to 1(3)-monoacyl-*sn*-glycerols occurs to some extent, and the enzyme can completely degrade these to glycerol and free fatty acids. Other lipases hydrolyze the phospholipids and other complex lipids in foods simultaneously.

This process is somewhat different in neonates and young infants, in which pancreatic lipase is less active but is effectively replaced by lipases in breast milk and an acid gastric lipase (pH optimum 4-6).

There is evidence that the regiospecific structure of dietary triacylglycerols affects the uptake of particular fatty acids and may further influence lipid metabolism in humans. Incorporation of palmitic acid into the position *sn*-2 of milk fat may benefit the human infant (as a source of energy for growth and development). However, it increases the atherogenic potential for adults. In addition, 2-monoacylglycerols and 2-oleoylglycerol especially have a signaling function in the intestines by activating a specific G-protein coupled receptor GPR119, sometimes called the fat sensor. When stimulated, this causes a reduction in food intake and body weight gain in rats and regulates glucose-stimulated insulin secretion. The free fatty acids released have a similar effect, though by a very different mechanism, via the receptor GPR40. Overall, it has become evident that triacylglycerol metabolism in the intestine has regulatory effects on the secretion of gut hormones and, subsequently, on systemic lipid metabolism and energy balance.

The intestinal cells rapidly take up the free fatty acids and 2-monoacyl-*sn*-glycerols, from the distal duodenum to the jejunum, via specific carrier molecules and passive diffusion. A specific fatty acid binding protein prevents a potentially toxic build-up of unesterified fatty acids and targets them for triacylglycerol biosynthesis. The long-chain fatty acids are converted to the CoA esters and esterified into triacylglycerols by the monoacylglycerol pathway as described above. In contrast, short and medium-chain fatty acids (C_{12} and below) are absorbed in unesterified form and pass directly into the portal bloodstream, where they are transported to the liver to be oxidized.

Subsequently, the triacylglycerols are incorporated into **lipoprotein complexes** termed **chylomicrons** in the enterocytes in the small intestines. In brief, these consist of a core of triacylglycerols together with some cholesterol esters that is stabilized and rendered compatible with an aqueous environment by a surface film consisting of phospholipids, free cholesterol, and one molecule of a truncated form of apoprotein B (called apo B48). A cartoon structure of a chylomicron is shown in Figure **21.2.11**.

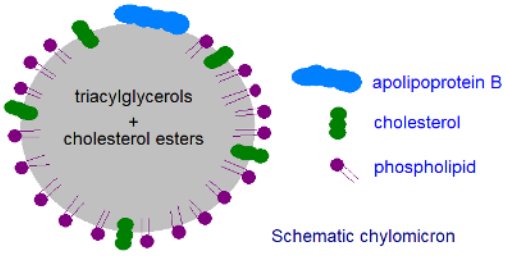


Figure **21.2.11**: Cartoon structure of a chylomicron

These particles are secreted into the lymph and the plasma for transport to the peripheral tissues for storage or structural purposes. Adipose tissue, in particular, exports appreciable amounts of the enzyme **lipoprotein lipase.** This enzyme binds to the luminal membrane of

endothelial cells facing into the blood, where it rapidly hydrolyses the passing triacylglycerols at the cell surface, releasing free fatty acids. Most of these are absorbed into the adjacent adipocytes and re-utilized for triacylglycerol synthesis within the cell.

The chylomicron remnants eventually reach the liver, where the remaining lipids are hydrolyzed at the external membranes by a hepatic lipase and absorbed. The fatty acids within the liver can be utilized for various purposes, from oxidation to synthesizing structural lipids. Still, a proportion is re-converted into triacylglycerols; some of this is stored as lipid droplets within the cytoplasm of the cells (see next section). In addition, phosphatidylcholine from the high-density lipoproteins is taken up by the liver, and a high proportion of this is eventually converted to triacylglycerols. In a healthy liver, the levels of triacylglycerols are low (<5% of the total lipids) because the acquisition rates of fatty acids from plasma and synthesis *de novo* within the liver are balanced by rates of oxidation and secretion into plasma. On the other hand, excessive accumulation of storage triacylglycerols is associated with fatty liver, insulin resistance, and type 2 diabetes.

Most of the newly synthesized triacylglycerols are exported into the plasma in the form of very-low-density lipoproteins (VLDL), consisting again of a triacylglycerol and cholesterol ester core, surrounded by phospholipids and free cholesterol, together with one molecule of full-length apoprotein B (100 kDa), apoprotein C, and sometimes apoprotein E. These particles, in turn, are transported to the peripheral tissues, where they are hydrolyzed and the free acids absorbed. Eventually, the remnants are returned to the liver.

In the **mammary gland**, triacylglycerols are synthesized in the endoplasmic reticulum, and large lipid droplets are produced with a monolayer of phospholipids derived from this membrane. These are transported to the plasma membrane and bud off into the milk with an envelope of the phospholipid membrane to form milk fat globules as food for the newborn. Thus, the process differs from that involved in the secretion of triacylglycerol-rich lipoproteins from other organs.

21.2.4: TRIACYLGLYCEROL SYNTHESIS AND CATABOLISM (LIPOLYSIS) IN ADIPOCYTES AND LIPID DROPLETS

Adipose tissue and the adipocytes are characterized by accumulations of triacylglycerols, which act as the main energy store for animals, although they also cushion and insulate the body. Large fat deposits occur around internal organs such as the liver and subcutaneously, and each may react differently to metabolic constraints. Thus, triacylglycerols stored in a surplus of nutrients are mobilized for energy production during starvation. Adipose tissue also functions as a reserve of bioactive lipids, such as eicosanoids and lipid-soluble vitamins, and when required, provides structural components, including fatty acids, cholesterol, and retinol, for membrane synthesis and repair. By buffering against fatty acid accumulation that might exceed their capacity, non-adipose cells defend themselves against lipotoxicity while providing a rapid source of energy and essential metabolites by sensing and responding rapidly to changes in systemic energy balance. Brown and beige fat have special properties and are discussed below, while bone marrow adipocytes (70% of the available space) also have distinctive functions.

Similarly, within most other animal cells, including most cell types in the brain, a proportion of the fatty acids taken up from the circulation is converted to triacylglycerols as described above and incorporated into cytoplasmic lipid droplets (also termed 'fat globules', 'oil bodies', 'lipid particles' or 'adiposomes'). In adipocytes, the lipid droplets can range from up to 200 μm in diameter, while other cell types contain smaller lipid droplets of 50 nm in diameter. The triacylglycerol droplets, cholesterol esters, and other neutral lipids are surrounded by a protective monolayer that includes phospholipids, cholesterol, and hydrophobic proteins. The phospholipid component of the monolayer consists mainly of phosphatidylcholine and phosphatidylethanolamine derived from cytosolic leaflets of the endoplasmic reticulum and plasma membrane. Many proteins function directly in lipid metabolism, including acyltransferases, lipases, perilipins, caveolins, and the Adipose Differentiation Related Protein (ADRP or adipophilin). Acting in concert with other cellular organelles, they function in many different metabolic processes, facilitating coordination and communication between different organelles and acting as vital hubs of cellular metabolism.

Cytosolic lipid droplets with similar metabolic activities are found in most eukaryotic cells, including those of the fruit fly *Drosophila melanogaster. Many* aspects of triacylglycerol processing and regulation parallel those in humans. They are also present in the cytoplasm of some prokaryotes and in the plastids and other organelles of plants (see below).

Lipid droplet assembly

This process takes place in sub-domains of the endoplasmic reticulum, where at least one isoform of each of the enzymes of triacylglycerol biosynthesis, from acyl-CoA synthetases through to glycerol-3-phosphate acyltransferases, is located, probably in a protein assembly or 'interactome'. As triacylglycerols accumulate, they reach a critical level when a spontaneous condensation or nucleation by phase separation occurs, leading to the formation of an oil blister within the hydrophobic bilayer region, attracting perilipins and other proteins that allow lipid droplets to grow further in patches of the membrane as lens-like swellings between the two membrane leaflets.

The protein **seipin** stabilizes the nascent droplets with minimal disruption to the membrane and enables them to mature. Seipin monomers assemble into a decameric cage-like structure and sit in the ER to provide a space that permits triacylglycerol molecules to interact with

each other rather than with phospholipid acyl chains. Transmembrane protein segments probably aid this process. This enables phase separation of the triacylglycerols, lens formation, and growth to a point where the seipin oligomer opens toward the cytoplasm so the lens can form a budding lipid droplet.

Figure **21.2.12** presents a cartoon that shows the role of ER membrane seipins and other proteins in the assembly of lipid droplets.

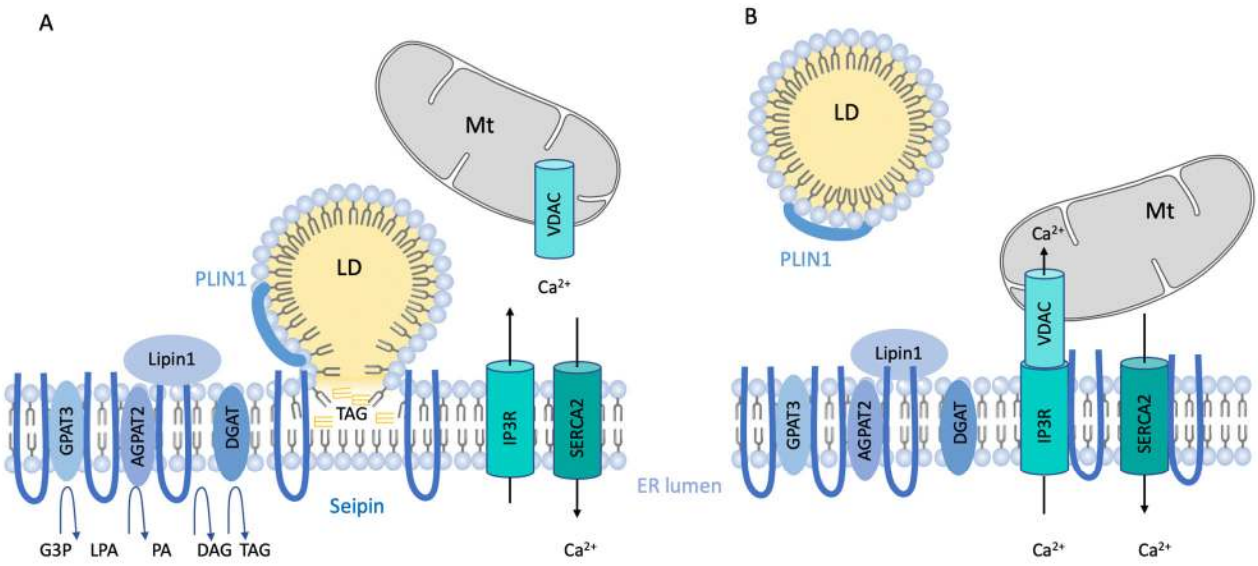
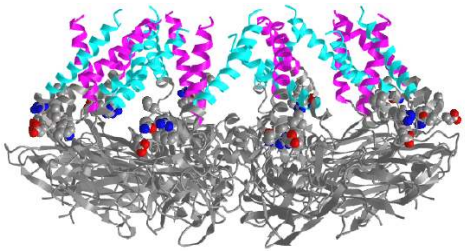


Figure **21.2.12**: Seipin function in mature adipocytes. Magré J, Prieur X. Seipin Deficiency as a Model of Severe Adipocyte Dysfunction: Lessons from Rodent Models and Teaching for Human Disease. Int J Mol Sci. 2022 Jan 11;23(2):740. doi: 10.3390/ijms23020740. Creative Commons Attribution (CC BY) license (https://creativecommons.org/licenses/by/4.0/

In panel (A), seipin is enriched at the endoplasmic reticulum (ER)/lipid droplet (LD) contact sites and is crucial in triglyceride (TAG) flow from the ER to the LD. Seipin interacts with Perilipin1 (PLIN1) and with several TAG synthetic enzymes such as glycerol-3-phosphate acyltransferase (GPAT3), 1-acyl-sn-glycerol-3-phosphate acyltransferase beta (AGPAT2), and LIPIN. No interaction with diacylglycerol acyltransferases (DGAT) has been formally reported. Magré J et al, Int J Mol Sci. 2022 Jan 11;23(2):740. doi: 10.3390/ijms23020740. Creative Commons Attribution (CC BY) license (https://creativecommons.org/licenses/by/4.0/

In panel (B), representing the fasting state, seipin is enriched at the ER/mitochondria (Mt) contact sites, also named mitochondria-associated membranes (MAM) and participates in ER/mitochondria calcium (Ca^{2+}) flux and mitochondrial activity. Seipin is near MAM Ca^{2+} regulators IP3(inositol 1,4,5-trisphosphate) receptor (IP3R), voltage-dependent anion channel (VDAC), and sarco-/ER Ca^{2+} ATPase 2 (SERCA2), as well as glycerol-3-phosphate (G3P), lysophosphatidic acid (LPA), phosphatidic acid (PA), and diacylglycerol (DAG).

Figure **21.2.13** shows an interactive iCn3D model of the S. cerevisiae seipin Homo 10-mer flexible cage at lipid droplet formation sites (7RSL).



NCBI iCn3D Figure **21.2.13**: S. cerevisiae seipin homo 10-mer flexible cage at lipid droplet formation sites (7RSL). Click the image for a popup or use this external link: https://structure.ncbi.nlm.nih.gov/i...BjYLiQXVJjBpk8

The N-terminal transmembrane segment (TMS) on each monomer is shown in cyan, while the C-terminal TMS is magenta. These form the cage sides and top, anchoring the complex in the ER membrane. The side chains of a conserved switch sequence (F_{232}xxGLR) on each monomer are shown in spacefill, CPK colors. The gray ribbons represent the part of the complex in the ER lumen.

Adjacent monomers in the homo 10-mer cage, even though they are identical in sequence, adopt different orientations for the two helices that enable a binary switch in the conformation of the complex. Two adjacent subunits, the A chain in blue and the B chain in orange, are shown, along with their overlap, in Figure **21.2.14**.



Figure **21.2.14**: Conformational flexibility in adjacent monomers in the seipin homo 10-mer.

A highly conserved "switch" region is shown in green with its highly conserved motif F_{232}xxGLR shown as sticks with CPK colors. Note the large conformational change in the switch region that occurs with the two helices' large conformational change. This suggests that there are two overall conformations of the complex, a closed form allowing accumulation of TAGs and an open form which allows the budding and release of lipid droplets. A possible model for the formation and budding of lipid droplets is illustrated in Figure **21.2.15**. As in the above figure, the A (open) chain is shown in blue while the B (closed) chain is shown in orange.

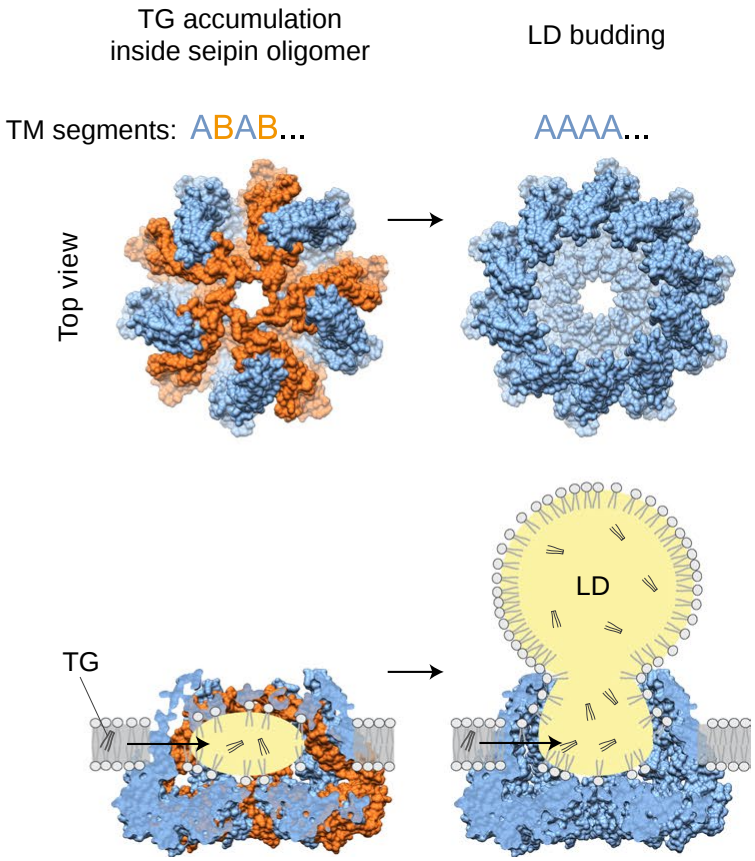


Figure **21.2.15**: Accumulation and phase separation of triacylglycerides (TG) and budding of lipid droplets (LD) from the seipin complex. Arlt et al. https://doi.org/10.1038/s41594-021-00718-y. Nature Structural & Molecular Biology, 194–202 (2022). Creative Commons Attribution 4.0 International License. http://creativecommons.org/licenses/by/4.0l. The left-hand side shows alternating monomer conformations (A in blue and B in orange, based on the solved structure), which forms an overall "closed" form of the complex, allowing the accumulation of TGs. The right-hand side shows a possible open form, with all monomers in the A or blue form, which allows lipid droplet formation and release.

Some surface proteins on lipid droplets can extend long helical hairpins of hydrophobic peptides deep into the lipid core. For example, perilipins constitute a family of at least five phosphorylated proteins that bind to animal droplets and share a common region, the so-called ‘PAT’ domain, named for the family's three original members, including perilipin and ADRP. Proteins related evolutionarily to these are found in more primitive organisms, including insects, slime molds, and fungi, but not in the nematode *Caenorhabditis elegans*. In mammals,

perilipin A (or 'PLIN1' or, more accurately, the splice variant 'PLIN1a') is a well-established regulator of lipolysis in adipocytes, and it is believed to be involved in the formation of the large lipid droplets in white adipose tissue. The perilipins PLIN1 and PLIN2 function in triacylglycerol metabolism in tissues other than adipocytes, and PLIN2 is the main perilipin in hepatocytes; PLIN5 operates in tissues that oxidize fatty acids, such as the heart. Other surface proteins of lipid droplets are enzymes intimately involved in triacylglycerol metabolism. However, there is a suggestion that cytoplasmic droplets may act as a storage organelle for hydrophobic proteins whose function is elsewhere in the cell.

Lipolysis

When fatty acids are required by other tissues for energy or other purposes, they are released from the triacylglycerols by the sequential actions of three cytosolic enzymes at neutral pH, i.e., adipose triacylglycerol lipase (ATGL), hormone-sensitive lipase (HSL) and monoacylglycerol lipase, which cycle between the cytoplasmic surfaces of the endoplasmic reticulum and the surface layer of lipid droplets. Simplistically, ATGL hydrolyses triacylglycerols to diacylglycerols, which HSL hydrolyses to monoacylglycerols before the monoacylglycerol lipase hydrolyses these to complete the process. Lipolysis proceeds in a highly ordered manner with stimulation through cell-surface receptors via neurotransmitters, hormones, and autocrine/paracrine factors that activate various intracellular signaling pathways and increase kinase activity. A protein perilipin (PLIN1) has been described as "the gatekeeper of the adipocyte lipid storehouse" that regulates lipolysis by acting as a barrier to lipolysis in non-stimulated cells. However, on β-adrenergic stimulation during fasting, it is phosphorylated by the cAMP-protein kinase, which changes its shape and reduces its hydrophobicity, and in the process, activates lipolysis. An isoform, perilipin A, is the main regulatory factor in white adipose tissue. However, many other proteins interact with the three enzymes to modulate their activity, location, and stability.

The **adipose triacylglycerol lipase**, which initiates the process, was recently discovered. It is structurally related to the plant acyl-hydrolases in that it has a patatin-like domain in the NH_2-terminal region (patatin is a non-specific acyl-hydrolase in potatoes). Specific transport mechanisms guide ATGL from the endoplasmic reticulum membrane to lipid droplets located on the surface in the basal and activated states. This lipase is specific for triacylglycerols containing long-chain fatty acids, preferentially cleaving ester bonds in the *sn*-1 or *sn*-2 position (but not *sn*-3), and it yields diacylglycerols and free fatty acids as the main products, with low activity only towards diacylglycerols and none towards monoacylglycerols and cholesterol esters. However, it also has transacylase and phospholipase activities and hydrolyses retinol esters in hepatic stellate cells. Adipose triacylglycerol lipase can be activated at the same time as hormone-sensitive lipase and is now believed to be rate-limiting for the first step in triacylglycerol hydrolysis. Figure **21.2.16** shows the sequential hydrolysis of TAGs in adipocytes and lipid droplets.

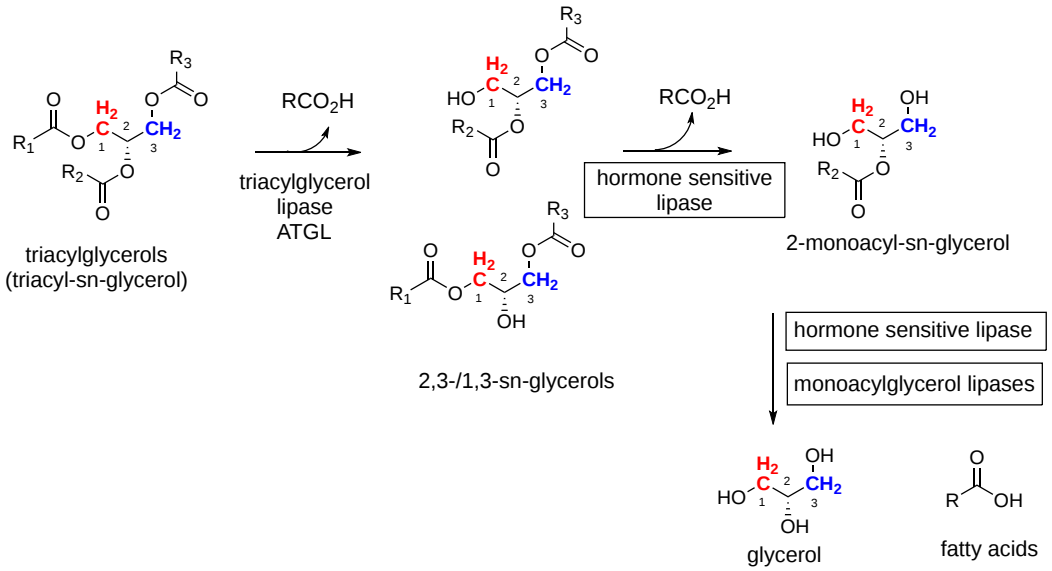


Figure **21.2.16**: Sequential hydrolysis of TAGs in adipocytes and lipid droplets

Regulation of the enzymatic activity is a complex process. For example, a lipid droplet protein designated Gene identification-58 (CGI-58 or ABHD5), is an important activating factor and is required for hydrolysis of fatty acids from position *sn*-1. In the resting state, this protein binds to perilipin (PLIN1). Still, on hormonal stimulation, the latter is phosphorylated, leading to dissociation and interaction of CGI-58 with phosphorylated ATGL to commence the first step in triacylglycerol hydrolysis. Mutations in adipose triacylglycerol lipase or CGI-58 are believed to be responsible for a human syndrome known as ‘neutral lipid storage disease’. A second protein (G0S2) inhibits the enzyme.

Hormone-sensitive lipase in various isoforms is a structurally unique member of the large Ser-lipase/esterase family of enzymes in animals. It is regulated by the action of the hormones insulin and noradrenaline by a mechanism that ultimately involves phosphorylation of

the enzyme by cAMP-protein kinase (as with perilipin), thereby increasing its activity and causing it to translocate from the cytosol to the lipid droplet to initiate the second step in hydrolysis. Its activity is further regulated by various proteins, including PLINs and fatty acid binding proteins (FABP). Hormone-sensitive lipase has a broad substrate specificity compared to other neutral lipases. In addition to its activity towards triacylglycerols, it will rapidly hydrolyze diacylglycerols, monoacylglycerols, retinol esters, and cholesterol esters. Diacylglycerols are hydrolyzed ten times as rapidly as triacylglycerols. Within the triacylglycerol molecule, hormone-sensitive lipase preferentially hydrolyses ester bonds in the *sn*-1 and *sn*-3 positions, leaving free acids and 2-monoacylglycerols as the main end products.

The **monoacylglycerol lipase** is believed to be the rate-limiting enzyme in lipolysis, i.e., the final step in triacylglycerol catabolism, releasing free glycerol and fatty acids, and it is found in the cytoplasm, the plasma membrane, and in lipid droplets. It is specific for monoacylglycerols but has no positional specificity and has no activity against di- or triacylglycerols. As it is the enzyme mainly responsible for deactivating the endocannabinoid **2-arachidonylglycerol** and is highly active in malignant cancers, it attracts pharmaceutical interest. A further enzyme, α/β hydrolase containing-6 (ABHD6), is located on the inner leaflet of the plasma membrane and preferentially hydrolyses fatty acids at the *sn*-1 position over the *sn*-2 position of monoacylglycerols. It also hydrolyses lysophospholipids and bis(monoacylglycerol)-phosphate. This has been associated with the development of insulin resistance and the progression of cancer. Additional lipolytic enzymes, including carboxyesterases, are believed to operate against triacylglycerols in cytoplasmic lipid droplets in the liver.

Unesterified fatty acids released by the combined action of these three lipases are exported into the plasma for transport to other tissues in the form of albumin complexes. In contrast, the released glycerol is transported to the liver for metabolism by either glycolysis or gluconeogenesis.

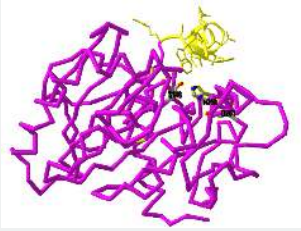
Eventually, the whole organelle, including the proteins, can disappear when they undergo a process of autophagy (**lipophagy**), i.e., the delivery of the organelles to lytic compartments for degradation. This can occur through direct lysosomal invagination or more often by a multistep process involving the formation of double-membrane vesicles termed 'autophagosomes' around droplets with subsequent lysosomal fusion and degradation of the triacylglycerols by the lysosomal acid lipase. This process is important for regulating cellular lipid levels in various tissues and disease conditions, especially during starvation. It is relevant to tumorigenesis and cancer metastasis and to neurodegenerative and neuroinflammatory diseases. While lipophagy is mechanistically distinct from lipolysis, there is cross-talk between the two.

THE STRUCTURE OF LIPASES

Lipases carry out hydrolysis reactions (nucleophilic substitution with water as the nucleophile), alcoholysis reactions (with an ROH as the nucleophile), and even transesterification reactions with other fatty acid esters. Lipases are critical enzymes, yet no good structures are available for hormone-sensitive lipase, for example. Yet, much is known about the structure and activity of lipases. Lipases have a catalytic Ser-His-Asp triad like serine proteases, which also catalyze hydrolysis reactions. However, the substrates for lipase are nonpolar and could be part of larger structures such as lipid droplets. As such, the lipases work at the interface between aqueous and non-aqueous interfaces. They are **interfacially** activated.

Lipases appear to have low activity in aqueous solutions but more in solutions that are more nonpolar. Many appear to have two conformations, a closed one with lower activity and poor lipid substrate binding properties, and an open one with higher activity and activation by nonpolar solvents. An alpha-helical lid appears to close off the active site in the closed conformation. In a more nonpolar solvent or bulk lipids, such as lipid droplets, the alpha-helical lid moves, exposing the enzyme's hydrophobic binding site to substrate interactions.

Figure **21.2.17** shows an interactive iCn3D model comparing the structure of a *Thermomyces lanuginosus* lipase in its closed (1DT3) and open conformation (1EIN).



NCBI iCn3D Figure **21.2.17**: The structure of a *Thermomyces lanuginosus* lipase in its closed (1DT3) and its open conformation (1EIN). Click the image for a popup or use this external link: https://structure.ncbi.nlm.nih.gov/icn3d/share.html?C9yEwy6SR6MZ9Q1S7

> The closed structure (1DT3) is shown in magenta, and the open (1EIN) is in cyan. The active site triad Ser146, His258, and Asp201 is shown in CPK-colored sticks and labeled for each. The lid is shown in yellow with its side chains as sticks. Toggle between the two states using the "a" key. Note how the lid covers the active site in the closed (1DT3) structure. You will have to rotate the molecule to see the optimal orientation. Also, close out menu boxes for a larger and more centered display.

Endocrine functions

Not only does the adipocyte provide a store of energy, but it is also an endocrine organ that manages the flow of energy through the formation of the hormone **leptin**, which signals through the adiponectin receptors (AdipoR)1 and AdipoR2 and binds to the non-signaling interacting protein T-cadherin. The result is the stimulation of signaling cascades to communicate with other tissues through the secretion of cytokines and other mediators. Adipocytes tightly control the synthesis of leptin. However, it is also produced by the stomach, placenta, and mammary gland, and its principal function is to provide information on the state of fat stores to other tissues. In so doing, it regulates food intake and energy expenditure. Leptin was initially described as an anti-obesity hormone. Still, it serves as an adiposity signal with a vital function in maintaining adipose tissue mass to ensure survival under conditions of negative energy balance and protect against either a deficit or an excess of adiposity. Lipid droplets have a role in this process, since perilipin is required for the sensing function.

Adiponectin is a potent insulin sensitizer and suppressor of cell death and inflammation, directly promoting anti-diabetic and anti-atherosclerotic outcomes. Insulin is the main hormone that affects metabolism, and its receptor at the plasma membrane is located in caveolae. Proinflammatory cytokines can stimulate lipolysis and cause insulin resistance, leading to dysfunction of adipose tissue and systemic disruption of metabolism. Thus, adipose tissue metabolism has profound effects on whole-body metabolism, and defects in these processes can have severe implications for such serious pathological conditions as diabetes, obesity, cardiovascular disease, fatty liver disease, and cancer in humans. It is hoped that developing specific inhibitors for hormone-sensitive lipase will improve the treatment of such metabolic complications. As **caveolae**, which contain the proteins caveolins (and presumably sphingolipids) and are particularly abundant in adipocytes, modulate the flux of fatty acids across the plasma membrane and are involved in signal transduction and membrane trafficking pathways, it is evident that they have a major role in this aspect of lipid metabolism.

White fat acts as an endocrine organ and can release a variety of hormones, including **adipokines** (analogous to cytokines, chemokines, and lymphokines), **adipsin,** and **leptin,** as well as tumor necrosis factor α (TNF-α), adiponectin, resistin, and RBP4.

Functions other than energy management

Lipid droplets accumulate within many cell types other than adipocytes, including leukocytes, epithelial cells, hepatocytes, and even astrocytes, especially during infections, cancer, and other inflammatory conditions. They are important for the cellular storage and release of hydrophobic vitamins, signaling precursors, and other lipids unrelated to energy homeostasis while reducing the dangers of lipotoxicity. On the other hand, excessive fatty acid accumulation is associated with lipotoxicity, endoplasmic reticulum stress, and mitochondrial damage and dysfunction, so lipid storage in lipid droplets must be balanced for health.

Various enzymes are associated with lipid droplets, including protein kinases, which are involved in many aspects of lipid metabolism, such as cell signaling, membrane trafficking, and control of the production of inflammatory mediators like the eicosanoids. Lipolysis enables the secretion of lipid species termed **lipokines** (more generally 'adipokines') from adipocytes that may signal in a hormone-like fashion to other tissues, thereby modulating gene expression and physiological function, including food intake, insulin sensitivity, insulin secretion, and related processes. These include **palmitoleic acid (9-16:1)** and **fatty acid esters of hydroxy fatty acids (FAHFA)**, though the circulating proteins adiponectin and leptin have been studied more intensively. Adiponectin is a powerful insulin sensitizer and suppressor of apoptosis and inflammation with anti-diabetic and anti-atherosclerotic functions, often operating through its effects on sphingolipids. At the same time, leptin exerts most of its effects on the brain to trigger behavioral, metabolic, and endocrine responses to control the body's fuel reserves.

Indeed, there are now suggestions that lipid droplets in all cell types are essential for the response mechanisms to cellular stress, including autophagy, inflammation, and immunity, and act as hubs to integrate metabolic and inflammatory processes. Via their lipolytic machinery, they regulate the availability of fatty acids to activate signaling pathways and produce oxylipins from polyunsaturated fatty acids. For example, triacylglycerols in cytoplasmic lipid droplets of human mast cells, which are potent mediators of immune reactions and influence many inflammatory diseases, have a high content of arachidonic acid, and this can be released by adipose triacylglycerol lipases as a substrate for the production of specific eicosanoids when the cells are stimulated appropriately. Active metabolism in lipid droplets is important for the differentiation of monocytes, and it is essential for the sustained functional activity of differentiated macrophages, especially in relation to inflammation.

During apoptosis, triacylglycerols enriched in polyunsaturated fatty acids accumulate in lipid droplets, possibly as a protective mechanism against membrane damage caused by oxidative stress and hydroperoxide formation in this process. Triacylglycerols in lipid droplets of the skin are a highly specific source of linoleic acid required to form the ***O*-acylceramides**, which are essential for epidermal barrier function.

An organelle termed the midbody in dividing cells in humans and rodents contains a unique triacylglycerol that is a single molecular species consisting of three fatty acids 16:1-12:0-18:1 (12:0 is especially rarely detected in human lipids), but its function is not known.

Vitamin E (tocopherols) and vitamin A in the form of retinyl esters are stored in cytoplasmic lipid droplets, and the latter are present in appreciable concentrations in the stellate cells of the liver, for example. In endocrine cells of the gonads and adrenals, cholesterol esters stored in lipid droplets are an important source of cholesterol for the mitochondrial biosynthesis of various steroid hormones. In addition to providing a reservoir of fatty acids for membrane remodeling in the cell's nucleus, lipid droplets can sequester transcription factors and chromatin components and generate the lipid ligands for certain nuclear receptors.

Lipid droplets participate in protein degradation and glycosylation in addition to their role in lipid biochemistry. Pathogenic viruses and bacteria, such as *Mycobacterium tuberculosis*, can manipulate their metabolism, with unfortunate consequences for the host. Still, they also serve as reservoirs for proteins that fight intracellular pathogens. Consequently, such lipid droplets and their enzyme systems may be markers for disease states and are also considered targets for pharmaceutical intervention.

Insects

In insects, the fat body is a multifunctional tissue, the main metabolic organ. It integrates signals that control the immune system, molting, metamorphosis, and synthesis of hormones that regulate innumerable aspects of metabolism. In fat, lipids, carbohydrates, and proteins are the substrates and products of many pathways for energy production. Fat also acts as a reserve for mobilization at the appropriate stage of life (diapause, metamorphosis, and flight). In relation to innate and acquired humoral immunity, the fat body produces bactericidal proteins and polypeptides, i.e., lysozyme. It is also important in the early stages of an insect's life due to the production of vitellogenin, the yolk protein needed to develop oocytes.

21.2.5: BROWN ADIPOSE TISSUE

Most adipose tissue depots ('white fat') serve primarily as storage and endocrine organs that provide a reservoir of nutrients for release when the food supply is low. However, a second specialized form of adipose tissue, brown fat, is multilocular, highly vascularized, and rich in mitochondria and the iron-containing pigments that transport oxygen and give the tissue its color and name. Brown adipocytes arise from progenitor cells closer to those of skeletal muscle than white adipocytes. In humans, these depots tend to be located in specific anatomical regions such as subcutaneous areas around the neck, where their function may be to supply warm venous blood directly to the spinal cord and brain and elsewhere to the heart, kidney, pancreas, and liver. Brown fat can oxidize fat so rapidly that heat is generated (“non-shivering thermogenesis”), and it is especially important in young animals and those recovering from hibernation.

In brief, during cold exposure, the release of noradrenaline and stimulation of β-adrenergic receptors in the nervous system initiates a catabolic program that commences with a rapid breakdown of cellular triacylglycerol stores and release of unesterified fatty acids and transient activation of a co-activator of peroxisome proliferator-activated receptor gamma (PPARγ). These set in motion a signaling process that results in the efficient **β-oxidation** of fatty acids to produce heat. The key molecule is believed to be the **uncoupling protein-1 (UCP1)**, which acts as a valve to uncouple electron transport in the respiratory chain from ATP production with a highly exothermic release of chemical energy, i.e., as heat rather than as ATP. Its actions are illustrated in Figure 21.2.18.

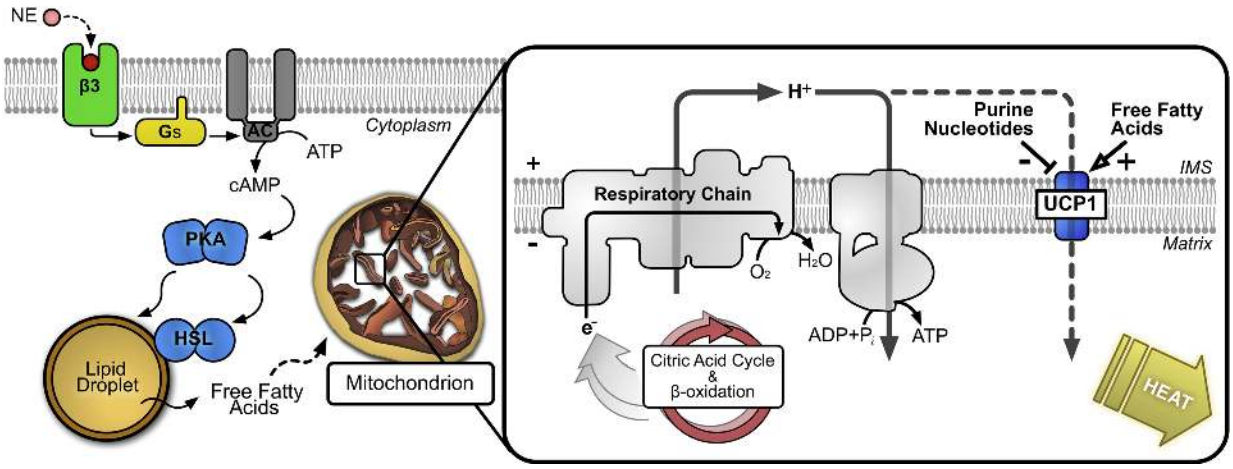


Figure 21.2.18: Role of UCP1 in generation of heat. https://commons.wikimedia.org/wiki/F...n_the_cell.jpg. Creative Commons Attribution-Share Alike 4.0 International

This is an example of a futile cycle that releases heat. Although many aspects of the mechanism are uncertain, it is clear that proton conductance by UCP1 is highly regulated and inducible. It is activated by free long-chain fatty acids and inhibited by purine nucleotides.

Fatty acids are the substrate for thermogenesis and act as self-regulating second messengers. The mitochondrial phospholipid **cardiolipin**, which is intimately involved in oxidative phosphorylation, is indispensable for stimulating and sustaining the function of thermogenic fat. Upon activation of brown adipose tissue, the dense vasculature increases the delivery of fatty acids and glucose to the brown adipocytes and warms the blood passing through the tissue.

Long-chain fatty acids bind to UCP1 and may be transported through the membrane along with a proton. Alternatively, it may just bind and activate the transport of a proton. Figure **21.2.19** shows an interactive iCn3D model of the AlphaFold predicted structure of human UCP1 (P25874).

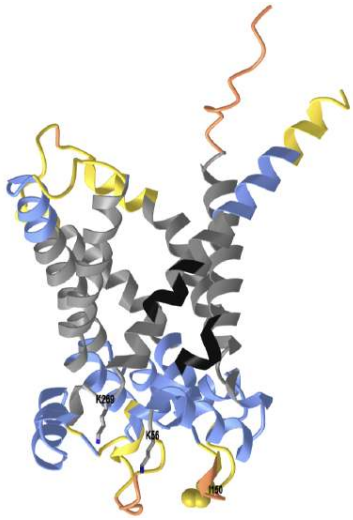


Figure **21.2.19**: AlphaFold predicted structure of human UCP1 (P25874). Click the image for a popup or use this external link: https://structure.ncbi.nlm.nih.gov/i...FkfrEqWE3D2dX6

Imagine a bilayer orienting perpendicularly to the gray helices representing the transmembrane helical segments that embed the protein into the inner mitochondrial membrane. The spacefill Ile150 denotes the matrix domain. Two key residues (K56, K29) involved in binding the carboxyl end of the fatty acids are shown on the matrix side of the protein, in CPK-colored sticks and labeled. The black faces of the helices in the inner membrane region show the most probable binding site for the acyl chain of the fatty acid. The lighter yellow/orange regions have greater predicted uncertainty in the AlphaFold computational model.

There is evidence that **acylcarnitines** produced in the liver from fatty acids released from white adipose tissue in response to cold exposure are transported in plasma to brown adipose tissue and can serve as a substrate for thermogenesis. Indeed, a wide array of circulating lipids, including free fatty acids and triacylglycerols, contribute to thermogenic potential.

The activities of acyl-CoA synthetases and acyl-CoA thioesterases determine the availability of substrates for β-oxidation and, consequently, the thermogenic capacity. Synthesis of the lipokine (or 'batokine') **octadecanoid** 12,13-dihydroxy-9*Z*-octadecenoic acid (12,13-diHOME), is induced by cold also, and this stimulates the activity of brown adipose tissue by promoting the uptake of fatty acids, acting via G-protein-coupled receptors. It increases cardiac function and cardiomyocyte respiration via enhanced calcium cycling. Similarly, there are suggestions that *n*-3 polyunsaturated fatty acids may promote adaptive thermogenesis, for example, through the activity of the 12-lipoxygenase metabolite and batokine 12-hydroxyeicosapentaenoic acid (12-HEPE) by improving glucose metabolism via increased glucose uptake into adipocytes and skeletal muscle. (**FAHFA**) are relevant in this context. Peroxisomal synthesis of **plasmenyl-phospholipids** is believed to regulate adipose tissue thermogenesis by mediating mitochondrial fission.

In hibernating mammals, brown adipose tissue is especially important metabolically, and even in laboratory animals such as mice, it can consume about 50% of dietary lipids and glucose when the animals are exposed to cold. Similarly, in humans, the activity of brown adipose tissue is induced acutely by cold. It is stimulated via the sympathetic nervous system, and the relevance of this tissue to human metabolism is now becoming apparent. For example, there are suggestions that brown adipose tissue can behave as an endocrine system to secrete endocrine factors ('batokines') that may be favorable in reducing cardiovascular risk. For obvious reasons, there are efforts to determine whether sustained activation of brown fat by pharmaceutical means could be beneficial for human disease states, including obesity, diabetes, and cardiovascular disease.

Such research has been stimulated by the observation that clusters of distinct adipocytes with thermogenic capacity and their storage function can be present in white adipose tissue and emerge in response to various physiological signals, especially reactive oxygen species. They are termed **beige** or brite adipocytes and arise from multipotent pre-adipocytes. Brown adipose tissue is a discrete organ in

animals, but beige adipose tissue is interspersed with white, and the two forms have different developmental origins. In adult humans, most deposits once thought to be classical brown adipose tissue do not contain the genetic markers for this tissue and are now recognized as beige/brite fat. However, brown adipose tissue *per se* is present in significant amounts in human newborns and infants. However, beige adipocytes utilize the same machinery to release heat by oxidizing fatty acids under β-adrenergic stimulation.

The uncoupler protein 1 (UCP1) appears to be expressed only in brown and beige fat cells and is a marker for those cells. It can be regulated transcriptionally and posttranscriptionally by ROS modification of a cysteine to produce a sulfenyl group. The more classical brown adipocyte arises developmentally from the skeletal muscle-like cell, whereas the beige appears to develop to some extent from vascular smooth muscle cells. The beige cells can differentiate into more white adipocytes or more brown ones by the factors described in Figure **21.2.20**.

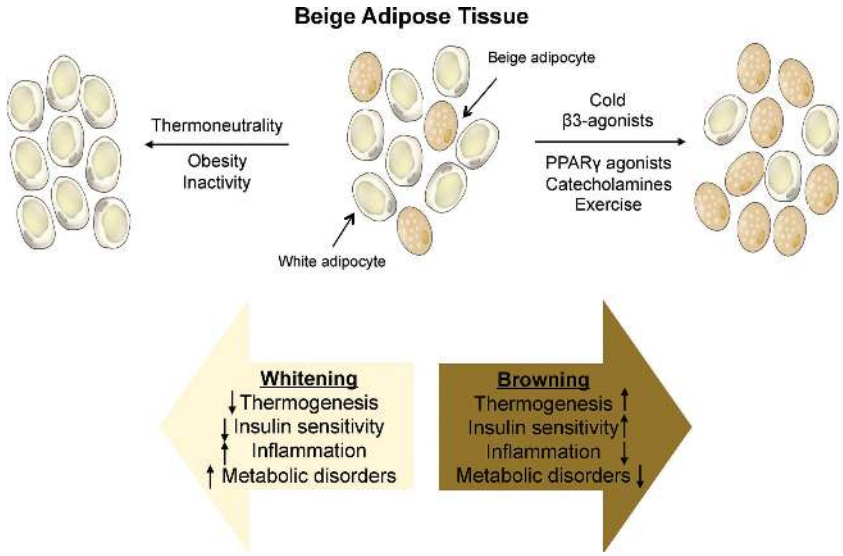


Figure (\PageIndex{20}\): Factors altering beige adipose tissue. Paul Cohen and Bruce M. Spiegelman. **Molecular Biology of the** Cell, 27, 2017. https://doi.org/10.1091/mbc.e15-10-0749. Attribution–Noncommercial–Share Alike 3.0 Unported Creative Commons License (http://creativecommons.org/licenses/by-nc-sa/3.0).

FAT CELL SIZE

In addition to the type of fat cell, the location and size of the adipocyte also affect health risks. Obesity, cardiovascular disease, type II diabetes, and nonalcoholic fatty liver disease all depend on and are correlated with fat cell dysfunction. The endocrine role of adipose tissue plays a key role in the development of dysfunction. The main depots of fat are the subcutaneous adipose tissue (SAT) and the visceral adipose tissue (VAT), the latter of which is associated with proinflammatory effects and greater health risks (type II diabetes, hypertension, metabolic syndrome, obesity, etc.). Figure (\PageIndex{21}\) below summarizes the health consequence as the size of the SAT and VAT adipocytes increases (in the direction of the red arrow).

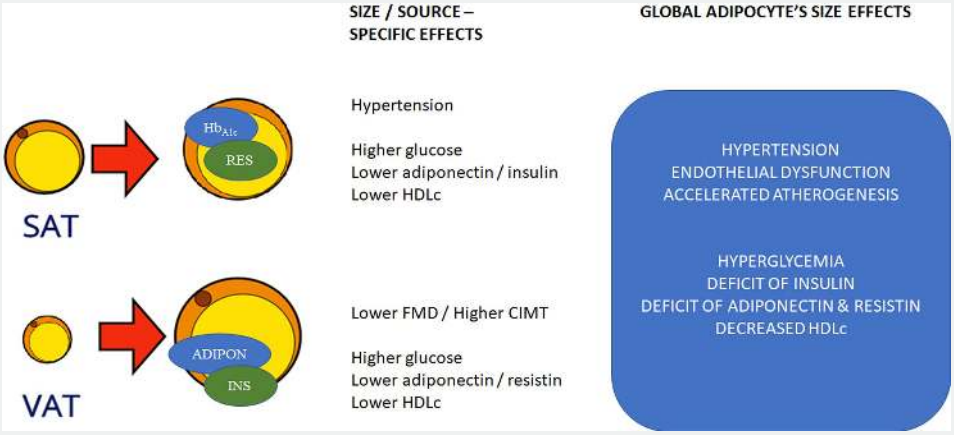


Figure (\PageIndex{2}\): Adipocyte characteristics and cardiovascular risk. The diagram describes a proposed model, based on the results of adipocyte size/source, potential interactions with metabolic mediators, and pathophysiological effects. SAT, subcutaneous adipose tissue; VAT, visceral adipose tissue; HbA1c, glycated hemoglobin (a marker of elevated blood sugar associated with diabetes); RES, resistin; ADIPON, adiponectin; INS, insulin; HDLc; high-density lipoprotein cholesterol; FMD, flow-mediated dilation; CIMT, carotid intima media thickness. Suárez-Cuenca et al. *Sci Rep* **11**, 1831 (2021). https://doi.org/10.1038/s41598-021-81289-2. Creative Commons Attribution 4.0 International License. http://creativecommons.org/licenses/by/4.0/.

It appears that the larger the adipocyte, the greater the inflammatory response. This condition is called adipocyte hypertrophy, and it may be more important than obesity per se as a risk factor for inflammation, as indicated by inflammatory cytokine levels and macrophage infiltration into adipose tissue. When released under normal conditions, the adipose-derived hormone leptin leads to appetite suppression and decreases liver and muscle fat. Higher fat storage is associated with increased blood leptin levels. It also correlates with greater lymphocyte size.

In contrast, the adipose hormone adiponectin leads to positive health consequences, including increased sensitivity to insulin, decreased inflammation, and the formation of adipocytes from stem cells (adipogenesis). The larger the fat cell, the lower the serum levels of adiponectin. However, the link between fat cell size and adiponectin levels may be determined more by obesity.

21.2.6: OTHER FUNCTIONS OF TRIACYLGLYCEROL DEPOTS

Subcutaneous depots act as a cushion around joints and serve as insulation against the cold in many terrestrial animals, as is obvious in the pig, which is surrounded by a layer of fat. It is especially true for marine mammals such as seals. Those adipocytes embedded in the skin differ from the general subcutaneous depots and support the growth of hair follicles and regenerating skin. They may also have a defensive role, both as a physical barrier and by responding metabolically to bacterial infection.

In marine mammals and fish, the fat depots are less dense than water and aid buoyancy. Hence, less energy is expended in swimming. More surprisingly, triacylglycerols, together with the structurally related glyceryl ether diesters and wax esters, are the main components of the sonar lens used in echolocation by dolphins and toothed whales. The triacylglycerols are distinctive in containing two molecules of 3-methylbutyric (isovaleric) acid with one long-chain fatty acid. It appears that the relative concentrations of the various lipids in an organ in the head of the animals (termed the ‘melon’) are arranged anatomically in a three-dimensional topographical pattern to enable them to focus sound waves.

In cold climates, many insects do not feed over winter and must manage their energy stores to meet the energetic demands of development and reproduction in the spring. Some insect species that are tolerant of freezing produce triacylglycerols containing acetic acid, which remain liquid at low temperatures; interacting with water may play a role in cryoprotection.

21.2.7: TRIACYLGLYCEROL METABOLISM IN PLANTS AND YEASTS

Fruit and seed oils are major agricultural products with appreciable economic and nutritional value to humans. The mesocarp of fruits is a highly nutritious energy source that attracts animals that help to disperse the seeds, and in plants such as the oil palm and olive trees, a high proportion of the fruit flesh contains triacylglycerols. Similarly, triacylglycerols are the main storage lipids in seeds and can comprise as much as 60% of their weight. Fruit lipids are not intended for use by the plant *per se* and are stored in lipid droplets in large, irregular structures that break down readily. Still, seed lipids are required to develop the plant embryo, so their metabolism is particularly important. However, triacylglycerol biosynthesis and metabolism are also required for pollen viability and to maintain lipid homeostasis in chloroplasts (see the note on plastoglobules below).

Seed oils: In seeds and other plant tissues, biosynthesis of fatty acids takes place in plastids, and these are stored in the form of triacylglycerols in lipid droplets with a coherent surface layer of proteins and lipids in the embryo (e.g., Arabidopsis, soybean, or sunflower) or endosperm (e.g., castor bean) tissues of seeds. In addition to the common range of fatty acids synthesized in plastids, mainly palmitate and oleate, some plant species produce novel fatty acids, including medium- and very-long-chain components and those with oxygenated and other functional moieties. A specific means of diverting these to seeds for triacylglycerol production exists to prevent disruption of the plant membranes. Seed development occurs in three stages: rapid cell division with no accumulation of storage material, rapid deposition of triacylglycerols and other energy-rich metabolites, and finally, desiccation.

During the period of oil accumulation in seeds, the newly formed ACP esters of fatty acids are first hydrolyzed by two different classes of acyl-ACP thioesterases at the inner plastid envelope membrane, before the unesterified fatty acids are transported to the endoplasmic reticulum (ER), by a family of fatty acid export proteins (FAX) of which there are seven isoforms in Arabidopsis, two of which (FAX2 and FAX4) are highly expressed during the early stage of seed development. The unesterified fatty acids are shuttled across the plastid outer envelope, probably by vectorial acylation by long-chain acyl-CoA synthases, which catalyze the formation of CoA esters.

In the ER, triacylglycerols and membrane lipids are synthesized by the Kennedy and other pathways described above. In yeast and plants, 1,2-diacyl-*sn*-glycerol esterification is the only committed step in triacylglycerol production, and this occurs by mechanisms that can be

both dependent and independent of acyl-CoA esters. The acyl-CoA-dependent route is catalyzed by diacylglycerol:acyl-CoA acyltransferases (DGATs) with acyl-CoA and diacylglycerols as substrates, and two membrane-bound isoenzymes (DGAT1 and DGAT2) and a cytosolic isoenzyme (DGAT3) are known. DGAT1 is a key enzyme involved in triacylglycerol formation in developing seeds. At the same time, DGAT2 is especially important in those plant species with unusual fatty acid compositions. In Arabidopsis, DGAT3 has some specificity for polyunsaturated fatty acids in seed development. Figure **21.2.22** summarizes TAG synthesis in plant ER.

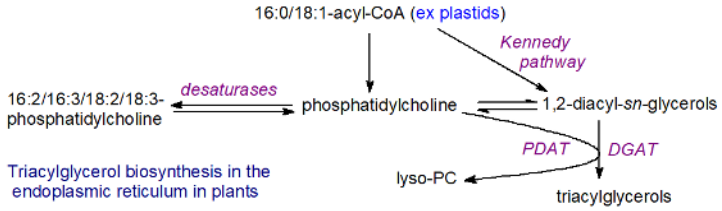


Figure **21.2.22**: TAG biosynthesis in plant ER

In addition, a substantial proportion of triacylglycerol biosynthesis in some plant species is synthesized by flux through the membrane phospholipid **phosphatidylcholine**, produced by what are sometimes termed inaccurately the 'eukaryotic and prokaryotic pathways' with differing positional distributions, in which diacylglycerols are generated from phosphatidic acid by the action of a phosphatidate phosphatase as an intermediate. In the acyl-CoA-independent reaction, the direct transfer of one fatty acid from phosphatidylcholine to diacylglycerol by the action of the phospholipid:1,2-diacyl-*sn*-glycerol-acyltransferase (PDAT) enzyme also occurs, with the formation of lysophosphatidylcholine as a byproduct, which can be re-esterified for further reaction. As phosphatidylcholine undergoes extensive remodeling and its fatty acid components are subject to modification, for example, by desaturation to form linoleic and linolenic acids, the compositions and especially the positional distributions of triacylglycerols produced in this way can be very different from those synthesized by the 'classical' pathways. Phosphatidylcholine may also function as a carrier for the trafficking of acyl groups between organelles and membrane subdomains, and it has been suggested that an assembly of interacting enzymes may facilitate the transfer of polyunsaturated fatty acids from this phospholipid to triacylglycerols in seeds. Both sterol and sphingolipid biosynthesis are important factors for efficient seed oil production.

As triacylglycerol synthesis continues, oil droplets accumulate between the leaflets of the endoplasmic reticulum. They are surrounded by a monolayer of phospholipids, sterols, and proteins, which in Arabidopsis include oleosins, a caleosin, a steroleosin, a putative aquaporin, and a glycosylphosphatidylinositol-anchored protein. Oleosins are the most abundant of these (~65%). They are small proteins (15-30 kDa) that contain cytosolic-facing N- and C-termini and a large hydrophobic domain necessary to target them to lipid droplets, where they are important for the control of their size and stability. Eventually, lipid droplets "bud off" from the endoplasmic reticulum with their monolayer of phospholipids and proteins, and they are released into the cytosol by a yet-to-be-defined mechanism.

Water is absorbed at the onset of germination, and esterases/lipases are activated. Lipolysis begins at the surface of oil bodies, where the oleosins, the most abundant structural proteins, are believed to assist in the docking of lipases and control the size and stability of lipid droplets in seeds. Several esterases/lipases have been cloned from various plant species and possess a conserved catalytic triad of Ser, His, and Asp or Glu, somewhat different from the animal lipases, as in patatin (an especially abundant lipolytic protein in potatoes), which can hydrolyze triacylglycerols but not phospho- or galactolipids. The most important of these is believed to be the 'sugar-dependent lipase 1 (SDP1)', which is a patatin-like lipase similar in function to the mammalian adipose triacylglycerol lipase discussed above and is located on the surface of the oil body. This is active mainly against triacylglycerols to generate diacylglycerols but presumably works in conjunction with di- and monoacylglycerol lipases to generate free fatty acids and glycerol.

Seed lipid droplets exist near glyoxysomes (broadly equivalent to peroxisomes). These are the membrane-bound organelles that contain most of the enzymes required to oxidize fatty acids derived from the triacylglycerols via acetyl-CoA to four-carbon compounds, such as succinate, which are then converted to soluble sugars to provide germinating seeds with energy to fuel the growth of the seedlings and to produce shoots and leaves. In addition, they supply structural elements before the seedlings develop the capacity to photosynthesize. How lipolysis products are transported to the glyoxysomes for further metabolism remains to be determined. Still, a specific 'ABC' transporter is required to import fatty acids into the glyoxysomes in Arabidopsis. The free acids are converted to their coenzyme A esters by two long-chain acyl-CoA synthetases located on the inner face of the peroxisome membrane before entry into the β-oxidation pathway. All these processes are controlled by an intricate regulatory network, involving transcription factors that crosstalk with signaling events from the seed maturation phase through to embryo development. After about two days of germination, the glyoxysomes begin to break down, but β-oxidation can continue in peroxisomes in leaf tissue.

Lipid droplets - plastoglobules: Triacylglycerol-rich lipid droplets (LD) have been observed in most cell types in vegetative tissues of plants as well as in seeds, and although their origin and function are poorly understood, they contain all the enzymes required for triacylglycerol metabolism together with phospholipases, lipoxygenases, and other oxidative enzymes. Instead of oleosins, these lipid

droplets in plants and algae contain a family of ubiquitously expressed 'LD-associated proteins' on the surface, together with a monolayer of phospholipids (mainly phosphatidylcholine), galactolipids such as sulfoquinovosyldiacylglycerol, and in some species, betaine lipids. As in yeast and humans, seipins (three in Arabidopsis) are necessary for normal LD biogenesis. Again, LDs form within the bilayer of the endoplasmic reticulum and pinch off into the cytoplasm. Abiotic stresses can induce the remodeling of lipid membranes through lipase action with the formation of toxic lipid intermediates. These can be sequestered in lipid droplets to inhibit membrane damage and potentially prevent cell death. While they are believed to be involved mainly in stress responses, lipid droplets may have other specialized roles, for example, in anther and pollen development, where triacylglycerols serve as a source of fatty acids for membrane biosynthesis. Fatty acids derived from triacylglycerols in lipid droplets are believed to be subjected to peroxisomal β-oxidation to produce the ATP required for stomatal opening and many other purposes.

In addition, lipid droplets that have been termed 'plastoglobules' are produced by a localized accumulation of triacylglycerols and other neutral lipids between the membrane leaflets of the thylakoid cisternae and then pinch off into the stroma, where they are involved in a wide range of biological functions from biogenesis to senescence via the recruitment of specific proteins. During senescence, for example, lipid droplets accumulate rapidly in the leaves of *A. thaliana*. It may have a more direct function in reproductive tissues by recruiting and transporting proteins for organ formation and successful pollination. Antifungal compounds such as **2-hydroxy-octadecatrienoic acid** and other oxylipins are produced from α-linolenic acid in these organelles, and it has been suggested that the latter function as intracellular factories to produce stable metabolites via unstable intermediates by concentrating the enzymes and hydrophobic substrates efficiently. Plastoglobules are also implicated in the biosynthesis and metabolism of vitamins E and K.

Microalgae: Triacylglycerol metabolism in lipid droplets in microalgae is under intensive study because of their potential for nutraceutical and biodiesel production. Similar processes seem to occur in higher plants, but with a simpler genome encoding few redundant proteins. In the unicellular green model microalga *Chlamydomonas reinhardtii*, key lipid droplet proteins, lipases, and enzymes of β-oxidation have been characterized.

Yeasts: Lipid droplets in yeast are a highly dynamic and functionally diverse hub that ensures stress resistance and cell survival by promoting membrane and organelle homeostasis. As most of the important biosynthetic and catabolic enzymes involved in triacylglycerol metabolism are conserved between yeasts and mammals, the former are useful models for studying triacylglycerol production. The size and triacylglycerol content of lipid droplets in yeasts change appreciably in different stages of growth and development, and *Saccharomyces cerevisiae* contains a single phosphatidic acid phosphatase (Pah1), which has an essential role in this process. During vegetative growth, Pah1 in the cytosol is phosphorylated by multiple protein kinases, enabling the synthesis of phospholipids rather than triacylglycerols. As cells progress into stasis, the Pah1 is dephosphorylated and translocates to the endoplasmic reticulum, leading to triacylglycerol synthesis for storage in lipid droplets. Some fatty acids derived from phospholipids are utilized for triacylglycerol biosynthesis at the inner nuclear membrane, which is important for nuclear integrity.

21.2.8: TRIACYLGLYCEROL METABOLISM IN PROKARYOTES

An awareness of the role of this lipid class in the pathogenesis of *Mycobacterium tuberculosis* and the relationship with antibiotic biosynthesis by *Streptomyces coelicolor has stimulated the study of the biosynthesis of triacylglycerols in bacteria*. For example, triacylglycerols are believed to be an energy reserve for the long-term survival of *M. tuberculosis* during the persistence phase of infection and a means by which unesterified fatty acids are detoxified. Increasing numbers of bacterial species, for example, from the genera *Mycobacterium*, *Nocardia*, *Rhodococcus*, *Micromonospora*, *Dietzia*, and *Gordonia*, are now known to produce triacylglycerols (sometimes wax esters), and these can be stored in lipid droplets in the organisms. The first three steps in triacylglycerol biosynthesis are catalyzed by GPAT, LPAT, and PAP enzymes comparable to those in other organisms. However, it has become apparent that the DGAT can be a dual-function CoA-dependent acyltransferase known as wax ester synthase/diacylglycerol acyltransferase, which accepts a broad diversity of acyl-CoA substrates for esterification of diacylglycerols or long-chain fatty alcohols for the synthesis of triacylglycerols or wax esters, respectively, depending on which intermediates are present in the organisms. Bacteria that lack such an enzyme are unable to produce these non-polar lipids.

21.2.9: SUMMARY

This chapter provides an in-depth exploration of triacylglycerol (TAG) metabolism, highlighting the biochemical pathways by which organisms synthesize, store, and mobilize these essential lipids. TAGs are not only a vital energy reserve and a source of fatty acids for membrane synthesis and signaling but also serve protective roles by sequestering potentially harmful lipids. The chapter spans multiple systems—including animal, plant, yeast, and prokaryotic pathways—underscoring both conserved mechanisms and tissue-specific adaptations.

Biosynthesis of Triacylglycerols:

The primary pathway for TAG formation in many eukaryotes is the Kennedy pathway, which begins with the generation of a glycerol

backbone (sn-glycerol-3-phosphate) either from glycolysis or via glyceroneogenesis. Sequential acylation steps—catalyzed by glycerol-3-phosphate acyltransferase (GPAT), acylglycerophosphate acyltransferase (AGPAT), and phosphatidic acid phosphohydrolases (PAPs, including the lipin family)—convert glycerol-3-phosphate into diacylglycerol. Finally, diacylglycerol acyltransferases (DGATs) catalyze the formation of TAGs. The chapter also outlines alternate pathways, such as the monoacylglycerol pathway in enterocytes and a diacylglycerol transacylase route observed in seeds.

Structural and Regulatory Aspects:
Lipid droplets, once thought to be inert fat deposits, are now recognized as dynamic organelles surrounded by a phospholipid monolayer embedded with specific proteins (e.g., perilipins in adipocytes, oleosins in seeds). These droplets coordinate TAG storage and mobilization, ensuring that excess lipids do not induce lipotoxicity. Key regulatory proteins, including seipin, facilitate lipid droplet biogenesis by organizing TAG accumulation within the endoplasmic reticulum, while lipases (such as ATGL, hormone-sensitive lipase, and monoacylglycerol lipase) mediate the controlled hydrolysis (lipolysis) of TAGs to release free fatty acids and glycerol for energy production or biosynthesis.

Tissue-Specific Pathways and Endocrine Functions:
The synthesis and catabolism of TAGs are finely tuned in various tissues. In the intestines, TAGs are resynthesized from dietary monoacylglycerols and packaged into chylomicrons for transport via the lymphatic system. In the liver, TAGs are incorporated into VLDL particles and exported to peripheral tissues, while in the mammary gland, TAGs are secreted as milk fat globules. Adipose tissue serves not only as an energy store but also as an endocrine organ, releasing hormones such as leptin and adiponectin that regulate appetite, insulin sensitivity, and systemic lipid metabolism.

Additional Roles in Plants, Yeasts, and Prokaryotes:
In plants, TAGs accumulate in seeds and fruit, serving as key energy reserves and precursors for membrane lipids during germination. Lipid droplets in plants, including plastoglobules in chloroplasts, also play roles in stress responses and the storage of hydrophobic vitamins. Yeasts exhibit dynamic changes in lipid droplet size and composition during different growth phases, offering a model for studying TAG metabolism. Similarly, certain prokaryotes, including Mycobacterium species, store TAGs as energy reserves and to detoxify excess fatty acids.

Integration with Metabolic Health and Disease:
The chapter emphasizes the physiological importance of maintaining balanced TAG metabolism. While essential for normal energy homeostasis, dysregulation of TAG synthesis and breakdown is linked to obesity, insulin resistance, fatty liver disease, and cardiovascular disorders. Additionally, the interplay between TAG storage, lipolysis, and signaling underscores the complex endocrine functions of adipose tissue and its impact on systemic metabolism.

In summary, this chapter integrates the biochemical pathways, structural organization, regulatory mechanisms, and physiological roles of triacylglycerol metabolism. It highlights how TAG synthesis and storage serve critical functions in energy management and cellular protection, while also linking disturbances in these processes to a range of metabolic diseases.

This page titled 21.2: Biosynthesis of Triacylglycerols is shared under a not declared license and was authored, remixed, and/or curated by Henry Jakubowski and Patricia Flatt.

- **Current page** by Henry Jakubowski and Patricia Flatt has no license indicated.
- **11.2: Diffusion Across a Membrane - Passive and Facilitated Diffusion** by Henry Jakubowski and Patricia Flatt has no license indicated.

21.3: BIOSYNTHESIS OF MEMBRANE GLYCEROLIPIDS

by William (Bill) W. Christie and Henry Jakubowski.

This section is an abbreviated and modified version of material from the Lipid Web, an introduction to the chemistry and biochemistry of individual lipid classes, written by William Christie.

LEARNING GOALS (CHATGPT O3-MINI)

1. **Describe the Structure and Function of Phosphatidic Acid:**
   - Explain the basic structure of phosphatidic acid (1,2-diacyl-sn-glycero-3-phosphate) and its dual role as a biosynthetic precursor for complex lipids (e.g., glycerophospholipids and triacylglycerols) and as a signaling molecule.
   - Discuss how its acidic, anionic properties influence membrane structure and protein interactions.
2. **Outline Biosynthetic Pathways for Phosphatidic Acid:**
   - Illustrate the glycerol-3-phosphate pathway for phosphatidic acid formation via sequential acylation reactions catalyzed by GPAT and LPAT enzymes.
   - Compare alternative routes (e.g., the dihydroxyacetone phosphate pathway and phospholipase D-mediated hydrolysis) that contribute to phosphatidic acid production.
3. **Explain the Role of Phosphatidic Acid in Lipid Biosynthesis and Signaling:**
   - Discuss how phosphatidic acid serves as a precursor for the synthesis of complex glycerolipids, including its conversion into diacylglycerol and subsequent products.
   - Analyze its role as a lipid mediator in regulating processes such as membrane curvature, vesicular trafficking, and protein recruitment (e.g., via binding to regulatory proteins like Opi1).
4. **Detail the Biosynthesis and Remodeling of Phosphatidylcholine (PC):**
   - Describe the CDP-choline pathway (Kennedy pathway) for de novo phosphatidylcholine synthesis, including the role of choline kinase and CTP:phosphocholine cytidylyltransferase.
   - Explain how the Lands cycle (deacylation–reacylation) remodels PC molecular species and alters fatty acid composition post-synthesis.
5. **Outline the Biosynthesis and Functions of Phosphatidylethanolamine (PE):**
   - Compare the two major pathways for PE synthesis: the CDP-ethanolamine pathway and the phosphatidylserine decarboxylase pathway.
   - Evaluate the physical and functional roles of PE in membranes, such as its effect on curvature, fusion, and mitochondrial function.
6. **Discuss the Biosynthesis and Biological Roles of Phosphatidylserine (PS):**
   - Explain how PS is synthesized in animal cells via calcium-dependent base-exchange reactions and its subsequent decarboxylation in mitochondria.
   - Analyze the functions of PS in cell signaling (e.g., as an “eat-me” signal during apoptosis), blood coagulation, and as a cofactor for protein activation.
7. **Examine the Biosynthesis and Signaling Functions of Phosphatidylinositol (PI) and Its Phosphorylated Derivatives:**
   - Outline the conversion of phosphatidic acid to PI via CDP-diacylglycerol and myo-inositol, and describe the structural features of PI.
   - Discuss the generation of polyphosphoinositides (e.g., PI(4)P, PI(4,5)P_2, PI(3)P, and PI(3,4,5)P_3) by specific kinases and phosphatases, and their roles in defining membrane identity and regulating intracellular signaling and trafficking.
8. **Understand the Concept of the Phosphatidylinositol Cycle:**
   - Describe the coordinated sequence of phosphorylation and dephosphorylation reactions that recycle PI and its derivatives between the endoplasmic reticulum and plasma membrane.
   - Evaluate the energy requirements and regulatory significance of this cycle in maintaining signaling dynamics.
9. **Identify Key Lipid-Binding Domains and Their Roles in Membrane Targeting:**
   - Recognize domains such as PH, PX, FYVE, and C2, and explain how they mediate specific interactions with phosphoinositides.
   - Discuss how these interactions influence the localization and activity of signaling proteins.
10. **Compare and Contrast Phospholipid Metabolism in Animals Versus Plants and Microorganisms:**

10. **Compare and Contrast Phospholipid Metabolism in Animals versus Plants and Microorganisms:**
    - Summarize the similarities and differences in the biosynthetic pathways for glycerophospholipids (e.g., differences in acyltransferase isoforms, compartmentalization, and remodeling processes).
    - Explain how these differences impact membrane composition, signaling, and cellular responses to stress in various organisms.
11. **Discuss the Role of Lysophospholipids (e.g., Lysophosphatidic Acid and Lysophosphatidylcholine):**
    - Describe how lysophospholipids are generated by phospholipase A enzymes and their conversion back to diacyl forms via acyltransferases.
    - Evaluate their functions as potent signaling molecules, including growth factor-like activities and roles in inflammation and cell migration.
12. **Integrate the Impact of Phospholipid Remodeling on Cellular Function:**
    - Explain how deacylation–reacylation cycles (Lands cycle) regulate the molecular species composition of major phospholipids.
    - Analyze how remodeling processes contribute to membrane fluidity, protein–lipid interactions, and the production of lipid-derived signaling molecules.

These goals provide a framework for students to master the complexities of glycerophospholipid synthesis, remodeling, and signaling, while connecting these processes to broader cellular functions and pathophysiological conditions.

21.3.1: INTRODUCTION

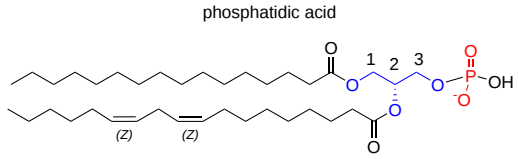
This section will explore the synthesis of membrane glycerophospholipids and their metabolic derivatives. We will start with the simplest one, phosphatidic acids, and end with phosphatidylinositol. To shorten the online text, details about the properties of each lipid are hidden but available for interested readers in boxes with links.

21.3.2: PHOSPHATIDIC ACIDS AND DERIVATIVES

Phosphatidic acid or 1,2-diacyl-*sn*-glycero-3-phosphate is a key intermediate in the biosynthesis of other glycerophospholipids and triacylglycerols. It is structurally one of the simplest of the phospholipids and was long thought to be important only as a precursor of other lipids, where it is indeed a key molecule. Still, it is now known to have many other functions in animals, plants, and other organisms by its influence on membrane structure and dynamics, and by its interactions with various proteins. As a lipid mediator, it modulates various signaling and cellular processes, such as membrane tethering, conformational changes, and enzymatic activities of specific proteins, and vesicular trafficking. Moreover, its metabolite **lysophosphatidic acid** is recognized as a key signaling molecule with many biological effects mediated through specific receptors.

21.3.2.1: PHOSPHATIDIC ACID – OCCURRENCE AND BIOSYNTHESIS

Phosphatidic acid is not an abundant lipid constituent of any living organism, seldom greater than picomolar concentrations in cells. Still, it is extremely important as an intermediate in the biosynthesis of other glycerophospholipids and triacylglycerols and as a signaling molecule or a precursor of signaling molecules. Indeed, it is often overestimated in tissues as it can arise by inadvertent enzymatic hydrolysis during inappropriate storage or extraction conditions during analysis. It is the simplest diacyl-glycerophospholipid, and the only one with a phosphomonoester as the head group. The molecule is acidic and carries a negative charge, i.e., it is an anionic lipid. The structure of phosphatidic acid is shown in Figure **21.3.1**.



1-hexadecanoyl,2-(9Z,12Z)-octadecadienoyl-sn-glycero-3-phosphate

Figure **21.3.1**: Phosphatidic acid

At least four important biosynthetic pathways for phosphatidic acid biosynthesis are found in different organelles under various stimuli. The main pathway involves the sequential acylation of *sn*-glycerol-3-phosphate, derived from the catabolism of glucose, by acyl-CoA derivatives of fatty acids. First, one acyltransferase catalyzes the acylation of position *sn*-1 to form lysophosphatidic acid (1-acyl-*sn*-glycerol-3-phosphate), and then a second specific acyltransferase catalyzes the acylation of position *sn*-2 to yield phosphatidic acid. The synthesis of phosphatidic acid from glycerol-3-phosphate is shown in Figure **21.3.2**.

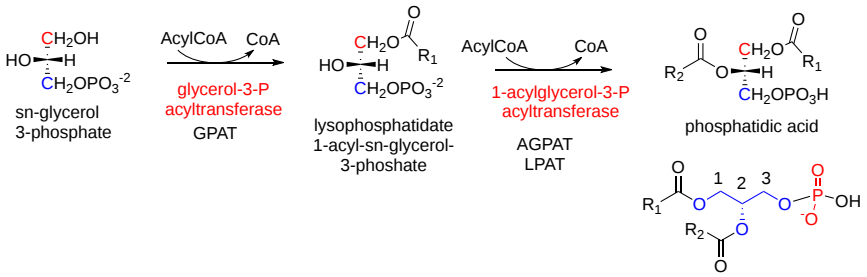


Figure **21.3.2**: Synthesis of phosphatidic acid from glycerol-3-phosphate

In **mammals**, the glycerol-3-phosphate acyltransferase that catalyses the first step exists in four isoforms, two in the mitochondrial outer membrane (designated GPAT1 and 2) and two in the endoplasmic reticulum (GPAT3 and 4); all are membrane-bound enzymes, which are believed to span the membranes. GPAT1 is highly expressed in the liver and adipose tissue, where it is responsive to changes in feeding status via the sterol regulatory element binding protein-1 (SREBP-1), a master transcriptional regulator of lipogenic enzymes. It is essential in directing fatty acyl-CoA esters toward glycerolipid synthesis instead of β-oxidation. GPAT3 is especially important for triacylglycerol storage in adipocytes, while GPAT4 is the main contributor to lysophosphatidic acid synthesis in the liver and brown adipose tissue.

For the second step in phosphatidic acid biosynthesis, five mammalian acyl-CoA:lysophosphatidic acid acyltransferases are known, of which three are in the endoplasmic reticulum (LPAAT or LPAT or AGPAT1, 2 and 3), with a further two (LPAT4 and 5) on the outer mitochondrial membrane. While LPAT1 and 2 have strict specificity for lysophosphatidic acid as acyl acceptor, other isoforms can esterify other lysophospholipids. Human LPAT1 showed higher activity with 14:0-, 16:0-, and 18:2-CoAs, while LPAT2 prefers 20:4-CoA and LPAT3 produces phosphatidic acid containing docosahexaenoic acid (22:6(*n*-3)); the last is especially important in the retina and testes. LPAT4 and 5 prefer oleoyl-CoA and polyunsaturated acyl-CoAs as the acyl donor, suggesting a dual role in glycerolipid synthesis and remodeling. The activity in the endoplasmic reticulum predominates in adipose tissue, but the mitochondrial forms are believed to be responsible for half the activity in the liver. However, as there is a traffic of phosphatidic acid between the mitochondria and endoplasmic reticulum for remodeling or synthesis of other lipids, the relative contributions of the two can be difficult to assess.

In **plants**, the *sn*-glycerol-3-phosphate pathway exists both in plastids and at the endoplasmic reticulum with multiple isoforms of the two acyltransferases and differences in the acyl substrates. In brief, most plant lipid biosynthesis begins with fatty acid biosynthesis in the chloroplasts. In plastids, the acyltransferase ATS1 transfers 18:1 acyl groups from acyl-acyl carrier protein (acyl-ACP) to position *sn*-1 of glycerol 3-phosphate before ATS2 transfers a palmitoyl group from ACP to position *sn*-2, producing phosphatidic acid at the inner leaflet of the chloroplast inner envelope membrane (IEM). Fatty acids intended for the endoplasmic reticulum are released from ACP in the chloroplast stroma by IEM-associated thioesterases, exported, and then activated by acyl-CoA synthetases of the outer envelope membrane to produce species with C18 fatty acids in both positions. Thus, acyl-CoAs are used for phosphatidic acid biosynthesis in the endoplasmic reticulum with marked differences in the specificity of the acyl substrates. Subsequently, phosphatidic acid in the plastids is utilized for the biosynthesis of galactosyldiacylglycerols, while that in the endoplasmic reticulum is used to synthesize triacylglycerols and phospholipids.

In **bacteria**, two families of enzymes are responsible for the acylation of position *sn*-1 of glycerol-3-phosphate. For example, one in *Escherichia coli* utilizes the acyl-acyl carrier protein (acyl-ACP) products of fatty acid synthesis as acyl donors and acyl-CoA derived from exogenous fatty acids. In a second wider group of bacteria, including cyanobacteria, there are enzymes (PlsX and PlsY) that use the unique acyl donors, **acyl-phosphates** derived partly from acyl-ACP, to acylate position *sn*-1. Acylation of position *sn*-2 in this instance is performed by a further family of enzymes (PlsC) that uses acyl-ACP as the acyl donor. However, some bacterial species may also use acyl-CoA.

In animals, a second biosynthetic pathway utilizes dihydroxyacetone phosphate (DHAP) as the primary precursor for the peroxisomal enzyme DHAP acyltransferase, which produces acyl-DHAP. This intermediate is converted to lysophosphatidic acid in an NADPH-dependent reaction catalyzed by acyl-DHAP reductase, and this is, in turn, acylated to form phosphatidic acid by the same LPAT as in the previous mechanism. This pathway is of particular importance in the biosynthesis of **ether lipids**. The synthesis of phosphatidic acid from dihydroxyacetone phosphate is shown in Figure **21.3.3**.

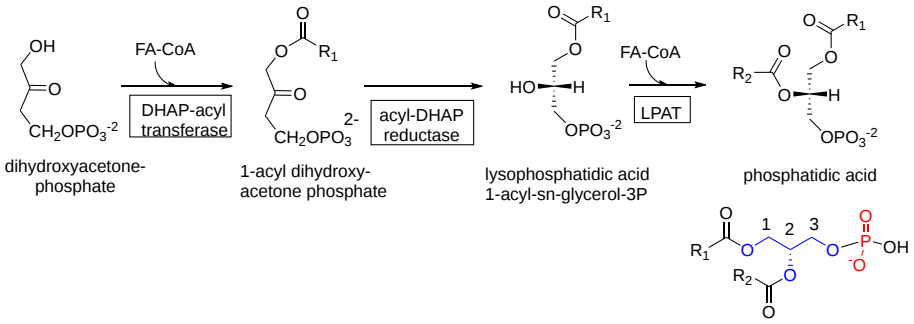


Figure **21.3.3**:Synthesis of phosphatidic acid from dihydroacetone phosphate

A third important route to phosphatidic acid is hydrolysis of other phospholipids, especially phosphatidylcholine, by the enzyme phospholipase D (or by a family or related enzymes of this kind). The enzyme is readily available for study in plants, where the special functions of phosphatidic acid have long been known. It is now recognized that phospholipase D is present in bacteria, yeasts, and most animal cells. In the last, it exists in two main isoforms with differing specificities and cellular locations; PLD1 is found mainly in the Golgi-lysosome continuum, while PLD2 is present mainly in the plasma membrane. They are phosphoproteins, the activity of which is regulated by kinases and phosphatases and by binding to phosphatidylinositol-4,5-bisphosphate. In mitochondria, a distinctive enzyme of this type utilizes cardiolipin as substrate. The mechanism involves using water as the nucleophile to catalyse the hydrolysis of phosphodiester bonds in phospholipids. Phospholipase D activity is dependent on and regulated by neurotransmitters, hormones, small monomeric GTPases, and lipids. The hydrolysis of phosphatidylcholine to phosphatidic acids by phospholipase D is shown in Figure **21.3.4**.

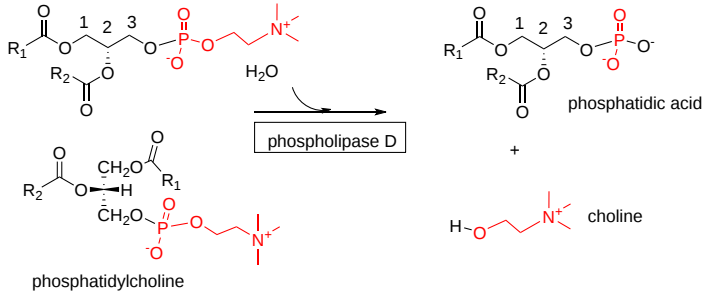


Figure **21.3.4**: Hydrolysis of phosphatidylcholine to phosphatidic acids by phospholipase D

In addition to its function in generating phosphatidic acid mainly for signaling purposes but also for the maintenance of membrane composition, phospholipase D is involved in intracellular protein trafficking, cytoskeletal dynamics, cell migration, and cell proliferation, partly through protein-protein interactions; it is considered to be important in inflammation and cancer growth and metastasis as a downstream transcriptional target of proteins involved in the pathophysiology of these diseases. It also has an unusual activity as a guanine nucleotide exchange factor. A transphosphatidylation reaction with ethanol generates **phosphatidylethanol**, a useful biomarker for human ethanol consumption.

Under some conditions, phosphatidic acid can be generated from 1,2-diacyl-*sn*-glycerols by **diacylglycerol kinases**, for example, those produced from other phospholipids by the action of phospholipase C. Such enzymes appear ubiquitous, although bacteria and yeast are structurally different from the mammalian enzymes. Diacylglycerol kinases, of which at least ten isoforms (DGKα to DGKκ) exist with different sub-cellular locations and functions in animals, use ATP as the phosphate donor. While the epsilon isoform (DGKε) utilizes the 1-stearoyl-2-arachidonoyl species of diacyl-*sn*-glycerols preferentially to produce phosphatidic acid for the biosynthesis of **phosphatidylinositol**, other isoenzymes phosphorylate diverse diacylglycerol species. Aside from producing phosphatidic acid for phospholipid production or signaling, these enzymes may attenuate the signaling effects of diacylglycerols. For example, diacylglycerol kinases can contribute to cellular asymmetry and control the polarity of cells by regulating the gradients in diacylglycerol and phosphatidic acid concentrations. Figure **21.3.5** shows the synthesis of phosphatidic acid via diacylglycerols and the reverse reaction.

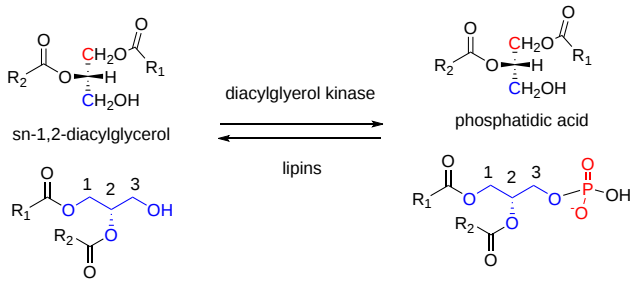


Figure **21.3.5**: Synthesis of phosphatidic acid via diacylglycerols and the reverse reaction

The reverse reaction, hydrolysis, is catalyzed by lipins. These enzymes are important in regulating the local concentrations of phosphatidic acid and, hence, its biological activity.

A further possible route to phosphatidic acid production for signaling is via acylation of lysophosphatidic acid, which can be produced independently for signaling purposes, as discussed below. This pathway may be especially relevant in membranes, where the protein endophilin has LPAT activity and is believed to generate phosphatidic acid from lysophosphatidic acid to alter the curvature of the membrane bilayer.

21.3.2.2: PHOSPHATIDIC ACID - ROLE AS A LIPID PRECURSOR

In summary, phosphatidic acid generated via 1-acyl-*sn*-glycerol-3-phosphate is the primary precursor of other glycerolipids, although other pathways may be more important for generating the lipid for signaling functions. Whether separate pools of this lipid exist for specific purposes is not certain since dynamic changes of intracellular distribution occur under various cellular conditions. These are attributed to inter-organelle transfer via vesicular transport or at membrane contact sites by lipid transfer proteins. Control of its concentration in membranes, especially in the endoplasmic reticulum, is therefore of great importance, and a transcriptional repressor 'Opi1', which binds specifically to phosphatidic acid in membranes, is a key regulatory factor. However, many other phosphatidic acid-binding proteins have been identified that influence how phosphatidic acid is used either as a biosynthetic precursor or for signaling purposes. The mechanisms for phosphatidic acid homeostasis differ among animals, plants, yeasts, and bacteria in response to the differing functional requirements in these organisms. Figure **21.3.6** shows the pathways for biosynthesis of complex glycerolipids.

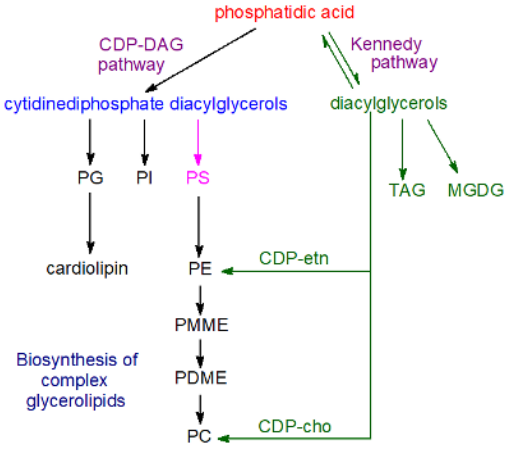


Figure **21.3.6**: Biosynthesis of complex glycerolipids

In addition to dietary, hormonal, and tissue-specific factors in animals, the extent to which fatty acids are channeled either into triacylglycerol synthesis for storage in lipid droplets and secretion in lipoproteins or into glycerophospholipids for membrane formation depends to a large extent upon the enzymes of the glycerol-3-phosphate pathway, their isoform expression, activities, and locations. On the other hand, phosphatidic acid is not only a biosynthetic precursor of other lipids but also a regulatory molecule in the transcriptional control of the genes for glycerolipid synthesis, and regulation of its concentration in cells for this purpose is similarly essential. For example, the local concentration of phosphatidic acid in the endoplasmic reticulum is an important factor in the biogenesis of lipid droplets.

The subsequent steps in using phosphatidic acid in the biosynthesis of triacylglycerols and the various glycerophospholipids are described in separate documents on this website. Thus, hydrolysis of phosphatidic acid by phosphatidate phosphatase enzymes (including lipins 1, 2, and 3) is the source of most other glycerolipids, e.g., ***sn*-1,2-diacylglycerols** (DG), which are the precursors for the biosynthesis of **triacylglycerols** (TAG), **phosphatidylcholine** (PC) and **phosphatidylethanolamine** (PE) via the so-called Kennedy pathway (also of **monogalactosyldiacylglycerols** in plants). Via reaction with cytidine triphosphate, phosphatidic acid is the precursor of **cytidine**

diphosphate diacylglycerol, which is the key intermediate in the synthesis of **phosphatidylglycerol** (PG), and thence of **cardiolipin** (CL), and of **phosphatidylinositol** (PI), and in prokaryotes and yeast but not animals **phosphatidylserine** (PS). Depending on the organism and other factors, phosphatidylserine can be a precursor for phosphatidylethanolamine, while the latter can give rise to phosphatidylcholine by way of mono- and dimethyl-phosphatidylethanolamine intermediates. The cytidine diphosphate diacylglycerol synthase is another enzyme that consumes phosphatidic acid and is important for modulating the concentration of phosphatidic acid in cells and for regulating processes mediated by this lipid.

While the fatty acid composition of phosphatidic acid can resemble that of the eventual products, the latter are generally much altered by remodeling after synthesis via deacylation-reacylation reactions.

? PHOSPHATIDIC ACID - ADDITIONAL BACKGROUND

Click for more details.

Link

Phosphatidic Acid - Biological Functions in Animals

In addition to its role as an intermediate in lipid biosynthesis, phosphatidic acid, especially that generated by the action of phospholipase D and by diacylglycerol kinases, may have signaling functions as a second messenger. However, it is not certain whether all the activities suggested by studies *in vitro* operate *in vivo*. Nonetheless, phosphatidic acid has been implicated in many aspects of animal cell biochemistry and physiology.

Some of the observed effects may be explained simply by the physical properties of phosphatidic acid, which tends to form a hexagonal II phase, especially in the presence of calcium ions. Thus, hydrolysis of phosphatidylcholine, a cylindrical non-fusogenic lipid, converts it into cone-shaped phosphatidic acid, which promotes negative membrane curvature and fusion of membranes. It differs from other anionic phospholipids in that its small anionic phosphomonoester head group lies very close to the hydrophobic interior of the lipid bilayer. In model systems, phosphatidic acid can cause membrane fusion, probably because of its ability to form non-bilayer phases. For example, the phosphatidic acid biosynthesis is believed to favor intraluminal budding of endosomal membranes with the formation of exosomes. In many cell types, vesicle trafficking, secretion, and endocytosis may require phosphatidic acid derived by the action of phospholipase D.

Also of relevance in this context is its overall negative charge, and it is not always clear whether some of the observed biological effects are specific to phosphatidic acid or to negatively charged phospholipids in general. In contrast to phosphoinositide-interacting proteins, which have defined structural folds, the binding motifs of effector proteins with phosphatidic acid are not highly conserved. However, it has been demonstrated that the positively charged lysine and arginine residues on proteins can bind with some specificity to phosphatidic acid through hydrogen bonding with the phosphate group, thus distinguishing it from other phospholipids. An ‘electrostatic-hydrogen bond switch model’ has been proposed in which the head group of phosphatidic acid forms a hydrogen bond to amino acid residues, leading to de-protonation of the head group, increasing its negative charge from -1 to -2, and thus enabling stronger interactions with basic residues and tight docking with the membrane-interacting protein. In this way, phosphatidic acid can tether certain proteins to membranes, and it can simultaneously induce conformational changes, hinder ligand binding, and/or oligomerize proteins to alter their catalytic activity, stability, and interactions with other molecules. It functions as a cellular pH sensor in that binding to proteins depends on intracellular pH and the protonation state of its phosphate head group.

One key target of phosphatidic acid is mTOR, a serine/threonine protein kinase with a signaling cascade that regulates cell growth, proliferation, motility, and survival, together with protein synthesis and transcription, by integrating nutrient and growth factor signals. This forms two distinct complexes of accessory proteins that regulate downstream targets. Of these, mTORC1 interacts directly with phosphatidic acid, and this interaction allosterically activates the enzyme complex to regulate protein synthesis, mitochondrial metabolism, and the transcription of enzymes involved in lipid synthesis. In contrast, phosphatidic acid appears to inhibit mTORC2 activity, for example, in relation to insulin signaling.

Phosphatidic acid is believed to regulate membrane trafficking events, and it is involved in activating the enzyme NADPH oxidase, which operates as part of the defence mechanism against infection and tissue damage during inflammation. It may increase or inhibit their activities by binding to targeted proteins, including protein kinases, protein phosphatases, and G-proteins. Effects on gene transcription have been observed linked to the inhibition of peroxisome proliferator-activated receptor (PPAR) activity. In yeast, phosphatidic acid in the endoplasmic reticulum binds directly to a specific transcriptional repressor to keep it inactive outside the nucleus; when the lipid precursor inositol is added, this phosphatidic acid is rapidly depleted, releasing the transcriptional factor

so that it can be translocated to the nucleus, where it can repress target genes. The overall effect is a mechanism to control phospholipid synthesis.

In addition, phosphatidic acid regulates many aspects of phosphoinositide function. For example, the murine phosphatidylinositol 4-phosphate 5-kinase, the main enzyme generating the lipid second messenger **phosphatidylinositol-4,5-bisphosphate**, does not appear to function unless phosphatidic acid is bound to it; this lipid, generated by the action of phospholipase D, recruits the enzyme to the membrane and induces a conformational change that regulates its activity. It may promote phospholipase A_2 activity, a key enzyme in eicosanoid production from phosphoinositide precursors.

In relation to signaling activities, it should be noted that phosphatidic acid can be metabolized to ***sn*-1,2-diacylglycerols** or lysophosphatidic acid (see next section), both of which have distinctive signaling functions in their own right. Conversely, conversion back to phosphatidic acid can effectively deactivate both compounds.

Phospholipase D isoforms and phosphatidic acid have been implicated in a variety of pathologies, including neurodegenerative diseases, blood disorders, late-onset Alzheimer's disease, and cancer, leading to attempts to develop specific inhibitors of the enzyme for therapeutic purposes. Similarly, the expression of LPAT isoforms can enhance the proliferation and chemoresistance of some cancer cells. Diacylglycerol kinase alpha (DGKα) is highly expressed in several refractory cancer cells, attenuating apoptosis and promoting proliferation. In addition, DGKα is highly abundant in T cells and induces a nonresponsive state, which enables advanced cancers to escape immune action. Inhibition of this enzyme is also seen as a promising treatment strategy.

Phosphatidic Acid - Biological Functions in Plants

Phosphatidic acid is present at higher levels in the roots of plants than in the leaves and is believed to have a function in root architecture. Similarly, its concentration is elevated in flowers and reproductive tissues, but its significance is unknown. In addition to its role as one of the central molecules in lipid biosynthesis, it facilitates the transport of lipids across plant membranes, and it is also the key plant lipid second messenger, which is rapidly and transiently generated in response to many different biotic and abiotic stresses. In contrast to animal metabolism, the **diacylglycerol** signaling pathway is believed to be relatively insignificant in plants.

The main source of phosphatidic acid for these purposes is the action of phospholipase D (PLD) on membrane phospholipids, such as phosphatidylcholine and phosphatidylethanolamine. Plants contain numerous related enzymes of this type, 12 in Arabidopsis and 17 in rice, compared with two in humans and one in yeast, and individual isozymes may elicit specific responses. The isoforms are grouped into six classes based on the genic architecture, sequence similarities, domain structures, and biochemical properties in the former. These depend mainly on their lipid-binding domains, with some homologous to the human and yeast enzymes and most containing a characteristic ‘C2’ (calcium- and lipid-binding) domain. The most widespread of these is PLDα, which does not require binding to phosphatidylinositol 4,5-bisphosphate, in contrast to other PLD isoforms and the mammalian enzyme, but millimolar levels of Ca^{2+} are necessary. Studies with fluorescent biosensors suggest that phosphatidic acid accumulates in the subapical region of the cytosolic leaflet of the plasma membrane.

Phosphatidic acid can also be produced by the sequential action of phospholipase C and diacylglycerol kinase on membrane inositol phospholipids, with diacylglycerols as an intermediate (there are seven isoenzymes in *A. thaliana*). One difference from animal metabolism is that diacylglycerol pyrophosphate can be synthesized from phosphatidic acid in plants (see below).

Phosphatidic acid is required to bind and allosterically activate the **monogalactosyldiacylglycerol synthase (MGDG1)**, located in the inner envelope membrane of the chloroplast. It may be a regulator of the biosynthesis of thylakoid membranes. Phospholipase D activity and the phosphatidic acid produced have long been recognized as important during germination and senescence, and they have an essential role in the response to stress damage and pathogen attack, both in higher plants and in green algae. A high content of phosphatidic acid induced by phospholipase D action during wounding or senescence brings about a loss of the membrane bilayer phase because of the conical shape of this negatively charged phospholipid in comparison to the cylindrical shape of structural phospholipids. This change in ionization properties has crucial effects upon lipid-protein interactions, "the electrostatic-hydrogen bond switch model" described above. Promoting negative curvature at the plasma membrane and binding to clathrin proteins is believed to facilitate the process of endocytosis. Similar phenomena may explain why phosphatidic acid is important in responding to other forms of stress, including osmotic stress (salinity or drought), cold, and oxidation. Although much remains to be learned of the mechanism by which it exerts its effects, it is believed to promote the response to the plant hormone abscisic acid. In addition, phosphatidic acid may interact with salicylic acid to mediate defence responses.

In plants, phosphatidic acid is involved in many different cell responses induced by hormones, stress, and developmental processes. In relation to cellular signaling, it often acts in concert with **phosphatidylinositol 4,5-bisphosphate** by binding to specific proteins rather than acting via a receptor. As in mammalian cells, targets for such signaling include protein kinases and phosphatases in addition to proteins involved in membrane trafficking and the organization of the cytoskeleton. It can both activate and inhibit enzymes. If the target protein is soluble, binding to phosphatidic acid can cause the protein to be sequestered into a membrane,

which affects downstream targets. For example, it promotes the growth of pollen tubes and root hairs, decreases peroxide-induced cell death, and mediates the signaling processes that lead to responses to ethylene and again to the hormone abscisic acid. Thus, in the 'model' plant *Arabidopsis*, phosphatidic acid interacts with a protein phosphatase to signal the closure of stomata promoted by abscisic acid; it interacts also with a further enzyme to mediate the inhibition of stomatal opening effected by abscisic acid. Together, these reactions constitute a signaling pathway that regulates plant water loss.

Notably, phosphatidic acid production can be initiated by opposing stress factors, such as cold and heat, as well as by hormones that are considered antagonistic, such as abscisic acid and salicylic acid. It is possible that phosphatidic acid molecules synthesized by the two main pathways differ in composition and cellular distributions and may produce different responses, but this is an open question. Certainly, during low temperature stress, phosphatidic acid is generated by the action of diacylglycerol kinase. It also seems likely that these differing activities are controlled by the cellular environment where the lipid is produced and by the availability of target proteins or other molecules with which it can act synergistically. Genes encoding enzymes involved in phosphatidic acid metabolism have been manipulated to explore their potential application for crop improvements, based on effects on plant growth, development, and stress responses.

As in animals, phosphatidic acid is catabolized, and its signaling functions are terminated by lipid phosphate phosphatases and phosphatidic acid hydrolases, and by acyl-hydrolases and lipoxygenases with the production of fatty acids and other small molecules, which are subsequently absorbed and recycled.

21.3.2.3: LYSOPHOSPHATIDIC ACID

Figure **21.3.7** shows the structure of a lysophosphatidic acid (note the absence of an acyl group at C2).

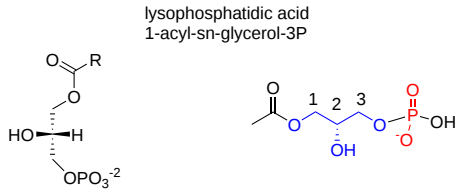


Figure **21.3.7**: lysophosphatidic acid

Lysophosphatidic acid (LPA) or 1-acyl-*sn*-glycerol-3-phosphate differs structurally from phosphatidic acid in having only one mole of fatty acid per mole of lipid. As such, it is one of the simplest possible glycerophospholipids. It exists in the form of many different molecular species, i.e., esterified to 16:0 to 22:6 fatty acids, and there is preliminary evidence that saturated and polyunsaturated species may differ in their biological properties in some circumstances. As the *sn*-1-acylated form is more stable thermodynamically, facile isomerization ensures this tends to predominate. It lacks one fatty acid compared to phosphatidic acid, so it is a much more hydrophilic molecule. At the same time, the additional hydroxyl group strengthens hydrogen bonding within membranes, properties that may be important for its function in cells.

Although lysophosphatidic acid is present at very low levels only in animal tissues, it is extremely important biologically, influencing many biochemical processes. It is a biosynthetic precursor of phosphatidic acid, but there is particular interest in its role as a lipid mediator with growth factor-like activities. For example, it is rapidly produced and released from activated platelets to influence target cells.

Biosynthesis: In the circulation, the most important source of lysophosphatidic acid is the activity of an enzyme with lysophospholipase D-like activity and known as '**autotaxin**' on **lysophosphatidylcholine** (200 μM in plasma) to yield LPA in an albumin-bound form, mainly, although it is relatively soluble in aqueous media because of its polarity and small size. This lipid is more abundant in serum (1 to 5 μM) than in plasma (100 nM) because its main precursor, lysophosphatidylcholine, is released from activated platelets during coagulation. Autotaxin is a member of the nucleotide pyrophosphatase-phosphodiesterase family. It is also present in cerebrospinal and seminal fluids and many other tissues, including cancer cell lines from which it was first isolated and characterized. Indeed, the name derives from the finding that it promoted chemo*taxis* in melanoma cells in an *auto*crine fashion. It binds to target cells via integrin and heparan sulfate proteoglycans, which may assist the delivery of lysophosphatidic acid to its receptors. Genetic deletion of the enzyme in mice results in aberrant vascular and neuronal development and soon leads to the death of the embryos. However, the overexpression of autotaxin also causes physical defects and is eventually lethal to embryos.

Figure **21.3.8** shows the pathways for lysophosphatidic acid synthesis.

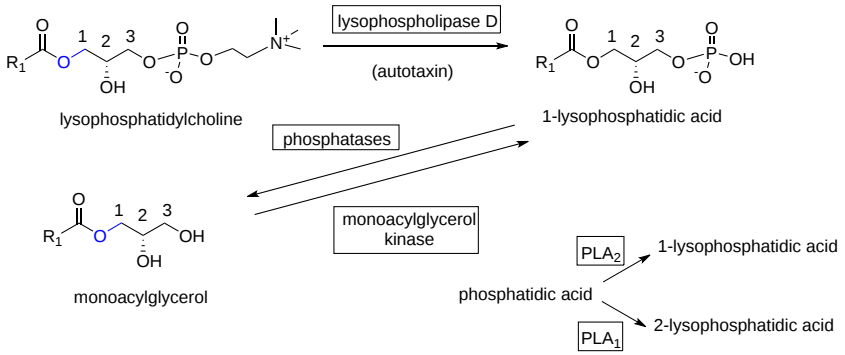


Figure **21.3.8**: Pathways for lysophosphatidic acid synthesis.

While autotaxin is the primary source of extracellular lysophosphatidic acid, it is now established that it is produced intracellularly by a wide variety of cell types by various mechanisms, often with phosphatidic acid derived from other phospholipids by the action of phospholipase D as the primary precursor. For example, the hydrolysis of phosphatidic acid by a phospholipase A_2 (PLA_2) is the main mechanism in platelets. Still, other cellular enzymes involved include a phosphatidic acid-selective phospholipase A_1 (PLA_1) producing *sn*-2-acyl-lysophosphatidic acid, a monoacylglycerol kinase (utilizing monoacylglycerols produced by the action of lipid phosphate phosphatases), and glycerol-3-phosphate acyltransferase (the first step in phosphatidic acid biosynthesis). In particular, secretory PLA_2-IIA (sPLA2-IIA) can induce the release of LPA from phosphatidic acid exposed on the surface of extracellular vesicles derived from platelets and Ca^{2+}-loaded erythrocytes upon stimulation by pro-inflammatory cytokines.

? LYSOPHOSPHOLIPIDS - ADDITIONAL BACKGROUND

Click the link below.

Link

General function: Although lysophospholipids are relatively small molecules, they carry a high content of information through the nature of the phosphate head group, the positional distribution of the fatty acids on the glycerol moiety, the presence of ether or ester linkages to the glycerol backbone, and the chain-length and degree and position of saturation of the fatty acyl chains. Lysophosphatidic acid acts upon nearly all cell types, often as a proliferative and pro-survival signal, inducing cellular invasion, migration, and differentiation while stimulating smooth muscle and fibroblast contraction, cytoskeletal rearrangement, secretion of cytokines/chemokines, and numerous other effects. The 1-*O*-alkyl- and alkenyl-ether forms also display many of these activities, which can be derived from the **platelet-activating factor**. On the other hand, much of the lysophosphatidic acid produced intracellularly may be used to synthesize other phospholipids rather than for signaling purposes.

Receptors: The informational content of the lysophosphatidic acid molecule leads to selectivity in the functional relationship with cell receptors. As most mammalian cells express receptors for lysophosphatidic acid, this lipid may initiate signaling in the cells in which it is produced and affect neighboring cells. Characterization of cloned lysophosphatidic acid receptors in combination with strategies of molecular genetics has allowed the determination of both signaling and biological effects dependent on receptor mechanisms. At least six G protein-coupled receptors that are specific for lysophosphatidic acid have now been identified in vertebrates, each found in particular organs and coupled to at least one or more of the four heterotrimeric G_α proteins and designated $LPAR_1$ to $LPAR_6$, of which $LPAR_1$ is virtually ubiquitous in tissues. These vary appreciably in amino acid sequences but are classified into two subgroups, the EDG (LPAR1-3) and P2Y (LPAR4-6) families, with differing tissue distributions. Most cell types express these receptors in different combinations. There is also some interaction with transient receptor potential cation channel V1 (TRPV1), peroxisome proliferator-activated receptor gamma (PPARγ), and other proteins. Plasma lysophosphatidic acid binds to its receptors while it is bound to albumin.

Experimental activation of the LPAR receptors has shown that a range of downstream signaling cascades are mediated by lysophosphatidic acid signaling via these receptors. These include activation of adenylyl cyclase, cAMP production, intracellular Ca^{2+} and K^+ production (by activating ion channels), protein kinases, phospholipase C, phosphatidylinositol 3-kinase, small GTPases (Ras, Rho, Rac), release of arachidonic acid, and much more. This way, lysophosphatidic acid regulates cell survival, proliferation, cytoskeleton re-arrangement, motility, cytokine secretion, cell differentiation, and many other vital cellular processes. Sometimes, lysophosphatidic acid appears to function in contradictory ways, and there is evidence that it is involved in cell survival in some circumstances and programmed cell death in others.

Signaling by lysophosphatidic acid has regulatory functions in the mammalian reproductive system, both male and female, facilitating oocyte maturation and spermatogenesis through the action of the receptors $LPAR_1$ to $LPAR_3$. During early gestation, it regulates vascular remodeling at the maternal-fetal interface. There is also evidence that lipids are involved in brain development through their activity in neural progenitor cells, neurons, glia, and vascular remodeling. In the central nervous system, these receptors are thought to play a central role in triggering and maintaining neuropathic pain by mechanisms that may involve the demyelination of damaged nerves.

Lysophosphatidic acid has been found in saliva in significant amounts, and it has been suggested that it is involved in wound healing in the upper digestive organs such as the mouth, pharynx, and oesophagus. When applied topically to skin wounds, it has similar effects, probably by stimulating the proliferation of new cells to seal the wound. Receptor $LPAR_6$, together with the phospholipase A1, is required for the development of hair follicles, and this receptor is also involved in the regulation of endothelial blood-brain barrier function. The proliferation and survival of stem cells and their progenitors are regulated by lysophosphatidic acid signaling. In contrast, in bone cells, acting via $LPAR_1$, lysophosphatidic acid is important for bone mineralization and repair.

Disease: There is particular interest in the activity of lysophosphatidic acid in various disease states and **cancer,** especially as increased expression of autotaxin and the subsequent increased levels of lysophosphatidic acid have been reported in several primary tumors. For example, a finding that lysophosphatidic acid is markedly elevated in the plasma and peritoneal fluid (ascites) of ovarian cancer patients compared to healthy controls may be especially significant. Also, elevated plasma levels were found in patients in the first stage of ovarian cancer, suggesting that it may represent a useful marker for the early detection of the disease. It is believed that the secretory form of phospholipase A_2 acts preferentially on lipids from damaged membranes or microvesicles, such as those produced by malignant cells, and this eventually results in increased levels of this lipid. Lysophosphatidic acid has been shown to stimulate the expression of genes for many different enzymes that lead to the proliferation of ovarian and other cancer cells and may induce cell migration via receptors $LPAR_1$ to $LPAR_3$ and possibly $LPAR_6$. At the same time, $LPAR_4$ and $LPAR_5$ have opposing effects. Autotaxin and LPARs have been implicated in resistance to chemotherapy and radiation treatment in cancer therapy.

As lysophosphatidic acid has growth-factor-like activities for many cell types that induce cell proliferation and migration, changes in cellular shape, and increase endothelial permeability, it is perhaps not surprising that it is relevant to tumor biology. Treatment of various cancer cell types with lysophosphatidic acid promotes the expression and release of interleukin 8 (IL-8), a potent angiogenic factor. Thus, it has a critical role in the growth and spread of cancers by enhancing the availability of nutrients and oxygen. There is evidence that signaling by lysophosphatidic acid is causally linked to hyperactive lipogenesis in cancer. For example, it activates the sterol regulatory element-binding protein (SREBP) together with the fatty acid synthase and AMP-activated protein kinase–ACC lipogenic cascades leading to elevated synthesis of lipids *de novo*. Increased autotaxin expression has been demonstrated in many cancer cell lines, and the expression of many of the surface receptors for lysophosphatidic acid in cancer cells is aberrant. Cancer cells must evade the immune system during metastasis, and lysophosphatidic acid facilitates this process by inhibiting the activation of T cells. Therefore, lysophosphatidic acid metabolism is a target of the pharmaceutical industry in the search for new drugs for cancer therapy, aided by a knowledge of the crystal structures of three of the receptors.

Signaling by lysophosphatidic acid has been implicated in many aspects of chronic inflammation, which it promotes by affecting the endothelium in several ways, for example, by stimulating endothelial cell migration, the secretion of chemokines and cytokines, and regulating the integrity of the endothelial barrier. Problems with lysophosphatidic acid signaling together with changes in autotaxin expression are believed to be factors in such metabolic and inflammatory disorders as obesity, insulin resistance, non-alcoholic fatty liver disease, rheumatoid arthritis, multiple sclerosis, and cardiovascular disease. Further, there is evidence that it contributes to neurological disorders, such as Alzheimer's disease and neuropathic pain, and asthma, fibrosis, and bone malfunction. Drugs that interact with the lysophosphatidic acid receptors are reported to be effective in attenuating symptoms of several diseases in animal models, and three have passed phase I and II clinical trials for idiopathic pulmonary fibrosis and systemic sclerosis in human patients. Drugs that target autotaxin production and catabolism of lysophosphatidic acid are also in development, and the steroidal anti-inflammatory agent, dexamethasone, appears to be especially useful.

Under certain conditions, lysophosphatidic acid can become athero- and thrombogenic and might aggravate cardiovascular disease. As oxidized low-density lipoproteins promote lysophosphatidic acid production, their content in atherosclerotic plaques is high, suggesting that it might serve as a biomarker for cardiovascular disease. Indeed, lysophosphatidic acid promotes pro-inflammatory events that lead to the development of atheroma and encourages the progression of the disease. It could lead to arterial thrombus formation by mediating platelet aggregation.

Related lipids: The sphingolipid analogue, **sphingosine-1-phosphate**, shows a similar range of activities to lysophosphatidic acid, and the two lipids are often discussed in the same contexts, although they may have opposing effects. Acute leukemia cells produce **methyl-lysophosphatidic acids** (the polar head-group is methylated). As these act as antigens to which a specific group of human T

cells react strongly, they might be a target for the immunotherapy of hematological malignancies. Other lysophospholipids are known to have distinctive biological functions.

Catabolism: Deactivation of lysophosphatidic acid is accomplished by dephosphorylation to produce monoacylglycerols by a family of three lipid phosphate phosphatases (LPP1, 2, and 3), which also dephosphorylate sphingosine-1-phosphate, phosphatidic acid, and ceramide 1-phosphate in a non-specific manner. These are integral membrane proteins with the active site in the plasma membrane facing the extracellular environment, enabling them to access and hydrolyse extracellular lysophosphatidic acid and other phospholipids. Mice with a constitutive LPP3 deficiency are not viable, but this is not true for LPP1 and LPP2 knockout mice. Lysophosphatidic acid can be converted back to phosphatidic acid by a membrane-bound *O*-acyltransferase (MBOAT2) specific for lysophosphatidic acid (and lysophosphatidylethanolamine) with a preference for oleoyl-CoA as substrate.

21.3.3: PHOSPHATIDYLCHOLINE AND RELATED LIPIDS

21.3.3.1: PHOSPHATIDYLCHOLINE - STRUCTURE AND OCCURRENCE

Phosphatidylcholine or 1,2-diacyl-*sn*-glycero-3-phosphocholine (once given the trivial name 'lecithin') is a neutral or zwitterionic phospholipid over a pH range from strongly acid to strongly alkaline. It is usually the most abundant phospholipid in animals and plants, often amounting to almost 50% of the complex lipids. As such, it is a key building block of membrane bilayers. In particular, it makes up a very high proportion of the lipids of the outer leaflet of the plasma membrane in animals. Virtually all the phosphatidylcholine in human erythrocyte membranes is in the outer leaflet. In the plasma membranes of nucleated cells, 80-90% of this lipid is located on the outer leaflet. Phosphatidylcholine is also the principal phospholipid circulating in plasma, where it is an integral component of the **lipoproteins**, especially the HDL. On the other hand, it is less often found in bacterial membranes, perhaps ~10% of species, but there is none in the 'model' organisms *Escherichia coli* and *Bacillus subtilis*. In animal tissues, some of its membrane functions appear to be shared with the structurally related sphingolipid, **sphingomyelin**, although the latter has many unique properties.

Figure **21.3.9** shows the structure of phosphatidylcholine

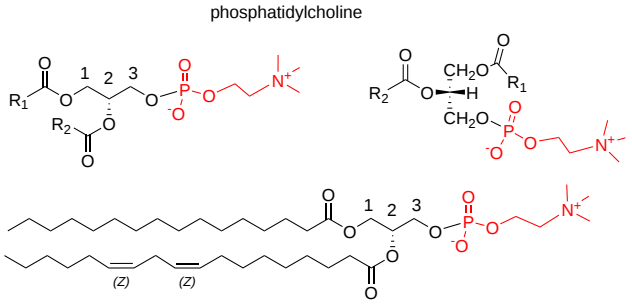


Figure **21.3.9**: Phosphatidylcholine

In animal tissues, phosphatidylcholine tends to exist mainly in the diacyl form. Still, small proportions (in comparison to phosphatidylethanolamine and phosphatidylserine) of alkyl, acyl, and alkenylacyl forms may also be present. As a generalization, animal phosphatidylcholine tends to contain lower proportions of arachidonic and docosahexaenoic acids and more of the C_{18} unsaturated fatty acids than the other zwitterionic phospholipid, phosphatidylethanolamine. Saturated fatty acids are most abundant in position *sn*-1, while polyunsaturated components are concentrated in position *sn*-2. Indeed, C_{20} and C_{22} polyenoic acids are exclusively in position *sn*-2, yet in the brain and retina, the unusual very-long-chain polyunsaturated fatty acids (C_{30} to C_{38}) of the *n*-6 and *n*-3 families occur in position *sn*-1. Dietary factors influence fatty acid compositions, but in comparing animal species, it would be expected that the structure of the phosphatidylcholine in the same metabolically active tissue would be somewhat similar in terms of the relative distributions of fatty acids between the two positions. Table **21.3.1** lists some representative data.

Table **21.3.1. Positional distribution of fatty acids in the phosphatidylcholine of some animal tissues.**

Position	Fatty acid						
	16:0	16:1	18:0	18:1	18:2	20:4	22:6
			Rat liver [1]				
***sn*-1**	23	1	65	7	1	trace	
***sn*-2**	6	1	4	13	23	39	7
			Rat heart [2]				
***sn*-1**	30	2	47	9	11	-	-
***sn*-2**	10	1	3	17	20	33	9
			Rat lung [3]				
***sn*-1**	72	4	15	7	3	-	-
***sn*-2**	54	7	2	12	11	10	1
			Human plasma [4]				
***sn*-1**	59	2	24	7	4	trace	-
***sn*-2**	3	1	1	26	32	18	5
			Human erythrocytes [4]				
***sn*-1**	66	1	22	7	2	-	-
***sn*-2**	5	1	1	35	30	16	4
			Bovine brain (gray matter) [5]				
***sn*-1**	38	5	32	21	1	-	-
***sn*-2**	33	4	trace	48	1	9	4
			Chicken egg [6]				
***sn*-1**	61	1	27	9	1	-	-
***sn*-2**	2	1	trace	52	33	7	4

1, Wood, R. and Harlow, R.D. *Arch. Biochem. Biophys*., **131**, 495-501 (1969); DOI.
2, Kuksis, A. *et al*. *J. Lipid Res*., **10**, 25-32 (1969); DOI.
3, Kuksis, A. *et al. Can. J. Physiol. Pharm*., **46**, 511-524 (1968); DOI.
4, Marai, L. and Kuksis, A. *J. Lipid Res*., **10**, 141-152 (1969); DOI.
5, Yabuuchi, H. and O'Brien, J.S. J. Lipid Res., 9, 65-67 (1968); DOI.
6, Kuksis, A. and Marai, L. *Lipids*, **2**, 217-224 (1967); DOI.

Some exceptions exist, as the phosphatidylcholine in some tissues or organelles contains relatively high proportions of disaturated molecular species. For example, it is well known that lung phosphatidylcholine in most, if not all, animal species studied to date contains a high proportion (50% or more) of dipalmitoylphosphatidylcholine.

The positional distributions of fatty acids in phosphatidylcholine in representative plants and yeast are listed in Table **21.3.2**. In the leaves of the model plant *Arabidopsis thaliana*, saturated fatty acids are concentrated in position *sn*-1, but monoenoic fatty acids are distributed approximately equally between the two positions, and there is a preponderance of di- and triunsaturated fatty acids in position *sn*-2; the same is true for soybean lecithin. The pattern is somewhat similar in the yeast *Lipomyces lipoferus*, except that much of the 16:1 is in position *sn*-1.

Table **21.3.2**: **Composition of fatty acids (mol%) in positions *sn*-1 and *sn*-2 in the phosphatidylcholine from plants and yeast.**

Position	Fatty acid					
	16:0	16:1	18:0	18:1	18:2	18:3
Arabidopsis thaliana (leaves) [1]						
***sn*-1**	42		4	5	23	26
***sn*-2**	1		trace	5	47	47
Soybean 'lecithin' [2]						
***sn*-1**	24		9	14	47	4
***sn*-2**	5		1	13	75	6
Lipomyces lipoferus [3]						
***sn*-1**	24	18	trace	37	16	4
***sn*-2**	4	5	trace	39	31	19
1, Browse, J., Warwick, N., Somerville, C.R., and Slack, C.R. *Biochem. J.*, **235**, 25-31 (1986); DOI. 2, Blank, M.L., Nutter, L.J. and Privett, O.S. *Lipids*, **1**, 132-135 (1966); DOI. 3, Haley, J.E. and Jack, R.C. *Lipids*, **9**, 679-681 (1974); DOI.						

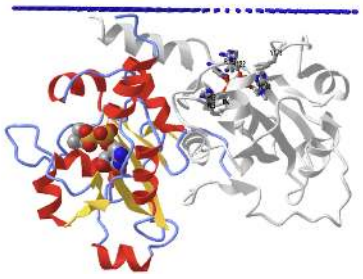
21.3.3.2: PHOSPHATIDYLCHOLINE – BIOSYNTHESIS

There are several mechanisms for the biosynthesis of phosphatidylcholine in animals, plants, and microorganisms. Choline itself is not synthesized by animal cells. It is an essential nutrient for phospholipid synthesis and cholinergic neurotransmission (acetylcholine synthesis), and it is a source of methyl groups for numerous other metabolites. It must be obtained from dietary sources or by degradation of existing choline-containing lipids, for example, those produced by the second pathway described below. Once taken across membranes and into cells by specific transporters, choline is immediately phosphorylated by a choline kinase (1) in the cytoplasm of the cell to produce phosphocholine, which is reacted with cytidine triphosphate (CTP) by the enzyme **CTP:phosphocholine cytidylyltransferase (CCT)** (2) to form cytidine diphosphocholine (CDP-choline).

$$\text{CTP} + \text{PC} \rightarrow \text{CDP-choline} + \text{Pi}$$

The latter enzyme exists in two isoforms, of which CCTα is the more important. It is a soluble protein found first in the nucleoplasm and then in the nucleoplasmic reticulum. This is considered the rate-limiting step in phosphatidylcholine biosynthesis, and the enzyme's activity is regulated by signals from a sensor in the membrane that reports on the relative abundance of the final product. However, choline kinase (ChoKα) also has regulatory functions.

Figure **21.3.10** shows an interactive iCn3D model of the mammalian (rat) CTP: Phosphocholine cytidylyltransferase catalytic domain (3HL4).



NCBI iCn3D Figure **21.3.10**: Mammalian (rat) CTP-Phosphocholine cytidylyltransferase catalytic domain (3HL4). Click the image for a popup or use this external link: https://structure.ncbi.nlm.nih.gov/i...tBYRYk7vPKD7f6

The biologically active homodimer is shown. The B chain is colored by secondary structure, and the A chain is shown in gray. Key active site residues (only shown in the A chain) are labeled and in CPK-colored sticks. A bound CDP-choline analog ((2-cytidylate-O'-phosphonyloxy)-ethyl-trimethylammonium) is shown in spacefill CPK colors.

This enzyme (CCT) catalyzes the key regulatory and rate-limiting step in PC synthesis. The C-terminal domain binds membrane lipids and regulates the enzyme. The iCn3D model above is for the catalytic domain with the regulatory domain deleted. Two nonconserved active site

side chains, His 168 and Tyr 173, interact with and position the phosphocholine. Other active site residues include Arg-196 in L6, Lys-122 in L2, and Asp-94. Figure **21.3.11** shows a simplified mechanism for the reaction

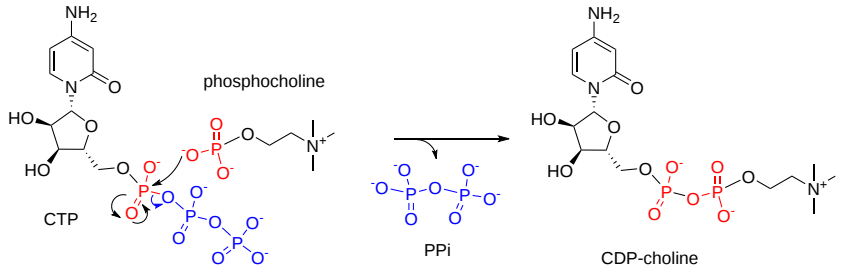


Figure **21.3.11**: Simplified mechanism for CTP-Phosphocholine cytidylyltransferase

In plants, nematodes, and certain parasites, most phosphocholine is synthesized by sequential methylation of phosphoethanolamine by phospho-base *N*-methyltransferases. Still, phosphatidylethanolamine is only methylated in this way in a few plant species. This is also the main route to free choline and betaine in plants.

The CDP-choline produced is acted upon by the membrane-bound enzyme CDP-choline:1,2-diacylglycerol choline/ethanolamine-phosphotransferase in the endoplasmic reticulum (CEPT1) and a related choline phosphotransferase 1 (CPT1) in the *trans*-Golgi, which catalyse the reaction with *sn*-1,2-diacylglycerols to form phosphatidylcholine. The first is responsible for most phosphatidylcholine biosynthesis, but with a somewhat different molecular species composition from the second, which prefers 1-alkyl precursors. This is the main pathway for the synthesis of phosphatidylcholine in animals and plants, and it is analogous to that for a major route to **phosphatidylethanolamine**; it is also found in a few bacterial species (e.g., *Sinorhizobium meliloti*). Phosphatidylcholine in mitochondria is obtained by transfer from the endoplasmic reticulum.

Figure **21.3.12** shows the main pathways for PC synthesis in plants and animals.

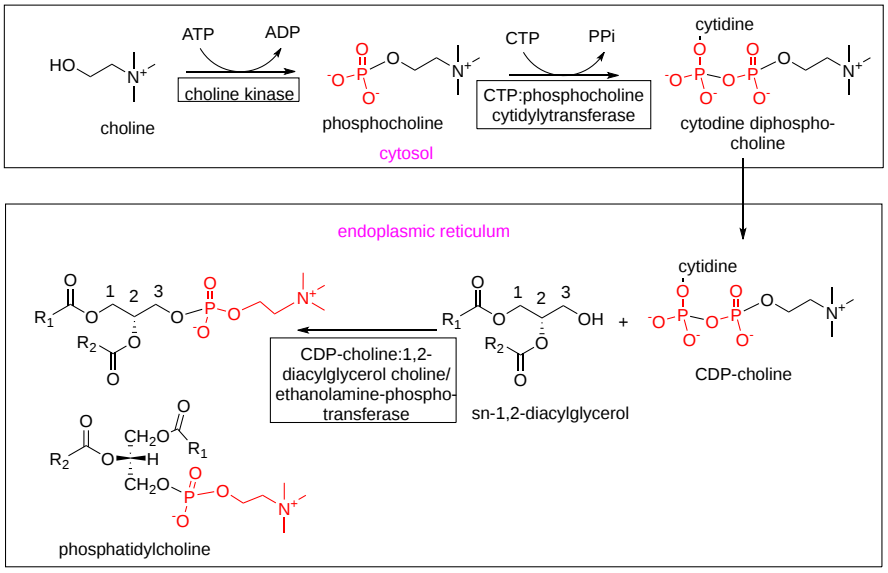


Figure **21.3.172**: Main pathways for PC synthesis in plants and animals.

The discovery of the importance of this pathway depended a little on serendipity. In experiments in Professor Eugene Kennedy's laboratory, samples of adenosine triphosphate (ATP) contained some cytidine triphosphate (CTP) as an impurity. However, luck is of little value without receptive minds, and Kennedy and co-workers demonstrated that the impurity was an important metabolite essential for the formation of phosphatidylcholine.

The above reaction and the biosynthetic mechanism for phosphatidylethanolamine are significantly different from those for phosphatidylglycerol, phosphatidylinositol, and cardiolipin. Both use nucleotides, but with the latter, the nucleotide is covalently linked directly to the lipid intermediate, **cytidine diphosphate diacylglycerol**. However, a comparable pathway to the latter for phosphatidylcholine biosynthesis occurs in bacteria (see below).

The source of the *sn*-1,2-diacylglycerol precursor, which is also a key intermediate in forming phosphatidylethanolamine and phosphatidylserine, and triacylglycerols, is **phosphatidic acid**. In this instance, the important enzyme is phosphatidic acid phosphatase (also known as lipin or phosphatidate phosphatase' or 'lipid phosphate phosphatase' or 'phosphatidate phosphohydrolase').

Figure **21.3.13** shows the biosynthesis of the diacyl precursor of PC

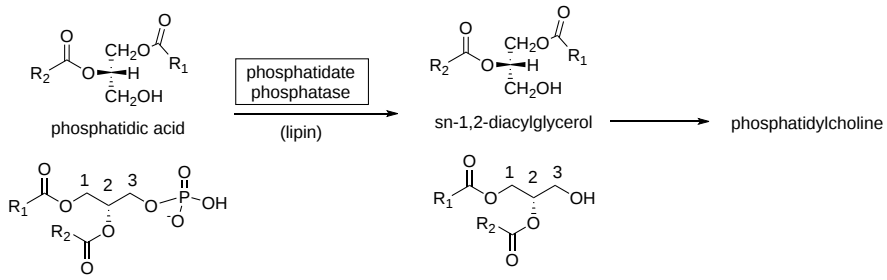


Figure **21.3.13**: Synthesis of the diacyl precursor of PC

This enzyme is also important for producing diacylglycerols as essential intermediates in the biosynthesis of triacylglycerols and **phosphatidylethanolamine**. Yeasts contain two such enzymes, one of which is Mg^{2+}-dependent (PAP1) and the other Mg^{2+}-independent (PAP2). Much of the phosphatidic acid phosphatase activity in mammals resides in three related cytoplasmic proteins, lipins-1, -2, and -3. Lipin-1 is found mainly in adipose tissue, while lipin-2 is present mainly in the liver. They are unique among biosynthetic enzymes for glycerolipids in that they can transit among cellular membranes rather than remain tethered to membranes. Of these, lipin-1 is the most important and exists in three isoforms, lipin-1α, lipin-1β, and lipin-1γ, with lipin-1α located mainly in the nucleus and lipin-1β in the cytoplasm. Lipin-1γ is present primarily in the brain.

The second pathway for biosynthesis of phosphatidylcholine involves sequential methylation of phosphatidylethanolamine, with *S*-adenosylmethionine (SAM) as the source of methyl groups, with **mono- and dimethylphosphatidylethanolamine** as intermediates, and catalyzed by the enzyme phosphatidylethanolamine *N*-methyltransferase. A single enzyme (~20 KDa) in two isoforms catalyses all three reactions in hepatocytes; the main form is located in the endoplasmic reticulum (ER), where it spans the membrane, while the second is found in the mitochondria-associated ER membrane. At least two *N*-methyltransferases are present in yeast. This is a major pathway in the liver, generating one-third of the phosphatidylcholine in this organ but not in other animal tissues or, in general, in higher organisms. It may be the main route to phosphatidylcholine in those bacterial species that produce this lipid and in yeasts, but it appears to operate in only a few species of higher plants. This liver pathway is especially important when choline is deficient in the diet.

Figure **21.3.14** shows PC synthesis via PE methylation.

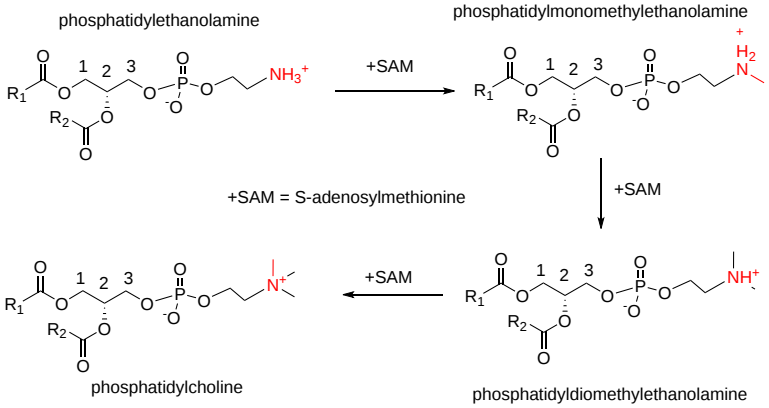


Figure **21.3.14**: synthesis of PC via methylation of PE

A by-product of the biosynthesis of phosphatidylcholine from phosphatidylethanolamine is the conversion of *S*-adenosylmethionine to *S*-adenosylhomocysteine, which is hydrolyzed in the liver to adenosine and homocysteine. An elevated level of the latter in plasma is a risk factor for cardiovascular disease and myocardial infarction.

Phosphatidylcholine biosynthesis by both pathways in the liver is necessary for normal secretion of the plasma lipoproteins (VLDL and HDL), and it is relevant to many human physiological conditions. It should be noted that all of these pathways for the biosynthesis of diacylphosphatidylcholine are very different and are separated spatially from those producing **alkyl, acyl- and alkenylacyl-phosphatidylcholines** *de novo*. Also, phosphatidylcholine synthesis does not occur uniformly throughout the endoplasmic reticulum. It occurs at membrane interfaces or where it meets other organelles, especially where the membrane is expanding dynamically.

The enzymes in the endoplasmic reticulum responsible for synthesizing all phospholipids are oriented so that their active sites are exclusively facing the cytosol. Problems would arise if there were a rapid expansion of the cytosolic leaflet while the luminal leaflet did not change, but a phospholipid transporter known as a scramblase enables a rapid bidirectional flip-flop of phospholipids between leaflets of the bilayer in an energy-independent manner. Compositional asymmetry is first seen in the *trans*-Golgi and is completed before the plasma

membrane is formed, with phosphatidylcholine and sphingolipids present mainly in the exofacial (outer) leaflet. Phosphatidylethanolamine and phosphatidylserine are enriched in the cytosolic leaflet.

Dietary phosphatidylcholine is rapidly hydrolyzed in the proximal small intestine by pancreatic enzymes with lysophosphatidylcholine (and free fatty acids) formation. Further hydrolysis can occur in the jejuno-ileal brush-border by the action of the membrane phospholipases, with the release of glycerophosphocholine. Still, much of the lysophosphatidylcholine is reacylated by the lyso-PC-acyl-CoA-acyltransferase 3 for export in chylomicrons.

In **plant** cells, phosphatidylcholine biosynthesis occurs mainly in the endoplasmic reticulum, and it is a major component of most membranes other than the internal membranes of plastids; it is absent from the thylakoids and the inner envelope membrane but is the main glycerolipid of the outer monolayer of the outer envelope membrane. Further complications arise in plants in that turnover or partial synthesis via lysophosphatidylcholine occurs in different organelles from different fatty acid pools or with enzymes with differing specificities. In addition, fatty acids esterified to phosphatidylcholine serve as substrates for desaturases. The result is that an appreciable pool of the diacylglycerols for the biosynthesis of **triacylglycerols**, **galactosyldiacylglycerols,** and other glycerolipids passes through phosphatidylcholine as an intermediate, so that the fatty acid compositions in different membranes change after the initial synthetic process. This mechanism differs from the remodeling of molecular species in animal tissues, which will be discussed next. However, a comparable exchange of acyl groups does occur, in part catalyzed by acyl transferases (see next section). Some phosphatidylcholine transfer *per se* from the endoplasmic reticulum to plastids may occur via contact points between the two membranes or may be facilitated by specific transport proteins.

While phosphatidylcholine is a major lipid in yeasts, recent work suggests that it is not essential if suitable alternative growth substrates are available, unlike higher organisms where perturbation of phosphatidylcholine synthesis can lead to inhibition of growth or even cell death.

21.3.3.3: REMODELING OF PHOSPHATIDYLCHOLINE - THE LANDS' CYCLE

Whatever the mechanism of biosynthesis of phosphatidylcholine in animal tissues, it is apparent that the fatty acid compositions and positional distributions on the glycerol moiety are determined post synthesis by extensive re-modeling involving orchestrated reactions of hydrolysis (phospholipase A_2 mainly) to lysophosphatidylcholine, acyl-CoA synthesis and re-acylation by lysophospholipid acyltransferases or transacylases, a series of reactions that is sometimes termed the 'Lands' Cycle' after its discoverer W.E.M. (Bill) Lands. Similar processes occur with all glycerophospholipid classes.

The final composition of the lipid is achieved by a mixture of de novo synthesis and the remodeling pathway. At least 15 groups of enzymes in the phospholipase A_2 super-family differ in calcium dependence, cellular location, and structure. All hydrolyze the *sn*-2 ester bond of phospholipids specifically, generating a fatty acid and lysophospholipid, which have important functions in addition to their role in the Lands cycle. There is also a phospholipase A_1 family of enzymes, which are esterases that can cleave the *sn*-1 ester bond but are less important in this context.

Figure **21.3.15** shows Land's cycle

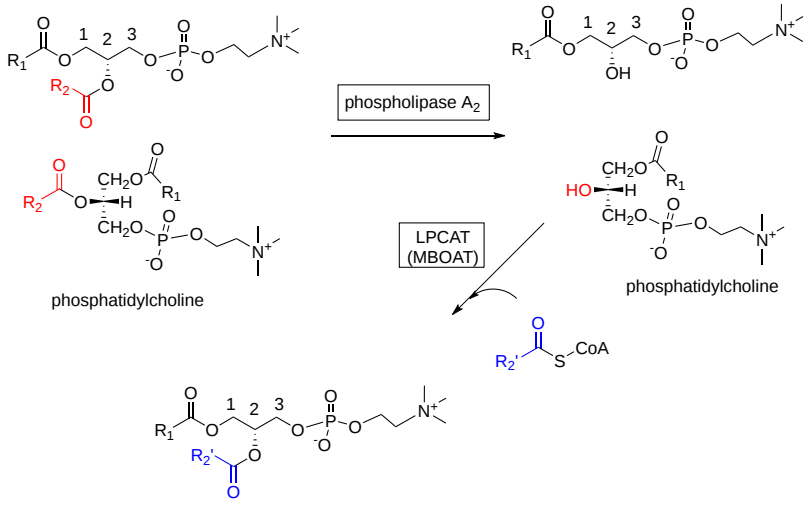


Figure **21.3.15**: Land's cycle - 1

The re-acylation step is catalyzed by membrane-bound coenzyme A-dependent lysophosphatidylcholine acyltransferases such as LPCAT3 (also designated ‘MBOAT5’), which is located chiefly within the endoplasmic reticulum, though also in mitochondria and the plasma membrane in organs such as the liver, adipose tissue, and pancreas. It maintains systemic lipid homeostasis by regulating lipid absorption and composition in the intestines, the secretion of lipoproteins, and lipogenesis *de novo* in the liver, and it is notable in that it incorporates

linoleoyl and arachidonoyl chains specifically into lysophosphatidylcholine (as does a related enzyme LPCAT2). There is also a CoA-independent acyltransferase in inflammatory cells that transfers arachidonic acid from phosphatidylcholine to ethanolamine-containing phospholipids. While LPCAT3 prefers 1-acyl lysophosphatidylcholine as an acyl acceptor, LPCAT2 utilizes 1-acyl and 1-alkyl precursors. LPCAT2 is highly expressed in inflammatory cells such as macrophages and neutrophils, which contain ether-phospholipids and contribute to the production of eicosanoid lipid mediators. The highly saturated molecular species of phosphatidylcholine found in lung surfactant are formed from species with a more conventional composition by remodeling by an acyltransferase with a high specificity for palmitoyl-CoA acid (LPCAT1). In other tissues, those species containing high proportions of polyunsaturated fatty acids depend more on de novo synthesis. These and further related enzymes are involved in remodeling all other phospholipids. Overexpression of the genes for these enzymes is associated with the progression of many different cancers and may be involved in other pathological conditions.

Phosphatidylcholine has a central role in glycerolipid metabolism in plants, and remodeling occurs for reasons and by mechanisms that are rather different from those in animal cells, as described briefly above. For example, there is extensive remodeling involving fatty acid desaturation, which is the main entry point for acyl groups exported from the plastid into the endoplasmic reticulum. In addition, the remodeling of phosphatidylcholine provides fatty acids for triacylglycerol synthesis in developing seeds and diacylglycerols for synthesizing thylakoid lipids such as **galactosyldiacylglycerols**. In Arabidopsis, two lysophosphatidylcholine acyltransferases, LPCAT1 and LPCAT2, are used in remodeling in developing seeds and leaves, with some preference for position *sn*-2 using fatty acids exported from the plastid. In some plant species, there is a strong preference for C_{18}-unsaturated acyl chains over 16:0. However, the lipases that generate lysophosphatidylcholine from phosphatidylcholine for this purpose are unknown. Some remodeling in plant membranes occurs in response to stress.

The yeast *Saccharomyces cerevisiae* can reacylate glycerophosphocholine, generated endogenously by the action of phospholipase B (an enzyme with both phospholipase A_1 and A_2 activities) on phosphatidylcholine, with acyl-CoA in the microsomal membranes using a glycerophosphocholine acyltransferase (Gpc1) to produces lysophosphatidylcholine, which can be converted back to phosphatidylcholine by the lysophospholipid acyltransferase (Ale1) with appreciable changes in the molecular species composition. The process is regulated in coordination with the other main lipid pathways and affects yeast growth. The enzyme Gpc1 does not affect other phospholipids in yeast. A similar mechanism appears to operate in some plant species. Figure **21.3.16** shows the Land's cycle variants.

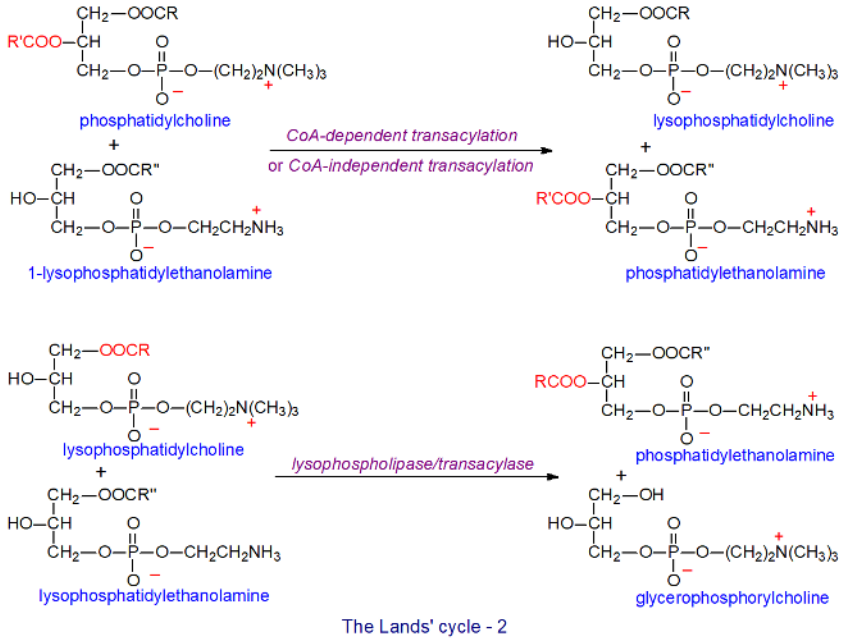


Figure **21.3.16**: Variants of the Land's cycle - 2

21.3.3.4: CATABOLISM

Phosphatidylcholine (and most other glycerophospholipids) in membranes can be metabolized by lipolytic enzymes, especially phospholipases, some isoforms specific for particular lipid classes in humans. For example, in addition to the action of phospholipase A (discussed above), phospholipase C (six families in mammals differing in expression and subcellular distribution) yields **diacylglycerols** together with phosphocholine by hydrolyzing glycerophospholipids at the phosphodiester bond. This process is especially important in relation to **phosphoinositide** metabolism. The **sphingomyelin synthases** also have phospholipase C activity (in the absence of ceramide). Phospholipase D generates **phosphatidic acid** and choline, while phospholipase B removes both fatty acids to yield glycerophosphocholine.

Figure **21.3.17** shows the activities of phospholipases on phosphatidylcholine.

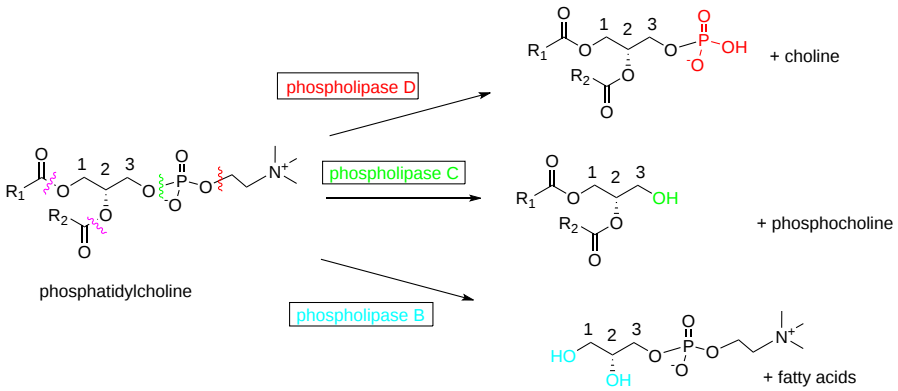


Figure **21.3.17**: Activities of phospholipases on phosphatidyl choline

On catabolism in this way, the lipid components are recycled, or they may have signaling functions. At the same time, much of the choline is reused for phosphatidylcholine biosynthesis, often after being returned to the liver (the CDP-choline cycle). Some choline is oxidized in the kidney and liver to betaine, which serves as a donor of methyl groups for *S*-adenosylmethionine production, and some is lost through the excretion of phosphatidylcholine in bile. A proportion is used in nervous tissues to produce acetylcholine, a neurotransmitter important to learning, memory, and sleep. The liver takes up phosphatidylcholine in the high-density lipoproteins of plasma, and perhaps surprisingly, a high proportion of this is eventually converted to triacylglycerols via diacylglycerol intermediates.

? PHOSPHATIDYL CHOLINE - ADDITIONAL BACKGROUND

Click the link below.

Link

Phosphatidylcholine – Biological Functions

Because of the generally cylindrical shape of the molecule, phosphatidylcholine organizes spontaneously into bilayers, so it is ideally suited to serve as the bulk structural element of biological membranes. As outlined above, it makes up a high proportion of the lipids in the outer leaflet of the plasma membrane. The unsaturated acyl chains are kinked and confer fluidity on the membrane. Such properties are essential to act as a balance to those lipids that do not form bilayers or that form specific micro-domains such as **rafts**. While phosphatidylcholine does not induce curvature of membranes, as may be required for membrane transport and fusion processes, it can be metabolized to form lipids that do.

In contrast, dipalmitoyl phosphatidylcholine is the main surface-active component of human lung surfactant. However, in other animals, the lung surfactant can be enriched in some combination of short-chain disaturated and monounsaturated species, mainly palmitoylmyristoyl- and palmitoylpalmitoleoyl- in addition to the dipalmitoyl-lipid. This is believed to provide alveolar stability by decreasing the surface tension at the alveolar surface to a very low level during inspiration while preventing alveolar collapse at the end of expiration. Also, the internal lipids of the animal cell nucleus (after the external membrane has been removed) contain a high proportion of disaturated phosphatidylcholine. This is synthesized entirely within the nucleus, unlike phosphatidylinositol, for example, and in contrast to other cellular lipids, its composition cannot be changed by extreme dietary manipulation; it has been suggested that it may have a role in stabilizing or regulating the structure of the chromatin, as well as being a source of diacylglycerols with a signaling function. A further unique molecular species, 1-oleoyl-2-palmitoyl-phosphatidylcholine, is located specifically at the protrusion tips of neuronal cells and appears essential for their function. 1-palmitoyl-2-arachidonoyl-phosphatidylcholine is important in regulating the progression of the cell cycle and cell proliferation, which is independent of eicosanoid production.

Phosphatidylcholine is bound non-covalently in many membrane proteins' crystal structures, including cytochrome c oxidase and yeast cytochrome bc_1. The ADP/ATP carrier protein has two binding sites for phosphatidylcholine, one on each side. In addition, it is known that the enzyme 3-hydroxybutyrate dehydrogenase must be bound to phosphatidylcholine before it can function optimally. Depending on the protein, the head group and the acyl chains may be involved in the interactions.

As noted above, phosphatidylcholine is the most abundant phospholipid component in plasma and all plasma **lipoprotein** classes. Although it is especially abundant in high-density lipoproteins (HDL), it strongly influences the levels of all circulating lipoproteins and especially of the very-low-density lipoproteins (VLDL), which are surrounded by a phospholipid monolayer. Indeed, phosphatidylcholine with polyunsaturated fatty acids in position *sn*-2 is essential for the assembly and secretion of VLDLs and

chylomicrons in the liver and the intestines, and it must be synthesized *de novo* in the latter. Similarly, phosphatidylcholine synthesis is required to stabilize the surface of lipid droplets in tissues where **triacylglycerols** are stored.

Some of the phosphatidylcholine synthesized in the liver is secreted into bile by a specific flippase together with bile acids, where it assists in the emulsification of dietary triacylglycerols in the intestinal lumen to facilitate their hydrolysis and uptake. Eventually, it is absorbed across the intestinal brush border membrane after hydrolysis to lysophosphatidylcholine, which may then be involved in initiating chylomicron formation in the endoplasmic reticulum of enterocytes by activating a protein kinase. In addition, phosphatidylcholine produced in enterocytes is secreted into the intestinal lumen, forming part of the hydrophobic mucus layer that protects the intestinal surface.

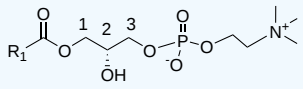
Phosphatidic acid generated from phosphatidylcholine by the action of phospholipase D in plants has key signaling functions. Similarly, phosphatidic acid generated in this way from phosphatidylcholine in animals is involved in the metabolism and signaling function of phosphoinositides by activating phosphatidylinositol 4-phosphate 5-kinase, the main enzyme generating the lipid second messenger **phosphatidylinositol-4,5-bisphosphate**. The plasmalogen form of phosphatidylcholine may also have a signaling function, as thrombin treatment of endothelial cells activates a selective hydrolysis (phospholipase A_2) of molecular species containing arachidonic acid in the *sn*-2 position, releasing this fatty acid for eicosanoid production. In contrast, the diacyl form of phosphatidylcholine may have a related function in signal transduction in other tissues. In addition, phosphatidylcholine may have a role in signaling via the generation of **diacylglycerols** by phospholipase C, especially in the nucleus. Although the precursor pool is so great in many tissues that turnover is not easily measured, the presence of phospholipases C and D that are specific for phosphatidylcholine and are activated by many agonists suggests such a function, especially in the cell nucleus. Diacylglycerols formed this way would be much more saturated than those derived from phosphatidylinositol and would not be expected to be as active in some functions.

Phosphatidylcholine is the biosynthetic precursor of **sphingomyelin** and, as such, must have some influence on the many metabolic pathways that constitute the sphingomyelin cycle. It is also a precursor for phosphatidic acid, lysophosphatidylcholine, and **platelet-activating factor**, each with important signaling functions, and of **phosphatidylserine**.

Because of the increased demand for membrane constituents, phosphatidylcholine synthesis is enhanced in cancer cells and solid tumors; the various biosynthetic and catabolic enzymes are potential targets for developing new therapeutic agents. Impaired phosphatidylcholine biosynthesis has been observed in many pathological conditions in the liver in humans, including the development of non-alcoholic fatty liver disease, liver failure, and impaired liver regeneration. Similarly, a deficiency in phosphatidylcholine or an imbalance in the ratio of phosphatidylcholine to phosphatidylethanolamine negatively affects insulin sensitivity and glucose homeostasis in skeletal muscle.

Plants and bacteria: In addition to its structural role in plant membranes, phosphatidylcholine levels at the shoot apex correlate with flowering time, and this lipid is believed to bind to the Flowering Locus T, a master regulator of flowering. Molecular species containing relatively low levels of α-linolenic acid are involved. Diacylglycerols formed by the action of a family of enzymes of the phospholipase C type on phosphatidylcholine, as opposed to phosphatidylinositol, may be more important in plants and especially during phosphate deprivation for the generation of precursors for galactolipid biosynthesis and perhaps for lipid remodeling more generally. In prokaryotes, phosphatidylcholine is essential for certain symbiotic and pathogenic microbe-host interactions. For example, in human pathogens such as *Brucella abortus* and *Legionella pneumophila*, this lipid is necessary for full virulence, and the same is true for plant pathogens such as *Agrobacterium tumefaciens*. Bacteria symbiotic with plants, e.g., the rhizobial bacterium *Bradyrhizobium japonicum*, require it to establish efficient symbiosis and root nodule formation.

Figure **21.3.18** shows the structure of lysophosphatidylcholine



lysophosphatidylcholine

Figure **21.3.18**: Lysophosphatidylcholine

Lysophosphatidylcholine (LPC)

Lysophosphatidylcholine (LPC), with one mole of fatty acid per mole of lipid in position *sn*-1, is found in trace amounts in most animal tissues. However, there are relatively high concentrations in plasma (150–500μM). It is produced by the hydrolysis of dietary and biliary phosphatidylcholine and is absorbed as such in the intestines, but it is re-esterified before being exported in the lymph. In addition, it is formed in most tissues by the hydrolysis of phosphatidylcholine using the superfamily of **phospholipase A_2** enzymes as part of the de-acylation/re-acylation cycle that controls the overall molecular species composition of the latter, as discussed above. Much of the LPC in the plasma of animal species is secreted by hepatocytes into the plasma in a complex with

albumin. Still, an appreciable amount is formed in plasma by the action of the enzyme **lecithin:cholesterol acyltransferase (LCAT)**, which is secreted by the liver. This catalyzes the transfer of fatty acids from position *sn*-2 of phosphatidylcholine to free cholesterol in plasma, with formation of cholesterol esters and, of course, lysophosphatidylcholine, which consists of a mixture of molecular species with predominantly saturated and mono- and dienoic fatty acid constituents. The action of an endothelial lipase on phosphatidylcholine in HDL forms some LPC.

At high concentrations, lysophosphatidylcholine can disrupt membranes, while some biological effects at low concentrations may be simply due to its ability to diffuse readily into membranes, altering their curvature and indirectly affecting the properties of membrane proteins. In plasma, it is bound to albumin and lipoproteins so that its effective concentration is reduced to a relatively safe level.

Lysophosphatidylcholine is considered to be an important factor in cardiovascular and neurodegenerative diseases. It is usually considered to have pro-inflammatory properties, and it is known to be a pathological component of oxidized lipoproteins (LDL) in plasma and of atherosclerotic lesions when generated by over-expression or enhanced activity of phospholipase A2. Its concentration is elevated in joint fluids from patients with rheumatoid arthritis. In addition, it is a major component of platelet-derived microvesicles and activates a specific receptor in platelets, ultimately leading to vascular inflammation and increasing the instability of atherosclerotic plaques. The intracellular acyltransferase LPCAT cannot remove lysophosphatidylcholine directly from plasma or lipoproteins, nor do there appear to be any enzymes with lysophospholipase A_1 activity in the circulation. Lysophosphatidylcholine blocks the formation of early hemifusion intermediates required for cell-cell fusions. Lysophosphatidylcholine in insect bites attracts inflammatory cells to the site, enhances parasite invasion, and inhibits nitric oxide production, for example, in Chagas disease. Elevated levels of 26:0-lysophosphatidylcholine in blood are reported to be characteristic of Zellweger spectrum disorders (the result of a defect in peroxisome biogenesis).

Elevated levels of lysophosphatidylcholine have been identified in cervical cancer and may be diagnostic for the disease. On the other hand, reduced concentrations of lysophosphatidylcholine are observed in some malignant cancers, and it has protective effects in patients undergoing chemotherapy. Stearoyl-lysophosphatidylcholine has an anti-inflammatory role in protecting against lethal sepsis in experimental animals by various mechanisms, including the stimulation of neutrophils to eliminate invading pathogens through a peroxide-dependent reaction. Similarly, there are reports that lysophosphatidylcholine may have beneficial effects in rheumatoid arthritis and other diseases. However, there are suggestions that some experimental studies *in vitro* of the activity of lysophosphatidylcholines may be flawed because insufficient levels of carrier proteins were used. A further point for consideration is that lysophosphatidylcholine is the precursor of the key lipid mediator **lysophosphatidic acid** via the action of the enzyme autotaxin in plasma, and this may be the true source of some of the effects described for the former, especially on cell migration and survival.

There is evidence to suggest that lysophosphatidylcholine containing docosahexaenoic (DHA) and eicosapentaenoic (EPA) acids, presumably in position *sn*-2, in plasma targets more of these fatty acids into the brain, via a specific receptor/transporter at the blood-brain barrier known as the sodium-dependent LPC symporter 1 (MFSD2A), than occurs from the corresponding fatty acids in unesterified form. Hepatic lipase is especially important for the generation of these lipids. This finding is now being explored in relation to potential therapeutic applications for neurological diseases, cognitive decline, and dementia. Similarly, at the maternal plasma/placental interface, phosphatidylcholine is taken up and hydrolyzed to *sn*-2-lysophosphatidylcholine, presumably by the endothelial lipase, to facilitate the transfer of polyunsaturated fatty acids across the basal membrane into the fetal circulation with the aid of the same LPC transporter.

Lysophosphatidylcholine has been found to have some functions in cell signaling, and specific receptors (coupled to G proteins) have been identified, i.e., GPR119, GPR40, and GPR55. It activates the specific phospholipase C that releases diacylglycerols and inositol triphosphate with resultant increases in intracellular Ca^{2+} and activation of protein kinase C. Increased glucose-stimulated insulin secretion has been observed in different cell systems. Lysophosphatidylcholine also activates the mitogen-activated protein kinase in certain cell types, promoting demyelination in the nervous system. The interaction of lysophosphatidylcholine with the TRPV4 ion channels of skin keratinocytes can cause persistent itching. Identifying a highly specific phospholipase A2γ in peroxisomes that is unique in generating *sn*-2-arachidonoyl lysophosphatidylcholine suggests that this may be relevant to eicosanoid generation and signaling. For example, there is reportedly an enrichment of 2-arachidonoyl-lysophosphatidylcholine in carotid atheroma plaque from type 2 diabetic patients. In vascular endothelial cells, it induces the important pro-inflammatory mediator **cyclooxygenase-2 (COX-2)**, a key enzyme in prostaglandin synthesis. However, it has beneficial effects on the innate immune system as it can activate macrophages and increase their phagocytic activity in the presence of T lymphocytes.

Lysophospholipids in general and lysophosphatidylcholine in particular are important signaling molecules within mammalian cells. Their levels are closely regulated, mainly by the action of the lysophospholipases A_1 and A_2 (LYPLA1 and LYPLA2), depending on

the position to which the fatty acid is esterified; these are cytosolic serine hydrolases with esterase and thioesterase activity. The glycerophosphocholine produced can enter the Lands' cycle or be further degraded.

In plants, amylose-rich starch granules of cereal grains contain lysophosphatidylcholine as virtually the only lipid in the form of inclusion complexes or lining channels in the starch macromolecules.

21.3.4: PHOSPHATIDYLETHANOLAMINE AND RELATED LIPIDS

21.3.4.1: PHOSPHATIDYLETHANOLAMINE – STRUCTURE AND OCCURRENCE

Phosphatidylethanolamine or 1,2-diacyl-*sn*-glycero-3-phosphoethanolamine (once given the trivial name 'cephalin') is usually the second most abundant phospholipid in animal and plant lipids, after phosphatidylcholine, and it is frequently the main lipid component of microbial membranes. It can amount to 20% of liver phospholipids and as much as 45% of those of the brain; higher proportions are found in mitochondria than in other organelles. As such, it is a key building block of membrane bilayers, and it is present exclusively in the inner leaflet of the plasma membrane in animal cells, for example. It is a neutral or zwitterionic phospholipid (at least in the pH range 2 to 7), with the structure shown (with one specific molecular species illustrated as an example).

Figure **21.3.19** shows the structure of phosphatidylethanolamine.

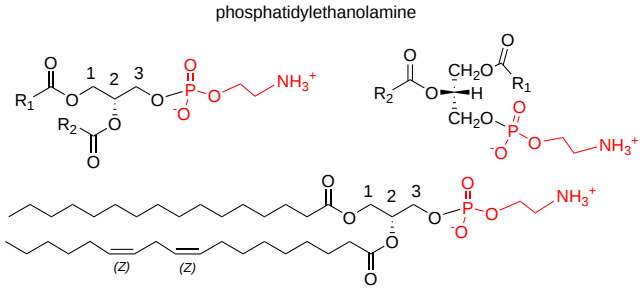


Figure **21.3.19**: Phosphatidylethanolamine

In animal tissues, phosphatidylethanolamine tends to exist in diacyl, alkyl, alkenyl, and acyl forms. As much as 70% of the phosphatidylethanolamine in some cell types (especially inflammatory cells, neurons, and tumor cells) can have an ether linkage. Still, in the liver, the plasmalogen form of phosphatidylethanolamine, i.e., with an O-alk-1'-enyl linkage, accounts for only 0.8% of total phospholipids. Generally, there is a much higher proportion of PE with ether linkages than of PC. If physiological conditions inhibit biosynthesis of the plasmalogen form, it is replaced by the diacyl form so that the overall content of the phospholipid remains constant.

Animal phosphatidylethanolamine tends to contain higher proportions of arachidonic and docosahexaenoic acids than the other zwitterionic phospholipid, phosphatidylcholine. These polyunsaturated components are concentrated in position *sn*-2 with saturated fatty acids most abundant in position *sn*-1, as illustrated for rat liver and chicken egg in Table **21.3.3**. In most other species, it would be expected that the structure of the phosphatidylethanolamine in the same metabolically active tissues would exhibit similar features.

Table **21.3.3**: **Positional distribution of fatty acids in phosphatidylethanolamine in animal tissues.**

Position	Fatty acid						
	14:0	16:0	18:0	18:1	18:2	20:4	22:6
Rat liver [1]							
***sn*-1**		25	65	8			
***sn*-2**	2	11	8	8	10	46	13
Chicken egg [2]							
***sn*-1**		32	59	7	1		
***sn*-2**		1	1	25	22	29	12
1, Wood, R. and Harlow, R.D., *Arch. Biochem. Biophys.*, **131**, 495-501 (1969); 2, Holub, B.J. and Kuksis, A. *Lipids*, **4**, 466-472 (1969);							

The *O*-alkyl and *O*-alkenyl chains at the *sn*-1 position of the analogous ether lipids generally consist of 16:0, 18:0 or 18:1 chains. In contrast, arachidonic and docosahexaenoic acids are the most abundant components at the *sn*-2 position.

The positional distributions of fatty acids in phosphatidylethanolamine from the model plant *Arabidopsis thaliana* leaves are listed in Table **21.3.4**. Here, saturated fatty acids are also concentrated in position *sn*-1, and there is a preponderance of di- and triunsaturated in position *sn*-2. The pattern is somewhat different for the yeast *Lipomyces lipoferus*, where the compositions of the two positions are relatively similar.

Table **21.3.4**: **Composition of fatty acids (mol%) in positions *sn*-1 and *sn*-2 in the phosphatidylethanolamine from leaves of *Arabidopsis thaliana* and from *Lipoferus lipoferus*.**

Position	Fatty acid					
	16:0	16:1	18:0	18:1	18:2	18:3
A. thaliana [1]						
***sn*-1**	58	trace	4	5	15	18
***sn*-2**	trace	trace	trace	2	60	38
L. lipoferus [2]						
***sn*-1**	29	18	4	28	13	6
***sn*-2**	23	15	3	34	17	6

1, Browse, J., Warwick, N., Somerville, C.R., and Slack, C.R. *Biochem. J.*, **235**, 25-31 (1986); DOI.
2, Haley, J.E. and Jack, R.C. *Lipids*, **9**, 679-681 (1974); DOI .

21.3.4.2: PHOSPHATIDYLETHANOLAMINE – BIOSYNTHESIS

The two main pathways employed by mammalian cells for the biosynthesis of phosphatidylethanolamine are the CDP-ethanolamine pathway, i.e., one of the general routes to phospholipid biosynthesis *de novo* in plants and animals, and the phosphatidylserine decarboxylase pathway, which occurs in two spatially separated organelles - the endoplasmic reticulum and mitochondria, respectively. Ethanolamine is obtained by decarboxylation of serine in plants, and in animals, most must come from dietary sources and require facilitated transport into cells. A small amount of ethanolamine phosphate comes from the catabolism of **sphingosine-1-phosphate**, which is essential for the survival of the protozoan *Trypanosoma brucei*. The initial steps in phosphatidylethanolamine biosynthesis occur in the cytosol, with the phosphorylation of ethanolamine by two specific ethanolamine kinases to produce ethanolamine phosphate; the reverse reaction can occur using the enzyme ethanolamine phosphate phosphorylase, and this may have a regulatory function in some tissues. The second step is rate-limiting, i.e., the reaction of the product with cytidine triphosphate (CTP) to form cytidine diphosphoethanolamine catalyzed by CTP:phosphoethanolamine cytidylyltransferase.

In the final step, a membrane-bound enzyme CDP-ethanolamine:diacylglycerol ethanolaminephosphotransferase catalyzes the reaction of cytidine diphosphoethanolamine with diacylglycerol to form phosphatidylethanolamine. There are two such enzymes, ethanolamine phosphotransferase 1 (EPT1) in the Golgi and choline/EPT1 (CEPT1) in the endoplasmic reticulum, but EPT1 is more important for the biosynthesis of the **plasmalogen form**, 1-alkenyl-2-acyl-glycerophosphoethanolamine, and especially molecular species containing polyunsaturated fatty acids. At the same time, CEPT1 produced species with shorter-chain fatty acids. The diacylglycerol precursor is formed from phosphatidic acid via the action of the enzyme phosphatidic acid phosphohydrolase.

Figure **21.3.20** shows the synthesis of phosphatidyethanolamine in the ER/Golgi.

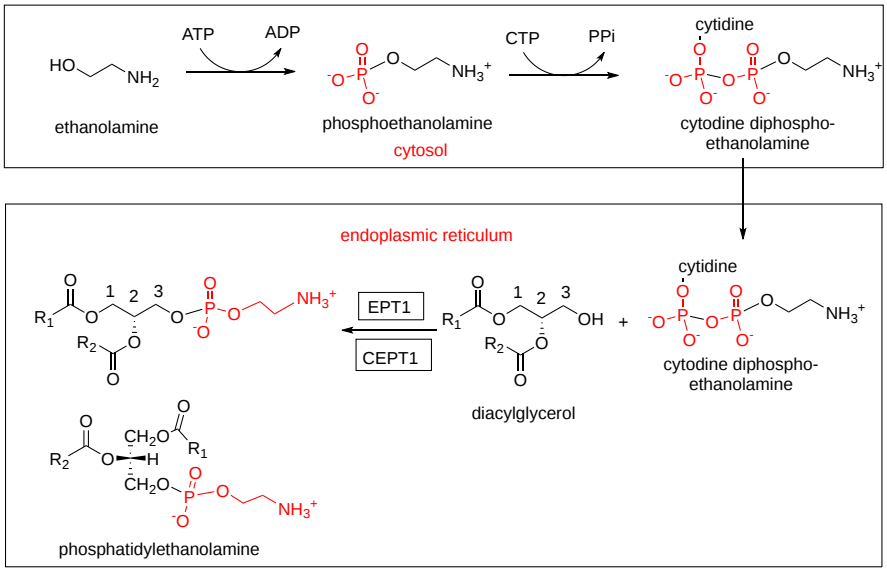


Figure **21.3.20**: Synthesis of phosphatidyethanolamine in the ER/Golgi

The second major pathway is the conversion of phosphatidylserine (decarboxylation) to phosphatidylethanolamine in mitochondria. The conservation of this pathway from bacteria to humans suggests that it has been preserved to optimize mitochondrial performance. Mitochondria are not connected with the rest of the cell's membrane network by classical vesicular routes but must receive and export small molecules through the nonvesicular transport at zones of proximity with other organelles at membrane contact sites, such as a specific domain of the endoplasmic reticulum termed the mitochondria-associated membrane (MAM). Lipid transport of phosphatidylserine is then enabled by tethers that bridge two membranes, lipid transfer proteins, and recruitment proteins. In this process, the lipid must traverse two aqueous compartments, the cytosol and the mitochondrial intermembrane space, to reach the inner mitochondrial membrane.

The phosphatidylserine decarboxylase is located on the external aspect of the mitochondrial inner membrane, and most of the phosphatidylethanolamine in mitochondria is derived from this pathway. While various isoforms of the phosphatidylserine decarboxylation exist in prokaryotes, yeasts, and mammals, the main forms designated 'PSD1' are found only in mitochondria and are related structurally. An isoform designated 'PSD2' is located in the endosomal membranes of yeasts, and the phosphatidylethanolamine formed is the preferred substrate for phosphatidylcholine biosynthesis. Cellular concentrations of phosphatidylethanolamine and phosphatidylserine are closely related and tightly regulated.

Figure **21.3.21** shows the synthesis of phosphatidyethanolamine in mitochondria.

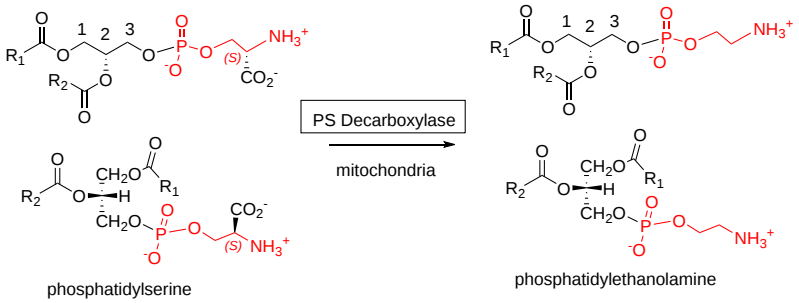


Figure **21.3.21**: Synthesis of phosphatidyethanolamine in mitochondria

In prokaryotic cells, such as *E. coli*, in which phosphatidylethanolamine is the most abundant membrane phospholipid, all of it is derived from phosphatidylserine decarboxylation. In this instance, the enzyme undergoes auto-cleavage for activation and utilizes a pyruvoyl moiety to form a Schiff base intermediate with phosphatidylserine to facilitate decarboxylation. This pathway is also important in mammalian cells and yeasts. However, the relative contributions of the two main pathways for phosphatidylethanolamine synthesis in mammalian cells appears to depend on the cell type. In cells in culture, more than 80% of the phosphatidylethanolamine is reported to be derived from the phosphatidylserine decarboxylase pathway. In hamster heart and rat hepatocytes, only ~5% of phosphatidylethanolamine synthesis comes from this route, and most is from the CDP-ethanolamine pathway. In yeast, 70% of the phosphatidylethanolamine is generated by PSD1. The spatially distinct pools within the cell are functionally distinct, but both are essential to life. For example, disruption of the phosphatidylserine decarboxylase gene causes misshapen mitochondria and has lethal consequences in embryonic mice, although

phosphatidylethanolamine synthesis continues for a time in other cellular regions. Similarly, the elimination of the endoplasmic reticulum route is embryonically lethal.

Three additional minor biosynthetic pathways are known. Phosphatidylethanolamine can be formed by the enzymatic exchange reaction of ethanolamine with phosphatidylserine or by re-acylation of lysophosphatidylethanolamine. The second is associated with the mitochondria-associated membrane, where the phosphatidylserine synthase II is located. Finally, the bacterial plant pathogen *Xanthomonas campestris* can synthesize phosphatidylethanolamine by condensing **cytidine diphosphate diacylglycerol** with ethanolamine.

Ether lipids: It should be noted that all of these pathways for the biosynthesis of diacyl-phosphatidylethanolamine are very different and are separated spatially from those producing **alkyl, acyl- and alkenyl,acyl-phosphatidylethanolamines**, suggesting that there may be functional differences. In the protozoon *T. brucei*, for example, it has been demonstrated that the diacyl and ether pools of phosphatidylethanolamine have separate functions and cannot substitute for each other.

Lands cycle: The various mechanisms produce different pools of phosphatidylethanolamine species, often in different cellular compartments with distinctive compositions. Studies with mammalian cell types *in vitro* suggest that the CDP-ethanolamine pathway produces molecular species with mono- or di-unsaturated fatty acids on the *sn*-2 position preferentially. At the same time, the phosphatidylserine decarboxylation reaction mainly generates species with polyunsaturated fatty acids on the *sn*-2 position. However, as with other phospholipids, the final fatty acid composition in animal tissues is attained by a process of remodeling known as the Lands cycle. The first step is hydrolysis by a phospholipase A_2 to lysophosphatidylethanolamine, followed by reacylation using various acyl-CoA:lysophospholipid acyltransferases. The enzymes LPCAT1, 2, and 3, which are involved in phosphatidylcholine biosynthesis, are also active with phosphatidylethanolamine, while LPEAT1 mainly utilizes lysophosphatidylethanolamine and is specific for oleoyl-CoA. Some of these isoforms appear to be confined to particular tissues. A CoA-independent acyltransferase in macrophages also transfers arachidonic acid from phosphatidylcholine to ethanolamine-containing phospholipids.

? PHOSPHTIDYLETHANOLAMINE - ADDITIONAL BACKGROUND

Click the link below for more information.

Link

21.3.4.3: PHOSPHATIDYLETHANOLAMINE – BIOLOGICAL FUNCTION

Physical properties: Although PE has sometimes been equated with PC in biological systems, there are significant differences in these lipids' chemistry and physical properties, and they have different functions in biochemical processes. Both are key components of membrane bilayers, and the ratio of the two may be important to many cellular functions. However, PE has a smaller head group, which gives the lipid a cone shape. On its own, it does not form bilayers but inverted hexagonal phases. With other lipids in a bilayer, it is believed to exert a lateral pressure that modulates membrane curvature and stabilizes membrane proteins in their optimum conformations. It can hydrogen bond to adjacent lipids and proteins through its polar head group. For example, the phosphate can be stabilized at the binding site by interactions with lysine and arginine side chains or with hydroxyls from tyrosine side chains. There can also be strong interactions with the acyl chains of the phospholipid.

In contrast to phosphatidylcholine, phosphatidylethanolamine is concentrated with phosphatidylserine in the inner leaflet of the plasma membrane. On the other hand, it is present in both the inner and outer membranes of mitochondria, but especially the former, where it is present at much higher levels than in other organelles and facilitates membrane fusion and protein movement across membranes in addition to many other essential mitochondrial functions, including oxidative phosphorylation via the electron transport chain. It is an important functional component of membrane contact sites between the endoplasmic reticulum and mitochondria. Studies suggest that eukaryotic cells, especially those of insects, have a similar function to cholesterol in membranes in that they increase the rigidity of the bilayer to maintain membrane fluidity. In bacterial membranes, it appears that a primary role for phosphatidylethanolamine is simply to dilute the high negative charge density of the anionic phospholipids.

Protein Interactions: Membrane proteins amount to 30% of the genome, and they carry out innumerable biochemical functions, including transport, energy production, biosynthesis, signaling, and communication. Within a membrane, most integral proteins consist of hydrophobic α-helical transmembrane domains that zigzag across it and are connected by hydrophilic loops. Of those parts of the proteins outwith the bilayer, positively charged residues are much more abundant on the cytoplasmic side of membrane proteins than on the trans side (the positive-inside rule). Phosphatidylethanolamine is believed to have a key function in that it inhibits the location of negative amino acids on the cytoplasmic side, supporting the positive-inside rule, and it has an appropriate charge density to balance that of the membrane surface and the protein. However, it can also permit the presence of negatively charged residues on the cytosolic surface in some circumstances in support of protein function.

Phosphatidylethanolamine is vital for mitochondrial functionality, as demonstrated by defects in the operation of oxidative phosphorylation in the absence of PSD1, and by the role of the lipid in the regulation of mitochondrial dynamics in general and the biogenesis of proteins in the outer mitochondrial membrane. Synthesis of phosphatidylethanolamine in the inner membrane of mitochondria is critical for the function of the cytochrome bc_1 complex (III), where there is a conserved binding site for the lipid in a specific subunit.

Phosphatidylethanolamine binds non-covalently to a superfamily of cytosolic proteins with multiple functions termed 'phosphatidylethanolamine-binding proteins'. While four members have been identified in mammals (PEBP1-4), more than 400 family members conserved during evolution are known from bacteria to higher eukaryotes. These have many different functions, including lipid binding, neuronal development, serine protease inhibition, and the regulation of several signaling pathways; in plants, they control shoot growth and flowering. PEBP4 is particularly interesting as it is highly expressed in many different cancers and can increase their resistance to therapy. In animal tissues, phosphatidylethanolamine is especially important in the sarcolemmal membranes of the heart during ischemia; it is involved in the secretion of the nascent very-low-density lipoproteins from the liver, and it has functions in membrane fusion and fission. It has a functional role in the Ca^{2+}-ATPase in that one molecule of phosphatidylethanolamine is bound in a cavity between two transmembrane helices, acting as a wedge to keep them apart. This is displaced when Ca^{2+} is bound to the enzyme. Many other important proteins bind non-covalently to phosphatidylethanolamine similarly, including rhodopsin and aquaporins.

The content of phosphatidylethanolamine in newly secreted VLDL particles and apoB-containing particles isolated from the lumen of the Golgi is much higher than that in circulating VLDLs, suggesting that this lipid is involved in VLDL assembly and/or secretion. However, it is rapidly and efficiently removed from the VLDL in circulation. With lipid droplets in cells, PE is believed to promote the coalescence of smaller droplets into larger ones.

Although the mechanism has yet to be fully elucidated, effects on protein conformation are believed to be behind a finding that phosphatidylethanolamine is the primary factor in the brain required for the propagation and infectivity of mammalian prions. Host defense peptides are antimicrobial agents produced by both prokaryotic and eukaryotic organisms, and many of these have a high affinity for phosphatidylethanolamine as a lipid receptor to modulate their activities. For example, the peptide antibiotics cinnamycin and duramycins from Streptomyces have a hydrophobic pocket that fits around phosphatidylethanolamine such that the binding is stabilized by ionic interaction between the ethanolamine group of the lipid and the carboxylate moiety of the peptide; this complex exhibits activity against other Gram-positive organisms, such as *Bacillus* species.

Much of the evidence for the unique properties of PE comes from studies of the biochemistry of the bacterium *E. coli*, where this lipid is a major component of the membranes. Gram-negative bacteria have two membrane bilayers in the cell wall. As much as 90% of the phospholipid in the inner leaflet of the outer membrane is phosphatidylethanolamine, with a high proportion in the cytoplasmic leaflet of the inner membrane also. In particular, PE has a specific involvement in supporting the active transport of lactose by the lactose permease, and other transport systems may require or be stimulated by it. There is evidence that phosphatidylethanolamine acts as a 'chaperone' during the assembly of this and other membrane proteins to guide the proteins' folding path and aid in the transition from the cytoplasmic to the membrane environment.

Autophagy and ferroptosis: A covalent conjugate of phosphatidylethanolamine with a protein designated 'Atg8' is formed by the action of cysteine protease ATG4 (belonging to the caspase family) and various other proteins, and is involved in the process of autophagy (controlled degradation of cellular components) in yeast by promoting the formation of membrane vesicles containing the components to be degraded (**phosphatidylinositol 3-phosphate** is also essential to this process). Similarly, oxidatively modified phosphatidylethanolamine is an important factor in **ferroptosis**, a form of apoptosis in which disturbances to iron metabolism lead to an accumulation of hydroperoxides.

Precursor of other lipids: Phosphatidylethanolamine is a precursor for the synthesis of *N*-acyl-phosphatidylethanolamine (see below) and thence of **anandamide** (*N*-arachidonoylethanolamine), and it is the donor of ethanolamine phosphate during the synthesis of the **glycosylphosphatidylinositol anchors** that attach many signaling proteins to the surface of the plasma membrane. In bacteria, it functions similarly in the biosynthesis of **lipid A** and other lipopolysaccharides. It is also the substrate for the hepatic enzyme phosphatidylethanolamine *N*-methyltransferase, which provides about a third of the **phosphatidylcholine** in the liver.

Miscellaneous other functions: Phosphatidylethanolamine is the precursor of an ethanolamine phosphoglycerol moiety bound to two conserved glutamate residues in eukaryotic elongation factor 1A, an essential component in protein synthesis. This unique modification appears to be of great importance for the resistance of plants to attack by pathogens. *Francisella tularensis* bacteria, the cause of tularemia, suppress host inflammation and the immune response when infecting mouse cells. The effect is due to a distinctive phosphatidylethanolamine species containing 10:0 and 24:0 fatty acids, and the synthetic lipid produces the same effects

in vitro in human cells infected with the dengue fever virus. It is hoped that this lipid will prove to be a potent anti-inflammatory therapeutic agent.

Plants: In the seeds of higher plants, a deficiency of phosphorylethanolamine cytidylyltransferase, a rate-limiting enzyme in the biosynthesis of phosphatidylethanolamine, profoundly affects embryo viability and maturation.

21.3.4.4: LYSOPHOSPHATIDYLETHANOLAMINE

Figure **21.3.22** shows the the structure of lysophosphatidyethanolamine

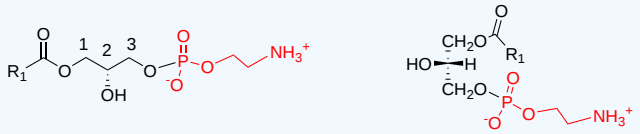


Figure **21.3.22**: Lysophosphatidyethanolamine

Lysophosphatidylethanolamine (LPE), with one mole of fatty acid per mole of lipid, is found in trace amounts only in animal tissues other than plasma (10 to 50μM, or ~1% of total serum phospholipids). It is formed by hydrolysis of phosphatidylethanolamine by the enzyme phospholipase A_2, as part of a de-acylation/re-acylation cycle that controls its overall molecular species composition as discussed above. A membrane-bound *O*-acyltransferase (MBOAT2) specific for LPE (and lysophosphatidic acid) has been characterized by a preference for an oleoyl-CoA substrate. There are reports of the involvement of LPE in cellular functions, such as the differentiation and migration of certain neuronal cells and various cancer cells. For example, oleoyl-LPE in the brain stimulates neurite outgrowth and protects against glutamate toxicity.

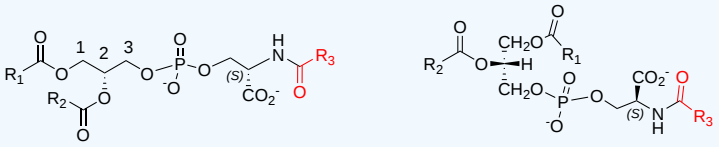
In plants, lysophosphatidylethanolamine is a specific inhibitor of phospholipase D, a key enzyme in the degradation of membrane phospholipids during the early stages of plant senescence. Through this action, it retards the senescence of leaves, flowers, and post-harvest fruits. Indeed, it has many horticultural applications when applied externally, e.g., to stimulate ripening and extend the shelf life of fruit, delay senescence, and increase the vase life of cut flowers. In bacteria, lysophosphatidylethanolamine displays chaperone-like properties, promoting the functional folding of citrate synthase and other enzymes. Some biological properties have been reported in animal tissues *in vitro*, but a specific receptor has yet to be identified.

Lysophospholipids, and especially lysophosphatidylethanolamines, are produced in the envelope membranes of bacteria by many different endogenous and exogenous factors. They must be transported back into the bacterial cell by flippases for conversion back to the diacyl forms by the action of a peripheral enzyme, acyl-ACP synthetase/LPL acyltransferase. Lysophosphatidylethanolamines produced by certain bacteria act synergistically with the **sulfonolipid** rosette-inducing factors (RIFs) to maximize the activity of the latter to induce choanoflagellates to move from a unicellular to a multicellular state.

21.3.4.5: *N*-ACYL PHOSPHATIDYLETHANOLAMINE

In *N*-Acyl phosphatidylethanolamine, the free amino group of phosphatidylethanolamine is acylated by a further fatty acid. This lipid has been detected in rather small amounts in several animal tissues (~0.01%), but especially brain, nervous tissues, and the epidermis, when the *N*-acyl chain is often palmitic or stearic acid (human plasma: N16:0-PE (40%), N18:1-PE (23.3%), N18:0-PE (19%), N18:2-PE (16.6%) and N20:4-PE (1.4%)). Under conditions of degenerative stress, it can accumulate in significant amounts, for example, as a result of ischemic injury, infarction, or cancer. It is present in plasma after feeding a high-fat diet to rats, and then it can cross into the brain, where it accumulates in the hypothalamus.

Figure **21.3.23** shows the structures of *N*-Acyl Phosphatidylethanolamine.



N-acylphosphatidylethanolamine

Figure **21.3.23**: *N*-Acyl Phosphatidylethanolamine

In animals, *N*-Acyl phosphatidylethanolamine is of particular importance as the precursor of **anandamide** and of other biologically important ethanolamides (e.g., ***N*-oleoylethanolamide**) in the brain and other tissues, but especially the intestines. In brief, it is formed biosynthetically by the action of a transferase (cytosolic phospholipase $A_2\varepsilon$), exchanging a fatty acid from the *sn*-1 position of a phospholipid (probably phosphatidylcholine) to the primary amine group of phosphatidylethanolamine (without a hydrolytic step). Both diacyl- and alkenylacyl-species of phosphatidylethanolamine can serve as acceptors. In addition, some transfer can also occur from phosphatidylethanolamine *per se* by an intramolecular reaction. However, it should be noted that some *N*-acyl phosphatidylethanolamine can be formed artefactually due to faulty extraction procedures during analysis.

In plants, *N*-acyl phosphatidylethanolamine is a common constituent of cereal grains (e.g., wheat, barley, and oats) and of some other seeds (1.9% of the phospholipids of cotton seeds, but 10-12% of oats). In other plant tissues, it is detected most often under conditions of physiological stress. In contrast to animals, synthesis involves direct acylation of phosphatidylethanolamine with a free fatty acid, catalyzed by a membrane-bound transferase in a reverse serine-hydrolase catalytic mechanism. The activation of *N*-acyl phosphatidylethanolamine metabolism in plants, with the release of *N*-acylethanolamines and phosphatidic acid formation, seems to be associated with cellular stresses. However, research is still in the early stages. However, both *N*-acyl lipid classes have been implicated in such physiological processes as the elongation of main and lateral roots, the regulation of seed germination, seedling growth, and defense from attacks by pathogens.

N-Acyl phosphatidylethanolamine has been found in many microbial species, while *N*-acetyl phosphatidylethanolamine was detected in a filamentous fungus, *Absidia corymbifera*, where it comprised 6% of the total membrane lipids. It was accompanied by an even more unusual lipid 1,2-diacyl-*sn*-glycero-3-phospho(*N*-ethoxycarbonyl)-ethanolamine.

In contrast, it inhibits the folding of some multi-helical proteins. Without this lipid, the transport membranes may not have the correct tertiary structure and will not function correctly. Whether the lipid is required once the protein is correctly assembled is not fully understood in all cases, but it may be needed to orient enzymes correctly in the inner membrane. Some studies suggest that life in this organism can be maintained without phosphatidylethanolamine, but life processes are inhibited.

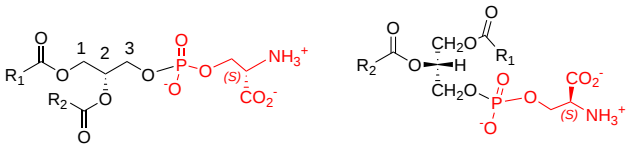
21.3.5: PHOSPHATIDYLSERINE AND RELATED LIPIDS

Phosphatidylserine or 1,2-diacyl-*sn*-glycero-3-phospho-L-serine is an important anionic phospholipid, bringing essential physical properties to membranes in eukaryotes and prokaryotes. Independent of this, it has many biological functions in cells, including effects on blood coagulation and apoptosis, and it is the biosynthetic precursor for phosphatidylethanolamine in prokaryotes and in eukaryotic mitochondria. Its metabolite, lysophosphatidylserine, has signaling functions and operates through specific receptors. Also, there is increasing interest in a structurally related lipid, phosphatidylthreonine, and other phospholipids linked to amino acids.

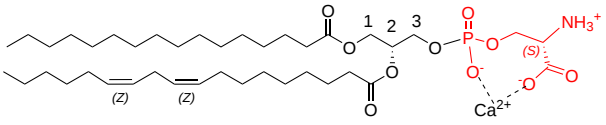
21.3.5.1: PHOSPHATIDYLSERINE - STRUCTURE AND OCCURRENCE

Although phosphatidylserine is distributed widely among animals, plants, and microorganisms, it is usually less than 10% of the total phospholipids, the greatest concentration being in myelin from brain tissue. For example, the brain and liver of mice contain 14% and 3% phosphatidylserine, respectively. However, it may comprise 10 to 20 mol% of the total phospholipids in the plasma membrane, where, under normal conditions, it is concentrated in the inner leaflet and the endoplasmic reticulum of cells. In the yeast *Saccharomyces cerevisiae*, it is a minor component of most cellular organelles other than the plasma membrane, where, surprisingly, it can amount to more than 30% of the total lipids. It is a minor membrane constituent in most bacteria, although it is important as an intermediate in phosphatidylethanolamine biosynthesis. The 1-octadecanoyl-2-docosahexaenoyl molecular species, especially important in brain tissue, is illustrated here.

Figure **21.3.24** shows the structure of phosphatidylserine



phosphatidylserine



1-hexadecanoyl,2-(9Z,12Z)-octadecadienoyl-sn-glycero-3-phosphoserine

Figure **21.3.24**: Phosphatidylserine

Phosphatidylserine is an acidic (anionic) phospholipid with three ionizable groups, i.e., the phosphate moiety, the amino group, and the carboxyl function. As with other acidic lipids, it exists in nature in salt form. However, it has a high propensity to chelate to calcium via the charged oxygen atoms of both the carboxyl and phosphate moieties, modifying the conformation of the polar head group. This interaction may be of considerable relevance to the biological function of phosphatidylserine, especially during bone formation.

In animal cells, the fatty acid composition of phosphatidylserine varies from tissue to tissue. Still, it does not appear to resemble the precursor phospholipids, either because of selective utilization of specific molecular species for biosynthesis or because of the remodeling of the lipid via deacylation-reacylation reactions with lysophosphatidylserine as an intermediate (see below). In human plasma, 1-stearoyl-

2-oleoyl and 1-stearoyl-2-arachidonoyl species predominate, but in the brain (especially grey matter), retina, and many other tissues, 1-stearoyl-2-docosahexaenoyl species are especially abundant and appear to be essential for the normal functioning of the nervous system. Indeed, the ratio of *n*-3 to *n*-6 fatty acids in brain phosphatidylserine is much higher than in most other lipids. The positional distribution of fatty acids in phosphatidylserine from rat liver and bovine brain are listed in Table **21.3.5**. As with most phospholipids, saturated fatty acids are concentrated in position *sn*-1 and polyunsaturated fatty acids in position *sn*-2.

Table **21.3.5**: **Positional distribution of fatty acids in phosphatidylserine from rat liver and bovine brain**

Position	Fatty acid					
	16:0	18:0	18:1	18:2	20:4	22:6
			Rat liver [1]			
***sn*-1**	5	93	1			
***sn*-2**	6	29	8	4	32	19
			Bovine brain [2]			
***sn*-1**	3	81	13			
***sn*-2**	2	1	25	trace	1	60

1. Wood, R. and Harlow, R.D. *Arch. Biochem. Biophys*., **135**, 272-281 (1969); DOI.
2. Yabuuchi, H. and O'Brien, J.S. *J. Lipid Res*., **9**, 65-67 (1968); DOI.

In the leaves of *Arabidopsis thaliana*, used as a 'model' plant in many studies, the fatty acid composition of phosphatidylserine resembles that of **phosphatidylethanolamine**. An intriguing report states that the chain lengths of the acyl groups increase with age and stress in phosphatidylserine quite specifically, and 22:0 and 24:0 fatty acids have been reported to occur in this lipid in the plasma membrane of some plant species.

Compared to PE, PS with ether-linked moieties (alkyl and alkenyl) is uncommon in animal tissues. However, they are reported to be relatively abundant in human retina and macrophages (they were first found in rat lung). As a general rule, the concentration of phosphatidylserine is highest in plasma membranes and endosomes but is very low in mitochondria. As it is located entirely on the inner monolayer surface of the plasma membrane (and of other cellular membranes) and is the most abundant anionic phospholipid, it may contribute to interfacial effects in membranes involving non-specific electrostatic interactions. This normal distribution is disturbed during platelet activation and cellular apoptosis.

***N*-Acylphosphatidylserine** is reportedly present in the frontal cortex of patients with schizophrenia as a minor component of the lipids of sheep erythrocytes, bovine brain, and the central nervous system of freshwater fish and Bryozoans, amongst others. The *N*-arachidonoyl form may be the precursor of the endocannabinoid ***N*-arachidonoylserine**.

21.3.5.2: BIOSYNTHESIS OF PHOSPHATIDYLSERINE

L-serine is a non-essential amino acid that is actively synthesized by most organisms. In animals, it is produced in nearly all cell types, although in the brain, it is synthesized by astrocytes but not by neurons. Neurons must be supplied with this amino acid for the biosynthesis of phosphatidylserine (and of sphingoid bases).

In animal tissues, phosphatidylserine is synthesized solely by calcium-dependent base-exchange reactions in which the polar head-group of an existing phospholipid is exchanged for L-serine. Two routes involve distinct enzymes (PS synthase I and II) with 30% homology and several membrane-spanning domains that can utilize different substrates. Both enzymes synthesize phosphatidylserine on the cytosolic face of the endoplasmic reticulum (ER) of the cell, but mainly in a specific domain of this termed the mitochondria-associated membrane ('MAM'), because it is tethered transiently to the mitochondrial outer membrane, presumably by a protein bridge. A complex of integrated proteins ('ERMES') has been characterized in yeast with a similar function. The reaction involves the exchange of L-serine with either phosphatidylcholine or phosphatidylethanolamine, catalyzed by PS synthase I (although it was long thought that only phosphatidylcholine was a substrate for this enzyme).

In contrast, PS synthase II catalyzes a similar exchange with diacyl-phosphatidylethanolamine and its plasmalogen form. Both enzymes are subject to feedback regulation by their product phosphatidylserine, thereby maintaining the correct amounts of this lipid. Figure **21.3.25** shows the synthesis and metabolism of phosphatidylserine in animals.

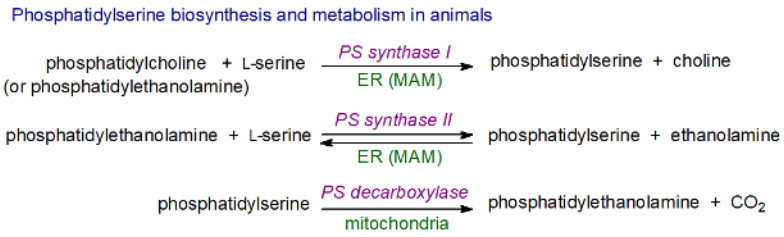


Figure **21.3.25**: Synthesis and metabolism of animal phosphatidylserine.

Phosphatidylserine synthase I is expressed in all mouse tissues, especially the kidney, liver, and brain, while phosphatidylserine synthase II is most active in the brain and testis and much less so in other tissues. The latter enzyme has a high specificity for molecular species containing docosahexaenoic acid. It is unknown why such a complex series of coupled reactions is necessary or why there should be two enzymes. Still, one virtue is that the free ethanolamine and choline formed are rapidly re-utilized for phospholipid synthesis. Thus, phosphatidylserine and phosphatidylethanolamine are produced without reducing the amount of phosphatidylcholine. The elimination of both enzymes is embryonically lethal in knockout mice. Still, each can be knocked out separately, and the mice survive, even though they have substantially reduced levels of phosphatidylserine and phosphatidylethanolamine.

As with other phospholipids, the final fatty acid composition in animal tissues is attained by remodeling, known as the Lands cycle. The first step is hydrolysis by a phospholipase A_2 to lysophosphatidylserine, followed by the reacylation by various acyl-CoA:lysophospholipid acyltransferases. One membrane-bound *O*-acyltransferase (LPCAT4 or MBOAT2) with a preference for oleoyl-CoA has been characterized, while a second (LPCAT3 or MBOAT5) incorporates linoleoyl and arachidonoyl chains (and also utilizes lysophosphatidylcholine).

Following synthesis, phosphatidylserine molecules can diffuse laterally in a concentration-dependent manner to different membrane regions to fulfill their physiological functions. In humans, cytosolic transport proteins transfer phosphatidylserine and other acidic phospholipids between membranes, and this can also occur by a vesicular transport mechanism.

Some of the newly synthesized phosphatidylserine is transferred to the plasma membrane. At the same time, a proportion is transported to the mitochondria, probably again via transient membrane contact (MAM), where it is decarboxylated to produce **phosphatidylethanolamine** by a specific decarboxylase in the inner mitochondrial membrane. In yeast, there is a preference for molecular species containing two monoenoic fatty acids for transport and metabolism; this process also occurs at the Golgi/endosome membranes. All the phosphatidylethanolamine in mitochondria is formed this way. Still, some can return to the endoplasmic reticulum, where it may be converted back to phosphatidylserine by the action of the PS synthases. The CDP-ethanolamine pathway does not fully complement the mitochondrial production of phosphatidylethanolamine from phosphatidylserine, as mice lacking the enzyme do not survive for long. Cellular concentrations of these two lipids are intimately related and tightly regulated. Figure **21.3.26** shows the mitochondrial metabolism of phosphatidylserine

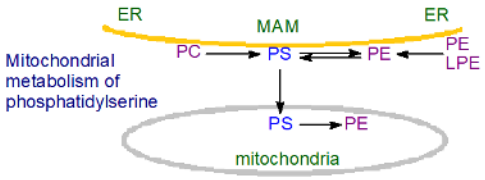


Figure **21.3.26**: Mitochondrial metabolism of phosphatidylserine

Thus, much of the phosphatidylserine is decarboxylated to phosphatidylethanolamine, which may be the major route to the latter in bacteria. As phosphatidylcholine in yeast is produced via methylation of phosphatidylethanolamine, phosphatidylserine is the primary precursor for this phospholipid in these organisms.

Bacteria and plants: In bacteria and other prokaryotic organisms and yeast, phosphatidylserine is synthesized by a mechanism comparable to that of most other phospholipids, i.e., by reaction of L-serine with CDP-diacylglycerol, and depends on Mg^{2+} or Mn^{2+}. Phosphatidylserine synthases belong to two different families: type I (non-integral membrane form) in the phospholipase D-like family, as in *E. coli*, and type II (integral membrane form) in the CDP-alcohol phosphotransferase family, as in *Bacillus* sp. and the yeast *S. cerevisiae*. However, the latter shows no homology with the bacterial enzymes.

In many plants, including in the model plant Arabidopsis, much of the phosphatidylserine is produced by a calcium-dependent base-exchange reaction in which the head group of an existing phospholipid is exchanged for L-serine in the luminal leaflet of the endoplasmic reticulum (i.e., mechanistically similar to PS synthase I). It is transferred to the cytoplasmic membrane leaflet by flippases and thence to the post-Golgi compartments before eventually accumulating at the plasma membrane. However, some vesicular transport may occur, or there

may be direct transfer at membrane contact sites. A CDP-diacylglycerol (prokaryotic-like) biosynthetic pathway exists in some species, e.g., wheat.

Let's explore the mechanism of the *Methanocaldococcus jannaschii* phosphatidylserine synthase (**MjPSS**). The organism is a hyperthermophilic methanogen. Figure **21.3.27** shows substrate binding by MjPSS.

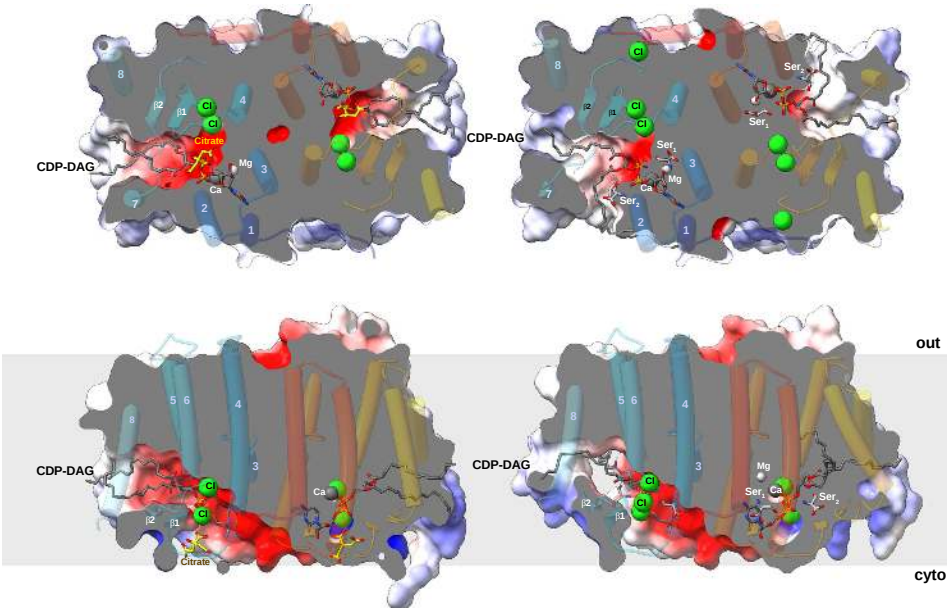


Figure **21.3.27**: Substrate binding by MjPSS. Centola, M., van Pee, K., Betz, H. *et al.* Crystal structures of phosphatidylserine synthase PSS reveal the catalytic mechanism of CDP-DAG alcohol O-phosphatidyl transferases. *Nat Commun* **12,** 6982 (2021). https://doi.org/10.1038/s41467-021-27281-w. Creative Commons Attribution 4.0 International License, http://creativecommons.org/licenses/by/4.0/.

The large binding pocket for CDP-DAG in MjPSS extends from the hydrophobic membrane core to the active site near the cytoplasmic surface in the center of the dimer. In the closed structures (left), both CDP-DAG alkyl chains adopt similar conformations within the binding pocket. In contrast, helices 7 and 8 positions in the open structures (right) allow one alkyl chain to reach the membrane via a different path. Serine molecules are only found in open structures (right). In one closed conformation, there is a citrate near the substrate-binding site, whereas in the other closed structures, this position is empty. A chain of three chloride ions extends parallel to the dimer interface from the active site to the cytoplasmic interface with the N-terminal helix hH from the other protomer.

Figure **21.3.28** shows the reaction cycle of MjPSS during the synthesis of PS from CDP-DAG and serine in the presence of Mg^{2+} and Ca^{2+}.

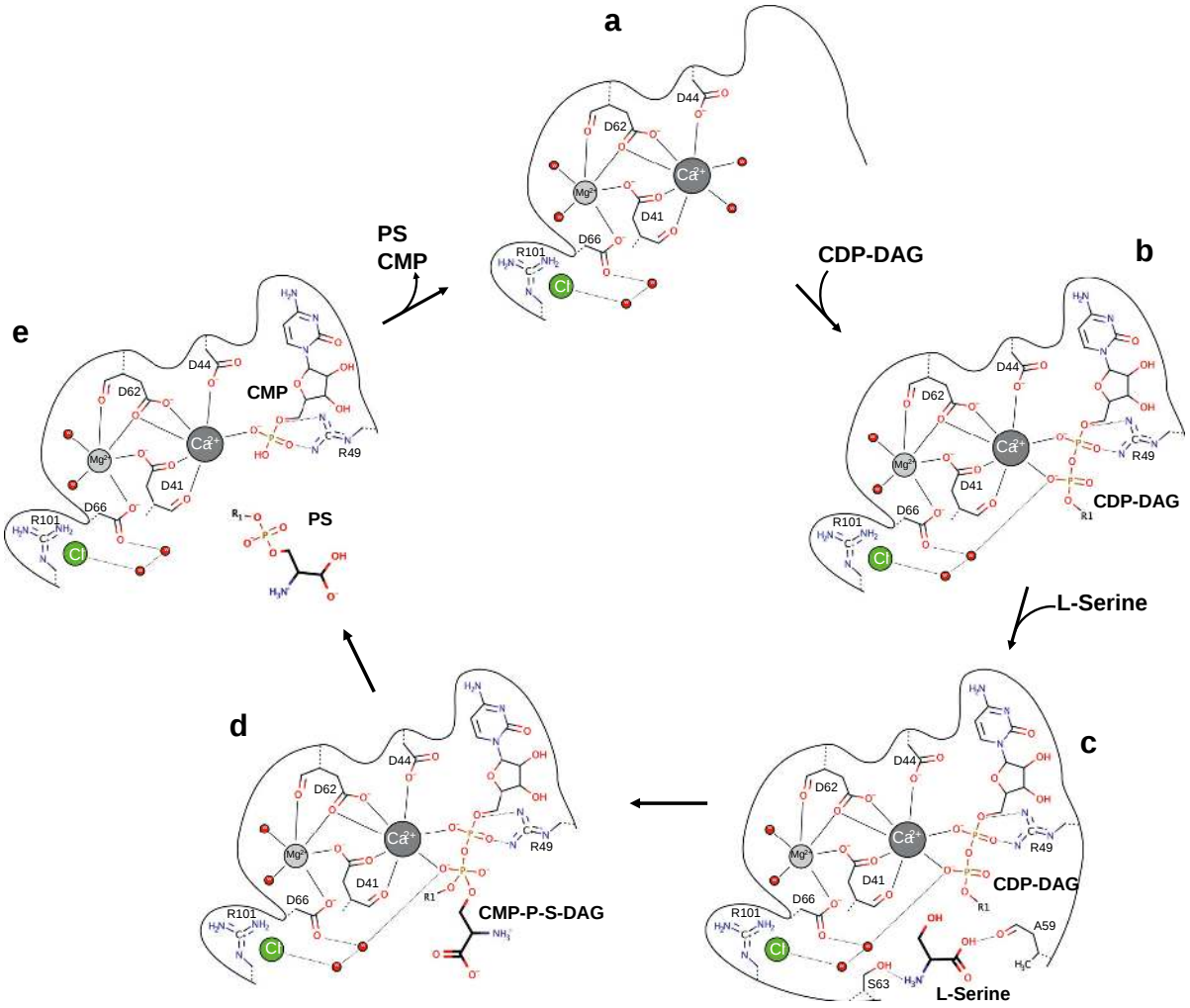
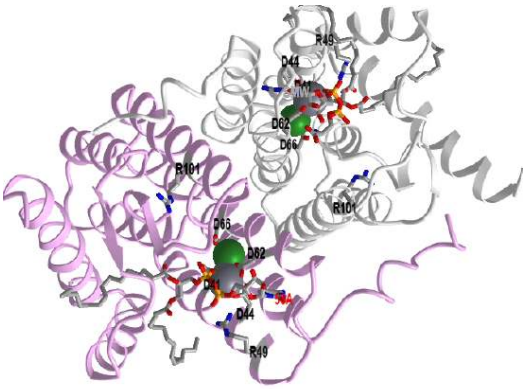


Figure **21.3.28**: Reaction mechanism for MjPss. Centola, M. et al., ibid

The CDPDAG binding site in MjPSS is formed and stabilized by the divalent cations Mg^{2+} and Ca^{2+} (a). In the absence of CDP-DAG, Ca^{2+} most likely is coordinated by water molecules, as shown in a, or by residues in nearby loops that would be flexible in the absence of CDP-DAG. The binding of CDP-DAG (b) is driven by the coordination of Ca^{2+} by the negatively charged phosphates. Serine binds to the binding pocket after CDP-DAG (c). For the nucleophilic attack, the serine molecule is positioned with its hydroxyl group near the β-phosphate of CDP-DAG. The serine molecule is activated by deprotonation, attacks the β-phosphate, and forms the penta-coordinated transition state (d). The proton of serine is probably removed by one of the water molecules located in the interaction network of Asp66, Arg101, and the nearby chloride ions. Hydrolysis of the CDP-DAG/serine complex from the transition state leads to the complex of MjPSS with the products PS and CMP (e). The next cycle starts after the release of the products and CDP-DAG binding. Structural data are available for the state with bound CDP-DAG (b), CDP-DAG, and serine (c), and for the transition state of the CDP-DAG/serine complex (d).

Figure **21.3.29** shows an interactive iCn3D model of the Methanocaldococcus jannaschii phosphatidylserine synthase (PSS) in the open state with bound CDP-DAG and serine (7B1L). The enzyme is also named CDP-diacylglycerol--serine O-phosphatidyltransferase.



NCBI iCn3D Figure **21.3.29**: Bacterial phosphatidylserine synthase (PSS) in the open state with bound CDP-DAG and serine (7B1L) (Note the actual PDB file title is for the closed state.) Click the image for a popup or use this external link: https://structure.ncbi.nlm.nih.gov/i...B3Rn3gVN4c4ge6

The A chain of the homodimer is shown in gray and the B in plum. The active site residues in the A chain in the above mechanism are shown in stick, CPK colors, and labeled. Hover over the large ligand (58A) in the gray subunit. Two free serines are shown near it, but only one is probably the substrate.

? PHOSPHATIDYLSERINE - ADDITIONAL BACKGROUND

Click the link below.

Link

Phosphatidylserine – Biological Function

Membrane location: Phosphatidylserine modulates membrane charge locally, enabling the recruitment of soluble cations and proteins, and so it contributes to the organization of processes within cell membranes. Its membrane distribution is tightly controlled as it facilitates signaling within the various cellular compartments. Thus, it undergoes a transition from the lumenal leaflet of the endoplasmic reticulum to the cytosolic leaflet in the trans-Golgi network, probably by the activity of flippases and scramblases in the Golgi, and it is highly enriched on the inner leaflet of the plasma membrane. Transport to the plasma membrane against a concentration gradient is aided in part by proteins designated 'ORP5' and 'ORP8' in humans (Osh 6 and Osh7 in yeast) with a 'PH' binding domain for **phosphatidylinositol 4,5-bisphosphate** and an 'ORD' domain for phosphatidylserine. At a membrane contact site between the endoplasmic reticulum and plasma membrane, phosphatidylserine is exchanged for phosphatidylinositol 4-phosphate. Such transfer requires an input of energy, which can be supplied in the form of ATP or by phosphoinositides. Although it does not take part in membrane **raft** formation, phosphatidylserine is present in **caveolae**, where it is believed to interact with caveolin-1. It is also present in appreciable amounts in the endosomal compartment.

The asymmetric structure of the plasma membrane with high concentrations of anionic lipids, such as phosphatidylserine in the cytosolic leaflet with zwitterionic lipids in the extracellular leaflet, generates two surfaces with greatly different electrostatic potentials that influence the association of proteins with the membrane surface and the activities of integral membrane proteins. This distribution is maintained and can be altered, after specific activation, by various flippases (transfer back into the cytoplasmic leaflet), floppases (transfer out of the cytoplasmic leaflet), and scramblases (bidirectional transfer), including ATP-dependent translocases selective for phosphatidylserine. Phosphatidylserine is highly enriched in the cytosolic leaflet of the membranes of recycling endosomes, which replenish the lipids and proteins of the plasma membrane, and it is essential for their function.

Enzyme activation: Besides its function as a component of cellular membranes and as a precursor for other phospholipids, phosphatidylserine is an essential cofactor that binds to and activates many proteins, especially those with signaling activities. The negative charge on the lipid facilitates the binding to proteins through electrostatic interactions or Ca^{2+} bridges. For example, the presence of appreciable amounts of phosphatidylserine on the cytosolic leaflet of endosomes and lysosomes enables these compartments to dock with proteins that possess specific phosphatidylserine-binding domains, including several important signaling and fusogenic effectors. The cytoskeletal protein spectrin binds to phosphatidylserine in this way, and it is also required by enzymes such as the neutral sphingomyelinase and the Na^+/K^+ ATPase, where the 18:0/18:1 molecular species is especially important. It is believed that the fatty acyl components of this species in the inner leaflet of the plasma membrane (and potentially other intracellular membranes) may interact (interdigitation or "hand-shake") with the very-long chains of sphingolipids in the outer

leaflet in raft microdomains, resulting in a high local concentration of the anionic phospholipid and an accumulation of negative surface charge to which specific poly-cationic proteins in the membranes can bind. This may then enable the transfer of signals across the membrane to the cytosol.

Similarly, phosphatidylserine participates directly in key signaling pathways in the brain by binding to the cytosolic proteins involved in neuronal signaling, activating them. At least three major pathways are affected, including phosphatidylinositol 3-kinase and protein kinase C. For example, most enzymes of the protein kinase C family contain a 'C2' calcium-dependent cysteine-rich region that recognizes phosphatidylserine, and in coordination with the 'C1' domain that binds to **diacylglycerols**, is essential for activating and locating them to the plasma membrane of appropriately stimulated cells. Phosphatidylserine is not involved in cell signaling through the formation of metabolites, as is the case with phosphatidylinositol.

Blood coagulation: Phosphatidylserine is an important element of the blood coagulation process in platelets, where it is transported from the inner to the outer surface of the plasma membrane in platelets activated by exposure to fibrin-binding receptors, for example. Here, the exposed phosphatidylserine enhances the activation of prothrombin to thrombin (the key molecule in the blood clotting cascade) by triggering a cascade of reactions and providing the negatively charged platform that enables calcium ions to form bridges with γ-carboxyglutamic acid-containing domains on the coagulation factors. Membrane vesicles with surface-exposed phosphatidylserine can also be released from platelets, promoting coagulation. Apolipoprotein A-1 in high-density lipoproteins has a controlling function. It neutralizes these procoagulant properties by arranging the phospholipid in surface areas that are too small to accommodate the prothrombinase complex. Blood coagulation is beneficial when it prevents blood loss from the circulatory system. Still, it is detrimental when it causes thrombosis, and the action of phosphatidylserine is essential to regulating the process.

Apoptosis: In addition, in response to particular calcium-dependent stimuli, phosphatidylserine is known to have an important role in regulating apoptosis or programmed cell death, the natural process by which aged or damaged cells are removed from tissues before they can exert harmful effects. When cells are damaged, a mechanism is initiated in which the normal distribution of this lipid on the inner leaflet of the plasma membrane bilayer is disrupted by the stimulation of scramblases, which are ATP-independent and can move the lipid across the membrane to the outer leaflet. This occurs with the inhibition of aminophospholipid translocases, which return the lipid to the inner side of the membrane. In erythrocytes, phosphatidylserine is located in the inner leaflet of the membrane bilayer under low Ca^{2+} conditions when a phospholipid scramblase is suppressed by membrane cholesterol. It is exposed to the outer leaflet under elevated Ca^{2+} concentrations, which activate the scramblase. After the collapse of this asymmetry and transfer of phosphatidylserine to the outer leaflet of an effete cell, it is believed that it is recognized by a cohort of receptors, either directly or indirectly, through bridging ligands on the surface of macrophages and related scavenger cells. These activate a family of cysteine-dependent aspartate-specific proteases, the caspases, and other enzymes to facilitate the engulfment of the apoptotic cells and their potentially toxic or immunogenic contents in a non-inflammatory manner. Notably, the transition from a pro-inflammatory to an anti-inflammatory state is defined by phagocytosis of neutrophils by macrophages via this phosphatidylserine-dependent process.

During apoptosis, the generation of reactive oxygen species occurs, mainly hydrogen peroxide, which together with the enzyme cytochrome c brings about rapid oxidation of the fatty acids in phosphatidylserine before this lipid is externalized. Indeed, it is now apparent that molecular species of phosphatidylserine with an oxidatively truncated *sn*-2 acyl group that incorporates terminal γ-hydroxy(or oxo)-α,β-unsaturated acyl moieties are especially potent signals for scavenger receptors in macrophages as a prerequisite for engulfment of apoptotic cells.

This has been described as "a dominant and evolutionarily conserved immunosuppressive signal that promotes tolerance and prevents local and systemic immune activation" or, more succinctly, as an "eat-me signal" (externalized phosphatidylinositol 3,4,5-trisphosphate (PI(3,4,5)P) may have a similar function). Phosphatidylserine binding to specific proteins, such as apolipoprotein H (β2-glycoprotein 1), enhances their recognition and clearance. This process is essential for the development of the lung and brain, and it is also relevant to clinical situations where apoptosis plays an important part, such as cancer, chronic autoimmunity, and infections. For example, phosphatidylserine is a necessary component of the TAM family of receptor tyrosine kinases and the receptor-ligand complex of particular importance in cancer cells, where phosphatidylserine-TAM signaling regulates many aspects of inflammation and immune resolution and is seen as a target for therapeutic intervention. Phosphatidylserine exposure is increased substantially on the surface of tumor cells or tumor cell-derived microvesicles, which have innate immunosuppressive properties and facilitate tumor growth and metastasis. Targeting phosphatidylserine is considered to be a promising strategy in cancer immunotherapy. In atherosclerosis, phosphatidylserine is believed to have anti-inflammatory and protective effects as a component of the high-density lipoproteins, probably mediated by the apoptosis mechanism. In contrast, as this mechanism is important for the turnover of erythrocytes, it is relevant to thrombus formation and the stabilization of blood clots. The innate immunosuppressive effect of externalized phosphatidylserine has been hijacked by numerous viruses and bacteria to facilitate infection.

A similar apoptotic mechanism operates in retinal pigment epithelial cells to remove the large amounts of photoreceptor cell debris generated continuously. In addition, appreciable amounts of phosphatidylserine are translocated by an analogous mechanism to the surface of T lymphocytes that express low levels of the transmembrane enzyme tyrosine phosphatase. This change in distribution acts as a signaling mechanism to modulate the activities of several membrane proteins. The anti-coagulant protein annexin V binds with high specificity to phosphatidylserine and is used as a probe to detect apoptotic cells. Notably, phosphatidylserine is a major component of the membranes of microvesicles in animal cells, and translocation to the outer leaflet upon cellular activation is essential for their biogenesis. In addition, exposure of phosphatidylserine on the cell surface is reported to be a factor in non-apoptotic forms of regulated inflammatory cell death, such as necroptosis.

Role in infections: Unfortunately, viruses such as Ebola and HIV can hijack this apoptosis machinery by incorporating phosphatidylserine into their viral envelopes, so conning cells into engulfing them; the viral glycoprotein/cellular receptor complex may then facilitate the entry of foreign organisms into other cells. Similarly, parasites ingested in this manner, including *Leishmania* and *Trypanosoma* species, utilize host phosphatidylserine to establish infections and facilitate disease progression, as they do not then elicit the production of proinflammatory cytokines. This mechanism has been termed 'apoptotic mimicry' and is critical for the survival of parasites within the macrophage.

Other activities: Phosphatidylserine is required for the transmembrane movement of excess cholesterol, derived initially from the lysosomal degradation of low-density lipoproteins, from the plasma membrane to the endoplasmic reticulum, thereby maintaining membrane integrity and ensuring cell survival. It is, therefore, an important element in **cholesterol homeostasis**. The mechanism is believed to involve proteins known as GRAMD1s embedded in the endoplasmic reticulum membrane at sites in contact with the plasma membrane. These have two functional domains: the StART-like domain that binds cholesterol and the GRAM domain that binds anionic lipids, such as phosphatidylserine, forming a link between the two membranes that enables the transfer of cholesterol.

A further unusual function of phosphatidylserine is that it is a key component of the lipid-calcium-phosphate complexes that act as nucleation centers for hydroxyapatite formation and initiate mineral deposition during the formation of bone. It has been established that phosphatidylserine and inorganic phosphate must be present before calcium ions are introduced, when the high affinity of phosphatidylserine for calcium ions becomes important. Nucleation is facilitated by the protein annexin V. Similarly, during bone repair and maintenance, the fusion of osteoclasts requires the non-apoptotic exposure of phosphatidylserine at the surface of fusion-committed cells with the aid of a transmembrane protein (DC-STAMP) expressed in dendrocytes. This activity is relevant to cardiovascular disease and, in particular, to the phenomenon of "hardening of the arteries," where atherosclerotic plaques can undergo mineralization with the deposition of hydroxyapatite.

Among many other functions of phosphatidylserine, it is believed to be an essential surface membrane component for the fusion of cell types other than osteoclasts, including during the formation of fibers in muscle cells, and the fusion of macrophages into inflammatory giant cells and myoblasts into myotubes. Such cell fusions require the non-apoptotic exposure of phosphatidylserine at the surface of fusing cells, where it interacts with phosphatidylserine-recognizing proteins to regulate the time and place of cell fusion. Phosphatidylserine provides stable membrane domains in spermatozoa that are essential for fertilization, and it is also an essential component of the plasma membrane microdomains known as **caveolae**, where it is required both for their formation and stability, possibly through specific binding to the cavin proteins.

The high concentrations of docosahexaenoic acid (DHA) in the brain and retinal phosphatidylserine are certainly important for the development and function of these tissues. Accumulation of phosphatidylserine in neuronal membranes is promoted by DHA. This is important for the maintenance of neuronal survival. Phosphatidylserine may also be a reservoir of DHA for **protectin** formation in neuronal tissue. On the other hand, the Food and Drug Administration in the USA considers that there is little scientific evidence to support claims that dietary supplements of phosphatidylserine reduce the risk of dementia or cognitive dysfunction in the elderly, and other nutritional claims appear to be dubious also. Antibodies to phosphatidylserine are formed in some disease states, including thrombosis and recurrent spontaneous pregnancy loss. A mutation in the phosphatidylserine synthase causes the rare genetic disease Lenz-Majewski syndrome I gene that greatly increases the enzyme's activity while preventing feedback inhibition. Abnormal phosphatidylserine metabolism has been implicated in other diseases.

In yeasts such as *Candida albicans*, phosphatidylserine and the enzyme phosphatidylserine decarboxylase, which generates phosphatidylethanolamine, are both essential for the organism's virulence toward a host species.

Lysophosphatidylserine

Figure **21.3.30** shows the structure of lysophosphatidylserine

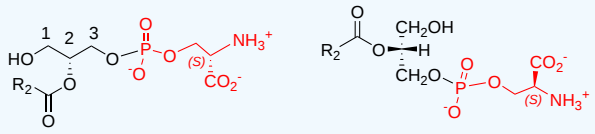


Figure **21.3.30**: lysophosphatidylserine

Lysophosphatidylserine, i.e., with a fatty acid in one position only, is known to mediate many biological processes, especially in the context of the immune system in animal tissues. It has been found in the thymus, peripheral lymphoid tissues, central nervous system, and colon but is barely detectable in plasma. Deacylation of the diacyl lipid by phospholipases is the primary source. For example, a secreted isoform that is phosphatidylserine-specific (PLA1A) removes the *sn*-1 acyl group of phosphatidylserine to generate *sn*-2-lysophosphatidylserine containing unsaturated fatty acids, and this is upregulated greatly by various inflammatory stimuli. This extracellular enzyme utilizes phosphatidylserine exposed on the cell membrane as a substrate, although other phospholipases may operate intracellularly and produce *sn*-1-lysophosphatidylserine. In addition, platelets in some species (not significantly in humans) secrete a phospholipase A_2 group IIA (ABHD16A), which generates saturated *sn*-1-lysophosphatidylserine (and other lysophospholipids).

Lysophosphatidylserine has been detected after injury to animal tissues (tumor growth, graft rejection, burns). It may have a similar function to **lysophosphatidic acid** in cell signaling, for example, in regulating calcium flux and stimulating immune cells through G protein-coupled receptors of which three (GPR34, P2Y10 and GPR174, LPS1-3) have been detected in mice and humans. For example, GPR174 mediates the suppression of T-cell proliferation induced *in vitro* by lysophosphatidylserine. When cells are damaged, lysophosphatidylserine can be generated by a reaction dependent on the activation of the NADPH oxidase. It can diffuse and transmit the information to other cells, especially mast cells, and it is produced to enhance the clearance of activated and dying neutrophils. It thus has a role in the resolution of inflammation. One specific molecular species, i.e., 1-(11*Z*-eicosenoyl)-glycero-3-phosphoserine, is reported to be a true agonist of the Toll-like receptor 2/6 heterodimer of importance to the immune response to pathogens; both its polar head group and the length of the acyl chain are required for this activity. On the other hand, *sn*-2-lysophosphatidylserine has proinflammatory reactions as it augments mast cell degranulation and mast cell-dependent anaphylactic shock; most other lysophospholipids have no such activity.

Deregulated lysophosphatidylserine metabolism has been linked to certain cancers, cardiometabolic disorders, night blindness, and the human genetic neurological disorder PHARC. High serum levels of PLA1A are associated with such autoimmune disorders as Graves' disease and systemic lupus erythematosus, and there is increased expression of the enzyme in metastatic melanomas. It is necessary to assemble the hepatitis C virus, and it can play a role in the antivirus innate immune response. In Schistosome infections, lysophosphatidylserine from the parasite is believed to be a key activator molecule in the host.

Negatively charged lysophosphatidylserine species tend to organize in non-bilayer structures and are believed to facilitate the folding of certain membrane proteins *in situ* better than bilayer-forming lipids.

21.3.6: PHOSPHATIDYLINOSITOL AND RELATED PHOSPHOINOSITIDES

Although it had long been recognized that phosphatidylinositol or 1,2-diacyl-*sn*-glycero-3-phospho-(1'-*myo*-inositol) was a key membrane constituent, it was initially something of a surprise when the manifold biological activities of this lipid, and then of the derived phosphatidylinositol phosphates and their hydrolysis products, were discovered in animals, plants, and microorganisms. Many years after the initial discoveries in the 1950s, these lipids remain a major focus for research efforts worldwide, with considerable relevance to human health. Phosphatidylinositol and its various metabolites and relevant enzymes can be located and function within different membrane regions in cells, and they form part of what have been termed phosphoinositide and phosphatidylinositol cycles, their versatility stemming from the inositol head group, a six-carbon hexahydroxy ring, which can be reversibly phosphorylated on the 3, 4, and 5 positions. In addition to their structural role in membranes, these lipids are intimately involved in innumerable aspects of membrane trafficking and signaling in eukaryotic cells. These functions are essential to cell growth and metabolism. Only a brief overview of such a highly complex topic is possible here. **Glycosyl-phosphatidylinositol (GPI)** is a related lipid that serves as an anchor for proteins.

21.3.6.1: PHOSPHATIDYLINOSITOL

Structure and Occurrence: Phosphatidylinositol is an important lipid, both as a membrane constituent and as a participant in essential metabolic processes in all plants and animals, both directly and via a number of its metabolites. It is an acidic (anionic) phospholipid with a phosphatidic acid backbone, linked via the phosphate group to inositol (hexahydroxycyclohexane). In most organisms, the stereochemical form of the last is *myo*-D-inositol (with one axial hydroxyl in position 2, with the remainder equatorial, i.e., a chair-like structure). However, other forms (*scyllo*- and *chiro*-) have occasionally been found in plants. The 1-stearoyl,2-arachidonoyl molecular species, which is of considerable biological importance in animals, is illustrated.

Figure **21.3.31** shows the structure of phosphatidylinositol.

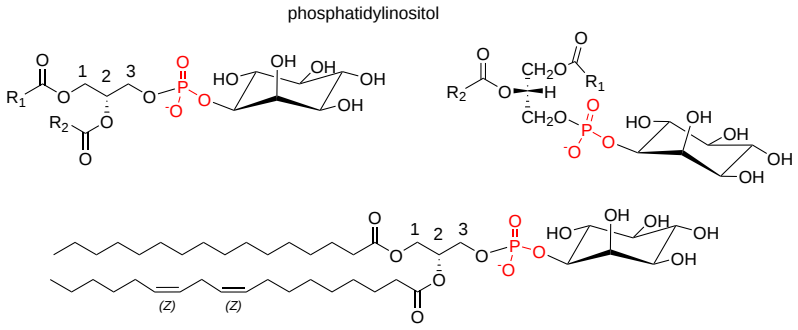


Figure **21.3.31**: Phosphatidylinositol

Phosphatidylinositol is especially abundant in brain tissue, where it can amount to 10% of the phospholipids. It is present in all tissues, cell types, and membranes at relatively low levels compared to many other phospholipids. In rat liver, it amounts to 1.7 micromoles/g, i.e., less than phosphatidylcholine, phosphatidylethanolamine, and phosphatidylserine. Under normal conditions, it is present entirely in the erythrocyte membrane's inner leaflet and the plasma membrane in nucleated cells. Phosphatidylinositol *per se* is rarely found in prokaryotes other than the *Actinomycetales*, although the thermophilic α-proteobacterium *Rhodothermus marinus* contains dialkylether glycerophosphoinositides.

The fatty acid composition of phosphatidylinositol is rather distinctive, as shown in Table **21.3.6**. Thus, in almost all animal tissues, the characteristic feature is a high content of stearic and arachidonic acids. All the stearic acid is linked to position *sn*-1 and all the arachidonic acid to position *sn*-2. As much as 78% of the total lipid may consist of the single molecular species *sn*-1-stearoyl-*sn*-2-arachidonoyl-glycerophosphorylinositol (see Table **21.3.7** below). Although 1-alkyl- and alkenyl- forms of phosphatidylinositol are known, they tend to be much less abundant than the diacyl form. In plant phosphatidylinositol, e.g., *Arabidopsis thaliana*, palmitic acid is the main saturated fatty acid in position *sn*-1, while linoleic and linolenic acids are the main unsaturated components in position *sn*-2. Similarly, in yeast, palmitic acid is in position *sn*-1 with oleic and palmitoleic acids in position *sn*-2 predominantly; the Amoebozoa have a C16 alkyl group in position *sn*-1 and *cis*-vaccenic acid in position *sn*-2.

Table **21.3.6**: **Fatty acid composition of phosphatidylinositol (wt % of the total) in animal and plant tissues.**

Tissue	Fatty acids									
	16:0	18:0	18:1	18:2	18:3	20:3	20:4	22:3	22:5	22:6
Bovine brain [1]	8	38	10	1	-	5	34	2	tr.	1
Bovine liver [2]	5	32	12	6	1	7	23	4	3	5
Rat liver [3]	5	49	2	2		4	35			1
A. thaliana [4]	48	3	2	24	24					

[1] = Holub, B.J. *et al.*. *J. Lipid Res.*., **11**, 558-564 (1970); DOI. [2] = Thompson, W. and MacDonald, G., *J. Biol. Chem*., **250**, 6779-6785 (1975); DOI. [3] = Wood, R. and Harlow, R.D. *Arch. Biochem. Biophys*., **135**, 272-281 (1969); DOI. [4] = Browse, J. *et al. Biochem. J*., **235**, 25-31 (1986); DOI.

Biosynthesis: The basic mechanism for the biosynthesis of phosphatidylinositol and phosphatidylglycerol is sometimes termed a branch point in phospholipid synthesis, as phosphatidylcholine and phosphatidylethanolamine are produced by a somewhat different route.

Phosphatidylinositol is found in all eukaryotes, which are, in general, able to synthesize inositol *de novo* via glucose-6-phosphate. As with **phosphatidylglycerol** (and hence cardiolipin), phosphatidylinositol is formed biosynthetically from **phosphatidic acid** via the intermediate **cytidine diphosphate diacylglycerol**, which is produced by the action of a CDP-diacylglycerol synthase believed to be the rate-limiting enzyme in phosphatidylinositol biosynthesis. Then, the enzyme CDP-diacylglycerol inositol phosphatidyltransferase ('phosphatidylinositol synthase' or 'PIS') catalyzes a reaction with *myo*-inositol to produce phosphatidylinositol.

Figure **21.3.32** shows the synthesis of phosphatidylinositol in eukaryotes.

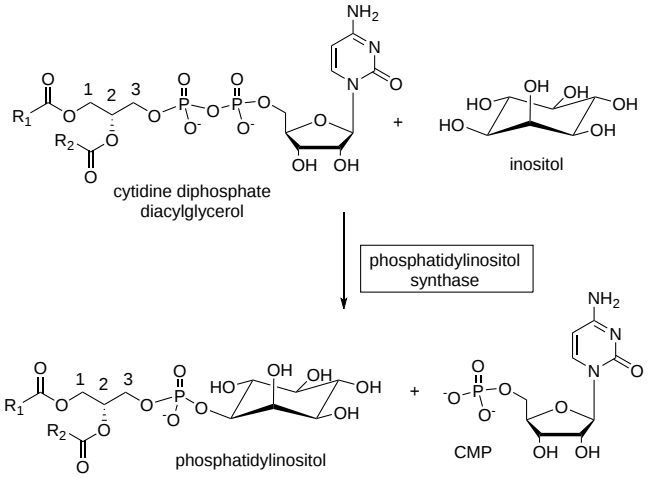


Figure 21.3.32: Synthesis of phosphatidylinositol in eukaryotes

In mammals, PIS is located in the endoplasmic reticulum, in part in a subcompartment associated with mitochondria (mitochondria-associated membranes - MAM) and in mitochondria *per se*. Indeed, it is reported that PIS is present in a mobile ER-derived subcompartment that makes transient contacts with other organelles, including the plasma membrane, and facilitates the distribution of phosphatidylinositol to other subcellular compartments. The other product of the reaction is cytidine monophosphate (CMP). As PIS catalyzes the reverse reaction, the phosphatidylinositol synthesis rate is determined by the relative concentrations of the precursors and product, and the latter must be transported away from the site of synthesis for the reaction to continue. Much of the phosphatidylinositol is delivered to other membranes by vesicular transport. A family of soluble phosphatidylinositol transfer proteins (PITPα, PITPβ, and PITPNC1) provides phosphatidylinositol from the ER to kinases for phosphorylation (see below).

Molecular species specificity: The phosphatidylinositol synthase *per se* does not exhibit the fatty acyl specificity observed in the final product, but earlier in the biosynthetic process, 1-stearoyl-2-arachidonoyl species of diacyl-*sn*-glycerols are converted preferentially into **phosphatidic acid** by the epsilon isoform of **diacylglycerol kinase** (DGKε), anchored to the membrane via its N-terminal hydrophobic helix segment; ATP is the phosphate donor. In addition, one of the CDP-diacylglycerol synthases (CDS2) has similar specificity in generating the immediate precursor CDP-diacylglycerols from phosphatidic acid. Some specificity may be introduced via lysophosphatidylinositol, formed as a by-product of eicosanoid formation (see below) or as an intermediate as part of the normal cycle of deacylation-acylation of phosphatidylinositol in tissues in which the fatty acid composition is remodeled to give the final distinctive composition. A membrane-bound *O*-acyltransferase (MBOAT7 or LPIAT1) specific for position *sn*-2 of lysophosphatidylinositol with a marked preference for arachidonoyl-CoA is ubiquitously expressed in animal tissues, and this may be one means by which free arachidonic acid and eicosanoid levels are regulated.

In macrophages subjected to inflammatory stimuli, phosphatidylinositol containing two molecules of arachidonate is produced by remodeling reactions, and there is evidence that it is a novel bioactive phospholipid regulating innate immune responses in these cells. Further specificity may be introduced by lysocardiolipin acyltransferase (LYCAT; also known as LCLAT1 or ALCAT1), which exhibits a preference for lysophosphatidylinositol and lysophosphatidylglycerol over other phospholipids *in vitro*, and incorporates 18:0 rather than shorter chain fatty acids into position *sn*-1 of phosphatidylinositol and other phosphoinositides, especially phosphatidylinositol-4,5-bisphosphate and phosphatidylinositol-3-phosphate; this enzyme may be located adjacent to the phosphatidylinositol synthase in the endoplasmic reticulum. Some of the phosphatidylinositol in membranes is derived from recycling polyphosphoinositides via the phosphatidylinositol cycle, which could influence the molecular species composition (see below).

The highly specific distribution of fatty acids on the glycerol moiety of phosphatidylinositol breaks down in some cancer cells, especially those with a mutation on the transcription factor p53 gene, one of the most highly mutated genes in cancer.

Plants and bacteria: In contrast to animals, **plants** have two phosphatidylinositol synthase isoforms, PIS1 and PIS2, which display specificities for particular species of the CDP-diacylglycerol substrate. PIS1 generates phosphatidylinositol with saturated or monounsaturated fatty acids preferentially, while PIS2 generates polyunsaturated species, the two forms possibly having different functions. In protozoan parasites, such as *Trypanosoma brucei*, phosphatidylinositol synthase's active site may be the endoplasmic reticulum's and the Golgi's lumen. There is evidence for two distinct pools of product in this organism: the bulk membrane form derived from inositol imported from the environment, and a second used for synthesizing GPI anchors, which uses *myo*-inositol synthesized *de novo*. In yeast, some biosynthesis may occur on the cytosolic side of the plasma membrane.

The enzyme is a transmembrane protein and uses CDP-diacylglycerol as a donor and either inositol (eukaryotes) or inositol phosphate (prokaryotes) as the acceptor alcohol. The structure of a similar enzyme, phosphatidylinositol-phosphate synthase from *Renibacterium salmoninarum*, is shown in Figure **21.3.33**.

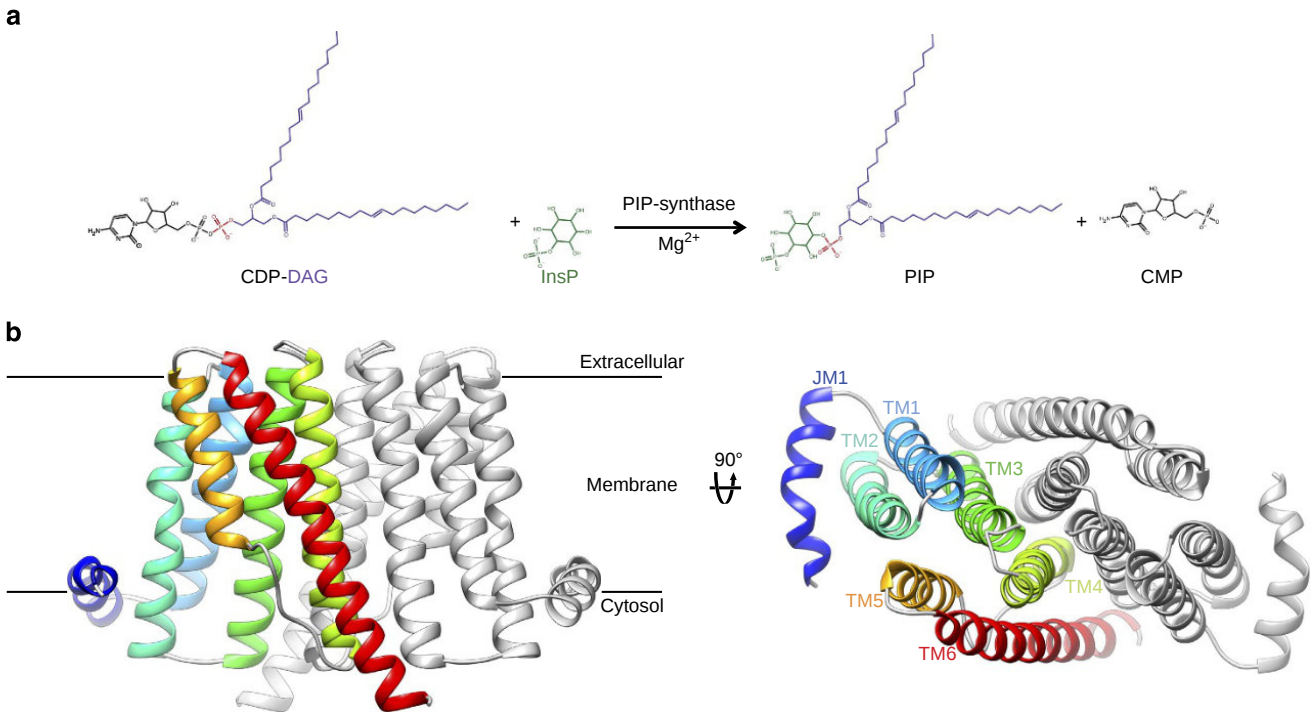


Figure **21.3.33**: Structure and reaction of phosphatidylinositol-phosphate synthase from *Renibacterium salmoninarum.* Clarke, O., Tomasek, D., Jorge, C. *et al.* Structural basis for phosphatidylinositol-phosphate biosynthesis. *Nat Commun* **6,** 8505 (2015). https://doi.org/10.1038/ncomms9505. Creative Commons Attribution 4.0 International License. http://creativecommons.org/licenses/by/4.0/

Panel A shows the reaction for PIP synthases, which involves the transfer of a diacylglycerol-substituted phosphate group (purple/red) from the CDP-DAG donor to the inositol phosphate acceptor (green), generating PIP and CMP. Panel B shows the structure of the *Rs*PIPS-Δ6N homodimer in ribbon representation viewed from two orthogonal orientations (in the plane of the membrane on the left; towards the cytosol down the dimer axis on the right). One protomer is colored grey, and the helices of the other are depicted in spectral coloring, from blue (JM1) to red (TM6). The *Af*2299 extramembrane domain used to facilitate crystallization is not shown here.

Figure **21.3.34** shows a large cavity that contains the active site of RsPIPS.

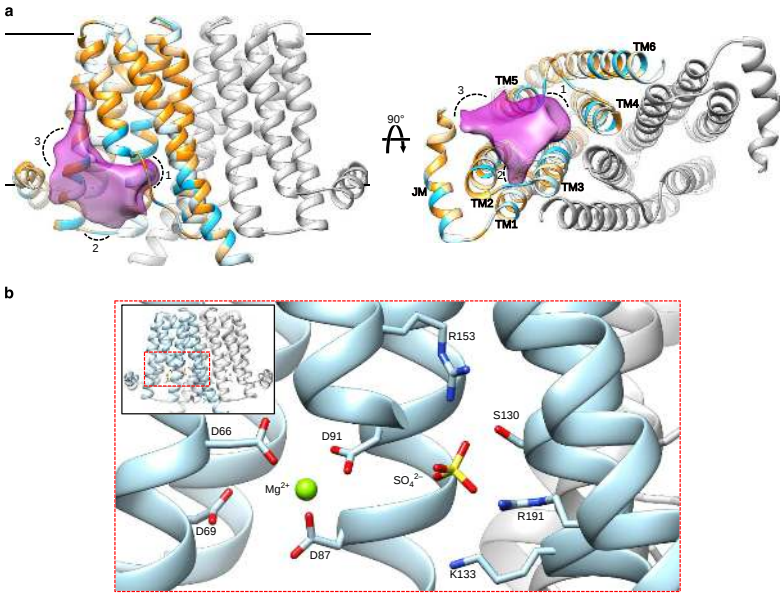
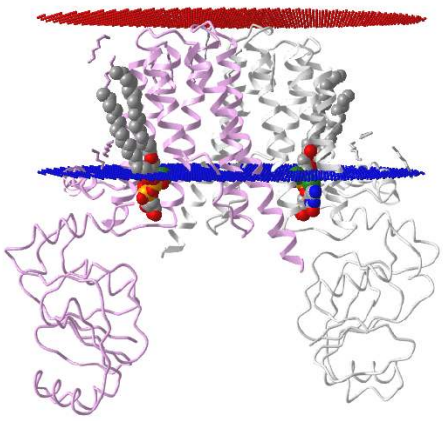


Figure **21.3.34**: Large cavity containing the active site of RsPIPS . Clarke, O., Tomasek, D., Jorge, C. *et al.* ibid.

Panel (**a**) shows the structure of *Rs*PIPS-Δ6N in ribbon representation, with one protomer colored grey and the other colored by the Kyte–Doolittle hydrophobicity scale, from −4.5 (most polar, light blue) to 4.5 (most hydrophobic, orange). Two orthogonal representations are shown; on the left is a view in the plane of the membrane, and on the right is a view from the cytosol along the dimer axis. A transparent purple surface delineates the borders of the interfacial cavity, which contains three subregions as follows: 1, the inositol phosphate acceptor-binding pocket; 2, the nucleotide-binding pocket between TM2 and TM3; and 3, a hydrophobic groove between TM2 and JM1. (**b**) Detail of the active site viewed in the plane of the membrane, with side chains that contact the bound Mg^{2+} and SO_4^{2-} ions labeled and depicted in stick representation.

A nucleotide-binding site formed from transmembrane segments 1, 2, and 3 contains 8 conserved residues (D_1xxD_2G_1xxAR… G_2xxxD_3xxxD_4). The first three aspartic acid side chains coordinate a metal ion, while the 4th is likely a general base in catalysis.

Figure **21.3.35** shows an interactive iCn3D model of the phosphatidylinositolphosphate (PIP) synthase with bound CDP-DAG from Renibacterium salmoninarum (5D92).



NCBI iCn3D Figure **21.3.35**: Phosphatidylinositolphosphate (PIP) synthase with bound CDP-DAG from Renibacterium salmoninarum (5D92).. Click the image for a popup or use this external link: https://structure.ncbi.nlm.nih.gov/i...i9nhSw9U32Man8

The two identical subunits of the homodimer are shown in gray and plum. The two CDP-DAGs are shown in spacefill and CPK colors.

Function: In addition to functioning as negatively charged building blocks of membranes, the inositol phospholipids (including the phosphatidylinositol phosphates or 'polyphosphoinositides' discussed below) have crucial roles in the interfacial binding of proteins and the regulation of protein activity at the cell interface. Phosphoinositides are polyanionic so that they can be very effective in non-specific electrostatic interactions with proteins. However, they are especially efficient in specific binding to so-called ‘PH’ domains of cellular proteins. At least three phosphatidylinositol molecules are present in the crystal structure of human erythrocyte glycophorin, for example,

and they are believed to influence binding to other proteins via their head groups. The lipid is a structural component of yeast cytochrome bc_1.

In animal tissues, phosphatidylinositol is the primary source of the arachidonic acid required for the biosynthesis of **eicosanoids**, including prostaglandins, via the action of the enzyme phospholipase A_2, which releases the fatty acids from position *sn*-2. The reverse reaction also occurs.

Figure **21.3.36**s shows the generation of arachidonic acid and eicosanoids from PI using phospholipase A2

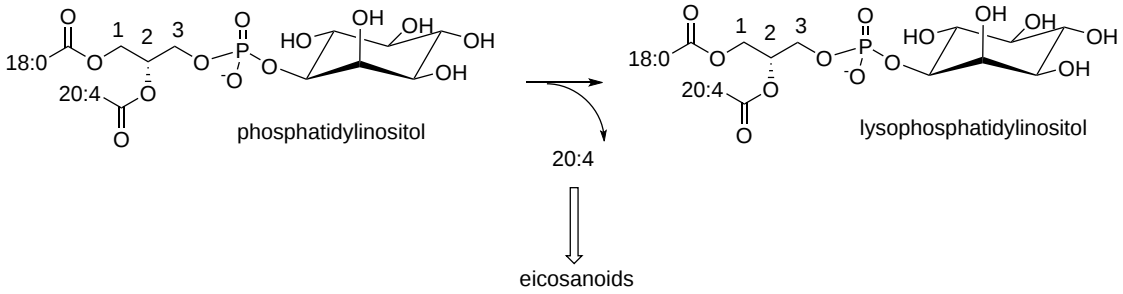


Figure **21.3.36**: Generation of arachidonic acid and eicosanoids from PI using phospholipase A2.

Similarly, phosphatidylinositol and the phosphatidylinositol phosphates are the main sources of diacylglycerols that serve as signaling molecules in animal and plant cells via the action of a family of highly specific enzymes collectively known as phospholipase C. In brief, diacylglycerols regulate the activity of a group of at least a dozen related enzymes known as protein kinase C, which control many key cellular functions, including differentiation, proliferation, metabolism, and apoptosis. Indeed, the biological actions of the various components released have been the subject of intensive study over many years. **2-Arachidonoylglycerol**, an endogenous cannabinoid receptor ligand, may also be a product of phosphatidylinositol catabolism.

21.3.6.2: PHOSPHATIDYLINOSITOL PHOSPHATES (POLYPHOSPHOINOSITIDES) IN ANIMALS

Structure and Occurrence: The pioneering work of Mable and Lowell Hokin in the 1950s led to the discovery that phosphatidylinositol was converted to polyphosphoinositides with important signaling and other functional activities, including cell communication via signal transduction, cell survival and proliferation, membrane trafficking, and modulation of gene expression. Phosphatidylinositol is now known to be phosphorylated by many substrate-selective kinases that place the phosphate moiety on positions 3, 4, and 5 of the inositol ring, with the balance among them maintained by distinct phosphatases and phospholipases. Seven different isomers are known (mono-, bis, and tris-phosphorylated), which are produced in a tightly coordinated manner, and all of these have characteristic biological activities. They each turn over much more rapidly than the parent phosphatidylinositol molecule. In addition, an array of molecular species of each of these isomers differs in the nature of the fatty acyl groups. Although the most significant in quantitative and possibly biological terms were long thought to be **phosphatidylinositol 4-phosphate** and **phosphatidylinositol 4,5-bisphosphate**, it is now recognized that **phosphatidylinositol 3-phosphate** and its metabolites are as important biologically.

Figure **21.3.37** shows the structures of phosphatidylinositol phosphates

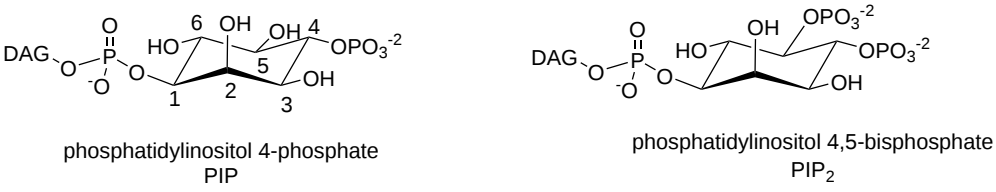


Figure **21.3.37**: Structures of phosphatidylinositol phosphates in animals

These lipids are usually present at low levels only in tissues, typically at about 0.5 to 1% of the total lipids of the inner leaflet of the plasma membrane, so they are unlikely to have an appreciable structural role. On the other hand, static measurements of lipids that turn over very rapidly do not provide a meaningful assessment of their cellular functions. The positional distributions of fatty acids in the phosphatidylinositol, phosphatidylinositol 4-phosphate, and phosphatidylinositol 4,5-bisphosphate of ox brain are listed in Table **21.3.7**. In each, the saturated fatty acids are concentrated in position *sn*-1 and polyunsaturated, especially arachidonate, in position *sn*-2; there are few differences among the three lipids in this instance.

Table **21.3.7**: **Distribution of fatty acids (mol% of the total) in positions *sn*-1 and *sn*-2 in phosphatidylinositol (PI) and the phosphatidylinositol mono- and diphosphates of ox brain.**

Fatty acids	PI		PI monophosphate		PI diphosphate	
	sn-1	*sn*-2	*sn*-1	*sn*-2	*sn*-1	*sn*-2
16:0	15		9		7	
18:0	74		69		69	
18:1	10	10	20	13	21	10
18:2	1	2	trace	1	1	1
20:3(*n*-9)		5		10		10
20:3(*n*-6)		5		11		12
20:4(*n*-6)		67		49		52
22:3		7		10		7
22:6(*n*-3)		trace		trace		trace

Data from Holub, B.J. *et al.*, *J. Lipid Res*., **11**, 558-564 (1970); DOI.
Molecular species data, see Traynor-Kaplan, A. *et al.*, *Biochim. Biophys. Acta*, **1862**, 513-522 (2017); DOI.

Biosynthesis: Phosphatidylinositol *per se* is the ultimate precursor of all phosphoinositides, the head groups of which have different charges and structures that directly impact membrane properties and, via metabolic interactions, can function as chemical switches. The individual phosphoinositides are maintained at steady state levels in membranes by a continuous and sequential series of phosphorylation and dephosphorylation reactions by specific kinases, phosphatases, and phospholipase C enzymes, which are regulated and/or relocated through cell surface receptors for extracellular ligands, the phosphoinositide cycle. While this has been termed a ‘futile cycle’, which can consume a significant proportion of cellular ATP production, it is only part of a wider pattern of reactions - the **phosphatidylinositol cycle** (see below). Controlled synthesis of these different phosphoinositides occurs in different intracellular compartments for distinct and independently regulated functions with spatially distinct target enzymes or receptors. In mammals, the complexity is such that 18 phosphoinositide inter-conversion reactions have been identified to date, and these are mediated by at least 20 phosphoinositide kinases and 34 phosphoinositide phosphatases that span 8 and 10 classes, respectively; some have yet to be characterized. Most of these enzymes are conserved across all of the eukaryota, and each has distinct functions and specificities that cannot be replaced by the activity of related isoforms.

Generally, most monophosphorylations occur in endomembranes, such as the endosomes and the Golgi network. In contrast, second and third phosphorylations occur primarily at the plasma membrane, which is reflected in each membrane's lipid composition. While these enzymes are believed to work independently and sequentially to produce a specific product, there remains a possibility that some participate in protein complexes to coordinate their activities. Specific transporters, especially the 'Nir2' protein, facilitate the exchange of phosphoinositides between membranes. It should be noted that there are links to the metabolism of **phosphatidylcholine**, which can be hydrolyzed by phospholipase D to phosphatidic acid, an important activator of key kinases. Figure **21.3.38** overviews polyphosphoinositide metabolism in animal tissues.

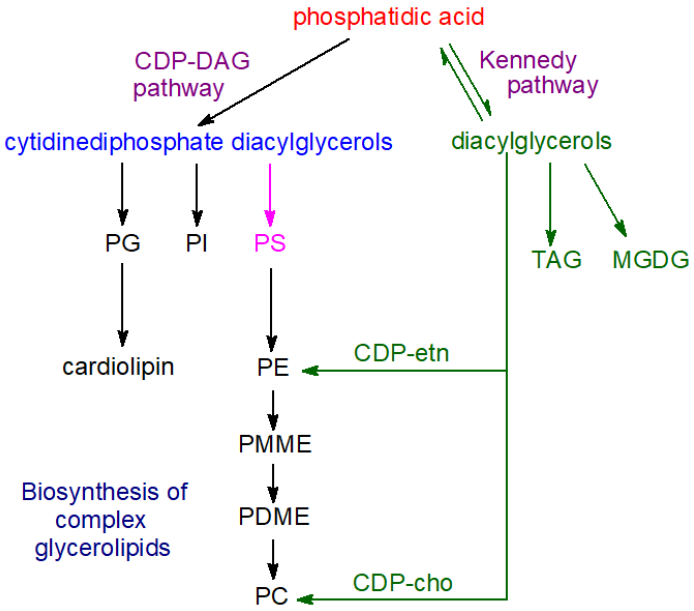


Figure **21.3.38**: Overview of polyphosphoinositide metabolism in animal tissues

Thus as an example, phosphatidylinositol 4-phosphate (PI(4)P) is produced by the action of a phosphatidylinositol 4-kinase (PI4K) in the Golgi, and is in turn phosphorylated by a phosphatidylinositol phosphate 5-kinase (PIPK I) to form phosphatidylinositol 4,5-bisphosphate (PI(4,5)P) at the plasma membrane. However, this can also be formed by phosphorylation of phosphatidylinositol 5-phosphate by a specific 4-kinase (PIPK II). Four isoforms of PI4K in two structural families operate in different subcellular membrane compartments to produce phosphatidylinositol 4-phosphate for particular signaling functions. Some selectivity in forming molecular species or remodeling may occur to enrich the arachidonic acid content further.

Subsequently, it was discovered that phosphatidylinositol is also phosphorylated by a 3-kinase (PI3K III or the VPS 34 complex) to produce phosphatidylinositol 3-phosphate (PI(3)P) in the early endosomes. Three phosphatidylinositol 3-kinases families (eight isoforms) have been described, each with distinct substrate specificities. A second phosphoinositide signaling pathway involves activation of two of these 3-kinases, stimulated by growth factors and hormones, which phosphorylate phosphatidylinositol 4,5-bisphosphate (by PI3K I - four isoforms) and phosphatidylinositol 4-phosphate (by PI3K II - three isoforms) to produce phosphatidylinositol 3,4,5-trisphosphate (PI(3,4,5)P) and phosphatidylinositol 3,4-bisphosphate (PI(3,4)P), respectively. While phosphatidylinositol 3-phosphate and other 3-phosphorylated metabolites amount to only about 0.5% of the total phosphoinositides in resting mammalian cells, they are now recognized as profoundly important for cellular metabolism.

In addition to the activity of kinases, the amounts of these various metabolites are regulated by the activities of specific phosphoinositide phosphatases, which are highly conserved in eukaryotes and dephosphorylate phosphoinositides at the 3, 4, and 5 positions of the inositol ring. For example, so-called ‘SHIP’ phosphatases convert phosphatidylinositol 4,5-bisphosphate back to phosphatidylinositol 4-phosphate by hydrolysis of the 5-phosphate group. 3-Phosphorylated phosphoinositides are only degraded by phosphatases, especially those of the PTEN family, and not by phospholipase C (see below).

The various organelles in cells have membranes with distinct functions and molecular compositions. Yet, all the phosphatidylinositol precursor is formed primarily at the endoplasmic reticulum, and the different membrane lipids must be transported between membrane sites via specific trafficking processes/proteins. There is selective recruitment of effector proteins to particular membranes by binding only to a single type of phosphoinositide, and this is followed by interactions between the phosphoinositide-binding proteins and various enzymes to channel phosphoinositide production to the required biological outcomes and to regulate signaling. For example, much of the phosphatidylinositol 4-phosphate and phosphatidylinositol 4,5-bisphosphate involved in signaling is believed to be formed at contact sites between the endoplasmic reticulum and plasma membrane.

A concept has emerged in which each phosphoinositide has its own role – **the ‘lipid code’ hypothesis**, in which defined lipids act as labels for each cellular membrane to organize cells into dynamic and responsive membrane-bound compartments and maintain the orderly flow required for the complexities of membrane trafficking and spatio-temporal signaling reactions. Thus, phosphatidylinositol 4-phosphate, phosphatidylinositol 4,5-bisphosphate, phosphatidylinositol 3-phosphate, and phosphatidylinositol 3,5-bisphosphate are found mainly on the Golgi, plasma membrane, early endosomes, and late endocytic organelles, respectively, where they are sometimes regarded as landmarks for these compartments. For example, phosphatidylinositol 4,5-bisphosphate is present throughout the plasma membrane and is considered a general marker. In contrast, phosphatidylinositol 3,4,5-triphosphate is a characteristic component of the basolateral region of this membrane

in a polarized cell but is absent from the apical part. On the other hand, it should be noted that this map of phosphoinositides to specific organelles is derived from their steady-state distributions. Still, the highly dynamic generation and consumption of different phosphoinositides in response to different stimuli in the various sub-cellular compartments in living cells by the action of kinases and phosphatases, together with lipase reactions, may lead to the formation of transient pools of distinct molecular forms. The precursors must be continuously replenished by new synthesis.

? PHOSPHATIDYL INOSITOL AND DERIVATIVES - ADDITIONAL BACKGROUND

Click the link below.

Link

Function: The distinctive subcellular location of the different phosphoinositide species and phosphorylation's rapid and reversible nature give them a central and general position in cell signaling cascades and intracellular membrane trafficking. The precise locations of particular phosphoinositides are factors that contribute a specific identity to each organelle and sometimes even to each face of an organelle, such as the *cis* and *trans* faces of the Golgi apparatus, and this enables directional transport of cellular constituents between organelles or membranes. Phosphoinositides can achieve signaling effects directly by binding to specific cytosolic domains of membrane proteins via their polar head groups, thereby triggering downstream signaling cascades, often in conjunction with an acidic phospholipid, such as phosphatidylserine or phosphatidic acid, at an adjacent-binding site. The term 'lipidon' has been coined to describe the unique collection of co-located lipids that distinguish biological membrane nano-environments and provide the context for PI recognition *in vivo*. In this way, they can regulate the function of innumerable proteins integral to membranes, for example, by relocating a protein from one area of the cell to another, e.g., from the cytosol to the inner leaflet of the plasma membrane, or they can attract cytoskeletal and signaling components to the membrane. Amongst the proteins that bind to phosphoinositides in this way are phospholipases, protein kinases, regulators of membrane trafficking, and cytoskeletal, scaffold, and ion channel proteins. Dysregulation of phosphoinositide metabolism and signaling is a factor in many diseases, including cancer.

Binding usually involves electrostatic interactions with the negative charges of the phosphate groups on the inositol ring, with characteristic clusters of basic amino acid residues in proteins to recruit them to intracellular membranes, often leading to specific folding and increased activity of unstructured peptides. At least 70 distinct types of phosphoinositide binding sites have been identified in proteins. In particular, a binding region termed the pleckstrin homology (PH) domain, consisting of ~100 amino acids, is the most abundant lipid-binding domain with more than 225 examples identified, and this can exhibit great specificity for particular polyphosphoinositides, often binding simultaneously with other proteins. While the interaction is initially driven by non-specific electrostatic interactions, it is followed by specific binding to increase the membrane residence time.The phox homology (PX) domain family with 49 members in humans is unique in that it can recognize all seven phosphoinositide forms, while proteins with a FYVE domain, which is enriched in cysteine and is stabilized by two zinc atoms, bind specifically to phosphatidylinositol 3-phosphate (PI(3)P). The protein kinase C family has C1 or C2 domains that recognize phosphatidylinositol 4,5-bisphosphate and phosphatidylinositol 3,4,5-trisphosphate specifically (and sometimes other lipids). The distinctive phosphoinositide composition of membranes in different organelles adds strength and specificity to the interactions by cooperative binding with other membrane proteins.

Phosphatidylinositol 3-phosphate and the other phosphatidylinositol monophosphates are present in cells at low levels, although their levels do not appear to fluctuate greatly. PI(3)P has been implicated in membrane trafficking by interacting with certain endosome proteins. In particular, it plays a pivotal role in initiating autophagy, i.e., cellular constituents' controlled internal degradation and turnover. At the same time, $PI(3,5)P_2$ is important in the autophagosome–lysosome fusion step and in the subsequent acidification of this organelle. After sorting of the lysosomal contents, components of the internalized cargo are recycled to the plasma membrane, and PI(3)P is dephosphorylated to phosphatidylinositol by a specific phosphatase, and this is, in turn, phosphorylated to PI(4)P. Thus, the processes of internalization, sorting, and trafficking of membrane proteins depend on the interconversion of phosphoinositide species by coordinated phosphorylation-dephosphorylation reactions.

PI(3)P generally controls cellular processes by recruiting effector proteins through low to moderate affinity interaction with specific PI(3)P binding domains. A protein designated Akt (protein kinase B) is recognized as a direct effector of the PI3K signaling cascade with receptor tyrosine kinases as the main upstream activators, for example, but it is now known that every phosphatidylinositol phosphate has a specific set of effector proteins that are recruited to target membranes or are allosterically regulated by the specific receptors; each function may require a different effector. A further function of PI(3)P is regulating the final stage of cell division (cytokinesis), and the lipid accumulates where cells divide. As the class I PI3K isoforms especially have been implicated in the etiology and maintenance of various diseases and metabolic disorders, including cancer, inflammation, and autoimmunity, drug

companies are actively pursuing the development of inhibitors. In particular, they mediate insulin-independent glucose transport and many of the physiological actions of insulin. In relation to lung cancer, especially, RAS proteins, which are key signaling switches essential for the control of proliferation, differentiation, and survival of eukaryotic cells, regulate the activity of type I phosphatidylinositol 3-kinase (PI3K); this is essential for tumor initiation and maintenance.

Phosphatidylinositol 4-phosphate is the precursor for the 4,5-bisphosphate, but it binds to a protein on the cell's cytoskeleton and has its own characteristic functions. It is the most widely distributed of the phosphoinositides, and in addition to the Golgi and the plasma membrane, it is present in late endosomes, lysosomes, secretory vesicles, and autophagosomes. As a part of protein-lipid complexes, it is believed to have a role in essential nuclear processes. In yeast, it has a function in the anterograde transport from the trans-Golgi and the retrograde transport from the Golgi to the endoplasmic reticulum; it is also necessary for the formation of secretory vesicles in the Golgi that are targeted to the plasma membrane. Some of that in the plasma membrane is exchanged for phosphatidylserine by the action of specific transport proteins at junctions with the endoplasmic reticulum.

In addition, PI(4)P is essential for the structure and function of the late endosomes, where it is required for the recruitment of specific proteins that control cargo exit (following hydrolysis of PI(3)P). Some of these participate in vesicle formation, while others like the oxysterol binding protein (OSBP) are involved in lipid transfer. After initiation of the process by PI(3)P, PI(4)P, $PI(4,5)P_2$, and their binding proteins are modulators of autophagy at most stages of the process. PI(4)P has been called the 'fuel' that drives cholesterol transport, as its hydrolysis provides the energy that enables the establishment of active sterol concentration gradients across membrane-bound compartments with the aid of OSBP, which is a key regulator of cholesterol, oxysterol, and PI(4)P concentrations in membranes. In the plasma membrane, PI(4)P can support the functions of ion channels, contributing to the anchoring of proteins with polybasic domains. However, it is not utilized to synthesize $PI(4,5)P_2$ in this membrane. On the other hand, PI(4)P derived from $PI(4,5)P_2$ in the membrane of primary cilia in the retina is important for vision. PI(4)P has an important influence on the progression of many diseases, especially virus replication, cancer, and various inflammatory diseases, and inhibitors of PI4-kinase are under study for their therapeutic potential.

While the biological properties of **phosphatidylinositol 5-phosphate** have taken longer to unravel because of the difficulties of separating this isomer, it is now apparent that it is involved in osmoregulation in plants and animals. It also has signaling functions, and although it is the least abundant phosphatidylinositol monophosphate, it is involved in signaling at the nucleus and in the cytoplasm, modulating cellular responses to various stresses, hormones, and growth factors. In the endosomes, it is a regulator of protein sorting.

Although **phosphatidylinositol 4,5-bisphosphate** (PI(4,5)P2) is found primarily in the inner leaflet of the plasma membrane, where it may define membrane identity in eukaryotic cells, it is also present in endosomes, the endoplasmic reticulum, and the nucleus. It is an essential precursor of lipid second messengers, such as diacylglycerols, with vital signaling functions that operate through plasma membrane G-protein coupled receptors, receptor tyrosine kinases, and immune receptors. Because of its large head group and multivalent negative charge, $PI(4,5)P_2$ has been described as an "electrostatic beacon" interacting with membrane proteins, other lipids, and cellular cations in various ways. In consequence and despite its relatively low concentration, it is a key regulator of innumerable events at the plasma membrane, including cell adhesion and motility, vesicle endocytosis and exocytosis, and the function of ion channels, especially those for potassium, calcium, and sodium. For example, ion channels appear to be an obligatory factor, increasing their activity by activating key proteins, while hydrolysis by phospholipase C reduces such activity.

$PI(4,5)P_2$ interacts with cationic residues of a large array of proteins in concert with cholesterol to form localized membrane domains distinct from the sphingolipid-enriched **rafts**. Indeed, it has a much higher concentration than other phosphoinositide species in cells, although most of this is, in effect, sequestered by binding proteins. Also, phosphatidylinositol 4,5-bisphosphate and its diacylglycerol metabolites are important for membrane vesicle formation. For example, the clathrin-coated vesicle pathway is a major cellular pathway to internalize cell surface proteins such as transferrin. $PI(4,5)P_2$ is essential to this process in that it binds to the machinery involved in the membrane, increasing the number of clathrin-coated pits and permitting the internalization of proteins. It has a related function in **caveolae**, where it is concentrated at the rim.

Through its attachment to the apical plasma membrane, phosphatidylinositol 4,5-bisphosphate is intimately involved in developing the actin cytoskeleton, thereby controlling cell shape, motility, and many other processes. In particular, it binds with high specificity to effectors such as vinculin, a membrane-cytoskeletal protein that links integrin adhesion molecules to the actin cytoskeleton. Dysregulation of this function has been implicated in the migration and metastasis of tumor cells. In yeast, stearic acid in position *sn*-1 appears to be essential for this function. In the cell nucleus, this lipid is believed to be involved in maintaining chromatin, the complex combination of DNA, RNA, and protein that makes up chromosomes in a transcriptionally active conformation, and is a precursor for further signaling molecules. It has a role in gene transcription and RNA processing, especially in the modulation of RNA polymerase activity, and in other nuclear processes.

The lipid is an essential component of the immune response of animal tissues to toxic bacterial **lipopolysaccharides** by binding to specific proteins. It is also involved in the pathophysiology of HIV via an interaction with the Tat protein secreted by infected cells.

$PI(4,5)P_2$ is the primary precursor of the endocannabinoid **2-arachidonoylglycerol** in neurons. It is also an essential cofactor for phospholipase D and affects phosphatidic acid's cellular production with its specific signaling functions. By binding specifically to ceramide kinase, the enzyme responsible for synthesizing **ceramide-1-phosphate**, it influences sphingolipid metabolism. Like ceramide-1-phosphate, it binds to and activates the Ca^{2+}-dependent phospholipase A_2, which generates the arachidonate for eicosanoid production. One molecule of phosphatidylinositol 4,5-bisphosphate is bound to each subunit of the protein of the mammalian GIRK2 potassium channel, enabling a conformational change that assists the transport function of the protein.

Perhaps the best characterized of the phosphoinositide signaling functions results from the hydrolysis of phosphatidylinositol phosphates by phospholipase C isoforms, in this instance to produce ***sn*-1,2-diacylglycerols** and inositol 3,4,5-trisphosphate (see below), which act as second messengers. Only those polyunsaturated diacylglycerol species derived from $PI(4,5)P_2$ can bind and activate protein kinase C (α, ε, δ) isoforms *in vitro* and *in vivo*. This lipid is important as it binds strongly to these enzymes via a basic patch distal to a Ca^{2+} binding site, which targets them selectively to the plasma membrane. The aberrant expression of phospholipase Cγ2 may be a factor in neurodegenerative diseases. Via the action of PI3 kinase, $PI(4,5)P_2$ is the precursor of $PI(3,4,5)P_3$ with its distinctive signaling properties.

Phosphatidylinositol 3,4-bisphosphate can be produced by two routes and regulates a variety of cellular processes with relevance to health and disease that include B cell activation and autoantibody production, insulin sensitivity, neuronal dynamics, endocytosis, and cell migration. It binds selectively to many proteins and acts as a secondary messenger by recruiting the protein kinases Akt (protein kinase B). It may influence the cell cycle, cell survival, angiogenesis, and glucose metabolism. During endocytosis in the endolysosomal system, it is produced from $PI(4,5)P_2$ and controls the maturation of endocytic-coated pits. Its synthesis and turnover are spatially segregated within the endocytic pathway. In epithelial cells, it is located on the apical membrane, i.e., facing the lumen, as opposed to the basolateral membranes, and it is believed to be a determinant of the identity and function of the apical membrane.

Phosphatidylinositol 3,5-bisphosphate is present at low levels only in cells (0.04-0.1% of the total phosphatidylinositides) unless stimulated by growth factors. Still, it is important in membrane and protein trafficking, especially in the late endosomes in eukaryotes and yeast vacuoles. For example, converting PI(3)P to $PI(3,5)P_2$ promotes endosomal maturation and degradative sorting. It mediates signaling in response to stress and hormonal cues and controls ion transport in membranes. Genetic studies confirm that it is essential for healthy embryonic development, especially in the nervous system.

Phosphatidylinositol 3,4,5-trisphosphate ($PI(3,4,5)P_3$) is almost undetectable in quiescent cells. Yet, its intracellular level rises very rapidly from synthesis at the plasma membrane in response to agonists such as extracellular growth factors and hormonal stimuli. By recruiting proteins with pleckstrin homology (PH) domains to the plasma membrane, it has been implicated in various cellular functions, including growth, cell survival, proliferation, cytoskeletal rearrangement, intracellular vesicle trafficking, and cell metabolism. In particular, it is an important component of a signaling pathway in the cell nucleus. In epithelial cells, it is located on the basolateral membrane, i.e., facing adjacent cells, where it may be a determinant of the identity and function of this membrane. In contrast to phosphatidylinositol 3-phosphate, it opposes autophagy by binding to and activating the PH domain of Akt, inducing cell proliferation. During feeding, various physiological responses lead to the secretion of insulin, which stimulates the phosphorylation of phosphatidylinositol 4,5-bisphosphate to phosphatidylinositol 3,4,5-trisphosphate and triggers a signaling cascade that leads to the suppression of autophagy. When impaired, this pathway has deleterious effects on insulin resistance associated with various metabolic diseases, including obesity and diabetes. It has been implicated in tumor cell migration and metastasis. $PI(3,4,5)P_3$ is also present in the nucleus and nucleoli of cells, where it is believed to have functions in RNA processing/splicing, cytokinesis, protein folding, and DNA repair. In contrast, like **phosphatidylserine**, it is reportedly transferred to the outer leaflet of the plasma membrane in aged or damaged cells as an 'eat-me' signal for phagocytes and apoptosis.

The human immune system utilizes neutrophils, which are highly mobile cells, to eliminate pathogens from infected tissue. The first step is to track and then pursue molecular signals, such as cytokines, emitted by pathogens. It has been established that two phospholipids operate in sequence to point the neutrophils in the correct direction. The first is phosphatidylinositol 3,4,5-trisphosphate, which binds to a specific protein, DOCK2, and enables it to translocate to the plasma membrane. Then, phosphatidic acid, generated by the action of phospholipase D on phosphatidylcholine, takes over and directs the DOCK2 to the leading edge of the plasma membrane. This causes the polymerization of actin within the cell and, in effect, reshapes the neutrophil and points it in the direction from which the pathogens' signals are coming. On the other hand, *Mycobacterium tuberculosis* can subvert phosphoinositide signaling to arrest phagosome maturation by dephosphorylation of phosphatidylinositol 3-phosphate.

21.3.6.3: WATER-SOLUBLE INOSITOL PHOSPHATES

As mentioned briefly above, hydrolysis of phosphatidylinositol phosphates by calcium-dependent phospholipase C (or 'phosphoinositidase C') leads to the generation of ***sn*-1,2-diacylglycerols**, which act as second messengers in animal cells and are of enormous metabolic importance. There are many different enzymes of this type, but the activity of the phosphoinositide-specific phospholipase C constitutes an essential step in the inositide signaling pathways. The enzyme exists in six families of at least 13 isoenzymes, all with conserved regions such as the plekstrin homology (PH) binding domain. Each has a distinctive role and can have a characteristic cell distribution linked to a specific function. The activity of these enzymes is stimulated by signaling molecules such as G-protein coupled receptors, receptor tyrosine kinases, Ras-like GTPases, and calcium ions, thus linking the hydrolysis of phosphatidylinositol phosphates to a wide range of other cellular signals. As phospholipase C is a soluble protein in the cytosol, translocation to the plasma membrane is crucial in signal transduction. Regulation of these isoenzymes and the form PLCγ1 in particular is vital for health, as they are associated with activating or inhibiting important pathophysiological processes, especially cancer.

Some phosphatidic acid is synthesized from the diacylglycerols produced within the plasma membrane through the activity of diacylglycerol kinases. This acid is transported back to the endoplasmic reticulum and ultimately can be re-utilized for phosphatidylinositol biosynthesis.

The other products of the phospholipase C reaction that are of special relevance because of their many essential functions are **water-soluble inositol phosphates**. Up to 60 different compounds of this type are possible, and at least 37 of these have been found in nature at the last count, all of which are extremely important biologically. However, polyphosphoinositides with a phosphate in position 3 are not substrates for phospholipase C.

Figure **21.3.39** shows the generation of inositol phosphates by phospholipase C.

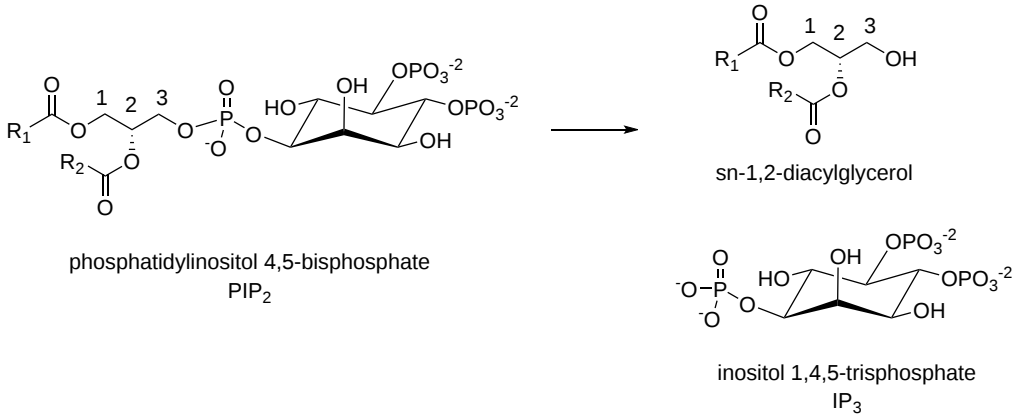


Figure **21.3.39**: Generation of inositol phosphates by phospholipase C

For example, under the action of various physiological stimuli in animals, including sphingosine-1-phosphate, and acting via various G-protein-coupled receptors, phosphatidylinositol 4,5-bisphosphate in the plasma membrane is hydrolyzed to release inositol 1,4,5-trisphosphate. This important cellular messenger diffuses into the cytosol and stimulates calcium release from an ATP-loaded store in the endoplasmic reticulum via ligand-gated calcium channels (the diacylglycerols remain in the membrane to recruit and activate members of the protein kinase C family). The increase in calcium concentration, together with the altered phosphorylation status, activates or deactivates many different protein targets, enabling cells to respond appropriately to the extracellular stimulus. To enable rapid replenishment of the phosphatidylinositol 4,5-bisphosphate used in this way, a cycle of reactions - the phosphatidylinositol cycle - must occur (see below). On the other hand, a recent publication suggests that phosphatidylinositol 4-phosphate in the plasma membrane may be a more important source of diacylglycerols following G protein–coupled receptors stimulation.

The various inositol phosphates appear to be involved in controlling cellular events in specific ways, but especially in the organization of key signaling pathways, the rearrangement of the actin cytoskeleton, or intracellular vesicle trafficking. They have been implicated in gene transcription, RNA editing, nuclear export, and protein phosphorylation. These remarkable compounds can be rapidly synthesized and degraded in discrete membrane domains or even sub-nuclear structures, so they are considered ideal regulators of dynamic cellular mechanisms. From structural studies of inositol polyphosphate-binding proteins, it is believed that the inositides may act, in part at least, by modifying protein function by acting as structural cofactors, ensuring that proteins adopt their optimum conformations. In addition, phosphoinositides and inositol polyphosphates are key components of the cell's nucleus, where they have many essential functions, including DNA repair, transcription regulation, and RNA dynamics. It is believed that they may be activity switches for the nuclear complexes responsible for such processes, with the phosphorylation state of the inositol ring being of primary importance. As different

isomers appear to have specific functions at each gene expression level, extracellular events must coordinate the production of these compounds in a highly synchronous manner.

In organisms from plants to mammals, kinases generate an extra tier of regulatory mechanisms by generating energetic diphosphate (pyrophosphate)- containing molecules from inositol phosphates. Conversely, these can be dephosphorylated by polyphosphate phosphohydrolase enzymes to regenerate the original inositol phosphates. These inositol pyrophosphates and the enzymes involved in their metabolism are also involved in regulating cellular processes by modulating the activity of proteins by various mechanisms.

It should be noted that the phospholipase C isoenzymes regulate the concentration of phosphatidylinositol 4,5-bisphosphate and related lipids and, hence, their activities, in addition to the generation of new biologically active metabolites.

21.3.6.4: PHOSPHATIDYLINOSITIDES IN PLANTS

In plants as in animals, phosphatidylinositol and polyphosphoinositides have essential biological functions, exerting their regulatory effects by acting as ligands that bind to protein targets via specific lipid-binding domains, altering the location of proteins and their enzymatic activities. However, it appears that polyphosphoinositide metabolism developed differently after the divergence of the animal and plant kingdoms. Hence, the details of each process are very different, not least because the subcellular locations of phosphoinositides differ appreciably between plants and animals. Phosphatidylinositol *per se* is the precursor of the phosphorylated forms and determines their fatty acid compositions. It also inhibits programmed cell death by acting as the biosynthetic precursor of the sphingolipid **ceramide phosphoinositol** and reducing the levels of ceramide.

As in animals, the various phosphoinositides (five in total) are produced and interconverted rapidly by a series of kinases and phosphatases (in many isoforms) in different cellular membranes in response to environmental or developmental cues. For example, phosphatidylinositol is generated mainly in the endoplasmic reticulum. At the same time, PI 4-kinases and their product are located in the trans-Golgi network and nucleus, and PI4P 5-kinases and their product are present in the plasma membrane. During the biosynthesis of polyphosphoinositides, the first phosphorylation occurs at the hydroxyl group at positions 3 or 4 of the inositol ring, catalyzed by the appropriate kinases, while the second phosphorylation then takes place at position 5; the action of a phosphatase on PI 3,5-bisphosphate produces PI 5-phosphate. Most other metabolites are produced via phosphatidylinositol 3-phosphate, and reports that some phosphatidylinositol 3,4,5-trisphosphate may be produced from phosphatidylinositol 4,5-bisphosphate require confirmation. In contrast to mammalian phosphatidylinositol 3-kinases, which accept phosphatidylinositol and its monophosphates as substrates, the plant enzyme acts only on the former.

Figure 21.3.40 shows polyphosphoinositide metabolism in plants

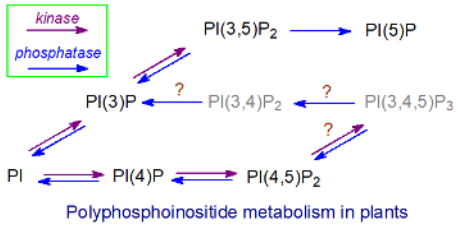


Figure 21.3.40: Polyphosphoinositide metabolism in plants

The reverse reaction in plants is accomplished by phosphoinositide phosphatases, which can be grouped into three main families: the phosphatase/tensin (PTEN) family, 5-phosphatases (5-PTases), and phosphatases containing Suppressor of Actin (SAC) domains, each with differing subcellular locations, substrate specificities, and regulatory mechanisms.

Although what might be considered normal levels of phosphatidylinositol 4-phosphate are present, the concentrations of phosphatidylinositol 4,5-bisphosphate and other phosphoinositides are extremely low in plants (10 to 20-fold lower than in mammalian cells), although they still have vital functions. There are differences between cell types, but in Arabidopsis epidermal root cells, $PI(4,5)P_2$ is present at the highest concentration in the plasma membrane (apex region) and nucleus. At the same time, PI4P slowly distributes between the plasma membrane and Golgi, with the highest concentration in the former. Multivesicular bodies/late endosomes accumulate PI3P and $PI(3,5)P_2$; the tonoplast and autophagosomes contain PI3P. How the various metabolites are transported between membranes has yet to be determined. Non-vesicular transport is believed to occur at membrane contact sites, and vesicular transport probably also occurs.

Highly polarized distributions of phosphoinositides are found within membranes, generally oriented toward the cytosolic leaflet, and they are believed to be organized in nanoclusters with other lipids and proteins. For example, phosphatidylinositol-4-phosphate is an important constituent of the plasma membrane in plant cells, where it controls the electrostatic state and is involved in cell division. It may control the location and function of many membrane proteins, including those required for development, reproduction, immunity, nutrition, and signaling. PI(4)P is the only phosphoinositide present at the cell plate, i.e., the membrane separating two daughter cells during cell division. In addition, PI(4)P may interact with salicylic acid in the plant immune response, and it is produced during salt stress. However, specific functions are now being discovered for each of the plant phosphoinositides, which are produced rapidly in response to osmotic and heat

stress, and it has become evident that a continuous turnover is essential for cell growth and development. For example, they have marked effects on the growth of many cell types and on guard cell function. In the nucleus, proteins have been identified that bind to phosphoinositides via the acyl chains, leaving the head group exposed for enzymatic modifications and signal transduction.

Phosphoinositides are of special importance in microdomains at the tip of growing tissues such as the shoot apical meristem, pollen tubes, and root hairs, where phosphatidylinositol 4,5-bisphosphate functions in stem cell maintenance and organogenesis. In the plasma membrane, it is enriched in the detergent-resistant component commonly equated with **'rafts. '** Although its concentration is low, PI(4,5)P_2 has been shown to have signaling functions by binding to many target proteins with characteristic binding domains. For example, with phosphatidic acid, PI(4,5)P_2 regulates the activity of many actin-binding proteins, which in turn control the activity of the actin cytoskeleton. This has a key role in plant growth, the movement of subcellular organelles, cell division and differentiation, and plant defense. In addition, this lipid exerts control over ion channels, ATPases, and phospholipase C-mediated lipid degradation and the production of further second messengers. It is an important factor in both clathrin-mediated endocytosis and exocytosis. The specificity of the interactions may be dependent on the fatty acid composition of the lipid and on the activity of phosphatidylinositol 4-phosphate 5-kinase.

As in animals, phosphoinositides have a role in endosomal sorting through the central vacuole, a plant-specific organelle with both lytic and storage functions. Phosphatidylinositol 3,5-bisphosphate is the least abundant of the phosphoinositides, but it is a crucial lipid for membrane trafficking systems. The PI to PI(3)P to PI(3,5)P_2 cascade, the second step requiring a kinase designated FAB1, is required for endosomal sorting events leading to membrane protein degradation or retrieval, vacuolar morphogenesis, and autophagy. PI(3,5)P_2 is involved in stomatal closure and the growth of root hairs, and it is also induced in salt stress.

Some different enzymes of the phospholipase C type that are specific for polyphosphoinositides have been isolated from higher plants; Ca^{2+} activates them, and unlike their mammalian counterparts, they are not regulated by G proteins. It is uncertain whether phosphatidylinositol is a substrate for these enzymes *in vivo*. Less is known about the metabolism of the water-soluble inositol phosphates produced compared to animals, and plants appear to lack a receptor for inositol 1,4,5-trisphosphate (IP_3). However, it is the most abundant metabolite of this type and is reported to induce the release of calcium ions to trigger stomatal closure. However, there is increasing evidence for lipid signaling mediated by phospholipase C in abiotic stress tolerance and development in plants. There is a general, if contested, belief that inositol hexakisphosphate (phytic acid or IP6), produced at least in part by sequential phosphorylation of inositol 1,4,5-trisphosphate, is a more important cellular messenger in plants and mobilizes an endomembrane store of calcium ions. Inositol-1,2,4,5,6-pentakisphosphate (IP_5) is a structural co-factor of the **jasmonic acid** receptor coronatine insensitive 1, linking phosphoinositide signaling with phytohormone-controlled pathways.

In contrast to animals, **diacylglycerols**, the other product of phospholipase C hydrolysis of phosphoinositides, are rapidly converted to **phosphatidic acid** by diacylglycerol kinases and have not been considered important in signal transduction in plants. Plants lack protein kinase C, but they do have proteins with related properties that appear to be influenced by diacylglycerols. Via the action of phospholipase D, inositol phospholipids are a source of phosphatidic acid with its well-characterized signaling functions in plants, especially in defence.

21.3.6.5: LYSO-PHOSPHOINOSITIDES

Figure **21.3.41** shows the structure of lysophosphatidylinositol

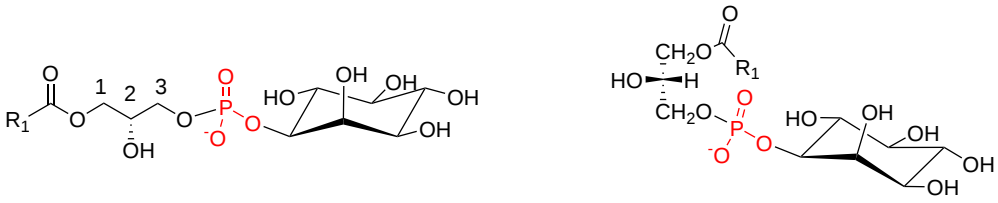


Figure **21.3.41**: Lysophosphatidylinositol

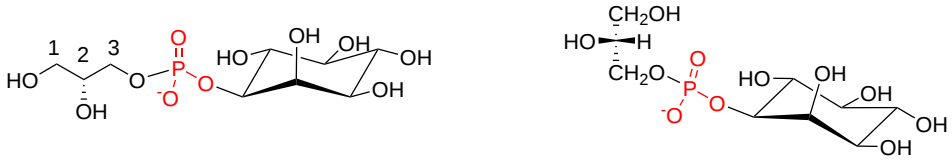
Lysophosphatidylinositols: Lysophosphatidylinositols (LPI), i.e., with a single fatty acid only linked to the glycerol moiety, are formed as intermediates in the remodeling of the fatty acid compositions of the lipids by the action of phospholipase A_1 or phospholipase A_2 (e.g., cPL$A_2\alpha$), and when arachidonic acid is released for eicosanoid biosynthesis (see above). In ovarian cancer, LPI is elevated appreciably to around 15µM in ascites, and it is also present at high levels in obese subjects.

It has become apparent relatively recently that, like other lysophospholipids, phosphatidylinositol and polyphospho-analogues may have messenger functions. For example, it has long been known to stimulate insulin release from pancreatic cells, suggesting a role in glucose homeostasis. *sn*-2-Arachidonoyl-lysophosphatidylinositol, in particular, is an endogenous ligand for a G protein-coupled receptor GPR55, and thereby can induce rapid phosphorylation of certain enzymes, including a protein kinase, which promote cancer cell proliferation, migration, and metastasis. Indeed, lysophosphatidylinositol is a biomarker for poor prognosis in cancer patients, and its concentration is

elevated significantly in highly proliferative cancer cells *in vitro*. GPR55 is expressed in many brain regions, the intestines, endocrine pancreas, and islets (where it may stimulate insulin release). It has been implicated in macrophage activation and inflammation. In addition to its role in cancer, lysophosphatidylinositol has been implicated in many metabolic diseases. It is reported to be a precursor of the endocannabinoid **2-arachidonoylglycerol** by the action of human glycerophosphodiesterase 3 as a lysophospholipase C. This enzyme suppresses the receptor for lysophosphatidylinositol, and so acts as a switch between GPR55 and endocannabinoid (CB2) signaling.

Glycerophosphoinositol: Sequential removal of both fatty acids from phosphatidylinositol by a specific phospholipase A_2 ($PLA_2IV\alpha$) with both phospholipase A_2 and lysophospholipase activities releases water-soluble glycerophosphoinositol. While this can be hydrolyzed by a glycerophosphodiester phosphodiesterase to inositol 1-phosphate, glycerophosphoinositol *per se* has distinctive biological activities and functions, as do related compounds derived from the phosphatidylinositol phosphates. In particular, glycerophosphoinositol has anti-inflammatory activity in that it inhibits the inflammatory and thrombotic responses induced by bacterial lipopolysaccharides (endotoxins).

Figure **21.3.42** shows the structure of glycerophosphoinositol



glycerophosphoinositol

Figure **21.3.42**: Glycerolphosphoinositol

21.3.6.6: THE PHOSPHATIDYLINOSITOL CYCLE

Phosphatidylinositol can be considered at the center of a cycle of reactions and intermediates involved in innumerable aspects of cellular signaling in animals (a similar cycle could be described for plants). These are discussed individually at length above, but it is useful to point out how each component forms part of a larger pattern. In brief as illustrated, the various synthetic and hydrolytic reactions involved in phosphoinositide metabolism can be considered to constitute a **phosphatidylinositol cycle** with enzymes located both in the endoplasmic reticulum and plasma membrane, so lipids have to be transferred across the cytosol in both directions between the two to complete the cycle, probably via adjacent membrane structures and facilitated by proteins of the phosphatidylinositol transfer protein membrane-associated family (PITPNM or nir2), which may channel phosphoinositide production to specific biological outcomes. Phospholipase C and phosphatidylinositol-4-phosphate 5-kinase (PI4P 5K) are located in the plasma membrane, while the cytidine diphosphate-diacylglycerol synthase (CDS2) and phosphatidylinositol synthase are in the endoplasmic reticulum. The epsilon isoform of diacylglycerol kinase (DGKε) is located at contact sites between the endoplasmic reticulum and plasma membrane. Still, nine further isoforms with differing cellular and subcellular locations may be involved in the cycle. Each turn of the cycle uses a great deal of energy and consumes three moles of ATP, together with cytidine triphosphate and inositol. If it is assumed that the pyrophosphate is hydrolyzed by endogenous pyrophosphatases to inorganic phosphate, the cycle can proceed in one direction only.

Figure **21.3.43** shows the phosphatidylinositol cycle.

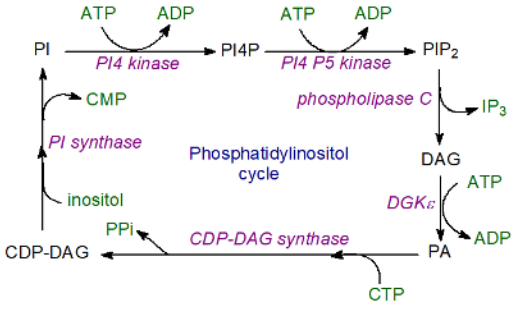


Figure **21.3.43**: Phosphatdylionositol cycle

Factors such as membrane curvature must be taken into account, and the diagram is of necessity a considerable over-simplification. In addition to participating in this cycle, many of the lipid intermediates can be precursors for other lipids; for example, diacylglycerols are potential precursors for triacylglycerols, while phosphatidic acid is a precursor for phosphatidylcholine and phosphatidylethanolamine. Each lipid intermediate is subject to remodeling of the acyl chains via the Lands cycle, and polyunsaturated fatty acids released can be utilized for eicosanoid production. A further byproduct of the cycle is inositol triphosphate, which regulates intracellular calcium levels.

It has been suggested that the unique molecular species composition of phosphoinositides (18:0-20:4) could influence their selective recycling back into phosphatidylinositol, as many of the enzymes involved have a preference for this substrate. A further proposal is that the phosphatidylinositol cycle could enrich this species through multiple passages around the cycle.

21.3.7: SUMMARY

This chapter provides an in-depth overview of the biosynthesis, remodeling, and functional roles of membrane glycerophospholipids, highlighting their importance as both essential structural components of cellular membranes and dynamic mediators of intracellular signaling. The discussion begins with phosphatidic acid (PA), the simplest diacylglycerophospholipid, which is synthesized primarily via the sequential acylation of glycerol-3-phosphate by acyltransferases. PA serves as a critical branching point in lipid metabolism: it is not only a precursor for the synthesis of complex glycerophospholipids and triacylglycerols via the Kennedy pathway but also functions as a lipid mediator, influencing membrane curvature and protein interactions.

From PA, the biosynthetic pathways diverge into the formation of major phospholipids:

- **Phosphatidylcholine (PC):** Produced mainly via the CDP-choline (Kennedy) pathway, PC is the most abundant phospholipid in eukaryotic membranes, particularly in the outer leaflet of the plasma membrane. Its synthesis and subsequent remodeling through the Lands cycle allow for the fine-tuning of fatty acid composition, impacting membrane fluidity and signaling.
- **Phosphatidylethanolamine (PE):** Synthesized via both the CDP-ethanolamine pathway in the endoplasmic reticulum and by decarboxylation of phosphatidylserine (PS) in mitochondria, PE is especially abundant in inner membranes. Its cone-shaped structure promotes negative curvature and is vital for processes like membrane fusion and mitochondrial function.
- **Phosphatidylserine (PS):** Generated by base-exchange reactions on existing PC or PE, PS is an anionic phospholipid predominantly located in the inner leaflet of the plasma membrane. It plays crucial roles in signaling—such as marking cells for apoptosis—and serves as a cofactor for many enzymes involved in coagulation and cellular homeostasis.
- **Phosphatidylinositol (PI) and Polyphosphoinositides:** PI is synthesized from PA through the CDP-diacylglycerol pathway and, despite its low abundance, is the precursor to a family of phosphorylated derivatives (PIPs) that are key regulators of signal transduction, vesicle trafficking, and membrane identity. The reversible phosphorylation of the inositol ring (at positions 3, 4, and 5) generates multiple signaling molecules (e.g., $PI(4,5)P_2$, $PI(3,4,5)P_3$) that interact with specific protein domains (PH, PX, FYVE) to direct processes such as endocytosis, cytoskeletal dynamics, and cell proliferation.

The chapter further details the mechanisms of acyl chain remodeling through deacylation–reacylation cycles (Lands cycle), which refine the molecular species of phospholipids to meet the functional requirements of different cellular membranes. It also discusses how lysophospholipids (such as lysophosphatidic acid and lysophosphatidylcholine) are generated by phospholipases and serve both as intermediates in lipid remodeling and as potent signaling molecules.

In plants and microorganisms, these pathways exhibit unique features, including additional isoforms of acyltransferases and distinct compartmentalization (e.g., in plastids or cell plate formation), underscoring the evolutionary adaptation of glycerophospholipid metabolism to specific cellular and environmental demands.

Overall, the synthesis and interconversion of glycerophospholipids not only sustain the structural integrity of membranes but also dynamically regulate a myriad of cellular processes—from energy metabolism and membrane trafficking to signal transduction and apoptosis—highlighting their central role in cellular physiology and pathology.

This page titled 21.3: Biosynthesis of Membrane Glycerolipids is shared under a not declared license and was authored, remixed, and/or curated by Henry Jakubowski and Patricia Flatt.

- **Current page** by Henry Jakubowski and Patricia Flatt has no license indicated.
- **11.2: Diffusion Across a Membrane - Passive and Facilitated Diffusion** by Henry Jakubowski and Patricia Flatt has no license indicated.

21.4: BIOSYNTHESIS OF MEMBRANE SPHINGOLIPIDS

by William (Bill) W. Christie and Henry Jakubowski.

This section is an abbreviated and modified version of material from the Lipid Web, an introduction to the chemistry and biochemistry of individual lipid classes, written by William Christie.

LEARNING GOALS (CHATGPT O3-MINI)

1. **Define Sphingolipids and Their Historical Context**
   - Explain what sphingolipids are, including the key structural element (the sphingoid base) and how it differs from glycerol-based lipids.
   - Describe the historical origins of the term “sphingolipid” and the contributions of early researchers (e.g., Thudichum and Carter).
2. **Describe the Structural Components of Sphingolipids**
   - Identify the basic building blocks of sphingolipids, such as sphingosine and ceramide.
   - Understand how variations in chain length, degree of hydroxylation, and unsaturation contribute to the diversity of sphingolipid structures.
3. **Explain the Biosynthesis of Sphingolipids**
   - Outline the de novo synthesis pathway of sphingoid bases (starting with serine and palmitoyl-CoA catalyzed by serine palmitoyltransferase).
   - Detail the enzymatic steps that convert sphingoid bases into ceramides (including the role of ceramide synthases, desaturases, and hydroxylases).
   - Discuss how the diversity of ceramide synthase isoforms influences the acyl chain composition of ceramides.
4. **Characterize the Formation of Complex Sphingolipids**
   - Describe the conversion of ceramides into complex sphingolipids such as sphingomyelin, glucosylceramide, and galactosylceramide.
   - Explain the role of glycosyl- and phosphoryl-transferases in modifying ceramides and the significance of these modifications.
5. **Understand Membrane Organization and Raft Formation**
   - Explain how sphingolipids, along with cholesterol, contribute to the formation of lipid rafts and nanodomains in cellular membranes.
   - Discuss the importance of the “sphingoid motif” in mediating intermolecular interactions (e.g., hydrogen bonding and van der Waals forces) within membranes.
6. **Interpret the Signaling Roles of Sphingolipid Metabolites**
   - Describe the functions of bioactive sphingolipid metabolites such as sphingosine, sphingosine-1-phosphate, and ceramide-1-phosphate.
   - Analyze how the balance (or “sphingolipid rheostat”) between pro-apoptotic (e.g., ceramide, sphingosine) and pro-survival (e.g., sphingosine-1-phosphate) lipids regulates cell fate.
7. **Examine the Sphingomyelin (Ceramide) Cycle**
   - Illustrate the sphingomyelin cycle, including the reversible interconversion between sphingomyelin and ceramide by sphingomyelinases and sphingomyelin synthases.
   - Discuss how this cycle contributes to rapid cellular responses to stress and regulates downstream signaling events.
8. **Relate Sphingolipid Metabolism to Human Disease**
   - Identify how dysregulation of sphingolipid metabolism is linked to pathological conditions such as lysosomal storage disorders (e.g., Gaucher and Niemann-Pick diseases), neurodegenerative disorders, diabetes, and cancer.
   - Evaluate the therapeutic potential of targeting sphingolipid metabolic pathways in disease treatment.
9. **Contrast Sphingolipid Metabolism in Different Organisms**
   - Compare and contrast sphingolipid compositions and metabolic pathways in animals, plants, fungi, and select bacteria.
   - Understand unique features in plant and microbial sphingolipid metabolism (e.g., the absence of sphingomyelin in plants).
10. **Analyze Techniques and Approaches in Sphingolipid Research**

- Review modern analytical methods (e.g., mass spectrometry, thin-layer chromatography) used for the identification and quantification of sphingolipids and their metabolites.
- Discuss how molecular biology techniques (such as gene knockout studies) have advanced our understanding of sphingolipid function.

These learning goals aim to build your ability to integrate structural, biochemical, and physiological aspects of sphingolipid metabolism and to appreciate its significance in health and disease.

21.4.1: SPHINGOLIPIDS

The sphingolipids comprise a wide range of complex lipids. The defining component is a long-chain or sphingoid base, usually linked to a fatty acid via an amide bond. J.L.W. Thudichum, a German chemist working in London, first coined the root term “sphingo-” in 1884 following his discovery of the first glycosphingolipids because the enigmatic nature of the molecules reminded him of the riddle of the sphinx. Regretfully, the importance of his work was not recognized until 25 years after his death, and it was 1947 before the term “sphingolipide” was introduced by Herbert Carter and colleagues. While they are much less enigmatic than they once were, sphingolipids are extremely versatile molecules that continue to fascinate as new knowledge is gained of their functions in healthy (and diseased) animal and plant tissues. They are found in only a few bacterial genera, notably *Sphingomonas*, *Sphingobacterium*, and a few other species. Many pathogenic species utilize host sphingolipids to promote infections. Novel sphingolipid structures continue to be reported, and as an example, at the last count, 188 of the complex sphingolipids classified as **gangliosides**, with variations in the complex carbohydrate component alone, had been characterized in vertebrates.

Long-chain or sphingoid bases, of which sphingosine is typical, are the basic elements and are the simplest possible functional sphingolipids. They vary in chain length and the presence of various functional groups, including double bonds of both the *cis*- and *trans*-configuration at different locations in the aliphatic chain. **Ceramides**, which contain sphingoid bases linked to fatty acids by amide bonds, vary appreciably in the compositions of both aliphatic components, depending on their biological origins. The structures of sphingosine and ceramide, the sphingolipid building blocks, are shown in Figure **21.4.1**.

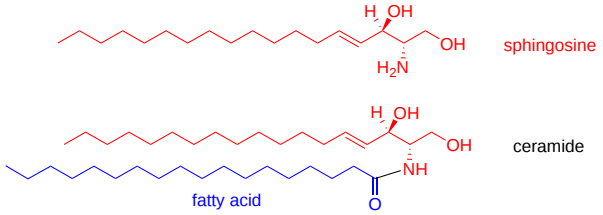


Figure **21.4.1**: Sphingolipid building blocks

Long-chain bases and ceramides have important biological properties in their own right, for example, in relation to intra- and intercellular molecular signaling, especially in animal cells. Another relatively simple sphingolipid, **sphingosine-1-phosphate**, is now recognized as a key factor in countless aspects of animal metabolism. The concentrations of these bioactive lipids respond rapidly to the action of specific stimuli and then regulate downstream effectors and targets.

Ceramides are the precursors of many sphingo-phospho- and sphingo-glycolipids with an immense range of functions in tissues. The properties and functions of these complex sphingolipids are quite distinct from those of the comparable glycerophospho- and glyceroglycolipids. For example, in animals, **sphingomyelin** has structural similarities to phosphatidylcholine but has very different physical and biological properties, while the complex **oligoglycosylceramides** and **gangliosides**(glycosphingolipids, of which **glucosylceramide** is the precursor) have no true parallels among the glyceroglycolipids. Figure **21.4.2** shows the complex sphingolipids sphingomyelin and glucosylceramide structures.

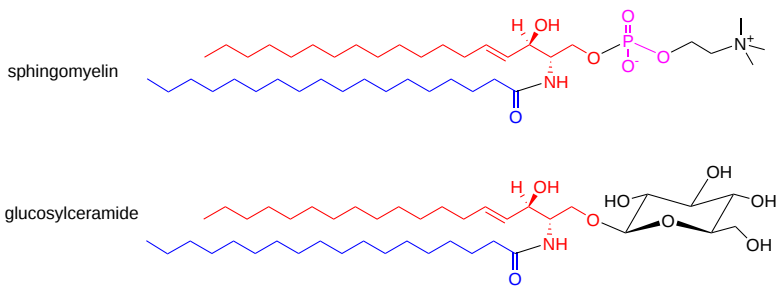


Figure **21.4.2**: Complex Sphingolipids

Complex sphingolipids are synthesized in the endoplasmic reticulum and Golgi. They are located mainly in the plasma membrane of most mammalian cells, where they have a structural function and also serve as adhesion sites for proteins from the extracellular tissue. The glycosphingolipids are especially important for myelin formation in the brain. However, sphingolipids have intracellular functions in all cellular compartments, including the nucleus. The first five carbon atoms of the sphingoid base in sphingolipids have a highly specific stereochemistry and constitute a key feature that has been termed the 'sphingoid motif', which, in comparison to other lipid species, facilitates a relatively large number of noncovalent interactions with other membrane lipids, via hydrogen-bonding, ion-ion interactions, and induced dipole-induced dipole interactions. A distinctive property of sphingolipids in membranes is that they spontaneously form transient nanodomains termed '**rafts**', usually in conjunction with cholesterol, where such proteins as enzymes and receptors congregate to carry out their signaling and other functions. Thus, in addition to their direct effects on metabolism, sphingolipids indirectly affect innumerable aspects of biochemistry via their physical properties.

While it may be obvious that a well-balanced sphingolipid metabolism is important for animal health, increasing evidence has been acquired to demonstrate that impaired sphingolipid metabolism and function are involved in the pathophysiology of many more common human diseases. These include diabetes, various cancers, microbial infections, Alzheimer's disease and other neurological syndromes, and diseases of the cardiovascular and respiratory systems. In humans, many important genetic defects in sphingolipid metabolism or sphingolipidoses have been detected, especially storage diseases associated with the lysosomal compartment, where sphingolipids are catabolized. Sphingolipids and their metabolism are likely to prove of ever-increasing interest to scientists.

There are appreciable differences in sphingolipid compositions and metabolism between animal and plant cells, with respect to the aliphatic components and especially the polar head groups. However, there are also some important similarities. While sphingomyelin is the most abundant sphingolipid in animals, it does not occur in plants and fungi. Although less is known of their role in plants, it has become apparent that complex sphingolipids are much more abundant in plant membranes than was once believed, and it is now recognized that they are key components of the plasma membrane and endomembrane system.

21.4.1.1: OVERVIEW OF SPHINGOLIPID METABOLISM

The biosynthesis and catabolism of sphingolipids involve many intermediate metabolites, all of which have distinctive biological activities. In animals, the relationships between these metabolites have been rationalized in terms of a 'sphingomyelin, sphingolipid or ceramide cycle', as shown in Figure **21.4.3**.

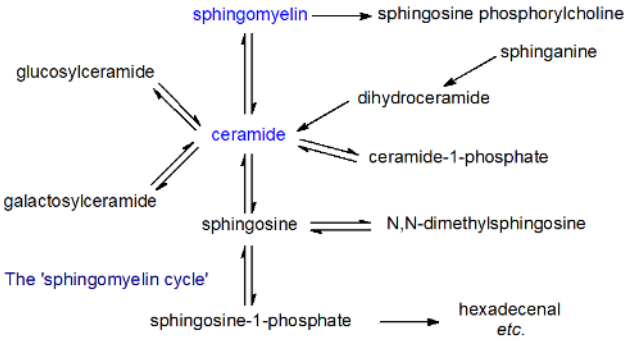


Figure **21.4.3**: Sphingomyelin, sphingolipid or ceramide cycle

Many different enzymes (and their isoforms) are involved, and their activities depend on many factors, including intracellular locations and mechanisms of activation. Each of the various compounds in these pathways has characteristic metabolic properties. Thus, free sphingosine and other **long-chain bases**, which are the primary precursors of ceramides and thence of all the complex sphingolipids, function as mediators of many cellular events, for example by inhibiting the important enzyme protein kinase C. **Ceramides** are involved in cellular signaling, and especially in the regulation of apoptosis, and cell differentiation, transformation and proliferation, and most stress conditions. In contrast, **sphingosine-1-phosphate** and **ceramide-1-phosphate** promote cellular division (mitosis) as opposed to apoptosis, so that the balance between these lipids and ceramide and/or sphingosine levels in cells is critical and necessitates exquisite control in each cellular compartment.

Similarly, the 'structural' sphingolipids, such as **sphingomyelin**, **monoglycosylceramides**, **oligoglycosylceramides,** and **gangliosides**, all have unique and characteristic biological functions, some of which are due to their physical properties and location within **rafts,** nanodomains of membranes. Most of the reactions in the sphingomyelin cycle are reversible, and the relevant enzymes are located in the endoplasmic reticulum, Golgi, plasma membrane, and mitochondria. The more complex sphingolipids are catabolized in the lysosomal compartment. Sphingolipids are especially important in providing the permeability barrier in the **skin**, where they are characterized by the presence of ultra-long fatty acyl components as well as fatty acyl groups linked to a hydroxyl group at the terminal end of the *N*-linked fatty acids (thereby generating a three-chain rather than a two-chain molecule).

Metabolic pathways comparable to the sphingomyelin cycle are believed to occur in plants, as shown in Figure **21.4.4**. However, they have not been studied as extensively as those in animals.

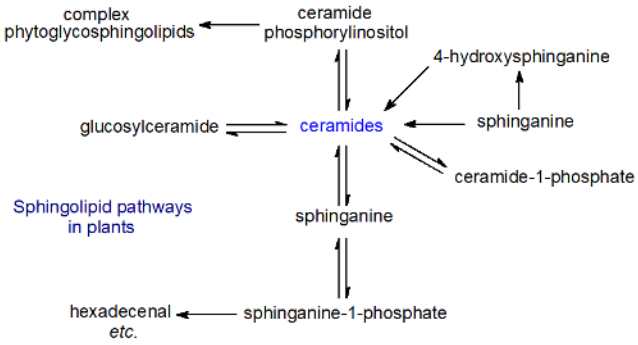


Figure **21.4.4**: Sphingomyelin, sphingolipid or ceramide cycle in plants

However, sphingolipid metabolites such as sphingosine-1-phosphate (or analogues) have been linked to programmed cell death, signal transduction, membrane stability, host-pathogen interactions, and stress responses. Plants also have a unique range of complex sphingolipids in their membranes, such as **ceramide phosphorylinositol and the phytoglycosphingolipids**, and these are now known to constitute a higher proportion of the total lipids than had hitherto been supposed. However, their functions have hardly been explored. While relatively few bacterial species produce sphingolipids, sulfono-analogues of long-chain bases and ceramides (capnoids) are produced by some species.

21.4.1.2: FATTY ACID COMPONENTS OF SPHINGOLIPIDS

The **fatty acids** of sphingolipids are very different from those of glycerolipids, consisting of very-long-chain (up to C_{26}) odd- and even-numbered saturated or monoenoic and related **2(*R*)-hydroxy** components, while even longer fatty acids (C_{28} to C_{36}) occur in spermatozoa and the epidermis. The dienoic acid 15,18-tetracosadienoate (24:2(*n*-6)), derived from the elongation of linoleic acid, is found in the ceramides and other sphingolipids of a number of different tissues, but at relatively low levels. Polyunsaturated fatty acids are only rarely present, although sphingomyelins of testes and spermatozoa are exceptions in that they contain such fatty acids, which are even longer in chain length (up to 34 carbon atoms) and include 28:4(*n*-6) and 30:5(*n*-6). Skin ceramides also contain unusual very-long-chain fatty acids, while yeast sphingolipids are distinctive in containing mainly C_{26} fatty acids. In plants and yeasts, a similar range of chain-lengths occurs as in animals, but 2-hydroxy acids predominate, sometimes accompanied by small amounts of 2,3-dihydroxy acids; saturated fatty acids are most abundant, but monounsaturated fatty acids are present in higher proportions in the Brassica family (including Arabidopsis) and a few other species. Some fungal species contain monoenoic fatty acids with a *trans*-3 double bond and/or a hydroxyl group. Figure **21.4.5** shows typical sphingolipid fatty acids.

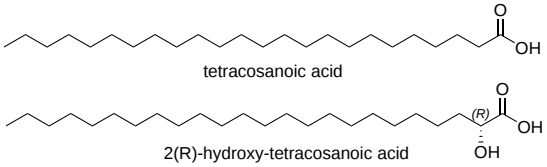


Figure **21.4.5**: Typical sphingolipid fatty acids

Very-long-chain saturated and monoenoic fatty acids for sphingolipid biosynthesis are produced from medium-chain precursors by **elongases (ELOVL)** in the endoplasmic reticulum of cells in mammals, and there is increasing evidence that specific isoforms are involved in the biosynthesis of certain ceramides. For example, ELOVL1 has been linked to the production of ceramides with C_{24} fatty acids (saturated and unsaturated), while ELOVL4 is responsible for the ultra-long-chain fatty acids in the skin. Yeasts possess three elongation enzymes: Elo1 (for medium to long-chain fatty acids), Elo2 (up to C_{22}), and Elo3 (up to C_{26}).

The hydroxyl group is believed to add to the hydrogen-bonding capacity of the sphingolipids, and it helps to stabilize membrane structures and strengthen the interactions with membrane proteins. Hydroxylation is carried out by a fatty acid 2-hydroxylase in mammals, i.e., an NAD(P)H-dependent monooxygenase, an integral membrane protein of the endoplasmic reticulum. It converts unesterified long-chain fatty acids to 2-hydroxy acids *in vitro* and probably *in vivo*. For example, experimental evidence has been obtained that is consistent with 2-hydroxylation occurring at the fatty acid level before incorporation into ceramides in the brain of mice, where the enzyme is expressed at high levels. A second enzyme of this kind is known to exist. It has yet to be characterized, and a proportion of the odd-chain fatty acids in the brain may be synthesized by Peroxisomal α-oxidation of the 2-hydroxy acids. Similarly, in skin, 2-hydroxy and non-hydroxy fatty acids as their CoA esters are used with equal facility for ceramide biosynthesis by ceramide synthases. As mutations in the fatty acid 2-hydroxylase in humans and mice give rise to demyelination disorders, such as leukodystrophy, it is evident that sphingolipids containing 2-hydroxy acids have unique functions in membranes that non-hydroxy analogues cannot substitute.

In plants, it appears that 2-hydroxyl groups are inserted into fatty acyl chains while they are linked to ceramide, as ceramide synthase does not accept hydroxy fatty acids *in vitro* at least. Two fatty acid 2-hydroxylases (di-iron-oxo enzymes) have been found in Arabidopsis, with one specific for very-long-chain fatty acids and one for palmitic acid. In fungi, a hydroxyl group is inserted at C2 of the fatty acid in a dihydroceramide intermediate.

Although the fatty acids are only occasionally considered in terms of the biological functions of sphingolipids, their influence is considerable, especially in relation to their physical properties and function in membranes. For example, very-long-chain fatty acids may play a role in stabilizing highly curved membrane domains, as is required during cell division. The hydrophobic nature of the fatty acyl groups (together with the long-chain bases) enables the hydrogen bonding essential for forming **raft nanodomains** in membranes. As a general rule, lipid bilayers containing sphingolipids with 2-hydroxy-fatty acyl or 4-hydroxy-sphingoid base moieties tend to generate condensed and more stable gel phases with higher melting temperatures than their non-hydroxylated equivalents because they have a more extended and strengthened intermolecular hydrogen bonding network. Changes in fatty acid composition are seen in some disease states; for example, increased concentrations of fatty acids >C24 are a feature of adrenoleukodystrophy, an X-linked genetic disorder.

Removal of very-long-chain fatty acids from sphingolipids in mutants of the model plant Arabidopsis inhibits the development of seedlings. As an example of a more specific interaction, it has been demonstrated that synthetic glycerolipids must contain very-long-chain fatty acids (C_{26}) to allow growth in yeast mutants lacking sphingolipids, probably by stabilizing the proton-pumping enzyme H^+-ATPase. Similarly, ceramides containing different fatty acids can be used in highly specific ways. Thus, in fungi, C_{16} or C_{18} hydroxy acids are used exclusively to synthesize glucosylceramide. Those containing very-long-chain C_{24} and C_{26} hydroxy acids are used only to synthesize **glycosyl inositol phosphorylceramide** anchors for proteins. In plants, sphingolipids containing 2-hydroxy acids are protective against oxidative and other biotic stresses.

21.4.1.3: LINKS BETWEEN GLYCEROLIPID AND SPHINGOLIPID METABOLISM

Sphingolipid and glycerolipid metabolism have been widely treated as separate sciences until relatively recently, partly for historical reasons and partly because the analysis of the two lipid groups required different approaches and skills. However, there are many areas where the two overlap, not least because phosphatidylcholine is the biosynthetic precursor of **sphingomyelin** in animal cells. In plants and fungi, phosphatidylinositol is the biosynthetic precursor of **ceramide phosphorylinositol**. In contrast, ethanolamine phosphate derived from the catabolism of sphingolipids via **sphingosine 1-phosphate** is recycled for the biosynthesis of **phosphatidylethanolamine**, and this is essential for survival in the protozoan parasite *Trypanosoma brucei*. In in vitro studies, sphingosine 1-phosphate is an activator of the phospholipase C involved in the hydrolysis of the lipid mediator **phosphatidylinositol 4,5-bisphosphate** with the formation of diacylglycerols and inositol triphosphate. The location and functions of glycerophospholipids in membranes are positively and negatively influenced by sphingolipid-rich domains or **rafts** in membranes.

In addition, there are several examples of phosphoinositides and other complex lipids binding to enzymes of sphingolipid metabolism, either as part of a regulatory function that controls their activity or to facilitate their location to various membranes. Thus, sphingosine kinase 2, one of the enzymes responsible for the biosynthesis of sphingosine 1-phosphate, binds to phosphatidylinositol monophosphate. The ceramide kinase responsible for the biosynthesis of **ceramide 1-phosphate** requires phosphatidylinositol 4,5-bisphosphate to function. Similarly, the CERT protein involved in **ceramide** transport has a binding site for phosphatidylinositol 4-phosphate. Sphingomyelin production at the trans-Golgi network triggers a signaling pathway leading to dephosphorylation of phosphatidylinositol 4-phosphate, interrupting transport of cholesterol and sphingomyelin. Again, the interactions are not solely in one direction as ceramide 1-phosphate (with phosphatidylinositol 4,5-bisphosphate) binds to the specific **phospholipase A_2 ($cPLA_2\alpha$)** responsible for the hydrolysis of phosphatidylinositol and thence the release of arachidonic acid for eicosanoid production. Other than the phosphoinositides, phosphatidylserine activates the neutral sphingomyelinase in the brain.

21.4.2: LONG-CHAIN (SPHINGOID) BASES

Long-chain/sphingoid bases are the characteristic and defining structural unit of the sphingolipids, which are important structural and signaling lipids of animals and plants and a few bacterial species. These are long-chain aliphatic amines, containing two or three hydroxyl groups and often a distinctive *trans*-double bond in position 4. To be more precise, they are 2-amino-1,3-dihydroxy-alkanes or alkenes with (2*S*,3*R*)-*erythro* stereochemistry, often with various further structural modifications in the alkyl chain. They are important for the physical and biological properties of the more complex sphingolipids, but free sphingoid bases are also bioactive and interact with specific receptors and target molecules. As discussed below, the mechanisms for biosynthesis of sphingoid bases and of the *N*-acylated form (ceramides) are intimately linked.

21.4.2.1: STRUCTURES AND OCCURRENCE

In animal tissues, the most common or abundant of the sphingoid bases is **sphingosine** ((2*S*,3*R*,4*E*)-2-amino-4-octadecene-1,3-diol) or sphing-4*E*-enine, i.e., with a C_{18} aliphatic chain, hydroxyl groups in positions 1 and 3, and an amine group in position 2; the double bond in

position 4 has the *trans* (or *E*) configuration. This was first characterized in 1947 by Professor Herbert Carter, who was also the first to propose the term “sphingolipides” for those lipids containing sphingosine. It is usually accompanied by the saturated analogue dihydrosphingosine (or sphinganine). Sphingoid bases are illustrated in Figure **21.4.6**.

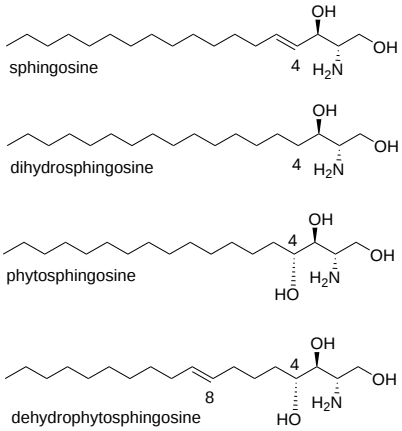


Figure **21.4.6**: Sphingoid Bases

For shorthand purposes, a nomenclature similar to that for fatty acids can be used; the chain length and number of double bonds are denoted in the same manner with the prefix 'd' or 't' to designate di- and trihydroxy bases, respectively. Thus, sphingosine is denoted as d18:1 and phytosphingosine is t18:0. A superscript may indicate the position of the double bond. For example, 4-sphingenine can be abbreviated as d18:1$^{\Delta 4t}$ or 4*E*-d18:1. While alternative nomenclatures are occasionally seen in publications, they are not recommended.

Long-chain bases found in animals, plants, and microorganisms now amount to over one hundred. Many of these may occur in a single tissue or organism, but almost always as part of a complex lipid with an *N*-acyl-linked fatty acid and often phosphate or carbohydrate functional groups. The aliphatic chains can contain from 14 to as many as 28 carbon atoms, and most often, they are saturated, monounsaturated, or diunsaturated, with double bonds of either the *cis* or *trans* configuration. For example, the main dienoic long-chain base (sphingadienine) in human plasma is D-erythro-1,3-dihydroxy-2-amino-4-*trans*,14-*cis*-octadecadiene, and this is especially abundant in the kidney, with more in women than in men. It is not present in zebra fish, which are widely used as a model species. Forms with three double bonds, such as sphinga-4*E*,8*E*,10*E*-trienine, sometimes with a methyl group in position 9, have been found in the sphingolipids of some marine invertebrates and a dinoflagellate. In addition, long-chain bases can have branched chains with methyl substituents in the *omega*-1 (*iso*), *omega*-2 (*anteiso*), or other positions; hydroxyl groups in positions 4, 5, or 6; ethoxy groups in position 3; and even a cyclopropane ring in the aliphatic chain in some organisms. *N*-Methyl, *N*,*N*-dimethyl, and *N*,*N*,*N*-trimethyl derivatives of sphingoid bases have been detected in mouse brains.

The main C_{18} components of long-chain bases of sphingomyelins of some animal tissues are accompanied by small amounts of C_{16} to C_{19} dihydroxy bases. The latter attain higher proportions in tissues of ruminant animals. In gangliosides from human brain and intestinal tissues, eicosasphingosine (2*S*,3*R*,4*E*-d20:1) occurs in appreciable concentrations with variable amounts in different regions and membranes. However, human skin contains many isomers, including saturated, monoenoic, 6-hydroxy bases, and phytosphingosines from C_{16} to C_{28} chain lengths. Shorter-chain bases are found in many insect species. In the fruit fly, *Drosophila melanogaster* is widely used as a model species in genetic and metabolic experiments, the main components are C_{14} bases. In contrast to higher animals, nematodes such as *Caenorhabditis elegans* produce C_{17} *iso*-methyl-branched sphingoid bases, essential for normal sphingolipid function in the organism.

The long-chain base composition of individual lipids can vary markedly between species, tissues, organelles, and even different membranes within a single organelle. For example, the data in Table **21.4.1** is perhaps from an extreme example. Still, it illustrates remarkable differences among lipids in one cellular component (rat liver mitochondria). Only part of the data from the paper cited is listed. It illustrates that 3-keto-sphinganine, produced in the first step of sphingosine biosynthesis (see below) and normally a minor component of sphingolipids - often not detectable- can vary from 28 to 100% of the sphingoid bases, depending on the lipid class and membrane within the organelle.

Table **21.4.1**: **Long chain base composition of some lipid components of mitochondria from rat liver.**

Type	Base (%)			
	d18:1	d18:0-3keto	t21:1 (phyto)	Unidentified
Ceramides[a]	18	28	53	-
Glucosylceramides[a]	3	95	-	3
Lactosylceramides[b]		100		

[a] whole mitochondria; [b] mitochondrial inner membrane
Data from Ardail, D. *et al. FEBS Letts*, **488**, 160-164 (2001).

Phytosphingosine or 4D-hydroxy-sphinganine ((2*S*,3*R*,4*R*)-2-amino-octadecanetriol) is a common long-chain base of mainly plant origin. It is a saturated C_{18}-trihydroxy compound, although unsaturated analogues, for example, with a *trans* (or occasionally a *cis* (*Z*)) double bond in position 8, i.e., dehydrophytosphingosine or 4D-hydroxy-8-sphingenine, tend to be much more abundant. In many plant species, there are lipid class preferences also, and dihydroxy long-chain bases are more enriched in glucosylceramides than in glycosylinositolphosphoceramides, for example. This is true in the model plant *Arabidopsis thaliana*, where the data listed for whole tissue is probably representative largely of the latter lipid, as shown in Table **21.4.2** below.

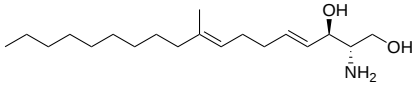
Table **21.4.2: Sphingolipid long-chain base composition of whole tissue and glucosylceramides from *Arabidopsis thaliana*.**

	Base (%)					
	t18:1 (8*Z*)	t18:1 (8*E*)	t18:0	d18:1 (8*Z*)	d18:1 (8*E*)	d18:0
Whole tissue	12	70	13		4	1
Glucosylceramides	44	22		5	28	2
Data from Sperling, P. *et al*. *Plant Physiol. Biochem*., **43**, 1032-1038 (2005)						

Other plant long-chain bases have double bonds in position 4, which can be of either the *cis* or *trans* configuration, although *trans*-isomers are far more common. In contrast, the base d18:2$\Delta^{4E,8Z/E}$ is relatively abundant in most plant species. In *A. thaliana* and related species, Δ^4 long-chain bases are found mainly in the flowers and pollen and then exclusively as a component of the glucosylceramides. In general, as with Brassica species, the composition is dependent on species. Still, typically it is composed of up to eight different C_{18}-sphingoid bases, with variable geometry of the double bond in position 8, i.e., (*E/Z*)-sphing-8-enine (d18:1Δ^8), (4*E*,8*E/Z*)-sphinga-4,8-dienine (d18:2$\Delta^{4,8}$) and (8*E/Z*)-4-hydroxy-8-sphingenine (t18:1Δ^8); d18:1Δ^4, d18:0 and t18:0 tend to be present in small amounts only.

Phytosphingosine is not restricted to plants but is found in significant amounts in intestinal cells and the skin of animals, with much smaller relative proportions in the kidneys. Although non-mammalian sphingoid bases generally tend to be poorly absorbed from the intestines, a small proportion of the phytosphingosine and related sphingoid bases found in animal tissues may enter via the food chain.

Yeasts and fungi tend to have distinctive and characteristic long-chain base compositions. For example, filamentous fungi have 9-methyl-4*E*,8*E*-sphingadienine as the main sphingoid base in the glucosylceramides, as shown in Figure **21.4.7**, but not in the ceramide phosphoinositol glycosides. At the same time, yeasts contain mainly the saturated C_{18} bases sphinganine and phytosphingosine, although some *trans*-4/8-unsaturated forms are usually present. Only a few bacterial species synthesize sphingolipids, but the family Bacteroidetes, abundant in the human gut, is an important exception; they usually contain saturated (and branched) long-chain bases. Other pathogenic bacteria may utilize sphingolipids and sphingoid bases from their hosts.



(4E,8E)-9-methylsphinga-4,8-dienine

Figure **21.4.7**: Main sphingoid base in filamentous fungi

Sphingoid bases are surface-active amphiphiles with critical micellar concentrations of about 20 μM in aqueous solutions; they probably exist in the gel phase at physiological temperatures. They are unusual among lipids because they bear a small positive charge at neutral pH. However, their pK_a (9.1) is lower than in simple amines due to intramolecular hydrogen bonding. Together with their relatively high solubility (> 1μM), they can easily cross or move between membranes. In so doing, they increase the permeability of membranes to small solutes. In esterified form in complex lipids, they form ordered lipid domains in membranes such as **rafts**.

In complex sphingolipids, the sphingoid base is linked via the amine group to a fatty acid, including very-long-chain saturated or monoenoic and 2-hydroxy components, to form **ceramides.** These can be attached to a polar head group, such as phosphate or a carbohydrate, via the primary hydroxyl moiety. An important exception is **sphingosine-1-phosphate**, which is not acylated and has signaling functions in cells akin to lysophospholipids.

21.4.2.2: BIOSYNTHESIS AND METABOLISM

Sphinganine biosynthesis

The basic mechanism for the biosynthesis of **sphinganine** involves the condensation of palmitoyl-coenzyme A with L-serine, catalyzed by the membrane-bound enzyme **serine palmitoyltransferase**, requiring pyridoxal 5'-phosphate as a cofactor, which binds to a specific lysine residue on the enzyme. The reaction occurs on the cytosolic side of the endoplasmic reticulum in animal, plant, and yeast cells with the formation of 3-keto-sphinganine, as illustrated in Figure **21.4.8**.

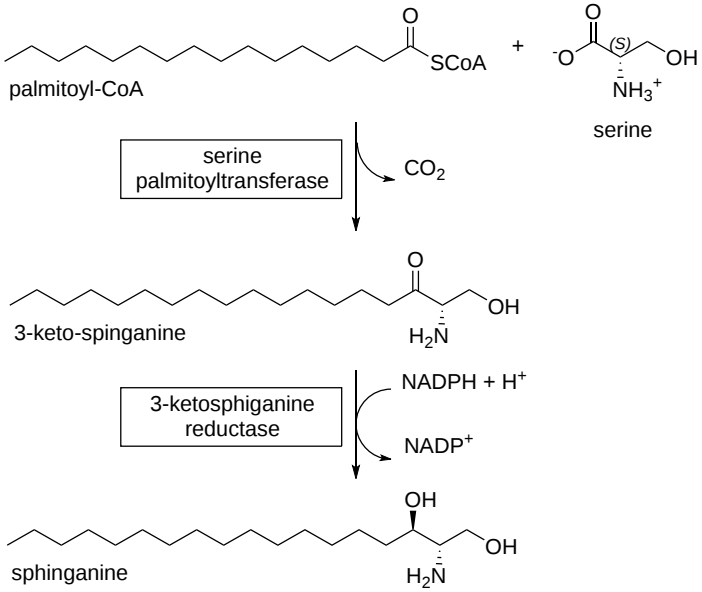


Figure **21.4.8**: Sphinganine synthesis

This is believed to be the key regulatory or rate-limiting step in sphingolipid biosynthesis and is conserved in all organisms studied to date. The elimination of this enzyme is embryonically fatal in mammals and fruit flies. In mammals, serine palmitoyltransferase is a heterotrimer composed of two main subunits, designated SPTLC1 with either SPTLC2 or SPTLC3 (sometimes termed SPTLC2a and SPTLC2b, respectively). SPTLC1 is essential for activity, and it is ubiquitously expressed, as is SPTLC2, while SPTLC3 is present in a relatively limited range of tissues and is most abundant in skin and placental tissue. In addition, there are two small subunits, ssSPTA and ssSPTB (again, other nomenclatures exist), which differ in a single amino acid residue and may have regulatory functions; the active site is at the interface between the two main subunits. ssSPTA is essential for serine palmitoyltransferase function during development and hematopoiesis.

A possible mechanism for the 1st step in the pathway, catalyzed by serine palmitotyltransferase, is shown in Figure **21.4.9**.

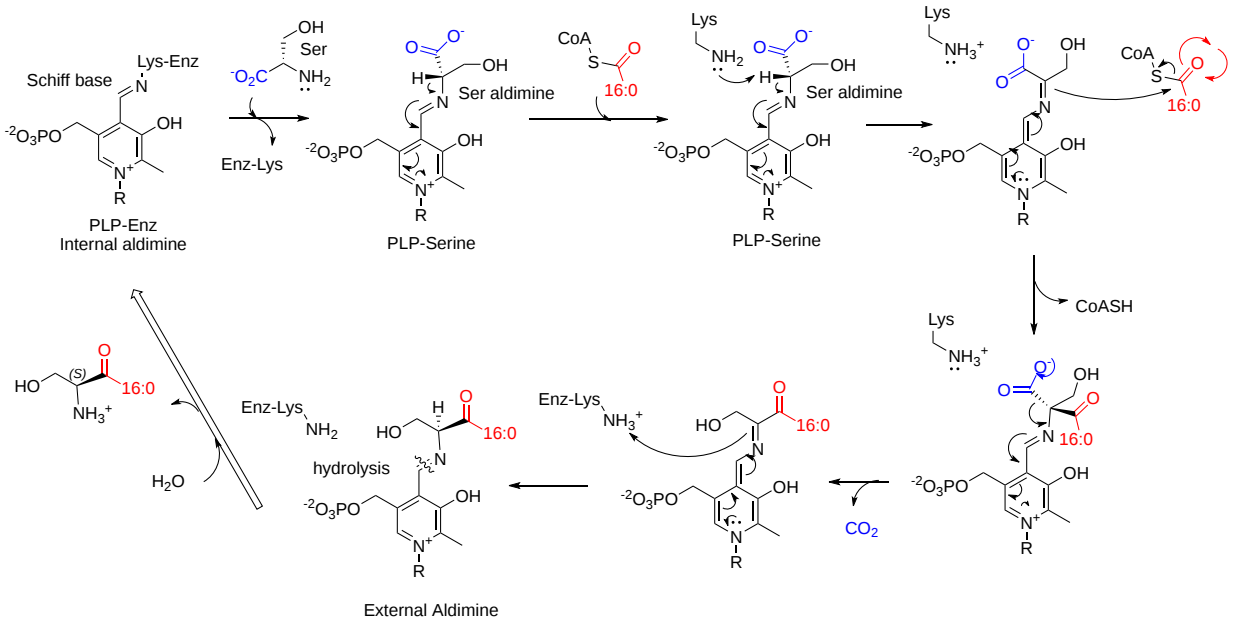
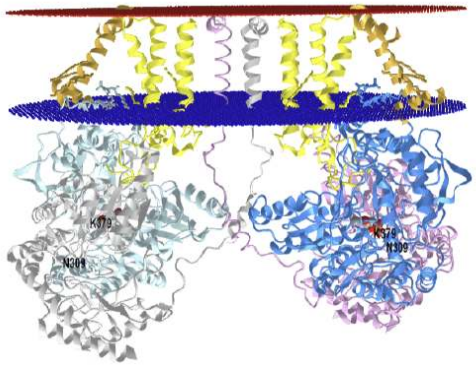


Figure **21.4.9**: Mechanism for serine palmitoyltransferase, the key regulatory step in sphingolipid metabolism

Adding either of the two small subunits to the complexes substantially changes the substrate preferences and enables the synthesis of a wide range of natural homologs. In mammals, the SPTLC1-SPTLC2 complex forms C_{18} sphingoid bases specifically (with some C_{19} and C_{20}), while the combination of SPTLC1 and SPTLC3 gives a broader product spectrum, including an *anteiso*-methylbranched-C_{18} isomer (from *anteiso*-methyl-palmitate as the precursor). Such branched bases are synthesized to a limited extent in human skin, but they are the main forms in lower invertebrates such as *C. elegans*. The activity of the serine palmitoyltransferase is governed by negative feedback and partly by orosomucoid (ORM-like or ORMDL) proteins, three in mammals (ORMDL1 to 3) and two in yeast (Orm1/2), which are ubiquitously expressed transmembrane proteins located in the endoplasmic reticulum. The availability of serine is also an important factor.

Figure **21.4.10** shows an interactive iCn3D model of the human serine palmitoyltransferase complex (7K0M).



NCBI iCn3D Figure **21.4.10**: Human serine palmitoyltransferase complex (7K0M).. Click the image for a popup or use this external link: https://structure.ncbi.nlm.nih.gov/i...tuGThTq9Vi4J58

- Gray and Plum (SPT1 A and E Chains
- Light Blue and Blue (SPT2 B and F Chains)
- Light Brown (small subunit A - ssA, C, and G chains)
- Yellow (ORM D and H)

The second step in sphinganine biosynthesis is the reduction of the keto group to a hydroxyl in an NADPH-dependent manner by a specific 3-ketodihydrosphingosine reductase ('3KSR'), also on the cytosolic side of the endoplasmic reticulum. This step must occur rapidly as the intermediate is rarely encountered in tissues. The enzymes are presumed to be in similar subcellular locations in plant cells.

In plants, serine palmitoyltransferase is a heterodimer composed of LCB1 and LCB2 subunits with some homology to the mammalian enzymes, while in the yeast *Saccharomyces cerevisiae*, there are three subunits: Lcb1, Lcb2, and Tsc3. Serine palmitoyltransferase is a

water-soluble homodimer in a few bacteria that synthesize sphingoid bases. The enzyme in the apicomplexan parasite *Toxoplasma gondii* is a homodimer located in the endoplasmic reticulum.

Free sphinganine formed in this way is rapidly *N*-acylated by acyl-CoA to form dihydroceramides by dihydroceramide synthases, which in animals are located primarily on the endoplasmic reticulum, presumably on the cytoplasmic surface. Animals and plants have multiple isoforms of this enzyme, for which the abbreviated term 'ceramide synthase' is now widely applied, as they utilize most other sphingoid bases, such as those produced by the hydrolysis of sphingolipids, as substrates. They are unique gene products, each located on a different chromosome and with considerable variation in the expression of the enzymes in different cell types within each tissue. Each isoenzyme has distinct specificities for the chain-length of the fatty acyl-CoA moieties, but to a limited extent only for the base, suggesting that ceramides containing different fatty acids have differing roles in cellular physiology. These enzymes have six membrane-spanning regions, but the only substantial difference is in an 11-residue sequence in a loop between the last two putative transmembrane domains. **Ceramides** are central to all elements of sphingolipid biochemistry. These steps are illustrated in Figure **21.4.11**.

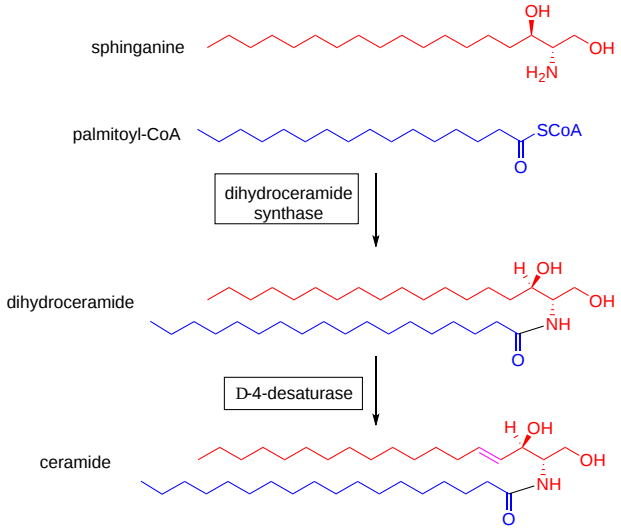


Figure **21.4.11**: Synthesis of ceramide from sphinganine.

Humans and mice have six ceramide synthases, which utilize subsets of acyl-CoAs and thus produce ceramides with specific acyl chain lengths. Of these, ceramide synthase 2 is most abundant and is specific for coA esters of very-long-chain fatty acids (C20 to C26); it is most active in the lungs, liver, and kidney. Ceramide synthase 1 is specific for 18:0 and is located mainly in the brain, with lower levels in skeletal muscle and testes. Ceramide synthase 3 is responsible for the unusual ceramides of skin and testes. It uses C26-CoA and higher, including polyunsaturated-CoAs, in the latter tissue, while ceramide synthase 4 (skin, liver, heart, adipose tissue, and leukocytes) uses C18 to C22-CoAs. Ceramide synthase 5 (lung epithelia and brain gray and white matter) generates C16 (mainly) and C18 ceramides, and ceramide synthase 6 (intestine, kidney, and lymph nodes) produces C14 and C16 ceramides. However, hydroxylation and the presence or otherwise of double bonds in the acyl-CoAs do not appear to influence the specificity of the ceramide synthases. Also, the expression of mRNA for ceramide synthases does not always correlate with the fatty acid composition of sphingolipids in a particular tissue, suggesting that other factors are involved in determining which molecular species are formed. One such is acyl-coenzyme A-binding protein (ACBP), which facilitates the synthesis of ceramides containing very-long fatty acids and stimulates ceramide synthases 2 and 3.

Insertion of the *trans*-double bond in position 4 to produce sphingosine occurs only **after** the sphinganine has been esterified in this way to form a ceramide, as illustrated in Figure **21.4.11**, with desaturation occurring at the cytosolic surface of the endoplasmic reticulum also. The desaturases were first characterized in plants, simplifying the isolation of the appropriate enzymes in humans and other organisms. Two dihydroceramide desaturases have been identified in animals and designated 'DEGS1 and DEGS2'. Both enzymes insert *trans* double bonds in position 4, but DEGS2 is a dual-function enzyme acting as a hydroxylase to generate phytoceramides, i.e., adding a hydroxyl group on position 4. Distribution of the enzymes in tissues is very different, with DEGS1 expressed ubiquitously but highest in the liver, Harderian gland, kidney, and lung. DEGS2 expression is largely restricted to the skin, intestine, and kidneys, where phytoceramides are more important. A considerable family of Δ^4-sphingolipid desaturases has now been identified, and an early study by Stoffel and colleagues demonstrated that Δ^4-desaturation involves first the *syn*-removal of the C(4)- H_R and then the C(5)-H_S hydrogens. This appears to have been the first evidence that desaturases in general operate in this stepwise fashion.

The enzyme inserting the *cis*-14 double bond into sphinga-4-*trans*,14-*cis*-dienine is the fatty acid desaturase 3 (FADS3), which utilizes ceramides containing sphingosine as the precursor. The only other known activity of this enzyme is inserting a *cis*-double bond in position 13 of the CoA ester of vaccenic acid (11*t*-18:1) to produce the conjugated diene 11*t*,13*c*-18:2.

Synthesis of sphingoid bases *de novo* is essential in most organisms, and inhibition of the biosynthetic pathways affects growth and viability. However, this can be tissue-specific, as deletion of the liver-specific SPTLC2 in mice did not affect liver function, while a comparable deletion of adipocyte-specific SPTLC1 caused major tissue defects. Presumably, the latter tissue cannot take up enough sphingolipid from the circulation to remedy the problem. Deficiencies in SPTLC3 are related to dermal pathologies, and genetic variants of SPTLC3 are associated with dyslipidemia and atherosclerosis. The essentiality of sphingoid base synthesis in plants has been demonstrated similarly in studies with mutants in which specific enzymes have been deleted.

? SPHINGOSINE AND DERIVATIVES - DETAILED BACKGROUND

Click the link below.

Link

Phytosphingosine and plant ceramides: Phytosphingosine is formed from sphinganine, produced as above, by hydroxylation in position 4, possibly via the free base in plants, although it can be formed both from sphinganine and a ceramide substrate in yeasts. A single sphinganine C4-hydroxylase is present in yeast, but Arabidopsis has two such enzymes (SBH1 and 2), which are critical for growth and viability. Much remains to be learned of the processes involved, but it is known that the enzyme responsible is closely related to a Δ^4 desaturase. Indeed, it has been shown that there are bifunctional Δ^4-desaturase/Δ^4-hydroxylases in *Candida albicans* and mammals, especially in keratinocytes (DEGS2 discussed above), with which either 4-hydroxylation or Δ^4-desaturation is initiated by removal of the pro*R* C-4 hydrogen. Sphinganine attached to ceramide is the substrate for 4-hydroxylation in intestinal cells.

In *Arabidopsis thaliana* leaves, 90% of the sphingoid bases are phytosphingosine with a Δ^8-double bond. In plants in general, in addition to Δ^4-desaturation, two distinct types (20 gene products) of sphingoid Δ^8-desaturase have been characterized that catalyse the introduction of a double bond at position 8,9 of phytosphingosine. These are evolutionarily distinct from the Δ^4-desaturases. One type produces the *trans (E)*-8 isomer mainly, and the other mostly the *cis (Z)*-8 isomer, with the *trans*-isomer tending to predominate overall but dependent upon plant species. It appears that the *trans* isomer is formed when the hydrogen on carbon 8 is removed first, and the *cis* isomer when carbon 9 is the point of attack. While the main group of Δ^8-desaturases requires a 4-hydroxysphinganine moiety as substrate, the second does not.

In Arabidopsis, three different isoforms of ceramide synthase have been identified and denoted LOH1, LOH2, and LOH3. Phytosphingosine is used efficiently by LOH1 and LOH3 (class II synthases), but only LOH2 (class I synthase) uses sphinganine efficiently; LOH2 and 3 prefer unsaturated long-chain bases. Marked fatty acid specificity is also observed with LOH2, showing almost complete specificity for palmitoyl-CoA and dihydroxy bases, while LOH1 shows greatest activity for 24:0- and 26:0-CoAs and trihydroxy bases; none utilize unsaturated acyl-CoA esters efficiently. In plants, fatty acid desaturases and hydroxylases are also closely related, and sphingolipid fatty acid α-hydroxylation is believed to occur on the ceramide, as opposed to the free acyl chain. It is believed that the Δ^8-desaturase utilizes ceramide as the substrate and channels the products selectively into synthesizing complex sphingolipids, while Δ^4-desaturation channels ceramides for glucosylceramide synthesis.

It has been established that long-chain bases with 4-hydroxyl groups are necessary for the viability of the filamentous fungus *Aspergillus nidulans* and growth in plants such as *A. thaliana*. The presence of an 8*E* double bond confers aluminium tolerance to yeasts and plants, and it is important for chilling resistance in tomatoes. However, a *trans*-4 double bond in the sphingoid base does not appear essential for Arabidopsis growth and development.

Fungal sphingoid bases: Fungi produce *trans* Δ^8-isomers only, but Δ^4- and Δ^8-desaturases do not occur in the widely studied yeast *S. cerevisiae*. In the biosynthesis of sphingoid bases in fungi, the double bonds in positions 4 and 8 and the methyl group in position 9 are inserted sequentially into the sphinganine portion of a ceramide, the last using an *S*-adenosylmethionine-dependent methyltransferase similar to plant and bacterial **cyclopropane fatty acid synthases**. In *S. cerevisiae*, the ceramide synthase is a heteromeric protein complex containing three subunits, Lag1, Lac1, and Lip1, of which the first two are homologous proteins that feature eight transmembrane domains. The yeast *Pichia pastoris* has a distinct ceramide synthase, which utilizes dihydroxy sphingoid bases and C_{16}/C_{18} acyl-coenzyme A as substrates to produce ceramides. The long-chain-base components of the ceramide are then desaturated *in situ* by a Δ^4-desaturase, and the fatty acid components are hydroxylated in position 2. Further desaturation of the long-chain base component by a Δ^8-(*trans*)- desaturase occurs before the methyl group in position 9 is introduced by an *S*-adenosylmethionine-dependent sphingolipid C-9 methyltransferase. As a final step, a *trans*-double bond may be introduced into position 3 of the fatty acid component. These ceramides are used exclusively for the production of **glucosylceramides**, and it is believed that a separate ceramide synthase encoded by a different gene produces the ceramide precursors for **ceramide phosphorylinositol mannosides**.

Viral sphingoid bases: The genome of an important marine virus (EhV) encodes for a novel serine palmitoyltransferase. This enzyme hijacks the metabolism of algal hosts to produce unusual hydroxylated C17 sphingoid bases; these accumulate in lytic cells of infected algae, such as the important bloom-forming species *Emiliania huxleyi*. While this may seem a rather esoteric topic, viruses constitute a high proportion of the marine biome, and their control of the growth of algal blooms has global consequences.

Unesterified sphingosine: A cycle of reactions occurs in tissues by which sphingoid bases are incorporated via ceramide intermediates into sphingolipids, which are utilized for innumerable functions, before being broken down again to their component parts. All the free sphingosine in tissues must arise by this route, particularly by the action of ceramidases on **ceramides**. Five ceramidases are known, each with differing pH optima and subcellular locations. The levels of free sphingoids and their capacities to function as lipid mediators, as shown in Figure **21.4.12**, are controlled mainly by enzymic re-acylation to form ceramides. However, some is acted upon by sphingosine kinases to produce sphingosine-1-phosphate.

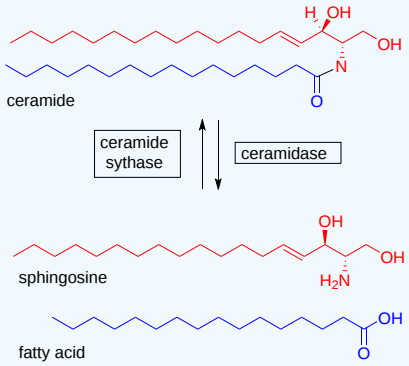


Figure **21.4.12**: Ceramide hydrolysis and resynthesis

Free sphingoid bases are absorbed by enterocytes following the digestion of dietary sphingolipids in animals (including some from gut microorganisms). While some of this is converted to complex sphingolipids, much is catabolized with the eventual formation of palmitic acid.

Catabolism of sphingosine and other long-chain bases occurs after conversion to **sphingosine-1-phosphate** and analogues. In yeast, an alternative means of detoxification has been reported. An excess of phytosphingosine is first acetylated and then converted to a vinyl ether before export from the cells.

21.4.2.3: BIOLOGICAL FUNCTIONS OF UNESTERIFIED SPHINGOID BASES

The primary function of sphingoid bases is to serve as a basic component of ceramides and complex sphingolipids, where variations in their compositions can influence the physical and biological properties of these lipids. Independent of this, in their free (unesterified) form, they are important mediators of many cellular events, even though they are present at low levels only in tissues (typically 25 and 50 nM in plasma), with intracellular levels determined by hydrolysis by ceramidases or by the action of sphingosine kinases (sphingosine-1-phosphate production). In animal cells, they indirectly inhibit protein kinase C, possibly by interfering with the binding of enzyme activators, such as diacylglycerols or phorbol esters. In addition, sphingoid bases are known to be potent inhibitors of cell growth, although they stimulate cell proliferation and DNA synthesis. They are involved in the process of apoptosis in a manner distinct from that of ceramides by binding to specific proteins and regulating their phosphorylation. While sphingosine does not appear to participate in membrane raft formation, it may rigidify pre-existing gel domains in mixed bilayers. However, any such effects will be dependent on local concentrations and pH. It should be noted that some of the biological effects observed experimentally may be due to conversion to sphingosine-1-phosphate.

Free sphingosine has been implicated in various pathological conditions; for example, plasma sphingosine levels are increased in hyperthyroidism and patients with type 2 diabetes. Lysosomal lipid storage is an initiating factor in Niemann Pick type C disease. This neurodegenerative disorder causes a change in calcium release, leading to a buildup of cholesterol and sphingolipids. In the human adrenal cortex, sphingosine produced *in situ* by the acid ceramidase has a function in steroid production by serving as a ligand for steroidogenic factor 1 at the cell nucleus, which controls the transcription of genes involved in the conversion of cholesterol to steroid hormones. Unesterified sphingoid bases may have a protective role against cancer of the colon in humans. Thus, *N*,*N*-dimethylsphingosine and dihydrosphingosine, like the deoxysphingoid bases, are known to induce cell death in various malignant cells. There is evidence that sphingadienes of plant and animal origin inhibit colorectal cancer in mouse models by reducing sphingosine-1-phosphate levels. Consequently, synthetic analogues of long-chain bases are being tested for their pharmaceutical properties.

Free sphingosine is believed to have a signaling role in plants by controlling pH gradients across membranes. In addition, free long-chain bases (and the balance with the 1-phosphate derivatives) are essential for regulating apoptosis in plants.

21.4.3: CERAMIDES

21.4.3.1: STRUCTURE AND OCCURRENCE

Figure **21.4.13** shows the ceramide structure again.

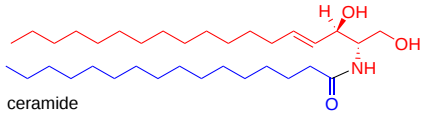


Figure **21.4.13**: Structure of ceramides (with varying fatty acids in ester link)

Ceramides consist of a long-chain or **sphingoid base** linked to a fatty acid via an amide bond. They are essential intermediates in the biosynthesis and metabolism of all sphingolipids, including the complex sphingolipids in which the terminal primary hydroxyl group is linked to carbohydrate, phosphate, and so forth (sphingomyelin, glycosphingolipids, and gangliosides), as shown in Figure **21.4.14**.

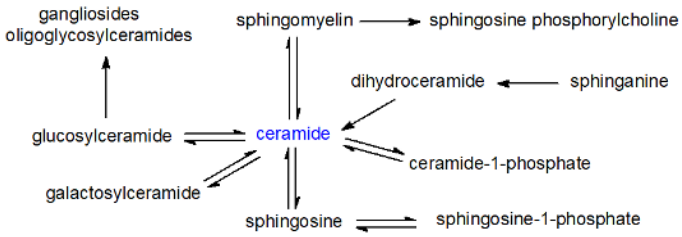


Figure **21.4.14**: Central role of ceramkin in sphingolipid biosynthesis and metabolism

They are also the primary source of unesterified sphingoid bases and the important biological mediators sphingosine-1-phosphate and ceramide-1-phosphate. At last count, 33 enzymes were known to participate in ceramide metabolism. While ceramides are rarely found as such at greater than trace amounts in tissues other than skin, they can exert important biological effects of their own at these low levels. They are present in membranes where they participate in the formation of raft domains.

Each organism and tissue may synthesize ceramides in which there are a variety of di- and trihydroxy long-chain bases linked to fatty acids. As discussed previously, the fatty acids consist mainly of longer-chain (up to C_{24} or greater) saturated and monoenoic (mainly (*n*-9)) components, sometimes with a hydroxyl group in position 2. Other than in certain testicular cells, polyunsaturated fatty acids do not occur. More than 200 structurally distinct molecular species of ceramides have been characterized from mammalian cells. In plants, 2-hydroxy acids predominate, sometimes accompanied by small amounts of 2,3-dihydroxy acids. Although small amounts of free ceramides are produced in all tissues as required for the specific biological functions described below, most are converted rapidly to more complex sphingolipids, including sphingomyelin (in animals) and the various glycosylceramides. The ceramides in skin are a remarkable exception to this rule, and as such, they are discussed separately below.

A shorthand nomenclature simply combines those used conventionally for fatty acids and long-chain bases to denote molecular species of ceramides, including those as components of more complex lipids, e.g., *N*-palmitoyl-sphingosine is d18:1-16:0. Ceramides containing sphinganine are sometimes termed ‘dihydroceramides’.

21.4.3.2: CERAMIDE BIOSYNTHESIS

Ceramide production is complex and involves at least three pathways. Biosynthesis *de novo* occurs in the endoplasmic reticulum with palmitoyl-CoA and serine as the precursors for the long-chain base component, which is converted to ceramide. Biosynthesis of the specific fatty acids in ceramides involving various chain elongases (ELOVL) also requires consideration. Alternative routes for ceramide production involve regeneration from complex sphingolipids. For example, in animals, in the sphingomyelinase pathway, conversion of sphingomyelin into ceramides (and *vice versa*) occurs in the plasma membrane, Golgi, and mitochondria. Finally, hydrolytic enzymes in the lysosomal compartment can remove the polar moieties of complex glycosphingolipids to recover the ceramides (or their parts) in a recycling/catabolic process. As these biosynthetic or metabolic pathways are located in different organelles, specific ceramide pools and sphingolipids have differing biological properties and functions.

Ceramide synthesis *de novo*: The first of these pathways is described in mechanistic terms. In brief, in animals, sphinganine is coupled to a long-chain fatty acid to form dihydroceramide using one of six ceramide synthases in the endoplasmic reticulum, mainly before the double bond is introduced into position 4 of the sphingoid base. Of these, ceramide synthase 2 is most abundant and is specific for CoA esters of

very-long-chain fatty acids (C_{20} to C_{26}); it is most active in the central nervous system. Ceramide synthase 1 is specific for 18:0 and is located exclusively in brain and skeletal muscle; ceramide synthases 5 and 6 generate 16:0-containing ceramides, and ceramide synthase 3 is responsible for the unusual ceramides of skin and testes.

Figure **21.4.15** shows again the synthesis of ceramide from sphinganine and palmitoyl-CoA (a repeat of Figure **21.4.11**

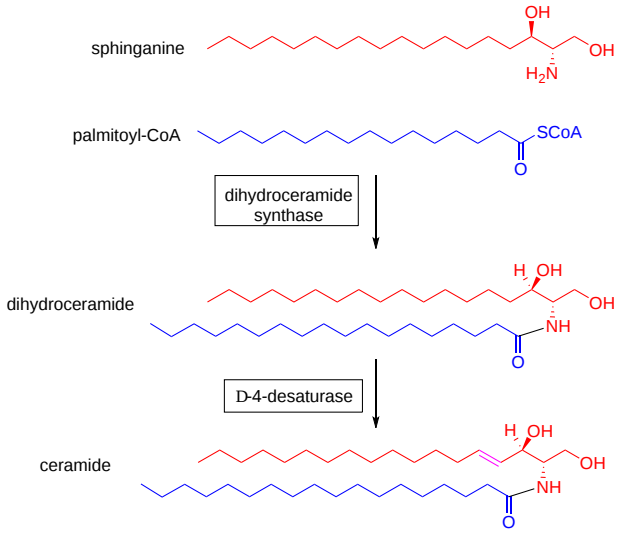


Figure **21.4.15**: Synthesis of ceramide from sphinganine and palmitoyl-CoA

Each synthase has six membrane-spanning domains and contains a characteristic motif with the specific structures required for catalysis and substrate binding that are essential for its activity. They have been shown to differ primarily in an 11-residue sequence in a loop between the last two putative transmembrane domains. In addition to the separate transcriptional regulation of each enzyme, ceramide synthase activity is modulated by many factors, including reversible dimerization. Ceramide synthase 2 has a **sphingosine-1-phosphate** binding motif, and this lipid may inhibit its activity. Acyl-coenzyme A-binding protein (ACBP) facilitates the synthesis of ceramides containing very-long fatty acids and stimulates ceramide synthases 2 and 3, especially.

Most ceramides generated in this way are rapidly utilized to synthesize complex sphingolipids, especially sphingomyelin and hexosylceramides, to regulate cellular ceramide concentrations and control their biological activities. In mammalian cells, most complex glycerolipids are synthesized in the endoplasmic reticulum before their transport to their final subcellular locations, but the process is rather different for sphingolipids. Ceramide is synthesized on the cytoplasmic leaflet of the endoplasmic reticulum. Subsequent formation of complex sphingolipids occurs in the Golgi apparatus, and a key cytoplasmic protein, ceramide transporter or '**CERT**' (CERamide Trafficking), mediates the transport of ceramide between these organelles in a non-vesicular manner. It has several distinct functional domains, including an N-terminal **phosphatidylinositol-4-monophosphate (PI(4)P)**-binding or Pleckstrin homology (PH) domain, which targets the Golgi apparatus, and a C-terminal 'START' domain, which can recognize ceramide species with the natural D-*erythro* stereochemistry, including dihydroceramide and phytoceramide (but not sphingosine). It holds them within a long amphiphilic cavity by hydrogen bonding with all three polar atoms of the sphingoid motif. A short peptide motif (FFAT) also recognizes a specific protein in the endoplasmic reticulum. There is sufficient flexibility in the body of the protein to enable the transfer of ceramide from the endoplasmic reticulum to the Golgi without free movement through the cytosol.

Very-long-chain ceramides containing 24:0 or 24:1 fatty acids turn over much more rapidly in animal cells than those containing 16:0 or 18:0 fatty acids because of the more rapid conversion of the former into complex sphingolipids, where they may regulate the levels and perhaps the biological functions of the latter. In contrast, ceramides containing d16:1 and d18:1 sphingoid bases turnover at similar rates and do not affect the flux of ceramides through these pathways. The CERT protein is a major factor in this specificity as it extracts ceramides from membrane bilayers with a preference for those required to synthesize complex sphingolipids. Removal of ceramide by this process provides the gradient that enables the process to continue and prevents an accumulation of ceramide in the endoplasmic reticulum that might otherwise be disruptive to the membrane and even cause cell death. While the transfer process itself is not dependent on ATP, the overall process requires ATP, possibly to keep PI(4)P in a phosphorylated form, and the multiple factors that control the biosynthesis of this lipid must also influence sphingolipid metabolism.

As a neutral lipid, ceramide can flip readily across membrane leaflets, and this is also necessary for the synthesis of sphingomyelin, which occurs in the lumen of the Golgi. The ceramide pool utilized for synthesizing **glycosylceramide** is delivered to the Golgi by a separate transport mechanism that does not require ATP. In addition, some ceramide synthesis occurs in mitochondria, although this has the potential

to lead to cell death. Regulation of ceramide and subsequent sphingolipid biosynthesis is crucial, as excess sphingolipids can be toxic, while reduced synthesis can inhibit cell proliferation.

Some ceramides are transported from the liver to other tissues in plasma **lipoproteins**, especially subclasses HDL2 and HDL3, which contain apolipoprotein B. There is a suggestion that the transport of ceramides via lipoproteins could be a paracrine mechanism to regulate the metabolism of other cells.

Ceramides are also produced during the catabolism of other complex sphingolipids, and especially by the action of one or other of the sphingomyelinases or phospholipase C on **sphingomyelin** in animal tissues as part of the 'sphingomyelin cycle' as shown in Figure **21.4.16**.

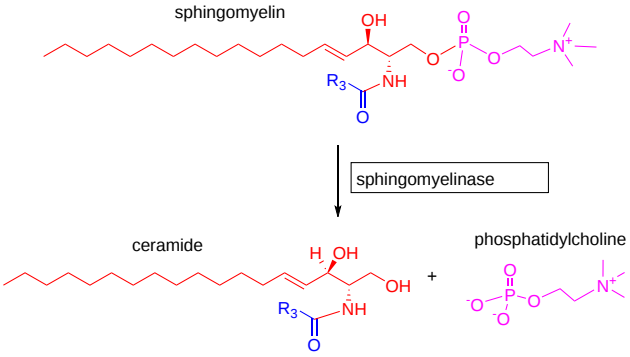


Figure **21.4.16**: Ceramide formation from sphinogmyelin

Many agonists, including chemotherapeutic agents, tumor necrosis factor-alpha, 1,25-dihydroxy-vitamin D3, endotoxin, gamma-interferon, interleukins, nerve growth factor, ionizing radiation, and heat, stimulate hydrolysis of sphingomyelin to produce ceramide. In addition, reversal of the sphingomyelin synthesis reaction may generate ceramide, and some may be produced by the reverse operation of the enzyme ceramidase (see next section). Such reactions are much more rapid than de novo synthesis, so they are of special relevance in signaling functions of ceramides, especially when they occur at the plasma membrane. For example, the acid sphingomyelinase may be especially important in this context because it generates the ceramides that initiate the train of events that lead to apoptosis (see below).

Glycosidases can also hydrolyze glycosphingolipids to ceramides in tissues, but the process tends to be less important in quantitative terms (other than in skin). The key enzymes of sphingolipid metabolism were first characterized in the yeast *Saccharomyces cerevisiae*, and these were found to be sufficiently similar to the corresponding enzymes in mammals to facilitate their study in the latter.

As discussed above, specific ceramide synthases utilize specific fatty acids for ceramide biosynthesis in animals, and knowledge is slowly being acquired of how these are compartmentalized and regulated within cells. Thus, the synthesis and subsequent catabolism of ceramides involve a complex web of at least 28 distinct enzymes, including six ceramide synthases and five sphingomyelinases, all products of different genes. Each of these enzymes may produce distinctive molecular species of ceramides with their characteristic biological properties. It has been determined that ceramide species containing very-long-chain fatty acids (C_{24}) turnover more rapidly than those containing $C_{16/18}$ components.

21.4.3.3: CERAMIDE CATABOLISM

In animals, ceramide metabolism and function are controlled in part by the action of **ceramidases**, which cause hydrolysis, forming sphingoid bases and free fatty acids, and indeed, this is the only route to the formation of unesterified sphingosine. This is illustrated in Figure **21.4.17**.

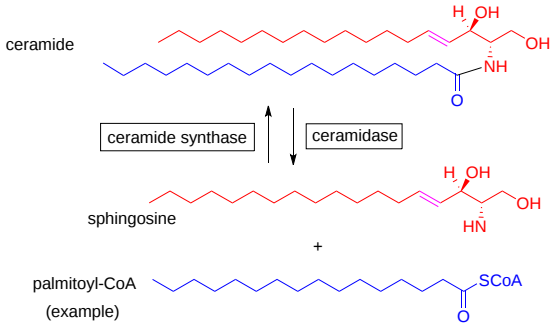


Figure **21.4.17**: Ceramide hydrolysis-resynthesis

Five such enzymes are known in humans, classified according to their pH optima, i.e. acid (‘ASAH1’), neutral (‘ASAH2’, which differs between humans and animals), and alkaline (three enzymes - ‘ACER1 to ACER3’), with differing cellular locations and fatty acid

specificities and with the potential to affect distinct signaling and metabolic events. The acid ceramidase is of particular importance, and aberrations in its synthesis or activity are involved in several human disease states, including the rare autosomal-recessive **Farber disease,** where the enzyme is deficient, so ceramide accumulates; ceramide containing 26:0 in the blood is considered to be a biomarker for diagnosis of the disease. ASAH1 is located in the lysosomes and hydrolyses ceramides with small to medium-chain fatty acid components (C_6 to C_{18}) most efficiently. The neutral ceramidase is located in the plasma membrane and Golgi, especially of intestinal epithelial cells and colorectal tissues, and prefers long-chain components (C_{16} to C_{18}); it also catalyzes the reverse reaction, and this may be a means of ceramide synthesis in mitochondria. ACER1 and ACER2 are found in the endoplasmic reticulum and Golgi, respectively, and they prefer species with very-long-chain acyl groups. ACER3 is present in both the endoplasmic reticulum and Golgi; it has a marked specificity for ceramides, dihydroceramides, and phytoceramides linked to unsaturated long-chain fatty acids (18:1, 20:1, or 20:4) *in vitro*, at least. Neutral/alkaline ceramidase activity has also been found in mitochondria and nuclei.

In Arabidopsis, an alkaline ceramidase (AtACER) can hydrolyze phytosphingosine-containing ceramides, and a related enzyme from rice has a preference for d18:1Δ4-ceramide; the latter can function in reverse to increase the content of C_{26}- and C_{28}-phytoceramides. Several neutral ceramidases (AtNCERs) have been identified, but there does not appear to be an equivalent to the acid ceramidase in plants. Ceramidases also exist in lower organisms such as *Pseudomonas aeruginosa* and slime molds. The enzymes are secreted and are not integral membrane enzymes. A neutral ceramidase is only found in prokaryotes, including some pathogenic bacteria.

Sphingoid bases released by the action of acid ceramidase can escape from the lysosomes and be re-utilized for ceramide biosynthesis through the action of a ceramide synthase. This has been termed the 'salvage' pathway and is important in quantitative and biological terms. For example, it has been estimated to contribute 50% to 90% of sphingolipid biosynthesis. The biological functions of ceramides are discussed below. There are reasons to believe that ceramides derived from the salvage pathway are spatially and functionally distinct from those synthesized *de novo*. In addition, sphingoid bases released in this way have their own biological functions, which include utilization for the synthesis of the biologically important metabolite **sphingosine-1-phosphate**. Therefore, the regulation of ceramidase action is central to the biological processes of innumerable animals.

? CERAMIDES - DETAILED OVERVIEW

See link below

Link

21.4.3.4: BIOLOGICAL FUNCTIONS OF CERAMIDES

The role of ceramides in the biosynthesis of complex glyco- and phospho-sphingolipids is discussed elsewhere in this text. Ceramides, like other lipid second messengers in signal transduction, are produced rapidly and transiently in response to specific stimuli to target specific proteins, for example, to activate certain serine/threonine protein kinases or phosphatases. They may also regulate cellular processes by influencing membrane properties. While they can be produced by synthesis *de novo* for such functions, activating one of the sphingomyelinases under physiological stress or other agents allows a more rapid generation in animal tissues. Ceramides appear to be formed under all conditions of cellular stress by a multiplicity of activators in eukaryotic organisms. However, it should be noted that ceramides with different fatty acid and long-chain base (molecular species) compositions are formed in different compartments or membranes of the cell by various mechanisms over different time scales and potentially with distinct functions. The biological functions of those ceramides containing medium-chain (up to C_{14}), long-chain (C_{16} and C_{18}), and very-long-chain (C_{20} and longer) fatty acids, in particular, may have to be considered separately.

Physical properties: Unsaturation in the sphingoid backbone augments intramolecular hydrogen bonding in the polar region, which permits a close packing of ceramide molecules and a tight intramolecular interaction in membranes. A further important factor in this context is the length of the fatty acyl moiety, as shorter-chain ceramides tend to produce a positive curvature in a lipid monolayer. Long-chain molecules have the opposite effect and possess a marked intrinsic negative curvature that facilitates the formation of inverted hexagonal phases and increases the order of the acyl chains in bilayers. By their interactions with ion channels, ceramides influence the permeability of membranes and render bilayers and cell membranes permeable to solutes that vary from small to protein size.

While ceramides are minor components of membranes in general, their physical properties ensure that they are concentrated preferentially into lateral liquid-ordered microdomains (a distinct form of '**raft**' termed 'ceramide-rich platforms'). However, these effects are again chain-length specific. These domains differ appreciably in composition from those rafts enriched in **sphingomyelin** and cholesterol, and ceramides containing C_{12} to C_{18} fatty acids can displace cholesterol from rafts to modify their physical properties. Ceramides are generated within rafts by the action of acid sphingomyelinase, causing small rafts to merge into larger units and modifying the membrane structure in a manner that is believed to permit the oligomerization of specific proteins such as

cytokines and death receptors. Ceramides are also essential for the formation and/or secretion of exosomes by facilitating or inducing membrane curvature. In contrast, sphingosine, sphingosine-1-phosphate, and ceramide-1-phosphate do not facilitate raft formation.

Ceramides can function in signal transduction through the medium of these modified rafts. Specific receptor molecules and signaling proteins are recruited and clustered within such domains, excluding potential inhibitory signals while initiating and greatly amplifying primary signals. Ceramide-rich platforms are believed to amplify both receptor- and stress-mediated signaling events and may influence various disease states. Ceramide-enriched membrane domains formed in response to sphingomyelinase activity are sites for endocytic uptake of pathogens because of a concentration of pathogen receptors and signaling complexes, and in particular, these can enhance viral infections, including Norovirus, Japanese encephalitis virus, Ebola, and possibly SARS-CoV-2. However, elevated levels of ceramide inhibit the cellular uptake of HIV.

Although ceramides and diacylglycerols have structural similarities, their occurrence, location, and behavior in membranes differ. Ceramides cross synthetic lipid bilayers relatively quickly *in vitro*. Still, it is unclear whether they can flip across more complex biological membranes equally readily, especially in the ceramide-rich platforms. Restricted flipping could have important effects on the signaling role of ceramides, in that those generated by different enzymes on each side of a membrane could have distinct functions.

Enzyme activation: Ceramides generally modify intracellular signaling pathways to slow anabolism and promote catabolism. Amongst a wide range of biological functions in relation to cellular signaling, ceramides are especially important in triggering apoptosis, and they have also been implicated in the activation of various protein kinase cascades, dependent on the site of generation. The mechanism of these interactions is the subject of intensive study at present, but in relation to the latter, two intracellular targets for ceramide action of special importance have been discovered – at least two protein phosphatases (ceramide-activated protein phosphatases) and a family of protein kinases (ceramide-activated protein kinases). For example, the phosphatase may regulate glycogen synthesis, insulin resistance, and response to apoptotic stimuli. Ceramides generated by the action of sphingomyelinase and by de novo synthesis are both important to the process. At the same time, ceramidases have contrasting effects in these and other biological effects of ceramides.

Apoptosis: The role of ceramides in regulating **apoptosis,** cell differentiation, transformation, and proliferation has received special attention. Apoptosis is a normal process that occurs in response to oxidative stress, in particular, in which a cell can be considered to commit suicide. It is essential for many aspects of normal development and maintaining tissue homeostasis. There are two pathways - 'extrinsic' initiated in the plasma membrane by ligation of so-called 'death factors', such as the tumor necrosis factor-α (TNF-α), and 'intrinsic' induced by external actions in mitochondria, e.g., by DNA damage, oxidation, or radiation injury. Although the mechanism of the ceramide interaction with these pathways is uncertain, it is clear that a cascade of reactions is initiated that culminates in the release of intracellular proteases of the caspase family to promote apoptosis. In dysfunctional mitochondria, one mechanism involves the formation of channels in the membrane that enable the release of specific mitochondrial proteins, including caspases. Ceramides with fatty acids of differing chain lengths are believed to function differently, and 16:0-ceramide generated by ceramide synthase 6 is especially pro-apoptotic, for example. In contrast, ceramides with very-long-chain fatty acids accumulate in necroptosis, a form of apoptosis. On the other hand, ceramides containing 2-hydroxy acids in keratinocytes appear to be protective against apoptosis. Ceramides also induce the related process of cellular senescence.

Failure to properly regulate apoptosis can have catastrophic consequences, and many disease states, including cancer, diabetes, neuropathies, Alzheimer's disease, Parkinson's disease, and atherosclerosis, are thought to arise from the deregulation of apoptosis. For example, ceramides have been implicated in the actions of TNF-α and in the cytotoxic responses to amyloid Aβ peptide, which are involved in Alzheimer’s disease and neurodegeneration. In addition, ceramides appear to be involved in many aspects of aging biology and male and female fertility. These effects may hold implications for diseases associated with obesity and insulin resistance, including diabetes and cardiovascular disease.

Similarly, ceramides are intimately involved in the induction of autophagy, the 'maintenance' process by which cellular proteins and excess or damaged organelles are removed from cells by engulfing them in a membrane-enclosed cellular compartment called the phagosome. In particular, maturing phagosomes are enriched in very-long-chain ceramides. While this process is beneficial in that it aids the recycling of cellular nutrients, the presence of excess ceramide can lead to unnecessary apoptosis.

As animals and plants have multiple isoforms of ceramide synthase specific for the base's chain length and fatty acid, it has been suggested that ceramides containing different fatty acids have distinct roles in cellular physiology. In particular, C_{16} ceramide appears to be especially important in apoptosis in non-neuronal tissues. In contrast, C_{18} ceramide has growth-arresting properties and may be involved in apoptosis in some carcinomas treated with chemotherapy agents. In addition, a transferase has been identified that transfers the acetyl group from **platelet-activating factor** to sphingosine with high specificity. The product, *N*-

acetylsphingosine - the simplest of all ceramides, has signaling functions that are distinct from those of the parent lipids or other ceramides; it does not enter the salvage pathway in cancer cells *in vitro* and is cytotoxic.

In contrast, the ceramide metabolite, **sphingosine-1-phosphate**, has opposing effects on cell survival and proliferation. As ceramide and sphingosine-1-phosphate are interconvertible via sphingosine as an intermediate, which also has pro-apoptotic activity, the balance between these lipids and ceramide-1-phosphate is obviously of great metabolic importance. It has been termed the 'sphingolipid-rheostat', as illustrated in Figure **21.4.18**.

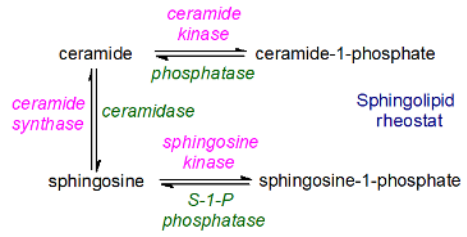


Figure **21.4.18**: Sphingolipid rheostat

Plants: Comparatively little information is available on the role of ceramides in cell signaling in plants, but there are suggestions that sphingolipid catabolic products may be linked to programmed cell death, signal transduction, membrane stability, host-pathogen interactions, and stress responses. For example, there is evidence that enhanced synthesis of ceramides with very-long-chain fatty acids and trihydroxy sphingoid bases by ceramide synthases LOH1 and LOH3 promotes cell division and growth, while, in contrast, accumulation of the ceramide species C_{16} fatty acid with a dihydroxy sphingoid base, due to LOH2 overexpression, leads to plant dwarfing and programmed cell death. Ceramides aggregate in rafts in plant membranes and other sphingolipids and sterols, as in animal tissues. Similarly, in the yeast *S. cerevisiae*, widely used as a model organism, it has been reported that ceramide species with different *N*-acyl chains and sphingoid bases regulate different sets of functionally related genes.

21.4.3.5: SKIN CERAMIDES

The mammalian skin forms the protective barrier between the internal tissues of the host and the hostile external environment, which can include chemicals, ultraviolet light, mechanical damage, and pathogenic microorganisms, while preventing the loss of water and electrolytes. It consists of stratified layers of increasingly differentiated cells or keratinocytes, of which the basal layer is responsible for the renewal of the tissue but begins to migrate upwards and differentiate while accumulating specific lipids and proteins that change the cellular architecture. Eventually, the keratinocytes lose their nucleus and become flattened structures of insoluble protein surrounded by lipids termed 'corneocytes' in the outermost impermeable layer or stratum corneum. By secreting peptides and proteins that possess antimicrobial activity, keratinocytes add to the defensive capability of skin against commensal microorganisms and opportunistic pathogens, and this is reinforced by lipid mediators such as free sphingoid bases and eicosanoids in the stratum corneum and free fatty acids in sebum.

The stratum corneum contains high levels of ceramides (as much as 50% of the total lipids), including *O*-acylceramides, which exist in the free form and are linked by ester bonds to structural proteins. They are present mainly in the extracellular domains (interstices). They are accompanied by nearly equimolar amounts of cholesterol and free fatty acids. This ratio is believed to be essential for normal tissue organization into the membrane structures responsible for the epidermal barrier's functioning. In contrast to other biological membranes, the lipid organization in the membranes of skin consists of two lamellar phases, which form crystalline lateral phases mainly, with repeat distances of approximately 6 and 13 nm. Small sub-domains of lipids in a liquid phase may also exist.

Some of these skin ceramides have distinctive structures not seen in other tissues; many forms are commonly recognized. They can contain the normal range of longer-chain fatty acids (a), e.g., formula 1 in the figure, some with hydroxyl groups in position 2 (a*), e.g., formula 2, linked both to dihydroxy bases with *trans*-double bonds in position 4 or to trihydroxy bases. This is illustrated in Figure **21.4.18**.

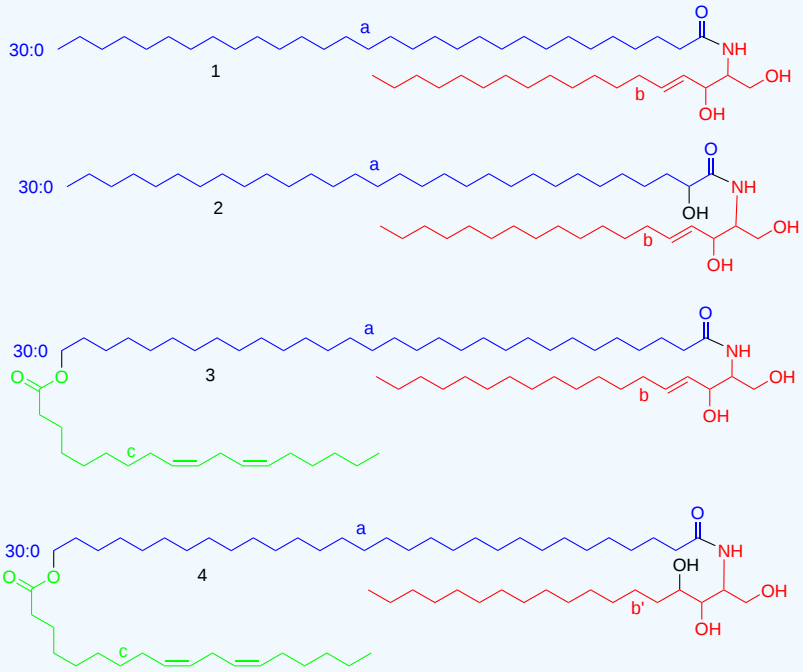
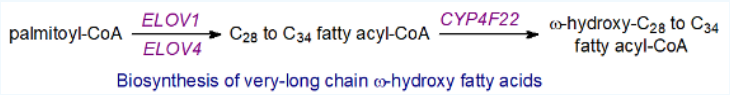


Figure **21.4.18**: Skin ceramides

In addition, there are *O*-acyl ceramides in which a unique very-long-chain fatty acid component (typically C_{30} or C_{32}) has a terminal hydroxyl group, and this may be in the free form or esterified with linoleate (**c**), e.g., formulae 3 and 4; the sphingoid base can be either di- (**b**) or trihydroxy (**b***), e.g., formula 4; the latter is not a common feature in sphingolipids of animal origin, and can include both phytosphingosine and the unique 6-hydroxy-4-sphingenine in human epidermis. Ceramides of type 1 (with the 1-*O*-hydroxyl group of the sphingoid base acylated by a very-long-chain fatty acid), are also present (1-*O*-acylceramides - illustrated above). These comprise 5% of the total ceramides in the epidermis of mice and humans and comprise as many as 700 molecular species. In all, 15 classes of free ceramides and three classes of covalently bound ceramides with up to 1700 distinct molecular species have been identified. Such lipids were first studied in detail in the pig's skin as a convenient experimental model, but they have been characterized in humans and rats. In addition, several molecular forms of **glucosylceramide**, based on similar ceramide structures, have been characterized in skin, and these are also essential for its proper function.

The lipid composition can vary depending on the particular layer of the skin (keratinocytes, stratum corneum, *etc.*). These lipids have an obvious role in the skin's barrier properties, limiting the loss of water and solutes and, at the same time, preventing the ingress of harmful substances. As the aliphatic chains in the ceramides and the fatty acids are mainly non-branched long-chain saturated compounds with a high melting point and a small polar head group, the lipid chains are mostly in a solid crystalline or gel state, which exhibits low lateral diffusional properties and low permeability at physiological temperatures. There is a report that the stratum corneum layer of the skin has a water permeability of only one-thousandth that of other biomembranes, for example. Natural and synthetic ceramides are now commonly added to cosmetics and other skin care preparations.

Most steps in the biosynthesis of ceramides linked to ω-*O*-acylated fatty acids occur in the endoplasmic reticulum of keratinocytes. First, fatty acid synthesis of very-long-chain (and ultra-long-chain, ≥C_{26}) acyl-CoA *de novo* must occur, requiring the chain-elongation enzymes **ELOVL1 and ELOVL4**. Desaturation and oxidation can occur in the 2 (α) and terminal (ω) positions. The ω-hydroxylation step requires an enzyme of the cytochrome P450 family, designated CYP4F22, of the kind involved in synthesizing **hydroxy-eicosatetraenoic acids** (HETE). Mutations are a cause of lamellar ichthyosis, and knockout mice deficient in the equivalent enzyme were found to die within 8 hours of birth.



Biosynthesis of very-long chain ω-hydroxy fatty acids

Ceramides are first synthesized by ceramide synthase 3 (CERS3), which has a high specificity for very-long-chain fatty acids (>C_{26}) with the incorporation of the ω-hydroxy fatty acid. This is acylated with linoleate by the action of an unusual enzyme related to the phospholipase A family, PNPLA1, which catalyzes esterification by first releasing linoleate from triacylglycerols in the skin

while acting as an acyltransferase to link the linoleate directly to the ω-hydroxyl moiety of the ultra-long chain fatty acid. PNPLA1 is unique among phospholipases in that it is involved in the metabolism of sphingolipids rather than glycerophospholipids and catalyzes transacylation rather than hydrolysis. In addition, some linoleate for this purpose is released from triacylglycerols by the action of the adipose tissue lipase aided by a protein ABHD5. This process is vital for proper skin barrier function and keratinocyte differentiation, as mice with defective triacylglycerol biosynthesis and metabolism, including a deficiency of the acyl-CoA synthase ACSL1, are unable to synthesize ω-*O*-acylceramides and have an impaired skin barrier. Mutations in the human *PNPLA1* gene are believed to cause the autosomal recessive disease, congenital ichthyosis.

The resulting ceramides are converted to the complex sphingolipids **sphingomyelin** and especially **glucosylceramide**, which are transferred with the aid of ATP-binding cassette (ABC) transporters together with degradative enzymes into the stratum corneum via specific organelles termed 'lamellar bodies.' These organelles must fuse with the apical plasma membrane of the outermost cell layer of the epidermis so that their contents can be secreted. It is only then that the final step of hydrolysis of the lipid precursors occurs in the extracellular spaces of the stratum corneum, i.e., ceramides are generated from sphingomyelin by the action of acid sphingomyelinase and from glucosylceramides by β-glucocerebrosidase. This mechanism ensures that ceramides, with their potentially harmful biological activities, never accumulate within nucleated cells.

Eventually, ceramides with a terminal ω-hydroxyl group in the fatty acyl moiety are bound covalently to the proteins of the cornified envelope, especially to involucrin. This is illustrated in Figure **21.4.19**.

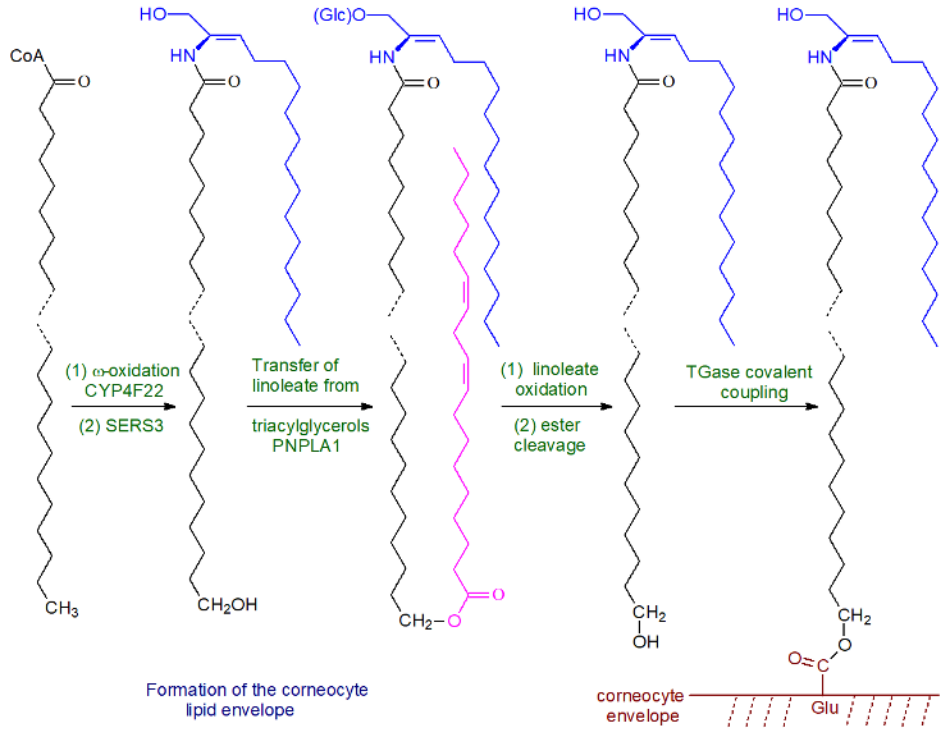
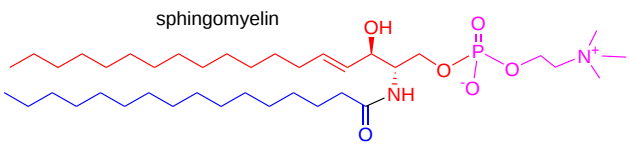


Figure **21.4.19**: Formation of the corneocyte lipid envelope

21.4.4: SPHINGOMYELIN AND RELATED SPHINGOPHOSPHOLIPIDS

21.4.4.1: STRUCTURE AND OCCURRENCE OF SPHINGOMYELIN

Sphingomyelin or ceramide 1-phosphocholine consists of a **ceramide** unit with a phosphorylcholine moiety attached to position 1 of the **sphingoid base** component. It is thus the sphingolipid analog of **phosphatidylcholine**, and like that lipid, it is zwitterionic. The d18:1/16:0 molecular species is illustrated as an example in Figure **21.4.20**.



N-(hexadecanolyl)-sphing-4-enine-1-phosphocholine

Figure **21.4.20**: Example of a sphingolipid

Sphingomyelin is primarily of animal origin and is a ubiquitous component of all animal cell membranes, from mammals to nematodes (and in a few protozoa), where it is, by far, the most abundant sphingolipid. Indeed, it can comprise as much as 50% or more of the lipids in certain tissues, though it is usually lower in concentration than phosphatidylcholine. For example, it makes up about 10% of the brain's lipids (especially in myelin) but 70% of the phospholipids of the human lens. Like phosphatidylcholine, sphingomyelin tends to be in the greatest concentration in the plasma membrane of cells (up to 20%), the endocytic recycling compartment, and the *trans* Golgi network. It is also abundant in the nucleus, where it is the main phospholipid associated with chromatin. Still, there is very little in the endoplasmic reticulum (2 to 4%) and even less in mitochondria. All the sphingomyelin in human erythrocyte membranes is in the outer leaflet, and ~90% of that in the plasma membrane of nucleated cells is in the outer leaflet. All lipoprotein fractions in plasma contain appreciable amounts of sphingomyelin, with a higher proportion in the VLDL/LDL. Sphingomyelin is the single most abundant lipid in the erythrocytes of most ruminant animals, where it replaces phosphatidylcholine entirely. In this instance, a highly active phospholipase A breaks down the glycerophospholipids but not sphingomyelin.

Sphingomyelin is not synthesized in plants or fungi, which produce the sphingophospholipid **ceramide phosphoinositol** and related lipids instead, or in bacteria, and its evolutionary significance is a matter for speculation. However, many bacteria and viruses utilize sphingomyelin or its metabolism in their hosts for growth and viability.

Sphingosine is usually the most abundant **long-chain base** constituent (along with sphinganine and C_{20} homologues), although other bases can be present, especially in ruminant animals. In contrast, sphinganine is the major sphingoid base in the sphingomyelin of human lens membranes, linked mainly to 16:0. Typically, the fatty acids are very-long-chain saturated and monounsaturated, including odd-numbered components. Compared to the glycosphingolipids, 2-hydroxy acids are rarely detected in small amounts. They are found in testes, spermatozoa, the kidney, and the skin sphingomyelin. The absolute proportions of each fatty acid and sphingoid base can vary markedly between tissues and species, and some of the variability in compositions can be seen from the data in Table 21.4.3 and Table 21.4.4 below.

Table 21.4.3: Fatty acid compositions of sphingomyelin (wt % of the total) in some animal tissues.

Source	Fatty acids									
	16:0	18:0	18:1	20:0	22:0	22:1	23:0	23:1	24:0	24:1
Egg	66	10	1	4	6	1	2	-	5	3
Bovine brain	3	42	-	6	7	3	3	3	6	27
Cow's milk	14	3	1	1	22	-	32	-	19	5

Adapted from Ramstedt, B. *et al*. Analysis of natural and synthetic sphingomyelins using high-performance thin-layer chromatography. *Eur. J. Biochem*., **266**, 997-1002 (1999); DOI.

Table 21.4.4: Long-chain base compositions of sphingomyelin (wt% of the total) in some animal tissues.

Source	Sphingoid base						
	d16:0*	d17:0	d17:1	d17:1-methyl	d18:0	d18:1	d19:0
Egg					7	93	
Bovine brain					19	81	
Cow's milk	9	15	8	11	10	44	3

Also from Ramstedt, B. *et al*. *Eur. J. Biochem*., **266**, 997-1002 (1999); DOI.
* d = dihydroxy base

Palmitic acid (16:0) is the most common fatty acid component of sphingomyelin in the peripheral cells of mammals. In contrast, stearic acid (18:0) is more abundant in neural tissue, but this only hints at the potential complexity, as there can be variability within tissues. For example, about 60% of the fatty acids of the sphingomyelin of the grey matter of the human brain consist of stearic acid (18:0). In comparison, lignoceric (24:0) and nervonic (24:1) acids make up 60% of the corresponding lipids of white matter. However, this is dependent on the stage of development. During the first two years of life, the 18:0 concentration in sphingomyelin of white matter decreases from 82% to 33%, while the proportions of 24:0 and 24:1 increase. This pronounced shift from long-chain to very-long-chain sphingomyelins does not apply to the cerebral cortex. Approximately 100 molecular species of sphingomyelin have been detected in human plasma. Although polyunsaturated fatty acids such as arachidonic acid are rarely present, they have sometimes been mistakenly identified in the literature. Exceptions are the sphingomyelins of testes and spermatozoa, which contain very-long-chain polyunsaturated fatty acids (up to 34 carbon atoms), the major components being 28:4(*n*-6) and 30:5(*n*-6) with a proportion having hydroxyl groups in position 2.

21.4.4.2: BIOSYNTHESIS, METABOLISM, AND FUNCTION OF SPHINGOMYELIN

The biosynthesis of sphingomyelin is distinct from that of **phosphatidylcholine**. It indeed depends upon it, as it involves the transfer of phosphorylcholine from phosphatidylcholine to ceramide, synthesized in the endoplasmic reticulum, with the liberation of 1,2-diacyl-*sn*-

glycerols, as illustrated in Figure **21.4.21**.

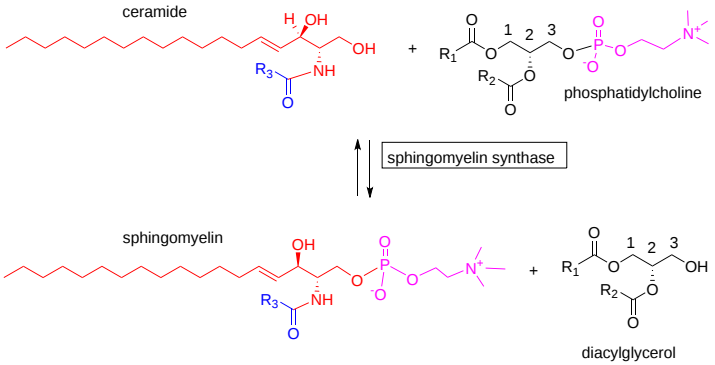
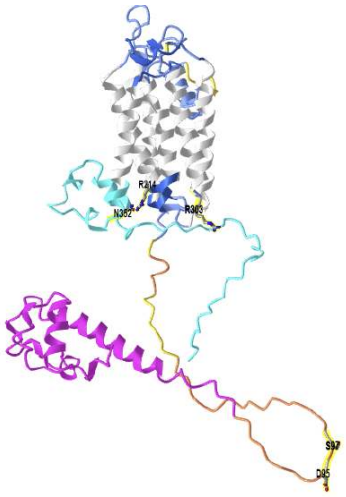


Figure **21.4.21**: Synthesis of sphingomyelin

The reaction is catalyzed by a ceramide choline-phosphotransferase (sphingomyelin synthase or SMS). It takes place primarily on the luminal side of the *trans*-Golgi but also in the plasma membrane, with two related enzymes, each with six transmembrane domains and their N- and C-termini facing the cytosol, i.e., SMS1 and SMS2. Both enzymes are present in the Golgi, but only SMS2 is in the plasma membrane (facing the extracellular space in this instance) and may be necessary to form raft domains (see below). SMS2 is also present in the membranes of nuclei from rat liver cells. Notably, in the absence of ceramide, both SMS1 and 2 have phospholipase C activity, which may regulate the steady-state levels of phosphatidylcholine, diacylglycerol, and sphingomyelin. The reaction does not use free phosphorylcholine or CDP-choline as a donor.

Figure **21.4.22** shows an interactive iCn3D model of the AlphaFold model of human Golgi membrane phosphatidylcholine:ceramide cholinephosphotransferase 1, also called sphingomyelin synthase 1 (Q86VZ5).



NCBI iCn3D Figure **21.4.22**: . Click the image for a popup or use this external link: https://structure.ncbi.nlm.nih.gov/i...v6s5wHRgPXKJC6

The gray helices are the transmembrane helices. A cytoplasmic protein:protein interaction domain called SAM (sterile alpha motif) is shown in magenta. The other cytoplasmic C-terminal domain is shown in cyan. Much of the cytoplasmic domain is disordered in this computational structure. Side chains involved in binding phosphatidylcholine are shown as sticks colored CPK. Note that two, D95 and S97, are located in a disordered section in this model but would close in the actual active site in the actual structure.

It has been proposed that Asp101 (95 in the AlphaFold structure) deprotonates Arg220 (214 in the model), which then acts as a nucleophile that attacks the phosphate group of phosphatidylcholine. Given the very high pKa of arginine, this mechanism, if true, is somewhat unique. Phosphocholine is linked to ceramide, which produces sphingomyelin. Three key and extremely conserved amino acids in the active site are Asp101, Arg220, and Asn358.

A specific ceramide transport molecule (CERT) is important to the reaction with SMS1 in that it transfers ceramide from the cytosolic surface of the endoplasmic reticulum to the *trans*-Golgi in an ATP-dependent and non-vesicular manner. A vesicular transport mechanism delivers much of the sphingomyelin produced in the Golgi to the apical plasma membrane. Sphingomyelin synthesis is partially regulated by phosphatidylinositide metabolism and is connected to sterol homeostasis through the oxysterol binding protein (OSBP).

SMS2 in the plasma membrane is not dependent on CERT-mediated ceramide delivery but is believed to convert ceramide produced locally by a sphingomyelinase back to sphingomyelin; this may be an important protective mechanism for the cell. The location of the enzymes explains the enrichment of sphingomyelin in specific membranes and the sidedness, i.e., the luminal *trans*-Golgi and the outer leaflet of the plasma membrane, while ceramide reaching the *cis*-Golgi is utilized for the synthesis of **glucosylceramide**. As the nature of the molecular species of sphingomyelin produced differs appreciably from that of the ceramide precursors, the sphingomyelin synthases must have considerable substrate specificity. The reaction can be reversible, using sphingomyelin to generate ceramide for specific signaling functions. Sphingomyelin biosynthesis links the sphingolipid signaling pathway (pro-apoptotic - see below) and that of glycerolipids via the mitogenic **diacylglycerol** by-products. Although the importance of this production relative to that via **phosphatidylinositol** is unknown, it may be significant locally at the external leaflet of the plasma membrane.

An alternative pathway of sphingomyelin synthesis has been demonstrated in the endoplasmic reticulum. In this pathway, ceramide is first converted to ceramide phosphoethanolamine via transfer of the head group from phosphatidylethanolamine, followed by stepwise methylation of the ethanolamine moiety. However, the physiological significance of this pathway has yet to be established.

It was long thought that the only function of sphingomyelin was to serve as a substitute for phosphatidylcholine as a building block of membranes, i.e., by forming a stable and chemically resistant outer leaflet of the plasma membrane lipid bilayer. For example, it may limit oxygen ingress and, hence, the oxidation of adjacent unsaturated acyl chains. While this is certainly one of its functions, the apparent similarity between PC and SM is superficial, and there are great differences in the two lipids' hydrogen bonding capacities and physical properties. For example, sphingomyelin has an amide bond at position 2 and a hydroxyl at position 3 of the sphingoid base, and both can participate in hydrogen bonding. At the same time, the *trans* double bond also appears to assist intermolecular interactions in membranes. Indeed, the first five carbon atoms of the sphingoid base in sphingolipids constitute a key feature that has been termed the ‘sphingoid motif’, which facilitates a relatively large number of molecular interactions with other membrane lipids via hydrogen-bonding, charge-pairing, hydrophobic, and van der Waals forces. In contrast, the two ester carbonyl groups can act only as hydrogen acceptors with phosphatidylcholine. The degree of unsaturation of the alkyl moieties in each lipid differs, giving them dissimilar membrane packing properties.

It is now recognized that sphingomyelin and other sphingolipids have a strong tendency to interact with proteins and cholesterol, often via strong van der Waals interactions and hydrogen bonding, to form transient nano-domains in membranes known as '**rafts**' and on the surface of lipoprotein particles. Initially, there was a view that saturated sphingomyelin formed a liquid-ordered phase with cholesterol or a gel phase with saturated ceramides to lead to lateral segregation within the membrane and that sphingomyelin and cholesterol metabolism were closely integrated, even that the sphingomyelin concentration might control the distribution of cholesterol in cells. On the other hand, understanding the mechanism of raft formation in membranes has changed substantially in recent years. While an interaction with cholesterol is important, it may not be the major factor *in vivo*. Ceramide can displace cholesterol from its association with sphingomyelin when formed in membranes by hydrolysis of the latter.

Other functions: Sphingomyelin *per se* is generally considered a relatively inert molecule, although modern molecular biology methods uncover potential regulatory functions via interactions with particular proteins. For example, it has been shown to inhibit the activity of **phospholipase $A_2\alpha$**, a key enzyme in eicosanoid production. Sphingomyelin in the plasma membrane may be essential for the internalization of transferrin and thence of iron into cells, and it appears to be required for the activity of many membrane-bound proteins, including those of certain ion channels and receptors. As the most abundant sphingolipid in the nucleus, it is intimately involved in chromatin assembly and dynamics and is an integral component of the nuclear matrix. A single molecular species of sphingomyelin with a C_{18} acyl chain binds specifically to a coat protein designated 'p24' to enable it to form membrane vesicles. In addition, sphingomyelin is selectively recognized and acts as a receptor for the actinoporins, which are pore-forming toxins produced by sea anemones.

There is a specific binding site for sphingomyelin on the amyloid beta-peptide (Aβ) in the brain, and there is evidence from studies *in vitro* that this may promote the aggregation of these proteins in Alzheimer's disease. In turn, this leads to the depletion of brain sphingomyelin by activating acid sphingomyelinase, which disrupts many protein–lipid interactions and downstream signaling pathways. In contrast, the ganglioside GM1 may be protective against Aβ aggregation.

As well as its role in membranes, it serves as a precursor for ceramides, long-chain bases, sphingosine-1-phosphate, and many other biologically important sphingolipids, as part of the 'sphingomyelin cycle' (also termed the ‘sphingolipid’ or ‘ceramide’ cycles depending on the context). Some metabolites are intracellular and intercellular messengers, while others are essential membrane constituents. The sphingomyelin cycle extends to other sphingolipids via the action of sphingomyelinases and enzymes such as glycosylhydrolases and glycosyltransferases in cells to produce innumerable new oligoglycosylceramides. It can also give rise to ***sn*-1,2-diacylglycerols**, central to many metabolic and signaling pathways. These molecular relationships are illustrated briefly in Figure **21.4.23**.

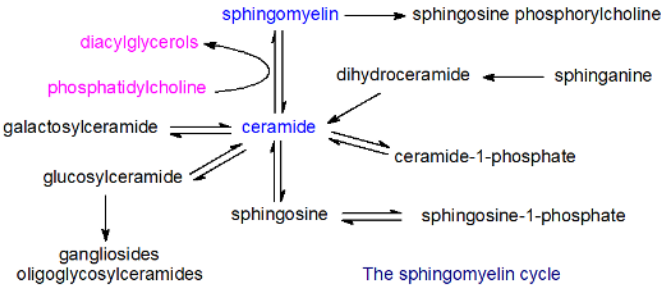


Figure **21.4.23**: The sphingomyelin cycle

In particular, sphingomyelin is a major source of **ceramides** in most cellular organelles, including the nucleus and even mitochondria, via the action of sphingomyelinases (see next section). In addition to being a source of other sphingolipids, these are required to trigger apoptosis and other metabolic changes. As ceramides do not mix well with glycerophospholipids and cholesterol, this conversion forms new membrane domains enriched in ceramide that exclude cholesterol and differ in composition from other sphingolipid rafts. This profoundly affects membrane function, especially of the plasma membrane, in that different proteins may be recruited or excluded depending on their relative affinities for cholesterol and ceramides. It may also influence disease states such as cancer.

Chlamydiae and other bacterial pathogens acquire sphingomyelin from their hosts' Golgi apparatus and plasma membrane, which is necessary for the viability and growth of the organisms. Other pathogenic bacteria, notably *Pseudomonas aeruginosa* and *Neisseria gonorrhoeae*, can hijack sphingomyelin catabolic enzymes with deleterious effects on the host. Likewise, human immunodeficiency virus (HIV) and the hepatitis C virus utilize host sphingomyelin for their nefarious purposes.

Nutrition: Although there is no known nutritional requirement for sphingomyelin and other sphingolipids, they are components of any diet containing egg, meat, or dairy products. Thus, it has been estimated that *per capita* sphingolipid consumption in the United States, for example, is of the order of 0.3-0.4 g/d. As sphingolipids constitute an appreciable proportion of the polar lipid constituents of milk, they may be significant if minor nutrients for infants and beneficial effects upon their development have been claimed. Animal experiments show that dietary sphingolipids can reduce the intestinal absorption of cholesterol and other lipids, reducing serum lipid concentrations. Feeding sphingolipids inhibits colon carcinogenesis and may alleviate some inflammatory bowel disease symptoms. 2-Hydroxyoleic acid suppresses the growth and induces autophagy in cancer cells by stimulating sphingomyelin synthesis and increasing the amount of this lipid in the plasma membrane. On the other hand, plasma sphingomyelin levels are considered an independent risk factor for atherosclerosis, possibly due to its ability to retain cholesterol in cells and the arterial wall with consequent diminished reverse cholesterol transfer via HDL.

21.4.4.3: SPHINGOMYELIN CATABOLISM

In contrast to the glycerolipids, dietary sphingolipids are not hydrolyzed by pancreatic enzymes only. Rather, most of the sphingomyelin in the diet is hydrolyzed in the brush border of the intestines by an **alkaline sphingomyelinase** (at a pH of 8.5–9 optimally) to ceramide and thence by a neutral ceramidase to free fatty acids and sphingosine. Some of this enzyme is also present in the liver, from which it is secreted in bile into the intestinal lumen, where it can hydrolyze sphingomyelin and other phospholipids with bile salts. The sphingosine released at the brush border is absorbed; some is re-*N*-acylated to form ceramides, and the remainder is converted via sphingosine-1-phosphate to palmitic acid, which is esterified into the triacylglycerol component of chylomicrons. Some of these sphingolipid intermediates may have signaling functions and anti-inflammatory properties in intestinal cells. The alkaline sphingomyelinase is unusual in that it is very different in its structure and other properties from intracellular enzymes with a related function; it is part of the (ecto)nucleotidepyrophosphatase-phosphodiesterase protein family (NPP) that includes **autotaxin**. The enzyme is believed to have a role in producing sphingolipid metabolites within the intestines and colon, which may influence some disease states. For example, it appears to inhibit colon cancer by generating ceramides. In addition, alkaline sphingomyelinase has phospholipase C activity towards the pro-inflammatory metabolite **platelet-activating factor** and lysophosphatidylcholine with potentially further beneficial effects. Reducing the level of endogenous sphingomyelin and increasing that of ceramides in intestinal cell membranes may reduce dietary cholesterol uptake.

Catabolism in other tissues: The key enzymes for the degradation of sphingomyelin to ceramides in most tissues are also sphingomyelinases (phosphodiesterases), as shown in Figure **21.4.24**.

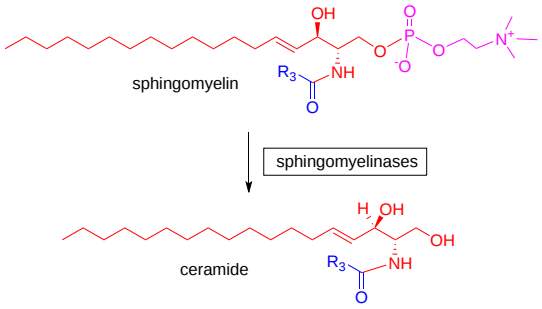


Figure **21.4.24**: Sphingomyelin catabolism

These function similarly to phospholipase C and generate ceramides, with their innumerable and important signaling properties being the main product. Many such enzymes with different pH optima and metal ion requirements operate in different cell regions and have potentially distinct biochemical roles. Thus, there is an acid sphingomyelinase in the endo-lysosomes and different neutral sphingomyelinases in the plasma membrane, endoplasmic reticulum, Golgi, and mitochondria, in addition to the alkaline sphingomyelinase in the intestines. It should not be forgotten that the other reaction product is phosphocholine, which is important as a nutrient. Bacterial sphingomyelinases are known to lyse red blood cells. Intriguingly, there is a sphingomyelinase in the bacterium *Pseudomonas aeruginosa* that can also act as a sphingomyelin synthase *in vitro* at least.

The lysosomal **acid sphingomyelinase** (pH optimum ca. 5) is expressed ubiquitously. It has a key housekeeping role in maintaining normal membrane turnover and remodeling of the sphingolipid constituents, especially those of lipoproteins. While other lysosomal sphingolipid hydrolases require a **saposin** activator protein for full activity, the acid sphingomyelinase has an N-terminal saposin domain. It also has the unique lysosomal phospholipid **bis(monoacylglycero)phosphate**.

There is a related secreted acid sphingomyelinase (Zn^{2+}-dependent), which can be transported to the outer membrane of the cell and is especially important in endothelial cells of the human coronary artery. The same gene produces this enzyme, but it differs from the lysosomal enzyme as it requires Zn^{2+} ions for activation and has a different glycosylation pattern. It can also operate at neutral pH and has multiple functions, in that it is involved in many aspects of cellular signaling and membrane sphingomyelin turnover. It acts at the plasma membrane to produce ceramides and regulate the trafficking of **palmitoylated proteins** from the Golgi to their new location.

Neutral sphingomyelinases (pH optima 7.4), of which four quite distinct enzymes are known, are located in membranes of the endoplasmic reticulum, Golgi, and plasma membrane, with one in mitochondria (MA-NSM), where they have signaling functions by generating ceramides and thence other biologically active sphingolipids. Human NSM-1 has 423 amino acid residues and a molecular weight of 47.6 kDa; it has two putative transmembrane domains in the C-terminus and resides mainly in the nucleus and endoplasmic reticulum. It has a broad specificity for choline phospholipids, but it is most active with sphingomyelin and may not have a significant role in cellular signaling. In contrast, NSM-2, which is located in the Golgi apparatus and plasma membrane, is activated by phosphatidylserine and is important for ceramide signaling. It is especially important in the brain and nervous tissue, where it is required for the secretion of hypothalamic-releasing hormones. However, it is relevant to many other tissues' cellular functions and physiological processes. Dysregulation of NMS-2 is reported to be a factor in many inflammation-related pathologies. Neutral sphingomyelinase-3 is found mainly in the plasma membrane of bone and cartilage, where it is vital for mineralization; it is also important in striated and cardiac muscle. Little is known about the function of the mitochondrial enzyme. Losses, mutations, and poor expression of the gene encoding neutral sphingomyelinase have been observed in several cancers. Still, exposure to ionizing irradiation led to rapid hydrolysis of sphingomyelin to ceramide by this enzyme, and thence to cancer cell death.

A diverse range of factors activate the enzymes, including chemotherapeutic agents, tumor necrosis factor-alpha, 1,25-dihydroxy-vitamin D_3, endotoxin, gamma-interferon, interleukins, nerve growth factor, and most conditions known to induce cellular stress, especially in relation to inflammation. As they utilize by far the most abundant sphingolipid in animal tissues to generate ceramides and other sphingolipid metabolites that have important signaling functions, sphingomyelinases are believed to function as regulators of signaling mechanisms, especially in the nucleus of the cell. Thus, they have a much wider metabolic role than simply the catabolism of sphingomyelin.

The **type A and B forms of Niemann-Pick disease** are lysosomal lipid storage disorders that are a consequence of a deficiency of acid sphingomyelinase with a resulting accumulation of sphingomyelin and smaller amounts of other sphingolipids, including gangliosides, in cells and tissues, especially in the monocyte/macrophage system to form the so-called “foam cells” that characterize the disease. A consequent lack of ceramide production may be involved in the pathology of the disease. Increasing sphingomyelin levels, in turn, results in elevated cholesterol concentrations. It is noteworthy that membranes containing ceramides have a much lower binding capacity for cholesterol, so that sphingomyelin degradation may play a part in cholesterol homeostasis. **Type C Niemann-Pick** disease differs from the A and B forms and is caused by defects in two distinct cholesterol-binding proteins (NPC1 and NPC2).

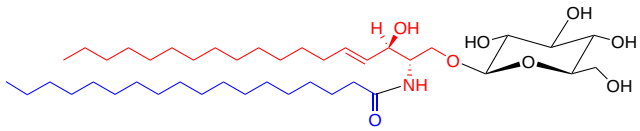
21.4.5: GLUCOSYL- AND GALACTOSYLCERAMIDES (CEREBROSIDES)

There are two natural monoglycosylceramides of special importance in animals, i.e., glucosylceramide and galactosylceramide. Both have biological functions in their own right, but especially as structural components of membranes, as in the brain, where galactosylceramide is required to maintain the structure and stability of myelin and the differentiation of oligodendrocytes. Glucosylceramide is a vital component of all cell types and is most abundant in human skin; it is the key intermediate in the biosynthesis of lactosylceramide and thence of complex oligoglycosphingolipids, including gangliosides. This monoglycosylceramide is also a major component of the membranes of plants and fungi. Although the two lipids have very similar structures in that D-galactose is an epimer of D-glucose and differ only in the configuration at C4, they have very different biological properties. A few other monoglycosylceramides are produced in nature, for example, by some bacteria of the order *Sphingomonadales* of α-proteobacteria.

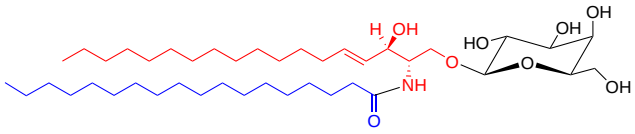
21.4.5.1: STRUCTURE AND OCCURRENCE

β-D-Galactosylceramide (Galβ1-1'Cer) is the principal glycosphingolipid in brain tissue, hence the trivial name "cerebroside", which was first conferred on it in 1874. Galactosylceramides are found in all nervous tissues and indeed at low levels in all organs, but in the brain they can amount to 2% of the dry weight of grey matter and 12% of white matter or 23% of myelin lipids, where they insulate the axons of neuronal cells and constitute a substantial component of the extended plasma membrane of oligodendrocytes. It is also present in some fungal species. While galactosylceramide can be sulfated to form a sulfatide or sialylated to form ganglioside GM_4, only a small proportion is subjected to further galactosylation to form Gal_2Cer as the precursor for the limited gala-series of oligoglycosphingolipids.

β-D-Glucosylceramide (Glcβ1-1'Cer), with the trivial name "glucocerebroside", is a major constituent of skin lipids, where it is essential for the maintenance of the water permeability barrier of the skin. Otherwise, it is most abundant in animal tissues such as the spleen and erythrocytes, and in nervous tissues, especially in the neurons if at low levels, and it is also found in plants. Higher than normal concentrations of this glycosphingolipid have been reported for the apical plasma membrane domain of epithelial cells from the intestines (especially the absorptive villous cells) and the urinary bladder. The d18:1/16:0 molecular species of the two lipids are illustrated in Figure **21.4.25**.



glucosylceramide



b- galactosylceramide

Figure **21.4.25**: gluco- and galactoceramides (cerebrosides)

However, of equal or greater importance to the natural occurrence of glucosylceramide *per se* is its role as the biosynthetic precursor of lactosylceramide in animals and, hence, of most of the complex **neutral oligoglycolipids** and **gangliosides**. In contrast, glucosylceramide is the end-product of the biosynthetic pathway in plants and fungi.

Interestingly, the proportion of galactosylceramides relative to glucosylceramides in myelin glycolipids increases greatly in the ascending phylogenic tree, and the ratio of hydroxy- to nonhydroxy fatty acids in cerebrosides increases with the complexity of the central nervous system. There is also an intriguing sex difference in the kidney, where it has been shown that galactosylceramide rather than glucosylceramide occurs in male mice only (or androgen-treated adult females). Only glucosylceramide is present in the nerves of the most primitive animals (protostomes).

In the brain, the galactosylceramides are enriched in very-long-chain fatty acids (C_{22}–C_{26}). The fatty acid and long-chain base compositions of cerebrosides from the intestines of the Japanese quail are listed in Table **21.4.5** for illustrative purposes. The fatty acid components resemble those of other sphingolipids, although the percentage of 2-hydroxy acids is higher than that in sphingomyelin. They are exclusively saturated in this instance, though a small proportion of monoenoic components may also be found in other tissues. Glucosylceramides tend to contain mainly non-hydroxylated fatty acids that are of relatively shorter chain length. The proportion of trihydroxy bases listed is perhaps higher than in many other tissues or species studied, probably reflecting the diet. Usually, sphingosine is the main long-chain base in cerebrosides of animal tissues.

Table **21.4.5**: **Composition of fatty acids and long-chain bases (wt % of the total) in cerebrosides of intestines from the Japanese quail.***

Long-chain bases		Fatty acids	Non-hydroxy acids	2-Hydroxy acids
Type	**%**		**%**	**%**
t18:0	43	16:0	5	6
d18:0	9	18:0	3	trace
d18:1	27	20:0	2	4
t20:0	6	21:0	trace	2
d20:0	3	22:0	4	43
d20:1	11	23:0	1	13
		24:0	3	12

* The cerebrosides comprised 81% galactosylceramide and 19% glucosylceramide.
From Hirabayashi, Y. *et al.*, *Lipids*, **21**, 710-714 (1986); DOI.

Plants: Glucosylceramide is the only glycosphingolipid common to plants, fungi, and animals. It has often been described incorrectly as the main sphingolipid in plants. However, this has been because the more polar complex **glycosylinositol phosphoceramides** are not easily extracted and, until relatively recently, were missed in conventional analyses. Nonetheless, glucosylceramide is abundant in photosynthetic tissues and constitutes approximately a third of the total sphingolipids, where the main long-chain bases are C_{18} 4,8-diunsaturated (*Z*/*Z* and *E*/*Z*) (not sphingosine as illustrated above); it is a major component of the outer layer of the plasma membrane and is also enriched in the late endosomes and plant tonoplast. Small amounts of monoglycosylceramides containing a β-D-mannopyranosyl unit may be present in non-photosynthetic tissues, but galactosylceramides have not been found in plants. Glucosylceramide is a common component of the lipids of yeast and other fungi, including most fungal pathogens. However, it does not occur in the yeast *Saccharomyces cerevisiae*, which is widely used as an experimental model, although trace galactosylceramide levels have been detected.

The fatty acid and long-chain base compositions of glucosylceramides from two plant sources are listed in Table **21.4.6**. Perhaps surprisingly, the fatty acid components are not very different from those in animal tissues, comprising mainly longer-chain saturated and monoenoic acids, with a high proportion being saturated and having a hydroxyl group in position 2. In the examples selected for the table, di- and tri-hydroxy long-chain bases were found, mainly diunsaturated (*Z*/*Z* and *E*/*Z*) and almost entirely C_{18} in chain length. Much higher concentrations of glucosylceramides are found in pollen than in leaves, with substantial compositional differences. For example, the long-chain bases in Arabidopsis leaves consist mainly of t18:1, with relatively little d18:1, t18:0, and d18:0 (with 16:0, 24:0, and 24:1 hydroxy fatty acids mainly), but no d18:2 base. However, this is 50% of those in pollen. While saturated 2-hydroxy acids predominate in most plants, some cereal glucosylceramides contain high proportions of monounsaturated, very-long-chain fatty acids of the *n*-9 family. Glucosylceramides from algae tend to resemble those from higher plants, although some novel structures have been reported from microalgae.

Table **21.4.6: Composition of fatty acids and long-chain bases (wt % of the total) in glucosylceramides of seeds from scarlet runner beans and kidney beans.**

	Fatty acids[a]			**Long-chain bases**[b]	
Type	**Runner beans**	**Kidney beans**		**Runner beans**	**Kidney beans**
	%	**%**		**%**	**%**
16:0	4	5	t18:0	trace	trace
Other non-hydroxy	1	2	t18:1-8*t*	13	11
14:0-OH	1	1	t18:1-8*c*	10	9
15:0-OH	1	1	d18:0	trace	trace
16:0-OH	58	58	d18:1-8*c*/*t*	1	3
18:0-OH	trace	trace	d18:1-4*t*	trace	trace
20:0-OH	trace	trace	d18:2-4*t*,8*t*	45	60
22:0-OH	7	6	d18:2-4*t*,8*c*	31	17
23:0-OH	2	1			
24:0-OH	23	23			
25:0-OH	1	1			
26:0-OH	1	1			

From Kojima, M. *et al*., *J. Agric. Food. Chem.*, **39**, 1709-1714 (1991); DOI, but see also Yamashita, S. *et al*. for further data: DOI
[a] including 2-hydroxy acids; [b] di- and tri-hydroxy bases with *cis* or *trans* double bonds in the positions indicated.

21.4.5.2: BIOSYNTHESIS

Ceramides synthesized both *de novo* and by catabolism of sphingomyelin are used for the biosynthesis of monoglycosylceramides in animal tissues. The biosynthetic mechanism resembles that of **glycosyldiacylglycerols**, i.e., there is a direct transfer of the carbohydrate moiety from a sugar-nucleotide, e.g., uridine 5-diphosphate(UDP)-galactose, UDP-glucose, etc, to a ceramide unit synthesized in the endoplasmic reticulum. This is illustrated in Figure **21.4.26**.

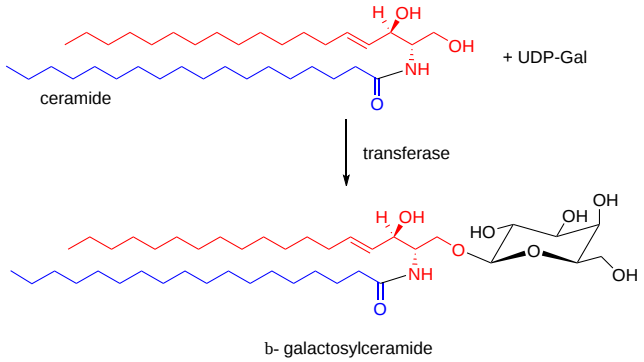


Figure **21.4.25**: Synthesis of galactosylceramide

During the transfer, which is catalyzed by specific glycosyl-transferases, inversion of the glycosidic bond occurs from the *alpha* to *beta* configuration. Synthesis of β-D-galactosylceramide takes place on the lumenal surface of the endoplasmic reticulum. However, it has free access to the cytosolic surface by an energy-independent flip-flop process. Expression of the UDP-galactose:ceramide galactosyl transferase (galactosylceramide synthase) is restricted to oligodendrocytes, Schwann cells, kidneys, and testes. Before **sulfation**, galactosylceramide is transported to the *trans*-Golgi compartment.

In contrast, after the transfer of the precursor **ceramides** from the endoplasmic reticulum to the cytosolic side of the early Golgi membranes with the aid of the CERT protein, glucosylceramide is produced by a glucosylceramide synthase present in this membrane (with the possible exception of neuronal tissues). Suppose it is to be converted to more complex **oligoglycosylceramides.** In that case, this must be translocated to the luminal leaflet of the *trans*-Golgi membranes, a process that occurs both by vesicular and non-vesicular transport. The latter is mediated by a conserved clade of integral membrane proteins, i.e., phospholipid flippases (P4-ATPases) designated ATP10A and ATP10D, together with the four phosphate adapter protein-2 (FAPP2) and glycolipid transfer protein (GLTP) in humans, with related enzymes in fungi, which utilize the energy from ATP catalysis to translocate lipids across cellular membranes. The human enzymes are entirely specific for glucosylceramide and not galactosylceramide. Indeed, the galactosyl- and glycosylceramide synthases have no significant sequence homology, indicating different evolutionary origins.

Both galactosyl- and glucosylceramide must be transported to and then across the plasma membrane for their functions in protein interactions and signaling. Some glucosylceramide is carried by lipoproteins (VLDL, LDL, and HDL) in the circulation and presumably requires active transport for absorption and distribution across the membranes of target tissues.

In plants, glucosylceramides are also formed by an evolutionarily conserved glucosylceramide synthase involving UDP-glucose in the endoplasmic reticulum. However, an alternative mechanism that utilizes sterol glucoside as the immediate glucose donor to ceramide has been described. There is also evidence for a requirement for ceramides containing Δ^4 *trans*-double bonds to synthesize glucosylceramides but not other sphingolipids in some plant and fungal tissues. However, there is a distinct ceramide synthase in the yeast *Pichia pastoris*, which produces ceramides of defined composition exclusively for the production of glucosylceramides. A separate ceramide synthase with different specificities produces the ceramide precursors for **phosphorylinositol**, which only contains phytosphingosine as the long-chain base. In fungi, glucosylceramide synthases have been characterized, but a galactosylceramide synthase has yet to be identified. Enzymes responsible for the biosynthesis of glucuronosylceramide and α-galactosylceramide in some bacterial species have been characterized.

21.4.5.3: FUNCTION

Galactosylceramides: A remarkable property of cerebrosides is that their melting point is well above physiological body temperature, so glycolipids have a para-crystalline structure at this temperature. Each cerebroside molecule may form up to eight inter- or intramolecular hydrogen bonds by lateral interaction between the polar hydrogens of the sugar and the hydroxy and amide groups of the sphingosine base of the ceramide moiety, and this dense network of hydrogen bonds is believed to contribute to the high transition temperature and the compact alignment of cerebrosides in membranes. As with sphingomyelin, monoglycosylceramides tend to be concentrated in the outer leaflet of the plasma membrane with cholesterol and thence in myelin in the specific membrane domains termed **rafts**. Indeed, the latter appear to facilitate segregation to a greater extent than sphingomyelin via the combination of hydrogen bonds and hydrophobic interactions,

and these forces are also of great importance for binding to the wide range of proteins, including enzymes and receptors, which are found in raft domains.

Galactosylceramide is essential to myelin structure and function and is involved in the differentiation of oligodendrocytes. While molecular species with 2'-hydroxy fatty acid constituents are not essential for myelin formation, they are critical for the long-term stability of myelin, presumably because increased hydrogen bonding with neighboring lipids in membranes stabilizes the phase structure. Galactosylceramide is important as a precursor of **3'-sulfo-galactosylceramide**, which is also essential to brain development and numerous functions in other tissues. By interacting with sulfatide located in the membrane of opposing layers in the myelin sheath by carbohydrate-carbohydrate interaction, it forms what is known as a glycosynapse, contributing to the long-term stability of myelin.

Glucosylceramides: Glucosylceramides have similar physical properties in membranes to the galactose analog, and they are also concentrated in raft domains in the outer leaflet of the plasma membrane. As mentioned briefly above, they are the primary precursor for most of the more complex oligoglycosphingolipids in animal tissues, especially in the brain, where synthesis is vital for producing most neuronal oligoglycosphingolipids. Glucosylceramide, *per se*, is essential for axonal growth. They are major constituents of skin lipids, essential for lamellar body formation in the stratum corneum and for maintaining the water permeability barrier of the skin. In addition, the epidermal glucosylceramides and sphingomyelin are the source of the unusual complex **ceramides** found in the stratum corneum, including those with terminal hydroxyl groups and estolide-linked fatty acids. Some of the glucosylceramide in the skin is linked covalently to proteins via terminal hydroxyl groups, presumably to strengthen the epidermal barrier.

Much of the evidence for the function of glycosylceramides in animals has been derived from cell lines in which lipid synthesis has been suppressed by various means *in vitro*. It appears that glucosylceramide is not essential for the viability of certain cell lines in culture. However, disruption of the global synthase gene in mice results in the death of embryos. It is essential for the survival of cancer cells, and deletion from other cell types can lead to abnormalities. In addition to being an intermediate in the biosynthesis of more complex glycosphingolipids and its role in the permeability barrier of the skin (discussed above), glucosylceramide is believed to be required for intracellular membrane transport, cell proliferation and survival, and various functions in the immune system. In contrast, there are indications that it may have adverse implications for various disease states. For example, the overexpression of glucosylceramide synthase in cancer cells has been linked to tumour progression with a reduction in ceramide concentration, resulting in increased resistance to chemotherapy. The lipid has also been associated with drug resistance in a wider context. In the nematode *Caenorhabditis elegans*, glucosylceramide containing the fatty acid 22:0 is reported to be a longevity metabolite that functions through the membrane localization of clathrin, a protein that regulates membrane budding.

In Arabidopsis, glucosylceramides are critical for cell differentiation and organogenesis but not necessarily for the viability of cells. It has been proposed that glycosphingolipids could impose positive curvature on membranes, facilitating vesicle fusion. There is evidence that glycosylceramides (but not glycosyldiacylglycerols), together with sterols, are located in rafts in plant membranes in an analogous manner to sphingolipids in animal tissues and that they are associated with specific proteins. Correlative studies suggest that glucosylceramides help the plasma membrane in plants to withstand stresses brought about by cold and drought. For example, glycosylceramides containing 2-hydroxy monounsaturated very-long-chain fatty acids and long-chain bases with 4-*cis* double bonds appear to be in higher concentrations in plants more tolerant of chilling and freezing. While fungal glucosylceramides with a 9-methyl group within the sphingosine backbone elicit defense responses in rice, cerebrosides with double bonds in positions 4 and/or 8 of the long-chain base appear to be involved in the defense of some plant species against fungal attack.

Less is known about the function of glucosylceramides in fungi, although they are major constituents of the plasma membrane and cell wall. They are believed to be involved in cell wall assembly, cell division and differentiation, and signaling. The presence of the methyl branch in the long-chain base is essential for cell division and alkali tolerance. In the case of fungal pathogens, glucosylceramides are recognized by the host immune system and regulate virulence, often after export into the external environment as extracellular vesicles. In contrast to animals, ceramide monohexosides are not precursors for oligoglycosylceramides in fungi. Some molecular species of this lipid from plants (a Δ^8 double bond in the long-chain base is essential) show fruiting-inducing activity in the fungus *Schizophyllum commune*.

α-D-Galactosylceramides: Cerebrosides linked to an α-D- rather than a β-D-galactosyl unit, such as that found in the marine sponge *Agelas mauritianus*, in human gut microflora, and even in cow's milk, are potent stimulators of mammalian immune systems by binding to the protein CD1d on the surface of antigen-presenting cells and activating invariant natural killer T cells. Indeed, this was one of the first pieces of evidence to show that glycolipids, like glycoproteins, could invoke an immune response. Subsequently, it was demonstrated that α-galactosylceramide with a 24:1 fatty acid, though present in very small amounts, is loaded onto the CD1d or CD40 protein and is presented as the natural endogenous ligand for NKT cells in the thymus and the periphery. Once activated, NKT cells secrete a range of pro- and anti-inflammatory cytokines to modulate innate and adaptive immune responses. The α-glucosyl and α-psychosine analogs show similar activity.

It is not certain whether α-galactosylceramide is synthesized in animal tissues, and it is likely derived primarily from members of the gut microbiome, such as *Bacteroides fragilis* and related species (although, in general, few bacterial species produce sphingolipids). Ceramide-

galactosyltransferases responsible for synthesizing this lipid in two species of bacteria from the intestinal microbiome have been identified. In the mouse gut, the main molecular form consisted of a 2-(*R*)-hydroxylated hexadecanoyl chain linked to C_{18}-sphinganine, while that in *B. fragilis* contained longer-chain components with *iso*-methyl-branches in the sphingoid base and often fatty acid moieties. The sphinganine chain branching is a critical determinant of NKT cell activation by the bacterial enzyme. A decrease in the production of this lipid was observed in mice exposed to stress conditions that alter the composition of the gut microbiota, including a Western-type diet, colitis, and influenza A virus infection, with potential consequences for the systemic immune responses. Catabolic enzymes control their concentration within animal tissues in a two-step mechanism: removal of the acyl chain by an acid ceramidase and hydrolysis of the sugar residue by an α-glycosidase. Initial studies with animal models suggest that treatment with α-D-galactosylceramides is effective against lung and colorectal cancers, melanomas, and leukemia, and pre-clinical trials of this lipid and its synthetic analogs so far have shown that these are safe and effective as anti-tumor immunotherapeutic agents and vaccine adjuvants. Indeed, a phase I trial with high-risk melanoma patients has given promising preliminary results.

21.4.5.4: CATABOLISM OF GLYCOSPHINGOLIPIDS

In animal tissues, the lysosomes are the main sites for the degradation of **all** glycosphingolipids, including the monoglycosylceramides, oligoglycosphingolipids, and gangliosides. These membrane-bound organelles comprise a limiting external membrane and internal lysosomal vesicles, which contain soluble digestive enzymes that are active at the acidic pH of this organelle. All membrane components are transported to the lysosomes to be broken down into their primary components. In the case of glycosphingolipids, this means fatty acids, sphingoid bases, and monosaccharides, which can be recovered for reuse or further degraded. Thus, sections of the plasma membrane enter the cell by endocytosis, and they are then transported through the endosomal compartment to the lysosomes. The compositional and physical arrangement of the lysosomal membranes is such that they are themselves resistant to digestion with **bis(monoacylglycero)phosphate** (lysobisphosphatidic acid) as a characteristic component of the inner membrane. A glycocalyx of highly *N*-glycosylated integral membrane proteins protects the perimeter membrane with the aid of the ganglioside GM3, which is resistant to degradation. This glycocalyx forms an efficient hydrophilic barrier at the luminal surface of the lysosomal perimeter membrane to protect it from degradation by proteases and hydrolases and to prevent lipids and their hydrolysis products from escaping from the lumen of the lysosome.

The degradation of oligoglycosylceramides and gangliosides occurs by the sequential removal of monosaccharide units via the action of specific exohydrolases from the non-reducing end until a monoglycosylceramide unit is reached, when glucosylceramide β-glucosidases or an analogous β-galactosidase (one isoform) removes the final carbohydrate moiety. Several glucosylceramidases are known; GBA1 is a lysosomal hydrolase, GBA2 is a ubiquitous non-lysosomal enzyme, and GBA3 is a cytosolic β-glucosidase. The last is found in the kidney, liver, spleen, and a few other tissues of mammals, but its function is unclear.

As glycolipids with fewer than four carbohydrate residues are embedded in intralysosomal membranes, while the degradative enzymes are soluble, the process requires the presence of negatively charged lipids and specific activator proteins, which are water-soluble glycoproteins of low molecular weight. These are not themselves active catalytically but are required as cofactors either by directing the enzyme to the substrate or activating the enzyme by binding it in some manner. Five such proteins are known: the GM2-activator protein (specific for gangliosides) and Sphingolipid Activator Proteins or **saposins A, B, C, and D**, which perturb the membranes sufficiently to enable the degradative enzymes to reach the glycolipid substrates. The four saposins are derived by proteolytic processing from a single precursor protein, prosaposin, which is synthesized in the endoplasmic reticulum, transported to the Golgi for glycosylation, and then to the lysosomes. Of these, saposin C is essential for the degradation of galactosyl- and glucosylceramide, while saposin B is required for the hydrolysis of sulfatide, globotriaosylceramide, and digalactosylceramide. The hydrolysis reaction products of monoglycosylceramides are ceramides and monosaccharides with net retention of the stereochemistry of the latter in the process. This is illustrated in Figure **21.4.26**.

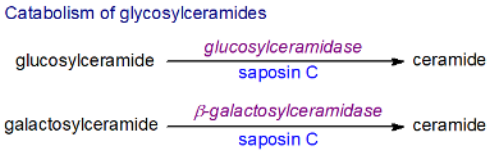


Figure **21.4.26**: Catabolism of glycosylceramide

The reactions are aided by anionic lipids such as bis(monoacylglycero)phosphate. In particular, this increases the ability of the GM2-activator to solubilize lipids and stimulates the hydrolysis of membrane-bound GM1, GM2, and some of the kidney sulfatides. Saposin D stimulates the degradation of lysosomal ceramide by acid ceramidase, and it is also involved in the solubilization of negatively charged lipids at an appropriate pH. Eventually, the ceramides can, in turn, be hydrolyzed by an acid ceramidase to fatty acids and sphingoid bases.

β-Glucosylceramidase and saposin C are also required to generate the structural **ceramides** from glucosylceramide in the outer region of the skin, a process essential for optimal skin barrier function and survival. Some glucosylceramide is hydrolyzed by the enzyme GBA2 at the plasma membrane, where the ceramide formed is rapidly converted to sphingomyelin by the sphingomyelinase 2, which may be co-located

with the glucosidase. In addition, it has been established that cellular β-glucosidases can transfer the glucose moiety from glucosylceramide to and from other lipids, as in the formation of **cholesterol glucoside**.

Small but significant amounts of glucosyl- and galactosylceramides are ingested in the human diet. They are not hydrolyzed by pancreatic enzymes but are degraded in the brush border of the intestines by the enzyme lactase-phlorizin hydrolase (which also hydrolyses the lactose in milk) to ceramides and thence to sphingosine.

An Arabidopsis homolog of human glucosylceramidase (AtGCD3) preferentially hydrolyses glucosylceramides that contain long acyl chains, and three further isoforms may exist based on sequence homology.

21.4.5.5: GENETIC DISORDERS AND DISEASE

Harmful quantities of glucosylceramide accumulate in the spleen, liver, lungs, bone marrow, and, in rare cases, the brain of patients with **Gaucher disease**, the most common of the inherited metabolic disorders (autosomal recessive) involving storage of excessive amounts of complex sphingolipids. Three clinical forms (phenotypes) of the disease are commonly recognized, of which the most dangerous are those affecting the brain (Types 2 and 3). All of the patients exhibit a deficiency in the activity of the lysosomal glucosylceramide-β-glucosidase (GBA1), which catalyzes the first step in the catabolism of glucosylceramide. The enzyme may be present, but a mutation prevents it from forming its correct conformation. However, other factors may be involved as patients with a defective saposin C, the lysosomal activator protein, develop similar symptoms.

In the brain, glucosylceramide accumulates when complex lipids turn over during brain development and the formation of the myelin sheath of nerves. The excess glucosylceramide arises mainly from the biodegradation of old red and white blood cells. The result is that the glucosylceramide remains stored within the lysosomes of macrophages, i.e., the specialized cells that remove worn-out cells by degrading them to simple molecules for recycling, thus preventing them from functioning normally and often leading to chronic inflammation. The enlarged macrophages containing undigested glucosylceramide are termed Gaucher cells. They overexpress and secrete certain proteins into the circulation, and some of these are used as biomarkers. In addition, glucosylceramide is converted more rapidly to **gangliosides** in these cells, leading to an increase in ganglioside GM3 in the plasma and spleen of patients with Gaucher disease. Fortunately, there are now effective enzyme replacement therapies for patients with the milder (non-neurological or Type 1) form of Gaucher disease that successfully reverse most manifestations of the disorder, including decreasing liver and spleen size and reducing skeletal abnormalities. Two oral drugs that inhibit glucosylceramide synthesis have also been approved.

Defective GBA1 enzyme activity in humans has been implicated in an increased risk of multiple myeloma and other cancers. Oligoglycosylceramides and gangliosides, in particular, are known to be involved in the pathology of many cancers, and glucosylceramide is an important precursor of these. Inhibition of glucosylceramide synthase, which is overexpressed in many human tumors, leads to a marked arrest of cell growth in cancer cells *in vitro*. This may have the potential to treat colorectal and other cancers.

A deficiency in glucocerebrosidase activity may predispose individuals to more common disorders such as Parkinson's disease and Lewy body dementia. Excess glucosylceramide production and more complex glycosphingolipids are factors in polycystic kidney disease. It appears to be a general rule that the mere process of lysosomal substrate accumulation in all lysosomal storage disorders impairs lysosome integrity and results in more general disruptions to lipid metabolism, membrane structure, and function. On the other hand, inhibition of glucosylceramidases may be of benefit in cystic fibrosis. Krabbe disease is discussed in the next section.

Galactosylceramide is believed to function as an initial receptor for the human immunodeficiency virus (HIV) in mucosal epithelial cells. It controls the early infection-independent phase of HIV transfer to T cells. Glucosylceramide levels regulate the uptake of viruses that rely upon the late endosomal compartment for fusion, including the influenza A and Ebola viruses.

21.4.6: GANGLIOSIDES

The name **ganglioside** was first applied by the German scientist Ernst Klenk in 1942 to a mixture of complex glycosphingolipids newly isolated from ganglion cells of the brain. Subsequently, he demonstrated that as part of an oligosaccharide chain, they contained an acidic carbohydrate component, which he named "neuraminic acid" - later termed "sialic acid" from the Greek "sialon" for saliva, from which they were first isolated. However, it was not until 1963 that the first ganglioside species was fully characterized. Innumerable sphingolipids are now known that differ in both the glycan (glucose, galactose, *N*-acetylgalactosamine, and sialic acid residues) and **ceramide** structures. They are present throughout the animal kingdom, from echinoderms up to higher animals, but not in plants. Such highly polar, acidic, and relatively hydrophilic molecules have distinctive physical properties, which are essential for the vital functions of gangliosides in the membranes of the central nervous system and other tissues.

21.4.6.1: SIALIC ACIDS AND GANGLIOSIDES

Sialic acids: Gangliosides are oligoglycosylceramides derived as a first step from lactosylceramide, and they are defined by the presence of one to as many as five **sialic acid** residues, i.e., carbohydrate molecules with a nine-carbon backbone and a carboxylic acid group, a

subclass of the superfamily of naturally occurring non-2-ulosonic acids. Of the many forms that have been characterized, only a few are relevant to gangliosides, and the most important of these is *N*-acetylneuraminic acid (‘NANA’ or ‘SA’ or 'Neu5Ac' or 'NeuAc'). Less often, the sialic acid component is *N*-glycolylneuraminic acid (Neu5Gc), which differs by only one oxygen atom at the C-5 *N*-acetyl group, or it can be a Neu5Ac analogue in which the amide group is replaced by a hydroxyl group, i.e., 3-deoxy-D-glycero-D-galacto-nonulosonic acid (ketodeoxynonulosonic acid or ‘KDN’). The sialic acids are joined via α-glycosidic linkages to one or more monosaccharide units, e.g., via the hydroxyl group on position 2 or to another sialic acid residue. The polar head groups of the lipids carry a net-negative charge at pH 7.0, and they are acidic. Their structures are shown in Figure **21.4.27**.

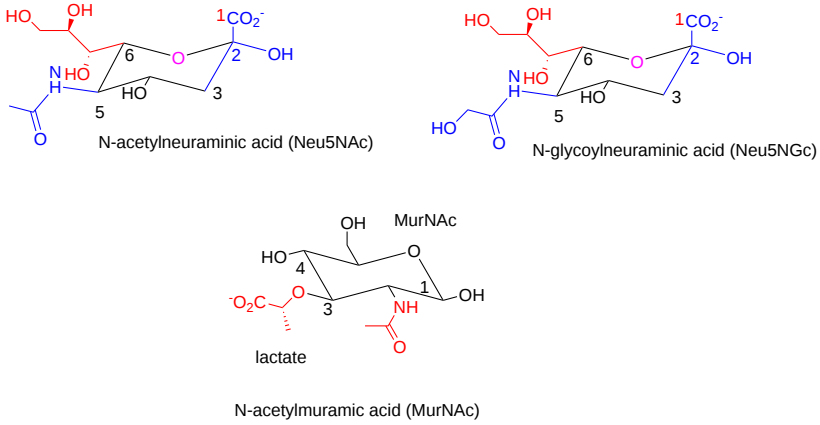


Figure **21.4.27**: Sialic acids

Humans lack Neu5Gc: Neu5Ac is the biosynthetic precursor of Neu5Gc, a component of gangliosides from most animal species, including mice, horses, sheep, and goats, via the action of the enzyme CMP-*N*-acetylneuraminic acid hydroxylase (CMAH). However, NeuGc is not synthesized in humans (or birds and New World monkeys), although it is present in other primates such as the great apes, and indeed, as it is a xenogeneic antigen, anti-NeuGc antibodies are produced normally in healthy humans (and especially after injection of NeuGc-containing glycoconjugates). The absence or irreversible inactivation of many relevant genes, but especially a critical exon in the *CMAH* gene, both for sialolipids and peptides in humans, suggests that this may have been a major biochemical branch-point in human evolution that occurred ~2 to 3 million years ago after the divergence of humans and chimpanzees from a common ancestor. It may even be a factor in the superior performance of the human brain, as the overexpression of Neu5Gc in the brains of transgenic mice was found to result in abnormal development. It could also mean that there might have been a fertility barrier between us and other hominids during evolution.

While these are speculations, there is some evidence that the loss of Neu5Gc in humans had complex effects on immunity, providing greater capabilities to clear sublethal bacterial challenges. Some NeuGc may be obtained from the diet in meat and milk, for example, and this may be incorporated into human gangliosides to a limited extent, especially in fetal tissues and some cancers. In the latter, the preferential expression of dietary Neu5Gc has been ascribed to their higher metabolic rate.

21.4.6.2: 2. STRUCTURE AND OCCURRENCE OF GANGLIOSIDES

Most of the common range of gangliosides are derived from the ganglio- and neolacto-series of **neutral oligoglycosphingolipids (Table 1)**, and they should be named systematically in the same way, with the position of the sialic acid residue(s) indicated as for branched structures. However, they are more conveniently defined by a short-hand nomenclature system proposed by Svennerholm in which M, D, T, and Q refer to mono-, di-, tri, and tetrasialogangliosides, respectively, and the numbers 1, 2, 3, etc refer to the order of migration of the gangliosides on thin-layer chromatography. For example, the order of migration of monosialogangliosides is GM3 > GM2 > GM1 (sometimes defined by subscripts, e.g., G_{M1} or GM_1). Further terms indicate variations within the basic structures, e.g., GM1a, GD1b, etc. Although alternatives have been proposed that are more systematic in structural terms, the Svennerholm nomenclature is the one approved by IUPAC-IUB. Ganglio-series glycosphingolipids having 0, 1, 2, and 3 sialic acid residues linked to the inner galactose unit are termed asialo- (or 0-), a-, b-, and c-series gangliosides, respectively, while gangliosides having sialic acid residues linked to the inner *N*-galactosamine residue are classified as α-series gangliosides. The structures for these groups are illustrated in the section on ganglioside **biosynthesis** below for practical convenience.

As of 2020, more than 200 gangliosides with variations in the carbohydrate chain had been characterized in vertebrates alone. One of the most studied monosialo-gangliosides and the first to be fully characterized is ganglioside GM1a (Neu5Acα2-3(Galβ1-3GalNAcβ1-4)Galβ1-4Glcβ1Cer), a major brain ganglioside of mammals and the preferred ligand of cholera toxin, illustrated in Figure **21.4.28**.

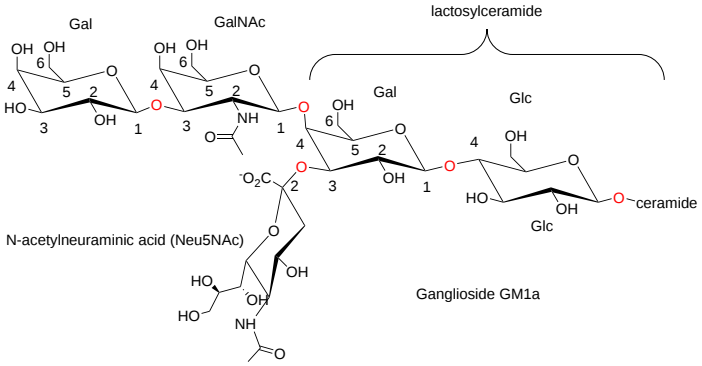


Figure 21.4.28: Ganglioside GM1a

It can also be depicted using the abbreviated structure in Figure 21.4.29.

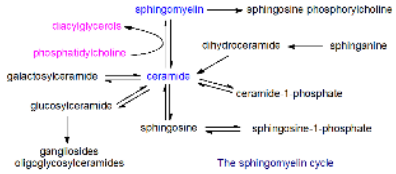


Figure 21.4.29: Abbreviated structure for Ganglioside GM1a

IUPAC-IUB recommends a less-used alternative nomenclature based upon the ganglion (Gg) root structure. This nomenclature employs Roman numerals to designate each hexose unit and the location of the Neu5Ac along the carbohydrate chain, with Arabic superscripts to designate the hydroxyl group to which this is linked. By this system, GM1a is defined as II^3-α-Neu5Ac-Gg_4Cer.

Brain gangliosides: Gangliosides can amount to 6% of the weight of lipids from the brain (20 to 500 times more than in other tissues), where they constitute 10 to 12% of the total lipid content (20-25% of the outer layer) of neuronal membranes, for example. Aside from this, they are synthesized and are present at low levels (1 to 2% of the total lipids) in all animal tissues, where, like the neutral oligoglycosphingolipids, they are concentrated in the outer leaflet of the plasma membrane in the nanodomains known as '**rafts**' or in related structures. Mammalian neurons actively primarily synthesize gangliosides of the ganglio-series. Still, oligodendrocytes in the brain produce myelin-forming glycosphingolipids, such as galactosylceramide and sulfatide, together with a minor amount of ganglioside GM4.

The brain contains as much as 20 to 500 times more gangliosides than most non-neural tissues, with three times as much gray as white matter. As the brain develops, there is an increase in the content of gangliosides and their degree of sialylation. There are large differences between species and tissues. For example, during embryogenesis and the postnatal period in the human central nervous system, the total amount of gangliosides increases approximately threefold, while that of GM1 and GD1a increases 12 to 15-fold. During the same period, the hemato-series gangliosides GM3, GD3, and 9-OAc-GD3, which lack a hexosamine residue, are the predominant ganglioside species. Still, they are present in much lower amounts in adults and in some areas of the brain only. In the mouse brain, the total amount of gangliosides is almost 8-fold greater in adults than in embryos, with a similar shift in composition from simple (GM3 and GD3) to more complex gangliosides. It is evident that the ganglioside changes during brain maturation are correlated with many neuro-developmental milestones, and there is no doubt that gangliosides play a crucial role in neuronal function and brain development, especially during infancy when there is high nutrient demand as the brain undergoes rapid restructuring.

The main gangliosides (~95%) of adult mammalian brain are ganglio series GM1, GD1a, GD1b, and GQ1b, while lactosyl series gangliosides such as GM3 (sialyllactosylceramide) are found mainly in the extra-neural tissues. The remaining ~5% consists of minor components in the brain, including gangliosides GM4, GM3, GD3, GM2, GD2, Fuc-GM1, Fuc-GD1b, GT1a, and GP1c, the proportions of which vary depending on species. On the other hand, modern mass spectrometric methodology (electrospray ionization ion mobility MS) has revealed a much higher degree of sialylation than was previously recognized, including a complete series of mono- to octasialylated gangliosides in fetal frontal lobe. Subsequently, this methodology found many previously unknown acetylated gangliosides in the fetal hippocampus. The content and composition of gangliosides in the brain also change with aging, with a substantial fall in the content of lipid-bound sialic acid but an increase in the proportion of the more complex forms in terms of carbohydrate structures in the elderly.

Gangliosides in other tissues and species: Among the extraneural tissues, lactosyl series gangliosides such as GM3 (sialyllactosylceramide) and monosialogangliosides, in general, tend to predominate. Relatively high concentrations of ganglioside GD1a are present in erythrocytes, bone marrow, testis, spleen, and liver. At the same time, GM4 is more abundant in the kidney, GM2 in the bone marrow, GM1 in erythrocytes, and GM3 in the intestine. In the germ cells of mice, there is a switch between gangliosides of the a- and 0-series upon differentiation when crossing the blood-testis barrier. Skin fibroblasts and many cells of visceral organs mainly generate

gangliosides of the globo series. Similarly, glob-o and lacto series gangliosides are characteristic components of the stage-specific embryonic antigens (SSEA), which underlie the development and differentiation of human embryonic stem cells. A sialyl-lactotetraosylceramide is present in the latter and the brains of children under two, but not in the tissues of adult humans. Gangliosides can cross the placental barrier into the fetus, and those in milk, derived from the apical plasma membrane of secretory cells of the mammary gland, may be of nutritional importance for the newborn. GD3 is the main ganglioside in human breast milk at an early stage of lactation, whereas GM3 is more abundant in the later stages (and in bovine milk). Unfortunately, gangliosides are poorly characterized and quantified in foods in general.

A 5-*N*-deacetylated form of ganglioside GM3 has been detected in human melanoma tumors. In addition, *O*-acetylation or lactonization of the sialic acid residue adds to the potential complexity. Gangliosides containing *O*-acetylated sialic acids, such as 9-*O*Ac-GD3, are expressed during embryonic development and in the retina and cerebellum of adult rats but not in other brain regions. They also occur in certain tumors and may protect them from apoptosis. Such gangliosides may be even more widespread, but they are missed after treatment with mild alkali during the isolation procedure, a common analytical practice. A further complexity is the occurrence of gangliosides with sulfate groups, which have been isolated from human, mouse, and monkey kidney cells. KDN-containing gangliosides are minor components of egg, ovarian fluid, sperm, and testis of fish and some mammalian tissues.

Gangliosides from marine invertebrates (echinoderms), such as starfish and sea cucumbers, are very different in structure from those in vertebrates and do not have a shorthand nomenclature. They include forms with distinctive ceramide compositions, untypical carbohydrate residues, sialic acids within the oligosaccharide chain, or glycosyl inositol-phosphoceramide structures. The mollusk, *Aplysia kurodai*, lacks gangliosides but produces complex oligoglycosylceramides with 2-aminoethylphosphonic acids and/or phosphoethanolamine groups attached that may serve as ganglioside surrogates.

Ceramide structures: In general, the ceramide structures of gangliosides tend to be relatively simple. Sphingosine is usually the main sphingoid base, accompanied by the C_{20} analog in the central nervous system gangliosides. Stearic acid (18:0) can be 80 to 90% of the fatty acid constituents in the brain, accompanied by small amounts of 16:0, 20:0, and 22:0, but with little or no polyunsaturated or 2-hydroxy acids, other than in some exceptional circumstances (e.g., some carcinomas). Palmitic acid is more abundant in the intestines and liver gangliosides, while 2-hydroxylated fatty acids are relatively abundant in the last and the kidney. There are also differences in the composition of the base and fatty acid components in different cells or regions of the brain. During development, the nature and concentrations of these constituents change markedly, and for example, the ratio of C_{20}/C_{18}-sphingosine in ganglioside GD1a of cerebellum increases 16-fold from 8-day-old to 2-year-old rats. In gangliosides outwith the nervous system, C_{20}-sphingosine is barely detectable, and there is often a much wider range of fatty acid constituents (C_{14} to C_{24}).

The nature of the ceramide component is relevant to the biological function of gangliosides, and changing the fatty acid component to α-linolenic acid by synthetic means dramatically alters the biological activity of gangliosides *in vitro*. However, the carbohydrate moiety is of primary importance for most of its functions, and a detailed discussion of these structures would take us into the realms of chemistry best left to carbohydrate experts (see the reading list below). The number of different gangliosides may be relatively small in any given cell type. Still, their nature and compositions may be characteristic and in some way related to the function of the cell. Notably, some terminal glycan structures of gangliosides are also present in the glycoproteins of membranes.

21.4.6.3: 3. BIOSYNTHESIS

Evidence shows that the pool of **glucosylceramide** and **lactosylceramide** utilized for ganglioside biosynthesis differs from the other neutral **oligoglycosylceramides**. This may explain differences between the two groups in the fatty acid and sphingoid base components, which will also depend on cell type. It is an open question of how the ganglioside precursors enter the Golgi and trans-Golgi network, where synthesis occurs at the luminal leaflet. Still, regulating intracellular sphingolipid traffic may be as important as controlling enzyme expression and activity in determining the final compositions of the various glycosphingolipid types.

In humans, sialic acid biosynthesis occurs through a series of reactions in the cytosol. The Neu5Ac produced is transferred to the nucleus and activated by the cytosine 5'-monophosphate *N*-acetylneuraminic acid synthetase (CMAS) to form CMP-Neu5Ac. This is transported to the Golgi apparatus by a family of sialyltransferases specific for particular glycosidic linkages (α2,3, α2,6, α2,8, and α2,9).

Thereafter, the pathways for the biosynthesis of the common series of gangliosides of the ganglio-series, for example, involve sequential activities of distinct membrane-spanning sialyltransferases and glycosyltransferases as illustrated in Figure **21.4.29** for the four main 0-, a-, b- and c-series of gangliosides.

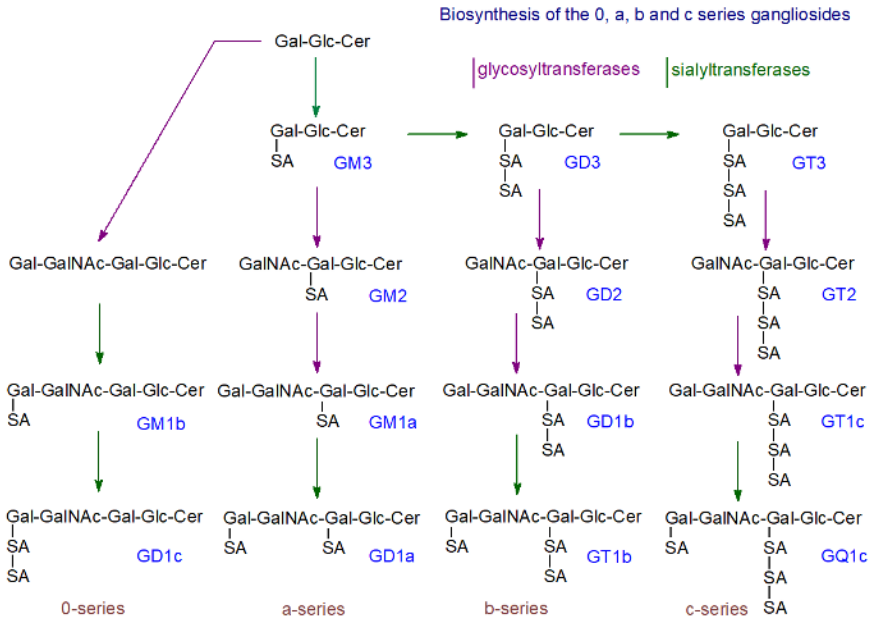


Figure **21.4.29**: Biosynthesis of gangliosides

The required enzymes are bound to the Golgi apparatus membranes in a sequence corresponding to the order of addition of the various carbohydrate components. Thus, the sialyltransferase that catalyzes the synthesis of the relatively simple ganglioside GM3 is located in the *cis*-region of the Golgi. In contrast, those that catalyse the terminal steps of ganglioside synthesis are located in the distal or *trans*-Golgi region. The GM3 synthase in particular, which catalyzes the transfer of Neu5Ac from cytidine monophosphate (CMP)-Neu5Ac onto the terminal galactose residue of lactosylceramide, has a unique specificity.

The simple ganglioside GM3 is synthesized by the addition of sialic acid to lactosylceramide by CMP:LacCer α2-3 sialyltransferase (or GM3 synthase), before GD3 and GT3 are produced in turn by the action of appropriate synthases. Subsequently, GM3, GD3, and GT3 serve as precursors of more complex gangliosides by the action of further glycosyl- and sialyl-transferases. An alternative theory with some supporting evidence proposes that a multiglycosyl-transferase complex synthesizes each ganglioside rather than a series of individual enzymes. Further sialylation of each of the a, b, and c series and in different positions in the carbohydrate chain can occur to give an increasingly complex and heterogeneous range of products, such as the α-series gangliosides with sialic acid residue(s) linked to the inner *N*-acetylgalactosamine residue (not illustrated). GM4 or NeuAcα2,3Gal-Ceramide, a minor component of the brain and present in a few other tissues at low levels, is an exception because galactosylceramide is its precursor. Finally, the newly synthesized gangliosides are transferred to the external leaflet of the plasma membrane via the luminal surface of transport vesicles. Gangliosides are also important constituents of nuclear membranes.

The changes that occur in the ganglioside compositions of brain and other tissues in the embryonic and postnatal stages are mainly governed by changes in the expression level and activity of the glycosyl- and sialyl-transferases, although the former can also be regulated by glycosylation and phosphorylation.

The presence of distinctive sialidases that differ from the catabolic lysosomal enzymes (see below) in raft-like regions of the plasma membrane bring about further changes in the composition of the cell surface gangliosides that can be specific to particular cell types, causing a shift from poly-sialylated species involving a decrease of GM3 and formation of GM2 then GM1 by hydrolysis of terminal sialosyl residues linked either α2-8 on another sialic acid or α2-3 on galactose. As GM1 is resistant to most sialidases, it tends to increase in concentration relative to oligosialo species as developmental and other GM1-requiring processes come into play. This may affect important cellular events, such as neuronal differentiation and apoptosis. Conversely, sialylation may occur in some neuronal membranes, increasing the proportions of poly-sialylated species. In particular, a CMP-NeuAc:GM3 sialyltransferase can sialylate GM3. Gangliosides GM1 and GD1a have been identified in both membranes of the nuclear envelope together with two neuraminidases.

Ganglioside lactones, where ester linkages connect the sialic acids, have been detected as minor components in brain tissues. Lactonization occurs at the plasma membrane. As lactonization profoundly influences the shape and biological properties of the original ganglioside, lactonization-delactonization in a membrane might trigger specific cellular reactions. Similarly, GD3 ganglioside can undergo *O*-acetylation at C9 of the outer sialic acid with important metabolic implications.

Gangliosides added to many types of cell preparations *in vitro* are rapidly taken up by the cells, while gangliosides injected into animals *in vivo* are rapidly internalized by tissues. They can cross the blood-brain barrier and enter the fetus via the placenta. Similarly, dietary

gangliosides are absorbed intact by intestinal cells. They can be broken down into their lipid and carbohydrate constituents for reuse. The sialic acids released by an intestinal sialidase are transported in plasma to the brain and other tissues, influencing ganglioside expression. Indeed, some experimental evidence shows that dietary gangliosides may improve cognitive functions in animals and humans.

21.4.6.4: CATABOLISM

The ganglioside degradation occurs at the surface of intralysosomal luminal vesicles, generated by an inward budding of the endosomal membrane, after endocytosis. In brief, in relation to gangliosides, soluble sialidases (neuraminidases) and exoglycohydrolases remove individual sialic acid and sugar residues sequentially from the non-reducing terminal unit, as illustrated for ganglioside GM1, with the eventual formation of ceramide, which is then split into long-chain base and fatty acids by ceramidases. This degradation occurs through the endocytosis-endosome-lysosome pathway, which requires an acidic pH inside the organelle. In addition to the sialidases and exoglycohydrolases, the various reactions have an absolute requirement for effector molecules, termed sphingolipid activator proteins, including saposins (Sap) and the specific GM2-activator protein (GM2-AP). Ganglioside GM3 is a component of the lysosomal membrane but is protected from degradation by a glycocalyx of the membrane facing the lysosome. Anionic lipids, especially **bis(monoacylglycero)phosphate** in the membranes, stimulate ganglioside degradation, while cholesterol is inhibitory. The catabolic pathway is shown in Figure **21.4.30**.

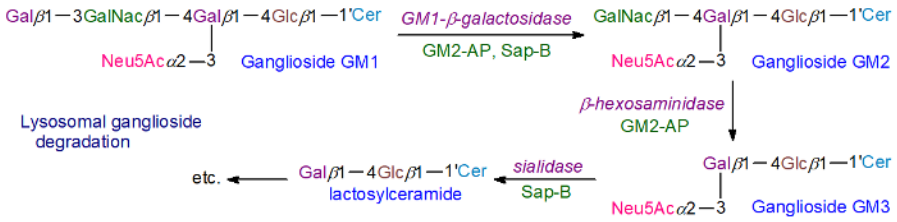


Figure **21.4.30**: Catabolism of gangliosides

This process constitutes a salvage mechanism important to the overall cellular economy since a high proportion of the various hydrolysis products are recycled for glycolipid biosynthesis. Generating ceramide and sphingosine may also be relevant to these lipids' regulatory and signaling functions. In addition, some partial hydrolysis of gangliosides occurs in the plasma membrane as part of the biosynthetic remodeling process discussed above. Defects in catabolism lead to the gangliosidoses, which will be discussed later.

21.4.6.5:

? GANGLIOSIDES - DETAILED BACKGROUND

Click the link below

Link

Ganglioside Function

Cell surface effects: In their natural biological environment, gangliosides have a negative charge because of sialic acids, which also add to the hydrophilicity of the polysaccharide constituent. This is balanced somewhat by the hydrophobic character of the ceramide moiety so that, overall, the molecules are amphiphilic but very different from the glycerophospholipids, which are essential for forming membrane bilayers. Indeed, a ganglioside such as GM1 is virtually soluble in water, where it can form large aggregates through hydrophilic effects. The nature of the ceramide unit, with its capacity to form hydrogen bonds with glycerophospholipids, is important in ensuring that gangliosides are inserted stably into the outer layer of the plasma membrane.

Thus, gangliosides are anchored in membranes by their ceramide units with the double-tailed sialoglycan components extending out from the cell surface, where they can participate in intermolecular interactions by a network of hydrogen bonds and hydrophobic interactions. For example, the glucose-ceramide bond of GM1 is oriented in the outer leaflet of the plasma membrane such that the glycan extends perpendicularly to the plane of the lipid bilayer. All gangliosides, but especially the simplest GM3 or Neu5Acα2-3Galβ1-4Glcβ1Cer, have a structural role, and they a natural propensity to segregate laterally and to associate with each other and with other sphingolipids, phospholipids and cholesterol into **raft** nano-domains or in related structures, such as the **caveolae**, where the very large surface area occupied by the oligosaccharide chain imparts a strong positive curvature to the membrane. In this environment, gangliosides can interact with each other through side-by-side hydrogen bonds mediated by water molecules that act as bridges between the chains.

Further, molecules of GM3 and other gangliosides self-aggregate into clusters on the surface of human peripheral blood lymphocytes, and there is evidence that the density of these clusters in membranes governs their reactivity as antigens. In addition, it is believed that gangliosides and other oligoglycosylceramides can cluster together through hydrogen donor-acceptor (*cis*)

interactions because of the presence of hydroxyl and acetamide groups to form glycosynaptic domains, which are related to but functionally distinct from raft signaling platforms (with lower cholesterol concentrations). Many of the biological functions of gangliosides are mediated through their location in these nanodomains, where they may have specialized functions in cell adhesion, growth, and motility through interactions with specific proteins and signal transduction pathways. However, not all gangliosides are present in such raft-like structures.

Receptor/signaling functions: Gangliosides can bind to membrane proteins directly by carbohydrate-carbohydrate or carbohydrate-amino acid interactions, usually involving specific ganglioside head groups, resulting in changes to the location of proteins within membrane microdomains for recruitment of signaling partners, or to dimerization or other effects upon receptors. In rafts and caveolae, especially, gangliosides can modulate cell signaling processes by interacting with specific receptors, adhesion molecules, and ion channels. Cell–cell (*trans*) interactions occur by sialoglycans on one cell binding to complementary binding proteins (lectins) on adjacent cells, bringing about adhesion of cells and enabling regulation of intracellular signaling pathways, e.g., myelin-associated glycoprotein on myelin sheaths binds to gangliosides present on axonal membranes.

In addition, gangliosides act as receptors of interferon, epidermal growth factor, nerve growth facto,r and insulin, and they may regulate cell signaling and control growth and differentiation of cells in this way. While intact gangliosides inhibit growth by rendering cells less sensitive to epidermal growth factor stimulation, removing the *N*-acetyl group of sialic acid enhances this reaction and stimulates growth. Gangliosides function as antigens or receptors by recognizing specific molecules (lectins), including bacterial toxins, at the cell surface and by modulating the charge density at the membrane surface (see the section on Gangliosides and Disease below). They also regulate the activities of proteins within the plasma membrane, especially receptor-type tyrosine kinases. For example, the phosphorylation state and activity of insulin receptors in caveolae and thence the insulin resistance of cells is controlled by the concentration of GM3, the main ganglioside in plasma and other extraneural tissues. GM3 also interacts with the epidermal growth factor receptor, leading to cell growth inhibition. GM1 strongly influences specific neuronal functions by interacting with specific receptors, such as the tropomyosin receptor kinase (Trk) A (TrkA) receptor, by altering its conformation to enable interaction with the nerve growth factor (NGF) ligand.

GM3 (SA-Gal-Glc-Cer) is a serum ganglioside that is highly enriched in a type of membrane microdomain termed a **glycosynapse**, and it forms complexes with co-localized cell signaling molecules. It has a function in the innate immune function of macrophages, and it has been demonstrated that molecular species of GM3 with differing acyl-chain structures and modifications can operate as pro- and anti-inflammatory modulators of Toll-like receptor 4 (TLR4); very-long-chain and α-hydroxy GM3 species increase TLR4 activation, while long-chain and unsaturated GM3 species have the opposite effect. In addition, gangliosides are cell-type-specific antigens that have key functions in immune defense. For example, a major immunological function of gangliosides and sialic acids is protecting cells from attack by our immune system and autoimmunity. They recognize and protect host organs and tissues from complement attack by binding to the complement regulatory protein factor H, which has the potential to exert strong cytotoxic and inflammation-inducing activity. In particular, sialic acids protect against complement killing of autologous cells by binding to this protein via the α2–3 linked sialic acid glycans of the GD3 ganglioside. On the other hand, the breakdown of this system can lead to autoimmune diseases.

Brain function: One of the first examples of a ganglioside influencing a signaling event to be studied in detail concerns the simple ganglioside GD3, which has a central role in early neurogenesis. GD3 binds to the epidermal growth factor receptor (EGFR) via a protein-carbohydrate interaction involving its terminal *N*-acetylneuraminic acid and a lysine residue in the transmembrane domain of the receptor and also by a carbohydrate-carbohydrate interaction, thereby maintaining the latter in its inactive monomeric state. EGFR then binds to the epidermal growth factor and stimulates the transition of the receptor from an inactive monomeric to an active homodimeric form, and this, in turn, triggers receptor auto-phosphorylation and activation of a signaling cascade that promotes cell proliferation. This has proven to be essential for the regulation of the stem cell self-renewal capacity in the brain. In contrast, the neutral oligoglycosphingolipid Gb4 exerts the opposite effect on EGFR by interacting directly with it to potentiate its auto-phosphorylation with activation of the downstream cascade.

The techniques of molecular biology, such as targeted gene deletion, which enable specific enzymes to be eliminated from experimental animals, are now leading to a better understanding of the function of each ganglioside. They are essential to central myelination, maintaining the integrity of axons and myelin, and transmitting nervous impulses. These effects may be mediated by interactions of gangliosides' negatively charged sialic acid residues with calcium ions, which are critical for neuronal responses. For example, a variant of GD3, 9-*O*-acetyl GD3, appears to be involved in glial-guided neuronal migration during brain development in the rat, while GM1 may have a similar function in humans; it determines which growth cone of unpolarized neurons becomes the axon. By stabilizing neuronal circuits, gangliosides function in memory, and conversely, disturbances in ganglioside synthesis can lead to neurodegenerative disorders (see below). Ganglioside GM3 in raft domains has been shown to have an indispensable role in the development, function, and viability of cochlear hair cells, and thence, it is essential for hearing. On the other hand, mice that

express GM3 primarily and are devoid of the typical complex gangliosides of the brain suffer weight loss, progressive motor and sensory dysfunction, and deterioration in spatial learning and memory with aging. GD3 is important for retinal structure and visual function in mice.

Nerve stimulation, environmental factors, or drug treatments can induce changes in ganglioside composition. The various interconvertible ganglioside types in the plasma membrane of neurons are particularly important for their development in that they regulate such processes as axonal determination and growth, signaling, and repair. In addition, gangliosides are believed to be functional ligands for maintaining myelin stability and controlling nerve regeneration by binding to a specific myelin-associated glycoprotein. The occurrence of gangliosides in cell nuclei suggests a possible involvement of gangliosides in the expression of genes relevant to neuronal function. For example, the monosialoganglioside **GM1** has been shown to promote the differentiation of various neuronal cell lines in culture. It has protective effects on the neural system by encouraging neural stem cell survival and proliferation while facilitating the stability and regeneration of axons and by inhibiting neurodegeneration through autophagy, for example, after ischemic stroke. Within membrane rafts, this ganglioside has key roles in several signaling systems through association with specific proteins that have glycolipid-binding domains, including those that modulate mechanisms such as ion transport, neuronal differentiation, G protein-coupled receptors (GPCRs), immune system reactivities, and neuroprotection. It is important for Ca^{2+} and Na^{+} homeostasis in the nucleus and plasma membrane, and in regulating the effects of platelet-derived growth factor. However, there have been unpleasant complications when GM1 has been administered for therapeutic purposes. GD1a is sometimes considered to be a reserve pool for GM1.

After nerve injury, toll-like receptor 2 (TLR2) signaling is important for the induction of neuropathic pain; ganglioside GT1b functions as a TLR2 agonist to produce mechanical and thermal hypersensitivity.

Other functions: The ganglioside GD3 is essential for the process of apoptosis by blocking the activation of specific transcription factors and disabling the induction of antiapoptotic genes. 9-*O*-Acetylation of the GD3 molecule prevents ganglioside oxidation and blocks its pro-apoptotic effects. Similarly, GD3 is a regulator of autophagy, i.e., the degradation and/or recycling of cellular components. Gangliosides are also important in reproduction, and in mice, GD1a is important to oocyte maturation, monospermic fertilization, and embryonic development, while GM1 is important in sperm-oocyte interactions and sperm maturation processes. Deletion of the GM2/GD2 synthase leads to infertility in male mice and the production of a novel fucosylated ganglioside containing very-long-chain polyunsaturated fatty acids. Related studies with gene knockout mice have revealed that b-series gangliosides are important in adipocyte leptin secretion. In contrast, a-series gangliosides interact with the leptin receptor in the hypothalamus to influence the energy balance.

Gangliosides and Disease

Bacterial toxins and viruses: In relation to adaptive immunity, a-series and o-series gangliosides in the plasma membrane are involved in the function and stimulation of receptors on certain subsets of T cells by acting as pattern-recognition receptors for invading pathogens. In particular, certain gangliosides bind specifically to viruses and to various bacterial toxins, such as those from botulinum, tetanus, and cholera, and to blood merozoites of the deadliest malaria parasite, *Plasmodium falciparum*, and they mediate interactions between microbes and host cells during infections, with NeuAc as the main recognition module. The best known example is the cholera toxin, an enterotoxin produced by *Vibrio cholerae*, where the specific cell surface receptor is ganglioside GM1; the five B-chains of cholera toxin each bind one molecule of GM1. Interestingly, the subsequent metabolism of the ganglioside-toxin complex depends on the nature of the fatty acid components of the ganglioside. It is believed that toxins utilize the gangliosides to hijack an existing retrograde transport pathway from the plasma membrane to the endoplasmic reticulum. For example, the passage of the cholera toxin through the epithelial barrier of the intestine is mediated by GM1, possibly by endocytosis of the toxin-GM1 complex via caveolae into the apical endosome and thence into the Golgi/endoplasmic reticulum, where the complex dissociates. The consequence is the persistent activation of adenylate cyclase by the toxin and the continuous production of cAMP that leads to the severe fluid loss typical of cholera infections. As a further example, the botulinus toxin binds to a complex of a polysialoganglioside with the protein synaptotagmin, which together act as a high-affinity receptor complex to enable the neurotoxic effects. Similarly, ganglioside GM2 binds to a toxin secreted by *Clostridium perfringens*.

Influenza viruses have two glycoproteins in their envelope membranes: hemagglutinin and neuraminidase. Hemagglutinin binds to cellular receptors such as gangliosides. After entering respiratory epithelial cells, the virus's sialidase (neuraminidase) cleaves the sialic acid from the receptors to prevent the entry of further viruses into the cell. Variations in the structure of these proteins force the development of new vaccines. The carbohydrate moiety of gangliosides is essential for the initial binding of viruses, but the lipid moiety is believed to be important for controlling their intracellular transport.

Some gangliosides, especially GD1a, have anti-inflammatory properties in that they inhibit the effects of bacterial lipopolysaccharides by preventing the activation of tumor necrosis factor (TNF) and other cytokines. In contrast, GM2 may increase

cytokine production in similar circumstances, while the heat-labile toxins of *Escherichia coli* bind to several gangliosides in macrophages, thus activating an inflammatory response.

Gangliosidoses and other neurodegenerative diseases: It appears to be a general rule that the mere process of lysosomal substrate accumulation in all lysosomal storage disorders impairs lysosome integrity and results in more general disruptions to lipid metabolism and membrane structure and function, inevitably triggering pathologic mechanisms. Endogenous generation of antibodies to gangliosides is often a factor, and it has been argued that gangliosides and their sialic acid components are at the border of immune tolerance.

As with the neutral **oligoglycosylceramides** and **ceramide monohexosides**, many unpleasant lipidoses have been identified that involve the storage of excessive amounts of gangliosides in tissues because of failures in the catabolic mechanism. The most important of these are the **GM2 gangliosidoses**, i.e., **Tay-Sachs disease** (and the similar Sandhoff disease), a fatal genetic disorder found mainly in Jewish populations in which harmful quantities of ganglioside GM2 accumulate in the nerve cells in the brain and other tissues. Lyso-GM2 (non-acylated) in plasma may serve as a marker. A modified GM2 derivative that contains taurine in amide linkage to the sialic acid carboxyl group has been identified in the brains of such patients. As infants with the most common form of the disease develop, the nerve cells become distended, and a relentless deterioration of mental and physical abilities occurs. The condition is caused by insufficient activity of specific enzymes, i.e., β-*N*-acetylhexosaminidase, which catalyzes the degradation of gangliosides by removing the terminal *N*-acetylgalactosamine residue from GM2 or the GM2 activator protein.

In addition, a generalized **GM1 gangliosidosis** (an autosomal recessive and neurodegenerative disease) has been characterized in which ganglioside GM1 accumulates in the nervous system, leading to mental retardation and enlargement of the liver. The condition results from a deficiency of the lysosomal β-galactosidase enzyme, which hydrolyses the terminal β-galactosyl residues from GM1 ganglioside to produce GM2. It appears that storage of substantial amounts of unwanted lipids in the lysosomal system leads to cellular starvation, so essential elements such as iron are depleted in brain tissue. The presence of lyso-GM1 in plasma is now seen as a useful aid to diagnosis. Small amounts of some gangliosides accumulate as secondary storage compounds in **Niemann–Pick** disease. The **Guillain–Barré syndrome** is an acute inflammatory disorder usually triggered by a severe infection affecting the peripheral nervous system. Antibodies to gangliosides are produced by the immune system, leading to damage to the axons, which can result in the patient's paralysis. Huntington’s disease is believed to involve disruption of the metabolic pathways between glycosylceramides and gangliosides, and a mutation to a sialyl transferase causes a human autosomal recessive infantile-onset epilepsy syndrome. Impaired ganglioside metabolism is also relevant to Alzheimer’s disease because complexation with ganglioside GM1 may cause aggregation of the amyloid β-protein deposits that characteristically accumulate in the brain in this condition (this explanation does not appear universally accepted). In general, in ganglioside deficiencies, natural or induced, progressive inflammatory reactions appear to occur, leading to neurodegeneration in part because of the deterioration of the architecture of lipid rafts.

On the other hand, at normal tissue concentrations, gangliosides such as GM1 are believed to have an anti-inflammatory and neuroprotective role in certain types of neuronal injury, Parkinsonism, and some related diseases. For example, in relation to Parkinson's disease, GM1 binds to α-synuclein and inhibits or eliminates fibril formation. It may have a protective role by preventing sphingomyelin-induced aggregation, but its beneficial effect decreases as the overall level of GM1 decreases during aging. For these reasons, the therapeutic properties of ganglioside GM1, the most accessible species, and derived molecules are under clinical investigation. However, there is no approved therapy for any gangliosidosis, although many different therapeutic strategies are being studied, including hematopoietic stem cell transplantation and gene therapy. For the moment, the blood-brain barrier remains a challenge.

Cancer: Gangliosides have essential functions in cancer, especially in regulating signal transduction induced by growth-factor receptors in a specific microdomain termed a 'glycosynapse' in the cancer cell membranes and interactions with glycan recognition molecules involved in cell adhesion and immune regulation. In particular, depending on the tissue, certain distinctive gangliosides are expressed at much higher levels in tumors than in normal healthy tissues, mainly by aberrant expression of glycosyltransferases and glycohydrolases. This enables tumor cells to escape immune surveillance and retain their malignancy. GM3 is not normally expressed in melanocytes but is detected in 60% of primary melanomas and 75% of metastatic melanomas, for example. Gangliosides can be shed from the surface of tumor cells into the local environment, where they can influence interactions between cancer cells, including the transition of tumors from a dormant to a malignant state (angiogenesis); when present in the circulation, they can be useful diagnostic aids. For example, the ganglioside GM3 is elevated in the serum of patients with breast cancer and may be a biomarker for the disease. In contrast, disialylated gangliosides GD2 and GD3 (Figure **21.4.31**) are considered to be markers of neuroectoderm origin in tumors (neuroblastoma).

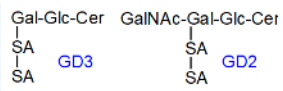


Figure 21.4.31: Structure GD2 and GD3

Specific gangliosides can have either positive or negative effects on regulating the malignant properties of cancer cells. Generally, disialyl glycosphingolipids or tandem-repeated sialic acid structures confer malignant properties in various cancer systems; they are not merely markers. For example, the disialo-gangliosides GD2 and GD3 are present in trace amounts only in normal tissues but are found at much higher concentrations in cancer cells, especially melanomas and neuroblastomas, with GD2 especially elevated in triple-negative breast cancer. These b-series gangliosides play a substantial part in the malignant properties of gliomas by mediating cell proliferation, migration, invasion, adhesion, and angiogenesis, and preventing immunosuppression. They are considered tumor-associated antigens, and the GD2 and GD3 synthases are important drug targets.

Ganglioside GM3(Neu5Gc), i.e., containing an abnormal sialic acid, is sometimes considered a tumor-specific antigen and a target for cancer immunotherapy. Aberrant sialylation is found in many malignant cancers, where the levels of neuraminidases are key factors for metastasis and survival of cancer cells, and there can be a significant accumulation of unusual gangliosides containing *N*-glycolyl sialic acid in some cancers. *N*-Glycolyl-GM3, normally absent from human tissues, is present in all stage II breast cancers, and many other less common complex gangliosides accompany it. Similarly, the 5-*N*-deacetylated form of GM3 is expressed in metastatic melanomas but not in healthy tissue or even in primary melanomas; it is considered a specific marker for the metastatic condition and a target for potential therapy. Increased synthesis of 9-*O*-acetyl-GD3, dependent on a sialyl-*O*-acetyltransferase - CAS1 Domain-Containing Protein 1, occurs in acute lymphoblastic leukemia and malignant melanomas, which appears to limit apoptosis. At the same time, *O*-acetylated GD2 (OAcGD2) is expressed in breast cancer and other tumors. A unique fucosyl-GM1 in which the terminal galactose is α-1,2-fucosylated at the non-reducing end is found circulating in the serum of patients with many cancers, especially with small-cell lung cancer, but rarely in normal conditions, and it is also considered to be a potential indicator of cancer and a candidate for immunotherapy.

Clinical trials with an antibody to GD2 have been carried out successfully against the rare childhood cancer neuroblastoma, and the USDA has approved the use of this in combination with other drugs to treat this often lethal cancer. However, this antibody can have painful side effects due to an interaction with GD2 on neurons, and modified antibodies, which may be safer, are now being tested in multiple clinical trials. A phase I clinical trial with an antibody to GD3 has shown promising results in patients with malignant melanoma. Similarly, antibodies to OAcGD2 and fucosyl-GM1 have shown anti-tumor effects *in vitro*, and studies with human patients are underway.

Other diseases: Aberrant production of the ganglioside GM3 has been linked to pathophysiological changes associated with obesity, metabolic disorders, and type 2 diabetes mellitus through its effects on insulin receptors. It has a role in autoimmune disorders such as multiple sclerosis. In epilepsy, it is believed that a deficiency in the enzyme ceramide synthase 1, which produces 18:0 ceramides, leads to reduced ganglioside formation. Gangliosides influence allergic responses and autoimmune diseases by their presence in certain T cell subsets. As gangliosides are present on the surface of vascular, vascular-associated, and inflammatory cells, they may have a role in atherosclerosis and aging.

In contrast, monosialyl gangliosides, such as GM1, GM2, and GM3, may suppress the malignant properties of various cancer cells. The mechanism is believed to involve complex formation at the cell surface with membrane proteins, such as growth factor receptors and adhesion receptors like those of the integrin family, leading to the modification of cell signals mediated by these receptors. Metastatic melanoma cells have high levels of GD3 compared to poorly metastatic cells or the normal counterpart, suggesting that GD3 may promote metastasis by suppressing the anti-tumor immune response.

21.4.7: SUMMARY

Sphingolipids are a diverse and biologically crucial class of lipids that are defined by the presence of a sphingoid (long-chain) base. Historically first noted by Thudichum for their “enigma” and later formally named by Carter, these lipids now stand recognized for their versatile structural and signaling roles across eukaryotic organisms—and even in select bacteria.

Key Structural Features and Diversity:

At their core, sphingolipids are built from long-chain sphingoid bases, with sphingosine being the archetypal example. These bases can vary in chain length, saturation, and degree of hydroxylation, which, when coupled to fatty acids via amide bonds, form ceramides. Ceramides serve as the central intermediates for the biosynthesis of more complex sphingolipids, such as sphingomyelin and glycosphingolipids (e.g., glucosylceramide, galactosylceramide, and gangliosides). The unique “sphingoid motif”—the first five carbons of the sphingoid base—enables extensive hydrogen bonding and electrostatic interactions, influencing membrane organization and the formation of dynamic nanodomains known as lipid rafts.

Biosynthesis and Metabolic Pathways:

Sphingolipid biosynthesis initiates at the endoplasmic reticulum (ER) with the enzyme serine palmitoyltransferase catalyzing the condensation of L-serine and palmitoyl-CoA, forming 3-keto-sphinganine, which is then reduced to sphinganine. Ceramide synthases subsequently acylate sphinganine to generate dihydroceramide, which is desaturated to produce ceramide. Ceramides are further processed through glycosylation or phosphorylation reactions to yield complex sphingolipids. A key metabolic cycle—the sphingomyelin cycle—reversibly interconverts sphingomyelin and ceramide via the action of sphingomyelin synthases and sphingomyelinases, enabling rapid cellular responses to various stimuli.

Functional Roles in Cells:

Sphingolipids are not only essential components of cellular membranes but also potent signaling molecules. They regulate processes such as apoptosis, cell proliferation, and differentiation. Ceramides often act as pro-apoptotic signals, while sphingosine-1-phosphate (S1P) promotes cell survival and proliferation; together, they form a "sphingolipid rheostat" that is critical for determining cell fate. Furthermore, sphingolipids contribute to the formation and stabilization of lipid rafts, which are microdomains that serve as platforms for receptor clustering and signal transduction.

Biological and Clinical Significance:

Dysregulation of sphingolipid metabolism is implicated in a range of human diseases—from lysosomal storage disorders (like Gaucher and Niemann-Pick diseases) to neurodegenerative conditions (such as Alzheimer's and Parkinson's), diabetes, and various cancers. Understanding the enzymes and pathways that regulate sphingolipid levels is therefore pivotal for developing new therapeutic strategies.

Comparative Aspects:

While animal cells predominantly contain sphingomyelin, plants and fungi synthesize distinct sphingolipids (e.g., ceramide phosphorylinositol and glycosylinositol phosphorylceramides). Even among bacteria, sphingolipid production is limited to a few genera, underscoring the evolutionary specialization of these molecules.

Analytical Advances:

Recent advances in mass spectrometry and molecular biology techniques have allowed researchers to unravel the complexity of sphingolipid molecular species, their biosynthetic regulation, and their roles in health and disease, making this an exciting and rapidly evolving field.

Overall, sphingolipids exemplify the intricate interplay between lipid structure and cellular function, offering insights into both the fundamental mechanisms of membrane organization and the regulation of key signaling pathways that affect organismal health.

This page titled 21.4: Biosynthesis of Membrane Sphingolipids is shared under a not declared license and was authored, remixed, and/or curated by Henry Jakubowski and Patricia Flatt.

- **Current page** by Henry Jakubowski and Patricia Flatt has no license indicated.
- **11.2: Diffusion Across a Membrane - Passive and Facilitated Diffusion** by Henry Jakubowski and Patricia Flatt has no license indicated.

21.5: BIOSYNTHESIS OF CHOLESTEROL AND STEROIDS

By William (Bill) W. Christie and Henry Jakubowski.

This section is an abbreviated and modified version of material from the Lipid Web, an introduction to the chemistry and biochemistry of individual lipid classes, written by William Christie.

LEARNING GOALS (CHATGPT O3-MINI)

1. **Structural Understanding:**
   - Describe the molecular structure of cholesterol, including its tetracyclic cyclopenta[a]phenanthrene nucleus, iso-octyl side chain, and functional groups (e.g., the 3β-hydroxyl group and the Δ5 double bond).
   - Explain how the structure of cholesterol relates to its orientation and interaction within the lipid bilayer (e.g., using the diamond lattice model to illustrate atomic positions and interactions).
2. **Membrane Organization and Function:**
   - Analyze the distribution of cholesterol among various cellular membranes (plasma membrane, endoplasmic reticulum, Golgi apparatus, mitochondria) and explain the functional significance of its uneven distribution.
   - Explain how cholesterol modulates membrane fluidity, thickness, and permeability by interacting with phospholipids (e.g., phosphatidylcholine, sphingomyelin) and how these interactions lead to the formation of ordered microdomains (rafts).
3. **Biosynthesis of Cholesterol:**
   - Outline the cholesterol biosynthetic pathway from acetyl-CoA via the mevalonate pathway, highlighting key intermediates (e.g., HMG-CoA, mevalonate, squalene, lanosterol) and the role of critical enzymes such as HMG-CoA reductase.
   - Discuss the energetic cost and oxygen requirements of cholesterol synthesis, and describe how this process is tightly regulated (including feedback by sterol levels and regulation via SREBP and SCAP).
4. **Cholesterol Esterification and Transport:**
   - Explain the biosynthesis and hydrolysis of cholesterol esters, including the roles of enzymes such as lecithin:cholesterol acyltransferase (LCAT) and acyl-CoA:cholesterol acyltransferase (ACAT).
   - Describe how cholesterol esters are packaged into lipoproteins (e.g., HDL, LDL, VLDL) and the importance of these processes in cholesterol transport and storage.
5. **Regulation and Homeostasis:**
   - Discuss the mechanisms that maintain cholesterol homeostasis in cells, including the roles of intracellular cholesterol pools, feedback inhibition of biosynthetic enzymes, and the regulation of cholesterol uptake (via LDL receptors) and efflux (via ABC transporters).
   - Evaluate the role of oxysterols (oxygenated cholesterol derivatives) in modulating cholesterol synthesis and immune responses through nuclear receptor activation (e.g., LXR).
6. **Pathophysiological Implications:**
   - Analyze how disruptions in cholesterol metabolism contribute to human diseases, such as cardiovascular disease, atherosclerosis, gallstone formation, and various neurodegenerative disorders.
   - Assess the impact of pharmacological agents (e.g., statins) on cholesterol biosynthesis and discuss current and emerging therapeutic targets within the cholesterol metabolic pathway.
7. **Comparative and Integrated Perspectives:**
   - Compare cholesterol metabolism in animals with that of plant sterols (phytosterols), noting both similarities and key differences in structure, biosynthesis, and functional roles.
   - Integrate knowledge of cholesterol structure, synthesis, regulation, and transport to predict how alterations in these processes may influence cell signaling, membrane dynamics, and overall human health.

These learning goals aim to ensure that students can critically analyze the multifaceted roles of cholesterol and its derivatives in cellular biochemistry and understand their broader implications for human physiology and disease.

21.5.1: STEROLS: CHOLESTEROL AND CHOLESTEROL ESTERS

In animal tissues, **cholesterol** (cholest-5-en-3β-ol) is by far the most abundant member of a family of polycyclic compounds known as **sterols**. It can also be described as a polyisoprenoid or a triterpene from its biosynthetic origin. Cholesterol was first recognized as a component of gallstones as early as 1769, while the great French lipid chemist Michel-Eugène Chevreul isolated it from animal fats in 1815. However, it was not until well into the 20th century that the structure was fully defined by the German Chemist Heinrich Wieland, who received the Nobel Prize in Chemistry for his work in 1927, the first of thirteen so honored for research on cholesterol and its metabolism.

Cholesterol plays a vital role in animal life, and it is essential for the normal functioning of cells both as a structural component of cell membranes and as a precursor of steroid hormones and other key metabolites, including vitamin D and bile acids. It is also important for cell signaling, transport processes, nerve conduction, and the regulation of gene transcription. Every cell in vertebrates is capable of both synthesizing and metabolizing cholesterol, and there is evidence that de novo synthesis is essential, regardless of dietary intake; this process is particularly vital in the brain. However, excess cholesterol can contribute to the pathology of various diseases, notably cardiovascular disease, so cholesterol levels must be balanced to ensure an adequate but not excessive supply.

21.5.1.1: CHOLESTEROL – STRUCTURE, OCCURRENCE, AND FUNCTION IN MEMBRANES

The structure of cholesterol is shown below in Figure **21.5.1**.

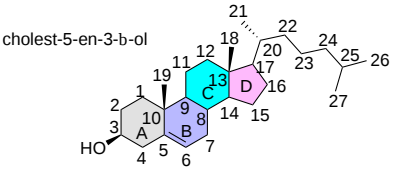


Figure **21.5.*xx***:

Cholesterol consists of a tetracyclic cyclopenta[a]phenanthrene structure with an *iso*-octyl side-chain at carbon 17. The four rings (A, B, C, D) have *trans* ring junctions, and the side chain and two methyl groups (C-18 and C-19) are at an angle to the rings above the plane with β stereochemistry (as for the hydroxyl group on C-3 also); there is a double bond between carbons 5 and 6. Thus, the molecule has a rigid planar four-ring nucleus with a flexible tail. Of the two recognized numbering systems in use, one originally described by Fieser and Fieser in 1959 and a second by IUPAC-IUB in 1989, the first appears to be preferred by most current authors.

Most of the atoms in cholesterol can be placed on the diamond lattice, which is the structure showing the position of each carbon atom in the network solid diamond. In that structure, each carbon is connected to four other carbons using sp^3-hybridized atomic orbitals and a tetrahedral geometry. A representation of the diamond lattice is shown below. It consists of a series of interconnected boat conformations of cyclohexane propagating in the xyz direction. The structures of two different fused cyclohexanes, trans- and cis-decalins, as well as the structure of three fused cyclohexanes, adamantane, are shown in Figure **21.5.2**. Superimposing sp^3-connected atoms onto a diamond lattice allows improved visualization of the real and allowed structures of more complicated molecules.

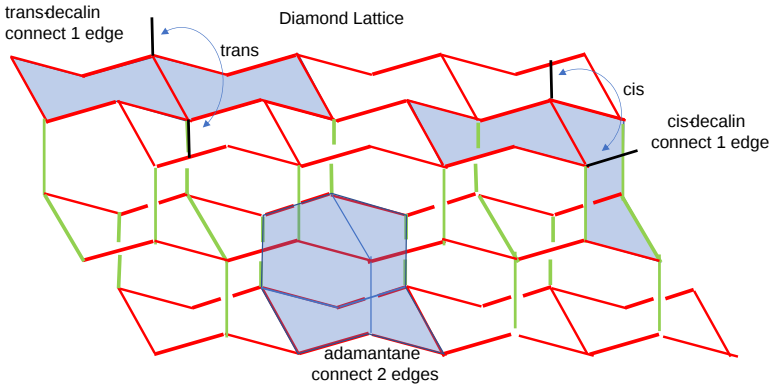


Figure **21.5.2**: The diamond lattice showing decalins and adamantane

Figure **21.5.3** shows a superposition of 5-α-cholestane, a reduced and non-hydroxylated form of cholesterol, onto the diamond lattice. The pink cyclopentane D ring of 5-α-cholestane, which is distorted from the 109^0 bond angle for sp^3-hybridized carbon atoms, does not fit exactly onto the lattice. Cholesterol, with its double bond, would also deviate from the ideal position on the diamond lattice, given the two sp^2-hybridized carbons in the double bond.

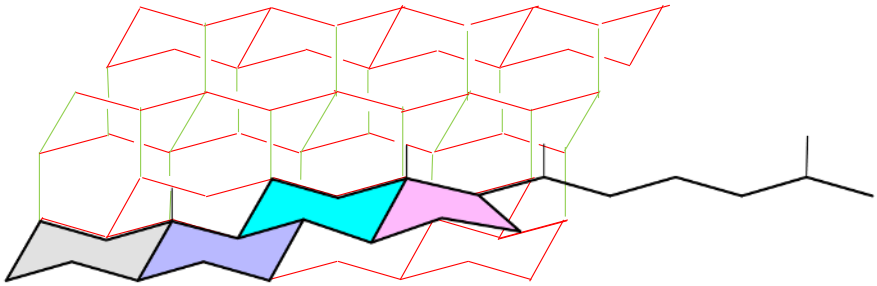


Figure **21.5.3**: The diamond lattice showing 5-α-cholestane

Cholesterol is a ubiquitous component of all animal tissues (and of some fungi), produced by every nucleated animal cell, where much of it is located in the membranes, although it is not evenly distributed. The highest proportion of unesterified cholesterol is found in the plasma membrane, accounting for roughly 30-50% of the lipid in the membrane or 60-80% of the cholesterol in the cell. In comparison, mitochondria and the endoplasmic reticulum contain significantly less (~5% in the latter), while the Golgi contains an intermediate amount. Cholesterol is also enriched in early and recycling endosomes, but not in late endosomes. It may surprise some to learn that the brain contains more cholesterol than any other organ, comprising roughly a quarter of the total free cholesterol in the human body, with 70-80% of this cholesterol found in the myelin sheath. Of all the organic constituents of blood, only glucose is present in a higher molar concentration than cholesterol. In animal tissues, it occurs in the free form, esterified to long-chain fatty acids (**such as cholesterol esters**), and in other covalent and non-covalent linkages, including associations with **plasma lipoproteins**. In plants, it tends to be a minor component only of a complex mixture of structurally related '**phytosterols**'. However, there are exceptions; nevertheless, it is important as a precursor to some plant hormones.

Animals in general synthesize a high proportion of their cholesterol requirement, but they can also ingest and absorb appreciable amounts from foods. On the other hand, many invertebrates, including insects, crustaceans, and some molluscs, are unable to synthesize cholesterol and must obtain it from their diet; for example, spiny lobsters must obtain exogenous cholesterol to produce essential sex hormones. Similarly, it must be supplied from exogenous sources to the primitive nematode *Caenorhabditis elegans*, where it does not appear to have a major role in membrane structure, other than perhaps in the function of ion channels, although it is essential for the production of steroidal hormones required for larval development; the novel lipid **phosphoethanolamine glucosylceramide regulates its uptake**. Some species can convert dietary plant sterols, such as β-sitosterol, into cholesterol. Prokaryotes lack cholesterol entirely except for some pathogens that acquire it from eukaryotic hosts to ensure their intracellular survival (e.g., *Borrelia sp.*); bacterial **hopanoids** are often considered to be sterol surrogates.

Cholesterol plays vital structural roles in membranes and lipid metabolism, with an extraordinary diversity of biological functions, including cell signaling, morphogenesis, lipid digestion and absorption in the intestines, reproduction, stress responses, sodium and water balance, and calcium and phosphorus metabolism. We can only touch on a few of these functions in this web page. It is a biosynthetic precursor of bile acids, vitamin D, and steroid hormones (glucocorticoids, estrogens, progesterones, androgens, and aldosterone), and it is found in covalent linkage to specific membrane proteins or **proteolipids** ('hedgehog' proteins), which have vital functions in embryonic development. Additionally, it plays a significant role in the development and functioning of the central nervous system. On the other hand, excess cholesterol in cells can be toxic, and a complex web of enzymes is essential to maintain the optimum concentrations. Because plasma cholesterol levels can be a major contributory factor to atherogenesis, media coverage has created what has been termed a 'cholesterophobia' in the population at large.

One of the primary functions of cholesterol is to regulate the fluidity of membranes by interacting with their complex lipid components, specifically phospholipids such as phosphatidylcholine and sphingomyelin. As an amphiphilic molecule, cholesterol can intercalate between phospholipids in lipid bilayers to span about half a bilayer. In its three-dimensional structure, it is, in essence, a planar molecule that can interact on both sides. The tetracyclic ring structure is compact and very rigid. Additionally, the location of the hydroxyl group facilitates the orientation of the molecule within a membrane bilayer. The positions of the methyl groups appear to maximize interactions with other lipid constituents. The structure of cholesterol as it would appear on the diamond lattice is shown in Figure **21.5.4**.

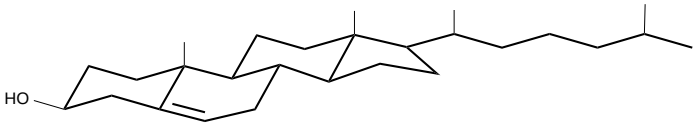


Figure **21.5.4**: "Diamond" lattice structure of cholesterol

As the α-face of the cholesterol nucleus (facing down) is 'smooth', it can make good contact with the saturated fatty-acyl chains of phospholipids down to about their tenth methylene group; the β-face (facing up) is made 'rough' by the projection of methyl groups from carbons 10 and 13. The interaction is primarily mediated by van der Waals and hydrophobic interactions, with a contribution from hydrogen bonding between the cholesterol hydroxyl group and the polar head group and interfacial regions of the phospholipids, especially sphingomyelin. Intercalated cholesterol may also disrupt electrostatic interactions between the ionic phosphocholine head groups of nearby membrane phospholipids, leading to increased mobility of the head groups. Indeed, there is evidence that cholesterol forms stoichiometric complexes with the saturated fatty acyl groups of sphingomyelin and, to a lesser extent, phosphatidylcholine.

Experiments with mutant cell lines and specific inhibitors of cholesterol biosynthesis suggest that an equatorial hydroxyl group at C-3 of sterols is essential for the growth of mammalian cells. The Δ5 double bond ensures that the molecule adopts a planar conformation, and this feature also appears to be essential for cell growth, as is the flexible *iso*-octyl side-chain. The C-18 methyl group is crucial for the proper orientation of the sterol. While plant sterols appear to be able to substitute for cholesterol in supporting many of the bulk properties of membranes in mammalian cells *in vitro*, cholesterol is essential for other purposes.

In the absence of cholesterol, a membrane composed of unsaturated lipids is in a fluid state that is characterized by a substantial degree of lipid chain disorder, i.e., it constitutes a *liquid-disordered* phase. The function of cholesterol is to increase the degree of order (cohesion and packing) in membranes, leading to the formation of a *liquid-ordered* phase. In contrast, it renders bilayers composed of more saturated lipids, which would otherwise be in a solid gel state, more fluid. Thus, cholesterol can promote and stabilize a liquid-ordered phase over a substantial range of temperatures and sterol concentrations. Further, high cholesterol concentrations in membranes reduce their passive permeability to solutes. These effects enable membranes to bend or withstand mechanical stresses, and they permit the fine-tuning of membrane lipid composition and organization, and regulate critical cell functions. Simplistically, the higher cholesterol concentrations in the plasma membrane support its barrier function by increasing membrane thickness and reducing its permeability to small molecules. In contrast, the endoplasmic reticulum has increased membrane flexibility due to its lower cholesterol concentration, which enables the insertion and folding of proteins into its lipid bilayer. While mitochondrial membranes have a low cholesterol content overall, this may be concentrated in nanodomains at regions of high curvature in the inner mitochondrial membrane, with links to nucleoprotein complexes (nucleoids).

In comparison to other lipids, it has been reported that cholesterol can flip rapidly between the leaflets in a bilayer; however, this is not universally accepted, leading to doubts about the trans-bilayer distribution of cholesterol in some biological membranes. However, much recent evidence suggests that the concentration of cholesterol in the inner leaflet of the plasma membrane is much lower than that in the outer leaflet in a range of mammalian cells. This distribution is significant because cholesterol promotes negative curvature of membranes and may be a crucial factor in facilitating membrane fusion during the process of exocytosis. It may also be relevant for regulating various cellular signaling processes at the plasma membrane.

Cholesterol also plays a key role in the lateral organization of membranes and their free volume distribution, which allows for more intimate protein-cholesterol interactions that may regulate the activities of membrane proteins. Many membrane proteins bind strongly to cholesterol, including some that are involved in cellular cholesterol homeostasis or trafficking, and contain a conserved region termed the ‘sterol-sensing domain’. Some proteins bind to cholesterol deep within the hydrophobic core of the membrane via binding sites on the membrane-spanning surfaces or in cavities or pores in the proteins, driven by hydrogen bond formation. Cholesterol has an intimate interaction with G-protein-coupled receptors (GPCRs) to affect ligand binding and activation, either by direct high-affinity binding to the receptor, by changing their oligomerization state, or by inducing changes in the properties of the membrane. For example, it is essential for the stability and function of the β2-adrenergic, oxytocin, and serotonin receptors by increasing the agonist affinities. The inactive state of rhodopsin is stabilized both through indirect effects on plasma membrane curvature and by a direct interaction between lipid and protein. The GPCR neurotransmitter serotonin 1A receptor has ten closely bound cholesterol molecules, which control its organization and positioning. The receptor senses membrane cholesterol via a lysine residue in a so-called 'CRAC' motif in transmembrane helix 2.

Ion pumps, such as the (Na^+-K^+)-ATPase, which have specific binding sites for cholesterol molecules, are the single most important consumers of ATP in cells and are responsible for the ion gradients across membranes that are essential for many cellular functions; depletion of cholesterol in the plasma membrane deactivates these ion pumps. In the brain, in addition to being essential for the structure of the myelin sheath, cholesterol is a major component of synaptic vesicles and controls their shape and functional properties. In the nucleus of cells, cholesterol plays an important role in the structure and function of chromatin.

The role of cholesterol, together with sphingolipids, in the formation of transient membrane nano-domains known as **rafts** is crucial for cell function, while the interaction of cholesterol with **ceramides** is essential for the skin's barrier function.

21.5.1.2: CHOLESTEROL BIOSYNTHESIS

Cholesterol biosynthesis involves a highly complex series of at least thirty different enzymatic reactions, which were largely unraveled by Konrad Bloch and Fyodor Lynen, who received the Nobel Prize for their work on the topic in 1964. When the various regulatory, transport,

and genetic studies of recent years are taken into account, it is clear that this subject cannot be treated in depth here. The bare bones of the mechanistic aspects are therefore delineated, which should serve as a guide for further study. In **plants**, cholesterol synthesis occurs by a somewhat different pathway with cycloartenol as the key intermediate. We will explore the reaction mechanisms of several enzymes on this complex pathway, given its medical importance.

Almost all nucleated cells can synthesize their full complement of cholesterol. The first steps involve the synthesis of the important intermediate mevalonic acid from acetyl-CoA and acetoacetyl-CoA, both of which are derived from acetate, in two enzymatic steps. These precursors are located in the cytosol, as is the first enzyme, **3-hydroxy-3-methylglutaryl (HMG)-CoA synthase**. The second enzyme, **HMG-CoA reductase,** is a particularly important control point and is widely regarded as the rate-limiting step in the overall synthesis of sterols. Its activity is regulated at the transcriptional level and by several additional factors, including a cycle of phosphorylation and dephosphorylation. This and subsequent enzymes are membrane-bound and are located in the endoplasmic reticulum. The enzyme HMG-CoA reductase is among the targets inhibited by the drugs known as 'statins', so that patients must then obtain much of their cholesterol from the diet. The first two reactions in the synthesis of cholesterol are shown in Figure **21.5.5**.

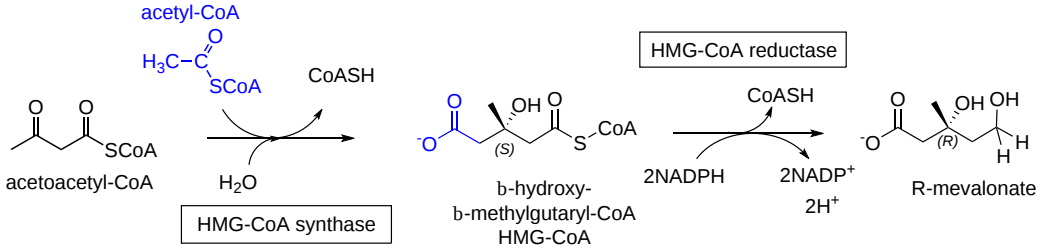


Figure **21.5.5**: First two reaction in the synthesis of cholesterol

HMG-CoA Synthase

We saw this reaction in the synthesis of ketone bodies in Chapter 17. This enzyme catalyzes the condensation of acetoacetyl-CoA–CoA (AcAc–CoA) and acetyl–CoA (Ac-CoA) to form 3-hydroxy-3-methylglutaryl (HMG)–CoA, and requires the formation of a C-C bond. HMG-CoA synthase forms a C-C bond by activating the methyl group of **acetyl-cysteine**. The acetyl group originates from an acyl-CoA donor. The enzyme catalyzes the first committed step in the formation of complex isoprenoids, such as cholesterol and ketone bodies. The product, 3-hydroxy-3-methylglutaryl HMG–CoA, can either be reduced by HMG-CoA reductase to form mevalonate, which leads to cholesterol synthesis, or cleaved by the enzyme HMG-CoA lyase to produce acetoacetate, a ketone body.

HMG-CoA synthase catalyzes a bisubstrate reaction that displays ping-pong kinetics, characteristic of a covalent enzyme intermediate. The first substrate binds to the enzyme and transfers an acetyl group to the nucleophilic Cys 111 in the active site, forming an acetyl-Cys 111 intermediate. Free CoA departs. Next, the second substrate, acetoacetyl-CoA, binds and condenses with the acetyl group donated by acetyl-Cys 111. This condensation involves an enolate. A plausible reaction mechanism is shown in Figure **21.5.6**.

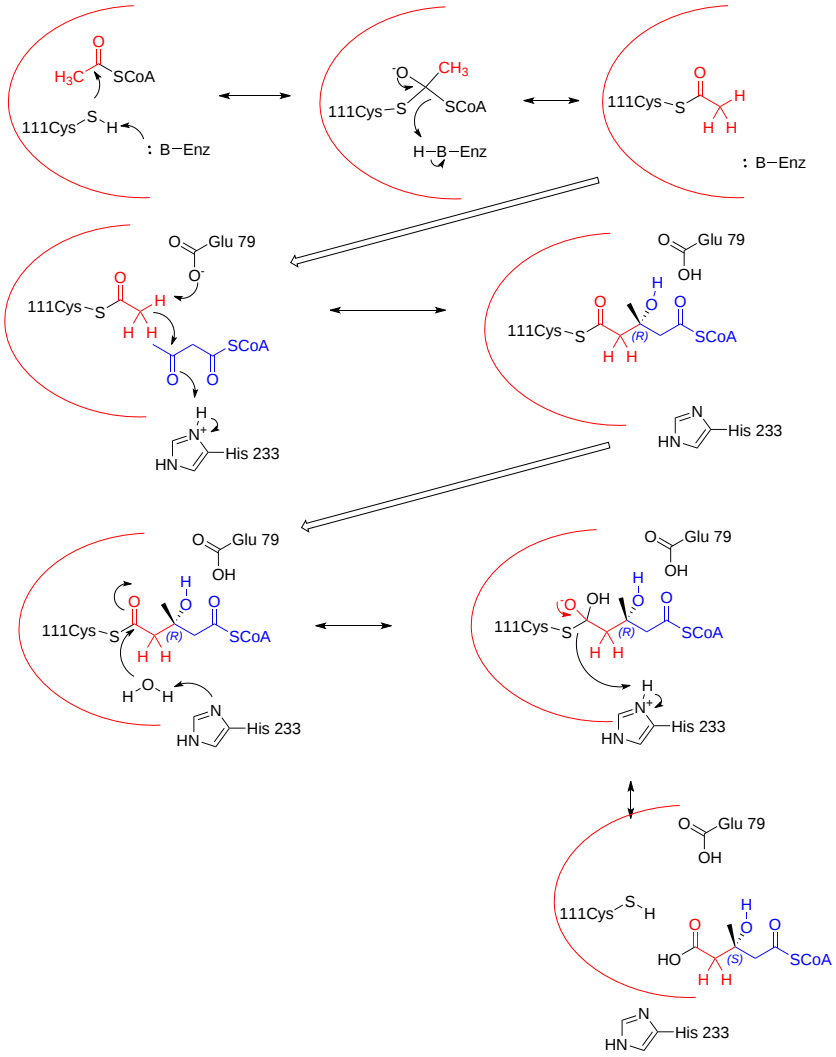


Figure 21.5.6: Reaction mechanism for HMG-CoA synthase

Hence, there are three parts of the reaction: acetylation/deacetylation, condensation/cleavage with an enolate intermediate, and C-C formation and hydrolysis/dehydration. Figure 21.5.7 shows an interactive iCn3D model of the Staphylococcus aureus HMG-COA Synthase with bound HMG-CoA and acetoacetyl-CoA (1XPK).

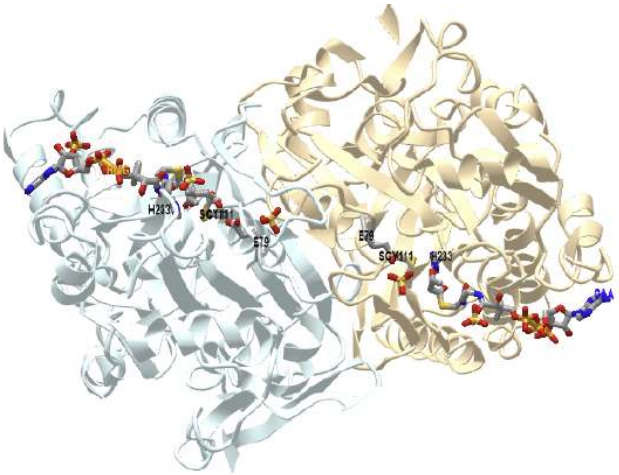


Figure 21.5.7: Staphylococcus aureus HMG-COA Synthase with bound HMG-CoA and acetoacetyl-CoA (1XPK). (Copyright; author via source). Click the image for a popup or use this external link: https://structure.ncbi.nlm.nih.gov/i...deiFs7JceE5H76

The biologically active unit (homodimer) is shown, with each monomer shown in a different color. The A chain (light cyan) has bound HMG-CoA (HMG) while the B chain (light gold) has acetoacetyl-CoA (CAA) bound. The Glu 79, Cys 111, and His 233 in each subunit are shown in CPK sticks and labeled. Note that Cys 111 is covalently modified in each subunit.

Figure **21.5.8** shows an interactive iCn3D model of the human 3-hydroxy-3-methylglutaryl CoA synthase I with bound CoASH (2P8U)

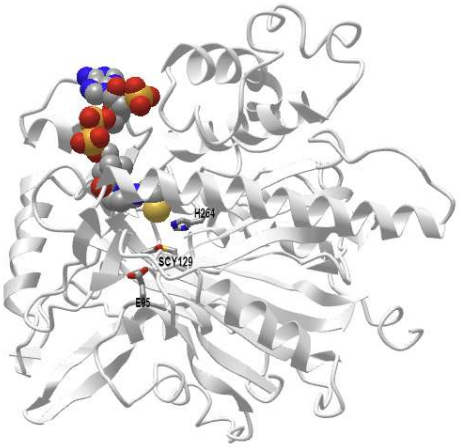


Figure **21.5.8**: Human 3-hydroxy-3-methylglutaryl CoA synthase I (monomer) with bound CoASH (2P8U). (Copyright; author via source). Click the image for a popup or use this external link: https://structure.ncbi.nlm.nih.gov/i...xxEoUfecTk3eL6

The active site side chains are numbered differently (Glu 95, Cys 129, and His 264) compared to the S. aureus protein. Only the monomer is shown in this model.

HMG-CoA Reductase

In this key rate-limiting step that commits HMG to the sterol and isoprenoid synthetic pathways, HMG is converted to mevalonate. A reducing agent, such as NADPH, is required for this biosynthetic reaction. A plausible mechanism is shown in Figure **21.5.9**.

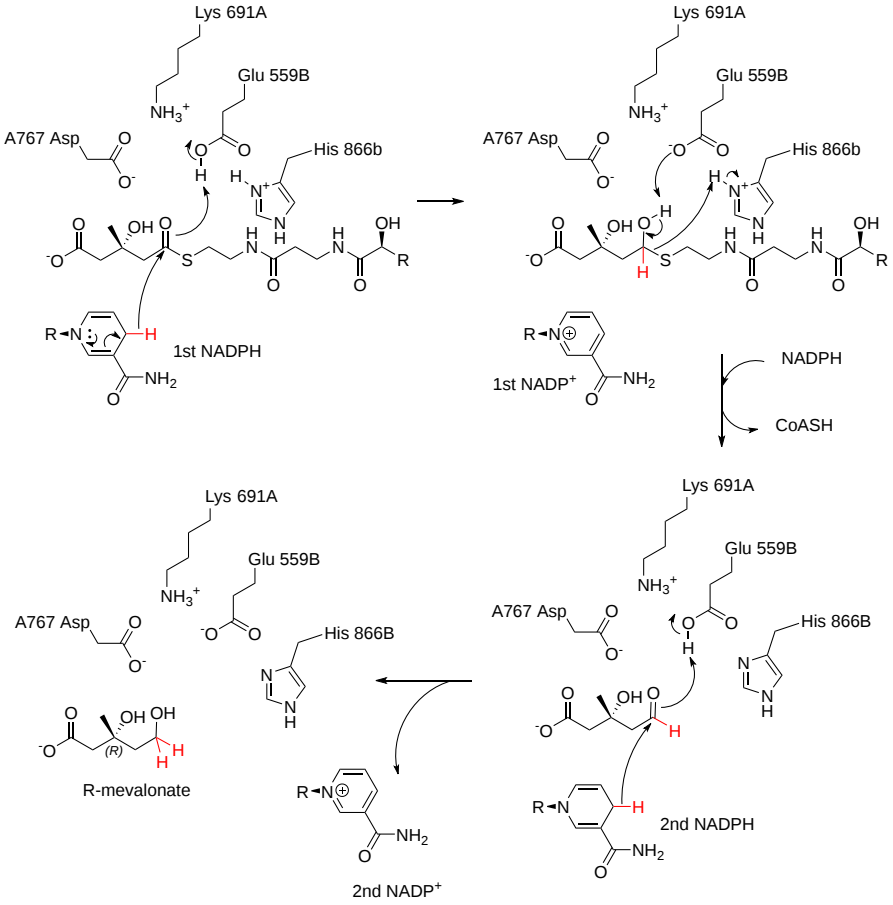
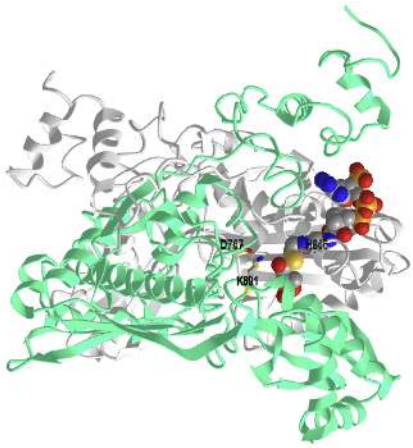


Figure **21.5.9**: Reaction mechanism for HMG-CoA reductase. Adapted from https://www.ebi.ac.uk/thornton-srv/m-csa/entry/93/. Creative Commons Attribution 4.0 International (CC BY 4.0) License.

Figure **21.5.10** shows an interactive iCn3D model of the catalytic domain of human HMG-CoA reductase with bound HMG-CoA (1DQ9).



NCBI iCn3D Figure **21.5.10**: Catalytic domain of human HMG-CoA reductase with bound HMG-CoA (1DQ9). (Copyright; author via source). Click the image for a popup or use this external link: https://structure.ncbi.nlm.nih.gov/i...dZvWzTocKhUzt8

Two of the four identical monomers in the biological unit, the C (gray) and D (cyan) chains, are shown. HMG-CoA is shown in spacefill and CPK colors. Three key catalytic residues, His 866 in the C chain (b chain in the mechanism above) and Lys 691 and Asp 767 in the D chain (A chain in the mechanism above), are shown in sticks, CPK colors, and labeled.

Synthesis of 5-isopentenyl and 2-isopentenyl pyrophosphate

The next sequence of reactions involves first the phosphorylation of mevalonic acid by a mevalonate kinase to form the 5-monophosphate ester, followed by further phosphorylation to yield an unstable pyrophosphate, which is rapidly decarboxylated to produce 5-isopentenyl

pyrophosphoric acid, the universal isoprene unit. An isomerase converts part of the latter to 3,3-dimethylallyl pyrophosphoric acid. These reactions are shown in Figure **21.5.11**.

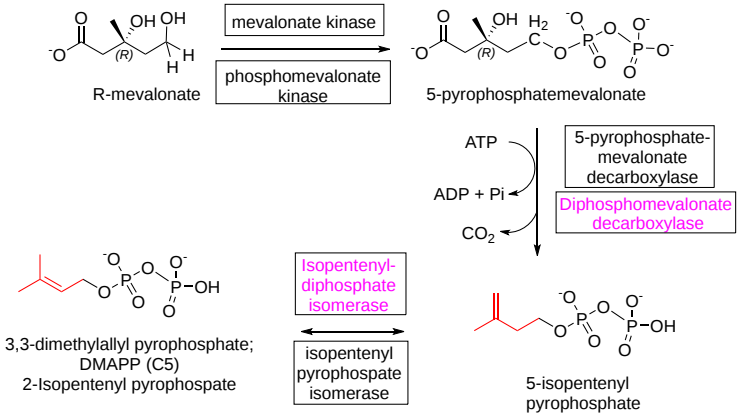


Figure **21.5.11**: Reactions for the synthesis of 5-isopentenyl and 2-isopentenyl pyrophosphate for the synthesis of sterols and isoprenoids

Two phosphorylations are required, one by mevalonate kinase, which proceeds by an ordered sequential binding of mevalonate as the first reactant and its phosphomevalonate as the first product released. The enzyme is inhibited by two downstream products of the reaction pathway, farnesyl pyrophosphate and geranyl pyrophosphate. A mechanism for mevalonate kinase is shown in Figure **21.5.12**.

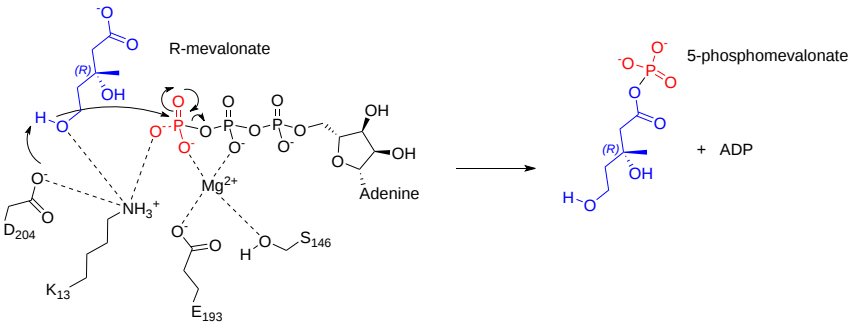


Figure **21.5.12**: Mechanism of mevalonate kinase (adapted from Fu et al. JBC. 277 (2002). https://doi.org/10.1074/jbc.M200912200

A reaction mechanism for the second kinase, phosphomevalonate kinase, showing progression through the transition state, is shown in Figure **21.5.13**. The reaction proceeds through direct phosphorylation through a dissociative mechanism.

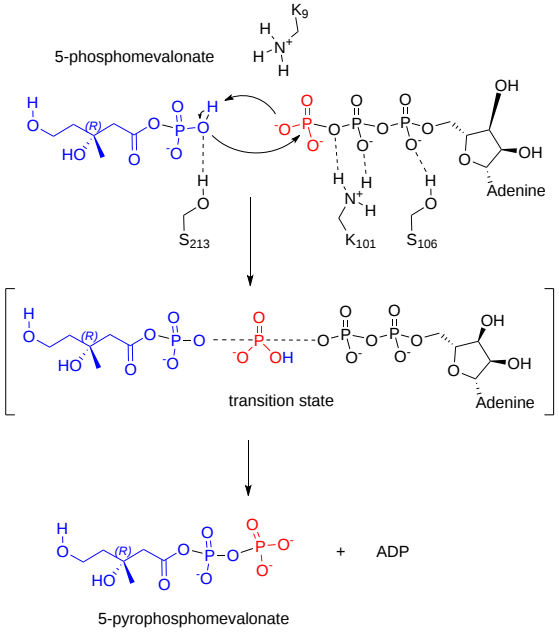


Figure **21.5.13**: Reaction mechanism for phosphomevalonate kinase (after Huang et al. J. Phys. Chem. B 2016, 120. DOI: 10.1021/acs.jpcb.6b08480)

Mevalonate diphosphate decarboxylase

This enzyme catalyzes the decarboxylation of 5-pyrophosphate mevalonate to 5-isopentenylpyrophosphate as shown in Figure **21.5.14**.

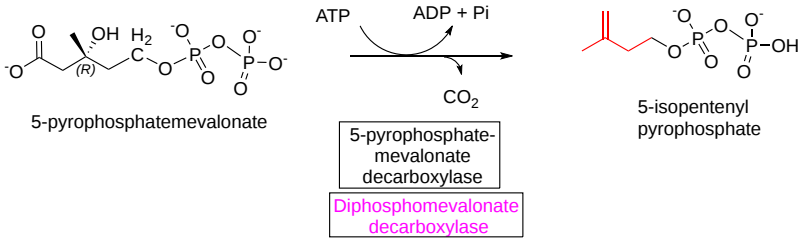


Figure **21.5.14**: Conversion of 5-pyrophosphaemevalonate to 5-isopentyl pyrophosphate

The binding of the two substrates, pyrophosphatemevalonate (or mevalonate pyrophosphate - MVAPP) and ATP to the enzyme (A), and a reaction mechanism (B, are shown in Figure **21.5.15**.

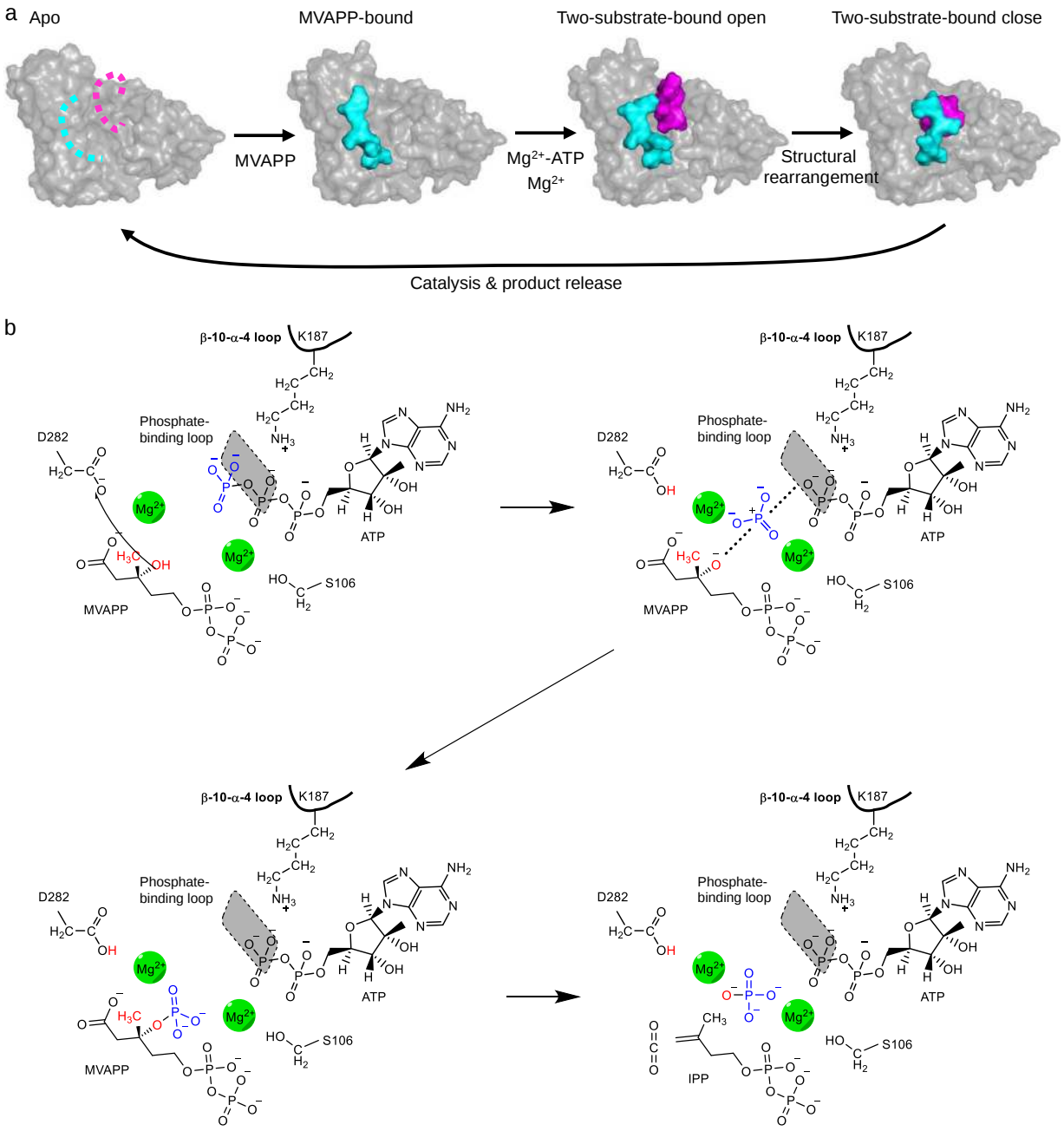


Figure **21.5.15**: Proposed model for the detailed MDD enzyme mechanism. Chen et al. Nature Communications. (2020) 11:3969 |https://doi.org/10.1038/s41467-020-17733-0. Creative Commons Attribution 4.0 International License. http://creativecommons.org/licenses/by/4.0/.

Panel (a) shows changes in the enzyme structure upon substrate binding. The apo-enzyme is shown on the left. The middle structure shows the enzyme after binding of the first substrate, MVAPP. A key loop (β10-α4) is shown as a cyan surface. The enzyme is then shown in an open conformation with the second substrate, ATP, also bound. An additional phosphate-binding loop is shown in magenta. At the far right, the enzyme is shown in a closed conformation, resulting from conformational changes in both loops, which trap substrates in the active site. These changes enable catalysis. Product release follows.

Panel (b) shows the dissociative phosphoryl transfer catalytic mechanism. At the top left, D282 is shown interacting with the 3′-OH group of MVAPP (red). The top right shows a dissociative phosphoryl (blue) transition state. In the bottom left, the phosphate attaches to the 3′ oxygen (red) of MVAPP. The bottom right shows the products after dephosphorylation and decarboxylation, which produce IPP, ADP, phosphate, and CO2. K187 from the β10-α4 loop and metal ions in the active site are involved in neutralizing the negatively charged environment and assist in catalysis.

Figure **21.5.16** shows an interactive iCn3D model of mevalonate diphosphate decarboxylase with mevalonate-5-diphosphate, AMPPCP, and Magnesium (6E2U).



Figure **21.5.16**: Mevalonate diphosphate decarboxylase with mevalonate-5-diphosphate, AMPPCP and Magnesium (6E2U) . (Copyright; author via source). Click the image for a popup or use this external link: https://structure.ncbi.nlm.nih.gov/i...SukmP1BTyNhH26

The correctly positioned substrates interact with two Mg^{2+} ions in the initial steps of the reaction. The conserved lysine facilitates the phosphoryl transfer.

21.5.1.3: POLYMERIZATION OF ISOPRENE

Isoprene, a small branched alkadiene, can polymerize into larger molecules containing isoprene monomer to form isoprenoids, often called terpenes. Instead of using isoprene as the polymerization monomer, either dimethylallyl pyrophosphate (DMAPP) or isopentenyl pyrophosphate (IPP) is used biologically.

Figure **21.5.*x*** below shows how DMAPP and IPP (both containing 5Cs) are used in a polymerization reaction to form geranyl-pyrophosphate (C10), farnesyl pyrophosphate (C15), and geranyl-geranyl pyrophosphate (C20). Figure **21.5.17**:

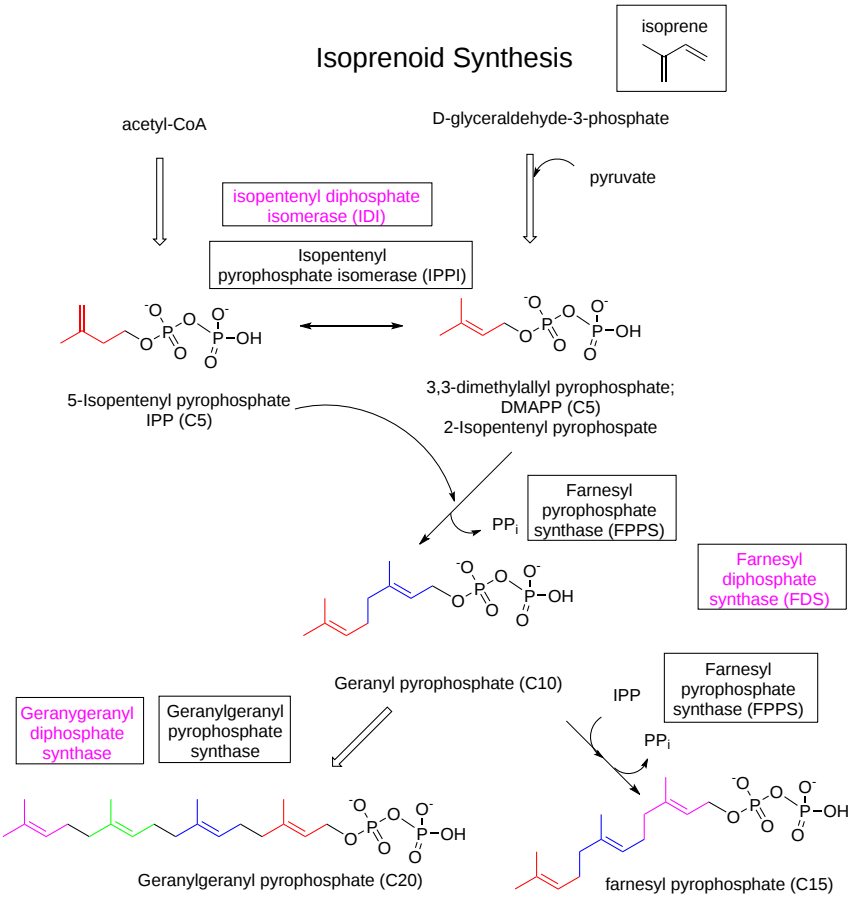


Figure 21.5.17: Synthesis of geranyl-pyrophosphate (C10), farnesyl pyrophosphate (C15) and geranyl-geranyl pyrophosphate (C20)

The condensation of IPP and DMAPP is a head-to-tail condensation reaction. Another IPP reacts with geranylpyrophosphate using the same enzyme to produce farnesylpyrophosphate. DMAPP is first formed by the isomerization of IPP to DMAPP catalyzed by isopentenyl-diphosphate delta-isomerase. It catalyzes the 1,3-allylic rearrangement of the homoallylic substrate isopentenyl (IPP). 5-isopentenyl pyrophosphate is a nucleophile, but its isomer, DMAPP, is highly electrophilic, which promotes the condensation of the two molecules.

A mechanism for the next reaction, the first condensation of DMAPP and IPP to form geranylpyrophosphate, catalyzed by farnesyl pyrophosphate (diphosphate) synthase, is shown in Figure 21.5.18.

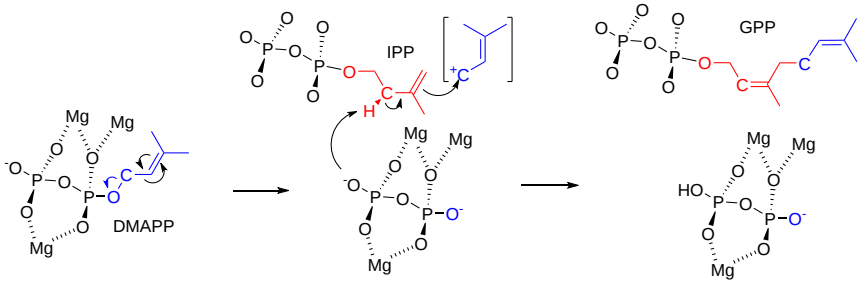
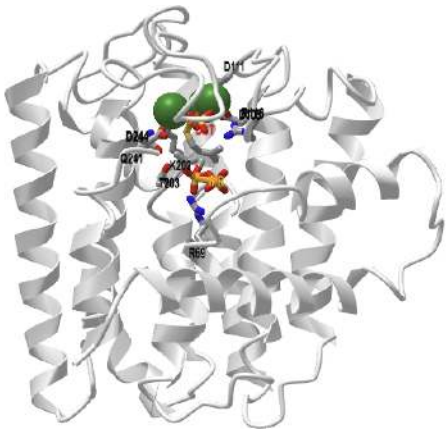


Figure 21.5.18: Mechanism for the condensation of DMAPP and IPP to form geranylpyrophosphate by farnesyl pyrophosphate (diphosphate) synthase

The reaction appears to proceed using a carbocation transition state, followed by the transfer of a hydrogen atom (not an ion) from IPP to pyrophosphate. Figure 21.5.19 shows an interactive iCn3D model of E. Coli farnesyl pyrophosphate synthase bound to isopentyl pyrophosphate and dimethylallyl S-thiolodiphosphate (1RQI).



NCBI iCn3D Figure **21.5.19**: Farnesyl pyrophosphate synthase Bound to isopentyl pyrophosphate (IPP) and dimethylallyl S-thiolodiphosphate (1RQI). (Copyright; author via source). Click the image for a popup or use this external link: https://structure.ncbi.nlm.nih.gov/i...kQBU5dNnKrCVt6

DST in the structure is dimethylallyl S-thiolodiphosphate, an analog of dimethylallyl diphosphate (DMAPP). Key conserved amino acids involved in substrate binding, transition state stabilization, and catalysis are shown as sticks, CPK colors. Thr203, Gln241, and Lys202 presumably stabilized the carbocation intermediate/transition state. Lys202 also forms a hydrogen bond with DMAPP. Two arginines (69, 116) form salt bridges with the pyrophosphates of IPP and DMAPP.

Many isoprenoid lipids are made from farnesyl pyrophosphate. For membrane purposes, the most important of these is cholesterol. Figure **21.5.20** shows an overview of the synthesis of cholesterol from two farnesyl pyrophosphates linking together in a "tail-to-tail" reaction to form squalene, a precursor of cholesterol. Each isoprene unit (5Cs) is shown in different colors to facilitate easier visualization.

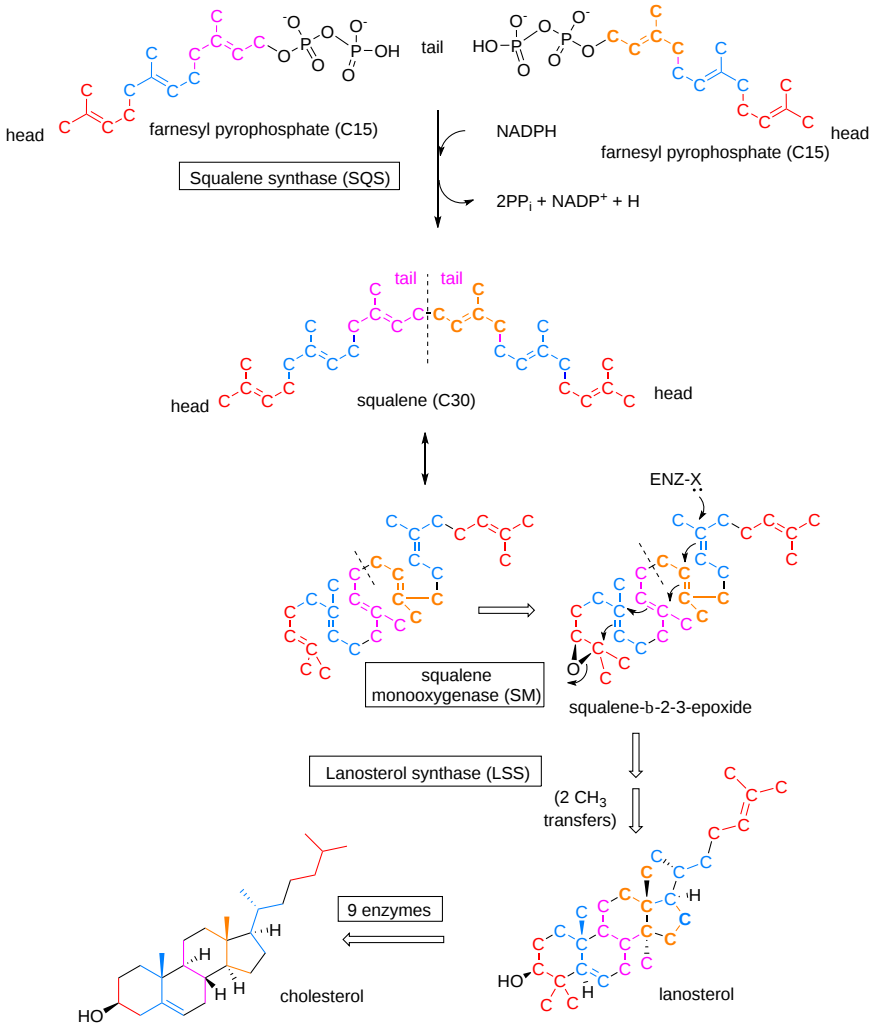


Figure 21.5.20: Synthesis of squalene from isoprene units.

Figure 21.5.21 shows reactants (two farnesyl pyrophosphate), intermediate (presqualene diphosphate), and product (squalene) in the reaction catalyzed by squalene synthase.

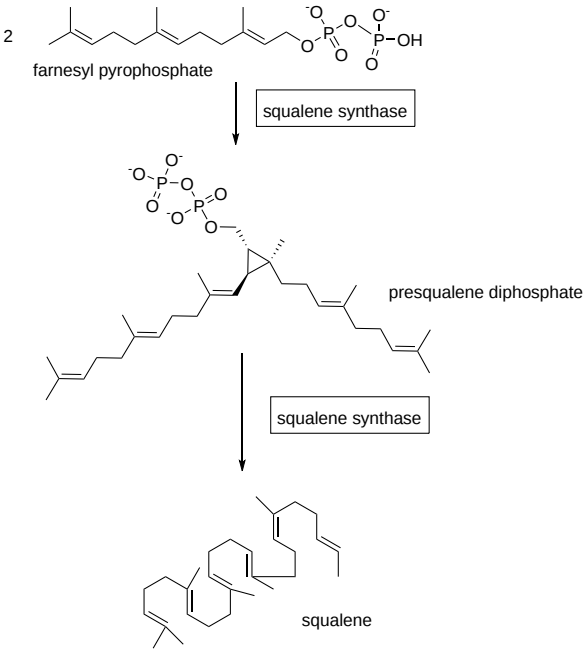


Figure **21.5.21**:

In the squalene synthase reaction, two molecules of farnesyl pyrophosphate condense to yield presqualene pyrophosphate. In turn, this is reduced by NADPH to produce the key intermediate **squalene**. The enzyme squalene synthase, which regulates the flow of metabolites into either the sterol or non-sterol pathways, with farnesyl pyrophosphate as the branch point, is considered the first committed enzyme in cholesterol biosynthesis.

Given the importance of this reaction, we will explore the unique mechanism of squalene synthase in some detail.

Part 1: Formation of the cyclopropyl presqualene intermediate

Figure 21.5.22 illustrates the mechanism for the first part of the reaction, which leads to the formation of the cyclopropyl intermediate, presqualene. The reaction proceeds through a series of carbocation intermediates.

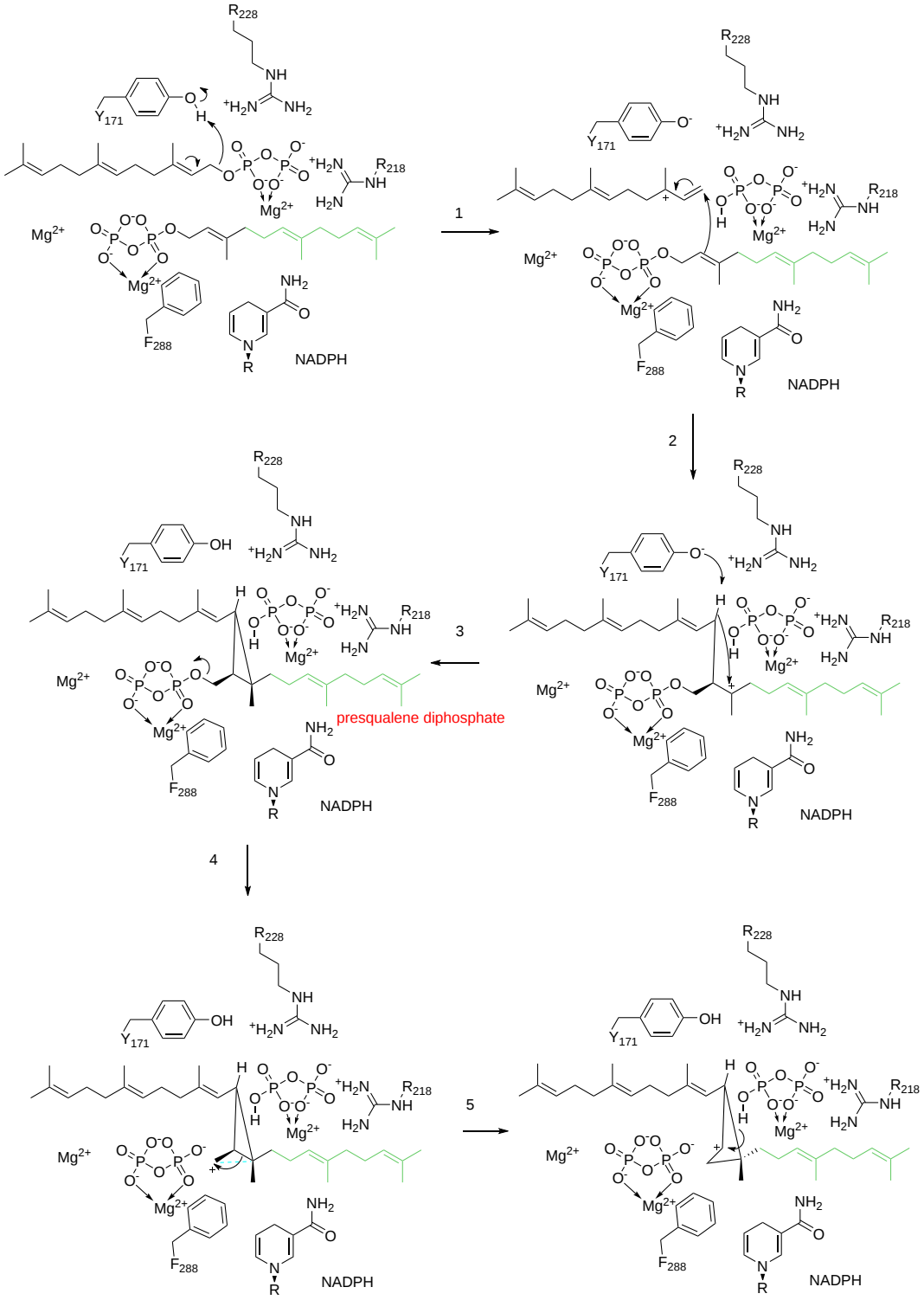


Figure **21.5.22**: Mechanism for the synthesis of presqualene by squalene synthase. https://www.ebi.ac.uk/thornton-srv/m-csa/entry/264/. Creative Commons Attribution 4.0 International (CC BY 4.0) License

Part 2: Conversion of cyclopropyl intermediate to squalene - reduction

The next part of the reaction involves the reductive formation of squalene, as shown in Figure **21.5.23**.

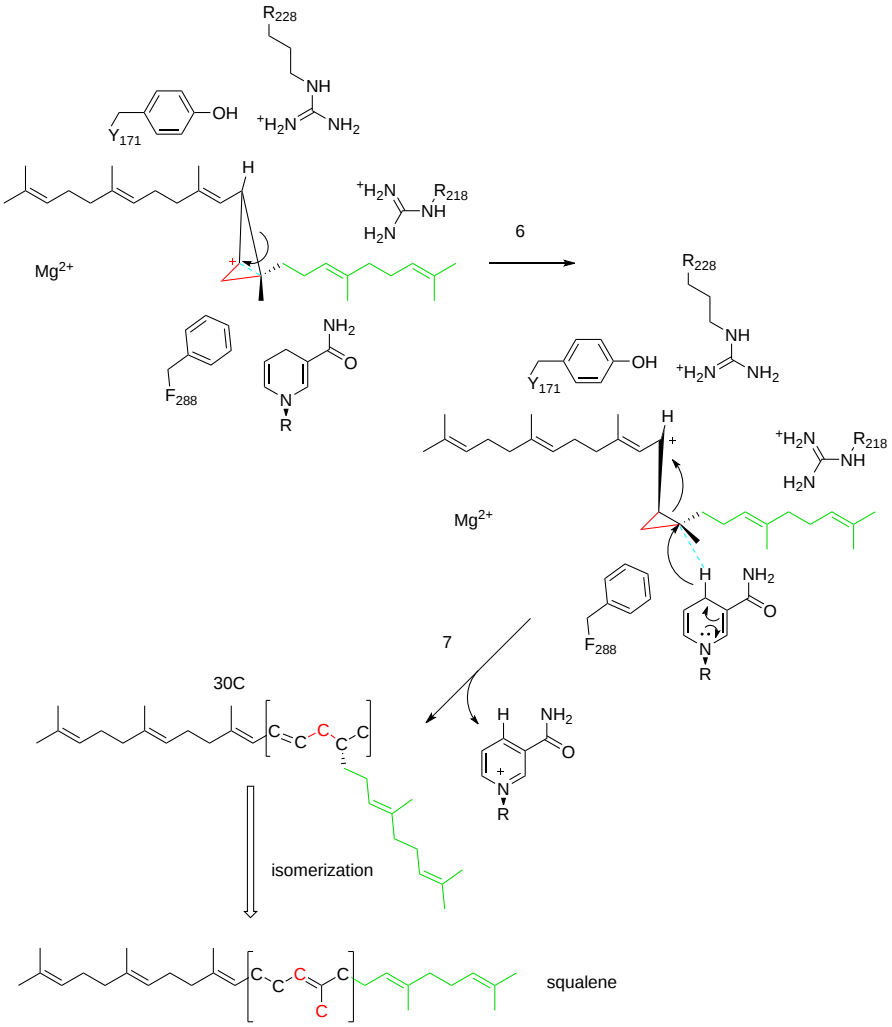
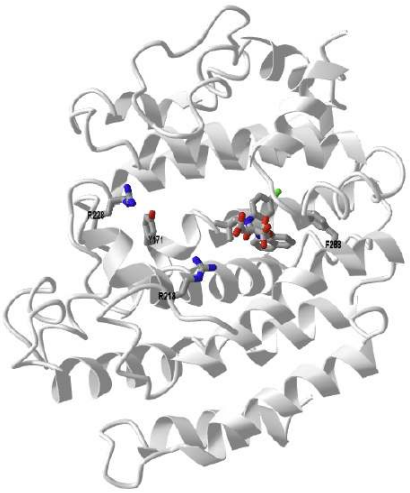


Figure **21.5.23**: Mechanism for conversion of presqualene to squalene by squalene synthase. https://www.ebi.ac.uk/thornton-srv/m-csa/entry/264/. Creative Commons Attribution 4.0 International (CC BY 4.0) License

Figure **21.5.24** shows an interactive iCn3D model of human squalene synthase with bound inhibitor (1EZF).



NCBI iCn3D Figure **21.5.24**: Human squalene synthase with bound inhibitor (1EZF). (Copyright; author via source). Click the image for a popup or use this external link: https://structure.ncbi.nlm.nih.gov/i...jLreHkvbftoFPA

Tyr 171 acts as a general acid/base in the first half of the reaction. Arg 218 and 228 stabilize the diphosphate in the transition state as it leaves. Phe 288 stabilizes the reactive carbocation.

The enzyme has a single domain that contains a large channel on one face, which extends from a solvent-exposed site to the hydrophobic interior. Two FPPs bind at the beginning of the channel, where key side chains for the first reaction are located. The cyclopropyl intermediate then moves into the hydrophobic end of the channel, where it reacts in the second half of the reaction without exposure to water.

In the next crucial step, squalene is oxidized by squalene monooxygenase to form squalene 2,3-epoxide, a key control point in the cholesterol synthesis pathway. This introduces the oxygen atom to squalene, which becomes the signature oxygen of the hydroxyl group in cholesterol. The epoxide then undergoes cyclization catalyzed by the enzyme squalene epoxide lanosterol-cyclase to form the first steroidal intermediate, lanosterol (or cycloartenol en route to **phytosterols** in photosynthetic organisms). This is illustrated in Figure **21.5.26**.

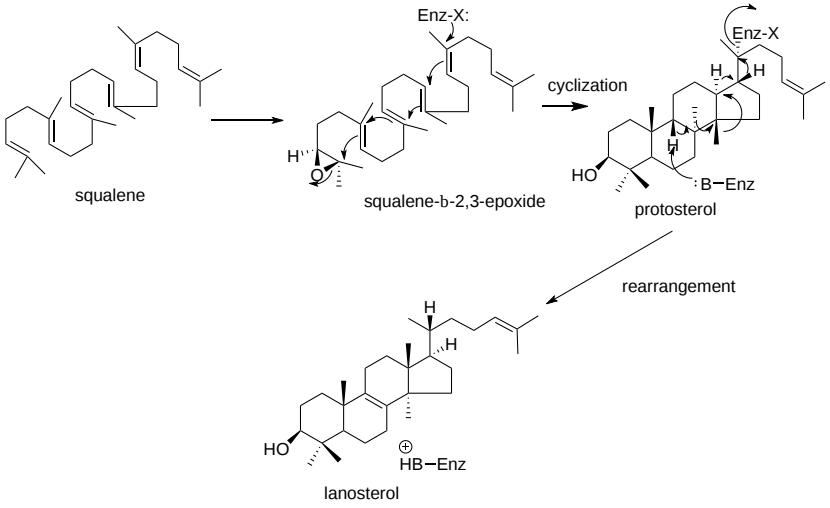


Figure **21.5.26**: Conversion of squalene to lanosterol

In this remarkable reaction, there is a series of concerted 1,2-methyl group and hydride shifts along the chain of the squalene molecule to bring about the formation of the four rings. No intermediate compounds have been found. This is believed to be one of the most complex single enzymatic reactions ever identified, despite the enzyme involved being only 90 kDa in size. Again, the reaction takes place in the endoplasmic reticulum. However, a cytosolic protein, sterol carrier protein 1, is required to bind squalene in an appropriate orientation in the presence of the cofactors NADPH, flavin adenine dinucleotide (FAD), and O_2; the presence of phosphatidylserine promotes the reactions.

The ring closure reaction, initiated by the epoxide, involves a concerted flow of electrons from a source to the epoxide oxygen atom, which acts as an electron sink. This brings to mind a reaction familiar to all students who have studied chemistry: the reaction of the pH indicator phenolphthalein with a base, which produces a pink-colored solution. That reaction, which produces a more conjugated molecule that absorbs at 553 nm (green), results in a magenta solution color and is illustrated for comparison (and fun) in Figure **21.5.27**.

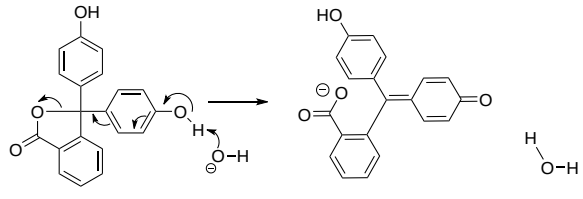


Figure **21.5.27**: Reaction of phenolphthalein with base

In subsequent steps, lanosterol is converted to cholesterol by a series of demethylations, desaturations, isomerizations, and reductions, involving nineteen separate reactions as illustrated in Figure **21.5.28**.

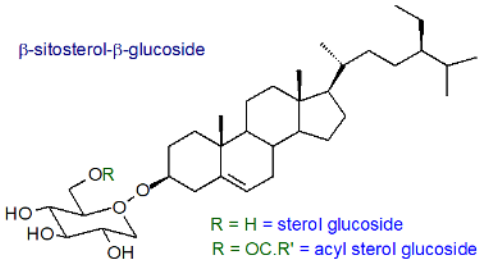


Figure **21.5.28**: Production of cholesterol from lanosterol

Thus, demethylation reactions produce zymosterol as an intermediate, and this is converted to cholesterol via a series of intermediates, all of which have been characterized, and by at least two pathways that utilize essentially the same enzymatic machinery but differ in the order of the various reactions, mainly at the point at which the Δ24 double bond is reduced. Desmosterol is the key intermediate in the so-called 'Bloch' pathway, while 7-dehydrocholesterol is the immediate precursor in the 'Kandutsch-Russell' pathway. While some tissues, such as adrenal glands and testis, use the Bloch pathway mainly, the brain synthesizes much of its cholesterol by the 'Kandutsch-Russell' pathway. This may enable the production of a variety of other minor sterols for specific biological purposes in different cell types and locations.

The energy cost of the synthesis of one cholesterol molecule is roughly one hundred ATP equivalents, and eleven oxygen molecules are required. Synthesis occurs mainly in the liver, although the brain, peripheral nervous system, and skin also synthesize their own considerable supplies. Cholesterol is exported from the liver and transported to other tissues in the form of low-density **lipoproteins** (LDL) for uptake via specific receptors. In animals, cells can obtain the cholesterol they require either from the diet via circulating LDL or synthesize it themselves, as outlined above. Cholesterol biosynthesis is highly regulated, with rates of synthesis varying over hundreds of fold depending on the availability of any external sources of cholesterol, and cholesterol homeostasis requires the actions of a complex web of enzymes, transport proteins, and membrane-bound transcription factors, as discussed below.

? REGULATION OF CHOLESTEROL HOMEOSTATIS - DETAILS

Click the link below.

Link

In humans, only about a third of the cholesterol is of dietary origin (mainly eggs and red meat), the remainder is produced by synthesis *de novo* in the endoplasmic reticulum. The latter must be tightly regulated as it is an energetically expensive process that requires appreciable amounts of acetyl-CoA, ATP, oxygen, and the reducing factors NADPH and NADH, especially since cholesterol cannot be catabolized for energy purposes (see below).

Many factors contribute to maintaining the significant differences in cholesterol concentrations among various membranes and organelles within cells, all within precise limits. To explain how cholesterol in the plasma membrane, where it is most abundant, can regulate cholesterol biosynthesis and uptake through enzymes in the endoplasmic reticulum, where it is least abundant, it has been suggested that a key to the process is that there are three pools of cholesterol in the plasma membrane with distinct functional roles. The first of these is “accessible” to receptor proteins for transport to the endoplasmic reticulum. In contrast, the second pool is sequestered by sphingomyelin and can be released by the action of sphingomyelinase if required. The third residual pool of cholesterol is essential for plasma membrane integrity. These correspond to about 16, 15, and 12 mol % of total plasma membrane lipids, respectively, in cholesterol-replete cells. Simplistically, when cholesterol in the plasma membrane is in excess for any reason, e.g., after LDL uptake by receptor-mediated endocytosis, there is a rise in accessible cholesterol, which is then transported to the endoplasmic reticulum to switch off cholesterol biosynthesis and expression of the LDL receptor. This process requires a host of regulatory proteins and mechanisms that can involve either vesicle formation or non-vesicular pathways, utilizing specific transport proteins, such as the ABC transporters.

Ultimately, post-translational control of the many different enzymes involved provides a rapid means for modifying flux through the biosynthetic pathway in the endoplasmic reticulum; some are rapidly degraded in response to tissue levels of cholesterol and its intermediates, while others have their activity altered through phosphorylation or acetylation mechanisms. For example, the second rate-limiting enzyme in cholesterol biosynthesis is squalene monooxygenase, which undergoes cholesterol-dependent proteasomal degradation when cholesterol is in excess. This degradation is guided by a 12-amino-acid hydrophobic sequence on the enzyme that can serve as a degradation signal. When the cholesterol concentration in the endoplasmic reticulum is high, the degradation sequence detaches from the membrane and is exposed, providing a signal for the enzyme to be degraded. Similarly, HMG-CoA reductase is recognized as the key enzyme in regulating cholesterol biosynthesis, and this process can be controlled by a feedback mechanism involving ubiquitin–proteasomal degradation. Further regulation of cholesterol biosynthesis is exerted by sterol

intermediates in cholesterol biosynthesis, such as lanosterol and 24,25-dehydrolanosterol (dimethyl-sterols), by accelerating the degradation of the biosynthetic enzymes, such as HMG-CoA reductase. It is noteworthy that ceramide downregulates cholesterol synthesis – another link between cholesterol and sphingolipid metabolism.

The regulatory element-binding proteins (mainly SREBP-1c and SREBP-2), which contain an N-terminal membrane domain and a C-terminal regulatory domain, play a crucial role in maintaining cholesterol levels. Each is synthesized as an inactive precursor that is inserted into the endoplasmic reticulum, where it can encounter an escort protein termed **SREBP cleavage-activating protein (SCAP)**, which is the cellular cholesterol sensor. When the latter recognizes that cellular cholesterol levels are inadequate, it binds to the regulatory domain of SREBP. The SCAP-SREBP complex then moves to the Golgi, where two specific proteases (designated site-1 and site-2 proteases) cleave the SREBP, enabling the *C*-terminal regulatory domain to enter the nucleus. There, it activates transcription factors, such as the nuclear liver X receptor (LXR), which stimulate the expression of the genes coding for the LDL receptor in the plasma membrane and for the key enzyme in cholesterol biosynthesis, HMG-CoA reductase. This, in turn, stimulates the rate of cholesterol uptake and synthesis. Conversely, when cholesterol in the endoplasmic reticulum exceeds a threshold, it binds to SCAP in a manner that prevents the SCAP-SREBP complex from leaving the membrane for the nucleus. As a result, cholesterol synthesis and uptake are repressed, and cholesterol homeostasis is restored. In effect, cholesterol exerts feedback inhibition by suppressing its own production by preventing the proteolytic cleavage and maturation of SREBP-2. **Oxysterols**, especially 25-hydroxycholesterol, are also inhibitors of this process.

Cholesterol in the endoplasmic reticulum is transferred to the Golgi and eventually to the plasma membrane by vesicular and non-vesicular transport mechanisms involving, in part, soluble sterol transport proteins, including the so-called 'START' domain proteins, and partly by binding to those proteins that are intimately involved in the transport and metabolism of polyphosphoinositides such as **phosphatidylinositol 4-phosphate (PI(4)P)**. In the latter mechanism, cholesterol is transported by binding to the ORD domain of oxysterol binding protein (OSBP) or Osh4 in yeast, before OSBP binds to PI(4)P in the plasma membrane to transfer its cargo. The key to this process is that cholesterol and PI(4)P are synthesized at two different locations: the endoplasmic reticulum for sterols and the trans-Golgi network and plasma membrane for PI(4)P. Therefore, the two lipids do not compete; instead, they can be exchanged. OSBP carries cholesterol in the forward direction to the trans-Golgi network and plasma membrane, and PI(4)P, which binds to a C-terminal PH domain in the protein, in the reverse direction. The subsequent hydrolysis of PI(4)P is the energy source for the reaction, and indeed PI(4)P has been termed "lipid ATP". As this reaction is irreversible, a gradient of cholesterol is established along the organelles of the secretory pathway. OSBP is thus a lipid transfer protein that enables two organelles to exchange cholesterol rapidly between them at membrane contact sites in a cycle of reactions involving membrane tethering, cholesterol transport, PI(4)P countertransport, and PI(4)P hydrolysis. A similar mechanism is involved in the transport of phosphatidylserine from the endoplasmic reticulum to the inner leaflet of the plasma membrane.

Subsequently, the ATP-binding cassette (ABC) transporters ABCA1 and ABCG1, located in the plasma membrane and containing a significant portion of the cellular cholesterol, are activated to export the excess. Nuclear factor erythroid 2-related factor-1 (NRF1) in the endoplasmic reticulum binds directly to cholesterol and senses when its level is high, thereby bringing about the derepression of genes involved in cholesterol removal, with mediation by the liver X receptor. Also, side-chain oxysterols, especially 25-hydroxycholesterol, can suppress the activation of SREBP by binding to an oxysterol-sensing protein in the endoplasmic reticulum.

Within cells, cholesterol derived initially from the lysosomal degradation of low-density lipoproteins is transferred first to the plasma membrane and thence to the endoplasmic reticulum, the latter step by a mechanism involving proteins known as GRAMD1s embedded in the endoplasmic reticulum membrane at sites in contact with the plasma membrane. These proteins have two functional domains: the START-like domain, which binds cholesterol, and the GRAM domain, which binds anionic lipids such as phosphatidylserine, thereby forming a link between the two membranes that enables the transfer of cholesterol.

In peripheral tissues, excess cholesterol is exported to high-density lipoproteins (HDL) in the circulation and returned to the liver, a process known as **reverse cholesterol transport**. The liver plays a crucial role in cholesterol synthesis, but it is equally essential for its elimination from the body through bile. Additionally, some lipoproteins containing cholesterol and cholesterol esters are delivered to lysosomes by endocytosis for degradation. Cholesterol is transported to the inner surface of the lysosomal membrane through the glycocalyx, via a transglycocalyx tunnel, with the aid of Niemann-Pick C1, C2, and other proteins, and then via contact sites between membranes to other organelles. Cholesterol in cellular membranes above the stoichiometric requirement can escape back into the cell, where it may serve as a feedback signal to downregulate cholesterol accumulation. Meanwhile, some is converted into the relatively inert storage form, i.e., cholesterol esters, while others are used for steroidogenesis.

The intestines play a crucial role in cholesterol homeostasis by absorbing dietary cholesterol and excreting it through feces, along with its metabolites. A specific transporter (Niemann-Pick C1-like 1 or NPC1L1)in the brush border membrane of enterocytes in the proximal jejunum of the small intestine is involved in the uptake of cholesterol from the intestinal contents. In contrast, the metabolism of sterols in the intestines is primarily controlled by an acetyl-CoA acetyltransferase (ACAT2), which facilitates

intracellular cholesterol esterification, and the microsomal triglyceride transfer protein (MTTP), which is involved in the assembly of chylomicrons for export into the lymphatic system. Some cholesterol can be transferred in the opposite direction (transintestinal cholesterol excretion), but the quantitative importance of this process is unclear. There is evidence that dietary or synthesized cholesterol is necessary to maintain intestinal integrity, as cholesterol derived from circulating lipoproteins is not sufficient for the purpose.

In the intestines, especially the colon, the intestinal microflora can hydrogenate cholesterol from bile, diet, and desquamated cells to form coprostanol with an efficiency dependent on the composition of microbial species. Coprastanol is not significantly absorbed by intestinal tissue, and it may inhibit the uptake of residual cholesterol. There are two mechanisms for this conversion in bacteria: one involving direct reduction and another via cholestenone and coprostanone as intermediates. As the relevant genes have now been identified, the therapeutic potential is under investigation.

Brain: There are substantial differences in cholesterol synthesis and metabolism in the brain in comparison to the liver and peripheral tissues. Trace amounts of cholesterol can cross the blood-brain barrier via transport in low-density lipoproteins. Therefore, virtually all the cholesterol in the brain must be synthesized *de novo*, mainly in astrocytes (glial cells). During the perinatal and adolescent years, especially, cholesterol is synthesized in large amounts to form the myelin that surrounds the axons. Afterward, the rate begins to decline, eventually reaching about 10% of its earlier values.

Cholesterol is transported to neurons in the form of Apo E complexes in discoidal HDL-like particles, for which seven main receptors have been identified in brain cells that take up cholesterol from these lipoproteins. Apo E is synthesized in the brain, and 24-hydroxy-cholesterol concentrations regulate its transcription. Similarly, in the brain and central nervous system, cholesterol synthesis is regulated independently of that in peripheral tissues, mainly by forms of the liver X receptor (LXR). As cholesterol and oxysterols are involved in providing neuroprotective effects and lowering neuroinflammation, dysregulation of their concentrations has been noted in many neurodegenerative disorders. Most of the lipoproteins in cerebrospinal fluid differ from the nascent poorly-lipidated HDL secreted by astrocytes, suggesting that the latter are modified during maturation.

21.5.1.4: CHOLESTEROL CATABOLISM

Cholesterol is not readily degraded in animal tissues, so it does not serve as a metabolic fuel to generate ATP. Only the liver possesses the enzymes to degrade significant amounts, and then via pathways that do not lead to energy production. Cholesterol and oxidized metabolites, known as oxysterols, are transferred back from peripheral tissues in lipoprotein complexes to the liver for catabolism by conversion to oxysterols and bile acids. The latter are exported into the intestines to aid in digestion, while leading to some loss that is essential for cholesterol homeostasis. Until recently, it was believed that approximately 90% of cholesterol elimination from the body in humans occurred via bile acids. However, experiments with animal models now suggest that a significant amount is secreted directly into the intestines by a process known as trans-intestinal cholesterol efflux. The mechanisms by which this occurs and its relevance to humans are under active investigation.

Gut bacteria reduce some of the cholesterol in the diet to highly insoluble 5β-cholestan-3β-ol (coprostanol), which is excreted and can be used as a biomarker for sewage in the environment. Certain bacterial species contain a 3β-hydroxysteroid:oxygen oxidoreductase (EC 1.1.3.6), commonly referred to as cholesterol oxidase, a flavoenzyme that catalyzes the oxidation of cholesterol to cholest-5-en-3-one, which is then rapidly isomerized to cholest-4-en-3-one, marking the first essential step in the catabolism of sterols. The enzyme is widespread in organisms that degrade organic wastes, but it is also present in pathogenic organisms where it influences the virulence of infections (see below). In biotechnology, it has been utilized for the production of various steroids, and it is employed in a clinical procedure for determining cholesterol levels in serum.

21.5.1.5: CHOLESTEROL ESTERS

Cholesterol esters, i.e., with long-chain fatty acids linked to the hydroxyl group, are much less polar than free cholesterol and appear to be the preferred form for transport in plasma and as a biologically inert storage or detoxification form to buffer an excess. They do not contribute to membrane structures but are packed into intracellular lipid droplets. Cholesterol esters are major constituents of the adrenal glands, and they accumulate in the fatty lesions of atherosclerotic plaques. Similarly, esters of steroidal hormones are also present in the adrenal glands, where they are concentrated in cytosolic lipid droplets adjacent to the endoplasmic reticulum; 17β-estradiol, the principal estrogen in fertile women, is transported in lipoproteins in the form of a fatty acid ester.

Because of the mechanism of synthesis (see below), plasma cholesterol esters tend to contain relatively high proportions of the polyunsaturated components typical of phosphatidylcholine, as shown in Table **21.5.1** below. Arachidonic and “adrenic” (20:4(n-6)) acids can be especially abundant in cholesterol esters from the adrenal gland.

Table **21.5.1. Fatty acid composition of cholesterol esters (wt% of the total) from various tissues.**

Form	Fatty acids						
	16:0	18:0	18:1	18:2	18:3	20:4	22:4
Human							
plasma	12	2	27	45		8	
liver	23	10	28	22		6	
Sheep							
plasma	10	2	27	35	7	-	-
liver	17	9	29	7	4	3	-
adrenals	13	7	35	18	2	4	2

Data from Christie, W.W. *et al. Lipids*, **10**, 649-651 (1975); DOI. Nelson, G.J. *Comp. Biochem. Physiol.*, **30**, 715-725 (1969); Horgan, D.J. and Masters, C.J. *Aust. J. Biol. Sci.*, **16**, 905-915 (1963); Nestel, P.J. and Couzens, E.A. *J. Clin. Invest.*, **45**, 1234-1240 (1966); DOI.

In plasma and the high-density lipoproteins (HDL) in particular, cholesterol esters are synthesized largely by the transfer of fatty acids to cholesterol from position *sn*-2 of phosphatidylcholine ('lecithin'), catalyzed by the enzyme **lecithin:cholesterol acyl transferase (LCAT)**; the other product is 1-acyl lysophosphatidylcholine. This is illustrated in Figure **21.5.29**.

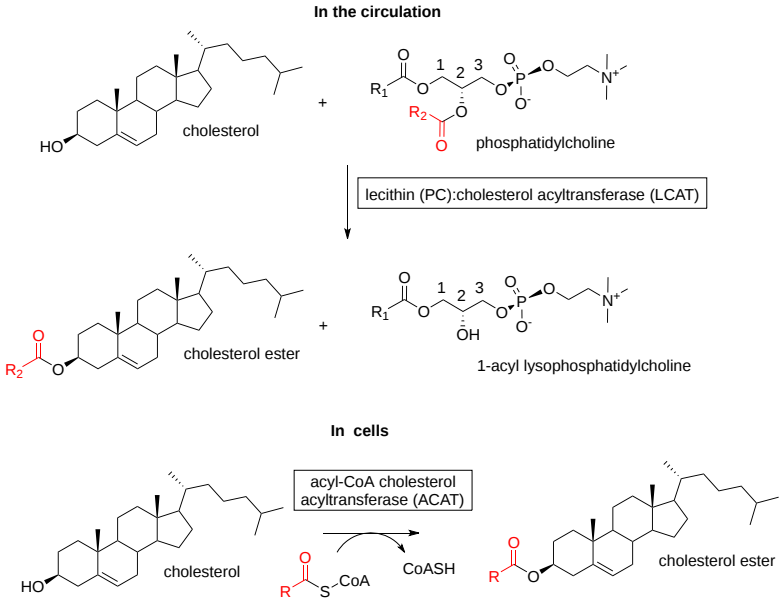


Figure **21.5.29**: Synthesis of cholesterol esters

The reaction occurs in several steps. First, apoprotein A1 in HDL acts to concentrate lipid substrates near LCAT and present them in the optimal conformation; simultaneously, it opens a lid on the enzyme, activating it by exposing the site of transesterification. Then, cleavage of the *sn*-2 ester bond of phosphatidylcholine occurs via the phospholipase activity of LCAT, releasing a fatty acyl moiety. This is transacylated to the sulfur atom of a cysteine residue, forming a thioester, and ultimately it is donated to the 3β-hydroxyl group of cholesterol to form the cholesterol ester. Some LCAT activity has also been detected in apolipoprotein B100-containing particles (β-LCAT activity as opposed to α-LCAT with HDL).

It has been established that human LCAT is a relatively small glycoprotein with a polypeptide mass of approximately 49 kDa, which increases to about 60 kDa due to the addition of four *N*-glycosylation and two *O*-glycosylation moieties. Most of the enzyme is produced in the liver and circulates in the bloodstream bound reversibly to HDL, where the main protein component of HDL, apolipoprotein A1, activates it. As cholesterol esters accumulate in the lipoprotein core, cholesterol is removed from its surface, thus promoting the flow of cholesterol from cell membranes into HDL. This, in turn, leads to morphological changes in HDL, resulting in larger and more spherical particles. Subsequently, cholesterol esters are transferred to the other lipoprotein fractions, LDL and VLDL, a reaction catalyzed by cholesterol ester transfer protein. This process promotes the efflux of cholesterol from peripheral tissues, known as reverse cholesterol transport, especially from macrophages in the arterial wall, for subsequent delivery to the liver. LCAT is often cited as the primary driving force behind this process, and it is of great importance for cholesterol homeostasis, making it a suggested target for therapeutic intervention against cardiovascular disease.

The stereospecificity of LCAT changes with molecular species of phosphatidylcholine containing arachidonic or docosahexaenoic acid, when 2-acyl lysophosphatidylcholines are formed. This reaction may be significant for the supply of these essential fatty acids to the brain in that such lysophospholipids are believed to cross the blood-brain barrier more readily than the free acids.

In other animal tissues, a further enzyme acyl-CoA:cholesterol acyltransferase (ACAT) synthesizes cholesterol esters from CoA esters of fatty acids and cholesterol. ACAT exists in two forms, both of which are intracellular enzymes found in the endoplasmic reticulum and are characterized by multiple transmembrane domains and a catalytic histidine residue in a hydrophobic domain; they are members of the *O*-acyltransferase (MBOAT) superfamily. ACAT1 is present in many tissues, but is especially abundant in macrophages and the adrenal and sebaceous glands, which store cholesterol esters in the form of cytoplasmic lipid droplets. It is responsible for the synthesis of cholesterol esters in arterial foam cells within human atherosclerotic lesions. ACAT2 is found only in the liver and small intestine, and it is believed to be involved in the supply of cholesterol esters to the nascent lipoproteins. Analogous enzymes are found in yeast, where ergosterol is the primary sterol; however, a very different process occurs in plants.

Oxidized Cholesterol Esters: All lipid classes containing polyunsaturated fatty acids are susceptible to oxidation. Under normal circumstances, cholesterol esters are considered to be relatively inert. However, when they contain oxidized polyunsaturated fatty acids, their properties change, and they acquire biological activity. A reaction with 15-lipoxygenase may form such oxidized cholesterol esters, but they can also be produced through free radical-induced lipid peroxidation. They have been detected in lipoproteins, particularly LDL, in human blood and atherosclerotic lesions. Those oxidized cholesterol esters in plasma are trafficked into cells and metabolized by the same mechanisms as the corresponding unoxidized lipids.

Such "minimally oxidized LDL" does not bind to CD36 but rather to CD14, a receptor that recognizes bacterial lipopolysaccharides. The result is stimulation of toll-like receptor 4 (TLR4), although the response differs from that of lipopolysaccharides. In addition, oxidized metabolites of cholesteryl arachidonate of this kind stimulate macrophages to express inflammatory cytokines of relevance to atherosclerosis, among other effects. Oxidized cholesterol esters can be hydrolyzed to release their fatty acids, which can then be incorporated into phospholipids, resulting in a different repertoire of activities.

Hydrolysis of cholesterol esters: Cholesterol ester hydrolases in animals liberate cholesterol and free fatty acids when required for membrane and lipoprotein formation, and they also provide cholesterol for hormone synthesis in adrenal cells. Several cholesterol ester hydrolases have been identified, including carboxyl ester hydrolase, lysosomal acid cholesterol ester lipase, hormone-sensitive lipase, and hepatic cytosolic cholesterol ester hydrolase. These are located in various tissues and organelles, serving multiple functions. A neutral cholesterol ester hydrolase has received special attention, as it is involved in the removal of cholesterol esters from macrophages, thereby reducing the formation of foam cells and, consequently, the development of fatty streaks within the arterial wall —a key event in the progression of atherosclerosis.

21.5.1.6: OTHER ANIMAL STEROLS

Cholesterol will slowly oxidize in tissues or foods to form a range of different products with additional hydroperoxy, epoxy, hydroxy, or keto groups, and these can enter tissues through the diet. There is increasing interest in these compounds from the standpoint of human health and nutrition, as the accumulation of oxo-sterols in plasma is associated with the inhibition of cholesterol and bile acid biosynthesis, as well as other abnormalities in plasma lipid metabolism.

Some other sterols occur in small amounts in tissues, most of which are intermediates in the pathway from lanosterol to cholesterol. However, some of them have distinct functions in their own right. **Lanosterol**, the first sterol intermediate in cholesterol biosynthesis, was first identified in wool wax, both in its free and esterified forms, and remains the primary commercial source. It is found at low levels only in most other animal tissues (typically 0.1% of the cholesterol concentration). As oxygen is required, lanosterol cannot be produced by primitive organisms; hence, its absence from prokaryotes has led to some speculation on its evolutionary significance. When sterols became available to eukaryotes, numerous new possibilities emerged for their continued evolution. The production of cholesterol from lanosterol is then seen as ‘molecular streamlining’ by evolution, removing protruding methyl groups that hinder the interaction between sterols and phospholipids in membranes.

Desmosterol (5,24-cholestadien-3β-ol), the last intermediate in the biosynthesis of cholesterol by the Bloch pathway, may be involved in the process of myelination, as it is found in relative abundance in the brains of young animals but not in those of adults, other than astrocytes. It is also found in appreciable amounts in testes and spermatozoa, together with another cholesterol intermediate, testis meiosis-activating sterol. In addition, there is evidence that desmosterol activates certain genes involved in lipid biosynthesis in macrophages and may deactivate others associated with the inflammatory response. There is a rare genetic disorder in which there is an impairment in the conversion of desmosterol to cholesterol, desmosterolosis, with serious consequences in terms of mental capacity. These and related sterols appear to be essential for human reproduction.

In human serum, the levels of **lathosterol** (5α-cholest-7-en-3β-ol) were found to be inversely related to the size of the bile acid pool, and in general, the concentration of serum lathosterol is strongly correlated with the cholesterol balance under most dietary conditions. The

isomeric saturated sterols, **cholestanol** and **coprastanol**, which differ in the stereochemistry of the hydrogen atom on carbon 5, are formed by microbial biohydrogenation of cholesterol in the intestines, and together with cholesterol are the main sterols in feces. Further examples of animal sterols include **7-dehydrocholesterol** (cholesta-5,7-dien-3β-ol), found in the skin, which, upon irradiation with UV light, is converted to **vitamin D3** (cholecalciferol). These sterols are shown in Figure **21.5.30**.

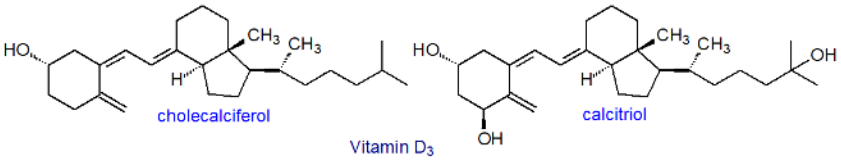


Figure **21.5.30**: Other animal sterols

Marine invertebrates produce a large number of novel sterols, featuring both unusual nuclei and unconventional side chains, some derived from cholesterol and others from plant sterols or alternative biosynthetic intermediates. For example, at least 80 distinct sterols have been isolated from echinoderms and 100 from sponges.

? CHOLESTEROL AND DISEASE

Click the link for more information.

Link

Elevated cholesterol and cholesterol ester levels are associated with the pathogenesis of cardiovascular disease, including atherosclerotic plaques, myocardial infarctions, and strokes, as is well known. The rate-limiting enzyme in cholesterol synthesis, HMG-CoA reductase, is the target of statins. However, drugs targeting other steps in the biosynthetic pathway, particularly squalene monooxygenase and lanosterol synthase, are also under investigation.

Cholelithiasis, or the presence of 'stones' in the gallbladder or bile ducts, which consist largely of cholesterol (~85%), is one of the most prevalent and costly digestive diseases in developed countries. The primary cause is the excessive excretion of cholesterol from the liver. Excess accumulation of cholesterol associated with the metabolism of **bis(monoacylglycero)phosphate** and causing disturbances in glycosphingolipid trafficking in cell membranes is involved in the pathogenesis of **Niemann-Pick C disease**, a lysosomal storage disease in which endocytosed cholesterol becomes sequestered in late endosomes/lysosomes because of gene mutations affecting two binding proteins (NPC1 and NPC2) thereby causing neuronal and visceral atrophy. In addition, deficiencies in cholesterol transport and metabolism are associated with many forms of neurodegeneration, including Alzheimer's disease, Huntington's disease, and related conditions associated with old age. These proteins are also key virulence factors for several viral and bacterial pathogens.

Several genetic disorders of cholesterol biosynthesis have been identified in recent years that can result in developmental malformations, including neurologic defects. As there is limited cholesterol transport across the placenta, the human fetus is highly dependent upon endogenous synthesis. While the molecular basis for the altered developmental pathways is not fully understood, impaired synthesis of the **hedgehog** family of signaling proteins, which require covalently linked cholesterol to function in membranes, is believed to be involved in many cases. In others, there are confirmed enzyme defects. For example, the recessive Smith-Lemli-Opitz syndrome in infants born with a decreased concentration of the enzyme 7-dihydrocholesterol reductase produces symptoms varying from mild autism to severe mental and often fatal physical problems. The effects are due to a lack of cholesterol and the accumulation of 7-dehydrocholesterol and its 27-hydroxy metabolite, as brain tissue cannot utilize dietary cholesterol or that produced peripherally. At least eight different inherited disorders of cholesterol biosynthesis result in congenital abnormalities in those affected. In animal models, deficiencies in SREBP-2 and genes encoding sterol biosynthetic enzymes display embryonic lethality. Deficiencies in the enzymes responsible for the hydrolysis of cholesterol esters, such as the lysosomal acid lipase, occur in Wolman disease and cholesterol ester storage disease.

Cholesterol and other sterols bind directly to several immune receptors, especially in macrophages and T cells. Dynamic changes in cholesterol biosynthesis directly impact innate and adaptive immune responses, such that functional coupling between sterol metabolism and immunity has implications for health and disease. For example, cholesterol binds directly to the αβ T cell antigen receptor (αβTCR) and has at least two opposing functions in its activation. By binding to the transmembrane domain of this receptor, it is maintained in an inactive, non-signaling conformation; however, when required, it can stimulate the formation of receptor nanoclusters to increase their avidity for the antigen. In cancer, there is a high demand for cholesterol to support the inherent nature of tumor cells to divide and proliferate, and perturbations of reverse cholesterol transport can have negative

consequences. Drugs that lower cholesterol levels in cancer cells by inhibiting the mevalonate pathway are undergoing clinical trials.

When increased levels of sterols other than cholesterol are detected in plasma, they typically serve as markers for abnormalities in lipid metabolism associated with specific disease states. For example, premature atherosclerosis and xanthomatosis occur in two rare lipid storage diseases, cerebrotendinous xanthomatosis and sitosterolemia. In the former, cholestanol is present in all tissues, while in the latter, the dietary plant sterols campesterol and sitosterol accumulate in plasma and red blood cells. Inhibition of cholesterol biosynthesis may be associated with the appearance of some of the precursor sterols in the plasma.

In infections with *Mycobacterium tuberculosis*, the organism utilizes host cholesterol as its primary carbon and energy source, thereby promoting persistent infection with significant effects on pathogenicity. Similarly, *Chlamydia trachomatis*, a gram-negative obligate intracellular bacterium and a significant cause of sexually transmitted diseases, requires host cholesterol for growth. Many viruses utilize cholesterol as part of their life cycle, and a reduction in cellular cholesterol is sometimes employed as an anti-viral strategy. However, this approach may not always be beneficial. For example, an HIV protein has a binding site for cholesterol, which it utilizes to facilitate fusion with raft regions in the host cell's membranes.

21.5.2: STEROLS: 2. OXYSTEROLS AND OTHER CHOLESTEROL DERIVATIVES

Oxysterols, as defined and discussed here, are oxygenated derivatives of **cholesterol** and its precursors, i.e., with additional hydroxyl, epoxyl, or keto groups, that are found in all animal tissues. Many of these have vital functions in animals. In contrast, others are important as short-lived intermediates or end products in the catabolism or excretion of cholesterol, as well as in the biosynthesis of steroid hormones, bile acids, and 1,25-dihydroxy-vitamin D_3. They are usually present in biological membranes and lipoproteins at trace levels, although they can exert profound biological effects at these concentrations. However, they are always accompanied by a significant excess (as much as 10^6-fold) of cholesterol *in itself*.

A variety of different oxysterols are synthesized in cells through sequential reactions catalyzed by specific oxygenases. However, due to the presence of the double bond in the 5,6-position, oxysterols can also be formed rapidly by non-enzymatic oxidation, or autoxidation, of cholesterol and cholesterol esters within tissues, resulting in the formation of various oxygenated derivatives. Simplistically, non-enzymatic oxidation leads mainly to the generation of products in which the sterol ring system is oxidized. At the same time, enzymatic processes typically produce metabolites with an oxidized side chain, with 7-hydroxylation being an important exception. Oxidized cholesterol molecules can also be generated by the gut microflora and be taken up through the enterohepatic circulation. Once an oxygen function is introduced into cellular cholesterol, the product can act as a biologically active mediator by interacting with specific receptors before it is metabolized to **bile acids** or further degraded, a process assisted by the fact that oxysterols can diffuse much more rapidly through membranes than cholesterol itself. Cholesterol metabolites of this kind are significant in the brain, which is a major site for *de novo* cholesterol synthesis, and they are crucial elements of cholesterol homeostasis.

21.5.2.1: ENZYMATIC OXIDATION OF CHOLESTEROL

Within animal cells, the oxidation of sterols is primarily an enzymatic process carried out by several enzymes from the cytochrome P450 family of oxygenases, named for their characteristic absorption at 450 nm. These comprise a disparate group of proteins that contain a single heme group and have a similar structural fold, though the amino acid sequences can differ appreciably. They are all mono-oxygenases. Oxysterol biosynthesis can be considered in terms of different pathways that depend on the position of the initial oxidation. These pathways tend to overlap and lead to a complex web of different oxysterols, eventually resulting in **bile acids**. As these enzymes, which include cytochrome P450, cholesterol hydroxylase, hydroxysteroid dehydrogenases, and squalene epoxidase, are specific to particular tissues and indeed animal species, there is considerable variation in oxysterol distributions between organs. A few examples only of the first steps in some of these pathways are illustrated in Figure **21.5.31**.

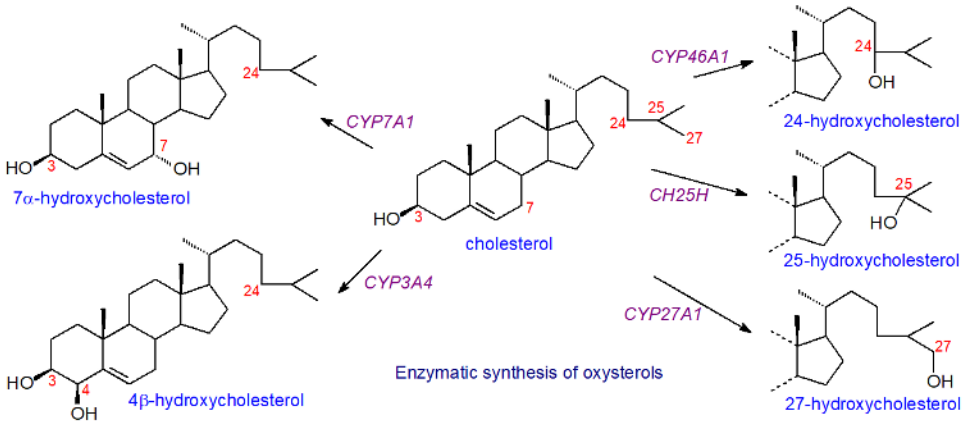


Figure **21.5.31**: Enzymatic synthesis of oxysterols

As an example, a primary product is **7α-hydroxycholesterol**, which is an important intermediate in the biosynthesis of bile acids by the 'neutral' pathway and of many other oxysterols, and it is produced in the liver by the action of cholesterol 7α-hydroxylase (CYP7A1). This enzyme plays a crucial role in maintaining cholesterol homeostasis. The reaction is under strict regulatory control, and the expression of CYP7A1 is controlled by the farnesoid X receptor (FXR) and is activated by cholic and chenodeoxycholic acids. Any circulating 7α-hydroxycholesterol represents leakage from the liver. Further oxidation of 7α-hydroxycholesterol can occur, and the action of CYP3A4 in humans generates 7α,25-dihydroxycholesterol as an important metabolite, for example, while oxidation by CYP27A1 yields 7α,27-dihydroxycholesterol; the latter is regarded as a key step in a further pathway to oxysterols and bile acids. On the other hand, the epimer **7β-hydroxycholesterol** is produced in the brain by the action of the toxic β-amyloid peptide and its precursor on cholesterol, but whether this is involved in the pathology of Alzheimer's disease has yet to be determined.

The hydroxysteroid 11-β-dehydrogenase 1 (HSD11B1) is responsible for the conversion of 7β-hydroxy-cholesterol to the important metabolite **7-keto-cholesterol**, while HS11B2 catalyzes the reverse reaction; 7-keto-cholesterol is also formed by autoxidation (see below). HSD11B1 is better known as the oxidoreductase that converts inactive cortisone to the active stress hormone cortisol in glucocorticoid target tissues.

An alternative ('acidic') pathway to bile acids starts with the synthesis of **27-hydroxycholesterol** (or more systematically named (25*R*)26-hydroxycholesterol), which is produced by the cytochrome P450 enzyme (CYP27A1) and introduces the hydroxyl group into the terminal methyl carbon (C27 or C26 - used interchangeably). While this enzyme is present in the liver, it is also found in many extrahepatic tissues, particularly the lung, which provides a steady flux of 27-oxygenated metabolites to the liver. As a multifunctional mitochondrial P450 enzyme in the liver, it generates both 27-hydroxycholesterol and 3β-hydroxy-5-cholestenoic acid, the bile acid precursor, which occurs in small but significant amounts in plasma. 27-Hydroxycholesterol is the most abundant circulating oxysterol, and its concentration in plasma correlates with that of total cholesterol. It can be oxidized to 7α,27-dihydroxycholesterol by the enzyme CYP7B1. **4β-Hydroxycholesterol** is also abundant in plasma and is relatively stable; it is produced in humans by the action of the cytochromes CYP3A4 and CYP3A5.

In humans, the specific cytochrome P450 that produces **24*S*-hydroxycholesterol** (cholest-5-ene-3β,24-diol) is cholesterol 24*S*-hydroxylase (CYP46A1) and is located almost entirely in the smooth endoplasmic reticulum of neurons in the brain, including those of the hippocampus and cortex, which are important for learning and memory. It is by far the most abundant oxysterol in the brain after parturition, but during development, many more oxysterols are produced. 24*S*-hydroxycholesterol is responsible for 98-99% of the turnover of cholesterol in the central nervous system, which is the source of most of this oxylipin found in plasma. A small amount of it is converted in the brain directly into 7α,24*S*-dihydroxycholesterol by the cytochrome CYP39A1 and thence via side-chain oxidation in peroxisomes to bile acids, such as cholestanoic acid. It is evident that constant passive fluxes of oxysterols cross the blood-brain barrier, but not cholesterol *per se*, due to their permissive chemical structures and concentration gradients. In plasma, it is transported via high-density lipoproteins, as discussed further below. In contrast to humans, CYP46A1 is present in the liver of rodents as well as the brain.

25-Hydroxycholesterol is a relatively minor but biologically important cholesterol metabolite that is produced rapidly by immune cells in response to inflammation resulting from bacterial or viral infections. The dioxygenase enzyme cholesterol 25-hydroxylase (CH25H in humans), which utilizes a diiron cofactor to catalyze hydroxylation, is the primary route to this metabolite *in vivo*. *However,* at least two cytochrome P450 enzymes, CYP27A1 and CYP3A4, can catalyze this conversion to a limited extent. Further oxidation by CYP7B1 is a second route to 7α,25-dihydroxycholesterol, and thus to additional oxysterols.

24(*S*),25-Epoxycholesterol is not produced by the pathways described above but is synthesized in a shunt of the mevalonate pathway using the same enzymes that produce cholesterol, specifically squalene mono-oxygenase and lanosterol synthase, in which a second epoxy group

is introduced on the other end of squalene from the initial epoxidation. A further mechanism in the brain is the action of CYP46A1 on desmosterol, another intermediate in cholesterol biosynthesis.

The oxysterols formed by both autoxidation and enzymatic routes can undergo further oxidation-reduction reactions, and they can be modified by many of the enzymes involved in the metabolism of cholesterol and steroidal hormones, such as esterification and sulfation of position 3, as illustrated for 7-keto-cholesterol as an example in Figure **21.5.32**.

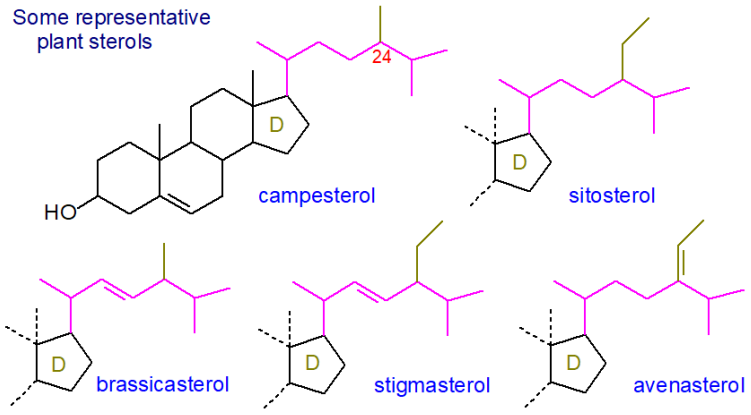


Figure **21.5.32**: Metabolism of 7-keto-cholesterol

In most tissues, esterification of the 3β-hydroxyl group only occurs and requires the activity of sterol *O*-acyltransferases 1/2 (SOAT1/2 or ACAT1/2) with the participation of cytosolic phospholipase A_2 (cPLA_2α) to liberate the required fatty acids from phospholipids. In plasma, oxysterols can be esterified by lecithin–cholesterol acyltransferase (LCAT) for transport in lipoproteins; however, in this instance, a diester can be specifically produced from 27-hydroxycholesterol. Whether such esters serve as an inert storage form for oxysterols, which can be liberated on demand by esterases, remains to be determined.

It is noteworthy that the important human pathogen *Mycobacterium tuberculosis* utilizes a cytochrome P450 enzyme (CYP125) to catalyze the C26/C27 hydroxylation of cholesterol, an essential early step in its catabolism as part of the infective process.

Catabolism: Because of their increased polarity relative to cholesterol, oxysterols produced by both enzymatic and non-enzymatic means can exit cells relatively easily. A proportion is oxidized further and converted to **bile acids**, while some are converted to sulfate esters (especially at the 3-hydroxyl group) or glucuronides (see below) for elimination via the kidneys.

21.5.2.2: NON-ENZYMATIC OXIDATION OF CHOLESTEROL

In biological systems in which both cholesterol and fatty acids are present, it would be expected that autoxidation of polyunsaturated fatty acids by free radical mechanisms would be favored thermodynamically, with the formation of isoprostanes from arachidonic acid in phospholipids. However, certain circumstances can favor cholesterol oxidation *in vivo*. For example, the concentration of cholesterol in low-density lipoprotein particles (LDL) is approximately three times higher than that of phospholipids, and the rate of cholesterol-hydroperoxide formation can be higher than that of phospholipid hydroperoxides. The rate and specificity of the reaction can also depend on whether it is initiated by free radical species, such as those arising from the superoxide/hydrogen peroxide/hydroxyl radical system (Type I autoxidation), or whether it occurs by non-radical but highly reactive oxygen species such as singlet oxygen, HOCl, or ozone (Type II autoxidation). As examples of the main types of products of non-enzymatic oxidation, the structures of a few of the more important of these oxysterols are illustrated in Figure **21.5.33**.

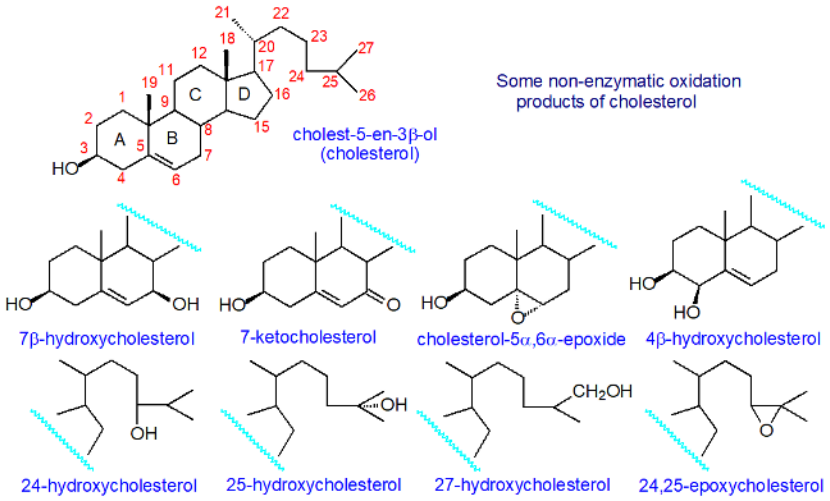


Figure **21.5.33**: Some non-ezymatic oxidation products of cholesterol

Oxysterols produced by this means can vary in type (hydroperoxy, hydroxy, keto, epoxy), number, and position of the oxygenated functions introduced, as well as the nature of their stereochemistry. Derivatives with the A and B rings and the *iso*-octyl side-chain oxidized are illustrated, but compounds with oxygen groups in position 15 (D ring) are also important biologically. Many are similar to those produced by enzymatic means, although the stereochemistry typically differs. Like the enzymic products, they are named according to their relationship to cholesterol, rather than by the strict systematic terminology.

Mechanisms of autoxidation have been studied intensively in relation to unsaturated fatty acids, and it appears that similar mechanisms also operate with sterols. The first event in lipid peroxidation by a radical mechanism is an initiation reaction, in which a carbon with a labile hydrogen undergoes hydrogen abstraction by reaction with a free radical, such as a non-lipid species, including transition metals, hydroxyl radicals, or peroxynitrite radicals. This is followed by oxygen capture. The resulting reactive species recruits further non-oxidized lipids, initiating a chain reaction known as the propagation phase. Finally, the reaction is terminated by the conversion of hydroperoxy intermediates into more stable hydroxy products through reaction with endogenous antioxidants, such as tocopherols.

As an example, the reaction mechanism leading to the production of 7-oxygenated cholesterol derivatives is illustrated in Figure **21.5.34**.

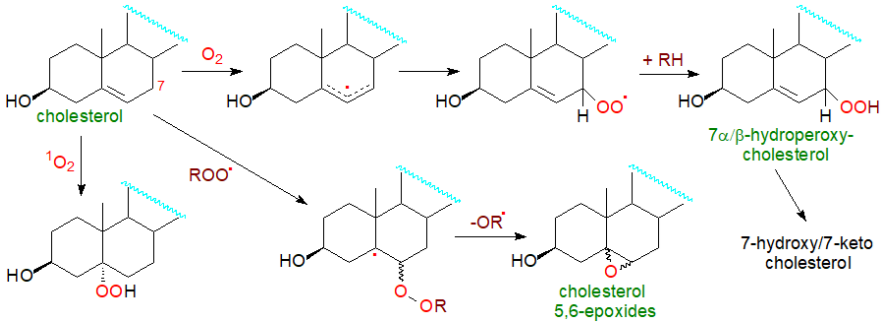


Figure **21.5.34**: Cholesterol non-enzymatic oxidation mechanisms

In aqueous dispersions, oxidation is initiated by a radical attack from a reactive-oxygen species such as a hydroxyl radical with the abstraction of hydrogen from the C-7 position to form a delocalized three-carbon allylic radical, which reacts with oxygen to produce 7α-hydroperoxycholesterol, which gradually isomerizes to the more thermodynamically stable 7β-hydroperoxycholesterol. Subsequent enzymic and non-enzymic reactions lead to the 7-hydroxy and 7-keto analogs, which tend to be the most abundant non-enzymatically generated oxysterols in tissues, often accompanied by epoxy-ene and ketodienoic secondary products. Reaction with singlet oxygen ($^1O_2$) produces 5α-hydroperoxycholesterol mainly together with some 6α- or 6β-hydroperoxycholesterol. The reaction does not occur readily at the other allylic carbon, 4, presumably due to steric hindrance. When cholesterol is in the solid state, the reaction occurs primarily at the tertiary carbon-25, though some products oxygenated at C-20 may also be produced.

Cholesterol hydroperoxides can be converted to stable diols only by the phospholipid hydroperoxide glutathione peroxidase-type 4 (GPx4) and then relatively slowly, but not by the type 1 glutathione peroxidase (GPx1) when in a membrane-bound state. However, in mammalian cells, monomeric GPx4 (~20 kDa), although present in several cellular compartments, including mitochondria, is much less abundant than tetrameric GPx1. Phospholipid-hydroperoxides are reduced most rapidly, followed by cholesterol 6β-OOH > 7α/β-OOH >> 5α-OOH. The

result is that cholesterol hydroperoxides are expected to have a relatively long half-life and can therefore be potentially quite hazardous in biological systems. Of these, 5α-OOH, with the lowest reduction rate, is the most cytotoxic of the hydroperoxides, unfortunately.

Epimeric 5,6-epoxy-cholesterols may be formed by a non-radical reaction involving the non-enzymatic interaction of a hydroperoxide with the double bond, a process believed to occur primarily in macrophages and low-density lipoproteins (LDL). In this instance, the initial peroxidation product is a polyunsaturated fatty acid. The hydroperoxide transfers an oxygen atom to cholesterol, producing the epoxide, and in doing so, is reduced to a hydroxyl. Other non-radical oxidation processes include reactions with singlet oxygen, which is especially important in the presence of light and photosensitizers, and can generate 5-hydroxy as well as 6- and 7-hydroxy products. Additionally, the reaction with ozone in the lungs can create a family of distinctive oxygenated cholesterol metabolites.

Similarly, a diverse range of oxidation products is generated by the peroxidation of the cholesterol and vitamin D precursor 7-dehydrocholesterol, which has the highest propagation rate constant known for any lipid in free-radical chain oxidation. These metabolites possess important biological properties.

Oxysterols occur in tissues both in the free state and esterified with long-chain fatty acids. For example, in human atherosclerotic lesions, 80–95% of all oxysterols are esterified. Appreciable amounts of oxysterols can be present in foods, especially those rich in cholesterol, such as meat, eggs, and dairy products, where they are most probably generated non-enzymically during cooking or processing when such factors as temperature, oxygen, light exposure, the associated lipid matrix, and the presence of antioxidants and water all play a part. Those present in foods can be absorbed from the intestines and transported into the circulation in chylomicrons. However, the extent to which dietary sources contribute to tissue levels of total oxysterols or individual isomers is not known and is likely to be highly variable, but relatively lower than that of cholesterol *itself*.

21.5.2.3: OXYSTEROLS – BIOLOGICAL ACTIVITY

General Functions: In vivo tissues, the very low oxysterol:cholesterol ratio means that oxysterols have a minimal impact on the primary role of cholesterol in cell membrane structure and function. However, it has been claimed that oxysterols could cause packing defects and, consequently, atheroma formation in vascular endothelial cells. It is often argued that there are few reliable measurements of cellular or subcellular oxysterol concentrations, because of the technical difficulties in the analysis of the very low concentrations of oxysterols in the presence of a vast excess of native cholesterol; the average levels of 26-, 24- and 7α-hydroxy-cholesterol in human plasma that are often quoted are 0.36, 0.16 and 0.14 μM, respectively. Autoxidation products of cholesterol, particularly 7-keto- and 7-hydroxy-cholesterol, are cytotoxic and may serve as useful markers of oxidative stress or for monitoring the progression of various diseases. However, experts in the field caution that it can be challenging to extrapolate from experiments *in vitro* to the in vivo situation, due to the rapidity with which cholesterol can autoxidize in experimental systems and the difficulty of conducting experiments with physiological levels of oxysterols.

Nonetheless, aside from their role as precursors of bile acids and some steroidal hormones, it is evident that oxysterols have a variety of roles in maintaining cholesterol homeostasis and perhaps in signaling, where those formed enzymatically are most significant. They can exert potent biological effects at physiologically relevant concentrations by binding to various receptors, thereby eliciting transcriptional programs that regulate gene and, consequently, protein expression. Among many cell membrane receptors for oxysterols that have been identified, nuclear receptors are especially important and include the liver X receptors (LXRs), retinoic acid receptor-related orphan receptors (RORs), estrogen receptors (ERs), and glucocorticoid receptors (GRs). In addition, *N*-methyl-D-aspartate receptors (NMDARs) are expressed in nerve cells and work over a short time scale to regulate excitatory synaptic function. In contrast, G protein-coupled receptors operate at the cell membrane and are activated by molecules outside the cell to initiate signaling pathways within the cell. As various isoforms of these receptors exist in different tissues and can interact with several oxysterols, only a summary of this complex topic is possible here.

A family of oxysterol-binding proteins (OSBP) transports and regulates the metabolism of sterols and targets oxysterols to specific membranes, especially to contact sites between organelles, with the transport of **phosphatidylinositol 4-phosphate** in the reverse direction (see our web page on the latter). In this way, they can enable oxysterols to regulate membrane composition and function, as well as mediate intracellular lipid transport. As with cholesterol, oxysterols can be eliminated from cells by transporters such as the ATP-binding cassette proteins ABCA1 and ABCG1. They are transported in the bloodstream within lipoproteins, especially in association with HDL and LDL, and are mainly present in the esterified form.

Cholesterol homeostasis: While cholesterol plays a key role in its own feedback regulation, there is some evidence that oxysterols are **regulators of cholesterol concentration** in cell membranes, and that **25-hydroxycholesterol** and **24(*S*),25-epoxycholesterol** may be especially effective, although the other side-chain oxysterols 22-, 24- and 27-hydroxycholesterol have been implicated. Several mechanisms appear to be involved, and it is suggested that 24(*S*),25-epoxycholesterol especially acts as a ligand for the liver X receptor, which forms a heterodimer with the retinoic X receptor, to inhibit the transcription of key genes in cholesterol biosynthesis, as well as directly inhibiting or accelerating the degradation of such important enzymes in the process as HMG-CoA reductase and squalene synthase. Similarly, both 26-hydroxylanosterol and 25-hydroxycholesterol inhibit HMG-CoA reductase. 25-Hydroxycholesterol inhibits the transfer of the 'sterol

regulatory element binding protein' (SREBP-2) to the Golgi for processing to its active form as a transcription factor for the genes of the cholesterol biosynthesis pathway, and it stimulates the enzyme acyl-CoA:cholesterol acyl transferase in the endoplasmic reticulum to esterify cholesterol. Through these mechanisms, oxysterols fine-tune cholesterol homeostasis, ensuring smooth regulation rather than substantial fluctuations in tissue concentration.

Oxysterols and the immune system: Oxysterols are known to have vital and diverse roles in immunity by regulating both the adaptive and innate immune responses to infection. For example, infection with viruses leads to the production of type I interferon. In macrophages, this induces the synthesis of **25-hydroxycholesterol**, which is generally regarded as anti-inflammatory and exerts broad antiviral activity by activating integrated stress response genes and reprogramming protein translation again via its interaction with LXR receptors. It is a potent inhibitor of SARS-CoV-2 replication, for example, possibly by a mechanism involving the blocking of cholesterol export from the late endosome/lysosome compartment and depletion of membrane cholesterol levels. However, the formation of 25-hydroxycholesterol may be detrimental in cases of influenza infections, as it can lead to the overproduction of inflammatory metabolites. Similarly, the biosynthesis of 25-hydroxycholesterol in macrophages is stimulated by the endotoxin **Kdo2-lipid A**, the active component of the lipopolysaccharide present on the outer membrane of Gram-negative bacteria, which acts as an agonist for Toll-like receptor 4 (TLR4). There is enhanced expression of the oxygenase CH25H in immune cells in response to bacterial and viral infection.

Many oxysterol species are active in a range of immune cell subsets, mediated through the control of LXR and SREBP signaling, as well as by acting as ligands for RORs and for the cell surface receptors G protein-coupled receptor 183 (GPR183) or CXCR2. Activation of LXR tends to dampen the immune response. In response to various stimuli, they can operate through ion channels to effect rapid changes in intracellular ion concentrations, especially of Ca^{2+}, which brings about changes in membrane potential, cell volume, cell death (including apoptosis, autophagy, and necrosis), gene expression, secretion, endocytosis, or motility. For example, 27-hydroxycholesterol in human milk is reported to be active against the pathogenic human rotavirus and rhinovirus, which are important in pediatrics. Additionally, 7-dehydrocholesterol also exhibits antiviral properties. While they can exert their immune functions within the cell in which they are generated, oxysterols can also operate in a paracrine fashion towards other immune cells.

25-Hydroxycholesterol, in particular, can have either pro- or anti-inflammatory effects, depending on the conditions; however, the enzyme CH25H, responsible for its biosynthesis, is induced markedly in macrophages activated by inflammatory agents. It is reported to have a regulatory effect on the biosynthesis of sphingomyelin, which is required in conjunction with cholesterol for the formation of **raft** subdomains in membranes, where signaling molecules are concentrated. Together with other oxysterols, such as 24*S*,25-epoxycholesterol, it regulates the activities of the **hedgehog proteins** involved in embryonic development. Metabolites of 25-hydroxycholesterol, such as 7α,25-dihydroxycholesterol, and further oxidation products, are pro-inflammatory and act as chemoattractants for lymphocytes, playing a role in the regulation of immunity in secondary lymphoid organs through interactions with the GPR183 receptor.

Oxysterols in the brain: Oxysterols are especially important for cholesterol homeostasis in the brain, which contains 25% of the total body cholesterol, virtually all of it in unesterified form, in only about 2% of the body volume. Cholesterol is a major component of the plasma membrane, particularly in its role of regulating fluidity and permeability. This membrane is produced in large quantities in the brain. It forms the basis of compacted myelin, which is essential for the conduction of electrical stimuli and contains approximately 70% of the brain's cholesterol. While this pool is relatively stable, the remaining 30% is present in the membranes of neurons and glial cells in the gray matter and is more metabolically active. Even in the fetus and the newborn infant, all the cholesterol required for growth is produced by synthesis *de novo* in the brain, not by transfer from the circulation across the blood-brain barrier, which consists of tightly opposed endothelial cells lining the extensive vasculature of the tissue. The fact that this pool of cholesterol in the brain is independent of circulating levels must reflect a requirement for constancy in the content of this lipid in membranes and myelin. In adults, although the membrane undergoes continuous turnover, cholesterol is efficiently recycled and has a remarkably high half-life, up to 5 years. The rate of cholesterol synthesis is a little greater than the actual requirement, so net movement of cholesterol out of the central nervous system must occur. A crucial component of this system is apolipoprotein E (Apo E), a 39-kDa protein highly expressed in the brain, which facilitates the cellular transport of cholesterol and contributes to cholesterol homeostasis. Apo E complexes with cholesterol are required for transport from the site of synthesis in astrocytes to neurons.

Hydroxylation by CYP46A1 of cholesterol to **24(*S*)-hydroxycholesterol** (cerebrosterol) is responsible for 50–60% of all cholesterol metabolism in the adult brain. If cholesterol itself cannot cross the blood-brain barrier, this metabolite can do so with relative ease. When the hydroxyl group is introduced into the side chain, this oxysterol causes a local reordering of membrane phospholipids, making it more favorable energetically to expel it at a rate that is orders of magnitude greater than that of cholesterol *alone*, although still only 3-7 mg per day. There is a continuous flow of metabolites from the brain into the circulation, much of which is in the form of inactive sterol esters, which are transported by lipoprotein particles to the liver for further catabolism. Specifically, it undergoes hydroxylation at position 7 and is then converted into **bile acids**. This is illustrated in Figure **21.5.35**.

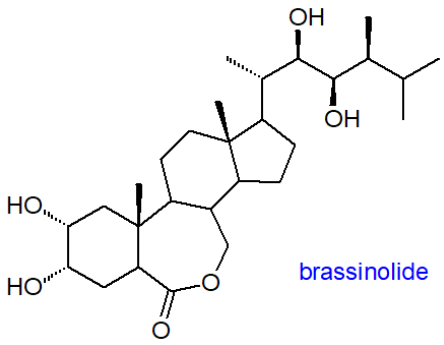


Figure **21.5.35**: Brain/Liver 27-carboxy and 27-OH steroid metabolism.

Both 24(*S*)-hydroxycholesterol and 24(*S*),25-epoxycholesterol are believed to play a role in regulating cholesterol homeostasis in the brain. They interact with the specific nuclear receptors involved in the expression and synthesis of proteins involved in sterol transport. For example, 24-hydroxycholesterol regulates the transcription of apolipoprotein E (ApoE). In particular, it is an agonist of the nuclear liver X receptors (LXRs), influencing the expression of those LXR target genes involved in cholesterol homeostasis and inflammatory responses. It is also a high-affinity ligand for the retinoic acid receptor-related orphan receptors α and γ (RORα and RORγ). In this way, it can act locally to affect the functioning of neurons, astrocytes, oligodendrocytes, and vascular cells.

24(*S*)-Hydroxycholesterol downregulates the trafficking of the amyloid precursor protein and may be a factor in preventing neurodegenerative diseases. Especially high levels of 24(*S*)-hydroxycholesterol are observed in the plasma of human infants and patients with brain trauma. In contrast, reduced levels are found in the plasma of patients with neurodegenerative diseases, including Parkinson's disease, multiple sclerosis, and Alzheimer's disease. In contrast, there are elevated levels in the brain and especially cerebrospinal fluid in patients with these conditions, where it may be a marker of neurodegeneration. Increased expression of cholesterol 24-hydroxylase (CYP46A1) is believed to improve cognition. At the same time, a reduction leads to poor cognitive performance, as occurs at advanced stages of the disease, likely reflecting a selective loss of neuronal cells. This may be a factor in age-related macular degeneration. An excess of 24(*S*)-hydroxycholesterol and especially of its ester form can lead to neuronal cell death, and elevated levels in plasma are reported to be a potential marker for Autism Spectrum Disorders in children. On the other hand, it may be protective against glioblastoma, the most common primary malignant brain tumour in adults, via activation of LXRs.

27-Hydroxy-cholesterol diffuses across the blood-brain barrier from the bloodstream into the brain (in the reverse direction to 24-hydroxycholesterol), where it does not accumulate but is further oxidized and then exported as steroidal acids. This flux may regulate certain key enzymes within the brain, and there are suggestions that the balance between the levels of 24- and 27-hydroxy-cholesterol, especially an excess of the latter, may be relevant to the generation of β-amyloid peptides in Alzheimer's disease by reducing insulin-mediated glucose uptake by neurons. While 7β-hydroxycholesterol is pro-apoptotic, any links with Alzheimer's disease are unproven. However, there is a school of thought that other oxidized cholesterol metabolites may be major factors behind the development of this disease. For example, seco-sterols such as 3β-hydroxy-5-oxo-5,6-secocholestan-6-al and its stable aldolization product, the main ozonolysis metabolites derived from cholesterol, have been detected in brain samples of patients who have died from Alzheimer's disease and Lewy body dementia; they are also found in atherosclerotic lesions. Oxidation products of the cholesterol precursor 7-dehydrocholesterol and especially those of 3β,5-dihydroxycholest-7-ene-6-one are involved in the pathophysiology of the human disease Smith-Lemli-Opitz syndrome.

Cell differentiation: Oxysterols can influence the differentiation of various cell types, a phenomenon first studied in the skin, where 22(*R*)- and 25(*R*)-hydroxycholesterol were shown to induce differentiation in human keratinocytes. Subsequently, by stimulating nuclear binding receptors, oxysterols were found to have similar effects on mesenchymal stem cells. There have been numerous reports of the involvement of oxysterols in various disease processes, including atherosclerosis and the formation of human atherosclerotic plaques, as well as cytotoxicity, necrosis, inflammation, immunosuppression, phospholipidosis, and gallstone formation. They have been implicated in the development of cancers, especially those of the breast, prostate, colon, and bile duct. For example, **27-hydroxycholesterol** is a component in the elimination of cholesterol from macrophages and arterial endothelial cells. Still, it is also an endogenous ligand for the human nuclear estrogen receptor (ERα) and the liver X receptor. It modulates their activities, with effects on various human disease states, including cardiovascular dysfunction and the progression of breast and prostate cancer, as well as involvement in the regulation of bone mineralization (osteoporosis). It has been linked to cancer metastasis through effects on immune cells, and there is hope that pharmacological inhibition of CYP27A1 and thence the formation of 27-hydroxycholesterol may be a useful strategy in the treatment of breast cancer; *CYP7A1* gene polymorphism has been associated with colorectal cancer. In contrast, oxysterols can interfere with the proliferation of several types of cancer cells (glioblastoma, leukemia, colon, breast, and prostate cancer).

Cholesterol 5,6-epoxide (with either 5α or 5β stereochemistry) is formed non-enzymatically in tissues, but it is also believed to be produced by an unidentified cytochrome P450 enzyme in the adrenal glands. While it was for some time believed to be a causative agent in cancer, it is now recognized that downstream metabolites are responsible. Thus, cholesterol epoxide hydrolase converts cholesterol 5,6-epoxide into cholestane-3β,5α,6β-triol, which is transformed by 11β-hydroxysteroid-dehydrogenase-type-2 into the oncometabolite 3β,5α-dihydroxycholestan-6-one (oncosterone). By binding to the glucocorticoid receptor, this oncosterone stimulates the growth of breast cancer cells, and it also acts as a ligand to the LXR receptors, which may mediate its pro-invasive effects. In contrast, in normal breast tissue, cholesterol 5,6-epoxide is metabolized to the tumor suppressor metabolite, a steroidal alkaloid designated dendrogenin A, which is a conjugation product with histamine and controls a nuclear receptor to trigger lethal autophagy in cancers; its synthesis is greatly reduced in cancer cells. Tamoxifen, a widely used drug against breast cancer, binds to the cholesterol 5,6-epoxide hydrolase, which is also a microsomal anti-estrogen binding site (AEBS), thereby inhibiting its activity.

7-Ketocholesterol is a major oxysterol produced during the oxidation of low-density lipoproteins and is one of the most abundant in plasma and atherosclerotic lesions; it accumulates in erythrocytes of heart failure patients. It exhibits a high pro-apoptotic potential and preferentially associates with membrane lipid **raft** domains. As it is not readily exported from macrophages, it impairs cholesterol efflux and promotes the development of the foam cell phenotype. In cardiomyocytes, this accumulation can lead to cell hypertrophy and death, and it has been suggested that oxysterols constitute a significant factor precipitating morbidity in atherosclerosis-induced cardiac diseases and inflammation-induced heart complications. Photooxidation in the retina, mediated by the action of free radicals or singlet oxygen, generates unstable cholesterol hydroperoxides, which may contribute to the development of age-related macular degeneration. For example, these compounds can be quickly converted to highly toxic 7α- and 7β-hydroxycholesterols and 7-ketocholesterol, depending on the status of tissue oxidases and reductases. Three separate enzymatic pathways have developed in the eye to neutralize their activities. Novel branches of the acidic pathway of bile acid biosynthesis metabolize these sterols.

Those oxysterols formed non-enzymatically can be particularly troublesome in disease. For example, they are enriched in pathologic cells and tissues, such as macrophage foam cells, atherosclerotic lesions, and cataracts. They may regulate some of the metabolic effects of cholesterol, but as cautioned above, effects observed *in vitro* may not necessarily be of physiological importance *in vivo*. Various oxysterols have been implicated in the differentiation of mesenchymal stem cells, as well as the signaling pathways involved in this process. High levels of 7-hydroxycholesterol and cholestane-3β,5α,6β-triol are characteristic of the lysosomal storage diseases Niemann-Pick types B and C, as well as lysosomal acid lipase deficiency.

Cholesterol hydroperoxides: With the aid of START domain proteins, cholesterol hydroperoxides can translocate from a membrane of origin to another membrane, such as mitochondria. Such a transfer of free radical-generated 7-hydroperoxycholesterol, for example, has adverse consequences, as it impairs cholesterol utilization in steroidogenic cells and the anti-atherogenic reverse-cholesterol transport in vascular macrophages. The antioxidant activity of GPx4 may be crucial for maintaining mitochondrial integrity and functionality in these cells.

21.5.2.4: VITAMIN D

Vitamin D encompasses two primary sterol metabolites that are essential for the regulation of calcium and phosphorus levels and hence for bone formation in animals. However, these have many other functions, including induction of cell differentiation, inhibition of cell growth, immunomodulation, and control of other hormonal systems. Vitamin D deficiency, often accompanied by calcium deficiency, is responsible for the disease rickets in children, characterized by weak and deformed bones. It is also associated with various types of cancer and autoimmune diseases. Ultraviolet light mediates the cleavage of 7-dehydrocholesterol, an important intermediate in cholesterol biosynthesis, by opening the second (B) ring in the skin to produce pre-vitamin D. This pre-vitamin D rearranges spontaneously to form the secosteroid vitamin D3, also known as cholecalciferol. Its structure is shown in Figure **21.5.36**.

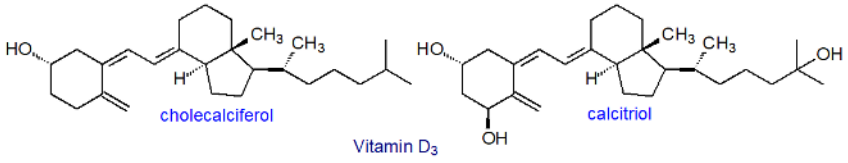


Figure **21.5.36**: Structure of Vitamin D_3

The newly generated vitamin D3 is transported to the liver, where it undergoes 25-hydroxylation and is subsequently transported to the kidney for 1α-hydroxylation to produce the active form, 1α,25-dihydroxyvitamin D3 (calcitriol). This is an actual hormone and serves as a high-affinity ligand for the vitamin D receptor in distant tissues. For transportation in plasma, it is bound to a specific glycoprotein, vitamin D-binding protein (BDP). Vitamin D_2 or ergocalciferol is derived from ergosterol, which is obtained from plant and fungal sources in the diet.

Vitamin D_3 functions by activating a cellular receptor, known as the vitamin D receptor (VDR), a transcription factor that binds to sites in the DNA called vitamin D response elements. There are thousands of such binding sites, which, together with co-modulators, regulate innumerable genes in a cell-specific manner. In this way, it enhances bone mineralization by promoting the absorption of dietary calcium and phosphate, as well as having direct effects on bone cells. In addition, it functions as a general development hormone in many different tissues, while together with Vitamin D_2 it has profound effects on immune responses in the defense against microbes.

21.5.2.5: STEROIDAL HORMONES AND THEIR ESTERS

Steroidal hormones cannot be discussed in depth here as their structures, biosynthesis, and functions comprise a rather substantial and specialized topic. In brief, animal tissues produce small amounts of vital steroidal hormones from cholesterol, the primary precursor, with 22*R*-hydroxycholesterol, produced by hydroxylation via the cholesterol side-chain cleavage enzyme (P450scc), as the first metabolite in the pathway. This step involves the 'STAR' protein, which enables the transport of cholesterol into mitochondria, where conversion to pregnenolone is rate-limiting and involves first hydroxylation and then cleavage of the side-chain. After export from the mitochondria, it can be converted directly to progesterone or, in several steps, to testosterone. 17β-Estradiol, for example, is the most potent and important of the endogenous estrogens; it is made mainly in the follicles of the ovaries and regulates menstrual cycles and reproduction, but it is also present in testicles, adrenal glands, fat, liver, breasts, and brain. Testosterone is the primary male sex hormone and an anabolic steroid, and it is produced mainly in the testes; it has a key function in the development of male reproductive tissues such as the testes and prostate, in addition to promoting secondary sexual characteristics. Pregnane neurosteroids are synthesized in the central nervous system. Cholesterol homeostasis is therefore vital to fertility and numerous bodily functions. The structures of key steroidal hormones are shown in Figure **21.5.37**.

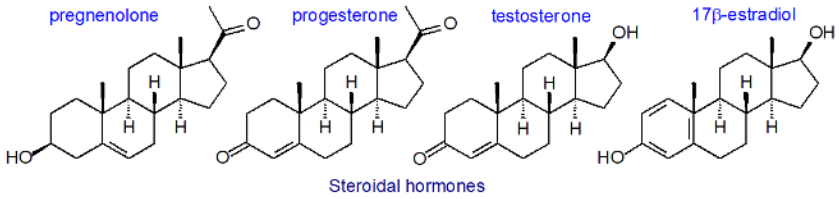


Figure **21.5.37**: Structures of key steroidal hormones

Steroidal esters accumulate in tissues, such as the adrenal glands, which synthesize corticosteroids like cortisol and aldosterone, and are responsible for releasing hormones in response to stress and other factors. It is also apparent that fatty acyl esters of estradiols, such as dehydroepiandrosterone, accumulate in adipose tissue in post-menopausal women. Small amounts of estrogens acylated with fatty acids at the C-17 hydroxyl are present in the plasma lipoproteins. In each instance, they appear to be biologically inert storage or transport forms of the steroid. Eventually, esterified steroids in low-density lipoproteins (LDL) particles are taken up by cells via lipoprotein receptors and then are hydrolyzed to release the active steroid.

21.5.3: STEROLS 3. STEROLS AND THEIR CONJUGATES FROM PLANTS AND LOWER ORGANISMS

21.5.3.1: PLANT STEROLS - STRUCTURES AND OCCURRENCE

Plants, algae, and fungi contain a somewhat different range of sterols from those in animals. Like **cholesterol**, to which they are structurally and biosynthetically related, plant sterols form a group of triterpenes with a tetracyclic cyclopenta[*a*]phenanthrene structure and a side chain at carbon 17, sometimes referred to as the $C_{30}H_{50}O$ triterpenome. The four rings (A, B, C, D) have *trans* ring junctions, and the side chain and two methyl groups (C-18 and C-19) are oriented at an angle to the rings above the plane, exhibiting β stereochemistry (similar to a hydroxyl group commonly located on C-3). The basic sterol from which other sterol structures are defined is 5α-cholestan-3β-ol with the numbering scheme recommended by IUPAC as shown in Figure **21.5.38**.

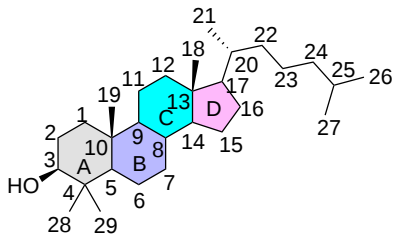


Figure **21.5.38**: IUPAC sterol numbing system

The phytosterols (as opposed to zoosterols) include campesterol, β-sitosterol, stigmasterol, and Δ5-avenasterol, some of which are illustrated in Figure **21.5.39**.

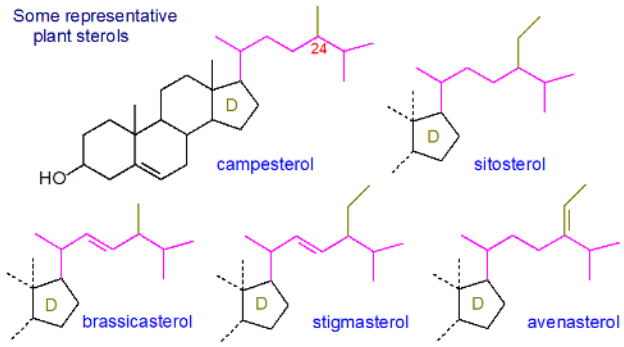


Figure **21.5.39**: Some common plant sterols

These more common plant sterols have a double bond in position 5, and a definitive feature – a one- or two-carbon substituent with variable stereochemistry in the side chain at C-24, which is preserved during subsequent metabolism. For example, campesterol is a 24-methylsterol, while β-sitosterol and stigmasterol are 24-ethylsterols. Occasionally, there is a double bond in this chain that can be of the *cis* or *trans* configuration, as in stigmasterol (at C22) or fucosterol (C24), the principal sterol in green algae.

Phytosterols can be further classified on a structural or biosynthetic basis as 4-desmethyl sterols (i.e., with no substituent on carbon-4), 4α-monomethyl sterols, and 4,4-dimethyl sterols. The most abundant group is the 4-desmethyl sterols, which may be subdivided into Δ5-sterols (illustrated above), Δ7-sterols (e.g., α-spinasterol), and Δ5,7-sterols depending on the position of the double bonds in the B ring. As the name suggests, brassicasterols (24-methyl-cholesta-5,22-dien-3β-ol and related sterols) are best known from the brassica family of plants, but they are also common constituents of marine algae (phytoplankton). Phytostanols (fully saturated) are normally present at trace levels only in plants, but they are relatively abundant in cereal grains.

Many different sterols may be present in photosynthetic organisms, and their amounts and relative proportions depend on the species. Over 250 different phytosterols have been recorded, with 60 in corn (maize) alone, for example. As a rough generalization, a typical plant sterol mixture would be 70% sitosterol, 20% stigmasterol, and 5% campesterol (or >70% 24-ethyl-sterols and <30% 24-methyl-sterols). However, this composition may vary with the stage of development and in response to stress. **Table 1** contains data on the main components from some representative commercial seed oils.

Table **21.5.2. Sterol composition in some seed oils of commercial importance (mg/Kg).**

	corn	cottonseed	olive	palm	rapeseed	safflower	soybean	sunflower
cholesterol	-	-	-	26	-	-	-	-
campesterol	2691	170	28	358	1530	452	720	313
stigmasterol	702	42	14	204	-	313	720	313
β-sitosterol	7722	3961	1310	1894	3549	1809	1908	2352
Δ5-avenasterol	468	85	29	51	122	35	108	156
Δ7-stigmasterol	117	-	58	25	306	696	108	588
Δ7-avenasterol	-	-	-	-	-	104	36	156
brassicasterol	-	-	-	-	612	-	-	-
other	-	-	-	-	-	69	-	39

Data adapted from Gunstone, F.D. *et al. The Lipid Handbook (Second Edition)* (Chapman & Hall, London) (1994).

Cholesterol is usually a minor component only of plant sterols (<1%). Still, it is unwise to generalize too much, as it can be the main sterol component of red algae and some families of higher plants, such as in the Solanaceae, Liliaceae, and Scrophulariaceae. It can also be a significant constituent sterol of chloroplasts, shoots, pollen, and leaf surface lipids in other plant families; wheat roots contain 10% and Arabidopsis cells 19% of the sterols as cholesterol. Yeasts and fungi typically contain ergosterol as their primary sterol (see below). **Ecdysteroids** (phytoecdysteroids) are polyhydroxylated plant sterols that can occur in appreciable amounts in some species. Sterols are also found in some bacterial groups, but not in archaea. Hopanoids in bacteria are considered functional counterparts of triterpenes.

Sterols can occur in plants in the 'free' state, i.e., in which the sterol hydroxyl group is not linked to any other moiety. Still, they are usually present as conjugates with the hydroxyl group covalently bound via an ester bond to a fatty acid, for example, as sterol esters, or via a glycosidic linkage to glucose (and occasionally other sugars), as steryl glycosides.

21.5.3.2: PLANT STEROLS - BIOSYNTHESIS

The biosynthetic route to plant sterols resembles that to cholesterol in many aspects in that it follows an isoprenoid biosynthetic pathway with isopentenyl pyrophosphate, derived primarily from mevalonate, as the key building block in the cytoplasm (but not plastids) at least. The main pathway for the biosynthesis of isopentenyl pyrophosphate and dimethylallyl pyrophosphate, the isoprene units, has been described previously and therefore need not be repeated here. It is known as the 'mevalonic acid (MVA) pathway' and functions in the cytosol, endoplasmic reticulum, and mitochondria.

However, an alternative pathway that does not use mevalonic acid as a precursor was first established for bacterial **hopanoids**, but has since been found in plant chloroplasts, algae, cyanobacteria, eubacteria, and some parasites (although not in animals). This route is variously termed the 'non-mevalonate', '1-deoxy-D-xylulose-5-phosphate' (DOXP), or better, the **2*C*-methyl-D-erythritol 4-phosphate (MEP)** pathway, as the last compound is presumed to be the first committed intermediate in sterol biosynthesis by this route. In the first step, pyruvate and glyceraldehyde phosphate are combined to form deoxyxylose phosphate, which is in turn converted to 2C-methyl-D-erythritol 4-phosphate. The pathway then proceeds via various erythritol intermediates until isopentenyl pyrophosphate and dimethylallyl pyrophosphate are formed. This pathway is illustrated in Figure **21.5.40**.

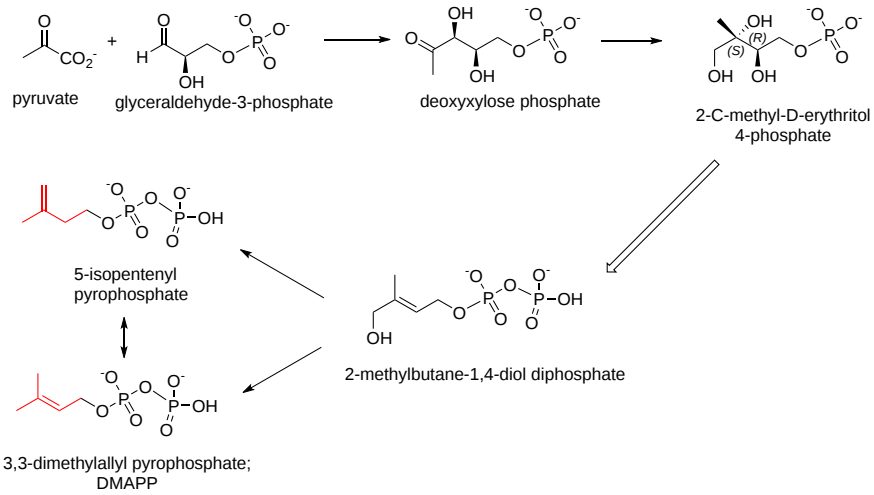


Figure **21.5.40**: Alternative 2*C*-methyl-D-erythritol 4-phosphate (MEP) pathway for synthesis of sterol and isoprenoid precursors in chloroplasts.

There is evidence that some of the isoprene units are exchanged between the cytoplasm and plastids. In much of the plant kingdom, both the MVA and MEP pathways operate in parallel, but green algae use the MEP pathway only. Thereafter, sterol biosynthesis continues via squalene and (3*S*)-2,3-oxidosqualene.

In photosynthetic organisms (as opposed to yeast and fungi), the subsequent steps in the biosynthesis of plant sterols differ from those for cholesterol in that the important intermediate in the route from squalene via 2,3-oxidosqualene is **cycloartenol**, rather than lanosterol, and this is produced by the action of a 2,3(*S*)-oxidosqualene-cycloartenol cyclase (cycloartenol synthase). Then, the enzyme sterol methyltransferase 1 is of special importance because it converts cycloartenol to 24-methylene cycloartenol, the first step in introducing the methyl group onto C-24. The enzyme cyclopropyl sterol isomerase is required to open the cyclopropane ring. Animals lack the sterol C24-methyltransferase gene. While this pathway is essentially linear up to the synthesis of 24-methylene lophenol, a bifurcation then occurs, resulting in two alternative pathways. One of these pathways leads to the synthesis of sitosterol and stigmasterol, while the other leads to the synthesis of campesterol. This pathway is shown in Figure **21.5.41**.

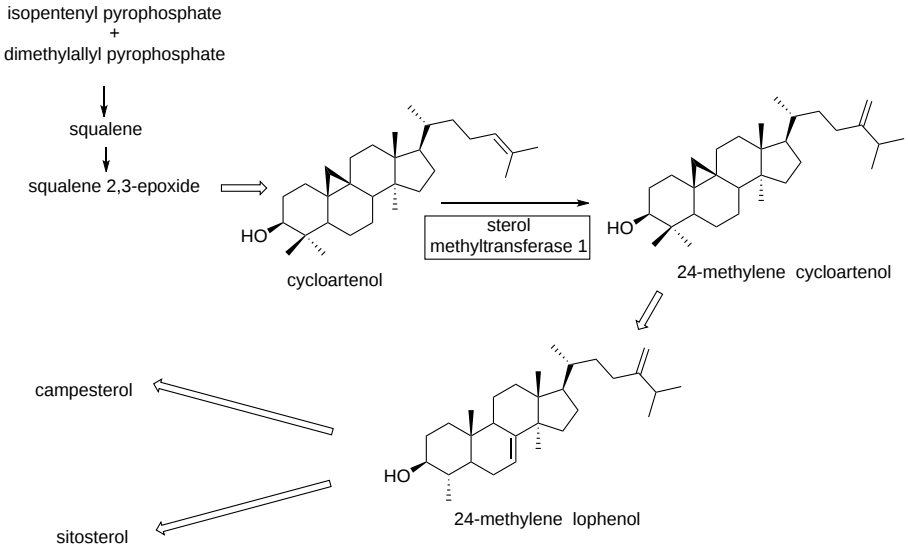


Figure **21.5.41**: Synthesis of plant sterols via the cycloartenol intermediate

There are more than thirty enzyme-catalyzed steps in the overall process of plant sterol biosynthesis, each of which is associated with membranes. We will describe a few here. The 4,4-dimethyl- and 4α-methylsterols are part of the biosynthetic pathway, but are only minor, if ubiquitous, sterol components of plants. New biosynthetic pathways are being discovered through genome analysis, revealing the complexity of sterol biosynthesis in various plant species.

Dinoflagellates produce a characteristic 4-methylsterol, termed dinosterol, as well as others, such as gorgosterol, via lanosterol as a precursor. Protozoans synthesize many different sterols related to those in plants. For example, some species of *Acanthamoeba* and *Naegleria* produce both lanosterol and cycloartenol. Still, only the latter is used for the synthesis of other sterols, especially ergosterol, but in other protozoan species, sterol biosynthesis occurs via lanosterol. The best-studied bacterial pathway is that of the methylotroph *Methylococcus capsulatus*, which produces several unique Δ18(14)-sterols and is known to possess a squalene epoxidase and a lanosterol 14-demethylase.

Cholesterol in plants is produced from cycloartenol as the key intermediate, with Sterol Side Chain Reductase 2 (SSR2) as the key enzyme. It is now established that the cholesterol biosynthetic pathway in tomato plants comprises 12 enzymes acting in 10 steps. Of these, half evolved through gene duplication and divergence from phytosterol biosynthetic enzymes, whereas others act reciprocally in both cholesterol and phytosterol metabolism. Algae can also produce cholesterol through a multi-step process from cycloartenol, as well as many other sterols, via 24-methylene lophenol as the key intermediate. It is hoped that genetic manipulation of these enzymes will lead to plants that synthesize high-value steroidal products.

Oxidation: Phytosterols can undergo non-enzymatic oxidation, resulting in the formation of **oxysterols** similar to those found in animals. This process results in ring products, including hydroxy, keto-, epoxy-, and triol-derivatives. Further enzymatic reactions can oxidize the side chain. However, photosensitized oxidation is more common in plants and is much faster (>1500 times); it starts with the *ene*-addition of singlet oxygen ($^1O_2$) on either side of the double bond in the B ring to generate 5α-/6α-/6β-hydroperoxysterols, of which 5α-OOH is the most abundant and rearranges to form the more stable 7α-OOH isomer. This is the main reaction in foods stored under LED lighting in food retailers.

21.5.3.3: PLANT STEROLS - FUNCTION

Like cholesterol, plant sterols are amphiphilic and are vital constituents of all membranes, and especially of the plasma membrane, the mitochondrial outer membrane, and the endoplasmic reticulum. The three-dimensional structure of the plant sterols is such that there are planar surfaces at both the top and the bottom of the molecules, which permit multiple hydrophobic interactions between the rigid sterol and the other components of membranes. Indeed, they must determine the physical properties of membranes to an appreciable extent. It is believed that campesterol, β-sitosterol, and 24-methylcholesterol, in this order, can regulate membrane fluidity and permeability in plant membranes by restricting the mobility of fatty acyl chains, similarly to cholesterol in mammalian cells. However, stigmasterol has a much less significant effect on lipid ordering and no effect on membrane permeability. In the plasma membrane, plant sterols associate with glycosphingolipids, such as **glucosylceramide** and **glycosylinositolphosphoceramides,** in **raft**-like subdomains, analogous to those in animal cells. These associations support the membrane localization and activities of many proteins with important functions in plant cells. The sterol glycosides are especially important in this context (see below).

Sterols (and their conjugates) are involved in plant membrane adaptations to changes in temperature and other biotic and abiotic stresses. For example, β-sitosterol is a precursor of stigmasterol via the action of a C22-sterol desaturase, and the ratio of these two sterols is important to the resistance of *A. thaliana* plants to low and high temperatures. In addition, plant sterols can modulate the activity of membrane-bound enzymes. Thus, stigmasterol and cholesterol regulate the activity of the Na^+/K^+-ATPase in plant cells, probably in a manner analogous to that of cholesterol in animal cells. Stigmasterol may be explicitly required for cell differentiation and proliferation. In addition to being the precursor of plant steroidal hormones, campesterol serves as a signaling molecule that regulates growth, development, and stress adaptation.

Perhaps surprisingly, cholesterol is a precursor for the biosynthesis of some steroidal saponins and alkaloids in plants, such as the well-known steroidal glycoalkaloid α-solanine in potatoes, as well as other steroids, including phytoecdysteroids, which are derived from lathosterol in some species. While the physiological roles of ecdysteroids in plants have yet to be confirmed, they are believed to enhance stress resistance by promoting health and vitality. Withanolides are complex oxysterols believed to serve as defense compounds against insect herbivores.

21.5.3.4: STEROIDAL PLANT HORMONES

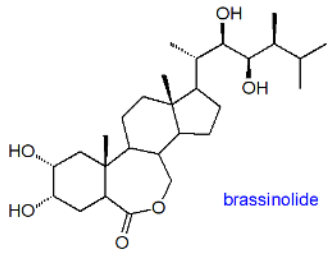


Figure **21.5.42**: Structure of brassinolide

They play a crucial role in plant growth processes, including cell elongation, division, differentiation, immunity, and the development of reproductive organs. They are involved in regulating numerous aspects of metabolism. Via signal transduction pathways, they interact with transcription factors through phosphorylation cascades to regulate the expression of target genes. Brassinosteroids are also signaling molecules in responses to abiotic stresses, including drought, salinity, high temperatures, low temperatures, and heavy metal stresses. They may have biomedical applications as anticancer drugs for endocrine-responsive cancers, inducing apoptosis and inhibiting growth. Some plant species produce small amounts of steroid hormones that are often considered to be of animal origin only, including progesterone and testosterone, and these may have physiological roles in plants.

21.5.3.5: STEROL ESTERS IN HIGHER PLANTS

Sterol esters are present in all plant tissues, but they are most abundant in tapetal cells of anthers, pollen grains, seeds, and senescent leaves. In general, they are minor components relative to the free sterols, other than in waxes. Typically, the sterol components of sterol esters are similar to those of free sterols, although there may be a relatively lower concentration of stigmasterol. The fatty acid components tend to resemble those of the other plant tissue lipids, but there can be significant differences on occasion. Sterol esters are presumed to serve as inert storage forms of sterols, as they are often enriched in the intermediates of sterol biosynthesis and can accumulate in **lipid droplets** within the cells. However, they have been found in some membranes, especially in microsomes and mitochondrial preparations, although their function in these locations is uncertain. They may also play a role in transport within cells and between tissues, as they can exist in the form of soluble lipoprotein complexes.

Biosynthesis of sterol esters in *A. thaliana* is known to occur in the endoplasmic reticulum by the action of a phospholipid:sterol acyltransferase, which catalyzes the transfer of a fatty acyl group to the sterol from position *sn*-2 of phospholipids - mainly phosphatidylethanolamine; the enzyme is very different from those in animals and yeasts. However, an acyl CoA:sterol acyltransferase closer in structure to the animal enzyme has also been characterized; it prefers saturated fatty acyl-CoAs as acyl donors and cycloartenol as the acceptor molecule. The enzymes responsible for the hydrolysis of sterol esters in *A. thaliana* are not yet known. Certain distinctive phytosterol esters occur in the aleurone cells of cereal grains, including *trans*-hydroxycinnamate, ferulate (4-hydroxy-3-methoxycinnamate), and *p*-coumarate esters. Similarly, rice bran oil is a rich source of esters of ferulic acid and a mixture of sterols and triterpenols, termed 'γ-orizanol'', and an example of one of these compounds is illustrated in Figure **21.5.43**.

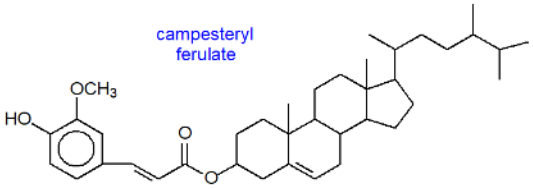


Figure **21.5.43**: Structure of campesteryl ferulate

This is sold as a health food supplement due to its claimed beneficial effects, including cholesterol-lowering and antioxidant activities, as well as enhancements to muscle growth and sports performance. However, none of these effects have been confirmed by rigorous clinical testing.

21.5.3.6: STEROL GLYCOSIDES

Leaf and other tissues in plants contain a range of **sterol glycosides** and **sterol acyl-glycosides** in which the hydroxyl group at C3 on the sterol is linked to the sugar by a glycosidic bond. Other than in the genus *Solanum*, where they can represent up to 85% of the sterol fraction in tomato fruit, as an example, they tend to be minor components relative to other lipids. Typical examples (glucosides of β-sitosterol) are illustrated in Figure **21.5.44**.

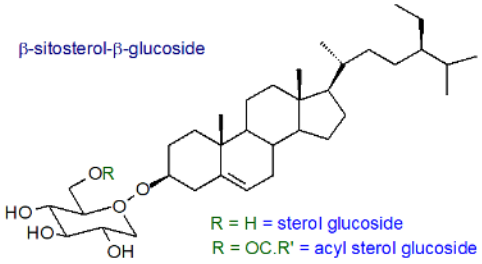


Figure **21.5.44**: Structure of β-sitosterol-β-glucoside

Most of the common plant sterols occur in this form, but Δ5 sterols are preferred (Δ7 in some genera). Glucose is the most common carbohydrate moiety, but galactose, mannose, xylose, and arabinose can also be present, depending on plant species; occasionally, complex carbohydrates with up to five hexose units linked linearly are present. Algae also contain sterol glycosides with a wide range of sterol and carbohydrate components. Plant, animal, fungal, and most bacterial steryl glycosides have a β-glycosidic linkage, but in a few bacterial species, there is an α-linkage.

Similarly, the nature of the fatty acid component in the acyl sterol glycosides can vary, as well as the hydroxyl group to which they are linked. However, it is usually position 6 of the glucose moiety. In potato tubers, for example, the 6'-palmitoyl-β-D-glucoside of β-sitosterol is the major species, while the corresponding linoleate derivative predominates in soybeans. Usually, the sterol acyl-glycosides are present at concentrations that are two- to tenfold greater than those of the non-acylated forms. They are known to be located in the plasma membrane, tonoplasts, and endoplasmic reticulum.

Biosynthesis involves the reaction of free sterols with a glucose unit catalyzed by a sterol glycosyltransferase, or by the reaction of the sterol with uridine diphosphoglucose (UDP-glucose) and UDP-glucose:sterol glucosyltransferase on the cytosolic side of the plasma membrane. The acyl donor for acyl sterol glycoside synthesis is not acyl-coenzyme A but is believed to be a glycerolipid. Steryl β-D-glycoside hydrolases have been characterized from plants that reverse this reaction, but no fatty acyl hydrolase activity for sterol acyl-glycosides is yet known. One route to the biosynthesis of **glucosylceramides** in plants involves the transfer of the glucose moiety of sterol glycosides to ceramide.

The functions of sterol glycosides and sterol acyl-glycosides are slowly being revealed, and they are believed to be significant components of the plasma membrane that associate with sphingolipids in **raft-like domains**; the esterified form, especially, may be involved in the adaptation of plant membranes to low temperatures and other stresses. It is possible that they have a role in signal transmission through membranes, and they are reported to be beneficial in the response to pathogens. It seems probable that sterol glycosides are oriented with the sterol moiety buried in the hydrophobic core of the lipid bilayer, with the sugar located in the plane of the polar head groups of the membrane, while with sterol acyl-glycosides, both the sterol moiety and the fatty acid chain are embedded in the hydrophobic core of the membrane. Sitosterol-β-D-glucoside in the plasma membrane is believed to be the primer molecule for cellulose synthesis in plants, as in cotton (*Gossypium arboreum*) fiber, where it may be required for the initiation of glucan polymerization. The sterol is eventually removed from the polymer by a specific cellulase enzyme; the multimeric cellulase synthase is believed to be stabilized by sterols in the plasma membrane.

Sterol glycosides appear to be essential for the pathogenicity of certain fungi and some bacteria, and ergosterol glycosides are especially troublesome components of plant fungal pathogens. Sterol glycosides have only rarely been reported from organisms other than plants and fungi. However, some bacteria, such as the gram-negative bacterium *Helicobacter pylori* and *Borrelia burgdorferi*, the causative agent of Lyme disease, produce **cholesterol glucoside** from host cholesterol. On the other hand, cholesteryl glucoside has been identified as a natural component of a few animal tissues. Acting as immunoadjuvants, sterol glycosides are reported to be efficacious in protecting animal hosts against lethal Cryptococcal infections. In the human diet, sterol glycosides offer potential benefits similar to those of free sterols, as they inhibit the absorption of cholesterol from the gut and reduce plasma cholesterol levels. The fatty acids are removed from sterol acyl-glycosides by enzymes in the intestine.

Some species of monocotyledons contain complex steroidal **saponins**, which consist of an aglycone based on a triterpenoid furostanol or spirostanol skeleton (derived from cholesterol) and an oligosaccharide chain of two to five hexose or pentose moieties attached to the 3β-hydroxyl group of the sterol. These can interact with cholesterol in plant membranes to form insoluble complexes, which increase membrane permeability.

21.5.3.7: ERGOSTEROL AND OTHER STEROLS IN YEASTS AND FUNGI

Yeasts and fungi, together with microalgae and protozoa, can contain a wide range of different sterols. However, **ergosterol** ((22*E*)-ergosta-5,7,22-trien-3β-ol) is the most common sterol in fungi and yeast. It is accompanied by other sterols not normally abundant in higher plants, including cholesterol, 24-methyl cholesterol, 24-ethyl cholesterol, and brassicasterol, depending on the species. In *Saccharomyces cerevisiae*, which is widely studied as a model species of yeasts, ergosterol is the most abundant sterol (ca. 12% of all lipids), with the highest levels in the plasma membrane (up to 40% of the lipids or 90% of the total cell sterols). Its structure is shown in Figure **21.5.45**.

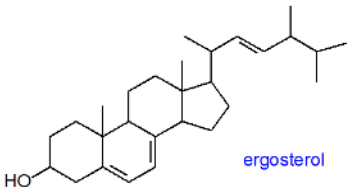


Figure **21.5.45**: Strurture of ergosterol

Like cholesterol, and in contrast to plant sterols, it is synthesized in the endoplasmic reticulum via lanosterol as the key intermediate, followed by zymosterol. However, the pathway diverges at this stage to produce fecosterol en route to ergosterol (see the reading list below for further details). Ergosterol is transported to other organelles within the cell in a non-vesicular manner by two families of evolutionarily conserved sterol-binding proteins - 'Osh' and 'Lam', which can optimize the sterol composition of cell membranes rapidly under conditions of stress. As in humans, a Niemann-Pick protein, NCR1, integrates sterols into the lysosomal membrane before further distribution as part of the mechanism of sterol homeostasis. Some antifungal drugs target ergosterol, either by binding to it to cause damaging cellular leakage or by preventing its synthesis from lanosterol.

Many mutants defective in ergosterol biosynthesis have been isolated, yielding a wealth of information on the features of the sterol molecule required for its structural role in the membranes of yeast and fungi. Ergosterol stabilizes the liquid-ordered phase in the same manner as cholesterol and also forms raft microdomains with sphingolipids in membranes, whereas lanosterol does not. It is also evident that ergosterol has multiple functions in regulating yeast growth.

Under some conditions, especially those that retard growth, a high proportion of the sterols in yeasts can be in esterified form, where they are stored in lipid droplets. Ergosterol esters are synthesized in yeast by enzymes (ARE1 and ARE2), which are related to ACAT-1 and ACAT-2 that perform this function in animals, and both transfer an activated fatty acid to the hydroxyl group at the C3-position of a sterol molecule. In addition, specific sterol ester hydrolases that catalyze the reverse reaction have been characterized in yeasts, with two enzymes located in lipid droplets and one at the plasma membrane. Many fungal species and slime molds contain steryl glycosides (ergosteryl β-monoglucopyranosides in the former). Still, they are present at very low levels only in the widely studied yeast *Saccharomyces cerevisiae*.

Most fungi conjugate the 3β-hydroxyl group of ergosterol with aspartate in an RNA-dependent reaction catalyzed by an ergosteryl-3β-*O*-L-aspartate synthase, with the reverse reaction using a dedicated hydrolase. A phylogenomic study has shown that this pathway is conserved across higher fungi (except *S. cerevisiae*), including pathogens. It has been suggested that these reactions constitute a homeostasis system with potential impacts on membrane remodeling, trafficking, antimicrobial resistance, and pathogenicity.

21.5.3.8: BACTERIAL STEROLS

Hopanoids replace sterols in many species of bacteria. It has long been recognized that some bacteria take up cholesterol and other sterols from host animals for use as membrane constituents. Indeed, an external source of sterols is required for growth in species of *Mycoplasma*. Additionally, numerous reports have been published regarding the biosynthesis of sterols by various bacterial species. However, a

significant proportion of these appear to have been discounted due to fungal contamination. In particular, the possibility of sterol biosynthesis in cyanobacteria has been a subject of controversy, and molecular biology studies have yet to detect the presence of the required enzyme, squalene epoxide cyclase.

That said, there is good evidence that at least a few species of prokaryotes can synthesize sterols *de novo*. Among the eubacteria, certain methylotrophs, *such as Methylobacterium* and *Methylosphaera* species, produce mono- and dimethyl sterols, including lanosterol. Similarly, some soil bacteria produce 4-desmethylsterols. It has now been established through gene sequence studies that a few bacteria contain enzymes of the sterol biosynthesis pathway, such as oxidosqualene cyclase. However, as these enzymes have no obvious evolutionary link, it seems probable that they were acquired via lateral transfer from eukaryotes.

21.5.3.9: PLANT STEROLS IN THE HUMAN DIET

The absorption of dietary plant sterols and stanols in humans is low, ranging from 0.02% to 3.5%, compared to cholesterol, which is absorbed at rates of 35-70%. Although there are similar amounts of plant sterols and stanols in an average Western diet, their absorption rates are significantly lower. The explanation is believed to be that the Niemann-Pick C1-like protein 1 (NPC1L1), which is responsible for cholesterol absorption in enterocytes, does not efficiently take up plant sterols. Two transporters, ABCG5 and ABCG8, redirect any that are absorbed back into the intestinal lumen. In rare cases, elevated levels of plant sterols in plasma serve as markers for a hereditary lipid storage disease (phytosterolemia) caused by mutations in the enterocyte transporters. Among many symptoms, accelerated atherosclerosis is often reported, although the reasons for this are not clear. There is evidence that while plant sterols can substitute for cholesterol in maintaining membrane function in mammalian cells, they can exert harmful effects by disrupting cholesterol homeostasis. This may be particularly relevant to the brain, as phytosterols can cross the blood-brain barrier; however, they cannot be enzymatically oxidized due to the alkyl moiety on carbon 24. In contrast, dietary supplements of plant sterols have been reported to have anti-cancer effects.

Substantial amounts of phytosterols are available as by-products of the refining of vegetable oils and of tall oil from the wood pulp industry. As it appears that they can inhibit the uptake of cholesterol from the diet and thereby reduce the levels of this in the plasma low-density lipoproteins, there is an increasing interest in such commercial sources of plant sterols to be added as "nutraceuticals" to margarines and other foods. Hydrogenated phytosterols or "**stanols**" are also used for this purpose. Studies suggest they are as effective as sterols in reducing LDL cholesterol. The consensus among experts in the field, including the FDA in the USA, is that such dietary supplements indeed have the effects claimed. Such claims can be used in the advertising of commercial products, with the important caveat that there are no randomized, controlled clinical trial data to establish the ensuing health benefits, especially concerning cardiovascular disease. Other pharmacological effects are under investigation, and there may be beneficial effects for the development of the human fetus and newborn, as well as for the treatment of non-alcoholic steatohepatitis, inflammatory bowel diseases, and allergic asthma.

It is unclear whether oxy-phytosterols are generated in animal tissues; however, those produced enzymatically or non-enzymatically can enter the food chain, particularly when they are formed during cooking. Although they are not efficiently absorbed, 7-keto-sitosterol and 7-keto-campesterol have been detected in human plasma and have the potential to exert various biological effects. For example, they have pro-atherogenic and pro-inflammatory properties in animal models.

21.5.4: SUMMARY

This chapter explores the central role of cholesterol—a key sterol in animal tissues—and its esterified forms in cellular structure, metabolism, and signaling. We begin by examining cholesterol's unique polycyclic structure, characterized by its rigid, planar tetracyclic nucleus, a flexible iso-octyl side chain, and a 3β-hydroxyl group. These structural features not only determine its orientation within lipid bilayers but also facilitate its interaction with other membrane lipids, influencing membrane fluidity, thickness, and the formation of specialized microdomains known as lipid rafts.

The biosynthesis of cholesterol occurs via the mevalonate pathway, starting from acetyl-CoA. Key intermediates include 3-hydroxy-3-methylglutaryl (HMG)-CoA, which is reduced by HMG-CoA reductase—the rate-limiting enzyme and target of statins—to form mevalonate. Subsequent reactions generate isopentenyl pyrophosphate, which polymerizes to form squalene. Squalene is then converted to lanosterol and ultimately to cholesterol through a series of demethylation, isomerization, and reduction reactions. This process is highly energy-demanding and tightly regulated to balance endogenous synthesis with dietary uptake.

Cholesterol is differentially distributed among cellular membranes: it is most abundant in the plasma membrane, where it can comprise 30–50% of the lipid content, and less so in the endoplasmic reticulum and mitochondria. This uneven distribution is critical for maintaining membrane properties and for regulating the lateral organization of proteins, including those involved in cell signaling. Cholesterol also modulates membrane permeability and interacts with sphingolipids to form liquid-ordered domains that serve as platforms for signaling and protein sorting.

To prevent the deleterious effects of cholesterol overaccumulation, cells employ sophisticated regulatory mechanisms. Cholesterol homeostasis is maintained via feedback regulation—mediated by sterol regulatory element-binding proteins (SREBPs) and their escort

protein SCAP—as well as through the action of oxysterols, which can act as ligands for nuclear receptors such as the liver X receptor (LXR). In addition, excess cholesterol is esterified by enzymes such as lecithin:cholesterol acyltransferase (LCAT) in the plasma and acyl-CoA:cholesterol acyltransferase (ACAT) within cells, forming cholesterol esters that are stored in lipid droplets or packaged into lipoproteins for transport throughout the body.

Cholesterol serves as the precursor for several vital biomolecules, including bile acids, vitamin D, and steroid hormones. For instance, in the skin, 7-dehydrocholesterol is converted into vitamin D3 under ultraviolet light, initiating a cascade that produces the active hormone calcitriol, essential for calcium and phosphorus homeostasis.

Overall, this chapter emphasizes the intricate balance of cholesterol synthesis, transport, and catabolism that is essential for cellular function and organismal health. Dysregulation of these processes is linked to a range of diseases—from cardiovascular disorders and neurodegeneration to metabolic and developmental abnormalities—highlighting the clinical significance of sterol metabolism and the potential of targeting these pathways for therapeutic intervention.

This page titled 21.5: Biosynthesis of Cholesterol and Steroids is shared under a not declared license and was authored, remixed, and/or curated by Henry Jakubowski and Patricia Flatt.

- **Current page** by Henry Jakubowski and Patricia Flatt has no license indicated.
- **11.2: Diffusion Across a Membrane - Passive and Facilitated Diffusion** by Henry Jakubowski and Patricia Flatt has no license indicated.

21.6: BIOSYNTHESIS AND METABOLISM OF ISOPRENOIDS

By William (Bill) W. Christie and Henry Jakubowski.

This section is an abbreviated and modified version of material from the Lipid Web, an introduction to the chemistry and biochemistry of individual lipid classes, written by William Christie.

LEARNING GOALS (CHATGPT O3-MINI)

Tocopherols and Tocotrienols (Vitamin E)

- **Structural Analysis**
  - Describe the chemical structures of tocopherols and tocotrienols, highlighting the differences in their side chains (saturated vs. unsaturated) and chiral centers.
  - Explain the nomenclature (α, β, γ, δ forms) and relate specific structural features to their antioxidant and vitamin activity.
- **Biosynthesis in Plants**
  - Outline the biosynthetic pathway for tocochromanols in chloroplasts, including the roles of tyrosine, p-hydroxyphenylpyruvate dioxygenase, and prenyl transferases.
  - Compare how tocopherol and tocotrienol pathways diverge based on the isoprenoid precursor (phytyl diphosphate vs. geranylgeranyl diphosphate).
- **Biological Function and Antioxidant Activity**
  - Explain how tocopherols act as lipid-soluble antioxidants by scavenging lipid peroxyl radicals in membranes.
  - Describe the regeneration cycle of tocopherols via interaction with other antioxidants (e.g., vitamin C, glutathione) and discuss the significance of this antioxidant network.
- **Absorption, Transport, and Metabolism in Animals**
  - Discuss the intestinal absorption of dietary tocopherols, the role of chylomicrons, and the selective uptake of α-tocopherol by the liver via the α-tocopherol transfer protein (α-TTP).
  - Explain how tocopherols are distributed among lipoproteins and how excess forms are catabolized to produce biologically active metabolites.
- **Physiological and Clinical Relevance**
  - Analyze the role of vitamin E in preventing deficiency diseases (e.g., ataxia) and its indirect functions in signal transduction and gene expression.
  - Evaluate the dietary sources and nutritional importance of tocopherols and tocotrienols in human health.

Retinoids (Vitamin A)

- **Structural and Metabolic Pathways**
  - Identify the structures of retinol, retinal, and retinoic acid and describe their interconversion.
  - Explain the oxidative cleavage of provitamin A carotenoids (e.g., β-carotene) to produce retinal, including the role of β-carotene-15,15'-oxygenase (BCO1).
- **Visual Cycle and Beyond**
  - Outline the retinoid (visual) cycle in the retina, detailing the conversion of 11-cis-retinal to all-trans-retinal and back, and the role of key proteins such as STRA6 and IRBP.
  - Discuss the non-visual roles of retinoids in gene regulation, embryonic development, immune function, and cell differentiation.
- **Transport and Storage**
  - Describe how retinoids are absorbed, transported (via retinol-binding proteins and transthyretin), and stored (primarily as retinyl esters in hepatic stellate cells) in animal tissues.
- **Clinical Implications**
  - Evaluate the impact of vitamin A deficiency on health (e.g., impaired vision, immune dysfunction) and the therapeutic use of retinoids in cancer and skin disorders.

Other Membrane-Associated Isoprenoids

- **Overview of Structural Diversity**

- Differentiate among various isoprenoids (e.g., phytol, plastoquinone, ubiquinone, vitamin K, dolichols/polyprenols) in terms of their chemical structures and biosynthetic origins.
- Explain how the mevalonate and non-mevalonate (MEP) pathways contribute to the synthesis of isoprenoid precursors.

- **Functional Roles in Cellular Metabolism**
  - Discuss the role of plastoquinone in photosynthetic electron transport and compare it to ubiquinone's function in the mitochondrial electron transport chain.
  - Describe the role of vitamin K (phylloquinone and menaquinones) in blood coagulation via the γ-carboxylation of glutamate residues.
  - Explain the function of dolichols and polyprenols as lipid carriers in protein glycosylation, including the synthesis and flipping of lipid-linked oligosaccharides (e.g., Lipid II in bacterial peptidoglycan synthesis).
- **Biological and Clinical Relevance**
  - Analyze how the structural diversity of isoprenoids contributes to their distinct roles in membrane organization, electron transport, and cellular signaling.
  - Evaluate the potential therapeutic applications of targeting isoprenoid pathways in diseases such as cardiovascular disorders, neurodegeneration, and infections.

Integration and Critical Analysis

- **Pathway Interconnections**
  - Synthesize how the biosynthetic pathways of various isoprenoids interrelate and diverge from common precursors (e.g., isopentenyl pyrophosphate).
  - Evaluate the impact of dietary isoprenoids and their metabolites on cellular function and overall health.
- **Application to Disease and Therapeutics**
  - Critically assess how dysregulation in isoprenoid metabolism can lead to human diseases (e.g., atherosclerosis, neurodegenerative disorders, vitamin deficiencies) and discuss current strategies for therapeutic intervention.

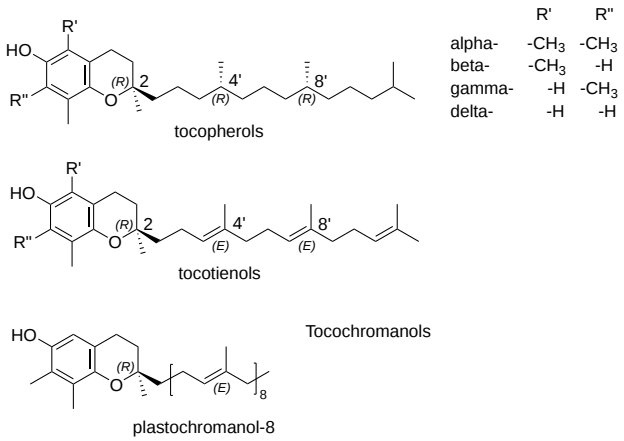
By mastering these learning goals, students will gain a comprehensive understanding of the structure, biosynthesis, function, and clinical significance of key isoprenoid compounds in both plants and animals.

21.6.1: ISOPRENOIDS: 1. TOCOPHEROLS AND TOCOTRIENOLS (VITAMIN E)

Tocopherols and tocotrienols constitute a series of related benzopyranols (or methyltocols) that are synthesized in plants and other photosynthetic organisms, where they have many important functions, but especially as part of a complex web of antioxidants that protect plants from the activities of reactive oxygen species (ROS). First described in 1922 as a dietary factor essential for preventing fetal reabsorption in rats, it was soon understood that plants contained a fat-soluble vitamin, vitamin E, which is essential for numerous aspects of animal development. Of these many related molecules, only one form, i.e., **α-tocopherol**, is recognized as having vitamin E activity in humans, as it prevents a spectrum of human deficiency diseases termed 'ataxia', which is characterized by very low concentrations of α-tocopherol in plasma. The progression of the disease can be prevented by the administration of α-tocopherol alone, although the pathogenic mechanism remains uncertain. While all tocopherols are known to be powerful lipid-soluble antioxidants *in vitro* at least, α-tocopherol has indirect roles in signal transduction and gene expression in animal tissues. On the other hand, specific functions (non-vitamin E) for other tocopherol forms and their metabolites in animal tissues are now being revealed. Vegetable oils are a major dietary source of vitamin E for humans.

21.6.1.1: STRUCTURE AND OCCURRENCE

In the tocopherols, the C_{16} side chain is saturated, and in the **tocotrienols** it contains three *trans* double bonds. Together, these two groups are collectively referred to as the **tocochromanols.** In essence, the tocopherols have a 20-carbon phytyl tail (including the pyranol ring) and four chiral centers in total, with variable numbers of methyl groups attached to the benzene ring, while the tocotrienols have a 20-carbon geranylgeranyl tail with double bonds at the 3', 7' and 11' positions relative to the ring system. Tocopherols contain three chiral carbons, one at C2 in the chromanol ring and two in the side chain at C4′ and C8′ with *R*,*R*,*R* stereochemistry. The four main constituents of the two classes are termed - *alpha* (5,7,8-trimethyl), *beta* (5,8-dimethyl), *gamma* (7,8-dimethyl), and *delta* (8-methyl). In contrast to the tocopherols, the tocotrienols have only one chiral center. **Plastochromanol-8** is an analog of γ-tocotrienol with a much longer side chain. Their structures are shown in Figure **21.6.1**.



	R'	R''
alpha-	$-CH_3$	$-CH_3$
beta-	$-CH_3$	-H
gamma-	-H	$-CH_3$
delta-	-H	-H

Figure **21.6.1**: Tocochromanols

The tocochromanols are only synthesized by plants and other oxygenic photosynthetic organisms, such as algae and some cyanobacteria, but they are essential components of the diet of animals. Of these, only natural *R*,*R*,*R*-α-tocopherol is now designated 'vitamin E', as explained below. However, the other tocopherols are sometimes termed 'vitamers' (some claim incorrectly - nor should all forms be termed isomers strictly speaking). In the United States, the current recommended dietary allowance (RDA) is 15 mg of α-tocopherol daily for adults. In plants, there is a wide range of tocochromanol contents and compositions, and photosynthetic plant tissues contain from 10 to 50 μg of tocochromanols per gram of fresh weight. α-Tocopherol is present only in photosynthetic membranes of plant leaves, while γ-tocopherol and other forms are found principally in fruits, seeds, and nuts. While tocopherols are present in all photosynthetic organisms, the tocotrienols are found only in certain plant families.

Seed oils are a significant source for the human diet, and the compositions of tocopherols in some unrefined oils are listed in **Table 1**. Sunflower and olive oils are good sources of α-tocopherol, and palm oil is a good source of the tocotrienols. In general, tocotrienols tend to be abundant only in seeds and fruits, especially those of monocots such as wheat, rice, and barley; however, a major commercial source is palm oil. In leaf tissue, α-tocopherol is often the main form, while γ-tocopherol is the primary tocopherol of many seeds. Plastochromanol-8 was first identified in the leaves of the rubber tree (*Hevea brasiliensis*) but has since been found in many other plants, including rapeseed and maize, typically at lower levels than the tocopherols. Additionally, tocopherol esters of fatty acids are found in plant tissues, where they may serve as a storage form. Unesterified tocopherols are not released during digestion in animals, so they may not contribute to vitamin E activity.

Table **21.6.1**: **Tocopherol and tocotrienol contents (mg/Kg) in some seed oils.**

	α-T*	β-T	γ-T	δ-T	α-TT*	β-TT	γ-TT	δ-TT
palm	89	-	18	-	128	-	323	72
soybean	100	8	1021	421	-	-	-	-
maize	282	54	1034	54	49	8	161	6
sunflower	670	27	11	1	-	-	-	-
rapeseed	202	65	490	9	-	-	-	-

* Abbreviations: T, tocopherol; TT, tocotrienol

Data from: Gunstone, F.D., Harwood, J.L. and Padley, F.B. *The Lipid Handbook (Second Edition)* (Chapman & Hall, London)(1994).

An unusual tocopherol, termed marine-derived α-tocomonoenol, is found in conjunction with α-tocopherol in a wide range of marine fish species, where it appears to be a more efficient scavenger of free radicals at low temperatures. A related isomer with a Δ11 double bond has been found in palm oil and kiwi fruit. While pumpkin seeds contain both α- and γ-tocomonoenols, other plant species contain β-, γ-, and δ-tocomonoenols with unsaturation in the terminal isoprene unit of their side chains. Tocochromenols or 3,4-dehydrotocopherols, i.e., with a double bond in the pyranol ring, are also known in addition to more complex tocopherol-like molecules. The structures of tocomonoenols are shown in Figure **21.6.2**.

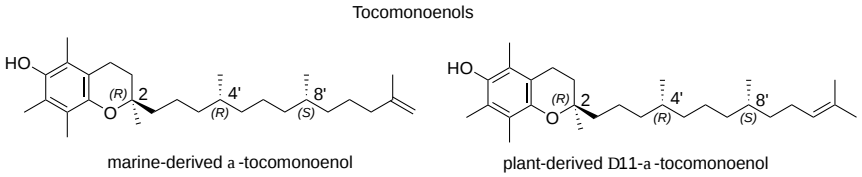


Figure **21.6.2**: Tocomonoenols

α-Tocopherol is a minor but ubiquitous component of the lipid constituents of animal cell membranes (non-raft domains), with estimates ranging from one molecule of tocopherol to 100 to 1000 molecules of phospholipids, depending on the membrane. The hydrophobic tail lies within the membrane, as might be expected, and the polar head group is oriented towards the surface but below the level of the phosphate moieties of the phospholipids. There may be some limited hydrogen bonding between the hydroxyl groups and phosphate, depending on the degree of hydration of the membrane. On the other hand, there is a strong affinity of α-tocopherol for polyunsaturated fatty acids, where the chromanol unit may interact with the double bonds, suggesting that tocopherol is located deep within the membrane.

α-Tocopheryl phosphate has recently been detected at low levels in plasma, liver, and adipose tissue. Its structure is shown in Figure **21.6.3**. Together with catabolic tocopherol metabolites, it has important biological properties.

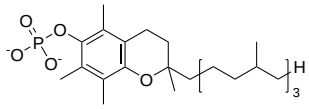


Figure **21.6.3**: α-Tocopheryl phosphate

During the refining of vegetable oils, much of the natural tocopherols are lost or destroyed. Most commercial vitamin E is therefore prepared by chemical synthesis with trimethylhydroquinone and phytyl bromide as the precursors. The resulting product is a mixture of eight stereoisomers (from *R,R,R-* to *S,S,S*-methyl groups) of α-tocopherol, with the various stereoisomers differing by a factor of two in biologic activity, as a consequence of the stereochemistry of position 2 in the chromanol ring (i.e., 2*S*-α- compared to 2*R*-α-tocopherol). It is usually administered as the acetate derivative *in vivo*. Tocopherols are not traditionally regarded as effective antioxidants in polyunsaturated seed oils. At higher concentrations, they can even act as pro-oxidants, although the reasons for this are not well understood.

21.6.1.2: BIOSYNTHESIS AND FUNCTIONS OF TOCOCHROMANOLS IN PLANTS

The mechanism of tocopherol biosynthesis has been elucidated and involves the coupling of phytyl diphosphate with homogentisic acid (2,5-dihydroxyphenylacetic acid), followed by cyclization and methylation reactions. The plant chloroplast is the site of biosynthesis, and most of the enzymes are located on the inner membrane of the chloroplast envelope. However, there is increasing evidence that **plastoglobules,** associated with the thylakoid membrane, may also be involved in this process. The pathway for biosynthesis of tocopherols is shown in Figure **21.6.4**.

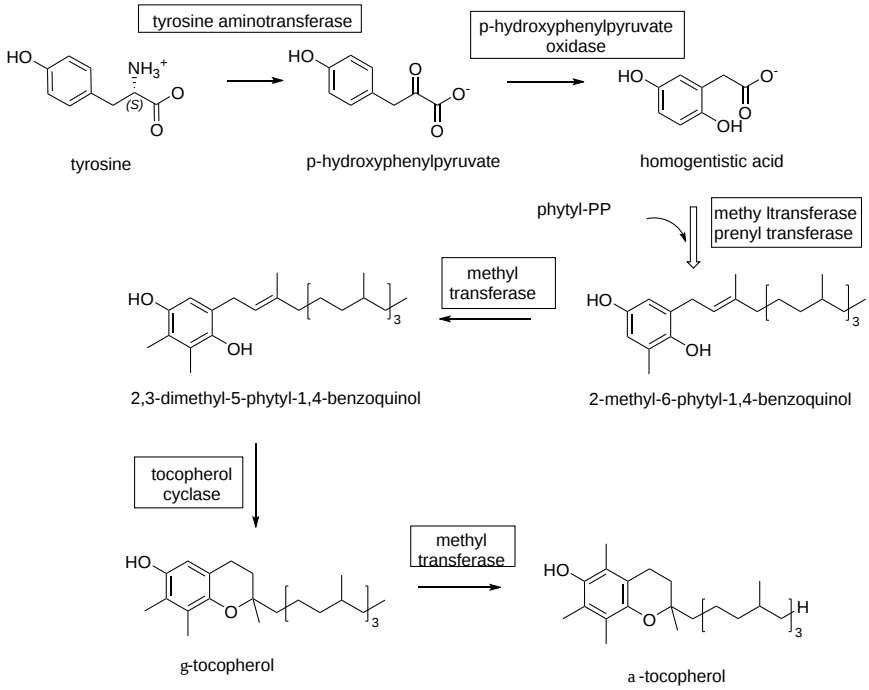


Figure **21.6.4**: Synthesis of tocopherols

The aromatic amino acid tyrosine can be considered the basic precursor, and this is oxidized to *p*-hydroxypyruvic acid, which in the first committed step is converted to homogentisic acid by the enzyme *p*-hydroxyphenylpyruvate dioxygenase. Homogentisic acid is condensed with phytyl diphosphate, derived from **phytol** obtained from hydrolysis of chlorophyll, in a reaction catalyzed by a prenyl transferase to yield 2-methyl-6-phytyl-plastoquinol, which is first methylated to form 2,3-dimethyl-5-phytyl-1,4-benzoquinol and then converted by the

enzyme tocopherol cyclase to γ-tocopherol. A further methylation reaction produces α-tocopherol, while modifications to the pathway produce β- and δ-tocopherols, as well as **plastoquinones,** which ultimately lead to the formation of plastochromanol-8. Tocotrienols and tocomonoenols result from a similar series of reactions but with geranylgeranyl diphosphate and tetrahydro-geranylgeraniol diphosphate, respectively, as substrates in the condensation step. The isoprenoid precursors are also synthesized in the plastid by the non-mevalonate or 'MEP' pathway.

In plants, tocopherols are found mainly in the chloroplasts of green tissues, but they are also present in seeds, fruits, roots, and tubers. They are especially important as antioxidant molecules, limiting the damage from photosynthesis-derived reactive oxygen species under conditions of oxidative stress, including high-intensity light stress. The mechanisms for this antioxidant activity are discussed below. However, recent studies suggest that they are just one of several components involved in photoprotection. Certainly, any tocochromanol peroxy radicals formed must be converted back to the original compounds by the concerted action of other plant antioxidants, for example, by ascorbate, glutathione, ubiquinol, or lipoic acid, and antioxidant enzymes, including superoxide dismutase, catalase, and peroxidases. Tocopherols are essential for controlling non-enzymatic lipid peroxidation during seed dormancy and seedling germination. In their absence, elevated levels of malondialdehyde and phytoprostanes are formed, and there can be inappropriate activation of plant defense responses.

There is evidence that tocopherols play a role in intracellular signaling in plants, regulating the amount of **jasmonic acid** in leaves by modulating lipid peroxidation and gene expression, thereby influencing plant development and stress responses. Thus, by controlling the degree of lipid peroxidation in chloroplasts (redox regulation), they limit the accumulation of lipid hydroperoxides required for the synthesis of jasmonic acid, which in turn regulates the expression of genes that affect various abiotic stress conditions, including drought, salinity, and extreme temperatures. The translocation of enzymes to the plasma membrane is regulated by tocopherols, possibly by modulating protein-membrane interactions, altering membrane microdomains (lipid **rafts**), or competing for common binding sites within lipid transport proteins. Additionally, tocopherols are essential for the development of cell walls in phloem transfer cells under cold conditions. It appears that α- and γ-tocopherol and the tocotrienols may each have distinct functions. For example, γ-tocopherol is reportedly more potent than α-tocopherol in protecting plants from the harmful effects of osmotic stress and is important for seed longevity. Efforts are underway to increase tocopherol levels in plants through selective breeding and genetic manipulation, to produce crops with enhanced health benefits for consumers and, potentially, for the plants *themselves*.

21.6.1.3: TOCOPHEROLS METABOLISM IN ANIMALS

In animals, the first step in the digestion of tocopherols is their dissolution with other lipids in mixed micelles in the intestines. All tocopherol forms are absorbed to a similar extent in the intestines using transporters in the enterocyte apical membrane that have a broad specificity for hydrophobic molecules, such as cholesterol, vitamin D, and carotenoids. These include scavenger receptor class B type I (SR-BI), the CD36 protein, and NPC1-like intracellular cholesterol transporter 1 (NPC1L1). However, some passive diffusion cannot be ruled out. Transport across the enterocyte may involve cytoplasmic transporters or clathrin-coated vesicles before the tocopherols are incorporated into chylomicrons in free form in the Golgi apparatus for release into the lymph. At the liver, α-tocopherol specifically is taken up from the chylomicrons by a receptor-mediated mechanism with the aid of a specific tocopherol-binding protein (the α-tocopherol transfer protein (α-TTP)), i.e., a 30,500 Da cytosolic protein that has a marked affinity for α-tocopherol and can enhance its transfer between membranes. This recognizes α-tocopherol by the three methyl groups and the hydroxyl on the chromanol ring, as well as by the structure and orientation of the phytyl side chain. It is the chief regulator of whole-body α-tocopherol status and is expressed primarily in the cytosol of hepatocytes in the liver, but has also been reported in other tissues, such as the placenta, at much lower concentrations.

α-TTP ultimately regulates the egress of α-tocopherol selectively from hepatocytes with the aid of the ATP-binding cassette proteins ABCA1 and ABCG for conveyance in the plasma **lipoproteins**, mainly in the very-low-density lipoproteins or VLDL (and thence to LDL) and HDL in humans, to the peripheral tissues (together with much smaller amounts of γ-tocopherol). Most of the other tocopherol forms are directed toward catabolism. Once in the circulation, tocopherol can exchange spontaneously between membranes and lipoproteins, and no specific transport protein for vitamin E in plasma has yet been described. The transfer of tocopherols from VLDL to peripheral tissues occurs as the enzyme lipoprotein lipase hydrolyzes triacylglycerols, whereas that in LDL is processed via the LDL receptor-mediated uptake pathway. Within cells of peripheral tissues, including the central nervous system, α-TTP functions in transporting α-tocopherol to wherever it is required in membranes. This process appears to be aided by **phosphatidylinositol** metabolites. In the brain, tocopherol is transported by apoE-rich lipoproteins. Concentrations of tocopherols can vary appreciably amongst tissues, with most in adipose tissue and adrenals, less in the kidney, heart, and liver, and least in the erythrocytes.

The "α-tocopherol salvage pathway" is partly due to this process and partly to selective oxidation (see below), resulting in a 20- to 30-fold enrichment of α-tocopherol in plasma (average concentration: 22-28 μM) relative to the other tocopherols. Thus, the process of conserving one specific tocopherol appears to determine the relative vitamin E activities of the tocopherols and tocotrienols *in vivo*, rather than their potencies as antioxidants, as measured in model systems *in vitro*. Only α-tocopherol (including synthetic material) or natural mixtures

containing this can be sold under the label 'Vitamin E'. γ-Tocopherol is the second most abundant form in plasma, and it is present in relatively greater proportions in the skin, adipose tissue, and skeletal muscle, where it has some specific biological properties that are distinct from those of α-tocopherol. Although tocotrienols are more potent antioxidants *in vitro*, they are not typically detected in tissues; however, they are believed to have some important functions.

Catabolism: The unwanted surplus of tocochromanols other than α-tocopherol may be excreted in the urine and feces in the form of carboxy-chromanols, including the so-called 'Simon metabolites' - tocopheronic acids (carboxyethylhydroxychromans, CEHC) and tocopheronolactones, after oxidative cleavage of much of the phytyl tail, although these are normally detected in the form of conjugates as sulfate or glucuronidate esters, the forms in which they are excreted in feces and urine. For example for illustrative purposes in liver cells, the first step in the catabolism of γ-tocopherol is ω-hydroxylation by cytochrome P450 (CYP4F2) at the 13' carbon to form γ-13'-hydroxychromanol in the endoplasmic reticulum, followed by ω-oxidation in the peroxisomes to produce γ-13'-carboxychromanol, and finally by stepwise β-oxidation in the mitochondria to cut off two or three carbon moieties from the phytyl chain in each cycle. These steps are shown in Figure **21.6.5**.

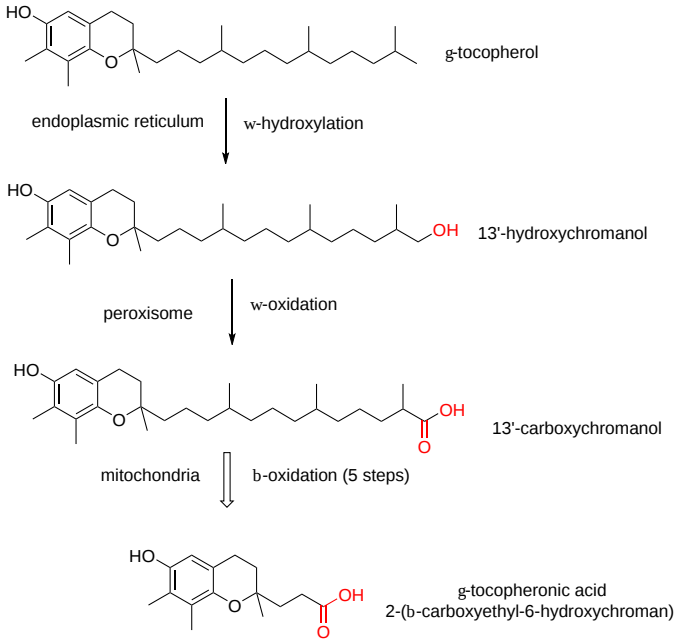


Figure **21.6.5**: Catabolism of γ-tocopherol

Various carboxychromanol intermediates have been identified for all tocopherols, as well as forms in which the hydroxyl group is sulfated in human cell cultures *in vitro*. Sulfated carboxychromanols are the primary tocopherol metabolites in the plasma of rodents. As the vitamin E ω-hydroxylase has a high affinity for the tocopherols other than the α-form and does not attack those bound to the α-tocopherol transfer protein, this provides a further specific enhancement of the α-tocopherol concentration in plasma relative to the others. Some of these catabolic metabolites may have some biological activity in their own right. For example, carboxyethylhydroxychromans derived from γ-tocopherol have been reported to induce apoptosis in cancer cells and exhibit anti-inflammatory effects by inhibiting cyclooxygenases and 5-lipoxygenase (see below). Tocotrienols are catabolized similarly, but with additional steps in which the double bonds are reduced before oxidation; the final carboxyethylchromanols are the same as for tocopherols.

21.6.1.4: TOCOPHEROLS AS ANTIOXIDANTS

Although the syndrome associated with a lack of vitamin E in animal diets has been known for decades, the mode of action and specific location of tocopherols in cell membranes remain unclear. Several theories have been proposed to explain the functions of vitamin E in animal cells. From *in vitro studies*, it has long been believed that a major task is to act as an **antioxidant,** inhibiting, decreasing, delaying, or preventing oxidative damage to unsaturated lipids or other membrane constituents, and thereby protecting tissues by scavenging free radicals. For example, vitamin E administration can prevent lipid peroxidation and hepatotoxicity upon exposure to the free radical-generating agent carbon tetrachloride. Lipid peroxidation is also a cause of **ferroptosis**, an iron-dependent form of nonapoptotic cell death. However, tocopherols have functions other than as antioxidants. In non-biological systems, such as food, cosmetics, and pharmaceutical preparations, tocopherols are invaluable as antioxidant additives.

Due to their lipophilic character, tocopherols are located in membranes or associated with storage lipids, where they can be readily available to interact with lipid hydroperoxides. In brief, **Reactive Oxygen Species (ROS)**, of which innumerable forms exist, can be derived by

enzymatic or non-enzymatic means and produce superoxide anions and other peroxyl radicals. Superoxide radicals ($O_2^{\bullet-}$) ultimately generate highly toxic hydroxyl ($^{\bullet}OH$) or alkoxyl radicals, which can abstract a hydrogen atom from *bis*-allylic methylene groups of polyunsaturated fatty acids under aerobic conditions *in vivo* in animals and plants to generate lipid peroxyl radicals ($LOO^{\bullet}$) and hydroperoxy-fatty acids. **Singlet oxygen** ($^1O_2$ or O=O) is an especially important ROS (non-radical) in photosynthetic tissues of plants. As the radical generation is not enzymatic, all methylene groups between two *cis* double bonds can potentially be involved in the reaction, although not necessarily to the same degree. Tocopherols react rapidly in a non-enzymic manner, unlike many other cellular antioxidants, which are dependent on enzymes, to scavenge lipid peroxyl radicals, i.e., the chain-carrying species that propagate lipid peroxidation. In model systems *in vitro*, all the tocopherols (α > γ > β > δ) and tocotrienols are good antioxidants, with the tocotrienols being the most potent.

In general, the oxidation of lipids is known to proceed by a chain process mediated by such free radicals, in which the lipid peroxyl radical serves as a chain carrier. In the initial step of chain propagation, a hydrogen atom is abstracted from the target lipid by the peroxyl radical, as shown in Figure **21.6.6**.

$$LOO^{\bullet} + LH \longrightarrow LOOH + L^{\bullet} \quad (1)$$

$$L^{\bullet} + O_2 \longrightarrow LOO^{\bullet} \quad (2)$$

- where LH is a lipid, $LOO^{\bullet}$ is the lipid peroxyl radical and LOOH is the lipid hydroperoxide

Figure **21.6.6**: Formation of lipid peroxyl radical

The main function of α-tocopherol is to scavenge the lipid peroxyl radical before it can react with the lipid substrate, as shown in Figure **21.6.7**.

$$LOO^{\bullet} + TOH \longrightarrow LOOH + TOO^{\bullet} \quad (3)$$

- where TOH is tocopherol and $TOO^{\bullet}$ is the tocopheroxyl radical

Figure **21.6.7**: Scavenging of free radicals by tocopherol

The potency of an antioxidant is determined by the relative rates of reactions (1) and (2). When a tocopheroxyl radical is formed, it is stabilized by the delocalization of the unpaired electron around the fully substituted chromanol ring system, rendering it relatively unreactive and thus preventing the propagation of the chain reaction. This also explains the high first-order rate constant for hydrogen transfer from α-tocopherol to peroxyl radicals, as studies of the relative rates of chain propagation to chain inhibition by α-tocopherol in model systems have demonstrated that α-tocopherol can scavenge peroxyl radicals much more rapidly than the peroxyl radical can react with a lipid substrate.

In biological systems, oxidant radicals can originate from various sources, including singlet oxygen, alkoxyl radicals, superoxide, peroxynitrite, nitrogen dioxide, and ozone. α-Tocopherol is most efficient at protecting against peroxyl radicals in a membrane environment.

The reaction of the tocopheroxyl radical with a lipid peroxyl radical, as illustrated, yields 8α-substituted tocopherones, which are readily hydrolyzed to 8α-hydroxy tocopherones that rearrange spontaneously to form α-tocopherol quinones. In an alternative pathway, the tocopheroxyl radical reacts with the lipid peroxyl radical to form epoxy-8α-hydroperoxytocopherones, which hydrolyze and rearrange to epoxyquinones. Tocopherol dimers and trimers may also be formed as minor products. These reactions are shown in Figure **21.6.8**.

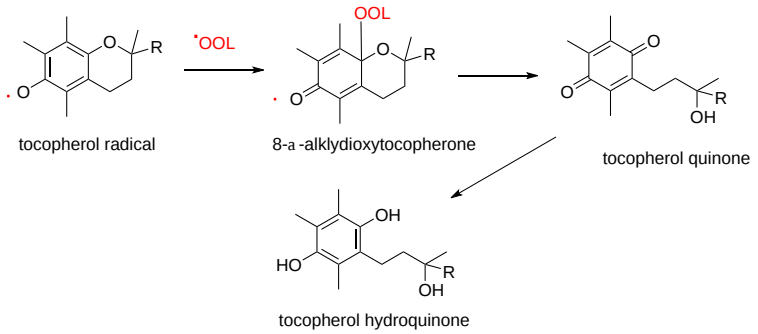


Figure **21.6.8**: Reaction of the tocopherol radical

Free radical-mediated lipid peroxidation is the primary pathway of lipid oxidation in humans, and α-tocopherol is a key antioxidant. Still, it does not scavenge the nitrogen dioxide radical, carbonate anion radical, and hypochlorite efficiently. Vitamin E forms with an unsubstituted 5-position, such as γ-tocopherol, are an exception to the rule that the various tocopherols have similar antioxidant properties in that they can trap electrophiles, including **Reactive Nitrogen Species (RNS)**, which are enhanced during inflammation. The enzyme nitric oxide synthase is capable of continuously producing a large amount of nitric oxide ($NO^{\bullet}$), which can react with superoxide to produce peroxynitrite ($ONOO^-$). This potent and versatile oxidant can attack a wide range of biological targets. It induces lipid peroxidation and nitrates aromatic

compounds and unsaturated fatty acids while isomerizing *cis*-double bonds in fatty acids to the *trans*-configuration. γ-Tocopherol is superior to α-tocopherol in detoxifying the NO_2 radical and peroxynitrite with formation of 5-nitro-γ-tocopherol, as shown in Figure **21.6.9**.

Figure **21.6.*xx***:

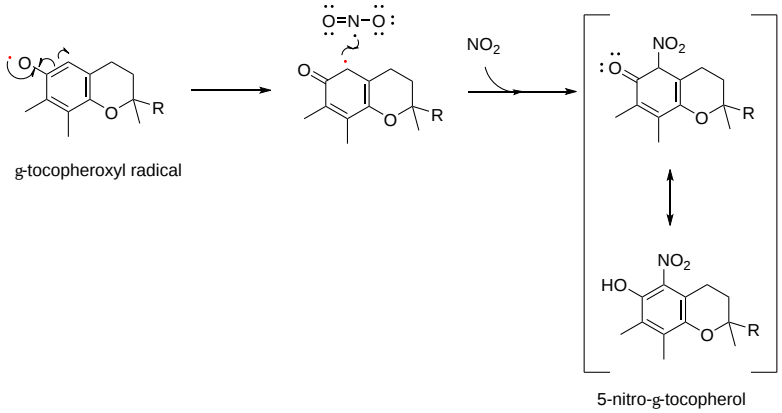


Figure **21.6.9**: Radical reaction with γ-Tocopherol

This occurs *in vivo*, and the concentrations of 5-nitro-γ-tocopherol are elevated in the plasma of subjects with coronary heart disease and in carotid-artery atherosclerotic plaque.

In plant and animal tissues, tocopherols can be regenerated from tocopheroxyl radicals in a redox cycle mediated by various endogenous antioxidants, including vitamins A and C, as well as coenzyme Q, which significantly extends their biological potency. Vitamin C (ascorbic acid) may be especially important in aqueous systems. However, it may also act at the surface of membranes to regenerate α-tocopherol, while being oxidized in turn to dehydroascorbic acid. This can be regenerated to its reduced form by glutathione (GSH), with the production of glutathione disulfide (GSSG), which can subsequently be enzymatically reduced by glutathione reductase using NAD(P)H as a cofactor. In plants, an NAD(P)H-dependent quinone oxidoreductase is involved at an early stage of the regeneration process. In contrast, tocopherol cyclase, an enzyme involved in tocopherol biosynthesis, reintroduces the chromanol ring. These linked cycles, known as the antioxidant network, are illustrated in Figure **21.6.10**.

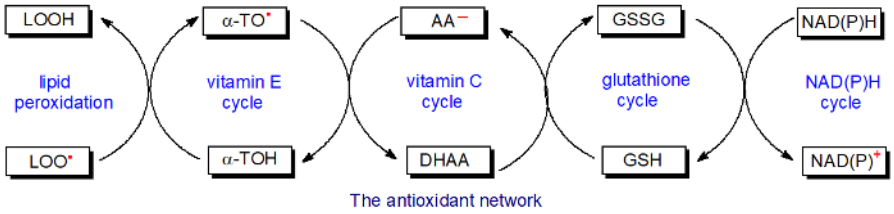


Figure **21.6.10**: The antioxidant network

Thus, tocopherols are only one component of a complex web of metabolites and enzymes in tissues that have antioxidant activities and act by various mechanisms, including the stimulation of genes involved in signaling responses to environmental stresses. One antioxidant mechanism involves the removal of free radicals and reactive species by enzymes such as superoxide dismutase, catalase, and glutathione peroxidase. Additionally, electron donors such as glutathione, tocopherols, ascorbic acid, vitamin K, coenzyme Q, and thioredoxin also scavenge free radicals. Metal-binding proteins, such as transferrin, metallothionein, haptoglobin, and ceruloplasmin, exhibit antioxidant activity by sequestering pro-oxidant metal ions, including iron and copper. However, some metals, such as selenium and zinc, exhibit antioxidant properties. Other antioxidants, including flavonoids, carotenoids, and phenolic acids, as well as tocopherols, enter animal tissues through the food chain. Although the discussion here has been limited to the effects upon lipids, free radicals can cause damage to proteins, DNA, and indeed virtually any native substance in living organisms.

21.6.1.5: BIOLOGICAL FUNCTIONS OF TOCOCHROMANOLS IN ANIMALS

Vitamin E deficiency has been detected in patients with fat malabsorption, cystic fibrosis, Crohn's disease, liver disease, pancreatic insufficiency, and premature infants. Impairment of the normal functions of the immune system has been demonstrated in animals and humans in vitamin E deficiency, and this can be corrected by vitamin E repletion. It also displays activity against nonalcoholic hepatosteatosis. Although there are various proposals for the pathogenic mechanism, none as yet appears to be generally accepted. Following the discovery of vitamin E's effects on fertility in laboratory animal studies, its importance was documented in the development of various tissues and organs, including the brain and nerves, muscles and bones, skin, bone marrow, and blood, most of which are specific to α-tocopherol. However, there is no evidence to support a vitamin E effect on fertility in humans, as was initially observed in rats. The rare

genetic disorder “Ataxia with Isolated Vitamin E Deficiency” or “AVED” is the result of mutations in the gene coding for α-TTP. The death of cerebellar Purkinje cells causes it, but administration of α-tocopherol prevents this and the subsequent development of clinical symptoms of the disease.

There appears to be little doubt that tocopherols inhibit many of the enzymes associated with inflammation *in vitro* in animals and may contribute to the amelioration and treatment of some chronic diseases. However, it has been argued that data on the effects of vitamin E on in vivo biomarkers of oxidative stress are inconsistent. Oxidized metabolites of vitamin E, i.e., those that have reacted as antioxidants, are barely detectable in tissues, and vitamin E maintenance *in vivo* does not appear to have been associated with its regeneration. There appear to be significant differences between the results obtained in studies using laboratory animals and those in humans. Thus, suggestions that dietary supplements of vitamin E may reduce the rate of oxidation of lipids in low-density lipoproteins in humans have not been confirmed in clinical intervention studies, which have not shown a reduction in the incidence or severity of atherosclerosis. However, benefits have been claimed in some conditions. Indeed, there are suggestions that excessive vitamin E supplementation may even be harmful. One study has suggested that relatively high doses of natural α-tocopherol over a long period are required to demonstrate a significant reduction in the levels in the urine of F_2 **isoprostanes**, which are considered to be the most reliable marker for oxidative stress *in vivo*. While there are many fat-soluble antioxidants in the diet, only α-tocopherol is a vitamin. It has even been suggested that tocopherol may be protected from functioning as an antioxidant in some tissues *in vivo* through a network of cellular antioxidant defenses, such that tocopherols are utilized only when other antioxidants are depleted. However, there is no experimental evidence to support this hypothesis.

At the cellular level, *RRR*-α-tocopherol has been shown to inhibit protein kinase C. In the process, it inhibits the assembly and radical-producing activity of NADPH oxidase in monocytes. Similarly, vitamin E suppresses the expression of xanthine oxidase, a source of reactive oxygen species, in the liver. It is thus possible that α-tocopherol can diminish the levels of free radicals by preventing their production, rather than by scavenging them. Its physical presence in membranes adjacent to polyunsaturated fatty acids may thus limit autoxidation.

With the discovery that the antioxidant effects of various tocopherols and tocotrienols have little relation to their vitamin E activities *in vivo*, has come the realization that they have other functions in tissues, most of which are specific to α-tocopherol. Most current research focuses on how vitamin E and its metabolites function in signaling and, controversially, in the regulation of gene activity. While it is certainly true that most other vitamins are essential cofactors for specific enzymes or transcription factors, no receptor that binds specifically to vitamin E has yet been discovered. By preventing the increase of peroxidized lipids that alter both metabolic pathways and gene expression profiles within tissues and cells, it may act indirectly as a regulator of genes connected with tocopherol catabolism, lipid uptake, collagen synthesis, cellular adhesion, inflammation, the immune response, and cell signaling. Vitamin E affects several transcription factors in this manner, including peroxisome proliferator-activated receptor gamma (PPARγ), nuclear factor erythroid-derived 2 (NRF2), nuclear factor kappa B (NFκB), RAR-related orphan receptor alpha (RORα), estrogen receptor beta (ERβ), and the pregnane X receptor (PXR).

α-Tocopherol and its metabolites are believed to modulate the activity of several enzymes involved in signal transduction, including protein kinases and phosphatases, as well as lipid kinases and phosphatases, and other enzymes involved in lipid metabolism, particularly those with inflammatory properties, such as lipoxygenases, cyclooxygenase-2, and phospholipase A_2. While the credentials of tocopherols as antioxidants *in vivo* have been questioned, this does not preclude a role in inhibiting oxidative enzymes, especially in relation to the immune system's function. For example, vitamin E regulates T cell function directly by affecting T cell membrane integrity, signal transduction, and cell division, and it also functions indirectly by influencing eicosanoids and related inflammatory mediators generated by other immune cells. Various tocopherols and tocotrienols have been shown to suppress COX-2 involvement in prostaglandin (PGD_2 and PGE_2) synthesis in lipopolysaccharide-activated macrophages.

In addition, it has been established that the 13'-carboxy metabolite of α-tocopherol (α-T-13'-COOH) and other tocopherol ω-carboxylates are potent allosteric inhibitors of 5-lipoxygenase, a key enzyme in the biosynthesis of the inflammatory **leukotrienes**. α-T-13'-COOH accumulates in immune cells and inflamed exudates, both *in vitro* and *in vivo*, in mice. It has even been suggested that the immune regulatory and anti-inflammatory functions of α-tocopherol depend on this endogenous metabolite. The structure of α-T-13'-COOH is shown in Figure **21.6.11**.

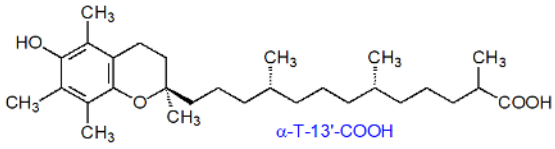


Figure **21.6.11**: Structure of α-T-13'-COOH

α-Tocopherol has a stimulatory effect on the dephosphorylation enzyme, protein phosphatase 2A, which cleaves phosphate groups from protein kinase C, leading to its deactivation. The mechanism may involve the direct binding of vitamin E to enzymes, thereby competing with their substrates, or it may alter their activities through redox regulation. It may also compete for common binding sites within lipid

transport proteins, thereby indirectly altering the traffic of lipid mediators and affecting their signaling functions and enzymatic metabolism. For example, it binds to albumin as well as to a specific α-tocopherol-associated protein (TAP), and in this latter form, it inhibits phosphoinositide 3-kinase. It has been suggested that vitamin E may have a secondary role in stabilizing the structure of membranes, or it may interact with enzymes in membranes to interfere with binding to specific membrane lipids, or it may affect membrane microdomains such as lipid **rafts**.

Evidence suggests that the biological activities of β-, γ-, and δ-tocopherols do not accurately reflect their behavior as chemical antioxidants; however, anti-inflammatory, antineoplastic, and natriuretic actions have been reported. Some non-antioxidant effects of **γ-tocopherol** in tissues, in relation to reactive nitrogen oxide species, have been observed; however, the specificity of these effects *in vivo* remains uncertain. In addition, anti-inflammatory properties have been attributed to a chain-shortened metabolite. Beneficial effects against cancer cells *in vitro* have been observed, which have been attributed to the scavenging of reactive nitrogen species, as these effects are not observed with α-tocopherol. On the other hand, vitamin E and its derivatives are believed to regulate tumor cells by activating the mitogen-activated protein kinase (MAPK) signaling pathway.

Tocotrienols have been shown to have neuroprotective effects and to inhibit cholesterol synthesis. They reduce the growth of breast cancer cells *in vitro*, possibly by influencing gene expression through interaction with the estrogen receptor-β. When administered in combination with either standard antitumor agents, such as those used in chemotherapy, or with natural compounds that exhibit anticancer activity, they are reported to exert a synergistic antitumor effect on cancer cells. γ-Tocotrienol is reported to be an inducer of apoptosis via endoplasmic reticulum stress, while α-tocotrienol may be neuroprotective by inhibition of lipoxygenase activity. Although anti-obesity and anti-diabetic effects have been observed in mice, clinical trials in humans have yielded inconclusive results. These properties are largely distinct from those of the tocopherols, and the pharmaceutical potential of tocotrienols against cancer, bone resorption, diabetes, and various diseases affecting the skin, cardiovascular system, and nervous system is currently being studied.

The biological functions of **α-tocopheryl phosphate** are slowly being revealed. In addition to serving as a possible storage or transport (water-soluble) form of tocopherol, it is involved in cellular signaling. It regulates many genes, including those involved in angiogenesis and vasculogenesis, in a manner distinct from α-tocopherol *per se*. As it lacks the free hydroxyl group, it cannot act directly as an antioxidant, and some consider it to be the biologically active form of the vitamin. It is certainly more active in several biological systems *in vitro* than α-tocopherol, so these effects cannot be attributed to the hydrolyzed molecule. In some instances, it is even antagonistic to α-tocopherol, for example, in its activity towards phosphatidylinositol 3-kinase. On the other hand, activation requires a kinase, while a phosphatase is needed to make the system reversible, but neither has yet been identified. Synthetic phosphate derivatives of γ-tocopherol and α-tocopheryl succinate are known to have potent anti-cancer properties.

21.6.2: ISOPRENOIDS: 2. RETINOIDS (VITAMIN A)

The ancient Egyptians and Greeks were aware of the role of dietary factors in visual acuity. Still, it was not until the 1930s that the importance of carotenoids and their metabolites was recognized, and β-carotene and retinol were fully characterized. It is now recognized that vitamin A activity resides in the metabolites retinol, retinal, and retinoic acid, and in several provitamin A carotenoids, most notably β-carotene. A share of the Nobel Prize for Medicine in 1967 was awarded to George Wald, who, over many years, demonstrated how retinol derivatives (named for their function in the retina) constituted the chemical basis of vision. Now, it is recognized that retinol, retinoic acid, and their numerous metabolites have innumerable other functions in human metabolism, from embryogenesis to adulthood, including growth and development, reproduction, cancer prevention, and resistance to infection. They are important natural antioxidants with health benefits, although some potentially harmful properties have been reported.

Carotenoids are a class of highly unsaturated terpenoids that occur in innumerable molecular forms (>1000). They are common, colorful pigments found in plants, fungi, and bacteria, and are vital to photosynthesis. As dietary constituents, they can add ornamentation to some animal species. Apart from acting as precursors of retinoids, carotenoids *themselves* appear to have a relatively limited range of functions in animal tissues; however, they are important for vision and as antioxidants, especially in the skin. They do, of course, have important functions in plants and lower organisms where they originate, but this topic can only be dealt with briefly here. Other fat-soluble vitamins **tocopherols (vitamin E)**, **vitamin K,** and **vitamin D** are discussed elsewhere.

21.6.2.1: OCCURRENCE AND BASIC METABOLISM OF CAROTENOIDS AND RETINOIDS

The term ‘vitamin A’ is used to denote **retinol** (or all-*trans*-retinol, sometimes termed 'vitamin A_1'), together with a family of biologically active C_{20} **retinoids** derived from this ('vitamers'). The structure of retinol is shown in Figure **21.6.12**.

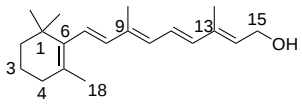


Figure **21.6.12**: All-trans-retinol

These are only found in animal tissues, where they are essential to innumerable biochemical processes. However, they cannot be synthesized *de novo* in animals, and their biosynthetic precursors are plant carotenoids with a β-ionone ring (provitamin A), which are C40 tetraterpenes; β-carotene is the most efficient. It is an orange-red pigment that occurs in the photosynthetic tissues of plants and seed oils. In the human diet in the developed world, plant sources tend to be less important than those from dairy products, meat, fish oils, and margarines, which provide vitamin A *per se*. *However,* carrots and spinach are good sources of the provitamin. In the U.K., for example, all vegetable spreads must be supplemented with the same level of vitamin A (synthetic retinol or β-carotene) as is found in butter. While most research efforts have been focused on retinoids, there is an increasing interest in the biological activities of intact carotenoids in animal tissues.

The biosynthesis of carotenoids in plants via isopentenyl diphosphate and dimethylallyl diphosphate has much in common with that of the **plant sterols**, but this is too specialized a topic to be treated at length here. They have many important functions in plants, for example, during photosynthesis or as precursors to plant hormones, which are discussed below. Some crop plants with increased carotene levels are being developed to prevent vitamin A deficiency in populations of developing countries, and further efforts are underway. Non-photosynthetic bacteria produce a different range of carotenoids, some with chain lengths other than C_{40} (C_{30} to C_{50}).

In animals, including humans, dietary carotenoids such as β-carotene are solubilized in mixed micelles with other dietary lipids, aided by bile acids. They are absorbed in the intestines in their intact form through a process facilitated by specific receptor proteins. Dietary retinol and retinol esters are absorbed similarly in the intestines, but the latter are first hydrolyzed by pancreatic lipase. Conversion to retinoids, leading ultimately to retinol esters occurs in the enterocytes, where dietary β-carotene is subjected to oxidative cleavage at its center, the first step of which is catalyzed by a cytosolic enzyme β-carotene-15,15'-oxygenase-1 (BCO1), which is specific for carotenes with a β-ionone ring, to yield two molecules of all-*trans*-retinal, which is reversibly reduced by a retinol reductase to retinol. Xanthophyll carotenoids are absorbed without cleavage mainly. These reactions are shown in Figure **21.6.13**.

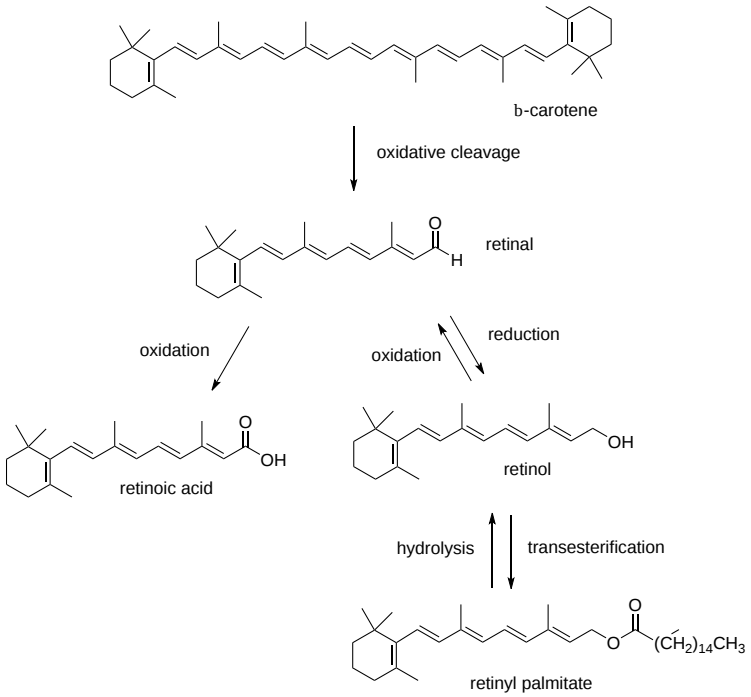


Figure **21.6.13**: Synthesis of all-trans retinoids in the intestines and liver

jbc: https://www.jbc.org/article/S0021-92...842-6/fulltext

Based on the incorporation of ^{18}O into the products. It appears that the enzyme that introduces the oxygen atom, β-carotene-15,15'-oxygenase-1 (BCO1), into the cleavage products is a **dioxygenase,** as both atoms of oxygen in dioxygen are incorporated into products. This is in contrast to a possible mechanism in which only one oxygen atom from dioxygen is added, with the other coming from H_2O if the enzyme acted as a monooxygenase. Figure **21.6.14** shows how oxygen could be introduced in the reaction catalyzed by BCO1 through both possible mechanisms.

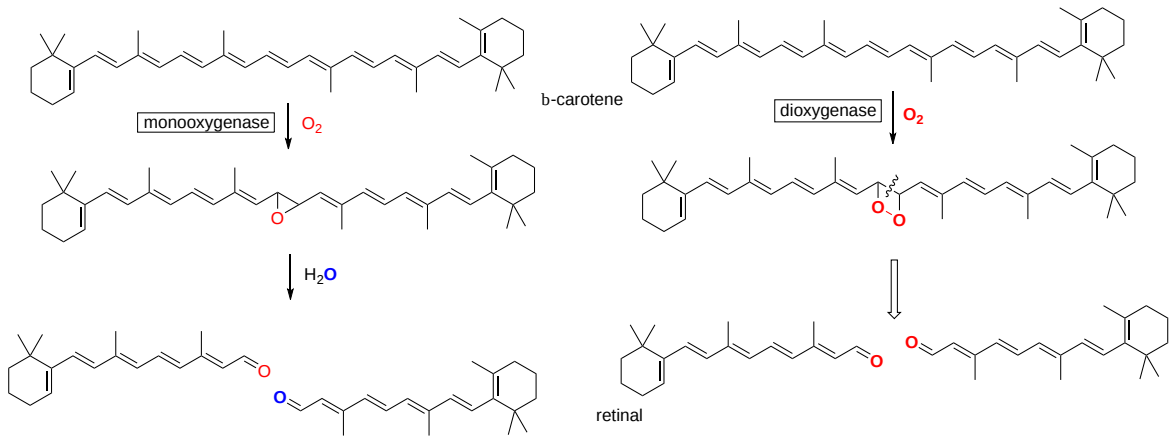
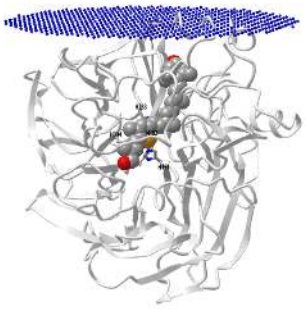


Figure **21.6.14**: Introduction of oxygen atoms into retinal through either mono- and dioxygenase actions of β-carotene-15,15'-oxygenase-1 (BCO1).

The dioxygenase mechanism on the right best accounts for the incorporation of ^{18}O isotope of oxygen in dioxygen.

Figure **21.6.15** shows an interactive iCn3D model of the apocarotenoid cleavage oxygenase from Synechocystis, a Retinal-Forming Carotenoid Oxygenase (2BIW)



NCBI iCn3D Figure **21.6.15**: Retinal-Forming Carotenoid Oxygenase from Synechocystis (2BIW). (Copyright; author via source). Click the image for a popup or use this external link: https://structure.ncbi.nlm.nih.gov...dttF958wFPAUP7

The enzyme has a bound carotene analog, (3R)-3-hydroxy-8'-apocarotenol. It contains an active site Fe^{2+} ion at the end of a hydrophobic tunnel. Four histidine side chains ligate the ion. On binding, three of the trans C=C bonds convert to a distorted cis-trans-cis conformation. The middle trans bond is proximal to the $Fe^{2+,}$ which is ligated by dioxygen, the source of the incorporated oxygen atoms on cleavage.

Any unchanged β-carotene and newly formed retinol esters in the enterocytes are incorporated into **chylomicrons** and released into the lymphatic system and thence into the bloodstream, where some is taken up by peripheral tissues before most is absorbed by the liver. Some intact carotene and other carotenoids are transferred to lipoproteins (LDL and HDL) for transport in plasma, with assistance from specific binding and transport proteins. For example, carotene can be absorbed at the placental barrier and transferred to the fetus for conversion to retinoids, which are essential for development. Within the hepatocytes, retinol esters are hydrolyzed in the late endosomes with the release of free retinol into the cytosol, from which it can be released back into the circulation, converted to retinoids or transferred to hepatic stellate cells for storage in lipid droplets, the main body reservoir of vitamin A. In these specialized cells, retinol is esterified to form retinyl palmitate by the transfer of fatty acids from position *sn*-1 of phosphatidylcholine, mainly via the action of a membrane-bound lecithin:retinol acyltransferase (LRAT) in the endoplasmic reticulum. There are also lesser acyl-CoA-dependent pathways, including an acyl-CoA:retinol acyltransferase and even the enzyme diacylglycerol acyltransferase 1 (DGAT1); esterification is facilitated by binding to cellular retinol-binding protein type II (CRBP2).

Both retinol and retinoic acid are precursors of many metabolites, known as retinoids, which are required for specific purposes in tissues through enzymatic modification of the functional groups and geometrical isomerization of the polyene chains. In the liver, activation of the retinol pathway involves first mobilization of the ester, followed by hydrolysis by retinol ester hydrolases, which include carboxylesterase ES-10. Then, the reversible oxidation of retinol to retinal is carried out by one of several enzymes, including dehydrogenases and various cytochrome P450s, before some retinal is irreversibly oxidized to retinoic acid by enzymes with retinal dehydrogenase activity. On-demand conversion of retinol to retinoic acid occurs through the same mechanisms in other tissues. However, for vision, retinol esters serve directly as the substrate for the formation of the visual chromophore 11-*cis*-retinal (see below). Retinyl-β-D-glucoside, retinyl-β-D-

glucuronide, and retinoyl-β-D-glucuronide are naturally occurring and biologically active metabolites of vitamin A, which are found in fish and mammals. Indeed, the last has similar activity to all-*trans*-retinoic acid without any of the unwanted side effects in some circumstances.

Cleavage of β-carotene at double bonds other than that in the center or of a wider range of other carotenoids occurs by the action of a related enzyme β-carotene-9',10'-dioxygenase (β-carotene-oxygenase-2 or BCO2) in mitochondria, which leads to the formation of similar molecules, i.e., β-apocarotenals and β-apocarotenones of variable chain length. While these may exert distinctive biological activities in their own right, there is evidence that they can also be metabolized to form retinal.

In the aqueous environment within cells, as well as in plasma, retinol, retinal, and retinoic acid are bound to retinoid-binding proteins (RBP), which solubilize, protect, and, in effect, detoxify them. These proteins also play a role in facilitating retinoid transport and metabolism; some are present only in specific tissues, and many are specific to particular retinoids and metabolic pathways. To prevent infiltration through the kidneys, retinol and holo-RBP form an association in blood with a protein termed transthyretin (TTR), which also serves as a carrier for thyroid hormones and is essential for their secretion. Normally, vitamin A circulates in plasma as a retinol:RBP:TTR complex with a 1:1:1 molar ratio. Unesterified retinol is the main form of the vitamin that is exported from the liver upon demand, and it is transported in the blood in this bound form in VLDL, LDL, and HDL, with some directly from the diet in the chylomicrons and their remnants. Peripheral tissues have specific receptors to take up what they require, likely after the hydrolysis of any esters to retinol by the enzyme lipoprotein lipase. Then, retinol dissociates from the protein as it forms a complex with a receptor (STRA6) at a target cell and diffuses through the plasma membrane, a process driven by retinol esterification.

The RBP-TTR complex does not bind to retinal and retinoic acid, although these do bind to RBP on their own, and most of the low levels of retinoic acid transported in the blood are bound to albumin. Local levels of retinoic acid are the result of an interplay between enzymes of synthesis, binding, and catabolism. For example, within cells, retinoic acid binding proteins (CRABP1 and CRABP2) bind to the newly synthesized retinoic acid, increase its rate of metabolism, and protect cells from an excess.

In skin, 3,4-dehydroretinoids are synthesized from all-*trans* retinoids by the desaturase Cytochrome P450 27C1 with the assistance of cellular retinol-binding proteins (CRBPs). 3,4-Dehydroretinol, which is sometimes termed vitamin A_2, is shown in Figure **21.6.16**.

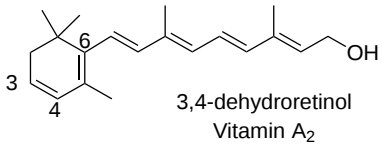


Figure **21.6.16**: 3,4-dehydroretinol (Vitamin A_2)

Its derivative, 3,4-dehydroretinal, is used as a visual chromophore in many cold-blooded vertebrates, including lampreys, fish, amphibians, and some reptiles (see below). Geranylgeranoic acid shares structural similarities with retinoic acid and is therefore termed an acyclic retinoid, although it lacks vitamin A activity. It is synthesized in animal tissues from mevalonate, and together with its 2,3-dihydro metabolite, has potent anticancer properties.

Retinol esters: A relatively small proportion of the cellular retinoids is located in membranes in tissues. Rather, retinol esters, mainly retinyl palmitate, are the main storage form of vitamin A, and they occur in many different organs, including adipose tissue and testes, but chiefly in stellate cells of the liver and pancreas. The mechanism by which retinol is directed specifically to these cells and enters them before esterification is not known. Although hepatic stellate cells are much smaller and less abundant than hepatocytes (only 5 to 8% of all liver cells), they are characterized by cytoplasmic lipid droplets that contain 90-95% of the hepatic retinoids (and up to 80% of the body pool) in addition to other non-retinoid lipids; the lecithin:retinol acyltransferase is the only retinol ester synthase in this instance. Additionally, specialized cells in the eye store retinoids, which are essential for vision, in the form of lipid droplets. When the supply of retinol in the diet is limited, hepatic stores of retinol esters are mobilized as retinol ester hydrolases are activated to maintain constant circulating retinol levels; hormone-sensitive lipase is the most important of these enzymes, although the adipose tissue triacylglycerol lipase and the lysosomal acid lipase are also involved.

Catabolism: All-*trans*-retinoic acid formation is irreversible, so its synthesis and degradation must be tightly regulated. As a first step in catabolism, the excess is cleared by conversion to more polar metabolites through oxidation by various enzymes of the cytochrome P450 family. Secondly, the water-soluble retinoic acid metabolites, including 4-hydroxy-, 4-oxo-, and 18-hydroxy-retinoic acids, conjugate with glucuronic acid and can then be rapidly removed from circulation and eliminated from the body via the kidney.

21.6.2.2: RETINOIDS AND VISION

The structure of 11-cis-retinal, which we discussed in Chapter 11, is shown in Figure **21.6.17**

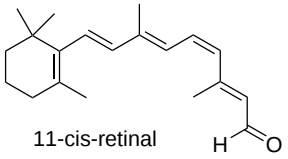


Figure **21.6.17**: 11-cis-retinal

Retinoids are essential for vision, and there is now a good appreciation of how this works at the molecular level. In the eye, uptake of retinol from the circulation is mediated by the transmembrane cell-surface STRA6 receptor of the retinal pigment epithelium, a pigmented monolayer of cells located between the photoreceptors and choroid that nourishes retinal visual cells and catalyzes the release of retinol from retinol-binding proteins and transports it to the cytosol. The process by which light is converted to a signal recognized by the brain, sometimes termed the '**retinoid (visual) cycle**', requires a two-cell system beginning in the retinal pigment epithelium and continuing in photoreceptor cells, i.e., retinal rod and cone cells in the eye that contain membranous vesicles that serve as light receptors. Roughly half of the proteins in these vesicles consist of the protein conjugate, rhodopsin, which consists of a protein, opsin, with the retinoid **11-*cis*-retinal**. Each step in the visual process requires specific binding or transport proteins, especially the interphotoreceptor retinoid-binding protein (IRBP).

All-*trans*-retinol is first converted to its ester by the enzyme lecithin:retinol acyltransferase as described above in the RPE, and the products coalesce into lipid droplets, i.e. dynamic organelles termed 'retinosomes'. The next step involves a dual-purpose enzyme (RPE65) in the endoplasmic reticulum, which cleaves the *O*-alkyl bond (not a conventional hydrolysis reaction) in the retinol ester and at the same time causes a change in the geometry of the double bond in position 11 of retinol from *trans* to *cis*. The 11-*cis*-retinol is then oxidized to 11-*cis*-retinal by 11-*cis*-retinal dehydrogenase (RDH5). The full cycle is shown in Figure \(\PageIndex{18}\) below.

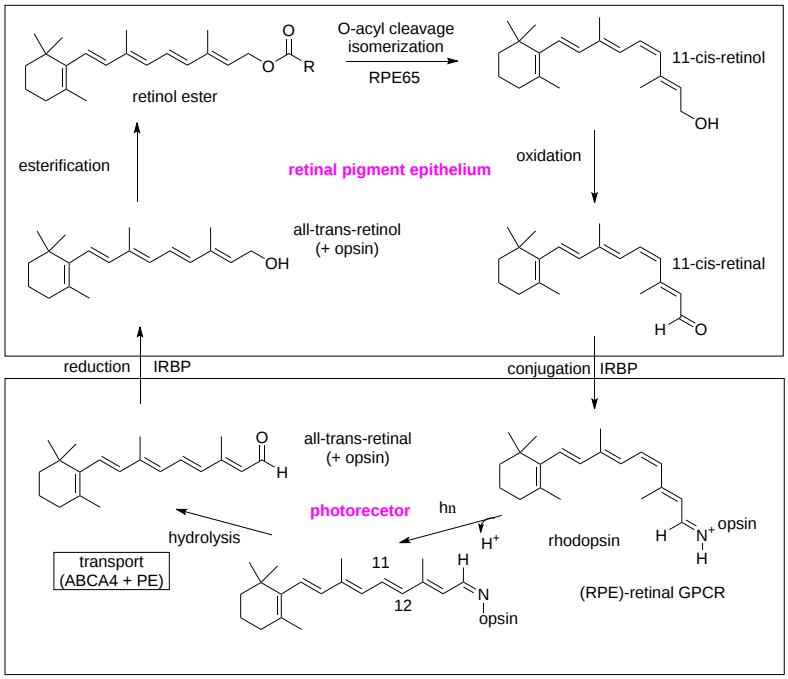


Figure **21.6.18**: Retinoid visual cycle

The final part of the cycle occurs in the photoreceptor, where first the 11-*cis*-retinal is reacted with opsin to produce the protein conjugate rhodopsin in a protonated form. When rhodopsin is activated by light, the *cis*-double bond in the retinoid component is isomerized non-enzymatically by the energy of a photon to the 11-*trans* form, with a change in conformation that, in turn, affects the permeability of the membrane and influences calcium transport. This results in further molecular changes that culminate in the release of opsin and all-*trans*-retinal, which is the trigger that sets off the nerve impulse, allowing the light to be perceived by the brain.

A second mechanism for 11-*cis*-retinal formation, which may function to ensure continuous visual responsiveness in bright light, involves the RPE-retinal G protein-coupled receptor (RGR), which can act as a retinaldehyde photoisomerase. As the enzyme RPE65 functions optimally under low-light conditions, it is believed that RGR prevents the saturation of photoreceptors under high-light levels, thereby facilitating vision in daylight. The isomerase, RPE65, and the photoisomerase, RGR, operate together to provide a sustained supply of the visual chromophore under different levels of illumination.

The all-*trans*-retinal is removed from the photoreceptor either by reduction to all-*trans*-retinol by all-*trans*-retinol dehydrogenase 8 expressed in the outer segments of photoreceptors or after transport using a specific transporter (ABCA4), which provides phosphatidylethanolamine (PE) for conversion to the Schiff-base adduct, i.e., *N*-retinylidene-phosphatidylethanolamine, as shown in Figure **21.6.19**.

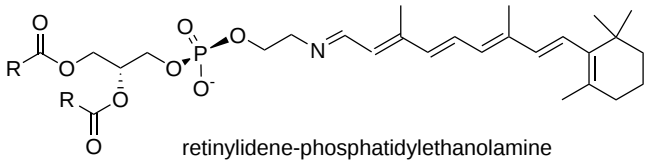


Figure **21.6.19**: *N*-retinylidene-phosphatidylethanolamine

It flips from the lumen to the cytosolic leaflet of the disc membrane. This process prevents non-specific aldehyde activity, thereby removing potentially toxic retinoid compounds from the photoreceptors. The adduct is a transient sink that dissociates, allowing the retinal to be reduced back to all-*trans*-retinol by cytoplasmic retinol dehydrogenase. All-trans-retinol exits the photoreceptor and enters the retinal pigment epithelium with the aid of binding to the retinoid-binding protein (IRBP), where it is converted back to a retinyl ester to complete the cycle and restore light sensitivity.

As a side reaction, some troublesome bis-retinoid adducts of PE (and further byproducts) may be produced by non-enzymatic mechanisms, and these can accumulate with age, potentially affecting vision. **Lower organisms:** Bacteriorhodopsin is the best studied of a family of opsins, found in archaea, eubacteria, fungi, and algae. It is a protein with seven transmembrane helices that acts as an opto-electrical transducer or light-gated active ion pump to capture photon energy via its covalently bound chromophore, all-*trans*-retinal, converting it to 13-*cis*-retinal, and moves protons against their electrochemical gradient from the cytoplasm to the extracellular space. In Archaea, it is known as the "purple membrane" and can occupy a significant proportion of the organism's surface area.

21.6.2.3: OTHER FUNCTIONS OF RETINOIDS IN HEALTH AND DISEASE

In addition to their role in vision, it is now recognized that retinoids play essential roles in growth and development, reproduction, and resistance to infection. They are particularly important for the function of epithelial cells in the digestive tract, lungs, nervous system, immune system, skin, and bone at all stages of life. They are required for the regeneration of damaged tissues, including the heart, and they appear to have some potential as chemopreventive agents for cancer and for the treatment of skin diseases such as acne. Under pathological conditions, stellate cells lose their retinoid content and transform into fibroblast-like cells, contributing to the fibrogenic response. A massive loss of retinoids accompanies cirrhosis of the liver, but it is not clear whether this is a cause or a symptom, and there appears to be confusion as to when supplementation may be helpful in this and other diseases of the liver. Like retinol and retinoic acid, the metabolite 9-*cis*-retinoic acid also has valuable pharmaceutical properties.

With such a large number of double bonds in conjugation, it is not surprising that carotenoids in general, and retinoids in particular, are efficient quenchers of singlet oxygen and scavengers of other reactive oxygen species. However, any direct antioxidant properties are not believed to be important in terms of general health *in vivo*, and it is unclear how relevant the physical properties of retinoids are to specific biochemical processes compared to their effects on signaling and gene transcription. There is a caveat that retinoids may stimulate certain antioxidant genes, thereby having an indirect antioxidant function. Nutritional studies with dietary supplements of carotenoids have sometimes suggested pro-oxidant activity. One explanation for detrimental effects may be that regeneration of the parent carotenoid or retinoid from the corresponding radical cation may be limited when concentrations of reductants such as ascorbic acid are low.

Many of the retinol metabolites function as ligands to activate specific transcription factors for particular receptors in the nucleus of the cell. Thus, they regulate the expression of a large number of genes (>500), including those essential for maintaining normal cell proliferation and differentiation, embryogenesis, a healthy immune system, and male and female reproduction. In the innate immune system, vitamin A is required for the differentiation of cells such as macrophages, neutrophils, and natural killer cells. All-*trans*-retinoic acid, on the other hand, is involved in differentiating the precursors of dendritic cells. **Retinoic acid** and its 9-*cis*-isomer are especially important in this context, and they are often considered the most important retinoids in terms of function other than in the eye. This structure of the cis-isomer is shown in Figure **21.6.20**.

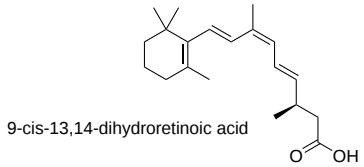


Figure **21.6.20**: Cis isomer of retinoic acid

In essence, retinoic acid moves to the nucleus with the aid of small intracellular lipid-binding proteins (CRABP2 and FABP5), which channel it to specific nuclear receptors, the **retinoic acid receptors (RAR)** of which there are three, RAR-α, β, and γ. These are ligand-dependent regulators of transcription, functioning *in vivo* as heterodimers with **retinoid X receptors (RXR)** to process the retinoic acid signal by acting through polymorphic retinoic acid response elements (RAREs) within the promoter regions of responsive genes. Similarly, 9-*cis*-retinoic acid and 9-*cis*-13,14-dihydroretinoic acid are high-affinity ligands for RXR in mice. Together with retinoic acid, these are also ligands for the farnesoid X receptor (FXR), which forms a heterodimer with RXR. The latter receptor complex is involved primarily in **bile acid** homeostasis, and conversely, there are suggestions that bile acids may have regulatory effects on vitamin A homeostasis.

In addition, other nuclear receptors, such as the peroxisome proliferator-activated receptor PPARγ, form a heterodimer with the retinoid X receptor and are activated by retinoic acid to recruit cofactors. This complex, in turn, binds to the peroxisome proliferator response element (PPRE) gene promoter, leading to the regulation mainly of those genes involved in lipid and glucose metabolism, including some involved in inflammation and cancer. To add to the complexity, retinoic acid has extra-nuclear, non-transcriptional effects, such as the activation of protein kinases and other signaling pathways.

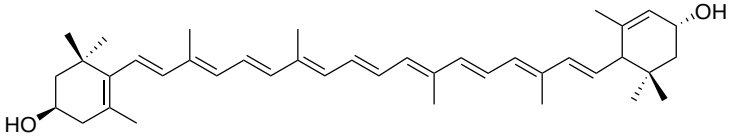
It has also become evident that many of the functions of retinoids are mediated via the action of specific binding proteins (as discussed briefly above), which control their metabolism *in vivo* by reducing the effective or free retinoid concentrations, by protecting them from unwanted chemical attack, and by presenting them to enzyme systems in an appropriate conformation. With some tissues, retinol-bound RBP in the blood is recognized by the membrane protein STRA6, which transports retinol into cells, where it binds to an intracellular retinol acceptor, cellular retinol-binding protein 1 (CRBP1), and activates a signaling cascade that targets specific genes. In addition, a specific retinol-binding protein (RBP4) secreted by adipose tissue is involved in the development of insulin resistance and type 2 diabetes, possibly by affecting glucose utilization by muscle tissue, with obvious application to controlling obesity. In the eye, the activity of retinoic acid during development is controlled by binding to apolipoprotein A1.

All-*trans*-retinoic acid is effective against various types of human cancers, particularly in model systems, and in some clinical trials, due to its specific effects on cell proliferation, differentiation, and apoptosis, where its relatively low toxicity at normal tissue levels is a benefit. For example, it induces complete remission in most cases of acute promyelocytic leukemia when administered in combination with other chemotherapy techniques. Similarly, 13-*cis*-retinoic acid has been used successfully in the treatment of children with high-risk neuroblastoma to reduce the risk of recurrence and increase long-term survival rates. However, the efficacy of similar treatments against other types of acute myeloid leukemia and solid tumors appears to be poor. It is hoped that current efforts to obtain a better understanding of the mechanism of the anti-cancer activities will lead to improved treatments. Synthetic analogs of retinoic acid, termed **rexinoids**, which activate retinoic X receptors, also hold promise as anti-cancer agents.

Vitamin A deficiency in children and adult patients is usually accompanied by impairment of the immune system, leading to a greater susceptibility to infection and an increased mortality rate, often with growth retardation and congenital malformations. However, vitamin A deficiency in malnourished children is the major reason for childhood mortality in the underdeveloped world, causing over 650,000 early childhood deaths annually and pediatric blindness. This is doubly tragic, as it is so easily preventable. In adults, vitamin A deprivation affects the reproductive system, inhibiting spermatogenesis in males and ovulation in females. Unfortunately, it is not always easy to distinguish between the effects of vitamin A deficiency and primary defects of retinoid signaling.

21.6.2.4: FUNCTIONS OF XANTHOPHYLLS AND OTHER CAROTENOIDS IN HUMANS

Xanthophylls are plant C_{40} tetraterpenes that differ from the carotenoids in having oxygen atoms in the ring structures (hydroxyl, oxo, or epoxyl). Lutein, zeaxanthin, and *meso*-zeaxanthin from dietary sources, such as green leafy vegetables and yellow and orange fruits and vegetables, are found specifically in the macula of the eye in humans and other primates, i.e. the functional center of the retina in a small central pit known as the *macula lutea*, where they enhance visual acuity and protect the eye from high-intensity, short-wavelength visible light. They are powerful antioxidants in a region vulnerable to light-induced oxidative stress. Binding proteins specific for lutein- and zeaxanthin mediate the highly selective uptake of these carotenoids into the retina, but *meso*-zeaxanthin is mainly a metabolite of dietary lutein. Macular xanthophylls decrease the risk of age-related macular degeneration. In the brain, they may stimulate and maintain cognitive function in the elderly and assist with brain development in infants. Hydroxylated xanthophylls such as lutein, shown in Figure **21.6.21**, occur both in the free form and esterified to fatty acids; the latter are hydrolyzed in the intestines when consumed by animals.



lutein

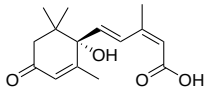
Figure **21.6.21**: Leutin

Many other carotenoids are absorbed from the diet. They are subject to oxidative cleavage or other catabolic processes, partly in the intestines and partly in other tissues, after being transported in lipoproteins. Some carotenoids remain intact and are believed to act as antioxidants, while others may have specific anti-inflammatory properties. For example, carotenoids accumulate in the skin of mammals, where they may have antioxidant and photoprotective roles, as well as effects on moisture content, texture, and elasticity. Lycopene may have protective effects against atherogenesis, coronary heart disease, and prostate cancer.

21.6.2.5: FUNCTIONS OF CAROTENOIDS IN PLANTS

As carotenoids have a polyene chain of 9 to 11 double bonds in conjugation, they can absorb light in the gap of chlorophyll absorption, and so function as additional light-harvesting pigments in plants. Their distinctive arrangement of electronic levels enables them to transfer excitation energy from the carotenoid excited state to chlorophyll in the light-harvesting complex (photosystem II). Energy can also be transferred back from chlorophyll to carotenoids as a photoprotection mechanism. During photosynthesis, damaging species are produced by both light and oxygen, with reactive oxygen species (ROS) of special concern. The energy is transferred from chlorophyll to the polyene tail of the carotenoid, where electrons are moved between the carotenoid bonds until the most balanced or lowest energy state is reached. While there is therefore appreciable potential for carotenoids to act as antioxidants in plants, it is uncertain how important this is from a practical functional standpoint. The length of the polyene tail of carotenoids determines which wavelengths of light will be absorbed by the plant; those not absorbed are reflected, thereby determining the coloration.

Carotenoids are precursors for two plant hormones and a diverse set of apocarotenoids. For example, **abscisic acid**, shown in Figure **21.6.21**, is a C_{15} isoprenoid plant hormone, which is synthesized in plastids from the C_{40} carotenoid zeaxanthin.



abscisic acid

Figure **21.6.21**:

A series of enzyme-catalyzed epoxidations and isomerizations is involved, followed by cleavage of the intermediate product by a dioxygenation reaction and further oxidations to yield, eventually, abscisic acid. Functioning via signaling cascades, abscisic acid regulates innumerable biological effects in plants, especially in relation to developmental processes that include plant growth, seed and bud dormancy, embryo maturation and germination, cell division and elongation, floral growth, and the control of stomatal closure. Plants must respond to environmental stresses, including drought, cold and heat stress, salinity, and tolerance to heavy metal ions. Similarly, strigolactones are C_{15} oxidation products of carotenoids that are involved in regulating symbiosis between plants and arbuscular mycorrhizal fungi, as well as interactions with plant parasites.

21.6.3: ISOPRENOIDS: 3. OTHER MEMBRANE-ASSOCIATED ISOPRENOIDS

Terpenes (isoprenoids) are one of the most varied and abundant natural products produced by animals, plants, and bacteria. They are generally defined based on their biosynthetic derivation from isoprene units (C5H8), with 55,000 different types characterized to date, according to a recent estimate. By most definitions, all isoprenoids should be classified as ‘lipids’, from simple monoterpenes such as geraniol, which is derived from two prenol units, to complex polymers such as natural rubber. Only those isoprenoids that have a **functional** role in cellular membranes will be discussed here. These include plastoquinone, ubiquinone (coenzyme Q), phylloquinone and menaquinone (vitamin K), dolichol and polyprenols, undecaprenyl phosphate and lipid II, and farnesyl pyrophosphate, together with some key biosynthetic precursors. The nature and function of **tocopherols and tocotrienols (vitamin E)** and **retinoids (vitamin A)** are relevant here, but have been discussed previously. Of course, sterols are also isoprenoids.

There are two basic mechanisms for the biosynthesis of the isoprene units that are the precursors for the biosynthesis of isoprenoids, i.e., isopentenyl pyrophosphate and dimethylallyl pyrophosphate. These are the mevalonate pathway, which is located in the cytosol of the cell, and the non-mevalonate pathway, found mainly in the plastids of plants. These have been discussed previously.

21.6.3.1: PHYTOL

Phytol or (2*E*,7*R*,11*R*)-3,7,11,15-tetramethyl-2-hexadecen-1-ol, i.e., with 20 carbons in a 16-carbon chain and one double bond, is an acyclic diterpene alcohol, which is synthesized in large amounts in plants as an essential component of chlorophyll, the most important photosynthetic pigment in plants and algae. Geranylgeranyl-diphosphate, synthesized in chloroplasts via the 4-methylerythritol-5-phosphate (non-mevalonate) pathway, is the primary precursor of phytol following reduction of three double bonds by geranylgeranyl reductase, and this can occur before or after attachment to chlorophyll, depending upon species. Chlorophyll dephytylase (CLD1) is the enzyme in plants responsible for chlorophyll hydrolysis and the release of phytol. The reactions are shown in Figure **21.6.22**.

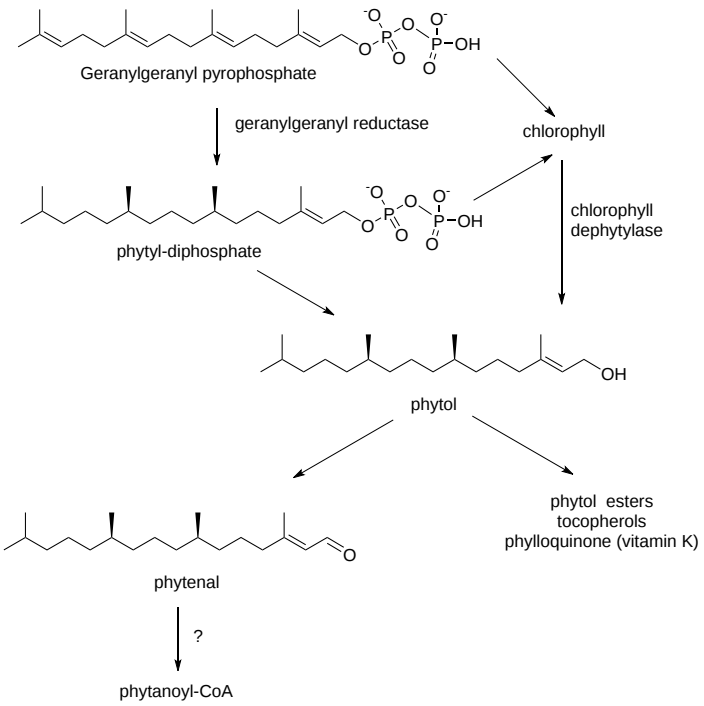


Figure **21.6.22**: Phytol synthesis and metabolism in plants

Little free phytol is present in plant tissues. However, some phytol esters of fatty acids may occur, especially when plants are stressed during nitrogen deprivation or in senescence, when chlorophyll is degraded, fatty acids are released from glycerolipids, and a phytol ester synthase is induced as part of a detoxification and recycling process. Bell peppers and rocket salad are especially rich sources under normal conditions. In addition, phytol, as its diphosphate, is utilized for the synthesis of **tocopherols** (vitamin E) and phylloquinol (vitamin K - see below), and the precursor geranylgeraniol and its fatty acid ester occur in small amounts in some plant species. It is the biosynthetic precursor of tocotrienols and the highly unsaturated carotenoids (and hence of **retinoids**). Phytenal has been isolated as an intermediate in the catabolism of phytol in plants, but further steps are uncertain, although phytanoyl-CoA has been detected in stressed plants. As phytenal is highly reactive and potentially toxic via its interaction with proteins, its accumulation must be kept at a low level by competing pathways.

In ruminant animals, chlorophyll is hydrolyzed by rumen microorganisms, releasing free phytol. This does not occur in humans, but some phytol may be ingested with plant foods, either in its free form or as phytol esters, and can be absorbed from the intestines. Within animal tissues, phytol is oxidized to **phytanic acid**. Phytol and/or its metabolites have been reported to activate the transcription factors PPARα and retinoid X receptor. In mice, oral phytol induces a substantial proliferation of peroxisomes in many organs.

21.6.3.2: PLASTOQUINONE

A molecule that is related to the tocopherols, **plastoquinone**, is found in cyanobacteria and plant chloroplasts, and it is produced in plants by analogous biosynthetic pathways to those of tocopherols in the inner chloroplast envelope with solanesol diphosphate as the biosynthetic precursor of the side chain; there appears to be a somewhat different mechanism in cyanobacteria. The molecule is sometimes designated - 'plastoquinone-n' (or PQ-n), where 'n' is the number of isoprene units, which can vary from 6 to 9. Its structure is shown in Figure **21.6.23**.

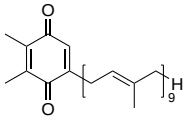


Figure **21.6.23**: Plastoquinone

Plastoquinone plays a crucial role in photosynthesis by serving as an electronic connection between photosystems I and II, thereby generating an electrochemical proton gradient across the thylakoid membrane. This provides energy for the synthesis of adenosine triphosphate (ATP). The reduced dihydroplastoquinone (plastoquinol) transfers further electrons to the photosynthesis enzymes before being re-oxidized by a specific cytochrome complex. The redox state of the plastoquinone pool regulates the expression of many genes encoding photosystem proteins. X-ray crystallography studies of photosystem II from cyanobacteria reveal that two molecules of plastoquinone form two membrane-spanning branches. In addition, plastoquinone has antioxidant activity comparable to that of the tocopherols, protecting especially against excess light energy and photooxidative damage. Similarly, in thylakoid membranes, plastoquinol can scavenge superoxide, producing H_2O_2. Plastoquinone is a cofactor participating in the desaturation of phytoene in carotenoid biosynthesis and the

biosynthetic precursor of plastochromanols. With its numerous functions, plastoquinone connects photosynthesis in plants with metabolism, light acclimation, and stress tolerance.

Plastoquinone-9, together with phylloquinone, tocopherol, and plastochromanol-8, is stored in plastoglobuli, lipoprotein-like micro-compartments, which enable exchange with the thylakoid membrane and are also involved in chlorophyll catabolism and recycling. It has been suggested that the redox state of the plastoquinone pool is the main redox sensor in chloroplasts that initiates many physiological responses to changes in the environment, and in particular to those related to light intensity by regulating the expression of chloroplast genes.

21.6.3.3: UBIQUINONE (COENZYME Q)

The **ubiquinones**, which are also known as coenzyme Q (CoQ) or mitoquinones, have obvious biosynthetic and functional relationships to plastoquinone and they are found in all the domains of life (hence the name). They have a 2,3-dimethoxy-5-methylbenzoquinone nucleus and a side chain of six to ten isoprenoid units; the human form illustrated below has ten such units (coenzyme Q_{10}), i.e., it is 2,3-dimethoxy-5-methyl-6-decaprenyl-1,4-benzoquinone, while that of the rat has nine, *Escherichia coli* has eight, and *Saccharomyces cerevisiae* has six. In plants, ubiquinones tend to have nine or ten isoprenoid units. Forms with a second chromanol ring, resembling the structures of tocopherols, are also produced (ubichromanols), but not in animal tissues. They are generated on an industrial scale for pharmaceutical purposes by yeast fermentation. Because of their hydrophobic properties, ubiquinones are located entirely in membrane bilayers in most eukaryotic organelles, probably at the mid-plane.

Ubiquinones are synthesized *de novo* in mitochondria in most cells in animal, plant, and bacterial tissues by a complex sequence of reactions from the essential amino acid phenylalanine and then tyrosine to generate *p*-hydroxybenzoic acid, which is the key precursor that is condensed with the polyprenyl unit (from the cholesterol synthesis pathway) via a specific transferase; this is followed by decarboxylation, hydroxylation, and methylation steps, depending on the specific organism, although some of the required enzymes have yet to be fully characterized. In *Escherichia coli*, biosynthesis does not occur in a membrane environment as had been thought. Rather, the seven proteins that catalyze the last six reactions of the biosynthetic pathway, following the attachment of the isoprenoid tail, form a stable complex, or metabolon, in the cytoplasm, enabling the modification of hydrophobic substrates in a hydrophilic environment.

In mitochondria, coenzyme Q is present both as the oxidized (ubiquinone) and reduced (ubiquinol) forms, as shown in Figure **21.6.24**.

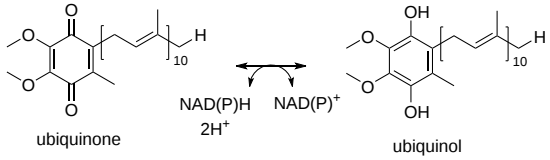


Figure **21.6.24**: Ubiquinone-ubiquinol interconversion

Ubiquinones are essential components of the respiratory electron transport system, possibly as part of supramolecular complexes, taking part in the oxidation of succinate or NADH via the cytochrome system to generate the protonmotive force used by the mitochondrial ATPase to synthesize ATP. In this process, coenzyme Q transfers electrons from the various primary donors, including complex I, complex II, and the oxidation of fatty acids and branched-chain amino acids, to the oxidase system (complex III), while simultaneously transferring protons to the outside of the mitochondrial membrane, resulting in a proton gradient across the membrane. As a consequence, it is reduced to ubiquinol. Thus, it is an essential component of the cycle that generates the proton motive force driving ATP production via oxidative phosphorylation. In yeast, one coenzyme Q binding protein (COQ10), and in humans, two related proteins (COQ10A and COQ10B) may serve as chaperones or transporters during this process. Mitochondrial coenzyme Q is also implicated in the production of reactive oxygen species through a mechanism involving the formation of superoxide from ubisemiquinone radicals, and in this way, it is responsible for causing some of the oxidative damage underlying many degenerative diseases. In this action, it is a pro-oxidant. It is most abundant in organs with a high metabolic rate, such as the heart, kidneys, and liver.

In its reduced form (ubiquinol), it acts as an endogenous antioxidant in non-mitochondrial cellular membranes and plasma lipoproteins, making it the only lipid-soluble antioxidant synthesized endogenously. It inhibits lipid peroxidation in biological membranes and serum low-density lipoproteins, and it may also protect membrane proteins and DNA against oxidative damage. The ferroptosis suppressor protein 1 (FSP1) replenishes ubiquinol, and this acts protectively by combating the lipid peroxidation that drives **ferroptosis**. The mechanism involves the recruitment of FSP1 to the plasma membrane following myristoylation, where this functions as an oxidoreductase that reduces ubiquinone to ubiquinol, which acts as a lipophilic radical-trapping antioxidant that halts the propagation of lipid peroxides. In this manner, it regulates cellular redox status and cytosolic oxidative stress, thereby serving as a controlling factor in apoptosis. Other NAD(P)H dehydrogenases with CoQ reductase activity include cytochrome b5 reductase and NQo1 (NAD(P)H:quinone oxidoreductase).

Although ubiquinone has only about one-tenth of the antioxidant activity of **vitamin E** (α-tocopherol), it can stimulate the effects of the latter by regenerating it from its oxidized form back to its active, fully reduced state (similarly with vitamin C). However, ubiquinones and tocopherols appear to exhibit both cooperative and competitive effects under different conditions. Similarly, in bacteria and other prokaryotes, ubiquinones participate in a large number of redox reactions, notably in the respiratory electron transport system but also in other enzyme reactions that require electron donation, including the formation of disulfide bonds.

Coenzyme Q has many other functions that are not related directly to its antioxidant function. Some coenzyme Q is used in mitochondria by enzymes that link the mitochondrial respiratory chain to other metabolic pathways, including fatty acid β-oxidation as an electron acceptor, nucleotide biosynthesis *de novo*, amino acid oxidation (glycine, proline, glyoxylate, and arginine), and detoxification of sulfide. Through these activities, coenzyme Q may indirectly modulate metabolic pathways located outside the mitochondria. There are also suggestions that coenzyme Q may be involved in the redox control of cell signaling and gene expression, particularly in repressing the expression of inflammatory genes. In relation to its anti-inflammatory properties, clinical studies suggest that supplementation with coenzyme Q_{10} significantly reduces the levels of inflammatory mediators, including C-reactive protein, interleukin-6, and tumor necrosis factor-alpha (TNF-α). Additionally, it serves as a regulator of mitochondrial permeability, and in relation to pyrimidine nucleotide biosynthesis, it is essential for DNA replication and repair.

Dietary ubiquinone, i.e., that in food or dietary supplements, is absorbed by enterocytes via a process of “passive facilitated diffusion”, probably requiring a carrier molecule, before incorporation into chylomicrons for transport to the liver. This eventually leads to elevated levels of ubiquinol in the blood, especially in the LDL and VLDL lipoproteins, presumably due to the reduction of the oxidized form in the lymphatic system. Consequently, there is reported to be enhanced protection against lipid peroxidation, with beneficial effects on health, particularly in relation to cardiac function, sperm motility, and neurodegenerative diseases. For example, CoQ levels in both plasma and the heart correlate with heart failure in patients, and clinical trials of dietary supplementation have shown promising results. This may be particularly important in the elderly or in patients taking statins, as endogenous synthesis declines. A CoQ_{10} deficiency syndrome is associated with inherited pathological diseases, defined by a decrease in the CoQ_{10} content in muscle and/or cultured skin fibroblasts. Early clinical trials with CoQ10 and a synthetic analog, idebenone, against various neurodegenerative diseases, including Alzheimer's disease, Parkinson's disease, Huntington's disease, and others, are encouraging.

21.6.3.4: PHYLLOQUINONE AND MENAQUINONES (VITAMIN K)

Phylloquinone or 2-methyl-3-phytyl-1,4-naphthoquinone is synthesized in the inner chloroplast envelope of cyanobacteria, algae, and higher plants by a mechanism analogous to that of the **tocopherols**, i.e., from chorismate in the shikimate pathway with a prenyl side chain derived from phytyldiphosphate. In this membrane, it is a key component of the photosystem I complex, where it receives an electron from the chlorophyll a acceptor molecule and then donates it to the membrane-associated iron-sulfur protein acceptor cluster within the complex. In an obvious parallel to the plastoquinones (above), two molecules of phylloquinone form two membrane-spanning branches, as demonstrated by X-ray crystallography studies of photosystem I from cyanobacteria. Plastoglobules associated with the thylakoid membrane are believed to function as a reservoir for excess phylloquinone and may also function in its metabolism. Edward A. Doisy and Henrik Dam received the Nobel Prize in Physiology or Medicine in 1943 for their discovery of vitamin K and its chemical structure. The structure of vitamin K is shown in Figure **21.6.25**.

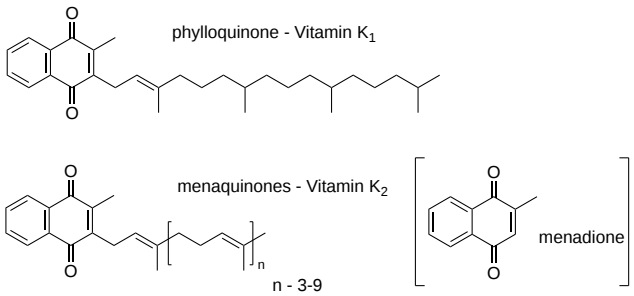


Figure **21.6.25**: Vitamin K

The menaquinones are related bacterial products, which function in the respiratory and photosynthetic electron transport chains of bacteria. They have a variable number (4 to 10) of isoprenoid units in the tail, and they are sometimes designated ‘MK-4’ to ‘MK-10’. In contrast to phylloquinone, these are usually highly unsaturated. In some species, methyl or other groups are attached to the naphthoquinone moiety. Remarkably high concentrations of menaquinones are present in membranes of some extremophiles such as the haloarchaea, where it has been suggested that they act as ion permeability barriers and as a powerful shield against oxidative stress in addition to their functions as electron and proton transporters.

Phylloquinone is an essential component of the diet of animals and is commonly referred to as '**vitamin K_1**'. It must be supplied by green plant tissues, where it occurs in the range 400-700 μg/100 g, or seed oils. The menaquinones, the main source of which in the human diet is cheese and yogurt, also have vitamin K activity and are termed '**vitamin K_2**'. They account for about 10-25% of the vitamin K content of the Western diet. A synthetic saturated form of this, which is used in animal feeds, is known as 'vitamin K_3 or menadione', though strictly speaking it is not a vitamin but a provitamin in that it can be converted to the menaquinone MK-4 in animal tissues by addition of a phytyl unit; it is too toxic for human nutrition. Vitamin K forms are absorbed from the intestines and transported in plasma in the form of lipoproteins in a similar manner to the other fat-soluble vitamins. Different tissues have different storage capacities and presumably requirements for the various forms of vitamin K. As a high proportion is excreted, there appears to be a requirement for a constant intake. Vitamin K_1 is taken up rapidly by the liver, but vitamin K_2 remains in the plasma for much longer and may be the main source of the vitamin in peripheral tissues. In addition, it has been established that some dietary phylloquinone is converted to menaquinone-4 in animals, although the quantitative significance has still to be established; the mechanism involves conversion to menadione in the intestines, followed by transport to tissues where a specific prenyl transferase attaches a geranylgeranyl side-chain.

The primary role of vitamin K in animal tissues is to act as a cofactor specific to the vitamin K-dependent enzyme γ-glutamyl carboxylase in the endoplasmic reticulum in the liver. Its function is the post-translational carboxylation of glutamate residues to form γ-carboxyglutamic acid in proteins, such as prothrombin. In this way, prothrombin and three related proteins are activated to promote blood clotting. The γ-carboxyglutamic acid residues are located at the binding site for Ca^{2+}, and are vital for the activity of the enzyme. Phylloquinone must first be converted to the reduced form, phylloquinol, which is the actual cofactor for the enzyme; molecular oxygen and carbon dioxide are also required. Phylloquinol donates hydrogen to the glutamic acid residue and is oxidized in the process to 2,3-epoxyphylloquinone. A further enzyme, vitamin K epoxide reductase, regenerates phylloquinone by reduction of the epoxide in a dithiol-dependent reaction so that this can be re-utilized many times ("the vitamin K cycle", shown below in Figure **21.6.26**).

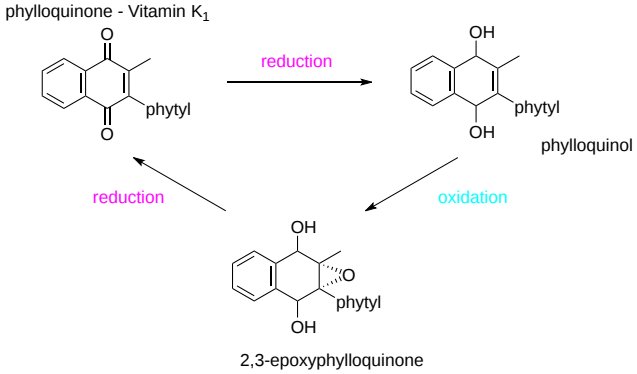


Figure **21.6.26**: The Vitamin K cycle

Menaquinones undergo the same reaction cycle. By interfering with the last step in the metabolic cycle, warfarin, the rodenticide, prevents blood clotting. Similarly, a deficiency in vitamin K results in the inhibition of blood clotting and can lead to brain hemorrhaging in malnourished newborn infants. However, this is not observed in adult humans, presumably because intestinal bacteria produce sufficient amounts to meet our needs. Vitamin K-dependent proteins also play important roles in the central and peripheral nervous systems, and vitamin K influences sphingolipid biosynthesis in the brain.

Unsaturated isoprene units, rather than phytol, are used for the biosynthesis of menaquinones, which differ from phylloquinone in terms of their chemical structure and pharmacokinetics. It is now apparent that vitamin K_2 (MK-4, especially) has several distinct actions, some of which are tissue-specific. For example, osteocalcin is a γ-carboxyglutamic acid-containing protein that forms a strong complex with the mineral hydroxyapatite (calcium phosphate) in bone; it must be carboxylated to function properly, and vitamin K_2 appears to be of particular importance in this process. Vitamin K_2 also regulates bone remodeling by osteoclasts to remove old or damaged bone and its replacement by new bone. Additionally, vitamin K_2 is involved in regulating vascular calcification, cell growth, and apoptosis. Side effects of using anticoagulants that interfere with vitamin K can include osteoporosis and an increased risk of vascular calcification. Although careful control of the dosage is necessary, vitamin K_2 may be a useful adjunct for the treatment of osteoporosis, and it may reduce morbidity and mortality in cardiovascular health by reducing vascular calcification.

Excess vitamin K_1 and the menaquinones are catabolized in the liver by a common degradative pathway in which the isoprenoid side chain is shortened to yield carboxylic acid aglycones such as menadiol, which can be excreted in bile and urine as glucuronides or sulfates.

21.6.3.5: DOLICHOLS AND POLYPRENOLS

Polyisoprenoid alcohols, such as dolichols, are ubiquitous, if minor components, relative to the glycerolipids, of membranes of most living organisms, from bacteria to mammals. They are hydrophobic linear polymers, consisting of up to twenty isoprene residues or a hundred

carbon atoms (or many more in plants, especially), linked head-to-tail, with a hydroxy group at one end (α-residue) and a hydrogen atom at the other (ω-end). In **dolichols** (or dihydropolyprenols), the double bond in the α-residue is hydrogenated, and this distinguishes them from the **polyprenols** with a double bond in the α-residue. Their structures are shown in Figure **21.6.27**.

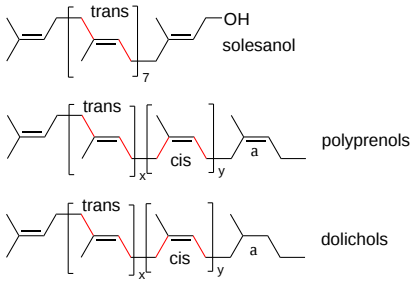


Figure **21.6.27**: Polyprenols and dolichols

Polyisoprenoid alcohols are further differentiated by the geometrical configuration of the double bonds into three subgroups, i.e., di-*trans*-poly-*cis*, tri-*trans*-poly-*cis*, and all-*trans*. For many years, it was assumed that polyprenols were only present in bacteria and plants, particularly in photosynthetic tissues, while dolichols were found in mammals and yeasts. Still, it is now known that dolichols can also occur at low levels in bacteria and plants, while polyprenols have been detected in animal cells. **Solanesol** is a related and distinctive plant product with *trans* double bonds only and serves as a precursor to plastoquinone.

Within a given species, components of one chain length may predominate, but other homologs are usually present. The chain length of the main polyisoprenoid alcohols varies from 11 isoprene units in eubacteria, to 16 or 17 in Drosophila, 15 and 16 in yeasts, 19 in hamsters, and 20 in pigs and humans. In plants, the range is from 8 to 22 units; however, some plant species have an additional class of polyprenols with up to 40 units. In tissues, polyisoprenoid alcohols can be present in the free form, esterified with acetate or fatty acids, phosphorylated, or monoglycosylated and phosphorylated (in various forms), depending on the species and tissue. Polyisoprenoid alcohols, *per se*, do not form bilayers in aqueous solution, but rather a type of lamellar structure. However, they are found in most membranes, especially the plasma membrane of liver cells and the chloroplasts of plants.

Dolichoic acids, i.e., related molecules with a terminal carboxyl group and containing 14–20 isoprene units, have been isolated from the substantia nigra of the human brain. However, they were barely detectable in the pig brain.

The biosynthesis of the basic building block of dolichols, such as isopentenyl diphosphate, follows either the mevalonate pathway or a more recently described methylerythritol phosphate pathway, as previously discussed in relation to **cholesterol biosynthesis**. Farnesyl pyrophosphate is the primary precursor in the biosynthesis of polyprenols and is the branch point in sterol/isoprene biosynthesis, depending on the nature of the organism (see a further note below). Subsequent formation of the linear prenyl chain is accomplished by *cis*-prenyl transferases that catalyze the condensation of isopentenyl pyrophosphate and farnesyl pyrophosphate and then the elongation of the allylic prenyl diphosphate chain. The end products are polyprenyl pyrophosphates, which are first dephosphorylated to polyprenol phosphate and then to the free alcohol. Finally, a specific reductase has been identified from human tissues that catalyzes the reduction of the double bond in position 2 to produce dolichols. There is a family of *cis*-prenyl transferases, present in both eukaryotes and bacteria, that in addition to the synthesis of dolichols, can catalyze the formation of isoprenoid carbon skeletons from neryl pyrophosphate (C_{10}) to natural rubber ($C_{>10,000}$), including the polyisoprenoid phosphates involved in protein glycosylation as discussed in the next section. The reactions in the synthesis of dolichol are shown in Figure **21.6.28**.

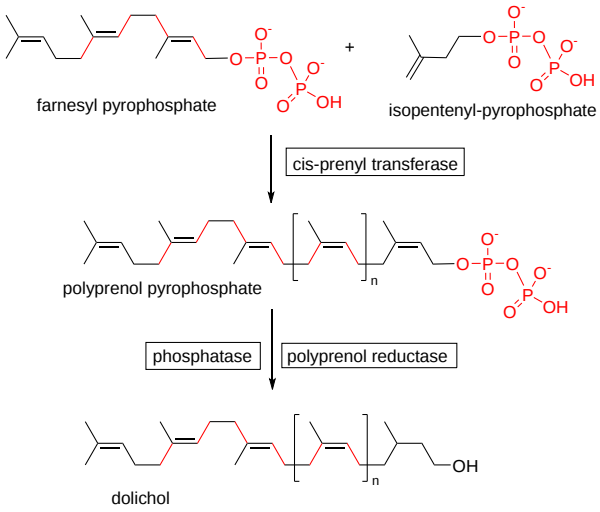


Figure **21.6.28**: Synthesis of dolichol

Although polyprenols and dolichols were initially regarded as secondary metabolites, they are now recognized to have significant biological functions. Glycosylation of asparagine residues is the primary protein modification in all three domains of life, and phosphorylated polyisoprenoids, including dolichols, are crucial to this process (see next section). There is also a suggestion that free dolichol may have a beneficial antioxidant function in cell membranes.

21.6.3.6: POLYISOPRENOID PHOSPHATES AND GLYCOSYLATION OF PROTEINS

Glycosylated phosphopolyisoprenoid alcohols are the carriers of oligosaccharide units for transfer to proteins. As glycosyl donors, they serve as substrates for glycosyl transferases in the biosynthesis of glycans, similar to cytosolic sugar nucleotides. They differ from the latter in their intracellular location, with the lipid portion located in the membrane of the endoplasmic reticulum and the oligosaccharide portion specifically located on either the cytosolic or lumenal face of the membrane. The degree of unsaturation and chain length of the product are important for recognition by the enzymes in the next stage of the pathway.

Dolichol phosphates: In eukaryotes, *N*-glycosylation begins on the cytoplasmic side of the endoplasmic reticulum with the transfer of carbohydrate moieties from nucleotide-activated sugar donors, such as uridine diphosphate *N*-acetylglucosamine, onto dolichol phosphate. Then, *N*-acetylglucosamine phosphate is added to give dolichol-pyrophosphate linked to *N*-acetylglucosamine, to which a further *N*-acetylglucosamine unit is added, followed by five mannose units, the last catalyzed by dolichol phosphate mannose synthase, which is also essential for **GPI-anchor** biosynthesis. The dolichol-PP glycan is shown in Figure **21.6.29**.

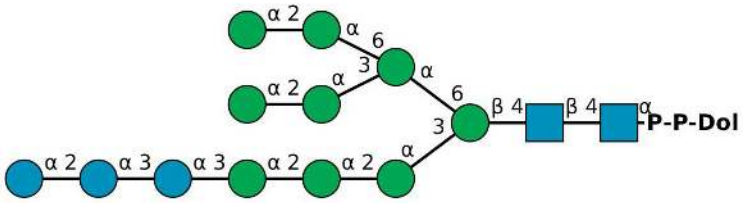


Figure **21.6.29**: Dolichol-pyrophosphate glycan. Blue squares GlcNAc, Green circles Man, blue circles Glc. Cheng, K. et al., 'DrawGlycan-SNFG: a robust tool to render glycans and glycopeptides with fragmentation information', Glycobiology 27(3): 200-205, 2017

The resulting dolichol-pyrophosphate heptasaccharide is then flipped across the endoplasmic reticulum membrane to the luminal face with the aid of a “flippase”. Four further mannose and three glucose residues are added to the oligosaccharide chain using glycosyltransferases, which utilize dolichol-phospho-mannose and dolichol-phospho-glucose as donors. These donors are also synthesized on the cytosolic face of the membrane and flipped across to the luminal face. In humans, the final lipid product is a C_{95}-dolichol pyrophosphate-linked tetradecasaccharide, the oligosaccharide unit of which is transferred from the dolichol carrier onto specific asparagine residues on a developing polypeptide in the membrane. The carrier dolichol-pyrophosphate is dephosphorylated to dolichol-phosphate, then diffuses or is flipped back across the endoplasmic reticulum to the cytoplasmic face.

The **Archaea** utilize dolichol in the synthesis of lipid-linked oligosaccharide donors, with both dolichol phosphate (Euryarchaeota) and pyrophosphate (Crenarchaeota) serving as carriers. These donors can have variable numbers of isoprene units, many of which can be saturated. In the haloarchaeon *Haloferax volcanii*, for example, a series of C_{55} and C_{60} dolichol phosphates with saturated isoprene subunits at the α- and ω-positions is involved in the glycosylation reaction of target proteins. At the same time, similar lipid carriers of oligosaccharide units are also present in methanogens. Archaea, of course, use **isoprenyl ethers linked to glycerol** as major membrane lipid

components in addition to unusual carotenoids such as the C50 bacterioruberins. In many of these species, isoprenoid biosynthesis occurs via the 'classical' mevalonate pathway; however, in other species, certain aspects of this pathway differ.

Undecaprenylphosphate: Most other bacteria use undecaprenyl-diphosphate-oligosaccharide as a glycosylation agent in a similar way for the biosynthesis of peptidoglycan, the main component of most bacterial cell walls and a structure unique to bacteria, of many other cell-wall polysaccharides, including lipopolysaccharides, *O*-antigenic polysaccharides, and capsular polysaccharides, and of *N*-linked protein glycosylation in both Gram-negative and Gram-positive bacteria. **Undecaprenyl phosphate** (a C_{55} isoprenoid), also referred to as bactoprenol, is the essential lipid intermediate. Its structure is shown in Figure **21.6.30**.

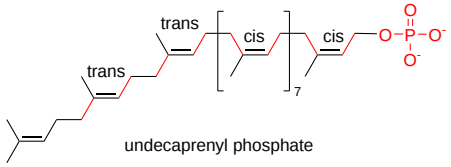


Figure **21.6.30**: Undecaprenyl phosphate

It differs from the dolichol phosphates mainly in that the terminal unit is unsaturated and is synthesized by the addition of eight units of isopentenyl pyrophosphate to farnesyl pyrophosphate, a reaction catalyzed by undecaprenyl pyrophosphate synthase in the cytoplasm, followed by the removal of a phosphate group. Undecaprenyl phosphate is required for the synthesis and transport of glycans for external polymer formation. Thus, glycans are covalently transferred to the carrier lipid by membrane-embedded or membrane-associated enzymes using nucleotide-activated precursors. For example, the carrier lipid with GlcNAc-MurNAc-peptide monomers, i.e., as lipid II, is hydrophilic and is then transported across the cytoplasmic membrane to external sites for peptidoglycan formation. Similarly, it is required for the synthesis of **lipoteichoic acids** and **lipopolysaccharide *O*-antigens**.

Lipid II: Undecaprenyl diphosphate-MurNAc-pentapeptide-GlcNAc, often termed **lipid II**, is the last significant lipid intermediate in the construction of the peptidoglycan cell wall in bacteria (Lipid I is the biosynthetic precursor lacking the *N*-acetylglucosamine residue). Its structure is shown below in Figure **21.6.31**.

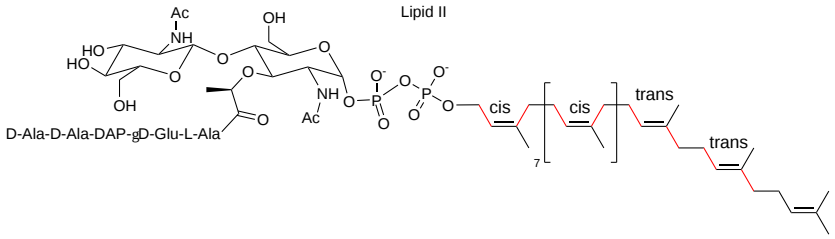


Figure **21.6.31**: Lipid II

This molecule must be translocated from the cytosolic to the exterior membrane of the organism, and three different protein classes have been identified that can accomplish this, of which ATP-binding cassette (ABC) transporters are best characterized. Once across the membrane, lipid II is cleaved to provide the MurNAc-pentapeptide-GlcNAc monomer, which undergoes polymerization and crosslinking to form the complex peptidoglycan polymer that provides strength and shape to bacteria. The undecaprenyl-pyrophosphate remaining is hydrolyzed to undecaprenyl phosphate by a membrane-integrated member of the type II phosphatidic acid phosphatase family and is recycled back to the interior of the membrane by an as-yet-unidentified transport mechanism. The turnover rate is very high, so the lipid II cycle is considered to be the rate-limiting step in peptidoglycan biosynthesis. There is also some evidence that lipid II has a function on the inner leaflet of the cytoplasmic membrane in organizing the proteins of the cytoskeleton. Due to its highly conserved structure and surface membrane accessibility, the proteins involved in the synthesis and transport of lipid II are considered important targets for the development of novel antibiotics. Figure **21.6.*xx***:

In a few prokaryotes, the membrane intermediate has a polyprenyl-monophosphate-glycan structure instead of lipid II, and undecaprenyl-phosphate-L-4-amino-4-deoxyarabinose is involved in **lipid A** modification in Gram-negative bacteria, for example. There are obvious parallels with the involvement of glycosylated phosphopolyisoprenoid alcohols as carriers of oligosaccharide units for transfer to proteins and as glycosyl donors in higher organisms (see above).

β-D-Mannosyl phosphomycoketide is an isoprenoid phosphoglycolipid found in the cell walls of *Mycobacterium tuberculosis*, the lipid component of which is a C_{32}-mycoketide, consisting of a saturated oligoisoprenoid chain with five chiral methyl branches. It acts as a potent antigen to activate T-cells upon presentation by the CD1c protein. Its structure is shown in Figure **21.6.32**.

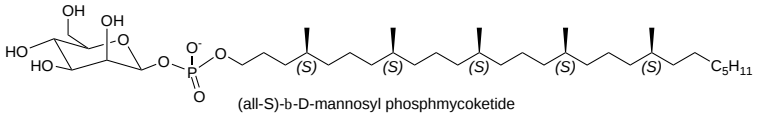


Figure **21.6.32**: β-D-Mannosyl phosphomycoketide

21.6.3.7: FARNESYL PYROPHOSPHATE AND RELATED COMPOUNDS

Farnesyl pyrophosphate is a key intermediate in the biosynthesis of sterols such as **cholesterol**, and it is the donor of the farnesyl group in the biosynthesis of dolichols and polyprenols (see above) as well as for the isoprenylation of many proteins (see the web page on **proteolipids**). However, it is also known to mediate various biological reactions in its own right via interaction with a specific receptor. It is synthesized through two successive phosphorylations of farnesol.

Presqualene diphosphate is unique among the isoprenoid phosphates in that it contains a cyclopropylcarbinyl ring. In addition to being a biosynthetic precursor of squalene and thence of cholesterol, it is a natural anti-inflammatory agent, which functions by inhibiting the activity of phospholipase D and the generation of superoxide anions in neutrophils.

Their structures are shown in Figure **21.6.32**.

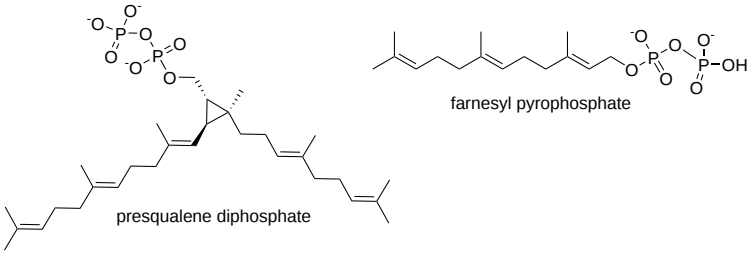


Figure **21.6.32**: Structures of farnesyl pyrophosphate and presqualene diphosphate

21.6.4: SUMMARY

This chapter explores the structure, biosynthesis, function, and metabolism of tocopherols and tocotrienols—the isoprenoid compounds collectively known as vitamin E—and their pivotal roles in both plant and animal systems.

Structural Diversity and Nomenclature:

Tocopherols and tocotrienols are benzopyranols (or methyltocols) that differ primarily in the saturation of their hydrophobic side chains. Tocopherols possess a saturated 20-carbon phytyl tail and three chiral centers, whereas tocotrienols have a 20-carbon side chain containing three trans double bonds and only one chiral center. The number and position of methyl groups on the chromanol ring distinguish the α, β, γ, and δ forms. Importantly, only the natural R,R,R-α-tocopherol is recognized as vitamin E in humans because it uniquely prevents deficiency diseases like ataxia.

Biosynthesis in Plants:

In photosynthetic organisms, tocochromanols are synthesized within chloroplasts—primarily along the inner envelope membrane. The process begins with the conversion of tyrosine to homogentisic acid, which then couples with either phytyl diphosphate (for tocopherols) or geranylgeranyl diphosphate (for tocotrienols). Subsequent methylation and cyclization reactions yield the various tocopherol isomers. This pathway not only underpins antioxidant defense in plants but also contributes to the quality and nutritional value of seed oils.

Biological Functions and Antioxidant Mechanisms:

Tocopherols and tocotrienols serve as lipid-soluble antioxidants that protect cellular membranes from oxidative damage. They do so by rapidly scavenging lipid peroxyl radicals, thereby interrupting the chain reactions of lipid peroxidation. When a tocopherol molecule donates a hydrogen atom to neutralize a free radical, it forms a relatively stable tocopheroxyl radical. This radical can be regenerated back to the active antioxidant form by other antioxidants (e.g., vitamin C or glutathione), integrating tocopherols into a broader antioxidant network.

Beyond antioxidant protection, vitamin E compounds influence signal transduction and gene expression, modulate inflammatory responses, and may indirectly affect the activity of enzymes like protein kinase C. These non-antioxidant roles have significant implications for cellular regulation and health.

Absorption, Transport, and Metabolism in Animals:

Dietary tocopherols are solubilized in mixed micelles in the intestine and absorbed by enterocytes, then incorporated into chylomicrons. In the liver, the α-tocopherol transfer protein (α-TTP) selectively enriches α-tocopherol in the plasma, while other forms are preferentially catabolized into various metabolites (such as carboxyethylhydroxychromans). These metabolites, sometimes excreted as conjugates, may

possess their own biological activities. The selective retention of α-tocopherol explains its predominance in plasma and underlies its designation as the active form of vitamin E.

Physiological and Clinical Relevance:

Adequate levels of vitamin E are essential for maintaining normal neurological function, immune response, and cellular integrity. Deficiency—often seen in disorders of fat absorption—leads to neurological degeneration (ataxia) and impaired immune function. Although all tocopherols are potent antioxidants in vitro, the unique metabolism and transport of α-tocopherol confer it with the specific biological activity required to meet human vitamin E needs. Current research continues to evaluate the therapeutic potential of vitamin E compounds in mitigating chronic diseases, including cardiovascular disorders, neurodegenerative conditions, and inflammatory diseases.

Integration with Broader Isoprenoid Metabolism:

Tocopherols and tocotrienols exemplify how isoprenoid biosynthesis, derived from common precursors like isopentenyl pyrophosphate, yields diverse compounds with specialized functions. Their interrelationships with other isoprenoids (e.g., sterols, carotenoids, ubiquinone) underscore the integrated network that governs cellular redox balance, membrane dynamics, and signaling.

In summary, this chapter provides an in-depth examination of vitamin E's chemical and biochemical attributes—from its plant-based synthesis and structural diversity to its essential roles in protecting membranes against oxidative stress and regulating cellular processes in animals. Understanding these mechanisms is critical for appreciating how dietary and endogenous vitamin E contribute to health and disease prevention.

This page titled 21.6: Biosynthesis and Metabolism of Isoprenoids is shared under a not declared license and was authored, remixed, and/or curated by Henry Jakubowski and Patricia Flatt.

- **Current page** by Henry Jakubowski and Patricia Flatt has no license indicated.
- **11.2: Diffusion Across a Membrane - Passive and Facilitated Diffusion** by Henry Jakubowski and Patricia Flatt has no license indicated.

CHAPTER OVERVIEW

22: BIOSYNTHESIS OF AMINO ACIDS, NUCLEOTIDES, AND RELATED MOLECULES

Return to Fundamentals of Biochemistry Search Fundamentals of Biochemistry

22.1: Overview of Nitrogen Metabolism - Nitrogenase
22.2: Biosynthesis of Amino Acids
22.3: Molecules Derived from Amino Acids
22.4: Biosynthesis and Degradation of Nucleotides

This page titled 22: Biosynthesis of Amino Acids, Nucleotides, and Related Molecules is shared under a not declared license and was authored, remixed, and/or curated by Henry Jakubowski and Patricia Flatt.

22.1: OVERVIEW OF NITROGEN METABOLISM - NITROGENASE

LEARNING GOALS (CHATGPT O3-MINI)

1. **Describe the Nitrogen Cycle:**
   - Explain the overall biological nitrogen cycle, including the roles of inorganic (e.g., ammonium, nitrate, nitrite) and organic (e.g., amino acids, nucleotides) nitrogen compounds.
   - Differentiate between aerobic and anaerobic processes (e.g., nitrification, denitrification, anammox, and ammonification) and discuss their ecological significance.
2. **Understand Nitrogen Fixation:**
   - Outline the process of nitrogen fixation by soil bacteria and archaea, including the conversion of atmospheric N_2 into biologically available ammonium (NH_4^+).
   - Compare biological nitrogen fixation with the industrial Haber–Bosch process, emphasizing the kinetic and thermodynamic challenges involved.
3. **Analyze Thermodynamic and Kinetic Challenges:**
   - Explain why, despite favorable room-temperature thermodynamics, N_2 is kinetically inert due to its strong triple bond.
   - Discuss how high pressure and the use of catalysts (in both industrial and biological systems) overcome these kinetic barriers.
4. **Examine the Structure of Nitrogenase:**
   - Identify the key protein components of the nitrogenase complex, including the reductase (Fe-protein) and the catalytic (MoFe-protein) subunits.
   - Describe the metal clusters (F-cluster, P-cluster, and the iron–molybdenum (M) cluster) and their proposed roles in electron transfer and N_2 reduction.
5. **Detail the Role of ATP and Electron Transfer:**
   - Explain how ATP hydrolysis in the Fe-protein drives the electron transfer necessary for nitrogen fixation.
   - Illustrate the coupling between ATP hydrolysis, conformational changes, and the sequential delivery of electrons from the reductase to the MoFe-protein.
6. **Interpret the Lowe–Thorneley Model:**
   - Summarize the stepwise accumulation of electrons and protons in nitrogenase as described by the Lowe–Thorneley kinetic model.
   - Define the E_4 “Janus” intermediate, and discuss its significance in binding N_2 and enabling reductive elimination of H_2.
7. **Apply Organometallic Reaction Principles:**
   - Describe the concepts of oxidative addition, reductive elimination, and migratory insertion as they apply to the nitrogenase mechanism.
   - Relate these reaction types to the biochemical transformations involved in the reduction of N_2 to NH_3.
8. **Evaluate Experimental Evidence and Mechanistic Models:**
   - Critically assess experimental data (e.g., isotope labeling and deuterium incorporation studies) that support the proposed intermediates and mechanisms in nitrogenase catalysis.
   - Discuss how mutations (e.g., at key amino acid residues) affect substrate access and the overall catalytic process.
9. **Connect Nitrogen Metabolism to Ecosystem Function:**
   - Explain how microbial nitrogen fixation impacts plant nutrition and overall ecosystem productivity.
   - Discuss the environmental implications of anthropogenic nitrogen inputs (e.g., fertilizer runoff) and how they disrupt the natural balance of the nitrogen cycle.
10. **Integrate Knowledge Across Disciplines:**
    - Synthesize concepts from organic chemistry, enzymology, and inorganic/organometallic chemistry to explain the biochemical challenges and solutions inherent in N_2 fixation.
    - Recognize the broader significance of studying nitrogen metabolism—not only in human biochemistry but also in understanding global ecological processes.

These learning goals aim to help students grasp both the biochemical mechanisms of nitrogen fixation and the broader environmental context in which these processes operate.

22.1.1: INTRODUCTION

Organic chemistry is usually described as the chemistry of carbon-containing molecules. But isn't that definition a bit carbon-centric, especially since the prevalence of oxygen-containing molecules is staggering? What about nitrogen? We live in a dinitrogen-rich atmosphere (80%), and all classes of biomolecules (lipids, carbohydrates, nucleic acids, and proteins) contain nitrogen. Dinitrogen is very stable due to its triple bond and nonpolar nature. We rely on a few organisms to fix N_2 from the atmosphere to form ammonium (NH_4^+), which, through nitrification and denitrification, can form nitrite (NO_2^-), nitrate (NO_3^-), nitric oxide (NO), and nitrous oxide (N_2O), the latter being a potent greenhouse gas. We'll concentrate on the metabolic fate of amino groups in amino acids and proteins in the next section. Before exploring their fates, look at Figure **22.1.1**, which shows an overall view of the biological nitrogen cycle. The study of biochemistry should encompass more than homo sapiens and expand to the ecosystem in which we are such a small but damaging part.

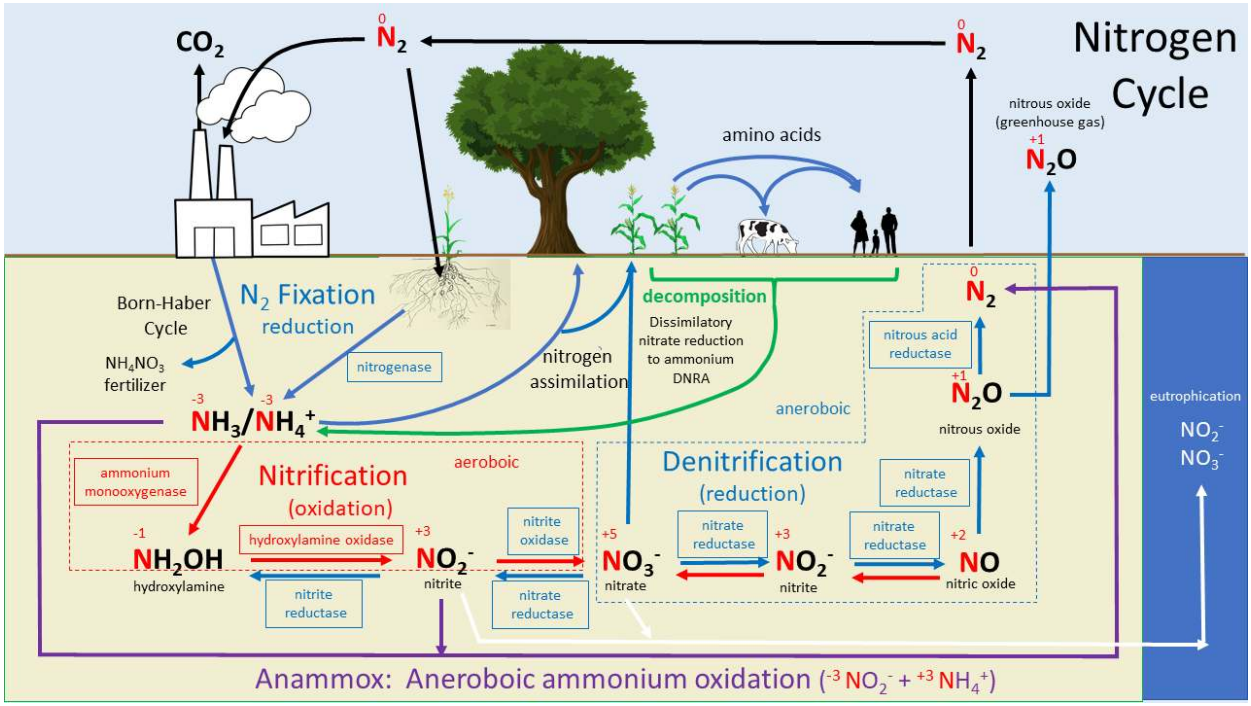


Figure **22.1.1**: Nitrogen Cycle

Let's break down the diagram from a biochemical perspective. There are aerobic and anaerobic processes (conducted by bacteria). Nitrogen-containing substances include both inorganic (ammonium, nitrate, nitrite) and organic (amino acids, nucleotides, etc) molecules. The reactions shown are both oxidative and reductive (note: the oxidation numbers of the nitrogen atoms in the molecules are shown in red). Most of the reactions are carried out underground by bacterial and Archaeal microorganisms.

Here are some of the major reactions:

- N_2 fixation (a reduction): N_2 from the air is converted by bacteria to ammonium (NH_4^+) by the enzyme nitrogenase of soil prokaryotes. The energetically disfavored reaction requires lots of ATPs. Ammonium that has been made can then be taken up by primary producers, such as plants, and incorporated into biomolecules like amino acids, which animals consume. For those who may still believe that people have marginal effects on our biosphere, consider this. We may soon fix more N_2 to NH_3 through the industrial Haber-Bosch reaction (used for fertilizer and explosive production), which is all made by the biosphere. Much of the nitrogen in use comes from the Haber-Bosch reaction. The excess NH_4^+ (upwards of 50%) produced industrially and entering the soil through fertilizers (mostly as NH_4NO_3) has overwhelmed nature's ability to balance the nitrogen cycle and is not taken up by plants. It is metabolized by microorganisms to nitrite and nitrate.
- Nitrification: Ammonium is converted to nitrite by ammonia-oxidizing aerobic microorganisms and further to nitrate by a separate group of nitrite-oxidizing aerobic bacteria. Here are the reactions (Rx 1 and 2) to produce nitrate through a hydroxylamine intermediate, followed by the formation of nitrate (Rx 3).

$$NH_3 + O_2 + 2e^- \rightarrow NH_2OH + H_2O \text{ Rx 1}$$

$$NH_2OH + H_2O \rightarrow NO_2^- + 5H^+ + 4e^- \text{ Rx 2}$$

$$NO_2^- + 1/2\ O_2 \rightarrow NO_3^- \text{ Rx 3}$$

These added ions exceed soil capacity and end up in runoff water, polluting our rivers and lakes.

- Denitrification: This anaerobic reaction pathway converts nitrate into N_2. Here is the net reaction:

$$2NO_3^- + 10e^- + 12H^+ \rightarrow 2N_2 + 6H_2O$$

- Anammox reaction: This recently discovered bacterial anaerobic reaction pathway converts ammonium and nitrate to nitrogen gas (N_2). Here is the net reaction

$$NO_2^- + NH_3^+ \rightarrow N_2 + 2H_2O$$

- Ammonification (not to be confused with mummification) occurs when plants and animals decompose, releasing ammonium back into the soil for reuse by plants and microbes.

These reactions are shown in the abbreviated Nitrogen Cycle shown in Figure **22.1.2**.

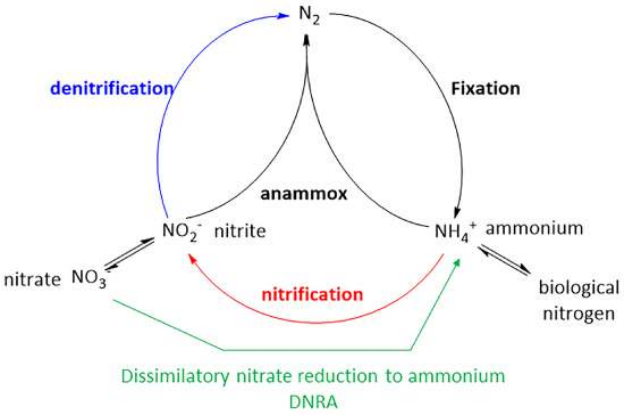


Figure **22.1.2**: Abbreviated Nitrogen Cycle

Nitrogen metabolites are essential nutrients for plants, playing a crucial role in regulating plant growth (primary productivity) and maintaining biodiversity in the biosphere. All living organisms require feedstocks to produce energy and as substrates for biosynthetic reactions. Which is used depends on the organism. Plants are primary producers, so they use their synthesized carbohydrates for both energy production and biosynthesis. For carnivores, proteins and their derived amino acids serve as an energy source through oxidation and as biosynthetic precursors for various cellular processes. For omnivorous organisms, the source of energy depends on the "fed" state. With abundant food resources, carbohydrates and lipids serve as the primary sources of energy. Unlike carbohydrates and lipids, which can be stored as glycogen and triacylglycerols for future use, excess protein and its associated amino acids can not be stored, so amino acids can be eliminated or used for oxidative energy.

In the fed state, carbohydrates are the main source, while in the unfed state, lipids take a predominant role. Under starving conditions, the organism's own proteins are broken down and utilized for oxidative energy production and any remaining biosynthesis. In diseased states like diabetes, which can be likened to a state of starvation in the presence of abundant carbohydrates, both lipids and amino acids become sources of energy.

How are amino acids in animals oxidatively metabolized? Several pathways could be employed to achieve this. Still, it would seem logical that NH_4^+ would be removed, and the carbons in the remaining molecule would eventually enter glycolysis or the TCA cycle in the form of ketoacids. NH_4^+ is toxic in high concentrations. Ammonium is not oxidized to nitrite or nitrates in humans, unlike what occurs in soil with the help of microorganisms. It can be recycled back into nucleotides or amino acids, and excess amounts are eliminated from the organism. Both processes must be highly controlled. We will turn our attention to the oxidation of amino acids in the next section.

22.1.2: NITROGENASE: AN INTRODUCTION

Beauty is in the eye of the beholder.

As the domain of biochemistry covers the entire biological world, the extent of coverage of a given topic in textbooks can depend, in part, on the interest and experiences of the author(s) presenting the material. Is relevance a metric that should determine coverage? If so, books focused on human or medical biochemistry would surely omit the topic of photosynthesis. If topics are selected based on their importance for life, then photosynthesis must surely be covered. If so, then nitrogenase must also be included. Considering the degree of chemical difficulty in a chemical reaction and the remarkable eloquence of the evolved biochemistry solution, both photosynthesis and nitrogen

fixation must be presented. Although nitrogen fixation is a reductive reaction, it shares strong similarities with the oxygen-evolving complex in photosynthesis. They catalyze enormously important redox reactions that involve an abundant atmospheric gas, utilizing a very complicated and unique inorganic metallic cofactor that evolution has selected as uniquely suited for the task.

Every first-year student of chemistry can draw the Lewis structure of dinitrogen, N_2, which contains a triple bond and a lone pair on each nitrogen. If Lewis structures resonate with them, they should be able to state that the triple bond makes N_2 extraordinarily stable, thus explaining why we can breathe an atmosphere containing 80% N_2 without dying. If they have taken biology, they are also aware that very few biological organisms can utilize N2 as a substrate, as this requires breaking bonds between the nitrogen atoms, a chemical process reserved for nitrogen-fixing bacteria found in rhizomes of certain plants. Lastly, they likely memorized that high pressure and temperature are needed in the Haber-Bosch process to convert N_2 and H_2 to ammonia, NH_3. As with any scientific advance, the Haber-Bosch process has brought both harm (it is used for explosive weapons) and benefit (in the form of fertilizers). This process now fixes enough N_2 in the form of fertilizers to support half of the world's population, with nitrogenase supporting the rest. Efforts are underway to genetically modify plants to produce nitrogenase, eliminating the need for fertilizers, but this may create unforeseen problems of its own.

You might be surprised to find out that at room temperature, the equilibrium constant favors ammonia formation, hence $\Delta G^0 < 0$. The reaction is favored enthalpically as it is exothermic at room temperature. It is disfavored entropically, as should be evident from the balanced equation:

$$\mathbf{N_2(g) + 3\,H_2(g) \longrightarrow 2\,NH_3(g).}$$

The thermodynamic parameters for the reaction (per mol) are $\Delta H° = –46.2$ kJ, $\Delta S° = –389$ J K–1, and $\Delta G° = –16.4$ kJ at 298 K

The entropy is negative since the reaction proceeds from 4 to 2 molecules. From an enthalpy perspective, raising the temperature of an exothermic reaction drives it in the reverse direction. If you increase the pressure, you shift the equilibrium to the side that has the fewest number of molecules.

If the reaction is favored thermodynamically at room temperature, why doesn't it proceed? This story sounds familiar, as this same descriptor applies to the oxidation of organic molecules with dioxygen. There, we showed using MO theory that the reaction is kinetically slow. Same with NH_3 formation. A superficial way to view this is that we must break bonds in the stable N_2 to initiate the reaction, resulting in a high activation energy and sluggish reaction kinetics.

One could jump-start the reaction by raising the temperature, but that would slow an exothermic reaction. The Keq (or K_D) and ΔG^0 are functions of temperature, and for this reaction, the reaction becomes disfavored at higher temperatures. The solution Bosch found was high pressure, forcing the reaction to the side that has fewer molecules of gas, and high temperature to overcome the activation energy barrier and make the reaction kinetically feasible. A complex metal catalyst (magnetite - Fe_3O_4 -with metal oxides like CaO and Al_2O_3, which prevent reduction of the Fe with H_2) provides an absorptive surface to bring reagents together and facilitate bond breaking in H_2 and N_2.

In photosynthesis, the **oxygen-evolving complex** (OEC), which contains Mn, Fe, S, and Ca, is used to oxidize another highly stable and ubiquitous molecule, H_2O. Now we explore the amazing mechanisms behind the nitrogenase complex, which fixes N_2 to form NH_3 in a reductive fashion.

What might be needed to drive this reaction biologically? You might surmise the list to include:

- a source of energy, most likely ATP, to facilitate this complex reaction;
- a source of electrons as the N atoms move from an oxidation state of 0 in elemental N to 3- in NH_3; this source turns out to be a protein called flavodoxin or ferredoxin. Of course, these electrons also have an interesting origin before they are in the electron carriers of these proteins.
- some pretty amazing metal centers to accept and donate electrons in a controlled way; these centers are mostly FeS clusters with an additional cluster containing molybdenum (Mo). The clusters are named F, P, and M
- a source of hydrogen; you might have guessed correctly that it's not H_2 gas (from where would that come?), but H^+ ions, which are pretty ubiquitously available.
- a net reaction that is different from the Haber-Bausch process ($N_2 + 3H_2 \rightarrow 2\ NH_3$).

Here is the actual reaction catalyzed by nitrogenase:

$$\mathbf{N_2 + 8\,e^- + 16\,ATP + 8\,H^+ \longrightarrow 2\,NH_3 + H_2 + 16\,ADP + 16\,P_i.}$$

Let's think a bit about the reaction. As electrons are added, the attraction between the nitrogen atoms must decrease. Eventually, bonds between them must be broken. Protons could be easily added to maintain charge neutrality. A basic mechanism might involve intermediates as shown in Figure **22.1.3**.

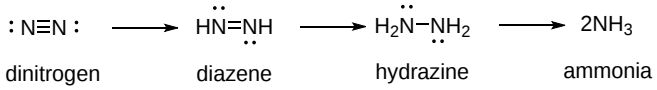


Figure **22.1.3**: Possible intermediates in the conversion of dinitrogen to ammonia by nitrogenase

Nitrogenase can also interact with other small molecules with triple bonds, including C≡O: and H-C≡C-H.

22.1.3: THE STRUCTURE OF NITROGENASE

Nitrogenase is a multiprotein complex in which the functional biological unit is built from **two** sets of the following dimeric structures:

- a homodimer of subunits, E and F, which have binding sites for the mobile carrier of electrons (the protein ferredoxin or flavodoxin), ATP, and an FeS cofactor (4Fe-4S, called the F cluster) that accepts electrons. These subunits are hence referred to as the nitrogenase reductase subunits.
- a heterodimer of alpha and beta subunits. The a (alpha chain) binds the 8Fe-7S F cluster and the Fe-S-Mo M cluster. These subunits comprise the (di)nitrogenase catalytic subunits. The iron-molybdenum M cluster is in the α subunit and is where N_2 reduction occurs. The P-cluster is between the α and β subunits and facilitates electron flow between the Fe-protein (F cluster) and FeMo-cofactor (M cluster)

For clarity, one-half of the overall structure of the protein complex with bound ATP and metal centers is shown in Figure **22.1.4**.

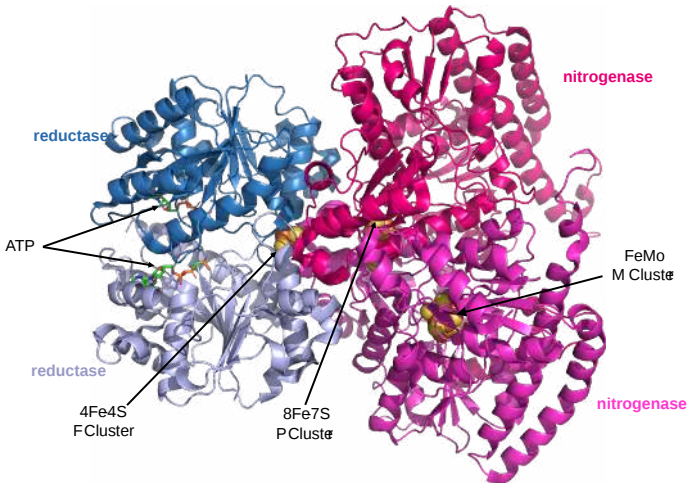
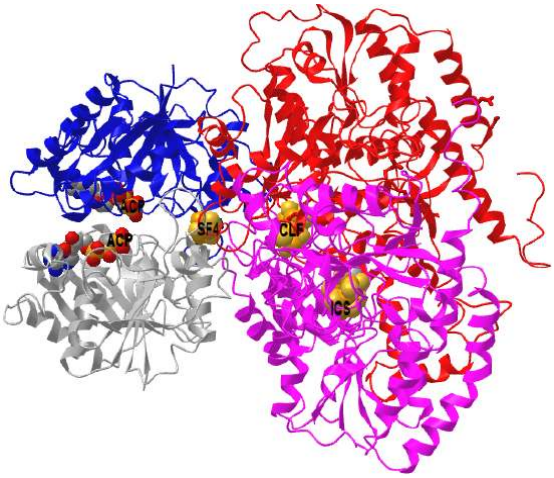


Figure **22.1.4**: Nitrogenase structure (4wzb)

This half-structure consists of a homodimer of the reductase monomers and a heterodimer of nitrogenase subunits.

Figure **22.1.5** shows an interactive iCn3D model of the half structure of nitrogenase complex from Azotobacter vinelandii (4WZB) (long load).



NCBI iCn3D Figure **22.1.5**: Nitrogenase complex from Azotobacter vinelandii (4WZB). (Copyright; author via source). Click the image for a popup or use this external link: https://structure.ncbi.nlm.nih.gov/i...zPNjfPRwq8MSeA (long load))

The structure is color-coded in a fashion similar to Figure 4. The F cluster is labeled as SF4, the P cluster as CLF (FE(8)-S(7) cluster), and the M cluster as ICS (iron-sulfur-molybdenum cluster with interstitial carbon).

The reductase subunits (called Av2 in *Azotobacter vinelandii*), accept electrons from ferredoxin and is where the ATP analog, ACP (phosphomethylphosphonic acid adenylate ester), and the 4Fe-4S F cluster is bound. The nitrogenase subunits (called Av1 in *Azotobacter vinelandii*) convert N_2 to NH_3, and it is where the 8Fe-7S P cluster, FeMo (C Fe_7 Mo S_9) M Cluster is bound.

An enhanced view of the bound cofactors and ATP is shown in the same spatial orientation in Figure **22.1.6**below.

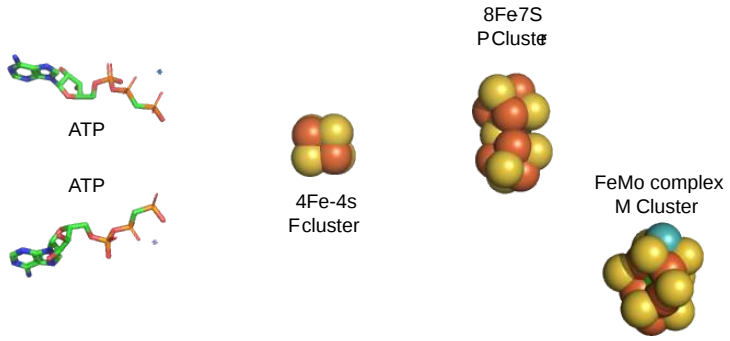


Figure **22.1.6**: Bound cofactor metal clusters and ATP in nitrogenase

You can easily imagine the direction of the flow of electrons from the F cluster to the P cluster to the M cluster.

The metal centers are shown in Figure **22.1.7** in more detail, both in line and space fill views.

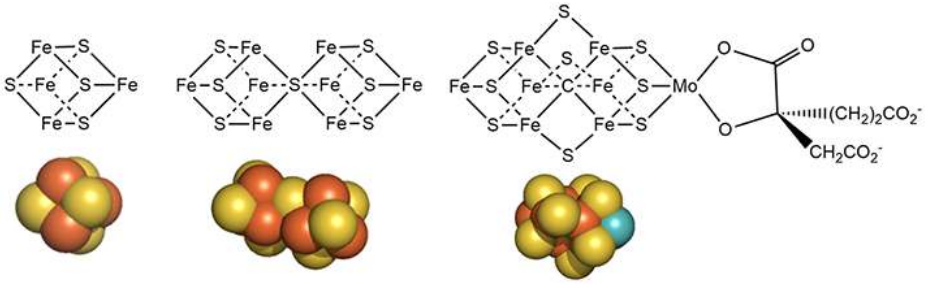


Figure **22.1.7**: Detailed structures of the metal cofactors in nitrogenase

Mo is bound to 3 sulfur ions and oxygen from 3-hydroxy-3-carboxy-adipic acid as shown in Figure 7 above.

The M cluster contains an interstitial carbide ion derived from the -CH_3 group attached to the sulfur of S-adenosyl-methionine (SAM), allowing the carbide to be labeled with either ^{13}C or ^{14}C for mechanistic studies. These labeled carbides are neither exchanged nor used as a substrate during the enzyme's catalytic turnover. Hence, it appears that the carbide likely stabilizes the M cluster. It will not be shown in the figures below, which provide more detailed mechanisms.

We will focus on two key features of the reaction mechanism: ATP hydrolysis and the flow of electrons and protons to N_2 as it is reduced to NH_3.

NITROGENASE IS NOT FOUND IN PLANTS! WHY?

The answer is that O_2 destroys the enzyme. Plants are aerobic. So how does it function? See Chapter 32.17: Part 4 - Fixing Nitrogen Fixation for details!

22.1.4: ATP HYDROLYSIS

ATP binds in the reductase subunit (AV2) where ferredoxin brings in electrons, and where the F metal cluster is bound. Much as GTP hydrolysis controls conformational change and subunit dissociation in the heterotrimeric $G_{\alpha\beta\gamma}$ in signal transductions, ATP hydrolysis in reductase (AV2) subunits drives not only electron transfer but also dissociation/reassociation of the reductase and nitrogenase catalytic subunits. It appears that two ATPs are hydrolyzed per electron transferred from the F cluster to the M cluster. Since the oxidation numbers of N are 0 and -3 in N_2 and NH_3, respectively, sequential rounds of ATP hydrolysis and dissociation/reassociation occur. Note that the Fe-protein hydrolyzes ATP only when bound to the MoFe-protein.

The overall reaction involves the reduction of N_2 to two molecules of NH_3 at the FeMo cofactor. It involves the reductive elimination of hydrides bridged by Fe ions (Fe-H-Fe) in a reaction that also produces H_2 as a by-product. We'll describe this complex reaction next.

22.1.5: NITROGENASE REACTION: PART 1 - ADDITION OF ELECTRONS AND PROTONS

The sequential path of electrons from the reductase subunit containing the F cluster to the P and M clusters in the nitrogenase subunit should be apparent from the figures above. We will concentrate on the binding of N_2 and how it receives electrons from the M cluster. Figure **22.1.8** shows the FeMo-cofactor and some adjacent amino acid residues. Mo is labeled but not shown in spacefill. HCA is a bound molecule of 3-hydroxy-3-carboxy-adipic acid, which interacts with Mo. The carbide is shown in the middle as the green sphere and labeled CX.

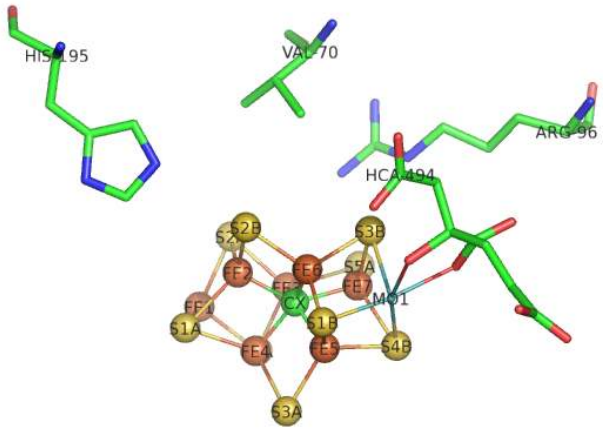


Figure **22.1.8**: Side chains near the M cluster

If Val 70 is mutated to Ile, a substrate appears not to access the cluster, suggesting that N_2 may interact with the top part of the structure, with the residues shown acting as gatekeepers. His side chains are often found at enzyme active sites, so you might expect His 195 to be a general acid/base. Mutations lead to drastic losses in the reduction of N_2. His 195 is involved in hydrogen bonds to sulfur S2B and bridges Fe2 and Fe3 in Figure 8, where reduction of N_2 likely occurs. If His 195 moves, it can form a short H bond between the imidazole N and an H bond to HFe2. If the ring is rotated 180^0, no proton transfer occurs from the surface. It appears that His195 might be involved in the first N_2 protonation event.

The Lowe and Thorneley (LT) model has been proposed as a mechanism for the reduction of dinitrogen. In this model, an electron and a proton are added to the oxidized form of the enzyme (E_o) to produce E_1. This is repeated three more times to form sequentially, E_2, E_3, and E_4. Only then does N_2 bind, and the reduction of N_2 occurs. Two of the added electrons are accepted by H^+ ions, which form H_2, which is liberated on N_2 binding. Hence, only 6 electrons are added to the actual N_2 molecule, in agreement with the change in oxidation numbers discussed above. The Lowe and Throneley model is shown in Figure **22.1.9**.

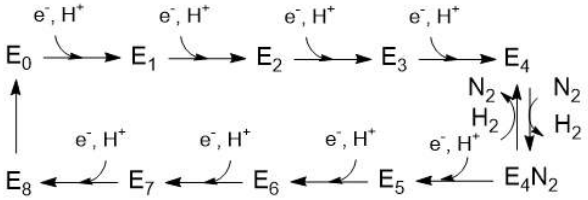


Figure **22.1.9**: Lowe and Throneley model for electron and proton additions in nitrogenase

The crystal structure shows 2 ATP analogs bound to the reductase subunit. The stoichiometry of the reaction indicates that 16 ATP are used. Simple math suggests that 2 ATP are cleaved to support the entry of one electron into the complex, assuming 8 electrons are transferred (6 to N_2 and 2 to protons to form H_2).

Part 1 - E1-E4: A potential structure for the E4 intermediate is shown in Figure **22.1.10**.

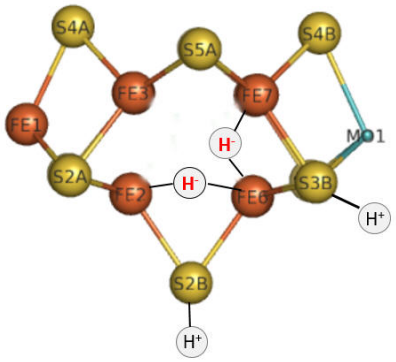


Figure **22.1.10**: The E4 Janus intermediate in the reduction of N_2.

Note that the central carbide is not shown. This is often referred to as the **Janus intermediate,** as it is situated halfway through the catalytic cycle. It is named after Janus, the Roman god of beginnings and transitions, and has been associated with gates, doors, doorways, and passages. Janus is typically shown with two faces, one looking to the future and one to the past (image below: DOI:10.1590/2177-6709.21.1.018-023.oin. License CC BY 4.0 Creative Commons Attribution 4.0 International)



The hydrides bridge 2 Fe ions, so these are examples of three-center, two-electron bonds. The H^+ ions in Figure 10 balance the charge from the hydrides.

How does this reaction occur? We must look to organometallic chemistry to help us understand the mechanism of this and subsequent steps. Hydride equivalents have been added to the metals, associated with the oxidation of metal ions in the center. This particular reaction is called an **oxidative addition**. Presumably, the sulfur ions act as Lewis bases as they gain protons from a Lewis acid, probably His 195.

Oxidative addition reactions

Figure **22.1.11** shows oxidative additions to metal centers for three different types of reactants. L is the ligand(s) and M is the metal.

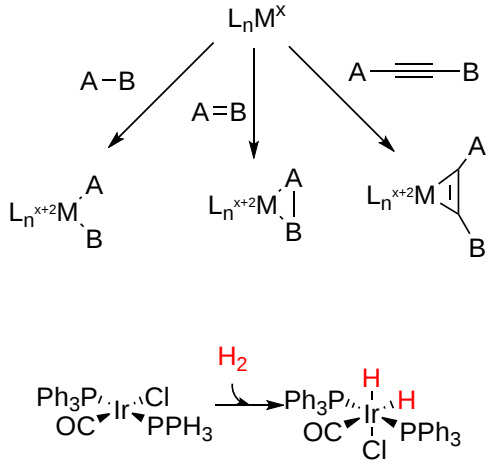


Figure **22.1.11**: Three different types of oxidative addition reactions (after Schaller, http://employees.csbsju.edu/cschaller/ROBI1.htm)

In oxidative insertion, the oxidation state of the metal ion increases, hence the name oxidative. The hydrogens are now hydrides. Note the example of H_2 insertion, which is similar to the proposed hydride additions to the M cluster. Oxidative reduction occurs most readily when the two oxidation states of the metal ion are stable. It is likewise favored for metal centers that are not sterically hindered (makes sense if A-B is to be added) and if A-B has a low bond dissociation energy.

One way to study reaction intermediates is to trap them in place. If N_2 can't access the binding site and the temperature is reduced, the accumulated hydrides (and for charge balance, the H^+s) in E4 might leave in the opposite reaction, reductive elimination. We will discuss this below, as the reaction goes back to E1. In the elimination, they can form H_2 as the metal gains back electrons in a reduction. The Val70Ile discussed above would allow an intermediate to be trapped.

22.1.6: NITROGENASE REACTION: PART 2 - REDUCTION OF N_2

Step E4 to E5 seems a bit bizarre as H_2 gas is released. This would seem to waste ATP, but we should trust that evolution has led to this mechanism for a reason. This mechanism, the reverse of oxidative addition, is another classic organometallic reaction, **reductive elimination**.

Reductive elimination reactions

In this reaction, a molecule is eliminated or expelled from the complex as the metal ion is reduced, gaining two electrons. Figure **22.1.12** shows reductive elimination. Reductive elimination occurs most readily in higher oxidation state metal centers, which can be stabilized on reduction. It occurs most readily from electron-rich ligands, and if the other surrounding ligands are bulky. The dissociating species must also be cis to each other in the transition metal complex so they can form a bond with each other when they leave.

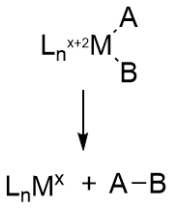


Figure **22.1.12**: Reductive Elimination reaction (after Schaller, ibid)

Oxidative addition and reductive elimination (OA/RE) reactions at metal centers are often coupled together in organometallic **catalytic cycles**, much like a histidine can act as a general acid and then accept a proton back as a general base to complete the catalytic cycle. In the OA/RE reactions at metal centers, some rearrangements or other modifications can also occur. Think about it. The FeS clusters must return to their original oxidation state after the complete LT cycle. We will encounter another organometallic reaction after the addition of N_2, **migratory insertion**, in the second half of the reaction. Another advantage of coupling OA/RE is that the positive charge or oxidation state on the transition metal complex does not become too high, which would be unstable. Making a cation with a positive charge more positive becomes more difficult, much as removing a second proton from a polyprotic acid is more difficult than removing the first (as reflected in the higher pKa for removal of the second proton).

Is H_2(g) released? To study this, investigators have used alternative substrates such as acetylene, HC≡CH (similar to N≡N), in the presence of D_2 and N_2 in an aqueous system. It is helpful to review Figure **22.1.9** again.

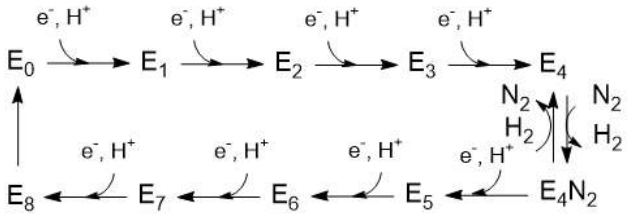


Figure **22.1.9**: Lowe and Throneley model for electron and proton additions in nitrogenase

The acetylene was reduced and formed $C_2H_2D_2$ and C_2H_3D. Hence, E4 must have had two Ds in it, and E2 probably had one. These results support the **reversible** reductive elimination mechanism for the E4 to E4:N_2 reaction above. Previously, it had been shown that H^+ are reduced by D_2 in the presence of D_2 and N_2 in an aqueous system, so these results are consistent. In addition, deuterium from D_2 is not incorporated into products ($C_2H_2D_2$, C_2H_3D, or HD) in the absence of N_2.

Let's return for a moment to the bridging hydrides as shown again Figure **22.1.10**.

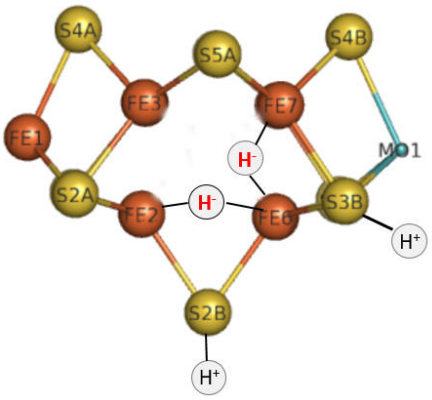


Figure **22.1.10**: The E4 Janus intermediate in the reduction of N_2

It appears likely that the reductive elimination of the two proximal bridging hydrides is the mechanism for the formation of H_2. The bridging hydrides, which are strong bases, are much less likely to be protonated than if the hydrides were terminal. A simple and competing protonation reaction could also form H_2, and if that occurred, the reducing equivalents of the bridging hydrides would be lost. Hence, the bridging hydrides (shared by two metal centers) are more stable and can "wait" for the incoming N_2 reactants before their reducing equivalents are lost. They may convert to terminal hydrides eventually to facilitate substrate reduction (hydrogenation).

The Janus intermediate E4 is now positioned to bind N_2 and release H_2. For each H^- that binds to the M cluster, two H^+s bind to the M cluster sulfides for electrostatic stabilization.

Migratory Insertions

We need to consider one last common type of reaction at a metal center, **migratory insertions (MI)**. In an MI reaction, a group attached to a metal ion center is transferred to another group attached to the same metal. Figure **22.1.13** shows four examples of MI reactions.

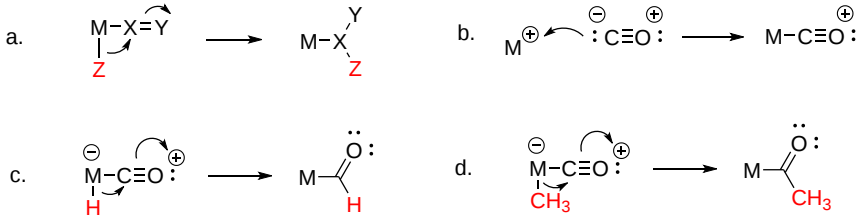


Figure **22.1.13**: Migratory insertion reactions at metal centers

Panel (a) shows a generic MI reaction. Panel (b) shows the interaction of carbon monoxide, :C≡O: (isoelectronic and analogous to :N≡N:), with a metal center. Panel (c) shows how a hydride could engage in 1:1 insertion as it shifts and covalently bonds to the first atom of another ligand bound to the metal center. Note that metal does not have to have a negative charge. This could theoretically be important for the reduction of N_2 bound as a ligand through a coordinate covalent (dative) bond to the metal. Panel (d) shows the migration of an alkyl group.

We will see that the MI reaction is involved in adding Hs to N_2, starting not with N_2 but with the N_2H_2 stage as the intermediates insert into an Fe-H bond. N_2 is not reactive to the insertion of a hydride, as is carbon monoxide, CO, which provides a positive oxygen to facilitate electron flow during the insertion. In addition, the oxygen becomes neutral after the reaction.

This provides a compelling explanation for how nature selected the FeMo cluster for nitrogen fixation. The interaction of two hydrides requires a 4 Fe face (coordinated with the carbon) that allows for the storage of reducing equivalents for the initial reduction of N_2. The large M cluster is more stable and effectively held together by a central carbide anion. This also allows the metal centers to never change their oxidation state by more than one charge unit.

The source of the protons to form N_2H_2 comes directly from the two H_2 attached to the two sulfurs. They can't come from the hydrides, which are released as H_2. The seemingly wasteful reductive elimination of H_2 and energy is required to allow the kinetically unreactive N_2 molecule to bind to the reduced and activate 4Fe face, which is also electrostatically facilitated by the two bound protons in what has been called a push (reductive)-pull (protonation) reaction. This first step in N_2 reduction to N_2H_2 is the hardest.

22.1.7: OXIDATION STATES OF NITROGENASE FE CENTERS

First Half: It would be difficult to assign specific oxidation states to each Fe ion in the M complex. Instead, we can assign relative changes in the oxidation states as the reaction proceeds from E0 to E4. In each step of the LT model, 1 electron is added. We will first assign this to an average Fe ion, M^0, with an arbitrarily assigned oxidation state of 0. Upon the addition of 1 electron, the oxidation state would go from

M^0 to M^{-1} as the metal is reduced. The M^{-1} state is then oxidized as an electron is transferred to H^+, and when 2 electrons are transferred, a single H^- is made. The diagram in Figure **22.1.14** illustrates the change in oxidation state as the system transitions from E0 to E4.

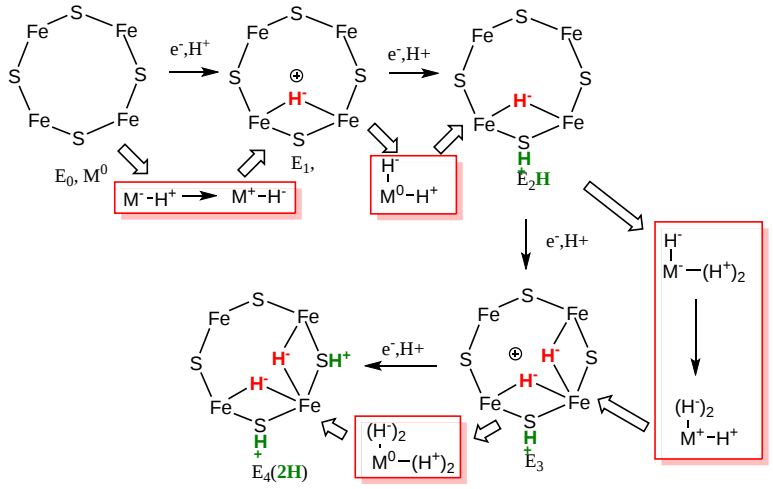


Figure **22.1.14**: Change in oxidation state in going from E0 to E4

The red boxes highlight thermodynamic cycle-like steps, which show how changes in the redox state of the Fe ions (M) could be visualized. Note that in going from E0 to E4, the actual oxidation state of M changes back and forth from 0 to +1 and finally back to 0. That is quite amazing given that 4 electrons have been added. Note also that in the red box going from step E0 to E1, M goes from -1 to +1, which corresponds to our description of an oxidative addition when the metal center loses two electrons. This mechanism suggests that nitrogenase can be considered a "hydride storage device."

Second Half (facing forward to production NH_3):

How does N_2 initially interact with E4? It must depend on how the hydrides are released as H_2, which evidence shows occurs by **reductive elimination** (re) and not hydride protonation (hp). On addition, the N_2 is very quickly converted to diazene, HN=NH, with the departing H_2 taking with it 2 H^+s and 2 electrons (or reducing equivalents). These events could occur as shown in Figure **22.1.15**.

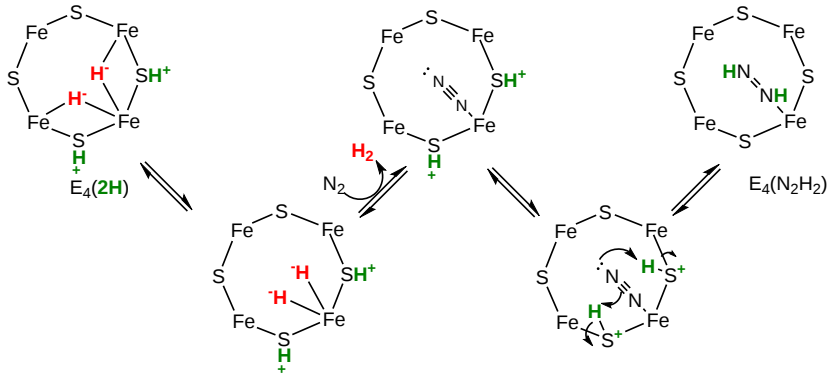


Figure **22.1.15**: Reaction mechanism for the formation of N_2H_2

Now, with N_2 bound as diazene (N_2H_2) and H_2 released, the rest of the reaction could occur as shown below. One new step, a migratory insertion, is shown in Figure **22.1.16**.

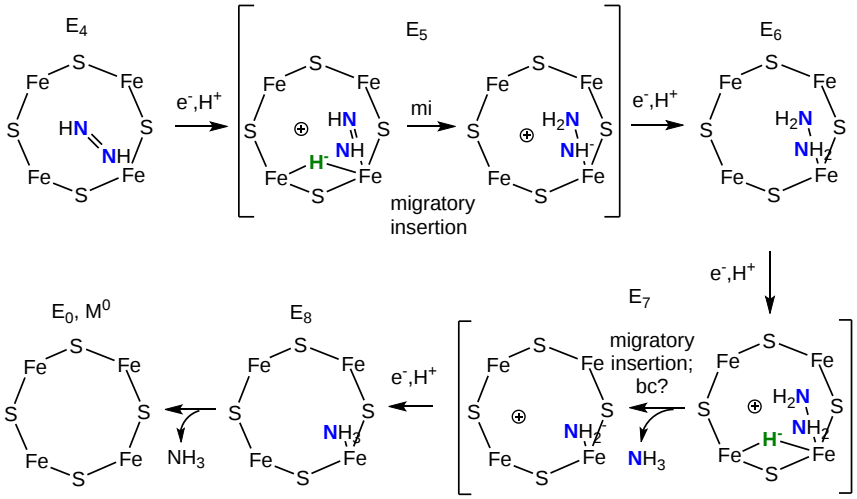


Figure **22.1.16**: Reaction mechanism for the conversion N_2H_2 to NH_3.

The two halves of the reaction are similar, with bridging hydrides utilized - the E4 Janus intermediate links the two halves together.

22.1.8: SUMMARY

This chapter explores the central role of nitrogen in biochemistry and ecology by examining the biological nitrogen cycle and, in depth, the mechanism of biological nitrogen fixation via nitrogenase.

Key Points:

- **The Nitrogen Cycle in Nature:**
  The chapter begins by challenging the carbon-centric view of organic chemistry, emphasizing that nitrogen—present in both inorganic forms (ammonium, nitrate, nitrite) and organic biomolecules (amino acids, nucleotides)—is equally essential. It provides an overview of the nitrogen cycle, highlighting how aerobic and anaerobic bacterial processes (nitrification, denitrification, anammox, and ammonification) transform atmospheric N_2 into bioavailable forms and back again, thereby supporting ecosystem productivity.
- **Biological Nitrogen Fixation:**
  Despite the thermodynamic favorability at room temperature (exothermic with a negative $\Delta G°$), the reduction of the highly stable N_2 molecule is kinetically hindered by its strong triple bond. Nitrogen fixation is accomplished by specialized prokaryotes that use the enzyme nitrogenase to convert atmospheric N_2 into ammonium (NH_4^+) under ambient conditions, powered by the hydrolysis of ATP.
- **Structure and Function of Nitrogenase:**
  Nitrogenase is a complex, multi-protein enzyme composed of two main components:
  - **The Reductase (Fe-protein):** A homodimer containing a 4Fe–4S cluster that accepts electrons from electron carriers (e.g., ferredoxin or flavodoxin) and hydrolyzes ATP to drive electron transfer.
  - **The Catalytic Component (MoFe-protein):** A heterodimer housing two key metal clusters—the P-cluster and the iron–molybdenum (M) cofactor. The M cluster, which includes molybdenum, iron, sulfur, and an interstitial carbide, is the site of N_2 binding and reduction.
- **Kinetic Mechanism and the Lowe–Thorneley Model:**
  The chapter details the stepwise accumulation of electrons and protons in nitrogenase, as described by the Lowe–Thorneley kinetic model. In this model, the enzyme cycles through intermediate states (E_0 to E_4), culminating in the “Janus” intermediate (E_4). At this stage, bridging hydrides accumulate and, upon N_2 binding, undergo reductive elimination to release H_2. This critical step “activates” N_2, allowing its reduction to ammonia.
- **Organometallic Reaction Principles in Nitrogenase:**
  The enzyme’s mechanism is illuminated by concepts from organometallic chemistry. Key reactions such as oxidative addition (where H_2 is “added” to the metal center, raising its oxidation state) and reductive elimination (where H_2 is released as the metal center is reduced) are central to the enzyme’s function. Additionally, migratory insertion may play a role during later steps of N_2 reduction. Together, these processes illustrate how nature has evolved a sophisticated strategy to overcome the kinetic barriers associated with breaking the strong N≡N bond.
- **Ecological and Biochemical Significance:**
  Finally, the chapter connects these biochemical processes to broader ecological implications. Nitrogen fixation by microorganisms

supplies essential nitrogen to plants, underpinning global primary productivity. This understanding also offers insight into the impact of human activities (such as industrial fertilizer use) on the natural nitrogen cycle.

In Summary:

This chapter integrates organic, inorganic, and organometallic chemistry principles to explain how nature fixes atmospheric nitrogen—a process essential for life on Earth. By dissecting the structure and mechanism of nitrogenase, the text illustrates how energy (from ATP), electrons, and sophisticated metal cofactors work together to overcome kinetic barriers and drive the reduction of N_2 to ammonia. Moreover, it places these biochemical insights within the context of global nutrient cycles and environmental sustainability, underscoring the interconnectedness of molecular-level processes and ecosystem dynamics.

This summary provides a comprehensive overview designed to help advanced undergraduate biochemistry students integrate concepts from thermodynamics, enzymology, and inorganic chemistry with ecological and environmental perspectives.

This page titled 22.1: Overview of Nitrogen Metabolism - Nitrogenase is shared under a not declared license and was authored, remixed, and/or curated by Henry Jakubowski and Patricia Flatt.

- **Current page** by Henry Jakubowski and Patricia Flatt has no license indicated.
- **11.2: Diffusion Across a Membrane - Passive and Facilitated Diffusion** by Henry Jakubowski and Patricia Flatt has no license indicated.

22.2: BIOSYNTHESIS OF AMINO ACIDS

LEARNING GOALS (CHATGPT O3-MINI)

1. **Classify Amino Acids by Nutritional Requirement:**
   - Define and differentiate essential versus nonessential amino acids.
   - Explain the metabolic interdependence of certain amino acids (e.g., how deficiencies in cysteine or tyrosine can affect methionine or phenylalanine levels).
2. **Map Biosynthetic Origins to Central Metabolic Intermediates:**
   - Identify glycolytic and TCA cycle intermediates (e.g., glucose-6-phosphate, 3-phosphoglycerate, pyruvate, α-ketoglutarate, and oxaloacetate) as precursors for amino acid synthesis.
   - Explain how these central metabolites channel into specific amino acid pathways.
3. **Describe Specific Pathways from Glycolytic Intermediates:**
   - Outline the pathway of histidine synthesis from a phosphorylated ribose derivative originating from glucose-6-phosphate.
   - Detail the synthesis of serine from 3-phosphoglycerate and its subsequent conversion into glycine and cysteine.
4. **Explain Aromatic Amino Acid Biosynthesis:**
   - Summarize the initial steps (from phosphoenolpyruvate and erythrose 4-phosphate) leading to chorismate.
   - Distinguish the branch pathways from chorismate that lead to the synthesis of tryptophan versus phenylalanine and tyrosine.
5. **Outline Branched-Chain Amino Acid (BCAA) Synthesis:**
   - Describe how pyruvate serves as the precursor for alanine and for the branched-chain amino acids (valine, leucine, isoleucine).
   - Discuss the role of transamination in converting pyruvate to alanine and the additional steps required for BCAA formation.
6. **Integrate TCA-Derived Amino Acid Biosynthesis:**
   - Explain the conversion of α-ketoglutarate into glutamate and glutamine via transamination and subsequent glutamine synthetase activity.
   - Describe how glutamate serves as a precursor for proline and arginine, and relate these pathways to the urea cycle.
7. **Examine Aspartate-Derived Pathways:**
   - Outline how oxaloacetate is transaminated to aspartate.
   - Describe downstream pathways that convert aspartate into asparagine, threonine, methionine, and lysine (highlighting the diaminopimelic acid pathway for lysine).
8. **Relate Amino Acid Metabolism to Energy and Nutrient Balance:**
   - Explain how the breakdown (catabolism) of amino acids contributes to energy production during fasting and supports gluconeogenesis and ketogenesis.
   - Discuss why excess dietary amino acids cannot be stored and must be oxidatively degraded or excreted.
9. **Contextualize Amino Acid Biosynthesis within Cellular and Ecosystem Metabolism:**
   - Summarize the Reactome “Cellular Metabolism of Amino Acids and Related Molecules” diagram to relate biosynthetic pathways to overall cellular metabolism.
   - Reflect on how the biosynthesis of amino acids supports primary productivity in plants and, by extension, the entire food web.

These learning goals are designed to encourage you to:

- Connect the individual pathways of amino acid synthesis with central metabolic processes.
- Appreciate the complexity and integration of nutrient utilization in different nutritional states.
- Understand how biosynthetic pathways are not only vital for protein synthesis but also for energy metabolism and overall cellular homeostasis.

By mastering these goals, you will be well-equipped to understand the biochemical logic behind amino acid synthesis and its broader implications for metabolism and physiology.

22.2.1: INTRODUCTION

By the time many students reach the study of amino acid biosynthesis, they have encountered numerous pathways that learning new pathways for the amino acids may seem daunting, even though they can be clustered into subpathways. Most students are aware that, from a nutritional perspective, amino acids can be categorized into two types: nonessential and essential (those that require external dietary supplementation). These are shown for humans below.

- Nonessential amino acids: Alanine, Asparagine, Aspartate, Cysteine, Glutamate, Glutamine, Glycine, Proline, Serine, Tyrosine
- Essential amino acids: Arginine*, Histidine, Isoleucine, Leucine, Lysine, Methionine*, Phenylalanine*, Threonine, Tryptophan, Valine

Three of the essential amino acids can be made in humans but need significant supplementation. Arginine is depleted in processing through the urea cycle. When cysteine levels are low, methionine is used to replace them, causing their levels to fall. If tyrosine is low, phenylalanine is used to replace it.

The amino acids can be synthesized from glycolytic and citric acid cycle intermediates as shown in Figure **22.2.1**

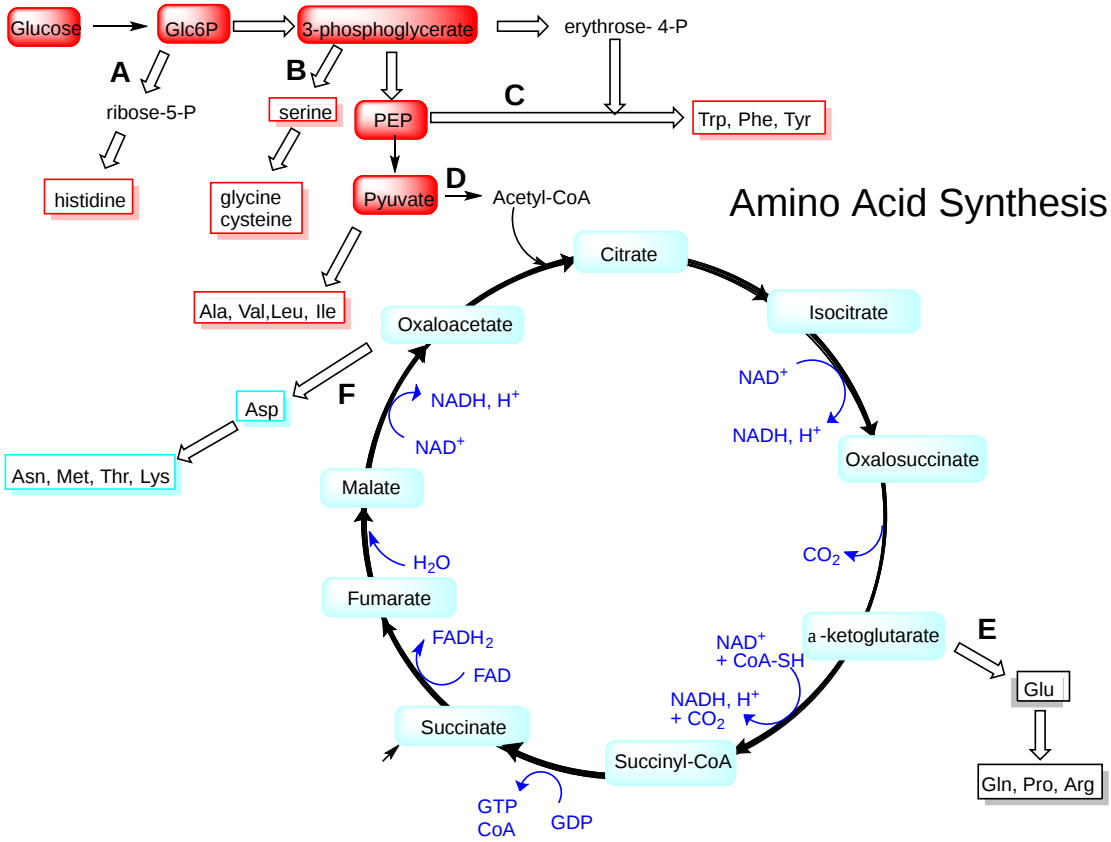


Figure **22.2.1**: Summary amino acid synthesis from glycolytic and TCA intermediates

For this chapter subsection, we will provide only the basic synthetic pathways in abbreviated form, without delving into mechanistic or structural details (likely to the relief of readers and authors alike).

22.2.2: AMINO ACID SYNTHESIS FROM GLYCOLYTIC INTERMEDIATES

22.2.2.1: FROM GLUCOSE-6-PHOSPHATE: HISTIDINE

The synthesis of histidine from a phosphorylated form of ribose (derived from glucose-6-phosphate) is shown in Figure **22.2.2**.

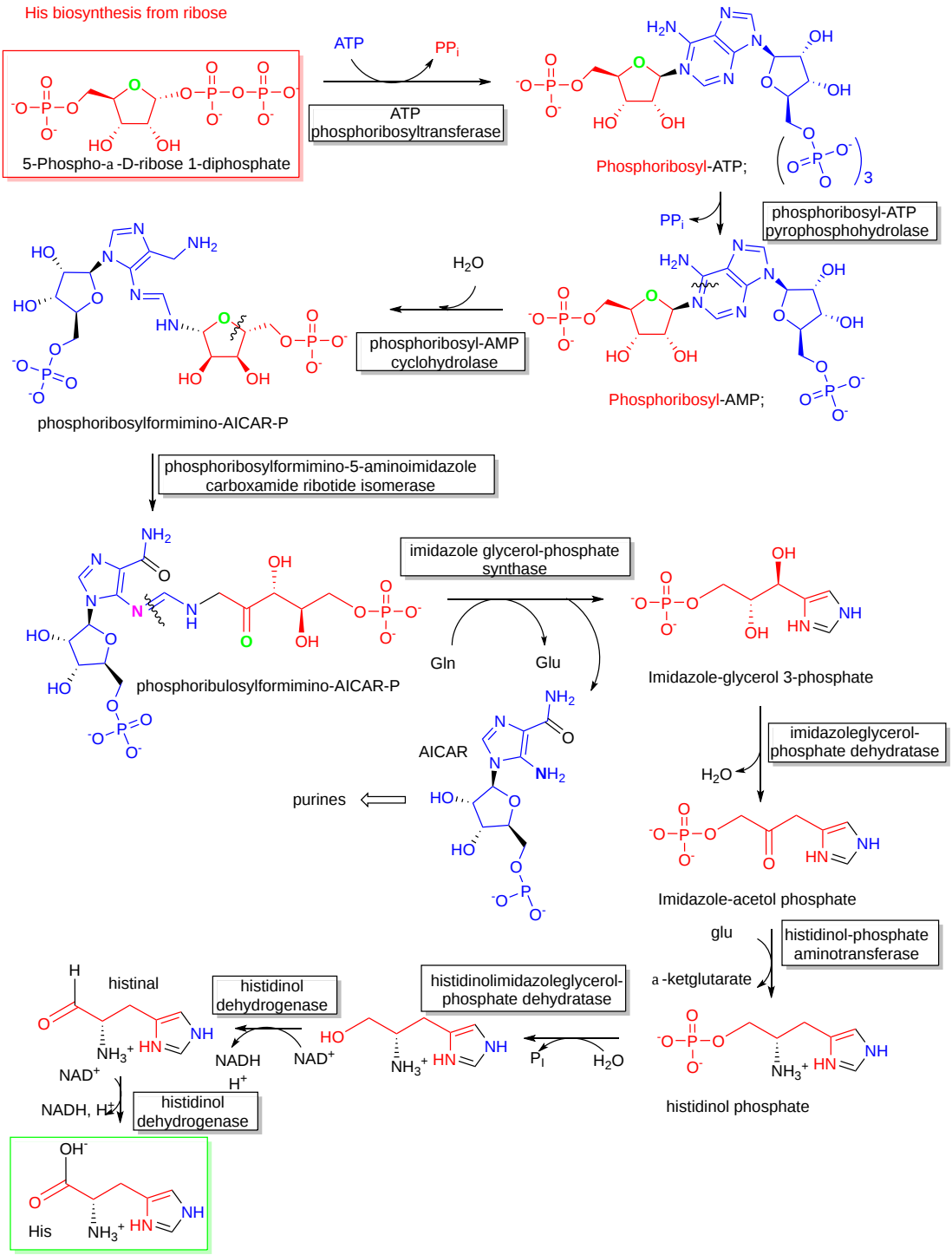


Figure **22.2.2**: Synthesis of histidine from a phosphorylated form of ribose

22.2.2.2: FROM 3-PHOSPHOGLYCERATE: SERINE, GLYCINE, AND CYSTEINE

The synthesis of serine, glycine, and cysteine from 3-phosphoglycerate is shown in Figure **22.2.3**.

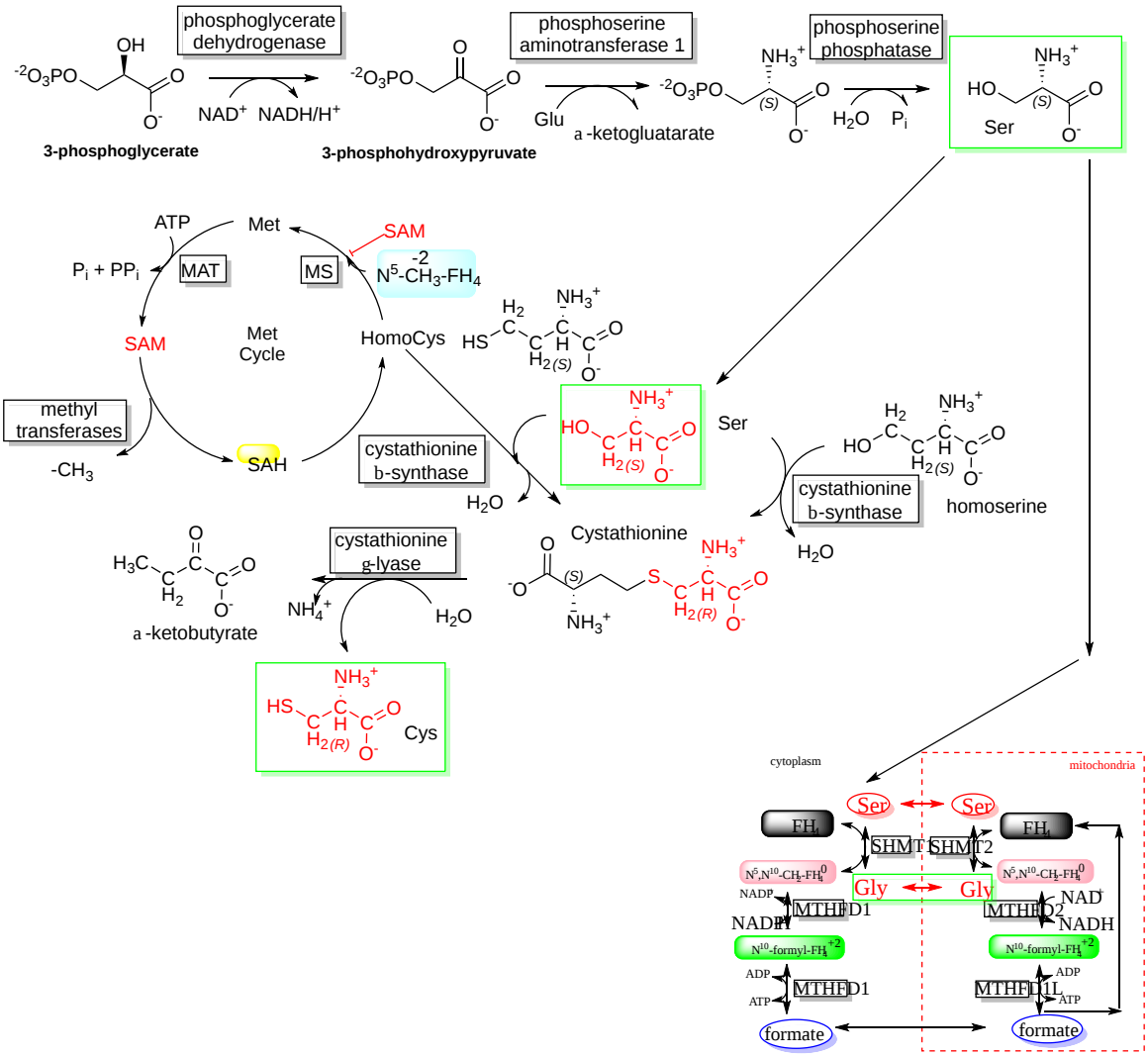


Figure **22.2.3**: The synthesis of serine, glycine, and cysteine from 3-phosphoglycerate

CYSTEINE AND CONTROL OF BODY WEIGHT

Recent studies have shown that inhibiting cysteine synthesis leads to significant body loss. The figure below shows simplified pathways for Cys synthesis (blue) and consumption (reversible, green; and irreversible, brown).

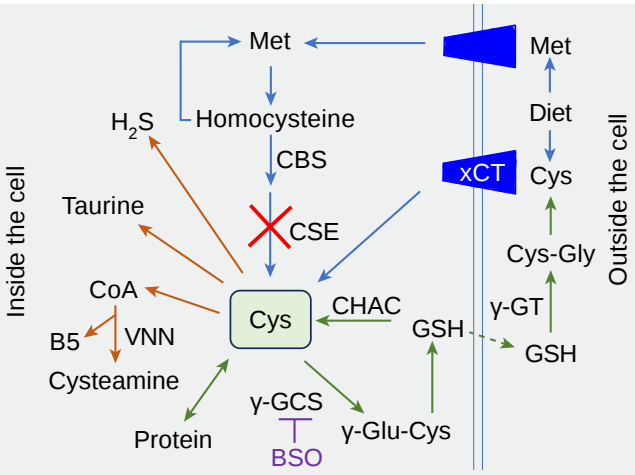


Figure: Simplified pathways for Cys synthesis (blue) and consumption (reversible, green; and irreversible, brown). **Cystathionine β-synthase (CBS)** and **cystathionine γ-lyase (CSE)** are involved in the *trans*-sulfuration pathway for cysteine synthesis. Varghese, A., Gusarov, I., Gamallo-Lana, B. *et al.* Unravelling cysteine-deficiency-associated rapid weight loss. *Nature* (2025). https://doi.org/10.1038/s41586-025-08996-y. Creative Commons Attribution-NonCommercial-NoDerivatives 4.0 International License. http://creativecommons.org/licenses/by-nc-nd/4.0/.

Dramatically decreasing cysteine leads to the depletion of **glutathionine** (γ-glutamylcysteinylglycine, **GSH**), the main reducing agent (and antioxidant) in the cell, and CoASH, which is needed for the citric acid cycle and oxidation of fatty acids. Deletions of the mouse gene for CSE (red cross) and the addition of the inhibitor BSO (purple) decrease GSH synthesis, which proceeds through VNN (vanin/pantetheinase), GT (glutamyl transferase, and GCS (glutamate–cysteine ligase). Cysteine is a nonessential amino acid, but can be made essential through the inhibitions described in the above figure. These inhibitions led to a 30% reduction in mouse body weight in just one week. White adipose tissue was lost and replaced with brown adipose tissue. Accompanying these changes were large changes in transcription and mitochondrial dysfunction. Ultimately, this results in malfunctions in both the cell's integrated stress response (ISR) and oxidative stress response (OSR), inhibiting mitochondrial function. Glycolytic and citric acid intermediates are lost in the urine, leading to weight loss.

What is so special about cysteine? It is cytotoxic in high concentrations as it alters the redox balance. Hence, has one of the lowest concentrations of free amino acids in the cell (typically 50–200 μM). As you know from the study of protein structure, cysteine, as a free thiol, is a redox reagent (like β-mercaptoethanol or βME). βME is used at a concentration of 5% or about 7 M in SDS-PAGE reducing sample preparation solutions. At these very high levels, it reduces disulfide bonds in proteins by forming mixed disulfides, and then, by further reaction with more βME, it forms free thiols in proteins. Hence, it acts as a **reducing** agent. At lower levels, it can form a persistent mixed disulfide with a cysteine or cystine in a target protein. It is an **oxidizing** agent under these conditions (typical of a cellular environment).

Given standard reduction potentials, cysteine can reduce Fe^{3+} to Fe^{2+}, as shown below:

$$\mathbf{2Cys-SH + 2Fe^{3+} \longrightarrow RSSR + 2Fe^{2+} + 2H^{+}} \tag{22.2.1}$$

The free Fe^{2+} is toxic to cells, in part by generating the hydroxy free radical through the Fenton Reaction, as shown below:

$$\mathbf{Fe^{2+} + H_2O_2 \longrightarrow Fe^{3+} + OH^{-} + \cdot OH} \tag{22.2.2}$$

This set of reactions becomes autocatalytic as the Fe^{3+} produced can re-enter the cycle. The hydroxy free radical oxidizes proteins, lipids, and nucleic acids and can also form more ROS.

It can also react with O_2 in an autooxidation reaction, giving cystine and ROS like H_2O_2.

$$\mathbf{2Cys-SH + O_2 \longrightarrow Cys-S-S-Cys + H_2O_2} \tag{22.2.3}$$

Normally, ingested cysteine is kept low by liver uptake and conversion to GSH and taurine, which are less toxic. In low cysteine diets, free intracellular cysteine is depleted as it is pulled into protein synthesis and used to maintain pools of CoASH and GSH. The inhibitions described above amplify the dysfunction and lead to the results described.

What's so special about GSH? It is the main mitochondrial antioxidant. It is much more abundant in cells (0.5–15 mM). The γ-glutamyl group helps protect this tripeptide from proteolytic cleavage. This helps contribute to its higher cellular concentration. An

enzyme, glutathione reductase, helps keep glutathione in reduced form and higher concentrations to act as a redox buffering agent in cells. It is also much less reactive in the Fenton reaction.

As shown below, GSH directly scavenges hydrogen peroxide (H_2O_2) and other peroxides using glutathione peroxidase.

$$2GSH + H_2O_2 \xrightarrow{\text{glutathione peroxidase}} GSSG + 2H_2O \quad (22.2.4)$$

and

$$2GSH + ROOH \xrightarrow{\text{glutathione peroxidase}} GSSG + ROH + H_2O \quad (22.2.5)$$

When GSH is depleted, increased reactive oxygen species (ROS) produced at Complex I and III inhibit their activity through oxidative damage. Further damage to mitochondrial proteins reduces electron flow and ultimately decreases ATP production. Key mitochondrial citric acid cycle enzymes are also damaged.

22.2.2.3: FROM PHOSPHENOL PYRUVATE: THE AROMATICS - TRP, PHE, AND TYR

The synthesis of the first of the biosynthetic pathways for the aromatic amino acids phenylalanine, tryptophan, and tyrosine from phosphoenolpyruvate up to chorismate is shown in Figure **22.2.4**.

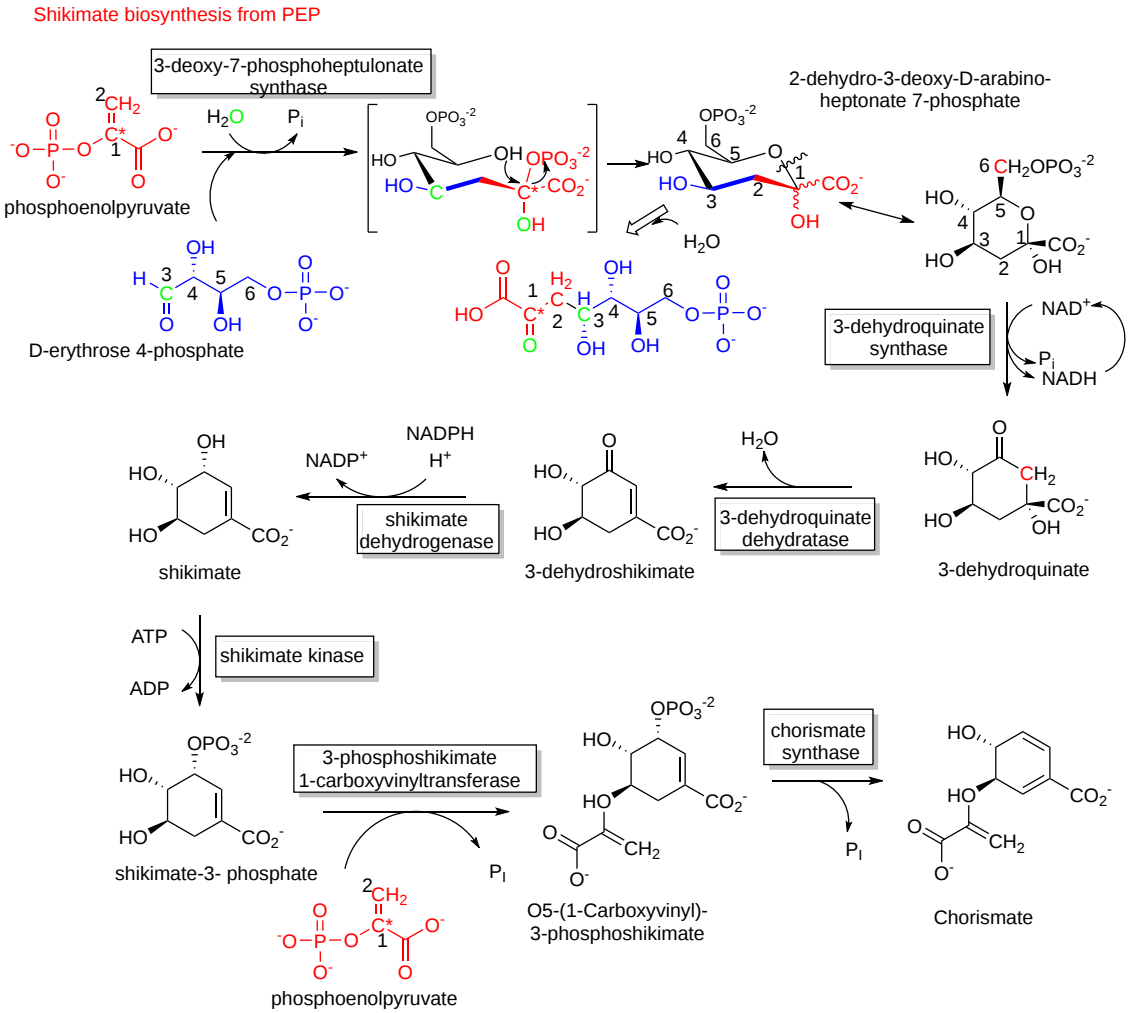


Figure **22.2.4**: Synthesis of the first of the biosynthetic pathways for the aromatic amino acids phenylalanine, tryptophan, and tyrosine from phosphoenolpyruvate up to chorismate

Chorismate to tryptophan

The synthesis of the second half of the biosynthetic pathway for tryptophan from chorismate is shown in Figure **22.2.5**

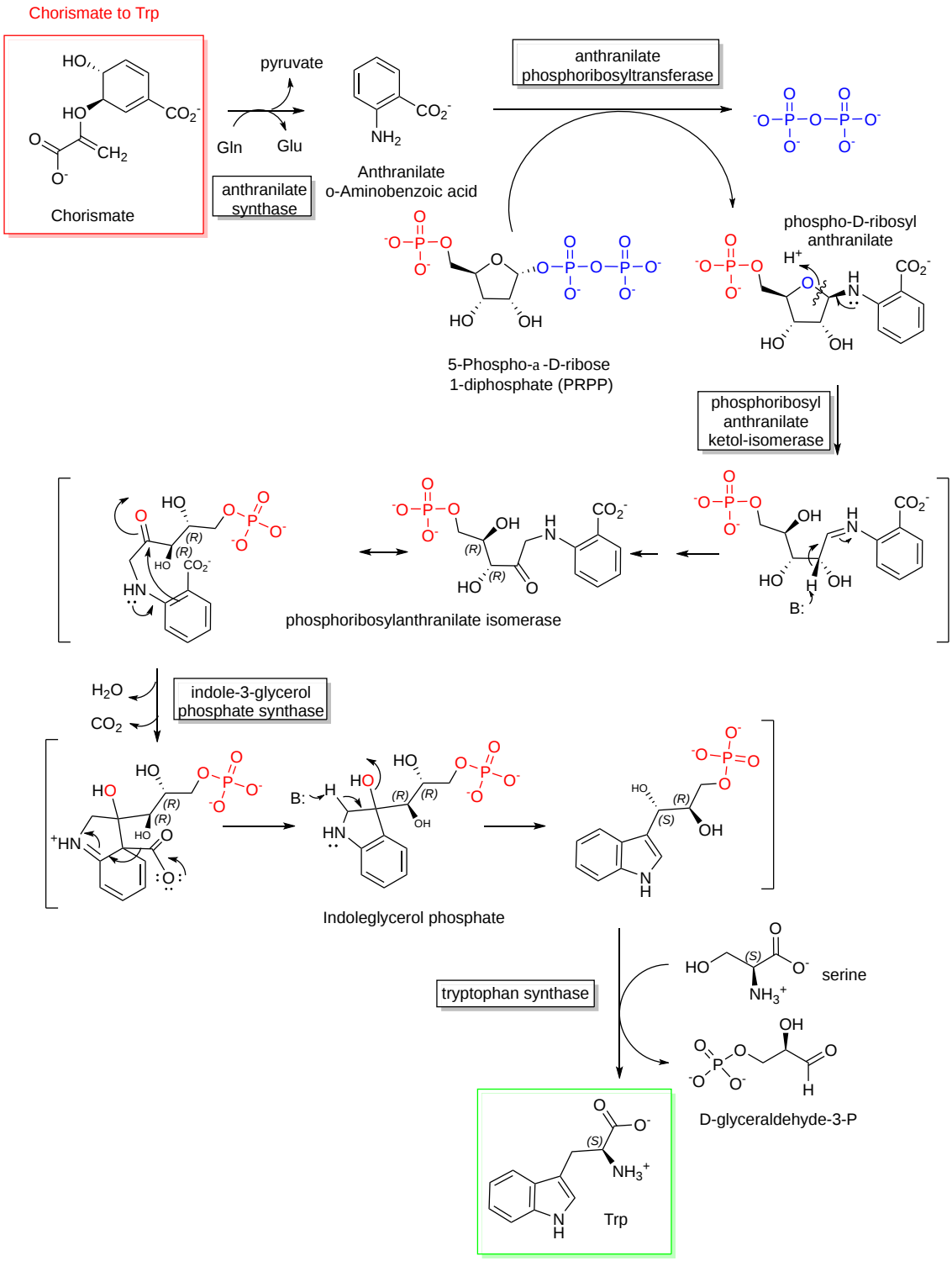


Figure (\PageIndex{5}\): Synthesis of the second half of the biosynthetic pathways for the aromatic amino acid tryptophan from chorismate

Chorismate to Phe and Tyr

The synthesis of the second half of the biosynthetic pathway for phenylalanine and tyrosine from chorismate is shown in Figure **22.2.6**

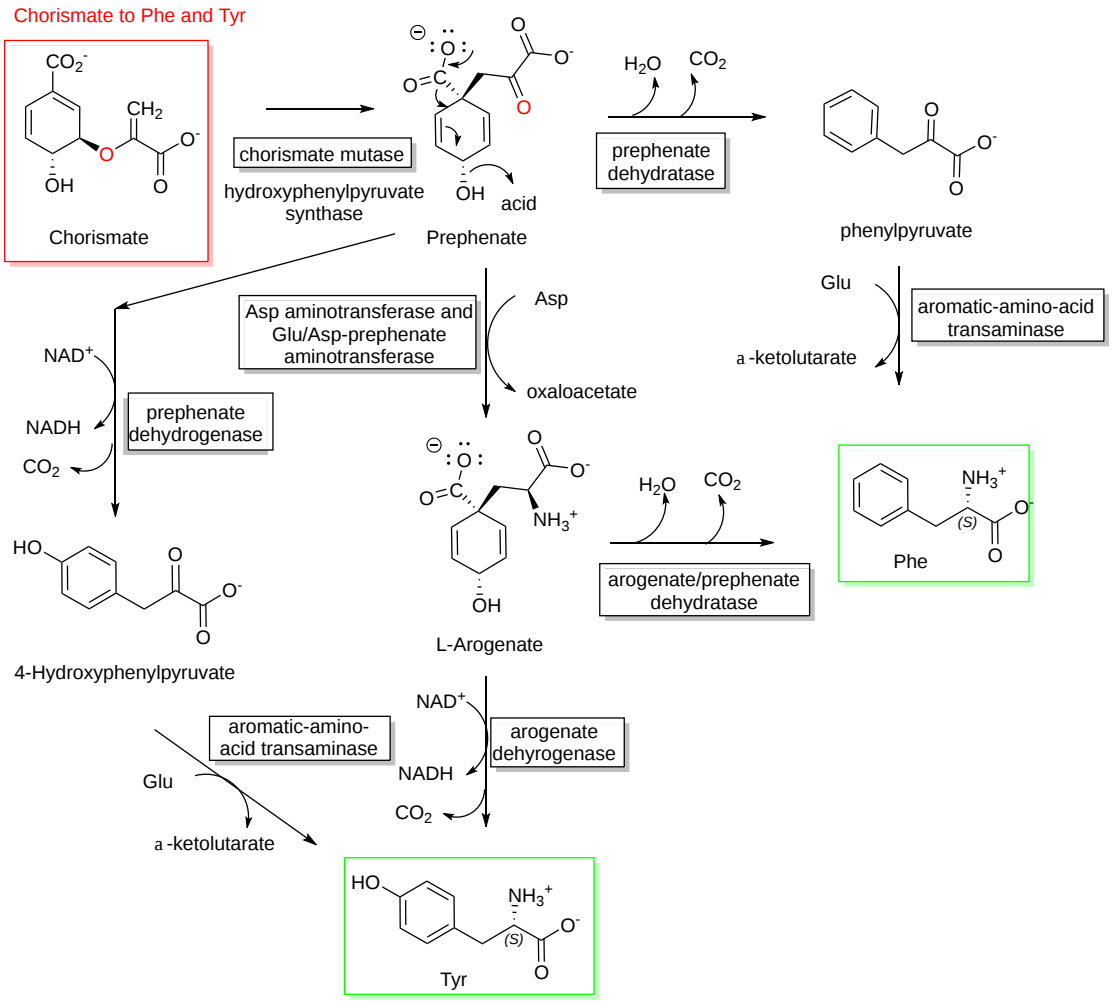


Figure 22.2.6: Synthesis of the second half of the biosynthetic pathway for phenylalanine and tyrosine from chorismate

22.2.2.4: FROM PYRUVATE: ALA, VAL, LEU, ILE

Alanine can be easily synthesized from the alpha-keto acid pyruvate through a transamination reaction; therefore, we will focus our attention on the other branched-chain nonpolar amino acids, Val, Leu, and Ile.

The synthesis of valine, leucine, and isoleucine from pyruvate is shown in Figure 22.2.7.

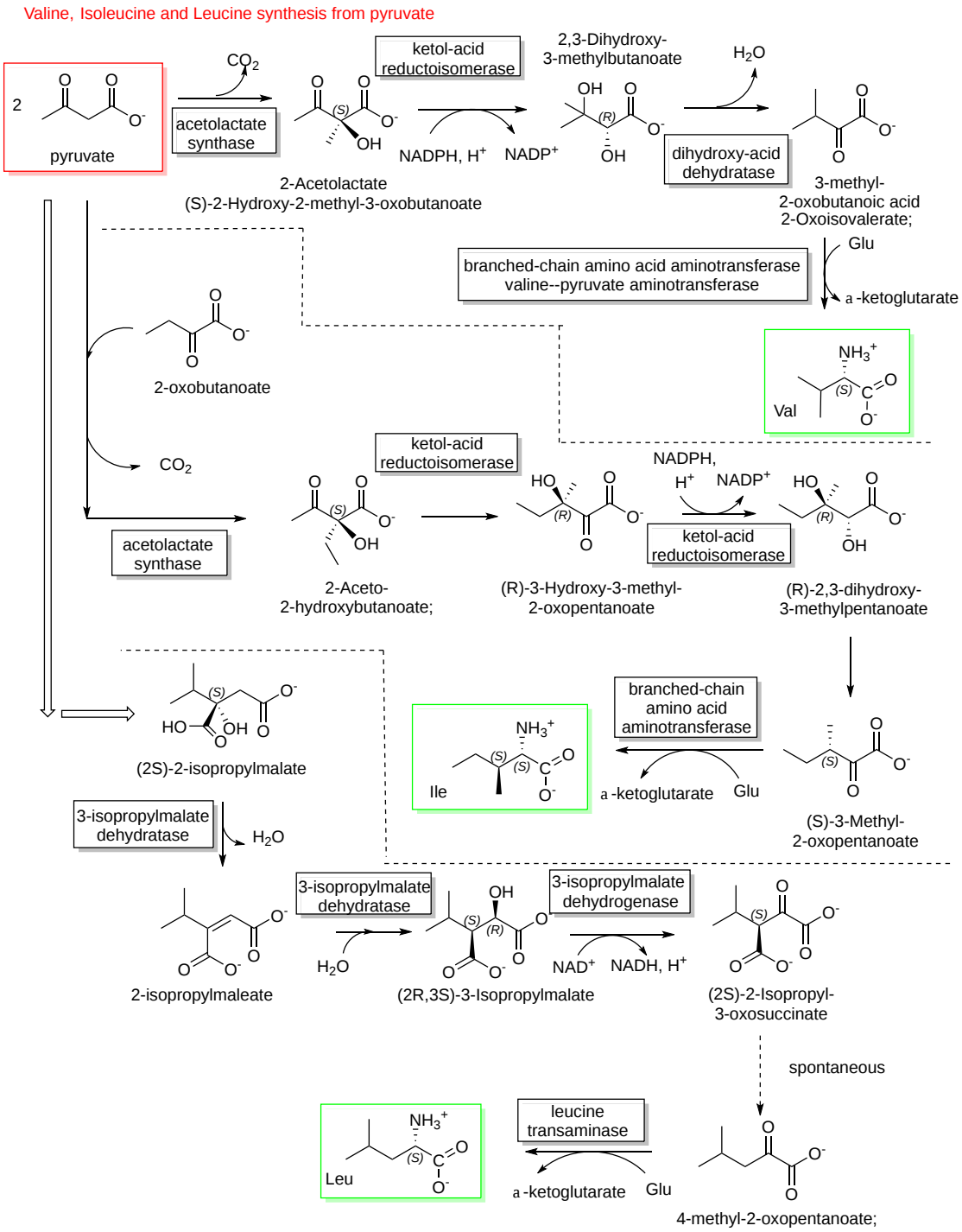


Figure **22.2.7**: The synthesis of valine, leucine, and isoleucine from pyruvate

22.2.3: TCA INTERMEDIATES

22.2.3.1: FROM A-KETOGLUATARATE: GLU, GLN, PRO, ARG

Since amino acid metabolism is so complex, it is essential to continually review past learning. Figure **22.2.8** from section 18.2 shows the relationship among Glu, Gln, and keto acids.

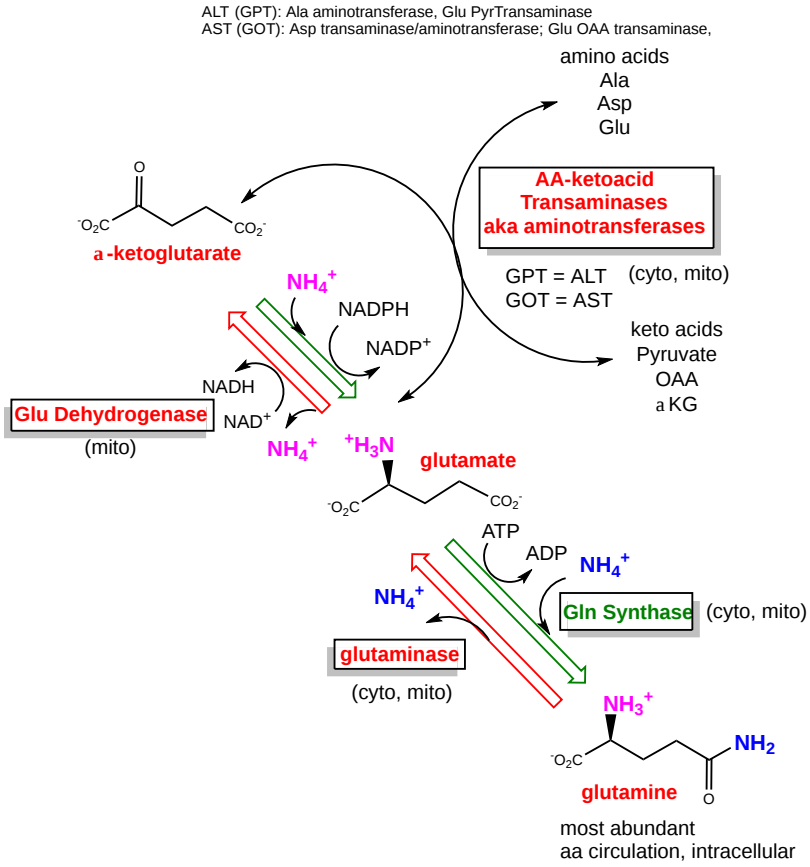


Figure **22.2.8**: Glutamate and glutamine synthesis from α-ketoglutarate

As is evident from the figure, glutamic acid can be made directly through the transamination of α-ketoglutarate by an ammonia donor. In contrast, glutamine can be made by the action of glutamine synthase on glutamic acid.

Arginine is synthesized in the urea cycle, as previously discussed. It can be made from α-ketoglutarate through the following sequential intermediates: N-acetylglutamate, N-acetylglutamate-phosphate, N-acetylglutamate-semialdehyde, N-acetylornithine to N-acetylcitruline. It is deacetylated and enters the urea cycle.

The pathway for conversion of α-ketoglutarate to proline is shown in Figure **22.2.9**.

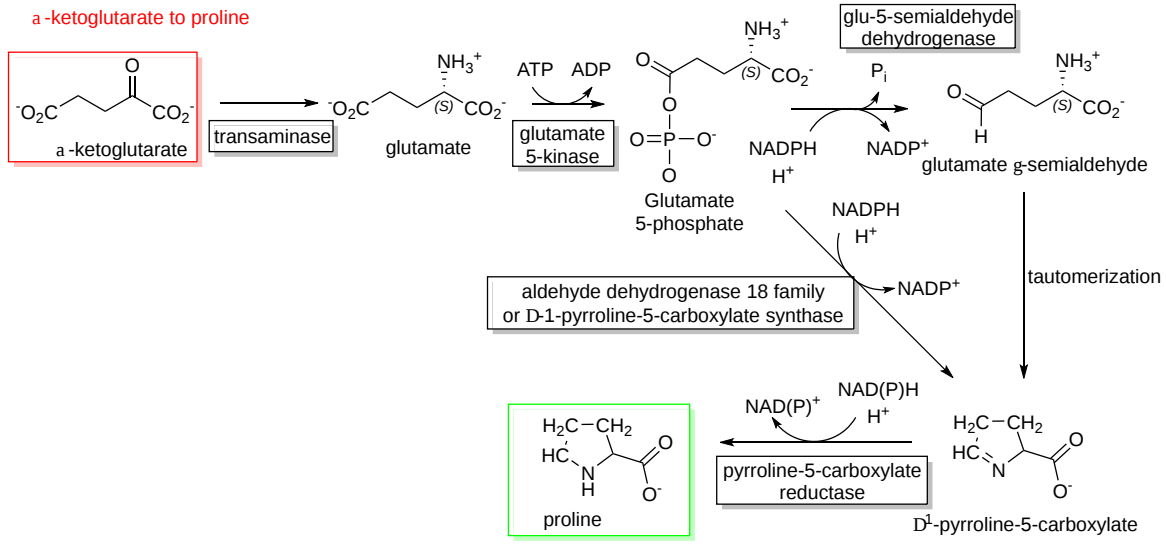


Figure **22.2.9**: Conversion of α-ketoglutarate to proline

22.2.3.2: FROM OXALACETATE: ASP, ASN, MET, THR, LYS

22.2.3.2.1: OAA TO ASPARTIC ACID

This is a simple transamination

22.2.3.2.2: ASPARTIC ACID TO ASPARAGINE

This is catalyzed by the enzyme Asparagine Synthase, as shown in the reaction equation below:

$$\text{Aspartate} + \text{Glutamine} + \text{ATP} + H_2O \rightarrow \text{Asparagine} + \text{Glutamic Acids} + \text{AMP} + PP_i$$

22.2.3.2.3: ASPARTIC ACID TO LYSINE

There are two pathways.

- The diaminopimelic acid (DAP) pathway utilizes aspartate and pyruvate, forming diaminopimelic acid as an intermediate. It is found in bacteria, some fungi, and archaea, as well as in plants.
- The aminoadipic acid (AAA) pathway utilizes α-ketoglutarate and acetyl-CoA to form aminoadipic acid as an intermediate. Fungi use it.

Here, we present the synthesis of lysine from aspartate and pyruvate using the diaminopimelic acid (DAP) pathway. The pathway is shown in Figure **22.2.10**.

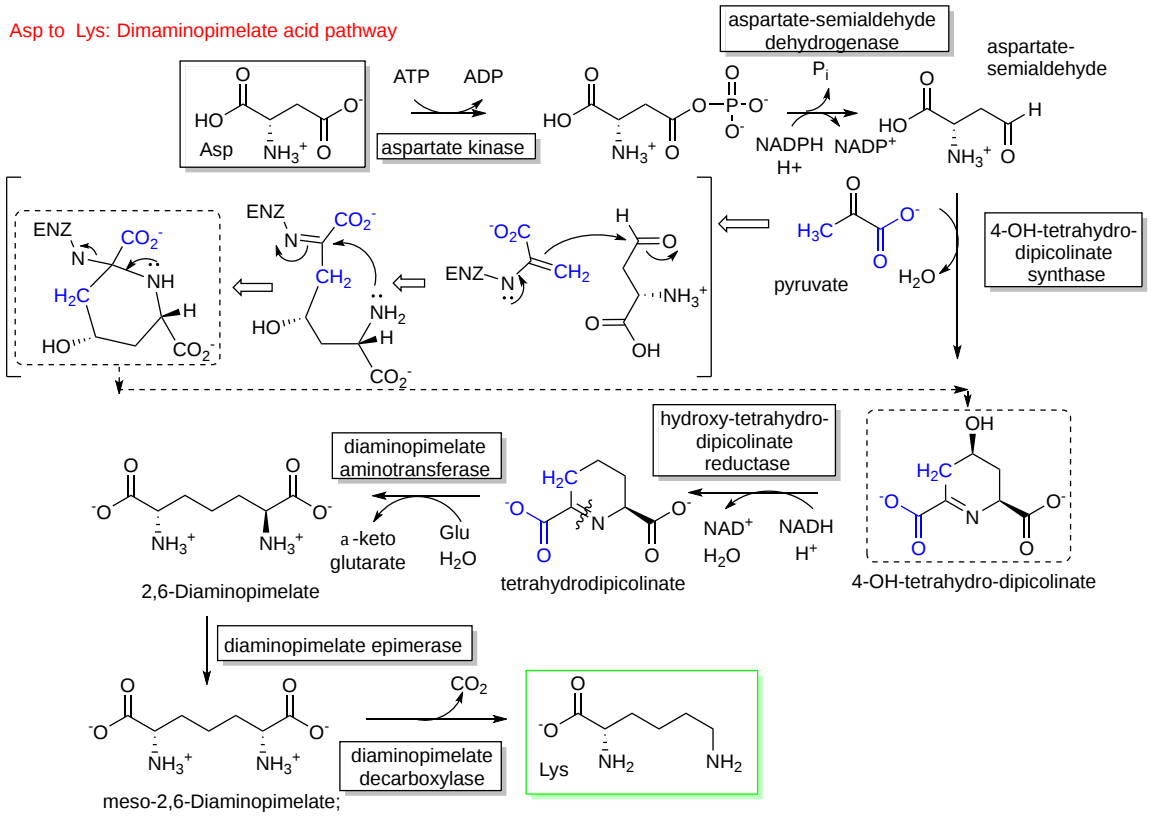


Figure **22.2.10**: The synthesis of lysine from aspartic acid in the diaminopimelic acid DAP pathway

.

22.2.3.2.4: ASPARTIC ACID TO THREONINE

The conversion of aspartic acid to threonine is shown in Figure **22.2.11**.

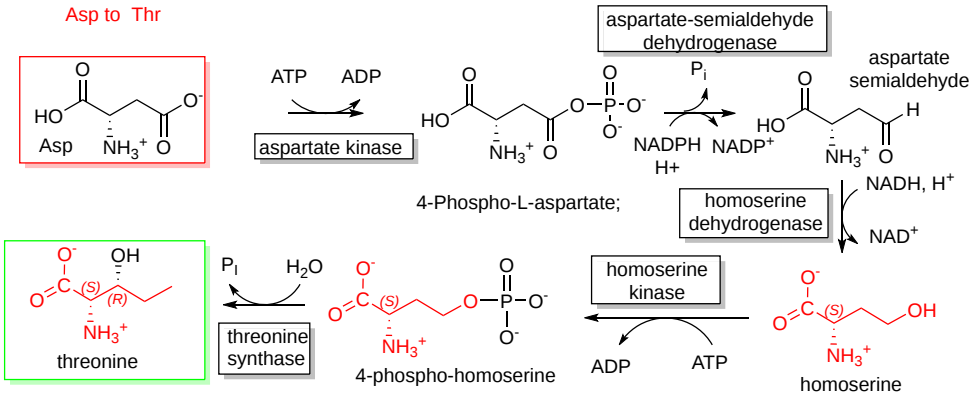


Figure **22.2.11**: The conversion of aspartic acid to threonine

22.2.3.2.5: ASPARTIC ACID TO METHIONINE

The conversion of aspartic acid to methionine is shown in Figure **22.2.12**.

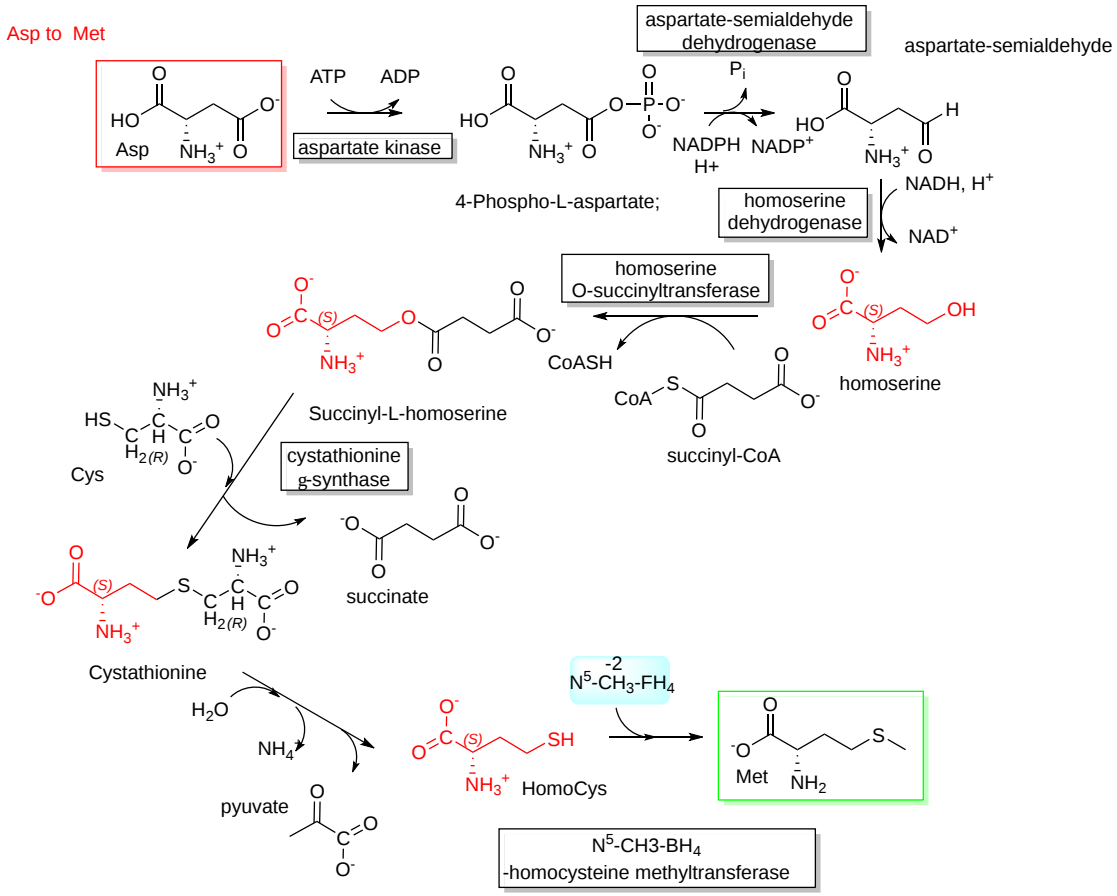
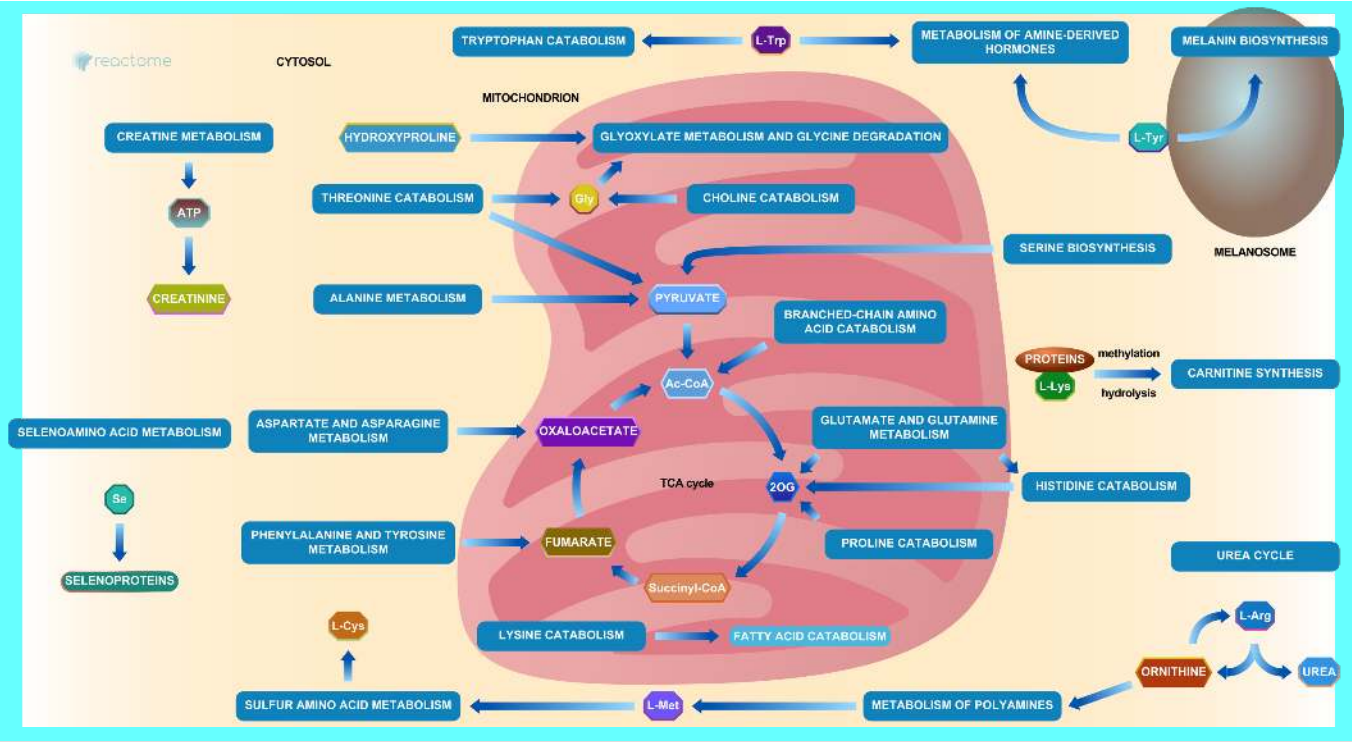


Figure **22.2.12**: The conversion of aspartic acid to methionine

This SUMMARY GRAPHIC From Reactome shows "Cellular metabolism of amino acids and related molecules includes the pathways for the catabolism of amino acids, the biosynthesis of the nonessential amino acids (alanine, arginine, aspartate, asparagine, cysteine, glutamate, glutamine, glycine, proline, and serine) and selenocysteine, the synthesis of urea, and the metabolism of carnitine, creatine, choline, polyamides, melanin, and amine-derived hormones. The metabolism of amino acids provides a balanced supply of amino acids for protein synthesis. In the fasting state, the catabolism of amino acids derived from the breakdown of skeletal muscle protein and other sources is coupled to the processes of gluconeogenesis and ketogenesis to meet the body's energy needs in the absence of dietary energy sources."



Provided by Reactome. Citation Accessed on Wed, May 15, 2024. Fabregat A, Sidiropoulos K, Viteri G, Marin-Garcia P, Ping P, Stein L, D'Eustachio P, Hermjakob H. Reactome diagram viewer: data structures and strategies to boost performance. Bioinformatics (Oxford, England). 2018 Apr;34(7) 1208-1214. doi: 10.1093/bioinformatics/btx752. PubMed PMID: 29186351. PubMed Central PMCID: PMC6030826. Image: https://reactome.org/PathwayBrowser/#/R-HSA-71291&PATH=R-HSA-1430728

22.2.4: SUMMARY

In this chapter, we integrate and summarize the biosynthetic pathways that produce the twenty standard amino acids, emphasizing how central metabolic intermediates from glycolysis and the tricarboxylic acid (TCA) cycle serve as key starting points. The amino acids are grouped into nonessential and essential categories, with the understanding that in humans some “conditionally essential” amino acids (such as arginine, methionine, and tyrosine) require supplementation under certain physiological conditions.

Key Concepts Covered:

- **Central Carbon Metabolism as a Precursor Source:**
  Glycolytic intermediates (e.g., glucose-6-phosphate, 3-phosphoglycerate, and phosphoenolpyruvate) and TCA cycle intermediates (e.g., α-ketoglutarate and oxaloacetate) provide the carbon skeletons for amino acid synthesis. This chapter demonstrates the elegant link between energy metabolism and the generation of biosynthetic precursors.
- **Pathways Originating from Glycolytic Intermediates:**
  - **From Glucose-6-Phosphate:** Histidine is synthesized via a pathway that starts from a phosphorylated ribose derivative.
  - **From 3-Phosphoglycerate:** Serine is produced and further serves as a precursor for glycine and cysteine.
  - **From Phosphoenolpyruvate:** The aromatic amino acids—tryptophan, phenylalanine, and tyrosine—are synthesized via the shikimate pathway up to chorismate, from which distinct branch pathways lead to each aromatic amino acid.
- **Pathways Originating from Pyruvate:**
  Alanine is formed directly from pyruvate by transamination, while the branched-chain amino acids (valine, leucine, and isoleucine) are generated through a series of reactions involving pyruvate condensation and further modifications.
- **TCA Cycle-Derived Pathways:**
  - **From α-Ketoglutarate:** Glutamate is synthesized by transamination and serves as a hub for the formation of glutamine, proline, and arginine. Arginine’s synthesis is closely linked to the urea cycle.
  - **From Oxaloacetate:** Aspartate, produced by transamination, is the precursor for several amino acids including asparagine, threonine, methionine, and lysine. Notably, lysine can be synthesized via the diaminopimelic acid (DAP) pathway in plants and bacteria or via the aminoadipic acid pathway in fungi.

- **Integration into Overall Metabolism:**
  The chapter also highlights that amino acids are not only the building blocks of proteins but are interwoven into energy metabolism. For example, during fasting or stress, when carbohydrates are scarce, amino acids can be catabolized (after removal of their amino groups) to feed into glycolysis or the TCA cycle. This interconversion is critical since, unlike carbohydrates and lipids, proteins cannot be stored in large quantities.
- **Systems-Level Perspective:**
  A summary graphic (provided by Reactome) encapsulates how amino acid metabolism connects with protein synthesis, urea cycle, and various other metabolic pathways, underscoring the central role of amino acids in both anabolic and catabolic processes.

Conclusion:

This chapter provides a cohesive overview of the multiple biosynthetic routes leading to amino acids, emphasizing the central role of glycolytic and TCA cycle intermediates as precursors. Understanding these pathways is crucial not only for grasping the fundamentals of cellular metabolism but also for appreciating how alterations in amino acid biosynthesis can affect overall metabolic homeostasis in both health and disease.

These learning goals and the summary serve to prepare you to:

- **Trace the Carbon Flow:** Map how central metabolic intermediates are diverted into specific amino acid biosynthetic pathways.
- **Differentiate Pathways:** Distinguish between the different precursor sources and understand the unique steps leading to various amino acid classes.
- **Integrate Metabolic Networks:** Appreciate how amino acid synthesis is interconnected with energy metabolism and nitrogen balance, which is essential for overall cellular function.
- **Apply Biochemical Principles:** Utilize principles such as transamination, redox reactions, and metabolic regulation in the context of amino acid biosynthesis.

This page titled 22.2: Biosynthesis of Amino Acids is shared under a not declared license and was authored, remixed, and/or curated by Henry Jakubowski and Patricia Flatt.

- **Current page** by Henry Jakubowski and Patricia Flatt has no license indicated.
- **11.2: Diffusion Across a Membrane - Passive and Facilitated Diffusion** by Henry Jakubowski and Patricia Flatt has no license indicated.
- **22.3: Molecules Derived from Amino Acids** by Henry Jakubowski and Patricia Flatt has no license indicated.

22.3: MOLECULES DERIVED FROM AMINO ACIDS

LEARNING GOALS (CHATGPT O3-MINI)

1. **Describe Diverse Metabolic Fates of Amino Acids:**
   - Explain how amino acids serve as building blocks for proteins and also feed into central metabolic pathways (e.g., TCA cycle and gluconeogenesis) by conversion into intermediates like oxaloacetate, α-ketoglutarate, or acetyl-CoA.
   - Discuss how branched-chain amino acids contribute to both energy production and lipid synthesis.
2. **Integrate Amino Acid Catabolism with Energy Metabolism:**
   - Analyze how amino acid catabolism provides substrates for energy production in different nutritional states (fed, fasting, or in metabolic diseases such as diabetes).
   - Relate the concept of anaplerosis (e.g., through glutamine conversion to α-ketoglutarate) to cancer cell metabolism and the Warburg effect.
3. **Explain Polyamine Biosynthesis and Function:**
   - Outline the pathway for polyamine synthesis from arginine and S-adenosylmethionine (SAM) and identify the main biological polyamines (putrescine, spermidine, spermine, and cadaverine).
   - Discuss the significance of polyamines in regulating nucleic acid structure, gene transcription, and cellular proliferation (including their role in tumor growth).
4. **Describe Glutathione Synthesis and Its Role in Redox Balance:**
   - Summarize the enzymatic steps in the synthesis of glutathione (GSH) from glutamate, cysteine, and glycine.
   - Explain how glutathione, in conjunction with NADPH (derived from pathways like the pentose phosphate pathway and the serine–glycine one-carbon cycle), maintains cellular redox homeostasis and defends against oxidative stress.
5. **Outline the Heme Biosynthetic Pathway:**
   - Describe the key steps in heme biosynthesis, including the rate-limiting reaction catalyzed by 5-aminolevulinic acid synthase (ALA-S) and the subsequent conversion of ALA to protoporphyrin IX, and finally insertion of iron to form heme.
   - Compare the C4 (used by mammals, fungi, and some bacteria) and C5 pathways (used by plants, archaea, and most bacteria) for ALA synthesis.
6. **Understand the Synthesis of Amino Acid-Derived Neurotransmitters:**
   - Identify which amino acids serve as neurotransmitters (e.g., glutamate, aspartate, glycine) and those that are precursors to amine neurotransmitters (e.g., tyrosine to catecholamines, tryptophan to serotonin).
   - Explain how compartmentalization of amino acids in neurons supports both their metabolic functions and their role in synaptic transmission.
7. **Explain Regulation and Mechanism of Catecholamine Synthesis:**
   - Describe the conversion of tyrosine to dihydroxyphenylalanine (DOPA) by tyrosine hydroxylase and outline subsequent steps leading to dopamine, norepinephrine, and epinephrine synthesis.
   - Discuss the feedback inhibition of tyrosine hydroxylase by dopamine and the regulatory role of serine 40 phosphorylation in modulating its activity.
8. **Integrate Amino Acid Metabolism with Broader Cellular Processes:**
   - Explain how the breakdown and conversion of amino acids not only provide energy but also supply precursors for the biosynthesis of nucleotides (to be discussed in a later chapter) and other critical metabolites such as polyamines, heme, and neurotransmitters.
   - Evaluate the importance of balancing amino acid utilization for energy versus biosynthesis in both normal physiology and in pathological conditions like cancer.

These learning goals are intended to help students build a systems-level understanding of how amino acids are not only the building blocks of proteins but also pivotal molecules that integrate and regulate energy metabolism, redox balance, and cell signaling.

22.3.1: INTRODUCTION

Once made or ingested, amino acids have many metabolic fates. Of course, they are used for the synthesis of proteins. Aspartate and glutamate (and indirectly glutamine) can be converted to oxaloacetate and α-ketoglutarate, respectively, and used in the citric acid cycle for energy production. They can also be used for gluconeogenesis, utilizing both mitochondrial and cytoplasmic enzymes. Branched-chain amino acids can be converted to acetyl-CoA and used in energy production or fat synthesis. A review summary of the use of amino acids in energy and biosynthetic metabolic pathways is shown in Figure **22.3.1**.

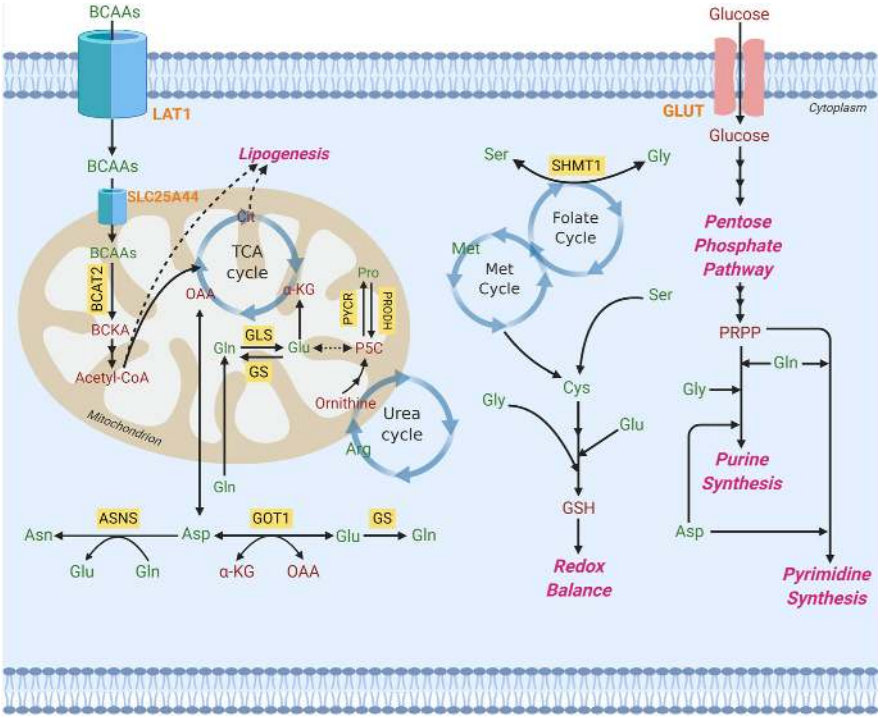


Figure **22.3.1**: Review summary of the use of amino acid in energy and biosynthetic metabolic pathways. Lieu, E.L., Nguyen, T., Rhyne, S., *et al*. Amino acids in cancer. *Exp Mol Med* **52,** 15–30 (2020). https://doi.org/10.1038/s12276-020-0375-3. Creative Commons Attribution 4.0 International License, http://creativecommons.org/licenses/by/4.0/.

Amino acids are shown in green, and other metabolites are in red. Orange represents transporters. Yellow boxes signify enzymes. Lesser known abbreviations for species include SHMT1 serine hydroxymethyltransferase, cytosolic, BCAT branched-chain amino acid transaminase, mitochondrial, BCAA branched-chain amino acid (valine, leucine, isoleucine), BCKA branched-chain ketoacid, GOT1 aspartate transaminase, cytosolic (AST), GLS glutaminase, GS glutamine synthetase (cytosolic and mitochondrial), ASNS asparagine synthetase, PRODH pyrroline-5-carboxylate dehydrogenase, PYCR pyrroline-5-carboxylate reductase, P5C pyrroline-5-carboxylate, GSH glutathione, PRPP phosphoribosyl pyrophosphate, LAT1 large-neutral amino acid transporter 1, SLC25A44 solute carrier family 25 member 44, GLUT glucose transporter,

Cancer cells have an increased need for fuels and biosynthetic intermediates. Both can be derived from amino acids, as described previously. Glutamine is a key amino acid, especially when glucose is depleted, as it is converted into α-ketoglutarate (α-KG) and subsequently into oxaloacetate (OAA), which powers the TCA cycle by increasing the levels of fumarate, malate, and citrate. Hence, it is both anaplerotic and a source of fuel.

Similar increases in citrate occur in hypoxia. Aerobic glycolysis, also known as the Warburg effect, occurs in cancer cells, which exhibit enhanced glucose uptake and conversion to lactate even in the presence of oxygen. This process can occur so rapidly that the amount of ATP produced in cancer cells through aerobic glycolysis can be comparable to that produced through oxidative metabolism in the mitochondria, despite being far less efficient. More information on cancer cell metabolism is found in Chapter 23.

In this chapter, we will discuss the conversion of amino acids to other molecules that are not directly involved in these metabolic pathways. We will focus on their use for the synthesis of polyamines, heme, and neurotransmitters. We will not discuss the detailed mechanisms or structures of the proteins and enzymes involved in these pathways. In the next chapter section (22.4), we will present amino acids as substrates in synthesizing pyrimidine and purine bases, which are essential for nucleotides and nucleic acids.

22.3.2: POLYAMINE SYNTHESIS

If a non-quaternary amine has a single positive charge when protonated, a polyamine can have multiple positive charges. Hence, they would be expected to bind to almost any negatively charged biomolecule, especially those with multiple negative charges. These include polyanions such as RNA and DNA, as well as proteins and lipid bilayers. They would then be able to regulate many features of cell life, including DNA replication and transcription, RNA translation, and a multitude of binding interactions. The question arises of whether these interactions are nonspecific or specific, and in which case they can be considered key regulators of cellular activity. Polyamine response elements have been found that regulate the transcription of genes, including c-Myc and c-Jun. Polyamines have been shown to affect tumor growth and aggressiveness.

The primary biological polyamines include putrescine, spermine, and spermidine. Another is cadaverine. Given their names, you can surmise that they smell horrible. The synthesis of three polyamines from arginine and SAM is shown in Figure **22.3.2**.

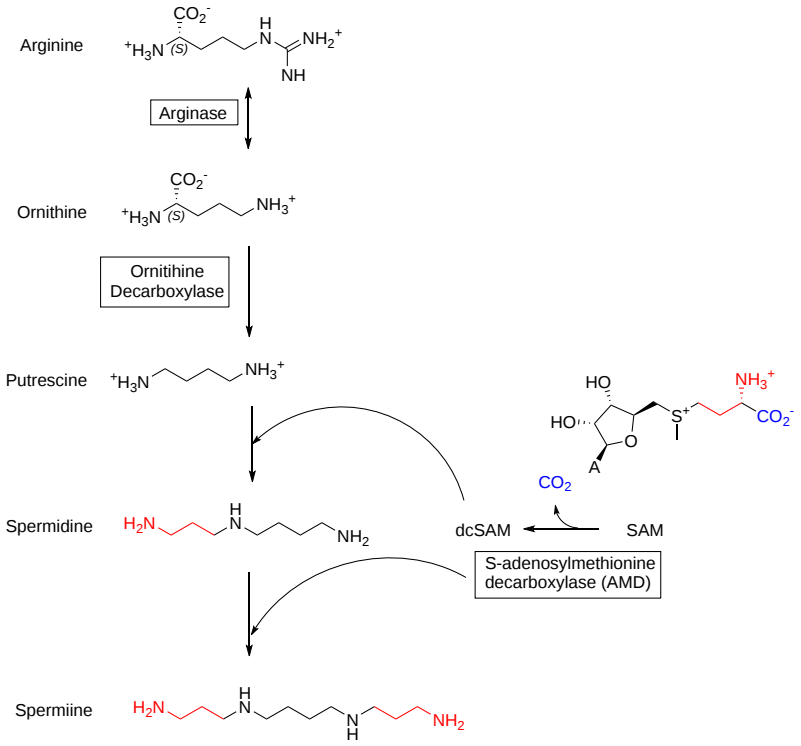


Figure **22.3.2**: Polyamine synthesis form arginine and SAM

22.3.3: GLUTATHIONE SYNTHESIS AND REDOX BALANCE

Glutathione, γ-glutamylcysteinylglycine (GSH), is a chief regulator of the oxidation state of a cell. As a disulfide bond can be cleaved and hence reduced by the excess concentration of a thiol (sulfhydryl) like β-mercaptoethanol (which gets oxidized in the process), the free thiol on glutathione can act as a reducing agent in the cell. Reactive oxygen species (ROS) production in normal cells, but especially in tumor cells, which have increased oxygen demand and utilization, is countered by generating an antioxidant defense state. This is partially characterized by increased levels of reductants such as NADPH, especially glutathione. It can react with H_2O_2 through the enzyme GSH peroxidase to form water and the oxidized disulfide form of GSH, GSSG. The GSSG is reduced back to GSH by glutathione reductase (GR) and NADPH. Figure **22.3.3** shows glutathione synthesis from glutamate, cysteine, and glycine.

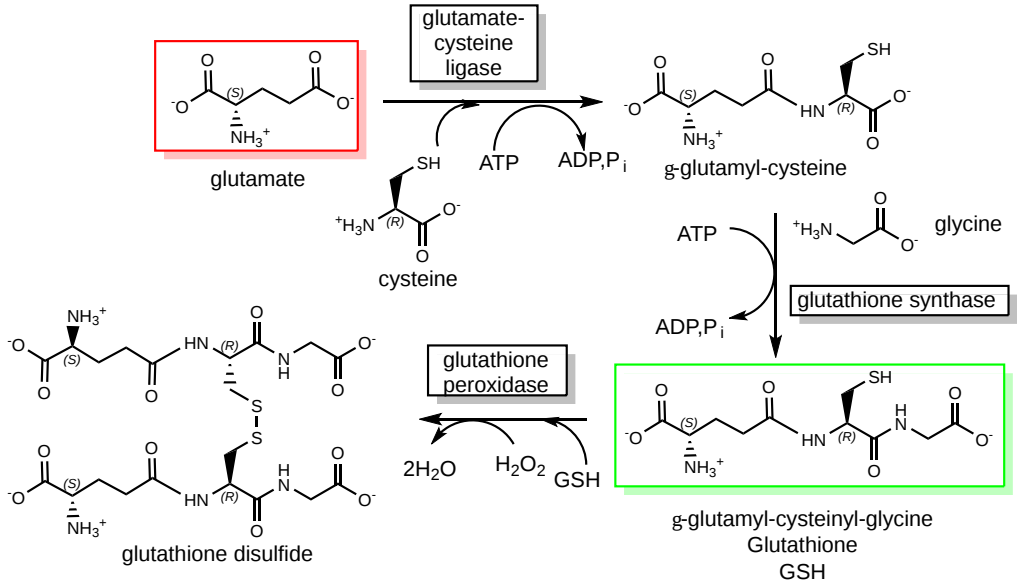


Figure **22.3.3**: Synthesis of glutathione

NADPH is generated in the cell by the phosphopentose pathway metabolism of glucose and malic enzyme. It can also be generated from the Ser-Glycine One Carbon Cycle (SGOT), which we saw in Chapter 18.4 and is shown again in Figure **22.3.4**. Under appropriate conditions, this cycle can produce NADPH.

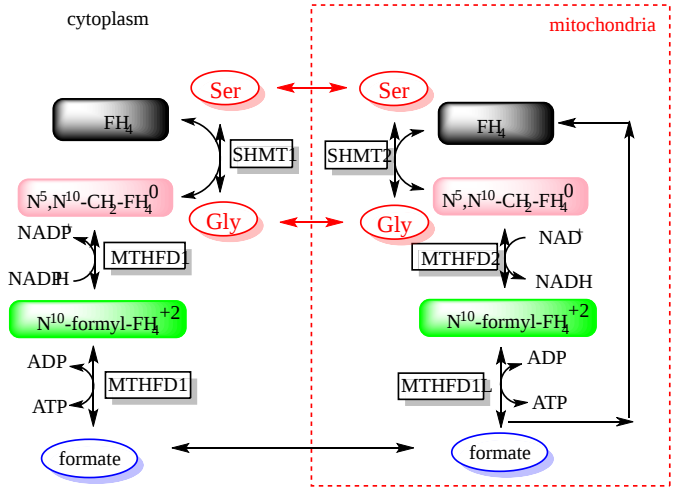


Figure **22.3.4**: The Ser-Gly One Carbon (SGOC) Cycle

HIF1α upregulates Serinehydroxymethyltransferase (SHMT) 2 and helps maintain the NADPH/$NADP^+$ ratio. Given the connection between the SGOC and the methionine cycle through folate, a decrease in serine concentration leads to a decrease in GSH.

22.3.4: HEME BIOSYNTHESIS

This section is derived from Aminat S. Ogun; Neena V. Joy; Menogh Valentine. https://www.ncbi.nlm.nih.gov/books/NBK537329/. Creative Commons Attribution 4.0 International License (http://creativecommons.org/licenses/by/4.0/)

Heme is a macrocyclic tetrapyrrole ring structure containing two nonpolar vinyl groups on one edge and two charged propionates on the other. It is extensively conjugated with 26 π electrons (4n+2 = 4(6)+2), so it is aromatic. The molecule without Fe^{2+} is called protoporphyrin IX. With a centrally coordinated Fe^{2+}, it is called heme. Both structures are shown in Figure **22.3.5**.

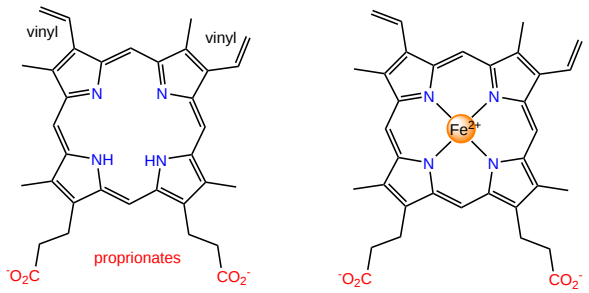


Figure **22.3.5**: Structure of protoporphyrin IX and heme

It is found in oxygen-binding proteins and as substrates and cofactors for enzymes involved in electron transport. It is synthesized in the bone marrow and liver. Alternative forms of heme include heme b (in hemoglobin), heme a (cytochrome a), and heme c (cytochrome c).

Its synthesis, as expected given its macrocyclic structure, is complicated. The key enzyme in the pathway for regulation is 5'-Aminolevulinic acid synthase (ALA-S). Liver and bone express ALAS2, while ALAS1 is expressed in all tissues. The synthesis process begins in the mitochondria and concludes in the cytosol. Figure **22.3.6** shows the overall pathway for heme synthesis.

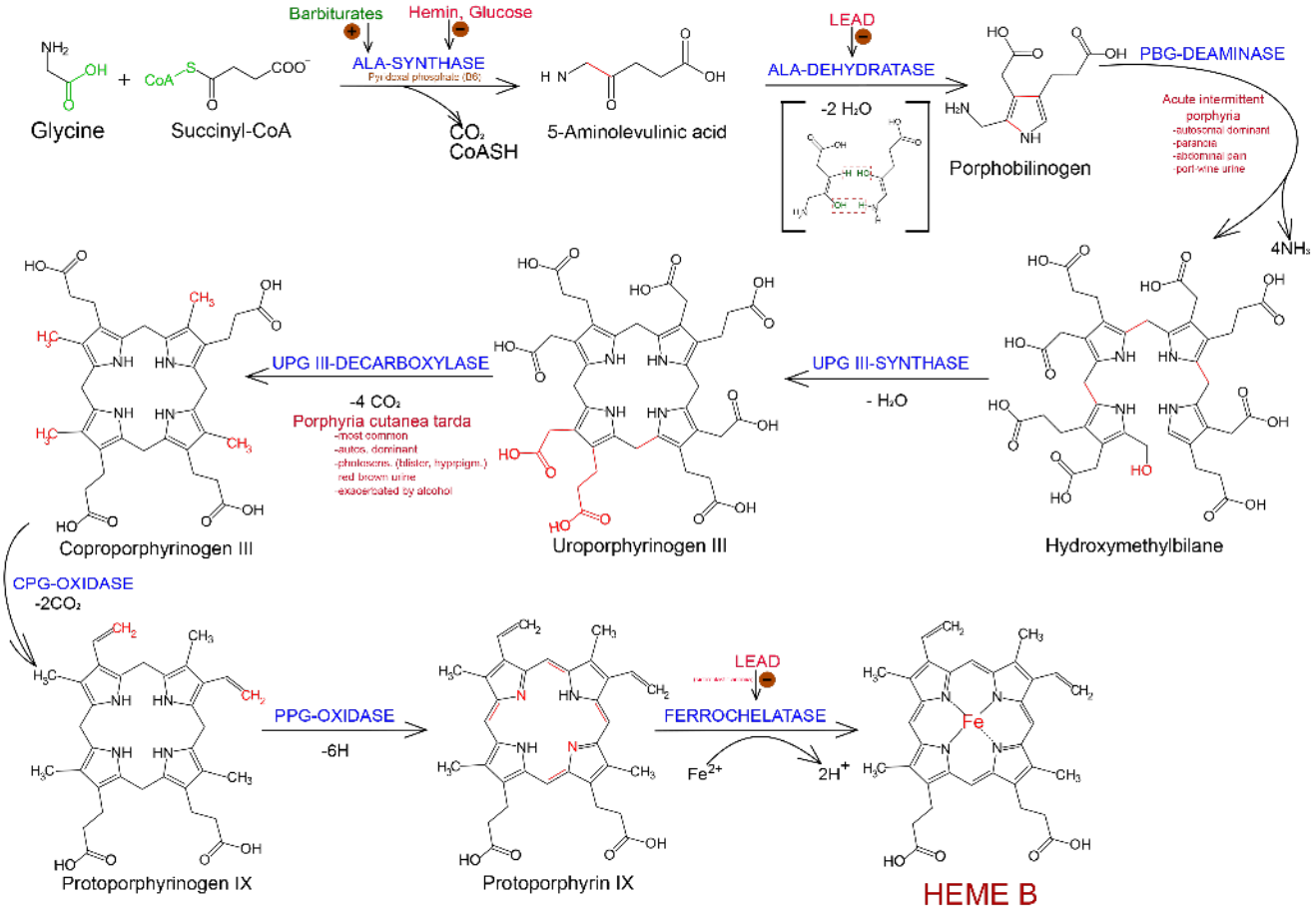


Figure **22.3.6**: Heme biosynthetic pathway. Wikimedia Commons file: Heme-Synthesis-Chemical-Details-Mirror.svg

5'-Aminolevulinic acid synthase (ALA-S), a pyridoxal phosphate-dependent enzyme, catalyzes the rate-limiting step in heme synthesis in the liver and erythroid cells. It is highly regulated. There are two forms of ALA Synthase, ALAS1 and ALAS2. All cells express ALAS1, while only the liver and bone marrow express ALAS2. The gene for ALAS2 is on the X chromosome. After the synthesis of ALA in the mitochondria, it moves into the cytoplasm for the remaining steps.

Figure **22.3.7** shows a likely mechanism for the first committed step, the production of ALA. This enzyme synthesizes all tetrapyrroles, including heme, chlorophyll, and cobalamin.

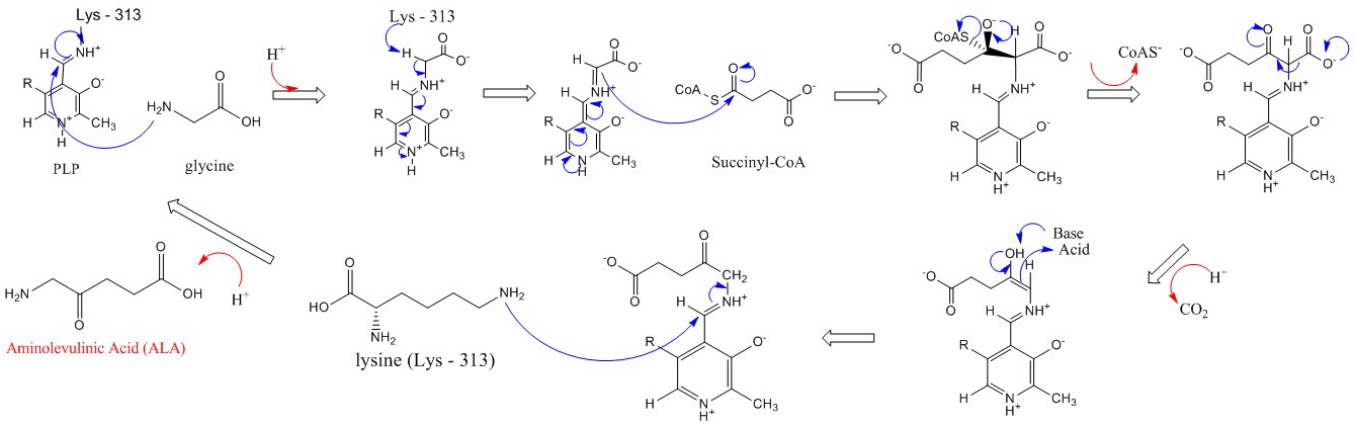


Figure **22.3.7**: Mechanism for 5'-Aminolevulinic acid synthesis by ALAS (Wikipedia. https://en.Wikipedia.org/wiki/Aminol..._acid_synthase)

The pathway shown in Figure 6 above is known as the C4 pathway and is found in mammals, fungi, and certain types of bacteria, including purple nonsulfur bacteria. A C5 pathway is found in most bacteria, all archaea, and plants. The biosynthetic pathway for heme synthesis in E. Coli is shown in Figure **22.3.8**.

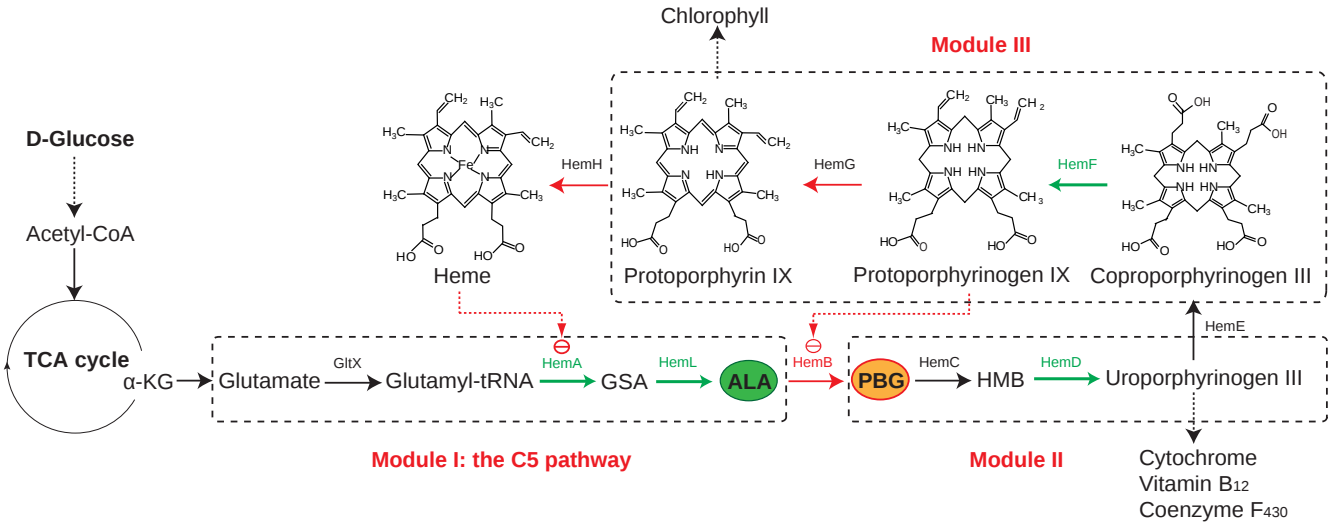


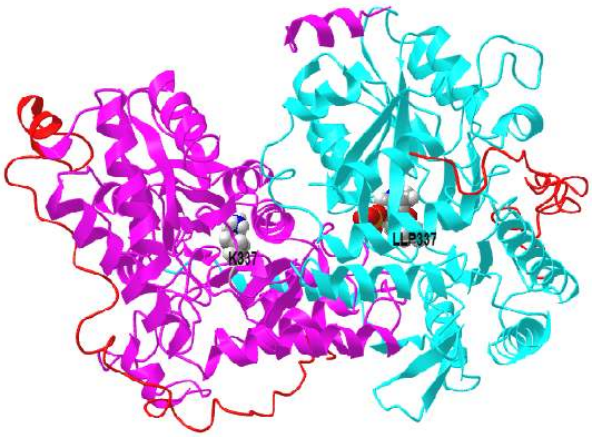
Figure **22.3.8**: Heme pathway in *E. coli*. Zhang, J., Kang, Z., Chen, J. *et al.* Optimization of the heme biosynthesis pathway for the production of 5-aminolevulinic acid in *Escherichia coli*. *Sci Rep* **5,** 8584 (2015). https://doi.org/10.1038/srep08584. Creative Commons Attribution 4.0 International License. http://creativecommons.org/licenses/by/4.0/

The pathway is divided into three modules: Module I, Module II, and Module III, as shown in the dotted box. The green and red arrows represent the positive and negative enzymes for ALA accumulation, respectively. Dotted red arrows represent the feedback inhibition. α-KG: α-ketoglutarate, GSA: glutamate-1-semialdehyde, ALA: 5-aminolevulinic acid, PBG: porphobilinogen, HMB: hydroxymethylbilane, GltX: glutamyl-tRNA synthetase, HemA: glutamyl-tRNA reductase, HemL: glutamate-1-semialdehyde aminotransferase, HemB: 5-aminolevulinic acid dehydratase, HemC: porphobilinogen deaminase, HemD: uroporphyrinogen III synthase, HemE: uroporphyrinogen decarboxylase, HemF: coproporphyrinogen III oxidase, HemG: protoporphyrin oxidase, HemH: ferrochelatase.

Heme increases globin protein synthesis in immature red blood cells (reticulocytes). The hormone erythropoietin increases heme synthesis. In the liver, heme is part of cytochrome P450s. An increased concentration of drugs causes an increase in ALAS1, which in turn produces the cytochrome P450s to metabolize them. Also, low heme concentration increases ALAS1 transcription. Mutations in ALAS2 can lead to X-linked sideroblastic anemia from decreased heme production, even as Fe^{2+} continues to enter the cell.

Yeast ALAS is a homodimer with PLP covalently attached through a Schiff base link to lysine 337 of just one of the monomers. The structures of a noncovalent complex of PLP with ALAS (pdb 5TXR) and the covalently bound one (5TXT) show large changes in the protein conformation. PLP, when covalently attached, reorders the active. A C-terminal extension not found in bacteria wraps around the dimer, binds near the active site, and is important for activity. Mutations in the tail can result in human diseases.

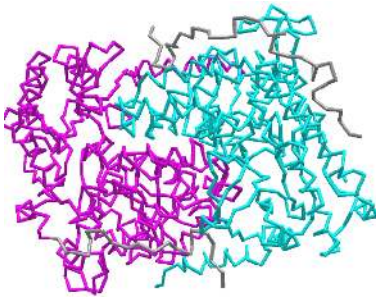
Figure **22.3.9** shows an interactive iCn3D model of the 5-aminolevulinic acid synthase with covalently attached PLP (5TXT).



NCBI iCn3D Figure **22.3.9**: 5-aminolevulinic acid synthase with covalently attached PLP (5TXT). (Copyright; author via source). Click the image for a popup or use this external link: https://structure.ncbi.nlm.nih.gov/icn3d/share.html?fTBbWuS3HPTP8uRm9

Lysine 337 (spacefill, CPK colors, labeled) is shown in the A chain (magenta, no bound PLP). Lys 337 in the B chain (cyan) is covalently linked to PLP. The side chain of lysine 337 covalently attached to PLP is shown in spacefill, CPK colors, and labeled. The C-terminal extension (493–548) is a red backbone chain. The very distal end of the extension is disordered and missing in the B chain (cyan).

Figure **22.3.10** shows an interactive iCn3D model of aligned 5-aminolevulinic acid synthase with free PLP (not covalently attached, 5TXR) and with covalently attached PLP (5TXT).



NCBI iCn3D Figure **22.3.11**: Alignment of 5-aminolevulinic acid synthase with free PLP (5TXR) and with covalently attached PLP (5TXT). (Copyright; author via source). Click the image for a popup or use this external link: https://structure.ncbi.nlm.nih.gov/i...aqN4Qpi2pSLkD7

The 5TXT structure contains two molecules of a stabilizing molecule, shown in stick form, which can be ignored. The A chain is magenta, and the B chain is cyan. Press "a" to toggle back and forth between the structures. The C-terminal extension is missing from the figure.

Figure **22.3.11** shows another view of heme synthesis, highlighting the roles of mitochondrial and cytoplasmic enzymes.

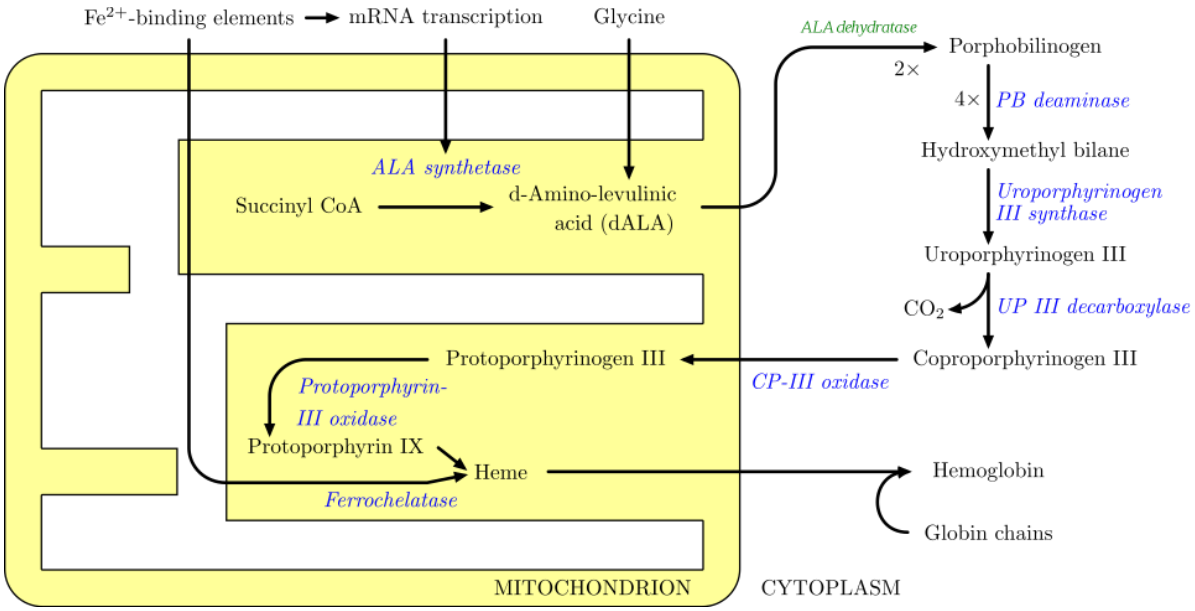


Figure **22.3.11**: Mitochondrial and cytosolic contributions to heme synthesis. https://commons.wikimedia.org/wiki/F..._synthesis.png

22.3.5: NEUROTRANSMITTERS

The section below is modified from Manorama Patri. **Synaptic Transmission and Amino Acid Neurotransmitters.** DOI: 10.5772/intechopen.82121. https://www.intechopen.com/books/neu...rotransmitters. Creative Commons Attribution 3.0 License,

Three major categories of amino acids and their derivatives act as neurotransmitters:

1. Amino acids: The neurotransmitters of this group are involved in fast synaptic transmission and are inhibitory and excitatory in action (primarily glutamic acid, GABA, aspartic acid, and glycine).
2. Amines: Amines are modified amino acids such as biogenic amines, e.g., catecholamines. The neurotransmitters of this group are involved in slow synaptic transmission and exhibit both inhibitory and excitatory actions (noradrenaline, adrenaline, dopamine, serotonin, and histamine).
3. Others: The ones that do not fit in any of these categories (acetylcholine and nitric oxide). Amino acids are among the most abundant of all neurotransmitters present within the central nervous system (CNS).

Amino acid transmitters provide the majority of excitatory and inhibitory neurotransmission in the nervous system. Amino acids used for synaptic transmission are compartmentalized (e.g., glutamate, compartmentalized from metabolic glutamate used for protein synthesis by packaging the transmitter into synaptic vesicles for subsequent Ca^{2+}-dependent release). Amino acid neurotransmitters are all products of intermediary metabolism except GABA. Unlike all the other amino acid neurotransmitters, GABA is not used in protein synthesis and is produced by an enzyme (glutamic acid decarboxylase; GAD) uniquely located in neurons.

Here is some more specific information:

- Glutamate: Glutamate is used at most fast excitatory synapses in the brain and spinal cord. Glutamate binds to glutamate receptors, of which there are many subtypes based on other molecules (some amino acid derivatives) that can bind to them. These other molecules include N-methyl-D-aspartate (NMDA), α-amino-3-hydroxy-5-methyl-4-isoxazolepropionate (AMPA), kainate, and quisqualate.
- Aspartate: Aspartate is the most abundant excitatory neurotransmitter in the CNS. Like glycine, aspartate is primarily localized to the ventral spinal cord. Note that the two major excitatory neurotransmitters both have carboxylic acid side chains.
- Gamma-aminobutyric acid (GABA): GABA, which is not one of the canonical amino acids used in protein biosynthesis, is the most ubiquitous inhibitory neurotransmitter in the brain.
- Glycine: these receptors are ligand-gated ion channels that increase Cl^- influx and hence are generally inhibitory. Hydroxymethyl transferase converts the amino acid serine to glycine. Glycine has been found to play a role in the functional modulation of NMDA receptors.

The pathways for synthesizing amino acid-derived bioactive amines and neurotransmitters are shown in Figure **22.3.12**.

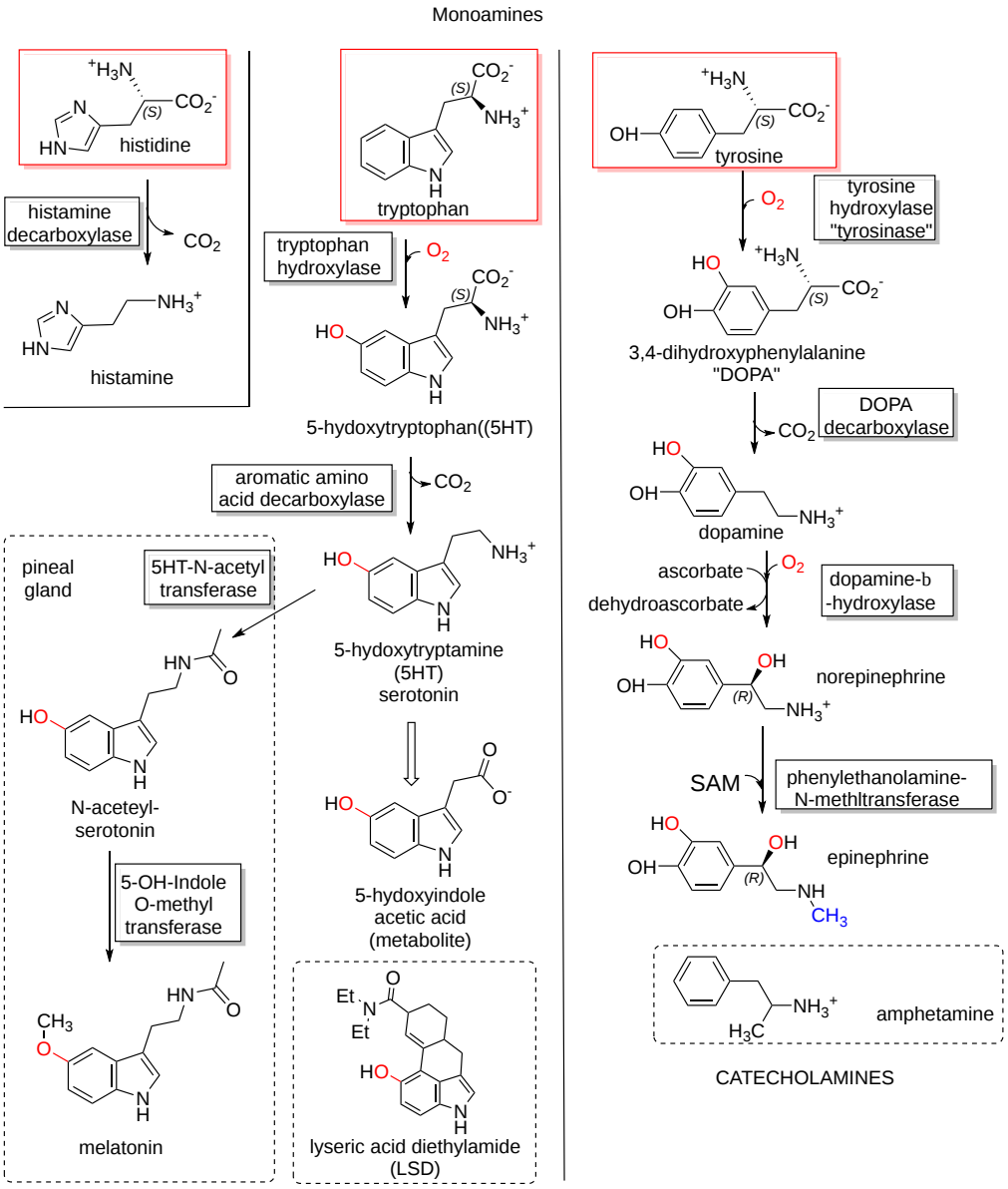


Figure **22.3.12**: Pathways for the synthesis of amino acid-derived bioactive amines and neurotransmitters

Note the structural similarity of the psychotropic and hallucinogenic drug LSD to serotonin (5HT), amphetamines to norepinephrine and epinephrine, and melatonin (a substance some take as a sleeping aid and which is formed in the dark at night in the brain. The name **catecholamines** derives from the common name of the 1,2-dihydroxybenzene group (catechol).

Tyrosine hydroxylase (TH) catalyzes the first and rate-limiting step in catecholamine synthesis. Al**though** it lacks heme, it contains Fe2+ and tetrahydrobiopterin as cofactors used in the synthesis of dihydroxyphenylalanine (DOPA). Tyrosine hydroxylase is also the rate-limiting enzyme for the synthesis of all three neurotransmitters.

Catecholamines, including dopamine, a downstream product, inhibit the enzyme, which is activated by phosphorylation on serine 40. The structures of TH in the absence of dopamine and the pSer40 state are known. The protein is a tetramer, consisting of a regulatory domain (a dimer) and a catalytic domain (also a dimer), separated by 15 Å.

The mammalian TH is a member of the aromatic amino acid hydroxylases (AAAHs), mainly found as homotetramers. Each subunit has three domains:

- The N-terminal **regulatory domain (RD)** consists of an unstructured, variable-length section followed by an ACT (aspartate kinase-chorismate mutase-TyrA) domain. The N-terminal tail contains serine 40, which, on phosphorylation, relieves the inhibition when dopamine is bound to the catalytic domain.
- a central **catalytic domain (CD)** that binds Fe^{2+}, aromatic amino acid substrates, and the tetrahydrobiopterin cofactor

- C-terminal oligomerization domain (OD) leads to the formation of dimers and tetramers.

Figure **22.3.13** illustrates a potential model that depicts dopamine (DA)-mediated feedback inhibition and its regulation by serine 40 phosphorylation, resulting from the interaction between the N-terminal tail of the regulatory domain (RD) and the catalytic domain. All forms containing bound dopamine (yellow star) are inactive.

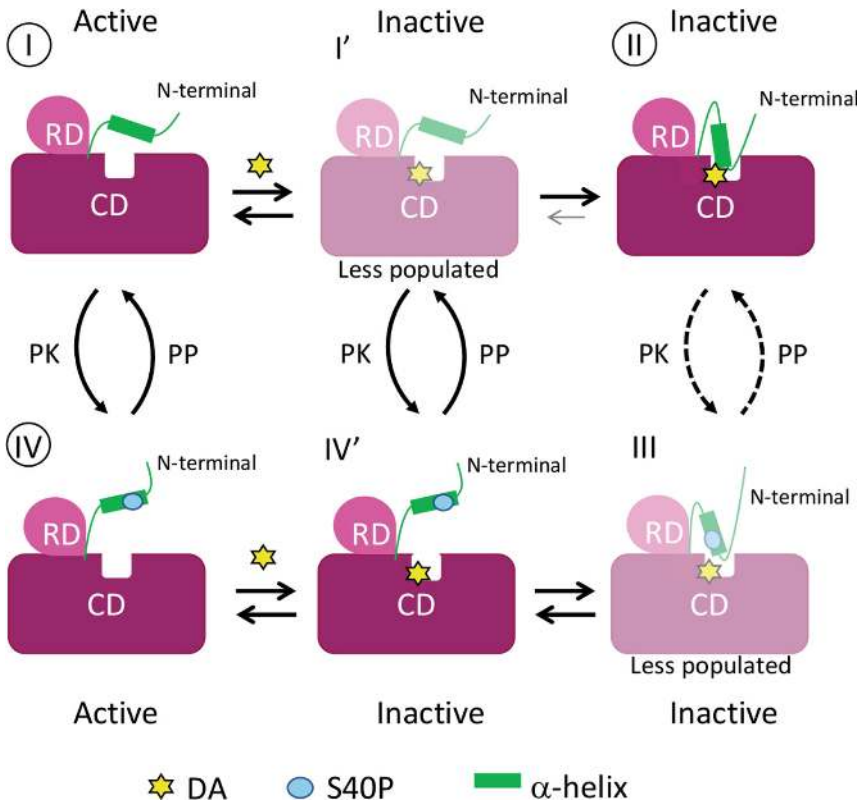


Figure **22.3.13**: Cartoon model of DA-mediated feedback inhibition and its regulation by S40 phosphorylation. Bueno-Carrasco, M.T., Cuéllar, J., Flydal, M.I. *et al.* Structural mechanism for tyrosine hydroxylase inhibition by dopamine and reactivation by Ser40 phosphorylation. *Nat Commun* **13,** 74 (2022). https://doi.org/10.1038/s41467-021-27657-y. Creative Commons Attribution 4.0 International License. http://creativecommons.org/licenses/by/4.0/.

In the active, apo, and non-phospho states, the 39−58 α-helix of the N-terminal regulatory domain of TH is detached from the main structure (I, apo-TH). The feedback inhibitor DA binds to the TH active site, most likely in the open conformation (I′, TH(DA)). DA-binding favors the interaction of the N-terminal α-helix with the same binding site, which blocks DA exit and contributes to the high-affinity binding and strong inhibition of TH activity (II, TH(DA)). Protein Kinase (PK) phosphorylation of S40 in TH(DA), leads to state III (THS40p(DA)), prompting the detachment of the α-helix from the TH active site (IV′), which opens up for DA-dissociation and activation (IV, THS40p). PKs and protein phosphatases (PPs) control the transition between THS40p and unphosphorylated TH for both DA-bound (I′ ↔ IV′ and II ↔ III) and apo-TH (I ↔ IV). States I′ and III are expected to be only transiently populated during DA binding, as states II and IV will be more stable. Hence, states I′ and III are faded. S40 is also expected to be less accessible in state II than in state I, as indicated by the stippled lines for phosphorylation of TH in state II. The case for dephosphorylation is unknown, but it could be expected that state III is a poorer substrate for PP than the open states IV′ and IV. The dephosphorylation reaction III → II is therefore also stippled. The states where we provide structural details in this work (I, II, and IV) are marked with circles.

Figure **22.3.14** shows a model of the TH active site changes on phosphorylation of serine 40 using structural and molecular dynamics approaches that led to the cartoon model above.

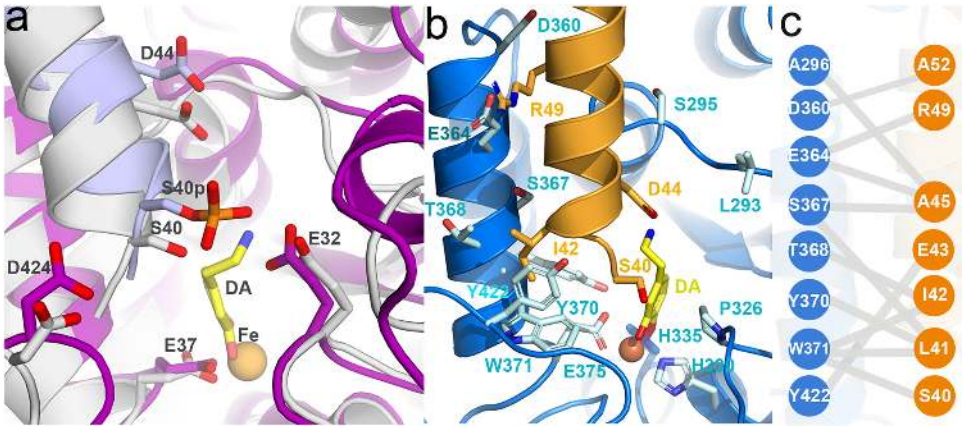


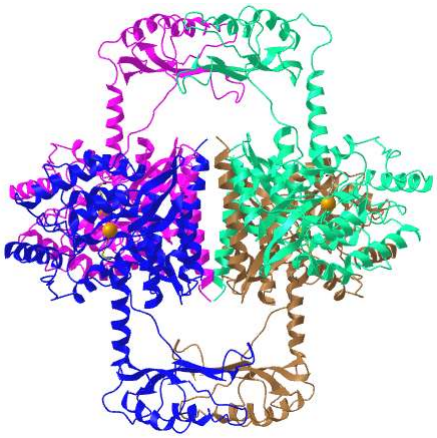
Figure **22.3.14**: **Modeling of the TH active site.**

Panel (a) shows models demonstrating the effect of serine 40 phosphorylation on the interaction of the N-terminal α-helix with bound dopamine (DA). Representative conformations from the last 50 ns of a 500 ns MD simulation for TH(DA) (grey ribbon) and pS40-TH(DA) (light blue ribbon) are shown. The resulting structures show a slight shift of the N-terminal α-helix upon phosphorylation, most probably due to electrostatic repulsion between the phosphate and E325, E375, and D424.

Panel (b) shows a detailed view of the atomic model of the TH(DA) active site. (left) The N-terminal α-helix (orange) establishes connections with the adjacent helix D360-E375 and with residues of the 290–297 and 420–429 loops (blue, right).

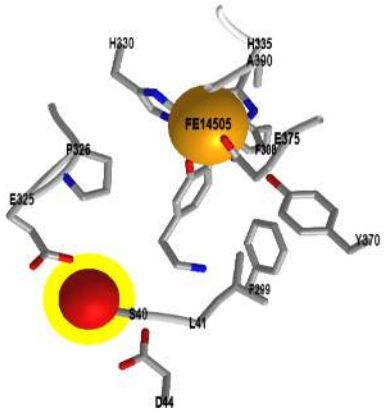
Pane (c) shows a cartoon depicting the interactions between N-terminal α-helix residues that enter the active site and residues of adjacent regions.

Figure \(\PageIndex{15\) below shows an interactive iCn3D model of the full-length tyrosine hydroxylase in complex with dopamine (residues 40-497) in which the regulatory domain (residues 40-165) has been included only with the backbone atoms (6zvp)



NCBI iCn3D Figure **22.3.15**: Tyrosine hydroxylase dopamine complex (6zvp). (Copyright; author via source). Click the image for a popup or use this external link: https://structure.ncbi.nlm.nih.gov/i...hu6vJn22eDkWw7

Finally, Figure **22.3.16** shows an interactive iCn3D model of the active site of tyrosine hydroxylase in complex with dopamine (6zvp)



NCBI iCn3D Figure **22.3.16**: Active site of tyrosine hydroxylase dopamine complex (6zvp). (Copyright; author via source). Click the image for a popup or use this external link: https://structure.ncbi.nlm.nih.gov/icn3d/share.html?sx5obQnzojmKXuLS9

The side chains binding the active site Fe^{2+} and the interaction of Fe^{2+} with dopamine (LDP) are shown in sticks and labeled. The oxygen of serine 40 is shown as a red sphere. Dopamine is the molecule containing 1,2-dihydroxybenzene.

Figure **22.3.17** shows a final summary presentation of the conversion of phenylalanine, tyrosine, and tryptophan to neurotransmitters.

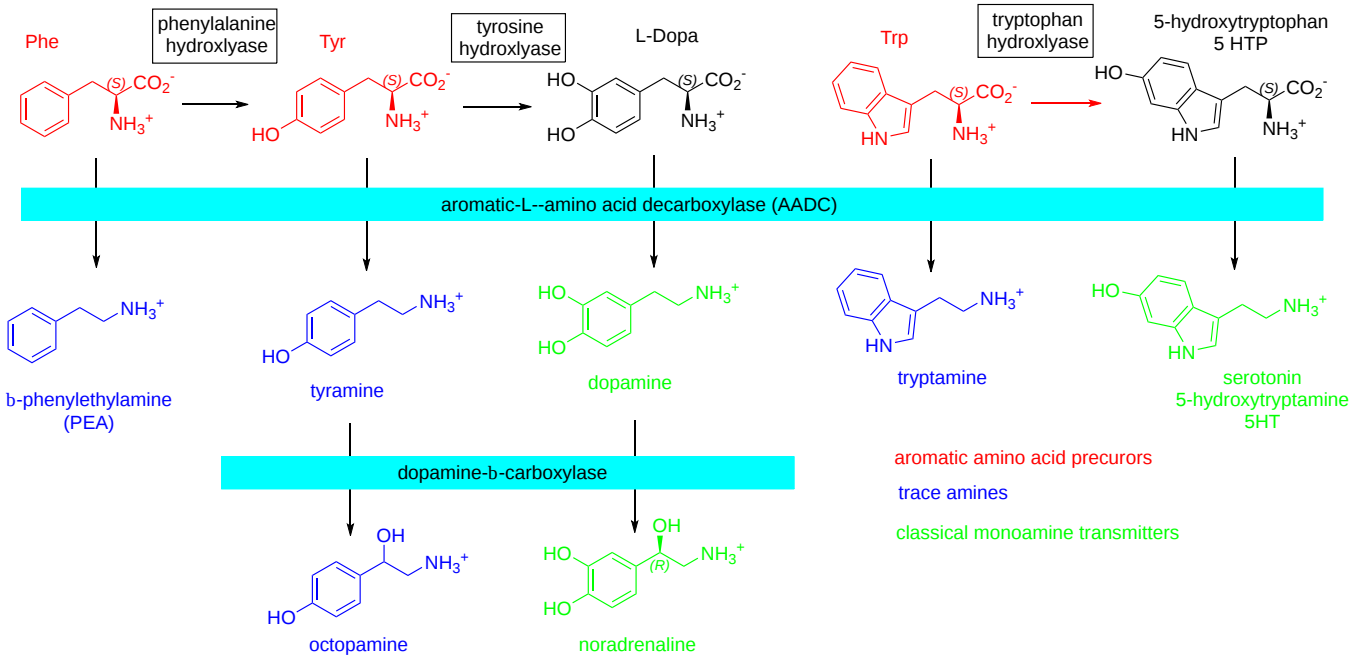


Figure **22.3.17**: Comparison of monoamine synthesis pathways. Adapted from Hochman, Shawn. (2015). Neural Regeneration Research. 10. 10.4103/1673-5374.169625. Creative Commons Attribution-NonCommercial-ShareAlike 4.0 International

22.3.6: SUMMARY

Amino acids, while famously known as the building blocks of proteins, play several pivotal roles in cellular metabolism. This chapter broadens the perspective by highlighting how amino acids serve as substrates for energy production, biosynthesis of vital small molecules, and regulation of cellular processes.

Energy Metabolism and Anaplerosis:

Amino acids can be converted into key intermediates of central metabolic pathways. For example, aspartate and glutamate (via glutamine) are transformed into oxaloacetate and α-ketoglutarate, respectively, which enter the tricarboxylic acid (TCA) cycle. Branched-chain amino acids (valine, leucine, and isoleucine) are metabolized to acetyl-CoA, thereby contributing to both energy production and lipid biosynthesis. The chapter also discusses how under different nutritional states—such as the fed state, fasting, or in metabolic diseases like diabetes—amino acids serve as critical fuel sources when carbohydrates and lipids are less available or in excess.

Biosynthesis of Specialized Metabolites:

Beyond energy, amino acids are precursors for several key biomolecules:

- **Polyamines:** Derived from arginine and S-adenosylmethionine (SAM), polyamines such as putrescine, spermidine, and spermine play crucial roles in stabilizing nucleic acids, regulating gene expression, and modulating cell proliferation. These polycations interact with negatively charged molecules (e.g., DNA, RNA) and are linked to the control of cell growth, with implications in cancer biology.
- **Glutathione and Redox Homeostasis:** The tripeptide glutathione (γ-glutamylcysteinylglycine) is synthesized from glutamate, cysteine, and glycine. It is a central antioxidant that maintains the cellular redox state by neutralizing reactive oxygen species (ROS). Glutathione functions in concert with NADPH, which is generated via the pentose phosphate pathway and the serine–glycine one-carbon cycle, to protect cells from oxidative stress.
- **Heme Biosynthesis:** Heme is a tetrapyrrole cofactor essential for oxygen transport and electron transfer. Its biosynthesis begins with the formation of 5-aminolevulinic acid (ALA) by ALA synthase—a rate-limiting, pyridoxal phosphate-dependent reaction in the mitochondria—and proceeds through both mitochondrial and cytosolic steps to yield protoporphyrin IX. Subsequent insertion of iron produces heme, with specific pathways differing between the C4 (mammals and fungi) and C5 (plants, archaea, most bacteria) routes for ALA synthesis.

Amino Acids as Neurotransmitter Precursors:

The chapter also covers how amino acids contribute to the nervous system:

- **Direct Neurotransmission:** Amino acids like glutamate, aspartate, glycine, and GABA serve directly as neurotransmitters in the central nervous system, mediating fast synaptic transmission.
- **Precursor Roles:** Other amino acids, particularly tyrosine and tryptophan, are precursors to biogenic amines (e.g., dopamine, norepinephrine, serotonin). The synthesis of catecholamines begins with tyrosine hydroxylase, a key regulatory enzyme whose activity is finely tuned by feedback inhibition (via dopamine) and by phosphorylation (notably at serine 40).

Integration and Regulation:

This chapter emphasizes that the fates of amino acids are tightly interconnected with broader metabolic networks. The balance between their use in energy production versus biosynthesis of compounds like polyamines, glutathione, heme, and neurotransmitters is critical for maintaining cellular homeostasis. The dynamic regulation of these pathways is essential not only under normal physiological conditions but also in disease states, such as cancer, where metabolic reprogramming occurs.

In summary, this chapter provides an integrated view of how amino acids are metabolically versatile, serving as both fundamental components for building macromolecules and as substrates for key biosynthetic and energy-producing pathways that underpin vital cellular functions.

This page titled 22.3: Molecules Derived from Amino Acids is shared under a not declared license and was authored, remixed, and/or curated by Henry Jakubowski and Patricia Flatt.

- **Current page** by Henry Jakubowski and Patricia Flatt has no license indicated.
- **11.2: Diffusion Across a Membrane - Passive and Facilitated Diffusion** by Henry Jakubowski and Patricia Flatt has no license indicated.

22.4: BIOSYNTHESIS AND DEGRADATION OF NUCLEOTIDES

LEARNING GOALS (CHATGPT O3-MINI)

1. **Describe the Biological Importance of Nucleotides**
   - Explain how nucleotides serve dual roles as building blocks for nucleic acids and as key carriers of biological energy (e.g., ATP, GTP) and signaling molecules.
   - Discuss the diverse metabolic fates of amino acids in relation to nucleotide synthesis and degradation.
2. **Identify the Precursors and Sources of Atoms in Nucleotide Synthesis**
   - Summarize the contributions of amino acids—such as glutamine, aspartate, glycine, and serine—to the synthesis of purine and pyrimidine rings.
   - Interpret Figure 1 to explain the origin of atoms in the nucleotide bases.
3. **Compare and Contrast Purine and Pyrimidine Biosynthesis Pathways**
   - Outline the key steps and enzymes involved in the de novo purine biosynthesis pathway (leading to IMP) including the role of multifunctional enzymes (e.g., TGART, PAICS, ATIC) and the importance of PRPP.
   - Explain how the salvage pathway recycles purine bases and how enzymes like APRT and HGPRT contribute to nucleotide homeostasis.
   - Describe the de novo pyrimidine biosynthesis pathway, highlighting how the nucleobase is synthesized directly as a ribonucleotide and the role of key substrates such as aspartate, carbamoyl phosphate, and 5,10-meTHF.
4. **Understand the Regulation of Nucleotide Biosynthesis**
   - Discuss the rate-limiting steps in both purine (e.g., PPAT) and pyrimidine (e.g., CAD complex) synthesis and how these pathways are regulated by substrate availability, feedback inhibition, and enzyme phosphorylation.
   - Explain the concept of the purinosome as a dynamic multienzyme complex that facilitates de novo purine synthesis and how its assembly is coordinated with mitochondrial metabolism.
5. **Outline Nucleotide Interconversion and Deoxynucleotide Formation**
   - Describe the enzymatic conversion of ribonucleotides to deoxynucleotides, emphasizing the role of ribonucleotide reductase (RNR) and its free-radical mechanism.
   - Recognize the importance of deoxynucleotide synthesis in DNA replication and repair, and how RNR activity is regulated through both allosteric effectors and transcriptional control.
6. **Summarize the Pathways for Nucleotide Degradation**
   - Detail the catabolic routes for purine degradation, including the conversion of nucleotides to uric acid.
   - Summarize the degradation pathway for pyrimidines and how these products are further processed and excreted.
   - Relate nucleotide turnover and salvage pathways to overall cellular metabolism and energy balance.
7. **Integrate Nucleotide Metabolism with Cellular Function and Disease**
   - Explain how disruptions in nucleotide synthesis, salvage, or degradation can affect energy production, signal transduction, and gene regulation.
   - Discuss the role of nucleotide metabolism in rapidly proliferating cells (e.g., cancer cells) and how targeting these pathways can be a therapeutic strategy.

These learning goals aim to equip you with a comprehensive understanding of the metabolic pathways of nucleotides, highlighting their synthesis from amino acids, regulatory mechanisms, and their critical roles in cellular physiology and pathology.

22.4.1: INTRODUCTION

We conclude our exploration of metabolic pathways with the biosynthesis and breakdown of nucleotides, the monomers that comprise nucleic acids. We cannot forget the important role of ATP as the universal carrier of biological free energy, as well as the nucleotides involved in signal transduction, such as GTP in heterotrimeric G proteins and small G proteins, and ATP as a substrate in protein phosphorylation by kinases. As with the other later sections on metabolism, we won't focus much on detailed reaction mechanisms or enzyme structures, with one exception: the enzyme that converts nucleotides to deoxynucleotides.

Nucleotide synthesis is often included in chapters on amino acid metabolism as almost every atom in the purine and pyrimidine ring derives from them, as shown in Figure **22.4.1**.

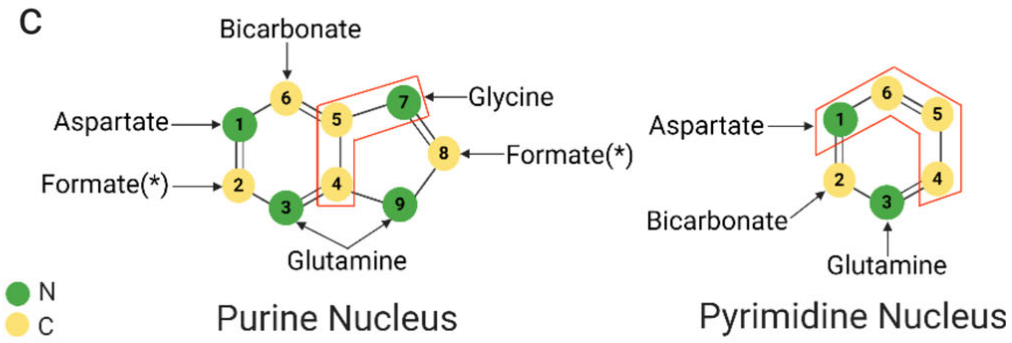


Figure **22.4.1**: Source of atoms in nucleotide bases. Lieu, E.L., Nguyen, T., Rhyne, S., *et al*. Amino acids in cancer. *Exp Mol Med* **52,** 15–30 (2020). https://doi.org/10.1038/s12276-020-0375-3. Creative Commons Attribution 4.0 International License, http://creativecommons.org/licenses/by/4.0/.

For purines, glutamine and aspartate provide the nitrogen for the nucleotide rings. They also provide the NH_3s for the ring substituents (glutamine for adenine and aspartate for guanine). Glycine and formate provide the carbon atoms for the rings. The one-carbon molecule formate, which derives from glycine, is also added to purine rings. Glycine provides a one-carbon unit indirectly through the main carrier of activated one-carbon units, 5,10-meTHF, which is converted to formate through 10-formyl THF.

Pyrimidines are much smaller, and their synthetic pathway reflects that. Instead of being synthesized as nucleobases, as in the case of purines, they are formed as ribonucleotides by being linked to phosphoribosyl pyrophosphate (PRPP). Glutamine and aspartate again provide the ring C and N atoms. The one-carbon unit derives from serine-to-glycine conversion. A methyl group from the activated 1C donor, 5,10-meTHF, is added to dUMP to make dTMP.

22.4.2: PURINE SYNTHESIS

The material below derives from De Vitto, H.; Arachchige, D.B.; Richardson, B.C.; French, J.B. The Intersection of Purine and Mitochondrial Metabolism in Cancer. Cells 2021, 10, 2603. https://doi.org/10.3390/cells10102603. **Creative Commons Attribution License**

Mammals have two pathways for purine synthesis: a de novo pathway and a salvage pathway, which allows for the recycling of nucleotide bases. The salvage pathway is typically sufficient, as purine bases are derived from nucleic acid breakdown. The resulting free bases (adenine, guanine, and hypoxanthine are connected to **phosphoribosyl pyrophosphate (PRPP)** to form nucleoside monophosphates (NMP) using either **adenine phosphoribosyltransferase (*APRT*)** to form AMP or hypoxanthine-guanine phosphoribosyltransferase (*HGRT*) to form IMP and GMP. PRPP is a substrate in both the salvage and de novo pathways. The overall de novo and salvage pathways for purine synthesis are described in detail in Figure **22.4.2**.

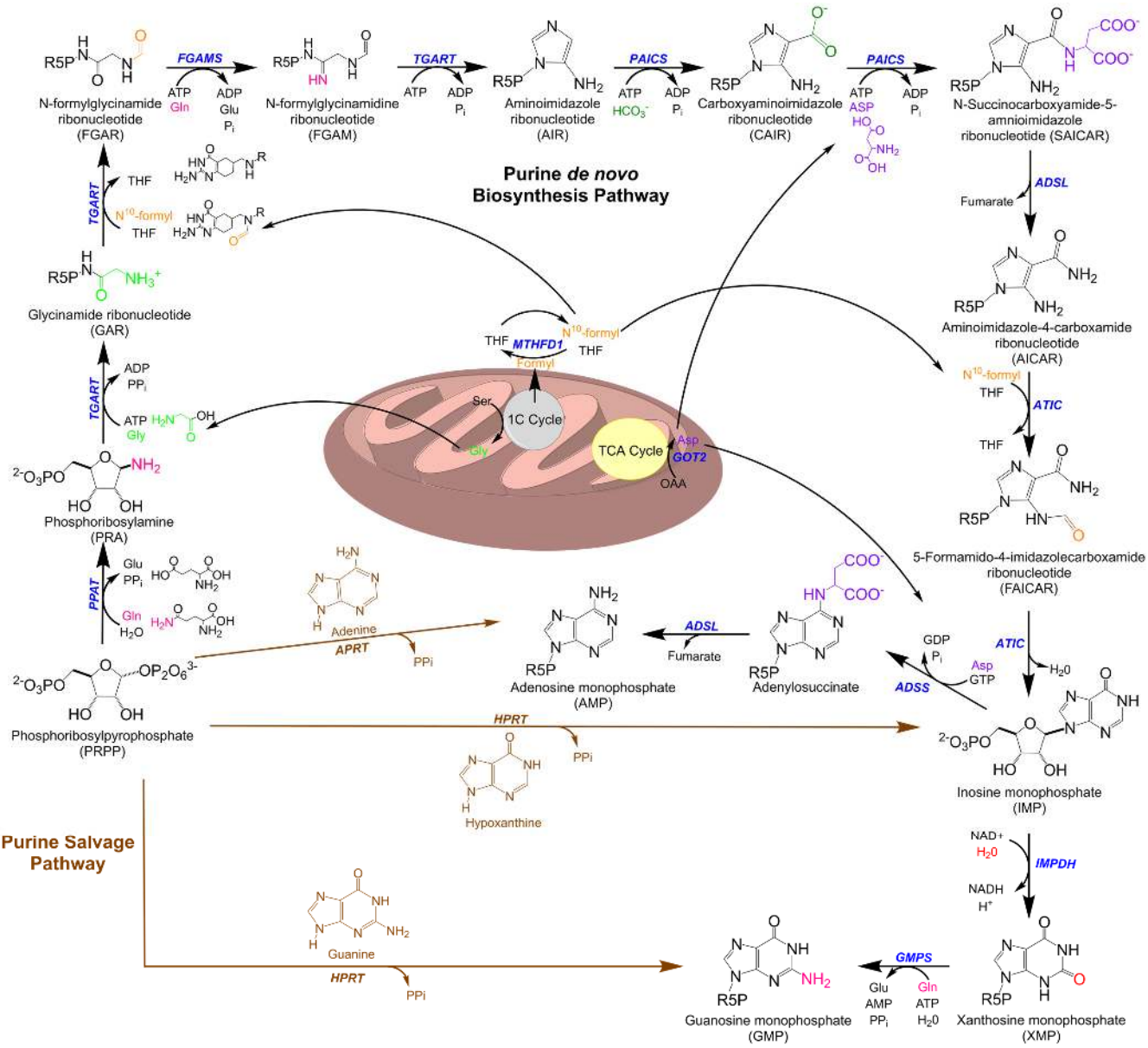


Figure **22.4.2**: Purine metabolic pathways. De Vitto, H.; Arachchige, D.B.; Richardson, B.C.; French, J.B. The Intersection of Purine and Mitochondrial Metabolism in Cancer. Cells 2021, 10, 2603. https://doi.org/10.3390/cells10102603. **Creative Commons Attribution License**

The conserved de novo biosynthesis pathway for generating IMP consists of 10 chemical steps, catalyzed by six gene products in humans. These include the trifunctional enzyme *TGART*, composed of GAR synthetase (GARS), GAR transformylase (GARTfase), and AIR synthetase (AIRS) domains; the bifunctional enzymes *PAICS*, composed of CAIR synthetase/AIR carboxylase (CAIRS) and SAICAR synthetase (SAICARS), and *ATIC*, composed of AICAR transformylase (AICART) and IMP cyclohydrolase (*IMPCH*); and three monofunctional enzymes, phosphoribosyl amidotransferase (*PPAT*), formyl glycin amidine ribonucleotide synthetase (*FGAMS*), and adenylosuccinate lyase (*ADSL*). Downstream IMP is converted to (1) GMP through stepwise reactions of IMP dehydrogenase (*IMPDH*) followed by GMP synthetase (*GMPS*) and (2) AMP via adenylosuccinate synthetase (*ADSS*) followed by *ADSL*. The salvage pathway requires PRPP to generate IMP and GMP through one-step reactions mediated by hypoxanthine phosphoribosyltransferase (*HPRT*), utilizing hypoxanthine and guanine bases. AMP is generated by adenine phosphoribosyltransferase (*APRT*), which utilizes the adenine base and PRPP as substrates. Mitochondria supply precursors for purine de novo biosynthesis, including glycine, N10-formyl THF, and aspartic acid, through their one-carbon cycle (1C cycle) and tricarboxylic acid cycle (TCA).

The de novo pathway kicks in when there is high demand for purines. Six enzymes are required for the 10-step pathway. Three of these are multifunctional enzymes catalyzing multiple steps in the pathway, comprising the two bifunctional enzymes phosphoribosylaminoimidazole

carboxylase (*PAICS)* and AICAR transformylase/inosine monophosphate cyclohydrolase (*ATIC)*, and the trifunctional enzyme glycinamide ribonucleotide transformylase (*TGART)*. When active, the pathway is limited by both substrate availability and the reaction rate of its initial step, the conversion of PRPP to phosphoribosylamine (PRA) by **phosphoribosylpyrophosphate amidotransferase (*PPAT*)**. The final product of the de novo biosynthesis pathway, IMP, is a substrate for the production of both AMP and GMP. Six ATPs are used to make one IMP from PRPP. None are required in the salvage pathway.

PPAT is also called Glutamine phosphoribosylpyrophosphate amidotransferase or amidophosphoribosyltransferase. It catalyzes the rate-limiting step and is tightly regulated. *PPAT* possesses two nucleotide-binding sites near the active site, allowing for feedback control by downstream purine nucleotides via allosteric inhibition.

Figure **22.4.3** shows an interactive iCn3D model of the Glutamine Phosphoribosylpyrophosphate Amidotransferase from Arabidopsis thaliana (6LBP)

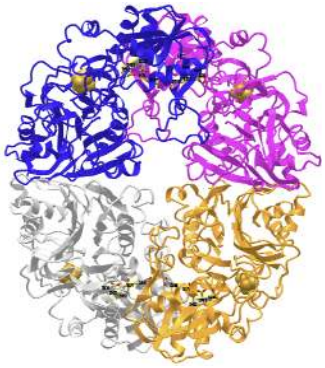


Figure **22.4.3**: Glutamine Phosphoribosylpyrophosphate Amidotransferase from Arabidopsis thaliana (6LBP). (Copyright; author via source). Click the image for a popup or use this external link: https://structure.ncbi.nlm.nih.gov/i...uWnf1bTq1odk88

The plant enzyme is a homotetramer, with each subunit having a Fe_4S_4 center (spacefill). The active site residues in each subunit (DDS 432-444 and DS 369-370) are shown as colored sticks and labeled.

Regulation of IMP production also occurs through enzyme phosphorylation. For example, Thr 397 on PPAT is phosphorylated by protein kinase B (PKB). PRPP concentrations also affect the rate. Another regulation of the flux through the de novo pathway involves the condensation of enzymes into the purinosome, which contains *PPAT*, *TGART*, formylglycinamidine ribonucleotide synthetase (*FGAMS*), *PAICS*, adenylosuccinate lyase (*ADSL*), and *ATIC*. The purinosome also interacts with the mitochondria, allowing for high local concentrations of ATP.

A cartoon view of the purinosome is shown in Figure **22.4.4**.

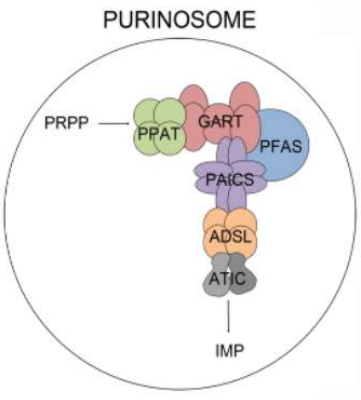


Figure **22.4.4**: Cartoon showing the purinosome. Baresova et al (2018) PLoS ONE 13(7): e0201432. https://doi.org/10.1371/journal.pone.0201432. Creative Commons Attribution License,

Figure **22.4.5** shows another view of de novo IMP synthesis in which the origin of each atom in the purine ring is shown in color.

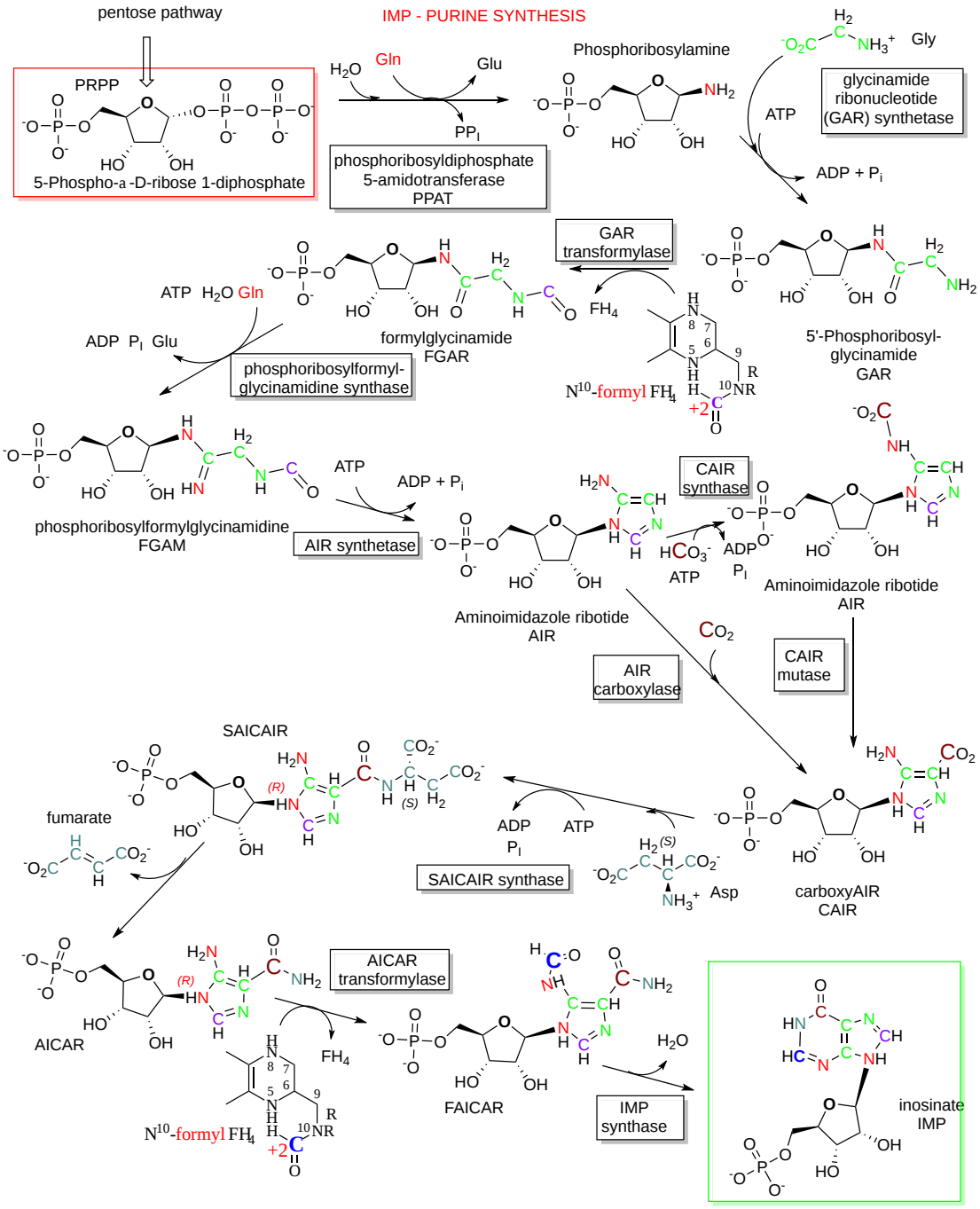


Figure **22.4.5**: De novo IMP synthesis showing the origin of atoms in IMP.

Figure **22.4.6** shows an expanded view of the conversion of IMP to GTP and ATP.

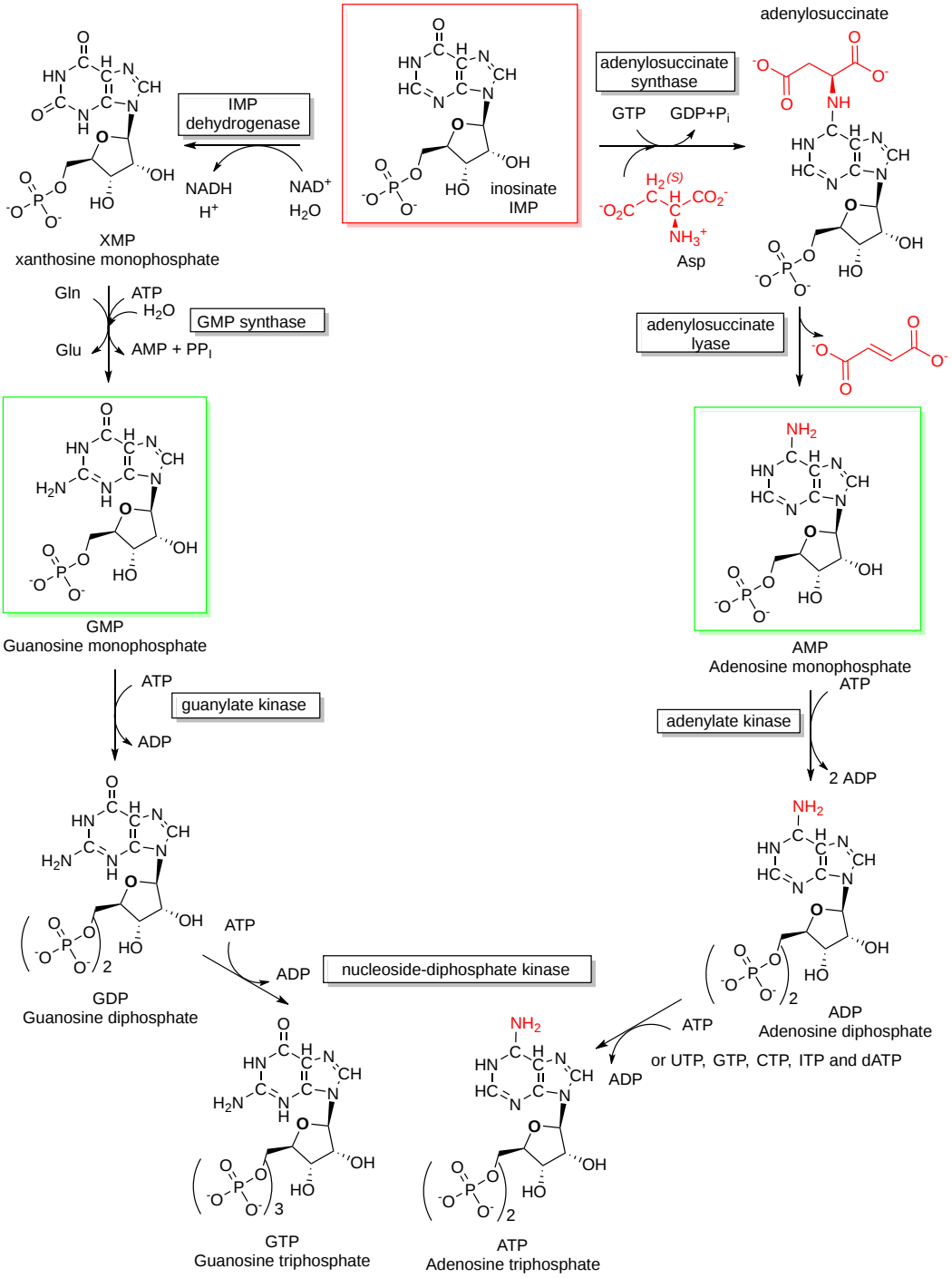


Figure **22.4.6**: Conversion of IMP to GTP and ATP

22.4.3: PYRIMIDINE SYNTHESIS

As mentioned in the introduction, pyrimidines have a much simpler biosynthetic pathway. Instead of being synthesized as nucleobases as in the case of purines, they are made as ribonucleotides as they are linked to phosphoribosyl pyrophosphate (PRPP). Glutamine and aspartate again provide the ring C and N atoms. The one-carbon unit derives from serine-to-glycine conversion. A methyl group from the activated 1C donor, 5,10-meTHF, is added to dUMP to make dTMP.

The first step in the pathway for pyrimidine synthesis is the condensation of aspartate and carbamoyl phosphate. We have seen the synthesis of carbamoyl phosphate in the urea cycle by the enzyme carbamoylphosphate synthase I (CPSI) in Chapter 18.3 but present the reaction again in Figure **22.4.7**.

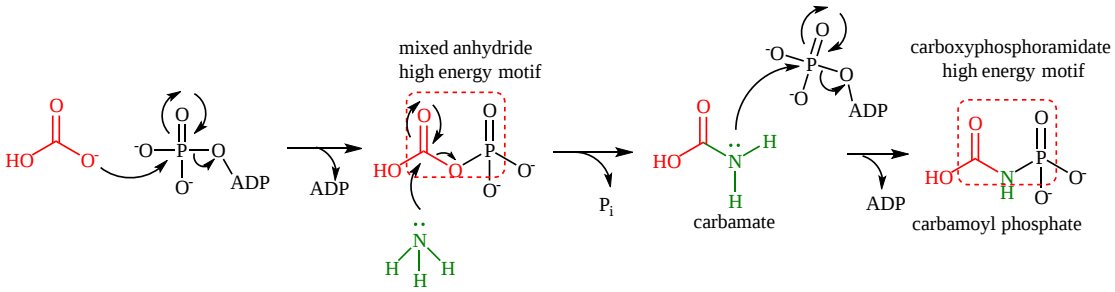


Figure **22.4.7**: Synthesis of carbamoyl phosphate

A different cytosolic version of the enzyme, CPS II, is used to synthesize both arginine and pyrimidine nucleotides. It uses glutamine as a donor of NH_3.

The pathway for the synthesis of UTP and CTP is shown in Figure **22.4.7**. It does not explicitly show the synthesis of carbamoylphosphate, which is an integral part of the pathway and a rate-limiting step in pyrimidine synthesis.

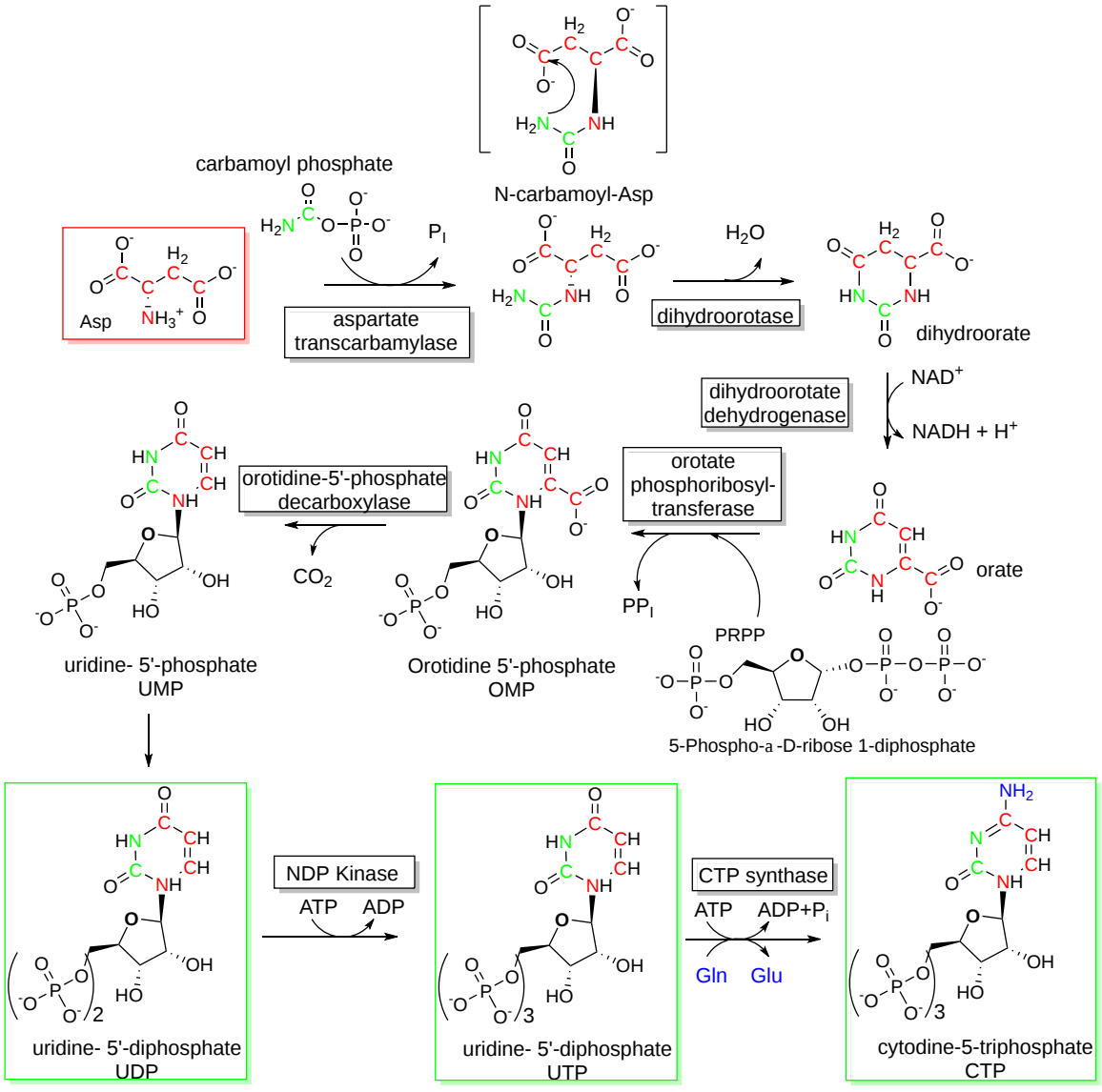


Figure **22.4.8**: De novo synthesis of UDP, UTP, and CTP

UDP and CDP can be converted to dCDP and dUDP, and then on to dCPT and dUTP, and to dTMP as shown in Figure **22.4.9**.

Deoxythymidine-5'-monophosphate Synthesis

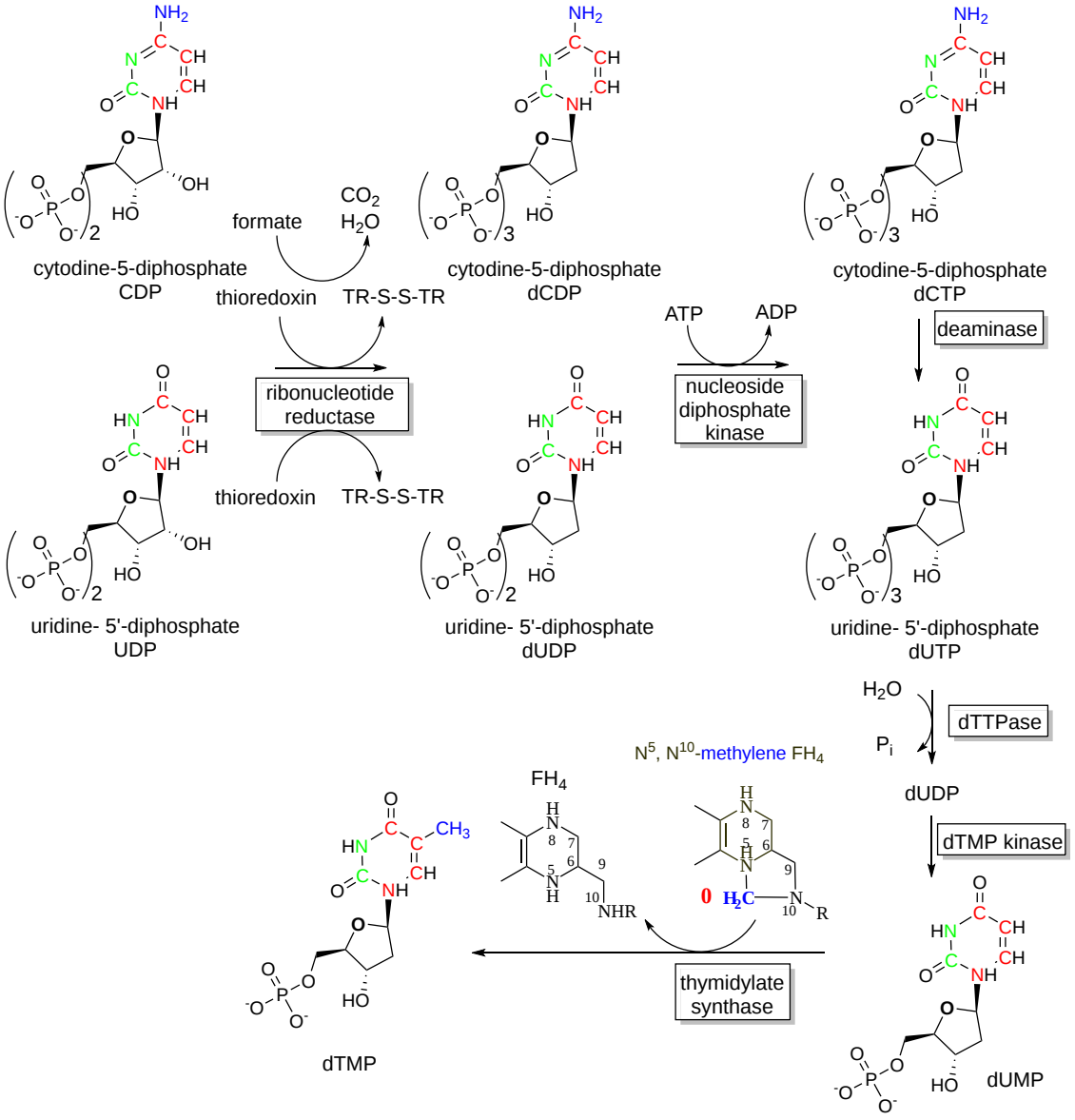


Figure **22.4.9**: Synthesis of dTMP

Some of the material below derives from Li et al. *Int. J. Mol. Sci.* **2021**, *22*(19), 10253; https://doi.org/10.3390/ijms221910253**.** Creative Commons Attribution (CC BY) license (https://creativecommons.org/licenses/by/4.0/)

In purine synthesis, we observed multifunctional enzymes that catalyze multiple steps, as well as the assembly of these enzymes into the purinosome within the de novo pathway. Analogously, three different enzyme activities that catalyze the first three combined rate-limiting steps of pyrimidine synthesis, **C**arbamoyl-phosphate synthetase, **A**spartate transcarbamoylase, and **D**ihydroorotase, are found in a single, multifunctional protein referred to as **CAD**. Its structure is a hexamer of a 243K monomer. It has four domains that include

- glutamine amidotransferase (GATase) which "moves" HCO_3^-, glutamine, and ATP to the CPSIIase domain
- carbamoylphosphate synthetase II (CPSIIase): This has two parts, CPSaseA, and CPSase B. They combine functionally with GATase to form a glutamine-dependent carbamoylphosphate synthase (CPSase)
- aspartate transcarbamylase (ATCase) acts as a homotrimer
- dihydroorotase (DHOase) catalyzes the reversible cyclization reaction.

The CAD protein is a fusion protein that encodes these four enzymatic activities of the pyrimidine pathway. Figure **22.4.10** shows the domain structure of the CAD protein.

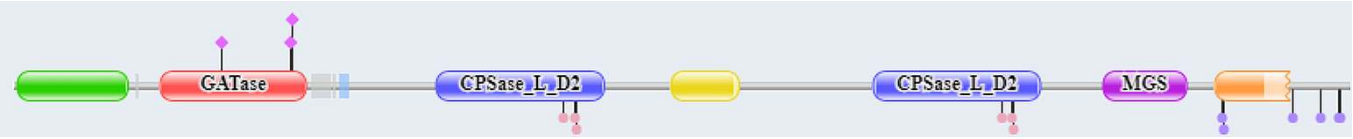
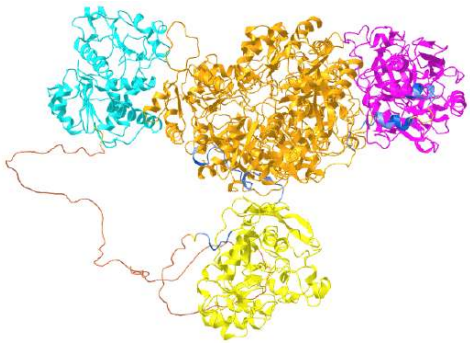


Figure 22.4.10: Domain structure of CAD

The red represents glutamine amidotransferase and the blue the carbamoyl phosphate synthase ATP binding domain. More specifically, the following amino acid stretches comprise the different domains: GATase (2-365), CPSase A (395-933), CPSase B (934-1455), DHOase (1456-1788), and ATCase (1918-2225)

Figure 22.4.11 shows an interactive iCn3D model of the AlphaFold predicted model of the CAD protein (P27708)



NCBI iCn3D Figure 22.4.11: AlphaFold predicted model of the CAD protein (P27708). (Copyright; author via source). Click the image for a popup or use this external link: https://structure.ncbi.nlm.nih.gov/i...5V2XUmfsz1qjZ6

The GATase domain is magenta, the CPSase domains are orange, the DHOase domain is yellow, and the ATCase domain is cyan. The structure of the disordered loops could not be modeled.

22.4.4: RIBONUCLEOTIDE REDUCTASES (RNRS)

Ruskoski and. Boal. J. Biol. Chem. (2021) 297(4) 101137. DOI:https://doi.org/10.1016/j.jbc.2021.101137. CC-BY license (http://creativecommons.org/licenses/by/4.0/).

Ribonucleotide reductases (RNRs), also called **ribonucleoside-diphosphate reductase,** catalyze the oxidation of the C2'-OH on the ribose ring to C2'-H through a free radical mechanism for the oxidation of all NDPs, including ADP, GDP, CDP, and UDP (which converts to dUDP and in a different reaction to dTDP). The reaction is as follows:

[thioredoxin]-dithiol + ribonucleoside 5'-diphosphate ↔ [thioredoxin]-disulfide + 2'-deoxyribonucleoside 5'-diphosphate + H_2O

To refresh your memory, thioredoxin is a small protein (12 kDa) that is part of a complex with thioredoxin reductase and thioredoxin-interacting protein. It has two key sulfhydryls at the active site, which act as reducing agents as they are converted to a disulfide, as shown in Figure 22.4.12.

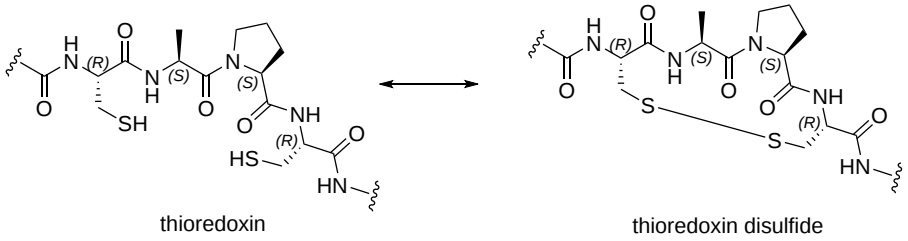


Figure 22.4.12: Reduced thioredoxin and its oxidized form

This single enzyme is so critical to cellular life that we will examine it more closely.

There are several classes of these enzymes, including Ia-Ie, II, and III. The class I enzymes generally use a di-transition metal complex as a cofactor, whereas class II enzymes use adenosylcobalamin. We will focus on class I enzymes, which have two subunits, designated as α and β, or M1 and M2, respectively. The NDP binds to an α/M1 subunit active site, which is only developed in the dimer. The β/M2 subunit is often referred to as the radical-generating subunit, as it contains the transition metal complex that generates a free tyrosyl radical cation, which is critical to the reaction.

Almost all class I ribonucleotide reductases (RNRs) use transition metal ions located in the β/M2 subunit in the catalytic cycle for the dehydroxylation of the 2' OH on the ribose ring of the nucleotide. The metal ion complex a β/M2 subunit tyrosine to a tyrosine free radical cation, which oxidizes an active site cysteine in the α/M1 subunit to form a thiol radical cation ($Cys^{\bullet+}$), called a thiyl radical. This abstracts a H• from the 3'C on the ribose of the substrate, forming a 3'C radical cation. This facilitates a dehydration reaction, which leads to the dehydroxylation of the 2' OH, regenerating the thiyl radical. Reducing equivalents to restore the catalytic function of the enzyme come from the oxidation of a thioredoxin disulfide bound in the other subunit of the protein or a formate.

Given the importance of these enzymes, they must be highly regulated. There are two regulatory sites:

- a specificity site: determines nucleotide (NDP) specificity
- an activity site: regulates catalytic activity

The specificity and activity sites are in the α/M1 subunit, where allosteric regulators dNTPs and ATP bind to different sites. When ATP is bound, the enzyme uses CDP and UDP as substrates. When dGTP is bound, ADP is the preferred substrate. Finally, when dTTP is bound, GDP is the preferred substrate. The enzyme is inhibited by dATP binding to the actual active site.

Figure **22.4.13**s shows an abbreviated mechanism and cartoon showing the activities of the two subunits.

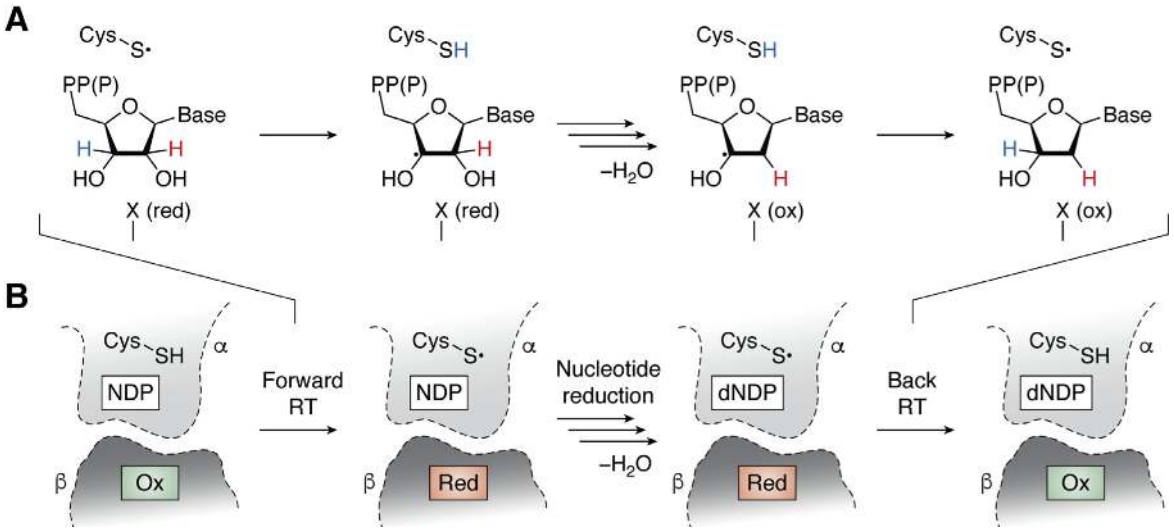


Figure **22.4.13**: Abbreviated mechanism and a cartoon showing the activities of the two subunits. in class I RNR. *A*, universal mechanism for nucleotide reduction in RNRs. *B*, diagram of the steps involved in radical translocation in class I RNRs. Ruskoski and. Boal. J. Biol. Chem. (2021) 297(4) 101137. DOI:https://doi.org/10.1016/j.jbc.2021.101137. CC-BY license (http://creativecommons.org/licenses/by/4.0/)

Radical formation starts at tyrosine 122 in the metal center site in the β/M2 subunit. Electron transfer then occurs across the two subunits from a very distant active site Cys 439 in the α subunit, which enables the formation of the thiyl radical cation ($Cys^{\bullet+}$).

The structure of an E. coli Type IA enzyme with bound ligands has been determined after considerable effort that involved trapping a long-lived intermediate. It required the replacement of Tyr 122 in both β chains with 2,3,5-trifluorotyrosine, which allowed the structure to be determined by cryo-EM. Tyr 122 in the β chain initiates the electron transfer process by becoming the Tyr $122^{\cdot+}$ radical cation.

A detailed mechanism showing both electron transfer to $Y122^{\cdot+}$ and accompanying proton transfer is shown in Figure **22.4.14**.

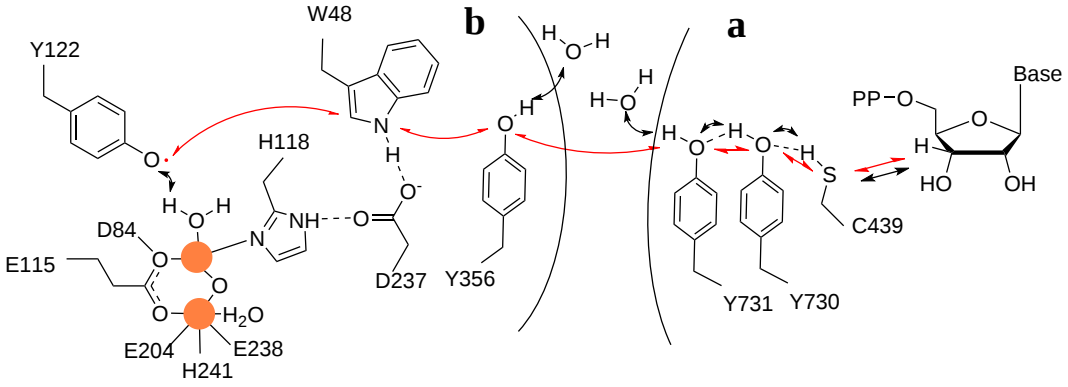
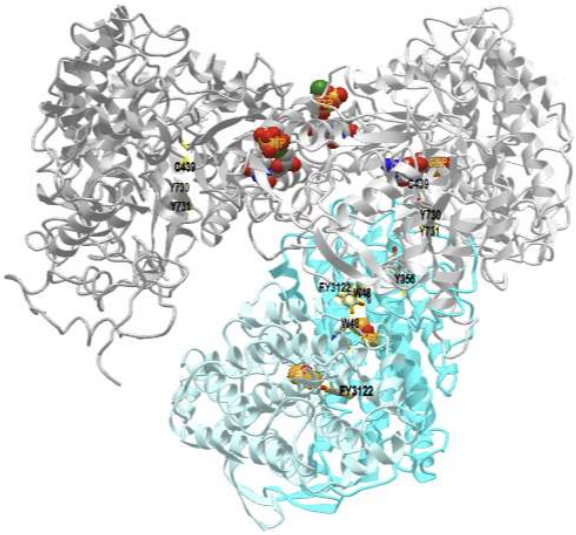


Figure 22.4.14: Pathway of electron and proton transfers for the formation of the thiyl radical cation (Cys•$^{+}$). after Kang et al. Science (2020). DOI: 10.1126/science.aba6794)

The path for electron flow from the sulfur of C439 in the β subunit to regenerate Y122 is shown. That electron transfer occurs over a very long distance of 35 Å as it hops from the original sulfur donor to the acceptor.

Figure 22.4.15 shows an interactive iCn3D model of the holocomplex of E. coli class Ia ribonucleotide reductase with GDP and TTP (6W4X).



NCBI iCn3D Figure 22.4.15: Holocomplex of E. coli class Ia ribonucleotide reductase with GDP and TTP (6W4X). (Copyright; author via source). Click the image for a popup or use this external link: https://structure.ncbi.nlm.nih.gov/i...71ubUDRovXURG8

The structure is a tetramer of two α chains (different shades of gray) and two β chains (different shades of cyan). The GDP and TTP in the α subunit, as well as the Fe cluster in the β subunit, are shown in CPK spacefill and labeled. The key side chains in the α and β chains that participate in electron transfer over the 35 Å distance are shown in CPK-colored sticks and labeled. The Fe^{2+} ions are in the form of a μ-oxo-diron complex (2 Fe ions coordinated by one oxide).

Figure 22.4.16 shows specificity and catalytic sites of the biologically active tetramer form for Class 1 RNR as well as the transition metal cofactors (Fe, Mn, or both) in various Class 1 RNRs.

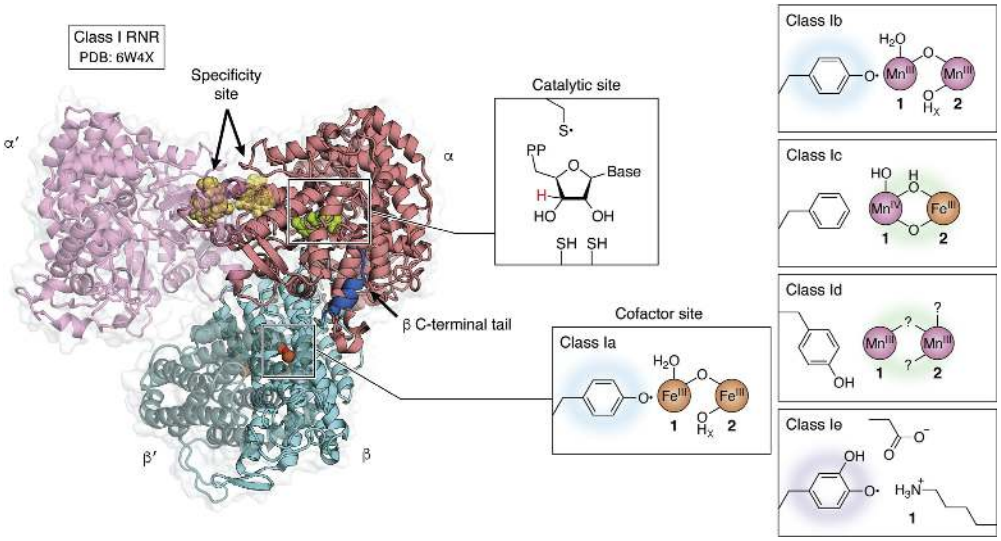


Figure 22.4.16: Quaternary structure of the active holoenzyme complex in class I RNR (PDB accession code 6W4X). *Insets* show the location of the active site in the catalytic α subunit (*middle top*) and the metallo- or radical cofactor (*middle bottom* and *far right*) in the β subunit.

The tyrosyl free radical forms on binding of dioxygen to the transition metal ion center electron and subsequent loss of an electron from tyrosine, as shown in Figure **22.4.17**:

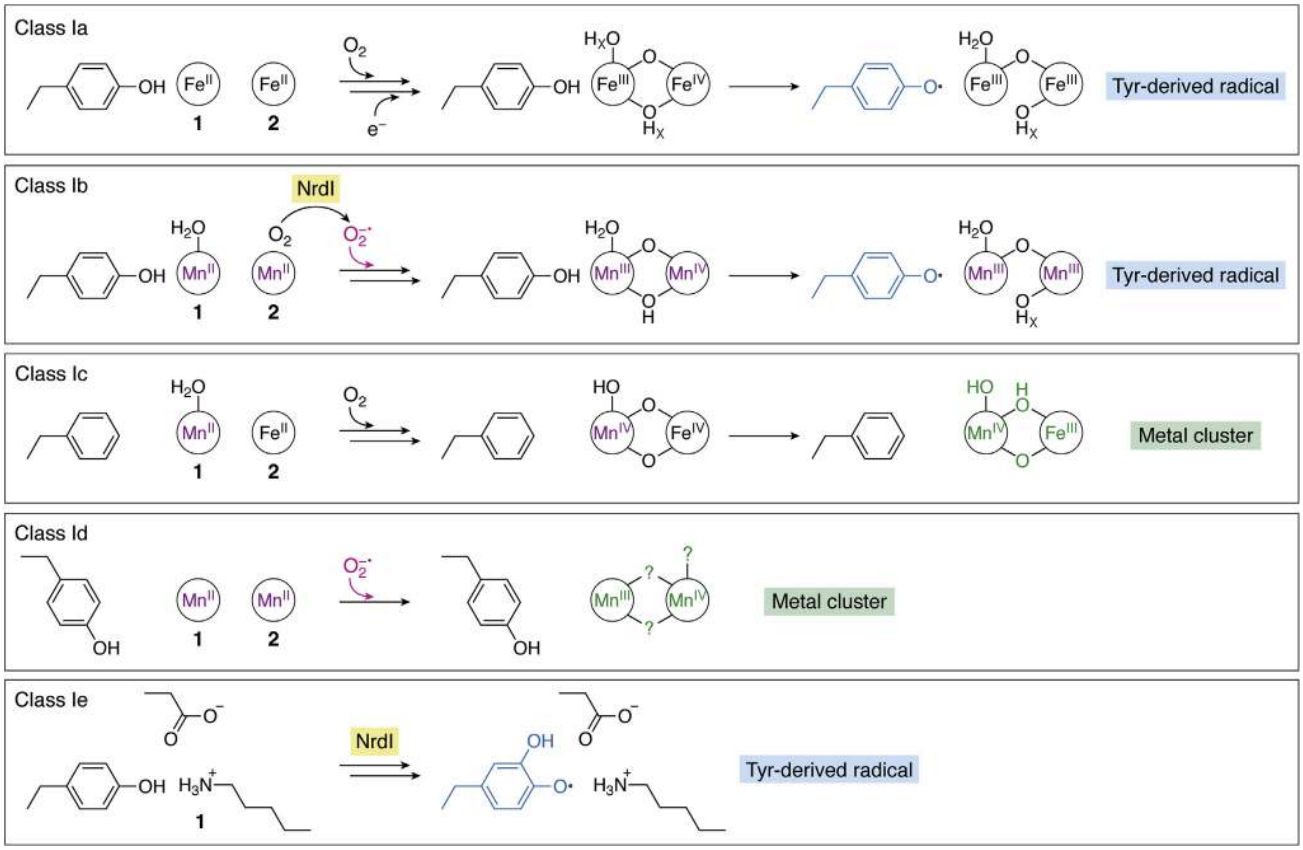


Figure **22.4.17**: Cofactor assembly mechanisms for class I RNRs. Manganese-dependent enzymes are highlighted in *purple*. Superoxide-dependent RNRs are highlighted in *hot pink*. Subclasses that require an NrdI activase are indicated with a *yellow box*. Metal-centered Cys oxidants are shown in *green*, and Tyr-derived radical Cys oxidants are shown in *blue*.

The mechanisms of cofactor actions are not fully understood. O_2 initially adds to the Fe^{2+}/Fe^{2+} cluster, forming a peroxo-Fe^{3+}/Fe^{3+} intermediate.

Structural features of the active site for different class I RNRs along with redox-active transition metal ions are shown in Figure **22.4.18**.

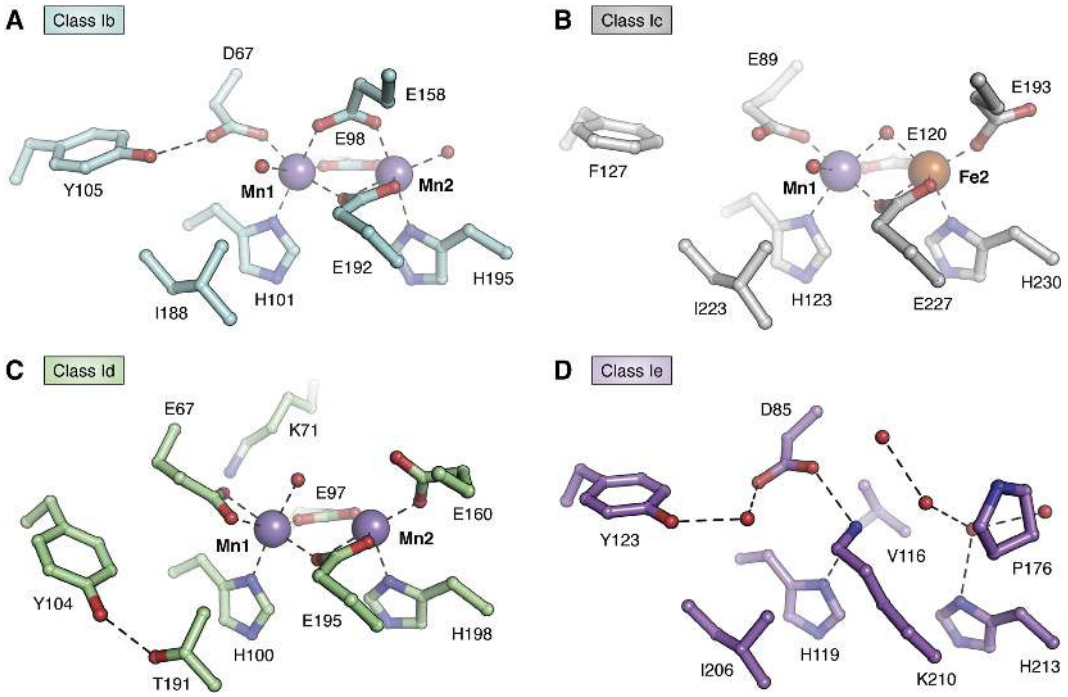


Figure **22.4.18**: Comparison of metal-binding sites in class I RNRs

The PDB codes for each structure are as follows: A (3N3A), B (4M1I), C (6CWP), and D (6EBO). Water molecules are shown as *red spheres*.

Now, let's examine the regulation of Class IA RNRs in more detail. Let's consider perhaps the most important allosteric regulators, which bind 15 Å from the active site and affect RNR enzymatic activity:

- dATP: inhibits RNRs when it binds to the α subunit
- ATP: reverses the inhibition by dATP

dATP/ATP also affects RNR enzyme specificity as they tilt the preference of RNR towards pyrimidine substrates, where TTP and dGTP promote purine substrate binding. These same rules apply to human and E. coli RNRs, with the locations of the active sites also being the same.

The allosteric regulators appear to affect the quaternary structure of the enzyme.

In E. Coli, the binding of dADP converts the structure of the enzyme from an active $\alpha_2\beta_2$ form to an inhibited $\alpha_4\beta_4$ ring structure. When dATP is bound, a "**cone**" domain in α forms interactions with the β subunit, leading to the formation of a dimer of the $\alpha_2\beta_2$ tetramer. ATP reverses this effect by displacing dATP and pushing the equilibrium towards the active $\alpha_2\beta_2$ form. This is shown in Panel A of Figure **22.4.19**.

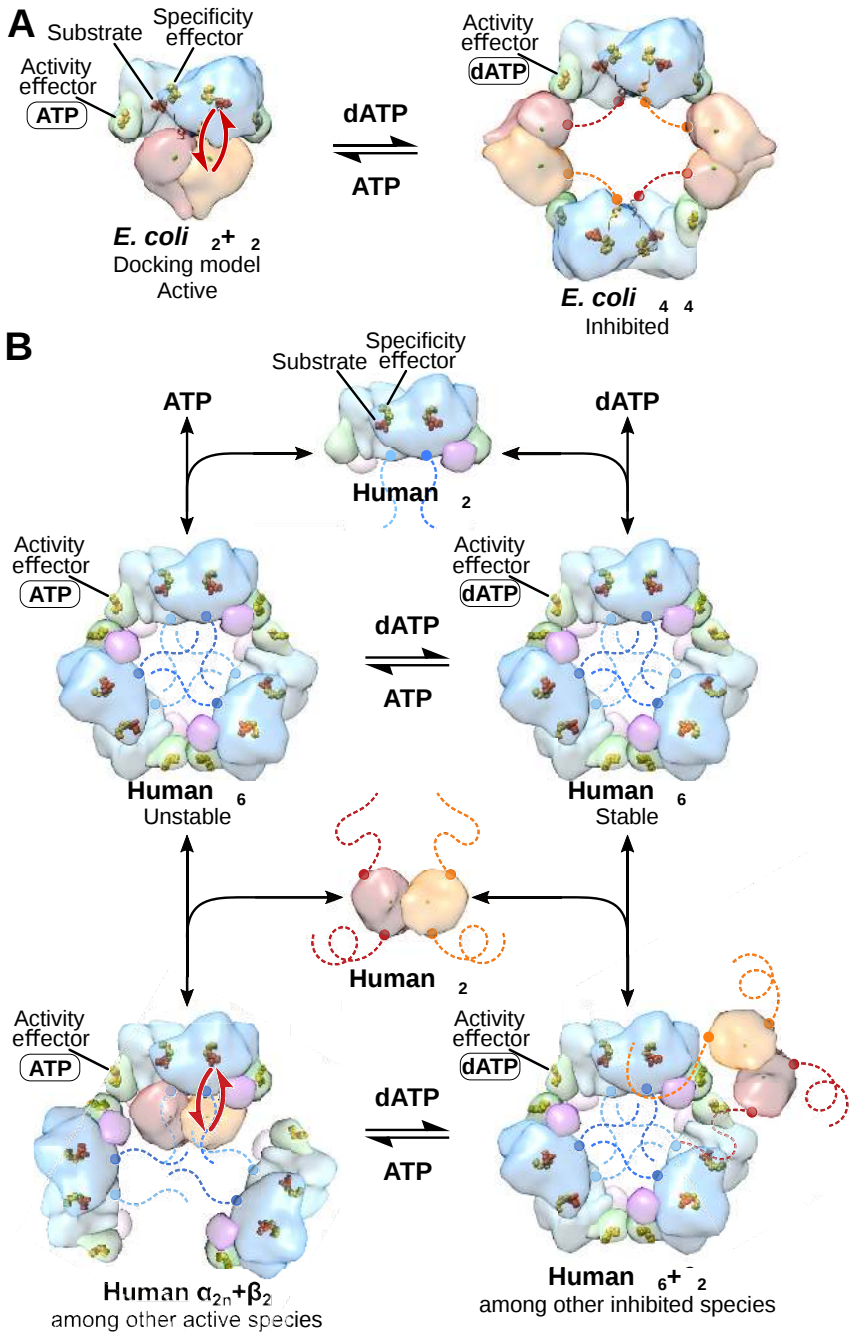


Figure 22.4.19: **Comparison of mechanisms of allosteric regulation of activity for *E. coli* and human RNRs.** Brignole et al. 3.3-Å resolution cryo-EM structure of human ribonucleotide reductase with substrate and allosteric regulators bound eLife 7:e31502. https://doi.org/10.7554/eLife.31502. Attribution 4.0 International (CC BY 4.0).

Panel B above illustrates the regulation of the human enzyme, which appears to be quite different. In the absence of either dATP or ATP, RNRs exist just as α_2 dimers. On binding either dATP or ATP, the α_2 dimer is converted to an α_6 (a trimer of dimers) structure. Both are inactive in the absence of β subunits (which provide the metal cofactor site)

- When β_2 is added to the dATP-bound α_6 hexamer, the hexamer becomes stabilized, but the resulting complex is inhibited.
- When β2 is added to the ATP-bound α6 hexamer, the hexamer becomes destabilized and breaks down into smaller, active structures.

Hence, the ratio of cellular dATP/ATP changes the aggregation state of the RNR and hence its activity in both E. Coli and humans.

Figure 22.4.20 shows an interactive iCn3D model of the Human ribonucleotide reductase large subunit (alpha) with dATP and CDP (6AUI).

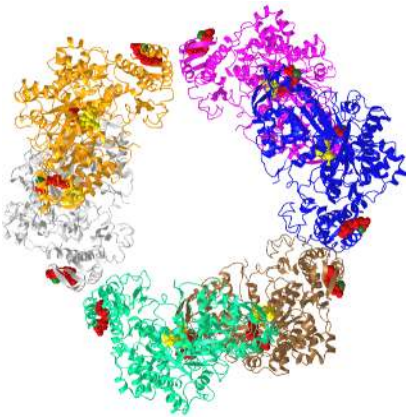


Figure **22.4.20**: Human ribonucleotide reductase large subunit (alpha) with dATP and CDP (6AUI). (Copyright; author via source). Click the image for a popup or use this external link:https://structure.ncbi.nlm.nih.gov/i...w1sFwwYSAD4nG6

Each of the α subunits in the hexamer is shown in a different color. dATPs (allosteric inhibitors) are shown in spacefill, red. CDPs (substrates) are shown in spacefill yellow.

The hole in the middle of the structure prevents β_2 from binding in a catalytically productive manner, rendering the structure inactive.

A specific loop, loop 2, assists in the determination of RNRs' specificity. It is between the base of dATP and the base of the substrate CDP. The backbone of the loop interacts with the adenine base and orients Gln 288 in the active site to interact with the cytosine of the substrate CDP. In both systems, backbone atoms of this loop 'read out' the adenine base and position Gln288 into the active site to recognize the cytosine of CDP. Figure **22.4.20** gives further details on the origin of substrate specificity.

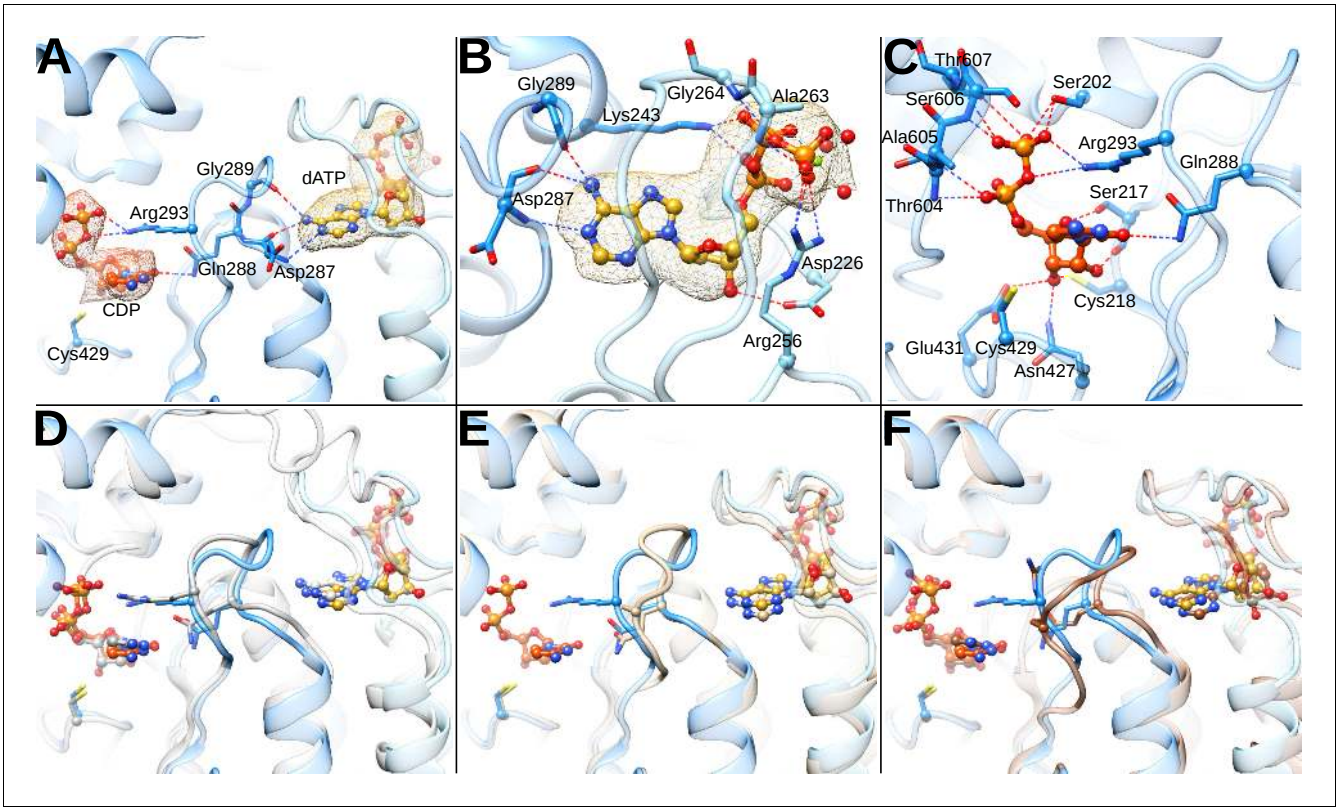


Figure **22.4.21**: Determinants of substrate specificity are conserved from *E. coli* to humans**.**

Panel (**A**) shows residues of human α (blue) interacting with CDP (carbons in orange) in the active site and dATP (carbons in yellow) in the specificity site. Density for CDP in the orange mesh and for dATP in the yellow mesh.

Panel (**B**) zooms in on dATP in the specificity site. Water molecules and oxygen atoms are in red, nitrogen in blue, magnesium in green, and phosphate in gold.

Panel (**C**) zooms in on CDP in the active site.

Panel (**D**) shows an overlay of human α from the α_6 EM structure in blue with *E. coli* α from the $\alpha_4\beta_4$-CDP-dATP cocrystal structure in gray (PDB: 5CNS) shows a nearly identical loop 2 conformation positioning Gln288 and Arg293 (Gln294 and Arg298 in *E. coli*).

Panel (**E**) shows an overlay of human α from the α_6 EM structure in blue with the crystal structure of human α with N- and C-termini truncated (residues 77–742) cocrystallized with dATP in tan (PDB: 2WGH) shows similar positioning of dATP but an altered conformation of loop 2 in the absence of bound CDP. The CDP shown is from the α_6 EM structure.

Panel (**F**) shows an overlay of human α from the α_6 EM structure in blue with equivalent residues of yeast α structure with CDP and AMPPNP in brown (PDB: 2CVU) and shows a conformation of loop 2 that is distinct from that seen in structures of *E. coli* and human α

22.4.4.1: TRANSCRIPTIONAL REGULATION OF RNRS

Given the importance of this key enzyme, it should come as no surprise that its levels are regulated at the transcription level. As the activity of RNR is determined by its polymeric quaternary state, the transcriptional activation of the genes for RNRs is controlled in bacteria by quaternary states of the RNR-specific transcriptional repressor NrdR. The transcription factors bind to a specific DNA sequence called an NrdR box, which precedes the transcription start site for RNR, where RNA polymerase binds.

The NrdR protein acts to repress the synthesis of RNR genes. DATP/ATP ratios control its aggregation state. When dATP is high, the NrdR binds to DNA and represses the synthesis of the RNR gene. In contrast, when ATP is high, the protein does not bind to DNA, and hence it can not repress transcription. The aggregation state of NrdR controls the association /dissociation of the repressor. When abundant, NrdR exists as a 12-mer complex with two molecules of ATP bound per monomer. This ATP-bound 12-mer can't bind DNA, so transcription of the gene for RNR is not repressed. As dATP increases, one ATP is displaced, so each monomer has one dATP and one ATP bound. This causes the NrdR to covet to an 8-mer. A 4-mer (tetrameric) version of this protein binds to the NrdR box sequence at the start of the RNR gene, repressing its synthesis.

Figure **22.4.22** illustrates the dodecameric, octameric, and tetrameric structures of NrdR, along with their corresponding functions.

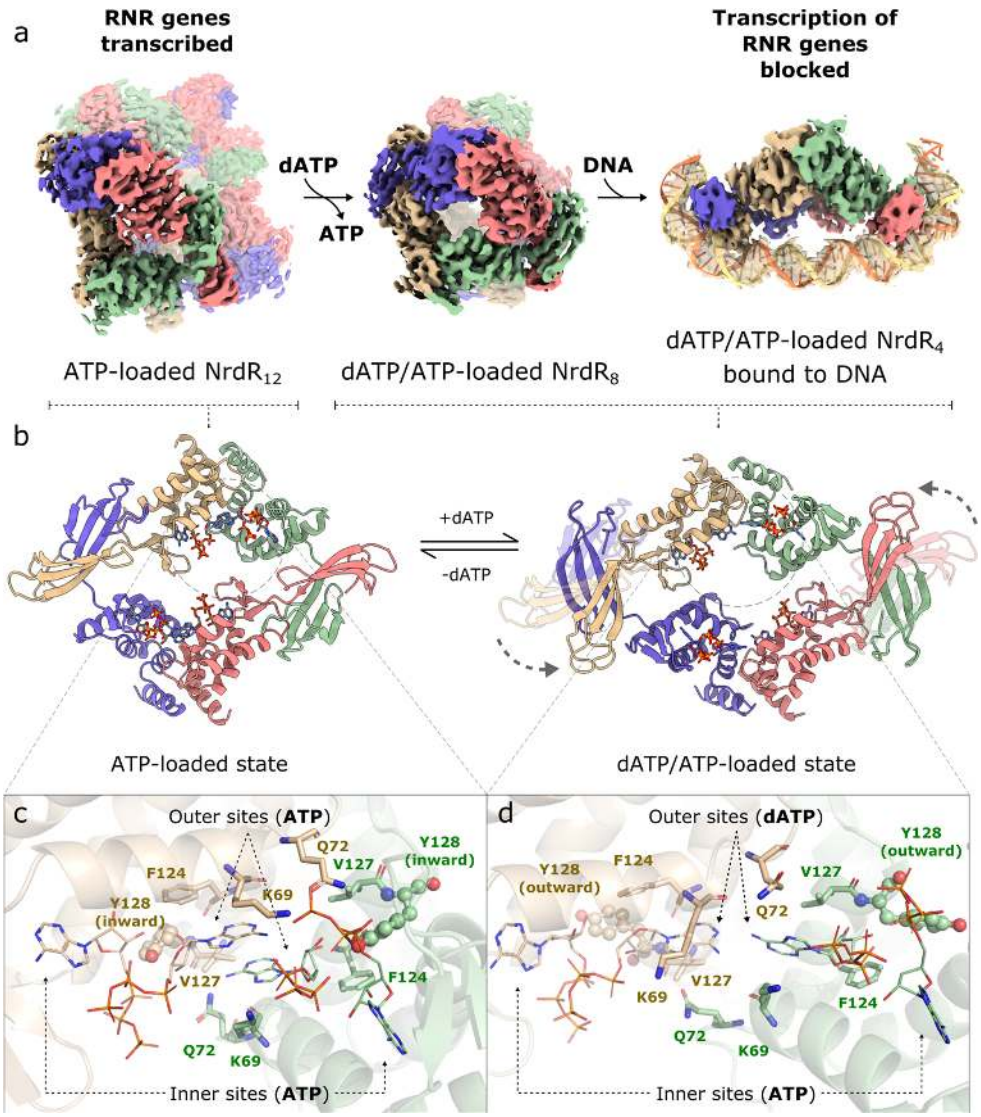


Figure 22.4.22: **Mechanism of NrdR function involving dodecameric, octameric, and tetrameric structures.** Rozman Grinberg, I., Martínez-Carranza, M., Bimai, O. *et al.* A nucleotide-sensing oligomerization mechanism that controls NrdR-dependent transcription of ribonucleotide reductases. *Nat Commun* **13,** 2700 (2022). https://doi.org/10.1038/s41467-022-30328-1. Creative Commons Attribution 4.0 International License. http://creativecommons.org/licenses/by/4.0/.

Panel (a) shows a surface representation of the cryo-EM maps for the dodecameric, octameric, and DNA-bound tetrameric NrdR structures.

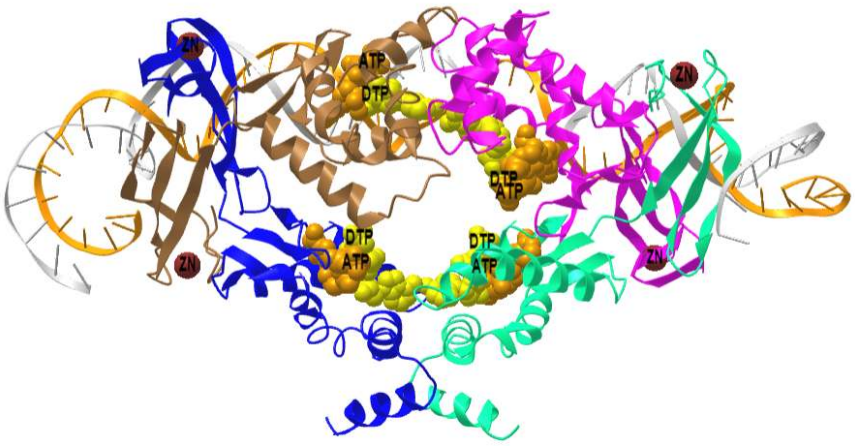
Panel (b) shows a cartoon representation of the ATP-loaded NrdR tetramer (left) and the dATP/ATP-loaded tetramer (right). Chains A, B, C, and D are colored beige, green, pink, and blue, respectively.

Panel (c) shows the interface between the ATP cones in chain A (beige) and chain B (green) in the ATP-loaded dodecamer.

Panel (**d**) shows the dATP/ATP-loaded tetramer.

Panels **c**, and **d** were made from the same perspective, based on an alignment of the ATP-cones in chains A and B in both structures.

Figure 22.4.23 shows an interactive iCn3D model of the Streptomyces coelicolor dATP/ATP-loaded NrdR in complex with its cognate DNA (7P3F)**.**



NCBI iCn3D Figure 22.4.23: Streptomyces coelicolor dATP/ATP-loaded NrdR in complex with its cognate DNA (7P3F). (Copyright; author via source). Click the image for a popup or use this external link: https://structure.ncbi.nlm.nih.gov/i...2u3HMRPmJHe9X9

The monomers of the NrdR tetramer are shown in different colors. The yellow spheres represent dATP, and the orange ones represent ATP.

22.4.5: PYRIMIDINE SALVAGE PATHWAY

There is also a salvage pathway as shown in Figure 22.4.24.

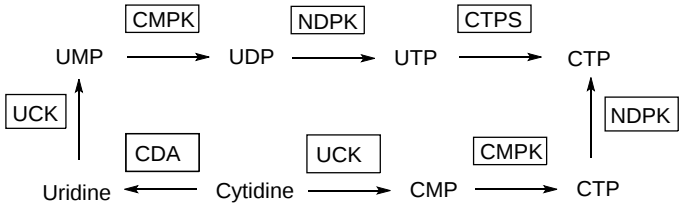


Figure 22.4.24: Pyrimidine salvage pathway (after Wang et al. Frontiers in Oncology, 11 (2021). https://www.frontiersin.org/article/...nc.2021.684961. DOI=10.3389/fonc.2021.684961

Cells at rest utilize the salvage pathway's reactants, which are derived from the degradation of nucleic acids.

22.4.6: NUCLEOTIDE DEGRADATION

22.4.6.1: PURINES

The pathway for purine degradation is shown in Figure 22.4.25.

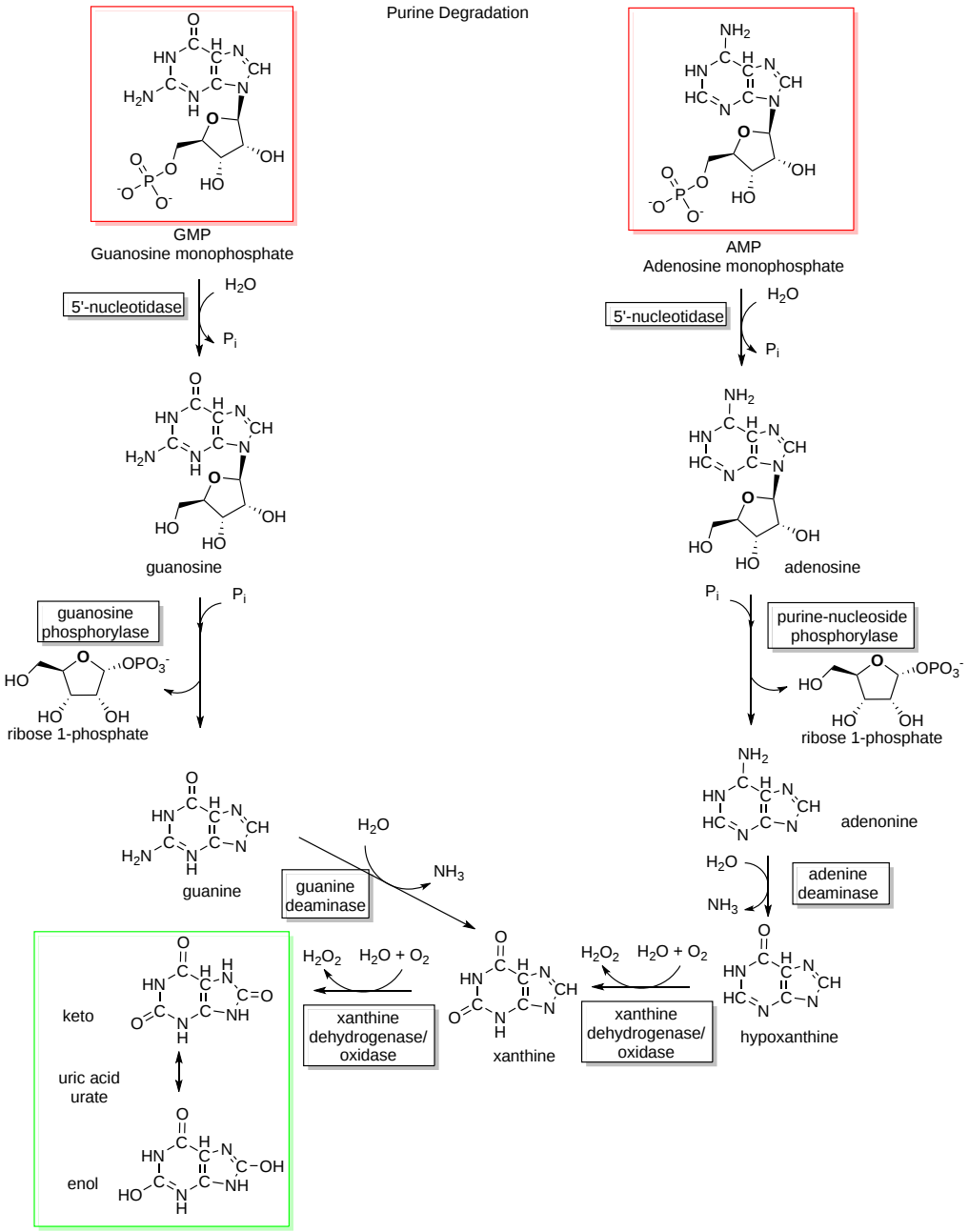


Figure **22.4.25**: Purine degradation

22.4.6.2: PYRIMIDINE DEGRADATION

The pathway for pyrimidine degradation is shown in Figure **22.4.26**.

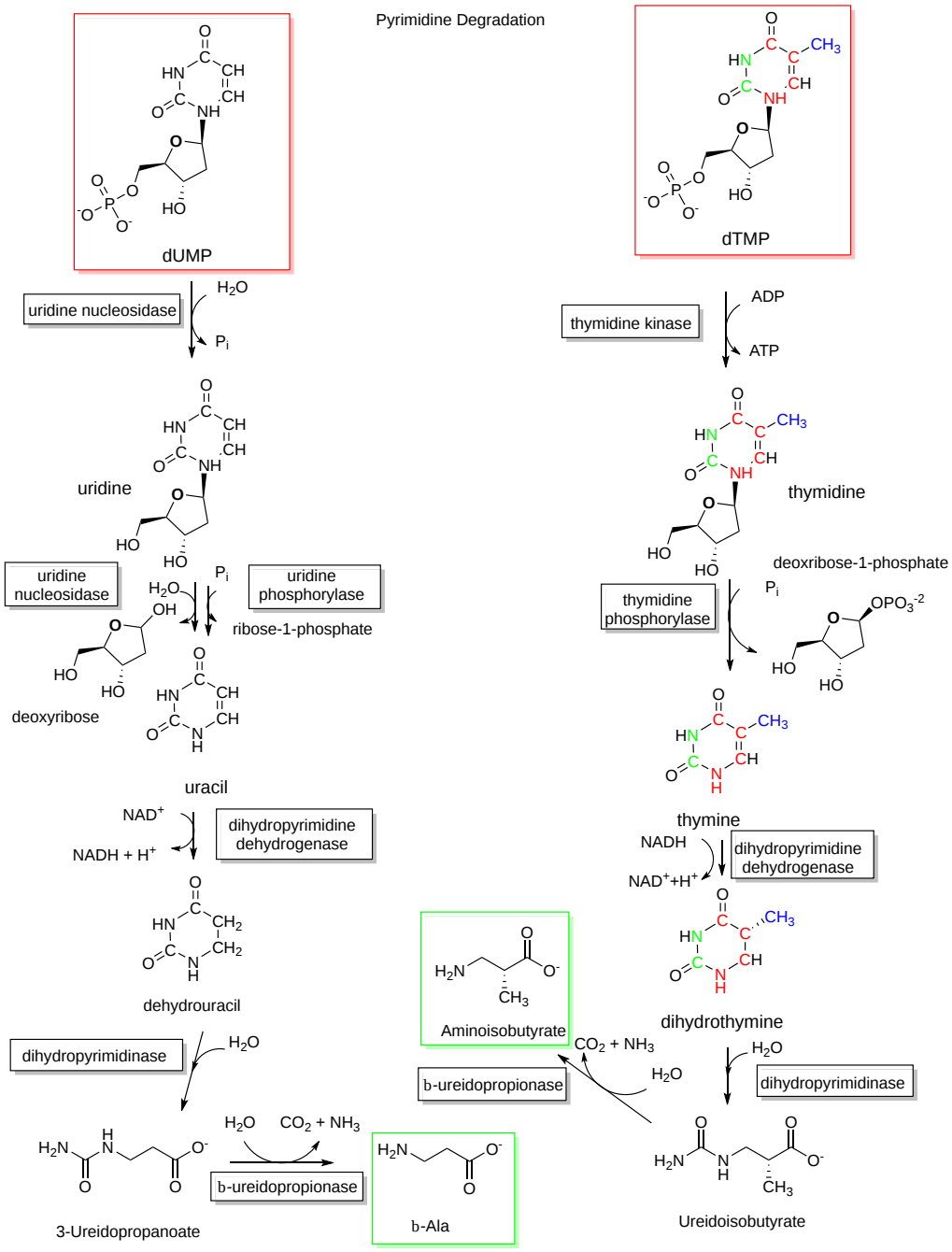


Figure **22.4.26**: Pyrimidine degradation

22.4.7: SUMMARY

This chapter concludes our exploration of metabolic pathways by focusing on the biosynthesis, interconversion, and degradation of nucleotides—the essential building blocks of nucleic acids—and their critical roles in energy metabolism and signal transduction.

1. Importance and Roles of Nucleotides

- **Fundamental Functions:**
  Nucleotides not only serve as the monomeric units of DNA and RNA but also function as universal energy carriers (e.g., ATP, GTP) and key signaling molecules. Their metabolism is intricately connected with the overall energy status and regulatory mechanisms of the cell.
- **Integration with Amino Acid Metabolism:**
  Many atoms in the purine and pyrimidine rings are derived from amino acids (e.g., glutamine, aspartate, glycine, serine). This link emphasizes the interconnectedness of amino acid and nucleotide metabolism.

2. Purine Biosynthesis

- **De Novo Pathway:**
  The purine de novo synthesis pathway builds the purine ring on a ribose-phosphate backbone (derived from PRPP) in a series of 10 steps catalyzed by multifunctional enzymes (such as the trifunctional TGART, bifunctional PAICS and ATIC, along with several monofunctional enzymes). Key nitrogen atoms come from glutamine and aspartate, while glycine and one-carbon units (from 5,10-methylenetetrahydrofolate) contribute essential carbon atoms. The end product, inosine monophosphate (IMP), serves as a branch point for the formation of both AMP and GMP.
- **Salvage Pathway:**
  To conserve energy, cells recycle free purine bases from nucleic acid turnover. Enzymes like adenine phosphoribosyltransferase (APRT) and hypoxanthine-guanine phosphoribosyltransferase (HGPRT) use PRPP to convert these bases back into nucleoside monophosphates.

3. Pyrimidine Biosynthesis

- **Direct Assembly as Ribonucleotides:**
  Unlike purines, pyrimidine rings are synthesized as part of the ribonucleotide. The pathway starts with the formation of carbamoyl phosphate (using CPS II, which uses glutamine as the nitrogen donor) and aspartate, leading to the production of UMP. Subsequent phosphorylation steps yield UTP and CTP, and the methylation of deoxy-UMP (using 5,10-meTHF) produces dTMP.

4. Deoxynucleotide Formation

- **Ribonucleotide Reductase (RNR):**
  RNR catalyzes the reduction of ribonucleotides to deoxyribonucleotides—a reaction critical for DNA synthesis and repair. This enzyme employs a radical mechanism and is tightly regulated through allosteric effectors (ATP, dATP, dGTP, dTTP) that modulate both substrate specificity and overall enzymatic activity. The regulation of RNR ensures balanced deoxynucleotide pools and prevents DNA damage.

5. Nucleotide Degradation

- **Purine and Pyrimidine Catabolism:**
  Nucleotide degradation involves a series of reactions that break down purine and pyrimidine bases into waste products (such as uric acid for purines) that are excreted. These pathways not only remove excess nucleotides but also recycle components for reuse in biosynthetic pathways.

6. Regulation and Integration with Cellular Metabolism

- **Feedback and Allosteric Regulation:**
  The de novo synthesis of purines is controlled by feedback inhibition (e.g., PPAT is allosterically inhibited by downstream nucleotides), and both purine and pyrimidine pathways are responsive to substrate availability and energy status. In addition, formation of multi-enzyme complexes like the purinosome optimizes metabolic flux by co-localizing pathway enzymes with mitochondrial sources of ATP and one-carbon units.
- **Interplay with Energy Metabolism:**
  Nucleotide metabolism is linked to the central energy-generating pathways, including glycolysis and the citric acid cycle. For example, intermediates from the TCA cycle (e.g., oxaloacetate and α-ketoglutarate) are precursors for amino acids that feed into nucleotide biosynthesis.
- **Clinical Relevance:**
  Disruptions in nucleotide metabolism can lead to imbalances in energy production and signal transduction, contributing to various diseases (such as cancer, where rapidly proliferating cells require robust nucleotide synthesis). Understanding these pathways also lays the groundwork for therapeutic strategies targeting nucleotide metabolism in disease.

This chapter integrates the biochemistry of nucleotide synthesis, interconversion, and degradation with broader cellular functions. It emphasizes how nucleotide metabolism is interwoven with amino acid metabolism, energy production, and regulatory networks that maintain cellular homeostasis and support growth, proliferation, and response to environmental cues.

This page titled 22.4: Biosynthesis and Degradation of Nucleotides is shared under a not declared license and was authored, remixed, and/or curated by Henry Jakubowski and Patricia Flatt.

- **Current page** by Henry Jakubowski and Patricia Flatt has no license indicated.
- **11.2: Diffusion Across a Membrane - Passive and Facilitated Diffusion** by Henry Jakubowski and Patricia Flatt has no license indicated.

INDEX

A

acetaldehyde
13.2: Fates of Pyruvate under Anaerobic Conditions-Fermentation

acetaldehyde toxicity
13.2: Fates of Pyruvate under Anaerobic Conditions-Fermentation

active transport
12.2: Phosphoryl Group Transfers and ATP

active transport systems
12.2: Phosphoryl Group Transfers and ATP

Acyltransferases
21.2: Biosynthesis of Triacylglycerols
21.3: Biosynthesis of Membrane Glycerolipids

adaptation
14.5: Metabolism and Signaling: The Steady State, Adaptation and Homeostasis

adaptive mechanisms
20.1: Light Absorption in Photosynthesis - An Overview

adaptive motifs
14.5: Metabolism and Signaling: The Steady State, Adaptation and Homeostasis

adipose tissue
17.1: Digestion, Mobilization, and Transport of Fats
21.2: Biosynthesis of Triacylglycerols

ADP
19.3: Regulation of Oxidative Phosphorylation

ADP/ATP ratio
19.3: Regulation of Oxidative Phosphorylation

aerobic glycolysis
14.3: The Flux Control Coefficient

aerobic metabolism
13.1: Glycolysis
14.3: The Flux Control Coefficient

aerobic processes
18.1: The Biochemistry of Nitrogen in the Biosphere

AGPAT
21.3: Biosynthesis of Membrane Glycerolipids

alanine cycle
18.2: Metabolic Fates of Amino Groups

alcohol dehydrogenase
13.2: Fates of Pyruvate under Anaerobic Conditions-Fermentation

alcohol metabolism
13.2: Fates of Pyruvate under Anaerobic Conditions-Fermentation

alcoholic liver damage
13.2: Fates of Pyruvate under Anaerobic Conditions-Fermentation

alcoholism treatment
13.2: Fates of Pyruvate under Anaerobic Conditions-Fermentation

aldehyde dehydrogenase
13.2: Fates of Pyruvate under Anaerobic Conditions-Fermentation

aldehydes
12.1: Biochemical Reactions and Energy Changes

allosteric effectors
15.5: Regulation of Gluconeogenesis
19.3: Regulation of Oxidative Phosphorylation

allosteric regulation
13.2: Fates of Pyruvate under Anaerobic Conditions-Fermentation
14.1: Regulation of Metabolic Pathways
14.5: Metabolism and Signaling: The Steady State, Adaptation and Homeostasis
15.4: Regulation of Glycolysis
16.3: Regulation of the Citric Acid Cycle
18.3: Nitrogen Excretion and the Urea Cycle

allosteric sites
14.1: Regulation of Metabolic Pathways

alpha oxidation
17.2: Oxidation of Fatty Acids

alternative oxidation pathways
17.2: Oxidation of Fatty Acids

amino acid catabolism
18.2: Metabolic Fates of Amino Groups
18.4: An Overview of Amino Acid Metabolism and the Role of Cofactors
18.5: Pathways of Amino Acid Degradation

amino acid degradation
18.4: An Overview of Amino Acid Metabolism and the Role of Cofactors
18.5: Pathways of Amino Acid Degradation

amino acid metabolism
18.4: An Overview of Amino Acid Metabolism and the Role of Cofactors

amino acids
13.3: Gluconeogenesis
18.1: The Biochemistry of Nitrogen in the Biosphere

ammonia detoxification
18.3: Nitrogen Excretion and the Urea Cycle

ammonia production
18.2: Metabolic Fates of Amino Groups

ammonia transport
18.2: Metabolic Fates of Amino Groups

ammonification
18.1: The Biochemistry of Nitrogen in the Biosphere

ammonium equivalents
18.2: Metabolic Fates of Amino Groups

AMP
15.4: Regulation of Glycolysis
19.3: Regulation of Oxidative Phosphorylation

anabolic reactions
13.4: Pentose Phosphate Pathway of Glucose Oxidation

anaerobic conditions
13.1: Glycolysis

anaerobic metabolism
13.2: Fates of Pyruvate under Anaerobic Conditions-Fermentation

anaerobic processes
18.1: The Biochemistry of Nitrogen in the Biosphere

anaerobic respiration
13.2: Fates of Pyruvate under Anaerobic Conditions-Fermentation

anammox reaction
18.1: The Biochemistry of Nitrogen in the Biosphere

anaplerotic reactions
16.2: Reactions of the Citric Acid Cycle

antenna proteins
20.1: Light Absorption in Photosynthesis - An Overview

antioxidant defenses
13.4: Pentose Phosphate Pathway of Glucose Oxidation

antioxidants
12.3: The Chemistry and Biochemistry of Dioxygen
20.1: Light Absorption in Photosynthesis - An Overview

antiport
12.2: Phosphoryl Group Transfers and ATP

apolipoproteins
17.1: Digestion, Mobilization, and Transport of Fats

arachidonic acid
21.1: Biosynthesis of Fatty Acids and Eicosanoids

arginase
18.3: Nitrogen Excretion and the Urea Cycle

argininosuccinate lyase
18.3: Nitrogen Excretion and the Urea Cycle

argininosuccinate synthase
18.3: Nitrogen Excretion and the Urea Cycle

atmospheric nitrogen
18.1: The Biochemistry of Nitrogen in the Biosphere

ATP
15.4: Regulation of Glycolysis
19.3: Regulation of Oxidative Phosphorylation

ATP hydrolysis
12.2: Phosphoryl Group Transfers and ATP

ATP production
13.1: Glycolysis
16.2: Reactions of the Citric Acid Cycle

ATP synthase
19.3: Regulation of Oxidative Phosphorylation

ATP synthesis
12.2: Phosphoryl Group Transfers and ATP
19.1: Electron-Transfer Reactions in Mitochondria
19.2: ATP Synthesis
19.3: Regulation of Oxidative Phosphorylation
20.1: Light Absorption in Photosynthesis - An Overview
20.3: Plant Electron Transport and ATP Synthesis

ATP usage
13.3: Gluconeogenesis

ATP utilization
18.3: Nitrogen Excretion and the Urea Cycle

B

basicity
12.1: Biochemical Reactions and Energy Changes

binding interactions
14.5: Metabolism and Signaling: The Steady State, Adaptation and Homeostasis

biochemical adaptation
16.4: Variants of the Citric Acid Cycle

biochemical mechanisms
15.2: Glycogenesis

biochemical pathways
15.2: Glycogenesis
16.1: Production of Acetyl-CoA (Activated Acetate)
16.2: Reactions of the Citric Acid Cycle
17.2: Oxidation of Fatty Acids
19.1: Electron-Transfer Reactions in Mitochondria
20.6: Biosynthesis of Starch, Sucrose and Cellulose
21.1: Biosynthesis of Fatty Acids and Eicosanoids

biochemical reactions
12.2: Phosphoryl Group Transfers and ATP
13.1: Glycolysis
14.4: Concentration Control and Elasticity Coefficients
18.1: The Biochemistry of Nitrogen in the Biosphere

biochemical regulation
20.3: Plant Electron Transport and ATP Synthesis

biochemical roles
12.4: Biological Oxidation-Reduction Reactions

biochemical strategies
18.2: Metabolic Fates of Amino Groups

biochemistry
12.1: Biochemical Reactions and Energy Changes
12.3: The Chemistry and Biochemistry of Dioxygen
12.4: Biological Oxidation-Reduction Reactions
13.1: Glycolysis
13.2: Fates of Pyruvate under Anaerobic Conditions-Fermentation
13.3: Gluconeogenesis
14.1: Regulation of Metabolic Pathways
14.3: The Flux Control Coefficient
14.4: Concentration Control and Elasticity Coefficients
14.5: Metabolism and Signaling: The Steady State, Adaptation and Homeostasis
15.1: Insulin Signaling in the Liver
15.3: Glycogenolysis and its Regulation by Glucagon and Epinephrine Signaling
15.4: Regulation of Glycolysis
15.5: Regulation of Gluconeogenesis
16.3: Regulation of the Citric Acid Cycle
16.4: Variants of the Citric Acid Cycle
17.1: Digestion, Mobilization, and Transport of Fats
17.2: Oxidation of Fatty Acids
17.3: Ketone Bodies
18.1: The Biochemistry of Nitrogen in the Biosphere
18.3: Nitrogen Excretion and the Urea Cycle
18.5: Pathways of Amino Acid Degradation
19.1: Electron-Transfer Reactions in Mitochondria
20.1: Light Absorption in Photosynthesis - An Overview
20.4: CO_2 uptake - Calvin Cycle and C3 organisms
20.6: Biosynthesis of Starch, Sucrose and Cellulose
21.2: Biosynthesis of Triacylglycerols

biochemistry education
15.2: Glycogenesis
19.2: ATP Synthesis

biochemistry learning goals
18.4: An Overview of Amino Acid Metabolism and the Role of Cofactors
19.2: ATP Synthesis
21.2: Biosynthesis of Triacylglycerols

bioenergetics
20.2: The Kok Cycle and Oxygen Evolving Complex of Photosystem II
20.3: Plant Electron Transport and ATP Synthesis
21.3: Biosynthesis of Membrane Glycerolipids

biological energy transformations
12.4: Biological Oxidation-Reduction Reactions

biological systems
12.4: Biological Oxidation-Reduction Reactions

biosynthesis
16.2: Reactions of the Citric Acid Cycle
18.1: The Biochemistry of Nitrogen in the Biosphere
18.5: Pathways of Amino Acid Degradation

biosynthetic processes
18.4: An Overview of Amino Acid Metabolism and the Role of Cofactors

biotin cofactor
13.3: Gluconeogenesis

blood glucose homeostasis
15.3: Glycogenolysis and its Regulation by Glucagon and Epinephrine Signaling

blood glucose regulation
15.1: Insulin Signaling in the Liver

blood urea nitrogen
18.3: Nitrogen Excretion and the Urea Cycle

bond breaking
12.1: Biochemical Reactions and Energy Changes

C

C3 plants
20.4: CO_2 uptake - Calvin Cycle and C3 organisms

C4 pathway
20.5: CO2 uptake - C4 and CAM Pathways

Calvin cycle
20.4: CO_2 uptake - Calvin Cycle and C3 organisms
20.5: CO2 uptake - C4 and CAM Pathways

CAM pathway
20.5: CO2 uptake - C4 and CAM Pathways

cancer risk
13.2: Fates of Pyruvate under Anaerobic Conditions-Fermentation

carbamoyl phosphate
18.3: Nitrogen Excretion and the Urea Cycle

carbohydrate biosynthesis
20.6: Biosynthesis of Starch, Sucrose and Cellulose

carbohydrate metabolism
13.1: Glycolysis

carbon capture
20.4: CO_2 uptake - Calvin Cycle and C3 organisms

carbon metabolism
18.2: Metabolic Fates of Amino Groups

carbon sequestration
20.5: CO2 uptake - C4 and CAM Pathways

carbon skeletons
18.4: An Overview of Amino Acid Metabolism and the Role of Cofactors

carbonic anhydrase
20.5: CO2 uptake - C4 and CAM Pathways

carbonyl reactions
12.1: Biochemical Reactions and Energy Changes

carboxylic acids
12.1: Biochemical Reactions and Energy Changes

carboxysome
20.4: CO_2 uptake - Calvin Cycle and C3 organisms

carboxysomes
20.5: CO2 uptake - C4 and CAM Pathways

cardioprotective alcohol effects
13.2: Fates of Pyruvate under Anaerobic Conditions-Fermentation

cardiovascular risk
17.1: Digestion, Mobilization, and Transport of Fats

catalysis
16.1: Production of Acetyl-CoA (Activated Acetate)

catalysts
12.1: Biochemical Reactions and Energy Changes

catalytic mechanism
21.1: Biosynthesis of Fatty Acids and Eicosanoids

cell physiology
21.2: Biosynthesis of Triacylglycerols

cellular biosynthesis
13.4: Pentose Phosphate Pathway of Glucose Oxidation

cellular compartmentalization
21.2: Biosynthesis of Triacylglycerols

cellular energetics
12.2: Phosphoryl Group Transfers and ATP

cellular energy
13.1: Glycolysis
17.2: Oxidation of Fatty Acids

cellular energy metabolism
16.1: Production of Acetyl-CoA (Activated Acetate)
16.3: Regulation of the Citric Acid Cycle
19.3: Regulation of Oxidative Phosphorylation

cellular energy production
19.2: ATP Synthesis

cellular homeostasis
14.5: Metabolism and Signaling: The Steady State, Adaptation and Homeostasis

cellular metabolism
12.4: Biological Oxidation-Reduction Reactions
14.3: The Flux Control Coefficient
14.4: Concentration Control and Elasticity Coefficients
16.2: Reactions of the Citric Acid Cycle
18.5: Pathways of Amino Acid Degradation
19.1: Electron-Transfer Reactions in Mitochondria
21.1: Biosynthesis of Fatty Acids and Eicosanoids

cellular regulation
13.4: Pentose Phosphate Pathway of Glucose Oxidation

cellulose structure
20.6: Biosynthesis of Starch, Sucrose and Cellulose

cellulose synthesis
20.6: Biosynthesis of Starch, Sucrose and Cellulose

Ceramide
21.4: Biosynthesis of Membrane Sphingolipids

CF1F0ATPase
20.3: Plant Electron Transport and ATP Synthesis

chlorophyll
20.1: Light Absorption in Photosynthesis - An Overview
20.2: The Kok Cycle and Oxygen Evolving Complex of Photosystem II

chlorophyll a and b
20.1: Light Absorption in Photosynthesis - An Overview

chloroplast
20.1: Light Absorption in Photosynthesis - An Overview
20.4: CO_2 uptake - Calvin Cycle and C3 organisms

chloroplasts
20.3: Plant Electron Transport and ATP Synthesis
Cholesterol Biosynthesis
21.5: Biosynthesis of Cholesterol and Steroids
cholesterol homeostasis
17.1: Digestion, Mobilization, and Transport of Fats
cholesterol metabolism
17.1: Digestion, Mobilization, and Transport of Fats
chronic alcohol effects
13.2: Fates of Pyruvate under Anaerobic Conditions-Fermentation
chronic drinking
13.2: Fates of Pyruvate under Anaerobic Conditions-Fermentation
citric acid cycle
16: The Citric Acid Cycle
16.1: Production of Acetyl-CoA (Activated Acetate)
16.2: Reactions of the Citric Acid Cycle
16.3: Regulation of the Citric Acid Cycle
16.4: Variants of the Citric Acid Cycle
18.3: Nitrogen Excretion and the Urea Cycle
19.3: Regulation of Oxidative Phosphorylation
clinical implications
17.1: Digestion, Mobilization, and Transport of Fats
CO2 fixation
20.4: CO_2 uptake - Calvin Cycle and C3 organisms
20.5: CO2 uptake - C4 and CAM Pathways
cofactor chemistry
16.1: Production of Acetyl-CoA (Activated Acetate)
cofactors in metabolism
18.4: An Overview of Amino Acid Metabolism and the Role of Cofactors
committed step enzymes
14.1: Regulation of Metabolic Pathways
committed steps
14.1: Regulation of Metabolic Pathways
complex I
19.1: Electron-Transfer Reactions in Mitochondria
complex II
19.1: Electron-Transfer Reactions in Mitochondria
complex III
19.1: Electron-Transfer Reactions in Mitochondria
complex IV
19.1: Electron-Transfer Reactions in Mitochondria
computational modeling
14.2: Basic Principles of Metabolic Control Analysis (MCA)
14.3: The Flux Control Coefficient
concentration control coefficient
14.4: Concentration Control and Elasticity Coefficients
14.5: Metabolism and Signaling: The Steady State, Adaptation and Homeostasis
Cori cycle
13.2: Fates of Pyruvate under Anaerobic Conditions-Fermentation
coupling
19.3: Regulation of Oxidative Phosphorylation
covalent modification
14.1: Regulation of Metabolic Pathways
covalent modifications
14.1: Regulation of Metabolic Pathways
cristae formation
19.3: Regulation of Oxidative Phosphorylation
cyclic pathways
16.2: Reactions of the Citric Acid Cycle
cyclooxygenases
21.1: Biosynthesis of Fatty Acids and Eicosanoids
cytochrome b6f complex
20.3: Plant Electron Transport and ATP Synthesis
cytochrome P450
12.4: Biological Oxidation-Reduction Reactions
21.1: Biosynthesis of Fatty Acids and Eicosanoids
cytoskeletal interaction
19.3: Regulation of Oxidative Phosphorylation

D

dark reactions
20.1: Light Absorption in Photosynthesis - An Overview
20.4: CO_2 uptake - Calvin Cycle and C3 organisms
deamination reactions
18.2: Metabolic Fates of Amino Groups
dehydrogenases
12.4: Biological Oxidation-Reduction Reactions
denitrification
18.1: The Biochemistry of Nitrogen in the Biosphere
DGAT enzymes
21.2: Biosynthesis of Triacylglycerols
diabetic ketoacidosis
17.3: Ketone Bodies
dioxygen
12.3: The Chemistry and Biochemistry of Dioxygen
dioxygen history
12.3: The Chemistry and Biochemistry of Dioxygen
dioxygen properties
12.3: The Chemistry and Biochemistry of Dioxygen
dioxygenases
12.4: Biological Oxidation-Reduction Reactions
disulfiram
13.2: Fates of Pyruvate under Anaerobic Conditions-Fermentation
DNA methylation
13.2: Fates of Pyruvate under Anaerobic Conditions-Fermentation
DNA oxidation
12.3: The Chemistry and Biochemistry of Dioxygen

E

ecosystem impact
18.1: The Biochemistry of Nitrogen in the Biosphere
eicosanoid biosynthesis
21.1: Biosynthesis of Fatty Acids and Eicosanoids
eicosanoids
21.1: Biosynthesis of Fatty Acids and Eicosanoids
elasticity coefficient
14.4: Concentration Control and Elasticity Coefficients
14.5: Metabolism and Signaling: The Steady State, Adaptation and Homeostasis
electrogenic transport
12.2: Phosphoryl Group Transfers and ATP
electron carriers
12.4: Biological Oxidation-Reduction Reactions
20.1: Light Absorption in Photosynthesis - An Overview
20.2: The Kok Cycle and Oxygen Evolving Complex of Photosystem II
electron transfer
12.1: Biochemical Reactions and Energy Changes
electron transport
20.1: Light Absorption in Photosynthesis - An Overview
electron transport chain
19.1: Electron-Transfer Reactions in Mitochondria
19.2: ATP Synthesis
19.3: Regulation of Oxidative Phosphorylation
20.2: The Kok Cycle and Oxygen Evolving Complex of Photosystem II
20.3: Plant Electron Transport and ATP Synthesis
electroneutral transport
12.2: Phosphoryl Group Transfers and ATP
energy changes
12.1: Biochemical Reactions and Energy Changes
energy conversion
13.1: Glycolysis
20.3: Plant Electron Transport and ATP Synthesis
energy coupling
12.2: Phosphoryl Group Transfers and ATP
energy deficit
17.3: Ketone Bodies
energy demand
15.4: Regulation of Glycolysis
energy dissipation
20.1: Light Absorption in Photosynthesis - An Overview
energy distribution
20.1: Light Absorption in Photosynthesis - An Overview
energy extraction
16.1: Production of Acetyl-CoA (Activated Acetate)
energy homeostasis
16.2: Reactions of the Citric Acid Cycle
17.3: Ketone Bodies
21.2: Biosynthesis of Triacylglycerols
energy metabolism
13.3: Gluconeogenesis
16.4: Variants of the Citric Acid Cycle
17.1: Digestion, Mobilization, and Transport of Fats
18.4: An Overview of Amino Acid Metabolism and the Role of Cofactors
19.1: Electron-Transfer Reactions in Mitochondria
19.3: Regulation of Oxidative Phosphorylation
energy mobilization
15.2: Glycogenesis
energy production
13.2: Fates of Pyruvate under Anaerobic Conditions-Fermentation
17.2: Oxidation of Fatty Acids
18.1: The Biochemistry of Nitrogen in the Biosphere
18.3: Nitrogen Excretion and the Urea Cycle
18.5: Pathways of Amino Acid Degradation

energy reserves
15.1: Insulin Signaling in the Liver
energy status
19.3: Regulation of Oxidative Phosphorylation
energy storage
15.2: Glycogenesis
21.2: Biosynthesis of Triacylglycerols
energy substrates
17.3: Ketone Bodies
energy transfer
20.1: Light Absorption in Photosynthesis - An Overview
environmental adaptation
20.5: CO2 uptake - C4 and CAM Pathways
enzymatic detoxification
12.3: The Chemistry and Biochemistry of Dioxygen
enzymatic mechanisms
20.5: CO2 uptake - C4 and CAM Pathways
21.2: Biosynthesis of Triacylglycerols
enzymatic regulation
15.3: Glycogenolysis and its Regulation by Glucagon and Epinephrine Signaling
enzyme abundance
14.1: Regulation of Metabolic Pathways
enzyme activity
14.1: Regulation of Metabolic Pathways
14.3: The Flux Control Coefficient
14.4: Concentration Control and Elasticity Coefficients
14.5: Metabolism and Signaling: The Steady State, Adaptation and Homeostasis
enzyme catalysis
12.1: Biochemical Reactions and Energy Changes
12.2: Phosphoryl Group Transfers and ATP
12.4: Biological Oxidation-Reduction Reactions
enzyme concentration
14.1: Regulation of Metabolic Pathways
enzyme condensates
14.1: Regulation of Metabolic Pathways
enzyme function
15.2: Glycogenesis
16.2: Reactions of the Citric Acid Cycle
17.1: Digestion, Mobilization, and Transport of Fats
enzyme importance
14.3: The Flux Control Coefficient
enzyme inhibition
14.2: Basic Principles of Metabolic Control Analysis (MCA)
enzyme kinetics
14.2: Basic Principles of Metabolic Control Analysis (MCA)
14.3: The Flux Control Coefficient
14.4: Concentration Control and Elasticity Coefficients
14.5: Metabolism and Signaling: The Steady State, Adaptation and Homeostasis
18.3: Nitrogen Excretion and the Urea Cycle
enzyme mechanisms
12.2: Phosphoryl Group Transfers and ATP
13.1: Glycolysis
13.2: Fates of Pyruvate under Anaerobic Conditions-Fermentation
13.3: Gluconeogenesis
13.4: Pentose Phosphate Pathway of Glucose Oxidation
16.2: Reactions of the Citric Acid Cycle
17.2: Oxidation of Fatty Acids
17.3: Ketone Bodies
18.3: Nitrogen Excretion and the Urea Cycle
18.5: Pathways of Amino Acid Degradation
20.6: Biosynthesis of Starch, Sucrose and Cellulose
enzyme modulation
14.1: Regulation of Metabolic Pathways
enzyme regulation
13.1: Glycolysis
13.2: Fates of Pyruvate under Anaerobic Conditions-Fermentation
14.1: Regulation of Metabolic Pathways
14.3: The Flux Control Coefficient
14.4: Concentration Control and Elasticity Coefficients
15.2: Glycogenesis
15.4: Regulation of Glycolysis
15.5: Regulation of Gluconeogenesis
16.3: Regulation of the Citric Acid Cycle
18.2: Metabolic Fates of Amino Groups
19.2: ATP Synthesis
20.4: CO_2 uptake - Calvin Cycle and C3 organisms
20.6: Biosynthesis of Starch, Sucrose and Cellulose
21.1: Biosynthesis of Fatty Acids and Eicosanoids
enzyme structure
16.1: Production of Acetyl-CoA (Activated Acetate)
enzyme structure and function
19.2: ATP Synthesis
epinephrine signaling
15.3: Glycogenolysis and its Regulation by Glucagon and Epinephrine Signaling
equilibrium
14.2: Basic Principles of Metabolic Control Analysis (MCA)
equilibrium enzymes
14.1: Regulation of Metabolic Pathways
ethanol fermentation
13.2: Fates of Pyruvate under Anaerobic Conditions-Fermentation
ethanol oxidation
13.2: Fates of Pyruvate under Anaerobic Conditions-Fermentation
ethanolic fermentation
13.2: Fates of Pyruvate under Anaerobic Conditions-Fermentation

F

F₁F₀ATPase
19.2: ATP Synthesis
FAD
16.1: Production of Acetyl-CoA (Activated Acetate)
FAD/FADH2
12.4: Biological Oxidation-Reduction Reactions
FADH2
16.2: Reactions of the Citric Acid Cycle
FAS
21.1: Biosynthesis of Fatty Acids and Eicosanoids
fasting
17.3: Ketone Bodies
fat digestion
17.1: Digestion, Mobilization, and Transport of Fats
fat synthesis
17.1: Digestion, Mobilization, and Transport of Fats
fatty acid biosynthesis
21.1: Biosynthesis of Fatty Acids and Eicosanoids
fatty acid degradation
16.4: Variants of the Citric Acid Cycle
fatty acid metabolism
17.3: Ketone Bodies
21.2: Biosynthesis of Triacylglycerols
fatty acid metabolism diseases
17.2: Oxidation of Fatty Acids
Fatty Acid Oxidation
17.2: Oxidation of Fatty Acids
fatty acid synthase
17.1: Digestion, Mobilization, and Transport of Fats
21.1: Biosynthesis of Fatty Acids and Eicosanoids
fatty acid synthase complex
21.1: Biosynthesis of Fatty Acids and Eicosanoids
fatty acids
17.1: Digestion, Mobilization, and Transport of Fats
21.1: Biosynthesis of Fatty Acids and Eicosanoids
Fe2+ reactivity
12.3: The Chemistry and Biochemistry of Dioxygen
feedback inhibition
15.4: Regulation of Glycolysis
16.3: Regulation of the Citric Acid Cycle
feedback loops
14.5: Metabolism and Signaling: The Steady State, Adaptation and Homeostasis
feedforward loops
14.5: Metabolism and Signaling: The Steady State, Adaptation and Homeostasis
feedforward stimulation
15.4: Regulation of Glycolysis
15.5: Regulation of Gluconeogenesis
Fenton reaction
12.3: The Chemistry and Biochemistry of Dioxygen
fermentation
13.2: Fates of Pyruvate under Anaerobic Conditions-Fermentation
ferredoxin
20.2: The Kok Cycle and Oxygen Evolving Complex of Photosystem II
ferritin
12.3: The Chemistry and Biochemistry of Dioxygen
flux control coefficient
14.3: The Flux Control Coefficient
folate cycle
18.4: An Overview of Amino Acid Metabolism and the Role of Cofactors
free energy
12.1: Biochemical Reactions and Energy Changes
12.2: Phosphoryl Group Transfers and ATP

fructokinase
15.4: Regulation of Glycolysis

fructose metabolism
15.4: Regulation of Glycolysis

fructose regulatory bypass
15.4: Regulation of Glycolysis
15.5: Regulation of Gluconeogenesis

fumarate
18.3: Nitrogen Excretion and the Urea Cycle

G

GABA shunt
16.4: Variants of the Citric Acid Cycle

gene expression
18.3: Nitrogen Excretion and the Urea Cycle

gene transcription
14.1: Regulation of Metabolic Pathways

Gibbs Free Energy
12.1: Biochemical Reactions and Energy Changes

glucagon
15.3: Glycogenolysis and its Regulation by Glucagon and Epinephrine Signaling
15.5: Regulation of Gluconeogenesis

glucagon signaling
15.3: Glycogenolysis and its Regulation by Glucagon and Epinephrine Signaling

glucogenic amino acids
18.4: An Overview of Amino Acid Metabolism and the Role of Cofactors
18.5: Pathways of Amino Acid Degradation

gluconeogenesis
13.3: Gluconeogenesis
15.4: Regulation of Glycolysis
15.5: Regulation of Gluconeogenesis
16.4: Variants of the Citric Acid Cycle
17.3: Ketone Bodies

gluconeogenesis regulation
13.3: Gluconeogenesis

glucose homeostasis
13.3: Gluconeogenesis
15.1: Insulin Signaling in the Liver

glucose metabolism
13.1: Glycolysis
13.4: Pentose Phosphate Pathway of Glucose Oxidation
15.2: Glycogenesis
15.3: Glycogenolysis and its Regulation by Glucagon and Epinephrine Signaling
15.4: Regulation of Glycolysis

glucose synthesis
13.3: Gluconeogenesis

gluDH isozymes
18.2: Metabolic Fates of Amino Groups

glutamate dehydrogenase
18.2: Metabolic Fates of Amino Groups

glutaminase
18.2: Metabolic Fates of Amino Groups

glutamine
18.3: Nitrogen Excretion and the Urea Cycle

glutamine synthetase
18.2: Metabolic Fates of Amino Groups

glycogen branching
15.1: Insulin Signaling in the Liver

glycogen branching enzyme
15.2: Glycogenesis

glycogen breakdown
15.3: Glycogenolysis and its Regulation by Glucagon and Epinephrine Signaling

glycogen debranching enzyme
15.3: Glycogenolysis and its Regulation by Glucagon and Epinephrine Signaling

glycogen metabolism
15.1: Insulin Signaling in the Liver
15.2: Glycogenesis

glycogen phosphorylase
15.3: Glycogenolysis and its Regulation by Glucagon and Epinephrine Signaling

glycogen structure
15.1: Insulin Signaling in the Liver

glycogen synthase
15.2: Glycogenesis

glycogen synthesis
15.1: Insulin Signaling in the Liver

glycogenesis
15.2: Glycogenesis

glycogenin
15.2: Glycogenesis

glycogenolysis
15.1: Insulin Signaling in the Liver
15.2: Glycogenesis
15.3: Glycogenolysis and its Regulation by Glucagon and Epinephrine Signaling

glycolate cycle
20.4: CO_2 uptake - Calvin Cycle and C3 organisms

glycolysis
13.1: Glycolysis
13.2: Fates of Pyruvate under Anaerobic Conditions-Fermentation
13.3: Gluconeogenesis
13.4: Pentose Phosphate Pathway of Glucose Oxidation
14.2: Basic Principles of Metabolic Control Analysis (MCA)
14.3: The Flux Control Coefficient
15.4: Regulation of Glycolysis
15.5: Regulation of Gluconeogenesis
16.1: Production of Acetyl-CoA (Activated Acetate)
19.3: Regulation of Oxidative Phosphorylation

glycolytic pathway
13.1: Glycolysis
14.3: The Flux Control Coefficient
15.4: Regulation of Glycolysis
15.5: Regulation of Gluconeogenesis

glycosidic bonds
15.1: Insulin Signaling in the Liver

glycosyltransferases
20.6: Biosynthesis of Starch, Sucrose and Cellulose

glyoxylate cycle
16.4: Variants of the Citric Acid Cycle

glyoxylate Shunt
16.4: Variants of the Citric Acid Cycle

gout
13.2: Fates of Pyruvate under Anaerobic Conditions-Fermentation

GPAT
21.3: Biosynthesis of Membrane Glycerolipids

grana
20.1: Light Absorption in Photosynthesis - An Overview

greenhouse gas
18.1: The Biochemistry of Nitrogen in the Biosphere

H

health and metabolism
17.2: Oxidation of Fatty Acids

hexokinase
15.4: Regulation of Glycolysis

hexokinase regulation
15.4: Regulation of Glycolysis
15.5: Regulation of Gluconeogenesis

histone acetylation
13.2: Fates of Pyruvate under Anaerobic Conditions-Fermentation

homeostasis
14.5: Metabolism and Signaling: The Steady State, Adaptation and Homeostasis

hormonal control
15.3: Glycogenolysis and its Regulation by Glucagon and Epinephrine Signaling

hormonal regulation
15.1: Insulin Signaling in the Liver
15.4: Regulation of Glycolysis
15.5: Regulation of Gluconeogenesis

hormone regulation
17.3: Ketone Bodies

hydroxyl radicals
12.3: The Chemistry and Biochemistry of Dioxygen

hyperammonemia
18.3: Nitrogen Excretion and the Urea Cycle

hyperbolic curves
14.5: Metabolism and Signaling: The Steady State, Adaptation and Homeostasis

hyperlipidemia
17.1: Digestion, Mobilization, and Transport of Fats

hypertriglyceridemia
15.4: Regulation of Glycolysis

hyperuricemia
13.2: Fates of Pyruvate under Anaerobic Conditions-Fermentation

I

immune response
12.3: The Chemistry and Biochemistry of Dioxygen

in vitro vs in vivo
14.2: Basic Principles of Metabolic Control Analysis (MCA)

inductive effects
12.1: Biochemical Reactions and Energy Changes

industrial fixation
18.1: The Biochemistry of Nitrogen in the Biosphere

inhibitors
19.1: Electron-Transfer Reactions in Mitochondria

insulin
15.1: Insulin Signaling in the Liver
15.5: Regulation of Gluconeogenesis

insulin receptor
15.1: Insulin Signaling in the Liver

insulin signaling
15.1: Insulin Signaling in the Liver
15.2: Glycogenesis

intermediates
16.2: Reactions of the Citric Acid Cycle

intracellular condensates
14.1: Regulation of Metabolic Pathways

ion gradients
12.2: Phosphoryl Group Transfers and ATP

isoenzymes
15.4: Regulation of Glycolysis

K

ketogenesis
17.3: Ketone Bodies

ketogenic amino acids
18.4: An Overview of Amino Acid Metabolism and the Role of Cofactors
18.5: Pathways of Amino Acid Degradation

ketogenic diet
17.3: Ketone Bodies

ketogenic pathway
17.3: Ketone Bodies

ketolysis
17.3: Ketone Bodies

Ketone bodies
13.2: Fates of Pyruvate under Anaerobic Conditions-Fermentation
17.3: Ketone Bodies

ketone body metabolism
17.3: Ketone Bodies

ketone body production
17.2: Oxidation of Fatty Acids

ketone body synthesis
17.3: Ketone Bodies

ketones
12.1: Biochemical Reactions and Energy Changes

key enzymes
21.1: Biosynthesis of Fatty Acids and Eicosanoids

kinetic equations
14.2: Basic Principles of Metabolic Control Analysis (MCA)

kinetic stability
12.2: Phosphoryl Group Transfers and ATP

kinetics
12.1: Biochemical Reactions and Energy Changes

Kok cycle
20.2: The Kok Cycle and Oxygen Evolving Complex of Photosystem II

Krebs cycle
16.2: Reactions of the Citric Acid Cycle
18.3: Nitrogen Excretion and the Urea Cycle

L

lactate dehydrogenase
13.2: Fates of Pyruvate under Anaerobic Conditions-Fermentation

lactate fermentation
13.2: Fates of Pyruvate under Anaerobic Conditions-Fermentation

lactate production
13.2: Fates of Pyruvate under Anaerobic Conditions-Fermentation

lactic acid bacteria
13.2: Fates of Pyruvate under Anaerobic Conditions-Fermentation

light absorption
20.1: Light Absorption in Photosynthesis - An Overview

light harvesting complex
20.1: Light Absorption in Photosynthesis - An Overview

light reactions
20.1: Light Absorption in Photosynthesis - An Overview
20.2: The Kok Cycle and Oxygen Evolving Complex of Photosystem II
20.4: CO_2 uptake - Calvin Cycle and C3 organisms

linkage of cycles
18.3: Nitrogen Excretion and the Urea Cycle

Lipid Biosynthesis
21.3: Biosynthesis of Membrane Glycerolipids

lipid droplets
21.2: Biosynthesis of Triacylglycerols

lipid metabolism
17.2: Oxidation of Fatty Acids
21.2: Biosynthesis of Triacylglycerols
21.5: Biosynthesis of Cholesterol and Steroids

lipid oxidation
12.3: The Chemistry and Biochemistry of Dioxygen

lipid regulation
21.2: Biosynthesis of Triacylglycerols

lipid storage
17.1: Digestion, Mobilization, and Transport of Fats

lipid transport
17.1: Digestion, Mobilization, and Transport of Fats

lipin proteins
21.2: Biosynthesis of Triacylglycerols

lipoic acid
16.1: Production of Acetyl-CoA (Activated Acetate)

lipoprotein metabolism
17.1: Digestion, Mobilization, and Transport of Fats

lipoprotein structure
17.1: Digestion, Mobilization, and Transport of Fats

lipoproteins
17.1: Digestion, Mobilization, and Transport of Fats

lipoxygenases
21.1: Biosynthesis of Fatty Acids and Eicosanoids

liver disease
13.2: Fates of Pyruvate under Anaerobic Conditions-Fermentation

liver function
21.2: Biosynthesis of Triacylglycerols

liver glycogen
15.1: Insulin Signaling in the Liver

liver metabolism
13.2: Fates of Pyruvate under Anaerobic Conditions-Fermentation
13.3: Gluconeogenesis
15.3: Glycogenolysis and its Regulation by Glucagon and Epinephrine Signaling
15.4: Regulation of Glycolysis

M

malate aspartate shuttle
18.3: Nitrogen Excretion and the Urea Cycle

malate dehydrogenase
20.5: CO2 uptake - C4 and CAM Pathways

mammalian target of rapamycin
19.3: Regulation of Oxidative Phosphorylation

mathematical framework
14.4: Concentration Control and Elasticity Coefficients

MCA
14.2: Basic Principles of Metabolic Control Analysis (MCA)

MCAD deficiency
17.2: Oxidation of Fatty Acids

Membrane Glycerolipids
21.3: Biosynthesis of Membrane Glycerolipids

membrane proteins
19.1: Electron-Transfer Reactions in Mitochondria

Membrane Sphingolipids
21.4: Biosynthesis of Membrane Sphingolipids

membrane transport
12.2: Phosphoryl Group Transfers and ATP

metabolic control
14.1: Regulation of Metabolic Pathways
14.5: Metabolism and Signaling: The Steady State, Adaptation and Homeostasis
15.4: Regulation of Glycolysis

metabolic control analysis
14.2: Basic Principles of Metabolic Control Analysis (MCA)
14.3: The Flux Control Coefficient
14.4: Concentration Control and Elasticity Coefficients

metabolic diseases
21.2: Biosynthesis of Triacylglycerols

metabolic disorders
18.5: Pathways of Amino Acid Degradation

metabolic efficiency
19.3: Regulation of Oxidative Phosphorylation

metabolic engineering
14.4: Concentration Control and Elasticity Coefficients

metabolic fate
18.1: The Biochemistry of Nitrogen in the Biosphere

metabolic flux
14.2: Basic Principles of Metabolic Control Analysis (MCA)
14.3: The Flux Control Coefficient
14.5: Metabolism and Signaling: The Steady State, Adaptation and Homeostasis

metabolic homeostasis
15.5: Regulation of Gluconeogenesis

metabolic integration
13.4: Pentose Phosphate Pathway of Glucose Oxidation
16.2: Reactions of the Citric Acid Cycle
21.2: Biosynthesis of Triacylglycerols

metabolic intermediates
18.5: Pathways of Amino Acid Degradation

metabolic intervention
15.4: Regulation of Glycolysis

metabolic networks
14.3: The Flux Control Coefficient

metabolic pathway
13.1: Glycolysis
16.2: Reactions of the Citric Acid Cycle

metabolic pathways
12.2: Phosphoryl Group Transfers and ATP
12.4: Biological Oxidation-Reduction Reactions
13.2: Fates of Pyruvate under Anaerobic Conditions-Fermentation
13.3: Gluconeogenesis
14.1: Regulation of Metabolic Pathways
14.2: Basic Principles of Metabolic Control Analysis (MCA)
14.3: The Flux Control Coefficient
14.4: Concentration Control and Elasticity Coefficients
14.5: Metabolism and Signaling: The Steady State, Adaptation and Homeostasis
15.1: Insulin Signaling in the Liver
15.4: Regulation of Glycolysis
15.5: Regulation of Gluconeogenesis
16.3: Regulation of the Citric Acid Cycle
16.4: Variants of the Citric Acid Cycle
18.2: Metabolic Fates of Amino Groups
18.3: Nitrogen Excretion and the Urea Cycle
18.4: An Overview of Amino Acid Metabolism and the Role of Cofactors
18.5: Pathways of Amino Acid Degradation
19.3: Regulation of Oxidative Phosphorylation
21.1: Biosynthesis of Fatty Acids and Eicosanoids
21.2: Biosynthesis of Triacylglycerols

metabolic processes
13.1: Glycolysis

Metabolic Regulation
14.3: The Flux Control Coefficient
14.5: Metabolism and Signaling: The Steady State, Adaptation and Homeostasis
15.2: Glycogenesis
16.1: Production of Acetyl-CoA (Activated Acetate)
16.2: Reactions of the Citric Acid Cycle
17.3: Ketone Bodies
18.3: Nitrogen Excretion and the Urea Cycle
18.5: Pathways of Amino Acid Degradation
19.1: Electron-Transfer Reactions in Mitochondria
20.6: Biosynthesis of Starch, Sucrose and Cellulose

metabolic shunts
16.4: Variants of the Citric Acid Cycle

metabolism
12.1: Biochemical Reactions and Energy Changes
13.3: Gluconeogenesis
13.4: Pentose Phosphate Pathway of Glucose Oxidation
21.3: Biosynthesis of Membrane Glycerolipids

metabolism efficiency
20.4: CO_2 uptake - Calvin Cycle and C3 organisms

metabolite concentration
14.4: Concentration Control and Elasticity Coefficients

metabolon
16.3: Regulation of the Citric Acid Cycle

methionine cycle
18.4: An Overview of Amino Acid Metabolism and the Role of Cofactors

Mevalonate Pathway
21.5: Biosynthesis of Cholesterol and Steroids

microbial metabolism
16.4: Variants of the Citric Acid Cycle

microbial processes
18.1: The Biochemistry of Nitrogen in the Biosphere

mitochondria
12.3: The Chemistry and Biochemistry of Dioxygen

mitochondrial ATP synthase
19.2: ATP Synthesis

mitochondrial electron transport
19.1: Electron-Transfer Reactions in Mitochondria
19.3: Regulation of Oxidative Phosphorylation

mitochondrial function
19.1: Electron-Transfer Reactions in Mitochondria
19.3: Regulation of Oxidative Phosphorylation

mitochondrial function regulation
19.3: Regulation of Oxidative Phosphorylation

mitochondrial genome
19.3: Regulation of Oxidative Phosphorylation

mitochondrial inner membrane
19.3: Regulation of Oxidative Phosphorylation

mitochondrial metabolism
17.2: Oxidation of Fatty Acids

mitochondrial permeability transition pore
19.3: Regulation of Oxidative Phosphorylation

mitochondrial signaling
19.3: Regulation of Oxidative Phosphorylation

mitogenesis
19.3: Regulation of Oxidative Phosphorylation

Mn4Ca cluster
20.2: The Kok Cycle and Oxygen Evolving Complex of Photosystem II

molecular level
20.1: Light Absorption in Photosynthesis - An Overview

molecular rotary motor
19.2: ATP Synthesis

monooxygenases
12.4: Biological Oxidation-Reduction Reactions

muscle glycogen
15.1: Insulin Signaling in the Liver

muscle metabolism
15.3: Glycogenolysis and its Regulation by Glucagon and Epinephrine Signaling
15.4: Regulation of Glycolysis

N

NAD+
16.1: Production of Acetyl-CoA (Activated Acetate)

NAD+ regeneration
13.2: Fates of Pyruvate under Anaerobic Conditions-Fermentation

NAD/NADH
12.4: Biological Oxidation-Reduction Reactions

NADH
16.2: Reactions of the Citric Acid Cycle

NADH/NAD+ ratio
13.2: Fates of Pyruvate under Anaerobic Conditions-Fermentation

NADPH
13.4: Pentose Phosphate Pathway of Glucose Oxidation
20.2: The Kok Cycle and Oxygen Evolving Complex of Photosystem II

NADPH formation
20.1: Light Absorption in Photosynthesis - An Overview

neurotransmitters
16.4: Variants of the Citric Acid Cycle

nitrification
18.1: The Biochemistry of Nitrogen in the Biosphere

nitrogen balance
18.3: Nitrogen Excretion and the Urea Cycle
18.4: An Overview of Amino Acid Metabolism and the Role of Cofactors
18.5: Pathways of Amino Acid Degradation

nitrogen cycle
18.1: The Biochemistry of Nitrogen in the Biosphere

nitrogen disposal
18.2: Metabolic Fates of Amino Groups
18.5: Pathways of Amino Acid Degradation

nitrogen excretion
18.3: Nitrogen Excretion and the Urea Cycle

nitrogen fixation
18.1: The Biochemistry of Nitrogen in the Biosphere

nitrogen metabolism
18.2: Metabolic Fates of Amino Groups
18.3: Nitrogen Excretion and the Urea Cycle

nitrogen metabolites
18.1: The Biochemistry of Nitrogen in the Biosphere

nitrogen transformations
18.1: The Biochemistry of Nitrogen in the Biosphere

nitrogenase
18.1: The Biochemistry of Nitrogen in the Biosphere

nonalcoholic fatty liver disease
17.1: Digestion, Mobilization, and Transport of Fats

nonoxidative branch
13.4: Pentose Phosphate Pathway of Glucose Oxidation

nucleophilic reactions
12.3: The Chemistry and Biochemistry of Dioxygen

nucleophilicity
12.1: Biochemical Reactions and Energy Changes

nucleotide biosynthesis
13.4: Pentose Phosphate Pathway of Glucose Oxidation

nutritional biochemistry
21.2: Biosynthesis of Triacylglycerols

O

obesity
21.2: Biosynthesis of Triacylglycerols

omega oxidation
17.2: Oxidation of Fatty Acids

organic chemistry
12.1: Biochemical Reactions and Energy Changes

ornithine
18.3: Nitrogen Excretion and the Urea Cycle
ornithine transcarbamylase
18.3: Nitrogen Excretion and the Urea Cycle
oxaloacetate
13.3: Gluconeogenesis
oxidant
12.3: The Chemistry and Biochemistry of Dioxygen
oxidases
12.4: Biological Oxidation-Reduction Reactions
oxidation numbers
12.1: Biochemical Reactions and Energy Changes
oxidation reactions
12.2: Phosphoryl Group Transfers and ATP
13.1: Glycolysis
oxidation states
18.1: The Biochemistry of Nitrogen in the Biosphere
oxidative aging
12.3: The Chemistry and Biochemistry of Dioxygen
oxidative and reductive reactions
16.4: Variants of the Citric Acid Cycle
oxidative branch
13.4: Pentose Phosphate Pathway of Glucose Oxidation
oxidative burst
12.3: The Chemistry and Biochemistry of Dioxygen
oxidative damage
12.3: The Chemistry and Biochemistry of Dioxygen
20.1: Light Absorption in Photosynthesis - An Overview
oxidative deamination
18.5: Pathways of Amino Acid Degradation
oxidative decarboxylation
16.1: Production of Acetyl-CoA (Activated Acetate)
oxidative phosphorylation
19.1: Electron-Transfer Reactions in Mitochondria
19.2: ATP Synthesis
19.3: Regulation of Oxidative Phosphorylation
oxidative phosphorylation regulation
19.3: Regulation of Oxidative Phosphorylation
oxidative processes
12.4: Biological Oxidation-Reduction Reactions
oxidative reactions
16.2: Reactions of the Citric Acid Cycle
oxidative stress
12.3: The Chemistry and Biochemistry of Dioxygen
19.1: Electron-Transfer Reactions in Mitochondria
oxidized state
20.3: Plant Electron Transport and ATP Synthesis
oxidizing agents
12.4: Biological Oxidation-Reduction Reactions

P

PDH complex
16.1: Production of Acetyl-CoA (Activated Acetate)
pentose phosphate pathway
13.4: Pentose Phosphate Pathway of Glucose Oxidation
peroxide
12.3: The Chemistry and Biochemistry of Dioxygen
peroxisomes
17.2: Oxidation of Fatty Acids
pH effects
14.1: Regulation of Metabolic Pathways
pharmaceutical interest
21.2: Biosynthesis of Triacylglycerols
phosphatase reactions
13.3: Gluconeogenesis
phosphatidic acid
21.2: Biosynthesis of Triacylglycerols
phosphoenolpyruvate
13.3: Gluconeogenesis
phosphoenolpyruvate carboxykinase
15.5: Regulation of Gluconeogenesis
phosphoenolpyruvate carboxylase
20.5: CO2 uptake - C4 and CAM Pathways
phosphoryl transfer
12.2: Phosphoryl Group Transfers and ATP
phosphoryl transfer reactions
12.2: Phosphoryl Group Transfers and ATP
phosphorylation
15.3: Glycogenolysis and its Regulation by Glucagon and Epinephrine Signaling
15.4: Regulation of Glycolysis
16.3: Regulation of the Citric Acid Cycle
20.1: Light Absorption in Photosynthesis - An Overview
photorespiration
20.4: CO_2 uptake - Calvin Cycle and C3 organisms
20.5: CO2 uptake - C4 and CAM Pathways
photosynthesis
20.1: Light Absorption in Photosynthesis - An Overview
20.2: The Kok Cycle and Oxygen Evolving Complex of Photosystem II
20.3: Plant Electron Transport and ATP Synthesis
20.4: CO_2 uptake - Calvin Cycle and C3 organisms
20.5: CO2 uptake - C4 and CAM Pathways
20.6: Biosynthesis of Starch, Sucrose and Cellulose
photosynthetic bacteria
20.1: Light Absorption in Photosynthesis - An Overview
photosynthetic processes
20.3: Plant Electron Transport and ATP Synthesis
photosystem I
20.1: Light Absorption in Photosynthesis - An Overview
20.2: The Kok Cycle and Oxygen Evolving Complex of Photosystem II
photosystem II
20.1: Light Absorption in Photosynthesis - An Overview
20.2: The Kok Cycle and Oxygen Evolving Complex of Photosystem II
physiological conditions
17.3: Ketone Bodies
physiological implications
18.5: Pathways of Amino Acid Degradation
physiological significance
20.5: CO2 uptake - C4 and CAM Pathways
plant biochemistry
20.5: CO2 uptake - C4 and CAM Pathways
plant biology
20.6: Biosynthesis of Starch, Sucrose and Cellulose
plant cell structure
20.6: Biosynthesis of Starch, Sucrose and Cellulose
plant growth
18.1: The Biochemistry of Nitrogen in the Biosphere
plant metabolism
20.4: CO_2 uptake - Calvin Cycle and C3 organisms
20.5: CO2 uptake - C4 and CAM Pathways
20.6: Biosynthesis of Starch, Sucrose and Cellulose
plant nutrition
18.1: The Biochemistry of Nitrogen in the Biosphere
plastocyanin
20.2: The Kok Cycle and Oxygen Evolving Complex of Photosystem II
plastoquinone
20.2: The Kok Cycle and Oxygen Evolving Complex of Photosystem II
polyunsaturated fatty acids
21.1: Biosynthesis of Fatty Acids and Eicosanoids
PPDK conformational changes
20.5: CO2 uptake - C4 and CAM Pathways
PPP
13.4: Pentose Phosphate Pathway of Glucose Oxidation
primary productivity
18.1: The Biochemistry of Nitrogen in the Biosphere
product inhibition
14.1: Regulation of Metabolic Pathways
protein complexes
19.1: Electron-Transfer Reactions in Mitochondria
protein digestion
18.2: Metabolic Fates of Amino Groups
protein expression
13.2: Fates of Pyruvate under Anaerobic Conditions-Fermentation
protein oxidation
12.3: The Chemistry and Biochemistry of Dioxygen
protein phosphorylation
15.1: Insulin Signaling in the Liver
proteolysis
14.1: Regulation of Metabolic Pathways
proton gradient
19.1: Electron-Transfer Reactions in Mitochondria
19.2: ATP Synthesis
19.3: Regulation of Oxidative Phosphorylation
20.2: The Kok Cycle and Oxygen Evolving Complex of Photosystem II
proton leak
19.3: Regulation of Oxidative Phosphorylation
proton motive force
19.2: ATP Synthesis
20.3: Plant Electron Transport and ATP Synthesis
proton translocation
19.3: Regulation of Oxidative Phosphorylation
pyrenoids
20.4: CO_2 uptake - Calvin Cycle and C3 organisms

pyridoxal phosphate
18.2: Metabolic Fates of Amino Groups
18.4: An Overview of Amino Acid Metabolism and the Role of Cofactors
pyruvate carboxylase
15.5: Regulation of Gluconeogenesis
pyruvate conversion
13.2: Fates of Pyruvate under Anaerobic Conditions-Fermentation
13.3: Gluconeogenesis
pyruvate dehydrogenase
16.1: Production of Acetyl-CoA (Activated Acetate)
16.2: Reactions of the Citric Acid Cycle
pyruvate dehydrogenase complex
16.3: Regulation of the Citric Acid Cycle
pyruvate kinase
15.4: Regulation of Glycolysis
pyruvate metabolism
16.1: Production of Acetyl-CoA (Activated Acetate)
pyruvate orthophosphate dikinase
20.5: CO2 uptake - C4 and CAM Pathways
pyruvate synthesis
13.1: Glycolysis
Pyuvate carboxylase
13.3: Gluconeogenesis

Q

quantitative tools
14.3: The Flux Control Coefficient
quantum mechanics
20.1: Light Absorption in Photosynthesis - An Overview

R

reaction center
20.1: Light Absorption in Photosynthesis - An Overview
reaction diagrams
12.1: Biochemical Reactions and Energy Changes
reaction intermediates
12.1: Biochemical Reactions and Energy Changes
reaction mechanisms
12.1: Biochemical Reactions and Energy Changes
12.2: Phosphoryl Group Transfers and ATP
12.4: Biological Oxidation-Reduction Reactions
18.1: The Biochemistry of Nitrogen in the Biosphere
reaction pathways
12.1: Biochemical Reactions and Energy Changes
reaction rates
14.5: Metabolism and Signaling: The Steady State, Adaptation and Homeostasis
reactive nitrogen species
19.3: Regulation of Oxidative Phosphorylation
reactive oxygen species
12.3: The Chemistry and Biochemistry of Dioxygen
13.2: Fates of Pyruvate under Anaerobic Conditions-Fermentation
19.1: Electron-Transfer Reactions in Mitochondria
19.3: Regulation of Oxidative Phosphorylation
20.1: Light Absorption in Photosynthesis - An Overview
reciprocal regulation
15.4: Regulation of Glycolysis
redox balance
13.4: Pentose Phosphate Pathway of Glucose Oxidation
16.1: Production of Acetyl-CoA (Activated Acetate)
16.2: Reactions of the Citric Acid Cycle
redox chemistry
18.1: The Biochemistry of Nitrogen in the Biosphere
redox reactions
12.1: Biochemical Reactions and Energy Changes
12.4: Biological Oxidation-Reduction Reactions
14.1: Regulation of Metabolic Pathways
19.1: Electron-Transfer Reactions in Mitochondria
20.1: Light Absorption in Photosynthesis - An Overview
reduced state
20.3: Plant Electron Transport and ATP Synthesis
Reduction
12.3: The Chemistry and Biochemistry of Dioxygen
Refsum disease
17.2: Oxidation of Fatty Acids
regulation
17.2: Oxidation of Fatty Acids
19.3: Regulation of Oxidative Phosphorylation
20.1: Light Absorption in Photosynthesis - An Overview
regulation mechanisms
13.4: Pentose Phosphate Pathway of Glucose Oxidation
regulation of lipid synthesis
21.2: Biosynthesis of Triacylglycerols
regulatory enzymes
13.1: Glycolysis
15.5: Regulation of Gluconeogenesis
regulatory mechanisms
14.4: Concentration Control and Elasticity Coefficients
21.1: Biosynthesis of Fatty Acids and Eicosanoids
regulatory motifs
14.5: Metabolism and Signaling: The Steady State, Adaptation and Homeostasis
resonance
12.1: Biochemical Reactions and Energy Changes
resonance energy transfer
20.1: Light Absorption in Photosynthesis - An Overview
respirasomes
19.1: Electron-Transfer Reactions in Mitochondria
reverse cholesterol transport
17.1: Digestion, Mobilization, and Transport of Fats
RNA degradation
14.1: Regulation of Metabolic Pathways
ROS
12.3: The Chemistry and Biochemistry of Dioxygen
rubisco
20.4: CO_2 uptake - Calvin Cycle and C3 organisms
20.5: CO2 uptake - C4 and CAM Pathways

S

scavenger receptors
12.3: The Chemistry and Biochemistry of Dioxygen
serine glycine cycle
18.4: An Overview of Amino Acid Metabolism and the Role of Cofactors
sigmoidal curves
14.5: Metabolism and Signaling: The Steady State, Adaptation and Homeostasis
signal transduction
12.2: Phosphoryl Group Transfers and ATP
14.5: Metabolism and Signaling: The Steady State, Adaptation and Homeostasis
signaling pathways
14.5: Metabolism and Signaling: The Steady State, Adaptation and Homeostasis
singlet oxygen
12.3: The Chemistry and Biochemistry of Dioxygen
slippage
19.3: Regulation of Oxidative Phosphorylation
solar energy conversion
20.1: Light Absorption in Photosynthesis - An Overview
Sphingolipid Biosynthesis
21.4: Biosynthesis of Membrane Sphingolipids
sphingolipids
21.4: Biosynthesis of Membrane Sphingolipids
standard reduction potential
12.4: Biological Oxidation-Reduction Reactions
starch storage
20.6: Biosynthesis of Starch, Sucrose and Cellulose
starch synthesis
20.6: Biosynthesis of Starch, Sucrose and Cellulose
steady state
14.2: Basic Principles of Metabolic Control Analysis (MCA)
14.5: Metabolism and Signaling: The Steady State, Adaptation and Homeostasis
stereochemistry
13.2: Fates of Pyruvate under Anaerobic Conditions-Fermentation
Steroid Biosynthesis
21.5: Biosynthesis of Cholesterol and Steroids
steroid hormones
21.5: Biosynthesis of Cholesterol and Steroids
Stn8 kinase
20.1: Light Absorption in Photosynthesis - An Overview
stoichiometry
18.1: The Biochemistry of Nitrogen in the Biosphere
structural biochemistry
16.1: Production of Acetyl-CoA (Activated Acetate)
structural biology
20.2: The Kok Cycle and Oxygen Evolving Complex of Photosystem II
structural components
20.1: Light Absorption in Photosynthesis - An Overview
substrate availability
14.1: Regulation of Metabolic Pathways
substrate channeling
21.1: Biosynthesis of Fatty Acids and Eicosanoids
substrate specificity
21.2: Biosynthesis of Triacylglycerols
sucrose metabolism
20.6: Biosynthesis of Starch, Sucrose and Cellulose

sucrose synthesis
20.6: Biosynthesis of Starch, Sucrose and Cellulose
summation theorem
14.3: The Flux Control Coefficient
superoxide
12.3: The Chemistry and Biochemistry of Dioxygen
symport
12.2: Phosphoryl Group Transfers and ATP
systems biology
14.2: Basic Principles of Metabolic Control Analysis (MCA)

T

TCA cycle
16.1: Production of Acetyl-CoA (Activated Acetate)
tetrahydrofolate
18.4: An Overview of Amino Acid Metabolism and the Role of Cofactors
thermodynamic comparison
20.5: CO2 uptake - C4 and CAM Pathways
thermodynamics
12.1: Biochemical Reactions and Energy Changes
12.2: Phosphoryl Group Transfers and ATP
14.1: Regulation of Metabolic Pathways
19.2: ATP Synthesis
thermogenesis
19.3: Regulation of Oxidative Phosphorylation
thiamine pyrophosphate
16.1: Production of Acetyl-CoA (Activated Acetate)
thylakoids
20.1: Light Absorption in Photosynthesis - An Overview
transaldolase
13.4: Pentose Phosphate Pathway of Glucose Oxidation
transaminases
18.2: Metabolic Fates of Amino Groups
transamination
18.3: Nitrogen Excretion and the Urea Cycle
18.5: Pathways of Amino Acid Degradation
transcriptional regulation
14.1: Regulation of Metabolic Pathways
transferrin
12.3: The Chemistry and Biochemistry of Dioxygen
transketolase
13.4: Pentose Phosphate Pathway of Glucose Oxidation
translational control
14.1: Regulation of Metabolic Pathways
transport proteins
12.2: Phosphoryl Group Transfers and ATP
triacylglycerides
17.1: Digestion, Mobilization, and Transport of Fats
triacylglycerol
21.2: Biosynthesis of Triacylglycerols
triacylglycerol biosynthesis
21.2: Biosynthesis of Triacylglycerols
tricarboxylic acid cycle
16.2: Reactions of the Citric Acid Cycle
triglycerides
15.4: Regulation of Glycolysis
17.1: Digestion, Mobilization, and Transport of Fats
triplet oxygen
12.3: The Chemistry and Biochemistry of Dioxygen
tyrosine 161
20.1: Light Absorption in Photosynthesis - An Overview

U

ubiquinone
19.1: Electron-Transfer Reactions in Mitochondria
uncoupling
19.3: Regulation of Oxidative Phosphorylation
uncoupling proteins
19.3: Regulation of Oxidative Phosphorylation
urea cycle
18.2: Metabolic Fates of Amino Groups
18.3: Nitrogen Excretion and the Urea Cycle
18.5: Pathways of Amino Acid Degradation

W

Warburg Effect
14.3: The Flux Control Coefficient
water oxidation
20.2: The Kok Cycle and Oxygen Evolving Complex of Photosystem II

Y

yeast glycolysis
14.3: The Flux Control Coefficient

Z

Z scheme
20.2: The Kok Cycle and Oxygen Evolving Complex of Photosystem II
Zellweger syndrome
17.2: Oxidation of Fatty Acids

GLOSSARY

Anaplerotic reactions | Chemical reactions that form intermediates of a metabolic pathway.

citric acid cycle | The citric acid cycle (CAC) – also known as the TCA cycle (tricarboxylic acid cycle) or the Krebs cycle – is a series of chemical reactions used by all aerobic organisms to release stored energy through the oxidation of acetyl-CoA derived from carbohydrates, fats, and proteins. In addition, the cycle provides precursors of certain amino acids, as well as the reducing agent NADH, that are used in numerous other reactions. [Wikipedia]

FISH | Fluorescence in situ hybridization is a cytogenetic technique used to detect and localize the specific DNA or RNA sequences. [boundless]

fluorescence | The emission of light (or other electromagnetic radiation) by a material when stimulated by the absorption of radiation or of a subatomic particle [boundless]

GABA | Gamma-Aminobutyric acid is the chief inhibitory neurotransmitter in the developmentally mature mammalian central nervous system. Its principal role is reducing neuronal excitability throughout the nervous system. [Wikipedia]

GABA shunt | The GABA shunt a closed loop that is involved in the production and conservation of the pool of GABA.

glyoxylate Shunt | The glyoxylate shunt is a two-step metabolic pathway (via isocitrate lyase, aceA and malate synthase, glcB) as an alternative to the citric acid cycle.

hybridize | To combine complementary subunits of multiple biological macromolecules. [boundless]

Krebs cycle | The citric acid cycle (CAC) – also known as the TCA cycle (tricarboxylic acid cycle) or the Krebs cycle – is a series of chemical reactions used by all aerobic organisms to release stored energy through the oxidation of acetyl-CoA derived from carbohydrates, fats, and proteins. In addition, the cycle provides precursors of certain amino acids, as well as the reducing agent NADH, that are used in numerous other reactions. [Wikipedia]

Pyruvate Dehydrogenase | Pyruvate dehydrogenase is an enzyme that catalyzes the reaction of pyruvate and a lipoamide to give the acetylated dihydrolipoamide and carbon dioxide. The conversion requires the coenzyme thiamine pyrophosphate. [Wikipedia]

TCA cycle | The citric acid cycle (CAC) – also known as the TCA cycle (tricarboxylic acid cycle) or the Krebs cycle – is a series of chemical reactions used by all aerobic organisms to release stored energy through the oxidation of acetyl-CoA derived from carbohydrates, fats, and proteins. In addition, the cycle provides precursors of certain amino acids, as well as the reducing agent NADH, that are used in numerous other reactions. [Wikipedia]

- **Glossary** has no license indicated.

Detailed Licensing

Overview

Title: Fundamentals of Biochemistry Vol. II - Bioenergetics and Metabolism

Webpages: 71

Applicable Restrictions: Noncommercial

All licenses found:

- Undeclared: 91.5% (65 pages)
- CC BY-SA 4.0: 2.8% (2 pages)
- CC BY-NC-SA 4.0: 2.8% (2 pages)
- CC BY 4.0: 2.8% (2 pages)

By Page

- Fundamentals of Biochemistry Vol. II - Bioenergetics and Metabolism - *CC BY-SA 4.0*
  - Front Matter - *Undeclared*
    - TitlePage - *Undeclared*
    - InfoPage - *Undeclared*
    - Table of Contents - *Undeclared*
    - Licensing - *Undeclared*
    - About the Authors - *Undeclared*
  - 12: Bioenergetics and Biochemical Reaction Types - *Undeclared*
    - 12.1: Biochemical Reactions and Energy Changes - *Undeclared*
    - 12.2: Phosphoryl Group Transfers and ATP - *Undeclared*
    - 12.3: The Chemistry and Biochemistry of Dioxygen - *Undeclared*
    - 12.4: Biological Oxidation-Reduction Reactions - *Undeclared*
  - 13: Glycolysis, Gluconeogenesis, and the Pentose Phosphate Pathway - *Undeclared*
    - 13.1: Glycolysis - *Undeclared*
    - 13.2: Fates of Pyruvate under Anaerobic Conditions-Fermentation - *Undeclared*
    - 13.3: Gluconeogenesis - *CC BY-SA 4.0*
    - 13.4: Pentose Phosphate Pathway of Glucose Oxidation - *Undeclared*
  - 14: Principles of Metabolic Regulation - *Undeclared*
    - 14.1: Regulation of Metabolic Pathways - *Undeclared*
    - 14.2: Basic Principles of Metabolic Control Analysis (MCA) - *Undeclared*
    - 14.3: The Flux Control Coefficient - *Undeclared*
    - 14.4: Concentration Control and Elasticity Coefficients - *Undeclared*
    - 14.5: Metabolism and Signaling: The Steady State, Adaptation and Homeostasis - *Undeclared*
  - 15: Glucose, Glycogen, and Their Metabolic Regulation - *Undeclared*
    - 15.1: Insulin Signaling in the Liver - *Undeclared*
    - 15.2: Glycogenesis - *Undeclared*
    - 15.3: Glycogenolysis and its Regulation by Glucagon and Epinephrine Signaling - *CC BY-NC-SA 4.0*
    - 15.4: Regulation of Glycolysis - *Undeclared*
    - 15.5: Regulation of Gluconeogenesis - *Undeclared*
  - 16: The Citric Acid Cycle - *Undeclared*
    - 16.1: Production of Acetyl-CoA (Activated Acetate) - *Undeclared*
    - 16.2: Reactions of the Citric Acid Cycle - *Undeclared*
    - 16.3: Regulation of the Citric Acid Cycle - *Undeclared*
    - 16.4: Variants of the Citric Acid Cycle - *Undeclared*
  - 17: Fatty Acid Catabolism - *Undeclared*
    - 17.1: Digestion, Mobilization, and Transport of Fats - *Undeclared*
    - 17.2: Oxidation of Fatty Acids - *CC BY 4.0*
    - 17.3: Ketone Bodies - *CC BY 4.0*
  - 18: Nitrogen - Amino Acid Catabolism - *Undeclared*
    - 18.1: The Biochemistry of Nitrogen in the Biosphere - *Undeclared*
    - 18.2: Metabolic Fates of Amino Groups - *Undeclared*
    - 18.3: Nitrogen Excretion and the Urea Cycle - *Undeclared*
    - 18.4: An Overview of Amino Acid Metabolism and the Role of Cofactors - *Undeclared*
    - 18.5: Pathways of Amino Acid Degradation - *Undeclared*
  - 19: Oxidative Phosphorylation - *Undeclared*

- 19.1: Electron-Transfer Reactions in Mitochondria - *Undeclared*
- 19.2: ATP Synthesis - *Undeclared*
- 19.3: Regulation of Oxidative Phosphorylation - *Undeclared*

- 20: Photosynthesis and Carbohydrate Synthesis in Plants - *Undeclared*
  - 20.1: Light Absorption in Photosynthesis - An Overview - *Undeclared*
  - 20.2: The Kok Cycle and Oxygen Evolving Complex of Photosystem II - *Undeclared*
  - 20.3: Plant Electron Transport and ATP Synthesis - *Undeclared*
  - 20.4: CO_2 uptake - Calvin Cycle and C3 organisms - *CC BY-NC-SA 4.0*
  - 20.5: CO2 uptake - C4 and CAM Pathways - *Undeclared*
  - 20.6: Biosynthesis of Starch, Sucrose and Cellulose - *Undeclared*
- 21: Lipid Biosynthesis - *Undeclared*
  - 21.1: Biosynthesis of Fatty Acids and Eicosanoids - *Undeclared*
  - 21.2: Biosynthesis of Triacylglycerols - *Undeclared*
  - 21.3: Biosynthesis of Membrane Glycerolipids - *Undeclared*
  - 21.4: Biosynthesis of Membrane Sphingolipids - *Undeclared*
  - 21.5: Biosynthesis of Cholesterol and Steroids - *Undeclared*
  - 21.6: Biosynthesis and Metabolism of Isoprenoids - *Undeclared*
- 22: Biosynthesis of Amino Acids, Nucleotides, and Related Molecules - *Undeclared*
  - 22.1: Overview of Nitrogen Metabolism - Nitrogenase - *Undeclared*
  - 22.2: Biosynthesis of Amino Acids - *Undeclared*
  - 22.3: Molecules Derived from Amino Acids - *Undeclared*
  - 22.4: Biosynthesis and Degradation of Nucleotides - *Undeclared*
- Back Matter - *Undeclared*
  - Index - *Undeclared*
  - Glossary - *Undeclared*
  - Detailed Licensing - *Undeclared*